SYNTHESIS OF STEREOENRICHED POLYCYCLIC SCAFFOLDS VIA PALLADIUM ENOLATES AND PROGRESS TOWARD THE TOTAL SYNTHESIS OF HYPERMOIN A

Thesis by

Ruby Pengjui Chen

In Partial Fulfillment of the Requirements

for the Degree of

Doctor of Philosophy



CALIFORNIA INSTITUTE OF TECHNOLOGY

Pasadena, California

2026

(Defended April 20, 2026)

© 2026

Ruby Pengjui Chen
ORCID: 0000-0002-3594-0081

All Rights Reserved

Dedicated to

my family, friends, and mentors

ACKNOWLEDGEMENTS

Writing the acknowledgments for my PhD thesis feels somewhat surreal. This challenging but immensely fruitful journey would not have been possible without the incredible support and guidance from so many people.

First and foremost, I want to thank my advisor, Professor Brian Stoltz. I truly could not have asked for a better mentor. Brian is an exceptionally talented and enthusiastic scientist who generously shares his wisdom, guiding his students through the inevitable challenges of graduate school. I am incredibly grateful for the research freedom he afforded me, which allowed me to explore diverse areas of chemistry and transformed me in ways I never expected before arriving at Caltech. Beyond chemistry, I deeply appreciate Brian's constant encouragement, his invaluable advice, and the great conversations we've shared. It is a rare privilege to work for an advisor who is genuinely invested in your personal well-being and professional success. I have never once regretted my decision to pursue my PhD at Caltech, and joining the Stoltz group has been the highlight of that experience. The opportunities, the education, and the welcoming environment that Brian has fostered made my time here so remarkable.

I am deeply grateful to Professor William (Bill) Goddard for serving as an invaluable second advisor in theoretical and computational chemistry. Having started my PhD with minimal experience in computational chemistry, I found Bill's mentorship to be truly transformative. I have learned an immense amount from his contagious enthusiasm and from our scientific meetings diving into computational work. I would also like to extend my sincere gratitude to my thesis committee. Professor Gregory Fu has been a very supportive committee chair, and his brilliant intellect and scientific rigor have continually

inspired me. Finally, I thank Professor Sarah Reisman for serving on my committee and for the insightful scientific discussions we have shared, both during my committee meetings and beyond.

I have received immense help from many staff members, without whom the research that I have performed would have been impossible. I am grateful for all the help I have received from Dr. Scott Virgil on various instruments on the third floor and on mass spectrometry. I would also like to thank Dr. David Vander Velde and Dr. Rajan Paranji for maintaining and running the NMR facility, Dr. Michael Takase for running the X-ray facility, and Dr. Mona Shahgholi for her expertise in mass spectrometry. I appreciate all the administrative help from Tomomi Kano and Beth Marshall throughout the past years.

During my time in the Stoltz lab, I have had the privilege of working alongside many fantastic chemists. I owe a huge thank you to Professor Alexander Cusumano and Dr. Kaylin Flesch, who were my rotation buddies and early mentors during my first year. Cus was a wonderful teacher who introduced me to the applications of computational chemistry in organic synthesis. Beyond being an inspiring mentor and project partner, he has been an understanding friend, and I will always appreciate his wise words and grad school survival tips. Kali is one of the kindest people I have ever met and played a fundamental role in my decision to join the lab. I am deeply grateful for our scientific discussions and her emotional support through both lab and life challenges, and I feel incredibly fortunate to have partnered with her on multiple projects throughout my graduate career.

I must also thank the rest of the [4+2] Diels–Alder “Corgi” team: Christian Strong and Emily Du. I vividly remember Cus joking “we really messed up putting two trolls on

the same project," once he realized how weird Christian and I were. Christian is an amazing chemist and an awesome person to talk to about absolutely anything. He consistently brings positive energy to the lab, and I will miss our random chats, scientific discussions, and our wild hypotheses.

In addition to Cus, I also had the pleasure of working with Drs Veronica Hubble and Stephen Sardini on the branched-selective alkylation project. Although I joined the project at a rather late stage, they were extremely welcoming and supportive. I appreciate all the discussions we've had, and their scientific vision and chemical intuition are amazing and have been something that I have always looked up to. I am also deeply grateful for all the career advice that I have received from them. It's interesting how the three of us have ended up in the same company and I can't wait to be colleagues with Veronica again when I start my job.

Finally, I have had the absolute pleasure of tackling the total synthesis of hypermoin A alongside "team grizzly": Kali, Madison Patch, Jameel Ahmad, Dr. Vaishnavi Nair, Zoe Grogan, and Sydney Bottcher. Working with such an incredible group of chemists has been a true privilege, and I am continually inspired by the creative ideas everyone brings to the table as the work advances. I feel especially fortunate that a chemist as talented as Madie joined the effort, and I cannot wait to see how this synthesis will be brought to the finish line.

I would also like to extend my thanks to all the members of the Stoltz and Reisman groups who have made my time here so memorable. A special thank you goes to Drs. Adrian Samkian and Kevin Gonzalez for their invaluable scientific discussions, helpful advice, and entertaining chats. I was incredibly fortunate to join Caltech as part of an

amazing cohort: Dr. Benjamin Gross, Kim Sharp, Christian Strong, Cami Suarez, Hao Yu, Marva Tariq, Ángel Hernández-Mejías, Matt Wong, and Yueming Long. I am deeply grateful for their friendship and unwavering support over the years. I also want to thank Omar Santiago Reyes for our collaboration on a palladium project, as he was such a fun and supportive person to work alongside. Finally, I am so thankful for the newer members of the lab, including Adrian de Almenara, Chloe Cerione, Jonathan Farhi, Bryce Gaskin, Sara Siddiqui, Eli Gonzalez, Madie Patch, Sean Corman, and Weicheng Xu. It has been a joy to share both scientific discussions and fun moments with all of them, and I cannot wait to see all the great things they will accomplish in the future.

My undergraduate research experience in the Burke lab at UIUC was incredibly inspiring, and I am deeply grateful for the mentorship and guidance I received from Professor Martin Burke. He was exceptionally generous to take a chance on a freshman undergraduate, and I deeply appreciate his continued support long after I left his lab. I must also express my sincere gratitude to my day-to-day mentors, Professor Daniel Blair and Dr. Andrew Blake. They not only introduced me to fundamental laboratory techniques and shared invaluable experimental tips, but they also provided the intellectual freedom to generate my own ideas and explore creative approaches. The foundational training they provided has remained crucial to my development as a scientist throughout my graduate career.

Beyond the lab, I have many friends to thank for their support throughout graduate school. I have always looked forward to sharing life updates and talking about grad school life with Elizabeth Murphy and Justin Ngai, my chemistry friends from college, and I'm so glad we stayed in touch. I am also immensely grateful for my food and tour group,

especially Will Chen, Eugene Li, and Stella Weng. They provided a tremendous amount of comfort during some of my darkest times, and I know I would not have made it to this point without them. I would also like to thank Jessica Yeh for her friendship and support. Finally, I want to thank my wonderful badminton community: Wenying Tang, Sherry Sun, Olive Cheng, Arabella Bai, Yunqing Wang, Shawn Yoshida, Ziyao Luo, and Jim Zhang. Hitting the courts, chatting about everything, getting food, and playing mahjong and random games with all of you was the absolute best way to decompress from research.

I want to thank my parents, Candy and Hermes, for their support throughout my PhD and everything that they have done for me. I appreciate all the snack items that they send me all the way from Taiwan, the suitcases packed with seafood when they come visit me, and the trips we were able to make in the US, Canada, and Europe. Pursuing a graduate degree so far away from home was challenging, and it would not have been possible without their love and support. Finally, my deepest thanks go to my boyfriend, Sean Hu, for being by my side and cheering me on through some of the toughest stages of graduate school and for his endless support during stressful times. I am grateful for all the adventures and fun moments we shared, and I am excited for the next steps of our lives together.

ABSTRACT

Research in the Stoltz lab is focused on the synergistic development of novel methodologies for the asymmetric formation of congested stereocenters and natural product total synthesis, while employing computations to aid mechanistic understanding. This thesis describes the development and mechanistic studies of novel asymmetric reactions from Pd enolates and progress toward the total synthesis of hypermoin A.

The first chapter details the development of an enantioselective intramolecular [4+2] cycloaddition from a chiral Pd enolate, allowing formation of highly stereoenriched polycyclic structures. Quantum mechanics calculations, Eyring analysis, and KIE studies allowed further mechanistic understanding of the reaction. The [4+2] cycloaddition was further investigated through molecular dynamics simulations, and studies of cyclohexenone-derived substrates are reported in chapter 2.

Chapter 3 describes the application of a chiral Pd enolate in an asymmetric intramolecular Michael spirocyclization, forging vicinal quaternary and tertiary stereocenters in a single step. Computational investigations provide mechanistic insights to the stereoselectivity of the process. In chapter 4, a branched-selective asymmetric decarboxylative allylic alkylation reaction is reported. The hypotheses informed by quantum mechanics calculations allow rational ligand design to achieve high regio-, diastereo-, and enantioselectivity in forming vicinal quaternary and tertiary stereocenters.

Chapter 5 outlines the ongoing progress toward the asymmetric total synthesis of hypermoin A. [2.2.2] bicycle formation through [4+2] cycloaddition or reductive Heck cyclization followed by ring expansion allows formation of a key [3.2.2] bicyclic core, and current efforts are focused on extending this approach to more elaborate substrates.

PUBLISHED CONTENT AND CONTRIBUTIONS

1. Flesch, K. N.‡; Cusumano, A. Q.‡; Chen. P.; Strong, C. S.; Sardini, S. R.; Du, Y. E.; Bartberger, M. D.; Goddard; W. A. III*; Stoltz, B. M. Divergent Catalysis: Catalytic Asymmetric [4+2] Cycloaddition of Palladium Enolates. *J. Am. Chem. Soc.* **2023**, *145*, 11301–11310. DOI: 10.1021/jacs.3c02104.

   R.P.C. participated in experimental work, computational investigations, data analysis, and manuscript preparation.

2. Chen, P.‡; Cusumano, A. Q.‡; Flesch, K. N.; Strong, C. S.; Goddard, W. A. III*; Stoltz, B. M.* Molecular Dynamics Investigation of Dienolate [4+2] Cycloadditions. *J. Am. Chem. Soc.* **2024**, *146*, 12758–12765. DOI: 10.1021/jacs.4c02681.

   R.P.C. participated in computational investigations, data analysis, and manuscript preparation.

3. Strong, C. S.; **Chen, P.**; Bissenali, S.; Goddard, W. A. III*; Stoltz, B. M.* Enantioselective Michael Spirocyclization of Palladium Enolates. *ACS Catal.* **2025***, 15,* 12231–12237. DOI*:* 10.1021/acscatal.5c02758.

   R.P.C. participated in computational investigations, data analysis, and manuscript preparation.

TABLE OF CONTENTS

Dedication iii
Acknowledgements iv
Abstract ix
Published Content and Contributions x
Table of Contents xi
List of Figures xv
List of Schemes xliv
List of Tables xlv
List of Abbreviations xlvi

CHAPTER 1 ***1***
Divergent Catalysis: Catalytic Asymmetric Intramolecular [4+2] Cycloaddition of Palladium Enolates

1.1 Introduction 1
1.2 Results and Discussion 3
1.2.1 Reaction Design and Optimization 3
1.2.2 Proposed Mechanism 9
1.2.3 Substrate Scope 10
1.2.4 [4+2] Cycloaddition 15
1.2.5 Catalyst Turnover 17
1.2.6 Further Mechanism-Based Developments 19
1.2.7 Product Derivatizations 21
1.3 Conclusions 23
1.4 Experimental Section 24
1.4.1 Materials and Methods 24
1.4.2 Experimental Procedures and Spectroscopic Data 25
1.4.3 Determination of Absolute and Relative Stereochemistry by VCD Spectroscopy 129
1.4.4 2D NMR Analysis of Select Compounds 154
1.4.5 General Computational Details 160
1.5 References and Notes 169

APPENDIX 1 ***181***
Spectra Relevant to Chapter 1

CHAPTER 2 ***413***
Molecular Dynamics Investigations of Dienolate [4+2] Reactions

2.1 Introduction 413
2.2 Experimental: Computational Methods....417
2.3 Results and Discussion....418
2.3.1 Reactions with Siloxy Dienes....420
2.3.2 Reactions of Conjugated Li Enolates....422
2.3.3 Reactions of Conjugated Pd Enolates 427
2.4 Conclusion....430
2.5 Experimental Section....431
2.5.1 General Notes – Quantum Mechanics Calculations 431
2.5.2 General Notes – Molecular Dynamics Simulations 433
2.5.3 Configuration and Parameters for Progdyn 434
2.5.4 Comparison of Computational Results from Different Functionals....436
2.6 References and Notes....439

CHAPTER 3 ***449***
Enantioselective Michael Spirocyclization of Palladium Enolates

3.1 Introduction 449
3.2 Results and Discussion....451
3.2.1 Reaction Optimization....451
3.2.2 Substrate Scope....452
3.2.3 Product Derivatization 454
3.2.4 Mechanistic Investigations 456
3.3 Conclusion....459
3.4 Experimental Section....460
3.4.1 Materials and Methods....460
3.4.2 Experimental Procedures and Spectroscopic Data....462
3.4.3 Computational Details 518
3.4.4 2D NMR Analysis of Select Compounds 526

3.5 References and Notes....530

APPENDIX 2 ***535***
Spectra Relevant to Chapter 3

CHAPTER 4 ***648***
A Pericyclic Strategy to the Enantio- and Diastereoselective Synthesis of Vicinal Quaternary/Tertiary Stereocenters from Chiral Palladium Enolates

4.1 Introduction....648
4.2 Results and Discussion....652
4.2.1 Reaction Design and Optimization....652
4.2.2 Substrate Scope and Product Derivatization....655
4.2.3 Inner-Sphere C–C Bond Formation....658
4.2.4 Reductive Elimination Pathways....660
4.2.5 Computational Investigation of Ligand Effects....662
4.3 Conclusion....666
4.4 Experimental Section....667
4.4.1 Materials and Methods....667
4.4.2 Experimental Procedures and Spectroscopic Data....668
4.4.3 Determination of Absolute and Relative Stereochemistry by VCD Spectroscopy....727
4.4.4 Computational Details....731
4.5 References and Notes....734

APPENDIX 3 ***743***
Spectra Relevant to Chapter 4

CHAPTER 5 ***880***
Progress Toward the Total Synthesis of Hypermoin A

5.1 Introduction....880
5.2 Retrosynthetic Analysis....884
5.3 Formation of the [3.2.2] Bicyclic Core....885
5.4 Summary and Future Directions....893
5.5 Experimental Section....895
5.5.1 Materials and Methods....895
5.5.2 Experimental Procedures and Spectroscopic Data....896

5.6 References 943

APPENDIX 4 ***947***
Spectra Relevant to Chapter 5

APPENDIX 5 ***1012***
Early Strategies Toward the Total Synthesis of Hypermoin A

A5.1 Introduction 1012
A5.2 Allylic Alkylation–Cyclization Sequence 1012
A5.3 Ring Expansion–Radical Cyclization Sequence 1015
A5.4 Investigation of [4+2] Cycloaddition Dienophiles....1018
A5.5 Experimental Section....1020
A5.5.1 Materials and Methods....1020
A5.5.2 Experimental Procedures and Spectroscopic Data....1021
A5.6 Preliminary X-ray crystallography analysis of **359**....1049
A5.7 References 1050

APPENDIX 6 ***1051***
Notebook Cross-Reference for New Compounds

ABOUT THE AUTHOR ***1058***

LIST OF FIGURES

CHAPTER 1

Divergent Catalysis: Catalytic Asymmetric Intramolecular [4+2] Cycloaddition of Palladium Enolates

Figure 1.1 Reactivity of chiral Pd enolates and proposed reaction 2

Figure 1.2 General reactivity paradigm from Pd enolate **13** 5

Figure 1.3 Sacrificial additives to enable catalyst turnover and additive-free reaction from prenyl ester **10a** 6

Figure 1.4 Eyring analysis of **11**/**19** product ratio for propylene and butylene tethered substrates **10a** and **10f** 13

Figure 1.5 Computational and experimental investigation of C–C bond formation 16

Figure 1.6 Computed lowest-energy pathways for catalyst turnover 18

Figure 1.7 KIE studies and modification of prenyl ester 20

Figure 1.8 Derivatization of [4+2] cycloadducts 22

Figure 1.9 Three diastereomers **11a**, **11q**, and **11q'** to be compared to spectra computed from all eight possible stereoisomers 131

Figure 1.10 Comparison of experimental VCD and IR spectra for product **11a** to computed spectra for **A_endo-trans** 132

Figure 1.11 Overlayed experimental and calculated VCD spectra for **11a** – assigned as ***ent*-A_endo-trans** 132

Figure 1.12 Comparison of experimental VCD and IR spectra for product **11a** to computed spectra for **A_exo-trans** 133

Figure 1.13 Comparison of experimental VCD and IR spectra for product **11a** to computed spectra for **A_endo-cis** 134

Figure 1.14 Comparison of experimental VCD and IR spectra for product **11a** to computed spectra for **A_exo-cis** 135

Figure 1.15 Comparison of experimental VCD and IR spectra for product **11q** to computed spectra for **A_endo-trans** 136

Figure 1.16 Comparison of experimental VCD and IR spectra for product **11q** to computed spectra for **A_exo-trans** 137

Figure 1.17 Comparison of experimental VCD and IR spectra for product **11q** to computed spectra for **A_endo-cis** 138

Figure 1.18 Overlayed experimental and calculated VCD spectra for **11q** – assigned as ***ent*-A_endo-cis**.....139
Figure 1.19 Comparison of experimental VCD and IR spectra for product **11q** to computed spectra for **A_exo-cis**.....139
Figure 1.20 Comparison of experimental VCD and IR spectra for product **11q'** to computed spectra for **A_endo-trans**.....140
Figure 1.21 Comparison of experimental VCD and IR spectra for product **11q'** to computed spectra for **A_exo-trans**.....141
Figure 1.22 Comparison of experimental VCD and IR spectra for product **11q'** to computed spectra for **A_endo-cis**.....142
Figure 1.23 Comparison of experimental VCD and IR spectra for product **11q'** to computed spectra for **A_exo-cis**.....143
Figure 1.24 Overlayed experimental and calculated VCD spectra for **11q'** – assigned as ***ent*-A_exo-cis**.....144
Figure 1.25 Three diastereomers **11k**, **11k'**, and **11k''** to be compared to spectra computed from all eight possible stereoisomers.....144
Figure 1.26 Experimental VCD and IR spectra for product **11k** compared to computed spectra for **B_endo-trans**.....145
Figure 1.27 Overlayed experimental and calculated VCD spectra for **11k** – assigned as **B_endo-trans**.....145
Figure 1.28 Experimental VCD and IR spectra for product **11k** compared to computed spectra for **B_exo-trans**.....146
Figure 1.29 Experimental VCD and IR spectra for product **11k** compared to computed spectra for **B_endo-cis**.....147
Figure 1.30 Experimental VCD and IR spectra for product **11k** compared to computed spectra for **B_exo-cis**.....148
Figure 1.31 Experimental IR spectrum for product **11k'** compared to computed spectra for isomers of **B**.....149
Figure 1.32 Experimental VCD and IR spectra for product **11k''** compared to computed spectra for **B_endo-trans**.....150
Figure 1.33 Experimental VCD and IR spectra for product **11k''** compared to computed spectra for **B_exo-trans**.....151
Figure 1.34 Experimental VCD and IR spectra for product **11k''** compared to computed spectra for **B_endo-cis**.....152

Figure 1.35 Overlayed experimental and calculated VCD spectra for **11k''** – assigned as **B_endo-cis** 153
Figure 1.36 Experimental VCD and IR spectra for product **11k''** compared to computed spectra for **B_exo-cis**..... 153
Figure 1.37 ^{1}H-^{1}H COSY NMR spectrum of **11a** (400 MHz, $CDCl_3$) 154
Figure 1.38 ^{1}H-^{13}C HSQC NMR spectrum of **11a** (400 MHz, $CDCl_3$) 154
Figure 1.39 ^{1}H-^{1}H NOESY NMR spectrum of **11a** (400 MHz, $CDCl_3$). 155
Figure 1.40 ^{1}H-^{1}H COSY NMR spectrum of **11p** (400 MHz, $CDCl_3$) 155
Figure 1.41 ^{1}H-^{13}C HSQC NMR spectrum of **11p** (400 MHz, $CDCl_3$) 156
Figure 1.42 ^{1}H-^{1}H NOESY NMR spectrum of **11p** (400 MHz, $CDCl_3$) 156
Figure 1.43 ^{1}H-^{1}H COSY NMR spectrum of **11q** (400 MHz, $CDCl_3$) 157
Figure 1.44 ^{1}H-^{13}C HSQC NMR spectrum of **11q** (400 MHz, $CDCl_3$) 157
Figure 1.45 ^{1}H-^{1}H NOESY NMR spectrum of **11q** (400 MHz, $CDCl_3$) 158
Figure 1.46 ^{1}H-^{1}H COSY NMR spectrum of **11q'** (400 MHz, $CDCl_3$) 158
Figure 1.47 ^{1}H-^{13}C HSQC NMR spectrum of **11q'** (400 MHz, $CDCl_3$) 159
Figure 1.48 ^{1}H-^{1}H NOESY NMR spectrum of **11q'** (400 MHz, $CDCl_3$) 159
Figure 1.49 Relative free energies for various inner-sphere reductive elimination transition states from allyl (**85**), cinnamyl (**86**), and prenyl (**87**) complexes 163
Figure 1.50 Relative free energies for various proton transfer transition states from post-cycloaddition enolate **26** 164
Figure 1.51 Relative free energies for various proton transfer transition states from pre-cycloaddition enolate **25** 165
Figure 1.52 IBO analysis of N-detached inner-sphere mechanism and corresponding derived arrow-pushing mechanism..... 166
Figure 1.53 Computed pKa values of cationic π-allyl Pd complex **88** and ketones **19a** and **11a**. 167
Figure 1.54 Comparison of internal versus external dienophile approach to both enantiotopic diene faces, select low energy conformers of **TS3** and space filling models..... 168

APPENDIX 1

Spectra Relevant to Chapter 1

Figure A1.1 ^{1}H NMR (400 MHz, $CDCl_3$) of compound **11a** 182
Figure A1.2 Infrared spectrum (Thin Film, NaCl) of compound **11a** 183
Figure A1.3 ^{13}C NMR (100 MHz, $CDCl_3$) of compound **11a**..... 183
Figure A1.4 ^{1}H NMR (400 MHz, $CDCl_3$) of compound **11b** 184

Figure A1.5 Infrared spectrum (Thin Film, NaCl) of compound **11b** 185
Figure A1.6 ^{13}C NMR (100 MHz, $CDCl_3$) of compound **11b** 185
Figure A1.7 ^{1}H NMR (400 MHz, $CDCl_3$) of compound **11c** 186
Figure A1.8 Infrared spectrum (Thin Film, NaCl) of compound **11c** 187
Figure A1.9 ^{13}C NMR (100 MHz, $CDCl_3$) of compound **11c** 187
Figure A1.10 ^{1}H NMR (400 MHz, $CDCl_3$) of compound **11d** 188
Figure A1.11 Infrared spectrum (Thin Film, NaCl) of compound **11d** 189
Figure A1.12 ^{13}C NMR (100 MHz, $CDCl_3$) of compound **11d** 189
Figure A1.13 ^{1}H NMR (400 MHz, $CDCl_3$) of compound **11f** 190
Figure A1.14 Infrared spectrum (Thin Film, NaCl) of compound **11f** 191
Figure A1.15 ^{13}C NMR (100 MHz, $CDCl_3$) of compound **11f** 191
Figure A1.16 ^{1}H NMR (400 MHz, $CDCl_3$) of compound **11j** 192
Figure A1.17 Infrared spectrum (Thin Film, NaCl) of compound **11j** 193
Figure A1.18 ^{13}C NMR (100 MHz, $CDCl_3$) of compound **11j** 193
Figure A1.19 ^{1}H NMR (400 MHz, $CDCl_3$) of compound **11k** 194
Figure A1.20 Infrared spectrum (Thin Film, NaCl) of compound **11k** 195
Figure A1.21 ^{13}C NMR (100 MHz, $CDCl_3$) of compound **11k** 195
Figure A1.22 ^{1}H NMR (400 MHz, $CDCl_3$) of compound **11k'** 196
Figure A1.23 Infrared spectrum (Thin Film, NaCl) of compound **11k'** 197
Figure A1.24 ^{13}C NMR (100 MHz, $CDCl_3$) of compound **11k'** 197
Figure A1.25 ^{1}H NMR (400 MHz, $CDCl_3$) of compound **11k''** 198
Figure A1.26 Infrared spectrum (Thin Film, NaCl) of compound **11k''** 199
Figure A1.27 ^{13}C NMR (100 MHz, $CDCl_3$) of compound **11k''** 199
Figure A1.28 ^{1}H NMR (400 MHz, $CDCl_3$) of compound **11l** 200
Figure A1.29 Infrared spectrum (Thin Film, NaCl) of compound **11l** 201
Figure A1.30 ^{13}C NMR (100 MHz, $CDCl_3$) of compound **11l** 201
Figure A1.31 ^{1}H NMR (400 MHz, $CDCl_3$) of compound **11m** 202
Figure A1.32 Infrared spectrum (Thin Film, NaCl) of compound **11m** 203
Figure A1.33 ^{13}C NMR (100 MHz, $CDCl_3$) of compound **11m** 203
Figure A1.34 ^{1}H NMR (400 MHz, $CDCl_3$) of compound **11m'** 204
Figure A1.35 Infrared spectrum (Thin Film, NaCl) of compound **11m'** 205
Figure A1.36 ^{13}C NMR (100 MHz, $CDCl_3$) of compound **11m'** 205
Figure A1.37 ^{1}H NMR (400 MHz, $CDCl_3$) of compound **11n** 206
Figure A1.38 Infrared spectrum (Thin Film, NaCl) of compound **11n** 207
Figure A1.39 ^{13}C NMR (100 MHz, $CDCl_3$) of compound **11n** 207

Figure A1.40 ^{1}H NMR (400 MHz, $CDCl_3$) of compound **11o** 208
Figure A1.41 Infrared spectrum (Thin Film, NaCl) of compound **11o** 209
Figure A1.42 ^{13}C NMR (100 MHz, $CDCl_3$) of compound **11o** 209
Figure A1.43 ^{1}H NMR (400 MHz, $CDCl_3$) of compound **11o'** 210
Figure A1.44 Infrared spectrum (Thin Film, NaCl) of compound **11o'** 211
Figure A1.45 ^{13}C NMR (100 MHz, $CDCl_3$) of compound **11o'** 211
Figure A1.46 ^{1}H NMR (400 MHz, $CDCl_3$) of compound **11p** 212
Figure A1.47 Infrared spectrum (Thin Film, NaCl) of compound **11p** 213
Figure A1.48 ^{13}C NMR (100 MHz, $CDCl_3$) of compound **11p** 213
Figure A1.49 ^{1}H NMR (400 MHz, $CDCl_3$) of compound **11p'** 214
Figure A1.50 Infrared spectrum (Thin Film, NaCl) of compound **11p'** 215
Figure A1.51 ^{13}C NMR (100 MHz, $CDCl_3$) of compound **11p'** 215
Figure A1.52 ^{1}H NMR (400 MHz, $CDCl_3$) of compound **11q** 216
Figure A1.53 Infrared spectrum (Thin Film, NaCl) of compound **11q** 217
Figure A1.54 ^{13}C NMR (100 MHz, $CDCl_3$) of compound **11q** 217
Figure A1.55 ^{1}H NMR (400 MHz, $CDCl_3$) of compound **11q'** 218
Figure A1.56 Infrared spectrum (Thin Film, NaCl) of compound **11q'** 219
Figure A1.57 ^{13}C NMR (100 MHz, $CDCl_3$) of compound **21q'** 219
Figure A1.58 ^{1}H NMR (400 MHz, $CDCl_3$) of compound **11r** 220
Figure A1.59 Infrared spectrum (Thin Film, NaCl) of compound **11r** 221
Figure A1.60 ^{13}C NMR (100 MHz, $CDCl_3$) of compound **11r** 221
Figure A1.61 ^{1}H NMR (400 MHz, $CDCl_3$) of compound **11s** 222
Figure A1.62 Infrared spectrum (Thin Film, NaCl) of compound **11s** 223
Figure A1.63 ^{13}C NMR (100 MHz, $CDCl_3$) of compound **11s** 223
Figure A1.64 ^{1}H NMR (400 MHz, $CDCl_3$) of compound **11t** 224
Figure A1.65 Infrared spectrum (Thin Film, NaCl) of compound **11t** 225
Figure A1.66 ^{13}C NMR (100 MHz, $CDCl_3$) of compound **11t** 225
Figure A1.67 ^{1}H NMR (400 MHz, $CDCl_3$) of compound **11t'** 226
Figure A1.68 Infrared spectrum (Thin Film, NaCl) of compound **11t'** 227
Figure A1.69 ^{13}C NMR (100 MHz, $CDCl_3$) of compound **11t'** 227
Figure A1.70 ^{1}H NMR (400 MHz, $CDCl_3$) of compound **11u** 228
Figure A1.71 Infrared spectrum (Thin Film, NaCl) of compound **11u** 229
Figure A1.72 ^{13}C NMR (100 MHz, $CDCl_3$) of compound **11u** 229
Figure A1.73 ^{1}H NMR (400 MHz, $CDCl_3$) of compound **D-11f** 230
Figure A1.74 Infrared spectrum (Thin Film, NaCl) of compound **D-11f** 231

Figure A1.75 ^{13}C NMR (100 MHz, $CDCl_3$) of compound **D-11f** 231
Figure A1.76 ^{2}H NMR (61 MHz, $CHCl_3$) of compound **D-11f** 232
Figure A1.77 ^{1}H NMR (400 MHz, $CDCl_3$) of compound **14** 233
Figure A1.78 Infrared spectrum (Thin Film, NaCl) of compound **14** 234
Figure A1.79 ^{13}C NMR (100 MHz, $CDCl_3$) of compound **14** 234
Figure A1.80 ^{1}H NMR (400 MHz, $CDCl_3$) of compound **10a** 235
Figure A1.81 Infrared spectrum (Thin Film, NaCl) of compound **10a** 236
Figure A1.82 ^{13}C NMR (100 MHz, $CDCl_3$) of compound **10a** 236
Figure A1.83 ^{1}H NMR (400 MHz, $CDCl_3$) of compound **10b** 237
Figure A1.84 Infrared spectrum (Thin Film, NaCl) of compound **10b** 238
Figure A1.85 ^{13}C NMR (100 MHz, $CDCl_3$) of compound **10b** 238
Figure A1.86 ^{1}H NMR (400 MHz, $CDCl_3$) of compound **10c** 239
Figure A1.87 Infrared spectrum (Thin Film, NaCl) of compound **10c** 240
Figure A1.88 ^{13}C NMR (100 MHz, $CDCl_3$) of compound **10c** 240
Figure A1.89 ^{1}H NMR (400 MHz, $CDCl_3$) of compound **10d** 241
Figure A1.90 Infrared spectrum (Thin Film, NaCl) of compound **10d** 242
Figure A1.91 ^{13}C NMR (100 MHz, $CDCl_3$) of compound **10d** 242
Figure A1.92 ^{1}H NMR (400 MHz, $CDCl_3$) of compound **10e** 243
Figure A1.93 Infrared spectrum (Thin Film, NaCl) of compound **10e** 244
Figure A1.94 ^{13}C NMR (100 MHz, $CDCl_3$) of compound **10e** 244
Figure A1.95 ^{1}H NMR (400 MHz, $CDCl_3$) of compound **10f** 245
Figure A1.96 Infrared spectrum (Thin Film, NaCl) of compound **10f** 246
Figure A1.97 ^{13}C NMR (100 MHz, $CDCl_3$) of compound **10f** 246
Figure A1.98 ^{1}H NMR (400 MHz, $CDCl_3$) of compound **D-10f** 247
Figure A1.99 Infrared spectrum (Thin Film, NaCl) of compound **D-10f** 248
Figure A1.100 ^{13}C NMR (100 MHz, $CDCl_3$) of compound **D-10f** 248
Figure A1.101 ^{2}H NMR (61 MHz, $CHCl_3$) of compound **D-10f** 249
Figure A1.102 ^{1}H NMR (400 MHz, $CDCl_3$) of compound **10g** 250
Figure A1.103 Infrared spectrum (Thin Film, NaCl) of compound **10g** 251
Figure A1.104 ^{13}C NMR (100 MHz, $CDCl_3$) of compound **10g** 251
Figure A1.105 ^{1}H NMR (400 MHz, $CDCl_3$) of compound **10h** 252
Figure A1.106 Infrared spectrum (Thin Film, NaCl) of compound **10h** 253
Figure A1.107 ^{13}C NMR (100 MHz, $CDCl_3$) of compound **10h** 253
Figure A1.108 ^{1}H NMR (400 MHz, $CDCl_3$) of compound **10i** 254
Figure A1.109 Infrared spectrum (Thin Film, NaCl) of compound **10i** 255

Figure A1.110 ^{13}C NMR (100 MHz, $CDCl_3$) of compound **10i** 255
Figure A1.111 ^{1}H NMR (400 MHz, $CDCl_3$) of compound **10j** 256
Figure A1.112 Infrared spectrum (Thin Film, NaCl) of compound **10j** 257
Figure A1.113 ^{13}C NMR (100 MHz, $CDCl_3$) of compound **10j** 257
Figure A1.114 ^{1}H NMR (400 MHz, $CDCl_3$) of compound **10k** 258
Figure A1.115 Infrared spectrum (Thin Film, NaCl) of compound **10k** 259
Figure A1.116 ^{13}C NMR (100 MHz, $CDCl_3$) of compound **10k** 259
Figure A1.117 ^{1}H NMR (400 MHz, $CDCl_3$) of compound **10l** 260
Figure A1.118 Infrared spectrum (Thin Film, NaCl) of compound **10l** 261
Figure A1.119 ^{13}C NMR (100 MHz, $CDCl_3$) of compound **10l** 261
Figure A1.120 ^{1}H NMR (400 MHz, $CDCl_3$) of compound **10m** 262
Figure A1.121 Infrared spectrum (Thin Film, NaCl) of compound **10m** 263
Figure A1.122 ^{13}C NMR (100 MHz, $CDCl_3$) of compound **10m** 263
Figure A1.123 ^{1}H NMR (400 MHz, $CDCl_3$) of compound **10n** 264
Figure A1.124 Infrared spectrum (Thin Film, NaCl) of compound **10n** 265
Figure A1.125 ^{13}C NMR (100 MHz, $CDCl_3$) of compound **10n** 265
Figure A1.126 ^{1}H NMR (400 MHz, $CDCl_3$) of compound **10o** 266
Figure A1.127 Infrared spectrum (Thin Film, NaCl) of compound **10o** 267
Figure A1.128 ^{13}C NMR (100 MHz, $CDCl_3$) of compound **10o** 267
Figure A1.129 ^{1}H NMR (400 MHz, $CDCl_3$) of compound **69** 268
Figure A1.130 Infrared spectrum (Thin Film, NaCl) of compound **69** 269
Figure A1.131 ^{13}C NMR (100 MHz, $CDCl_3$) of compound **69** 269
Figure A1.132 ^{1}H NMR (400 MHz, $CDCl_3$) of compound **10p** 270
Figure A1.133 Infrared spectrum (Thin Film, NaCl) of compound **10p** 271
Figure A1.134 ^{13}C NMR (100 MHz, $CDCl_3$) of compound **10p** 271
Figure A1.135 ^{1}H NMR (400 MHz, $CDCl_3$) of compound **10q** 272
Figure A1.136 Infrared spectrum (Thin Film, NaCl) of compound **10q** 273
Figure A1.137 ^{13}C NMR (100 MHz, $CDCl_3$) of compound **10q** 273
Figure A1.138 ^{1}H NMR (400 MHz, $CDCl_3$) of compound **10r** 274
Figure A1.139 Infrared spectrum (Thin Film, NaCl) of compound **10r** 275
Figure A1.140 ^{13}C NMR (100 MHz, $CDCl_3$) of compound **10r** 275
Figure A1.141 ^{1}H NMR (400 MHz, $CDCl_3$) of compound **10s** 276
Figure A1.142 Infrared spectrum (Thin Film, NaCl) of compound **10s** 277
Figure A1.143 ^{13}C NMR (100 MHz, $CDCl_3$) of compound **10s** 277
Figure A1.144 ^{1}H NMR (400 MHz, $CDCl_3$) of compound **10t** 278

Figure A1.145 Infrared spectrum (Thin Film, NaCl) of compound **10t**.....279
Figure A1.146 ^{13}C NMR (100 MHz, $CDCl_3$) of compound **10t**.....279
Figure A1.147 ^{1}H NMR (400 MHz, $CDCl_3$) of compound **10u**.....280
Figure A1.148 Infrared spectrum (Thin Film, NaCl) of compound **10u**.....281
Figure A1.149 ^{13}C NMR (100 MHz, $CDCl_3$) of compound **10u**.....281
Figure A1.150 ^{1}H NMR (400 MHz, $CDCl_3$) of compound **12**.....282
Figure A1.151 Infrared spectrum (Thin Film, NaCl) of compound **12**.....283
Figure A1.152 ^{13}C NMR (100 MHz, $CDCl_3$) of compound **12**.....283
Figure A1.153 ^{1}H NMR (400 MHz, $CDCl_3$) of compound **17**.....284
Figure A1.154 Infrared spectrum (Thin Film, NaCl) of compound **17**.....285
Figure A1.155 ^{13}C NMR (100 MHz, $CDCl_3$) of compound **17**.....285
Figure A1.156 ^{1}H NMR (400 MHz, $CDCl_3$) of compound **33**.....286
Figure A1.157 Infrared spectrum (Thin Film, NaCl) of compound **33**.....287
Figure A1.158 ^{13}C NMR (100 MHz, $CDCl_3$) of compound **33**.....287
Figure A1.159 ^{1}H NMR (400 MHz, $CDCl_3$) of compound **34**.....288
Figure A1.160 Infrared spectrum (Thin Film, NaCl) of compound **34**.....289
Figure A1.161 ^{13}C NMR (100 MHz, $CDCl_3$) of compound **34**.....289
Figure A1.162 ^{1}H NMR (400 MHz, $CDCl_3$) of compound **35**.....290
Figure A1.163 Infrared spectrum (Thin Film, NaCl) of compound **35**.....291
Figure A1.164 ^{13}C NMR (100 MHz, $CDCl_3$) of compound **35**.....291
Figure A1.165 ^{1}H NMR (400 MHz, $CDCl_3$) of compound **36**.....292
Figure A1.166 Infrared spectrum (Thin Film, NaCl) of compound **36**.....293
Figure A1.167 ^{13}C NMR (100 MHz, $CDCl_3$) of compound **36**.....293
Figure A1.168 ^{1}H NMR (400 MHz, $CDCl_3$) of compound **37**.....294
Figure A1.169 Infrared spectrum (Thin Film, NaCl) of compound **37**.....295
Figure A1.170 ^{13}C NMR (100 MHz, $CDCl_3$) of compound **37**.....295
Figure A1.171 ^{1}H NMR (400 MHz, $CDCl_3$) of compound **71**.....296
Figure A1.172 Infrared spectrum (Thin Film, NaCl) of compound **71**.....297
Figure A1.173 ^{13}C NMR (100 MHz, $CDCl_3$) of compound **71**.....297
Figure A1.174 ^{1}H NMR (400 MHz, $CDCl_3$) of compound **72**.....298
Figure A1.175 Infrared spectrum (Thin Film, NaCl) of compound **72**.....299
Figure A1.176 ^{13}C NMR (100 MHz, $CDCl_3$) of compound **72**.....299
Figure A1.177 ^{1}H NMR (400 MHz, $CDCl_3$) of compound **55**.....300
Figure A1.178 Infrared spectrum (Thin Film, NaCl) of compound **55**.....301
Figure A1.179 ^{13}C NMR (100 MHz, $CDCl_3$) of compound **55**.....301

Figure A1.180 ^{1}H NMR (400 MHz, $CDCl_3$) of compound **56** 302
Figure A1.181 Infrared spectrum (Thin Film, NaCl) of compound **56** 303
Figure A1.182 ^{13}C NMR (100 MHz, $CDCl_3$) of compound **56** 303
Figure A1.183 ^{1}H NMR (400 MHz, $CDCl_3$) of compound **D-56** 304
Figure A1.184 Infrared spectrum (Thin Film, NaCl) of compound **D-56** 305
Figure A1.185 ^{13}C NMR (100 MHz, $CDCl_3$) of compound **D-56** 305
Figure A1.186 ^{2}H NMR (61 MHz, $CHCl_3$) of compound **D-56** 306
Figure A1.187 ^{1}H NMR (400 MHz, $CDCl_3$) of compound **57** 307
Figure A1.188 Infrared spectrum (Thin Film, NaCl) of compound **57** 308
Figure A1.189 ^{13}C NMR (100 MHz, $CDCl_3$) of compound **57** 308
Figure A1.190 ^{1}H NMR (400 MHz, $CDCl_3$) of compound **63** 309
Figure A1.191 Infrared spectrum (Thin Film, NaCl) of compound **63** 310
Figure A1.192 ^{13}C NMR (100 MHz, $CDCl_3$) of compound **63** 310
Figure A1.193 ^{1}H NMR (400 MHz, $CDCl_3$) of compound **58** 311
Figure A1.194 Infrared spectrum (Thin Film, NaCl) of compound **58** 312
Figure A1.195 ^{13}C NMR (100 MHz, $CDCl_3$) of compound **58** 312
Figure A1.196 ^{1}H NMR (400 MHz, $CDCl_3$) of compound **59** 313
Figure A1.197 Infrared spectrum (Thin Film, NaCl) of compound **59** 314
Figure A1.198 ^{13}C NMR (100 MHz, $CDCl_3$) of compound **59** 314
Figure A1.199 ^{1}H NMR (400 MHz, $CDCl_3$) of compound **60** 315
Figure A1.200 Infrared spectrum (Thin Film, NaCl) of compound **60** 316
Figure A1.201 ^{13}C NMR (100 MHz, $CDCl_3$) of compound **60** 316
Figure A1.202 ^{1}H NMR (400 MHz, $CDCl_3$) of compound **61** 317
Figure A1.203 Infrared spectrum (Thin Film, NaCl) of compound **61** 318
Figure A1.204 ^{13}C NMR (100 MHz, $CDCl_3$) of compound **61** 318
Figure A1.205 ^{1}H NMR (400 MHz, $CDCl_3$) of compound **62** 319
Figure A1.206 Infrared spectrum (Thin Film, NaCl) of compound **62** 320
Figure A1.207 ^{13}C NMR (100 MHz, $CDCl_3$) of compound **62** 320
Figure A1.208 ^{1}H NMR (400 MHz, $CDCl_3$) of compound **64** 321
Figure A1.209 Infrared spectrum (Thin Film, NaCl) of compound **64** 322
Figure A1.210 ^{13}C NMR (100 MHz, $CDCl_3$) of compound **64** 322
Figure A1.211 ^{1}H NMR (400 MHz, $CDCl_3$) of compound **65** 323
Figure A1.212 Infrared spectrum (Thin Film, NaCl) of compound **65** 324
Figure A1.213 ^{13}C NMR (100 MHz, $CDCl_3$) of compound **65** 324
Figure A1.214 ^{1}H NMR (400 MHz, $CDCl_3$) of compound **66** 325

Figure A1.215 Infrared spectrum (Thin Film, NaCl) of compound **66**.....326
Figure A1.216 ^{13}C NMR (100 MHz, $CDCl_3$) of compound **66**.....326
Figure A1.217 ^{1}H NMR (400 MHz, $CDCl_3$) of compound **67**.....327
Figure A1.218 Infrared spectrum (Thin Film, NaCl) of compound **67**.....328
Figure A1.219 ^{13}C NMR (100 MHz, $CDCl_3$) of compound **67**.....328
Figure A1.220 ^{1}H NMR (400 MHz, $CDCl_3$) of compound **68**.....329
Figure A1.221 Infrared spectrum (Thin Film, NaCl) of compound **68**.....330
Figure A1.222 ^{13}C NMR (100 MHz, $CDCl_3$) of compound **68**.....330
Figure A1.223 ^{1}H NMR (400 MHz, $CDCl_3$) of compound **70**.....331
Figure A1.224 Infrared spectrum (Thin Film, NaCl) of compound **70**.....332
Figure A1.225 ^{13}C NMR (100 MHz, $CDCl_3$) of compound **70**.....332
Figure A1.226 ^{1}H NMR (400 MHz, $CDCl_3$) of compound **D-70**.....333
Figure A1.227 Infrared spectrum (Thin Film, NaCl) of compound **D-70**.....334
Figure A1.228 ^{13}C NMR (100 MHz, $CDCl_3$) of compound **D-70**.....334
Figure A1.229 ^{2}H NMR (61 MHz, $CHCl_3$) of compound **D-70**.....335
Figure A1.230 ^{1}H NMR (400 MHz, $CDCl_3$) of compound **73**.....336
Figure A1.231 Infrared spectrum (Thin Film, NaCl) of compound **73**.....337
Figure A1.232 ^{13}C NMR (100 MHz, $CDCl_3$) of compound **73**.....337
Figure A1.233 ^{1}H NMR (400 MHz, $CDCl_3$) of compound **75**.....338
Figure A1.234 Infrared spectrum (Thin Film, NaCl) of compound **75**.....339
Figure A1.235 ^{13}C NMR (100 MHz, $CDCl_3$) of compound **75**.....339
Figure A1.236 ^{1}H NMR (400 MHz, $CDCl_3$) of compound **76**.....340
Figure A1.237 Infrared spectrum (Thin Film, NaCl) of compound **76**.....341
Figure A1.238 ^{13}C NMR (100 MHz, $CDCl_3$) of compound **76**.....341
Figure A1.239 ^{1}H NMR (400 MHz, $CDCl_3$) of compound **77**.....342
Figure A1.240 Infrared spectrum (Thin Film, NaCl) of compound **77**.....343
Figure A1.241 ^{13}C NMR (100 MHz, $CDCl_3$) of compound **77**.....343
Figure A1.242 ^{1}H NMR (400 MHz, $CDCl_3$) of compound **83**.....344
Figure A1.243 Infrared spectrum (Thin Film, NaCl) of compound **83**.....345
Figure A1.244 ^{13}C NMR (100 MHz, $CDCl_3$) of compound **83**.....345
Figure A1.245 ^{1}H NMR (400 MHz, $CDCl_3$) of compound **74**.....346
Figure A1.246 Infrared spectrum (Thin Film, NaCl) of compound **74**.....347
Figure A1.247 ^{13}C NMR (100 MHz, $CDCl_3$) of compound **74**.....347
Figure A1.248 ^{1}H NMR (400 MHz, $CDCl_3$) of compound **78**.....348
Figure A1.249 Infrared spectrum (Thin Film, NaCl) of compound **78**.....349

Figure A1.250 ^{13}C NMR (100 MHz, $CDCl_3$) of compound **78** 349
Figure A1.251 ^{1}H NMR (400 MHz, $CDCl_3$) of compound **79** 350
Figure A1.252 Infrared spectrum (Thin Film, NaCl) of compound **79** 351
Figure A1.253 ^{13}C NMR (100 MHz, $CDCl_3$) of compound **79** 351
Figure A1.254 ^{1}H NMR (400 MHz, $CDCl_3$) of compound **80** 352
Figure A1.255 Infrared spectrum (Thin Film, NaCl) of compound **80** 353
Figure A1.256 ^{13}C NMR (100 MHz, $CDCl_3$) of compound **80** 353
Figure A1.257 ^{1}H NMR (400 MHz, $CDCl_3$) of compound **81** 354
Figure A1.258 Infrared spectrum (Thin Film, NaCl) of compound **81** 355
Figure A1.259 ^{13}C NMR (100 MHz, $CDCl_3$) of compound **81** 355
Figure A1.260 ^{1}H NMR (400 MHz, $CDCl_3$) of compound **82** 356
Figure A1.261 Infrared spectrum (Thin Film, NaCl) of compound **82** 357
Figure A1.262 ^{13}C NMR (100 MHz, $CDCl_3$) of compound **82** 357
Figure A1.263 ^{1}H NMR (400 MHz, $CDCl_3$) of compound **19a** 358
Figure A1.264 Infrared spectrum (Thin Film, NaCl) of compound **19a** 359
Figure A1.265 ^{13}C NMR (100 MHz, $CDCl_3$) of compound **19a** 359
Figure A1.266 ^{1}H NMR (400 MHz, $CDCl_3$) of compound **19d** 360
Figure A1.267 Infrared spectrum (Thin Film, NaCl) of compound **19d** 361
Figure A1.268 ^{13}C NMR (100 MHz, $CDCl_3$) of compound **19d** 361
Figure A1.269 ^{1}H NMR (400 MHz, $CDCl_3$) of compound **19e** 362
Figure A1.270 Infrared spectrum (Thin Film, NaCl) of compound **19e** 363
Figure A1.271 ^{13}C NMR (100 MHz, $CDCl_3$) of compound **19e** 363
Figure A1.272 ^{1}H NMR (400 MHz, $CDCl_3$) of compound **19f** 364
Figure A1.273 Infrared spectrum (Thin Film, NaCl) of compound **19f** 365
Figure A1.274 ^{13}C NMR (100 MHz, $CDCl_3$) of compound **19f** 365
Figure A1.275 ^{1}H NMR (400 MHz, $CDCl_3$) of compound **D-19f** 366
Figure A1.276 Infrared spectrum (Thin Film, NaCl) of compound **D-19f** 367
Figure A1.277 ^{13}C NMR (100 MHz, $CDCl_3$) of compound **D-19f** 367
Figure A1.278 ^{D}H NMR (61 MHz, $CHCl_3$) of compound **D-19f** 368
Figure A1.279 ^{1}H NMR (400 MHz, $CDCl_3$) of compound **19g** 369
Figure A1.280 Infrared spectrum (Thin Film, NaCl) of compound **19g** 370
Figure A1.281 ^{13}C NMR (100 MHz, $CDCl_3$) of compound **19g** 370
Figure A1.282 ^{1}H NMR (400 MHz, $CDCl_3$) of compound **19h** 371
Figure A1.283 Infrared spectrum (Thin Film, NaCl) of compound **19h** 372
Figure A1.284 ^{13}C NMR (100 MHz, $CDCl_3$) of compound **19h** 372

Figure A1.285 ^{1}H NMR (400 MHz, $CDCl_3$) of compound **19i** 373
Figure A1.286 Infrared spectrum (Thin Film, NaCl) of compound **19i** 374
Figure A1.287 ^{13}C NMR (100 MHz, $CDCl_3$) of compound **19i** 374
Figure A1.288 ^{1}H NMR (400 MHz, $CDCl_3$) of compound **19m** 375
Figure A1.289 Infrared spectrum (Thin Film, NaCl) of compound **19m** 376
Figure A1.290 ^{13}C NMR (100 MHz, $CDCl_3$) of compound **19m** 376
Figure A1.291 ^{1}H NMR (400 MHz, $CDCl_3$) of compound **19r** 377
Figure A1.292 Infrared spectrum (Thin Film, NaCl) of compound **19r** 378
Figure A1.293 ^{13}C NMR (100 MHz, $CDCl_3$) of compound **19r** 378
Figure A1.294 ^{1}H NMR (400 MHz, $CDCl_3$) of compound **19t** 379
Figure A1.295 Infrared spectrum (Thin Film, NaCl) of compound **19t** 380
Figure A1.296 ^{13}C NMR (100 MHz, $CDCl_3$) of compound **19t** 380
Figure A1.297 ^{1}H NMR (400 MHz, $CDCl_3$) of compound **19u** 381
Figure A1.298 Infrared spectrum (Thin Film, NaCl) of compound **19u** 382
Figure A1.299 ^{13}C NMR (100 MHz, $CDCl_3$) of compound **19u** 382
Figure A1.300 ^{1}H NMR (400 MHz, $CDCl_3$) of compound **53** 383
Figure A1.301 Infrared spectrum (Thin Film, NaCl) of compound **53** 384
Figure A1.302 ^{13}C NMR (100 MHz, $CDCl_3$) of compound **53** 384
Figure A1.303 ^{1}H NMR (400 MHz, $CDCl_3$) of compound **54** 385
Figure A1.304 Infrared spectrum (Thin Film, NaCl) of compound **54** 386
Figure A1.305 ^{13}C NMR (100 MHz, $CDCl_3$) of compound **54** 386
Figure A1.306 ^{1}H NMR (400 MHz, $CDCl_3$) of compound **29** 387
Figure A1.307 Infrared spectrum (Thin Film, NaCl) of compound **29** 388
Figure A1.308 ^{13}C NMR (100 MHz, $CDCl_3$) of compound **29** 388
Figure A1.309 ^{1}H NMR (400 MHz, $CDCl_3$) of compound **38** 389
Figure A1.310 Infrared spectrum (Thin Film, NaCl) of compound **38** 390
Figure A1.311 ^{13}C NMR (100 MHz, $CDCl_3$) of compound **38** 390
Figure A1.312 ^{1}H NMR (400 MHz, $CDCl_3$) of compound **84** 391
Figure A1.313 Infrared spectrum (Thin Film, NaCl) of compound **84** 392
Figure A1.314 ^{13}C NMR (100 MHz, $CDCl_3$) of compound **77** 392
Figure A1.315 ^{1}H NMR (400 MHz, $CDCl_3$) of compound **39** 393
Figure A1.316 Infrared spectrum (Thin Film, NaCl) of compound **39** 394
Figure A1.317 ^{13}C NMR (100 MHz, $CDCl_3$) of compound **39** 394
Figure A1.318 ^{1}H NMR (400 MHz, $CDCl_3$) of compound **40** 395
Figure A1.319 Infrared spectrum (Thin Film, NaCl) of compound **40** 396

Figure A1.320 ^{13}C NMR (100 MHz, $CDCl_3$) of compound **40** 396
Figure A1.321 ^{1}H NMR (400 MHz, $CDCl_3$) of compound **45** 397
Figure A1.322 Infrared spectrum (Thin Film, NaCl) of compound **45** 398
Figure A1.323 ^{13}C NMR (100 MHz, $CDCl_3$) of compound **45** 398
Figure A1.324 ^{1}H NMR (400 MHz, $CDCl_3$) of compound **46** 399
Figure A1.325 Infrared spectrum (Thin Film, NaCl) of compound **46** 400
Figure A1.326 ^{13}C NMR (100 MHz, $CDCl_3$) of compound **46** 400
Figure A1.327 ^{1}H NMR (400 MHz, $CDCl_3$) of compound **47** 401
Figure A1.328 Infrared spectrum (Thin Film, NaCl) of compound **47** 402
Figure A1.329 ^{13}C NMR (100 MHz, $CDCl_3$) of compound **47** 402
Figure A1.330 ^{1}H NMR (400 MHz, $CDCl_3$) of compound **48** 403
Figure A1.331 Infrared spectrum (Thin Film, NaCl) of compound **48** 404
Figure A1.332 ^{13}C NMR (100 MHz, $CDCl_3$) of compound **48** 404
Figure A1.333 ^{1}H NMR (400 MHz, $CDCl_3$) of compound **49** 405
Figure A1.334 Infrared spectrum (Thin Film, NaCl) of compound **49** 406
Figure A1.335 ^{13}C NMR (100 MHz, $CDCl_3$) of compound **49** 406
Figure A1.336 ^{1}H NMR (400 MHz, $CDCl_3$) of compound **50** 407
Figure A1.337 Infrared spectrum (Thin Film, NaCl) of compound **50** 408
Figure A1.338 ^{13}C NMR (100 MHz, $CDCl_3$) of compound **50** 408
Figure A1.339 ^{1}H NMR (400 MHz, $CDCl_3$) of compound **51** 409
Figure A1.340 Infrared spectrum (Thin Film, NaCl) of compound **51** 410
Figure A1.341 ^{13}C NMR (100 MHz, $CDCl_3$) of compound **51** 410
Figure A1.342 ^{1}H NMR (400 MHz, $CDCl_3$) of compound **52** 411
Figure A1.343 Infrared spectrum (Thin Film, NaCl) of compound **52** 412
Figure A1.344 ^{13}C NMR (100 MHz, $CDCl_3$) of compound **52** 412

CHAPTER 2

Molecular Dynamics Investigations of Dienolate [4+2] Reactions

Figure 2.1 Concerted and stepwise [4+2] reaction pathways and [4+2] reactions of cyclohexenone-derived substrates. 414
Figure 2.2 *Example PES of a stepwise, a concerted, and a dynamically stepwise (one-step two-stage) [4+2] reaction* 416
Figure 2.3 Previously studied [4+2] reactions and stereochemical outcome of stepwise [4+2] reactions 419
Figure 2.4 Computational investigations of **TS22** of siloxy diene 421

Figure 2.5 Thermodynamics investigations of **TS23** and **TS24** of Li dienolates 424
Figure 2.6 Molecular dynamics investigations of **TS23** and **TS24** of Li dienolates 425
Figure 2.7 Computational investigations of **TS2** of conjugated Pd enolate..... 428
Figure 2.8 Computational investigations of **TS19** using different functionals 437
Figure 2.9 Computational investigations of **TS25** using different functionals 438

CHAPTER 3
Enantioselective Michael Spirocyclization of Palladium Enolates

Figure 3.1 Reactivity of chiral Pd enolates and proposed reaction..... 450
Figure 3.2 Substrate scope and reaction limitations 453
Figure 3.3 Asymmetric enone difunctionalization and product derivatization..... 455
Figure 3.4 Proposed catalytic cycle 457
Figure 3.5 Computational investigations of possible Michael addition transition states (**TS26**) 458
Figure 3.6 Relative free energies for transition states explored for the selectivity-determining Michael addition process..... 522
Figure 3.7 Relative free energies for Pd intermediates explored..... 523
Figure 3.8 Relative free energies for proton transfer pathways studied..... 524
Figure 3.9 Proposed reaction pathway for Michael addition and proton transfer and the computed relative energies of relevant intermediates and transition states 525
Figure 3.10 ^{1}H–^{1}H COSY NMR spectrum of **132** (400 MHz, $CDCl_3$)..... 526
Figure 3.11 ^{1}H–^{13}C HSQC NMR spectrum of **132** (400 MHz, $CDCl_3$) 527
Figure 3.12 ^{1}H–^{13}C HMBC NMR spectrum of **132** (400 MHz, $CDCl_3$)..... 527
Figure 3.13 ^{1}H–^{1}H COSY NMR spectrum of **136** (400 MHz, $CDCl_3$)..... 528
Figure 3.14 ^{1}H–^{13}C HSQC NMR spectrum of **136** (400 MHz, $CDCl_3$) 528
Figure 3.15 ^{1}H–^{13}C HMBC NMR spectrum of **136** (400 MHz, $CDCl_3$)..... 529

APPENDIX 2
Spectra Relevant to Chapter 3

Figure A2.1 ^{1}H NMR (600 MHz, $CDCl_3$) of compound **127a** 536
Figure A2.2 Infrared spectrum (Thin Film, NaCl) of compound **127a** 537
Figure A2.3 ^{13}C NMR (100 MHz, $CDCl_3$) of compound **127a**..... 537
Figure A2.4 ^{1}H NMR (400 MHz, $CDCl_3$) of compound **127b** 538

Figure A2.5 Infrared spectrum (Thin Film, NaCl) of compound **127b** 539
Figure A2.6 ^{13}C NMR (100 MHz, $CDCl_3$) of compound **127b** 539
Figure A2.7 ^{1}H NMR (400 MHz, $CDCl_3$) of compound **127c** 540
Figure A2.8 Infrared spectrum (Thin Film, NaCl) of compound **127c** 541
Figure A2.9 ^{13}C NMR (100 MHz, $CDCl_3$) of compound **127c** 541
Figure A2.10 ^{1}H NMR (400 MHz, $CDCl_3$) of compound **127d** 542
Figure A2.11 Infrared spectrum (Thin Film, NaCl) of compound **127d** 543
Figure A2.12 ^{13}C NMR (100 MHz, $CDCl_3$) of compound **127d** 543
Figure A2.13 ^{1}H NMR (400 MHz, $CDCl_3$) of compound **127e** 544
Figure A2.14 Infrared spectrum (Thin Film, NaCl) of compound **127e** 545
Figure A2.15 ^{13}C NMR (100 MHz, $CDCl_3$) of compound **127e** 545
Figure A2.16 ^{1}H NMR (400 MHz, $CDCl_3$) of compound **127f** 546
Figure A2.17 Infrared spectrum (Thin Film, NaCl) of compound **127f** 547
Figure A2.18 ^{13}C NMR (100 MHz, $CDCl_3$) of compound **127f** 547
Figure A2.19 ^{1}H NMR (400 MHz, $CDCl_3$) of compound **127g** 548
Figure A2.20 Infrared spectrum (Thin Film, NaCl) of compound **127g** 549
Figure A2.21 ^{13}C NMR (100 MHz, $CDCl_3$) of compound **127g** 549
Figure A2.22 ^{1}H NMR (400 MHz, $CDCl_3$) of compound **127h (d1)** 550
Figure A2.23 Infrared spectrum (Thin Film, NaCl) of compound **127h (d1)** 551
Figure A2.24 ^{13}C NMR (100 MHz, $CDCl_3$) of compound **127h (d1)** 551
Figure A2.25 ^{1}H NMR (400 MHz, $CDCl_3$) of compound **127h (d2)** 552
Figure A2.26 Infrared spectrum (Thin Film, NaCl) of compound **127h (d2)** 553
Figure A2.27 ^{13}C NMR (100 MHz, $CDCl_3$) of compound **127h (d2)** 553
Figure A2.28 ^{1}H NMR (400 MHz, $CDCl_3$) of compound **127i (d1)** 554
Figure A2.29 Infrared spectrum (Thin Film, NaCl) of compound **127i (d1)** 555
Figure A2.30 ^{13}C NMR (100 MHz, $CDCl_3$) of compound **127i (d1)** 555
Figure A2.31 ^{1}H NMR (600 MHz, $CDCl_3$) of compound **127i (d2)** 556
Figure A2.32 Infrared spectrum (Thin Film, NaCl) of compound **127i (d2)** 557
Figure A2.33 ^{13}C NMR (100 MHz, $CDCl_3$) of compound **127i (d2)** 557
Figure A2.34 ^{1}H NMR (400 MHz, $CDCl_3$) of compound **127j** 558
Figure A2.35 Infrared spectrum (Thin Film, NaCl) of compound **127j** 559
Figure A2.36 ^{13}C NMR (100 MHz, $CDCl_3$) of compound **127j** 559
Figure A2.37 ^{1}H NMR (400 MHz, $CDCl_3$) of compound **127k** 560
Figure A2.38 Infrared spectrum (Thin Film, NaCl) of compound **127k** 561
Figure A2.39 ^{13}C NMR (100 MHz, $CDCl_3$) of compound **127k** 561

Figure A2.40 ^{1}H NMR (400 MHz, $CDCl_3$) of compound **129** 562
Figure A2.41 Infrared spectrum (Thin Film, NaCl) of compound **129** 563
Figure A2.42 ^{13}C NMR (100 MHz, $CDCl_3$) of compound **129** 563
Figure A2.43 ^{1}H NMR (400 MHz, $CDCl_3$) of compound **146a** 564
Figure A2.44 Infrared spectrum (Thin Film, NaCl) of compound **146a** 565
Figure A2.45 ^{13}C NMR (100 MHz, $CDCl_3$) of compound **146a** 565
Figure A2.46 ^{1}H NMR (400 MHz, $CDCl_3$) of compound **146b** 566
Figure A2.47 Infrared spectrum (Thin Film, NaCl) of compound **146b** 567
Figure A2.48 ^{13}C NMR (100 MHz, $CDCl_3$) of compound **146b** 567
Figure A2.49 ^{1}H NMR (400 MHz, $CDCl_3$) of compound **146c** 568
Figure A2.50 Infrared spectrum (Thin Film, NaCl) of compound **146c** 569
Figure A2.51 ^{13}C NMR (100 MHz, $CDCl_3$) of compound **146c** 569
Figure A2.52 ^{1}H NMR (600 MHz, $CDCl_3$) of compound **146d** 570
Figure A2.53 Infrared spectrum (Thin Film, NaCl) of compound **146d** 571
Figure A2.54 ^{13}C NMR (100 MHz, $CDCl_3$) of compound **146d** 571
Figure A2.55 ^{1}H NMR (600 MHz, $CDCl_3$) of compound **131a** 572
Figure A2.56 Infrared spectrum (Thin Film, NaCl) of compound **131a** 573
Figure A2.57 ^{13}C NMR (100 MHz, $CDCl_3$) of compound **131a** 573
Figure A2.58 ^{1}H NMR (400 MHz, $CDCl_3$) of compound **131b** 574
Figure A2.59 Infrared spectrum (Thin Film, NaCl) of compound **131b** 575
Figure A2.60 ^{13}C NMR (100 MHz, $CDCl_3$) of compound **131b** 575
Figure A2.61 ^{1}H NMR (400 MHz, $CDCl_3$) of compound **126a** 576
Figure A2.62 Infrared spectrum (Thin Film, NaCl) of compound **126a** 577
Figure A2.63 ^{13}C NMR (100 MHz, $CDCl_3$) of compound **126a** 577
Figure A2.64 ^{1}H NMR (400 MHz, $CDCl_3$) of compound **126b** 578
Figure A2.65 Infrared spectrum (Thin Film, NaCl) of compound **126b** 579
Figure A2.66 ^{13}C NMR (100 MHz, $CDCl_3$) of compound **126b** 579
Figure A2.67 ^{1}H NMR (400 MHz, $CDCl_3$) of compound **126c** 580
Figure A2.68 Infrared spectrum (Thin Film, NaCl) of compound **126c** 581
Figure A2.69 ^{13}C NMR (100 MHz, $CDCl_3$) of compound **126c** 581
Figure A2.70 ^{1}H NMR (400 MHz, $CDCl_3$) of compound **126d** 582
Figure A2.71 Infrared spectrum (Thin Film, NaCl) of compound **126d** 583
Figure A2.72 ^{13}C NMR (100 MHz, $CDCl_3$) of compound **126d** 583
Figure A2.73 ^{1}H NMR (400 MHz, $CDCl_3$) of compound **126e** 584
Figure A2.74 Infrared spectrum (Thin Film, NaCl) of compound **126e** 585

Figure A2.75 ^{13}C NMR (100 MHz, $CDCl_3$) of compound **126e** 585
Figure A2.76 ^{1}H NMR (400 MHz, $CDCl_3$) of compound **126f** 586
Figure A2.77 Infrared spectrum (Thin Film, NaCl) of compound **126f** 587
Figure A2.78 ^{13}C NMR (100 MHz, $CDCl_3$) of compound **126f** 587
Figure A2.79 ^{1}H NMR (400 MHz, $CDCl_3$) of compound **126g** 588
Figure A2.80 Infrared spectrum (Thin Film, NaCl) of compound **126g** 589
Figure A2.81 ^{13}C NMR (100 MHz, $CDCl_3$) of compound **126g** 589
Figure A2.82 ^{1}H NMR (400 MHz, $CDCl_3$) of compound **126h** 590
Figure A2.83 Infrared spectrum (Thin Film, NaCl) of compound **126h** 591
Figure A2.84 ^{13}C NMR (100 MHz, $CDCl_3$) of compound **126h** 591
Figure A2.85 ^{1}H NMR (400 MHz, $CDCl_3$) of compound **128** 592
Figure A2.86 Infrared spectrum (Thin Film, NaCl) of compound **128** 593
Figure A2.87 ^{13}C NMR (100 MHz, $CDCl_3$) of compound **128** 593
Figure A2.88 ^{1}H NMR (400 MHz, $CDCl_3$) of compound **126i** 594
Figure A2.89 Infrared spectrum (Thin Film, NaCl) of compound **126i** 595
Figure A2.90 ^{13}C NMR (100 MHz, $CDCl_3$) of compound **126i** 595
Figure A2.91 ^{1}H NMR (400 MHz, $CDCl_3$) of compound **148** 596
Figure A2.92 Infrared spectrum (Thin Film, NaCl) of compound **148** 597
Figure A2.93 ^{13}C NMR (100 MHz, $CDCl_3$) of compound **148** 597
Figure A2.94 ^{1}H NMR (400 MHz, $CDCl_3$) of compound **126j** 598
Figure A2.95 Infrared spectrum (Thin Film, NaCl) of compound **126j** 599
Figure A2.96 ^{13}C NMR (100 MHz, $CDCl_3$) of compound **126j** 599
Figure A2.97 ^{1}H NMR (400 MHz, $CDCl_3$) of compound **126k** 600
Figure A2.98 Infrared spectrum (Thin Film, NaCl) of compound **126k** 601
Figure A2.99 ^{13}C NMR (100 MHz, $CDCl_3$) of compound **126k** 601
Figure A2.100 ^{1}H NMR (400 MHz, $CDCl_3$) of compound **145a** 602
Figure A2.101 Infrared spectrum (Thin Film, NaCl) of compound **145a** 603
Figure A2.102 ^{13}C NMR (100 MHz, $CDCl_3$) of compound **145a** 603
Figure A2.103 ^{1}H NMR (400 MHz, $CDCl_3$) of compound **145b** 604
Figure A2.104 Infrared spectrum (Thin Film, NaCl) of compound **145b** 605
Figure A2.105 ^{13}C NMR (100 MHz, $CDCl_3$) of compound **145b** 605
Figure A2.106 ^{1}H NMR (400 MHz, $CDCl_3$) of compound **145c** 606
Figure A2.107 Infrared spectrum (Thin Film, NaCl) of compound **145c** 607
Figure A2.108 ^{13}C NMR (100 MHz, $CDCl_3$) of compound **145c** 607
Figure A2.109 ^{1}H NMR (400 MHz, $CDCl_3$) of compound **145d** 608

Figure A2.110 Infrared spectrum (Thin Film, NaCl) of compound **145d** 609
Figure A2.111 ^{13}C NMR (100 MHz, $CDCl_3$) of compound **145d** 609
Figure A2.112 ^{1}H NMR (400 MHz, $CDCl_3$) of compound **130a** 610
Figure A2.113 Infrared spectrum (Thin Film, NaCl) of compound **130a** 611
Figure A2.114 ^{13}C NMR (100 MHz, $CDCl_3$) of compound **130a** 611
Figure A2.115 ^{1}H NMR (400 MHz, $CDCl_3$) of compound **130b** 612
Figure A2.116 Infrared spectrum (Thin Film, NaCl) of compound **130b** 613
Figure A2.117 ^{13}C NMR (100 MHz, $CDCl_3$) of compound **130b** 613
Figure A2.118 ^{1}H NMR (400 MHz, $CDCl_3$) of compound **147a** 614
Figure A2.119 Infrared spectrum (Thin Film, NaCl) of compound **147a** 615
Figure A2.120 ^{13}C NMR (100 MHz, $CDCl_3$) of compound **147a** 615
Figure A2.121 ^{1}H NMR (400 MHz, $CDCl_3$) of compound **147b** 616
Figure A2.122 Infrared spectrum (Thin Film, NaCl) of compound **147b** 617
Figure A2.123 ^{13}C NMR (100 MHz, $CDCl_3$) of compound **147b** 617
Figure A2.124 ^{1}H NMR (400 MHz, $CDCl_3$) of compound **147c** 618
Figure A2.125 Infrared spectrum (Thin Film, NaCl) of compound **147c** 619
Figure A2.126 ^{13}C NMR (100 MHz, $CDCl_3$) of compound **147c** 619
Figure A2.127 ^{1}H NMR (400 MHz, $CDCl_3$) of compound **147d** 620
Figure A2.128 Infrared spectrum (Thin Film, NaCl) of compound **147d** 621
Figure A2.129 ^{13}C NMR (100 MHz, $CDCl_3$) of compound **147d** 621
Figure A2.130 ^{1}H NMR (400 MHz, $CDCl_3$) of compound **147e** 622
Figure A2.131 Infrared spectrum (Thin Film, NaCl) of compound **147e** 623
Figure A2.132 ^{13}C NMR (100 MHz, $CDCl_3$) of compound **147e** 623
Figure A2.133 ^{1}H NMR (400 MHz, $CDCl_3$) of compound **147f** 624
Figure A2.134 Infrared spectrum (Thin Film, NaCl) of compound **147f** 625
Figure A2.135 ^{13}C NMR (100 MHz, $CDCl_3$) of compound **147f** 625
Figure A2.136 ^{1}H NMR (400 MHz, $CDCl_3$) of compound **147g** 626
Figure A2.137 Infrared spectrum (Thin Film, NaCl) of compound **147g** 627
Figure A2.138 ^{13}C NMR (100 MHz, $CDCl_3$) of compound **147g** 627
Figure A2.139 ^{1}H NMR (400 MHz, $CDCl_3$) of compound **147h** 628
Figure A2.140 Infrared spectrum (Thin Film, NaCl) of compound **147h** 629
Figure A2.141 ^{13}C NMR (100 MHz, $CDCl_3$) of compound **147h** 629
Figure A2.142 ^{1}H NMR (400 MHz, $CDCl_3$) of compound **147i** 630
Figure A2.143 Infrared spectrum (Thin Film, NaCl) of compound **147i** 631
Figure A2.144 ^{13}C NMR (100 MHz, $CDCl_3$) of compound **147i** 631

Figure A2.145 ^{1}H NMR (400 MHz, $CDCl_3$) of compound **147j** 632
Figure A2.146 Infrared spectrum (Thin Film, NaCl) of compound **147j** 633
Figure A2.147 ^{13}C NMR (100 MHz, $CDCl_3$) of compound **147j** 633
Figure A2.148 ^{1}H NMR (400 MHz, $CDCl_3$) of compound **132** 634
Figure A2.149 Infrared spectrum (Thin Film, NaCl) of compound **132** 635
Figure A2.150 ^{13}C NMR (100 MHz, $CDCl_3$) of compound **132** 635
Figure A2.151 ^{1}H NMR (400 MHz, $CDCl_3$) of compound **134** 636
Figure A2.152 Infrared spectrum (Thin Film, NaCl) of compound **134** 637
Figure A2.153 ^{13}C NMR (100 MHz, $CDCl_3$) of compound **134** 637
Figure A2.154 ^{1}H NMR (400 MHz, $CDCl_3$) of compound **135** 638
Figure A2.155 Infrared spectrum (Thin Film, NaCl) of compound **135** 639
Figure A2.156 ^{13}C NMR (100 MHz, $CDCl_3$) of compound **135** 639
Figure A2.157 ^{1}H NMR (400 MHz, $CDCl_3$) of compound **133** 640
Figure A2.158 Infrared spectrum (Thin Film, NaCl) of compound **133** 641
Figure A2.159 ^{13}C NMR (100 MHz, $CDCl_3$) of compound **133** 641
Figure A2.160 ^{1}H NMR (400 MHz, $CDCl_3$) of compound **136** 642
Figure A2.161 Infrared spectrum (Thin Film, NaCl) of compound **136** 643
Figure A2.162 ^{13}C NMR (100 MHz, $CDCl_3$) of compound **136** 643
Figure A2.163 ^{1}H NMR (400 MHz, $CDCl_3$) of compound **137** 644
Figure A2.164 Infrared spectrum (Thin Film, NaCl) of compound **137** 645
Figure A2.165 ^{13}C NMR (100 MHz, $CDCl_3$) of compound **137** 645
Figure A2.166 ^{1}H NMR (400 MHz, $CDCl_3$) of compound **138** 646
Figure A2.167 Infrared spectrum (Thin Film, NaCl) of compound **138** 647
Figure A2.168 ^{13}C NMR (100 MHz, $CDCl_3$) of compound **138** 647

CHAPTER 4

A Pericyclic Strategy to the Enantio- and Diastereoselective Synthesis of Vicinal Quaternary/Tertiary Stereocenters from Chiral Palladium Enolates

Figure 4.1 *Enantio- and diastereoselective allylic alkylation of tetrasubstituted nucleophiles to forge vicinal quaternary/tertiary stereocenters* 651
Figure 4.2 Branched- and linear-selective reductive elimination and hypothesis for ligand design 653
Figure 4.3 Substrate scope of branched-selective allylic alkylation 656
Figure 4.4 Gram-scale synthesis and product derivatization 658
Figure 4.5 Computational investigation of inner-sphere reductive elimnation 659

Figure 4.6 Potential outer-sphere reductive elimination pathway and effects of ligand electronics and solvent polarities 661
Figure 4.7 Proposed catalytic cycle and computational studies of decarboxylation pathways. 663
Figure 4.8 Computational investigations of intermediates potentially involved in outer-sphere pathways 664
Figure 4.9 Comparison of experimental VCD and IR spectra for product **186** to computed spectra for **A_anti** 729
Figure 4.10 Overlayed experimental and calculated VCD spectra for **(R,S)-186** 729
Figure 4.11 Comparison of experimental VCD and IR spectra for product **186** to computed spectra for **A_syn** 730
Figure 4.12 Relative Gibbs free energies for various inner-sphere reductive elimination transition states with **L1** and **L2** 733

APPENDIX 3

Spectra Relevant to Chapter 4

Figure A3.1 ^{1}H NMR (600 MHz, $CDCl_3$) of compound **169** 744
Figure A3.2 Infrared spectrum (Thin Film, NaCl) of compound **169** 745
Figure A3.3 ^{13}C NMR (100 MHz, $CDCl_3$) of compound **169** 745
Figure A3.4 ^{1}H NMR (400 MHz, $CDCl_3$) of compound **170** 746
Figure A3.5 Infrared spectrum (Thin Film, NaCl) of compound **170** 747
Figure A3.6 ^{13}C NMR (100 MHz, $CDCl_3$) of compound **170** 747
Figure A3.7 ^{1}H NMR (400 MHz, $CDCl_3$) of compound **171** 748
Figure A3.8 Infrared spectrum (Thin Film, NaCl) of compound **171** 749
Figure A3.9 ^{13}C NMR (100 MHz, $CDCl_3$) of compound **171** 749
Figure A3.10 ^{1}H NMR (400 MHz, $CDCl_3$) of compound **172** 750
Figure A3.11 Infrared spectrum (Thin Film, NaCl) of compound **172** 751
Figure A3.12 ^{13}C NMR (100 MHz, $CDCl_3$) of compound **172** 751
Figure A3.13 ^{1}H NMR (400 MHz, $CDCl_3$) of compound **173** 752
Figure A3.14 Infrared spectrum (Thin Film, NaCl) of compound **173** 753
Figure A3.15 ^{13}C NMR (100 MHz, $CDCl_3$) of compound **173** 753
Figure A3.16 ^{1}H NMR (400 MHz, $CDCl_3$) of compound **174** 754
Figure A3.17 Infrared spectrum (Thin Film, NaCl) of compound **174** 755
Figure A3.18 ^{13}C NMR (100 MHz, $CDCl_3$) of compound **174** 755
Figure A3.19 ^{1}H NMR (400 MHz, $CDCl_3$) of compound **175** 756
Figure A3.20 Infrared spectrum (Thin Film, NaCl) of compound **175** 757

Figure A3.21 ^{13}C NMR (100 MHz, $CDCl_3$) of compound **175** 757
Figure A3.22 ^{1}H NMR (400 MHz, $CDCl_3$) of compound **176** 758
Figure A3.23 Infrared spectrum (Thin Film, NaCl) of compound **176** 759
Figure A3.24 ^{13}C NMR (100 MHz, $CDCl_3$) of compound **176** 759
Figure A3.25 ^{1}H NMR (400 MHz, $CDCl_3$) of compound **177** 760
Figure A3.26 Infrared spectrum (Thin Film, NaCl) of compound **177** 761
Figure A3.27 ^{13}C NMR (100 MHz, $CDCl_3$) of compound **177** 761
Figure A3.28 ^{1}H NMR (400 MHz, $CDCl_3$) of compound **178** 762
Figure A3.29 Infrared spectrum (Thin Film, NaCl) of compound **178** 763
Figure A3.30 ^{13}C NMR (100 MHz, $CDCl_3$) of compound **178** 763
Figure A3.31 ^{1}H NMR (600 MHz, $CDCl_3$) of compound **179** 764
Figure A3.32 Infrared spectrum (Thin Film, NaCl) of compound **179** 765
Figure A3.33 ^{13}C NMR (100 MHz, $CDCl_3$) of compound **179** 765
Figure A3.34 ^{1}H NMR (400 MHz, $CDCl_3$) of compound **180** 766
Figure A3.35 Infrared spectrum (Thin Film, NaCl) of compound **180** 767
Figure A3.36 ^{13}C NMR (100 MHz, $CDCl_3$) of compound **180** 767
Figure A3.37 ^{1}H NMR (400 MHz, $CDCl_3$) of compound **182** 768
Figure A3.38 Infrared spectrum (Thin Film, NaCl) of compound **182** 769
Figure A3.39 ^{13}C NMR (100 MHz, $CDCl_3$) of compound **182** 769
Figure A3.40 ^{1}H NMR (500 MHz, $CDCl_3$) of compound **181** 770
Figure A3.41 Infrared spectrum (Thin Film, NaCl) of compound **181** 771
Figure A3.42 ^{13}C NMR (100 MHz, $CDCl_3$) of compound **181** 771
Figure A3.43 ^{1}H NMR (400 MHz, $CDCl_3$) of compound **183** 772
Figure A3.44 Infrared spectrum (Thin Film, NaCl) of compound **183** 773
Figure A3.45 ^{13}C NMR (100 MHz, $CDCl_3$) of compound **183** 773
Figure A3.46 ^{19}F NMR (282 MHz, $CDCl_3$) of compound **183** 774
Figure A3.47 ^{1}H NMR (400 MHz, $CDCl_3$) of compound **186** 775
Figure A3.48 Infrared spectrum (Thin Film, NaCl) of compound **186** 776
Figure A3.49 ^{13}C NMR (100 MHz, $CDCl_3$) of compound **186** 776
Figure A3.50 ^{19}F NMR (282 MHz, $CDCl_3$) of compound **186** 777
Figure A3.51 ^{1}H NMR (400 MHz, $CDCl_3$) of compound **184** 778
Figure A3.52 Infrared spectrum (Thin Film, NaCl) of compound **184** 779
Figure A3.53 ^{13}C NMR (100 MHz, $CDCl_3$) of compound **184** 779
Figure A3.54 ^{19}F NMR (282 MHz, $CDCl_3$) of compound **184** 780
Figure A3.55 ^{1}H NMR (600 MHz, $CDCl_3$) of compound **185** 781

Figure A3.56 Infrared spectrum (Thin Film, NaCl) of compound **185** 782
Figure A3.57 ^{13}C NMR (100 MHz, $CDCl_3$) of compound **185** 782
Figure A3.58 ^{19}F NMR (282 MHz, $CDCl_3$) of compound **185** 783
Figure A3.59 ^{1}H NMR (500 MHz, $CDCl_3$) of compound **187** (mixture) 784
Figure A3.60 ^{1}H NMR (400 MHz, $CDCl_3$) of compound **187** 785
Figure A3.61 Infrared spectrum (Thin Film, NaCl) of compound **187** 786
Figure A3.62 ^{13}C NMR (100 MHz, $CDCl_3$) of compound **187** 786
Figure A3.63 ^{19}F NMR (282 MHz, $CDCl_3$) of compound **187** 787
Figure A3.64 ^{1}H NMR (400 MHz, $CDCl_3$) of compound **163** 788
Figure A3.65 Infrared spectrum (Thin Film, NaCl) of compound **163** 789
Figure A3.66 ^{13}C NMR (100 MHz, $CDCl_3$) of compound **163** 789
Figure A3.67 ^{1}H NMR (400 MHz, $CDCl_3$) of compound **202b** 790
Figure A3.68 Infrared spectrum (Thin Film, NaCl) of compound **202b** 791
Figure A3.69 ^{13}C NMR (100 MHz, $CDCl_3$) of compound **202b** 791
Figure A3.70 ^{1}H NMR (400 MHz, $CDCl_3$) of compound **202** 792
Figure A3.71 Infrared spectrum (Thin Film, NaCl) of compound **202** 793
Figure A3.72 ^{13}C NMR (100 MHz, $CDCl_3$) of compound **202** 793
Figure A3.73 ^{1}H NMR (400 MHz, $CDCl_3$) of compound **203** 794
Figure A3.74 Infrared spectrum (Thin Film, NaCl) of compound **203** 795
Figure A3.75 ^{13}C NMR (100 MHz, $CDCl_3$) of compound **203** 795
Figure A3.76 ^{1}H NMR (600 MHz, $CDCl_3$) of compound **204** 796
Figure A3.77 Infrared spectrum (Thin Film, NaCl) of compound **204** 797
Figure A3.78 ^{13}C NMR (100 MHz, $CDCl_3$) of compound **204** 797
Figure A3.79 ^{1}H NMR (600 MHz, $CDCl_3$) of compound **205** 798
Figure A3.80 Infrared spectrum (Thin Film, NaCl) of compound **205** 799
Figure A3.81 ^{13}C NMR (100 MHz, $CDCl_3$) of compound **205** 799
Figure A3.82 ^{1}H NMR (400 MHz, $CDCl_3$) of compound **206** 800
Figure A3.83 Infrared spectrum (Thin Film, NaCl) of compound **206** 801
Figure A3.84 ^{13}C NMR (100 MHz, $CDCl_3$) of compound **206** 801
Figure A3.85 ^{1}H NMR (400 MHz, $CDCl_3$) of compound **207** 802
Figure A3.86 Infrared spectrum (Thin Film, NaCl) of compound **207** 803
Figure A3.87 ^{13}C NMR (100 MHz, $CDCl_3$) of compound **207** 803
Figure A3.88 ^{1}H NMR (400 MHz, $CDCl_3$) of compound **208** 804
Figure A3.89 Infrared spectrum (Thin Film, NaCl) of compound **208** 805
Figure A3.90 ^{13}C NMR (100 MHz, $CDCl_3$) of compound **208** 805

Figure A3.91 ^{1}H NMR (400 MHz, $CDCl_3$) of compound **209** 806
Figure A3.92 Infrared spectrum (Thin Film, NaCl) of compound **209** 807
Figure A3.93 ^{13}C NMR (100 MHz, $CDCl_3$) of compound **209** 807
Figure A3.94 ^{1}H NMR (400 MHz, $CDCl_3$) of compound **210** 808
Figure A3.95 Infrared spectrum (Thin Film, NaCl) of compound **210** 809
Figure A3.96 ^{13}C NMR (100 MHz, $CDCl_3$) of compound **210** 809
Figure A3.97 ^{1}H NMR (400 MHz, $CDCl_3$) of compound **211** 810
Figure A3.98 Infrared spectrum (Thin Film, NaCl) of compound **211** 811
Figure A3.99 ^{13}C NMR (100 MHz, $CDCl_3$) of compound **211** 811
Figure A3.100 ^{1}H NMR (400 MHz, $CDCl_3$) of compound **212** 812
Figure A3.101 Infrared spectrum (Thin Film, NaCl) of compound **212** 813
Figure A3.102 ^{13}C NMR (100 MHz, $CDCl_3$) of compound **212** 813
Figure A3.103 ^{1}H NMR (400 MHz, $CDCl_3$) of compound **213** 814
Figure A3.104 Infrared spectrum (Thin Film, NaCl) of compound **213** 815
Figure A3.105 ^{13}C NMR (100 MHz, $CDCl_3$) of compound **213** 815
Figure A3.106 ^{1}H NMR (500 MHz, $CDCl_3$) of compound **214** 816
Figure A3.107 Infrared spectrum (Thin Film, NaCl) of compound **214** 817
Figure A3.108 ^{13}C NMR (100 MHz, $CDCl_3$) of compound **214** 817
Figure A3.109 ^{1}H NMR (400 MHz, $CDCl_3$) of compound **215** 818
Figure A3.110 Infrared spectrum (Thin Film, NaCl) of compound **215** 819
Figure A3.111 ^{13}C NMR (100 MHz, $CDCl_3$) of compound **215** 819
Figure A3.112 ^{19}F NMR (282 MHz, $CDCl_3$) of compound **215** 820
Figure A3.113 ^{1}H NMR (400 MHz, $CDCl_3$) of compound **216** 821
Figure A3.114 Infrared spectrum (Thin Film, NaCl) of compound **216** 822
Figure A3.115 ^{13}C NMR (100 MHz, $CDCl_3$) of compound **216** 822
Figure A3.116 ^{19}F NMR (282 MHz, $CDCl_3$) of compound **216** 823
Figure A3.117 ^{1}H NMR (400 MHz, $CDCl_3$) of compound **217** 824
Figure A3.118 Infrared spectrum (Thin Film, NaCl) of compound **217** 825
Figure A3.119 ^{13}C NMR (100 MHz, $CDCl_3$) of compound **217** 825
Figure A3.120 ^{19}F NMR (282 MHz, $CDCl_3$) of compound **217** 826
Figure A3.121 ^{1}H NMR (400 MHz, $CDCl_3$) of compound **218** 827
Figure A3.122 Infrared spectrum (Thin Film, NaCl) of compound **218** 828
Figure A3.123 ^{13}C NMR (100 MHz, $CDCl_3$) of compound **218** 828
Figure A3.124 ^{19}F NMR (282 MHz, $CDCl_3$) of compound **218** 829
Figure A3.125 ^{1}H NMR (400 MHz, $CDCl_3$) of compound **219** 830

Figure A3.126 Infrared spectrum (Thin Film, NaCl) of compound **219** 831
Figure A3.127 ^{13}C NMR (100 MHz, $CDCl_3$) of compound **219** 831
Figure A3.128 ^{19}F NMR (282 MHz, $CDCl_3$) of compound **219** 832
Figure A3.129 ^{1}H NMR (600 MHz, $CDCl_3$) of compound **204a** 833
Figure A3.130 Infrared spectrum (Thin Film, NaCl) of compound **204a** 834
Figure A3.131 ^{13}C NMR (100 MHz, $CDCl_3$) of compound **204a** 834
Figure A3.132 ^{1}H NMR (400 MHz, $CDCl_3$) of compound **205a** 835
Figure A3.133 Infrared spectrum (Thin Film, NaCl) of compound **205a** 836
Figure A3.134 ^{13}C NMR (100 MHz, $CDCl_3$) of compound **205a** 836
Figure A3.135 ^{1}H NMR (400 MHz, $CDCl_3$) of compound **206a** 837
Figure A3.136 Infrared spectrum (Thin Film, NaCl) of compound **206a** 838
Figure A3.137 ^{13}C NMR (100 MHz, $CDCl_3$) of compound **206a** 838
Figure A3.138 ^{1}H NMR (400 MHz, $CDCl_3$) of compound **210a** 839
Figure A3.139 Infrared spectrum (Thin Film, NaCl) of compound **210a** 840
Figure A3.140 ^{13}C NMR (100 MHz, $CDCl_3$) of compound **210a** 840
Figure A3.141 ^{1}H NMR (400 MHz, $CDCl_3$) of compound **211a** 841
Figure A3.142 Infrared spectrum (Thin Film, NaCl) of compound **211a** 842
Figure A3.143 ^{13}C NMR (100 MHz, $CDCl_3$) of compound **211a** 842
Figure A3.144 ^{1}H NMR (400 MHz, $CDCl_3$) of compound **212a** 843
Figure A3.145 Infrared spectrum (Thin Film, NaCl) of compound **212a** 844
Figure A3.146 ^{13}C NMR (100 MHz, $CDCl_3$) of compound **212a** 844
Figure A3.147 ^{1}H NMR (400 MHz, $CDCl_3$) of compound **214a** 845
Figure A3.148 Infrared spectrum (Thin Film, NaCl) of compound **214a** 846
Figure A3.149 ^{13}C NMR (100 MHz, $CDCl_3$) of compound **214a** 846
Figure A3.150 ^{1}H NMR (400 MHz, $CDCl_3$) of compound **213a** 847
Figure A3.151 Infrared spectrum (Thin Film, NaCl) of compound **213a** 848
Figure A3.152 ^{13}C NMR (100 MHz, $CDCl_3$) of compound **213a** 848
Figure A3.153 ^{1}H NMR (400 MHz, $CDCl_3$) of compound **222** 849
Figure A3.154 Infrared spectrum (Thin Film, NaCl) of compound **222** 850
Figure A3.155 ^{13}C NMR (100 MHz, $CDCl_3$) of compound **222** 850
Figure A3.156 ^{1}H NMR (400 MHz, $CDCl_3$) of compound **189** 851
Figure A3.157 Infrared spectrum (Thin Film, NaCl) of compound **189** 852
Figure A3.158 ^{13}C NMR (100 MHz, $CDCl_3$) of compound **189** 852
Figure A3.159 ^{1}H NMR (400 MHz, $CDCl_3$) of compound **190** 853
Figure A3.160 Infrared spectrum (Thin Film, NaCl) of compound **190** 854

Figure A3.161 ^{13}C NMR (100 MHz, $CDCl_3$) of compound **190** 854
Figure A3.162 ^{1}H NMR (400 MHz, $CDCl_3$) of compound **191** 855
Figure A3.163 Infrared spectrum (Thin Film, NaCl) of compound **191** 856
Figure A3.164 ^{13}C NMR (100 MHz, $CDCl_3$) of compound **191** 856
Figure A3.165 ^{1}H NMR (400 MHz, $CDCl_3$) of compound **192** 857
Figure A3.166 Infrared spectrum (Thin Film, NaCl) of compound **192** 858
Figure A3.167 ^{13}C NMR (100 MHz, $CDCl_3$) of compound **192** 858
Figure A3.168 ^{1}H NMR (300 MHz, $CDCl_3$) of compound **L4** 859
Figure A3.169 Infrared spectrum (Thin Film, NaCl) of compound **L4** 860
Figure A3.170 ^{13}C NMR (100 MHz, $CDCl_3$) of compound **L4** 860
Figure A3.171 ^{19}F NMR (282 MHz, $CDCl_3$) of compound **L4** 861
Figure A3.172 ^{31}P NMR (121 MHz, $CDCl_3$) of compound **L4** 861
Figure A3.173 ^{1}H NMR (400 MHz, $CDCl_3$) of compound **L6** 862
Figure A3.174 Infrared spectrum (Thin Film, NaCl) of compound **L6** 863
Figure A3.175 ^{13}C NMR (100 MHz, $CDCl_3$) of compound **L6** 863
Figure A3.176 ^{19}F NMR (282 MHz, $CDCl_3$) of compound **L6** 864
Figure A3.177 ^{31}P NMR (121 MHz, $CDCl_3$) of compound **L6** 864
Figure A3.178 ^{1}H NMR (500 MHz, $CDCl_3$) of compound **L5** 865
Figure A3.179 Infrared spectrum (Thin Film, NaCl) of compound **L5** 866
Figure A3.180 ^{13}C NMR (100 MHz, $CDCl_3$) of compound **L5** 866
Figure A3.181 ^{19}F NMR (282 MHz, $CDCl_3$) of compound **L5** 867
Figure A3.182 ^{31}P NMR (121 MHz, $CDCl_3$) of compound **L5** 867
Figure A3.183 ^{1}H NMR (300 MHz, $CDCl_3$) of compound **L7** 868
Figure A3.184 Infrared spectrum (Thin Film, NaCl) of compound **L7** 869
Figure A3.185 ^{13}C NMR (100 MHz, $CDCl_3$) of compound **L7** 869
Figure A3.186 ^{19}F NMR (282 MHz, $CDCl_3$) of compound **L7** 870
Figure A3.187 ^{31}P NMR (121 MHz, $CDCl_3$) of compound **L7** 870
Figure A3.188 ^{1}H NMR (300 MHz, $CDCl_3$) of compound **223** 871
Figure A3.189 Infrared spectrum (Thin Film, NaCl) of compound **223** 872
Figure A3.190 ^{13}C NMR (100 MHz, $CDCl_3$) of compound **223** 872
Figure A3.191 ^{19}F NMR (282 MHz, $CDCl_3$) of compound **223** 873
Figure A3.192 ^{31}P NMR (162 MHz, $CDCl_3$) of compound **223** 873
Figure A3.193 ^{1}H NMR (400 MHz, $CDCl_3$) of compound **224** 874
Figure A3.194 Infrared spectrum (Thin Film, NaCl) of compound **224** 875
Figure A3.195 ^{13}C NMR (100 MHz, $CDCl_3$) of compound **224** 875

Figure A3.196 ^{19}F NMR (282 MHz, $CDCl_3$) of compound **224** 876
Figure A3.197 ^{31}P NMR (162 MHz, $CDCl_3$) of compound **224** 876
Figure A3.198 ^{1}H NMR (400 MHz, $CDCl_3$) of compound **226** 877
Figure A3.199 Infrared spectrum (Thin Film, NaCl) of compound **226** 878
Figure A3.200 ^{13}C NMR (100 MHz, $CDCl_3$) of compound **226** 878
Figure A3.201 ^{19}F NMR (282 MHz, $CDCl_3$) of compound **226** 879
Figure A3.202 ^{31}P NMR (162 MHz, $CDCl_3$) of compound **226** 879

CHAPTER 5

Progress Toward the Total Synthesis of Hypermoin A

Figure 5.1 Examples of common PPAPs 881
Figure 5.2 Hypermoin A and its proposed biosynthesis 882
Figure 5.3 Previously developed approaches to access [3.2.2] bicycles 883
Figure 5.4 Retrosynthetic analysis 884
Figure 5.5 Synthesis of bicycle **259** and proposed ring expansion cascade 885
Figure 5.6 Proposed functionalization of [3.2.2] bicycle **259** 886
Figure 5.7 Synthesis of cyclopentyl fragment **270** 887
Figure 5.8 Challenging 1,2-addition and synthesis of alternative cyclopentyl fragment **277** 888
Figure 5.9 Challenging [4+2] cycloaddition from **281** and successful reaction with **284** 889
Figure 5.10 Cycloaddition using ynone **286** and succeeding functionalization sequence 890
Figure 5.11 Cycloaddition of diene **281** and ynone **286** and attempted optimization 891
Figure 5.12 Reductive Heck cyclization and attempted installation of an isopropyl group 892
Figure 5.13 Attempted hydrogenation and ring expansion to form **306** and proposed ring expansion on oxidized substrate **307** 893
Figure 5.14 Proposed endgame toward the synthesis of hypermoin A 894

APPENDIX 4

Spectra Relevant to Chapter 5

Figure A4.1 ^{1}H NMR (400 MHz, $CDCl_3$) of compound **258** 948
Figure A4.2 Infrared spectrum (Thin Film, NaCl) of compound **258** 949
Figure A4.3 ^{13}C NMR (100 MHz, $CDCl_3$) of compound **258** 949
Figure A4.4 ^{1}H NMR (400 MHz, $CDCl_3$) of compound **259** 950
Figure A4.5 Infrared spectrum (Thin Film, NaCl) of compound **259** 951
Figure A4.6 ^{13}C NMR (100 MHz, $CDCl_3$) of compound **259** 951
Figure A4.7 ^{1}H NMR (400 MHz, $CDCl_3$) of compound **314** 952

Figure A4.8 Infrared spectrum (Thin Film, NaCl) of compound **314** 953
Figure A4.9 ^{13}C NMR (100 MHz, $CDCl_3$) of compound **314** 953
Figure A4.10 ^{1}H NMR (400 MHz, $CDCl_3$) of compound **315** 954
Figure A4.11 Infrared spectrum (Thin Film, NaCl) of compound **315** 955
Figure A4.12 ^{13}C NMR (100 MHz, $CDCl_3$) of compound **315** 955
Figure A4.13 ^{1}H NMR (400 MHz, $CDCl_3$) of compound **283** 956
Figure A4.14 Infrared spectrum (Thin Film, NaCl) of compound **283** 957
Figure A4.15 ^{13}C NMR (100 MHz, $CDCl_3$) of compound **283** 957
Figure A4.16 ^{1}H NMR (600 MHz, $CDCl_3$) of compound **285-d1** 958
Figure A4.17 Infrared spectrum (Thin Film, NaCl) of compound **285-d1** 959
Figure A4.18 ^{13}C NMR (100 MHz, $CDCl_3$) of compound **285-d1** 959
Figure A4.19 ^{1}H NMR (400 MHz, $CDCl_3$) of compound **285-d2** 960
Figure A4.20 Infrared spectrum (Thin Film, NaCl) of compound **285-d2** 961
Figure A4.21 ^{13}C NMR (100 MHz, $CDCl_3$) of compound **285-d2** 961
Figure A4.22 ^{1}H NMR (600 MHz, $CDCl_3$) of compound **285-d3** 962
Figure A4.23 Infrared spectrum (Thin Film, NaCl) of compound **285-d3** 963
Figure A4.24 ^{13}C NMR (100 MHz, $CDCl_3$) of compound **285-d3** 963
Figure A4.25 ^{1}H NMR (400 MHz, $CDCl_3$) of compound **287** 964
Figure A4.26 Infrared spectrum (Thin Film, NaCl) of compound **287** 965
Figure A4.27 ^{13}C NMR (100 MHz, $CDCl_3$) of compound **287** 965
Figure A4.28 ^{1}H NMR (400 MHz, $CDCl_3$) of compound **288** 966
Figure A4.29 Infrared spectrum (Thin Film, NaCl) of compound **288** 967
Figure A4.30 ^{13}C NMR (100 MHz, $CDCl_3$) of compound **288** 967
Figure A4.31 ^{1}H NMR (600 MHz, $CDCl_3$) of compound **290** 968
Figure A4.32 Infrared spectrum (Thin Film, NaCl) of compound **290** 969
Figure A4.33 ^{13}C NMR (100 MHz, $CDCl_3$) of compound **290** 969
Figure A4.34 ^{1}H NMR (400 MHz, $CDCl_3$) of compound **291** 970
Figure A4.35 Infrared spectrum (Thin Film, NaCl) of compound **291** 971
Figure A4.36 ^{13}C NMR (100 MHz, $CDCl_3$) of compound **291** 971
Figure A4.37 ^{1}H NMR (400 MHz, $CDCl_3$) of compound **298** 972
Figure A4.38 Infrared spectrum (Thin Film, NaCl) of compound **298** 973
Figure A4.39 ^{13}C NMR (100 MHz, $CDCl_3$) of compound **298** 973
Figure A4.40 ^{1}H NMR (500 MHz, $CDCl_3$) of compound **299** 974
Figure A4.41 Infrared spectrum (Thin Film, NaCl) of compound **299** 975
Figure A4.42 ^{13}C NMR (100 MHz, $CDCl_3$) of compound **299** 975

Figure A4.43 ^{1}H NMR (400 MHz, $CDCl_3$) of compound **294** 976
Figure A4.44 Infrared spectrum (Thin Film, NaCl) of compound **294** 977
Figure A4.45 ^{13}C NMR (100 MHz, $CDCl_3$) of compound **294** 977
Figure A4.46 ^{1}H NMR (400 MHz, $CDCl_3$) of compound **295** 978
Figure A4.47 Infrared spectrum (Thin Film, NaCl) of compound **295** 979
Figure A4.48 ^{13}C NMR (100 MHz, $CDCl_3$) of compound **295** 979
Figure A4.49 ^{1}H NMR (400 MHz, $CDCl_3$) of compound **296** 980
Figure A4.50 Infrared spectrum (Thin Film, NaCl) of compound **296** 981
Figure A4.51 ^{13}C NMR (100 MHz, $CDCl_3$) of compound **296** 981
Figure A4.52 ^{1}H NMR (400 MHz, $CDCl_3$) of compound **301** 982
Figure A4.53 Infrared spectrum (Thin Film, NaCl) of compound **301** 983
Figure A4.54 ^{13}C NMR (100 MHz, $CDCl_3$) of compound **301** 983
Figure A4.55 ^{1}H NMR (400 MHz, $CDCl_3$) of compound **302** 984
Figure A4.56 Infrared spectrum (Thin Film, NaCl) of compound **302** 985
Figure A4.57 ^{13}C NMR (100 MHz, $CDCl_3$) of compound **302** 985
Figure A4.58 ^{1}H NMR (500 MHz, $CDCl_3$) of compound **305** 986
Figure A4.59 ^{1}H NMR (400 MHz, $CDCl_3$) of compound **268** 987
Figure A4.60 Infrared spectrum (Thin Film, NaCl) of compound **268** 988
Figure A4.61 ^{13}C NMR (100 MHz, $CDCl_3$) of compound **268** 988
Figure A4.62 ^{1}H NMR (400 MHz, $CDCl_3$) of compound **269** 989
Figure A4.63 Infrared spectrum (Thin Film, NaCl) of compound **269** 990
Figure A4.64 ^{13}C NMR (100 MHz, $CDCl_3$) of compound **269** 990
Figure A4.65 ^{1}H NMR (400 MHz, $CDCl_3$) of compound **270** 991
Figure A4.66 Infrared spectrum (Thin Film, NaCl) of compound **270** 992
Figure A4.67 ^{13}C NMR (100 MHz, $CDCl_3$) of compound **270** 992
Figure A4.68 ^{1}H NMR (400 MHz, $CDCl_3$) of compound **273** 993
Figure A4.69 Infrared spectrum (Thin Film, NaCl) of compound **273** 994
Figure A4.70 ^{13}C NMR (100 MHz, $CDCl_3$) of compound **273** 994
Figure A4.71 ^{1}H NMR (600 MHz, $CDCl_3$) of compound **274** 995
Figure A4.72 Infrared spectrum (Thin Film, NaCl) of compound **274** 996
Figure A4.73 ^{13}C NMR (100 MHz, $CDCl_3$) of compound **274** 996
Figure A4.74 ^{1}H NMR (400 MHz, $CDCl_3$) of compound **275** 997
Figure A4.75 Infrared spectrum (Thin Film, NaCl) of compound **275** 998
Figure A4.76 ^{13}C NMR (100 MHz, $CDCl_3$) of compound **275** 998
Figure A4.77 ^{1}H NMR (400 MHz, $CDCl_3$) of compound **276** 999

Figure A4.78 Infrared spectrum (Thin Film, NaCl) of compound **276** 1000
Figure A4.79 ^{13}C NMR (100 MHz, $CDCl_3$) of compound **276** 1000
Figure A4.80 ^{1}H NMR (400 MHz, $CDCl_3$) of compound **277** 1001
Figure A4.81 Infrared spectrum (Thin Film, NaCl) of compound **277** 1002
Figure A4.82 ^{13}C NMR (100 MHz, $CDCl_3$) of compound **277** 1002
Figure A4.83 ^{1}H NMR (400 MHz, $CDCl_3$) of compound **272** 1003
Figure A4.84 Infrared spectrum (Thin Film, NaCl) of compound **272** 1004
Figure A4.85 ^{13}C NMR (100 MHz, $CDCl_3$) of compound **272** 1004
Figure A4.86 ^{1}H NMR (400 MHz, $CDCl_3$) of compound **278** 1005
Figure A4.87 Infrared spectrum (Thin Film, NaCl) of compound **278** 1006
Figure A4.88 ^{13}C NMR (100 MHz, $CDCl_3$) of compound **278** 1006
Figure A4.89 ^{1}H NMR (400 MHz, $CDCl_3$) of compound **279** 1007
Figure A4.90 Infrared spectrum (Thin Film, NaCl) of compound **279** 1008
Figure A4.91 ^{13}C NMR (100 MHz, $CDCl_3$) of compound **279** 1008
Figure A4.92 ^{1}H NMR (400 MHz, $CDCl_3$) of compound **280** 1009
Figure A4.93 Infrared spectrum (Thin Film, NaCl) of compound **280** 1010
Figure A4.94 ^{13}C NMR (100 MHz, $CDCl_3$) of compound **280** 1010
Figure A4.95 ^{1}H NMR (600 MHz, $CDCl_3$) of compound **292** 1011

APPENDIX 5

Early Strategies Toward the Total Synthesis of Hypermoin A

Figure A5.1 First generation retrosynthetic analysis: allylic alkylation–cyclization 1012
Figure A5.2 Attempted asymmetric allylic alkylation to access **323** for Sakurai reaction 1013
Figure A5.3 Synthesis of enone **336** and attempted intramolecular cyclization 1014
Figure A5.4 Synthesis of aldehyde **343** and attempted radical cyclization 1015
Figure A5.5 Second generation retrosynthetic analysis: radical cascade 1016
Figure A5.6 Synthesis of precursor **348a** and attempted radical cascade 1017
Figure A5.7 Synthesis of precursor **348b** and attempted radical cascade 1017
Figure A5.8 Investigation of alternative [4+2] dienophiles 1018
Figure A5.9 Stereoselective installation of isopropyl group and stereochemical assignment 1019
Figure A5.10 *Preliminary picture of the structure of **359** (racemic) determined by X-ray crystallography* 1049

LIST OF SCHEMES

CHAPTER 1

Divergent Catalysis: Catalytic Asymmetric Intramolecular [4+2] Cycloaddition of Palladium Enolates

Scheme 1.1 Proposed divergent catalytic cycle..... 9

LIST OF TABLES

CHAPTER 1

Divergent Catalysis: Catalytic Asymmetric Intramolecular [4+2] Cycloaddition of Palladium Enolates

Table 1.1 Optimization of [4+2] reaction conditions 7

Table 1.2 Substrate scope of the [4+2] reaction 11

CHAPTER 3

Enantioselective Michael Spirocyclization of Palladium Enolates

Table 3.1 Optimization of Michael spirocyclization reaction conditions 451

CHAPTER 4

A Pericyclic Strategy to the Enantio- and Diastereoselective Synthesis of Vicinal Quaternary/Tertiary Stereocenters from Chiral Palladium Enolates

Table 4.1 Optimization of branched-selective asymmetric allylic alkylation 655

APPENDIX 6

Notebook Cross-Reference for New Compounds

Table A6.1 Notebook cross-reference for Chapter 1 1052

Table A6.2 Notebook cross-reference for Chapter 3 1054

Table A6.3 Notebook cross-reference for Chapter 4 1055

Table A6.4 Notebook cross-reference for Chapter 5 1056

Table A6.5 Notebook cross-reference for Appendix 5 1057

LIST OF ABBREVIATIONS

Å	Ångstrom
λ	wavelength
μ	micro
μwave	microwave
$[\alpha]_D$	specific rotation at wavelength of sodium D line
°C	degrees Celsius
Ac	acetyl
AcOH	acetic acid
An	*para*-anisoyl
APCI	atmospheric pressure chemical ionization
aq	aqueous
Ar	aryl
atm	atmosphere
Bn	benzyl
Boc	*tert*-butyloxycarbonyl
bp	boiling point
br	broad
Bu	butyl
Bz	benzoyl
c	concentration for specific rotation measurements (g/100 mL)
calc'd	calculated
CAN	ceric ammonium nitrate
cat	catalytic

cm^{-1}	wavenumber(s)
COD	1,5-cyclooctadiene
Cp	cyclopentadienyl
Cy	cyclohexyl
d	doublet
D	deuterium
dba	dibenzylideneacetone
DBU	1,8-diazabicyclo[5.4.0]undec-7-ene
DCE	1,2-dichloroethane
DIBAL	diisobutylaluminum hydride
DMA	*N*,*N*-dimethylacetamide
DMAP	4-dimethylaminopyridine
DMF	*N*,*N*-dimethylformamide
DMP	Dess-Martin periodinane
DMSO	dimethyl sulfoxide
dr	diastereomeric ratio
e.g.	for example (Latin exempli gratia)
ee	enantiomeric excess
equiv	equivalent(s)
ESI	electrospray ionization
Et	ethyl
EtOAc	ethyl acetate
FAB	fast atom bombardment
FD	field desorption
g	gram(s)
GC	gas chromatography
h	hour(s)

HE	Hantzsch ester
HFIP	1,1,1,3,3,3-hexafluoropropan-2-ol
HMDS	1,1,1,3,3,3-hexamethyldisilazane
HMPA	hexamethylphosphoramide
HPLC	high-performance liquid chromatography
HRMS	high-resolution mass spectroscopy
Hz	hertz
i-Bu	isobutyl
i.e.	that is (Latin id est)
IBX	2-iodoxybenzoic acid
IPA	isopropanol, 2-propanol
i-Pr	isopropyl
IR	infrared (spectroscopy)
J	coupling constant
K	Kelvin(s) (absolute temperature)
kcal	kilocalorie
L	liter; neutral ligand
LC–MS	liquid chromatography–mass spectrometry
LDA	lithium diisopropylamide
m	multiplet; milli
m	meta
M	metal; molar; molecular ion
m/z	mass to charge ratio
m-CPBA	*meta*-chloroperoxybenzoic acid
Me	methyl
mg	milligram(s)
MHz	megahertz

min	minute(s)
MM	mixed method
mol	mole(s)
mp	melting point
Ms	methanesulfonyl (mesyl)
MS	molecular sieves
MTBE	methyl *tert*-butyl ether
NBS	*N*-bromosuccinimide
n-Bu	butyl
NCS	*N*-chlorosuccinimide
ND	not determined
NMP	*N*-methyl-2-pyrrolidone
NMR	nuclear magnetic resonance
NR	no reaction detected
Nu^-	nucleophile
o	ortho
p	para
Pd/C	palladium on carbon
PG	protecting group
Ph	phenyl
pH	hydrogen ion concentration in aqueous solution
Phth	phthaloyl
Piv	pivaloyl
ppm	parts per million
Pr	propyl
p-TsOH	*para*-toluenesulfonic acid
Py	pyridine

q	quartet
R	generic for any atom or functional group
Ref.	reference
s	singlet
t	triplet
TBAF	tetrabutylammonium fluoride
TBS	*tert*-butyldimethylsilyl
t-Bu	*tert*-butyl
Tf	trifluoromethanesulfonyl (triflyl)
TFA	trifluoroacetic acid
TFAA	trifluoroacetic anhydride
TFE	2,2,2-trifluoroethanol
THF	tetrahydrofuran
TLC	thin-layer chromatography
TMP	2,2,6,6-tetramethylpiperidine
TMS	trimethylsilyl
TOF	time-of-flight
TosMIC	*para*-toluenesulfonylmethyl isocyanide
t_R	retention time
Ts	*p*-toluenesulfonyl (tosyl)
UV	ultraviolet
v/v	volume to volume
w	weak
w/v	weight to volume
w/w	weight to weight
X	anionic ligand or electronegative element

CHAPTER 1

Divergent Catalysis: Catalytic Asymmetric Intramolecular [4+2] Cycloaddition of Palladium Enolates†

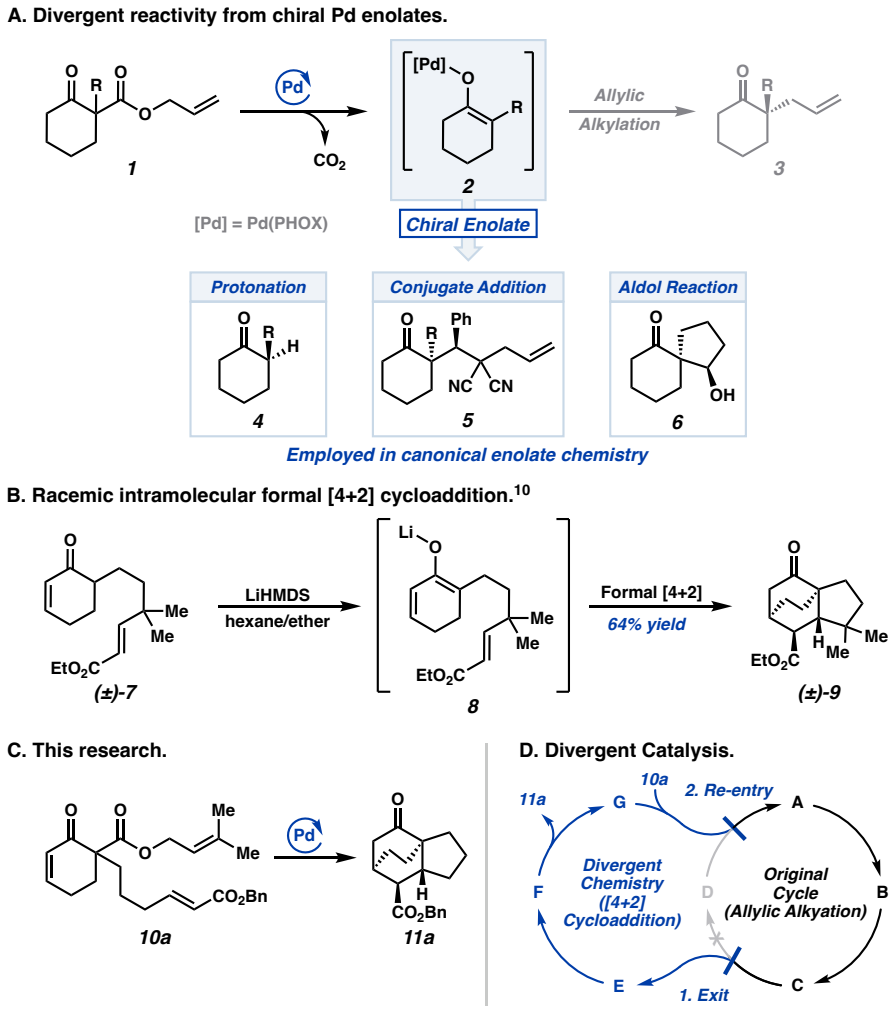
1.1 INTRODUCTION

Enantioselective construction of all-carbon quaternary stereogenic centers represents a central and ongoing challenge in synthetic organic chemistry.[1] The asymmetric allylic alkylation of enolate nucleophiles serves as a powerful strategy for accessing such motifs.[2]

A unique aspect of the Pd-catalyzed allylic alkylation methods developed by our group is the inner-sphere reductive elimination from a chiral O-bound Pd enolate intermediate (**2**), yielding enantioenriched ketones (**3**) (Figure 1.1A).[3,4] This intermediate is generated catalytically from achiral or racemic enolate precursors, such as allyl enol carbonates[5] and β-ketoesters[6] (**1**). The Pd enolate is accessed in the absence of a base, under neutral conditions, and in a regiospecific fashion. Conversely, canonical conditions for enolate formation are plagued by regioselectivity challenges and typically require the use of a strong base or Lewis acid. Given the inherent advantages of Pd enolates, we sought to exploit their reactivity beyond simple allylic alkylations in more general asymmetric transformations.

†This research was performed in collaboration with Flesch, K. N.; Cusumano, A. Q.; Strong, C. S.; Du, Y. E.. Portions of this chapter have been reproduced with permission from Stoltz, et al. *J. Am. Chem. Soc.* **2023**, *145*, 11301–11310. © 2023 American Chemical Society.

Figure 1.1. *(A) Examples of chiral Pd enolate reactivity. (B) Lithium base-promoted intramolecular formal [4+2] cycloaddition. (C) Proposed asymmetric intramolecular [4+2] reaction. (D) Divergent catalytic cycle.*



Highlighting the utility of this concept, our lab has demonstrated the enantioselective protonation of Pd enolates as a valuable strategy to access ketones with tertiary stereocenters (**4**).[7] Building upon this success, we subsequently developed methods to construct quaternary centers via enantioselective conjugate additions [8] (**5**) and

intramolecular aldol reactions (**6**).[9] Taken together, these advances underscore the feasibility of employing Pd enolates as pro-stereogenic nucleophiles.

In a unique example of enolate reactivity, Fukumoto and coworkers reported a formal [4+2] reaction from in situ generated conjugated lithium enolate **8**, forging tricyclic adduct **9** in a racemic fashion (Figure 1.1B).[10] We envisioned that an analogous asymmetric transformation would be tractable from a chiral, conjugated Pd enolate – derived from the decarboxylation of unsaturated β-ketoester **10a** using an asymmetric ligand on Pd (Figure 1.1C).

To realize this transformation, we sought to develop a conceptual framework based on our mechanistic understanding to expand the general utility of the Pd enolate. As such, we employed a strategy of divergent catalysis (Figure 1.1D), where deviation occurs at the common Pd enolate (*i.e.*, **C**, Figure 1.1D, cf. Scheme 1.1, vide infra), allowing for desired alternative reactivity in the diverged cycle. Subsequent re-entry into the original catalytic cycle turns over the catalyst allowing regeneration of the Pd enolate.

Applying this strategy of divergent catalysis, we developed a catalytic decarboxylative asymmetric intramolecular [4+2] cycloaddition from conjugated Pd enolates. Mechanistic studies including quantum mechanics calculations, Eyring analysis, and KIE studies offer insights into the reaction mechanism. This transformation enables access to tricyclic scaffolds bearing at least four contiguous stereocenters, at least one of which is quaternary.

1.2 RESULTS AND DISCUSSION

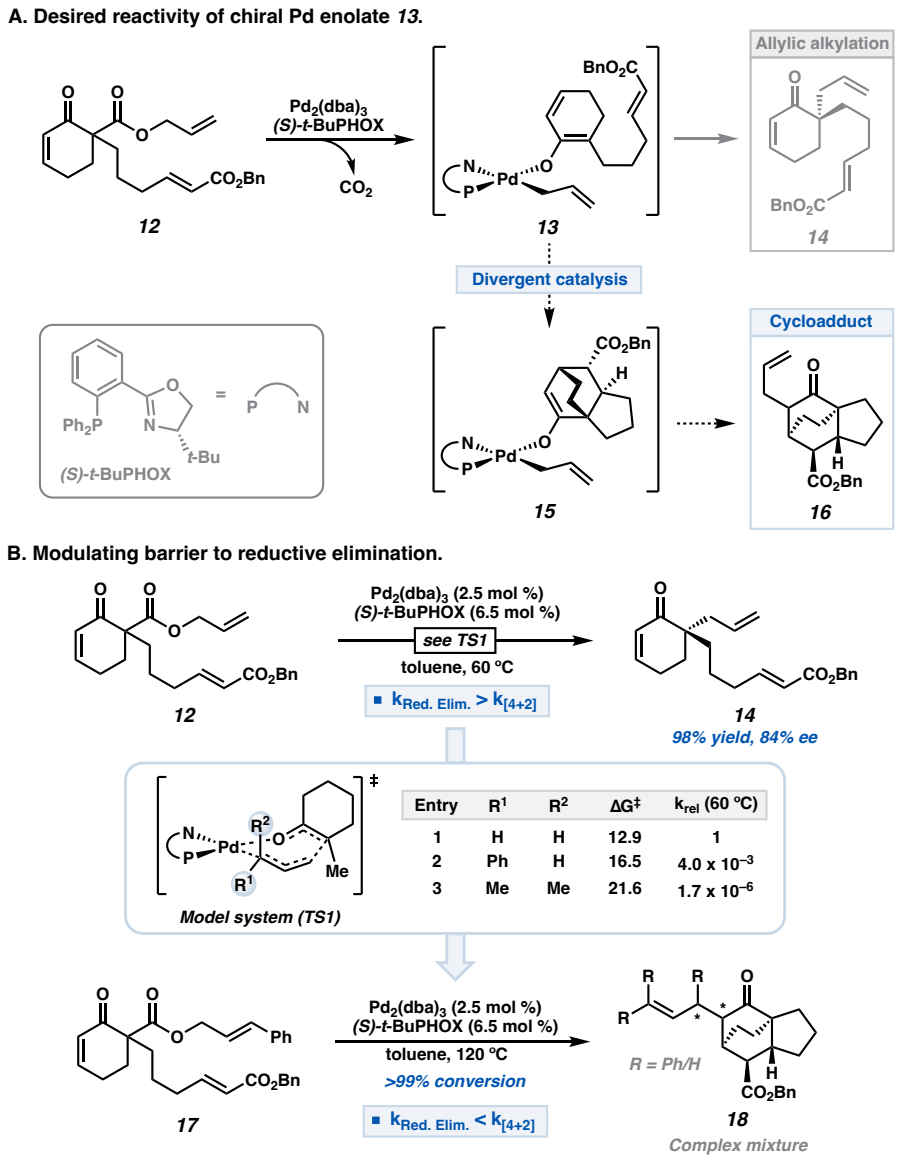
1.2.1 REACTION DESIGN AND OPTIMIZATION

Employing unsaturated β-ketoester **12** as a precursor for conjugated Pd enolate **13**, we hypothesized that the precedented allylic alkylation forming **14** could be interrupted by a [4+2] cycloaddition to generate **15** (Figure 1.2A). Alkylation of the transposed enolate (**15**) would then turn over the catalyst and forge tricyclic product **16**.

Unfortunately, the rate of direct allylic alkylation of enolate **13** supersedes the desired divergent reactivity. Treatment of β-ketoester **12** under our standard conditions produces ketone **14** in 98% yield and 84% ee (Figure 1.2B). This prompted us to redesign our exit strategy (Figure 1.1D). Increasing the rate of the cycloaddition through modification of the diene or dienophile could circumvent formation of premature allylic alkylation product **14** but would limit the generality of this transformation. Therefore, we sought to impede alkylation through modification of the allyl moiety.

Computational investigation of a model system (**TS1**) suggested that introducing terminal substitution on the allyl group raises the barrier to reductive elimination, decreasing the rate of allylic alkylation (Figure 1.2B, see 1.4 Experimental Section for computational details).[11] For example, phenyl substitution (entry 2, Figure 1.2B) slows the rate of inner-sphere reductive elimination by roughly three orders of magnitude. Inspired by these computational results, we explored the efficacy of cinnamyl ester substrate **17** in the transformation. In line with our hypothesis, the desired tricyclic core was observed (**18**), albeit as a complex mixture of isomers – hampering the synthetic utility. To this end, we sought to develop an alternative strategy for catalyst turnover that could potentially simplify the product outcomes.

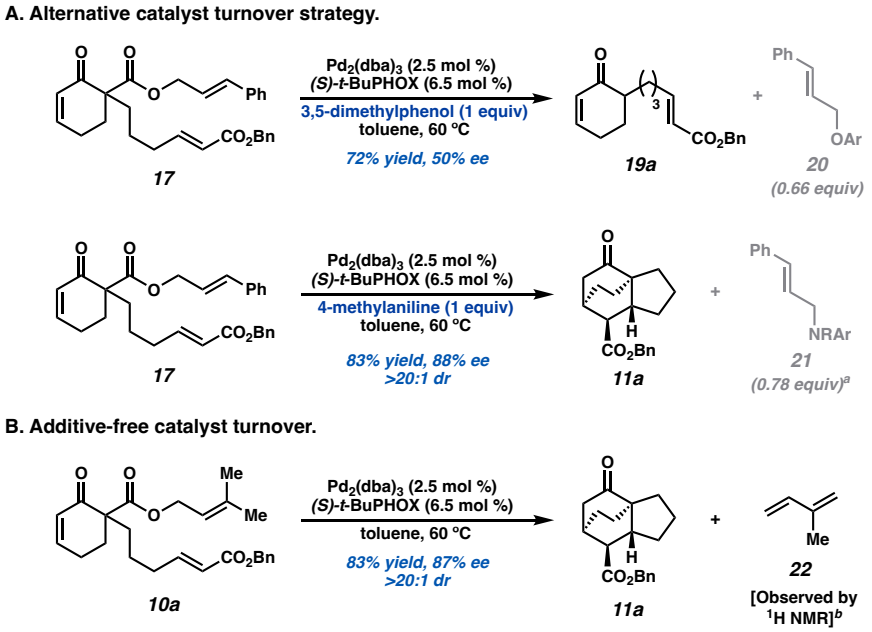
Figure 1.2. *(A) General reactivity paradigm from Pd enolate* ***13****. (B) Computed substituent effects on the rate of C–C bond formation and successful application.*[a]



[a] See 1.4 Experimental Section for computational details and discussion of other isomeric transition states. Yield determined by ^{1}H NMR with respect to 1,3,5-trimethoxybenzene as internal standard. Enantiomeric excess determined by chiral SFC.

Building upon previous findings from our group, we sought to employ stoichiometric acidic additives for catalyst turnover. The exogenous acid serves the dual purpose of protonating the final enolate (analogous to **15**) and turning over the catalyst by trapping the cinnamyl group. Addition of 3,5-dimethylphenol[9] exclusively yielded undesired protonation product **19a** along with aryl ether **20** (Figure 1.3A). To our delight, replacing the phenol additive with 4-methylaniline afforded the desired *endo* [4+2] cycloadduct (**11a**) as a single diastereomer in 83% yield and 88% ee.

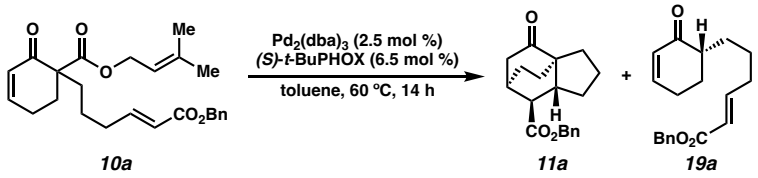
Figure 1.3. *(A) Sacrificial additives to enable catalyst turnover.*[a] *(B) Additive-free reaction with prenyl ester* ***10a****.*[b]



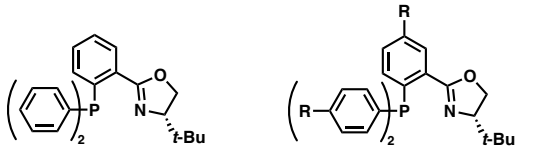
[a] Equivalents includes mixture of branched and linear constitutional isomers, as well as double-alkylation of aniline. [b] Isoprene (**22**) observed in 0.94:1 ratio with **11a** by ^{1}H NMR (J Young tube, toluene-d_8).

Seeking to improve the reaction yield, the competency of β-ketoester **10a**, derived from the commodity chemical prenyl alcohol, was explored. According to our computations, a substrate containing a di-substituted allyl fragment would be similarly effective in hindering premature allylic alkylation by increasing the barrier to reductive elimination (Figure 1.2B, entry 3). Perplexingly, while the desired tricyclic product was generated in 73% isolated yield and 88% ee, no alkylated 4-methylaniline (analogous to **21**) was observed as a byproduct (entry 8, Table 1.1).

Table 1.1. *Optimization of [4+2] reaction conditions.*[a]



Entry	Deviation from standard conditions	Yield *11a* (%)[b]	ee *11a* (%)	Yield *19a* (%)[b]	ee *19a* (%)
1	none	96 (83)	87 (87)	–	–
2	THF	86	81	–	–
3	benzene	92	87	–	–
4	1,4-dioxane	12	–	63	49
5	40 °C	51	89	–	–
6	*(S)*-$(CF_3)_3$-*t*-BuPHOX	12	89	66	62
7	*(S)*-$(OMe)_3$-*t*-BuPHOX	40	88	26	65
8	4-methylaniline (1 equiv)	93 (73)	87 (88)	–	–
9	4-methylaniline (2 equiv)	78	87	–	–
10	3,5-dimethylphenol (1 equiv)	0	–	100	71



[a] Conditions: 0.02 mmol **10a**, 2.5 mol % $Pd_2(dba)_3$, 6.5 mol % ligand, in 1.0 mL of solvent (0.02 M). [b] Yields determined by ^{1}H NMR with respect to 1,3,5-trimethoxybenzene as internal standard. Isolated yields on 0.2 mmol scale in parentheses.

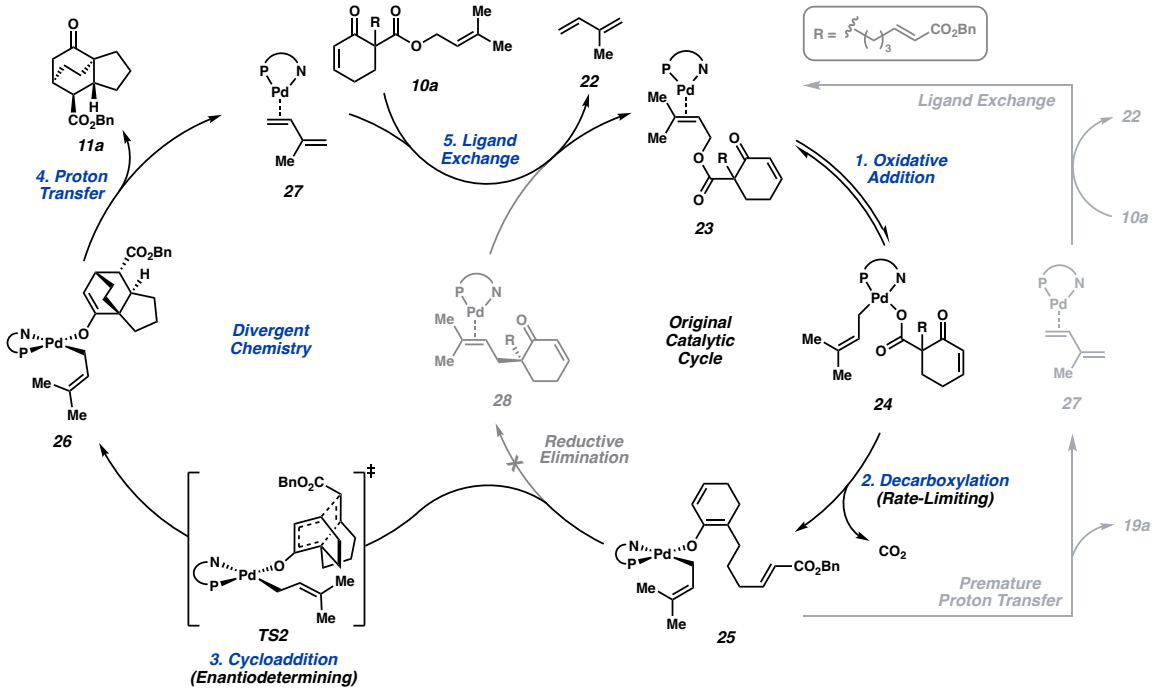
A control reaction excluding 4-methylaniline was carried out, and surprisingly, desired product **11a** was formed in 83% yield and 87% ee (Figure 1.3B). This suggests that an alternative catalyst turnover mechanism is operative. Further NMR experiments revealed the stoichiometric evolution of isoprene (**22**) accompanying formation of product **11a**. Intrigued by this unexpected finding and clean reaction profile, we pursued optimization of additive-free reaction conditions.

The reaction proceeds in THF and benzene albeit in slightly diminished yield and enantioselectivity (entries 2–3, Table 1.1). Employing 1,4-dioxane as the solvent, protonation product **19a** was obtained as the major product in 63% yield and 49% ee, while cycloadduct **11a** was observed in only 12% yield (entry 4, Table 1.1). Lowering the temperature to 40 ºC slightly improved the ee to 89% at the cost of decreased conversion (entry 5, Table 1.1). Modification of the electronic properties of the PHOX ligand deleteriously impacted the product distribution (entries 6–7, Table 1.1). Phenol and aniline additives do not improve the reaction (entries 8–10, Table 1.1). Ultimately, optimized reaction conditions were determined to be additive-free with *(S)-t*-BuPHOX in toluene at 60 ºC. The reaction affords **11a**, a bridged bicycle with a pendant fused ring, in 83% isolated yield and 87% ee. The transformation allows for the simultaneous construction of four contiguous stereocenters, including one all-carbon quaternary center. Gratifyingly, the reaction can be performed with reduced catalyst loading (0.625 mol %) on 1.0 mmol scale to afford **11a** in 59% yield and 89% ee. The ability to efficiently construct these complex building blocks on scale highlights the synthetic utility of this transformation.

1.2.2 PROPOSED MECHANISM

We sought to capitalize on these initial exciting results by constructing a mechanistic framework to inform rational design. Based on our lab's prior investigations of Pd-catalyzed decarboxylative asymmetric allylic alkylation reactions, we propose that oxidative addition of Pd^0 to β-ketoester **10a** proceeds through complex **23** to afford the η^1-allyl carboxylate resting state **24** (Scheme 1.1).[12] Rate-limiting decarboxylation ensues, affording O-bound Pd enolate **25**.[3,12] This chiral conjugated enolate then serves as the diene in a [4+2] cycloaddition (**TS2**) with the pendant dienophile to form tricyclic enolate **26**.

Scheme 1.1. *Proposed divergent catalytic cycle. Undesired reaction pathways in grey.*



Subsequent proton transfer would generate product **11a**. Concomitant isoprene generation, followed by ligand exchange, allows for re-entry into the original catalytic cycle at **23**. We

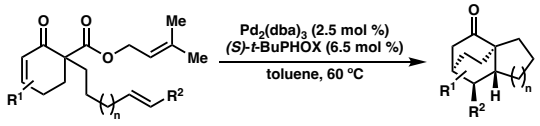
posit that the formation of undesired ketone **19a** arises from an off-cycle pathway, where catalyst turnover occurs prior to cycloaddition via premature proton transfer to **25**.

1.2.3 SUBSTRATE SCOPE

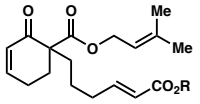
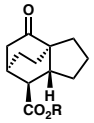
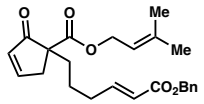
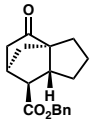
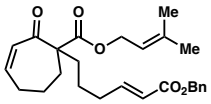
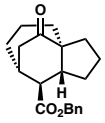
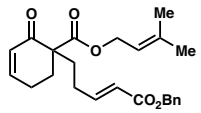
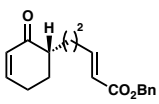
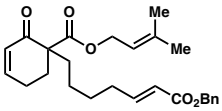
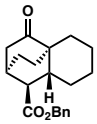
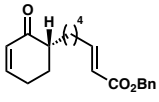
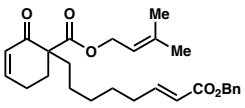
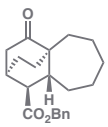
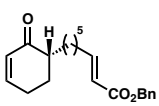
With a working mechanistic hypothesis in hand, we sought to draw further mechanistic insights from substrate design, while simultaneously exploring limits of the reaction. Considering the inverse relationship between diene ring size and Diels–Alder reaction rate, [2, 13] we explored whether this trend impacts the generality of our transformation. However, with cyclopentyl diene derived from enone **10c**, a decrease in yield and ee, relative to six-membered parent substrate **10a**, was noted (Table 1.2). In comparison to smaller ring sizes, seven-membered cyclic dienes require increased distortion energy to reach the desired transition state.[Error! Bookmark not defined.] Despite this, seven-membered ring substrate **10d** leads to a high yield and improved ee. Thus, this transformation represents a powerful method to synthesize various challenging bicyclic cores.

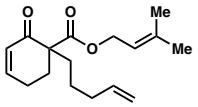
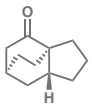
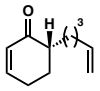
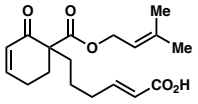
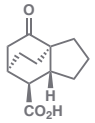
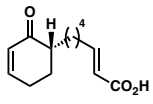
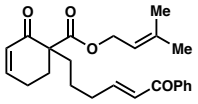
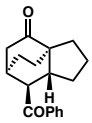
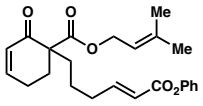
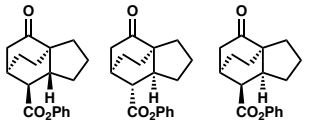
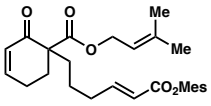
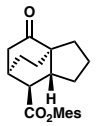
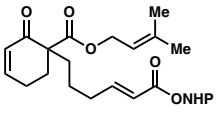
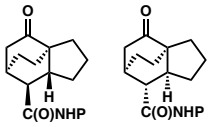
The dienophile tether length was subsequently modulated to test its influence on product distribution. The ethylene tethered substrate **10e** yields solely the premature protonation product **19e**, likely due to insurmountable developing ring strain in the cycloaddition transition state. In contrast to the propylene tethered substrate **10a**, the butylene tethered substrate **10f** leads to a near equal distribution of cycloadduct **11f** (42% yield) and premature protonation product **19f** (45% yield). Following this trend, the pentylene tethered substrate **10g** leads only to protonation product **19g**. Rationalizing this phenomenon, we propose that lengthening the tether increases conformational flexibility

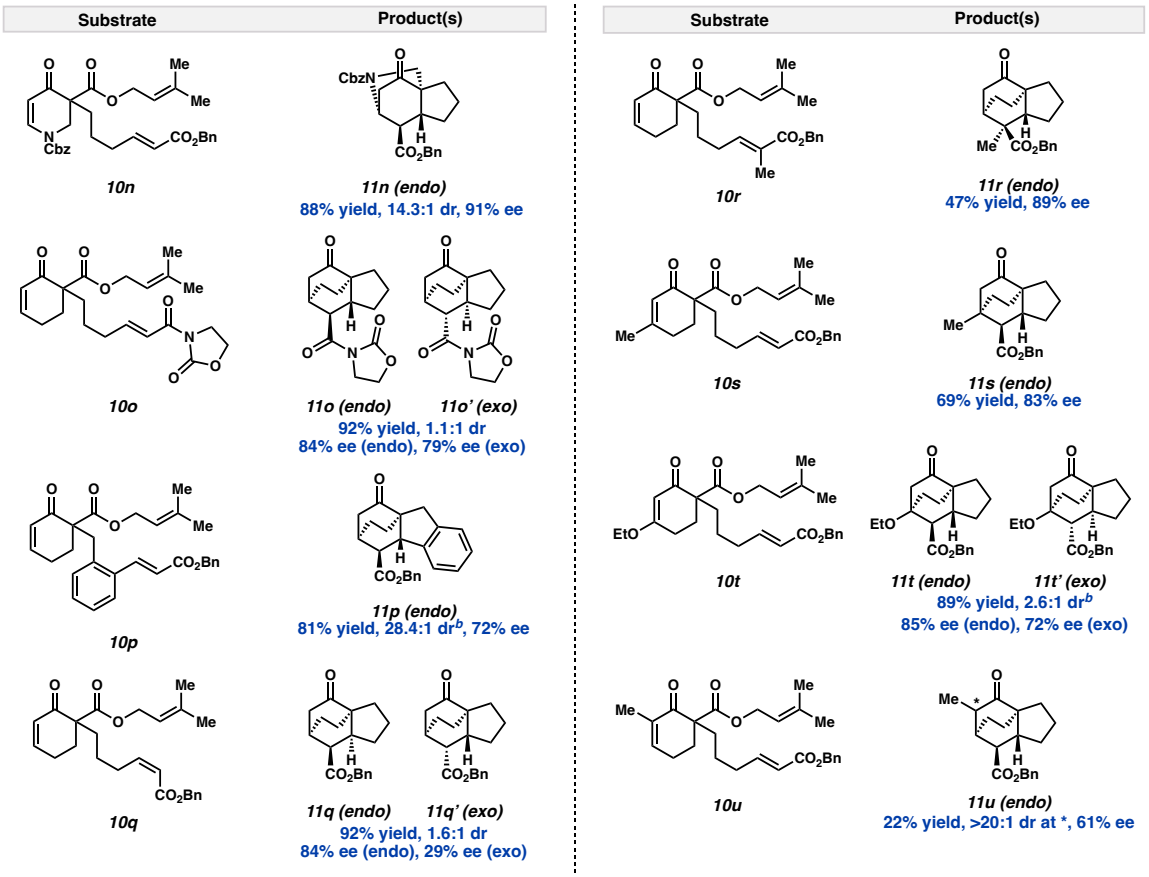
Table 1.2. *Substrate scope of the [4+2] reaction.*[a]



10a-u ***11a-u***

Substrate	Product(s)
 R = Bn ***10a*** R = Et ***10b***	 ***11a (endo)*** 83% yield, 87% ee ***11b (endo)*** 85% yield, 88% ee
 ***10c***	 ***11c (endo)*** 65% yield, 65% ee
 ***10d***	 ***11d (endo)*** 83% yield, 97% ee
 ***10e***	 ***11e (endo)*** (not observed)  ***19e*** 81% yield, 47% ee
 ***10f***	 ***11f (endo)*** 42% yield, 92% ee  ***19f*** 45% yield, 51% ee
 ***10g***	 ***11g (endo)*** (not observed)  ***19g*** 74% yield, 56% ee

Substrate	Product(s)
 ***10h***	 ***11h (endo)*** (not observed)  ***19h*** 33% yield, 58% ee
 ***10i***	 ***11i (endo)*** (not observed)  ***19i*** 80% yield, 7% ee
 ***10j***	 ***11j (endo)*** 50% yield, 87% ee
 ***10k***	 ***11k (endo)*** ***11k' (exo)*** ***11k'' (other)*** 82% yield, 10.4:1.4:1 dr, 88% ee (endo)
 ***10l***	 ***11l (endo)*** 90% yield, 89% ee
 ***10m***	 ***11m (endo)*** ***11m' (exo)*** 65% yield, 1.4:1 dr[b] 62% ee (endo), 62% ee (exo)



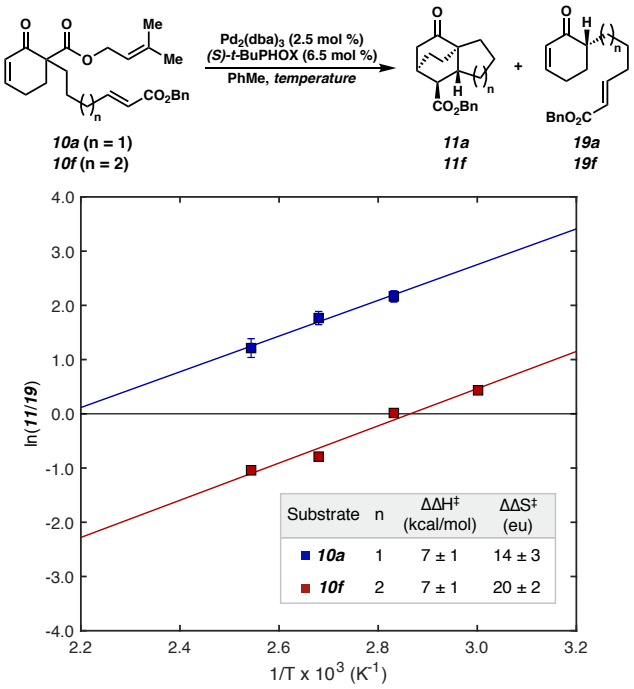
[a] Conditions: 0.2 mmol **10a**, 2.5 mol % $Pd_2(dba)_3$, 6.5 mol % ligand, in toluene (10 mL, 0.02 M), isolated yields, dr determined by ^1H NMR analysis of reaction crude. [b] dr determined by isolated yields of endo/exo products.

and imposes a greater entropic penalty to the highly organized [4+2] transition state. In contrast, increased tether length is inconsequential to the protonation process, which does not involve the dienophile.

Eyring analysis of product distributions from reactions of **10a** and **10f** further supports the hypothesis of an entropic preference for the formation of **19a/f** over **11a/f** (Figure 1.4). With **10a**, cycloaddition (**11a**) is enthalpically favored ($\Delta\Delta H^{\ddagger}$ = 7 kcal/mol) but entropically disfavored ($\Delta\Delta S^{\ddagger}$ = 14 eu) over protonation (**19a**). As anticipated,

increasing the tether length to four methylene units (**10f**) further increases the relative entropic penalty for cycloaddition ($\Delta\Delta S^{\ddagger}$ = 20 eu), while the differential enthalpy of activation remains similar ($\Delta\Delta H^{\ddagger}$ = 7 kcal/mol). Hence, entropy differences associated with tether length lead to the formation of differential amounts of undesired ketones **19a** and **19f**.

Figure 1.4. *Eyring analysis of **11**/**19** product ratio for propylene and butylene tethered substrates **10a** and **10f**.*[a]



T (°C)	*11a* : *19a*	*11f* : *19f*
60	–	1.5 : 1.0
80	8.7 : 1.0	1.0 : 1.0
100	5.9 : 1.0	1.0 : 2.2
120	3.4 : 1.0	1.0 : 2.8

[a] All data points collected in triplicate, error bars and ranges reflect a 95% confidence interval.[14] Reactions carried out on 0.02 mmol scale with product ratios determined by crude ^{1}H NMR analysis.

We then surveyed the scope of functional groups that are tolerated in this reaction (Table 1.2). The cycloaddition does not proceed in the absence of a π-acceptor (**10h**), and carboxylic acid **10i** exclusively affords undesired ketone **19i**. To our delight, a variety of functional groups are compatible, including ethyl ester **10b**, phenyl ketone **10j**, phenyl ester **10k**, mesityl ester **10l**, N-hydroxyphthalimido (NHP) ester **10m**, enecarbamate **10n**, and *N*-acyl oxazolidinone **10o**. Additionally, further conjugated cinnamic ester dienophile **10p** affords tetracycle **11p**. These results demonstrate the ability to tolerate varying dienophile electronics, incorporate additional functional handles, and access alternate ring systems.

The majority of the substrate scope is reflective of a stereospecific process, yielding only *endo* and *exo* diastereomers. We sought to exploit this property of the reaction to access other diastereomers of **11a** by employing *(Z)*-olefin dienophile **10q**. Gratifyingly, desired cycloadducts **11q** (*endo*) and **11q'** (*exo*) are furnished in a 1.6:1 ratio with a 92% combined yield, in 84% and 29% ee, respectively.

Further substitution patterns on the substrate were explored with the aim of increasing the stereochemical complexity of the products. Trisubstituted benzyl ester dienophile **10r** furnished cycloadduct **11r**, featuring two all-carbon quaternary centers, in 47% yield and 90% ee. β-Methyl (**10s**) and β-ethoxy (**10t**) α,β-unsaturated enones are also competent substrates, forging additional tetrasubstituted bridgehead stereocenters. Finally, we explored α-methyl substituted enone **10u**. The corresponding product **11u** was produced, bearing five contiguous stereocenters in >20:1 dr.

In summary, the transformation described herein represents a versatile method for the preparation of a variety of enantioenriched polycyclic scaffolds. Inspired by these

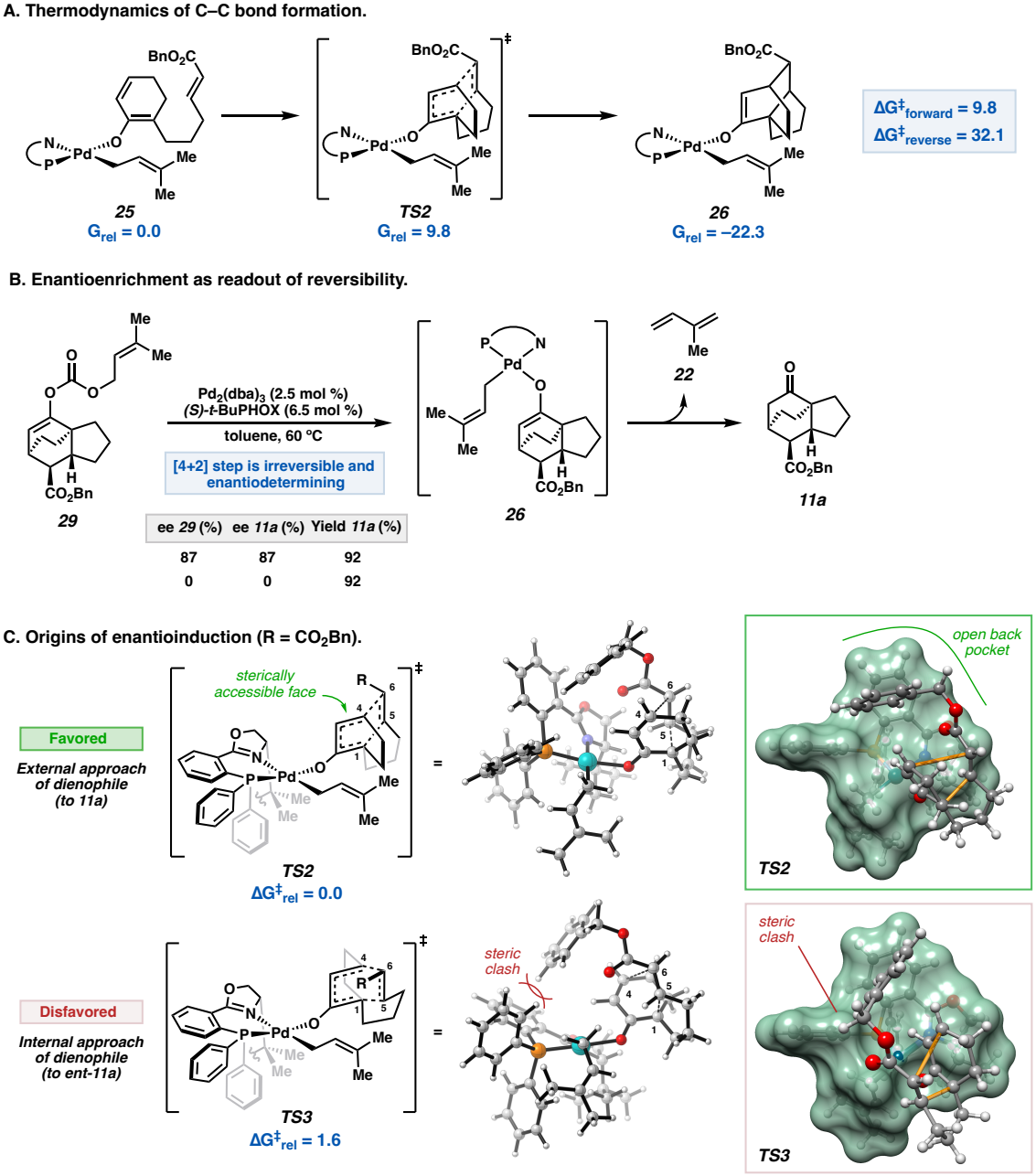
results, we sought to explore the origins of enantioinduction and the mechanism by which catalyst turnover is achieved.

1.2.4 [4+2] CYCLOADDITION

In order to probe the origins of enantioinduction in the transformation, we first aimed to elucidate the enantiodetermining step in the catalytic cycle. We hypothesized that either the cycloaddition is irreversible and dictates the stereochemical outcome, or a reversible [4+2] is coupled to a subsequent enantiodetermining step. First, we computationally evaluated the energetics of the [4+2] process. Cycloaddition directly from conjugated enolate **25** to transposed enolate **26** via **TS2** is achieved with a $\Delta G^{\ddagger}$ of 9.8 and ΔG of –22.3 kcal/mol (Figure 1.5A). The 32.1 kcal/mol barrier to the reverse process renders the cycloaddition step irreversible under the reaction conditions. Hence, our computations suggest that the cycloaddition step is enantiodetermining.

To assess this hypothesis experimentally, reaction product **11a** was converted to its corresponding prenyl enol carbonate **29**. Under the standard reaction conditions, Pd^0 undergoes oxidative addition to **29**, and decarboxylation affords target common intermediate **26** (Figure 1.5B).[5] When enantioenriched or racemic **29** is subjected to the reaction conditions, cycloadduct **11a** is obtained in high yield and identical enantiopurity to that of the respective enol carbonate precursor (**29**) (Figure 1.5B). No stereochemical resolution in product **11a** is observed from racemic enol carbonate **29**, indicating that a post-cycloaddition process is not responsible for enantioinduction. In addition to verifying the irreversibility of the cycloaddition step, these experiments also support the viability of enolate **26** as an intermediate in the catalytic cycle (Scheme 1.1).

Figure 1.5. *(A) Computed barriers.[a] (B) Experimentally verifying irreversibility of the C–C bond formation. (C) Origins of enantioinduction in the [4+2] cycloaddition step.*



[a] Gibbs free energies in kcal/mol. See Experimental Section in section 1.4 for details.

Considering the [4+2] cycloaddition as the enantiodetermining process, the origin of enantioinduction in this step was investigated. As such, the lowest energy *endo* transition states giving rise to each enantiomer of **11a** were evaluated (Figure 1.5C). The minimum energy pathway to each enantiomer of product features a transition state in which the dienophile tether is *syn* to the *t*-Bu group of the PHOX ligand – in accord with prior observations in inner-sphere allylic alkylation transition states.[3,15] From this orientation, the dienophile preferentially approaches the externally-exposed enantiotopic face of the diene to avoid steric clash between the benzyl ester and the phenyl groups of the PHOX ligand scaffold (Figure 1.5C). A 1.6 kcal/mol preference for external (**TS2**) over internal (**TS3**) approach is calculated, in accord with the experimentally observed 87% ee.[16] The major enantiomer of product (**11a**) predicted by computations matches that of the major enantiomer obtained experimentally, as confirmed by vibrational circular dichroism (VCD) spectroscopy (see 1.4 Experimental Section for details).

In summary, our investigations reveal C–C bond formation to be the enantiodetermining step, with enantioselectivity achieved by biasing *external* over *internal* dienophile approach (Figure 1.5).

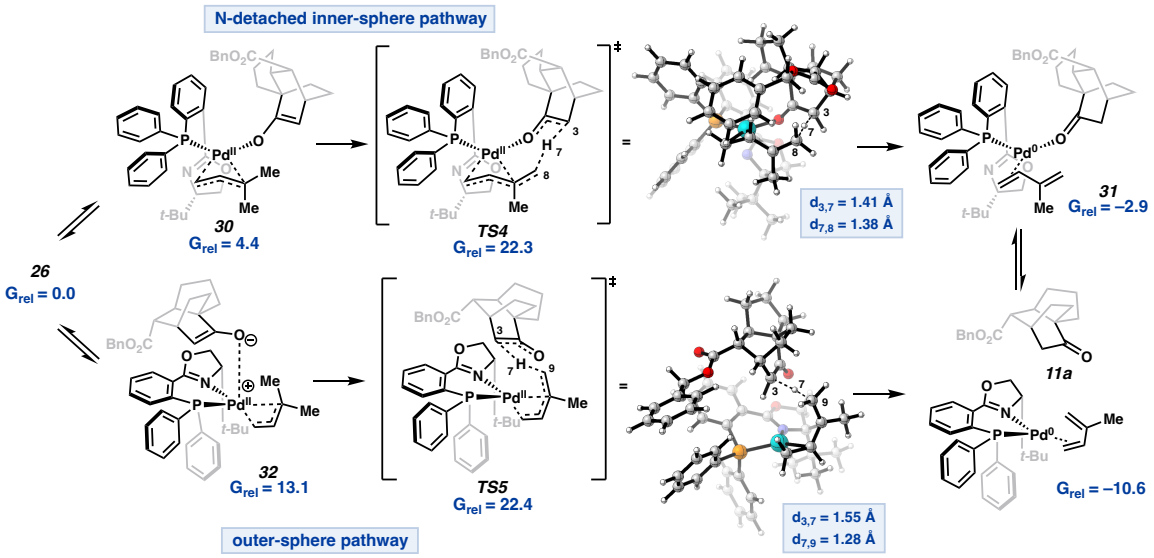
1.2.5 CATALYST TURNOVER

Our [4+2] transformation is rendered catalytic by a unique reduction of Pd^{II} to Pd^{0} that occurs concomitantly with formation of isoprene (**22**) and ketone **11a**. This observation motivated computational investigations to elucidate the catalyst turnover mechanism.

Of the numerous mechanisms explored, the minimum energy pathway involves isomerization of **26** to an N-detached π-allyl Pd species (**30**) and subsequent inner-sphere

proton transfer (**TS4**) (Figure 1.6). Additionally, a pathway featuring outer-sphere proton transfer (**TS5**) was found to be highly competitive for catalyst turnover. These two processes present very similar free energy barriers of 22.3 and 22.4 kcal/mol, respectively, which are readily surmountable at 60 °C. A single favored pathway is not identified as the energy difference between the two mechanisms is within error of computations (approximately 1 kcal/mol). In both pathways, subsequent ligand exchange of isoprene (**22**) for starting material **10a** completes the catalytic cycle. Analysis of Intrinsic Bonding Orbitals (IBOs) [17] along the reaction coordinate suggest these processes are best conceptualized as the transfer of a proton, rather than a hydride, to the Pd enolate (see 1.4 Experimental Section for details).[18] Analogous mechanisms were found to be operative from pre-cycloaddition enolate **25**, giving rise to premature protonation product **19a**.

Figure 1.6. *Two lowest-energy pathways for catalyst turnover.*[a]



[a] Gibbs free energies in kcal/mol. See section 1.4 Experimental Section for details.

1.2.6 FURTHER MECHANISM-BASED DEVELOPMENTS

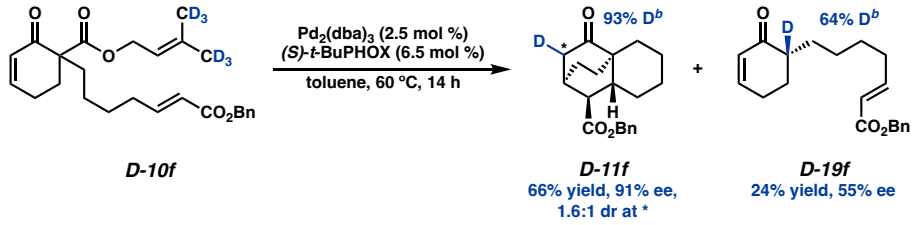
While this method allows access to a variety of complex scaffolds, premature protonation remains an outstanding challenge we sought to address. As such, we aimed to leverage our mechanistic insights surrounding this process to inhibit byproduct formation.

To that end, we turned our attention to butylene tethered substrate **10f** given its similar yield of desired **11f** (44%) and byproduct **19f** (42%). We envisioned favoring the formation of **11f** by modification of the ancillary prenyl moiety. By introducing a kinetic isotope effect, we aimed to slow down the protonation processes. To our delight, employing hexa-deutero prenyl ester **D-10f** (Figure 1.7A) increases the yield of desired cycloadduct **D-11f** to 66%, with 91% ee.[19] Next, cyclic analogs of the prenyl ester **10f** were prepared (Figure 1.7B). At one extreme, seven-membered exocycle **36** affords a product distribution which closely mirrors that of parent substrate **10f** (entry 5). Excitingly, contracting the ring by one methylene (**35**) shifts the distribution favorably toward **11f** (entry 4, 3:1 ratio of **11f**:**19f**). However, five- and four-membered exocycles (**34** and **33**), as well as acyclic bis-benzylic allylic ester **37**, afford unfavorable product distributions.

In summary, we find appropriate modification of the prenyl moiety to be effective in suppressing deleterious side reactions. This is particularly important as the ring system generated in this reaction is a scaffold relevant to natural product synthesis.

Figure 1.7. *(A) KIE study. (B) Prenyl ester modification.*

A. Leveraging kinetic isotope effect (KIE) to slow proton transfer.[a]

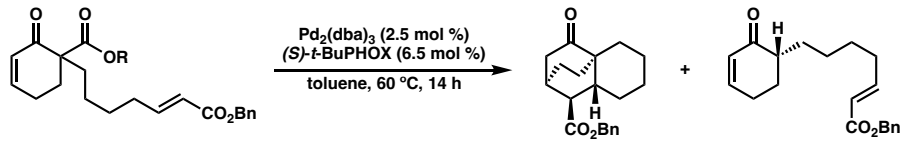


D-10f

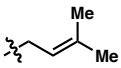
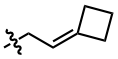
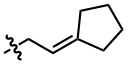
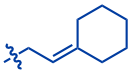
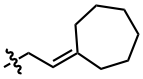
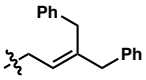
D-11f
66% yield, 91% ee,
1.6:1 dr at *

D-19f
24% yield, 55% ee

B. Modification of prenyl ester via cyclic and benzylic analogs.[c]



11f *19f*

Entry	R		Yield 11f (%)	ee 11f (%)	Yield 19f (%)	ee 19f (%)
1		*(10f)*	44	91	42	40
2[d]		*(33)*	25	92	44	46
3		*(34)*	8	–	89	48
4		*(35)*	63	92	21	44
5		*(36)*	48	92	46	38
6[e]		*(37)*	14	94	86	60

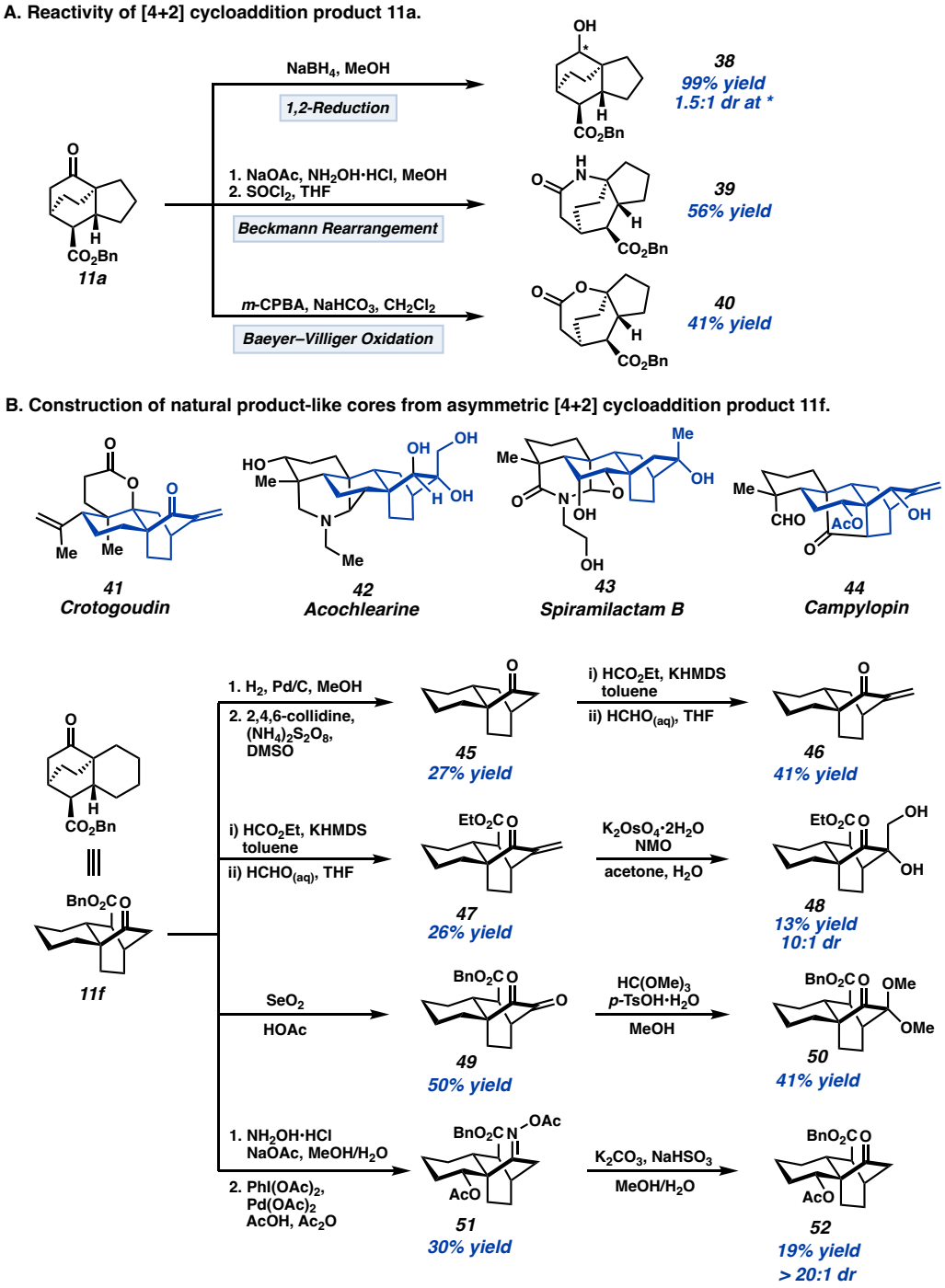
[a] Conditions: 0.20 mmol **D-10f**, 2.5 mol % $Pd_2(dba)_3$, 6.5 mol % ligand, in 10 mL of solvent (0.02 M). [b] Deuterium incorporation determined by HRMS. [c] Conditions: 0.02 mmol substrate, 2.5 mol % $Pd_2(dba)_3$, 6.5 mol % ligand, in 1.0 mL of solvent (0.02 M). Yield determined by ^1H NMR with respect to 1,3,5-trimethoxybenzene as internal standard. [d] 21% of allylic alkylation product was also observed. [e] The corresponding benzylic diene was also observed (see 1.4 Experimental Section for details).

1.2.7 PRODUCT DERIVATIZATIONS

To assess the utility of the asymmetric intramolecular [4+2] products, we started by altering the oxidation state of ketone **11a** (Figure 1.8A) through a 1,2-reduction, which provided alcohol **38** in quantitative yield and in 1.5:1 dr. Subsequently, we explored ring expansion strategies to incorporate heteroatoms and to furnish different ring systems (Figure 1.8A). From ketone **11a**, oxime condensation and subsequent Beckmann rearrangement afforded lactam **39** as a single isomer in 56% yield over two steps. Analogously, Baeyer–Villiger oxidation furnished lactone **40** in 41% yield as a single isomer.

Furthermore, the tricyclic cycloaddition products closely resemble many members of the atisane family of diterpenoids (Figure 1.8B, **41**-**44**). Therefore, reactions to further functionalize these scaffolds were explored. First, hydrogenolysis followed by persulfate-mediated radical decarboxylation of **11f** afforded ketone **45** in 27% yield over two steps.[20] We were delighted to find that the exo-cyclic methylene motif presented in both crotogoudin (**41**) and campylopin (**44**) could be achieved through aldol condensations from both **45** and **11f** to yield crotogoudin-like enone **46** in 41% yield and analogous enone **47** in 26% yield.[21] Enone **47** can be further functionalized through dihydroxylation to furnish the primary and tertiary alcohol centers of the acochlearine (**42**) core in 13% yield and 10:1 dr (**48**).[22] A wider spectrum of natural product cores could also be accessed through

Figure 1.8. *(A) Oxidation state alterations, ring system adjustments, and heteroatom incorporation on* ***11a****. (B) Reaction sequences to construct natural product-like cores.*



oxidation at different sites of the tricyclic hydrocarbon backbone. For example, Riley oxidation of **11f** provided diketone **49** in 50% yield,[23] which can then be selectively mono-protected as acetal **50** in 41% yield.[24] Further manipulations to the exposed ketone of **50** could yield spiramilactam B (**43**)-like oxidation patterns. To that end, directed C–H oxidation following an oxime condensation of **11f** yielded oxime **51** in 30% yield. Deprotection of the oxime afforded the desired acetate on campylopin (**44**)-like tricycle **52** in 19% yield as a single diastereomer.[25] Overall, derivatization of cycloadduct **11f** allowed access to four natural product-like motifs, demonstrating the potential of applying this transformation to asymmetric natural product syntheses.

1.3 CONCLUSIONS

We developed an asymmetric decarboxylative [4+2] cycloaddition employing a key catalytically-generated chiral Pd enolate intermediate – analogous to those implicated in inner-sphere allylic alkylation reactions. To enable this transformation, we first systematically modified the allyl moiety to disfavor undesired allylic alkylation. This allows the conjugated Pd enolate to engage in a [4+2] cycloaddition with a pendant dienophile. Computational and experimental analysis supports the role of C–C bond formation as the enantiodetermining step. Further computational investigation reveals that the catalyst turnover occurs through a proton transfer from the prenyl group directly to the transposed enolate, forming the desired product and releasing isoprene. Building upon these mechanistic insights, we were able to further favor the desired [4+2] cycloaddition over premature protonation for challenging substrates relevant to complex natural product synthesis. In summary, our approach of divergent catalysis serves as a powerful framework

for rational design in asymmetric catalytic reactions. Studies applying this strategy more broadly in other synthetically relevant transformations are currently underway.

1.4 EXPERIMENTAL SECTION

1.4.1 MATERIALS AND METHODS

Unless otherwise stated, reactions were performed in flame-dried glassware under an argon or nitrogen atmosphere using dry, deoxygenated solvents. Solvents were dried by passage through an activated alumina column under argon.[26] Reaction progress was monitored by thin-layer chromatography (TLC) or Agilent 1290 UHPLC-MS. TLC was performed using E. Merck silica gel 60 F254 precoated glass plates (0.25 mm) and visualized by UV fluorescence quenching or $KMnO_4$ staining. Silicycle Silia*Flash*® P60 Academic Silica gel (particle size 40–63 nm) was used for flash chromatography. ^{1}H NMR spectra were recorded on a Bruker 400 MHz spectrometer and are reported relative to residual $CHCl_3$ (δ 7.26 ppm). ^{13}C NMR spectra were recorded on a Bruker 400 MHz spectrometer (100 MHz) and are reported relative to $CHCl_3$ (δ 77.16 ppm). ^{2}H NMR spectra were recorded on a Bruker 400 MHz (61 MHz) spectrometer and are reported relative to residual $CDCl_3$ (δ 7.26 ppm). Data for ^{1}H NMR are reported as follows: chemical shift (δ ppm) (multiplicity, coupling constant (Hz), integration). Multiplicities are reported as the peaks appear as follows: s = singlet, d = doublet, t = triplet, q = quartet, p = pentet, sept = septuplet, m = multiplet, br s = broad singlet, br d = broad doublet. Data for ^{13}C NMR are reported in terms of chemical shifts (δ ppm). Some reported spectra include minor solvent impurities of water (δ 1.56 ppm), ethyl acetate (δ 4.12, 2.05, 1.26 ppm), methylene chloride (δ 5.30 ppm), acetone (δ 2.17 ppm), grease (δ 1.26, 0.86 ppm), and/or

silicon grease (δ 0.07 ppm), which do not impact product assignments. ^{13}C NMR spectra of deuterated compounds are complicated by the low intensity of peaks of deuterium-substituted carbon atoms. IR spectra were obtained by use of a Perkin Elmer Spectrum BXII spectrometer or Nicolet 6700 FTIR spectrometer using thin films deposited on NaCl plates and reported in frequency of absorption (cm^{-1}). Optical rotations were measured with a Jasco P-2000 polarimeter operating on the sodium D-line (589 nm), using a 100 mm path-length cell. Analytical SFC was performed with a Mettler SFC supercritical CO_2 analytical chromatography system utilizing Chiralpak (AD-H or IC) or Chiralcel (OD-H, OJ-H, or OB-H) columns (4.6 mm x 25 cm) obtained from Daicel Chemical Industries, Ltd. High resolution mass spectra (HRMS) were obtained from the Caltech Mass Spectral Facility using a JEOL JMS-600H High Resolution Mass Spectrometer in Field Desorption (FD+) mode. Absolute stereochemical assignments were made by vibrational circular dichroism analysis for select compounds with related compounds assigned by analogy.

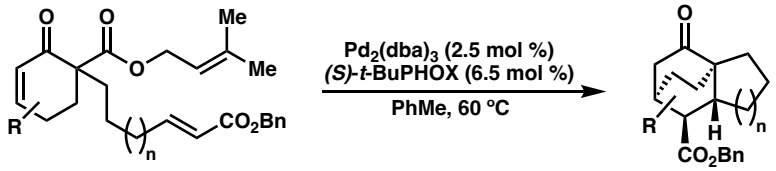
Reagents were purchased from commercial sources and used as received unless otherwise stated. Ligands were prepared according to literature procedures.[27]

List of Abbreviations: ee – enantiomeric excess, SFC – supercritical fluid chromatography, TLC – thin-layer chromatography, IPA – isopropanol, VCD – vibrational circular dichroism.

1.4.2 EXPERIMENTAL PROCEDURES AND SPECTROSCOPIC DATA

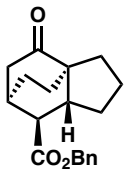
Pd-Catalyzed Decarboxylative Cycloadditions

General Procedure 1A: Asymmetric Pd-Catalyzed Decarboxylative Cycloadditions.



10 ***11***

In a nitrogen filled glovebox, an oven-dried 20 mL vial was charged with a stir bar, $Pd_2(dba)_3$ (4.6 mg, 0.005 mmol, 2.5 mol %), *(S)*-*t*-BuPHOX (5.0 mg, 0.013 mmol, 6.5 mol %), and toluene (5 mL). The catalyst solution was stirred at 23 ºC for 20 min. A solution of substrate **10** (0.2 mmol, 1 equiv) in toluene (5 mL) was added to the vial. The resultant solution was then heated to 60 ºC for 14 h. The solution was then cooled to 23 ºC and concentrated under reduced pressure. The crude reaction mixture was loaded directly onto a flash column and the product (**11**) was isolated by silica gel flash column chromatography.



11a

benzyl (3a*R*,6*R*,7*S*,7a*R*)-4-oxooctahydro-3a,6-ethanoindene-7-carboxylate (11a)

Prepared from **10a** following General Procedure 1A. Purification by flash column chromatography (0–35% EtOAc/hexanes) afforded the title compound as a colorless oil (49.7 mg, 0.167 mmol, 83% yield, 87% ee). Absolute and relative stereochemistry were assigned by VCD (vida infra). 2D NMR studies independently confirm the relative stereochemistry (vida infra).

^{1}H NMR (400 MHz, $CDCl_3$): δ 7.40 – 7.31 (m, 5H), 5.14 (d, *J* = 1.6 Hz, 2H), 2.54 (dt, *J* = 18.8, 2.3 Hz, 1H), 2.51 – 2.47 (m, 2H), 2.21 (dddd, *J* = 10.6, 8.7, 7.2, 1.7 Hz, 1H), 2.14 – 2.04 (m, 3H), 1.86 (ddd, *J* = 13.0, 11.1, 6.8 Hz, 1H), 1.81 – 1.72 (m, 2H), 1.70 – 1.52 (m, 3H), 1.44 (ddt, *J* = 12.9, 10.9, 1.8 Hz, 1H), 1.22 (ddd, *J* = 13.9, 9.2, 4.9 Hz, 1H).

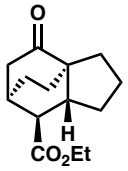
^{13}C NMR (100 MHz, $CDCl_3$): δ 215.1, 174.7, 136.0, 128.8, 128.5, 128.2, 66.7, 54.2, 47.5, 43.3, 41.3, 32.9, 29.1, 27.4, 26.5, 25.1, 22.6.

IR (Neat Film, NaCl): 2947, 2873, 1726, 1455, 1267, 1160 cm^{-1}.

HRMS (MM: FD+): *m/z* calc'd for $C_{19}H_{22}O_3$ $[M]^+$: 298.1564, found 298.1576.

Optical Rotation: $[\alpha]_D^{21}$ –20.3 (c 1.00, $CHCl_3$).

SFC conditions: 15% IPA, 2.5 mL/min, Chiralpak AD-H column, λ = 210 nm, t_R (min): minor = 4.21, major = 5.30



11b

ethyl (3a*R*,6*R*,7*S*,7a*R*)-4-oxooctahydro-3a,6-ethanoindene-7-carboxylate (11b)

Prepared from **10b** following General Procedure 1A. Purification by flash column chromatography (5–30% EtOAc/hexanes) afforded the title compound as a colorless oil (39.9 mg, 0.169 mmol, 84% yield, 88% ee).

^{1}H NMR (400 MHz, $CDCl_3$): δ 4.15 (q, *J* = 7.1 Hz, 2H), 2.55 (dt, *J* = 18.8, 2.6 Hz, 1H), 2.49 – 2.44 (m, 1H), 2.42 (d, *J* = 8.6 Hz, 1H), 2.23 – 2.14 (m, 1H), 2.15 – 2.04 (m, 3H),

1.91 – 1.71 (m, 3H), 1.71 – 1.52 (m, 3H), 1.50 – 1.40 (m, 1H), 1.26 (t, J = 7.1 Hz, 3H), 1.21 (dt, J = 9.2, 4.9 Hz, 1H).

^{13}C NMR (100 MHz, $CDCl_3$): δ 215.2, 174.9, 60.8, 54.2, 47.5, 43.3, 41.3, 32.9, 29.1, 27.4, 26.5, 25.1, 22.6, 14.4.

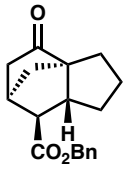
IR (Neat Film, NaCl): 2947, 2873, 1725, 1270, 1170 cm^{-1}.

HRMS (MM: FD+): *m/z* calc'd for $C_{14}H_{20}O_3$ $[M]^+$: 236.1412, found 236.1415.

Optical Rotation: $[\alpha]_D^{21}$ –34.2 (c 1.00, $CHCl_3$).

Enantiomeric excess determined by converting ethyl ester to benzyl ester through saponification and Steglish esterification.

SFC conditions: 15% IPA, 2.5 mL/min, Chiralpak AD-H column, λ = 210 nm, t_R (min): minor = 4.21, major = 5.30



11c

benzyl (3a*R*,6*R*,7*S*,7a*R*)-4-oxooctahydro-3a,6-methanoindene-7-carboxylate (11c)

Prepared from **10c** following General Procedure 1A. Purification by flash column chromatography (0–30% EtOAc/hexanes) afforded the title compound as a colorless oil (37.0 mg, 0.130 mmol, 65% yield, 65% ee).

^{1}H NMR (400 MHz, $CDCl_3$): δ 7.42 – 7.29 (m, 5H), 5.13 (dd, J = 12.3, 7.9 Hz, 2H), 2.96 (t, J = 4.2, 1H), 2.92 (ddd, J = 5.2, 3.7, 1.4, 1H), 2.42 – 2.35 (m, 1H), 2.22 – 2.17 (m, 1H),

2.16 – 2.05 (m, 3H), 1.95 (ddtd, *J* = 12.9, 8.4, 5.1, 2.2 Hz, 1H), 1.90 – 1.80 (m, 2H), 1.66 (dt, *J* = 10.6, 1.6 Hz, 1H), 1.52 – 1.37 (m, 2H).

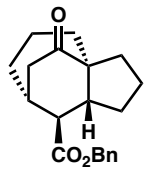
^{13}C NMR (100 MHz, $CDCl_3$): δ 213.9, 173.3, 136.0, 128.8, 128.5, 128.3, 67.8, 66.6, 52.4, 48.5, 41.8, 40.6, 40.5, 32.2, 27.5, 22.1.

IR (Neat Film, NaCl): 2960, 2358, 1739, 1164, 730, 668 cm^{-1}.

HRMS (MM: FD+): *m/z* calc'd for $C_{18}H_{20}O_3$ $[M]^+$: 284.1414, found 284.1407.

Optical Rotation: $[\alpha]_D^{21}$ +20.0 (c 1.00, $CHCl_3$).

SFC conditions: 15% IPA, 2.5 mL/min, Chiralpak AD-H column, λ = 210 nm, t_R (min): minor = 3.97, major = 4.33.



11d

benzyl (3a*R*,7*R*,8*S*,8a*R*)-10-oxooctahydro-1*H*-3a,7-ethanoazulene-8-carboxylate (11d)

Prepared from **10d** following General Procedure 1A. Purification by flash column chromatography (0–35% EtOAc/hexanes) afforded the title compound as a colorless oil (51.8 mg, 0.166 mmol, 83% yield, 97% ee).

^{1}H NMR (400 MHz, $CDCl_3$): δ 7.40 – 7.31 (m, 5H), 5.16 (d, *J* = 12.4 Hz, 1H), 5.12 (d, *J* = 12.3 Hz, 1H), 2.70 – 2.63 (m, 2H), 2.64 – 2.56 (m, 1H), 2.25 (ddd, *J* = 18.5, 2.0, 1.0 Hz, 1H), 2.08 (td, *J* = 10.5, 7.8 Hz, 1H), 2.03 – 1.94 (m, 1H), 1.93 – 1.79 (m, 3H), 1.78 – 1.60 (m, 4H), 1.59 – 1.43 (m, 4H).

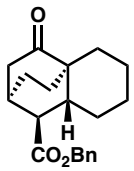
^{13}C NMR (100 MHz, $CDCl_3$): δ 215.7, 175.8, 136.0, 128.8, 128.5, 128.3, 66.7, 58.0, 50.2, 45.4, 41.0, 35.7, 33.6, 33.3, 32.0, 28.0, 21.8, 21.2.

IR (Neat Film, NaCl): 2934, 2873, 1727, 1713, 1455, 1161 cm^{-1}.

HRMS (MM: FD+): *m/z* calc'd for $C_{20}H_{24}O_3$ $[M+H]^+$: 312.1720, found 312.1734.

Optical Rotation: $[\alpha]_D^{21}$ +21.4 (c 1.00, $CHCl_3$).

SFC conditions: 15% IPA, 2.5 mL/min, Chiralpak AD-H column, λ = 210 nm, t_R (min): minor = 4.70, major = 6.23.



11f

benzyl (1*S*,2*R*,4a*R*,8a*R*)-4-oxooctahydro-2*H*-2,4a-ethanonaphthalene-1-carboxylate (11f).

Prepared from **10f** following General Procedure 1A. Purification by flash column chromatography (0–35% EtOAc/hexanes) afforded the title compound as a colorless oil (26.3 mg, 0.084 mmol, 42% yield, 92% ee).

^{1}H NMR (400 MHz, $CDCl_3$): δ 7.39 – 7.29 (m, 5H), 5.16 (d, *J* = 12.4 Hz, 1H), 5.10 (d, *J* = 12.2 Hz, 1H), 2.47 (dt, *J* = 17.0, 2.8 Hz, 2H), 2.28 – 2.19 (m, 2H), 2.14 (ddd, *J* = 19.7, 3.8, 1.8 Hz, 1H), 2.01 (dddd, *J* = 11.8, 6.8, 4.5, 1.7 Hz, 1H), 1.87 (ddtd, *J* = 12.8, 4.5, 3.4, 1.6 Hz, 1H), 1.83 – 1.71 (m, 1H), 1.71 – 1.56 (m, 4H), 1.51 – 1.11 (m, 5H).

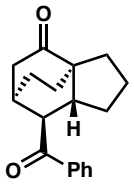
^{13}C NMR (100 MHz, $CDCl_3$): δ 216.3, 174.5, 136.0, 128.7, 128.4, 128.2, 66.7, 49.8, 45.1, 40.5, 37.1, 30.9, 30.0, 28.9, 26.2, 25.6, 21.7, 21.1.

IR (Neat Film, NaCl): 2928, 2856, 1721, 1170 cm^{-1}.

HRMS (MM: FD+): *m/z* calc'd for $C_{20}H_{24}O_3$ $[M]^+$: 312.1720, found 312.1732.

Optical Rotation: $[\alpha]_D^{21}$ –15.5 (c 1.00, $CHCl_3$).

SFC conditions: 15% IPA, 2.5 mL/min, Chiralpak AD-H column, λ = 210 nm, t_R (min): minor = 4.70, major = 6.23.



11j

(3a*R*,6*R*,7*S*,7a*R*)-7-benzoylhexahydro-3a,6-ethanoinden-4(1*H*)-one (11j)

Prepared from **10j** following General Procedure 1A. Purification by flash column chromatography (0–30% EtOAc/hexanes) afforded the title compound as a colorless oil (27.1 mg, 0.101 mmol, 50% yield, 87% ee).

^{1}H NMR (400 MHz, $CDCl_3$): δ 7.97 – 7.94 (m, 2H), 7.61 – 7.56 (m, 1H), 7.51 – 7.46 (m, 2H), 3.42 (d, *J* = 8.5 Hz, 1H), 2.58 – 2.50 (m, 2H), 2.41 – 2.38 (m, 1H), 2.16 (ddd, *J* = 13.7, 11.1, 6.2 Hz, 1H), 2.08 – 1.87 (m, 4H), 1.82 – 1.74 (m, 1H), 1.70 – 1.50 (m, 4H), 1.25 (ddd, *J* = 14.0, 9.2, 5.1 Hz, 1H).

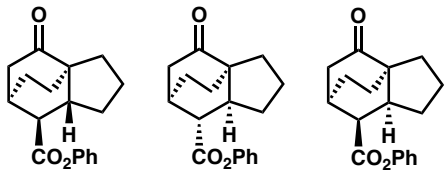
^{13}C NMR (100 MHz, $CDCl_3$): δ 214.9, 201.0, 136.4, 133.4, 128.9, 128.5, 54.2, 49.4, 41.4, 40.8, 34.1, 28.9, 27.8, 26.5, 25.6, 22.7.

IR (Neat Film, NaCl): 2945, 2871, 1720, 1677, 1447, 1217 cm^{-1}.

HRMS (MM: FD+): *m/z* calc'd for $C_{18}H_{20}O_2$ $[M]^+$: 268.1463, found 268.1463.

Optical Rotation: $[\alpha]_D^{21}$ –32.7 (c 1.00, $CHCl_3$).

SFC conditions: 30% IPA, 2.5 mL/min, Chiralpak AD-H column, λ = 210 nm, t_R (min): minor = 2.55, major = 3.40.



phenyl (3a*R*,6*R*,7*S*,7a*R*)-4-oxooctahydro-3a,6-ethanoindene-7-carboxylate (11k, 11k' and 11k'')

Prepared from **10k** following General Procedure 1A. Purification by flash column chromatography (0–35% EtOAc/hexanes) afforded the title compound as a colorless oil (47.2 mg, 0.166 mmol, 83% yield, 14.8:1.6:1.0 *endo-trans*/*endo-cis*/*exo-trans*, 88% ee (*endo-trans*)). Crude analysis by ^{1}H NMR affords a 10.4:1.4:1.0 ratio of *endo-trans*/*exo-trans/endo-cis*. The diastereomers were subsequently separated by preparative HPLC (15% IPA/hexanes, 25 mL/min, Chiralpak AD-H column) for independent characterization. Absolute and relative stereochemistry were assigned/confirmed by VCD where applicable (vida infra) in addition to 2D NMR.

11k (endo-trans):

^{1}H NMR (400 MHz, $CDCl_3$): δ 7.41 – 7.34 (m, 2H), 7.25 – 7.20 (m, 1H), 7.09 – 7.04 (m, 2H), 2.70 (d, *J* = 8.7 Hz, 1H), 2.67 – 2.60 (m, 2H), 2.31 (dddd, *J* = 10.6, 8.8, 7.3, 1.7 Hz, 1H), 2.23 – 2.09 (m, 3H), 1.97 – 1.76 (m, 3H), 1.67 (ddddd, *J* = 13.5, 11.1, 9.0, 6.2, 4.5 Hz, 3H), 1.50 (ddt, *J* = 12.5, 10.6, 1.7 Hz, 1H), 1.31 – 1.17 (m, 1H).

^{13}C NMR (100 MHz, $CDCl_3$): δ 214.8, 173.4, 150.7, 129.6, 126.0, 121.5, 54.2, 47.5, 43.4, 41.2, 32.9, 29.1, 27.3, 26.5, 25.0, 22.5.

IR (Neat Film, NaCl): 2948, 2872, 1750, 1721, 1592, 1492, 1192, 1144 cm^{-1}.

HRMS (MM: FD+): *m/z* calc'd for $C_{18}H_{20}O_3$ $[M]^+$: 284.1412, found 284.1411.

Optical Rotation: $[\alpha]_D^{21}$ –16.7 (c 0.20, $CHCl_3$). *(single major enantiomer of 11j)*

SFC conditions: 15% IPA, 2.5 mL/min, Chiralpak AD-H column, λ = 210 nm, t_R (min): minor = 4.09, major = 6.08.

11k' (exo-trans):

^{1}H NMR (400 MHz, $CDCl_3$): δ 7.39 – 7.34 (m, 2H), 7.25 – 7.19 (m, 1H), 7.06 – 7.01 (m, 2H), 3.30 (dt, *J* = 12.0, 2.3 Hz, 1H), 3.08 (dt, *J* = 19.5, 2.8 Hz, 1H), 2.58 (h, *J* = 2.8 Hz, 1H), 2.47 – 2.33 (m, 2H), 2.21 (dt, *J* = 19.6, 2.4 Hz, 1H), 2.08 – 2.01 (m, 2H), 1.93 – 1.71 (m, 5H), 1.70 – 1.59 (m, 1H), 1.04 (ddd, *J* = 12.8, 11.4, 6.7 Hz, 1H).

^{13}C NMR (100 MHz, $CDCl_3$): δ 215.2, 171.8, 150.6, 129.6, 126.0, 121.7, 54.6, 45.8, 44.0, 40.1, 31.4, 28.4, 28.2, 27.0, 26.3, 21.8.

IR ($CDCl_3$ solution): 2951, 2870, 1751, 1717, 1194, 1163, 1146 cm^{-1}.

HRMS (MM: FD+): *m/z* calc'd for $C_{18}H_{20}O_3$ $[M]^+$: 284.1412, found 284.1417.

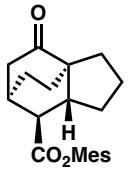
11k'' (endo-cis):

^{1}H NMR (400 MHz, $CDCl_3$): δ 7.43 – 7.36 (m, 2H), 7.27 – 7.22 (m, 1H), 7.12 – 7.07 (m, 2H), 2.76 – 2.67 (m, 1H), 2.58 (dt, *J* = 8.3, 1.7 Hz, 1H), 2.48 – 2.33 (m, 4H), 2.12 – 2.01 (m, 2H), 1.91 – 1.63 (m, 5H), 1.10 (ddd, *J* = 13.0, 11.2, 6.5 Hz, 1H), 1.01 (ddd, *J* = 12.4, 9.5, 2.8 Hz, 1H).

^{13}C NMR (100 MHz, $CDCl_3$): δ 215.1, 172.9, 150.9, 129.6, 126.1, 121.6, 53.8, 49.4, 46.0, 44.2, 32.7, 32.0, 28.6, 27.4, 22.6, 21.5.

IR ($CDCl_3$ solution): 2945, 2872, 1751, 1717, 1194, 1163, 1130 cm^{-1}.

HRMS (MM: FD+): *m/z* calc'd for $C_{18}H_{20}O_3$ $[M]^+$: 284.1412, found 284.1407.



11l

mesityl (3a*R*,6*R*,7*S*,7a*R*)-4-oxooctahydro-3a,6-ethanoindene-7-carboxylate (11l)

Prepared from **10l** following General Procedure 1A. Purification by flash column chromatography (0–35% EtOAc/hexanes) afforded the title compound as a colorless oil (58.6 mg, 0.180 mmol, 90% yield, 89% ee).

^{1}H NMR (400 MHz, $CDCl_3$):) δ 6.87 (s, 2H), 2.75 (d, *J* = 8.8 Hz, 1H), 2.72 – 2.65 (m, 2H), 2.36 (dddd, *J* = 10.6, 8.9, 7.3, 1.6 Hz, 1H), 2.26 (s, 3H), 2.24 – 2.09 (m, 3H), 2.08 (s, 6H), 1.98 – 1.78 (m, 3H), 1.75 – 1.61 (m, 3H), 1.55 – 1.48 (m, 1H), 1.31 – 1.24 (m, 1H).

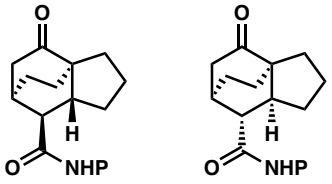
^{13}C NMR (100 MHz, $CDCl_3$): δ 214.8, 172.8, 145.9, 135.6, 129.5, 129.5, 54.2, 47.4, 43.5, 41.3, 33.2, 29.2, 27.5, 26.5, 25.1, 22.6, 20.9, 16.4.

IR (Neat Film, NaCl): 2946, 2873, 1747, 1723, 1485, 1458, 1189, 1137 cm^{-1}.

HRMS (MM: FD+): *m/z* calc'd for $C_{21}H_{26}O_3$ $[M]^+$: 326.1877, found 326.1886.

Optical Rotation: $[\alpha]_D^{21}$ –25.8 (c 1.00, $CHCl_3$).

SFC conditions: 15% IPA, 2.5 mL/min, Chiralpak AD-H column, λ = 210 nm, t_R (min): minor = 4.06, major = 4.33.



11m **(endo)** **11m'** **(exo)**

1,3-dioxoisoindolin-2-yl(3a*R*,6*R*,7*S*,7a*R*)-4-oxooctahydro-3a,6-ethanoindene-7-carboxylate (11m and 11m')

Prepared from **10m** following General Procedure 1A. Purification by flash column chromatography (0–35% EtOAc/hexanes) afforded the title compounds as colorless oils (**Endo**: 37.7 mg, 0.106 mmol, 53% yield, 62% ee; **Exo**: 8.6 mg, 0.024 mmol, 12% yield, 62% ee).

11m (endo):

^{1}H NMR (400 MHz, $CDCl_3$): δ 7.92 – 7.85 (m, 2H), 7.83 – 7.75 (m, 2H), 2.84 (dd, *J* = 8.7, 1.3 Hz, 1H), 2.71 (m, 1H), 2.64 (dt, *J* = 18.9, 2.5 Hz, 1H), 2.46 – 2.28 (m, 1H), 2.28 – 2.18 (m, 2H), 2.13 (m, 1H), 1.98 – 1.76 (m, 3H), 1.76 – 1.60 (m, 3H), 1.56 – 1.48 (m, 1H), 1.34 – 1.19 (m, 1H).

^{13}C NMR (100 MHz, $CDCl_3$): δ 214.0, 171.4, 162.1, 135.0, 129.0, 124.2, 54.1, 44.8, 43.3, 41.0, 33.2, 28.9, 27.2, 26.4, 24.9, 22.4.

IR (Neat Film, NaCl): 2948, 2873, 1782, 1742, 1718, 1466, 1362, 1185 cm^{-1}.

HRMS (MM: FD+): *m/z* calc'd for $C_{20}H_{19}NO_5$ $[M]^+$: 353.1263, found 353.1251.

Optical Rotation: $[\alpha]_D^{21}$ –0.2 (c 1.00, $CHCl_3$).

SFC conditions: 30% IPA, 2.5 mL/min, Chiralpak IC column, l = 210 nm, t_R (min): minor = 4.03, major = 3.00

11m' (exo):

^{1}H NMR (400 MHz, $CDCl_3$): δ 7.90 (dd, *J* = 5.5, 3.1 Hz, 2H), 7.81 (dd, *J* = 5.5, 3.1 Hz, 2H), 2.77 (tt, *J* = 3.9, 2.2 Hz, 1H), 2.73 (d, *J* = 8.4 Hz, 1H), 2.47 – 2.28 (m, 4H), 2.19 – 2.02 (m, 2H), 1.92 – 1.71 (m, 4H), 1.71 – 1.61 (m, 1H), 1.11 (ddd, *J* = 13.1, 11.2, 6.6 Hz, 1H), 1.08 – 0.95 (m, 1H).

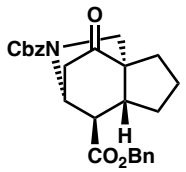
^{13}C NMR (100 MHz, $CDCl_3$): δ 214.2, 170.8, 162.1, 135.0, 129.1, 124.2, 53.7, 46.7, 46.0, 44.1, 32.9, 31.8, 28.4, 27.2, 22.5, 21.2.

IR (Neat Film, NaCl): 2947, 2868, 1809, 1784, 1743, 1717, 1466, 1362, 1185 cm^{-1}.

HRMS (MM: FD+): *m/z* calc'd for $C_{20}H_{19}NO_5$ $[M]^+$: 353.1263, found 353.1261.

Optical Rotation: $[\alpha]_D^{21}$ –13.6 (c 0.81, $CHCl_3$).

SFC conditions: 30% IPA, 2.5 mL/min, Chiralpak IC column, l = 210 nm, t_R (min): minor = 4.98, major = 4.29.



11n

dibenzyl (3aR,4R,5R,7aS)-7-oxooctahydro-5,7a-(epiminomethano)indene-4,9-dicarboxylate (11n)

Prepared from **10n** following General Procedure 1A. Purification by flash column chromatography (0–40 % EtOAc/hexanes) afforded the title compound as a colorless oil (76.1 mg, 0.176 mmol, 88% yield, 14.3:1 endo/exo, 91% ee (endo)).

^{1}H NMR (400 MHz, $CDCl_3$): δ 7.35 (dd, *J* = 7.1, 4.9 Hz, 10H), 5.21 – 5.07 (m, 4H), 4.90 – 4.74 (m, 1H), 3.49 (dd, *J* = 12.1, 5.8 Hz, 1H), 3.40 – 3.27 (m, 1H), 2.88 (t, *J* = 8.9 Hz, 1H), 2.66 – 2.42 (m, 2H), 2.30 (p, *J* = 9.3 Hz, 1H), 2.23 – 2.10 (m, 2H), 1.91 – 1.56 (m, 3H), 1.33 – 1.14 (m, 1H).

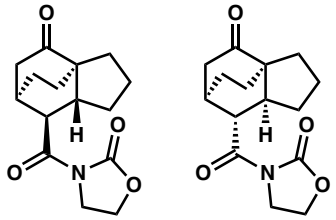
^{13}C NMR (100 MHz, $CDCl_3$): δ 210.1, 209.7, 172.2, 154.4, 136.3, 135.5, 128.9, 128.7, 128.7, 128.4, 128.4, 128.4, 128.3, 128.2, 128.1, 67.6, 67.2, 55.9, 55.8, 50.4, 50.0, 48.8, 48.6, 45.7, 45.6, 42.6, 42.6, 41.7, 41.6, 29.0, 28.9, 24.1, 22.9.

IR (Neat Film, NaCl): 3399, 2963, 2874, 2357, 1729, 1700, 1652, 1414, 1288, 1156, 1115, 748, 681 cm^{-1}.

HRMS (MM: FD+): *m/z* calc'd for $C_{26}H_{27}NO_5$ $[M]^+$: 433.1889, found 433.1874.

Optical Rotation: $[\alpha]_D^{21}$ –39.8 (c 0.75, $CHCl_3$).

SFC conditions: 15% IPA, 2.5 mL/min, Chiralpak AD-H column, l = 210 nm, t_R (min): minor = 9.19, major = 11.59.



11o (endo) ***11o' (exo)***

3-((3a*R*,6*R*,7*S*,7a*R*)-4-oxooctahydro-3a,6-ethanoindene-7-carbonyl)oxazolidin-2-one (11o and 11o')

Prepared from **10o** following General Procedure 1A. Purification by flash column chromatography (0–90 % EtOAc/hexanes) afforded the title compound as a colorless oil

(51.2 mg, 0.185 mmol, 92% yield, 1.1:1 endo/exo (ratio from crude ^{1}H NMR analysis), 84% ee (endo), 79% ee (exo)).

11o (endo):

^{1}H NMR (400 MHz, $CDCl_3$): δ 4.43 (t, *J* = 8.1 Hz, 2H), 4.15 – 4.00 (m, 2H), 3.54 – 3.47 (m, 1H), 2.66 (ddd, *J* = 12.4, 8.3, 6.9 Hz, 1H), 2.52 – 2.25 (m, 4H), 1.92 – 1.68 (m, 5H), 1.67 – 1.53 (m, 2H), 1.08 (ddd, *J* = 12.9, 11.2, 6.4 Hz, 1H), 0.89 (tt, *J* = 12.3, 9.5 Hz, 1H).

^{13}C NMR (100 MHz, $CDCl_3$): δ 215.5, 173.8, 153.4, 62.1, 53.7, 48.3, 44.1, 44.0, 43.1, 33.8, 31.3, 28.7, 27.3, 22.8, 20.8.

IR (Neat Film, NaCl): 2942, 2867, 1775, 1714, 1693, 1387, 1267, 1222, 1040 cm^{-1}.

HRMS (MM: FD+): *m/z* calc'd for $C_{15}H_{19}NO_4$ $[M]^+$: 277.1314, found 277.1321.

Optical Rotation: $[\alpha]_D^{21}$ –39.5 (c 1.00, $CHCl_3$).

SFC conditions: 20% IPA, 2.5 mL/min, Chiralpak AD-H column, λ = 210 nm, t_R (min): minor = 4.15, major = 5.17.

11o' (exo):

^{1}H NMR (400 MHz, $CDCl_3$): δ 4.43 (t, *J* = 8.1 Hz, 2H), 4.13 – 3.97 (m, 2H), 3.71 (d, *J* = 8.8 Hz, 1H), 2.59 – 2.41 (m, 2H), 2.35 (dd, *J* = 3.5, 2.3 Hz, 1H), 2.19 – 1.84 (m, 5H), 1.81 – 1.41 (m, 6H), 1.27 – 1.18 (m, 1H).

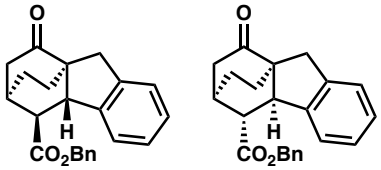
^{13}C NMR (100 MHz, $CDCl_3$): δ 214.9, 174.6, 153.5, 62.13, 54.1, 45.6, 43.1, 41.2, 40.6, 34.5, 28.4, 27.3, 26.5, 25.3, 22.7.

IR (Neat Film, NaCl): 2949, 2872, 1775, 1718, 1692, 1387, 1221,1040, 759 cm^{-1}.

HRMS (MM: FD+): *m/z* calc'd for $C_{15}H_{19}NO_4$ $[M]^+$: 277.1314, found 277.1317.

Optical Rotation: $[\alpha]_D^{21}$ –5.8 (c 1.00, $CHCl_3$).

SFC conditions: 15% IPA, 2.5 mL/min, Chiralpak AD-H column, λ = 210 nm, t_R (min): minor = 6.80, major = 6.38.



11p (endo) ***11p' (exo)***

benzyl (3*R*,4*S*,4a*S*,9a*S*)-1-oxo-1,2,3,4,4a,9-hexahydro-3,9a-ethanofluorene-4-carboxylate (11p and 11p')

Prepared from **10p** following General Procedure 1A. Purification by flash column chromatography (0–35% EtOAc/hexanes) afforded the title compounds as colorless oils (**Endo**: 56.8 mg, 0.156 mmol, 78% yield, 72% ee; **Exo**: 2.0 mg, 5.48 μmol, 3% yield).

11p (endo):

^{1}H NMR (400 MHz, $CDCl_3$): δ 7.28 – 7.20 (m, 5H), 7.14 – 7.05 (m, 4H), 5.13 (d, *J* = 2.4 Hz, 2H), 3.53 (dd, *J* = 9.4, 1.0 Hz, 1H), 3.16 (d, *J* = 15.7 Hz, 1H), 2.74 (dt, *J* = 9.3, 1.1 Hz, 1H), 2.61 (dt, *J* = 18.8, 2.4 Hz, 1H), 2.51 (ttd, *J* = 3.5, 2.2, 1.1 Hz, 1H), 2.31 (d, *J* = 15.8 Hz, 1H), 2.11 (ddd, *J* = 18.8, 3.5, 1.2 Hz, 1H), 1.70 – 1.56 (m, 2H), 1.54 – 1.45 (m, 1H), 1.42 – 1.34 (m, 1H).

^{13}C NMR (100 MHz, $CDCl_3$): δ 214.0, 174.6, 142.3, 140.6, 135.8, 128.8, 128.6, 128.4, 127.3, 127.0, 125.5, 124.3, 67.1, 56.6, 47.8, 45.6, 42.1, 35.0, 33.2, 27.0, 24.8.

IR (Neat Film, NaCl): 2942, 2869, 1726, 1457, 1164 cm^{-1}.

HRMS (MM: FD+): *m/z* calc'd for $C_{23}H_{22}O_3$ $[M+H]^+$: 346.1564, found 346.1571.

Optical Rotation: $[\alpha]_D^{21}$ +1.4 (c 1.00, $CHCl_3$).

SFC conditions: 15% IPA, 2.5 mL/min, Chiralpak AD-H column, λ = 210 nm, t_R (min): minor = 6.74, major = 6.28.

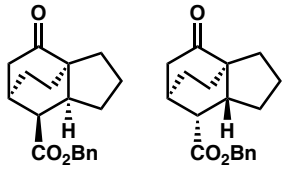
11p' (exo):

^{1}H NMR (400 MHz, $CDCl_3$): δ 7.41 – 7.34 (m, 5H), 7.24 (d, *J* = 7.1 Hz, 1H), 7.14 – 7.07 (m, 3H), 5.30 (d, *J* = 12.3 Hz, 1H), 5.25 (d, *J* = 12.3 Hz, 1H), 3.85 (d, *J* = 9.4 Hz, 1H), 3.46 (d, *J* = 14.7 Hz, 1H), 2.75 (d, *J* = 9.3 Hz, 1H), 2.69 – 2.65 (m, 1H), 2.44 (d, *J* = 14.9 Hz, 1H), 2.37 (dd, *J* = 18.7, 2.1 Hz, 1H), 2.19 (ddd, *J* = 18.6, 3.4, 2.1 Hz, 1H), 2.15 – 2.07 (m, 2H), 1.90 – 1.84 (m, 1H), 1.81 – 1.76 (m, 1H).

^{13}C NMR (100 MHz, $CDCl_3$): δ 213.5, 174.0, 143.8, 142.7, 135.9, 128.8, 128.6, 128.4, 127.2, 126.6, 124.8, 122.5, 67.1, 56.4, 49.9, 48.3, 44.1, 35.3, 31.9, 27.5, 21.8.

IR (Neat Film, NaCl): 2918, 1727, 1161 cm^{-1}.

HRMS (MM: FD+): *m/z* calc'd for $C_{23}H_{22}O_3$ $[M+H]^+$: 346.1569, found 346.1568.



11q (endo) *11q' (exo)*

benzyl (3a*R*,6*R*,7*S*,7a*S*)-4-oxooctahydro-3a,6-ethanoindene-7-carboxylate (11q and 11q')

Prepared from **10q** following General Procedure 1A. Purification by flash column chromatography (0–35% EtOAc/hexanes) afforded the title compound as a colorless oil (54.9 mg, 0.183 mmol, 92% yield, 1.6:1 endo/exo, 84% ee (endo), 29% ee (exo)). The *endo* (**11q**) and *exo* (**11q'**) diastereomers were subsequently separated by preparative TLC (25%

EtOAc/hexanes) for independent characterization. Absolute and relative stereochemistry were assigned/confirmed by VCD (see below).

11q (endo):

^{1}H NMR (400 MHz, $CDCl_3$): δ 7.39 – 7.31 (m, 5H), 5.13 – 5.02 (m, 2H), 3.10 – 2.99 (m, 2H), 2.47 (h, *J* = 2.9 Hz, 1H), 2.36 – 2.21 (m, 2H), 2.15 (dt, *J* = 19.3, 2.3 Hz, 1H), 1.86 – 1.63 (m, 6H), 1.56 – 1.48 (m, 1H), 1.06 – 0.92 (m, 2H).

^{13}C NMR (100 MHz, $CDCl_3$): δ 215.5, 172.9, 135.9, 128.7, 128.7, 128.5, 66.3, 54.4, 45.9, 44.0, 40.2, 31.4, 28.3, 28.1, 27.0, 26.4, 21.8.

IR (Neat Film, NaCl): 2940, 2868, 1728, 1456, 1174, 1166, 1146 cm^{-1}.

HRMS (MM: FD+): *m/z* calc'd for $C_{19}H_{22}O_3$ $[M]^+$: 298.1564, found 298.1578.

Optical Rotation: $[\alpha]_D^{21}$ –32.4 (c 1.00, $CHCl_3$).

SFC conditions: 15% IPA, 2.5 mL/min, Chiralpak AD-H column, λ = 210 nm, t_R (min): minor = 5.44, major = 6.53.

11q' (exo):

^{1}H NMR (400 MHz, $CDCl_3$): δ 7.40 – 7.31 (m, 5H), 5.14 (d, *J* = 12.3 Hz, 1H), 5.09 (d, *J* = 12.2 Hz, 1H), 3.01 (ddd, *J* = 11.7, 3.3, 1.4 Hz, 1H), 2.46 (h, *J* = 3.3 Hz, 1H), 2.35 – 2.25 (m, 3H), 2.14 (tdd, *J* = 11.6, 7.9, 1.6 Hz, 1H), 2.07 – 1.94 (m, 2H), 1.88 – 1.69 (m, 3H), 1.63 – 1.57 (m, 1H), 1.47 – 1.34 (m, 2H), 1.16 (ddd, *J* = 13.9, 9.1, 5.0 Hz, 1H).

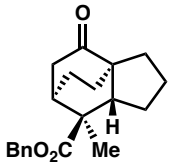
^{13}C NMR (100 MHz, $CDCl_3$): δ 215.5, 173.1, 136.0, 128.8, 128.5, 128.5, 66.3, 53.6, 45.4, 42.7, 41.2, 32.0, 26.4, 25.3, 24.4, 22.3, 21.8.

IR (Neat Film, NaCl): 2946, 2847, 1720, 1457, 1154 cm^{-1}.

HRMS (MM: FD+): *m/z* calc'd for $C_{19}H_{22}O_3$ $[M]^+$: 298.1564, found 298.1578.

Optical Rotation: $[\alpha]_D^{21}$ –5.1 (c 1.00, $CHCl_3$).

SFC conditions: 15% IPA, 2.5 mL/min, Chiralpak IC column, $\lambda = 210$ nm, t_R (min): minor = 7.01, major = 7.42.



11r

benzyl (3a*R*,6*R*,7*S*,7a*S*)-7-methyl-4-oxooctahydro-3a,6-ethanoindene-7-carboxylate (11r)

Prepared from **10r** following General Procedure 1A. Purification by flash column chromatography (0–30% EtOAc/hexanes) afforded the title compound as a colorless oil (29.4 mg, 0.094 mmol, 47% yield, 89% ee).

^{1}H NMR (400 MHz, $CDCl_3$): δ 7.39 – 7.29 (m, 5H), 5.16 (d, *J* = 12.4 Hz, 1H), 5.10 (d, *J* = 12.4 Hz, 1H), 2.49 – 2.38 (m, 2H), 2.32 (dt, *J* = 18.9, 2.8 Hz, 1H), 2.19 – 2.10 (m, 2H), 2.01 – 1.92 (m, 1H), 1.85 – 1.66 (m, 4H), 1.65 – 1.55 (m, 1H), 1.49 – 1.31 (m, 5H), 1.13 (ddd, *J* = 14.5, 9.1, 6.0 Hz, 1H).

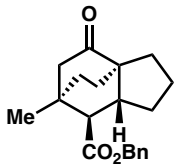
^{13}C NMR (100 MHz, $CDCl_3$): δ 215.2, 177.8, 136.1, 128.7, 128.4, 128.0, 66.8, 54.37, 45.8, 44.7, 43.4, 37.3, 26.5, 24.4, 24.1, 22.7, 22.4, 20.8.

IR (Neat Film, NaCl): 2951, 2875, 1723, 1454, 1239, 1212, 1106 cm^{-1}.

HRMS (MM: FD+): *m/z* calc'd for $C_{20}H_{24}O_3$ $[M]^+$: 312.1725, found 312.1732.

Optical Rotation: $[\alpha]_D^{21}$ –15.3 (c 1.00, $CHCl_3$).

SFC conditions: 40% IPA, 2.5 mL/min, Chiralpak IC column, $\lambda = 210$ nm, t_R (min): minor = 2.68, major = 3.51.



11s

benzyl (3aR,6R,7R,7aR)-6-methyl-4-oxooctahydro-3a,6-ethanoindene-7-carboxylate (11s)

Prepared from **10s** following General Procedure 1A. Purification by flash column chromatography (0–25% EtOAc/hexanes) afforded the title compound as a colorless oil (43.6 mg, 0.140 mmol, 69% yield, 83% ee).

^{1}H NMR (400 MHz, $CDCl_3$): δ 7.42 – 7.29 (m, 5H), 5.13 (d, *J* = 1.1 Hz, 2H), 2.86 (dd, *J* = 18.5, 3.5 Hz, 1H), 2.37 (dd, *J* = 8.8, 1.4 Hz, 1H), 2.29 – 2.15 (m, 1H), 2.15 – 2.04 (m, 1H), 2.01 – 1.70 (m, 3H), 1.84 (dd, *J* = 18.7, 1.4 Hz, 1H), 1.68 – 1.36 (m, 4H), 1.30 – 1.15 (m, 2H), 0.94 (s, 3H).

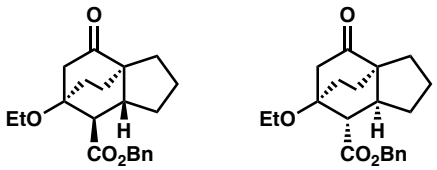
^{13}C NMR (100 MHz, $CDCl_3$): δ 214.5, 174.9, 135.9, 128.8, 128.5, 128.5, 66.7, 54.2, 52.6, 47.0, 44.9, 38.0, 36.0, 28.7, 26.3, 26.0, 23.8, 22.8.

IR (Neat Film, NaCl): 2949, 2873, 1750, 1498, 1454, 1384, 1324, 1155, 1114, 977, 754, 698, 678, 556 cm^{-1}.

HRMS (MM: FD+): *m/z* calc'd for $C_{20}H_{24}O_3$ $[M]^+$: 312.1703, found 312.1720.

Optical Rotation: $[\alpha]_D^{21}$ –68.2 (c 0.75, $CHCl_3$).

SFC conditions: 15% IPA, 2.5 mL/min, Chiralpak IC column, λ = 210 nm, t_R (min): minor = 10.23, major = 12.31.



11t (endo) ***11t' (exo)***

benzyl (3a*R*,6*S*,7*R*,7a*R*)-6-ethoxy-4-oxooctahydro-3a,6-ethanoindene-7-carboxylate (11t and 11t')

Prepared from **10t** following General Procedure 1A. Purification by flash column chromatography (0–50% EtOAc/hexanes) afforded the title compounds as colorless oils (**Endo**: 44.0 mg, 0.128 mmol, 64% yield, 85% ee; **Exo**: 17.0 mg, 0.050 mmol, 25% yield, 72% ee). Absolute and relative stereochemistry were assigned/confirmed by VCD (see below).

11t (endo):

^{1}H NMR (400 MHz, $CDCl_3$): δ 7.38 – 7.28 (m, 5H), 5.16 (d, *J* = 1.5 Hz, 2H), 3.55 – 3.32 (m, 2H), 3.17 (dd, *J* = 18.5, 3.1 Hz, 1H), 2.86 (dd, *J* = 8.5, 1.5 Hz, 1H), 2.38 – 2.25 (m, 2H), 2.16 – 2.02 (m, 1H), 2.02 – 1.86 (m, 3H), 1.87 – 1.39 (m, 5H), 1.20 (ddd, *J* = 14.1, 9.1, 5.1 Hz, 1H), 1.03 (t, *J* = 7.0 Hz, 3H).

^{13}C NMR (100 MHz, $CDCl_3$): δ 210.8, 173.7, 136.0, 128.7, 128.4, 128.3, 78.2, 66.8, 58.0, 54.2, 51.9, 45.1, 45.1, 30.7, 28.8, 25.8, 24.8, 22.9, 15.8.

IR (Neat Film, NaCl): 2944, 2875, 1726, 1458, 1390, 1320, 1282, 1153, 1110, 1039, 746, 700 cm^{-1}.

HRMS (MM: FD+): *m/z* calc'd for $C_{21}H_{26}O_4$ $[M]^+$: 342.1832, found 342.1826.

Optical Rotation: $[\alpha]_D^{21}$ –47.4 (c 0.75, $CHCl_3$).

SFC conditions: 15% IPA, 2.5 mL/min, Chiralpak AD-H column, λ = 210 nm, t_R (min): minor = 4.73, major = 5.13.

11t' (exo):

^{1}H NMR (400 MHz, $CDCl_3$): δ 7.42 – 7.28 (m, 5H), 5.19 (d, *J* = 1.1 Hz, 2H), 3.57 – 3.35 (m, 2H), 2.69 (dd, *J* = 7.8, 1.7 Hz, 1H), 2.60 – 2.47 (m, 1H), 2.47 – 2.44 (m, 2H), 2.39 (ddd, *J* = 12.5, 7.9, 6.9 Hz, 1H), 2.28 (ddd, *J* = 13.5, 9.4, 4.6 Hz, 1H), 1.92 – 1.78 (m, 3H), 1.77 – 1.66 (m, 1H), 1.67 – 1.58 (m, 1H), 1.11 (ddd, *J* = 11.3, 6.6, 3.7 Hz, 1H), 1.03 (t, *J* = 6.9 Hz, 3H), 0.89 (tt, *J* = 12.4, 9.6 Hz, 1H).

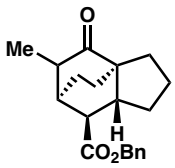
^{13}C NMR (100 MHz, $CDCl_3$): δ 211.5, 173.4, 136.0, 128.7, 128.4, 128.3, 66.9, 58.1, 54.1, 52.8, 47.5, 46.8, 31,0, 27.7, 26.5, 25.9, 23.1, 15.7.

IR (Neat Film, NaCl): 2946, 1721, 1451, 1390, 1328, 1154, 1117, 767, 698 cm^{-1}.

HRMS (MM: FD+): *m/z* calc'd for $C_{21}H_{26}O_4$ $[M]^+$: 342.1833, found 342.1826.

Optical Rotation: $[\alpha]_D^{21}$ +1.8 (c 0.75, $CHCl_3$).

SFC conditions: 15% IPA, 2.5 mL/min, Chiralpak IC column, λ = 210 nm, t_R (min): minor = 3.29, major = 4.04.



11u

benzyl (3a*R*,6*R*,7*S*,7a*R*)-5-methyl-4-oxooctahydro-3a,6-ethanoindene-7-carboxylate (11u)

Prepared from **10u** following General Procedure 1A. Purification by flash column chromatography (0–25% EtOAc/hexanes) afforded the title compound as a colorless oil (13.6 mg, 0.044 mmol, 22% yield, 61% ee).

^{1}H NMR (400 MHz, $CDCl_3$): δ 7.39 – 7.32 (m, 5H), 5.14 (ddd, *J* = 17.8, 12.2 Hz, 2H), 2.61 (dd, *J* = 3.7, 2.1 Hz, 1H), 2.45 – 2.30 (m, 3H), 2.21 – 2.06 (m, 4H), 1.90 – 1.63 (m, 3H), 1.61 – 1.35 (m, 2H), 1.32 – 1.16 (m, 1H), 0.97 (d, *J* = 7.7 Hz, 3H).

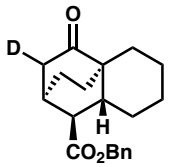
^{13}C NMR (100 MHz, $CDCl_3$): δ 217.7, 174.8, 135.9, 128.7, 128.6, 128.5, 66.8, 54.2, 48.3, 46.9, 42.2, 38.1, 29.7, 28.9, 26.6, 24.1, 22.5, 15.8.

IR (Neat Film, NaCl): 2943, 2873, 1718, 1455, 1197, 1171 cm^{-1}.

HRMS (MM: FD+): *m/z* calc'd for $C_{20}H_{24}O_3$ $[M]^+$: 312.1725, found 312.1730.

Optical Rotation: $[\alpha]_D^{21}$ +10.9 (c 0.75, $CHCl_3$).

SFC conditions: 15% IPA, 2.5 mL/min, Chiralpak AD-H column, λ = 210 nm, t_R (min): minor = 5.84, major = 5.43.



D-11f

benzyl (1*S*,2*R*,4a*R*,8a*R*)-4-oxooctahydro-2*H*-2,4a-ethanonaphthalene-1-carboxylate-3-*d* (*D*-11f)

Prepared from ***D*-10f** following General Procedure 1A. Purification by flash column chromatography (0–30% EtOAc/hexanes) afforded the title compound as a colorless oil (41.3 mg, 0.132 mmol, 66% yield, 91% ee).

^{1}H NMR (400 MHz, $CDCl_3$): δ 7.39 – 7.30 (m, 5H), 5.16 (d, *J* = 12.4 Hz, 1H), 5.11 (d, *J* = 12.2 Hz, 1H), 2.51 – 2.41 (m, 1.6H), 2.36 – 2.10 (m, 2.7H), 2.02 (dddd, *J* = 11.8, 9.1, 5.3, 2.9 Hz, 1H), 1.91 – 1.83 (m, 1H), 1.82 – 1.71 (m, 1H), 1.70 – 1.55 (m, 4H), 1.52 – 1.11 (m, 5H).

^{13}C NMR (100 MHz, $CDCl_3$): δ 216.4, 174.5, 136.0, 128.8, 128.4, 128.2, 77.5, 77.2, 76.8, 66.7, 49.9, 45.1, 40.5, 37.1, 31.0, 30.9, 30.8, 30.0, 28.9, 26.2, 25.6, 21.8, 21.2.

**Partial deuteration complicates ^{13}C NMR spectrum. Peaks are listed as they appear.*

^{2}H NMR (61 MHz, $CHCl_3$): δ 2.46, 2.14.

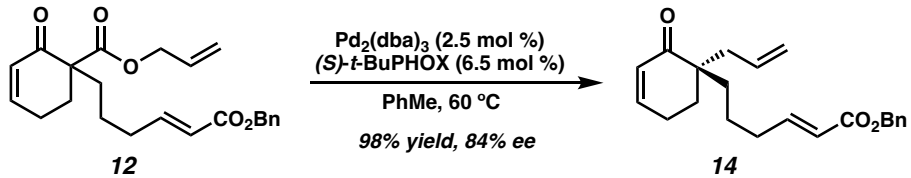
**Trace D-exchanged water observed in spectrum.*

IR (Neat Film, NaCl): 2928, 2858, 1723, 1169 cm^{-1}.

HRMS (MM: FD+): *m/z* calc'd for $C_{20}H_{23}DO_3$ $[M+H]^+$: 313.1783, found 313.1795.

Optical Rotation: $[\alpha]_D^{21}$ –21.3 (c 1.00, $CHCl_3$).

SFC conditions: 15% IPA, 2.5 mL/min, Chiralpak AD-H column, λ = 210 nm, t_R (min): minor = 5.07, major = 6.38.



12 14

benzyl (*S*,*E*)-6-(1-allyl-2-oxocyclohex-3-en-1-yl)hex-2-enoate (14)

Prepared from **12** (0.02 mmol) following General Procedure 1A. Purification by preparatory thin layer chromatography (25% EtOAc/hexanes) afforded the title compound as a colorless oil (10.1 mg, 0.0196 mmol, 98% yield, 84 % ee).

^{1}H NMR (400 MHz, $CDCl_3$): δ 7.40 – 7.29 (m, 5H), 6.97 (dt, *J* = 15.6, 6.9 Hz, 1H), 6.85 (dt, *J* = 10.1, 3.9 Hz, 1H), 5.91 (dt, *J* = 10.0, 2.0 Hz, 1H), 5.85 (dt, *J* = 15.7, 1.6 Hz, 1H), 5.69 (ddt, *J* = 16.6, 10.5, 7.3 Hz, 1H), 5.17 (s, 2H), 5.09 – 5.00 (m, 2H), 2.41 – 2.29 (m, 3H), 2.26 – 2.13 (m, 3H), 1.87 (t, *J* = 6.1 Hz, 2H), 1.63 – 1.23 (m, 4H).

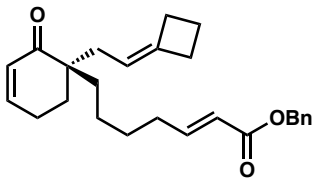
^{13}C NMR (100 MHz, $CDCl_3$): δ 202.9, 166.6, 149.6, 148.7, 136.3, 134.0, 129.0, 128.7, 128.3, 128.3, 121.4, 118.3, 66.2, 47.6, 39.1, 33.9, 32.9, 30.8, 23.1, 22.4.

IR (Neat Film, NaCl): 2936, 2358, 1718, 1669, 1262, 992 cm^{-1}.

HRMS (MM: FD+): *m/z* calc'd for $C_{22}H_{26}O_3$ $[M]^+$: 338.1881, found 338.1877.

Optical Rotation: $[\alpha]_D^{21}$ –0.69 (c 0.62, $CHCl_3$).

SFC conditions: 15% IPA, 2.5 mL/min, Chiralpak IC column, λ = 210 nm, t_R (min): minor = 14.49, major = 11.94.



53

benzyl (*E*)-7-(1-(2-cyclobutylideneethyl)-2-oxocyclohex-3-en-1-yl)hept-2-enoateenoate (53)

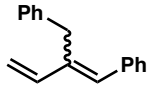
Prepared from **33** following General Procedure 1A, with the modification of being on 0.1 mmol scale. Purification by preparatory thin layer chromatography (20% EtOAc/hexanes) afforded the title compound as a clear oil (2.4 mg, 0.006 mmol, 6% yield).

^{1}H NMR (400 MHz, $CDCl_3$): δ 7.41 – 7.29 (m, 5H), 6.99 (dt, *J* = 15.6, 6.9 Hz, 1H), 6.83 (dt, *J* = 10.0, 3.9 Hz, 1H), 5.92 – 5.81 (m, 2H), 5.17 (s, 2H), 5.01 – 4.92 (m, 1H), 2.67 – 2.54 (m, 3H), 2.40 – 2.30 (m, 2H), 2.27 – 1.99 (m, 4H), 1.96 – 1.82 (m, 3H), 1.63 – 1.49 (m, 3H), 1.49 – 1.36 (m, 3H), 1.32 – 1.13 (m, 2H).

^{13}C NMR (100 MHz, $CDCl_3$): δ 203.6, 166.6, 150.1, 148.5, 143.1, 136.3, 129.1, 128.7, 128.3, 128.3, 121.1, 115.4, 66.2, 48.3, 34.1, 33.1, 32.3, 31.2, 30.8, 29.6, 28.8, 23.6, 23.2, 17.1.

IR (Neat Film, NaCl): 2929, 1720, 1670, 1185 cm^{-1}.

HRMS (MM: FD+): *m/z* calc'd for $C_{26}H_{32}O_3$ $[M]^+$: 392.2351, found 392.2341.



54

(2-vinylprop-1-ene-1,3-diyl)dibenzene (54)

Prepared from **37** following General Procedure 1A, with the modification of being on 0.1 mmol scale. Purification by flash column chromatography (0–35% EtOAc/hexanes) afforded the title compound as a colorless oil (6.5 mg, 0.03 mmol, 29% yield).

^{1}H NMR (400 MHz, $CDCl_3$): δ 7.39 – 7.18 (m, 11.5H), 6.91 – 6.80 (m, 1.15H), 6.56 (ddd, *J* = 17.4, 10.8, 0.9 Hz, 0.15H), 6.45 (s, 1H), 5.42 – 5.33 (m, 1H), 5.19 – 5.13 (m, 1.15H), 5.11 – 5.06 (m, 0.15H), 3.90 (s, 0.3H), 3.73 (s, 2H).

**Isolated as an apparent 1:0.15 mixture of alkene isomers.*

^{13}C NMR (100 MHz, $CDCl_3$): δ 140.5, 140.2, 139.9, 137.7, 137.5, 137.3, 134.2, 133.8, 131.8, 129.6, 128.9, 128.8, 128.7, 128.5, 128.2, 128.2, 127.3, 127.0, 126.2, 126.1, 116.4, 114.8, 40.3, 33.2.

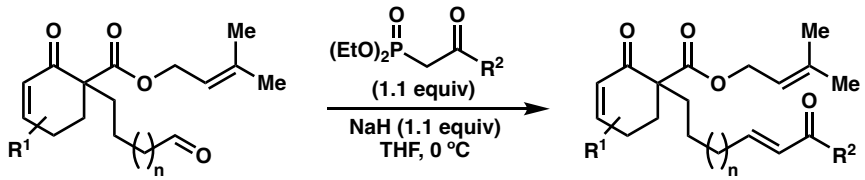
**Isolated as an apparent 1:0.15 mixture of alkene isomers.*

IR (Neat Film, NaCl): 3060, 3023, 2919, 1601, 1493, 1455, 1165, 1074 cm^{-1}.

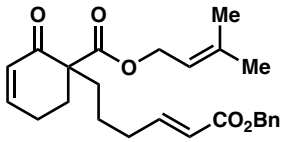
HRMS (MM: FD+): *m/z* calc'd for $C_{17}H_{16}$ $[M]^+$: 220.1252, found 220.1257.

Preparation of Unsaturated β-Ketoester Starting Materials

General Procedure 1B: Horner–Wadsworth–Emmons Olefination



To a suspension of NaH (60% by weight in mineral oil, 1.1 equiv) in THF (0.5 M) at 0 ºC was dropwise added a solution of the appropriate phosphonate ester (1.1 equiv) in THF (1.0 M). Stirred at 0 ºC was continued for 30 minutes. To the reaction was then dropwise added a solution of aldehyde **55** (1.0 equiv) in THF (0.5 M). Upon complete consumption of starting material (as determined by TLC), the reaction mixture was diluted with a saturated solution of $NaHCO_3$ and extracted with EtOAc (3x). The combined organic layers were dried over Na_2SO_4, filtered, and concentrated under reduced pressure. The product (**10**) was purified by silica gel flash column chromatography.



10a

3-methylbut-2-en-1-yl (*E*)-1-(6-(benzyloxy)-6-oxohex-4-en-1-yl)-2-oxocyclohex-3-ene-1-carboxylate (10a)

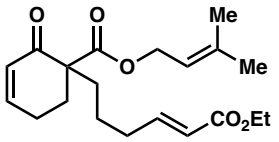
Prepared from **55** and benzyl 2-(diethoxyphosphoryl)acetate [28] following General Procedure 1B. Purification by flash column chromatography (20% EtOAc/hexanes) afforded the title compound as a colorless oil (0.410 g, 1.00 mmol, 67 % yield).

^{1}H NMR (400 MHz, $CDCl_3$): δ 7.38 – 7.29 (m, 5H), 6.98 (dt, *J* = 15.7, 6.9 Hz, 1H), 6.90 – 6.84 (m, 1H), 6.02 (ddd, *J* = 10.1, 2.5, 1.5 Hz, 1H), 5.87 (dt, *J* = 15.6, 1.6 Hz, 1H), 5.31 – 5.24 (m, 1H), 5.17 (s, 2H), 4.58 (dt, *J* = 7.2, 1.0 Hz, 2H), 2.55 – 2.41 (m, 2H), 2.37 – 2.27 (m, 1H), 2.22 (qd, *J* = 7.3, 1.6 Hz, 2H), 1.97 – 1.86 (m, 2H), 1.77 – 1.69 (m, 4H), 1.67 (d, *J* = 1.4 Hz, 3H), 1.55 – 1.38 (m, 2H).

^{13}C NMR (100 MHz, $CDCl_3$): δ 196.3, 171.6, 166.5, 149.3, 149.3, 139.7, 136.3, 129.4, 128.7, 128.3, 128.3, 121.5, 118.3, 66.2, 62.3, 57.0, 33.5, 32.7, 30.5, 25.8, 23.9, 23.2, 18.2.

IR (Neat Film, NaCl): 3034, 2938, 1723, 1684, 1653, 1455, 1384, 1246, 1174, 1166 cm^{-1}.

HRMS (MM: FD+): *m/z* calc'd for $C_{25}H_{30}O_5$ $[M]^+$: 410.2088, found 410.2097.



10b

3-methylbut-2-en-1-yl (*E*)-1-(6-(benzyloxy)-6-oxohex-4-en-1-yl)-2-oxocyclohex-3-ene-1-carboxylate (10b)

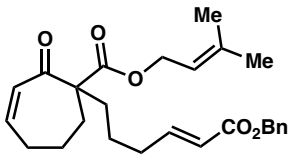
Prepared from **55** and ethyl 2-(diethoxyphosphoryl)acetate following General Procedure 1B. Purification by flash column chromatography (20% EtOAc/hexanes) afforded the title compound as a colorless oil (0.291 g, 0.835 mmol, 47 % yield).

^{1}H NMR (400 MHz, $CDCl_3$): δ 6.97 – 6.85 (m, 2H), 6.02 (ddd, *J* = 10.0, 2.6, 1.5 Hz, 1H), 5.81 (dt, *J* = 15.6, 1.6 Hz, 1H), 5.31 – 5.24 (m, 1H), 4.64 – 4.54 (m, 2H), 4.18 (q, *J* = 7.1 Hz, 2H), 2.55 – 2.41 (m, 2H), 2.37 – 2.27 (m, 1H), 2.21 (qd, *J* = 7.3, 1.6 Hz, 2H), 1.98 – 1.87 (m, 2H), 1.78 – 1.69 (m, 4H), 1.68 (s, 3H), 1.55 – 1.37 (m, 2H), 1.28 (t, *J* = 7.1 Hz, 3H).

^{13}C NMR (100 MHz, $CDCl_3$): δ 196.3, 171.6, 166.8, 149.3, 148.5, 139.7, 129.4, 121.8, 118.3, 62.3, 60.3, 57.0, 33.5, 32.6, 30.5, 25.8, 23.9, 23.3, 18.2, 14.4.

IR (Neat Film, NaCl): 2934, 1714, 1682, 1168 cm^{-1}.

HRMS (MM: FD+): *m/z* calc'd for $C_{20}H_{28}O_5$ $[M]^+$: 348.1937, found 348.1943.



10d

3-methylbut-2-en-1-yl (*E*)-1-(6-(benzyloxy)-6-oxohex-4-en-1-yl)-2-oxocyclohept-3-ene-1-carboxylate (10d)

Prepared from cyclohept-2-en-1-one following General Procedures 1B–D. Note that inseparable impurities plagued the β-ketoester and aldehyde intermediates. Fortunately, these intermediates could be brought through the sequence in sub-optimal purity to still

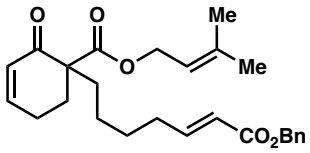
afford the title compound **10d** as a colorless oil (265 mg, 0.62 mmol, 3.2% yield from cyclohept-2-en-1-one) after a final purification by flash column chromatography (20% EtOAc/hexanes).

^{1}H NMR (400 MHz, $CDCl_3$): δ 7.39 – 7.30 (m, 5H), 6.97 (dt, *J* = 15.6, 6.9 Hz, 1H), 6.36 (ddd, *J* = 12.3, 5.5, 3.9 Hz, 1H), 5.98 (ddd, *J* = 12.3, 2.4, 1.4 Hz, 1H), 5.86 (dt, *J* = 15.6, 1.6 Hz, 1H), 5.28 (ddp, *J* = 8.6, 5.7, 1.4 Hz, 1H), 5.17 (s, 2H), 4.57 (d, *J* = 7.2 Hz, 2H), 2.47 – 2.27 (m, 3H), 2.19 (qd, *J* = 7.2, 1.6 Hz, 2H), 1.99 – 1.79 (m, 3H), 1.77 – 1.69 (m, 4H), 1.69 – 1.61 (m, 4H), 1.43 – 1.32 (m, 2H).

^{13}C NMR (100 MHz, $CDCl_3$): δ 201.1, 172.9, 166.5, 149.3, 143.2, 139.7, 136.3, 131.6, 128.7, 128.3, 128.3, 121.5, 118.2, 66.2, 63.9, 62.2, 36.5, 32.6, 32.3, 31.2, 25.8, 24.3, 23.0, 18.2.

IR (Neat Film, NaCl): 2927, 1720, 1686, 1453, 1162 cm^{-1}.

HRMS (MM: FD+): *m/z* calc'd for $C_{26}H_{32}O_5$ $[M]^+$: 424.2244, found 424.2241.



10f

3-methylbut-2-en-1-yl (*E*)-1-(7-(benzyloxy)-7-oxohept-5-en-1-yl)-2-oxocyclohex-3-ene-1-carboxylate (10f)

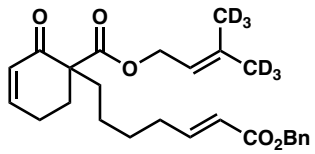
Prepared from **56** and benzyl 2-(diethoxyphosphoryl)acetate[28] following General Procedure 1B. Purification by flash column chromatography (15–20% EtOAc/hexanes) afforded the title compound as a colorless oil (652 mg, 1.54 mmol, 69% yield).

^{1}H NMR (400 MHz, $CDCl_3$): δ 7.39 – 7.30 (m, 5H), 6.99 (ddd, *J* = 15.5, 7.3, 6.3 Hz, 1H), 6.90 – 6.84 (m, 1H), 6.01 (d, *J* = 10.1 Hz, 1H), 5.85 (d, *J* = 15.6 Hz, 1H), 5.30 – 5.25 (m, 1H), 5.17 (s, 2H), 4.58 (d, *J* = 6.6 Hz, 2H), 2.55 – 2.40 (m, 2H), 2.36 – 2.26 (m, 1H), 2.24 – 2.16 (m, 2H), 1.96 – 1.86 (m, 2H), 1.77 – 1.65 (m, 7H), 1.47 (p, *J* = 7.4 Hz, 2H), 1.38 – 1.24 (m, 2H).

^{13}C NMR (100 MHz, $CDCl_3$): δ 196.2, 171.6, 166.5, 149.7, 149.2, 139.4, 136.2, 129.2, 128.6, 128.2, 128.2, 121.1, 118.2, 66.0, 62.1, 56.9, 33.5, 32.0, 30.2, 28.4, 25.7, 24.2, 23.7, 18.1.

IR (Neat Film, NaCl): 2932, 2861, 1722, 1684, 1653, 1456, 1263, 1181 cm^{-1}.

HRMS (MM: FD+): *m/z* calc'd for $C_{26}H_{32}O_5$ $[M]^+$: 424.2244, found 424.2247.



***D*-10f**

3-(methyl-d_3)but-2-en-1-yl-4,4,4-d_3 (*E*)-1-(7-(benzyloxy)-7-oxohept-5-en-1-yl)-2-oxocyclohex-3-ene-1-carboxylate (*D*-10f)

Prepared from ***D*-56** and benzyl 2-(diethoxyphosphoryl)acetate[28] following General Procedure 1B. Purification by flash column chromatography (15–20% EtOAc/hexanes) afforded the title compound as a colorless oil (201 mg, 0.467 mmol, 48 % yield).

^{1}H NMR (400 MHz, $CDCl_3$): δ 7.39 – 7.30 (m, 5H), 6.99 (dt, *J* = 15.6, 6.9 Hz, 1H), 6.90 – 6.85 (m, 1H), 6.01 (ddd, *J* = 10.1, 2.6, 1.5 Hz, 1H), 5.85 (dt, *J* = 15.6, 1.5 Hz, 1H), 5.27 (t, *J* = 7.1 Hz, 1H), 5.17 (s, 2H), 4.58 (dd, *J* = 7.2, 1.7 Hz, 2H), 2.55 – 2.41 (m, 2H), 2.36

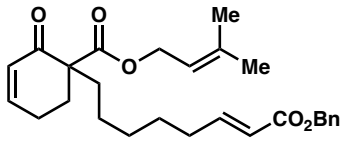
– 2.27 (m, 1H), 2.25 – 2.15 (m, 2H), 1.98 – 1.85 (m, 2H), 1.73 (ddd, *J* = 13.6, 11.2, 5.3 Hz, 1H), 1.51 – 1.42 (m, 2H), 1.37 – 1.25 (m, 2H).

^{13}C NMR (100 MHz, $CDCl_3$): δ 196.4, 171.7, 166.6, 149.8, 149.3, 139.4, 136.3, 129.4, 128.7, 128.3, 128.3, 121.2, 118.4, 66.2, 62.3, 57.0, 33.6, 32.2, 30.3, 28.5, 24.3, 23.9.

^{2}H NMR (61 MHz, $CHCl_3$): δ 1.69, 1.65.

IR (Neat Film, NaCl): 2930, 1720, 1683, 1264, 1167 cm^{-1}.

HRMS (MM: FD+): *m/z* calc'd for $C_{26}H_{26}D_6O_5$ $[M]^+$: 430.2621, found 430.2622.



10g

3-methylbut-2-en-1-yl (*E*)-1-(8-(benzyloxy)-8-oxooct-6-en-1-yl)-2-oxocyclohex-3-ene-1-carboxylate (10g)

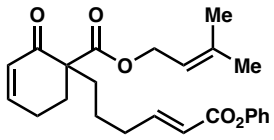
Prepared from **57** and benzyl 2-(diethoxyphosphoryl)acetate[28] following General Procedure 1B. Purification by flash column chromatography (10–25% EtOAc/hexanes) afforded the title compound as a colorless oil (773 mg, 1.76 mmol, 65 % yield).

^{1}H NMR (400 MHz, $CDCl_3$): δ 7.40 – 7.29 (m, 5H), 6.99 (dt, *J* = 15.6, 6.9 Hz, 1H), 6.89 – 6.84 (m, 1H), 6.01 (ddd, *J* = 10.0, 2.5, 1.5 Hz, 1H), 5.85 (dt, *J* = 15.6, 1.6 Hz, 1H), 5.28 (ddp, *J* = 8.6, 5.7, 1.4 Hz, 1H), 5.17 (s, 2H), 4.63 – 4.53 (m, 2H), 2.55 – 2.40 (m, 2H), 2.36 – 2.26 (m, 1H), 2.19 (qd, *J* = 7.1, 1.6 Hz, 2H), 1.98 – 1.84 (m, 2H), 1.77 – 1.69 (m, 4H), 1.67 (s, 3H), 1.49 – 1.41 (m, 2H), 1.36 – 1.23 (m, 4H).

^{13}C NMR (100 MHz, $CDCl_3$): δ 196.5, 171.7, 166.6, 150.1, 149.3, 139.5, 136.3, 129.4, 128.7, 128.3, 128.3, 121.2, 118.4, 66.2, 62.2, 57.1, 33.7, 32.3, 30.3, 29.6, 27.8, 25.8, 24.4, 23.9, 18.2.

IR (Neat Film, NaCl): 2929, 2858, 1721, 1684, 1654, 1456, 1264, 1168 cm^{-1}.

HRMS (MM: FD+): *m/z* calc'd for $C_{27}H_{34}O_5$ $[M]^+$: 438.2401, found 438.2396.



10k

3-methylbut-2-en-1-yl (*E*)-2-oxo-1-(6-oxo-6-phenoxyhex-4-en-1-yl)cyclohex-3-ene-1-carboxylate (10k)

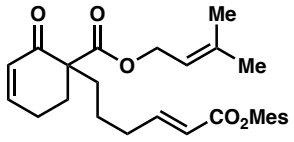
Prepared from **55** and benzyl 2-(diethoxyphosphoryl)acetate [29] following General Procedure 1B. Purification by flash column chromatography (20% EtOAc/hexanes) afforded the title compound as a colorless oil (409 mg, 1.03 mmol, 57 % yield).

^{1}H NMR (400 MHz, $CDCl_3$): δ 7.38 (t, *J* = 8.0 Hz, 2H), 7.22 (t, *J* = 7.4 Hz, 1H), 7.18 – 7.10 (m, 3H), 6.91 – 6.87 (m, 1H), 6.05 – 6.00 (m, 2H), 5.29 (tt, *J* = 7.1, 1.3 Hz, 1H), 4.61 (d, *J* = 7.1 Hz, 2H), 2.56 – 2.44 (m, 2H), 2.37 – 2.27 (m, 3H), 2.00 – 1.92 (m, 2H), 1.82 – 1.73 (m, 4H), 1.69 (s, 3H), 1.63 – 1.46 (m, 2H).

^{13}C NMR (100 MHz, $CDCl_3$): δ 196.3, 171.6, 165.1, 150.9, 150.9, 149.3, 139.7, 129.5, 129.4, 125.8, 121.8, 121.1, 118.3, 62.4, 57.0, 33.6, 32.8, 30.5, 25.8, 23.9, 23.2, 18.2.

IR (Neat Film, NaCl): 2930, 1732, 1684, 1652, 1458, 1245, 1195 cm^{-1}.

HRMS (MM: FD+): *m/z* calc'd for $C_{24}H_{28}O_5$ $[M]^+$: 396.1931, found 396.1945.



10l

3-methylbut-2-en-1-yl (*E*)-1-(6-(mesityloxy)-6-oxohex-4-en-1-yl)-2-oxocyclohex-3-ene-1-carboxylate (10l)

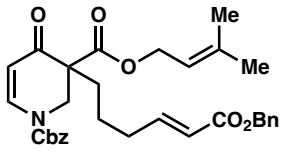
Prepared from **55** and mesityl 2-(diethoxyphosphoryl)acetate [30] following General Procedure 1B. Purification by flash column chromatography (20% EtOAc/hexanes) afforded the title compound as a colorless oil (597 mg, 1.36 mmol, 76% yield).

^{1}H NMR (400 MHz, $CDCl_3$): δ 7.17 (dt, *J* = 15.7, 6.8 Hz, 1H), 6.92 – 6.84 (m, 3H), 6.09 – 6.01 (m, 2H), 5.32 – 5.26 (m, 1H), 4.61 (d, *J* = 5.6 Hz, 2H), 2.57 – 2.43 (m, 2H), 2.39 – 2.27 (m, 3H), 2.26 (s, 3H), 2.09 (s, 6H), 2.01 – 1.92 (m, 2H), 1.79 (ddd, *J* = 13.6, 11.9, 4.8 Hz, 1H), 1.73 (s, 3H), 1.69 (s, 3H), 1.64 – 1.46 (m, 2H).

^{13}C NMR (100 MHz, $CDCl_3$): δ 196.3, 171.6, 164.6, 150.7, 149.3, 146.0, 139.7, 135.3, 130.0, 129.4, 129.3, 120.7, 118.3, 62.4, 57.0, 33.6, 32.8, 30.5, 25.8, 23.9, 23.2, 20.9, 18.2, 16.4.

IR (Neat Film, NaCl: 2920, 1733, 1684, 1458, 1248, 1192, 1140 cm^{-1}.

HRMS (MM: FD+): *m/z* calc'd for $C_{27}H_{34}O_5$ $[M]^+$: 438.2401, found 438.2401.



10n

1-benzyl 3-(3-methylbut-2-en-1-yl) (*E*)-3-(6-(benzyloxy)-6-oxohex-4-en-1-yl)-4-oxo-3,4-dihydropyridine-1,3(2*H*)-dicarboxylate (10n)

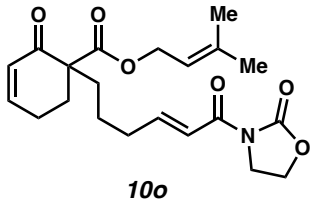
Prepared from **58** and benzyl 2-(diethoxyphosphoryl)acetate[28] following General Procedure 1B. Purification by flash column chromatography (20-30% EtOAc/hexanes) afforded the title compound as a colorless oil (181.3 mg, 0.332 mmol, 55% yield).

^{1}H NMR (400 MHz, $CDCl_3$): δ 7.79 (s, 1H), 7.44 – 7.28 (m, 10H), 6.94 (dt, *J* = 15.5, 6.8 Hz, 1H), 5.85 (dt, *J* = 15.7, 1.6 Hz, 1H), 5.42 – 5.21 (m, 4H), 5.17 (s, 2H), 4.67 – 4.51 (m, 3H), 3.71 (d, *J* = 13.6 Hz, 1H), 2.20 (q, *J* = 7.3 Hz, 2H), 2.07 – 1.92 (m, 1H), 1.69 – 1.58 (m, 1H), 1.71 (s, 3H), 1.66 (s, 3H), 1.49 – 1.40 (m, 2H).

^{13}C NMR (100 MHz, $CDCl_3$): δ 190.5, 169.5, 166.4, 148.7, 142.7, 140.1, 136.2, 135.0, 129.0, 128.9, 128.7, 128.6, 128.4, 128.3, 121.7, 118.0, 106.5, 69.4, 66.2, 62.8, 55.3, 48.3, 32.4, 31.3, 25.8, 23.0, 18.2.

IR (Neat Film, NaCl): 2938, 2338, 1726, 1676, 1604, 1456, 1388, 1303, 1201, 975 cm^{-1}.

HRMS (MM: FD+): *m/z* calc'd for $C_{32}H_{35}NO_7$ $[M]^+$: 545.2414, found 545.2408.



10o

3-methylbut-2-en-1-yl (*E*)-2-oxo-1-(6-oxo-6-(2-oxooxazolidin-3-yl)hex-4-en-1-yl)cyclohex-3-ene-1-carboxylate (10o)

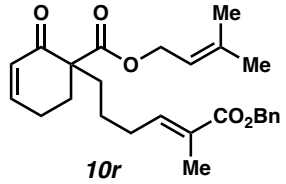
Prepared from **55** and diethyl (2-oxo-2-(2-oxooxazolidin-3-yl)ethyl)phosphonate [31] following General Procedure 1B. Purification by flash column chromatography (0-80% EtOAc/hexanes) afforded the title compound as a colorless oil (275.1 mg, 0.706 mmol, 71% yield).

^{1}H NMR (400 MHz, $CDCl_3$): δ 7.23 (d, *J* = 15.6 Hz, 1H), 7.12 (dt, *J* = 15.4, 6.7 Hz, 1H), 6.87 (ddd, *J* = 7.8, 6.0, 3.9 Hz, 1H), 6.01 (dt, *J* = 10.3, 2.0 Hz, 1H), 5.28 (tt, *J* = 7.2, 1.3 Hz, 1H), 4.62 – 4.54 (m, 2H), 4.41 (dd, *J* = 8.5, 7.6 Hz, 2H), 4.11 – 4.02 (m, 2H), 2.55 – 2.40 (m, 2H), 2.38 – 2.25 (m, 3H), 2.00 – 1.86 (m, 2H), 1.82 – 1.69 (m, 2H), 1.73 (s, 3H), 1.68 (s, 3H), 1.50 (dtd, *J* = 17.3, 12.4, 7.6 Hz, 2H).

^{13}C NMR (100 MHz, $CDCl_3$): δ 196.3, 171.6, 165.3, 153.6, 150.9, 149.4, 139.6, 129.3, 120.5, 118.3, 62.3, 62.2, 57.0, 42.8, 33.4, 33.1, 30.3, 25.8, 23.9, 23.3, 18.2.

IR (Neat Film, NaCl): 2927, 1774, 1724, 1684, 1636, 1385, 1359, 1222, 1042 cm^{-1}.

HRMS (MM: FD+): *m/z* calc'd for $C_{21}H_{27}NO_6$ $[M]^+$: 389.1838, found 389.1827.



10r

3-methylbut-2-en-1-yl (*E*)-1-(6-(benzyloxy)-5-methyl-6-oxohex-4-en-1-yl)-2-oxocyclohex-3-ene-1-carboxylate (10r)

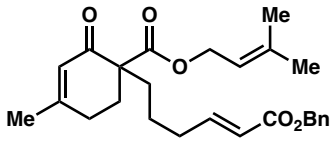
Prepared from **55** and benzyl 2-(diethoxyphosphoryl)propanoate [32] following General Procedure 1B. Purification by flash column chromatography (0–30% EtOAc/hexanes) afforded the title compound as a colorless oil (220 mg, 0.518 mmol, 29% yield).

^{1}H NMR (400 MHz, $CDCl_3$): δ 7.39 – 7.29 (m, 5H), 6.87 (dddd, *J* = 10.1, 4.9, 3.0, 1.1 Hz, 1H), 6.78 (tq, *J* = 7.5, 1.5 Hz, 1H), 6.01 (ddd, *J* = 10.1, 2.5, 1.5 Hz, 1H), 5.31 – 5.24 (m, 1H), 5.18 (s, 2H), 4.58 (d, *J* = 6.9 Hz, 2H), 2.55 – 2.41 (m, 2H), 2.36 – 2.26 (m, 1H), 2.19 (qd, *J* = 7.5, 1.1 Hz, 2H), 1.98 – 1.87 (m, 2H), 1.85 (s, 3H), 1.79 – 1.69 (m, 4H), 1.67 (s, 3H), 1.53 – 1.37 (m, 2H).

^{13}C NMR (100 MHz, $CDCl_3$): δ 196.3, 171.6, 168.0, 149.3, 142.3, 139.6, 136.5, 129.3, 128.6, 128.2, 128.1, 128.1, 118.3, 66.3, 62.3, 57.0, 33.7, 30.4, 29.2, 25.8, 23.9, 23.9, 18.2, 12.6.

IR (Neat Film, NaCl): 2930, 1711, 1686, 1452, 1265, 1180 cm^{-1}.

HRMS (MM: FD+): *m/z* calc'd for $C_{26}H_{32}O_5$ $[M]^+$: 424.2250, found 424.2250.



10s

3-methylbut-2-en-1-yl (*E*)-1-(6-(benzyloxy)-6-oxohex-4-en-1-yl)-4-methyl-2-oxocyclohex-3-ene-1-carboxylate (10s)

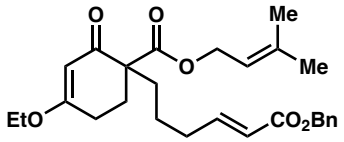
Prepared from **59** and benzyl 2-(diethoxyphosphoryl)acetate[28] following General Procedure 1B. Purification by flash column chromatography (15–20–25% EtOAc/hexanes) afforded the title compound as a colorless oil (827.2 mg, 2.16 mmol, 64% yield).

^{1}H NMR (400 MHz, $CDCl_3$): δ 7.39 – 7.28 (m, 5H), 6.98 (dt, *J* = 15.6, 6.8 Hz, 1H), 5.87 (dq, *J* = 2.7, 1.3 Hz, 1H), 5.86 (dt, *J* = 15.6, 1.6 Hz, 1H), 5.27 (tp, *J* = 7.1, 1.4 Hz, 1H), 5.16 (s, 2H), 4.64 – 4.51 (m, 2H), 2.52 – 2.36 (m, 2H), 2.28 – 2.14 (m, 3H), 1.98 – 1.83 (m, 5H), 1.72 (s, 4H), 1.67 (s, 3H), 1.54 – 1.34 (m, 2H).

^{13}C NMR (100 MHz, $CDCl_3$): δ 195.9, 171.7, 166.5, 161.4, 149.3, 139.6, 136.3, 128.7, 128.3, 128.3, 126.1, 121.5, 118.4, 66.2, 62.3, 55.9, 33.5, 32.7, 30.2, 28.8, 25.8, 24.2, 23.3, 18.2.

IR (Neat Film, NaCl): 3032, 2938, 1723, 1674, 1438, 1379, 1264, 1212, 1168, 1013, 741, 698 cm^{-1}.

HRMS (MM: FD+): *m/z* calc'd for $C_{26}H_{32}O_5$ $[M]^+$: 424.2235, found 424.2244.



10t

3-methylbut-2-en-1-yl (*E*)-1-(6-(benzyloxy)-6-oxohex-4-en-1-yl)-4-ethoxy-2-oxocyclohex-3-ene-1-carboxylate (10t)

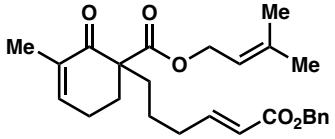
Prepared from **60** and benzyl 2-(diethoxyphosphoryl)acetate[28] following General Procedure 1B. Purification by flash column chromatography (30% EtOAc/hexanes) afforded the title compound as a colorless oil (814.7 mg, 1.79 mmol, 88% yield).

^{1}H NMR (400 MHz, $CDCl_3$): δ 7.40 – 7.28 (m, 5H), 6.98 (dt, *J* = 15.6, 6.8 Hz, 1H), 5.86 (dt, *J* = 15.7, 1.6 Hz, 1H), 5.34 (d, *J* = 1.2 Hz, 1H), 5.28 (dddt, *J* = 7.0, 5.6, 2.8, 1.4 Hz, 1H), 5.16 (s, 2H), 4.66 – 4.52 (m, 2H), 3.89 (qd, *J* = 7.1, 1.6 Hz, 2H), 2.61 (dddd, *J* = 17.9, 10.1, 4.9, 1.2 Hz, 1H), 2.46 – 2.27 (m, 2H), 2.21 (qd, *J* = 7.3, 1.6 Hz, 2H), 2.02 – 1.83 (m, 2H), 1.82 – 1.72 (m, 1H), 1.71 (s, 3H), 1.67 (s, 3H), 1.45 (dddd, *J* = 13.3, 11.2, 6.4, 2.7 Hz, 2H), 1.35 (t, *J* = 7.0 Hz, 3H).

^{13}C NMR (100 MHz, $CDCl_3$): δ 195.8, 176.6, 171.8, 166.5, 149.4, 139.5, 136.3, 128.7, 128.3, 128.3, 121.4, 118.5, 102.3, 66.2, 64.5, 62.3, 56.0, 33.8, 32.7, 28.7, 26.6, 25.8, 23.3, 18.2, 14.3.

IR (Neat Film, NaCl): 2939, 1721, 1655, 1608, 1446, 1380, 1314, 1242, 1190, 1026, 736 cm^{-1}.

HRMS (MM: FD+): *m/z* calc'd for $C_{27}H_{34}O_6$ $[M]^+$: 454.2349, found 454.2350.



10u

3-methylbut-2-en-1-yl (*E*)-1-(6-(benzyloxy)-6-oxohex-4-en-1-yl)-3-methyl-2-oxocyclohex-3-ene-1-carboxylate (10u)

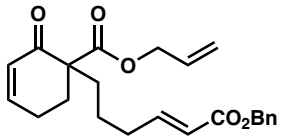
Prepared from **61** and benzyl 2-(diethoxyphosphoryl)acetate[28] following General Procedure 1B. Purification by flash column chromatography (10–25% EtOAc/hexanes) afforded the title compound as a colorless oil (1176.8 mg, 2.77 mmol, 71% yield).

^{1}H NMR (400 MHz, $CDCl_3$): δ 7.41 – 7.26 (m, 5H), 6.98 (dt, *J* = 15.6, 6.8 Hz, 1H), 6.59 (ddt, *J* = 4.7, 3.1, 1.3 Hz, 1H), 5.87 (dt, *J* = 15.6, 1.6 Hz, 1H), 5.27 (tdq, *J* = 7.1, 2.8, 1.5 Hz, 1H), 5.17 (s, 2H), 4.57 (d, *J* = 6.7 Hz, 2H), 2.50 – 2.36 (m, 2H), 2.33 – 2.16 (m, 3H), 1.98 – 1.83 (m, 2H), 1.78 (q, *J* = 1.7 Hz, 3H), 1.77 – 1.64 (m, 1H), 1.72 (s, 3H), 1.67 (s, 3H) 1.61 – 1.34 (m, 3H).

^{13}C NMR (100 MHz, $CDCl_3$): δ 197.0, 171.9, 166.5, 149.4, 143.8, 139.6, 136.3, 135.4, 128.7, 128.3, 128.3, 121.5, 118.3, 66.2, 62.2, 56.9, 33.6, 32.7, 30.9, 25.8, 23.6, 23.4, 18.2, 16.6.

IR (Neat Film, NaCl): 2921, 1721, 1677, 1450, 1377, 1248, 1168, 728 cm^{-1}.

HRMS (MM: FD+): *m/z* calc'd for $C_{26}H_{32}O_5$ $[M]^+$: 424.2244, found 424.2244.



12

allyl (*E*)-1-(6-(benzyloxy)-6-oxohex-4-en-1-yl)-2-oxocyclohex-3-ene-1-carboxylate (12)

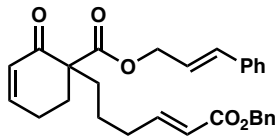
Prepared from **62** and benzyl 2-(diethoxyphosphoryl)acetate[28] following General Procedure 1B. Purification by flash column chromatography (20–25% EtOAc/hexanes) afforded the title compound as a colorless oil (599.1 mg, 1.41 mmol, 46% yield).

^{1}H NMR (400 MHz, $CDCl_3$): δ 7.41 – 7.26 (m, 5H), 6.98 (dt, *J* = 15.6, 6.9 Hz, 1H), 6.89 (dddd, *J* = 10.1, 4.8, 3.1, 1.0 Hz, 1H), 6.03 (ddd, *J* = 10.1, 2.5, 1.6 Hz, 1H), 5.93 – 5.77 (m, 2H), 5.27 (dq, *J* = 17.2, 1.5 Hz, 1H), 5.21 (dq, *J* = 10.4, 1.3 Hz, 1H), 5.17 (s, 2H), 4.60 (dq, *J* = 5.6, 1.6 Hz, 2H), 2.57 – 2.42 (m, 2H), 2.39 – 2.27 (m, 1H), 2.22 (qd, *J* = 7.3, 1.6 Hz, 2H), 2.02 – 1.87 (m, 2H), 1.77 (ddd, *J* = 13.7, 11.7, 5.2 Hz, 1H), 1.57 – 1.40 (m, 2H).

^{13}C NMR (100 MHz, $CDCl_3$): δ 196.0, 171.2, 166.5, 149.5, 149.1, 136.2, 131.7, 129.3, 128.7, 128.3, 128.3, 127.8, 127.1, 121.6, 118.7, 66.2, 65.9, 57.0, 33.4, 32.6, 30.3, 23.8, 23.2.

IR (Neat Film, NaCl): 2937, 2357, 1723, 1684, 1456, 1262, 1165, 992 cm^{-1}.

HRMS (MM: FD+): *m/z* calc'd for $C_{23}H_{27}O_5$ $[M]^+$: 383.1871, found 383.1853.



17

cinnamyl 1-((*E*)-6-(benzyloxy)-6-oxohex-4-en-1-yl)-2-oxocyclohex-3-ene-1-carboxylate (17)

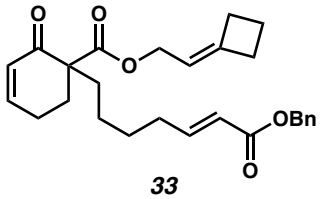
Prepared from **63** and benzyl 2-(diethoxyphosphoryl)acetate[28] following General Procedure 1B. Purification by flash column chromatography (20% EtOAc/hexanes) afforded the title compound as a colorless oil (569 mg, 1.24 mmol, 67% yield).

^{1}H NMR (400 MHz, $CDCl_3$): δ 7.37 – 7.34 (m, 6H), 7.34 – 7.29 (m, 3H), 7.27 – 7.24 (m, 1H), 6.97 (dt, *J* = 15.6, 6.9 Hz, 1H), 6.89 (dddd, *J* = 10.1, 4.8, 3.1, 1.0 Hz, 1H), 6.62 (d, *J* = 15.9 Hz, 1H), 6.22 (dt, *J* = 15.9, 6.4 Hz, 1H), 6.04 (ddd, *J* = 10.1, 2.5, 1.6 Hz, 1H), 5.86 (dt, *J* = 15.7, 1.6 Hz, 1H), 5.16 (s, 2H), 4.76 (dt, *J* = 6.4, 1.4 Hz, 2H), 2.56 – 2.45 (m, 2H), 2.37 – 2.28 (m, 1H), 2.22 (ddd, *J* = 7.4, 7.4, 1.6 Hz, 2H), 1.95 (ddt, *J* = 16.8, 7.9, 5.7 Hz, 2H), 1.78 (ddd, *J* = 13.7, 11.7, 5.0 Hz, 1H), 1.56 – 1.42 (m, 2H).

^{13}C NMR (100 MHz, $CDCl_3$): δ 196.0, 171.4, 166.5, 149.5, 149.1, 136.2, 136.2, 134.7, 129.3, 128.7, 128.7, 128.3, 128.3, 126.8, 122.6, 121.6, 66.2, 65.9, 57.0, 33.4, 32.6, 30.3, 23.8, 23.2.

IR (Neat Film, NaCl): 3034, 2942, 1718, 1700, 1684, 1247, 1166 cm^{-1}

HRMS (MM: FD+): *m/z* calc'd for $C_{29}H_{30}O_5$ $[M]^+$: 458.2088, found 458.2082.



33

22-cyclobutylideneethyl (*E*)-1-(7-(benzyloxy)-7-oxohept-5-en-1-yl)-2-oxocyclohex-3-ene-1-carboxylatecarboxylate (33)

Prepared from **64** and benzyl 2-(diethoxyphosphoryl)acetate[28] following General Procedure 1B. Purification by flash column chromatography (5–60% EtOAc/hexanes) afforded the title compound as a colorless oil (354 mg, 0.81 mmol, 39.8% yield).

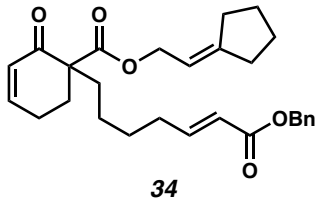
^{1}H NMR (400 MHz, $CDCl_3$): δ 7.40 – 7.29 (m, 5H), 6.99 (dt, *J* = 14.9, 1.0 Hz, 1H), 6.91 – 6.84 (m, 1H), 6.02 (d, *J* = 1.2 Hz, 1H), 5.86 (d, *J* = 15.7 Hz, 1H), 5.24 – 5.13 (m, 3H), 4.51 – 4.41 (m, 2H), 2.75 – 2.62 (m, 4H), 2.56 – 2.39 (m, 2H), 2.36 – 2.27 (m, 1H), 2.25 –

2.16 (m, 2H), 2.02 – 1.84 (m, 4H), 1.73 (ddd, J = 13.6, 11.2, 5.3 Hz, 1H), 1.47 (p, J = 7.5 Hz, 2H), 1.40 – 1.23 (m, 2H).

^{13}C NMR (100 MHz, $CDCl_3$): δ 196.4, 171.6, 166.6, 149.8, 149.3, 148.8, 136.3, 129.4, 128.7, 128.3, 128.3, 121.2, 114.0, 66.2, 62.3, 57.1, 33.6, 32.2, 31.2, 30.3, 29.6, 28.5, 24.3, 23.9, 17.1.

IR (Neat Film, NaCl): 2945, 1722, 1687, 1446, 1169 cm^{-1}.

HRMS (MM: FD+): *m/z* calc'd for $C_{27}H_{32}O_5$ $[M]^+$: 436.2250, found 436.2222.



34

2-cyclopentylideneethyl (*E*)-1-(7-(benzyloxy)-7-oxohept-5-en-1-yl)-2-oxocyclohex-3-ene-1-carboxylate (34)

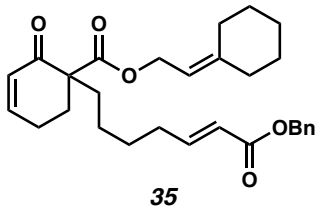
Prepared from **65** and benzyl 2-(diethoxyphosphoryl)acetate[28] following General Procedure 1B. Purification by flash column chromatography (10–60% EtOAc/hexanes) afforded the title compound as a colorless oil (1.40 g, 4.41 mmol, 38.9% yield).

^{1}H NMR (400 MHz, $CDCl_3$): δ 7.40 – 7.28 (m, 5H), 6.99 (dt, J = 15.6, 6.9 Hz, 1H), 6.91 – 6.83 (m, 1H), 6.01 (ddd, J = 10.1, 2.6, 1.5 Hz, 1H), 5.85 (dt, J = 15.6, 1.6 Hz, 1H), 5.37 (tp, J = 7.0, 2.2 Hz, 1H), 5.17 (s, 2H), 4.60 – 4.53 (m, 2H), 2.56 – 2.39 (m, 2H), 2.37 – 2.15 (m, 7H), 1.98 – 1.85 (m, 2H), 1.78 – 1.54 (m, 5H), 1.53 – 1.41 (m, 2H), 1.40 – 1.22 (m, 2H).

^{13}C NMR (100 MHz, $CDCl_3$): δ 196.4, 171.7, 166.6, 151.1, 149.8, 149.3, 136.3, 129.4, 128.7, 128.3, 128.3, 121.2, 113.8, 66.2, 63.7, 57.1, 33.9, 33.6, 32.2, 30.3, 29.0, 28.5, 26.4, 26.2, 24.3, 23.9.

IR (Neat Film, NaCl): 2946, 1719, 1686, 1457, 1165 cm^{-1}.

HRMS (MM: FD+): *m/z* calc'd for $C_{28}H_{34}O_5$ $[M]^+$: 450.2406, found 450.2394.



35

2-cyclohexylideneethyl (*E*)-1-(7-(benzyloxy)-7-oxohept-5-en-1-yl)-2-oxocyclohex-3-ene-1-carboxylate (35)

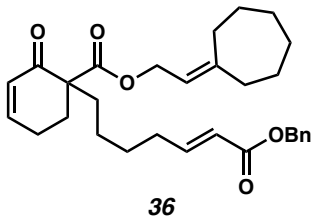
Prepared from **66** and benzyl 2-(diethoxyphosphoryl)acetate[28] following General Procedure 1B. Purification by flash column chromatography (10–60% EtOAc/hexanes) afforded the title compound as a colorless oil (81 mg, 0.17 mmol, 32.9% yield).

^{1}H NMR (400 MHz, $CDCl_3$): δ 7.41 – 7.27 (m, 5H), 6.99 (dt, *J* = 15.6, 6.9 Hz, 1H), 6.87 (dddd, *J* = 10.1, 5.2, 2.5, 1.1 Hz, 1H), 6.01 (ddd, *J* = 10.1, 2.6, 1.5 Hz, 1H), 5.85 (dt, *J* = 15.6, 1.6 Hz, 1H), 5.23 (tp, *J* = 7.3, 1.2 Hz, 1H), 5.17 (s, 2H), 4.59 (d, *J* = 7.2 Hz, 2H), 2.56 – 2.39 (m, 2H), 2.36 – 2.26 (m, 1H), 2.25 – 2.13 (m, 4H), 2.12 – 2.03 (m, 2H), 1.98 – 1.84 (m, 2H), 1.78 – 1.66 (m, 1H), 1.63 – 1.42 (m, 8H), 1.41 – 1.21 (m, 2H).

^{13}C NMR (100 MHz, $CDCl_3$): δ 196.4, 171.6, 166.6, 149.8, 149.3, 147.7, 136.3, 129.4, 128.7, 128.3, 128.3, 121.2, 114.9, 66.2, 61.5, 57.0, 37.1, 33.6, 32.2, 30.4, 29.2, 28.5, 28.5, 27.9, 26.7, 24.3, 23.9.

IR (Neat Film, NaCl): 2929, 2853, 1723, 1681, 1456, 1385, 1266, 1184 cm^{-1}.

HRMS (MM: FD+): *m/z* calc'd for $C_{29}H_{36}O_5$ $[M]^+$: 464.2563, found 464.2543.



36

2-cycloheptylideneethyl (*E*)-1-(7-(benzyloxy)-7-oxohept-5-en-1-yl)-2-oxocyclohex-3-ene-1-carboxylate (36)

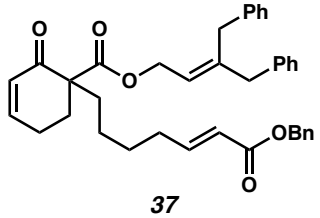
Prepared from **67** and benzyl 2-(diethoxyphosphoryl)acetate[28] following General Procedure 1B. Purification by flash column chromatography (5–70% EtOAc/hexanes) afforded the title compound as a colorless oil (135 mg, 0.28 mmol, 30% yield).

^{1}H NMR (400 MHz, $CDCl_3$): δ 7.43 – 7.29 (m, 5H), 6.99 (dt, *J* = 15.7, 6.9 Hz, 1H), 6.91 – 6.82 (m, 1H), 6.01 (ddd, *J* = 10.2, 2.6, 1.5 Hz, 1H), 5.85 (dt, *J* = 15.6, 1.6 Hz, 1H), 5.27 (tt, *J* = 7.1, 1.3 Hz, 1H), 5.17 (s, 2H), 4.59 (d, *J* = 7.1 Hz, 2H), 2.57 – 2.39 (m, 2H), 2.36 – 2.16 (m, 7H), 1.98 – 1.84 (m, 2H), 1.73 (ddd, *J* = 13.6, 11.3, 5.2 Hz, 1H), 1.61 – 1.43 (m, 10H), 1.31 (dddd, *J* = 13.2, 11.8, 8.6, 6.2 Hz, 2H).

^{13}C NMR (100 MHz, $CDCl_3$): δ 196.4, 171.7, 166.6, 149.8, 149.3, 149.0, 136.3, 129.4, 128.7, 128.3, 128.3, 121.2, 118.4, 66.2, 62.0, 57.0, 37.7, 33.6, 32.2, 30.4, 30.2, 29.8, 29.1, 28.9, 28.5, 27.3, 24.3, 23.9.

IR (Neat Film, NaCl): 2919, 2361, 1722, 1682, 1651, 1443, 1234, 1187 cm^{-1}.

HRMS (MM: FD+): *m/z* calc'd for $C_{30}H_{38}O_5$ $[M]^+$: 478.2719, found 478.2716.



37

3-benzyl-4-phenylbut-2-en-1-yl (*E*)-1-(7-(benzyloxy)-7-oxohept-5-en-1-yl)-2-oxocyclohex-3-ene-1-carboxylate (37)

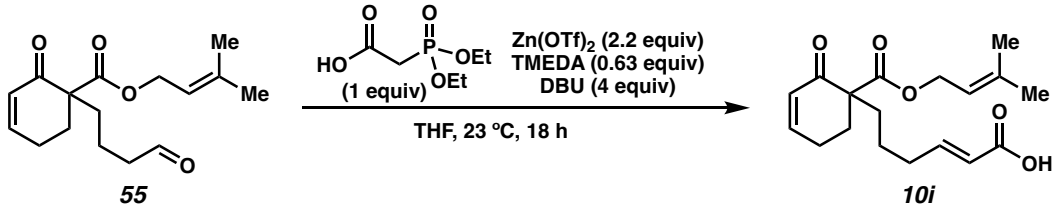
Prepared from **68** and benzyl 2-(diethoxyphosphoryl)acetate[28] following General Procedure 1B. Purification by flash column chromatography (5–70% EtOAc/hexanes) afforded the title compound as a colorless oil (205 mg, 0.36 mmol, 39% yield).

^{1}H NMR (400 MHz, $CDCl_3$): δ 7.39 – 7.24 (m, 9H), 7.23 – 7.17 (m, 2H), 7.09 (dd, *J* = 11.6, 7.3 Hz, 4H), 6.98 (dt, *J* = 15.6, 6.9 Hz, 1H), 6.89 – 6.80 (m, 1H), 6.02 (d, *J* = 10.1 Hz, 1H), 5.85 (d, *J* = 16.1 Hz, 1H), 5.51 (t, *J* = 7.2 Hz, 1H), 5.17 (s, 2H), 4.83 – 4.69 (m, 2H), 3.36 (s, 2H), 3.23 (s, 2H), 2.55 – 2.40 (m, 2H), 2.37 – 2.24 (m, 1H), 2.18 (q, *J* = 7.2 Hz, 2H), 2.00 – 1.85 (m, 2H), 1.75 (ddd, *J* = 13.5, 11.1, 5.2 Hz, 1H), 1.46 (p, *J* = 7.4 Hz, 1H), 1.38 – 1.22 (m, 2H).

^{13}C NMR (100 MHz, $CDCl_3$): δ 196.2, 171.6, 166.6, 149.8, 149.3, 144.8, 139.0, 138.8, 136.3, 129.4, 129.3, 128.8, 128.7, 128.7, 128.5, 128.3, 128.3, 126.5, 126.4, 121.7, 121.3, 66.2, 61.9, 57.1, 42.9, 35.8, 33.6, 32.1, 30.3, 28.5, 24.3, 23.9.

IR (Neat Film, NaCl): 3027, 2931, 1722, 1682, 1493, 1387, 1264, 1165 cm^{-1}.

HRMS (MM: FD+): *m/z* calc'd for $C_{38}H_{40}O_5$ $[M]^+$: 576.2876, found 576.2857.



(*E*)-6-(1-(((3-methylbut-2-en-1-yl)oxy)carbonyl)-2-oxocyclohex-3-en-1-yl)hex-2-enoic acid (10i)[33]

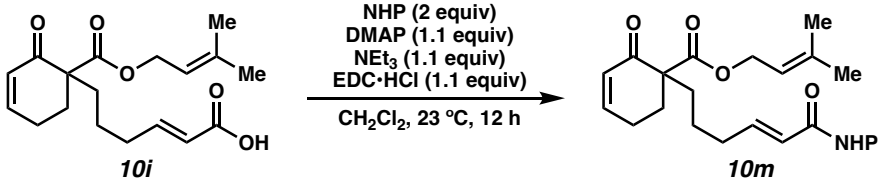
To a suspension of $Zn(OTf)_2$ (6.6 mmol, 2.2 equiv) in THF (15 mL) was added (diethoxyphosphinyl)acetic acid (3 mmol, 1 equiv), followed by the addition of TMEDA (1.89 mmol, 0.63 equiv), DBU (12 mmol, 4 equiv), and then a solution of aldehyde **55** (3 mmol, 1 equiv) in THF (2 mL). The solution was stirred at 23 ºC for 18 h, and the reaction was diluted with 1 M HCl and extracted with dichloromethane (4x). The combined organic layers were dried over Na_2SO_4, filtered, and concentrated under reduced pressure. Purification by silica gel flash column chromatography (35% EtOAc/hexanes with 3% AcOH) afforded the title compound as a white solid (137.4 mg, 0.43 mmol, 43% yield).

^{1}H NMR (400 MHz, $CDCl_3$): δ 7.04 (dt, *J* = 15.7, 6.8 Hz, 1H), 6.93 – 6.84 (m, 1H), 6.03 (ddd, *J* = 10.2, 2.6, 1.5 Hz, 1H), 5.83 (dt, *J* = 15.6, 1.6 Hz, 1H), 5.28 (tp, *J* = 7.2, 1.4 Hz, 1H), 4.66 – 4.53 (m, 2H), 2.58 – 2.40 (m, 2H), 2.37 – 2.28 (m, 1H), 2.25 (qd, *J* = 7.3, 1.6 Hz, 2H), 1.98 – 1.87 (m, 2H), 1.80 – 1.68 (m, 1H), 1.73 (s, 3H), 1.68 (s, 3H), 1.61 – 1.37 (m, 3H).

^{13}C NMR (100 MHz, $CDCl_3$): δ 196.3, 171.6, 170.2, 151.4, 149.3, 139.7, 129.4, 120.8, 118.3, 62.4, 57.0, 33.5, 32.7, 30.5, 25.8, 23.9, 23.1, 18.2.

IR (Neat Film, NaCl): 2929, 1725, 1694, 1424, 1384, 1236, 1171 cm^{-1}.

HRMS (MM: FD+): *m/z* calc'd for $C_{18}H_{24}O_5$ $[M]^+$: 320.1624, found 320.1636.



3-methylbut-2-en-1-yl (*E*)-1-(6-((1,3-dioxoisoindolin-2-yl)oxy)-6-oxohex-4-en-1-yl)-2-oxocyclohex-3-ene-1-carboxylate (10m)[34]

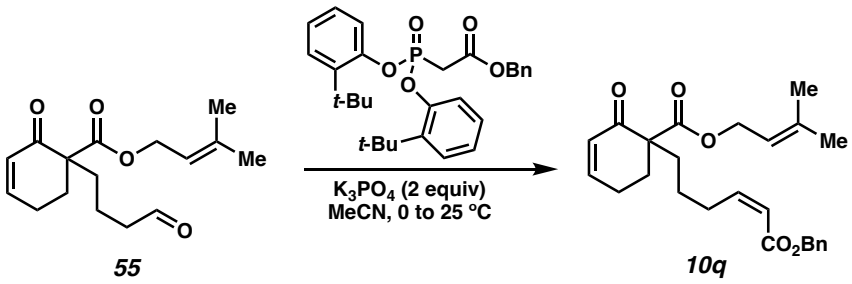
To a round bottom flask was added crude acid **10i** (assumed quantitative yield from previous reaction, 1 mmol, 1 equiv), DMAP (1.1 mmol, 1.1 equiv), NHP (2 mmol, 2 equiv), dichloromethane (9.5 mL), and triethylamine (1.1 mmol, 1.1 equiv). EDC•HCl (1.1 mmol, 1.1 equiv) was then added under N_2 atmosphere in a single portion, and the reaction was stirred vigorously at 23 ºC for 12 h. The reaction mixture was diluted with dichloromethane and washed with 0.5 N HCl, saturated aqueous $NaHCO_3$, and brine. The combined organic layers were dried over Na_2SO_4 and concentrated under reduced pressure. Purification by flash column chromatography (30–35% EtOAc/hexanes) afforded the title compound as a colorless oil (109.6 mg, 0.48 mmol, 24% yield over two steps).

^{1}H NMR (400 MHz, $CDCl_3$): δ 7.96 – 7.84 (m, 2H), 7.79 (dd, *J* = 5.5, 3.1 Hz, 2H), 7.30 (dd, *J* = 15.8, 6.7 Hz, 1H), 6.89 (dddd, *J* = 10.1, 4.9, 3.0, 1.1 Hz, 1H), 6.10 (dt, *J* = 15.8, 1.6 Hz, 1H), 6.04 (ddd, *J* = 10.1, 2.5, 1.5 Hz, 1H), 5.29 (tdt, *J* = 5.7, 2.8, 1.4 Hz, 1H), 4.67 – 4.55 (m, 2H), 2.58 – 2.40 (m, 2H), 2.35 (m, 3H), 2.03 – 1.89 (m, 2H), 1.87 – 1.74 (m, 1H), 1.74 (s, 3H), 1.69 (d, *J* = 1.3 Hz, 3H), 1.66 – 1.45 (m, 3H).

^{13}C NMR (100 MHz, $CDCl_3$): δ 196.2, 162.4, 162.2, 155.2, 149.3, 139.8, 134.8, 129.4, 129.1, 124.1, 118.3, 116.0, 62.4, 57.0, 33.5, 33.3, 30.6, 25.9, 23.9, 23.0, 18.3.

IR (Neat Film, NaCl): 1771, 1744, 1682, 1185 cm^{-1}.

HRMS (MM: FD+): *m/z* calc'd for $C_{26}H_{27}NO_7$ $[M]^+$: 465.1788, found 465.1779.



3-methylbut-2-en-1-yl (*Z*)-1-(6-(benzyloxy)-6-oxohex-4-en-1-yl)-2-oxocyclohex-3-ene-1-carboxylate (10q)

To a solution of benzyl 2-(bis(2-(*tert*-butyl)phenoxy)phosphoryl)acetate[35] (890 mg, 1.80 mmol, 1.00 equiv) in MeCN (18 mL, 0.1 M) was added K_2CO_3 (783 mg, 3.69 mmol, 2.05 equiv). The reaction was cooled to 0 ºC and a solution of **55** (500 mg, 1.80 mmol, 1.00 equiv) in MeCN (18 mL, 0.1 M) was dropwise added. The reaction was gradually warmed to 25 ºC and stirring was continued until consumption of **55** as determined by TLC (around 16 h). The reaction mixture was filtered through a plug of Celite® to remove solids and volatiles were removed in vacuo. Purification by flash column chromatography (0–40% EtOAc/hexanes) afforded the title compound as a colorless oil (482 mg, 1.17 mmol, 65 % yield).

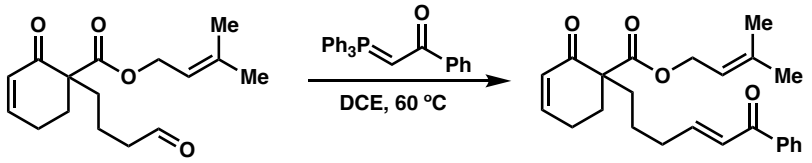
^{1}H NMR (400 MHz, $CDCl_3$): δ 7.39 – 7.29 (m, 5H), 6.90 – 6.84 (m, 1H), 6.24 (dt, *J* = 11.5, 7.4 Hz, 1H), 6.01 (ddd, *J* = 10.1, 2.5, 1.6 Hz, 1H), 5.83 (dt, *J* = 11.5, 1.7 Hz, 1H), 5.28 (ddp, *J* = 8.6, 5.7, 1.4 Hz, 1H), 5.15 (s, 2H), 4.59 (d, *J* = 7.2 Hz, 2H), 2.68 (qd, *J* =

7.4, 1.8 Hz, 2H), 2.53 – 2.41 (m, 2H), 2.35 – 2.26 (m, 1H), 1.98 – 1.87 (m, 2H), 1.79 – 1.71 (m, 4H), 1.67 (s, 3H), 1.52 – 1.37 (m, 2H).

^{13}C NMR (100 MHz, $CDCl_3$): δ 196.4, 171.7, 166.2, 150.5, 149.3, 139.5, 136.3, 129.3, 128.7, 128.3, 128.3, 119.9, 118.4, 65.9, 62.3, 57.1, 33.4, 30.3, 29.4, 25.8, 24.2, 23.8, 18.2.

IR (Neat Film, NaCl): 2918, 1714, 1447, 1178, 1161 cm^{-1}.

HRMS (MM: FD+): *m/z* calc'd for $C_{25}H_{30}O_5$ $[M]^+$: 410.2093, found 410.2108.



55 ***10j***

3-methylbut-2-en-1-yl (*E*)-2-oxo-1-(6-oxo-6-phenylhex-4-en-1-yl)cyclohex-3-ene-1-carboxylate (10j)

(2-oxo-2-phenylethyl)triphenylphosphonium bromide[36] (996 mg, 2.16 mmol, 1.2 equiv) was stirred in 26 mL of a 3:2 CH_2Cl_2/2 M aq. NaOH mixture for 30 minutes at 23 ºC. The layers were separated, and the aqueous layer was extracted twice with CH_2Cl_2. The combined organic layers were washed with brine, dried over Na_2SO_4, filtered, and solvent was removed in vacuo. To a solution of this crude ylide in DCE (22 mL, 0.1 M) was added aldehyde **55** (500 mg, 1.80 mmol, 1 equiv). The reaction was stirred at 65 ºC for 36 hours. Upon complete consumption of **55**, as determined by TLC, volatiles were removed in vacuo. Purification by flash column chromatography (30% EtOAc/hexanes) afforded the title compound as a colorless oil (330 mg, 0.867 mmol, 48% yield).

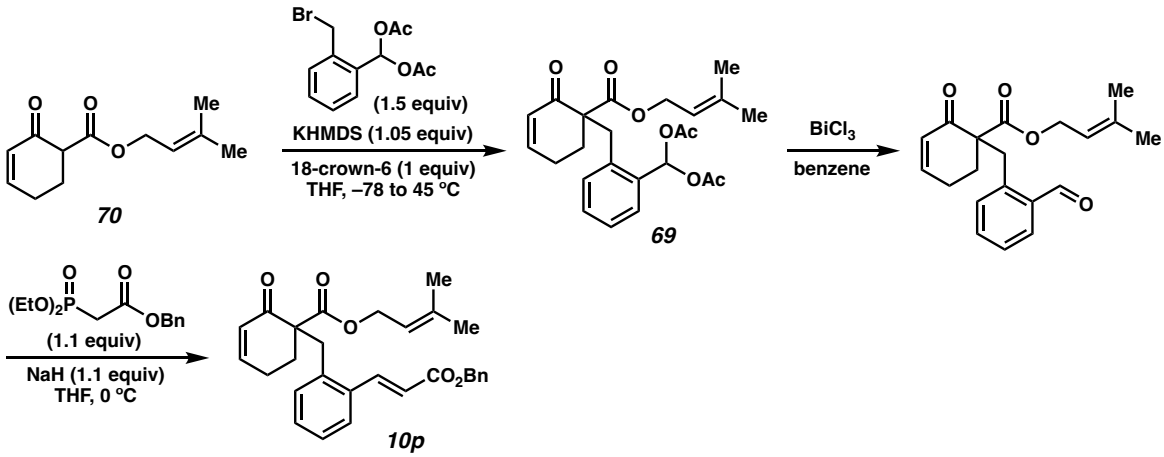
^{1}H NMR (400 MHz, $CDCl_3$): δ 7.95 – 7.90 (m, 2H), 7.60 – 7.51 (m, 1H), 7.46 (tt, *J* = 6.8, 1.5 Hz, 2H), 7.02 (dt, *J* = 15.4, 6.7 Hz, 1H), 6.93 – 6.85 (m, 2H), 6.03 (ddd, *J* = 10.2, 2.6,

1.5 Hz, 1H), 5.30 – 5.25 (m, 1H), 4.59 (d, J = 7.1 Hz, 2H), 2.55 – 2.43 (m, 2H), 2.38 – 2.27 (m, 3H), 2.01 – 1.91 (m, 2H), 1.80 (ddd, J = 13.6, 12.0, 4.7 Hz, 1H), 1.72 (s, 3H), 1.67 (s, 3H), 1.63 – 1.47 (m, 2H).

^{13}C NMR (100 MHz, $CDCl_3$): δ 196.3, 191.0, 171.6, 149.3, 149.1, 139.7, 138.1, 132.8, 129.4, 128.7, 128.7, 126.4, 118.3, 62.4, 57.0, 33.6, 33.2, 30.5, 25.8, 23.9, 23.4, 18.2.

IR (Neat Film, NaCl): 2931, 1724, 1671, 1619, 1447, 1229, 1177 cm^{-1}.

HRMS (MM: FD+): *m/z* calc'd for $C_{24}H_{28}O_4$ $[M]^+$: 380.1988, found 380.1982.



(2-((1-(((3-methylbut-2-en-1-yl)oxy)carbonyl)-2-oxocyclohex-3-en-1-yl)methyl)phenyl)methylene diacetate (69)

An oven dried round bottom flask was charged with KHMDS (837 mg, 4.20 mmol, 1.05 equiv), 18-crown-6 (1.06 g, 4.00 mmol, 1.0 equiv), and THF (21 mL). The mixture was cooled to –78 ºC and a solution of enone **70** (830 mg, 4.00 mmol, 1.0 equiv) in THF (10 mL) was added. The reaction mixture was stirred for 15 minutes then (2-(bromomethyl)phenyl)methylene diacetate[37] (1.86 g, 6.00 mmol, 1.5 equiv) was added in a minimal amount of THF (*ca* 5 mL). The solution was slowly warmed to 45 ºC and stirred

for 14 h. Upon complete consumption of starting material (as determined by TLC), the solution was cooled to 23 ºC, diluted with a saturated aqueous solution of NH_4Cl, and the reaction mixture was extracted thrice with EtOAc. The combined organic layers were dried over Na_2SO_4, filtered, and concentrated under reduced pressure. Purification by flash column chromatography (20–60% EtOAc/hexanes) afforded the title compound as a colorless oil (1.00 g, 2.33 mmol, 58% yield).

^{1}H NMR (400 MHz, $CDCl_3$): δ 7.87 (s, 1H), 7.58 – 7.52 (m, 1H), 7.30 – 7.24 (m, 2H), 7.21 – 7.16 (m, 1H), 6.88 – 6.82 (m, 1H), 6.07 (ddd, *J* = 10.1, 2.8, 1.3 Hz, 1H), 5.24 (ddq, *J* = 8.6, 5.7, 1.4 Hz, 1H), 4.56 (d, *J* = 7.2 Hz, 2H), 3.52 (d, *J* = 14.8 Hz, 1H), 3.45 (d, *J* = 14.8 Hz, 1H), 2.53 – 2.41 (m, 1H), 2.36 (dddd, *J* = 13.6, 4.9, 2.6, 1.3 Hz, 1H), 2.29 – 2.19 (m, 1H), 2.12 (s, 3H), 2.10 (s, 3H), 1.86 (ddd, *J* = 13.6, 10.4, 5.3 Hz, 1H), 1.73 (s, 3H), 1.67 (s, 3H).

^{13}C NMR (100 MHz, $CDCl_3$): δ 195.4, 171.1, 168.8, 168.8, 149.6, 139.7, 135.5, 134.9, 131.5, 129.6, 129.5, 127.6, 127.2, 118.2, 88.4, 62.5, 58.2, 34.2, 30.2, 25.9, 24.1, 21.0, 21.0, 18.2.

IR (Neat Film, NaCl): 2935, 1759, 1731, 1682, 1447, 1371, 1236, 1206 cm^{-1}.

HRMS (MM: FD+): *m/z* calc'd for $C_{24}H_{28}O_7$ $[M]^+$: 428.1835, found 428.1833.

3-methylbut-2-en-1-yl (*E*)-1-(6-(benzyloxy)-6-oxohex-4-en-1-yl)-2-oxocyclohept-3-ene-1-carboxylate (10p)

To a solution of diacetate **69** (500 mg, 1.17 mmol, 1 equiv) in benzene (11.7 mL, 0.1 M) was added bismuth chloride (38 mg, 0.12 mmol, 0.1 equiv). The reaction mixture was heated to 35 ºC for 3 hours. Upon cooling to 25 ºC, the reaction mixture was diluted with

water and the layers were separated. The aqueous layer was extracted twice with chloroform. The combined organic layers were washed with brine, dried over Na_2SO_4, and volatiles were removed in vacuo. The crude aldehyde was used directly in the subsequent Horner–Wadsworth–Emmons olefination.

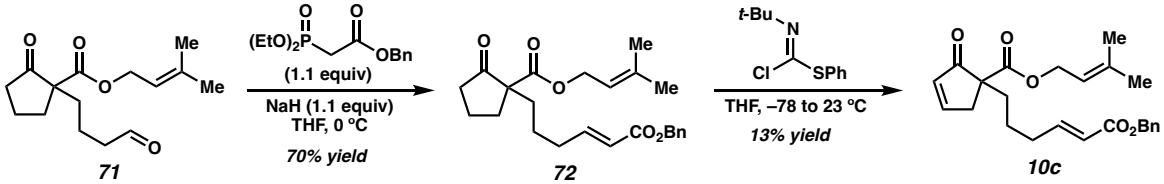
To a suspension of NaH (52 mg, 1.29 mmol, 60% by weight in mineral oil, 1.1 equiv) in THF (2.6 mL, 0.5 M) at 0 ºC was dropwise added a solution of benzyl 2-(diethoxyphosphoryl)acetate[28] (369 mg, 1.29 mmol, 1.1 equiv) in THF (1.3 mL, 1.0 M). Stirring at 0 ºC was continued for 30 minutes. To the reaction was then dropwise added a solution of the crude aldehyde in THF (2.4 mL, 0.5 M). Upon complete consumption of starting material (as determined by TLC), the reaction mixture was diluted with a saturated solution of $NaHCO_3$ and extracted with EtOAc (3x). The combined organic layers were dried over Na_2SO_4, filtered, and concentrated under reduced pressure. Purification by flash column chromatography (5–40% EtOAc/hexanes) afforded the title compound as a colorless oil (230 mg, 0.502 mmol, 43% yield).

^{1}H NMR (400 MHz, $CDCl_3$): δ 8.08 (d, *J* = 15.7 Hz, 1H), 7.57 (dd, *J* = 7.5, 1.9 Hz, 1H), 7.44 – 7.31 (m, 5H), 7.27 – 7.17 (m, 3H), 6.85 – 6.80 (m, 1H), 6.40 (d, *J* = 15.7 Hz, 1H), 6.06 (ddd, *J* = 10.1, 2.9, 1.2 Hz, 1H), 5.28 – 5.21 (m, 3H), 4.56 – 4.49 (m, 2H), 3.57 (d, *J* = 14.3 Hz, 1H), 3.31 (d, *J* = 14.4 Hz, 1H), 2.51 – 2.39 (m, 1H), 2.30 – 2.16 (m, 2H), 1.82 – 1.70 (m, 4H), 1.65 (s, 3H).

^{13}C NMR (100 MHz, $CDCl_3$): δ 195.1, 170.4, 166.7, 149.7, 143.2, 139.7, 136.7, 136.2, 134.7, 132.1, 130.0, 129.3, 128.7, 128.4, 128.3, 127.5, 126.8, 119.4, 118.2, 66.5, 62.5, 58.4, 35.4, 30.2, 25.9, 24.1, 18.2.

IR (Neat Film, NaCl): 3028, 2927, 1720, 1686, 1629, 1168 cm^{-1}.

HRMS (MM: FD+): *m/z* calc'd for $C_{29}H_{30}O_5$ $[M]^+$: 458.2088, found 458.2086.



3-methylbut-2-en-1-yl (*E*)-1-(6-(benzyloxy)-6-oxohex-4-en-1-yl)-2-oxocyclopentane-1-carboxylate (72)

Prepared from **71** and benzyl 2-(diethoxyphosphoryl)acetate[28] following General Procedure 1B. Purification by flash column chromatography (15% EtOAc/hexanes) afforded the title compound as a colorless oil (1.40 g, 3.51 mmol, 70% yield).

^{1}H NMR (400 MHz, $CDCl_3$): δ 7.76 (dt, *J* = 5.6, 2.7 Hz, 1H), 7.42 – 7.26 (m, 5H), 6.95 (dt, *J* = 15.6, 6.9 Hz, 1H), 6.16 (dt, *J* = 5.8, 2.2 Hz, 1H), 5.85 (dt, *J* = 15.6, 1.6 Hz, 1H), 5.27 (tdq, *J* = 7.2, 2.9, 1.5 Hz, 1H), 5.16 (s, 2H), 4.59 (d, *J* = 7.1 Hz, 2H), 3.33 – 3.19 (m, 1H), 2.68 – 2.51 (m, 1H), 2.21 (qd, *J* = 7.3, 1.6 Hz, 2H), 1.99 (ddd, *J* = 13.7, 12.3, 4.5 Hz, 1H), 1.82 – 1.70 (m, 1H), 1.73 (s, 3H), 1.67 (s, 3H), 1.53 – 1.23 (m, 3H).

^{13}C NMR (100 MHz, $CDCl_3$): δ 205.7, 170.6, 166.4, 163.9, 148.9, 139.6, 136.2, 132.4, 128.7, 128.4, 128.3, 121.7, 118.3, 66.2, 62.7, 58.0, 39.5, 34.0, 32.4, 25.9, 23.2, 18.2.

IR (Neat Film, NaCl): 2932, 2356, 1715, 1263, 1164, 976, 754 cm^{-1}.

HRMS (MM: FD+): *m/z* calc'd for $C_{24}H_{28}O_5$ $[M]^+$: 396.1920, found 396.1931.

3-methylbut-2-en-1-yl (*E*)-1-(6-(benzyloxy)-6-oxohex-4-en-1-yl)-2-oxocyclopent-3-ene-1-carboxylate (10c)

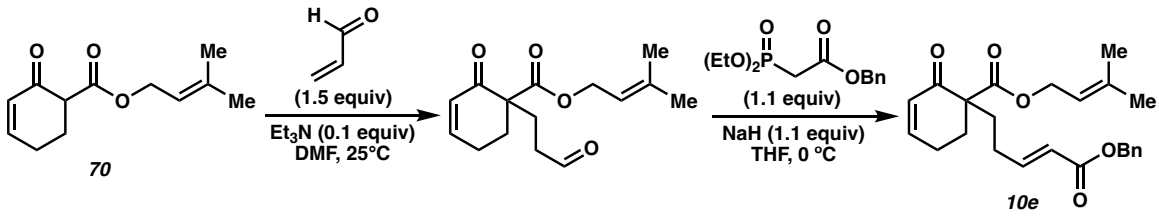
A flame dried round bottom flask was charged with *i*-Pr_2NH (0.35 mL, 2.5 mmol, 1.25 equiv) and THF (8.0 mL, 0.25 M). The solution was cooled to –78 ºC and *n*-BuLi (0.96 mL, 2.4 mmol, 1.2 equiv) was added dropwise and the resultant solution was stirred for 30 min. Ketoester **72** (797 mg, 2.00 mmol, 1.0 equiv) in THF (8.0 mL, 0.25 M) was added dropwise and the mixture was stirred for 1 h. *N-tert*-Butylbenzenesulfinimidoyl chloride[38] (560.9 mg, 2.6 mmol, 1.3 equiv) in THF (4.0 mL, 0.5 M) was added dropwise and the solution was slowly warmed to 23 ºC. Upon complete consumption of starting material (as determined by TLC), the reaction mixture was diluted with saturated aqueous $NaHCO_3$ solution and extracted with Et_2O (25 mL x 3). The combined organic layers were dried with Na_2SO_4, filtered, and concentrated under reduced pressure. The crude product was purified by column chromatography (SiO_2, 0–40% EtOAc/Hexanes) to afford enone **10b** as a colorless oil (100 mg, 0.25 mmol, 13% yield).

^{1}H NMR (400 MHz, $CDCl_3$): δ 7.76 (dt, *J* = 5.6, 2.7 Hz, 1H), 7.42 – 7.26 (m, 5H), 6.95 (dt, *J* = 15.6, 6.9 Hz, 1H), 6.16 (dt, *J* = 5.8, 2.2 Hz, 1H), 5.85 (dt, *J* = 15.6, 1.6 Hz, 1H), 5.27 (tdq, *J* = 7.2, 2.9, 1.5 Hz, 1H), 5.16 (s, 2H), 4.59 (d, *J* = 7.1 Hz, 2H), 3.33 – 3.19 (m, 1H), 2.68 – 2.51 (m, 1H), 2.21 (qd, *J* = 7.3, 1.6 Hz, 2H), 1.99 (ddd, *J* = 13.7, 12.3, 4.5 Hz, 1H), 1.82 – 1.70 (m, 1H), 1.73 (s, 3H), 1.67 (s, 3H), 1.53 – 1.23 (m, 3H).

^{13}C NMR (100 MHz, $CDCl_3$): δ 205.7, 170.6, 166.4, 163.9, 148.9, 139.6, 136.2, 132.4, 128.7, 128.4, 128.3, 121.7, 118.3, 66.2, 62.7, 58.0, 39.5, 34.0, 32.4, 25.9, 23.2, 18.2.

IR (Neat Film, NaCl): 2932, 2356, 1715, 1263, 1164, 976, 754 cm^{-1}.

HRMS (MM: FD+): *m/z* calc'd for $C_{24}H_{28}O_5$ $[M]^+$: 396.1920, found 396.1931.



3-methylbut-2-en-1-yl (*E*)-1-(5-(benzyloxy)-5-oxopent-3-en-1-yl)-2-oxocyclohex-3-ene-1-carboxylate (10e)

To a solution of enone **70** (1.04 g, 5.00 mmol, 1.0 equiv) in DMF (10 mL, 0.5 M) at 25°C was added dropwise triethylamine (0.07 mL, 0.50 mmol, 0.1 equiv) followed by acrolein (0.50 mL, 7.50 mmol, 1.5 equiv). Upon consumption of starting material (as determined by TLC), the reaction mixture was diluted with water and extracted thrice with diethyl ether. The combined organic layers were washed with water followed by brine, dried over Na_2SO_4, and volatiles were removed in vacuo. The crude aldehyde was used directly in the subsequent Horner–Wadsworth–Emmons olefination. To a suspension of NaH (132 mg, 3.30 mmol, 60% by weight in mineral oil, 1.1 equiv) in THF (6 mL, 0.5 M) at 0 ºC was dropwise added a solution of benzyl 2-(diethoxyphosphoryl)acetate (945 mg, 3.30 mmol, 1.1 equiv) in THF (3.0 mL, 1.0 M). Stirred at 0 ºC was continued for 30 minutes. To the reaction was then dropwise added a solution of the crude aldehyde in THF (6.0 mL, 0.5 M). Upon complete consumption of starting material (as determined by TLC), the reaction mixture was diluted with a saturated solution of $NaHCO_3$ and extracted with EtOAc (3x). The combined organic layers were dried over Na_2SO_4, filtered, and concentrated under reduced pressure. Purification by flash column chromatography (10–20% EtOAc/hexanes) afforded the title compound as a colorless oil (490 mg, 1.24 mmol, 41% yield).

^{1}H NMR (400 MHz, $CDCl_3$): δ 7.41 – 7.29 (m, 5H), 6.99 (dt, *J* = 15.7, 6.8 Hz, 1H), 6.93 – 6.84 (m, 1H), 6.03 (ddd, *J* = 10.1, 2.5, 1.5 Hz, 1H), 5.88 (dt, *J* = 15.6, 1.6 Hz, 1H), 5.27 (ddt, *J* = 7.2, 5.8, 1.4 Hz, 1H), 5.17 (s, 2H), 4.59 (d, *J* = 7.1 Hz, 2H), 2.56 – 2.41 (m, 2H), 2.38 – 2.13 (m, 3H), 2.08 – 1.81 (m, 3H), 1.73 (s, 3H), 1.67 (s, 3H).

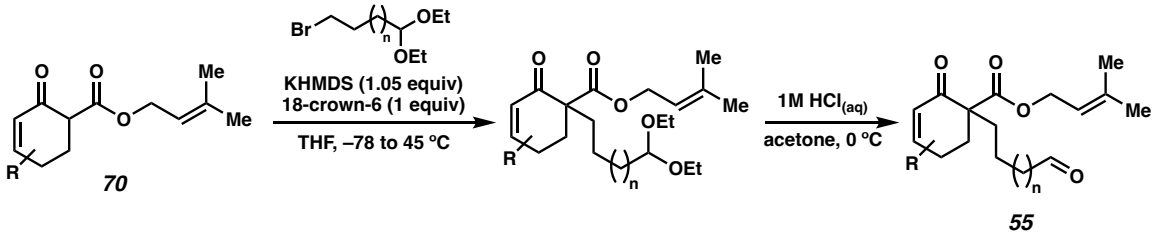
^{13}C NMR (100 MHz, $CDCl_3$): δ 196.0, 171.4, 166.4, 149.3, 148.9, 139.9, 136.2, 129.4, 128.7, 128.3, 121.5, 118.2, 66.2, 62.4, 56.6, 32.2, 30.7, 27.6, 25.8, 23.8, 18.2.

IR (Neat Film, NaCl): 3032, 2934, 1737, 1681, 1445, 1384, 1265, 1175, 1137 cm^{-1}.

HRMS (MM: FD+): *m/z* calc'd for $C_{24}H_{28}O_5$ $[M]^+$: 396.1937, found 396.1926.

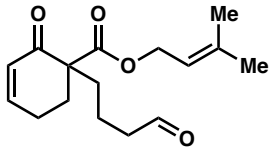
Preparation of Aldehyde Precursors

General Procedure 1C: Alkylation of β-Ketoesters



An oven dried round bottom flask was charged with KHMDS (1.05 equiv), 18-crown-6 (1.0 equiv), and THF (0.2 M with respect to KHMDS). The mixture was cooled to –78 ºC and a solution of acyclated enone **70** (1.0 equiv) in THF (0.4 M) was added. The reaction mixture was stirred for 15 minutes and then the appropriate alkyl bromide (1.5 equiv) was added neat dropwise. The solution was slowly warmed to 45 ºC and stirred for 14 h. Upon complete consumption of starting material (as determined by TLC), the solution was cooled to 23 ºC, diluted with a saturated aqueous solution of NH_4Cl and the reaction mixture was

extracted thrice with EtOAc. The combined organic layers were dried over Na_2SO_4, filtered, and concentrated under reduced pressure to afford the crude diethyl acetal which was used directly in the next step. A round bottom flask was charged with the crude acetal and acetone (0.5 M), then cooled to 0 ºC. Aqueous 1 M HCl (1:1 volume with respect to acetone) was added and stirring was continued for 1 h. Upon complete consumption of starting material (as determined by TLC), the reaction mixture was extracted with EtOAc (3x). The combined organic layers were washed with brine, dried over Na_2SO_4, filtered, and concentrated under reduced pressure. The crude product was purified by silica gel flash column chromatography to afford the respective aldehyde product (**55**).



55

3-methylbut-2-en-1-yl 2-oxo-1-(4-oxobutyl)cyclohex-3-ene-1-carboxylate (55)

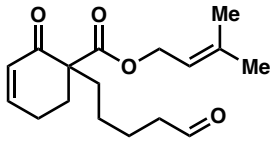
Prepared from **70** and 4-bromo-1,1-diethoxybutane[39] following General Procedure 1C. Purification by flash column chromatography (25% EtOAc/hexanes) afforded the title compound as a colorless oil (1.81 g, 6.50 mmol, 49% yield).

^{1}H NMR (400 MHz, $CDCl_3$): δ 9.75 (t, *J* = 1.5 Hz, 1H), 6.89 (dddd, *J* = 10.1, 4.4, 3.1, 1.1 Hz, 1H), 6.02 (ddd, *J* = 10.1, 2.5, 1.6 Hz, 1H), 5.31 – 5.25 (m, 1H), 4.59 (d, *J* = 6.8 Hz, 2H), 2.55 – 2.43 (m, 4H), 2.39 – 2.30 (m, 1H), 2.02 – 1.94 (m, 1H), 1.89 (ddd, *J* = 12.5, 11.7, 4.5 Hz, 1H), 1.78 (dd, *J* = 11.6, 4.9 Hz, 1H), 1.73 (s, 3H), 1.71 – 1.59 (m, 5H)

^{13}C NMR (100 MHz, $CDCl_3$): δ 202.2, 196.2, 171.5, 149.5, 139.7, 129.3, 118.3, 62.4, 57.0, 44.2, 33.2, 30.3, 25.8, 23.8, 18.2, 17.5.

IR (Neat Film, NaCl): 2942, 1732, 1716, 1456, 1180 cm^{-1}

HRMS (MM: FD+): *m/z* calc'd for $C_{16}H_{22}O_4$ $[M]^+$: 278.1518, found 278.1509.



56

3-methylbut-2-en-1-yl 2-oxo-1-(5-oxopentyl)cyclohex-3-ene-1-carboxylate (56)

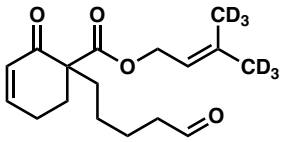
Prepared from **70** and 5-bromo-1,1-diethoxypentane[39] following General Procedure 1C. Purification by flash column chromatography (10–25% EtOAc/hexanes) afforded the title compound as a colorless oil (648 mg, 2.22 mmol, 38% yield).

^{1}H NMR (400 MHz, $CDCl_3$): δ 9.75 (s, 1H), 6.91 – 6.84 (m, 1H), 6.01 (ddd, *J* = 10.1, 2.6, 1.6 Hz, 1H), 5.27 (tdq, *J* = 7.1, 2.8, 1.4 Hz, 1H), 4.58 (d, *J* = 7.1 Hz, 2H), 2.54 – 2.40 (m, 4H), 2.36 – 2.27 (m, 1H), 1.98 – 1.86 (m, 2H), 1.78 – 1.60 (m, 10H), 1.40 – 1.26 (m, 2H).

^{13}C NMR (100 MHz, $CDCl_3$): δ 202.6, 196.4, 171.7, 149.4, 139.6, 129.3, 118.3, 62.3, 57.0, 43.7, 33.6, 30.4, 25.8, 24.3, 23.8, 22.5, 18.2.

IR (Neat Film, NaCl): 2941, 1733, 1717, 1456, 1219 cm^{-1}

HRMS (MM: FD+): *m/z* calc'd for $C_{16}H_{22}O_4$ $[M]^+$: 293.1747, found 293.1768.



D-56

3-(methyl-d_3)but-2-en-1-yl-4,4,4-d_3 2-oxo-1-(5-oxopentyl)cyclohex-3-ene-1-carboxylate (*D*-56)

Prepared from ***D*-70** and 5-bromo-1,1-diethoxypentane[39] following General Procedure 1C. Purification by flash column chromatography (10–25% EtOAc/hexanes) afforded the title compound as a colorless oil (290 mg, 0.971 mmol, 42% yield).

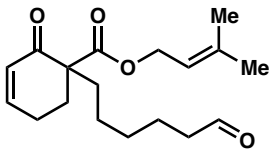
^{1}H NMR (400 MHz, $CDCl_3$): δ 9.75 (t, *J* = 1.7 Hz, 1H), 6.90 – 6.85 (m, 1H), 6.01 (ddd, *J* = 10.1, 2.6, 1.6 Hz, 1H), 5.27 (t, *J* = 7.2 Hz, 1H), 4.58 (dd, *J* = 7.2, 1.8 Hz, 2H), 2.55 – 2.41 (m, 4H), 2.36 – 2.26 (m, 1H), 1.97 – 1.86 (m, 2H), 1.74 (ddd, *J* = 13.6, 11.6, 5.1 Hz, 1H), 1.68 – 1.60 (m, 2H), 1.40 – 1.24 (m, 2H).

^{13}C NMR (100 MHz, $CDCl_3$): δ 202.6, 196.4, 171.7, 149.4, 139.4, 129.3, 118.4, 62.3, 57.0, 43.7, 33.6, 30.4, 24.3, 23.9, 22.5.

^{2}H NMR (61 MHz, $CHCl_3$): δ 1.69, 1.65.

IR (Neat Film, NaCl): 2941, 1726, 1682, 1238, 1186 cm^{-1}

HRMS (MM: FD+): *m/z* calc'd for $C_{17}H_{18}D_6O_4$ $[M]^+$: 298.2051, found 298.2052.



57

3-methylbut-2-en-1-yl 2-oxo-1-(6-oxohexyl)cyclohex-3-ene-1-carboxylate (57)

Prepared from **70** and 6-bromo-1,1-diethoxyhexane[39] following General Procedure 1C. Purification by flash column chromatography (10–25% EtOAc/hexanes) afforded the title compound as a colorless oil (838 mg, 2.73 mmol, 32% yield).

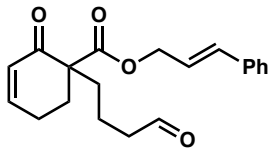
^{1}H NMR (400 MHz, $CDCl_3$): δ 9.75 (t, *J* = 1.8 Hz, 1H), 6.90 – 6.85 (m, 1H), 6.01 (ddd, *J* = 10.0, 2.5, 1.5 Hz, 1H), 5.30 – 5.25 (m, 1H), 4.62 – 4.55 (m, 2H), 2.54 – 2.39 (m, 4H),

2.36 – 2.27 (m, 1H), 1.98 – 1.84 (m, 2H), 1.73 (t, J = 1.2 Hz, 4H), 1.69 – 1.59 (m, 5H), 1.39 – 1.24 (m, 4H).

^{13}C NMR (100 MHz, $CDCl_3$): δ 202.8, 196.5, 171.7, 149.3, 139.5, 129.4, 118.4, 62.3, 57.1, 43.9, 33.6, 30.3, 29.6, 25.8, 24.4, 23.9, 21.9, 18.2.

IR (Neat Film, NaCl): 2934, 2864, 1733, 1717, 1684, 1456, 1220 cm^{-1}

HRMS (MM: FD+): *m/z* calc'd for $C_{18}H_{26}O_4$ $[M]^+$: 306.1831, found 306.1854.



63

cinnamyl 2-oxo-1-(4-oxobutyl)cyclohex-3-ene-1-carboxylate (63)

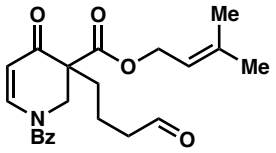
Prepared from **73** and 4-bromo-1,1-diethoxybutane[39] following General Procedure 1C. Purification by flash column chromatography (10–25% EtOAc/hexanes) afforded the title compound as a colorless oil (0.607 g, 1.86 mmol, 49% yield).

^{1}H NMR (400 MHz, $CDCl_3$): δ 9.74 (t, J = 1.5 Hz, 1H), 7.38 – 7.35 (m, 2H), 7.35 – 7.30 (m, 2H), 7.28 – 7.24 (m, 1H), 6.91 (dddd, J = 10.1, 4.3, 3.1, 1.1 Hz, 1H), 6.63 (dt, J = 16.0, 1.4 Hz, 1H), 6.23 (dt, J = 15.8, 6.4 Hz, 1H), 6.05 (ddd, J = 10.1, 2.4, 1.7 Hz, 1H), 4.77 (dt, J = 6.5, 1.1 Hz, 2H), 2.57 – 2.45 (m, 4H), 2.42 – 2.32 (m, 1H), 2.05 – 1.98 (m, 1H), 1.93 (ddd, J = 13.2, 11.7, 5.1 Hz, 1H), 1.80 (ddd, J = 13.2, 11.1, 5.5 Hz, 1H), 1.73 – 1.63 (m, 2H).

^{13}C NMR (100 MHz, $CDCl_3$): δ 202.1, 196.0, 171.3, 149.7, 136.2, 134.7, 129.2, 128.8, 128.3, 126.8, 122.7, 66.0, 57.1, 44.1, 33.3, 30.1, 23.8, 17.5.

IR (Neat Film, NaCl): 2941, 1732, 1717, 1700, 1181, 734, 701 cm^{-1}

HRMS (MM: FD+): *m/z* calc'd for $C_{20}H_{22}O_4$ $[M]^+$: 326.1513, found 326.1510.



58

1-benzyl 3-(3-methylbut-2-en-1-yl) 4-oxo-3-(4-oxobutyl)-3,4-dihydropyridine-1,3(2*H*)-dicarboxylate (58)

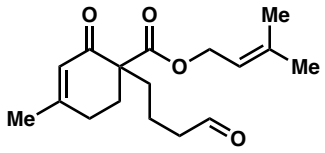
Prepared from **74** and 4-bromo-1,1-diethoxybutane[39] following General Procedure 1C. Purification by flash column chromatography (15–30% EtOAc/hexanes) afforded the title compound as a colorless oil (603.9 mg, 1.46 mmol, 60% yield).

^{1}H NMR (400 MHz, $CDCl_3$): δ 9.73 (t, *J* = 1.4 Hz, 1H), 7.80 (s, 1H), 7.40 (d, *J* = 3.5 Hz, 5H), 5.27 (m, 4H), 4.61 (m, 3H), 3.78 (d, *J* = 13.6 Hz, 1H), 2.45 (tt, *J* = 6.8, 1.7 Hz, 2H), 2.03 – 1.90 (m, 1H), 1.72 (s, 3H), 1.67 (s, 3H), 1.70 – 1.60 (m, 1H).

^{13}C NMR (100 MHz, $CDCl_3$): δ 201.6, 190.5, 169.4, 142.7, 140.1, 135.0, 129.0, 128.9, 128.6, 118.0, 106.5, 69.4, 62.8, 55.4, 48.2, 43.9, 31.1, 25.8, 18.2, 17.2.

IR (Neat Film, NaCl): 2945, 2338, 1727, 1670, 1604, 1389, 1302, 1201, 932 cm^{-1}.

HRMS (MM: FD+): *m/z* calc'd for $C_{23}H_{27}NO_6$ $[M]^+$: 413.1838, found 413.1852.



59

3-methylbut-2-en-1-yl 4-methyl-2-oxo-1-(4-oxobutyl)cyclohex-3-ene-1-carboxylate (59)

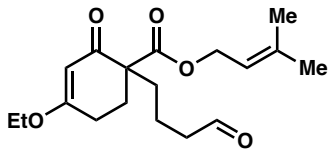
Prepared from **75** and 4-bromo-1,1-diethoxybutane[39] following General Procedure 1C. Purification by flash column chromatography (25–50% EtOAc/hexanes) afforded the title compound as a colorless oil (1141.4 mg, 3.90 mmol, 78% yield).

^{1}H NMR (400 MHz, $CDCl_3$): δ 9.74 (s, 1H), 5.87 (dt, *J* = 2.6, 1.2 Hz, 1H), 5.27 (tp, *J* = 7.1, 1.4 Hz, 1H), 4.58 (d, *J* = 7.2 Hz, 2H), 2.45 (ddd, *J* = 8.0, 4.8, 1.7 Hz, 4H), 2.29 – 2.18 (m, 1H), 1.92 (s, 3H), 2.00 – 1.84 (m, 2H), 1.72 (s, 3H), 1.67 (s, 3H), 1.79 – 1.54 (m, 3H).

^{13}C NMR (100 MHz, $CDCl_3$): δ 202.2, 195.9, 171.7, 161.6, 139.6, 126.0, 118.3, 62.3, 56.0, 44.2, 33.2, 30.0, 28.7, 25.8, 24.2, 18.2, 17.5.

IR (Neat Film, NaCl): 3426, 2936, 2730, 1725, 1672, 1637, 1440, 1380, 1348, 1311, 1272, 1233, 1214, 1177, 1104, 1050, 1016, 986, 939, 870, 842, 820, 776 cm^{-1}.

HRMS (MM: FD+): *m/z* calc'd for $C_{17}H_{24}O_4$ $[M]^+$: 292.1682, found 292.1669.



60

3-methylbut-2-en-1-yl 4-ethoxy-2-oxo-1-(4-oxobutyl)cyclohex-3-ene-1-carboxylate (60)

Prepared from **76** and 4-bromo-1,1-diethoxybutane[39] following General Procedure 1C. Purification by flash column chromatography (30–40% EtOAc/hexanes) afforded the title compound as a colorless oil (653.2 mg, 2.03 mmol, 21% yield).

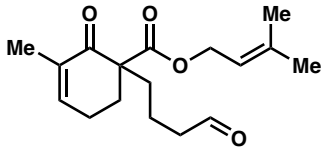
^{1}H NMR (400 MHz, $CDCl_3$): δ 9.75 (t, *J* = 1.5 Hz, 1H), 5.34 (d, *J* = 1.1 Hz, 1H), 5.29 (tp, *J* = 7.2, 1.4 Hz, 1H), 4.66 – 4.53 (m, 2H), 3.86 (q, *J* = 7.18, 2H), 2.61 (dddd, *J* = 17.8, 10.3,

4.7, 1.3 Hz, 1H), 2.50 – 2.30 (m, 4H), 2.02 – 1.87 (m, 2H), 1.82 – 1.73 (m, 1H), 1.72 (s, 3H), 1.68 (s, 3H), 1.67 – 1.58 (m, 2H), 1.35 (t, J = 7.0 Hz, 3H).

^{13}C NMR (100 MHz, $CDCl_3$): δ 201.9, 195.5, 176.5, 171.5, 139.1, 118.1, 101.9, 64.3, 62.0, 55.7, 43.9, 33.1, 28.2, 26.3, 25.5, 17.9, 17.2, 13.9.

IR (Neat Film, NaCl): 2939, 2728, 1723, 1659, 1608, 1447, 1380, 1315, 1242, 1179, 1108, 1027, 942, 816, 769 cm^{-1}.

HRMS (MM: FD+): *m/z* calc'd for $C_{18}H_{26}O_5$ $[M]^+$: 322.1790, found 322.1775.



61

3-methylbut-2-en-1-yl 3-methyl-2-oxo-1-(4-oxobutyl)cyclohex-3-ene-1-carboxylate (61)

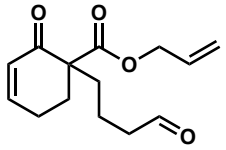
Prepared from **77** and 4-bromo-1,1-diethoxybutane[39] following General Procedure 1C. Purification by flash column chromatography (15–20% EtOAc/hexanes) afforded the title compound as a colorless oil (1.14 g, 3.90 mmol, 70% yield).

^{1}H NMR (400 MHz, $CDCl_3$): δ 9.75 (s, 1H), 6.64 – 6.57 (m, 1H), 5.27 (tt, J = 7.1, 1.4 Hz, 1H), 4.64 – 4.51 (m, 2H), 2.51 – 2.36 (m, 4H), 2.36 – 2.22 (m, 1H), 2.01 – 1.92 (m, 1H), 1.87 (m, 1H), 1.83-1.53 (m, 3H) 1.78 (s, 3H), 1.73 (s, 3H), 1.67 (d, J = 1.3 Hz, 3H).

^{13}C NMR (100 MHz, $CDCl_3$): δ 202.2, 196.9, 171.9, 143.9, 139.6, 135.3, 118.3, 62.2, 57.0, 44.2, 33.3, 30.7, 25.8, 23.5, 18.2, 17.7, 16.6.

IR (Neat Film, NaCl): 3500, 2925, 2333, 1725, 1681, 1449, 1361, 1182 cm^{-1}.

HRMS (MM: FD+): *m/z* calc'd for $C_{17}H_{24}O_4$ $[M]^+$: 292.1680, found 292.1669.



62

allyl 2-oxo-1-(4-oxobutyl)cyclohex-3-ene-1-carboxylate (62)

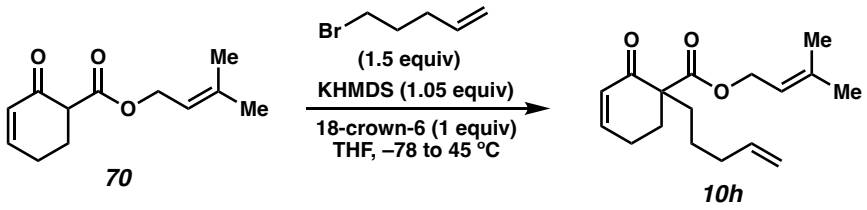
Prepared from allyl 2-oxocyclohex-3-ene-1-carboxylate [40] and 4-bromo-1,1-diethoxybutane[39] following General Procedure 1C. Purification by flash column chromatography (15–30% EtOAc/hexanes) afforded the title compound as a colorless oil (773.2 mg, 3.09 mmol, 21% yield).

^{1}H NMR (400 MHz, $CDCl_3$): δ 9.75 (t, *J* = 1.4 Hz, 1H), 6.91 (dddd, *J* = 10.1, 4.4, 3.1, 1.1 Hz, 1H), 6.03 (dt, *J* = 10.1, 2.0 Hz, 1H), 5.86 (ddt, *J* = 17.1, 10.2, 5.6 Hz, 1H), 5.28 (dq, *J* = 17.2, 1.6 Hz, 1H), 5.22 (dq, *J* = 10.4, 1.3 Hz, 1H), 4.60 (dq, *J* = 5.4, 1.6 Hz, 2H), 2.58 – 2.43 (m, 4H), 2.43 – 2.30 (m, 1H), 2.07 – 1.95 (m, 1H), 1.91 (ddd, *J* = 13.2, 11.6, 5.2 Hz, 1H), 1.79 (ddd, *J* = 13.2, 10.9, 5.6 Hz, 1H), 1.75 – 1.56 (m, 2H).

^{13}C NMR (100 MHz, $CDCl_3$): δ 202.1, 196.0, 171.2, 149.7, 131.7, 129.2, 118.7, 65.9, 57.1, 44.1, 33.1, 30.1, 23.7, 17.4.

IR (Neat Film, NaCl): 2947, 2732, 1726, 1680, 1238, 1184 cm^{-1}.

HRMS (MM: FD+): *m/z* calc'd for $C_{14}H_{19}O_4$ $[M]^+$: 251.1281, found 251.1278.



70 ***10h***

3-methylbut-2-en-1-yl 2-oxo-1-(pent-4-en-1-yl)cyclohex-3-ene-1-carboxylate (10h)

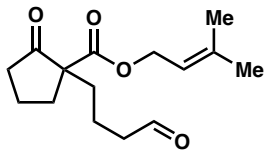
Prepared from **70** and 5-bromopent-1-ene following General Procedure 1C (without hydrolysis step). Purification by flash column chromatography (0-20% EtOAc/hexanes) afforded the title compound as a colorless oil (93.8 mg, 0.34 mmol, 23% yield).

^{1}H NMR (400 MHz, $CDCl_3$): δ 6.87 (dddd, *J* = 10.1, 4.8, 3.1, 1.1 Hz, 1H), 6.01 (ddd, *J* = 10.1, 2.5, 1.6 Hz, 1H), 5.78 (ddt, *J* = 16.9, 10.2, 6.6 Hz, 1H), 5.28 (tdq, *J* = 7.1, 2.9, 1.4 Hz, 1H), 5.00 (dq, *J* = 17.1, 1.6 Hz, 1H), 4.94 (ddt, *J* = 10.2, 2.2, 1.2 Hz, 1H), 4.59 (dd, *J* = 7.2, 3.7 Hz, 1H), 4.64 – 4.53 (m, 2H), 2.57 – 2.41 (m, 2H), 2.38 – 2.24 (m, 2H), 2.12 – 2.01 (m, 2H), 2.00 – 1.86 (m, 2H), 1.77 – 1.69 (m, 1H), 1.73 (s, 3H), 1.68 (s, 3H), 1.51 – 1.28 (m, 2H).

^{13}C NMR (100 MHz, $CDCl_3$): δ 196.5, 171.7, 149.3, 139.5, 138.4, 129.4, 118.4, 114.9, 62.2, 57.1, 34.2, 33.4, 30.3, 25.8, 24.0, 23.9, 18.2.

IR (Neat Film, NaCl): 2928, 1726, 1683, 1440, 1383, 1186, 912 cm^{-1}.

HRMS (MM: FD+): *m/z* calc'd for $C_{17}H_{24}O_3$ $[M]^+$: 276.1725, found 276.1718.



71

3-methylbut-2-en-1-yl 2-oxo-1-(4-oxobutyl)cyclopentane-1-carboxylate (71)

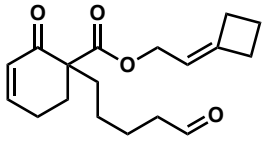
Prepared from 3-methylbut-2-en-1-yl 2-oxocyclopentane-1-carboxylate[41] and 4-bromo-1,1-diethoxybutane[39] following General Procedure 1C. Purification by flash column chromatography (20–25% EtOAc/hexanes) afforded the title compound as a colorless oil (1.86 g, 6.97 mmol, 87% yield).

^{1}H NMR (400 MHz, $CDCl_3$): δ 9.74 (t, *J* = 1.4 Hz, 1H), 5.29 (tp, *J* = 7.3, 1.4 Hz, 1H), 4.59 (d, *J* = 7.2 Hz, 2H), 2.58 – 2.47 (m, 1H), 2.44 (tt, *J* = 7.0, 1.5 Hz, 2H), 2.44 – 2.36 (m, 1H), 2.31 – 2.18 (m, 1H), 2.11 – 1.85 (m, 4H), 1.74 (s, 3H), 1.68 (s, 3H), 1.67 – 1.48 (m, 3H).

^{13}C NMR (100 MHz, $CDCl_3$): δ 214.8, 201.9, 171.0, 139.7, 118.2, 62.5, 60.4, 44.0, 38.0, 33.2, 33.0, 25.9, 19.8, 18.2, 17.6.

IR (Neat Film, NaCl): 3456, 2954, 2724, 1745, 1721, 1446, 1406, 1384, 1154, 953 cm^{-1}.

HRMS (MM: FD+): *m/z* calc'd for $C_{15}H_{22}O_4$ $[M]^+$: 266.1525, found 266.1513.



64

2-cyclobutylideneethyl 2-oxo-1-(5-oxopentyl)cyclohex-3-ene-1-carboxylate (64)

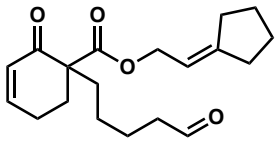
Prepared from **78** and 5-bromo-1,1-diethoxypentane[39] following General Procedure 1C. Purification by flash column chromatography (10–60% EtOAc/hexanes) afforded the title compound as a colorless oil (649 mg, 2.13 mmol, 29% yield).

^{1}H NMR (400 MHz, $CDCl_3$): δ 9.75 (t, *J* = 1.7 Hz, 1H), 6.94 – 6.83 (m, 1H), 6.02 (ddd, *J* = 10.1, 2.6, 1.5 Hz, 1H), 5.20 (tp, *J* = 7.1, 2.3 Hz, 1H), 4.46 (ddt, *J* = 7.4, 2.3, 1.1 Hz, 2H), 2.69 (dt, *J* = 16.0, 8.4 Hz, 4H), 2.56 – 2.40 (m, 4H), 2.37 – 2.26 (m, 1H), 2.03 – 1.84 (m, 4H), 1.75 (ddd, *J* = 13.6, 11.6, 5.1 Hz, 1H), 1.64 (p, *J* = 7.5 Hz, 2H), 1.42 – 1.26 (m, 2H).

^{13}C NMR (100 MHz, $CDCl_3$): δ 202.6, 196.4, 171.6, 149.4, 148.9, 129.4, 114.0, 62.3, 57.0, 43.7, 33.6, 31.2, 30.4, 29.6, 24.3, 23.9, 22.5, 17.1.

IR (Neat Film, NaCl): 2941, 1726, 1681, 1446, 1387, 1240, 1171, 1103 cm^{-1}.

HRMS (MM: FD+): *m/z* calc'd for $C_{18}H_{24}O_4$ $[M]^+$: 304.1675, found 304.1677.



65

2-cyclopentylideneethyl 2-oxo-1-(5-oxopentyl)cyclohex-3-ene-1-carboxylate (65)

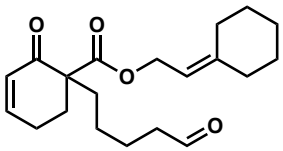
Prepared from **79** and 5-bromo-1,1-diethoxypentane[39] following General Procedure 1C. Purification by flash column chromatography (10–60% EtOAc/hexanes) afforded the title compound as a colorless oil (1.40 g, 4.40 mmol, 39% yield).

^{1}H NMR (400 MHz, $CDCl_3$): δ 9.75 (t, *J* = 1.7 Hz, 3H), 6.92 – 6.83 (m, 1H), 6.02 (ddd, *J* = 10.1, 2.6, 1.6 Hz, 1H), 5.41 – 5.32 (m, 1H), 4.64 – 4.50 (m, 2H), 2.56 – 2.39 (m, 4H), 2.37 – 2.20 (m, 5H), 1.99 – 1.83 (m, 2H), 1.80 – 1.57 (m, 7H), 1.45 – 1.22 (m, 2H).

^{13}C NMR (100 MHz, $CDCl_3$): δ 202.6, 196.4, 171.7, 151.1, 149.4, 129.4, 113.8, 63.8, 57.0, 43.7, 33.9, 33.6, 30.4, 29.0, 26.4, 26.2, 24.3, 23.9, 22.5.

IR (Neat Film, NaCl): 2947, 2725, 1729, 1697, 1456, 1356, 1215 cm^{-1}.

HRMS (MM: FD+): *m/z* calc'd for $C_{19}H_{26}O_4$ $[M]^+$: 318.1831, found 318.1809.



66

2-cyclohexylideneethyl 2-oxo-1-(5-oxopentyl)cyclohex-3-ene-1-carboxylate (66)

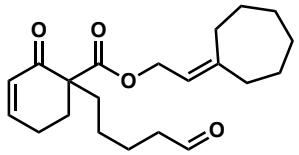
Prepared from **80** and 5-bromo-1,1-diethoxypentane[39] following General Procedure 1C. Purification by flash column chromatography (10–50% EtOAc/hexanes) afforded the title compound as a colorless oil (177 mg, 0.53 mmol, 25% yield).

^{1}H NMR (400 MHz, $CDCl_3$): δ 9.75 (t, *J* = 1.7 Hz, 1H), 6.93 – 6.83 (m, 1H), 6.02 (ddd, *J* = 10.1, 2.6, 1.6 Hz, 1H), 5.23 (tt, *J* = 7.2, 1.2 Hz, 1H), 4.60 (d, *J* = 7.2 Hz, 2H), 2.56 – 2.39 (m, 4H), 2.37 – 2.26 (m, 1H), 2.20 – 2.13 (m, 2H), 2.12 – 2.05 (m, 2H), 1.99 – 1.85 (m, 2H), 1.74 (ddd, *J* = 13.6, 11.7, 5.0 Hz, 1H), 1.64 (p, *J* = 7.5 Hz, 2H), 1.58 – 1.46 (m, 6H), 1.43 – 1.20 (m, 2H).

^{13}C NMR (100 MHz, $CDCl_3$): δ 202.6, 196.4, 171.6, 149.3, 147.7, 129.4, 114.8, 61.5, 57.0, 43.7, 37.1, 33.6, 30.4, 29.2, 28.5, 27.9, 26.7, 24.3, 23.9, 22.5.

IR (Neat Film, NaCl): 2929, 2858, 1731, 1446, 1170, 938 cm^{-1}.

HRMS (MM: FD+): *m/z* calc'd for $C_{20}H_{28}O_4$ $[M]^+$: 332.1988, found 332.1991.



67

2-cycloheptylideneethyl 2-oxo-1-(5-oxopentyl)cyclohex-3-ene-1-carboxylate (67)

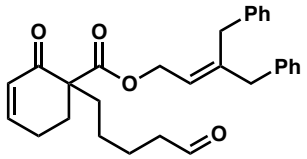
Prepared from **81** and 5-bromo-1,1-diethoxypentane[39] following General Procedure 1C. Purification by flash column chromatography (10–70% Et_2O/hexanes) afforded the title compound as a colorless oil (349 mg, 1.01 mmol, 15% yield).

^{1}H NMR (400 MHz, $CDCl_3$): δ 9.75 (t, *J* = 1.7 Hz, 1H), 6.91 – 6.84 (m, 1H), 6.02 (ddd, *J* = 10.1, 2.6, 1.6 Hz, 1H), 5.28 (tt, *J* = 7.1, 1.3 Hz, 1H), 4.60 (d, *J* = 7.1 Hz, 2H), 2.56 – 2.40 (m, 4H), 2.38 – 2.20 (m, 5H), 1.98 – 1.87 (m, 2H), 1.76 (ddd, *J* = 13.7, 12.0, 4.8 Hz, 1H), 1.65 (p, *J* = 7.5 Hz, 2H), 1.57 (q, *J* = 5.4 Hz, 4H), 1.50 (dt, *J* = 5.2, 2.4 Hz, 4H), 1.42 – 1.27 (m, 2H).

^{13}C NMR (100 MHz, $CDCl_3$): δ 202.6, 196.4, 171.7, 149.4, 149.0, 129.4, 118.4, 62.1, 57.0, 43.7, 37.7, 33.6, 30.4, 30.2, 29.8, 29.1, 28.9, 27.3, 24.3, 23.9, 22.5.

IR (Neat Film, NaCl): 2923, 2854, 1737, 1681, 1443, 1385, 1235, 1172 cm^{-1}.

HRMS (MM: FD+): *m/z* calc'd for $C_{21}H_{30}O_4$ $[M]^+$: 346.2144, found 346.2139.



68

3-benzyl-4-phenylbut-2-en-1-yl 2-oxo-1-(5-oxopentyl)cyclohex-3-ene-1-carboxylate (68)

Prepared from **82** and 5-bromo-1,1-diethoxypentane[39] following General Procedure 1C. Purification by flash column chromatography (10–60% Et_2O/hexanes) afforded the title compound as a colorless oil (425 mg, 0.955 mmol, 18% yield).

^{1}H NMR (400 MHz, $CDCl_3$): δ 9.73 (t, *J* = 1.7 Hz, 1H), 7.32 – 7.27 (m, 4H), 7.21 (tt, *J* = 7.5, 2.3 Hz, 2H), 7.15 – 7.03 (m, 4H), 6.90 – 6.82 (m, 1H), 6.02 (ddd, *J* = 10.2, 2.5, 1.6 Hz, 1H), 5.51 (d, *J* = 7.4 Hz, 1H), 4.83 – 4.70 (m, 2H), 3.36 (s, 2H), 3.24 (s, 2H), 2.54 – 2.24 (m, 5H), 2.00 – 1.86 (m, 2H), 1.77 (ddd, *J* = 13.6, 11.6, 5.1 Hz, 1H), 1.63 (p, *J* = 7.5 Hz, 2H), 1.44 – 1.22 (m, 2H).

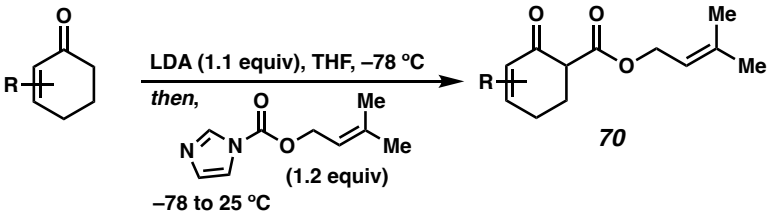
^{13}C NMR (100 MHz, $CDCl_3$): δ 202.5, 196.2, 171.6, 149.4, 144.8, 139.0, 138.8, 129.4, 129.3, 128.8, 128.7, 128.5, 126.5, 126.4, 121.7, 62.0, 57.0, 43.7, 42.9, 35.8, 33.6, 30.4, 24.3, 23.9, 22.5.

IR (Neat Film, NaCl): 2923, 1723, 1684, 1493, 1451, 1386, 1231 cm^{-1}.

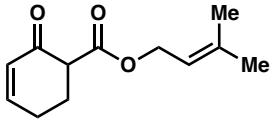
HRMS (MM: FD+): *m/z* calc'd for $C_{29}H_{32}O_4$ $[M]^+$: 444.2301, found 444.2300.

β-Ketoesters Synthesis

General Procedure 1D: Prenyl β-ketoesters Synthesis through Acylation



A flame dried round bottom flask was charged with iPr_2NH (1.1 equiv) and THF (1.75 M). The solution was cooled to 0 ºC and *n*-BuLi (2.5 M in hexanes, 1.05 equiv) was added dropwise. The resultant solution was stirred for 30 min at 0 ºC. The corresponding cyclohexenone (1.0 equiv) in THF (1.25 M) was added dropwise and stirring was continued at 0 ºC for 30 minutes. The solution was cooled to –78 ºC, and the appropriate N-acyl imidazole (1.2 equiv) in THF (3.25 M) was added dropwise. After 2 h, the reaction was gradually warmed to 23 ºC and diluted with 2 M aqueous HCl until reaching a pH < 7. The reaction mixture was extracted three times with EtOAc. The combined organic layers were washed with brine, dried over Na_2SO_4, filtered, and concentrated under reduced pressure. The crude product was purified by flash silica gel column chromatography to afford the corresponding acylated enone.



70

3-methylbut-2-en-1-yl 2-oxocyclohex-3-ene-1-carboxylate (70)

Prepared from 2-cyclohexen-1-one and 3-methylbut-2-en-1-yl 1H-imidazole-1-carboxylate [42] following General Procedure 1D. Purification by flash column

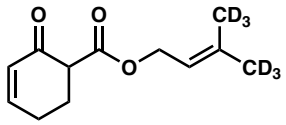
chromatography (25% EtOAc/hexanes) afforded the title compound as a colorless oil (6.65 g, 31.9 mmol, 41% yield).

^{1}H NMR (400 MHz, $CDCl_3$): δ 7.02 – 6.97 (m, 1H), 6.07 (dt, *J* = 10.2, 2.0 Hz, 1H), 5.37 – 5.32 (m, 1H), 4.65 (d, *J* = 7.1 Hz, 2H), 3.42 – 3.39 (m, 1H), 2.55 – 2.45 (m, 1H), 2.44 – 2.34 (m, 2H), 2.26 – 2.18 (m, 1H), 1.75 (s, 3H), 1.71 (s, 3H).

^{13}C NMR (100 MHz, $CDCl_3$): δ 194.1, 170.2, 150.7, 139.6, 129.3, 118.4, 62.3, 53.6, 25.9, 25.8, 24.5, 18.2.

IR (Neat Film, NaCl): 3033, 2934, 1736, 1682, 1447, 1387, 1302, 1233, 1159, 1123 cm^{-1}

HRMS (MM: FD+): *m/z* calc'd for $C_{12}H_{16}O_3$ $[M]^+$: 208.1099, found 208.1090.



D-70

3-(methyl-*d*$_3$)but-2-en-1-yl-4,4,4-*d*$_3$ 2-oxocyclohex-3-ene-1-carboxylate (D-70)

Prepared from 2-cyclohexen-1-one and 3-(methyl-*d*$_3$)but-2-en-1-yl-4,4,4-*d*$_3$ 1*H*-imidazole-1-carboxylate [43] following General Procedure 1D. Purification by flash column chromatography (25% EtOAc/hexanes) afforded the title compound as a colorless oil (1.00 g, 4.67 mmol, 37% yield). *Note that 1.0 equiv of the N-acyl imidazole can be employed*.

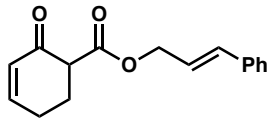
^{1}H NMR (400 MHz, $CDCl_3$): δ 6.99 (dt, *J* = 10.0, 3.7 Hz, 1H), 6.06 (dt, *J* = 10.2, 2.1 Hz, 1H), 5.34 (t, *J* = 7.2 Hz, 1H), 4.65 (d, *J* = 7.2 Hz, 2H), 3.40 (dd, *J* = 9.7, 5.0 Hz, 1H), 2.54 – 2.44 (m, 1H), 2.44 – 2.32 (m, 2H), 2.22 (ddt, *J* = 13.7, 8.8, 3.0 Hz, 1H).

^{13}C NMR (100 MHz, $CDCl_3$): δ 194.1, 170.2, 150.7, 139.4, 129.3, 118.4, 62.3, 53.6, 25.8, 24.5.

^{2}H NMR (61 MHz, $CHCl_3$): δ 1.72, 1.67.

IR (Neat Film, NaCl): 2942, 1736, 1681, 1388, 1164 cm^{-1}

HRMS (MM: FD+): *m/z* calc'd for $C_{12}H_{10}D_6O_3$ $[M]^+$: 214.1476, found 214.1476.



73

cinnamyl 2-oxocyclohex-3-ene-1-carboxylate (73)

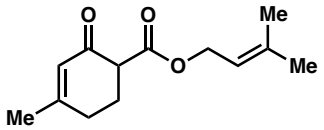
Prepared from 2-cyclohexen-1-one and cinnamyl 1*H*-imidazole-1-carboxylate[42] following General Procedure 1D. Purification by flash column chromatography (15–25% EtOAc/hexanes) afforded the title compound as a colorless oil (0.98 g, 3.82 mmol, 39% yield).

^{1}H NMR (400 MHz, $CDCl_3$): δ 7.40 – 7.37 (m, 2H), 7.34 – 7.30 (m, 2H), 7.28 – 7.24 (m, 1H), 7.01 (dt, *J* = 10.3, 3.8 Hz, 1H), 6.67 (dt, *J* = 15.9, 1.3 Hz, 1H), 6.29 (dt, *J* = 15.9, 6.4 Hz, 1H), 6.09 (dt, *J* = 10.2, 2.0 Hz, 1H), 4.83 (d, *J* = 6.5 Hz, 2H), 3.47 (dd, *J* = 10.2, 4.9 Hz, 1H), 2.57 – 2.47 (m, 1H), 2.47 – 2.34 (m, 2H), 2.28 – 2.21 (m, 1H).

^{13}C NMR (100 MHz, $CDCl_3$): δ 193.9, 169.9, 150.8, 136.3, 134.6, 129.3, 128.7, 128.2, 126.8, 122.9, 65.9, 53.6, 25.8, 24.5.

IR (Neat Film, NaCl): 3024, 2940, 1734, 1676, 1304, 1223, 1157, 1123, 969 cm^{-1}

HRMS (MM: FD+): *m/z* calc'd for $C_{16}H_{16}NaO_3$ $[M+Na]^+$: 279.0997, found 279.0983.



75

3-methylbut-2-en-1-yl 4-methyl-2-oxocyclohex-3-ene-1-carboxylate (75)

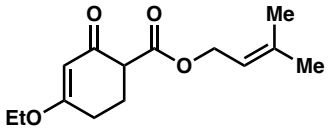
Prepared from 3-methylcyclohex-2-en-1-one and 3-methylbut-2-en-1-yl 1H-imidazole-1-carboxylate[42] following General Procedure 1D. Purification by flash column chromatography (10–20% EtOAc/hexanes) afforded the title compound as a colorless oil (2.95 g, 13.3 mmol, 17% yield).

^{1}H NMR (400 MHz, $CDCl_3$): δ 5.91 (h, *J* = 1.4 Hz, 1H), 5.35 (tp, *J* = 7.1, 1.6 Hz, 1H), 4.65 (d, *J* = 7.2 Hz, 2H), 3.37 – 3.27 (m, 1H), 2.48 – 2.24 (m, 3H), 2.21 – 2.15 (m, 1H), 1.97 (s, 3H), 1.75 (d, *J* = 1.3 Hz, 3H), 1.70 (s, 3H).

^{13}C NMR (100 MHz, $CDCl_3$): δ 193.9, 170.5, 163.0, 139.5, 126.0, 118.5, 62.3, 52.6, 29.5, 25.9, 25.7, 24.5, 18.2.

IR (Neat Film, NaCl): 2938, 1732, 1668, 1632, 1434, 1378, 1357, 1302, 1246, 1216, 1170, 1152, 1018 cm^{-1}.

HRMS (MM: FD+): *m/z* calc'd for $C_{13}H_{18}O_3$ $[M]^+$: 222.1257, found 222.1251.



76

3-methylbut-2-en-1-yl 4-ethoxy-2-oxocyclohex-3-ene-1-carboxylate (76)

Prepared from 3-ethoxycyclohex-2-en-1-one and 3-methylbut-2-en-1-yl 1H-imidazole-1-carboxylate[42] following General Procedure 1D. Purification by flash column

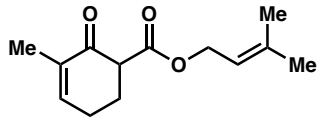
chromatography (25–30% EtOAc/hexanes) afforded the title compound as a colorless oil (2.84 g, 9.51 mmol, 19% yield).

^{1}H NMR (400 MHz, $CDCl_3$): δ 5.38 (s, 1H), 5.37 – 5.32 (m, 1H), 4.72 – 4.59 (m, 2H), 3.91 (qd, *J* = 7.0, 2.3 Hz, 2H), 3.36 – 3.27 (m, 1H), 2.56 (ddd, *J* = 16.6, 6.2, 4.5 Hz, 1H), 2.47 – 2.27 (m, 2H), 2.24 – 2.08 (m, 1H), 1.75 (s, 3H), 1.70 (s, 3H), 1.36 (t, *J* = 7.0 Hz, 3H).

^{13}C NMR (100 MHz, $CDCl_3$): δ 194.0, 177.7, 170.6, 139.4, 118.5, 102.3, 64.6, 62.3, 52.5, 27.5, 25.9, 24.3, 18.2, 14.2.

IR (Neat Film, NaCl): 2980, 2357, 1730, 1648, 1605, 1380, 1192, 1026, 668 cm^{-1}.

HRMS (MM: FD+): *m/z* calc'd for $C_{14}H_{20}O_4$ $[M]^+$: 252.1363, found 252.1356.



77

3-methylbut-2-en-1-yl 3-methyl-2-oxocyclohex-3-ene-1-carboxylate (77)

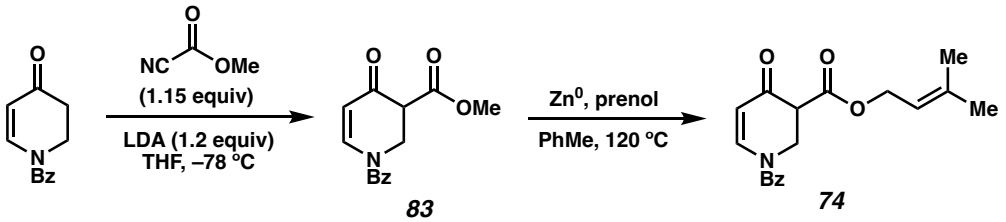
Prepared from 2-methylcyclohex-2-en-1-one[44] and 3-methylbut-2-en-1-yl 1H-imidazole-1-carboxylate[42] following General Procedure 1D. Purification by flash column chromatography (10–20% EtOAc/hexanes) afforded the title compound as a colorless oil (1.09 g, 4.90 mmol, 23% yield).

^{1}H NMR (400 MHz, $CDCl_3$): δ 6.78 – 6.69 (m, 1H), 5.35 (tdq, *J* = 7.2, 2.9, 1.5 Hz, 1H), 4.65 (d, *J* = 7.2 Hz, 2H), 3.42 – 3.36 (m, 1H), 2.48 – 2.11 (m, 5H), 1.79 (d, *J* = 1.6 Hz, 3H), 1.75 (s, 3H), 1.70 (s, 3H).

^{13}C NMR (100 MHz, $CDCl_3$): δ 194.7, 170.6, 145.5, 139.5, 135.4, 118.5, 62.2, 53.8, 26.3, 25.9, 24.6, 18.2, 16.2.

IR (Neat Film, NaCl): 2925, 1736, 1676, 1449, 1381, 1249, 1151 cm^{-1}.

HRMS (MM: FD+): *m/z* calc'd for $C_{13}H_{18}O_3$ $[M]^+$: 222.1255, found 222.1251.



1-benzyl 3-methyl 4-oxo-3,4-dihydropyridine-1,3(2*H*)-dicarboxylate (83)

A flame dried round bottom flask was charged with *i*-Pr_2NH (2.52 mL, 18.0 mmol, 1.2 equiv) and THF (167 mL, 0.1 M). The solution was cooled to –78 ºC and *n*-BuLi (7.20 mL, 18.0 mmol, 1.2 equiv) was added dropwise. The resultant solution was slowly warmed to 0 ºC over 1 h and then cooled to – 78 ºC. The LDA solution was added dropwise to a solution of 1-benzoyl-2,3-dihydropyridin-4(1*H*)-one[45] (3.47 g, 15.0 mmol, 1.0 equiv) in THF (239 mL, 0.06 M) at –78 ºC. The resultant solution was stirred for 1 h. Then methyl cyanoformate (1.37 mL, 17.25 mmol, 1.15 equiv) was added dropwise. Upon complete consumption of starting material (as determined by TLC), the reaction was diluted with a saturated solution of NH_4Cl and the product was extracted with EtOAc (3 x 200 mL). The combined organic layers were dried over Na_2SO_4, filtered, and concentrated under reduced pressure. The crude product was purified by column chromatography (SiO_2, 20–30% EtOAc/Hexanes) to afford acylated enone **83** (1.17 g, 4.05 mmol, 27% yield).

^{1}H NMR (400 MHz, $CDCl_3$): δ 7.88 (s, 1H), 7.39 (d, *J* = 2.3 Hz, 5H), 5.40 (s, 1H), 5.28 (s, 1H), 4.39 (dd, *J* = 13.6, 8.9 Hz, 1H), 4.18 (dd, *J* = 13.6, 5.4 Hz, 1H), 3.76 (s, 3H), 3.51 (dd, *J* = 8.9, 5.4 Hz, 1H).

^{13}C NMR (100 MHz, $CDCl_3$): δ 187.8, 168.2, 143.6, 134.8, 129.1, 128.9, 128.8, 128.7, 106.8, 69.6, 52.9, 50.6, 44.4.

IR (Neat Film, NaCl): 2952, 2332, 1734, 1670, 1601, 1388, 1293, 1213 cm^{-1}.

HRMS (MM: FD+): *m/z* calc'd for $C_{15}H_{15}NO_5$ $[M]^+$: 289.0950, found 289.0948.

1-benzyl 3-(3-methylbut-2-en-1-yl) 4-oxo-3,4-dihydropyridine-1,3(2*H*)-dicarboxylate (74)

A flame dried round bottom flask equipped with a reflux condenser was charged with Zn^0 dust (51.5 mg, 0.787 mmol, 0.2 equiv), acylated enone **83** (1.14 g, 3.40 mmol, 1.0 equiv), and toluene (19.7 mL, 0.2 M). To the stirred solution, prenyl alcohol was added neat (2.00 mL, 19.68 mmol, 5.0 equiv). The resultant solution was heated to reflux for 3 days. The solution was cooled to 23 ºC, filtered through a celite plug and eluted with CH_2Cl_2, and concentrated under reduced pressure. The crude product was purified by column chromatography (SiO_2, 15–25% EtOAc/Hexanes) to afford acylated enone **74** (883 mg, 2.57 mmol, 65% yield).

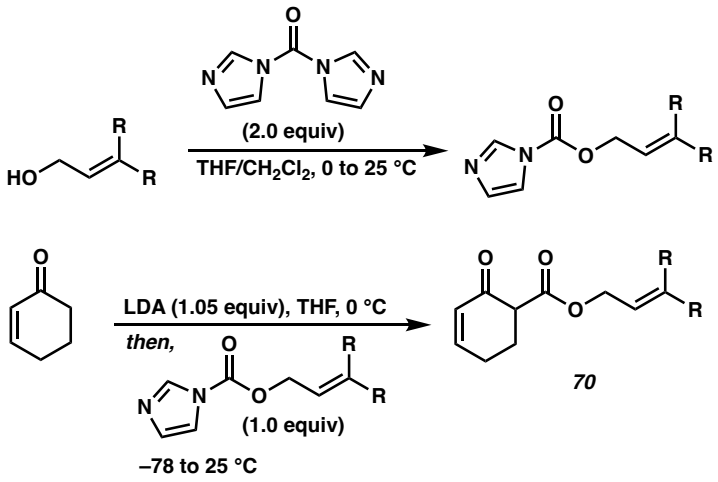
^{1}H NMR (400 MHz, $CDCl_3$): δ 7.86 (s, 1H), 7.39 (m, 5H), 5.39 (s, 1H), 5.32 (tp, *J* = 7.3, 1.4 Hz, 1H), 5.27 (s, 2H), 4.65 (dd, *J* = 7.3, 2.9 Hz, 2H), 4.38 (dd, *J* = 13.6, 8.9 Hz, 1H), 4.17 (dd, *J* = 13.5, 5.4 Hz, 1H), 3.48 (dd, *J* = 9.1, 5.3 Hz, 1H), 1.74 (s, 3H), 1.69 (s, 3H).

^{13}C NMR (100 MHz, $CDCl_3$): δ 187.9, 167.8, 143.5, 140.1, 134.9, 129.0, 128.9, 128.8, 128.7, 118.0, 106.9, 69.5, 62.8, 50.8, 44.5, 25.9, 18.2.

IR (Neat Film, NaCl): 2965, 1727, 1676, 1599, 1388, 1293, 1209, 940 cm^{-1}.

HRMS (MM: FD+): *m/z* calc'd for $C_{19}H_{21}HO_5$ $[M]^+$: 343.1420, found 343.1420.

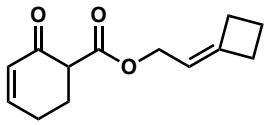
General Procedure 1E: Substituted β-Ketoesters Synthesis through Acylation[42]



To a solution of di(1*H*-imidazol-1-yl)methanone (2.0 equiv) in THF (2.0 M) at 0 °C was added dropwise a solution of the corresponding alcohol (1.0 equiv) in CH_2Cl_2 (1.0 M). After 3 h, the reaction mixture was gradually warmed to 25 °C. Upon consumption of starting material (as determined by TLC), the reaction mixture was concentrated under reduced pressure then filtered through a silica plug and eluted with 50% EtOAc/Hexanes. The resulting solution was concentrated under reduced pressure.

A flame dried round bottom flask was charged with iPr_2NH (1.1 equiv) and THF (1.75 M). The solution was cooled to 0 ºC and *n*-BuLi (2.5 M in hexanes, 1.05 equiv) was added dropwise. The resultant solution was stirred for 30 min at 0 ºC. 2-cyclohexen-1-one (1.0 equiv) in THF (1.25 M) was added dropwise and stirring was continued at 0 ºC for 30 minutes. The solution was cooled to –78 ºC, and the corresponding crude 1*H*-imidazole-1-carboxylate (1.2 equiv) in THF (3.25 M) was added dropwise. After 2 h, the reaction was

gradually warmed to 23 ºC and diluted with 2 M aqueous HCl until reaching a pH < 7. The reaction mixture was extracted three times with EtOAc. The combined organic layers were washed with brine, dried over Na_2SO_4, filtered, and concentrated under reduced pressure. The crude product was purified by column chromatography to afford the corresponding acylated enone.



78

2-cyclobutylideneethyl 2-oxocyclohex-3-ene-1-carboxylate (78)

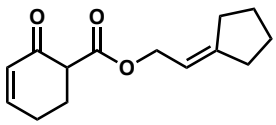
Prepared from 2-cyclohexen-1-one and 2-cyclobutylideneethan-1-ol[46] following General Procedure 1E. Purification by flash column chromatography (5–50% EtOAc/hexanes) afforded the title compound as a colorless oil (2.02 g, 9.19 mmol, 31.7% yield).

^{1}H NMR (400 MHz, $CDCl_3$): δ 7.00 (dt, *J* = 10.1, 3.7 Hz, 1H), 6.07 (dt, *J* = 10.2, 2.0 Hz, 1H), 5.27 (tp, *J* = 6.9, 2.2 Hz, 1H), 4.53 (d, *J* = 7.2 Hz, 2H), 3.45 – 3.36 (m, 1H), 2.80 – 2.65 (m, 4H), 2.56 – 2.31 (m, 3H), 2.28 – 2.15 (m, 1H), 1.98 (p, *J* = 8.0 Hz, 2H).

^{13}C NMR (100 MHz, $CDCl_3$): δ 194.1, 170.1, 150.7, 148.9, 129.3, 114.1, 62.3, 53.6, 31.2, 29.6, 25.8, 24.5, 17.1.

IR (Neat Film, NaCl): 2947, 1737, 1681, 1457, 1397, 1301, 1229, 1163, 1123 cm^{-1}.

HRMS (MM: FD+): *m/z* calc'd for $C_{13}H_{16}O_3$ $[M]^+$: 220.1099, found 220.1093.



79

2-cyclopentylideneethyl 2-oxocyclohex-3-ene-1-carboxylate (79)

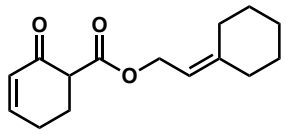
Prepared from 2-cyclohexen-1-one and 2-cyclopentylideneethan-1-ol[47] following General Procedure 1E. Purification by flash column chromatography (5–50% EtOAc/hexanes) afforded the title compound as a colorless oil (2.69 g, 11.46 mmol, 31.9% yield).

^{1}H NMR (400 MHz, $CDCl_3$): δ 6.99 (dt, *J* = 10.1, 3.8 Hz, 1H), 6.07 (dt, *J* = 10.2, 2.0 Hz, 1H), 5.50 – 5.40 (m, 1H), 4.64 (dt, *J* = 7.2, 1.1 Hz, 2H), 3.45 – 3.37 (m, 1H), 2.57 – 2.15 (m, 8H), 1.75 – 1.58 (m, 4H).

^{13}C NMR (100 MHz, $CDCl_3$): δ 194.1, 170.2, 151.2, 150.7, 129.3, 113.8, 63.8, 53.6, 34.0, 29.0, 26.4, 26.2, 25.8, 24.5.

IR (Neat Film, NaCl): 2946, 2869, 1782, 1681, 1455, 1387, 1304, 1224, 1156 cm^{-1}.

HRMS (MM: FD+): *m/z* calc'd for $C_{14}H_{18}O_3$ $[M]^+$: 234.1256, found 234.1255.



80

2-cyclohexylideneethyl 2-oxocyclohex-3-ene-1-carboxylate (80)

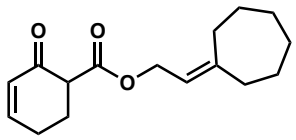
Prepared from 2-cyclohexen-1-one and 2-cyclohexylideneethan-1-ol[47] following General Procedure 1E, with the modification of 1.5 equiv of di(1*H*-imidazol-1-yl)methanone and 1.2 equiv of 2-cyclohexylideneethyl 1*H*-imidazole-1-carboxylate being used. Purification by flash column chromatography (5–30% EtOAc/hexanes) afforded the title compound as a colorless oil (535 mg, 2.15 mmol, 28% yield).

^{1}H NMR (400 MHz, $CDCl_3$): δ7.04 – 6.95 (m, 1H), 6.07 (dt, J = 10.1, 2.0 Hz, 1H), 5.29 (tt, J = 7.2, 1.2 Hz, 1H), 4.67 (d, J = 7.2 Hz, 2H), 3.45 – 3.36 (m, 1H), 2.56 – 2.30 (m, 3H), 2.27 – 2.15 (m, 3H), 2.14 – 2.08 (m, 2H), 1.60 – 1.48 (m, 6H).

^{13}C NMR (100 MHz, $CDCl_3$): δ 194.1, 170.2, 150.6, 147.5, 129.3, 115.0, 61.5, 53.6, 37.1, 29.2, 28.5, 27.9, 26.7, 25.8, 24.5.

IR (Neat Film, NaCl): 2930, 2852, 1735, 1683, 1447, 1388, 1298, 1169, 1122 cm^{-1}.

HRMS (MM: FD+): *m/z* calc'd for $C_{15}H_{20}O_3$ $[M]^+$: 248.1412, found 248.1418.



81

2-cycloheptylideneethyl 2-oxocyclohex-3-ene-1-carboxylate (81)

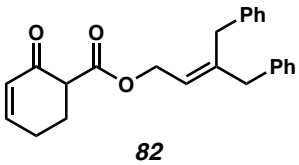
Prepared from 2-cyclohexen-1-one and 2-cycloheptylideneethan-1-ol[48] following General Procedure 1E. Purification by flash column chromatography (5–50% EtOAc/hexanes) afforded the title compound as a colorless oil (1.73 g, 5.43 mmol, 28.1% yield).

^{1}H NMR (400 MHz, $CDCl_3$): δ 6.99 (dt, *J* = 10.0, 3.8 Hz, 1H), 6.07 (dt, *J* = 10.1, 2.0 Hz, 1H), 5.34 (tt, *J* = 7.1, 1.3 Hz, 1H), 4.66 (d, *J* = 7.0 Hz, 2H), 3.45 – 3.37 (m, 1H), 2.57 – 2.15 (m, 8H), 1.63 – 1.44 (m, 8H).

^{13}C NMR (100 MHz, $CDCl_3$): δ 194.1, 170.2, 150.6, 148.8, 129.3, 118.5, 62.1, 53.6, 37.8, 30.2, 29.9, 29.1, 28.8, 27.3, 25.8, 24.5.

IR (Neat Film, NaCl): 2923, 2853, 1736, 1681, 1442, 1388, 1300, 1231, 1155, 1122, 1076 cm^{-1}.

HRMS (MM: FD+): *m/z* calc'd for $C_{26}H_{22}O_3$ $[M]^+$: 262.1569, found 262.1577.



82

3-benzyl-4-phenylbut-2-en-1-yl 2-oxocyclohex-3-ene-1-carboxylate (82)

Prepared from 2-cyclohexen-1-one and 3-benzyl-4-phenylbut-2-en-1-ol [49] following General Procedure 1E. Purification by flash column chromatography (5–50% EtOAc/hexanes) afforded the title compound as a colorless oil (1.96 g, 5.43 mmol, 21.3% yield).

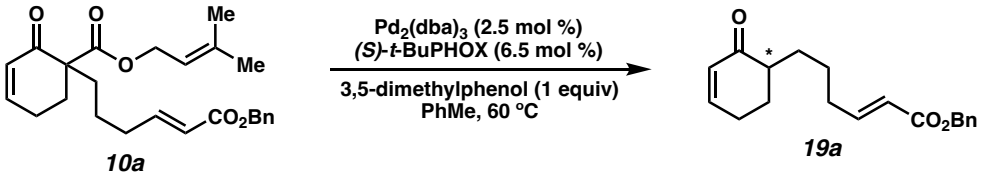
^{1}H NMR (400 MHz, $CDCl_3$): δ 7.33 – 7.25 (m, 4H), 7.24 – 7.18 (m, 2H), 7.17 – 7.07 (m, 4H), 7.03 – 6.97 (m, 1H), 6.08 (dt, *J* = 10.1, 2.0 Hz, 1H), 5.59 (tt, *J* = 7.1, 1.1 Hz, 1H), 4.86 – 4.80 (m, 2H), 3.48 – 3.35 (m, 3H), 3.26 (s, 2H), 2.55 – 2.32 (m, 3H), 2.30 – 2.15 (m, 1H).

^{13}C NMR (100 MHz, $CDCl_3$): δ 193.9, 170.1, 150.7, 144.4, 139.0, 138.9, 129.3, 129.3, 128.9, 128.7, 128.5, 126.5, 126.4, 121.9, 62.0, 53.6, 42.9, 35.9, 25.8, 24.5.

IR (Neat Film, NaCl): 3026, 2927, 1738, 1681, 1493, 1388, 1304, 1230, 1157, 1123 cm^{-1}.

HRMS (MM: FD+): *m/z* calc'd for $C_{24}H_{24}O_3$ $[M]^+$: 360.1725, found 360.17302.

Protonated Enone Byproducts



benzyl (*R*,*E*)-6-(2-oxocyclohex-3-en-1-yl)hex-2-enoate (19a)

In a nitrogen filled glovebox, an oven-dried 20 mL vial was charged with a stir bar, $Pd_2(dba)_3$ (0.46 mg, 0.50 μmol, 2.5 mol %), *(S)-t*-BuPHOX (0.50 mg, 1.3 μmol, 6.5 mol %), and toluene (0.5 mL). The catalyst solution was stirred at 23 ºC for 20 min. A solution of

substrate **10a** (8.2 mg, 0.020 mmol, 1 equiv) and 3,5-dimethylphenol (2.4 mg, 0.020 mmol, 1 equiv) in toluene (0.5 mL) was added to the vial. The resultant solution was then heated to 60 ºC for 14 h. The solution was then cooled to 23 ºC and concentrated under reduced pressure. NMR analysis of the crude reaction mixture affords an NMR yield of 100% (with respect to 1,3,5-trimethoxybenzene as an internal standard). The sample was purified by preparatory TLC (25% EtOAc/hexanes) to afford **19a** (71% ee).

^{1}H NMR (400 MHz, $CDCl_3$): δ 7.39 – 7.29 (m, 5H), 7.01 (dt, *J* = 15.7, 6.9 Hz, 1H), 6.92 (dddd, *J* = 10.1, 4.5, 3.5, 0.9 Hz, 1H), 5.98 (ddd, *J* = 10.1, 2.3, 1.7 Hz, 1H), 5.88 (dt, *J* = 15.6, 1.6 Hz, 1H), 5.17 (s, 2H), 2.46 – 2.34 (m, 2H), 2.32 – 2.20 (m, 3H), 2.09 (dqd, *J* = 13.3, 4.8, 1.0 Hz, 1H), 1.89 – 1.80 (m, 1H), 1.75 (dddd, *J* = 13.3, 11.0, 8.4, 5.8 Hz, 1H), 1.55 – 1.35 (m, 3H).

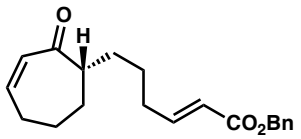
^{13}C NMR (100 MHz, $CDCl_3$): δ 201.6, 166.6, 149.7, 149.6, 136.3, 129.7, 128.7, 128.3, 128.3, 121.4, 66.2, 46.5, 32.5, 29.0, 28.0, 25.6, 25.3.

IR (Neat Film, NaCl): 2921, 1712, 1673, 1257 cm^{-1}.

HRMS (MM: FD+): *m/z* calc'd for $C_{19}H_{22}O_3$ $[M]^+$: 298.1569, found 298.1565.

Optical Rotation: $[\alpha]_D^{21}$ +3.5 (c 0.20, $CHCl_3$).

SFC conditions: 40% IPA, 2.5 mL/min, Chiralpak IC column, λ = 210 nm, t_R (min): minor = 3.81, major = 4.34.



19d

benzyl (*R*,*E*)-7-(2-oxocyclohex-3-en-1-yl)hept-2-enoate (19d)

Isolated as a byproduct from the reaction of **10d** to **11d** as a colorless oil (10.4 mg, 0.0332 mmol, 17% yield, 67% ee).

^{1}H NMR (400 MHz, $CDCl_3$): δ 7.32 – 7.22 (m, 5H), 6.93 (dt, *J* = 15.7, 6.9 Hz, 1H), 6.53 (ddd, *J* = 12.0, 6.7, 4.0 Hz, 1H), 5.94 (ddd, *J* = 11.9, 2.5, 0.9 Hz, 1H), 5.80 (dt, *J* = 15.6, 1.6 Hz, 1H), 5.10 (s, 3H), 2.59 – 2.49 (m, 1H), 2.42 – 2.25 (m, 2H), 2.14 (tdd, *J* = 7.7, 4.8, 1.4 Hz, 2H), 1.90 – 1.48 (m, 5H), 1.44 – 1.29 (m, 4H).

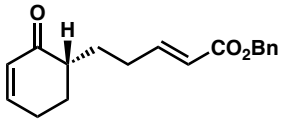
^{13}C NMR (100 MHz, $CDCl_3$): δ 205.7, 166.5, 149.6, 146.0, 136.2, 132.8, 128.6, 128.2, 128.2, 121.2, 66.0, 51.7, 32.4, 31.1, 29.9, 29.5, 25.8, 25.4.

IR (Neat Film, NaCl): 2917, 1719, 1671, 1266, 1165 cm^{-1}.

HRMS (MM: FD+): *m/z* calc'd for $C_{20}H_{24}O_3$ $[M]^+$: 312.1720, found 312.1734.

Optical Rotation: $[\alpha]_D^{21}$ –0.6 (c 1.00, $CHCl_3$).

SFC conditions: 15% IPA, 2.5 mL/min, Chiralpak AD-H column, λ = 210 nm, t_R (min): minor = 8.23, major = 7.63.



19e

benzyl (*S*,*E*)-5-(2-oxocyclohex-3-en-1-yl)pent-2-enoate (19e)

Isolated as the major byproduct from the reaction of **10e** to **11e**. Purification by flash column chromatography (0–45% EtOAc/hexanes) afforded the title compound as a colorless oil (46.1 mg, 0.16 mmol, 81% yield, 47% ee).

^{1}H NMR (400 MHz, $CDCl_3$): δ 7.42 – 7.28 (m, 5H), 7.01 (dt, *J* = 15.6, 6.9 Hz, 1H), 6.92 (dddd, *J* = 10.0, 4.4, 3.6, 1.0 Hz, 1H), 5.98 (dt, *J* = 10.0, 2.0 Hz, 1H), 5.90 (dt, *J* = 15.7,

1.6 Hz, 1H), 5.17 (s, 2H), 2.44 – 2.24 (m, 5H), 2.15 – 1.96 (m, 2H), 1.82 – 1.69 (m, 1H), 1.62 – 1.44 (m, 1H).

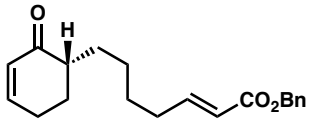
^{13}C NMR (100 MHz, $CDCl_3$): δ 201.3, 166.5, 149.6, 149.4, 136.2, 129.7, 128.7, 128.3, 128.3, 121.6, 66.2, 45.9, 29.7, 28.2, 27.8, 25.4.

IR (Neat Film, NaCl): 3032, 2932, 1719, 1675, 1455, 1386, 1265, 1171 cm^{-1}.

HRMS (MM: FD+): *m/z* calc'd for $C_{18}H_{20}O_3$ $[M]^+$: 284.1412, found 284.1407.

Optical Rotation: $[\alpha]_D^{21}$ +11.8 (c 1.00, $CHCl_3$).

SFC conditions: 10% IPA, 2.5 mL/min, Chiralpak AS-H column, λ = 210 nm, t_R (min): minor = 5.69, major = 6.54.



19f

benzyl (*R*,*E*)-7-(2-oxocyclohex-3-en-1-yl)hept-2-enoate (19f)

Isolated as a byproduct from the reaction of **10f** to **11f** as a colorless oil (28.1 mg, 0.090 mmol, 45% yield, 51% ee). Absolute stereochemistry proposed based on VCD analysis (vide infra).

^{1}H NMR (400 MHz, $CDCl_3$): δ 7.42 – 7.29 (m, 5H), 7.00 (dt, *J* = 15.6, 6.9 Hz, 1H), 6.90 (dddd, *J* = 10.0, 4.5, 3.5, 0.9 Hz, 1H), 5.97 (dt, *J* = 10.1, 2.0 Hz, 1H), 5.86 (dt, *J* = 15.6, 1.6 Hz, 1H), 5.17 (s, 2H), 2.42 – 2.33 (m, 2H), 2.29 – 2.18 (m, 3H), 2.08 (dqd, *J* = 13.3, 4.8, 0.9 Hz, 1H), 1.88 – 1.80 (m, 1H), 1.78 – 1.69 (m, 1H), 1.52 – 1.29 (m, 5H).

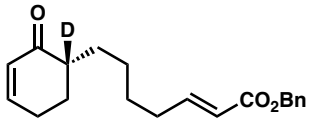
^{13}C NMR (100 MHz, $CDCl_3$): δ 201.8, 166.6, 150.0, 149.5, 136.3, 129.6, 128.6, 128.3, 128.3, 121.2, 66.1, 46.6, 32.2, 29.0, 28.2, 27.9, 26.6, 25.2.

IR (Neat Film, NaCl): 2927, 2859, 1716, 1675, 1652, 1262, 1172 cm^{-1}

HRMS (MM: FD+): *m/z* calc'd for $C_{20}H_{24}O_3$ $[M]^+$: 312.1725, found 312.1737.

Optical Rotation: $[\alpha]_D^{21}$ +4.1 (c 1.00, $CHCl_3$).

SFC conditions: 15% IPA, 2.5 mL/min, Chiralpak AD-H column, λ = 210 nm, t_R (min): minor = 7.77, major = 8.44.



D-19f

benzyl (*R*,*E*)-7-(2-oxocyclohex-3-en-1-yl-1-*d*)hept-2-enoate (*D*-19f)

Isolated as a byproduct from the reaction of ***D*-10f** to ***D*-11f** as a colorless oil (14.9 mg, 0.0475 mmol, 24% yield, 55% ee).

^{1}H NMR (400 MHz, $CDCl_3$): δ 7.39 – 7.29 (m, 5H), 7.00 (dt, *J* = 15.6, 7.0 Hz, 1H), 6.91 (dddd, *J* = 10.1, 4.5, 3.5, 0.9 Hz, 1H), 5.97 (dddd, *J* = 10.0, 2.3, 1.6, 0.6 Hz, 1H), 5.86 (dt, *J* = 15.6, 1.6 Hz, 1H), 5.17 (s, 2H), 2.44 – 2.33 (m, 2H), 2.28 – 2.18 (m, 2.5H), 2.09 (ddt, *J* = 13.3, 5.8, 4.5 Hz, 1H), 1.87 – 1.70 (m, 2H), 1.53 – 1.27 (m, 5H).

^{13}C NMR (100 MHz, $CDCl_3$): δ 201.9, 166.6, 150.0, 149.6, 129.7, 129.7, 128.7, 128.3, 128.3, 121.2, 66.2, 46.6, 32.3, 29.0, 28.9, 28.2, 27.9, 27.8, 26.7, 26.6, 25.3, 25.2.

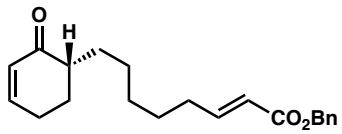
^{2}H NMR (61 MHz, $CHCl_3$): δ 2.25.

IR (Neat Film, NaCl): 2929, 2857, 1714, 1697, 1267, 1174 cm^{-1}.

HRMS (MM: FD+): *m/z* calc'd for $C_{20}H_{23}DO_3$ $[M+H]^+$: 313.1783, found 313.1788.

Optical Rotation: $[\alpha]_D^{21}$ +5.8 (c 0.50, $CHCl_3$).

SFC conditions: 15% IPA, 2.5 mL/min, Chiralpak AD-H column, λ = 210 nm, t_R (min): minor = 7.96, major = 8.67.



19g

benzyl (*R*,*E*)-8-(2-oxocyclohex-3-en-1-yl)oct-2-enoate (19g)

Isolated as the major product from the reaction of **10g** to **11g** as a colorless oil (50.5 mg, 0.155 mmol, 77% yield, 56% ee).

^{1}H NMR (400 MHz, $CDCl_3$): δ 7.40 – 7.29 (m, 5H), 7.01 (dt, *J* = 15.6, 6.9 Hz, 1H), 6.91 (dddd, *J* = 10.0, 4.5, 3.5, 0.9 Hz, 1H), 5.97 (dt, *J* = 10.0, 2.0 Hz, 1H), 5.86 (dt, *J* = 15.6, 1.6 Hz, 1H), 5.17 (s, 2H), 2.45 – 2.33 (m, 2H), 2.30 – 2.16 (m, 3H), 2.09 (dqd, *J* = 14.5, 5.0, 0.9 Hz, 1H), 1.86 – 1.70 (m, 2H), 1.51 – 1.42 (m, 2H), 1.41 – 1.28 (m, 5H).

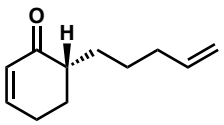
^{13}C NMR (100 MHz, $CDCl_3$): δ 202.0, 166.7, 150.2, 149.5, 136.3, 129.7, 128.7, 128.3, 128.3, 121.1, 66.1, 46.6, 32.3, 29.3, 29.1, 28.0, 27.9, 26.8, 25.2.

IR (Neat Film, NaCl): 2927, 2859, 1718, 1677, 1555, 1450, 1257, 1165 cm^{-1}

HRMS (MM: FD+): *m/z* calc'd for $C_{21}H_{26}O_3$ $[M]^+$: 326.1877, found 326.1891.

Optical Rotation: $[\alpha]_D^{21}$ +7.0 (c 1.00, $CHCl_3$).

SFC conditions: 15% IPA, 2.5 mL/min, Chiralpak AD-H column, λ = 210 nm, t_R (min): minor = 9.70, major = 10.46.



19h

6-(pent-4-en-1-yl)cyclohex-2-en-1-one (19h)

Isolated as the major product from the reaction of **10h** to **11h** as a colorless oil. Purification by flash column chromatography (0–15% EtOAc/hexanes) afforded the title compound as a colorless oil (11.0 mg, 0.067 mmol, 33% yield, 58% ee).

^{1}H NMR (400 MHz, $CDCl_3$): δ 6.91 (dddd, *J* = 10.1, 4.4, 3.5, 0.9 Hz, 1H), 5.97 (dt, *J* = 10.0, 2.1 Hz, 1H), 5.81 (ddt, *J* = 16.9, 10.2, 6.6 Hz, 1H), 5.01 (dq, *J* = 17.2, 1.8 Hz, 1H), 4.94 (dd, *J* = 10.1, 1.3 Hz, 1H), 2.45 – 2.24 (m, 3H), 2.16 – 1.98 (m, 2=3H), 1.95 – 1.69 (m, 2H), 1.55 – 1.31 (m, 3H).

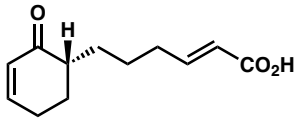
^{13}C NMR (100 MHz, $CDCl_3$): δ 202.0, 149.5, 138.8, 129.7, 114.7, 46.6, 34.0, 28.8, 27.9, 26.4, 25.2.

IR (Neat Film, NaCl): 2925, 2859, 1677, 1639, 1456, 1387, 1215, 912 cm^{-1}.

HRMS (MM: FD+): *m/z* calc'd for $C_{11}H_{16}O$ $[M]^+$: 164.1201, found 164.1201.

Optical Rotation: $[\alpha]_D^{21}$ –111.5 (c 1.00, $CHCl_3$).

SFC conditions: 3% IPA, 2.5 mL/min, Chiralpak AD-H column, λ = 210 nm, t_R (min): minor = 4.41, major = 4.11.



19i

(*E*)-6-(2-oxocyclohex-3-en-1-yl)hex-2-enoic acid (19i)

Isolated as the major product from the reaction of **10i** to **11i** as a colorless oil. Purification by flash column chromatography (35% EtOAc/hexanes with 3% AcOH) afforded the title compound as a white solid (33.2 mg, 0.16 mmol, 80% yield, 9% ee).

^{1}H NMR (400 MHz, $CDCl_3$): δ 7.07 (dtd, *J* = 15.5, 7.0, 1.5 Hz, 1H), 6.97 – 6.87 (m, 1H), 5.98 (dq, *J* = 10.1, 1.9 Hz, 1H), 5.84 (dt, *J* = 15.6, 1.6 Hz, 1H), 2.49 – 2.35 (m, 2H), 2.34 – 2.19 (m, 3H), 2.16 – 2.04 (m, 1H), 1.92 – 1.81 (m, 1H), 1.81 – 1.70 (m, 1H), 1.63 – 1.48 (m, 2H), 1.48 – 1.35 (m, 1H).

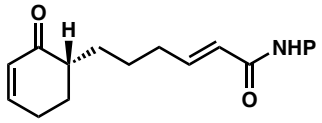
^{13}C NMR (100 MHz, $CDCl_3$): δ 201.7, 171.5, 151.9, 149.7, 129.7, 120.9, 46.5, 32.5, 29.0, 28.0, 25.5.

IR (Neat Film, NaCl): 2928, 2857, 1731, 1454, 1155 cm^{-1}

HRMS (MM: FD+): *m/z* calc'd for $C_{12}H_{17}O_3$ $[M]^+$: 209.1178, found 209.1168.

Optical Rotation: $[\alpha]_D^{21}$ 2.2 (c 1.00, $CHCl_3$).

SFC conditions: 30% IPA, 2.5 mL/min, Chiralpak IC column, l = 210 nm, t_R (min): minor = 3.30, major = 4.02



19m

1,3-dioxoisoindolin-2-yl (*E*)-6-(2-oxocyclohex-3-en-1-yl)hex-2-enoate (19m)

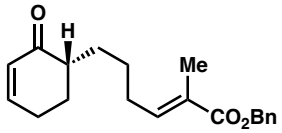
Isolated as a byproduct product from the reaction of **10m** to **11m** as a colorless oil. Purification by flash column chromatography (0–35% EtOAc/hexanes) afforded the title compound as a white solid (7.7 mg, 0.022 mmol, 11% yield).

^{1}H NMR (400 MHz, $CDCl_3$): δ 7.89 (dd, *J* = 5.5, 3.1 Hz, 2H), 7.79 (dd, *J* = 5.5, 3.1 Hz, 2H), 7.32 (dt, *J* = 15.8, 6.9 Hz, 1H), 6.93 (dddd, *J* = 10.1, 4.5, 3.5, 1.0 Hz, 1H), 6.10 (dt, *J* = 15.8, 1.6 Hz, 1H), 5.99 (ddd, *J* = 10.0, 2.3, 1.7 Hz, 1H), 2.50 – 2.25 (m, 5H), 2.12 (m, 1H), 1.95 – 1.84 (m, 1H), 1.78 (m, 1H), 1.59 (m, 2H), 1.45 (m, 1H).

^{13}C NMR (100 MHz, $CDCl_3$): δ 201.5, 162.5, 162.2, 155.6, 149.7, 134.9, 129.7, 129.1, 124.1, 115.9, 46.5, 33.2, 29.1, 28.1, 25.4, 25.3.

IR (Neat Film, NaCl): 2931, 1770, 1745, 1673, 1466, 1360, 1186 cm^{-1}.

HRMS (MM: FD+): *m/z* calc'd for $C_{20}H_{19}NO_5$ $[M]^+$: 353.1263, found 353.1242.



19r

benzyl (*R*,*E*)-2-methyl-6-(2-oxocyclohex-3-en-1-yl)hex-2-enoate (19r)

Isolated as a byproduct from the reaction of **10r** to **11r** as a colorless oil (23.2 mg, 0.0743 mmol, 37% yield, 59% ee).

^{1}H NMR (400 MHz, $CDCl_3$): δ 7.40 – 7.29 (m, 5H), 6.91 (dddd, *J* = 10.1, 4.5, 3.5, 0.9 Hz, 1H), 6.81 (td, *J* = 7.5, 1.5 Hz, 1H), 5.97 (dt, *J* = 10.0, 1.9 Hz, 1H), 5.18 (s, 2H), 2.45 – 2.34 (m, 2H), 2.32 – 2.17 (m, 3H), 2.09 (dqd, *J* = 13.4, 4.9, 1.0 Hz, 1H), 1.90 – 1.81 (m, 4H), 1.80 – 1.71 (m, 1H), 1.55 – 1.36 (m, 3H).

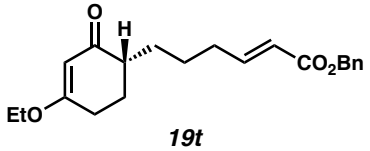
^{13}C NMR (100 MHz, $CDCl_3$): δ 201.7, 168.1, 149.6, 142.7, 136.6, 129.7, 128.6, 128.2, 128.1, 127.9, 66.3, 46.6, 29.2, 29.0, 28.0, 26.2, 25.2, 12.6.

IR (Neat Film, NaCl): 3033, 2932, 2861, 1710, 1677, 1256 cm^{-1}.

HRMS (MM: FD+): *m/z* calc'd for $C_{20}H_{24}O_3$ $[M]^+$: 312.1725, found 312.1729.

Optical Rotation: $[\alpha]_D^{21}$ +8.6 (c 1.00, $CHCl_3$).

SFC conditions: 15% IPA, 2.5 mL/min, Chiralpak AD-H column, λ = 210 nm, t_R (min): minor = 5.89, major = 6.22.



19t

benzyl (*E*)-6-(4-ethoxy-2-oxocyclohex-3-en-1-yl)hex-2-enoate (19t)

Isolated as a byproduct from the reaction of **10t** to **11t** as a colorless oil (5.2 mg, 0.015 mmol, 8% yield, 45% ee).

^{1}H NMR (400 MHz, $CDCl_3$): δ 7.41 – 7.27 (m, 5H), 7.01 (dt, *J* = 15.6, 6.9 Hz, 1H), 5.87 (dt, *J* = 15.6, 1.6 Hz, 1H), 5.31 (s, 1H), 5.17 (s, 2H), 3.88 (qd, *J* = 7.1, 1.4 Hz, 2H), 2.41 (dd, *J* = 7.2, 5.3 Hz, 2H), 2.29 – 2.13 (m, 3H), 2.06 (dq, *J* = 13.2, 5.2 Hz, 1H), 1.86 (ddt, *J* = 13.3, 11.1, 5.2 Hz, 1H), 1.78 – 1.64 (m, 1H), 1.59 – 1.37 (m, 3H), 1.35 (t, *J* = 7.0 Hz, 3H).

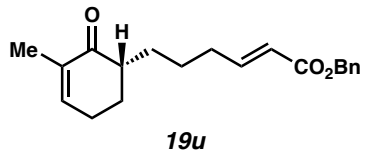
^{13}C NMR (100 MHz, $CDCl_3$): δ 201.4, 176.9, 166.6, 149.7, 136.3, 128.7, 128.3, 128.3, 121.3, 102.3, 66.1, 64.4, 45.1, 32.5, 29.3, 28.2, 26.4, 25.7, 14.3.

IR (Neat Film, NaCl): 2919, 1718, 1648, 1605, 1456, 1377, 1260, 1190, 732 cm^{-1}.

HRMS (MM: FD+): *m/z* calc'd for $C_{21}H_{26}O_4$ $[M]^+$: 342.1828, found 342.1826.

Optical Rotation: $[\alpha]_D^{21}$ –5.5 (c 0.34, $CHCl_3$).

SFC conditions: 15% IPA, 2.5 mL/min, Chiralpak AD-H column, λ = 210 nm, t_R (min): minor = 10.17, major = 11.69.



19u

benzyl (*E*)-6-(3-methyl-2-oxocyclohex-3-en-1-yl)hex-2-enoate (19u)

Isolated as a byproduct from the reaction of **10u** to **11u** as a colorless oil (23.6 mg, 0.075 mmol, 37% yield, 46% ee).

^{1}H NMR (400 MHz, $CDCl_3$): δ 7.41 – 7.28 (m, 5H), 7.01 (dt, *J* = 15.5, 6.9 Hz, 1H), 6.71 – 6.63 (m, 1H), 5.88 (dt, *J* = 15.6, 1.6 Hz, 1H), 5.17 (s, 2H), 2.33 (ddq, *J* = 6.3, 4.8, 2.0 Hz, 2H), 2.29 – 2.19 (m, 3H), 2.10 – 2.01 (m, 1H), 1.88 – 1.77 (m, 1H), 1.76 (q, *J* = 1.7 Hz, 3H), 1.74 – 1.69 (m, 1H), 1.56 – 1.34 (m, 3H).

^{13}C NMR (100 MHz, $CDCl_3$): δ 201.9, 166.6, 149.8, 144.5, 136.3, 135.3, 128.68, 128.3, 128.3, 121.3, 66.2, 46.6, 32.5, 29.2, 28.4, 25.7, 25.2, 16.3.

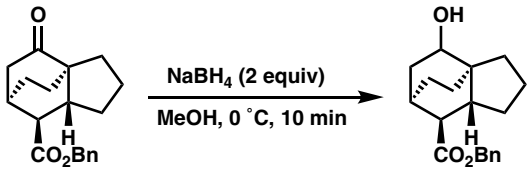
IR (Neat Film, NaCl): 2925, 1718, 1670, 1455, 1262, 1172, 1013 cm^{-1}.

HRMS (MM: FD+): *m/z* calc'd for $C_{20}H_{24}O_3$ $[M]^+$: 312.1725, found 312.1721.

Optical Rotation: $[\alpha]_D^{21}$ –14.7 (c 0.35, $CHCl_3$).

SFC conditions: 10% IPA, 2.5 mL/min, Chiralpak OJ-H column, λ = 210 nm, t_R (min): minor = 7.18, major = 7.62.

Product Derivatizations



11a ***38***

benzyl (3a*R*,6*R*,7*S*,7a*R*)-4-hydroxyoctahydro-3a,6-ethanoindene-7-carboxylate (38)

To a solution of ketone **11a** (0.125 mmol, 1 equiv) in methanol (4.4 mL) was added $NaBH_4$ (0.25 mmol, 2 equiv) at 0 ºC. The reaction was allowed to stir for 10 min at 0 ºC and then

was diluted with water. The aqueous layer was extracted with dichloromethane (3x), and the combined organic layers were dried over Na_2SO_4. Concentration under reduced pressure afforded the title compound as a colorless oil (37.6 mg, 0.125 mmol, 99% yield).

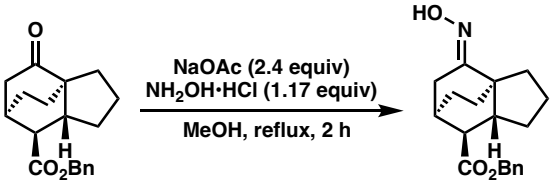
^{1}H NMR (400 MHz, $CDCl_3$): δ 7.42 – 7.30 (m, 5H), 5.19 – 5.05 (m, 2H), 3.76 (dd, *J* = 8.9, 5.3 Hz, 0.4H, minor), 3.69 (dt, *J* = 8.9, 1.5 Hz, 0.6H, major), 2.35 – 2.24 (m, 1H), 2.15 – 1.95 (m, 2H), 1.95 – 1.83 (m, br, 1H), 1.83 – 1.56 (m, 6H), 1.53 – 1.23 (m, 5H), 1.15 – 1.01 (m, 1H).

^{13}C NMR (100 MHz, $CDCl_3$): δ 175.8, 175.6, 136.3, 128.6, 128.2, 128.2, 128.0, 128.0, 75.6, 70.3, 66.3, 66.3, 49.21, 48.1, 44.5, 44.2, 43.2, 36.8, 35.0, 34.9, 34.0, 30.5, 30.3, 30.1, 29.6, 29.0, 26.7, 26.3, 22.8, 22.8, 20.3.

IR (Neat Film, NaCl): 3438, 3032, 2942, 2865, 1730, 1455, 1162 cm^{-1}

HRMS (MM: FD+): *m/z* calc'd for $C_{19}H_{24}O_3$ $[M]^+$: 300.1725, found 300.1730.

Optical Rotation: $[\alpha]_D^{21}$ –31.1 (c 1.00, $CHCl_3$).



11a ***84***

benzyl (3a*R*,6*R*,7*S*,7a*R*,*E*)-4-(hydroxyimino)octahydro-3a,6-ethanoindene-7-carboxylate (84)

To a stirred solution of ketone **11a** (0.125 mmol, 1 equiv) in methanol (1.25 mL) was added NaOAc (0.3 mmol, 2.4 equiv), NH_2OH•HCl (0.15 mmol. 1.17 equiv), and water (0.05 mL). The reaction was brought to reflux for 2 h and was subsequently cooled to 23 ºC and

concentrated under reduced pressure. The crude mixture was then diluted with water and extracted with EtOAc (3x), washed with a saturated aqueous solution of $NaHCO_3$ and brine, dried with Na_2SO_4, and concentrated under reduced pressure. The material was used in the next step without further purification assuming quantitative yield.

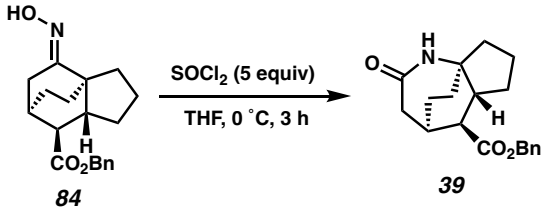
^{1}H NMR (400 MHz, $CDCl_3$): δ 7.42 – 7.28 (m, 5H), 5.20 – 5.06 (m, 2H), 2.52 – 2.46 (m, 2H), 2.43 – 2.39 (m, 1H), 2.39 – 2.36 (m, 1H), 2.15 (dtd, *J* = 10.2, 8.2, 1.8 Hz, 1H), 2.07 (ddt, *J* = 11.9, 8.3, 4.1 Hz, 1H), 1.98 (ddd, *J* = 13.0, 11.0, 8.0 Hz, 1H), 1.82 – 1.71 (m, 3H), 1.67 (ddd, *J* = 10.9, 3.6, 1.8 Hz, 1H), 1.48 (dddd, *J* = 12.5, 7.8, 6.5, 3.7 Hz, 2H), 1.36 (dddd, *J* = 23.6, 11.1, 8.8, 2.6 Hz, 2H).

^{13}C NMR (100 MHz, $CDCl_3$): δ 174.8, 165.4, 136.2, 128.7, 128.4, 128.2, 66.5, 48.2, 45.7, 44.4, 30.6, 29.2, 28.9, 28.1, 27.2, 25.5, 22.6.

IR (Neat Film, NaCl): 2945, 1731, 1161 cm^{-1}.

HRMS (MM: FD+): *m/z* calc'd for $C_{19}H_{23}NO_3$ $[M]^+$: 313.1678, found 313.1676.

Optical Rotation: $[\alpha]_D^{21}$ –22.0 (c 0.37, $CHCl_3$).



84 ***39***

benzyl (4*R*,5*S*,5a*R*,8a*R*)-2-oxooctahydro-1*H*-4,8a-ethanocyclopenta[*b*]azepine-5-carboxylate (39)

To a solution of **84** (0.125 mmol, 1 equiv) in THF (1.25 mL) at 0 ºC was added a solution of $SOCl_2$ (0.625 mmol, 5 equiv) in THF (0.23 mL). The reaction was stirred for 3 h at 0

ºC, followed by dilution with water. Aqueous solution NH_4OH was added to the reaction mixture until neutral, and the aqueous layer was extracted with dichloromethane (3x). The combined organic layers were washed with water and brine, dried over Na_2SO_4, and concentrated under reduced pressure. Purification by flash column chromatography (35% EtOAc/hexanes) afforded the title compound as a colorless oil (22 mg, 0.167 mmol, 56% yield over two steps).

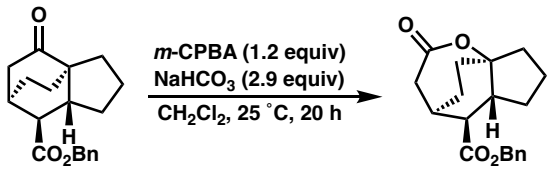
^{1}H NMR (400 MHz, $CDCl_3$): δ 7.41 – 7.27 (m, 5H), 6.67 (s, 1H, br), 5.15 (q, *J* = 12.3 Hz, 2H), 2.73 (dt, *J* = 18.1, 1.6 Hz, 1H), 2.62 (tdd, *J* = 9.9, 8.0, 1.4 Hz, 1H), 2.48 (dd, *J* = 18.4, 6.9 Hz, 1H), 2.40 – 2.32 (m, 2H), 2.29 – 2.16 (m, 1H), 1.95 (dtd, *J* = 12.7, 8.7, 2.2 Hz, 1H), 1.82 – 1.62 (m, 7H), 1.62 – 1.52 (m, 1H), 1.44 – 1.30 (m, 1H).

^{13}C NMR (100 MHz, $CDCl_3$): δ 174.6, 174.2, 135.9, 128.8, 128.4, 128.3, 66.7, 59.9, 48.8, 48.5, 39.2, 33.3, 31.1, 29.8, 25.1, 23.3.

IR (Neat Film, NaCl): 3182, 3055, 2934, 1727, 1648, 1456, 1398, 1167 cm^{-1}.

HRMS (MM: FD+): *m/z* calc'd for $C_{19}H_{23}NO_3$ $[M]^+$: 313.1678, found 313.1678.

Optical Rotation: $[\alpha]_D^{21}$ –5.5 (c 0.89, $CHCl_3$).



11a ***40***

benzyl (4*R*,5*S*,5a*R*,8a*R*)-2-oxooctahydro-4,8a-ethanocyclopenta[*b*]oxepine-5-carboxylate (40)

To a solution ketone **11a** (37 mg, 0.13 mmol, 1 equiv) in CH_2Cl_2 (1.25 mL, 0.1 M) at 0°C was added $NaHCO_3$ (30.8 mg, 0.37 mmol, 2.9 equiv). Subsequently, *m*-CPBA (31 mg, 0.15 mmol, 1.2 equiv) was added and the reaction was allowed to warm to 25 °C. Upon complete consumption of starting material (as determined by TLC), the reaction mixture was diluted with a saturated solution of $Na_2S_2O_3$ and extracted with Et_2O (3x). The combined organic layers were washed with a saturated solution of $NaHCO_3$ followed by brine, dried over Na_2SO_4, and volatiles were removed in vacuo. Purification by preparatory thin layer chromatography (30% EtOAc/hexanes) afforded the title compound as a clear oil (16 mg, 0.05 mmol, 41% yield).

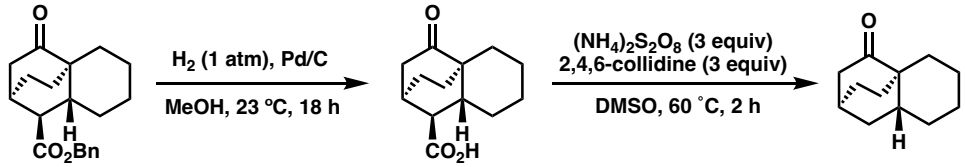
^{1}H NMR (400 MHz, $CDCl_3$): δ 7.43 – 7.29 (m, 5H), 5.22 – 5.10 (m, 2H), 2.97 (ddd, *J* = 19.0, 2.5, 1.4 Hz, 1H), 2.83 – 2.61 (m, 2H), 2.41 – 2.32 (m, 2H), 2.28 – 2.09 (m, 3H), 2.05 – 1.93 (m, 1H), 1.81 – 1.56 (m, 5H), 1.40 – 1.26 (m, 1H).

^{13}C NMR (100 MHz, $CDCl_3$): δ 173.9, 172.9, 135.7, 128.8, 128.6, 128.3, 88.4, 66.9, 47.8, 46.5, 39.6, 39.1, 32.8, 30.4, 29.7, 24.9, 22.7.

IR (Neat Film, NaCl): 2943, 2873, 1722, 1255, 1189, 1167 cm^{-1}.

HRMS (MM: FD+): *m/z* calc'd for $C_{19}H_{22}O_4$ $[M]^+$: 314.1518, found 314.1521.

Optical Rotation: $[\alpha]_D^{21}$ –15.8 (c 1.00, $CHCl_3$).



11f ***45***

(2*S*,4a*R*,8a*R*)-octahydro-2*H*-2,4a-ethanonaphthalen-9-one (45)

A vial containing ketone **11f** (0.72 mmol, 1 equiv) and Pd/C (10 wt. % with 67% H_2O, 0.072 mmol, 0.1 equiv) was evacuated and backfilled with H_2. Methanol (1.06 mL) was subsequently added, and the reaction was stirred at 23 ºC overnight. The crude reaction mixture was filtered through a silica plug and concentrated under reduced pressure to afford the corresponding acid as a white solid, which was used without further purification.

To a solution of the crude acid (0.62 mmol, 1 equiv) in DMSO (1.24 mL) was added $(NH_4)_2S_2O_8$ (1.86 mmol, 3 equiv) and 2,4,6-collidine (1.86 mmol, 3 equiv). The mixture was purged with N_2 for 5 min and was subsequently sealed and heated to 60 ºC for 2 h with stirring. The reaction mixture was diluted with dichloromethane, washed with brine (1x), and the aqueous layer was extracted with dichloromethane (3x). The combined organic layers were washed with brine (3x), dried over Na_2SO_4, and concentrated under reduced pressure. Purification by flash column chromatography (15% EtOAc/hexanes) afforded the title compound as a white solid (30.2 mg, 0.167 mmol, 27% yield).

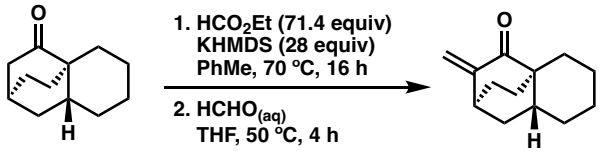
^{1}H NMR (400 MHz, $CDCl_3$): δ 2.33 – 2.21 (m, 3H), 2.13 – 2.07 (m, 1H), 1.93 (dddd, *J* = 13.3, 10.6, 3.8, 2.8 Hz, 1H), 1.75 – 1.58 (m, 6H), 1.53 (dd, *J* = 13.6, 4.0 Hz, 1H), 1.47 – 1.38 (m, 2H), 1.38 – 1.28 (m, 1H), 1.27 – 1.17 (m, 1H), 1.17 – 1.05 (m, 2H).

^{13}C NMR (100 MHz, $CDCl_3$): δ 218.6, 44.9, 43.9, 34.5, 34.1, 30.6, 29.0, 27.7, 25.9, 25.9, 21.8, 21.4.

IR (Neat Film, NaCl): 2925, 1716 cm^{-1}

HRMS (MM: FI+): *m/z* calc'd for $C_{12}H_{18}O$ $[M]^+$: 178.1358, found 178.1359.

Optical Rotation: $[\alpha]_D^{21}$ –59.9 (c 0.89, $CHCl_3$).



45 ***46***

(2*S*,4a*R*,8a*R*)-10-methyleneoctahydro-2*H*-2,4a-ethanonaphthalen-9-one (46)

To a solution of ketone **45** (0.056 mmol, 1 equiv) and ethyl formate (4 mmol, 71.4 equiv) in toluene (3.2 mL) was added a solution of KHMDS (0.5 M in toluene, 1.6 mmol, 28 equiv) at 23 ºC. The reaction mixture was stirred at 70 ºC for 16 h. Upon cooling to 0 ºC, THF (6.4 mL) and formalin (37% in water, 3.2 mL) was added, and then the reaction was heated to 50 ºC for 4 h. The reaction mixture was diluted with a saturated aqueous solution of NH_4Cl, extracted with EtOAc (3x), dried over Na_2SO_4, and concentrated under reduced pressure. Purification by preparatory thin layer chromatography (30% EtOAc/hexanes, 2x) afforded the title compound as a yellow oil (4.4 mg, 0.023 mmol, 41% yield).

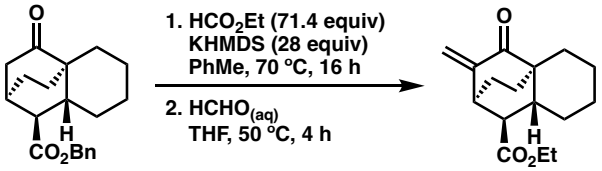
^{1}H NMR (400 MHz, $CDCl_3$): δ 5.93 (d, *J* = 1.8 Hz, 1H), 5.15 (d, *J* = 1.8 Hz, 1H), 2.66 (p, *J* = 3.0 Hz, 1H), 2.39 – 2.19 (m, 1H), 1.98 (dddd, *J* = 13.2, 10.6, 3.9, 2.8 Hz, 1H), 1.81 – 1.61 (m, 6H), 1.51 – 1.42 (m, 2H), 1.41 – 1.31 (m, 2H), 1.23 – 1.15 (m, 2H), 1.11 (dt, *J* = 12.9, 3.6 Hz, 1H).

^{13}C NMR (100 MHz, $CDCl_3$): δ 205.3, 147.9, 116.3, 45.0, 36.1, 35.0, 34.7, 30.8, 29.0, 26.5, 26.0, 21.6, 21.3.

IR (Neat Film, NaCl): 2926, 2859, 1708, 1630, 1464, 1449 cm^{-1}

HRMS (MM: FD+): *m/z* calc'd for $C_{13}H_{18}O$ $[M]^+$: 190.1358, found 190.1353.

Optical Rotation: $[\alpha]_D^{21}$ –34.2 (c 0.29, $CHCl_3$).



11f ***47***

ethyl (1*S*,2*S*,4a*R*,8a*R*)-3-methylene-4-oxooctahydro-2*H*-2,4a-ethanonaphthalene-1-carboxylate (47)

To a solution of **11f** (0.192 mmol, 1 equiv) and ethyl formate (13.71 mmol, 71.4 equiv) in toluene (11.1 mL) was added a solution of KHMDS (0.5 M in toluene, 5.49 mmol, 28 equiv) at 23 ºC. The reaction mixture was stirred at 70 ºC for 16 h. Upon cooling to 0 ºC, THF (22.2 mL) and formalin (37% in water, 11.1 mL) was added, and then the reaction was heated to 50 ºC for 4 h. The reaction mixture was diluted with a saturated aqueous solution of NH_4Cl, extracted with EtOAc (3x), dried over Na_2SO_4, and concentrated under reduced pressure. Purification by preparatory thin layer chromatography (30% EtOAc/hexanes, 2x) afforded the title compound as a yellow oil (13.1 mg, 0.05 mmol, 26% yield).

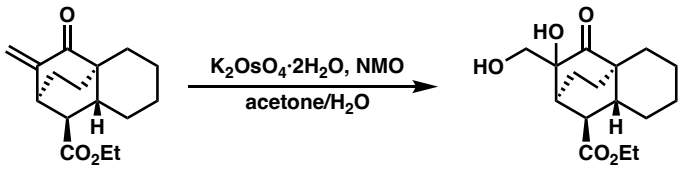
^{1}H NMR (400 MHz, $CDCl_3$): δ 5.99 (d, *J* = 1.7 Hz, 1H), 5.17 (d, *J* = 1.7 Hz, 1H), 4.21 – 4.01 (m, 2H), 3.04 (td, *J* = 3.1, 2.0 Hz, 1H), 2.27 (ddd, *J* = 14.2, 11.4, 5.4 Hz, 1H), 2.21 (dd, *J* = 6.8, 2.0 Hz, 1H), 2.01 (dddd, *J* = 11.6, 6.5, 4.4, 1.7 Hz, 1H), 1.92 – 1.75 (m, 3H), 1.73 – 1.65 (m, 2H), 1.56 – 1.50 (m, 1H), 1.47 – 1.31 (m, 2H), 1.29 – 1.16 (m, 6H).

^{13}C NMR (100 MHz, $CDCl_3$): δ 203.7, 173.8, 144.3, 119.0, 60.8, 51.1, 45.0, 39.1, 37.2, 30.3, 28.9, 26.2, 25.8, 21.3, 21.1, 14.4.

IR (Neat Film, NaCl): 2927, 2867, 1732, 1708, 1449, 1180 cm^{-1}.

HRMS (MM: FD+): *m/z* calc'd for $C_{16}H_{22}O_3$ $[M]^+$: 262.1569, found 262.1576.

Optical Rotation: $[\alpha]_D^{21}$ –3.9 (c 0.38, $CHCl_3$).



47 ***48***

ethyl (1*R*,2*S*,4a*R*,8a*R*)-3-hydroxy-3-(hydroxymethyl)-4-oxooctahydro-2*H*-2,4a-ethanonaphthalene-1-carboxylate (48)

A flame dried vial was charged with enone **47** (14.7 mg, 0.056 mmol, 1 equiv) and acetone (2.3 mL, 0.024 M) and water (0.6 mL, 0.094 M). NMO (50 wt. % in H_2O) (23 μL, 0.112 mmol, 2 equiv) was added and the solution was cooled to 0 ºC. $K_2OsO_4 \cdot 2H_2O$ (2.1 mg, 0.006 mmol, 0.1 equiv) was added to the solution. The resultant solution was slowly warmed to 23 ºC. Upon complete consumption of starting material (as determined by TLC), the reaction was quenched with a saturated solution of $Na_2S_2O_3$ and stirred for 30 min. The mixture was then diluted with CH_2Cl_2 and the product was extracted with CH_2Cl_2 (2 x). The combined organic layers were washed with brine, dried over Na_2SO_4, filtered, and concentrated under reduced pressure. Purification by preparatory thin layer chromatography (50% EtOAc/hexanes) afforded the title compound as a colorless oil (2.1 mg, 0.007 mmol,13% yield, 10:1 dr). In the ^1H NMR, peaks that correspond to the minor diastereomer closely resemble the major diastereomer. dr was determine through integration of ^1H NMR peaks 2.69 ppm (major) and 2.96 ppm (minor).

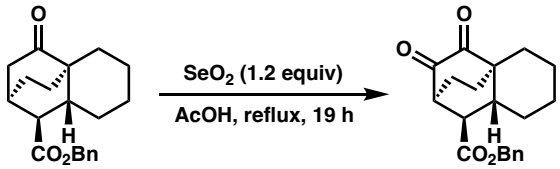
^{1}H NMR (400 MHz, $CDCl_3$): δ 4.15 (q, *J* = 7.1 Hz, 2H), 3.81 (dd, *J* = 11.8, 2.6 Hz, 1H), 3.54 (dd, *J* = 11.9, 2.7 Hz, 1H), 2.71 – 2.67 (m, 1H), 2.38 – 2.24 (m, 2H), 2.10 (d, *J* = 7.3 Hz, 1H), 1.94 – 1.64 (m, 7H), 1.47 – 1.18 (m, 9H).

^{13}C NMR (100 MHz, $CDCl_3$): δ 218.4, 174.8, 75.8, 65.8, 61.0, 48.9, 45.4, 37.3, 37.2, 30.3, 28.3, 25.6, 22.5, 21.0, 14.3.

IR (Neat Film, NaCl): 3468, 2930, 2355, 1716, 1197, 1033 cm^{-1}.

HRMS (MM: FD+): *m/z* calc'd for $C_{16}H_{24}O_5$ $[M]^+$: 296.1624, found 296.1619.

Optical Rotation: $[\alpha]_D^{21}$ 2.1 (c 0.24, $CHCl_3$).



11f *49*

benzyl (1*R*,2*S*,4a*R*,8a*R*)-3,4-dioxooctahydro-2*H*-2,4a-ethanonaphthalene-1-carboxylate (49)

To a solution of **11f** (0.064 mmol, 1 equiv) in glacial acetic acid (0.1 mL) was added SeO_2 (0.077 mmol, 1.2 equiv). The reaction was brought to reflux for 19 h. After cooling to 23 ºC, the reaction mixture was filtered and concentrated under reduced pressure. The resulting crude mixture was dissolved in EtOAc and washed with water (5x), dried over Na_2SO_4, and concentrated under reduced pressure. Purification by preparatory thin layer chromatography (30% EtOAc/hexanes) afforded the title compound as a yellow oil (10.4 mg, 0.031 mmol, 48% yield).

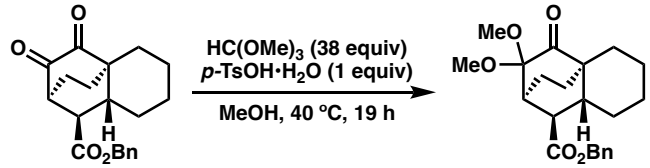
^{1}H NMR (400 MHz, $CDCl_3$): δ 7.41 – 7.28 (m, 5H), 5.19 – 5.04 (m, 2H), 3.00 (m, 1H), 2.54 (dd, *J* = 6.4, 2.3 Hz, 1H), 2.40 (ddd, *J* = 14.6, 10.3, 6.9 Hz, 1H), 2.02 (m, 3H), 1.80 – 1.69 (m, 2H), 1.68 – 1.50 (m, 3H), 1.48 – 1.38 (m, 1H), 1.33 (dt, *J* = 13.4, 3.5 Hz, 1H), 1.29 – 1.15 (m, 2H).

^{13}C NMR (100 MHz, $CDCl_3$): δ 198.7, 196.1, 173.2, 135.4, 128.8, 128.6, 128.4, 67.4, 49.9, 48.0, 46.3, 37.9, 30.2, 28.3, 25.5, 22.7, 20.5, 20.2.

IR (Neat Film, NaCl): 2932, 2857, 1731, 1454, 1155 cm^{-1}.

HRMS (MM: FD+): *m/z* calc'd for $C_{20}H_{22}O_4$ $[M]^+$: 326.1518, found 326.1532.

Optical Rotation: $[\alpha]_D^{21}$ –49.2 (c 1.04, $CHCl_3$).



49 ***50***

benzyl (1*R*,2*S*,4a*R*,8a*R*)-3,3-dimethoxy-4-oxooctahydro-2*H*-2,4a-ethanonaphthalene-1-carboxylate (50)

To a solution of diketone **49** (0.031 mmol, 1 equiv) in methanol (0.13 mL) was added $HC(OMe)_3$ (1.2 mmol, 38 equiv) and *p*-TsOH•H_2O (0.031 mmol, 1 equiv). The reaction was stirred for 19 h at 40 ºC, followed by dilution with a saturated aqueous solution of $NaHCO_3$. The aqueous layer was extracted with EtOAc (4x), dried over Na_2SO_4, and concentrated under reduced pressure. Purification by preparatory thin layer chromatography (30% EtOAc/hexanes) afforded the title compound as a yellow oil (4.7 mg, 0.013 mmol, 41% yield).

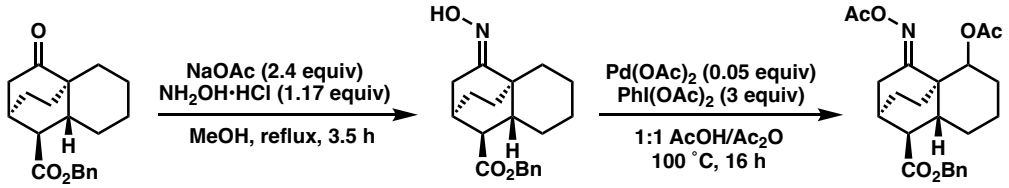
^{1}H NMR (400 MHz, $CDCl_3$): δ 7.42 – 7.29 (m, 5H), 5.26 (d, *J* = 12.3 Hz, 1H), 5.02 (d, *J* = 12.3 Hz, 1H), 3.20 (s, 3H), 3.06 (s, 3H), 2.93 (dt, *J* = 4.2, 2.2 Hz, 1H), 2.29 – 2.11 (m, 3H), 1.98 – 1.89 (m, 1H), 1.83 (dddd, *J* = 13.8, 11.4, 6.7, 2.4 Hz, 1H), 1.70 – 1.58 (m, 4H), 1.54 (d, *J* = 3.9 Hz, 1H), 1.31 (dd, *J* = 10.8, 2.4 Hz, 1H), 1.27 – 1.19 (m, 3H).

^{13}C NMR (100 MHz, $CDCl_3$): δ 209.0, 173.5, 136.5, 128.6, 128.5, 128.2, 97.4, 66.4, 50.4, 48.8, 48.4, 45.5, 36.4, 34.9, 30.0, 29.1, 25.5, 23.1, 21.0, 21.0.

IR (Neat Film, NaCl): 2933, 2855, 1736, 1449, 1172 cm^{-1}

HRMS (MM: FD+): *m/z* calc'd for $C_{22}H_{28}O_5$ $[M]^+$: 372.1937, found 372.1931.

Optical Rotation: $[\alpha]_D^{21}$ –26.2 (c 0.42, $CHCl_3$).



benzyl (1*S*,2*R*,4a*S*,8a*R*,*E*)-5-acetoxy-4-(acetoxyimino)octahydro-2*H*-2,4a-ethanonaphthalene-1-carboxylate (51)

To a stirred solution of ketone **11f** (0.096 mmol, 1 equiv) in methanol (0.93 mL) was added NaOAc (0.23 mmol, 2.4 equiv), NH_2OH•HCl (0.111 mmol, 1.17 equiv), and water (0.033 mL). The reaction was brought to reflux for 3.5 h and was subsequently cooled to 23 ºC and concentrated under reduced pressure. The crude mixture was then diluted with water and extracted with EtOAc (3x), washed with a saturated aqueous solution of $NaHCO_3$ and brine, dried with Na_2SO_4, and concentrated under reduced pressure. The crude oxime was dissolved in a 1:1 mixture of AcOH/Ac_2O (0.78 mL). The reaction vessel was sealed and

stirred at 23 ºC for 2 h. $Pd(OAc)_2$ (0.0048 mmol, 0.05 equiv) and $PhI(OAc)_2$ (0.288 mmol, 3 equiv) were subsequently added, and the reaction was heated to 100 ºC for 16 h. The reaction mixture was cooled to 23 ºC, filtered through a silica plug, and the filtrate was diluted with EtOAc. The organic layer was washed with a saturated solution of $NaHCO_3$ until not acidic, washed with brine, dried over Na_2SO_4, and concentrated under reduced pressure. Purification by preparatory thin layer chromatography (30% EtOAc/hexanes) afforded the title compound (**51**) as a yellow oil (12.3 mg, 0.0288 mmol, 30% yield over two steps).

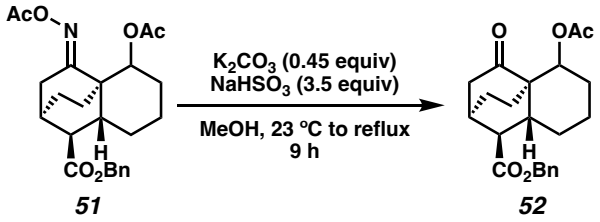
^{1}H NMR (400 MHz, $CDCl_3$): δ 7.43 – 7.27 (m, 5H), 5.31 – 5.20 (m, 1H), 5.20 – 5.02 (m, 2H), 2.62 (dt, *J* = 20.2, 3.5 Hz, 1H), 2.40 – 2.29 (m, 2H), 2.27 – 2.17 (m, 1H), 2.14 (s, 3H), 2.02 (s, 3H), 1.89 (m, 1H), 1.83 – 1.69 (m, 4H), 1.62 (t, *J* = 2.8 Hz, 2H), 1.46 – 1.28 (m, 4H).

^{13}C NMR (100 MHz, $CDCl_3$): δ 173.9, 170.6, 170.4, 168.9, 135.9, 128.8, 128.5, 128.2, 71.7, 66.9, 49.6, 42.2, 39.1, 29.5, 28.9, 28.6, 26.9, 25.5, 23.0, 21.4, 20.2, 16.7.

IR (Neat Film, NaCl): 2930, 1764, 1731, 1456, 1371, 1248, 1210 cm^{-1}.

HRMS (MM: FD+): *m/z* calc'd for $C_{24}H_{29}NO_6$ $[M]^+$: 427.1995, found 427.2017.

Optical Rotation: $[\alpha]_D^{21}$ –27.6 (c 1.00, $CHCl_3$).



51 ***52***

benzyl (1*S*,2*R*,4a*R*,8a*R*)-5-acetoxy-4-oxooctahydro-2*H*-2,4a-ethanonaphthalene-1-carboxylate (52)

To a solution of **51** (0.029 mmol, 1 equiv) in methanol (0.06 mL) in a loosely capped vial was added K_2CO_3 (0.013 mmol, 0.45 equiv) at 23 ºC in three portions over 6 h. $NaHSO_3$ (0.1 mmol, 3.5 equiv) and water (0.06 mL) were subsequently added, and the vial was sealed and heated to 80 ºC for 3 h. The reaction mixture was diluted with $CHCl_3$, rinsed with 1 M HCl, and the aqueous layer was extracted with $CHCl_3$ (3x). The combined organic layers were neutralized with a saturated solution of $NaHCO_3$, washed with brine, dried over Na_2SO_4, and concentrated under reduced pressure. Purification by preparatory thin layer chromatography (35% EtOAc/hexanes) afforded the title compound as a colorless oil (1.8 mg, 0.0056 mmol, 19% yield).

^{1}H NMR (400 MHz, $CDCl_3$): δ 7.41 – 7.30 (m, 5H), 5.19 – 5.06 (m, 3H), 2.48 (m, 1H), 2.41 (dt, *J* = 19.2, 2.8 Hz, 1H), 2.29 (dt, *J* = 6.9, 2.0 Hz, 1H), 2.16 – 2.04 (m, 3H), 1.98 (s, 3H), 1.94 – 1.89 (m, 1H), 1.87 – 1.79 (m, 3H), 1.78 – 1.73 (m, 1H), 1.71 (m, 2H), 1.46 – 1.29 (m, 3H).

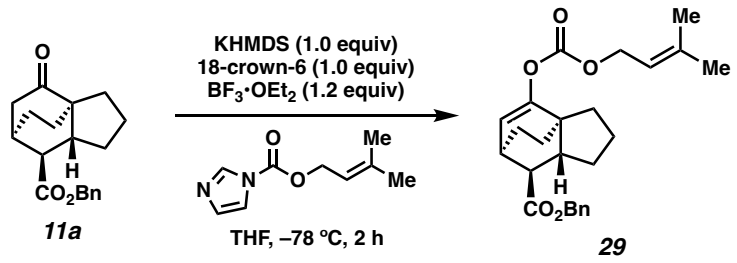
^{13}C NMR (100 MHz, $CDCl_3$): δ 212.2, 173.9, 170.2, 135.9, 128.8, 128.5, 128.3, 70.8, 66.9, 49.4, 48.5, 40.5, 37.9, 30.7, 29.0, 26.7, 25.8, 22.9, 21.3, 15.7.

IR (Neat Film, NaCl): 2928, 1781, 1375, 1246, 1173 cm^{-1}.

HRMS (MM: FD+): *m/z* calc'd for $C_{22}H_{26}O_5$ $[M]^+$: 370.1780, found 370.1774.

Optical Rotation: $[\alpha]_D^{21}$ –18.3 (c 0.18, $CHCl_3$).

Preparation of Additional Compounds



benzyl (3a*R*,6*R*,7*S*,7a*R*)-4-oxooctahydro-3a,6-ethanoindene-7-carboxylate (29)[42]

To a solution of KHMDS (40 mg, 0.20 mmol, 1.0 equiv) and 18-crown-6 (53 mg, 0.20 mmol, 1 equiv) in THF (2.0 mL) at –78 ºC was added a solution of **11a** (60 mg, 0.20 mmol, 1 equiv). Stirring was continued at –78 ºC for 30 minutes, then a pre-mixed solution of 3-methylbut-2-en-1-yl 1*H*-imidazole-1-carboxylate (43 mg, 0.24 mmol, 1.2 equiv) and boron trifluoride diethyl etherate (30 μL, 0.24 mmol, 1.2 equiv) in THF (1.2 mL) was added dropwise. After two additional hours of stirring at –78 ºC, EtOAc and saturated aqueous NH_4Cl were added. The layers were separated, and the aqueous layer was extracted twice with EtOAc. The combined organic layers were washed with brine, dried over Na_2SO_4, filtered, and solvent was removed in vacuo. The crude mixture was purified by silica gel flash column chromatography (0–40% EtOAc/hexanes) to afford enol carbonate **29** as a colorless oil (44 mg, 0.11 mmol, 55% yield).

^{1}H NMR (400 MHz, $CDCl_3$): δ 7.39 – 7.29 (m, 5H), 5.70 (d, *J* = 6.8 Hz, 1H), 5.42 – 5.36 (m, 1H), 5.09 (d, *J* = 3.6 Hz, 2H), 4.65 (d, *J* = 7.3 Hz, 2H), 3.08 – 2.96 (m, 1H), 2.25 (d, *J* = 5.6 Hz, 1H), 2.07 – 1.97 (m, 2H), 1.91 – 1.79 (m, 3H), 1.77 (s, 3H), 1.73 (s, 3H), 1.63 – 1.54 (m, 2H), 1.52 – 1.38 (m, 3H), 1.35 – 1.28 (m, 1H).

^{13}C NMR (100 MHz, $CDCl_3$): δ 174.9, 155.6, 153.5, 140.6, 136.4, 128.7, 128.2, 128.0, 117.9, 112.8, 66.3, 65.3, 51.3, 48.1, 48.1, 35.5, 28.4, 28.4, 27.3, 25.9, 24.6, 22.8, 18.3.

IR (Neat Film, NaCl): 2953, 2870, 1754, 1735, 1241, 1226, 1150 cm^{-1}

HRMS (MM: FD+): *m/z* calc'd for $C_{25}H_{30}O_5$ $[M]^+$: 410.2093, found 410.2094.

SFC conditions: 20% IPA, 2.5 mL/min, Chiralpak IC column, λ = 210 nm, t_R (min): minor = 3.05, major = 3.40.

1.4.3 DETERMINATION OF ABSOLUTE AND RELATIVE STEREOCHEMISTRY BY VCD SPECTROSCOPY

Experimental Protocol: A solution of the compound of interest (50 mg/mL) in $CDCl_3$ was loaded into a front-loading SL-4 cell (International Crystal Laboratories) possessing BaF_2 windows and a 100 mm path length. Infrared (IR) and VCD spectra were acquired on a BioTools ChiralIR-2X VCD spectrometer as a set of 24 one-hour blocks (24 blocks, 3120 scans per block) in dual PEM mode. A 15-minute acquisition of neat (+)-α-pinene control yielded a VCD spectrum in agreement with literature spectra. IR and VCD spectra were background corrected using a 30-minute block IR acquisition of the empty instrument chamber under gentle N_2 purge, and were solvent corrected using a 16-hour (16 blocks, 3120 scans per block) IR/VCD acquisition of $CDCl_3$ in the same 100 μm BaF2 cell. The reported spectra represent the result of block averaging.

Both enantiomers of compounds **11a**, **11q**, and **11q'** were prepared from the *(S)* and *(R)* enantiomers of the *t*-BuPHOX ligand. Data were collected for both enantiomers of

compounds at identical concentration and the final reported VCD spectra are the half-difference of the spectra of the compounds derived from the *(S)* minus *(R)* enantiomer of ligand. Due to limited sample size, spectra of cycloadducts **11k'** and **11k''** were collected at concentrations of 11.7 and 9.3 mg/mL, respectively.

Computational Protocol: An arbitrarily chosen enantiomer of the compound of interest was subjected to an exhaustive initial molecular mechanics-based conformational search (OPLS_2005 force field, $CHCl_3$ solvent, 10.0 kcal/mol cutoff, "Enhanced" torsional sampling) as implemented in MacroModel program.[50] The resulting ensemble of conformers was subsequently optimized using the B3PW91 functional, cc-pVTZ(-f) basis, and implicit PBF solvation model for chloroform using the Jaguar program.[51] Harmonic frequencies computed at the B3PW91/cc-pVTZ(-f)/PBF(chloroform) level were scaled by 0.98. The resultant structurally unique conformers possessing all positive Hessian eigenvalues were Boltzmann weighted by relative free energy at 298.15 K. The predicted IR and VCD frequencies and intensities of the retained conformers were convolved using Lorentzian line shapes (γ = 4 cm^{-1}) and summed using the respective Boltzmann weights to yield the final predicted IR and VCD spectra. The predicted VCD of the opposite enantiomer was generated by inversion of sign.

VCD Analysis for diastereomers 11a, 11q, and 11q'

Figure 1.9. *Three diastereomers* ***11a***, ***11q***, *and* ***11q'*** *to be compared to spectra computed from all eight possible stereoisomers.*

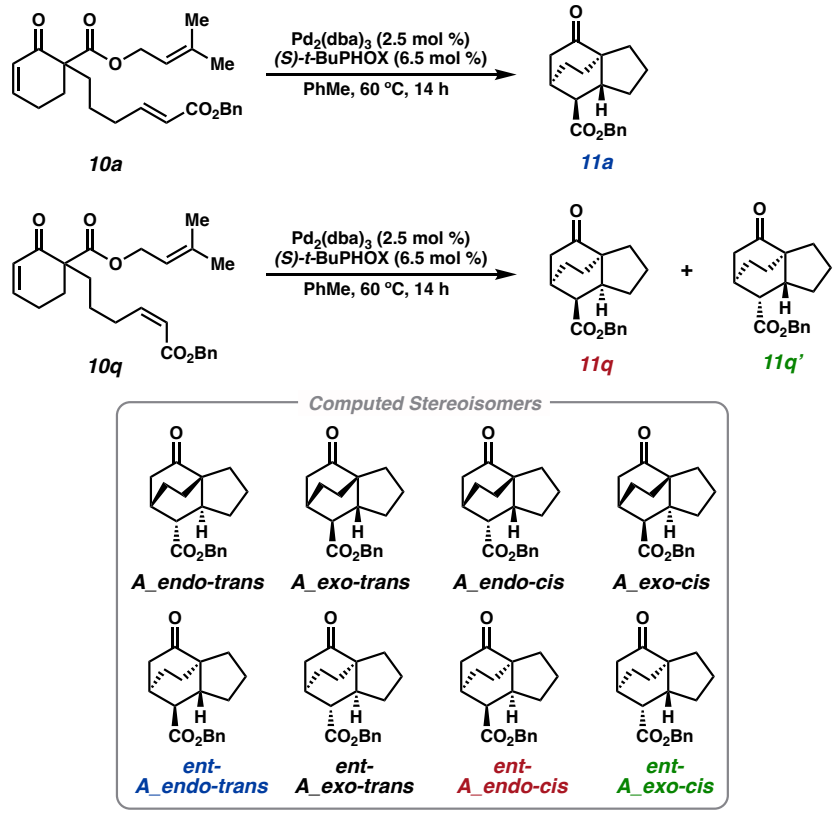
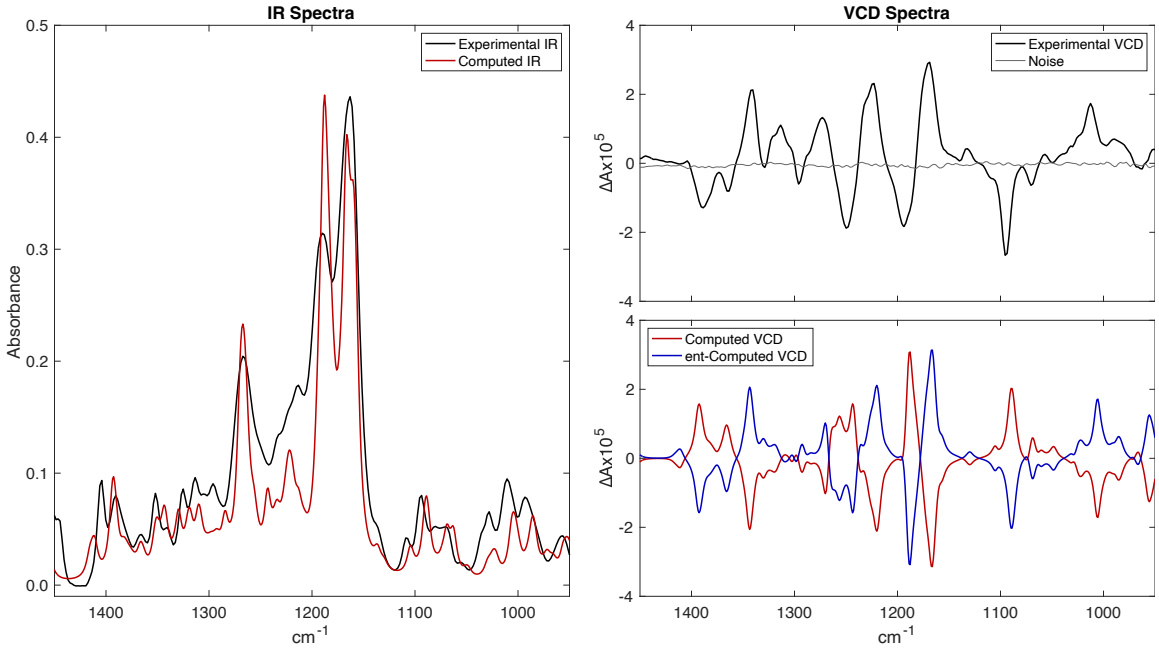


***Figure 1.10**. Comparison of experimental VCD and IR spectra for product **11a** to computed spectra for **A_endo-trans**.*[a]



[a] Experimental IR spectrum in good agreement with computed spectrum. Experimental VCD spectrum for **11a** is in excellent agreement with computed spectrum for ***ent*-A_endo-trans**.

***Figure 1.11**. Overlayed experimental and calculated VCD spectra for **11a** – assigned as **ent-A_endo-trans**.*

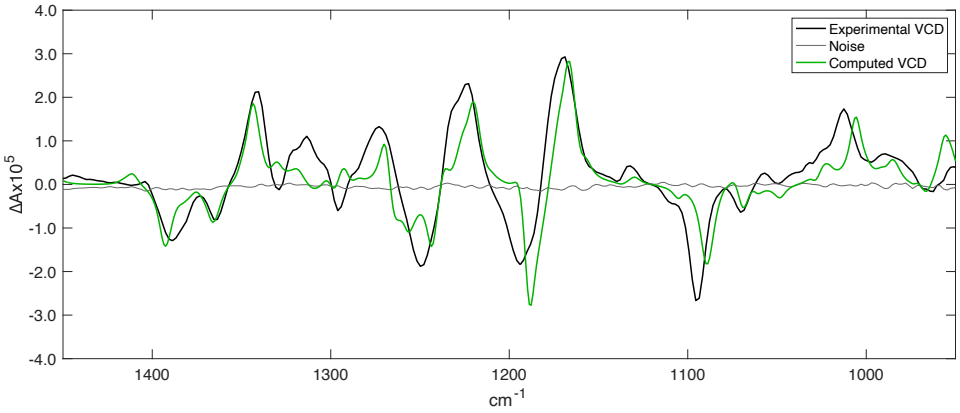
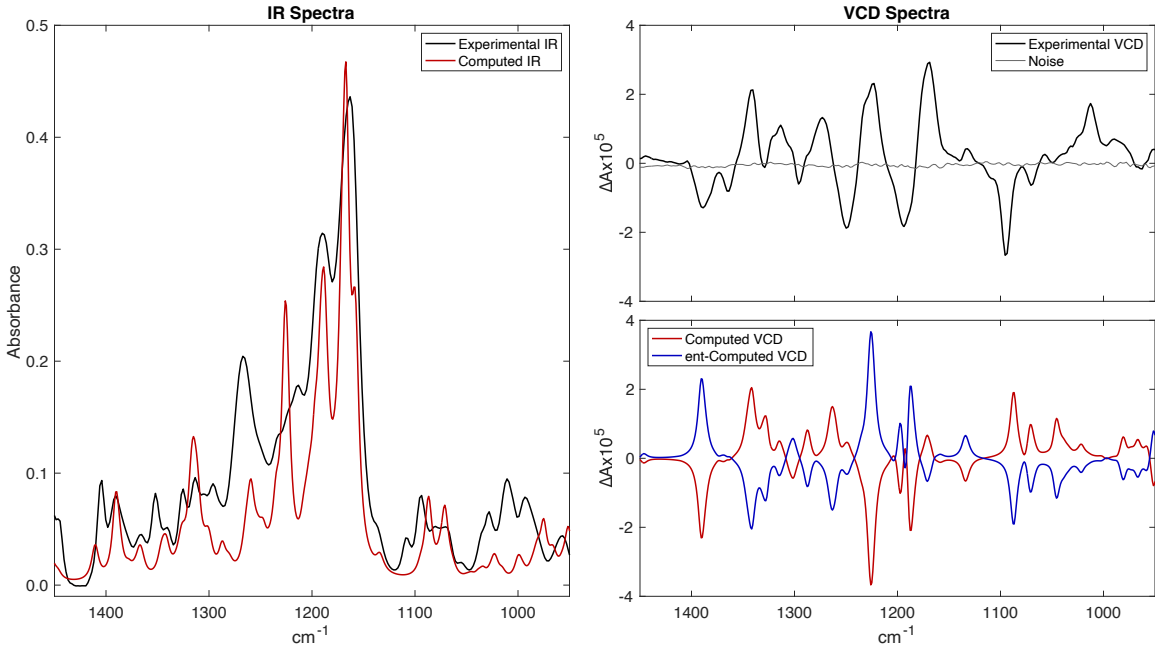
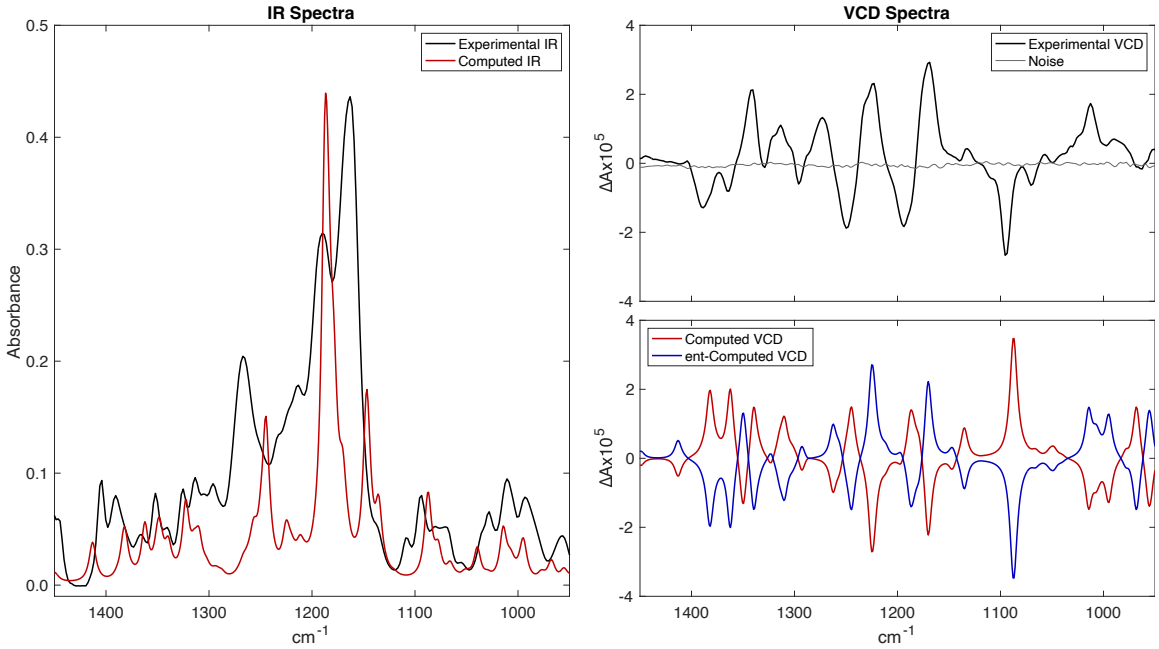


***Figure 1.12**. Comparison of experimental VCD and IR spectra for product **11a** to computed spectra for **A_exo-trans**.*[a]



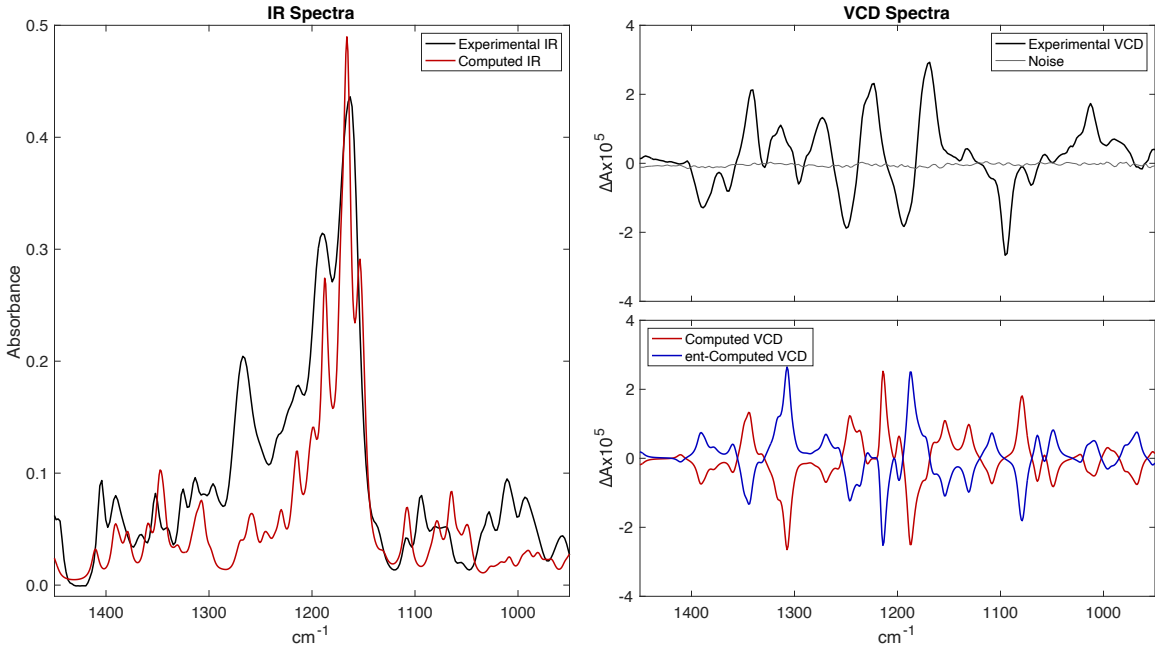
[a] A shift of –3 cm^{-1} along x-axis applied to computed spectra in fitting. Experimental data from **11a** do not match computed data of **A_exo-trans**.

Figure 1.13. *Comparison of experimental VCD and IR spectra for product* ***11a*** *to computed spectra for* ***A_endo-cis***.[a]



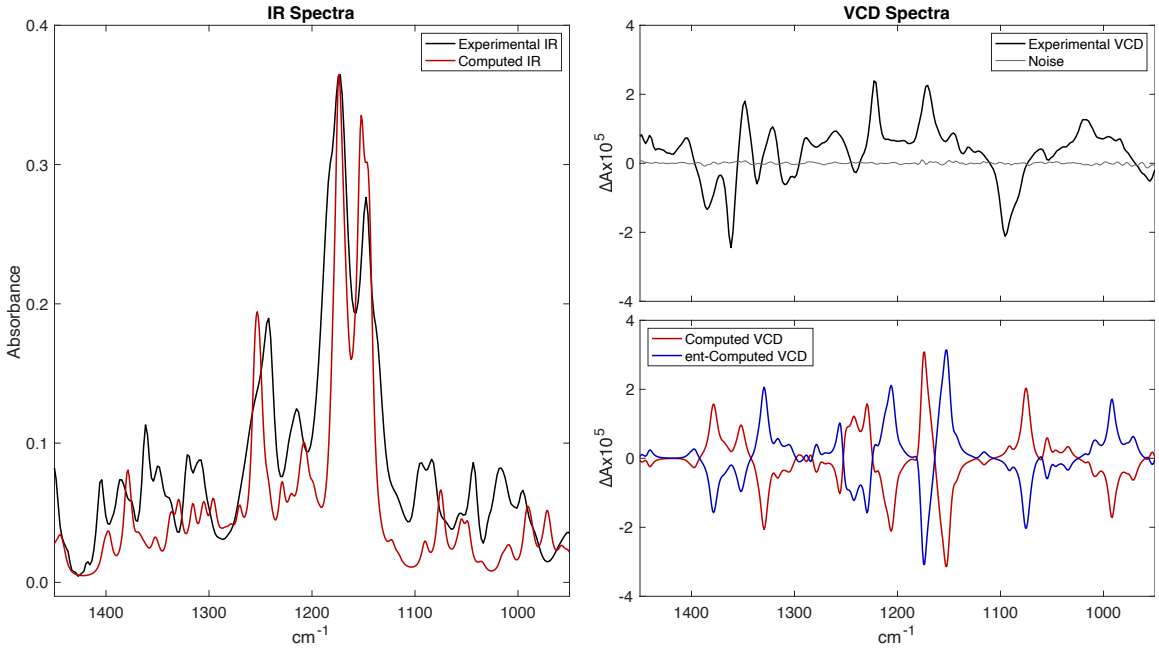
[a] Experimental data from **11a** do not match computed data of **A_endo-cis**.

***Figure 1.14**. Comparison of experimental VCD and IR spectra for product **11a** to computed spectra for **A_exo-cis**.*[a]



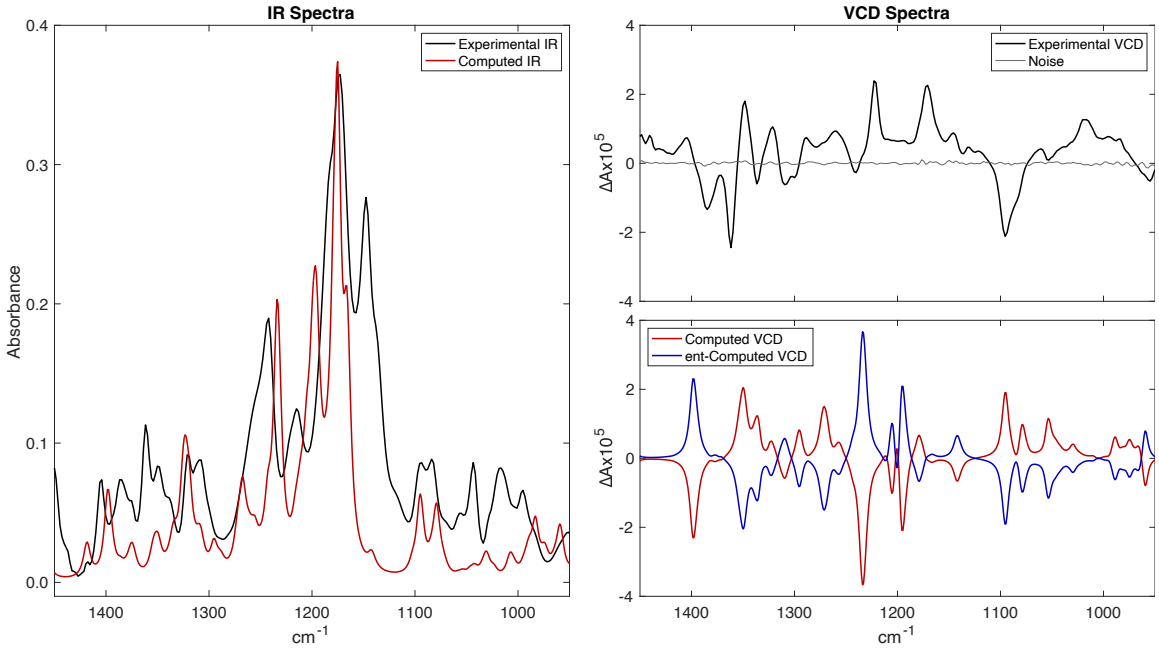
[a] A shift of –3 cm-1 along x-axis applied to computed spectra in fitting. Experimental data from **11a** do not match computed data of **A_exo-cis**.

***Figure 1.15**. Comparison of experimental VCD and IR spectra for product **11q** to computed spectra for **A_endo-trans**.*[a]



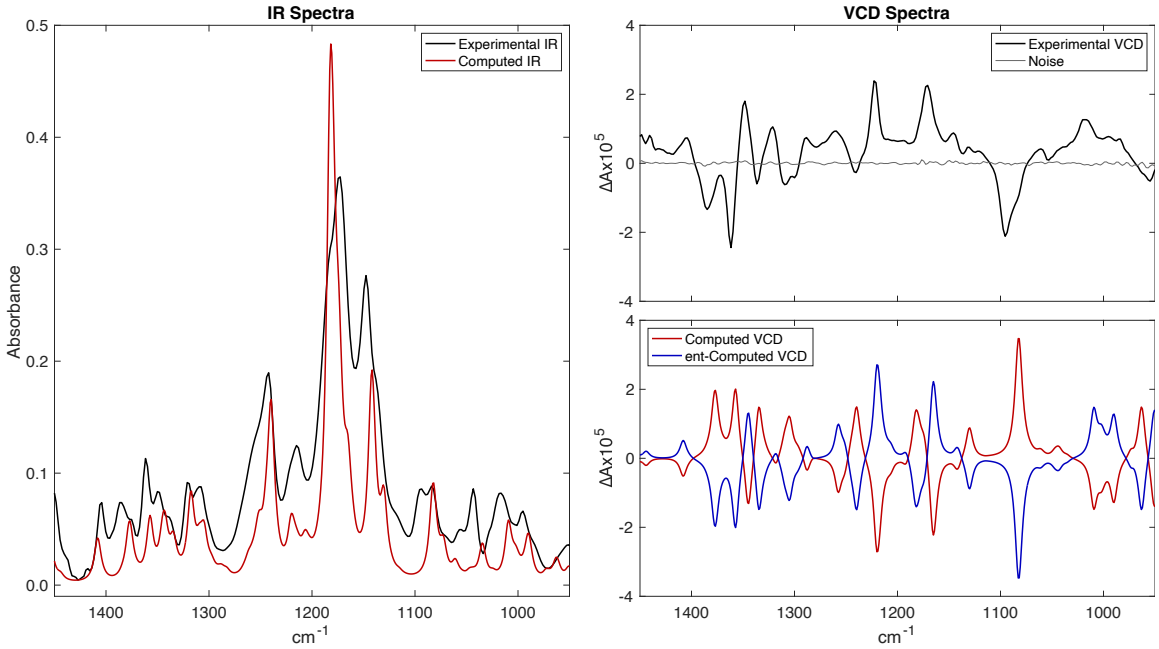
[a] A shift of +14 cm^{-1} along x-axis applied to computed spectra in fitting. The IR spectrum of **11q** contains similar features to the calculated spectrum for **A_endo-trans**; however, the VCD spectrum displays large discrepancies at 1174, 1152, 1330, 1076, and 992 cm^{-1}. **11q** is <u>not</u> assigned as **A_endo-trans**.

***Figure 1.16**. Comparison of experimental VCD and IR spectra for product **11q** to computed spectra for **A_exo-trans**.*



[a] Experimental data from **11q** do not match computed data of **A_exo-trans**.

Figure 1.17. *Comparison of experimental VCD and IR spectra for product* ***11q*** *to computed spectra for* ***A_endo-cis****.*



[a] A shift of +5 cm^{-1} along x-axis applied to computed spectra in fitting. The IR spectrum of **11q** is in good agreement with that of the computed IR spectrum of **A_endo-cis**. Experimental VCD spectrum for **11q** is in excellent agreement with computed spectrum for ***ent*-A_endo-cis**.

Figure 1.18. *Overlayed experimental and calculated VCD spectra for* ***11q*** *– assigned as* ***ent-A_endo-cis****.*

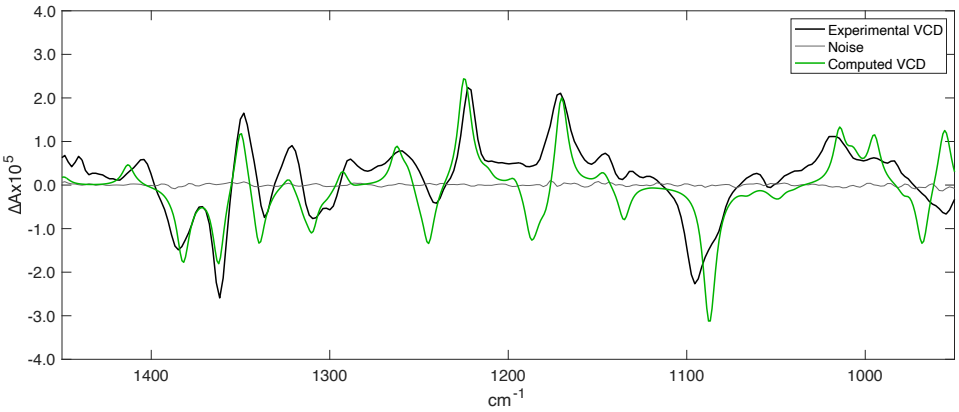
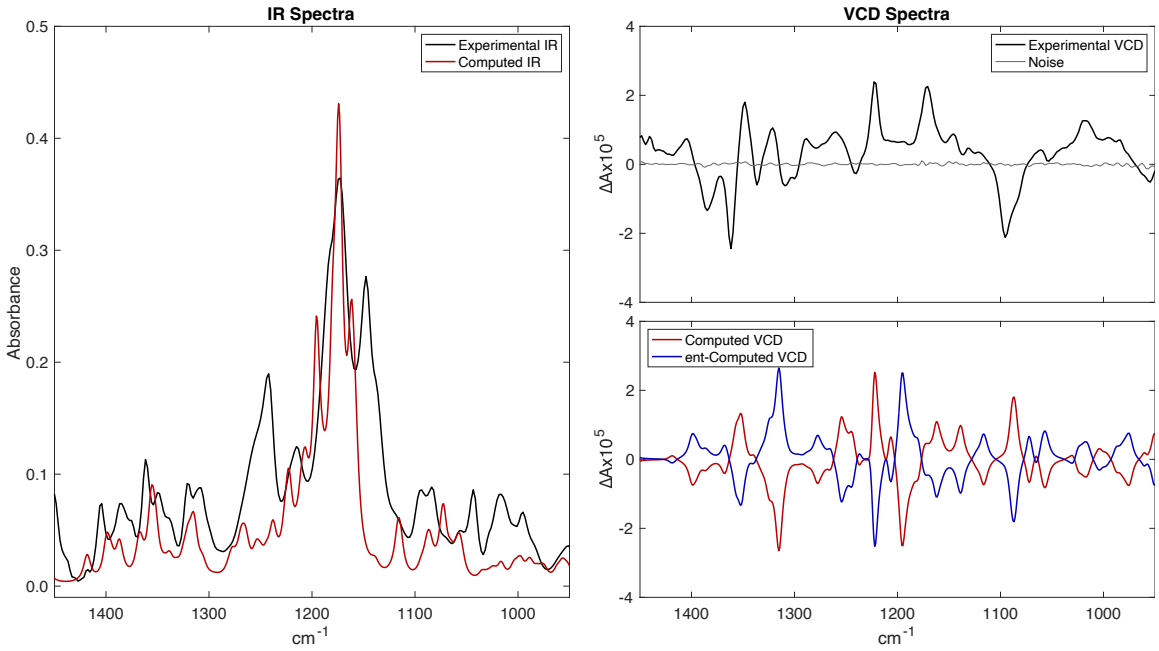
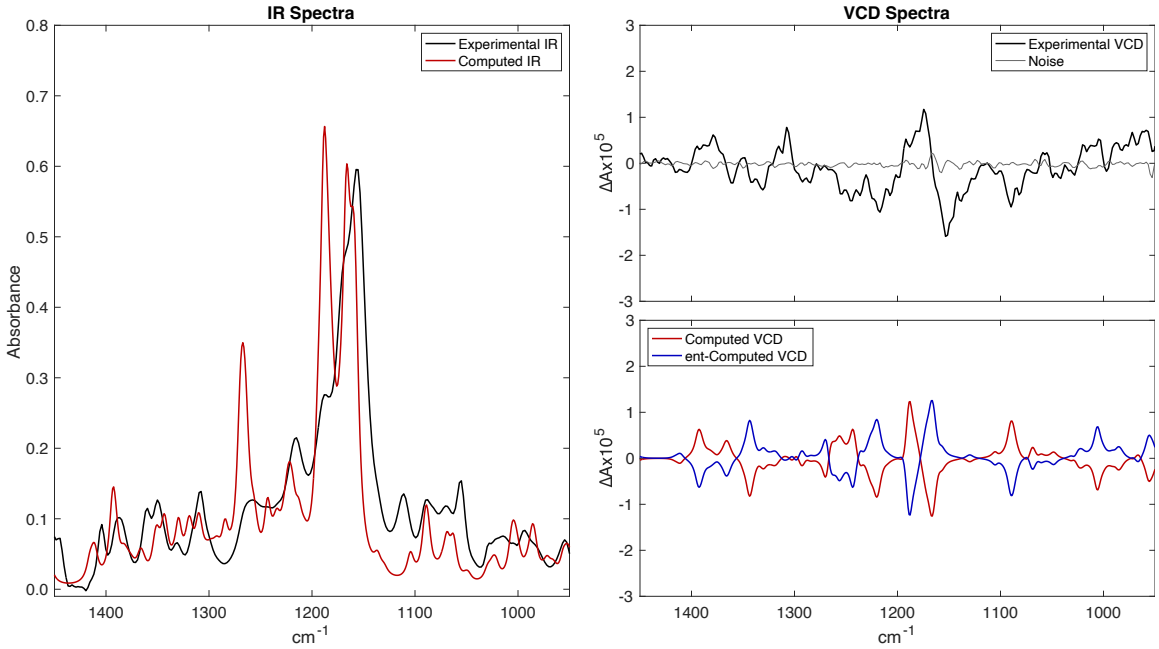


Figure 1.19*. Comparison of experimental VCD and IR spectra for product* ***11q*** *to computed spectra for* ***A_exo-cis****.*[a]



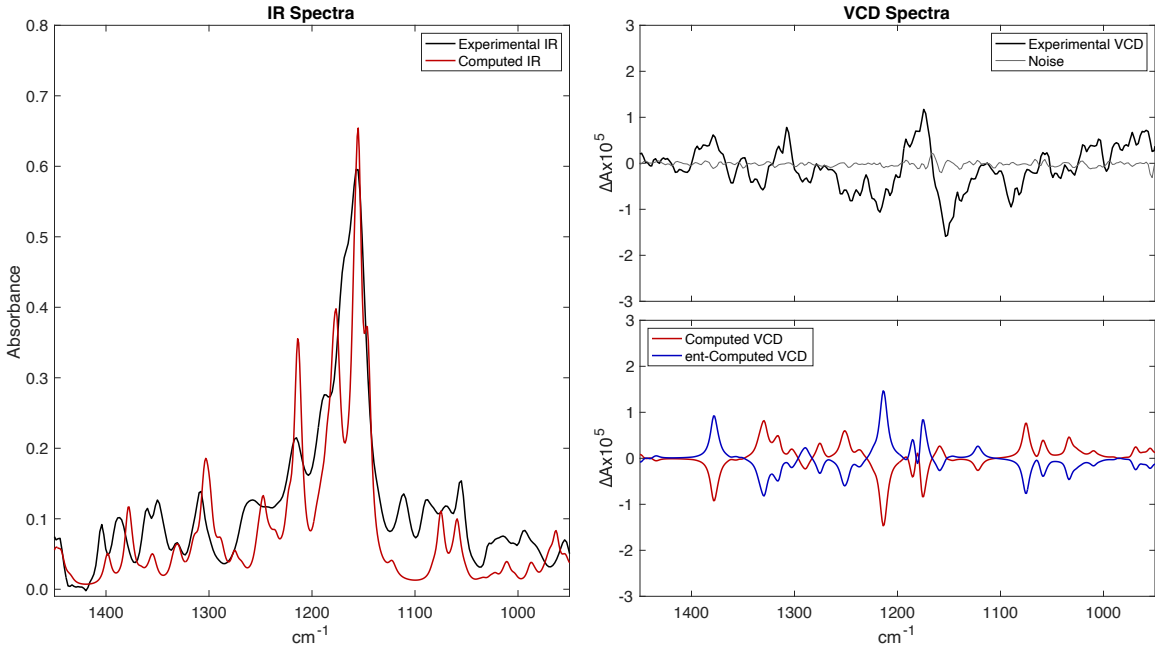
[a] Experimental data from **11q** do not match computed data of **A_exo-cis**.

***Figure 1.20**. Comparison of experimental VCD and IR spectra for product **11q'** to computed spectra for **A_endo-trans**.*[a]



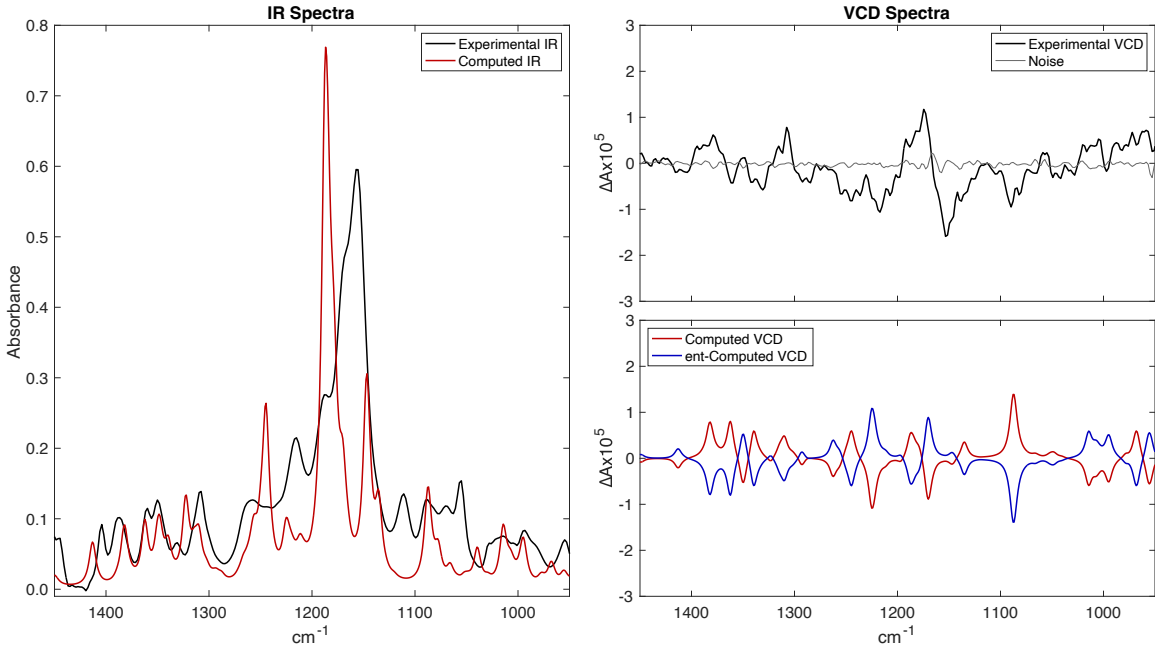
[a] The VCD spectrum was baseline-corrected with a shift of +7 cm^{-1} along y-axis. Experimental data from **11q'** do not match computed data of **A_endo-trans**.

***Figure 1.21**. Comparison of experimental VCD and IR spectra for product **11q'** to computed spectra for **A_exo-trans**.*[a]



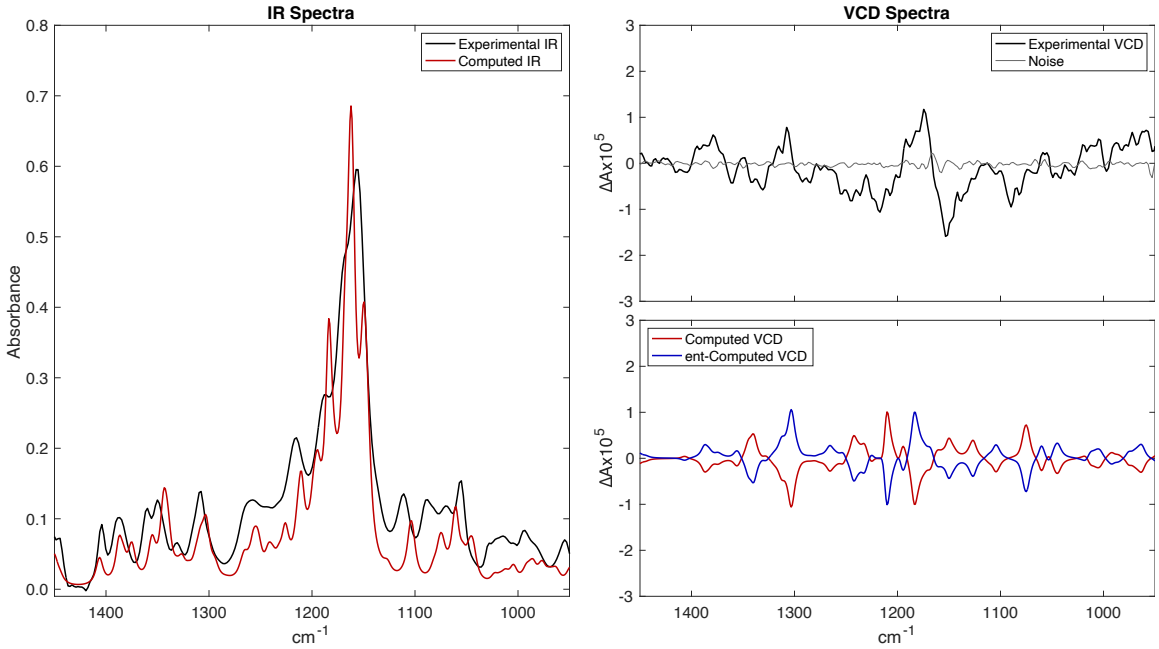
[a] The VCD spectrum of **11q'** was baseline-corrected with a shift of +7 cm^{-1} along y-axis. A shift of -15 cm^{-1} along x-axis applied to computed spectra in fitting. Experimental data from **11q'** do not match computed data of **A_exo-trans**.

Figure 1.22. *Comparison of experimental VCD and IR spectra for product* ***11q'*** *to computed spectra for* ***A_endo-cis****.*[a]



[a] The VCD spectrum of **11q'** was baseline-corrected with a shift of +7 cm^{-1} along y-axis. Experimental data from **11q'** do not match computed data of **A_endo-cis**.

Figure 1.23. *Comparison of experimental VCD and IR spectra for product* ***11q'*** *to computed spectra for* ***A_exo-cis****.*[a]



[a] The VCD spectrum of **11q'** was baseline-corrected with a shift of +7 cm^{-1} along y-axis. A shift of +7 cm^{-1} along x-axis applied to computed spectra in fitting. Experimental VCD spectrum for **11q'** is in good agreement with computed spectrum for ***ent*-A_exo-cis**.

Figure 1.24. *Overlayed experimental and calculated VCD spectra for* ***11q'*** *– assigned as* ***ent-A_exo-cis****.*

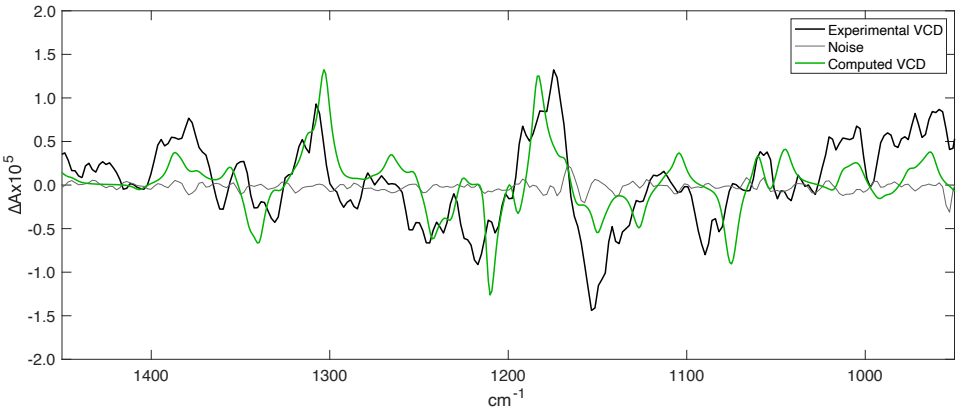


Figure 1.25. *Three diastereomers* ***11k****,* ***11k'****, and* ***11k''*** *to be compared to spectra computed from all eight possible stereoisomers.*

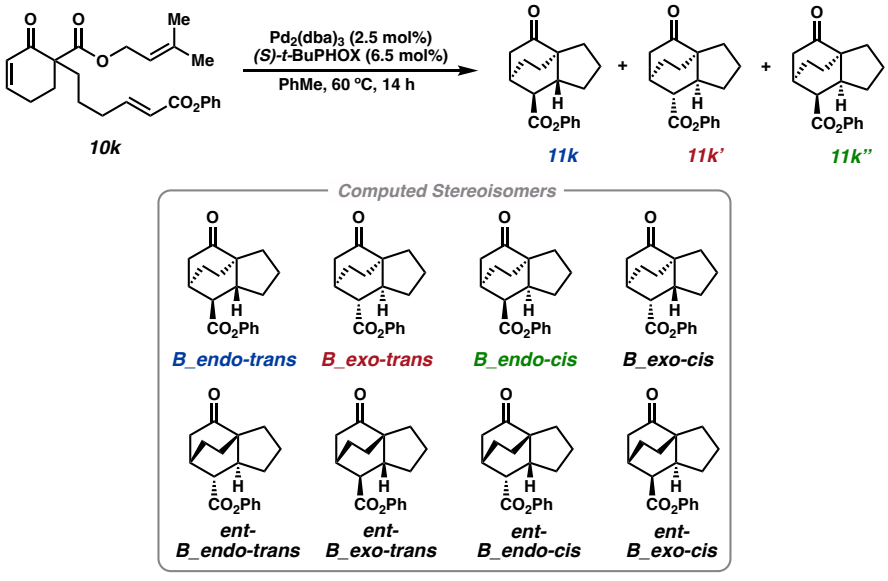
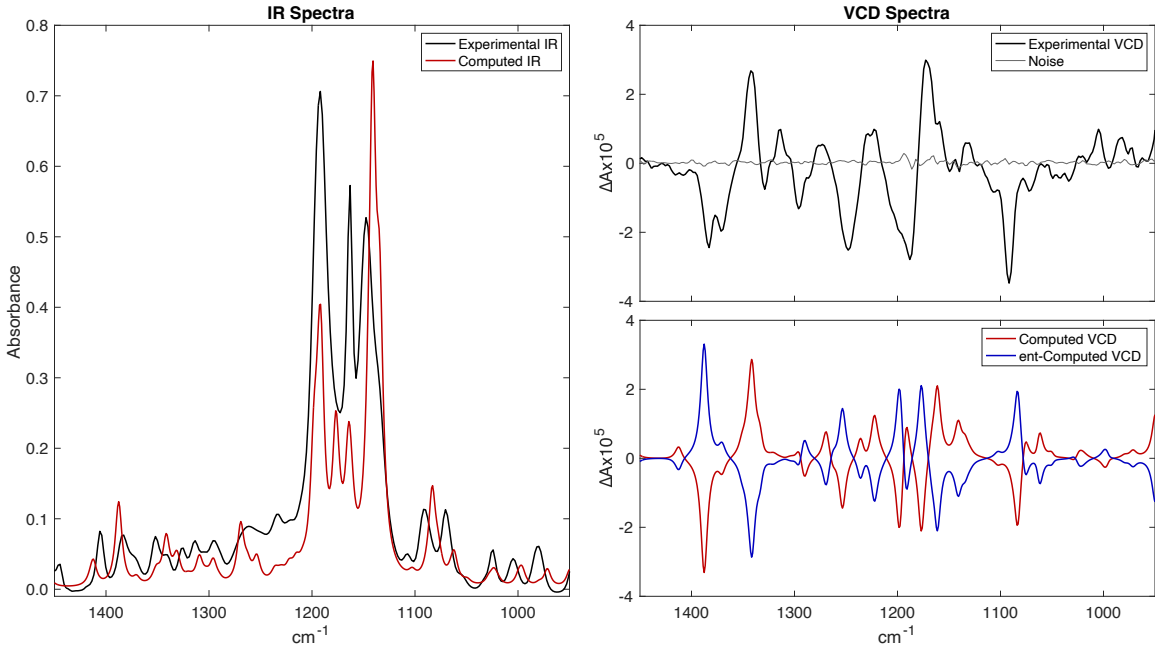


Figure 1.26. *Experimental VCD and IR spectra for product* ***11k*** *compared to computed spectra for* ***B_endo-trans****.*[a]



[a] Experimental IR spectrum in good agreement with computed spectrum. Experimental VCD spectrum for **11k** is in excellent agreement with computed spectrum for **B_endo-trans**.

Figure 1.27. *Overlayed experimental and calculated VCD spectra for* ***11k*** *– assigned as* ***B_endo-trans****.*

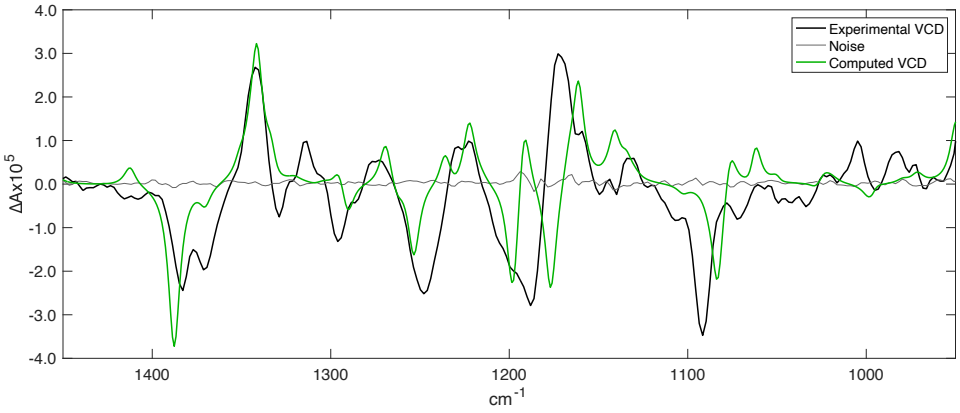
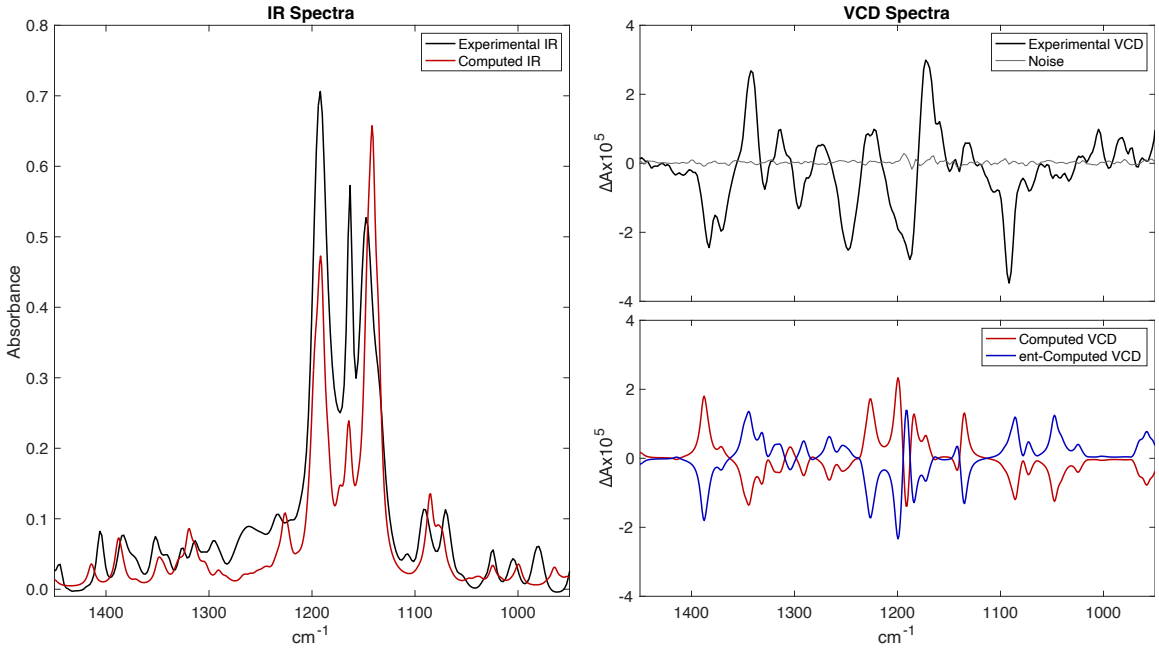
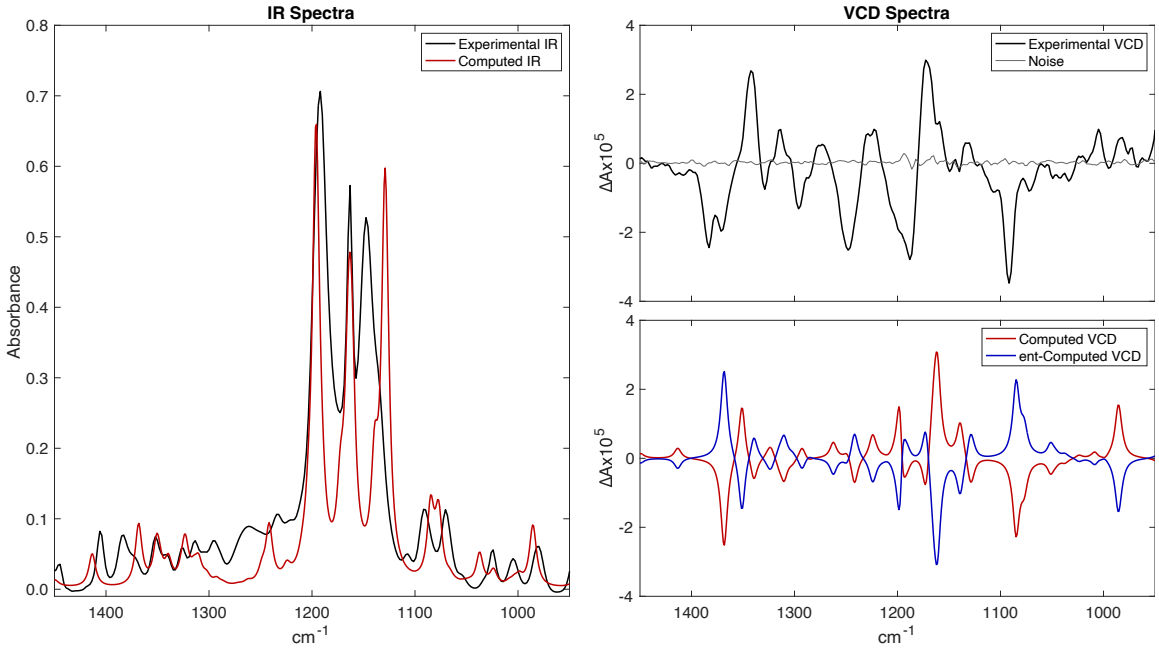


Figure 1.28. *Experimental VCD and IR spectra for product* ***11k*** *compared to computed spectra for* ***B_exo-trans***.[a]



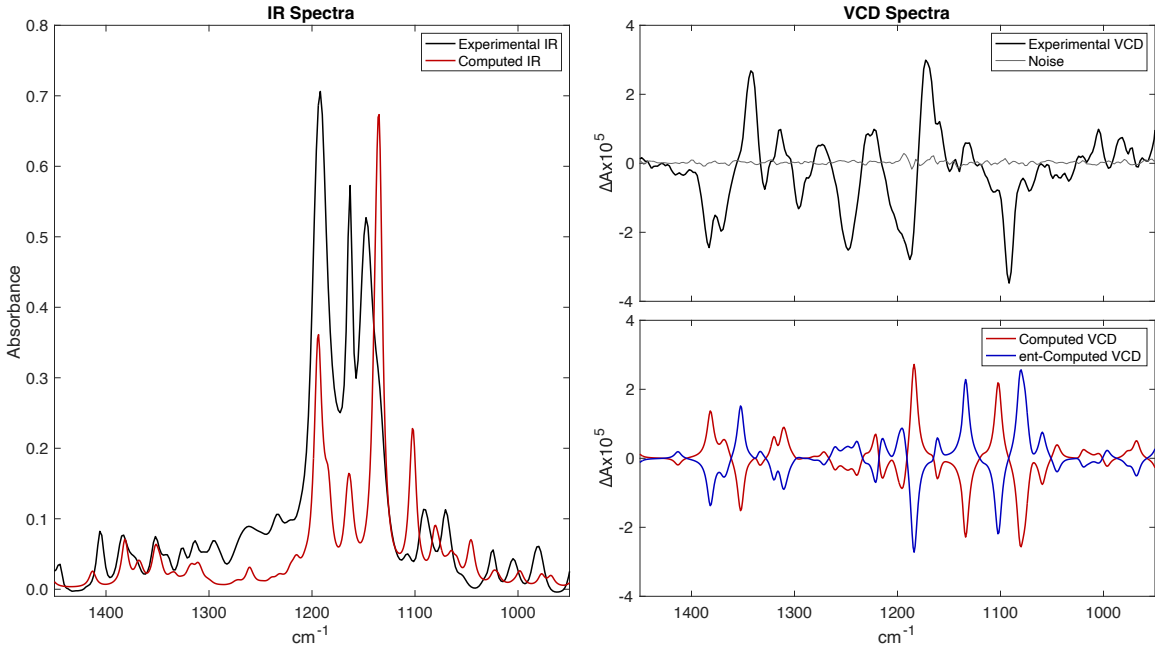
[a] Experimental IR spectrum in good agreement with computed spectrum. However, VCD spectrum contain key sign mismatches in regions around 1400 and 1100 cm^{-1}. Hence, **11k** is not assigned as **B_exo-trans**.

Figure 1.29. *Experimental VCD and IR spectra for product* ***11k*** *compared to computed spectra for* ***B_endo-cis***.[a]



[a] Experimental data do not match computed data and **11k** is not assigned as **B_endo-cis**.

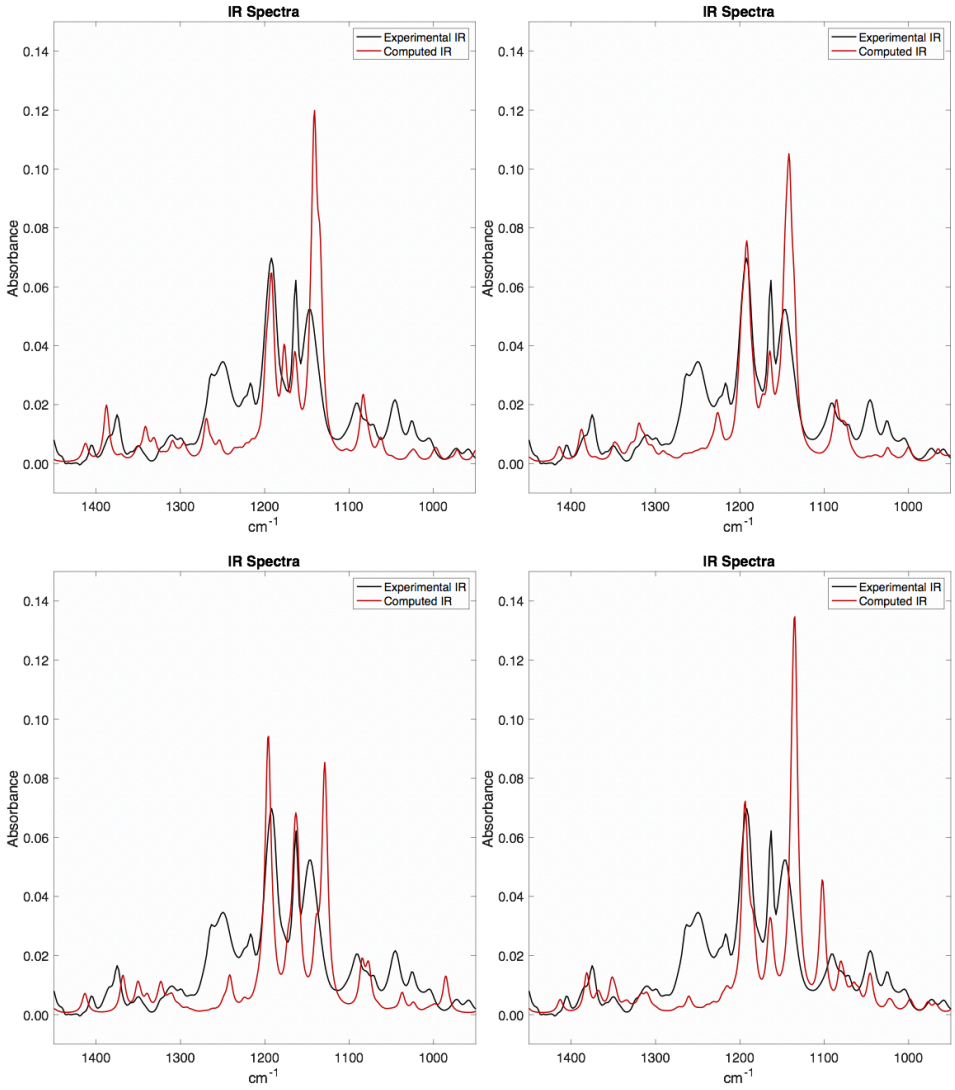
***Figure 1.30**. Experimental VCD and IR spectra for product **11k** compared to computed spectra for **B_exo-cis**.*[a]



[a] Experimental data do not match computed data and **11k** is not assigned as **B_exo-cis**.

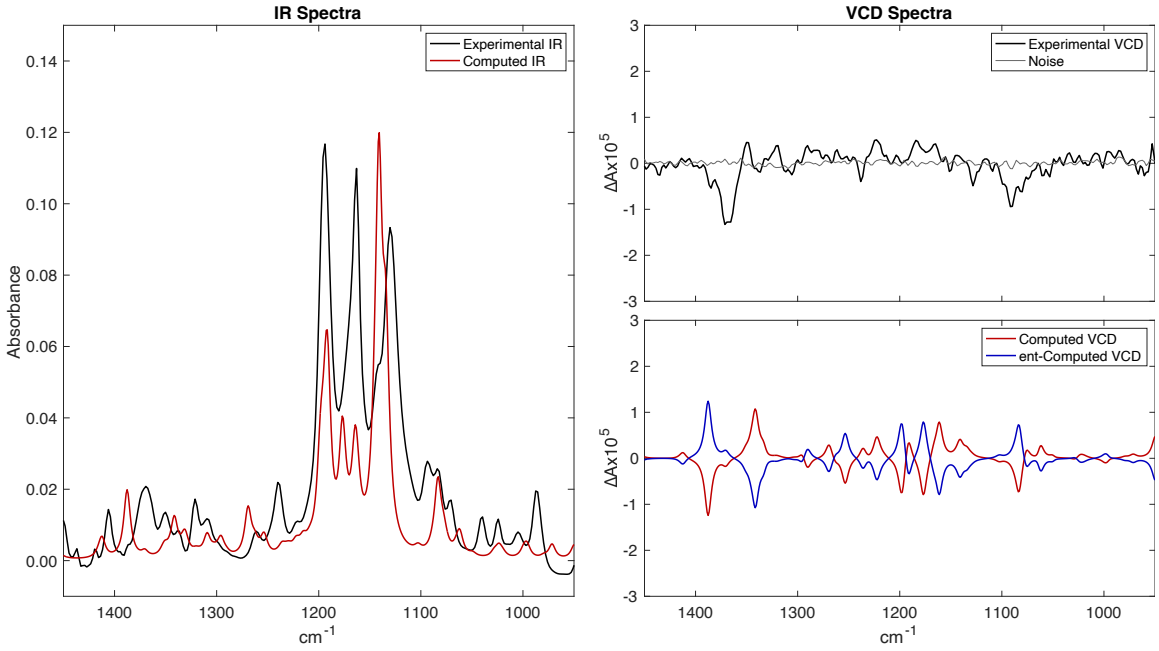
Due to limited sample size (< 3 mg), useful VCD spectra of **11k'** were unable to be obtained. Enantiomeric series was assigned by analogy to the **11a**, **11q** and **11q'** series. The 1000–1500 cm^{-1} region of the IR spectra are still analyzed to support relative stereochemical assignments made by 2D NMR.

Figure 1.31. *Experimental IR spectrum for product* ***11k'*** *compared to computed spectra for* ***B_endo-trans*** *(top left),* ***B_exo-trans*** *(top right),* ***B_endo-cis*** *(bottom left),* ***B_exo-cis*** *(bottom right).*[a]



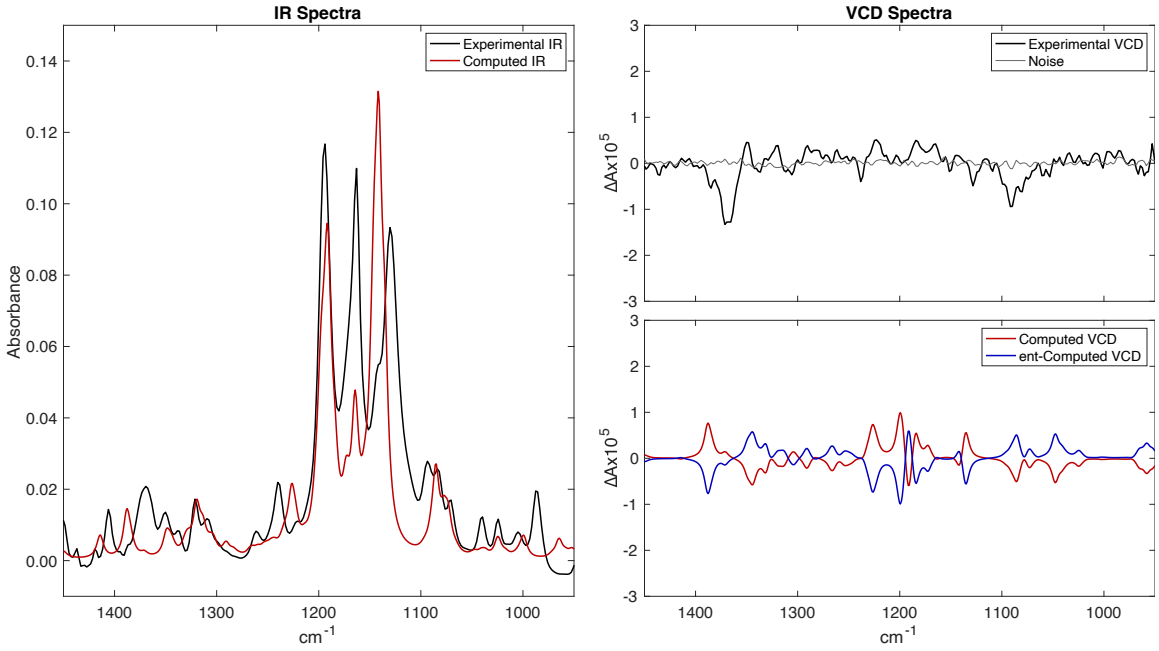
[a] The trans relationship is supported, in accord with 2D NMR data. In contrast to endo-cis and exo-cis, the computed IR spectra for both endo-trans and exo-trans are similar and do not offer key features for distinguishing the two. Given the trans stereochemistry, with **11k** known as **B_endo-trans**, **11k'** is assigned as **B_exo-trans** with absolute stereochemistry assigned based on analogy to **11q'**.

Figure 1.32. *Experimental VCD and IR spectra for product* ***11k″*** *compared to computed spectra for* ***B_endo-trans****.*[a]



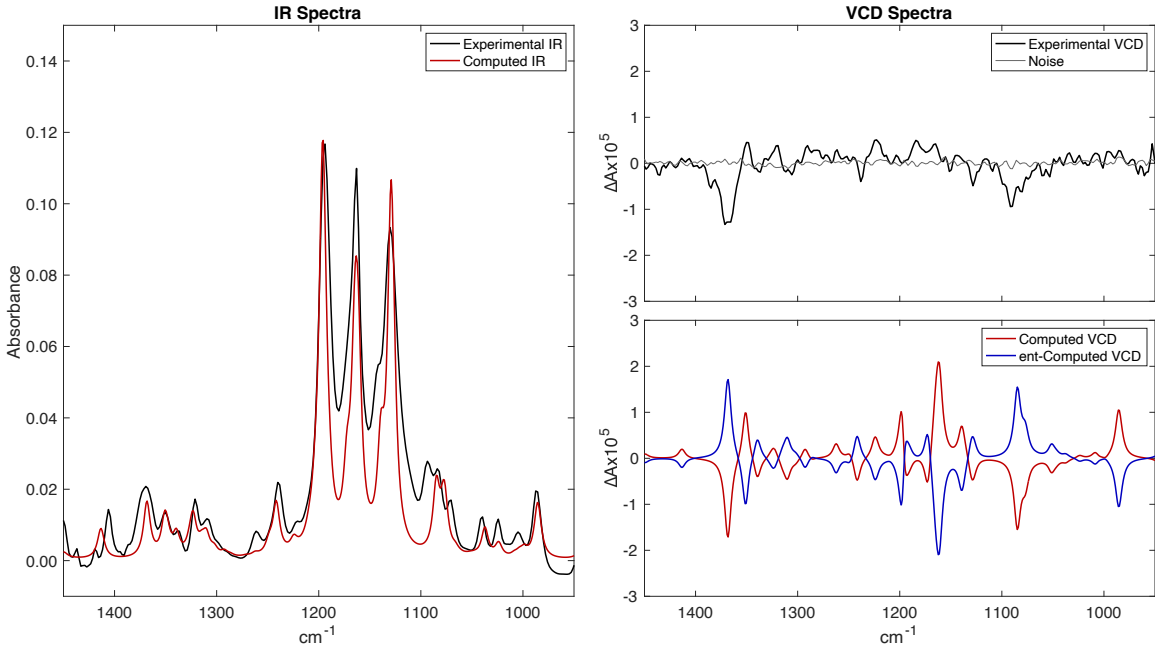
[a] Experimental data do not match computed data and **11k″** is not assigned as **B_endo-trans**.

Figure 1.33. *Experimental VCD and IR spectra for product* ***11k″*** *compared to computed spectra for* ***B_exo-trans***.[a]



[a] Experimental data do not match computed data and **11k″** is not assigned as **B_exo-trans**.

Figure 1.34. *Experimental VCD and IR spectra for product* ***11k″*** *compared to computed spectra for* ***B_endo-cis***.[a]



[a] Experimental IR spectrum is in agreement with the computed spectrum of **B_endo-cis**. Assignment of absolute stereochemistry is based the on the sign of the three most intense peaks in VCD spectrum, 1368, 1350, and 1085 cm^{-1}. These match **B_endo-cis**, the same enantiomeric series as **11k**.

Figure 1.35. *Overlayed experimental and calculated VCD spectra for* ***11k″*** *– assigned as* ***B_endo-cis****.*

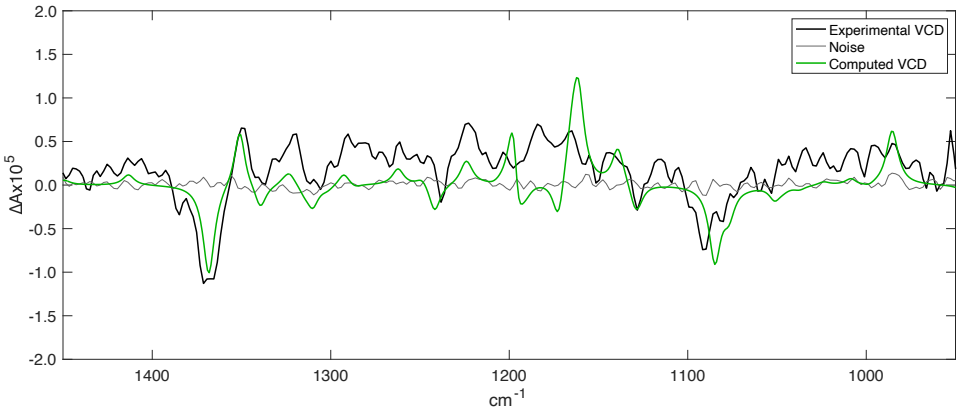
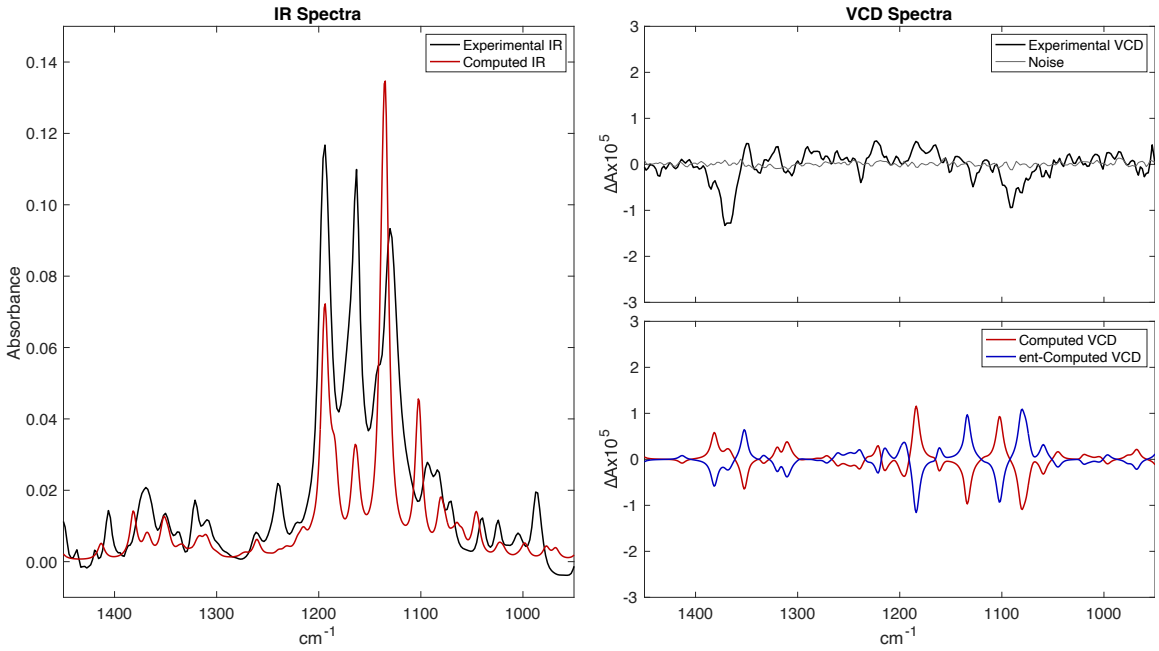


Figure 1.36. *Experimental VCD and IR spectra for product* ***11k″*** *compared to computed spectra for* ***B_exo-cis****.*[a]



[a] Experimental data do not match computed data and **11k″** is not assigned as **B_exo-cis**.

1.4.4 2D NMR ANALYSIS OF SELECT COMPOUNDS

Figure 1.37. *^{1}H-^{1}H COSY NMR spectrum of* ***11a*** *(400 MHz, $CDCl_3$).*

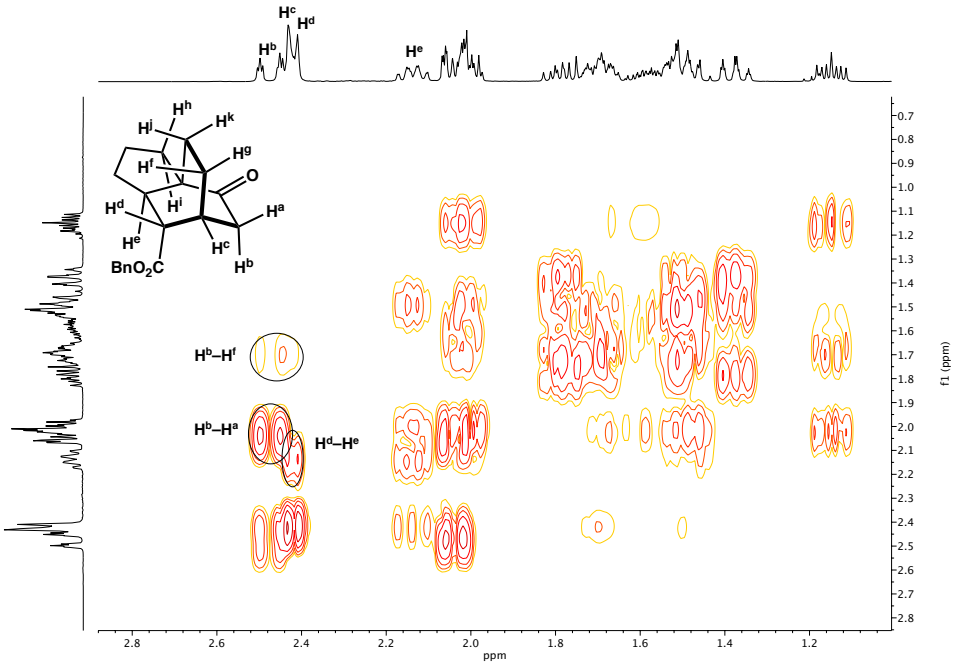


Figure 1.38. *^{1}H-^{13}C HSQC NMR spectrum of* ***11a*** *(400 MHz, $CDCl_3$).*

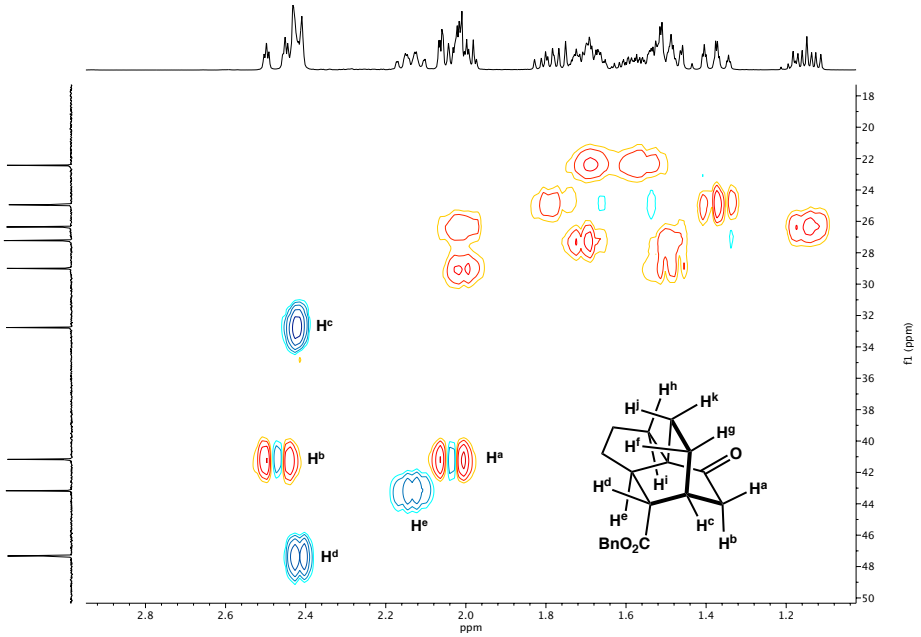


Figure 1.39. *^{1}H-^{1}H NOESY NMR spectrum of* ***11a*** *(400 MHz, $CDCl_3$).*

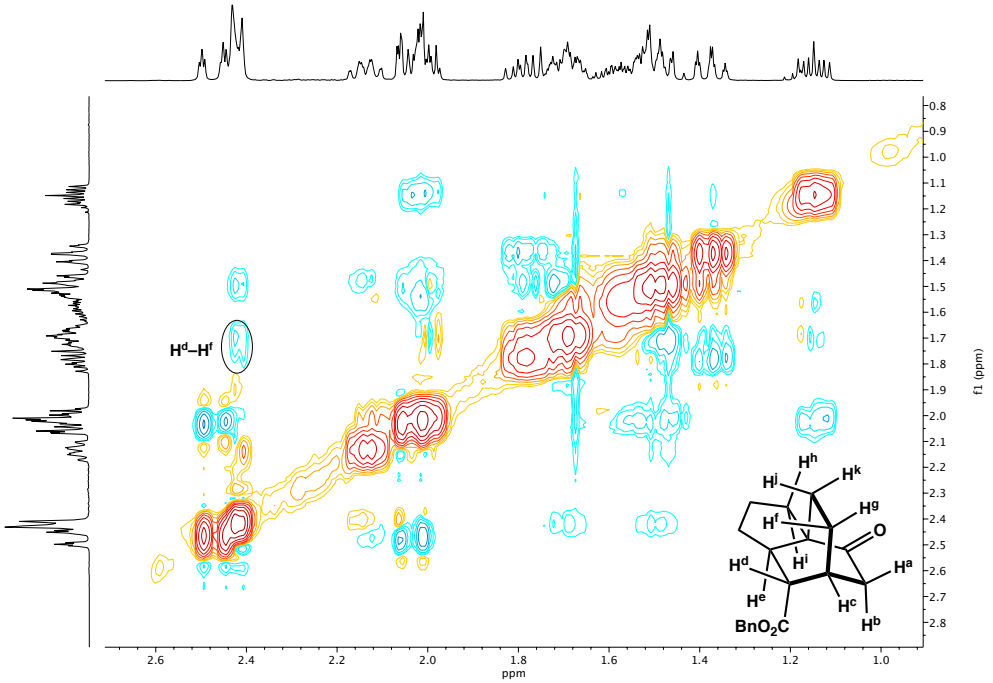


Figure 1.40. *^{1}H-^{1}H COSY NMR spectrum of* ***11p*** *(400 MHz, $CDCl_3$).*

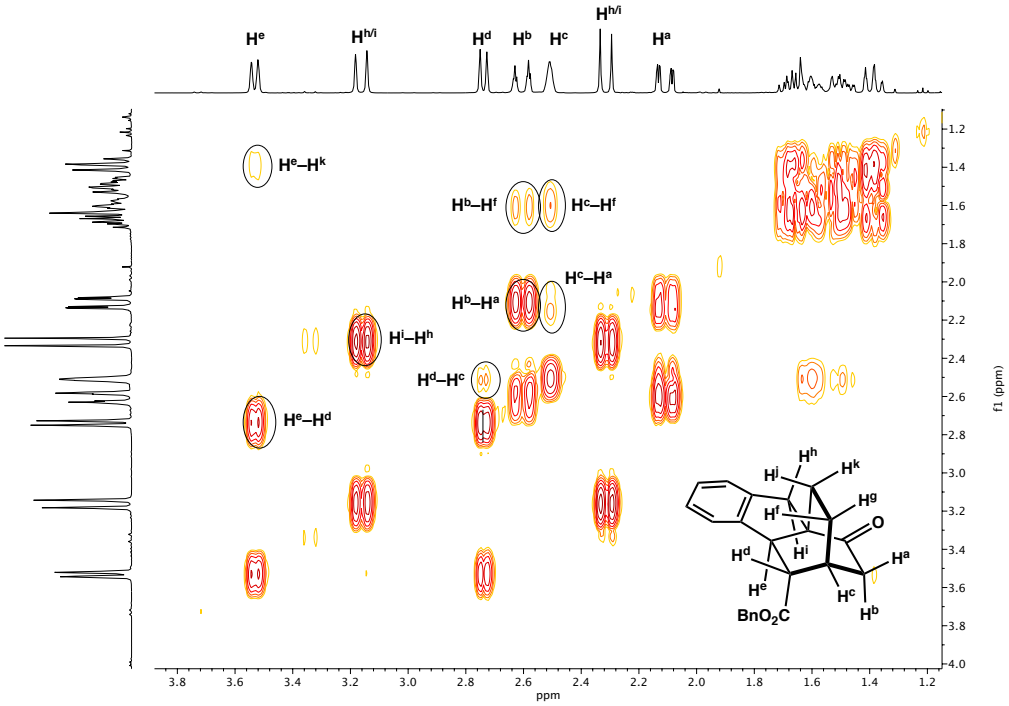


Figure 1.41. *^{1}H-^{13}C HSQC NMR spectrum of* ***11p*** *(400 MHz, $CDCl_3$).*

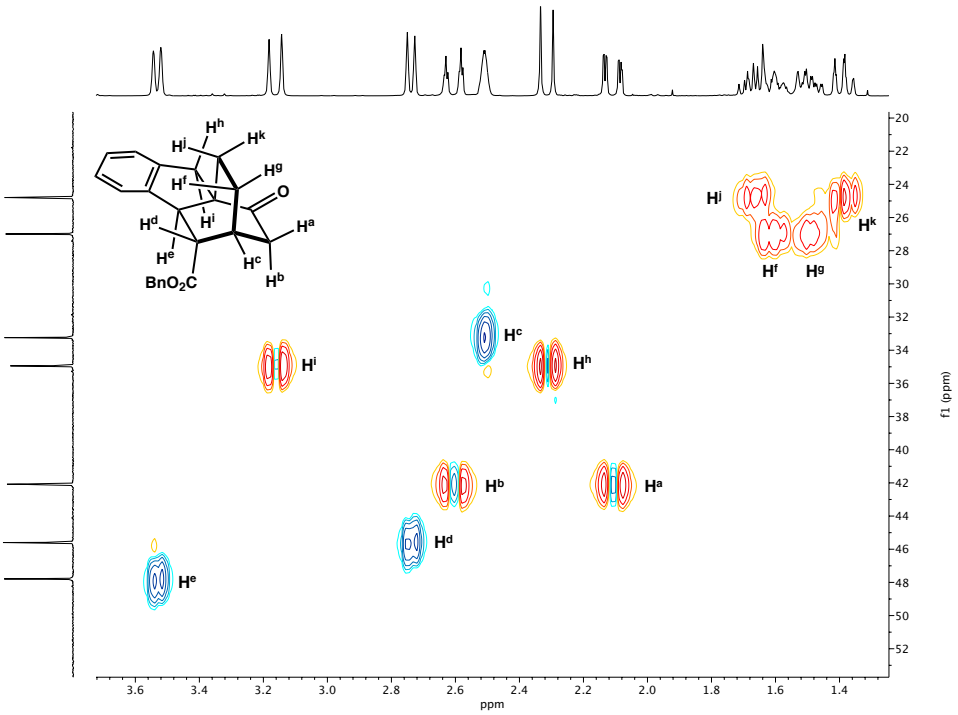


Figure 1.42. *^{1}H-^{1}H NOESY NMR spectrum of* ***11p*** *(400 MHz, $CDCl_3$).*

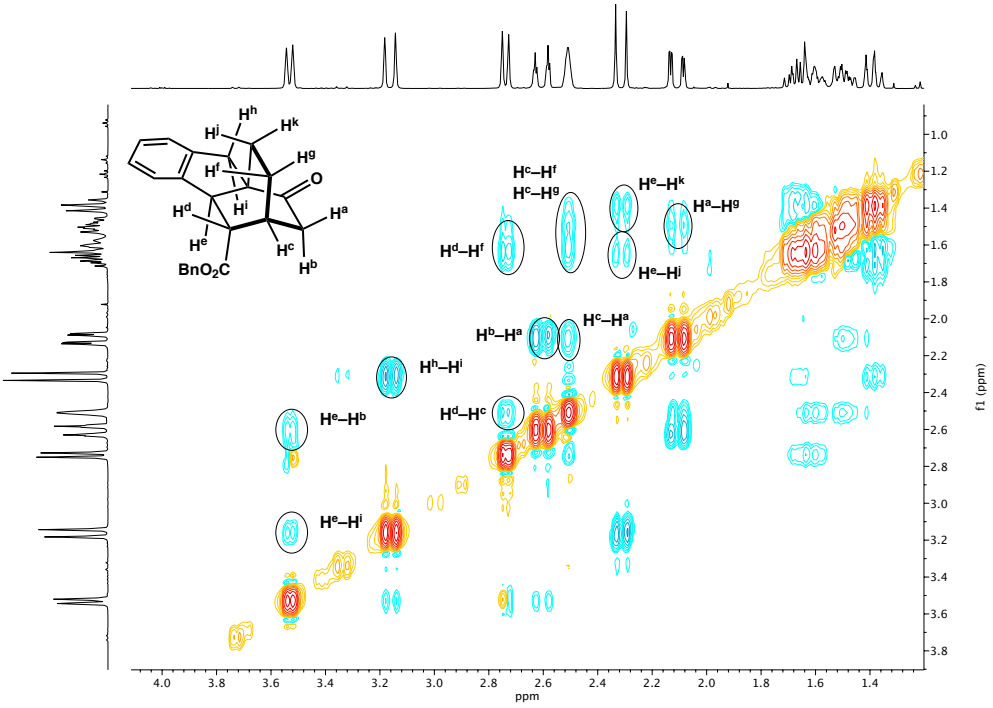


Figure 1.43. *^{1}H-^{1}H COSY NMR spectrum of* ***11q*** *(400 MHz, $CDCl_3$).*

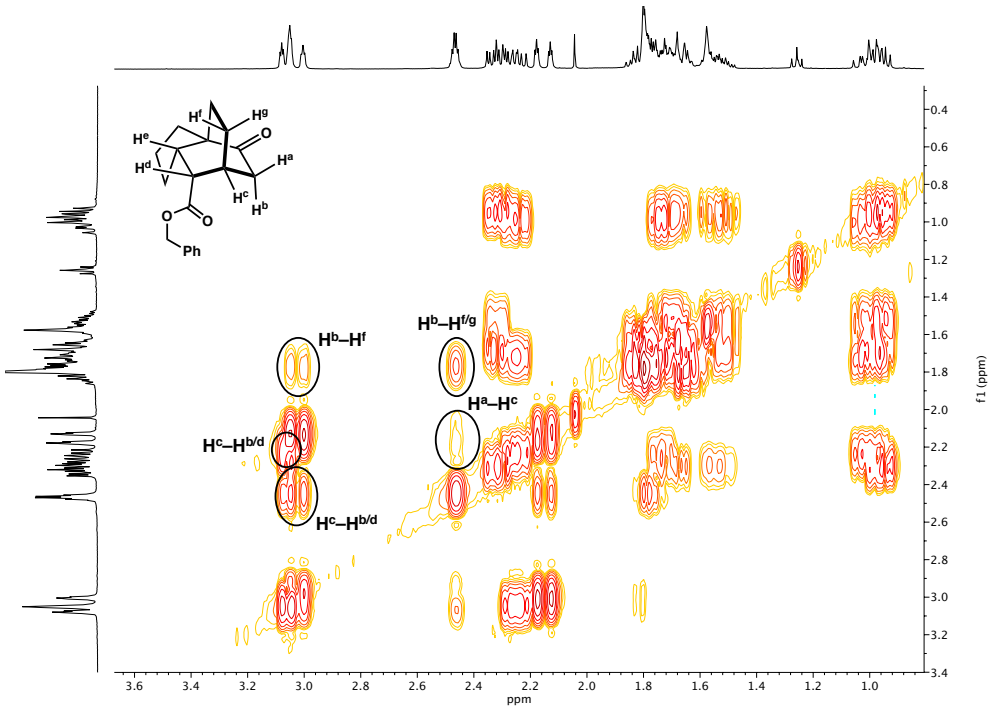


Figure 1.44. *^{1}H-^{13}C HSQC NMR spectrum of* ***11q*** *(400 MHz, $CDCl_3$).*

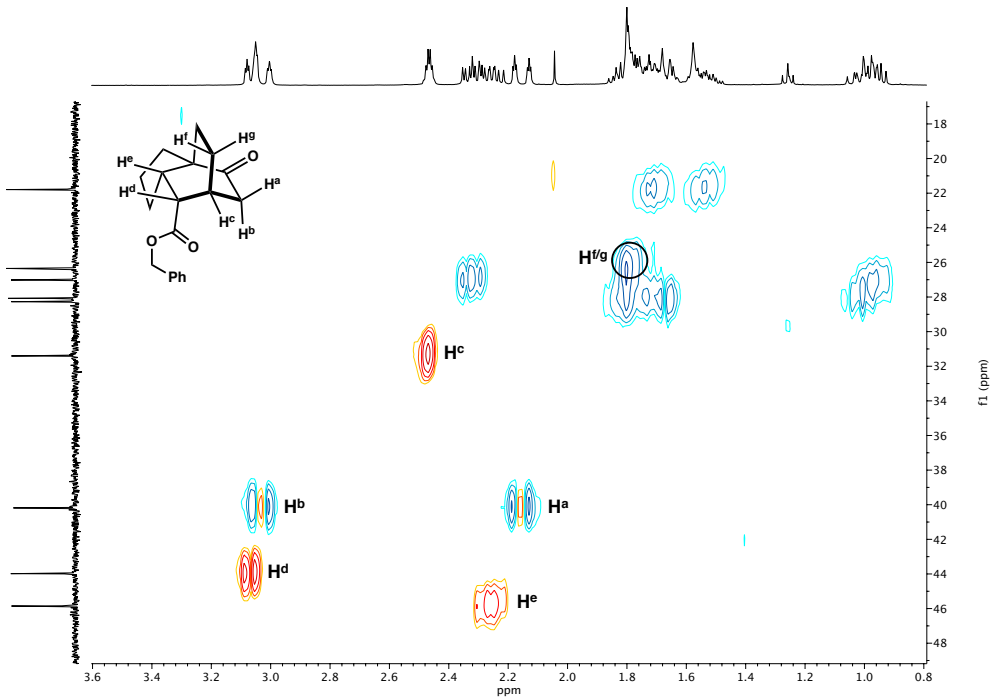


Figure 1.45. *^{1}H-^{1}H NOESY NMR spectrum of* ***11q*** *(400 MHz, $CDCl_3$).*

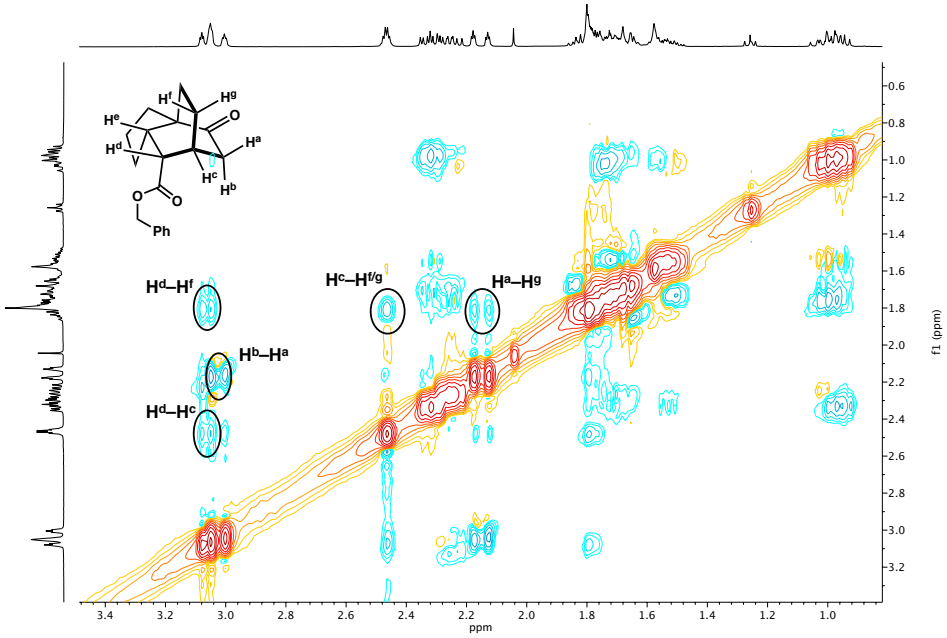


Figure 1.46. *^{1}H-^{1}H COSY NMR spectrum of* ***11q'*** *(400 MHz, $CDCl_3$).*

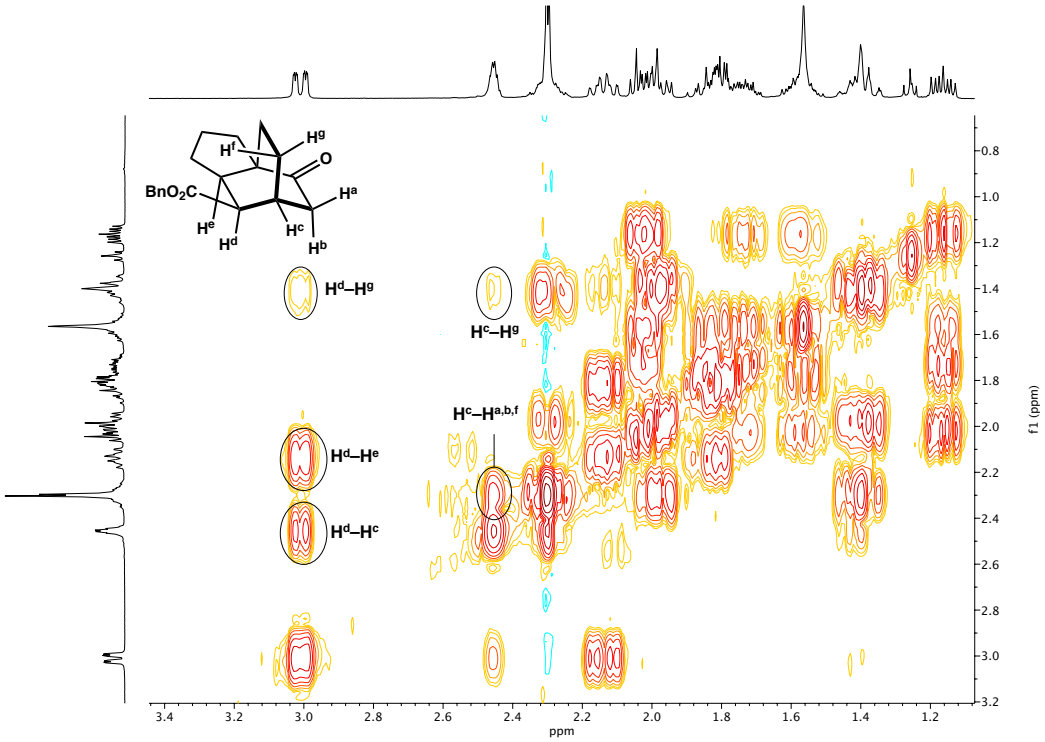


Figure 1.47. *^{1}H-^{13}C HSQC NMR spectrum of* ***11q'*** *(400 MHz, $CDCl_3$).*

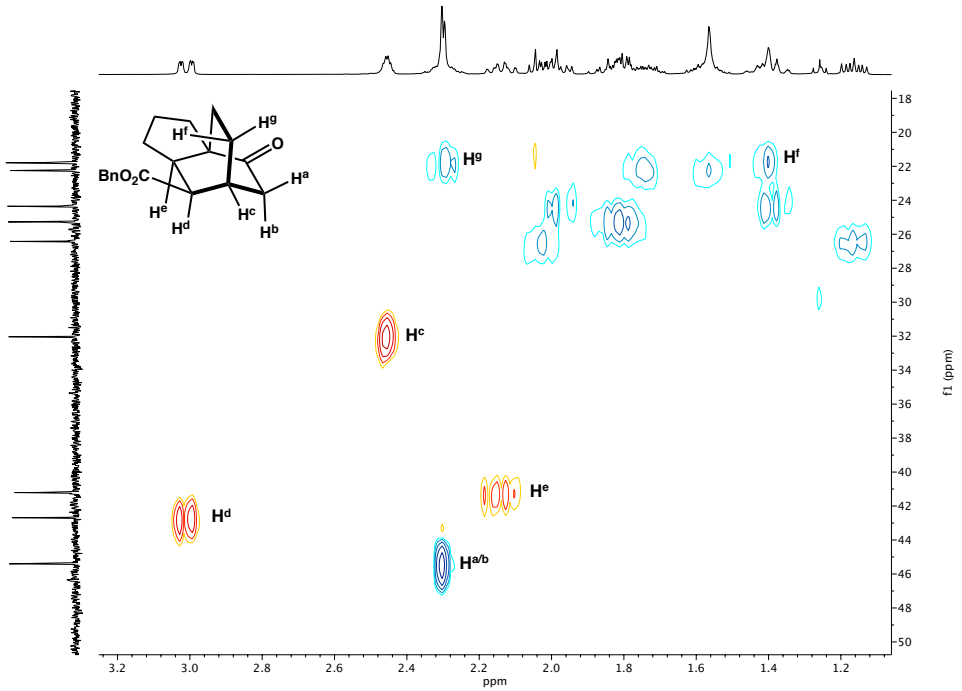
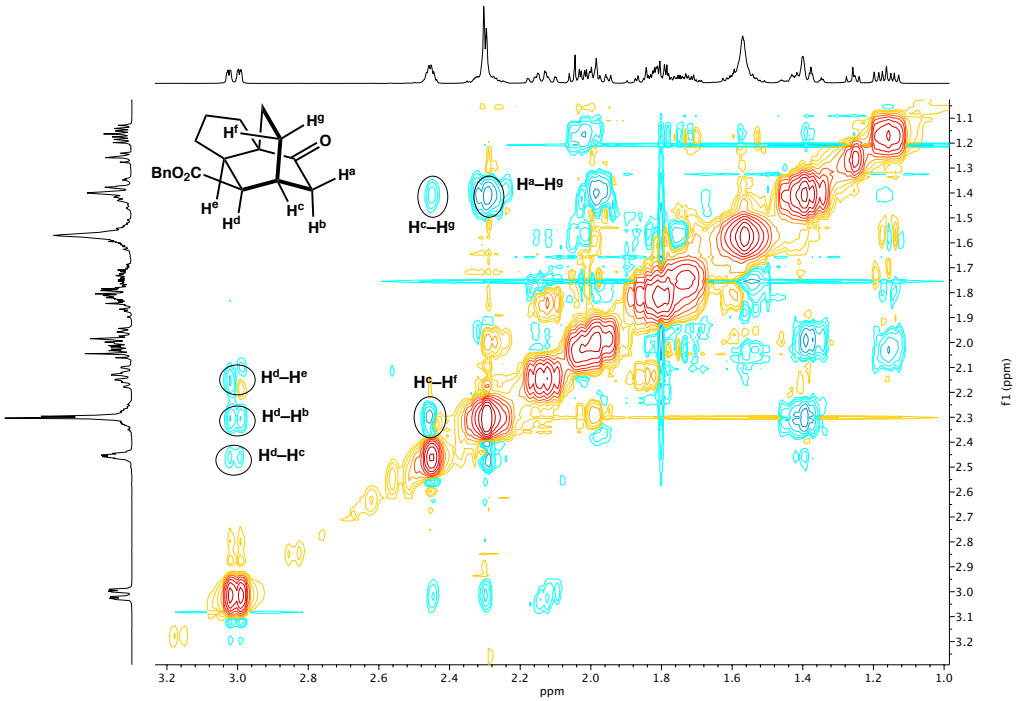


Figure 1.48. *^{1}H-^{1}H NOESY NMR spectrum of* ***11q'*** *(400 MHz, $CDCl_3$).*



1.4.5 GENERAL COMPUTATIONAL DETAILS

General Notes

All quantum mechanics calculations were carried out with the ORCA program.[52] Geometry optimizations, harmonic frequency calculations, and single-point energy evaluations were carried out with density functional theory (DFT). The PBE0 functional[53] paired with Becke–Johnson damped D4 dispersion corrections[54], henceforth referred to as PBE0-D4, was used as it has proven a robust method for such systems in our prior studies.[55] For geometry optimization and harmonic frequency calculations, Pd is described by the def2-TZVP basis set[56] and the ECP28MWB small-core (18 explicit valence electrons) quasi-relativistic pseudopotential,[57] while C, H, N, and P are assigned the def2-SVP basis. Diffuse functions are added to oxygen (ma-def2-SVP). Herein, we refer to this composite basis set as BS1. Geometry optimization and harmonic frequency calculations were carried out with the CPCM implicit solvation model for toluene (PhMe, $\varepsilon = 2.4$). For all calculations employing CPCM, surface charges are described by the improved Gaussian charge scheme of Neese and coworkers with a scaled Van der Waals cavity ($\alpha = 1.2$).[58] All Hessians were computed analytically. Stationary points are characterized by the correct number of imaginary vibrational modes (zero for minima and one for saddle points). Intrinsic reaction coordinate (IRC) analysis confirms the nature of transition states.[59] Cartesian coordinates of all optimized structures are included as ".xyz" files are available online in a compressed in a zip file format.

Electronic energies are further refined with single-point calculations employing the PBE0-D4 functional[60] and the def2-TZVPP basis set on all atoms (with the ECP28MWB

pseudopotential for Pd) with additional diffuse functions on O (ma-def2-TZVPP). This mixed basis is henceforth referred to as BS2. Solvation was accounted for with CPCM as mentioned above (PhMe, ε = 2.4). Final Gibbs free energies were obtained by applying thermodynamic corrections obtained at the optimization level of theory to these refined electronic energies. Thermodynamic corrections from harmonic frequency calculations employ the quasi-ridged rotor harmonic oscillator approach to correct for the breakdown of the harmonic oscillator approximation at low vibrational frequencies.[61] Note that free energies are adjusted to a 1 M standard state. The translational (S_{trans}) and rotational entropy (S_{rot}) contributions to the Gibbs free energy calculated for a complex in condensed phase are *ca.* 40–60% of the values obtained assuming an ideal gas.[62] As suggested in the literature, S_{trans} and S_{rot} obtained by ideal gas treatment are scaled by a factor of 0.5 to obtain the final condensed phase values.[63] Hence, the Gibbs free energy at 333.15 K is calculated as:

$$G^*_{solv} = E^{BS2}_{el,solv} + ZPE + E_{trans} + E_{rot} + E_{vib} + k_bT - T\left(S_{el} + S_{vib} + \frac{1}{2}S_{trans} + \frac{1}{2}S_{rot}\right) + \Delta G^{0\rightarrow *}$$

The resolution of identity (RI) and Chain-of-Spheres (COS) approximations are employed for efficient evaluation of Coulomb and exchange integrals, respectively.[64] The def2/J auxiliary basis[65] is employed for all atoms except oxygen, for which a suitable auxiliary was obtained via the automatic generation algorithm in the ORCA program (keyword: *AutoAux*).[66] Very fine grid settings are employed in all calculations (optimization/frequency calculations: DefGrid2, single point calculations: DefGrid3).

Conformer searching was carried out for each stationary point using the meta-dynamics-based CREST program (using GNF-FF) from the Grimme group. Duplicate conformers were removed, and low energy conformers were subsequently optimized and energies evaluated at the cheaper PBE0-D4/def2-TZVP (Pd), ma-def2-SVP (O), def2-SVP/CPCM(PhMe)//PBE-D4/def2-TZVP (Pd), ma-def2-SV(P) (O), def2-SV(P) level of theory. The final low energy conformers were further optimized at the level of theory mentioned prior. Note that for enantiodetermining transition states (such as TS2 and TS3) conformer searching also explicitly includes rotation about the Pd–O–C–C(enolate) dihedral, consideration of s-cis and s-trans ester conformations, as well as all permutations of the considered stereochemical elements.

Finally, conformational entropy [67] (entropy arising from multiple low energy thermally populated conformers) is accounted for by the *mixture of components* model of DeTar.[68] Conformational entropy (S_{conf}) is defined as:

$$S_{conf} = -R \sum \chi_i \ln (\chi_i)$$

where χ_i is the mole fraction (thermal population) of the ith conformer based on its relative free energy within the conformer ensemble. Given the computational demand for computing free energies for large ensembles of conformers, χ_i was derived from the free energies initially computed during the conformer screening process (PBE0-D4/def2-TZVP (Pd), ma-def2-SVP (O), def2-SVP/CPCM(PhMe)//PBE-D4/def2-TZVP (Pd), ma-def2-SV(P) (O), def2-SV(P))

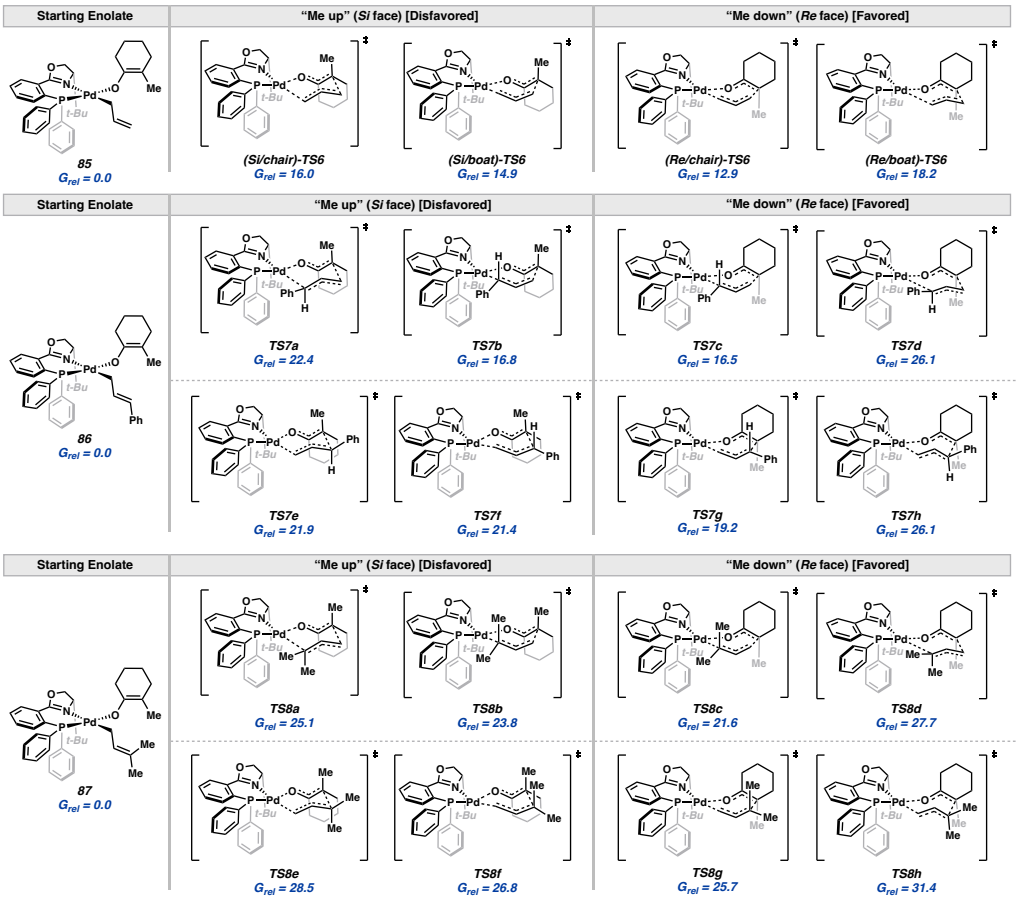
$$G_{final} = G^*_{solv} - TS_{conf}$$

For the systems at hand, values of TS_{conf} (at 333.15 K) can be on the order of magnitude of a few kcal/mol.

Comparison of Barrier Heights to Inner-sphere Reductive Elimination

Employing cyclohexanone-derived Pd enolate as a model system (**85, 86, 87**), the barrier to inner-sphere reductive elimination was investigated while varying substitution on the allyl moiety (Figure 1.49).

Figure 1.49. *Relative free energies for various inner-sphere reductive elimination transition states from allyl (**85**), cinnamyl (**86**), and prenyl (**87**) complexes.*[a]

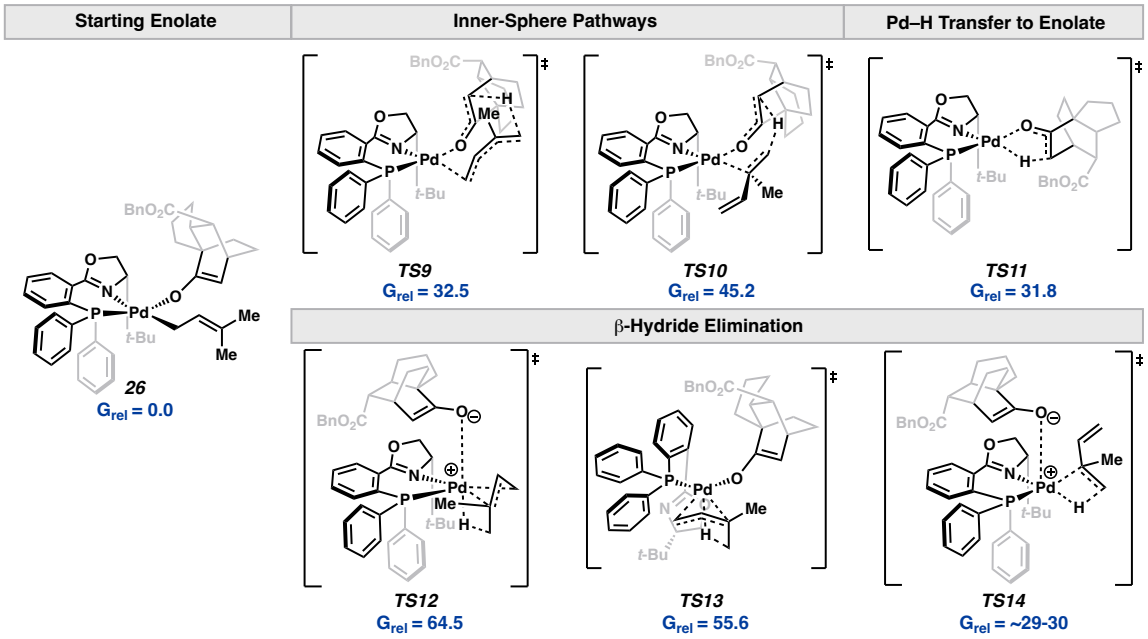


[a] Gibbs free energies in kcal/mol computed at the PBE0-D4/BS2/CPCM(PhMe)//PBE0-D4/BS1/CPCM(PhMe) level of theory at 333.15 K.

Mechanism of Catalyst Turnover

Of all the sampled transition states, we found the outer-sphere and N-detached inner-sphere pathways to be highly competitive and lowest in energy. Additional transition states were also explored, and the lowest energy pathway of each type of mechanism are shown in the following table.

Figure 1.50. *Relative free energies for various proton transfer transition states from post-cycloaddition enolate* ***26****.*[a]



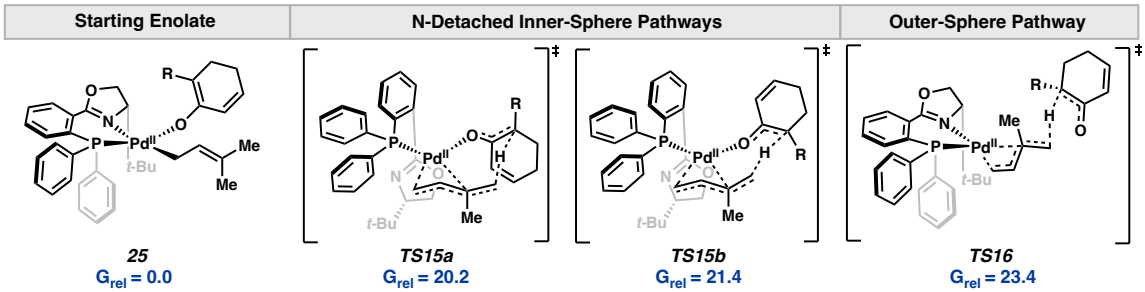
[a] Gibbs free energies in kcal/mol computed at the PBE0-D4/BS2/CPCM(PhMe)//PBE0-D4/BS1/CPCM(PhMe) level of theory at 333.15 K.

Mechanism of Premature Protonation

Analogous to the catalyst turnover mechanism, N-detached inner-sphere pathways were found to be lowest-energy for premature protonation. Of these transition states (**TS15a** and **TS15b**) that would yield enantiomeric protonation products, the lowest-energy **TS15a**

provides the enantiomer consistent with the major reaction product. In addition, an outer-sphere pathway (**TS16**) was also found to be competitive.

Figure 1.51. *Relative free energies for various proton transfer transition states from pre-cycloaddition enolate* ***25****.*[a]

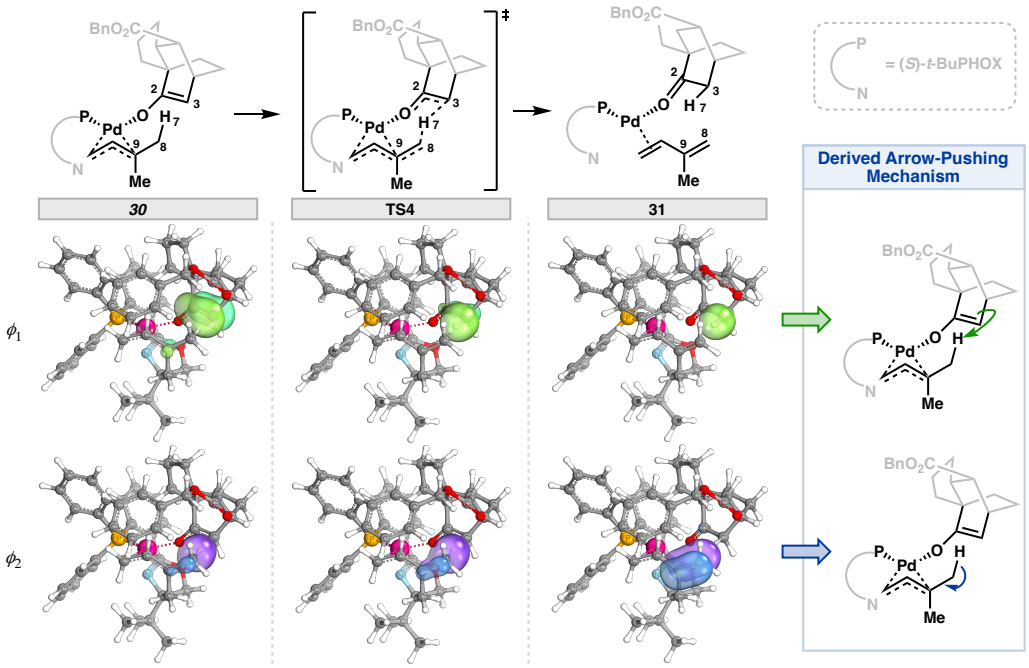


[a] Gibbs free energies in kcal/mol computed at the PBE0-D4/BS2/CPCM(PhMe)//PBE0-D4/BS1/CPCM(PhMe) level of theory at 333.15 K.

Intrinsic Bonding Orbital (IBO) Analysis of Inner-sphere Proton Transfer

IBO analysis along the reaction coordinate of the N-detached inner-sphere proton transfer to post-cycloaddition enolate confirms the role of prenyl as a proton source.

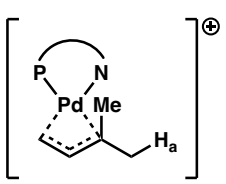
Figure 1.52. *IBO analysis of N-detached inner-sphere mechanism and corresponding derived arrow-pushing mechanism.*



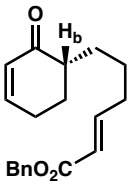
pKa Calculations and Thermodynamics of Outer-Sphere Proton Transfer

The pK_a values of the π-allyl Pd complex **88** and ketones were calculated, and the results verify that the proton transfers to both pre- and post-cycloaddition enolates are thermodynamically favorable.

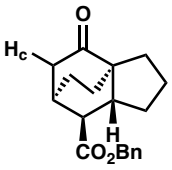
Figure 1.53. *Computed pKa values of cationic π-allyl Pd complex* ***88*** *and ketones* ***19a*** *and* ***11a****.*



88

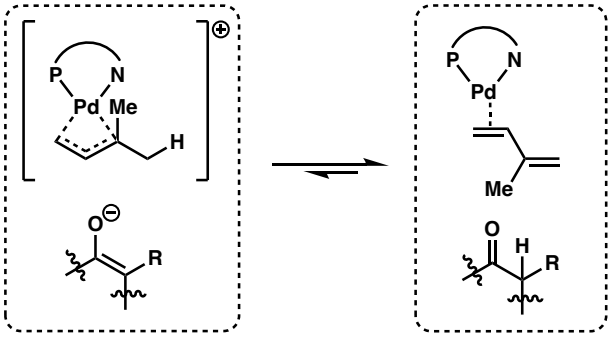


19a



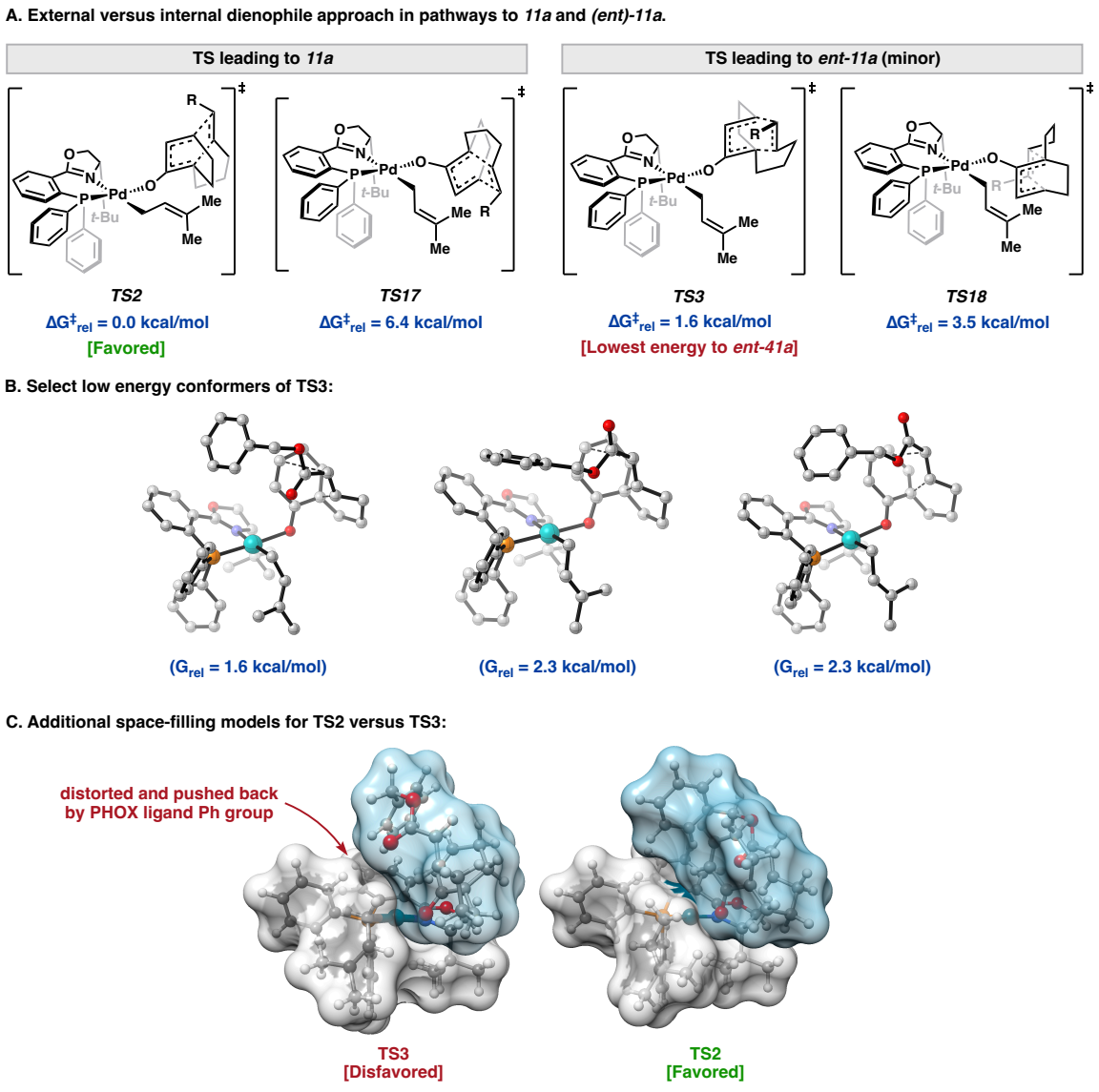
11a

Compound	Proton	pK_a in water	pK_a in DMSO
88	H_a	20.0	19.5
19a	H_b	30.1	30.3
11a	H_c	31.3	30.8



Enantiodetermining [4+2] cycloaddition

Figure 1.54. *(A) Comparison of internal versus external dienophile approach to both enantiotopic diene faces. (B) Select low energy conformers of* ***TS3*** *(allyl isomers not pictured). (C) Additional space-filling models for* ***TS2*** *and* ***TS3****.*



1.5 REFERENCES AND NOTES

(1) (a) Christoffers, J.; Mann, A. Enantioselective Construction of Quaternary Stereocenters. *Angew. Chem. Int. Ed.* **2001**, *40*, 4591–4597. (b) Douglas, C. J.; Overman, L. E. Catalytic Asymmetric Synthesis of All-Carbon Quaternary Stereocenters. *Proc. Natl. Acad. Sci. U.S.A.* **2004**, *101*, 5363–5367.

(2) (a) Liu, Y.; Han, S.-J.; Liu, W.-B.; Stoltz, B. M. Catalytic Enantioselective Construction of Quaternary Stereocenters: Assembly of Key Building Blocks for the Synthesis of Biologically Active Molecules. *Acc. Chem. Res.* **2015**, *48*, 740–751. (b) Trost, B. M.; Crawley, M. L. Asymmetric Transition-Metal-Catalyzed Allylic Alkylations: Applications in Total Synthesis. *Chem. Rev.* **2003**, *103*, 2921–2944.

(3) Cusumano, A. Q.; Stoltz, B. M.; Goddard, W. A. Reaction Mechanism, Origins of Enantioselectivity, and Reactivity Trends in Asymmetric Allylic Alkylation: A Comprehensive Quantum Mechanics Investigation of a $C(sp^3)$–$C(sp^3)$ Cross-Coupling. *J. Am. Chem. Soc.* **2020**, *142*, 13917–13933.

(4) (a) Keith, J. A.; Behenna, D. C.; Mohr, J. T.; Ma, S.; Marinescu, S. C.; Oxgaard, J.; Stoltz, B. M.; Goddard, W. A. The Inner-Sphere Process in the Enantioselective Tsuji Allylation Reaction with *(S)*-*t*-Bu-Phosphinooxazoline Ligands. *J. Am. Chem. Soc.* **2007**, *129*, 11876–11877. (b) Keith, J. A.; Behenna, D. C.; Sherden, N.; Mohr, J. T.; Ma, S.; Marinescu, S. C.; Nielsen, R. J.; Oxgaard, J.; Stoltz, B. M.; Goddard, W. A. The Reaction Mechanism of the Enantioselective Tsuji Allylation: Inner-

Sphere and Outer-Sphere Pathways, Internal Rearrangements, and Asymmetric C–C Bond Formation. *J. Am. Chem. Soc.* **2012**, *134*, 19050–19060. (C) McPherson, K. E.; Croatt, M. P.; Morehead, A. T.; Sargent, A. L. DFT Mechanistic Investigation of an Enantioselective Tsuji–Trost Allylation Reaction. *Organometallics* **2018**, *37*, 3791–3802.

(5) Behenna, D. C.; Stoltz, B. M. The Enantioselective Tsuji Allylation. *J. Am. Chem. Soc.* **2004**, *126*, 15044–15045.

(6) Mohr, J. T.; Behenna, D. C.; Harned, A. M.; Stoltz, B. M. Deracemization of Quaternary Stereocenters by Pd-Catalyzed Enantioconvergent Decarboxylative Allylation of Racemic β-Ketoesters. *Angew. Chem. Int. Ed.* **2005**, *44*, 6924–6927.

(7) (a) Mohr, J. T.; Nishimata, T.; Behenna, D. C.; Stoltz, B. M. Catalytic Enantioselective Decarboxylative Protonation. *J. Am. Chem. Soc.* **2006**, *128*, 11348–11349. (b) Marinescu, S. C.; Nishimata, T.; Mohr, J. T.; Stoltz, B. M. Homogeneous Pd-Catalyzed Enantioselective Decarboxylative Protonation. *Org. Lett.* **2008**, *10*, 1039–1042.

(8) Streuff, J.; White, D. E.; Virgil, S. C.; Stoltz, B. M. A Palladium-Catalysed Enolate Alkylation Cascade for the Formation of Adjacent Quaternary and Tertiary Stereocentres. *Nature Chem* **2010**, *2*, 192–196.

(9) Inanaga, K.; Wollenburg, M.; Bachman, S.; Hafeman, N. J.; Stoltz, B. M. Catalytic Enantioselective Synthesis of Carbocyclic and Heterocyclic Spiranes via a Decarboxylative Aldol Cyclization. *Chem. Sci.* **2020**, *11*, 7390–7395.

(10) (a) Ihara, M.; Ishida, Y.; Abe, M.; Toyota, M.; Fukumoto, K.; Kametani, T. Stereocontrolled Synthesis of the CDF Part of Aconitum Alkaloids via Intramolecular Double Michael Reaction. *J. Chem. Soc., Perkin Trans. 1* **1988**, 5, 1155–1163. See also: (b) Ihara, M.; Makita, K.; Tokunaga, Y.; Fukumoto, K. Stereoselective Formation of Three Carbon-Carbon Bonds by Cascade Reaction with Enolate Anion: Synthesis of Tricyclo[6.2.2.$0^{1,6}$]Dodecane and Tricyclo[5.3.1.$0^{3,8}$]Undecane Derivatives. *J. Org. Chem.* **1994**, *59*, 6008–6013. (c) Ihara, M.; Toyota, M.; Fukumoto, K.; Kametani, T. Intramolecular Double Michael Reaction. Part II. Synthesis of Isoatisirene Type Compound. *Tetrahedron Lett.* **1984**, *25*, 3235–3238. (d) Ihara, M.; Suzuki, M.; Fukumoto, K.; Kabuto, C. Asymmetric Total Synthesis of Atisine via Intramolecular Double Michael Reaction. *J. Am. Chem. Soc.* **1990**, *112*, 1164–1171.

(11) All quantum mechanics calculations were carried out with the ORCA program. Neese, F. Software Update: The ORCA Program System—Version 5.0. *WIREs Computational Molecular Science* **2022**, *12*, e1606.

(12) Sherden, N. H.; Behenna, D. C.; Virgil, S. C.; Stoltz, B. M. Unusual Allylpalladium Carboxylate Complexes: Identification of the Resting State of Catalytic Enantioselective Decarboxylative Allylic Alkylation Reactions of Ketones. *Angew. Chem. Int. Ed.* **2009**, *48*, 6840–6843.

(13) Paton, R. S.; Kim, S.; Ross, A. G.; Danishefsky, S. J.; Houk, K. N. Experimental Diels–Alder Reactivities of Cycloalkenones and Cyclic Dienes Explained through

Transition-State Distortion Energies. *Angew. Chem. Int. Ed.* **2011**, *50*, 10366–10368.

(14) Error bars are present for **10f** to **11f**/**19f** – they are smaller than the marker size in the figure.

(15) Bennett, N. B.; Duquette, D. C.; Kim, J.; Liu, W.-B.; Marziale, A. N.; Behenna, D. C.; Virgil, S. C.; Stoltz, B. M. Expanding Insight into Asymmetric Palladium-Catalyzed Allylic Alkylation of N-Heterocyclic Molecules and Cyclic Ketones. *Chem. Eur. J.* **2013**, *19*, 4414–4418.

(16) Unfortunately, attempts to further disfavor **TS3** by ortho-substitution of the PHOX ligand phenyl groups thwarted reactivity.

(17) (a) Knizia, G. Intrinsic Atomic Orbitals: An Unbiased Bridge between Quantum Theory and Chemical Concepts. *J. Chem. Theory Comput.* **2013**, *9*, 4834–4843. (b) Knizia, G.; Klein, J. E. M. N. Electron Flow in Reaction Mechanisms—Revealed from First Principles. *Angew. Chem. Int. Ed.* **2015**, *54*, 5518–5522.

(18) (a) Trost, B. M. When Is a Proton Not a Proton? *Chem. Eur. J.* **1998**, *4*, 2405–2412. See also: (b) Xu, L.; Hilton, M. J.; Zhang, X.; Norrby, P.-O.; Wu, Y.-D.; Sigman, M. S.; Wiest, O. Mechanism, Reactivity, and Selectivity in Palladium-Catalyzed Redox-Relay Heck Arylations of Alkenyl Alcohols. *J. Am. Chem. Soc.* **2014**, *136*, 1960–1967.

(19) Note that on smaller scales (0.02 mmol) the ratio of ***D*-11f** to ***D*-19f** is 6.7:1 – in accord with a primary KIE. We hypothesize this may arise from the highly

temperature-dependent nature of the product distribution paired with less homogenous reaction solution temperature on larger scales.

(20) McLean, E. B.; Mooney, D. T.; Burns, D. J.; Lee, A.-L. Direct Hydrodecarboxylation of Aliphatic Carboxylic Acids: Metal- and Light-Free. *Org. Lett.* **2022**, *24* 686–691.

(21) Nishiyama, Y.; Han-ya, Y.; Yokoshima, S.; Fukuyama, T. Total Synthesis of (–)-Lepenine. *J. Am. Chem. Soc.* **2014**, *136*, 6598–6601.

(22) Kim, K. E.; Sakazaki, Y.; Stoltz, B. M. Synthesis of Non-Natural Cyanthiwigin–Gagunin Hybrids through Late-Stage Diversification of the Cyanthiwigin Natural Product Core. *Tetrahedron* **2020**, *76*, 130755.

(23) Yang, T.-F.; Chang, C.-Y.; Lin, W.-F. Rearrangement of Acyclic-Alkyl [3.2.1]Bicyclic Alcohols to Free Methylene Dimethyl Alkyl [2.2.2]Bicyclic Octanes: Application to Preparation of Stereospecific Novel Sesquiterpene and Terpenoids. *Tetrahedron Letters* **2015**, *56*, 801–804.

(24) Song, L.; Zhu, G.; Liu, Y.; Liu, B.; Qin, S. Total Synthesis of Atisane-Type Diterpenoids: Application of Diels–Alder Cycloadditions of Podocarpane-Type Unmasked *Ortho*- Benzoquinones. *J. Am. Chem. Soc.* **2015**, *137*, 13706–13714.

(25) Neufeldt, S. R.; Sanford, M. S. O-Acetyl Oximes as Transformable Directing Groups for Pd-Catalyzed C–H Bond Functionalization. *Org. Lett.* **2010**, *12*, 532–535.

(26) Pangborn, A. M.; Giardello, M. A.; Grubbs, R. H.; Rosen, R. K.; Timmers, F. J. Safe and Convenient Procedure for Solvent Purification. *Organometallics* **1996**, *15*, 1518–1520.

(27) McDougal, N. T.; Streuff, J.; Mukherjee, H.; Virgil, S. C.; Stoltz, B. M. Rapid synthesis of an electron-deficient *t*-BuPHOX ligand: cross-coupling of aryl bromides with secondary phosphine oxides. *Tetrahedron Lett*. **2010**, *51*, 5550–5554.

(28) Ando, K.; Narumiya, K.; Takada, H.; Teruya, T. Z-Selective Intramolecular Horner−Wadsworth−Emmons Reaction for the Synthesis of Macrocyclic Lactones. *Org. Lett.* **2010**, *12*, 1460–1463.

(29) Shelkov, R.; Nahmany, M.; Melman, A. Selective Esterifications of Alcohols and Phenols through Carbodiimide Couplings. *Org. Biomol. Chem.* **2004**, *2*, 397–401.

(30) Taguchi, T.; Sasaki, H.; Shibuya, A.; Morikawa, T. Regio- and Stereoselective Synthesis of Gem-Difluorocyclopropanes Using 4-Bromo-4,4-Difluorocrotonate. *Tetrahedron Lett.* **1994**, *35*, 913–916.

(31) Fornicola, R. S.; Subburaj, K.; Montgomery, J. A New Entry to the Isogeissoschizoid Skeleton. *Org. Lett.* **2002**, *4*, 615–617.

(32) Fillion, E.; Dumas, A. M. Synthesis of Fused 4,5-Disubstituted Indole Ring Systems by Intramolecular Friedel−Crafts Acylation of 4-Substituted Indoles. *J. Org. Chem.* **2008**, *73*, 2920–2923.

(33) Brandt, D.; Dittoo, A.; Bellosta, V.; Cossy, J. Synthetic Approach to Wortmannilactone C. *Org. Lett.* **2015**, *17*, 816–819.

(34) Fulton, T. J.; Cusumano, A. Q.; Alexy, E. J.; Du, Y. E.; Zhang, H.; Houk, K. N.; Stoltz, B. M. Global Diastereoconvergence in the Ireland–Claisen Rearrangement of Isomeric Enolates: Synthesis of Tetrasubstituted α-Amino Acids. *J. Am. Chem. Soc.* **2020**, *142*, 21938–21947.

(35) Touchard, F. P.; Capelle, N.; Mercier, M. Efficient and Scalable Protocol for the Z-Selective Synthesis of Unsaturated Esters by Horner–Wadsworth–Emmons Olefination. *Adv. Synth. Catal.* **2005**, *347*, 707–711.

(36) Romano, C.; Fiorito, D.; Mazet, C. Remote Functionalization of α,β-Unsaturated Carbonyls by Multimetallic Sequential Catalysis. *J. Am. Chem. Soc.* **2019**, *141*, 16983–16990.

(37) Sureshbabu, R.; Saravanan, V.; Dhayalan, V.; Mohanakrishnan, A. K. Lewis Acid Mediated One-Pot Synthesis of Aryl/Heteroaryl-Fused Carbazoles Involving a Cascade Friedel–Crafts Alkylation/Electrocyclization/Aromatization Reaction Sequence. *Eur. J. Org. Chem.* **2011**, 922–935.

(38) Mukaiyama, T.; Matsuo, J.; Yanagisawa, M. A New and Efficient Method for Oxidation of Various Alcohols by Using N-Tert-Butyl Phenylsulfinimidoyl Chloride. *Chem. Lett.* **2000**, *29*, 1072–1073.

(39) Inanaga, K.; Wollenburg, M.; Bachman, S.; Hafeman, N. J.; Stoltz, B. M. Catalytic Enantioselective Synthesis of Carbocyclic and Heterocyclic Spiranes via a Decarboxylative Aldol Cyclization. *Chem. Sci.* **2020**, *11*, 7390–7395.

(40) Mohr, J. T.; Behenna, D. C.; Harned, A. M.; Stoltz, B. M. Deracemization of Quaternary Stereocenters by Pd-Catalyzed Enantioconvergent Decarboxylative Allylation of Racemic β-Ketoesters. *Angew. Chem. Int. Ed.* **2005**, *44*, 6924–6927.

(41) Hierold, J.; Lupton, D. W. Synthesis of Spirocyclic γ-Lactones by Cascade Beckwith–Dowd Ring Expansion/Cyclization. *Org. Lett.* **2012**, *14*, 3412–3415.

(42) Trost, B. M.; Xu, J. The O-Acylation of Ketone Enolates by Allyl 1H-Imidazole-1-Carboxylate Mediated with Boron Trifluoride Etherate: A Convenient Procedure for the Synthesis of Substituted Allyl Enol Carbonates. *J. Org. Chem.* **2007**, *72*, 9372–9375.

(43) Prepared following ref. 42 with 3-(methyl-d_3)but-2-en-4,4,4-d_3-1-ol (Mosaferi, S.; Jelley, R. E.; Fedrizzi, B.; Barker, D. Scalable Synthesis of the Aroma Compounds D6-β-Ionone and D6-β-Cyclocitral for Use as Internal Standards in Stable Isotope Dilution Assays. *Tetrahedron Lett.* **2020**, *61*, 152642.

(44) Shimizu, I.; Tsuji, J. Palladium-Catalyzed Decarboxylation-Dehydrogenation of Allyl β-Oxo Carboxylates and Allyl Enol Carbonates as a Novel Synthetic Method for α-Substituted α,β-Unsaturated Ketones. *J. Am. Chem. Soc.* **1982**, *104*, 5844–5846.

(45) Knapp, S.; Yang, C.; Pabbaraja, S.; Rempel, B.; Reid, S.; Withers, S. G. Synthesis and Kinetic Analysis of the N-Acetylhexosaminidase Inhibitor XylNAc-Isofagomine. *J. Org. Chem.* **2005**, *70*, 7715–7720.

(46) Szczesńiak, P.; Pieczykolan, M.; Steck, S. The Synthesis of α,α-Disubstituted α-Amino Acids via Ichikawa Rearrangement. *J. Org. Chem.* **2016**, *81*, 1057–1074.

(47) Srikrishna, A.; Kumar, P.P. Claisen Rearrangement Based Methodology for the Spiroannulation of a Cyclopentane Ring. Formal Total Synthesis of (±)-Acorone and Isoacorones. *Tetrahedron* **2000**, *56*, 8189–8195.

(48) Yang, J.; Lu, K.; Li, C.; Zhao, Z.; Zhang, X.; Zhang, F.; Tu, Y. Chiral 1,2,3-Triazolium Salt Catalyzed Asymmetric Mono- and Dialkylation of 2,5-Diketopiperazines with the Construction of Tetrasubstituted Carbon Centers. *Angew. Chem. Int. Ed.* **2022**, *61*, e202114129.

(49) Hou, H.; Xu, Y.; Yang, H.; Chen, X.; Yan, C.; Shi, Y.; Zhu, S. Visible-Light Mediated Hydrosilylative and Hydrophosphorylative Cyclizations of Enynes and Dienes. *Org. Lett.* **2020**, *22*, 1748-1753.

(50) **Schrödinger Release 2021-4:** MacroModel, Schrödinger, LLC, New York, NY, 2021.

(51) Bochevarov, A.D.; Harder, E.; Hughes, T.F.; Greenwood, J.R.; Braden, D.A.; Philipp, D.M.; Rinaldo, D.; Halls, M.D.; Zhang, J.; Friesner, R.A., Jaguar: A high-performance quantum chemistry software program with strengths in life and materials sciences, *Int. J. Quantum Chem.*, **2013**, *113*, 2110-2142.

(52) (a) Neese, F. Software Update: The ORCA Program System, Version 4.0. *Wiley Interdiscip. Rev.: Comput. Mol. Sci.* **2018,** *8*, No. e1327. (b) Neese, F. The ORCA Program System. *Wiley Interdiscip. Rev.: Comput. Mol. Sci.* **2012**, *2*, 73−78.

(53) Adamo, C.; Barone, V. Toward Reliable Density Functional Methods without Adjustable Parameters: The PBE0 Model. *J. Chem. Phys.* **1999**, *110*, 6158−6170.

(54) (a) Caldeweyher, E.; Ehlert, S.; Hansen, A.; Neugebauer, H.; Spicher, S.; Bannwarth, C.; Grimme, S. A Generally Applicable Atomic-Charge Dependent London Dispersion Correction. *J. Chem. Phys.* **2019**, *150*, 154122. (b) Caldeweyher, E.; Bannwarth, C.; Grimme, S. Extension of the D3 Dispersion Coefficient Model. *J. Chem. Phys.* **2017**, *147*, 034112.

(55) Cusumano, A. Q.; Goddard, W. A. I.; Stoltz, B. M. The Transition Metal Catalyzed [σ2s + σ2s + π2s + π2s] Pericyclic Reaction: Woodward–Hoffmann Rules, Aromaticity, and Electron Flow. *J. Am. Chem. Soc.* **2020**, *142*, 19033–19039.

(56) Weigend, F.; Ahlrichs, R. Balanced Basis Sets of Split Valence, Triple Zeta Valence and Quadruple Zeta Valence Quality for H to Rn: Design and Assessment of Accuracy. *Phys. Chem. Chem. Phys.* **2005**, *7*, 3297–3305.

(57) Peterson, K. A.; Figgen, D.; Goll, E.; Stoll, H.; Dolg, M. Systematically Convergent Basis Sets with Relativistic Pseudopotentials. II. Small-Core Pseudopotentials and Correlation Consistent Basis Sets for the Post- *d* Group 16–18 Elements. *J. Chem. Phys.* **2003**, *119*, 11113–11123.

(58) Garcia-Ratés, M.; Neese, F. Effect of the Solute Cavity on the Solvation Energy and Its Derivatives within the Framework of the Gaussian Charge Scheme. *J. Comput. Chem.* **2020**, *41*, 922–939.

(59) Ishida, K.; Morokuma, K.; Komornicki, A. The Intrinsic Reaction Coordinate. An Ab Initio Calculation for HNC→HCN and H−+CH4→CH4+H−. *J. Chem. Phys.* **1977**, *66*, 2153−2156.

(60) Zhao, Y.; Truhlar, D. G. The M06 Suite of Density Functionals for Main Group Thermochemistry, Thermochemical Kinetics, Noncovalent Interactions, Excited States, and Transition Elements: Two New Functionals and Systematic Testing of Four M06-Class Functionals and 12 Other Functionals. *Theor. Chem. Account.* **2008**, *120*, 215–241.

(61) Grimme, S. Supramolecular Binding Thermodynamics by Dispersion-Corrected Density Functional Theory. *Chem. Eur. J.* **2012**, *18*, 9955–9964.

(62) Izato, Y.; Matsugi, A.; Koshi, M.; Miyake, A. A Simple Heuristic Approach to Estimate the Thermochemistry of Condensed-Phase Molecules Based on the Polarizable Continuum Model. *Phys. Chem. Chem. Phys.* **2019**, *21*, 18920–18929.

(63) Finkelstein, A. V.; Janin, J. The Price of Lost Freedom: Entropy of Bimolecular Complex Formation. *Protein Eng. Des. Sel.* **1989**, *3*, 1–3.

(64) Neese, F.; Wennmohs, F.; Hansen, A.; Becker, U. Efficient, Approximate and Parallel Hartree-Fock and Hybrid DFT Calculations. A 'Chain-of-Spheres' Algorithm for the Hartree-Fock Exchange. *Chem. Phys.* **2009**, *356*, 98–109.

(65) Weigend, F. Accurate Coulomb-Fitting Basis Sets for H to Rn. *Phys. Chem. Chem. Phys.* **2006**, *8*, 1057–1065.

(66) Stoychev, G. L.; Auer, A. A.; Neese, F. Automatic Generation of Auxiliary Basis Sets. *J. Chem. Theory Comput.* **2017**, *13*, 554–562.

(67) (a) Pracht, P.; Grimme, S. Calculation of Absolute Molecular Entropies and Heat Capacities Made Simple. *Chem. Sci.* **2021**, *12*, 6551–6568. (b) Gorges, J.; Grimme, S.; Hansen, A.; Pracht, P. Towards Understanding Solvation Effects on the Conformational Entropy of Non-Rigid Molecules. *Phys. Chem. Chem. Phys.* **2022**, *24*, 12249–12259.

(68) (a) DeTar, D. F. Theoretical Ab Initio Calculation of Entropy, Heat Capacity, and Heat Content. *J. Phys. Chem. A* **1998**, *102*, 5128–5141. See also: (b) Guthrie, J. P. Use of DFT Methods for the Calculation of the Entropy of Gas Phase Organic Molecules: An Examination of the Quality of Results from a Simple Approach. *J. Phys. Chem. A* **2001**, *105*, 8495–8499.

APPENDIX 1

Spectra Relevant to Chapter 1: Divergent Catalysis: Catalytic Asymmetric Intramolecular [4+2] Cycloaddition of Palladium Enolates

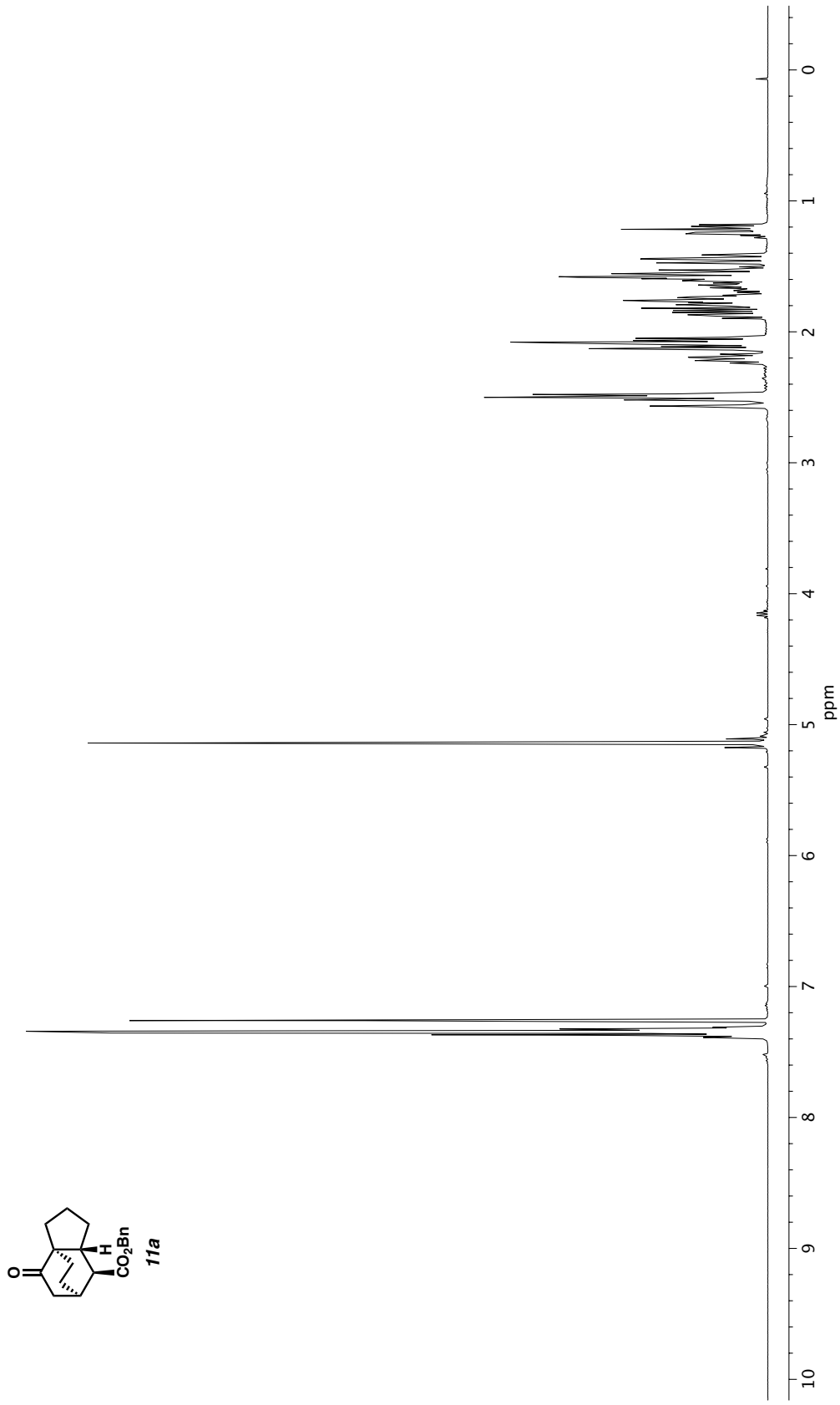


Figure A1.1. *^1H NMR (400 MHz, $CDCl_3$) of compound* ***11a****.*

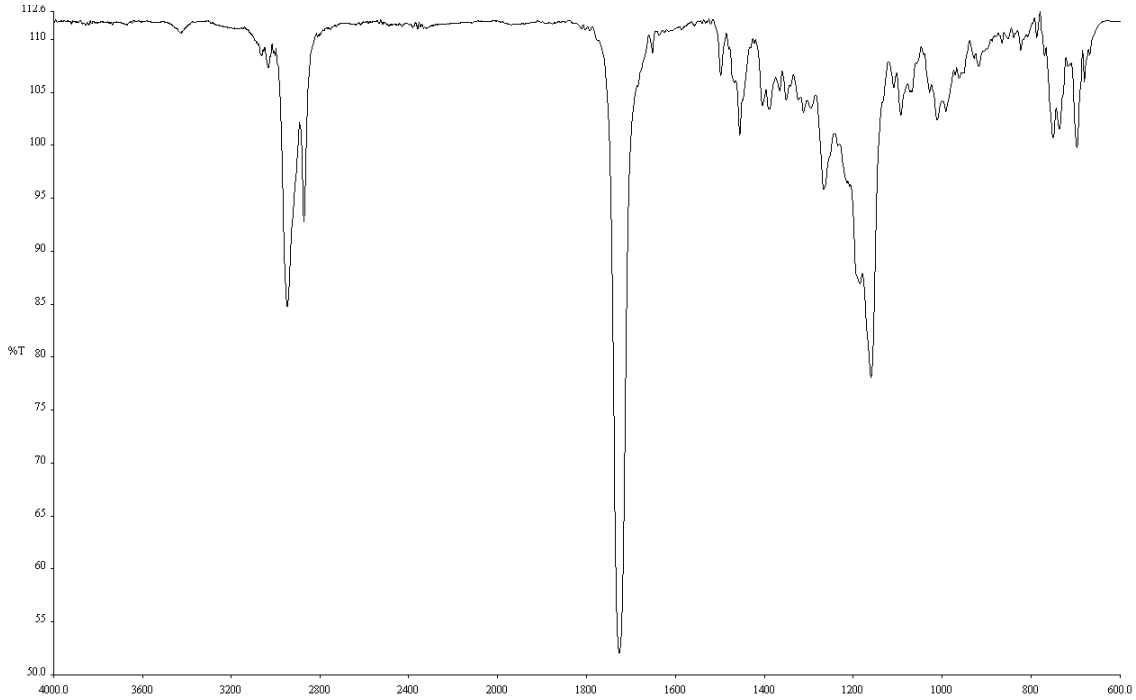


Figure A1.2. *Infrared spectrum (Thin Film, NaCl) of compound* ***11a****.*

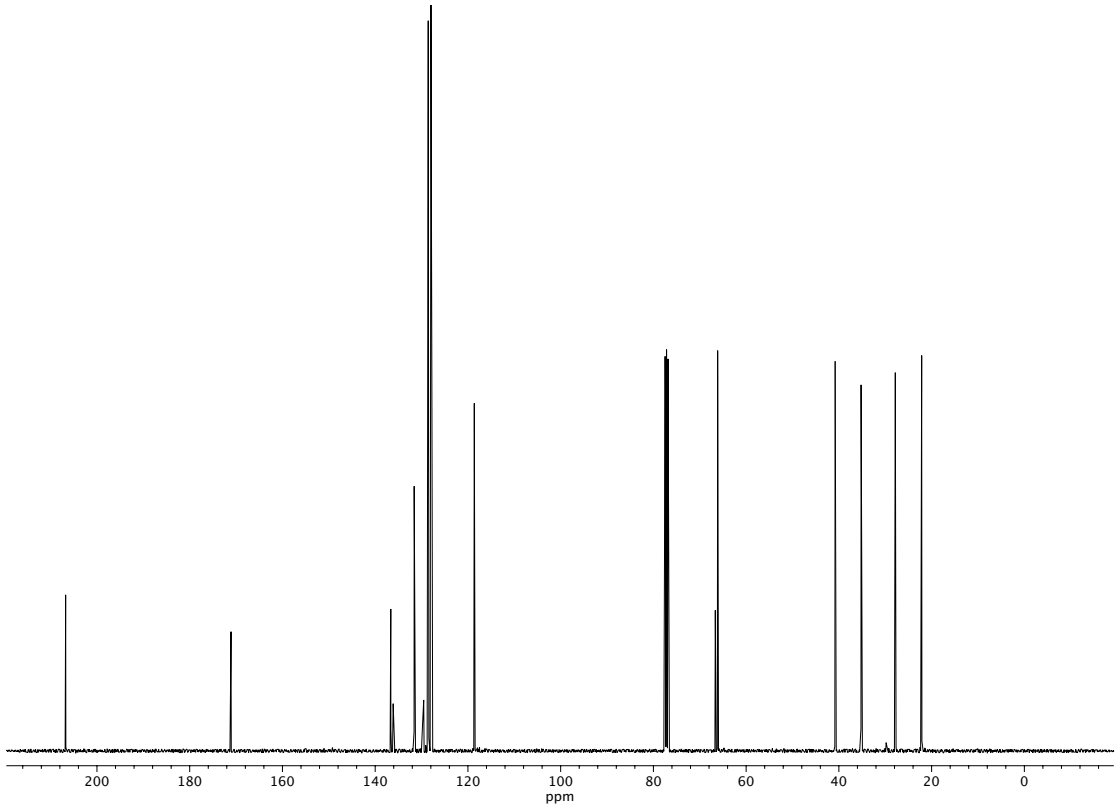
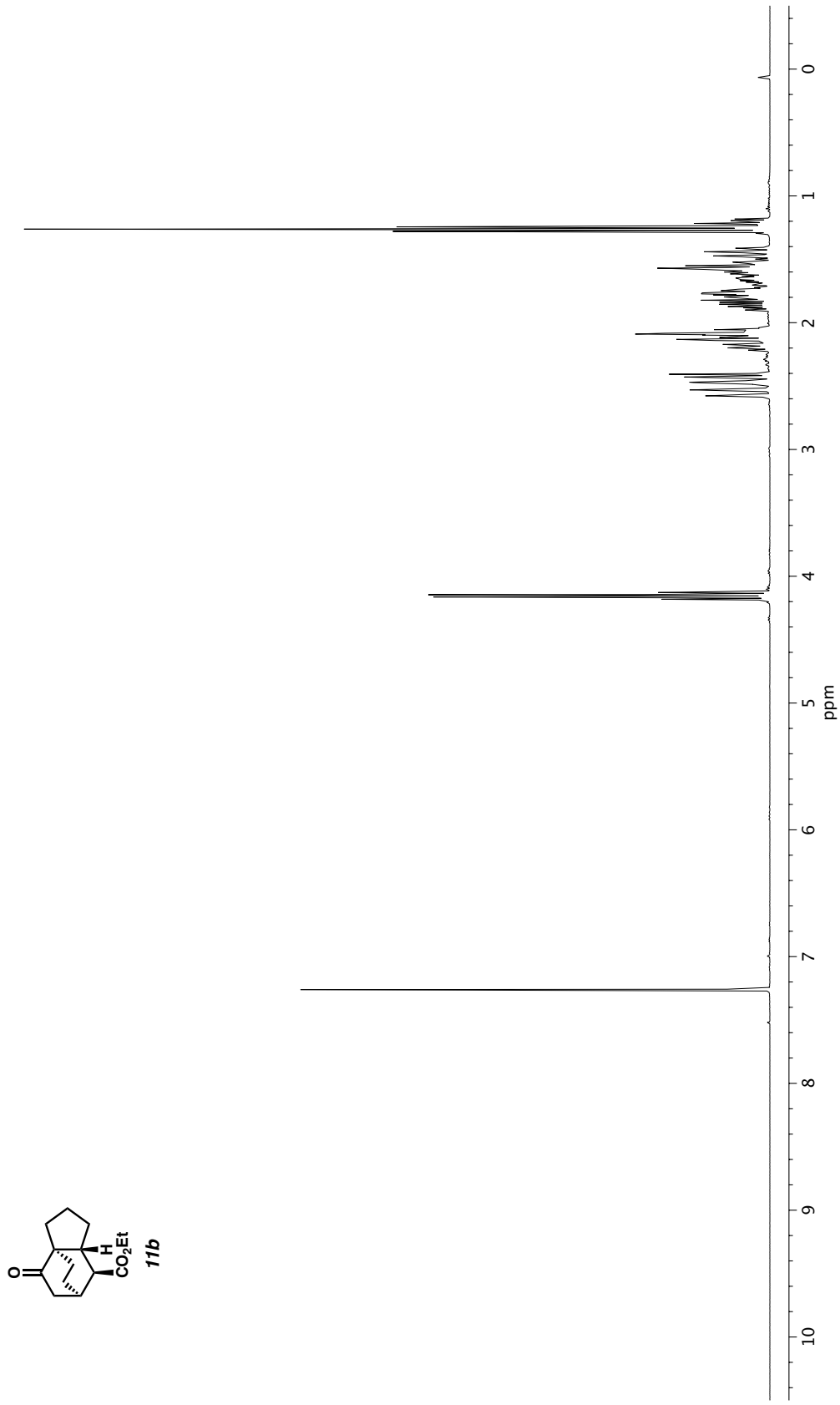


Figure A1.3. *^{13}C NMR (100 MHz, $CDCl_3$) of compound* ***11a****.*



11b

Figure A1.4. *^1H NMR (400 MHz, $CDCl_3$) of compound* ***11b***.

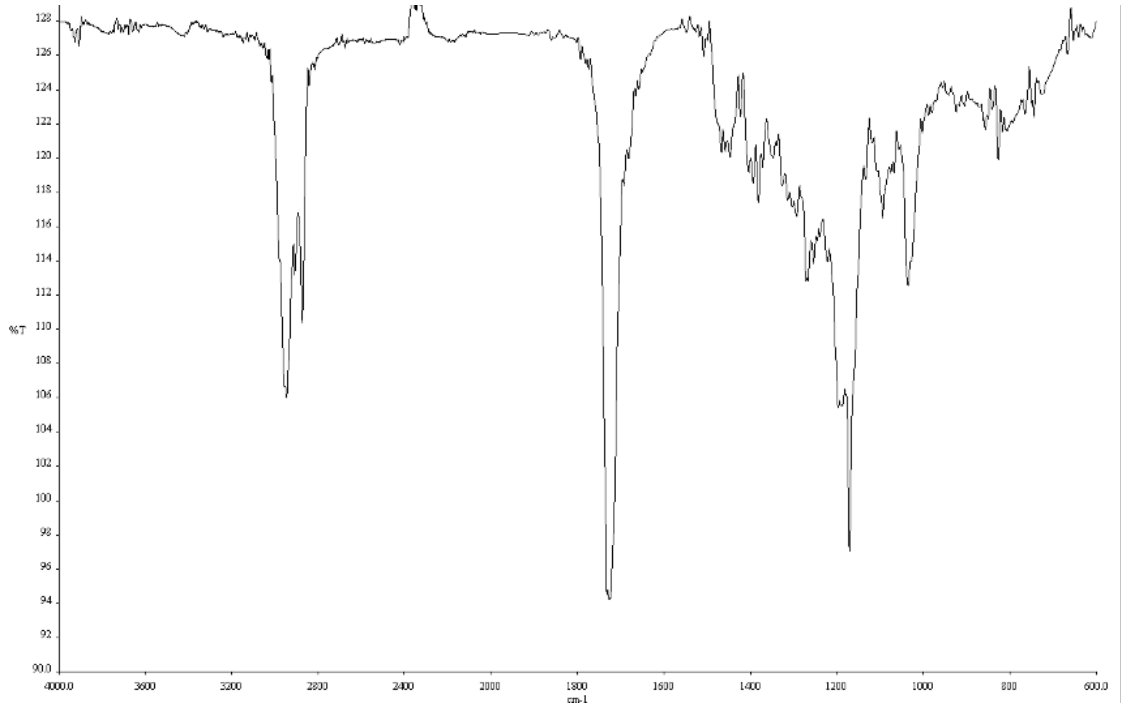


Figure A1.5. *Infrared spectrum (Thin Film, NaCl) of compound* ***11b****.*

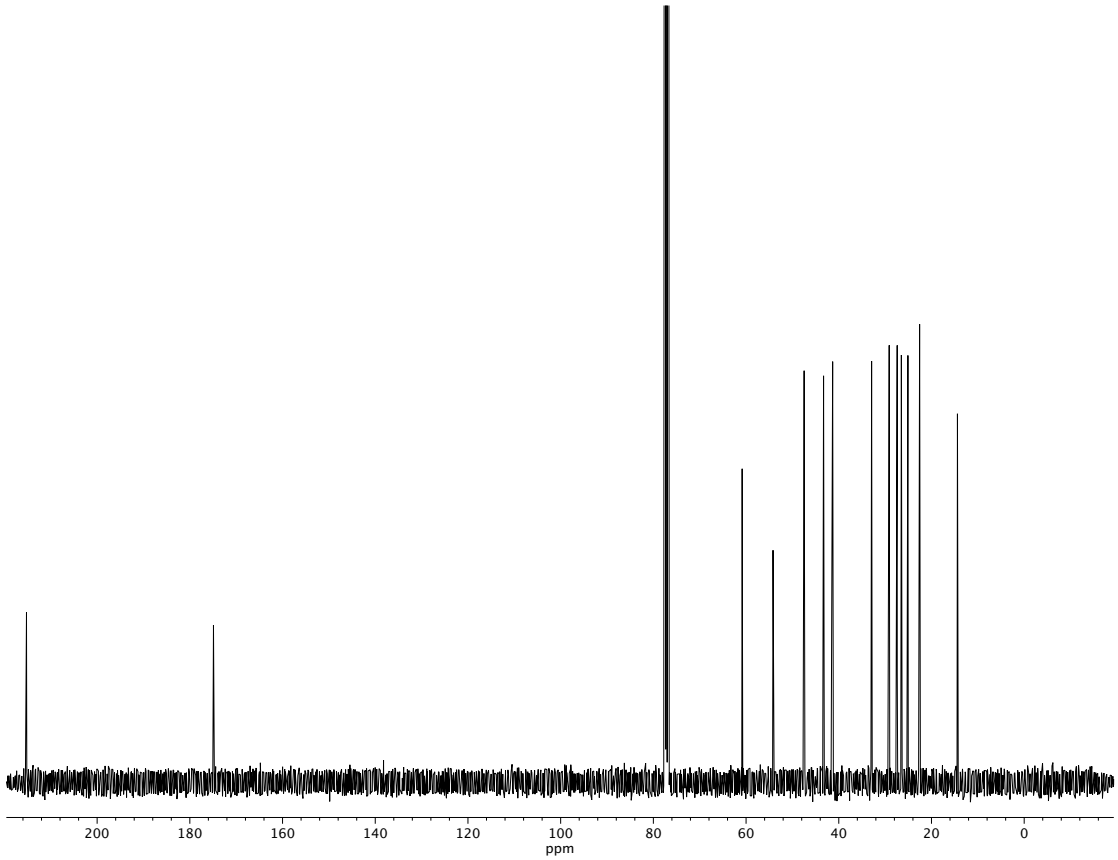


Figure A1.6. *^{13}C NMR (100 MHz, $CDCl_3$) of compound* ***11b****.*

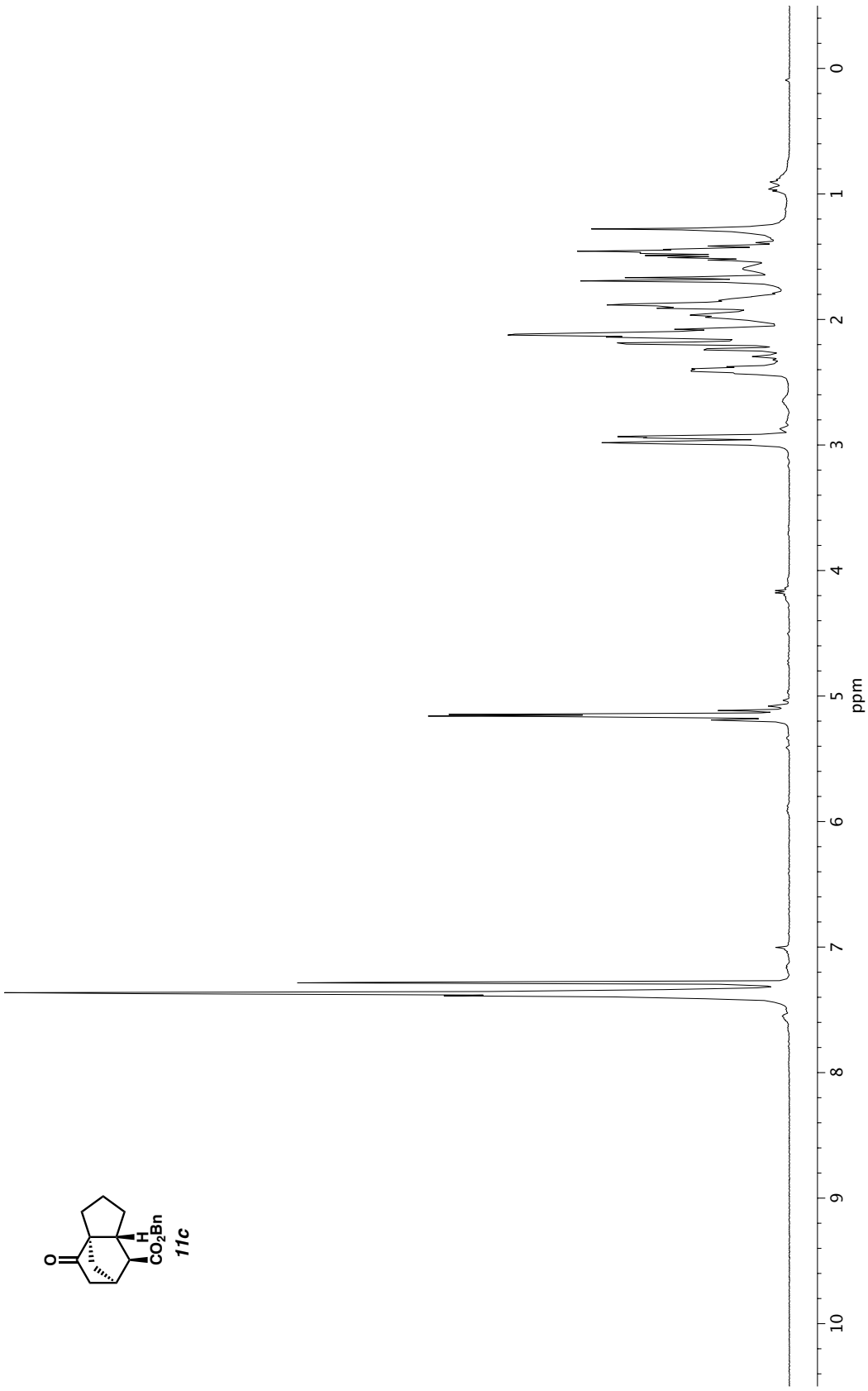


Figure A1.7. *^1H NMR (400 MHz, $CDCl_3$) of compound **11c**.*

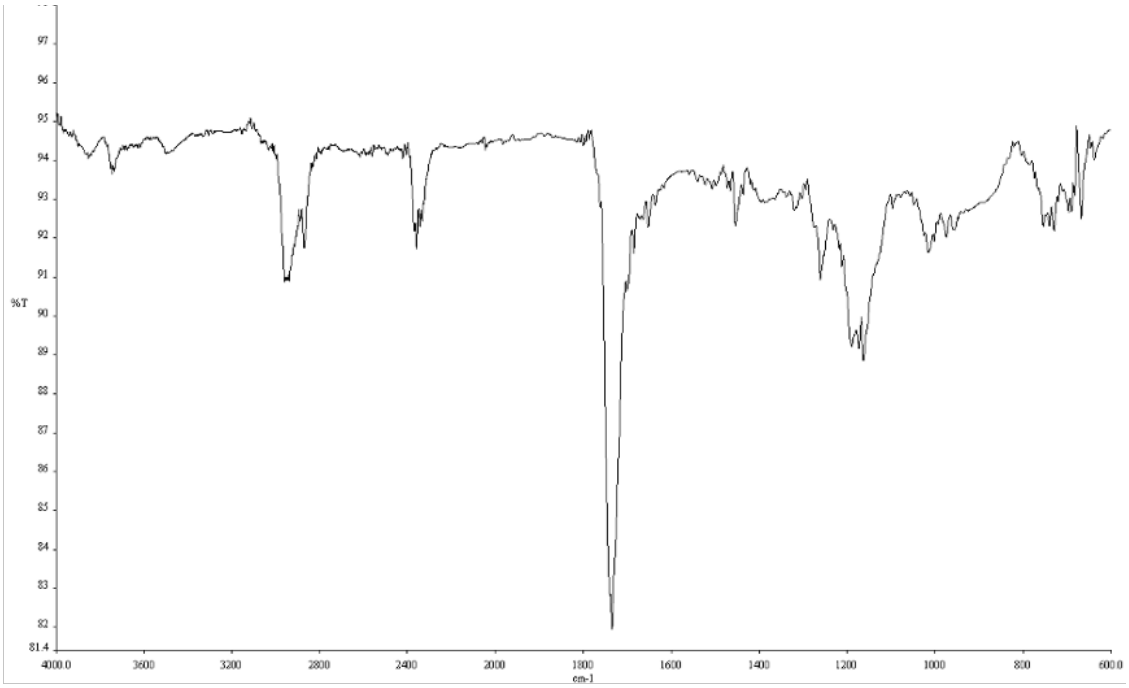


Figure A1.8. *Infrared spectrum (Thin Film, NaCl) of compound* ***11c****.*

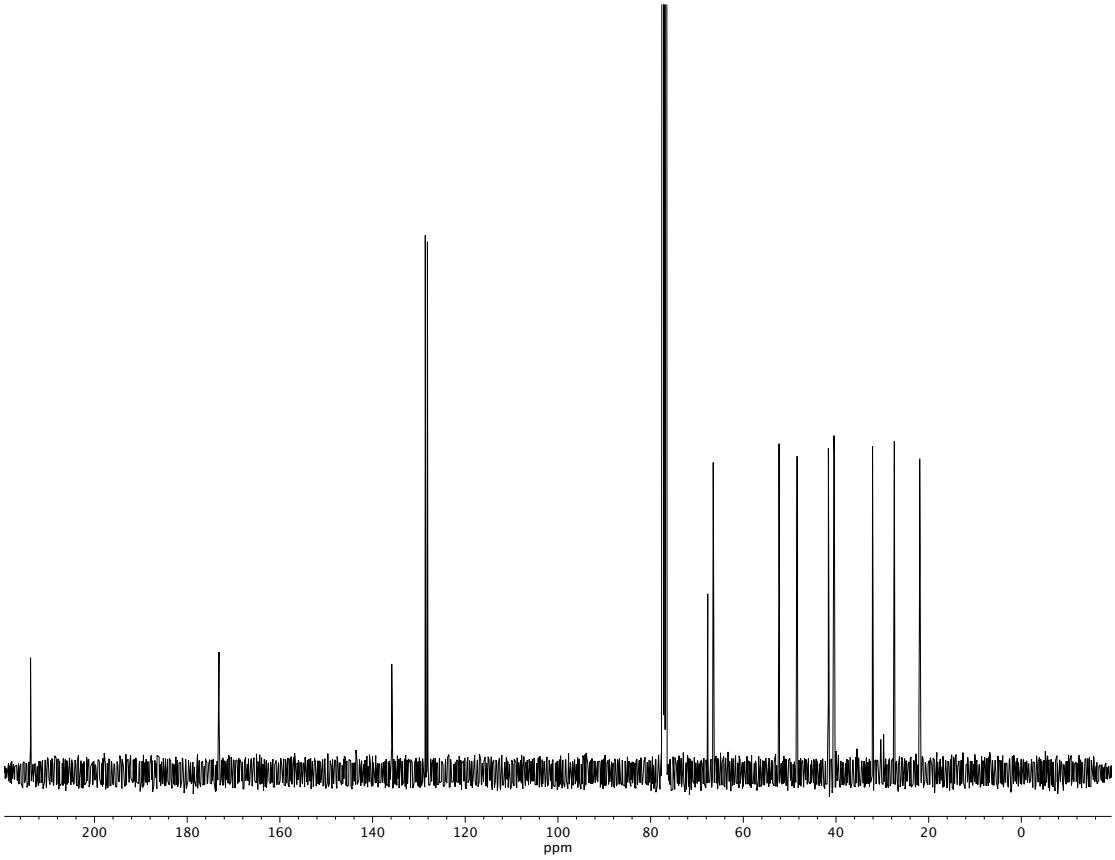


Figure A1.9. *^{13}C NMR (100 MHz, $CDCl_3$) of compound* ***11c****.*

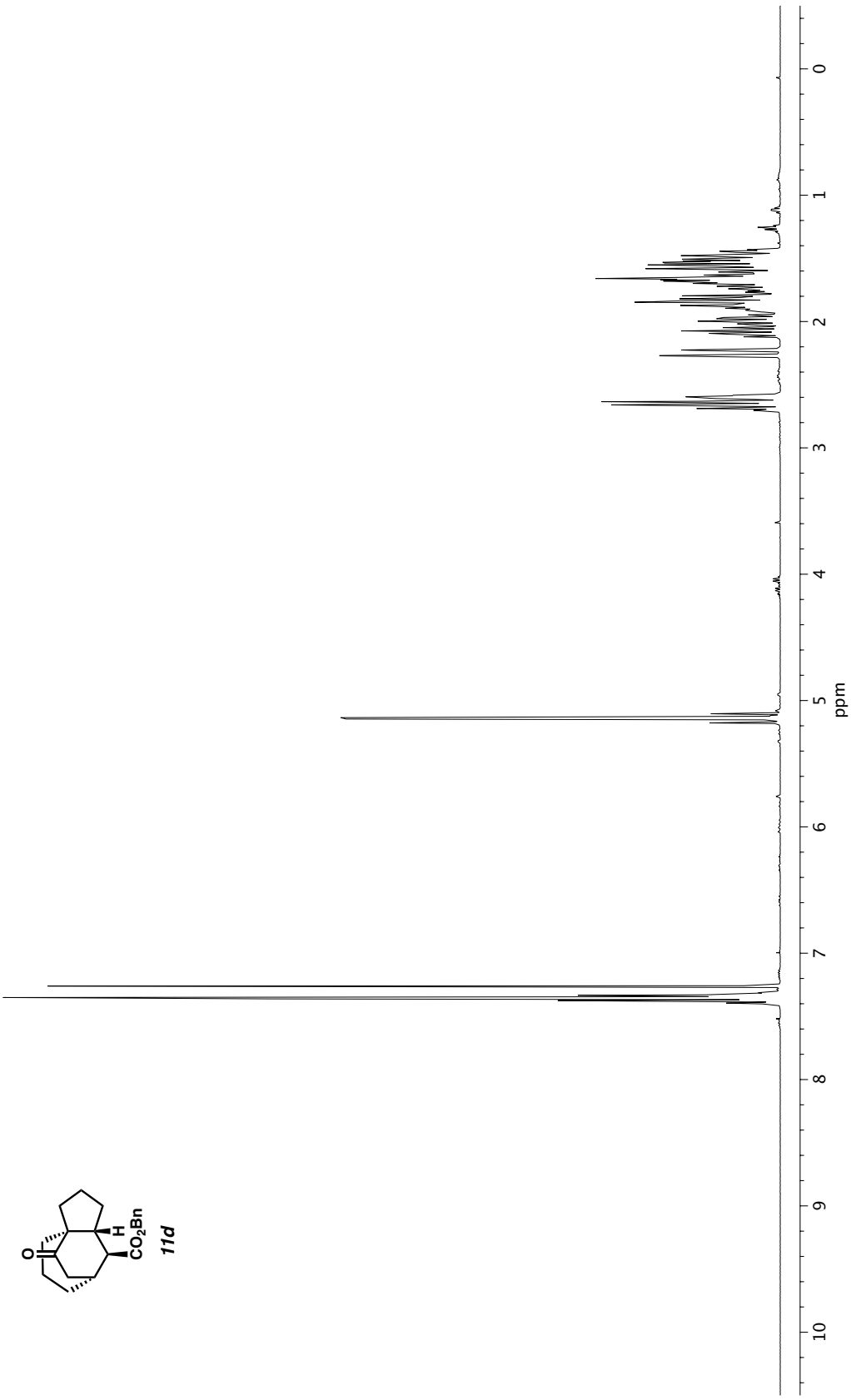


Figure A1.10. *^1H NMR (400 MHz, $CDCl_3$) of compound* ***11d****.*

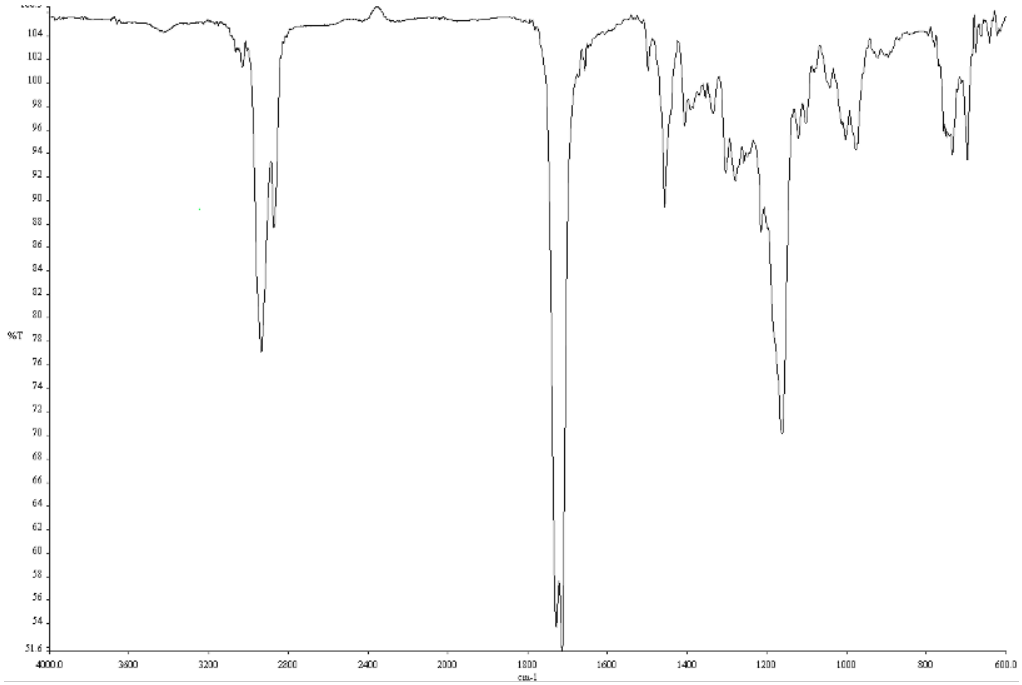


Figure A1.11. *Infrared spectrum (Thin Film, NaCl) of compound* ***11d****.*

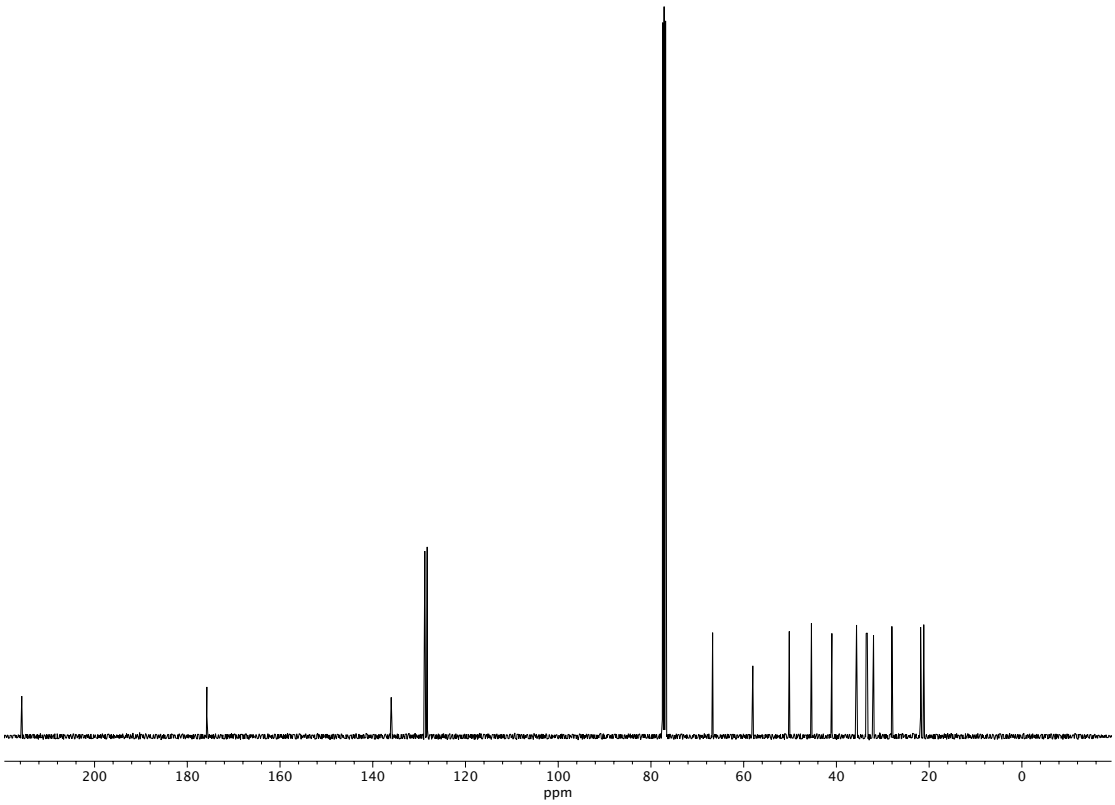


Figure A1.12. *^{13}C NMR (100 MHz, $CDCl_3$) of compound* ***11d****.*

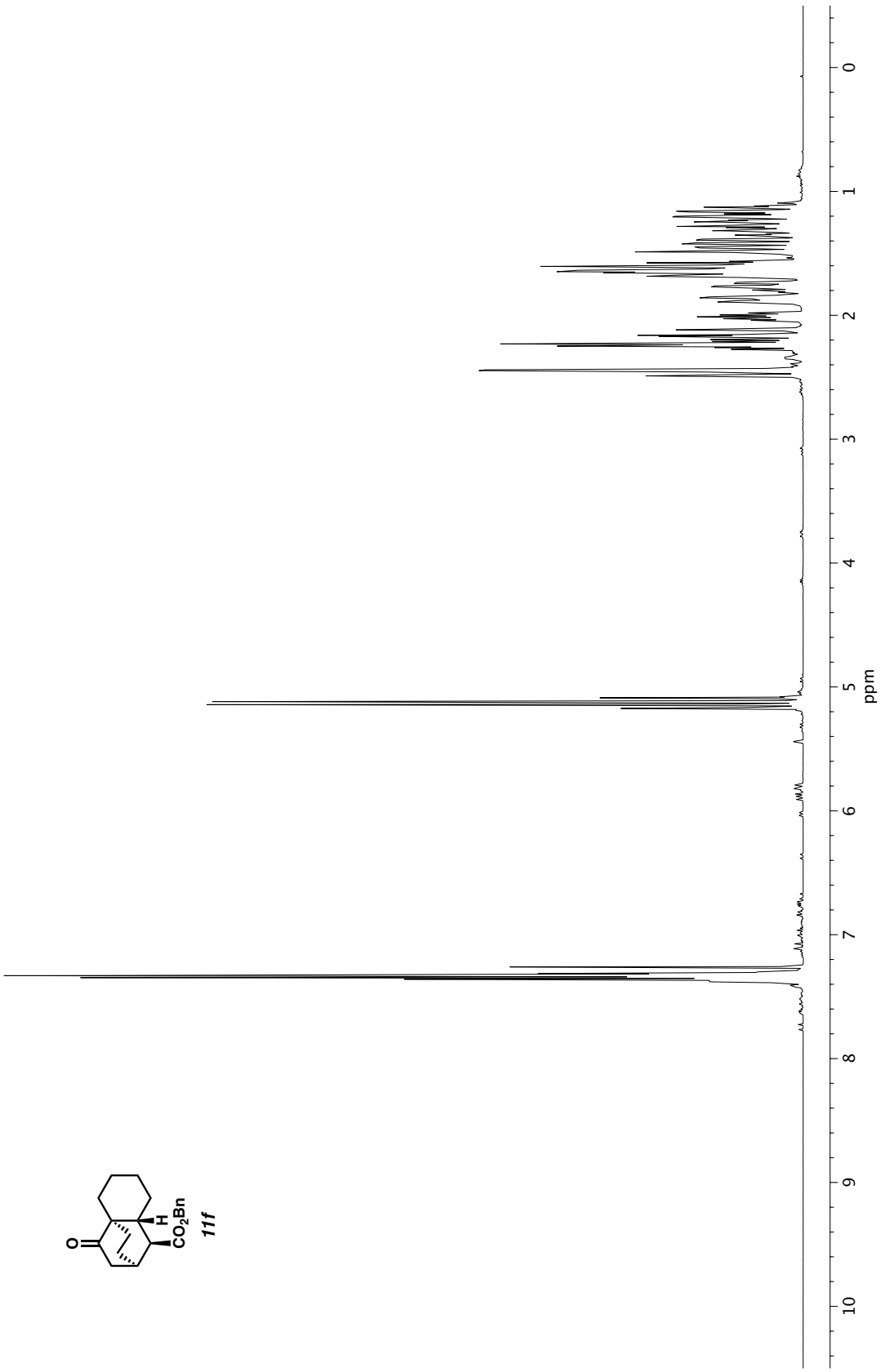


Figure A1.13. *^{1}H NMR (400 MHz, $CDCl_3$) of compound* ***11f****.*

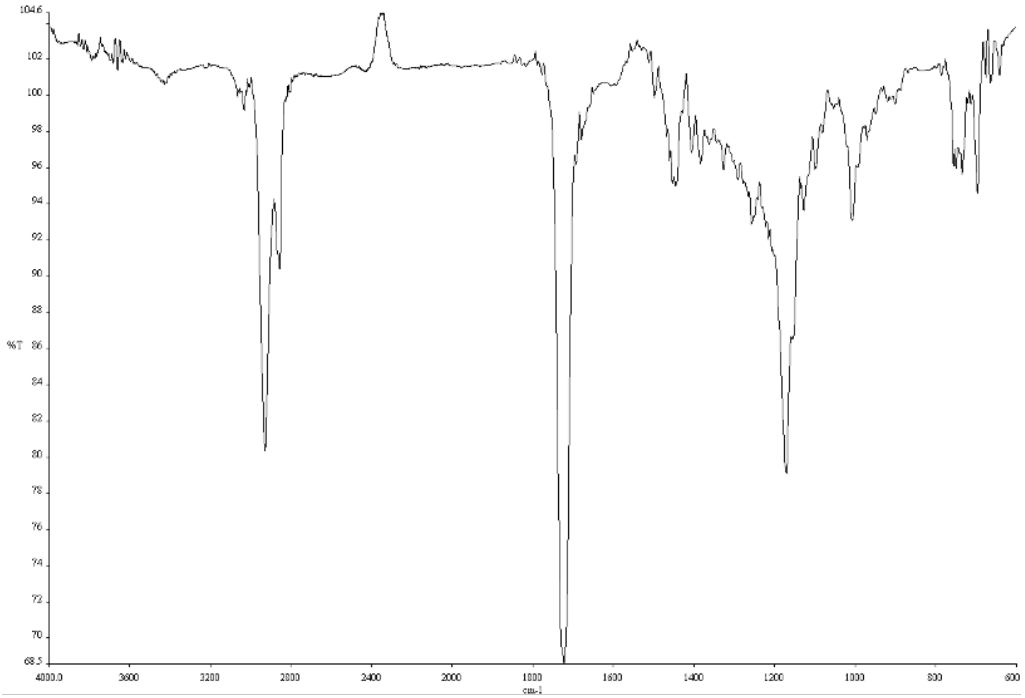


Figure A1.14. *Infrared spectrum (Thin Film, NaCl) of compound* ***11f****.*

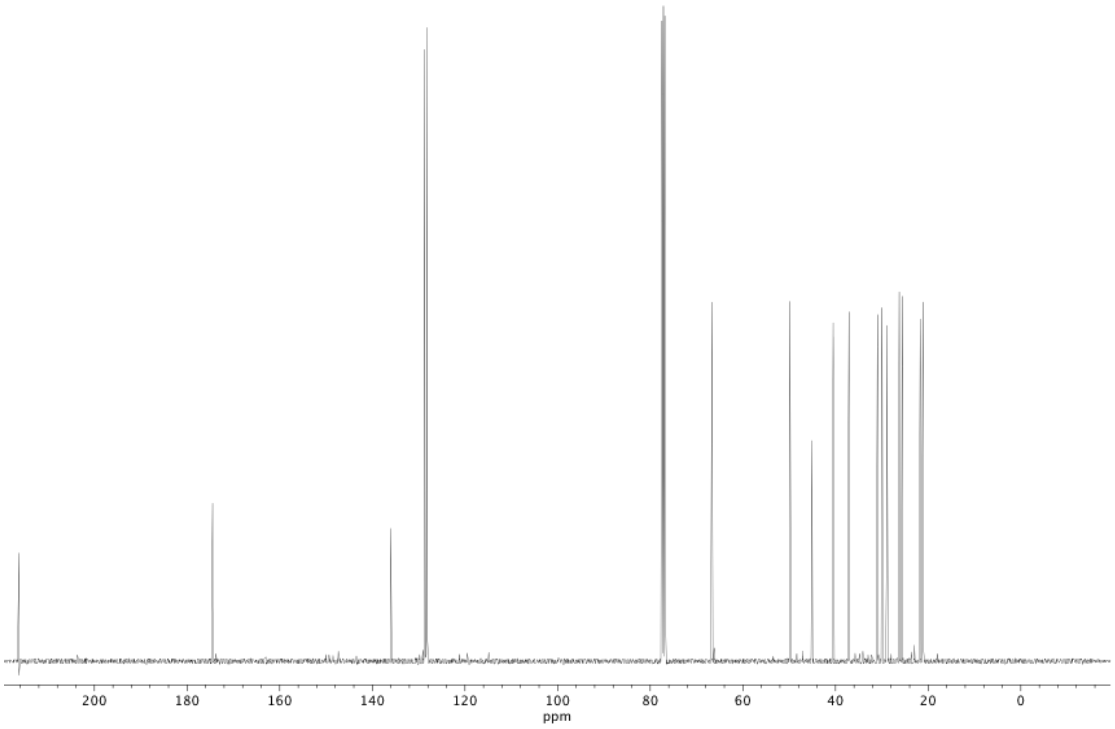


Figure A1.15. *^{13}C NMR (100 MHz, $CDCl_3$) of compound* ***11f****.*

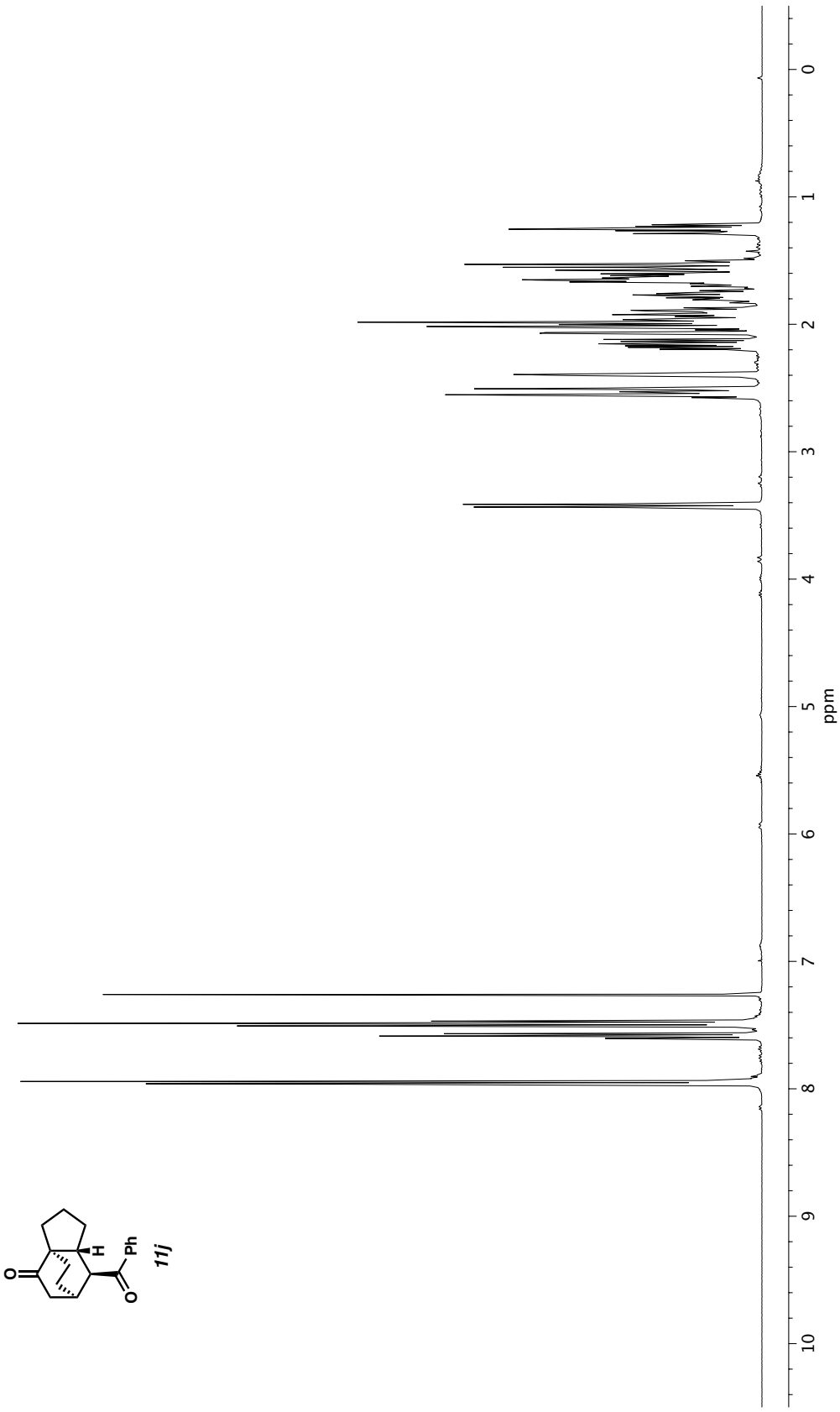


Figure A1.16. *^{1}H NMR (400 MHz, $CDCl_3$) of compound* ***11j****.*

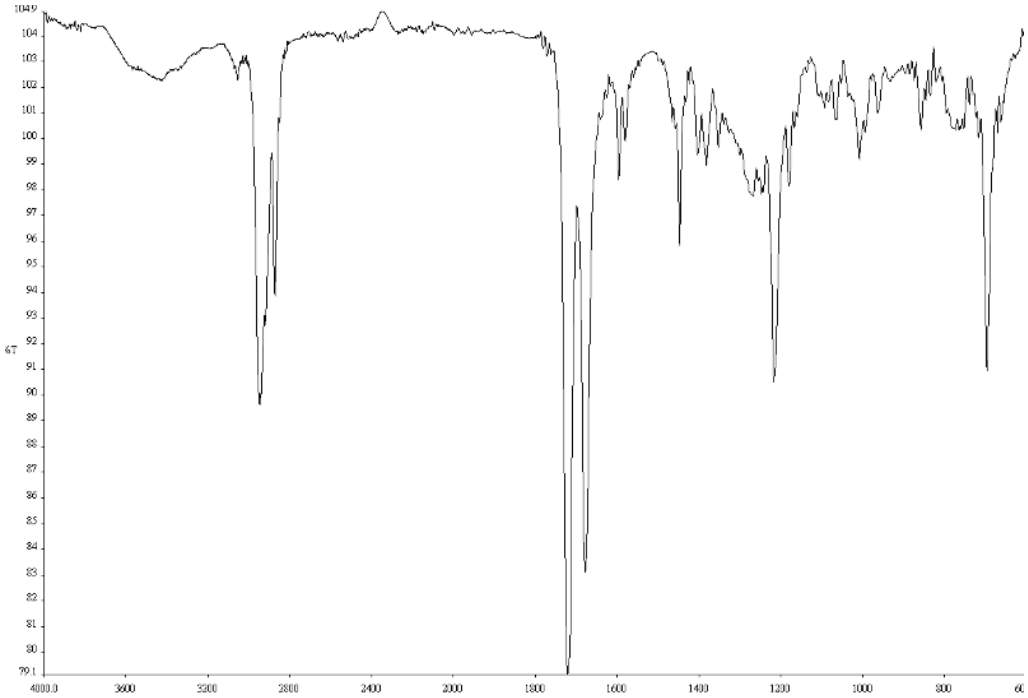


Figure A1.17. *Infrared spectrum (Thin Film, NaCl) of compound* ***11j****.*

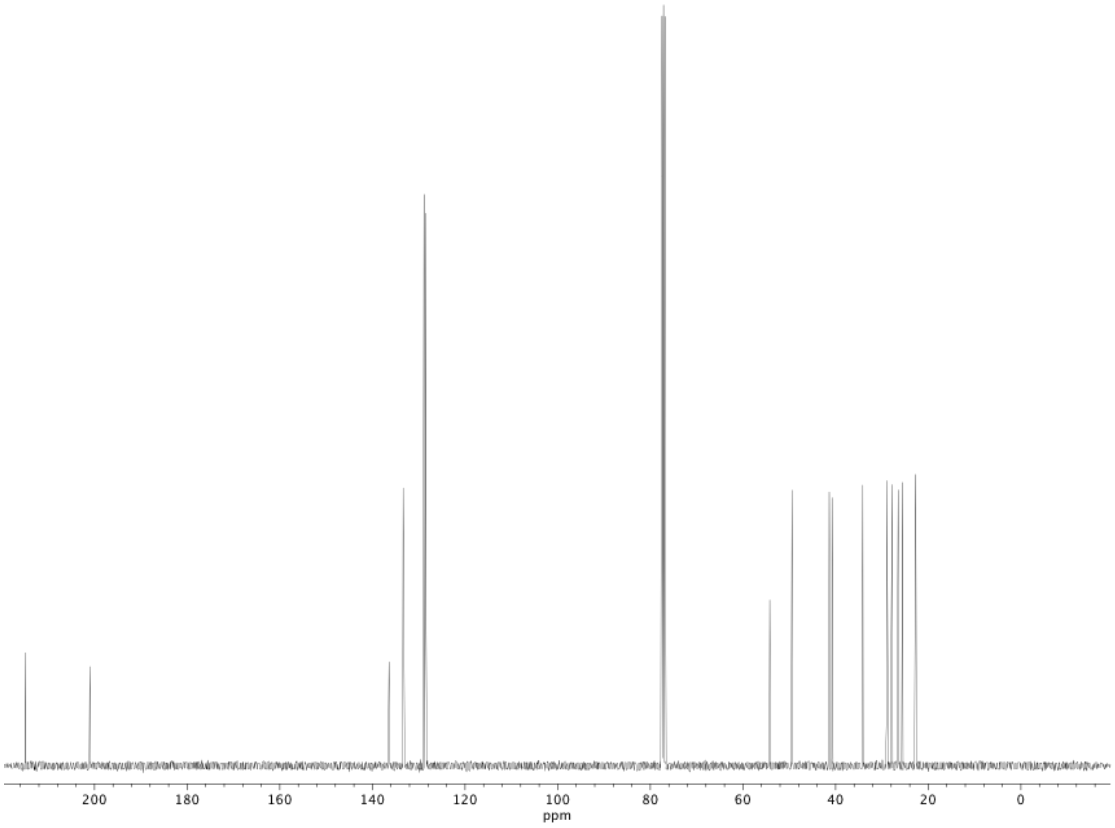


Figure A1.18. *^{13}C NMR (100 MHz, $CDCl_3$) of compound* ***11j****.*

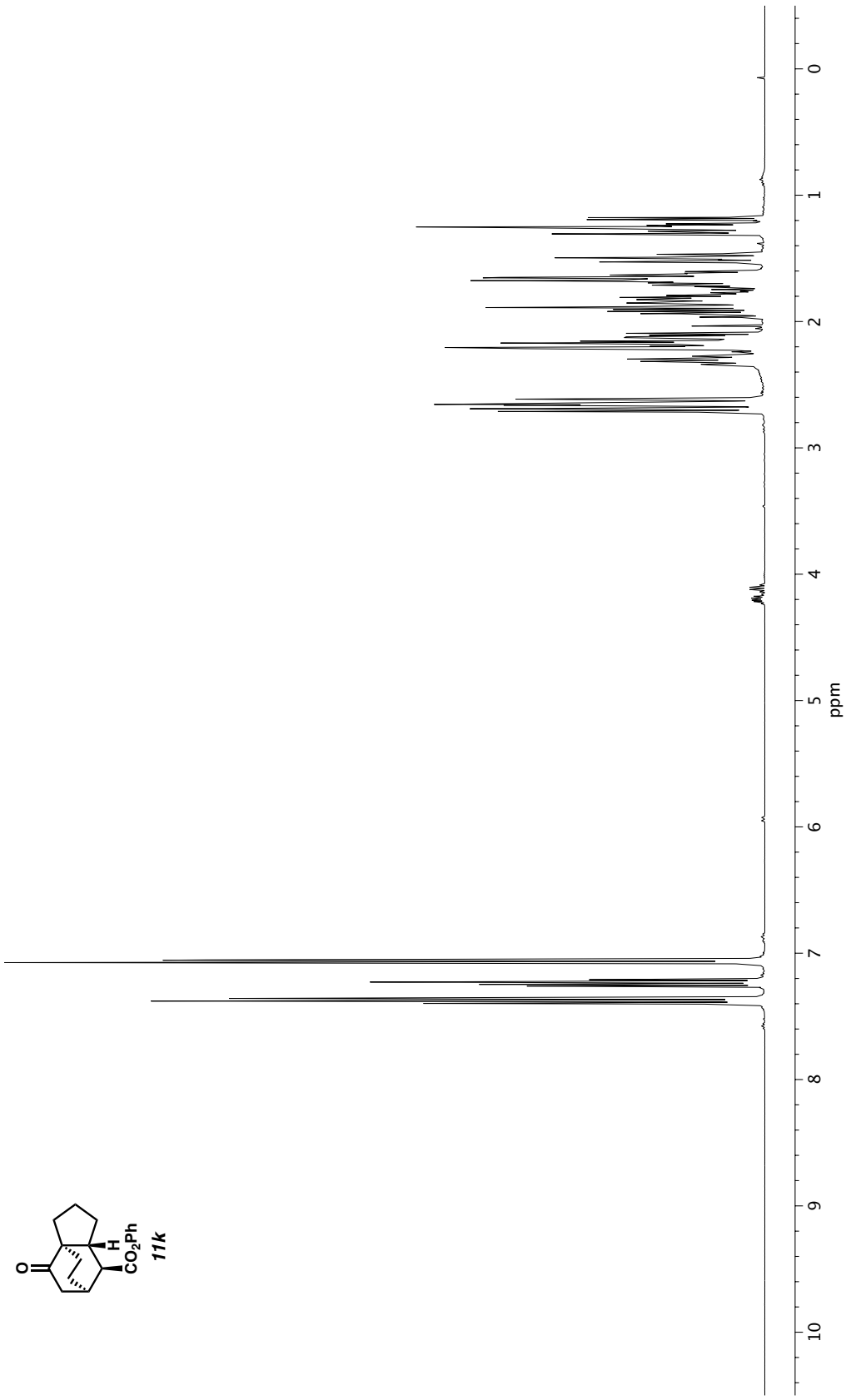


Figure A1.19. *^{1}H NMR (400 MHz, $CDCl_3$) of compound* ***11k****.*

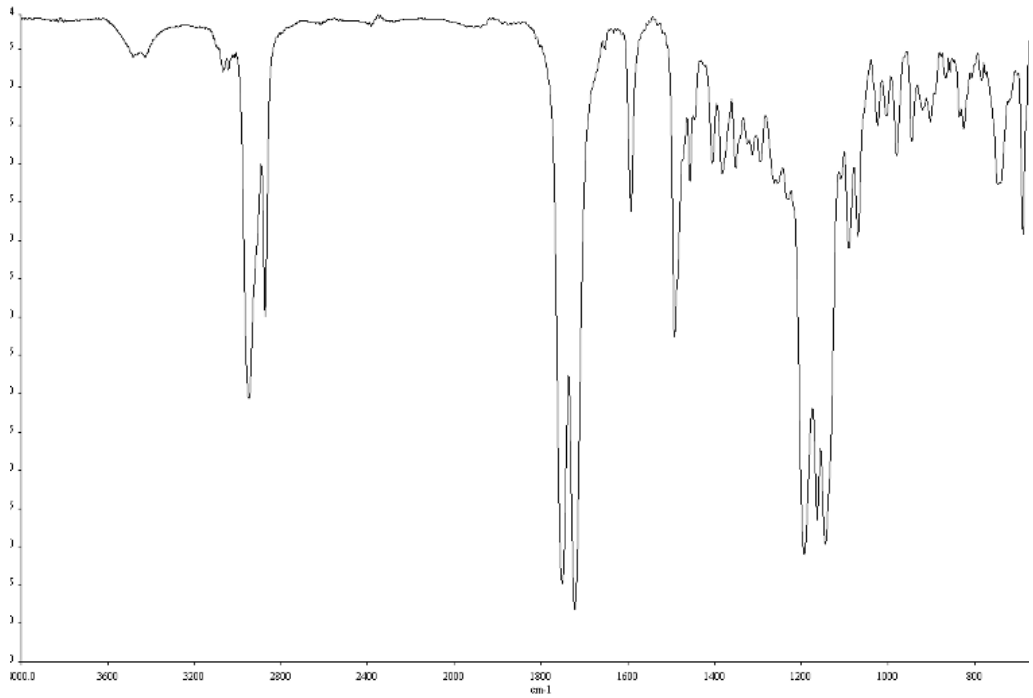


Figure A1.20. *Infrared spectrum (Thin Film, NaCl) of compound* ***11k****.*

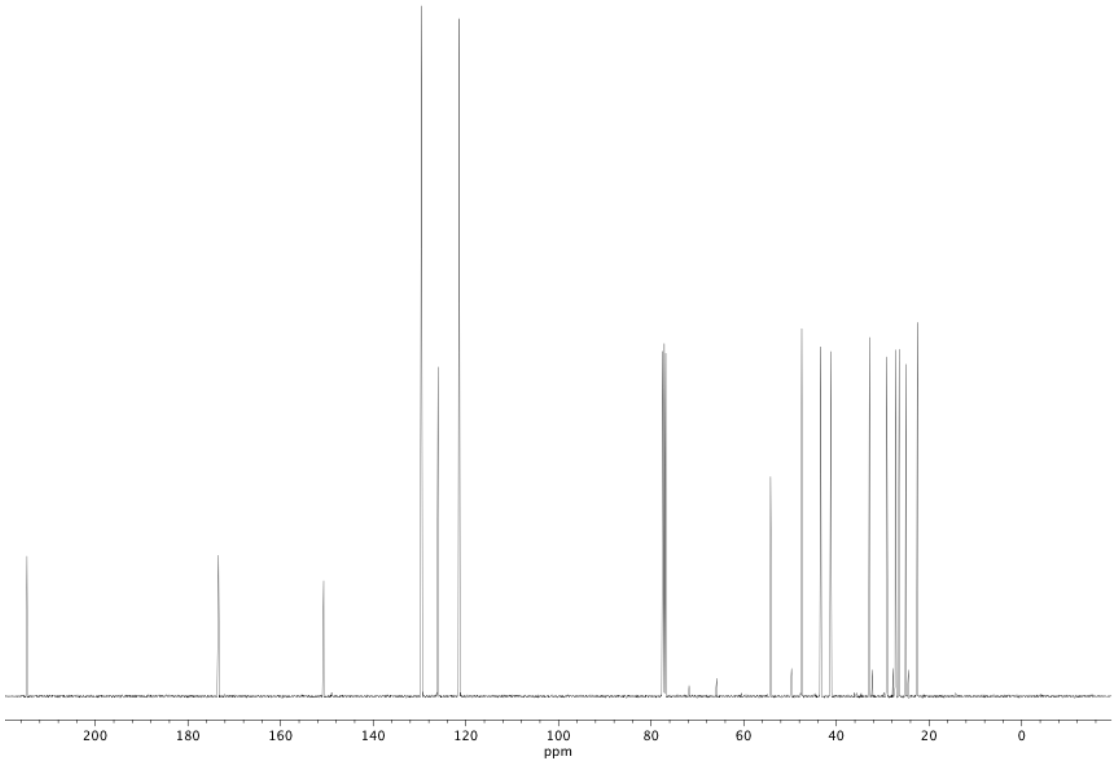


Figure A1.21. *^{13}C NMR (100 MHz, $CDCl_3$) of compound* ***11k****.*

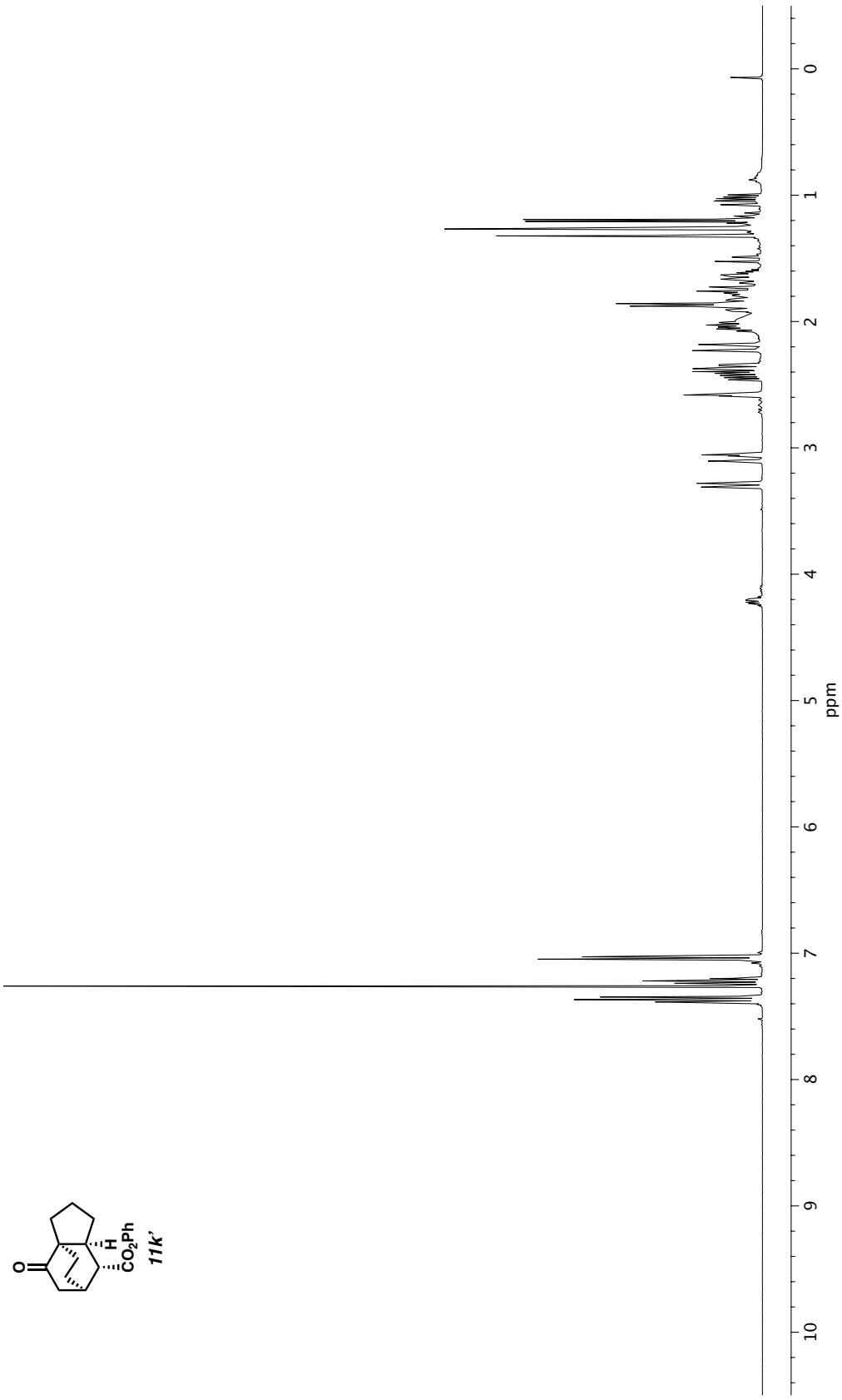


Figure A1.22. *^1H NMR (400 MHz, $CDCl_3$) of compound* ***11k'*** *.*

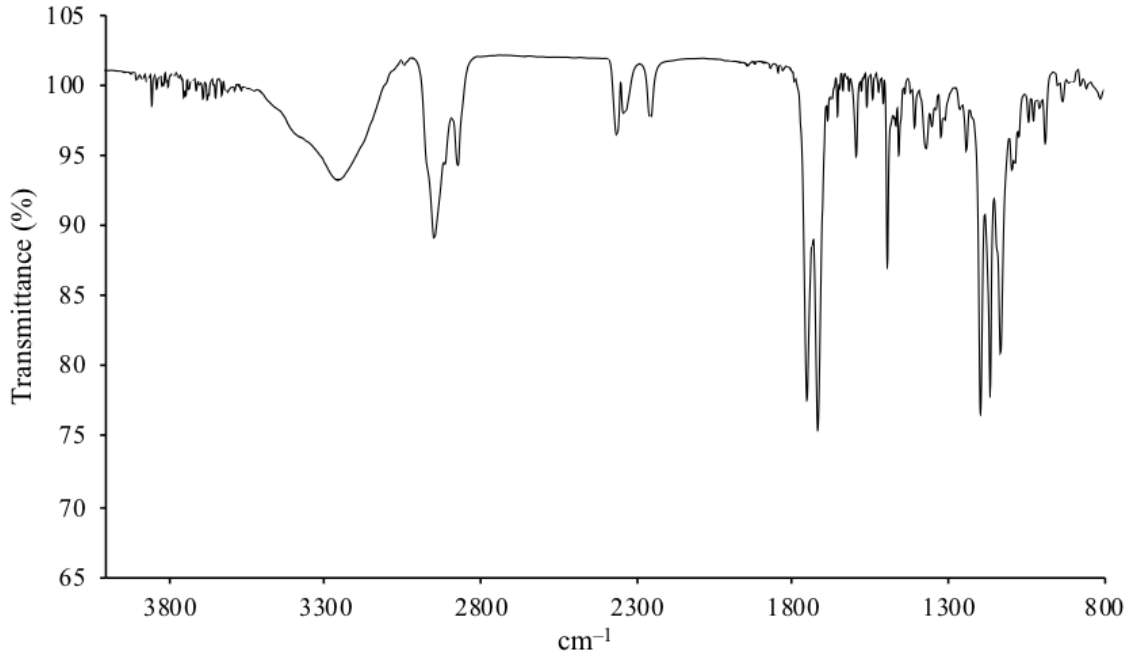


Figure A1.23. *Infrared spectrum ($CDCl_3$ solution) of compound* ***11k'***.

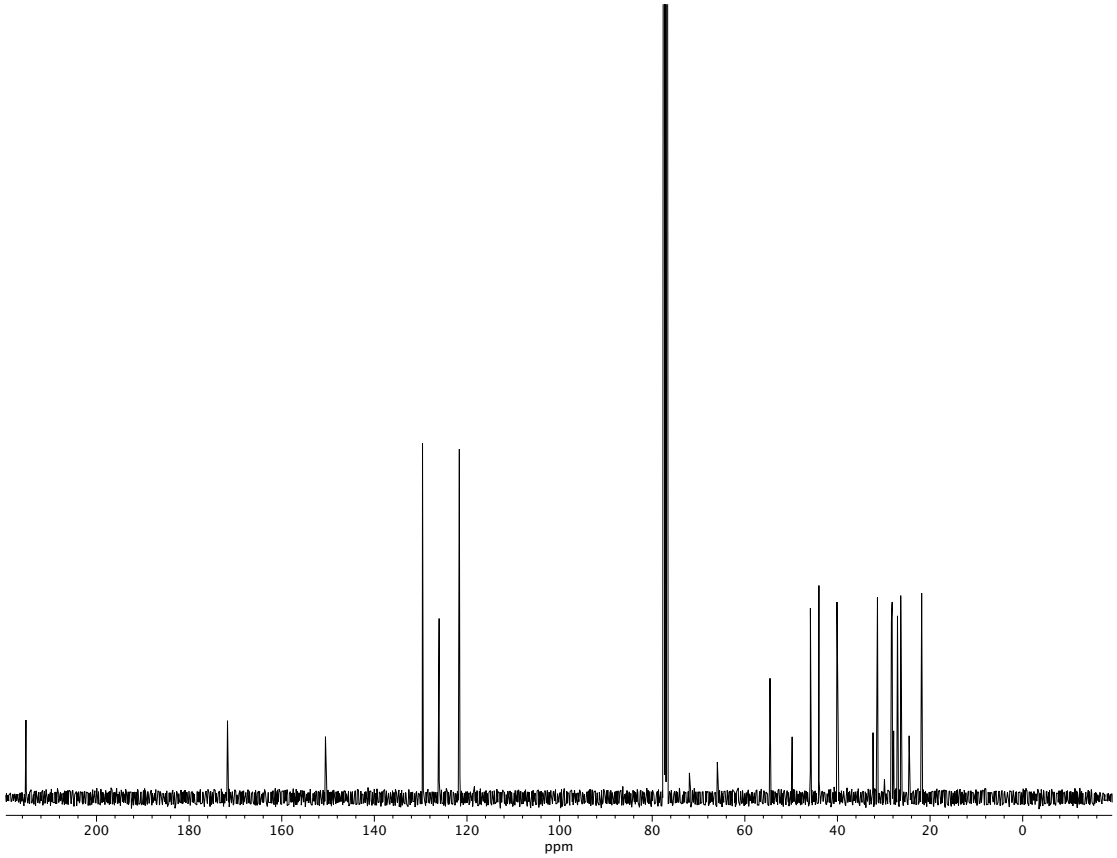


Figure A1.24. *^{13}C NMR (100 MHz, $CDCl_3$) of compound* ***11k'***.

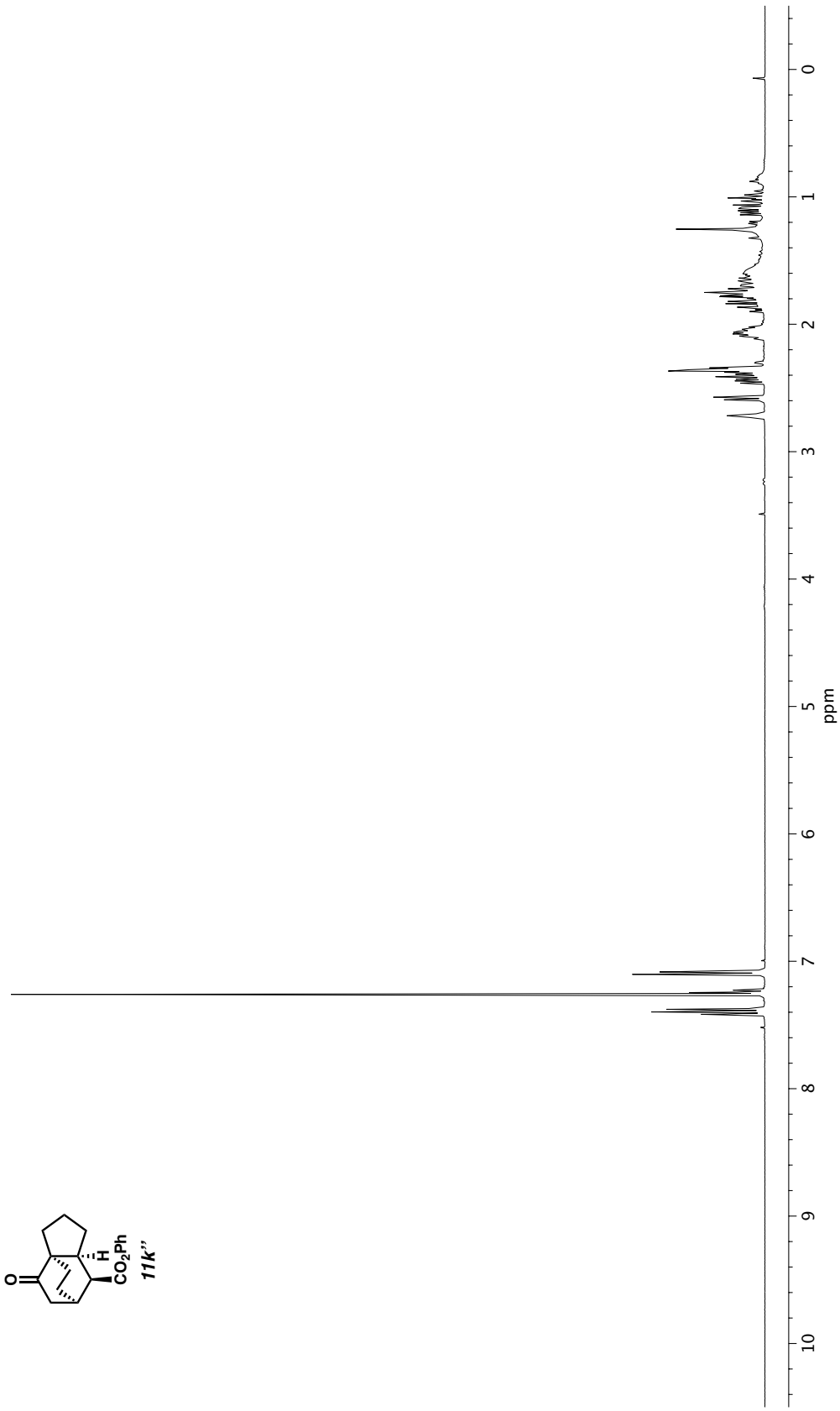


Figure A1.25. *^1H NMR (400 MHz, $CDCl_3$) of compound* ***11k''*** *.*

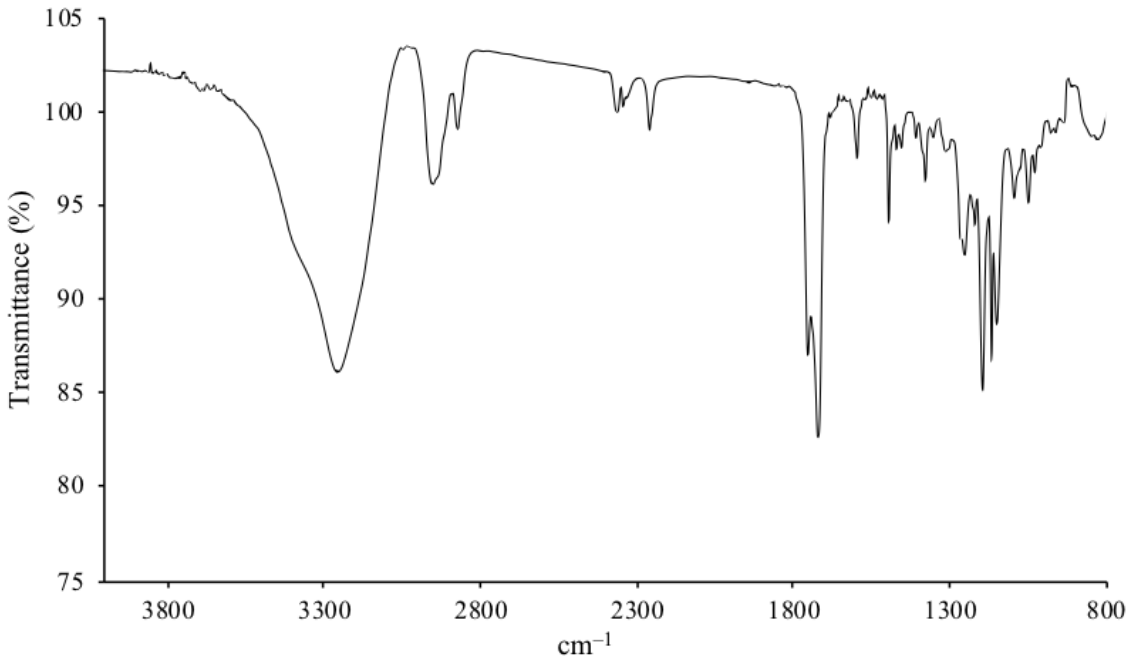


Figure A1.26. *Infrared spectrum ($CDCl_3$ solution) of compound* ***11k''***.

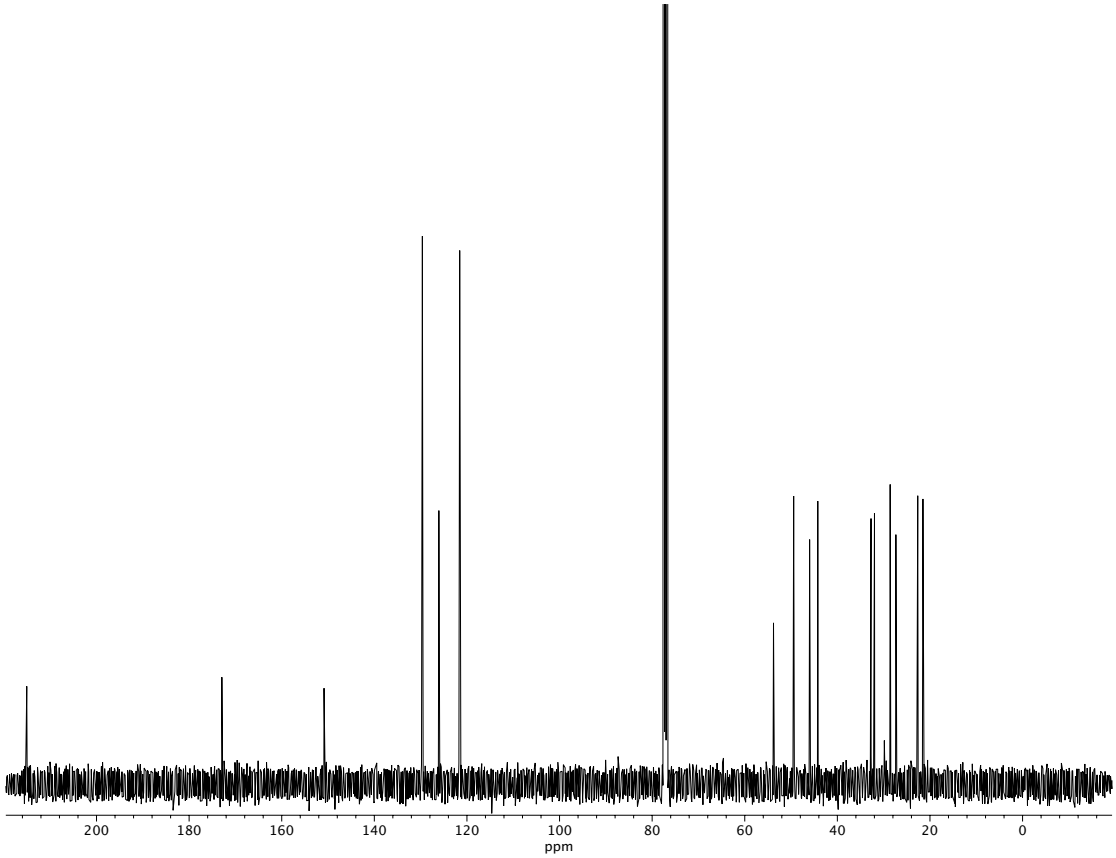


Figure A1.27. *^{13}C NMR (100 MHz, $CDCl_3$) of compound* ***11k''***.

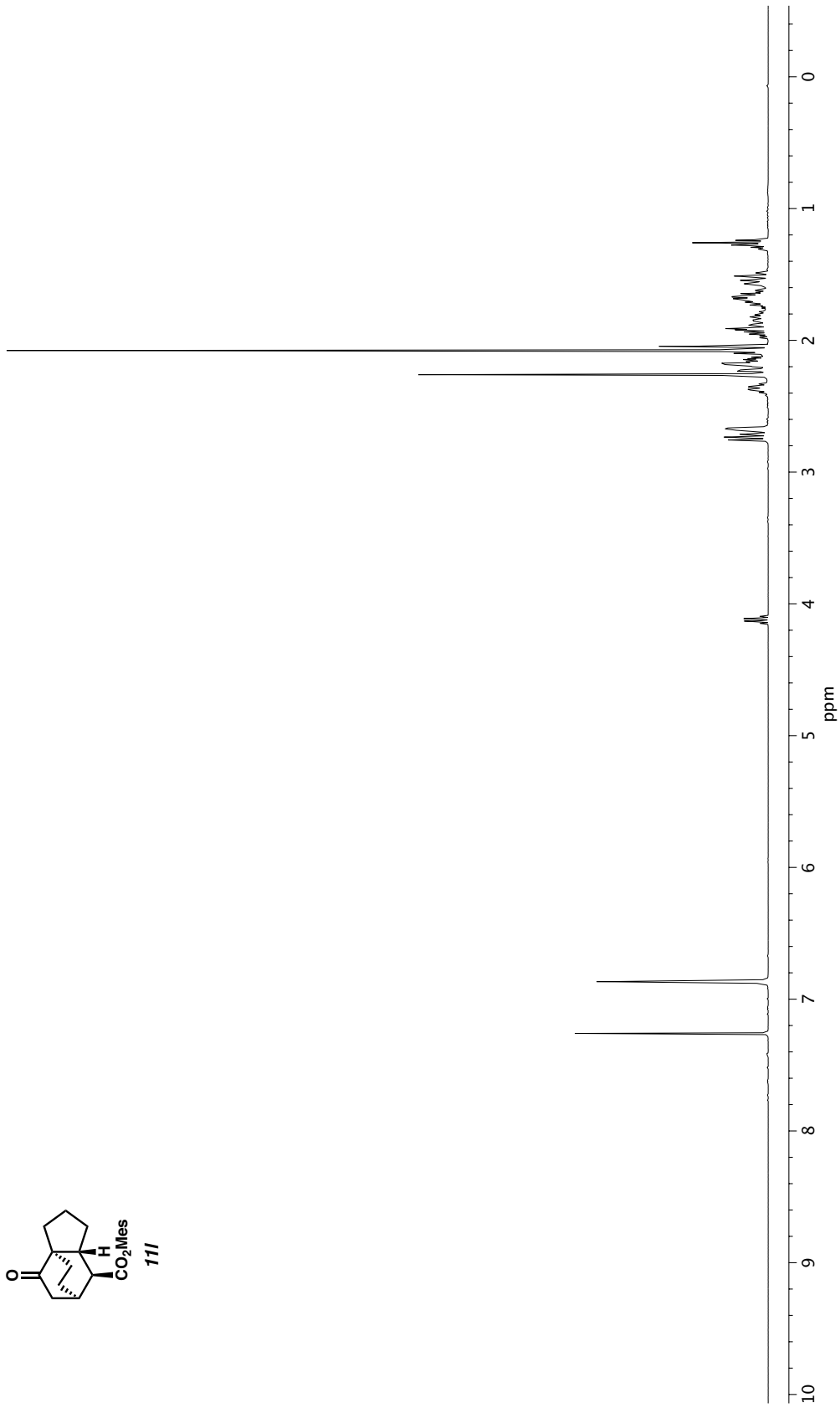


Figure A1.28. *^{1}H NMR (400 MHz, $CDCl_3$) of compound* ***11l****.*

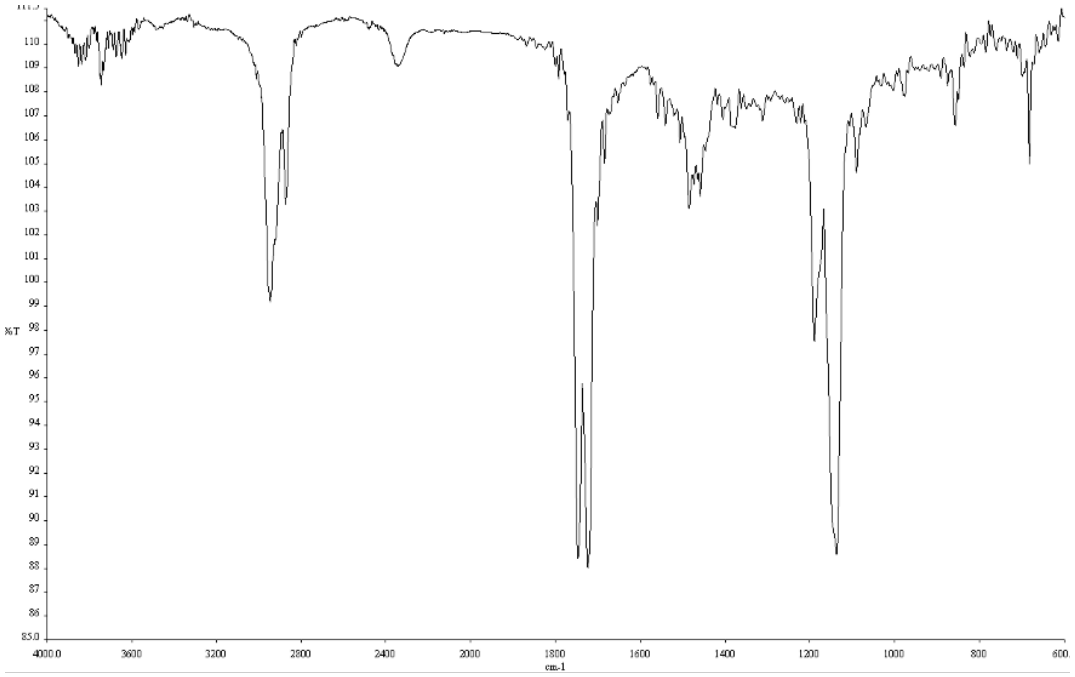


Figure A1.29. *Infrared spectrum (Thin Film, NaCl) of compound* ***11l****.*

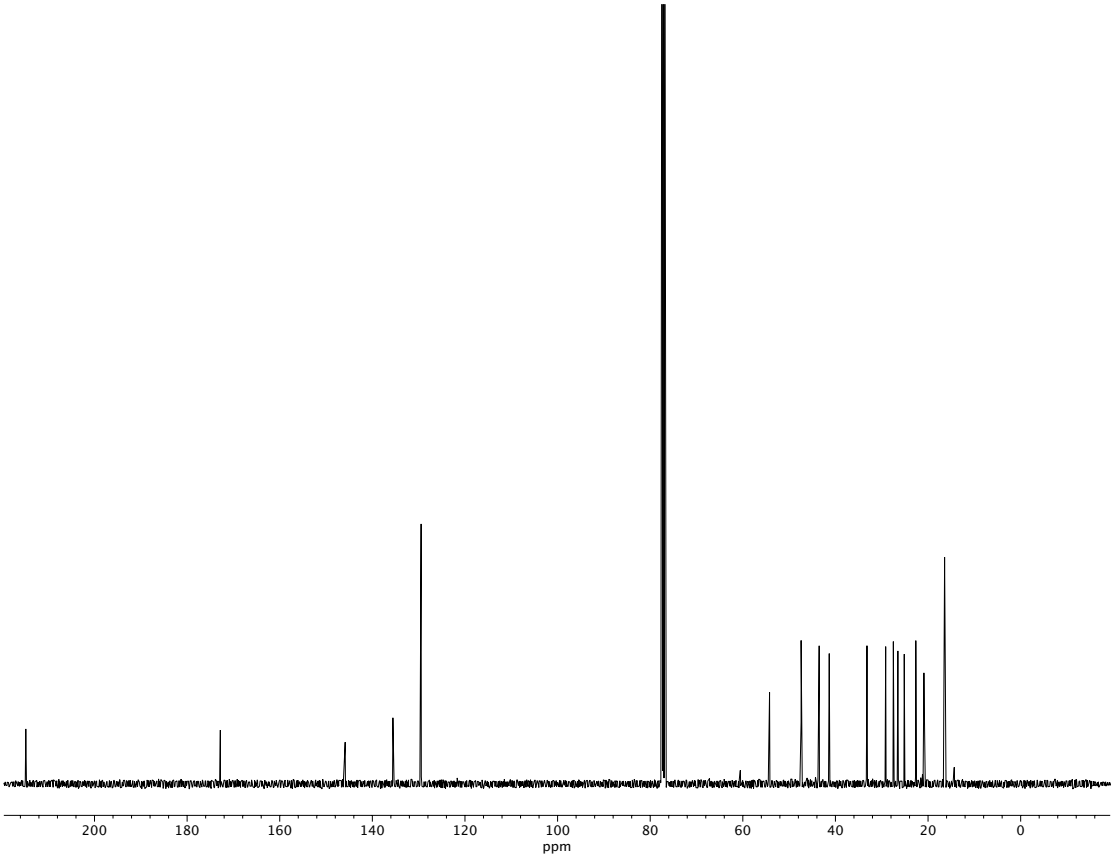


Figure A1.30. *^{13}C NMR (100 MHz, $CDCl_3$) of compound* ***11l****.*

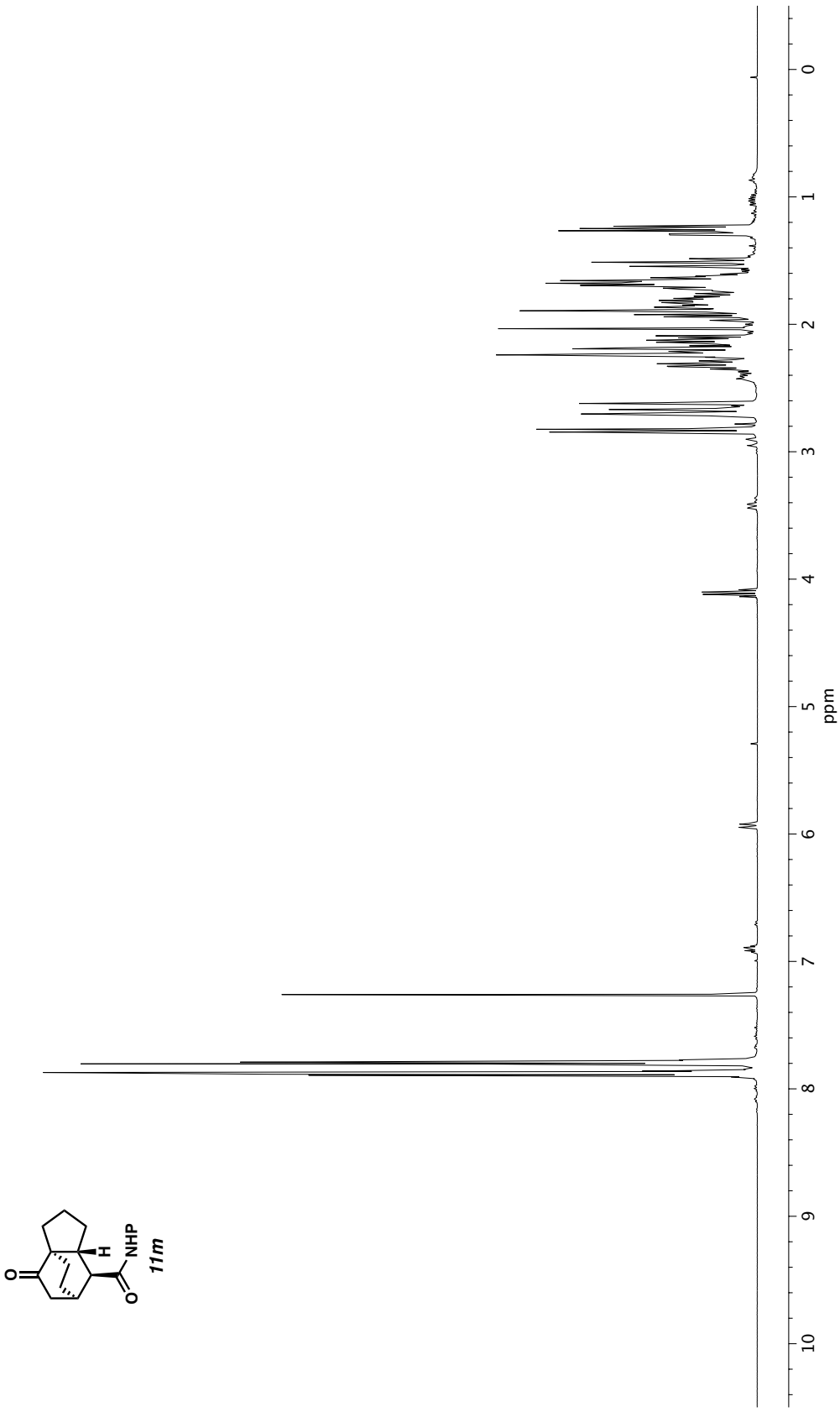


Figure A1.31. *^1H NMR (400 MHz, $CDCl_3$) of compound* ***11m****.*

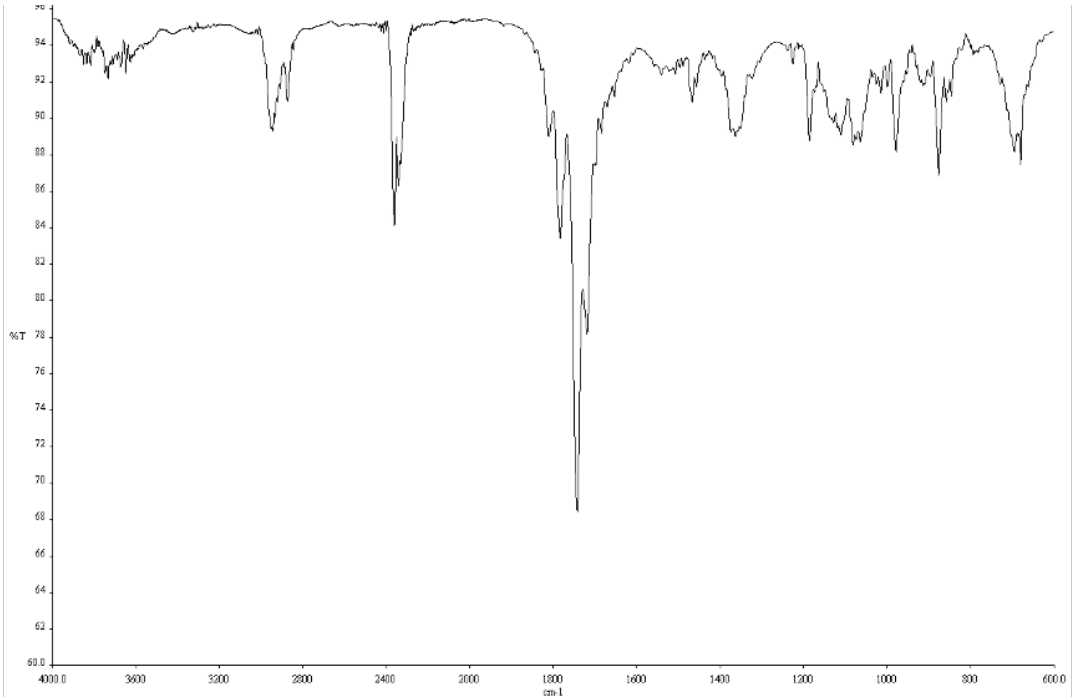


Figure A1.32. *Infrared spectrum (Thin Film, NaCl) of compound* ***11m****.*

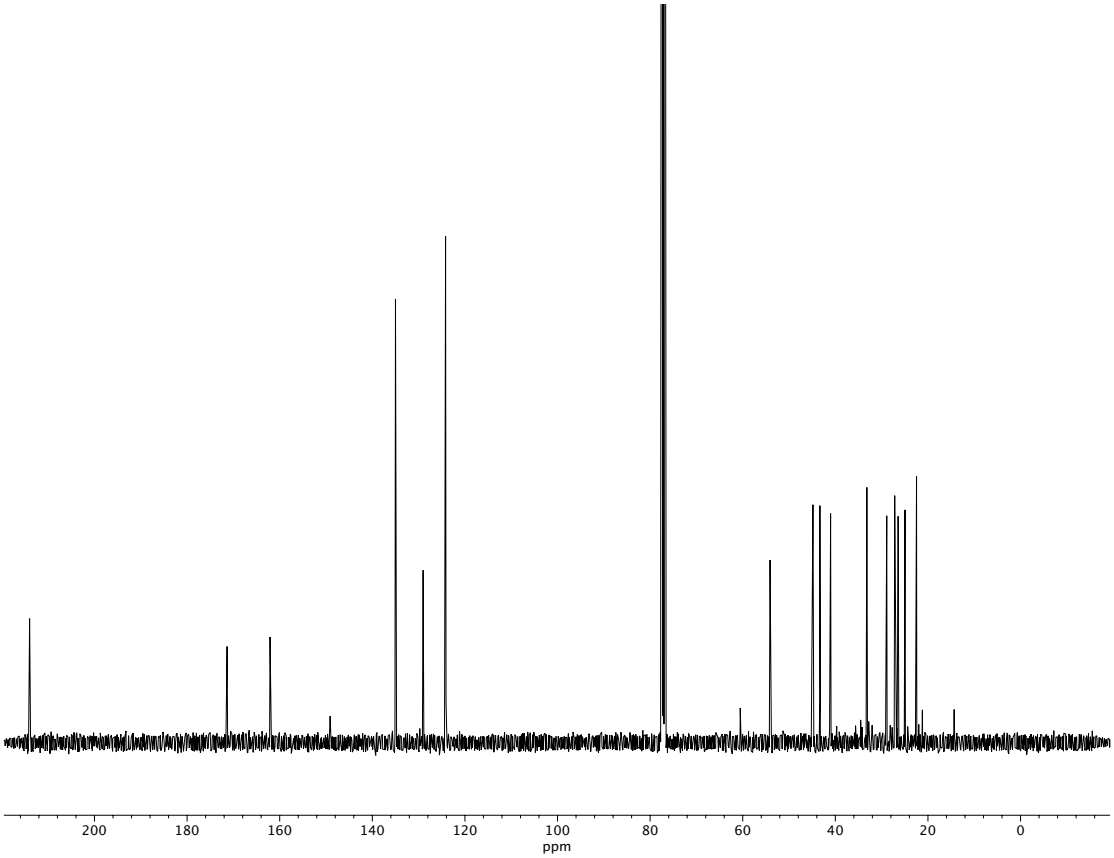


Figure A1.33. *^{13}C NMR (100 MHz, $CDCl_3$) of compound* ***11m****.*

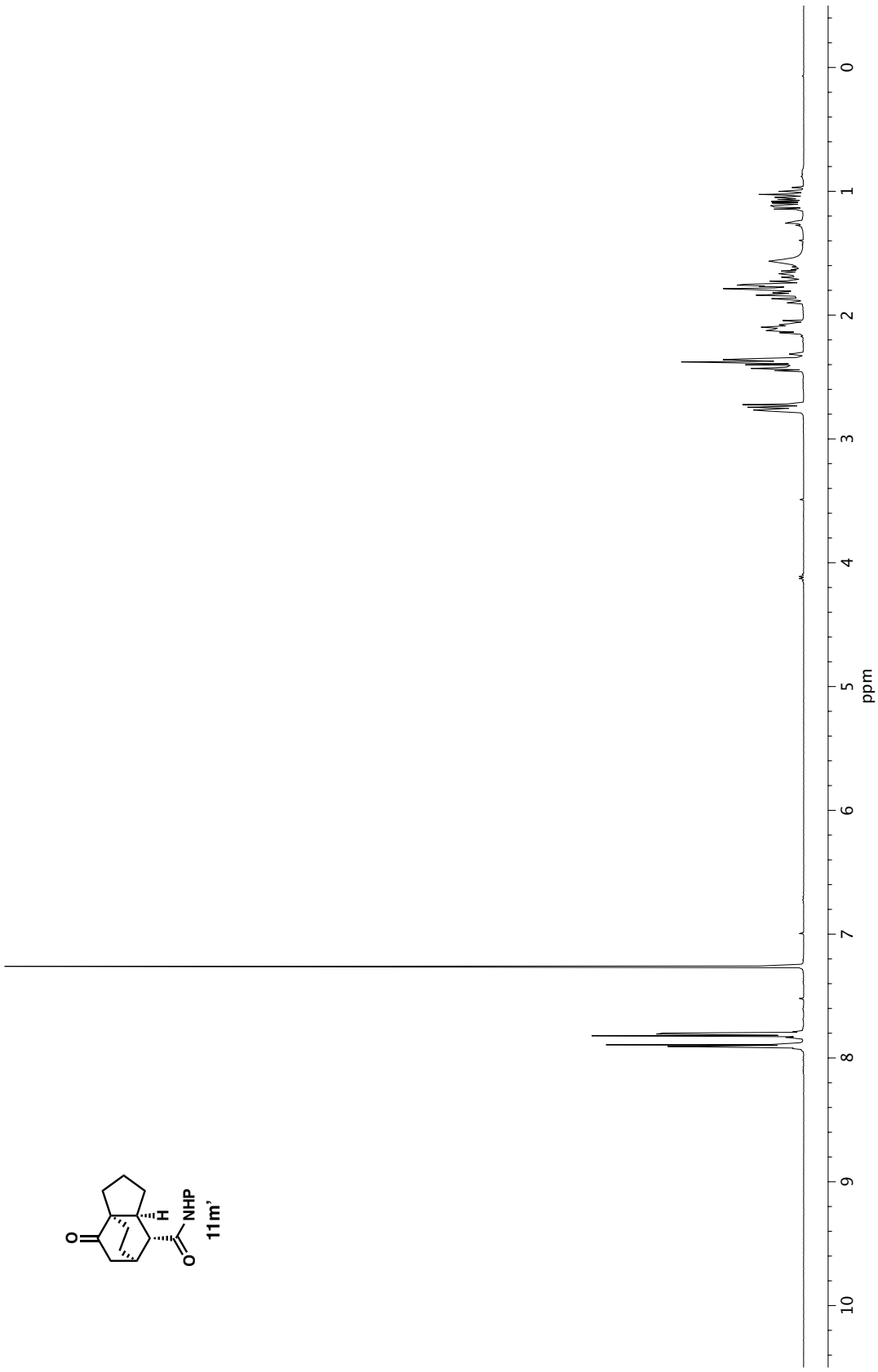


Figure A1.34. *^{1}H NMR (400 MHz, $CDCl_3$) of compound* ***11m'*** .

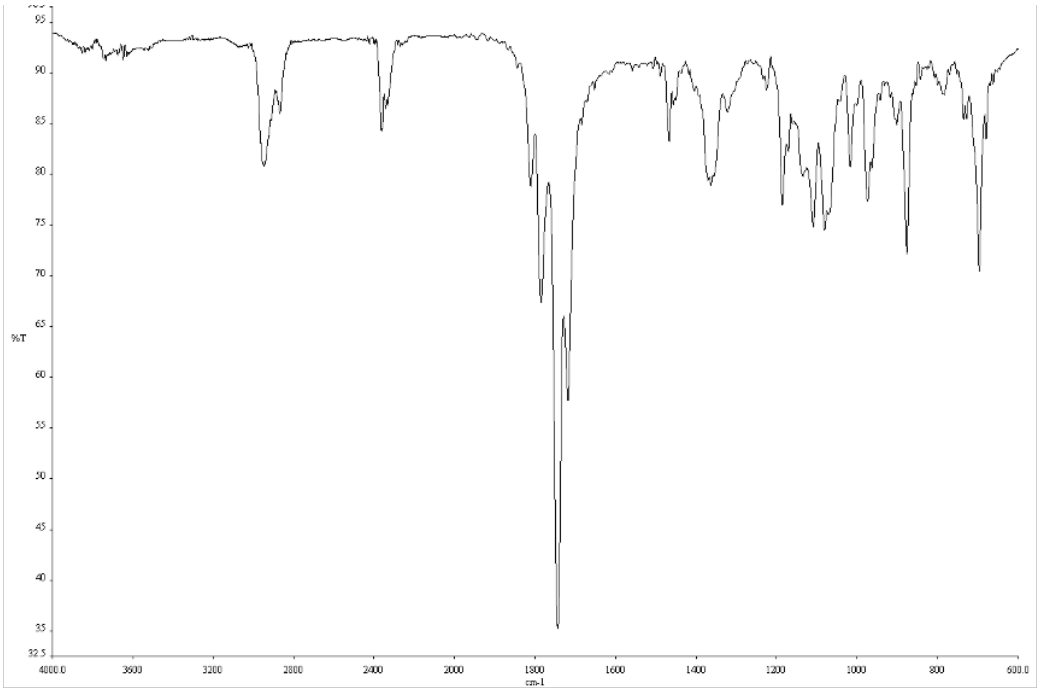


Figure A1.35. *Infrared spectrum (Thin Film, NaCl) of compound* ***11m′****.*

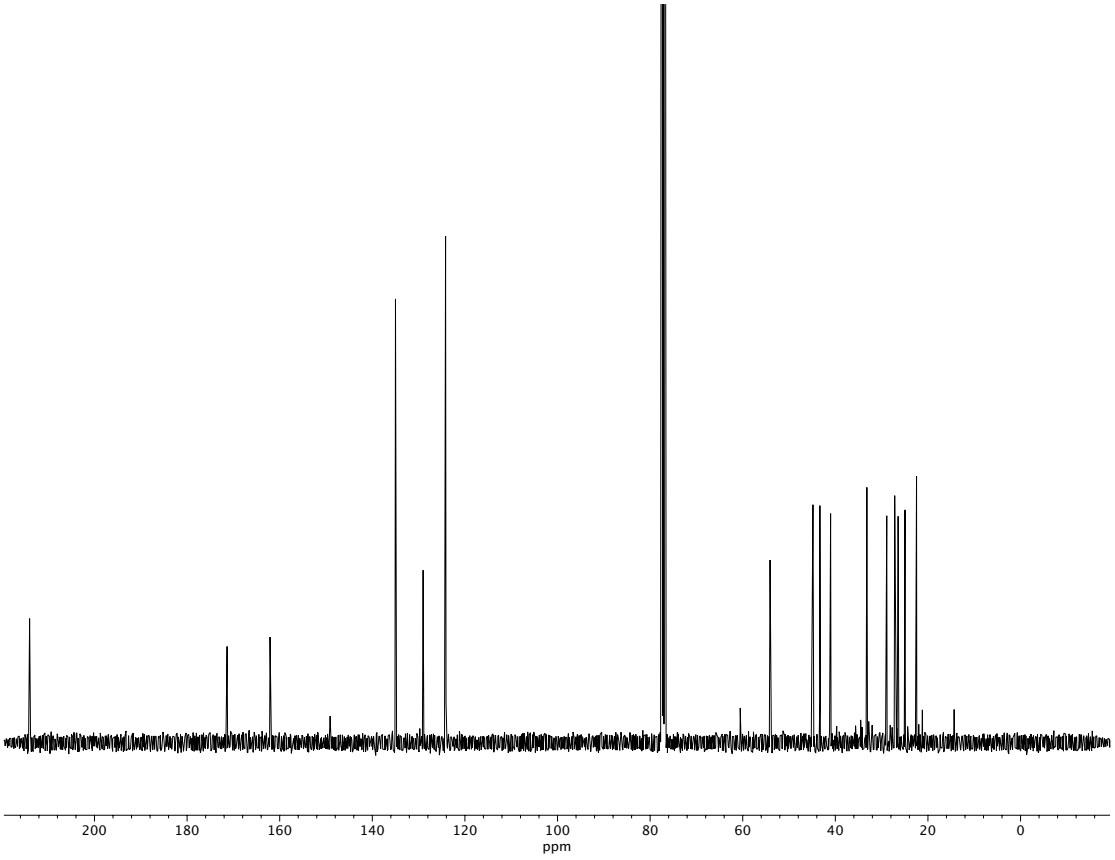


Figure A1.36. *^{13}C NMR (100 MHz, $CDCl_3$) of compound* ***11m′****.*

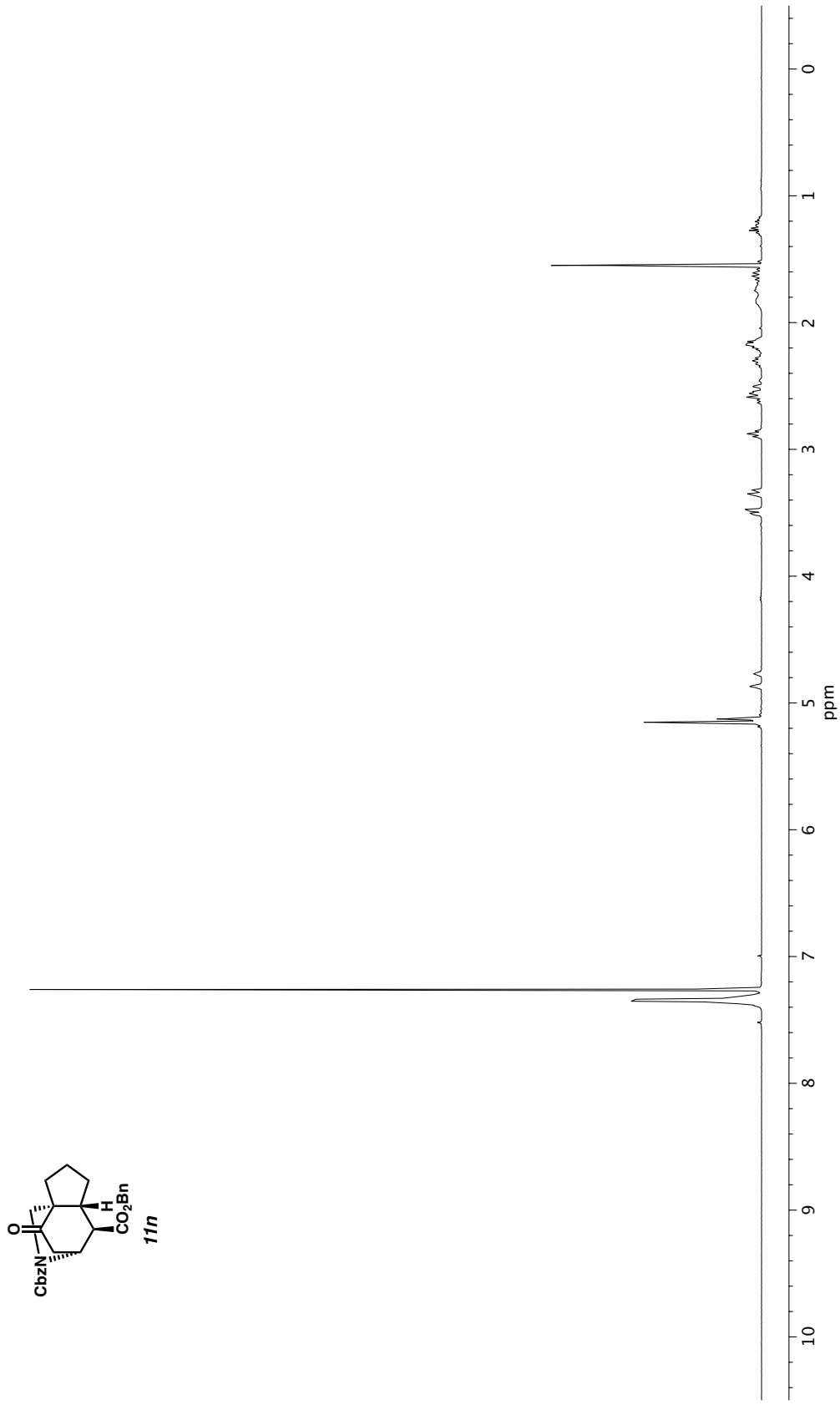


Figure A1.37. *^{1}H NMR (400 MHz, $CDCl_3$) of compound* ***11n***.

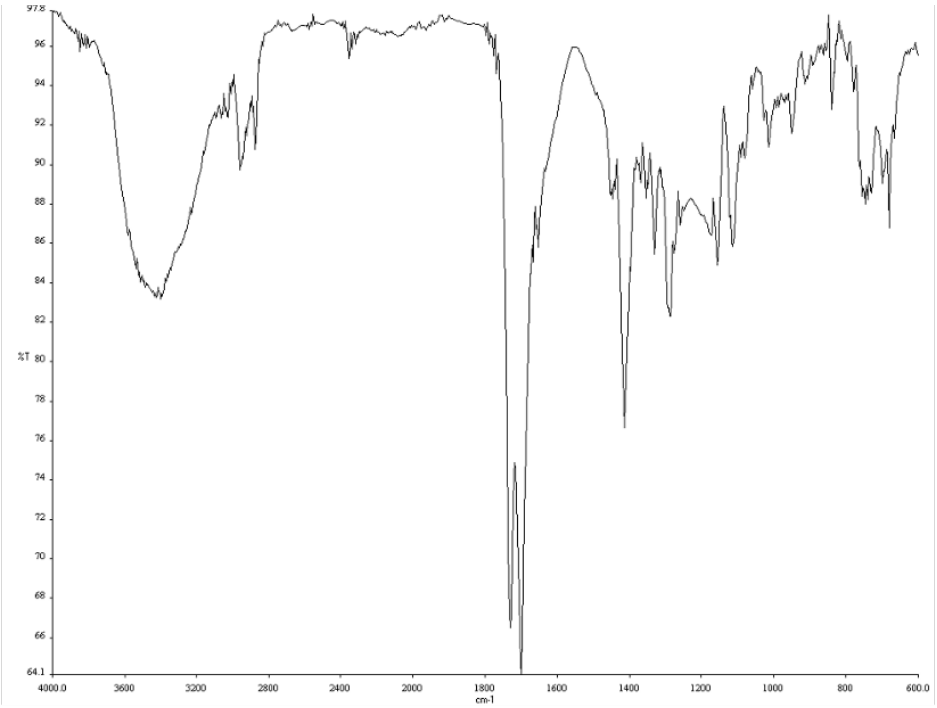


Figure A1.38. *Infrared spectrum (Thin Film, NaCl) of compound* ***11n****.*

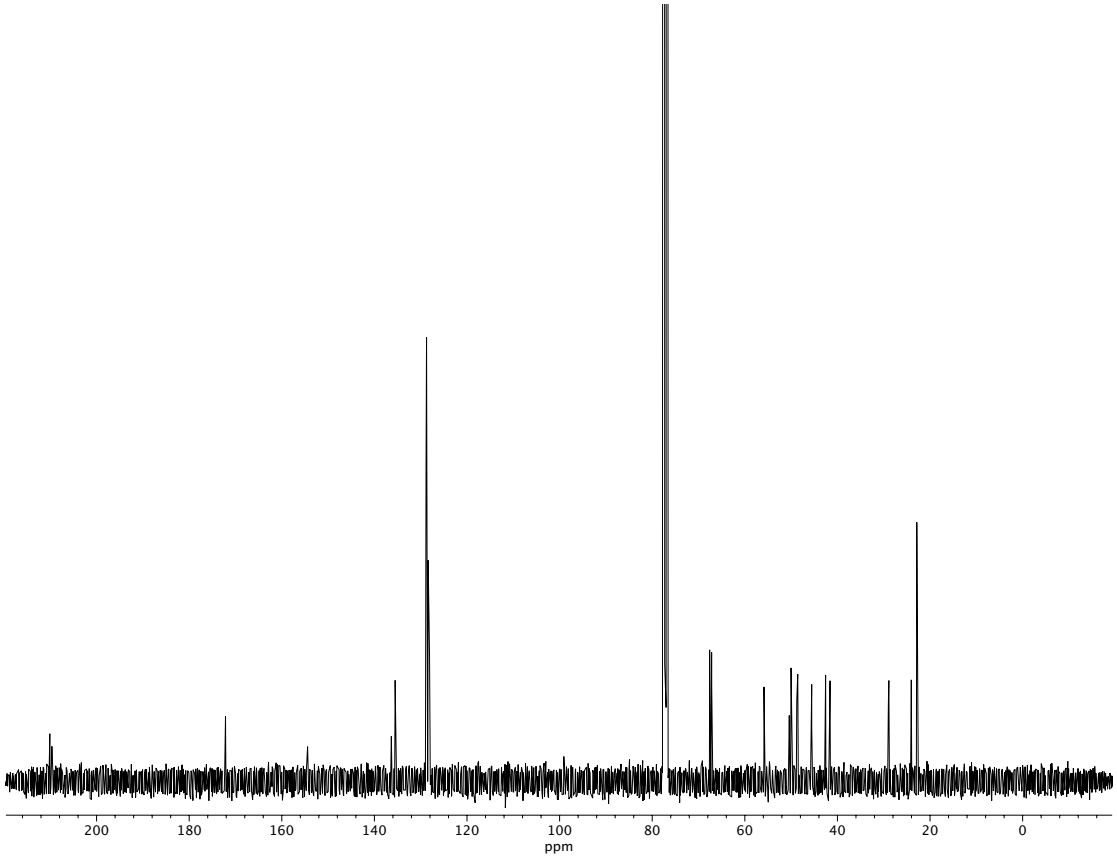
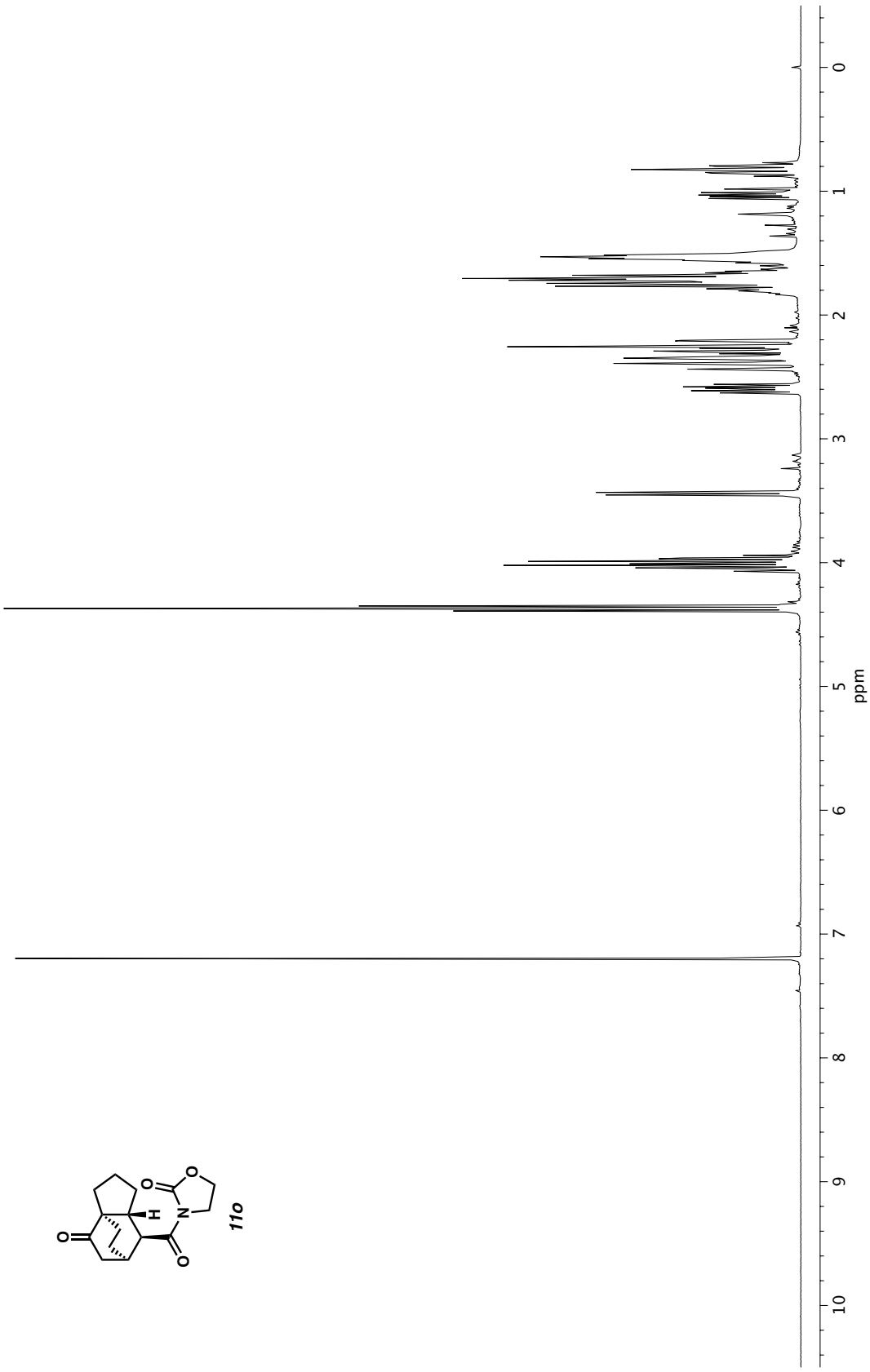


Figure A1.39. *^{13}C NMR (100 MHz, $CDCl_3$) of compound* ***11n****.*



11o

Figure A1.40. *^{1}H NMR (400 MHz, $CDCl_3$) of compound **11o**.*

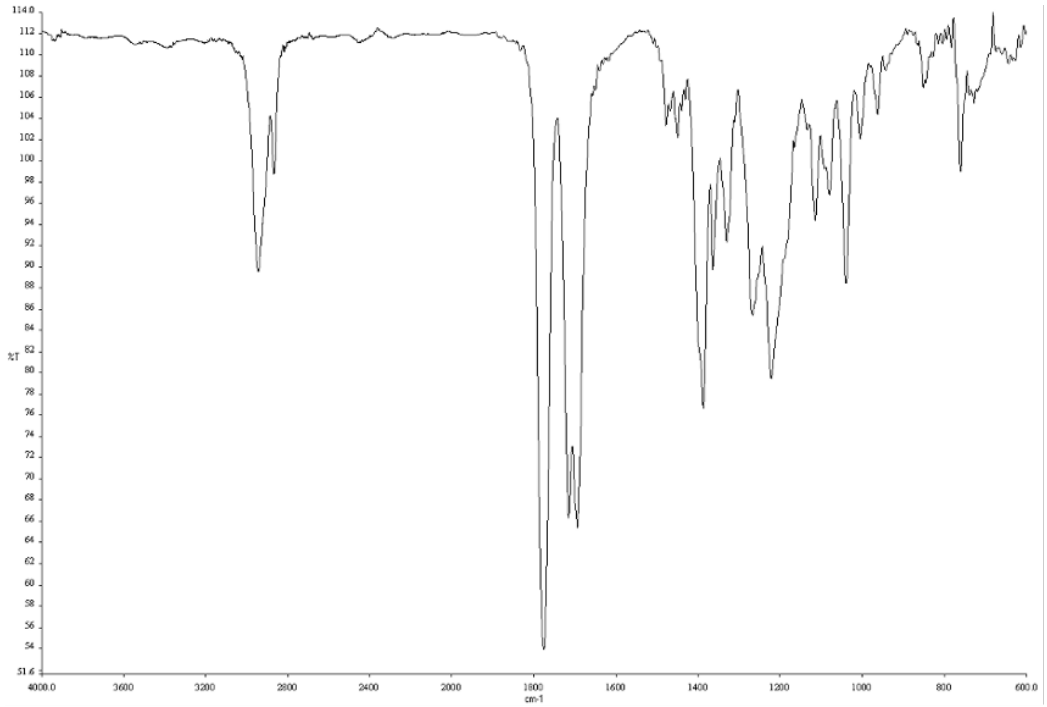


Figure A1.41. *Infrared spectrum (Thin Film, NaCl) of compound* ***11o****.*

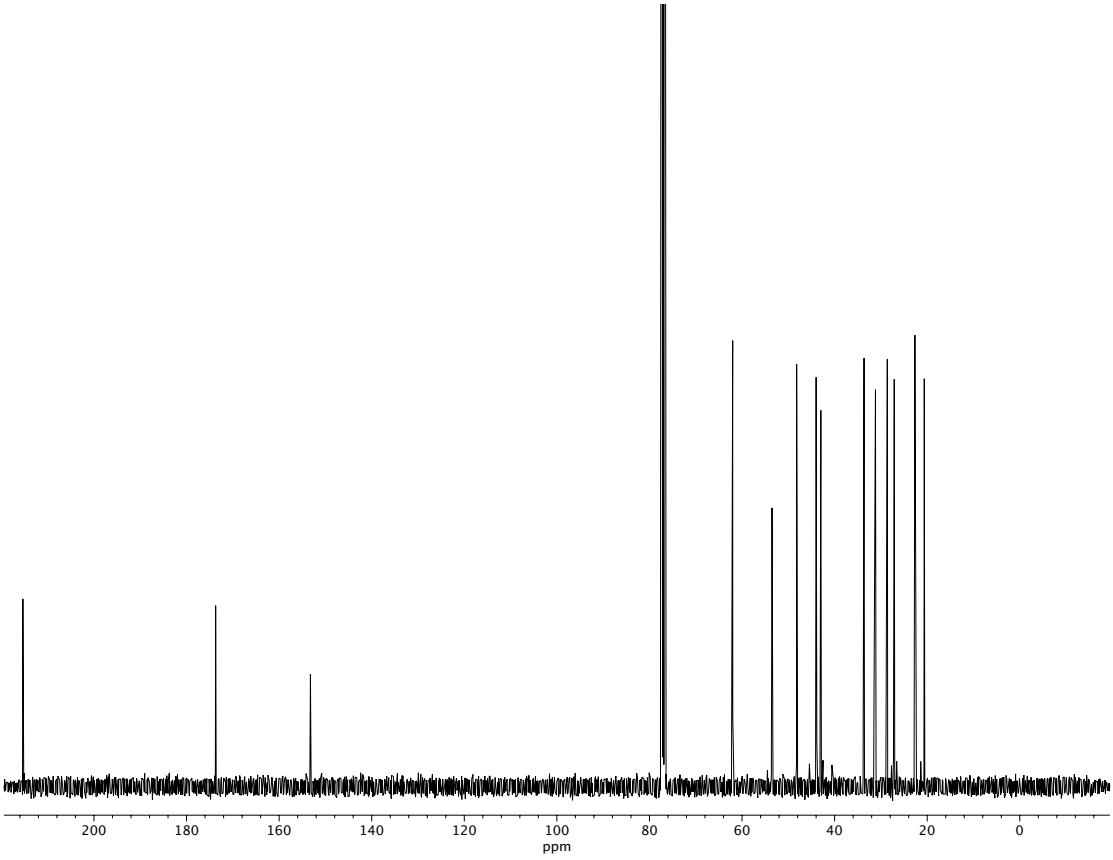


Figure A1.42. *^{13}C NMR (100 MHz, $CDCl_3$) of compound* ***11o****.*

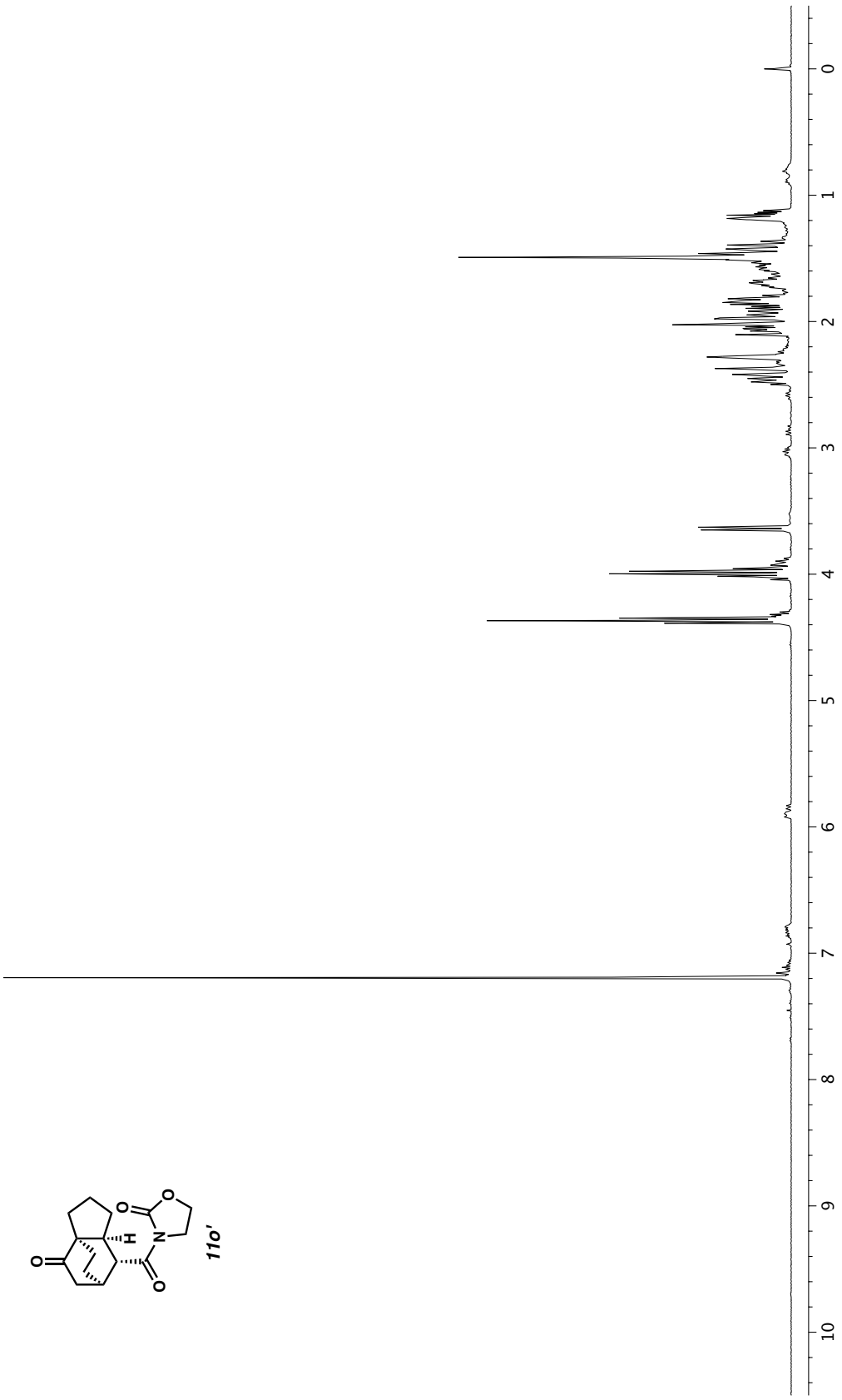


Figure A1.43. *^1H NMR (400 MHz, $CDCl_3$) of compound* ***11o'*** .

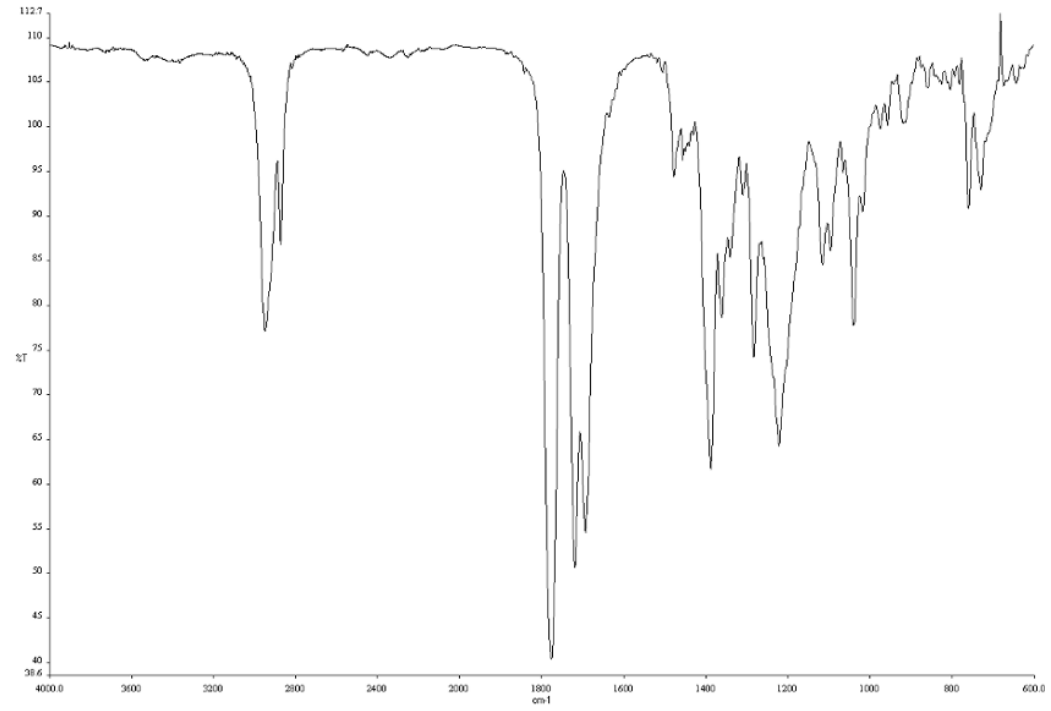


Figure A1.44. *Infrared spectrum (Thin Film, NaCl) of compound* ***11o′****.*

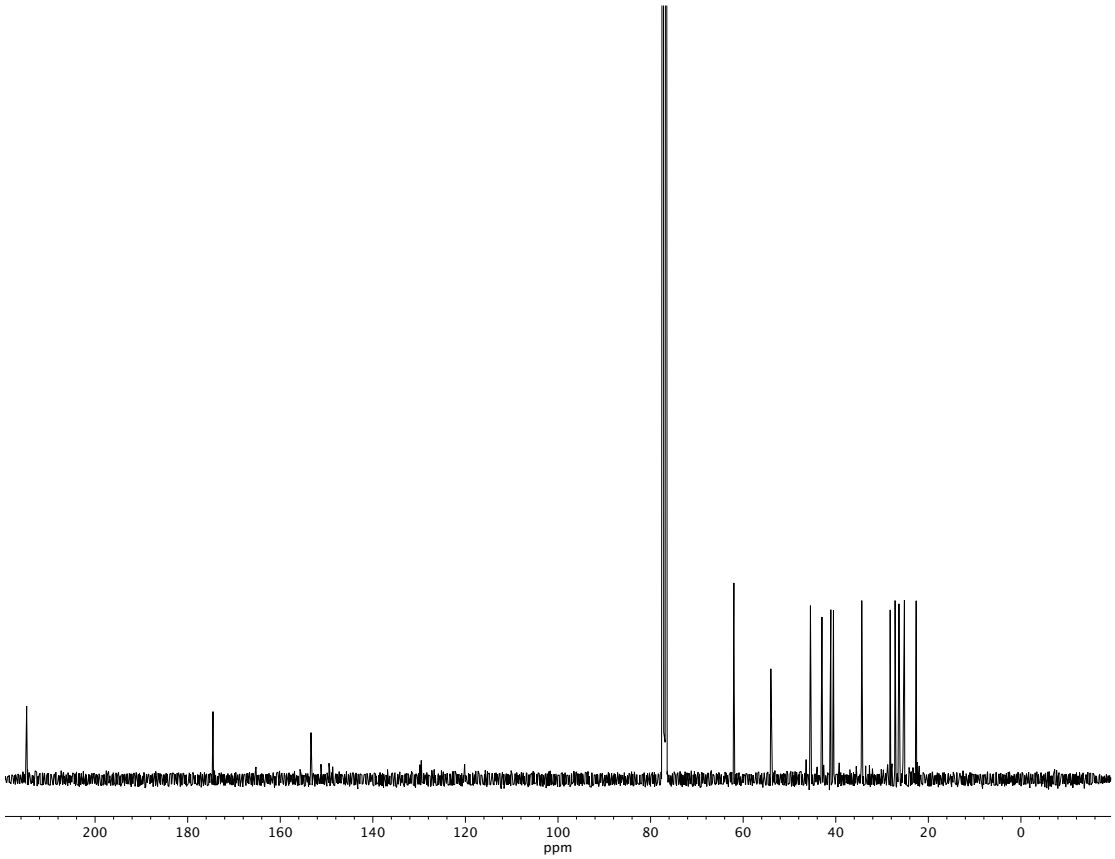


Figure A1.45. *^{13}C NMR (100 MHz, $CDCl_3$) of compound* ***11o′****.*

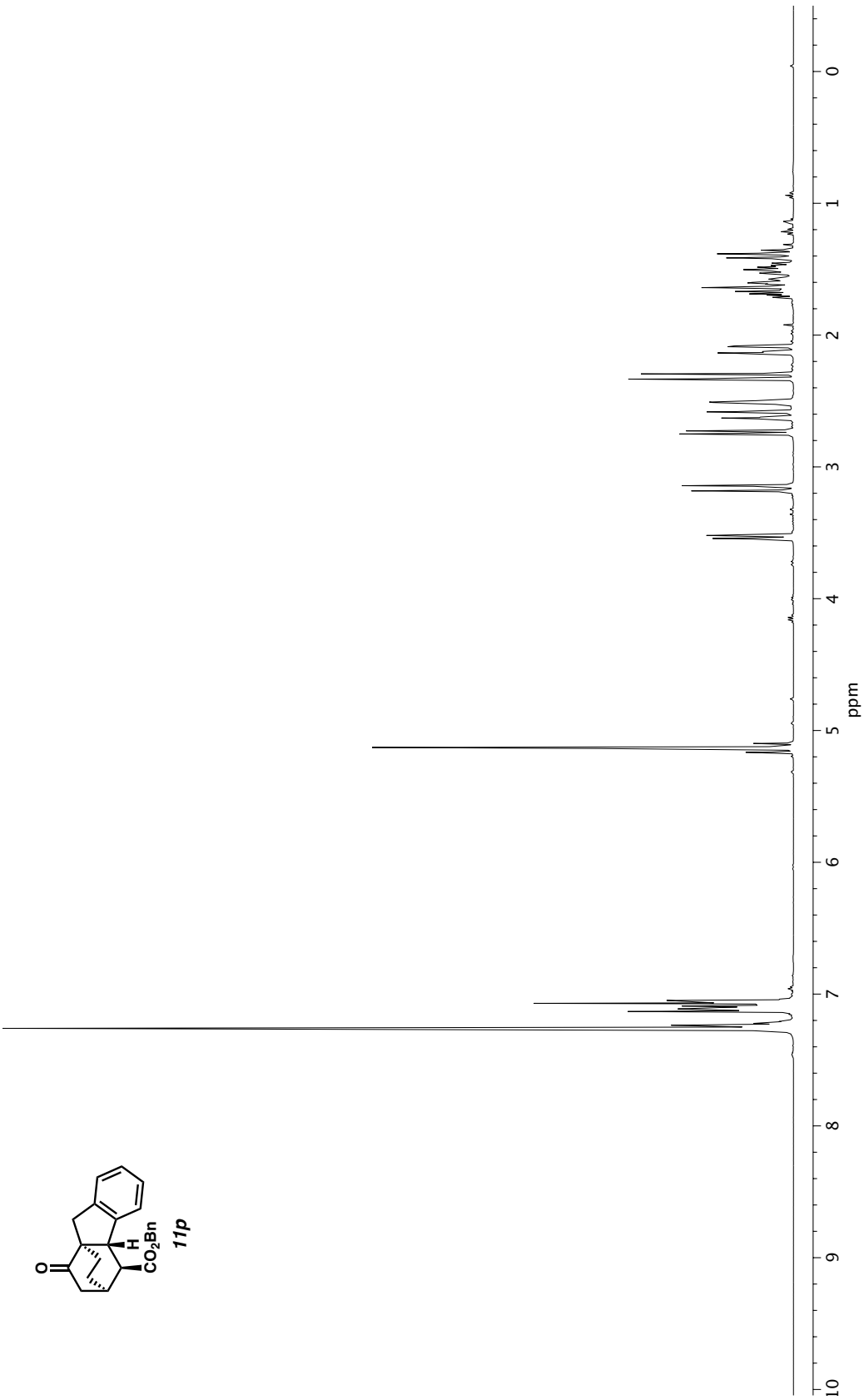


Figure A1.46. *^1H NMR (400 MHz, $CDCl_3$) of compound **11p**.*

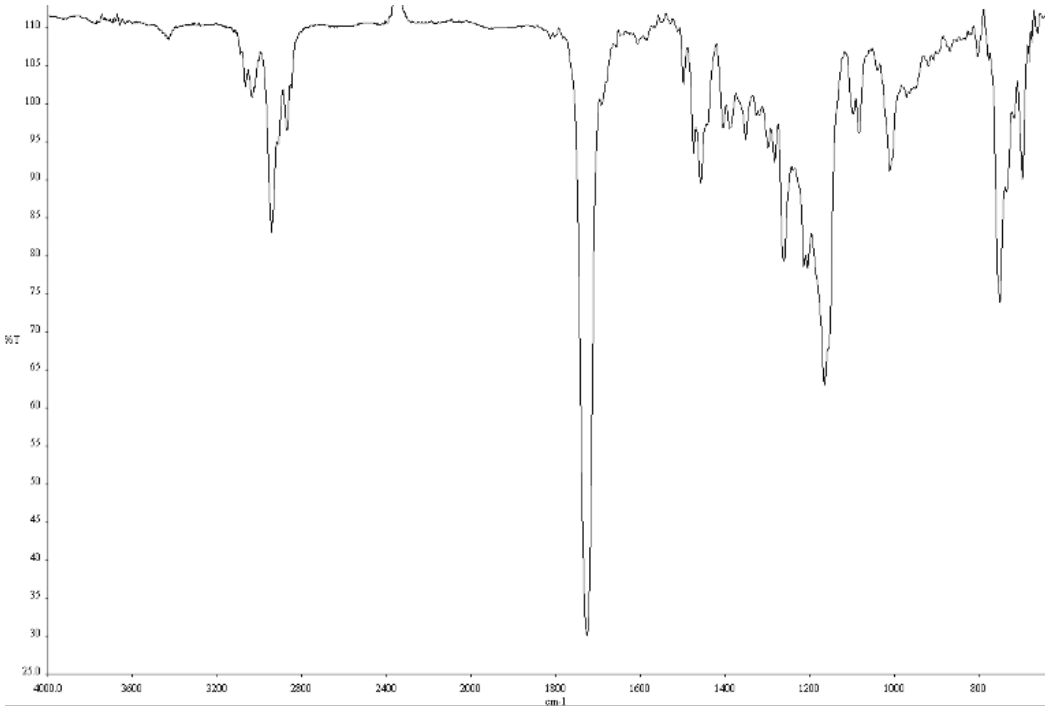


Figure A1.47. *Infrared spectrum (Thin Film, NaCl) of compound* ***11p****.*

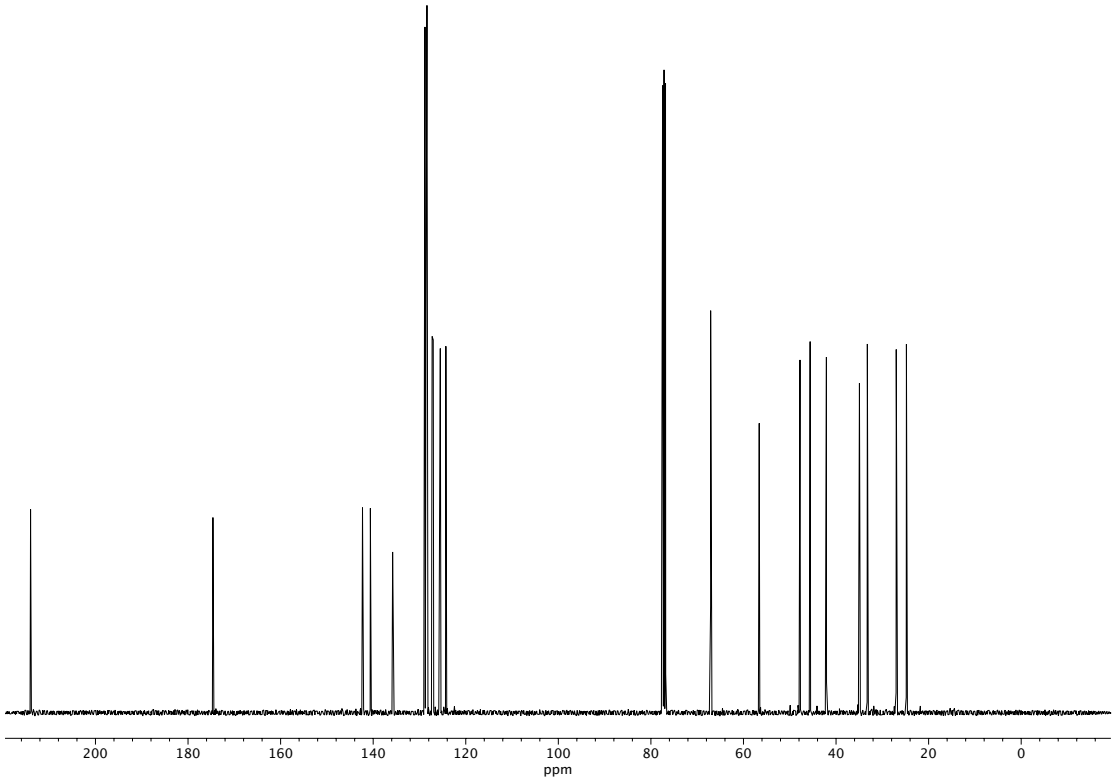


Figure A1.48. *^{13}C NMR (100 MHz, $CDCl_3$) of compound* ***11p****.*

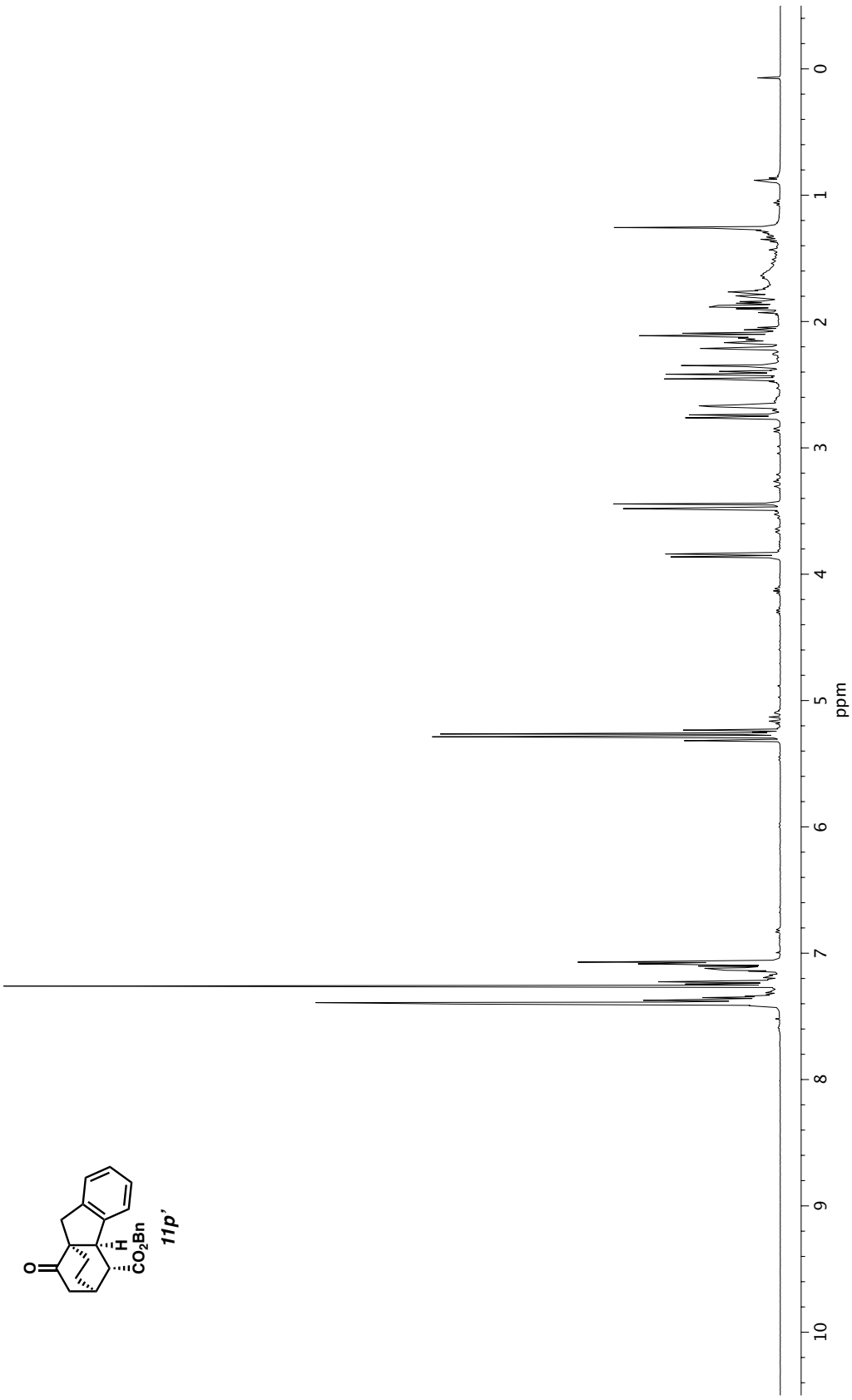


Figure A1.49. *^1H NMR (400 MHz, $CDCl_3$) of compound* ***11p'*** .

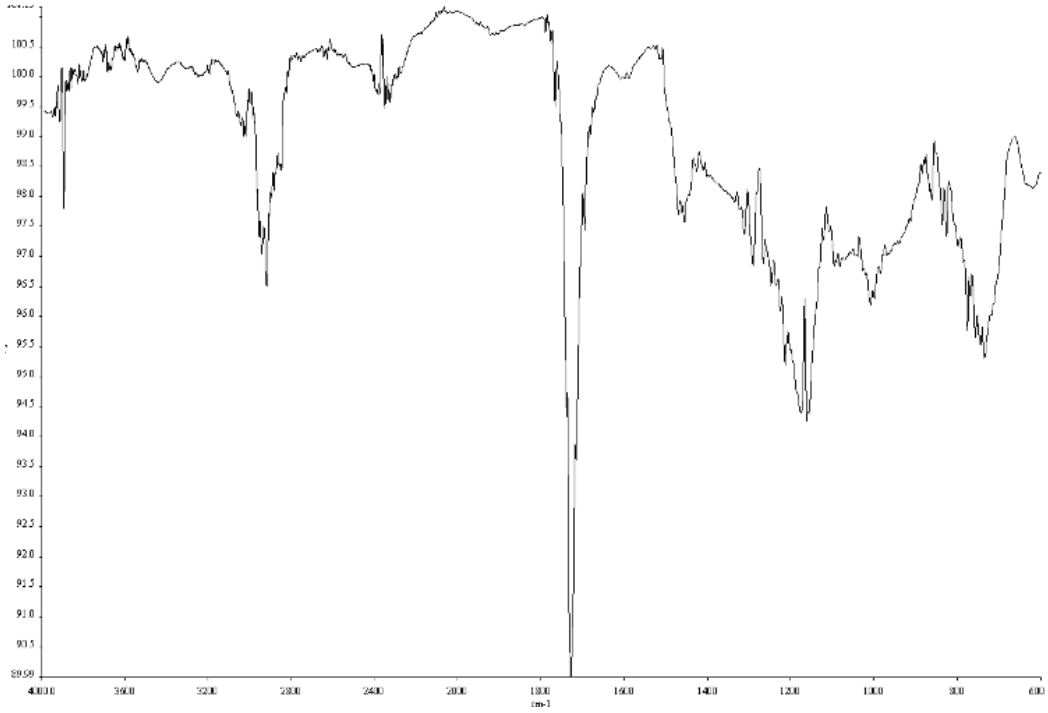


Figure A1.50. *Infrared spectrum (Thin Film, NaCl) of compound* ***11p′****.*

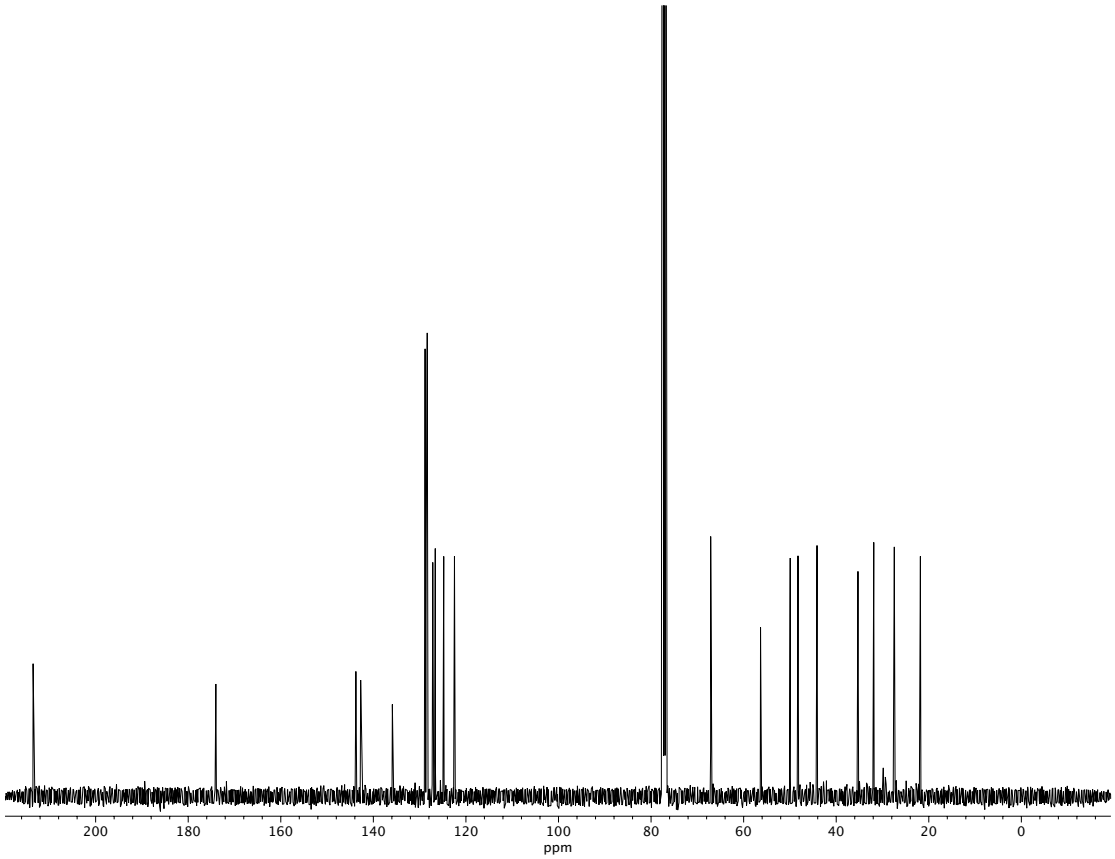


Figure A1.51. *^{13}C NMR (100 MHz, $CDCl_3$) of compound* ***11p′****.*

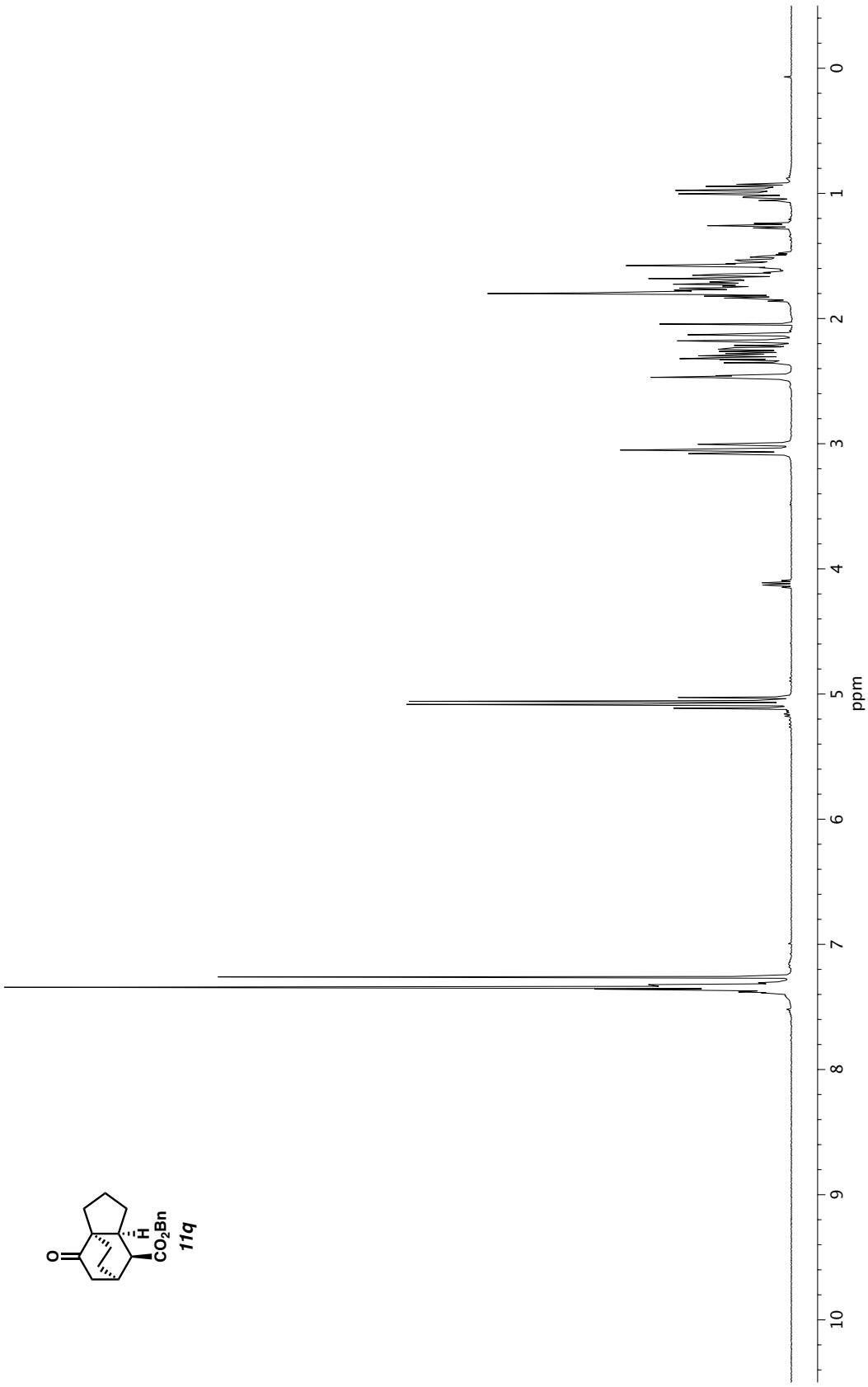


Figure A1.52. *^1H NMR (400 MHz, $CDCl_3$) of compound* ***11q***.

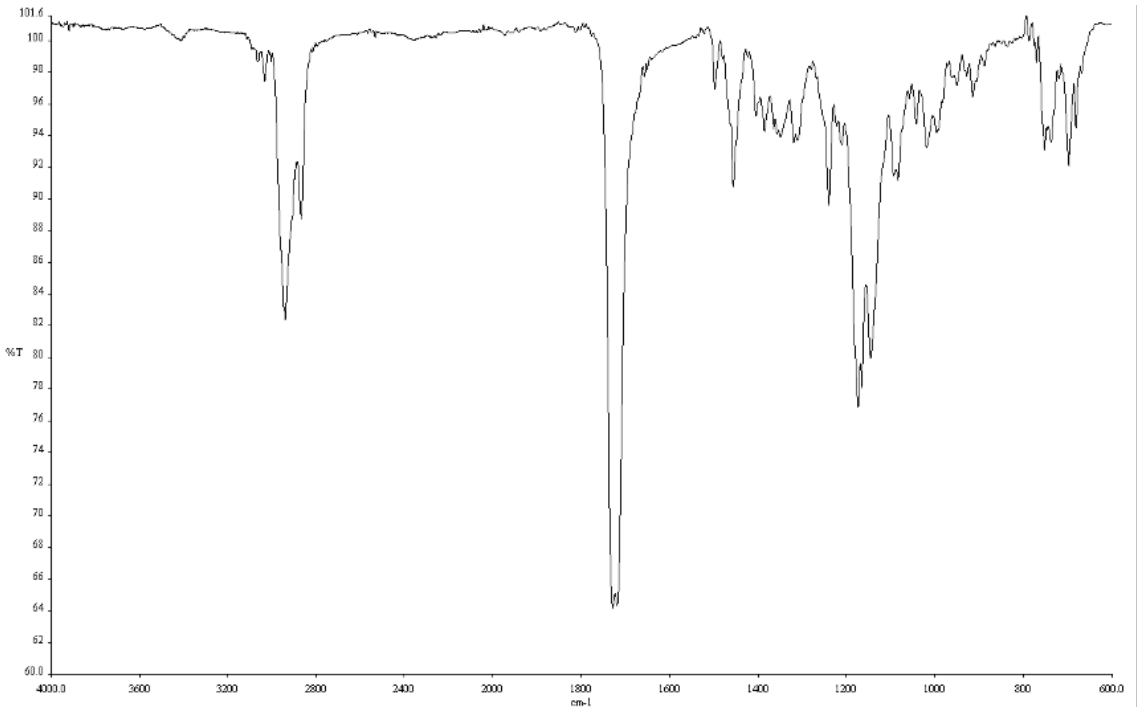


Figure A1.53. *Infrared spectrum (Thin Film, NaCl) of compound* ***11q****.*

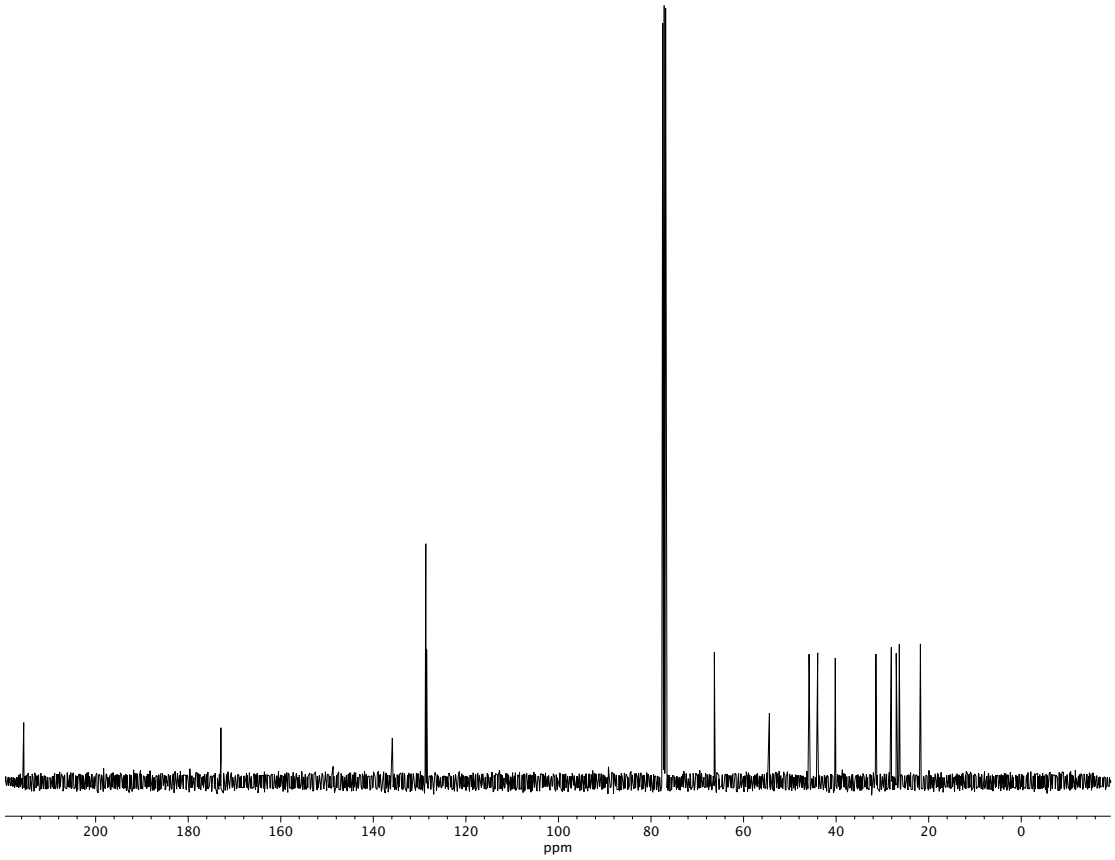


Figure A1.54. *^{13}C NMR (100 MHz, $CDCl_3$) of compound* ***11q****.*

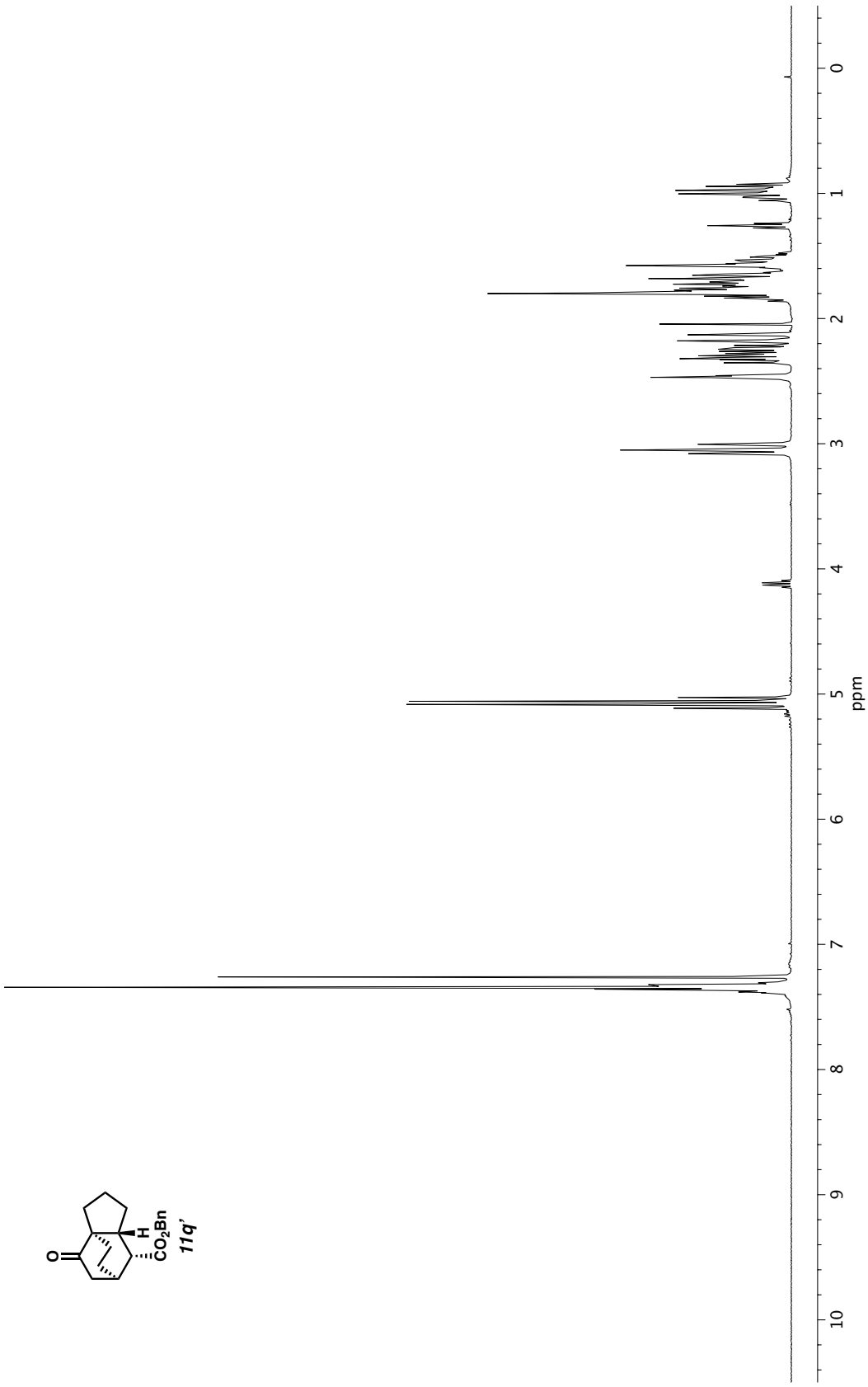


Figure A1.55. *^1H NMR (400 MHz, $CDCl_3$) of compound* ***11q'*** *.*

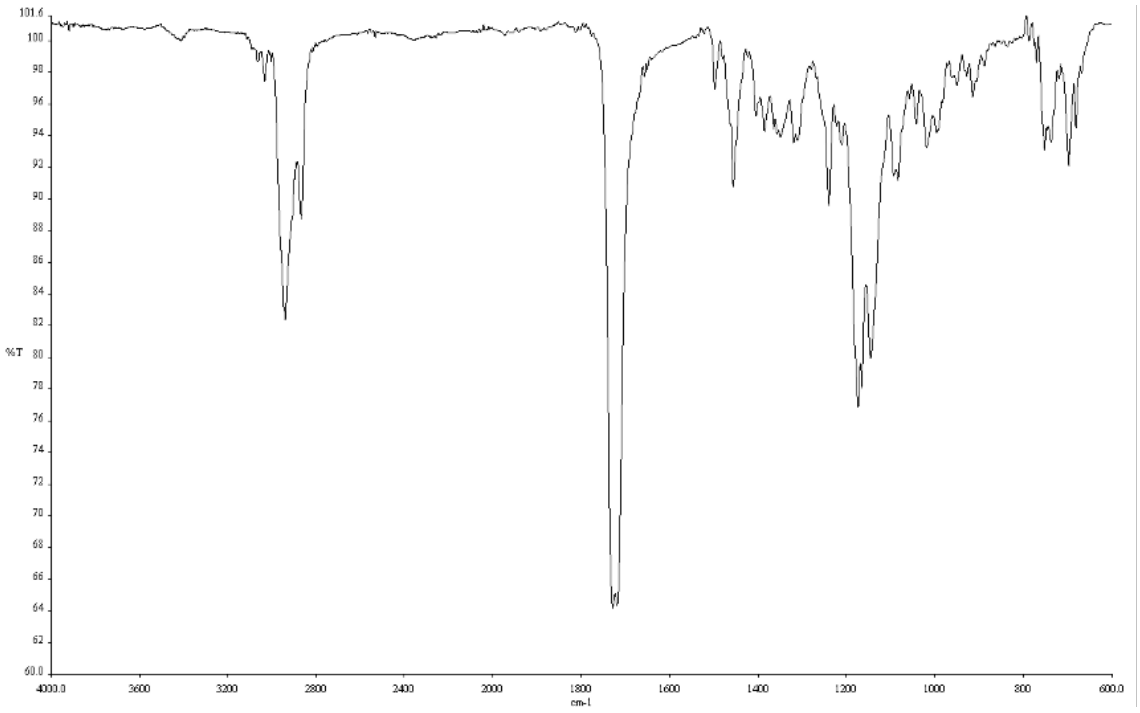


Figure A1.56. *Infrared spectrum (Thin Film, NaCl) of compound* ***11q'****.*

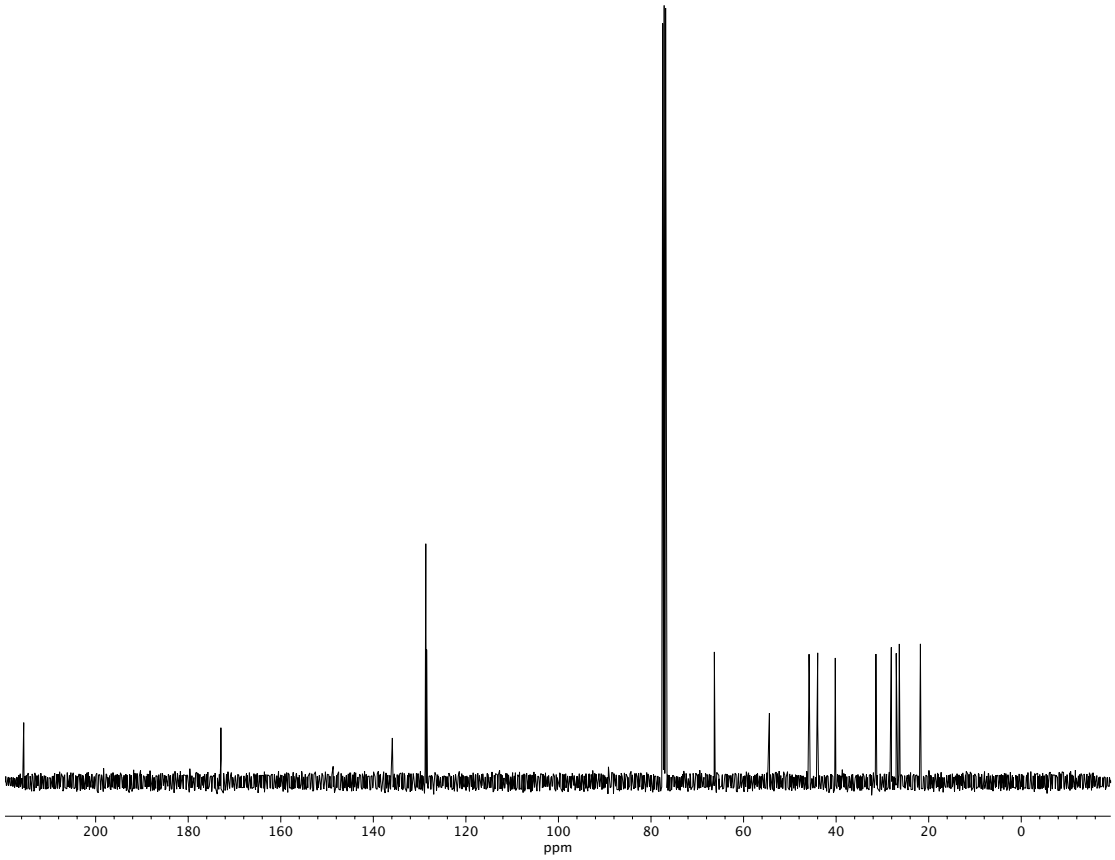


Figure A1.57. *^{13}C NMR (100 MHz, $CDCl_3$) of compound* ***11q'****.*

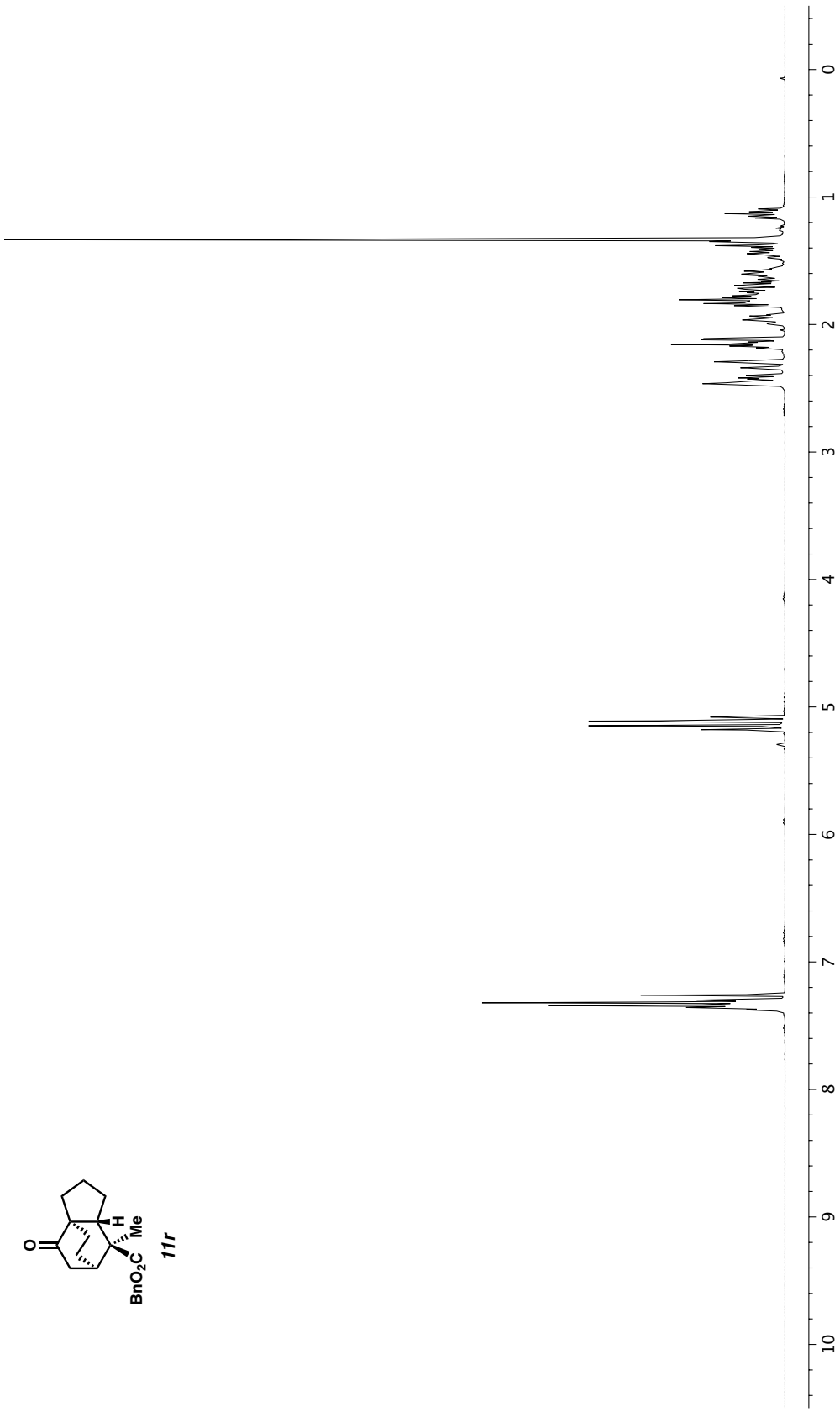


Figure A1.58. *^{1}H NMR (400 MHz, $CDCl_3$) of compound* ***11r****.*

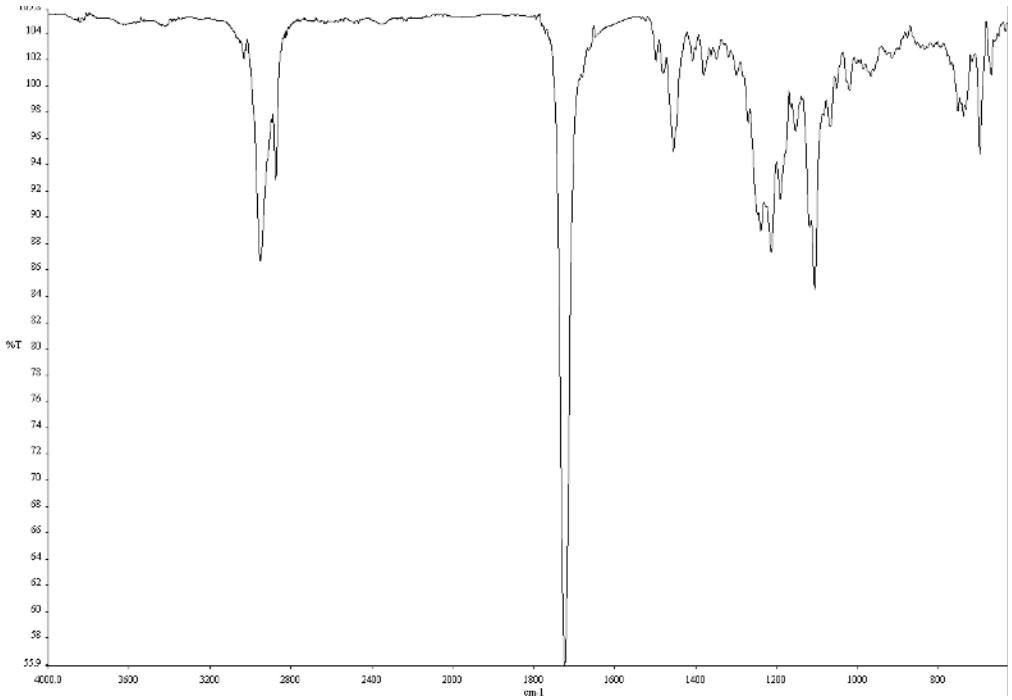


Figure A1.59. *Infrared spectrum (Thin Film, NaCl) of compound* ***11r****.*

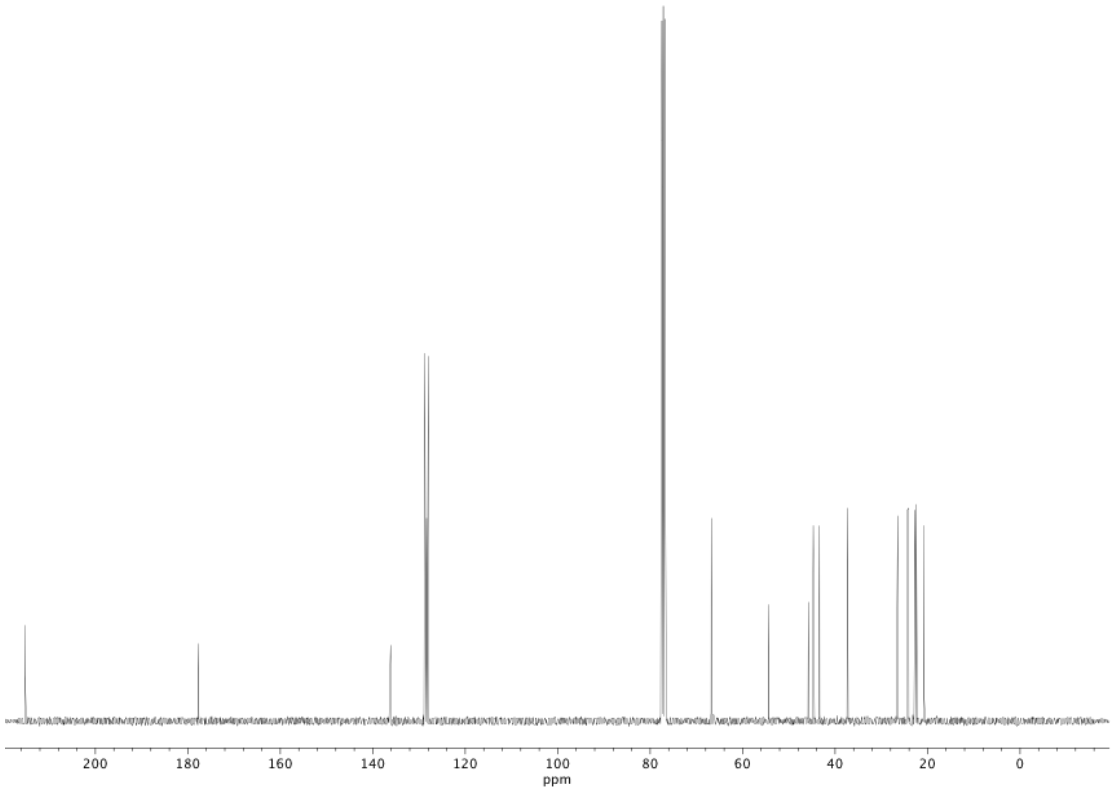


Figure A1.60. *^{13}C NMR (100 MHz, $CDCl_3$) of compound* ***11r****.*

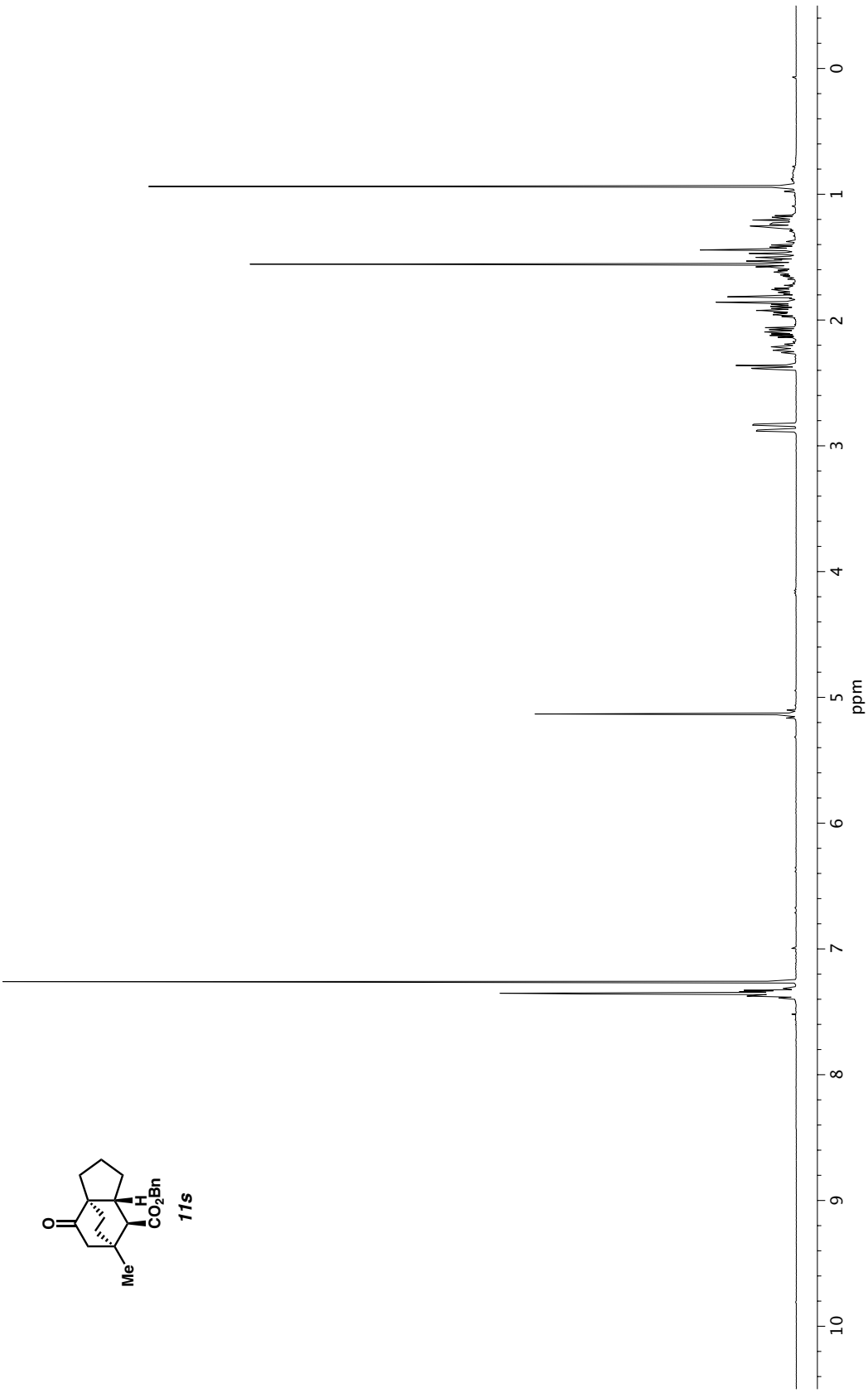


Figure A1.61. *^{1}H NMR (400 MHz, $CDCl_3$) of compound **11s**.*

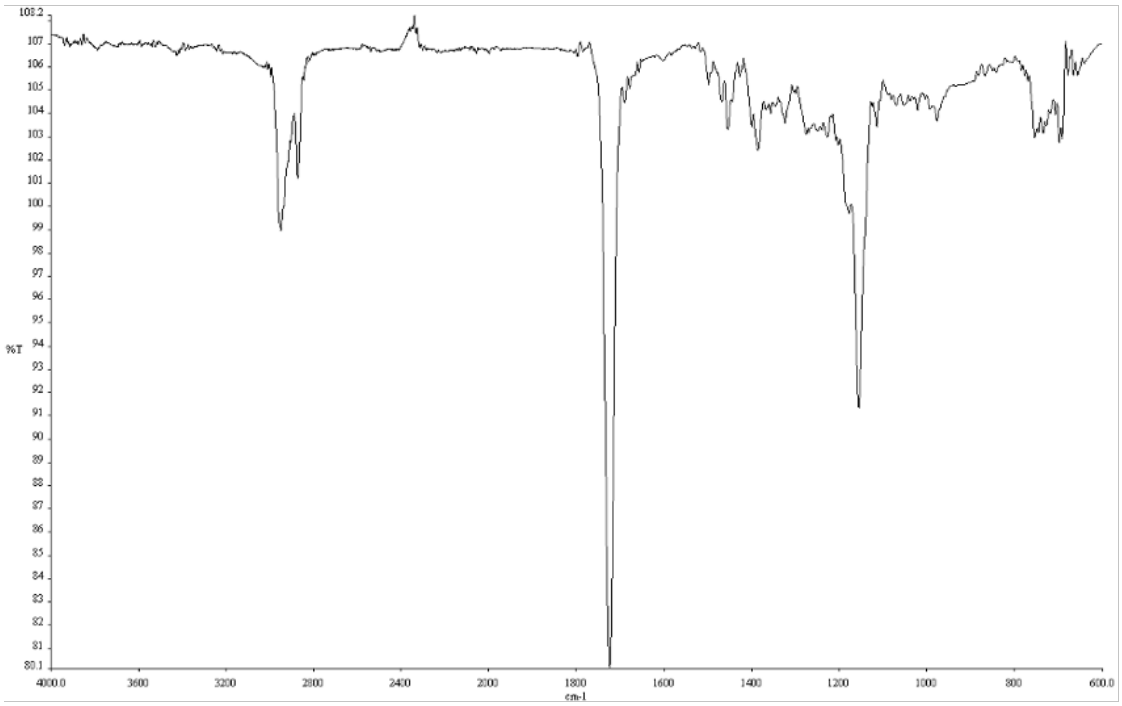


Figure A1.62. *Infrared spectrum (Thin Film, NaCl) of compound* ***11s****.*

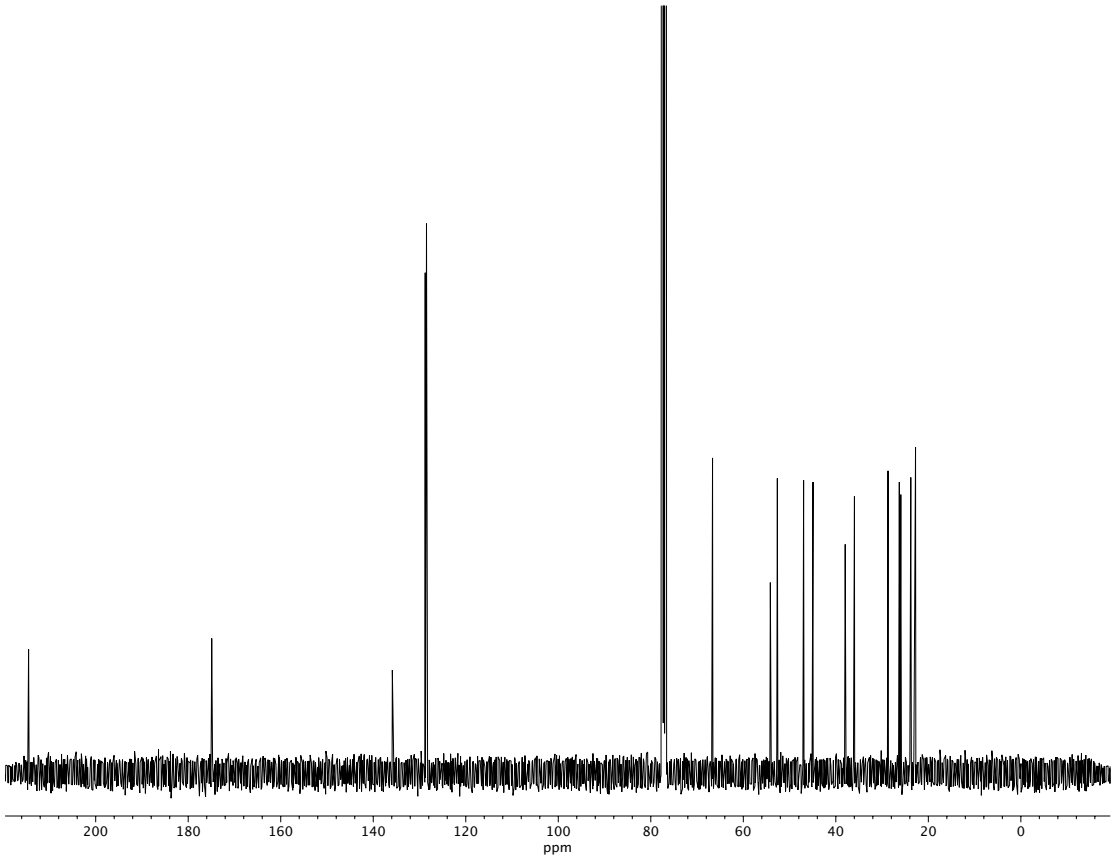


Figure A1.63. *^{13}C NMR (100 MHz, $CDCl_3$) of compound* ***11s****.*

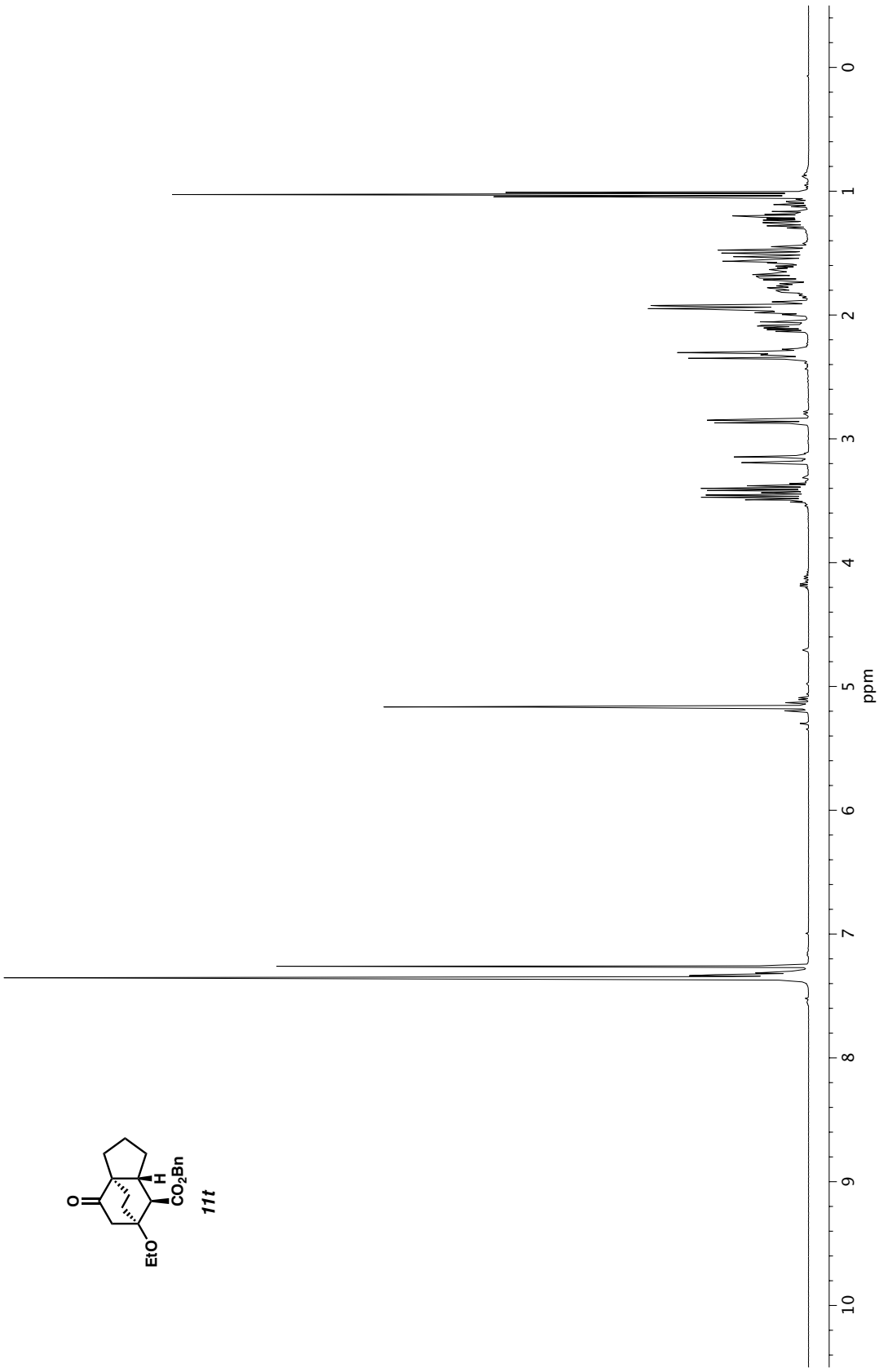


Figure A1.64. *^{1}H NMR (400 MHz, $CDCl_3$) of compound* ***11t****.*

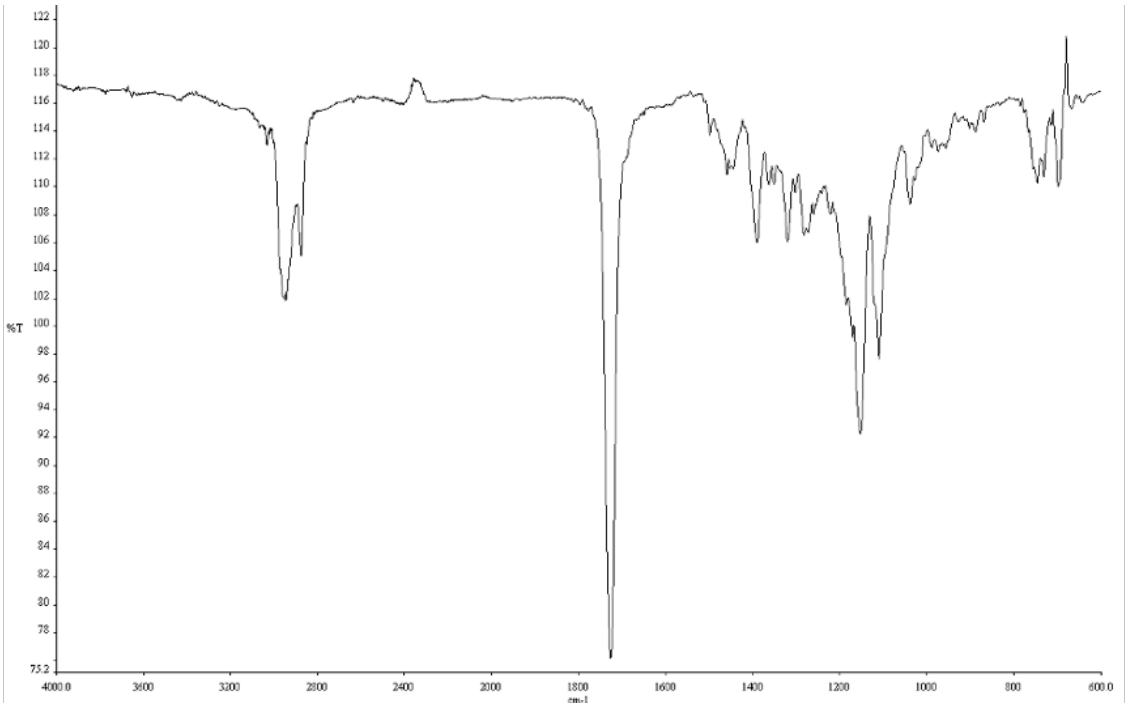


Figure A1.65. *Infrared spectrum (Thin Film, NaCl) of compound* ***11t****.*

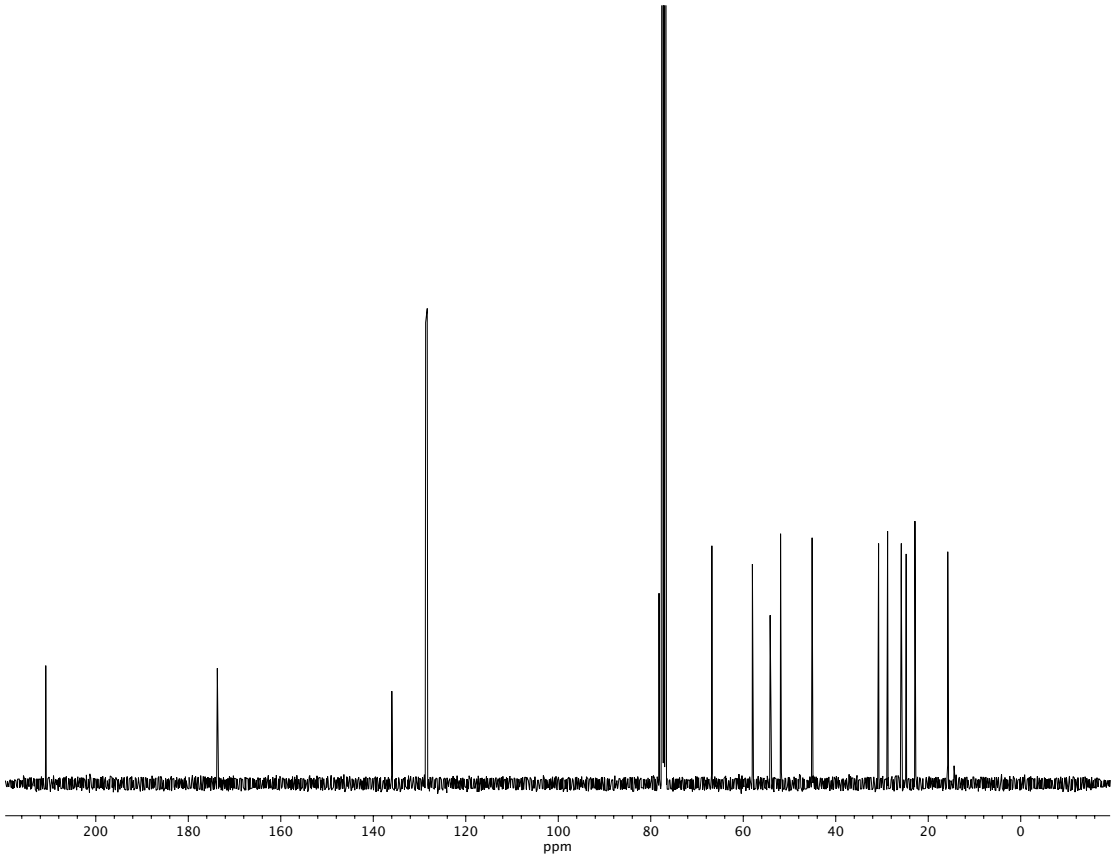


Figure A1.66. *^{13}C NMR (100 MHz, $CDCl_3$) of compound* ***11t****.*

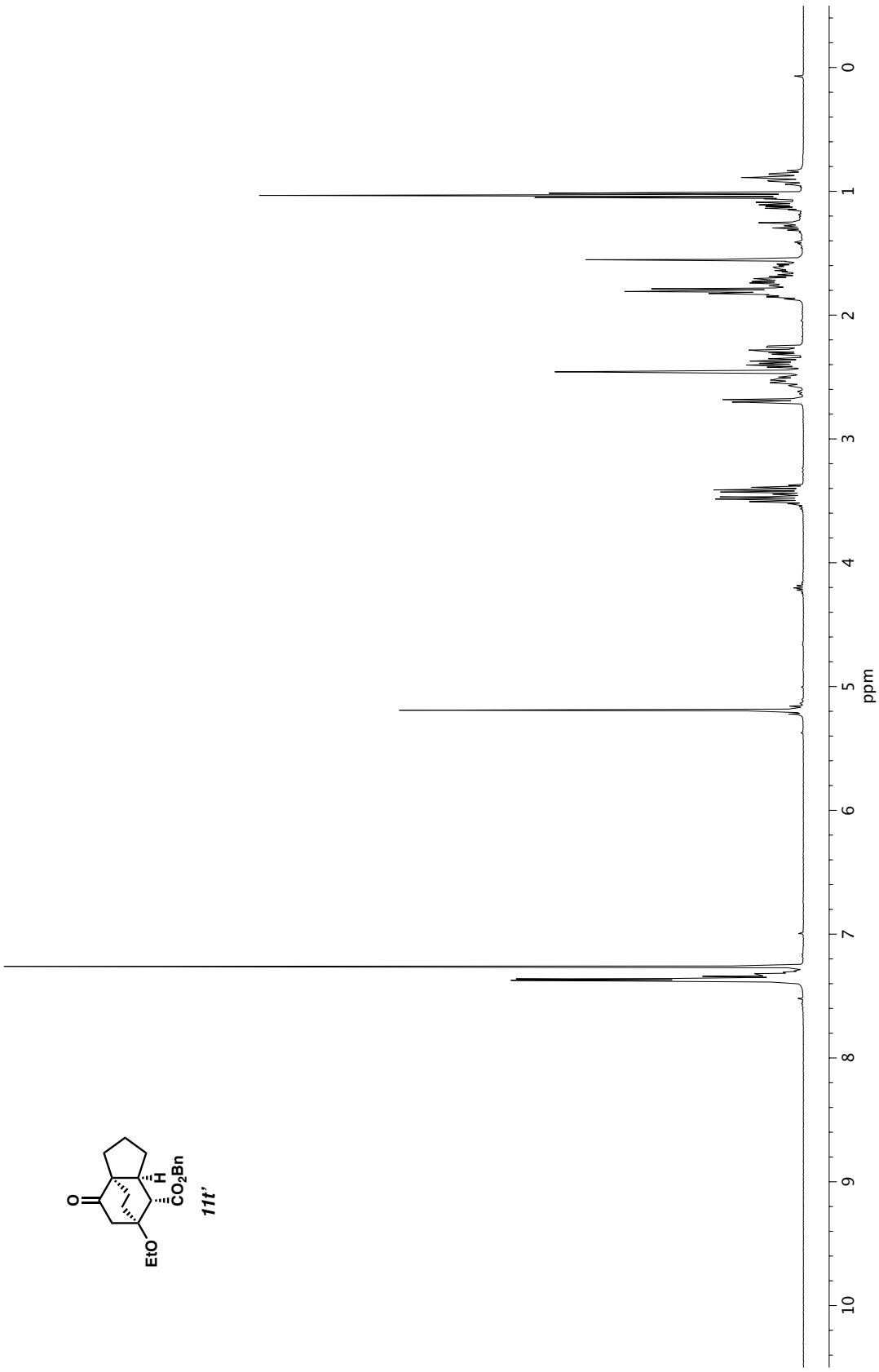


Figure A1.67. *^1H NMR (400 MHz, $CDCl_3$) of compound* ***11t'*** *.*

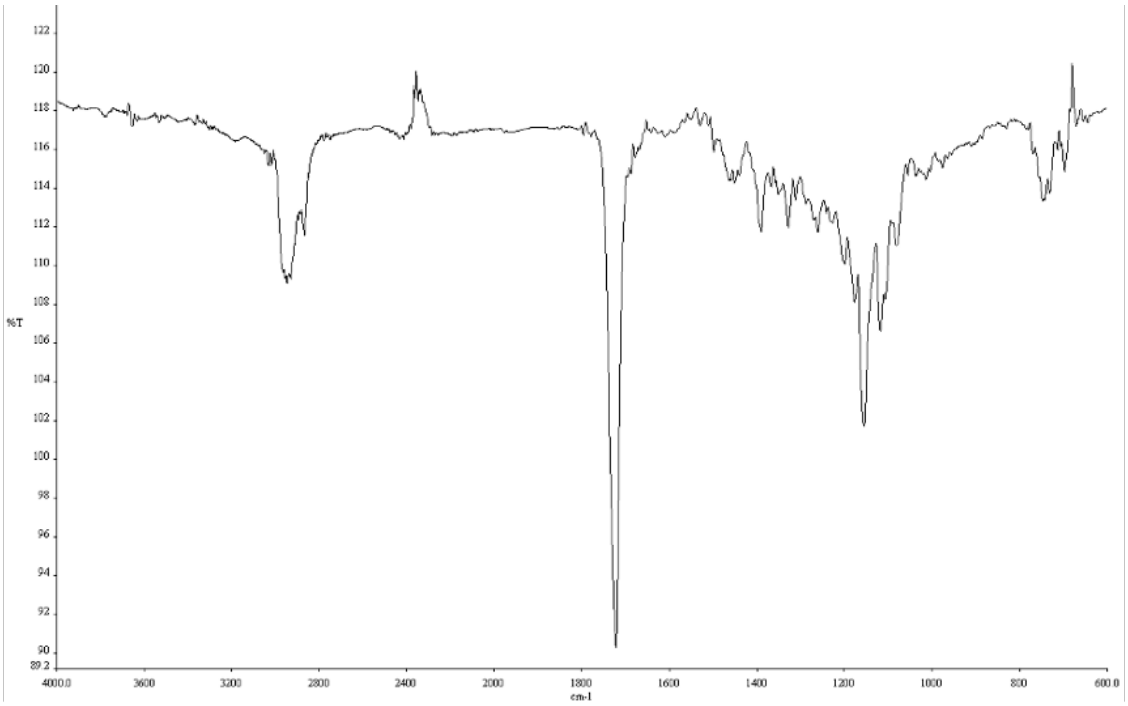


Figure A1.68. *Infrared spectrum (Thin Film, NaCl) of compound* ***11t'****.*

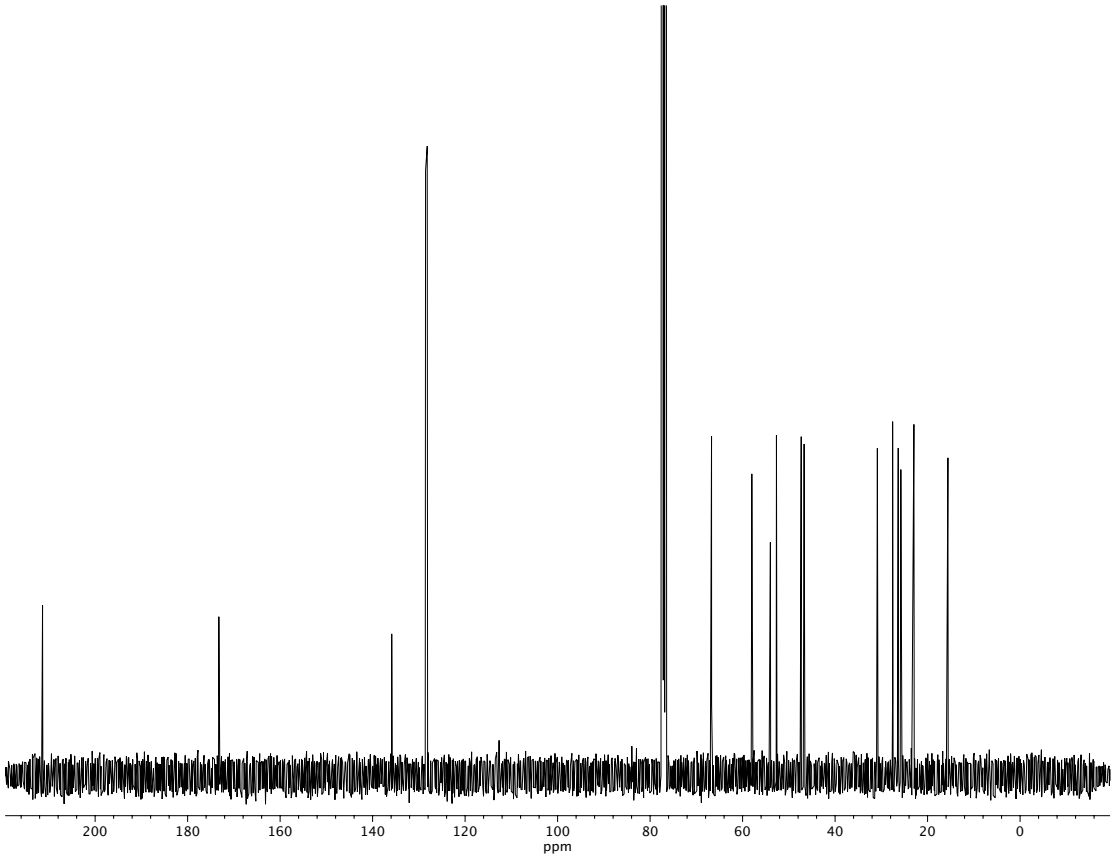


Figure A1.69. *^{13}C NMR (100 MHz, $CDCl_3$) of compound* ***11t'****.*

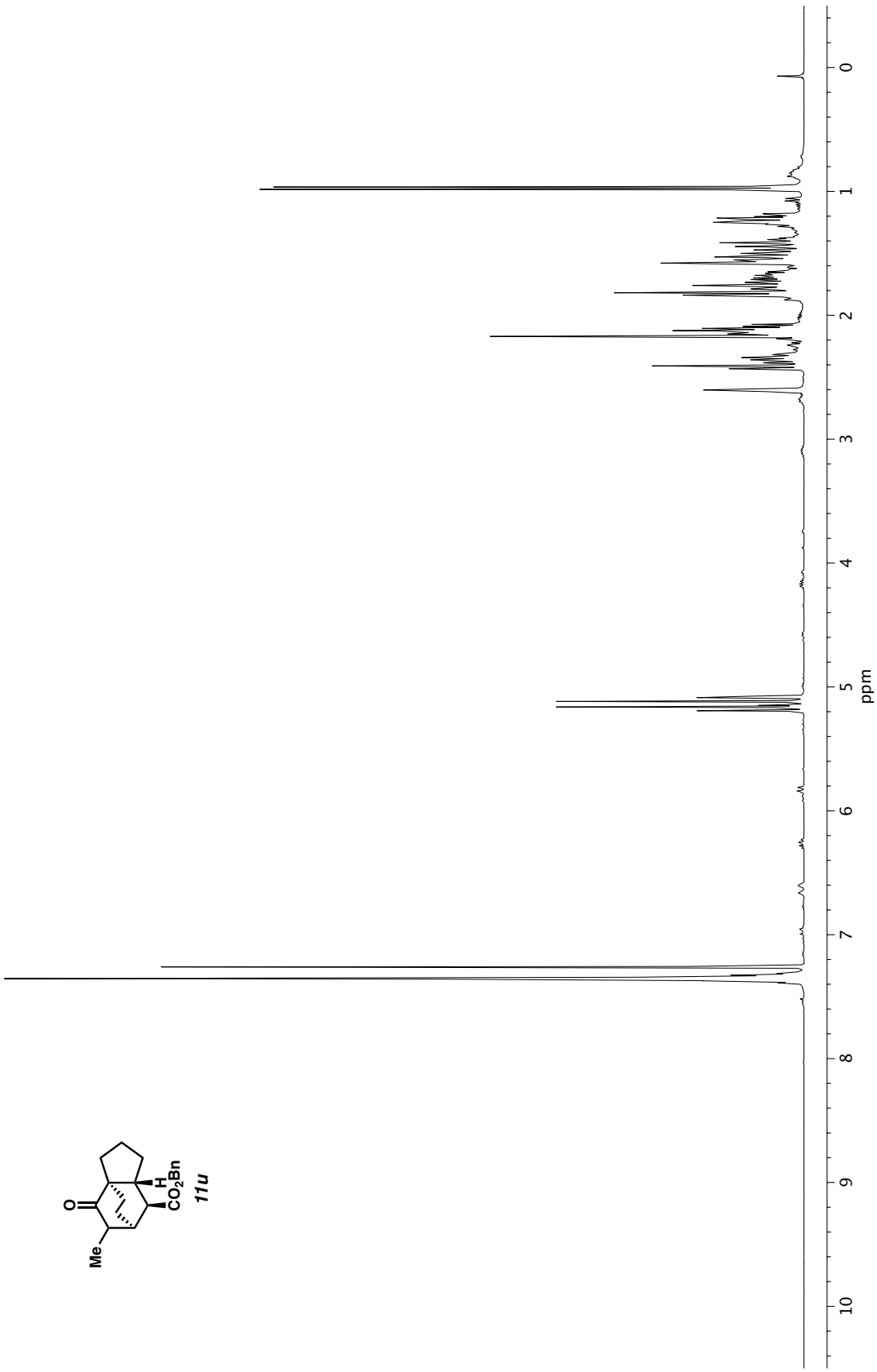


Figure A1.70. *^{1}H NMR (400 MHz, $CDCl_3$) of compound* ***11u****.*

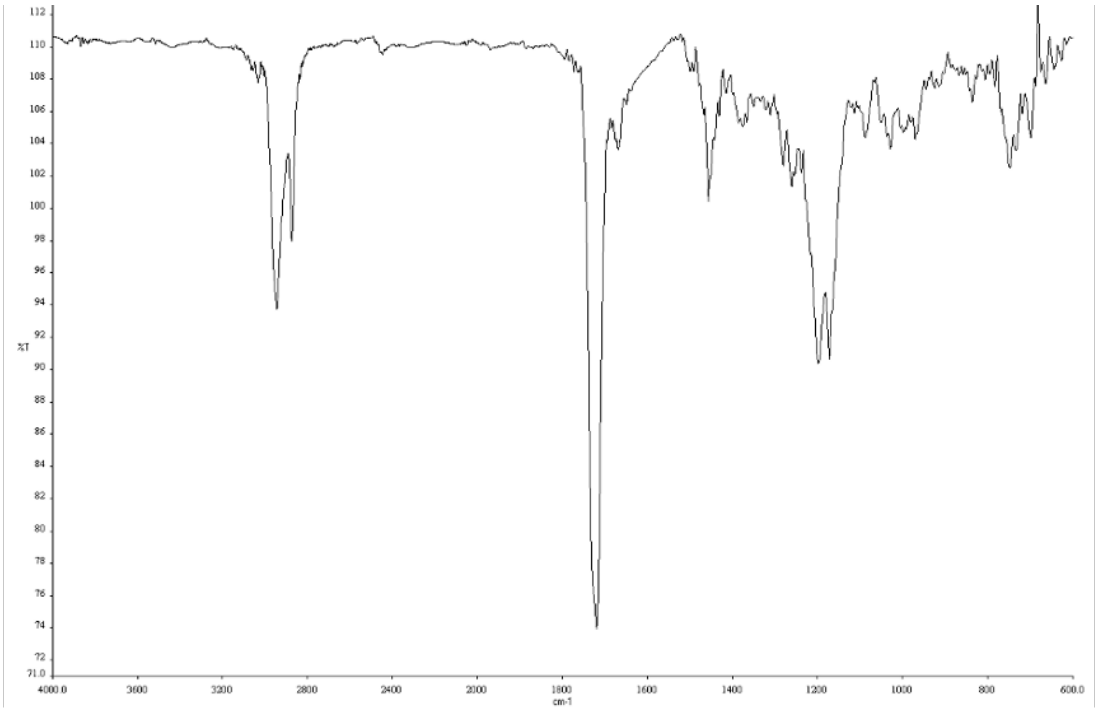


Figure A1.71. *Infrared spectrum (Thin Film, NaCl) of compound* ***11u****.*

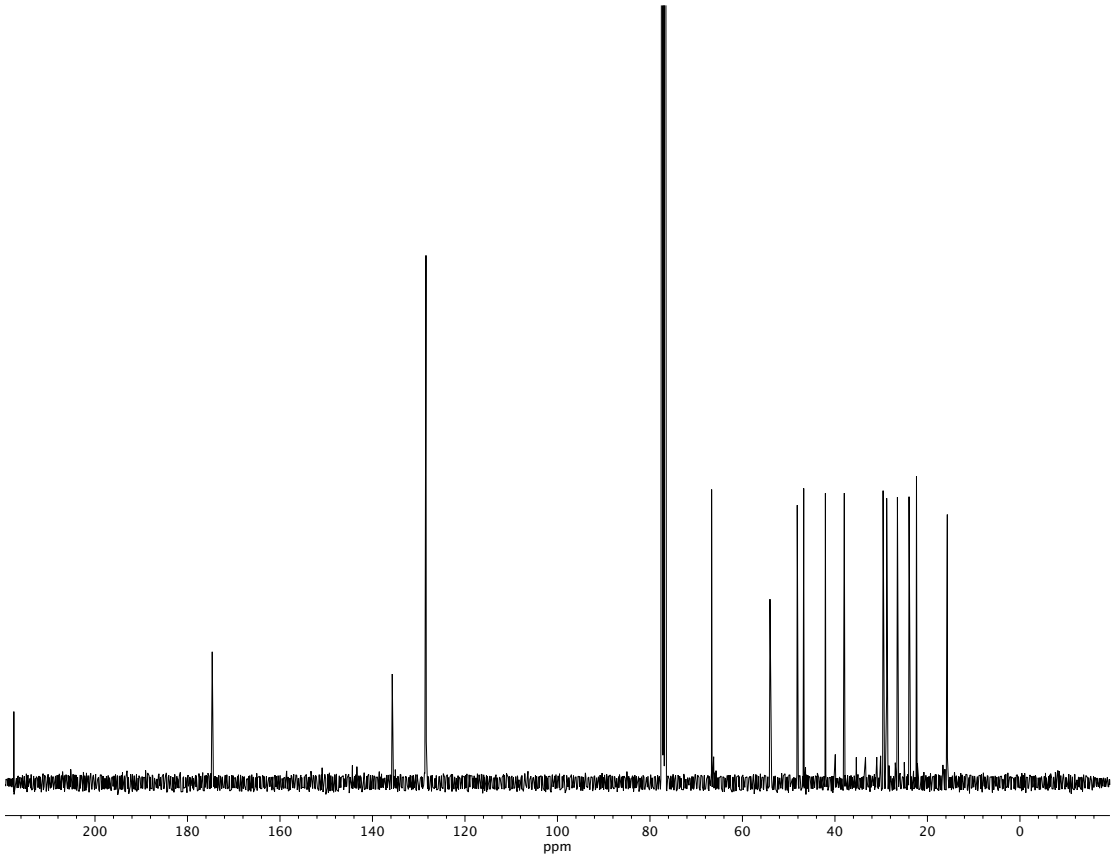


Figure A1.72. *^{13}C NMR (100 MHz, $CDCl_3$) of compound* ***11u****.*

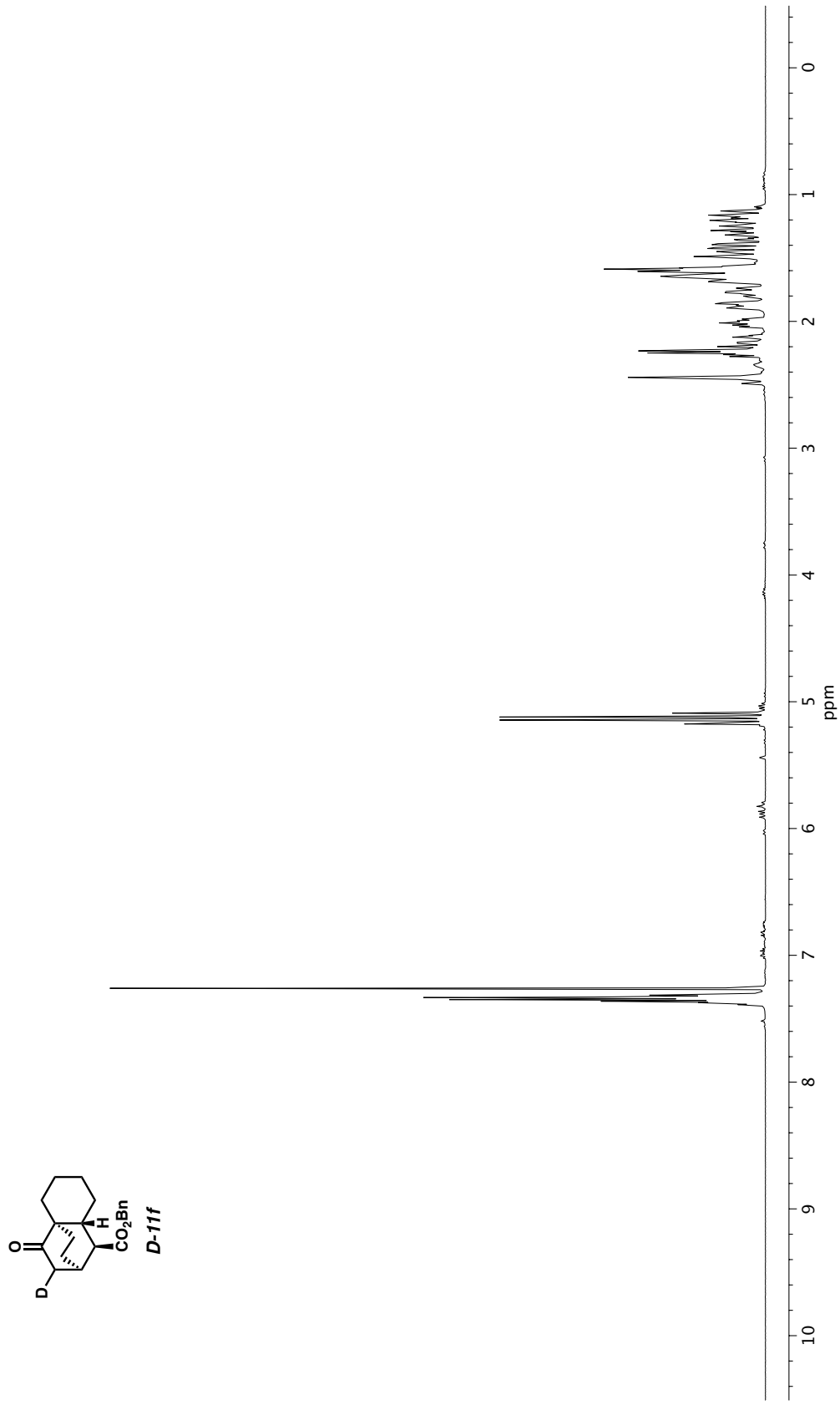


Figure A1.73. *^1H NMR (400 MHz, $CDCl_3$) of compound* ***D-11f****.*

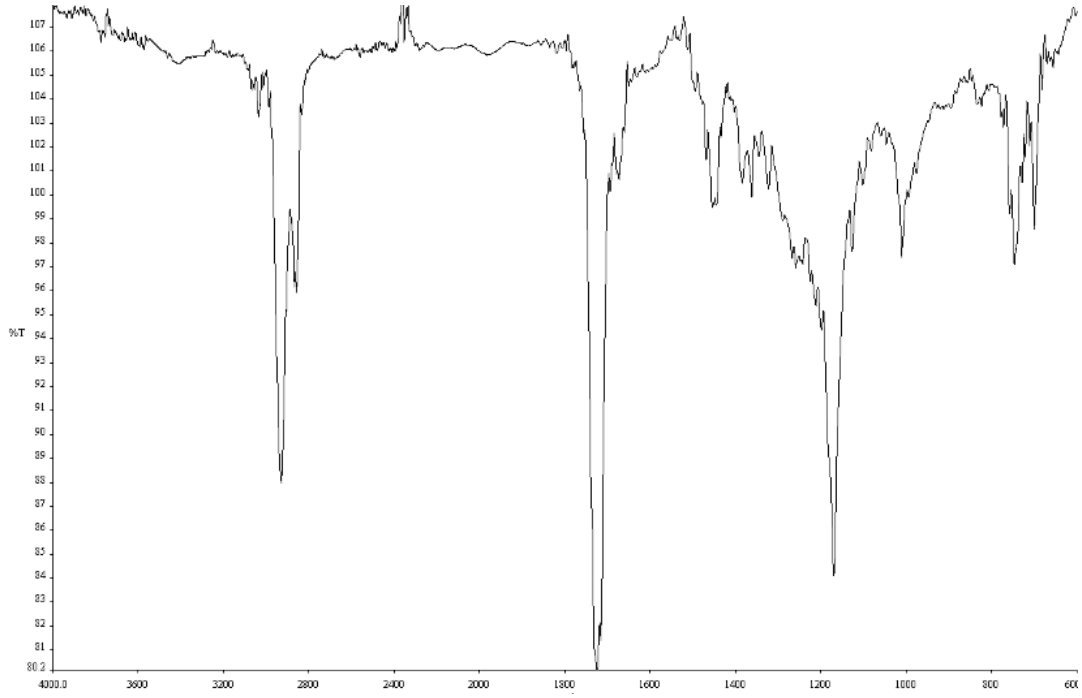


Figure A1.74. *Infrared spectrum (Thin Film, NaCl) of compound* ***D-11f****.*

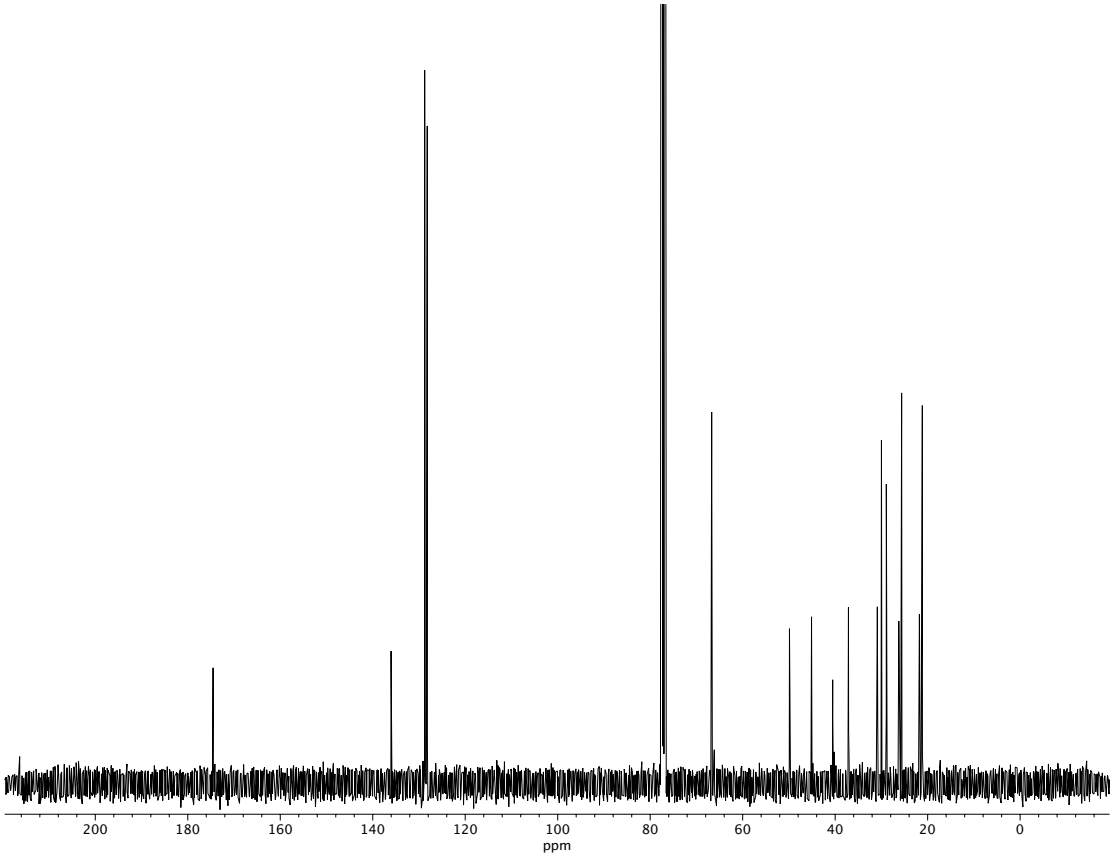


Figure A1.75. *^{13}C NMR (100 MHz, $CDCl_3$) of compound* ***D-11f****.*

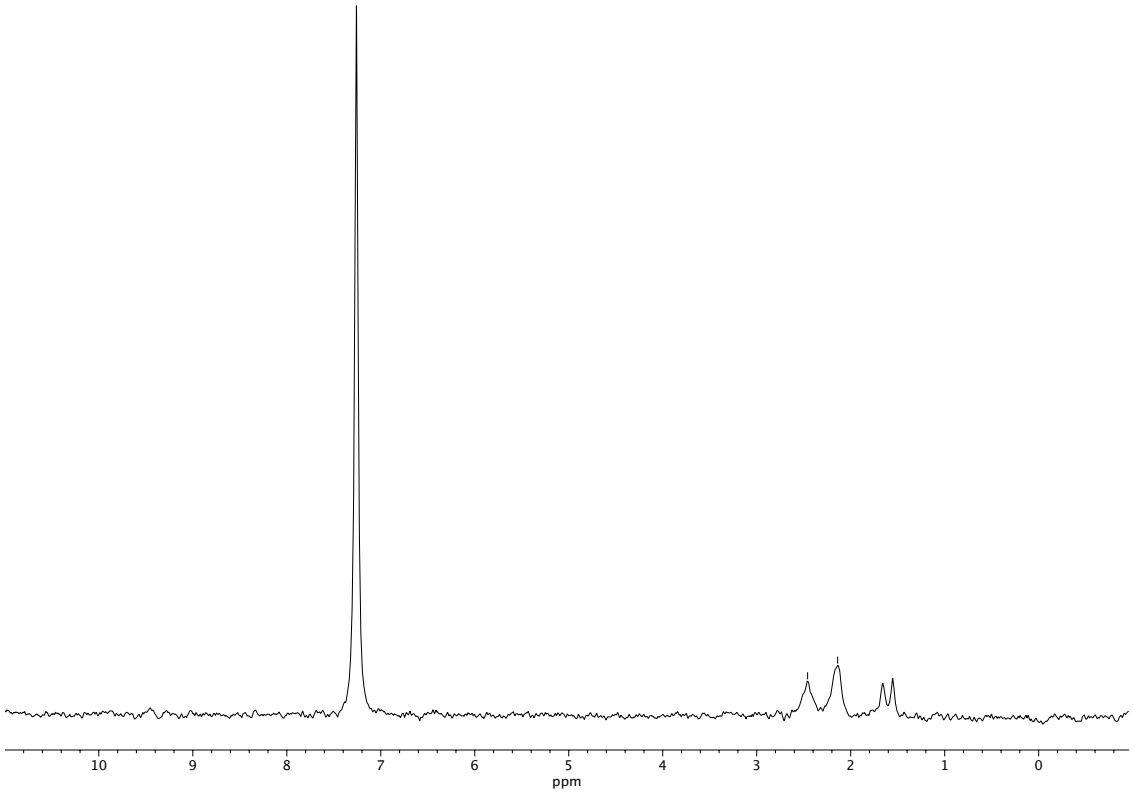


Figure A1.76. *^{2}H NMR (61 MHz, $CDCl_3$) of compound* ***D-11f****.*

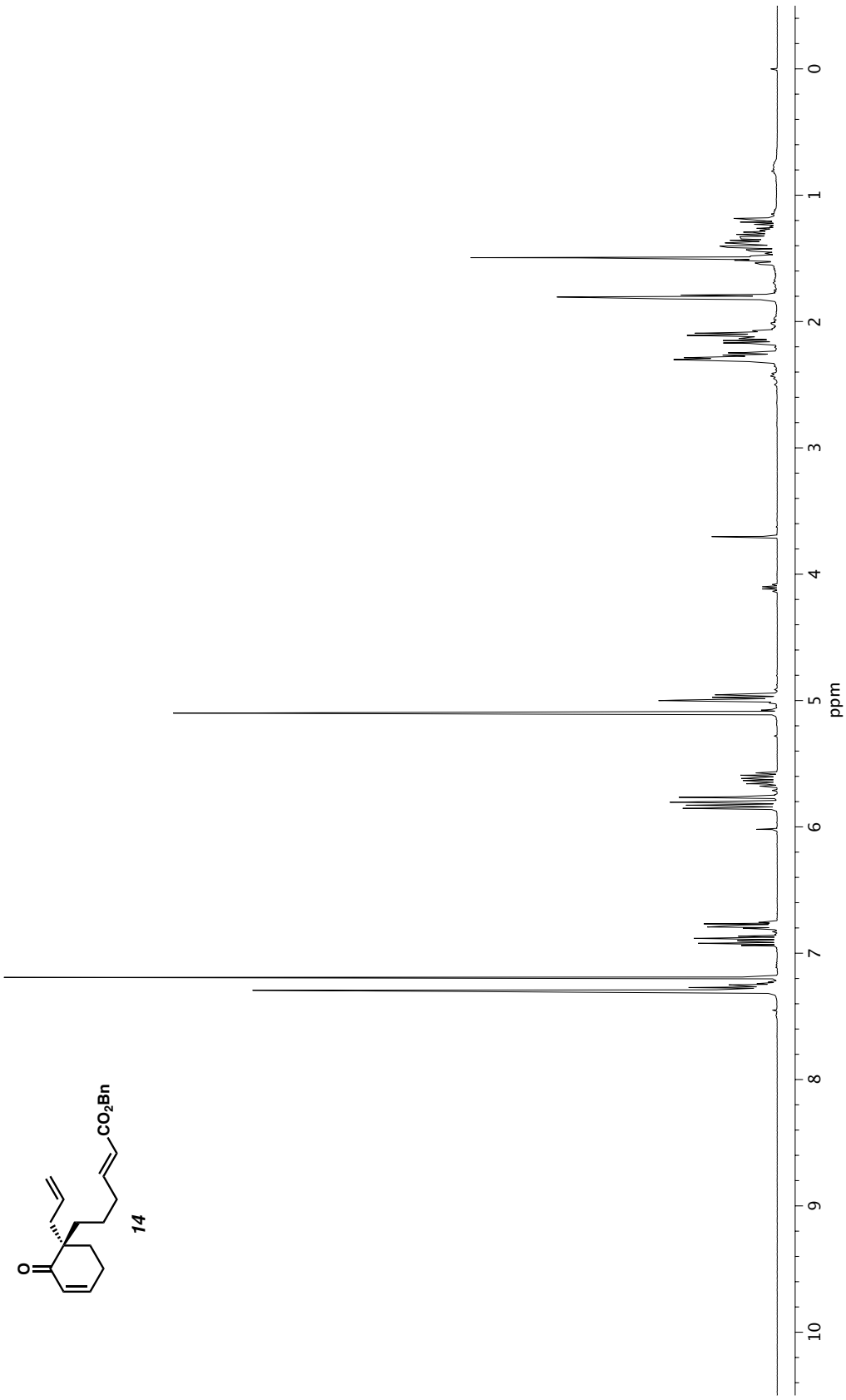


Figure A1.77. *^{1}H NMR (400 MHz, $CDCl_3$) of compound **14**.*

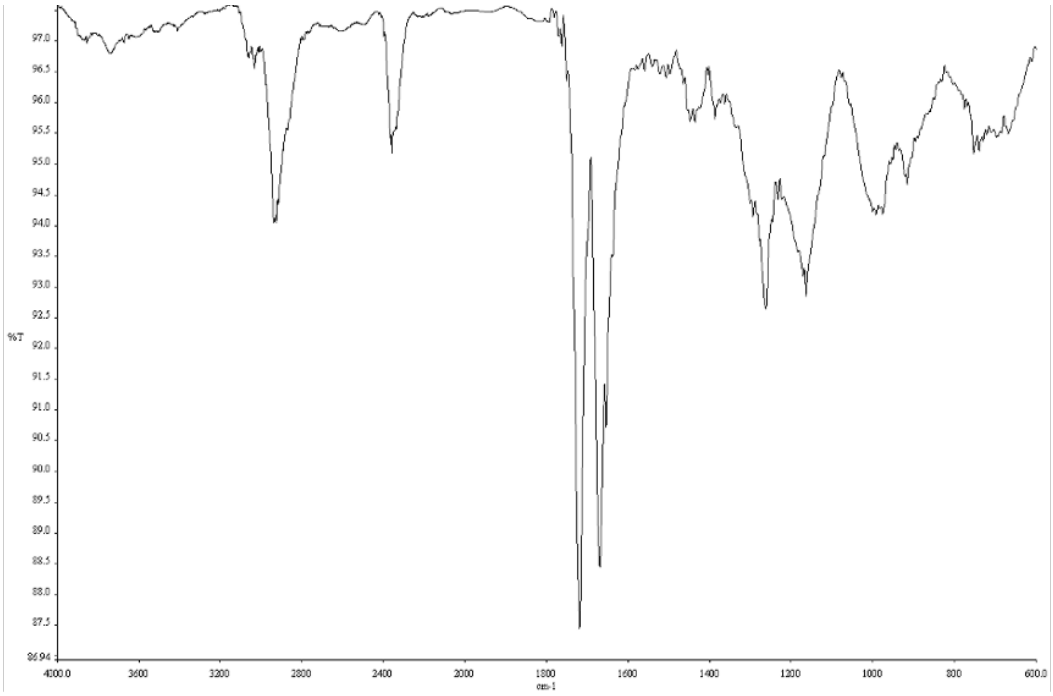


Figure A1.78. *Infrared spectrum (Thin Film, NaCl) of compound* ***14****.*

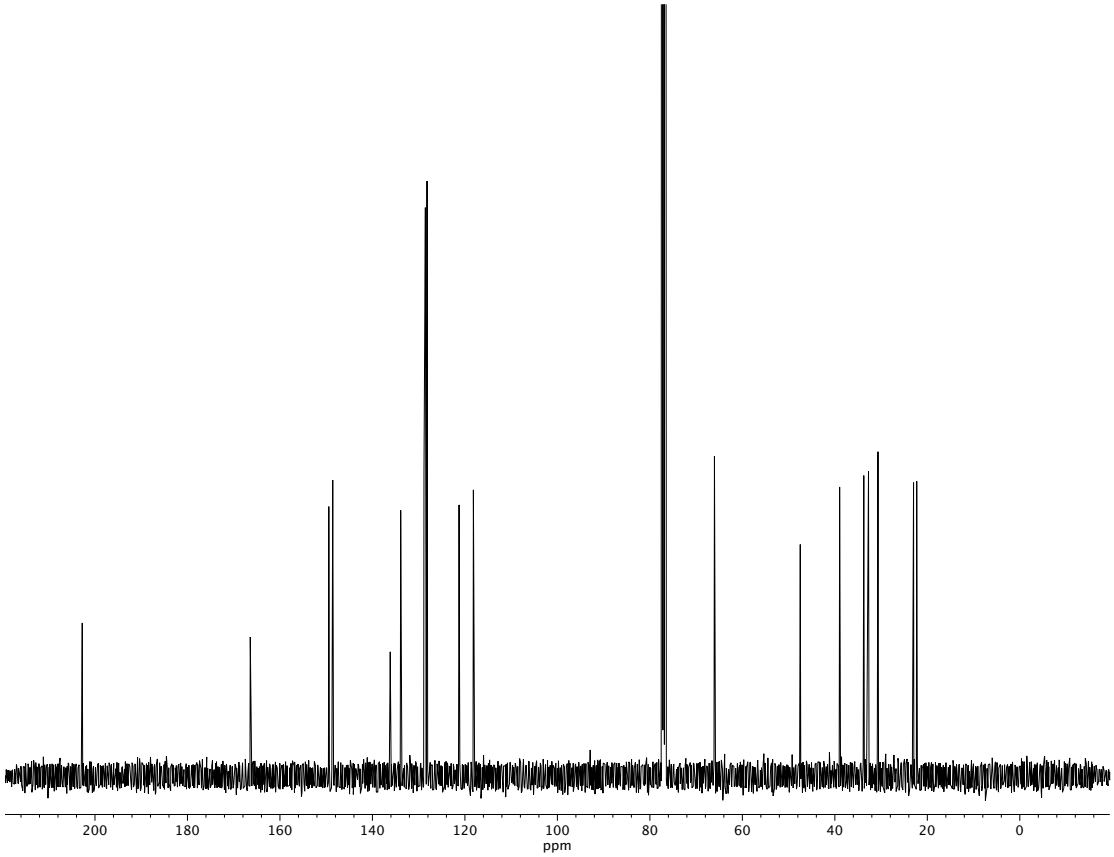


Figure A1.79. *^{13}C NMR (100 MHz, $CDCl_3$) of compound* ***14****.*

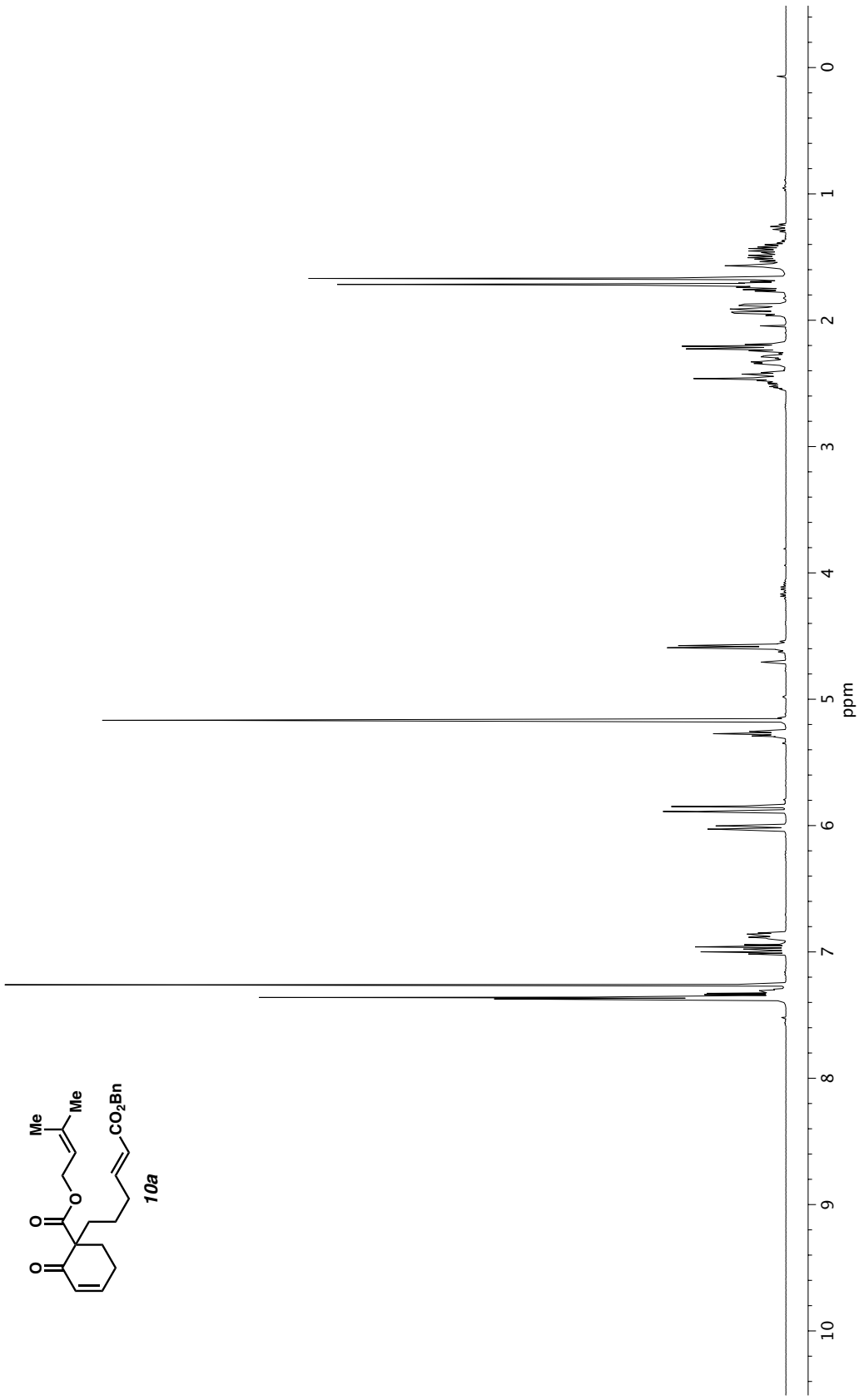


Figure A1.80. *^1H NMR (400 MHz, $CDCl_3$) of compound* ***10a****.*

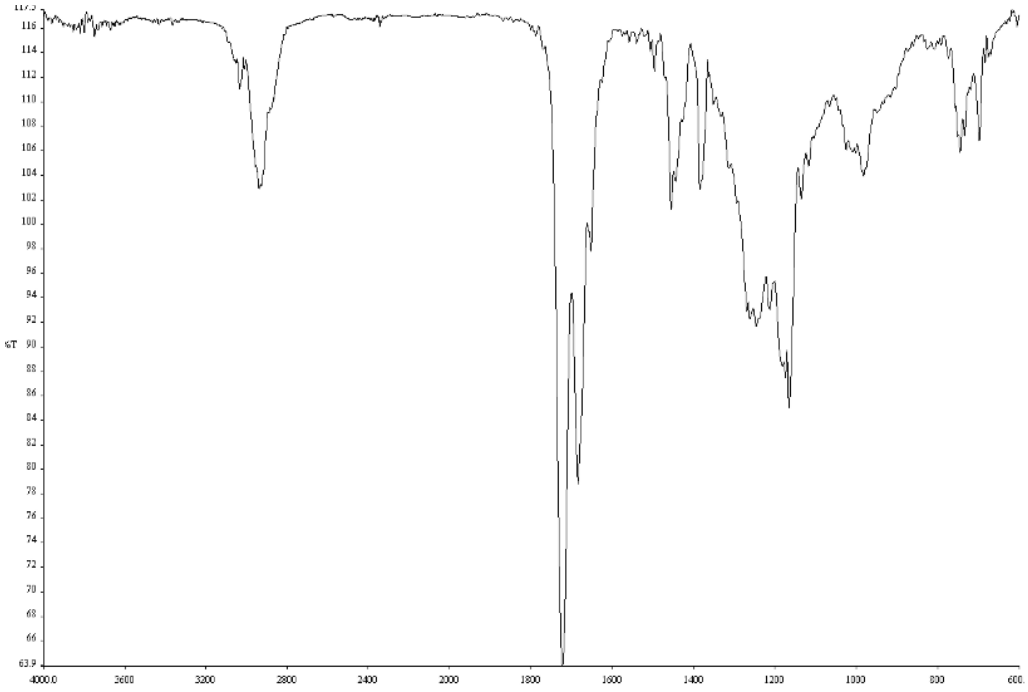


Figure A1.81. *Infrared spectrum (Thin Film, NaCl) of compound* ***10a****.*

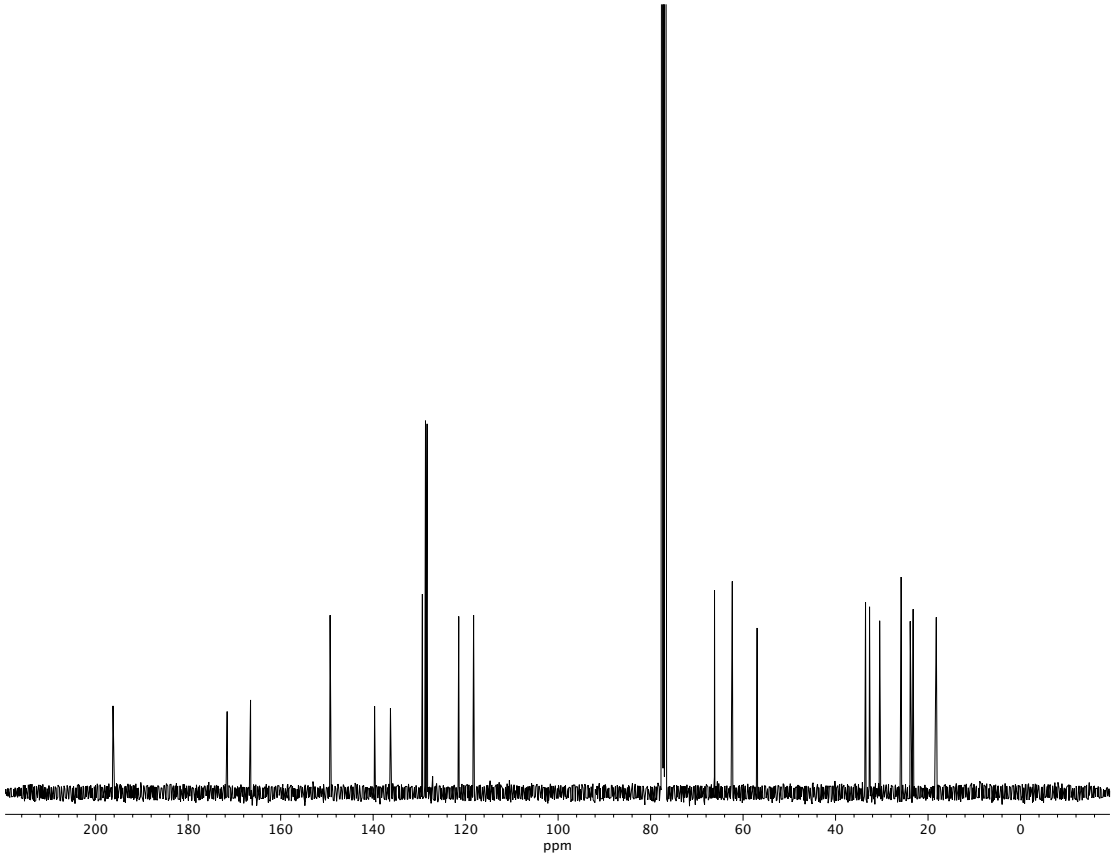


Figure A1.82. *^{13}C NMR (100 MHz, $CDCl_3$) of compound* ***10a****.*

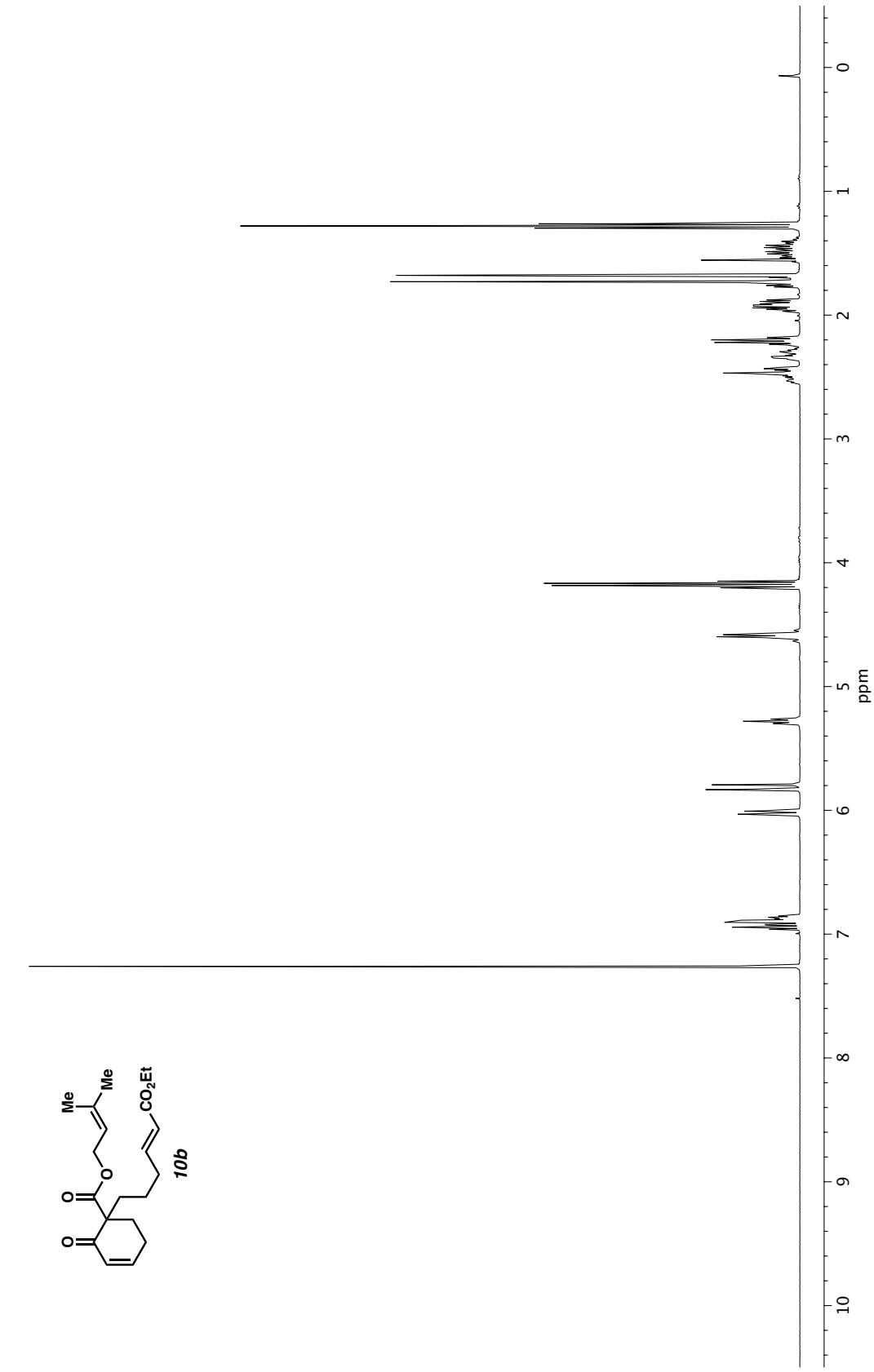


Figure A1.83. *^{1}H NMR (400 MHz, $CDCl_3$) of compound* ***10b****.*

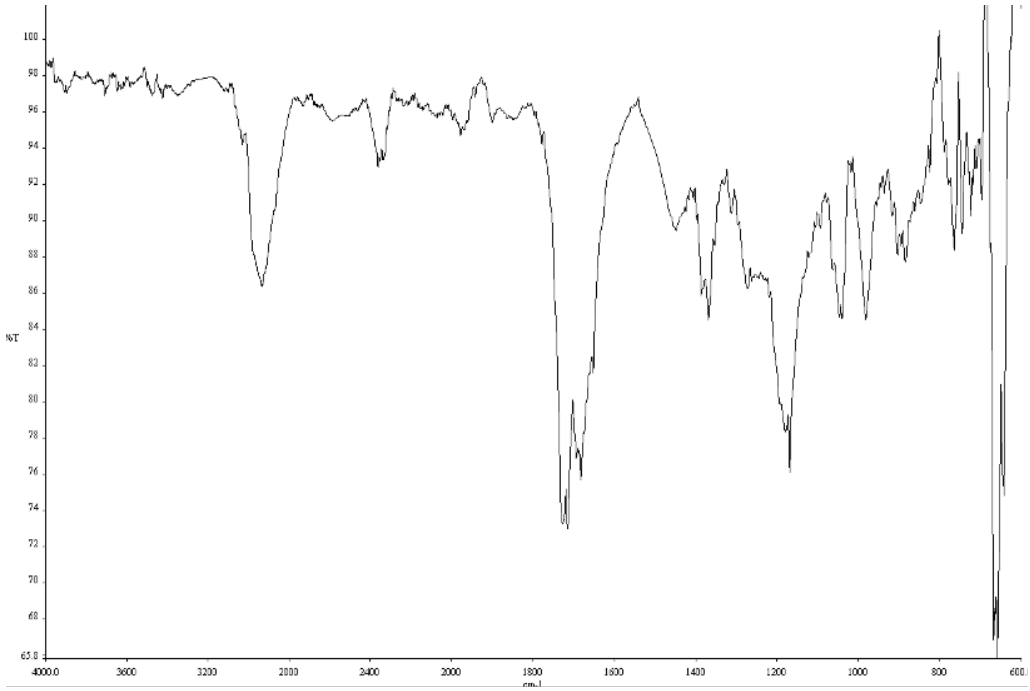


Figure A1.84. *Infrared spectrum (Thin Film, NaCl) of compound* ***10b****.*

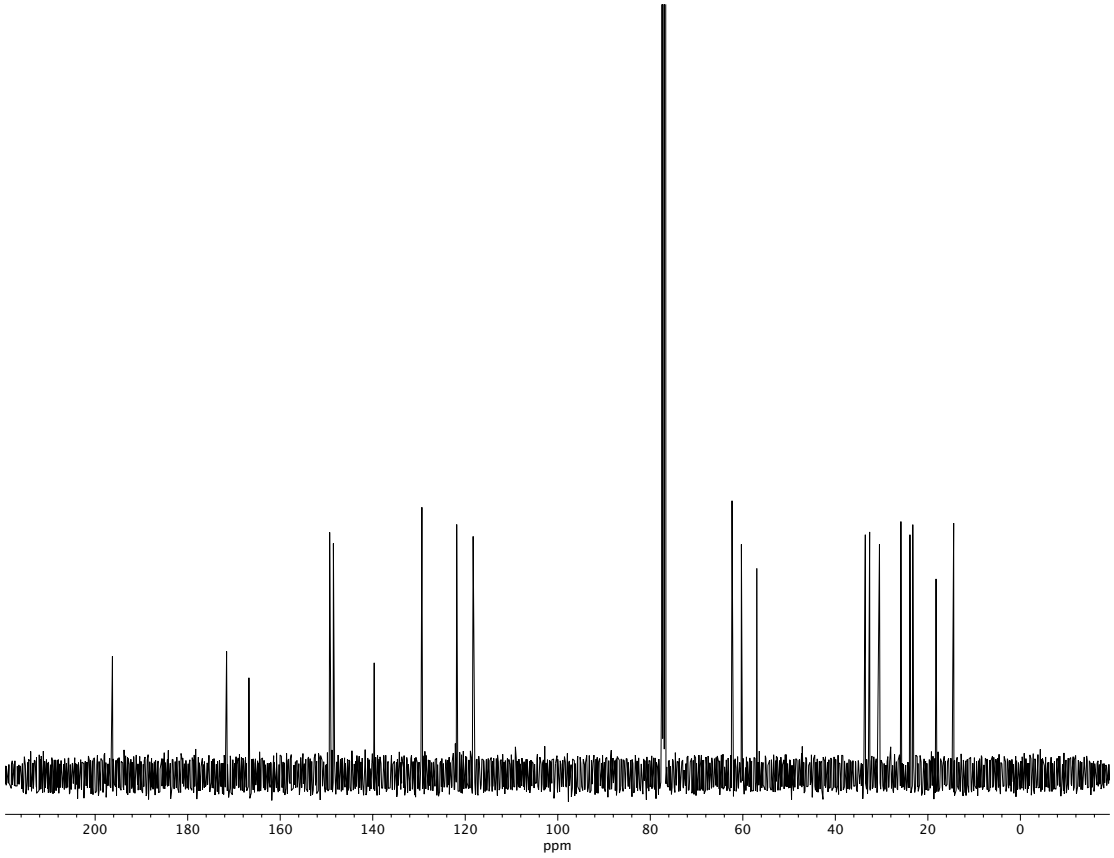


Figure A1.85. *^{13}C NMR (100 MHz, $CDCl_3$) of compound* ***10b****.*

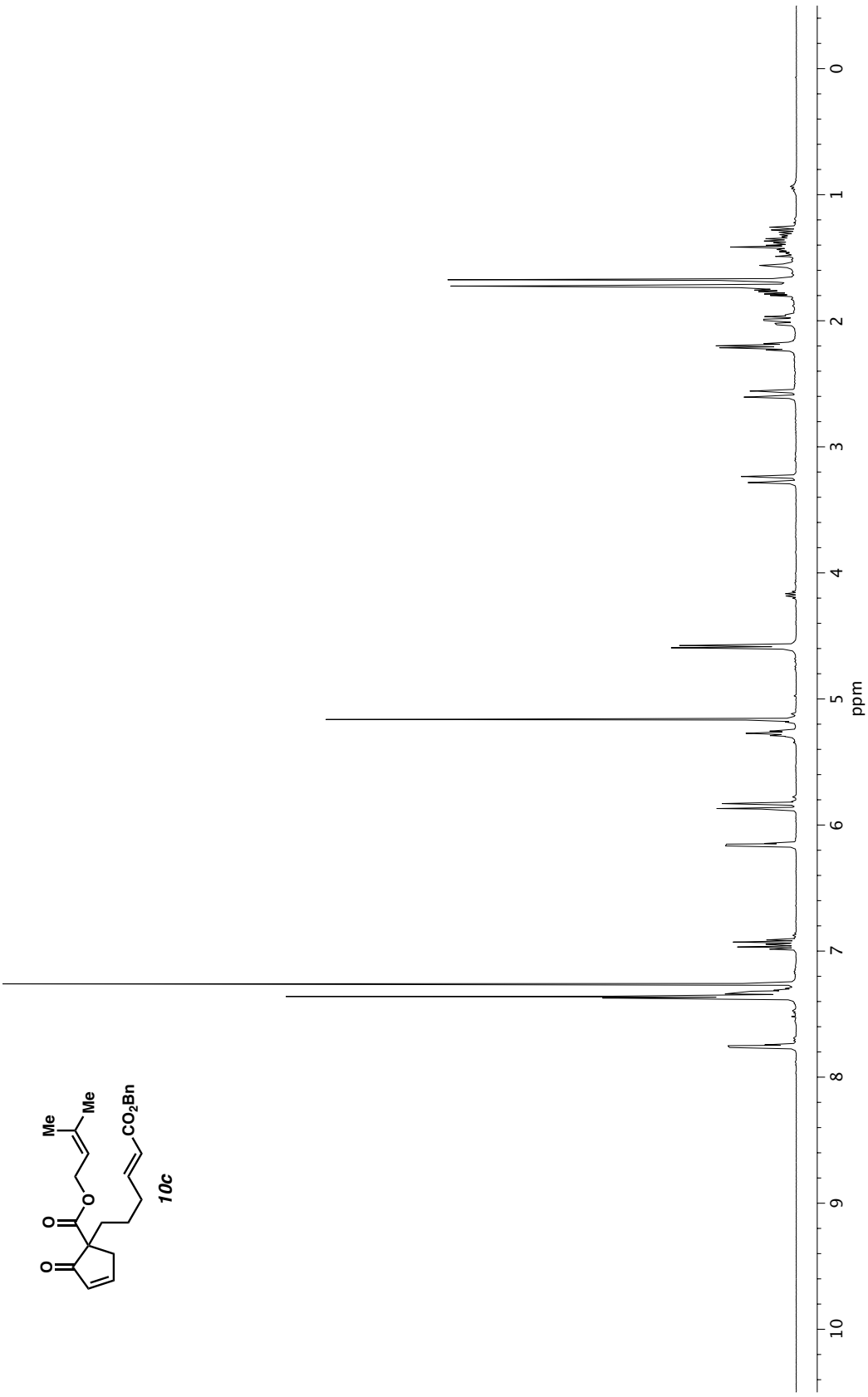


Figure A1.86. *^{1}H NMR (400 MHz, $CDCl_3$) of compound* ***10c****.*

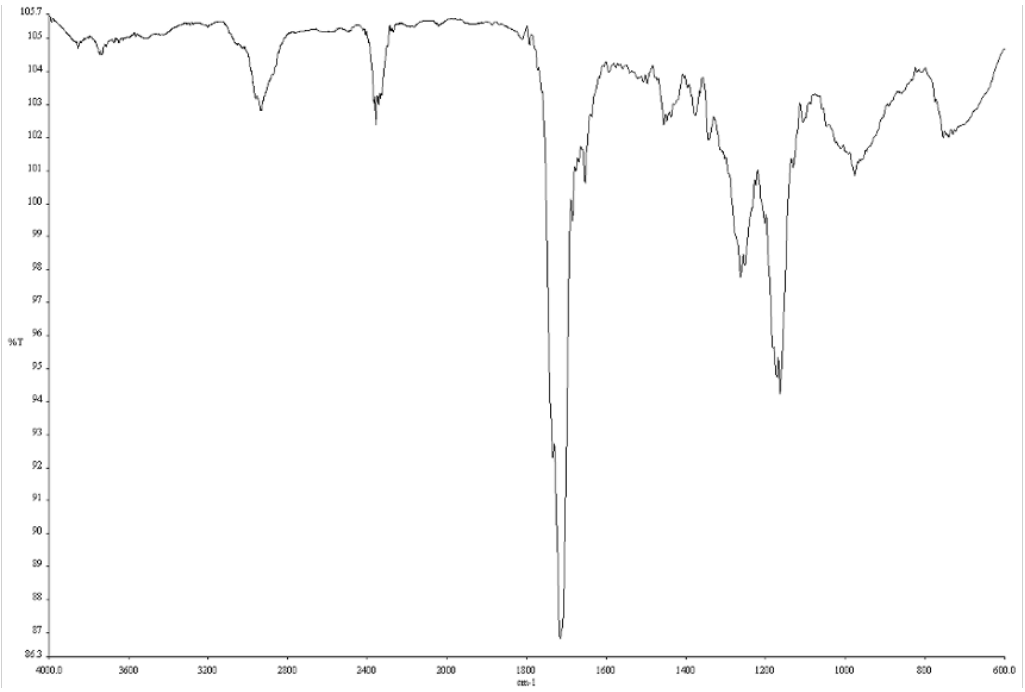


Figure A1.87. *Infrared spectrum (Thin Film, NaCl) of compound* ***10c****.*

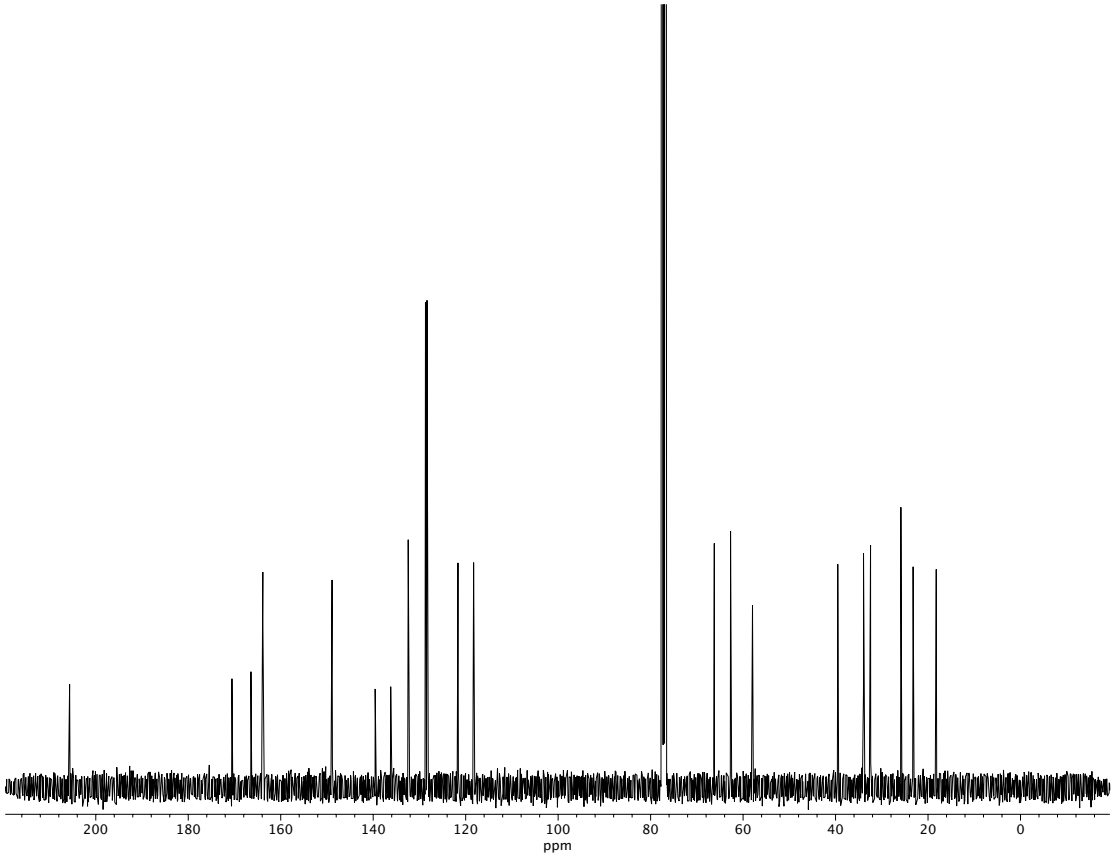


Figure A1.88. *^{13}C NMR (100 MHz, $CDCl_3$) of compound* ***10c****.*

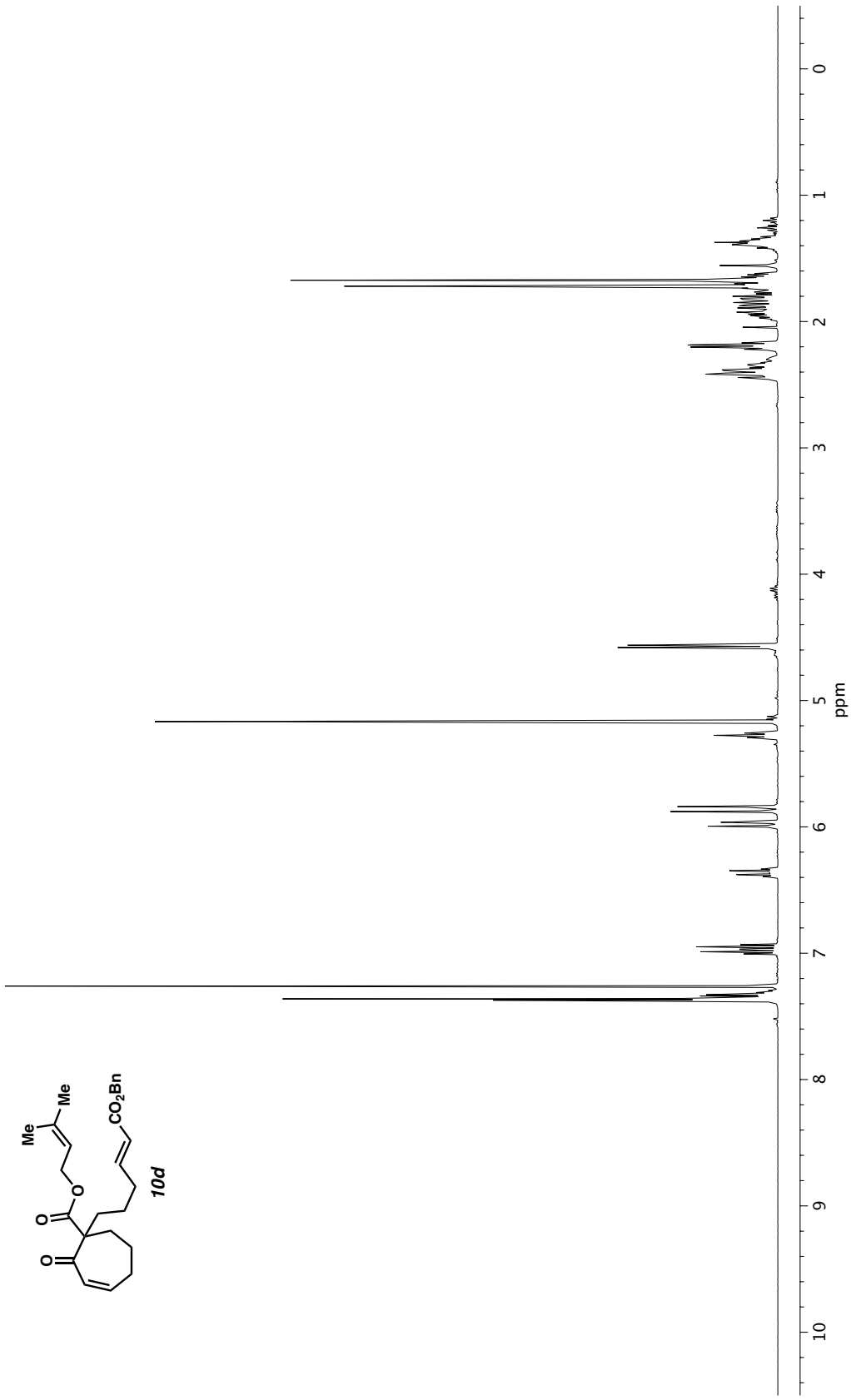


Figure A1.89. *^1H NMR (400 MHz, $CDCl_3$) of compound* ***10d****.*

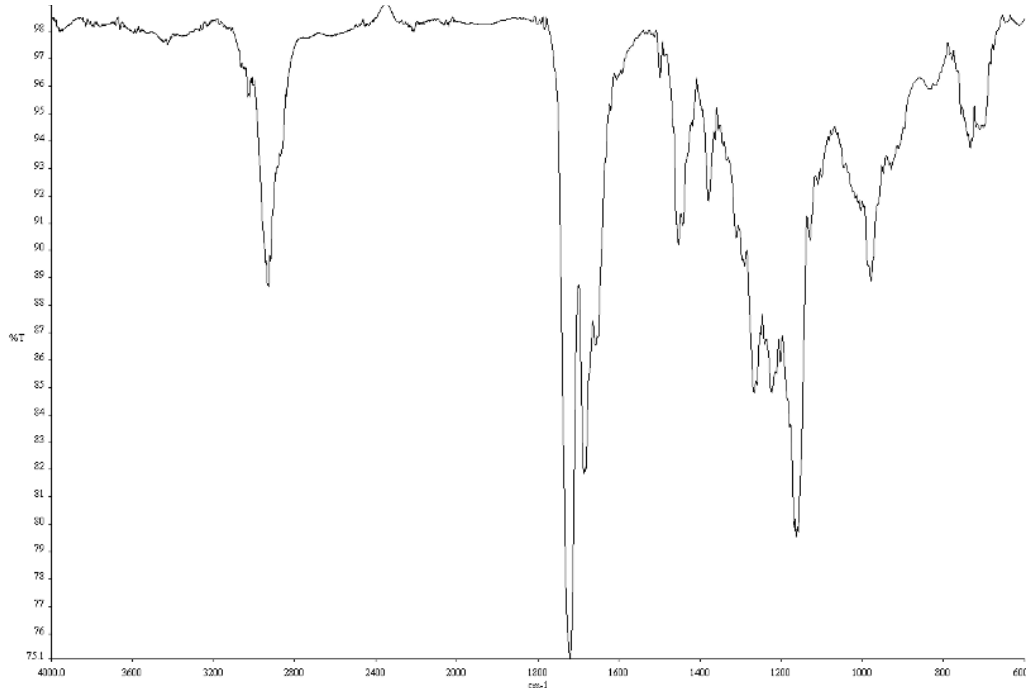


Figure A1.90. *Infrared spectrum (Thin Film, NaCl) of compound* ***10d****.*

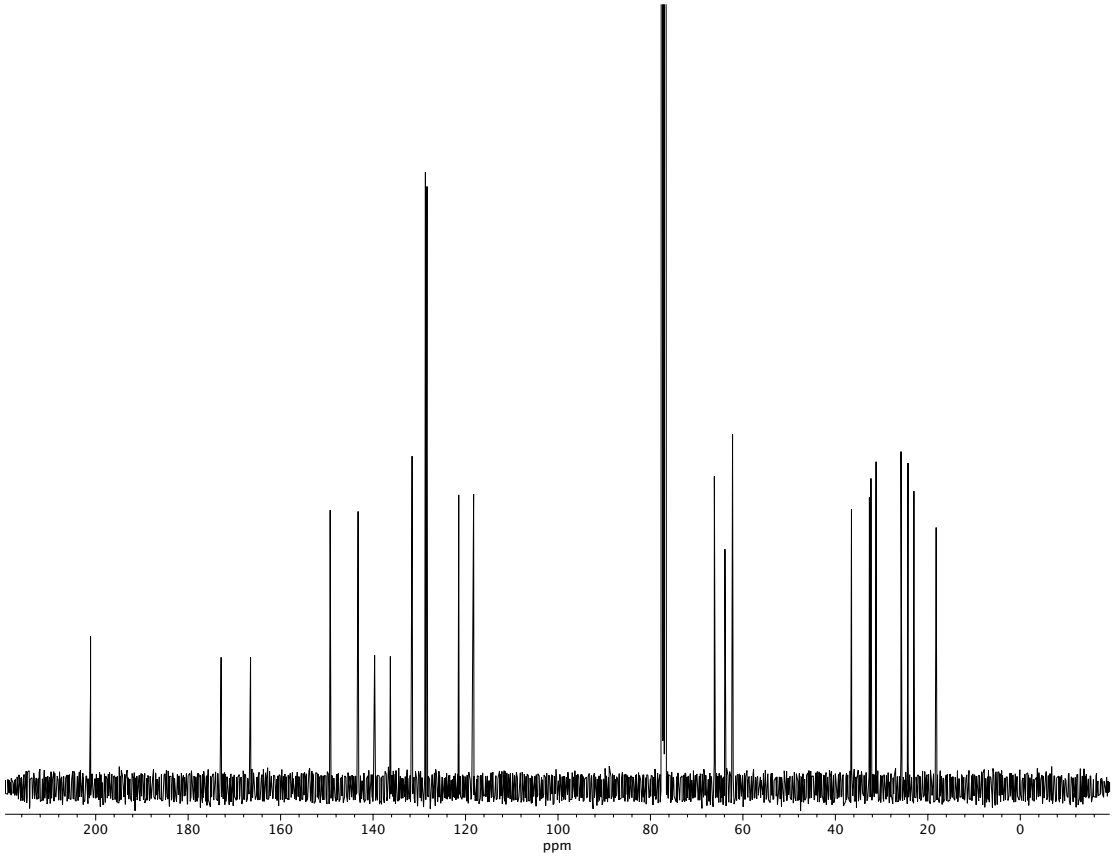


Figure A1.91. *^{13}C NMR (100 MHz, $CDCl_3$) of compound* ***10d****.*

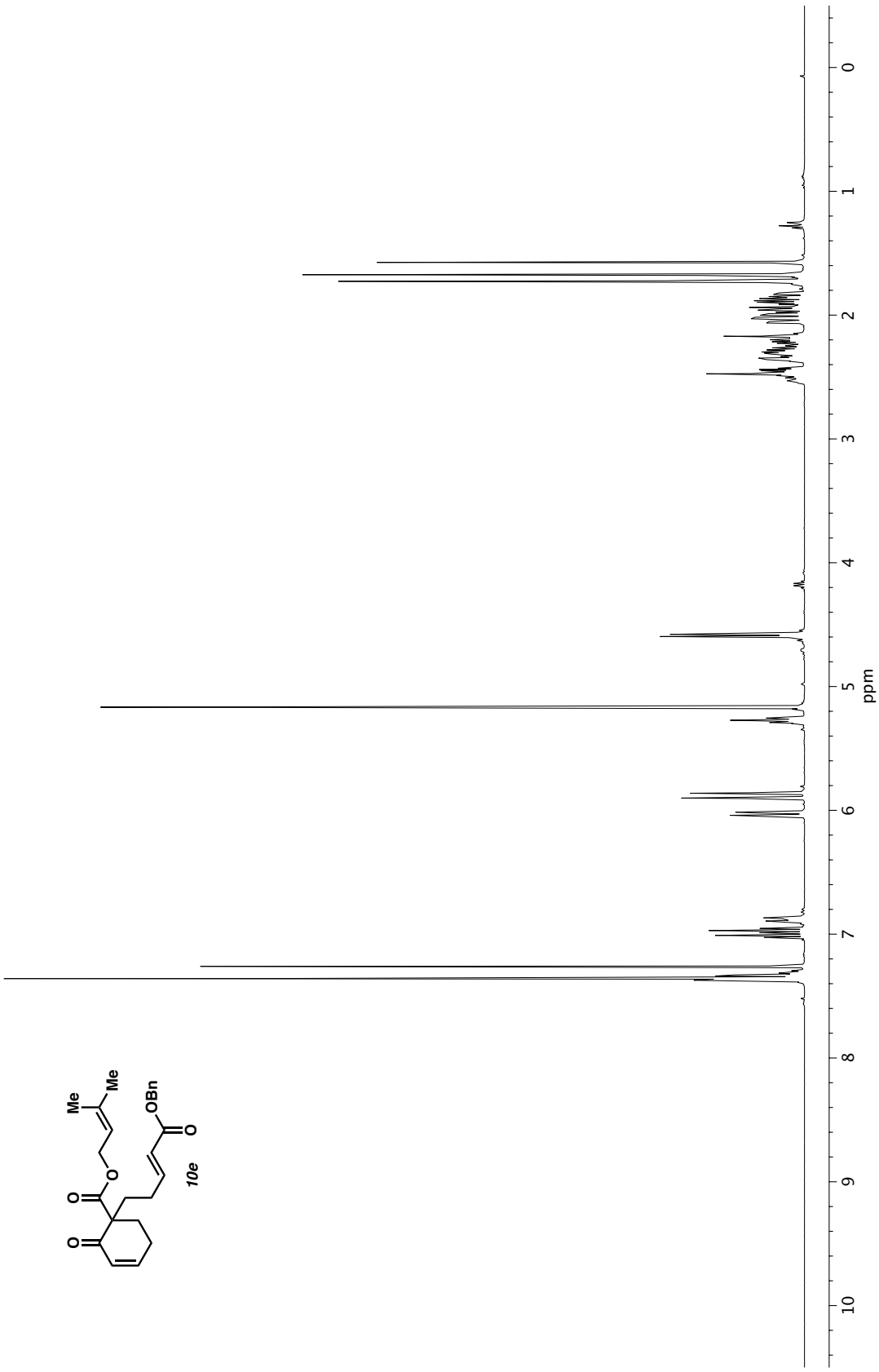


Figure A1.92. *^1H NMR (400 MHz, $CDCl_3$) of compound* ***10e****.*

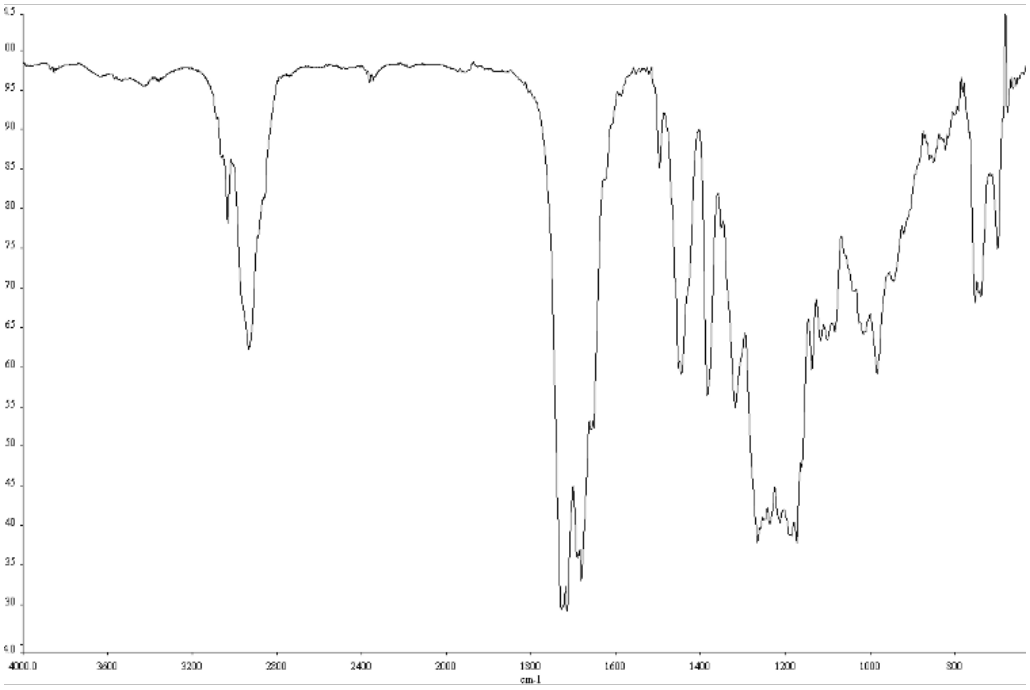


Figure A1.93. *Infrared spectrum (Thin Film, NaCl) of compound* ***10e****.*

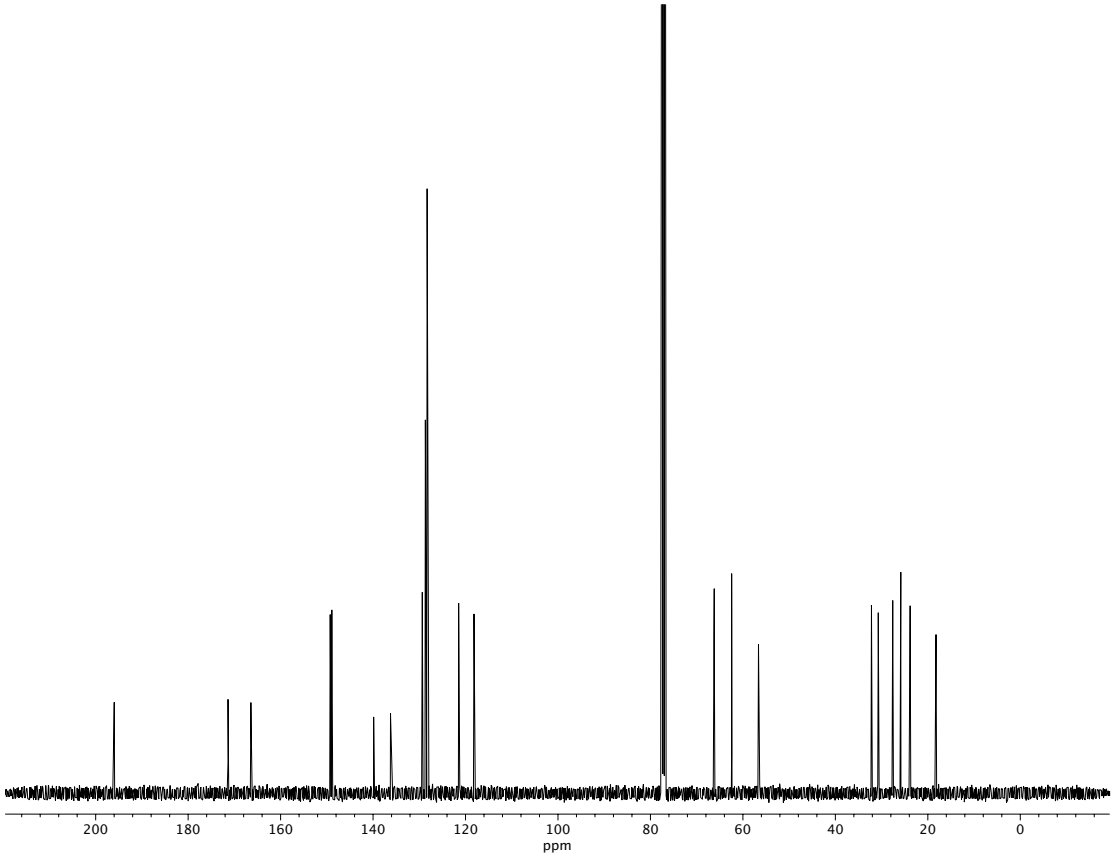


Figure A1.94. *^{13}C NMR (100 MHz, $CDCl_3$) of compound* ***10e****.*

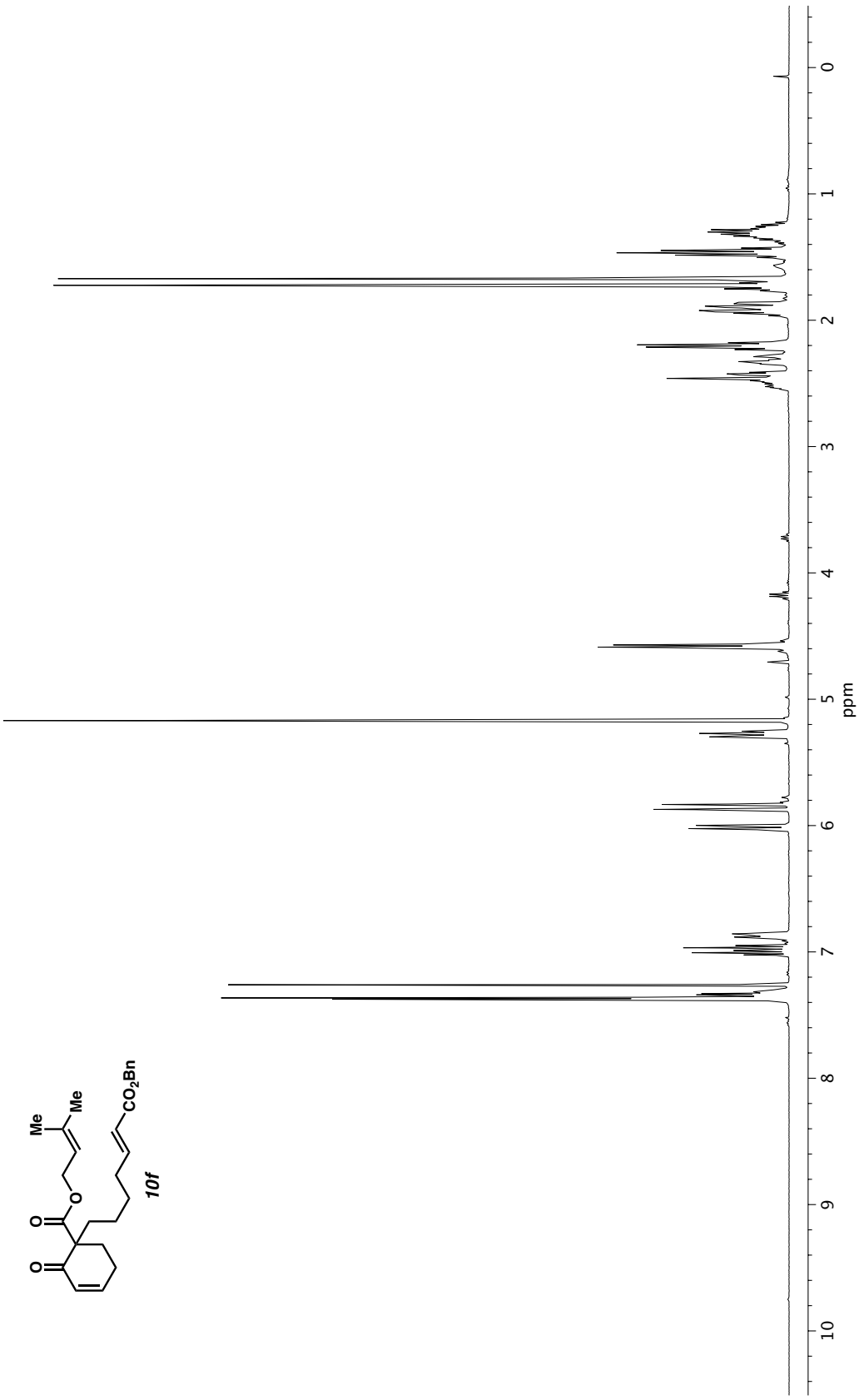


Figure A1.95. *^{1}H NMR (400 MHz, $CDCl_3$) of compound* ***10f****.*

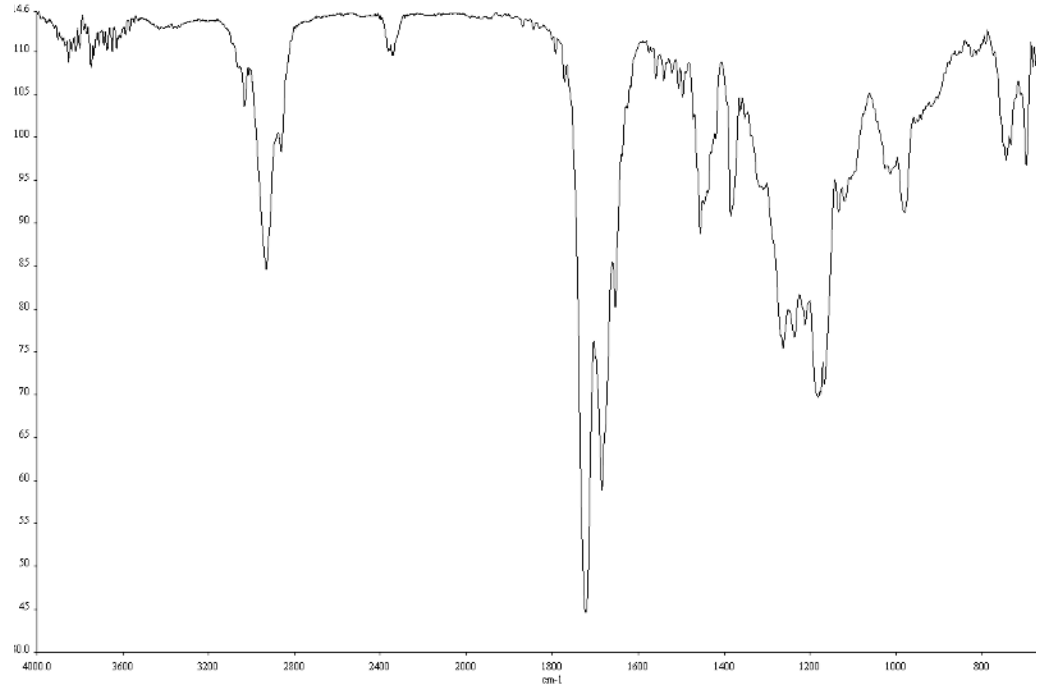


Figure A1.96. *Infrared spectrum (Thin Film, NaCl) of compound* ***10f****.*

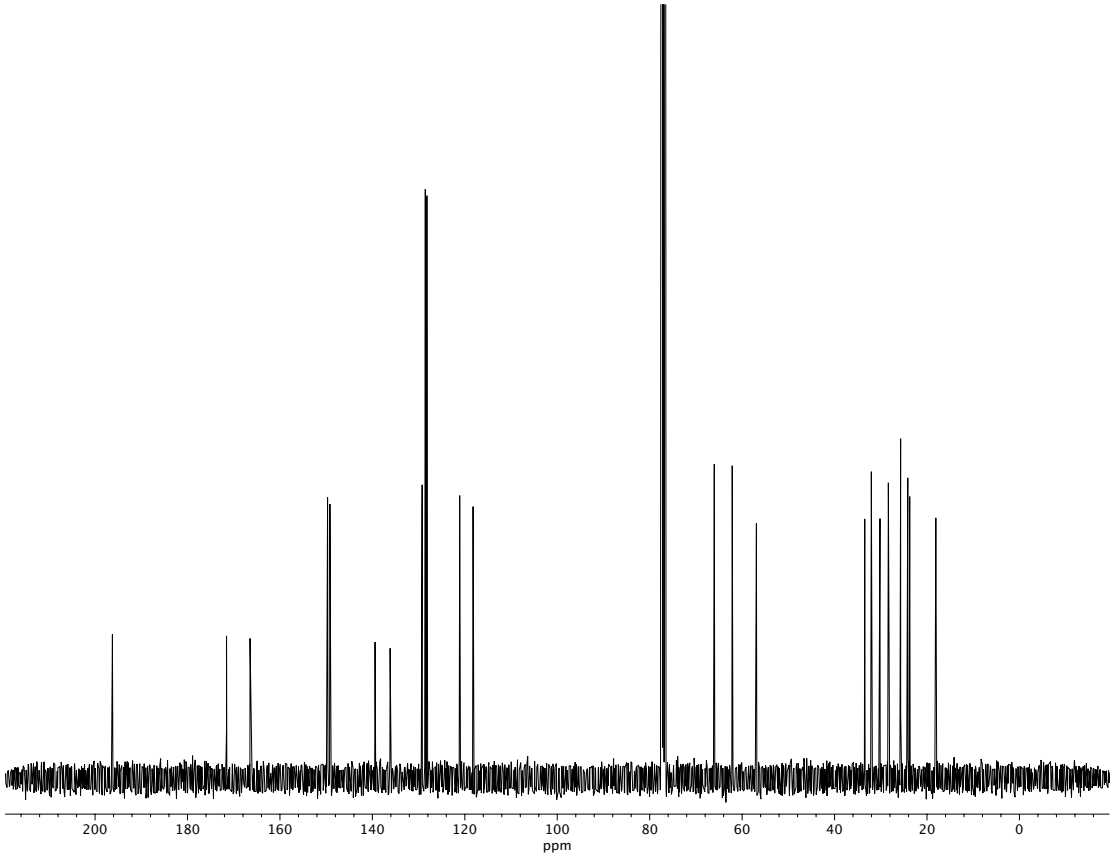


Figure A1.97. *^{13}C NMR (100 MHz, $CDCl_3$) of compound* ***10f****.*

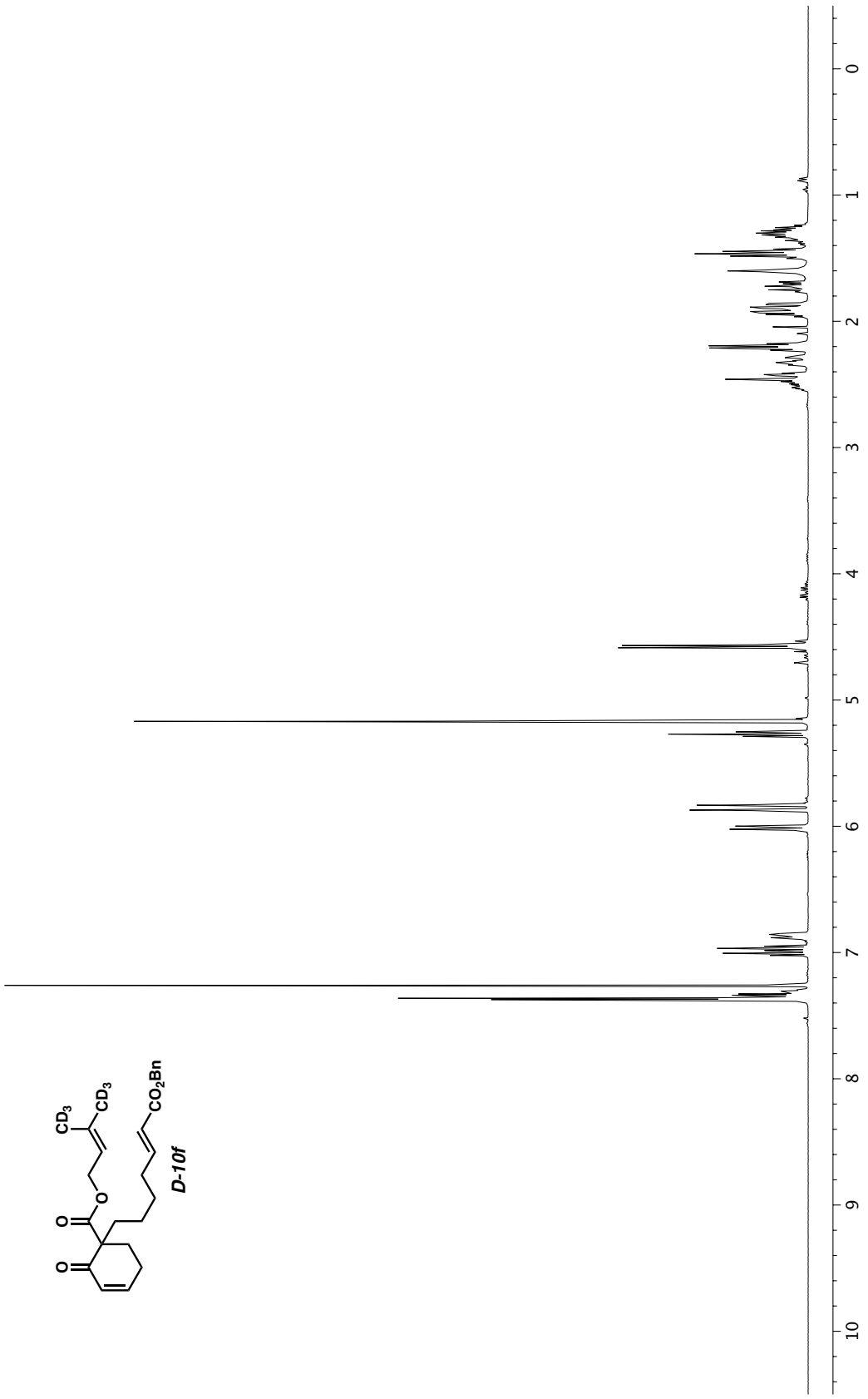


Figure A1.98. *^1H NMR (400 MHz, $CDCl_3$) of compound* ***D-10f****.*

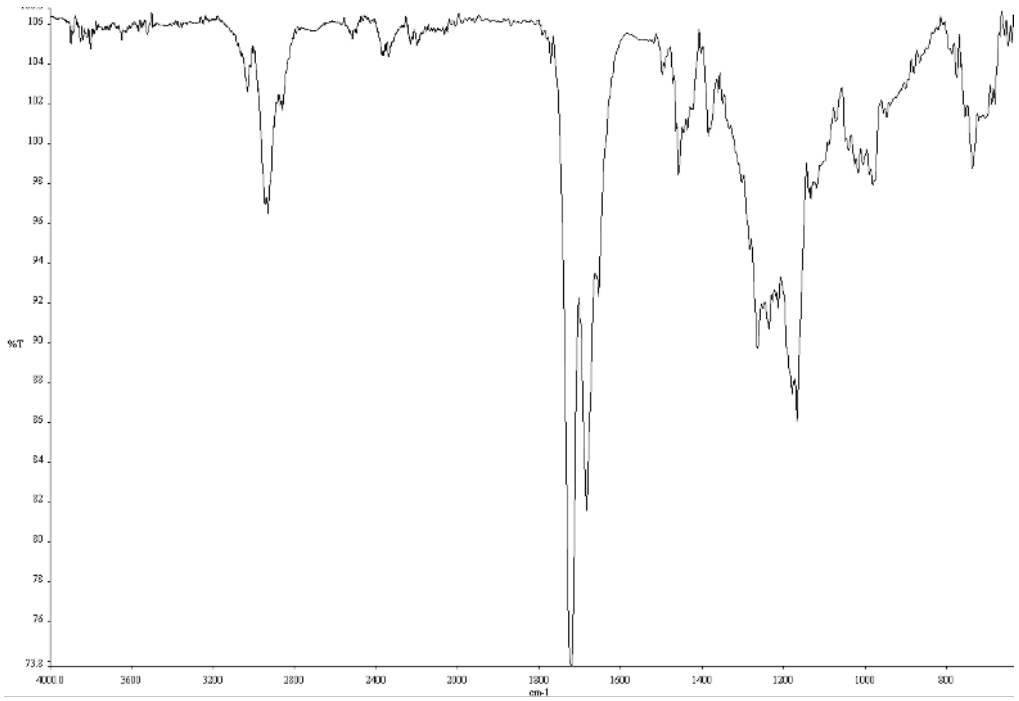


Figure A1.99. *Infrared spectrum (Thin Film, NaCl) of compound* ***D-10f****.*

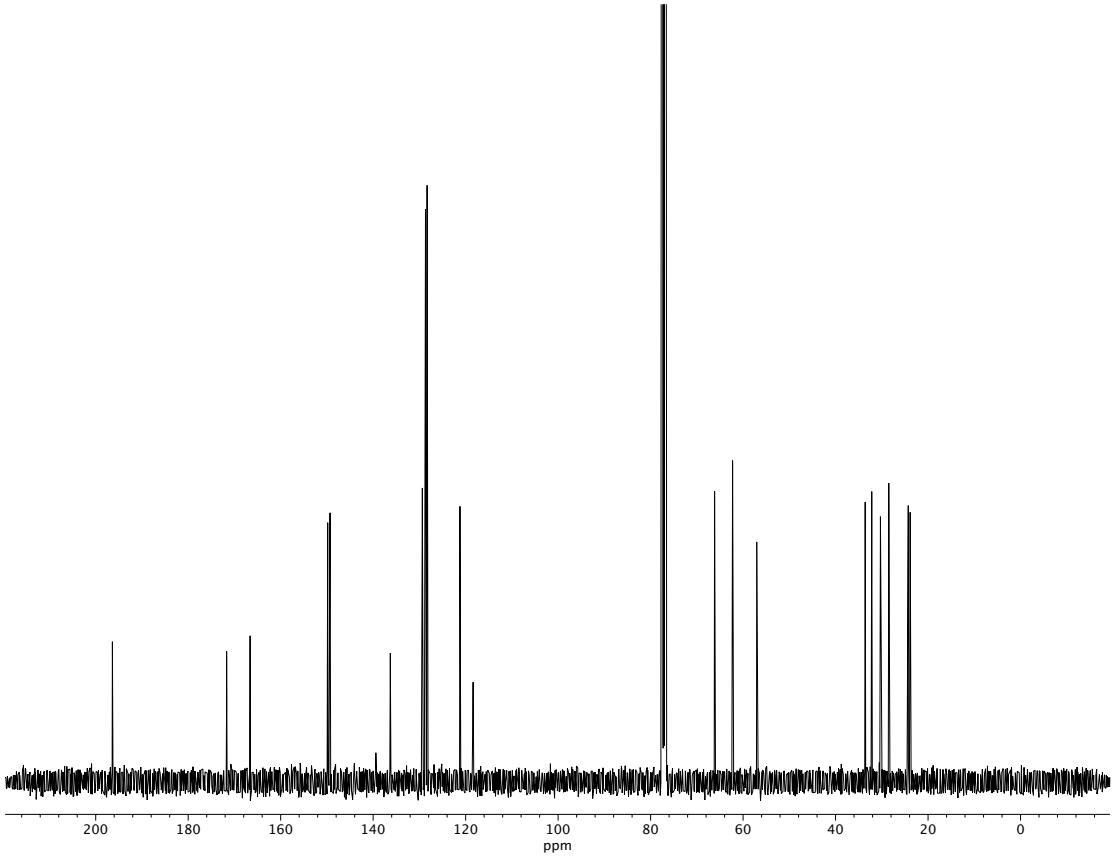


Figure A1.100. *^{13}C NMR (100 MHz, $CDCl_3$) of compound* ***D-10f****.*

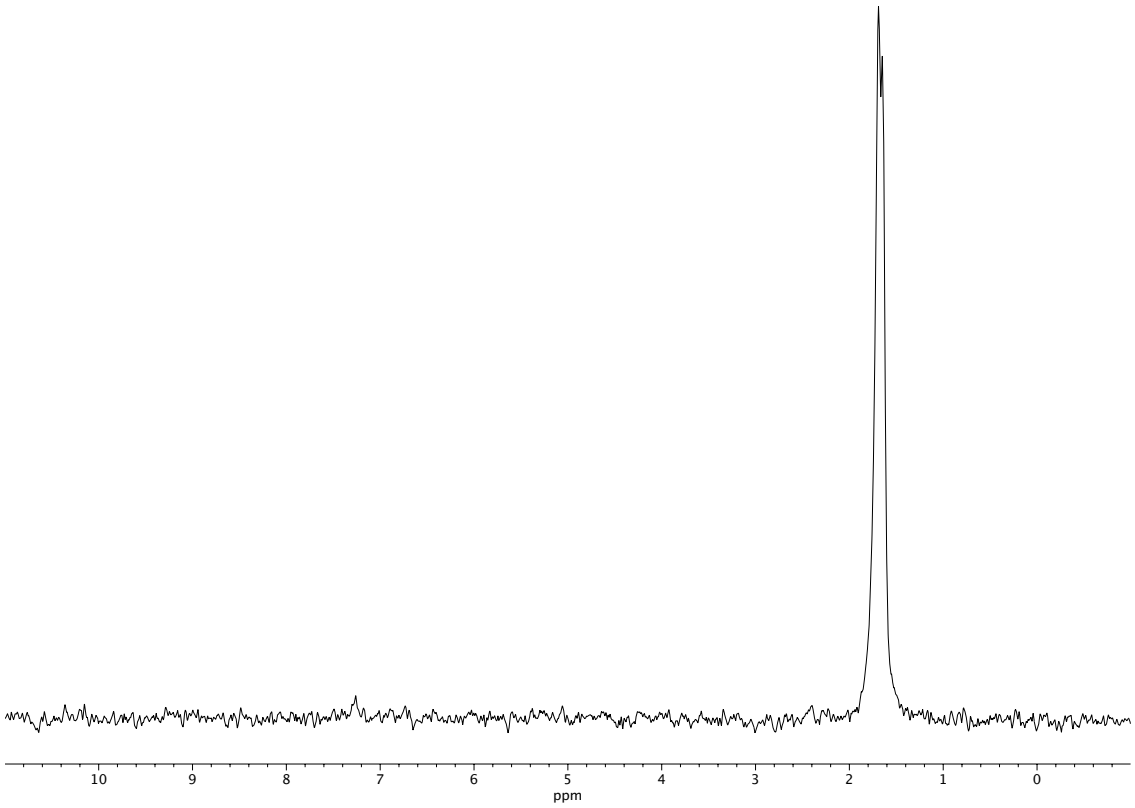


Figure A1.101. *^{2}H NMR (61 MHz, $CDCl_3$) of compound* ***D-10f****.*

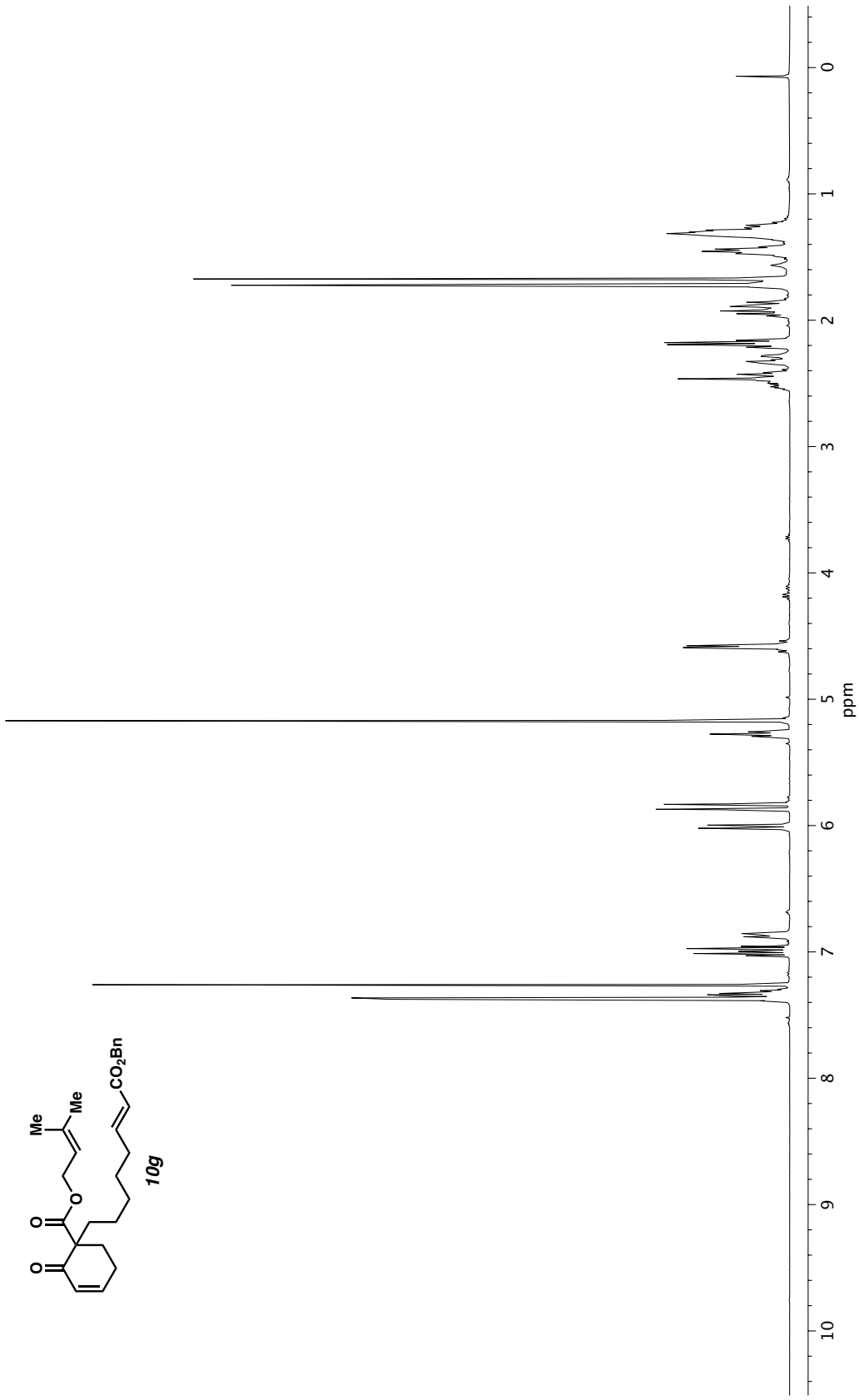


Figure A1.102. *^1H NMR (400 MHz, $CDCl_3$) of compound* ***10g****.*

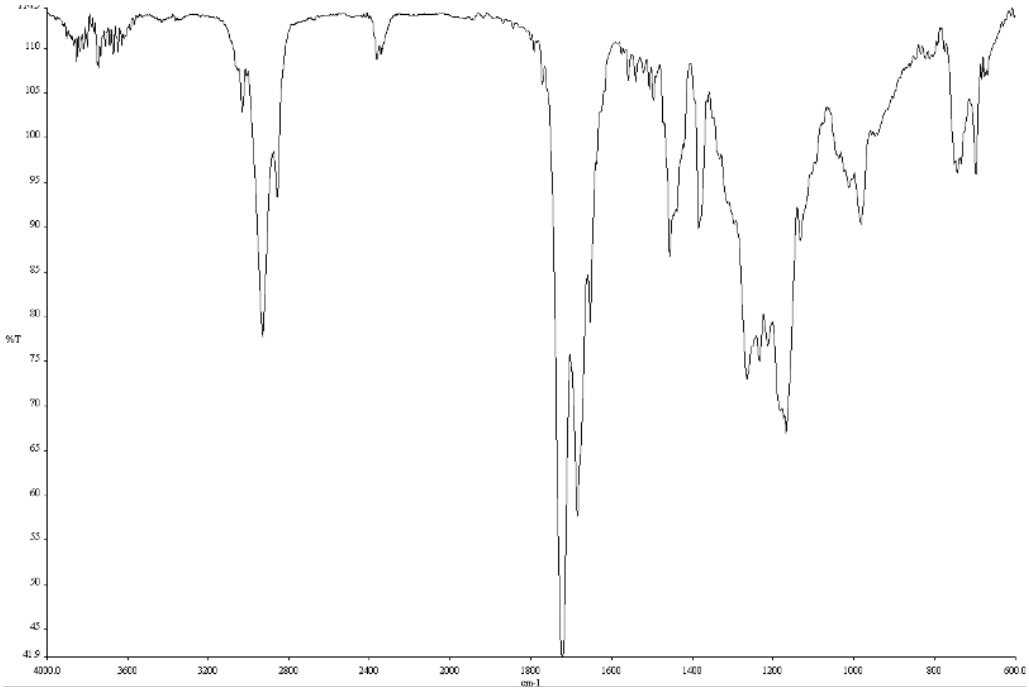


Figure A1.103. *Infrared spectrum (Thin Film, NaCl) of compound* ***10g****.*

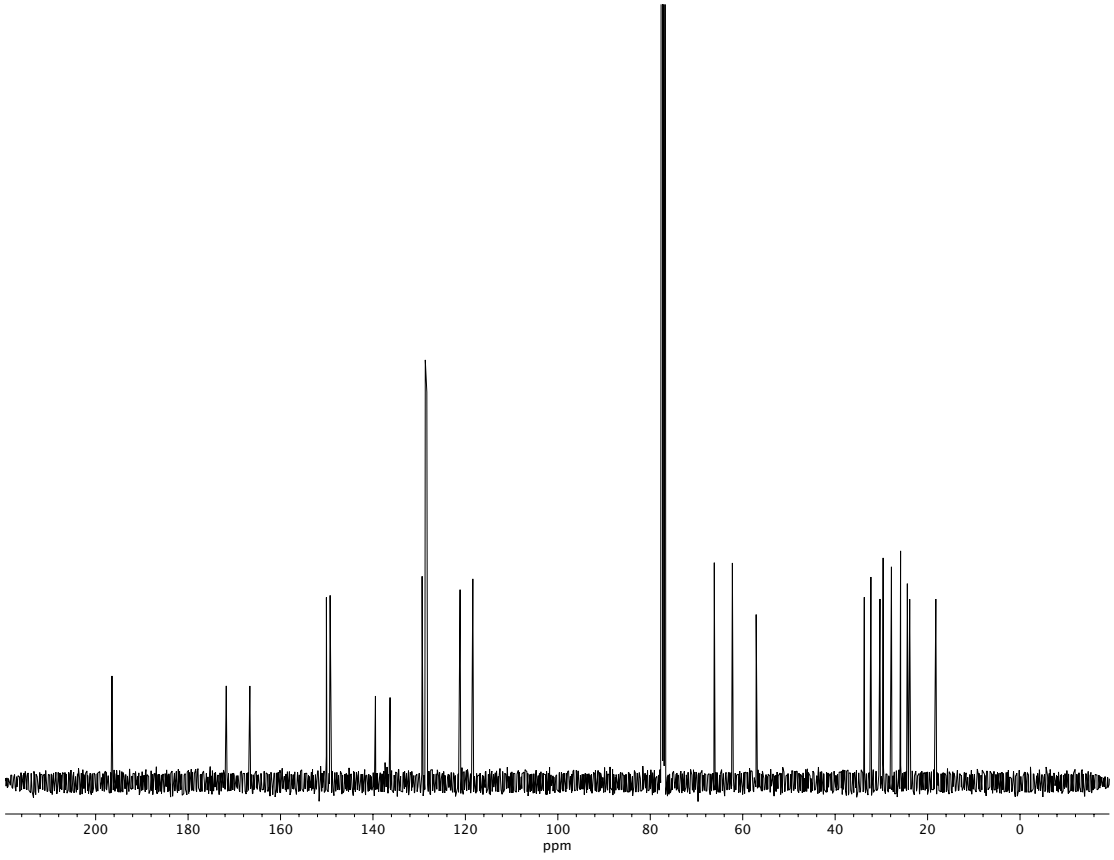


Figure A1.104. *^{13}C NMR (100 MHz, $CDCl_3$) of compound* ***10g****.*

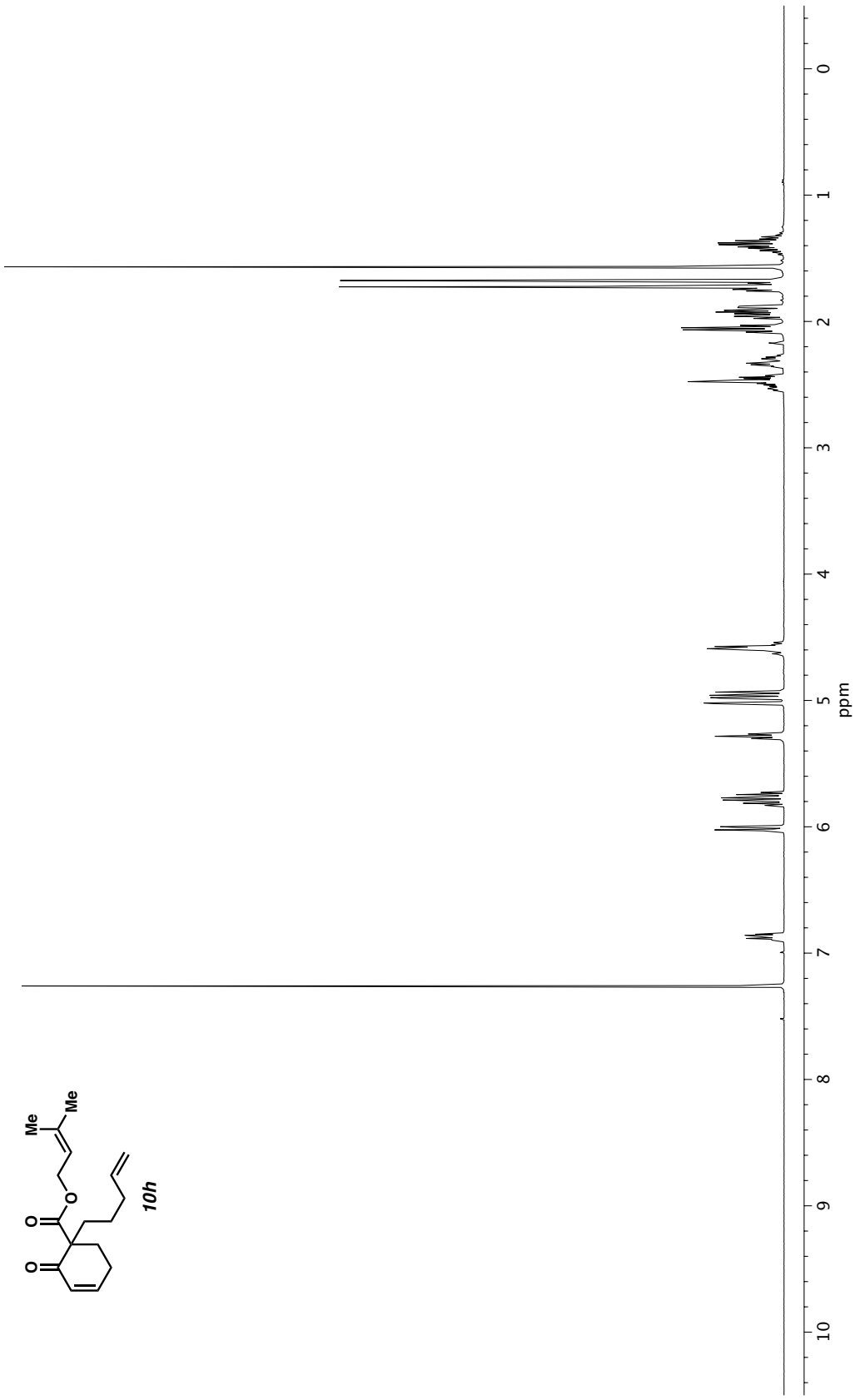


Figure A1.105. *^{1}H NMR (400 MHz, $CDCl_3$) of compound* ***10h****.*

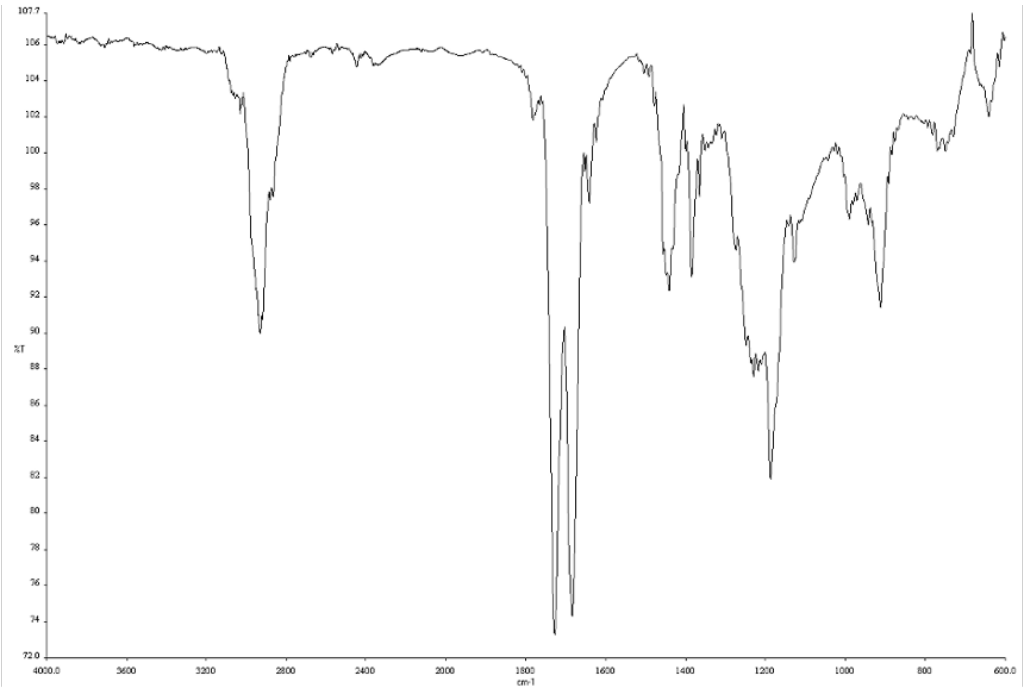


Figure A1.106. *Infrared spectrum (Thin Film, NaCl) of compound* ***10h****.*

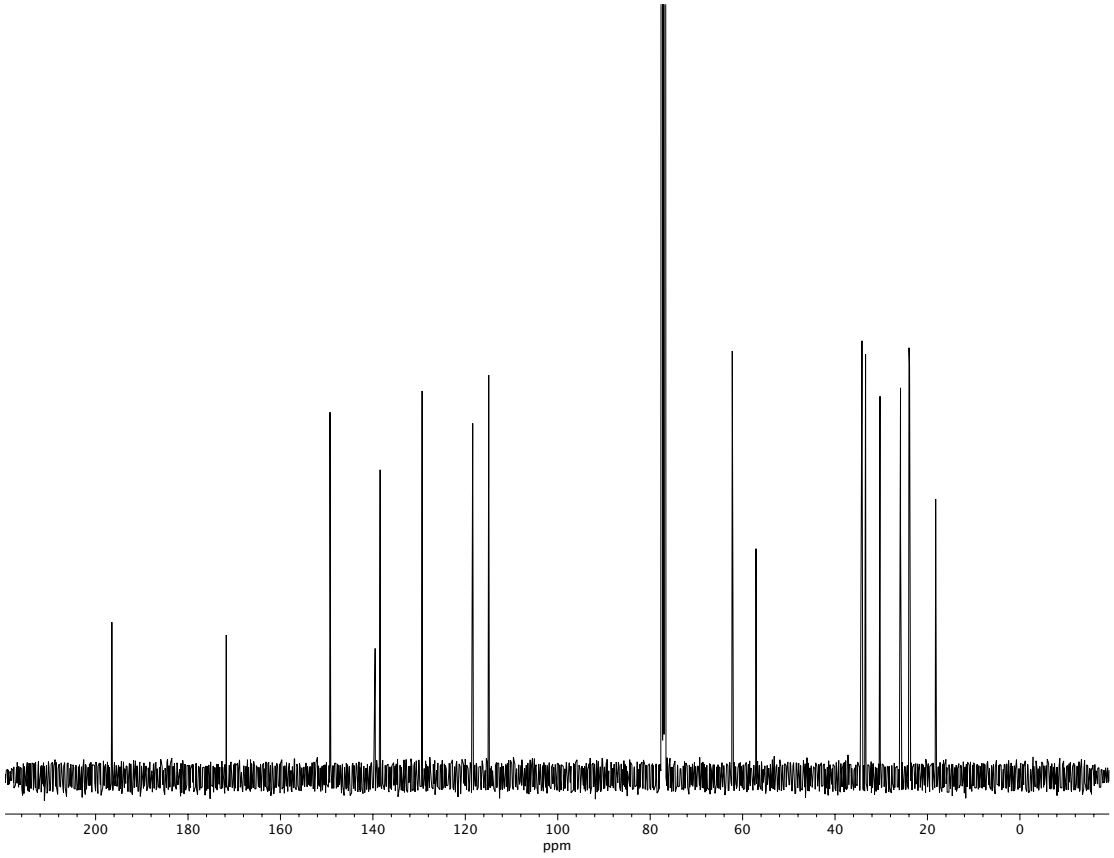


Figure A1.107. *^{13}C NMR (100 MHz, $CDCl_3$) of compound* ***10h****.*

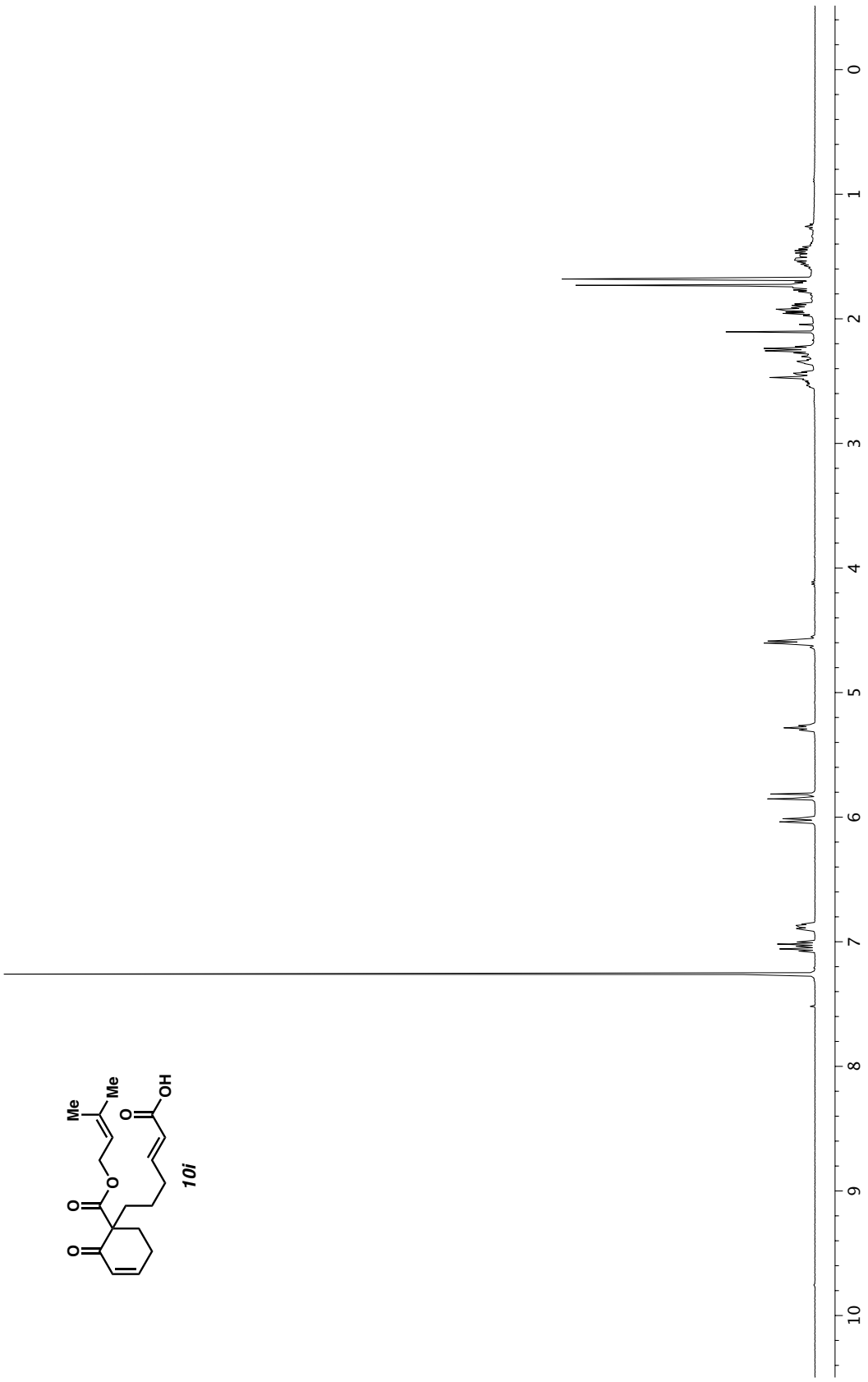


Figure A1.108. *^1H NMR (400 MHz, $CDCl_3$) of compound* ***10i****.*

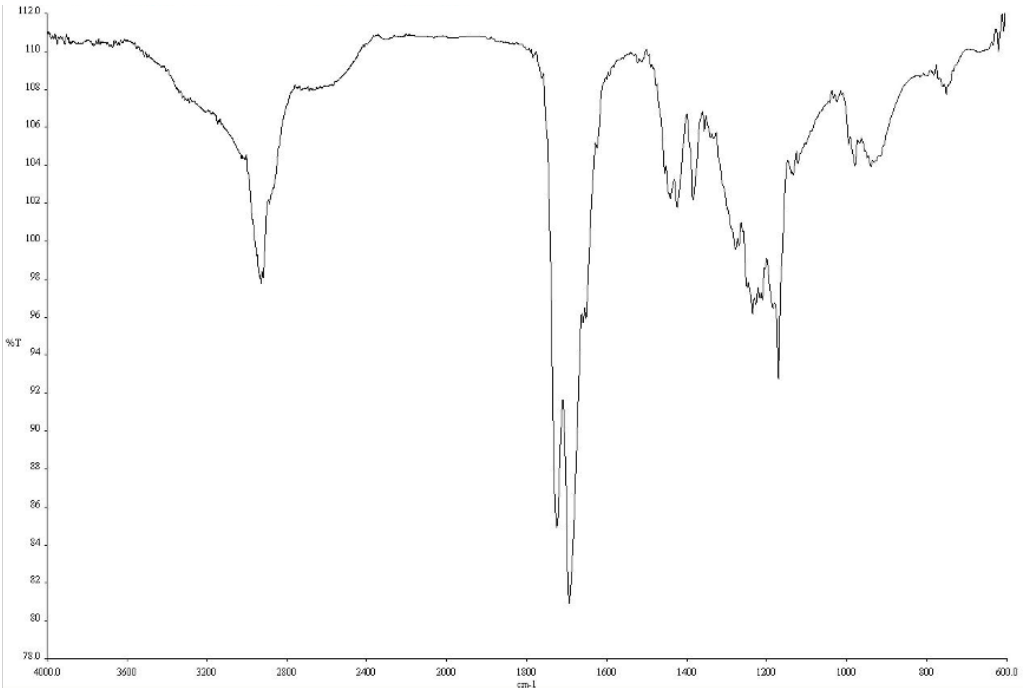


Figure A1.109. *Infrared spectrum (Thin Film, NaCl) of compound* ***10i****.*

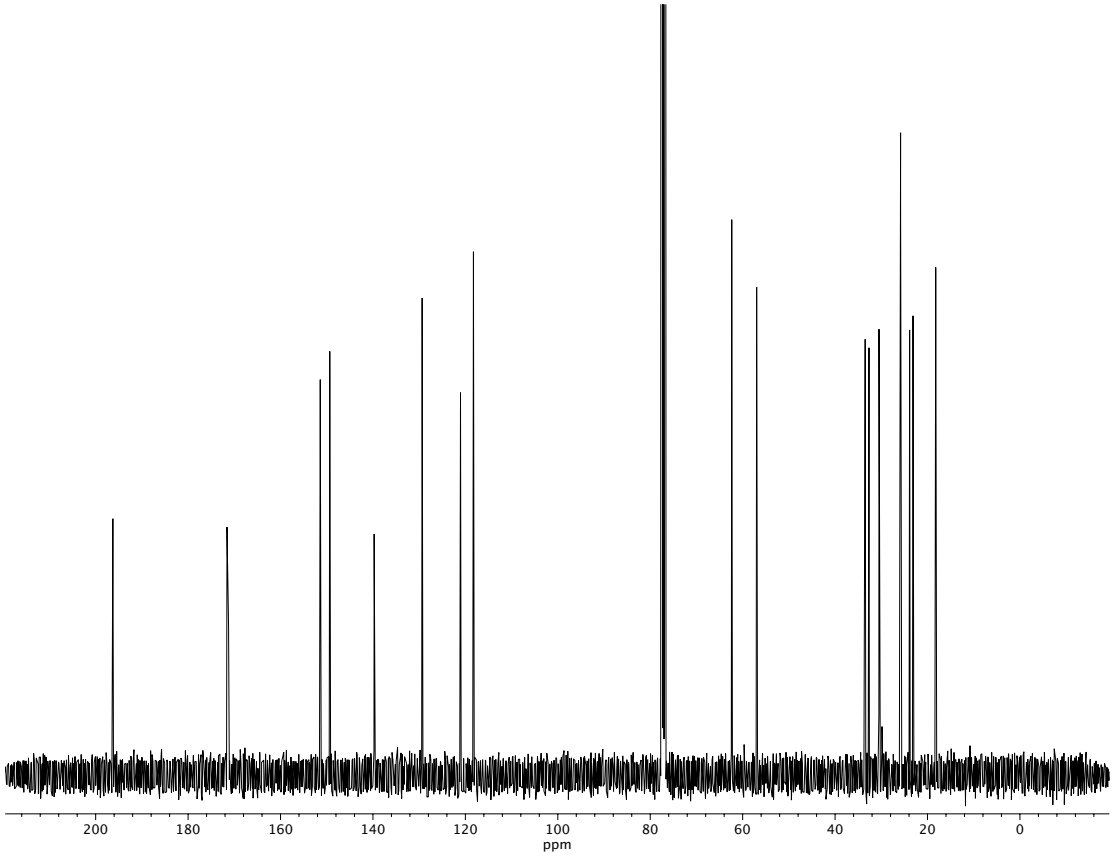


Figure A1.110. *^{13}C NMR (100 MHz, $CDCl_3$) of compound* ***10i****.*

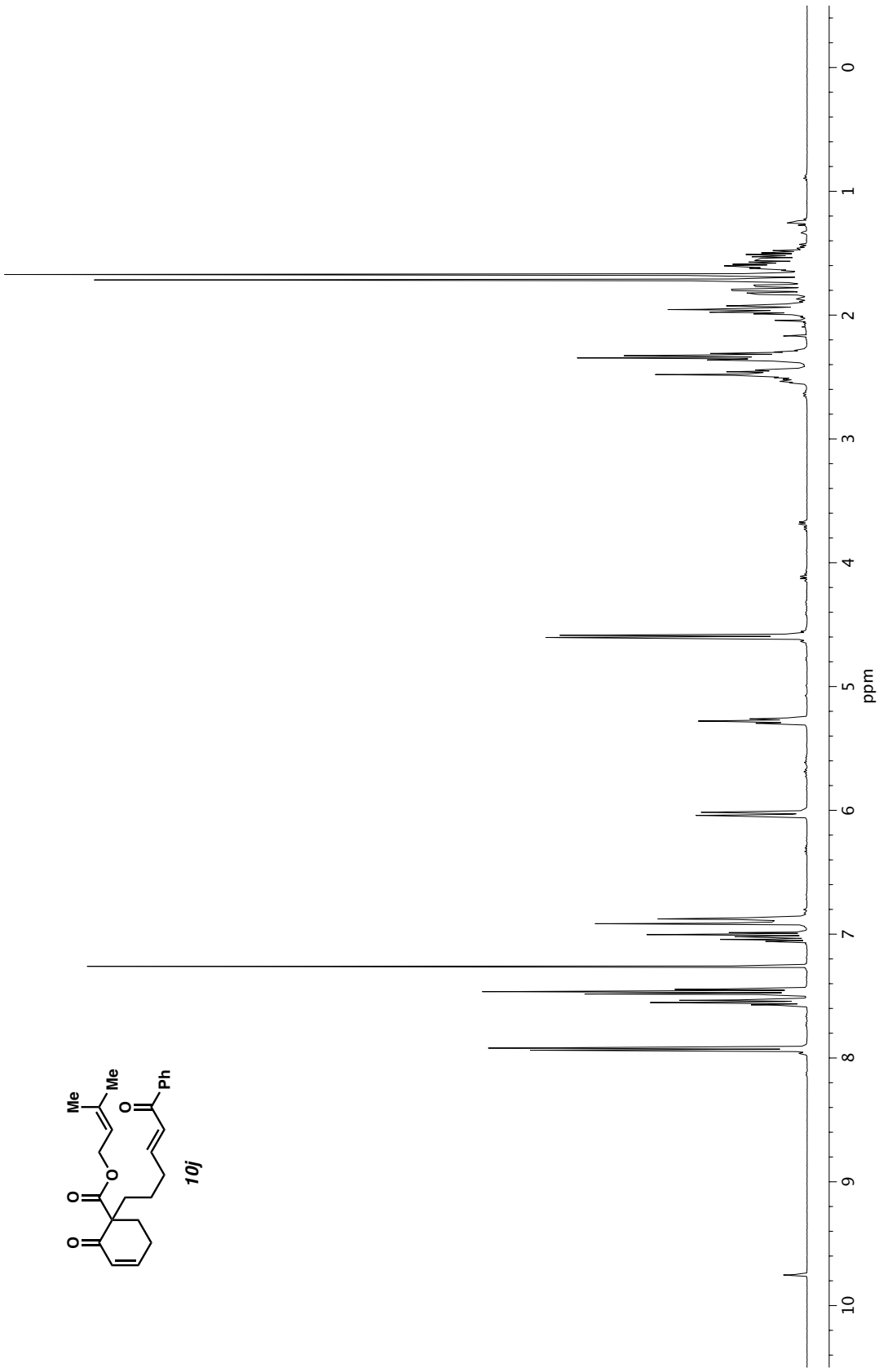


Figure A1.111. *^1H NMR (400 MHz, $CDCl_3$) of compound* ***10j****.*

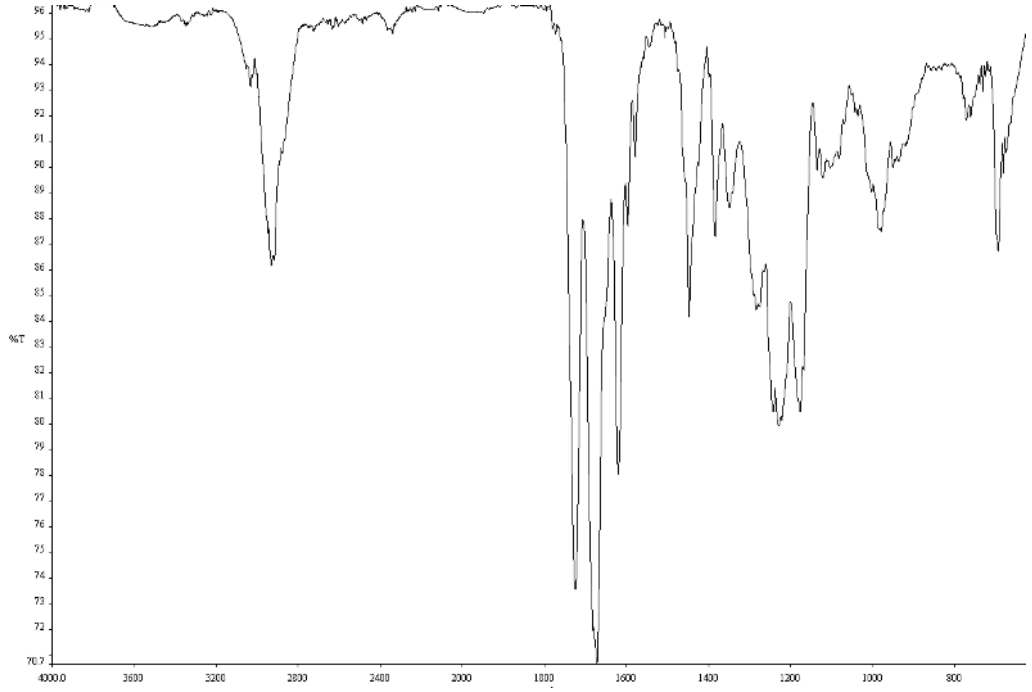


Figure A1.112. *Infrared spectrum (Thin Film, NaCl) of compound* ***10j****.*

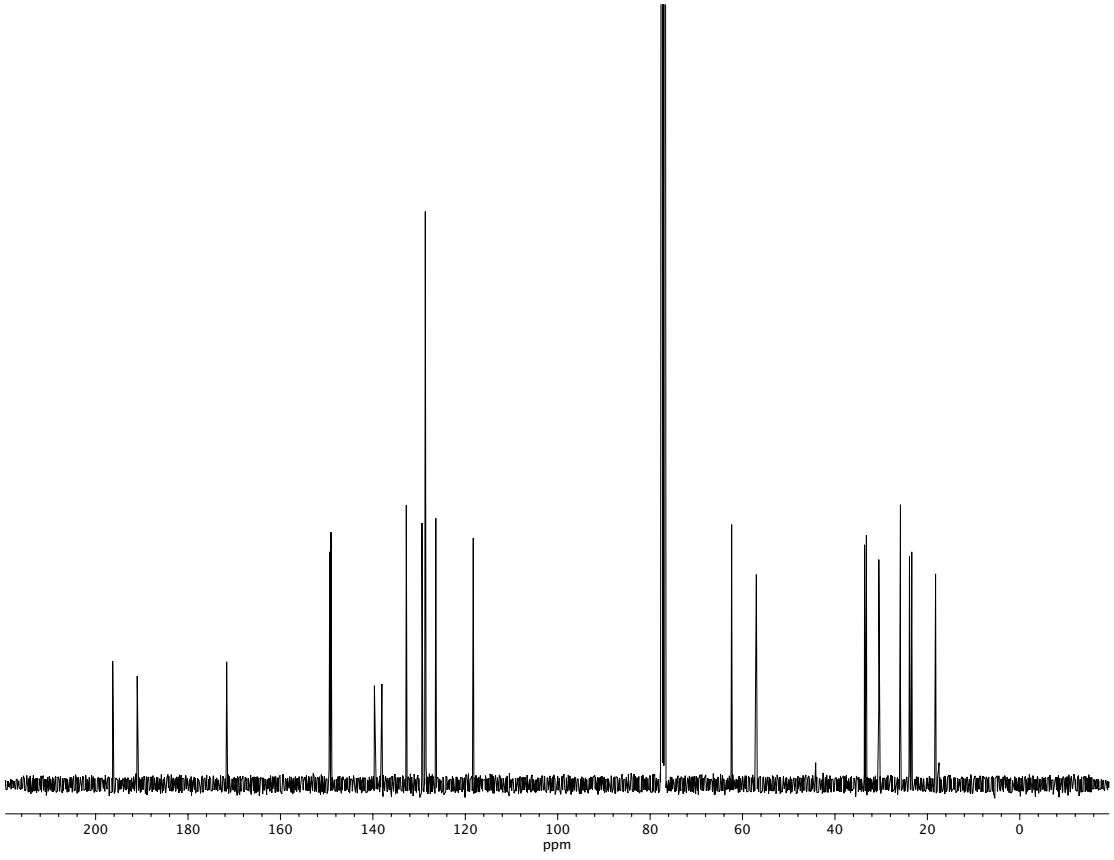


Figure A1.113. *^{13}C NMR (100 MHz, $CDCl_3$) of compound* ***10j****.*

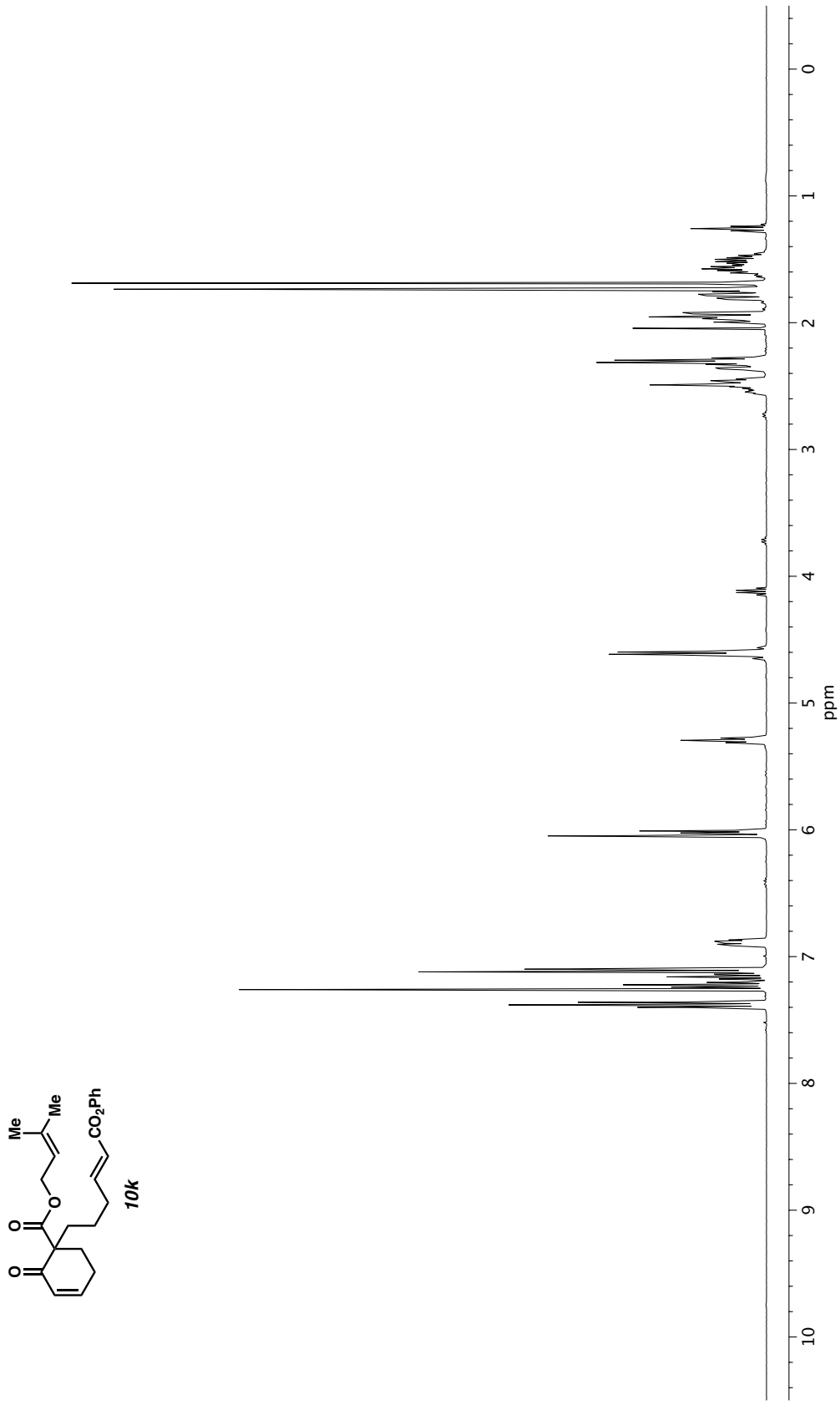


Figure A1.114. *^1H NMR (400 MHz, $CDCl_3$) of compound* ***10k****.*

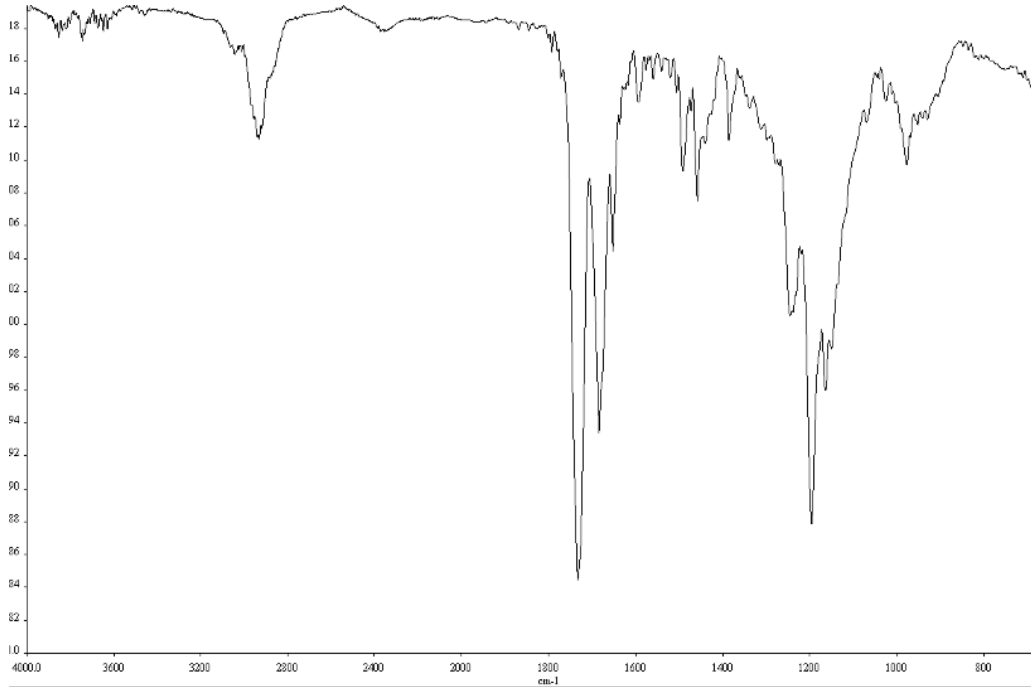


Figure A1.115. *Infrared spectrum (Thin Film, NaCl) of compound* ***10k****.*

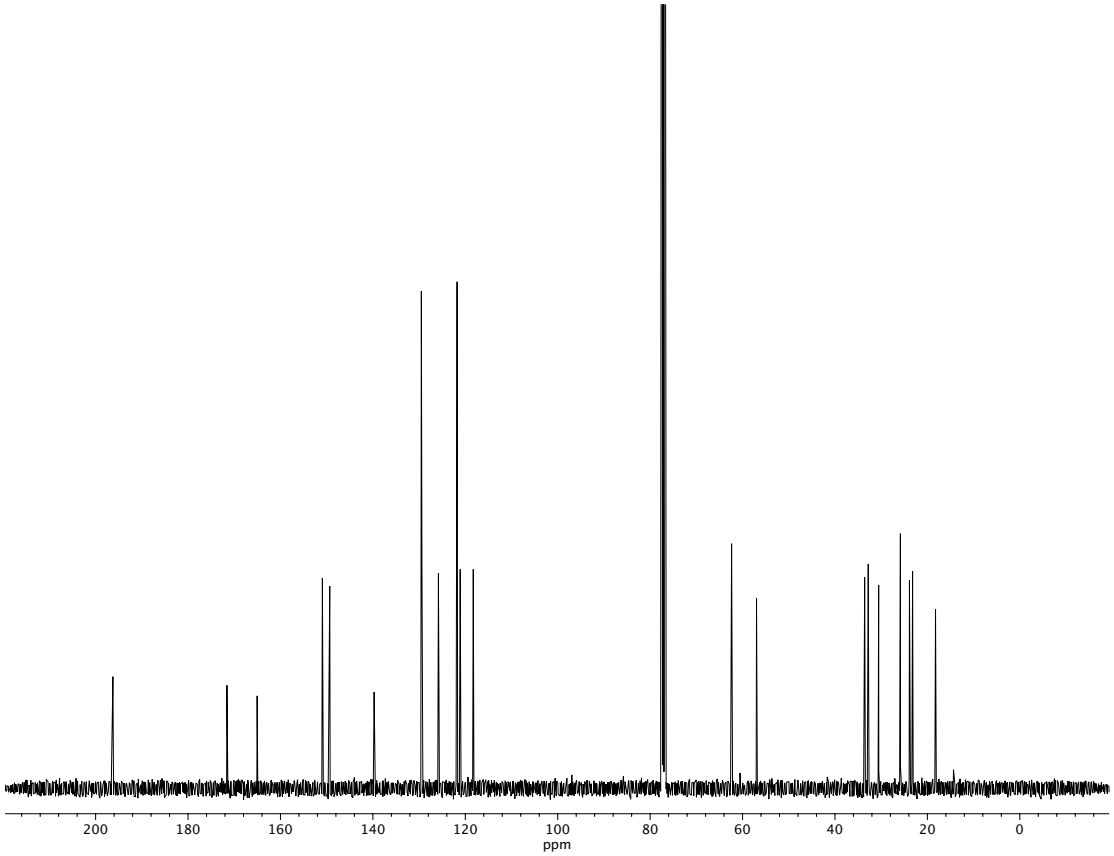


Figure A1.116. *^{13}C NMR (100 MHz, $CDCl_3$) of compound* ***10k****.*

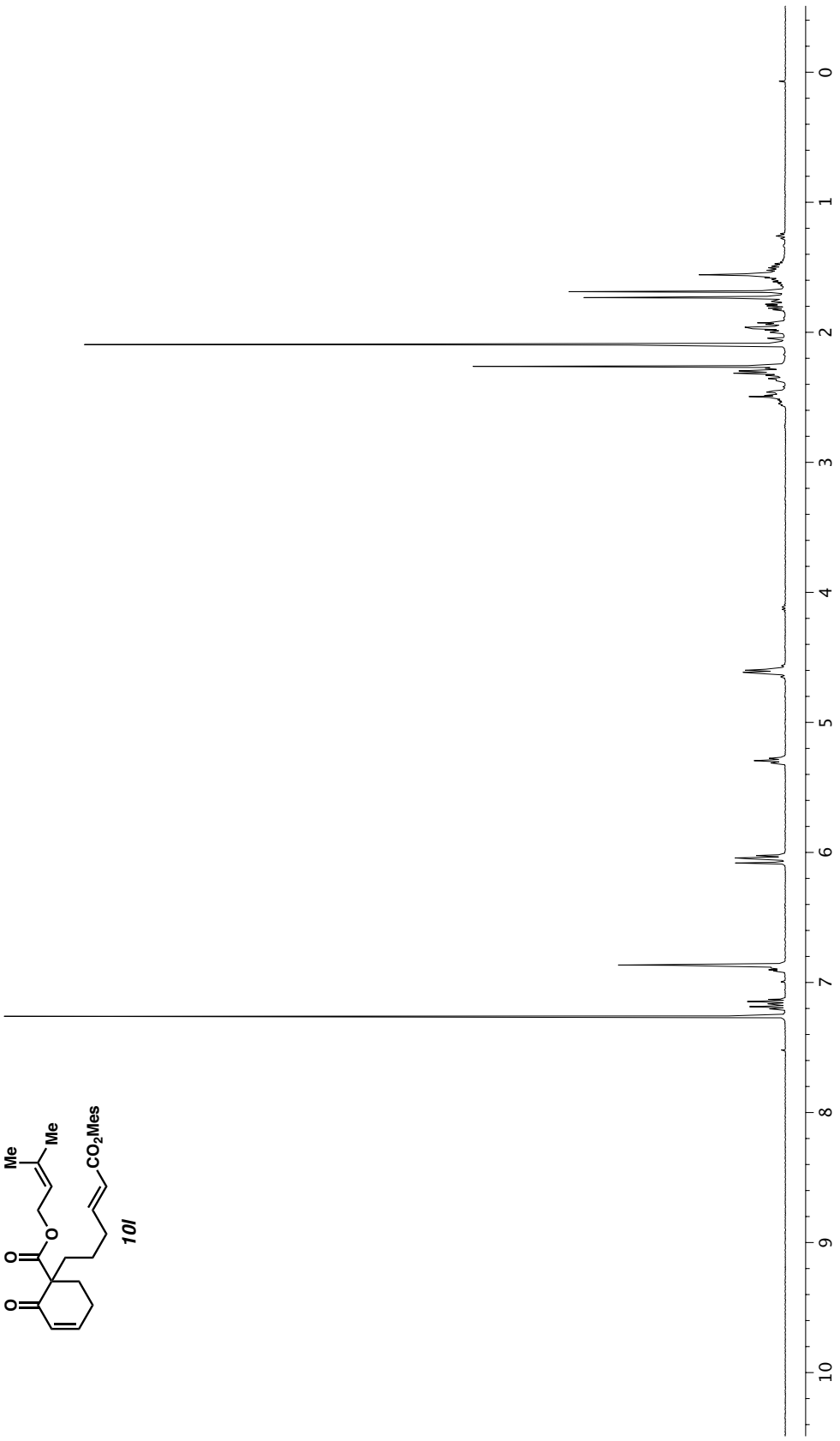


Figure A1.117. *^1H NMR (400 MHz, $CDCl_3$) of compound* ***10l****.*

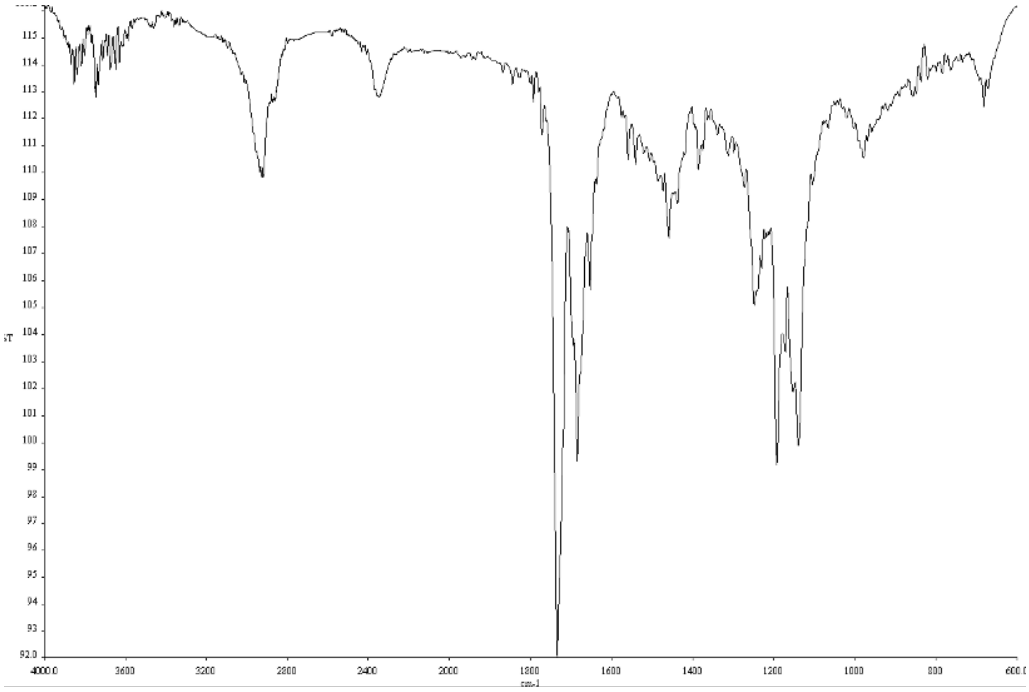


Figure A1.118. *Infrared spectrum (Thin Film, NaCl) of compound* ***10l****.*

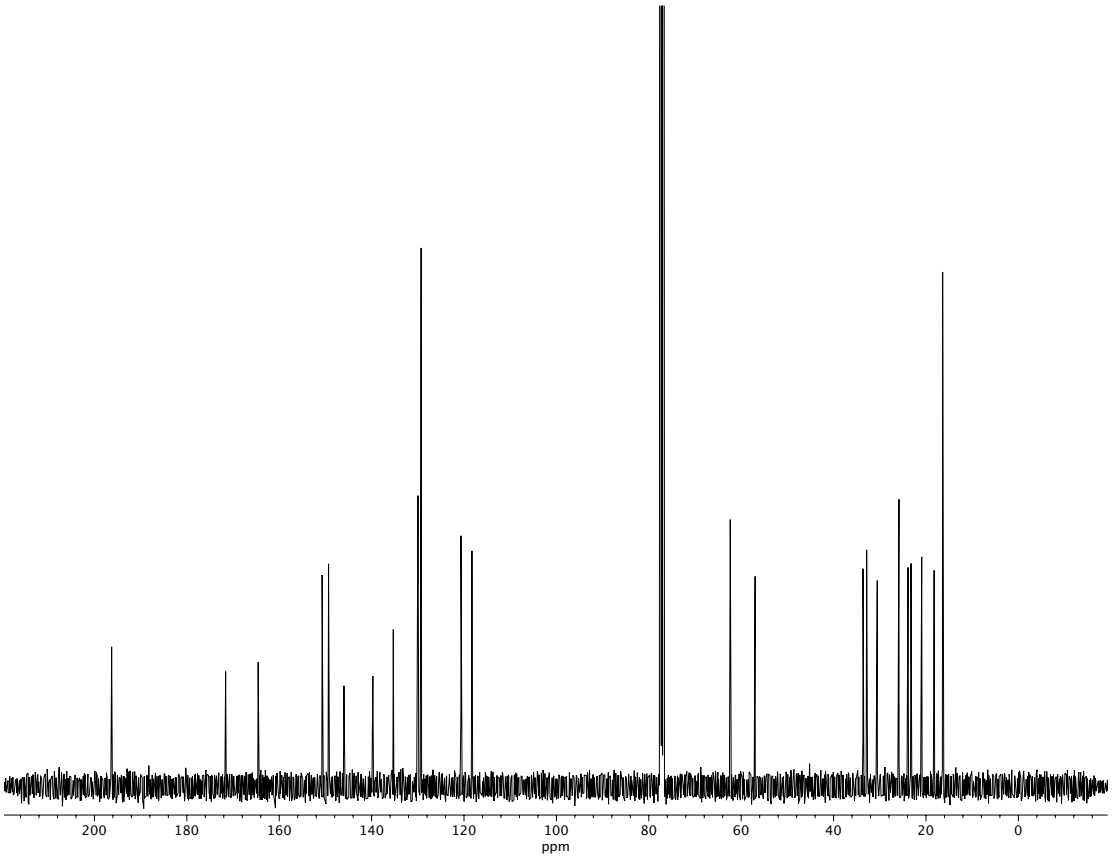


Figure A1.119. *^{13}C NMR (100 MHz, $CDCl_3$) of compound* ***10l****.*

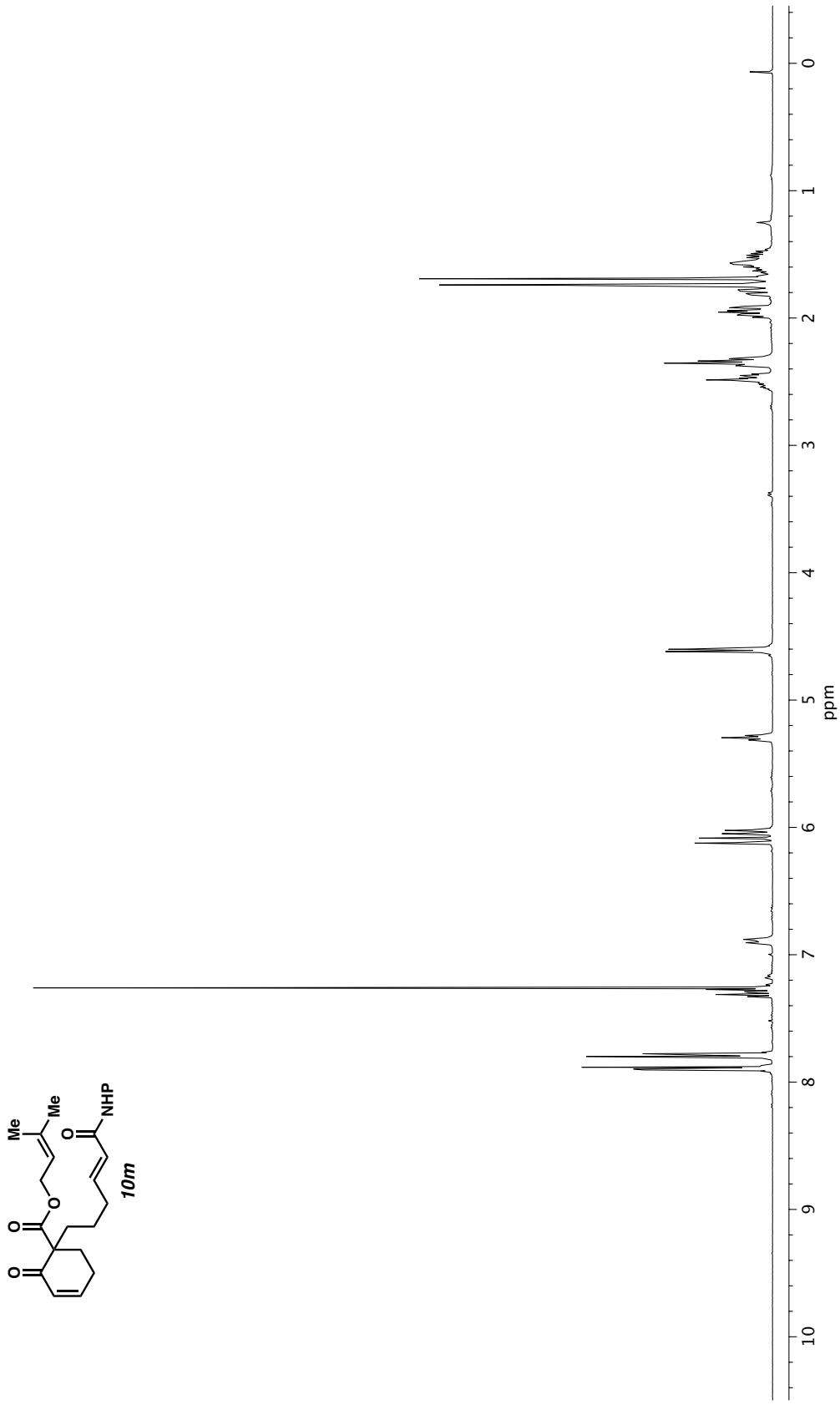


Figure A1.120. *^{1}H NMR (400 MHz, $CDCl_3$) of compound* ***10m****.*

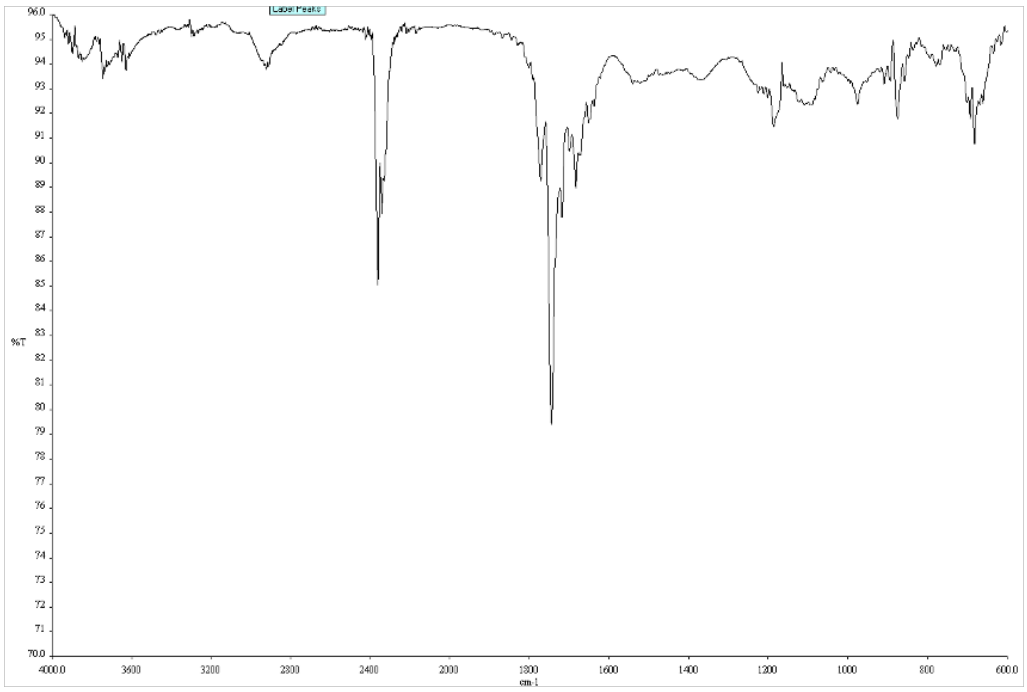


Figure A1.121. *Infrared spectrum (Thin Film, NaCl) of compound* ***10m****.*

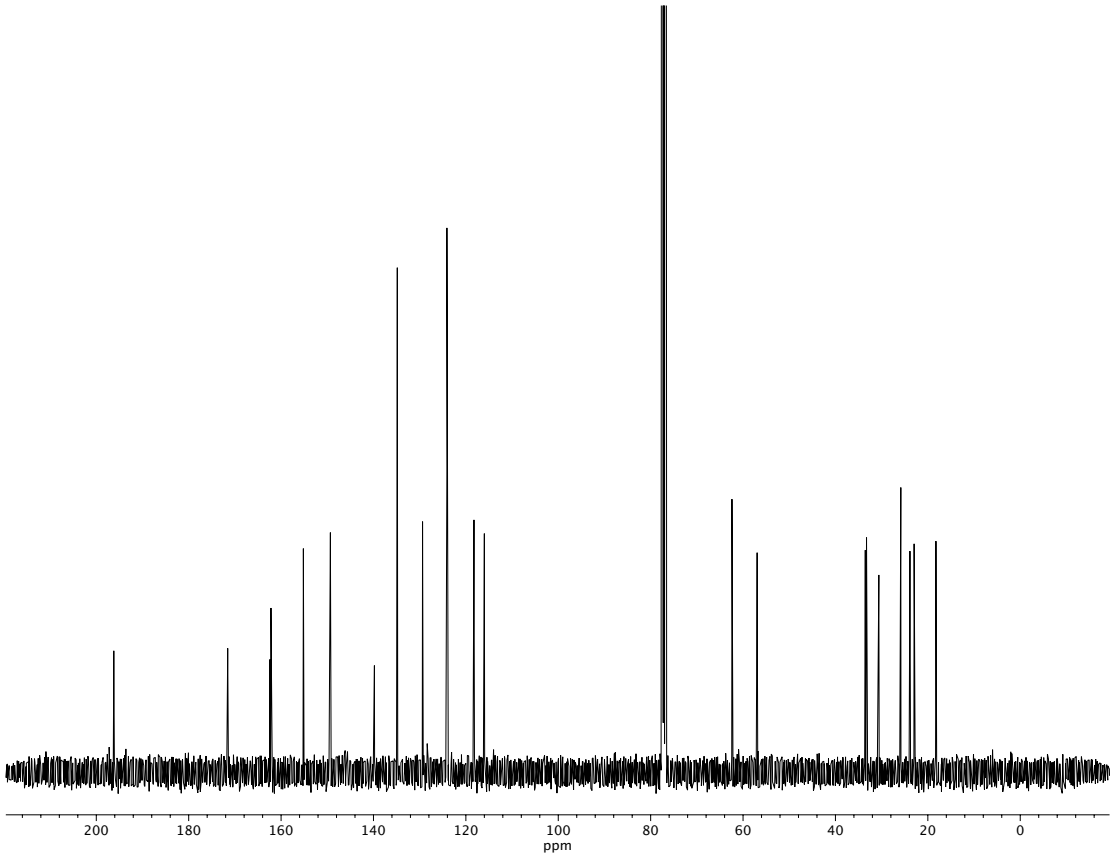


Figure A1.122. *^{13}C NMR (100 MHz, $CDCl_3$) of compound* ***10m****.*

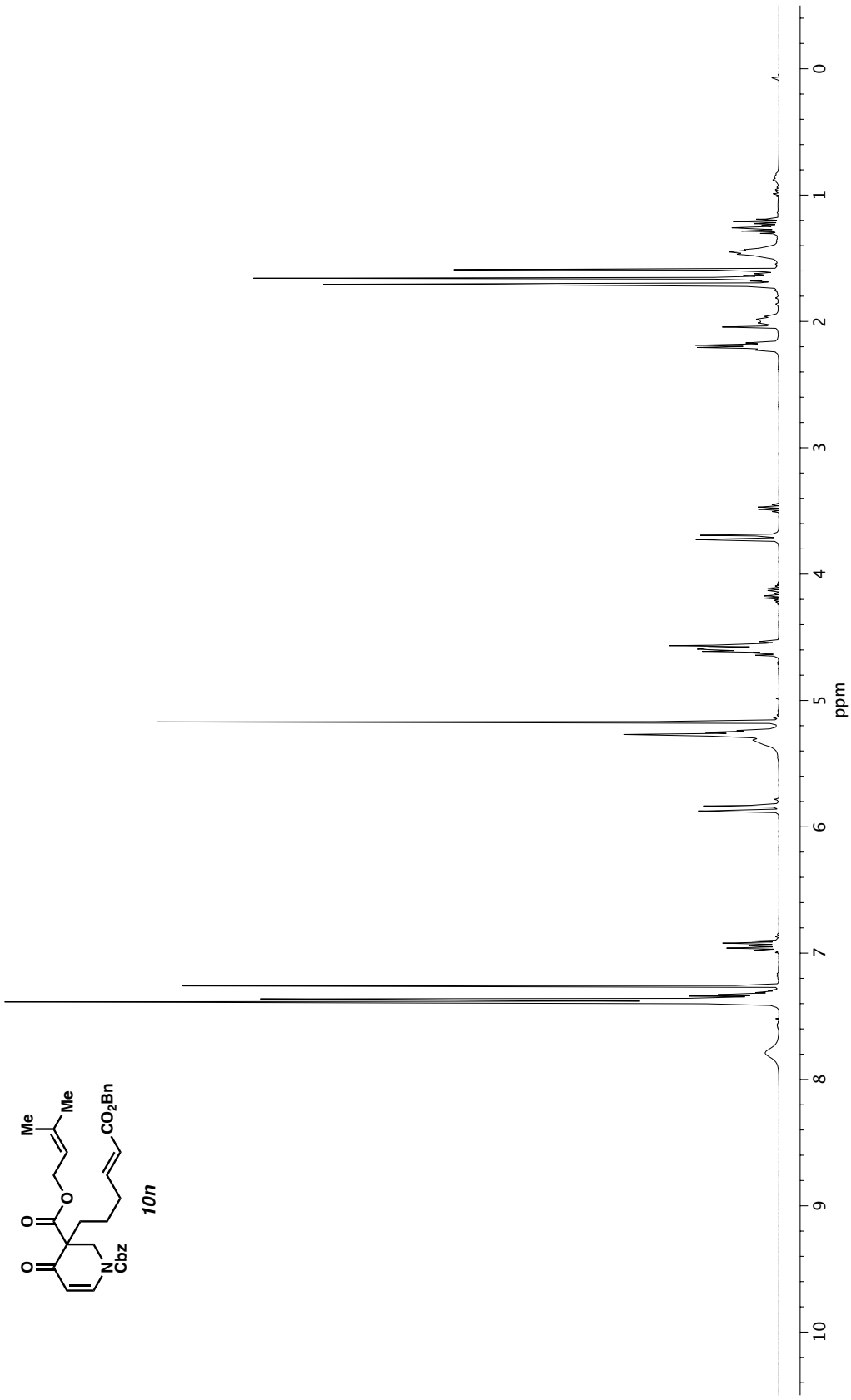


Figure A1.123. *^{1}H NMR (400 MHz, $CDCl_3$) of compound* ***10n****.*

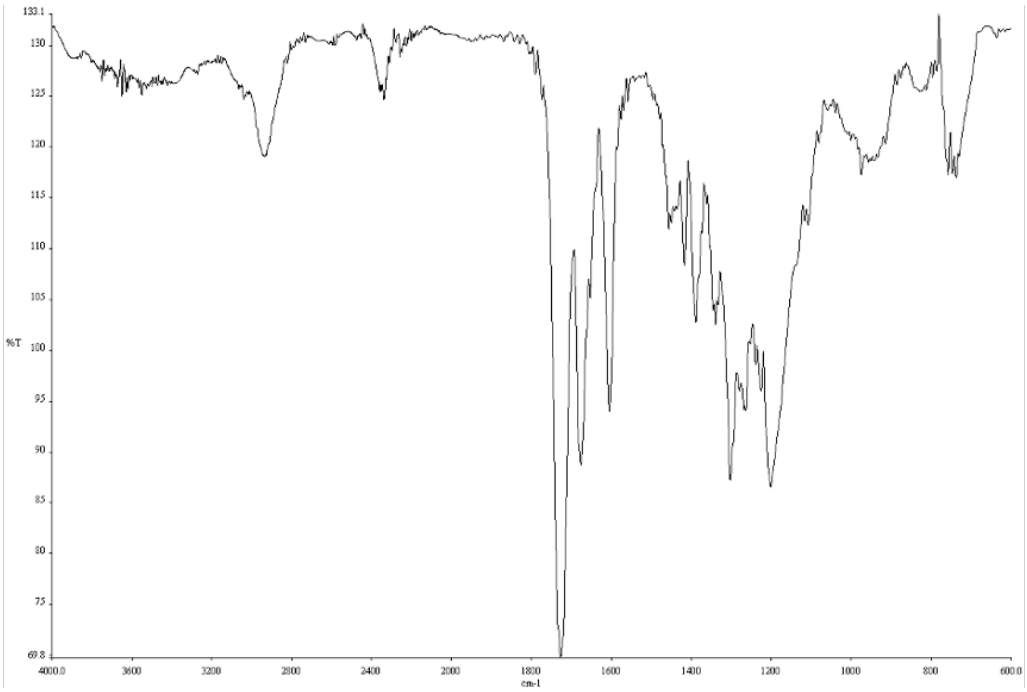


Figure A1.124. *Infrared spectrum (Thin Film, NaCl) of compound* ***10n****.*

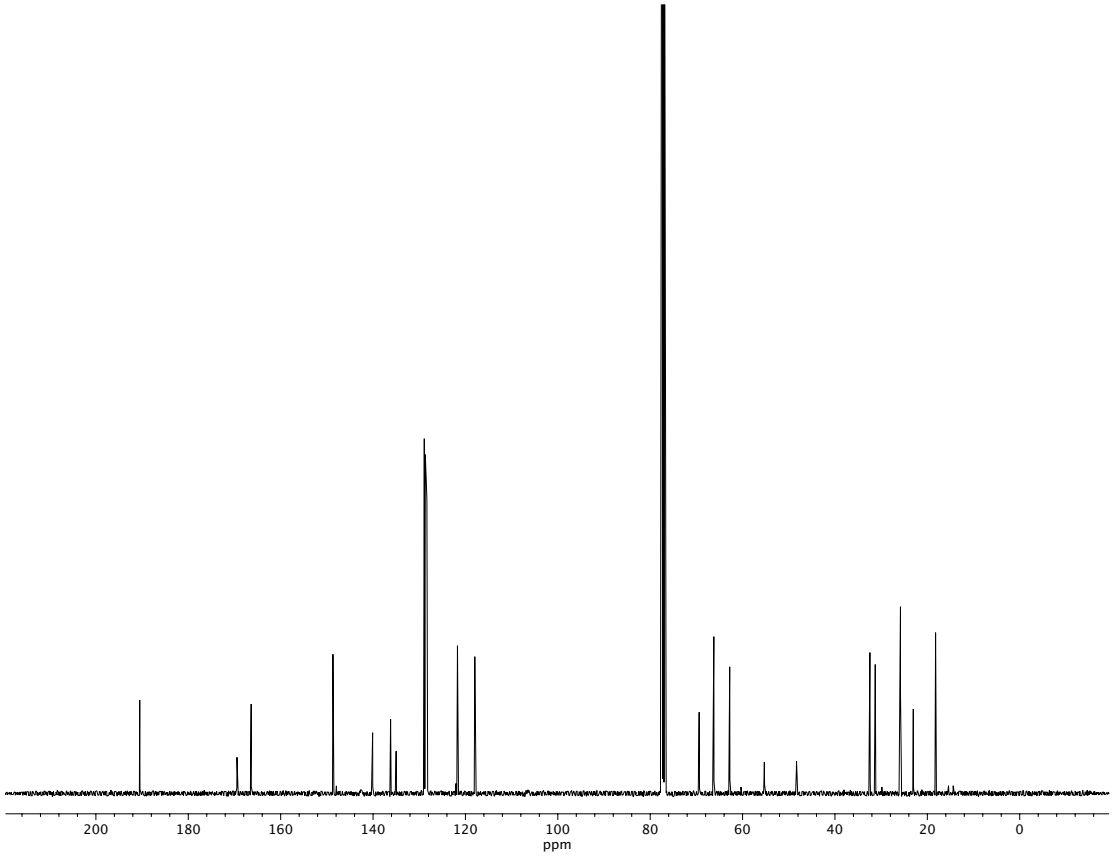


Figure A1.125. *^{13}C NMR (100 MHz, $CDCl_3$) of compound* ***10n****.*

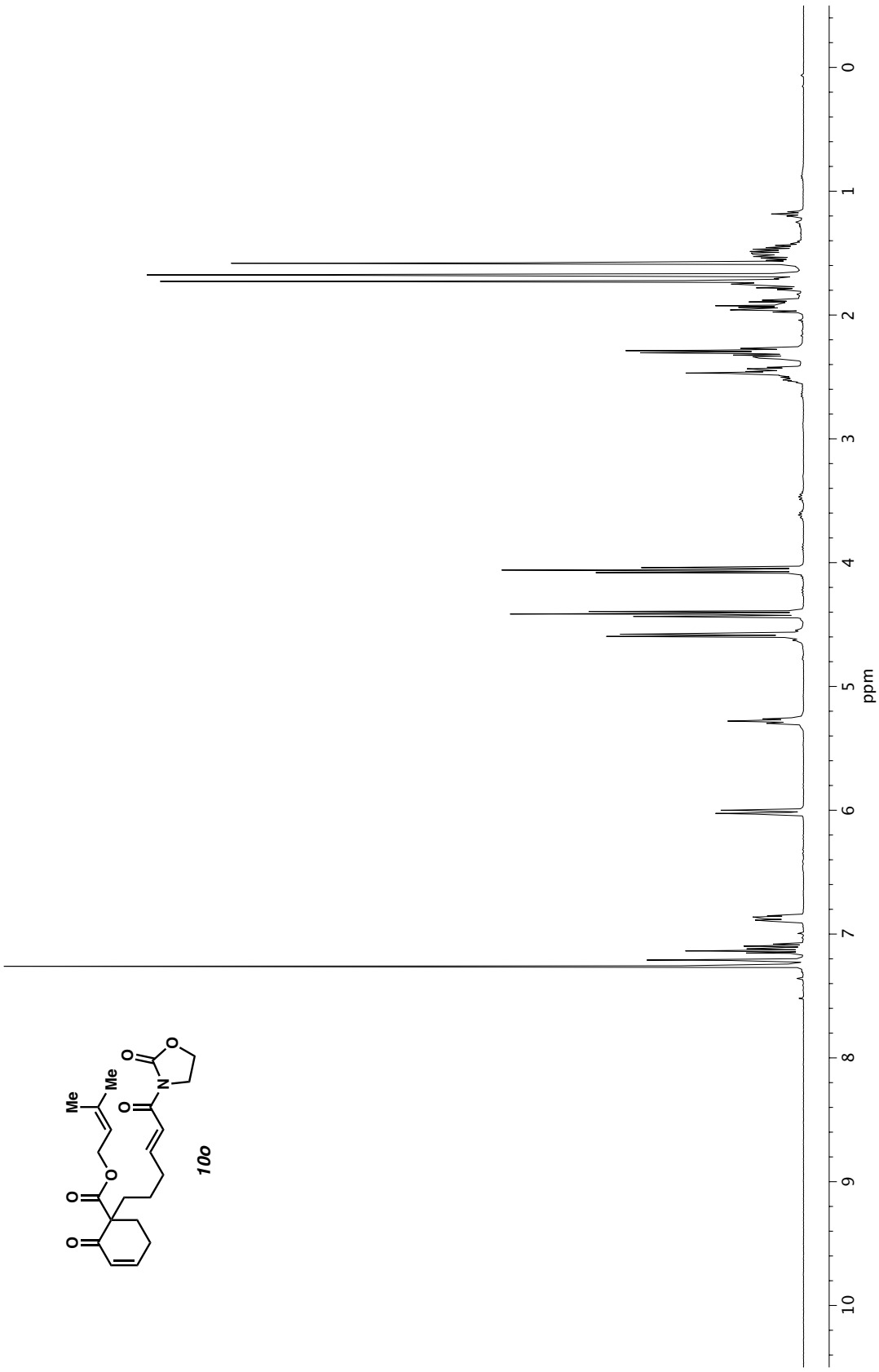


Figure A1.126. *^{1}H NMR (400 MHz, $CDCl_3$) of compound* ***10o***.

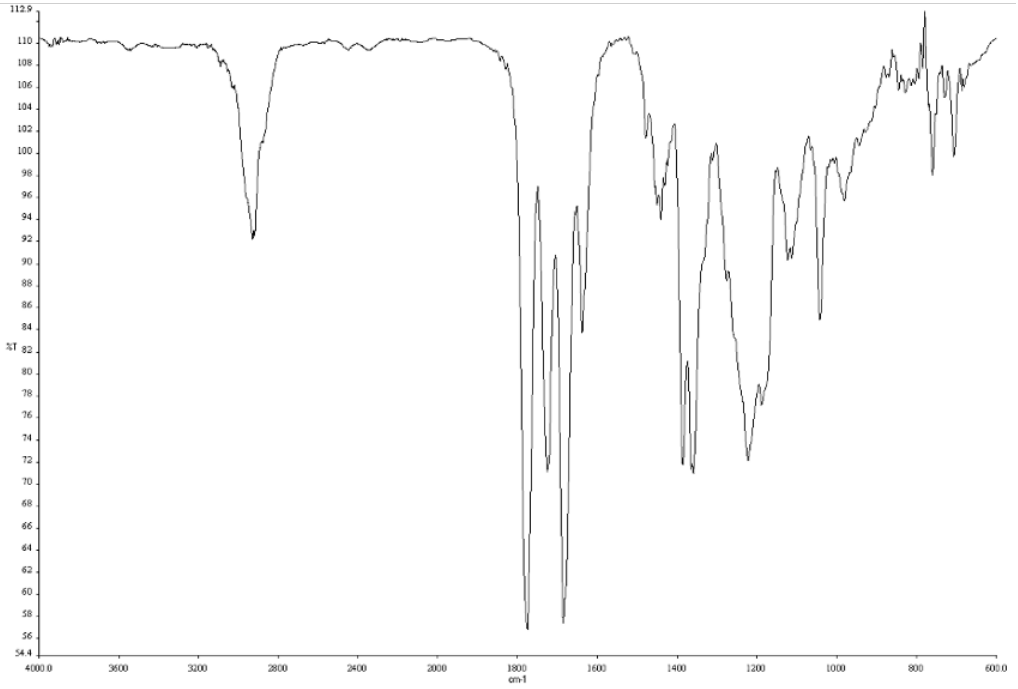


Figure A1.127. *Infrared spectrum (Thin Film, NaCl) of compound* ***10o****.*

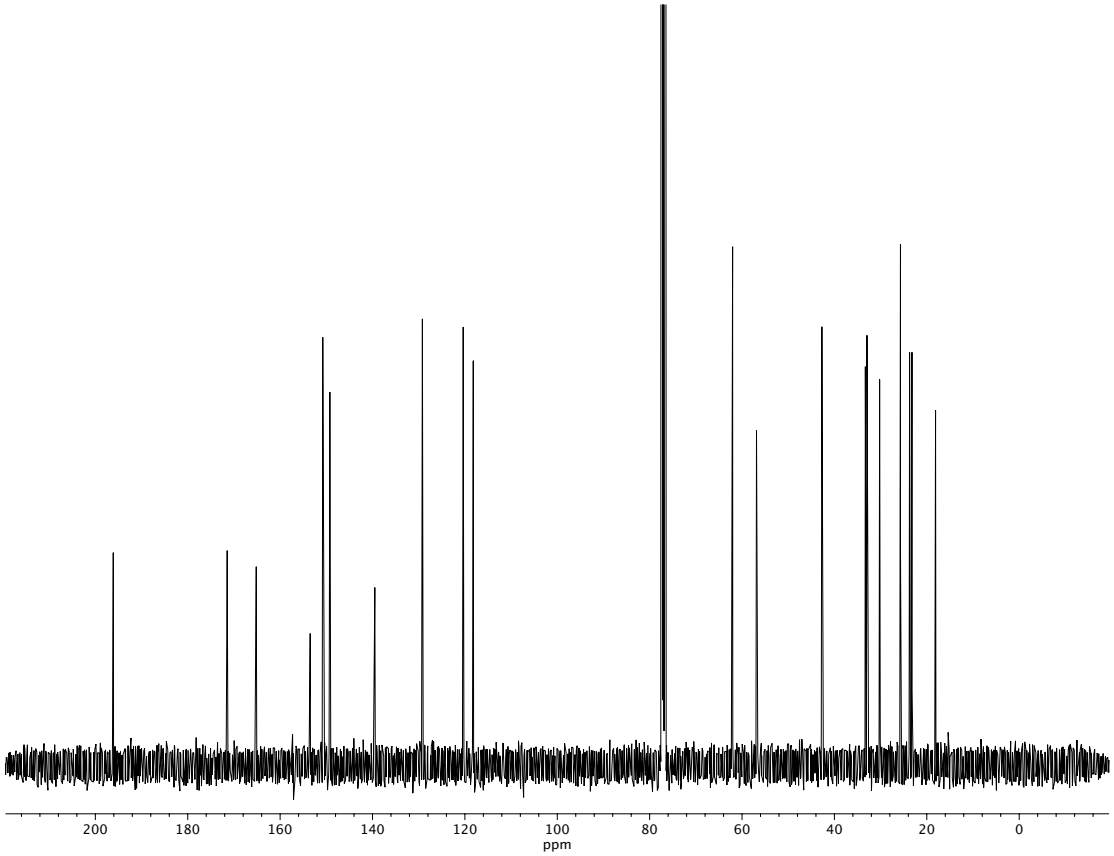


Figure A1.128. *^{13}C NMR (100 MHz, $CDCl_3$) of compound* ***10o****.*

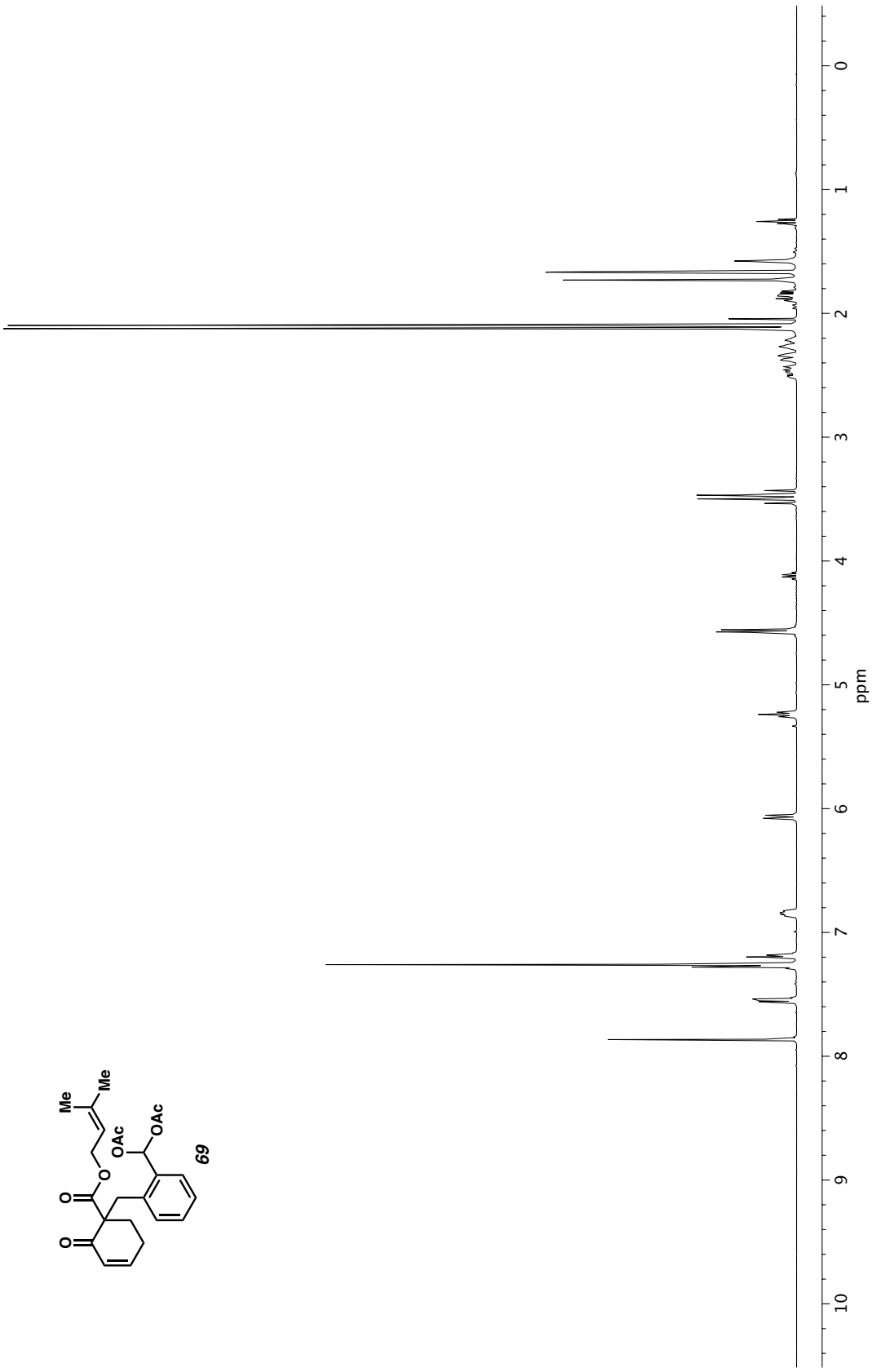


Figure A1.129. *^1H NMR (400 MHz, $CDCl_3$) of compound* ***69****.*

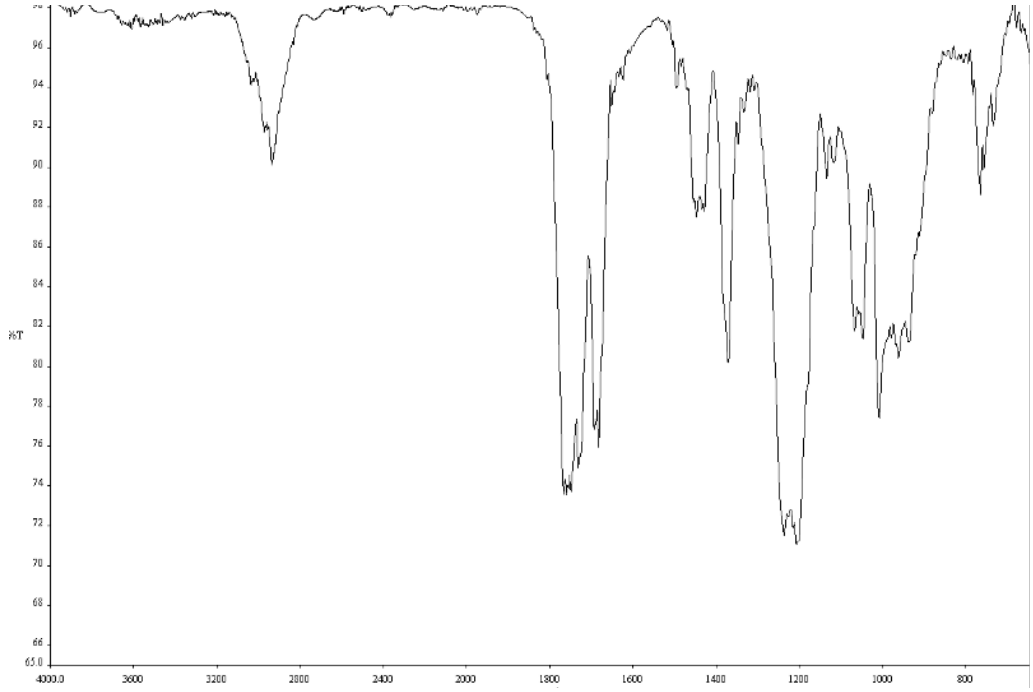


Figure A1.130. *Infrared spectrum (Thin Film, NaCl) of compound* ***69****.*

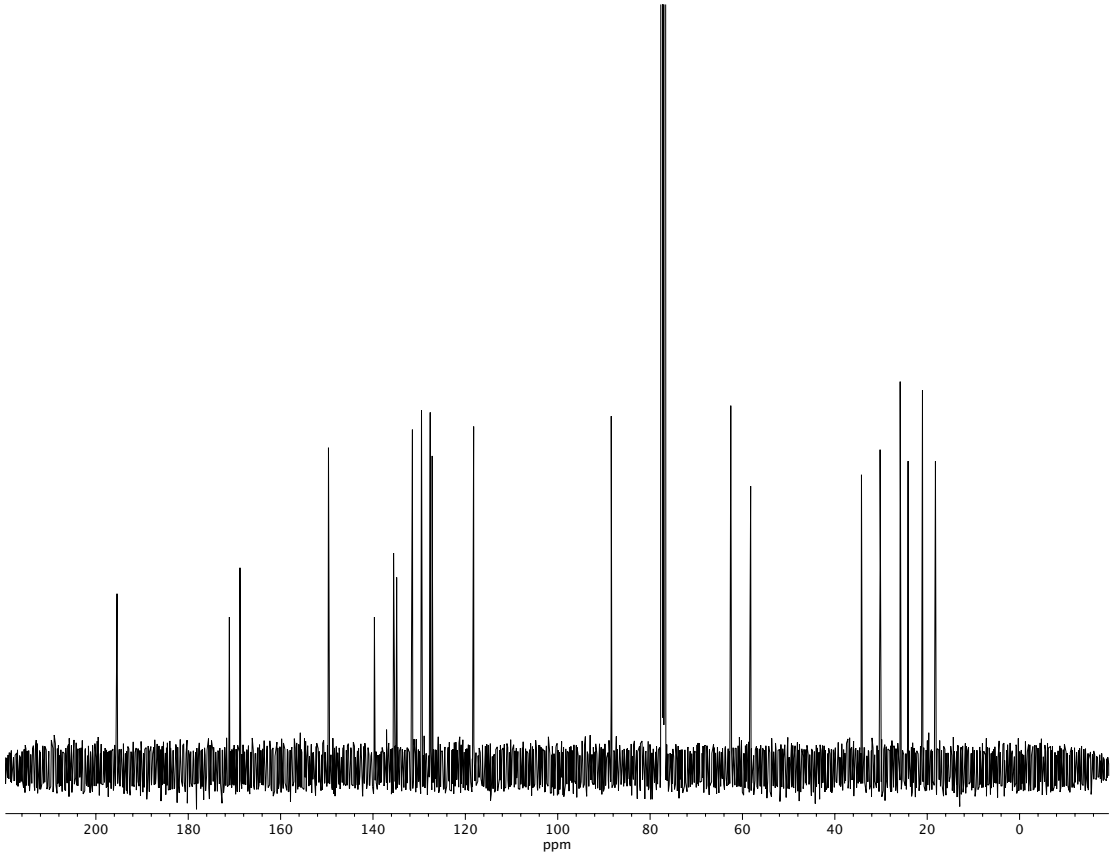


Figure A1.131. *^{13}C NMR (100 MHz, $CDCl_3$) of compound* ***69****.*

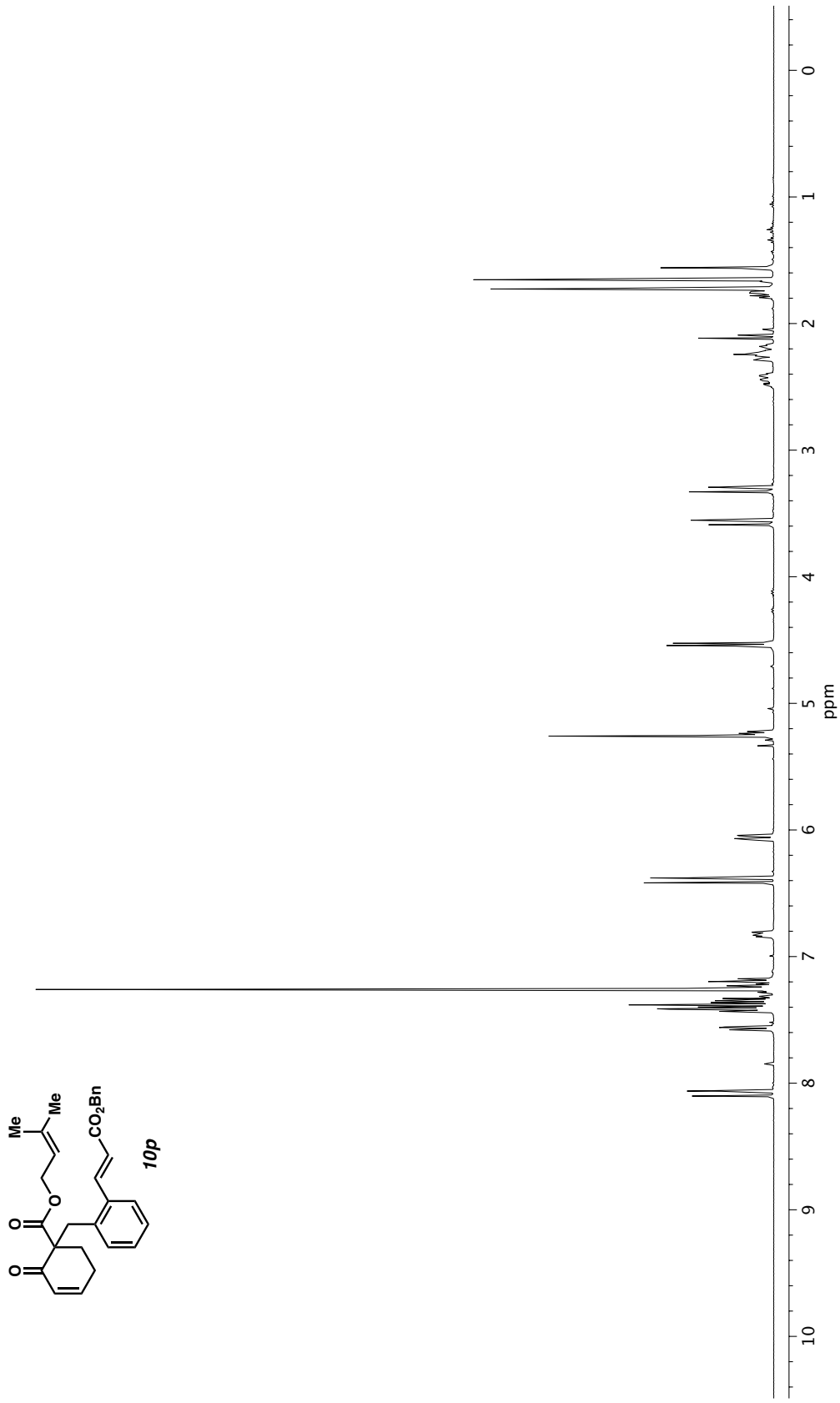


Figure A1.132. *^{1}H NMR (400 MHz, $CDCl_3$) of compound* ***10p****.*

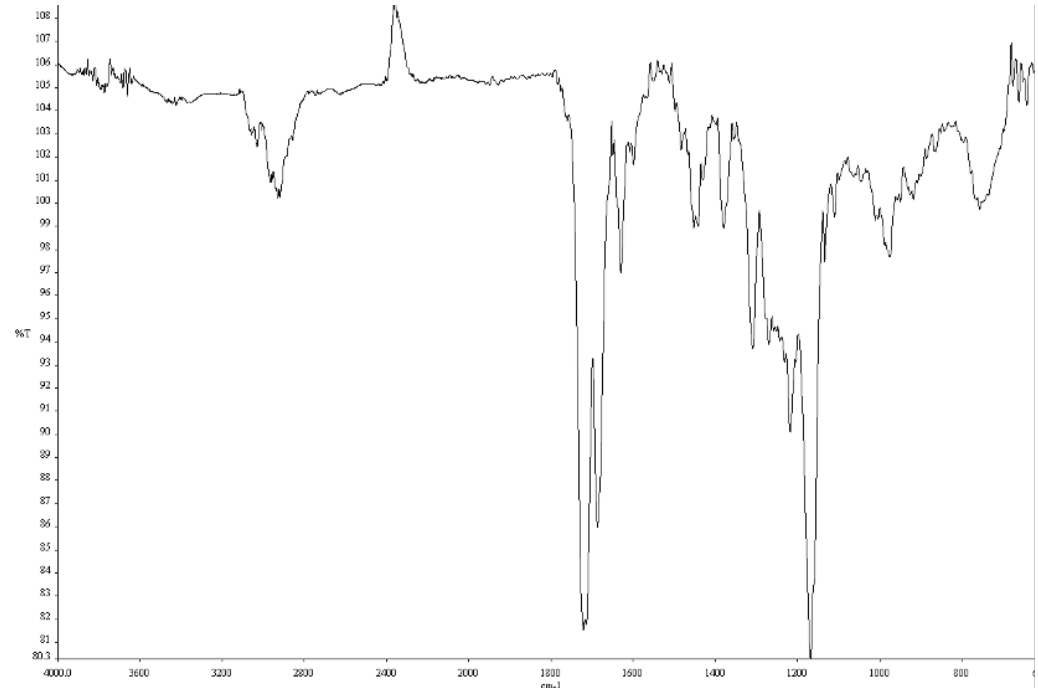


Figure A1.133. *Infrared spectrum (Thin Film, NaCl) of compound* ***10p****.*

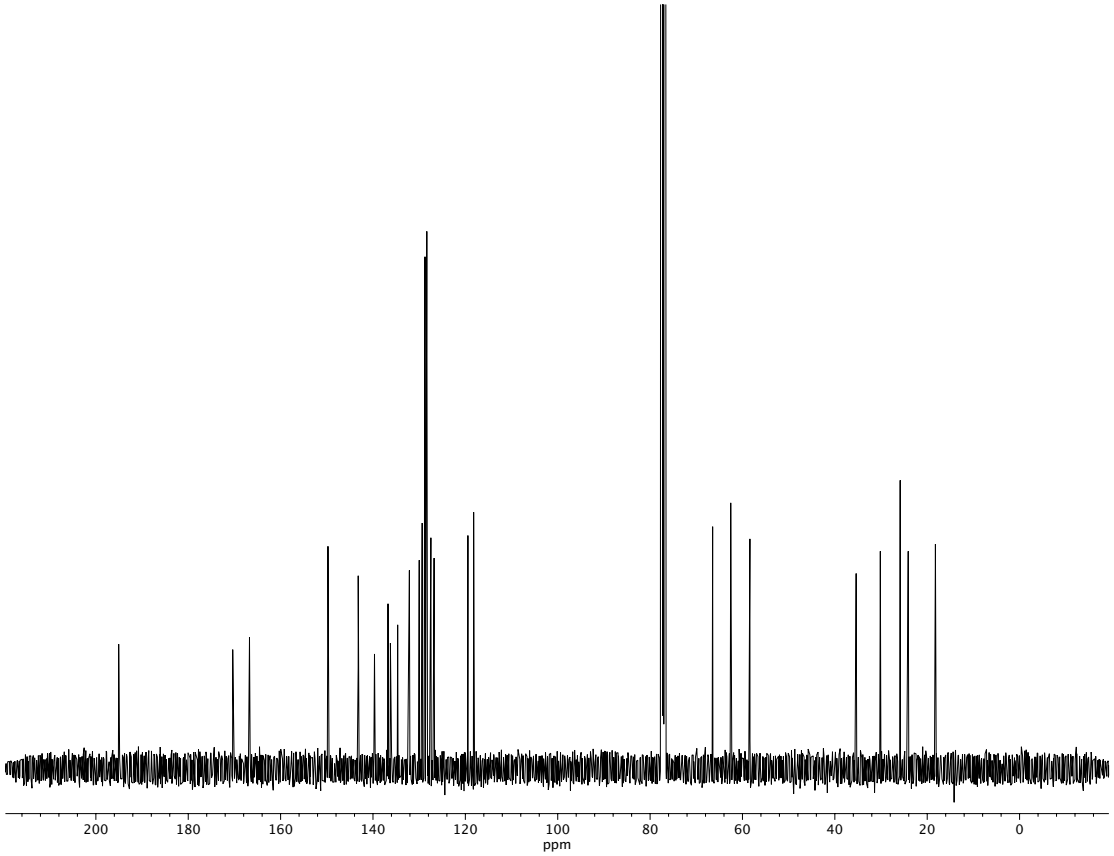


Figure A1.134. *^{13}C NMR (100 MHz, $CDCl_3$) of compound* ***10p****.*

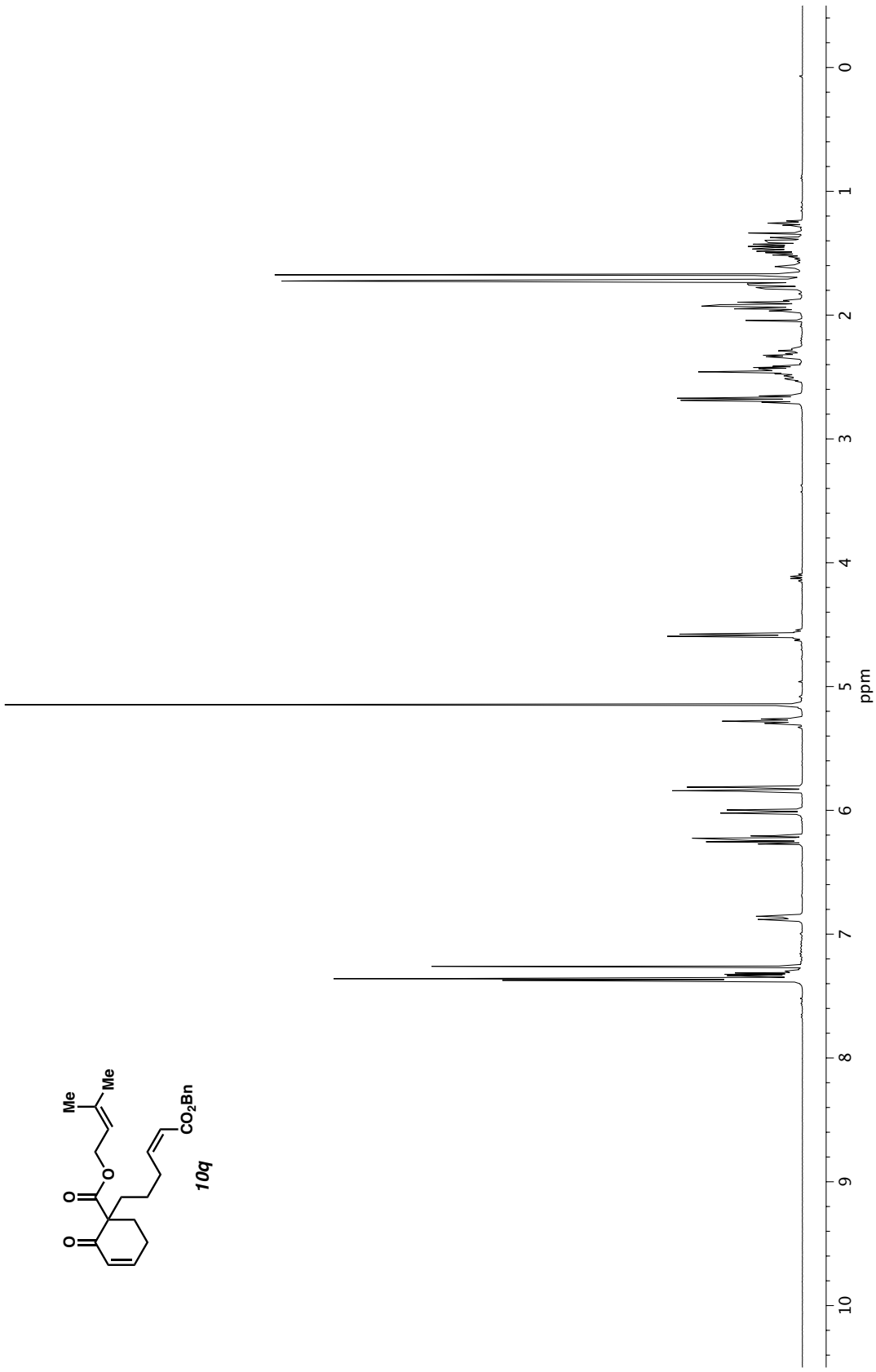


Figure A1.135. *^1H NMR (400 MHz, $CDCl_3$) of compound* ***10q***.

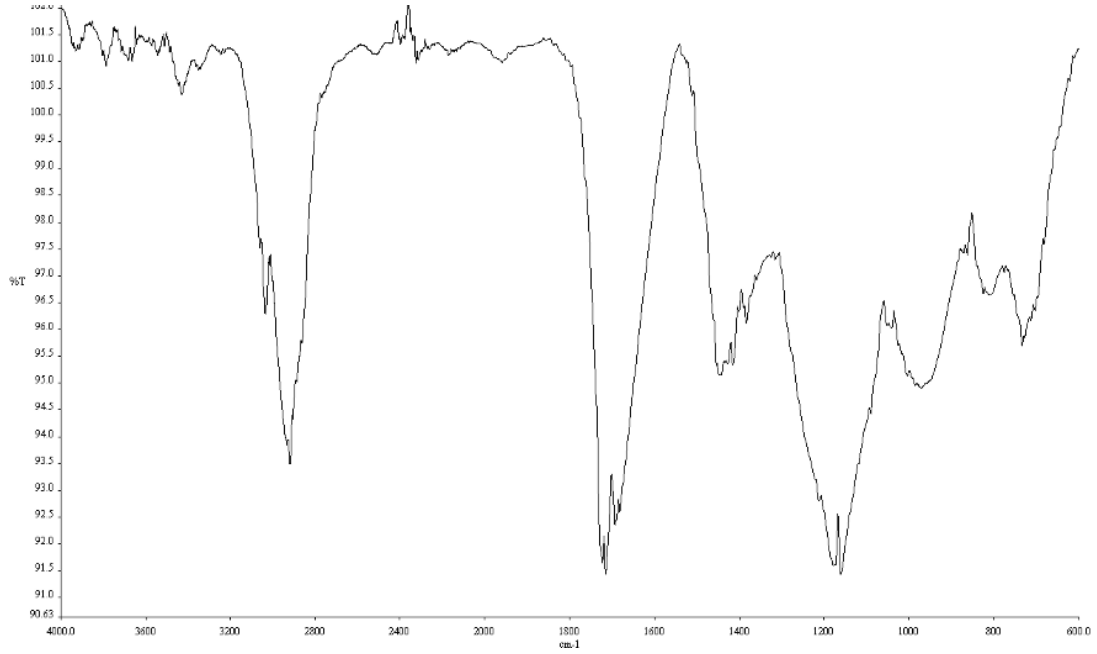


Figure A1.136. *Infrared spectrum (Thin Film, NaCl) of compound* ***10q****.*

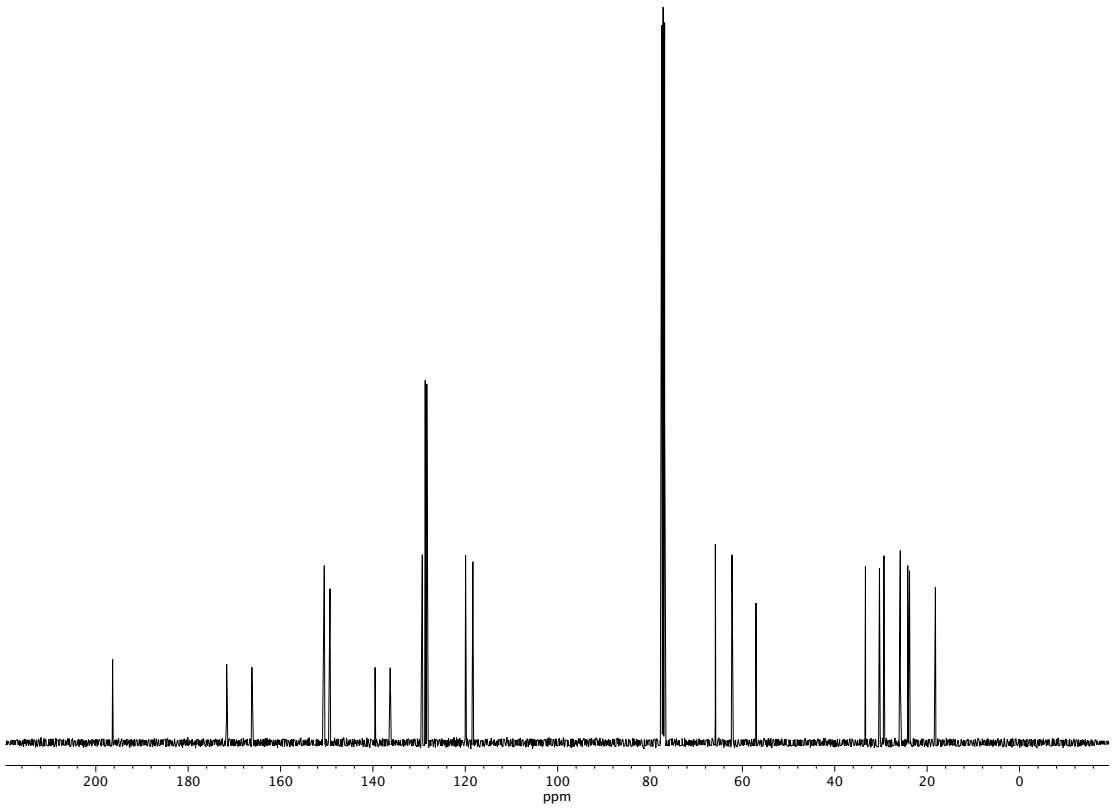


Figure A1.137. *^{13}C NMR (100 MHz, $CDCl_3$) of compound* ***10q****.*

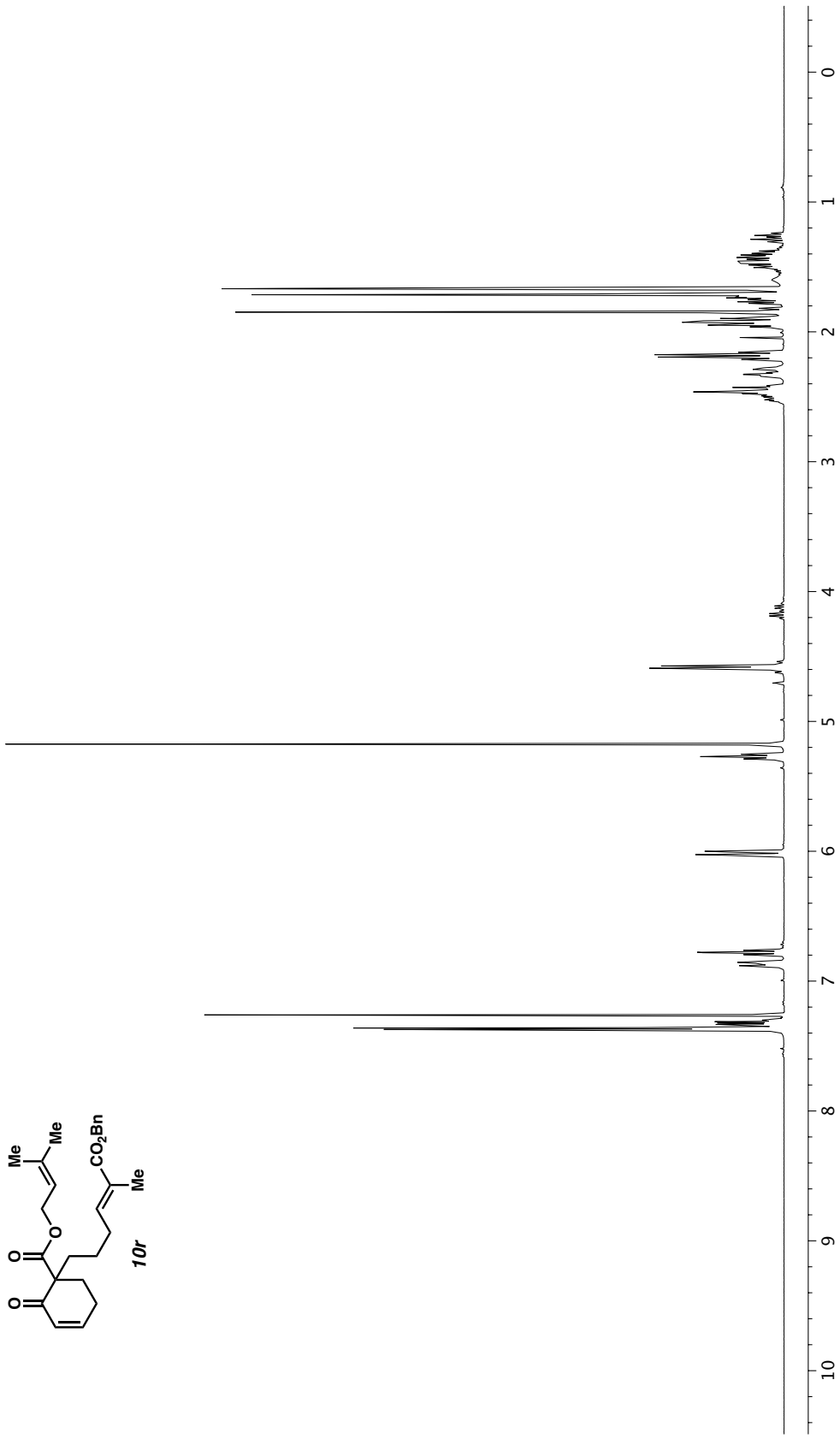


Figure A1.138. *^1H NMR (400 MHz, $CDCl_3$) of compound* ***10r****.*

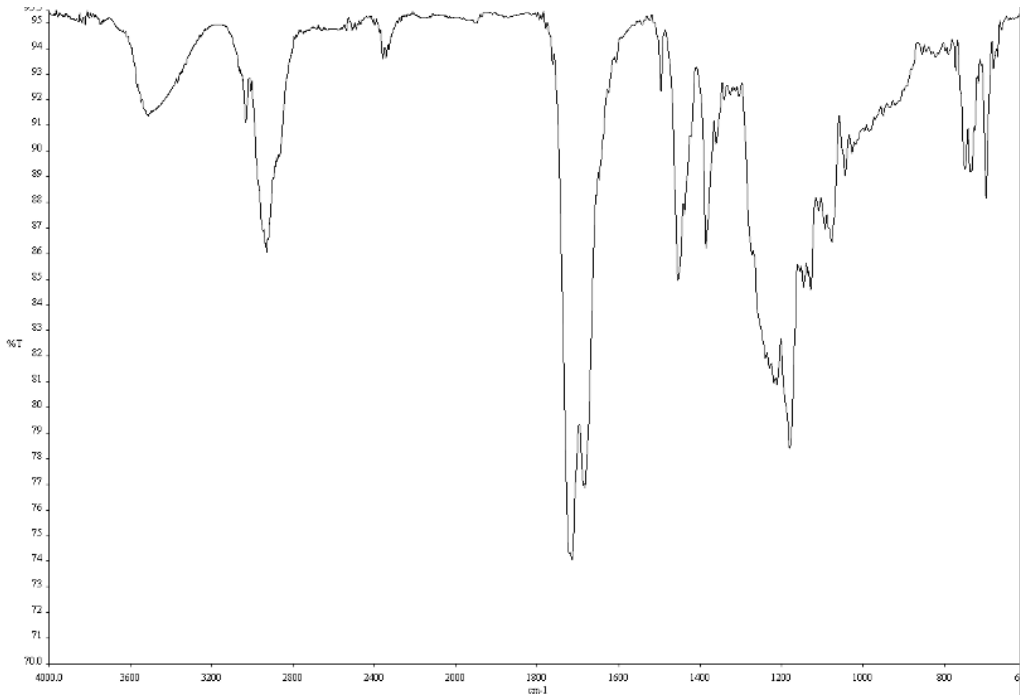


Figure A1.139. *Infrared spectrum (Thin Film, NaCl) of compound* ***10r****.*

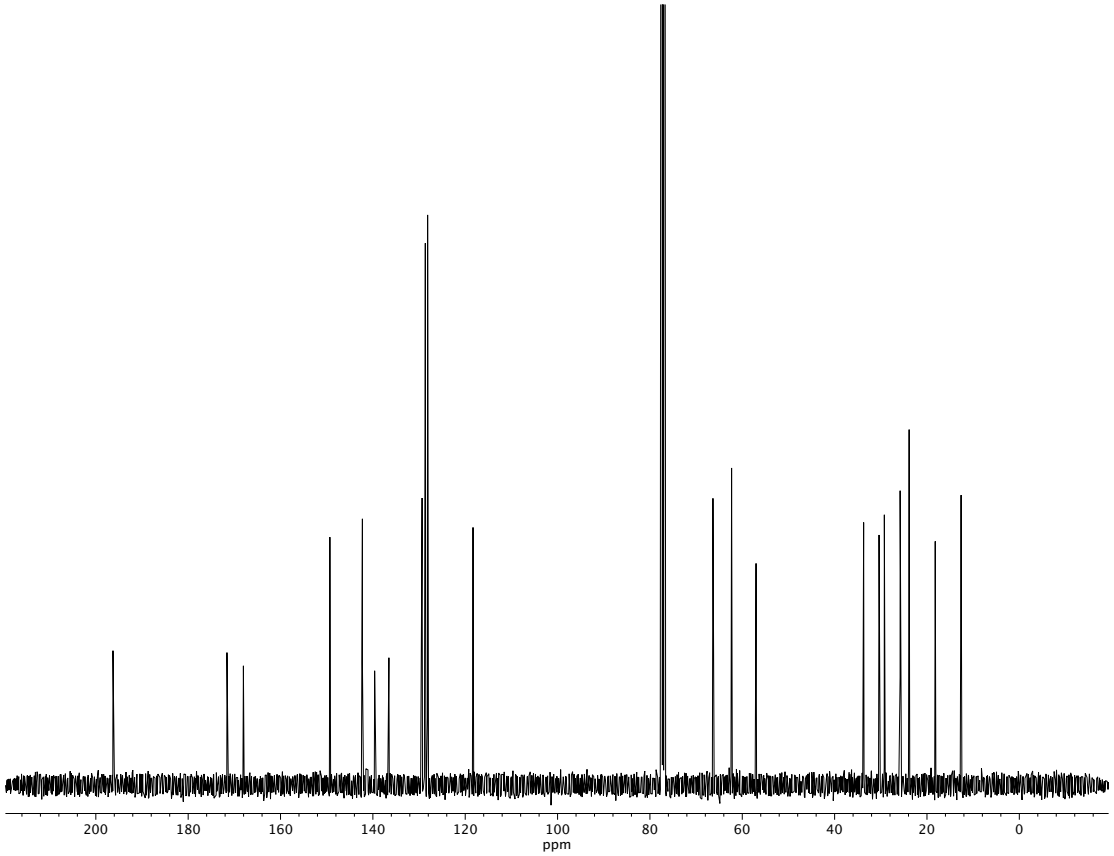


Figure A1.140. *^{13}C NMR (100 MHz, $CDCl_3$) of compound* ***10r****.*

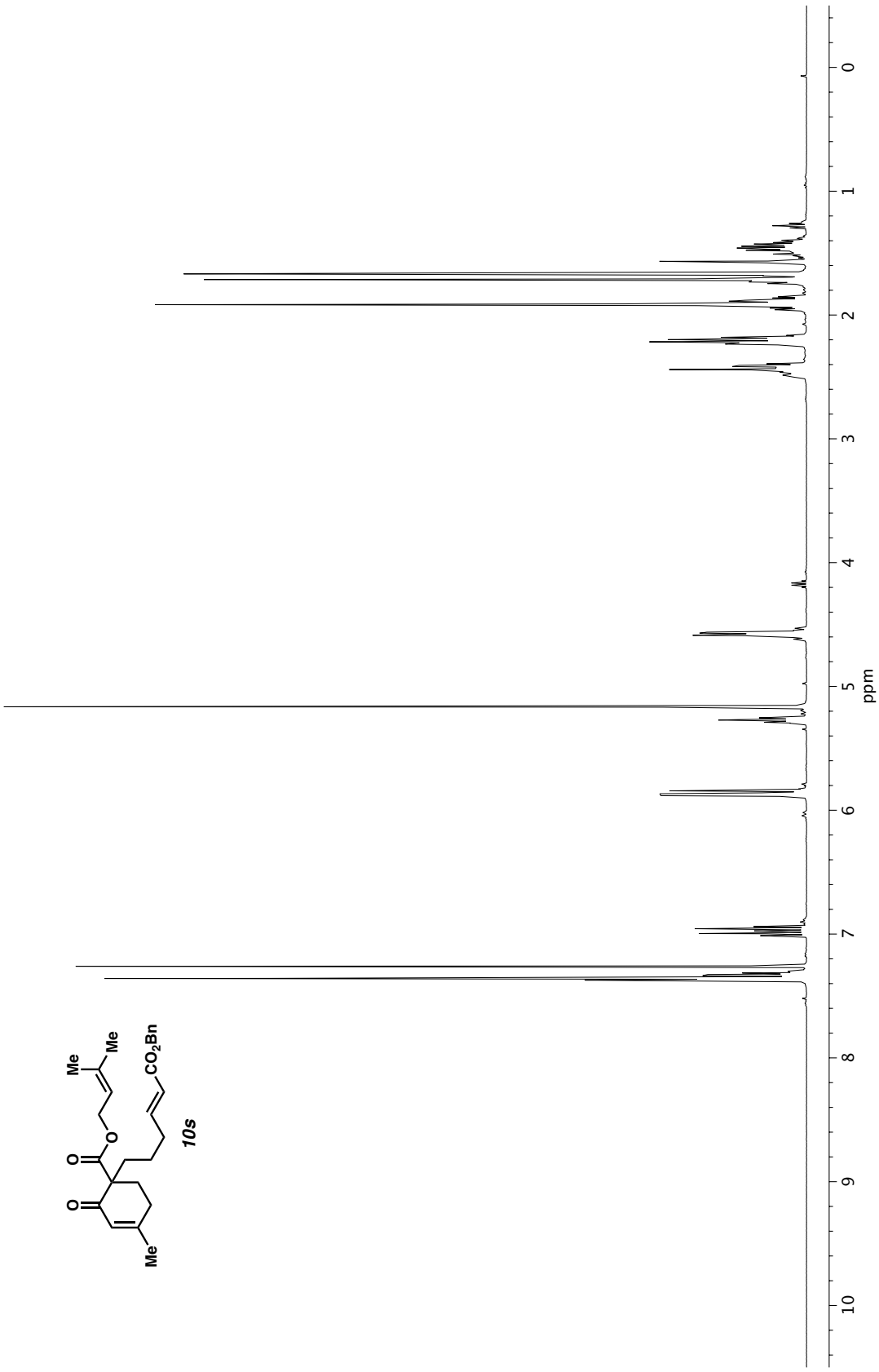


Figure A1.141. *^1H NMR (400 MHz, $CDCl_3$) of compound* ***10s****.*

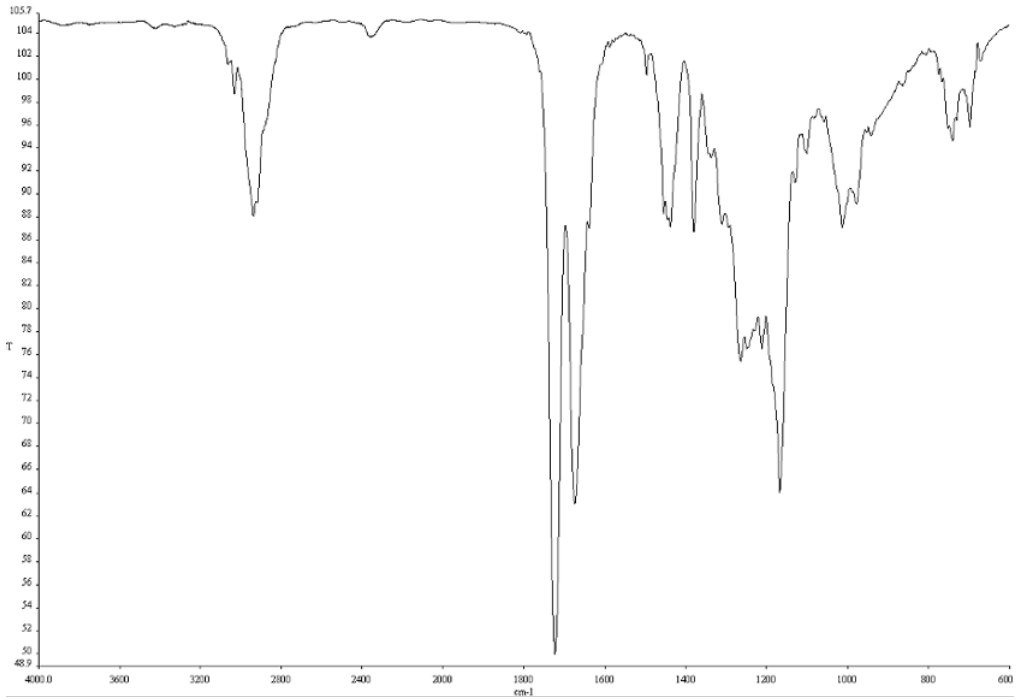


Figure A1.142. *Infrared spectrum (Thin Film, NaCl) of compound* ***10s****.*

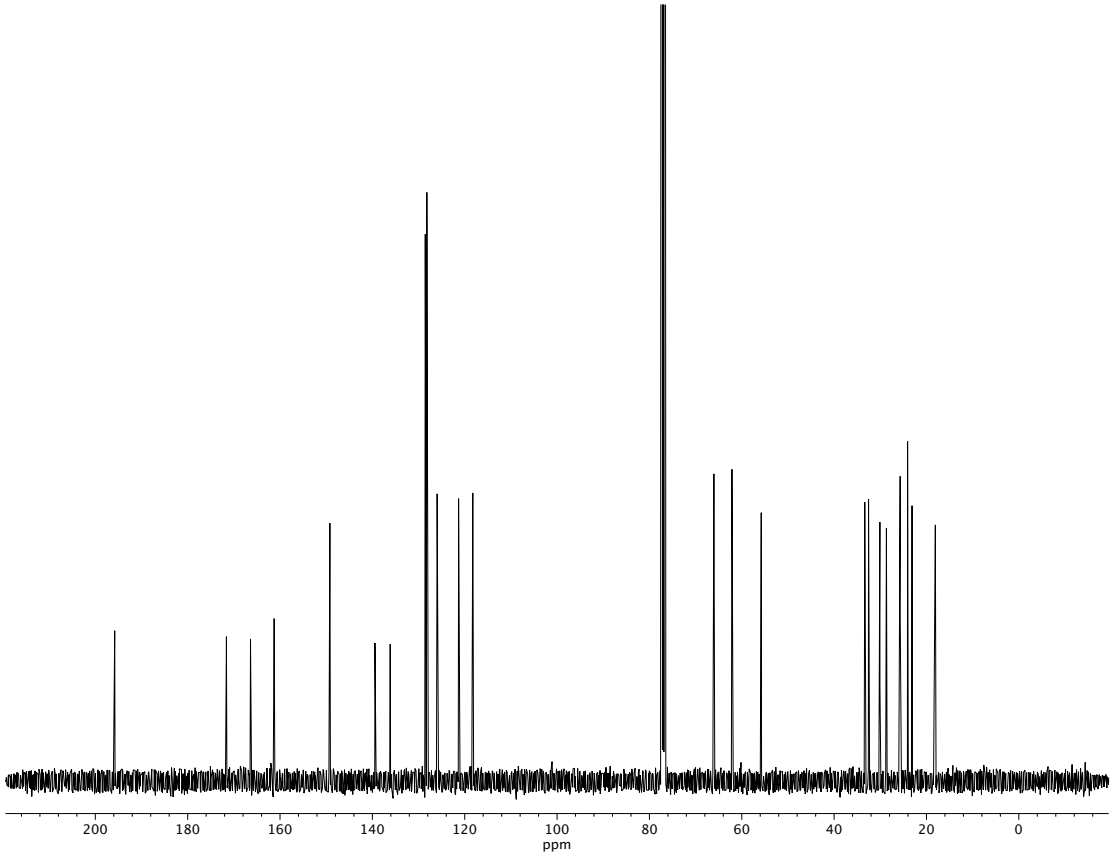


Figure A1.143. *^{13}C NMR (100 MHz, $CDCl_3$) of compound* ***10s****.*

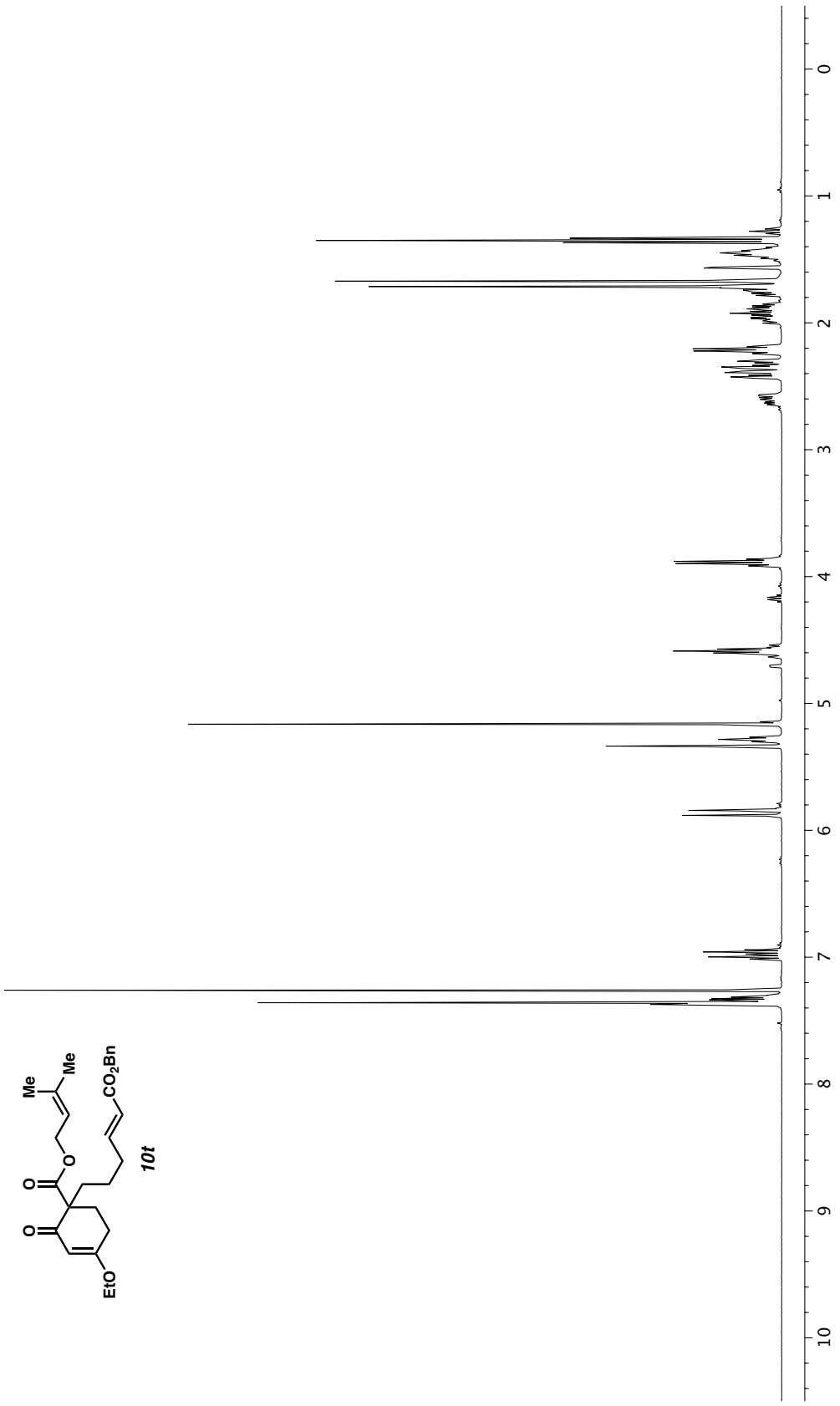


Figure A1.144. *^1H NMR (400 MHz, $CDCl_3$) of compound* ***10t****.*

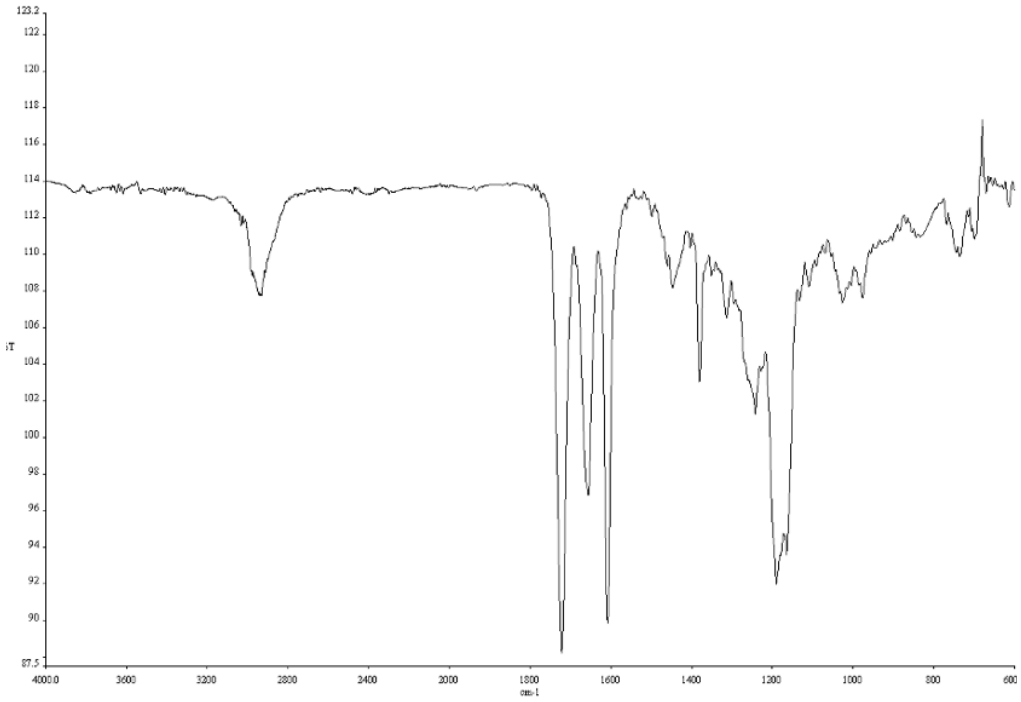


Figure A1.145. *Infrared spectrum (Thin Film, NaCl) of compound* ***10t****.*

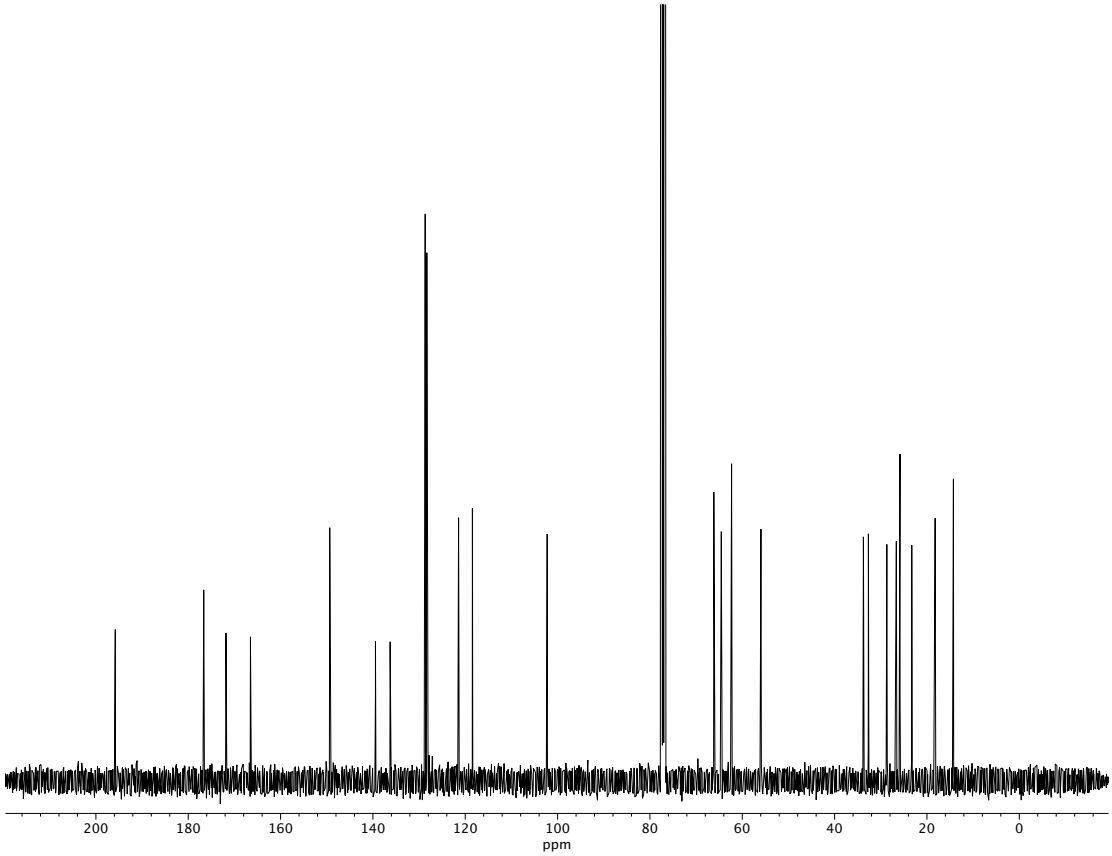


Figure A1.146. *^{13}C NMR (100 MHz, $CDCl_3$) of compound* ***10t****.*

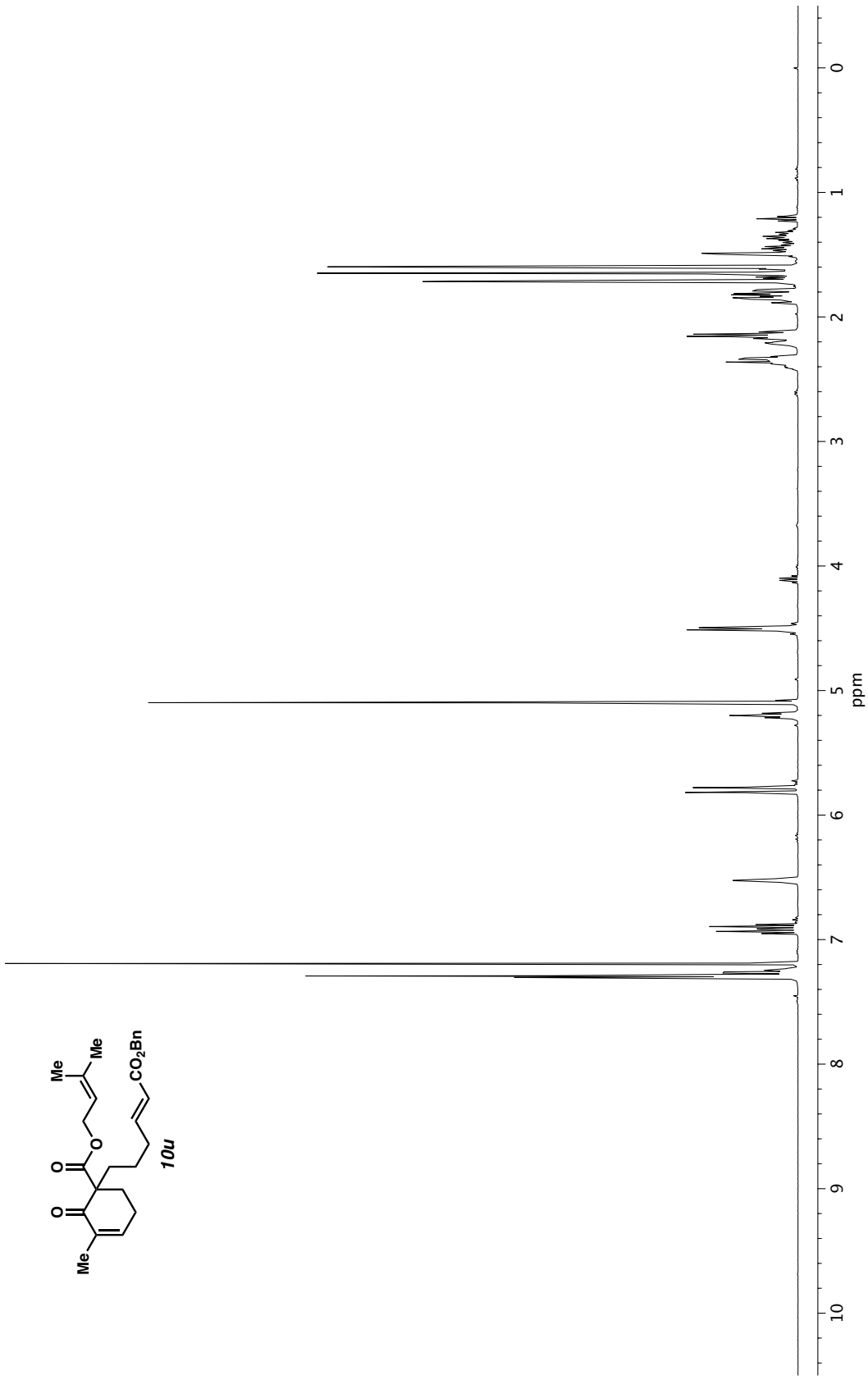


Figure A1.147. *^{1}H NMR (400 MHz, $CDCl_3$) of compound* ***10u****.*

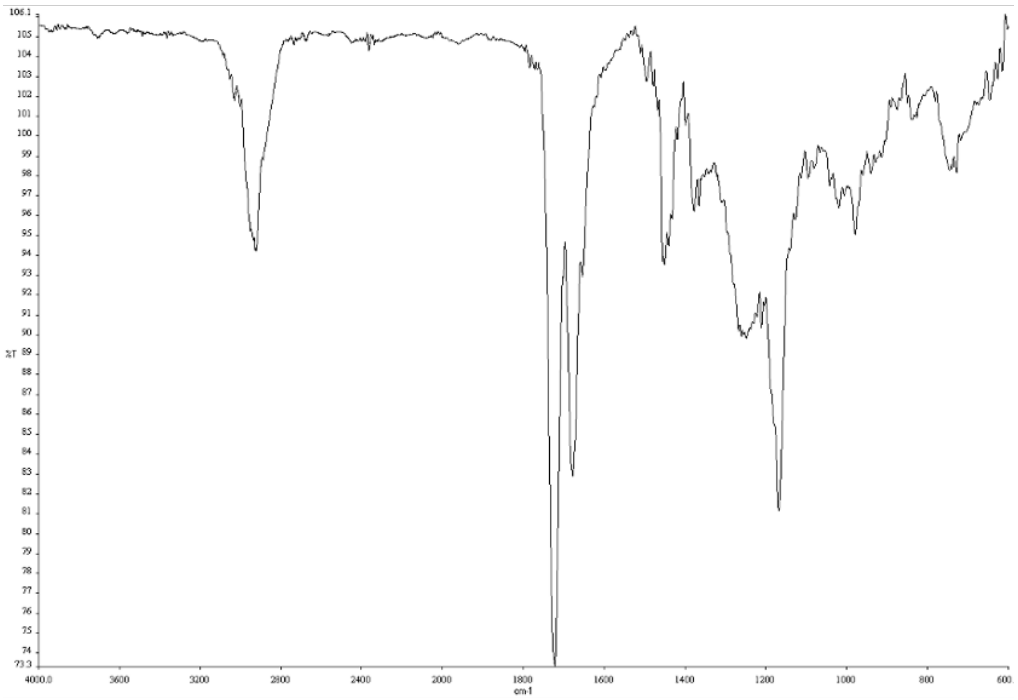


Figure A1.148. *Infrared spectrum (Thin Film, NaCl) of compound* ***10u****.*

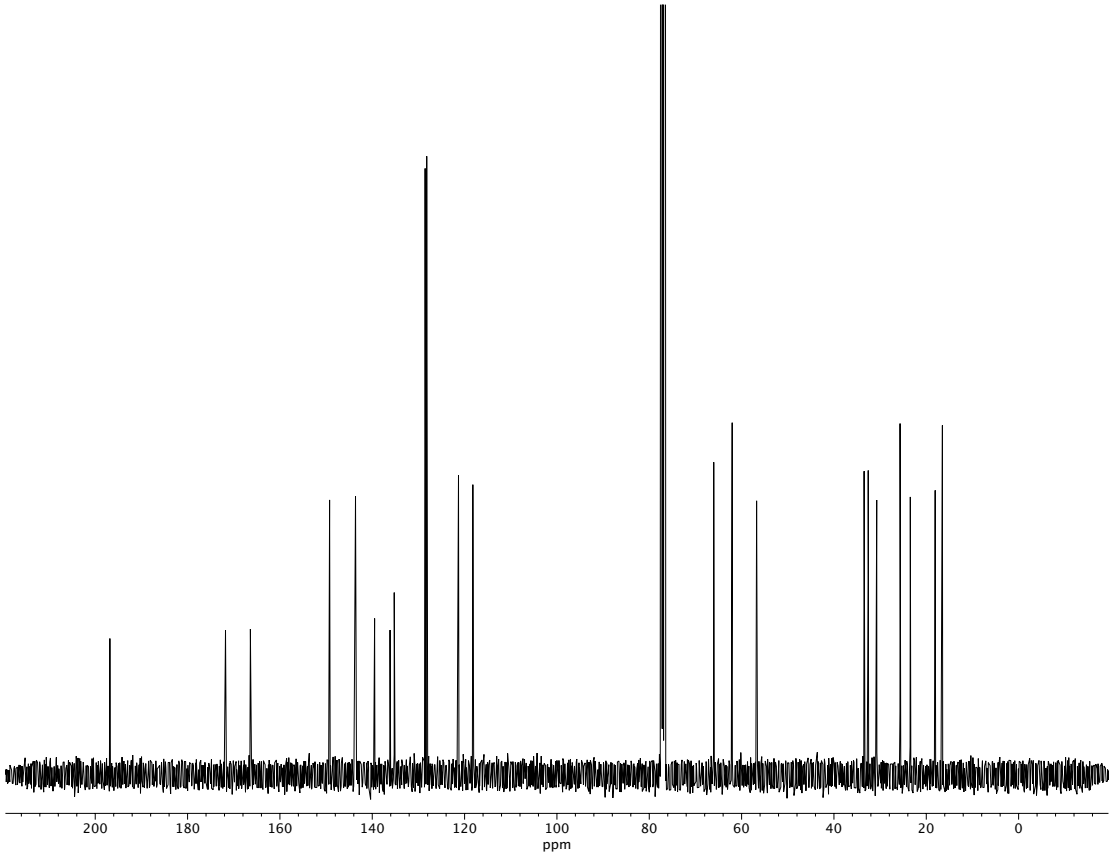


Figure A1.149. *^{13}C NMR (100 MHz, $CDCl_3$) of compound* ***10u****.*

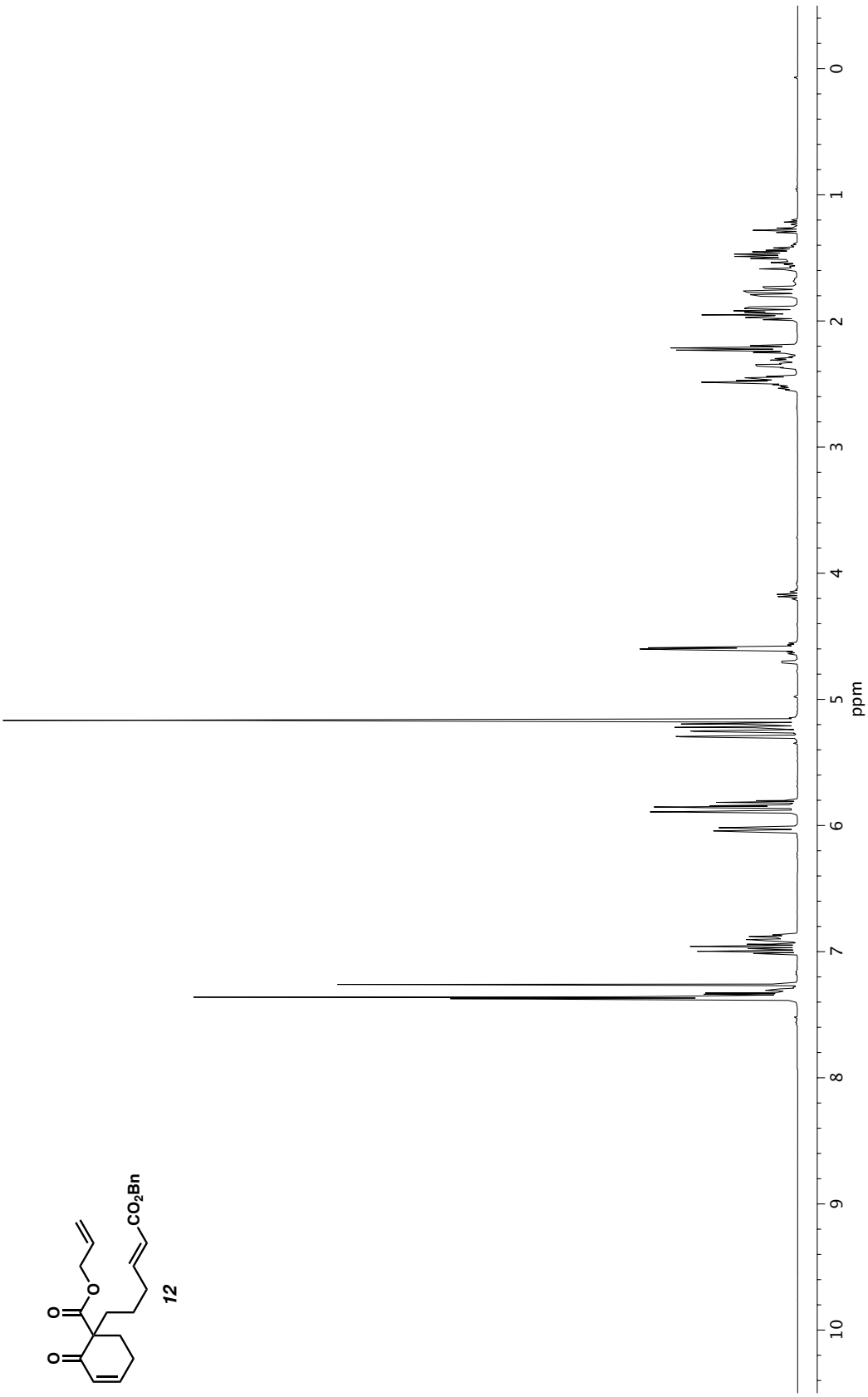


Figure A1.150. *^1H NMR (400 MHz, $CDCl_3$) of compound* ***12****.*

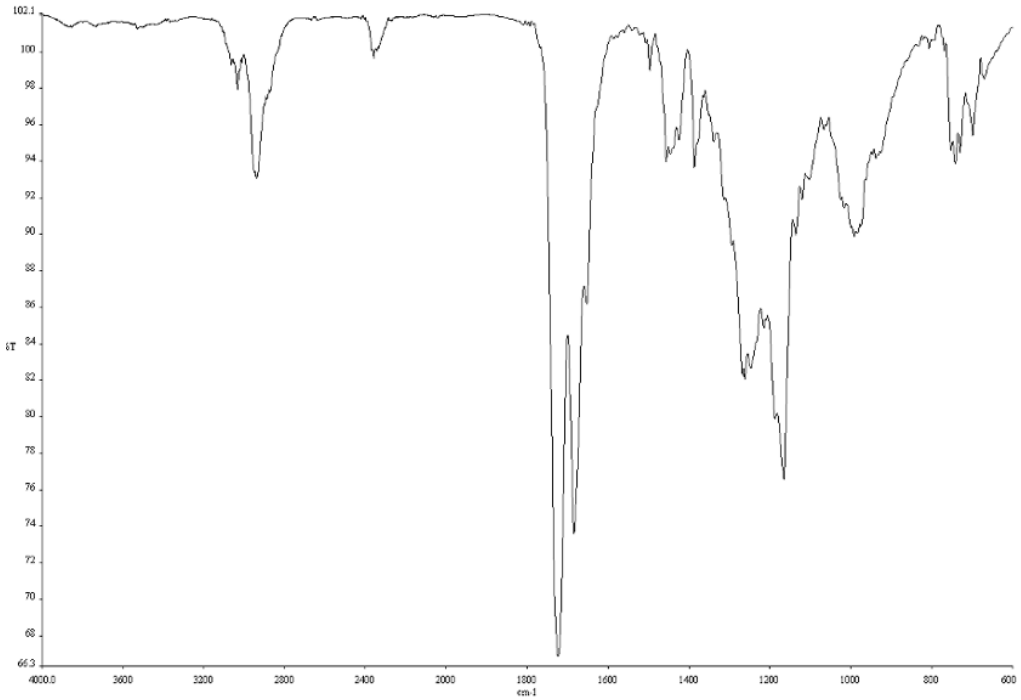


Figure A1.151. *Infrared spectrum (Thin Film, NaCl) of compound* ***12****.*

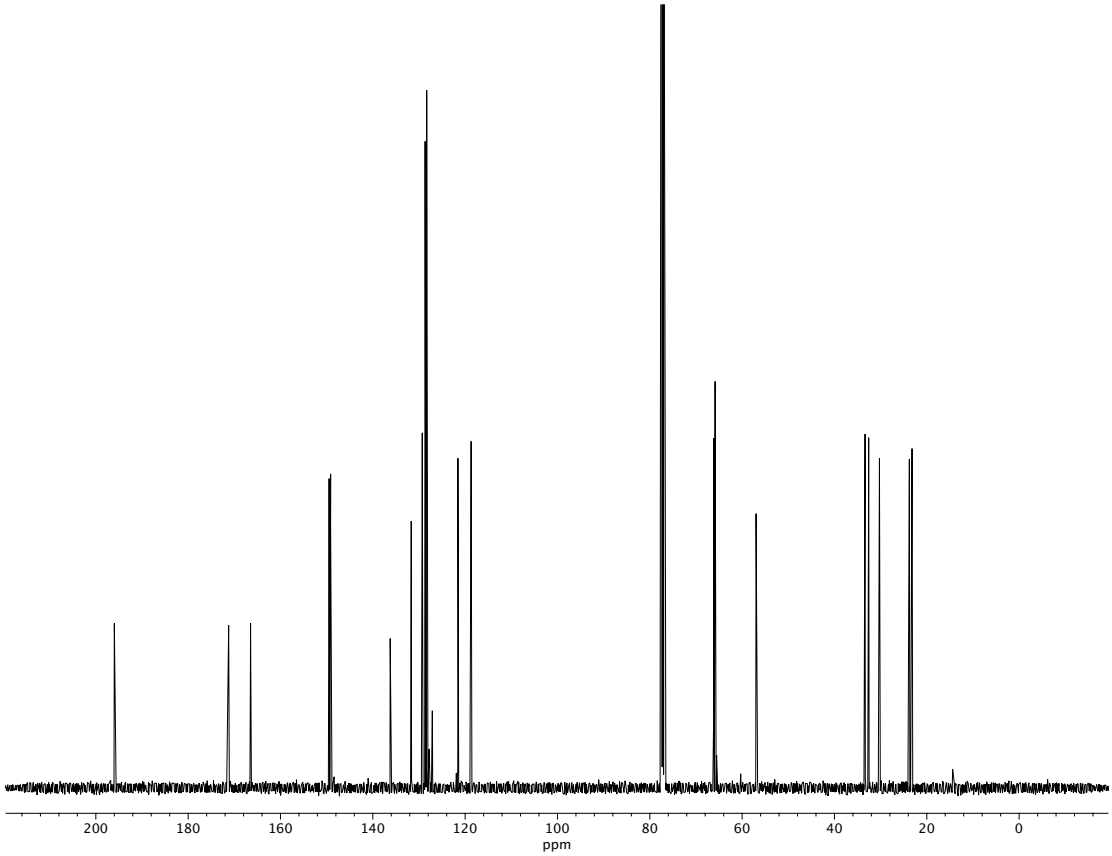


Figure A1.152. *^{13}C NMR (100 MHz, $CDCl_3$) of compound* ***12****.*

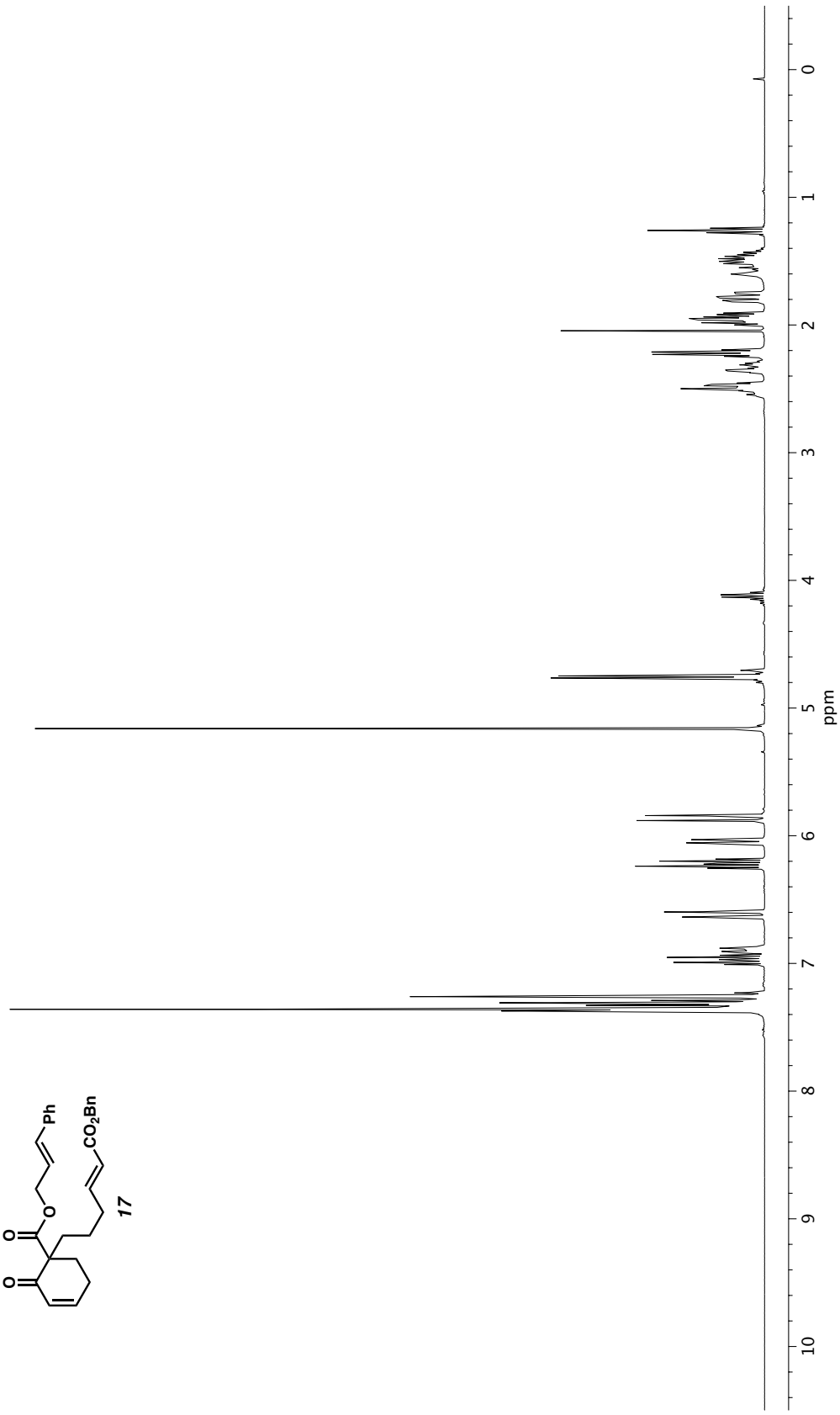


Figure A1.153. *^1H NMR (400 MHz, $CDCl_3$) of compound **17**.*

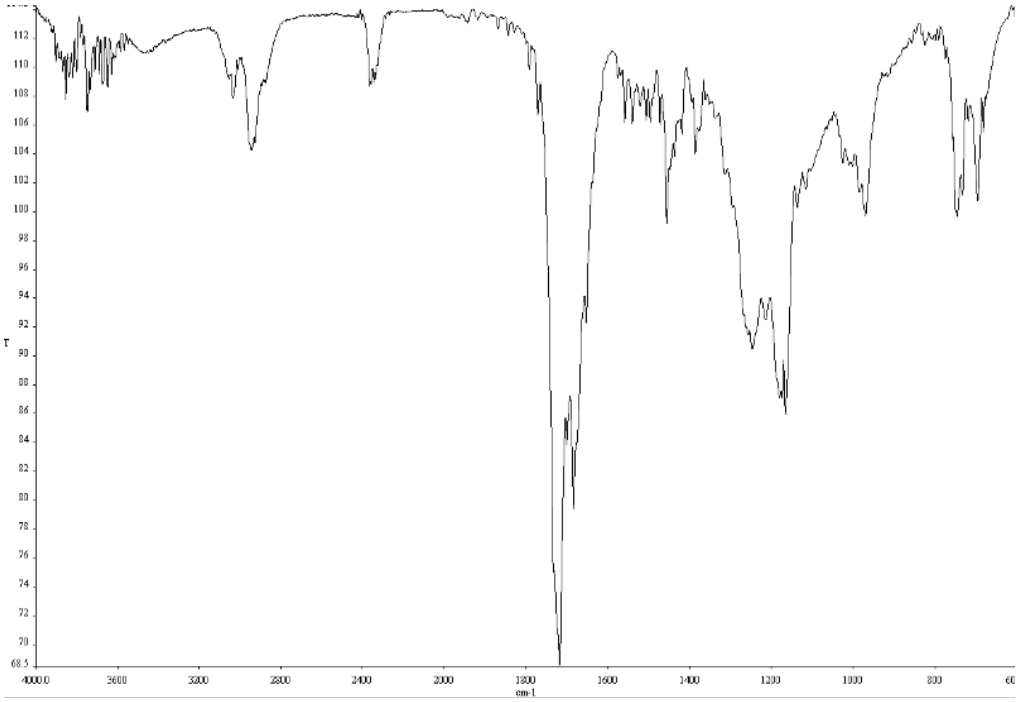


Figure A1.154. *Infrared spectrum (Thin Film, NaCl) of compound* ***17****.*

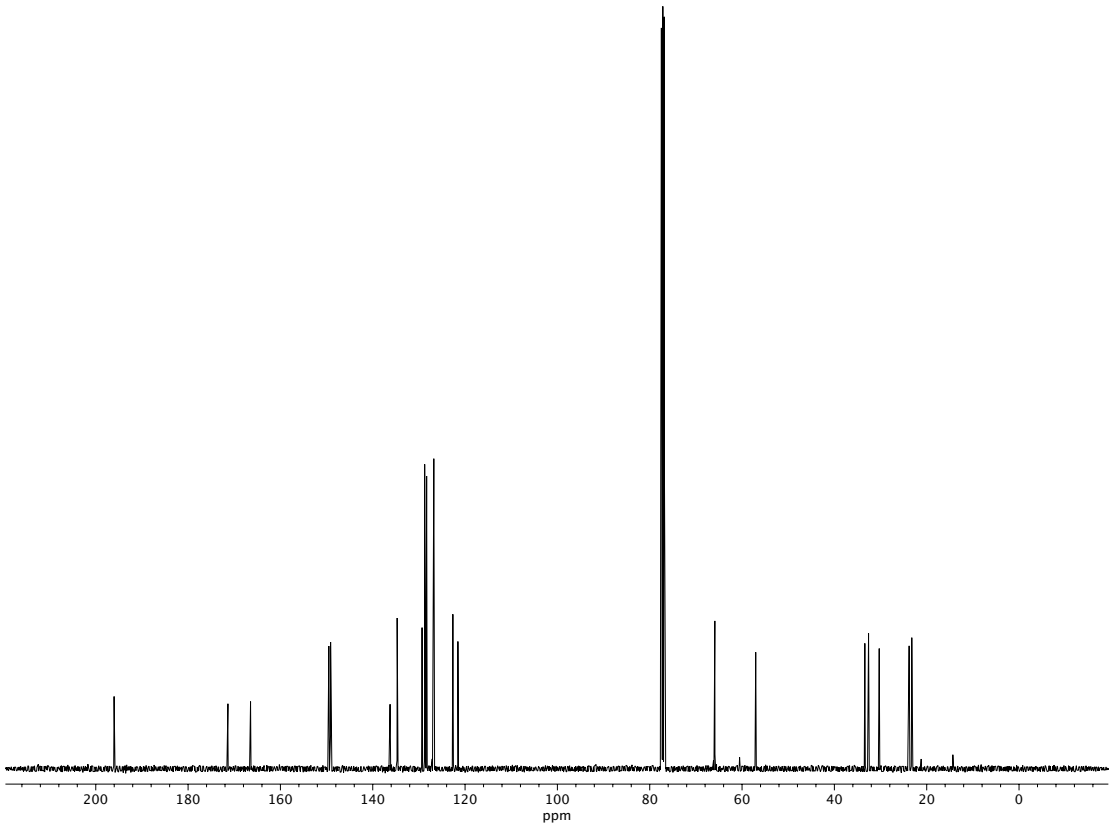


Figure A1.155. *^{13}C NMR (100 MHz, $CDCl_3$) of compound* ***17****.*

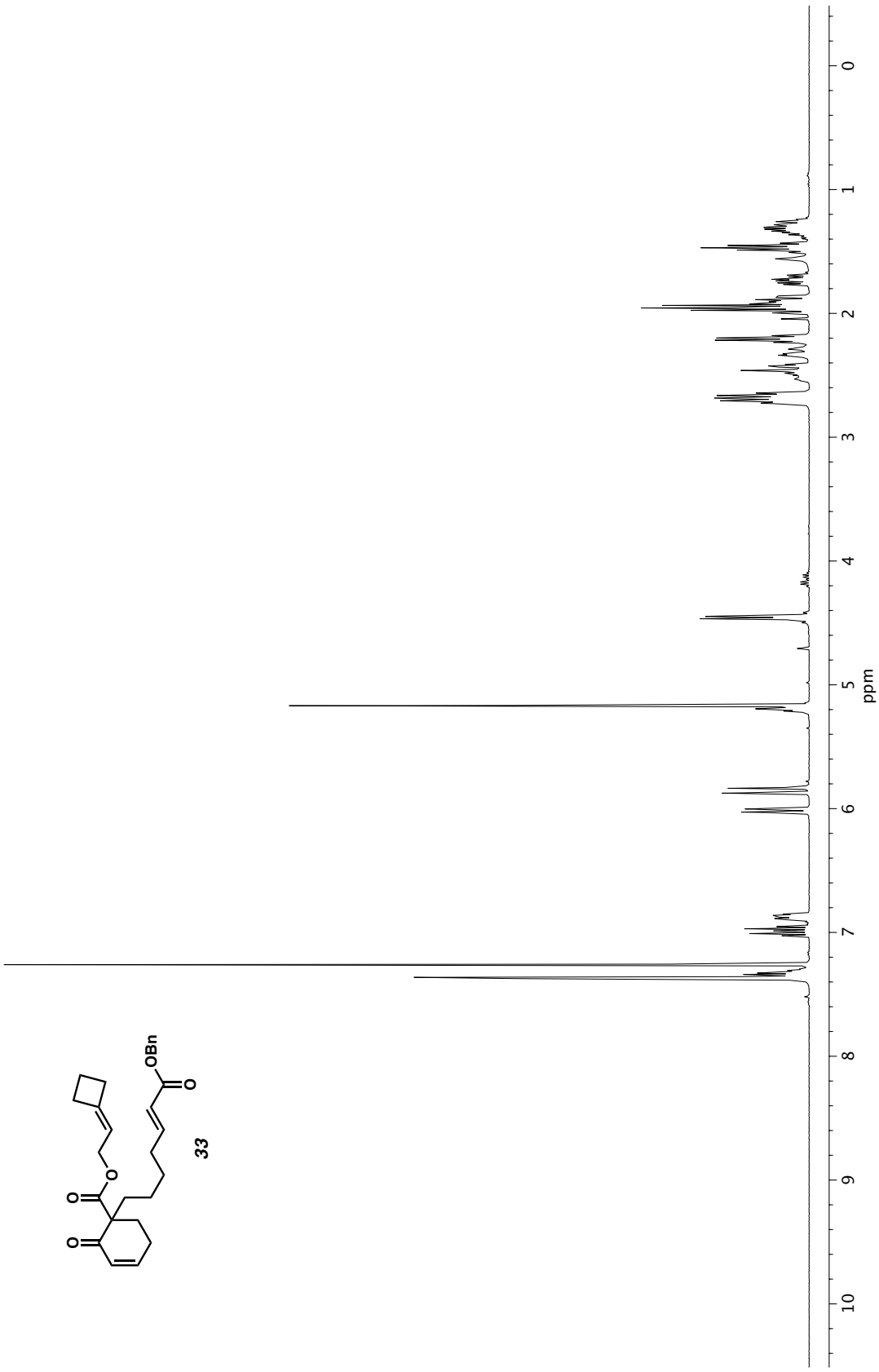


Figure A1.156. *^1H NMR (400 MHz, $CDCl_3$) of compound **33**.*

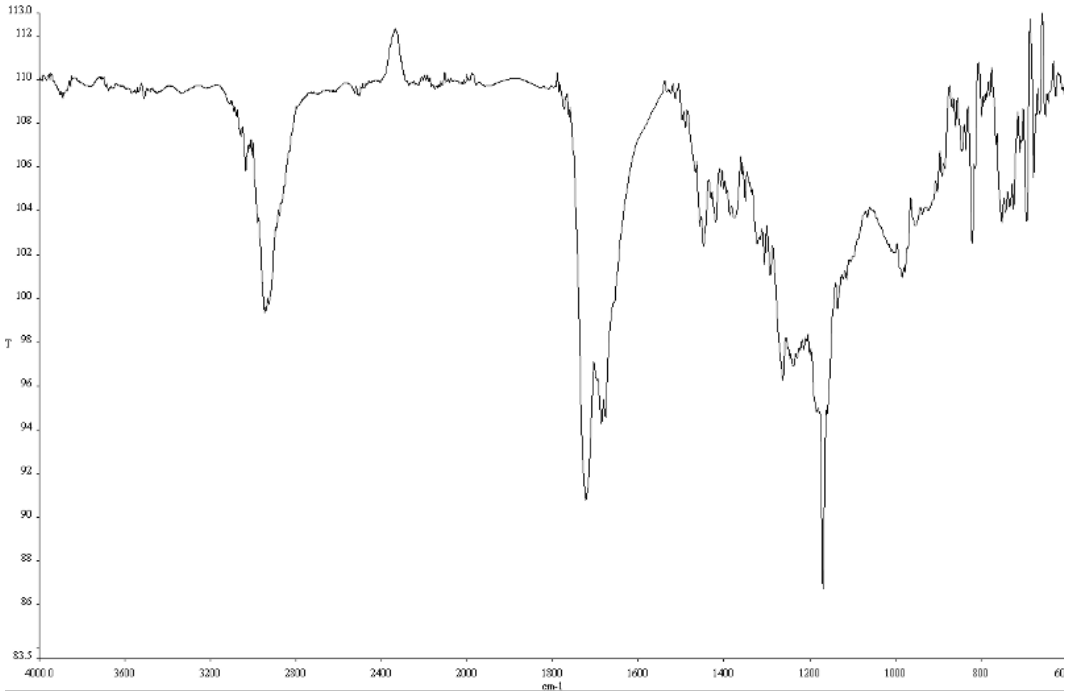


Figure A1.157. *Infrared spectrum (Thin Film, NaCl) of compound* ***33****.*

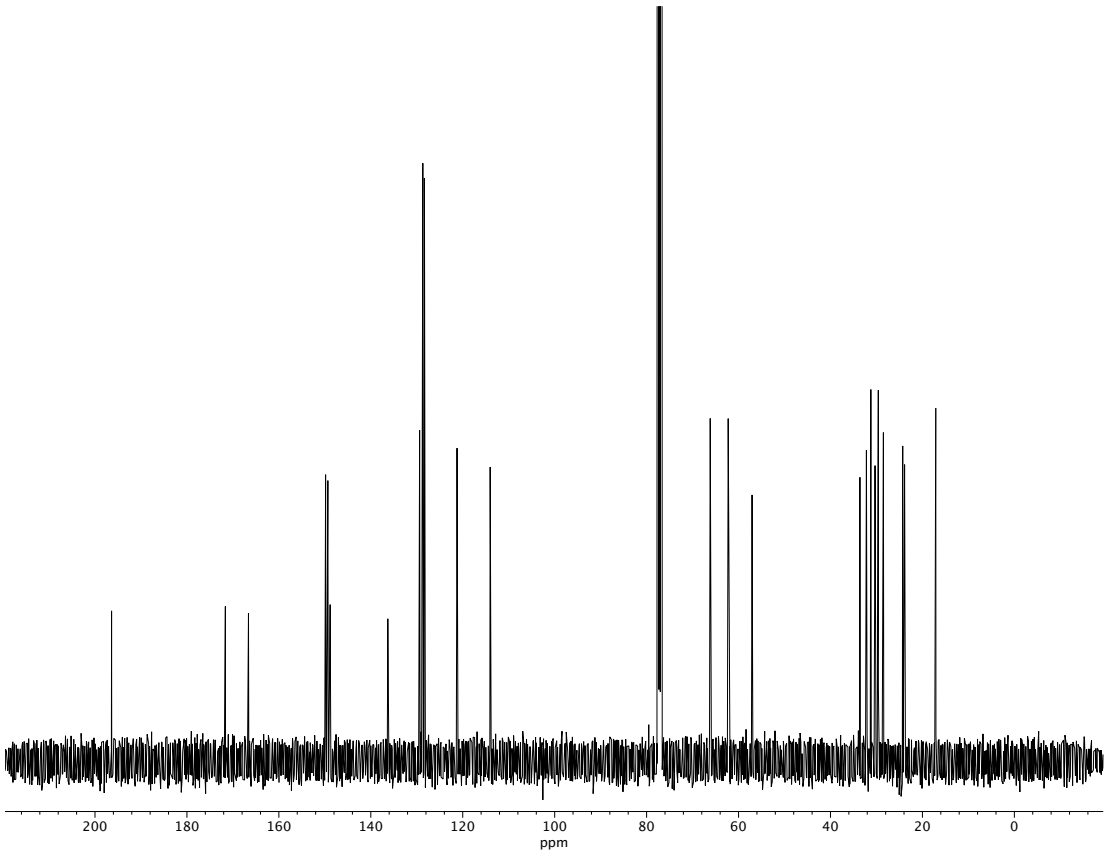


Figure A1.158. *^{13}C NMR (100 MHz, $CDCl_3$) of compound* ***33****.*

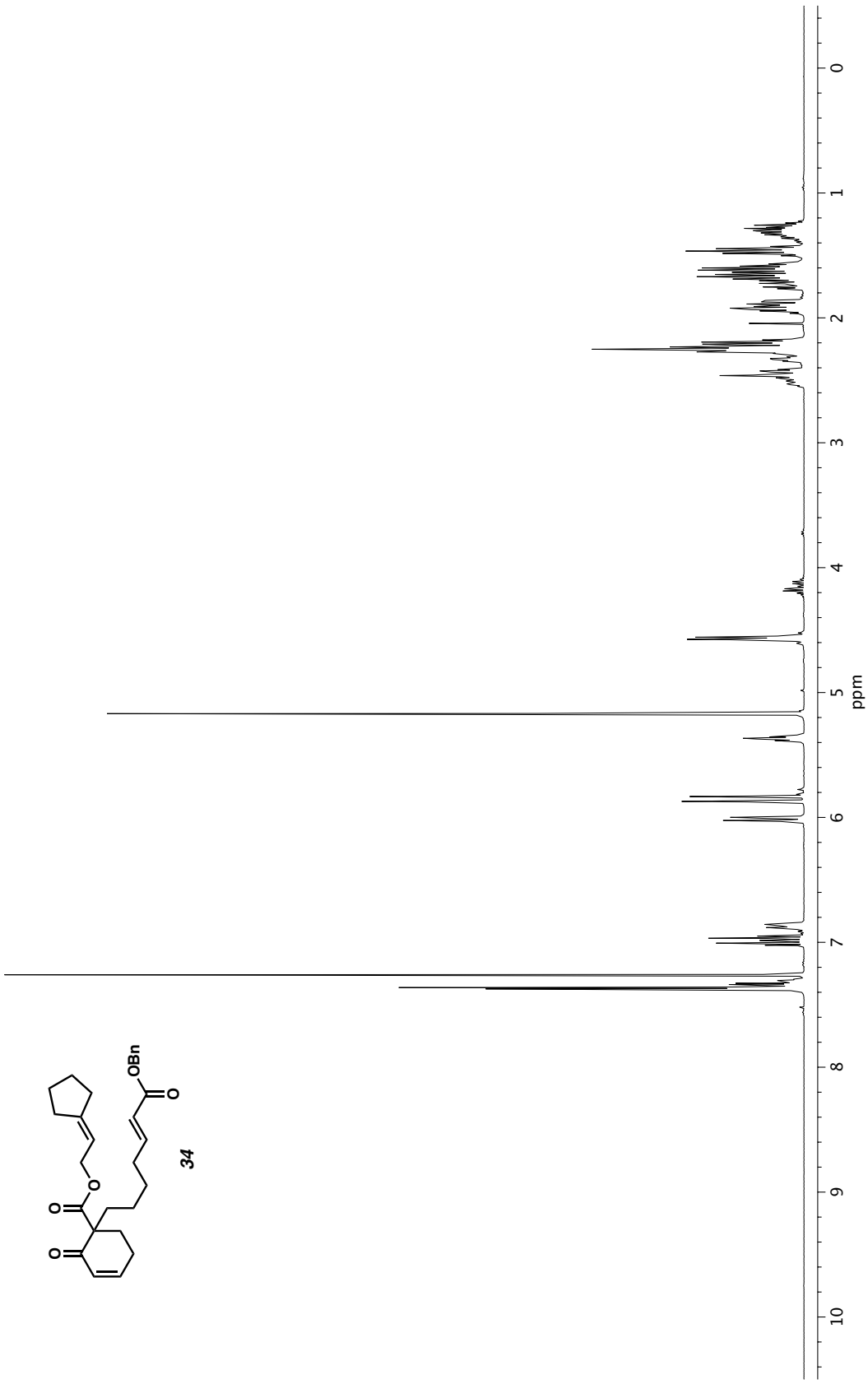


Figure A1.159. *^1H NMR (400 MHz, $CDCl_3$) of compound **34**.*

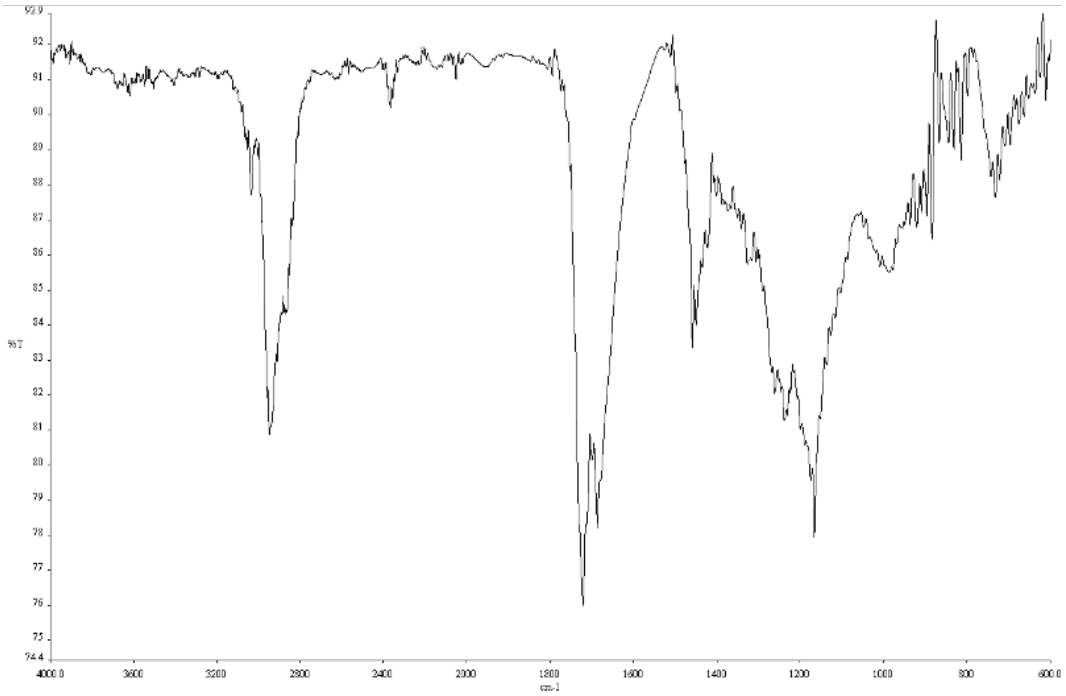


Figure A1.160. *Infrared spectrum (Thin Film, NaCl) of compound* ***34****.*

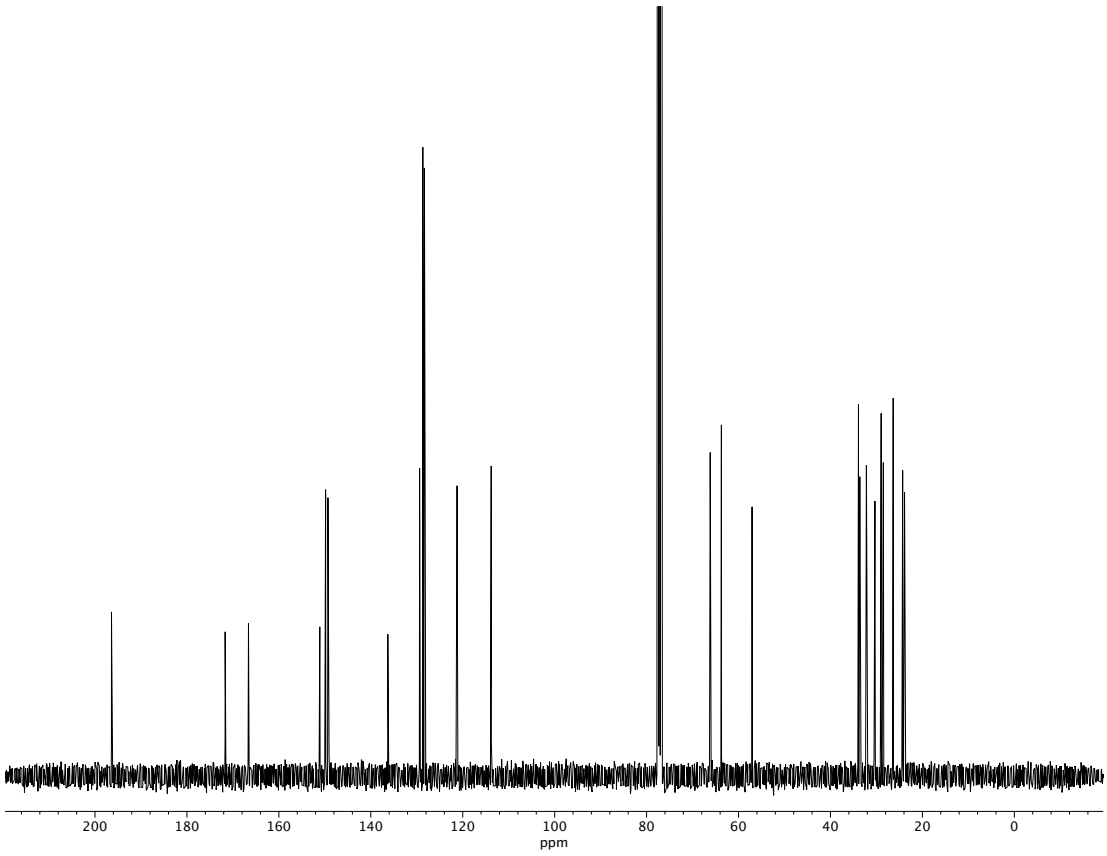


Figure A1.161. *^{13}C NMR (100 MHz, $CDCl_3$) of compound* ***34****.*

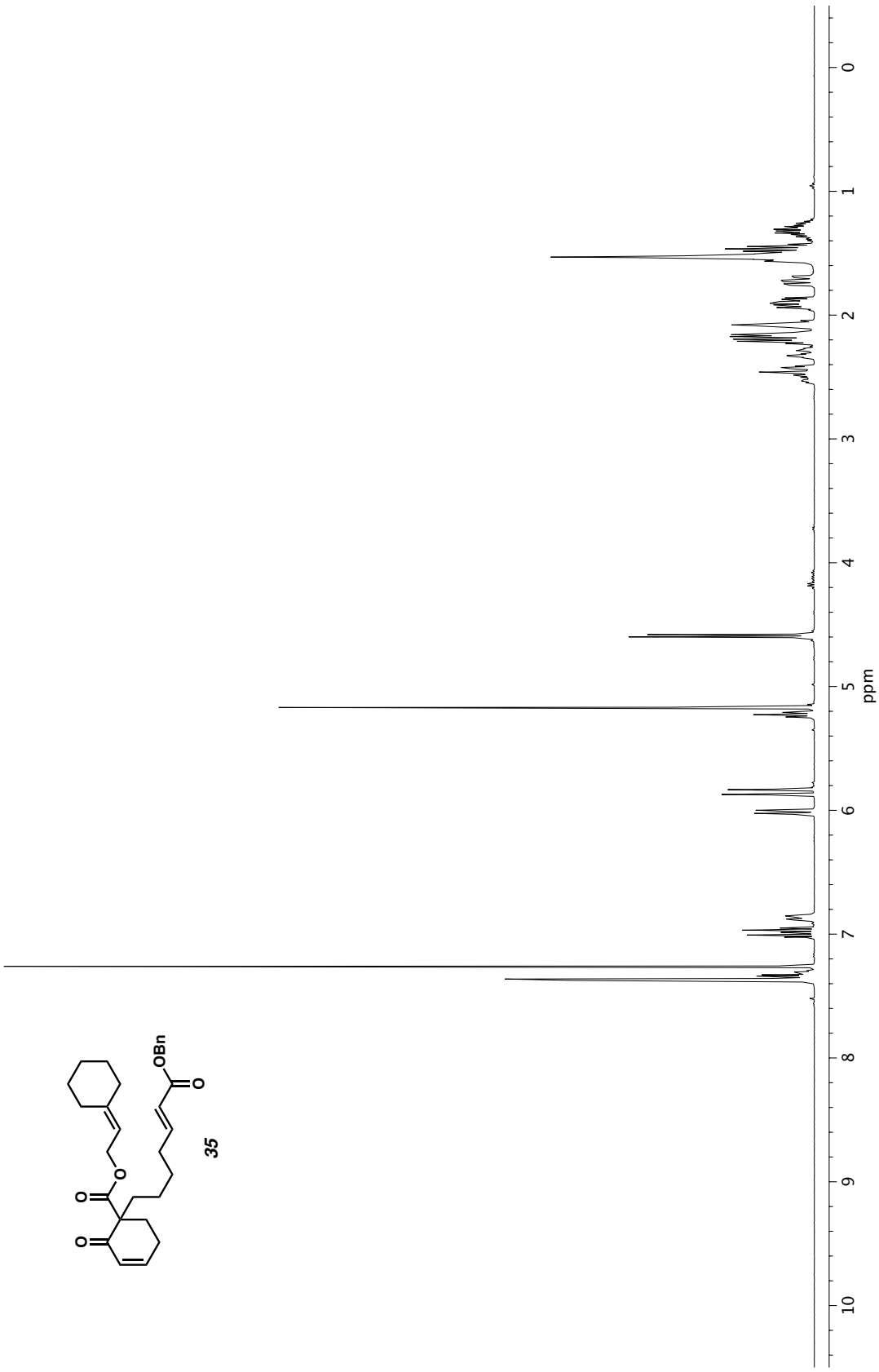


Figure A1.162. *^1H NMR (400 MHz, $CDCl_3$) of compound **35**.*

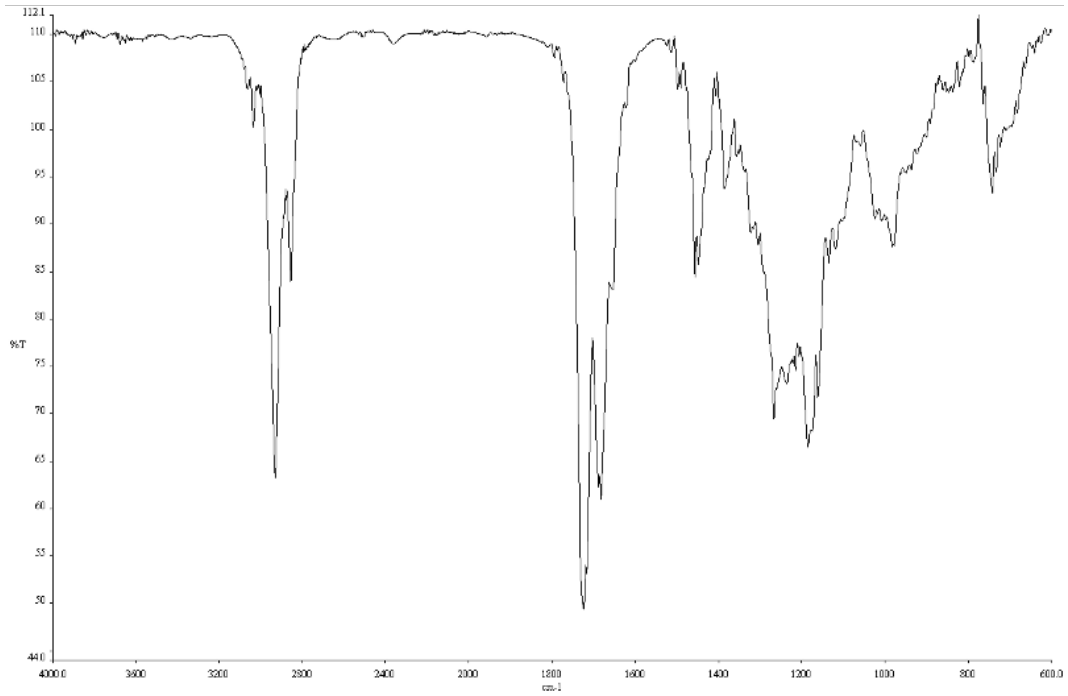


Figure A1.163. *Infrared spectrum (Thin Film, NaCl) of compound* ***35****.*

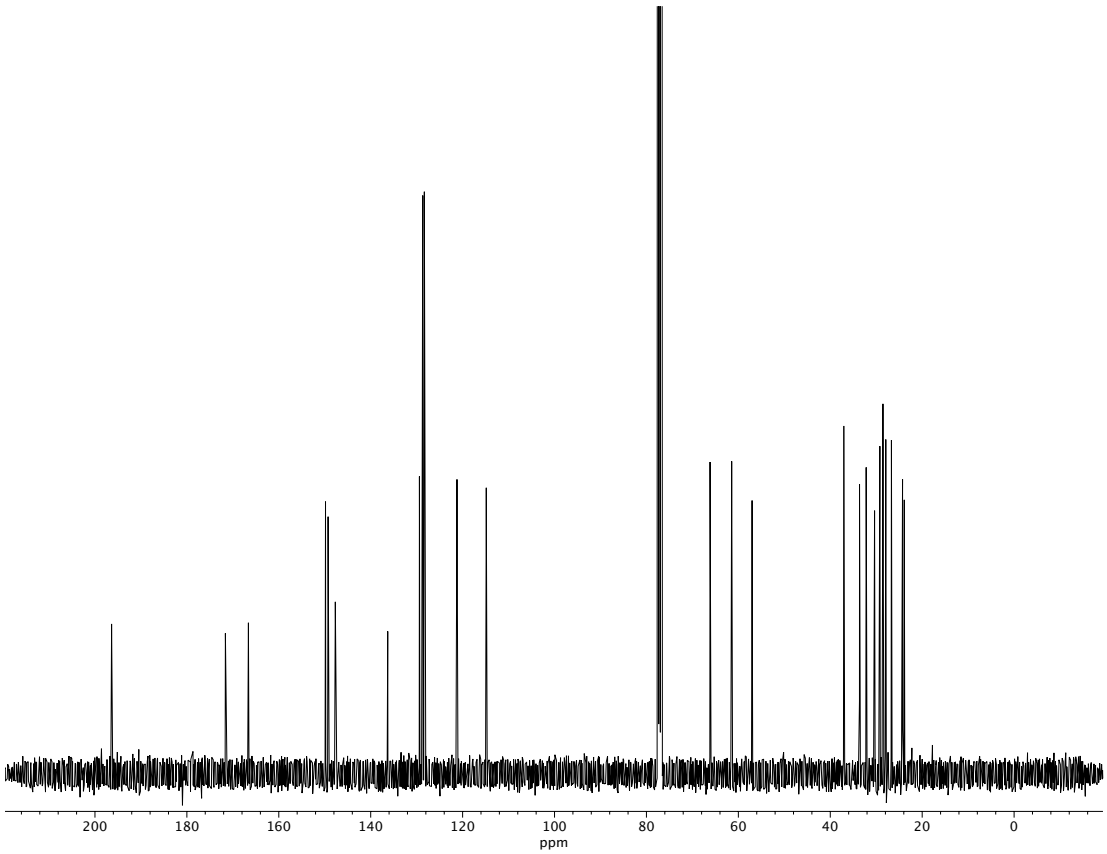


Figure A1.164. *^{13}C NMR (100 MHz, $CDCl_3$) of compound* ***35****.*

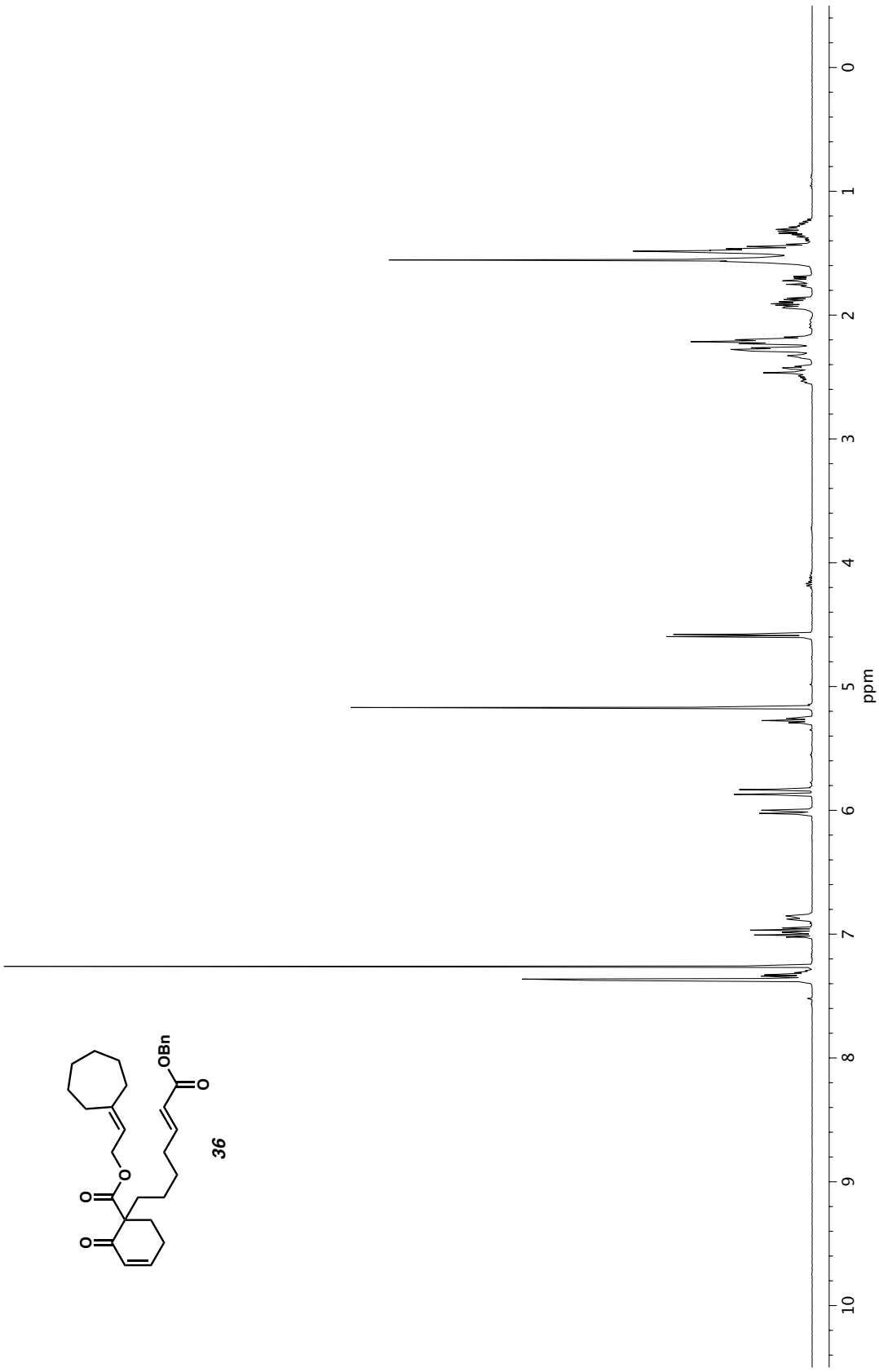


Figure A1.165. *^1H NMR (400 MHz, $CDCl_3$) of compound **36**.*

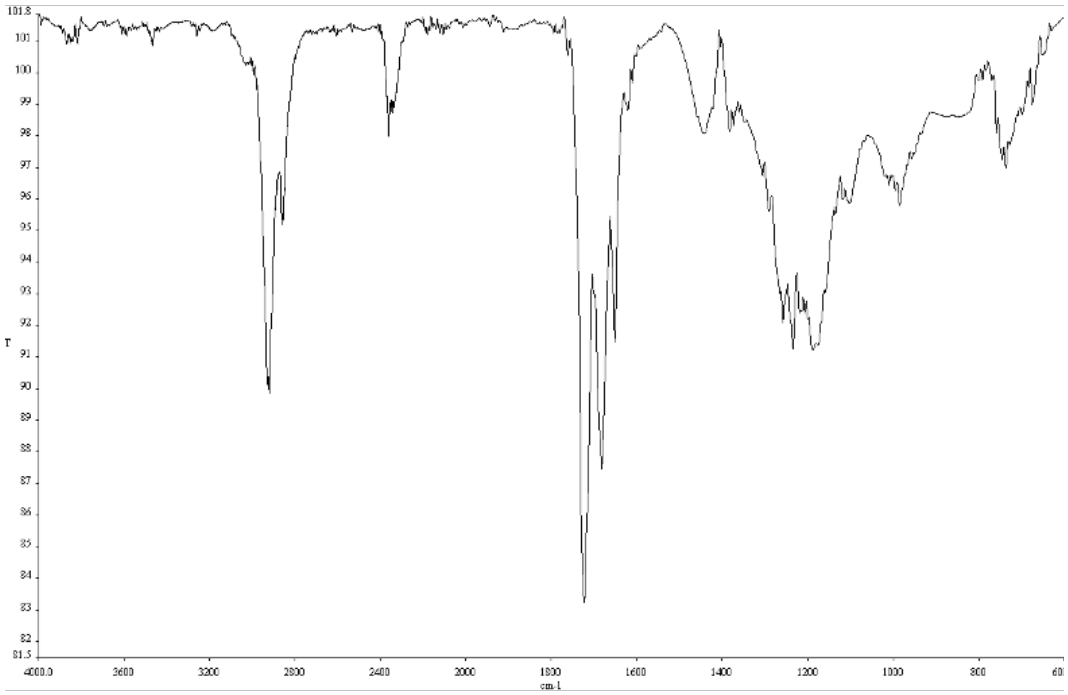


Figure A1.166. *Infrared spectrum (Thin Film, NaCl) of compound* ***36****.*

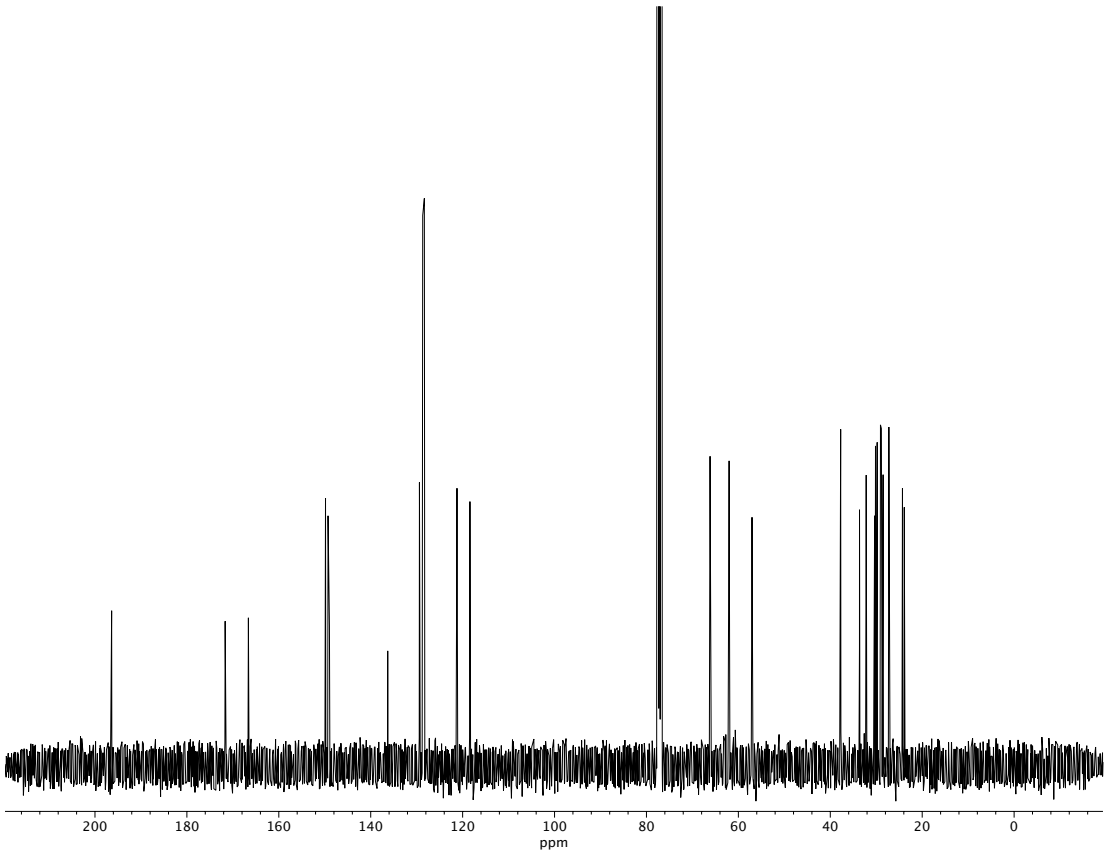


Figure A1.167. *^{13}C NMR (100 MHz, $CDCl_3$) of compound* ***36****.*

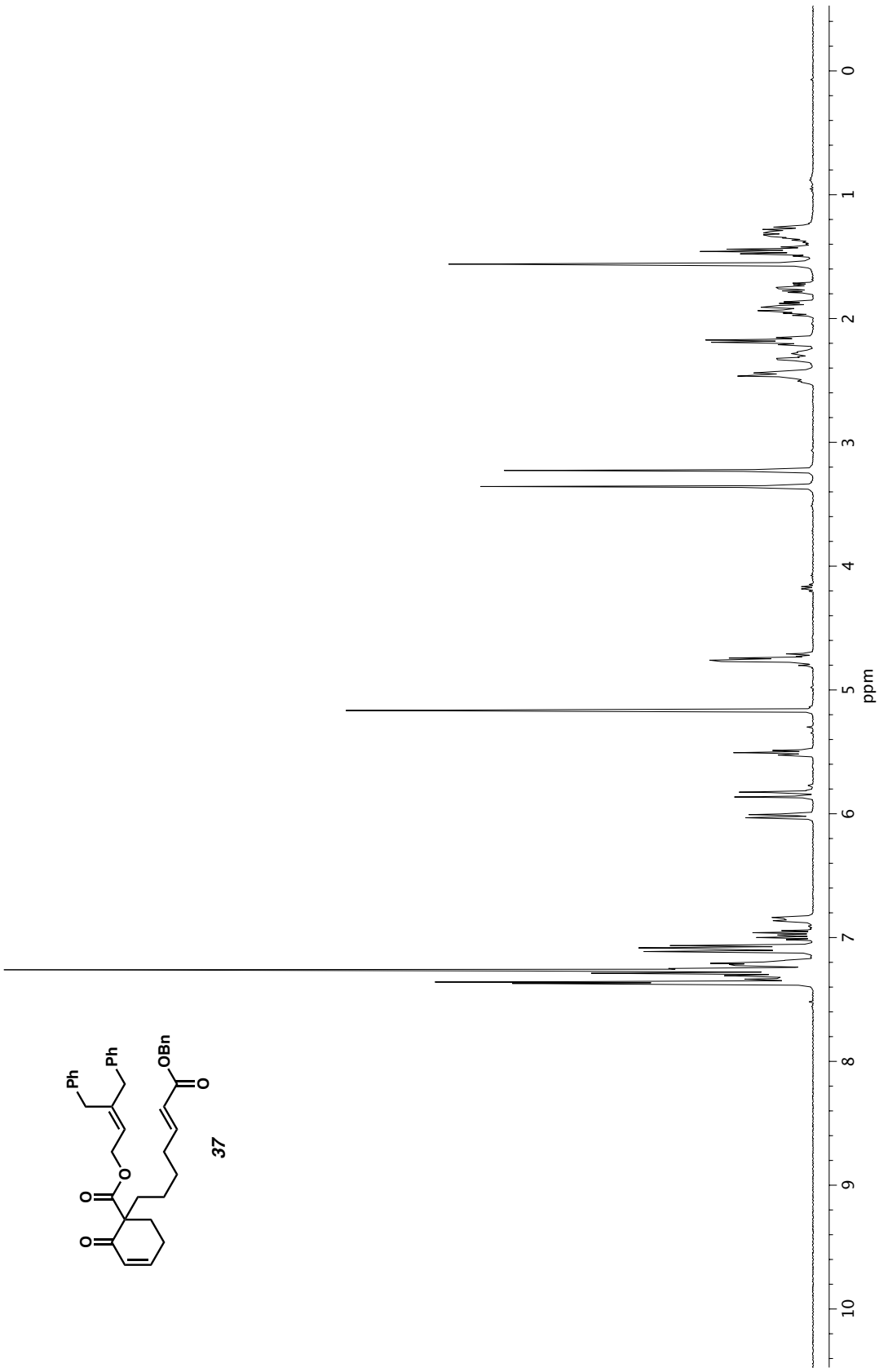


Figure A1.168. *^1H NMR (400 MHz, $CDCl_3$) of compound **37**.*

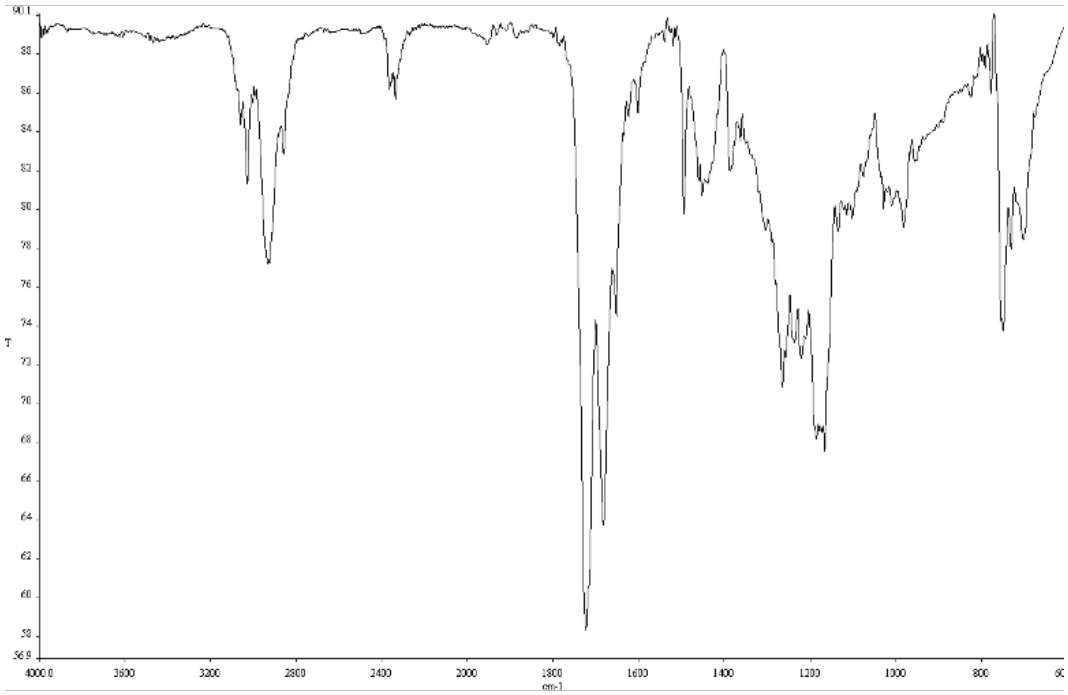


Figure A1.169. *Infrared spectrum (Thin Film, NaCl) of compound* ***37****.*

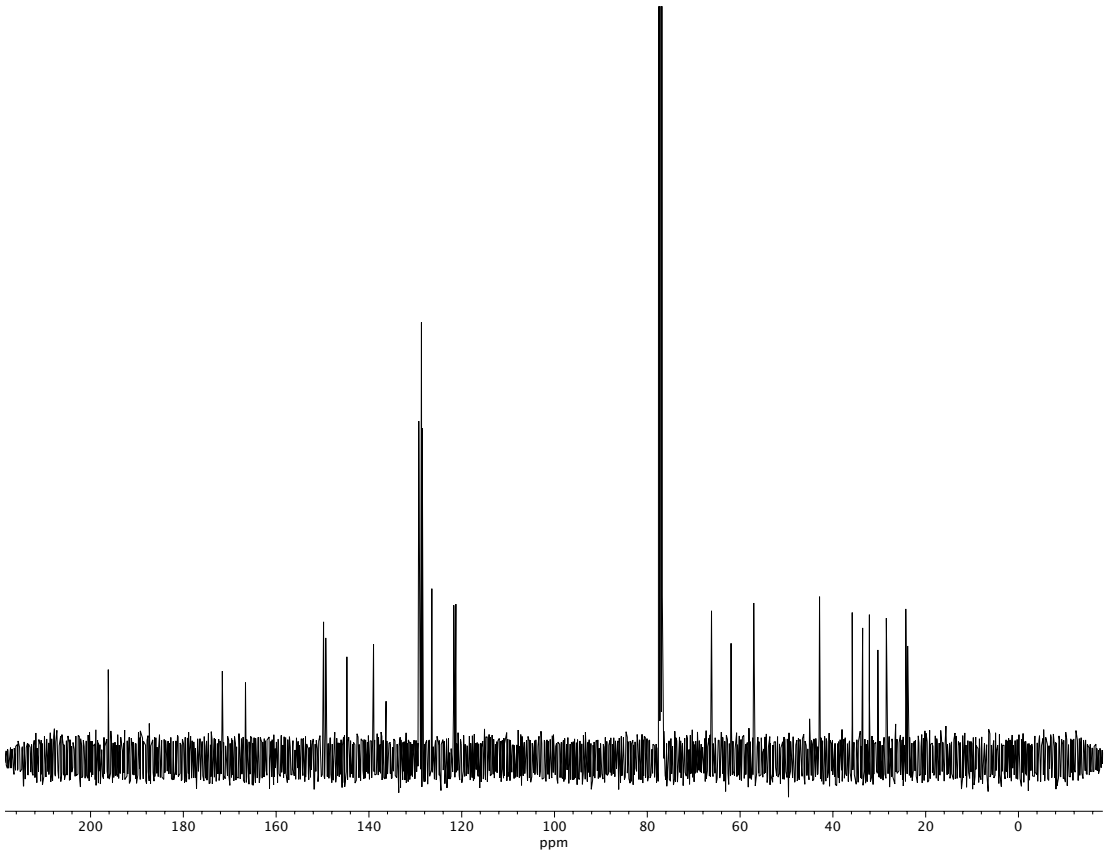


Figure A1.170. *^{13}C NMR (100 MHz, $CDCl_3$) of compound* ***37****.*

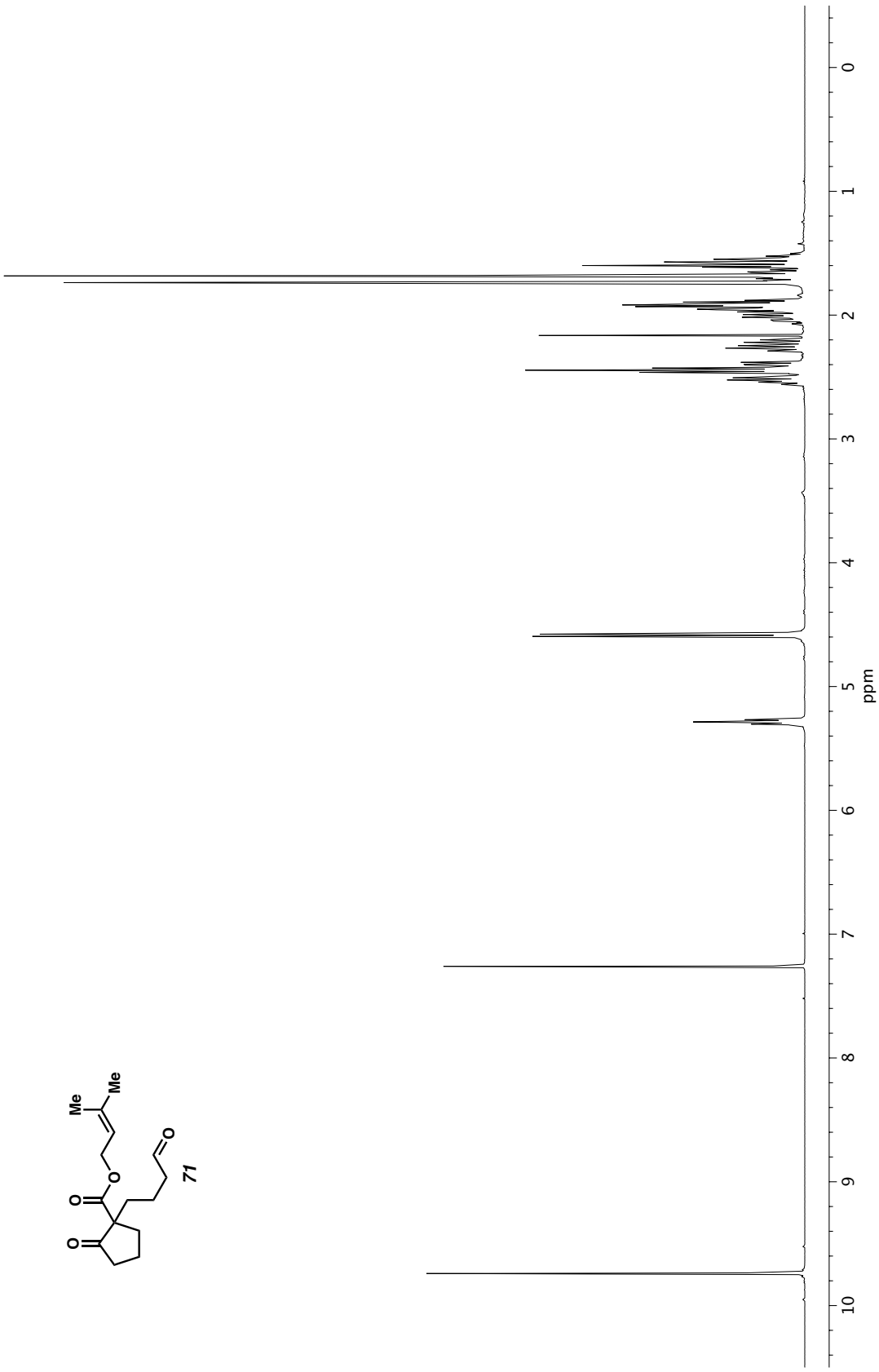


Figure A1.171. *^1H NMR (400 MHz, $CDCl_3$) of compound **71**.*

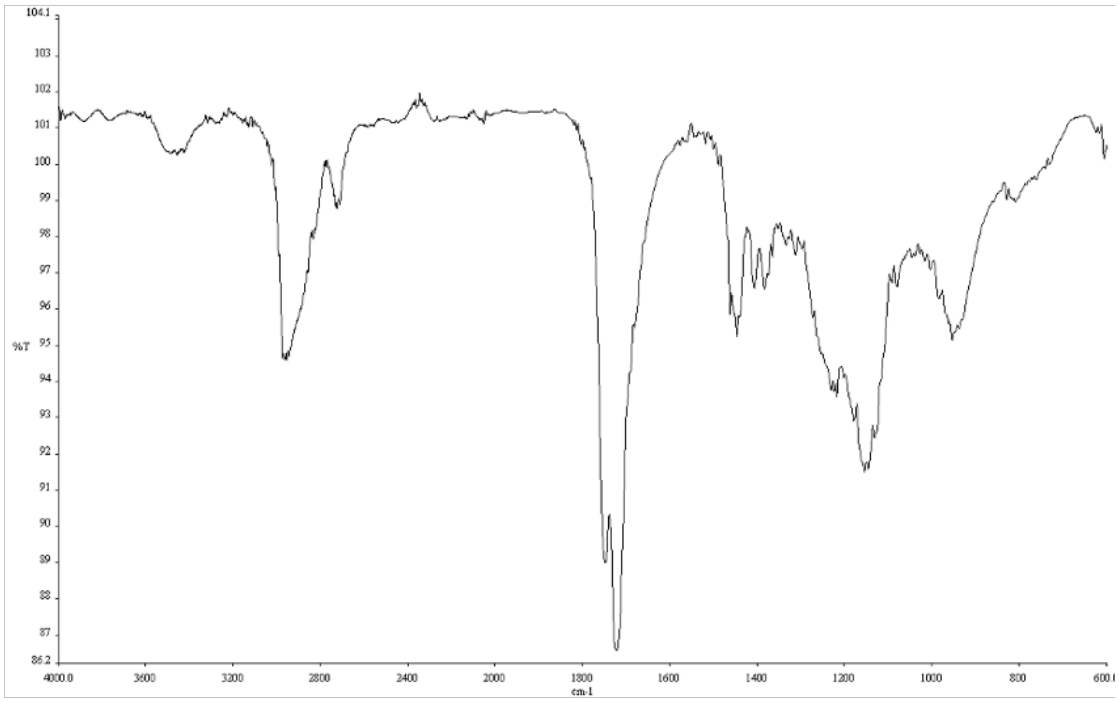


Figure A1.172. *Infrared spectrum (Thin Film, NaCl) of compound* ***71****.*

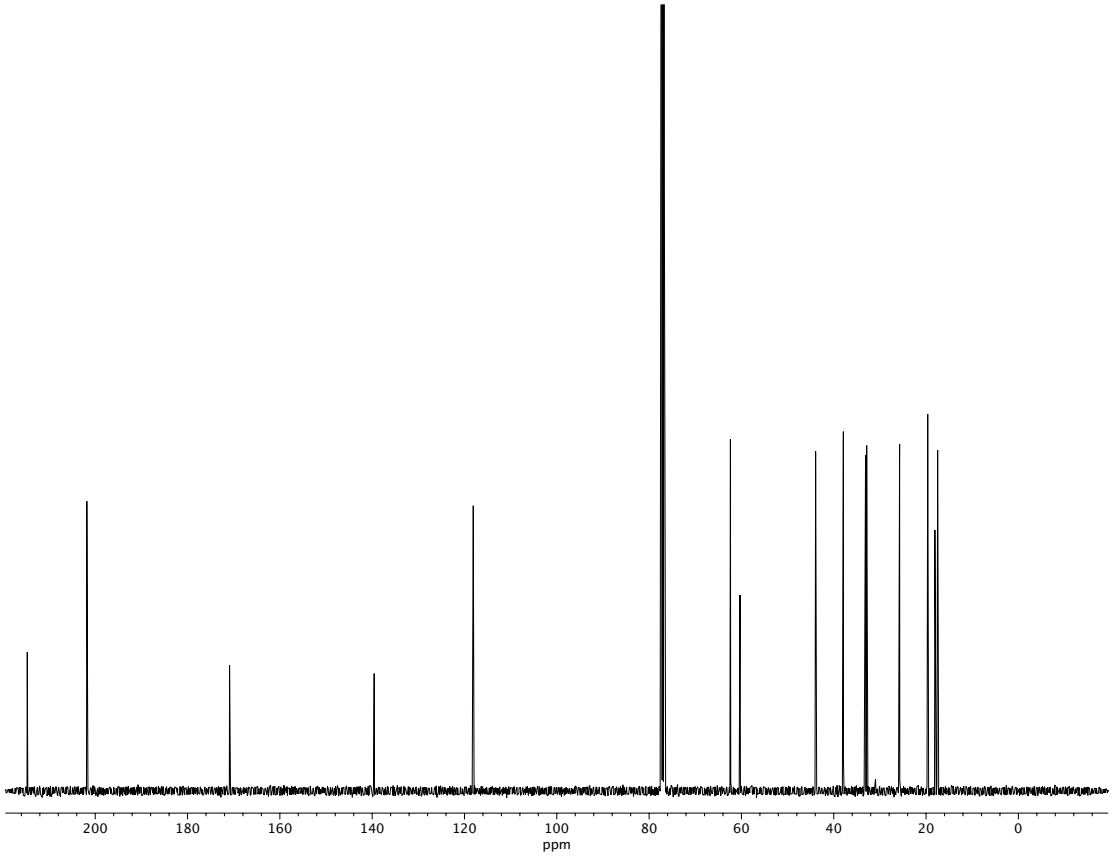


Figure A1.173. *^{13}C NMR (100 MHz, $CDCl_3$) of compound* ***71****.*

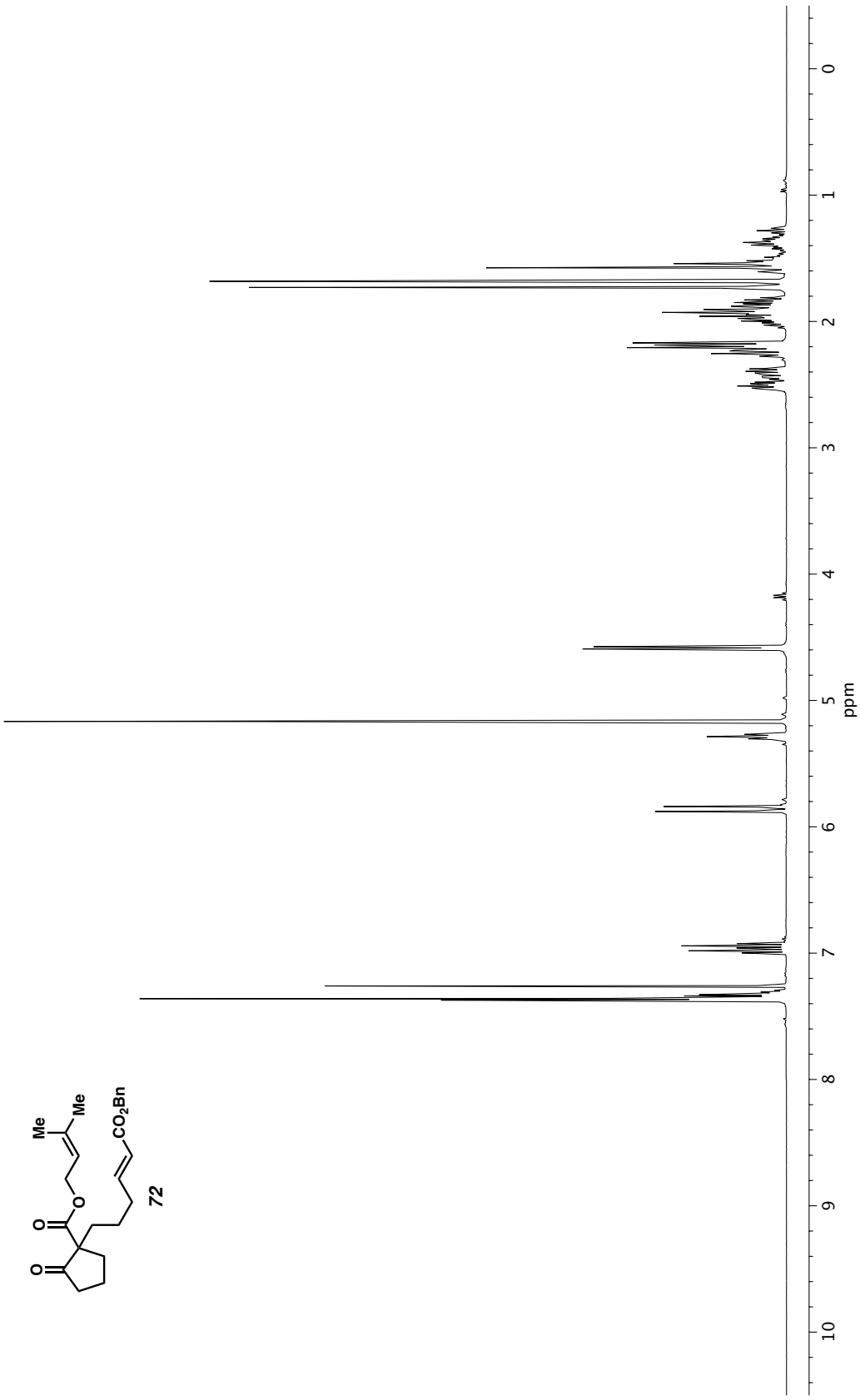


Figure A1.174. *^1H NMR (400 MHz, $CDCl_3$) of compound* ***72****.*

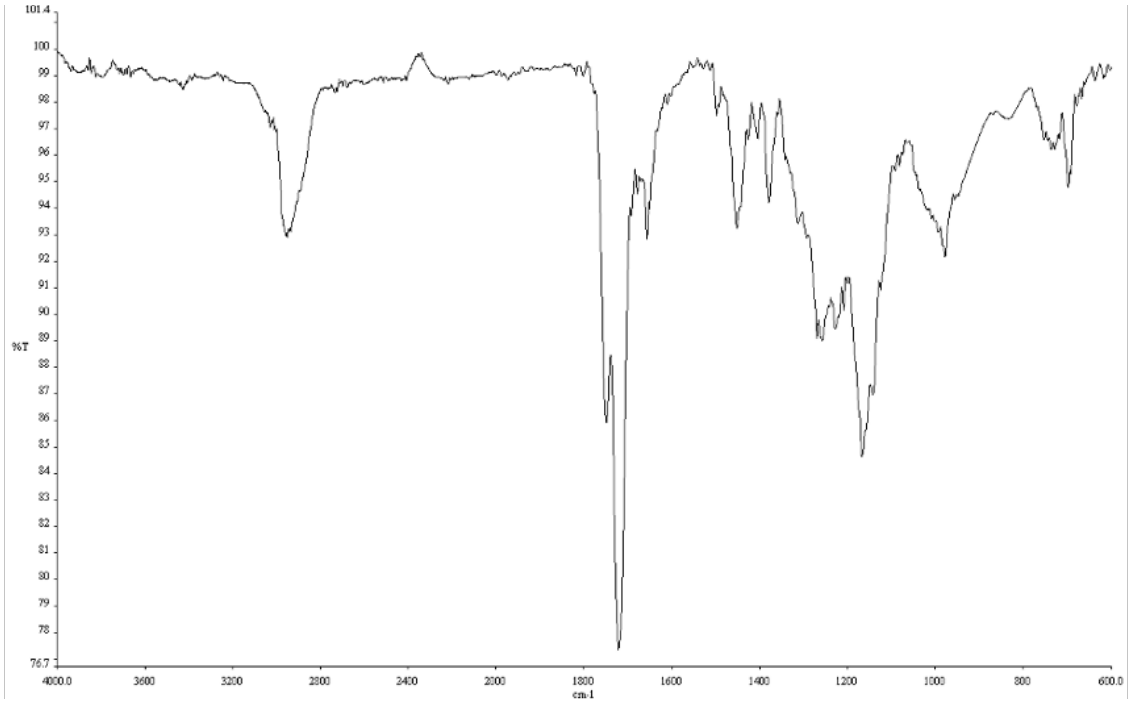


Figure A1.175. *Infrared spectrum (Thin Film, NaCl) of compound* ***72****.*

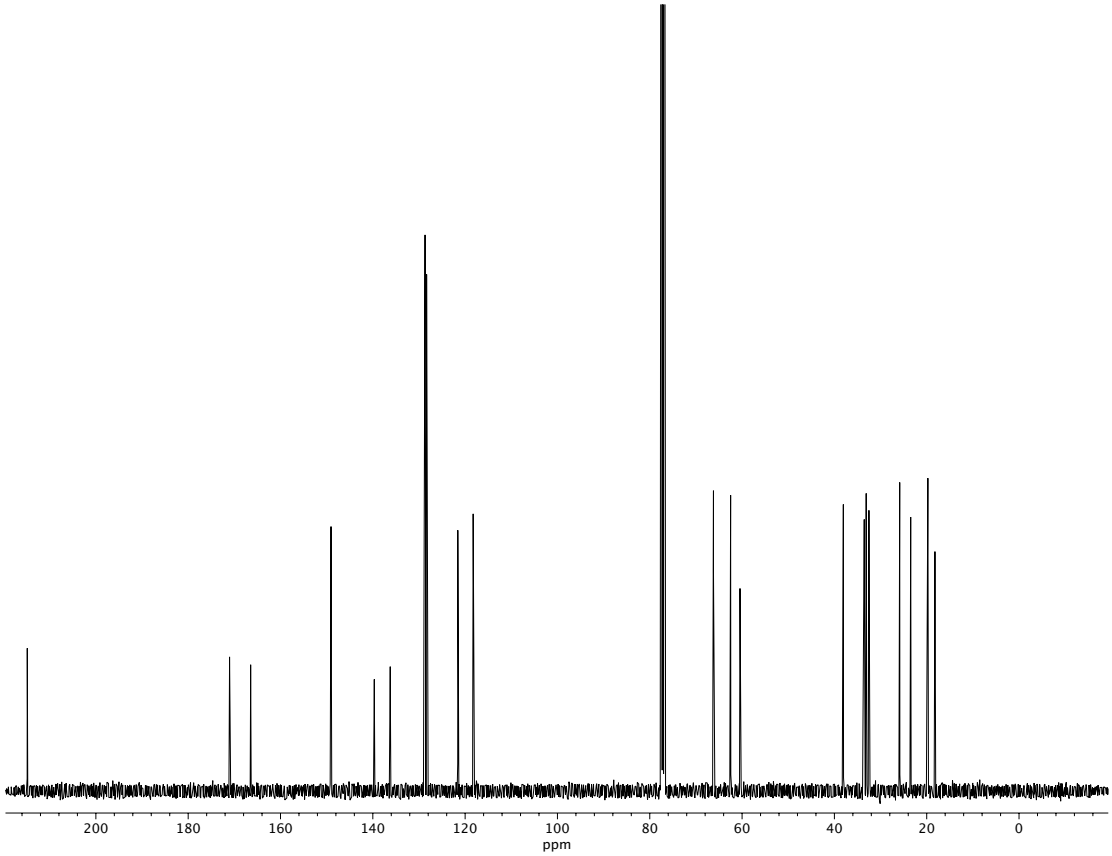


Figure A1.176. *^{13}C NMR (100 MHz, $CDCl_3$) of compound* ***72****.*

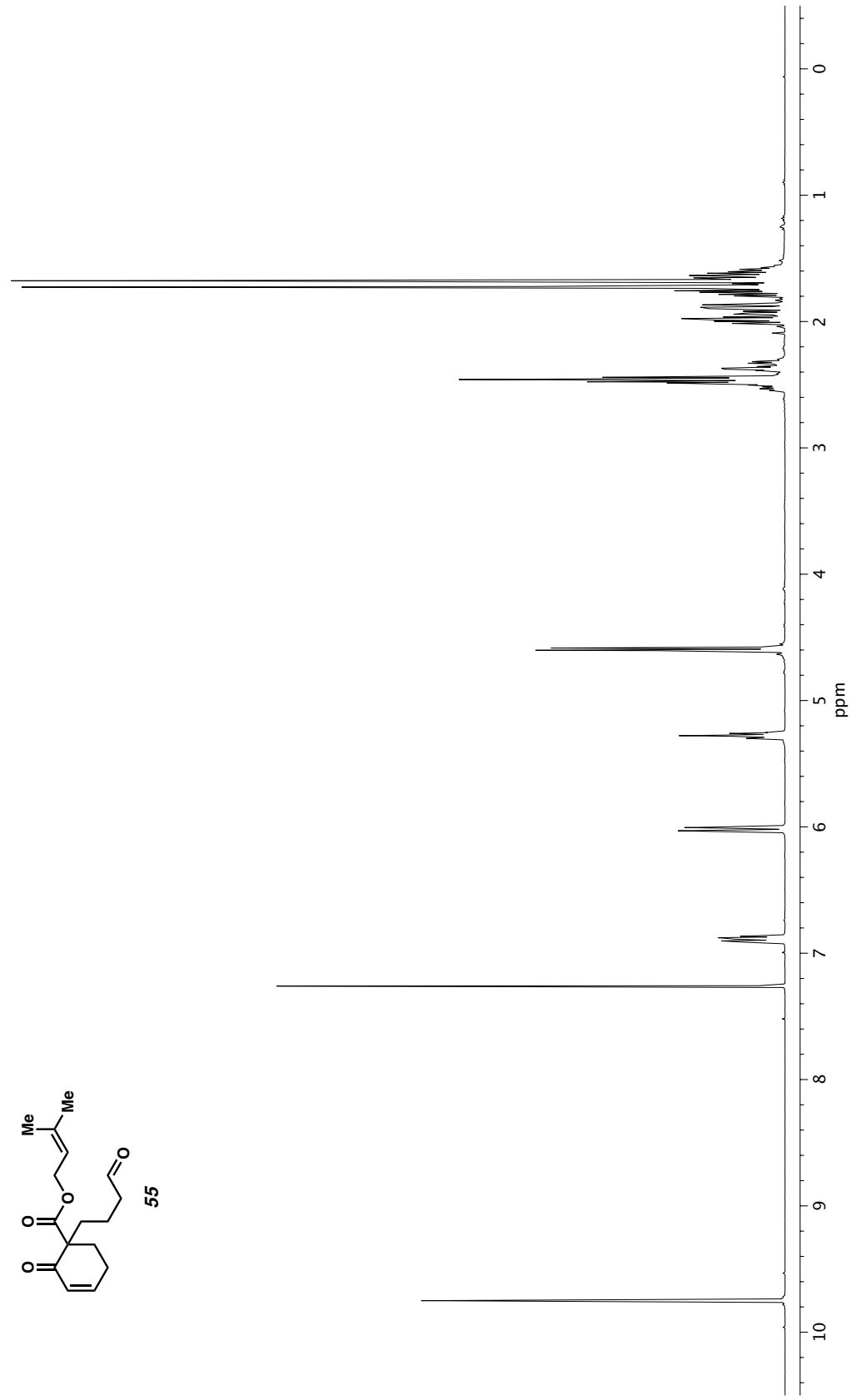


Figure A1.177. *^{1}H NMR (400 MHz, $CDCl_3$) of compound **55**.*

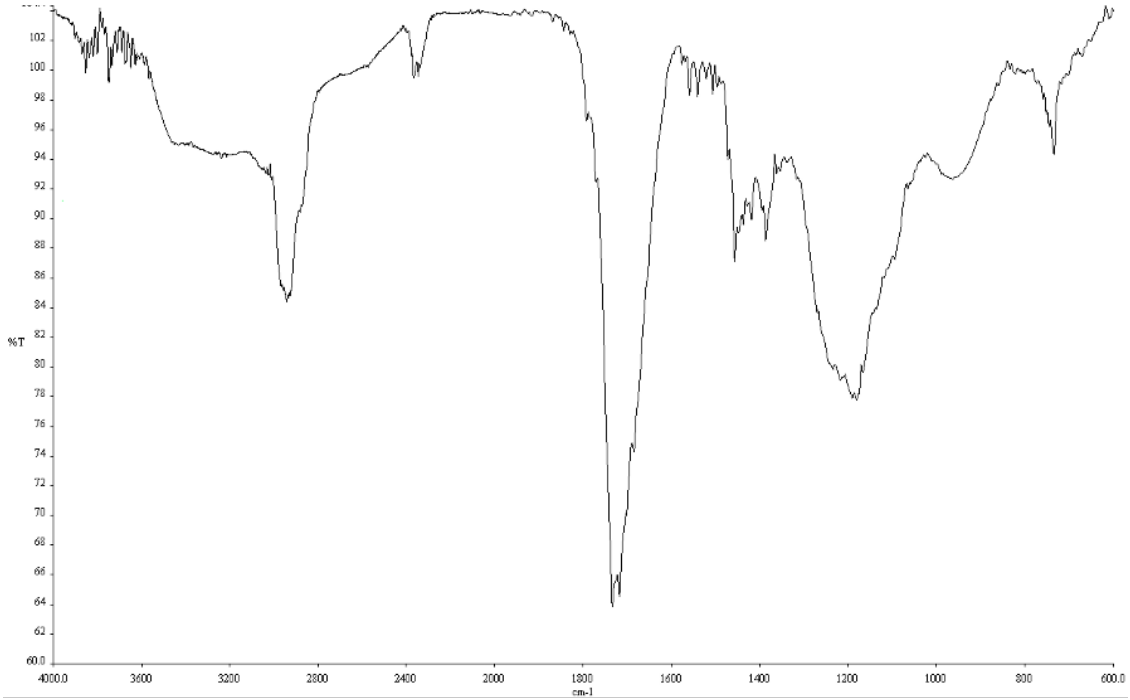


Figure A1.178. *Infrared spectrum (Thin Film, NaCl) of compound* ***55****.*

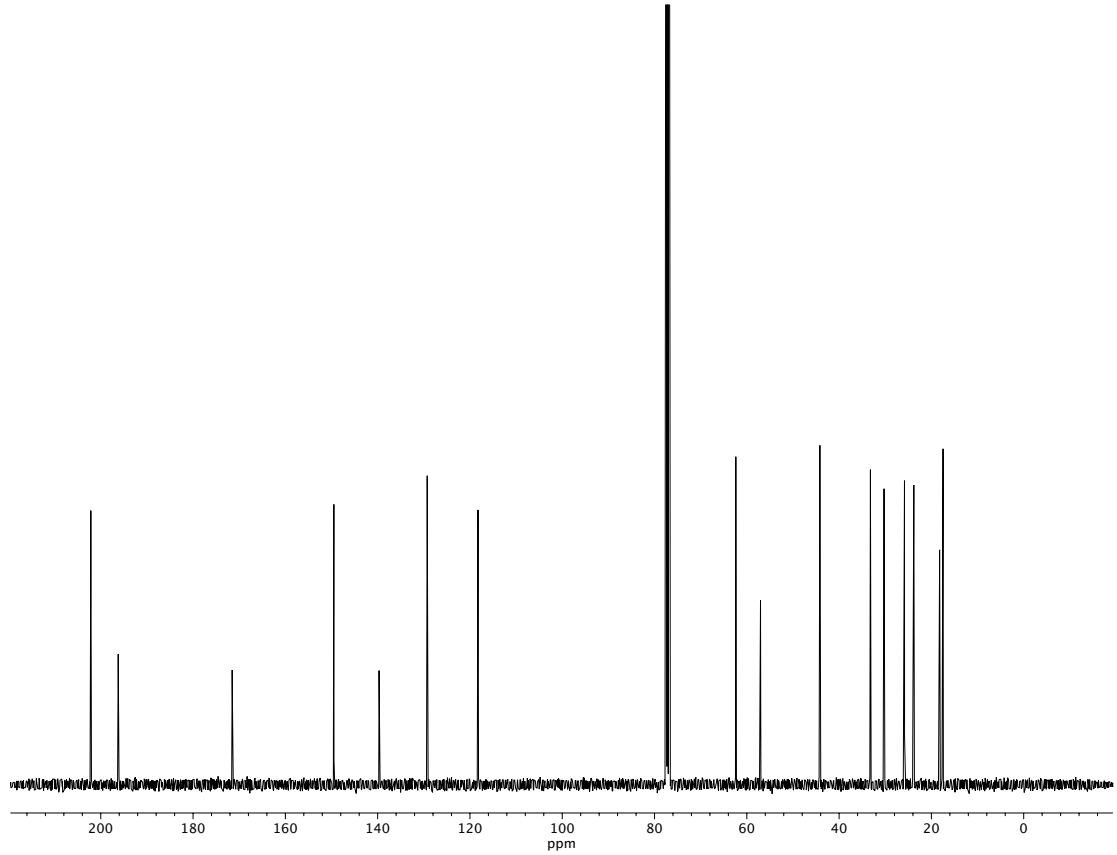


Figure A1.179. *^{13}C NMR (100 MHz, $CDCl_3$) of compound* ***55****.*

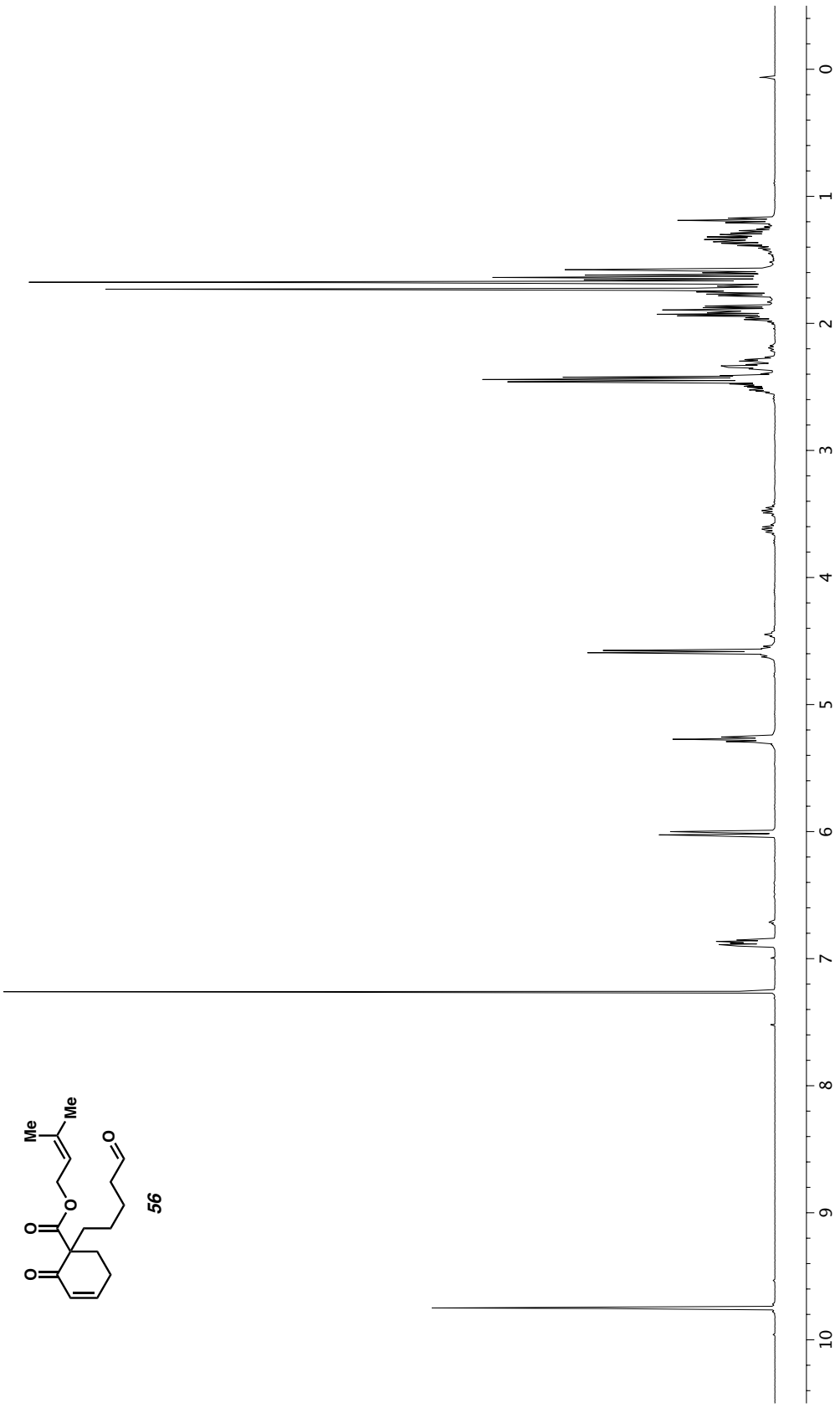


Figure A1.180. *^1H NMR (400 MHz, $CDCl_3$) of compound **56**.*

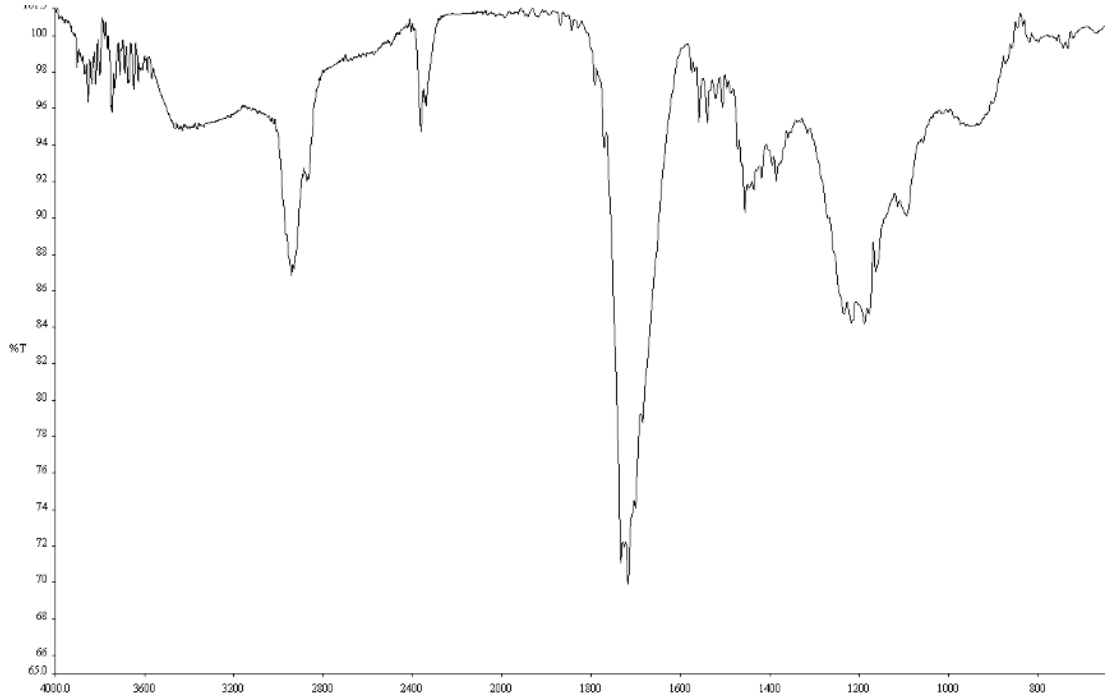


Figure A1.181. *Infrared spectrum (Thin Film, NaCl) of compound* ***56****.*

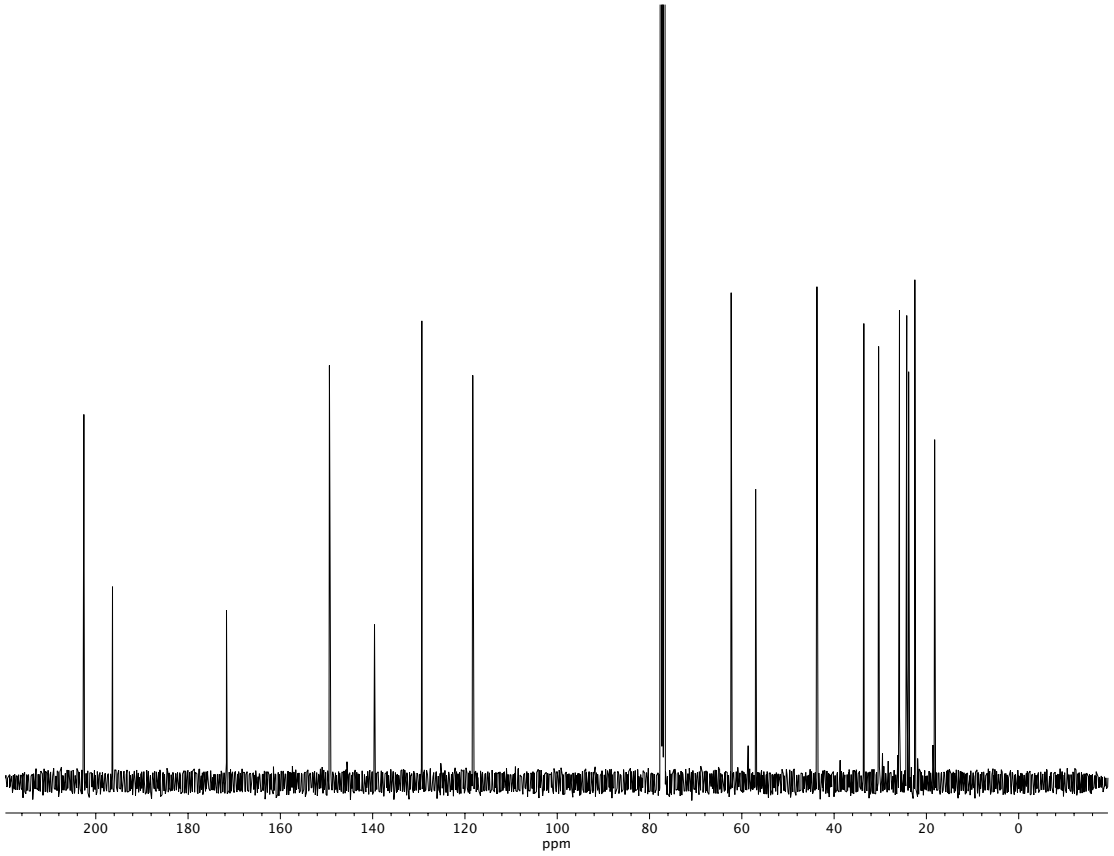


Figure A1.182. *^{13}C NMR (100 MHz, $CDCl_3$) of compound* ***56****.*

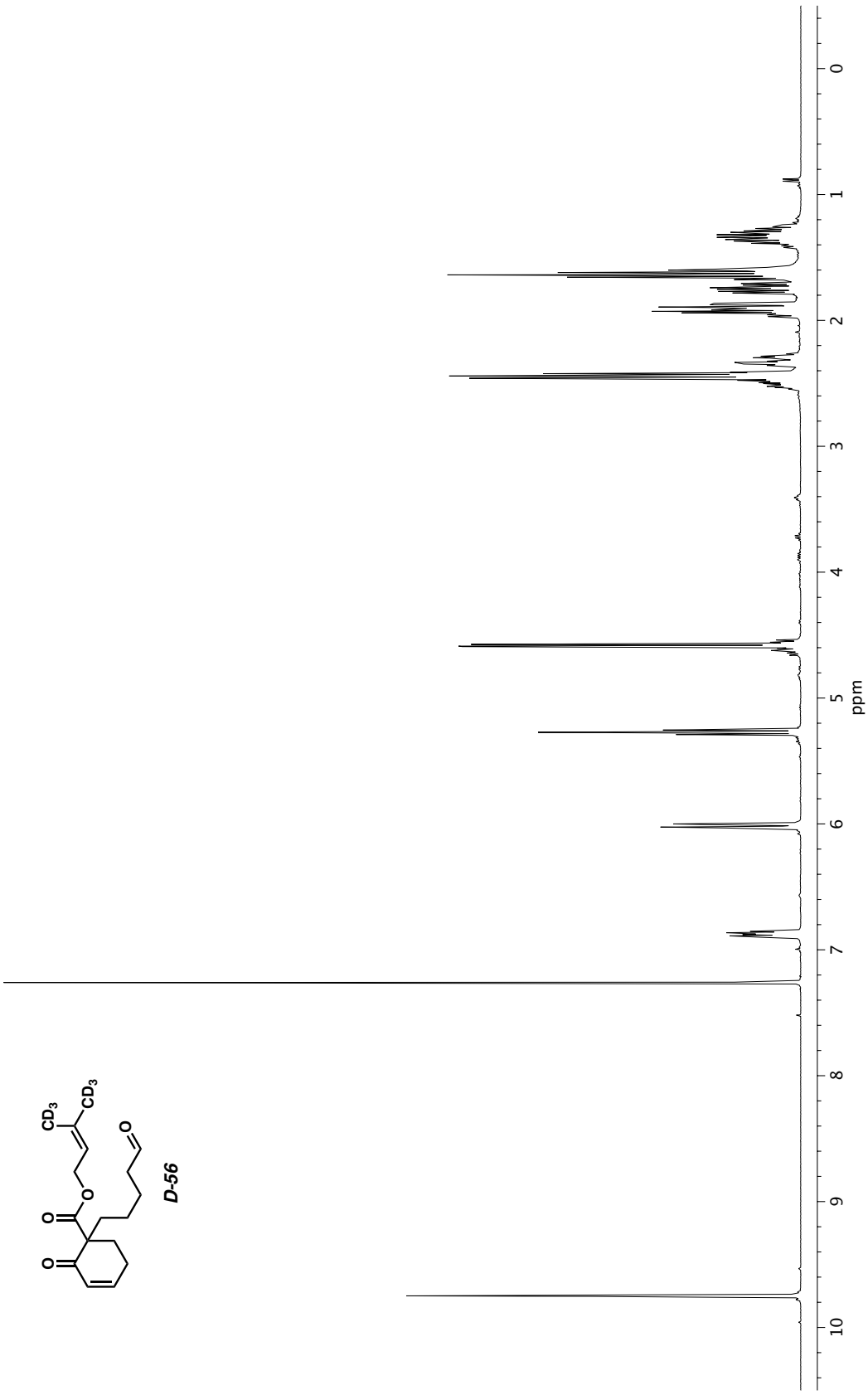


Figure A1.183. *^1H NMR (400 MHz, $CDCl_3$) of compound* ***D-56****.*

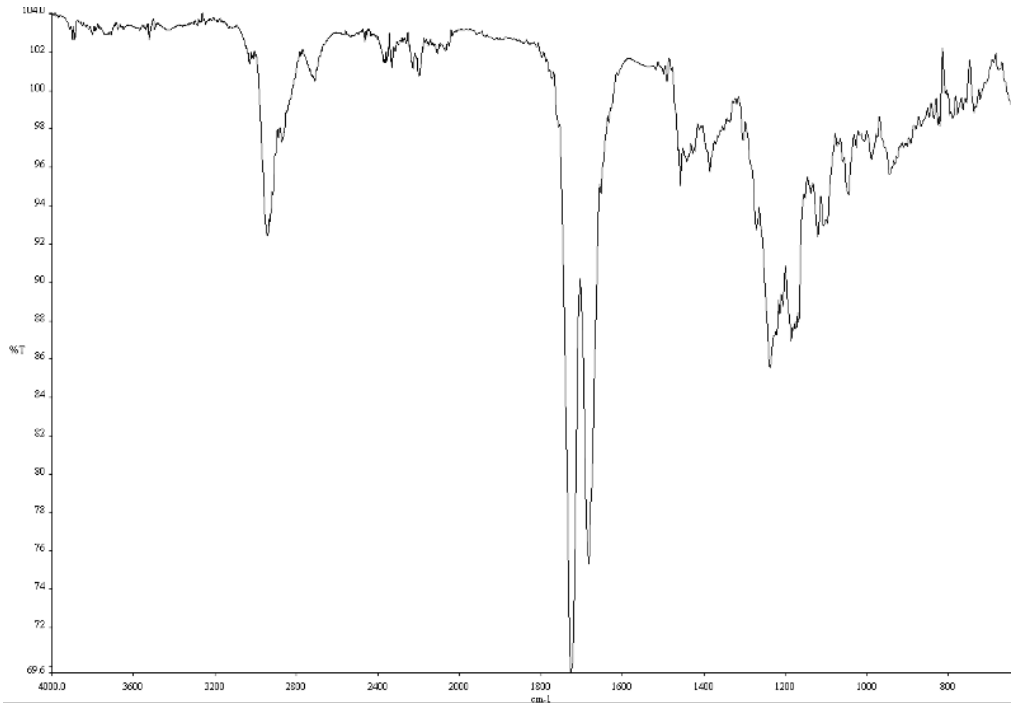


Figure A1.184. *Infrared spectrum (Thin Film, NaCl) of compound* ***D-56***.

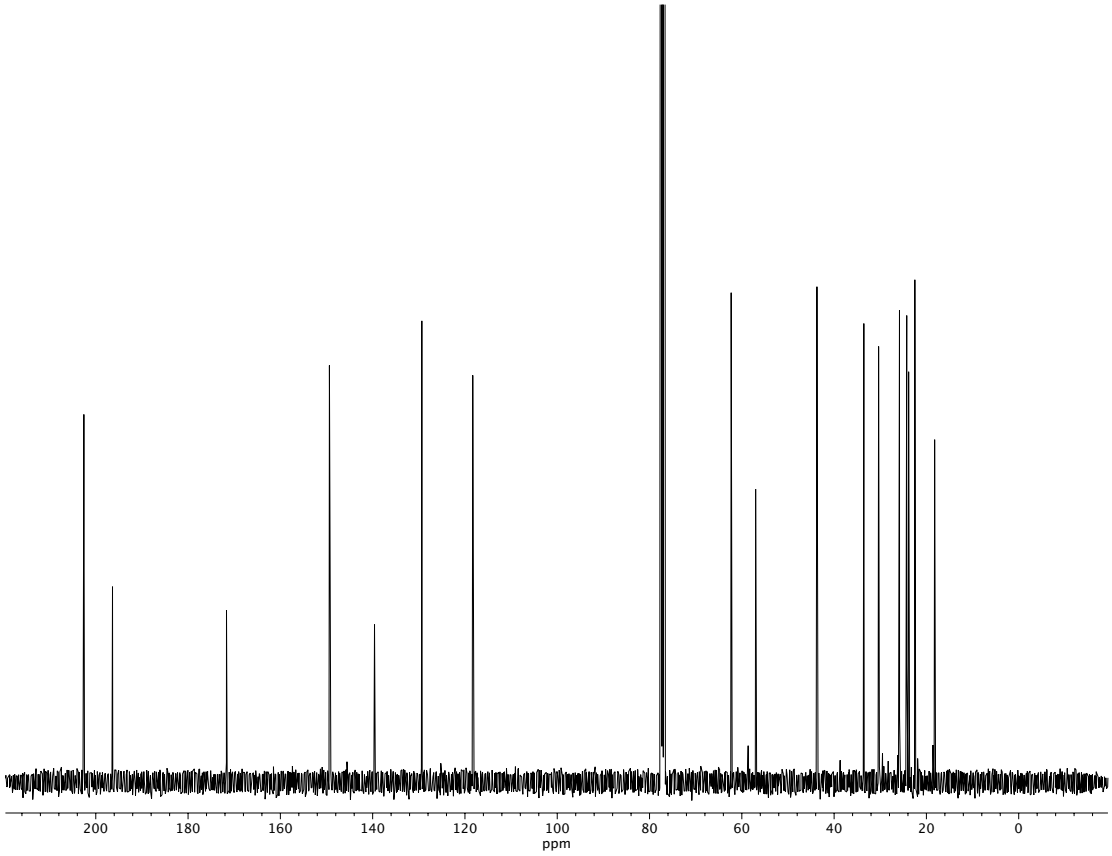


Figure A1.185. *^{13}C NMR (100 MHz, $CDCl_3$) of compound* ***D-56***.

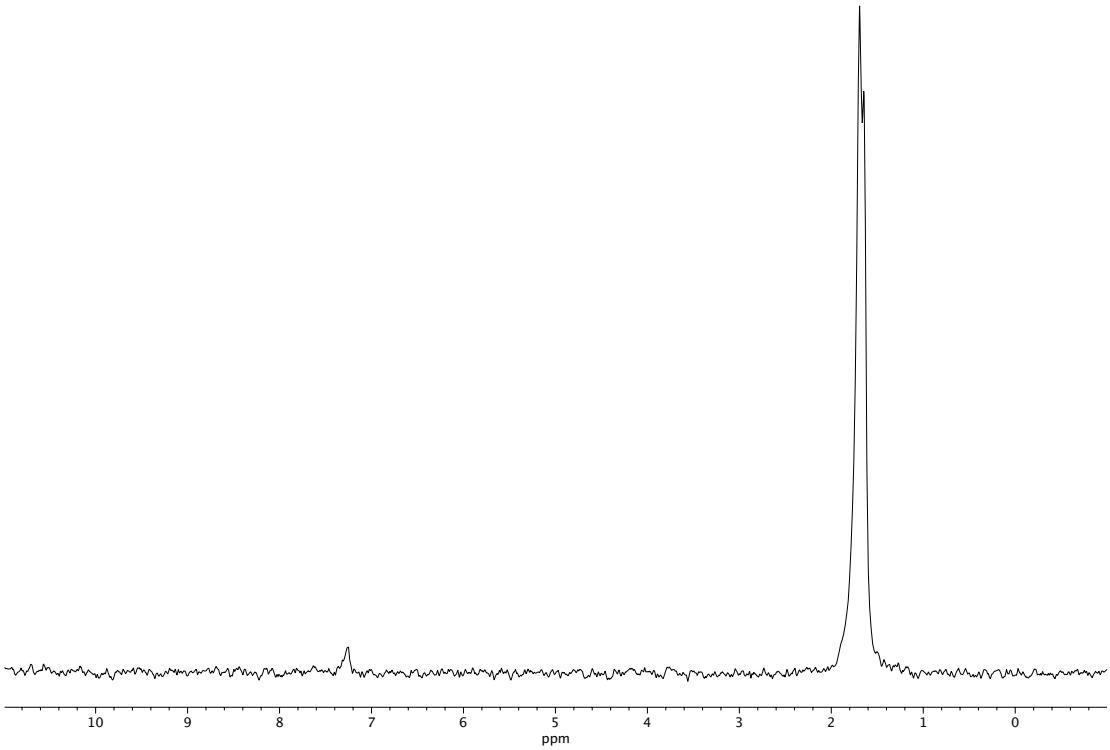


Figure A1.186. *^{2}H NMR (61 MHz, $CHCl_3$) of compound* ***D-56***.

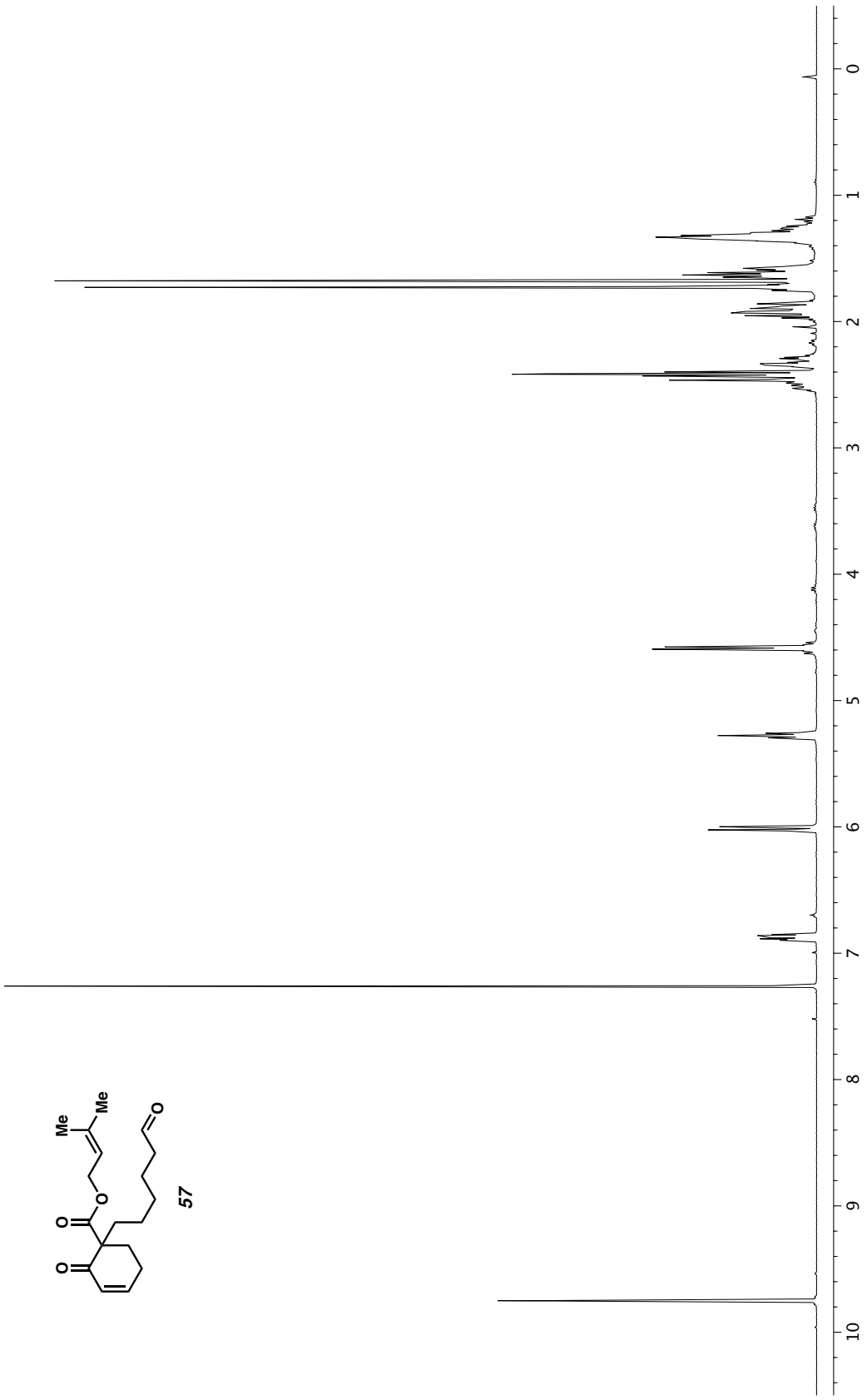


Figure A1.187. *^1H NMR (400 MHz, $CDCl_3$) of compound **57**.*

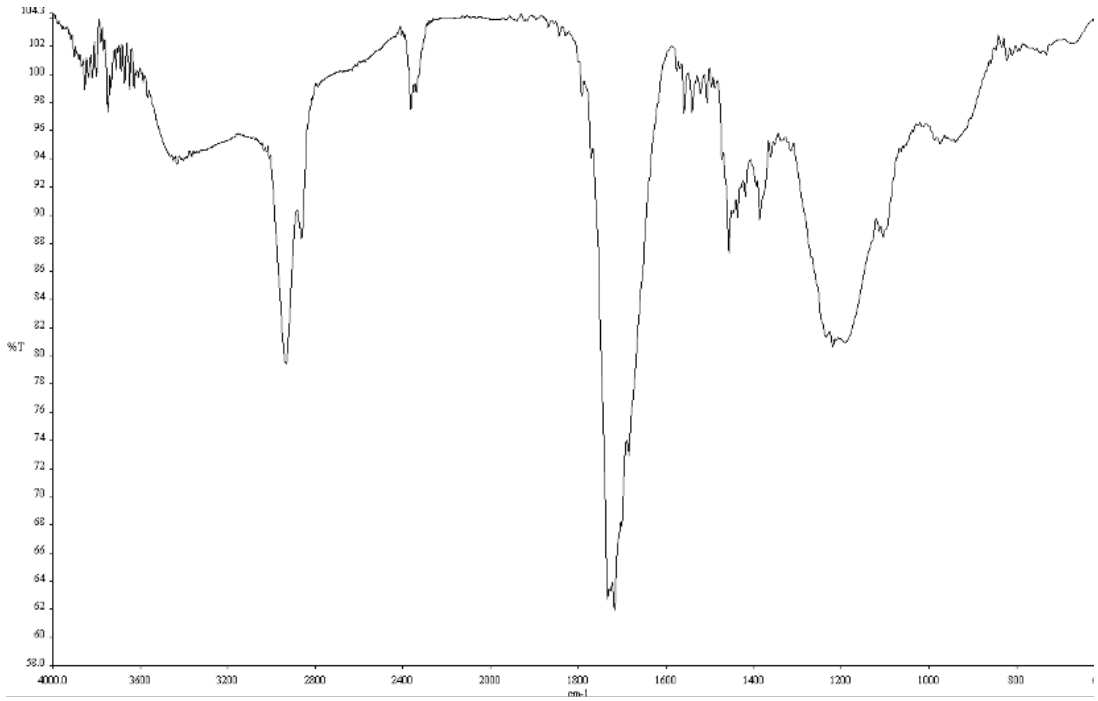


Figure A1.188. *Infrared spectrum (Thin Film, NaCl) of compound* ***57****.*

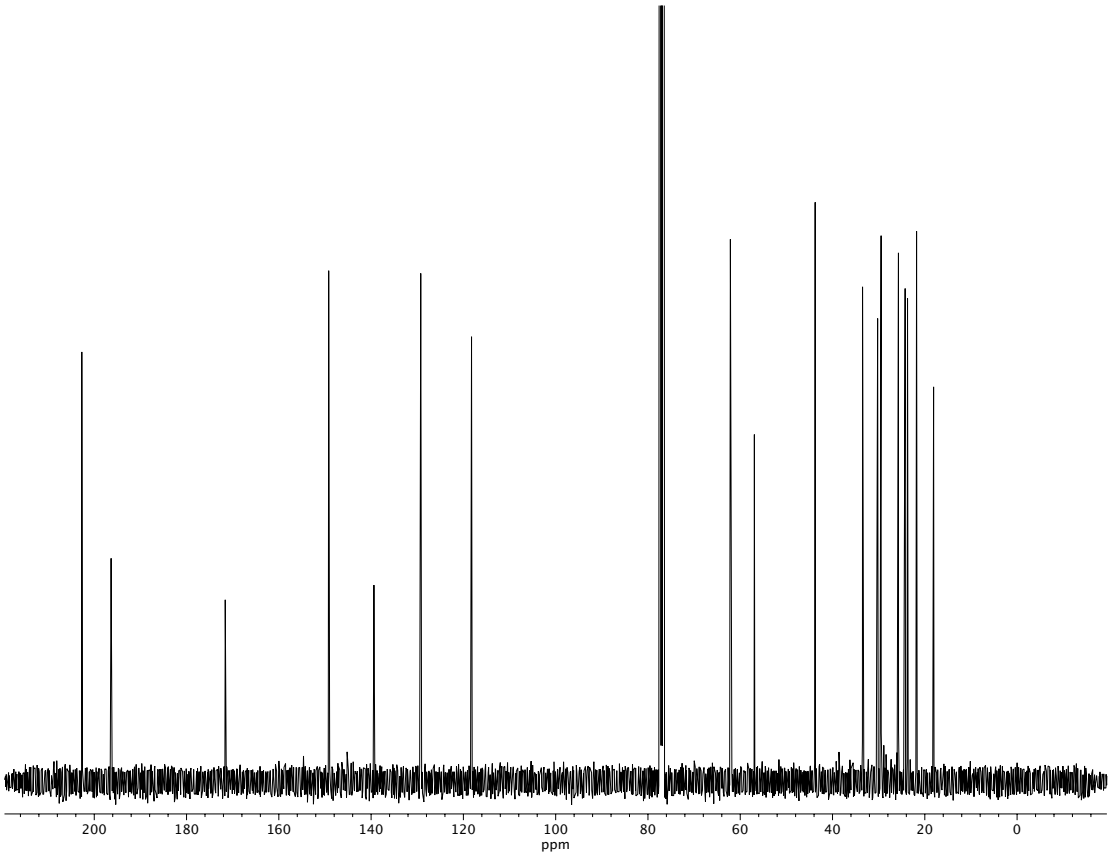


Figure A1.189. *^{13}C NMR (100 MHz, $CDCl_3$) of compound* ***57****.*

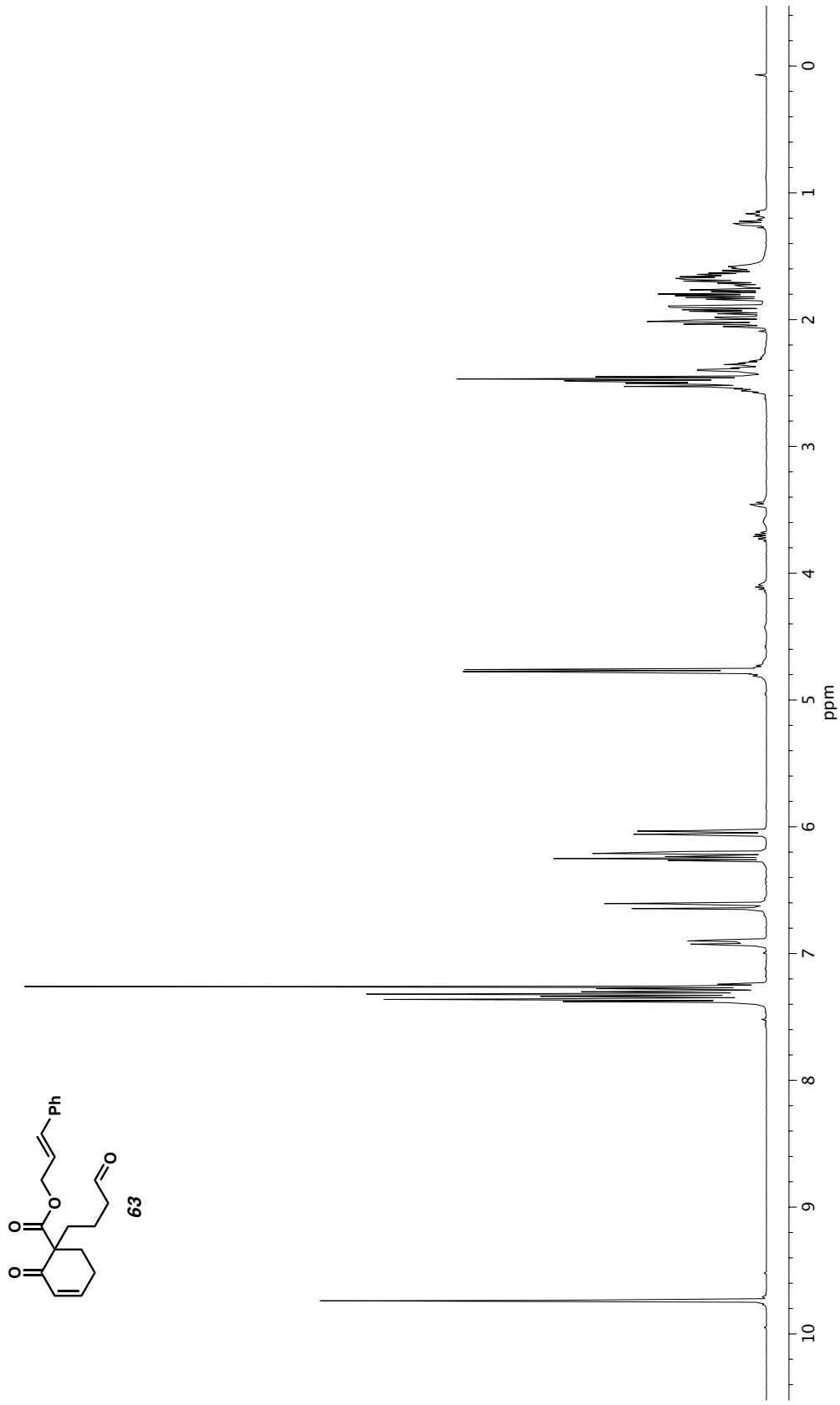


Figure A1.190. *^1H NMR (400 MHz, $CDCl_3$) of compound* ***63****.*

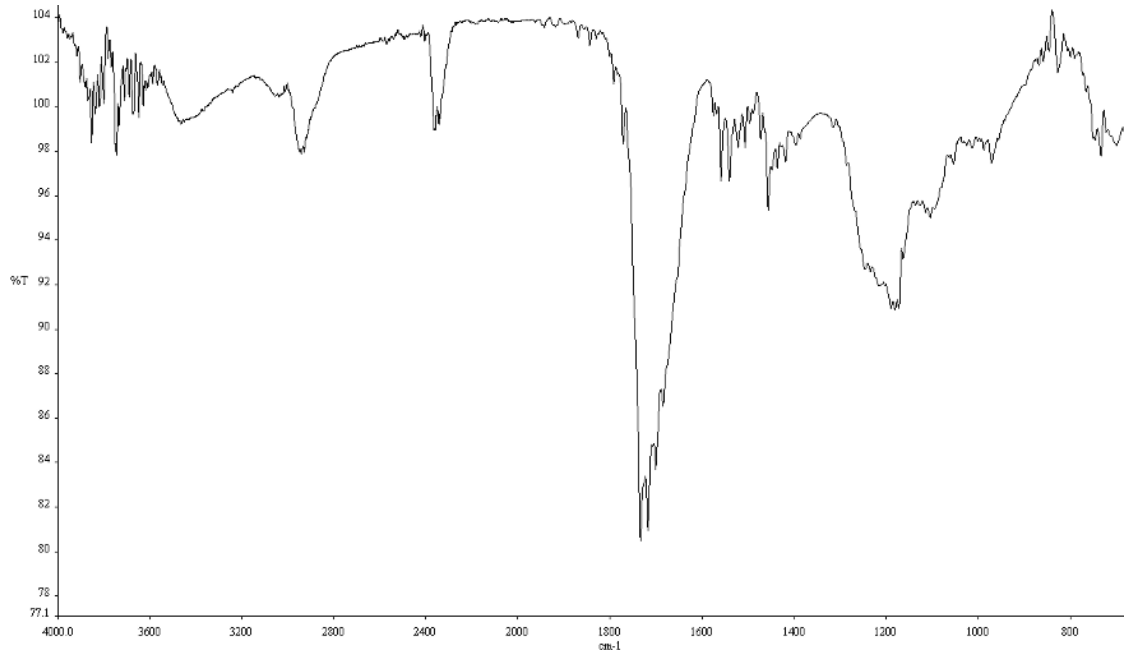


Figure A1.191. *Infrared spectrum (Thin Film, NaCl) of compound* ***63****.*

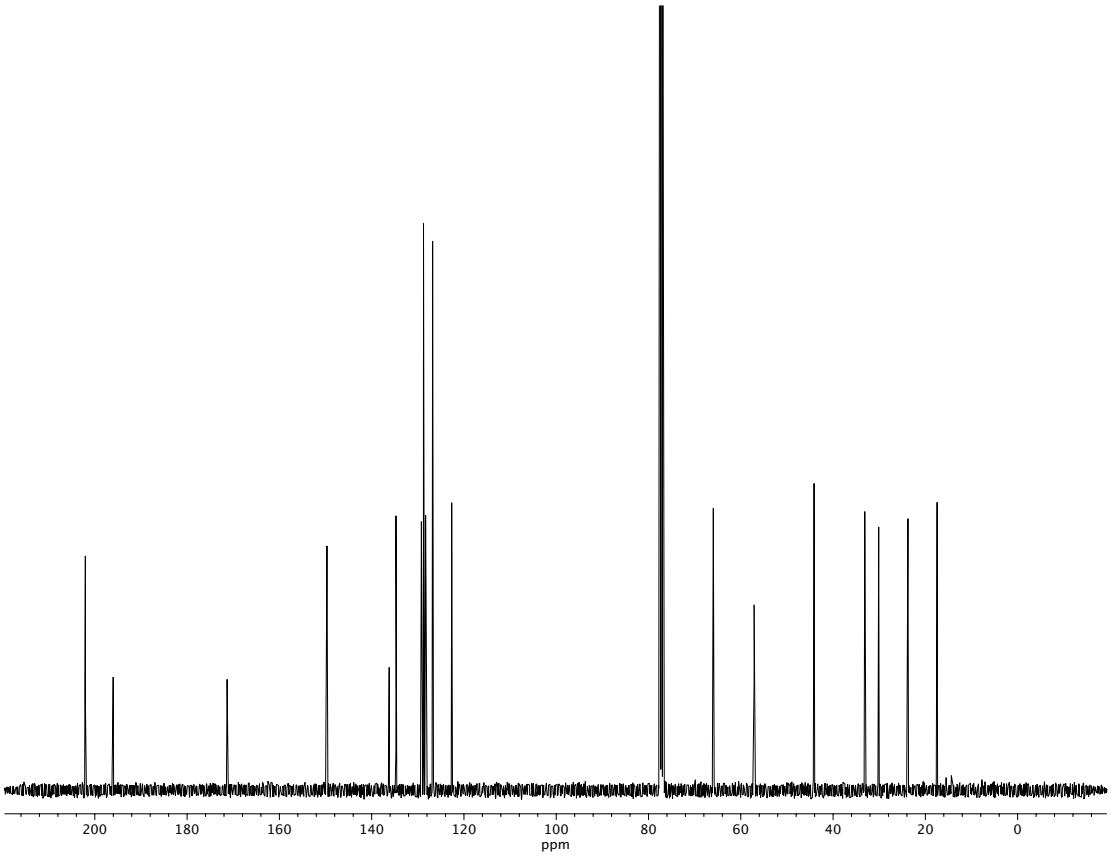


Figure A1.192. *^{13}C NMR (100 MHz, $CDCl_3$) of compound* ***63****.*

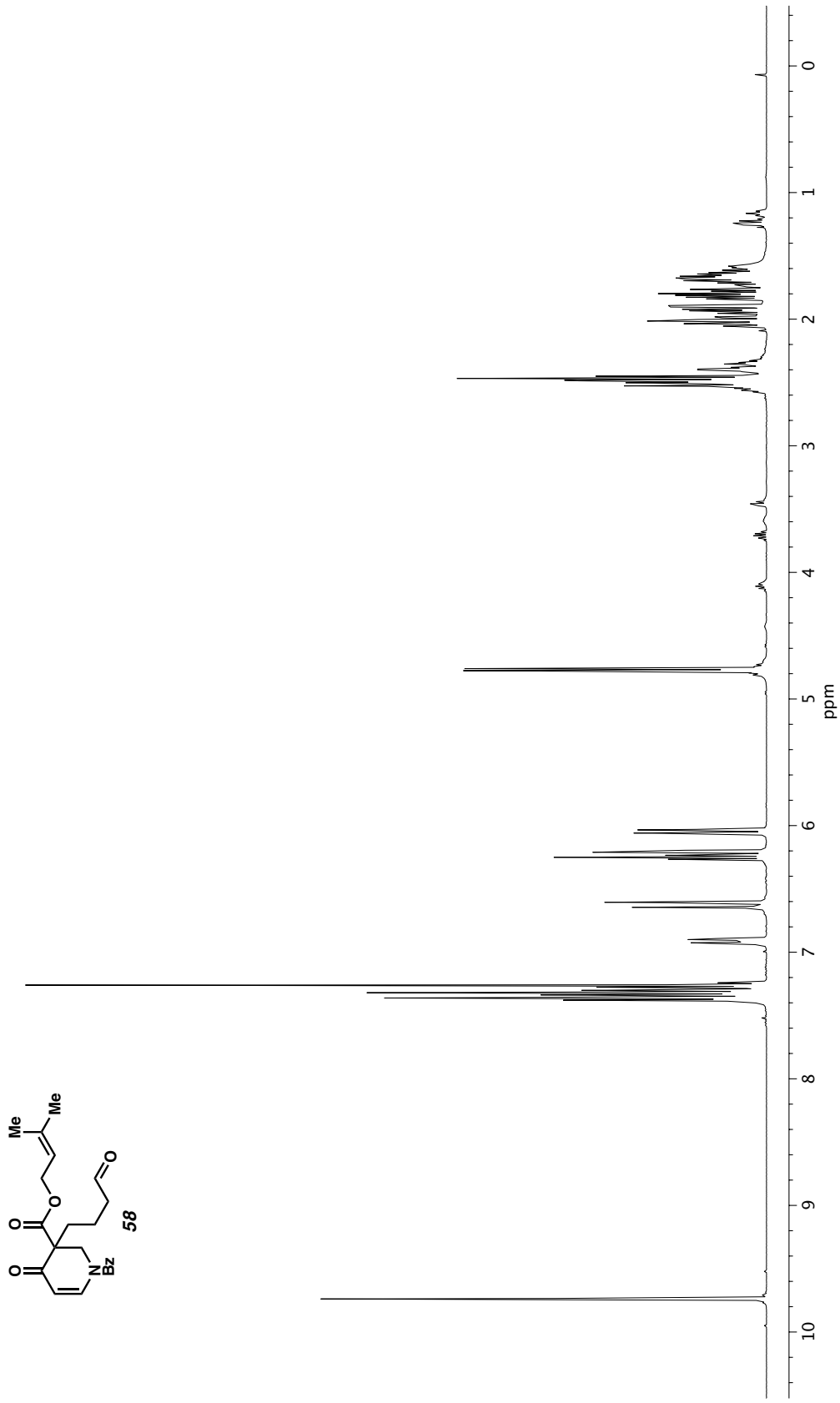


Figure A1.193. *^1H NMR (400 MHz, $CDCl_3$) of compound **58**.*

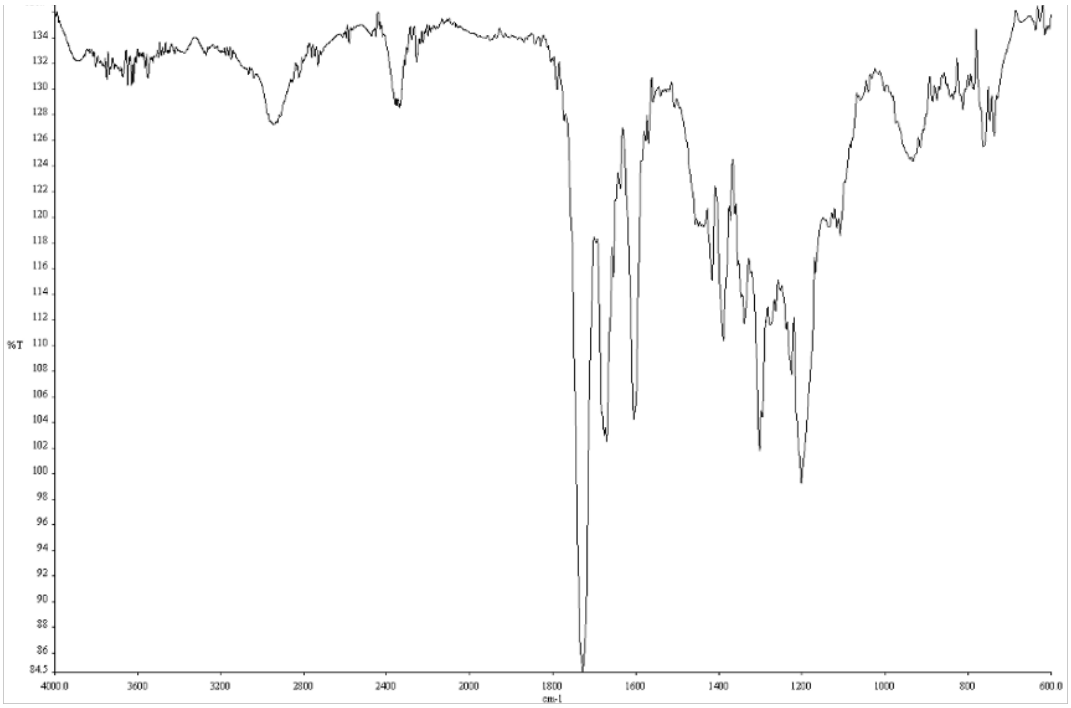


Figure A1.194. *Infrared spectrum (Thin Film, NaCl) of compound* ***58****.*

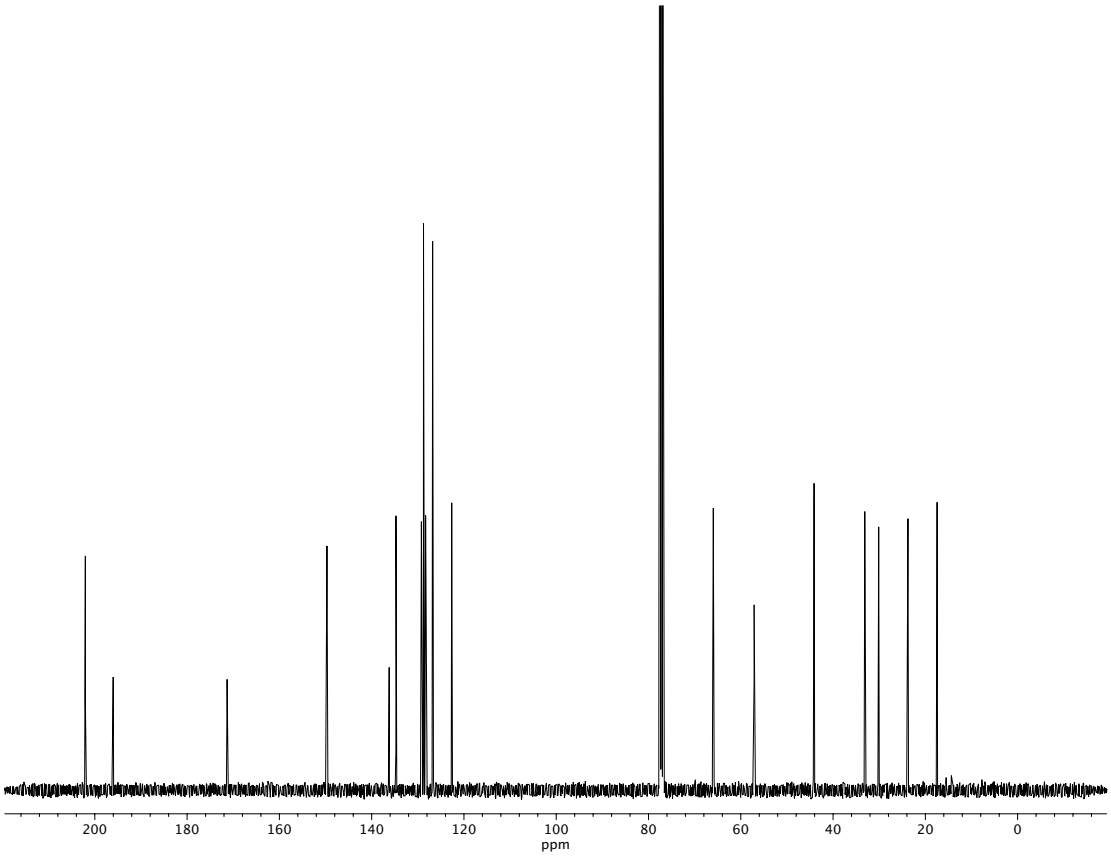


Figure A1.195. *^{13}C NMR (100 MHz, $CDCl_3$) of compound* ***58****.*

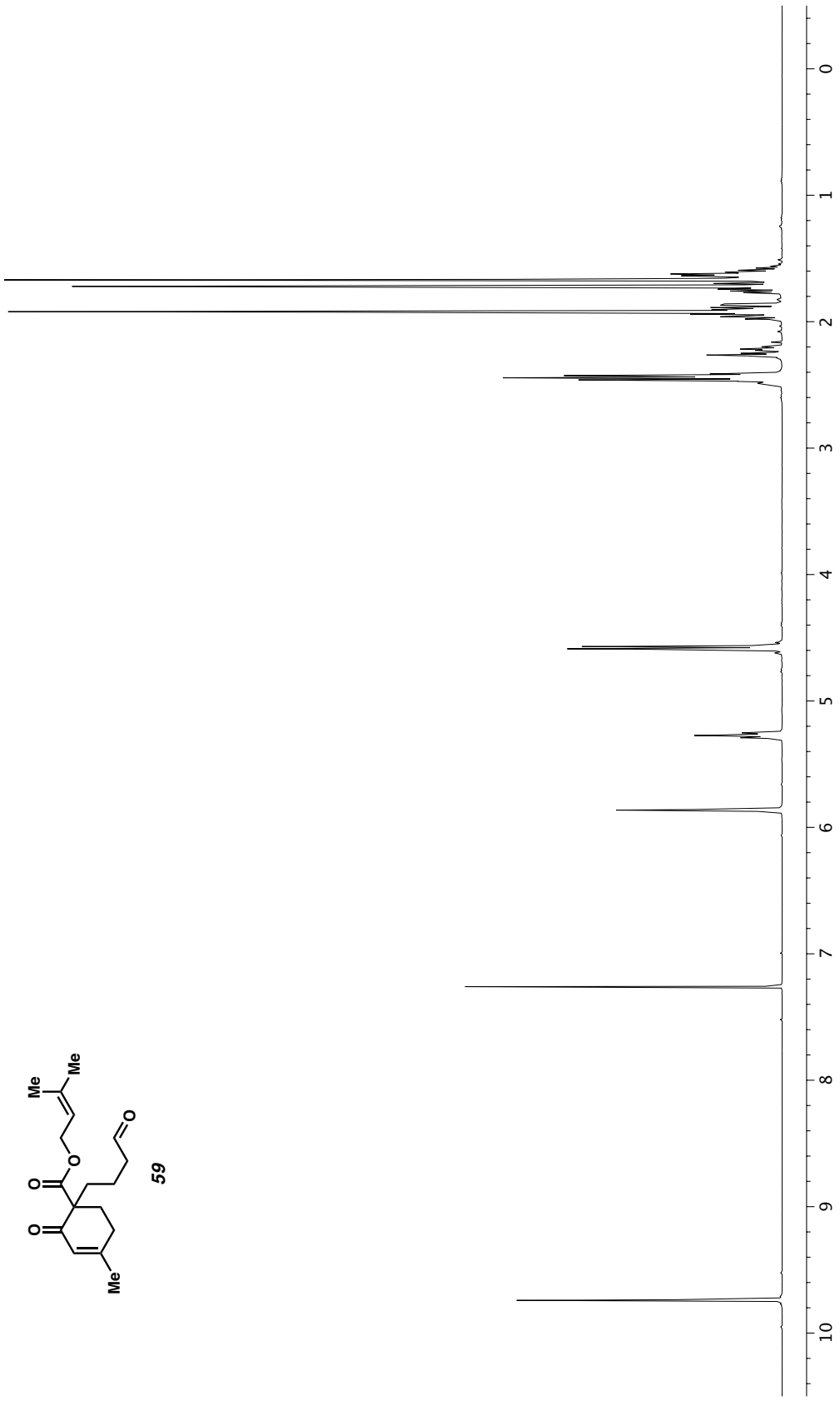


Figure A1.196. *^1H NMR (400 MHz, $CDCl_3$) of compound **59**.*

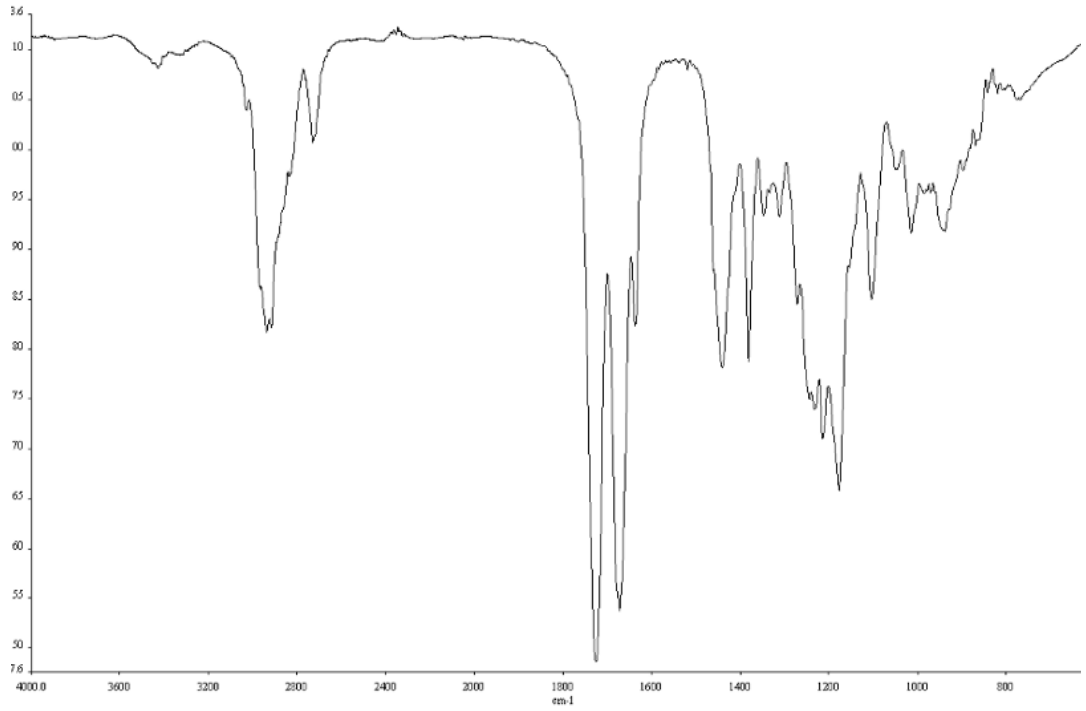


Figure A1.197. *Infrared spectrum (Thin Film, NaCl) of compound* ***59****.*

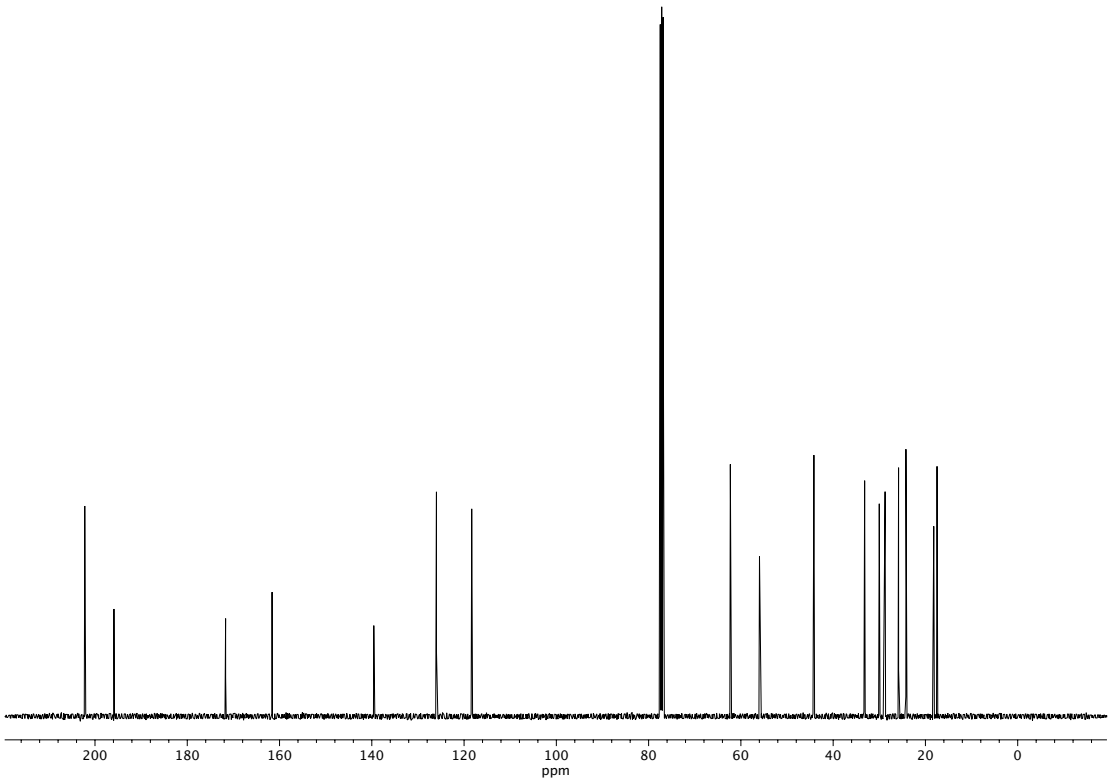
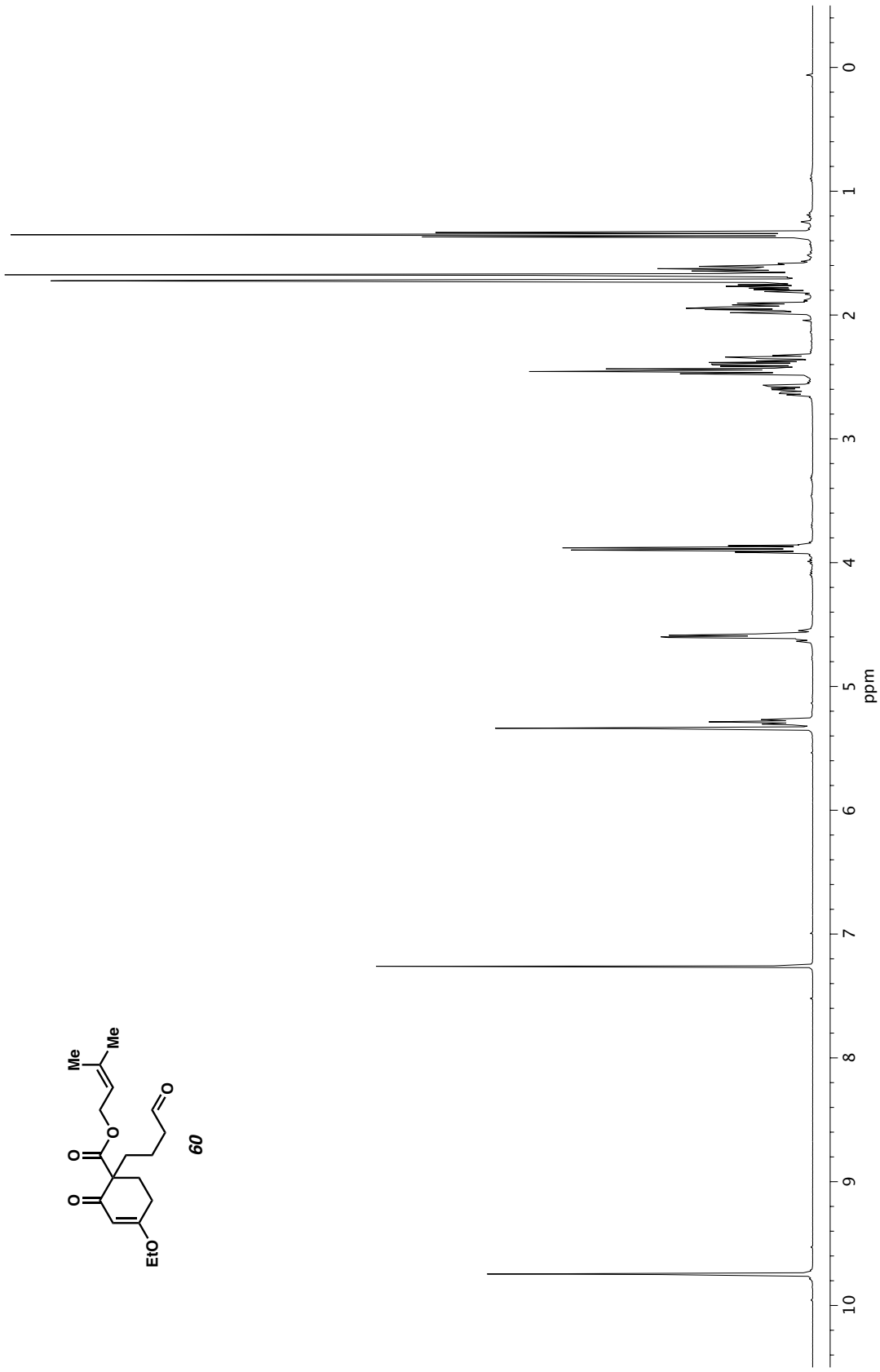


Figure A1.198. *^{13}C NMR (100 MHz, $CDCl_3$) of compound* ***59****.*



60

Figure A1.199. *^1H NMR (400 MHz, $CDCl_3$) of compound* ***60****.*

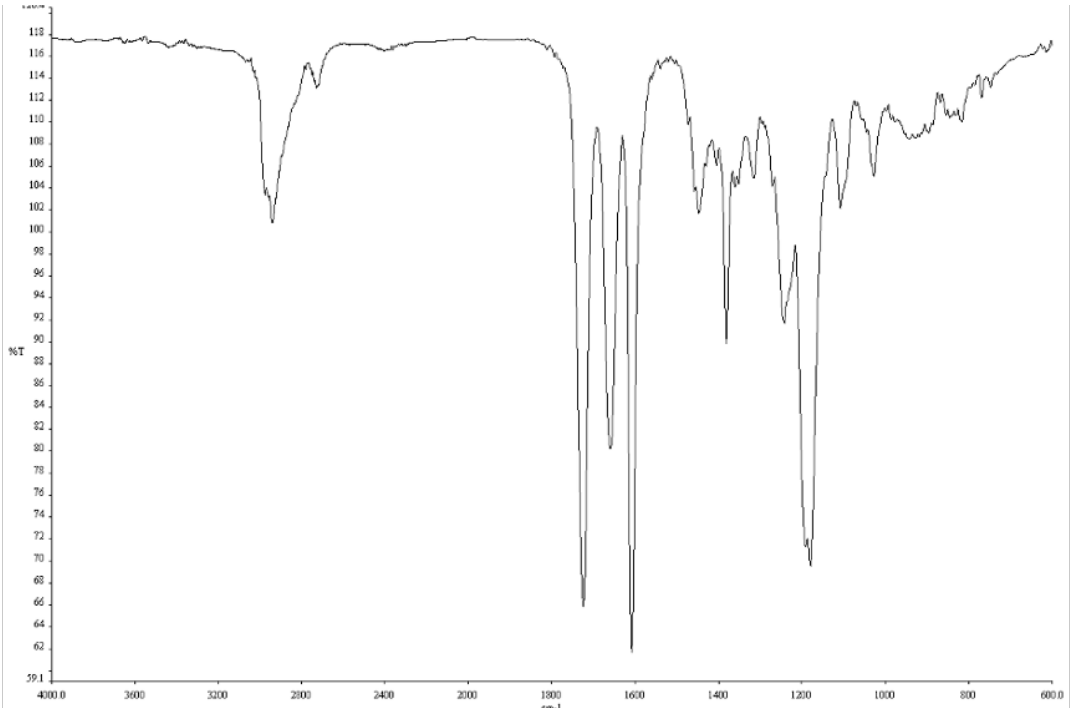


Figure A1.200. *Infrared spectrum (Thin Film, NaCl) of compound* ***60****.*

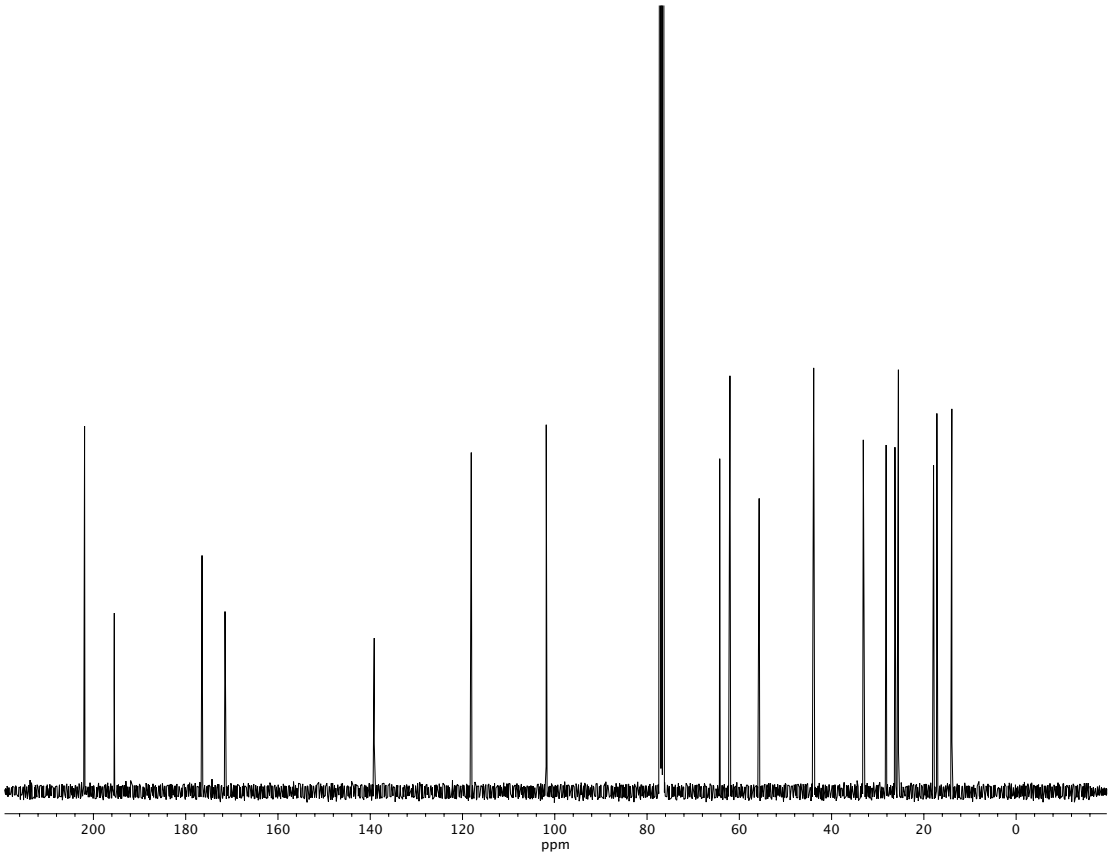


Figure A1.201. *^{13}C NMR (100 MHz, $CDCl_3$) of compound* ***60****.*

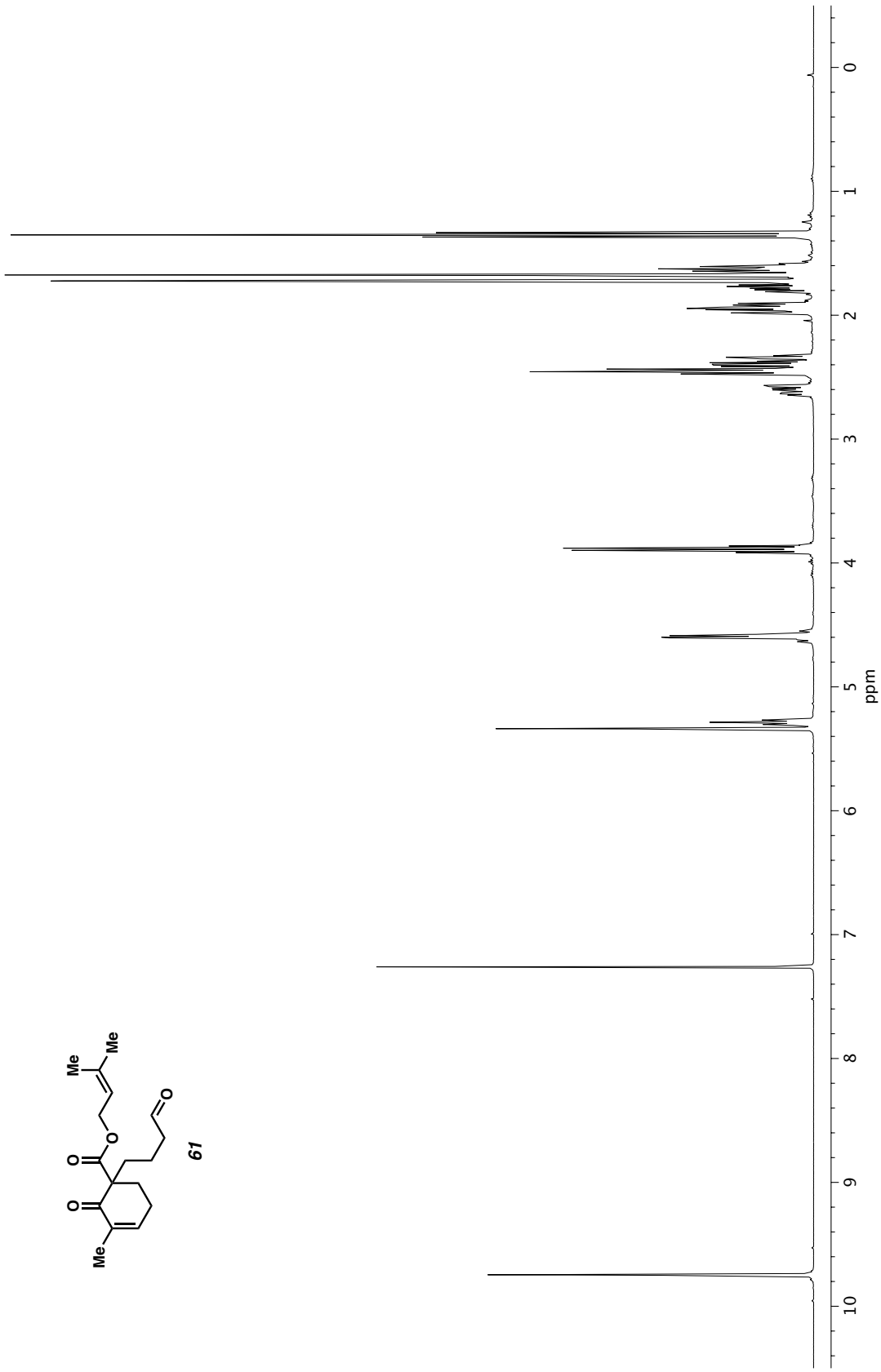


Figure A1.202. *^1H NMR (400 MHz, $CDCl_3$) of compound **61**.*

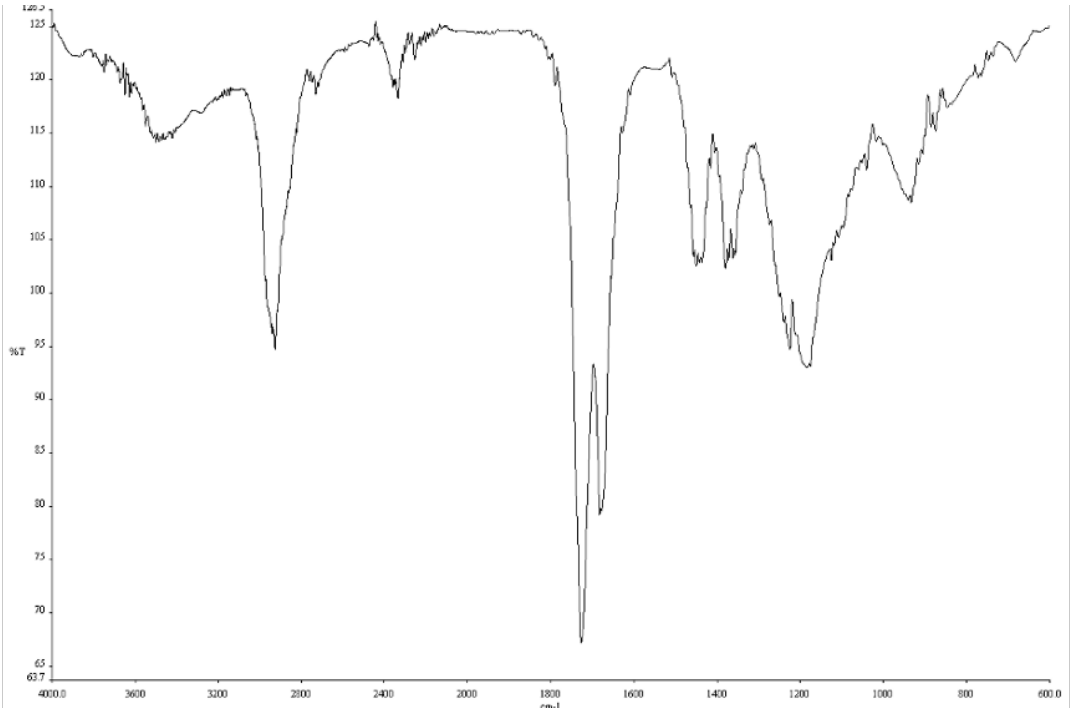


Figure A1.203. *Infrared spectrum (Thin Film, NaCl) of compound* ***61****.*

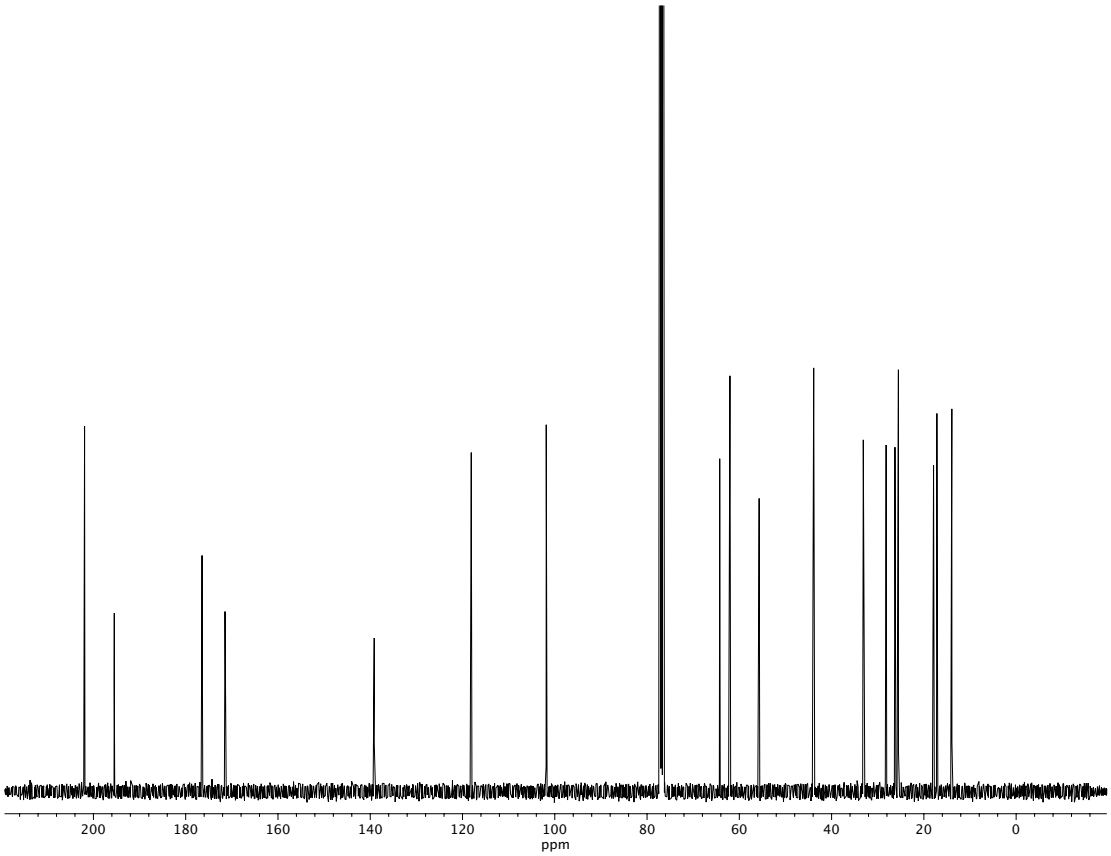


Figure A1.204. *^{13}C NMR (100 MHz, $CDCl_3$) of compound* ***61****.*

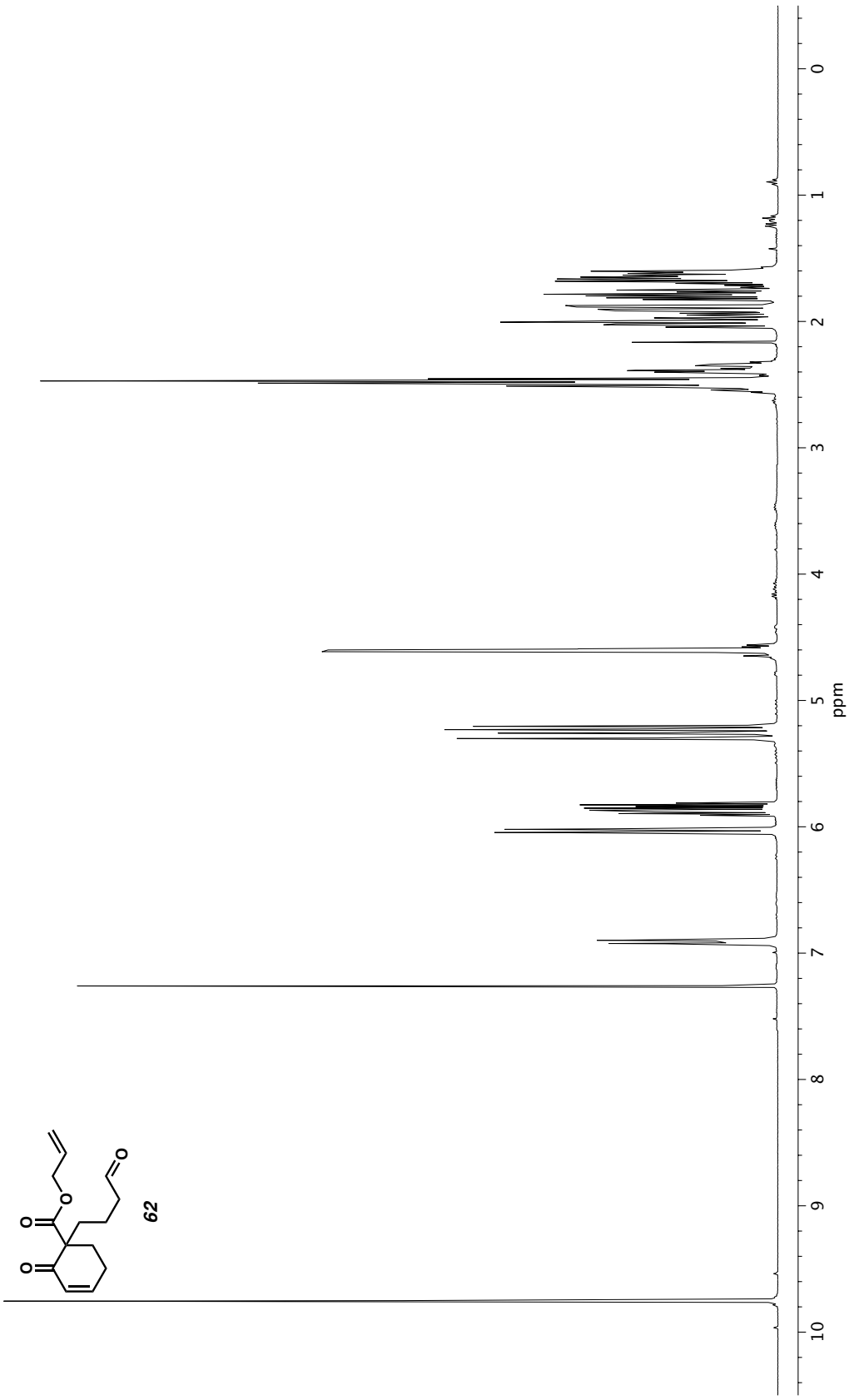


Figure A1.205. *^1H NMR (400 MHz, $CDCl_3$) of compound* ***62****.*

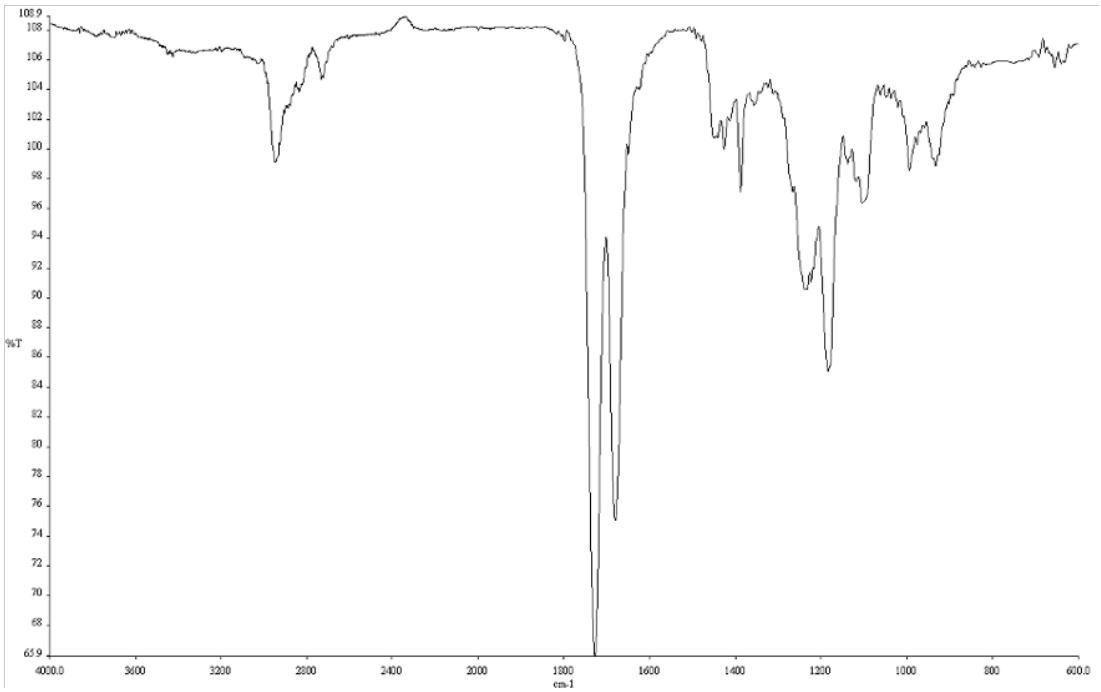


Figure A1.206. *Infrared spectrum (Thin Film, NaCl) of compound* ***62****.*

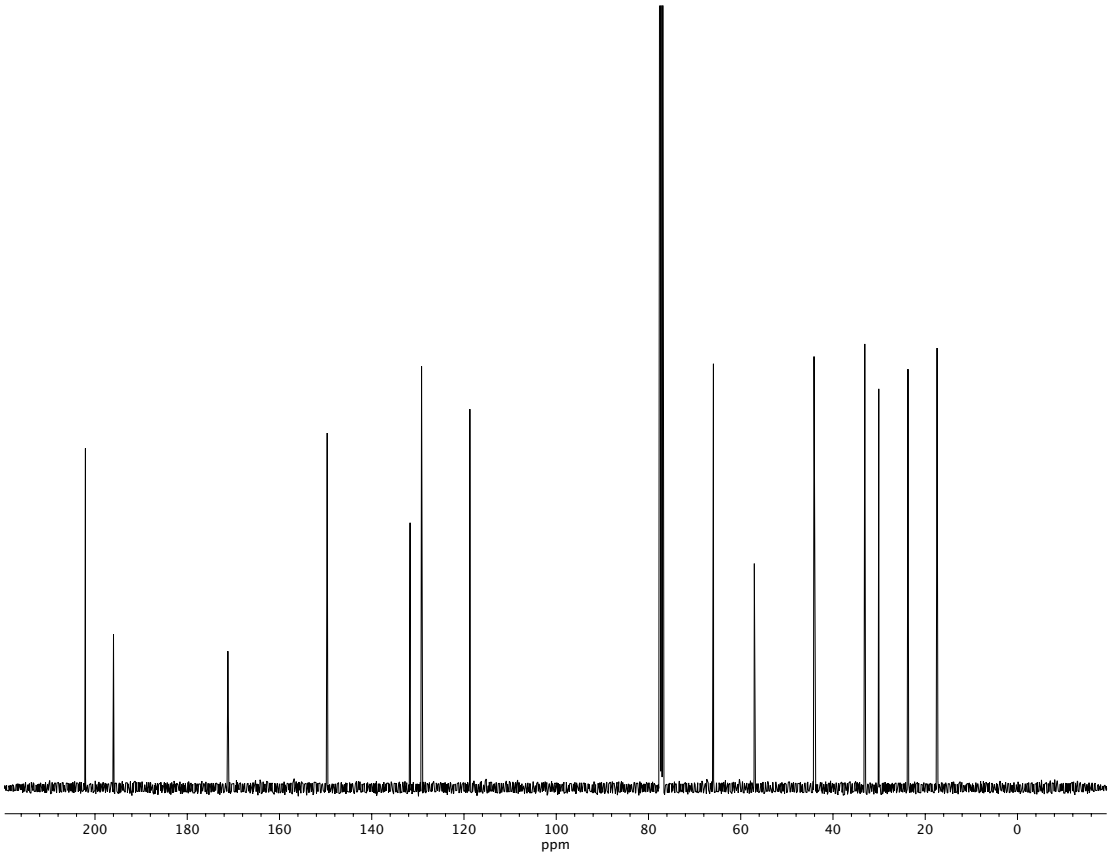


Figure A1.207. *^{13}C NMR (100 MHz, $CDCl_3$) of compound* ***62****.*

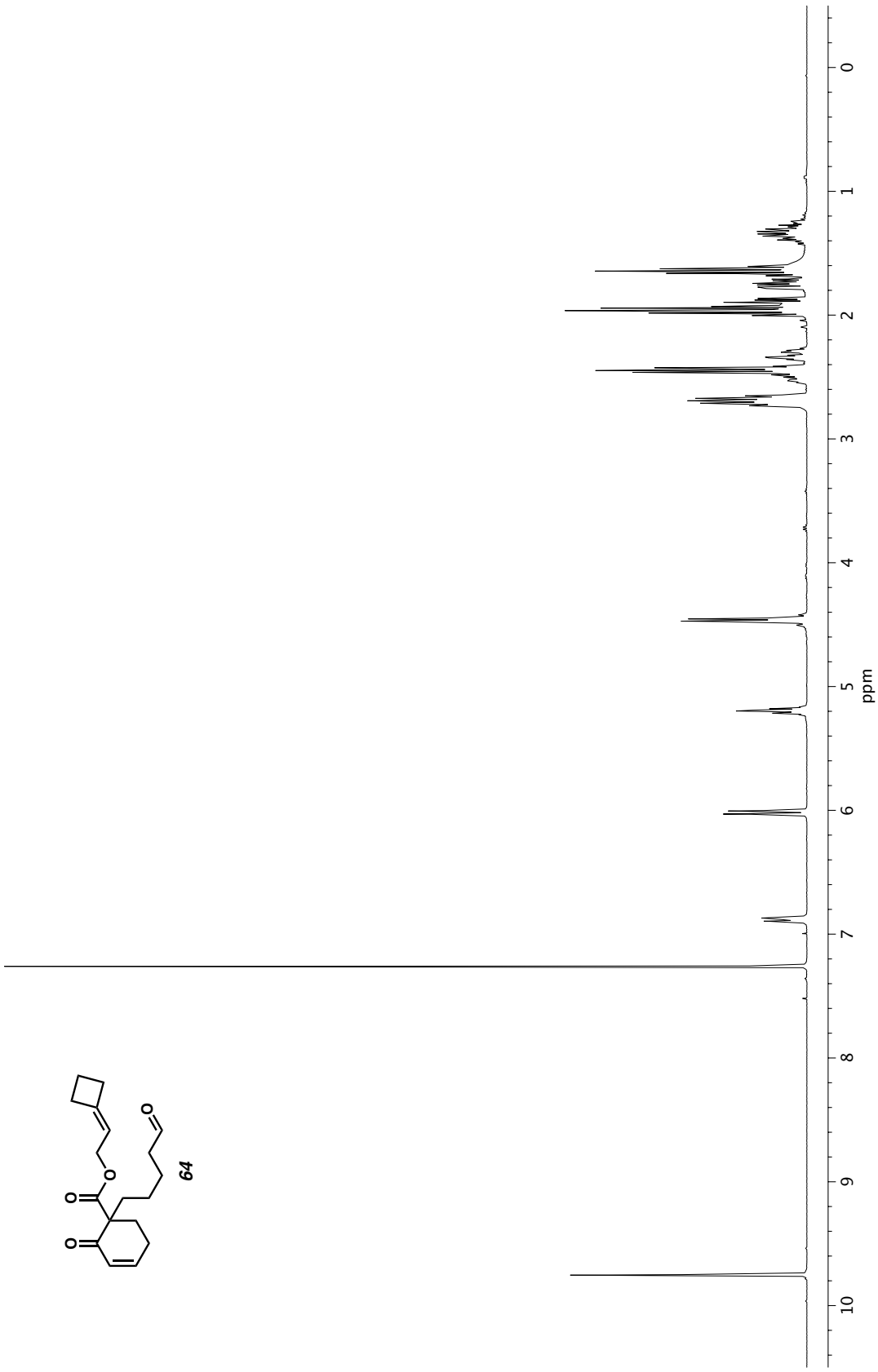


Figure A1.208. *^1H NMR (400 MHz, $CDCl_3$) of compound* ***64****.*

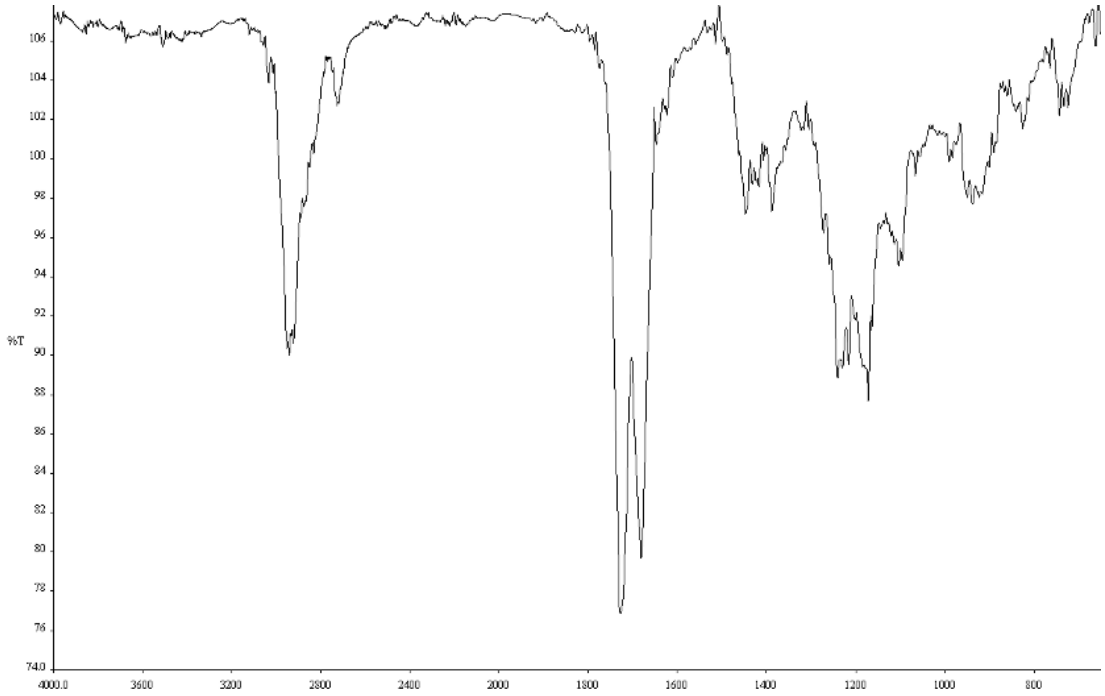


Figure A1.209. *Infrared spectrum (Thin Film, NaCl) of compound* ***64****.*

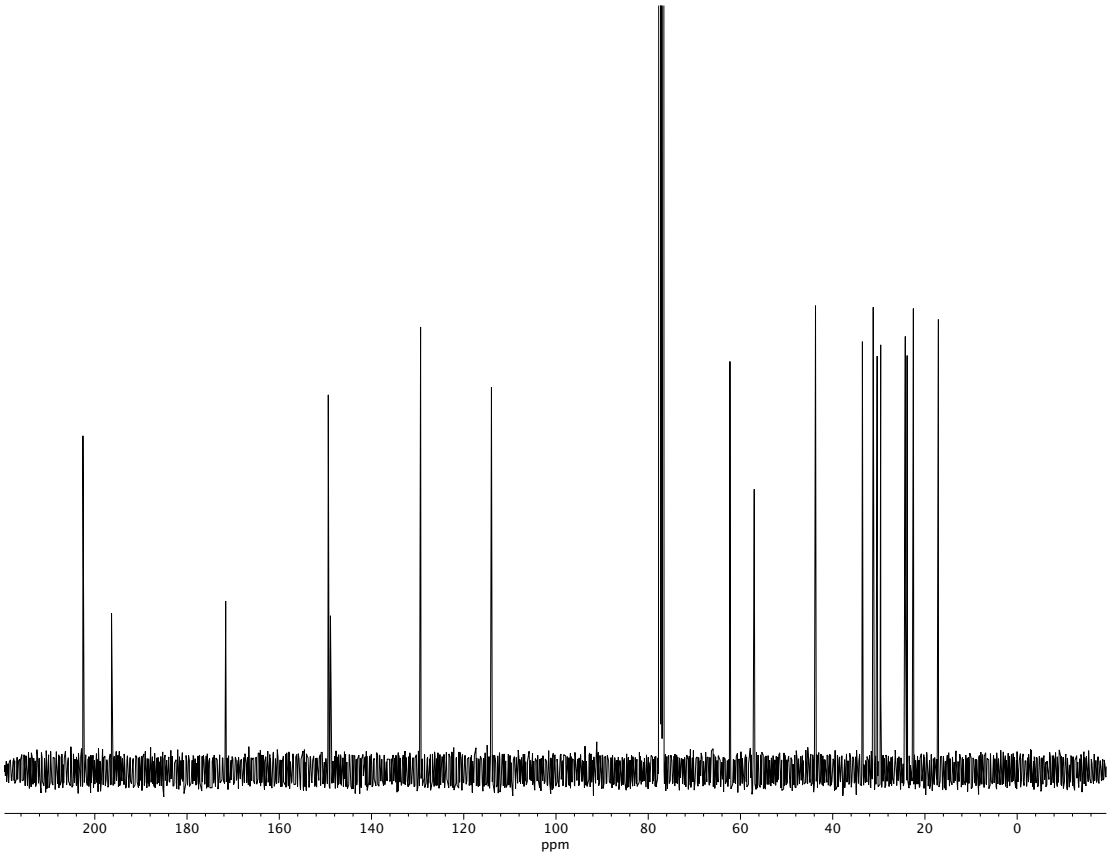


Figure A1.210. *^{13}C NMR (100 MHz, $CDCl_3$) of compound* ***64****.*

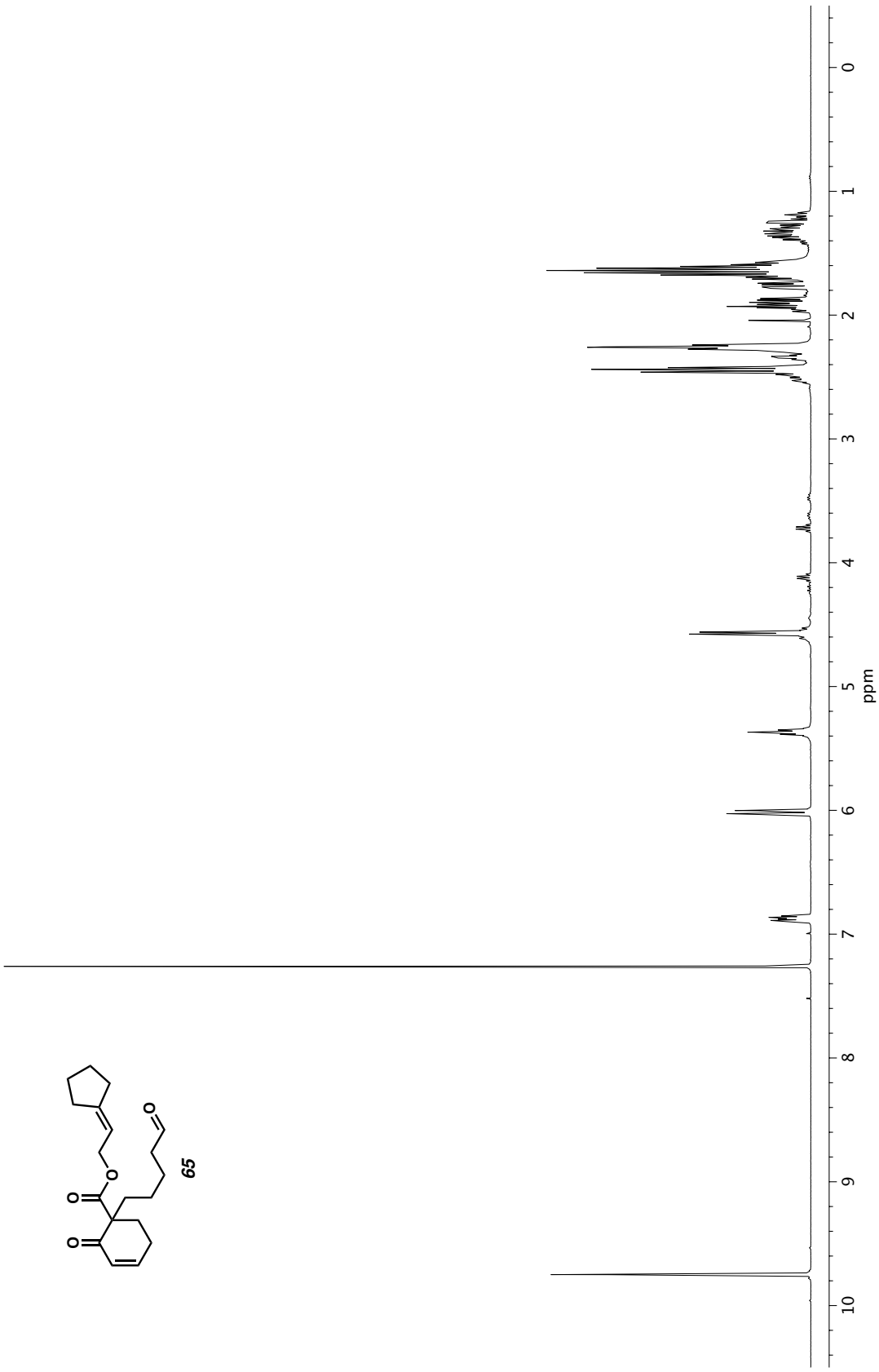


Figure A1.211. *^1H NMR (400 MHz, $CDCl_3$) of compound* ***65****.*

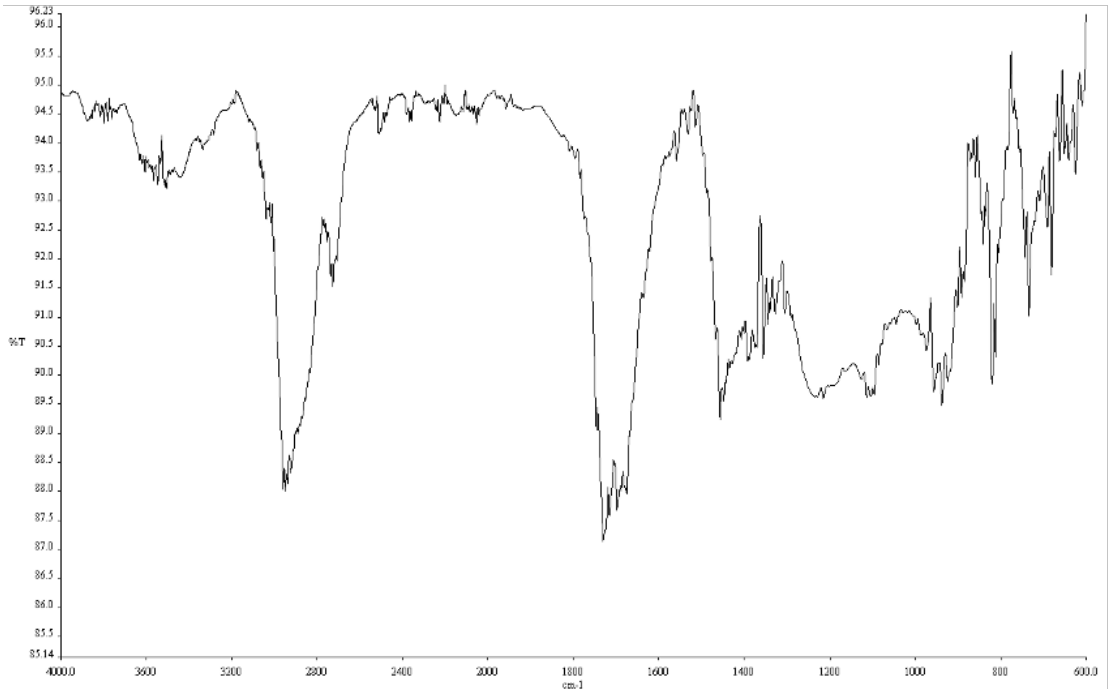


Figure A1.212. *Infrared spectrum (Thin Film, NaCl) of compound* ***65****.*

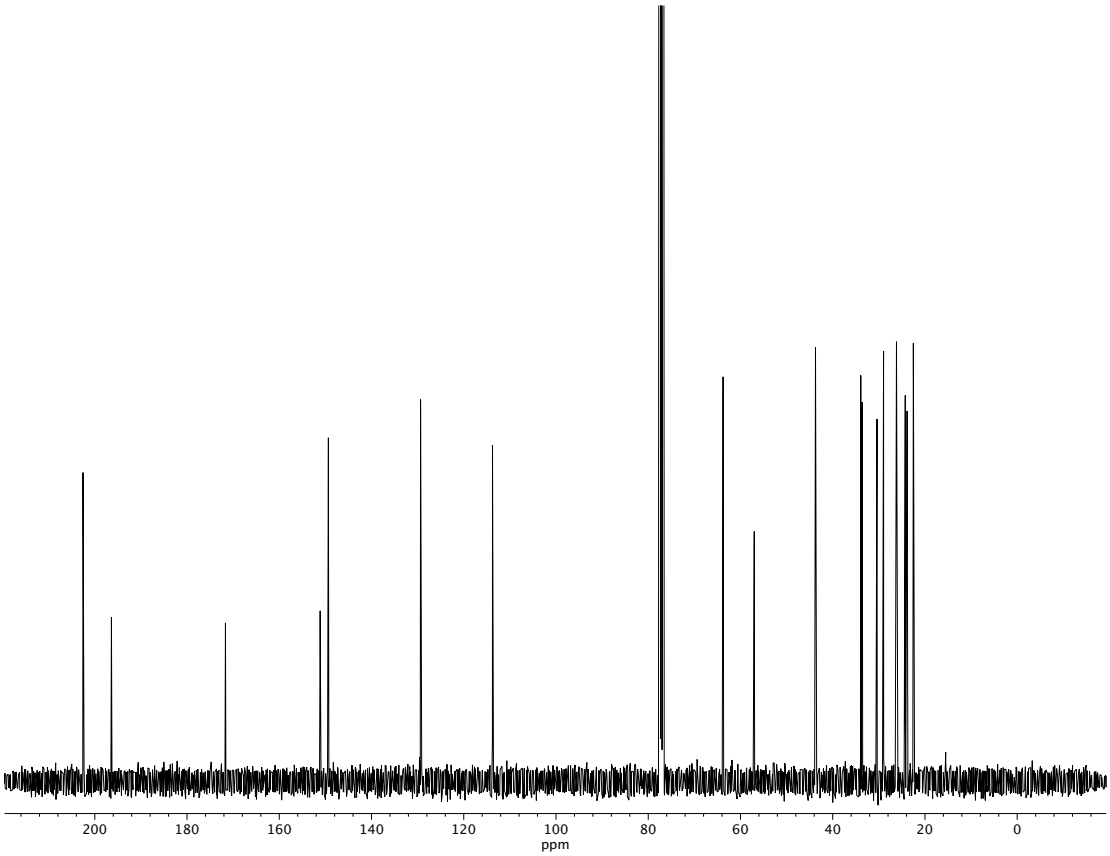


Figure A1.213. *^{13}C NMR (100 MHz, $CDCl_3$) of compound* ***65****.*

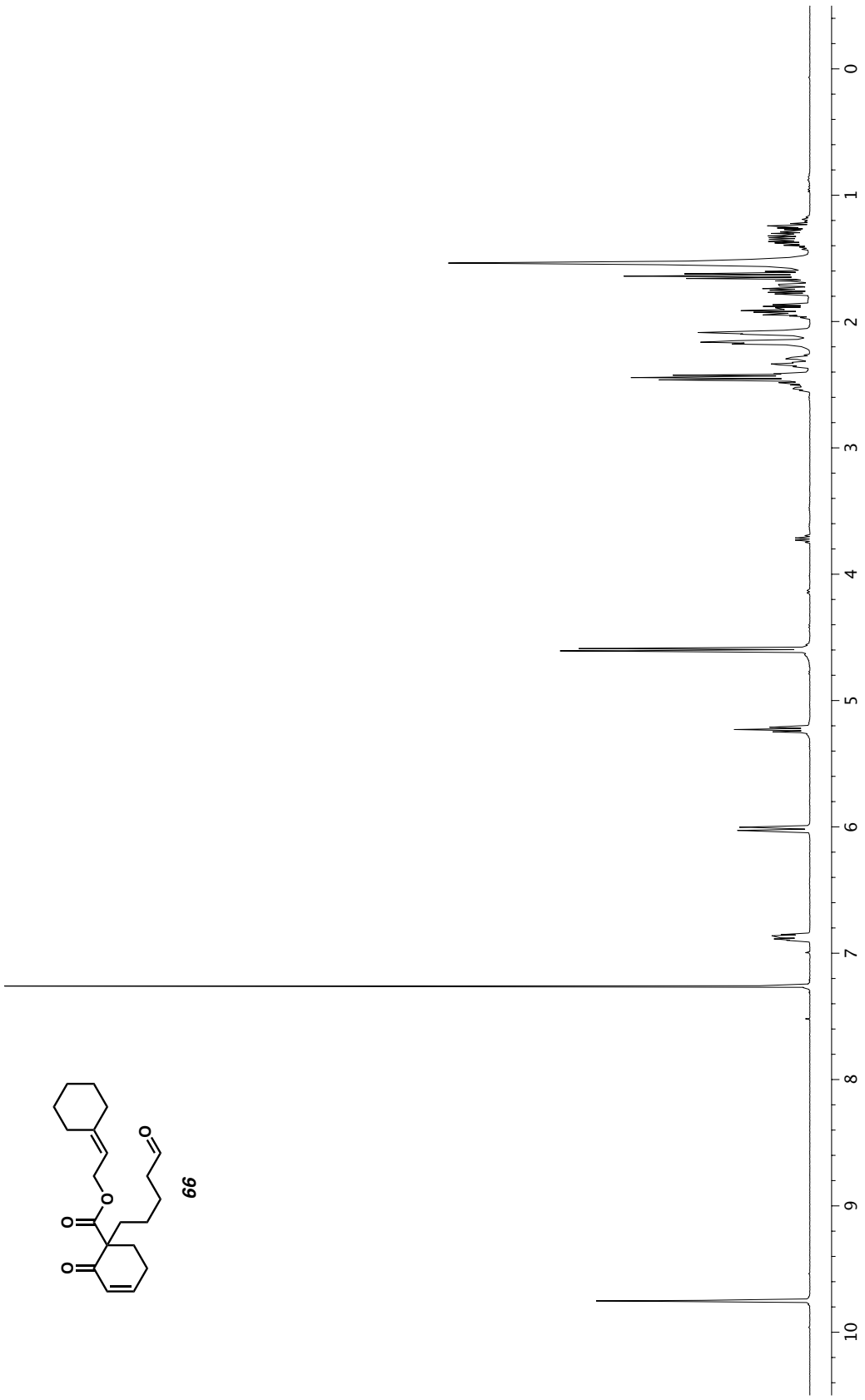


Figure A1.214. *^1H NMR (400 MHz, $CDCl_3$) of compound* ***66****.*

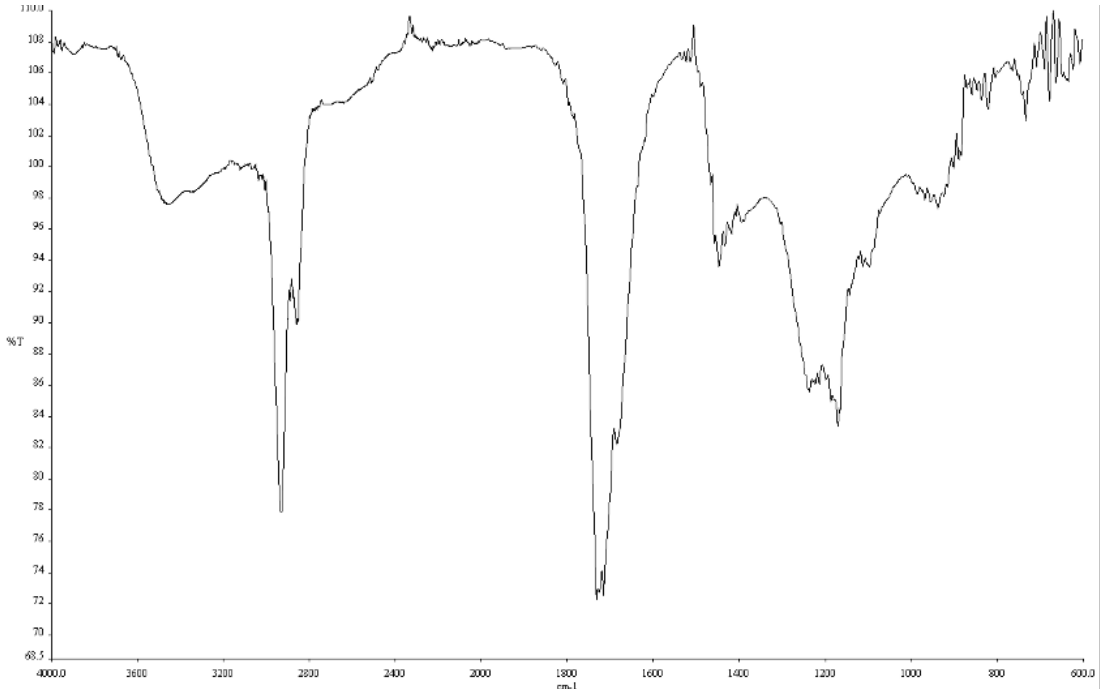


Figure A1.215. *Infrared spectrum (Thin Film, NaCl) of compound* ***66****.*

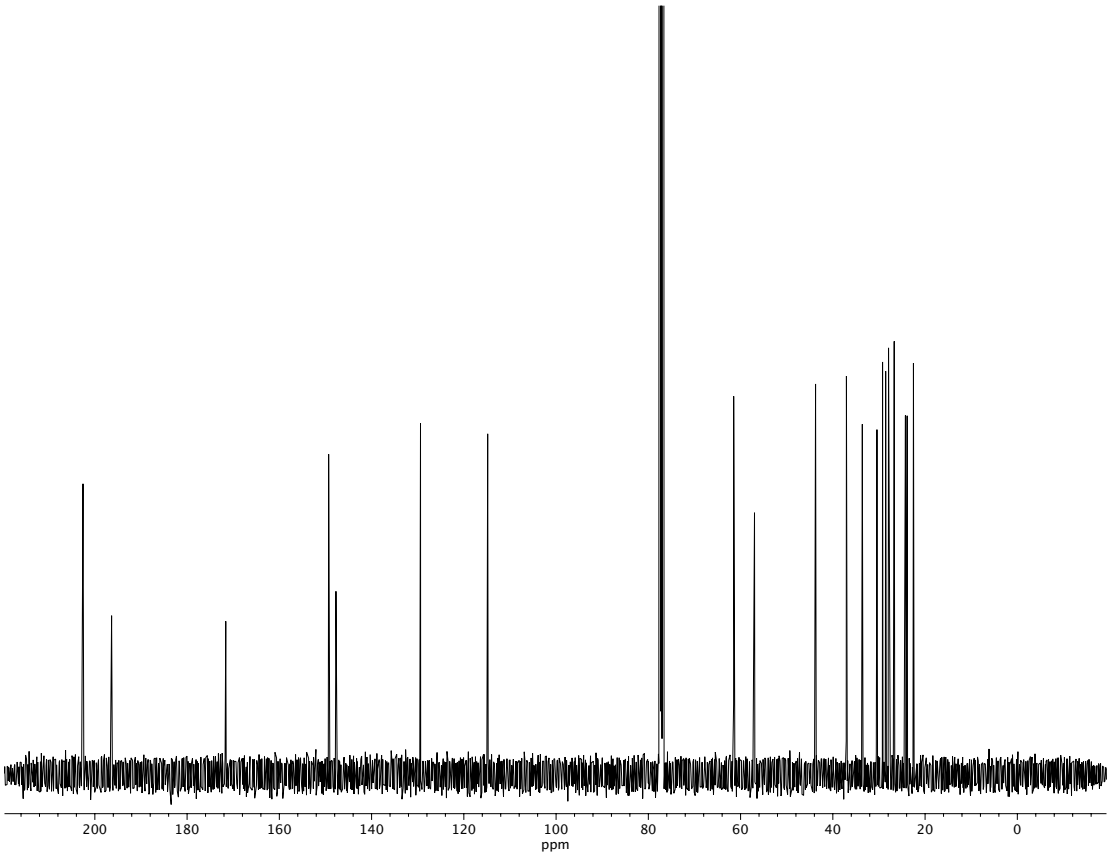


Figure A1.216. *^{13}C NMR (100 MHz, $CDCl_3$) of compound* ***66****.*

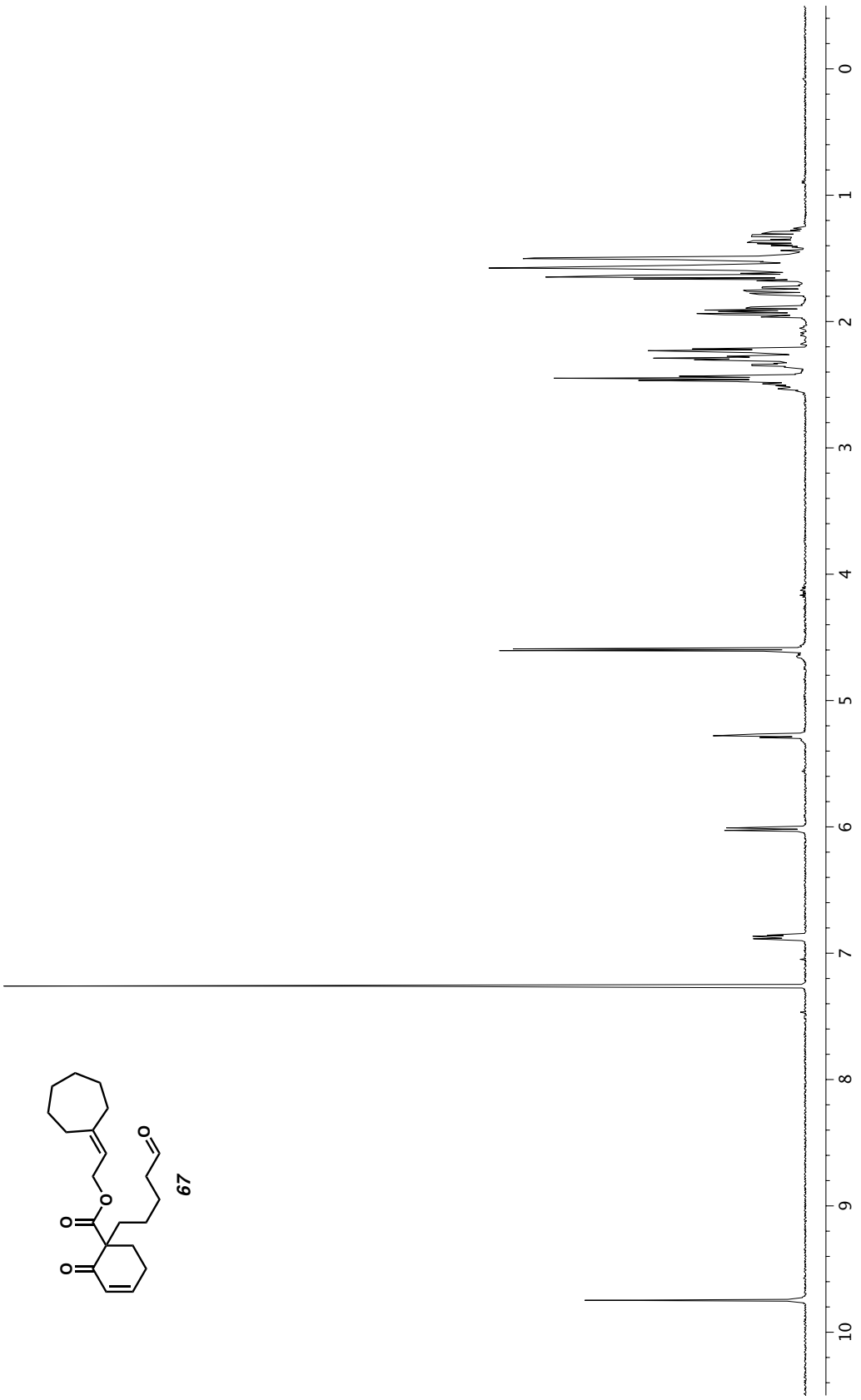


Figure A1.217. *^1H NMR (400 MHz, $CDCl_3$) of compound **67**.*

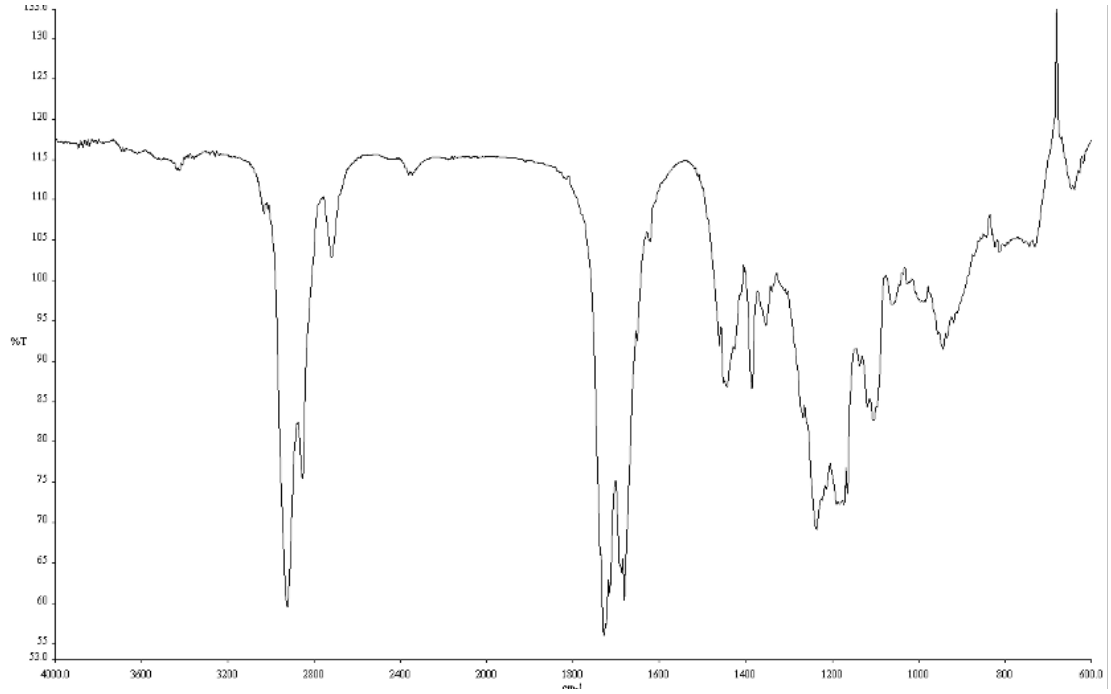


Figure A1.218. *Infrared spectrum (Thin Film, NaCl) of compound* ***67****.*

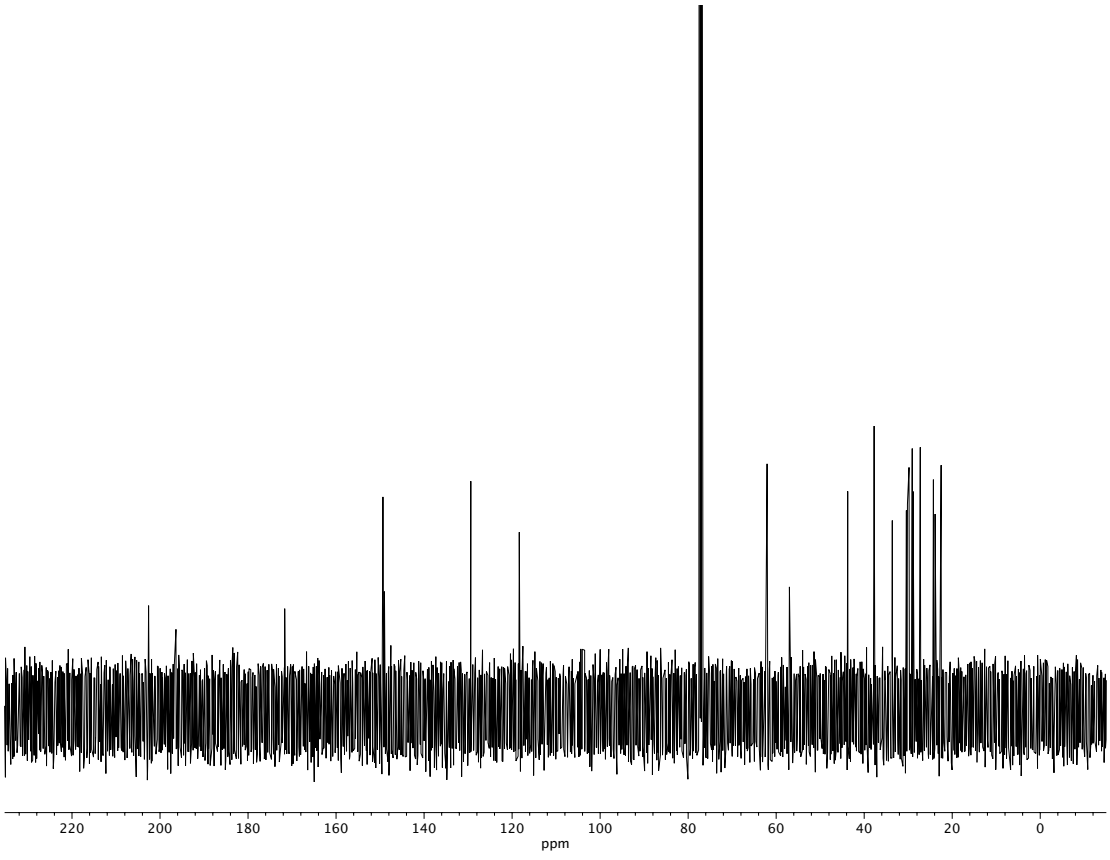


Figure A1.219. *^{13}C NMR (100 MHz, $CDCl_3$) of compound* ***67****.*

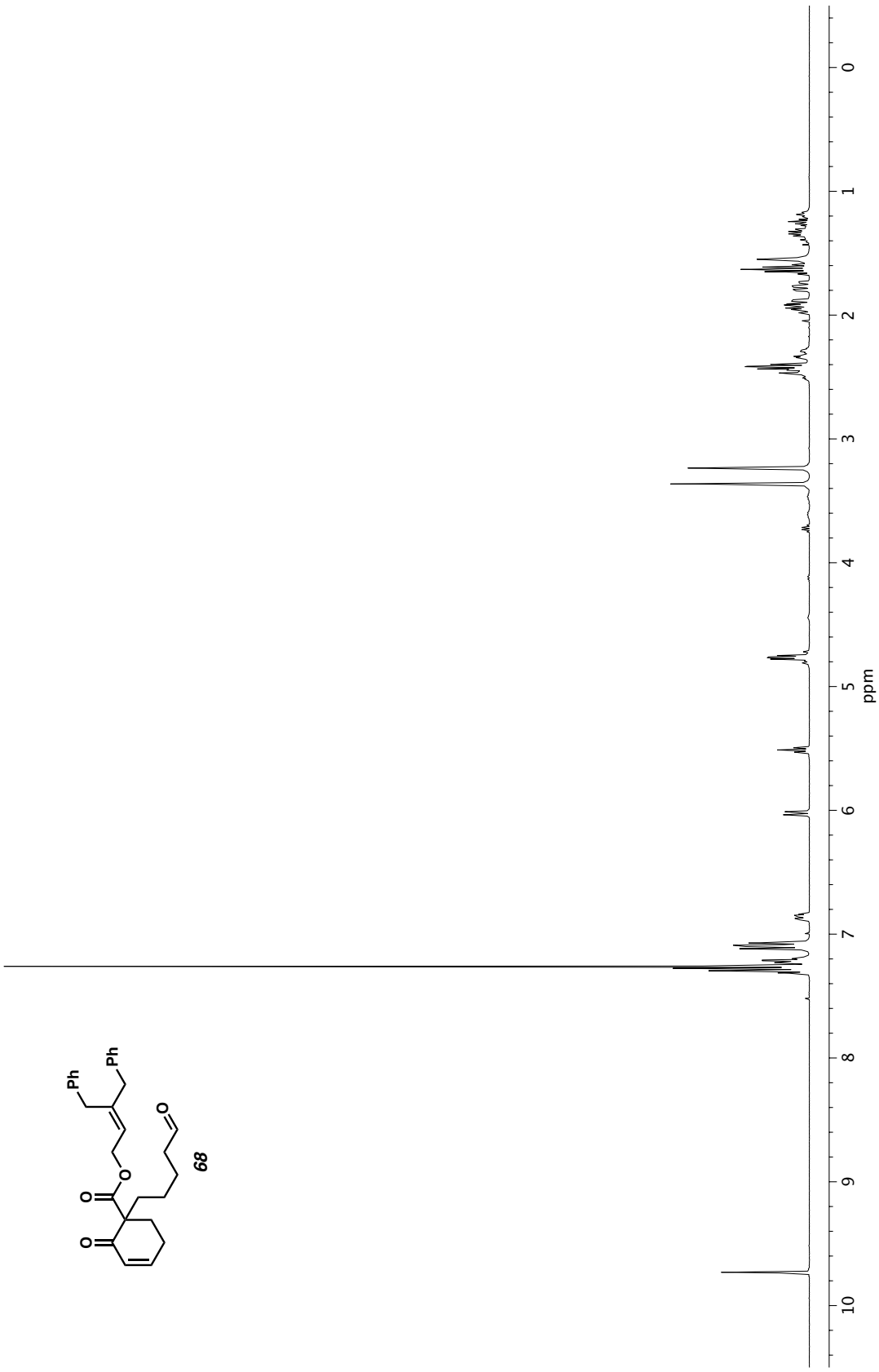


Figure A1.220. *^1H NMR (400 MHz, $CDCl_3$) of compound **68**.*

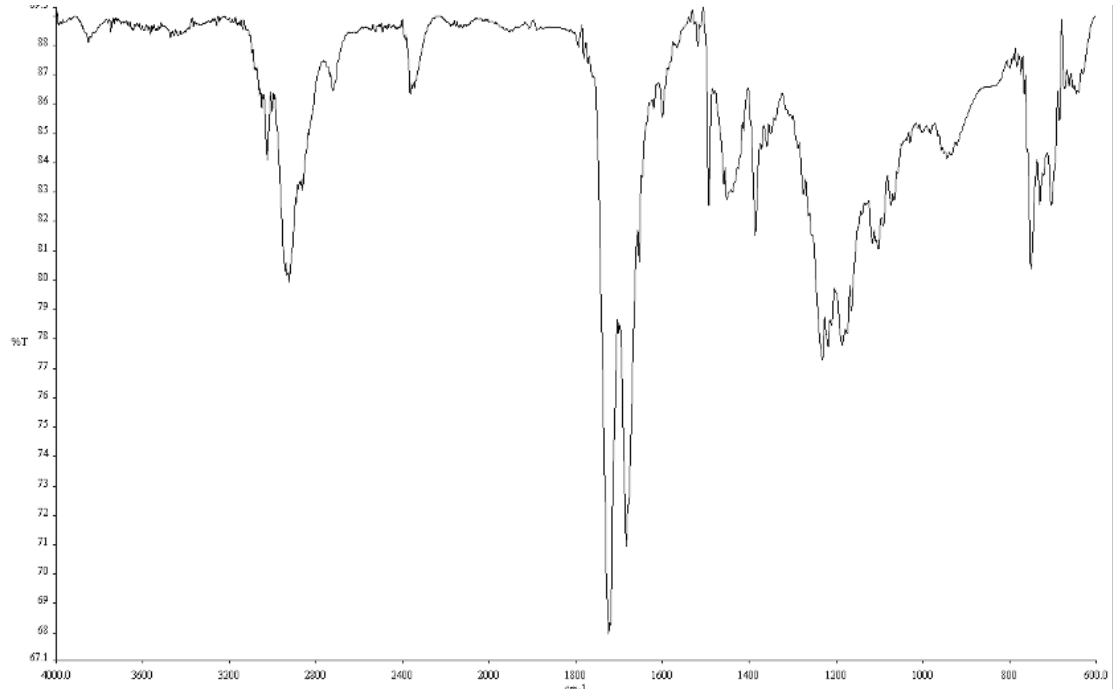


Figure A1.221. *Infrared spectrum (Thin Film, NaCl) of compound* ***68****.*

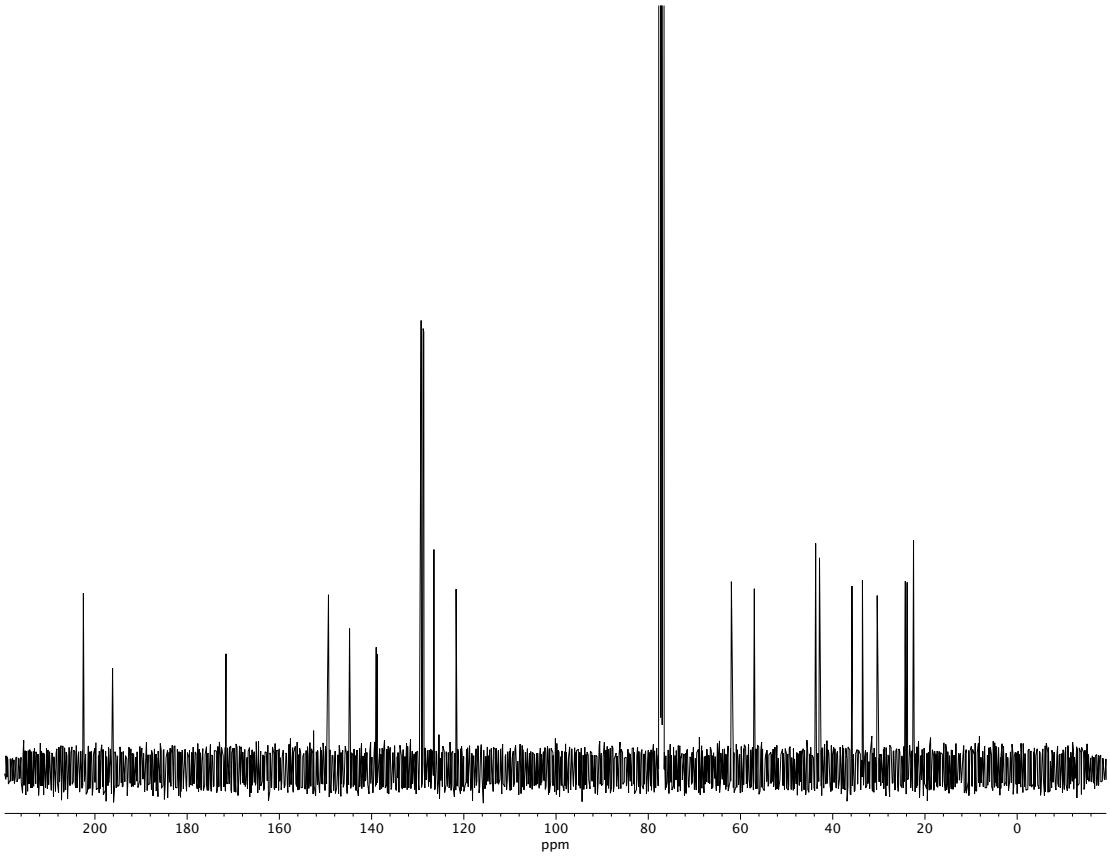
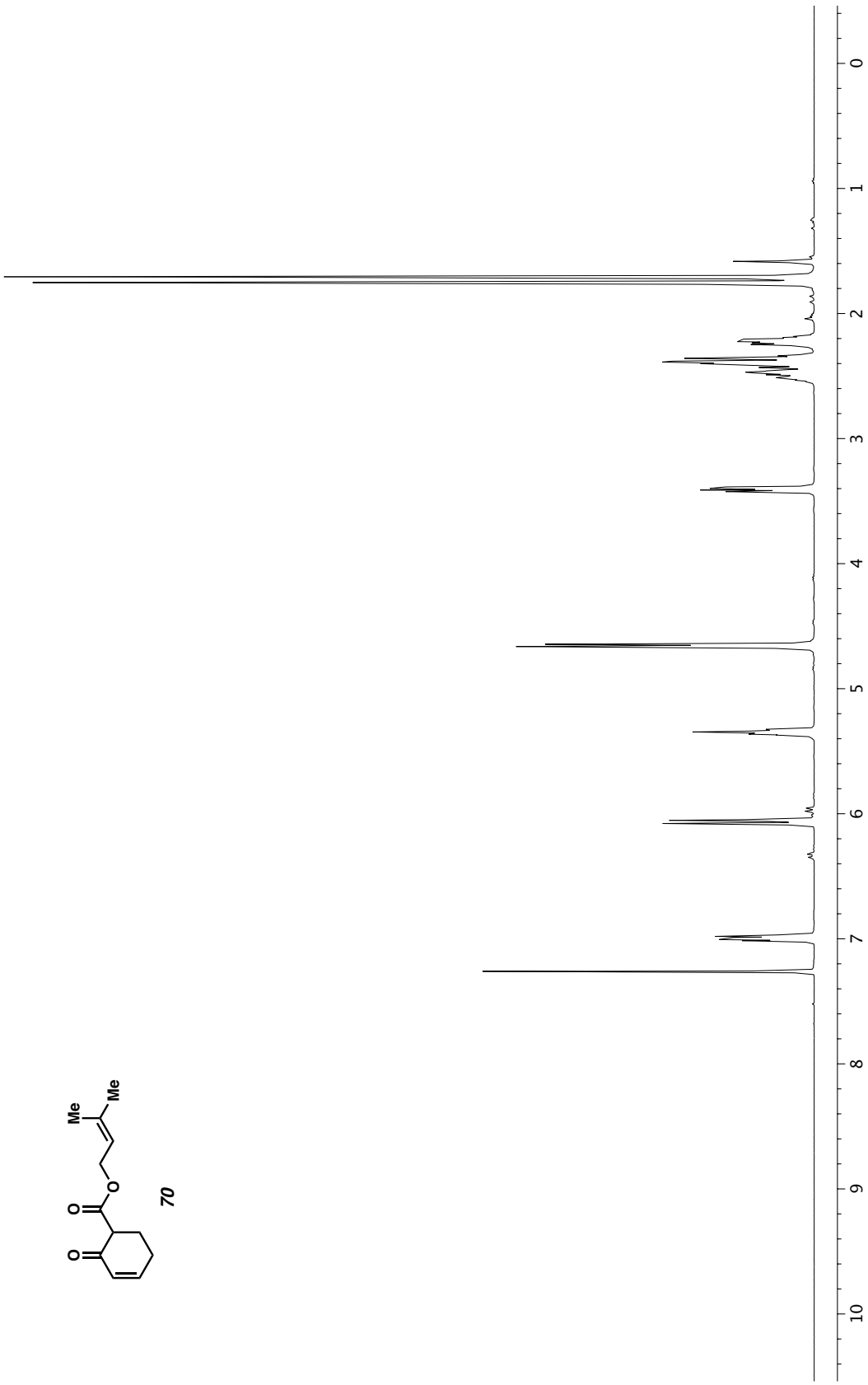


Figure A1.222. *^{13}C NMR (100 MHz, $CDCl_3$) of compound* ***68****.*



70

Figure A1.223. *^1H NMR (400 MHz, $CDCl_3$) of compound* ***70****.*

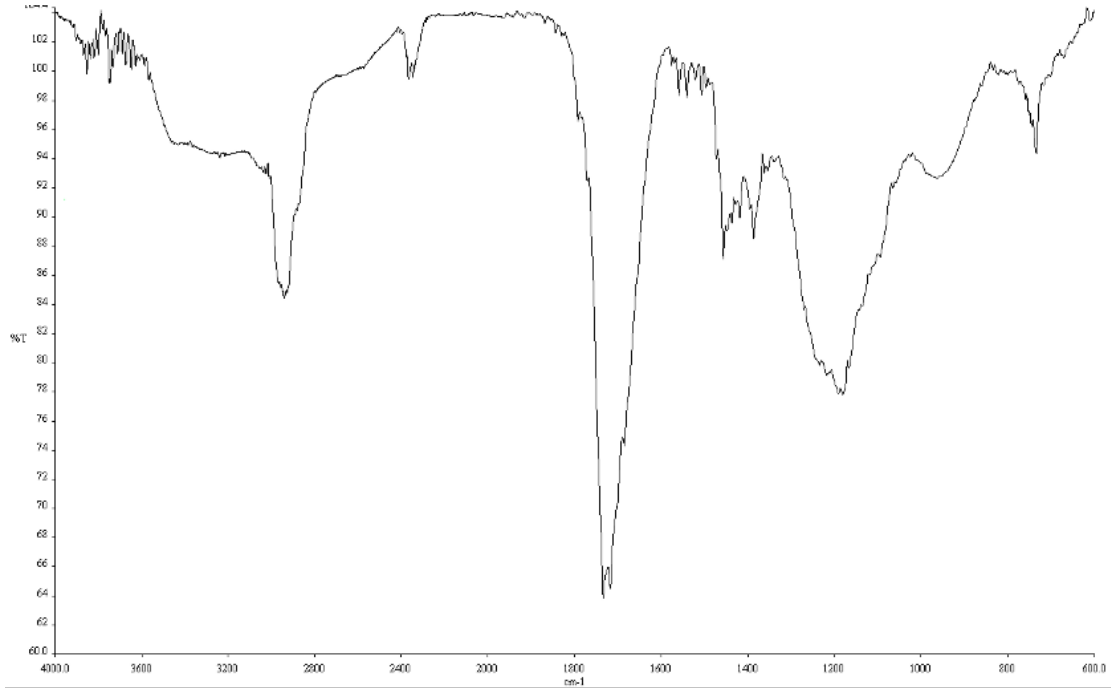


Figure A1.224. *Infrared spectrum (Thin Film, NaCl) of compound* ***70****.*

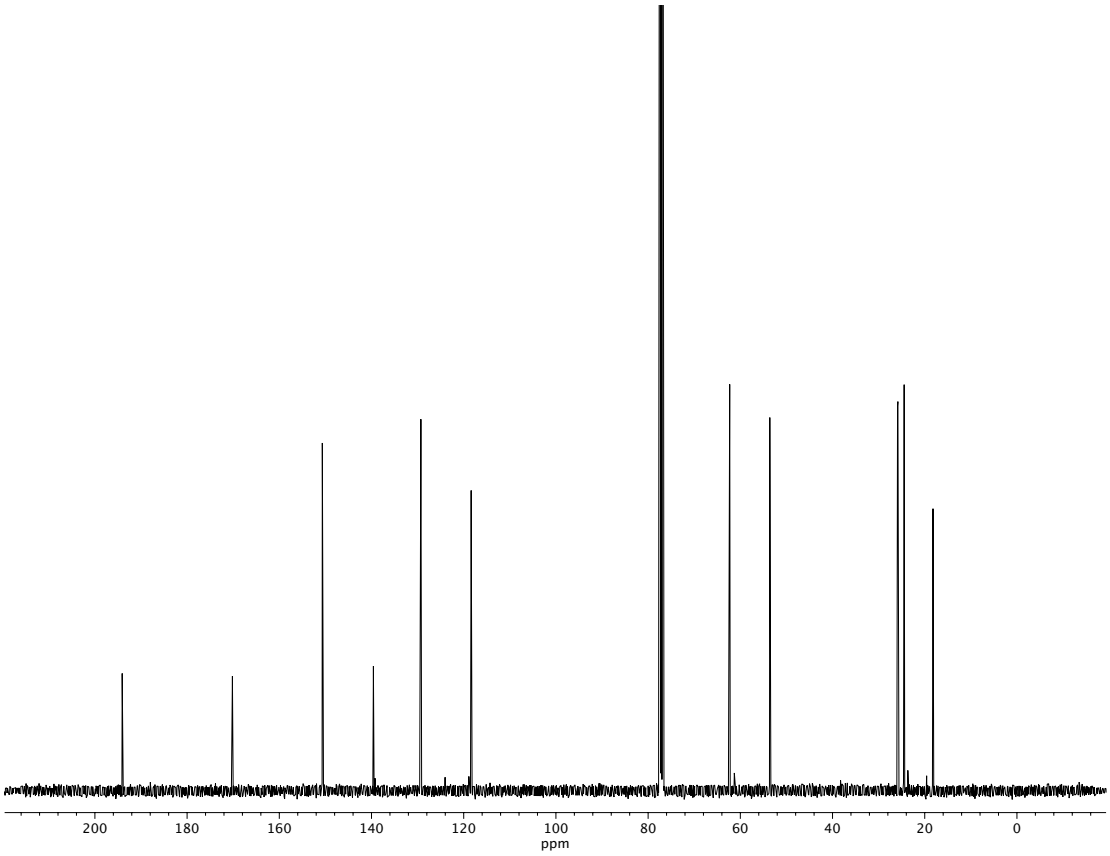


Figure A1.225. *^{13}C NMR (100 MHz, $CDCl_3$) of compound* ***70****.*

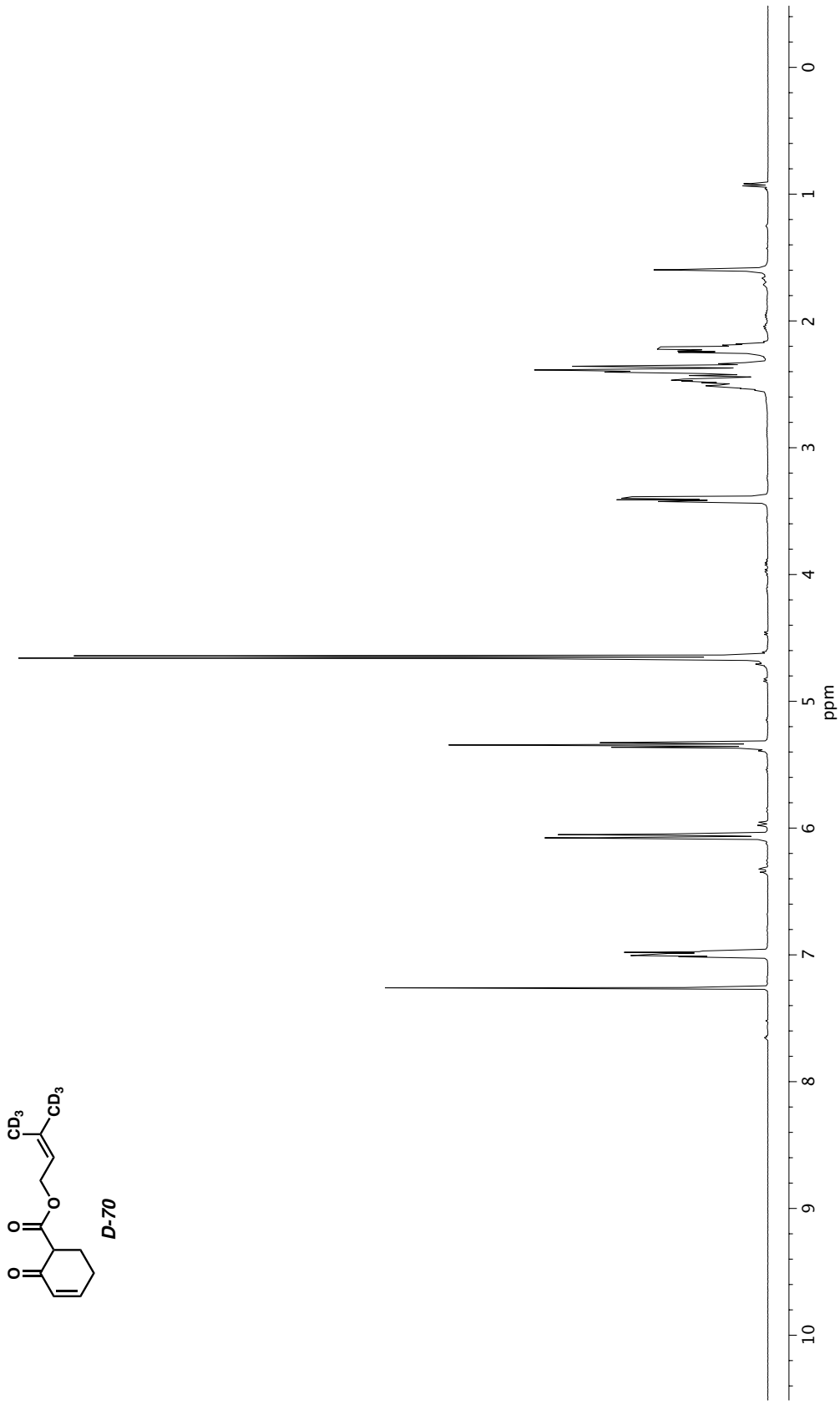


Figure A1.226. *^1H NMR (400 MHz, $CDCl_3$) of compound* ***D-70****.*

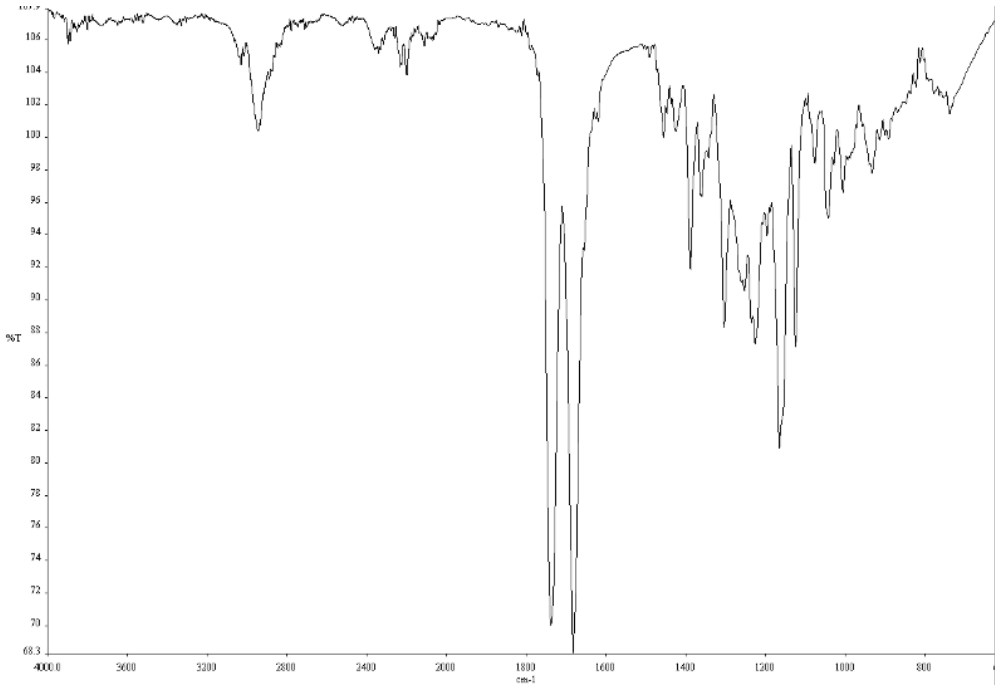


Figure A1.227. *Infrared spectrum (Thin Film, NaCl) of compound* ***D-70****.*

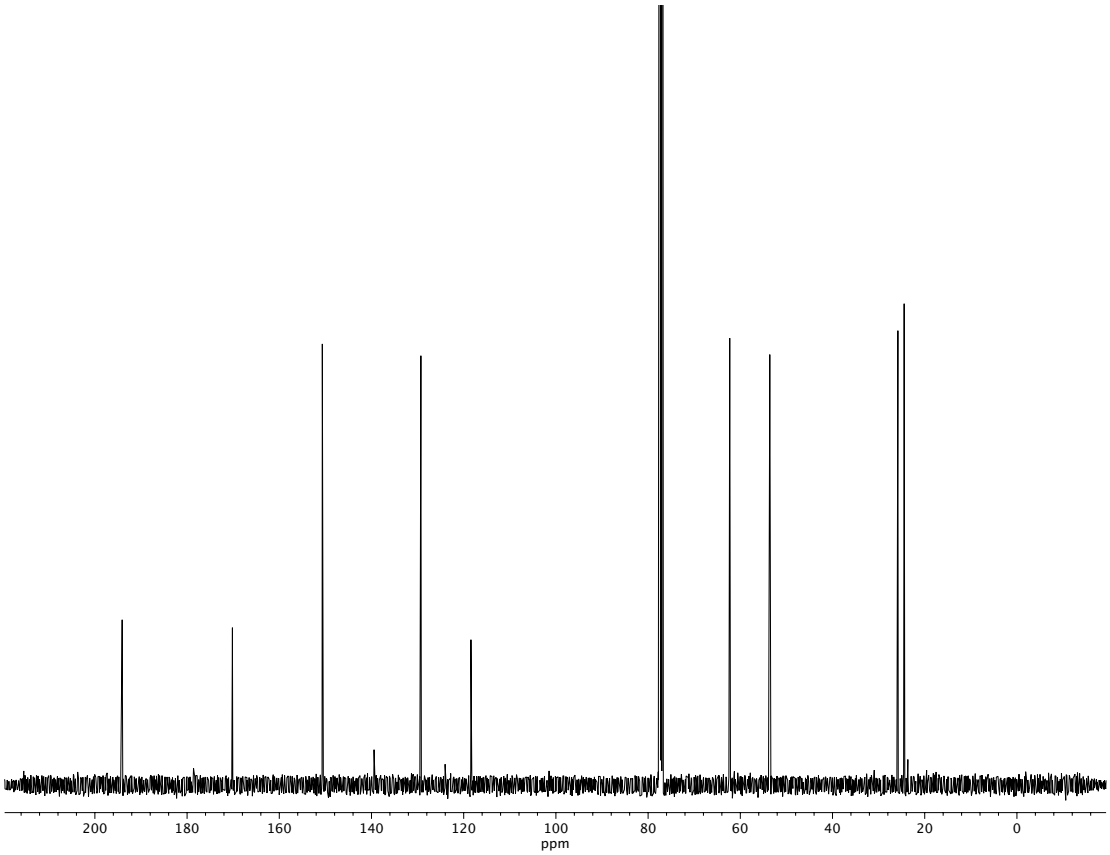


Figure A1.228. *^{13}C NMR (100 MHz, $CDCl_3$) of compound* ***D-70****.*

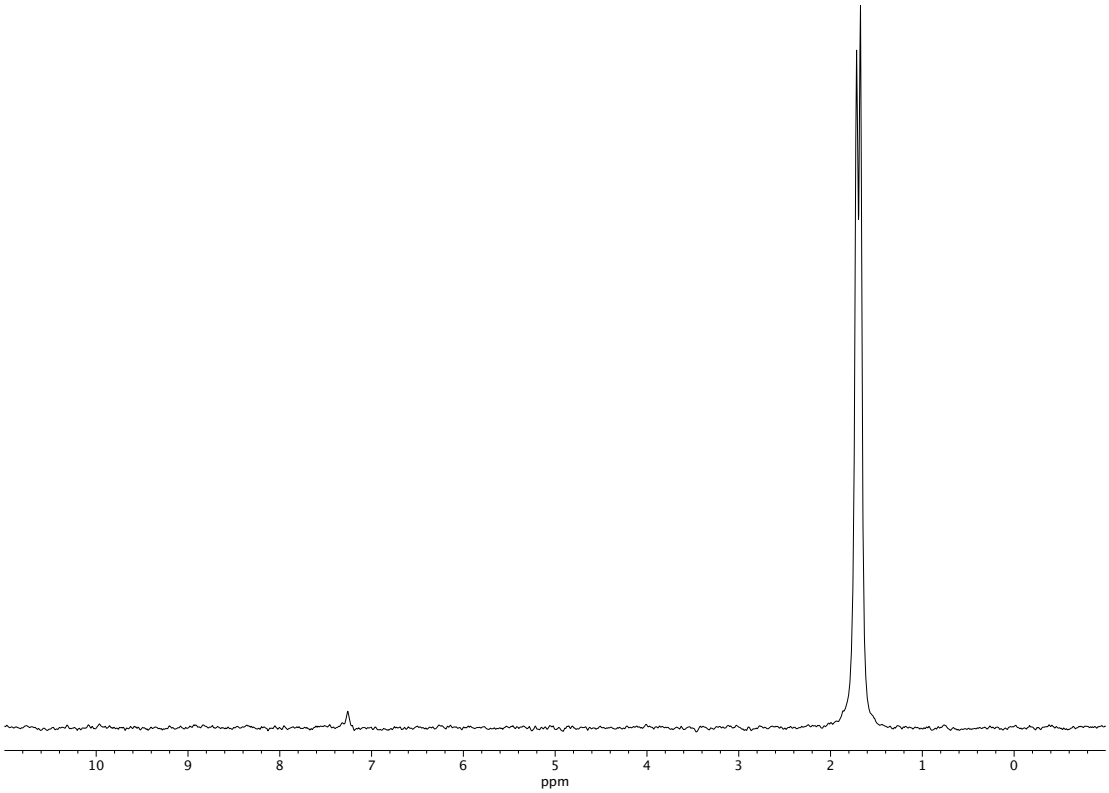


Figure A1.229. *^{2}H NMR (61 MHz, $CHCl_3$) of compound* ***D-70****.*

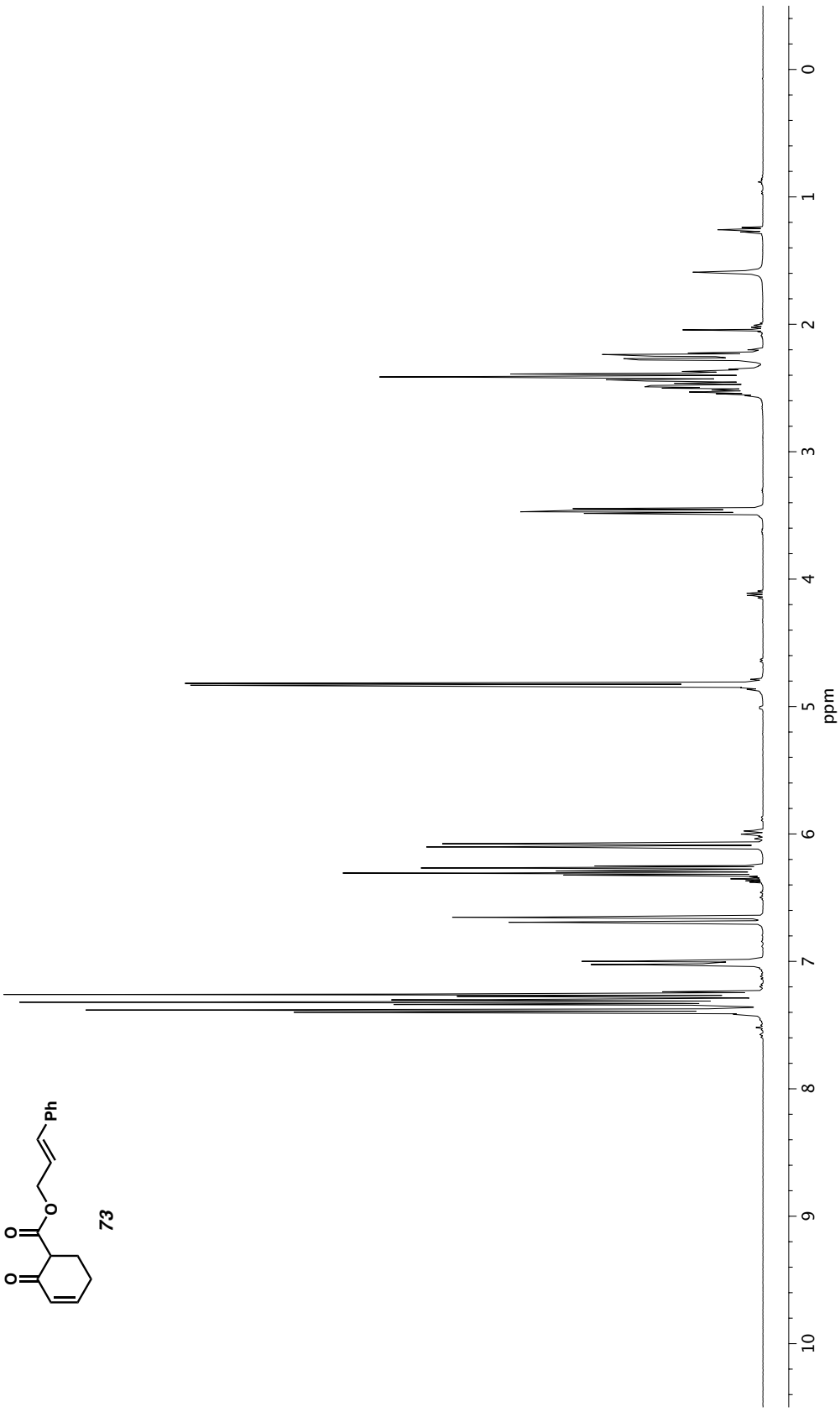


Figure A1.230. *^1H NMR (400 MHz, $CDCl_3$) of compound* ***73****.*

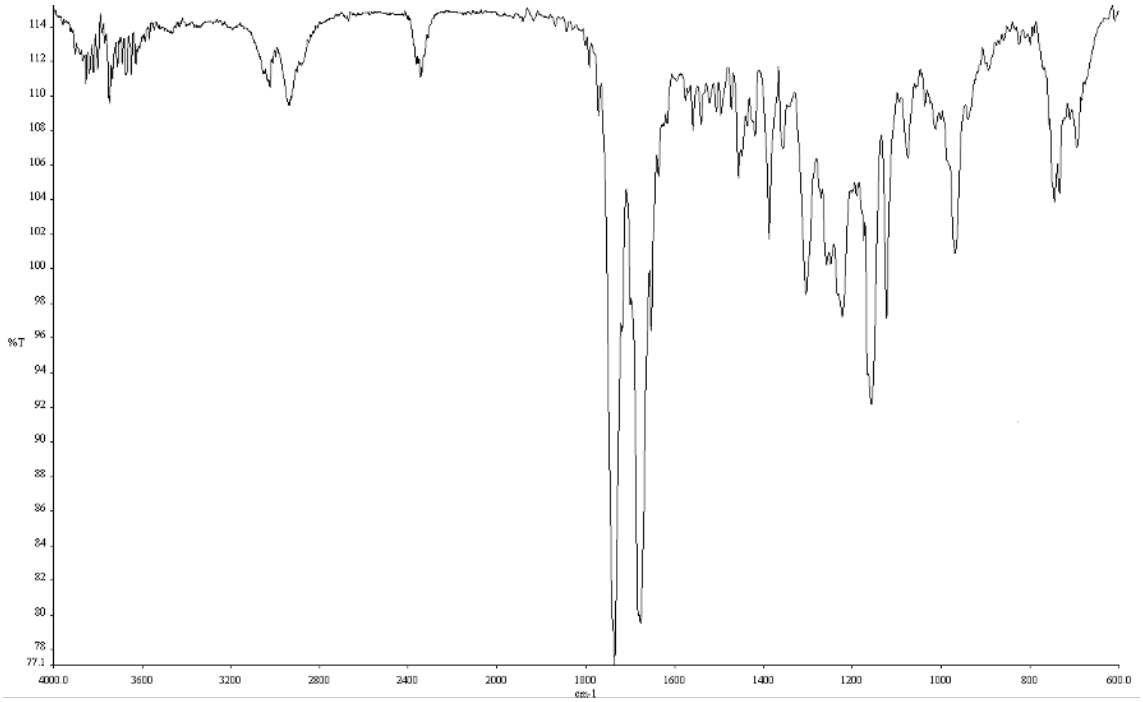


Figure A1.231. *Infrared spectrum (Thin Film, NaCl) of compound* ***73****.*

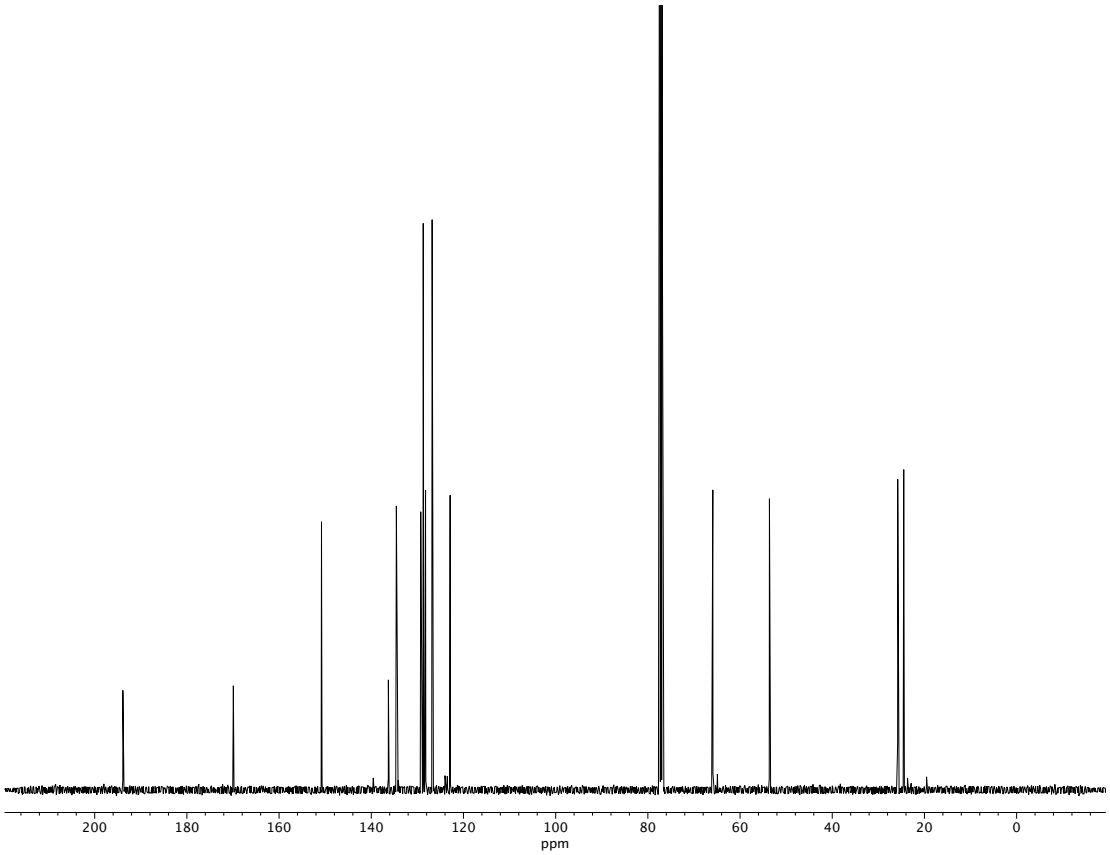


Figure A1.232. *^{13}C NMR (100 MHz, $CDCl_3$) of compound* ***73****.*

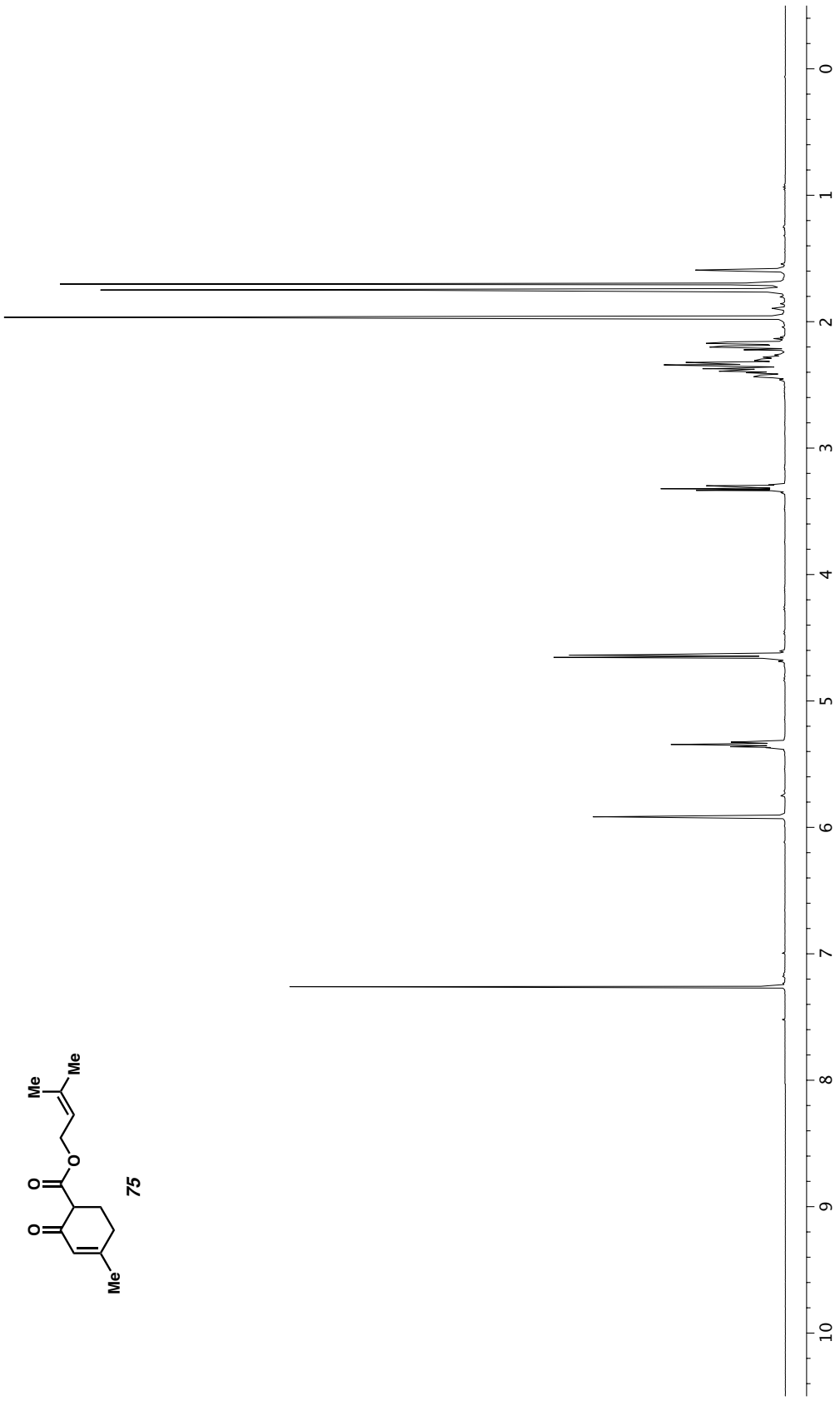


Figure A1.233. *^1H NMR (400 MHz, $CDCl_3$) of compound **75**.*

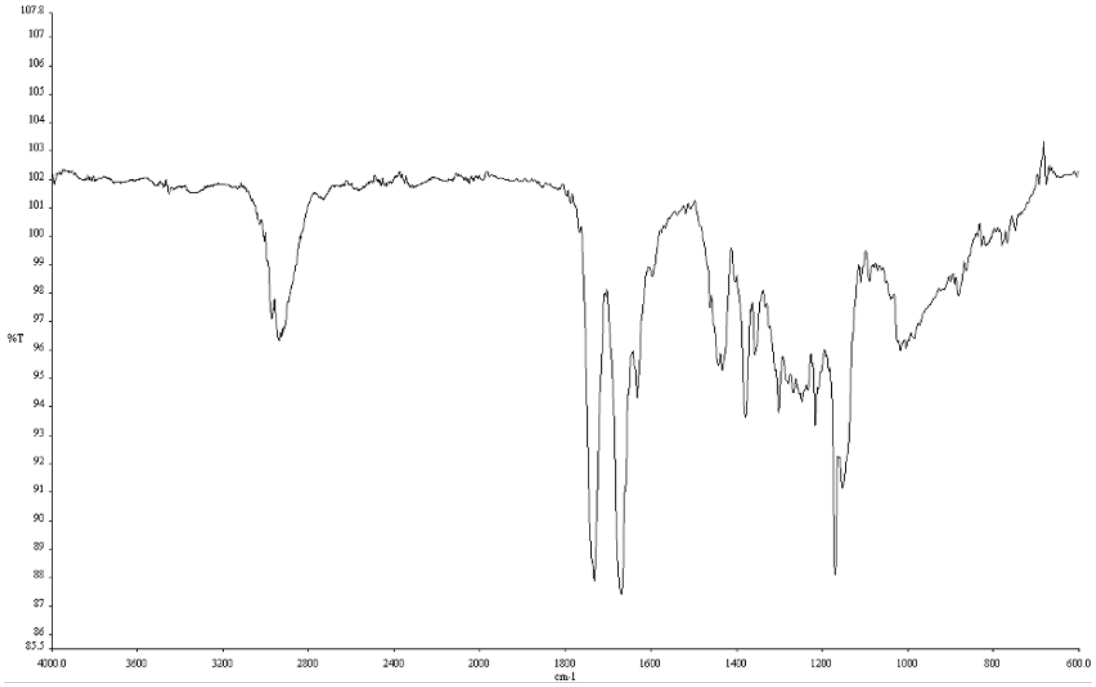


Figure A1.234. *Infrared spectrum (Thin Film, NaCl) of compound* ***75****.*

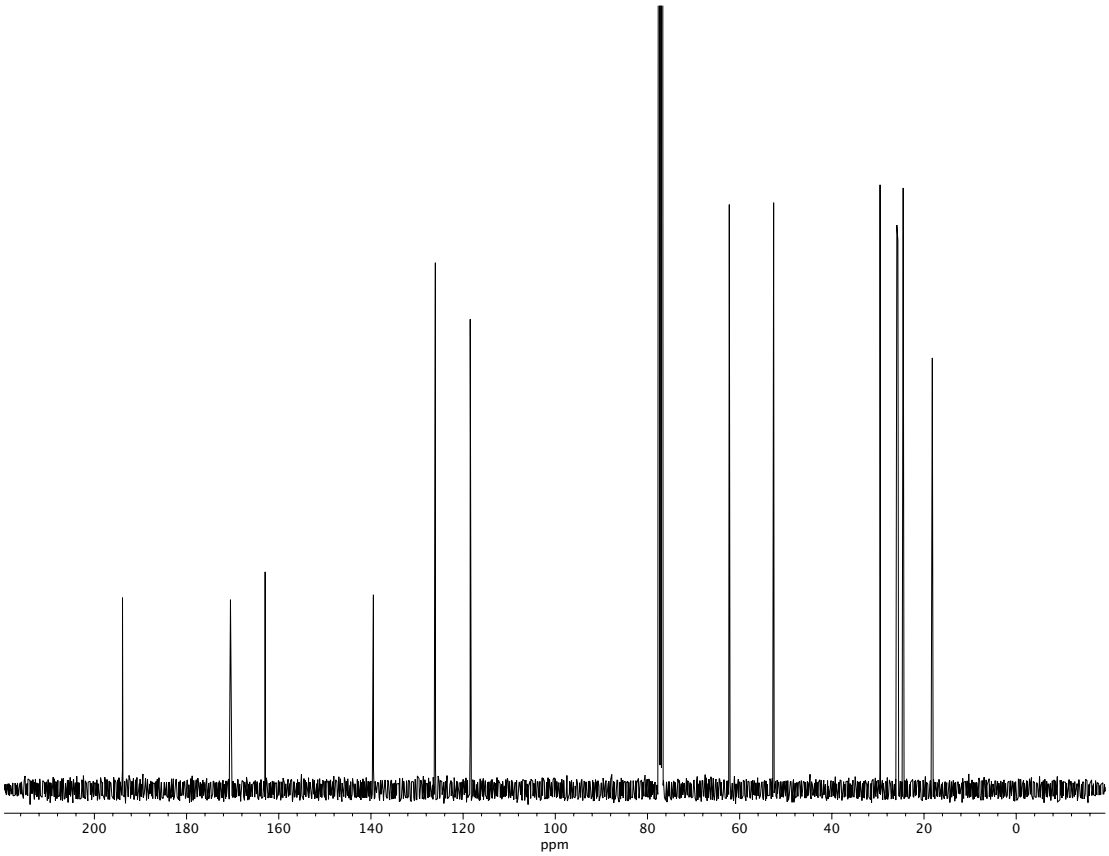


Figure A1.235. *^{13}C NMR (100 MHz, $CDCl_3$) of compound* ***75****.*

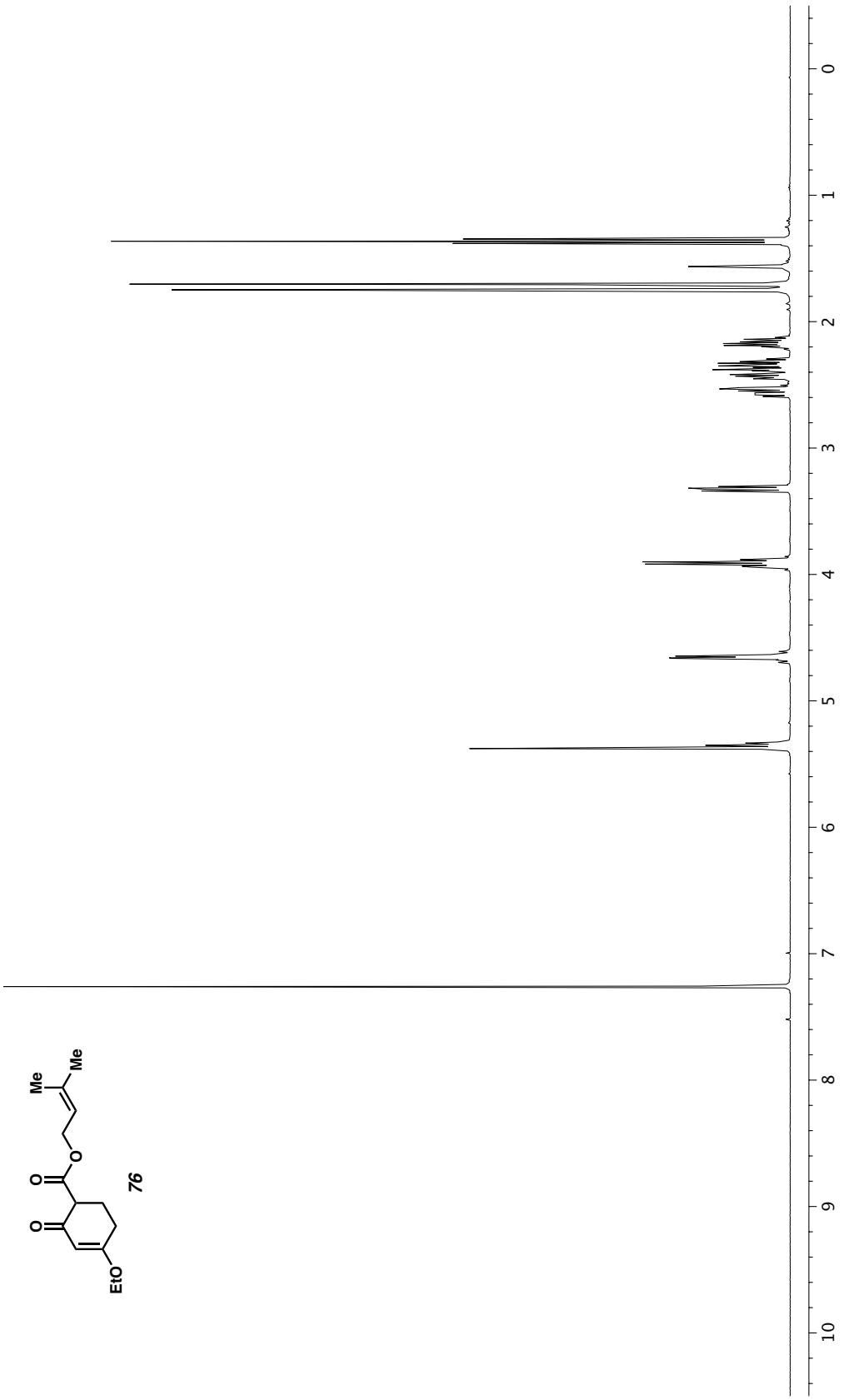


Figure A1.236. *^1H NMR (400 MHz, $CDCl_3$) of compound **76**.*

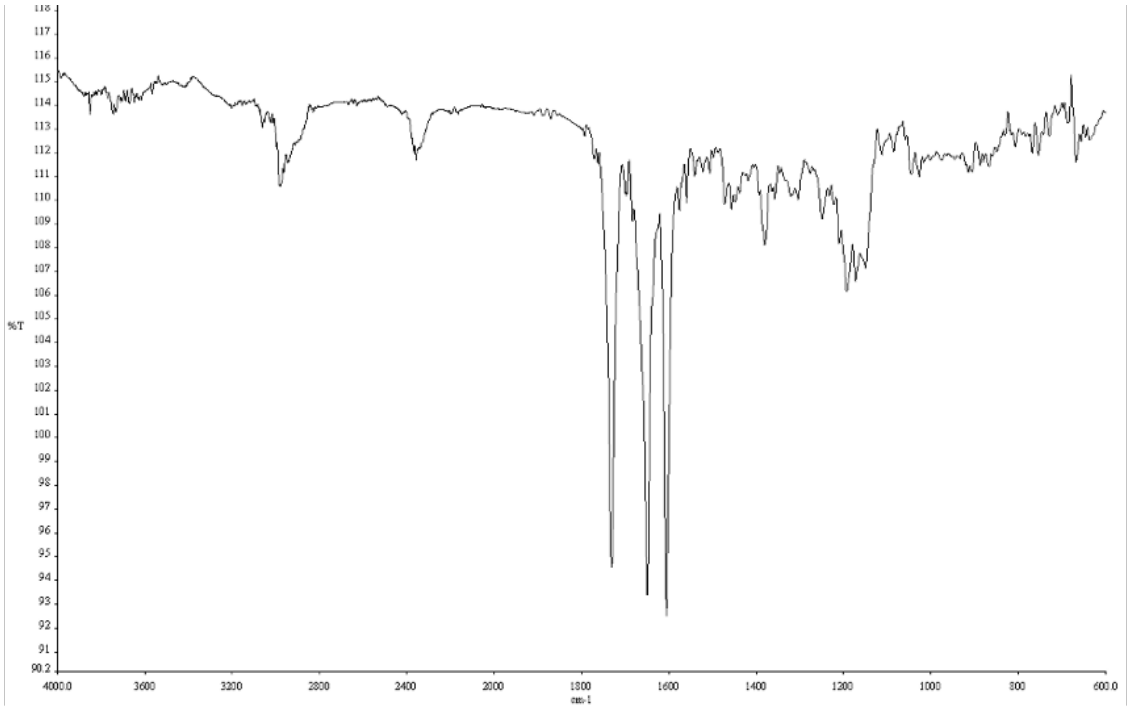


Figure A1.237. *Infrared spectrum (Thin Film, NaCl) of compound* ***76****.*

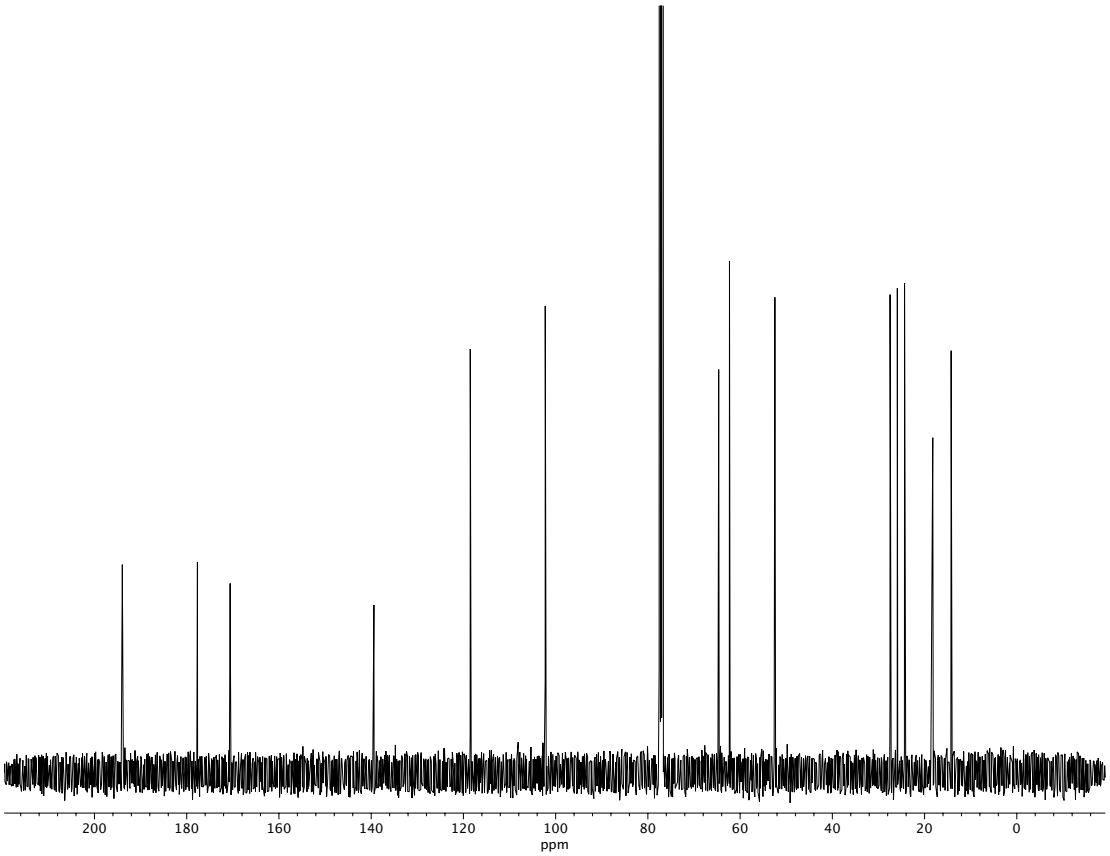


Figure A1.238. *^{13}C NMR (100 MHz, $CDCl_3$) of compound* ***76****.*

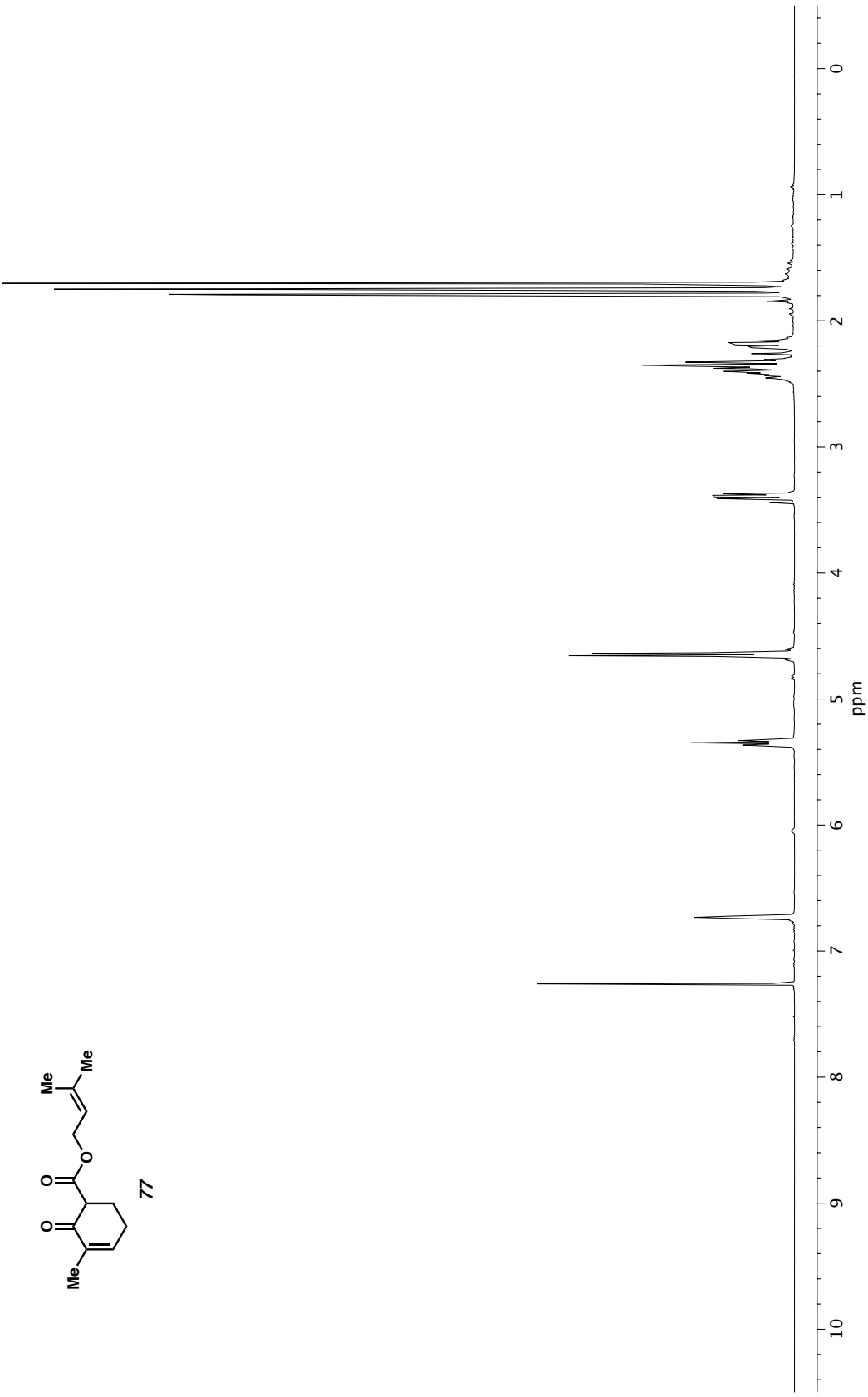


Figure A1.239. *^1H NMR (400 MHz, $CDCl_3$) of compound **77**.*

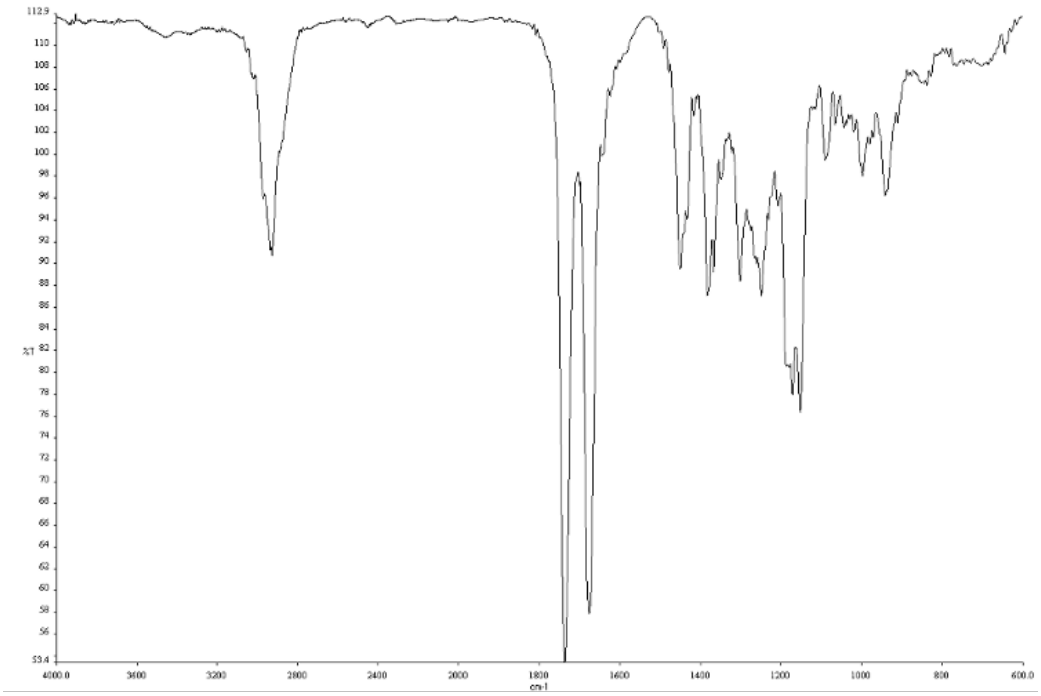


Figure A1.240. *Infrared spectrum (Thin Film, NaCl) of compound* ***77****.*

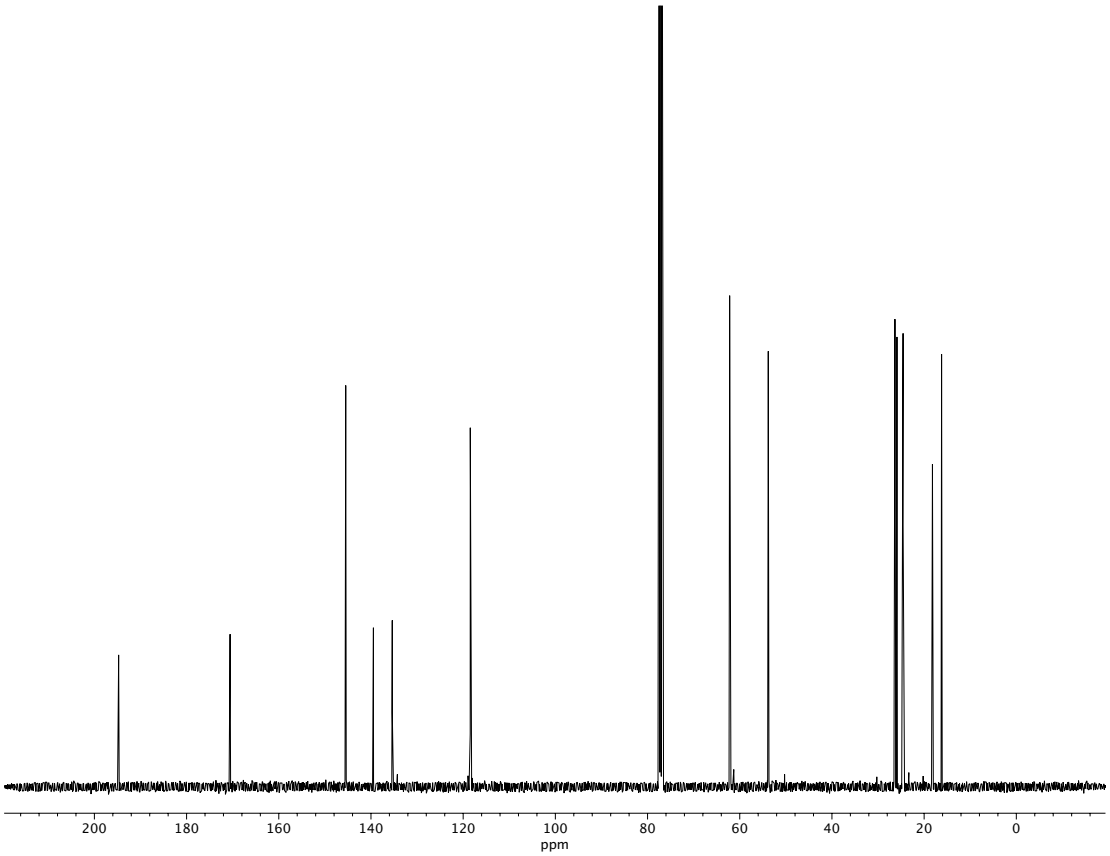


Figure A1.241. *^{13}C NMR (100 MHz, $CDCl_3$) of compound* ***77****.*

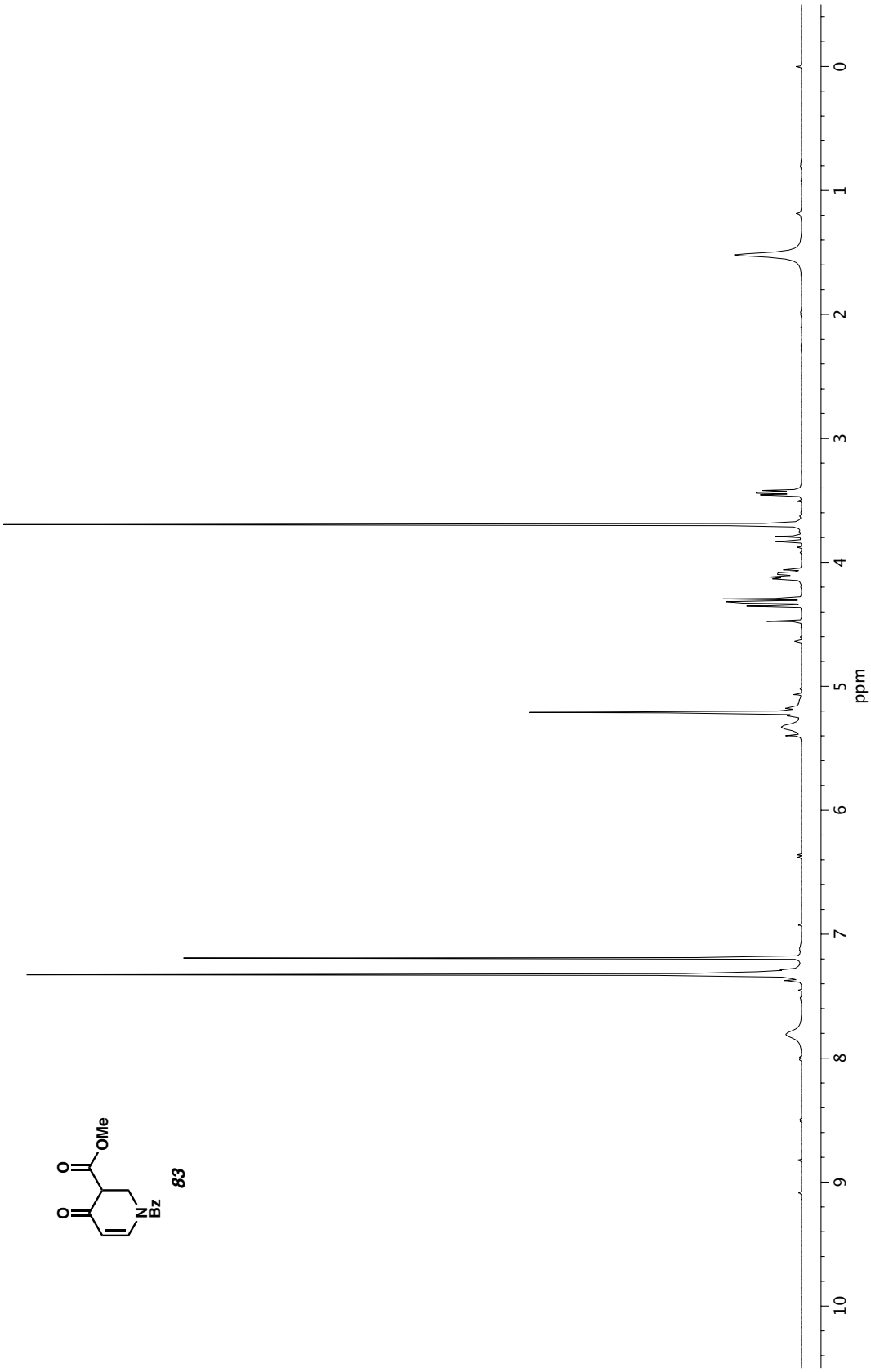


Figure A1.242. *^1H NMR (400 MHz, $CDCl_3$) of compound* ***83****.*

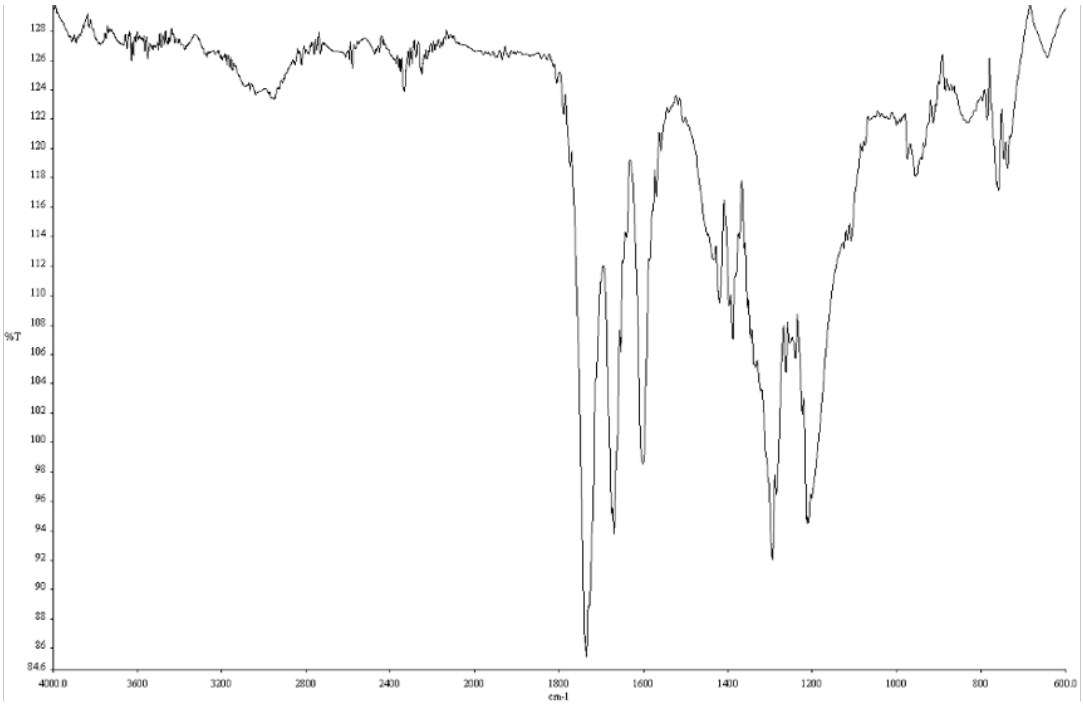


Figure A1.243. *Infrared spectrum (Thin Film, NaCl) of compound* ***83****.*

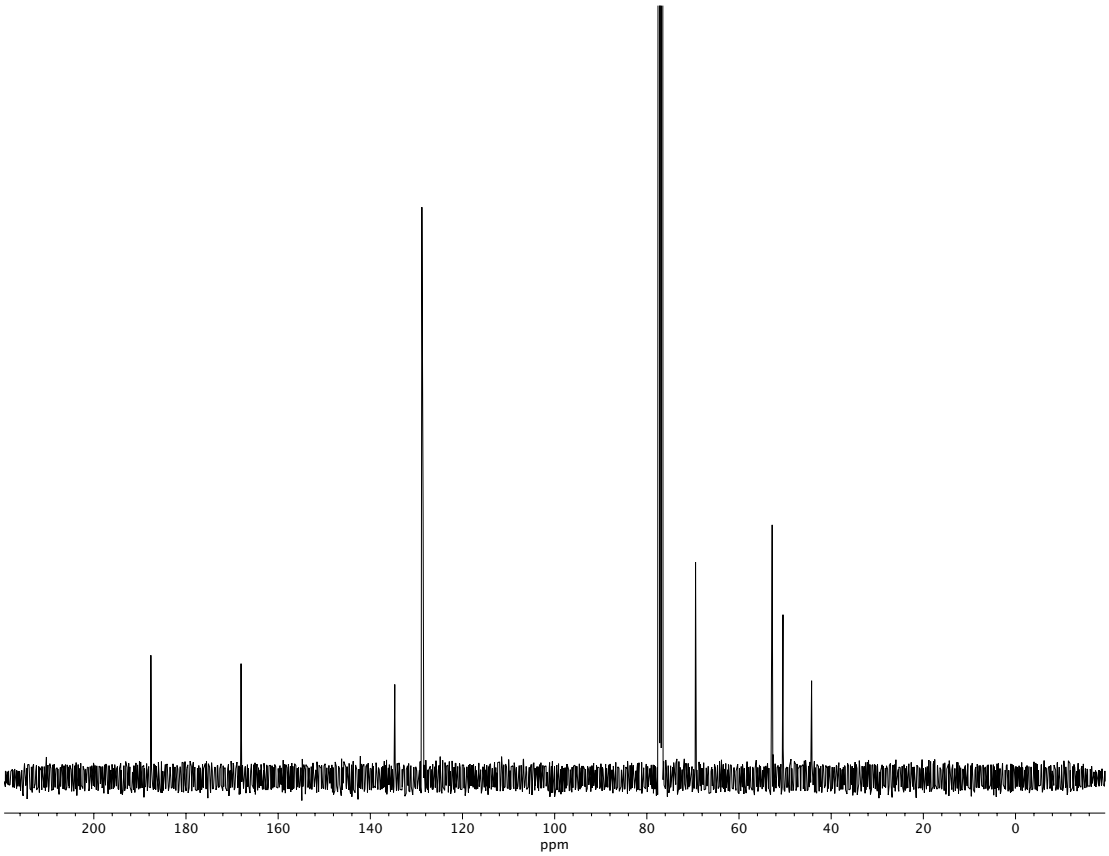


Figure A1.244. *^{13}C NMR (100 MHz, $CDCl_3$) of compound* ***83****.*

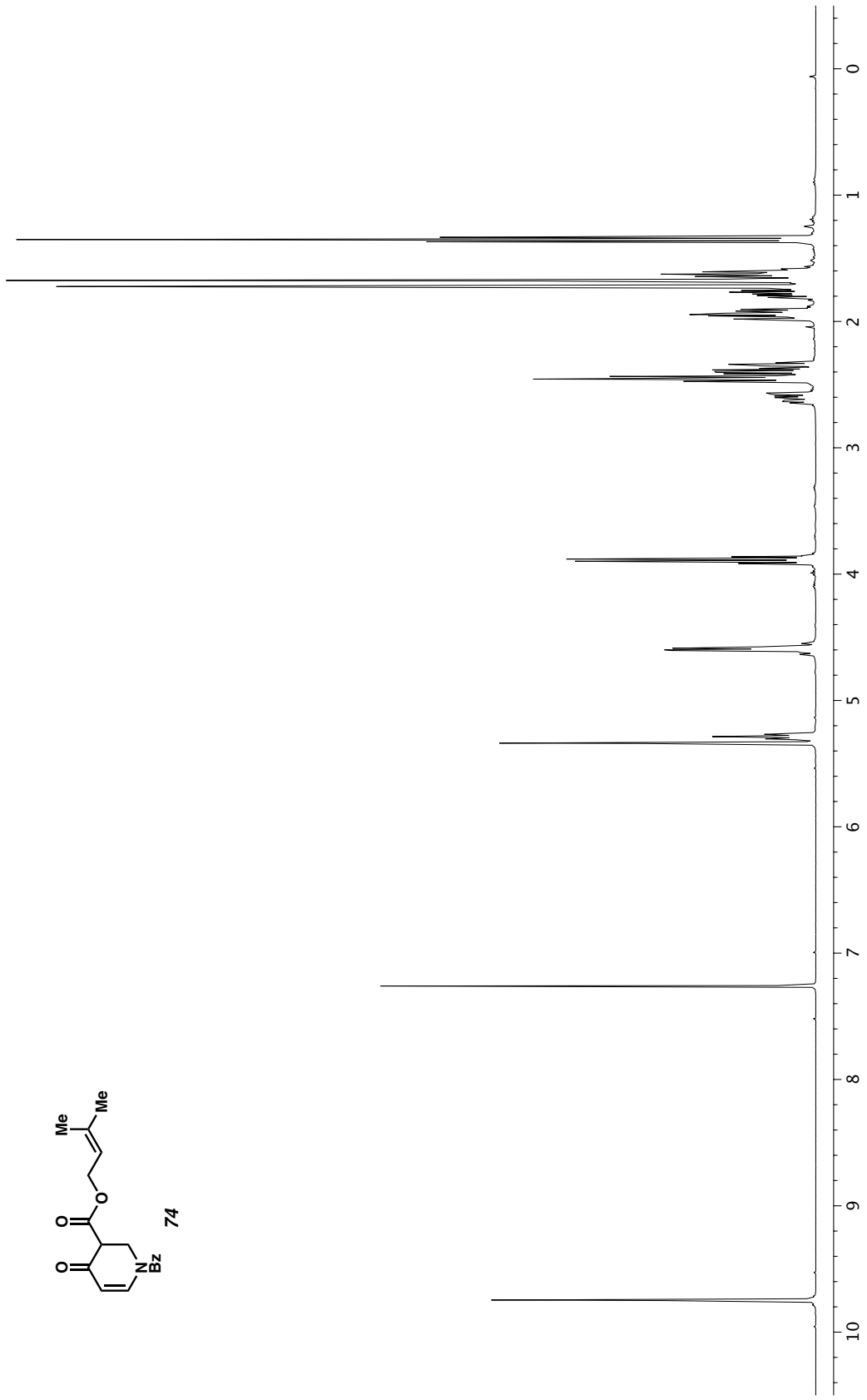


Figure A1.245. *^1H NMR (400 MHz, $CDCl_3$) of compound **74**.*

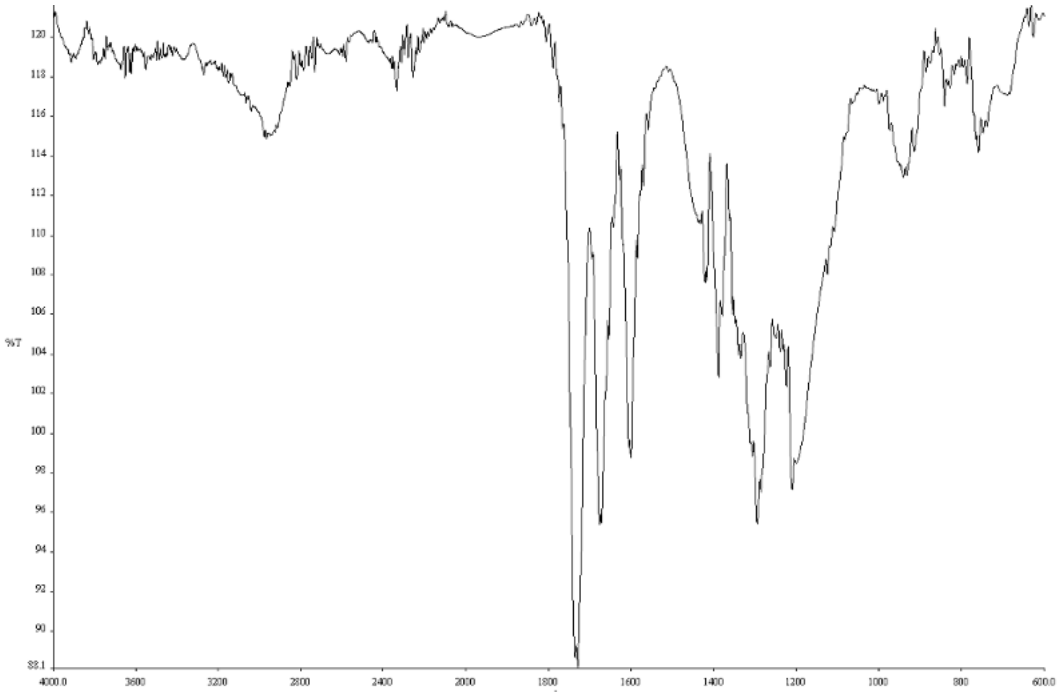


Figure A1.246. *Infrared spectrum (Thin Film, NaCl) of compound* ***74****.*

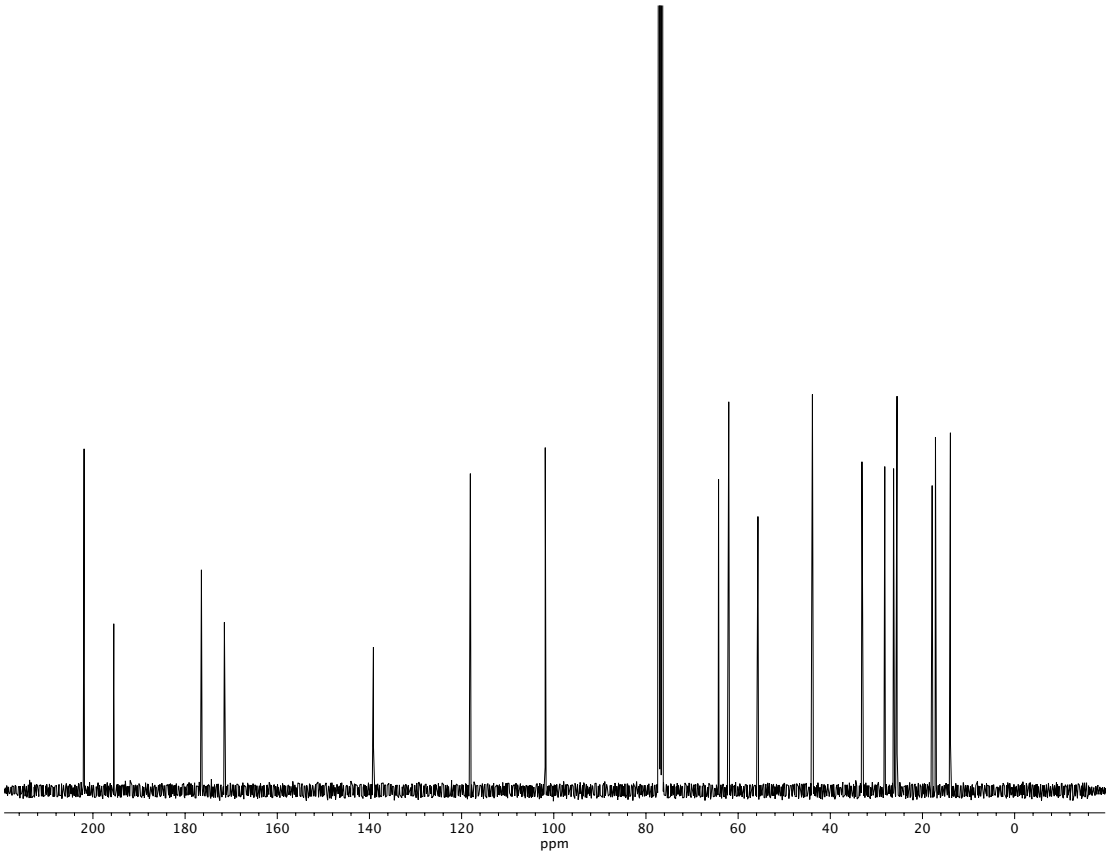


Figure A1.247. *^{13}C NMR (100 MHz, $CDCl_3$) of compound* ***74****.*

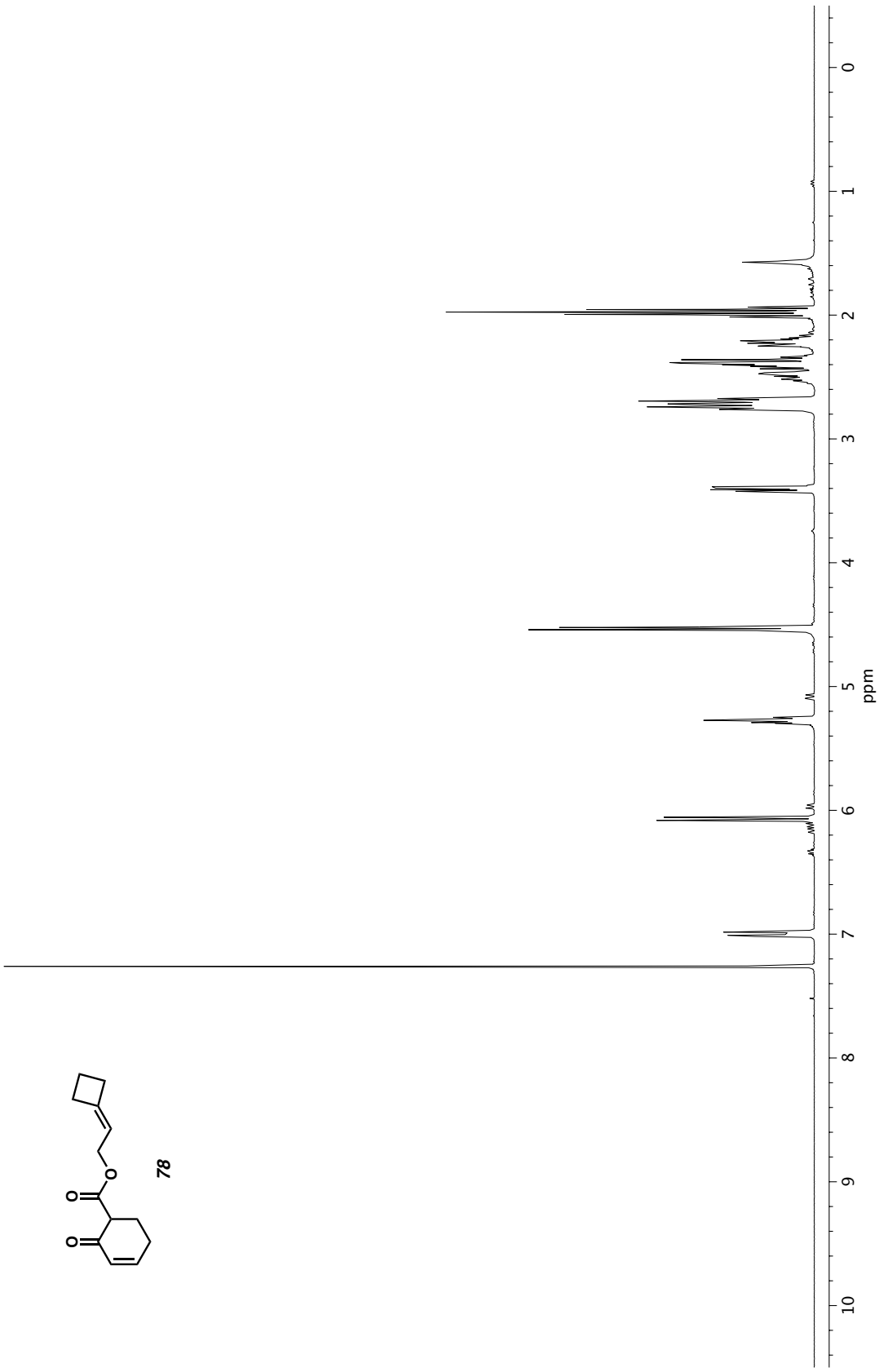


Figure A1.248. *^1H NMR (400 MHz, $CDCl_3$) of compound **78**.*

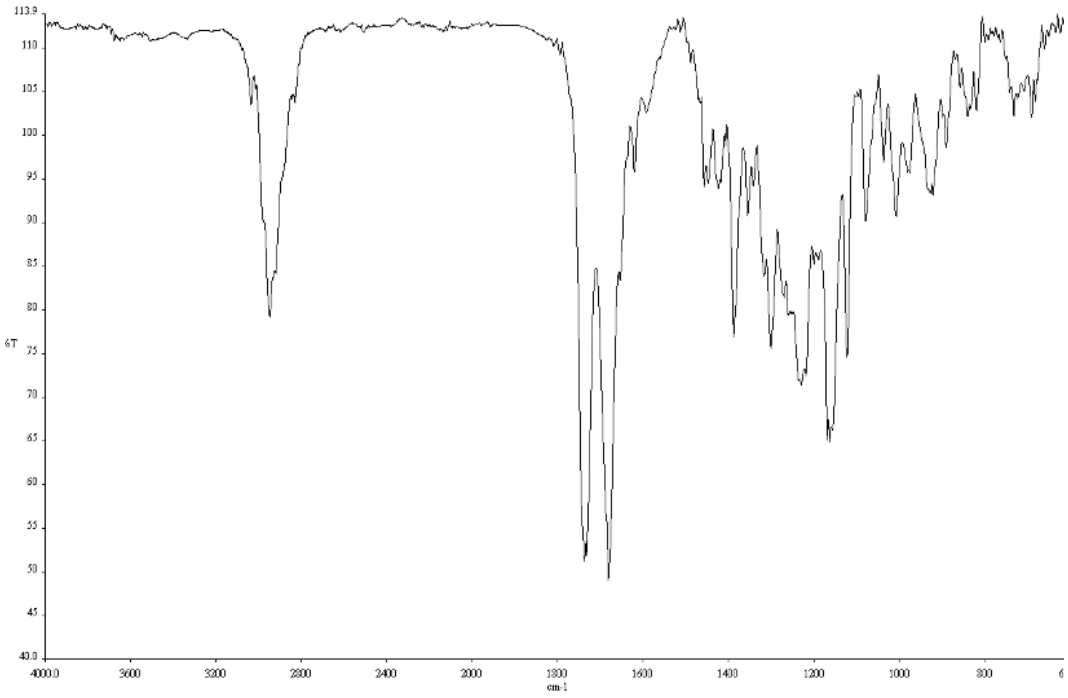


Figure A1.249. *Infrared spectrum (Thin Film, NaCl) of compound* ***78****.*

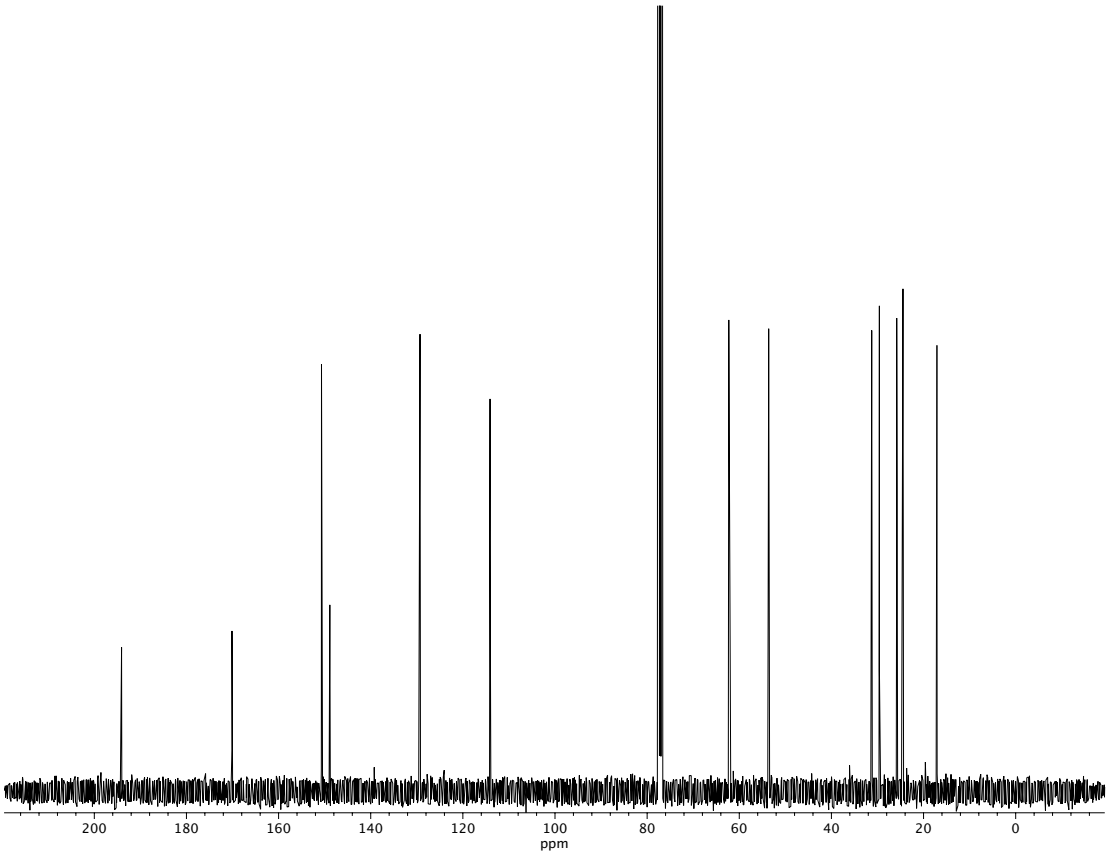
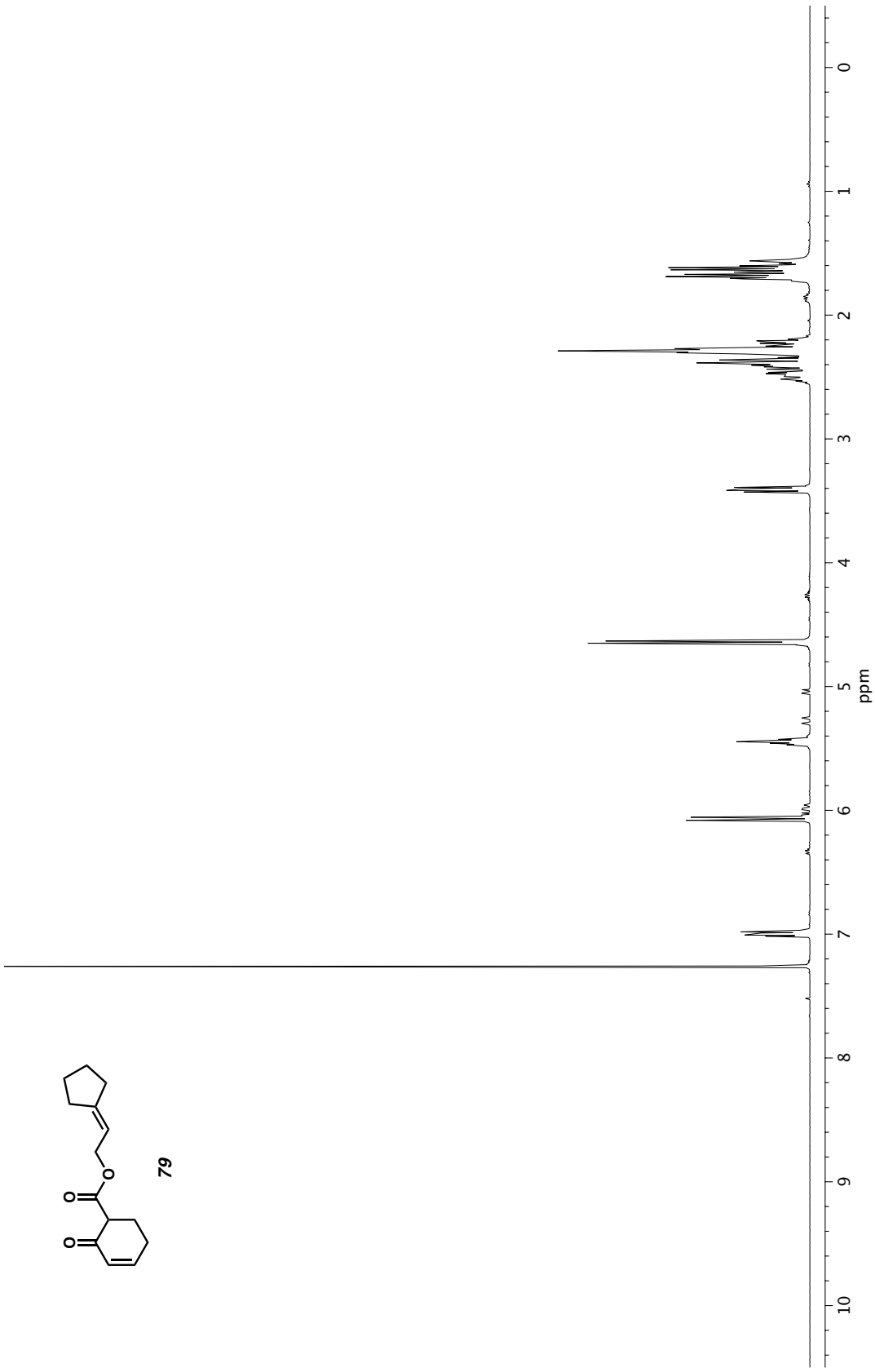


Figure A1.250. *^{13}C NMR (100 MHz, $CDCl_3$) of compound* ***78****.*



79

Figure A1.251. *^1H NMR (400 MHz, $CDCl_3$) of compound **79**.*

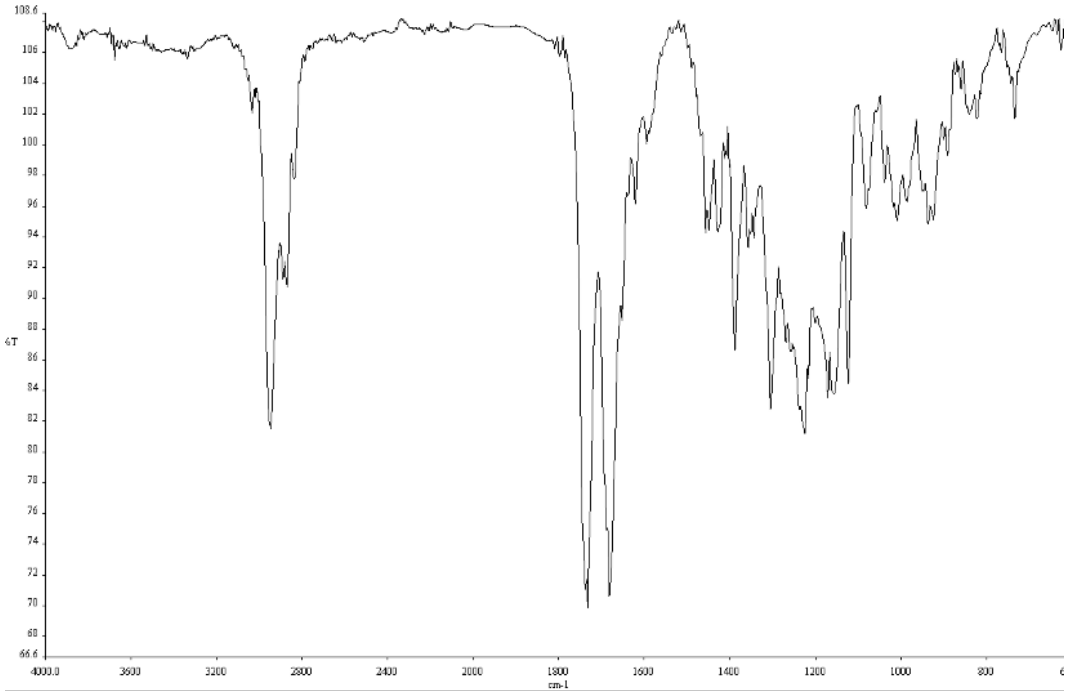


Figure A1.252. *Infrared spectrum (Thin Film, NaCl) of compound* ***79****.*

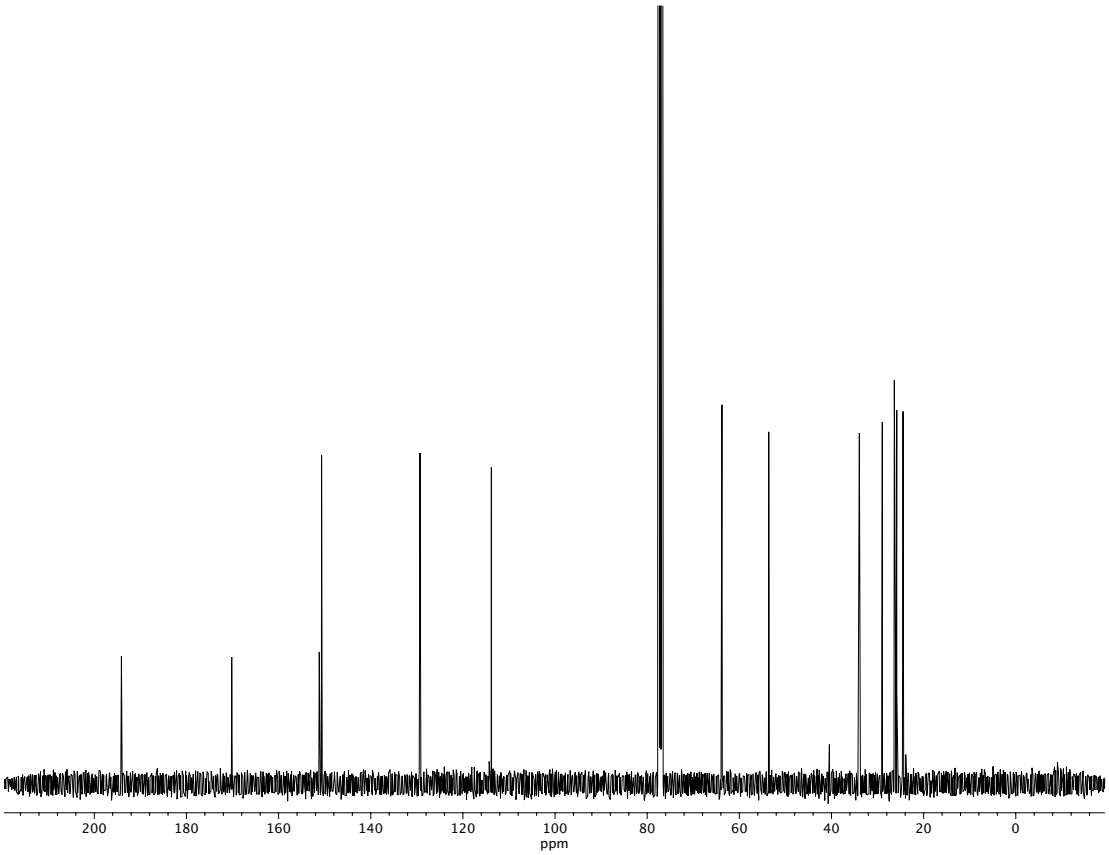


Figure A1.253. *^{13}C NMR (100 MHz, $CDCl_3$) of compound* ***79****.*

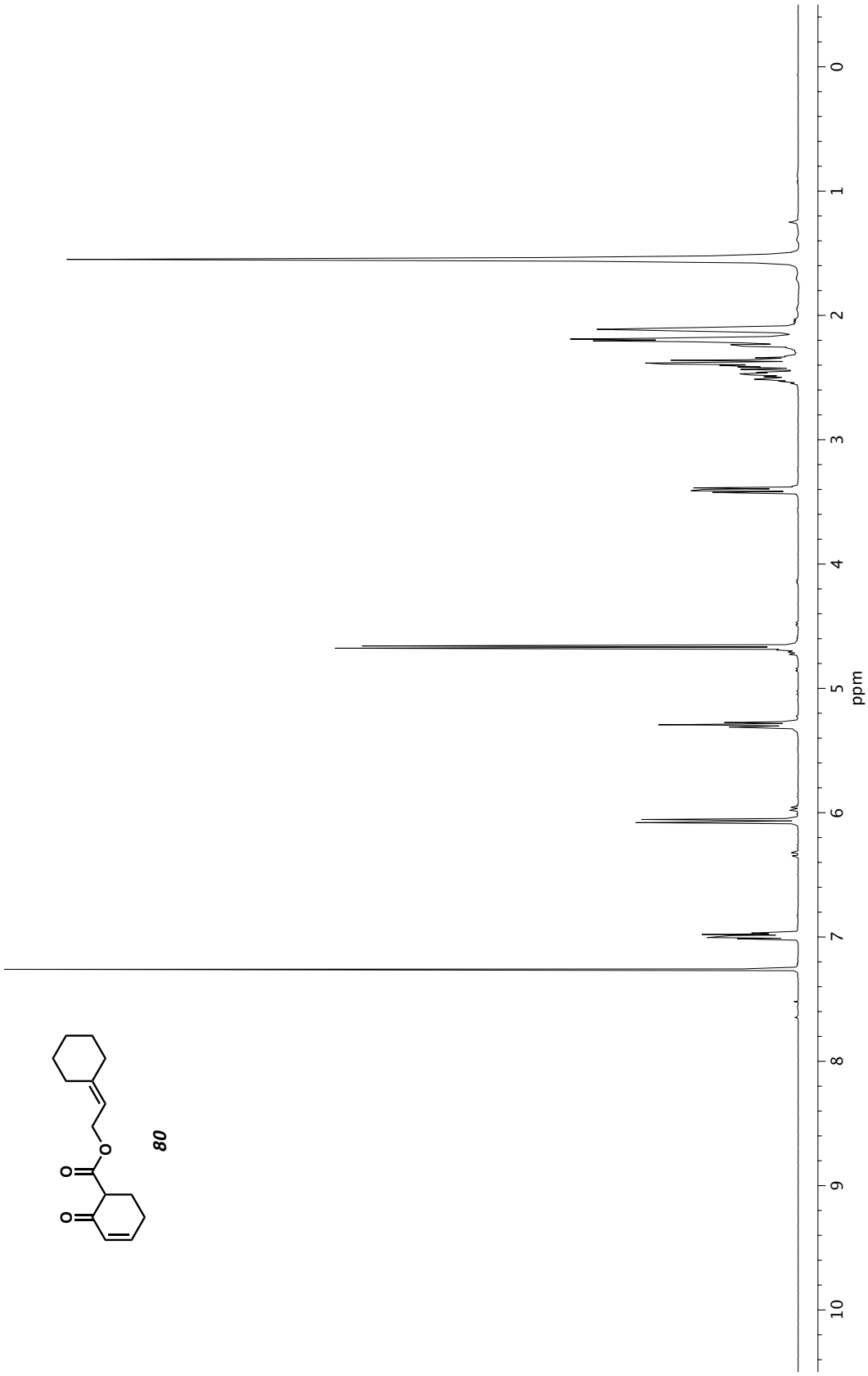


Figure A1.254. *^1H NMR (400 MHz, $CDCl_3$) of compound* ***80****.*

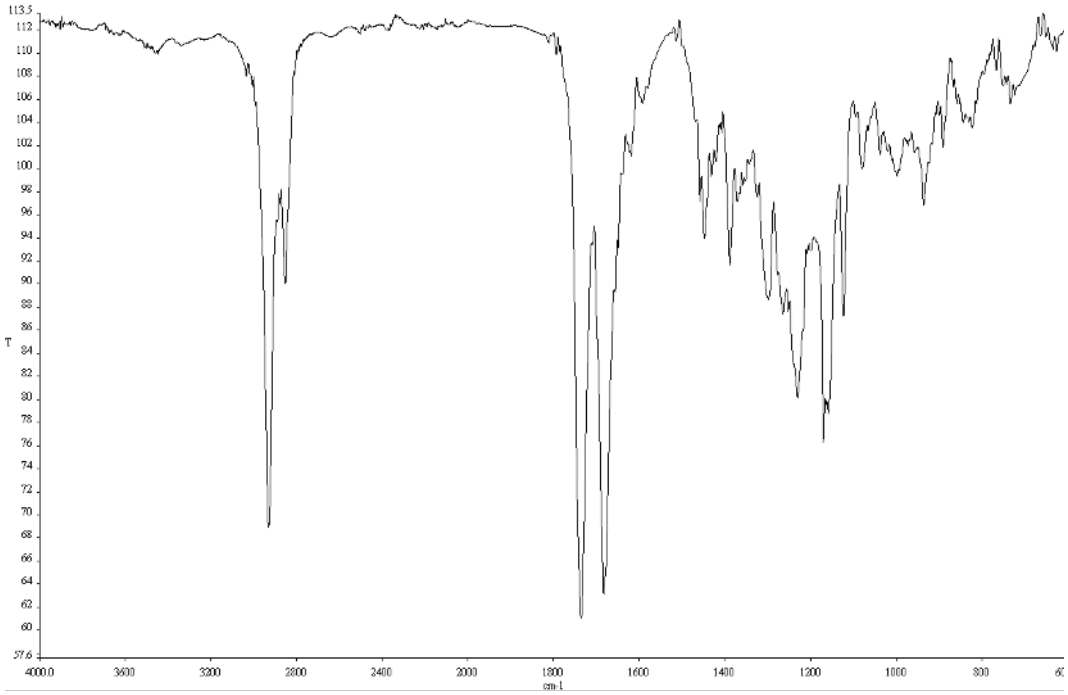


Figure A1.255. *Infrared spectrum (Thin Film, NaCl) of compound* ***80****.*

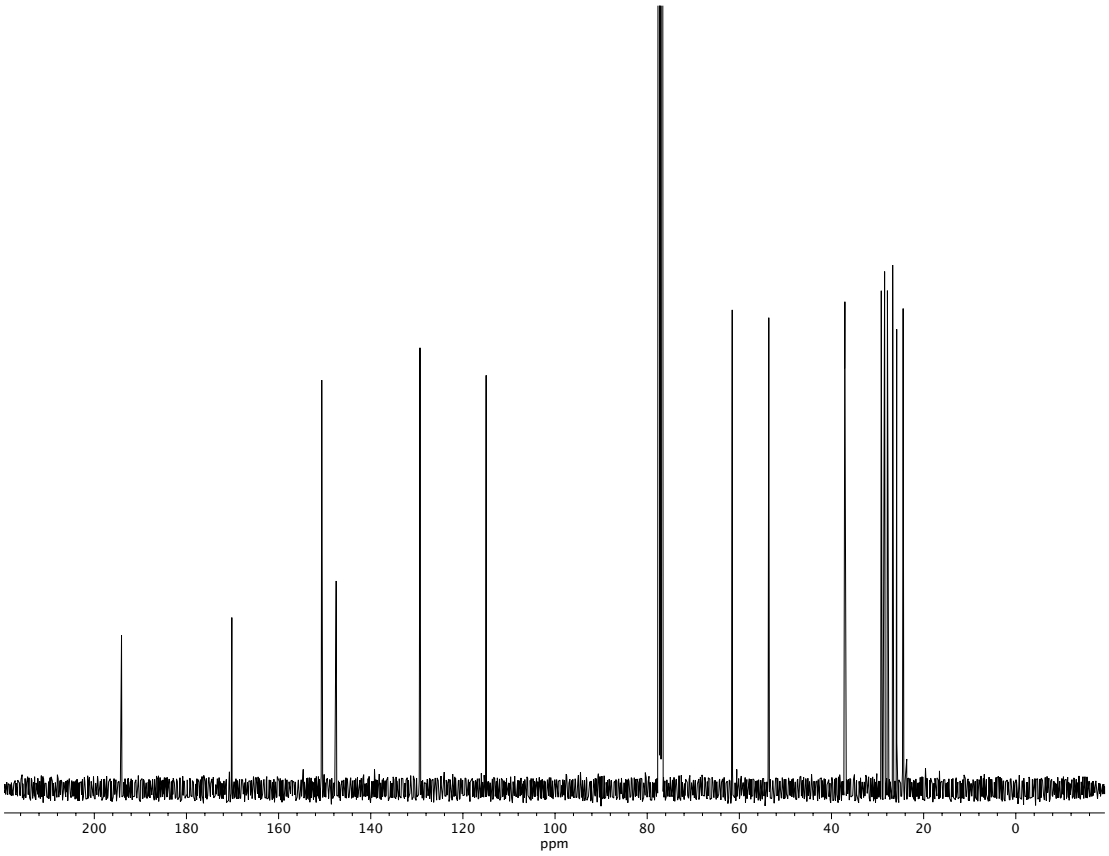


Figure A1.256. *^{13}C NMR (100 MHz, $CDCl_3$) of compound* ***80****.*

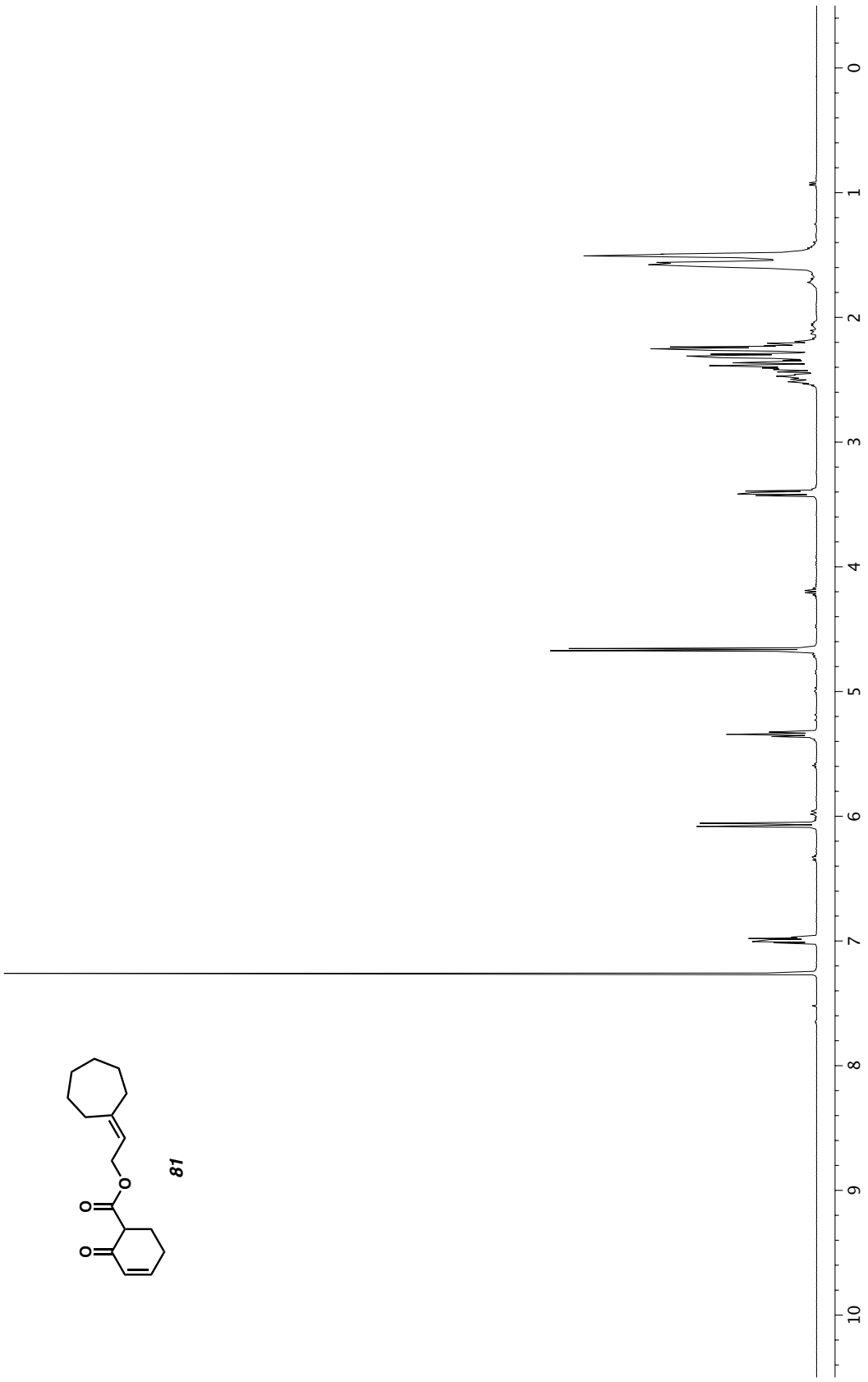


Figure A1.257. *^1H NMR (400 MHz, $CDCl_3$) of compound* ***81****.*

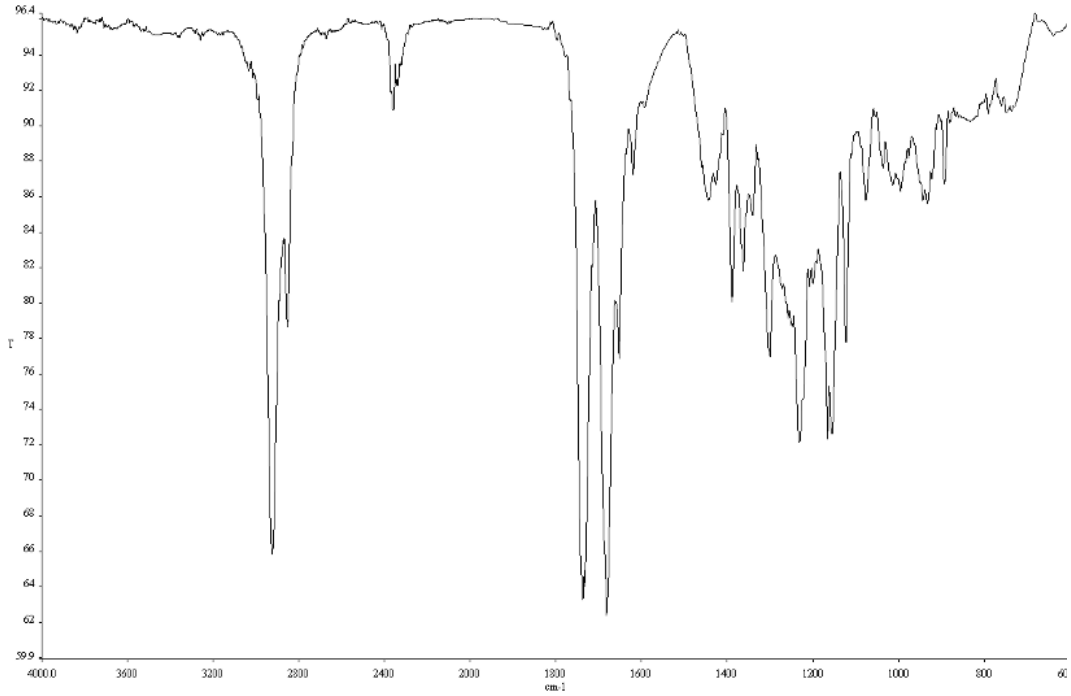


Figure A1.258. *Infrared spectrum (Thin Film, NaCl) of compound* ***81***.

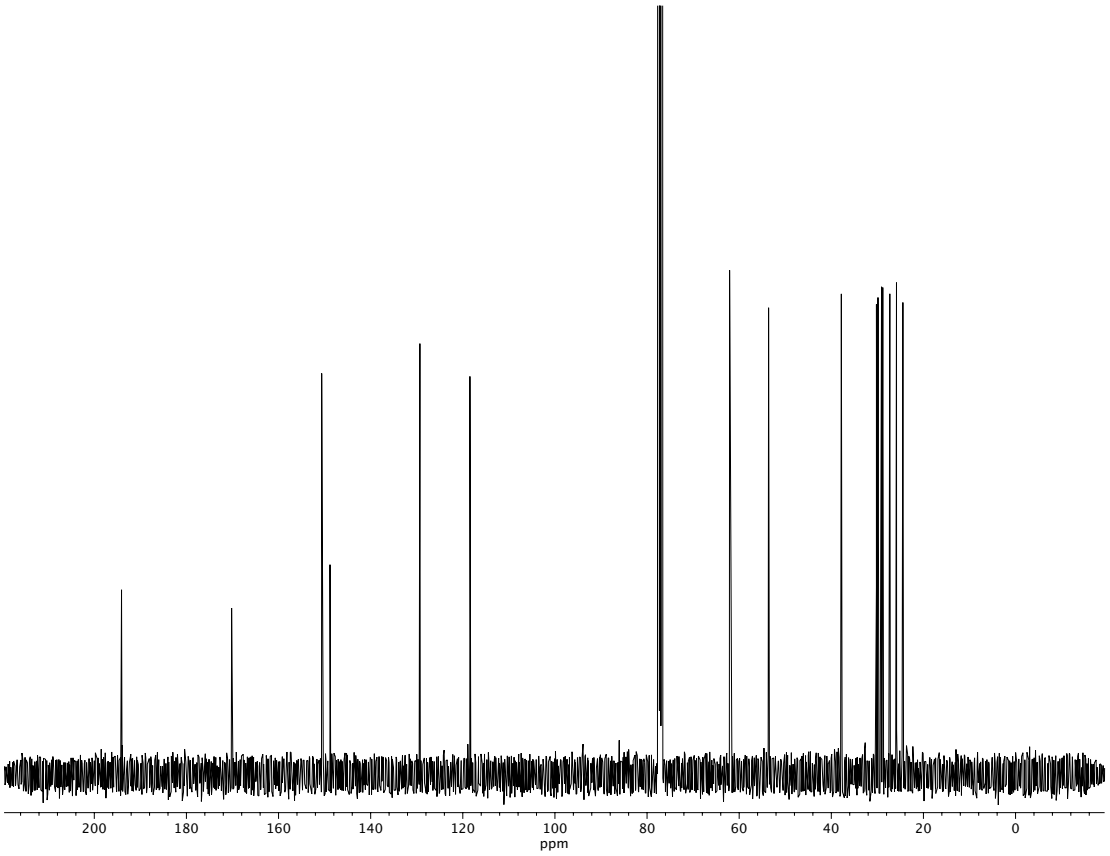


Figure A1.259. *^{13}C NMR (100 MHz, $CDCl_3$) of compound* ***81***.

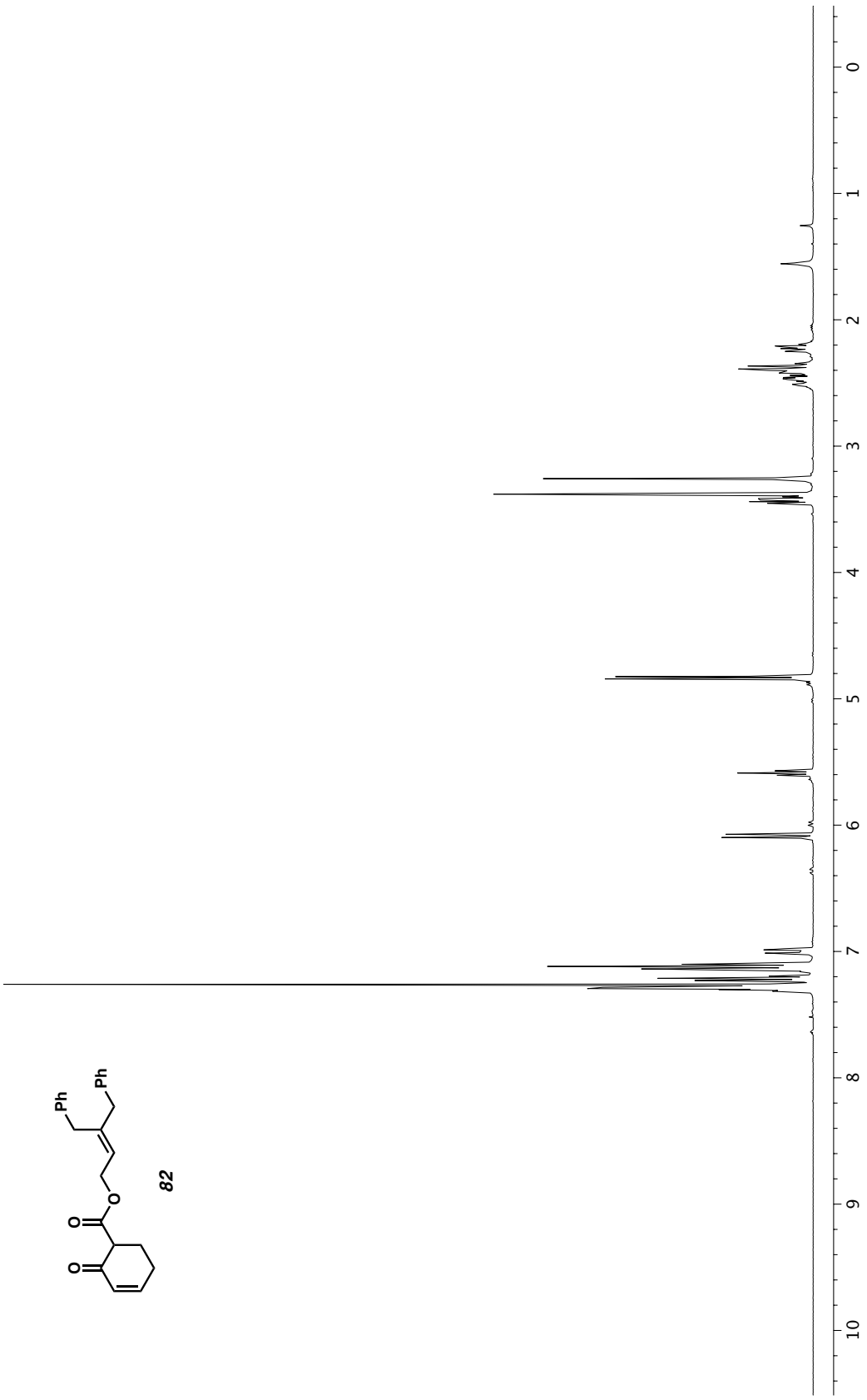


Figure A1.260. *^1H NMR (400 MHz, $CDCl_3$) of compound* ***82****.*

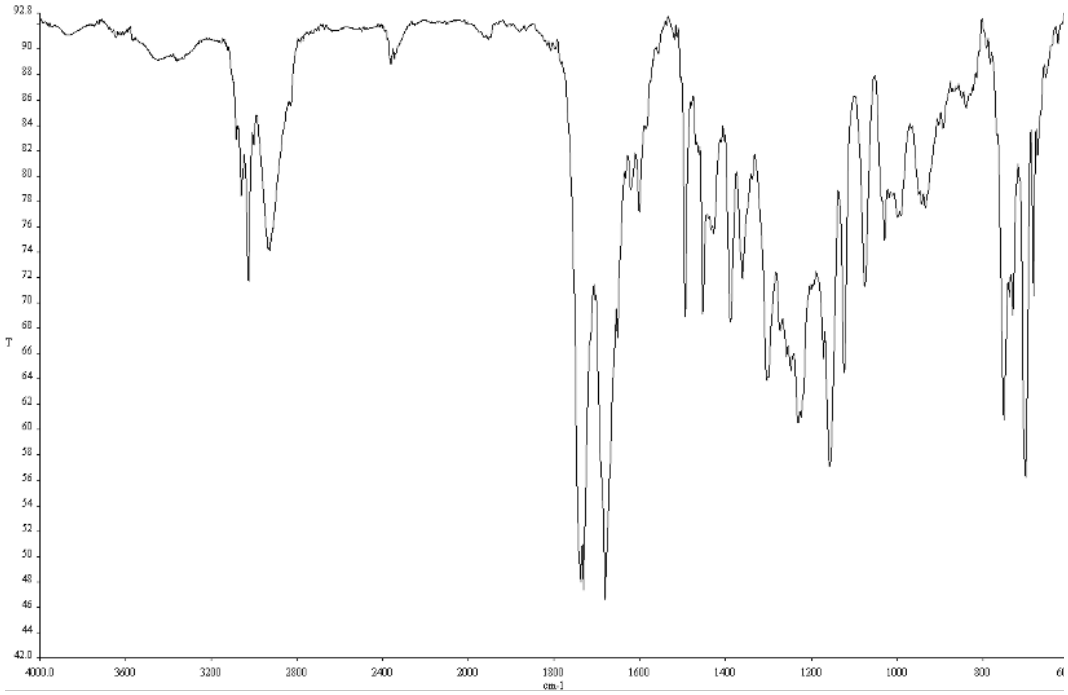


Figure A1.261. *Infrared spectrum (Thin Film, NaCl) of compound* ***82****.*

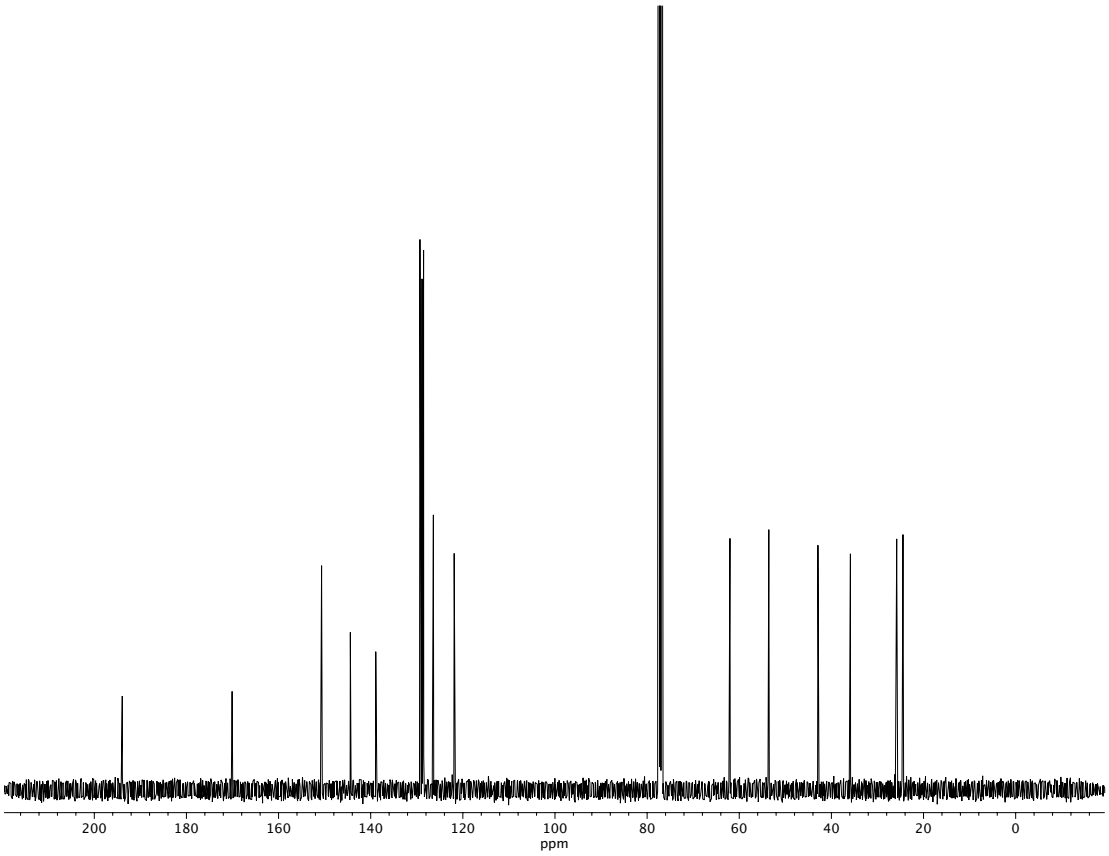


Figure A1.262. *^{13}C NMR (100 MHz, $CDCl_3$) of compound* ***82****.*

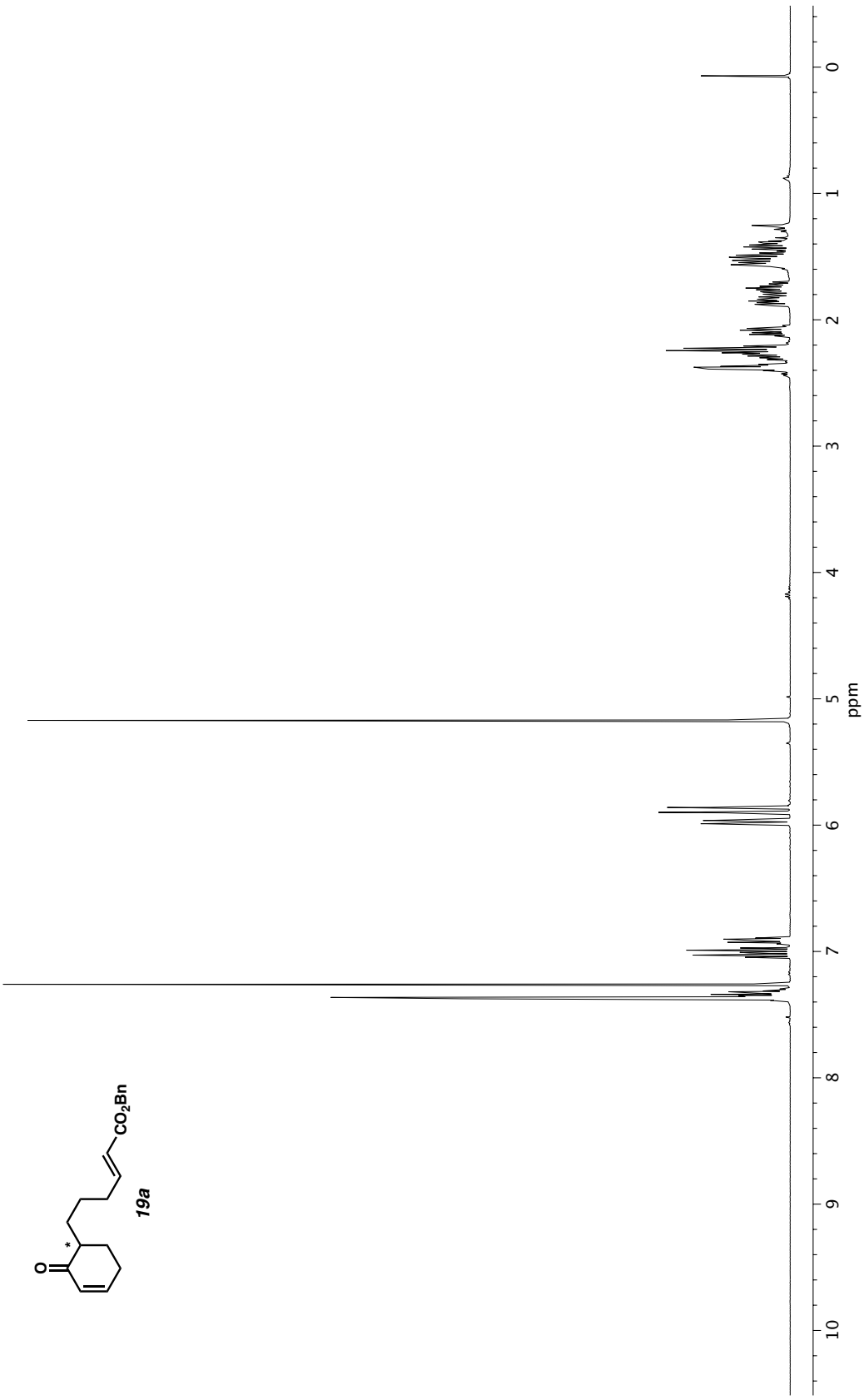


Figure A1.263. *^{1}H NMR (400 MHz, $CDCl_3$) of compound* ***19a****.*

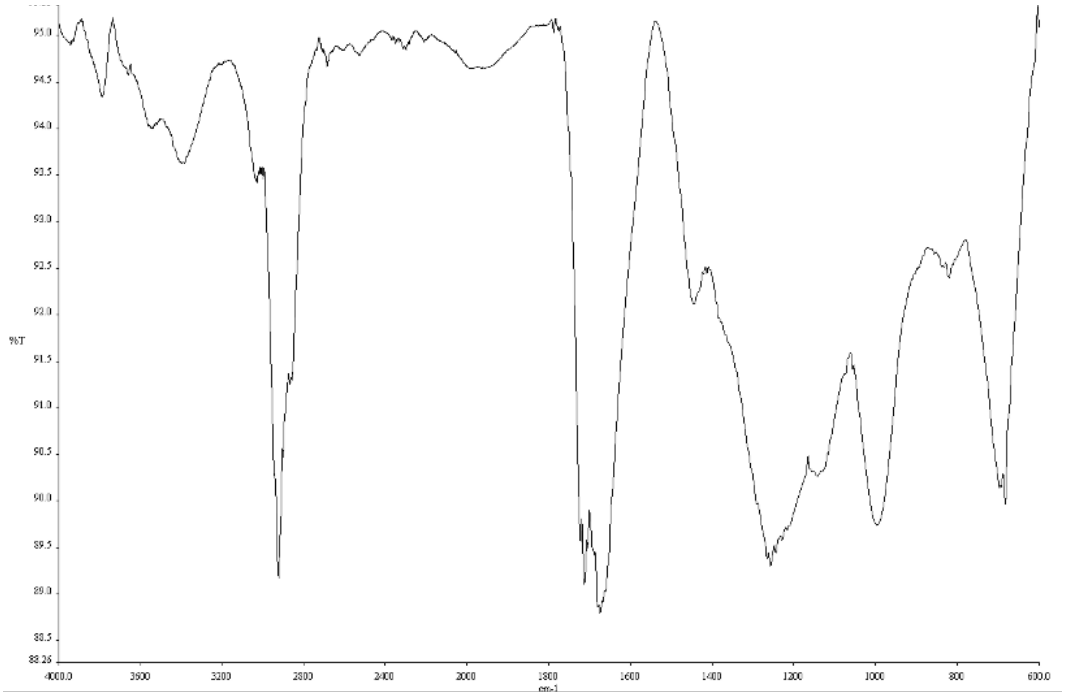


Figure A1.264. *Infrared spectrum (Thin Film, NaCl) of compound* ***19a****.*

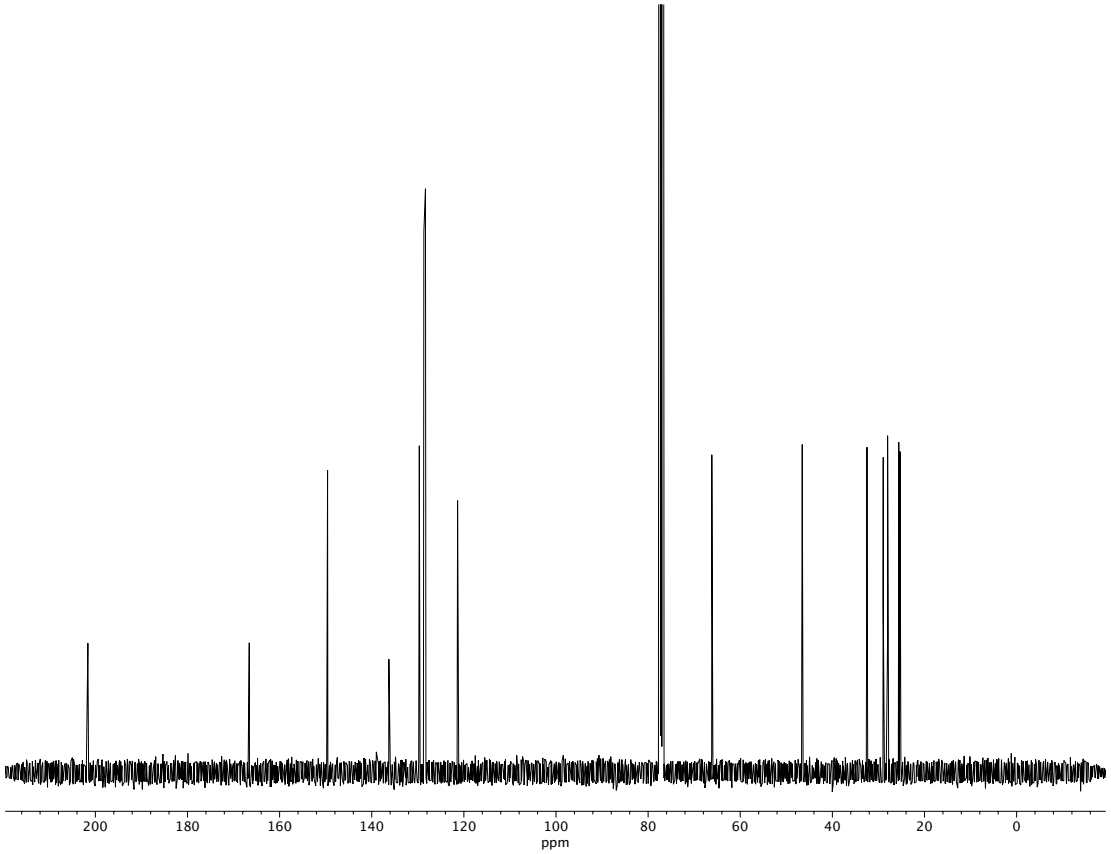


Figure A1.265. *^{13}C NMR (100 MHz, $CDCl_3$) of compound* ***19a****.*

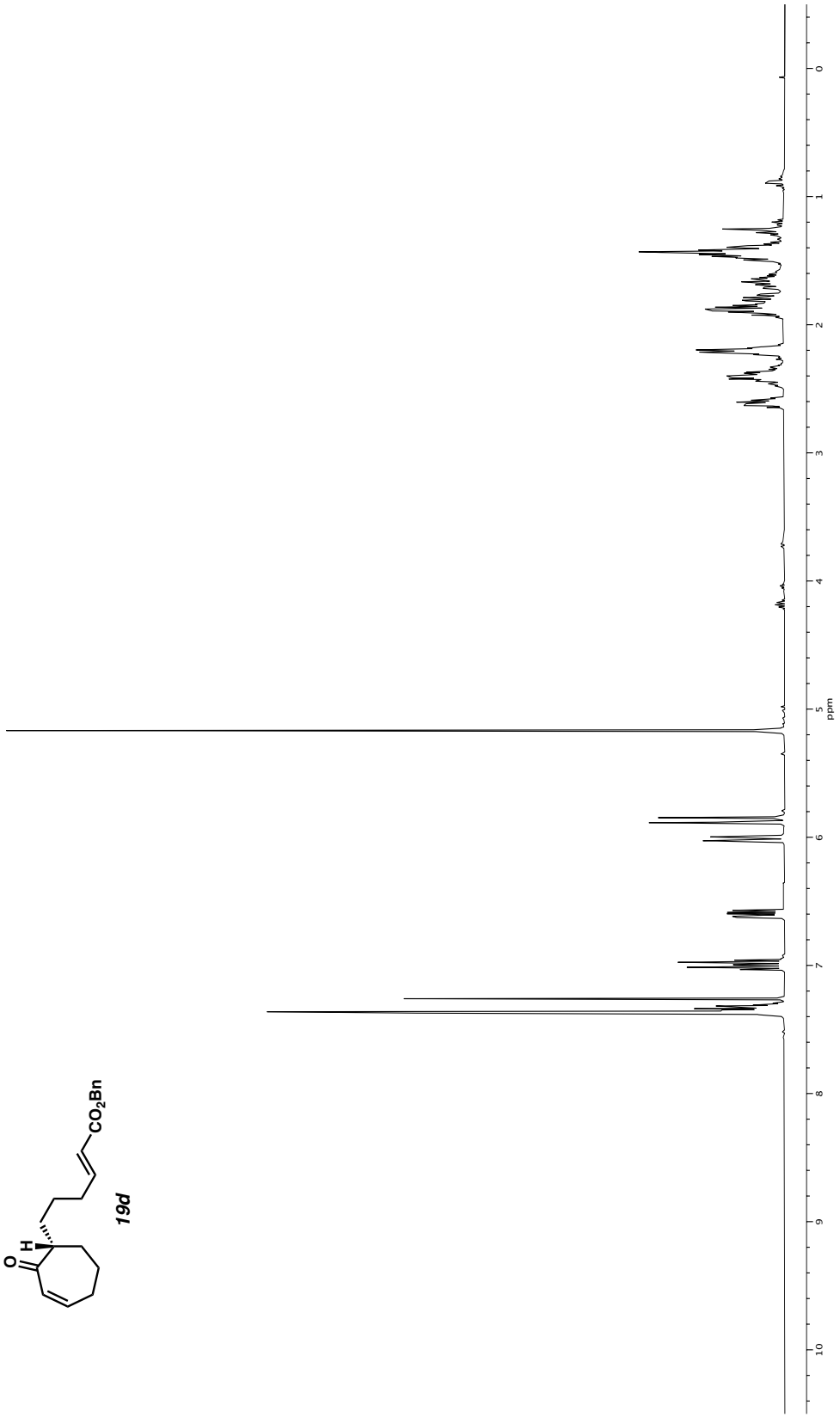


Figure A1.266. *^1H NMR (400 MHz, $CDCl_3$) of compound* ***19d****.*

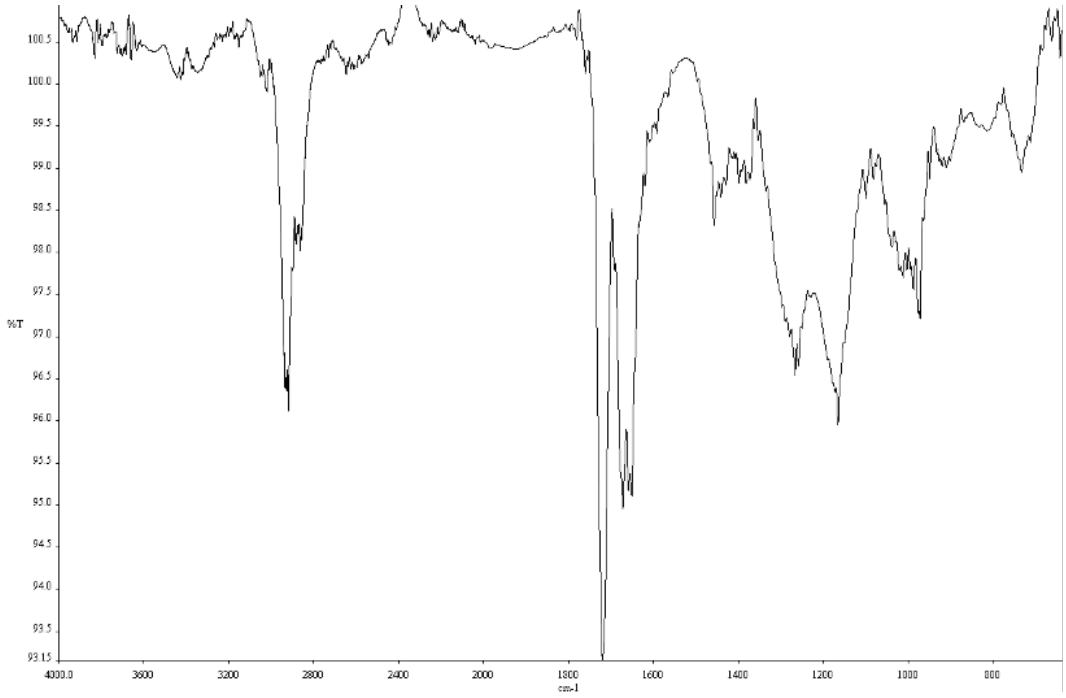


Figure A1.267. *Infrared spectrum (Thin Film, NaCl) of compound* ***19d****.*

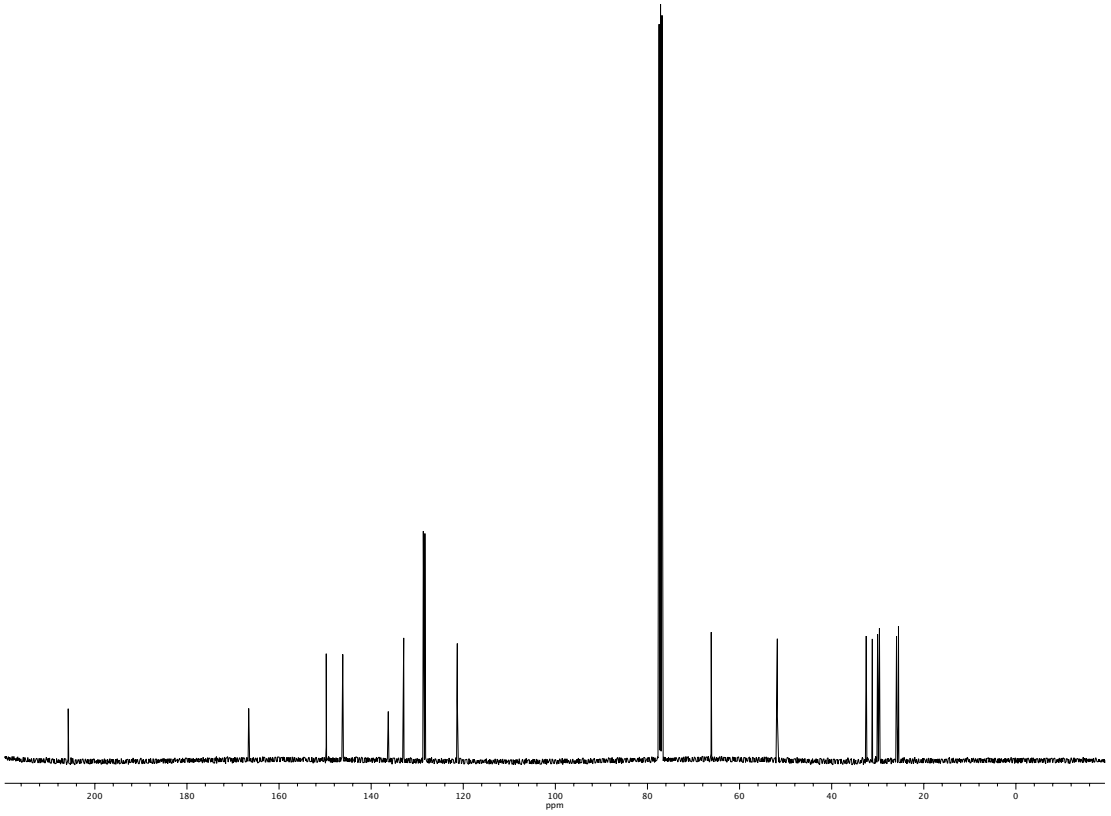


Figure A1.268. *^{13}C NMR (100 MHz, $CDCl_3$) of compound* ***19d****.*

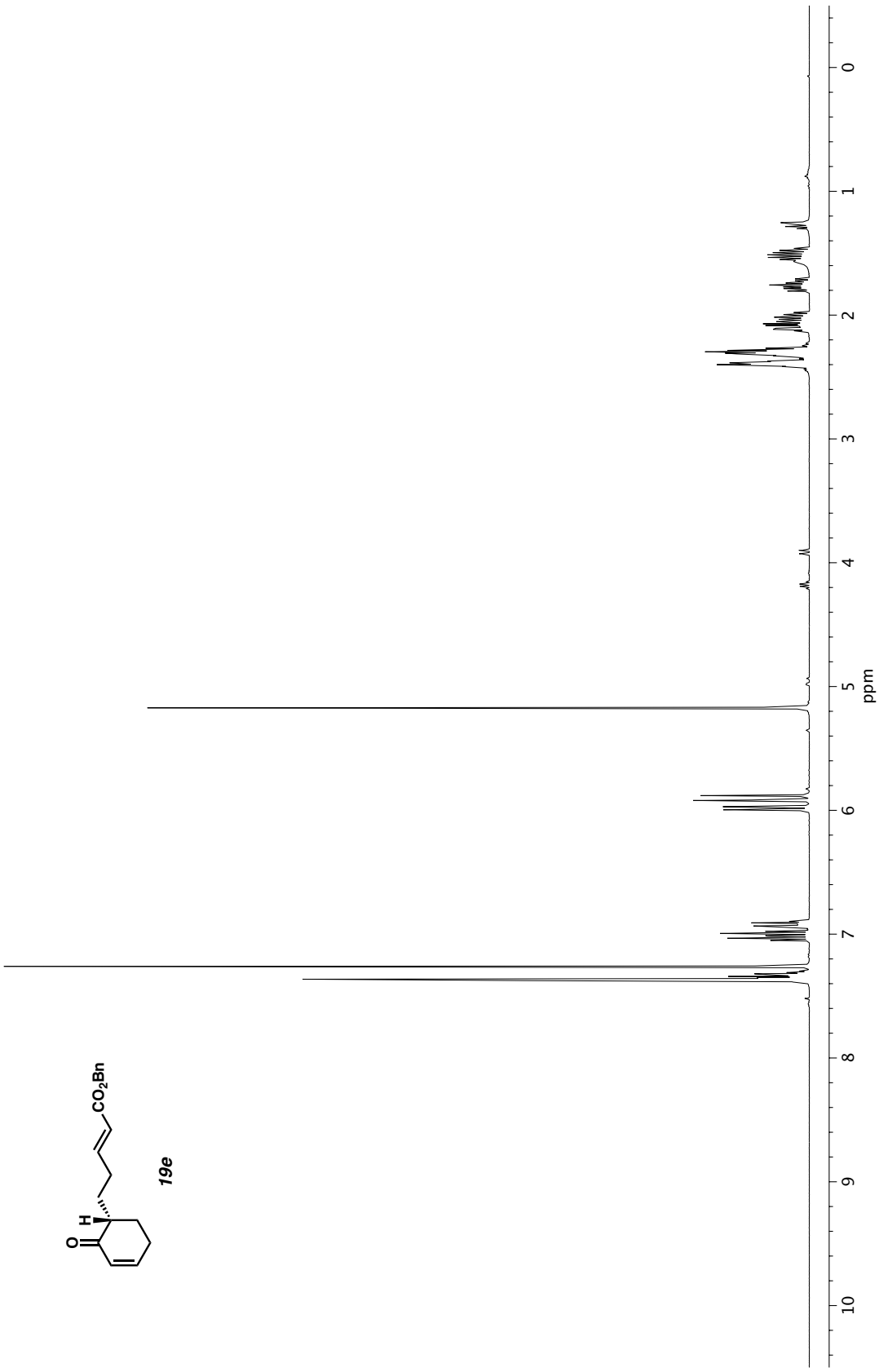


Figure A1.269. *^{1}H NMR (400 MHz, $CDCl_3$) of compound* ***19e****.*

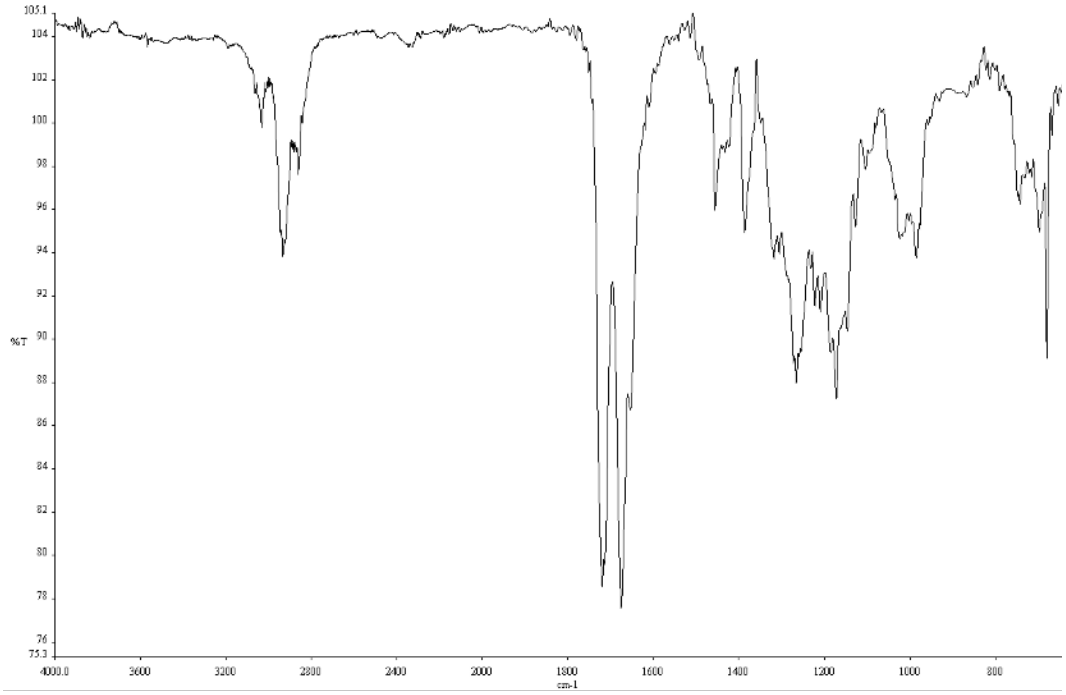


Figure A1.270. *Infrared spectrum (Thin Film, NaCl) of compound* ***19e****.*

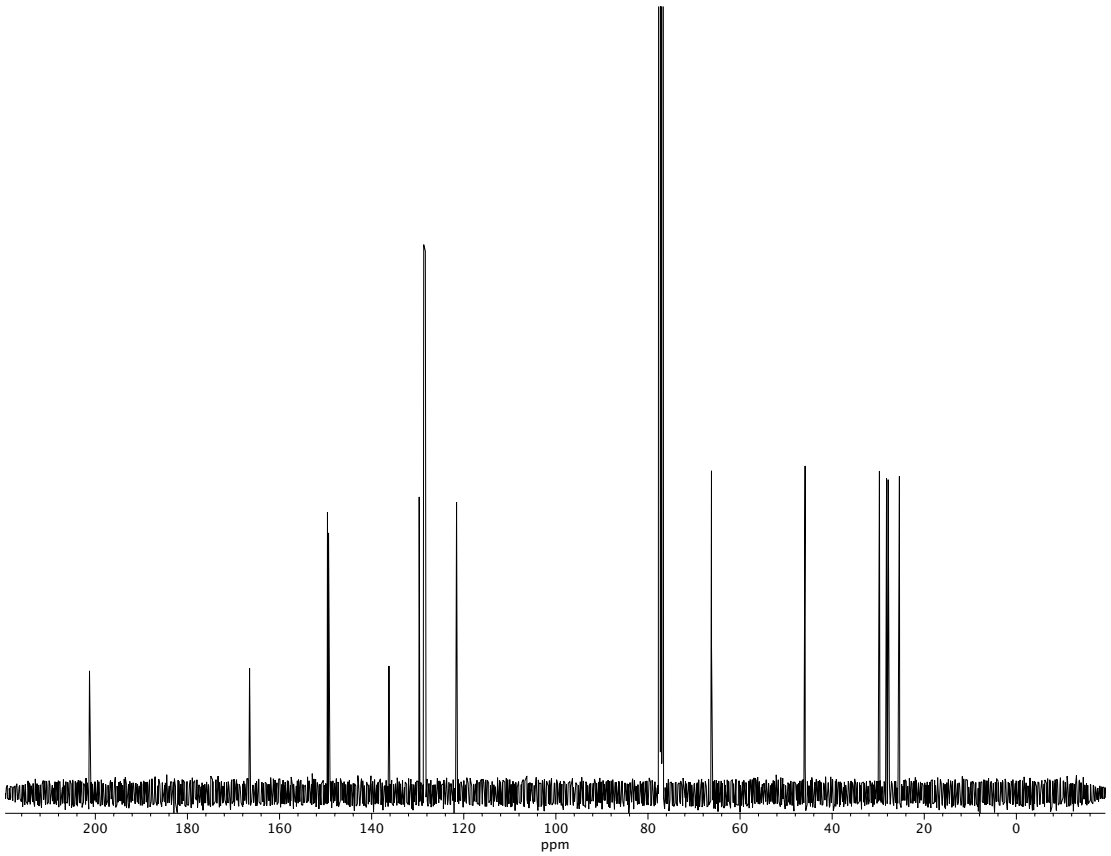


Figure A1.271. *^{13}C NMR (100 MHz, $CDCl_3$) of compound* ***19e****.*

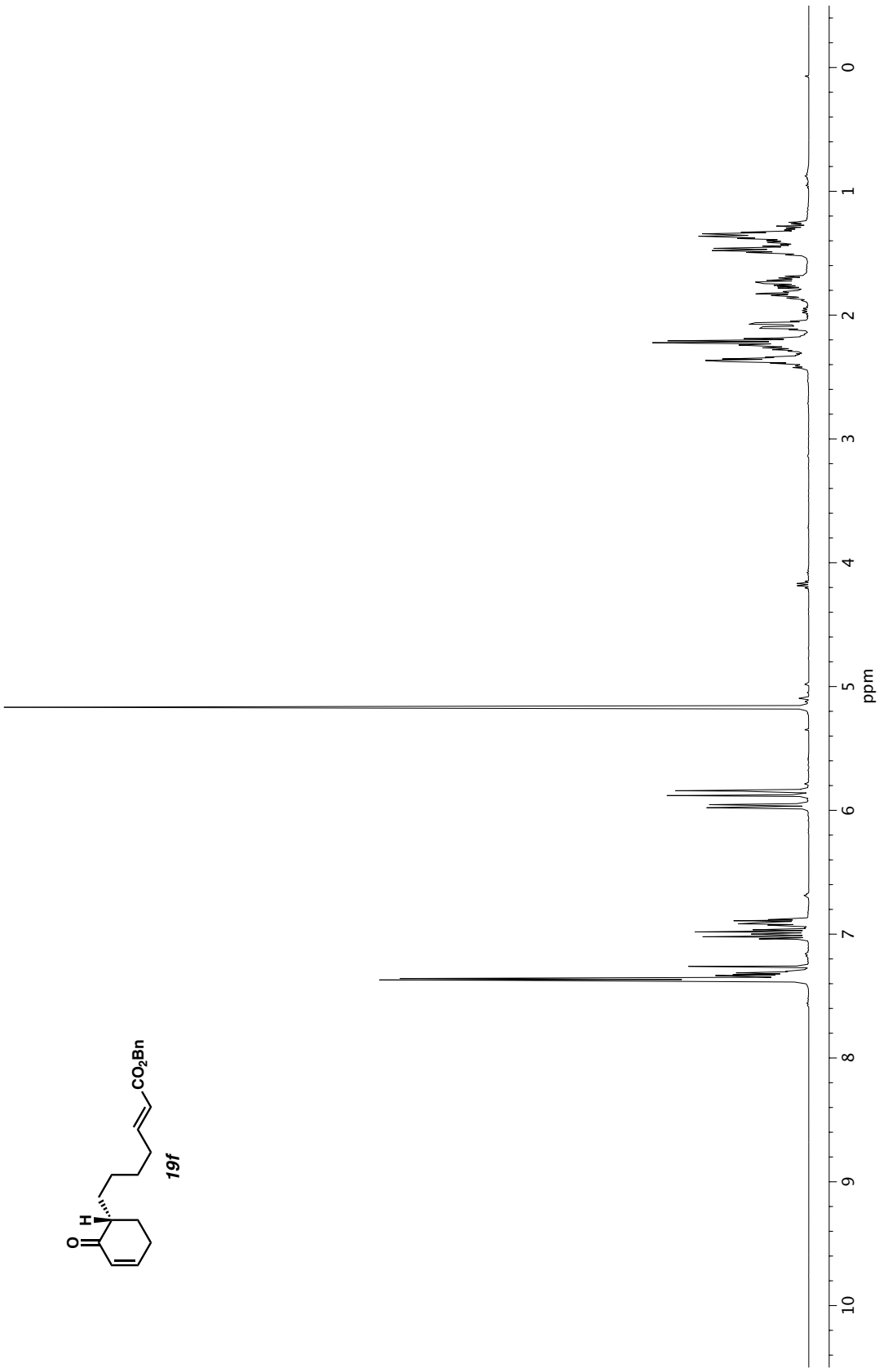


Figure A1.272. *^1H NMR (400 MHz, $CDCl_3$) of compound* ***19f****.*

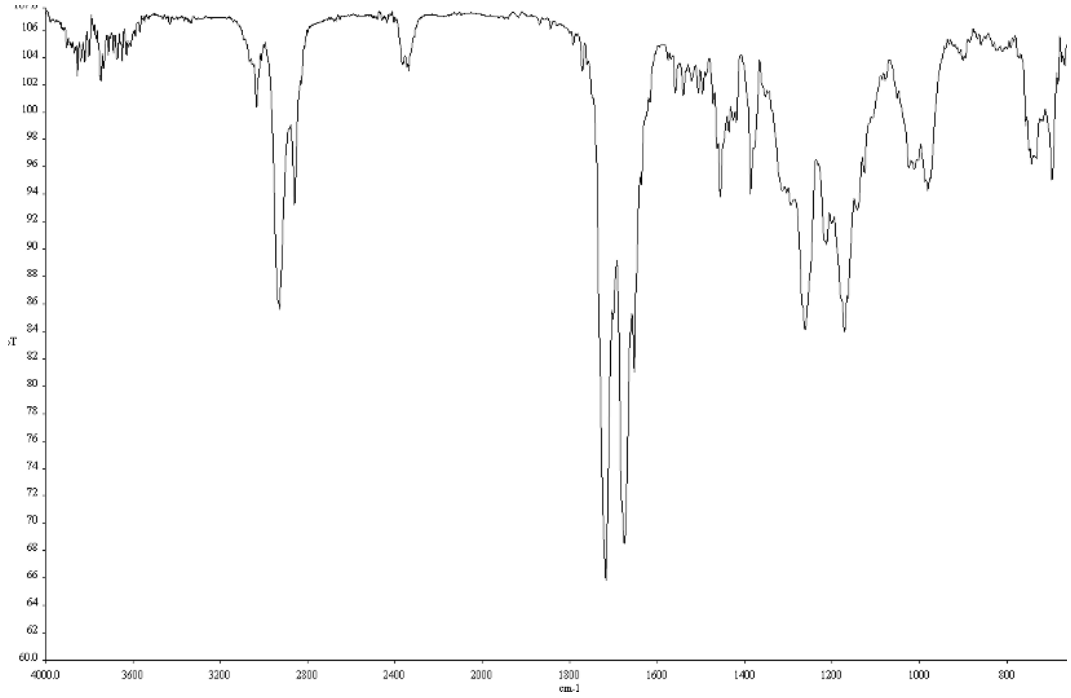


Figure A1.273. *Infrared spectrum (Thin Film, NaCl) of compound* ***19f****.*

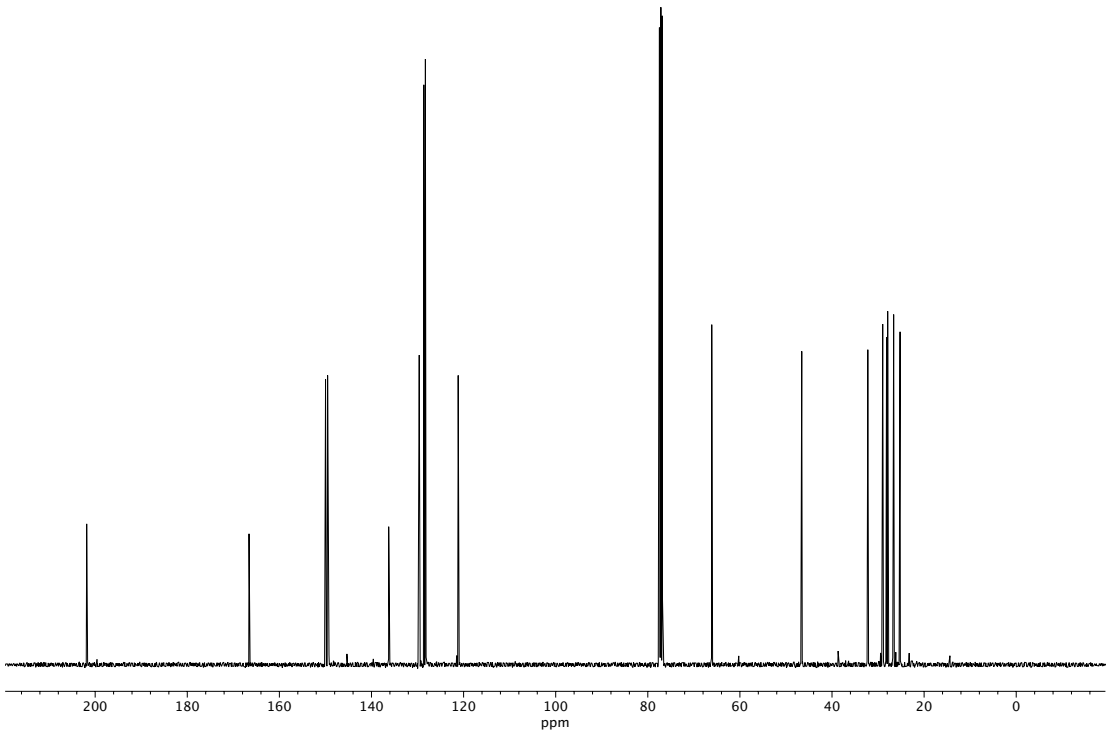


Figure A1.274. *^{13}C NMR (100 MHz, $CDCl_3$) of compound* ***19f****.*

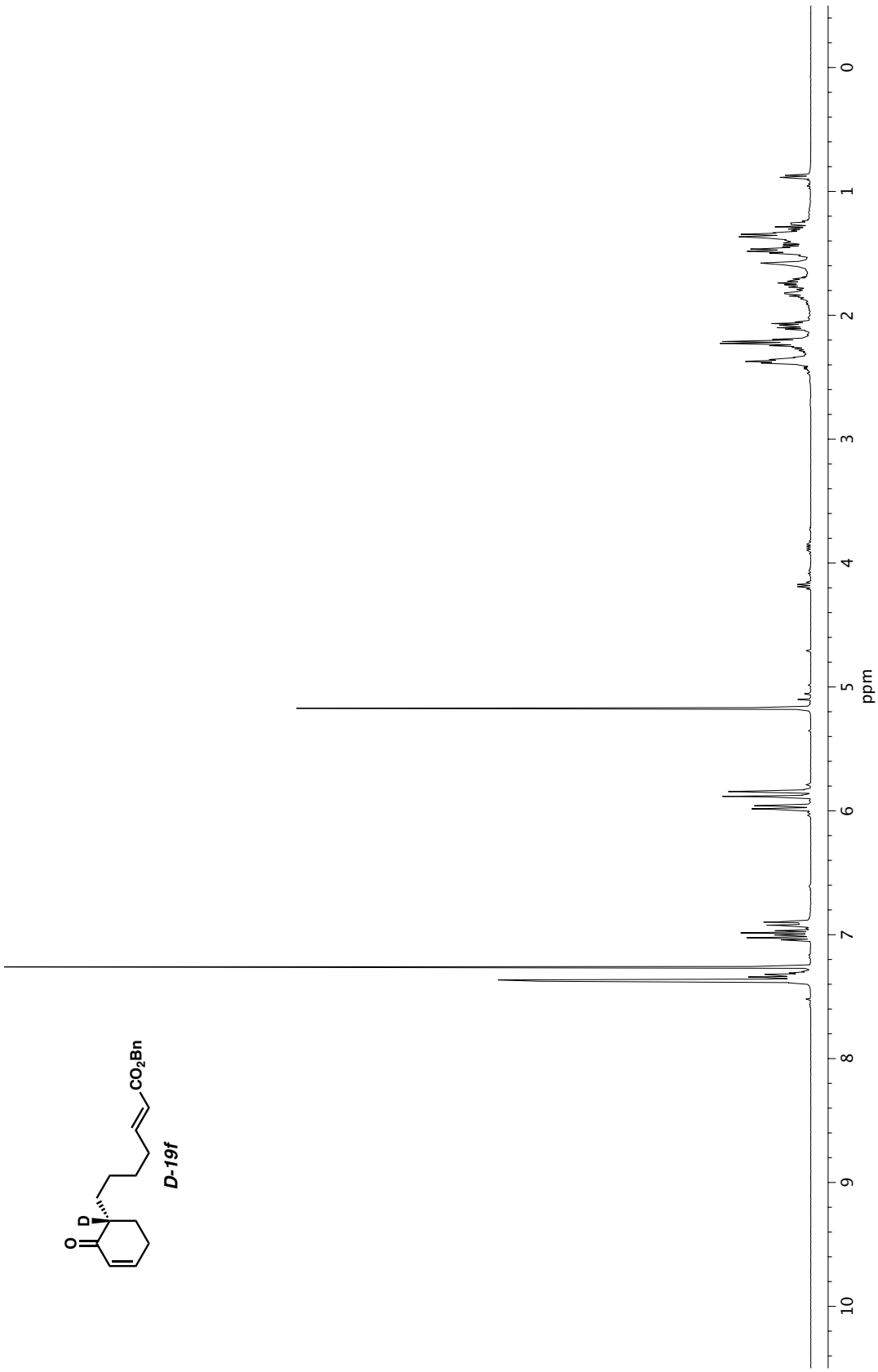


Figure A1.275. *^1H NMR (400 MHz, $CDCl_3$) of compound* ***D-19f****.*

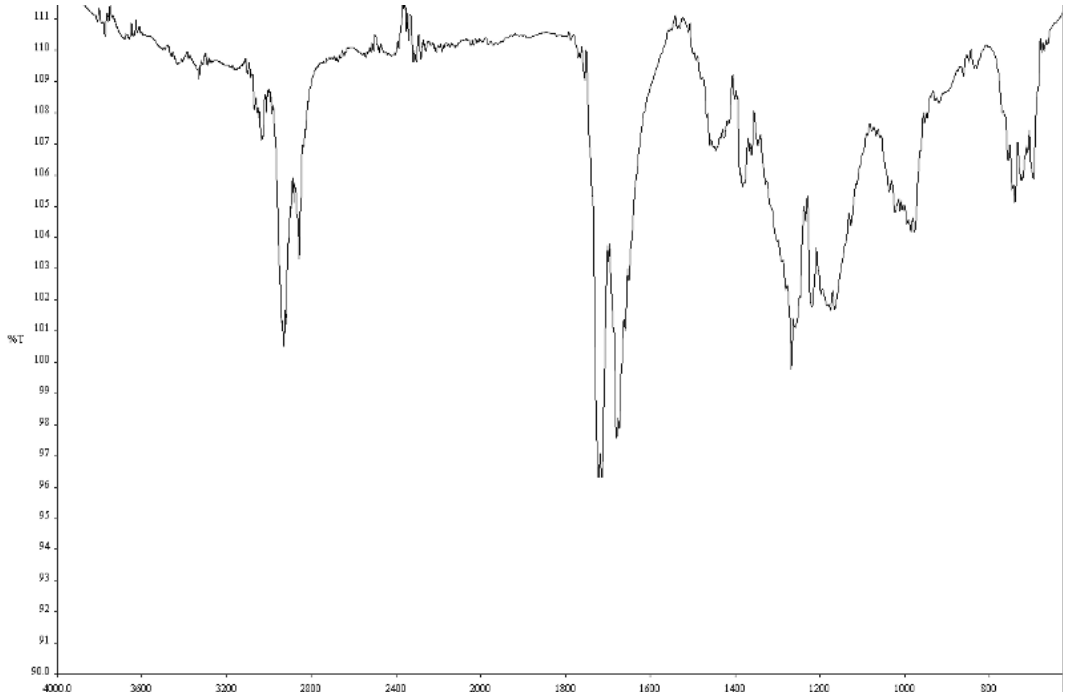


Figure A1.276. *Infrared spectrum (Thin Film, NaCl) of compound* ***D-19f****.*

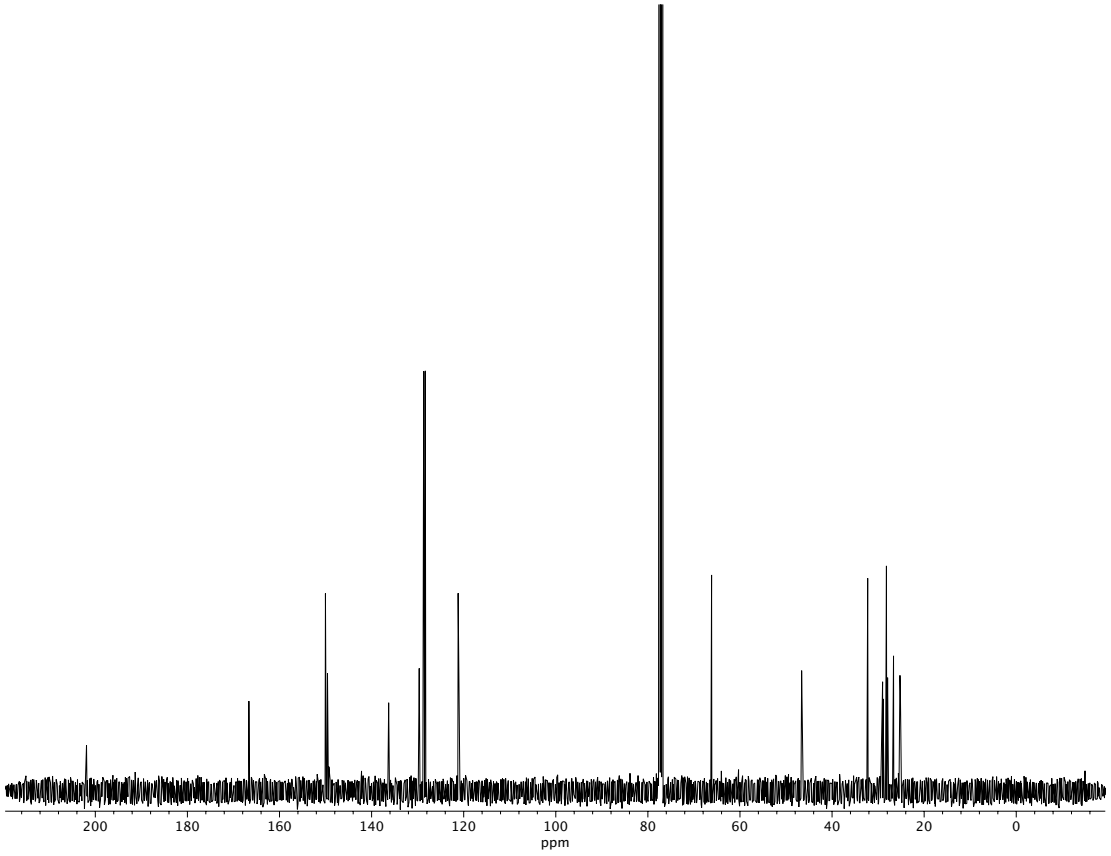


Figure A1.277. *^{13}C NMR (100 MHz, $CDCl_3$) of compound* ***D-19f****.*

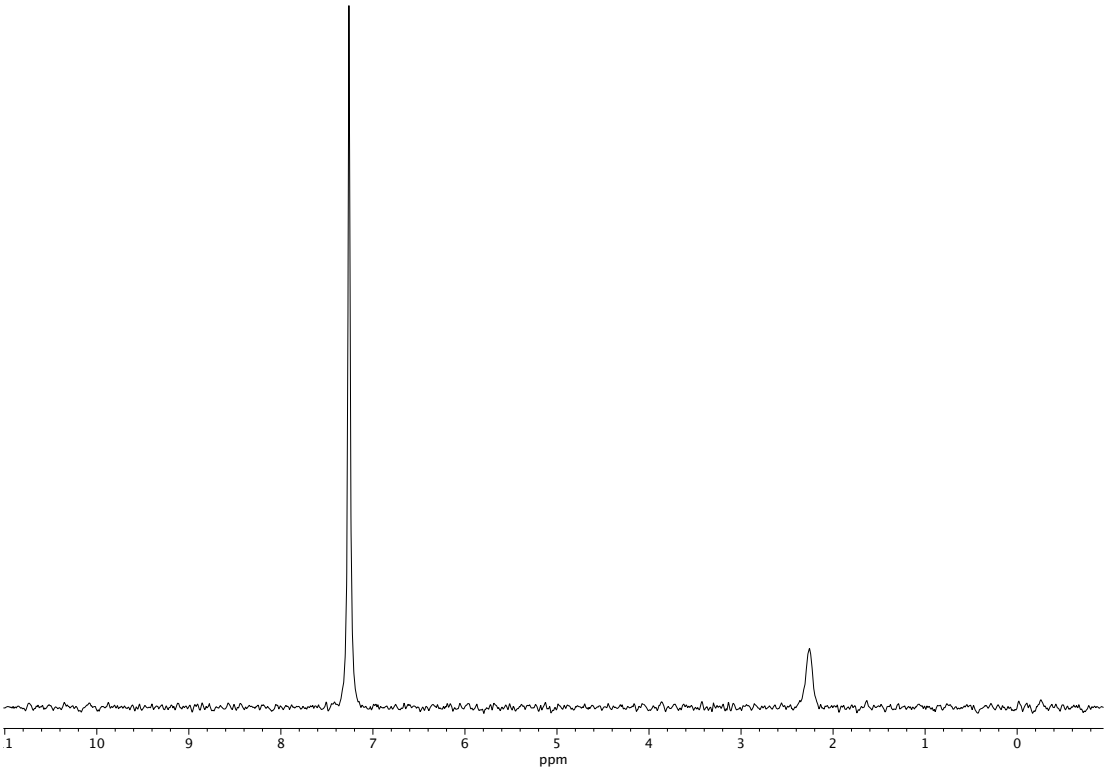


Figure A1.278. *^{2}H NMR (61 MHz, $CHCl_3$) of compound* ***D-19f****.*

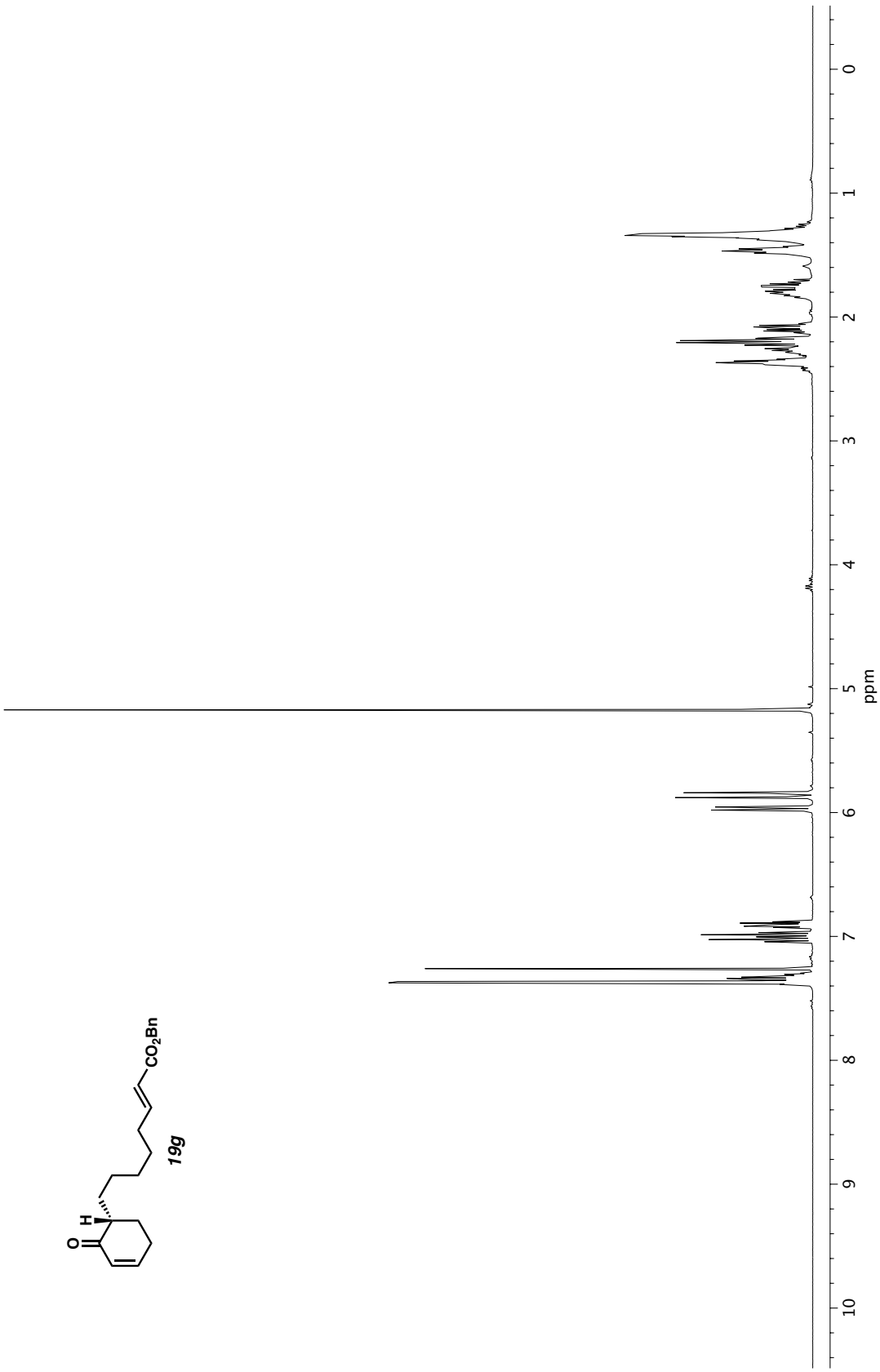


Figure A1.279. *^1H NMR (400 MHz, $CDCl_3$) of compound* ***19g****.*

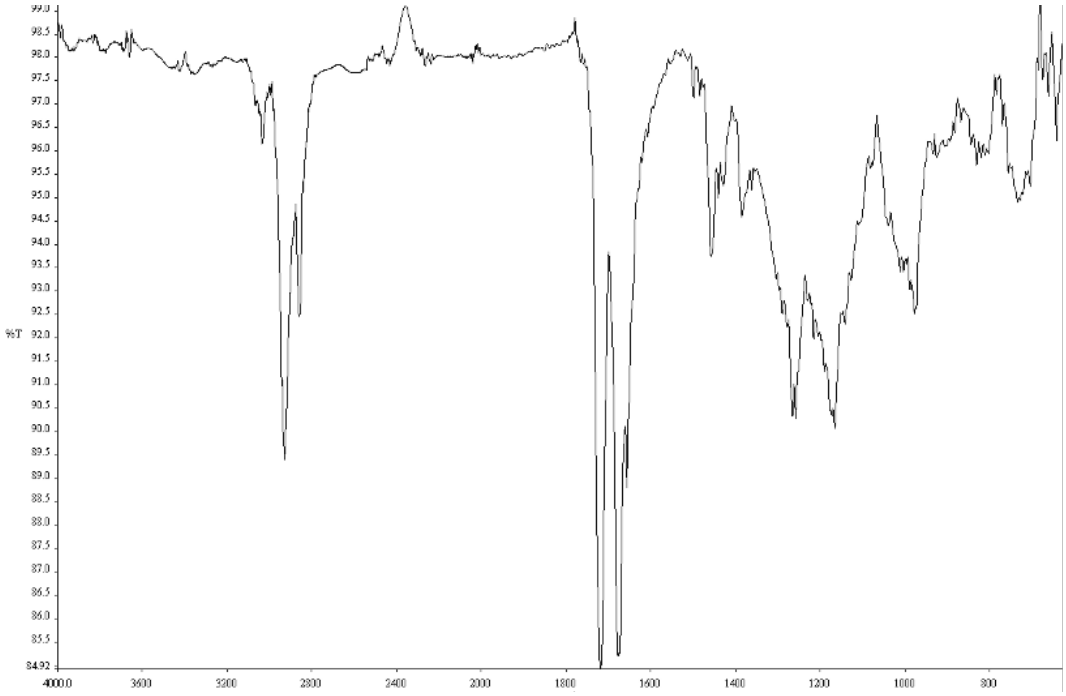


Figure A1.280. *Infrared spectrum (Thin Film, NaCl) of compound* ***19g****.*

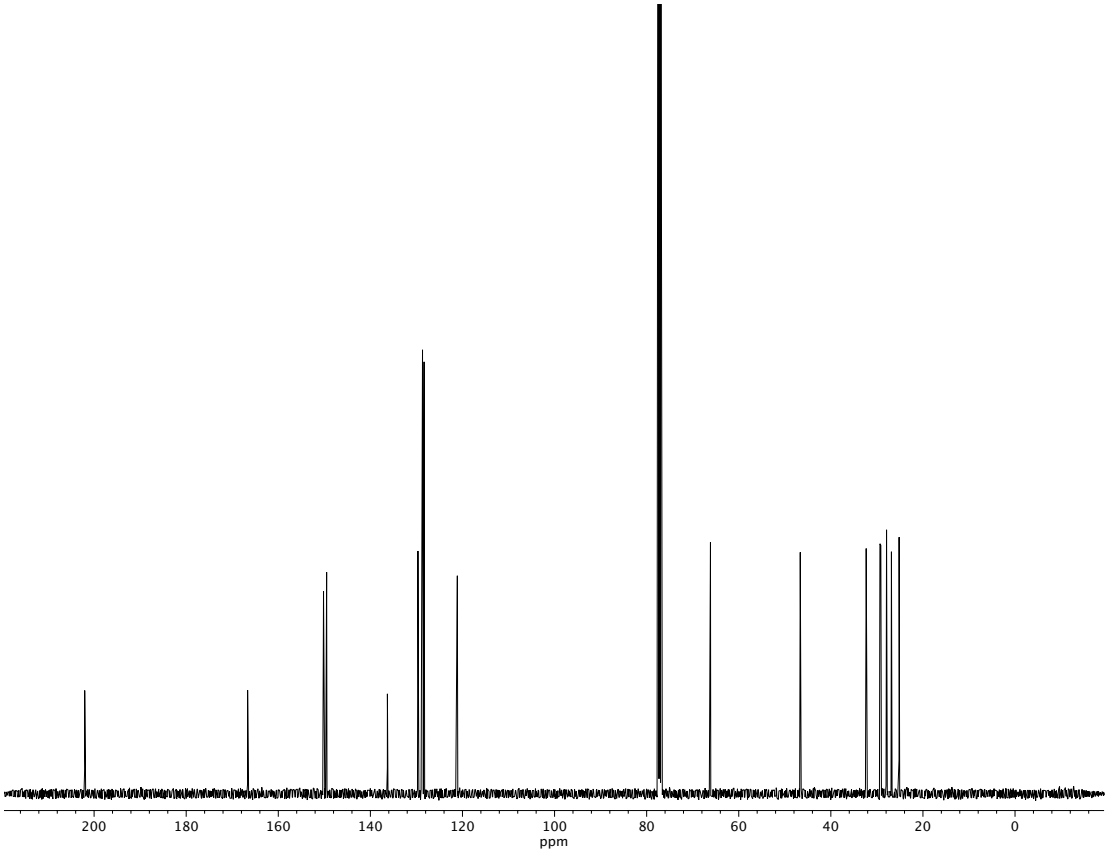


Figure A1.281. *^{13}C NMR (100 MHz, $CDCl_3$) of compound* ***19g****.*

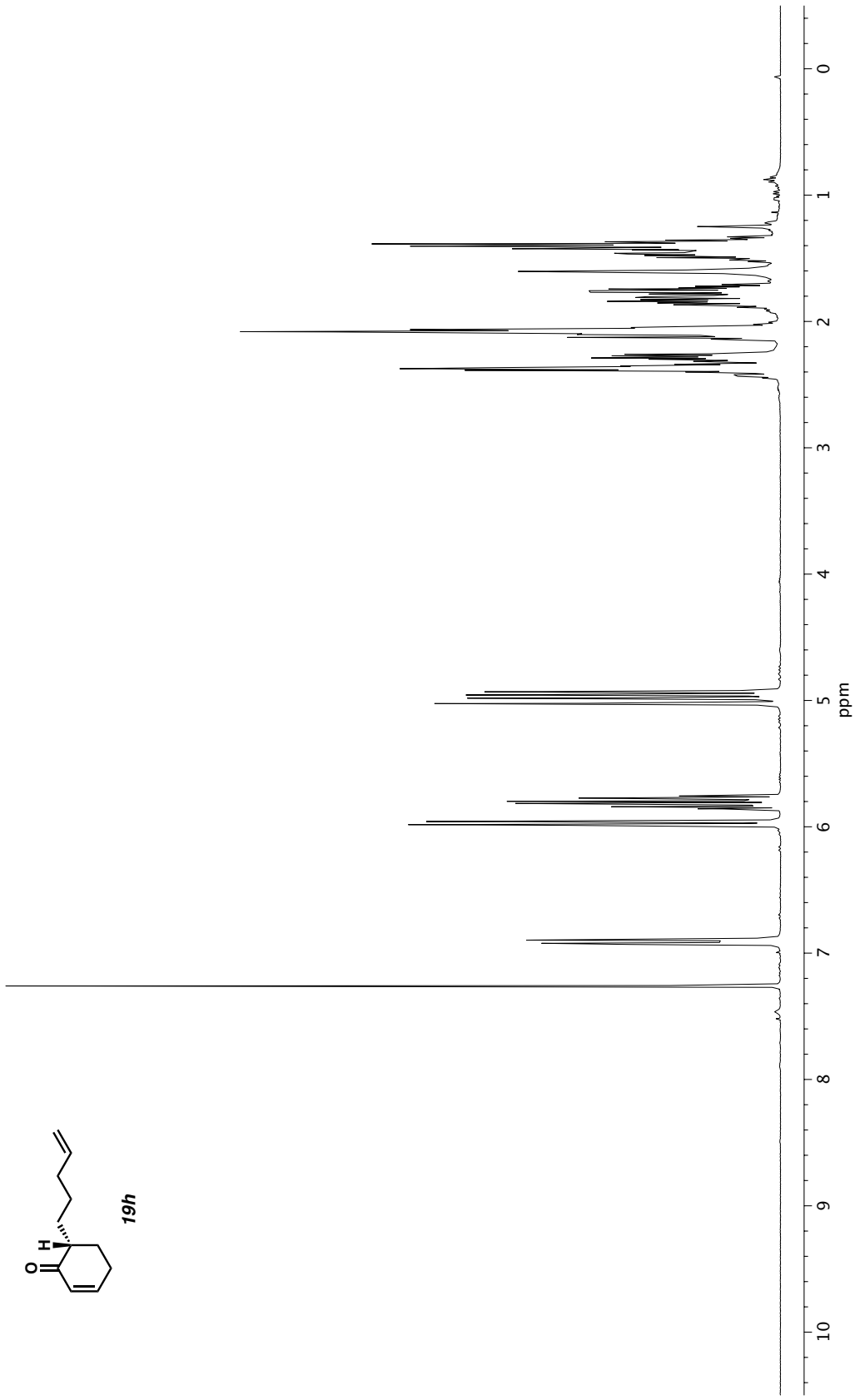


Figure A1.282. *^1H NMR (400 MHz, $CDCl_3$) of compound* ***19h****.*

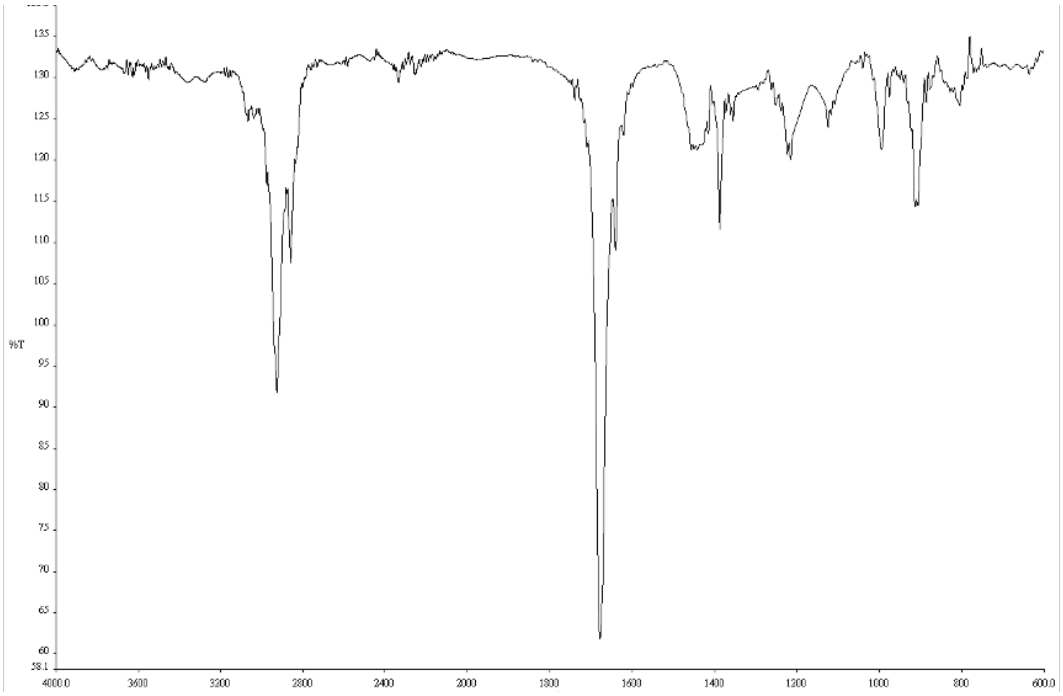


Figure A1.283. *Infrared spectrum (Thin Film, NaCl) of compound* ***19h****.*

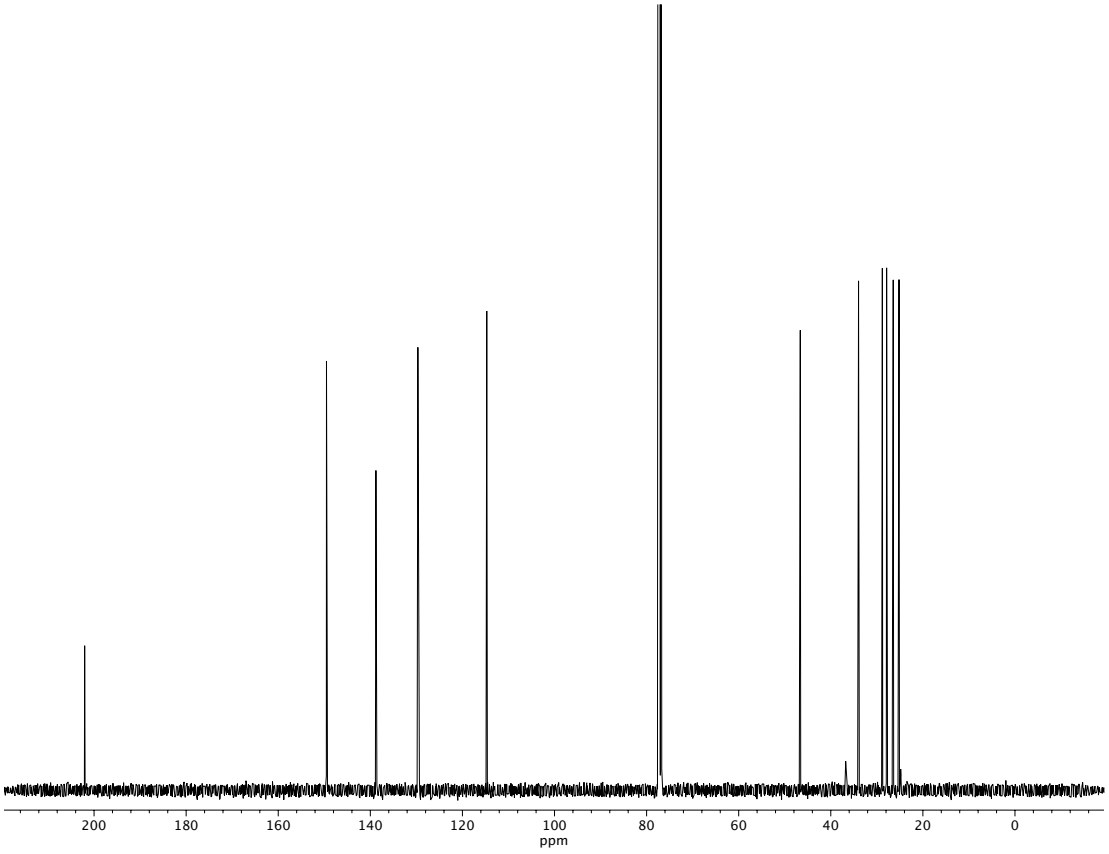


Figure A1.284. *^{13}C NMR (100 MHz, $CDCl_3$) of compound* ***19h****.*

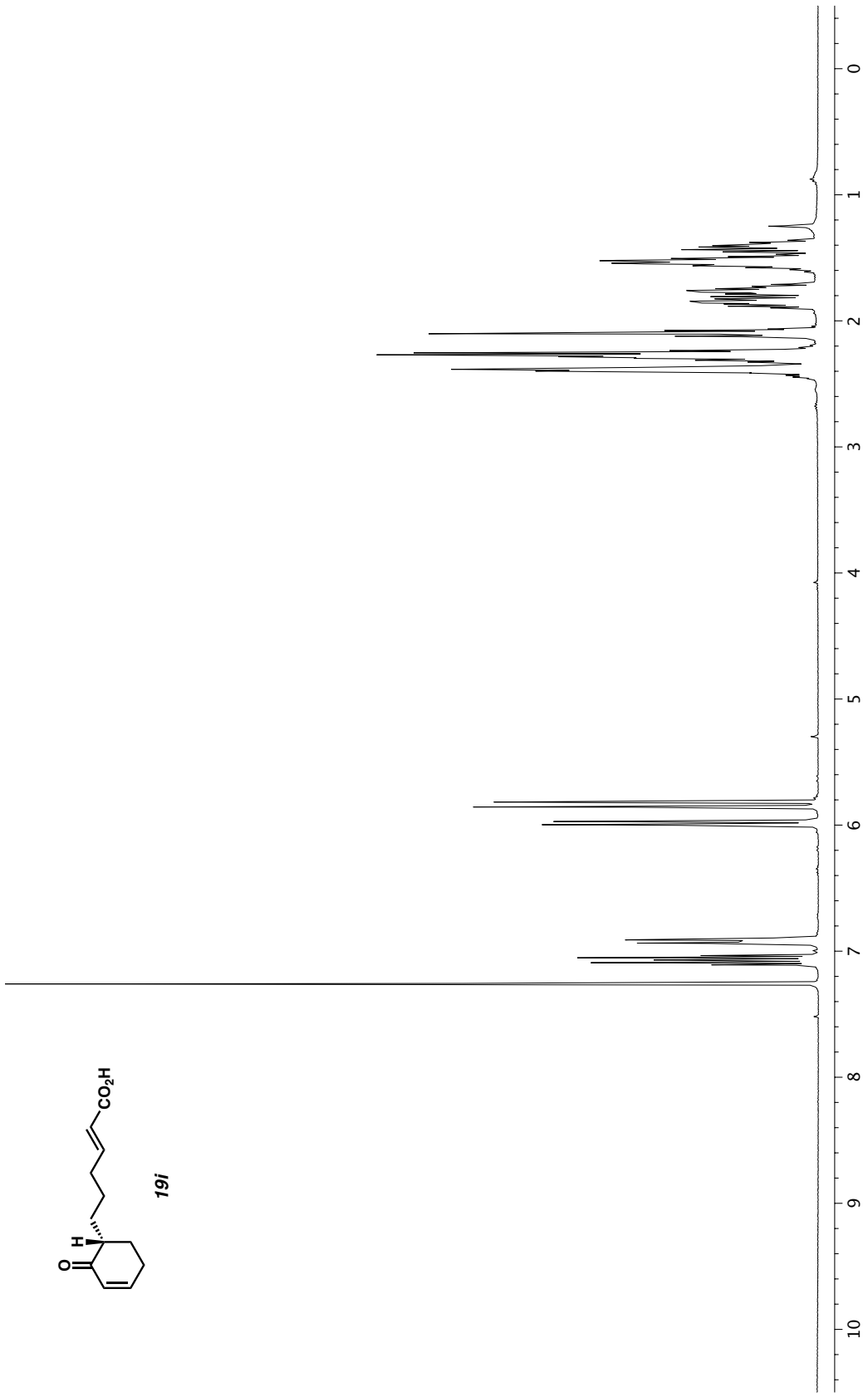


Figure A1.285. *^1H NMR (400 MHz, $CDCl_3$) of compound* ***19i****.*

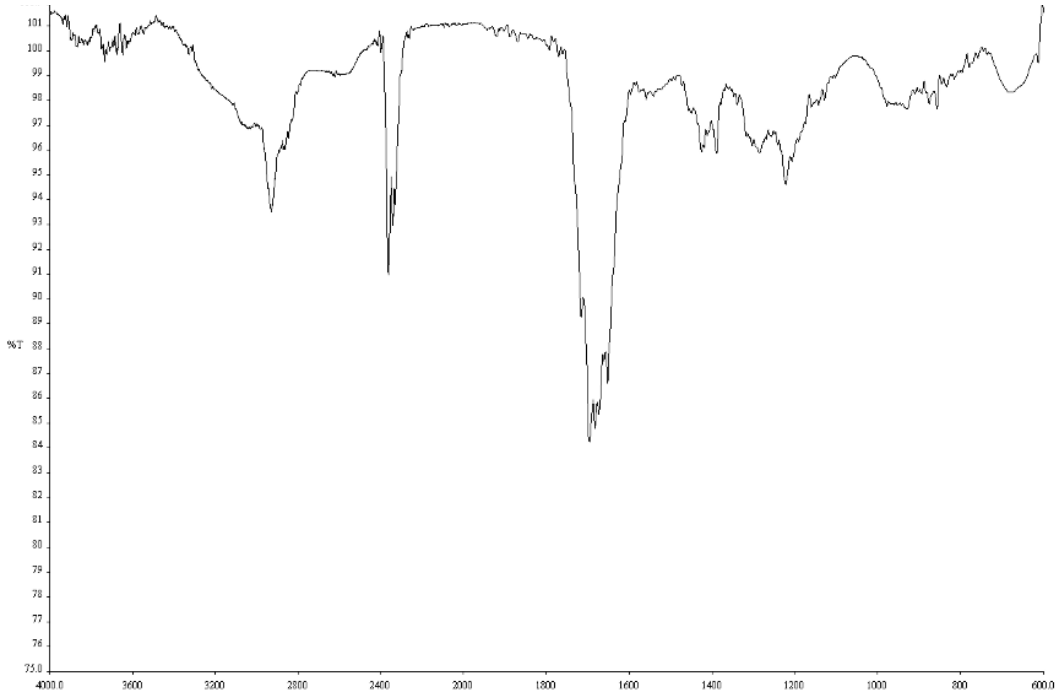


Figure A1.286. *Infrared spectrum (Thin Film, NaCl) of compound* ***19i****.*

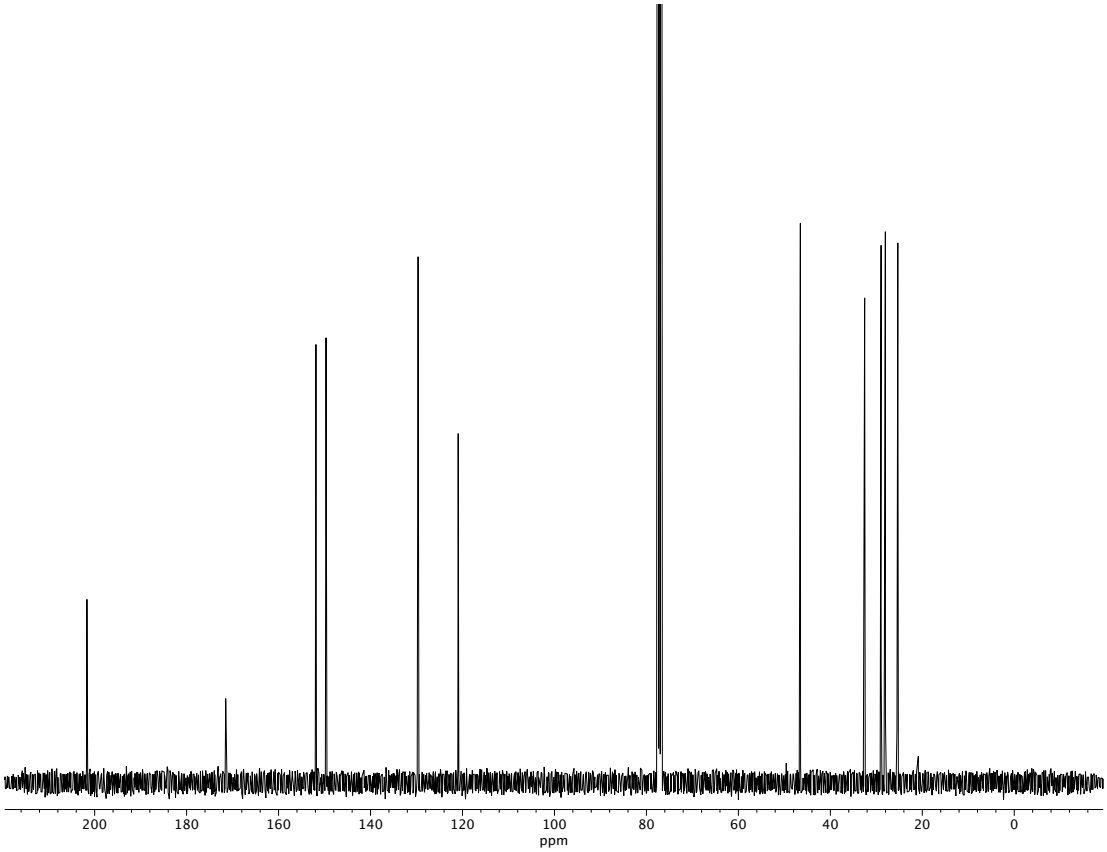


Figure A1.287. *^{13}C NMR (100 MHz, $CDCl_3$) of compound* ***19i****.*

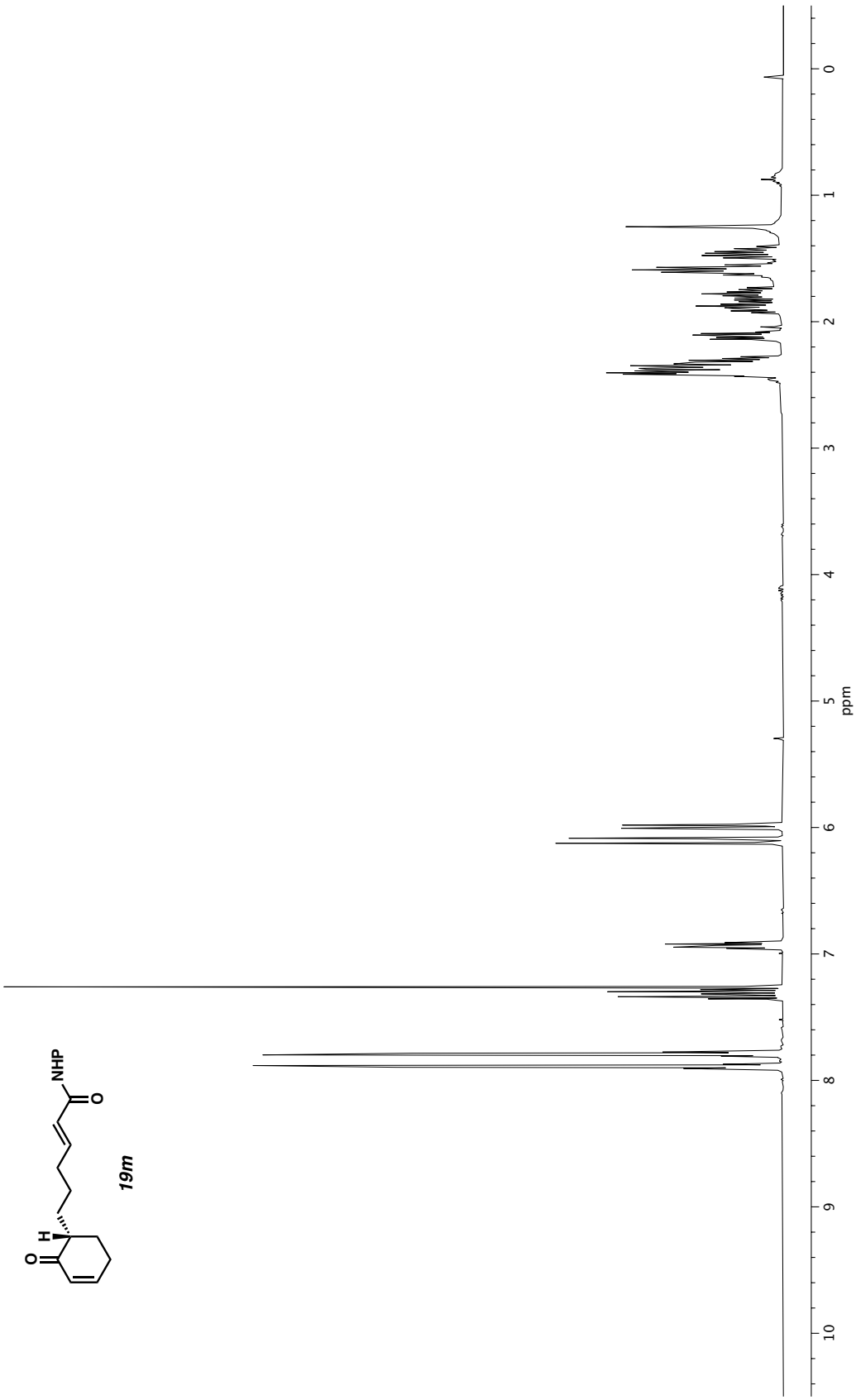


Figure A1.288. *^{1}H NMR (400 MHz, $CDCl_3$) of compound* ***19m****.*

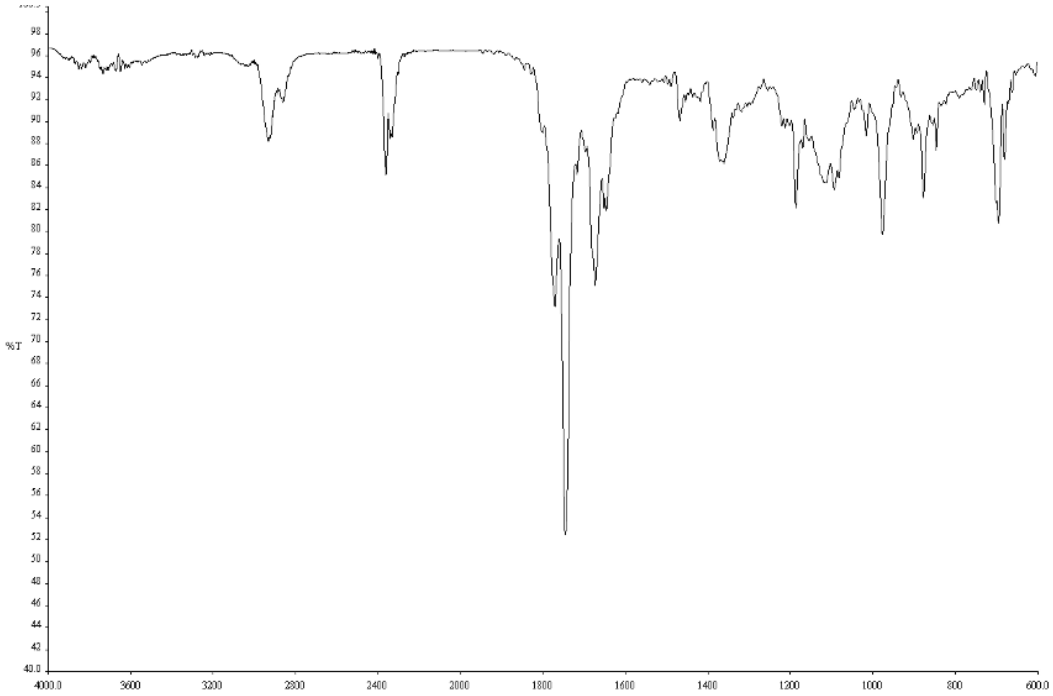


Figure A1.289. *Infrared spectrum (Thin Film, NaCl) of compound* ***19m****.*

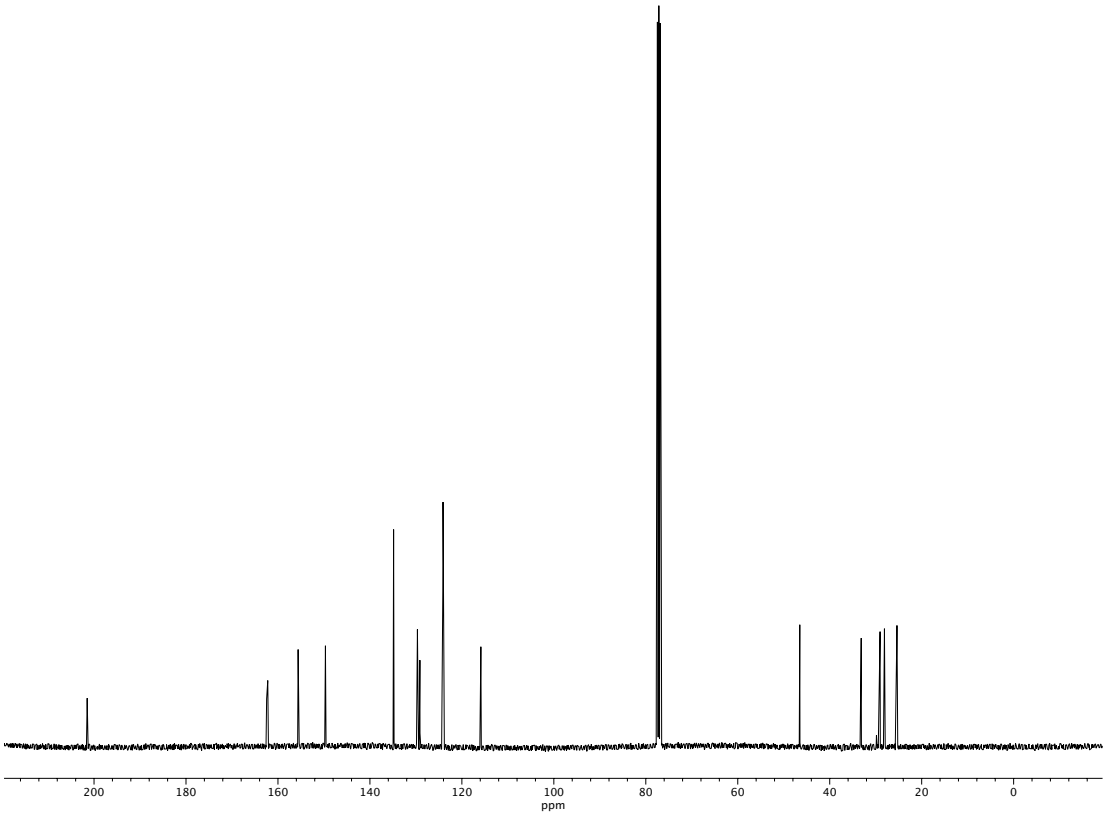


Figure A1.290. *^{13}C NMR (100 MHz, $CDCl_3$) of compound* ***19m****.*

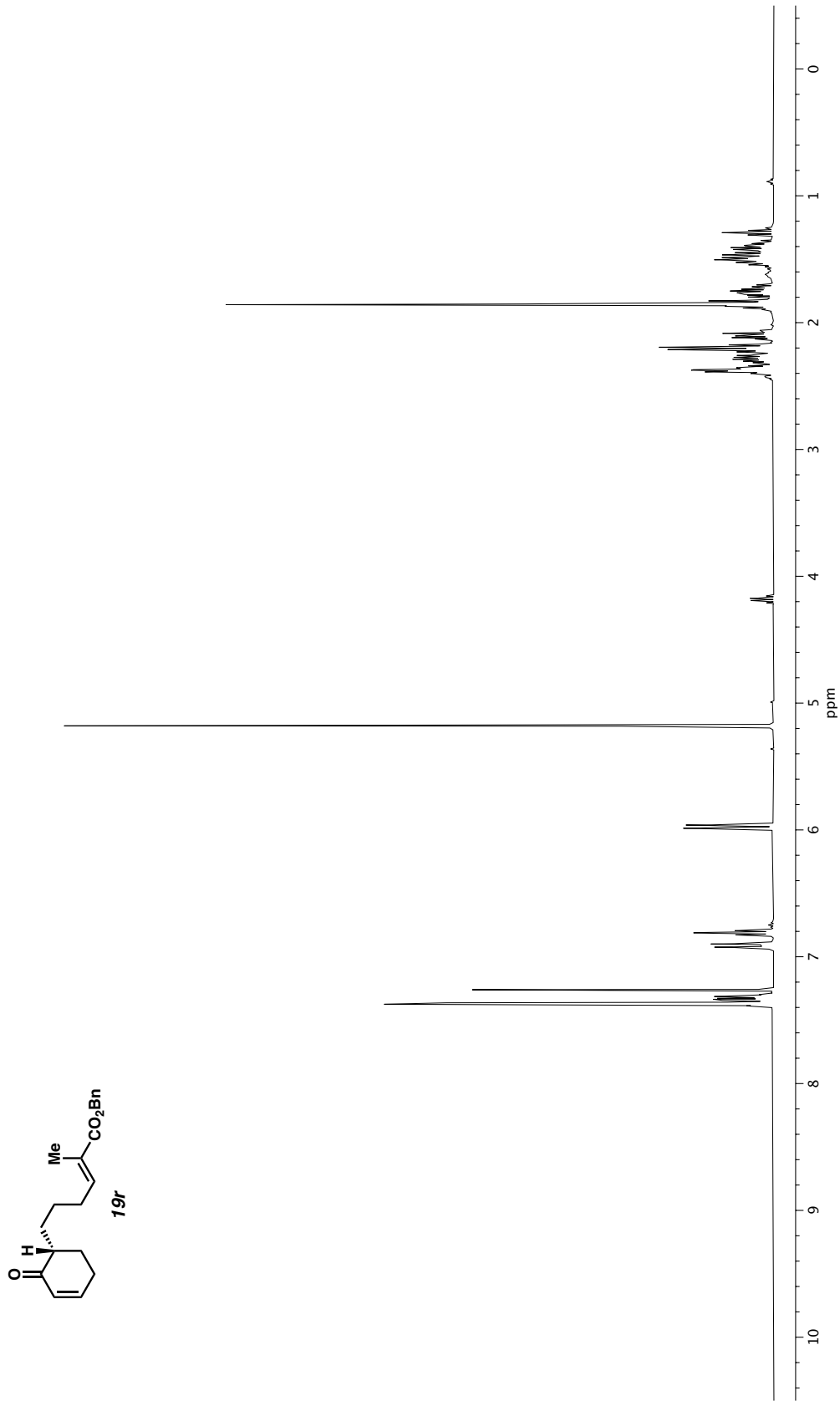


Figure A1.291. *^1H NMR (400 MHz, $CDCl_3$) of compound* ***19r****.*

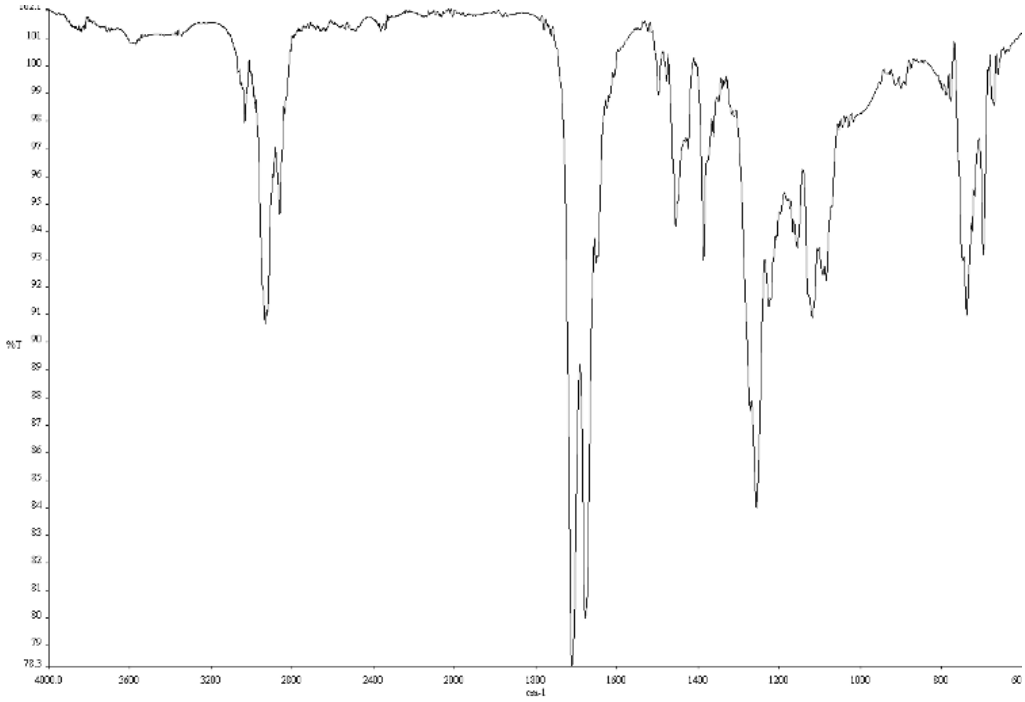


Figure A1.292. *Infrared spectrum (Thin Film, NaCl) of compound* ***19r****.*

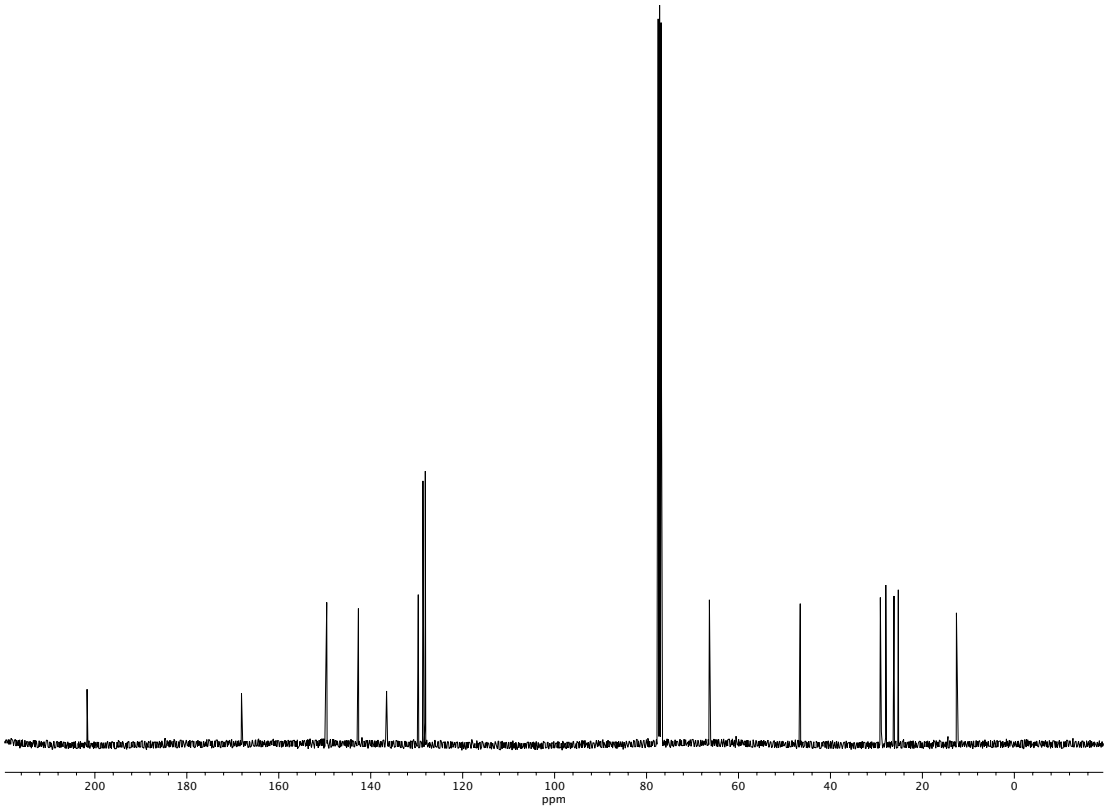


Figure A1.293. *^{13}C NMR (100 MHz, $CDCl_3$) of compound* ***19r****.*

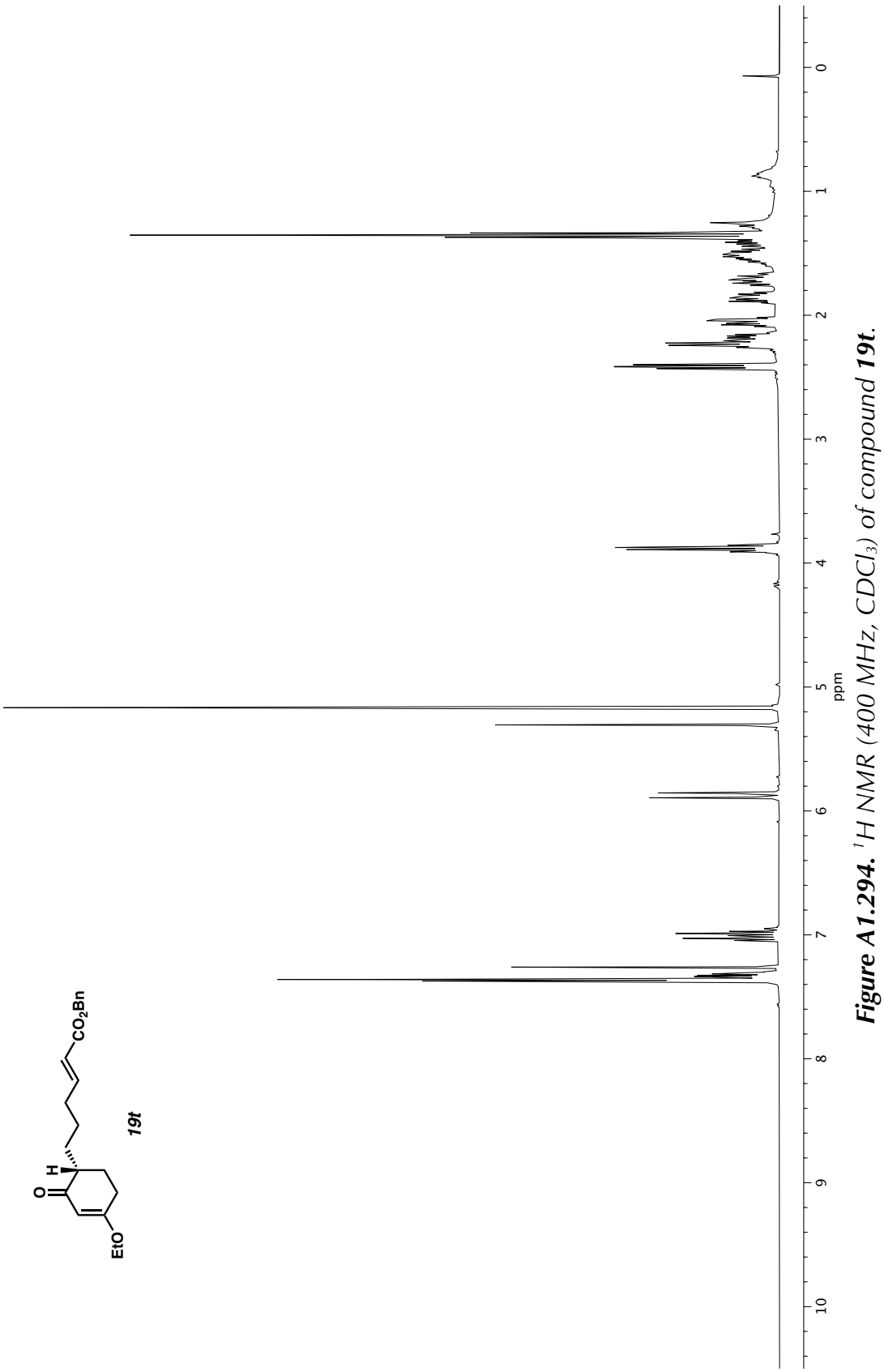


Figure A1.294. *^1H NMR (400 MHz, $CDCl_3$) of compound* ***19t****.*

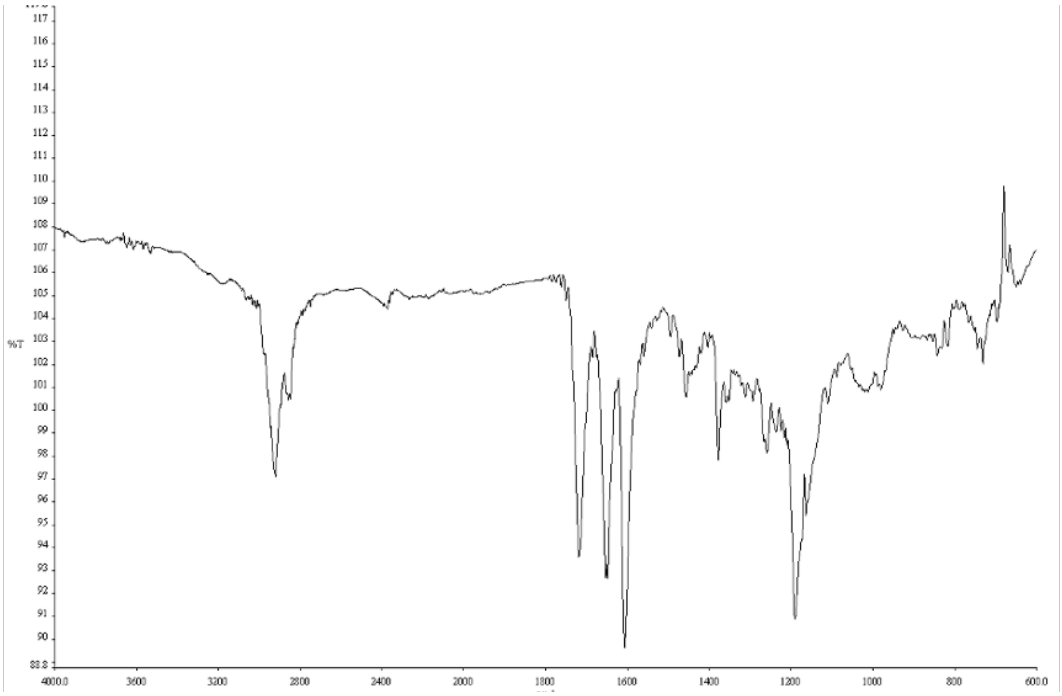


Figure A1.295. *Infrared spectrum (Thin Film, NaCl) of compound* ***19t****.*

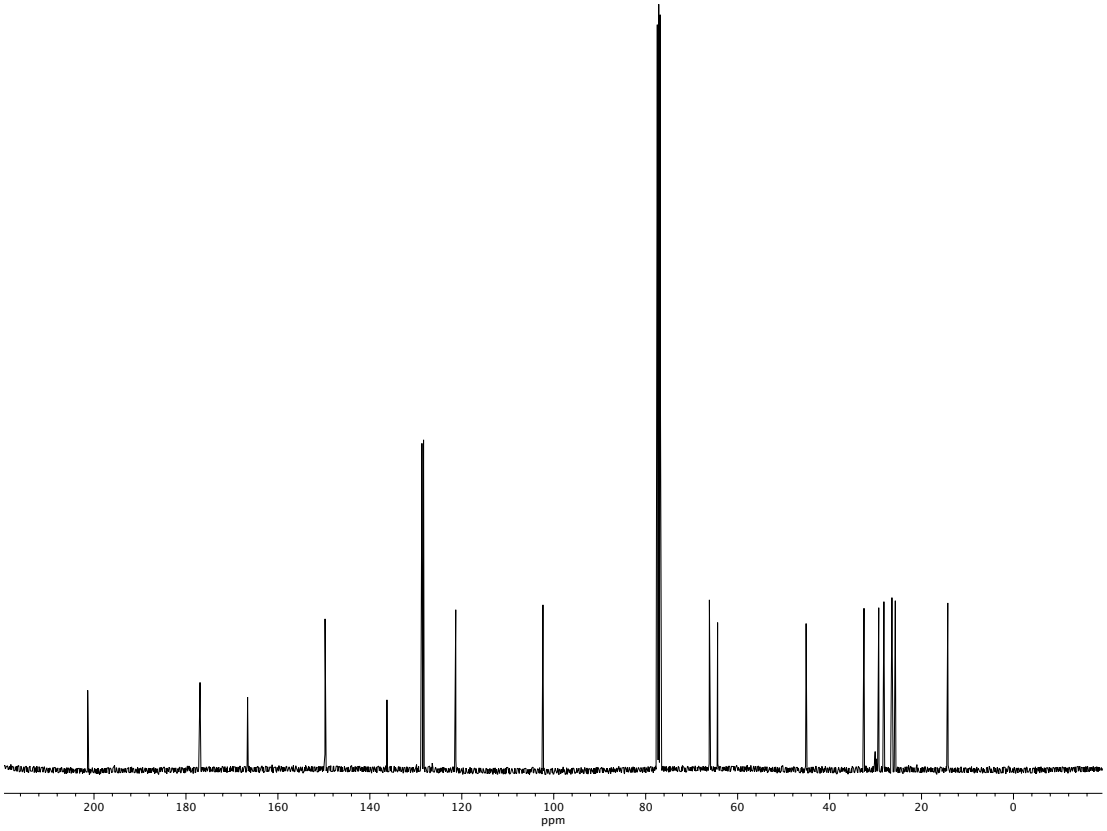


Figure A1.296. *^{13}C NMR (100 MHz, $CDCl_3$) of compound* ***19t****.*

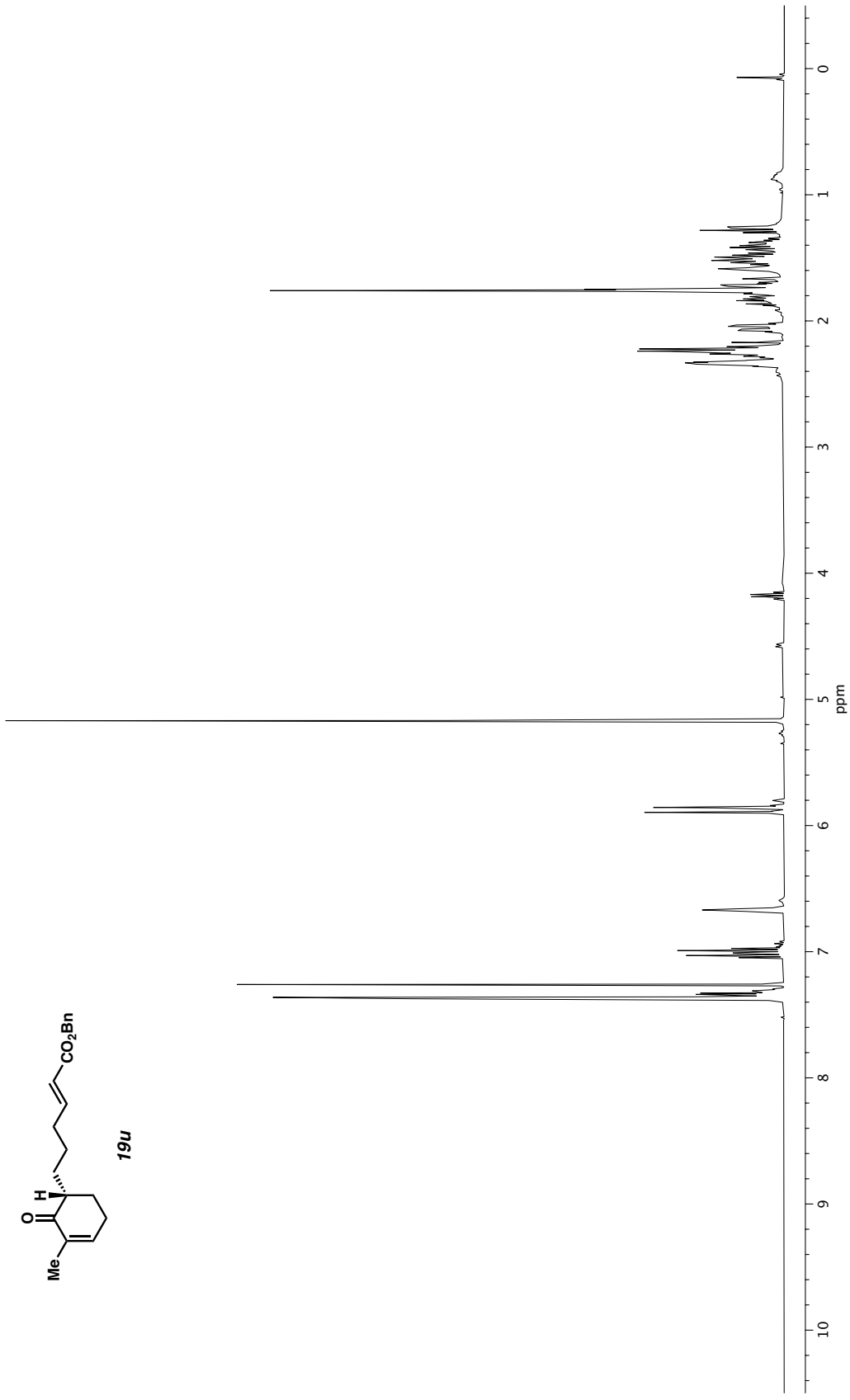


Figure A1.297. *^1H NMR (400 MHz, $CDCl_3$) of compound* ***19u****.*

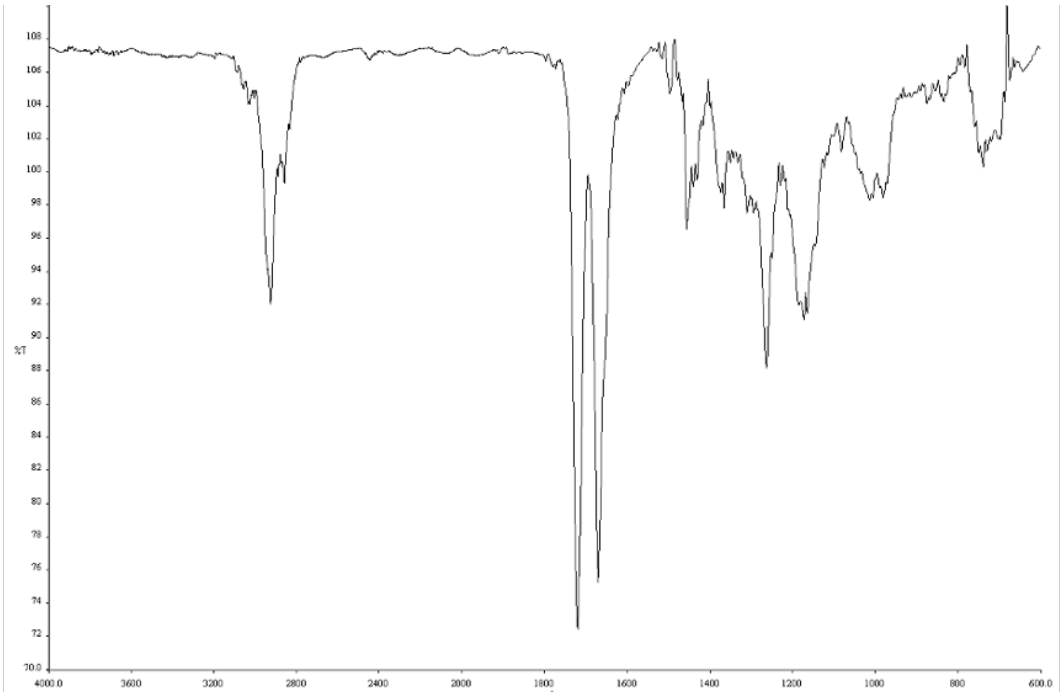


Figure A1.298. *Infrared spectrum (Thin Film, NaCl) of compound* ***19u****.*

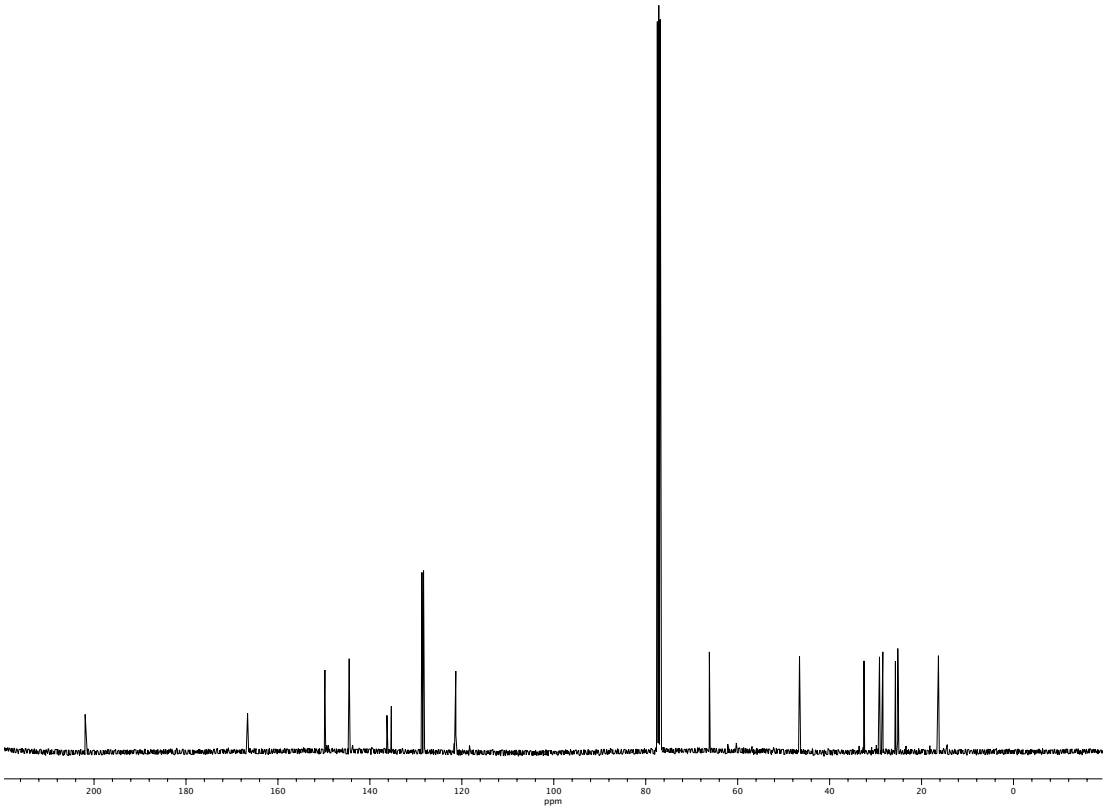


Figure A1.299. *^{13}C NMR (100 MHz, $CDCl_3$) of compound* ***19u****.*

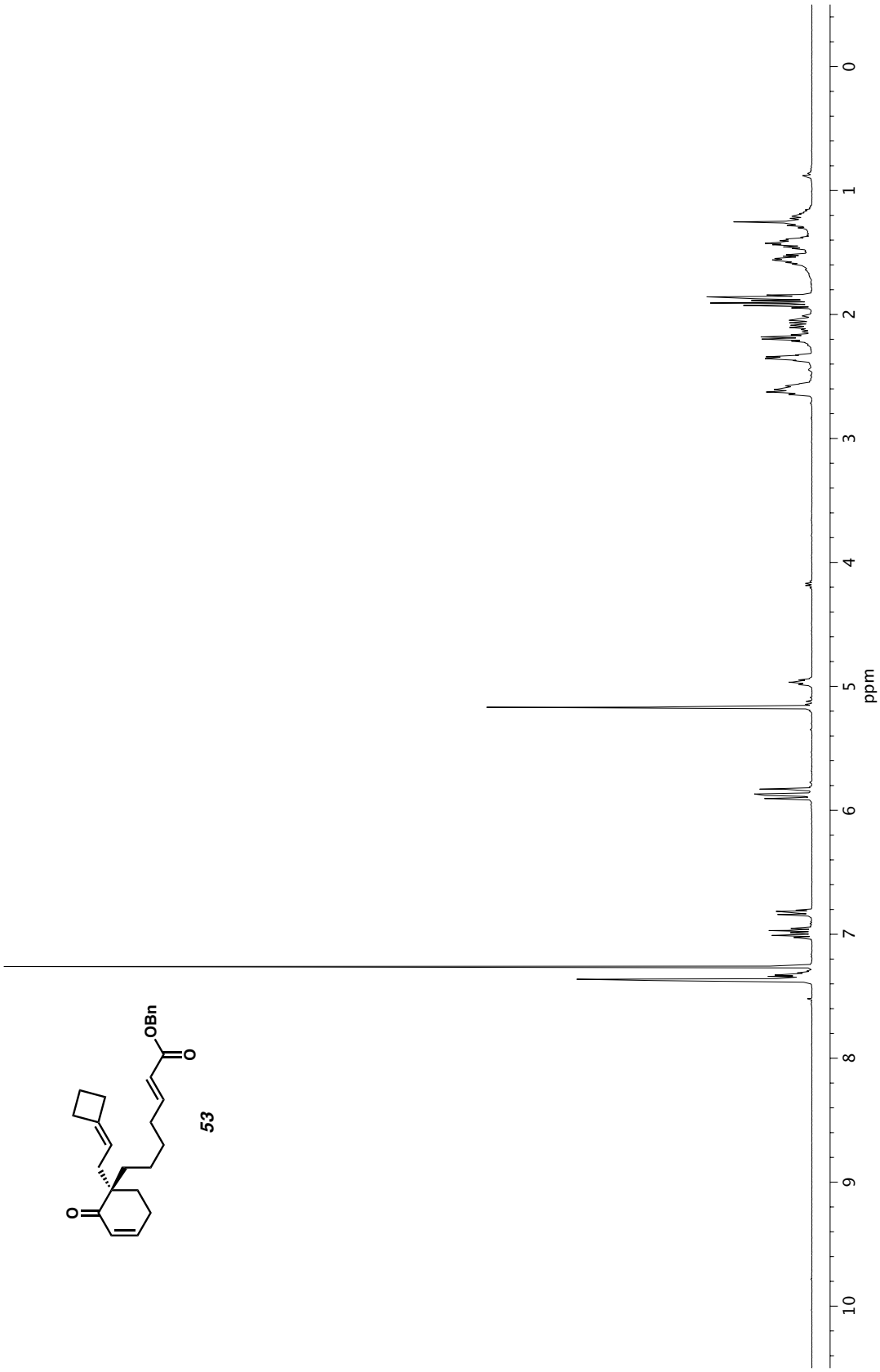


Figure A1.300. *^1H NMR (400 MHz, $CDCl_3$) of compound **53**.*

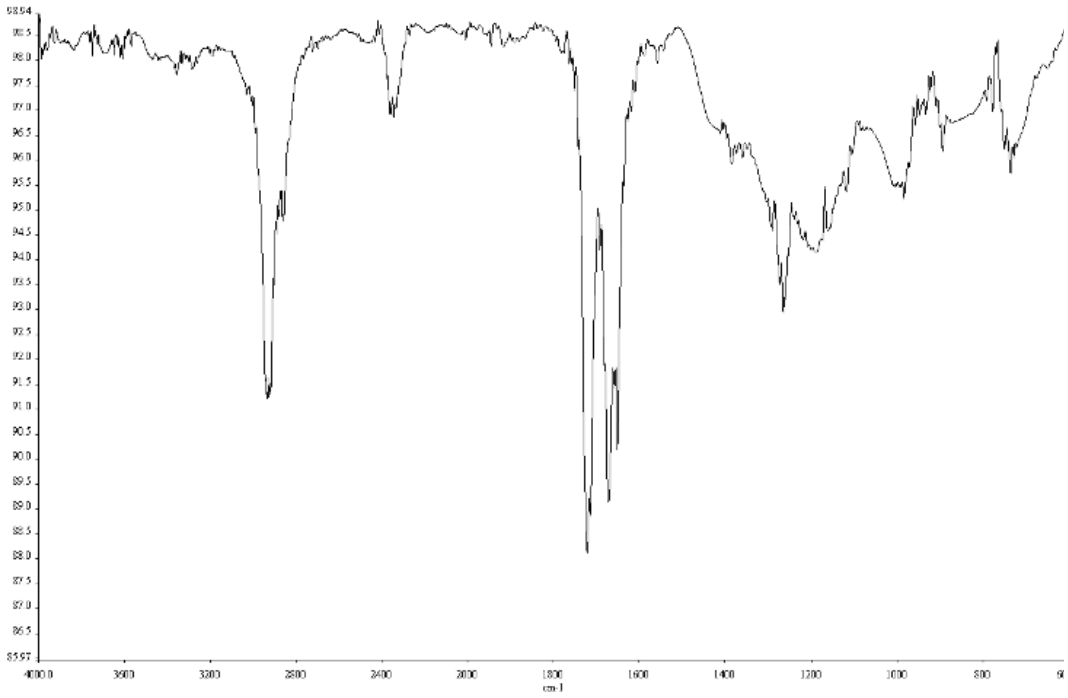


Figure A1.301. *Infrared spectrum (Thin Film, NaCl) of compound* ***53****.*

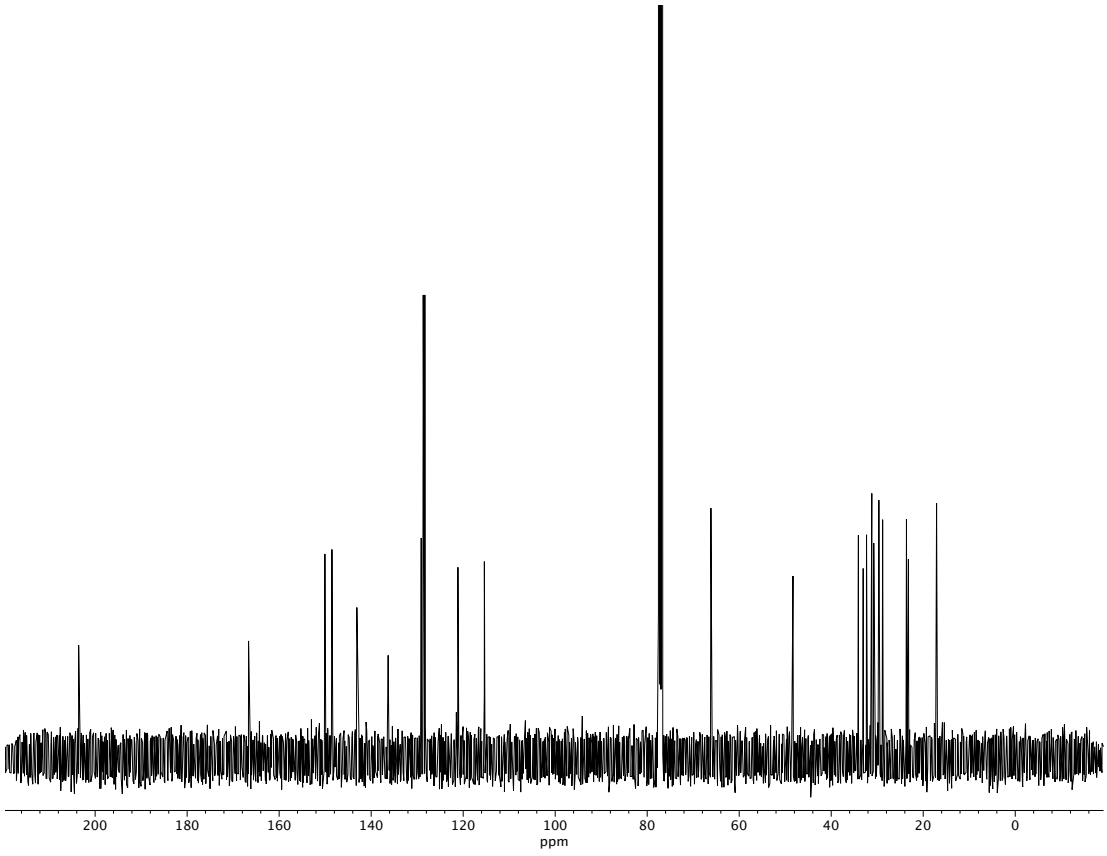


Figure A1.302. *^{13}C NMR (100 MHz, $CDCl_3$) of compound* ***53****.*

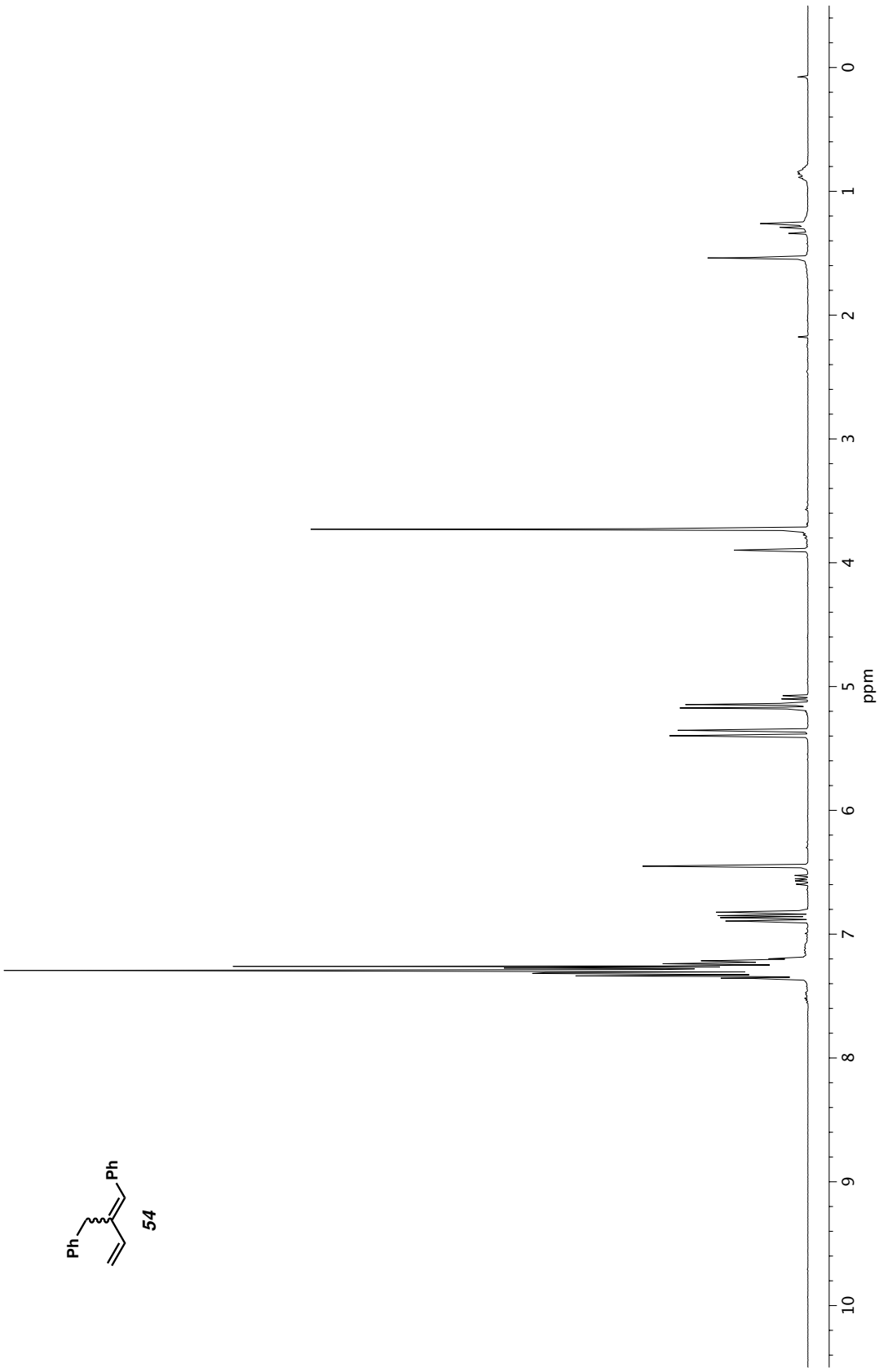


Figure A1.303. *^1H NMR (400 MHz, $CDCl_3$) of compound **54**.*

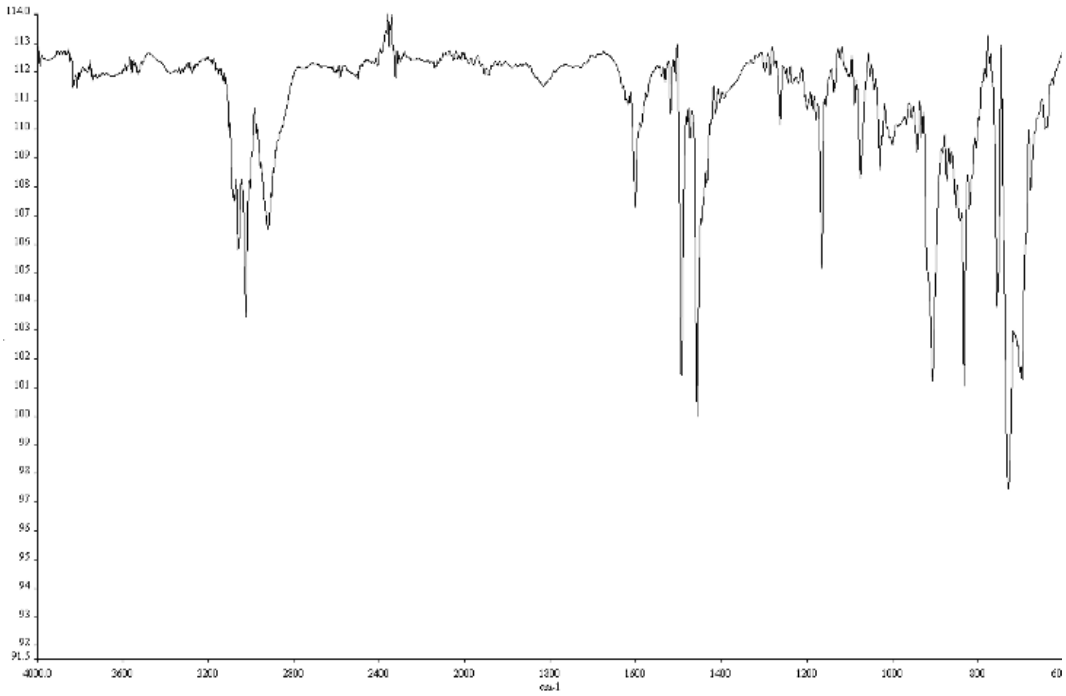


Figure A1.304. *Infrared spectrum (Thin Film, NaCl) of compound* ***54****.*

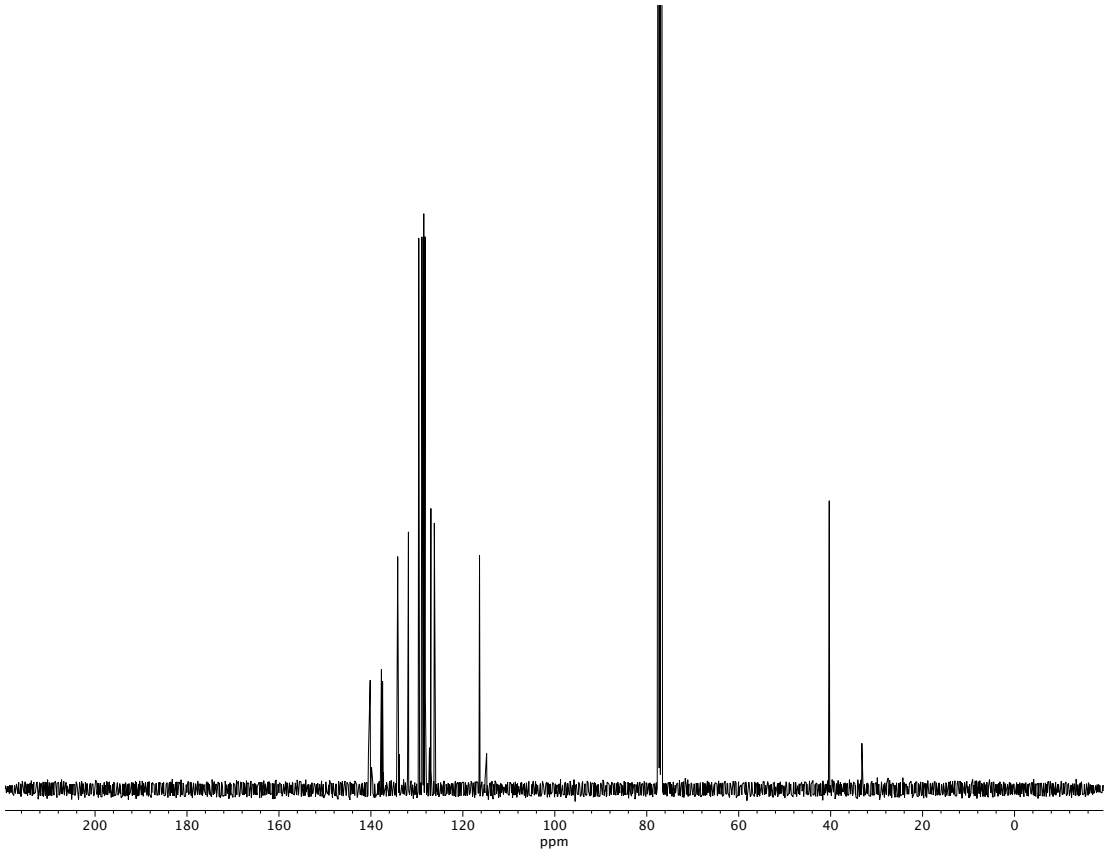


Figure A1.305. *^{13}C NMR (100 MHz, $CDCl_3$) of compound* ***54****.*

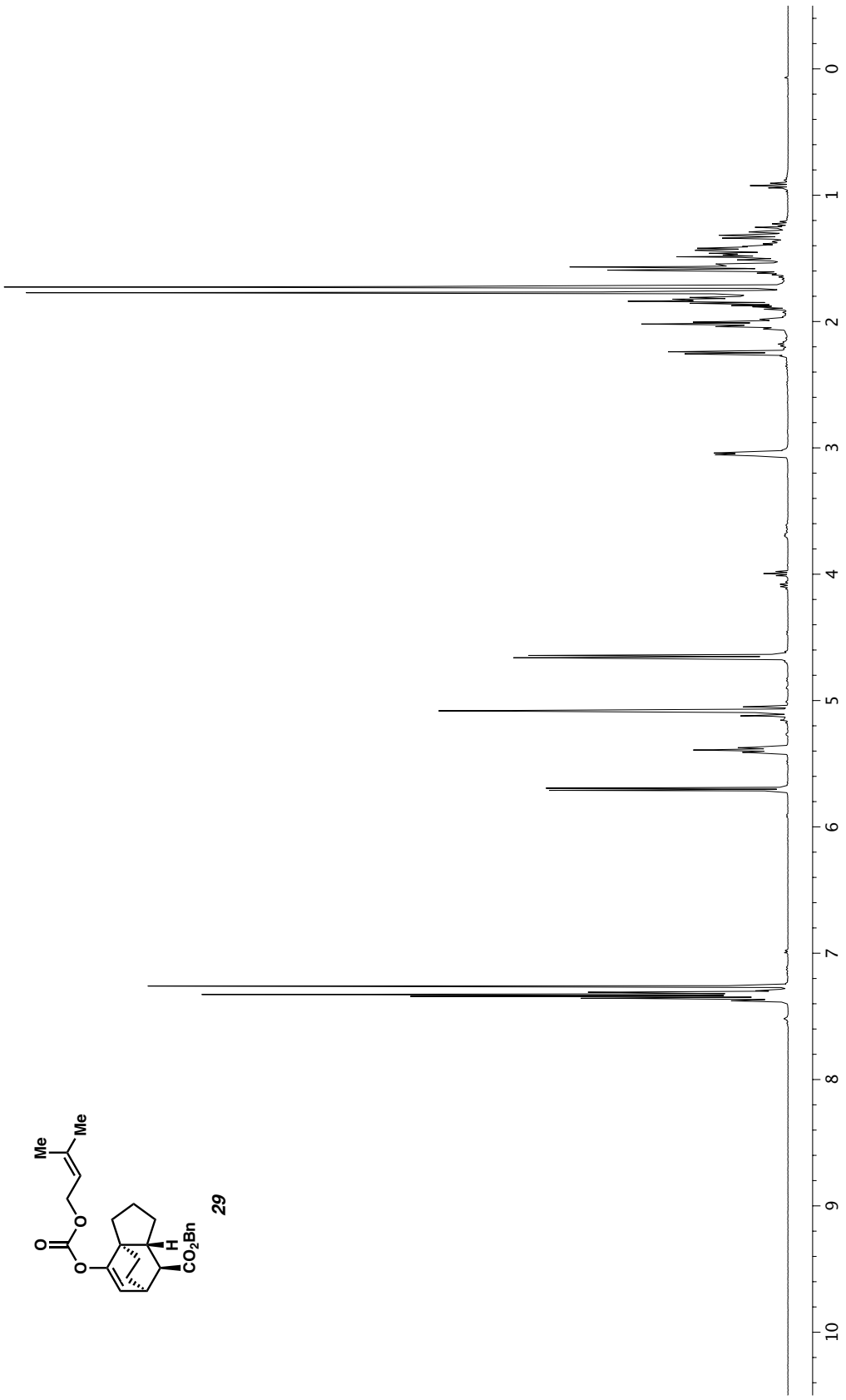


Figure A1.306. *^1H NMR (400 MHz, $CDCl_3$) of compound* ***29****.*

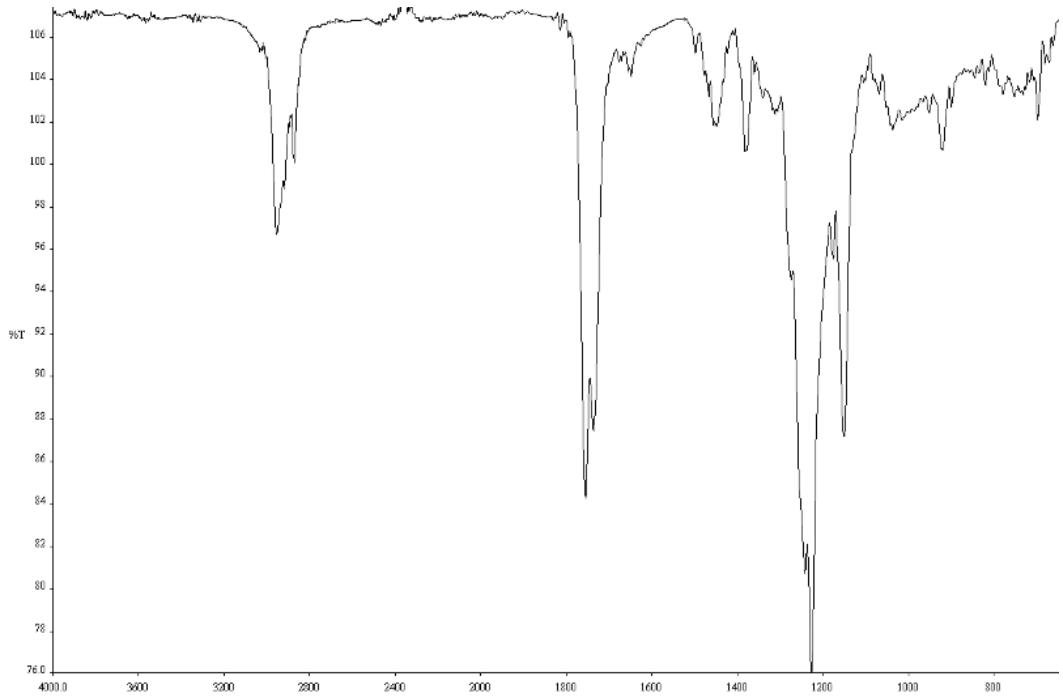


Figure A1.307. *Infrared spectrum (Thin Film, NaCl) of compound* ***29****.*

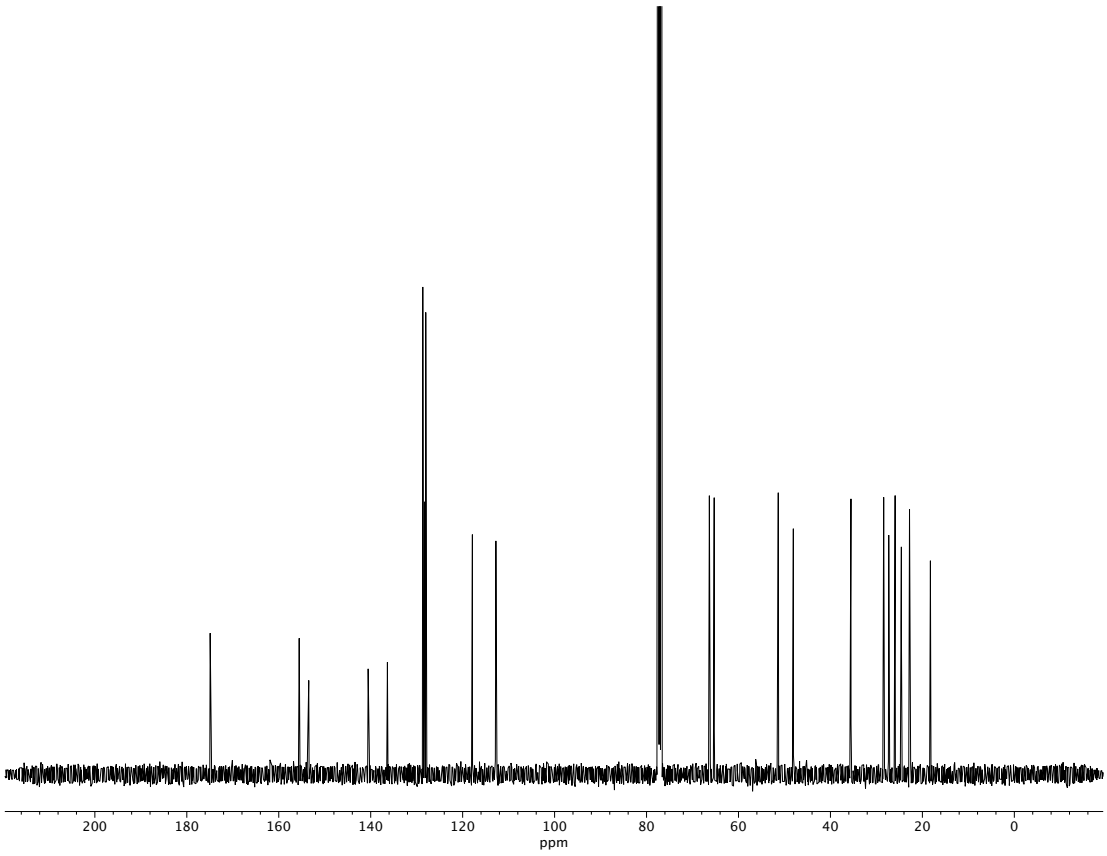


Figure A1.308. *^{13}C NMR (100 MHz, $CDCl_3$) of compound* ***29****.*

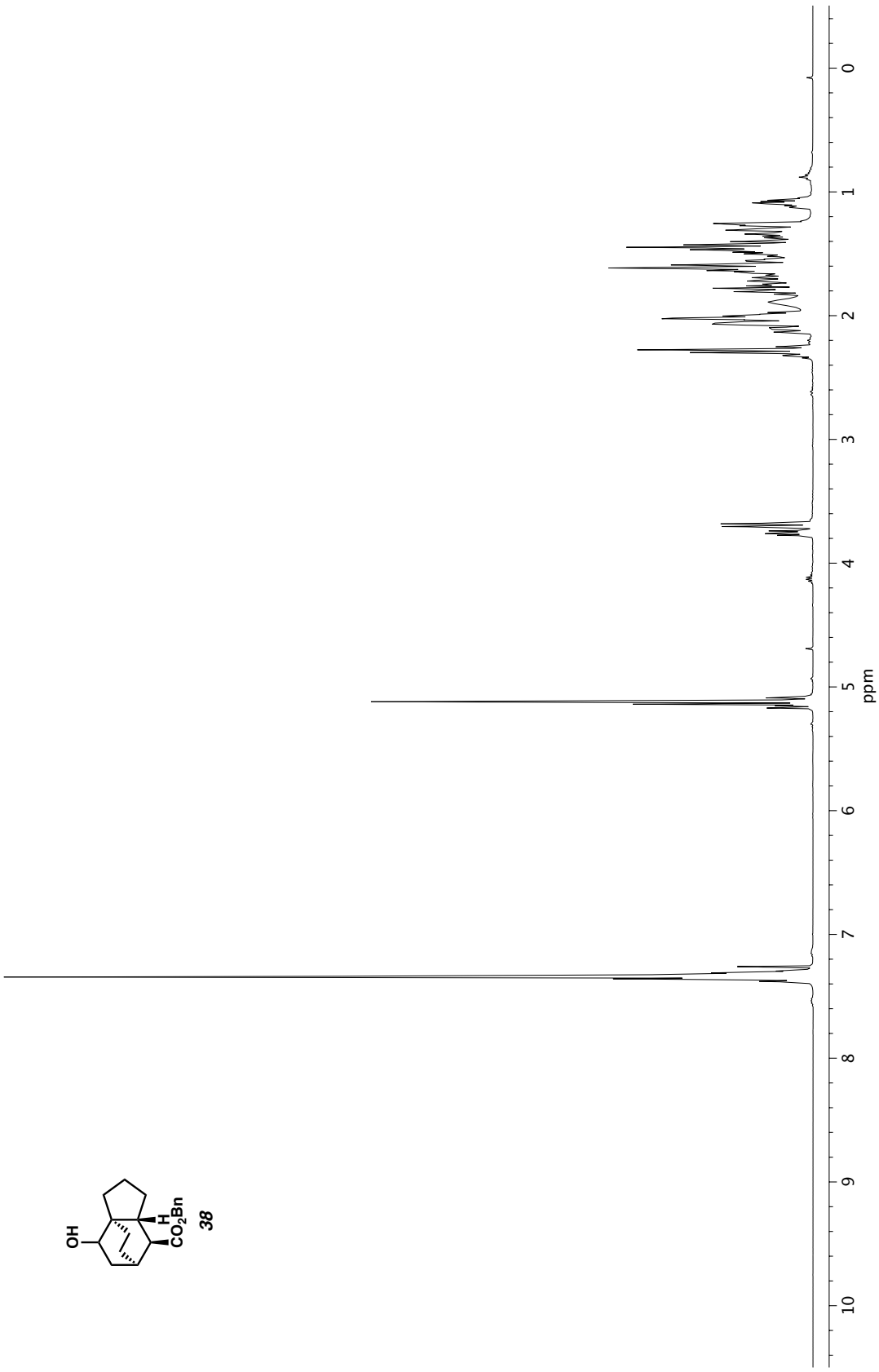


Figure A1.309. *^1H NMR (400 MHz, $CDCl_3$) of compound **38**.*

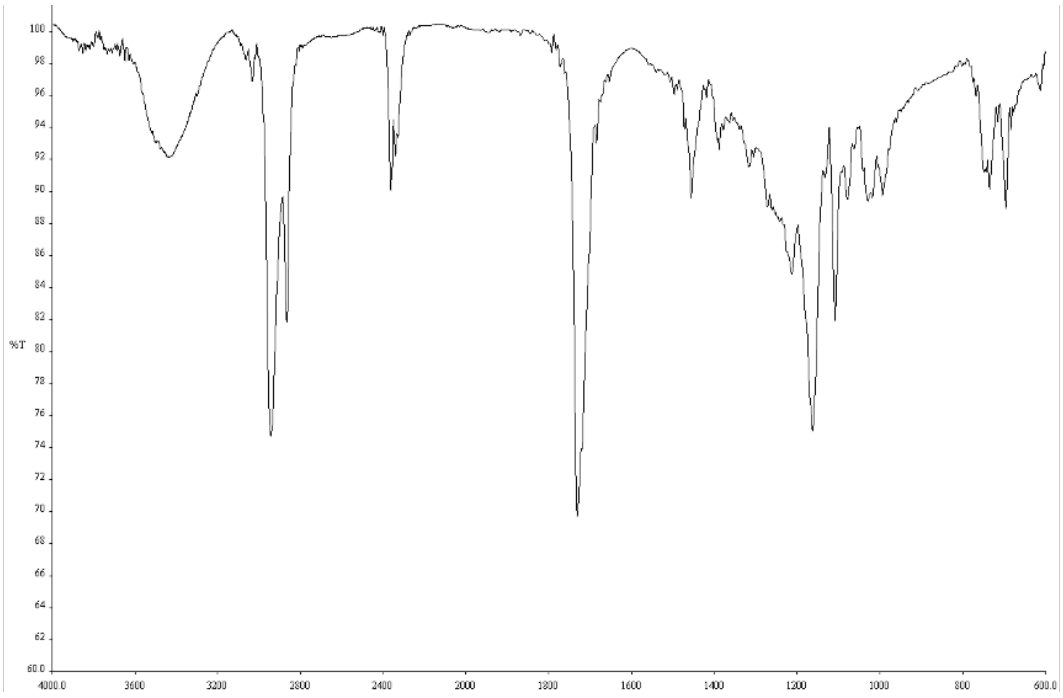


Figure A1.310. *Infrared spectrum (Thin Film, NaCl) of compound* ***38****.*

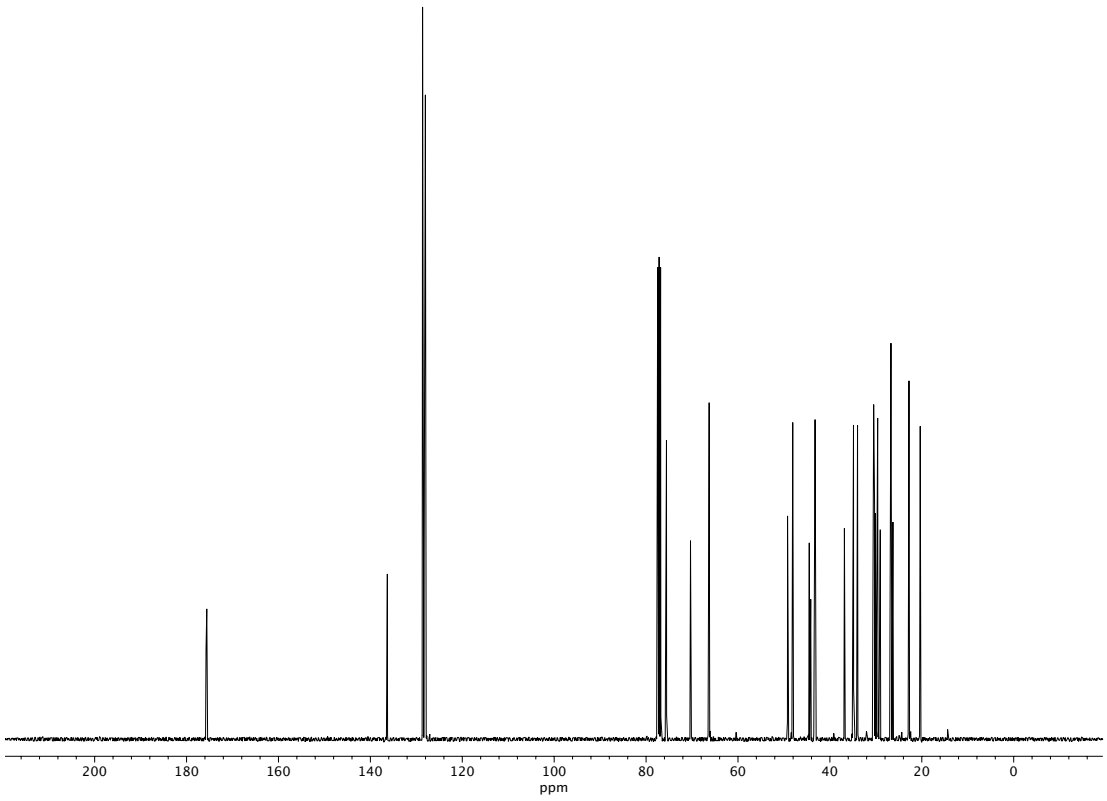


Figure A1.311. *^{13}C NMR (100 MHz, $CDCl_3$) of compound* ***38****.*

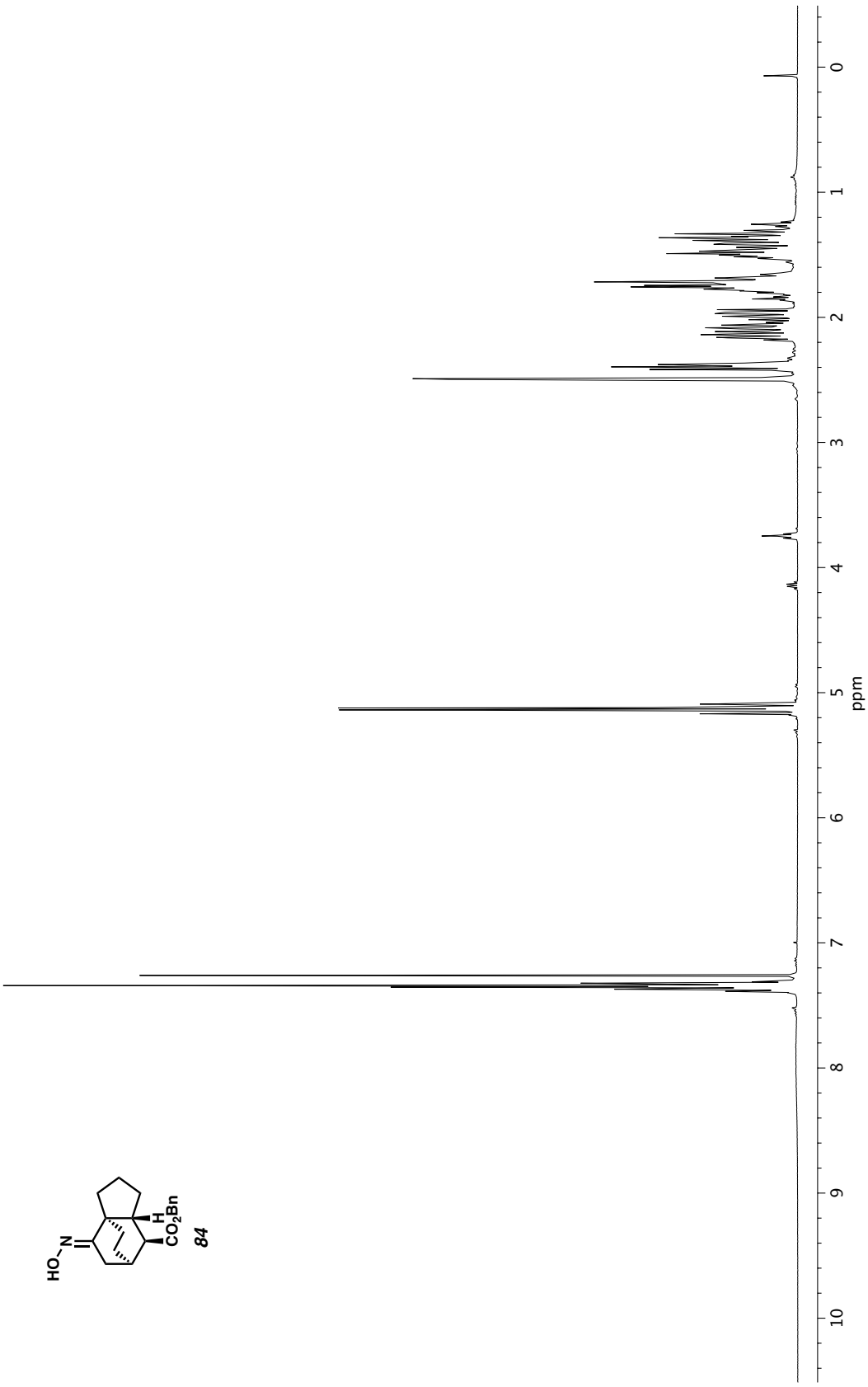


Figure A1.312. *^1H NMR (400 MHz, $CDCl_3$) of compound* ***84****.*

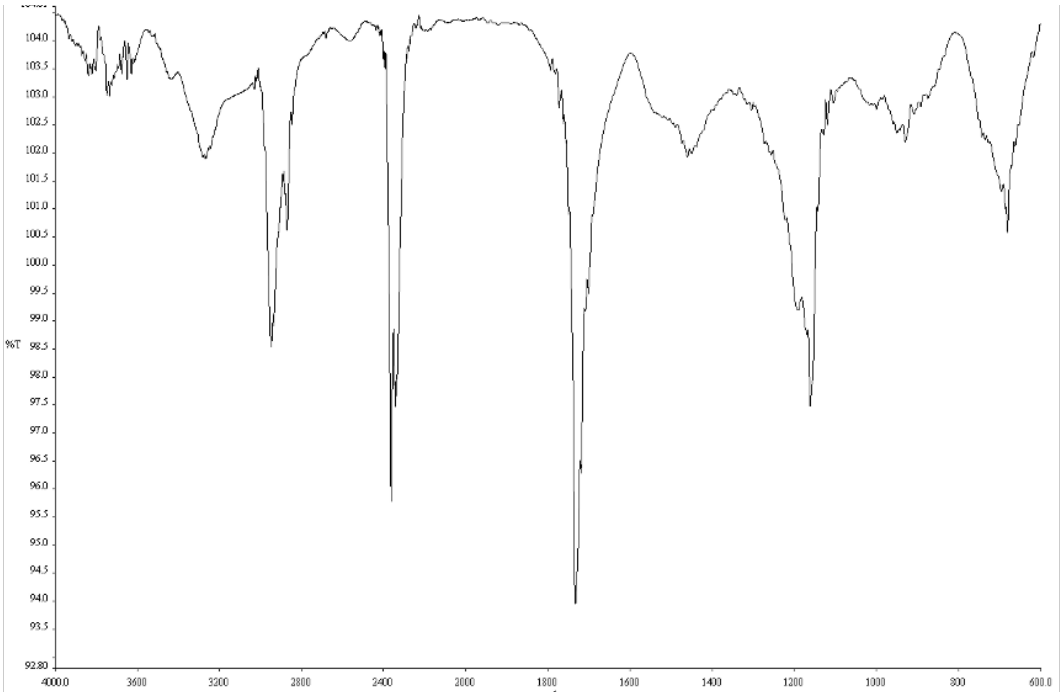


Figure A1.313. *Infrared spectrum (Thin Film, NaCl) of compound* ***84****.*

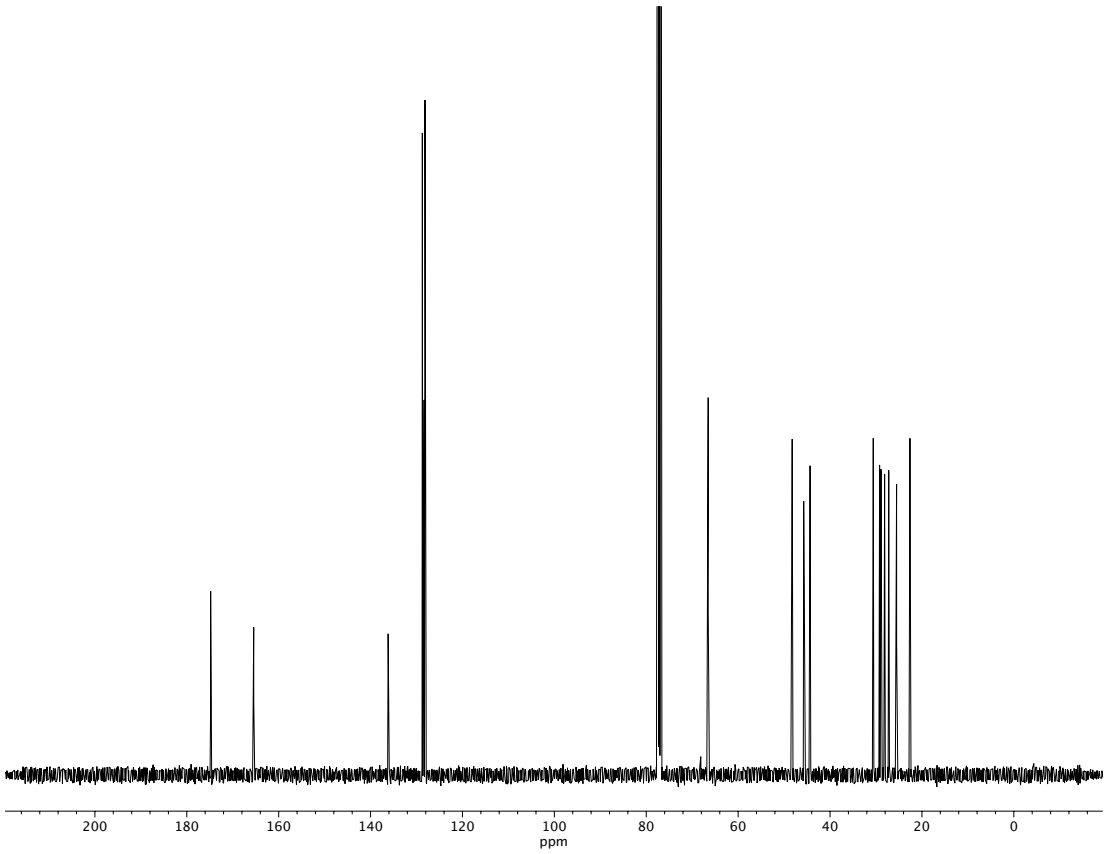
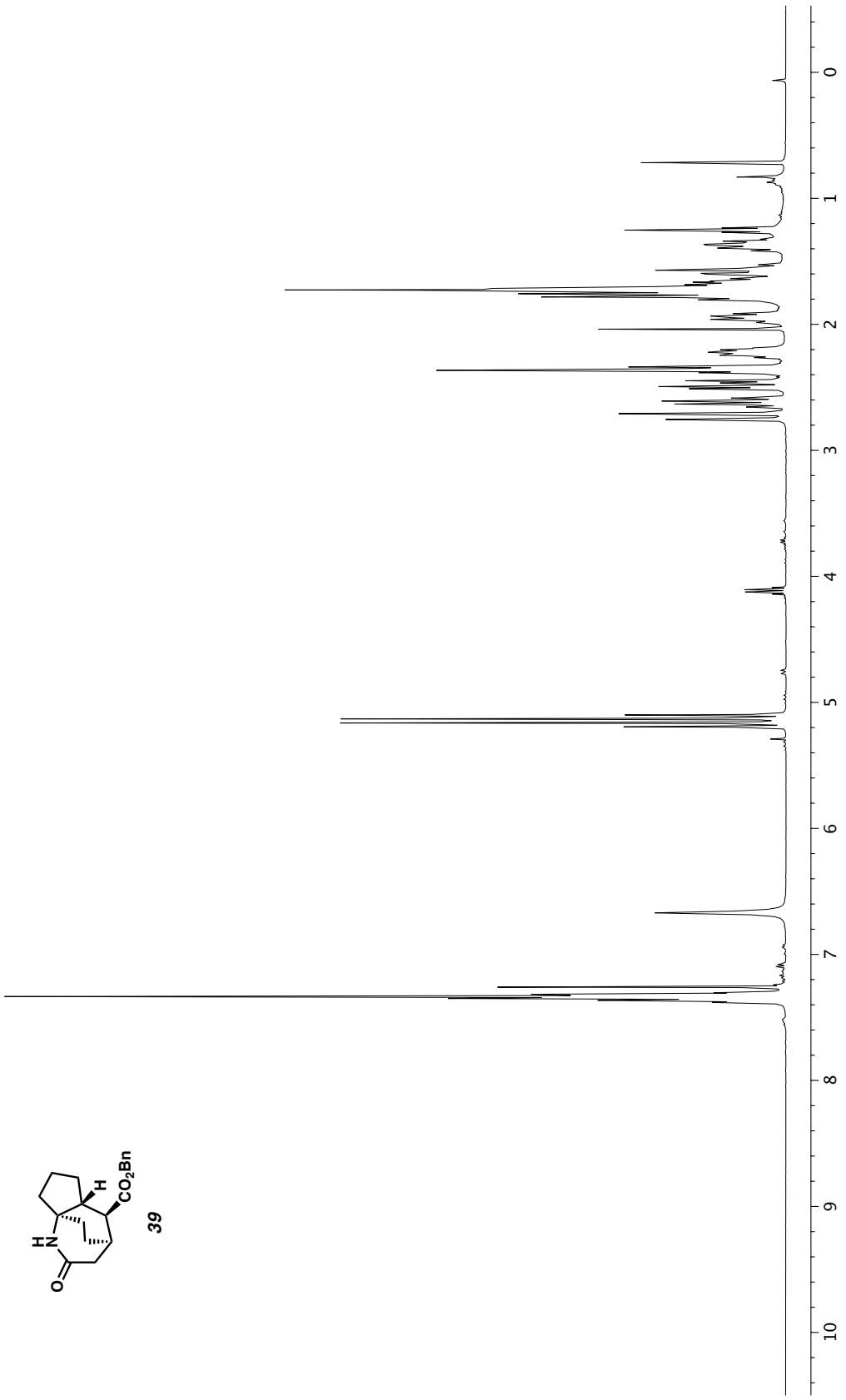


Figure A1.314. *^{13}C NMR (100 MHz, $CDCl_3$) of compound* ***84****.*



39

Figure A1.315. *^1H NMR (400 MHz, $CDCl_3$) of compound **39**.*

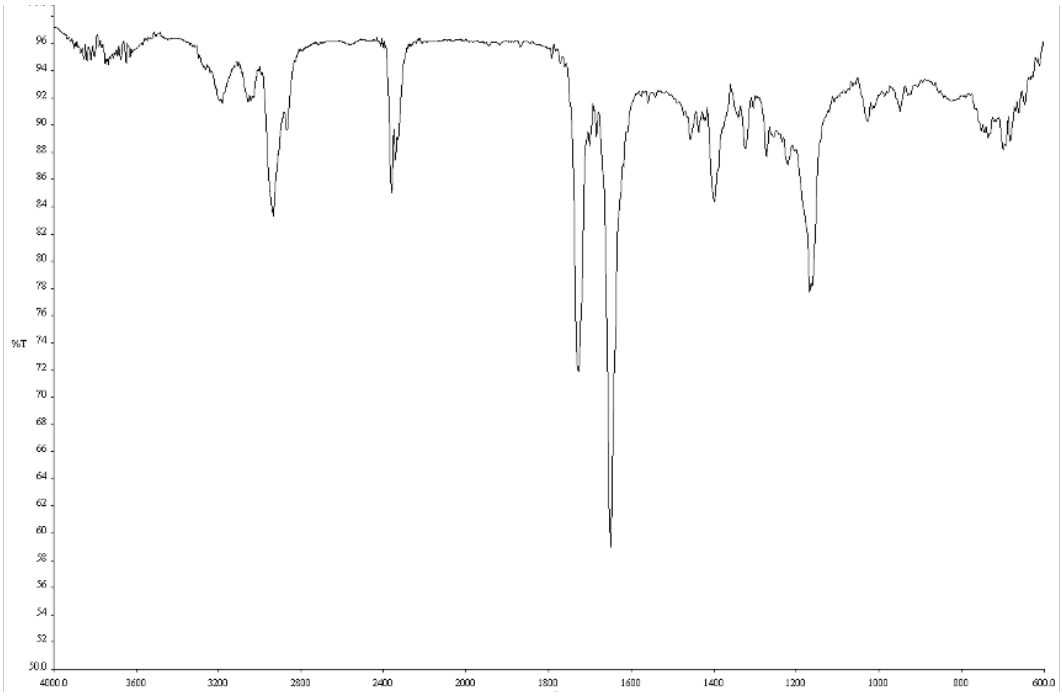


Figure A1.316. *Infrared spectrum (Thin Film, NaCl) of compound* ***39****.*

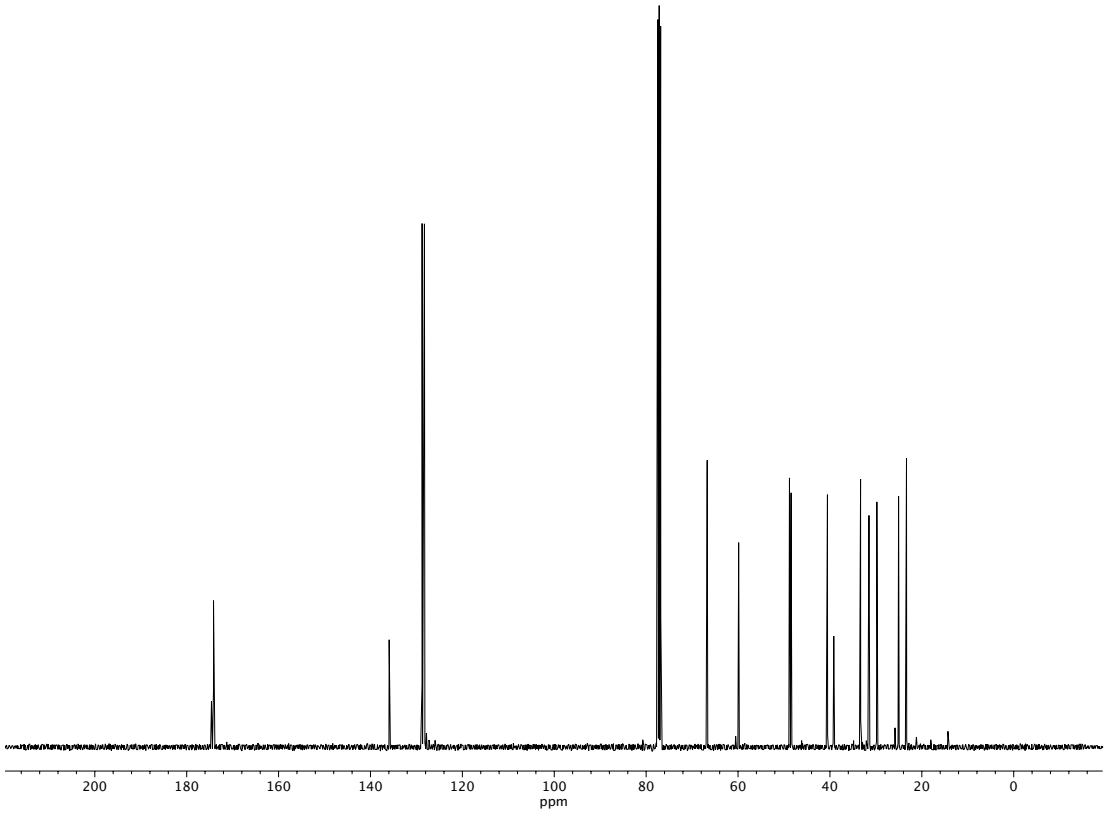


Figure A1.317. *^{13}C NMR (100 MHz, $CDCl_3$) of compound* ***39****.*

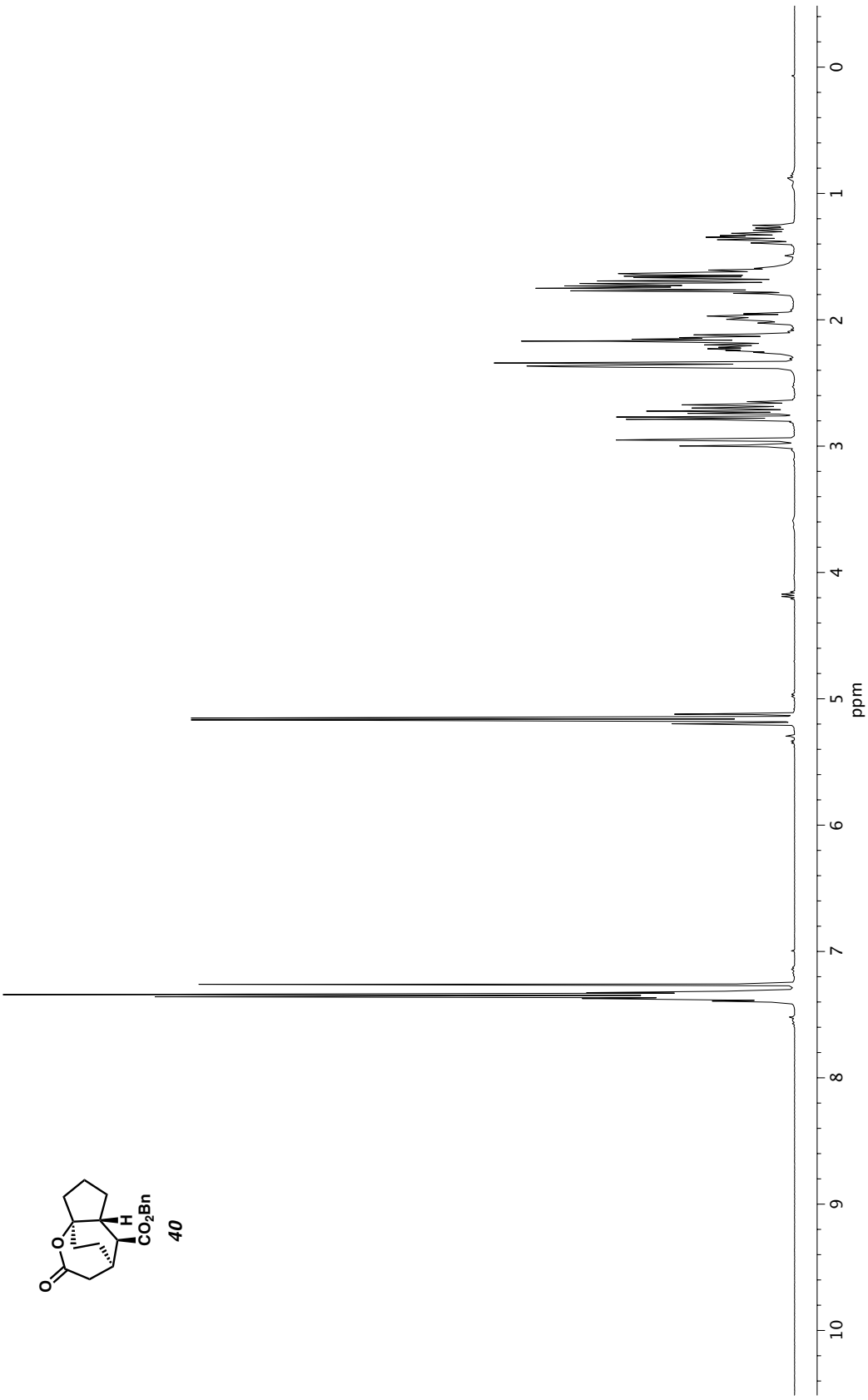


Figure A1.318. *^1H NMR (400 MHz, $CDCl_3$) of compound **40**.*

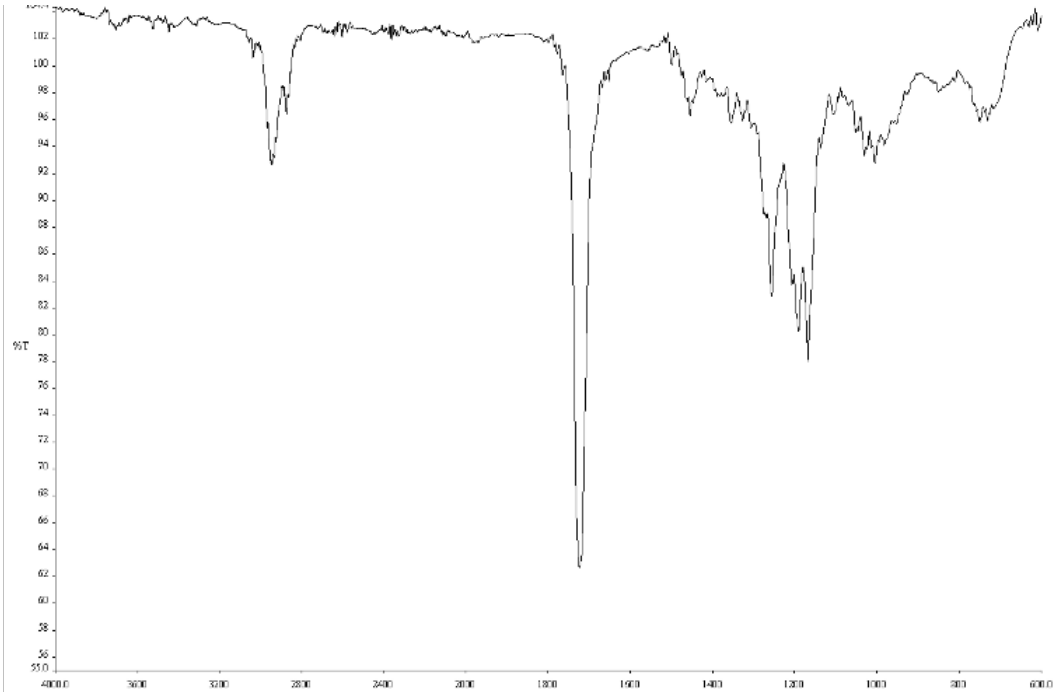


Figure A1.319. *Infrared spectrum (Thin Film, NaCl) of compound* ***40****.*

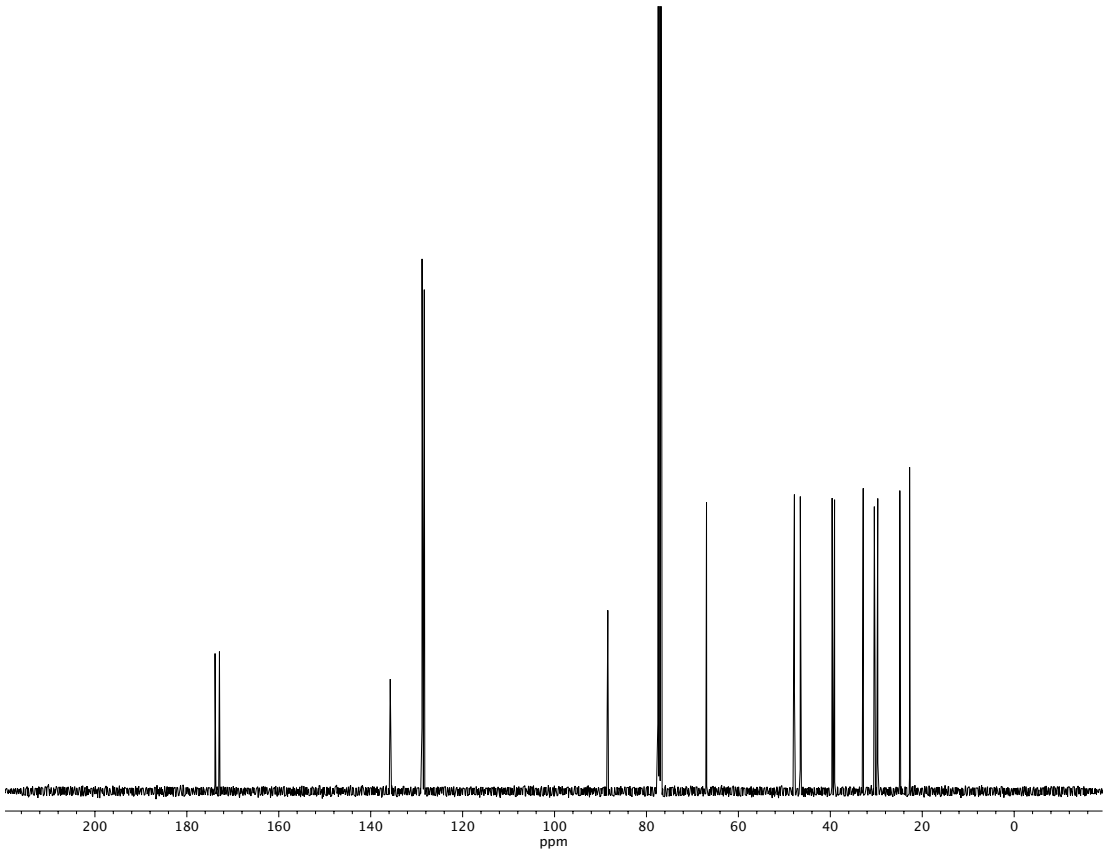


Figure A1.320. *^{13}C NMR (100 MHz, $CDCl_3$) of compound* ***40****.*

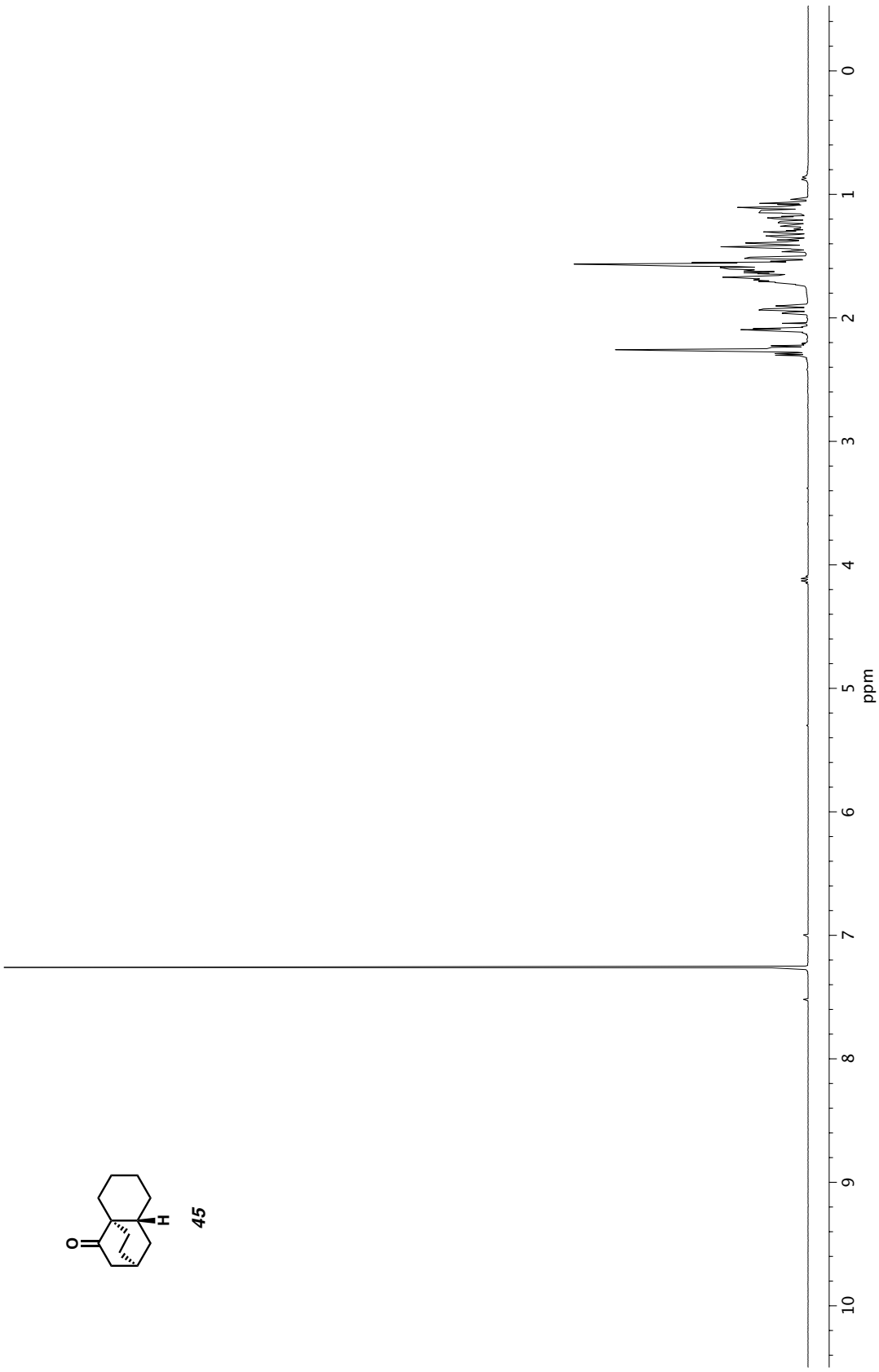


Figure A1.321. *^1H NMR (400 MHz, $CDCl_3$) of compound **45**.*

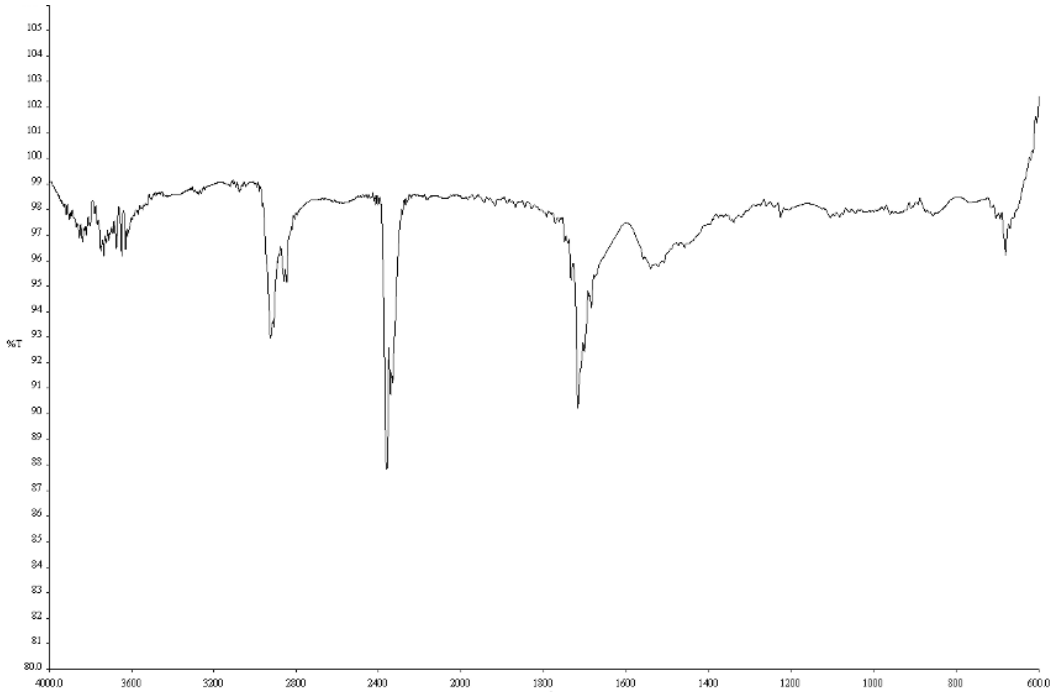


Figure A1.322. *Infrared spectrum (Thin Film, NaCl) of compound* ***45****.*

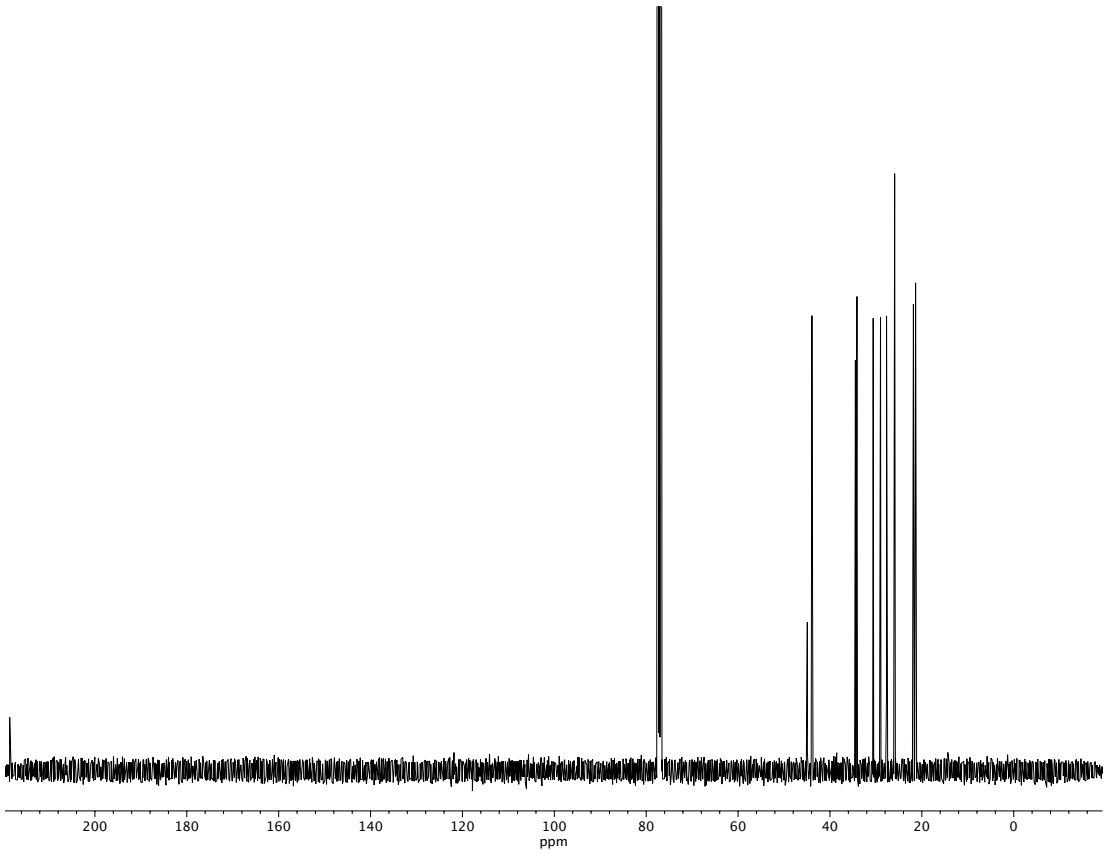


Figure A1.323. *^{13}C NMR (100 MHz, $CDCl_3$) of compound* ***45****.*

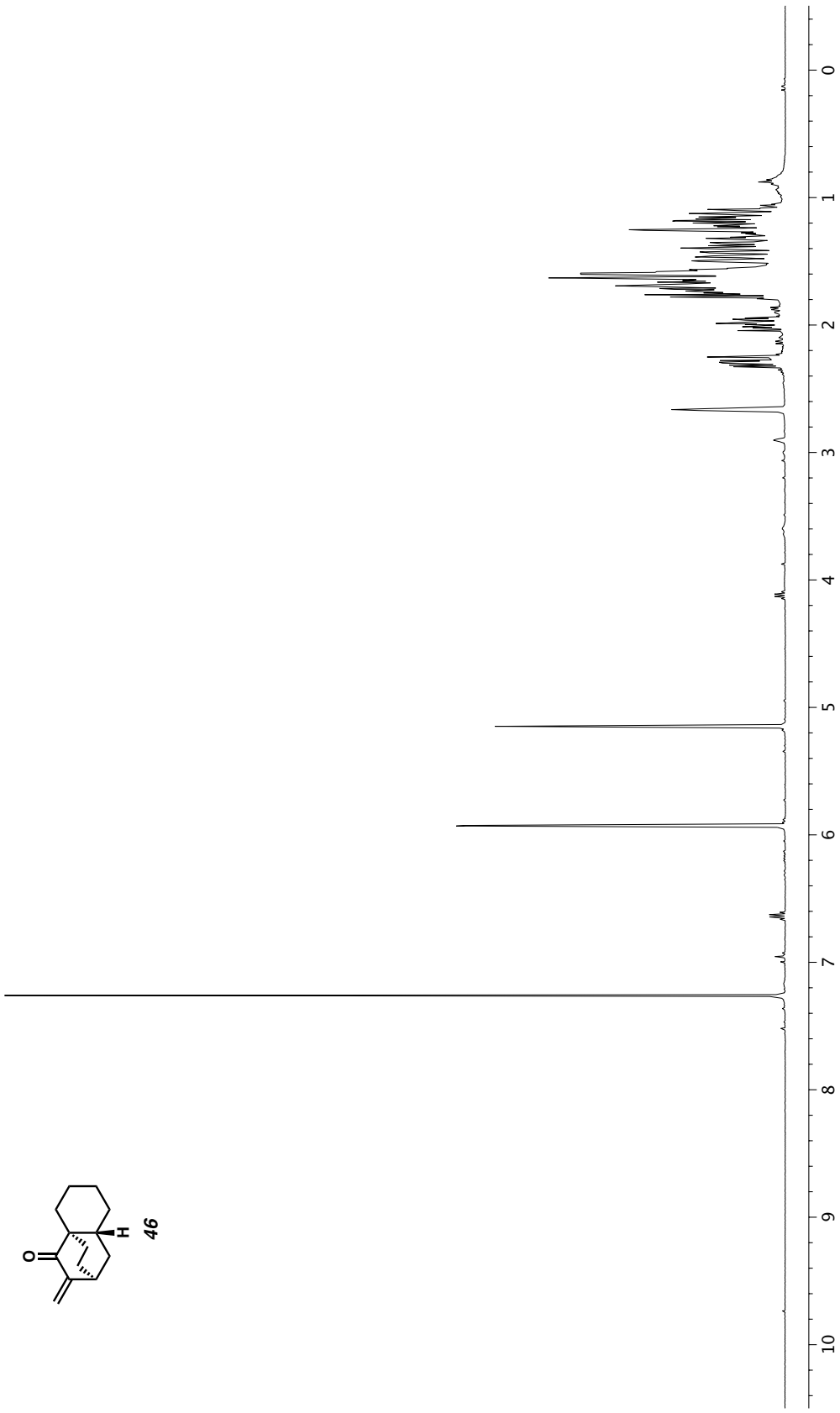


Figure A1.324. *^1H NMR (400 MHz, $CDCl_3$) of compound **46**.*

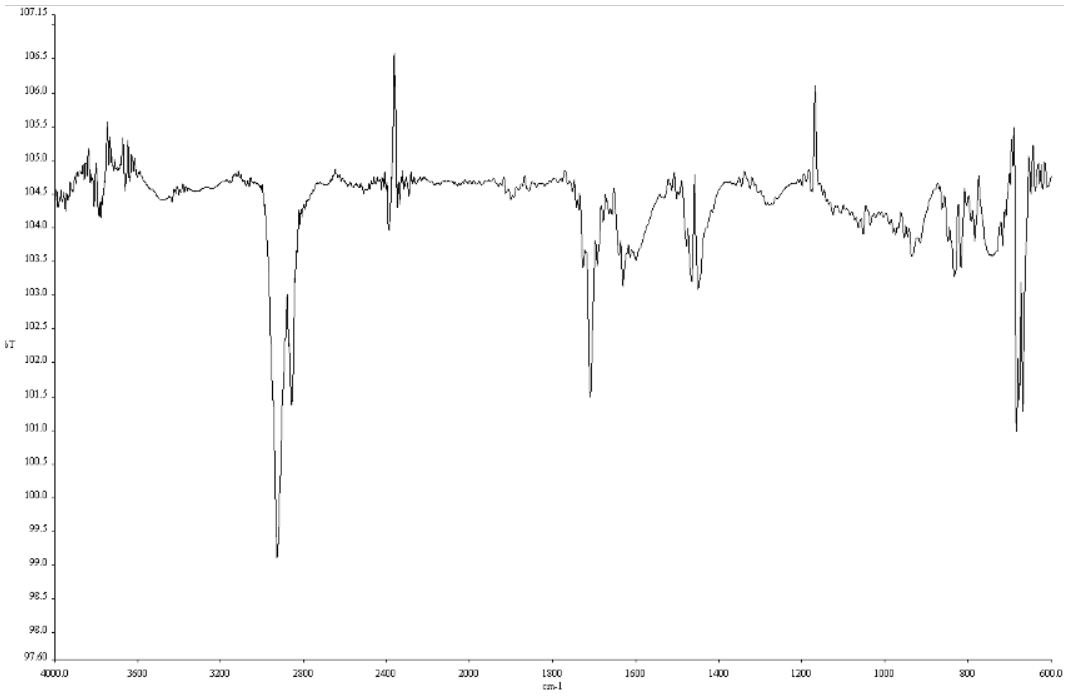


Figure A1.325. *Infrared spectrum (Thin Film, NaCl) of compound* ***46****.*

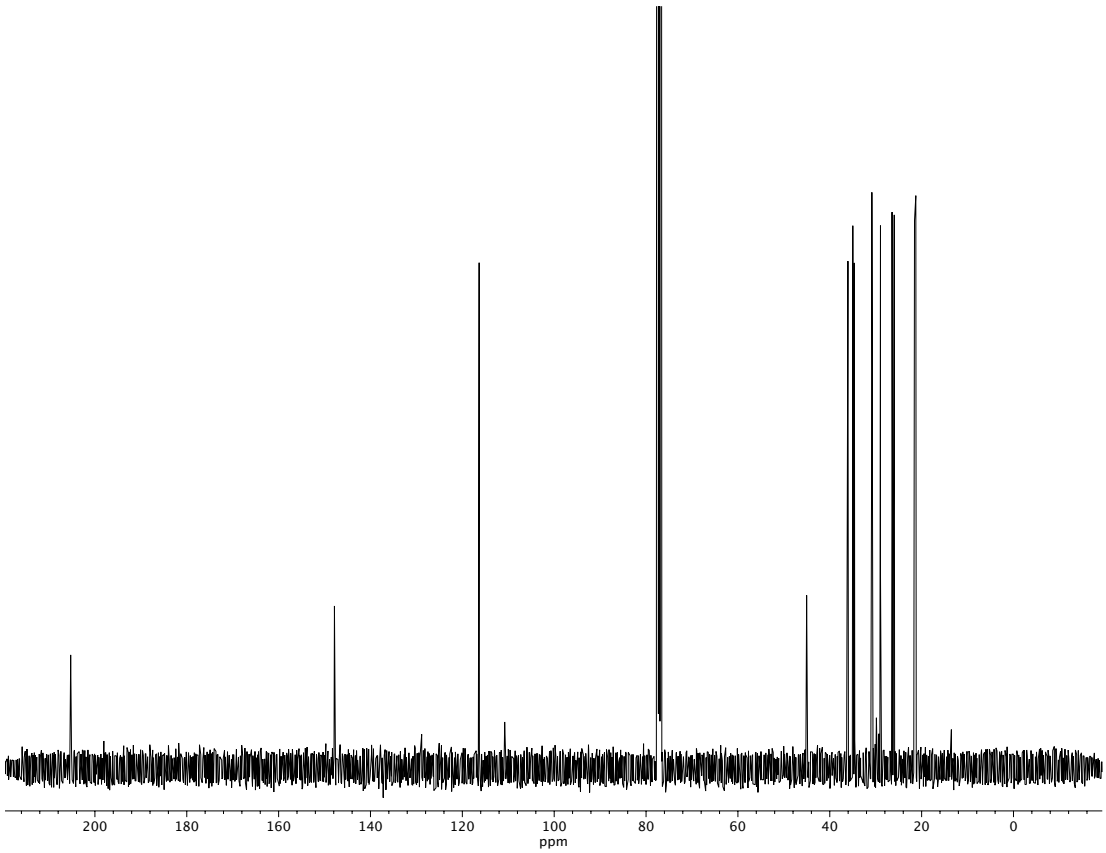


Figure A1.326. *^{13}C NMR (100 MHz, $CDCl_3$) of compound* ***46****.*

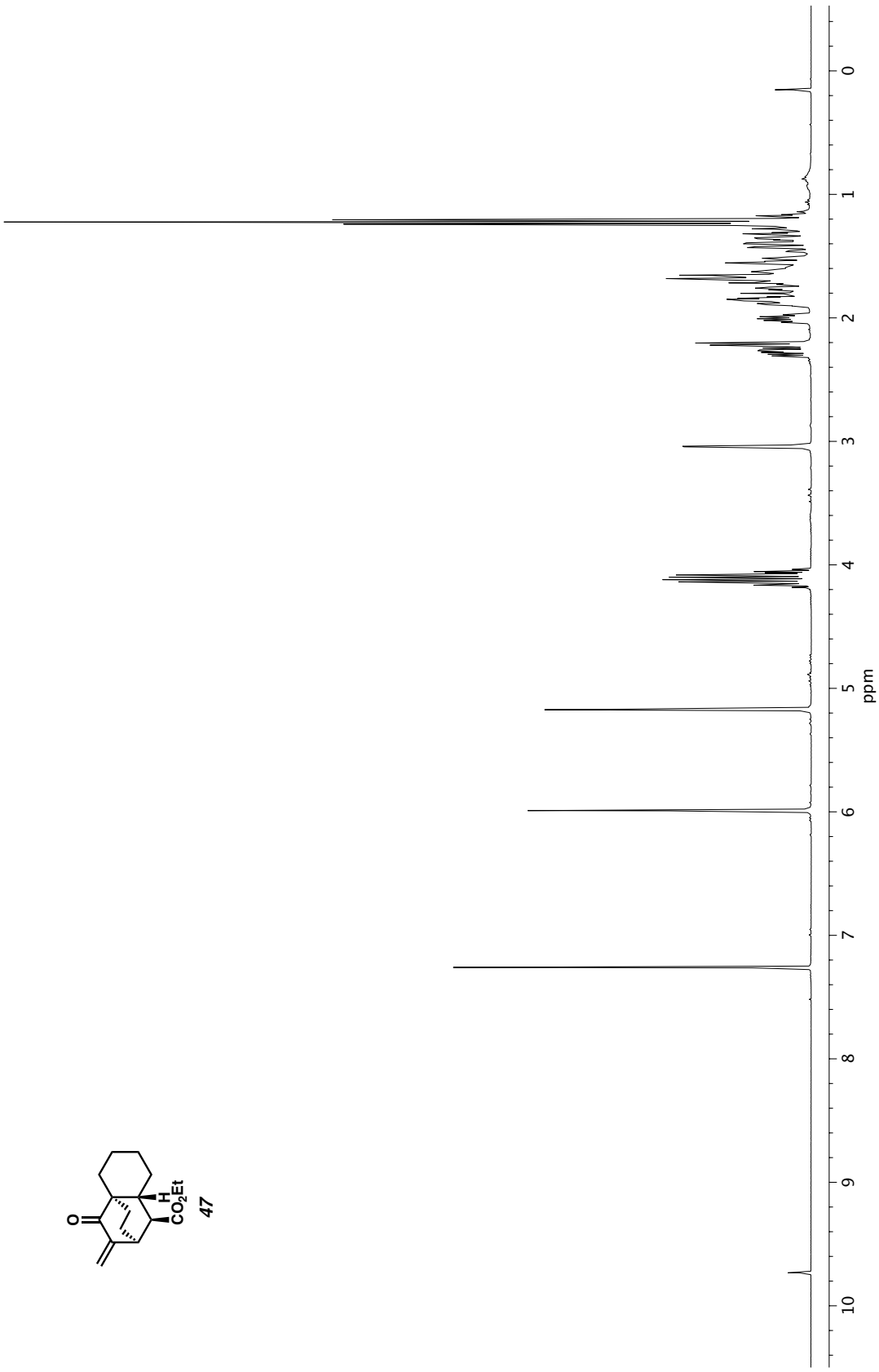


Figure A1.327. *^1H NMR (400 MHz, $CDCl_3$) of compound **47**.*

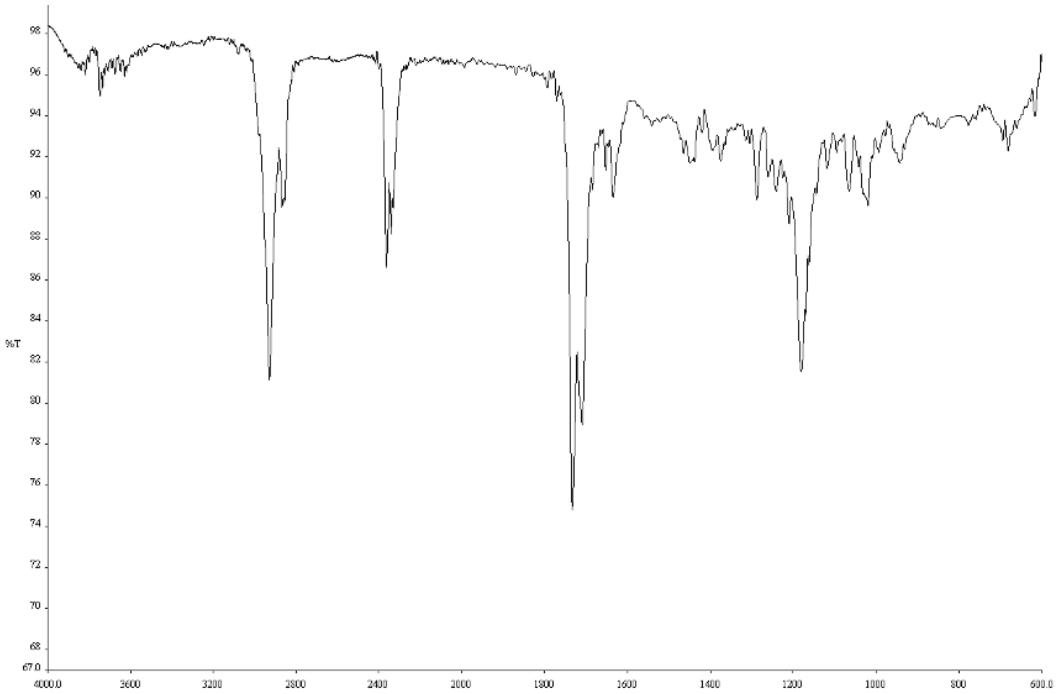


Figure A1.328. *Infrared spectrum (Thin Film, NaCl) of compound* ***47****.*

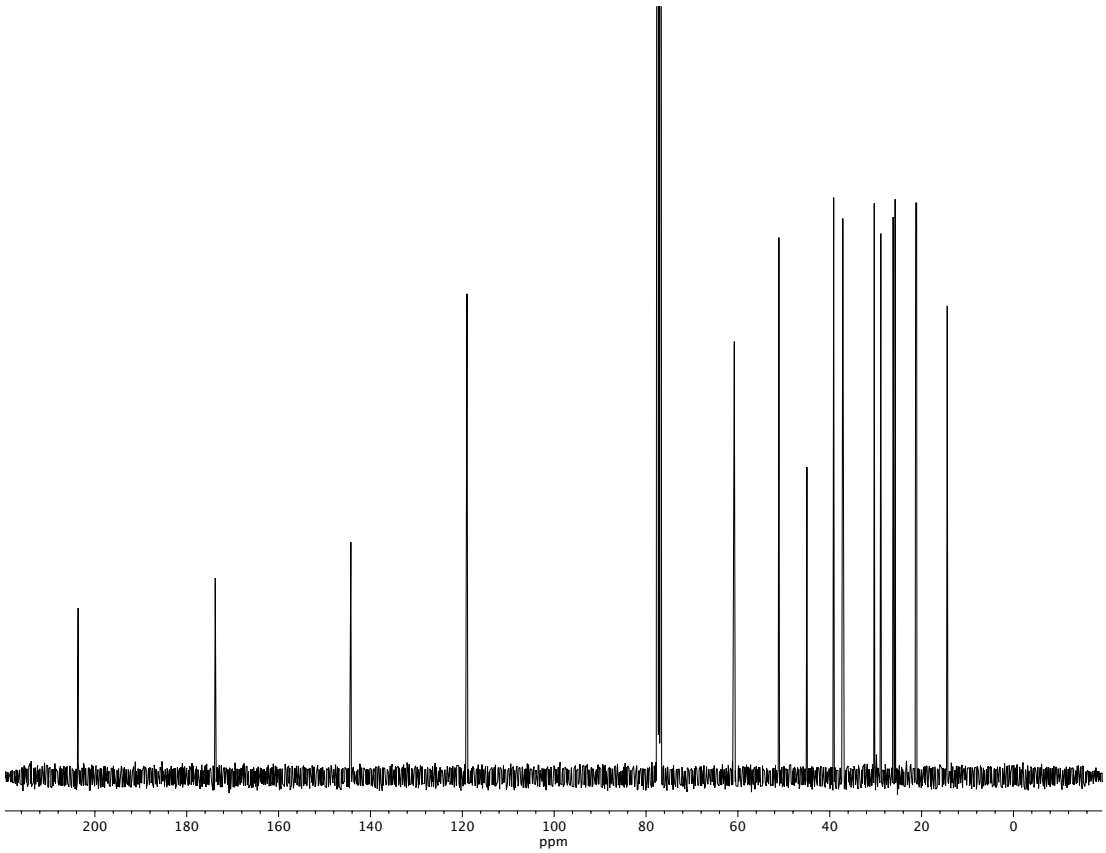


Figure A1.329. *^{13}C NMR (100 MHz, $CDCl_3$) of compound* ***47****.*

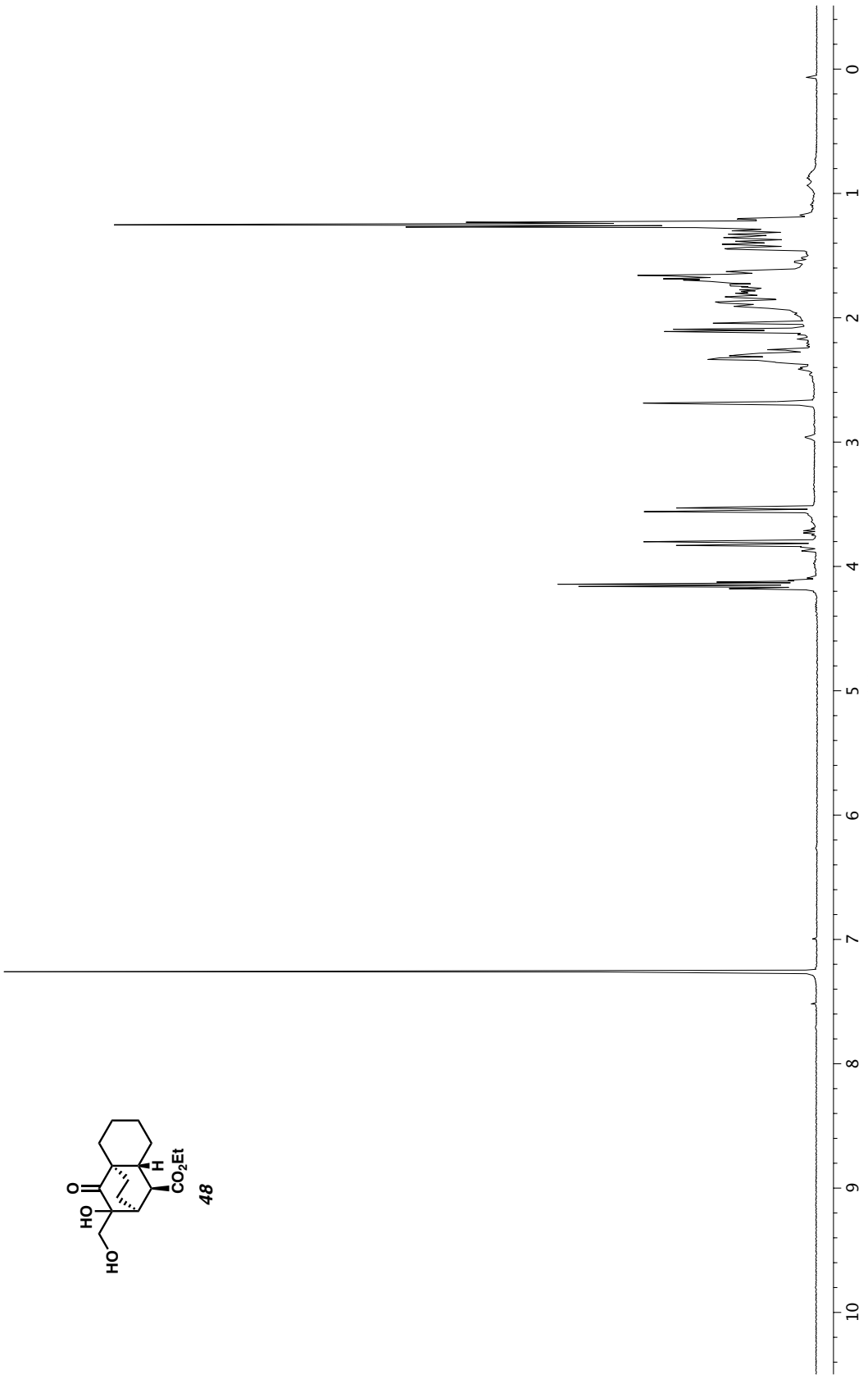


Figure A1.330. *^1H NMR (400 MHz, $CDCl_3$) of compound **48**.*

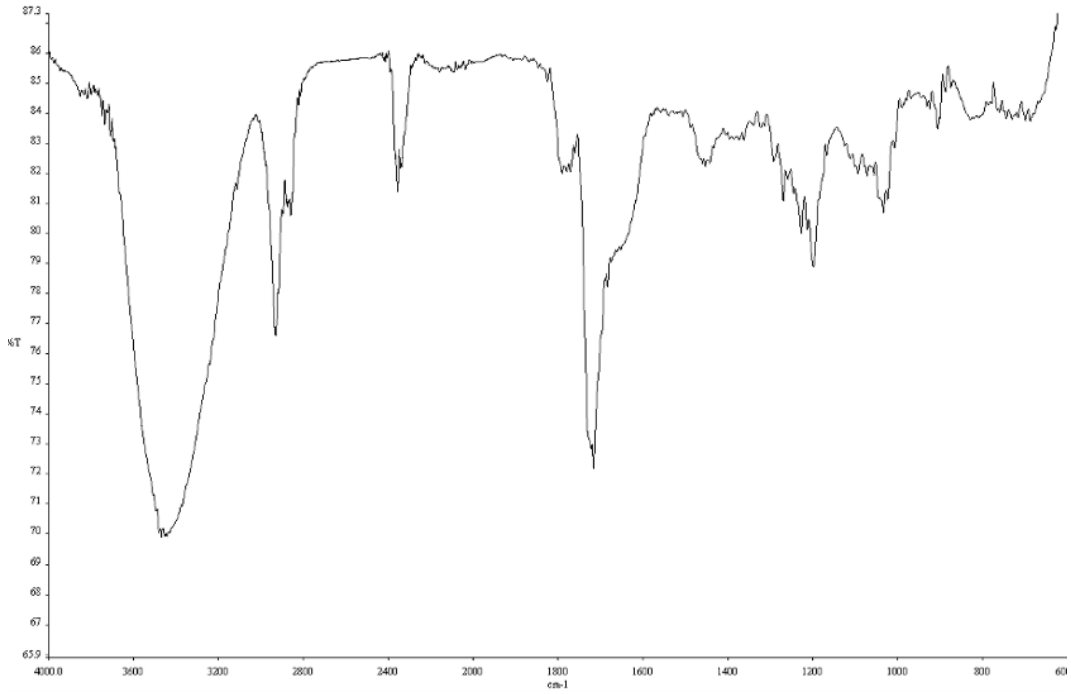


Figure A1.331. *Infrared spectrum (Thin Film, NaCl) of compound* ***48****.*

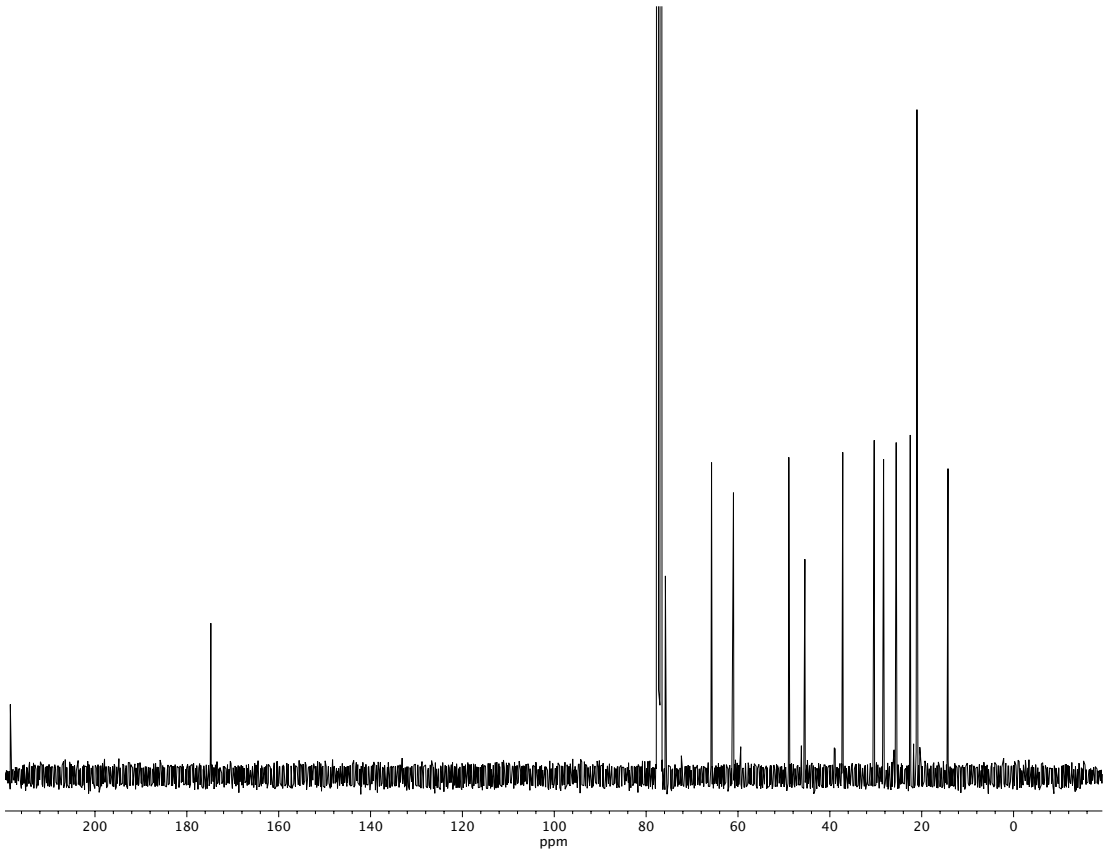


Figure A1.332. *^{13}C NMR (100 MHz, $CDCl_3$) of compound* ***48****.*

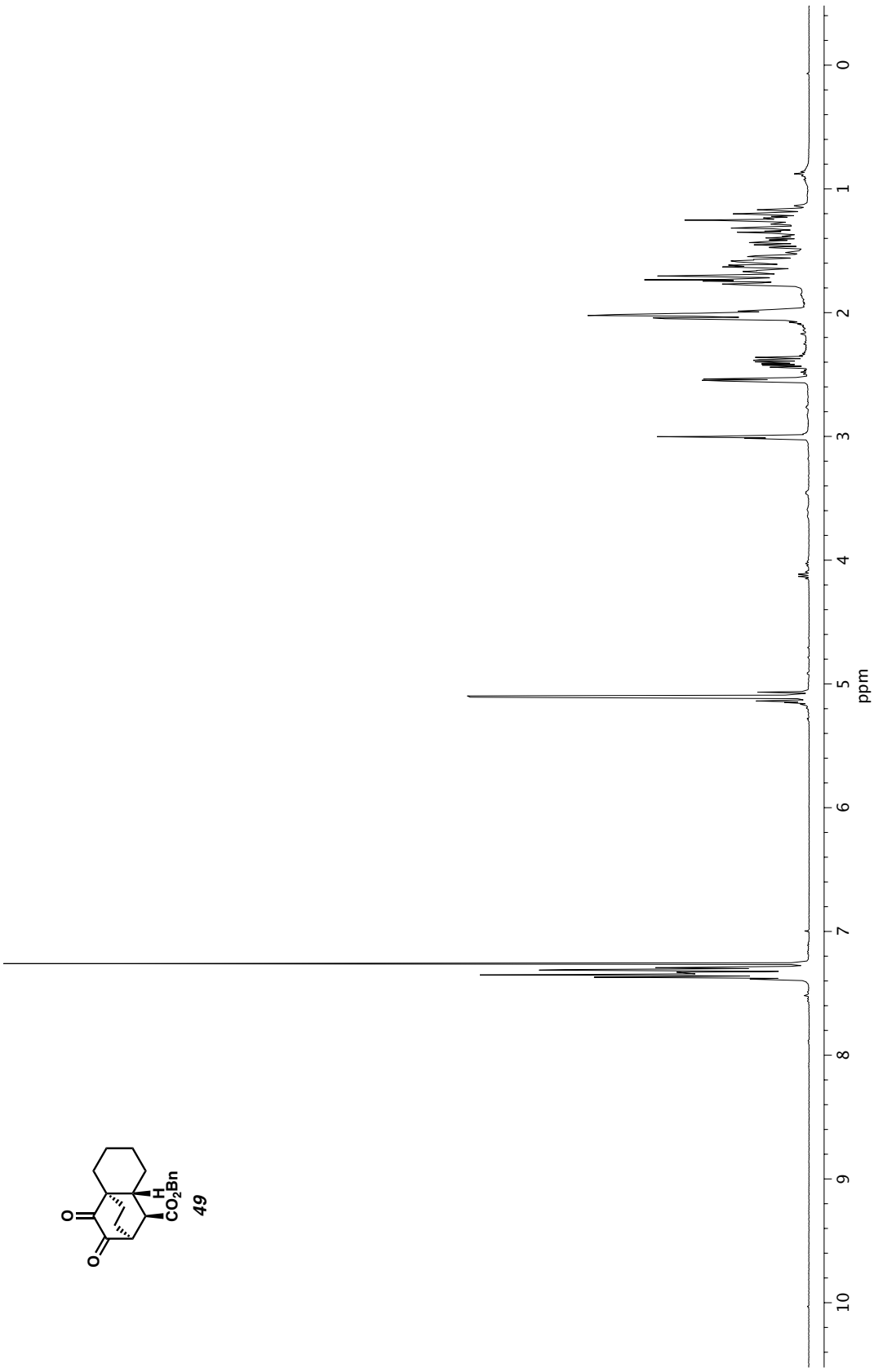


Figure A1.333. *^1H NMR (400 MHz, $CDCl_3$) of compound **49**.*

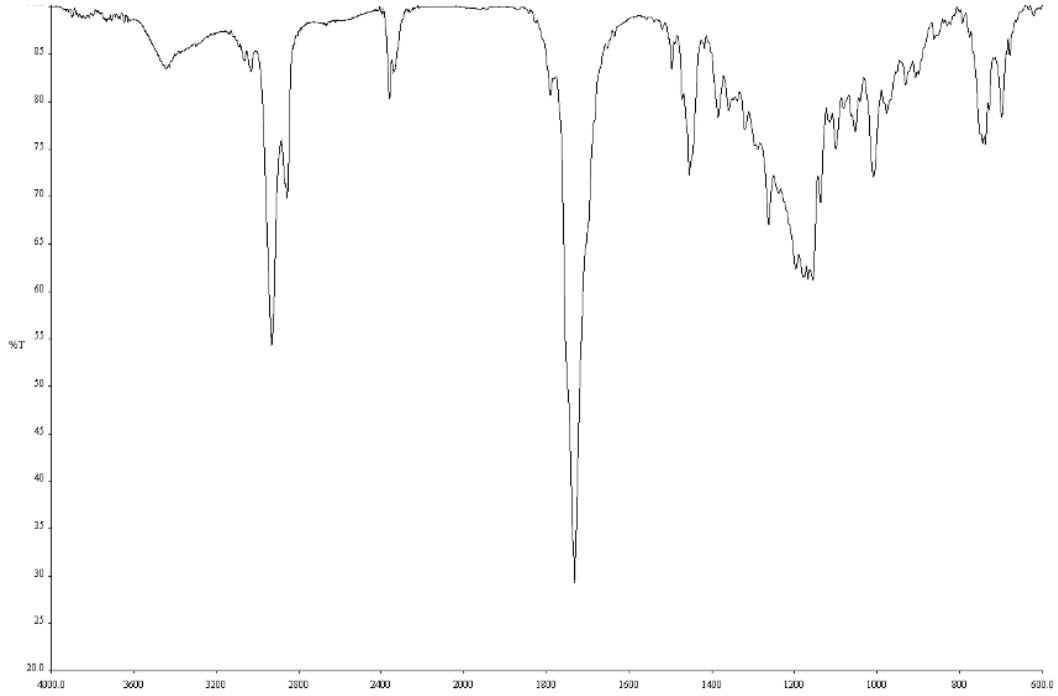


Figure A1.334. *Infrared spectrum (Thin Film, NaCl) of compound* ***49****.*

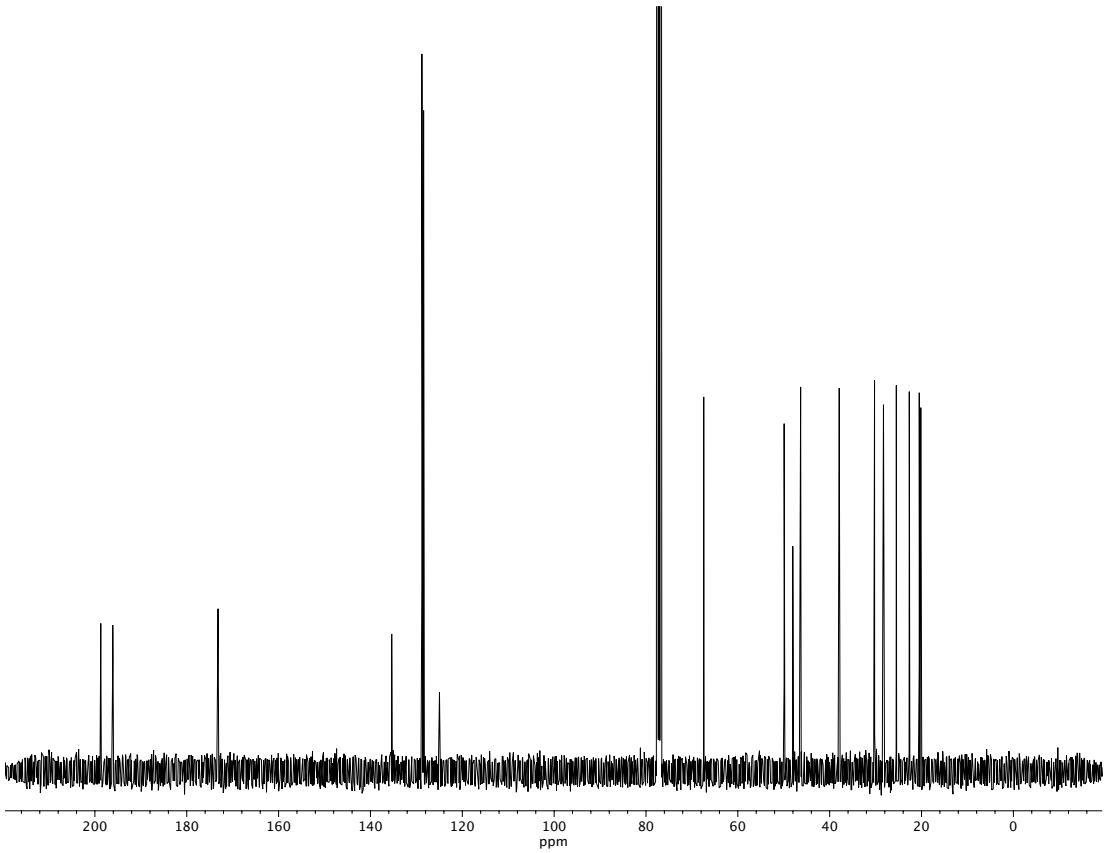


Figure A1.335. *^{13}C NMR (100 MHz, $CDCl_3$) of compound* ***49****.*

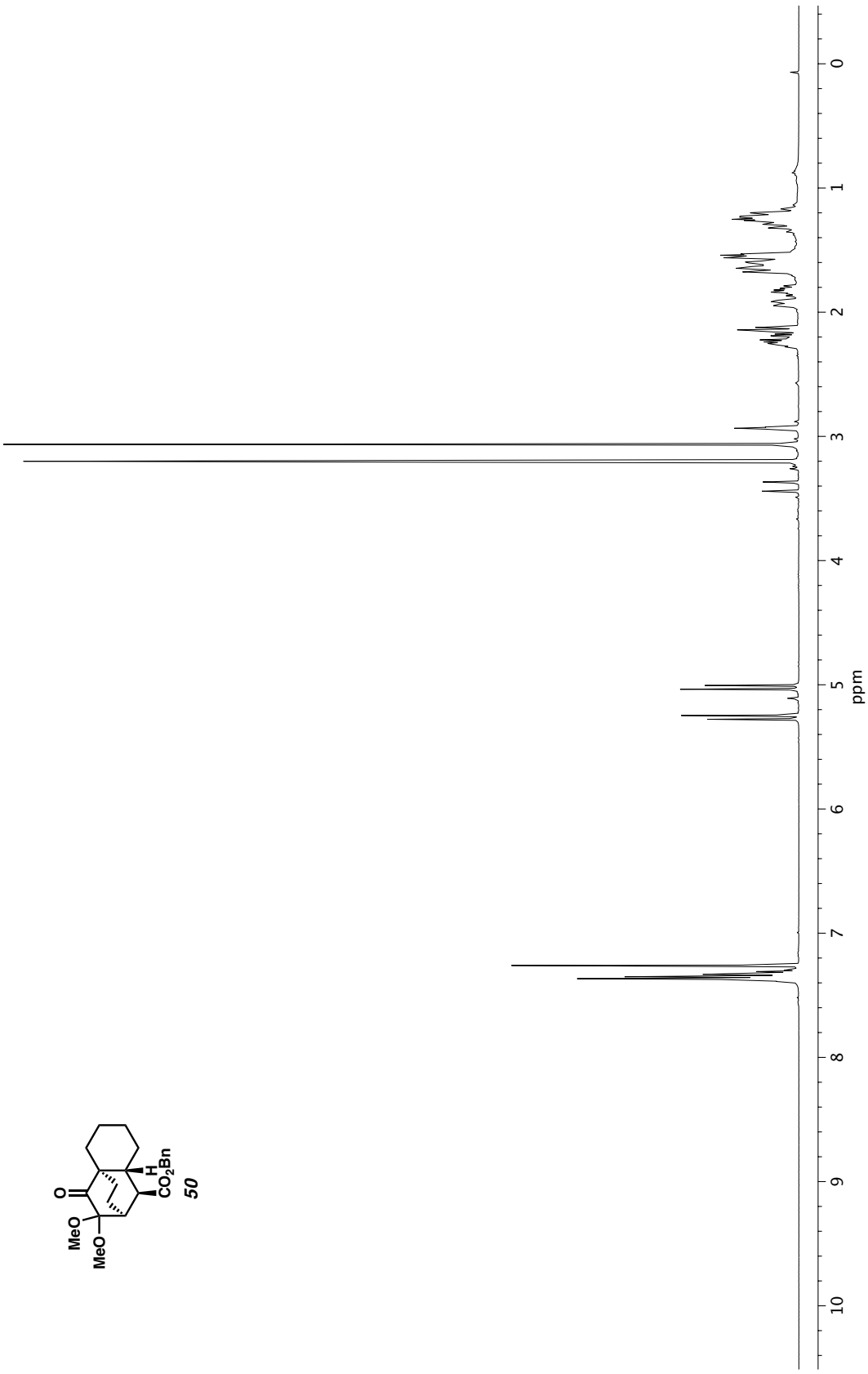


Figure A1.336. *^1H NMR (400 MHz, $CDCl_3$) of compound* ***50****.*

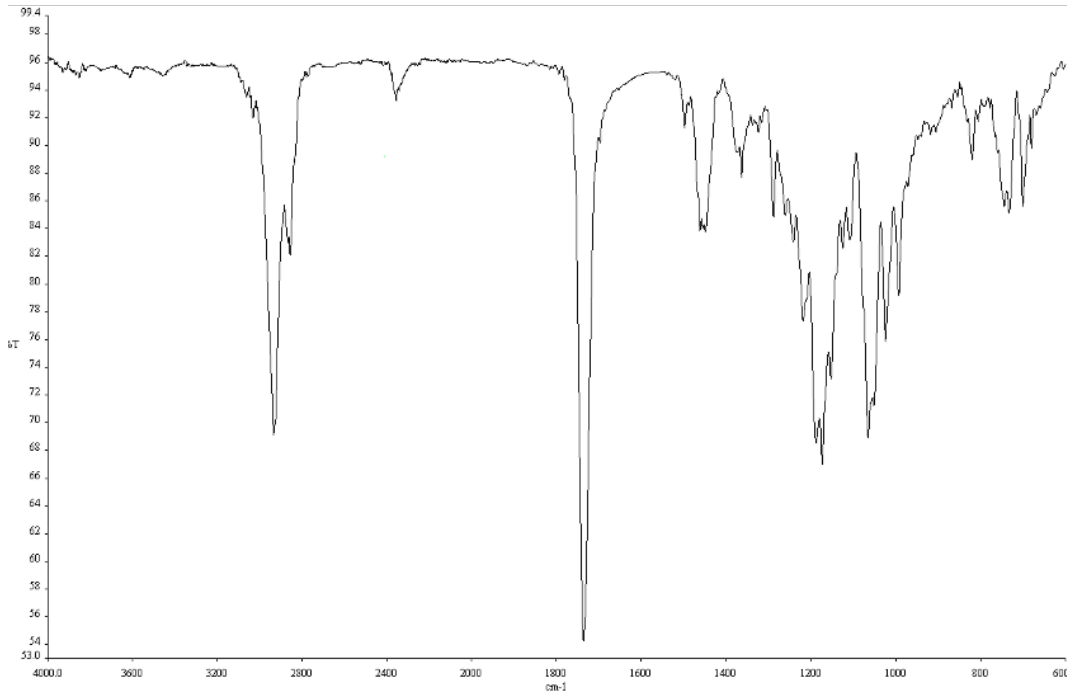


Figure A1.337. *Infrared spectrum (Thin Film, NaCl) of compound* ***50****.*

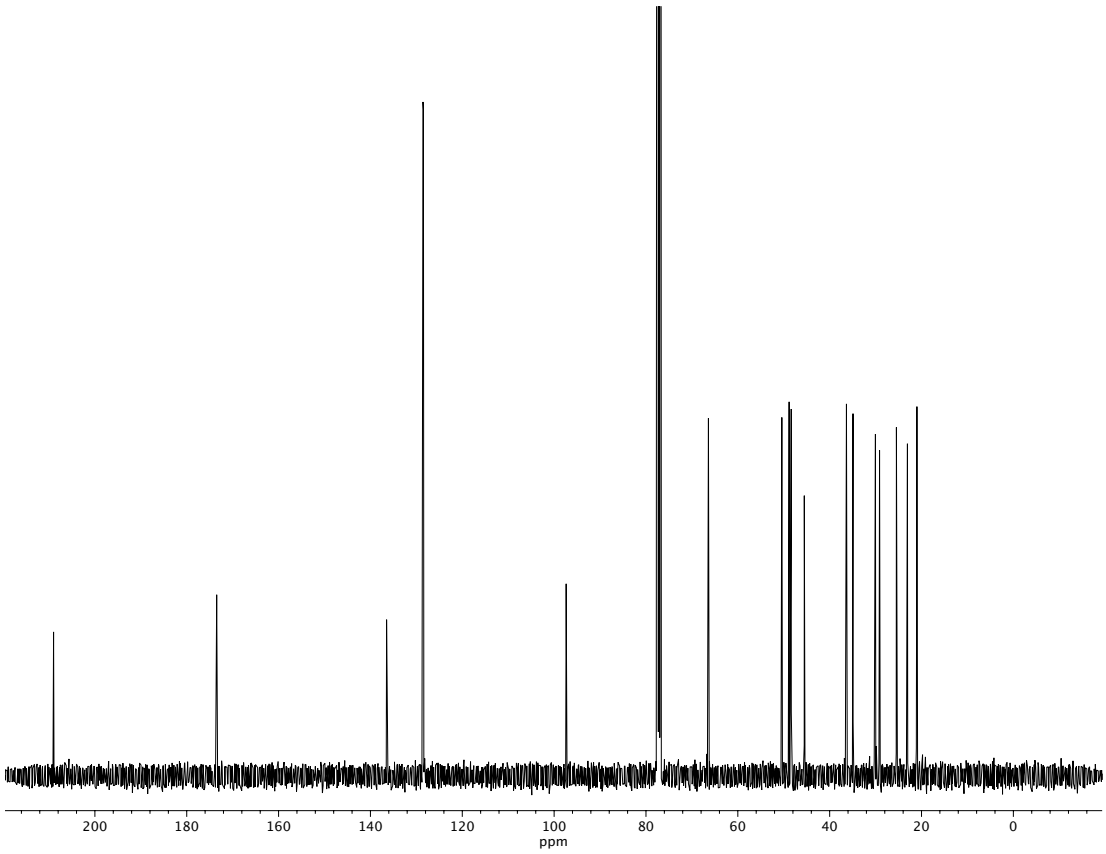


Figure A1.338. *^{13}C NMR (100 MHz, $CDCl_3$) of compound* ***50****.*

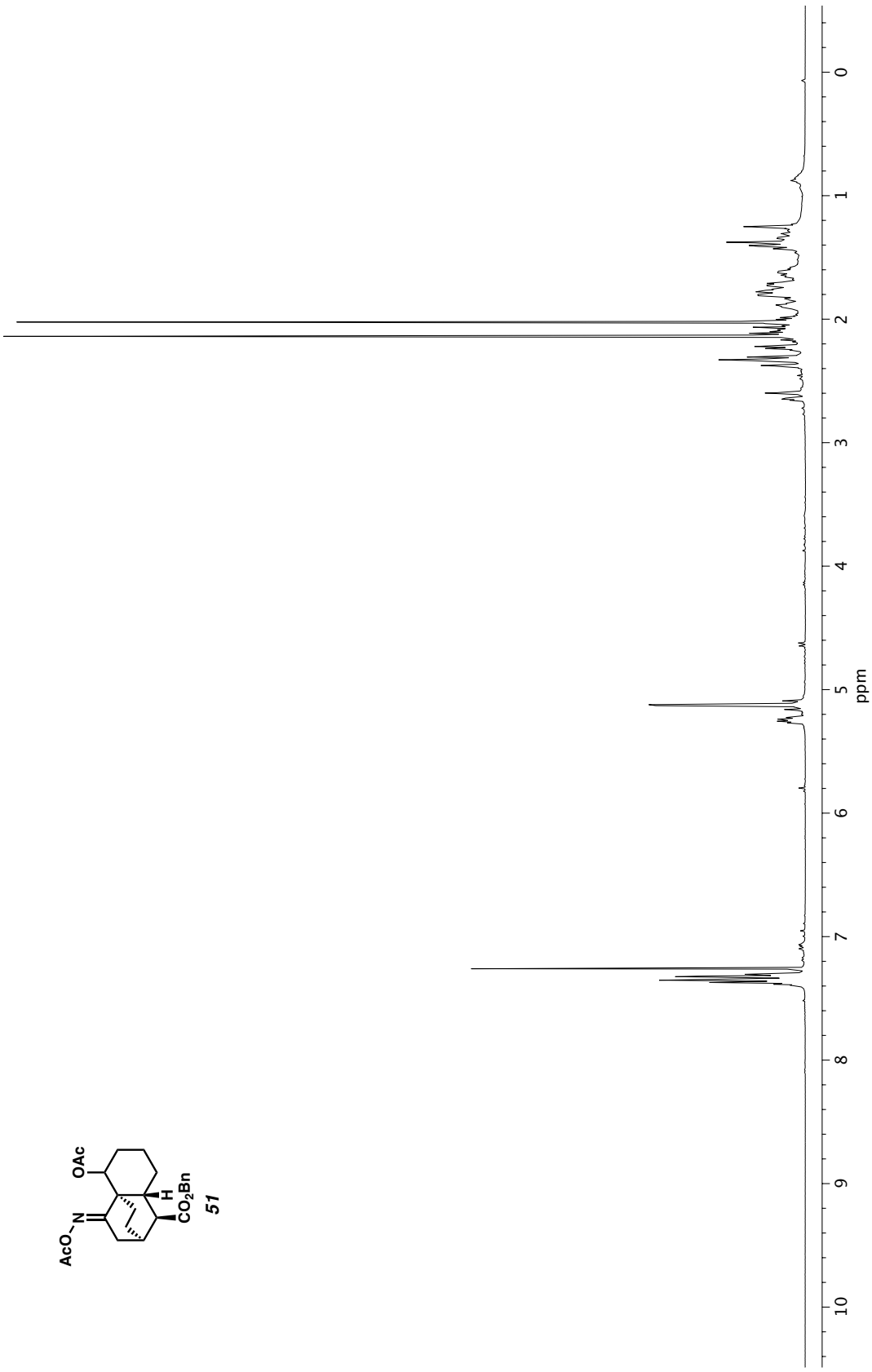


Figure A1.339. *^{1}H NMR (400 MHz, $CDCl_3$) of compound **51**.*

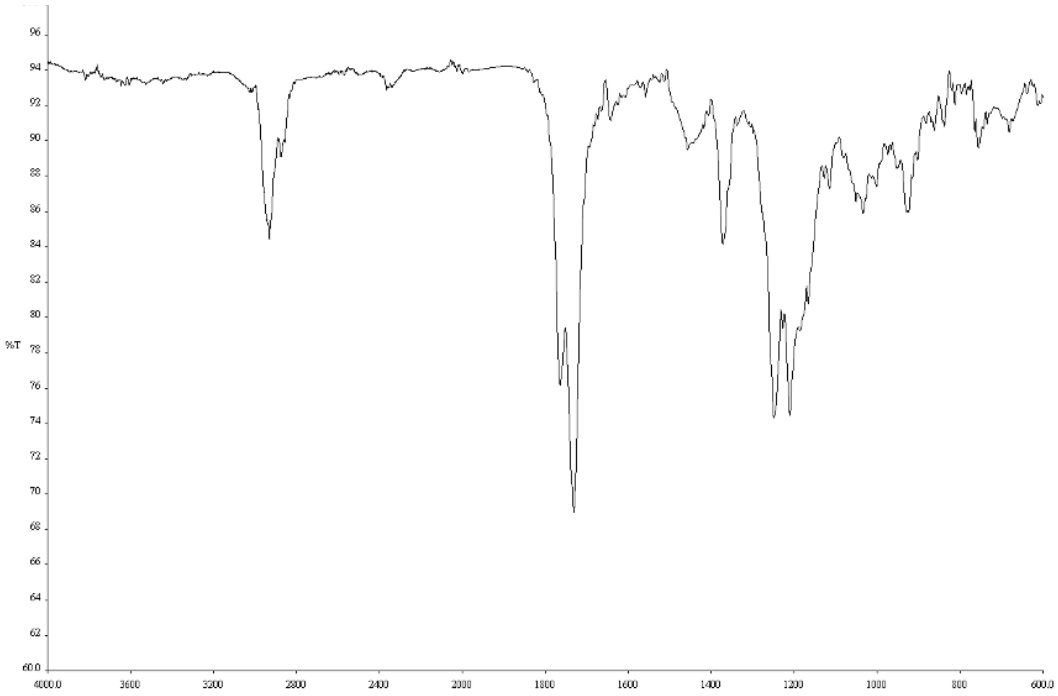


Figure A1.340. *Infrared spectrum (Thin Film, NaCl) of compound* ***51****.*

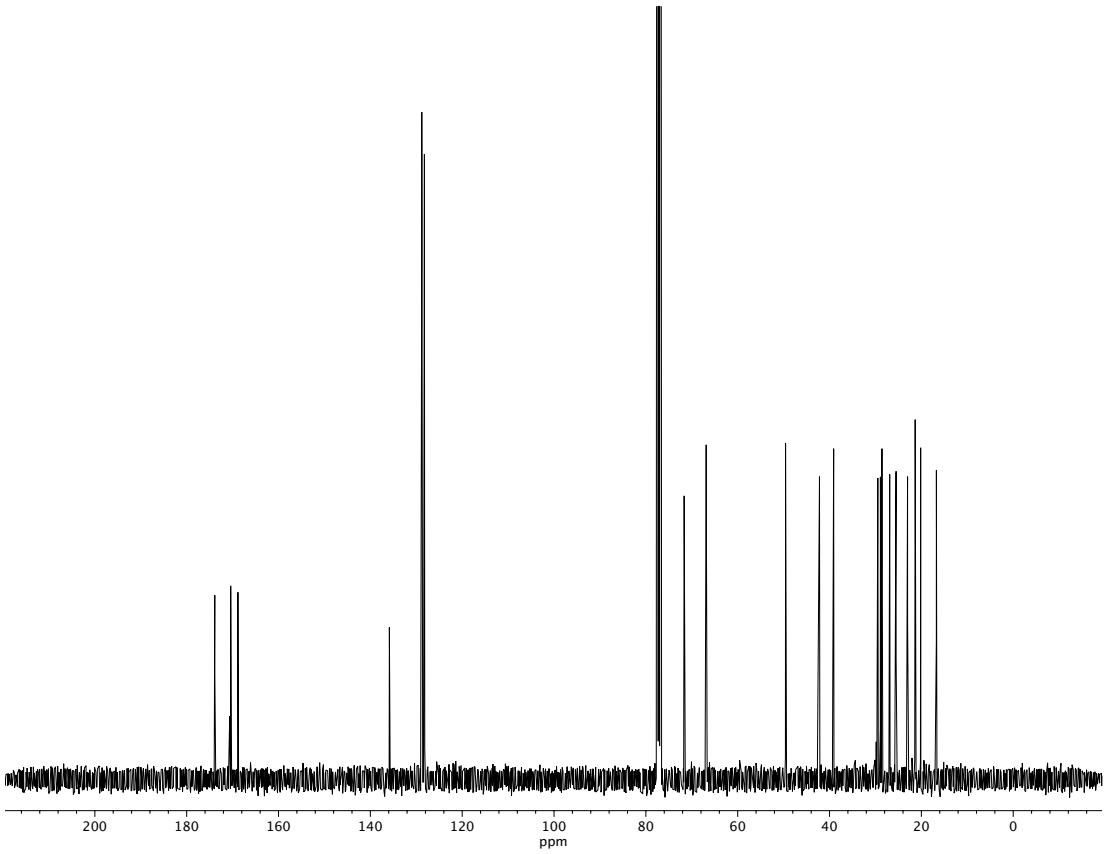


Figure A1.341. *^{13}C NMR (100 MHz, $CDCl_3$) of compound* ***51****.*

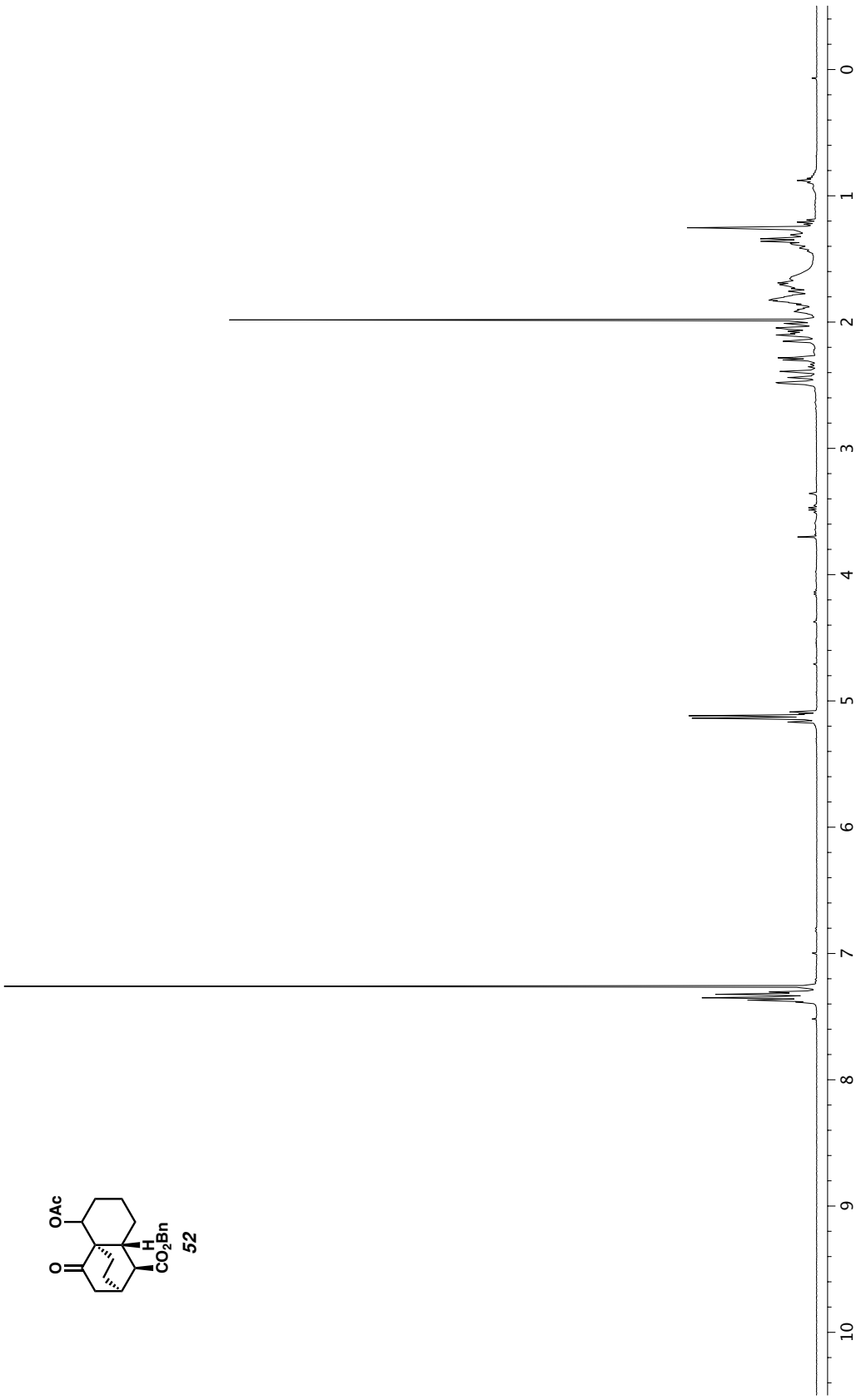


Figure A1.342. *^1H NMR (400 MHz, $CDCl_3$) of compound* ***52****.*

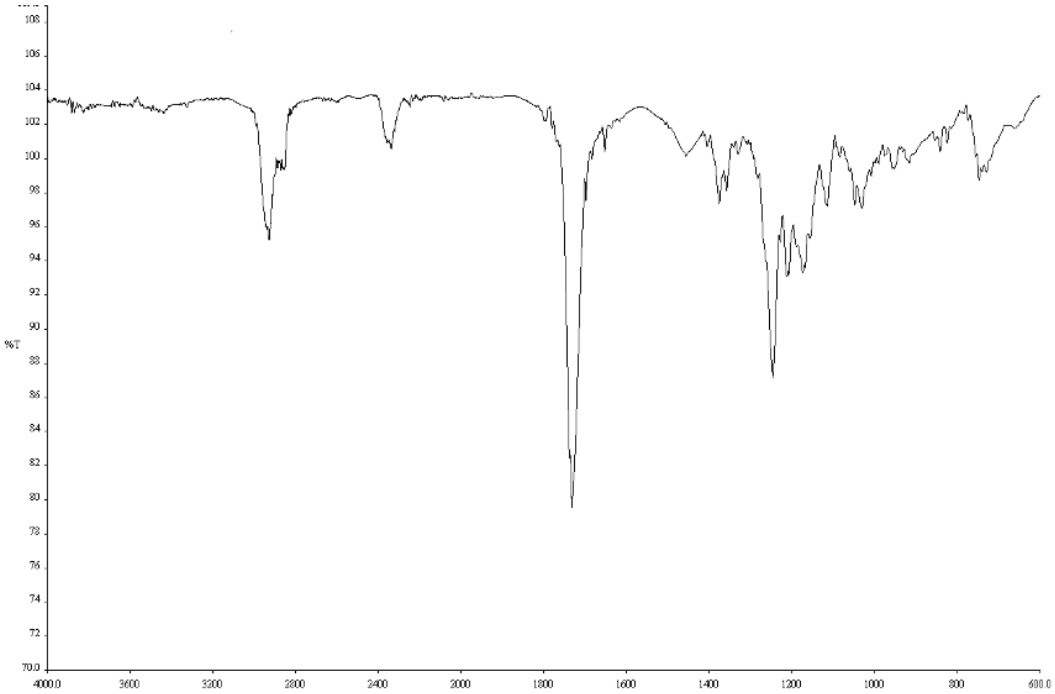


Figure A1.343. *Infrared spectrum (Thin Film, NaCl) of compound* ***52****.*

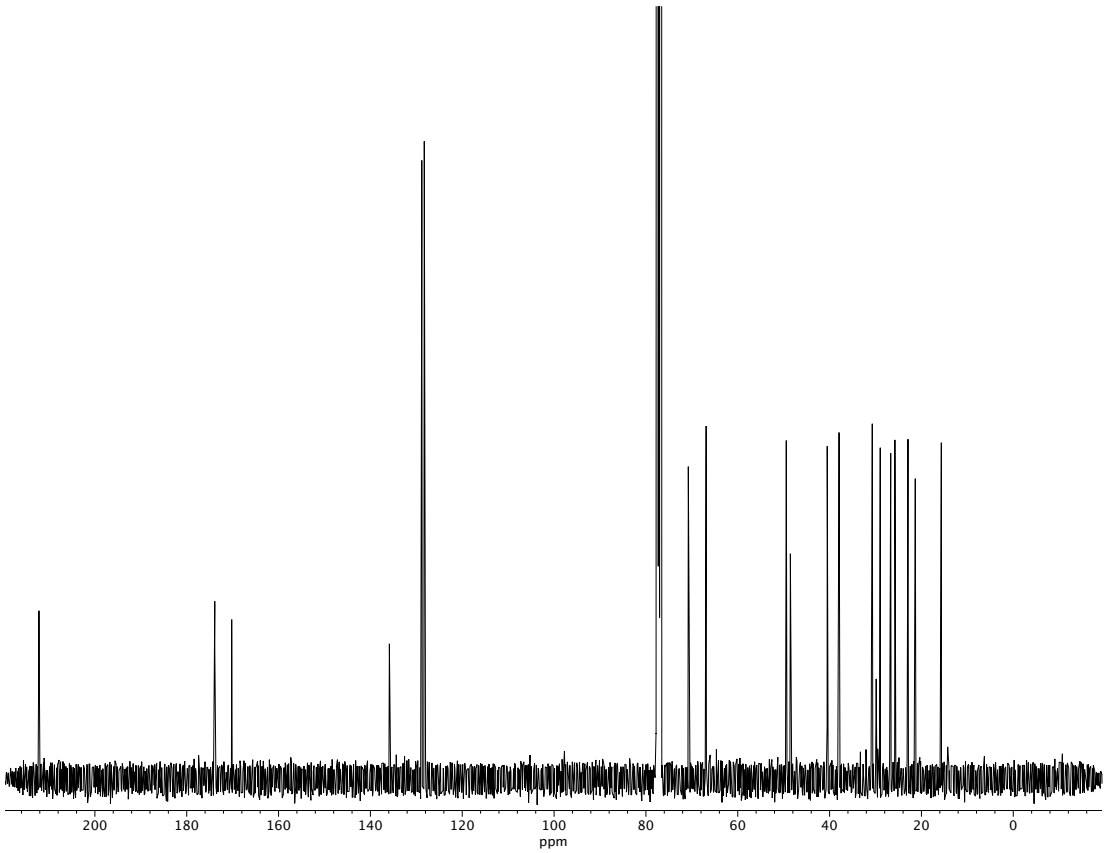


Figure A1.344. *^{13}C NMR (100 MHz, $CDCl_3$) of compound* ***52****.*

CHAPTER 2

Molecular Dynamics Investigations of Dienolate [4+2] Reactions†

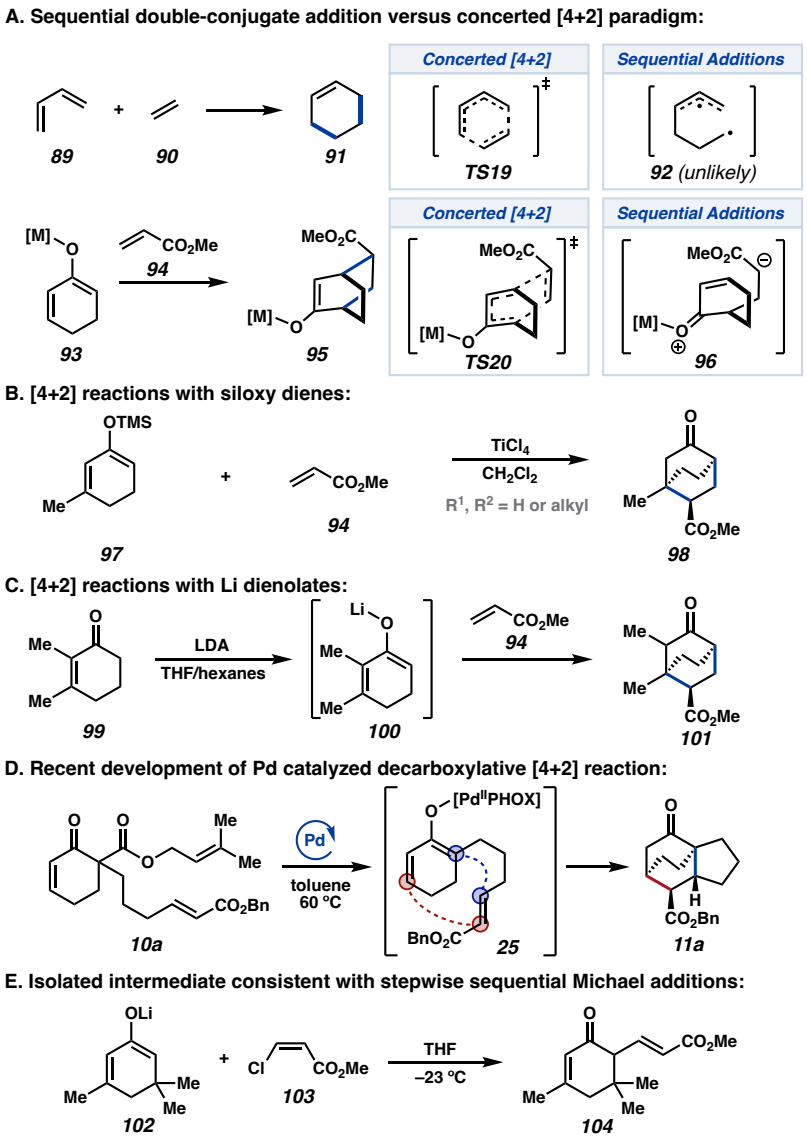
2.1 INTRODUCTION

[4+2] cycloadditions are among the most widely utilized reactions in organic synthesis owing to their ability to readily construct complex motifs through the concomitant formation of two C–C bonds and up to four stereocenters.[1] An important feature of canonical Diels–Alder reactions is its stereospecificity, guaranteeing control over relative stereochemistry at two centers of point chirality. Additionally, when the diene is suitably substituted, there is an additional element of stereoselectivity that must be considered regarding the relative facial bias of the two reactive partners. Fortunately, many [4+2] cycloadditions proceed with high levels of stereoselectivity, often favoring the so-called "endo" product.[1,2]

[4+2] reactions involving non-polarized or symmetrically polarized substrates generally follow a concerted and stereospecific mechanism (**TS19**).[3] In contrast, polarized dienes and dienophiles can electronically support charge-separated intermediates (**96**), and thus reactions with polarized substrates may proceed via two separate C–C bond forming events, and the stereochemical outcome in such processes may be determined by the stereoselectivity of the system (Figure 2.1.A).[4]

†This research was performed in collaboration with Cusumano, A. Q.; Flesch, K. N.; Strong, C. S.. Portions of this chapter have been reproduced with permission from Stoltz, et al. *J. Am. Chem. Soc.* **2024**, *146*, 12758–12765. © 2024 American Chemical Society.

Figure 2.1. *(A) Potential concerted and stepwise [4+2] reaction pathways of non-polarized and polarized dienes. (B) Siloxy diene [4+2] reactions. (C) Lithium base promoted [4+2] reactions. (D) Pd-catalyzed asymmetric [4+2] cycloaddition. (E) Isolated intermediate from intended [4+2] reaction with Li dienolate.*



Cyclohexenone-derived dienes are common polarized substrates utilized in [4+2] reactions for rapid access to ketone containing [2.2.2] bicycles (e.g., **98**, **101**, and **11a**,

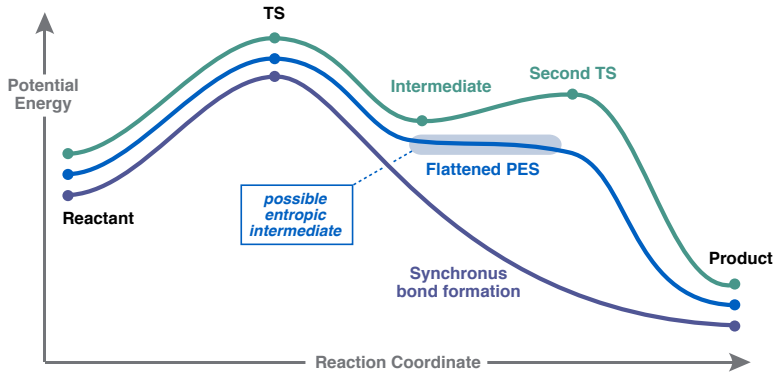
Figure 2.1.B–D), which are ubiquitous motifs in various complex natural products.[5] Representative substrates include siloxy dienes (**97**)[6], Li dienolates (**100**)[7], and more recently, chiral conjugated Pd enolates reported by our lab (**25**, Figure 2.1.D).[8]

Siloxy diene Diels–Alder cycloadditions are believed to afford [2.2.2] bicyclic products in a stereospecific manner with respect to the stereochemistry of the dienophile,[9] which is consistent with a concerted pathway that lacks long-lived intermediates. Conversely, despite nearly identical reaction and stereochemical outcomes from [4+2] reactions with Li dienolates, Li dienolate reactions have typically been considered to involve stepwise double Michael additions due to their mild reaction conditions (e.g., –78 ºC)[10] and the observation of single Michael adducts (**104**) in certain reactions (Figure 2.1.E) consistent with sequential conjugate addition pathways.[11] Recently, our lab reported the catalytic asymmetric synthesis of [2.2.2] bicycles, proceeding via chiral conjugated Pd enolates.[8] While the stereochemistry of most products were consistent with those expected from Diels–Alder reactions (i.e., stereospecific with respect to the dienophile olefin geometry and coupled to high endo:exo diastereoselectivity), it was ambiguous whether the reaction is indeed concerted and stereospecific, or completely stereoselective.

One possible delineation between concerted and stepwise pathways depends on whether an intermediate and a second transition state is featured. On the potential energy surface (PES), a stepwise pathway would be characterized by two local maxima (transition structures) connected by a local minimum (intermediate) along the reaction coordinate (Figure 2.2, top PES). However, analysis solely based on electronic energy (i.e., the PES) can be misleading.[12] For various pericyclic reactions, flat regions may exist along the

reaction coordinate PES (Figure 2.2., middle PES). Molecules may spend extended amounts of time in these regions as long-lived intermediates, despite the absence of a local potential energy minimum.[13,14] Such scenarios can arise from the entropic penalty associated with the progression along the reaction coordinate, and consequently these intermediates are often described as entropic intermediates, which exhibit shallow free energy minima but no potential energy minima. While these reactions appear concerted due to the lack of an intermediate on the PES, they can be dynamically stepwise if long-lived entropic intermediates are present.

Figure 2.2. *Example PES of a stepwise [4+2] reaction (top), concerted [4+2] reaction (bottom), and a dynamically stepwise (one-step two-stage) [4+2] reaction (middle).*



As entropic intermediates are not potential energy minima, they are challenging to identify based on transition structure and PES studies. This also leads to difficulty in characterizing dynamically stepwise reactions. Complementary to transition state analysis, molecular dynamics simulations have been shown effective in describing reactions in a time-resolved manner, which is key to discerning dynamically concerted and stepwise processes.[14,15]

In the context of the Diels–Alder reaction, Houk and coworkers demonstrate that highly asynchronous transition structures (i.e., those with large differences in bond distances in the two forming bonds) may undergo two temporally distinct bond forming steps, even in the absence of an intermediate on the PES. However, as the time gap between these steps is generally less than or equal to the period of a typical C–C bond stretch (~30–60 fs), the authors defined these processes to be "dynamically concerted".[16]

In this chapter, we present the results of molecular dynamics simulations of [4+2] reactions involving cyclohexenone derived diene substrates, describing a spectrum of mechanisms from synchronous and dynamically concerted to asynchronous and dynamically stepwise. Our findings are consistent with the usual classifications of [4+2] reactions with siloxy dienes and Li dienolates and demonstrate the influence of substrate choice on possible stereochemical outcomes.

2.2 EXPERIMENTAL: COMPUTATIONAL METHODS

All quantum mechanics calculations were carried out with the ORCA program.[17] Geometry optimizations, harmonic frequency calculations, and single-point energy evaluations were carried out with density functional theory (DFT). To locate saddle points of the reactions and propagate trajectories, the PBE functional[18] paired with Becke–Johnson damped D4 dispersion corrections[19] (PBE-D4) and implicit Conductor-like Polarizable Continuum model (CPCM) for the respective solvents[20] were used. For geometry optimization and harmonic frequency calculations, Pd is described by the def2-TZVP basis set[21] and the ECP28MWB small-core (18 explicit valence electrons) quasi-

relativistic pseudopotential[22], while C, H, N, and P are assigned the def2-SV(P) basis. Diffuse functions are added to oxygen (ma-def2-SV(P)).

Quasiclassical trajectories were initialized by normal mode sampling at the saddle points in which each normal mode includes zero-point energy, as well as a Boltzmann sampling of geometries corresponding to thermal energy available at the respective reaction temperatures with a randomized phase. Trajectories were propagated in the forward and reverse directions with a velocity-Verlet algorithm in 1.0 fs timesteps, as implemented in Singleton's Progdyn program[23], until either formation of cycloadduct (forming both C–C bond lengths < 1.5 Å), formation of starting material (the shorter C–C bond length > 3 Å and the longer > 4Å), or reaching max time (500 fs).

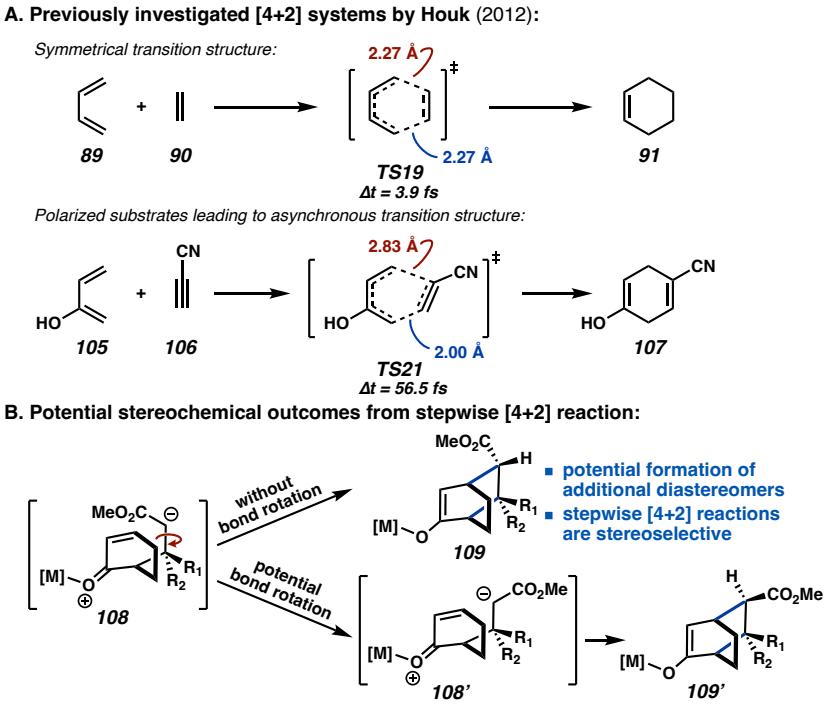
Considering the size of the system, a hundred trajectories were sampled to maintain tractability, and we limited the DFT to the generalized gradient approximation (GGA) functional PBE for the dynamic simulations. To investigate the influence of DFT functional choice on simulation results, a suite of control experiments was performed on a model reaction using hybrid, meta-hybrid, and range separated functionals. While simulations with different functionals yield slightly variable results, all simulation results described in this report were performed with the same functionals for comparison. For additional details and discussion see experimental sections 2.5.1 and 2.5.2.

2.3 RESULTS AND DISCUSSION

Molecular dynamics simulations provide time-resolved studies of pericyclic reactions, which enables identification of long-lived entropic intermediates in reactions where bond formations are not synchronous.[13,14] Herein, we define the average time gap (Δt) as the

difference in time between formation of the two developing C–C bonds and adopt 60 fs, approximately the period for a typical C–C bond stretch, as the time criteria to discern dynamically concerted and stepwise reactions, as proposed by Houk and coworkers.[13] Previously, the Houk lab reported an average time gap of 3.9 fs in the symmetrical [4+2] reaction of butadiene and ethylene (**TS19**, Figure 2.3.A).[16] While more asynchronous transition structures led to time gaps of up to 56.5 fs (**TS21**, Figure 2.3.A), the reported reactions are all deemed dynamically concerted.

Figure 2.3. *(A) Examples of previously studied [4+2] reactions. (B) Rotation of dienophile bond in dynamical intermediates can lead to formation of diastereomers.*



Conversely, highly polarized systems, such as cyclohexenone derived dienolates, may lead to dynamically stepwise reactions. Dynamically stepwise [4+2] reactions would feature long-lived intermediates, analogous to sequential Michael additions. These

reactions are considered stereoselective, rather than stereospecific, as bond rotation of the intermediate about the dienophile is potentially allowed, which can lead to formation of additional diastereomers (Figure 2.3.B).

To investigate the timing of the bond formations in [4+2] reactions with different cyclohexenone derived substrates, we report the molecular dynamics simulations of three different cyclohexenone systems: siloxy dienes, Li dienolates, and conjugated Pd enolates.

2.3.1 REACTIONS WITH SILOXY DIENES

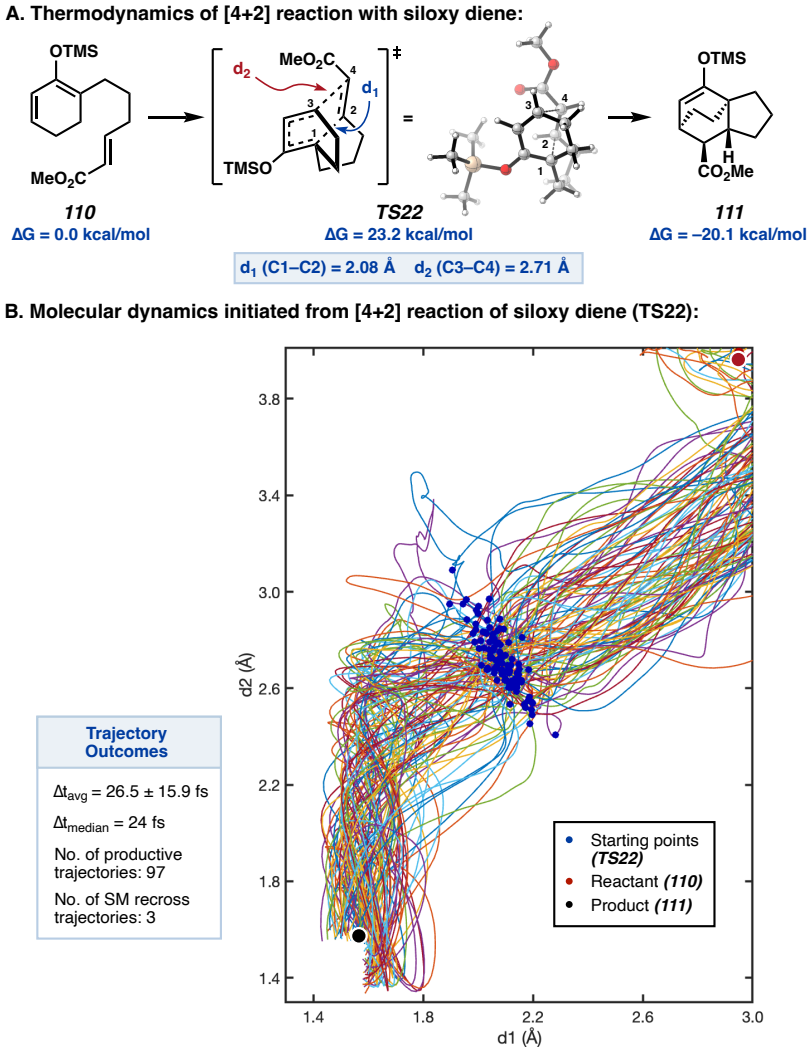
[4+2] reactions of siloxy dienes and dienophiles are generally considered to be concerted processes and are referred to as Diels–Alder reactions in literature. Aiming to investigate whether these reactions are concerted in a dynamical sense, we studied the model intramolecular reaction of siloxy cyclohexadiene **110** (Figure 2.4.A).

Reported examples of [4+2] reactions with siloxy dienes are typically performed in the presence of Lewis acid catalysts or in high boiling solvents at elevated temperatures. To eliminate potential influences of exogenous additives, our computations were performed for the additive-free reaction with the CPCM implicit solvation model for toluene. The vibrational frequency calculations and trajectory initialization in molecular dynamics simulation are in accord with thermal energies available at 383.15 K.

Quantum mechanical (QM) calculations revealed an asynchronous transition state (**TS22**) for the modeled reaction with an imaginary frequency of 323 cm^{-1}. Bond distances of C1–C2 ($\mathbf{d_1}$) and C3–C4 ($\mathbf{d_2}$) were found to be 2.08 and 2.71 Å, respectively. Comparison of the free energies of the transition state to the corresponding reactant indicates an activation energy barrier of 23.2 kcal/mol. From the identified transition state structure,

molecular dynamics simulations were employed to further investigate the synchronicity of bond formations.

Figure 2.4. *(A) Computed thermodynamics of intramolecular [4+2] reaction with siloxydiene. (B) Trajectories derived from molecular dynamics simulation originating from* ***TS22****.*



In practice, molecules will be found with geometries distributed along the dividing surface defined by the calculated transition structure, depending on the available thermal

energy. To simulate this distribution, weighted Boltzmann sampling was performed to yield a set of starting points, represented by the blue dots in Figure 2.4.B. From these starting points, trajectories are propagated in both directions, meaning that the atoms are assigned initial velocities of opposite signs for the two directions. The trajectories are subsequently plotted on a 2D potential energy surface defined by $\mathbf{d_1}$ and $\mathbf{d_2}$. Productive trajectories lead to formation of cycloadduct in one direction and separation of reactants in the other, while unproductive trajectories yield separated starting material (SM) in both propagated directions. These unproductive pathways are termed recrossing to starting material (SM) and are omitted from the analysis of Δt.

For the modeled [4+2] reaction with siloxy diene (**TS22**), unproductive trajectories leading to SM recross were found to be minimal (3%). An average time gap of 26.5 fs (median of 24 fs, range of 0–73 fs) was derived from the 97 productive trajectories. The short Δt for the C–C bond formations suggests a highly synchronous reaction, indicating that the reaction is dynamically concerted. Since bond rotations generally occur on picosecond timescales, rotation at the dienophile is extremely unlikely to occur during this time gap, and the stereochemistry of the reactants are relayed to that of the product through a perfectly stereoselective mechanism.

2.3.2 REACTIONS OF CONJUGATED LI ENOLATES

Reported [4+2] reactions of Li dienolates have generally been thought of as stepwise processes through sequential Michael additions.[24] This classification originates from the usually mild reaction conditions and specific examples in which intermediates with only one C–C σ bond formed were isolated.[11] Herein, we attempt to discuss the degree to which

both intramolecular and intermolecular Li base initiated [4+2] reactions (**TS23–24**) are concerted through molecular dynamics simulations.

Lithium enolates are known to form aggregates in organic solvents.[25] Consequently, a description of the solvated Li dienolate species is required to depict the [4+2] reactions more accurately. As such reactions are typically performed in a mixture of hexanes and ethereal solvents, we considered a cubic Li tetramer structure, reported for similar species in ethereal solvents.[26]

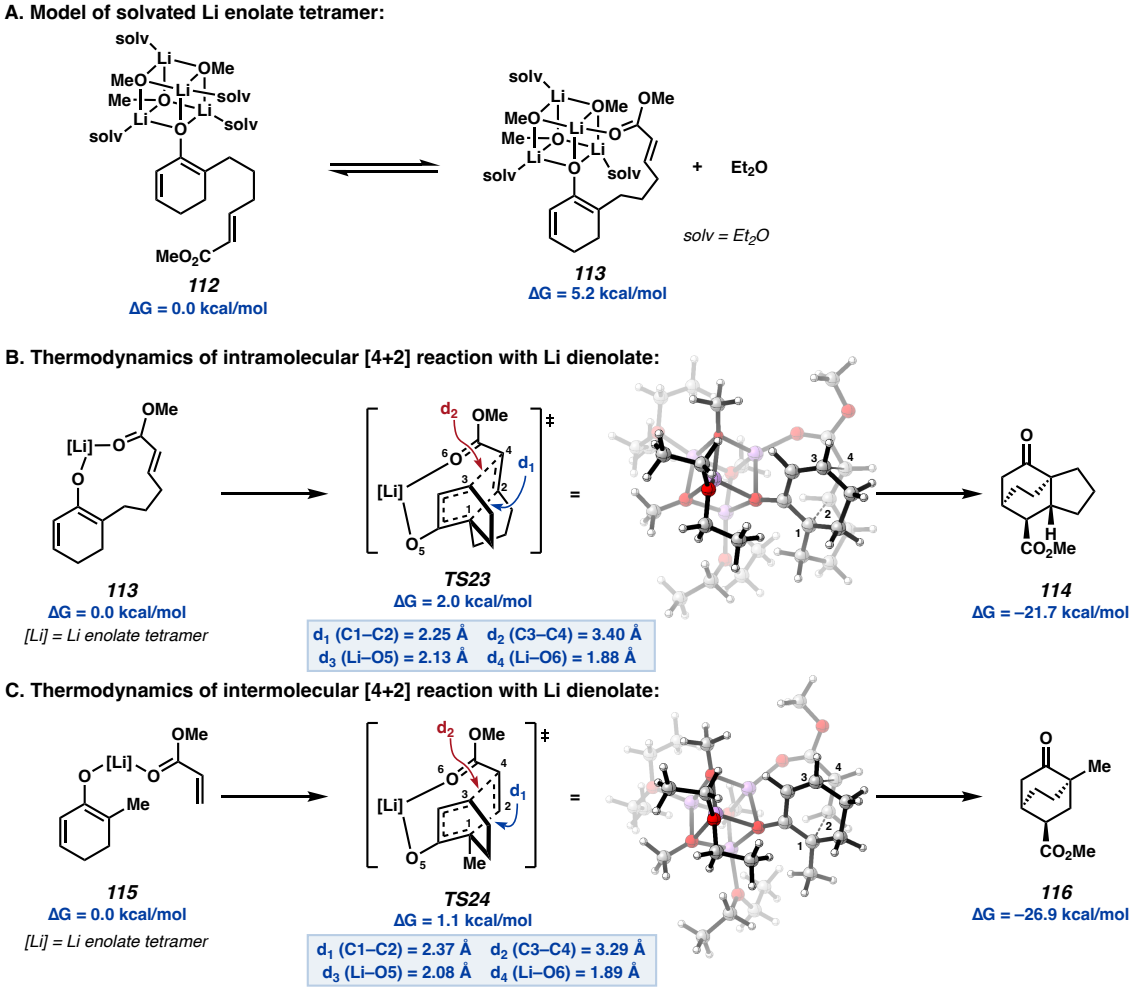
Computationally, this was achieved through explicit expression of Li-coordinated species (**112**, Figure. 2.5.A). In addition to four diethyl ether molecules, the reactive dienolate and three methoxy anions were coordinated. These methoxy anions are used as surrogates for additional enolate species for computational simplicity. This Li enolate tetramer (**112**) is proposed to be in equilibrium with thermodynamically favored tetramer **113**, where the reactive dienophile displaces coordinated solvent.

The reaction environment was subsequently simulated with the reactive Li tetramer **113** using the CPCM implicit solvation model. The dielectric constant of the solvent was chosen to be 2.3, which corresponds to a 5:1 mixture of hexanes and diethyl ether.[27] As low temperatures are generally required for such reactions, computations are in accord with thermal energies available at 195.15 K.

TS23 and **TS24** were found to have small energy barriers compared to the respective reactants, which is consistent with the typical low reaction temperatures. Similar to **TS22** of siloxy diene, Li dienolate reactions exhibited asynchronous transition structures, with

bond distances of $\mathbf{d_1}$ and $\mathbf{d_2}$ in **TS23** found to be 2.25 and 3.40 Å, and $\mathbf{d_1}$ and $\mathbf{d_2}$ in **TS24** to be 2.37 and 3.29 Å, respectively (Figure 2.5.B–C).

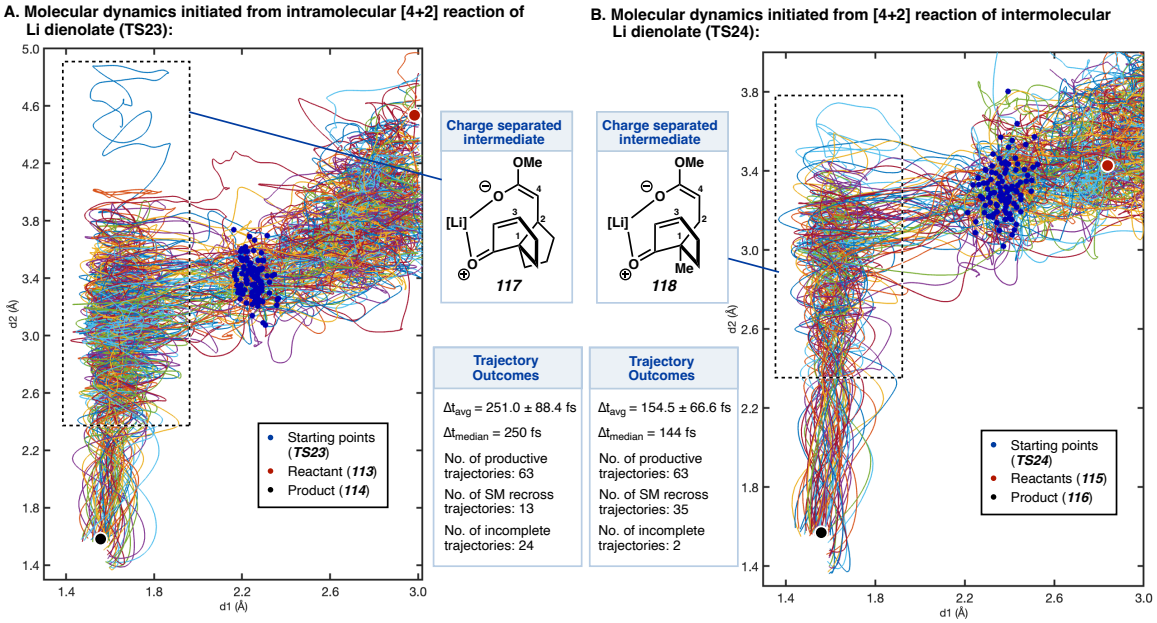
Figure 2.5. *(A) Model of solvated Li enolate tetramer in ethereal solvent (formal charges are removed for simplicity and clarity). (B) Computed thermodynamics of intramolecular [4+2] reaction with Li dienolate. (C) Computed thermodynamics of intermolecular [4+2] reaction with Li dienolate.*



Subsequent molecular dynamics simulations initiated from **TS23** and **TS24** revealed significantly different behavior from the reaction of siloxy diene **110**. Both Li dienolate

reactions exhibit substantially larger Δt, with Δt of the intramolecular reaction (Figure 2.6.A) found to be 251.0 fs and Δt of intermolecular reaction (Figure 2.6.B) 154.5 fs. These large time gaps indicate that Li dienolate systems tend to spend significant amounts of time as charge separated intermediates **117** and **118** (Figure 2.6.A–B), suggestive of dynamically stepwise processes. During the lifetime of charge separated intermediates **117** and **118**, free rotation of the C2–C4 σ bond can lead to formation of diastereomers. Since bond rotations typically occur on a picosecond timescale, C3–C4 bond formation generally outcompetes bond rotation to afford the formal [4+2] adduct with stereochemistry analogous to the products of concerted mechanisms. Therefore, such processes are considered stereoselective, rather than stereospecific as a concerted pathway.

Figure 2.6. *(A) Trajectories derived from molecular dynamics simulation originating from* ***TS23****. (B) Trajectories derived from molecular dynamics simulation originating from* ***TS24****.*



Subsequent molecular dynamics simulations initiated from **TS23** and **TS24** revealed significantly different behavior from the reaction of siloxy diene **110**. Both Li dienolate reactions exhibit substantially larger Δt, with Δt of the intramolecular reaction (Figure 2.6.A) found to be 251.0 fs and Δt of intermolecular reaction (Figure 2.6.B) 154.5 fs. These large time gaps indicate that Li dienolate systems tend to spend significant amounts of time as charge separated intermediates **117** and **118** (Figure 2.6.A–B), suggestive of dynamically stepwise processes. During the lifetime of charge separated intermediates **117** and **118**, free rotation of the C2–C4 σ bond can lead to formation of diastereomers. Since bond rotations typically occur on a picosecond timescale, C3–C4 bond formation generally outcompetes bond rotation to afford the formal [4+2] adduct with stereochemistry analogous to the products of concerted mechanisms. Therefore, such processes are considered stereoselective, rather than stereospecific as a concerted pathway.

Trajectory outcome distributions from **TS23** and **TS24** are also significantly different, despite the same ratio (63%) of productive trajectories. The majority of trajectories that were not productive for the intramolecular reaction (Figure 2.6.A) led to long-lived intermediate **117** that persisted through the duration of the simulation, which was 500 fs. The previously calculated Δt does not include these 24 incomplete trajectories, and therefore the Δt of the intramolecular reaction is likely to be even larger in reality. The remaining 13 trajectories from **TS23** were found to reform reactant. In contrast, significant recrossing (35%) to starting material was observed from **TS24** of the intermolecular reaction[28], and only 2 trajectories were incomplete.

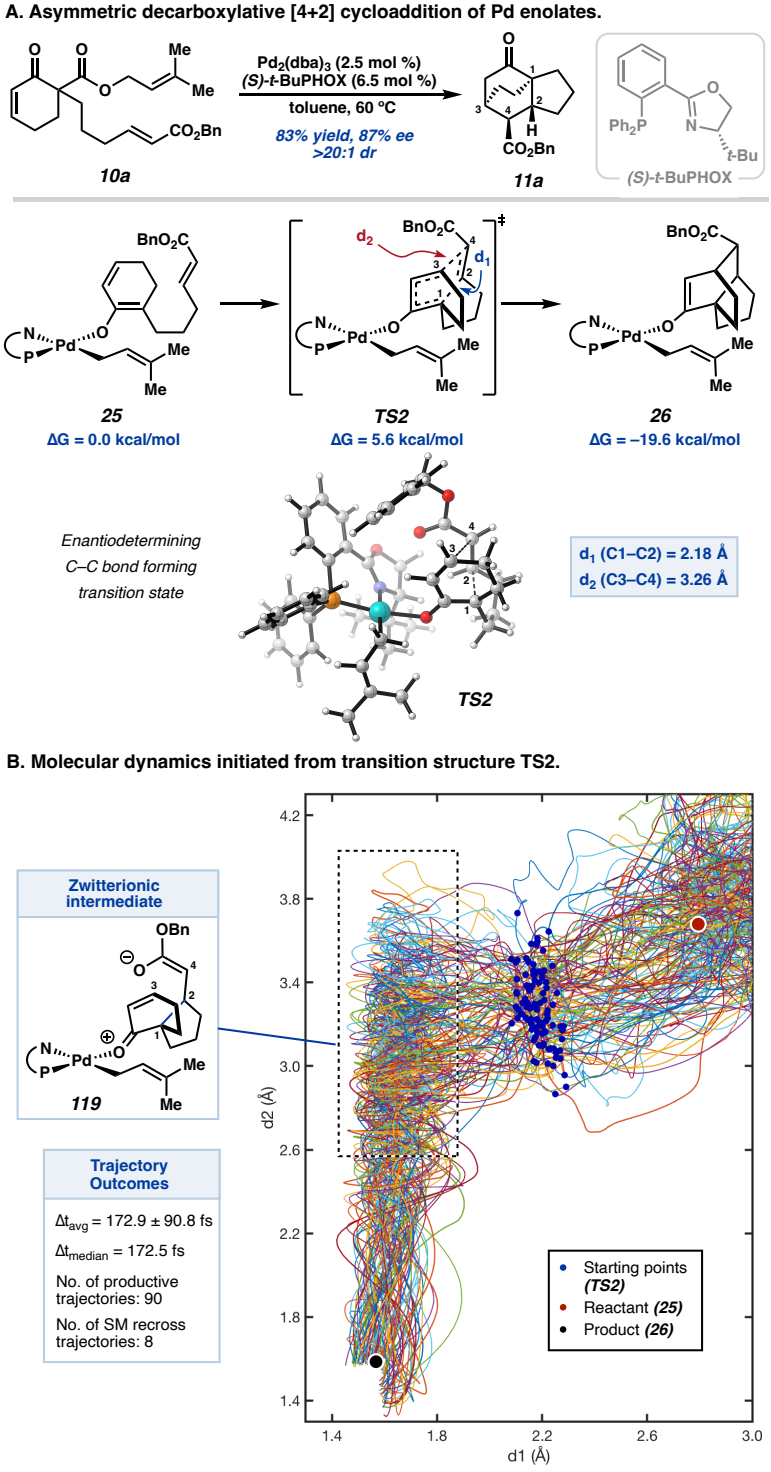
Differences in various features of both the PES analysis and the molecular dynamics simulation were also observed as a consequence of whether the Li dienolate and dienophile were tethered. The initial bond length difference of $\mathbf{d_1}$ and $\mathbf{d_2}$ was found to be 1.15 Å for **TS23**, while this difference decreased to 0.92 Å for **TS24**. The two transition states were both characterized by a negative curvature on the PES, but with magnitudes of 161 (**TS23**) and 119 cm^{-1} (**TS24**), respectively. While the distribution of the molecular dynamics simulation starting point geometries for **TS23** and **TS24** appear similar with regard to the initial $\mathbf{d_2}$, a tighter distribution along $\mathbf{d_1}$ is observed in intramolecular **TS23**.

In summary, our computational analysis of the intermolecular and intramolecular reactions with Li dienolates suggests that these reactions follow dynamically stepwise mechanisms, with long-lived charge separated intermediates having lifetimes of at least 154.5 fs for the intermolecular reaction and 251.0 fs for the intramolecular reaction. While the long intermediate lifetimes can potentially allow dienophile C–C σ bond rotation, the C4 stereochemistry of the reactants is transferred to that of the [4+2] adducts in a stereoselective fashion. It was also observed that the presence of a tether between diene and dienophile leads to decreased time gap, significantly less recrossing to starting material, and substantially more incomplete trajectories.

2.3.3 REACTIONS OF CONJUGATED Pd ENOLATES

Recently, our group reported the asymmetric decarboxylative [4+2] cycloaddition from catalytically generated Pd enolates as a unique approach to enantioenriched [2.2.2] bicyclic ketones (**11a**). This reaction is envisioned to proceed via the intermediacy of a conjugated O-bound Pd enolate (**25**) that undergoes a formal intramolecular [4+2] cycloaddition with

Figure 2.7. *(A) The decarboxylative asymmetric [4+2] cycloaddition of Pd enolates. (B) Trajectories derived from MD analysis of the bond forming processes.*



a pendant dienophile (Figure 2.7.A). While the net transformation mirrors that of the Li enolates and siloxy dienes discussed previously, the chiral Pd enolate enables unprecedented control of absolute stereochemistry. Similar to both Li enolates and silyl enol ethers, the dienophile olefin geometry is generally reflected in the relative stereochemistry in the product of the Pd-catalyzed transformation (**11a**). Our investigations of Li enolates and silyl enol ethers exemplify that analysis of product stereochemical outcome alone does not delineate between the possibilities of concerted stereospecific and dynamically stepwise stereoselective processes. Hence, while our initial report uncovered the origins enantioselectivity, understanding the origin of the C2/C4 relative stereochemistry requires a time-resolved picture of bond formation.

In analogy to the propylene-tethered intramolecular Li enolate cycloaddition (**TS23**), the transition structure for the net [4+2] reaction of conjugated Pd enolate **25** to transposed enolate **26** is highly asynchronous. The PES connecting **25** to **26** bears no minima between **TS2** and **26**. With C1–C2 ($\mathbf{d_1}$) and C3–C4 ($\mathbf{d_2}$) distances of 2.18 and 3.26 Å, respectively, **TS2** has a Δd value of 1.08 Å – smaller than that of Li enolate **TS23** (Δd = 1.15 Å) but significantly greater than silyl enol ether **TS22** (Δd = 0.63 Å). **TS2** is characterized by a negative curvature of the PES corresponding to –212 cm^{-1}, compared to the flatter curvature of **TS23** (–161 cm^{-1}).

Quasiclassical dynamics were initiated from the normal-mode sampled **TS2** starting points with thermal energy corresponding to 333.15 K (Figure 2.7.B). Our dynamics simulations reveal an average time difference between the C1–C2 and C3–4 bond formations (Δt) of 172.9 fs for the 90 productive trajectories (**25** to **26**). Of these trajectories,

81 present time gaps of >60 fs, while nine are classified as dynamically concerted ($\Delta t \leq 60$ fs). The Δt values range from 19 to 405 fs, with a standard deviation of 90.8 fs. Only eight trajectories display recrossing of the transition region to return to starting enolate **25**.

As with Li enolates **113** and **115**, significant time (up to 400 fs) is spent as a zwitterionic intermediate (i.e. **119**, Figure 2.7.B). While this time corresponds to several C–C bond vibrational stretching periods, it remains a shorter timescale than that of C2–C4 bond rotation ($\geq$ 1 ps). Hence, the dienophile olefin stereochemistry of **25** is relayed to that of product **26**. Overall, the Pd enolate [4+2] is more concerted in nature than its Li enolate counterparts (**113**, **115**), yet more stepwise than the analogous reaction from siloxy diene **110**.

2.4 CONCLUSIONS

We report molecular dynamics simulations of the [4+2] reactions of three classes of polarized dienes: siloxy dienes, Li dienolates, and conjugated Pd enolates. Analysis of the trajectories from our simulations demonstrates the reaction of a siloxy diene to be the most synchronous, with a time gap of only 26.5 fs and minimal recrossing to starting material (3%). The intramolecular [4+2] reaction with conjugated Pd enolate exhibited more asynchronous behavior, with a time gap of 172.9 fs and 90% of the productive trajectories classified as dynamically stepwise. Finally, the reactions of Li dienolates were found to be the most asynchronous in nature. Both intramolecular and intermolecular [4+2] reactions of Li enolates were found to give time gaps of at least 154.5 and 251.0 fs, with 95% and 100% of trajectories being considered dynamically stepwise, respectively.

In summary, these results affirm the tendency of certain polarized dienes to undergo [4+2] reactions with significant time differences between formation of the two new bonds. As long as this delay is shorter than the time required for a C–C σ bond rotation, stereochemical information is preserved, matching the stereospecificity of a concerted process. Understanding this time-resolved nature of bond formations is key to interpreting the stereochemical outcome of these processes and will aid the further developments and applications of [4+2] reactions.

2.5 EXPERIMENTAL SECTION

2.5.1 GENERAL NOTES – QUANTUM MECHANICS CALCULATIONS

All quantum mechanics calculations were carried out with the ORCA program.[29] Geometry optimizations, harmonic frequency calculations, and single-point energy evaluations were carried out with density functional theory (DFT). While PBE0-D4, the PBE0 hybrid functional[30] paired with Becke–Johnson damped D4 dispersion corrections[31], proved to be a robust method for Pd-catalyzed reactions in our prior studies,[32] generalized gradient approximation (GGA) functional PBE paired with D4 corrections was utilized in this study as a compromise between robustness and computational efficiency due to the size of the systems of interest. For geometry optimization and harmonic frequency calculations, Pd is described by the def2-TZVP all electron basis set[33] and the ECP28MWB small-core (18 explicit valence electrons) quasi-relativistic pseudopotential,[34] while C, H, N, and P are assigned the def2-SV(P) basis. Diffuse functions are added to oxygen (ma-def2-SVP). Herein, we refer to this composite basis set as BS1. Geometry optimization and harmonic frequency calculations were carried out with the CPCM implicit solvation model

for respective solvents and their corresponding dielectric constants. For all calculations employing CPCM, surface charges are described by the improved Gaussian charge scheme of Neese and coworkers with a scaled Van der Waals cavity ($\alpha = 1.2$).[35] All Hessians were computed analytically. Stationary points are characterized by the correct number of imaginary vibrational modes (zero for minima and one for saddle points). Cartesian coordinates of all optimized structures are included as ".xyz" files, available online in a compressed zip file format.

Final Gibbs free energies were obtained by applying thermodynamic corrections to the calculated electronic energies. Thermodynamic corrections from harmonic frequency calculations employ the quasi-ridged rotor harmonic oscillator approach to correct for the breakdown of the harmonic oscillator approximation at low vibrational frequencies.[36] Note that free energies are adjusted to a 1 M standard state. The translational (S_{trans}) and rotational entropy (S_{rot}) contributions to the Gibbs free energy calculated for a complex in condensed phase are *ca.* 40–60% of the values obtained assuming an ideal gas.[37] As suggested in the literature, S_{trans} and S_{rot} obtained by ideal gas treatment are scaled by a factor of 0.5 to obtain the final condensed phase values.[38] Hence, the final Gibbs free energy at 333.15 K is calculated as:

$$G^{*}_{solv} = E^{BS2}_{el,solv} + ZPE + E_{trans} + E_{rot} + E_{vib} + k_b T - T\left(S_{el} + S_{vib} + \frac{1}{2}S_{trans} + \frac{1}{2}S_{rot}\right) + \Delta G^{0\rightarrow *}$$

The resolution of identity (RI) and Chain-of-Spheres (COS) approximations are employed for efficient evaluation of Coulomb and exchange integrals, respectively.[39] The def2/J auxiliary basis[40] is employed for all atoms except oxygen, for which a suitable

auxiliary was obtained via the automatic generation algorithm in the ORCA program (keyword: *AutoAux*). [41] Very fine grid settings are employed in all calculations (optimization/frequency calculations: DefGrid2).

Transition states of the intramolecular Li dienolate [4+2] reaction and conjugated Pd enolate [4+2] reaction were computed through a relaxed surface scan and subsequent geometry optimization to a saddle point with a single imaginary frequency (keyword: *optTS*). The observed bond distances in these transition states were then exploited in the transition state search for the intermolecular Li dienolate and siloxy diene [4+2] reactions. The reactive bond distances in these two systems were constrained to the bond distances of the intramolecular Li dienolate [4+2] transition state, and the resulting structures were directly optimized to the respective transition states.

Conformer searching was carried out for the stationary points of siloxy diene and conjugated Pd enolate reactions using the meta-dynamics-based CREST program (using GNF-FF) from the Grimme group.[42] Duplicate conformers were removed, low energy conformers were subsequently optimized, and energies were evaluated at the level of theory mentioned prior. The lowest energy conformer of the two reactions were subsequently used as starting points in molecular dynamics simulations.

2.5.2 GENERAL NOTES – MOLECULAR DYNAMICS SIMULATIONS

Quasiclassical trajectories were initialized by normal mode sampling at the saddle points. Starting geometries were derived that correspond to a Boltzmann distribution (corresponding to thermal energy available at the respective reaction temperatures) of geometries along each normal mode. The result is a weighted distribution of starting

structures along the dividing surface at the saddle point. Normal modes are given vibrational zero-point energy and a randomized phase. Trajectories were propagated in the forward and reverse directions with a velocity-Verlet algorithm in 1.0 fs timesteps, as implemented in Singleton's Progdyn program.[43] Trajectories were propagated until either formation of cycloadduct (forming both C–C bond lengths < 1.5 Å), formation of reactant (the shorter C–C bond length > 3 Å and the longer > 4Å), or of a maximum simulation time of 500 fs was reached.

Considering the size of the system, 100 randomized trajectories were sampled to maintain tractability, and we employed the efficient generalized gradient approximation (GGA) functional PBE for the QM energies and forces. To investigate the influence of DFT functional choice on simulation results, a suite of control experiments was performed on a model reaction using hybrid, meta-hybrid, and range separated functionals. While simulations with different functionals yield slightly variable results, all simulation results described in this report were performed with the same functionals for comparison. Most importantly, the same qualitative results are obtained between polarized and non-polarized systems (vide infra).

The initial configurations for Progdyn are described below and samples of the remaining supporting files are provided online.

2.5.3 CONFIGURATION AND PARAMETERS FOR PROGDYN

A sample *progdyn.conf* file for the Pd enolate [4+2] cycloaddition is provided below for reference.

```
method PBE
basis def2-SV(P)
charge 0
multiplicity 1
processors 16
memory 2000
diagnostics 3
title G
initialdis 2
timestep 1E-15
scaling 1.0
temperature 333.15
method2 D4
method3 Def2/J
method4 CPCM(Toluene)
methodfile 6
numimag 1
searchdir positive
classical 0
keepevery 1
```

```
keepevery 1
highlevel 999
boxon 0
boxsize 7.5
etolerance 10
damping 1
reversetraj true
#JAN 2020 1.0 version, based on 2010 version progdyn
```

Note that the value of *etolerance* must be increased for the large conformationally flexible system. A value of 10 still leads to several initial trajectories being rejected. This value is adjusted accordingly for each system. The *methodfile* contains additional input information, such as basis set assignments. For the system above as an example:

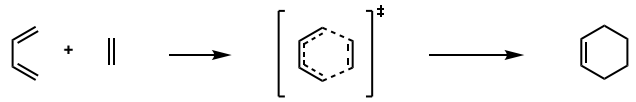
```
%basis
NewGTO Pd "def2-TZVP" end
NewECP Pd "def2-ECP" end
NewGTO O "ma-def2-SV(P)" end
NewAuxJGTO O "AutoAux" end
end
```

The value of 6 for the *methodfile* input in the *progdyn.conf* file corresponds to the six lines in the *methodfile* file.

2.5.4 COMPARISON OF COMPUTATIONAL RESULTS FROM DIFFERENT FUNCTIONALS

Limited by the size of the system of interest, generalized gradient approximation (GGA) functional PBE-D4 was utilized to maintain computational efficiency. To investigate the effect of the lack of terms describing Hartree–Fock exchange energy, a suite of control experiments, each consisted of 100 trajectories initiated from the transition state for molecular dynamics simulation, was performed on non-polarized and polarized model systems (Figure 2.7. and 2.8.) using different functionals, including hybrid functionals PBE0,[30] B3LYP,[44] and M06-2X.[45] In addition, range-separated functional wB97x-D3 was also sampled (keyword in ORCA: *wB97X-D3BJ*).[46] In this study, PBE0 and B3LYP were paired with Becke–Johnson damped D4 dispersion corrections. For comparison, calculations in vacuum at different temperatures were also conducted with the PBE-D4 functional. The computed transition structures, PES features, and molecular dynamics simulation results are summarized in Figures 2.7. and 2.8. It was observed that the absence of the Hartree–Fock exchange term generally led to more asynchronous transition structures and longer average Δt. In addition, flatter potential energy surfaces with

Figure 2.8. *Comparison of transition structures, PES features, and molecular dynamics simulation results of non-polarized [4+2] reaction from different functionals.* [a] *Imaginary vibrational frequencies were multiplied by the corresponding scaling factors at the level of theory utilized.*[47] [b] *Bond distance cutoff of 1.6 Å used for fully formed C–C bond.*

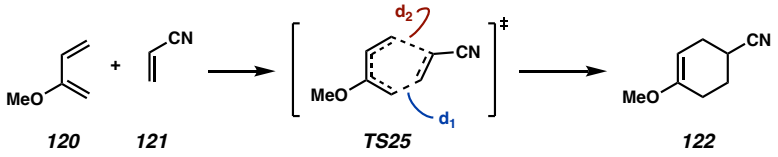


89 ***90*** ***TS19*** ***91***

Method	Solvent	Temperature (K)	d_1 (Å)	d_2 (Å)	Imaginary Vibrational Frequency (cm^{-1})[a]	Average Δt (fs)[b]	Median Δt (fs)	Stepwise Trajectories (%)	Concerted Trajectories (%)
PBE-D4	PhMe	333.15	2.35	2.35	–410.52	4.5	4	0	100
PBE-D4	gas	298.15	2.35	2.35	–408.58	4.1	3	0	100
PBE-D4	gas	333.15	2.35	2.35	–408.58	4.8	4	0	100
PBE0-D4	PhMe	333.15	2.31	2.31	–477.82	4.0	3	0	100
B3LYP-D4	PhMe	333.15	2.28	2.28	–518.23	3.7	4	0	100
M06-2X	PhMe	333.15	2.27	2.27	–497.06	2.8	3	0	100

imaginary vibrational frequencies of smaller magnitudes at the transition state were observed in the absence of Hartree–Fock exchange term.[48] Performing the calculations in vacuum led to slightly less flat PES and shorter Δt, but the effect was not significant.

Figure 2.9. *Comparison of transition structures, PES features, and molecular dynamics simulation results of polarized [4+2] reaction from different functionals.* [a] *Imaginary vibrational frequencies were multiplied by the corresponding scaling factors at the level of theory utilized.*[47] [b] *Bond distance cutoff of 1.6 Å used for fully formed C–C bond.*



120 ***121*** ***TS25*** ***122***

Method	Solvent	Temperature (K)	d_1 (Å)	d_2 (Å)	Imaginary Vibrational Frequency (cm^{-1})[a]	Average Δt (fs)[b]	Median Δt (fs)	Stepwise Trajectories (%)	Concerted Trajectories (%)
PBE-D4	PhMe	333.15	2.06	2.90	–354.86	45.9	38.0	19	81
PBE-D4	gas	298.15	2.06	2.85	–369.77	40.6	36.0	14	86
PBE-D4	gas	333.15	2.06	2.85	–369.77	37.0	34.0	11	89
PBE0-D4	PhMe	333.15	2.03	2.74	–422.32	25.3	24.0	3	97
B3LYP-D4	PhMe	333.15	1.99	2.72	–442.18	26.2	23.0	1	99
M06-2X	PhMe	333.15	2.04	2.50	–543.29	10.2	10.0	0	100
ωB97x-D3	PhMe	333.15	2.00	2.59	–544.25	14.1	12.5	0	100

2.6 REFERENCES AND NOTES

(1) (a) Nicolaou, K. C.; Snyder, S. A.; Montagnon, T.; Vassilikogiannakis, G. The Diels–Alder Reaction in Total Synthesis. *Angew. Chem. Int. Ed.* **2002**, *41*, 1668–1698. (b) Takao, K.; Munakata, R.; Tadano, K. Recent Advances in Natural Product Synthesis by Using Intramolecular Diels–Alder Reactions. *Chem. Rev.* **2005**, *105*, 4779–4807. (c) Wan, C.; Deng, J.; Liu, H.; Bian, M.; Li, A. Recent Advances of Intermolecular Diels-Alder Reaction in Bio-Inspired Synthesis of Natural Products. *Sci. China Chem.* **2014**, *57*, 926–929. (d) Heravi, M. M.; Vavsari, V. F. Recent Applications of Intramolecular Diels–Alder Reaction in Total Synthesis of Natural Products. *RSC Adv.* **2015**, *5*, 50890–50912.

(2) (a) Martin, J. G.; Hill, R. K. Stereochemistry of the Diels-Alder Reaction. *Chem. Rev.* **1961**, *61*, 537–562. (b) Fernández, I.; Bickelhaupt, F. M. Origin of the "Endo Rule" in Diels–Alder Reactions. *J. Comput. Chem.* **2014**, *35*, 371–376.

(3) (a) Li, Y.; Houk, K.N. Diels–Alder Dimerization of 1,3-Butadiene: An ab Initio CASSCF Study of the Concerted and Stepwise Mechanisms and Butadiene–Ethylene Revisited. *J. Am. Chem. Soc.* **1993**, *115*, 7478–7485. (b) Beno, B. R.; Houk, K. N.; Singleton, D. A. Synchronous or Asynchronous? An "Experimental" Transition State from a Direct Comparison of Experimental and Theoretical Kinetic Isotope Effects for a Diels–Alder Reaction. *J. Am. Chem. Soc.* **1996**, *118*, 9984–9985. (c) Dewar, M. J. S. Multibond Reactions Cannot Normally Be Synchronous. *J. Am. Chem. Soc.* **1984**, *106*, 209–219.

(4) (a) Loncharich, R. J.; Brown, F. K.; Houk, K. N. Transition Structures of the Diels-Alder Reaction of Butadiene with Acrolein. *J. Org. Chem.* **1989**, *54*, 1129–1134. (b) Birney, D. M.; Houk, K. N. Transition Structures of the Lewis Acid-Catalyzed Diels–Alder Reaction of Butadiene with Acrolein. The Origins of Selectivity. *J. Am. Chem. Soc.* **1990**, *112*, 4127–4133. (c) Jasiński, R. On the Question of Stepwise [4+2] Cycloaddition Reactions and Their Stereochemical Aspects. *Symmetry* **2021**, *13*, 1911.

(5) (a) Pepper, H. P.; Lam, H. C.; Bloch, W. M.; George, J. H. Biomimetic Total Synthesis of (±)-Garcibracteatone. *Org. Lett.* **2012**, *14*, 5162–5164. (b) Breitler, S.; Carreira, E. M. Total Synthesis of (+)-Crotogoudin. *Angew. Chem. Int. Ed.* **2013**, *52*, 11168–11171. (c) Xie, S.; Chen, G.; Yan, H.; Hou, J.; He, Y.; Zhao, T.; Xu, J. 13-Step Total Synthesis of Atropurpuran. *J. Am. Chem. Soc.* **2019**, *141*, 3435–3439.

(6) Asaoka, M.; Ishibashi, K.; Takahashi, W.; Takei, H. Synthesis of Sterically Hindered Bicyclo[2.2.2]Octanes by Lewis Acid Catalyzed Reaction of 2-(Trimethylsiloxy)-1,3-Cyclohexadienes with 4-Methyl-3-Penten-2-One. *BCSJ* **1987**, *60*, 2259–2260.

(7) White, K. B.; Reusch, W. The Synthesis of Bicyclo[2.2.2]Octan-2-Ones by Sequential Michael Reactions. *Tetrahedron* **1978**, *34*, 2439–2444.

(8) Flesch, K. N.; Cusumano, A. Q.; Chen, P.-J.; Strong, C. S.; Sardini, S. R.; Du, Y. E.; Bartberger, M. D.; Goddard, W. A. I.; Stoltz, B. M. Divergent Catalysis: Catalytic Asymmetric [4+2] Cycloaddition of Palladium Enolates. *J. Am. Chem. Soc.* **2023**, *145*, 11301–11310.

(9) Harada, S.; Nishida, A. Catalytic and Enantioselective Diels-Alder Reaction of Siloxydienes. *Asian J. Org. Chem.* **2019**, *8*, 732–745.

(10) (a) Lee, R. A. Reactions of a′ Dienolates with Michael Acceptors: A Synthesis of Bicyclo [2,2,2] Octan-2-Ones. *Tetrahedron Lett.* **1973**, *14*, 3333–3336. (b) White, K. B.; Reusch, W. The Synthesis of Bicyclo[2.2.2]Octan-2-Ones by Sequential Michael Reactions. *Tetrahedron* **1978**, *34*, 2439–2444. (c) Ihara, Masataka.; Suzuki, Makoto.; Fukumoto, Keiichiro.; Kametani, Tetsuji.; Kabuto, Chizuko. Stereoselective Total Synthesis of (±)-Atisine via Intramolecular Double Michael Reaction. *J. Am. Chem. Soc.* **1988**, *110*, 1963–1964.

(11) Gibbons, E. G. One-Step Synthesis of Tricyclo[5.2.2.0]Undecane Derivatives: Precursors to Pleuromutilin. *J. Org. Chem.* **1980**, *45*, 1540–1541.

(12) (a) de Souza, M. A. F.; Ventura, E.; do Monte, S. A.; Riveros, J. M.; Longo, R. L. Revisiting the Concept of the (a)Synchronicity of Diels-Alder Reactions Based on the Dynamics of Quasiclassical Trajectories. *J. Comput. Chem.* **2016**, *37*, 701–711. (b) Isamura, B. K.; Lobb, K. A. New Insights into the (A)Synchronicity of Diels–Alder Reactions: A Theoretical Study Based on the Reaction Force Analysis and Atomic Resolution of Energy Derivatives. *Molecules* **2022**, *27*, 1546.

(13) Yang, Z.; Jamieson, C. S.; Xue, X.-S.; Garcia-Borràs, M.; Benton, T.; Dong, X.; Liu, F.; Houk, K. N. Mechanisms and Dynamics of Reactions Involving Entropic Intermediates. *Trends in Chemistry* **2019**, *1*, 22–34.

(14) (a) Gonzalez-James, O. M.; Kwan, E. E.; Singleton, D. A. Entropic Intermediates and Hidden Rate-Limiting Steps in Seemingly Concerted Cycloadditions.

Observation, Prediction, and Origin of an Isotope Effect on Recrossing. *J. Am. Chem. Soc.* **2012**, *134*, 1914–1917. (b) Yang, Z.; Zou, L.; Yu, Y.; Liu, F.; Dong, X.; Houk, K. N. Molecular Dynamics of the Two-Stage Mechanism of Cyclopentadiene Dimerization: Concerted or Stepwise? *Chem. Phys.* **2018**, *514*, 120–125. (c) Houk, K. N.; Xue, X.-S.; Liu, F.; Chen, Y.; Chen, X.; Jamieson, C. Computations on Pericyclic Reactions Reveal the Richness of Ambimodal Transition States and Pericyclases. *Isr. J. Chem.* **2022**, *62*, e202100071.

15. Yang, Z.; Houk, K. N. The Dynamics of Chemical Reactions: Atomistic Visualizations of Organic Reactions, and Homage to van 't Hoff. *Chemistry – A European Journal* **2018**, *24*, 3916–3924.

(16) Black, K.; Liu, P.; Xu, L.; Doubleday, C.; Houk, K. N. Dynamics, Transition States, and Timing of Bond Formation in Diels–Alder Reactions. *Proc. Natl. Acad. Sci.* **2012**, *109*, 12860–12865.

(17) (a) Neese, F. Software Update: The ORCA Program System—Version 5.0. *WIREs Computational Molecular Science* **2022**, *12*, e1606. (b) Neese, F. The ORCA Program System. *Wiley Interdiscip. Rev.: Comput. Mol. Sci.* **2012**, *2*, 73–78.

(18) Perdew, J. P.; Burke, K.; Ernzerhof, M. Generalized Gradient Approximation Made Simple. *Phys. Rev. Lett.* **1996**, *77*, 3865–3868.

(19) (a) Caldeweyher, E.; Ehlert, S.; Hansen, A.; Neugebauer, H.; Spicher, S.; Bannwarth, C.; Grimme, S. A Generally Applicable Atomic-Charge Dependent London Dispersion Correction. *J. Chem. Phys.* **2019**, *150*, 154122. (b)

Caldeweyher, E.; Bannwarth, C.; Grimme, S. Extension of the D3 Dispersion Coefficient Model. *J. Chem. Phys.* **2017**, *147*, 034112.

(20) Barone, V.; Cossi, M. Quantum Calculation of Molecular Energies and Energy Gradients in Solution by a Conductor Solvent Model. *J. Phys. Chem. A* **1998**, *102*, 1995–2001.

(21) Weigend, F.; Ahlrichs, R. Balanced Basis Sets of Split Valence, Triple Zeta Valence and Quadruple Zeta Valence Quality for H to Rn: Design and Assessment of Accuracy. *Phys. Chem. Chem. Phys.* **2005**, *7*, 3297–3305.

(22) Peterson, K. A.; Figgen, D.; Goll, E.; Stoll, H.; Dolg, M. Systematically Convergent Basis Sets with Relativistic Pseudopotentials. II. Small-Core Pseudopotentials and Correlation Consistent Basis Sets for the Post- *d* Group 16–18 Elements. *J. Chem. Phys.* **2003**, *119*, 11113–11123.

(23) Aziz, H. R.; Singleton, D. A. Concert along the Edge: Dynamics and the Nature of the Border between General and Specific Acid–Base Catalysis. *J. Am. Chem. Soc.* **2017**, *139*, 5965–5972.

(24) Little, R. D.; Masjedizadeh, M. R.; Wallquist, O.; Mcloughlin, J. I. The Intramolecular Michael Reaction. In *Organic Reactions*; John Wiley & Sons, Ltd, 2004; pp 315–552.

(25) Jackman, L. M.; Lange, B. C. Structure and Reactivity of Alkali Metal Enolates. *Tetrahedron* **1977**, *33*, 2737–2769.

(26) (a) Abbotto, A.; Streitwieser, A.; Schleyer, P. V. R. Ab Initio and Semiempirical Study of the Effect of Ethereal Solvent on Aggregation of a Lithium Enolate. *J. Am.*

Chem. Soc. **1997**, *119*, 11255–11268. (b) Houghton, M. J.; Biok, N. A.; Huck, C. J.; Algera, R. F.; Keresztes, I.; Wright, S. W.; Collum, D. B. Lithium Enolates Derived from Pyroglutaminol: Aggregation, Solvation, and Atropisomerism. *J. Org. Chem.* **2016**, *81*, 4149–4157. (c) Jackman, L. M.; Szeverenyi, N. M. Studies in Nuclear Resonance Spectroscopy. 14. Characterization and Structures of Lithioisobutyrophenone Aggregates in Ether Solvents. *J. Am. Chem. Soc.* **1977**, *99*, 4954–4962.

(27) The dielectric constant of the solvent mixture was calculated as the weighted average of dielectric constants of hexanes and diethyl ether based on the respective concentrations. This method for approximating dielectric constants of solvent mixtures is precedented in several studies including: (a) Prakongpan, S.; Nagai, T. Solubility of Acetaminophen in Cosolvents. *Chem. Pharm. Bull.* **1984**, *32*, 340–343. (b) Held, C.; Reschke, T.; Mohammad, S.; Luza, A.; Sadowski, G. ePC-SAFT Revised. *Chem. Eng. Res. Des.* **2014**, *92*, 2884–2897. (c) Ascani, M.; Held, C. Prediction of Salting-out in Liquid-Liquid Two-Phase Systems with ePC-SAFT: Effect of the Born Term and of a Concentration-Dependent Dielectric Constant. *Z. Anorg. Allg. Chem.* **2021**, *647*, 1305–1314.

(28) The trajectories leading to separation of reactants to starting material do not feature the charge separated intermediate (**33**), meaning that no bond formation (characterized by either C–C bond distance < 1.6 Å) was observed in these trajectories.

(29) (a) Neese, F. Software Update: The ORCA Program System, Version 4.0. *Wiley Interdiscip. Rev.: Comput. Mol. Sci.* **2018,** *8*, No. e1327. (b) Neese, F. The ORCA Program System. *Wiley Interdiscip. Rev.: Comput. Mol. Sci.* **2012**, *2*, 73−78.

(30) Adamo, C.; Barone, V. Toward Reliable Density Functional Methods without Adjustable Parameters: The PBE0 Model. *J. Chem. Phys.* **1999**, *110*, 6158−6170.

(31) (a) Caldeweyher, E.; Ehlert, S.; Hansen, A.; Neugebauer, H.; Spicher, S.; Bannwarth, C.; Grimme, S. A Generally Applicable Atomic-Charge Dependent London Dispersion Correction. *J. Chem. Phys.* **2019**, *150* (15), 154122. (b) Caldeweyher, E.; Bannwarth, C.; Grimme, S. Extension of the D3 Dispersion Coefficient Model. *J. Chem. Phys.* **2017**, *147*, 034112.

(32) (A) Cusumano, A. Q.; Goddard, W. A. I.; Stoltz, B. M. The Transition Metal Catalyzed [π2s + π2s + s2s + s2s] Pericyclic Reaction: Woodward–Hoffmann Rules, Aromaticity, and Electron Flow. *J. Am. Chem. Soc.* **2020**, *142*, 19033–19039. (B) Cusumano, A. Q.; Stoltz, B. M.; Goddard, W. A. Reaction Mechanism, Origins of Enantioselectivity, and Reactivity Trends in Asymmetric Allylic Alkylation: A Comprehensive Quantum Mechanics Investigation of a C(sp3)–C(sp3) Cross-Coupling. *J. Am. Chem. Soc.* **2020**, *142*, 13917–13933.

(33) Weigend, F.; Ahlrichs, R. Balanced Basis Sets of Split Valence, Triple Zeta Valence and Quadruple Zeta Valence Quality for H to Rn: Design and Assessment of Accuracy. *Phys. Chem. Chem. Phys.* **2005**, *7*, 3297–3305.

(34) Peterson, K. A.; Figgen, D.; Goll, E.; Stoll, H.; Dolg, M. Systematically Convergent Basis Sets with Relativistic Pseudopotentials. II. Small-Core Pseudopotentials and

Correlation Consistent Basis Sets for the Post- *d* Group 16–18 Elements. *J. Chem. Phys.* **2003**, *119*, 11113–11123.

(35) Garcia-Ratés, M.; Neese, F. Effect of the Solute Cavity on the Solvation Energy and Its Derivatives within the Framework of the Gaussian Charge Scheme. *J. Comput. Chem.* **2020**, *41*, 922–939.

(36) Grimme, S. Supramolecular Binding Thermodynamics by Dispersion-Corrected Density Functional Theory. *Chem. Eur. J.* **2012**, *18*, 9955–9964.

(37) Izato, Y.; Matsugi, A.; Koshi, M.; Miyake, A. A Simple Heuristic Approach to Estimate the Thermochemistry of Condensed-Phase Molecules Based on the Polarizable Continuum Model. *Phys. Chem. Chem. Phys.* **2019**, *21*, 18920–18929.

(38) Finkelstein, A. V.; Janin, J. The Price of Lost Freedom: Entropy of Bimolecular Complex Formation. *Protein Engineering, Design and Selection* **1989**, *3*, 1–3.

(39) Neese, F.; Wennmohs, F.; Hansen, A.; Becker, U. Efficient, Approximate and Parallel Hartree-Fock and Hybrid DFT Calculations. A 'Chain-of-Spheres' Algorithm for the Hartree-Fock Exchange. *Chemical Physics* **2009**, *356*, 98–109.

(40) Weigend, F. Accurate Coulomb-Fitting Basis Sets for H to Rn. *Phys. Chem. Chem. Phys.* **2006**, *8*, 1057–1065.

(41) Stoychev, G. L.; Auer, A. A.; Neese, F. Automatic Generation of Auxiliary Basis Sets. *J. Chem. Theory Comput.* **2017**, *13*, 554–562.

(42) Grimme, S. Exploration of Chemical Compound, Conformer, and Reaction Space with Meta-Dynamics Simulations Based on Tight-Binding Quantum Chemical Calculations. *J. Chem. Theory Comput.* **2019**, *15*, 2847–2862.

(43) Aziz, H. R.; Singleton, D. A. Concert along the Edge: Dynamics and the Nature of the Border between General and Specific Acid–Base Catalysis. *J. Am. Chem. Soc.* **2017**, *139*, 5965–5972.

(44) Stephens, P. J.; Devlin, F. J.; Chabalowski, C. F.; Frisch, M. J. Ab Initio Calculation of Vibrational Absorption and Circular Dichroism Spectra Using Density Functional Force Fields. *J. Phys. Chem.* **1994**, *98*, 11623–11627.

(45) Zhao, Y.; Truhlar, D. G. The M06 Suite of Density Functionals for Main Group Thermochemistry, Thermochemical Kinetics, Noncovalent Interactions, Excited States, and Transition Elements: Two New Functionals and Systematic Testing of Four M06-Class Functionals and 12 Other Functionals. *Theor Chem Account* **2008**, *120*, 215–241.

(46) Najibi, A.; Goerigk, L. The Nonlocal Kernel in van Der Waals Density Functionals as an Additive Correction: An Extensive Analysis with Special Emphasis on the B97M-V and ωB97M-V Approaches. *J. Chem. Theory Comput.* **2018**, *14*, 5725–5738.

(47) Kesharwani, M. K.; Brauer, B.; Martin, J. M. L. Frequency and Zero-Point Vibrational Energy Scale Factors for Double-Hybrid Density Functionals (and Other Selected Methods): Can Anharmonic Force Fields Be Avoided? *J. Phys. Chem. A* **2015**, *119*, 1701–1714.

(48) See: Yepes, D.; Valenzuela, J.; Martínez-Araya, J. I.; Pérez, P.; Jaque, P. Effect of the Exchange–Correlation Functional on the Synchronicity/Nonsynchronicity in

Bond Formation in Diels–Alder Reactions: A Reaction Force Constant Analysis. *Phys. Chem. Chem. Phys.* **2019**, *21*, 7412–7428.

CHAPTER 3

Enantioselective Michael Spirocyclization of Palladium Enolates†

3.1 INTRODUCTION

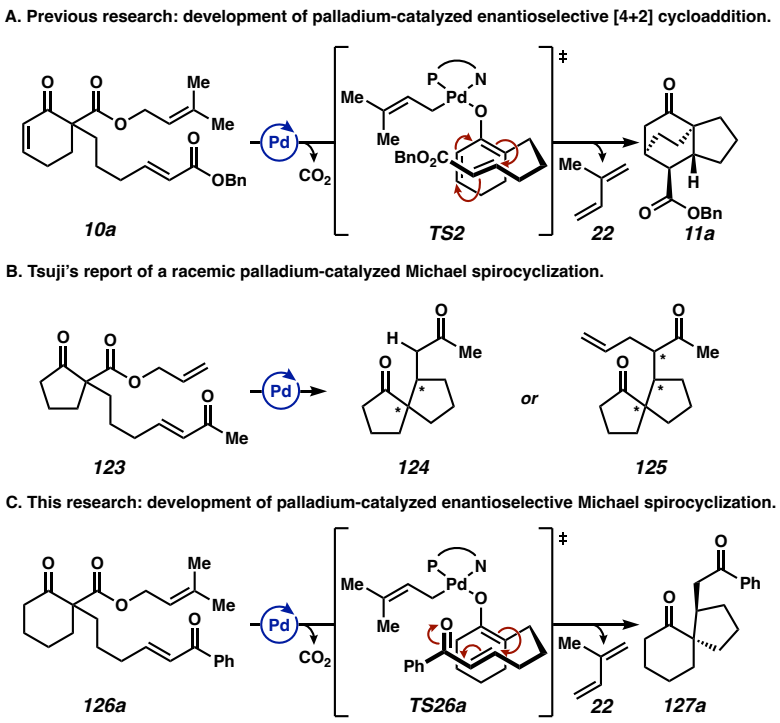
The enantio- and diastereoselective construction of spirocycles bearing all-carbon quaternary centers remains a persistent challenge in synthetic organic chemistry.[1] The prevalence of these motifs in complex natural products and other medicinally relevant molecules necessitates the development of new stereoselective reactions that can form these ring systems effectively.[2] The enantioselective Pd-catalyzed decarboxylative allylic alkylation reaction has proven to be a valuable tool for the construction of sterically congested all-carbon quaternary centers from racemic or prochiral starting materials.[3,4] Following extensive experimental and computational mechanistic studies, we have become interested in employing the chiral *O*-bound Pd enolate implicated in these transformations in the context of other reactions beyond allylic alkylation.[5]

Recently, our group reported a Pd-catalyzed decarboxylative [4+2] cycloaddition of Pd dienolates with tethered dienophiles (**TS2**), resulting in the formation of tricyclic scaffolds in high yield and good enantio- and diastereoselectivities (Figure 3.1.A).[6] In 1989 Tsuji and coworkers reported a non-enantioselective Pd-catalyzed Michael spirocyclization reaction which, depending on conditions, could favor formation of either protonolysis product **124** or allylated product **125** (Figure 3.1.B).[7] The diastereomeric outcome,

†This research was performed in collaboration with Strong, C. S.; Bissenali, S.. Portions of this chapter have been reproduced with permission from Stoltz, et al. *ACS Catal.* **2025**, *15*, 12231–12237. © 2025 American Chemical Society.

mechanism of catalyst turnover, and broader scope beyond a 5/5 spirane were not discussed.

Figure 3.1. *(A) Pd-catalyzed enantioselective [4+2] cycloaddition. (B) Racemic Pd-catalyzed Michael spirocyclization reported by Tsuji et al. (C) Development of a new Pd-catalyzed enantio- and diastereoselective Michael spirocyclization.*



Inspired by these findings, we sought to develop an enantio- and diastereoselective spirocyclization that could efficiently forge vicinal quaternary and tertiary stereocenters (Figure 3.1.C). We envisioned that enantioselectivity could be induced in a similar manner to the previously studied [4+2] cycloaddition.[5,6] On the other hand, the development of Michael cyclizations can be challenging due to the various diastereoselectivity considerations, in contrast to the well-established endo rule of Diels–Alder reactions.[8,9] For this reason, generating stereoenriched spiranes through a Pd-catalyzed Michael cyclization

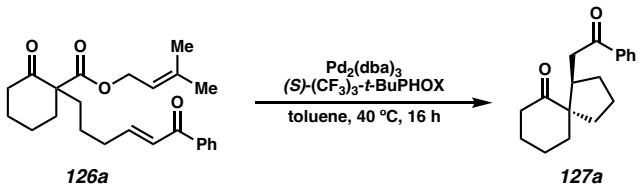
via an unstabilized enolate would represent a significant advance, complementary to other approaches.[10]

3.2 RESULTS AND DISCUSSION

3.2.1 REACTION OPTIMIZATION

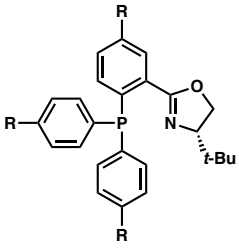
Designing the reaction substrate, we proposed applying our previously developed prenyl β-ketoester technology to achieve additive-free catalyst turnover.[6] Consequently, we synthesized the corresponding racemic substrate **126a** with a tethered phenyl enone as a Michael acceptor to evaluate reaction conditions. We found that performing the reaction at 0.025 mmol scale with $Pd_2(dba)_3$ (2.5 mol %) and *(S)*-$(CF_3)_3$-*t*-BuPHOX ligand (6.5 mol %) in toluene (0.1 M) at 40 ºC for 16 hours is optimal, affording **127a** in 89% ^{1}H NMR

Table 3.1. *Optimization of spirocyclization conditions. Conditions: 0.025 mmol* ***126a****, 2.5 mol % $Pd_2(dba)_3$, 6.5 mol % ligand, in 0.25 mL of solvent (0.1 M).* [a]*Yields determined by ^{1}H NMR with respect to 1,3,5-trimethoxybenzene as internal standard.*[12] [b]*Incomplete conversion was observed.*[11] [c]*Isolated yield on 0.1 mmol scale.*



126a *127a*

entry	variation from standard conditions	yield (%)[a]	ee (%)
1	none	89%	93%
2	THF	83%	89%
3	21 °C	56%[b]	95%
4	60 °C	75%	92%
5	*(S)*-*t*-BuPHOX	76%	93%
6	0.05 M	83%	94%
7	0.1 mmol scale	81%[c]	94%



R = CF_3; *(S)*-$(CF_3)_3$-*t*-BuPHOX

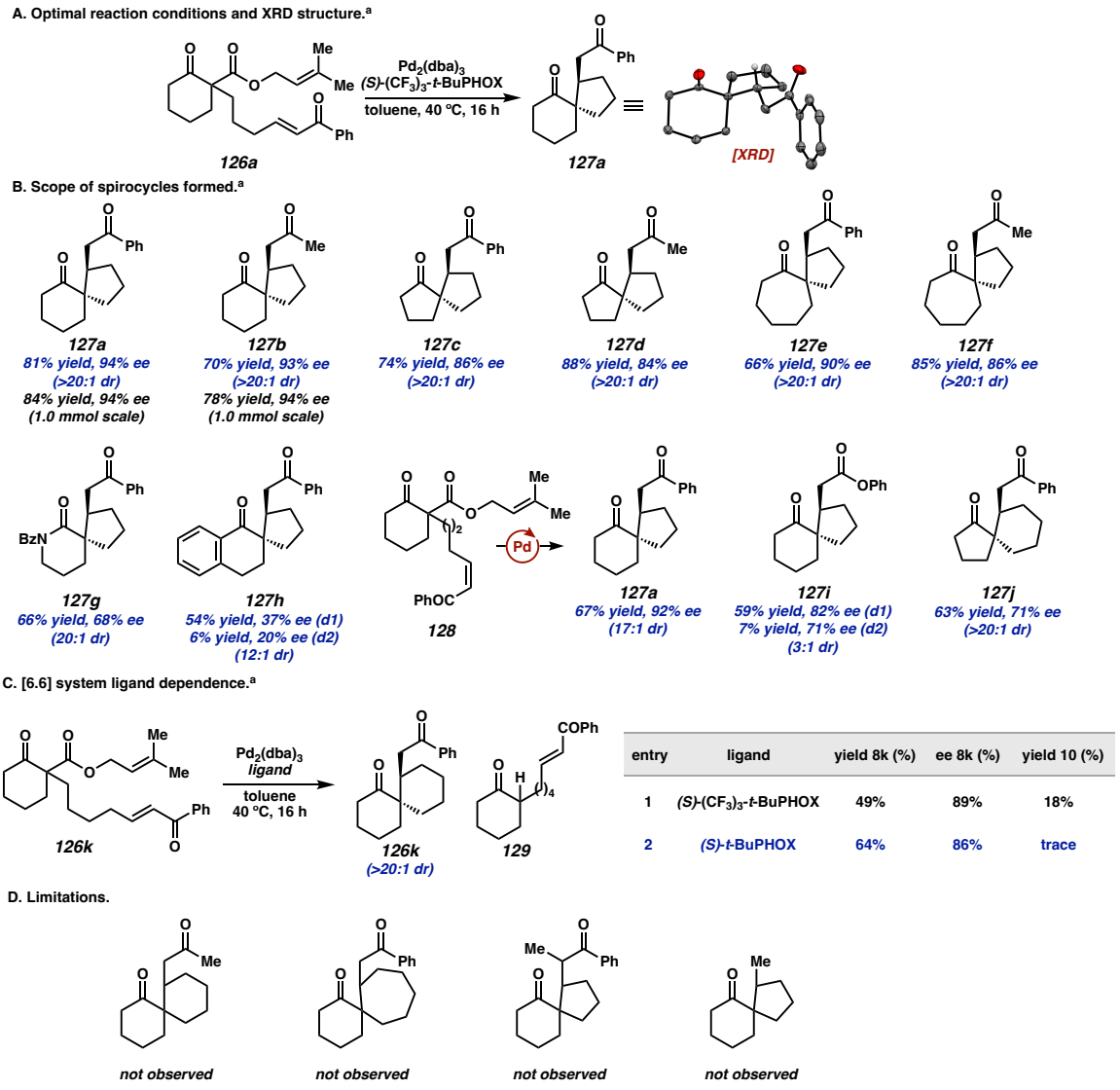
R = H; *(S)*-*t*-BuPHOX

yield, 93% ee, and >20:1 dr (Table 3.1., entry 1). The reaction proceeds similarly in THF albeit with slightly diminished yield and selectivity (entry 2). At 21 °C the conversion is reduced, although the enantioselectivity is marginally higher (entry 3).[11] Raising reaction temperature to 60 ºC proves detrimental to both yield and selectivity (entry 4). Employing the more electron-rich *(S)-t*-BuPHOX results in similar selectivity but lower yield (entry 5). Further dilution of the reaction is inconsequential (entry 6). When the reaction is performed at a 0.1 mmol scale, the isolated yield and ee are comparable to what is observed on smaller scale (entry 7). The absolute configuration of **127a** was assigned via an X-ray crystal structure (Figure 3.2.A, XRD).

3.2.2 SUBSTRATE SCOPE

With optimal conditions in hand, we began exploring the generality of this transformation (Figure 3.2.B). The phenyl enone can be replaced with a methyl enone to form spirocycle **127b** in good yield and similar selectivity. Gratifyingly, reactions of both substrates can be scaled to 1.0 mmol, resulting in slightly improved yields with maintained selectivities. 5/5 spirocycles can be accessed (**127c** and **127d**), albeit in slightly lowered enantioselectivity. In addition, 7/5 systems can also be formed (**127e** and **127f**). Spirolactam **127g** is formed in modest yield and lowered enantioselectivity, and tetralone-derived spirocycles are generated in slightly diminished dr and low ee (**127h d1** and **127h d2**, 12:1 dr based on crude NMR).[13] When Z-enone **128** is employed, the same diastereomer of product (**127a**) is obtained in modest yield with similar selectivity.[14] Employing a phenyl enoate, diastereoselectivity is greatly eroded (**127i d1** and **127i d2**, 3:1 dr based on crude NMR)[13], while moderate levels of enantioselectivity are maintained.

Figure 3.2. *[a]Conditions: 0.1 mmol* ***7****, 2.5 mol % $Pd_2(dba)_3$, 6.5 mol % ligand, in 0.25 mL of solvent (0.1 M). Isolated yields reported followed by dr's based on NMR ratios of unpurified reaction mixtures. (A) Generic reaction scheme and XRD structure. (B) Scope of spirocycles formed via Michael spirocyclization reaction. (C) Ligand-dependent product distribution for 6/6 system (D) Limitations of this transformation.*



The 5/6 system (derived from a cyclopentanone starting material) forms in modestly lower yield and ee (**127j**). Interestingly, when employing the optimal ligand toward the 6/6

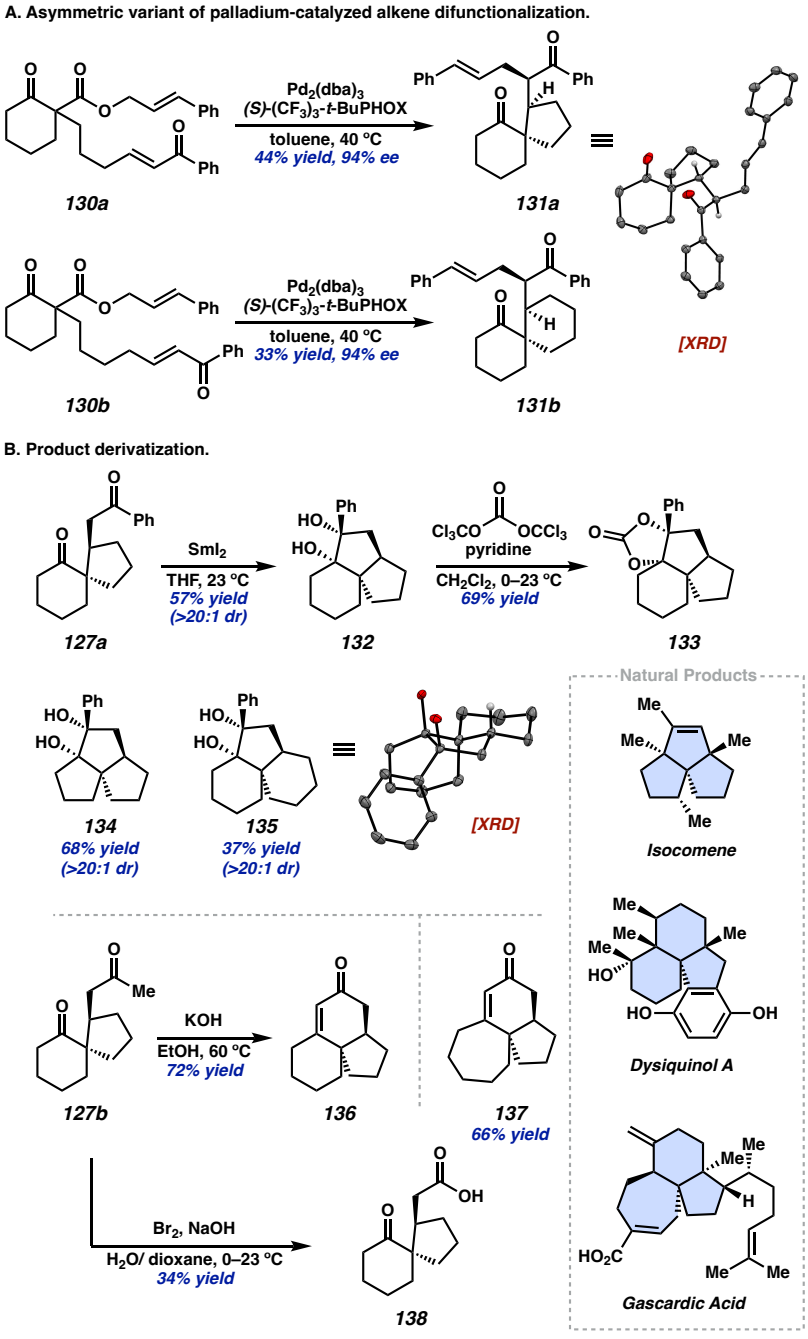
system (Figure 3.2.C, entry 1, **126k** → **127k**), some undesired protonation of the initial Pd-enolate occurs, generating **129**. This can be suppressed however, by employing the more electron-rich *(S)-t*-BuPHOX ligand (entry 2). There were several systems investigated in which appreciable amounts of spirocycle are not clearly observed (Figure 3.2.D). In these cases, direct protonation of the initial Pd-enolate is observed as the major product.

Inspired by Tsuji's enone difunctionalization (**125**, Figure 3.1.B), we opted to investigate whether it would be possible to selectively form a stereotriad by employing a cinnamyl β-ketoester (**130a**, Figure 3.3.A).[7] We found that employing the same catalytic conditions with **130a** resulted in formation of the desired difunctionalized spirocycle **131a**, isolated as a single diastereomer in 44% yield.[15] The absolute configuration was confirmed via X-ray crystallography (Figure 3.3.A, XRD). Additionally, the corresponding 6/6 spirane (**131b**) was also formed under the same conditions. Through this cascade transformation, racemic cinnamyl β-ketoesters were transformed to spirocycles bearing vicinal stereotriads. Further studies on these systems are currently underway.

3.2.3 PRODUCT DERIVATIZATION

With a diverse range of Michael adducts bearing dicarbonyls in hand, we sought to explore the utility of these scaffolds (Figure 3.3.B). Treatment of spirane **127a** with stoichiometric samarium diiodide generates pinacol product **132**.[16] The *cis* diol is formed in this process, as suggested by the successful formation of cyclic carbonate **133** upon subjection of **132** to triphosgene and pyridine. In addition to the 6/5/5 system (**132**), 5/5/5 and 6/5/6 angular ring systems (**134** and **135**) are also accessible using this method with the latter's structure (**135**) confirmed via XRD. These ring systems bear four contiguous

Figure 3.3. *(A) Application of this reaction system to asymmetric enone difunctionalization. (B) Product derivatizations toward versatile functional groups and diverse tricycles.*



stereocenters, three of which are fully substituted. Additionally, an aldol condensation was performed on methyl ketone **127b**, resulting in tricyclic enone **136**. This allows for differentiation of the carbonyls and access to the corresponding 6/6/5 (**136**) and 7/6/5 (**137**) angular ring systems. Lastly, methyl ketone **127b** can be converted to the corresponding carboxylic acid **138** through a haloform reaction, providing two orthogonal functionalities. These carbocyclic ring systems are found in numerous natural products such as isocomene, dysiquinol A, gascardic acid, and others.[2,17]

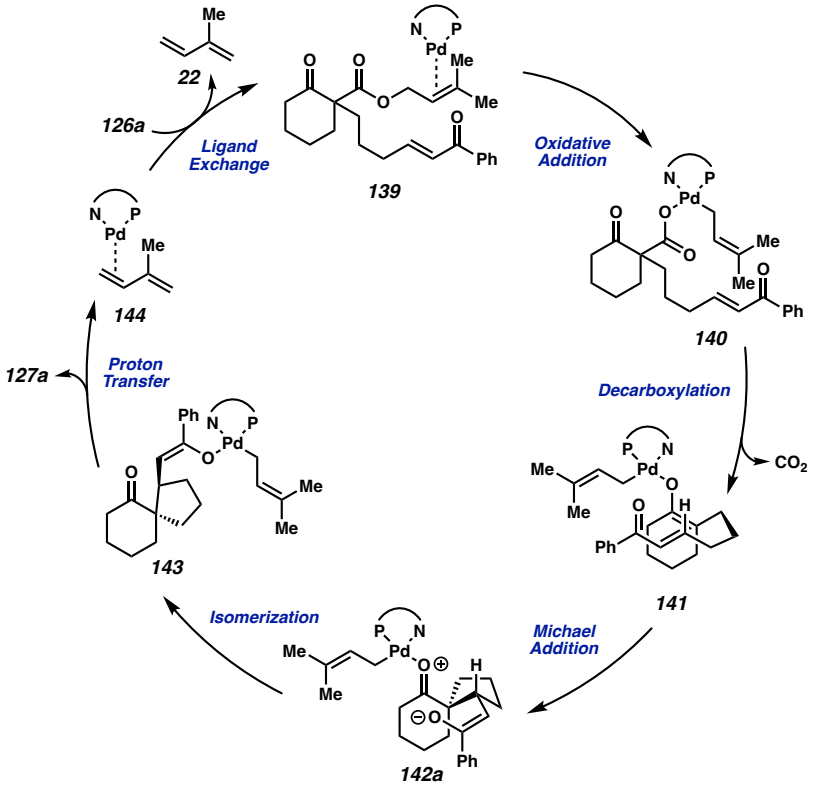
3.2.4 MECHANISTIC INVESTIGATIONS

Interested in the utility of this Michael spirocyclization, we sought to further understand the mechanism through which it proceeds by proposing a potential catalytic cycle. Using previous studies[4–6] as a starting point, we propose that the mechanism begins with oxidative addition to prenyl β-ketoester **139** to generate Pd-carboxylate **140** (Figure 3.4). Subsequent decarboxylation generates *O*-bound Pd enolate **141**, which can undergo intramolecular Michael spirocyclization to provide enolate **142a**. Following this, isomerization might occur to form *O*-bound Pd enolate **143** before a proton transfer liberates product **8a** and concomitantly generates isoprene bound to Pd^0 (**144**). Upon ligand exchange with another equivalent of substrate (**126a**), catalyst turnover can be achieved.

Intrigued by the Michael spirocyclization proposed in this cycle and the influence of our chiral ligand in this process, we opted to investigate potential Michael addition transition states leading to four possible stereoisomers **142a**–**d** through DFT calculations (Figure 3.5.). Computations were performed at the PBE0-D4/def2-TZVPP (Pd), ma-def2-TZVPP (O), def2-TZVPP/CPCM(PhMe)//PBE0-D4/def2-TZVP (Pd), ma-def2-SVP (O),

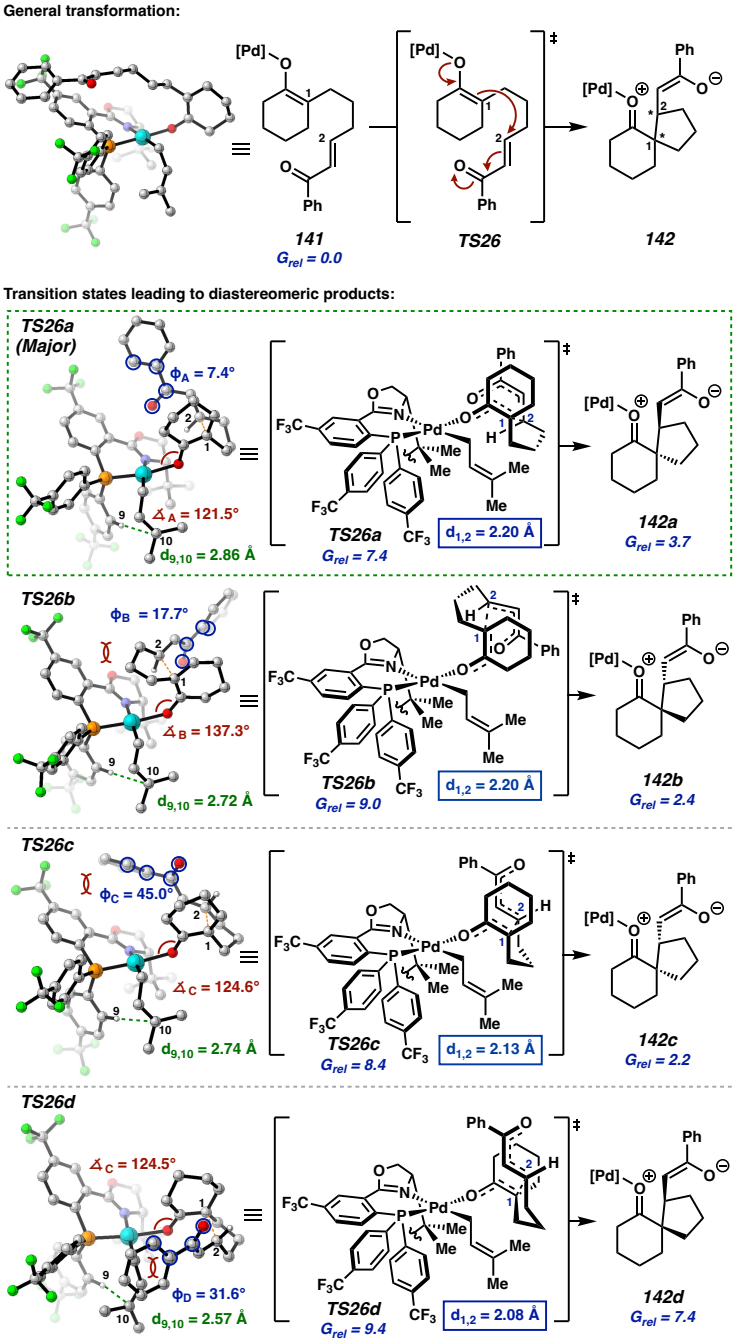
def2-SVP level of theory as it has proven to be a robust method in our prior studies of similar Pd systems[4] (see SI for more details on computational methods and additional preliminary results).

Figure 3.4. *Proposed catalytic cycle.*



Notably, the minimum energy transition structure to each product features an *s*-cis geometry of the Michael acceptor, resulting in Z-enolate geometries of intermediates **142a**–**d**. The lowest energy transition state **TS26a** features *syn* alignment of the Michael acceptor tether relative to the *t*-Bu substituent of the PHOX ligand, and the electrophile approaches from the more sterically accessible *external* face of the enolate. These characteristics are consistent with observations in our previously studied allylic alkylation and Diels–Alder transformations.[4,6] In comparison, **TS26b** requires the dienophile tether

Figure 3.5. *Computational evaluation of the four possible Michael addition transition states leading to the formation of stereoisomers at the PBE0-D4/def2-TZVPP (Pd), ma-def2-TZVPP (O), def2-TZVPP/CPCM(PhMe)//PBE0-D4/def2-TZVP (Pd), ma-def2-SVP (O), def2-SVP level of theory.*



be placed *anti* to the *t*-Bu group of the PHOX ligand to prevent steric clashing that would result from *internal* electrophile approach (see SI for more details). As such, interaction of the tether and the ligand backbone in **TS26b** leads to a distortion of 15.8º at the Pd–O–C bond angle (∢) relative to **TS26a**, reflecting an increased level of steric congestion that contributes to an increased energy barrier of 9.0 kcal/mol (ΔΔG = 1.6 kcal/mol).

Steric interactions between the phenyl ketone of the Michael acceptor and the ligand backbone in **TS26c** lead to a distorted dihedral angle (ϕ_c) of 45º between the planes of the carbonyl and the phenyl ring. The *internal* electrophile approach in **TS26d** results in steric clash with the Pd complex, which is reflected by the shortened interatomic distance ($d_{9,10}$ = 2.57 Å) between the ligand aryl group and the prenyl moiety. These undesired interactions contribute to the increased 8.4 and 9.4 kcal/mol energy barriers in **TS26c** and **TS26d**, respectively. These computational studies predict **142a** to be the major stereoisomer, which aligns with the experimentally observed product. The calculated 1.6 kcal/mol preference for **TS26a** over **TS26b** is in good agreement with experimentally observed 94% ee (which corresponds to a 2.1 kcal/mol difference in energy barriers). Further computational and experimental investigations related to the mechanism of catalyst turnover and the reversibility of the Michael addition are currently underway and will be reported in due course.

3.3 CONCLUSIONS

In summary, we report an asymmetric Pd-catalyzed Michael spirocyclization reaction that allows for the efficient construction of vicinal quaternary and tertiary stereodiads. This reaction provides access to a broad scope of bicyclic scaffolds in good

yield, dr, and ee. The diversification of these products toward complex tricycles relevant to natural product synthesis is also disclosed. Furthermore, our mechanistic understanding allowed for the development of a cinnamyl-based cascade reaction that generates a third stereocenter. We evaluated a stereochemical model of the Michael addition transition states, which suggest that the stereoselectivity of C–C bond formation could be governed by the Michael acceptor's conformation, placement of the Michael acceptor tether relative to the *t*-Bu substituent of the PHOX ligand, and the bias toward *external* versus *internal* approach of the electrophile.

By applying the rational design framework previously established,[5,6] we were able to expand the utility of Pd enolates through their application in a highly stereoselective Michael spirocyclization. We envision this discovery will expedite the synthesis of stereochemically complex and medicinally relevant polycyclic scaffolds. The insights gained from this study broaden our knowledge regarding the stereochemical interactions of different enolate substrates with the Pd–PHOX catalyst system, which will be leveraged to accelerate the future development of synthetically useful asymmetric transformations.

3.4 EXPERIMENTAL SECTION

3.4.1 MATERIALS AND METHODS

Unless otherwise stated, reactions were performed in flame-dried glassware under a nitrogen atmosphere using dry, deoxygenated solvents. Solvents were dried by passage through an activated alumina column under argon. Reaction progress was monitored by thin-layer chromatography (TLC) or Agilent 1290 UHPLC-MS. TLC was performed using E. Merck silica gel 60 F254 precoated glass plates (0.25 mm) and visualized by UV

fluorescence quenching, $KMnO_4$ staining, or *p*-anisaldehyde staining. Silicycle Silia*Flash*® P60 Academic Silica gel (particle size 40–63 nm) was used for flash chromatography. The absolute configurations of **127a** and **131a** were determined by X-ray crystallography, and all other products were assigned by analogy. Reagents were purchased from commercial sources and used as received unless otherwise stated. Ligands were prepared according to literature procedures.[1] HG-II was graciously provided by Umicore.

^{1}H NMR spectra were recorded on Varian Inova 600 MHz and Bruker 400 MHz spectrometers and are reported relative to residual non-deuterated solvent $CHCl_3$ (δ 7.26 ppm) or C_6H_6 (δ 7.16 ppm). ^{13}C NMR spectra were recorded on a Bruker 400 MHz spectrometer (100 MHz) and are reported relative to solvent $CDCl_3$ (δ 77.16 ppm) or C_6D_6 (δ 128.06 ppm). Data for ^{1}H NMR are reported as follows: chemical shift (δ ppm) (multiplicity, coupling constant (Hz), integration). Multiplicities are reported as the peaks appear as follows: s = singlet, d = doublet, t = triplet, q = quartet, p = pentet, sept = septuplet, m = multiplet, br s = broad singlet, br d = broad doublet. Some reported spectra include minor impurities of water (δ 1.56 ppm), ethyl acetate (δ 4.12, 2.05, 1.26 ppm), methylene chloride (δ 5.30 ppm), acetone (δ 2.17 ppm), grease (δ 1.26, 0.86 ppm), and/or silicon grease (δ 0.07 ppm), which do not impact product assignments. Data for ^{13}C NMR are reported in terms of chemical shifts (δ ppm).

IR spectra were obtained by use of a Perkin Elmer Spectrum BXII spectrometer or Nicolet 6700 FTIR spectrometer using thin films deposited on NaCl plates and reported in frequency of absorption (cm^{-1}). Optical rotations were measured with a Jasco P-2000 polarimeter operating on the sodium D-line (589 nm), using a 100 mm path-length cell. Analytical SFC and SFC-MS studies were performed with an Agilent 1260 Infinity II

G6125B SFC-MS supercritical CO_2 analytical chromatography system utilizing Chiralpak (IC-3, AD-3, ID-3, IF-3, IG-3, IH-3) or Chiralcel (OD-3, OJ-3) columns (4.6 mm x 25 cm) obtained from Daicel Chemical Industries, Ltd.[2] High resolution mass spectra (HRMS) were obtained from the Caltech Mass Spectral Facility using a JEOL JMS-T2000GC AccuTOFTM GC-Alpha High Resolution Mass Spectrometer in field ionization (FI+) or field desorption (FD+) mode, or an Agilent 6230 Series TOF with an Agilent Jet Stream ion source in electrospray ionization (ESI+).

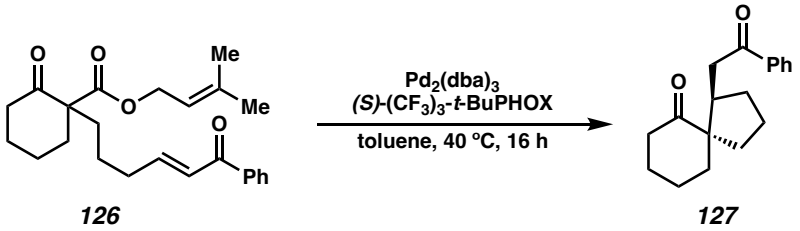
Low-temperature diffraction data (ϕ-and ω-scans) were collected on a Bruker AXS D8 VENTURE KAPPA diffractometer coupled to a PHOTON II CPAD detector with Cu K_α radiation (λ = 1.54178 Å) from an IμS micro-source for the structure of compound V25038. The structure was solved by direct methods using SHELXS[3] and refined against F^2 on all data by full-matrix least squares with SHELXL-2019[4] using established refinement techniques.[5] All non-hydrogen atoms were refined anisotropically. All hydrogen atoms were included into the model at geometrically calculated positions and refined using a riding model. The isotropic displacement parameters of all hydrogen atoms were fixed to 1.2 times the U value of the atoms they are linked to (1.5 times for methyl groups).

List of Abbreviations: ee – enantiomeric excess, dr – diastereomeric ratio, SFC – supercritical fluid chromatography, HPLC – high-performance liquid chromatography, TLC – thin-layer chromatography, IPA – isopropanol, EtOAc – ethyl acetate.

3.4.2 EXPERIMENTAL PROCEDURES AND SPECTROSCOPIC DATA

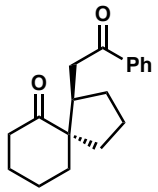
Pd-Catalyzed Decarboxylative Michael Cyclization:

General Procedure 3A: Asymmetric Pd-Catalyzed Decarboxylative Michael Cyclization



126 ***127***

In a nitrogen filled glovebox, an oven-dried 4 mL vial was charged with a stir bar, $Pd_2(dba)_3$ (2.3 mg, 0.0025 mmol, 2.5 mol %), *(S)*-$(CF_3)_3$-*t*-BuPHOX (3.8 mg, 0.0065 mmol, 6.5 mol %), and toluene (0.6 mL). The catalyst solution was stirred at 23 ºC for 20 min. A solution of substrate **126** (0.1 mmol, 1 equiv) in toluene (0.4 mL) was added to the catalyst solution. The resulting mixture was sealed, pumped out of the glovebox, and then heated to 40 ºC for 16 h. The solution was then cooled to 23 ºC and concentrated under reduced pressure. The crude mixture was purified by silica gel flash column chromatography to yield **127**.



127a

(1*R*,5*S*)-1-(2-oxo-2-phenylethyl)spiro[4.5]decan-6-one (127a)

Prepared from **126a** following General Procedure 3A. Purification by flash column chromatography (0–60% Et_2O/hexanes) afforded the title compound as a white crystalline solid (21.9 mg, 0.081 mmol, 81% yield, 94% ee). Absolute and relative stereochemistry were assigned by X-ray crystallography (vide infra).

^{1}H NMR (600 MHz, $CDCl_3$): δ 8.12 – 8.07 (m, 2H), 7.58 – 7.53 (m, 1H), 7.51 – 7.45 (m, 2H), 3.21 (dd, *J* = 14.0, 3.6 Hz, 1H), 3.01 – 2.92 (m, 1H), 2.52 (dd, *J* = 13.9, 11.2 Hz, 1H), 2.47 – 2.38 (m, 2H), 2.07 – 2.00 (m, 1H), 1.99 – 1.92 (m, 1H), 1.89 – 1.82 (m, 1H), 1.82 – 1.55 (m, 8H), 1.38 – 1.30 (m, 1H).

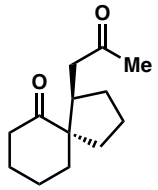
^{13}C NMR (100 MHz, $CDCl_3$): δ 214.3, 200.8, 136.9, 133.1, 128.71, 128.69, 58.8, 40.5, 40.2, 39.9, 34.9, 31.5, 29.3, 27.3, 21.8, 21.7.

IR (Neat Film, NaCl): 2938, 2862, 1699, 1684, 1448, 1279, 1213, 1128 cm^{-1}.

HRMS (ESI+): *m/z* calc'd for $C_{18}H_{23}O_2$ $[M+H]^+$: 271.1693, found 271.1681.

Optical Rotation: $[\alpha]_D^{23}$ –23.9 (c = 0.69, $CHCl_3$).

SFC conditions: 20% IPA, 2.5 mL/min, Chiralpak IC-3 column, λ = 254 nm, t_R (min): minor = 6.99, major = 8.67



127b

(1*R*,5*S*)-1-(2-oxopropyl)spiro[4.5]decan-6-one (127b)

Prepared from **126b** following General Procedure 3A. Purification by flash column chromatography (0–60% Et_2O/hexanes) afforded the title compound as a pale yellow crystalline solid (14.5 mg, 0.070 mmol, 70% yield, 93% ee). Absolute and relative stereochemistry were assigned by X-ray crystallography (vide infra).

^{1}H NMR (400 MHz, $CDCl_3$): δ 2.95 – 2.79 (m, 1H), 2.49 (dd, *J* = 14.9, 4.2 Hz, 1H), 2.44 – 2.31 (m, 2H), 2.21 – 2.10 (m, 4H), 2.04 – 1.95 (m, 1H), 1.94 – 1.81 (m, 2H), 1.80 – 1.71 (m, 2H), 1.71 – 1.45 (m, 6H), 1.27 – 1.14 (m, 1H).

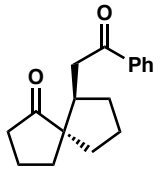
^{13}C NMR (100 MHz, $CDCl_3$): δ 214.0, 209.2, 58.3, 45.0, 40.3, 38.8, 35.1, 31.5, 30.0, 29.7, 27.1, 21.9, 21.7.

IR (Neat Film, NaCl): 2941, 2864, 1701, 1447, 1355, 1164, 1129 cm^{-1}.

HRMS (ESI+): *m/z* calc'd for $C_{13}H_{21}O_2$ $[M+H]^+$: 209.1536, found 209.1526.

Optical Rotation: $[\alpha]_D^{23}$ –5.3 (c = 0.49, $CHCl_3$).

SFC conditions: 30% IPA, 2.5 mL/min, Chiralpak IC-3 column, MSD1 TIC[2], t_R (min): major = 3.39, minor = 3.98



127c

(5*R*,6*R*)-6-(2-oxo-2-phenylethyl)spiro[4.4]nonan-1-one (127c)

Prepared from **126c** following General Procedure 3A. Purification by flash column chromatography (0–60% Et_2O/hexanes) afforded the title compound as a colorless oil (18.9 mg, 0.074 mmol, 74% yield, 86% ee).

^{1}H NMR (400 MHz, $CDCl_3$): δ 7.96 – 7.88 (m, 2H), 7.58 – 7.51 (m, 1H), 7.49 – 7.42 (m, 2H), 2.98 – 2.83 (m, 2H), 2.82 – 2.69 (m, 1H), 2.42 – 2.30 (m, 1H), 2.29 – 2.15 (m, 1H), 2.10 – 2.01 (m, 1H), 2.00 – 1.92 (m, 1H), 1.92 – 1.78 (m, 2H), 1.77 – 1.65 (m, 4H), 1.63 – 1.51 (m, 1H), 1.41 – 1.29 (m, 1H).

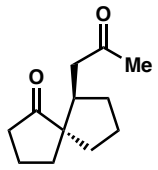
^{13}C NMR (100 MHz, $CDCl_3$): δ 222.9, 199.8, 136.9, 133.2, 128.8, 128.3, 58.8, 41.2, 40.5, 38.0, 37.8, 32.2, 31.5, 23.1, 19.6.

IR (Neat Film, NaCl): 2955, 2870, 1729, 1683, 1596, 1448, 1213, 1157 cm^{-1}.

HRMS (ESI+): *m/z* calc'd for $C_{17}H_{20}O_2Na$ $[M+Na]^+$: 279.1356, found 279.1345.

Optical Rotation: $[\alpha]_D^{23}$ +44.9 (c = 0.74, $CHCl_3$).

SFC conditions: 20% IPA, 2.5 mL/min, Chiralpak IC-3 column, λ = 254 nm, t_R (min): minor = 7.78, major = 10.03



127d

(5*R*,6*R*)-6-(2-oxopropyl)spiro[4.4]nonan-1-one (127d)

Prepared from **126d** following General Procedure 3A. Purification by flash column chromatography (0–60% Et_2O/hexanes) afforded the title compound as a colorless oil (17.1 mg, 0.088 mmol, 88% yield, 84% ee).

^{1}H NMR (400 MHz, $CDCl_3$): δ 2.64 – 2.51 (m, 1H), 2.42 – 2.23 (m, 3H), 2.19 – 2.07 (m, 4H), 2.06 – 1.97 (m, 1H), 1.97 – 1.87 (m, 1H), 1.85 – 1.73 (m, 2H), 1.73 – 1.60 (m, 4H), 1.59 – 1.47 (m, 1H), 1.30 – 1.13 (m, 1H).

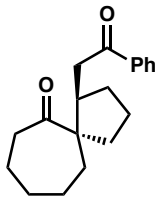
^{13}C NMR (100 MHz, $CDCl_3$): δ 222.9, 208.5, 58.7, 45.6, 40.6, 37.9, 37.7, 32.1, 31.2, 29.9, 22.9, 19.5.

IR (Neat Film, NaCl): 2955, 2872, 1730, 1406, 1357, 1158 cm^{-1}.

HRMS (ESI+): *m/z* calc'd for $C_{12}H_{19}O_2$ $[M+H]^+$: 195.1380, found 195.1370.

Optical Rotation: $[\alpha]_D^{23}$ +66.6 (c = 0.59, $CHCl_3$).

SFC conditions: 25% IPA, 2.5 mL/min, Chiralpak IC-3 column, MSD1 TIC[2], t_R (min): major = 4.16, minor = 4.78



127e

(1*R*,5*S*)-1-(2-oxo-2-phenylethyl)spiro[4.6]undecan-6-one (127e)

Prepared from **126e** following General Procedure 3A. Purification by flash column chromatography (0–60% Et_2O/hexanes) afforded the title compound as a colorless oil (18.7 mg, 0.066 mmol, 66% yield, 90% ee).

^{1}H NMR (400 MHz, $CDCl_3$): δ 8.06 – 7.99 (m, 2H), 7.60 – 7.52 (m, 1H), 7.51 – 7.43 (m, 2H), 3.25 (dd, *J* = 14.5, 4.3 Hz, 1H), 2.85 – 2.72 (m, 1H), 2.67 – 2.52 (m, 3H), 2.01 – 1.79 (m, 3H), 1.78 – 1.55 (m, 9H), 1.54 – 1.46 (m, 1H), 1.44 – 1.30 (m, 1H).

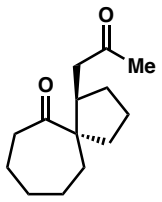
^{13}C NMR (100 MHz, $CDCl_3$): δ 217.2, 200.3, 136.9, 133.1, 128.7, 128.5, 60.7, 42.7, 42.7, 40.3, 37.5, 31.5, 31.0, 30.2, 26.4, 25.8, 22.2.

IR (Neat Film, NaCl): 2931, 2858, 1686, 1596, 1579, 1448, 1287, 1215 cm^{-1}.

HRMS (ESI+): *m/z* calc'd for $C_{19}H_{25}O_2$ $[M+H]^+$: 285.1849, found 285.1841.

Optical Rotation: $[\alpha]_D^{23}$ +16.2 (c = 1.56, $CHCl_3$).

SFC conditions: 20% IPA, 2.5 mL/min, Chiralpak IC-3 column, λ = 254 nm, t_R (min): major = 10.28, minor = 11.76



127f

(1*R*,5*S*)-1-(2-oxopropyl)spiro[4.6]undecan-6-one (127f)

Prepared from **126f** following General Procedure 3A. Purification by flash column chromatography (0–60% Et_2O/hexanes) afforded the title compound as a colorless oil (18.8 mg, 0.085 mmol, 85% yield, 86% ee).

^{1}H NMR (400 MHz, $CDCl_3$): δ 2.70 – 2.46 (m, 4H), 2.23 (dd, *J* = 15.2, 9.9 Hz, 1H), 2.14 (s, 3H), 2.02 – 1.85 (m, 2H), 1.81 – 1.72 (m, 1H), 1.72 – 1.44 (m, 10H), 1.30 – 1.17 (m, 1H).

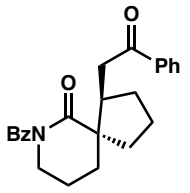
^{13}C NMR (100 MHz, $CDCl_3$): δ 217.1, 208.7, 60.5, 45.3, 42.7, 42.1, 37.1, 31.3, 31.0, 30.6, 30.0, 26.3, 25.7, 22.3.

IR (Neat Film, NaCl): 2931, 2858, 1713, 1697, 1453, 1354, 1159 cm^{-1}.

HRMS (ESI+): *m/z* calc'd for $C_{14}H_{23}O_2$ $[M+H]^+$: 223.1693, found 223.1683.

Optical Rotation: $[\alpha]_D^{23}$ +30.9 (c = 0.73, $CHCl_3$).

SFC conditions: 30% IPA, 2.5 mL/min, Chiralpak IC-3 column, MSD1 TIC[2], t_R (min): major = 3.90, minor = 6.06



127g

(1*R*,5*R*)-7-benzoyl-1-(2-oxo-2-phenylethyl)-7-azaspiro[4.5]decan-6-one (127g)

Prepared from **126g** following General Procedure 3A. Purification by flash column chromatography (0–80% Et_2O/hexanes) afforded the title compound as a white foam (24.6 mg, 0.066 mmol, 66% yield, 68% ee).

^{1}H NMR (600 MHz, $CDCl_3$): δ 7.93 – 7.89 (m, 2H), 7.59 – 7.55 (m, 2H), 7.54 – 7.50 (m, 1H), 7.47 – 7.40 (m, 3H), 7.37 (t, *J* = 7.7 Hz, 2H), 3.96 (dtd, *J* = 12.7, 4.5, 1.7 Hz, 1H),

3.70 (ddd, *J* = 12.7, 10.9, 4.8 Hz, 1H), 3.19 – 3.11 (m, 1H), 3.06 (dd, *J* = 15.0, 5.2 Hz, 1H), 2.80 (dd, *J* = 15.0, 9.6 Hz, 1H), 2.11 – 1.93 (m, 5H), 1.89 – 1.82 (m, 1H), 1.80 – 1.71 (m, 3H), 1.40 – 1.32 (m, 1H).

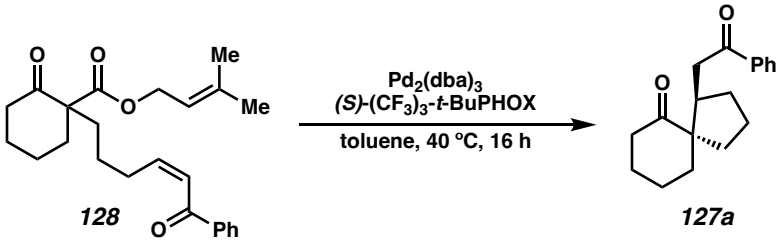
^{13}C NMR (100 MHz, $CDCl_3$): δ 199.6, 178.5, 175.5, 136.8, 136.8, 133.1, 131.4, 128.7, 128.3, 128.3, 127.6, 53.8, 46.5, 41.9, 39.7, 38.4, 29.9, 27.4, 22.3, 20.1.

IR (Neat Film, NaCl): 3059, 2951, 2872, 1681, 1597, 1475, 1448, 1386, 1277, 1169, 1151 cm^{-1}.

HRMS (ESI+): *m/z* calc'd for $C_{24}H_{26}NO_3$ $[M+H]^+$: 376.1907, found 376.1907.

Optical Rotation: $[\alpha]_D^{23}$ +51.6 (c = 2.05, $CHCl_3$).

SFC conditions: 40% IPA, 2.5 mL/min, Chiralpak IC-3 column, λ = 254 nm, t_R (min): minor = 5.93, major = 9.07

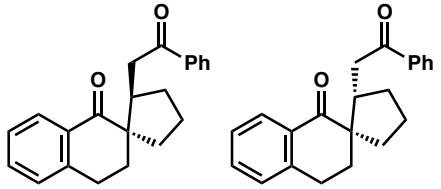


(1*R*,5*S*)-1-(2-oxo-2-phenylethyl)spiro[4.5]decan-6-one (127a)

Prepared from **128** following General Procedure 3A. Purification by flash column chromatography (0–55% Et_2O/hexanes) afforded the title compound as a colorless oil (18.2 mg, 0.067 mmol, 67% yield, 92% ee).

*Note: see NMR, IR, HRMS, Optical Rotation data in reaction of **126a** to **127a** earlier in SI.*

SFC conditions: 20% IPA, 2.5 mL/min, Chiralpak IC-3 column, λ = 254 nm, t_R (min): minor = 6.82, major = 8.44



127h (d1) ***127h (d2)***

(1*R*,2*R*)-2-(2-oxo-2-phenylethyl)-3',4'-dihydro-1'*H*-spiro[cyclopentane-1,2'-naphthalen]-1'-one (127h, *d1* and *d2*)

Prepared from **126h** following General Procedure 3A. Crude analysis by ^{1}H NMR affords a 12:1 ratio of *d1* to *d2*. The diastereomers were subsequently separated by flash column chromatography (0–60% Et_2O/hexanes) to afford the *d1* as a colorless oil (17.3 mg, 0.054 mmol, 54% yield, 37% ee) and *d2* as a colorless oil (1.9 mg, 0.006 mmol, 6% yield, 20% ee). The absolute configuration of 8h *d1* is assigned by analogy to **127a**. The relative configuration of **127h *d2*** is assigned by comparison to ^{1}H NMR of **127h *d1***, the absolute configuration is not determined.

127h (*d1*):

^{1}H NMR (400 MHz, $CDCl_3$): δ 8.08 (dd, *J* = 7.8, 1.4 Hz, 1H), 8.05 – 7.97 (m, 2H), 7.60 – 7.52 (m, 1H), 7.51 – 7.43 (m, 3H), 7.32 (t, *J* = 7.6 Hz, 1H), 7.24 (d, *J* = 7.8 Hz, 1H), 3.40 – 3.29 (m, 1H), 3.21 – 3.09 (m, 2H), 3.00 – 2.89 (m, 1H), 2.68 (dd, *J* = 14.5, 10.6 Hz, 1H), 2.14 – 1.89 (m, 4H), 1.82 – 1.68 (m, 2H), 1.68 – 1.60 (m, 1H), 1.50 – 1.35 (m, 1H).

^{13}C NMR (100 MHz, $CDCl_3$): δ 201.3, 200.2, 143.3, 136.9, 133.3, 133.1, 132.6, 128.8, 128.7, 128.5, 128.1, 126.8, 55.1, 40.8, 40.0, 33.6, 29.8, 27.1, 25.8, 22.5.

IR (Neat Film, NaCl): 3061, 2933, 2868, 1679, 1597, 1448, 1288, 1224 cm^{-1}.

HRMS (ESI+): *m/z* calc'd for $C_{22}H_{23}O_2$ $[M+H]^+$: 319.1693, found 319.1687.

Optical Rotation: $[\alpha]_D^{23}$ –9.7 (c = 1.44, $CHCl_3$).

SFC conditions: 25% IPA, 2.5 mL/min, Chiralpak IC-3 column, λ = 210 nm, t_R (min): major = 8.97, minor = 10.37

127h (*d2*):

^{1}H NMR (400 MHz, $CDCl_3$): δ 8.04 (dd, *J* = 7.9, 1.5 Hz, 1H), 7.94 – 7.80 (m, 2H), 7.55 – 7.36 (m, 4H), 7.36 – 7.28 (m, 1H), 7.24 – 7.19 (m, 1H), 3.27 (dd, *J* = 17.1, 10.0 Hz, 1H), 3.04 (t, *J* = 6.2 Hz, 2H), 2.84 (dd, *J* = 17.1, 3.5 Hz, 1H), 2.58 – 2.46 (m, 1H), 2.34 – 2.21 (m, 2H), 2.20 – 2.08 (m, 1H), 1.94 (dt, *J* = 13.5, 5.3 Hz, 1H), 1.84 – 1.62 (m, 4H).

^{13}C NMR (100 MHz, $CDCl_3$): δ 201.7, 200.2, 143.6, 137.4, 133.3, 133.0, 132.6, 128.8, 128.6, 128.2, 127.8, 126.8, 55.7, 44.6, 40.2, 36.0, 35.3, 32.8, 27.0, 22.8.

Note: A grease signal is observed in the ^{1}H and ^{13}C spectra.

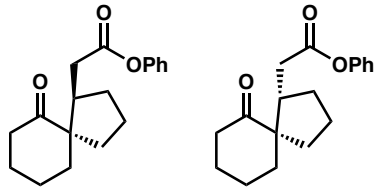
IR (Neat Film, NaCl): 2922, 2851, 1681, 1598, 1448, 1279, 1219 cm^{-1}.

HRMS (FD+): *m/z* calc'd for $C_{22}H_{22}O_2$ $[M]^{+\cdot}$: 318.16143, found 318.16025.

Note: The optical rotation measurement for this compound had a standard deviation greater than its magnitude (3.76) and is therefore unreliable.

Optical Rotation: $[\alpha]_D^{23}$ +0.04 (c = 0.16, $CHCl_3$).

SFC conditions: 25% IPA, 2.5 mL/min, Chiralpak IC-3 column, λ = 210 nm, t_R (min): minor = 3.85, major = 4.15



127i (d1) ***127i (d2)***

phenyl 2-((1*R*,5*S*)-6-oxospiro[4.5]decan-1-yl)acetate (127i, *d1* and *d2*)

Prepared from **126i** following General Procedure 3A. Crude analysis by ^{1}H NMR affords a 3:1 ratio of *d1* to *d2*. The diastereomers were subsequently separated by flash column chromatography (0–60% Et_2O/hexanes) to afford the *d1* as a colorless oil (16.9 mg, 0.059 mmol, 59% yield, 82% ee) and, after subsequent preparative TLC purification (5% Et_2O, 47.5% toluene, 47.5% hexanes) *d2* as a colorless oil (1.9 mg, 0.007 mmol, 7% yield, 71% ee). The absolute configuration of **127i *d1*** is assigned by analogy to **127a**. The relative configuration of **127i *d2*** is assigned by comparison to ^{1}H NMR of **127i *d1***, the absolute configuration is not determined.

127i (*d1*):

^{1}H NMR (400 MHz, $CDCl_3$): δ 7.42 – 7.32 (m, 2H), 7.25 – 7.16 (m, 1H), 7.14 – 7.06 (m, 2H), 3.12 – 3.00 (m, 1H), 2.64 (dd, *J* = 14.6, 5.4 Hz, 1H), 2.49 – 2.28 (m, 3H), 2.09 – 1.85 (m, 3H), 1.83 – 1.54 (m, 8H), 1.49 – 1.35 (m, 1H).

^{13}C NMR (100 MHz, $CDCl_3$): δ 213.5, 171.6, 150.8, 129.4, 125.7, 121.7, 58.1, 40.0, 39.4, 35.3, 35.3, 31.5, 29.9, 26.9, 21.8, 21.7.

IR (Neat Film, NaCl): 2938, 2865, 1757, 1702, 1593, 1492, 1455, 1230, 1195, 1126 cm^{-1}.

HRMS (ESI+): *m/z* calc'd for $C_{18}H_{23}O_3$ $[M+H]^+$: 287.1642, found 287.1629.

Optical Rotation: $[\alpha]_D^{23}$ +5.0 (c = 1.41, $CHCl_3$).

SFC conditions: 20% IPA, 2.5 mL/min, Chiralpak OD-3 column, λ = 210 nm, t_R (min): major = 2.80, minor = 2.99

127i (*d2*):

^{1}H NMR (600 MHz, $CDCl_3$): δ 7.37 (t, *J* = 7.8 Hz, 2H), 7.22 (t, *J* = 7.4 Hz, 1H), 7.10 – 7.03 (m, 2H), 2.80 (dd, *J* = 15.9, 10.6 Hz, 1H), 2.61 – 2.45 (m, 2H), 2.29 (dt, *J* = 14.9, 5.6

Hz, 1H), 2.25 – 2.15 (m, 2H), 2.13 – 2.03 (m, 1H), 1.96 (ddd, *J* = 13.7, 9.8, 3.8 Hz, 1H), 1.92 – 1.80 (m, 2H), 1.79 – 1.64 (m, 5H), 1.63 – 1.58 (m, 1H), 1.53 – 1.47 (m, 1H).

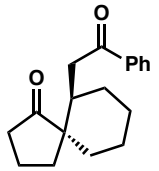
^{13}C NMR (100 MHz, $CDCl_3$): δ 213.9, 172.2, 150.8, 129.4, 125.7, 121.6, 59.3, 44.6, 40.4, 38.2, 36.3, 35.3, 30.3, 26.5, 22.6, 21.5.

IR (Neat Film, NaCl): 2925, 2855, 1756, 1697, 1592, 1492, 1197, 1126 cm^{-1}.

HRMS (FD+): *m/z* calc'd for $C_{18}H_{22}O_3$ $[M]^{+\cdot}$: 286.15635, 286.15495 found.

Optical Rotation: $[\alpha]_D^{23}$ –7.9 (c = 0.16 $CHCl_3$).

SFC conditions: 10% IPA, 2.5 mL/min, Chiralpak OD-3 column, λ = 210 nm, t_R (min): major = 3.99, minor = 4.23



127j

(5*R*,6*R*)-6-(2-oxo-2-phenylethyl)spiro[4.5]decan-1-one (127j)

Prepared from **126j** following General Procedure 3A. Purification by flash column chromatography (0–60% Et_2O/hexanes) afforded the title compound as a colorless oil (16.9 mg, 0.063 mmol, 63% yield, 71% ee).

^{1}H NMR (400 MHz, $CDCl_3$): δ 7.99 – 7.88 (m, 2H), 7.59 – 7.51 (m, 1H), 7.50 – 7.42 (m, 2H), 2.70 (dd, *J* = 13.6, 2.9 Hz, 1H), 2.57 – 2.32 (m, 3H), 2.23 – 2.11 (m, 1H), 2.06 – 1.83 (m, 4H), 1.72 – 1.51 (m, 4H), 1.43 – 1.18 (m, 3H), 1.13 – 0.99 (m, 1H).

^{13}C NMR (100 MHz, $CDCl_3$): δ 223.9, 199.6, 136.7, 133.2, 128.7, 128.6, 54.0, 42.1, 38.9, 38.1, 33.4, 28.4, 27.7, 25.7, 21.8, 19.1.

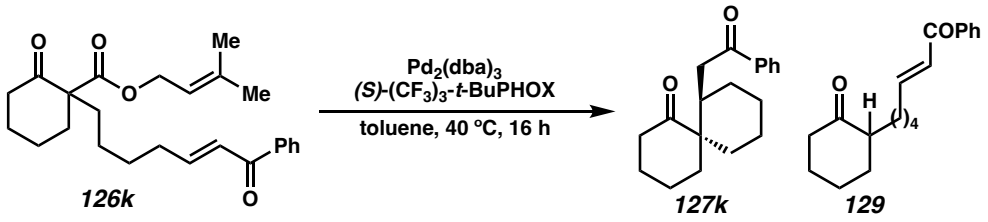
IR (Neat Film, NaCl): 2929, 2854, 1728, 1683, 1447, 1291, 1209 cm^{-1}.

HRMS (ESI+): *m/z* calc'd for $C_{18}H_{23}O_2$ $[M+H]^+$: 271.1693, found 271.1681.

Note: The optical rotation measurement for this compound had a standard deviation greater than its magnitude (0.73) and is therefore unreliable.

Optical Rotation: $[\alpha]_D^{23}$ –0.38 (c = 0.97, $CHCl_3$).

SFC conditions: 20% IPA, 2.5 mL/min, Chiralpak IC-3 column, λ = 230 nm, t_R (min): minor = 4.95, major = 8.16



(6*R*,7*R*)-7-(2-oxo-2-phenylethyl)spiro[5.5]undecan-1-one (127k) and (*E*)-2-(7-oxo-7-phenylhept-5-en-1-yl)cyclohexan-1-one (129)

Prepared from **126k** following General Procedure 3A. Purification by flash column chromatography (0–60% Et_2O/hexanes) afforded the compound **127k** as a colorless oil (13.8 mg, 0.049 mmol, 49% yield, 89% ee) and compound **129** as a colorless oil (5.1 mg, 0.018 mmol, 18% yield).

127k:

^{1}H NMR (400 MHz, $CDCl_3$): δ 8.16 – 8.07 (m, 2H), 7.58 – 7.52 (m, 1H), 7.51 – 7.44 (m, 2H), 3.03 (dd, *J* = 14.1, 2.5 Hz, 1H), 2.69 (tt, *J* = 11.1, 3.2 Hz, 1H), 2.60 – 2.41 (m, 2H), 2.37 – 2.26 (m, 1H), 2.19 – 1.96 (m, 3H), 1.82 – 1.70 (m, 2H), 1.70 – 1.59 (m, 2H), 1.59 – 1.46 (m, 4H), 1.28 – 1.08 (m, 3H).

^{13}C NMR (100 MHz, $CDCl_3$): δ 215.9, 200.7, 137.1, 133.0, 128.7, 128.6, 52.2, 41.8, 38.7, 36.8, 33.1, 27.2, 26.6, 26.4, 25.4, 20.8, 20.3.

IR (Neat Film, NaCl): 2931, 2858, 1697, 1596, 1447, 1287, 1126 cm^{-1}.

HRMS (ESI+): *m/z* calc'd for $C_{19}H_{25}O_2$ $[M+H]^+$: 285.1849, found 285.1841.

Optical Rotation: $[\alpha]_D^{23}$ –2.5 (c = 0.425, $CHCl_3$).

SFC conditions: 20% IPA, 2.5 mL/min, Chiralpak IC-3 column, λ = 210 nm, t_R (min): minor = 7.13, major = 11.24

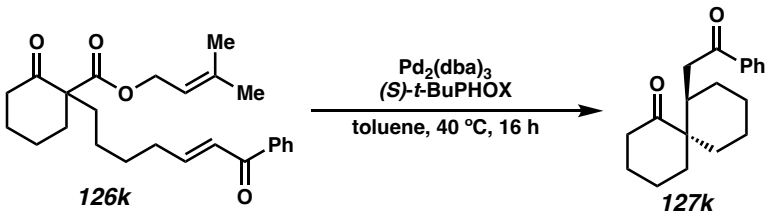
129:

^{1}H NMR (400 MHz, $CDCl_3$): δ 7.96 – 7.90 (m, 2H), 7.59 – 7.52 (m, 1H), 7.51 – 7.43 (m, 2H), 7.05 (dt, *J* = 15.3, 6.9 Hz, 1H), 6.87 (dt, *J* = 15.4, 1.4 Hz, 1H), 2.44 – 2.21 (m, 5H), 2.15 – 1.97 (m, 2H), 1.92 – 1.75 (m, 2H), 1.73 – 1.62 (m, 2H), 1.57 – 1.48 (m, 2H), 1.41 – 1.29 (m, 3H), 1.27 – 1.16 (m, 1H).

^{13}C NMR (100 MHz, $CDCl_3$): δ 213.5, 191.1, 150.0, 138.1, 132.7, 128.7, 128.7, 126.1, 50.8, 42.2, 34.1, 32.9, 29.3, 28.5, 28.2, 27.0, 25.1.

IR (Neat Film, NaCl): 2931, 2857, 1707, 1669, 1618, 1447, 1338, 1286, 1224, 1128 cm^{-1}.

HRMS (ESI+): *m/z* calc'd for $C_{19}H_{25}O_2$ $[M+H]^+$: 285,1849, found 285.1835.



(6*R*,7*R*)-7-(2-oxo-2-phenylethyl)spiro[5.5]undecan-1-one (127k)

In a nitrogen filled glovebox, an oven-dried 4 mL vial was charged with a stir bar, $Pd_2(dba)_3$ (2.3 mg, 0.0025 mmol, 2.5 mol %), *(S)-t*-BuPHOX (2.5 mg, 0.0065 mmol, 6.5 mol %), and toluene (0.6 mL). The catalyst solution was stirred at 23 ºC for 20 min. A solution of

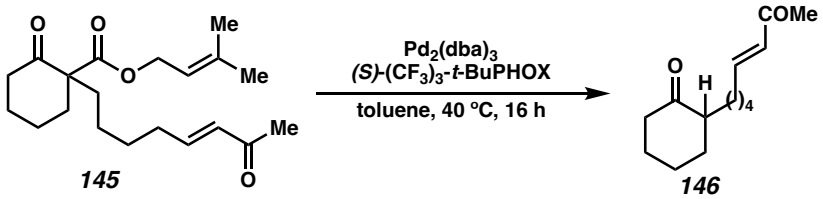
substrate **126k** (0.1 mmol, 1 equiv) in toluene (0.4 mL) was added to the catalyst solution. The resulting mixture was sealed, pumped out of the glovebox, and then heated to 40 ºC for 16 h. The solution was then cooled to 23 ºC and concentrated under reduced pressure. Purification by flash column chromatography (0–60% Et_2O/hexanes) afforded the compound **127k** as a colorless oil (18.3 mg, 0.064 mmol, 64% yield, 86% ee).

*Note: see NMR, IR, HRMS, Optical Rotation data in reaction of **126k** to **127k** and **129** earlier in SI.*

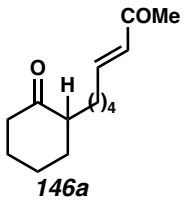
SFC conditions: 20% IPA, 2.5 mL/min, Chiralpak IC-3 column, λ = 210 nm, t_R (min): minor = 7.23, major = 11.41

Protonated Byproducts:

General Procedure 3B: Undesired Pd-Catalyzed Decarboxylative Protonation



In a nitrogen filled glovebox, an oven-dried 4 mL vial was charged with a stir bar, $Pd_2(dba)_3$ (2.3 mg, 0.0025 mmol, 2.5 mol %), *(S)*-$(CF_3)_3$-*t*-BuPHOX (3.8 mg, 0.0065 mmol, 6.5 mol %), and toluene (0.6 mL). The catalyst solution was stirred at 23 ºC for 20 min. A solution of substrate **145** (0.1 mmol, 1 equiv) in toluene (0.4 mL) was added to the catalyst solution. The resulting mixture was sealed, pumped out of the glovebox, and then heated to 40 ºC for 16 h. The solution was then cooled to 23 ºC and concentrated under reduced pressure. The crude reaction mixture was loaded directly onto a flash column and the product (**146**) was isolated by silica gel flash column chromatography.



146a

(*E*)-2-(7-oxooct-5-en-1-yl)cyclohexan-1-one (146a)

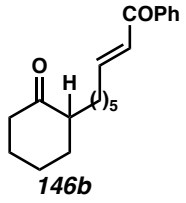
Prepared from **145a** following General Procedure 3B. Purification by flash column chromatography (0–60% Et_2O/hexanes) afforded the title compound as a colorless oil (13.8 mg, 0.062 mmol, 62% yield).

^{1}H NMR (400 MHz, $CDCl_3$): δ 6.78 (dt, *J* = 15.9, 6.8 Hz, 1H), 6.05 (dt, *J* = 16.0, 1.5 Hz, 1H), 2.43 – 2.34 (m, 1H), 2.33 – 2.16 (m, 7H), 2.14 – 1.96 (m, 2H), 1.91 – 1.71 (m, 2H), 1.70 – 1.57 (m, 2H), 1.54 – 1.41 (m, 2H), 1.39 – 1.13 (m, 4H).

^{13}C NMR (100 MHz, $CDCl_3$): δ 213.4, 198.9, 148.5, 131.5, 50.8, 42.2, 34.1, 32.5, 29.3, 28.4, 28.2, 27.0, 26.9, 25.1.

IR (Neat Film, NaCl): 2931, 2858, 1707, 1673, 1625, 1430, 1360, 1253, 1127 cm^{-1}.

HRMS (ESI+): *m/z* calc'd for $C_{14}H_{22}O_2$ $[M+H]^+$: 223.1693, found 223.1686.



146b

(*E*)-2-(8-oxo-8-phenyloct-6-en-1-yl)cyclohexan-1-one (146b)

Prepared from **145b** following General Procedure 3B. Purification by flash column chromatography (0–60% Et_2O/hexanes) afforded the title compound as a colorless oil (17.7 mg, 0.059 mmol, 59% yield).

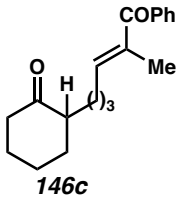
^{1}H NMR (400 MHz, $CDCl_3$): δ 7.97 – 7.88 (m, 2H), 7.59 – 7.51 (m, 1H), 7.49 – 7.42 (m, 2H), 7.05 (dt, *J* = 15.5, 6.9 Hz, 1H), 6.87 (dt, *J* = 15.4, 1.4 Hz, 1H), 2.46 – 2.18 (m, 5H), 2.16 – 1.94 (m, 2H), 1.92 – 1.58 (m, 4H), 1.57 – 1.47 (m, 2H), 1.44 – 1.11 (m, 6H).

Note: 2 carbon signals appear to be coincident.

^{13}C NMR (100 MHz, $CDCl_3$): δ 213.6, 191.1, 150.1, 138.1, 132.7, 128.7, 128.6, 126.1, 50.8, 42.1, 34.1, 32.9, 29.5, 29.5, 28.2, 27.1, 25.0.

IR (Neat Film, NaCl): 2930, 2856, 1708, 1669, 1619, 1447, 1338, 1282, 1222, 1127 cm^{-1}.

HRMS (ESI+): *m/z* calc'd for $C_{20}H_{26}O_2$ $[M+H]^+$: 299.2006, found 299.2002.



146c

(*E*)-2-(8-oxo-8-phenyloct-6-en-1-yl)cyclohexan-1-one (146c)

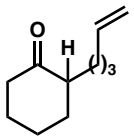
Prepared from **145c** following General Procedure 3B. Purification by flash column chromatography (0–60% Et_2O/hexanes) afforded the title compound as a colorless oil (13.4 mg, 0.047 mmol, 47% yield).

^{1}H NMR (600 MHz, $CDCl_3$): δ 7.62 (d, *J* = 7.6 Hz, 2H), 7.49 (t, *J* = 7.4 Hz, 1H), 7.41 (t, *J* = 7.6 Hz, 2H), 6.28 (t, *J* = 7.4 Hz, 1H), 2.42 – 2.34 (m, 1H), 2.33 – 2.23 (m, 4H), 2.11 – 2.01 (m, 2H), 1.96 (s, 3H), 1.89 – 1.76 (m, 2H), 1.70 – 1.61 (m, 2H), 1.47 – 1.33 (m, 3H), 1.24 – 1.17 (m, 1H).

^{13}C NMR (100 MHz, $CDCl_3$): δ 213.2, 199.2, 146.6, 138.9, 136.7, 131.5, 129.4, 128.2, 50.7, 42.2, 34.2, 29.5, 29.5, 28.2, 26.5, 25.1, 12.6.

IR (Neat Film, NaCl): 2929, 2856, 1707, 1646, 1446, 1284, 1167 cm^{-1}.

HRMS (ESI+): *m/z* calc'd for $C_{19}H_{25}O_2$ $[M+H]^+$: 285.1849, found 285.1841.



146d

2-(pent-4-en-1-yl)cyclohexan-1-one (146d)

Prepared from **145d** following General Procedure 3B. Purification by flash column chromatography (0–60% Et_2O/hexanes) afforded the title compound as a colorless oil (5.4 mg, 0.032 mmol, 32% yield).

^{1}H NMR (400 MHz, $CDCl_3$): δ 5.80 (ddt, *J* = 16.9, 10.2, 6.6 Hz, 1H), 5.06 – 4.88 (m, 2H), 2.44 – 2.35 (m, 1H), 2.34 – 2.20 (m, 2H), 2.16 – 1.94 (m, 3H), 1.90 – 1.73 (m, 2H), 1.66 (tddd, *J* = 14.0, 11.6, 7.7, 5.2 Hz, 2H), 1.45 – 1.31 (m, 3H), 1.28 – 1.14 (m, 1H).

Note: 2 carbon signals appear to be coincident.

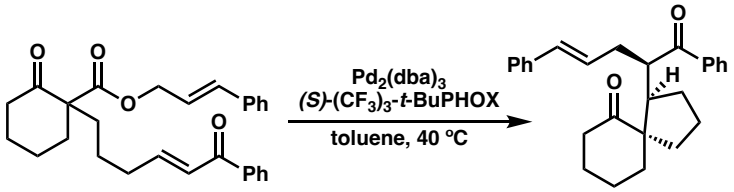
^{13}C NMR (100 MHz, $CDCl_3$): δ 213.6, 138.9, 114.6, 50.8, 42.2, 34.0, 29.1, 28.2, 26.7, 25.0.

IR (Neat Film, NaCl): 2931, 2859, 1710, 1639, 1447, 1125 cm^{-1}.

HRMS (FI+): *m/z* calc'd for $C_{11}H_{18}O$ $[M]^{+\cdot}$: 166.13522, found 166.13526.

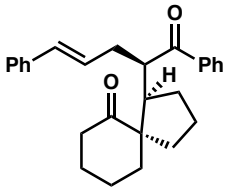
Pd-Catalyzed Decarboxylative Alkene Difunctionalization:

General Procedure 3C: Asymmetric Pd-Catalyzed Decarboxylative Alkene Difunctionalization



130 ***131***

In a nitrogen filled glovebox, an oven-dried 4 mL vial was charged with a stir bar, $Pd_2(dba)_3$ (2.3 mg, 0.0025 mmol, 2.5 mol %), *(S)*-$(CF_3)_3$-*t*-BuPHOX (3.8 mg, 0.0065 mmol, 6.5 mol %), and toluene (0.6 mL). The catalyst solution was stirred at 23 ºC for 20 min. A solution of substrate **130** (0.1 mmol, 1 equiv) in toluene (0.4 mL) was added to the catalyst solution. The resulting mixture was sealed, pumped out of the glovebox, and then heated to 40 ºC for 16 h. The solution was then cooled to 23 ºC and concentrated under reduced pressure. The crude reaction mixture was purified via preparative TLC to yield product **131**.



131a

(1*R*,5*S*)-1-((*R*,*E*)-1-oxo-1,5-diphenylpent-4-en-2-yl)spiro[4.5]decan-6-one (131a)

Prepared from **130a** following General Procedure 3C. Purification by preparative TLC (10% Et_2O, 45% toluene, 4% hexanes) afforded the title compound as a white crystalline solid (16.9 mg, 0.044 mmol, 44% yield, 94% ee). Absolute and relative stereochemistry were assigned by X-ray crystallography (vide infra).

^{1}H NMR (600 MHz, $CDCl_3$): δ 7.93 (dd, *J* = 7.6, 1.6 Hz, 2H), 7.55 – 7.50 (m, 1H), 7.44 (t, *J* = 7.7 Hz, 2H), 7.24 – 7.10 (m, 5H), 6.31 (d, *J* = 15.7 Hz, 1H), 6.02 (dt, *J* = 15.2, 7.3

Hz, 1H), 3.55 (ddd, *J* = 9.2, 7.5, 3.6 Hz, 1H), 3.14 (dt, *J* = 10.4, 7.5 Hz, 1H), 2.76 (dddd, *J* = 14.3, 9.1, 7.1, 1.4 Hz, 1H), 2.53 – 2.44 (m, 1H), 2.40 – 2.24 (m, 2H), 2.07 – 1.95 (m, 1H), 1.87 – 1.79 (m, 1H), 1.79 – 1.72 (m, 3H), 1.72 – 1.47 (m, 6H), 1.37 – 1.27 (m, 1H).

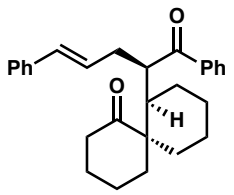
^{13}C NMR (100 MHz, $CDCl_3$): δ 213.2, 203.6, 138.0, 137.5, 132.8, 131.9, 128.7, 128.7, 128.5, 127.6, 127.2, 126.2, 58.3, 47.4, 44.2, 39.4, 38.5, 34.6, 33.0, 28.7, 25.4, 22.7, 21.6.

IR (Neat Film, NaCl): 2932, 2858, 1697, 1681, 1596, 1493, 1446, 1221 cm^{-1}.

HRMS (ESI+): *m/z* calc'd for $C_{27}H_{31}O_2$ $[M+H]^+$: 387.2319, found 387.2319.

Optical Rotation: $[\alpha]_D^{23}$ –10.7 (c = 0.53, $CHCl_3$).

SFC conditions: 30% IPA, 2.5 mL/min, Chiralpak AD-3 column, λ = 254 nm, t_R (min): major = 5.07, minor = 6.14



131b

(6*R*,7*R*)-7-((*R*,*E*)-1-oxo-1,5-diphenylpent-4-en-2-yl)spiro[5.5]undecan-1-one (131b)

Prepared from **130b** following General Procedure 3C. Purification by preparative TLC (5% Et_2O, 47.5% toluene, 47.5% hexanes) afforded the title compound as a colorless oil (13.3 mg, 0.033 mmol, 33% yield, 94% ee).

^{1}H NMR (400 MHz, $CDCl_3$): δ 7.96 – 7.89 (m, 2H), 7.56 – 7.48 (m, 1H), 7.46 – 7.39 (m, 2H), 7.23 – 7.16 (m, 2H), 7.15 – 7.05 (m, 3H), 6.30 (dd, *J* = 15.8, 1.6 Hz, 1H), 5.93 (dt, *J* = 15.7, 7.2 Hz, 1H), 3.48 (ddd, *J* = 10.9, 3.4, 2.3 Hz, 1H), 2.70 (dddd, *J* = 14.1, 10.9, 7.1, 1.4 Hz, 1H), 2.56 – 2.39 (m, 3H), 2.34 – 2.16 (m, 2H), 2.11 – 1.90 (m, 3H), 1.82 – 1.62 (m, 5H), 1.55 – 1.36 (m, 3H), 1.31 – 1.20 (m, 1H), 1.13 (td, *J* = 12.6, 4.9 Hz, 1H).

^{13}C NMR (100 MHz, $CDCl_3$): δ 215.2, 205.1, 138.1, 137.5, 132.7, 131.4, 128.9, 128.6, 128.5, 128.4, 127.1, 126.1, 54.1, 47.3, 40.7, 38.5, 33.8, 33.5, 28.5, 26.1, 26.0, 22.8, 21.1, 20.3.

IR (Neat Film, NaCl): 2929, 2855, 1698, 1673, 1596, 1446, 1222 cm^{-1}.

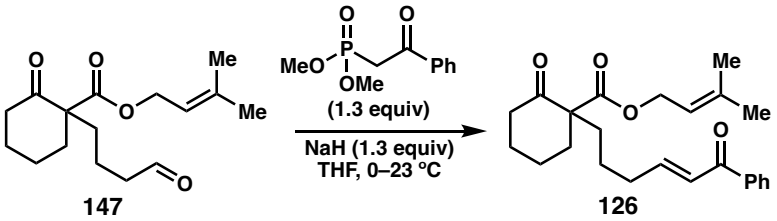
HRMS (ESI+): *m/z* calc'd for $C_{28}H_{33}O_2$ $[M+H]^+$: 401.2475, found 401.2471.

Optical Rotation: $[\alpha]_D^{23}$ –18.2 (c = 0.23, $CHCl_3$).

SFC conditions: 30% IPA, 2.5 mL/min, Chiralpak AD-3 column, λ = 254 nm, t_R (min): minor = 5.29, minor = 6.18

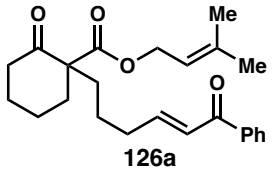
Preparation of Enone Starting Materials:

General Procedure 3D: Horner–Wadsworth–Emmons Olefination



To a suspension of NaH (60% by weight in mineral oil, 1.3 equiv) in THF (0.65 M) at 23 ºC was added dropwise a solution of the corresponding phosphonate ester (1.3 equiv) in THF (1.3 M). *Note: Caution, hydrogen evolution occurs.* This is stirred at 23 ºC for 30 minutes before cooling to 0 ºC. To this reaction was then added a solution of aldehyde **147** (1.0 equiv) in THF (0.35 M) dropwise. The reaction is gradually warmed to 23 ºC. Upon complete consumption of starting material by TLC, the reaction mixture was cooled to 0 ºC, diluted with a saturated solution of $NaHCO_3$, and extracted with EtOAc (3x). The

combined organic layers were dried over Na_2SO_4, filtered, and concentrated under reduced pressure. Product **126** was purified by silica gel flash column chromatography.



126a

3-methylbut-2-en-1-yl (*E*)-2-oxo-1-(6-oxo-6-phenylhex-4-en-1-yl)cyclohexane-1-carboxylate (126a)

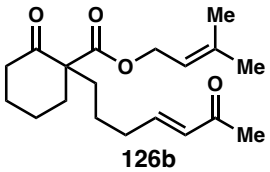
Prepared from **147a** and dimethyl (2-oxo-2-phenylethyl)phosphonate[6] following General Procedure 3D. Purification by flash column chromatography (0–50% EtOAc/hexanes) afforded the title compound as a colorless oil (1.41 g, 3.68 mmol, 64% yield).

^{1}H NMR (400 MHz, $CDCl_3$): δ 7.96 – 7.89 (m, 2H), 7.58 – 7.51 (m, 1H), 7.50 – 7.42 (m, 2H), 7.01 (dt, *J* = 15.5, 6.7 Hz, 1H), 6.88 (d, *J* = 15.4 Hz, 1H), 5.31 (tt, *J* = 7.3, 1.4 Hz, 1H), 4.70 – 4.55 (m, 2H), 2.57 – 2.37 (m, 3H), 2.37 – 2.22 (m, 2H), 2.01 (ddq, *J* = 12.4, 6.3, 3.2 Hz, 1H), 1.91 (td, *J* = 12.2, 3.1 Hz, 1H), 1.71 (dd, *J* = 12.7, 1.3 Hz, 7H), 1.67 – 1.48 (m, 4H), 1.48 – 1.32 (m, 2H).

^{13}C NMR (100 MHz, $CDCl_3$): δ 208.1, 191.0, 172.1, 149.2, 140.1, 138.1, 132.7, 128.7, 128.6, 126.3, 118.1, 62.2, 60.9, 41.3, 36.6, 34.6, 33.2, 27.8, 25.8, 23.1, 22.8, 18.2.

IR (Neat Film, NaCl): 2937, 2864, 1712, 1670, 1620, 1447, 1340, 1289, 1208, 1173, 1135 cm^{-1}.

HRMS (ESI+): *m/z* calc'd for $C_{24}H_{30}O_4Na$ $[M+Na]^+$: 405.2036, found 405.2045.



126b

3-methylbut-2-en-1-yl (*E*)-2-oxo-1-(6-oxohept-4-en-1-yl)cyclohexane-1-carboxylate (126b)

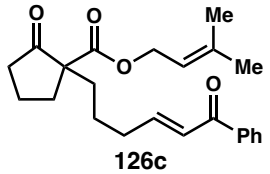
Prepared from **147a** and dimethyl acetylmethylphosphonate following General Procedure 3D. Purification by flash column chromatography (0–50% EtOAc/hexanes) afforded the title compound as a colorless oil (406 mg, 1.27 mmol, 71% yield).

^{1}H NMR (400 MHz, $CDCl_3$): δ 6.76 (dt, *J* = 16.0, 6.8 Hz, 1H), 6.06 (dt, *J* = 16.0, 1.6 Hz, 1H), 5.37 – 5.27 (m, 1H), 4.69 – 4.57 (m, 2H), 2.55 – 2.37 (m, 3H), 2.27 – 2.17 (m, 4H), 2.06 – 1.95 (m, 1H), 1.86 (td, *J* = 12.6, 3.6 Hz, 1H), 1.79 – 1.72 (m, 4H), 1.70 (s, 3H), 1.69 – 1.27 (m, 7H).

^{13}C NMR (100 MHz, $CDCl_3$): δ 208.1, 198.8, 172.1, 147.8, 140.2, 131.7, 118.1, 62.2, 60.9, 41.3, 36.6, 34.5, 32.8, 27.8, 27.0, 25.9, 23.1, 22.8, 18.2.

IR (Neat Film, NaCl): 2937, 2865, 1708, 1675, 1625, 1438, 1362, 1253, 1207, 1173, 1135 cm^{-1}.

HRMS (ESI+): *m/z* calc'd for $C_{19}H_{28}O_4Na$ $[M+Na]^+$: 343.1880, found 343.1884.



126c

3-methylbut-2-en-1-yl (*E*)-2-oxo-1-(6-oxo-6-phenylhex-4-en-1-yl)cyclopentane-1-carboxylate (126c)

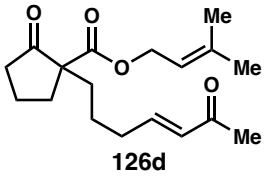
Prepared from **147b** and dimethyl (2-oxo-2-phenylethyl)phosphonate[6] following General Procedure 3D. Purification by flash column chromatography (0–50% EtOAc/hexanes) afforded the title compound as a colorless oil (631 mg, 2.37 mmol, 47% yield).

^{1}H NMR (400 MHz, $CDCl_3$): δ 8.00 – 7.84 (m, 2H), 7.60 – 7.51 (m, 1H), 7.51 – 7.41 (m, 2H), 7.01 (dt, *J* = 15.4, 6.7 Hz, 1H), 6.88 (dt, *J* = 15.4, 1.4 Hz, 1H), 5.33 – 5.23 (m, 1H), 4.60 (d, *J* = 7.1 Hz, 2H), 2.58 – 2.49 (m, 1H), 2.48 – 2.37 (m, 1H), 2.37 – 2.17 (m, 3H), 2.09 – 1.83 (m, 4H), 1.73 (s, 3H), 1.70 – 1.57 (m, 5H), 1.52 – 1.38 (m, 1H).

^{13}C NMR (100 MHz, $CDCl_3$): δ 214.9, 190.9, 171.1, 148.9, 139.7, 138.0, 132.8, 128.7, 128.7, 126.4, 118.3, 62.5, 60.5, 38.1, 33.6, 33.2, 33.1, 25.9, 23.6, 19.8, 18.2.

IR (Neat Film, NaCl): 2961, 1749, 1718, 1670, 1618, 1447, 1379, 1284, 1224, 1159 cm^{-1}.

HRMS (ESI+): *m/z* calc'd for $C_{23}H_{28}O_4Na$ $[M+Na]^+$: 391.1880, found 391.1879.



126d

3-methylbut-2-en-1-yl (*E*)-2-oxo-1-(6-oxohept-4-en-1-yl)cyclopentane-1-carboxylate (126d)

Prepared from **147b** and dimethyl acetylmethylphosphonate following General Procedure 3D. Purification by flash column chromatography (0–50% EtOAc/hexanes) afforded the title compound as a colorless oil (120 mg, 0.390 mmol, 52% yield).

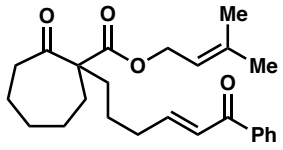
^{1}H NMR (400 MHz, $CDCl_3$): δ 6.75 (dt, *J* = 15.9, 6.8 Hz, 1H), 6.06 (dt, *J* = 16.1, 1.6 Hz, 1H), 5.34 – 5.24 (m, 1H), 4.59 (d, *J* = 7.1 Hz, 2H), 2.57 – 2.36 (m, 2H), 2.30 – 2.15 (m,

6H), 2.08 – 1.81 (m, 4H), 1.74 (s, 3H), 1.69 (s, 3H), 1.64 – 1.57 (m, 1H), 1.56 – 1.48 (m, 1H), 1.39 (qdd, J = 11.9, 8.2, 4.5 Hz, 1H).

^{13}C NMR (100 MHz, $CDCl_3$): δ 214.9, 198.7, 171.1, 147.4, 139.7, 131.8, 118.2, 62.5, 60.4, 38.1, 33.5, 33.2, 32.7, 27.1, 25.9, 23.6, 19.8, 18.2.

IR (Neat Film, NaCl): 2962, 1750, 1718, 1675, 1626, 1448, 1362, 1253, 1225, 1161 cm^{-1}.

HRMS (ESI+): *m/z* calc'd for $C_{18}H_{26}O_4Na$ $[M+Na]^+$: 329.1723, found 329.1722.



126e

3-methylbut-2-en-1-yl (*E*)-2-oxo-1-(6-oxo-6-phenylhex-4-en-1-yl)cycloheptane-1-carboxylate (126e)

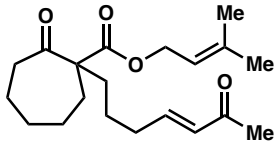
Prepared from **147c** and dimethyl (2-oxo-2-phenylethyl)phosphonate[6] following General Procedure 3D. Purification by flash column chromatography (0–50% EtOAc/hexanes) afforded the title compound as a colorless oil (494 mg, 1.24 mmol, 73% yield).

^{1}H NMR (400 MHz, $CDCl_3$): δ 7.97 – 7.87 (m, 2H), 7.59 – 7.52 (m, 1H), 7.51 – 7.42 (m, 2H), 7.01 (dt, J = 15.5, 6.7 Hz, 1H), 6.88 (dt, J = 15.4, 1.3 Hz, 1H), 5.38 – 5.23 (m, 1H), 4.71 – 4.54 (m, 2H), 2.71 – 2.59 (m, 1H), 2.50 – 2.41 (m, 1H), 2.38 – 2.23 (m, 2H), 2.21 – 2.10 (m, 1H), 2.08 – 1.96 (m, 1H), 1.80 – 1.71 (m, 5H), 1.71 – 1.58 (m, 7H), 1.56 – 1.37 (m, 4H).

^{13}C NMR (100 MHz, $CDCl_3$): δ 209.6, 191.0, 172.6, 149.2, 139.9, 138.1, 132.8, 128.7, 128.7, 126.4, 118.2, 62.9, 62.1, 42.3, 35.3, 33.2, 33.2, 29.9, 25.8, 25.6, 25.0, 23.5, 18.2.

IR (Neat Film, NaCl): 2932, 2860, 1707, 1670, 1619, 1447, 1377, 1344, 1286, 1222, 1165 cm^{-1}.

HRMS (ESI+): *m/z* calc'd for $C_{25}H_{32}O_4Na$ $[M+Na]^+$: 419.2193, found 419.2194.



126f

3-methylbut-2-en-1-yl (*E*)-2-oxo-1-(6-oxohept-4-en-1-yl)cycloheptane-1-carboxylate (126f)

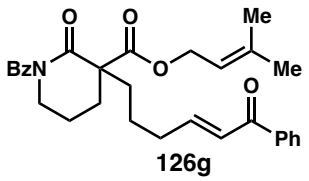
Prepared from **147c** and dimethyl acetylmethylphosphonate following General Procedure 3D. Purification by flash column chromatography (0–50% EtOAc/hexanes) afforded the title compound as a colorless oil (409 mg, 1.22 mmol, 72% yield).

^{1}H NMR (400 MHz, $CDCl_3$): δ 6.76 (dt, *J* = 16.0, 6.8 Hz, 1H), 6.06 (dt, *J* = 16.0, 1.5 Hz, 1H), 5.38 – 5.24 (m, 1H), 4.69 – 4.53 (m, 2H), 2.74 – 2.54 (m, 1H), 2.52 – 2.38 (m, 1H), 2.30 – 2.06 (m, 6H), 2.05 – 1.90 (m, 1H), 1.83 – 1.72 (m, 4H), 1.70 (d, *J* = 1.4 Hz, 4H), 1.66 – 1.49 (m, 5H), 1.49 – 1.31 (m, 3H).

^{13}C NMR (100 MHz, $CDCl_3$): δ 209.6, 198.8, 172.5, 147.7, 139.9, 131.7, 118.2, 62.8, 62.1, 42.3, 35.2, 33.2, 32.9, 29.9, 27.0, 25.8, 25.6, 25.0, 23.5, 18.2.

IR (Neat Film, NaCl): 2930, 2862, 1707, 1675, 1626, 1445, 1359, 1253, 1219, 1166 cm^{-1}.

HRMS (ESI+): *m/z* calc'd for $C_{20}H_{30}O_4Na$ $[M+Na]^+$: 357.2036, found 357.2041.



126g

3-methylbut-2-en-1-yl (*E*)-1-benzoyl-2-oxo-3-(6-oxo-6-phenylhex-4-en-1-yl)piperidine-3-carboxylate (126g)

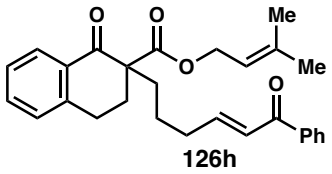
Prepared from **147d** and dimethyl (2-oxo-2-phenylethyl)phosphonate[6] following General Procedure 3D. Purification by flash column chromatography (0–50% EtOAc/hexanes) afforded the title compound as a colorless oil (317 mg, 0.650 mmol, 61% yield).

^{1}H NMR (400 MHz, $CDCl_3$): δ 7.96 – 7.84 (m, 2H), 7.78 – 7.70 (m, 2H), 7.59 – 7.51 (m, 1H), 7.50 – 7.40 (m, 3H), 7.40 – 7.33 (m, 2H), 6.97 (dt, *J* = 15.5, 6.6 Hz, 1H), 6.85 (dt, *J* = 15.4, 1.4 Hz, 1H), 5.49 – 5.35 (m, 1H), 4.81 – 4.64 (m, 2H), 3.90 – 3.70 (m, 2H), 2.51 – 2.39 (m, 1H), 2.28 (q, *J* = 7.2 Hz, 2H), 2.04 – 1.82 (m, 5H), 1.79 (s, 3H), 1.75 (s, 3H), 1.70 – 1.60 (m, 1H), 1.51 – 1.37 (m, 1H).

^{13}C NMR (100 MHz, $CDCl_3$): δ 190.9, 175.1, 172.3, 172.2, 148.8, 140.7, 138.0, 136.0, 132.8, 131.8, 128.7, 128.6, 128.3, 128.2, 126.4, 117.8, 63.0, 56.7, 46.6, 35.4, 33.0, 30.9, 26.0, 23.5, 20.5, 18.3.

IR (Neat Film, NaCl): 2937, 1724, 1701, 1676, 1618, 1447, 1386, 1348, 1277, 1189, 1166, 1149 cm^{-1}.

HRMS (ESI+): *m/z* calc'd for $C_{30}H_{33}NO_5Na$ $[M+Na]^+$: 510.2251, found 510.2264.



126h

3-methylbut-2-en-1-yl (*E*)-1-oxo-2-(6-oxo-6-phenylhex-4-en-1-yl)-1,2,3,4-tetrahydronaphthalene-2-carboxylate (126h)

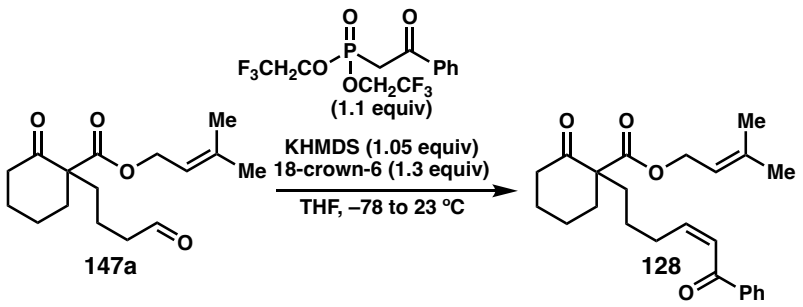
Prepared from **147e** and dimethyl (2-oxo-2-phenylethyl)phosphonate[6] following General Procedure 3D. Purification by flash column chromatography (0–50% EtOAc/hexanes) afforded the title compound as a colorless oil (248 mg, 0.576 mmol, 58% yield).

^{1}H NMR (400 MHz, $CDCl_3$): δ 8.04 (dd, *J* = 7.9, 1.4 Hz, 1H), 7.97 – 7.88 (m, 2H), 7.59 – 7.51 (m, 1H), 7.50 – 7.42 (m, 3H), 7.31 (t, *J* = 7.6 Hz, 1H), 7.20 (d, *J* = 7.7 Hz, 1H), 7.04 (dt, *J* = 15.5, 6.6 Hz, 1H), 6.91 (dt, *J* = 15.3, 1.4 Hz, 1H), 5.26 – 5.14 (m, 1H), 4.63 – 4.49 (m, 2H), 3.07 (ddd, *J* = 15.5, 10.4, 4.7 Hz, 1H), 2.91 (dt, *J* = 17.4, 4.9 Hz, 1H), 2.56 (dt, *J* = 13.7, 4.9 Hz, 1H), 2.36 (q, *J* = 7.5 Hz, 2H), 2.22 – 2.09 (m, 1H), 2.07 – 1.88 (m, 2H), 1.80 – 1.64 (m, 4H), 1.63 – 1.56 (m, 4H).

^{13}C NMR (100 MHz, $CDCl_3$): δ 195.6, 191.0, 172.0, 149.1, 143.1, 139.9, 138.1, 133.5, 132.8, 132.3, 128.8, 128.7, 128.7, 128.2, 126.9, 126.4, 118.2, 62.3, 57.6, 33.9, 33.3, 31.1, 26.1, 25.8, 23.5, 18.1.

IR (Neat Film, NaCl): 2931, 1725, 1685, 1670, 1618, 1599, 1447, 1351,1292,1230, 1174 cm^{-1}.

HRMS (ESI+): *m/z* calc'd for $C_{28}H_{30}O_4Na$ $[M+Na]^+$: 453.2036, found 453.2035.



3-methylbut-2-en-1-yl (*Z*)-2-oxo-1-(6-oxo-6-phenylhex-4-en-1-yl)cyclohexane-1-carboxylate (128)

An oven dried 100 mL round bottom flask was charged with 18-crown-6 (610 mg, 2.31 mmol, 1.3 equiv). To this a solution of bis(2,2,2-trifluoroethyl) (2-oxo-2-phenylethyl)phosphonate[7] (714 mg, 1.96 mmol, 1.1 equiv) in THF (10 mL, 0.2 M) was added. This was cooled to –78 ºC for 10 minutes before a solution of KHMDS (373 mg, 1.87 mmol, 1.05 equiv) in THF (2mL, 0.9 M) was added dropwise. The solution was stirred for 20 minutes at –78 ºC before a solution of **147a** (500 mg, 1.78 mmol, 1.0 equiv) in THF (10 mL, 0.18 M) was added dropwise. The reaction was warmed gradually to 23 ºC. Upon complete consumption of starting material by TLC, the reaction mixture was cooled to 0 ºC, diluted with a saturated solution of NH_4Cl (20 mL), and extracted with Et_2O (3x). The combined organic layers were dried over Na_2SO_4, filtered, and concentrated under reduced pressure. The crude reaction mixture was purified by silica gel flash column chromatography (15% Et_2O/hexanes) to afford **128** as a colorless oil (101 mg, 0.264 mmol, 15% yield).

^{1}H NMR (400 MHz, $CDCl_3$): δ 7.91 – 7.84 (m, 2H), 7.13 – 7.02 (m, 3H), 6.53 (dt, *J* = 11.5, 1.7 Hz, 1H), 6.05 (dt, *J* = 11.6, 7.4 Hz, 1H), 5.31 (tdt, *J* = 7.2, 2.9, 1.4 Hz, 1H), 4.55

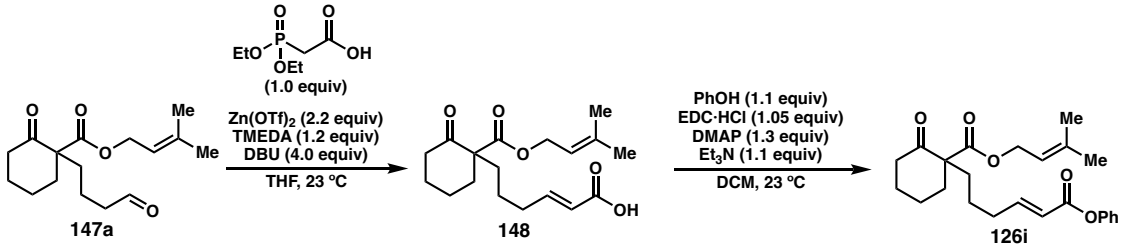
(d, J = 7.2 Hz, 2H), 2.82 – 2.65 (m, 2H), 2.48 – 2.26 (m, 3H), 2.14 – 2.01 (m, 1H), 1.75 – 1.46 (m, 8H), 1.44 (s, 3H), 1.37 – 1.06 (m, 3H).

^{13}C NMR (100 MHz, C_6D_6): δ 206.2, 191.0, 172.1, 148.7, 139.4, 139.2, 132.4, 128.6, 128.6, 124.8, 119.0, 61.8, 61.1, 41.2, 36.4, 34.9, 30.5, 27.7, 25.6, 24.6, 22.9, 17.9.

*Note: It was noted that upon standing in basified (K_2CO_3) or neutral deuterochloroform, Z-enone **128** isomerizes to **126a**.*

IR (Neat Film, NaCl): 2938, 2865, 1711, 1664, 1610, 1448, 1227, 1174, 1134 cm^{-1}.

HRMS (ESI+): *m/z* calc'd for $C_{24}H_{34}NO_4$ $[M+NH_4]^+$: 400.2482, found 400.2490.



(*E*)-6-(1-(((3-methylbut-2-en-1-yl)oxy)carbonyl)-2-oxocyclohexyl)hex-2-enoic acid (148)

To a flame dried 50 mL round bottom flask was added zinc triflate (2.09 g, 5.74 mmol, 2.2 equiv) followed by THF (9.5 mL, 0.6 M). 2-(diethoxyphosphoryl)acetic acid was then added (0.42 mL, 2.61 mmol, 1.0 equiv) followed by TMEDA (0.47 mL, 3.13 mmol, 1.2 equiv) and DBU (1.56 mL, 10.4 mmol, 4.0 equiv). To this a solution of **147a** (805 mg, 2.87 mmol, 1.1 equiv) in THF (6.6 mL, 0.43 M) was added dropwise. Upon complete consumption of starting material by TLC, the reaction was diluted with 1 M HCl (27 mL), extracted with CH_2Cl_2 (3x). The combined organic layers were dried over Na_2SO_4, filtered, and concentrated under reduced pressure. The crude reaction mixture was purified by silica

gel flash column chromatography (0–50% EtOAc/hexanes) to afford **148** as an amorphous white solid (610 mg, 1.89 mmol, 72% yield).

^{1}H NMR (400 MHz, $CDCl_3$): δ 7.06 (dt, *J* = 15.6, 6.8 Hz, 1H), 5.84 (dt, *J* = 15.7, 1.6 Hz, 1H), 5.38 – 5.30 (m, 1H), 4.66 (d, *J* = 7.3 Hz, 2H), 2.59 – 2.40 (m, 3H), 2.33 – 2.18 (m, 2H), 2.08 – 1.97 (m, 1H), 1.90 (td, *J* = 12.5, 3.5 Hz, 1H), 1.83 – 1.72 (m, 7H), 1.72 – 1.23 (m, 6H).

*Note: OH proton not observed for **S4** in ^{1}H NMR.*

^{13}C NMR (100 MHz, $CDCl_3$): δ 208.1, 172.1, 171.2, 151.6, 140.2, 120.9, 118.1, 62.2, 60.9, 41.3, 36.6, 34.5, 32.6, 27.8, 25.8, 22.9, 22.8, 18.2.

IR (Neat Film, NaCl): 2937, 2865, 1711, 1653, 1437, 1275, 1208, 1168 cm^{-1}.

HRMS (ESI+): *m/z* calc'd for $C_{18}H_{25}O_5$ $[M–H]^-$: 321.1707, found 321.1710.

3-methylbut-2-en-1-yl (*E*)-2-oxo-1-(6-oxo-6-phenoxyhex-4-en-1-yl)cyclohexane-1-carboxylate (126i)

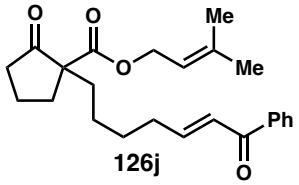
To a flame dried scint vial was added **148** (220 mg, 0.68 mmol, 1.0 equiv), phenol (70.6 mg, 0.75 mmol, 1.1 equiv), EDC·HCl (144 mg, 0.75 mmol, 1.1 equiv), followed by CH_2Cl_2 (3.4 mL, 0.2 M). Following this, Et_3N (0.10 mL, 0.75 mmol, 1.1 equiv) and DMAP (8.3 mg, 0.068 mmol, 0.1 equiv) were added successively. Upon complete consumption of starting material by TLC, the reaction was diluted with CH_2Cl_2, followed by a 1 M HCl (4 mL) rinse, and sat. $NaHCO_3$ solution (4 mL) rinse, and then rinsed with brine. The combined organic layers were dried over Na_2SO_4, filtered, and concentrated under reduced pressure. The crude reaction mixture was purified by silica gel flash column chromatography (0–35% Et_2O/hexanes) to afford **126i** as an amorphous white solid (144 mg, 0.36 mmol, 53% yield).

^{1}H NMR (400 MHz, $CDCl_3$): δ 7.42 – 7.34 (m, 2H), 7.25 – 7.19 (m, 1H), 7.17 – 7.07 (m, 3H), 6.02 (dt, *J* = 15.7, 1.6 Hz, 1H), 5.37 – 5.29 (m, 1H), 4.65 (d, *J* = 6.7 Hz, 2H), 2.58 – 2.38 (m, 3H), 2.34 – 2.20 (m, 2H), 2.07 – 1.97 (m, 1H), 1.91 (td, *J* = 12.5, 3.4 Hz, 1H), 1.80 – 1.71 (m, 7H), 1.70 – 1.57 (m, 3H), 1.55 – 1.32 (m, 3H).

^{13}C NMR (100 MHz, $CDCl_3$): δ 208.1, 172.1, 165.1, 151.1, 150.9, 140.2, 129.5, 125.8, 121.8, 121.0, 118.1, 62.2, 60.9, 41.3, 36.6, 34.5, 32.8, 27.8, 25.8, 23.0, 22.8, 18.2.

IR (Neat Film, NaCl): 2938, 2864, 1734, 1711, 1651, 1593, 1491, 1450, 1310, 1243, 1197 cm^{-1}.

HRMS (ESI+): *m/z* calc'd for $C_{24}H_{34}NO_5$ $[M+NH_4]^+$: 416.2431, found 416.2433.



126j

3-methylbut-2-en-1-yl (*E*)-2-oxo-1-(7-oxo-7-phenylhept-5-en-1-yl)cyclopentane-1-carboxylate (126j)

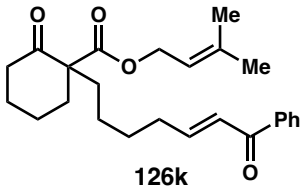
Prepared from **147f** and dimethyl (2-oxo-2-phenylethyl)phosphonate[6] following General Procedure 3D. Purification by flash column chromatography (0–50% EtOAc/hexanes) afforded the title compound as a colorless oil (392 mg, 1.03 mmol, 58% yield)

^{1}H NMR (400 MHz, $CDCl_3$): δ 7.96 – 7.88 (m, 2H), 7.59 – 7.53 (m, 1H), 7.51 – 7.41 (m, 2H), 7.03 (dt, *J* = 15.4, 6.8 Hz, 1H), 6.87 (dt, *J* = 15.4, 1.4 Hz, 1H), 5.34 – 5.22 (m, 1H), 4.58 (dt, *J* = 7.2, 1.0 Hz, 2H), 2.57 – 2.48 (m, 1H), 2.47 – 2.37 (m, 1H), 2.36 – 2.16 (m, 3H), 2.07 – 1.82 (m, 4H), 1.73 (s, 3H), 1.68 (s, 3H), 1.64 – 1.47 (m, 3H), 1.46 – 1.34 (m, 1H), 1.33 – 1.20 (m, 1H).

^{13}C NMR (100 MHz, $CDCl_3$): δ 215.1, 191.0, 171.2, 149.5, 139.5, 138.1, 132.8, 128.7, 128.7, 126.2, 118.3, 62.5, 60.6, 38.1, 33.7, 33.0, 32.6, 28.6, 25.9, 24.6, 19.8, 18.2.

IR (Neat Film, NaCl): 2930, 2859, 1750, 1719, 1670, 1618, 1597, 1447, 1335, 1278, 1223, 1166 cm^{-1}.

HRMS (ESI+): *m/z* calc'd for $C_{24}H_{30}O_4Na$ $[M+Na]^+$: 405.2036, found 405.2043.



126k

3-methylbut-2-en-1-yl (*E*)-2-oxo-1-(7-oxo-7-phenylhept-5-en-1-yl)cyclohexane-1-carboxylate (126k)

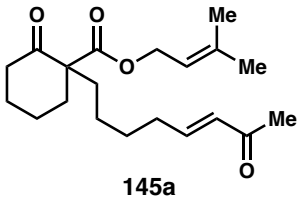
Prepared from **147g** and dimethyl (2-oxo-2-phenylethyl)phosphonate[6] following General Procedure 3D. Purification by flash column chromatography (0–50% EtOAc/hexanes) afforded the title compound as a colorless oil (273 mg, 0.69 mmol, 69% yield).

^{1}H NMR (400 MHz, $CDCl_3$): δ 7.95 – 7.89 (m, 2H), 7.59 – 7.52 (m, 1H), 7.50 – 7.43 (m, 2H), 7.03 (dt, *J* = 15.4, 6.8 Hz, 1H), 6.87 (dt, *J* = 15.4, 1.4 Hz, 1H), 5.34 – 5.26 (m, 1H), 4.67 – 4.55 (m, 2H), 2.56 – 2.37 (m, 3H), 2.36 – 2.23 (m, 2H), 2.07 – 1.95 (m, 1H), 1.94 – 1.80 (m, 1H), 1.77 – 1.68 (m, 7H), 1.67 – 1.59 (m, 2H), 1.57 – 1.47 (m, 3H), 1.46 – 1.37 (m, 1H), 1.36 – 1.21 (m, 2H).

^{13}C NMR (100 MHz, $CDCl_3$): δ 208.2, 191.1, 172.2, 149.7, 140.0, 138.1, 132.7, 128.69, 128.65, 126.2, 118.2, 62.1, 61.0, 41.3, 36.4, 34.7, 32.7, 28.7, 27.8, 25.8, 24.1, 22.8, 18.2.

IR (Neat Film, NaCl): 2929, 2854, 1728, 1683, 1596, 1447, 1291, 1209, 1185, 1160 cm^{-1}.

HRMS (ESI+): *m/z* calc'd for $C_{25}H_{32}O_4Na$ $[M+Na]^+$: 419.2193, found 419.2201.



145a

3-methylbut-2-en-1-yl (*E*)-2-oxo-1-(7-oxooct-5-en-1-yl)cyclohexane-1-carboxylate (145a)

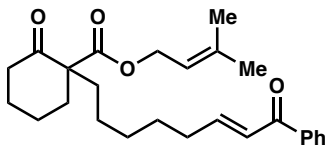
Prepared from **147g** and acetylmethylphosphonate following General Procedure 3D. Purification by flash column chromatography (0–50% EtOAc/hexanes) afforded the title compound as a colorless oil (222 mg, 0.66 mmol, 68% yield).

^{1}H NMR (400 MHz, $CDCl_3$): δ 6.77 (dt, *J* = 15.9, 6.9 Hz, 1H), 6.05 (dt, *J* = 16.0, 1.5 Hz, 1H), 5.35 – 5.26 (m, 1H), 4.69 – 4.55 (m, 2H), 2.54 – 2.35 (m, 3H), 2.26 – 2.15 (m, 5H), 2.06 – 1.95 (m, 1H), 1.85 (ddd, *J* = 13.6, 12.2, 4.7 Hz, 1H), 1.78 – 1.67 (m, 7H), 1.67 – 1.36 (m, 6H), 1.35 – 1.13 (m, 2H).

^{13}C NMR (100 MHz, $CDCl_3$): δ 208.2, 198.9, 172.2, 148.3, 140.0, 131.5, 118.1, 62.1, 61.0, 41.3, 36.4, 34.6, 32.4, 28.6, 27.8, 27.0, 25.8, 24.1, 22.8, 18.2.

IR (Neat Film, NaCl): 2938, 2863, 1709, 1674, 1626, 1449, 1361, 1309, 1253, 1208, 1170, 1135, 1100 cm^{-1}.

HRMS (ESI+): *m/z* calc'd for $C_{20}H_{30}O_4Na$ $[M+Na]^+$: 357.2036, found 357.2035.



145b

3-methylbut-2-en-1-yl (*E*)-2-oxo-1-(8-oxo-8-phenyloct-6-en-1-yl)cyclohexane-1-carboxylate (145b)

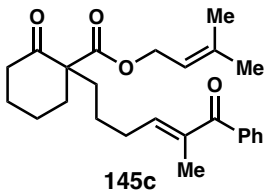
Prepared from **147h** and dimethyl (2-oxo-2-phenylethyl)phosphonate[6] following General Procedure 3D. Purification by flash column chromatography (0–50% EtOAc/hexanes) afforded the title compound as a colorless oil (493 mg, 1.20 mmol, 74% yield).

^{1}H NMR (400 MHz, $CDCl_3$): δ 7.97 – 7.89 (m, 2H), 7.59 – 7.51 (m, 1H), 7.50 – 7.42 (m, 2H), 7.04 (dt, *J* = 15.4, 6.9 Hz, 1H), 6.86 (dt, *J* = 15.4, 1.4 Hz, 1H), 5.36 – 5.25 (m, 1H), 4.68 – 4.56 (m, 2H), 2.56 – 2.36 (m, 3H), 2.33 – 2.24 (m, 2H), 2.03 – 1.93 (m, 1H), 1.86 (ddd, *J* = 13.5, 12.0, 4.5 Hz, 1H), 1.78 – 1.68 (m, 7H), 1.67 – 1.47 (m, 5H), 1.46 – 1.30 (m, 3H), 1.29 – 1.13 (m, 2H).

^{13}C NMR (100 MHz, $CDCl_3$): δ 208.3, 191.1, 172.2, 150.0, 139.9, 138.2, 132.7, 128.7, 128.6, 126.1, 118.2, 62.1, 61.0, 41.3, 36.4, 34.8, 32.9, 29.7, 28.1, 27.8, 25.9, 24.1, 22.8, 18.2.

IR (Neat Film, NaCl): 2935, 2859, 1710, 1670, 1618, 1447, 1378, 1340, 1279, 1221, 1167 cm^{-1}.

HRMS (ESI+): *m/z* calc'd for $C_{26}H_{34}O_4Na$ $[M+Na]^+$: 433.2349, found 433.2360.



145c

3-methylbut-2-en-1-yl (*E*)-1-(5-methyl-6-oxo-6-phenylhex-4-en-1-yl)-2-oxocyclohexane-1-carboxylate (145c)

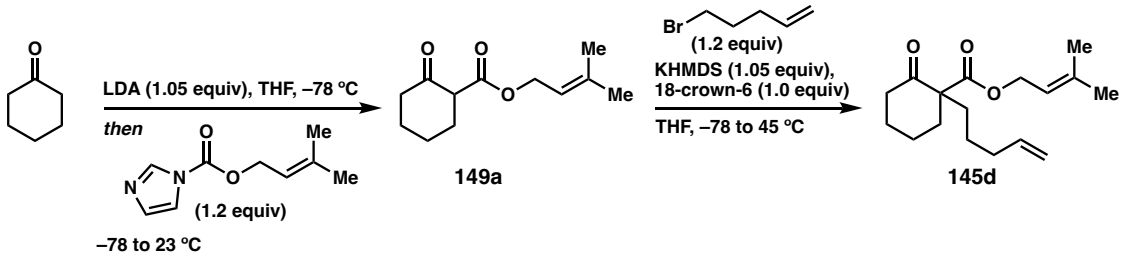
Prepared from **147a** and dimethyl (1-oxo-1-phenylpropan-2-yl)phosphonate[8] following General Procedure 3D. Purification by flash column chromatography (20% Et_2O/hexanes) afforded the title compound as a colorless oil (72.4 mg, 0.18 mmol, 26% yield).

^{1}H NMR (400 MHz, $CDCl_3$): δ 7.64 – 7.59 (m, 2H), 7.52 – 7.46 (m, 1H), 7.44 – 7.38 (m, 2H), 6.24 (td, *J* = 7.3, 1.4 Hz, 1H), 5.33 – 5.23 (m, 1H), 4.68 – 4.52 (m, 2H), 2.54 – 2.35 (m, 3H), 2.31 – 2.22 (m, 2H), 2.05 – 1.93 (m, 4H), 1.93 – 1.82 (m, 1H), 1.79 – 1.66 (m, 8H), 1.66 – 1.57 (m, 2H), 1.48 – 1.36 (m, 2H), 1.35 – 1.22 (m, 1H).

^{13}C NMR (100 MHz, $CDCl_3$): δ 208.1, 199.1, 172.1, 146.1, 140.1, 138.8, 136.9, 131.5, 129.5, 128.2, 118.1, 62.2, 60.9, 41.3, 36.6, 34.8, 29.6, 27.8, 25.8, 23.7, 22.8, 18.2, 12.7.

IR (Neat Film, NaCl): 2938, 2864, 1711, 1647, 1445, 1381, 1280, 1208, 1185 cm^{-1}.

HRMS (ESI+): *m/z* calc'd for $C_{25}H_{32}O_4Na$ $[M+Na]^+$: 419.2193, found 419.2203.



3-methylbut-2-en-1-yl 2-oxo-1-(pent-4-en-1-yl)cyclohexane-1-carboxylate (145d)

To a flame dried 250 mL round bottom flask was added *i*Pr$_2$NH (4.6 mL, 33 mmol, 1.1 equiv) followed by THF (17 mL, 1.9 M) before the solution was cooled to 0 °C. To this, *n*-BuLi (2.5 M in hexanes, 12.6 mL, 31.5 mmol, 1.05 equiv) was added dropwise before the solution was allowed to stir at 0 °C for 15 minutes. To this, a solution of cyclohexanone (3.1 mL, 30 mmol, 1.0 equiv) in THF (24 mL, 1.25 M) was added dropwise before the solution was allowed to stir at 0 °C for 30 minutes. The solution was then cooled to –78 °C, and a solution of 3-methylbut-2-en-1-yl 1*H*-imidazole-1-carboxylate[9] (6.48 g, 36 mmol, 1.2 equiv) in THF (9 mL, 4 M) was added dropwise. The reaction was warmed gradually to 23 °C. Upon complete consumption of starting material by TLC, the reaction was cooled to 0 °C, the pH was adjusted to 1.0 using 1 M HCl, and the mixture was extracted with EtOAc (3x). The combined organic layers were rinsed with brine, dried over Na_2SO_4, filtered, and concentrated under reduced pressure. The crude reaction mixture was purified by silica gel flash column chromatography (0–20% EtOAc/hexanes) to afford **149a** as a mixture of tautomers (4.18 g, 19.9 mmol, 66% yield), which was used directly in the next step.

To a flame dried 250 mL round bottom flask was added KHMDS (796 mg, 4.0 mmol, 1.05 equiv), and 18-crown-6 (1.00 g, 3.8 mmol, 1.0 equiv) followed by THF (20 mL, 0.19 M) before the solution was cooled to –78 °C. A solution of β-ketoester **149a** (884 mg, 3.8 mmol, 1.0 equiv) in THF (10 mL, 0.38 M) was added dropwise at –78 °C. The solution was stirred at this temperature for 15 minutes before 5-bromopent-1-ene was added neat (0.54 mL, 4.6 mmol, 1.2 equiv). The reaction was then warmed to 45 °C. Upon complete consumption of starting material by TLC, the reaction was cooled to 0 °C, and diluted with EtOAc (10 mL), followed by a saturated solution of NH_4Cl (20 mL). This mixture was then

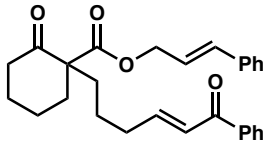
extracted with EtOAc (3x). The combined organic layers were rinsed with brine, dried over Na_2SO_4, filtered, and concentrated under reduced pressure. The crude reaction mixture was purified by silica gel flash column chromatography (0–20% EtOAc/hexanes) to afford **145d** as a colorless oil (601 mg, 2.16 mmol, 57% yield).

^{1}H NMR (400 MHz, $CDCl_3$): δ 5.77 (ddt, *J* = 16.9, 10.2, 6.6 Hz, 1H), 5.37 – 5.24 (m, 1H), 5.04 – 4.89 (m, 2H), 4.62 (d, *J* = 7.3 Hz, 2H), 2.56 – 2.35 (m, 3H), 2.08 – 1.94 (m, 3H), 1.86 (ddd, *J* = 13.7, 12.3, 4.6 Hz, 1H), 1.78 – 1.47 (m, 10H), 1.46 – 1.19 (m, 3H).

^{13}C NMR (100 MHz, $CDCl_3$): δ 208.2, 172.2, 140.0, 138.5, 118.2, 114.8, 62.1, 61.0, 41.3, 36.4, 34.4, 34.2, 27.8, 25.8, 23.7, 22.8, 18.2.

IR (Neat Film, NaCl): 2938, 2864, 1713, 1639, 1449, 1379, 1339, 1308, 1210, 1186, 1143 cm^{-1}.

HRMS (ESI+): *m/z* calc'd for $C_{17}H_{26}O_3Na$ $[M+Na]^+$: 301.1774, found 301.1761.



130a

cinnamyl 2-oxo-1-((*E*)-6-oxo-6-phenylhex-4-en-1-yl)cyclohexane-1-carboxylate (130a)

Prepared from **147i** and dimethyl (2-oxo-2-phenylethyl)phosphonate[6] following General Procedure 3D. Purification by flash column chromatography (0–50% EtOAc/hexanes) afforded the title compound as a colorless oil (533 mg, 1.24 mmol, 81% yield).

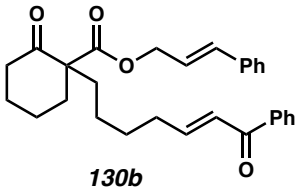
^{1}H NMR (400 MHz, $CDCl_3$): δ 7.95 – 7.87 (m, 2H), 7.58 – 7.51 (m, 1H), 7.49 – 7.42 (m, 2H), 7.40 – 7.34 (m, 2H), 7.33 – 7.27 (m, 2H), 7.26 – 7.21 (m, 1H), 7.00 (dt, *J* = 15.4, 6.7 Hz, 1H), 6.86 (dt, *J* = 15.4, 1.4 Hz, 1H), 6.71 – 6.62 (m, 1H), 6.26 (dt, *J* = 15.9, 6.6 Hz,

1H), 4.87 – 4.73 (m, 2H), 2.59 – 2.39 (m, 3H), 2.38 – 2.23 (m, 2H), 2.08 – 1.87 (m, 2H), 1.82 – 1.57 (m, 4H), 1.55 – 1.36 (m, 3H).

^{13}C NMR (100 MHz, $CDCl_3$): δ 207.9, 191.0, 171.9, 149.0, 138.1, 136.1, 135.4, 132.7, 128.8, 128.7, 128.6, 128.4, 126.8, 126.3, 122.4, 66.0, 61.0, 41.3, 36.4, 34.5, 33.2, 27.7, 23.2, 22.8.

IR (Neat Film, NaCl): 2942, 2865, 1711, 1669, 1619, 1448, 1339, 1288, 1218, 1170, 1135, 1101 cm^{-1}.

HRMS (ESI+): *m/z* calc'd for $C_{28}H_{30}O_4Na$ $[M+Na]^+$: 453.2036, found 453.2031.



130b

cinnamyl 2-oxo-1-((*E*)-7-oxo-7-phenylhept-5-en-1-yl)cyclohexane-1-carboxylate (130b)

Prepared from **147j** and dimethyl (2-oxo-2-phenylethyl)phosphonate[6] following General Procedure 3D. Purification by flash column chromatography (0–50% EtOAc/hexanes) afforded the title compound as a colorless oil (504 mg, 1.13 mmol, 76% yield).

^{1}H NMR (400 MHz, $CDCl_3$): δ 7.95 – 7.87 (m, 2H), 7.59 – 7.51 (m, 1H), 7.50 – 7.41 (m, 2H), 7.39 – 7.35 (m, 2H), 7.35 – 7.29 (m, 2H), 7.30 – 7.23 (m, 1H), 7.00 (dt, *J* = 15.4, 6.8 Hz, 1H), 6.82 (dt, *J* = 15.4, 1.5 Hz, 1H), 6.65 (dt, *J* = 15.8, 1.4 Hz, 1H), 6.25 (dt, *J* = 15.8, 6.5 Hz, 1H), 4.78 (dd, *J* = 6.6, 1.3 Hz, 2H), 2.59 – 2.50 (m, 1H), 2.49 – 2.38 (m, 2H), 2.34 – 2.20 (m, 2H), 2.05 – 1.87 (m, 2H), 1.81 – 1.59 (m, 4H), 1.57 – 1.41 (m, 3H), 1.38 – 1.20 (m, 2H).

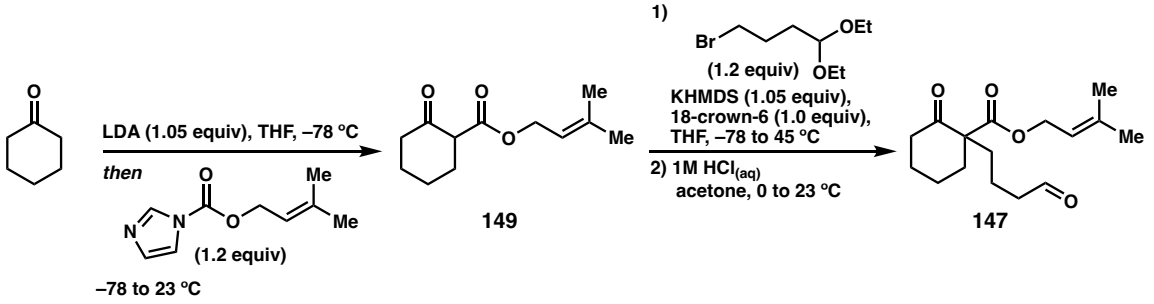
^{13}C NMR (100 MHz, $CDCl_3$): δ 208.0, 191.0, 172.0, 149.6, 138.1, 136.1, 135.3, 132.7, 128.8, 128.7, 128.6, 128.4, 126.8, 126.1, 122.5, 65.8, 61.1, 41.3, 36.3, 34.6, 32.7, 28.6, 27.7, 24.1, 22.7.

IR (Neat Film, NaCl): 2939, 2862, 1711, 1668, 1620, 1578, 1495, 1447, 1338, 1284, 1214, 1168 cm^{-1}.

HRMS (ESI+): *m/z* calc'd for $C_{29}H_{32}O_4$ $[M+Na]^+$: 467.2193, found 467.2200.

Preparation of Aldehyde Precursors:

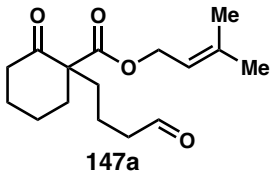
General Procedure 3E: Acylation, Alkylation of Carbonyls and Hydrolysis of Acetals



To a flame dried 250 mL round bottom flask was added *i*Pr_2NH (1.1 equiv) followed by THF (1.9 M) before the solution was cooled to 0 °C. To this, *n*-BuLi (2.5 M in hexanes, 1.05 equiv) was added dropwise before the solution was allowed to stir at 0 °C for 15 minutes. To this, a solution of the appropriate carbonyl compound (1.0 equiv) in THF (1.25 M) was added dropwise before the solution was allowed to stir at 0 °C for 30 minutes. The solution was then cooled to –78 °C, before a solution of 3-methylbut-2-en-1-yl 1*H*-imidazole-1-carboxylate[9] (1.2 equiv) in THF (4 M) was added dropwise. The reaction was warmed gradually to 23 °C. Upon complete consumption of starting material by TLC, the reaction was cooled to 0 °C, the pH was adjusted to 1.0 using 1 M HCl and the mixture

was extracted with EtOAc (3x). The combined organic layers were rinsed with brine, dried over Na_2SO_4, filtered, and concentrated under reduced pressure. The crude reaction mixture was purified by silica gel flash column chromatography to afford **149** as a mixture of tautomers, which was used directly in the next step.

To a flame dried 250 mL round bottom flask was added KHMDS (1.05 equiv), and 18-crown-6 (1.0 equiv) followed by THF (0.19 M) before the solution was cooled to –78 °C. A solution of β-ketoester **149** (1.0 equiv) in THF (0.38 M) was added dropwise at –78 °C. The solution was stirred at this temperature for 15 minutes before the appropriate alkyl bromide was added neat (1.2 equiv). The reaction was then warmed to 45 °C. Upon complete consumption of starting material by TLC, the reaction was cooled to 0 °C, and diluted with EtOAc followed by a saturated solution of NH_4Cl. This mixture was then extracted with EtOAc (3x). The combined organic layers were rinsed with brine, dried over Na_2SO_4, filtered, and concentrated under reduced pressure to afford the corresponding diethyl acetal which was used directly in the next step. A round bottom flask was charged with the corresponding diethyl acetal as a solution in acetone (0.5 M) before being cooled to 0 °C, and 1 M HCl was added (in a 2:1 volume ratio of 1 M HCl:acetone). The reaction was gradually warmed to 23 °C. Upon complete consumption of starting material by TLC, the reaction was diluted with EtOAc, extracted with EtOAc (3x), rinsed with brine, dried with Na_2SO_4, filtered, and concentrated under reduced pressure. The crude reaction mixture was purified by silica gel flash column chromatography to afford **147**. *Note: Yields are reported based on alkylation and hydrolysis sequence. This is done because the corresponding β-keto esters were sometimes used to prepare multiple substrates.*



147a

3-methylbut-2-en-1-yl 2-oxo-1-(4-oxobutyl)cyclohexane-1-carboxylate (147a)

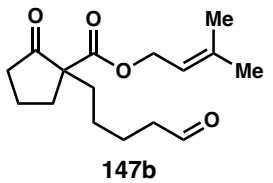
Prepared from cyclohexanone and 4-bromo-1,1-diethoxybutane[10] according to General Procedure 3E. Purification by flash column chromatography (0–60% EtOAc/hexanes) afforded the title compound as a colorless oil (715 mg, 2.55 mmol, 43% yield).

^{1}H NMR (400 MHz, $CDCl_3$): δ 9.73 (t, *J* = 1.6 Hz, 1H), 5.36 – 5.28 (m, 1H), 4.70 – 4.57 (m, 2H), 2.56 – 2.37 (m, 5H), 2.05 – 1.95 (m, 1H), 1.91 – 1.79 (m, 1H), 1.79 – 1.73 (m, 4H), 1.71 (s, 3H), 1.69 – 1.49 (m, 5H), 1.49 – 1.39 (m, 1H).

^{13}C NMR (100 MHz, $CDCl_3$): δ 208.0, 202.2, 172.0, 140.2, 118.1, 62.3, 60.9, 44.2, 41.2, 36.4, 34.3, 27.8, 25.8, 22.7, 18.2, 17.3.

IR (Neat Film, NaCl): 2939, 2866, 1713, 1450, 1380, 1211, 1179, 1137, 1096 cm^{-1}.

HRMS (ESI+): *m/z* calc'd for $C_{16}H_{24}O_4Na$ $[M+Na]^+$: 303.1567, found 393.1564.



147b

3-methylbut-2-en-1-yl 2-oxo-1-(5-oxopentyl)cyclopentane-1-carboxylate (147b)

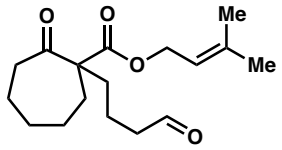
Prepared from cyclopentanone and 4-bromo-1,1-diethoxybutane[10] according to General Procedure 3E. Purification by flash column chromatography (0–50% EtOAc/hexanes) afforded the title compound as a colorless oil (631 mg, 2.37 mmol, 47% yield).

^{1}H NMR (400 MHz, $CDCl_3$): δ 9.75 (t, *J* = 1.4 Hz, 1H), 5.35 – 5.24 (m, 1H), 4.63 – 4.54 (m, 2H), 2.60 – 2.35 (m, 4H), 2.32 – 2.17 (m, 1H), 2.09 – 1.84 (m, 4H), 1.74 (s, 3H), 1.72 – 1.49 (m, 6H).

^{13}C NMR (100 MHz, $CDCl_3$): δ 214.9, 201.9, 171.0, 139.7, 118.2, 62.5, 60.4, 44.1, 38.1, 33.3, 33.0, 25.9, 19.8, 18.2, 17.6.

IR (Neat Film, NaCl): 2960, 1748, 1719, 1448, 1380, 1335, 1157 cm^{-1}.

HRMS (ESI+): *m/z* calc'd for $C_{15}H_{22}O_4Na$ $[M+Na]^+$: 289.1410, found 289.1408.



147c

3-methylbut-2-en-1-yl 2-oxo-1-(4-oxobutyl)cycloheptane-1-carboxylate (147c)

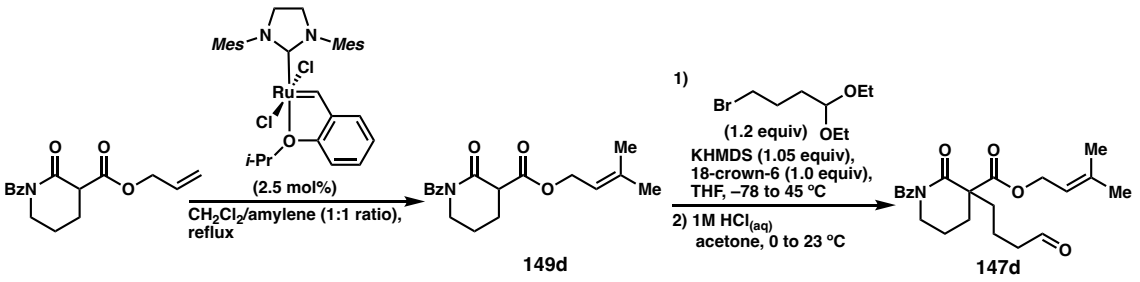
Prepared from cycloheptanone and 4-bromo-1,1-diethoxybutane[10] according to General Procedure 3E. Purification by flash column chromatography (0–50% EtOAc/hexanes) afforded the title compound as a colorless oil (1.34 g, 4.56 mmol, 57% yield).

^{1}H NMR (400 MHz, $CDCl_3$): δ 9.73 (t, *J* = 1.6 Hz, 1H), 5.37 – 5.24 (m, 1H), 4.62 (dd, *J* = 7.3, 3.1 Hz, 2H), 2.71 – 2.56 (m, 1H), 2.52 – 2.34 (m, 3H), 2.22 – 2.06 (m, 1H), 2.06 – 1.87 (m, 1H), 1.83 – 1.72 (m, 5H), 1.72 – 1.49 (m, 10H), 1.48 – 1.35 (m, 1H).

^{13}C NMR (100 MHz, $CDCl_3$): δ 209.6, 202.2, 172.4, 139.9, 118.2, 62.8, 62.2, 44.2, 42.3, 34.9, 33.0, 29.9, 25.8, 25.6, 25.0, 18.2, 17.6.

IR (Neat Film, NaCl): 2931, 2862, 1708, 1457, 1379, 1220, 1168 cm^{-1}.

HRMS (ESI+): *m/z* calc'd for $C_{17}H_{26}O_4Na$ $[M+Na]^+$: 317.1723, found 317.1719.



3-methylbut-2-en-1-yl 1-benzoyl-2-oxo-3-(4-oxobutyl)piperidine-3-carboxylate (147d)

To a flame dried 2-neck 250 mL round bottom flask equipped with a reflux condenser was added HG-II (54.5 mg, 0.09 mmol, 0.025 equiv). Allyl 1-benzoyl-2-oxopiperidine-3-carboxylate[11] (1.00 g, 3.5 mmol, 1.0 equiv) was added as a solution in CH_2Cl_2 (35 mL, 0.1 M) followed by amylene (35 mL, 1:1 volume ratio with CH_2Cl_2). The reaction mixture was heated to reflux and monitored via NMR. Upon complete consumption of allyl 1-benzoyl-2-oxopiperidine-3-carboxylate, the reaction was cooled to 23 °C and concentrated under reduced pressure. The crude reaction mixture was purified by silica gel flash column chromatography (0–50% EtOAc/hexanes) to afford **149d** (953 mg, 3.02 mmol, 87% yield), which was used directly in the next step.

To a flame dried 100 mL round bottom flask was added KHMDS (622 mg, 3.1 mmol, 1.05 equiv), and 18-crown-6 (784 mg, 3.0 mmol, 1.0 equiv) followed by THF (15 mL, 0.2 M) before the solution was cooled to –78 °C. A solution of β-ketoester **149d** (936 mg, 3.0 mmol, 1.0 equiv) in THF (7.5 mL, 0.4 M) was added dropwise at –78 °C. The solution was stirred at this temperature for 15 minutes before 4-bromo-1,1-diethoxybutane[10] was added neat (801 mg, 3.6 mmol, 1.2 equiv). The reaction was then warmed to 45 °C. Upon complete consumption of starting material by TLC, the reaction was cooled to 0 °C, and

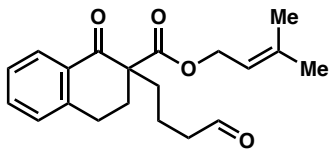
diluted with EtOAc (10 mL) followed by a saturated solution of NH_4Cl (20 mL). This mixture was then extracted with EtOAc (3x). The combined organic layers were rinsed with brine, dried over Na_2SO_4, filtered, and concentrated under reduced pressure to afford the corresponding diethyl acetal which was used directly in the next step. A 50 mL round bottom flask was charged with the corresponding diethyl acetal as a solution in acetone (6 mL, 0.5 M) before being cooled to 0 °C, and 1 M HCl was added (in a 1:1 volume ratio of 1 M HCl:acetone). The reaction was gradually warmed to 23 °C. Upon complete consumption of starting material by TLC, the reaction was diluted with EtOAc, extracted with EtOAc (3x), rinsed with brine, dried with Na_2SO_4, filtered, and concentrated under reduced pressure. The crude reaction mixture was purified by silica gel flash column chromatography (0–50% EtOAc/hexanes) to afford **147d** as a colorless oil (409 mg, 1.06 mmol, 36% yield).

^{1}H NMR (400 MHz, $CDCl_3$): δ 9.71 (t, *J* = 1.4 Hz, 1H), 7.78 – 7.68 (m, 2H), 7.51 – 7.43 (m, 1H), 7.41 – 7.34 (m, 2H), 5.47 – 5.38 (m, 1H), 4.81 – 4.65 (m, 2H), 3.88 – 3.69 (m, 2H), 2.54 – 2.30 (m, 3H), 2.07 – 1.95 (m, 2H), 1.93 – 1.85 (m, 2H), 1.84 – 1.79 (m, 3H), 1.79 – 1.69 (m, 4H), 1.67 – 1.43 (m, 2H).

^{13}C NMR (100 MHz, $CDCl_3$): δ 201.9, 175.1, 172.1, 172.1, 140.7, 136.0, 131.8, 128.2, 128.2, 117.8, 63.0, 56.7, 46.6, 44.0, 35.0, 30.7, 26.0, 20.5, 18.3, 17.5.

IR (Neat Film, NaCl): 2941, 1718, 1684, 1448, 1387, 1272, 1190, 1148 cm^{-1}.

HRMS (ESI+): *m/z* calc'd for $C_{22}H_{27}NO_5Na$ $[M+Na]^+$: 408.1781, found 408.1786.



147e

3-methylbut-2-en-1-yl 1-oxo-2-(4-oxobutyl)-1,2,3,4-tetrahydronaphthalene-2-carboxylate (147e)

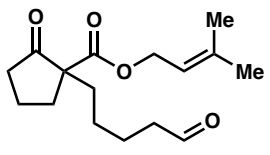
Prepared from 1-tetralone and 4-bromo-1,1-diethoxybutane[10] according to General Procedure 3E. Purification by flash column chromatography (0–50% EtOAc/hexanes) afforded the title compound as a colorless oil (531 mg, 1.62 mmol, 20% yield).

^{1}H NMR (400 MHz, $CDCl_3$): δ 9.76 (t, *J* = 1.5 Hz, 1H), 8.03 (dd, *J* = 7.9, 1.5 Hz, 1H), 7.46 (td, *J* = 7.5, 1.4 Hz, 1H), 7.30 (t, *J* = 7.6 Hz, 1H), 7.21 (d, *J* = 7.7 Hz, 1H), 5.26 – 5.17 (m, 1H), 4.64 – 4.49 (m, 2H), 3.07 (ddd, *J* = 17.4, 10.1, 4.7 Hz, 1H), 2.93 (dt, *J* = 17.4, 5.0 Hz, 1H), 2.57 (dt, *J* = 13.8, 5.0 Hz, 1H), 2.48 (t, *J* = 7.1 Hz, 2H), 2.23 – 2.11 (m, 1H), 2.03 – 1.86 (m, 2H), 1.86 – 1.72 (m, 1H), 1.72 – 1.62 (m, 4H), 1.58 (s, 3H).

^{13}C NMR (100 MHz, $CDCl_3$): δ 202.2, 195.6, 171.9, 143.2, 139.9, 133.6, 132.2, 128.8, 128.2, 126.9, 118.2, 62.4, 57.6, 44.2, 33.5, 30.9, 26.1, 25.8, 18.1, 17.7.

IR (Neat Film, NaCl): 2935, 2724, 1724, 1687, 1600, 1453, 1453, 1379, 1294, 1231, 1184, 1096 cm^{-1}.

HRMS (ESI+): *m/z* calc'd for $C_{20}H_{24}O_4Na$ $[M+Na]^+$: 351.1567, found 351.1571.



147f

3-methylbut-2-en-1-yl 2-oxo-1-(5-oxopentyl)cyclopentane-1-carboxylate (147f)

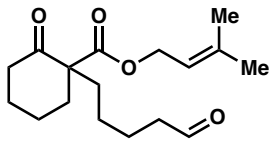
Prepared from cyclopentanone and 5-bromo-1,1-diethoxypentane[10] according to General Procedure 3E. Purification by flash column chromatography (0–40% EtOAc/hexanes) afforded the title compound as a colorless oil (886 mg, 3.16 mmol, 63% yield).

^{1}H NMR (400 MHz, $CDCl_3$): δ 9.75 (t, *J* = 1.7 Hz, 1H), 5.34 – 5.23 (m, 1H), 4.62 – 4.53 (m, 2H), 2.56 – 2.36 (m, 4H), 2.29 – 2.17 (m, 1H), 2.07 – 1.80 (m, 4H), 1.74 (s, 3H), 1.69 (s, 3H), 1.67 – 1.53 (m, 3H), 1.44 – 1.32 (m, 1H), 1.31 – 1.18 (m, 1H).

^{13}C NMR (100 MHz, $CDCl_3$): δ 215.0, 202.4, 171.1, 139.6, 118.3, 62.5, 60.5, 43.7, 38.1, 33.6, 33.1, 25.9, 24.5, 22.4, 19.8, 18.2.

IR (Neat Film, NaCl): 2947, 2725, 1748, 1722, 1451, 1380, 1224, 1159, 1127 cm^{-1}.

HRMS (ESI+): *m/z* calc'd for $C_{16}H_{24}O_4Na$ $[M+Na]^+$: 303.1567, found 303.1571.



147g

3-methylbut-2-en-1-yl 2-oxo-1-(5-oxopentyl)cyclohexane-1-carboxylate (147g)

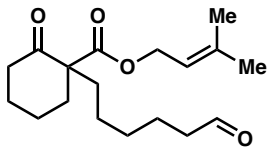
Prepared from cyclohexanone and 5-bromo-1,1-diethoxypentane[10] according to General Procedure 3E. Purification by flash column chromatography (0–60% EtOAc/hexanes) afforded the title compound as a colorless oil (617 mg, 2.10 mmol, 44% yield).

^{1}H NMR (400 MHz, $CDCl_3$): δ 9.74 (t, *J* = 1.7 Hz, 1H), 5.35 – 5.25 (m, 1H), 4.70 – 4.53 (m, 2H), 2.56 – 2.33 (m, 5H), 2.05 – 1.95 (m, 1H), 1.92 – 1.80 (m, 1H), 1.74 (s, 3H), 1.73 – 1.67 (m, 4H), 1.66 – 1.48 (m, 5H), 1.47 – 1.35 (m, 1H), 1.34 – 1.14 (m, 2H).

^{13}C NMR (100 MHz, $CDCl_3$): δ 208.2, 202.6, 172.1, 140.0, 118.1, 62.2, 60.9, 43.8, 41.3, 36.4, 34.6, 27.8, 25.8, 24.0, 22.7, 22.5, 18.2.

IR (Neat Film, NaCl): 2939, 2865, 2724, 1712, 1449, 1380, 1297, 1173, 1136, 1097 cm^{-1}.

HRMS (ESI+): *m/z* calc'd for $C_{17}H_{26}O_4Na$ $[M+Na]^+$: 317.1723, found 317.1719.



147h

3-methylbut-2-en-1-yl 2-oxo-1-(6-oxohexyl)cyclohexane-1-carboxylate (147h)

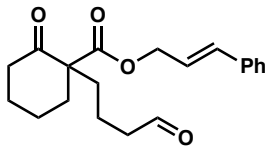
Prepared from cyclohexanone and 6-bromo-1,1-diethoxyhexane[10] according to General Procedure 3E. Purification by flash column chromatography (0–60% EtOAc/hexanes) afforded the title compound as a colorless oil (515 mg, 1.67 mmol, 44% yield).

^{1}H NMR (400 MHz, $CDCl_3$): δ 9.75 (t, *J* = 1.8 Hz, 1H), 5.40 – 5.23 (m, 1H), 4.70 – 4.54 (m, 2H), 2.57 – 2.32 (m, 5H), 2.06 – 1.95 (m, 1H), 1.85 (ddd, *J* = 13.3, 12.1, 4.1 Hz, 1H), 1.79 – 1.67 (m, 7H), 1.67 – 1.56 (m, 4H), 1.54 – 1.37 (m, 2H), 1.36 – 1.11 (m, 4H).

^{13}C NMR (100 MHz, $CDCl_3$): δ 208.3, 202.8, 172.2, 140.0, 118.2, 62.1, 61.0, 43.9, 41.3, 36.5, 34.7, 29.6, 27.8, 25.9, 24.1, 22.8, 21.9, 18.2.

IR (Neat Film, NaCl): 2936, 2862, 2720, 1712, 1450, 1380, 1270, 1200, 1170, 1136, 1098 cm^{-1}.

HRMS (ESI+): *m/z* calc'd for $C_{18}H_{28}O_4Na$ $[M+Na]^+$: 331.1880, found 331.1880.



147i

cinnamyl 2-oxo-1-(4-oxobutyl)cyclohexane-1-carboxylate (147i)

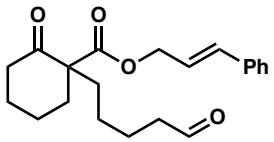
Prepared from cyclohexanone, cinnamyl 1*H*-imidazole-1-carboxylate (in place of 3-methylbut-2-en-1-yl 1*H*-imidazole-1-carboxylate), and 4-bromo-1,1-diethoxybutane[10] according to General Procedure 3E. Purification by flash column chromatography (0–60% EtOAc/hexanes) afforded the title compound as a colorless oil (1.81 g, 5.50 mmol, 37% yield).

^{1}H NMR (400 MHz, $CDCl_3$): δ 9.77 – 9.65 (m, 1H), 7.41 – 7.36 (m, 2H), 7.36 – 7.30 (m, 2H), 7.30 – 7.26 (m, 1H), 6.67 (d, *J* = 15.8 Hz, 1H), 6.27 (dtd, *J* = 15.9, 6.6, 0.8 Hz, 1H), 4.87 – 4.74 (m, 2H), 2.59 – 2.36 (m, 5H), 2.04 – 1.96 (m, 1H), 1.92 – 1.82 (m, 1H), 1.82 – 1.43 (m, 7H).

^{13}C NMR (100 MHz, $CDCl_3$): δ 207.8, 202.1, 171.8, 136.1, 135.4, 128.8, 128.4, 126.8, 122.4, 66.0, 61.0, 44.1, 41.2, 36.2, 34.2, 27.7, 22.7, 17.3.

IR (Neat Film, NaCl): 2944, 2866, 1713, 1495, 1450, 1242, 1206, 1178, 1137, 1098 cm^{-1}.

HRMS (ESI+): *m/z* calc'd for $C_{20}H_{24}O_4Na$ $[M+Na]^+$: 351.1567, found 351.1562.



147j

cinnamyl 2-oxo-1-(5-oxopentyl)cyclohexane-1-carboxylate (147j)

Prepared from cyclohexanone, cinnamyl 1*H*-imidazole-1-carboxylate (in place of 3-methylbut-2-en-1-yl 1*H*-imidazole-1-carboxylate), and 5-bromo-1,1-diethoxypentane[10] according to General Procedure 3E. Purification by flash column chromatography (0–60%

EtOAc/hexanes) afforded the title compound as a colorless oil (767 mg, 2.24 mmol, 45% yield).

^{1}H NMR (600 MHz, $CDCl_3$): δ 9.69 (t, *J* = 1.7 Hz, 1H), 7.41 – 7.36 (m, 2H), 7.36 – 7.31 (m, 2H), 7.30 – 7.26 (m, 1H), 6.66 (dd, *J* = 15.9, 1.6 Hz, 1H), 6.26 (dt, *J* = 15.9, 6.6 Hz, 1H), 4.79 (dd, *J* = 6.6, 1.3 Hz, 2H), 2.56 – 2.41 (m, 3H), 2.40 – 2.31 (m, 2H), 2.04 – 1.96 (m, 1H), 1.90 (ddd, *J* = 13.5, 12.2, 4.6 Hz, 1H), 1.80 – 1.72 (m, 1H), 1.71 – 1.53 (m, 5H), 1.46 (ddd, *J* = 13.6, 12.0, 4.2 Hz, 1H), 1.34 – 1.18 (m, 2H).

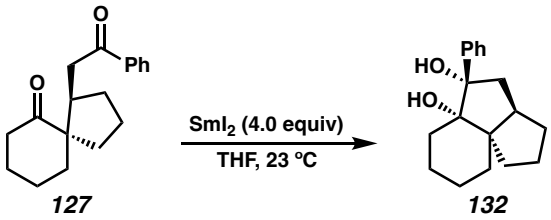
^{13}C NMR (100 MHz, $CDCl_3$): δ 207.9, 202.5, 171.9, 136.1, 135.4, 128.8, 128.5, 126.8, 122.4, 65.9, 61.0, 43.7, 41.3, 36.3, 34.6, 27.7, 24.1, 22.7, 22.5.

IR (Neat Film, NaCl): 2944, 2865, 1713, 1495, 1451, 1240, 1310, 1240, 1206, 1174, 1135, 1098 cm^{-1}.

HRMS (ESI+): *m/z* calc'd for $C_{21}H_{26}O_4Na$ $[M+Na]^+$: 365.1723, found 365.1721.

Product Derivatizations:

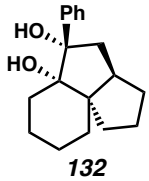
General Procedure 3F: Samarium Mediated Pinacol Coupling[12]



127 ***132***

To a flame dried round bottom flask was added a solution of SmI_2 (0.1 M in THF, 4.0 equiv), followed by a solution of the corresponding diketone (1.0 equiv) in THF (0.1 M). Upon complete consumption of starting material by TLC, the reaction was diluted with Et_2O, followed by further dilution with a saturated aqueous solution of $NaHCO_3$. The mixture was extracted with Et_2O (3x), rinsed with brine, dried with Na_2SO_4, filtered, and

concentrated under reduced pressure. The crude reaction mixture was purified by silica gel flash column chromatography or preparative TLC to afford the corresponding diol.



132

(3a*R*,5*S*,5a*S*,9a*S*)-5-phenyldecahydro-5a*H*-cyclopenta[*c*]indene-5,5a-diol (132)

Prepared from diketone **127a** according to General Procedure 3F. Purification by flash column chromatography (0–40% Et_2O/hexanes) afforded the title compound as a colorless oil (23 mg, 0.084 mmol, 56% yield). Structure assigned via 1D ^1H and ^{13}C NMR, 2D NMR studies (see below), and comparison with compounds found in the literature. Cis configuration was assigned via carbonate formation[12] (see **133** below).

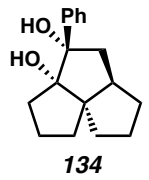
^1H NMR (400 MHz, $CDCl_3$): δ 7.64 – 7.58 (m, 2H), 7.38 – 7.31 (m, 2H), 7.29 – 7.22 (m, 1H), 4.12 (s, 1H), 2.73 (s, 1H), 2.65 – 2.47 (m, 2H), 2.12 – 1.94 (m, 2H), 1.72 – 1.58 (m, 3H), 1.55 – 1.47 (m, 1H), 1.41 – 1.11 (m, 7H), 1.07 – 0.96 (m, 1H), 0.12 – -0.05 (m, 1H).

^{13}C NMR (100 MHz, $CDCl_3$): δ 144.3, 127.9, 127.6, 127.2, 90.7, 79.3, 58.6, 47.0, 37.6, 35.3, 26.4, 25.7, 25.0, 22.3, 21.9, 20.8.

IR (Neat Film, NaCl): 3307, 2946, 2871, 1494, 1445, 1394, 1221, 1050, 1019 cm^{-1}.

HRMS (FD+): *m/z* calc'd for $C_{18}H_{24}O_2$ $[M]^{+\cdot}$: 272.17708, found 272.17608.

Optical Rotation: $[\alpha]_D^{23}$ –30.0 (c = 1.53, $CHCl_3$).



134

(3a*S*,4*S*,5a*R*,8a*R*)-4-phenyloctahydrocyclopenta[*c*]pentalene-3a,4(1*H*)-diol (134)

Prepared from diketone **127c** according to General Procedure 3F. Purification by preparative TLC (40% Et_2O/hexanes) afforded the title compound as a colorless oil (7.0 mg, 0.027 mmol, 68% yield).

^{1}H NMR (400 MHz, $CDCl_3$): δ 7.49 – 7.42 (m, 2H), 7.38 – 7.31 (m, 2H), 7.31 – 7.27 (m, 1H), 3.29 (s, 1H), 3.12 (s, 1H), 2.52 – 2.36 (m, 1H), 2.16 (dd, *J* = 13.5, 12.1 Hz, 1H), 2.12 – 2.02 (m, 1H), 2.01 – 1.88 (m, 1H), 1.82 (dd, *J* = 12.2, 4.5 Hz, 1H), 1.72 – 1.58 (m, 2H), 1.57 – 1.48 (m, 2H), 1.47 – 1.35 (m, 2H), 1.34 – 1.21 (m, 3H), 1.16 – 1.01 (m, 1H).

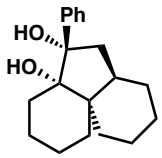
^{13}C NMR (100 MHz, $CDCl_3$): δ 144.5, 128.3, 127.6, 126.5, 90.0, 87.3, 64.3, 47.4, 39.5, 35.9, 34.0, 31.1, 26.6, 22.6, 22.1.

Note: A grease and water signal are observed in the ^{1}H and ^{13}C spectra.

IR (Neat Film, NaCl): 3334, 2953, 2873, 1446, 1376, 1128, 1100, 1046 cm^{-1}.

HRMS (FD+): *m/z* calc'd for $C_{17}H_{22}O_2$ $[M]^{+\cdot}$: 258.16143, found 258.16203.

Optical Rotation: $[\alpha]_D^{23}$ –36.0 (c = 0.58, $CHCl_3$).



135

(4a*S*,5*S*,6a*R*,10a*R*)-5-phenyldecahydrobenzo[*c*]indene-4a,5(5*H*)-diol (135)

Prepared from diketone **8k** according to General Procedure 3F. Purification by preparative TLC (40% Et_2O/hexanes) afforded the title compound as a colorless crystalline solid (5.2 mg, 0.018 mmol, 37% yield). Absolute and relative stereochemistry were assigned by X-ray crystallography (vide infra).

^{1}H NMR (400 MHz, $CDCl_3$): δ 7.64 – 7.55 (m, 2H), 7.38 – 7.30 (m, 2H), 7.30 – 7.21 (m, 1H), 3.92 (s, 1H), 2.77 (s, 1H), 2.58 (t, *J* = 13.4 Hz, 1H), 2.20 – 2.05 (m, 1H), 1.82 – 1.66

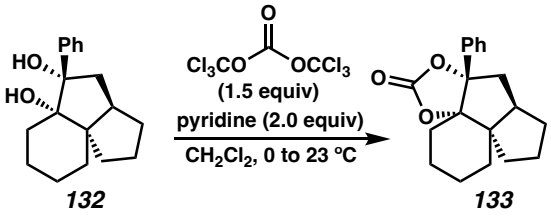
(m, 4H), 1.61 (dd, J = 11.6, 2.9 Hz, 1H), 1.55 – 1.43 (m, 3H), 1.43 – 1.14 (m, 6H), 1.13 – 0.96 (m, 2H), 0.20 – 0.02 (m, 1H).

^{13}C NMR (100 MHz, $CDCl_3$): δ 144.6, 127.9, 127.6, 127.2, 83.7, 83.2, 46.6, 42.2, 41.7, 34.1, 28.2, 26.3, 24.7, 22.2, 21.4, 20.9, 19.2.

IR (Neat Film, NaCl): 3310, 2924, 2857, 1495, 1444, 1391, 1143, 1038, 1028 cm^{-1}.

HRMS (FD+): *m/z* calc'd for $C_{19}H_{26}O_2$ $[M]^{+\cdot}$: 286.19273, found 286.19351.

Optical Rotation: $[\alpha]_D^{23}$ –27.4 (c = 0.43, $CHCl_3$).



132 ***133***

(3a*S*,4a*R*,7a*S*,11a*S*)-3a-phenyldecahydrocyclopenta[3,3a]indeno[1,7a-*d*][1,3]dioxol-2-onediol (133)

To a flame dried 2-dram vial was added a solution of diol **132** (5.0 mg, 0.02 mmol, 1.0 equiv) in CH_2Cl_2 (0.02 M, 1.0 mL) then the solution was cooled to 0 °C. Pyridine (3 μL, 0.04 mmol, 2.0 equiv) was added before a solution of triphosgene (8.9 mg, 0.03 mmol, 1.5 equiv) in CH_2Cl_2 (0.06 M, 0.5 mL) was added dropwise at 0 °C. *Note: serious caution must be taken when working with triphosgene due to its high toxicity. Review MSDS information before using.* Upon complete consumption of starting material by TLC, the reaction was diluted with saturated aqueous NH_4Cl, extracted with Et_2O (3x), rinsed with 1 M HCl, saturated aqueous $NaHCO_3$, and brine. Following this the organic layer was dried with Na_2SO_4, filtered, and concentrated under reduced pressure. Purification of the crude compound via flash column chromatography (0–50% Et_2O/hexanes) afforded the title

compound as a colorless oil (4.1 mg, 0.014 mmol, 69% yield). Successful formation of the carbonate (assigned via ^{1}H and ^{13}C NMR) is consistent with **132** being the cis-diol. This is due to the high degree of ring strain associated with the corresponding trans-fused [3.3.0] ring system.[12]

^{1}H NMR (400 MHz, $CDCl_3$): δ 7.54 – 7.48 (m, 2H), 7.46 – 7.34 (m, 3H), 2.59 (t, *J* = 13.6 Hz, 1H), 2.48 – 2.36 (m, 1H), 2.19 – 2.03 (m, 3H), 1.76 – 1.65 (m, 2H), 1.64 – 1.56 (m, 2H), 1.54 – 1.30 (m, 4H), 1.29 – 1.15 (m, 3H), 0.36 – 0.20 (m, 1H).

Note: A grease and water signal are observed in the ^{1}H spectrum.

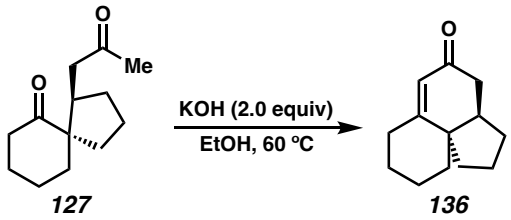
^{13}C NMR (100 MHz, $CDCl_3$): δ 154.9, 136.4, 129.0, 128.5, 127.0, 102.4, 91.7, 58.2, 47.1, 35.2, 30.3, 26.6, 25.9, 25.2, 22.3, 21.0, 20.4.

IR (Neat Film, NaCl): 2948, 2877, 1794, 1447, 1298, 1272, 1241, 1060 cm^{-1}.

HRMS (FD+): *m/z* calc'd for $C_{19}H_{22}O_3$ $[M]^{+\cdot}$: 298.15635, found 298.15641.

Optical Rotation: $[\alpha]_D^{23}$ –12.2 (c = 0.34, $CHCl_3$).

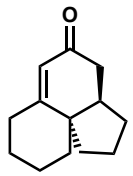
General Procedure 3G: Aldol Condensation[13]



127 ***136***

To a flame dried round bottom flask was added a solution of KOH (2.3 equiv) in EtOH (0.14 M) followed by a solution of the corresponding ketone (1.0 equiv) in EtOH (0.1 M). The reaction was heated to 60 °C. Upon complete consumption of starting material by TLC, the reaction was quenched with AcOH (2.3 equiv) and concentrated under reduced pressure.

The crude reaction mixture was purified by silica gel flash column chromatography to afford the corresponding enone.



136

(3a*R*,10a*S*)-2,3,3a,4,7,8,9,10-octahydrocyclopenta[*d*]naphthalen-5(1*H*)-one (136)

Prepared from diketone **127b** according to General Procedure 3G. Purification by flash column chromatography (0–45% Et_2O/hexanes) afforded the title compound as a colorless oil (13.1 mg, 0.069 mmol, 72% yield).

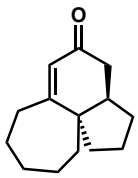
^{1}H NMR (400 MHz, $CDCl_3$): δ 5.77 (s, 1H), 2.42 (dd, *J* = 16.5, 3.7 Hz, 1H), 2.35 – 2.15 (m, 3H), 2.15 – 1.94 (m, 3H), 1.83 – 1.67 (m, 5H), 1.62 – 1.53 (m, 1H), 1.51 – 1.27 (m, 4H).

^{13}C NMR (100 MHz, $CDCl_3$): δ 200.6, 175.7, 123.2, 48.4, 44.8, 37.9, 35.1, 32.3, 31.7, 30.6, 26.2, 21.9, 20.0.

IR (Neat Film, NaCl): 2937, 2870, 1668, 1607, 1445, 1369, 1277, 1250, 1213, 1164, 1133, 1101 cm^{-1}.

HRMS (FI+): *m/z* calc'd for $C_{13}H_{18}O$ $[M]^{+\cdot}$: 190.13522, found 190.13552.

Optical Rotation: $[\alpha]_D^{23}$ +127.5 (c = 1.09, $CHCl_3$).



137

(3a*R*,11a*S*)-2,3,3a,4,8,9,10,11-octahydro-1*H*-cyclohepta[*d*]inden-5(7*H*)-one (137)

Prepared from diketone **127f** according to General Procedure 3G. Purification by preparative TLC (30% Et_2O/hexanes) afforded the title compound as a colorless oil (6.1 mg, 0.030 mmol, 66% yield).

^{1}H NMR (400 MHz, $CDCl_3$): δ 5.71 (s, 1H), 2.63 – 2.52 (m, 1H), 2.45 (dd, *J* = 17.6, 4.8 Hz, 1H), 2.39 – 2.27 (m, 2H), 2.19 – 1.99 (m, 2H), 1.87 – 1.53 (m, 8H), 1.53 – 1.36 (m, 3H), 1.32 – 1.15 (m, 2H).

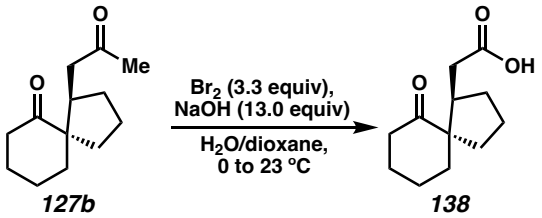
^{13}C NMR (100 MHz, $CDCl_3$): δ 201.4, 174.0, 127.1, 49.4, 47.7, 38.2, 34.9, 30.7, 30.7, 26.6, 26.3, 26.2, 25.5, 20.5.

Note: A grease and water signal are observed in the ^{1}H and ^{13}C spectra.

IR (Neat Film, NaCl): 2929, 2870, 1665, 1600, 1443, 1368, 1283, 1254 cm^{-1}.

HRMS (FI+): *m/z* calc'd for $C_{13}H_{18}O$ $[M]^{+\cdot}$: 204.15087, found 204.15113.

Optical Rotation: $[\alpha]_D^{23}$ +41.7 (c = 0.51, $CHCl_3$).



127b ***138***

2-((1*R*,5*S*)-6-oxospiro[4.5]decan-1-yl)acetic acid (138)

To a dried 2-dram vial was added a solution of diketone **127b** (20 mg, 0.096 mmol, 1.0 equiv) in 1,4-dioxane (0.1 M, 1.0 mL) and water (0.5 M, 0.2 mL) before being cooled to 0 °C. A solution of NaOBr in water was then prepared: NaOH (50 mg, 1.25 mmol, 13.0 equiv) was dissolved in water (2.6 M, 0.48 mL) and cooled to 0 °C. Bromine (16.5 μL, 0.32 mmol, 3.3 equiv) was then added dropwise at 0 °C. The NaOBr solution was then added dropwise to the solution of **127b** at 0 °C. The reaction was allowed to gradually

warm to 23 °C. Upon complete consumption of starting material by TLC, the reaction was diluted with 2 mL of water and then quenched by slow addition of concentrated HCl (until pH was 1.0). The mixture was then extracted with EtOAc (3x), rinsed with brine, dried with Na_2SO_4, filtered, and concentrated under reduced pressure. Purification of the crude mixture via preparative TLC purification (79% Et_2O, 20% hexanes, 1% AcOH) afforded the title compound as a white solid (6.9 mg, 0.033 mmol, 34% yield).

^{1}H NMR (400 MHz, $CDCl_3$): δ 2.95 – 2.82 (m, 1H), 2.50 – 2.35 (m, 3H), 2.11 (dd, *J* = 15.0, 10.4 Hz, 1H), 2.04 – 1.92 (m, 2H), 1.92 – 1.80 (m, 1H), 1.80 – 1.48 (m, 8H), 1.39 – 1.26 (m, 1H).

^{13}C NMR (100 MHz, $CDCl_3$): δ 213.9, 178.6, 58.3, 40.1, 39.3, 35.1, 35.0, 31.7, 29.9, 27.1, 21.8, 21.8.

IR (Neat Film, NaCl): 3021, 2941, 2865, 1705, 1444, 1420, 1281, 1235, 1164, 1129 cm^{-1}.

HRMS (FD+): *m/z* calc'd for $C_{12}H_{18}O_3$ $[M]^{+\cdot}$: 210.12505, found 210.12518.

Optical Rotation: $[\alpha]_D^{23}$ +7.7 (c = 0.58, $CHCl_3$).

3.4.3 COMPUTATIONAL DETAILS

General Notes – Quantum Mechanics Calculations:

All quantum mechanics calculations were carried out with the ORCA program.[14] Geometry optimizations, harmonic frequency calculations, and single-point energy evaluations were carried out with density functional theory (DFT). The PBE0 hybrid functional[15] paired with Becke–Johnson damped D4 dispersion corrections[16], henceforth

referred to as PBE0-D4, was used in this study. For geometry optimization and harmonic frequency calculations, Pd is described by the def2-TZVP all electron basis set[17] and the ECP28MWB small-core (18 explicit valence electrons) quasi-relativistic pseudopotential,[18] while C, H, N, and P are assigned the def2-SVP basis. Diffuse functions are added to oxygen ma-def2-SVP. Herein, we refer to this composite basis set as BS1. The combination of functional and basis set was chosen as it has been shown to be reliable in initial benchmarking studies, and has subsequently been employed to study various Pd-catalyzed reactions reported by our group and has remained robust, providing results in good agreement with experimental observations.[19] Geometry optimization and harmonic frequency calculations were carried out with the CPCM implicit solvation model for toluene (PhMe, $\varepsilon = 2.4$). For all calculations employing CPCM, surface charges are described by the improved Gaussian charge scheme of Neese and coworkers with a scaled Van der Waals cavity ($\alpha = 1.2$).[20] All Hessians were computed analytically. Stationary points are characterized by the correct number of imaginary vibrational modes (zero for minima and one for saddle points). Intrinsic reaction coordinate (IRC) analysis confirms the nature of transition states.[21] Cartesian coordinates of all optimized structures are included as ".xyz" files, available online in a compressed zip file format.

Electronic energies are further refined with single-point calculations employing the PBE0-D4 functional[22] and the def2-TZVPP basis set on all atoms (with the ECP28MWB pseudopotential for Pd) with additional diffuse functions on O (ma-def2-TZVPP). This mixed basis is henceforth referred to as BS2. Solvation was accounted for with CPCM as mentioned above (PhMe, $\varepsilon = 2.4$). Final Gibbs free energies were obtained by applying

thermodynamic corrections to the calculated electronic energies. Thermodynamic corrections from harmonic frequency calculations employ the quasi-ridged rotor harmonic oscillator approach to correct for the breakdown of the harmonic oscillator approximation at low vibrational frequencies.[23] The translational (S_{trans}) and rotational entropy (S_{rot}) contributions to the Gibbs free energy calculated for a complex in condensed phase are *ca.* 40–60% of the values obtained assuming an ideal gas.[24] As suggested in the literature, S_{trans} and S_{rot} obtained by ideal gas treatment are scaled by a factor of 0.5 to obtain the final condensed phase values.[25] Hence, the final Gibbs free energy at 333.15 K is calculated as:

$$G^*_{solv} = E^{BS2}_{el,solv} + ZPE + E_{trans} + E_{rot} + E_{vib} + k_bT$$
$$- T\left(S_{el} + S_{vib} + \frac{1}{2}S_{trans} + \frac{1}{2}S_{rot}\right)$$

The resolution of identity (RI) and Chain-of-Spheres (COS) approximations are employed for efficient evaluation of Coulomb and exchange integrals, respectively.[26] The def2/J auxiliary basis[27] is employed for all atoms except oxygen, for which a suitable auxiliary was obtained via the automatic generation algorithm in the ORCA program (keyword: *AutoAux*).[28] Very fine grid settings are employed in all calculations (optimization/frequency calculations: DefGrid2, single point calculations: DefGrid3).

Conformer searching was carried out for each stationary point individually using the meta-dynamics-based CREST program (using GNF-FF) from the Grimme group.[29] Duplicate conformers were removed, low energy conformers were subsequently optimized, and energies were evaluated at the cheaper PBE0-D4/def2-TZVPP (Pd), ma-def2-TZVPP (O), def2-TZVPP/CPCM(PhMe)//PBE-D4/def2-TZVP (Pd), ma-def2-SV(P) (O), def2-SV(P) level of theory. The final low energy conformers were further optimized at the level

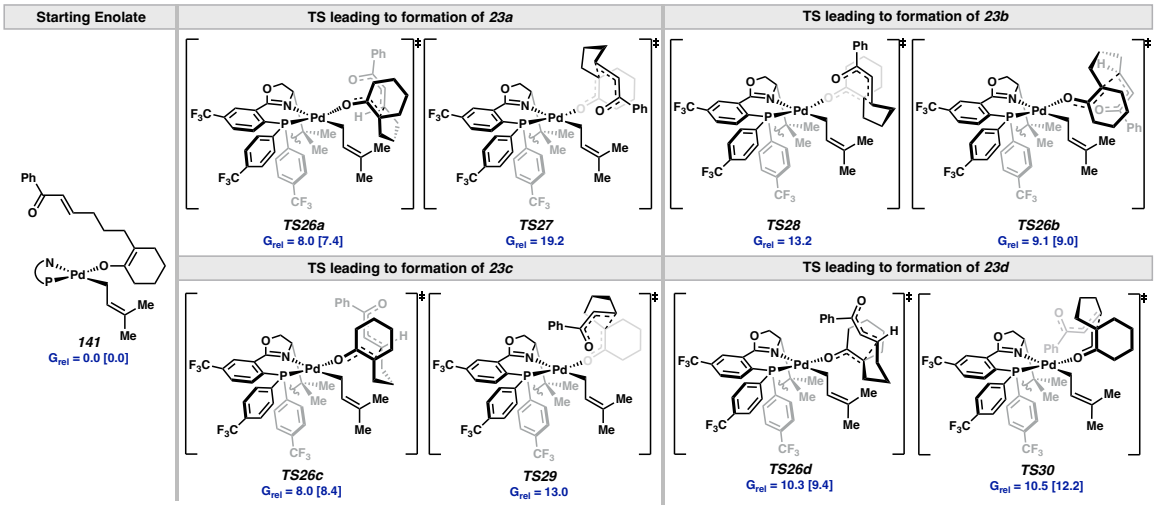
of theory mentioned prior, and the free energies and the optimized structures of the lowest-energy conformers are reported. It is assumed that interconversion of conformers of a single stationary point is low barrier compared to bond formation and breakage processes and is inconsequential to the evaluation of reaction pathways.

Comparison of Michael Addition Transition State Barriers:

Explicit conformer searching for rotation about the Pd–O–C–C(enolate) dihedral was performed for the selectivity-determining Michael addition transition states (Figure 3.6.). A strong preference for placement of the enolate electrophile tether *syn* to the ligand *t*-Bu group is observed for transition states to form *S* stereocenters at the spirocyclic quaternary carbon (Figure 3.6. **TS26a** and **TS26c**). This arrangement not only avoids undesired steric interactions of the rather bulky cyclohexyl group and the ligand *t*-Bu group but also places the *Re* face in the more sterically accessible orientation, external of the Pd complex.

In contrast, to form the *R* spirocyclic stereocenters in products **142b** and **142d**, either internal electrophile approach to the sterically hindered *Si* face of the enolate or positioning the bulky cyclohexyl group *syn* to the ligand *t*-Bu substituent is required. These destabilizing steric interactions contribute to the increase in energy barriers of **TS26b**, **TS26d**, **TS28**, and **TS30**. Between **TS26b** and **TS28**, steric clash resulting from internal electrophile approach outweighs preference for placement of electrophile tether *syn* to the ligand *t*-Bu group, leading to **TS26b** being the lower energy conformer. On the other hand, these two steric interactions cause energy increase of similar magnitudes in both **TS26d** and **TS30**.

Figure 3.6. *Relative free energies for transition states explored for the selectivity-determining Michael addition process. Gibbs free energies in kcal/mol computed at the PBE0-D4/BS2/CPCM(PhMe)//PBE-D4/def2-TZVP (Pd), ma-def2-SV(P) (O), def2-SV(P) level of theory, and in brackets are energies calculated at the PBE0-D4/BS2/CPCM(PhMe)//PBE0-D4/BS1/CPCM(PhMe) level of theory at 313.15 K.*



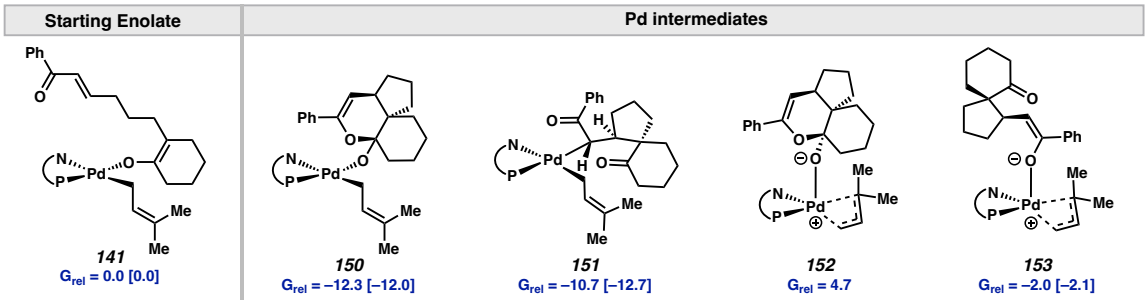
The major stereoisomer predicted based on these calculations is consistent with the major stereoisomer observed in all compounds which were structurally elucidated via x-ray crystallography (**127a**, **127b**, **131a**, **135**). Although additional computational and experimental evidence would be required to explain other observations regarding distinct substrate classes, we hypothesize that more general insights can potentially be taken from this stereochemical model. For instance, N-benzoyl lactam **127g** is modestly enantioselective but has good diastereoselectivity. Looking at **TS26a**, we imagine that the N-benzoyl moiety might have a destabilizing steric interaction with our ligand, potentially raising the energy of that transition state and thus decreasing the energy gap with the transition state leading to formation of the enantiomeric product. Tetralone **127h** has good

diastereoselectivity but poor enantioselectivity for both diastereomers. Electronically and sterically, tetralones are a unique substrate class and it is speculated that this fused aryl ring could influence the energies of many of the transition structures investigated. In addition, phenyl ester **127i** is formed in poor diastereoselectivity with decent levels of enantioselectivity, which is potentially due to altered geometrical elements (i.e. enolate conformation) and steric interactions with the ligand.

Computed Energies for Intermediates Post Michael Addition:

We propose that following formation of intermediate **142a** from Michael addition, isomerization to lower-energy Pd intermediates can occur. In addition to intermediates **143** and **143**, various Pd intermediates were explored and are shown in Figure 3.7.

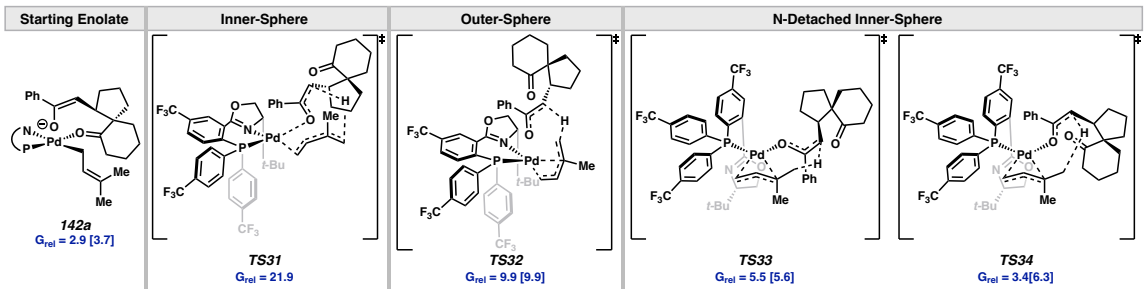
Figure 3.7. *Relative free energies for Pd intermediates explored. Gibbs free energies in kcal/mol computed at the PBE0-D4/BS2/CPCM(PhMe)//PBE-D4/def2-TZVP (Pd), ma-def2-SV(P) (O), def2-SV(P) level of theory, and in brackets are energies calculated at the PBE0-D4/BS2/CPCM(PhMe)//PBE0-D4/BS1/CPCM(PhMe) level of theory at 313.15 K.*



Mechansim of Proton Transfer:

We hypothesized that in analogy to previously investigated systems,[30] catalyst turnover can be achieved through the proton transfer from the prenyl group to a Pd enolate and the concomitant reduction of Pd. We therefore sampled the inner-sphere, outer-sphere, and N-detached inner-sphere proton transfer transition states (Figure 3.8.) analogous to the lowest energy pathways of each type of mechanism observed in previously investigated systems.[30] Proton transfer to both *Si* and *Re* face of the enolates were sampled for the N-detached inner-sphere pathway.

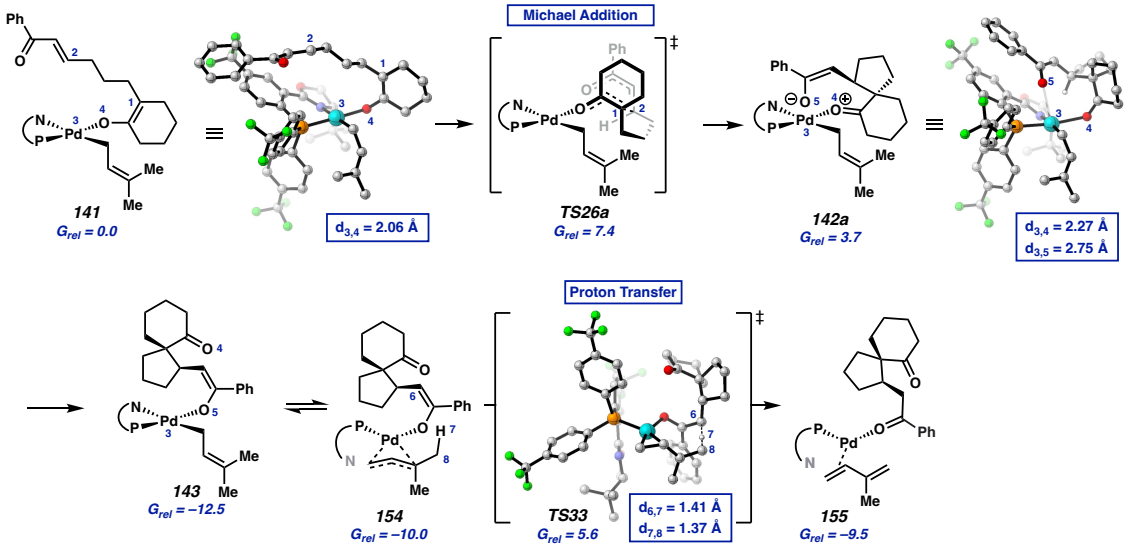
Figure 3.8. *Relative free energies for proton transfer pathways studied. Gibbs free energies in kcal/mol computed at the PBE0-D4/BS2/CPCM(PhMe)//PBE-D4/def2-TZVP (Pd), ma-def2-SV(P) (O), def2-SV(P) level of theory, and energies calculated at the PBE0-D4/BS2/CPCM(PhMe)//PBE0-D4/BS1/CPCM(PhMe) level of theory at 313.15 K are in brackets. The lowest-energy conformer for* ***TS34*** *at the PBE0-D4/BS2/CPCM(PhMe)//PBE-D4/def2-TZVP (Pd), ma-def2-SV(P) (O), def2-SV(P) level of theory failed to converge in geometry optimization at the PBE0-D4/BS2/CPCM(PhMe)//PBE0-D4/BS1/CPCM(PhMe) level of theory (due to a small imaginary mode corresponding to CF_3 rotation that we were unable to eliminate), and therefore the* ***TS34*** *energy shown in brackets is of a different conformer.*



Computational Investigation of Reversibility of Michael Addition:

We propose that simultaneous control of vicinal stereocenters can occur either via an irreversible Michael addition or a reversible C–C bond formation coupled to a subsequent irreversible proton transfer. We began by investigating the energetics of the Michael addition (Figure S4). Computationally, we found that the Michael addition of Pd enolate **141** to form spirocycle **142a** proceeds with a $\Delta G^{\ddagger}$ of 7.4 kcal/mol. Further isomerization of Pd-bound ketone **142a** to Pd enolate **143** releases an additional 16.2 kcal/mol of energy (Figure S4), leading to an overall exothermic process with a ΔG of –12.5 kcal/mol from intermediate **141**. The reverse process displays a 19.9 kcal/mol energy barrier, which is likely still achievable at the reaction temperature. Hence, we proceeded

Figure 3.9. *Proposed reaction pathway for Michael addition and proton transfer and the computed relative energies of relevant intermediates and transition states. Gibbs free energies in kcal/mol computed at the PBE0-D4/BS2/CPCM(PhMe)//PBE0-D4/BS1/CPCM(PhMe) level of theory at 313.15 K.*



to study the subsequent proton transfer process. Upon surveying various reaction pathways (Figure 3.9.), an *N*-detached inner-sphere pathway was found to be the most energetically favorable, with $\Delta G^{\ddagger}$ of 5.6 kcal/mol and ΔG of –9.5 kcal/mol. Under the assumption that isomerization of Pd intermediates is facile relative to the proton transfer and Michael addition processes, these results are consistent with the Michael addition being irreversible and selectivity-determining.

3.4.4 2D NMR ANALYSIS OF SELECT COMPOUNDS

Figure 3.10. *^{1}H–^{1}H COSY NMR spectrum of* ***132*** *(400 MHz, $CDCl_3$).*

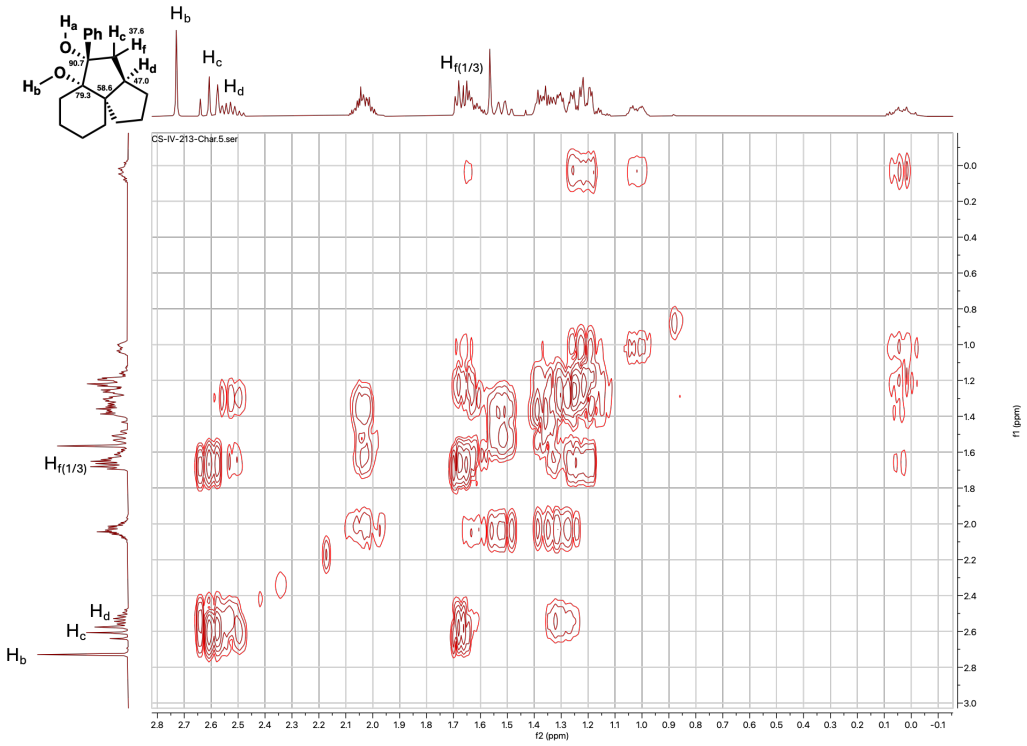


Figure 3.11. *$^{1}H–^{13}C$ HSQC NMR spectrum of* ***132*** *(400 MHz, $CDCl_3$)*

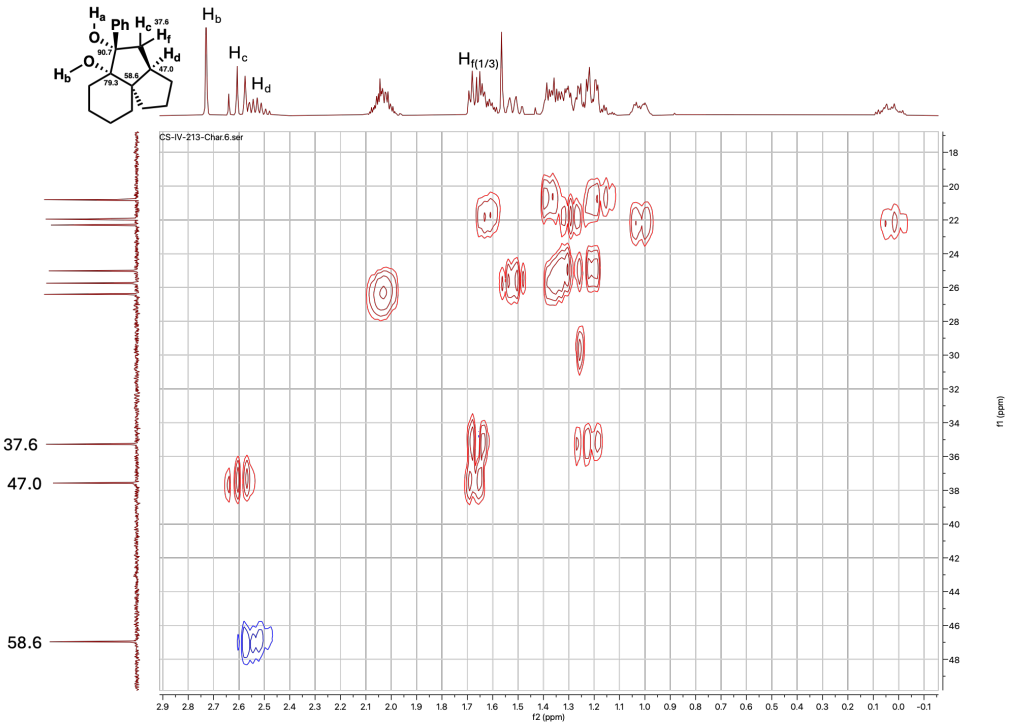


Figure 3.12. *$^{1}H–^{13}C$ HMBC NMR spectrum of* ***132*** *(400 MHz, $CDCl_3$)*

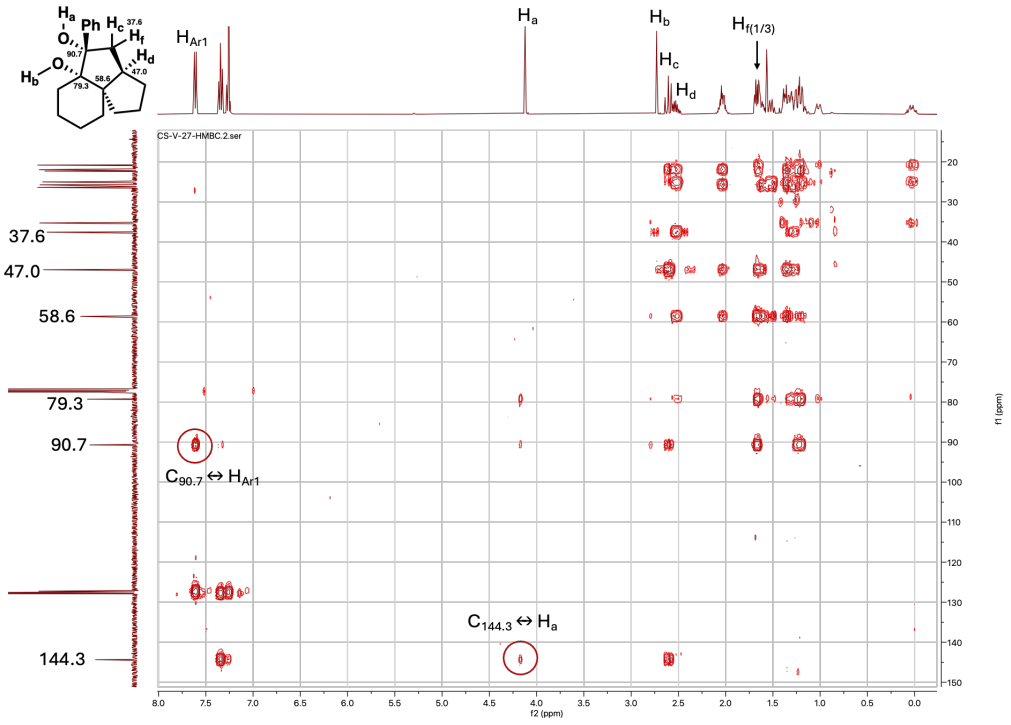


Figure 3.13. *$^{1}H–^{1}H$ COSY NMR spectrum of* ***136*** *(400 MHz, $CDCl_3$)*

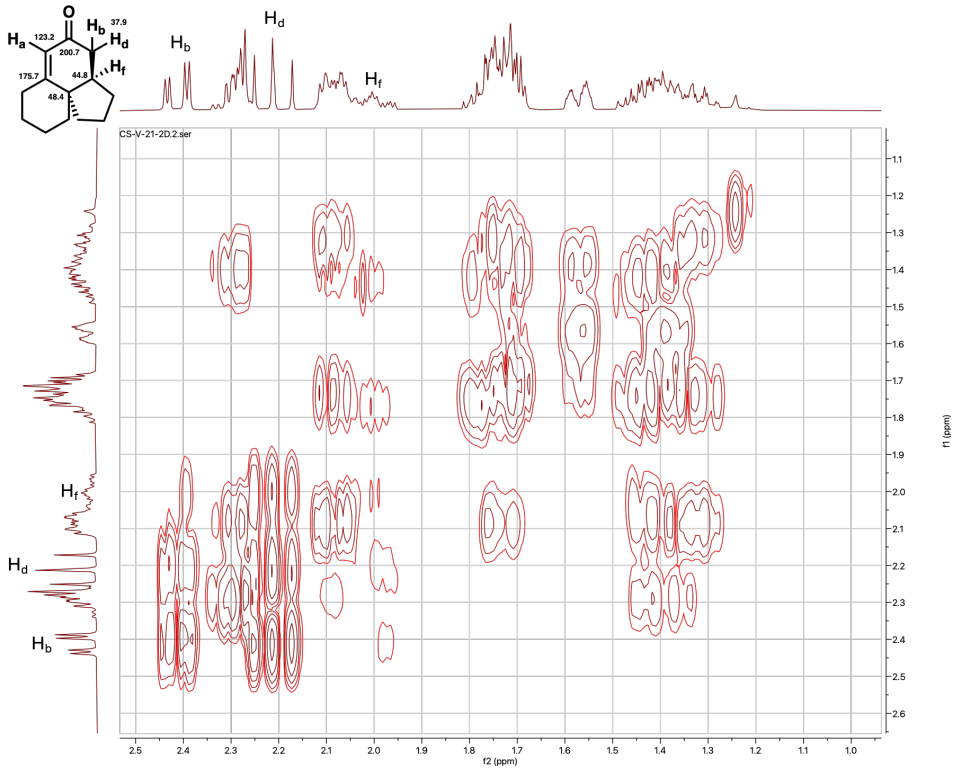


Figure 3.14. *$^{1}H–^{13}C$ HSQC NMR spectrum of* ***136*** *(400 MHz, $CDCl_3$)*

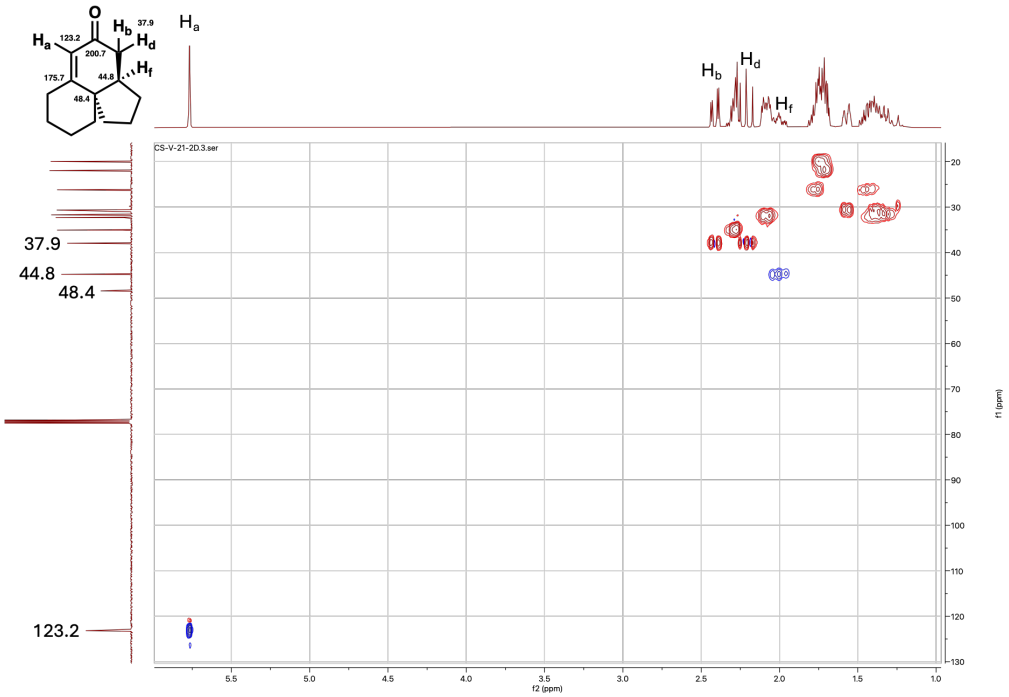
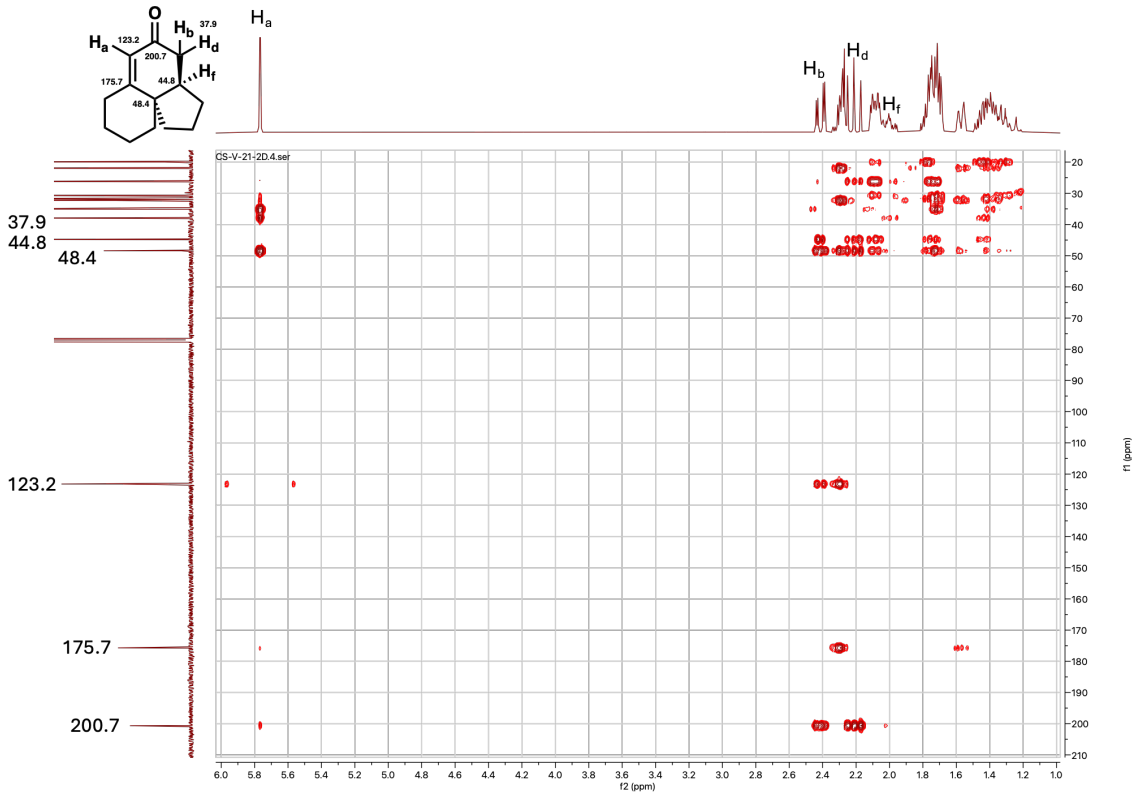


Figure 3.15. *^{1}H–^{13}C HMBC NMR spectrum of* ***136*** *(400 MHz, $CDCl_3$)*



3.5 REFERENCES AND NOTES

(1) (a) Krout, M. R.; Mohr, J. T.; Stoltz, B. M. Preparation of (*S*)-*tert*-ButylPHOX (Oxazole, 4-(1,1-dimethylethyl)-2-[2-(diphenylphosphino)phenyl]-4,5- dihydro-(4*S*)-). *Org. Synth.* **2009**, *86*, 181–193. (b) McDougal, N. T.; Streuff, J.; Mukherjee, H.; Virgil, S. C.; Stoltz, B. M. Rapid synthesis of an electron-deficient *t*-BuPHOX ligand: cross-coupling of aryl bromides with secondary phosphine oxides. *Tetrahedron Lett*. **2010**, *51*, 5550–5554.

(2) Wagen, C. C.; McMinn, S. E.; Kwan, E. E.; Jacobsen, E. N. Screening for Generality in Asymmetric Catalysis. *Nature*, **2022**, *610*, 680–686.

(3) Sheldrick, G. M. *Acta Cryst.* **1990**, A46, 467-473.

(4) Sheldrick, G. M. *Acta Cryst.* **2015**, C71, 3-8.

(5) Müller, P. *Crystallography Reviews* **2009**, *15*, 57-83.

(6) Milburn, R. R; McRae, K.; Chan, Johann, Tedrow, J.; Larsen, R.; Faul, M. A practical preparation of aryl β-ketophosphonates. *Tetrahedron Lett.* **2009**, *50*, 870–872.

(7) Sano, S.; Okubo, Y.; Hanada, A.; Nakao, M.; Kitaike, S.; Nagao, Y.; Nakegawa, H. Reinvestigation of the Synthesis of Isoliquiritigenin: Application of Horner–Wadsworth–Emmons Reaction and Claisen–Schmidt Condensation. *Chem. Pharm. Bull.* **2011**, *59*, 885–888.

(8) Murai, M.; Nakamura, M.; Takai, K. Rhenium-Catalyzed Synthesis of 2H-1,2-Oxaphosphorin 2-Oxides via the Regio- and Stereoselective Addition Reaction of β-Keto Phosphonates with Alkynes. *Org. Lett.* **2014**, *16*, 5784–5787.

(9) Trost, B. M.; Xu, J. The O-Acylation of Ketone Enolates by Allyl 1H-Imidazole-1-carboxylate Mediated with Boron Trifluoride Etherates–A Convenient Procedure for the Synthesis of Substituted Allyl Enol Carbonates. *J. Org. Chem.* **2007**, *72*, 9372–9375.

(10) Inanaga, K.; Wollenburg, M.; Bachman, S.; Hafeman, N. J.; Stoltz, B. M. Catalytic Enantioselective Synthesis of Carbocyclic and Heterocyclic Spiranes via a Decarboxylative Aldol Cyclization. *Chem. Sci.* **2020**, *11*, 7390–7395.

(11) Behenna, D. C.; Liu, Y.; Yurino, T.; Kim, J.; White, D. E.; Virgil, S. C.; Stoltz, B. M. Enantioselective Construction of Quaternary N-heterocycles by Palladium-Catalysed Decarboxylative Allylic Alkylation of Lactams. *Nat. Chem.* **2012**, *4*, 130–133.

(12) Kawato, Y.; Takahashi, N.; Kumagai, N.; Shibasaki, M. Catalytic Asymmetric Conjugate Addition of α-Cyanoketones for the Construction of a Quaternary Stereogenic Center. *Org. Lett.* **2010**, *12*, 1484–1487.

(13) Behenna, D. C.; Mohr, J. T.; Sherden N. H.; Marinescu, S. C., Harned, A. M.; Tani, K.; Seto, M.; Ma, S.; Novák, Z.; Krout, M. R.; McFadden, R. M.; Roizen, J. L.; Enquist jr.; J. A.; White, D. E.; Levine, S. R.; Petrova, K. V.; Iwashita, A.; Virgil, S. C.; Stoltz, B. M. Enantioselective Decarboxylative Alkylation Reactions: Catalyst Development, Substrate Scope, and Mechanistic Studies. *Chem. Eur. J.* **2011**, *17*, 14199–14223.

(14) (a) Neese, F. Software Update: The ORCA Program System, Version 5.0. *Wiley Interdiscip. Rev.: Comput. Mol. Sci.* **2022,** *12*, No. e1606. (b) Neese, F. The ORCA Program System. *Wiley Interdiscip. Rev.: Comput. Mol. Sci.* **2012**, *2*, 73−78.

(15) Adamo, C.; Barone, V. Toward Reliable Density Functional Methods without Adjustable Parameters: The PBE0 Model. *J. Chem. Phys.* **1999**, *110*, 6158−6170.

(16) (a) Caldeweyher, E.; Ehlert, S.; Hansen, A.; Neugebauer, H.; Spicher, S.; Bannwarth, C.; Grimme, S. A Generally Applicable Atomic-Charge Dependent London Dispersion Correction. *J. Chem. Phys.* **2019**, *150* (15), 154122. (b) Caldeweyher, E.; Bannwarth, C.; Grimme, S. Extension of the D3 Dispersion Coefficient Model. *J. Chem. Phys.* **2017**, *147*, 034112.

(17) Weigend, F.; Ahlrichs, R. Balanced Basis Sets of Split Valence, Triple Zeta Valence and Quadruple Zeta Valence Quality for H to Rn: Design and Assessment of Accuracy. *Phys. Chem. Chem. Phys.* **2005**, *7*, 3297–3305.

(18) Peterson, K. A.; Figgen, D.; Goll, E.; Stoll, H.; Dolg, M. Systematically Convergent Basis Sets with Relativistic Pseudopotentials. II. Small-Core Pseudopotentials and Correlation Consistent Basis Sets for the Post- *d* Group 16–18 Elements. *The Journal of Chemical Physics* **2003**, *119*, 11113–11123.

(19) (A) Cusumano, A. Q.; Goddard, W. A. I.; Stoltz, B. M. The Transition Metal Catalyzed [π2s + π2s + s2s + s2s] Pericyclic Reaction: Woodward–Hoffmann Rules, Aromaticity, and Electron Flow. *J. Am. Chem. Soc.* **2020**, *142*, 19033–19039. (B) Cusumano, A. Q.; Stoltz, B. M.; Goddard, W. A. Reaction Mechanism, Origins of Enantioselectivity, and Reactivity Trends in Asymmetric Allylic Alkylation: A

Comprehensive Quantum Mechanics Investigation of a C(sp3)–C(sp3) Cross-Coupling. *J. Am. Chem. Soc.* **2020**, *142*, 13917–13933. (C) Flesch, K. N.; Cusumano, A. Q.; Chen, P.-J.; Strong, C. S.; Sardini, S. R.; Du, Y. E.; Bartberger, M. D.; Goddard, W. A.; Stoltz, B. M. Divergent Catalysis: Catalytic Asymmetric [4+2] Cycloaddition of Palladium Enolates. *J. Am. Chem. Soc.* **2023**, *145*, 11301–11310.

(20) Garcia-Ratés, M.; Neese, F. Effect of the Solute Cavity on the Solvation Energy and Its Derivatives within the Framework of the Gaussian Charge Scheme. *J. Comput. Chem.* **2020**, *41*, 922–939.

(21) Ishida, K.; Morokuma, K.; Komornicki, A. The Intrinsic Reaction Coordinate. An Ab Initio Calculation for HNC→HCN and H−+CH4→CH4+H−. *J. Chem. Phys.* **1977**, *66 (5)*, 2153−2156.

(22) Zhao, Y.; Truhlar, D. G. The M06 Suite of Density Functionals for Main Group Thermochemistry, Thermochemical Kinetics, Noncovalent Interactions, Excited States, and Transition Elements: Two New Functionals and Systematic Testing of Four M06-Class Functionals and 12 Other Functionals. *Theor Chem Account* **2008**, *120* (1), 215–241.

(23) Grimme, S. Supramolecular Binding Thermodynamics by Dispersion-Corrected Density Functional Theory. *Chem. Eur. J.* **2012**, *18*, 9955–9964.

(24) Izato, Y.; Matsugi, A.; Koshi, M.; Miyake, A. A Simple Heuristic Approach to Estimate the Thermochemistry of Condensed-Phase Molecules Based on the Polarizable Continuum Model. *Phys. Chem. Chem. Phys.* **2019**, *21*, 18920–18929.

(25) Finkelstein, A. V.; Janin, J. The Price of Lost Freedom: Entropy of Bimolecular Complex Formation. *Protein Engineering, Design and Selection* **1989**, *3*, 1–3.

(26) Neese, F.; Wennmohs, F.; Hansen, A.; Becker, U. Efficient, Approximate and Parallel Hartree-Fock and Hybrid DFT Calculations. A 'Chain-of-Spheres' Algorithm for the Hartree-Fock Exchange. *Chemical Physics* **2009**, *356*, 98–109.

(27) Weigend, F. Accurate Coulomb-Fitting Basis Sets for H to Rn. *Phys. Chem. Chem. Phys.* **2006**, *8*, 1057–1065.

(28) Stoychev, G. L.; Auer, A. A.; Neese, F. Automatic Generation of Auxiliary Basis Sets. *J. Chem. Theory Comput.* **2017**, *13*, 554–562.

(29) Grimme, S. Exploration of Chemical Compound, Conformer, and Reaction Space with Meta-Dynamics Simulations Based on Tight-Binding Quantum Chemical Calculations. *J. Chem. Theory Comput.* **2019**, *15*, 2847–2862.

(30) Flesch, K. N.; Cusumano, A. Q.; Chen, P.-J.; Strong, C. S.; Sardini, S. R.; Du, Y. E.; Bartberger, M. D.; Goddard, W. A.; Stoltz, B. M. Divergent Catalysis: Catalytic Asymmetric [4+2] Cycloaddition of Palladium Enolates. *J. Am. Chem. Soc.* **2023**, *145*, 11301–11310.

APPENDIX 2

Spectra Relevant to Chapter 3:

Enantioselective Michael Spirocyclization of Palladium Enolates

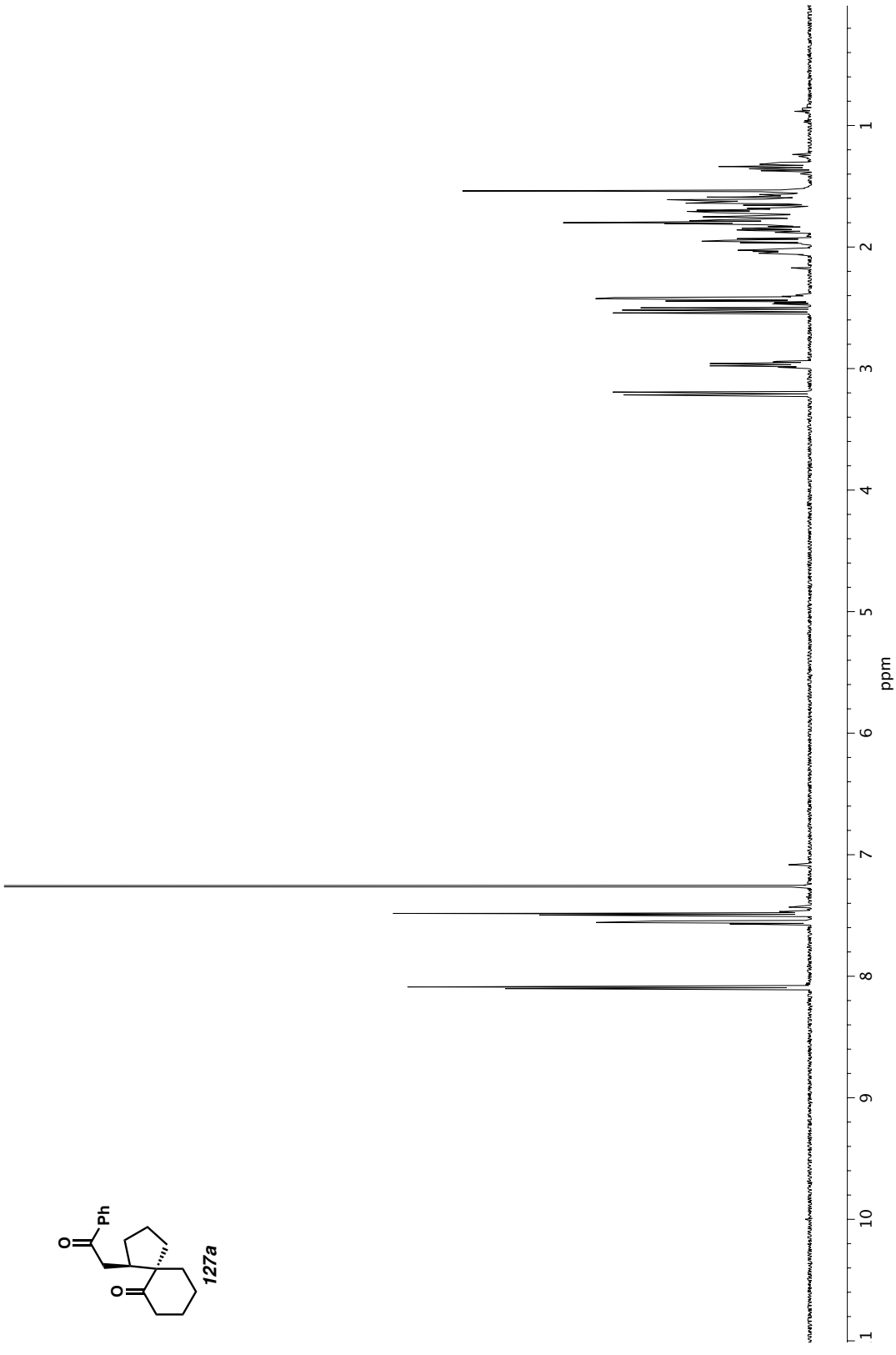


Figure A2.1. *^1H NMR (600 MHz, $CDCl_3$) of compound* ***127a****.*

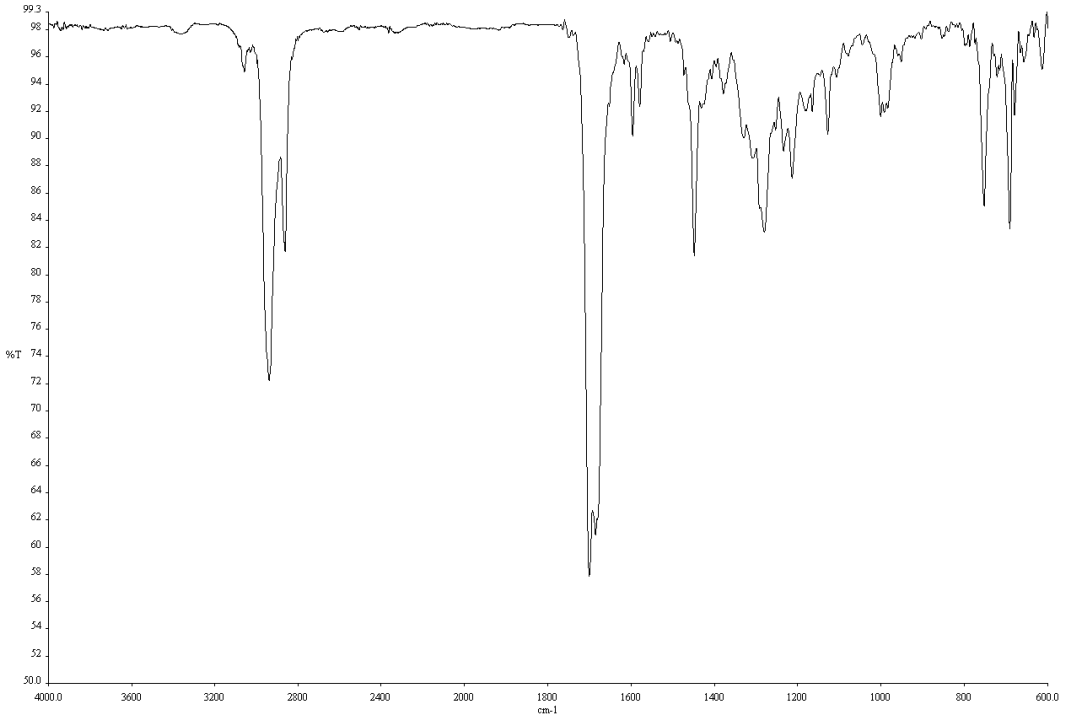


Figure A2.2. *Infrared spectrum (Thin Film, NaCl) of compound* ***127a****.*

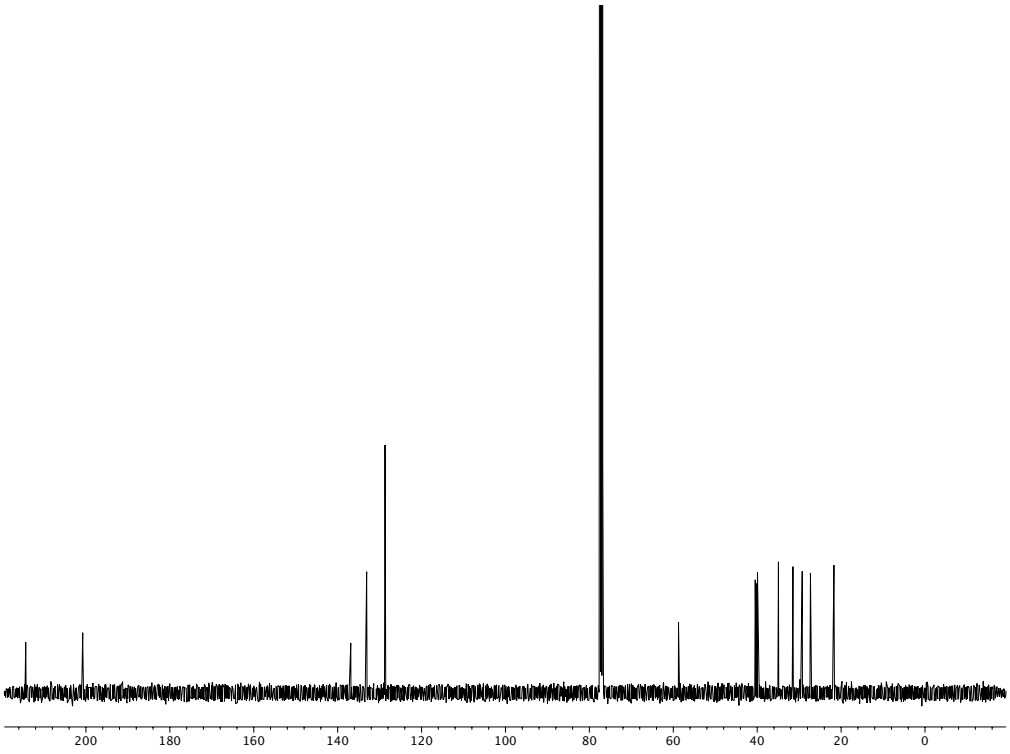


Figure A2.3. *^{13}C NMR (100 MHz, $CDCl_3$) of compound* ***127a****.*

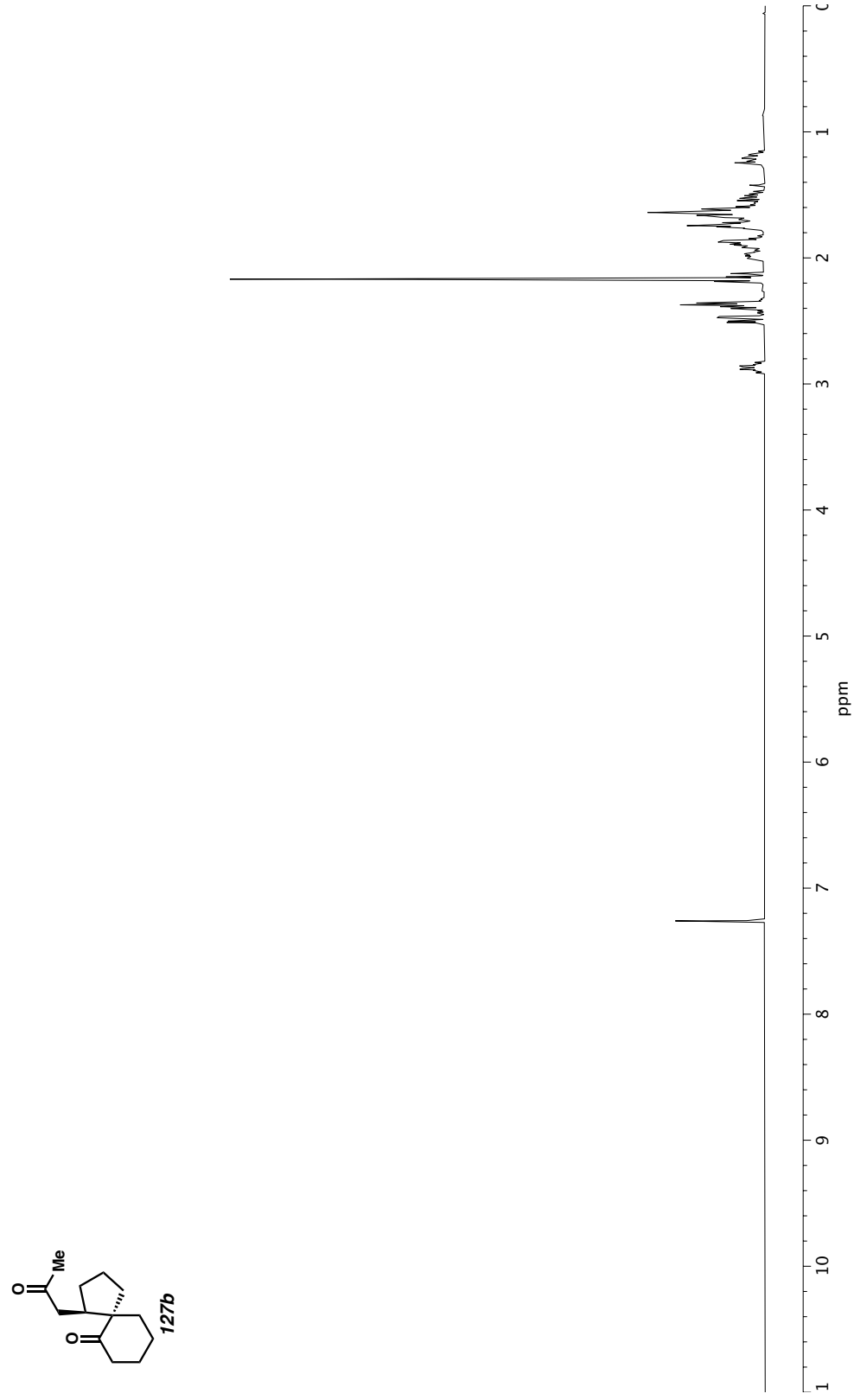


Figure A2.4. *^1H NMR (400 MHz, $CDCl_3$) of compound* ***127b****.*

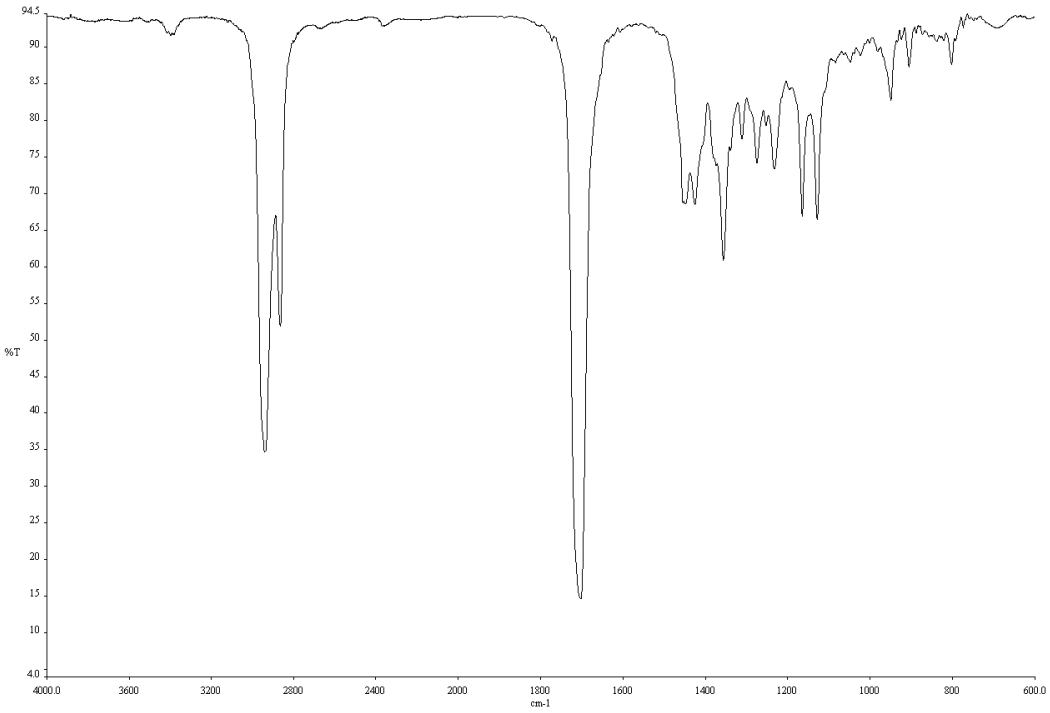


Figure A2.5. *Infrared spectrum (Thin Film, NaCl) of compound* ***127b****.*

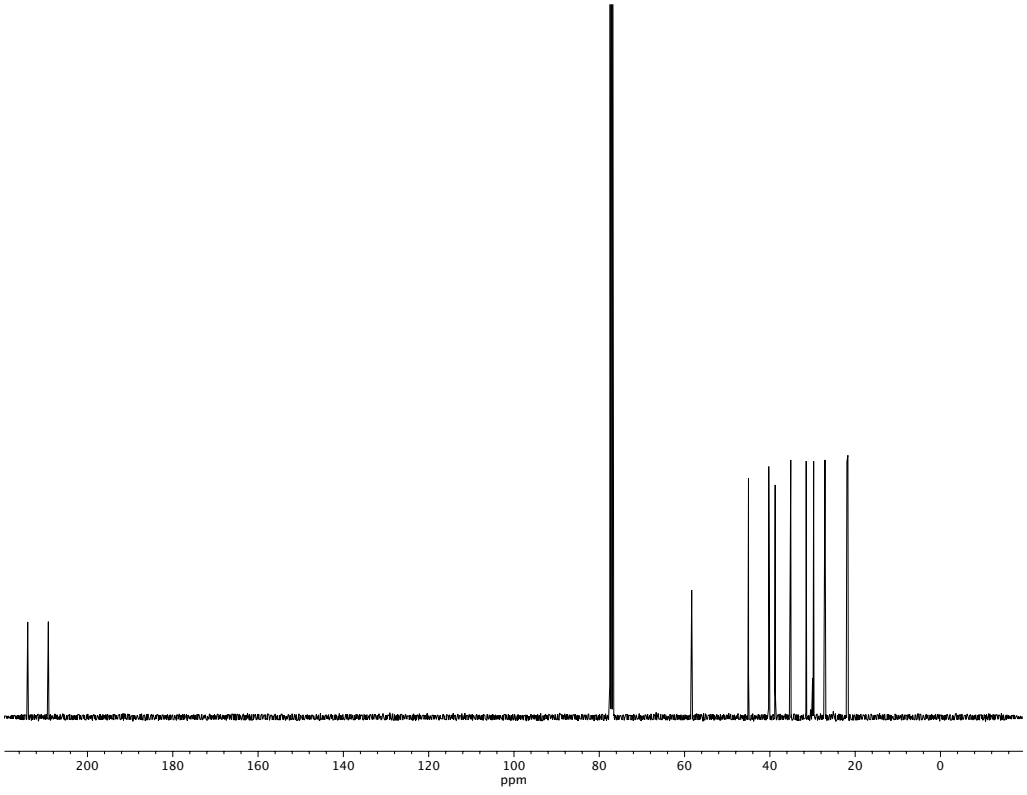


Figure A2.6. *^{13}C NMR (100 MHz, $CDCl_3$) of compound* ***127b****.*

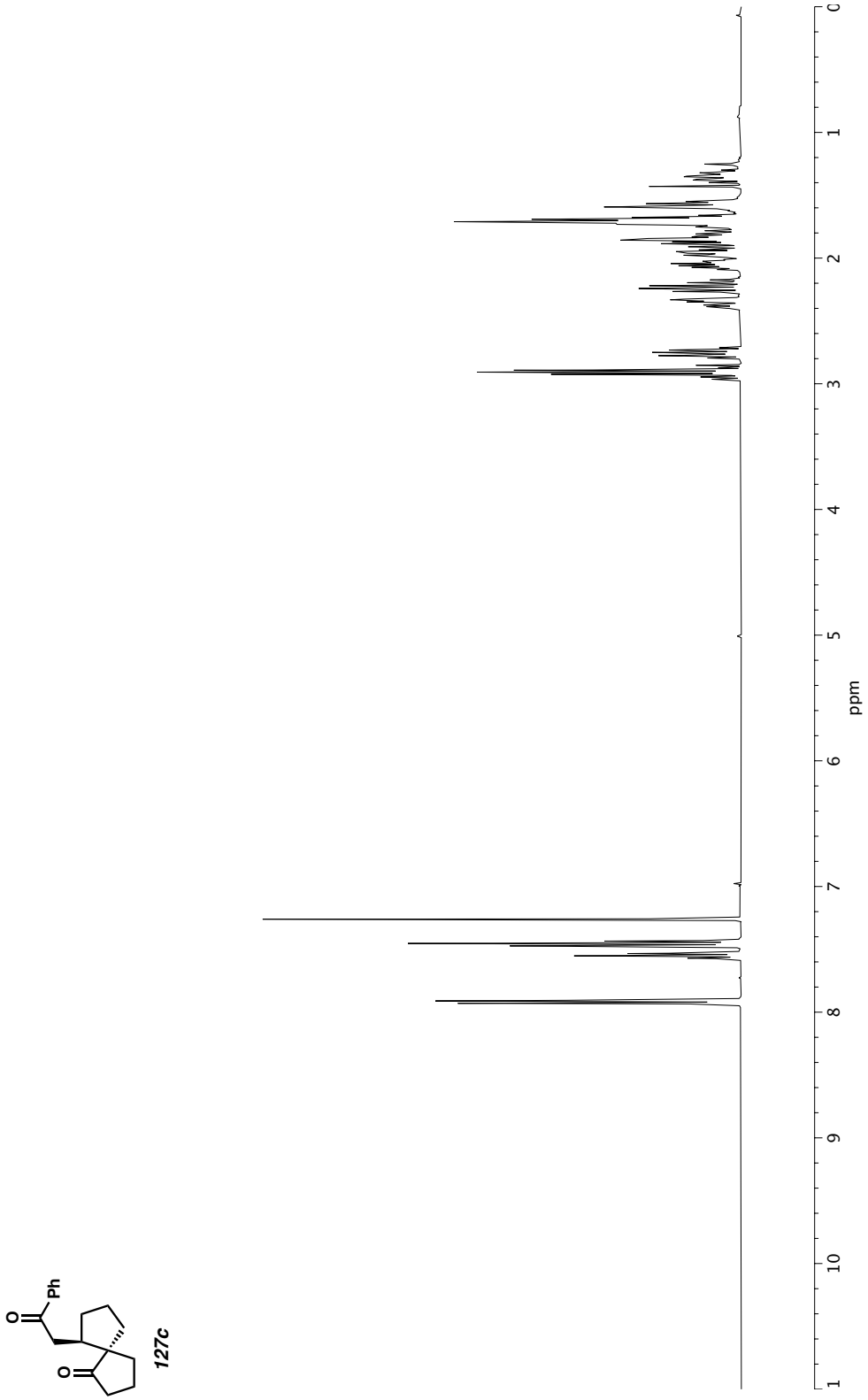


Figure A2.7. *^1H NMR (400 MHz, $CDCl_3$) of compound* ***127c****.*

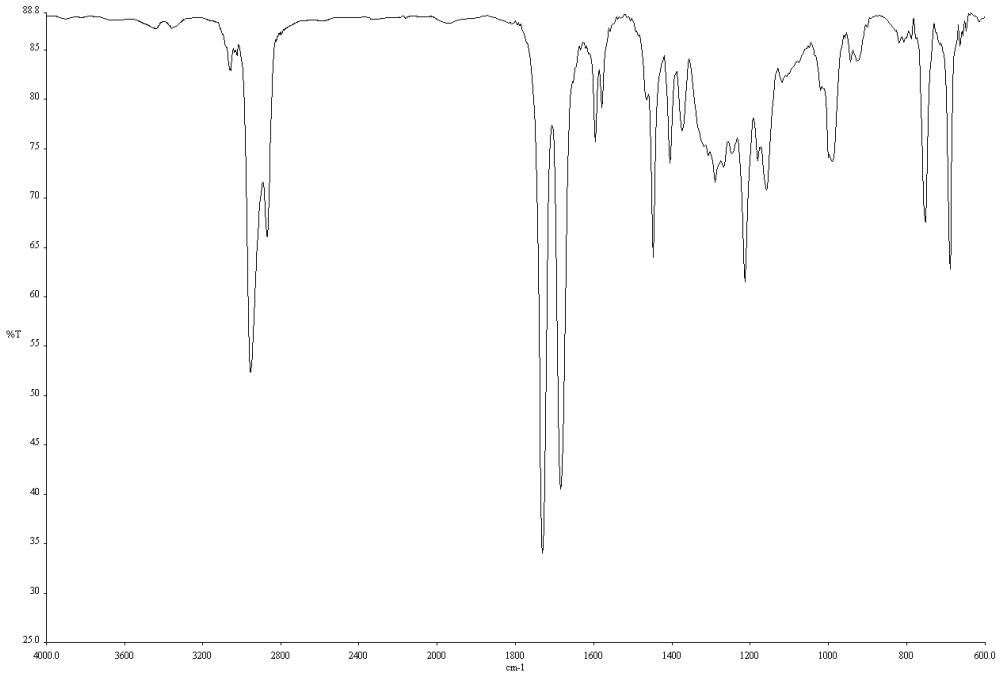


Figure A2.8. *Infrared spectrum (Thin Film, NaCl) of compound* ***127c****.*

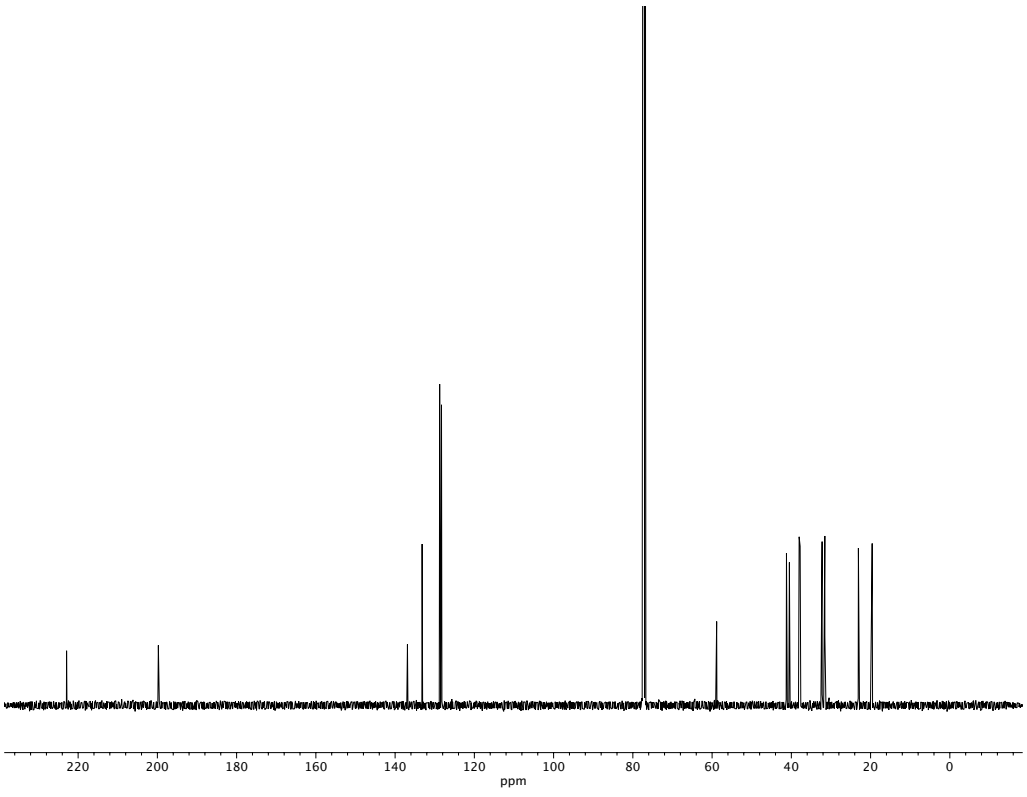


Figure A2.9. *^{13}C NMR (100 MHz, $CDCl_3$) of compound* ***127c****.*

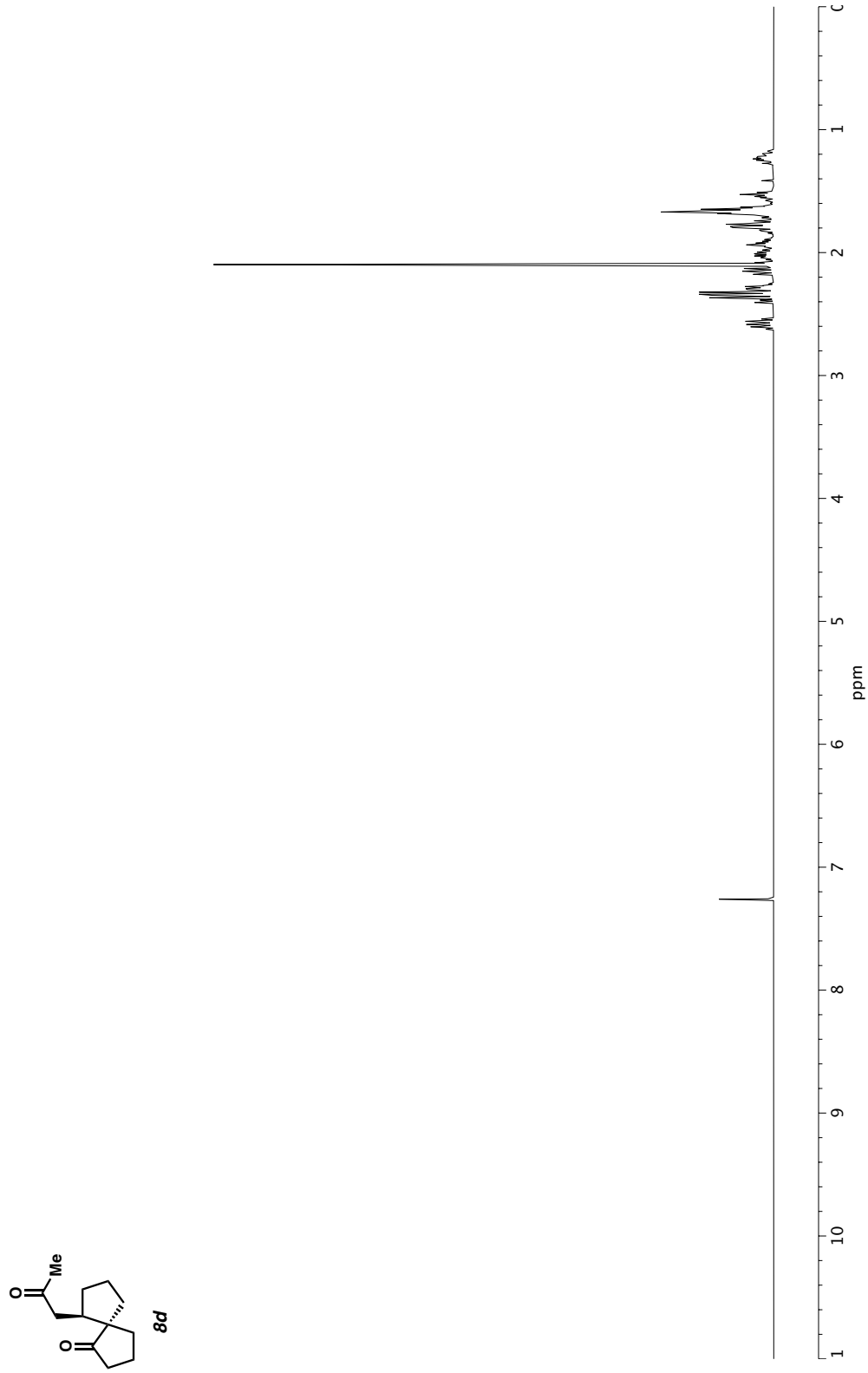


Figure A2.10. *^1H NMR (400 MHz, $CDCl_3$) of compound* ***127d****.*

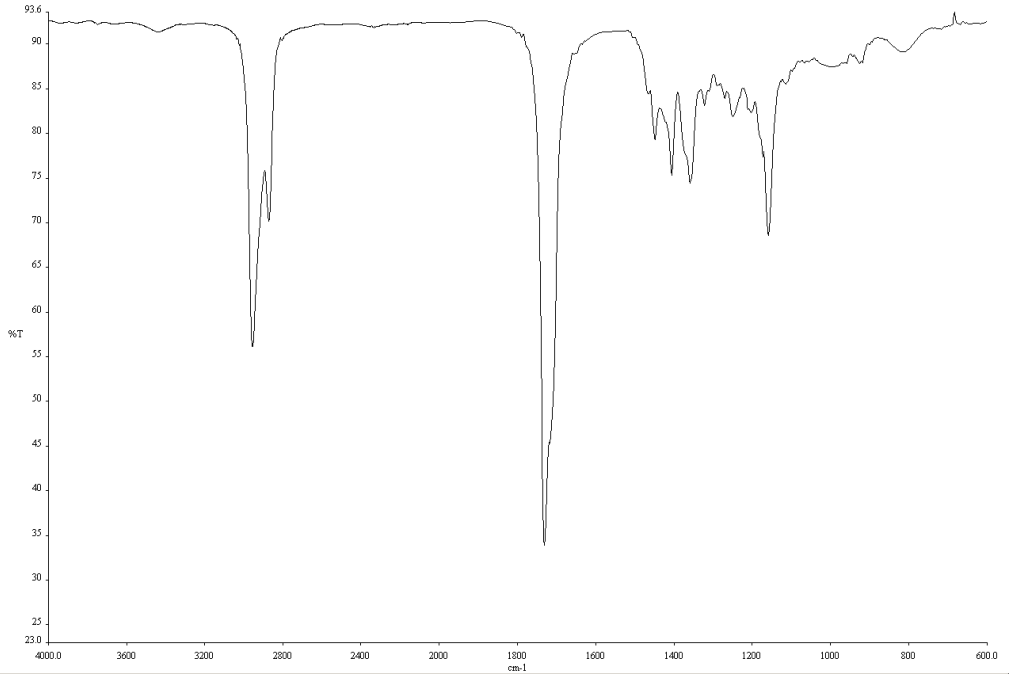


Figure A2.11. *Infrared spectrum (Thin Film, NaCl) of compound* ***127d****.*

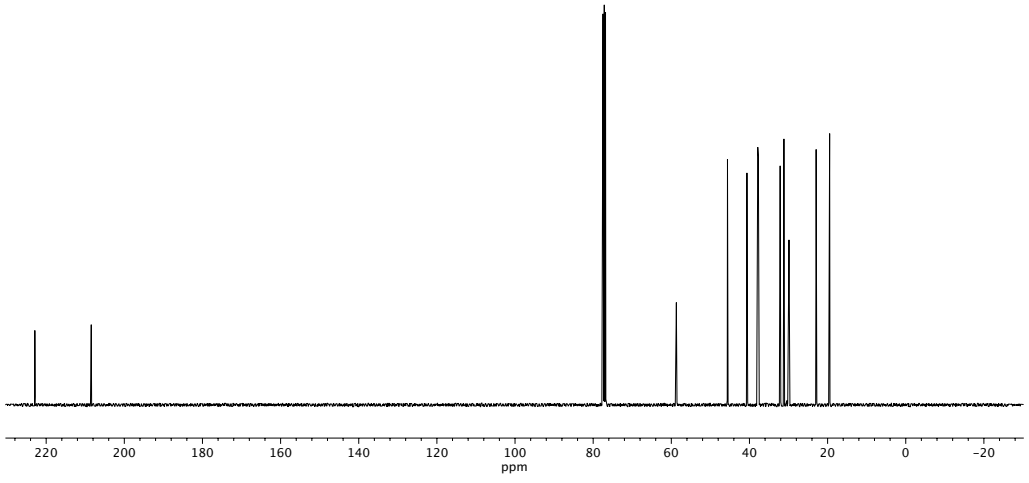


Figure A2.12. *^{13}C NMR (100 MHz, $CDCl_3$) of compound* ***127d****.*

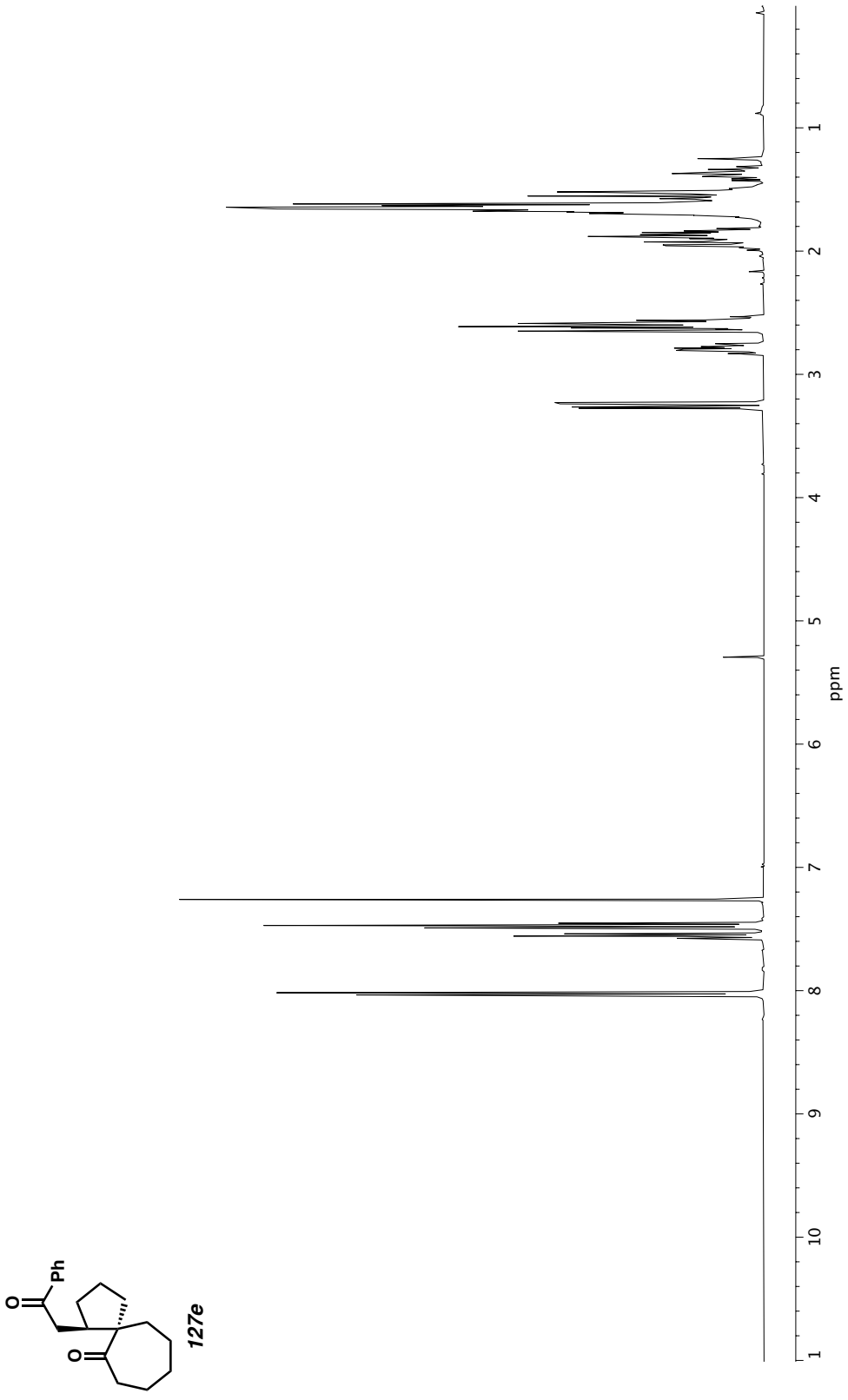


Figure A2.13. *^1H NMR (400 MHz, $CDCl_3$) of compound* ***127e****.*

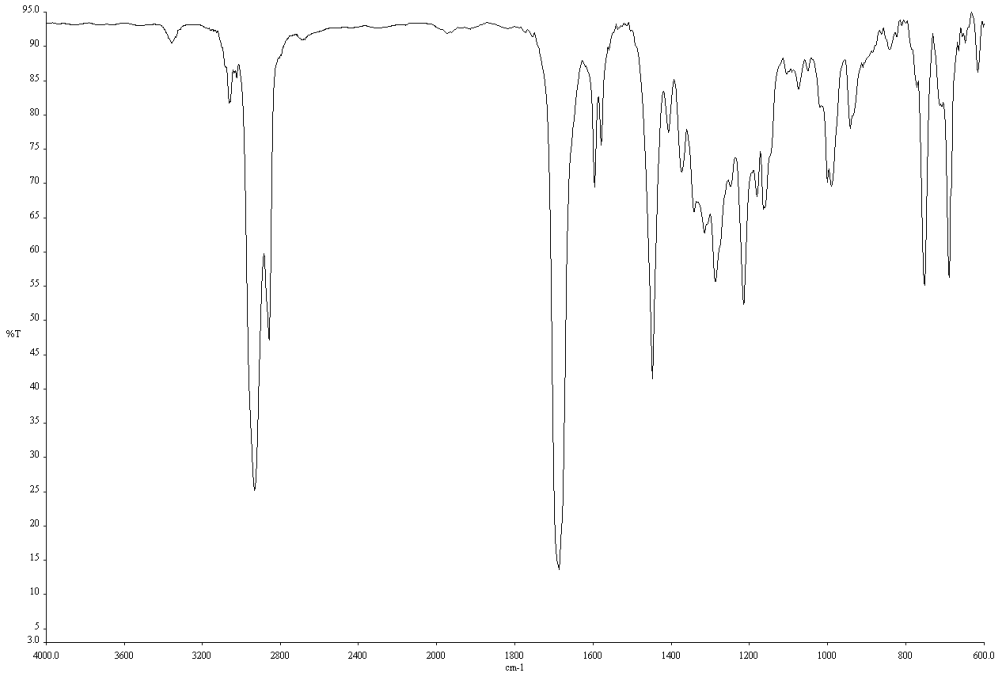


Figure A2.14. *Infrared spectrum (Thin Film, NaCl) of compound* ***127e****.*

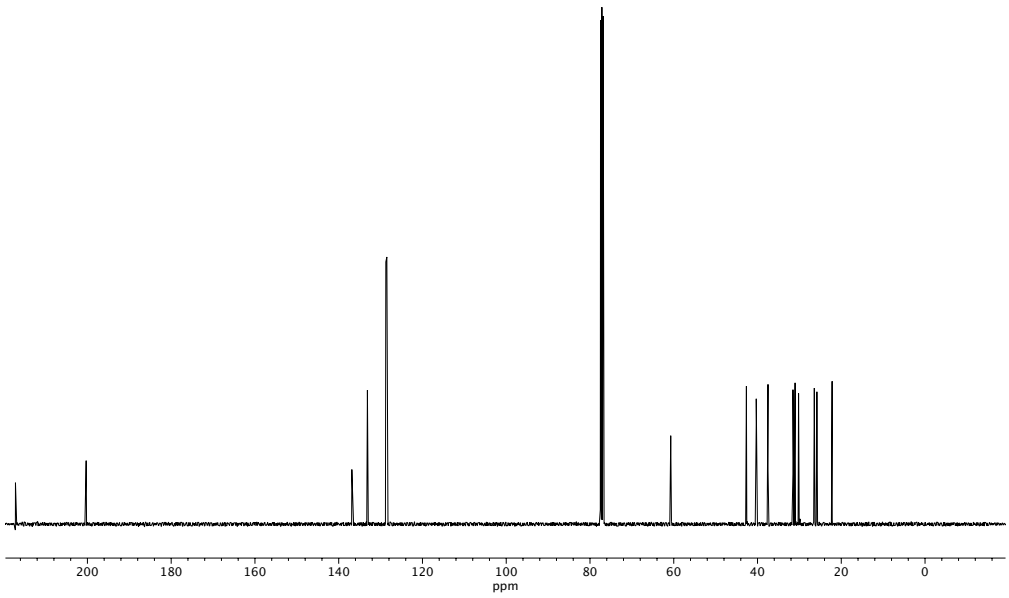


Figure A2.15. *^{13}C NMR (100 MHz, $CDCl_3$) of compound* ***127e****.*

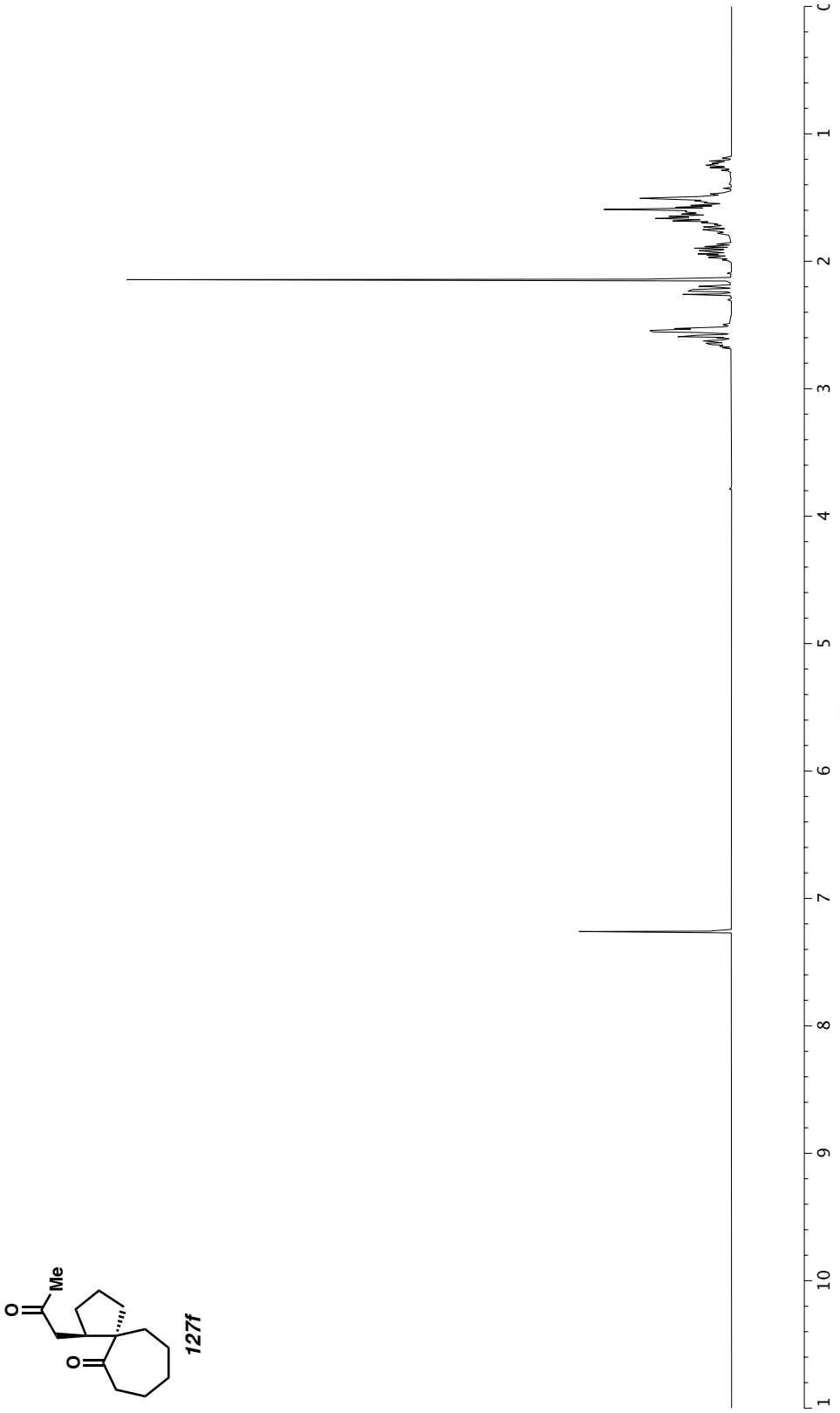


Figure A2.16. *^1H NMR (400 MHz, $CDCl_3$) of compound* ***127f****.*

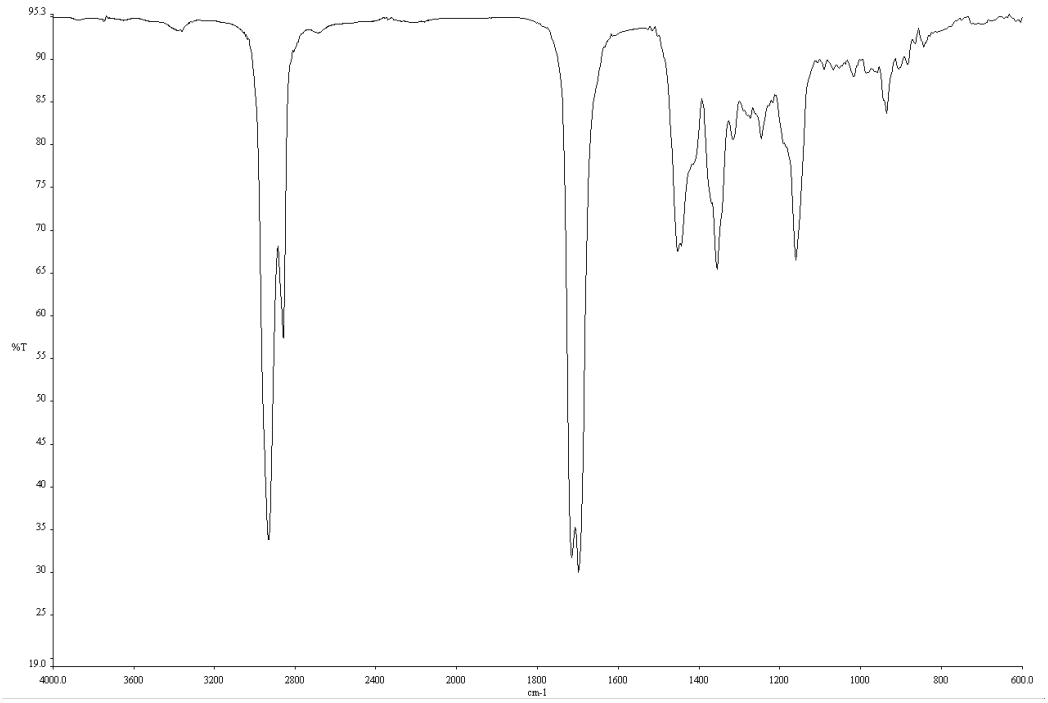


Figure A2.17. *Infrared spectrum (Thin Film, NaCl) of compound* ***127f****.*

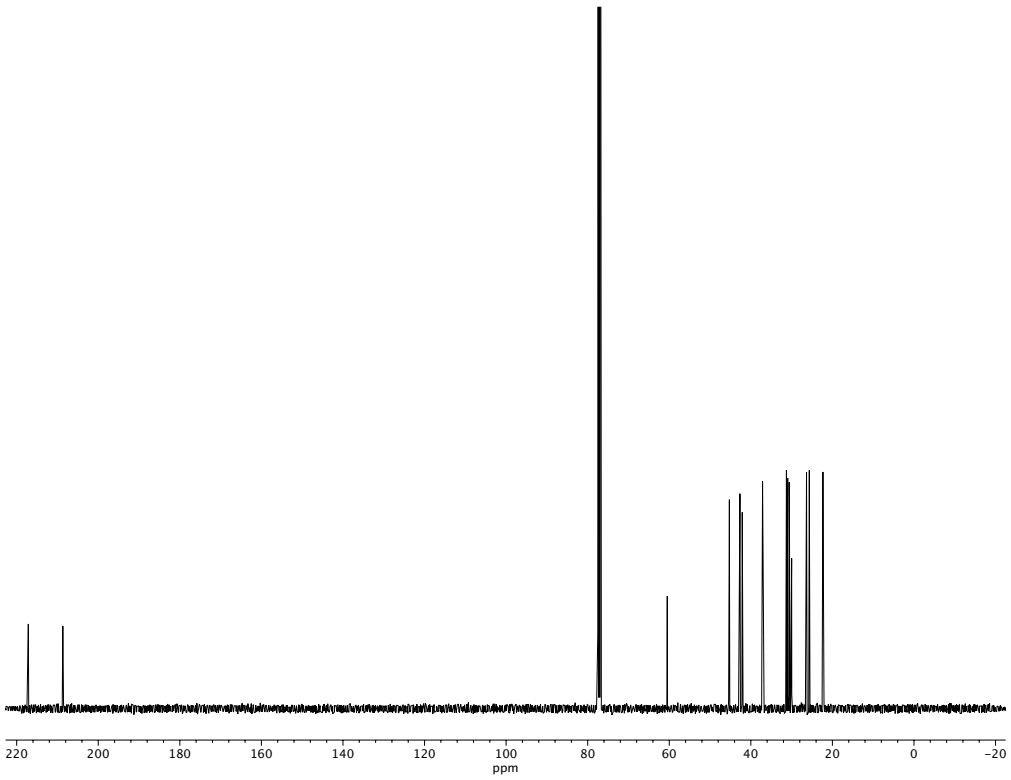


Figure A2.18. *^{13}C NMR (100 MHz, $CDCl_3$) of compound* ***127f****.*

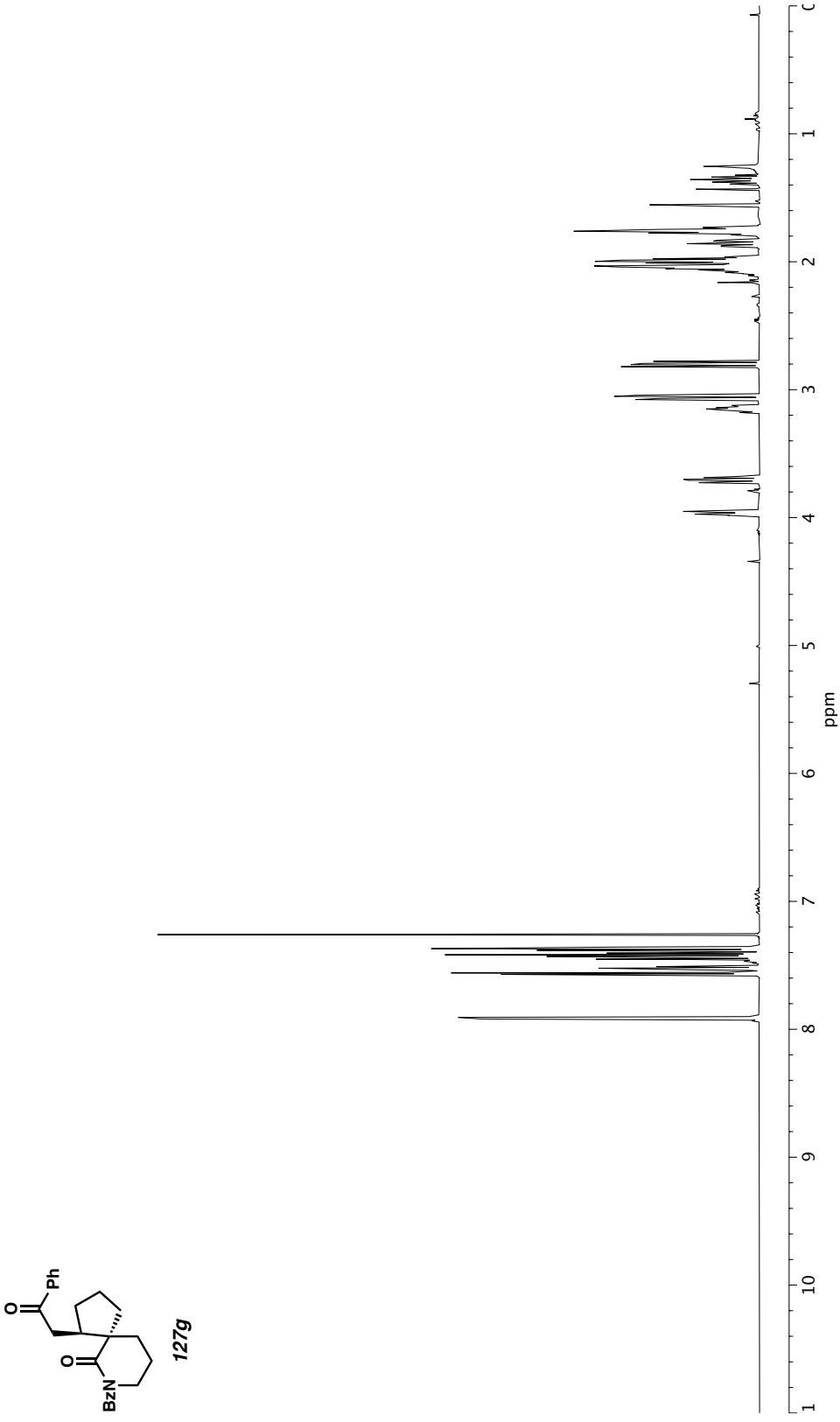


Figure A2.19. *^1H NMR (400 MHz, $CDCl_3$) of compound* ***127g****.*

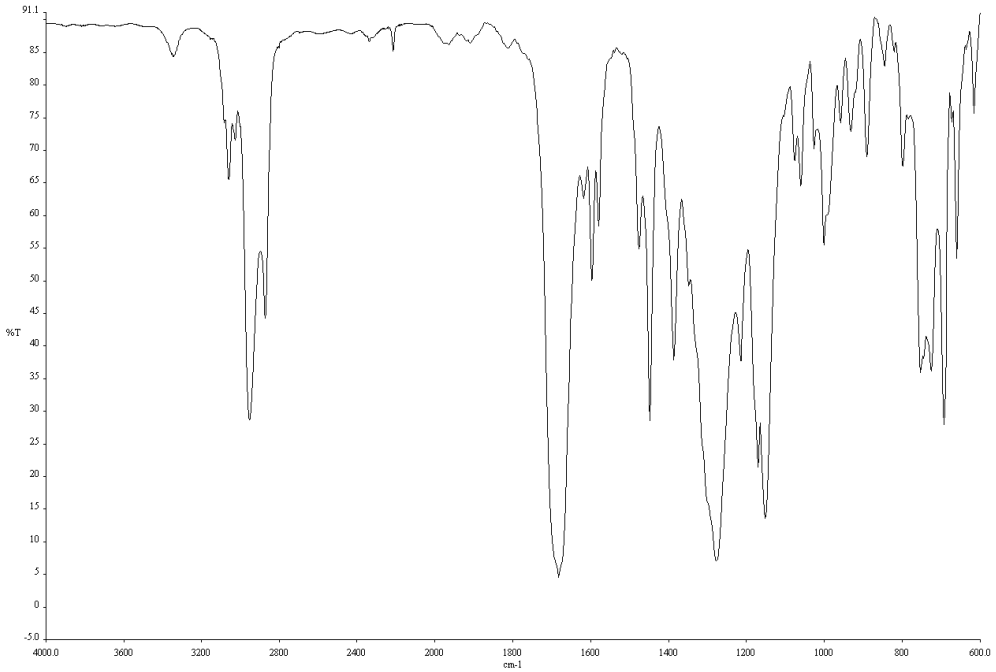


Figure A2.20. *Infrared spectrum (Thin Film, NaCl) of compound* ***127g****.*

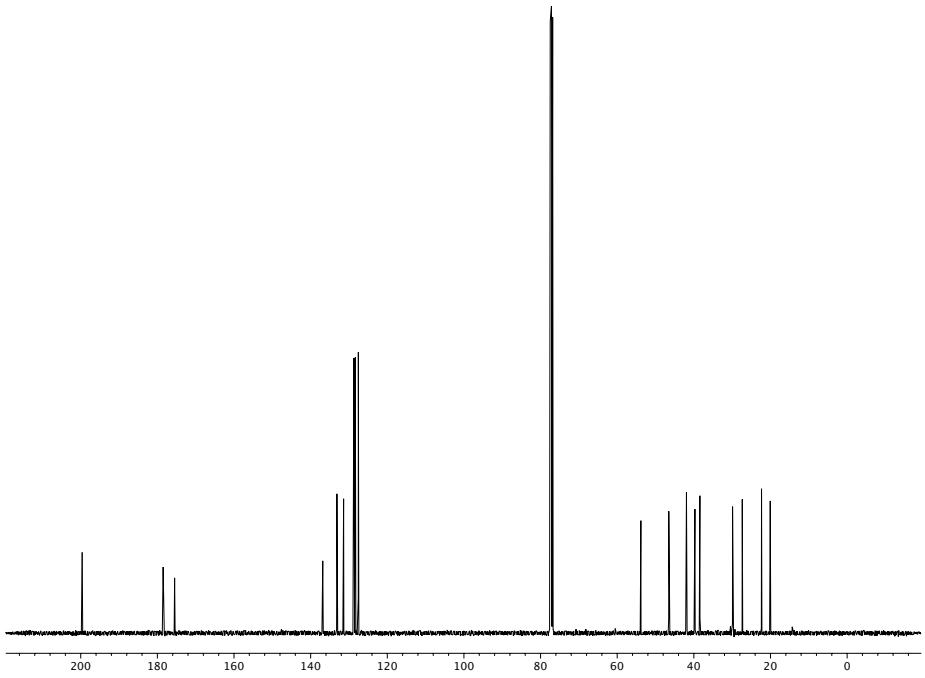


Figure A2.21. *^{13}C NMR (100 MHz, $CDCl_3$) of compound* ***127g****.*

Figure A2.22. *^1H NMR (400 MHz, $CDCl_3$) of compound* ***127h (d1)****.*

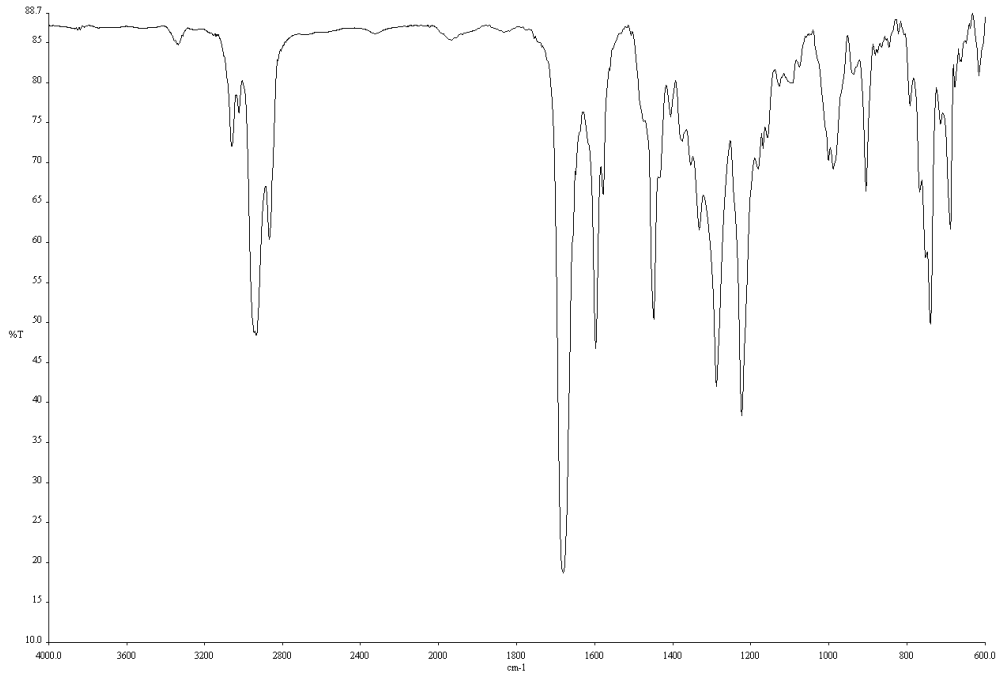


Figure A2.23. *Infrared spectrum (Thin Film, NaCl) of compound* ***127h (d1)****.*

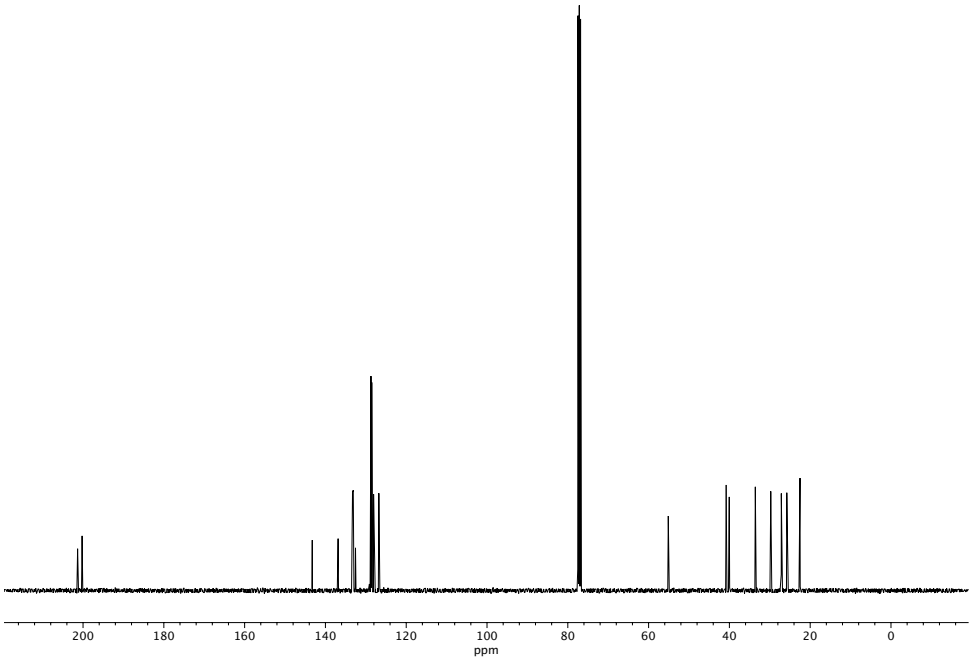


Figure A2.24. *^{13}C NMR (100 MHz, $CDCl_3$) of compound* ***127h (d1)****.*

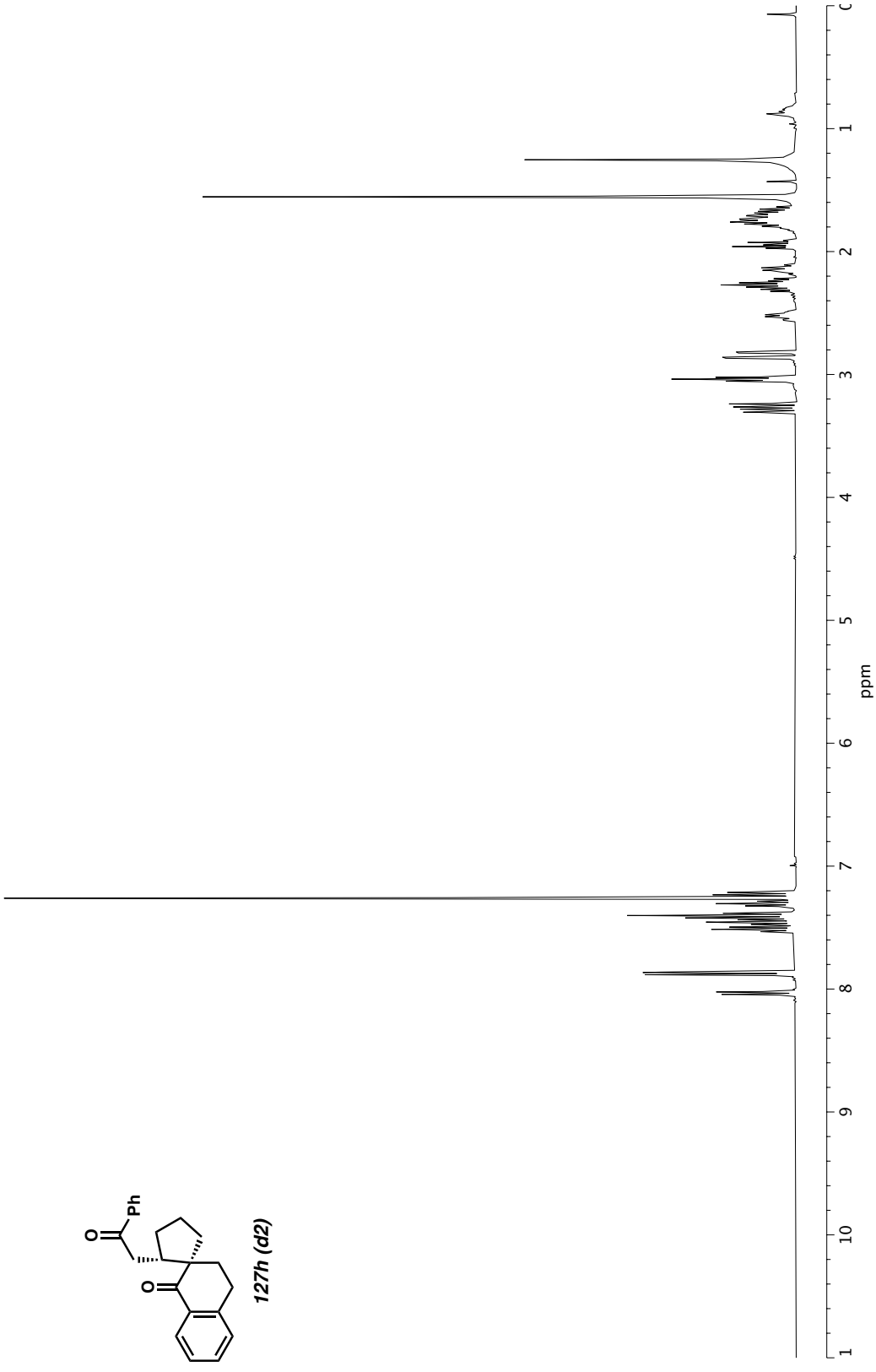


Figure A2.25. *^1H NMR (400 MHz, $CDCl_3$) of compound* ***127h (d2)****.*

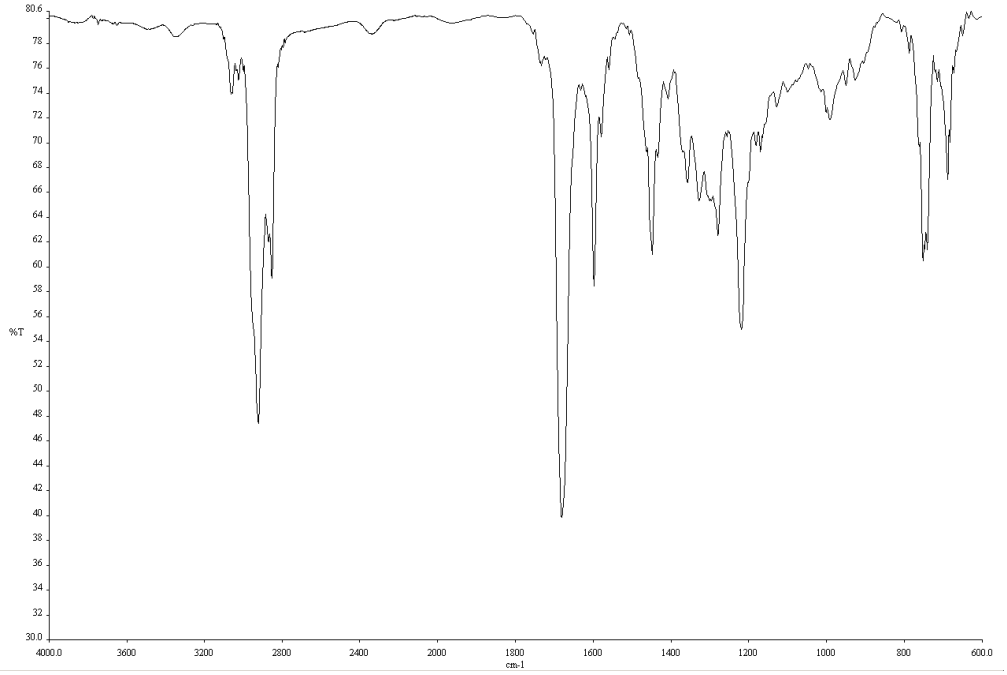


Figure A2.26. *Infrared spectrum (Thin Film, NaCl) of compound* ***127h (d2)****.*

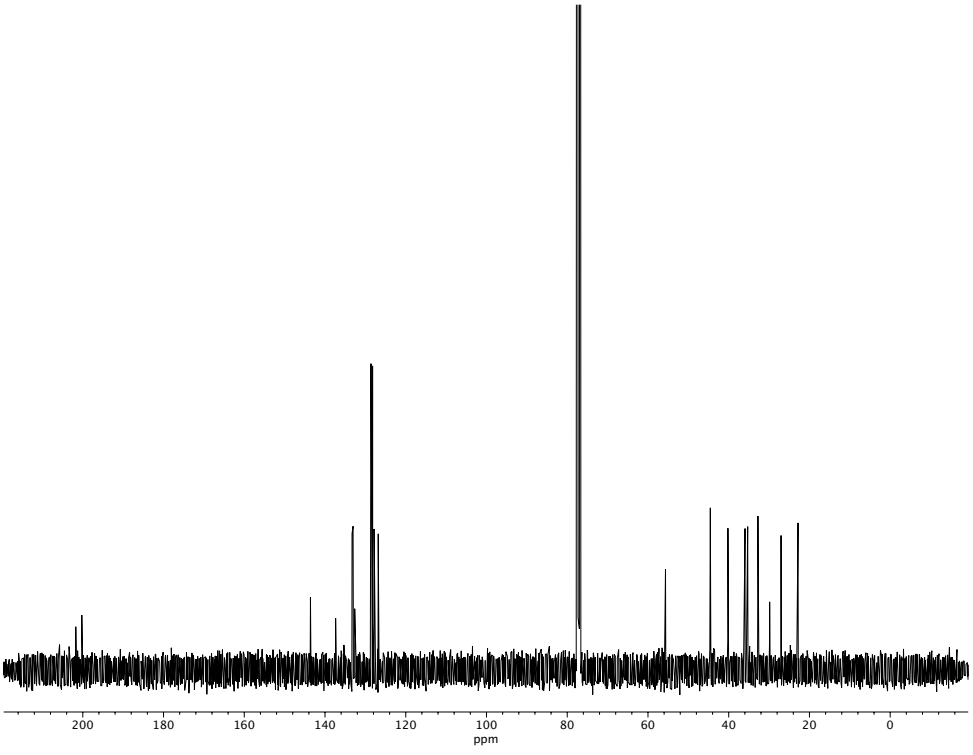


Figure A2.27. *^{13}C NMR (100 MHz, $CDCl_3$) of compound* ***127h (d2)****.*

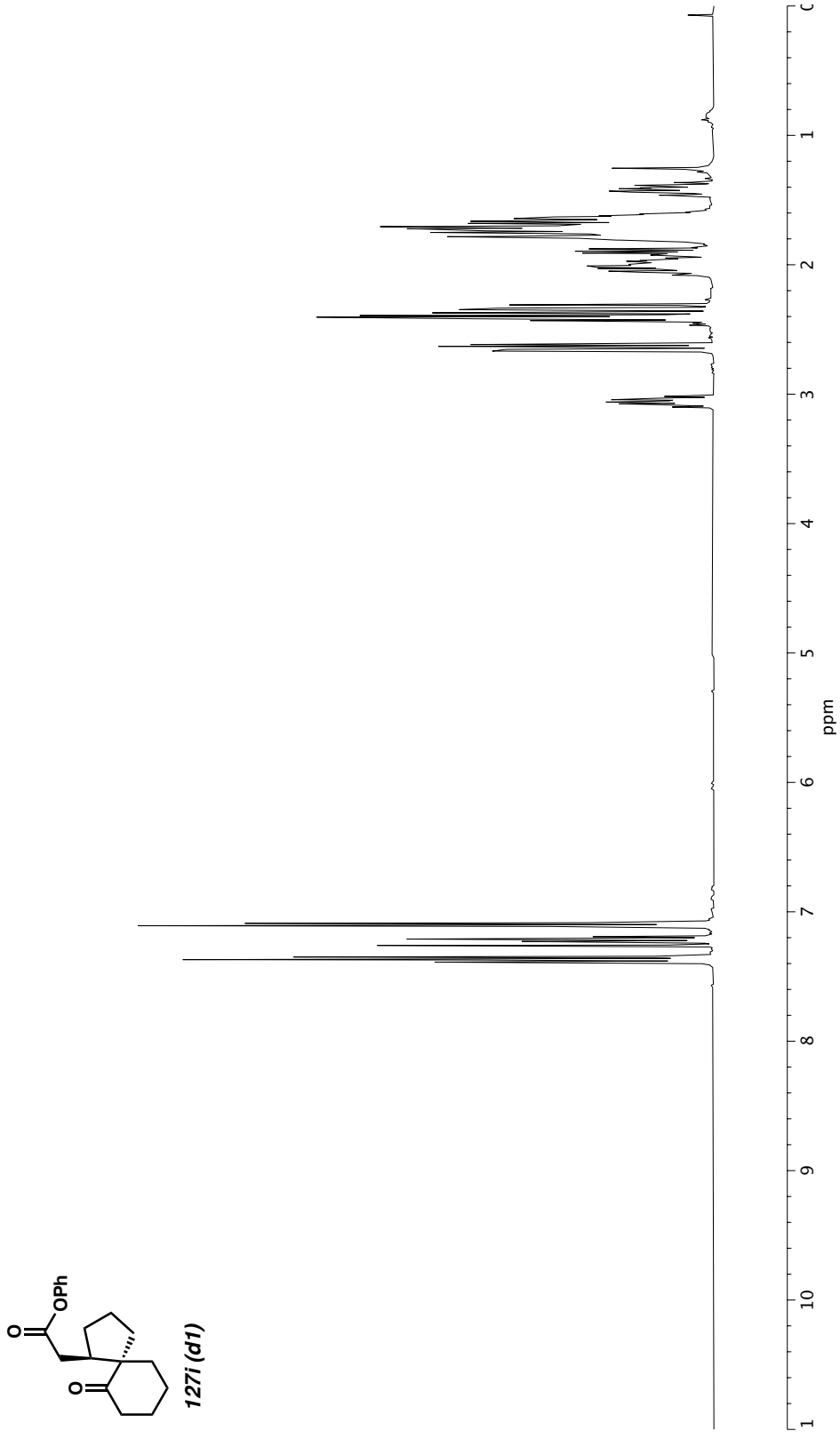


Figure A2.28. *^1H NMR (400 MHz, $CDCl_3$) of compound* ***127i (d1)****.*

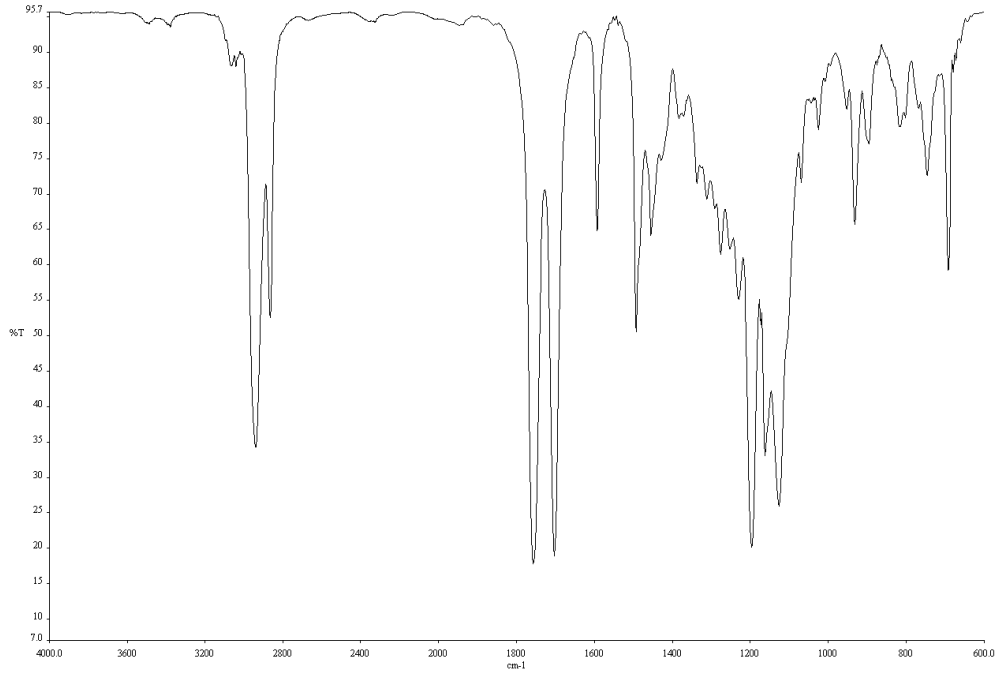


Figure A2.29. *Infrared spectrum (Thin Film, NaCl) of compound* ***127i (d1)***.

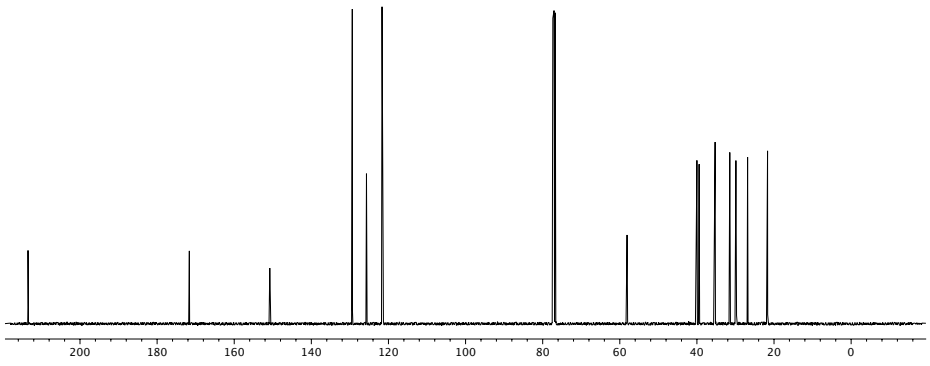


Figure A2.30. *^{13}C NMR (100 MHz, $CDCl_3$) of compound* ***127i (d1)***.

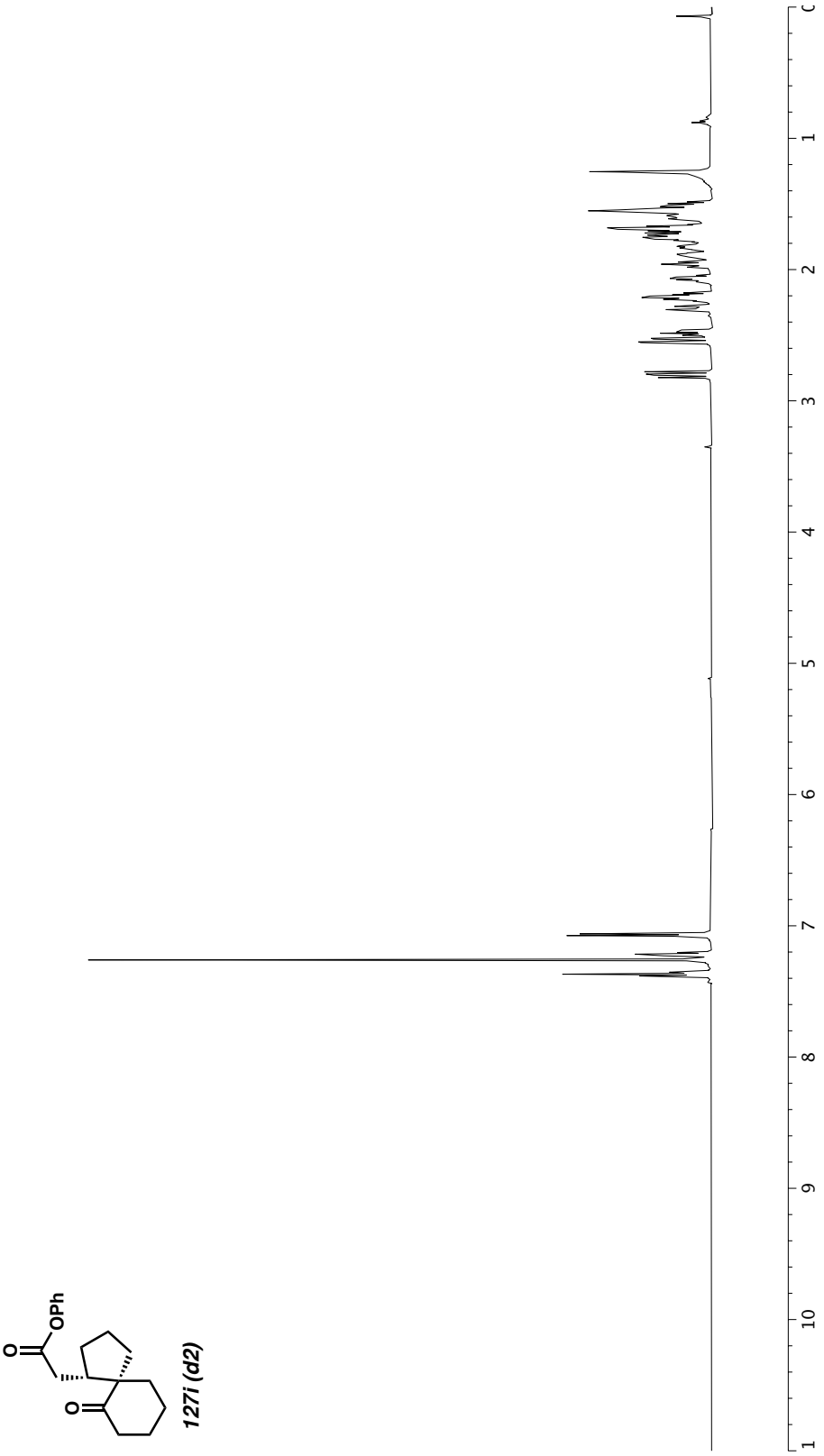


Figure A2.31. *^1H NMR (600 MHz, $CDCl_3$) of compound* ***127i (d2)****.*

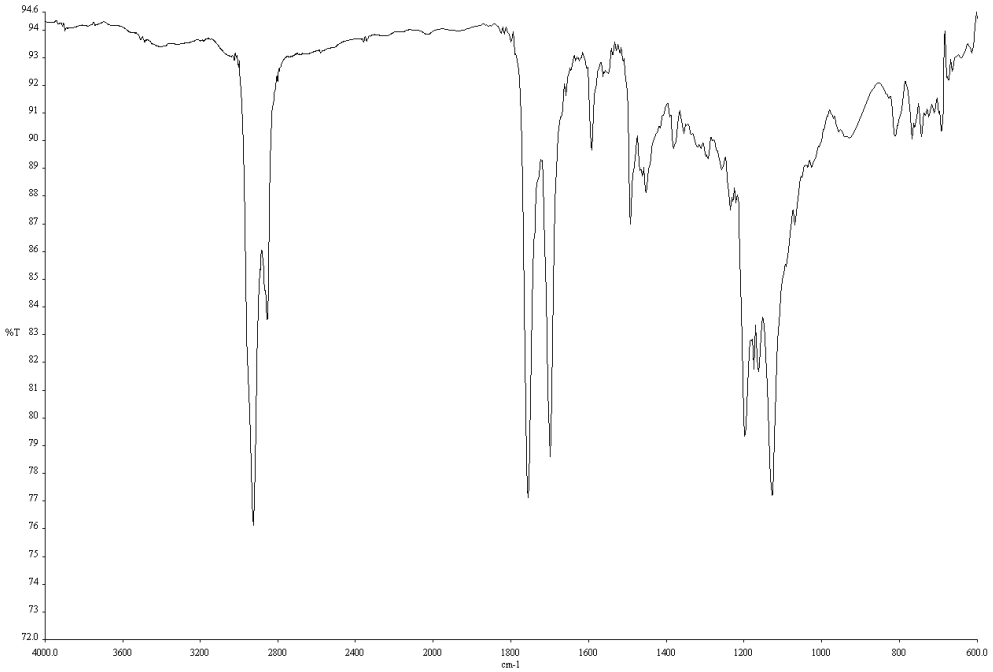


Figure A2.32. *Infrared spectrum (Thin Film, NaCl) of compound* ***127i (d2)***.

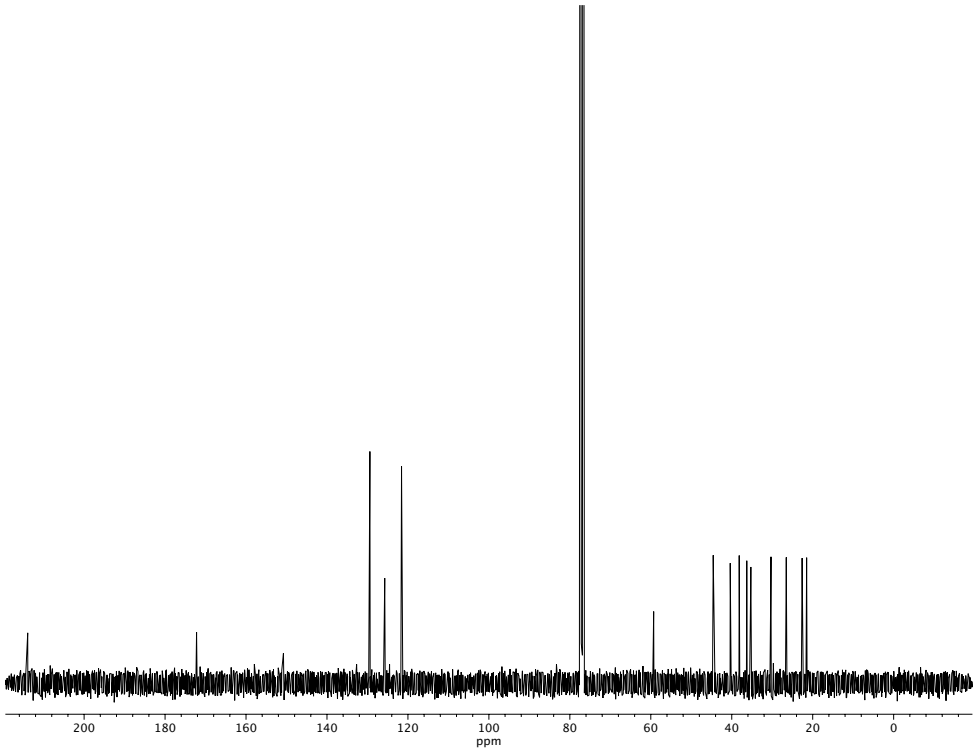


Figure A2.33. *^{13}C NMR (100 MHz, $CDCl_3$) of compound* ***127i (d2)***.

Figure A2.34. *^1H NMR (600 MHz, $CDCl_3$) of compound* ***127j****.*

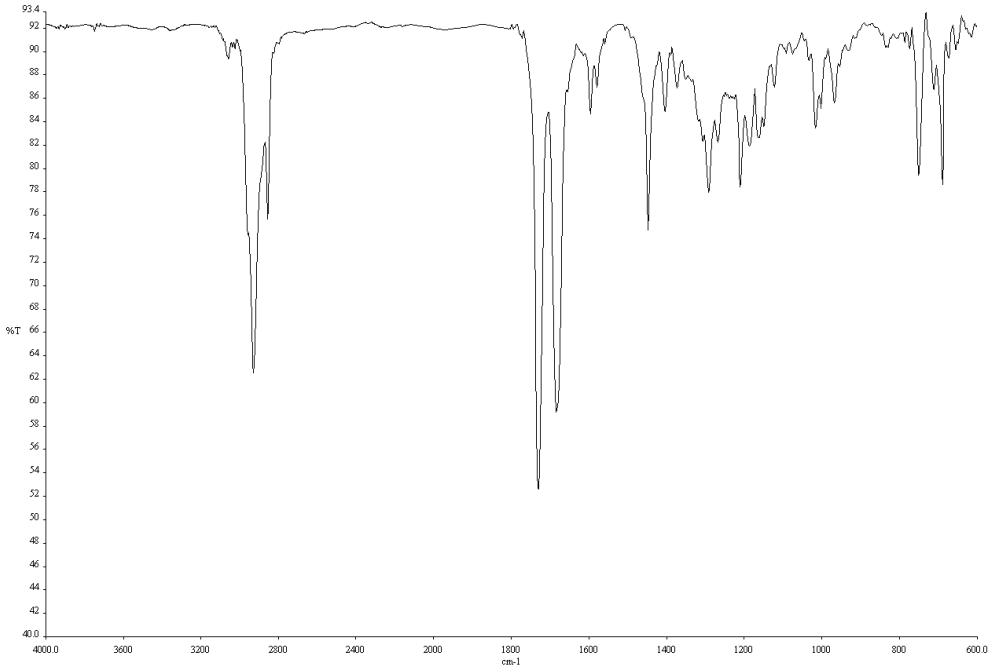


Figure A2.35. *Infrared spectrum (Thin Film, NaCl) of compound* ***127j****.*

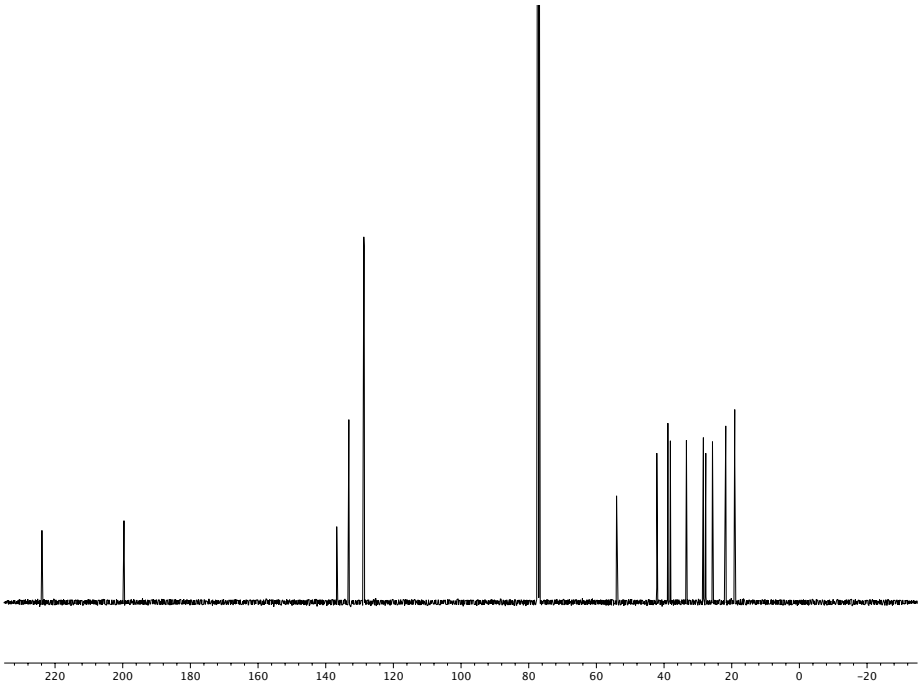


Figure A2.36. *^{13}C NMR (100 MHz, $CDCl_3$) of compound* ***127j****.*

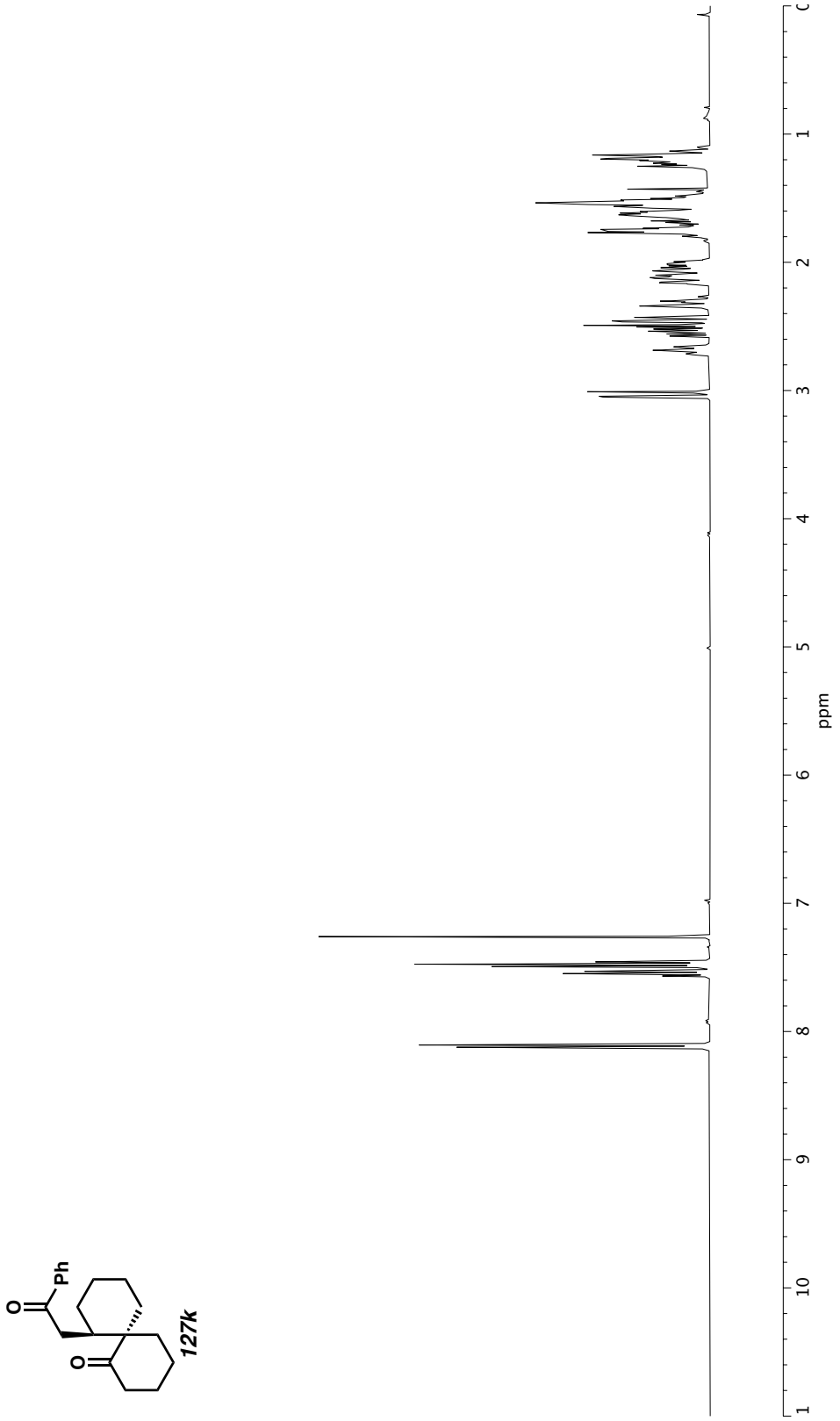


Figure A2.37. *^1H NMR (400 MHz, $CDCl_3$) of compound* ***127k****.*

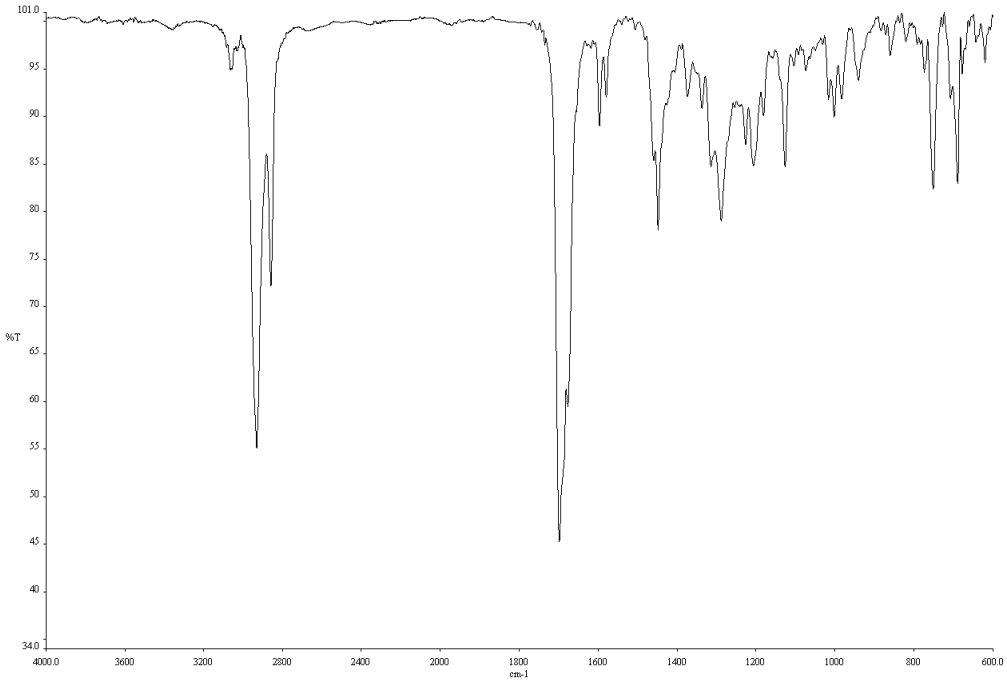


Figure A2.38. *Infrared spectrum (Thin Film, NaCl) of compound* ***127k****.*

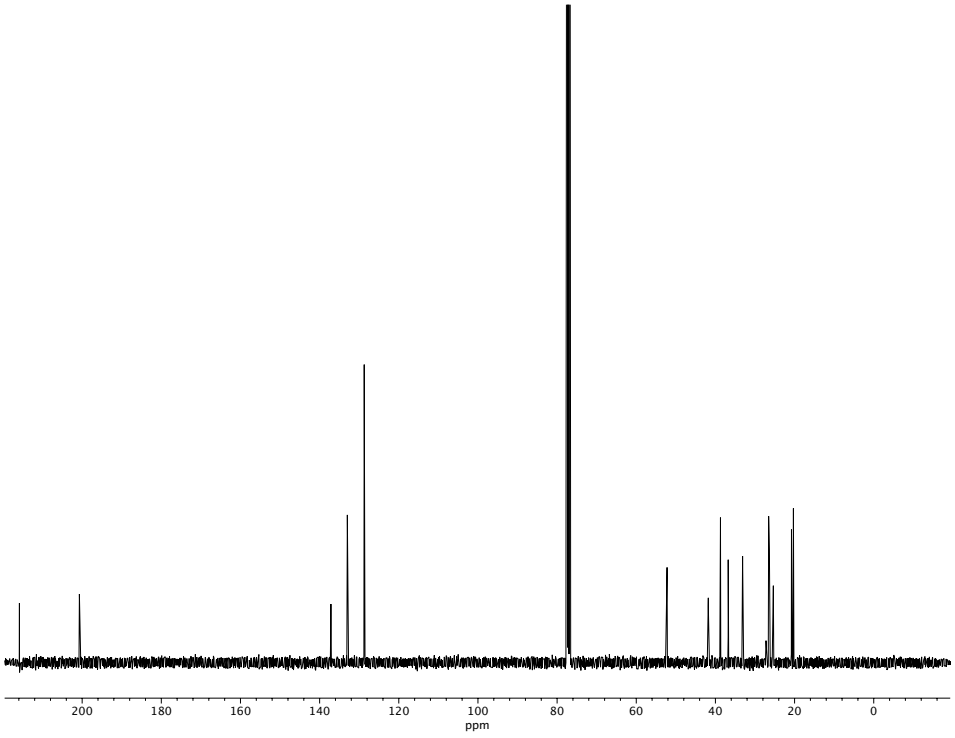


Figure A2.39. *^{13}C NMR (100 MHz, $CDCl_3$) of compound* ***127k****.*

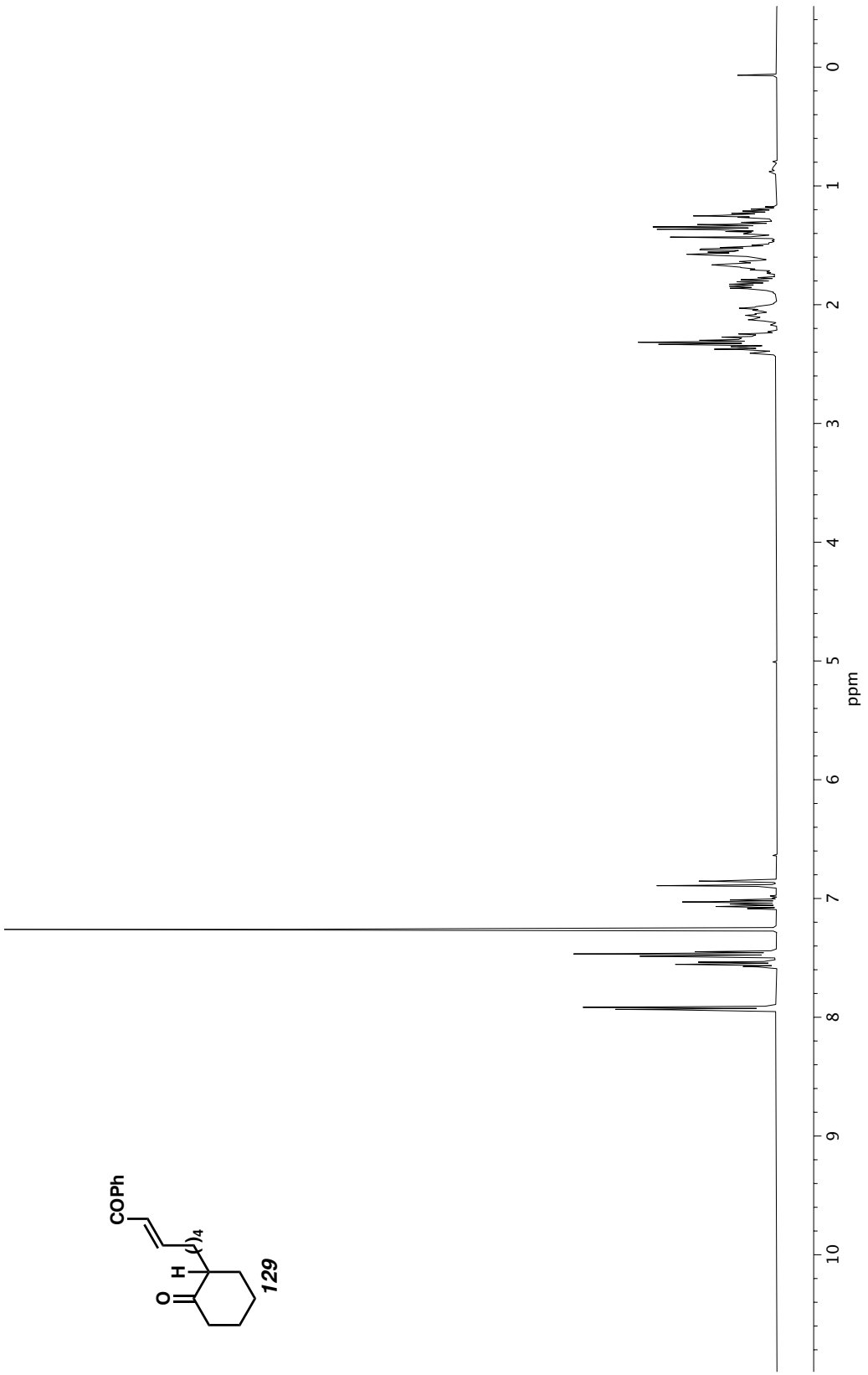


Figure A2.40. *^{1}H NMR (400 MHz, $CDCl_3$) of compound* ***129***.

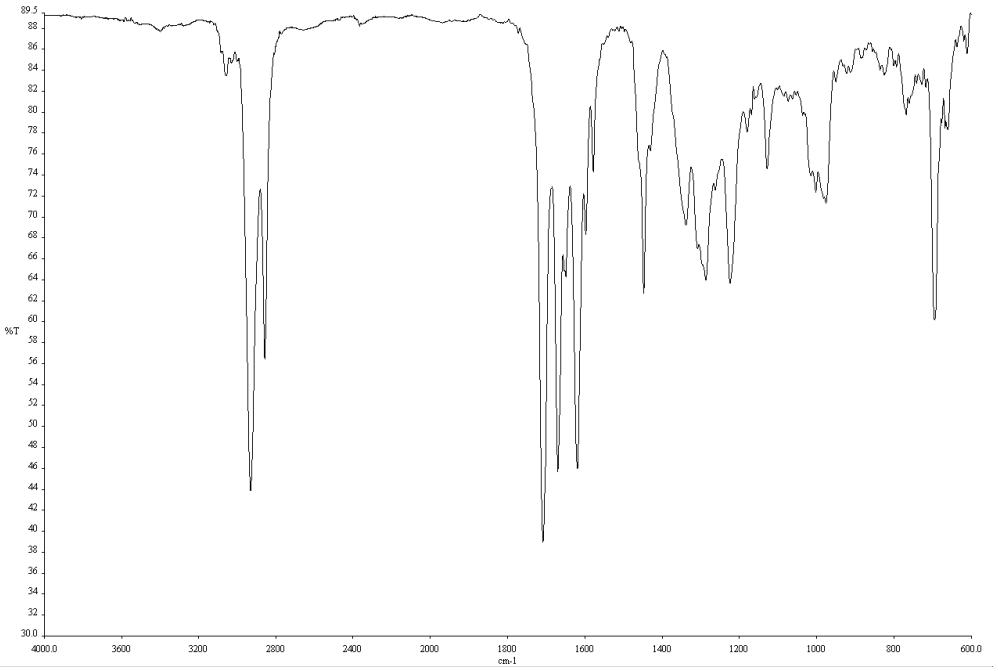


Figure A2.41. *Infrared spectrum (Thin Film, NaCl) of compound* ***129****.*

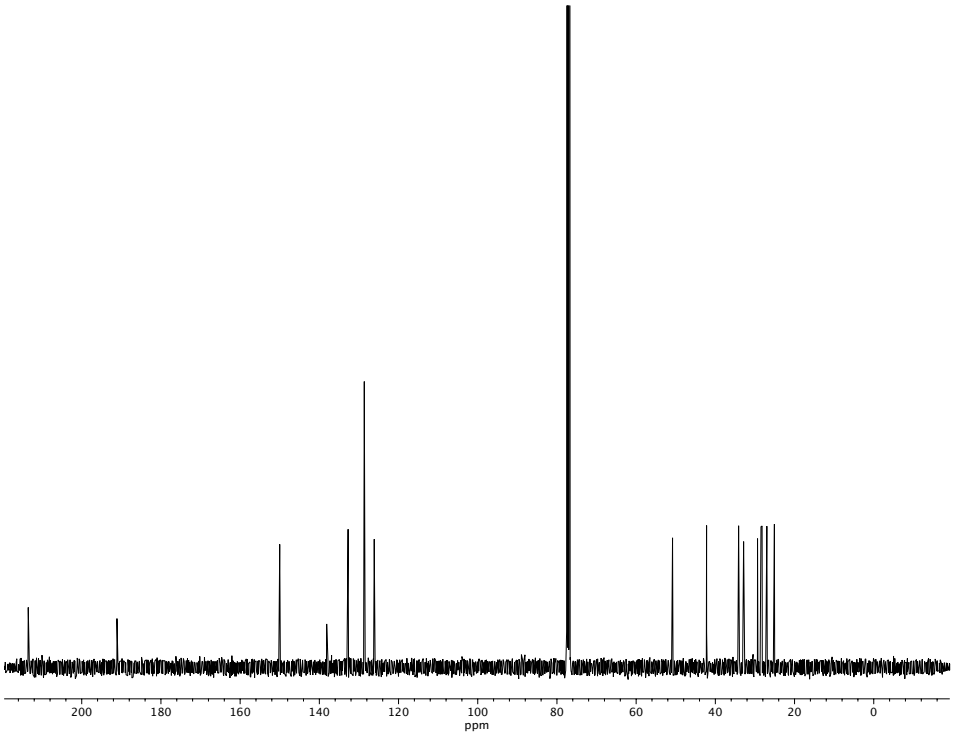


Figure A2.42. *^{13}C NMR (100 MHz, $CDCl_3$) of compound* ***129****.*

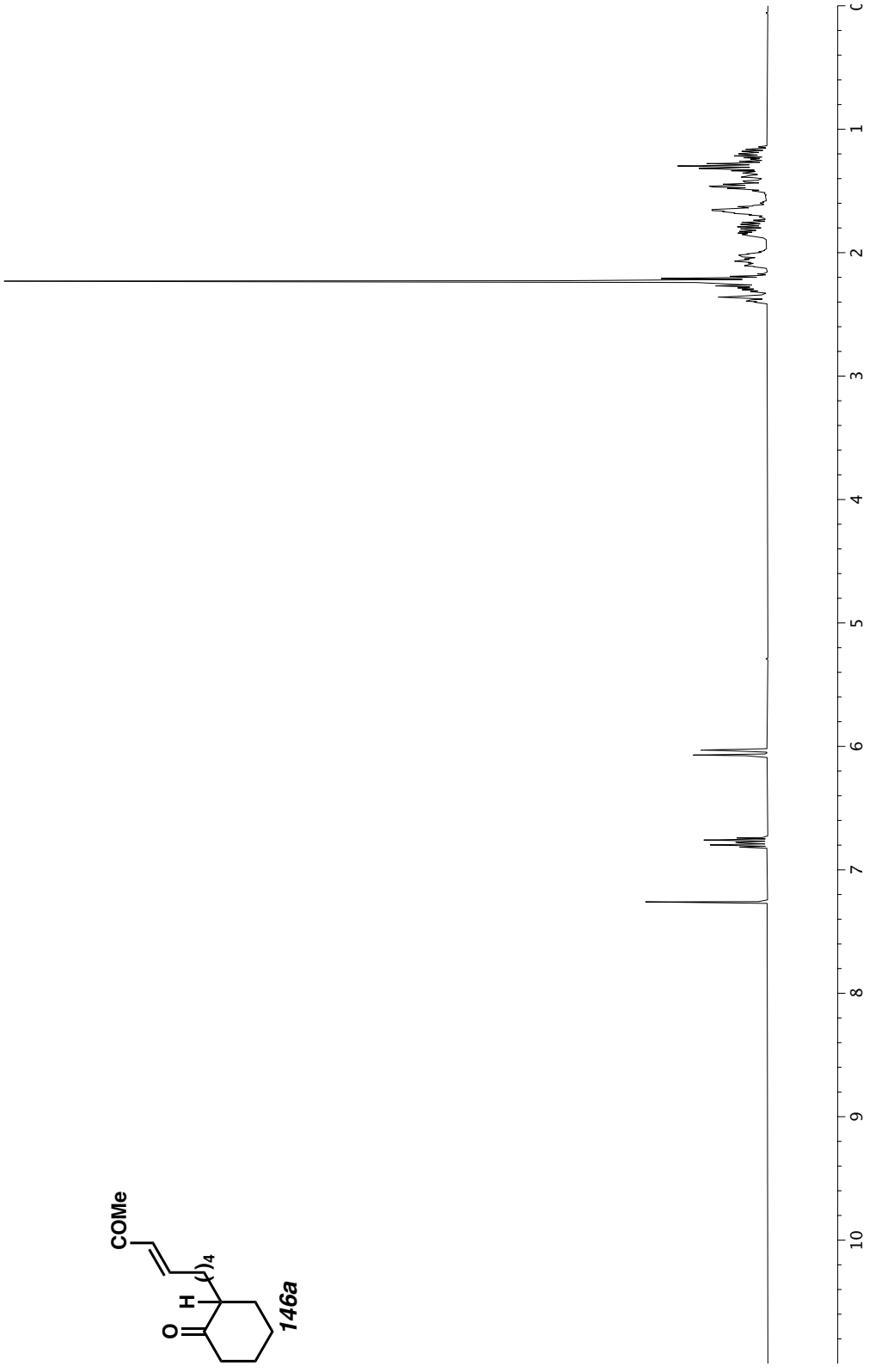


Figure A2.43. *^1H NMR (400 MHz, $CDCl_3$) of compound* ***146a****.*

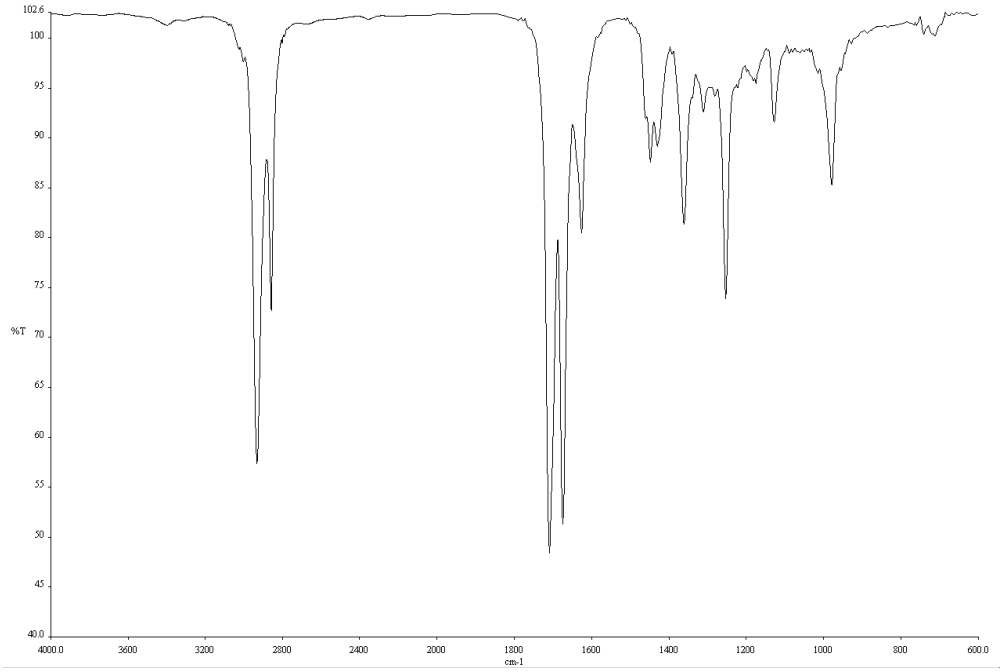


Figure A2.44. *Infrared spectrum (Thin Film, NaCl) of compound* ***146a****.*

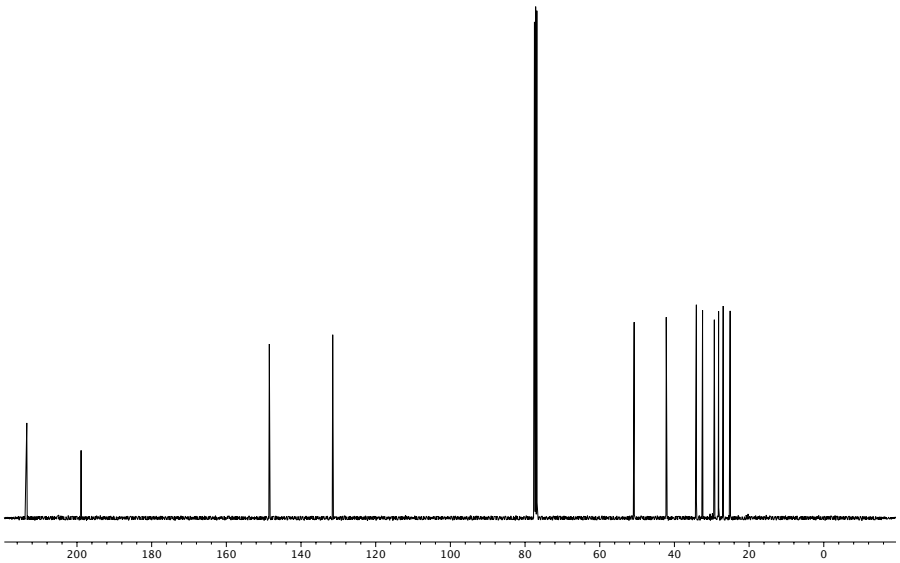


Figure A2.45. *^{13}C NMR (100 MHz, $CDCl_3$) of compound* ***146a****.*

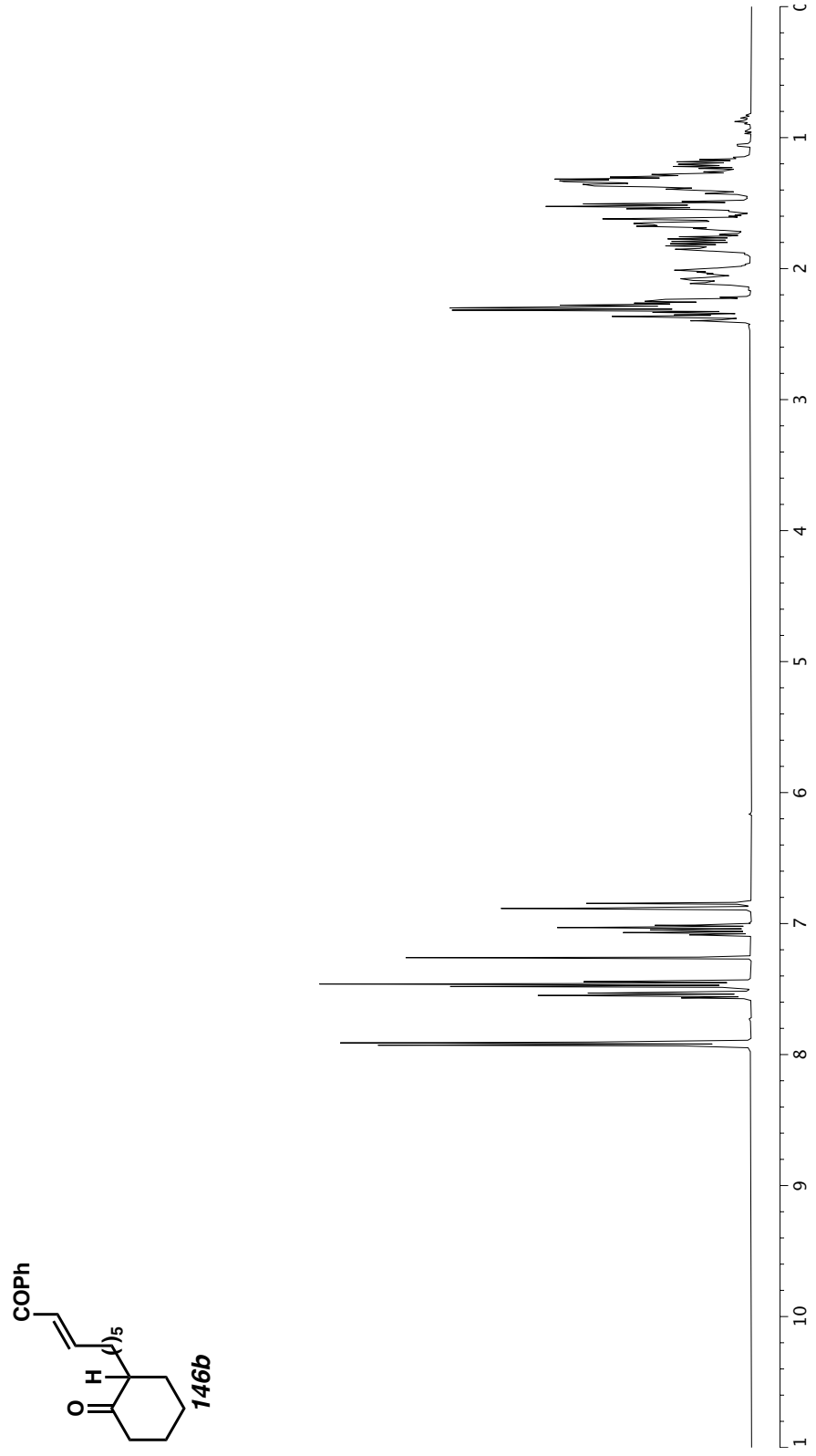


Figure A2.46. *^{1}H NMR (400 MHz, $CDCl_3$) of compound* ***146b***.

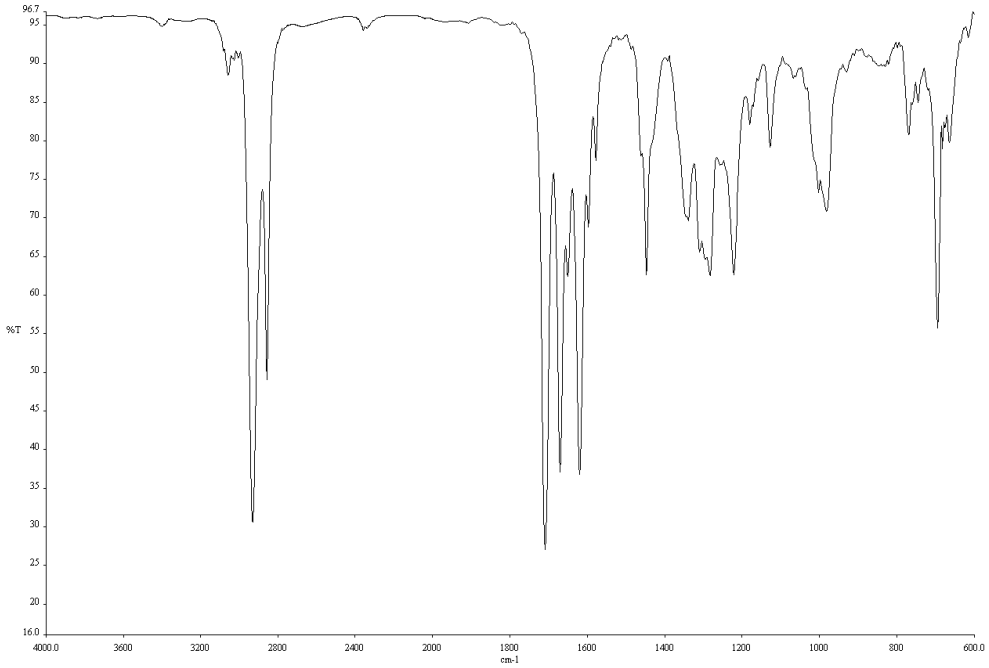


Figure A2.47. *Infrared spectrum (Thin Film, NaCl) of compound* ***146b****.*

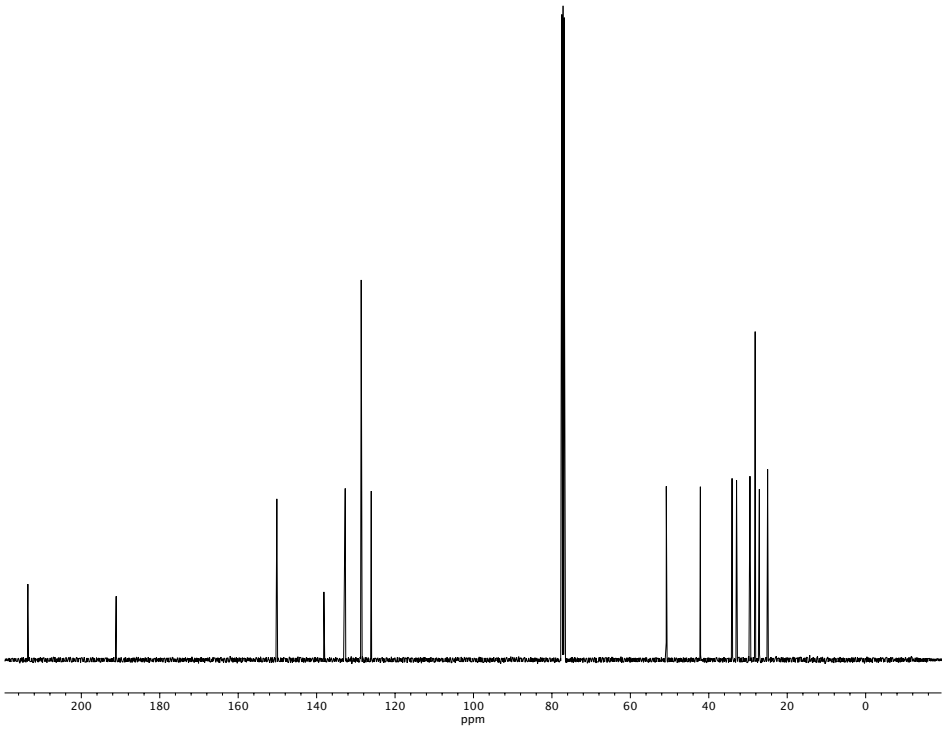


Figure A2.48. *^{13}C NMR (100 MHz, $CDCl_3$) of compound* ***146b****.*

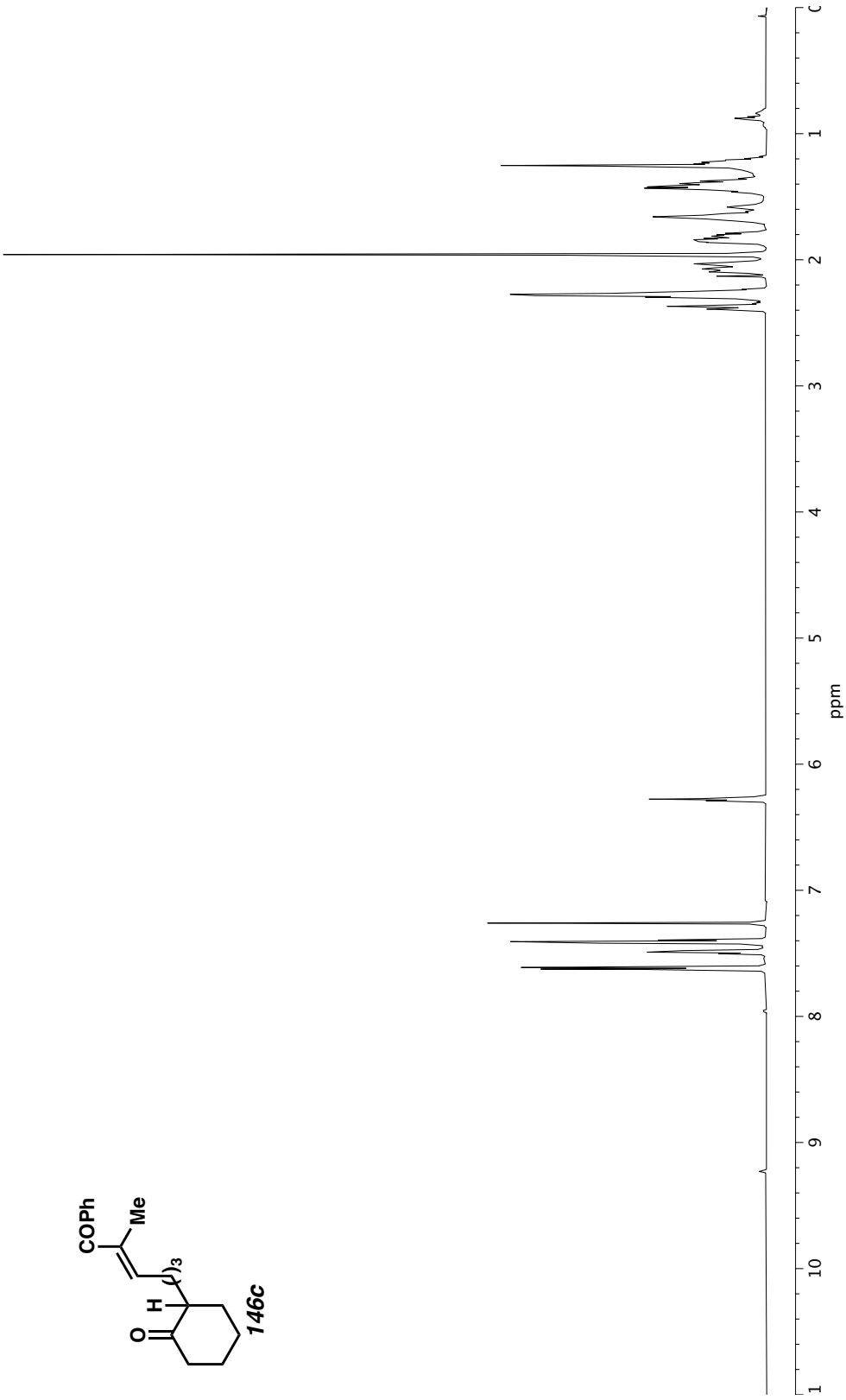


Figure A2.49. *^1H NMR (400 MHz, $CDCl_3$) of compound* ***146c****.*

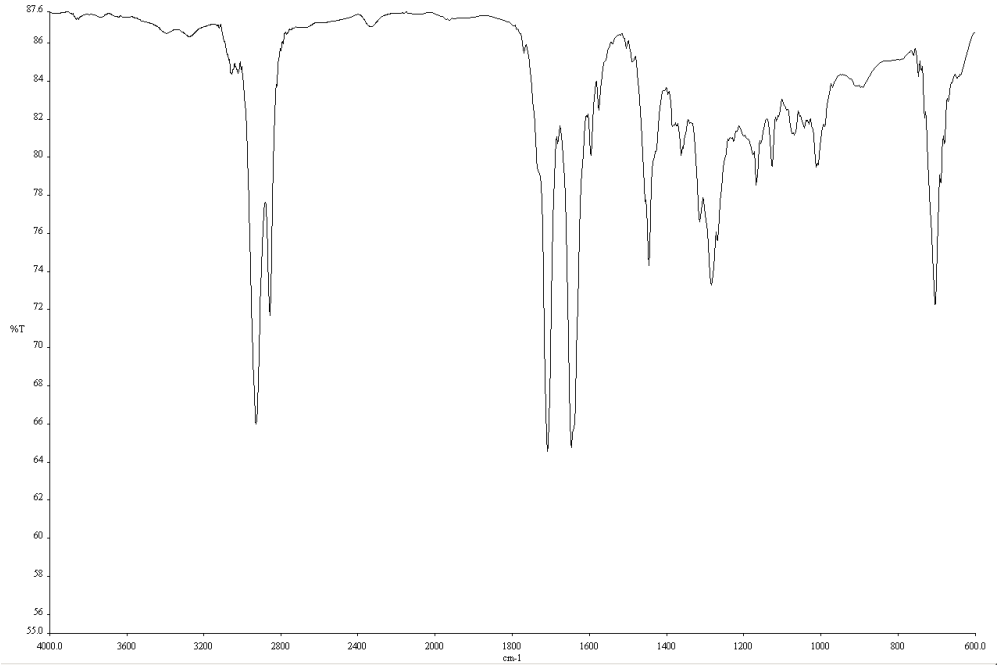


Figure A2.50. *Infrared spectrum (Thin Film, NaCl) of compound* ***146c****.*

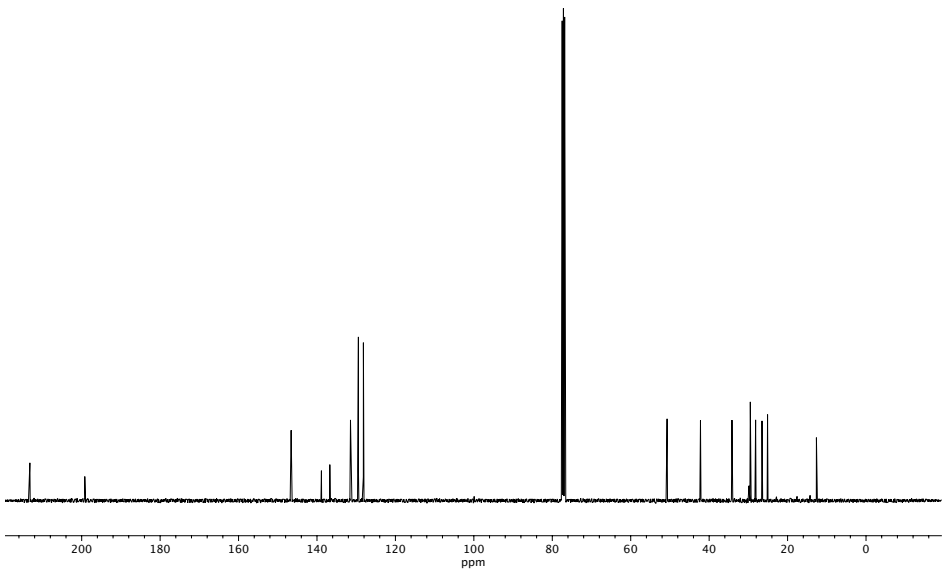


Figure A2.51. *^{13}C NMR (100 MHz, $CDCl_3$) of compound* ***146c****.*

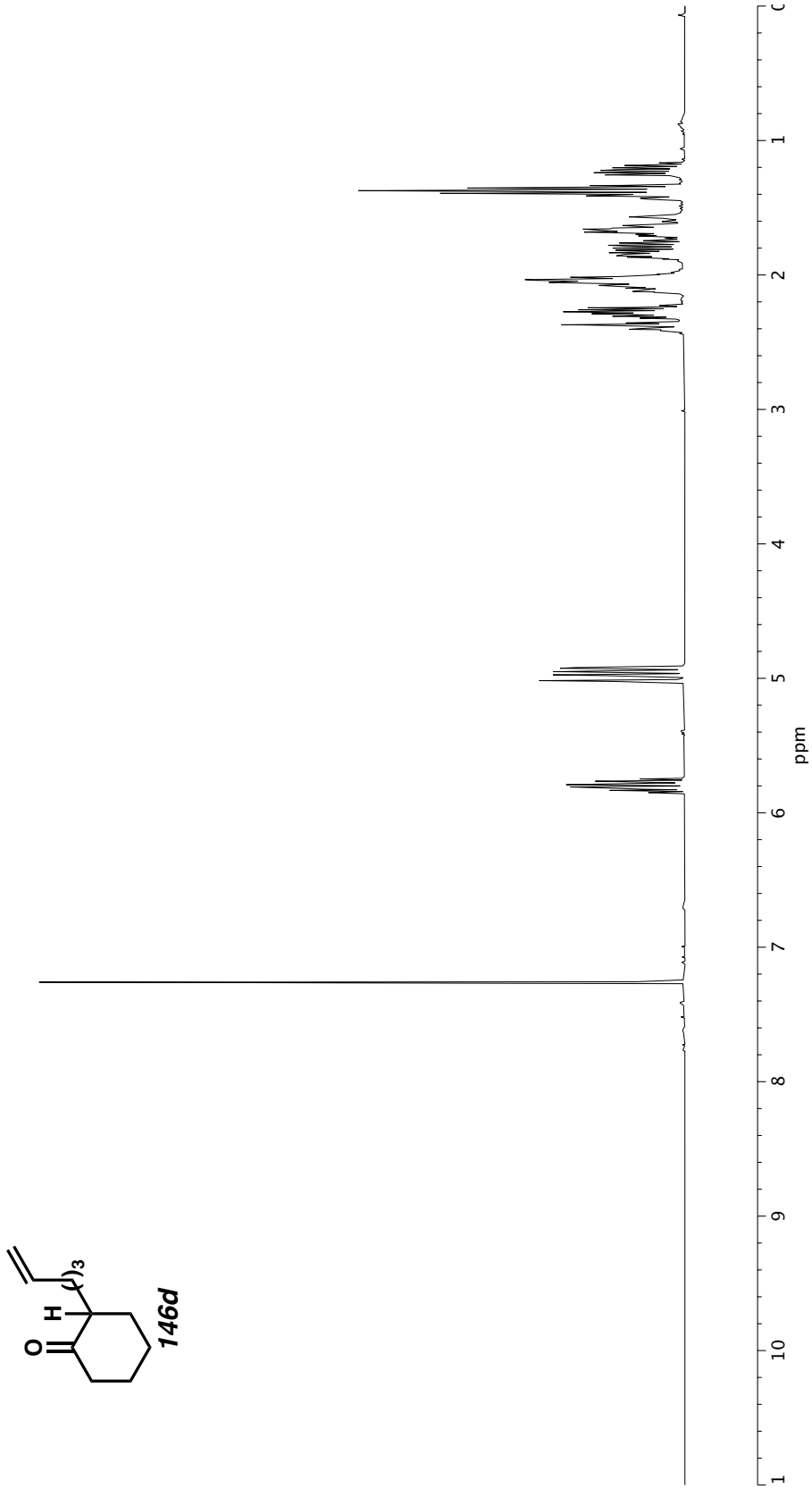


Figure A2.52. *^1H NMR (600 MHz, $CDCl_3$) of compound* ***146d****.*

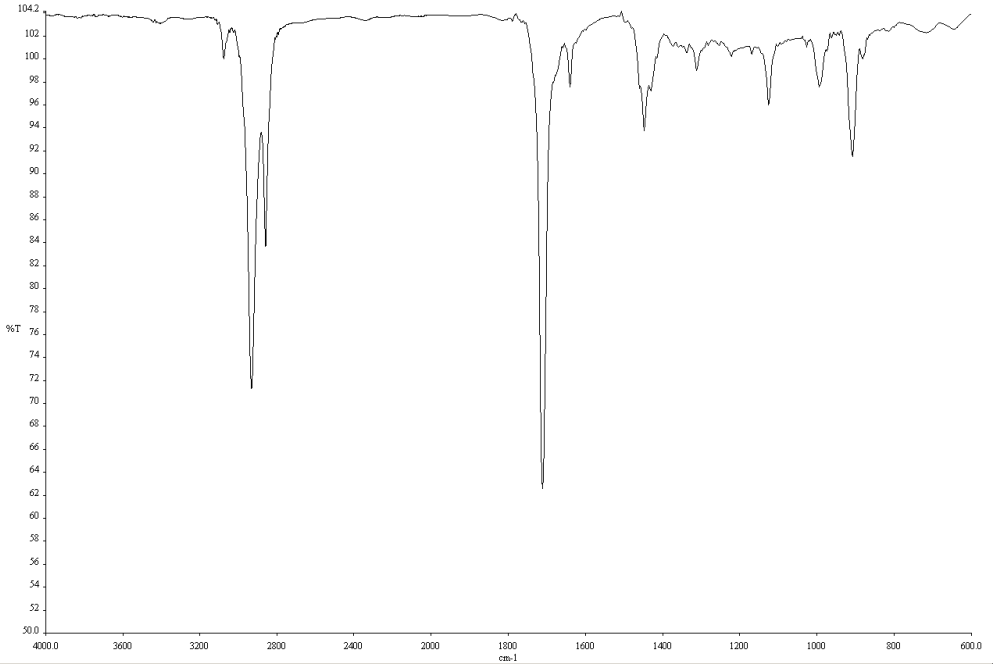


Figure A2.53. *Infrared spectrum (Thin Film, NaCl) of compound* ***146d****.*

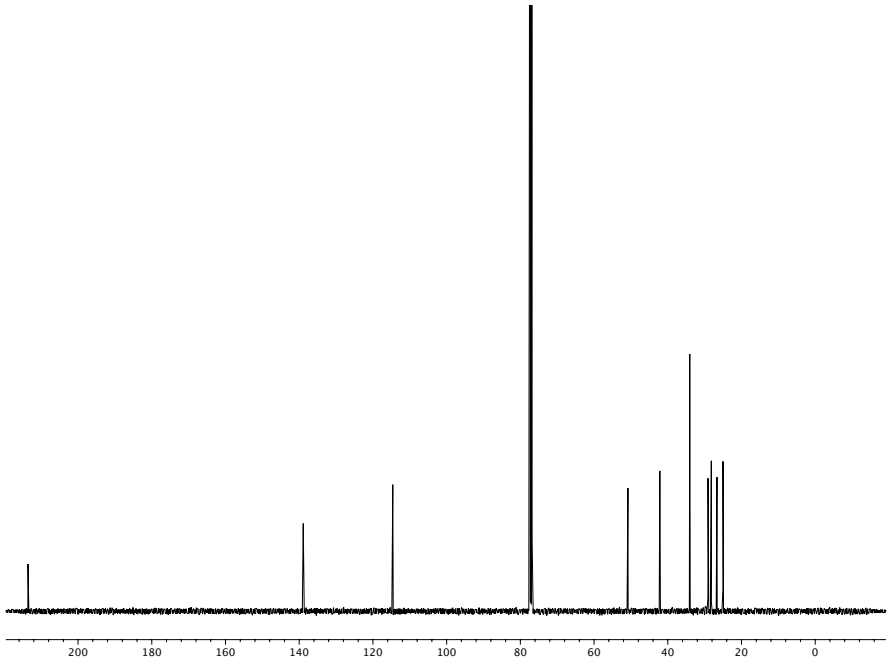


Figure A2.54. *^{13}C NMR (100 MHz, $CDCl_3$) of compound* ***146d****.*

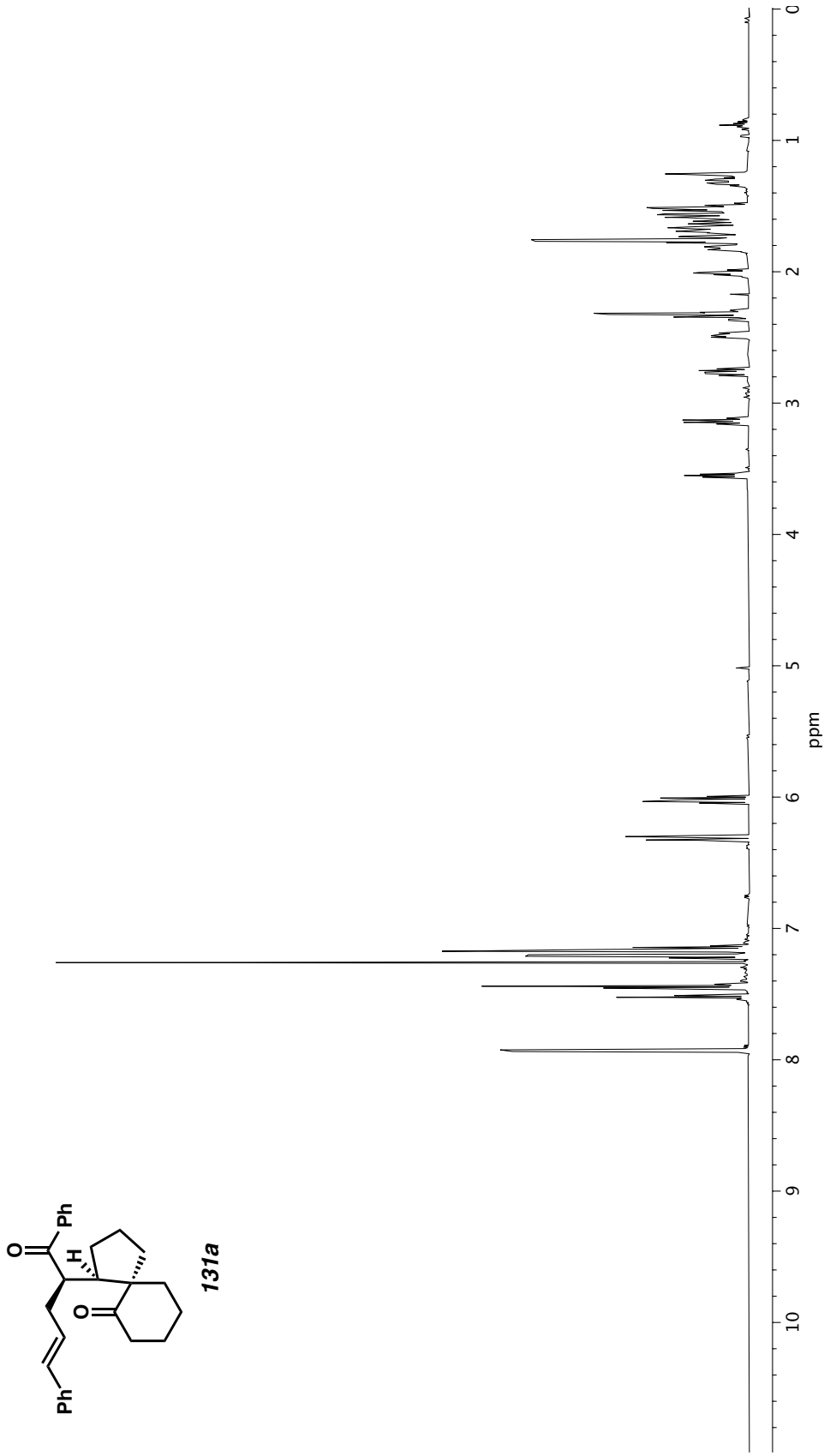


Figure A2.55. *^1H NMR (600 MHz, $CDCl_3$) of compound* ***131a****.*

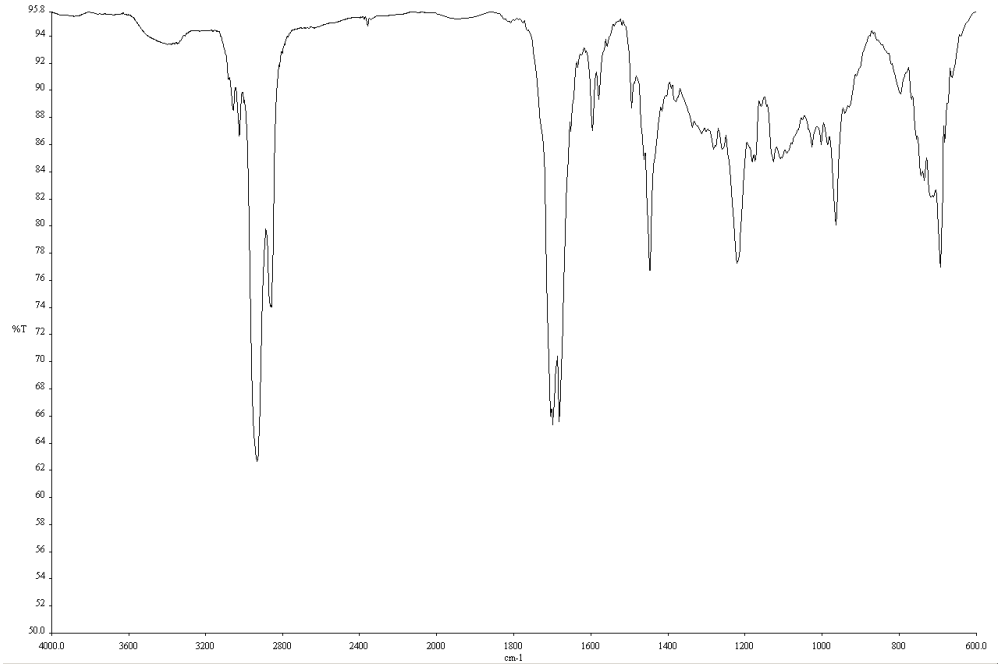


Figure A2.56. *Infrared spectrum (Thin Film, NaCl) of compound* ***131a****.*

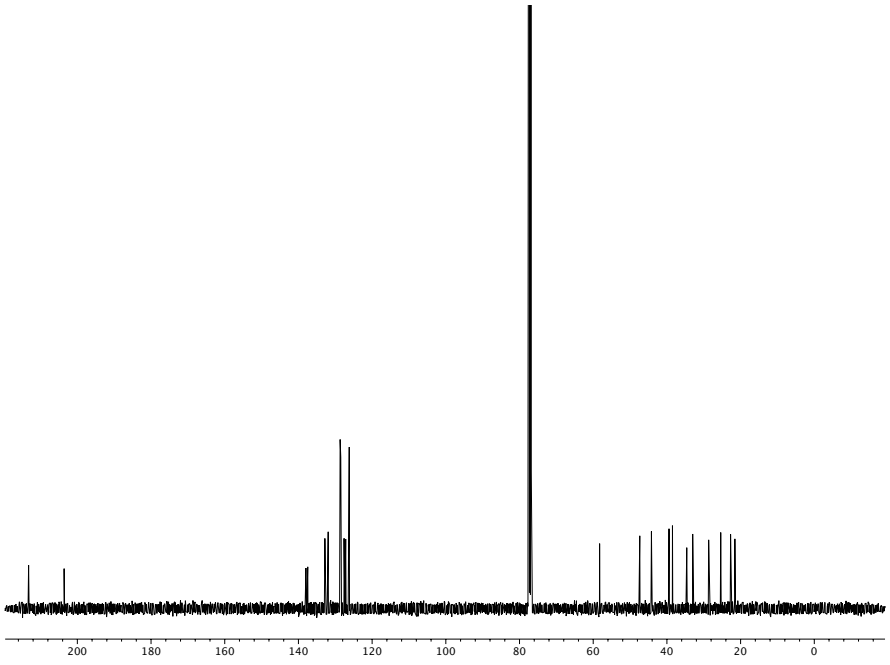


Figure A2.57. *^{13}C NMR (100 MHz, $CDCl_3$) of compound* ***131a****.*

Figure A2.58. *^1H NMR (400 MHz, $CDCl_3$) of compound **131b**.*

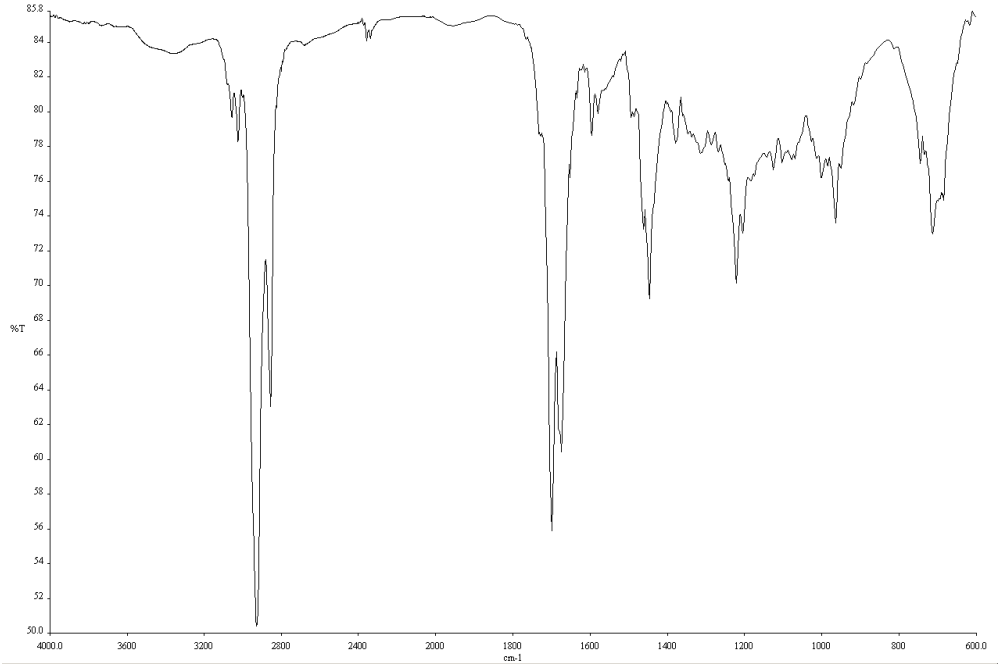


Figure A2.59. *Infrared spectrum (Thin Film, NaCl) of compound* ***131b****.*

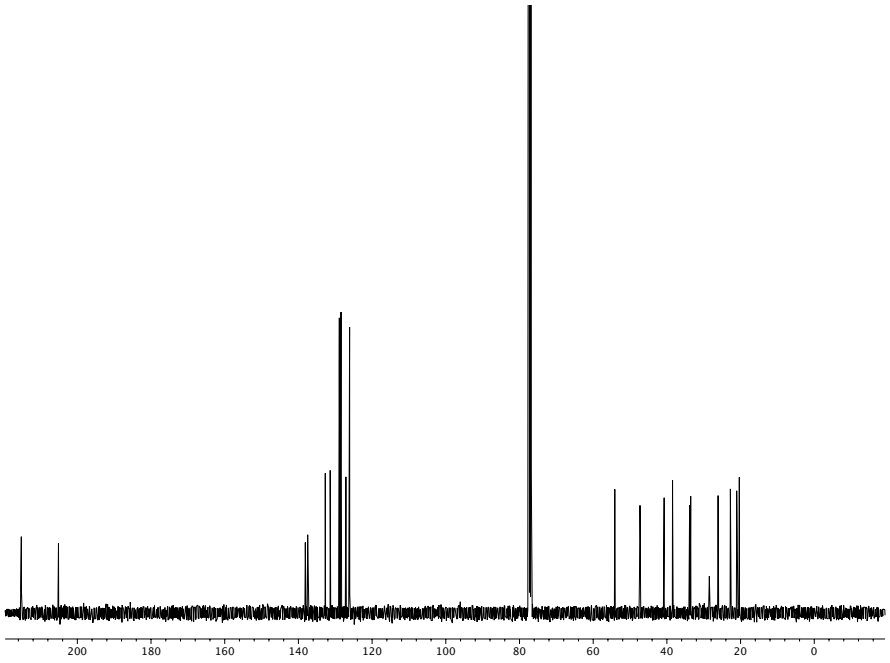


Figure A2.60. *^{13}C NMR (100 MHz, $CDCl_3$) of compound* ***131b****.*

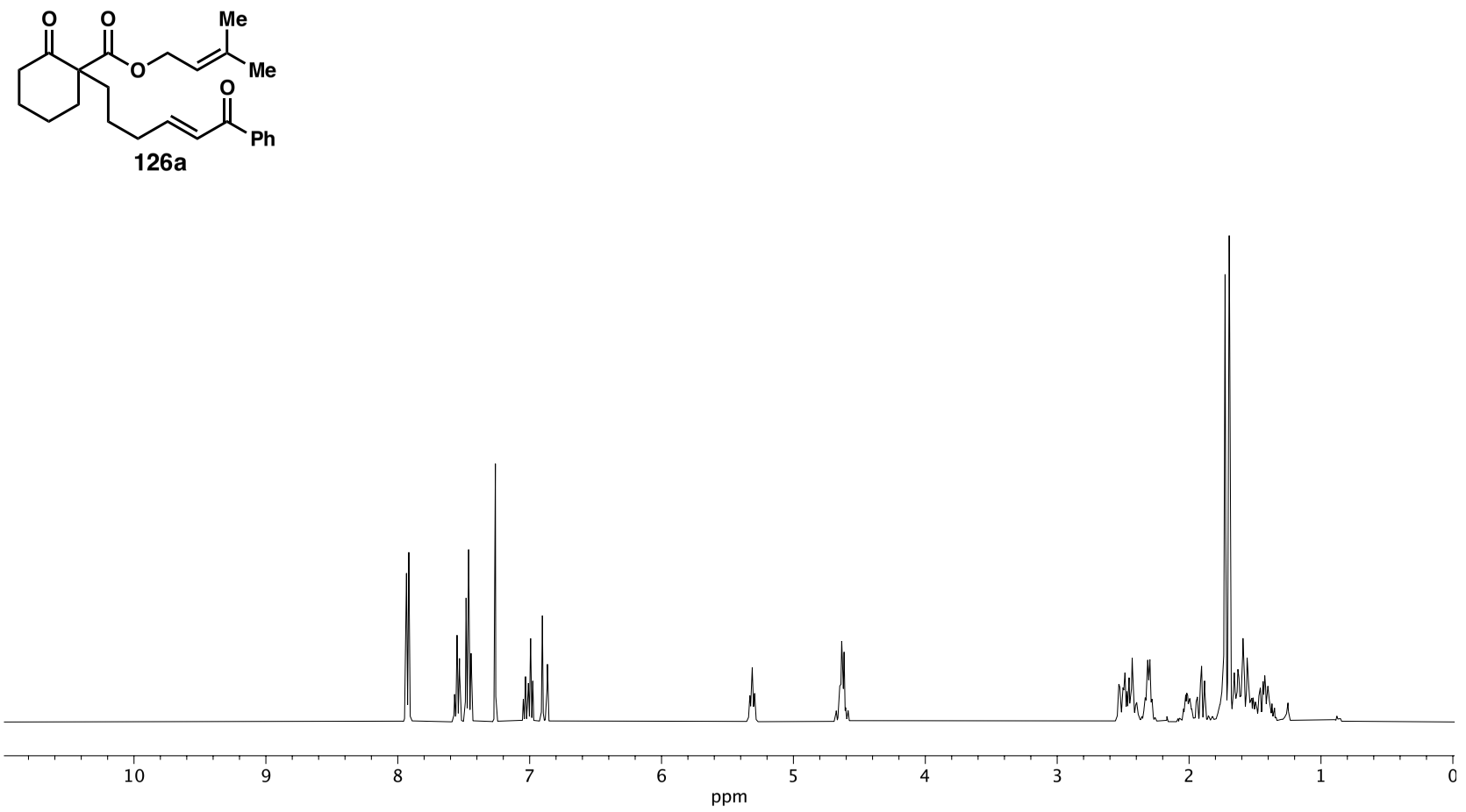


Figure A2.61. *^{1}H NMR (400 MHz, $CDCl_3$) of compound* ***126a****.*

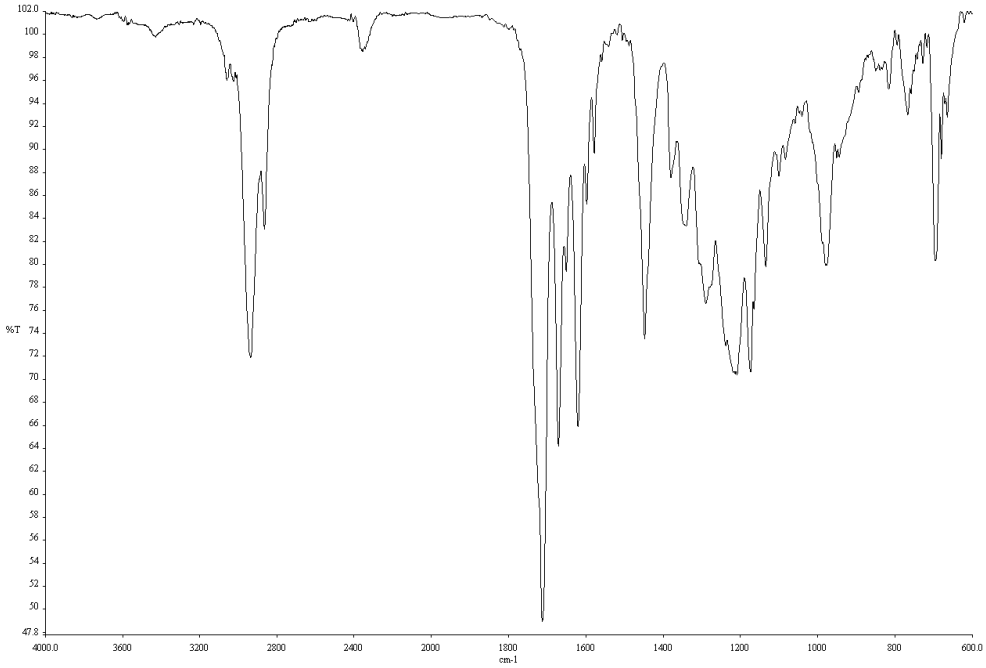


Figure A2.62. *Infrared spectrum (Thin Film, NaCl) of compound* ***126a****.*

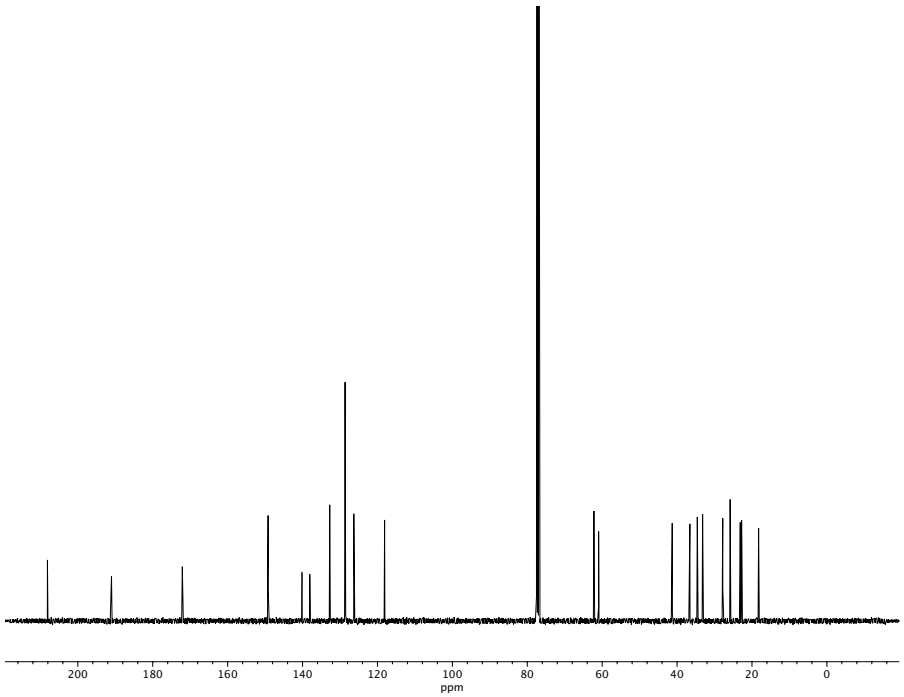


Figure A2.63. *^{13}C NMR (100 MHz, $CDCl_3$) of compound* ***126a****.*

Figure A2.64. *^1H NMR (400 MHz, $CDCl_3$) of compound* ***126b***.

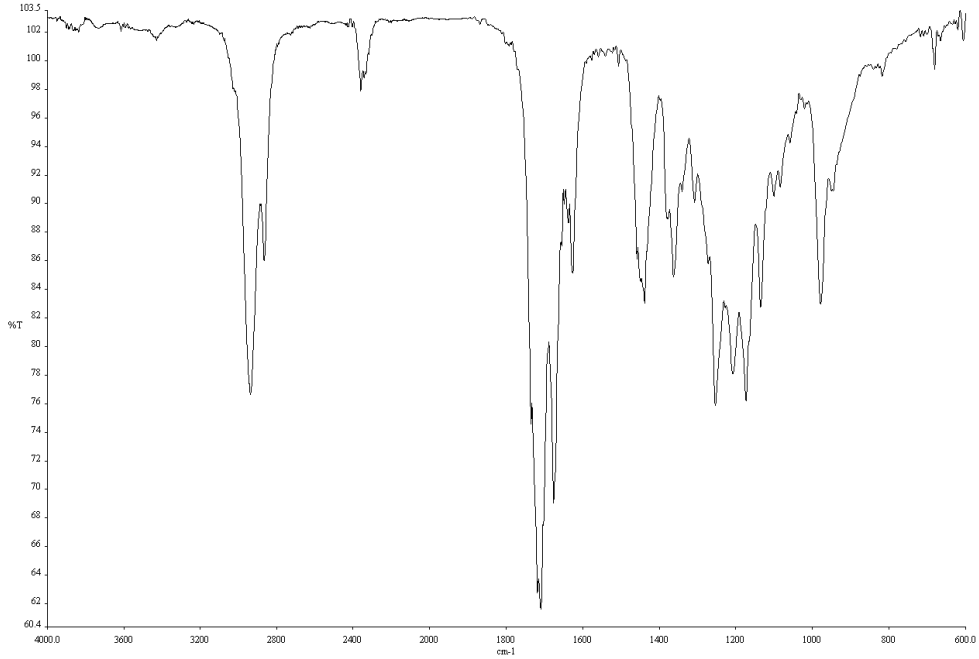


Figure A2.65. *Infrared spectrum (Thin Film, NaCl) of compound* ***126b****.*

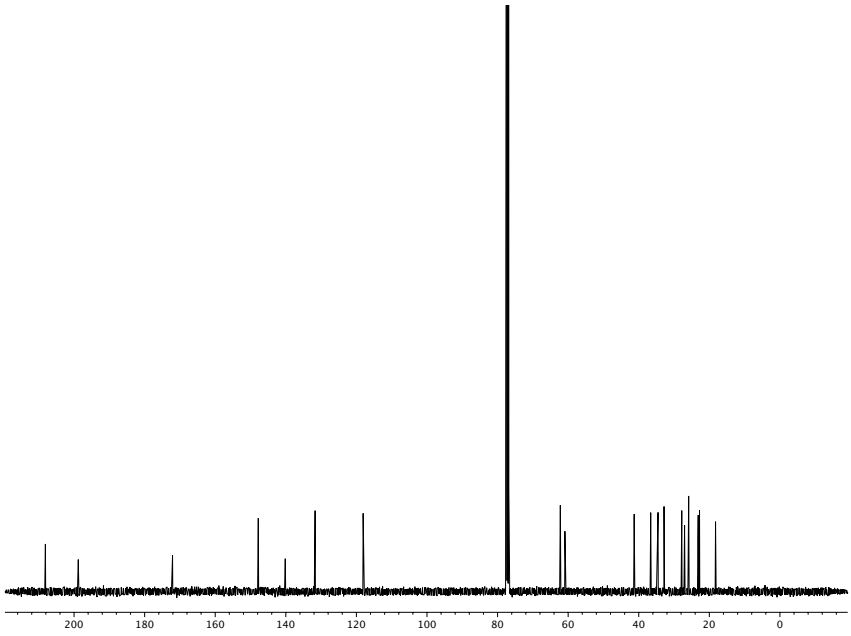


Figure A2.66. *^{13}C NMR (100 MHz, $CDCl_3$) of compound* ***126b****.*

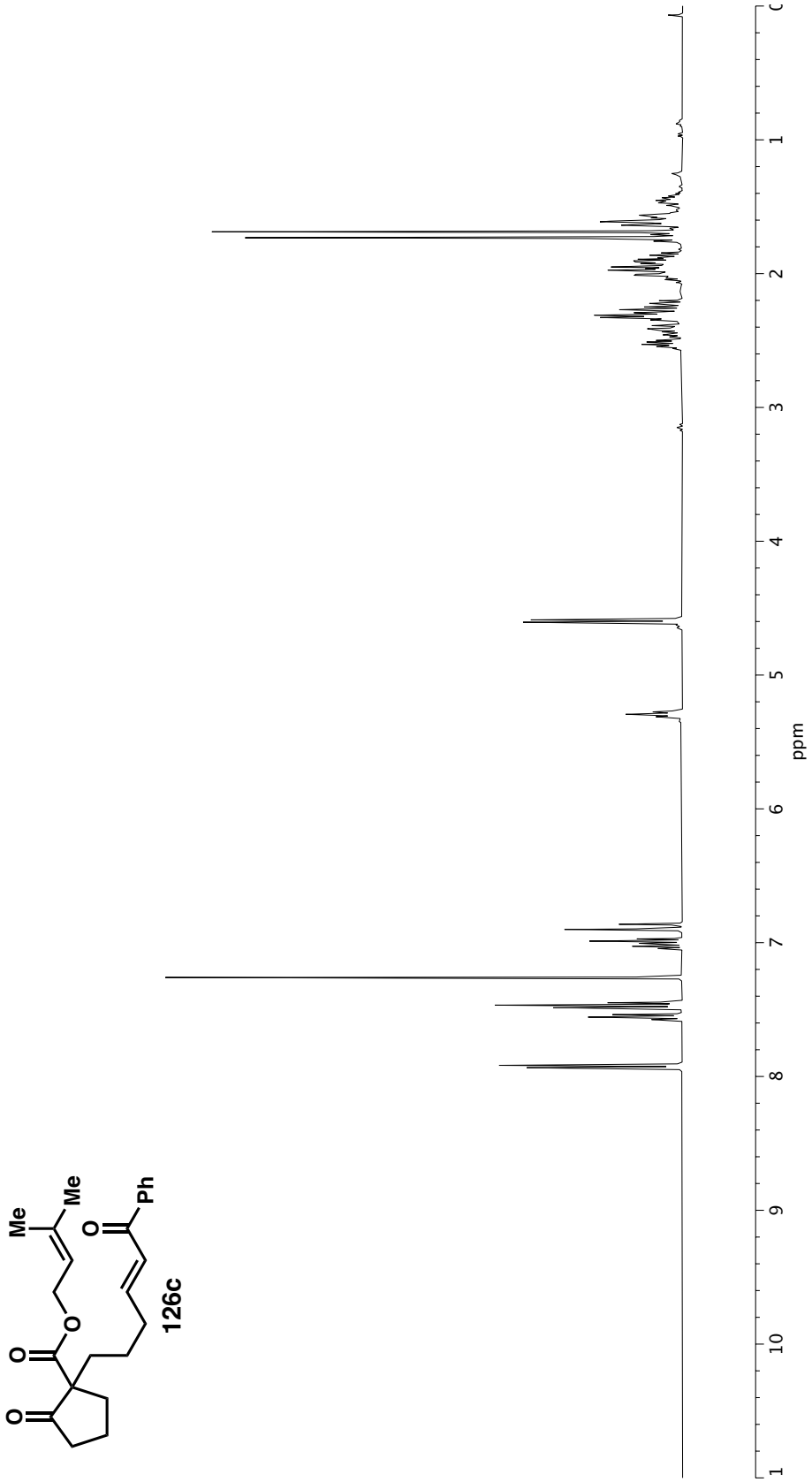


Figure A2.67. *^1H NMR (400 MHz, $CDCl_3$) of compound* ***126c****.*

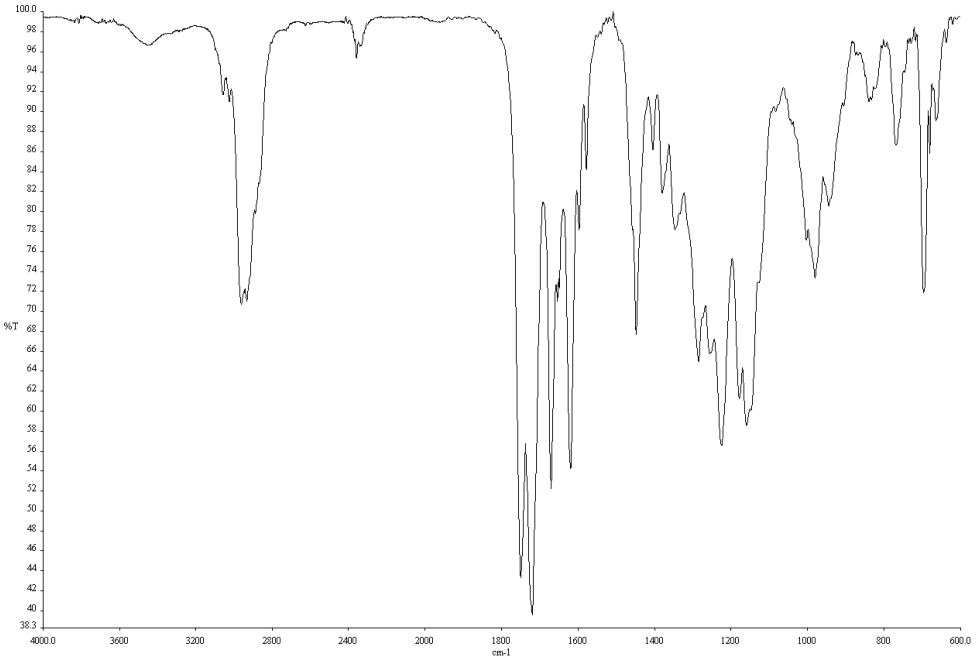


Figure A2.68. *Infrared spectrum (Thin Film, NaCl) of compound* ***126c****.*

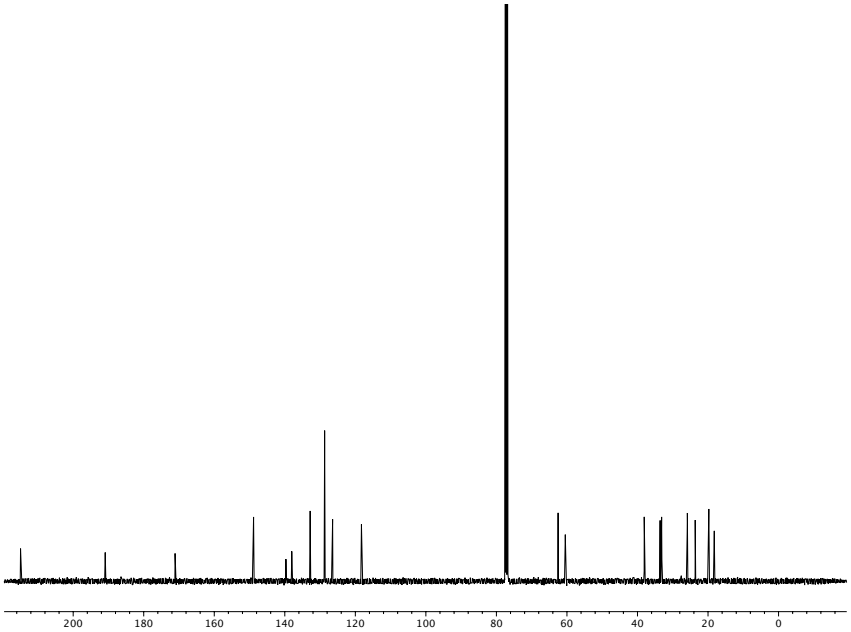


Figure A2.69. *^{13}C NMR (100 MHz, $CDCl_3$) of compound* ***126c****.*

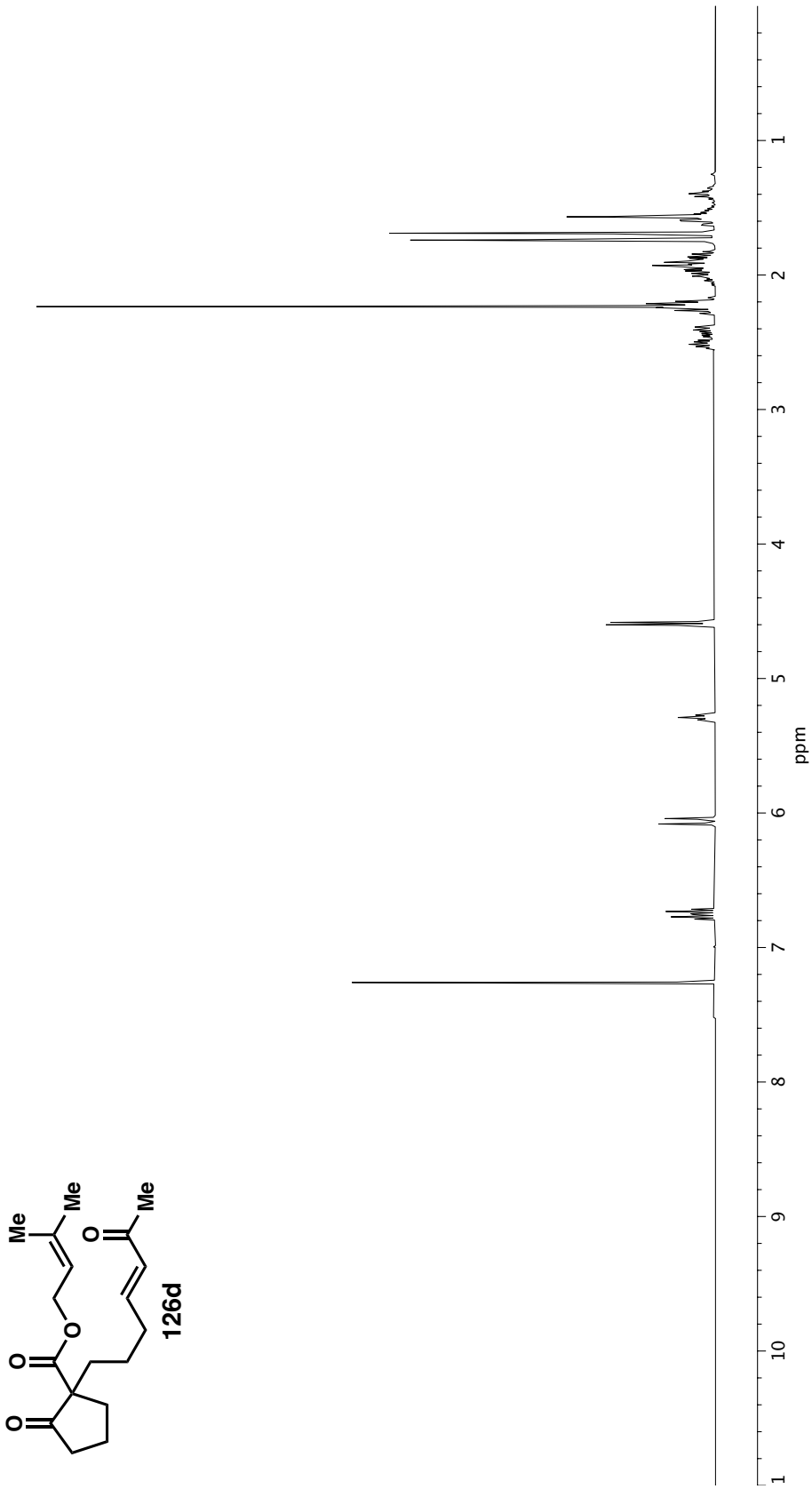


Figure A2.70. *^1H NMR (400 MHz, $CDCl_3$) of compound* ***126d****.*

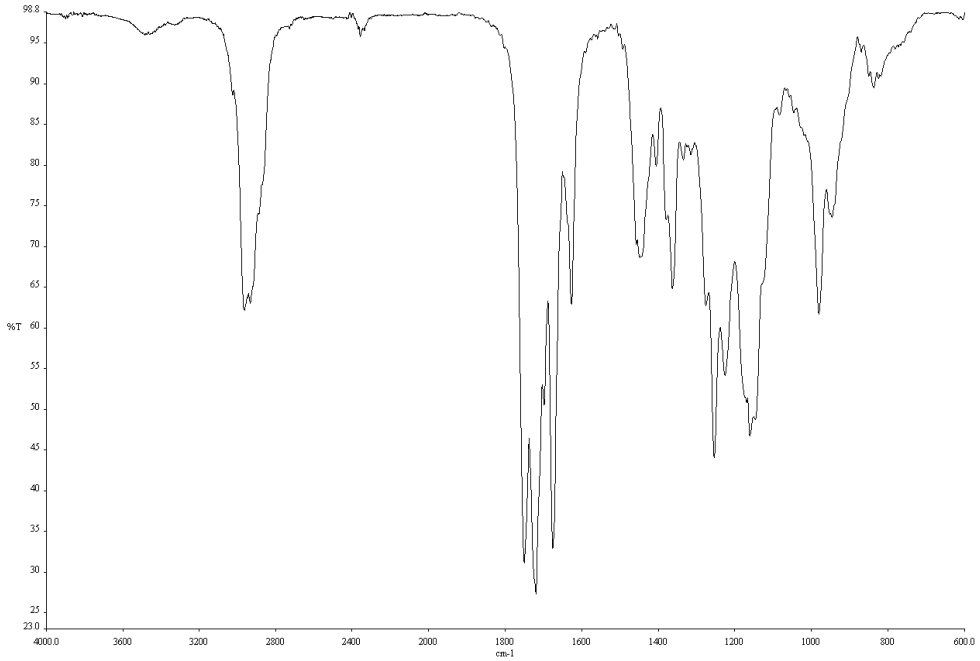


Figure A2.71. *Infrared spectrum (Thin Film, NaCl) of compound* ***126d****.*

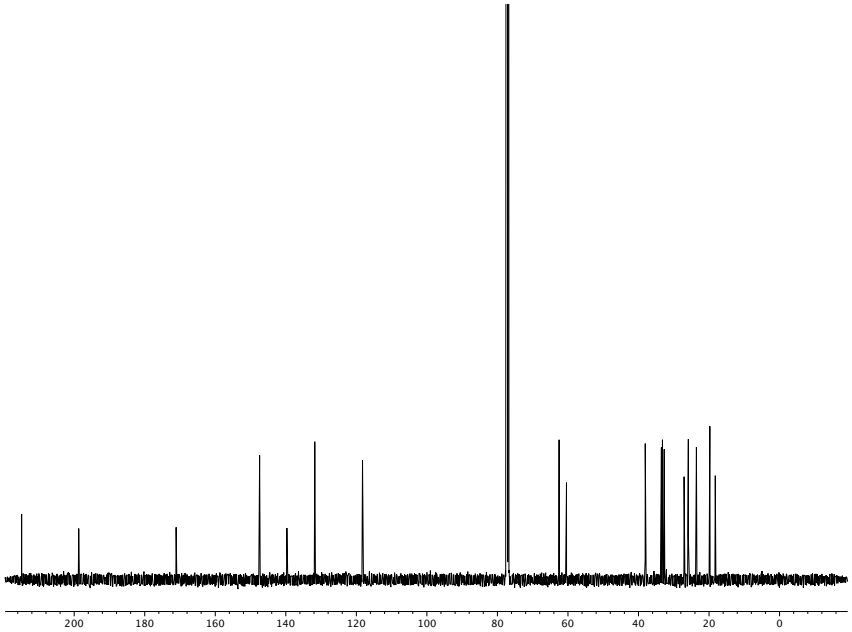


Figure A2.72. *^{13}C NMR (100 MHz, $CDCl_3$) of compound* ***126d****.*

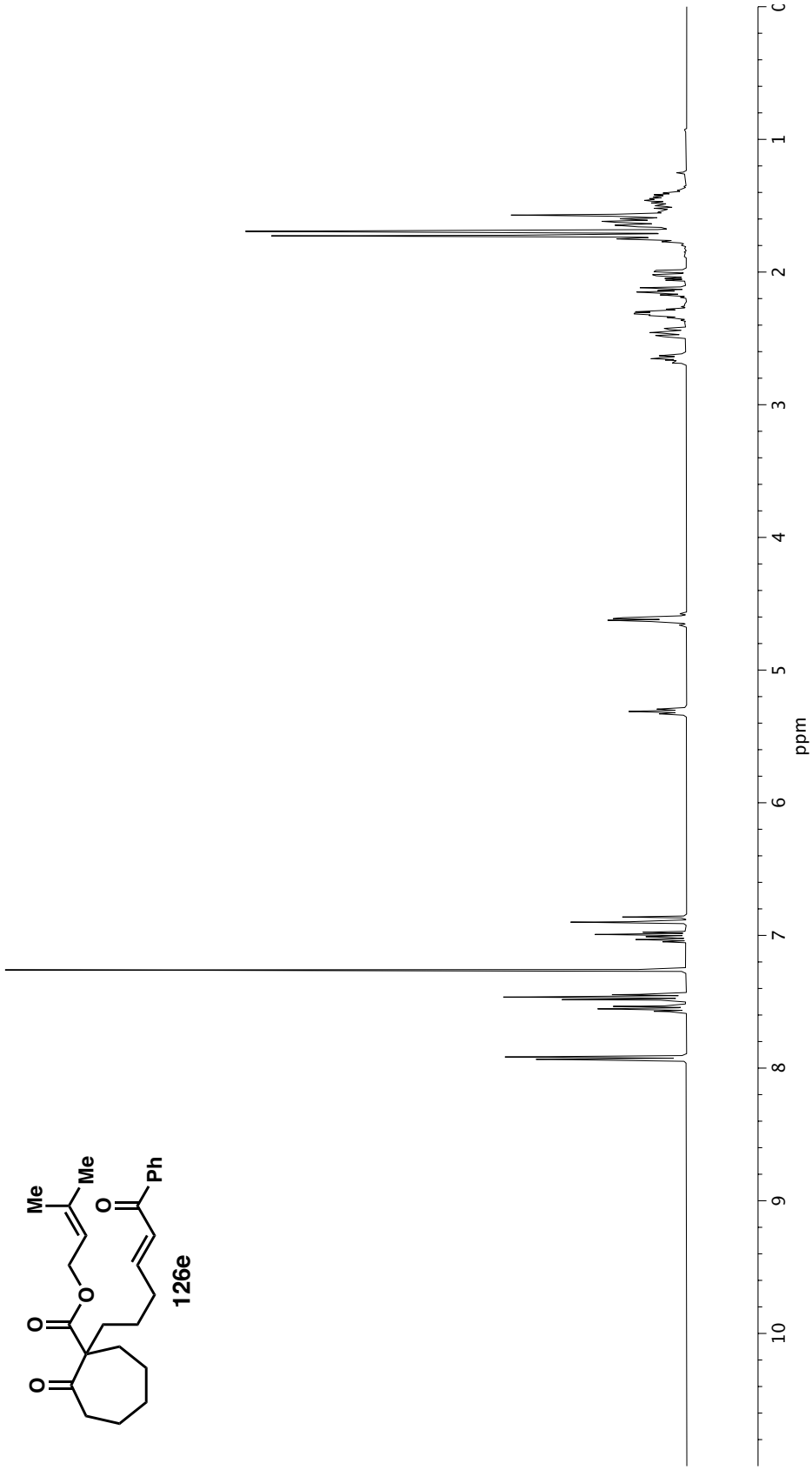


Figure A2.73. *^1H NMR (400 MHz, $CDCl_3$) of compound* ***126e****.*

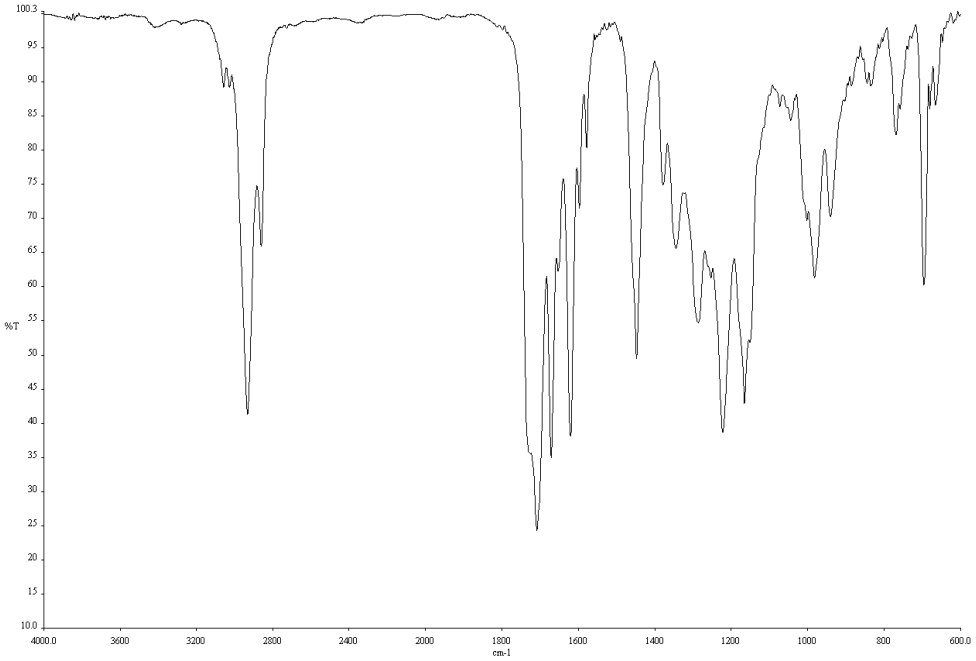


Figure A2.74. *Infrared spectrum (Thin Film, NaCl) of compound* ***126e****.*

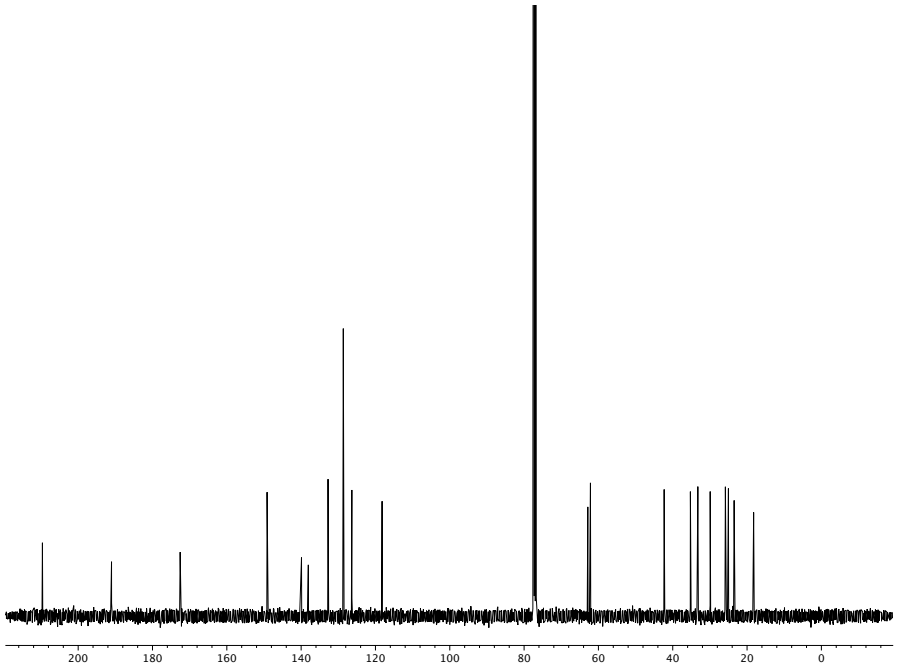


Figure A2.75. *^{13}C NMR (100 MHz, $CDCl_3$) of compound* ***126e****.*

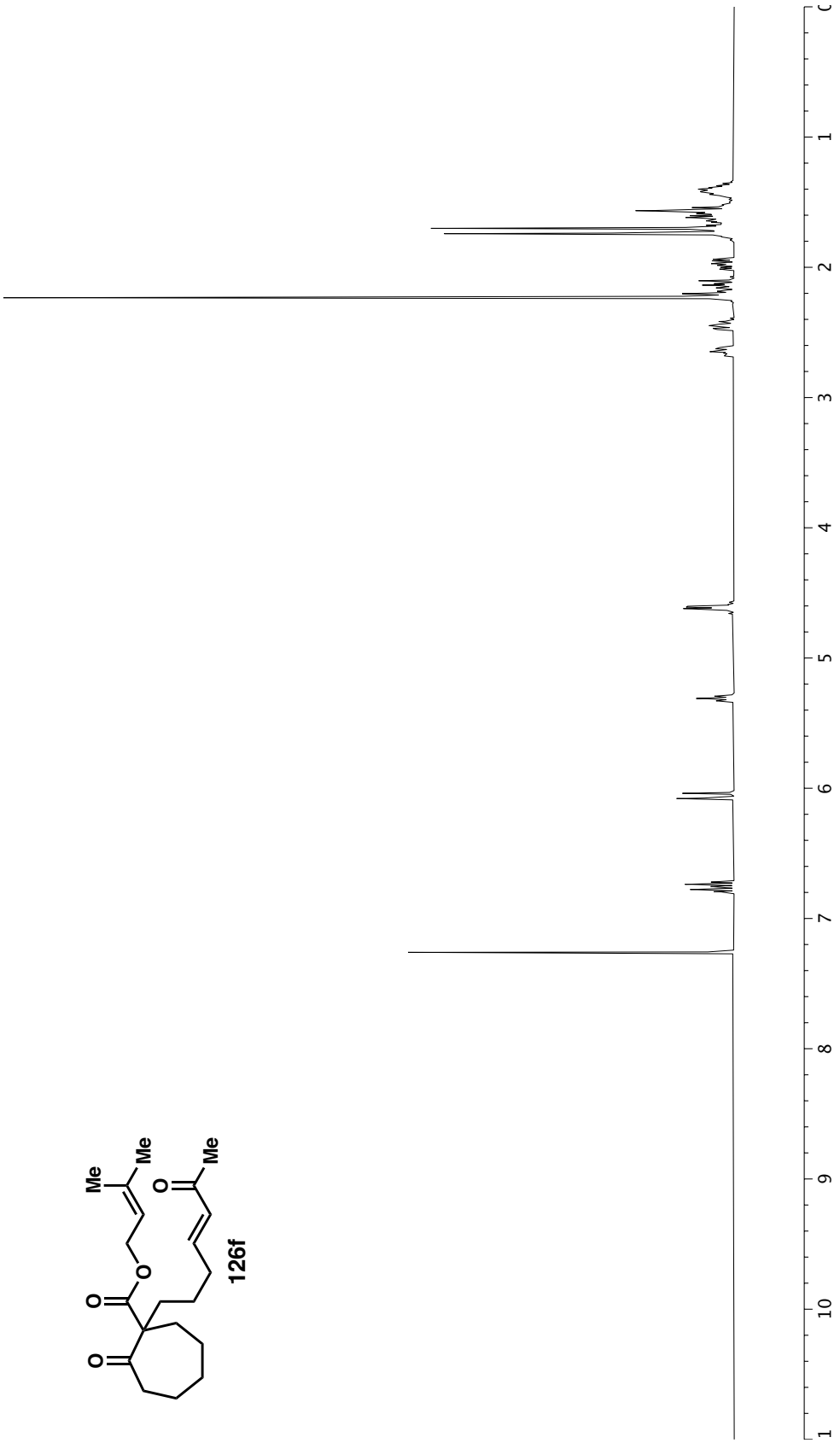


Figure A2.76. *^1H NMR (400 MHz, $CDCl_3$) of compound **126f**.*

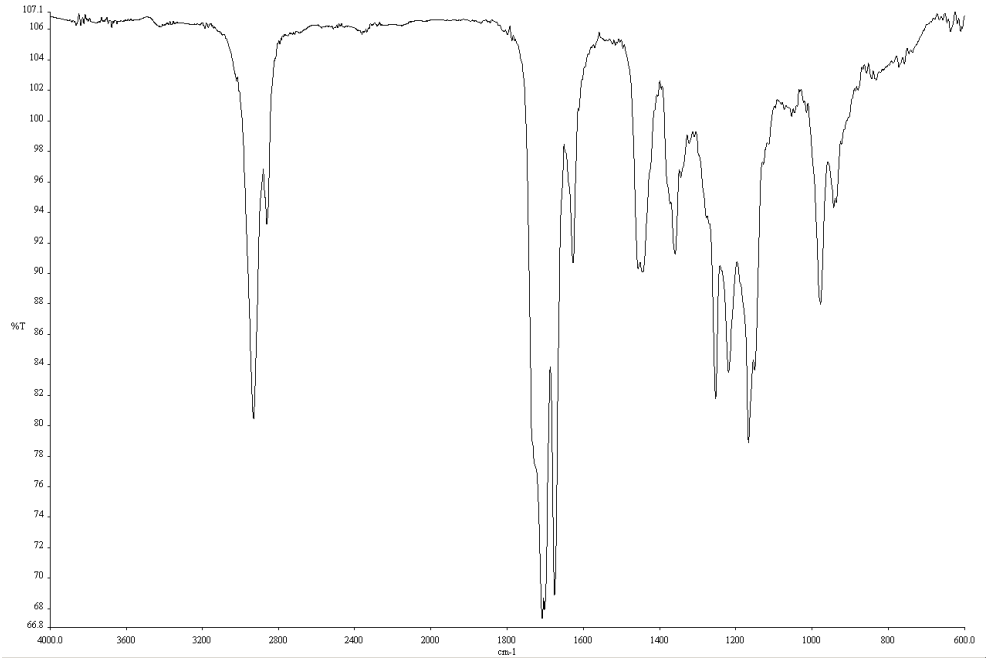


Figure A2.77. *Infrared spectrum (Thin Film, NaCl) of compound* ***126f****.*

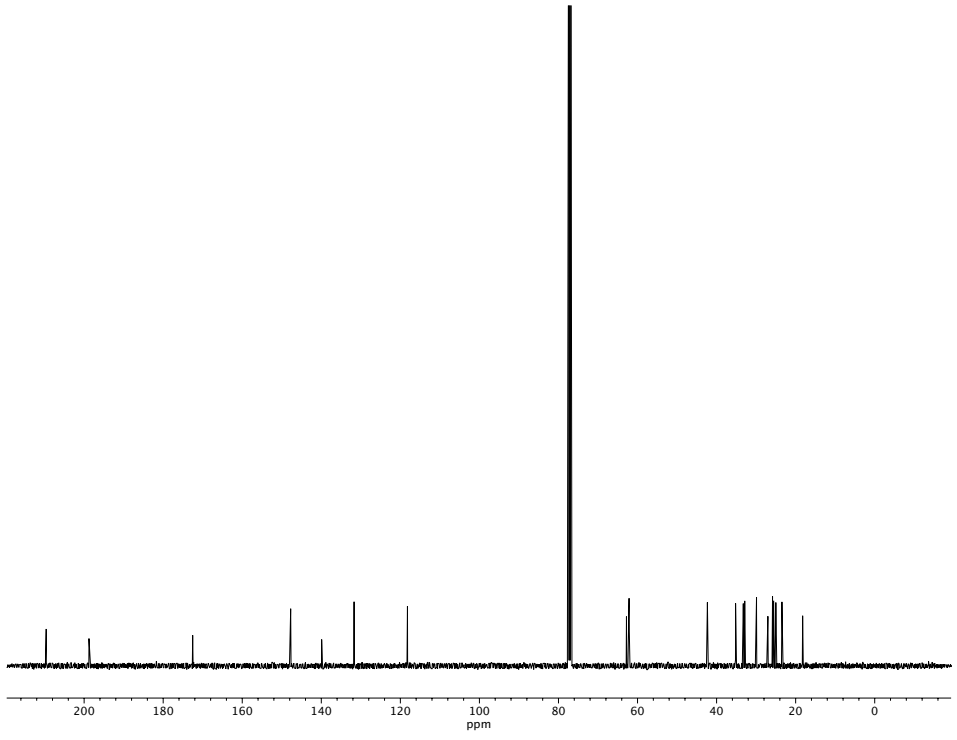


Figure A2.78. *^{13}C NMR (100 MHz, $CDCl_3$) of compound* ***126f****.*

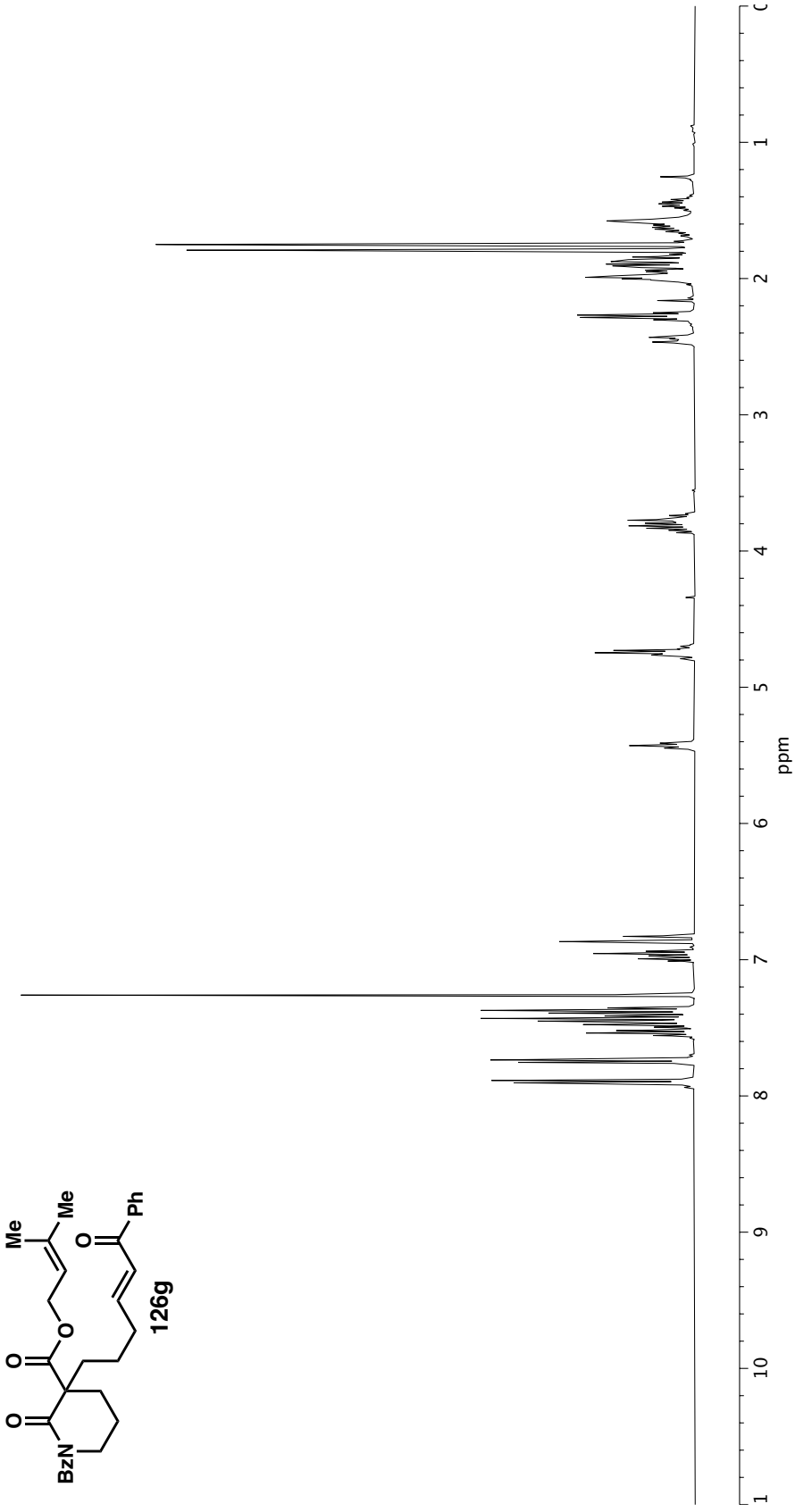


Figure A2.79. *^1H NMR (400 MHz, $CDCl_3$) of compound* ***126g****.*

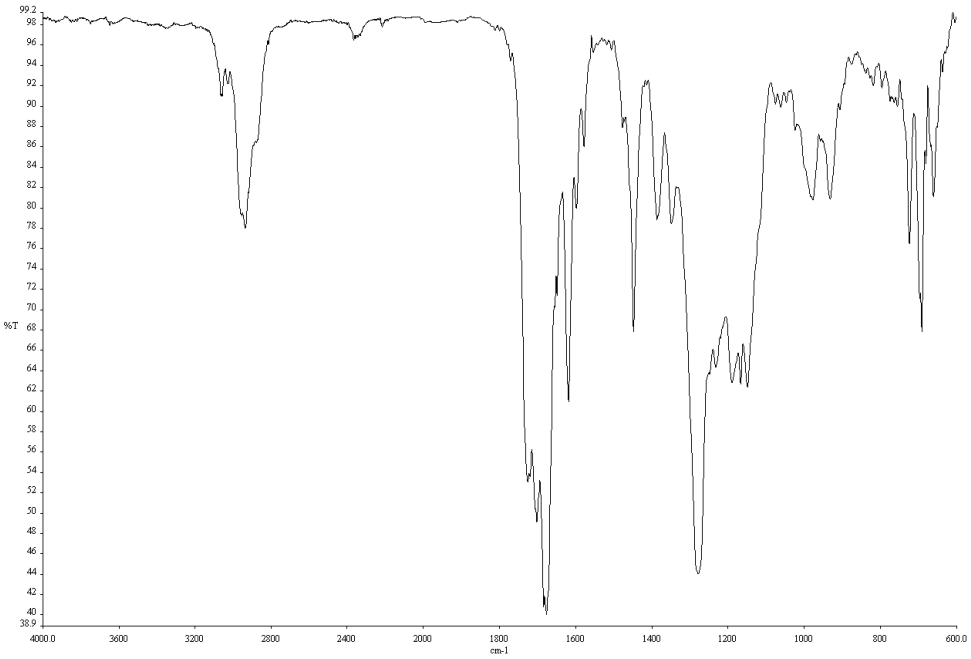


Figure A2.80. *Infrared spectrum (Thin Film, NaCl) of compound* ***126g****.*

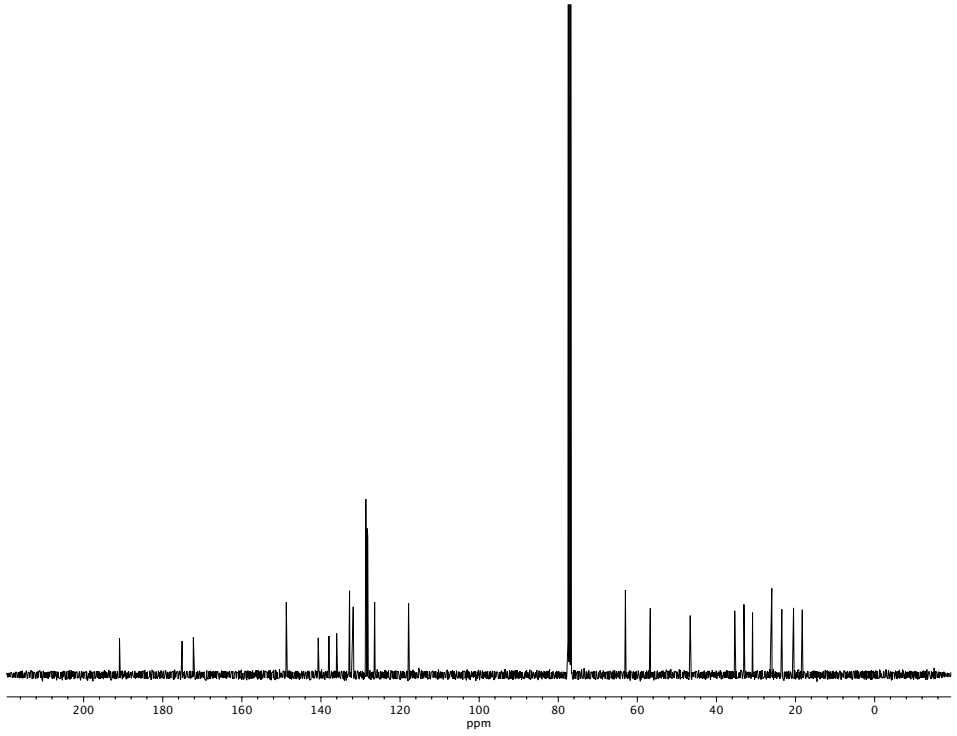


Figure A2.81. *^{13}C NMR (100 MHz, $CDCl_3$) of compound* ***126g****.*

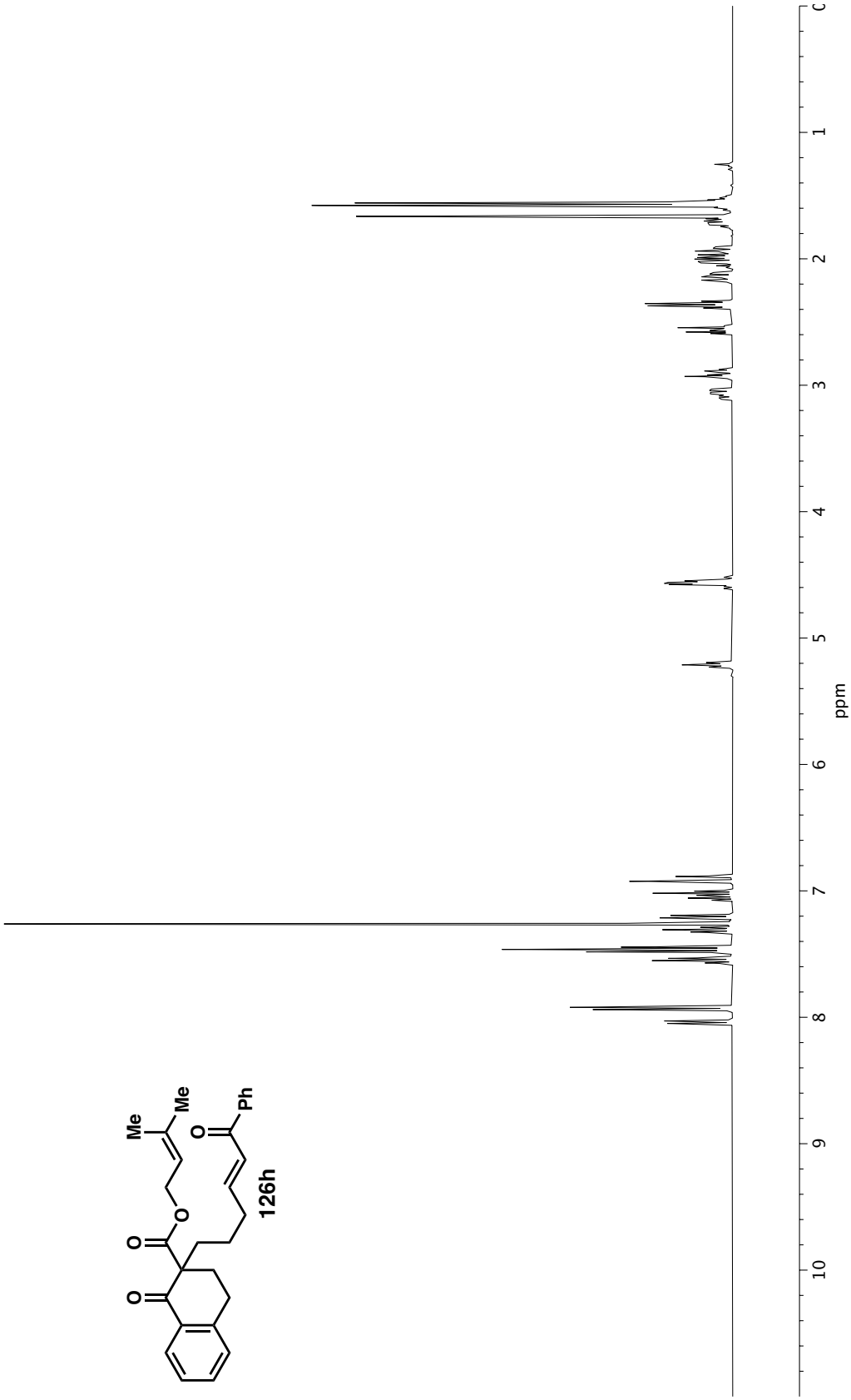


Figure A2.82. *^1H NMR (400 MHz, $CDCl_3$) of compound* ***126h****.*

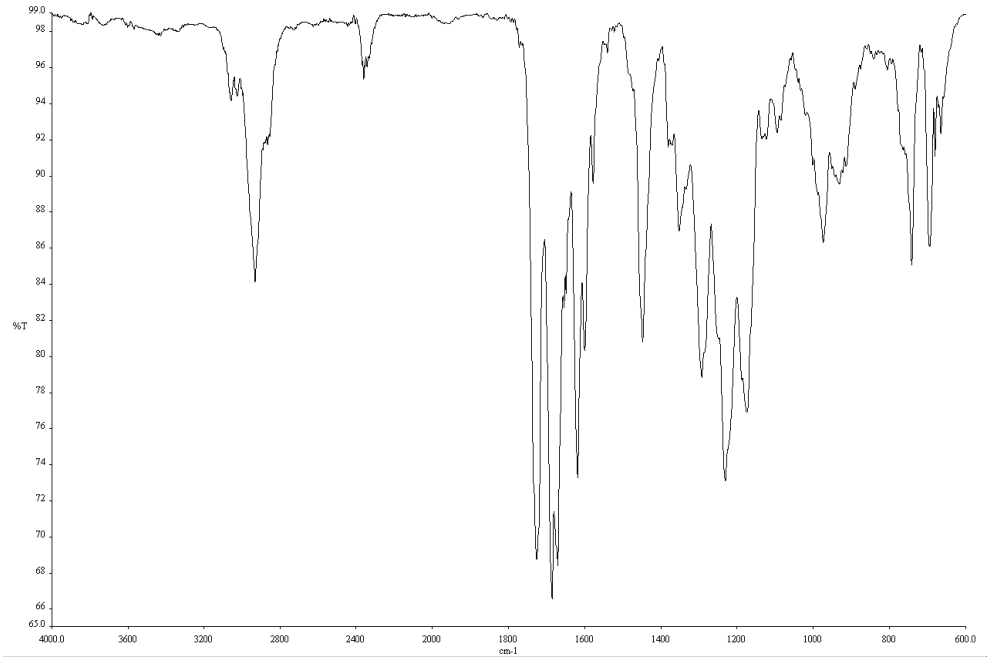


Figure A2.83. *Infrared spectrum (Thin Film, NaCl) of compound* ***126h****.*

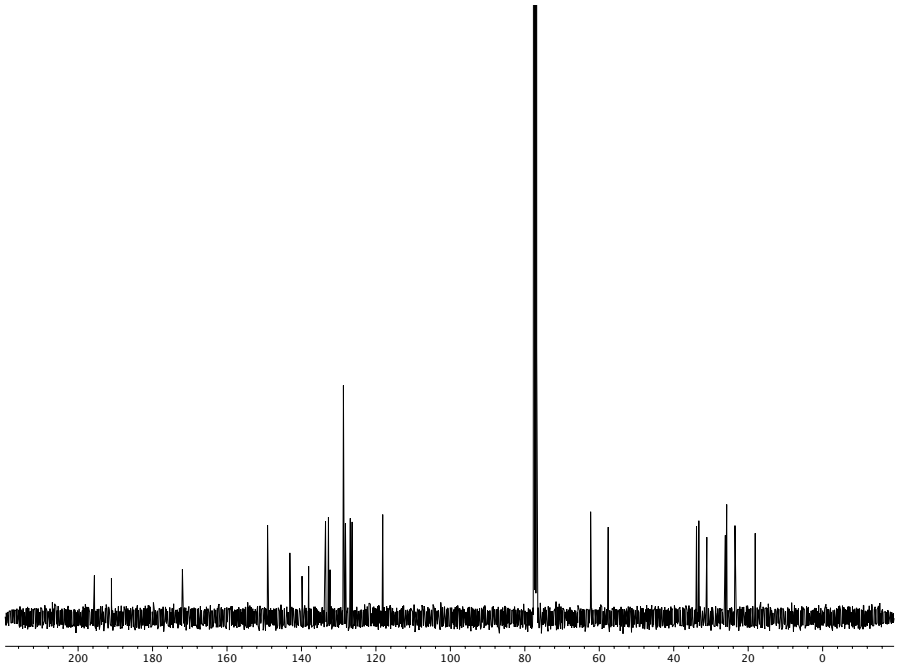


Figure A2.84. *^{13}C NMR (100 MHz, $CDCl_3$) of compound* ***126h****.*

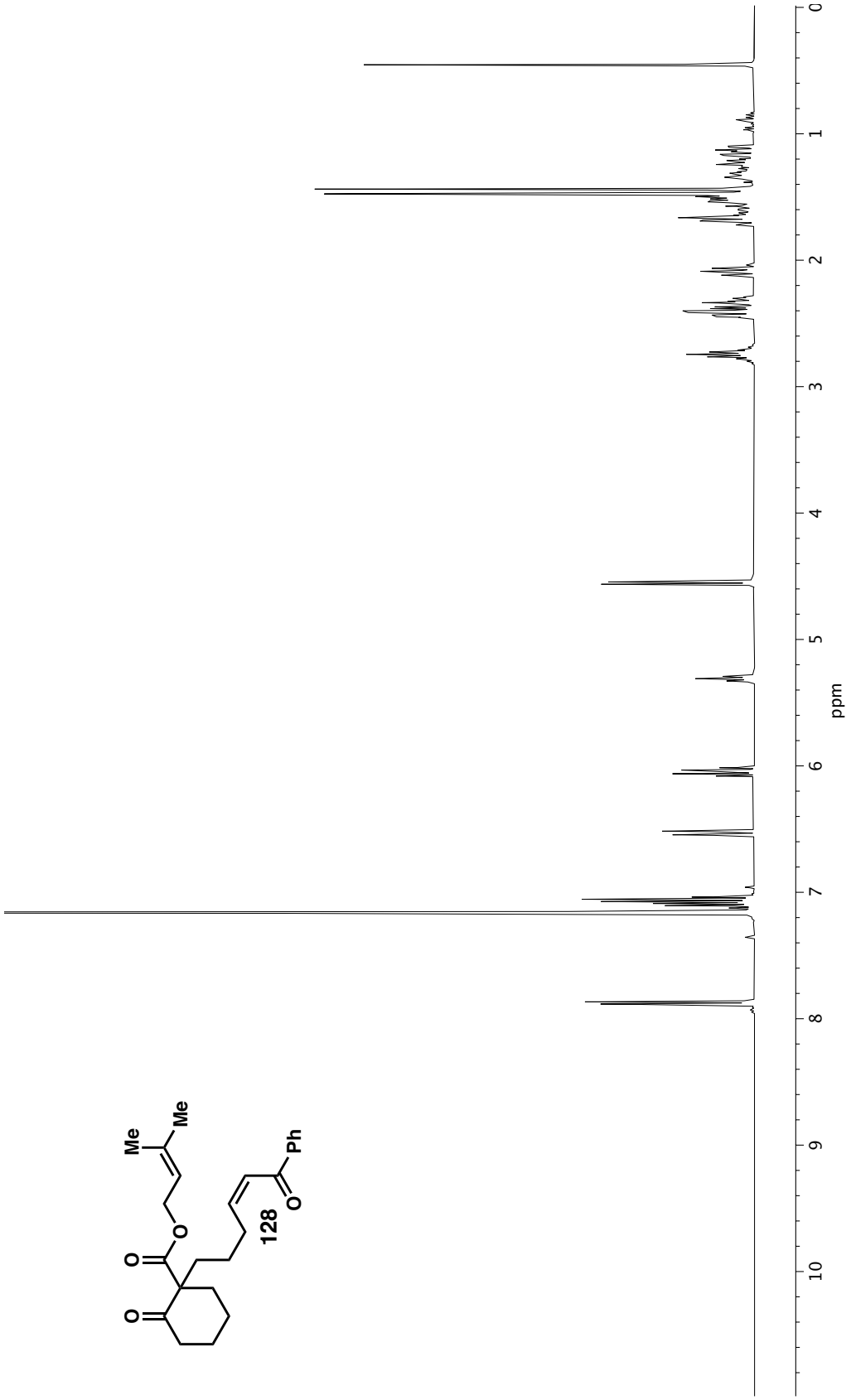


Figure A2.85. *^1H NMR (400 MHz, C_6D_6) of compound* ***128****.*

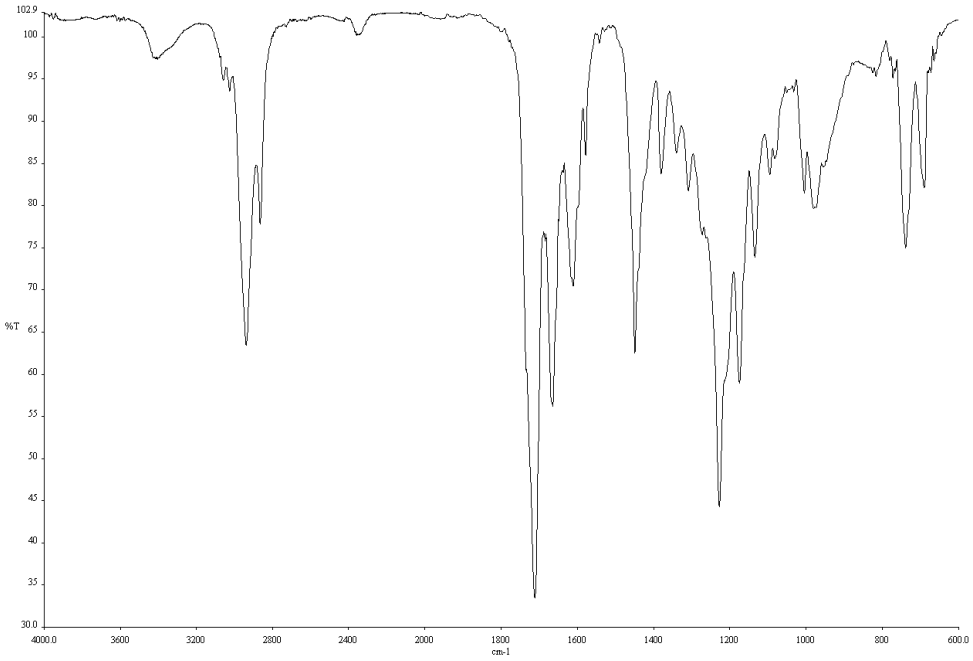


Figure A2.86. *Infrared spectrum (Thin Film, NaCl) of compound* ***128****.*

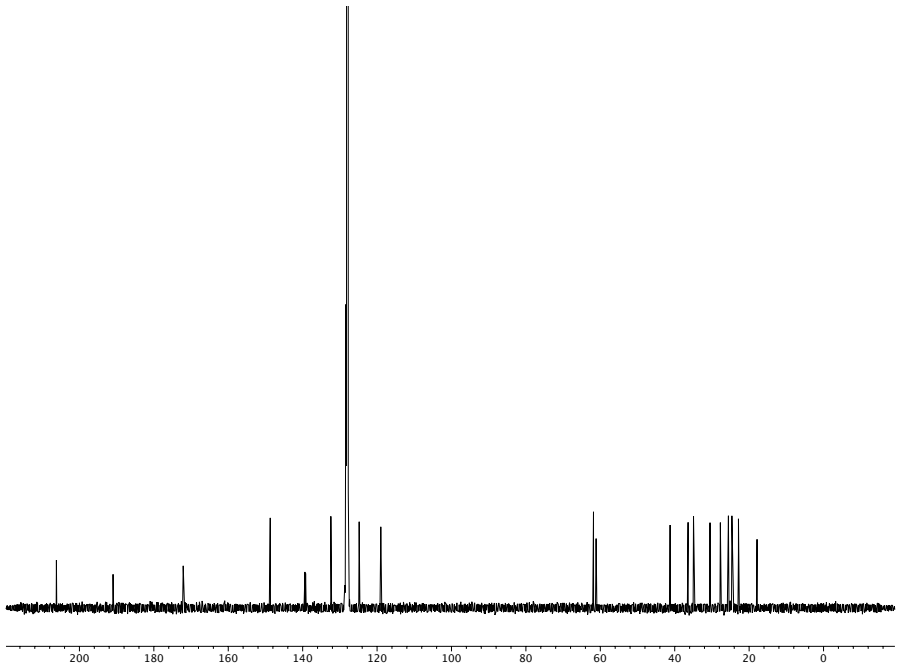


Figure A2.87. *^{13}C NMR (100 MHz, C_6D_6) of compound* ***128****.*

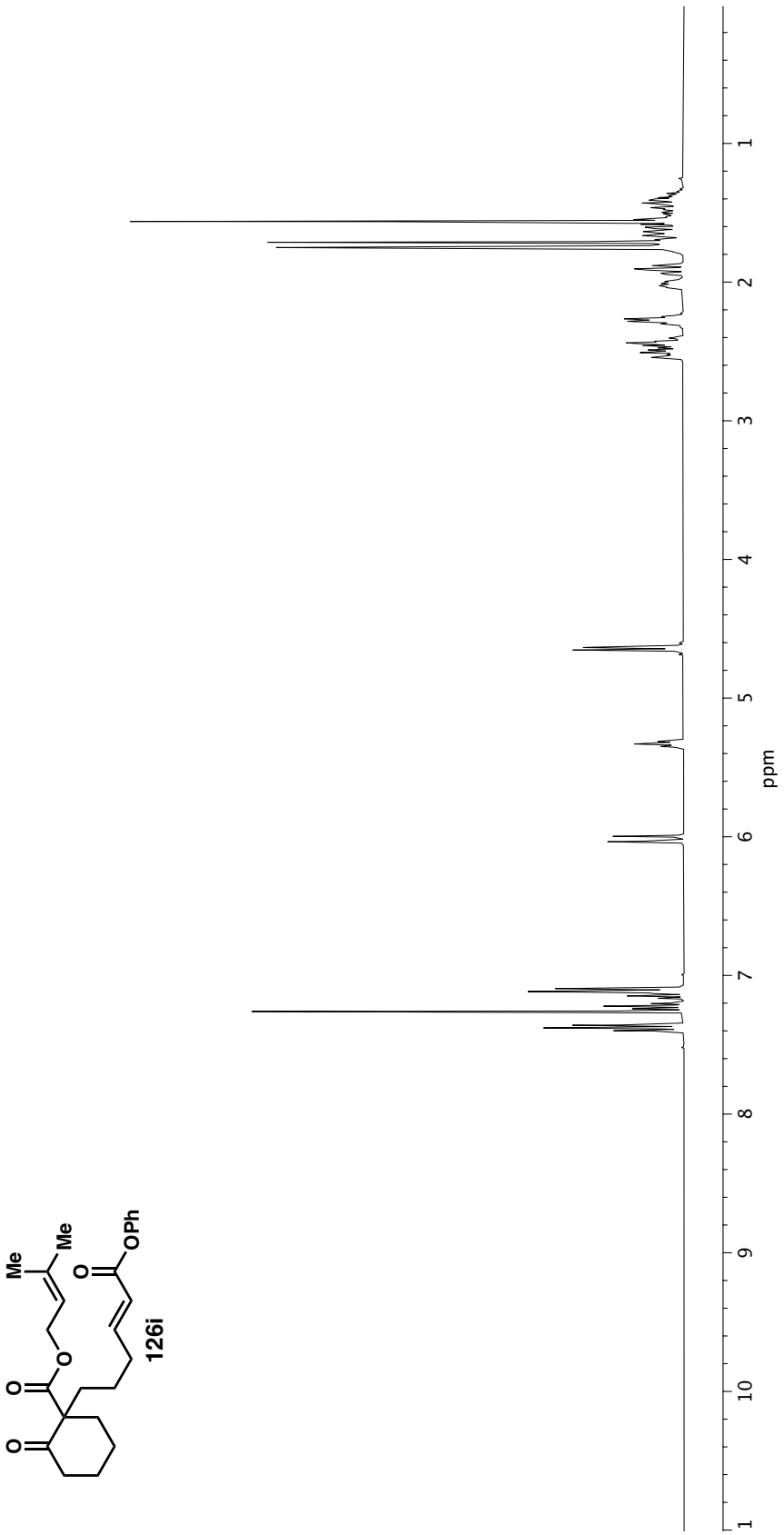


Figure A2.88. *^1H NMR (400 MHz, $CDCl_3$) of compound* ***126i****.*

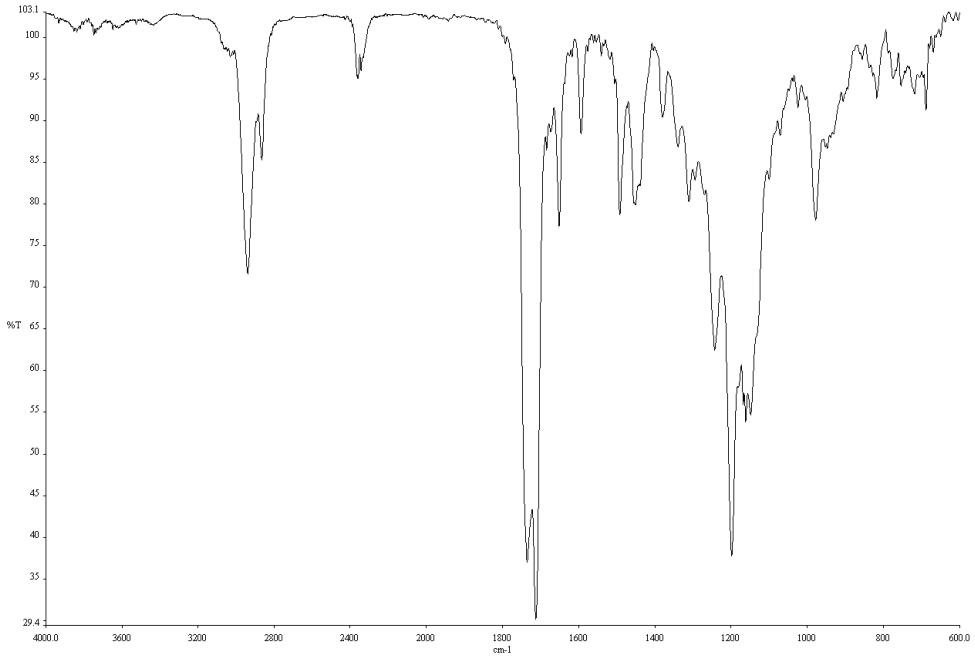


Figure A2.89. *Infrared spectrum (Thin Film, NaCl) of compound* ***126i****.*

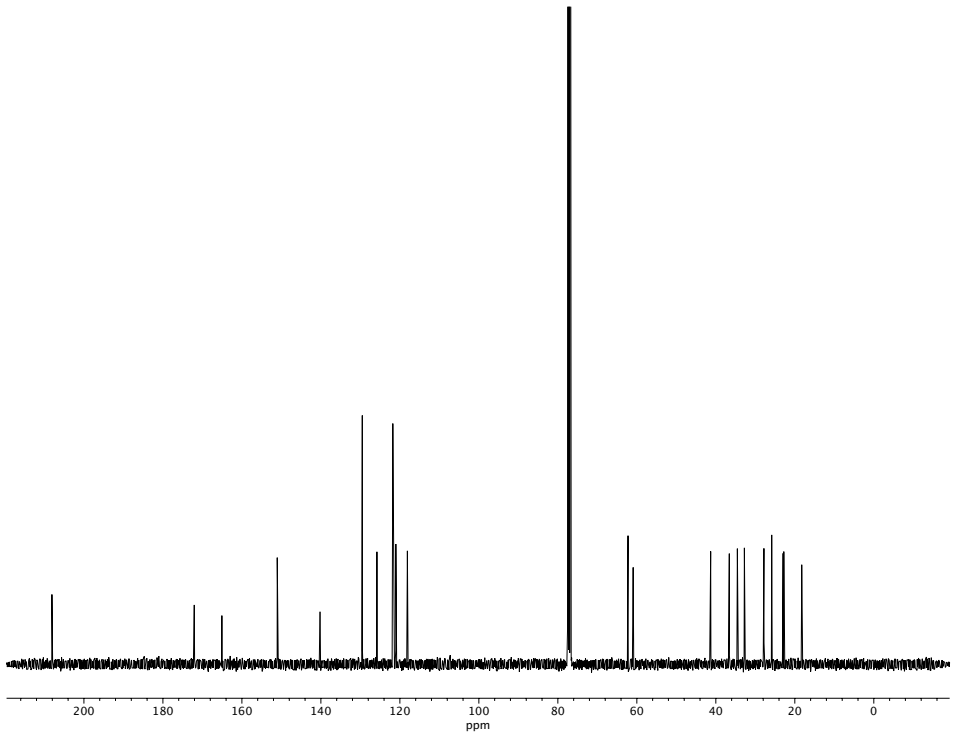


Figure A2.90. *^{13}C NMR (100 MHz, $CDCl_3$) of compound* ***126i****.*

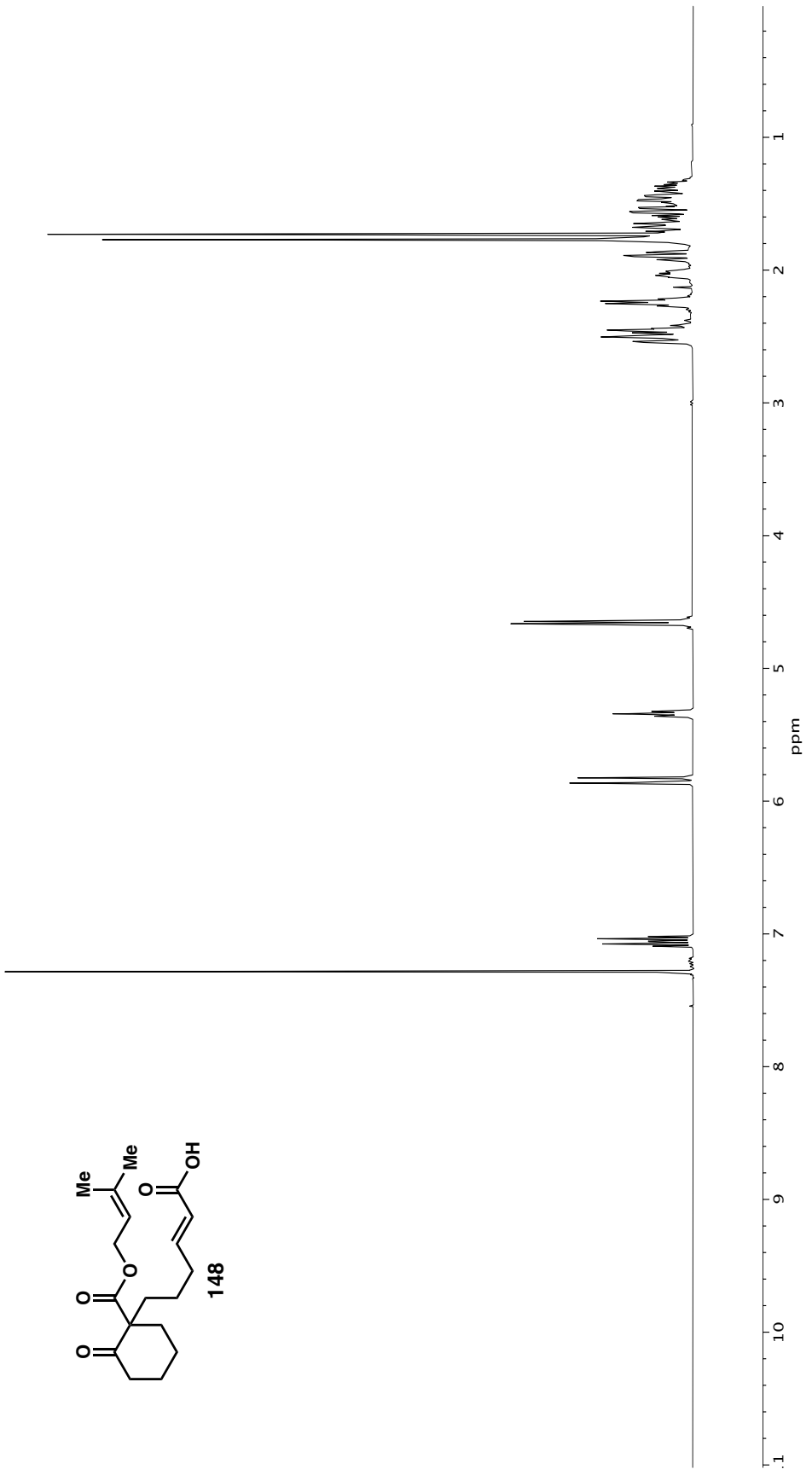


Figure A2.91. *^{1}H NMR (400 MHz, $CDCl_3$) of compound **148**.*

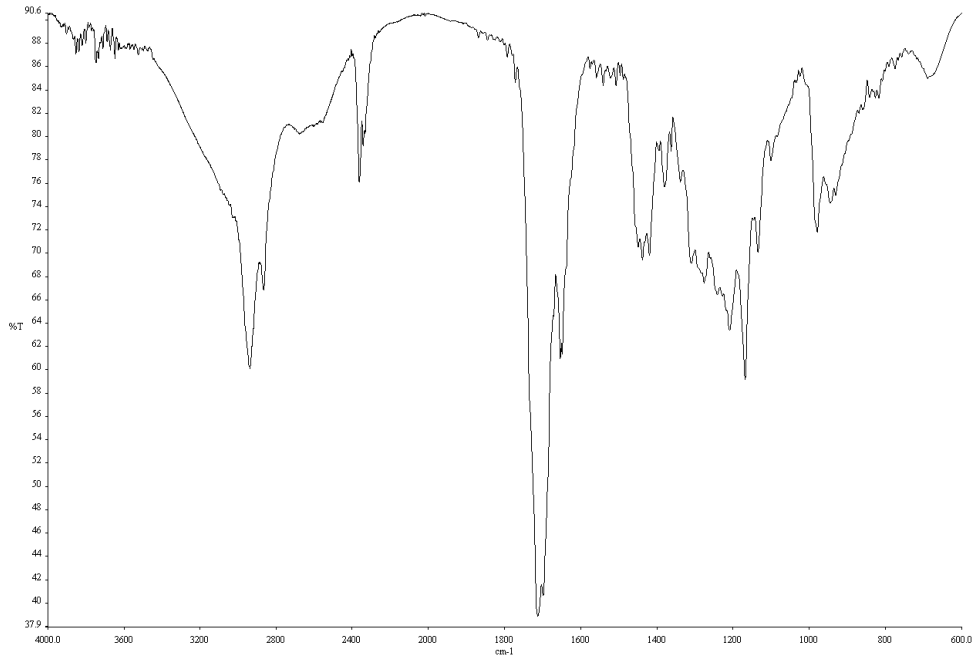


Figure A2.92. *Infrared spectrum (Thin Film, NaCl) of compound* ***148****.*

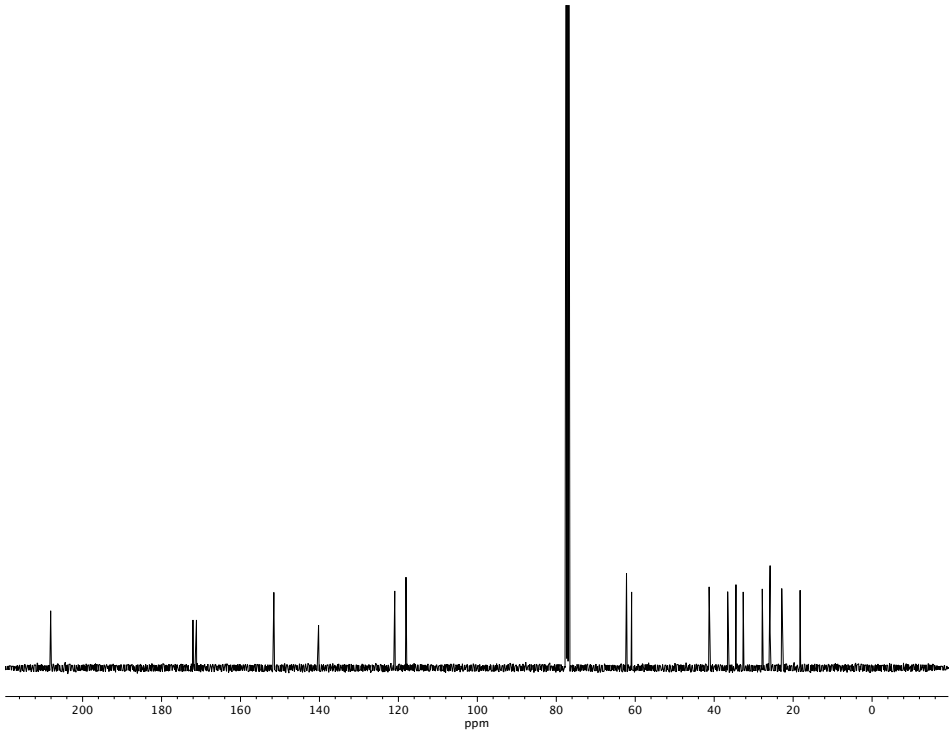


Figure A2.93. *^{13}C NMR (100 MHz, $CDCl_3$) of compound* ***148****.*

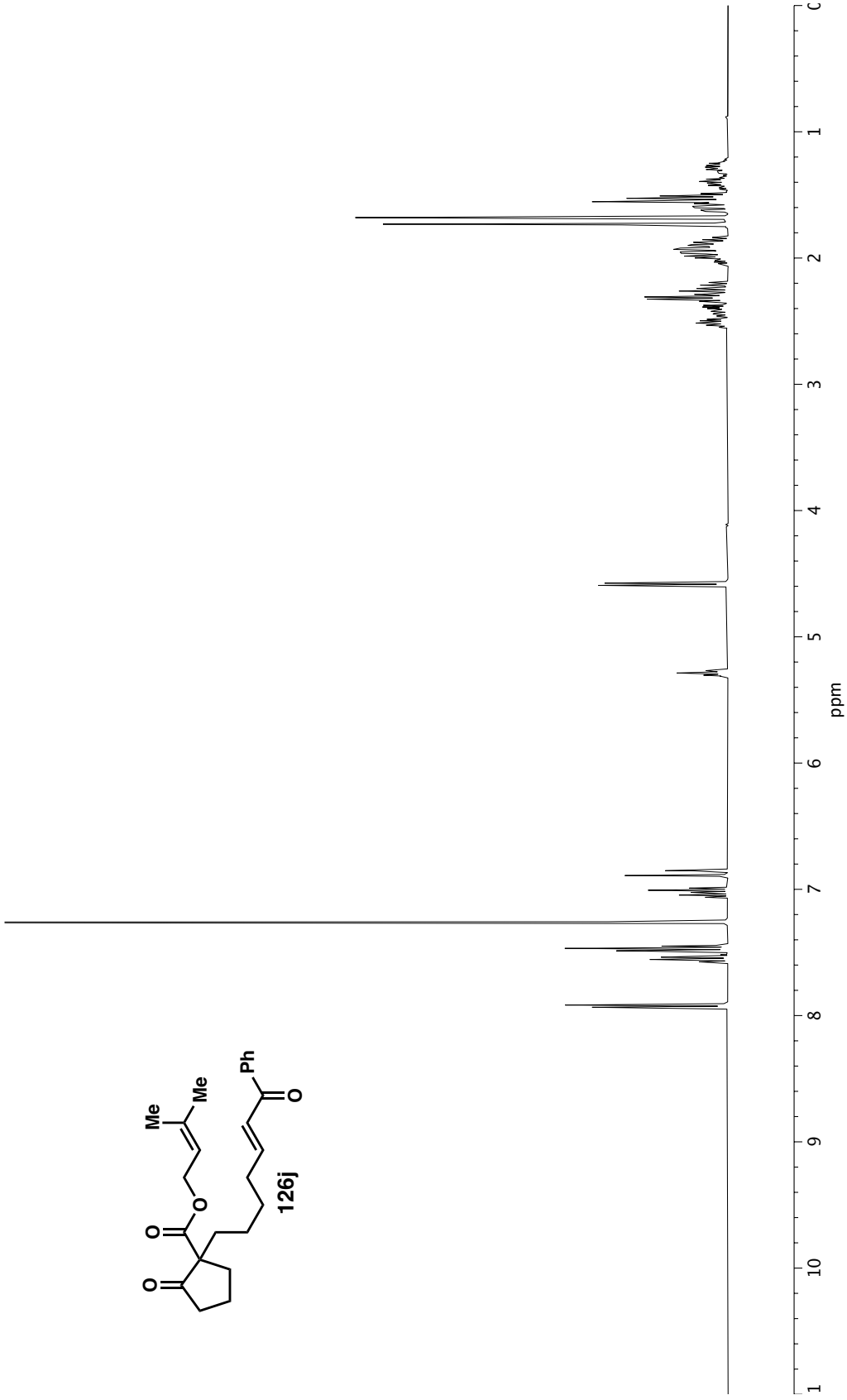


Figure A2.94. *^1H NMR (400 MHz, $CDCl_3$) of compound **126j**.*

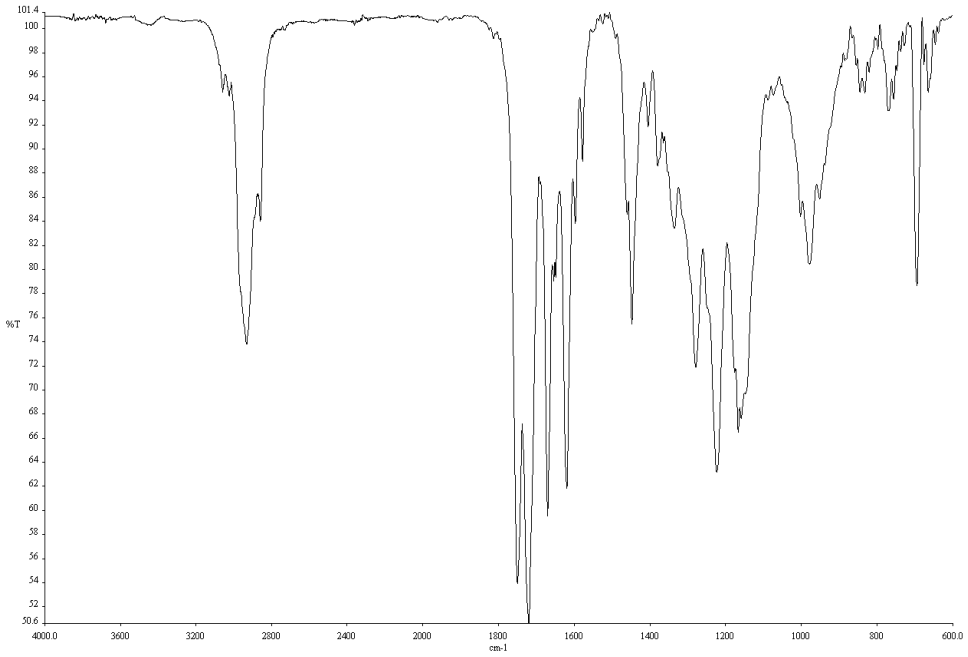


Figure A2.95. *Infrared spectrum (Thin Film, NaCl) of compound* ***126j****.*

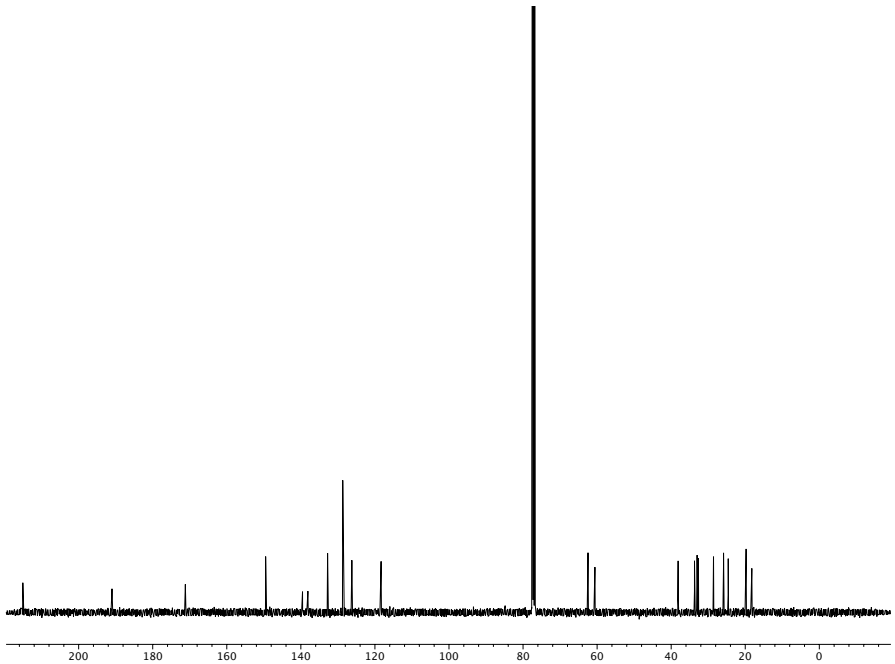


Figure A2.96. *^{13}C NMR (100 MHz, $CDCl_3$) of compound* ***126j****.*

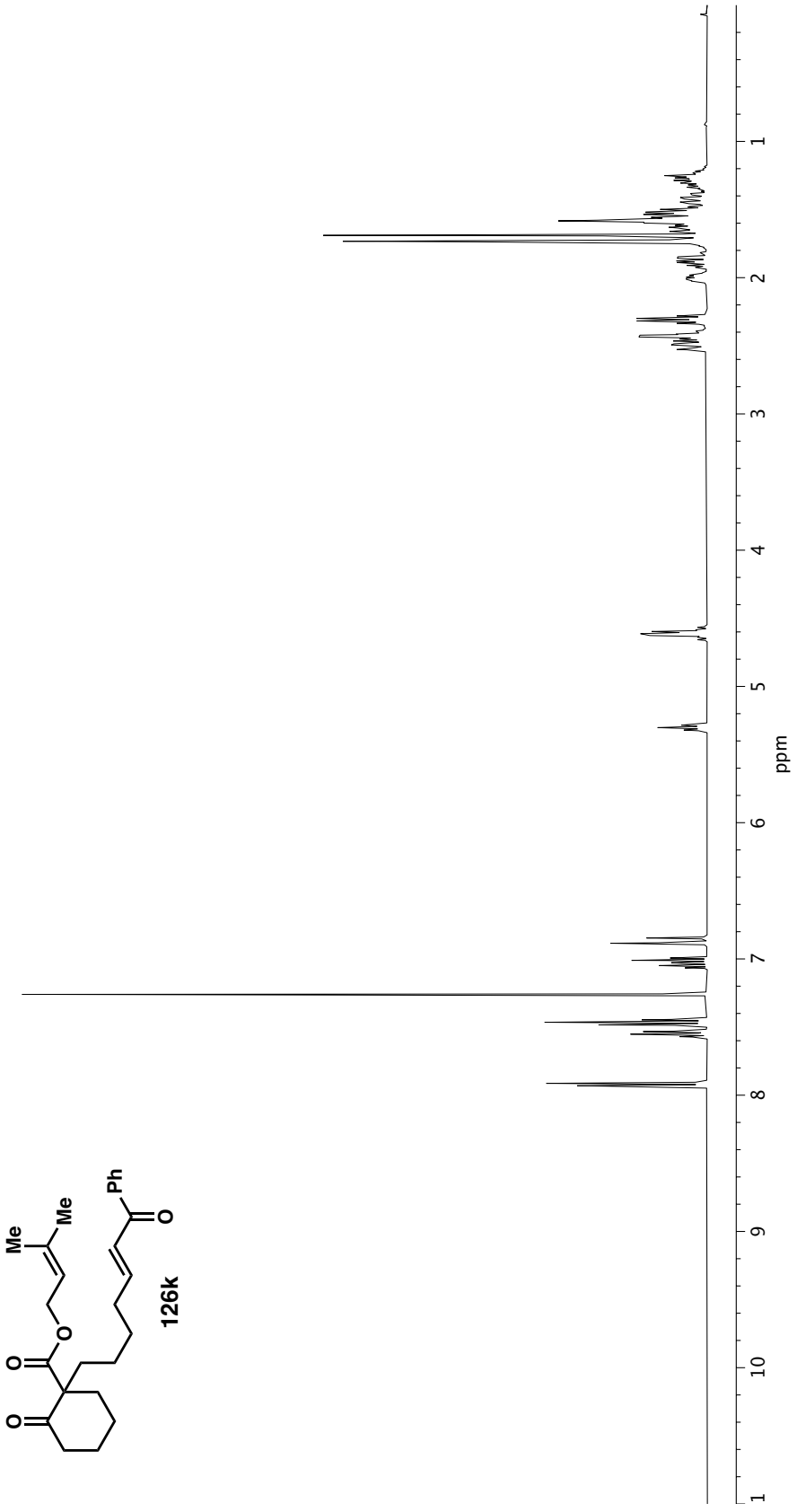


Figure A2.97. *^1H NMR (400 MHz, $CDCl_3$) of compound* ***126k****.*

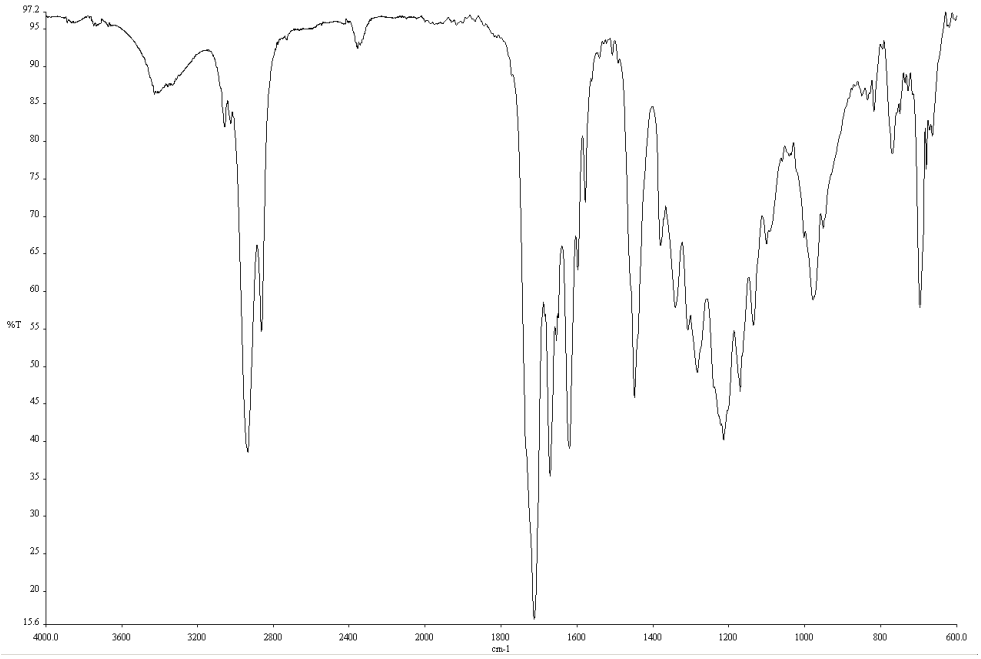


Figure A2.98. *Infrared spectrum (Thin Film, NaCl) of compound* ***126k****.*

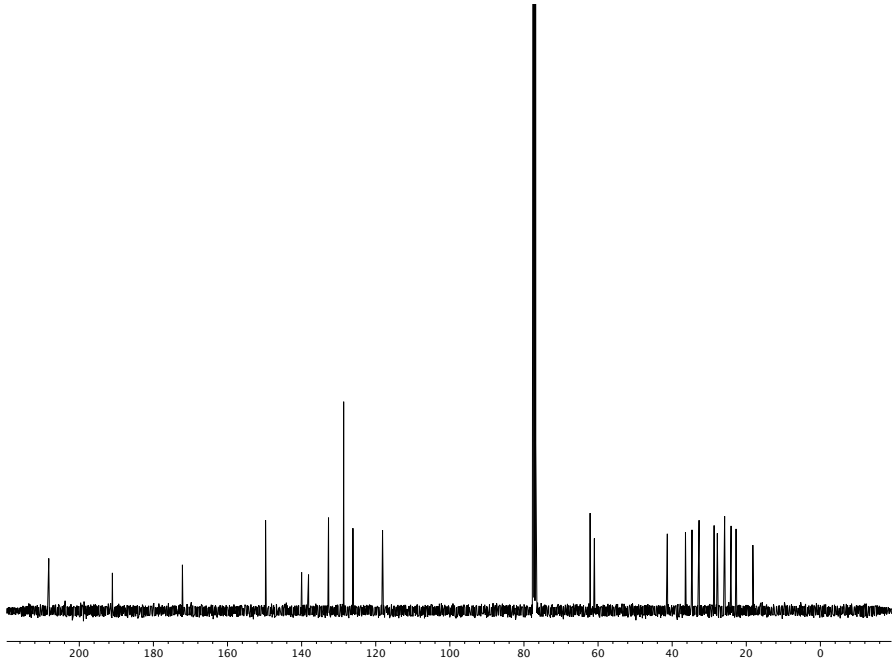


Figure A2.99. *^{13}C NMR (100 MHz, $CDCl_3$) of compound* ***126k****.*

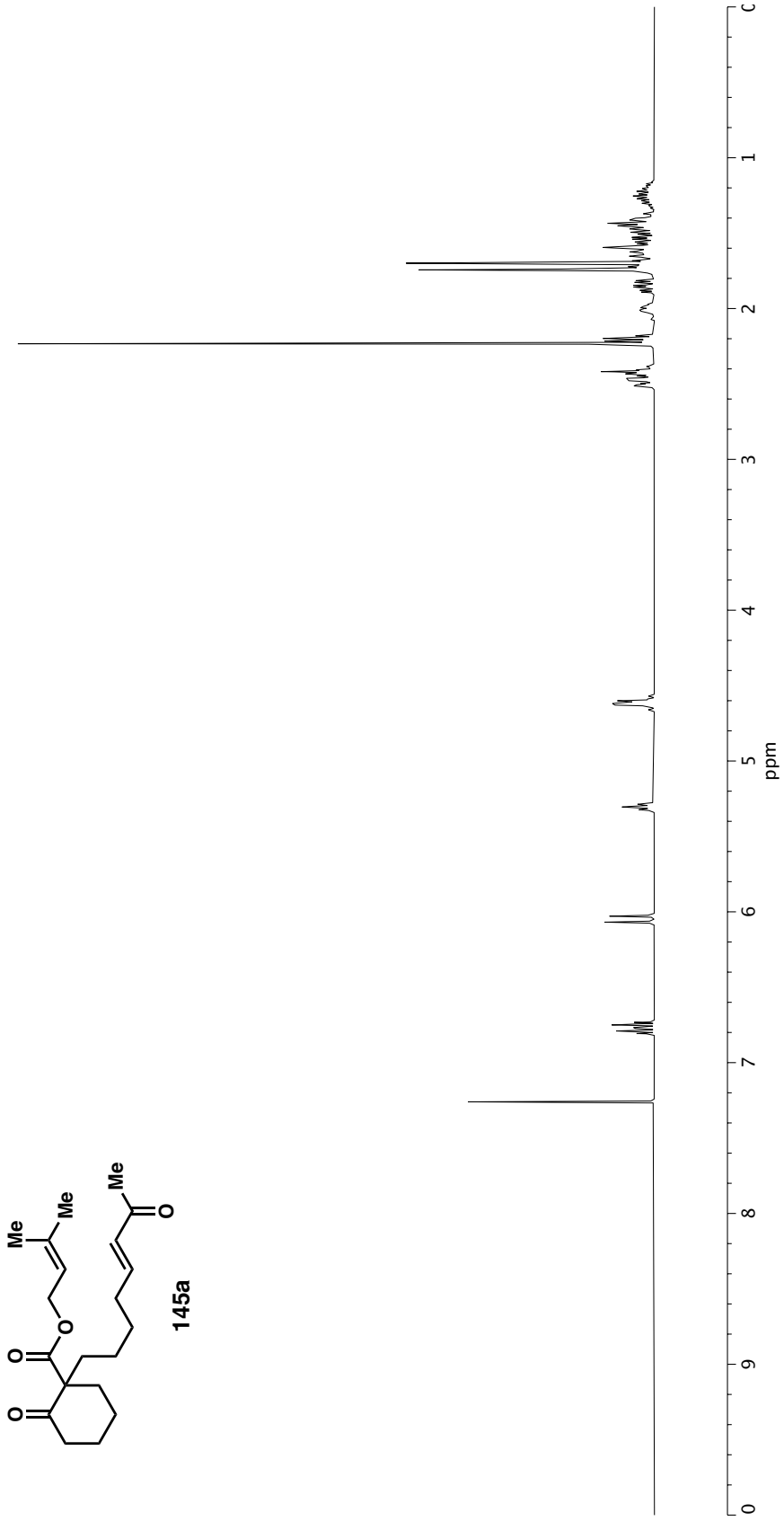


Figure A2.100. *^{1}H NMR (400 MHz, $CDCl_3$) of compound* ***145a****.*

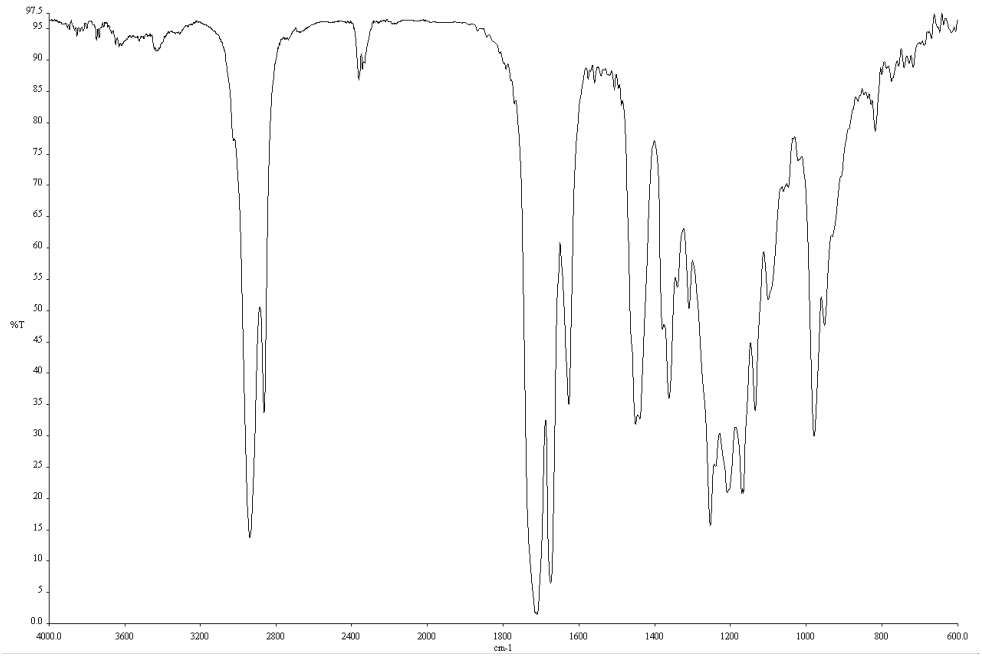


Figure A2.101. *Infrared spectrum (Thin Film, NaCl) of compound* ***145a****.*

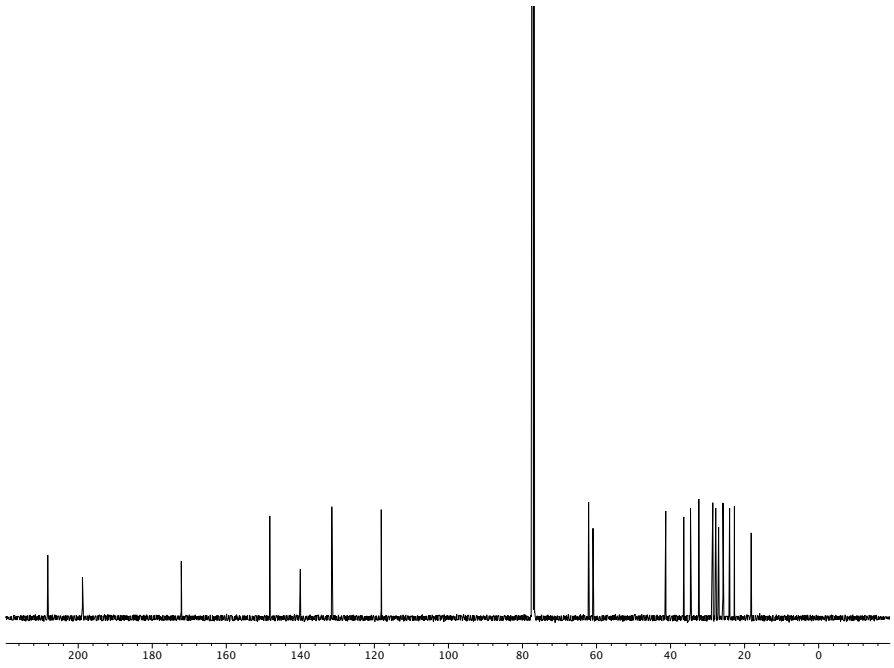


Figure A2.102. *^{13}C NMR (100 MHz, $CDCl_3$) of compound* ***145a****.*

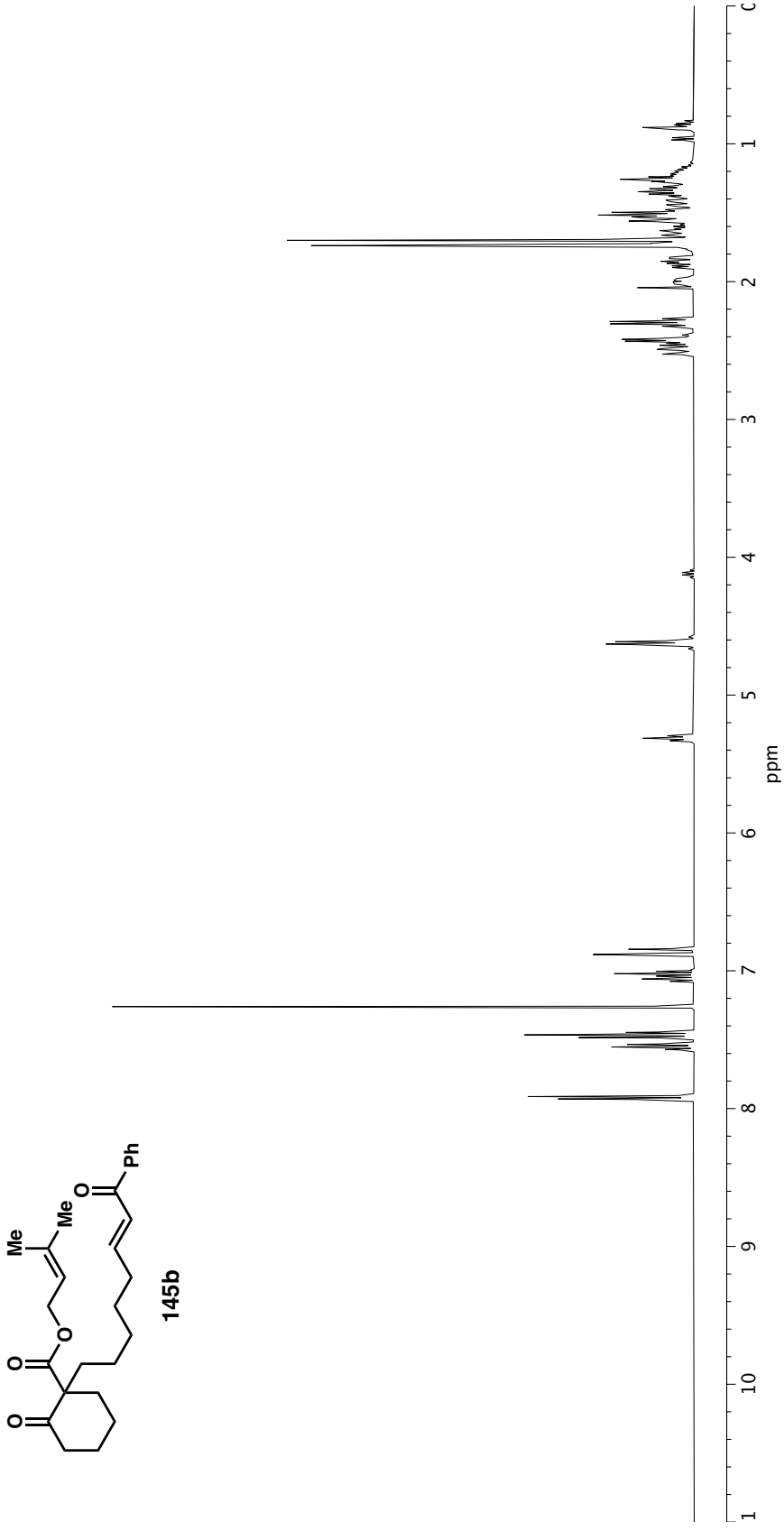


Figure A2.103. *^{1}H NMR (400 MHz, $CDCl_3$) of compound* ***145b***.

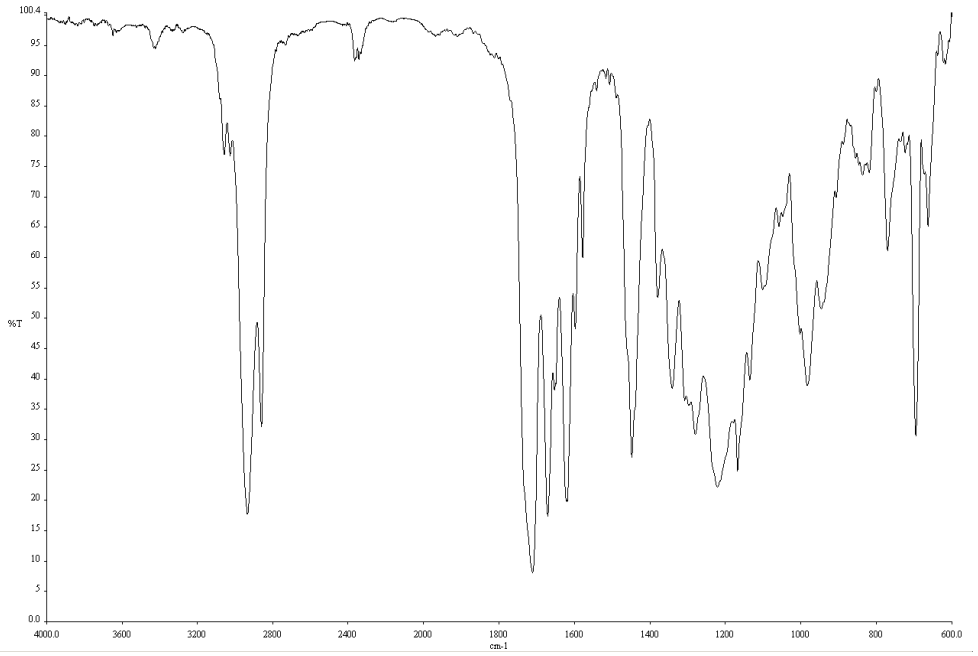


Figure A2.104. *Infrared spectrum (Thin Film, NaCl) of compound* ***145b****.*

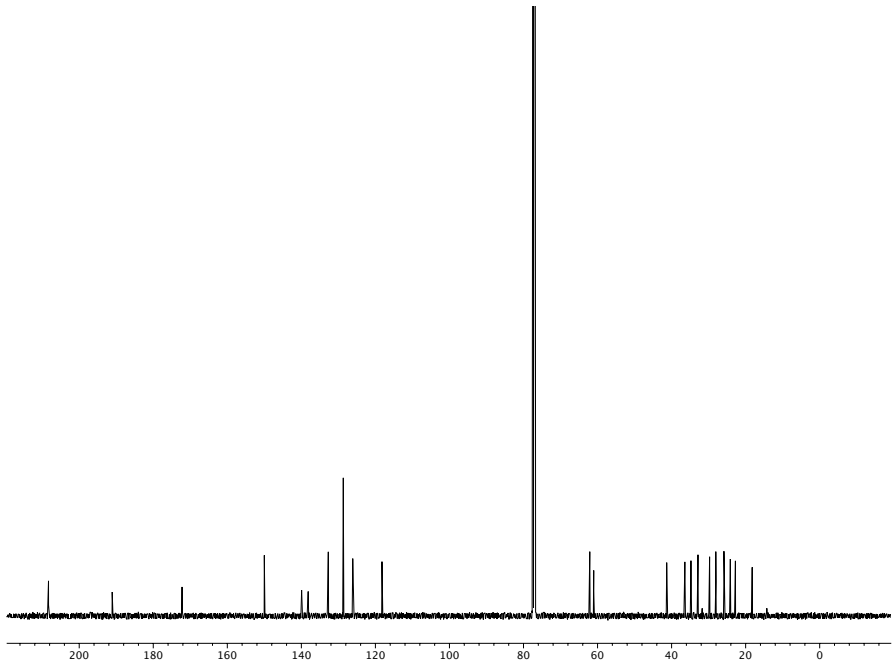


Figure A2.105. *^{13}C NMR (100 MHz, $CDCl_3$) of compound* ***145b****.*

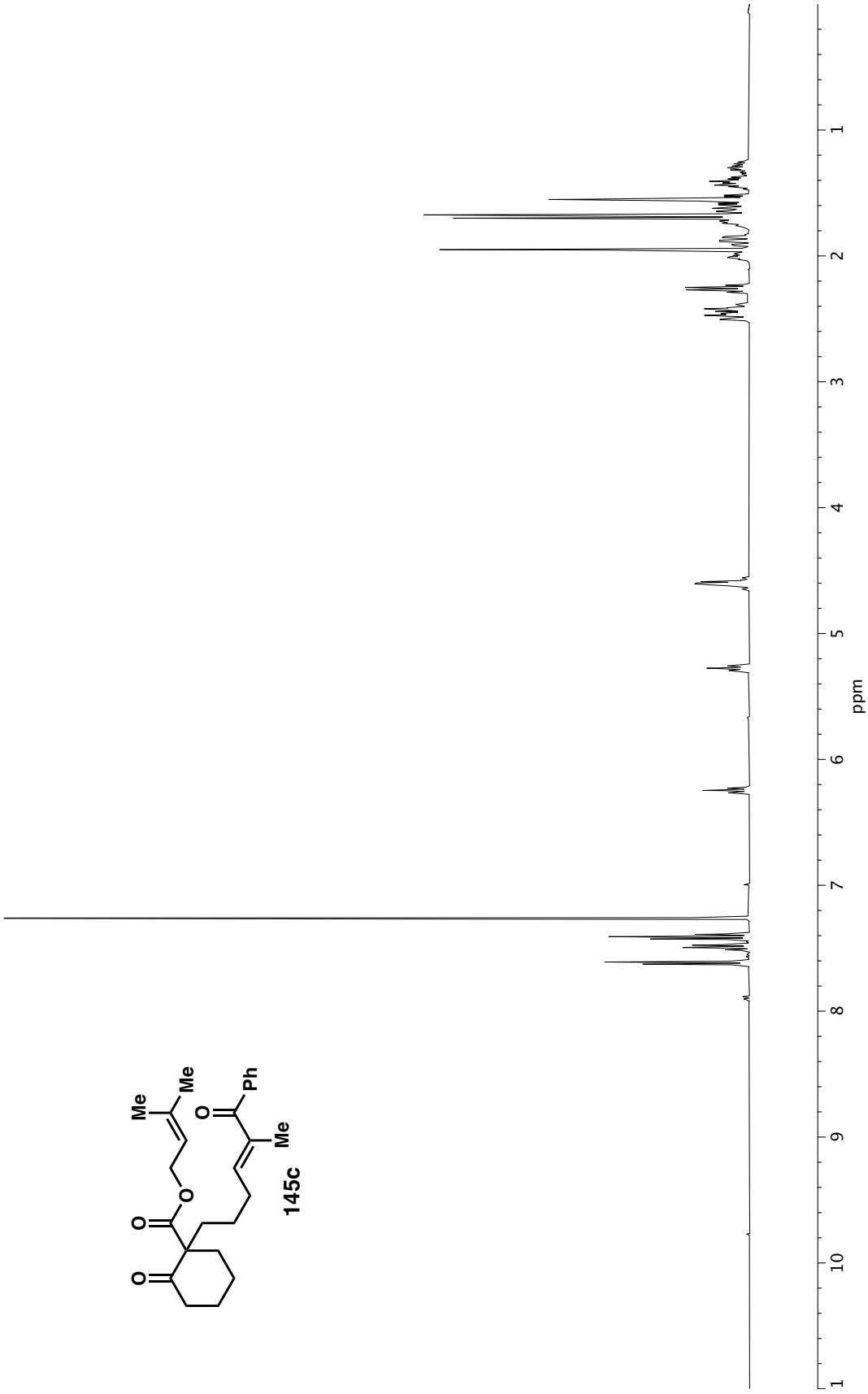


Figure A2.106. *^1H NMR (400 MHz, $CDCl_3$) of compound **145c**.*

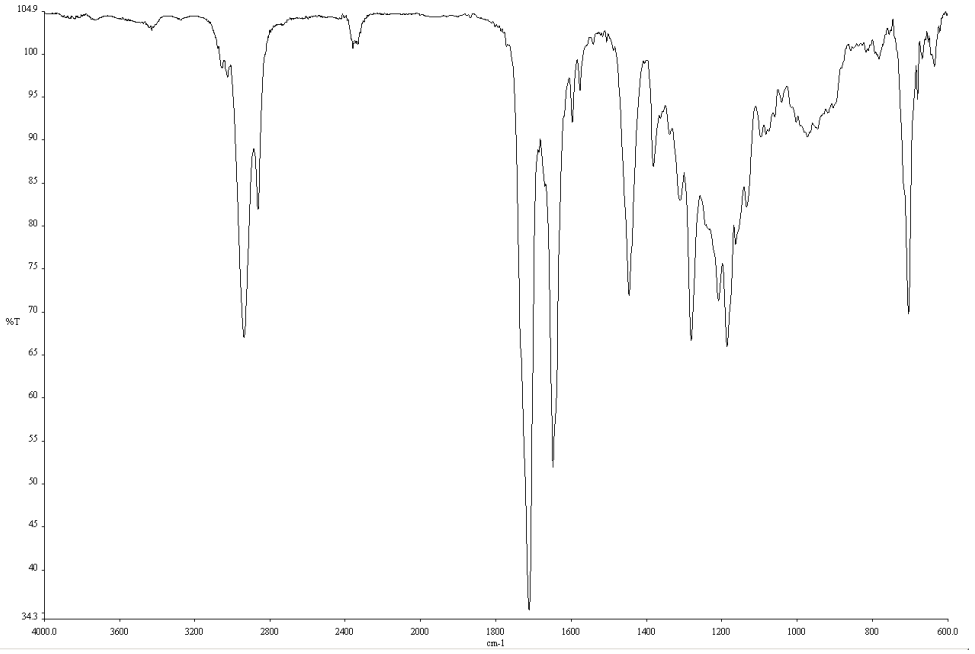


Figure A2.107. *Infrared spectrum (Thin Film, NaCl) of compound* ***145c****.*

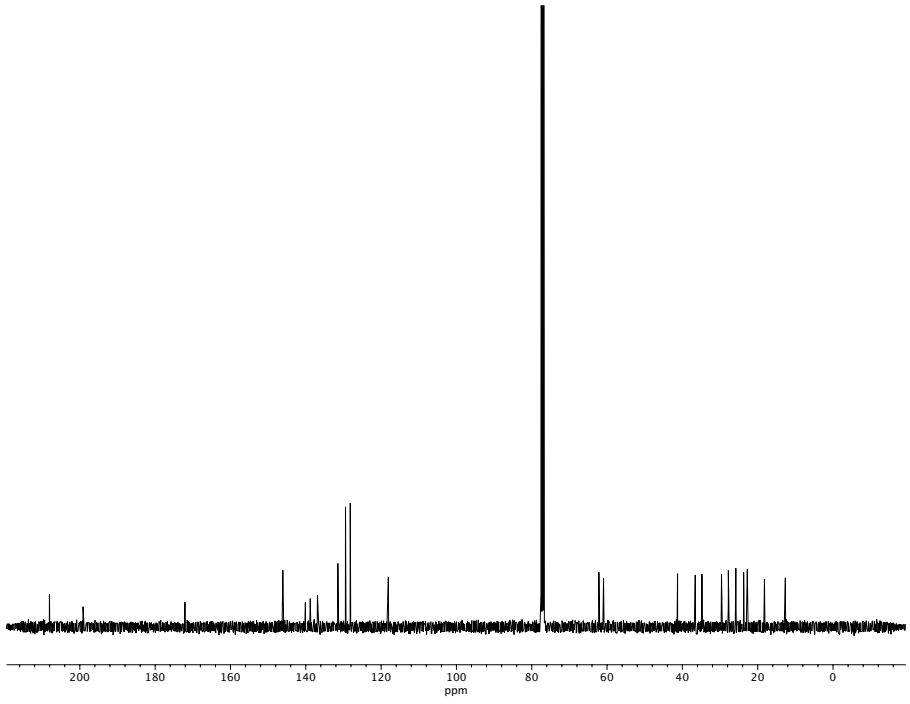


Figure A2.108. *^{13}C NMR (100 MHz, $CDCl_3$) of compound* ***145c****.*

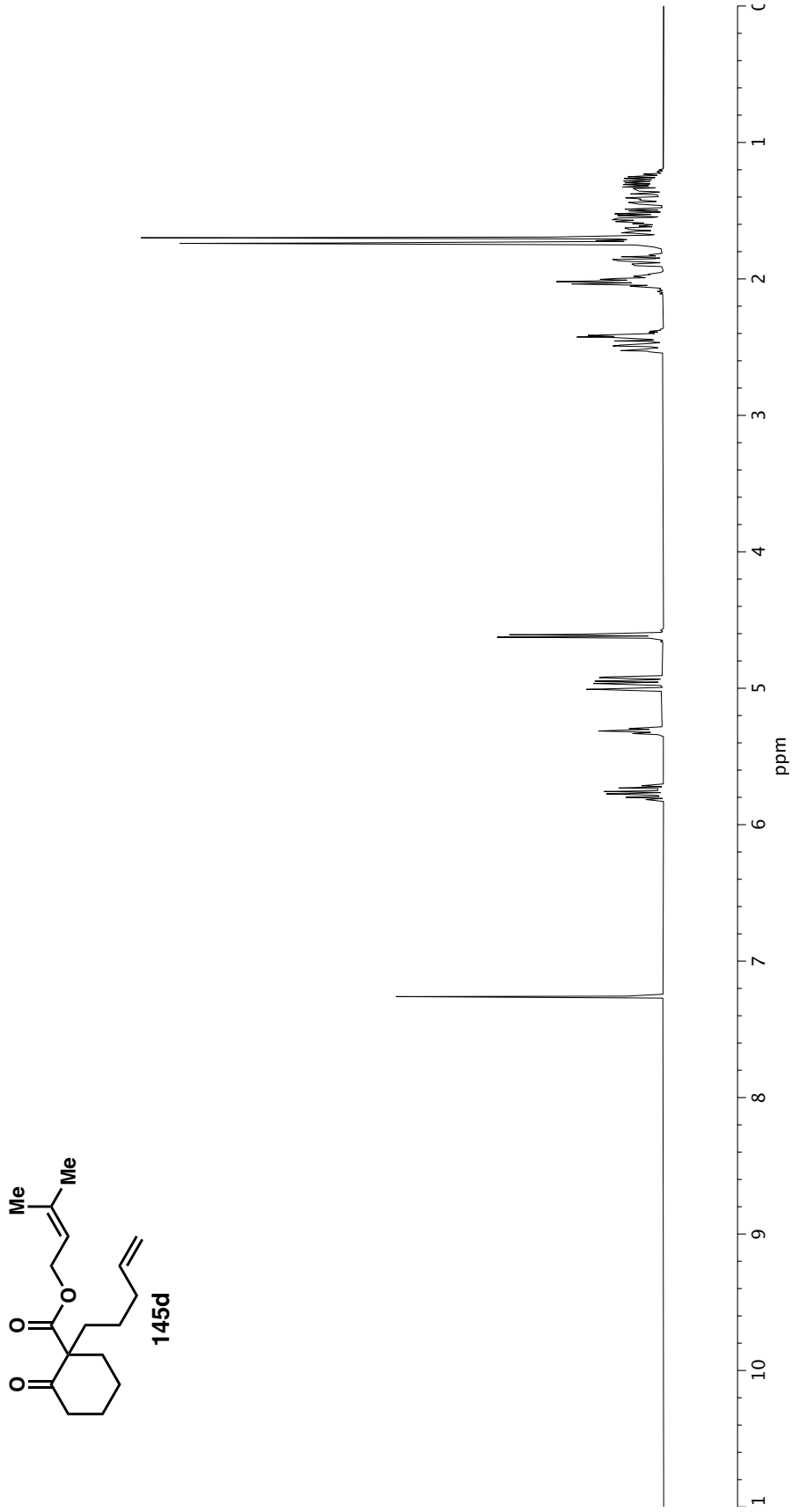


Figure A2.109. *^{1}H NMR (400 MHz, $CDCl_3$) of compound* ***145d***.

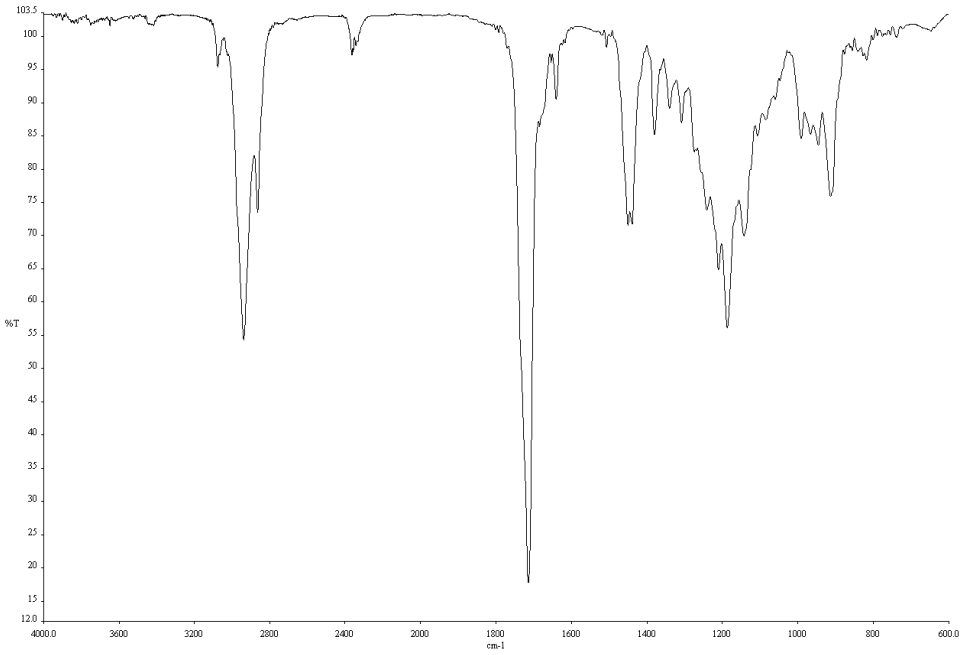


Figure A2.110. *Infrared spectrum (Thin Film, NaCl) of compound* ***145d****.*

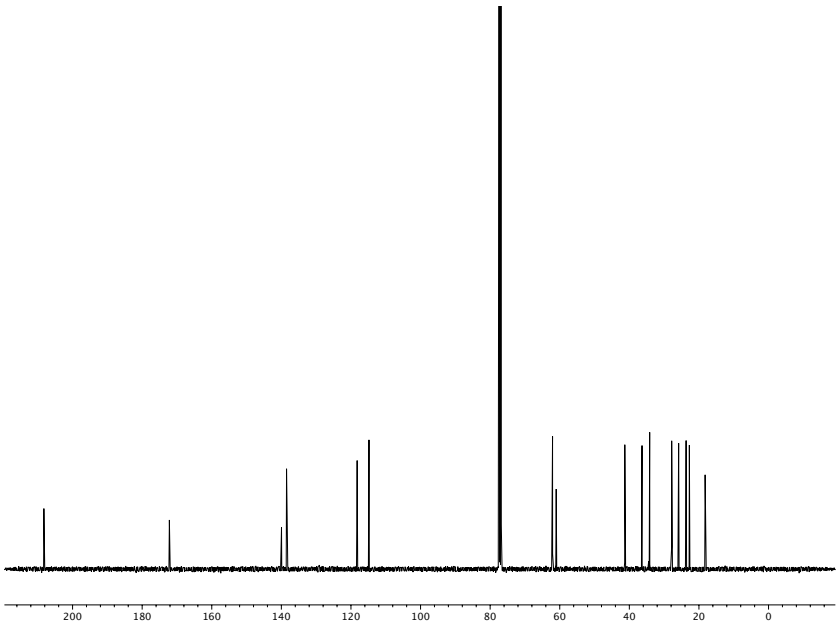


Figure A2.111. *^{13}C NMR (100 MHz, $CDCl_3$) of compound* ***145d****.*

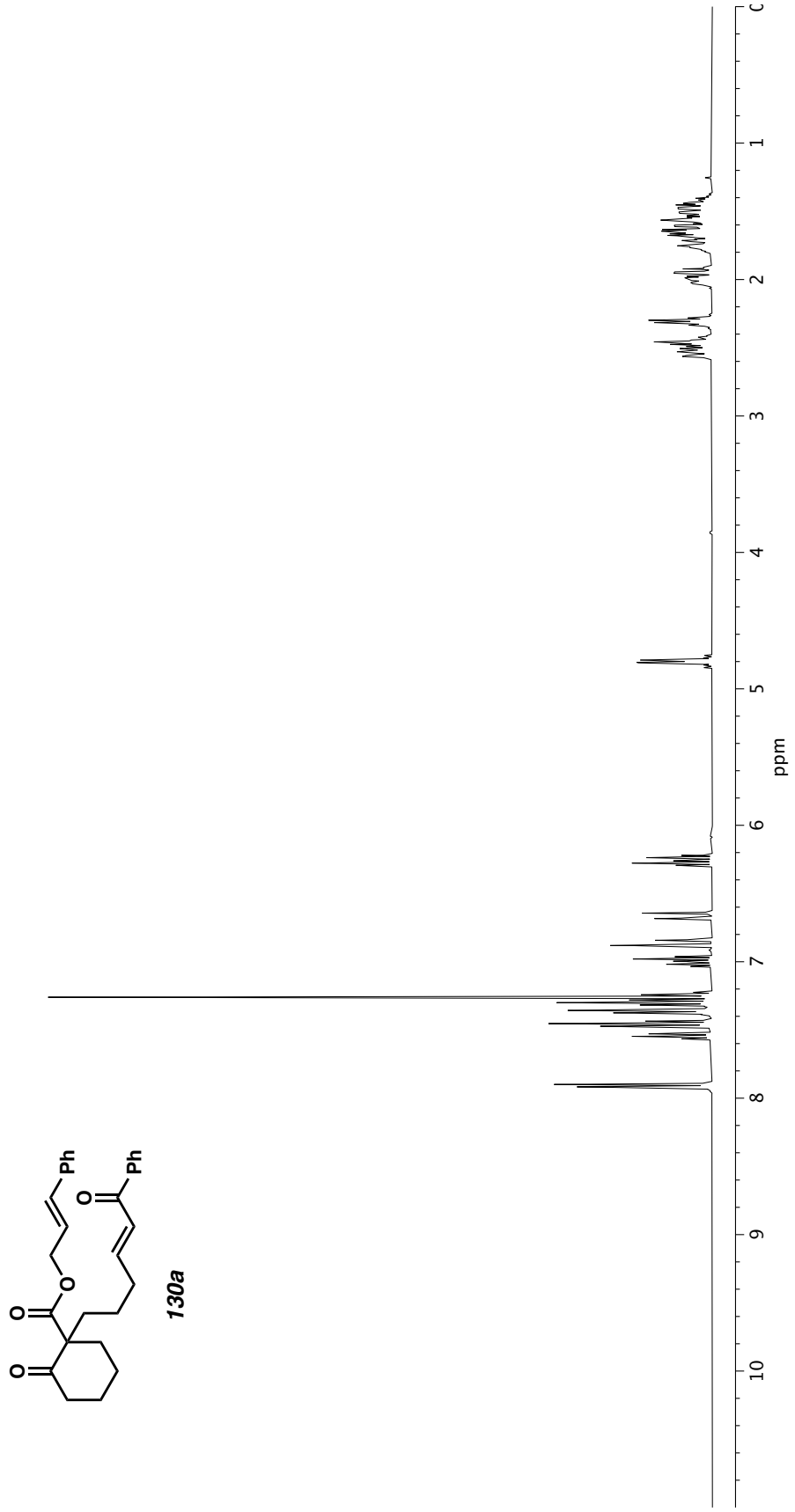


Figure A2.112. *^{1}H NMR (400 MHz, $CDCl_3$) of compound* ***130a***.

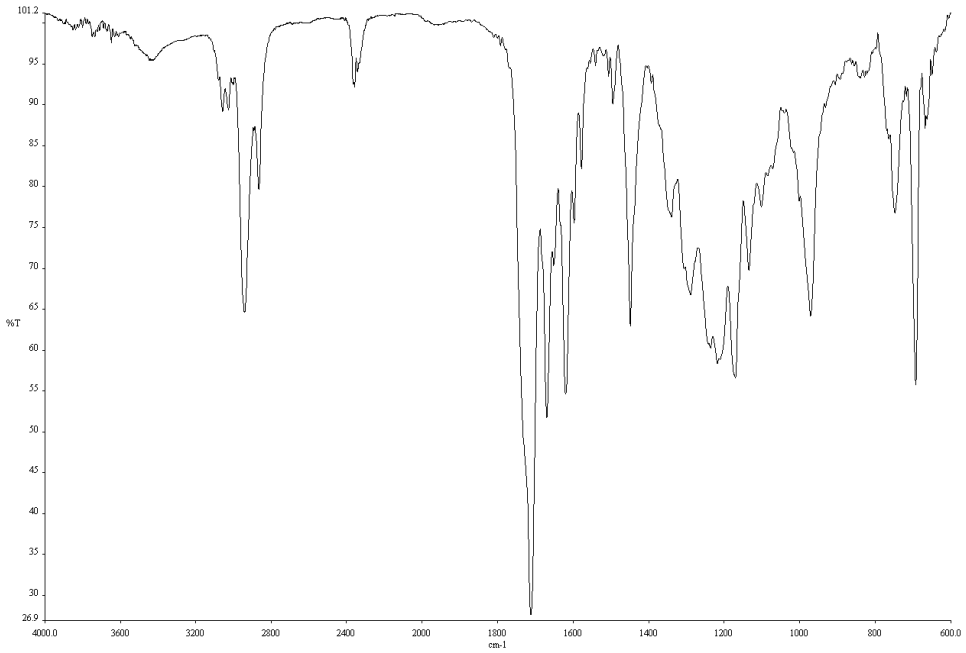


Figure A2.113. *Infrared spectrum (Thin Film, NaCl) of compound* ***130a****.*

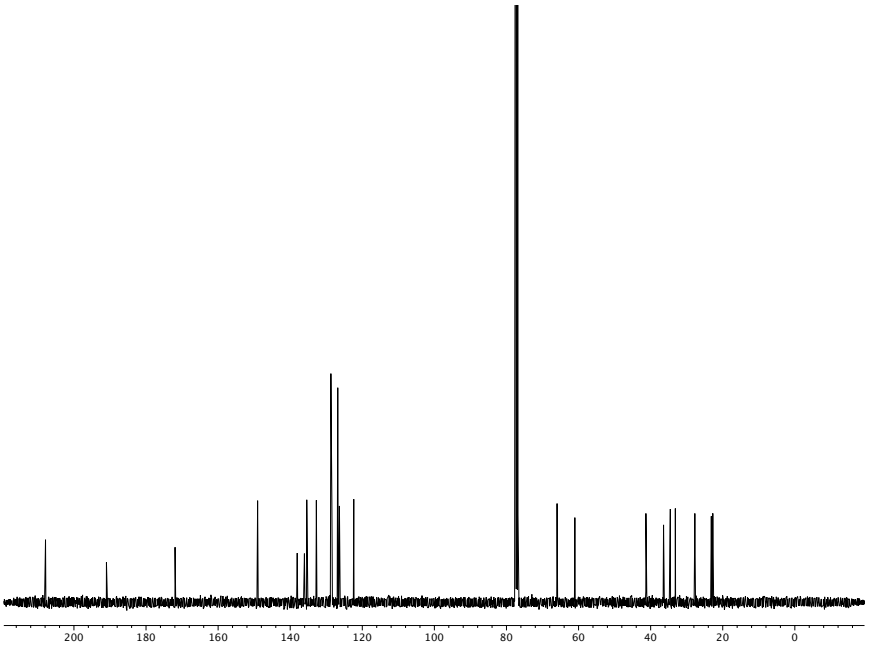


Figure A2.114. *^{13}C NMR (100 MHz, $CDCl_3$) of compound* ***130a****.*

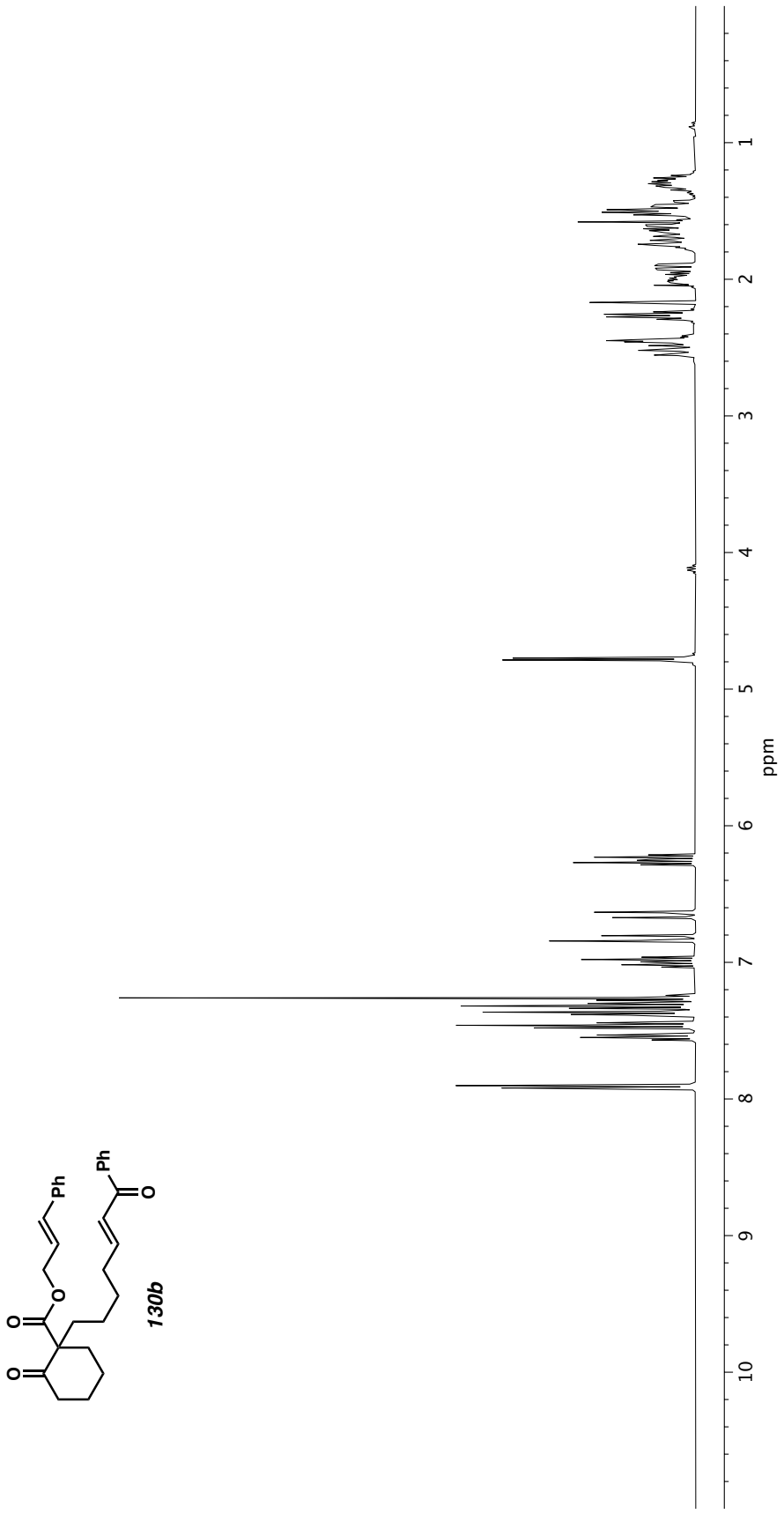


Figure A2.115. *^1H NMR (400 MHz, $CDCl_3$) of compound **130b**.*

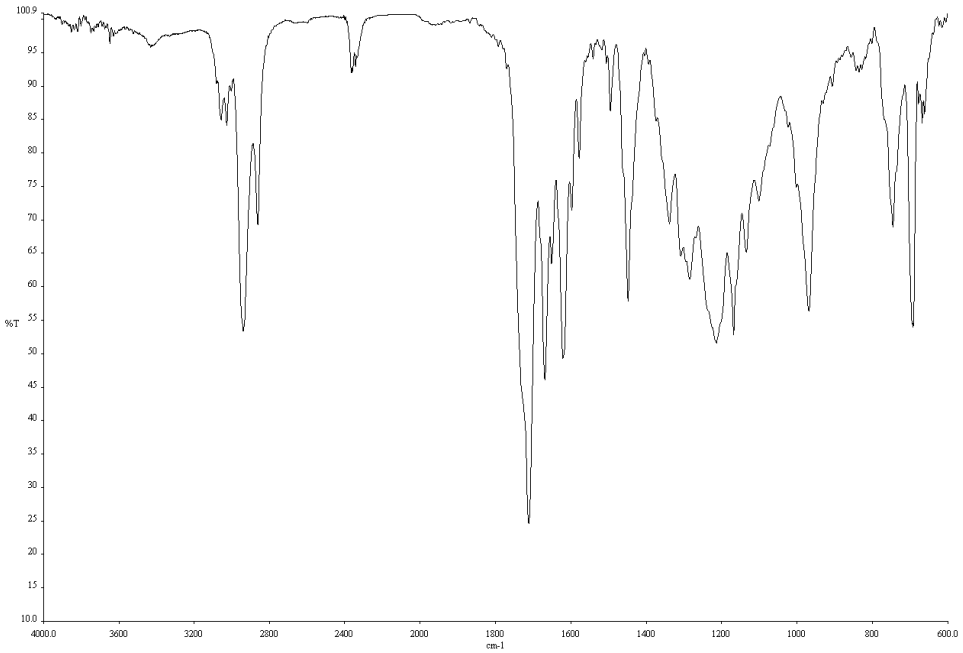


Figure A2.116. *Infrared spectrum (Thin Film, NaCl) of compound* ***130b****.*

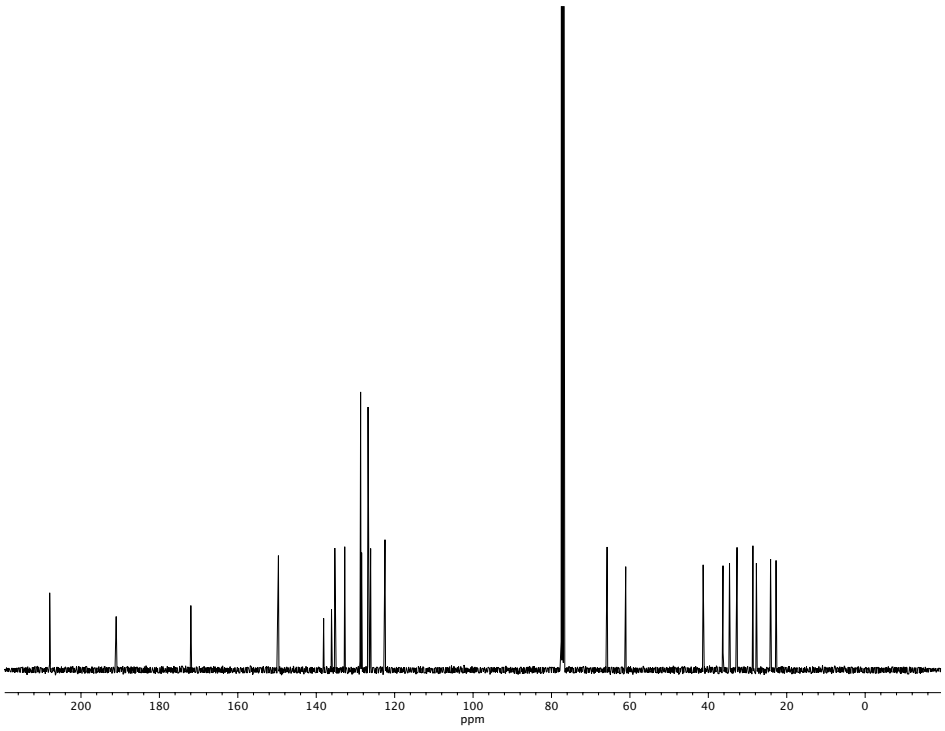


Figure A2.117. *^{13}C NMR (100 MHz, $CDCl_3$) of compound* ***130b****.*

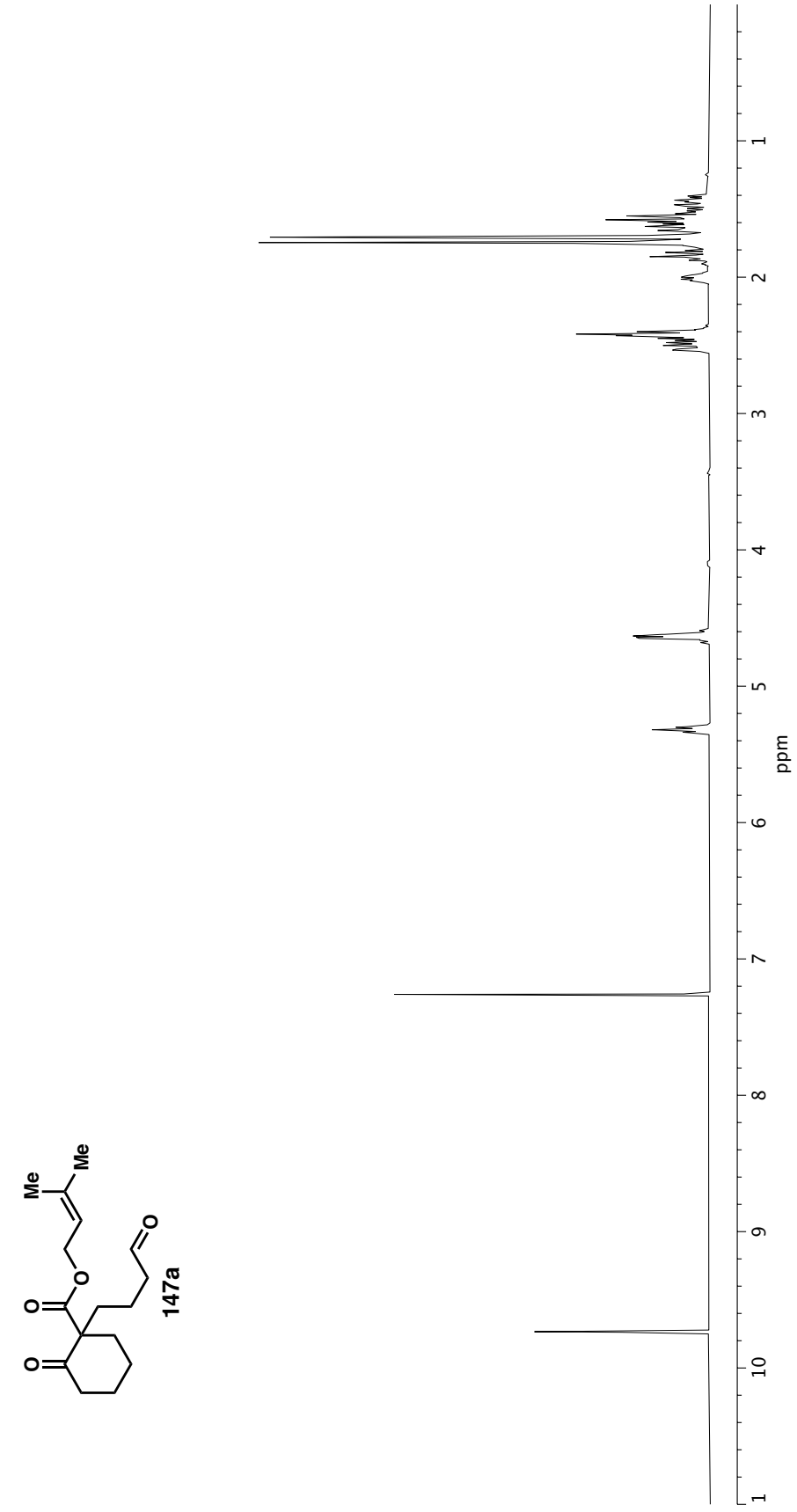


Figure A2.118. *^{1}H NMR (400 MHz, $CDCl_3$) of compound* ***147a****.*

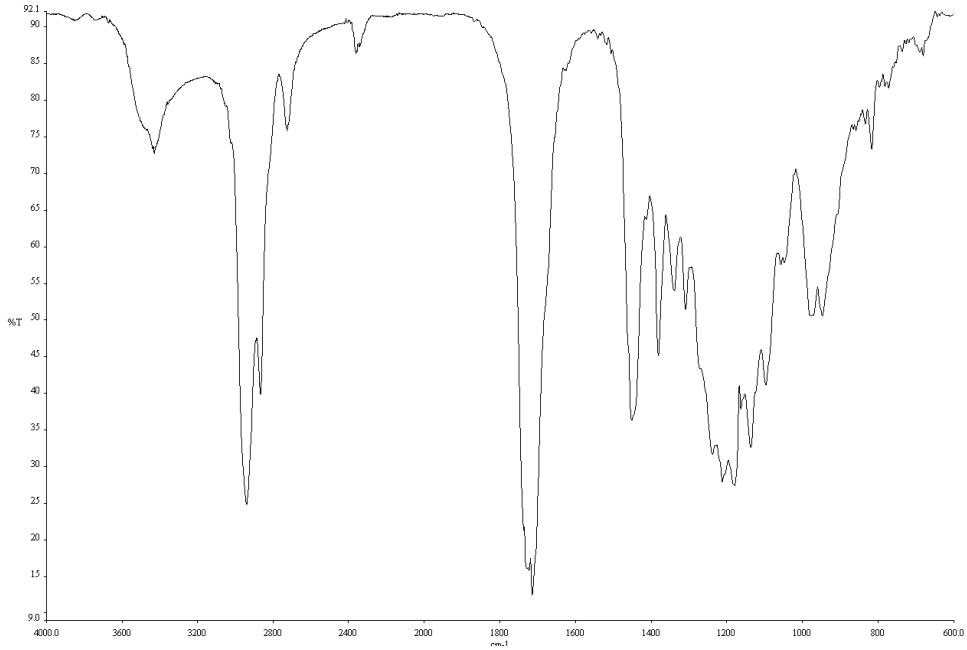


Figure A2.119. *Infrared spectrum (Thin Film, NaCl) of compound* ***147a****.*

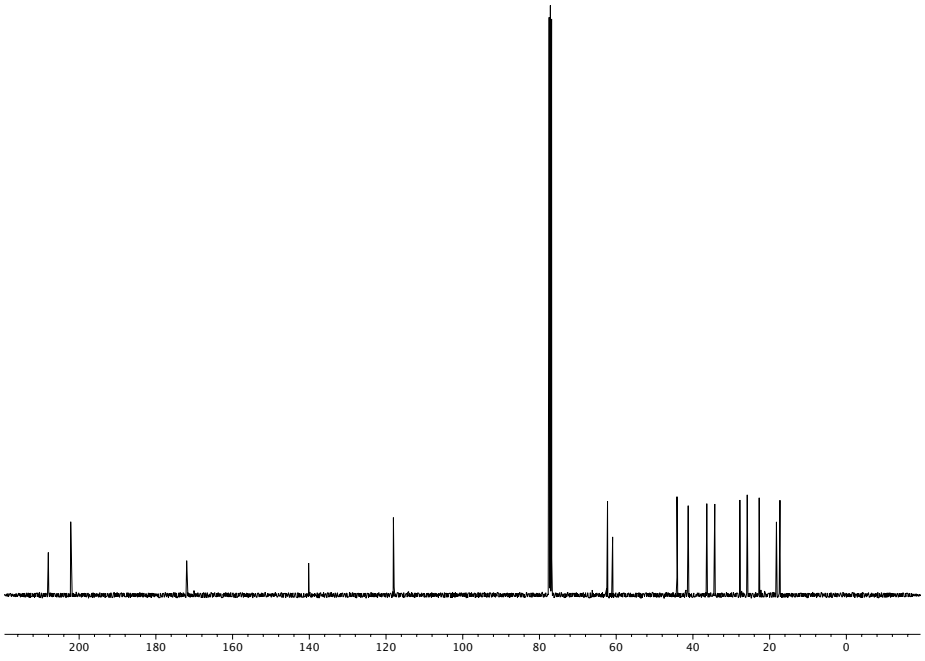


Figure A2.120. *^{13}C NMR (100 MHz, $CDCl_3$) of compound* ***147a****.*

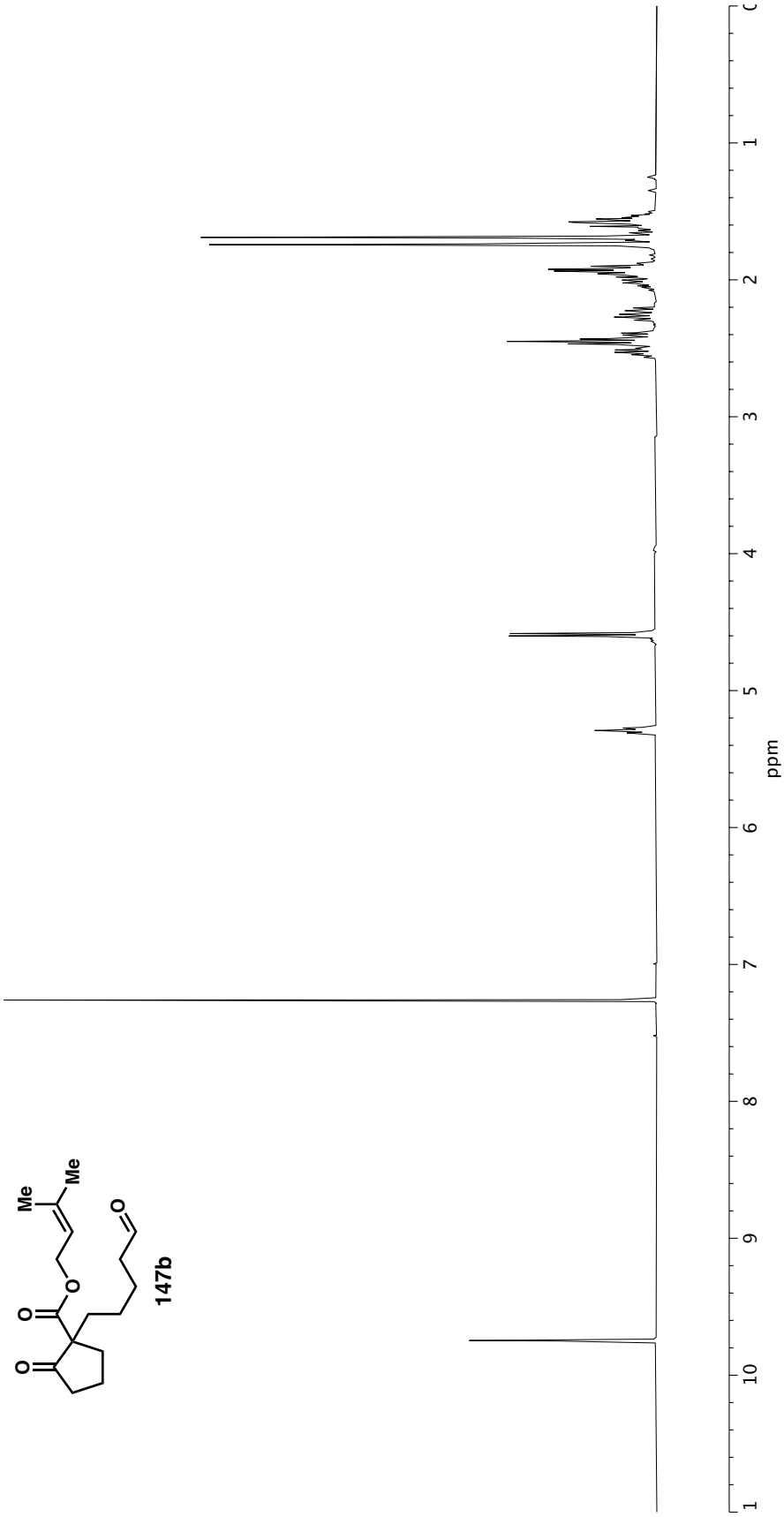


Figure A2.121. *^{1}H NMR (400 MHz, $CDCl_3$) of compound* ***147b****.*

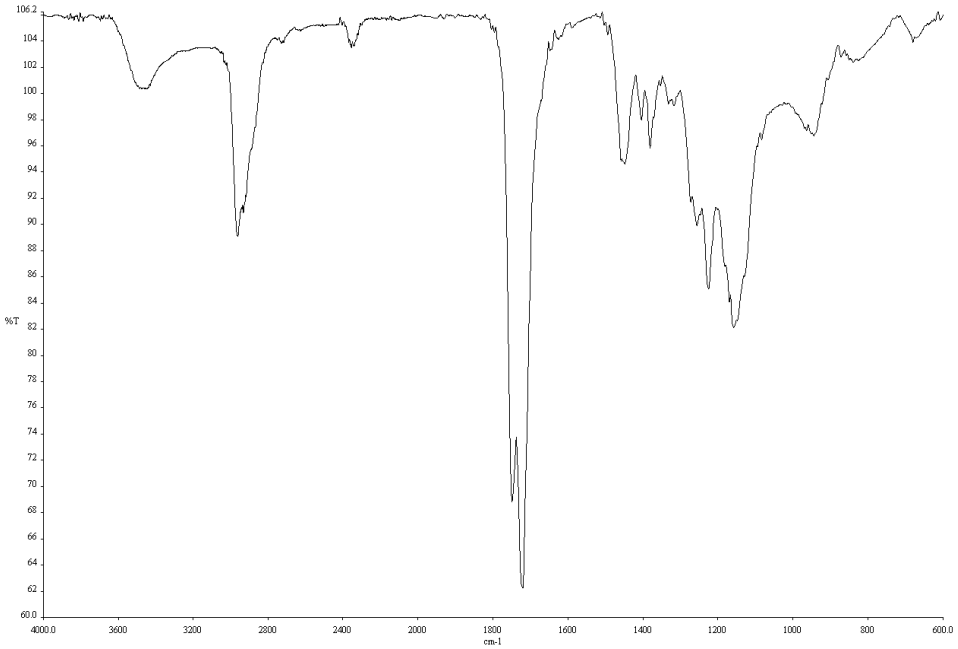


Figure A2.122. *Infrared spectrum (Thin Film, NaCl) of compound* ***147b****.*

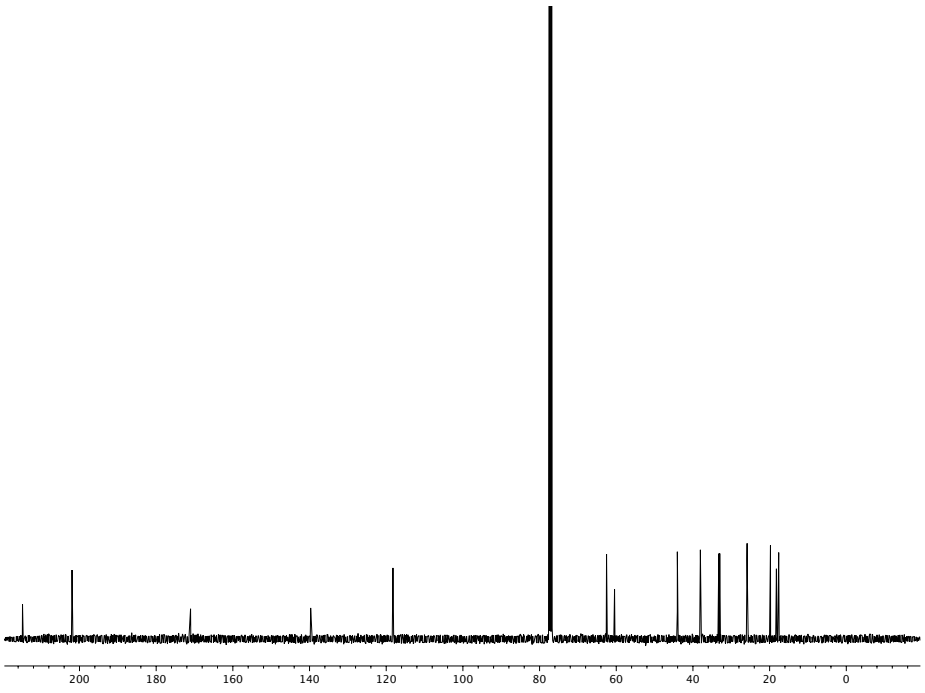


Figure A2.123. *^{13}C NMR (100 MHz, $CDCl_3$) of compound* ***147b****.*

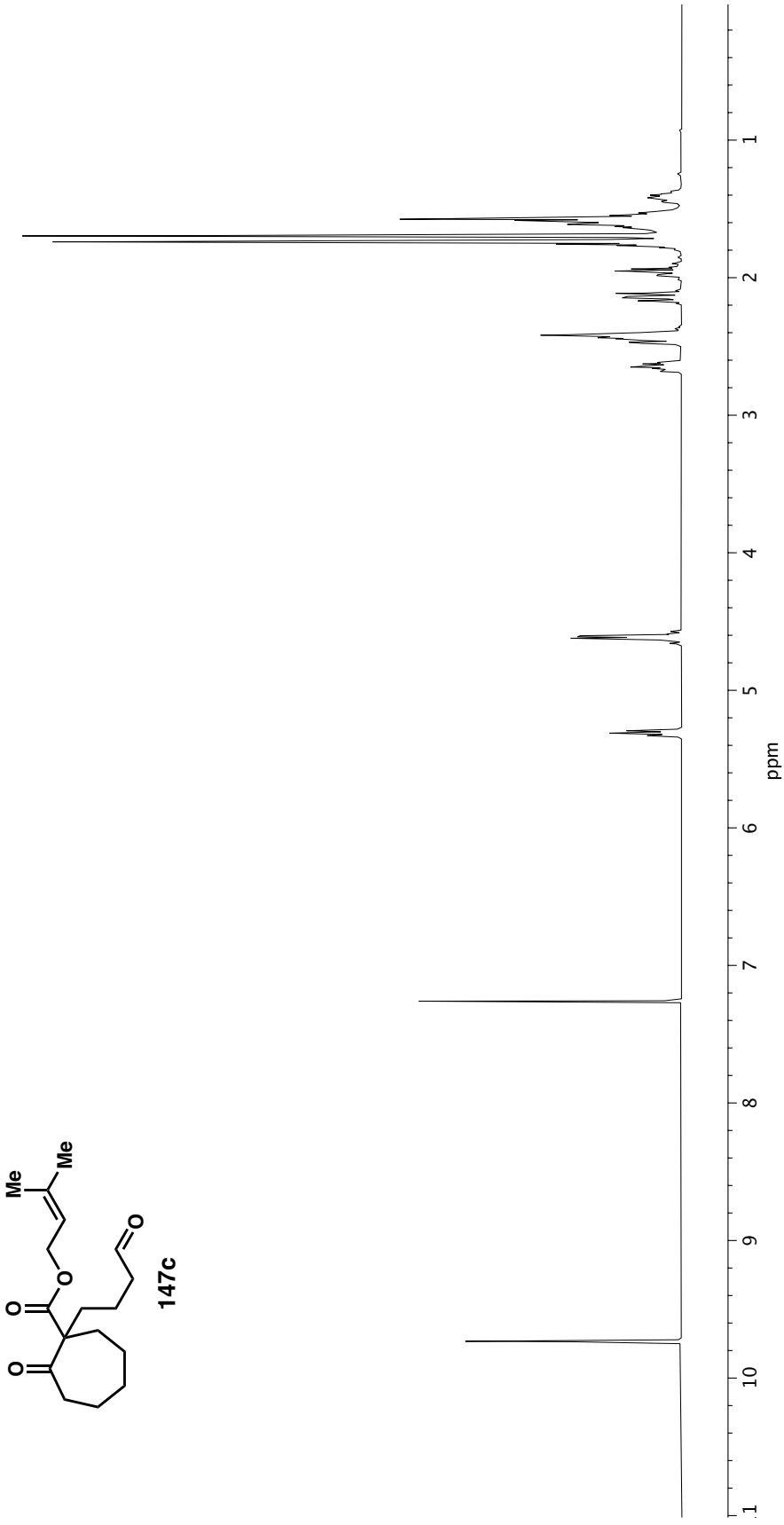


Figure A2.124. *^{1}H NMR (400 MHz, $CDCl_3$) of compound* ***147c****.*

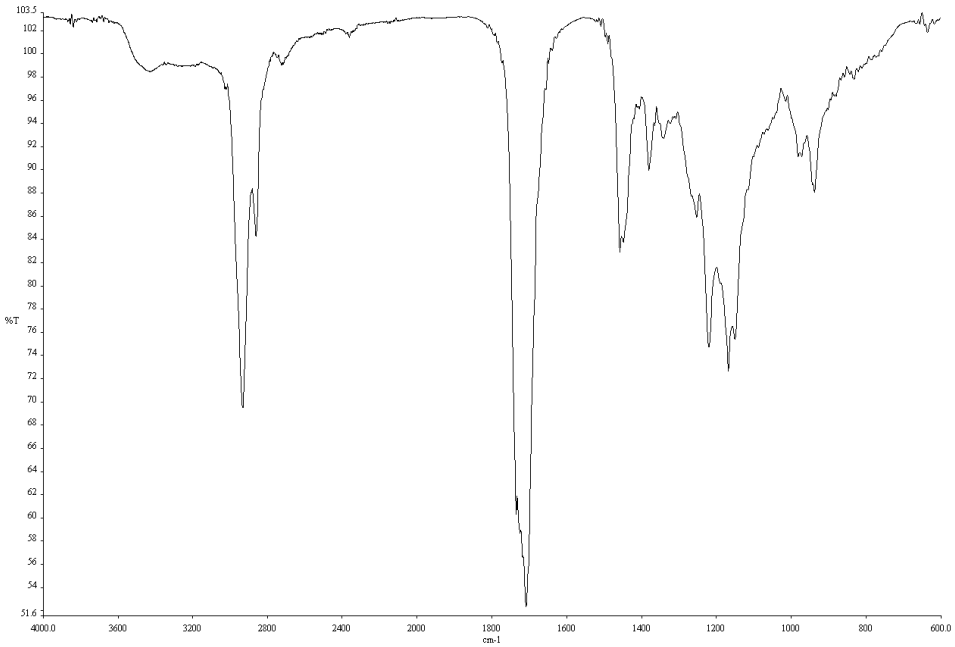


Figure A2.125. *Infrared spectrum (Thin Film, NaCl) of compound* ***147c****.*

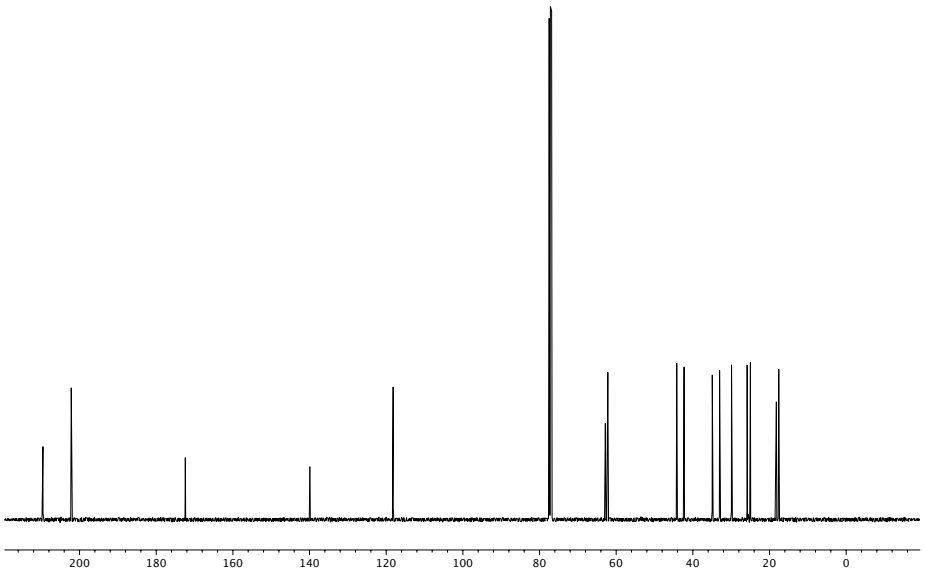


Figure A2.126. *^{13}C NMR (100 MHz, $CDCl_3$) of compound* ***147c****.*

Figure A2.127. *^1H NMR (400 MHz, $CDCl_3$) of compound* ***147d****.*

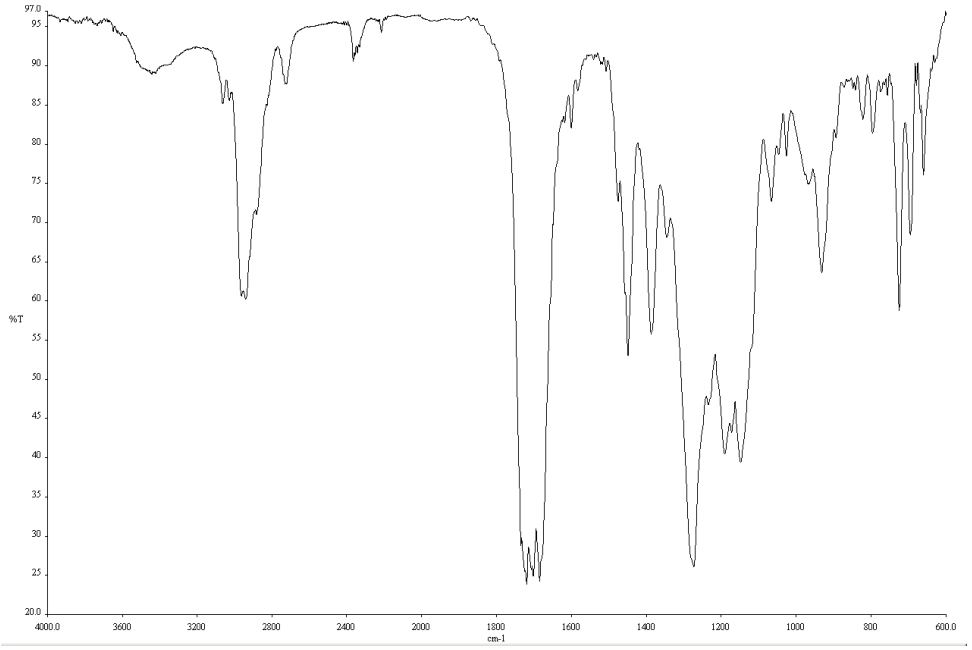


Figure A2.128. *Infrared spectrum (Thin Film, NaCl) of compound* ***147d****.*

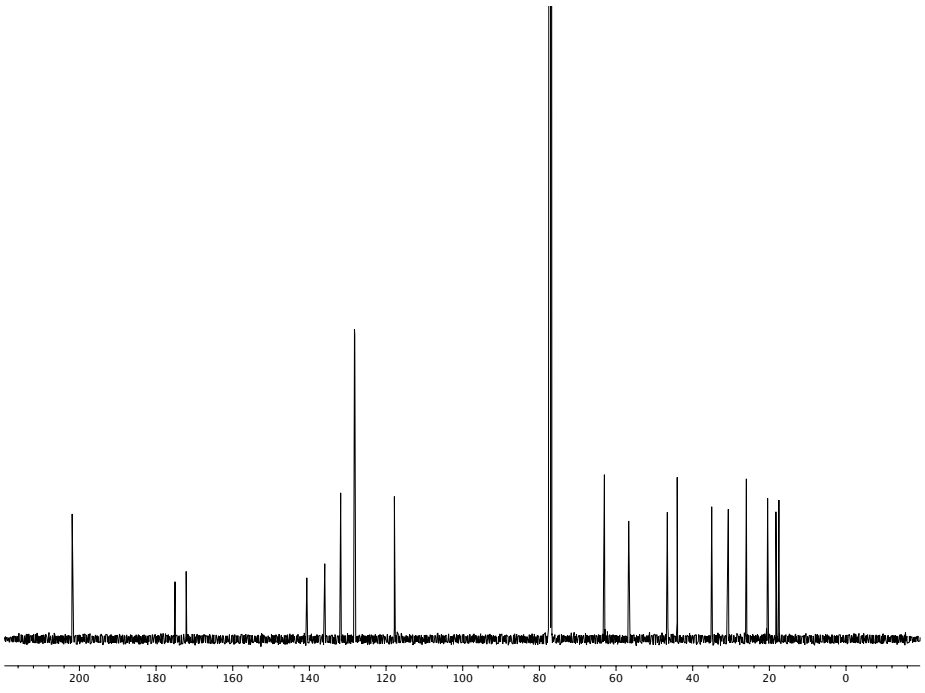


Figure A2.129. *^{13}C NMR (100 MHz, $CDCl_3$) of compound* ***147d****.*

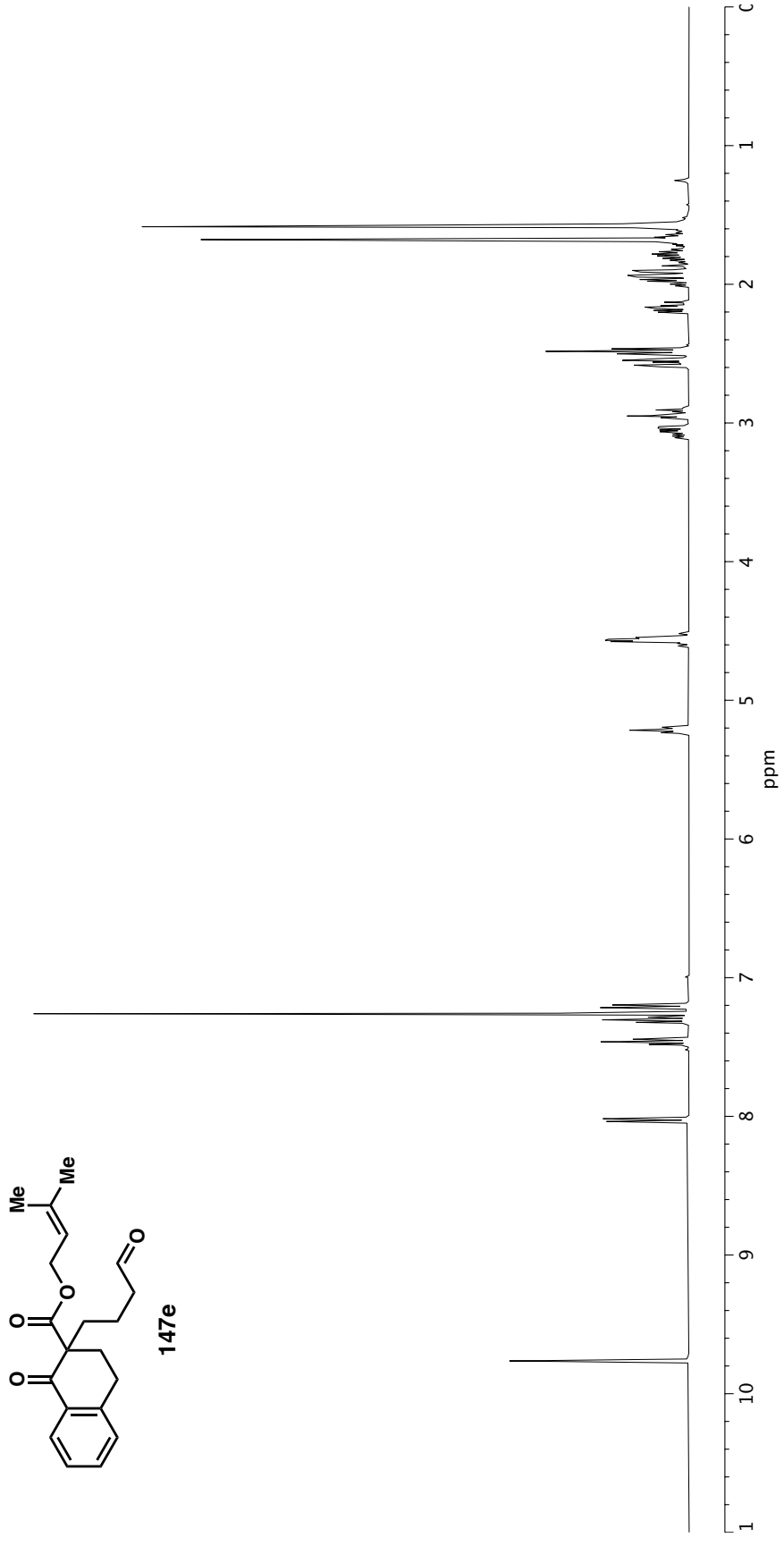


Figure A2.130. *^{1}H NMR (400 MHz, $CDCl_3$) of compound* ***147e****.*

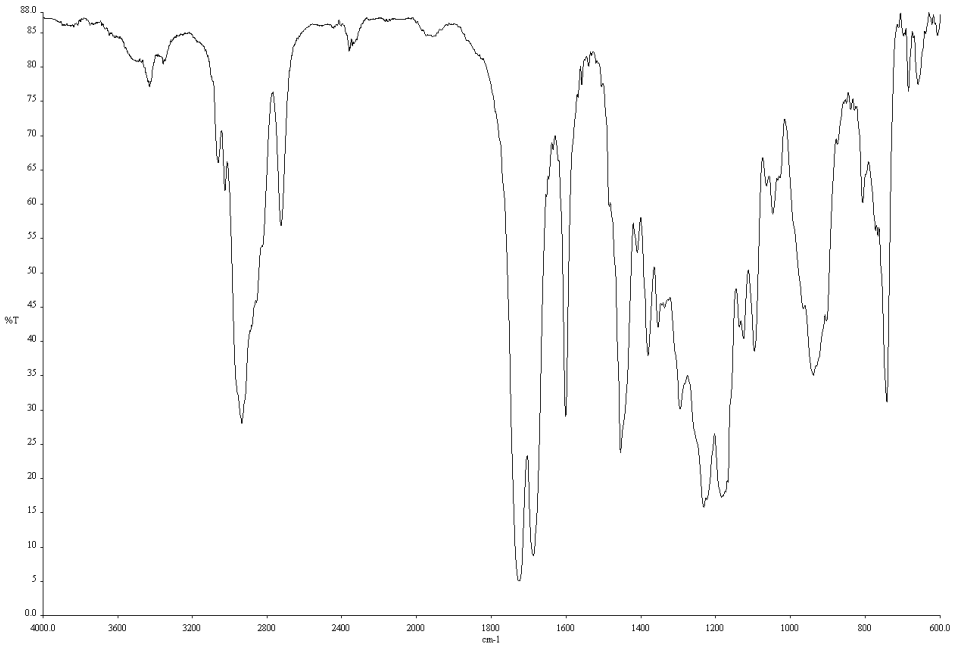


Figure A2.131. *Infrared spectrum (Thin Film, NaCl) of compound* ***147e****.*

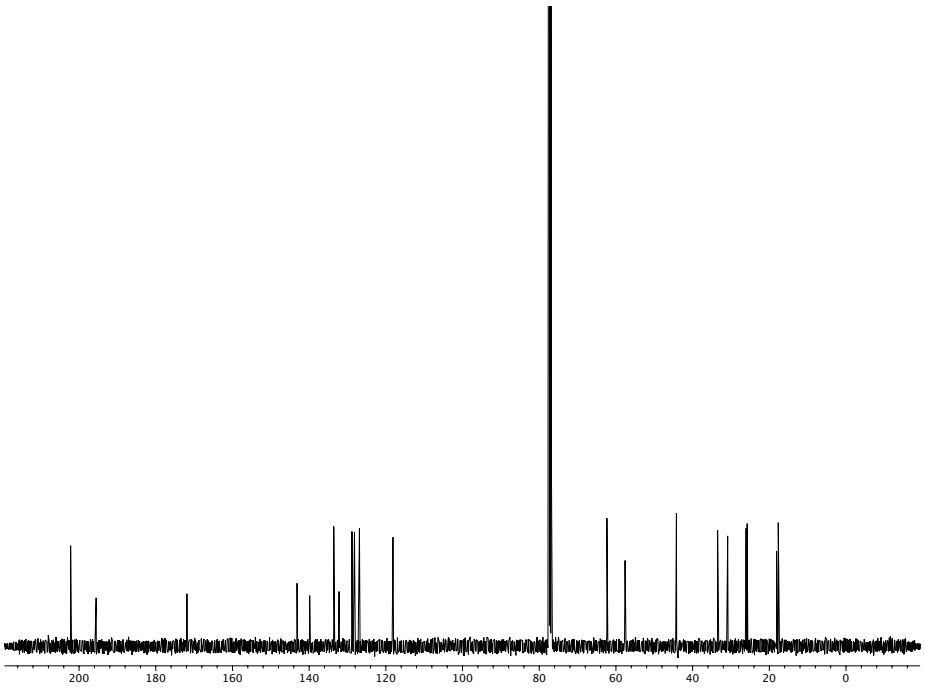


Figure A2.132. *^{13}C NMR (100 MHz, $CDCl_3$) of compound* ***147e****.*

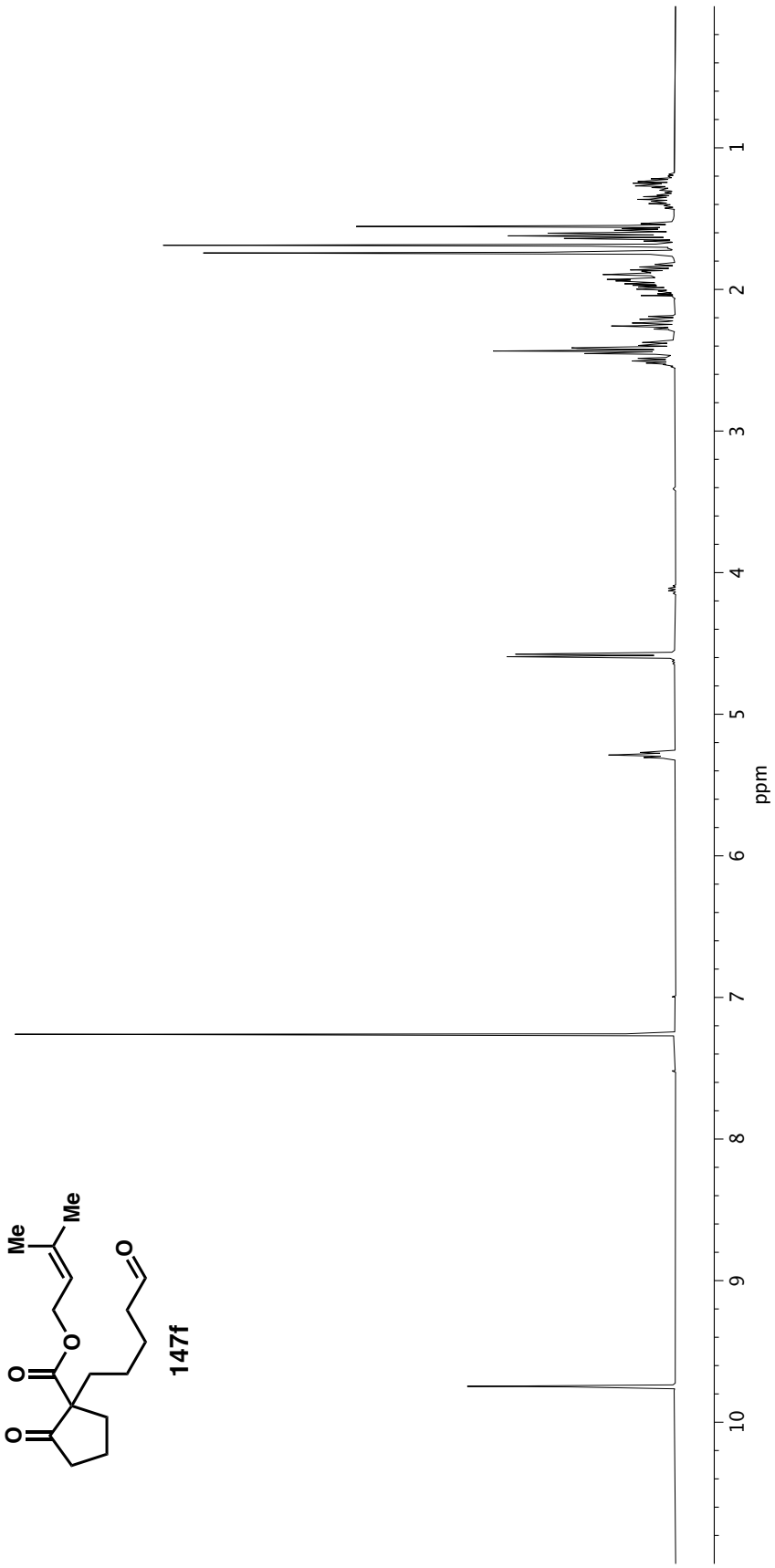


Figure A2.133. *^{1}H NMR (400 MHz, $CDCl_3$) of compound* ***147f****.*

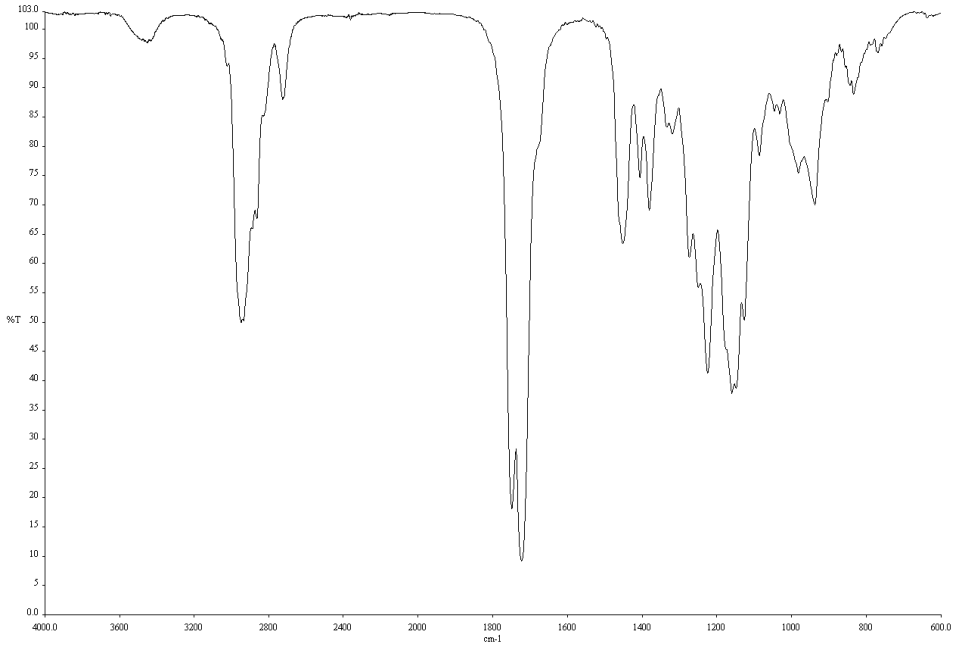


Figure A2.134. *Infrared spectrum (Thin Film, NaCl) of compound* ***147f****.*

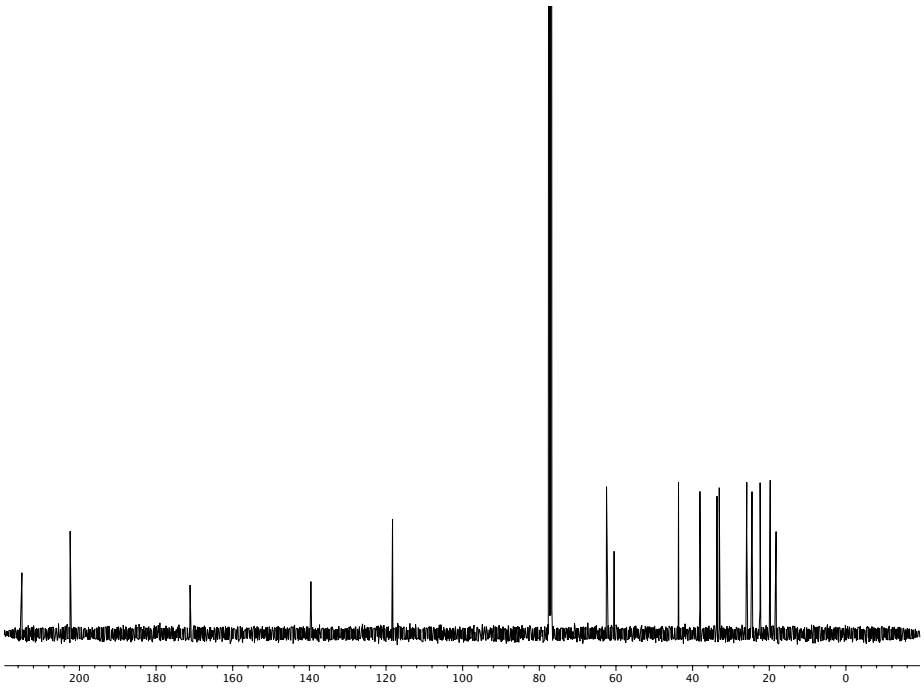


Figure A2.135. *^{13}C NMR (100 MHz, $CDCl_3$) of compound* ***147f****.*

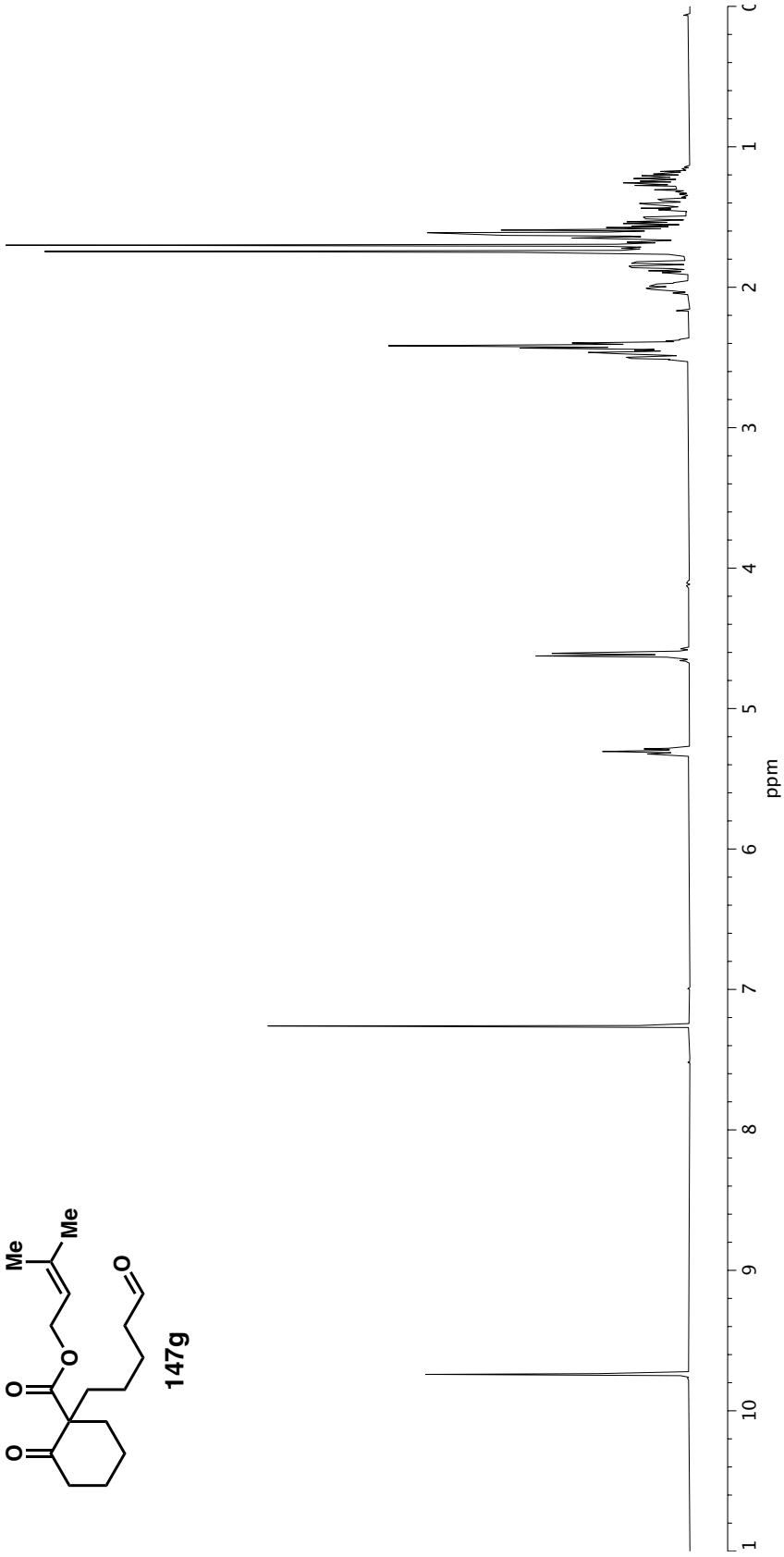


Figure A2.136. *^{1}H NMR (400 MHz, $CDCl_3$) of compound* ***147g****.*

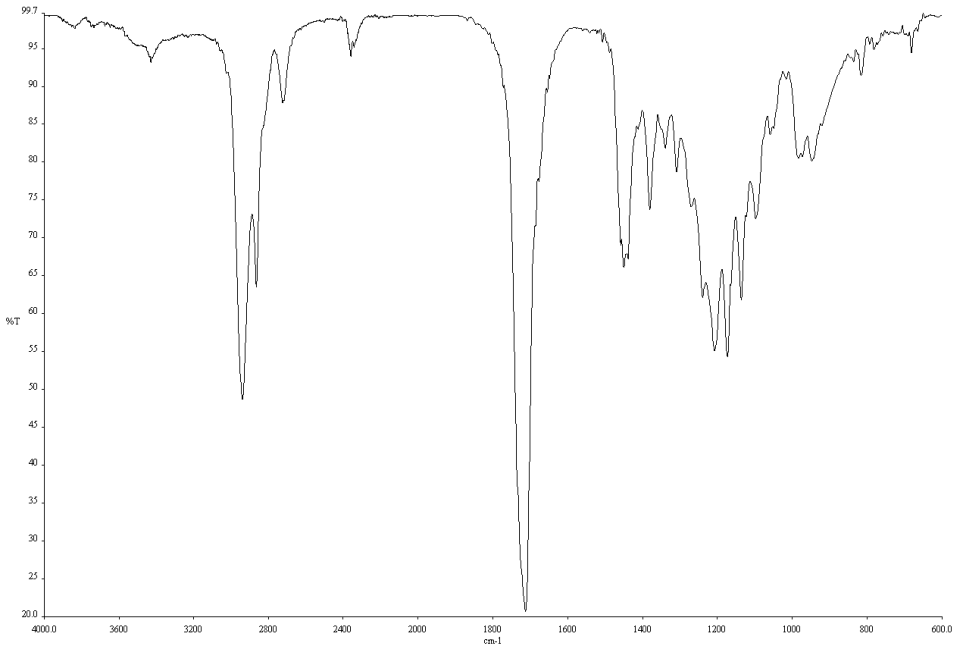


Figure A2.137. *Infrared spectrum (Thin Film, NaCl) of compound* ***147g****.*

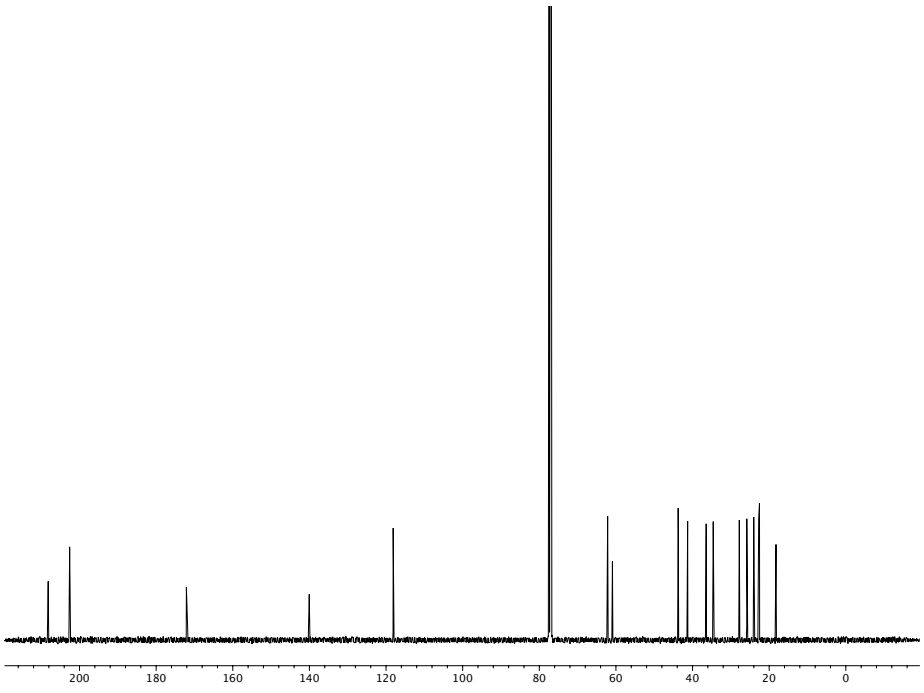


Figure A2.138. *^{13}C NMR (100 MHz, $CDCl_3$) of compound* ***147g****.*

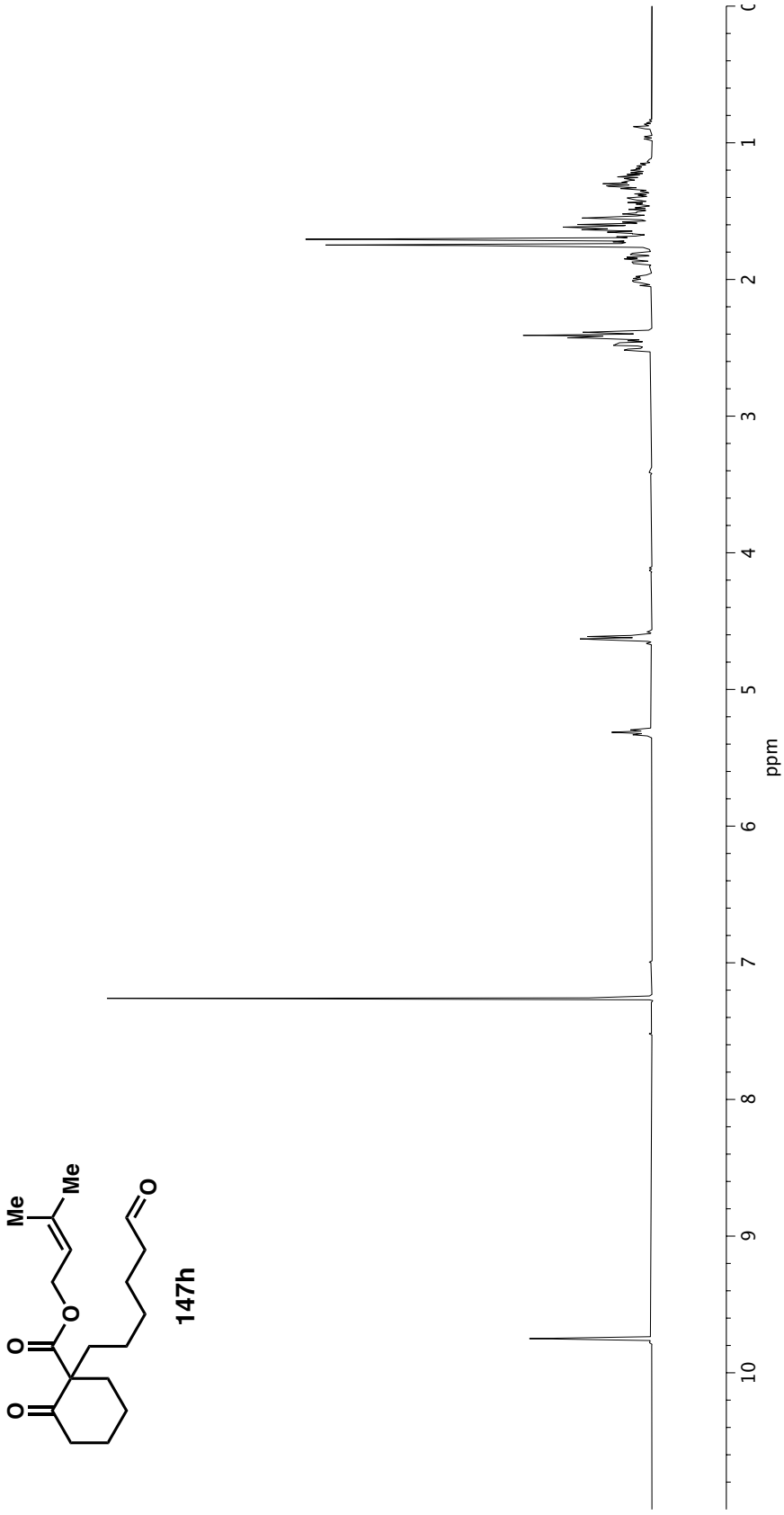


Figure A2.139. *^{1}H NMR (400 MHz, $CDCl_3$) of compound* ***147h****.*

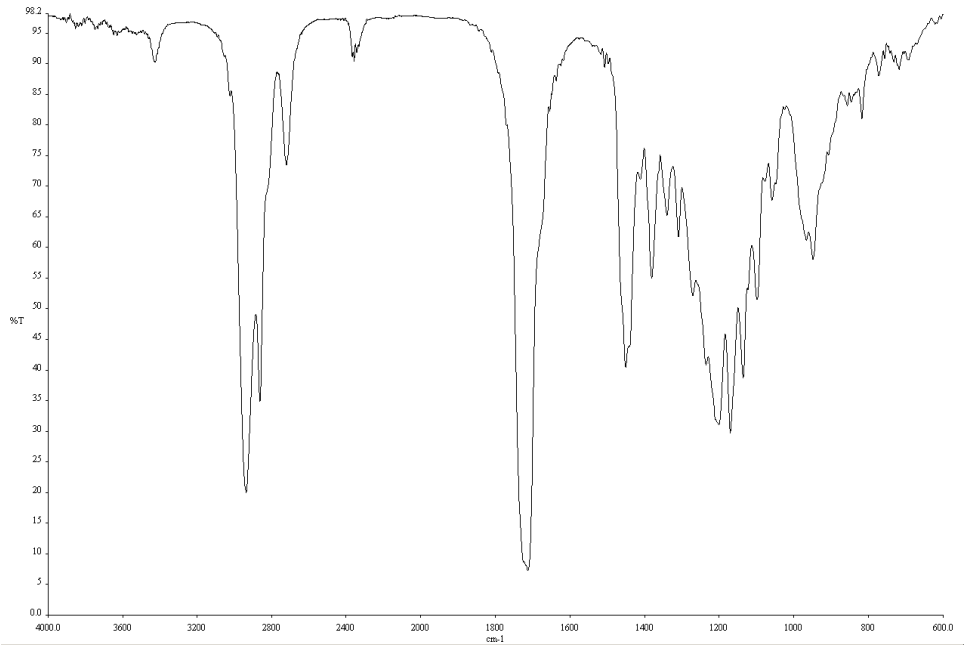


Figure A2.140. *Infrared spectrum (Thin Film, NaCl) of compound* ***147h****.*

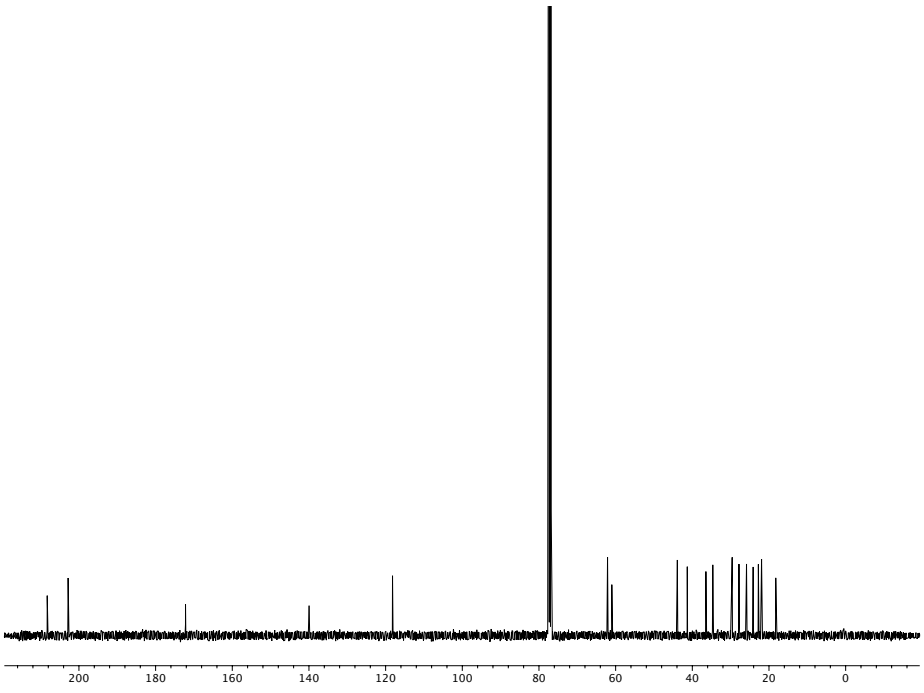


Figure A2.141. *^{13}C NMR (100 MHz, $CDCl_3$) of compound* ***147h****.*

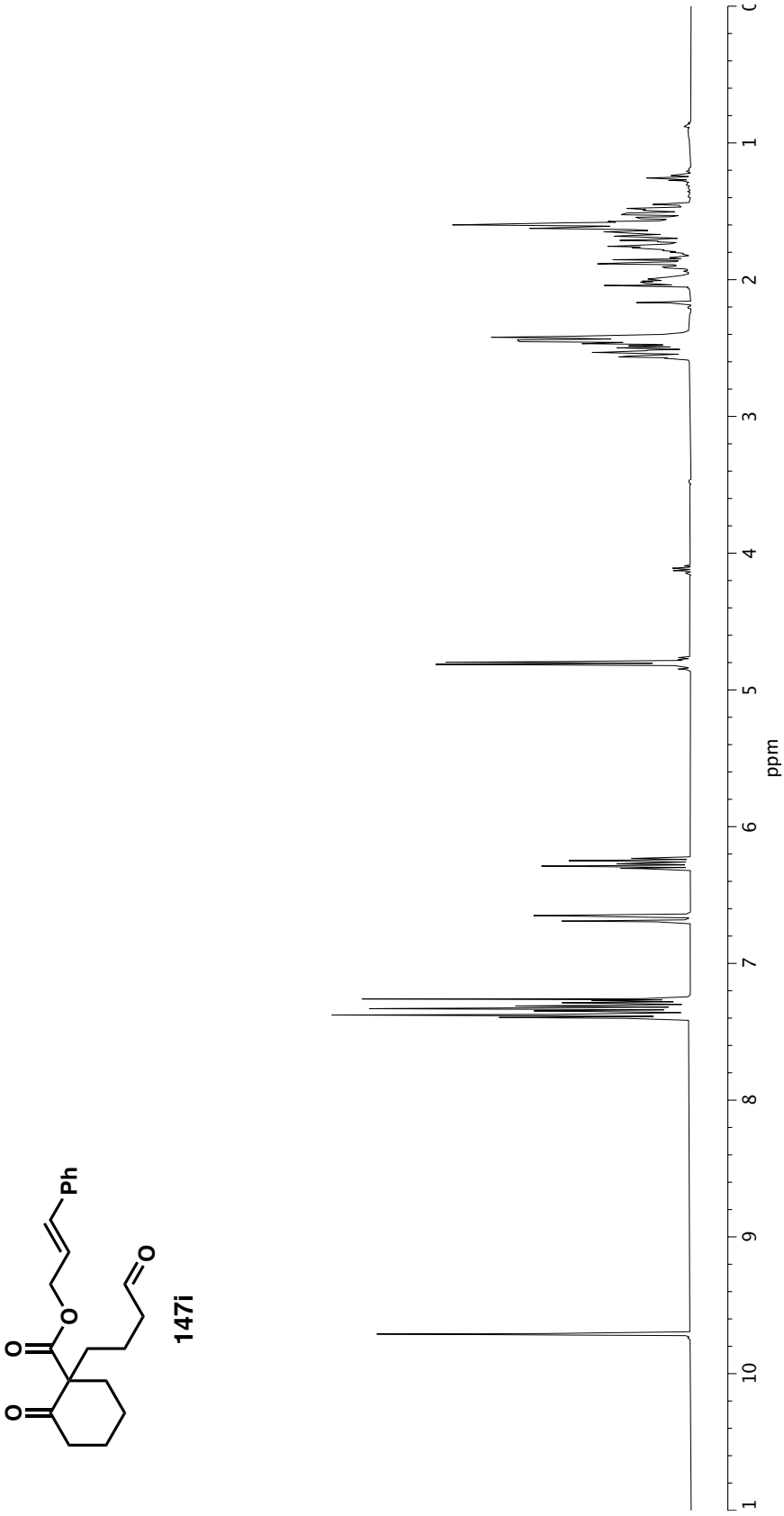


Figure A2.142. *^{1}H NMR (400 MHz, $CDCl_3$) of compound* ***147i****.*

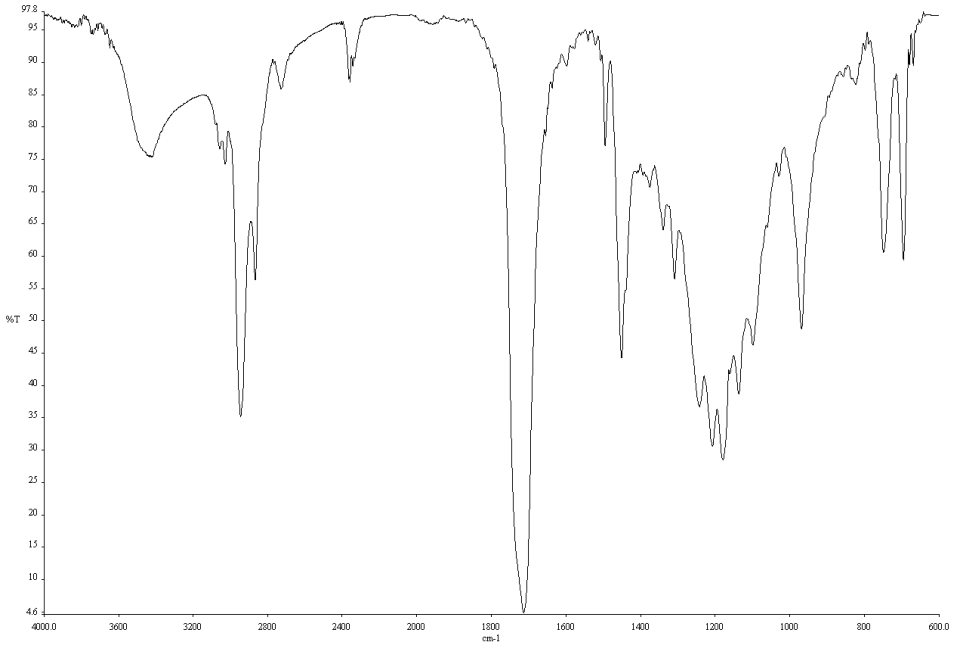


Figure A2.143. *Infrared spectrum (Thin Film, NaCl) of compound* ***147i****.*

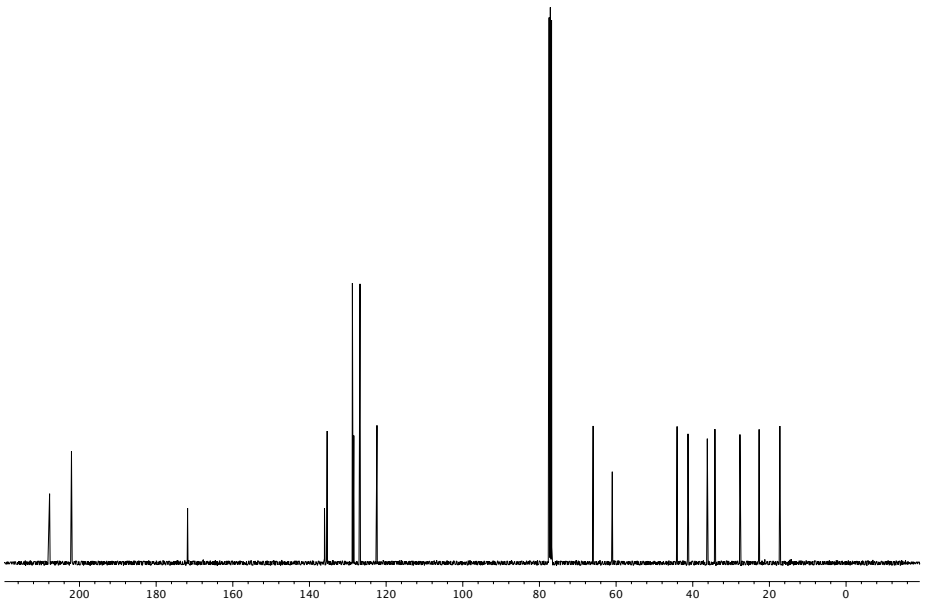


Figure A2.144. *^{13}C NMR (100 MHz, $CDCl_3$) of compound* ***147i****.*

Figure A2.145. *^{1}H NMR (600 MHz, $CDCl_3$) of compound* ***147j****.*

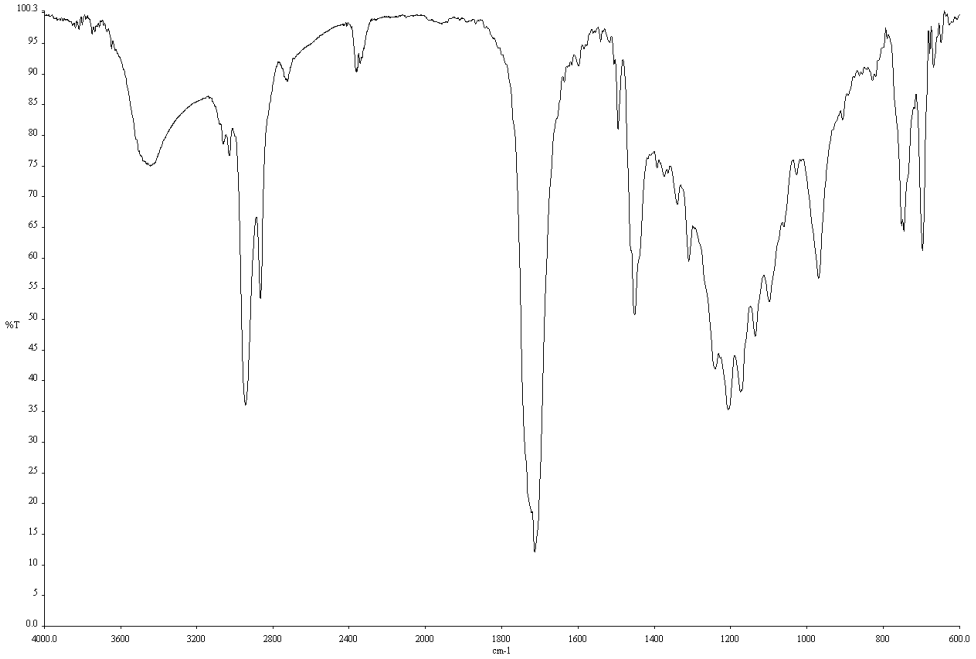


Figure A2.146. *Infrared spectrum (Thin Film, NaCl) of compound* ***147j****.*

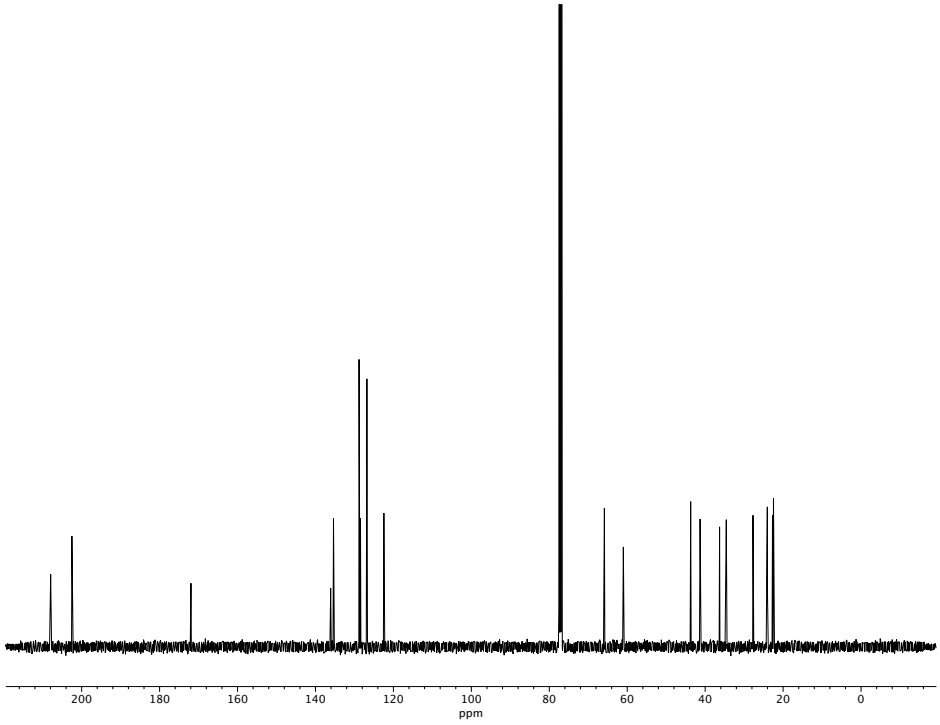


Figure A2.147. *^{13}C NMR (100 MHz, $CDCl_3$) of compound* ***147j****.*

Figure A2.148. *^{1}H NMR (400 MHz, $CDCl_3$) of compound* ***132***.

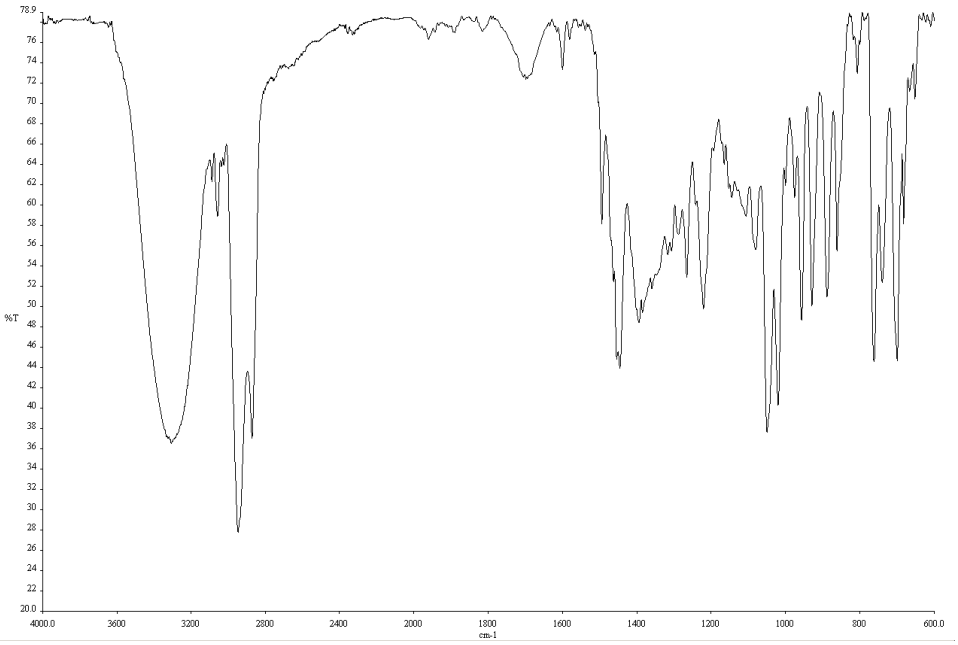


Figure A2.149. *Infrared spectrum (Thin Film, NaCl) of compound* ***132****.*

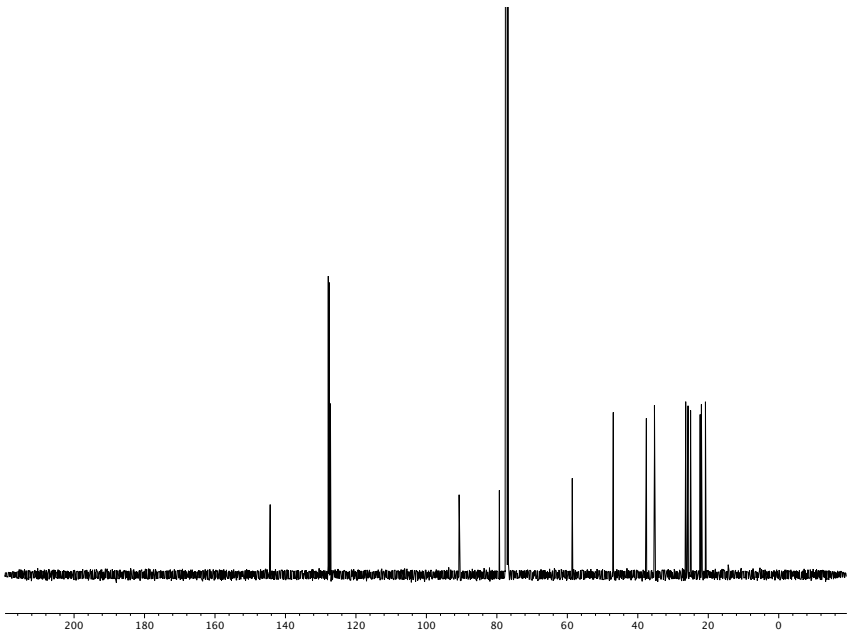


Figure A2.150. *^{13}C NMR (100 MHz, $CDCl_3$) of compound* ***132****.*

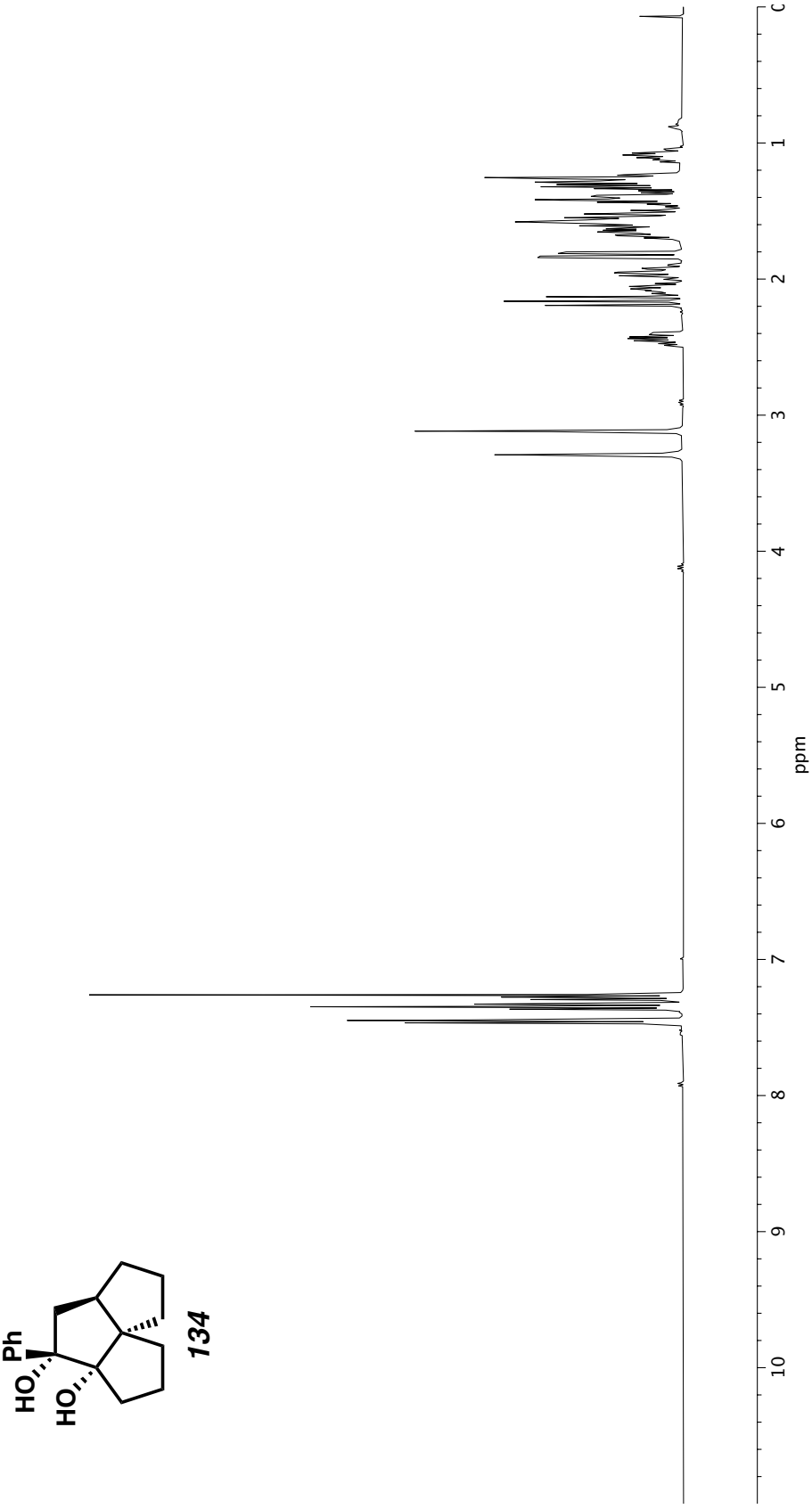


Figure A2.151. *^1H NMR (400 MHz, $CDCl_3$) of compound **134**.*

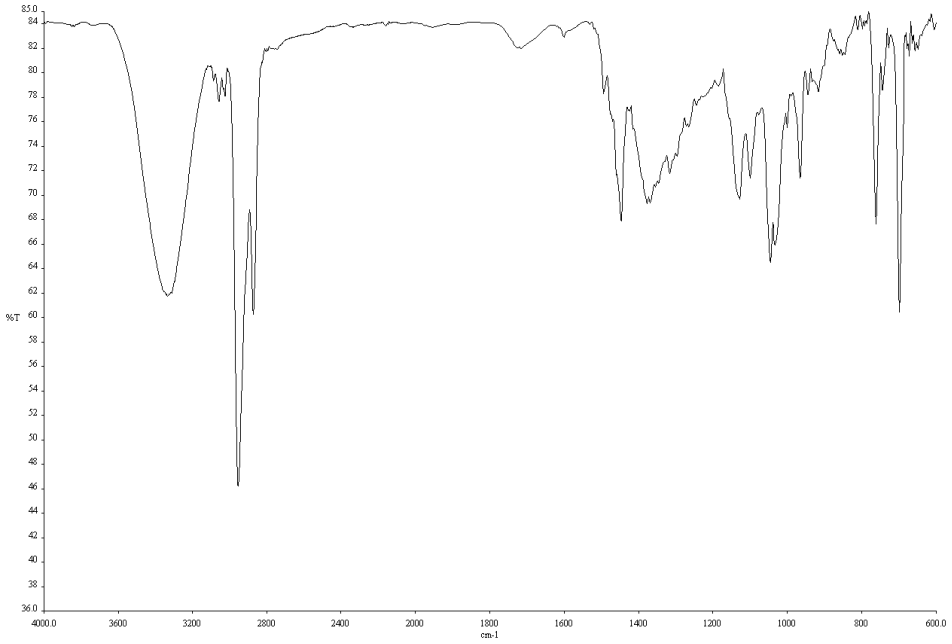


Figure A2.152. *Infrared spectrum (Thin Film, NaCl) of compound* ***134****.*

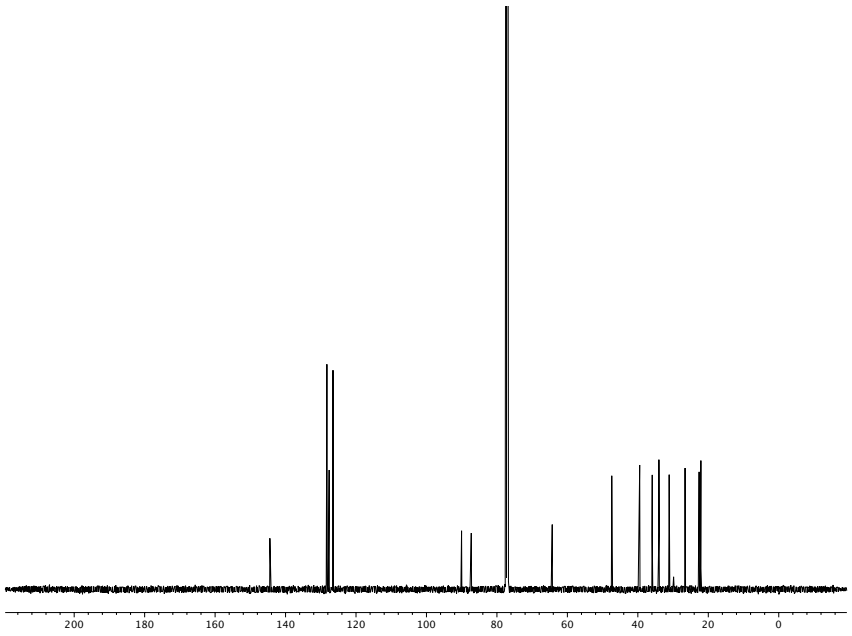


Figure A2.153. *^{13}C NMR (100 MHz, $CDCl_3$) of compound* ***134****.*

Figure A2.154. *^1H NMR (400 MHz, $CDCl_3$) of compound **135**.*

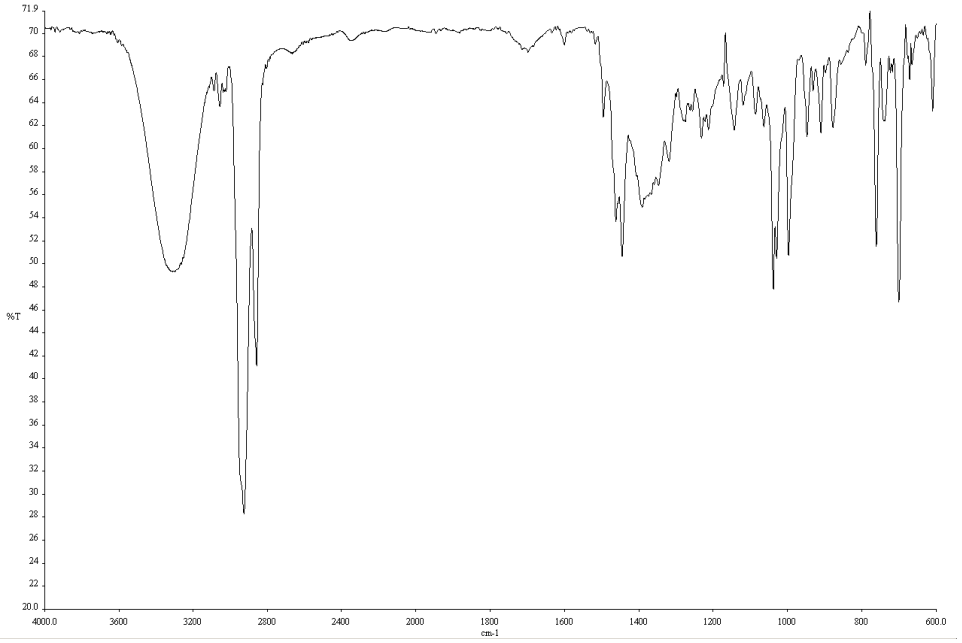


Figure A2.155. *Infrared spectrum (Thin Film, NaCl) of compound* ***135****.*

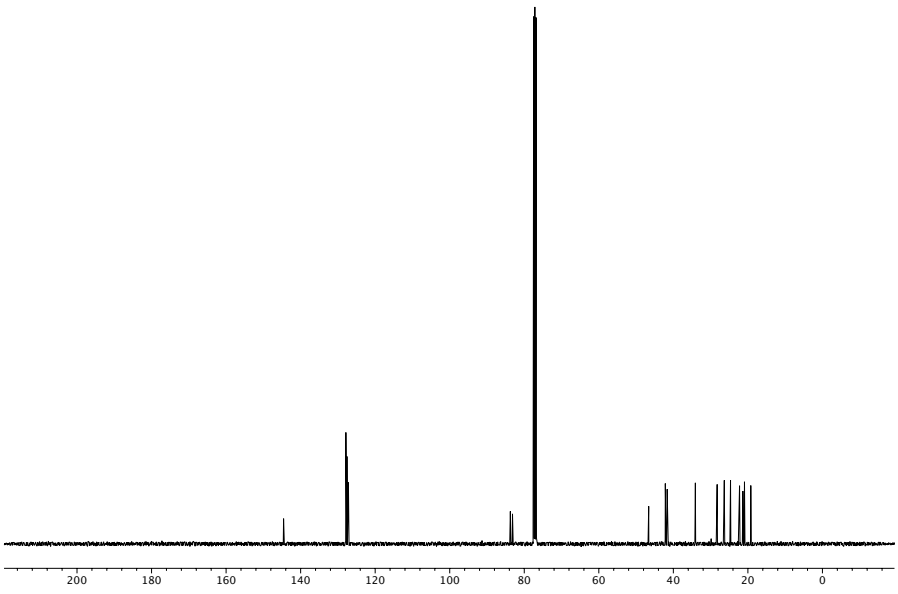


Figure A2.156. *^{13}C NMR (100 MHz, $CDCl_3$) of compound* ***135****.*

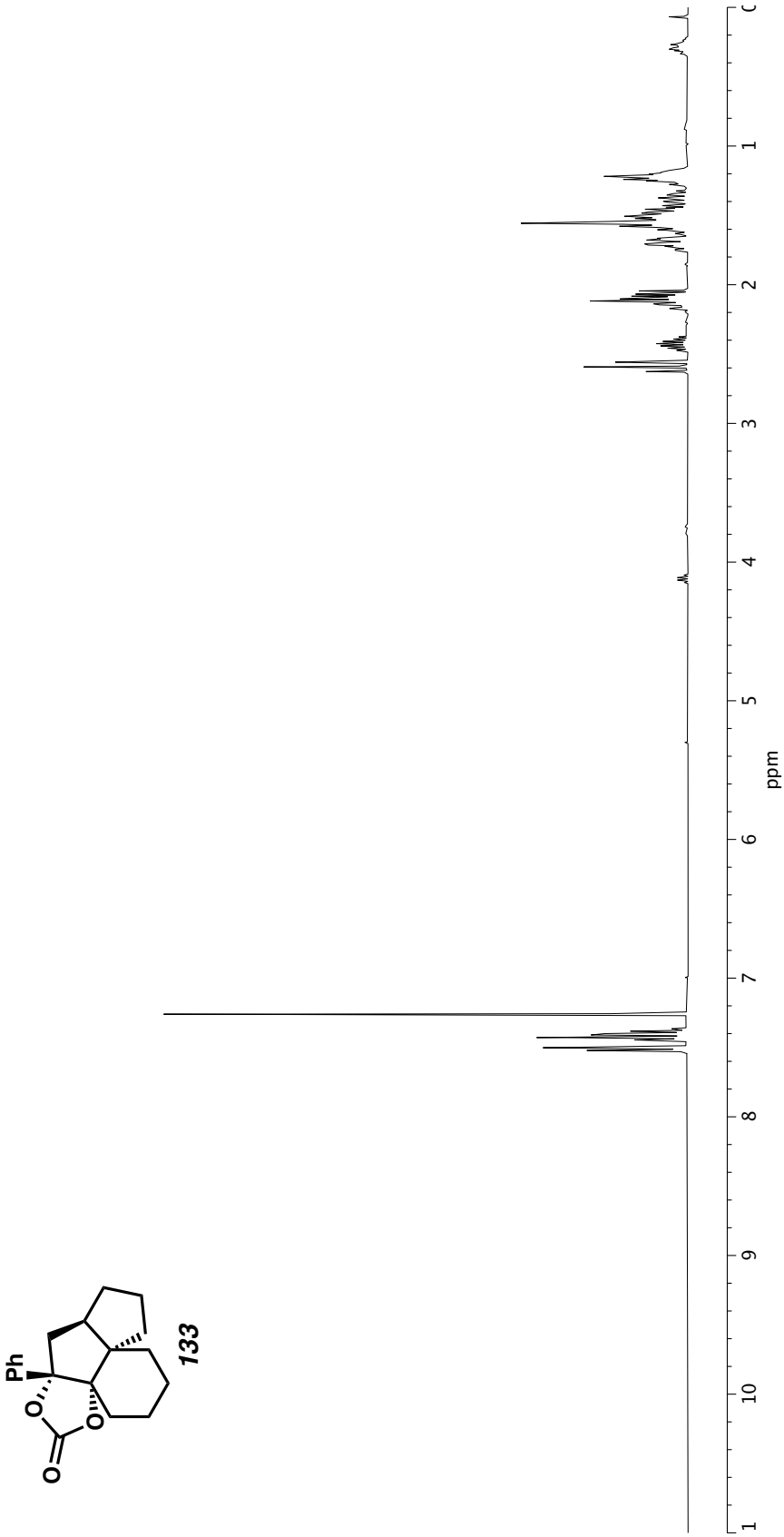


Figure A2.157. *^{1}H NMR (400 MHz, $CDCl_3$) of compound **133**.*

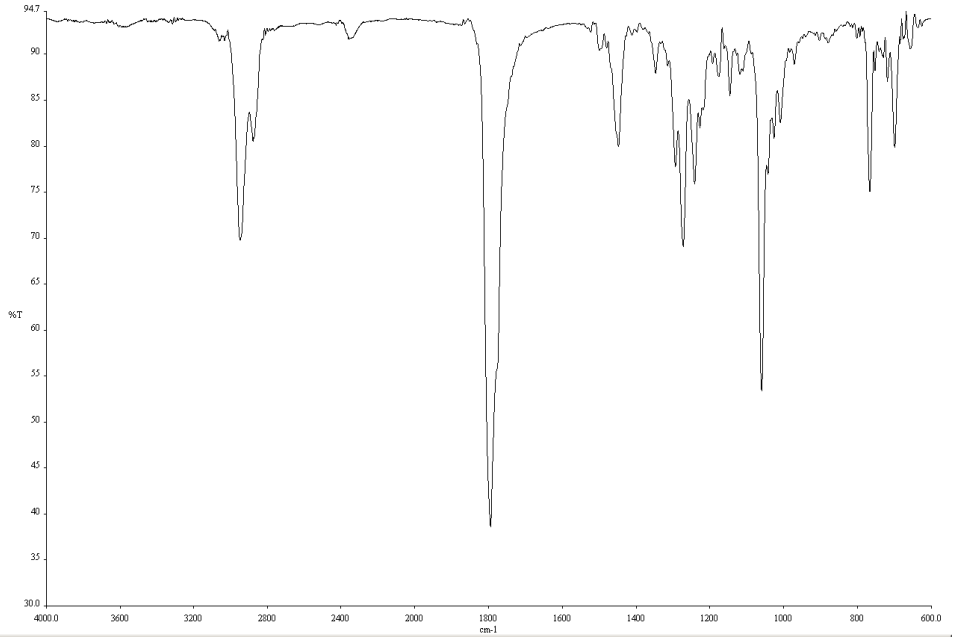


Figure A2.158. *Infrared spectrum (Thin Film, NaCl) of compound* ***133***.

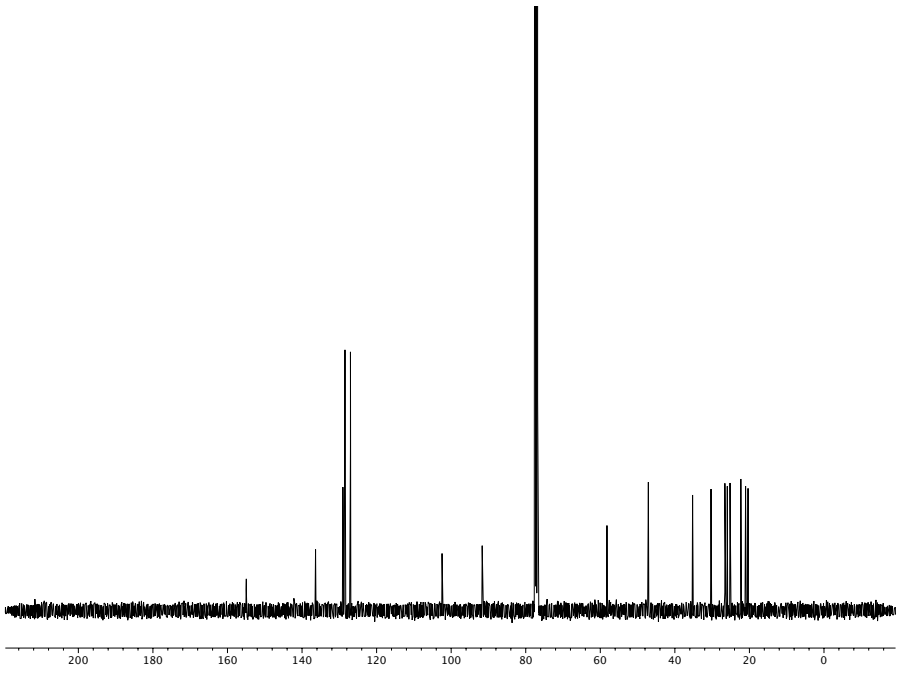


Figure A2.159. *^{13}C NMR (100 MHz, $CDCl_3$) of compound* ***133***.

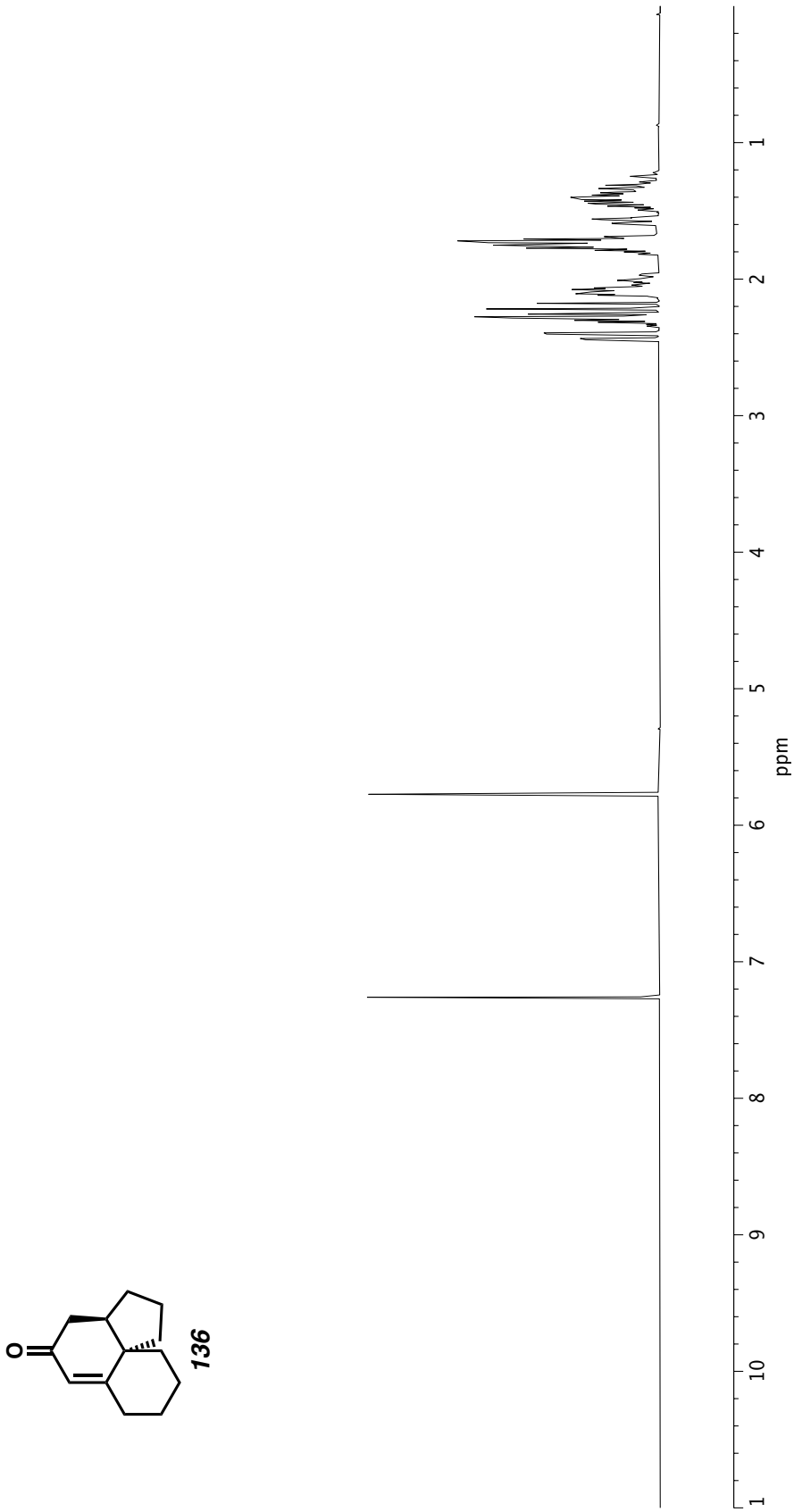


Figure A2.160. *^1H NMR (400 MHz, $CDCl_3$) of compound **136**.*

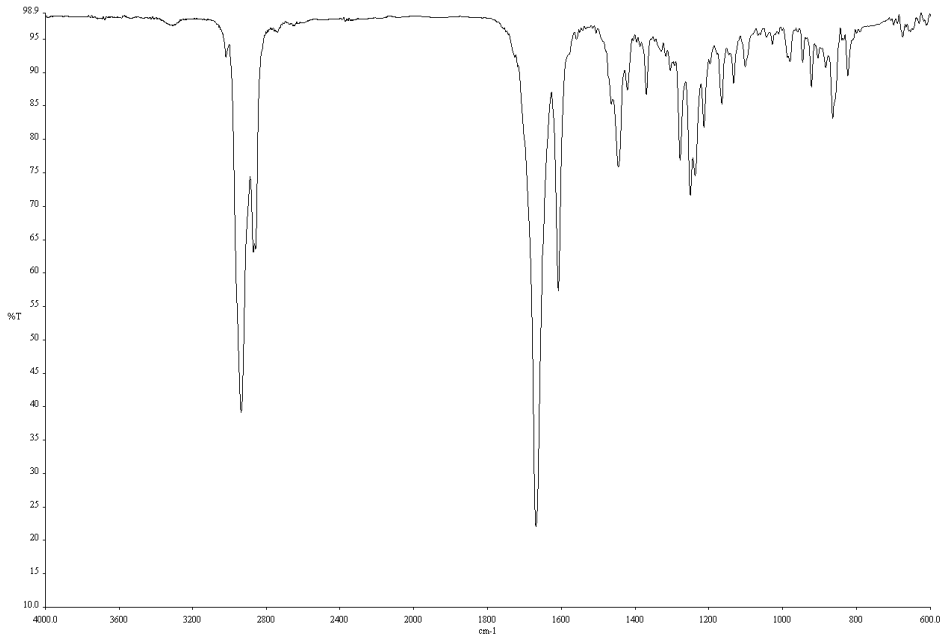


Figure A2.161. *Infrared spectrum (Thin Film, NaCl) of compound* ***136****.*

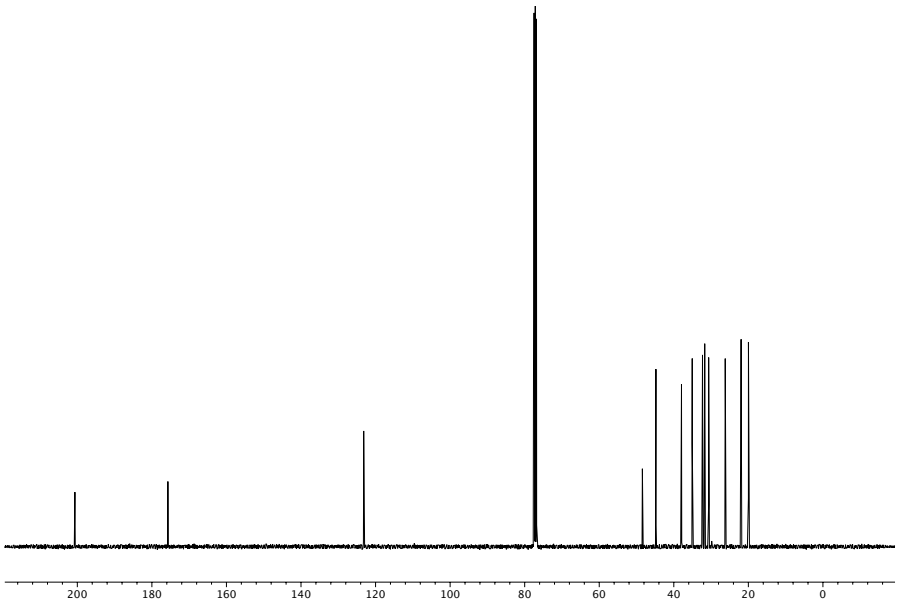


Figure A2.162. *^{13}C NMR (100 MHz, $CDCl_3$) of compound* ***136****.*

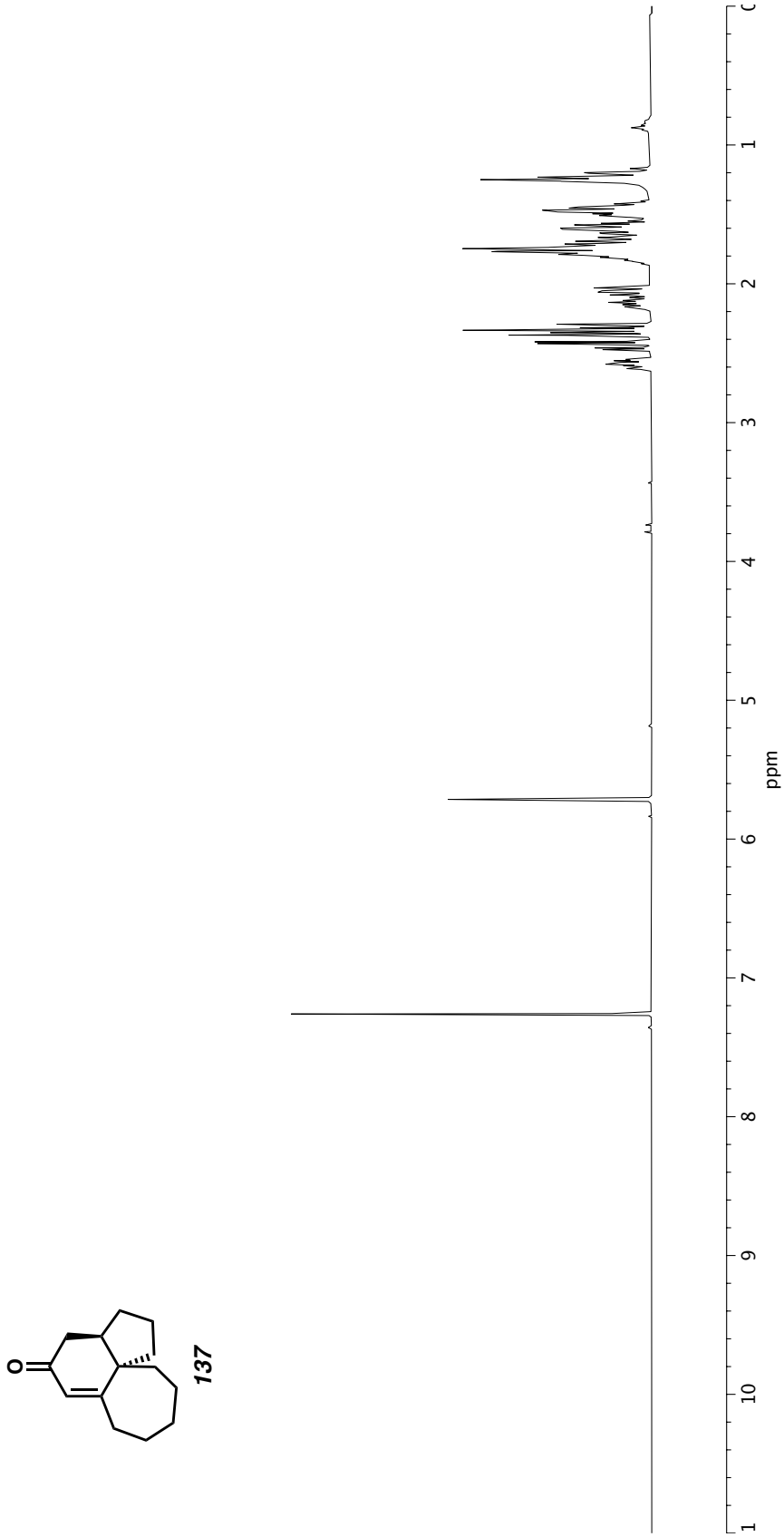


Figure A2.163. *^{1}H NMR (400 MHz, $CDCl_3$) of compound **137**.*

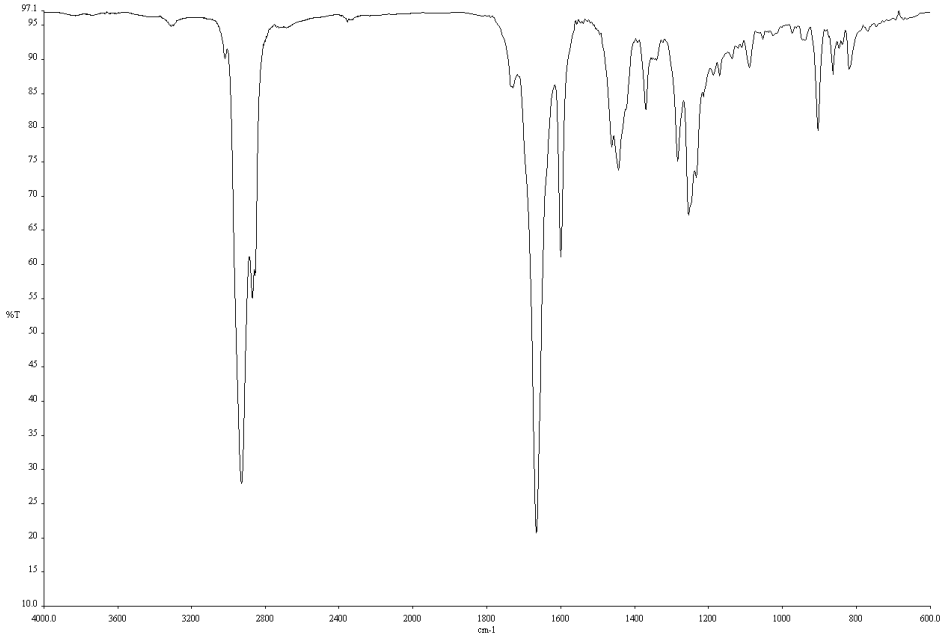


Figure A2.164. *Infrared spectrum (Thin Film, NaCl) of compound* ***137****.*

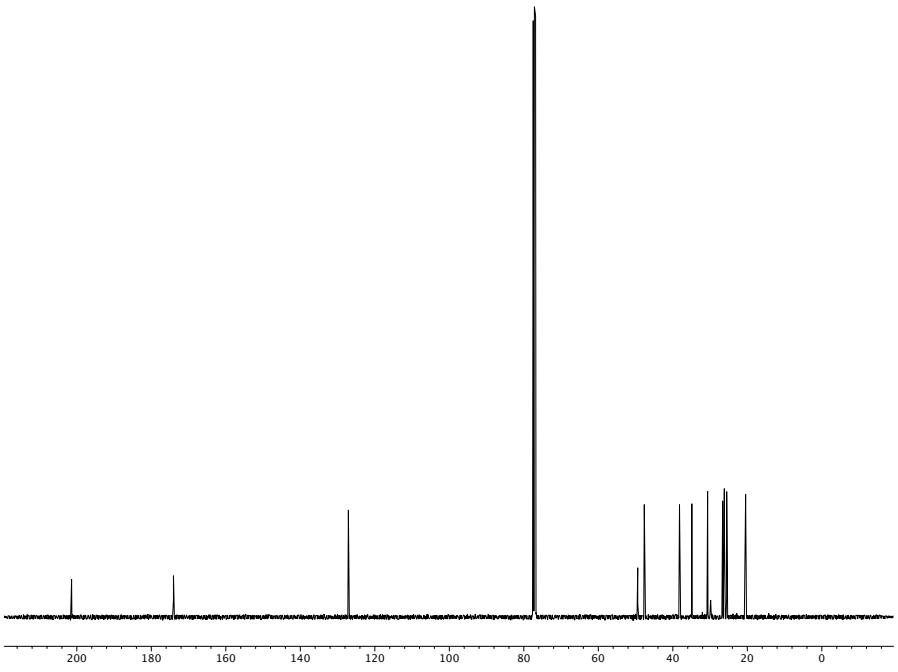


Figure A2.165. *^{13}C NMR (100 MHz, $CDCl_3$) of compound* ***137****.*

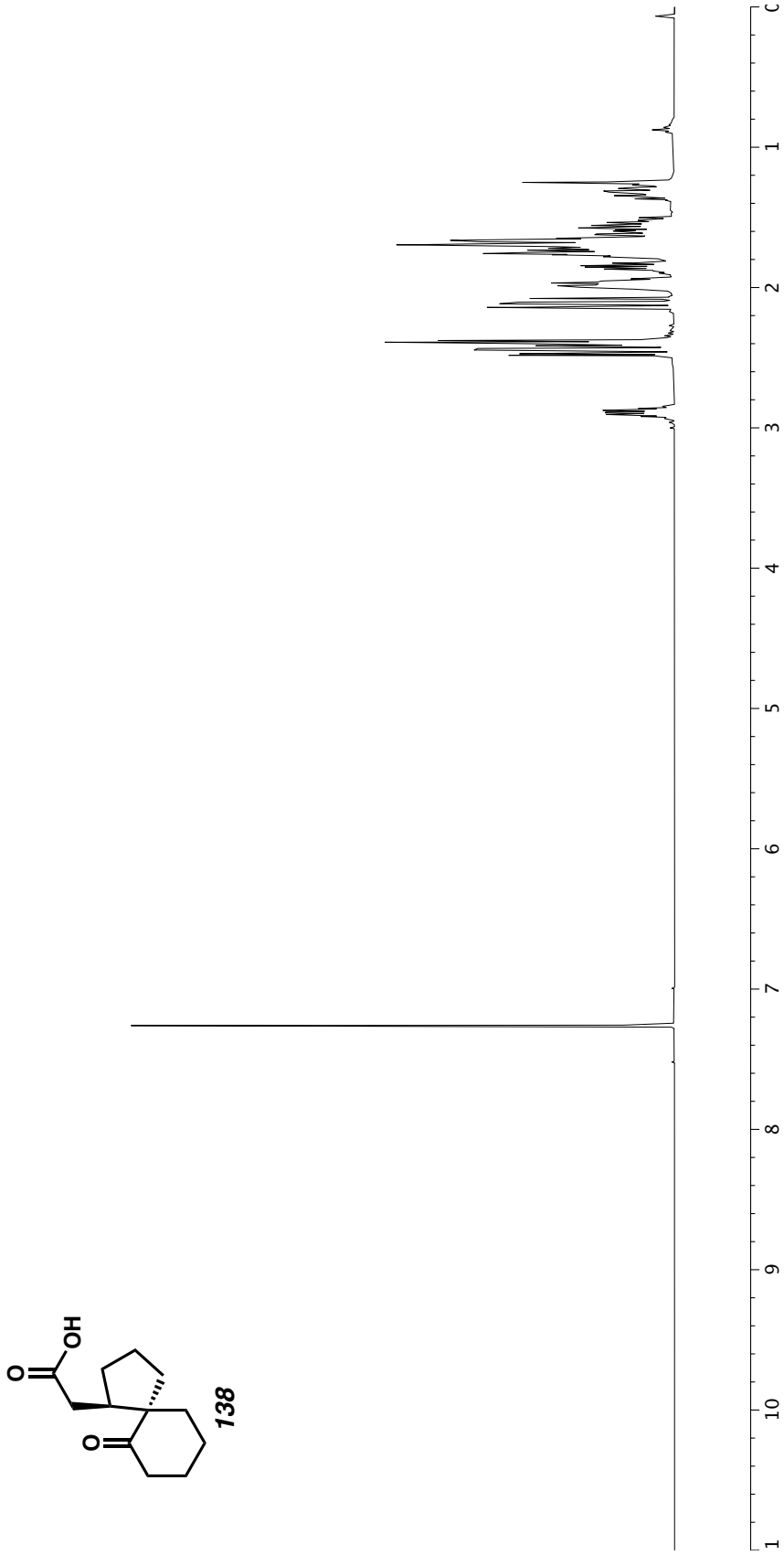


Figure A2.166. *^{1}H NMR (400 MHz, $CDCl_3$) of compound **138**.*

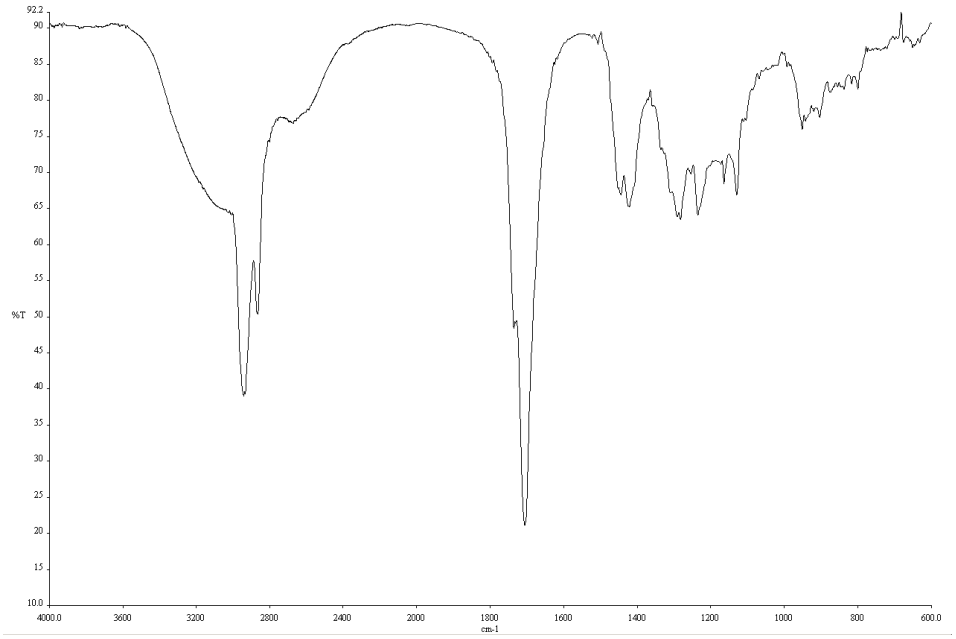


Figure A2.167. *Infrared spectrum (Thin Film, NaCl) of compound* ***138****.*

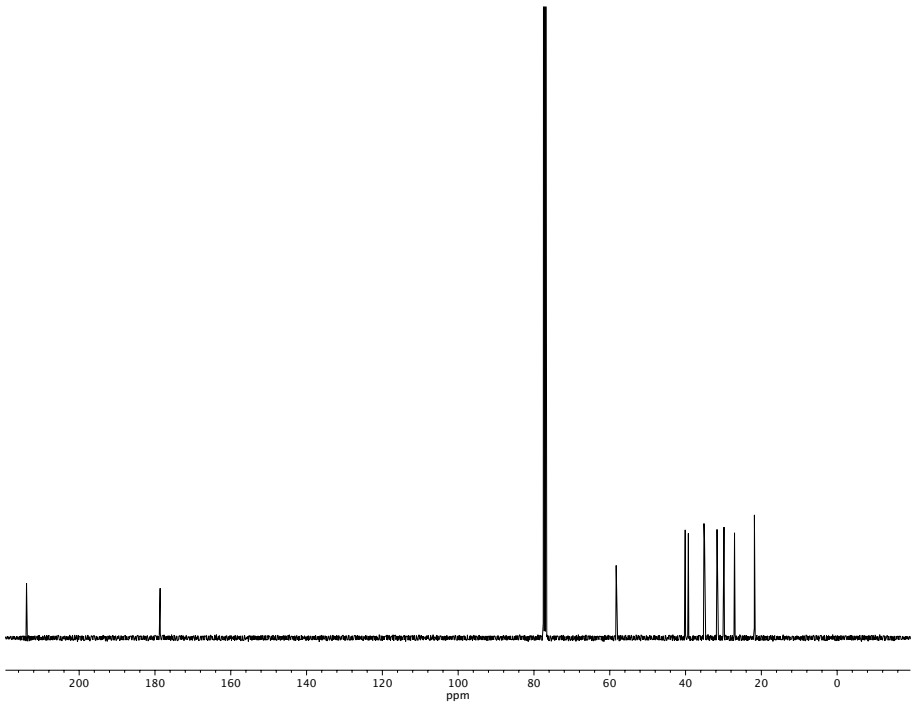


Figure A2.168. *^{13}C NMR (100 MHz, $CDCl_3$) of compound* ***138****.*

CHAPTER 4

A Pericyclic Strategy to the Enantio- and Diastereoselective Synthesis of Vicinal Quaternary/Tertiary Stereocenters from Chiral Palladium Enolates†

4.1 INTRODUCTION

The construction of chiral all-carbon quaternary centers featuring vicinal tertiary stereocenters exemplifies a prevalent challenge in synthetic chemistry (Figure 4.1.A). Strategies that forge the adjoining bond must simultaneously control stereochemistry at each of the two coupling centers.

Pericyclic reactions are particularly well suited for such a task – with the constrained, cyclic nature of the transition state eliminating complexity derived from the high degree of conformational freedom of an acyclic counterpart. Moreover, permutations of each stereochemical element (*e.g.*, chair versus boat) enable independent control of enantio- and diastereoselectivity. Lastly, pericyclic construction of a $C(sp^3)$–$C(sp^3)$ σ-bond through the union of two planar $C(sp^2)$ fragments is an ideal mechanism to minimize the enthalpic barrier to constructing a sterically encumbered bond.

Such pericyclic bond construction is key to $C(sp^3)$–$C(sp^3)$ bond formation in the Pd(PHOX)-catalyzed decarboxylative asymmetric allylic alkylation (DAAA). In contrast to traditional outer-sphere mechanisms, computational and mechanistic studies support that the critical C–C bond formation occurs through a concerted

†Unpublished research performed in collaboration with Cusumano, A. Q.; Hubble, V. B.; Sardini, S. R.

inner-sphere reductive elimination pathway in the Pd(PHOX) catalyst system (**TS35**, Figure 4.1.B).[1] We propose that this pericyclic allylation pathway could serve as an ideal platform to realize an enantio- and diastereoselective formation of vicinal quaternary and tertiary stereocenters from a substituted η^1-allyl *O*-bound Pd enolate.[2]

As a complicating matter, we envisioned a facile equilibration between constitutional isomers **160** and **161**, reaction from which leads to either the desired *branched* (**162**) or undesired *linear* (**159**) isomers of product, respectively (Figure 4.1.C). While we have established a likely inner-sphere mechanism to be operative in the Pd(PHOX)-catalyzed decarboxylative allylic alkylation of β-ketoesters, outer-sphere mechanisms may represent competing pathways, and are the predominant pathways for other ligand scaffolds, such as with Trost-type ligands. Concerningly, the Pd-catalyzed decarboxylative allylic alkylation of model substrate **163** with such ligand classes exclusively affords the undesired *linear* constitutional isomer of product (**164**, Figure 4.1.D).[3] Hence, in addition to designing a reaction that proceeds through a highly selective inner-sphere mechanism, preventing competing outer-sphere pathways is likely crucial to achieving high *branched* selectivity.

While examples of ligand design to promote branched-selective allylic alkylation of *soft* (*i.e.*, stabilized) enolate nucleophiles are known,[4-5] these transformations generally proceed through outer-sphere mechanisms and are not translatable to *hard* (*i.e.*, non-stabilized) enolate nucleophiles. Hartwig and coworkers demonstrated that Ba enolates of α-tetralones are competent nucleophile coupling partners in an Ir-catalyzed branched-selective allylic alkylation with cinnamyl carbonate

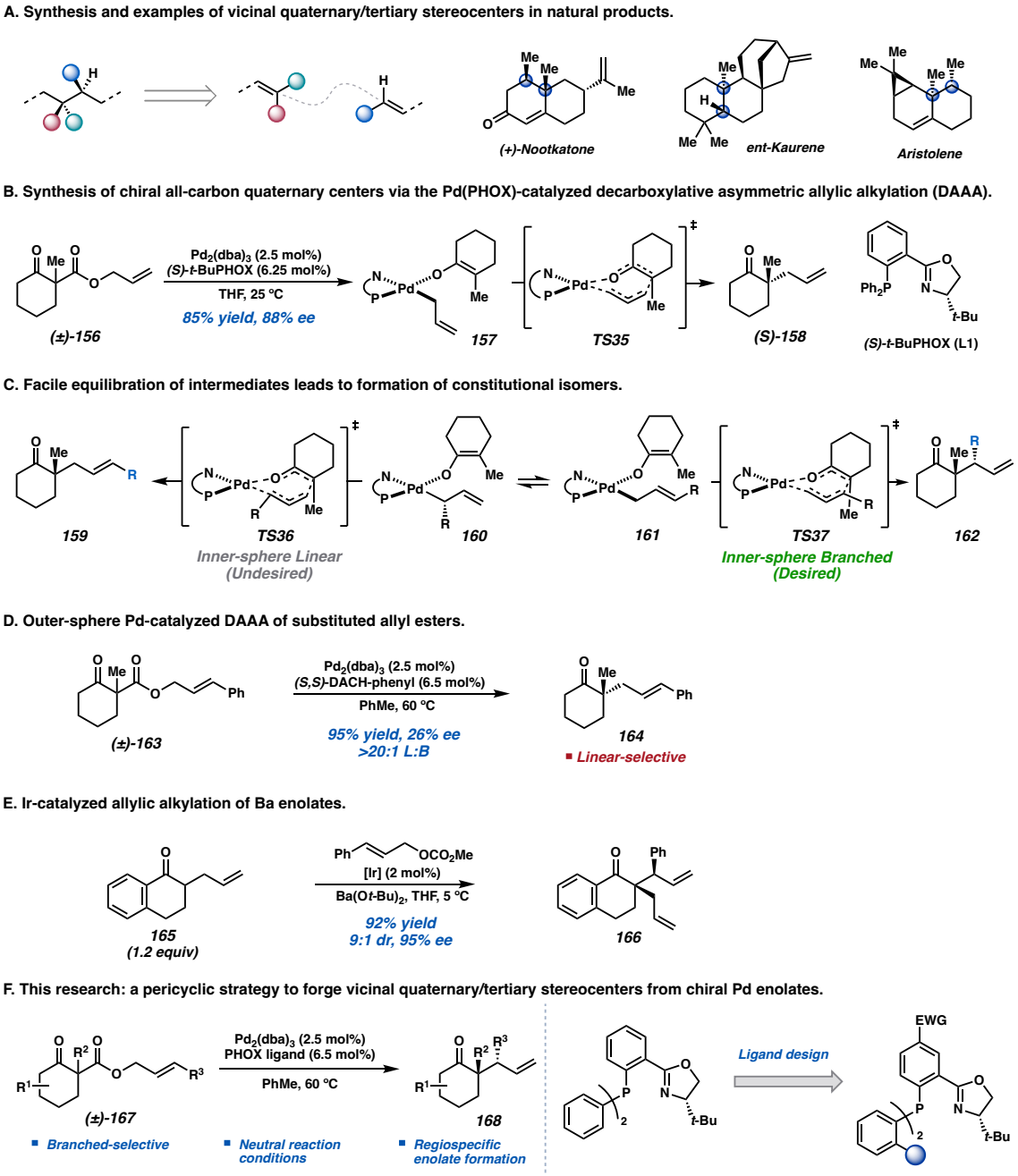
electrophiles (Figure 4.1.E).[6] While good yields and excellent enantioselectivities are observed, this approach is limited in the enolate nucleophile scope by the regioselectivity of the deprotonation, with related transformations subject to similar constraints.[7] Hence, we reasoned that regiospecific enolate generation through decarboxylation must remain a core component of our strategy.[8]

With this in mind, we aimed to develop a stereoselective DAAA strategy that biases formation of *branched* product **168** through rational ligand design (Figure 4.1.F). We posited that the requisite stereocontrol could be achieved through a [σ2s + σ2s + π2s + π2s] pericyclic reductive elimination from *O*-bound Pd enolate **161** (**TS37**). A chiral phosphinooxazoline (PHOX) ligand (**L1**) would promote enantiofacial control, while the boat/chair preference instills diastereoselectivity. Moreover, intermediate **161** could be catalytically unveiled through the decarboxylation of a β-ketoester substrate (**167**). To approach the challenge of regioselectivity, we envision destabilizing the transition state leading to formation of the *linear* product (**TS36**) by introducing additional steric bulk to the PHOX ligand to induce unfavorable steric interactions with the allyl substituent.

Aided by mechanistic insights, we designed a new class of PHOX ligands that promote a branched-selective, inner-sphere C–C bond formation. We demonstrate the ability of this approach to construct products bearing a stereogenic all-carbon quaternary center with a vicinal tertiary stereocenter (Figure 4.1.F). High diastereo- (>20:1) and enantioselectivity (>80% ee) are obtained, with the majority of products featuring >20:1 *branched/linear* selectivity. Experimental and computational studies were performed to investigate pathways that contribute to the various

elements of selectivity in this transformation. Subsequent derivatization of the reaction products highlights their broader utility as synthetic building blocks.

Figure 4.1. *Enantio- and diastereoselective allylic alkylation of tetrasubstituted nucleophiles to forge vicinal quaternary/tertiary stereocenters.*



4.2 RESULTS AND DISCUSSION

4.2.1 REACTION DESIGN AND OPTIMIZATION

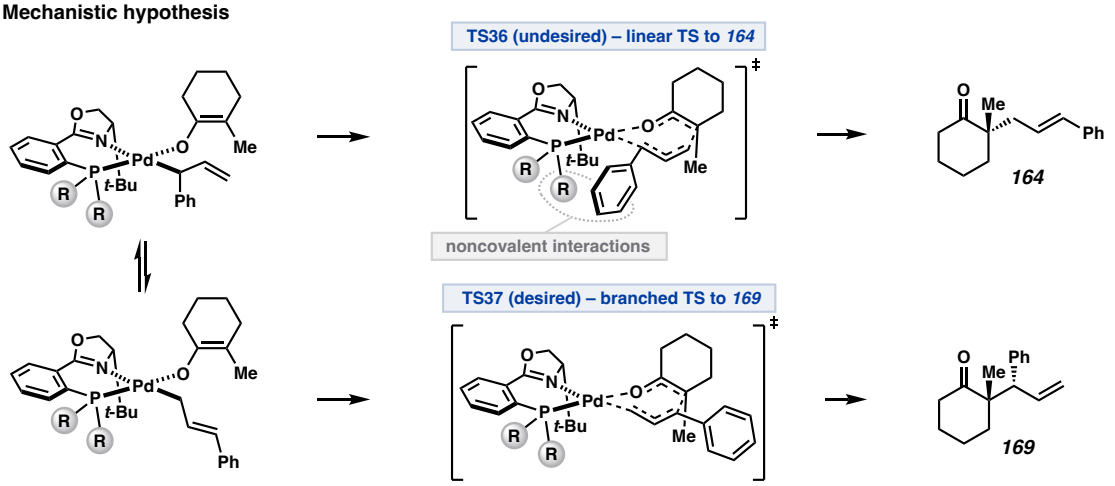
Under canonical conditions, employing Trost's *(S,S)*-DACH-phenyl ligand, the Pd-catalyzed decarboxylative allylic alkylation of β-ketoester **(±)-163** affords exclusively linear product **164** (Fig 4.1.D). Proceeding predominantly via an outer-sphere mechanism, linear selectivity likely arises from preferred nucleophilic attack at the less sterically hindered, unsubstituted allyl terminus. Substantial progress has been made in rendering outer-sphere processes in Pd catalysis branched-selective allylations via ligand design.[9]

In contrast, evidence suggests that the C–C bond forming step in Pd(PHOX)-catalyzed allylic alkylation of β-ketoesters proceeds via an inner-sphere mechanism, featuring a seven-centered C–C bond-forming transition state. We sought to capitalize on elements of cyclic stereocontrol offered by this distinct mechanistic paradigm to achieve regio-, enantio-, and diastereoselectivity in the branched-selective allylic alkylation from **163**. We began our investigation by computationally considering the C–C bond forming step in the mechanism, by which the desired branched (**169**) and undesired linear (**164**) products are derived from β-ketoester **(±)-163** (Figure 4.2.A). With a substituted allyl fragment, two isomeric transition states may be derived in which the substituent is poised either adjacent or distant to the forming C–C bond. Computationally, the two lowest energy transition states leading to linear (**164**) and branched (**169**) products are **TS36** and **TS37**, respectively. Unfortunately, with the prototypical *(S)-t*-BuPHOX ligand (**L1**), linear **TS36** is favored by 2.5 kcal/mol over its branched counterpart (**TS37**). This hypothesis is experimentally validated in the reaction of **(±)-163** promoted by *(S)-t*-BuPHOX (Table 4.1, entry 1).

Noting the proximity of the allyl substituent to the phenyl group of the PHOX ligand in **TS36** (R in Figure 4.2.A), we became interested in exploring di-*ortho* substitution of the ligand aryl groups as a means to disfavor **TS36** via non-covalent steric interactions.

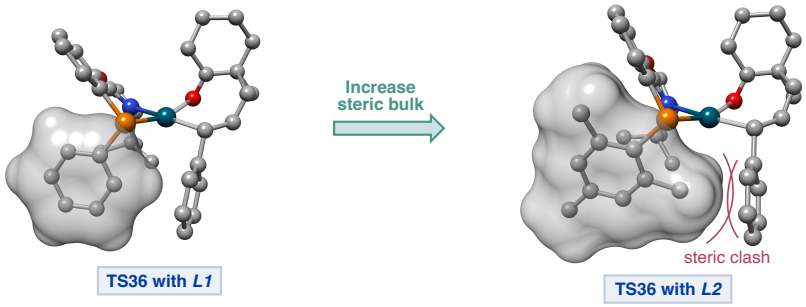
Figure 4.2. *(A) Branched and linear product outcomes from an inner-sphere reductive elimination. (B) Modifying ligand steric profile to disfavor* ***TS36****, hence favoring branched-product (****169****) formation via* ***TS37****.* Gibbs free energies at the PBE0-D4/def2-TZVPP/CPCM(PhMe)//PBE0-D4/def2-TZVP(Pd), def2-SVP/CPCM(PhMe) level of theory. See section 4.4.4 for more details.

A. Mechanistic hypothesis



B. Favoring TS37 by increasing the steric profile of R.

Substitution	Ligand	$\Delta G^{\ddagger}_{rel}$ TS36 (kcal/mol)	$\Delta G^{\ddagger}_{rel}$ TS37 (kcal/mol)
R = Ph	*(S)*-*t*-BuPHOX *(L1)*	0.0	2.5
Mes	*(S)*-Mes-*t*-BuPHOX *(L2)*	3.4	0.0



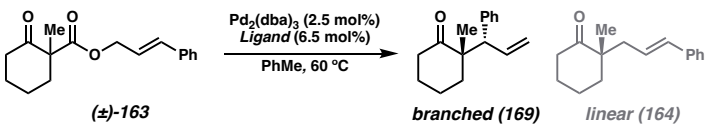
Accordingly, we modeled the possible reductive elimination pathways with *(S)*-Mes-*t*-BuPHOX (**L2**) (Figure 4.2.B). The more sterically demanding mesityl group disfavors **TS36** such that **TS37** now becomes favored by 3.4 kcal/mol. Enantioselectivity of the branched product (**169**) from inner-sphere reactivity is computed to remain high, with $\Delta\Delta G^{\ddagger}$ between diastereomeric transition states of 1.2 and 3.1 kcal/mol with **L1** and **L2**, respectively. Moreover, 3.8 and 2.3 kcal/mol preferences for the chair-like over the boat-like transition states ensures good diastereoselectivity (see 4.4.4 for complete transition state analysis). In summary, our preliminary *in silico* studies highlight that (1) *ortho* substitution of the ligand arenes will introduce a bias for the desired branched product (**169**), and (2) a purely inner-sphere reaction will maintain both high diastereo- and enantioselectivity.

Based on our computational analysis, we synthesized **L2**, which disappointingly resulted in only a modest improvement in branched/linear selectivity, and the branched product was formed with significantly diminished ee. This result indicates that the mechanism may not proceed exclusively through an inner-sphere process due to the electron rich nature of **L2** (Table 4.1, entry 2).[1c] As noted above, C–C bond formation via a competing outer-sphere mechanism will likely favor formation of the linear product (Figure 4.1.D). To test this hypothesis, we used a more electron-deficient ligand *(S)*-$(CF_3)_3$-*t*-BuPHOX (**L3**) which, as expected, favored the linear isomer (**164**); however, the branched product (i.e., **169**) that was formed was obtained in high diastereo- and enantioselectivity (Table 4.1, entry 3). Thus, we envisioned that a ligand featuring both *ortho*-substituents and electron deficient characteristics could allow for the simultaneous

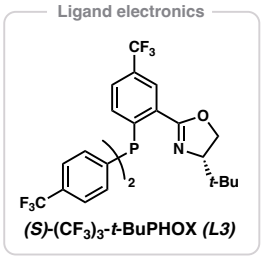
control of regio- and stereoselectivity. Therefore, we focused our ligand design on utilizing electron-deficient *ortho*-substituted PHOX ligands (**L4**–**L7**). Ultimately, use of an *ortho*-trifluoromethyl ether (**L7**) led to the best balance of regio- and enantioselectivities (Table 4.1, entry 7), which was further improved by conducting the reaction at lower temperature (Table 4.1, entry 8).

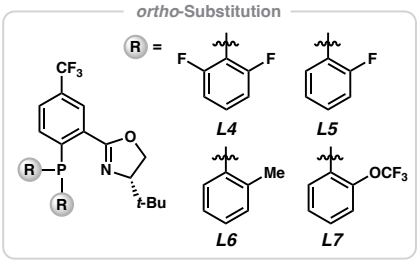
Table 4.1. *Optimization of Pd-catalyzed branched-selective asymmetric allylic alkylation.* [a]*Reaction conditions:* ***163*** *(0.05 mmol),* $Pd_2(dba)_3$ *(2.5 mol%), ligand (6.5 mol%), and PhMe (2 mL) at 60 °C for 14 h. NMR yield determined with 1,3,5-trimethoxybenzene as an internal standard. B:L and dr determined by crude* ^1H *NMR analysis. Enantioselectivity was measured by chiral SFC analysis.* [b]*Isolated yield from 0.1 mmol of* ***163*** *at 50 °C.*

Reaction optimization.[a]



Entry	Ligand	Yield (%)	B:L (169:164)	dr	% ee
1	(S)-t-BuPHOX (L1)	97	1 : 2	7 : 1	65
2	(S)-Mes-t-BuPHOX (L2)	38	1 : 1	2 : 1	6
3	(S)-$(CF_3)_3$-t-BuPHOX (L3)	86	1 : 1	14 : 1	80
4	L4	25	3 : 1	12 : 1	68
5	L5	78	2 : 1	16 : 1	82
6	L6	90	11 : 1	14 : 1	70
7	L7	62	6 : 1	>20 : 1	76
8[b]	L7	62	9 : 1	>20 : 1	82

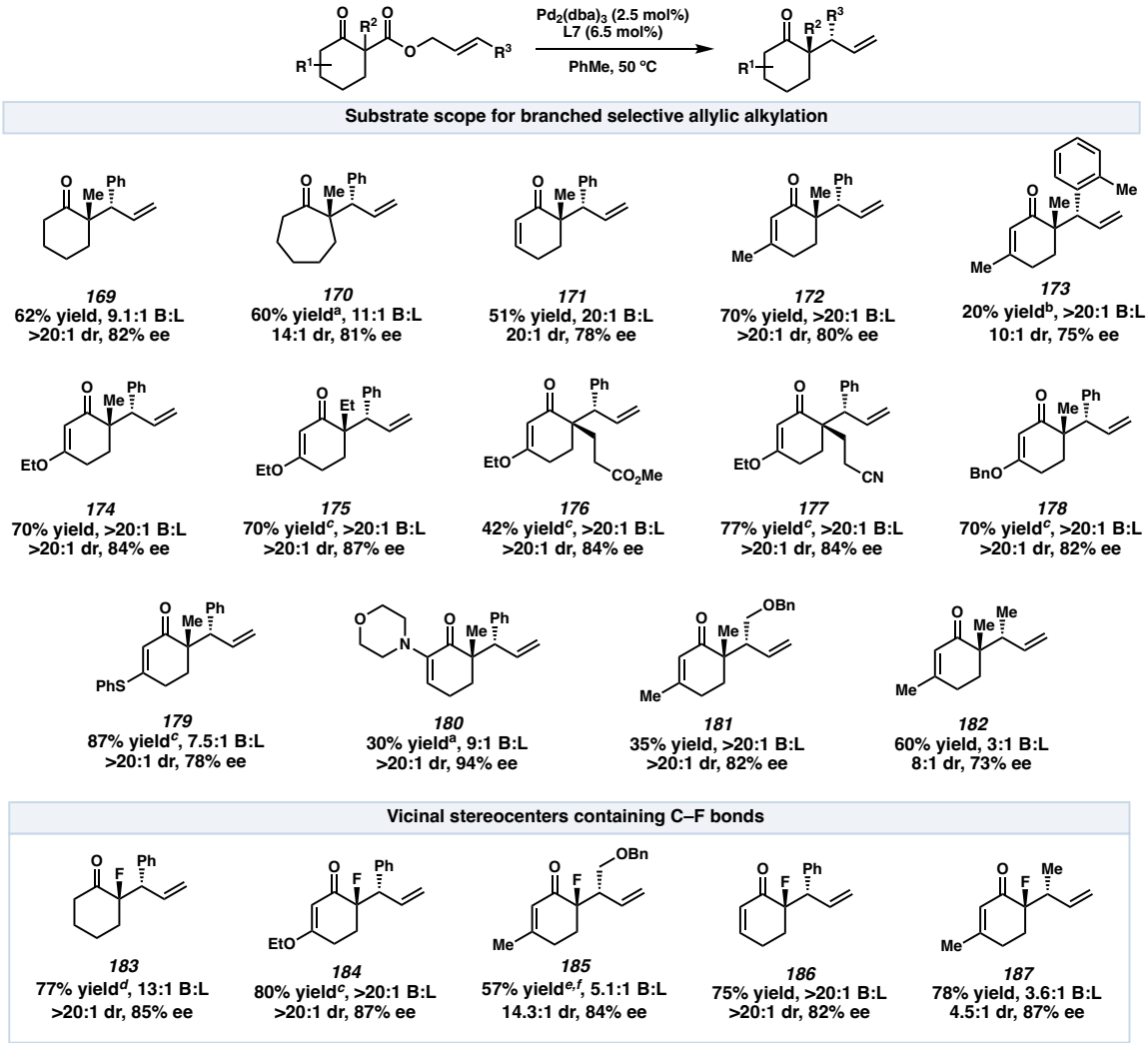




4.2.2 SUBSTRATE SCOPE AND PRODUCT DERIVATIZATION

With optimized conditions in hand, we then investigated the substrate scope of the transformation (Figure 4.3). Six-, and seven-membered rings were well tolerated under the

Figure 4.3. *Substrate scope of branched-selective allylic alkylation.* [a]*Reaction performed with* ***L3*** *instead of* ***L7***. [b]*Reaction performed with* ***L6*** *instead of* ***L7***. [c]*Reaction performed with* ***L5*** *instead of* ***L7***. [d]*B and L separable.* ***183*** *could be isolated as a >20:1 B:L in a 71% yield.* [e] *Reaction performed at 60 ºC instead of 50 ºC.* [f]*B and L separable.* ***185*** *could be isolated as a >20:1 B:L in a 48% yield.*



optimized reaction conditions (products **169** and **170**).[10] Decreasing the steric size of the α' position by incorporating unsaturation led to an increase in the ratio of branched product

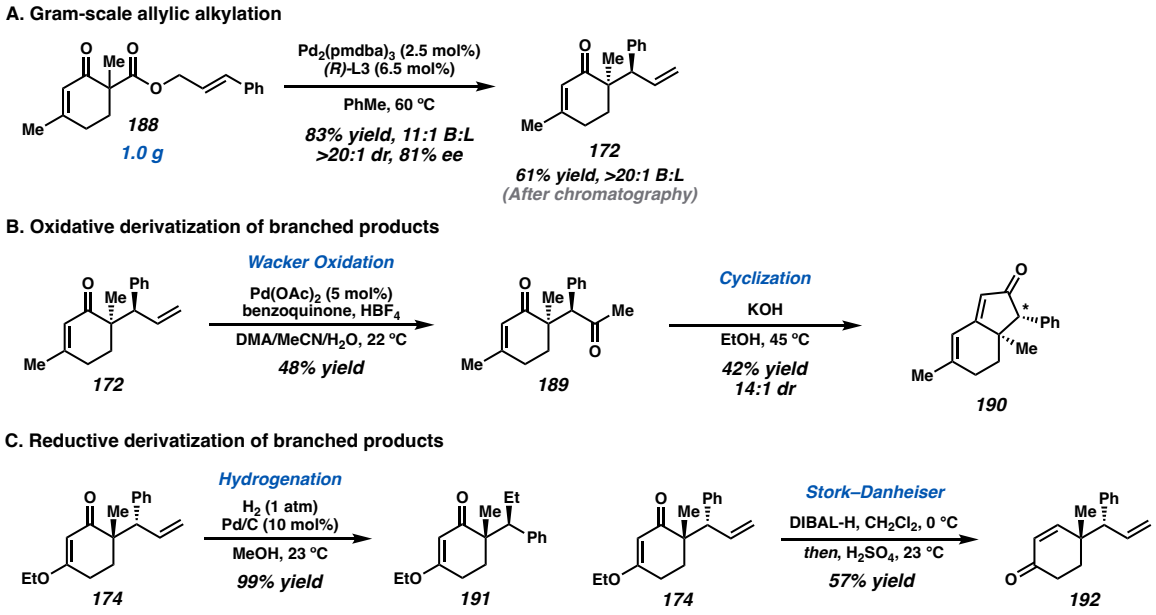
(products **171** and **172**) at a slight cost in enantioselectivity. To our delight, *ortho*-methyl substituted cinnamyl derivatives generate the corresponding branched product despite the increased steric congestion (product **173**). Excitingly, synthetically useful vinylogous esters were excellent substrates in the transformation, generally yielding products with >20:1 regio- and diastereoselectivity (products **174**-**178**). In the reaction of vinylogous ester substrates, **L5** could also be substituted in place of **L7**.[11]

Additionally, the mild nature of the reaction conditions allowed for the application of potentially base-sensitive functional groups such as a methyl ester and nitrile (products **176** and **177**). Enaminone **180** could also be generated with our optimized conditions with excellent levels of enantioselectivity. Moreover, alkyl-substituted allyl β-ketoesters smoothly undergo branched-selective allylic alkylation (products **181**, and **182**), signifying a successful departure from the privileged cinnamyl scaffold. Finally, α-fluoro-substituted β-ketoesters undergo branched selective allylic alkylation with excellent levels of regio- and stereoselectivity (products **183**–**187**).

The corresponding allylic alkylation reaction could also be performed on gram-scale without significant erosion of regio- or stereoselectivities (Figure 4.4.A).[12] Employing **L3** allows for the formation of product **172**, which could be isolated as the pure branched isomer after chromatography, albeit in overall lower regioselectivity.[13] We were then able to showcase the synthetic utility of the corresponding allylic alkylation products. Oxidative transformations of the newly installed alkene generally proceed smoothly to generate methyl ketone **189** via a Wacker oxidation.[14] Exposure of this material to base-promoted aldol condensation

grants access to the corresponding fused ring system **190** (Figure 4.4.B).[15] Hydrogenation of **174** results in the formation of enone **191**, which contains a stereodiad that is traditionally difficult to forge. Finally, we can showcase the synthetic utility of the vinylogous ester functionality by performing a Stork–Danheiser transposition on **174** to generate the corresponding enantioenriched γ-quaternary enone (**192**) (Figure 4.4.C).

Figure 4.4. *(A) Gram-scale synthesis of branched allylic alkylation product. (B) Oxidative functionalization reactions of the branched allylic alkylation products. (C) Reductive functionalization reactions of the branched allylic alkylation products.*

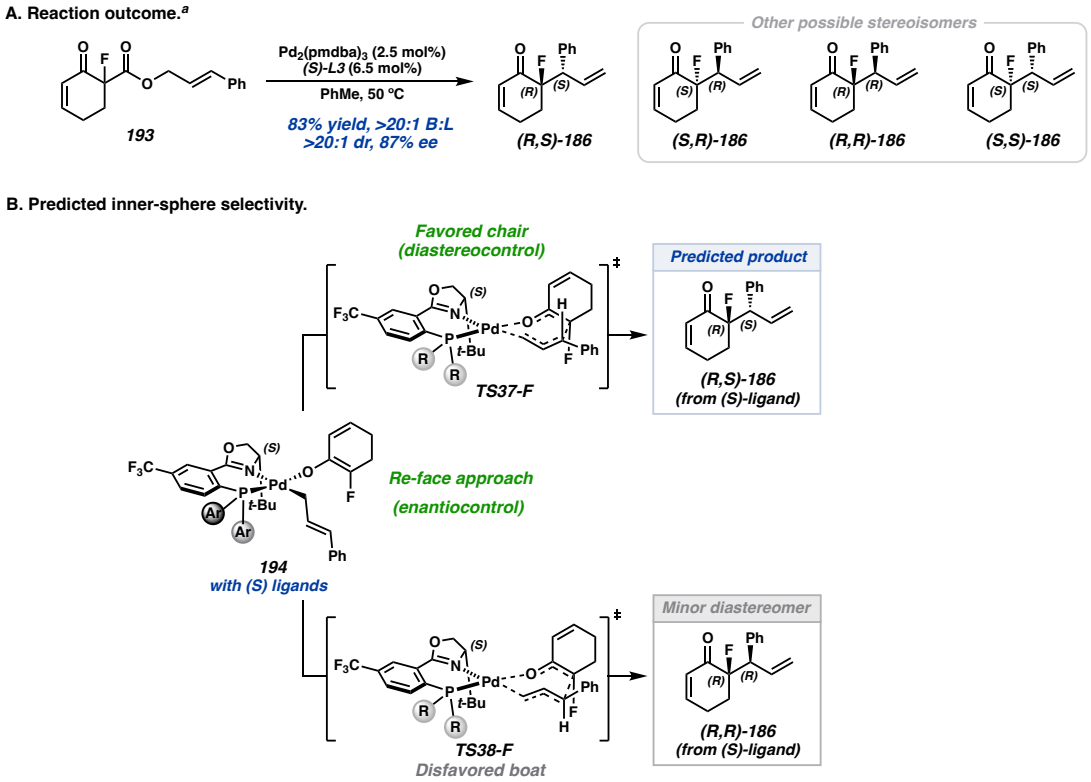


4.2.3 INNER-SPHERE C–C BOND FORMATION

Ultimately, our rational ligand design strategy was enabled by our mechanistic understanding of C–C bond formation in the Pd(PHOX) catalyst systems – namely the

inner-sphere enantiodetermining seven-centered pericyclic transition state, through which reductive elimination occurs. Our computational data suggest that branched product formation occurs preferentially from the enolate *Re* face (Figure 4.2.A, **TS36** and **TS37**).

Figure 4.5. *(A) Experimental outcome of reaction using substrate* ***193*** *and other possible stereoisomers. (B) Chair and boat-like transition states that can lead to formation of different stereoisomers.* [a]*Reaction conditions:* ***193*** *(0.10 mmol),* $Pd_2(pmdba)_3$ *(2.5 mol%),* ***(S)-L3*** *(6.5 mol%), and PhMe (4 mL) at 50 °C for 14 h. Isolated yield from 0.10 mmol of* ***193****. B:L and dr determined by crude* ^1H *NMR analysis. Enantioselectivity was measured by chiral SFC analysis.*

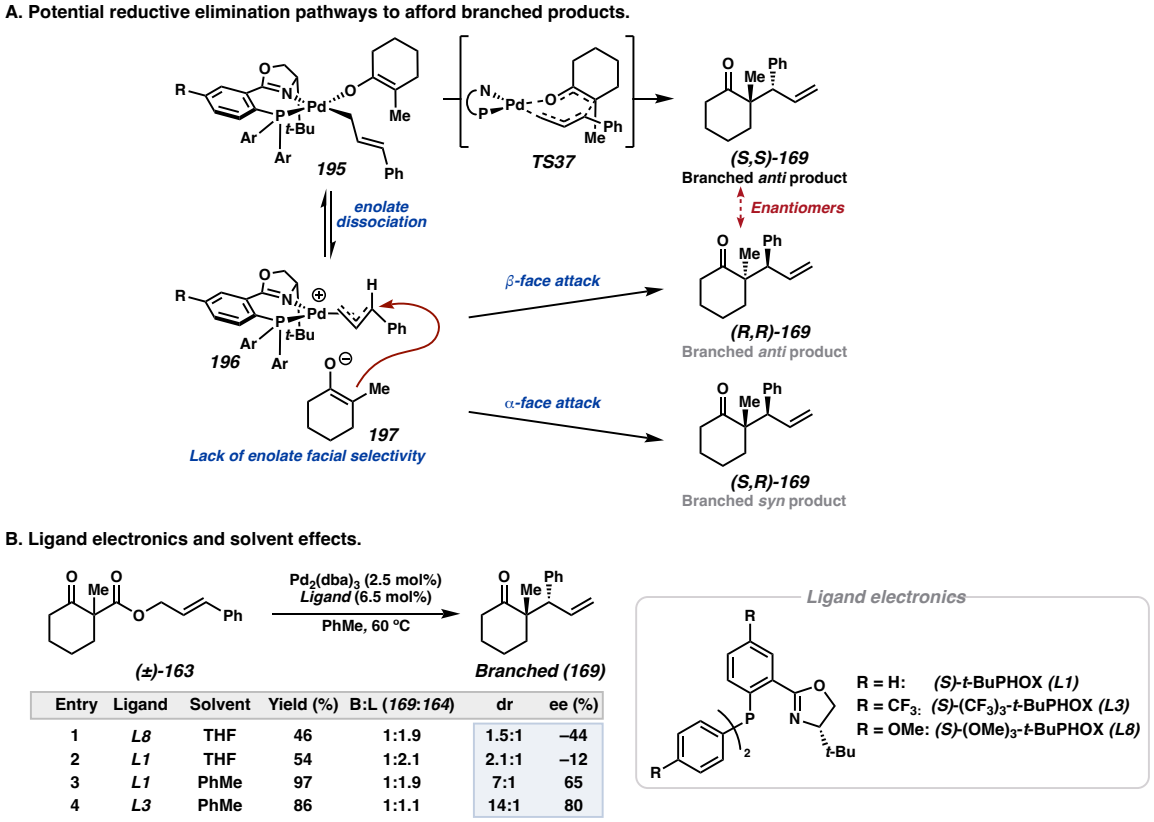


This can occur via a chair-like transition state with a pseudo-equatorial phenyl group to generate ***(R,S)*-186** (Figure 4.5.B, **TS37-F**). Alternatively, a boat-like transition state with the phenyl group place in a pseudo-equatorial position would give rise to ***(R,R)*-186** as the major stereoisomer (Figure 4.5.B, **TS38-F**). Computational analysis of the possible transition states from the reaction of **(±)-163** suggests that the chair-like transition state (**TS37-F**) would likely be the most favorable pathway, and thus ***(R,S)*-186** is expected to be the stereoisomer formed in the reaction (See 4.4.4 for additional discussion). In short, the enolate facial selectivity paired with the preference for a chair- over boat-like transition state control enantio- and diastereoselectivity, respectively. To further corroborate our inner-sphere transition state model, we experimentally determined the absolute and relative stereochemistry of α-fluoro enone **186** with vibrational circular dichroism (VCD) spectroscopy (see 4.4.3 for more details) and found that ***(R,S)*-186** is indeed the major product from the reaction of **193** with the *(S)* enantiomer of **L3** (Figure 4.5.A). This stereochemical outcome agrees with our inner-sphere reductive elimination model.

4.2.4 REDUCTIVE ELIMINATION PATHWAYS

As previously noted, application of a more sterically bulky ligand **L2** leads to poor branched/linear selectivity and diminished branched product (i.e., **169**) ee, in contrast to the predictions based on computational results. We hypothesize that the reductive elimination potentially proceeds partially through a competitive outer-sphere pathway that can lead to both branched and linear products. While attack at the carbon *trans* to the ligand phosphorus furnishes desired branched product **169** in an outer-sphere mechanism, there is very little facial bias for stereocontrol at the

Figure 4.6. *(A) Inner- and outer-sphere reductive elimination pathways that lead to branched product formation. (B) Reaction outcomes with varying ligand electronics and solvent polarities.*



Entry	Ligand	Solvent	Yield (%)	B:L (*169*:*164*)	dr	ee (%)
1	*L8*	THF	46	1:1.9	1.5:1	–44
2	*L1*	THF	54	1:2.1	2.1:1	–12
3	*L1*	PhMe	97	1:1.9	7:1	65
4	*L3*	PhMe	86	1:1.1	14:1	80

enolate nucleophile component (i.e., **197**), resulting in low selectivity at the forming quaternary stereocenter (Figure 4.6.A). Furthermore, β-face attack of the enolate would afford the *anti* branched product ***(R,R)*-169**, in contrast to the expected ***(S,S)*-169** from an inner-sphere reductive elimination. Thus, the ee of the formed *anti* branched product is diminished in a reaction where both inner-sphere and outer-sphere alkylation pathways are competitive. Based on this finding, we propose that the ee of the *anti* branched product can be correlated to participation of the outer-sphere pathway.

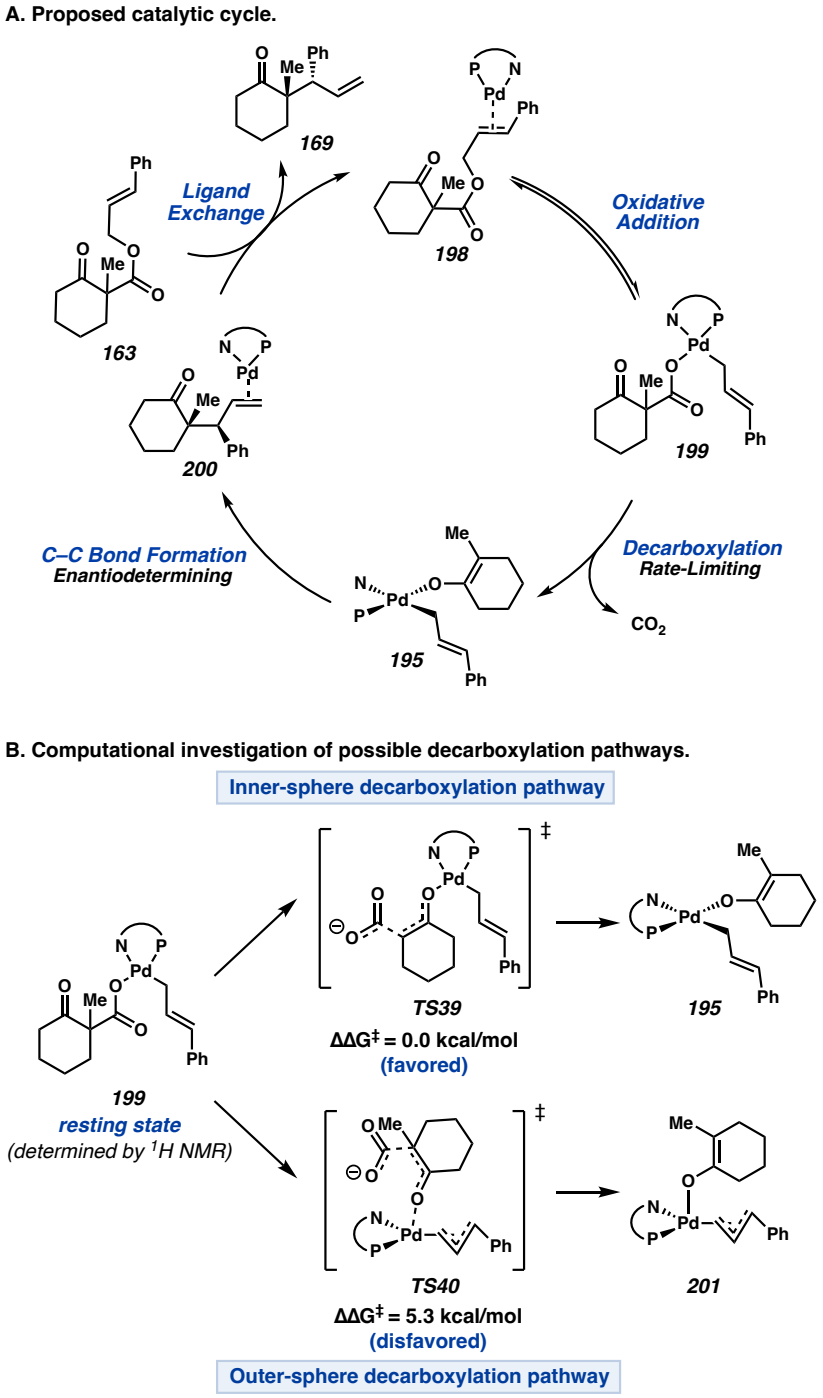
To experimentally assess our hypothesis, we elected to explore the effects of solvent polarity and ligand electronics, envisioning that stabilization of polarized intermediates could facilitate outer-sphere reductive elimination. In the absence of *ortho* substituents, branched/linear selectivities remain similar among all entries (Figure 4.6.B). In contrast, the stereoselectivities of **169** were greatly improved when apolar solvents and electron-deficient ligands were employed, which is consistent with our hypothesis that competitive outer-sphere pathways can be correlated with diminished ee.

4.2.5 COMPUTATIONAL INVESTIGATION OF LIGAND EFFECTS

Considering the effects of ligand electronics on the reductive elimination pathways, we subsequently sought to investigate the influence of ligand sterics computationally. We propose that allylic alkylation of cyclohexanones with a cinnamyl group proceeds through a similar reaction mechanism as previously reported allylations by our lab (Figure 4.7.A). The resting state of the catalyst, oxidative addition intermediate **199**, was utilized as a starting point for the computational investigations. We envisioned that the subsequent decarboxylation potentially proceeds through either inner-sphere or outer-sphere pathways (Figure 4.7.B). The lowest-energy outer-sphere decarboxylation transition state **TS40** was found to have an energy barrier 5.3 kcal/mol higher than that of inner-sphere **TS39**, suggesting that decarboxylation likely proceeds predominantly through an inner-sphere pathway, leading to the immediate formation of η^1 Pd complex **195**, rather than apical enolate π-allyl intermediate **201**.

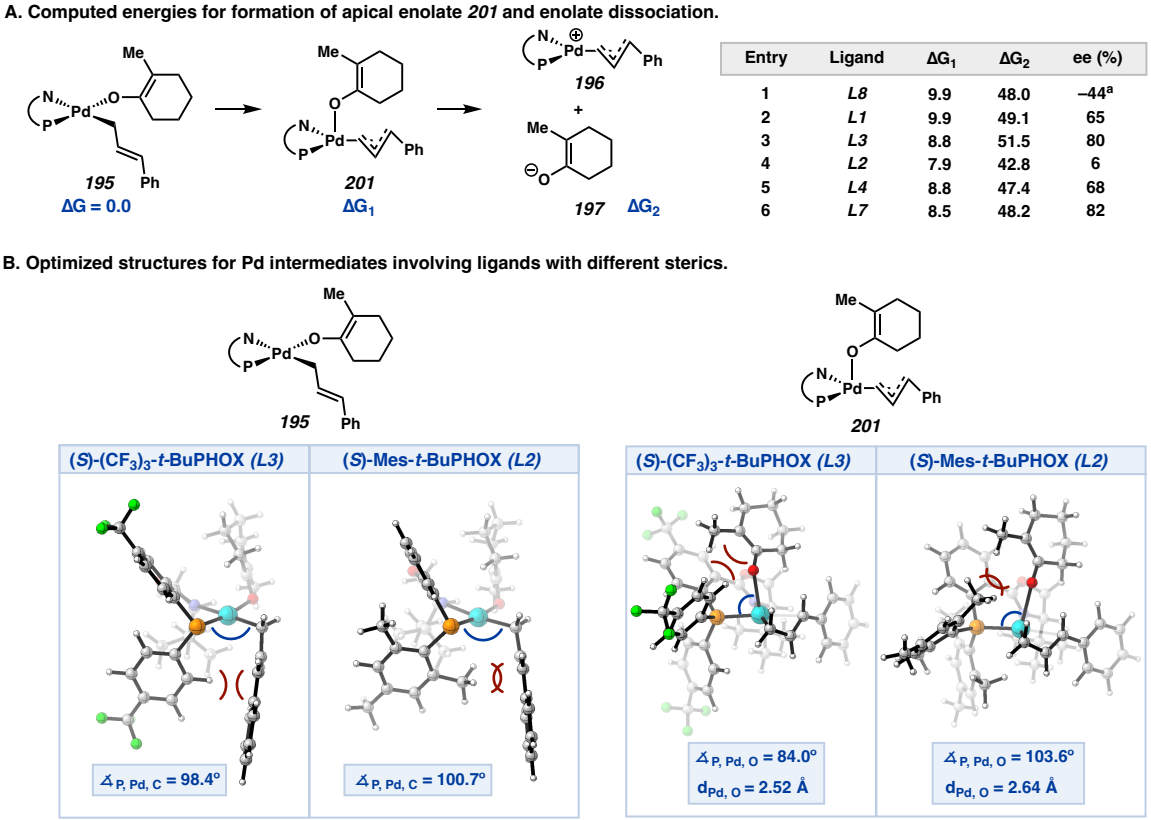
Diverging from intermediate **195**, the inner-sphere reductive elimination transition state (**TS37**) leading to branched product **169** can be reached without further isomerization.

Figure 4.7. *(A) Proposed catalytic cycle. (B) Quantum mechanics calculations of decarboxylation pathways.*



Conversely, isomerization to apically *O*-bound Pd-enolate **201** followed by enolate dissociation is likely necessary to access outer-sphere reductive elimination transition states, and we therefore investigated the energies of these relevant intermediates (Figure 4.8.A).[16]

Figure 4.8. *(A) Comparison of relative energies of apical enolate* ***201*** *and dissociated enolate-Pd complex ion pair (****196*** *and* ***197****) with different ligands. Enantioselectivies were measured under identical, optimized reaction conditions. (B) Differences in optimized geometries of Pd complexes under different ligand steric environments.* [a] *Reaction performed with THF instead of toluene.*



Entry	Ligand	ΔG_1	ΔG_2	ee (%)
1	*L8*	9.9	48.0	–44[a]
2	*L1*	9.9	49.1	65
3	*L3*	8.8	51.5	80
4	*L2*	7.9	42.8	6
5	*L4*	8.8	47.4	68
6	*L7*	8.5	48.2	82

It was discovered that isomerization to apically bound enolate **201** from enolate **195** is more favorable when electron-deficient ligands (entries 3 and 5–6, Figure 4.8.A) are employed. Notably, even without electron-withdrawing groups, complex **201** with **L2** was found to be significantly more energetically favorable than complexes with other ligands.

Analogously, dissociation of the enolate to ion pair **196** and **197** features a lower energy difference when **L2** is used as a ligand. It was also observed that ligands with larger dissociation energies generally provide better enantioselectivity. More electron-rich ligands with similar sterics tend to result in lower dissociation energies (entries 1–3, Figure 4.8.A), while mono-*ortho* substituted **L7** provides better enantioselectivity and lower dissociation energy than the electronically similar but more sterically bulky di-*ortho* substituted **L4** (entries 5–6, Figure 4.8.A).

Seeking to understand the influence of sterics, we analyzed the optimized geometries of Pd enolate **195** and apical enolate intermediate **201** using non-*ortho* substituted **L3** and sterically demanding tri-substituted **L2** (Figure 4.8.B). The influence of *ortho* substituents on the ligand aryl group is shown by the distortion of the P–Pd–C bond angle in complex **195**, in which the bond angle is increased by 2.3º using **L2**. This effect is further amplified in apical enolate intermediate **201**, in which the P–Pd–O bond angle is distorted by 19.6º due to steric clash between the apically bound enolate and the *ortho* substituent of **L2**. In addition, the Pd–O bond between the Pd center and the enolate oxygen lengthened from 2.52 Å (**L3**) to 2.64 Å (**L2**). These destabilizing steric interactions potentially facilitate dissociation of the enolate from Pd and thus favors outer-sphere pathways, leading to diminished enantioselectivity.

In summary, we propose that the rate-limiting decarboxylation of oxidative addition intermediate **199** proceeds through an inner-sphere pathway, leading to formation of Pd enolate **195**. Subsequent isomerization and enolate dissociation can allow for outer-sphere reductive elimination processes to take place, which can lead to diminished ee and branched/linear selectivity. Investigation of the impact of ligand sterics and electronics highlights the importance of balancing both factors to favor inner-sphere reductive elimination. Introducing sufficient sterics to bias branched selectivity without excessive hindrance that would promote outer-sphere pathways is also found key to achieving high selectivities.

4.3 CONCLUSIONS

In conclusion, we present a novel branched-selective Pd-catalyzed decarboxylative asymmetric allylic alkylation. Key to the development of the reaction was the use of in silico generated transition state models to guide the rational design of a new PHOX ligand to promote the desired transformation. Determination of the absolute stereochemistry via vibrational circular dichroism spectroscopy (VCD) represents a union between our computation models and experimental observations. Mechanistic analysis of the interplay between inner- and outer-sphere reductive elimination processes and the effect on regio- and stereoselectivity is also discussed. We believe the insights gained regarding the influence of stereochemical environment of Pd–PHOX systems will facilitate future development of synthetically useful stereoselective transformations.

4.4 EXPERIMENTAL SECTION

4.4.1 MATERIALS AND METHODS

Unless otherwise stated, reactions were performed in flame-dried glassware under an argon or nitrogen atmosphere using dry, deoxygenated solvents. Solvents were dried by passage through an activated alumina column under argon.[17] Reaction progress was monitored by thin-layer chromatography (TLC), or Agilent 1290 UHPLC-MS. TLC was performed using E. Merck silica gel 60 F254 precoated glass plates (0.25 mm) and visualized by UV fluorescence quenching or $KMnO_4$ staining. Silicycle Silia*Flash*® P60 Academic Silica gel (particle size 40–63 μm) was used for flash chromatography. ^{1}H NMR spectra were recorded on a Bruker 400 MHz spectrometer or a Varian 600 MHz spectrometer and are reported relative to residual $CHCl_3$ (δ 7.26 ppm). ^{13}C NMR spectra were recorded on a Bruker 400 MHz spectrometer (100 MHz) and are reported relative to $CHCl_3$ (δ 77.16 ppm). Data for ^{1}H NMR are reported as follows: chemical shift (δ ppm) (multiplicity, coupling constant (Hz), integration). Multiplicities are reported as the peaks appear as follows: s = singlet, d = doublet, t = triplet, q = quartet, p = pentet, sept = septuplet, m = multiplet, br s = broad singlet, br d = broad doublet. Data for ^{13}C NMR are reported in terms of chemical shifts (δ ppm). Some reported spectra include minor solvent impurities of water (δ 1.56ppm), ethyl acetate (δ 4.12, 2.05, 1.26 ppm), methylene chloride (δ 5.30 ppm), acetone (δ 2.17 ppm), grease (δ 1.26, 0.86 ppm), and/or silicon grease (δ 0.07 ppm), which do not impact product assignments. ^{13}C NMR spectra of deuterated compounds are complicated by the low intensity of peaks of deuterium-substituted carbon atoms. IR spectra were obtained by use of a Perkin Elmer Spectrum BXII spectrometer or Nicolet

6700 FTIR spectrometer using thin films deposited on NaCl plates and reported in frequency of absorption (cm^{-1}). Optical rotations were measured with a Jasco P-2000 polarimeter operating on the sodium D-line (589 nm), using a 100 mm path-length cell. Analytical SFC was performed with a Mettler SFC supercritical CO_2 analytical chromatography system utilizing Chiralpak (AD-H or IC) or Chiralcel (OD-H, OJ-H, or OB-H) columns (4.6 mm x 25 cm) obtained from Daicel Chemical Industries, Ltd. High resolution mass spectra (HRMS) were obtained from the Caltech Mass Spectral Facility using a JEOL JMS-600H High Resolution Mass Spectrometer in Field Desorption (FD+) mode. Absolute stereochemical assignments were made by vibrational circular dichroism (VCD) analysis for select compounds with related compounds assigned by analogy.

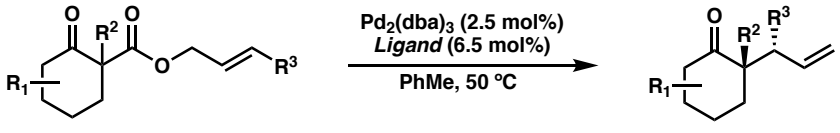
Reagents were purchased from commercial sources and used as received unless otherwise stated. Ligands were prepared according to literature procedures.[18]

List of Abbreviations: ee – enantiomeric excess, SFC – supercritical fluid chromatography, TLC – thin-layer chromatography, IPA – isopropanol, VCD – vibrational circular dichroism, pmdba – bis(4-methoxybenzylidene)acetone. B:L refers to the ratio of branched (B) and linear (L) products.

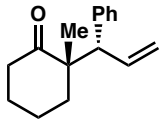
4.4.2 EXPERIMENTAL PROCEDURES AND SPECTROSCOPIC DATA

Pd-Catalyzed Decarboxylative Asymmetric Allylic Alkylation

General Procedure 4A: Asymmetric Pd-Catalyzed Decarboxylative Allylic Alkylation



In a nitrogen filled glovebox, an oven-dried 1 dram vial was charged with a stir bar, $Pd_2(dba)_3$ or $Pd_2(pmdba)_3$ (2.5 μmol, 2.5 mol%), ligand (6.5 μmol, 6.5 mol%), and toluene (1.0 mL). The catalyst solution was stirred at 23 ºC for 20 min, then added to a solution of substrate in toluene (3 mL) in a 2-dram vial. The reaction vial was then sealed with electrical tape, removed from the glovebox, and heated to 50 ºC or 60 °C for 14 h. The reaction mixture was let cool to ambient temperature, passed through a plug of silica gel, and concentrated under reduced pressure. The crude reaction mixture was loaded directly onto a flash column and the product was isolated by silica gel flash column chromatography.



169

(*S*)-2-methyl-2-((*S*)-1-phenylallyl)cyclohexan-1-one (169)

Prepared from **163** (27.2 mg, 100 μmol) following General Procedure 4A using $Pd_2(pmdba)_3$ and **L7**. Purification by flash column chromatography (0–15% EtOAc/hexanes) afforded the title compound as a colorless oil (14.2 mg, 62.2 μmol, 62% yield, 9.1:1 B/L, >20:1 dr (B), 82% ee(B)).

**Crude ^1H NMR analysis reveals a B:L of 5.9:1 prior to chromatography.*

^1H NMR (400 MHz, $CDCl_3$): δ 7.35 – 7.28 (m, 2H), 7.25 – 7.19 (m, 3H), 6.21 – 6.07 (m, 1H), 5.09 – 5.03 (m, 2H), 3.93 (d, *J* = 9.4 Hz, 1H), 2.56 – 2.32 (m, 2H), 2.10 – 1.98 (m, 2H), 1.87 – 1.62 (m, 3H), 1.35 – 1.24 (m, 1H), 0.98 (s, 3H).

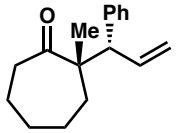
^{13}C NMR (100 MHz, $CDCl_3$): δ 215.0, 140.0, 136.6, 129.8, 128.2, 126.9, 117.2, 53.0, 52.5, 39.7, 37.4, 27.8, 21.1, 19.6.

IR (Neat Film, NaCl): 3062, 3027, 2933, 2863, 1704, 1453, 1124 cm^{-1}.

HRMS (MM: EI+): *m/z* calc'd for $C_{16}H_{20}O$ $[M]^{+\bullet}$: 228.1514, found 228.1515.

Optical Rotation: $[\alpha]_D^{21}$ –25.1 (c 1.00, $CHCl_3$).

SFC conditions: 10% IPA, 2.5 mL/min, Chiralpak OJ-H column, l = 210 nm, t_R (min): minor = 3.59, major = 2.81.



170

(*S*)-2-methyl-2-((*S*)-1-phenylallyl)cycloheptan-1-one (170)

Prepared from **202** (28.6 mg, 0.1 mmol) following General Procedure 4A using $Pd_2(dba)_3$ and **L3**. Purification by flash column chromatography (0–10% EtOAc/hexanes) afforded the title compound as a colorless oil (14.5 mg, 0.06 mmol, 60% yield, 11:1 B:L, 14:1 dr (B), 81% ee(B)).

**Crude ^{1}H NMR analysis reveals a B:L of 9:1 prior to chromatography.*

Ligand **L7 afforded higher B:L (>20:1), though lower enantioselectivity (77% ee).*

^{1}H NMR (400 MHz, $CDCl_3$): δ 7.33 – 7.25 (m, 2H), 7.25 – 7.20 (m, 1H), 7.19 – 7.15 (m, 2H), 6.16 (dt, *J* = 16.9, 10.0 Hz, 1H), 5.10 (dd, *J* = 10.2, 1.8 Hz, 1H), 5.03 (ddd, *J* = 16.9, 1.8, 0.8 Hz, 1H), 3.45 (d, *J* = 9.7 Hz, 1H), 2.34 – 2.23 (m, 1H), 2.17 – 2.09 (m, 1H), 1.88 – 1.68 (m, 4H), 1.47 (dd, *J* = 14.4, 8.4 Hz, 1H), 1.38 – 1.21 (m, 2H), 1.17 – 1.09 (m, 1H), 1.08 (s, 3H).

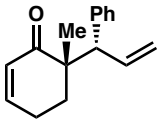
^{13}C NMR (101 MHz, $CDCl_3$): δ 217.7, 140.1, 136.8, 129.5, 128.3, 126.9, 117.6, 58.9, 55.2, 41.6, 35.1, 30.7, 26.9, 24.1, 19.7.

IR (Neat Film, NaCl): 3028, 2930, 2857, 1637, 1452, 1167, 919 cm^{-1}.

HRMS (MM: FD+): *m/z* calc'd for $C_{17}H_{22}O$ $[M]^{+\bullet}$: 242.16707, found 242.16667.

Optical Rotation: $[\alpha]_D^{23}$ –45.2 ° (c 1.21, $CHCl_3$). (From 81% ee sample using **L3**)

SFC conditions: 20% IPA, 2.5 mL/min, Chiralpak OJ-H column, l = 210 nm, t_R (min): minor = 3.03, major = 3.34.



171

(*S*)-6-methyl-6-((*S*)-1-phenylallyl)cyclohex-2-en-1-one (171)

Prepared from **203** (27.2 mg, 0.1 mmol) following General Procedure 4A using $Pd_2(pmdba)_3$ and **L7**. Purification by flash column chromatography (0–100% CH_2Cl_2/hexanes) afforded the title compound as a colorless oil (11.5 mg, 51 μmol, 51% yield, 20:1 B/L, >20:1 dr (B), 78% ee(B)).

**Crude ^{1}H NMR analysis reveals a B/L of 4.3:1 prior to chromatography.*

^{1}H NMR (400 MHz, $CDCl_3$): δ 7.32 – 7.17 (m, 5H), 6.84 (dt, *J* = 10.0, 3.9 Hz, 1H), 6.20 (dt, *J* = 16.8, 9.9 Hz, 1H), 5.91 (dt, *J* = 10.0, 2.1 Hz, 1H), 5.12 – 4.98 (m, 2H), 3.86 (d, *J* = 9.7 Hz, 1H), 2.56 – 2.46 (m, 1H), 2.40 – 2.29 (m, 1H), 1.85 (dt, *J* = 13.8, 5.7 Hz, 1H), 1.73 (ddd, *J* = 13.9, 7.3, 5.5 Hz, 1H), 1.10 (s, 3H).

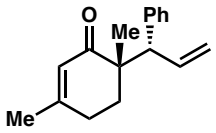
^{13}C NMR (101 MHz, $CDCl_3$): δ 203.0, 148.2, 140.8, 137.0, 129.8, 129.1, 128.1, 126.6, 117.4, 52.9, 48.8, 31.1, 23.4, 20.5.

IR (Neat Film, NaCl): 3028, 2935, 2343, 2357, 1699, 1670, 1636, 1387, 1222, 695 cm^{-1}.

HRMS (MM: FD+): *m/z* calc'd for $C_{16}H_{19}O$ $[M+H]^{+\bullet}$: 227.14359, found 227.14317.

Optical Rotation: $[\alpha]_D^{22}$ +39.0° (c 0.48, $CHCl_3$).

SFC conditions: 20% IPA, 2.5 mL/min, Chiralpak OJ-H column, l = 210 nm, t_R (min): minor = 3.70, major = 3.22.



172

(*S*)-3,6-dimethyl-6-((*S*)-1-phenylallyl)cyclohex-2-en-1-one (172)

Prepared from **204** (28.4 mg, 100 μmol) following General Procedure 4A using $Pd_2(pmdba)_3$ and **L7**. Purification by flash column chromatography (0–20% EtOAc/hexanes) afforded the title compound as a colorless oil (16.8 mg, 69.9 μmol, 70% yield, >20:1 B/L, >20:1 dr, 80% ee).

^{1}H NMR (400 MHz, $CDCl_3$): δ 7.37 – 7.24 (m, 5H), 6.28 (dt, *J* = 16.8, 9.9 Hz, 1H), 5.83 (q, *J* = 1.4 Hz, 1H), 5.17 (dd, *J* = 10.0, 1.8 Hz, 1H), 5.11 (ddd, *J* = 16.8, 1.8, 0.9 Hz, 1H), 3.94 (d, *J* = 9.7 Hz, 1H), 2.51 – 2.42 (m, 1H), 2.37 – 2.28 (m, 1H), 1.98 (s, 3H), 1.92 (ddd, *J* = 13.8, 6.9, 5.4 Hz, 1H), 1.78 (ddd, *J* = 13.8, 7.0, 5.4 Hz, 1H), 1.16 (s, 3H).

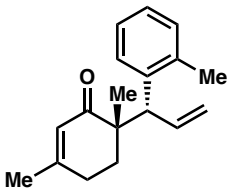
^{13}C NMR (100 MHz, $CDCl_3$): δ 202.8, 159.9, 141.0, 137.1, 129.8, 128.1, 126.5, 126.0, 117.4, 53.1, 47.5, 30.9, 28.3, 24.1, 20.8.

IR (Neat Film, NaCl): 3062, 3028, 2969, 2932, 1663, 1637, 1452, 1377, 1213 cm^{-1}.

HRMS (MM: FD+): *m/z* calc'd for $C_{17}H_{20}O$ $[M]^{+\bullet}$: 240.1514, found 240.1522.

Optical Rotation: $[\alpha]_D^{21}$ +38.1 (c 1.00, $CHCl_3$)

SFC conditions: 10% IPA, 2.5 mL/min, Chiralpak AD-H column, l = 210 nm, t_R (min): minor = 2.95, major = 3.31.



173

(*S*)-3,6-dimethyl-6-((*S*)-1-(*o*-tolyl)allyl)cyclohex-2-en-1-one (173)

Prepared from **205** (14.2 mg, 0.05 mmol) following General Procedure 4A using $Pd_2(dba)_3$ and **L6**. Purification by preparatory thin layer chromatography (0–10% EtOAc/hexanes) afforded the title compound as a colorless oil (2.6 mg, 10 μmol, 20% yield, >20:1 B:L, 10:1 dr (B), 75% ee(B)).

**Reaction does not reach full conversion; crude ^1H NMR analysis reveals remaining starting material (18% based on internal standard).*

^{1}H NMR (400 MHz, $CDCl_3$): δ 7.40 – 7.33 (m, 1H), 7.17 – 7.04 (m, 3H), 6.07 (ddd, *J* = 17.1, 10.1, 8.4 Hz, 1H), 5.75 (q, *J* = 1.4 Hz, 1H), 5.06 – 4.98 (m, 1H), 4.85 (dt, *J* = 17.0, 1.5 Hz, 1H), 3.95 (d, *J* = 8.3 Hz, 1H), 2.38 (s, 3H), 2.28 – 2.08 (m, 3H), 1.90 (s, 3H), 1.83 – 1.73 (m, 1H), 1.22 (s, 3H).

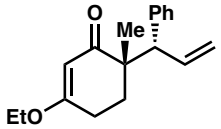
^{13}C NMR (101 MHz, $CDCl_3$): δ 203.0, 159.8, 139.9, 138.6, 136.9, 131.1, 128.8, 126.3, 125.8, 125.6, 116.3, 49.2, 47.4, 32.6, 28.6, 24.0, 21.4, 20.6.

IR (Neat Film, NaCl): 3071, 2970, 2934, 2906, 1667, 1452, 1379, 1210, 1007, 922 cm^{-1}.

HRMS [MM:FD+]: *m/z* calc'd for $C_{18}H_{22}O$ $[M]^{+\bullet}$: 254.16707, found 254.16692.

Optical Rotation: $[\alpha]_D^{24}$ +62.0 ° (c 0.21, $CHCl_3$).

SFC conditions: 10% IPA, 2.5 mL/min, Chiralpak OJ-H column, l = 210 nm, t_R (min): minor = 2.44, major = 2.84.



174

(*S*)-3-ethoxy-6-methyl-6-((*S*)-1-phenylallyl)cyclohex-2-en-1-one (174)

Prepared from **206** (31.4 mg, 100 μmol) following General Procedure 4A using $Pd_2(dba)_3$ and **L7**. Purification by flash column chromatography (0–40% EtOAc/hexanes) afforded the title compound as a colorless oil (18.8 mg, 70 μmol, 70% yield, >20:1 dr, 84% ee). Ligand **L5** afforded identical results.

^{1}H NMR (400 MHz, $CDCl_3$): δ 7.28 – 7.16 (m, 5H), 6.23 (dt, *J* = 16.8, 9.9 Hz, 1H), 5.23 (s, 1H), 5.12 (dd, *J* = 10.1, 1.8 Hz, 1H), 5.06 (ddd, *J* = 16.8, 1.9, 0.9 Hz, 1H), 3.90 (d, *J* = 9.7 Hz, 1H), 3.87 (dd, *J* = 7.0, 2.8 Hz, 1H), 3.83 (dd, *J* = 7.0, 2.7 Hz, 1H), 2.48 (ddd, *J* = 18.1, 7.0, 5.6 Hz, 1H), 2.44 – 2.34 (m, 1H), 1.87 (ddd, *J* = 13.4, 7.6, 5.6 Hz, 1H), 1.73 – 1.66 (m, 2H), 1.33 (t, *J* = 7.0 Hz, 3H), 1.11 (s, 3H).

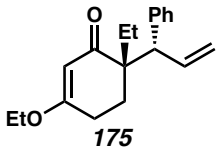
^{13}C NMR (100 MHz, $CDCl_3$): δ 202.8, 175.5, 141.2, 137.1, 129.8, 128.1, 126.5, 117.4, 102.0, 64.3, 53.5, 47.5, 29.5, 26.1, 21.3, 14.3.

IR (Neat Film, NaCl): 2942, 1647, 1611, 1377, 1190 cm^{-1}.

HRMS (MM: FD+): *m/z* calc'd for $C_{18}H_{22}O_2$ $[M]^{+\bullet}$: 270.1620, found 270.1628.

Optical Rotation: $[\alpha]_D^{21}$ –1.3 (c 1.00, $CHCl_3$).

SFC conditions: 10% IPA, 2.5 mL/min, Chiralpak OJ-H column, λ = 254 nm, t_R (min): minor = 2.70, major = 3.25.



175

(*S*)-3-ethoxy-6-ethyl-6-((*S*)-1-phenylallyl)cyclohex-2-en-1-one (175)

Prepared from **207** (34.4 mg, 104 μmol) following General Procedure 4A using $Pd_2(dba)_3$ and **L5**. Purification by flash column chromatography (5–20% EtOAc/hexanes) afforded the title compound as a colorless oil (21.0 mg, 74 mmol, 70% yield, >20:1 dr, 87% ee).

^{1}H NMR (400 MHz, $CDCl_3$): δ 7.26 – 7.21 (m, 4H), 7.19 – 7.13 (m, 1H), 6.26 (dt, *J* = 16.8, 10.1 Hz, 1H), 5.22 (s, 1H), 5.14 – 5.07 (m, 2H), 4.02 (d, *J* = 10.0 Hz, 1H), 3.86 – 3.78 (m, 2H), 2.47 – 2.33 (m, 2H), 1.96 – 1.74 (m, 3H), 1.50 (dq, *J* = 14.5, 7.4 Hz, 1H), 1.31 (t, *J* = 7.0 Hz, 3H), 0.83 (t, *J* = 7.4 Hz, 3H).

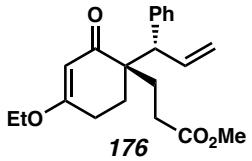
^{13}C NMR (100 MHz, $CDCl_3$): δ 201.0, 175.2, 141.6, 137.0, 130.1, 128.0, 126.3, 117.3, 103.0, 64.2, 51.7, 50.7, 26.7, 26.3, 26.0, 14.3, 8.3.

IR (Neat Film, NaCl): 2978, 2937, 1650, 1612, 1380, 1189 cm^{-1}.

HRMS (MM: ESI+): *m/z* calc'd for $C_{19}H_{25}O_2$ $[M+H]^{+\bullet}$: 285.1849, found 285.1859.

Optical Rotation: $[\alpha]_D^{21}$ +16.0 (c 1.00, $CHCl_3$).

SFC conditions: 10% IPA, 2.5 mL/min, Chiralpak OJ-H column, λ = 254 nm, t_R (min): minor = 2.93, major = 3.50.



176

methyl 3-((*R*)-4-ethoxy-2-oxo-1-((*S*)-1-phenylallyl)cyclohex-3-en-1-yl)propanoate (176)

Prepared from **208** (38.2 mg, 98.9 mmol) following General Procedure 4A using $Pd_2(dba)_3$ and **L5**. Purification by flash column chromatography (5–20% EtOAc/hexanes) afforded the title compound as a colorless oil (14.3 mg, 41.8 mmol, 42% yield, >20:1 dr, 84% ee).

^{1}H NMR (400 MHz, $CDCl_3$): δ 7.26 – 7.20 (m, 4H), 7.18 – 7.13 (m, 1H), 6.25 (dt, *J* = 16.8, 10.1 Hz, 1H), 5.20 (s, 1H), 5.19 – 5.10 (m, 2H), 4.07 (d, *J* = 10.1 Hz, 1H), 3.86 – 3.77 (m, 2H), 3.63 (s, 3H), 2.52 – 2.33 (m, 3H), 2.25 (ddd, *J* = 16.3, 11.4, 4.8 Hz, 1H), 2.00 (ddd, *J* = 14.0, 11.5, 5.2 Hz, 1H), 1.95 – 1.79 (m, 3H), 1.31 (t, *J* = 7.0 Hz, 3H).

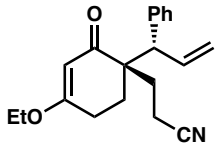
^{13}C NMR (100 MHz, $CDCl_3$): δ 200.2, 175.3, 174.3, 141.0, 136.2, 130.0, 128.0, 126.4, 117.9, 102.6, 64.2, 51.6, 51.0, 49.6, 28.3, 28.1, 27.0, 25.7, 14.1.

IR (Neat Film, NaCl): 2980, 2946, 1737, 1643, 1610, 1381, 1191 cm^{-1}.

HRMS (MM: ESI+): *m/z* calc'd for $C_{21}H_{27}O_4$ $[M+H]^{+\bullet}$: 343.1904, found 343.1909.

Optical Rotation: $[\alpha]_D^{21}$ +24.6 (c 1.00, $CHCl_3$).

SFC conditions: 10% IPA, 2.5 mL/min, Chiralpak OJ-H column, l = 254 nm, t_R (min): minor = 2.54, major = 3.00.



177

3-((*S*)-4-ethoxy-2-oxo-1-((*S*)-1-phenylallyl)cyclohex-3-en-1-yl)propanenitrile (177)

Prepared from **209** (35.3 mg, 100 μmol) following General Procedure 4A using $Pd_2(dba)_3$ and **L5**. Purification by flash column chromatography (5–40% EtOAc/hexanes) afforded the title compound as a colorless oil (23.9 mg, 77.2 μmol, 77% yield, >20:1 B/L, >20:1 dr, 84% ee).

^{1}H NMR (400 MHz, $CDCl_3$): δ 7.29 – 7.23 (m, 2H), 7.19 (td, *J* = 7.8, 1.4 Hz, 3H), 6.23 (dt, *J* = 16.9, 10.1 Hz, 1H), 5.24 (s, 1H), 5.20 (d, *J* = 10.2 Hz, 1H), 5.13 (d, *J* = 16.9 Hz, 1H), 3.97 (d, *J* = 9.9 Hz, 1H), 3.89 – 3.80 (m, 2H), 2.51 – 2.39 (m, 3H), 2.28 – 2.12 (m, 2H), 1.93 – 1.76 (m, 3H), 1.33 (t, *J* = 7.0 Hz, 3H).

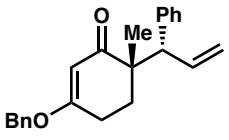
^{13}C NMR (100 MHz, $CDCl_3$): δ 199.5, 175.8, 140.2, 135.8, 129.8, 128.3, 126.9, 120.4, 118.5, 102.6, 64.6, 51.0, 49.8, 29.3, 26.7, 25.7, 14.2, 12.1.

IR (Neat Film, NaCl): 2980, 2937, 2246, 1643, 1606, 1381, 1190 cm^{-1}.

HRMS (MM: ESI+): *m/z* calc'd for $C_{20}H_{24}O_2N$ $[M+H]^{+\bullet}$: 310.1802, found 310.1804.

Optical Rotation: $[\alpha]_D^{21}$ +13.1 (c 1.00, $CHCl_3$).

SFC conditions: 20% IPA, 2.5 mL/min, Chiralpak OJ-H column, l = 254 nm, t_R (min): minor = 2.06, major = 3.05.



178

(*S*)-3-(benzyloxy)-6-methyl-6-((*S*)-1-phenylallyl)cyclohex-2-en-1-one (178)

Prepared from **210** following General Procedure 4A using $Pd_2(dba)_3$ and **L5**. Purification by flash column chromatography (0–40% EtOAc/hexanes) afforded the title compound as a colorless oil (23.4 mg, 0.704 mmol, 70% yield, >20:1 dr, 82% ee).

^{1}H NMR (400 MHz, $CDCl_3$): δ 7.42 – 7.32 (m, 5H), 7.30 – 7.24 (m, 4H), 7.19 (ddd, *J* = 8.4, 5.3, 2.2 Hz, 1H), 6.24 (dt, *J* = 16.8, 9.9 Hz, 1H), 5.37 (s, 1H), 5.12 (dd, *J* = 10.1, 1.9 Hz, 1H), 5.06 (d, *J* = 16.8 Hz, 1H), 4.87 – 4.80 (m, 2H), 3.92 (d, *J* = 9.7 Hz, 1H), 2.55 (dt,

J = 18.1, 6.1 Hz, 1H), 2.45 (ddd, *J* = 18.1, 7.5, 5.6 Hz, 1H), 1.91 (ddd, *J* = 13.3, 7.6, 5.6 Hz, 1H), 1.73 (ddd, *J* = 13.7, 7.0, 5.6 Hz, 1H), 1.14 (s, 3H).

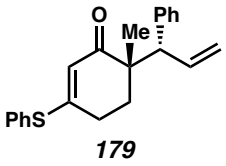
^{13}C NMR (100 MHz, $CDCl_3$): δ 202.6, 175.0, 141.1, 137.0, 135.2, 129.8, 128.8, 128.7, 128.1, 128.0, 126.5, 117.5, 102.6, 70.5, 53.5, 47.6, 29.4, 26.1, 21.3.

IR (Neat Film, NaCl): 2932, 1652, 1610, 1362, 1186 cm^{-1}.

HRMS (MM: FD+): *m/z* calc'd for $C_{23}H_{24}O_2$ $[M]^{+\bullet}$: 332.1776, found 332.1773.

Optical Rotation: $[\alpha]_D^{21}$ –5.0 (c 1.00, $CHCl_3$).

SFC conditions: 25% IPA, 2.5 mL/min, Chiralpak OD-H column, l = 254 nm, t_R (min): minor = 4.10, major = 3.72.



179

(*S*)-6-methyl-6-((*S*)-1-phenylallyl)-3-(phenylthio)cyclohex-2-en-1-one (179)

Prepared from **211** following General Procedure 4A using $Pd_2(dba)_3$ and **L5**. Purification by flash column chromatography (0–40% EtOAc/hexanes) afforded the title compound as a colorless oil (29.2 mg, 0.873 mmol, 87% yield, 7.5:1 B/L, >20:1 dr, 78% ee).

^{1}H NMR (400 MHz, $CDCl_3$): δ 7.47 – 7.38 (m, 5H), 7.27 – 7.18 (m, 5H), 6.18 (dt, *J* = 16.8, 9.9 Hz, 1H), 5.37 (s, 1H), 5.11 (dd, *J* = 10.1, 1.9 Hz, 1H), 5.05 (d, *J* = 16.8 Hz, 1H), 3.91 (d, *J* = 9.7 Hz, 1H), 2.63 – 2.46 (m, 2H), 1.94 (ddd, *J* = 13.3, 7.7, 5.3 Hz, 1H), 1.78 (ddd, *J* = 13.7, 6.7, 5.2 Hz, 1H), 1.11 (s, 3H).

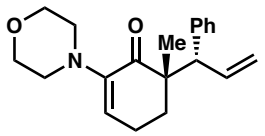
^{13}C NMR (100 MHz, $CDCl_3$): δ 199.3, 164.0, 143.5, 140.9, 136.8, 135.6, 130.2, 129.9, 129.8, 128.1, 126.5, 120.3, 117.6, 53.3, 47.9, 31.0, 27.2, 21.3.

IR (Neat Film, NaCl): 2927, 1650, 1579, 1212 cm^{-1}.

HRMS (MM: FD+): *m/z* calc'd for $C_{22}H_{22}O_2S$ $[M]^{+\bullet}$: 334.1391, found 334.1392.

Optical Rotation: $[\alpha]_D^{21}$ –64.9 (c 1.00, $CHCl_3$).

SFC conditions: 20% IPA, 2.5 mL/min, Chiralpak OJ-H column, l = 210 nm, t_R (min): minor = 4.45, major = 4.08.



180

***(S)*-6-methyl-2-morpholino-6-(*(S)*-1-phenylallyl)cyclohex-2-en-1-one (180)**

Prepared from **212** following General Procedure 4A using $Pd_2(dba)_3$ and **L3**. Purification by preparatory TLC (10% acetone/PhMe) afforded the title compound as a colorless oil (9.2 mg, 0.030 mmol, 30% yield, 9.1:1 B/L, >20:1 dr, 94% ee).

^{1}H NMR (400 MHz, C_6D_6): δ 7.18 – 7.16 (m, 3H), 7.14 – 7.08 (m, 2H), 7.06 – 7.01 (m, 1H), 6.13 (dt, *J* = 16.8, 9.9 Hz, 1H), 5.24 (t, *J* = 4.4 Hz, 1H), 4.98 – 4.90 (m, 2H), 3.90 (d, *J* = 9.6 Hz, 1H), 3.77 – 3.58 (m, 4H), 2.91 – 2.83 (m, 2H), 2.39 – 2.32 (m, 2H), 2.22 – 2.10 (m, 1H), 1.96 – 1.84 (m, 1H), 1.61 (dt, *J* = 13.8, 5.4 Hz, 1H), 1.33 (ddd, *J* = 13.8, 8.2, 5.6 Hz, 1H), 1.08 (s, 3H).

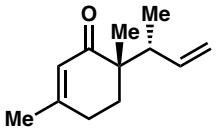
^{13}C NMR (100 MHz, C_6D_6): δ 198.3, 146.3, 141.1, 137.6, 130.0, 128.2, 126.8, 121.6, 117.2, 67.0, 53.4, 50.5, 49.4, 31.5, 22.0, 20.5.

IR (Neat Film, NaCl): 3027, 2928, 2853, 1681, 1615, 1450, 1263, 1210, 1119 cm^{-1}.

HRMS (MM: ESI+): *m/z* calc'd for $C_{20}H_{27}O_2N$ $[M+H]^{+\bullet}$: 312.1958, found 312.1961.

Optical Rotation: $[\alpha]_D^{21}$ +8.9 (c 0.90, $CHCl_3$).

SFC conditions: 30% IPA, 2.5 mL/min, Chiralpak OJ-H column, l = 280 nm, t_R (min): minor = 3.89, major = 2.05.



182

***(S)*-6-methyl-2-morpholino-6-(*(S)*-1-phenylallyl)cyclohex-2-en-1-one (182)**

Prepared from **213** (16.8 mg, 94 μmol) following General Procedure 4A using $Pd_2(pmdba)_3$ and **L5**. Purification by preparatory TLC (25% Et_2O/hexanes) afforded the title compound as a colorless oil (10.0 mg, 56 μmol, 60% yield, 2.5:1 B/L, 9.0:1 dr, 73% ee).

^{1}H NMR (400 MHz, C_6D_6): δ 5.81 – 5.75 (m, 1.4H (linear + both branched)), 5.69 (ddd, *J* = 16.5, 10.7, 8.4 Hz, 0.9H (branched)), 5.62 – 5.53 (m, 0.4H (linear)), 5.39 – 5.29 (m, 0.4H (linear)), 5.08 – 4.95 (m, 2H (branched major + branched minor)), 2.75 – 2.63 (m, 0.9H(branched major)), 2.64 – 2.56 (m, 0.1H (branched minor)), 2.31 – 2.21 (m, 3.6H), 2.01 (ddd, *J* = 13.7, 7.3, 6.3 Hz, 1H), 1.95 – 1.87 (m, 5H), 1.76 – 1.58 (m, 3.3H), 1.06 (s, 1.2H (linear)), 0.99 (s, 2.7H (branched major)), 0.98 (s, 0.4H (branched minor)), 0.94 (d, *J* = 6.8 Hz, 2.7H (branched major)), 0.88 (d, *J* = 7.0 Hz, 0.4H (branched minor)).

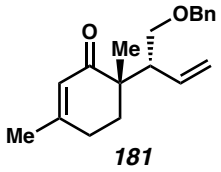
^{13}C NMR (100 MHz, $CDCl_3$): δ 204.0, 203.8, 160.5, 160.2, 140.4, 139.9, 126.8, 126.1, 125.8, 125.6, 125.5, 115.6, 115.4, 46.3, 46.0, 43.9, 41.6, 40.2, 33.8, 33.1, 31.9, 30.5, 29.8, 29.5, 28.4, 28.1, 28.0, 24.2, 24.1, 24.1, 21.9, 20.3, 18.1, 15.3, 14.4, 13.1.

IR (Neat Film, NaCl): 2965, 2930, 1666, 1638, 1433, 1378, 1213 cm^{-1}.

HRMS (MM: FI+): *m/z* calc'd for $C_{12}H_{18}O$ $[M]^{+\bullet}$: 178.1358, found 178.1362.

Optical Rotation: $[\alpha]_D^{21}$ +2.3 (c 1.00, $CHCl_3$).

SFC conditions: 4% IPA, 2.5 mL/min, Chiralpak IC column, l = 210 nm, t_R (min): minor = 7.16, major = 8.11.



181

***(S)*-6-methyl-2-morpholino-6-(*(S)*-1-phenylallyl)cyclohex-2-en-1-one (181)**

Prepared from **214** (29.9 mg, 105 μmol) following General Procedure 4A using $Pd_2(pmdba)_3$ and **L7**. Purification by flash column chromatography (0–20% EtOAc/hexanes) afforded the title compound as a colorless oil (10.6 mg, 37 μmol, 35% yield, >20:1 B/L, >20:1 dr, 82% ee).

^{1}H NMR (500 MHz, $CDCl_3$): δ 7.35 – 7.28 (m, 4H), 7.28 – 7.23 (m, 1H), 5.79 (s, 1H), 5.67 (dt, *J* = 16.9, 9.9 Hz, 1H), 5.19 – 5.10 (m, 2H), 4.47 (d, *J* = 2.4 Hz, 2H), 3.57 – 3.40 (m, 2H), 2.97 (ddd, *J* = 9.4, 7.4, 5.6 Hz, 1H), 2.37 – 2.17 (m, 2H), 2.08 – 1.97 (m, 1H), 1.91 (s, 3H), 1.70 – 1.61 (m, 2H), 1.02 (s, 3H).

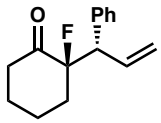
^{13}C NMR (101 MHz, $CDCl_3$): δ 202.7, 159.9, 138.6, 136.0, 128.3, 127.5, 127.4, 125.9, 118.5, 72.8, 70.6, 48.1, 45.1, 29.7, 28.0, 24.1, 20.9.

IR (Neat Film, NaCl): 3026, 2918, 1665, 1453, 1214, 1096 cm^{-1}.

HRMS (MM: ESI+): *m/z* calc'd for $C_{19}H_{24}O_2$ $[M]^{+\bullet}$: 284.1766, found 284.1776.

Optical Rotation: $[\alpha]_D^{21}$ +33.2 (c 1.05, $CHCl_3$).

SFC conditions: 10% IPA, 2.5 mL/min, Chiralpak OJ-H column, l = 210 nm, t_R (min): minor = 3.77, major = 2.81.



183

(*S*)-2-fluoro-2-((*S*)-1-phenylallyl)cyclohexan-1-one (183)

Prepared from **215** (28.6 mg, 103 mmol) following General Procedure 4A using $Pd_2(pmdba)_3$ and **L7**. Purification by flash column chromatography (0–15% EtOAc/hexanes) afforded the title compound as a colorless crystalline solid (17.1 mg, 73.6 mmol, 71% yield, >20:1 B/L, >20:1 dr, 85% ee) as well as a fraction (1.5 mg, 6.5 mmol, 6% yield) containing mixed E/Z linear isomers with trace of the major diastereomer of the branched isomer. Overall yield: 18.6 mg, 80.1 mmol, 77% yield, 13:1 B/L, >20:1 dr (B), 85% ee (B).

**Crude ^{1}H NMR analysis reveals a B/L of 12.5:1 prior to chromatography.*

^{1}H NMR (400 MHz, $CDCl_3$): δ 7.39 – 7.24 (m, 5H), 6.18 (ddd, *J* = 17.1, 10.3, 8.8 Hz, 1H), 5.12 (d, *J* = 10.3 Hz, 1H), 5.08 (d, *J* = 17.1 Hz, 1H), 3.88 (dd, *J* = 32.4, 8.8 Hz, 1H), 2.71 – 2.63 (m, 1H), 2.54 – 2.45 (m, 1H), 2.06 – 1.98 (m, 1H), 1.86 – 1.68 (m, 5H).

**Trace isolated peaks of minor diastereomer (<5%) observed as 5.26 – 5.19 (m, 2H), 2.88 – 2.75 (m, 2H), 2.43 – 2.30 (m, 2H). Others overlap with major diastereomer.*

^{13}C NMR (100 MHz, $CDCl_3$): δ 207.5 (d, $J_{C–F}$ = 18.2 Hz), 137.9, 135.3 (d, $J_{C–F}$ = 5.4 Hz), 129.6 (d, *J* = 2.6 Hz), 128.8, 127.5, 117.9, 100.7 (d, $J_{C–F}$ = 194.8 Hz), 53.1 (d, $J_{C–F}$ = 20.0 Hz), 40.3, 36.7 (d, $J_{C–F}$ = 21.7 Hz), 27.8, 22.2 (d, $J_{C–F}$ = 9.1 Hz).

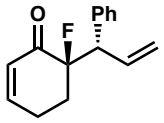
^{19}F NMR (282 MHz, $CDCl_3$): δ –166.45 (d, *J* = 32.5 Hz).

IR (Neat Film, NaCl): 2948, 1724, 1454, 1047 cm^{-1}.

HRMS (MM: EI+): *m/z* calc'd for $C_{15}H_{17}OF$ $[M]^{+\bullet}$: 232.1263, found 232.1259.

Optical Rotation: $[\alpha]_D^{21}$ –23.3 (c 1.00, $CHCl_3$).

SFC conditions: 10% IPA, 2.5 mL/min, Chiralpak OJ-H column, l = 210 nm, t_R (min): minor = 3.23, major = 2.65.



186

(*S*)-2-fluoro-2-((*S*)-1-phenylallyl)cyclohexan-1-one (186)

Prepared from **216** (27.0 mg, 98.4 μmol) following General Procedure 4A using $Pd_2(pmdba)_3$ and **L7**. Purification by flash column chromatography (0–20% EtOAc/hexanes) afforded the title compound as a colorless oil (17.1 mg, 74.3 μmol, 75% yield, >20:1 B/L, >20:1 dr, 82% ee).

^{1}H NMR (400 MHz, $CDCl_3$): δ 7.37 – 7.27 (m, 5H), 6.95 – 6.90 (m, 1H), 6.23 (ddd, *J* = 17.0, 10.1, 8.7 Hz, 1H), 6.06 (dddd, *J* = 10.0, 4.0, 2.8, 1.3 Hz, 1H), 5.11 (d, *J* = 10.1 Hz, 1H), 4.96 (d, *J* = 17.0 Hz, 1H), 3.67 (dd, *J* = 31.1, 8.7 Hz, 1H), 2.58 – 2.38 (m, 2H), 2.19 – 2.07 (m, 1H), 2.00 – 1.92 (m, 1H).

^{13}C NMR (100 MHz, $CDCl_3$): δ 195.6 (d, $J_{C–F}$ = 17.2 Hz), 149.0, 138.5, 135.3 (d, $J_{C–F}$ = 5.5 Hz), 129.2 (d, $J_{C–F}$ = 2.8 Hz), 128.9, 128.2, 127.6, 118.0, 97.4 (d, $J_{C–F}$ = 194.5 Hz), 53.0 (d, $J_{C–F}$ = 20.2 Hz), 31.2 (d, $J_{C–F}$ = 22.1 Hz), 25.1 (d, $J_{C–F}$ = 11.3 Hz).

^{19}F NMR (282 MHz, $CDCl_3$): –168.84 (d, *J* = 31.5 Hz).

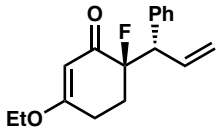
IR (Neat Film, NaCl): 3031, 2922, 1695, 1489, 1452, 1425, 1383, 1219, 1060 cm^{-1}.

HRMS (MM: EI+): *m/z* calc'd for $C_{15}H_{15}OF$ $[M]^{+\bullet}$: 230.1107, found 230.1113.

Optical Rotation: $[\alpha]_D^{21}$ +41.1 (c 1.00, $CHCl_3$).

SFC conditions: 10% IPA, 2.5 mL/min, Chiralpak OJ-H column, l = 210 nm, t_R (min): minor = 4.74, major = 3.92.

**Note racemic trace from (±)-$(CF_3)_3$-t-BuPHOX contains traces of minor branched diastereomer at 5.87 and 6.59 min.*



184

(*R*)-3-ethoxy-6-fluoro-6-((*S*)-1-phenylallyl)cyclohex-2-en-1-one (184)

Prepared from **217** (31.8 mg, 100 μmol) following General Procedure 4A using $Pd_2(dba)_3$ and **L5**. Purification by flash column chromatography (5–20% EtOAc/hexanes) afforded the title compound as a colorless oil (21.9 mg, 79.8 μmol, 80% yield, >20:1 B:L, >20:1 dr, 87% ee).

^{1}H NMR (400 MHz, $CDCl_3$): δ 7.37 – 7.26 (m, 5H), 6.36 – 6.22 (m, 1H), 5.35 – 5.32 (m, 1H), 5.13 (d, *J* = 10.2 Hz, 1H), 4.97 (d, *J* = 17.0 Hz, 1H), 3.92 (q, *J* = 7.1 Hz, 2H), 3.71 (dd, *J* = 29.7, 8.5 Hz, 1H), 2.61 – 2.50 (m, 1H), 2.45 – 2.36 (m, 1H), 2.16 – 2.03 (m, 1H), 1.94 – 1.85 (m, 1H), 1.38 (t, *J* = 7.1 Hz, 3H).

^{13}C NMR (100 MHz, $CDCl_3$): δ 194.4 (d, $J_{C–F}$ = 18.1 Hz), 194.3, 175.6 (d, $J_{C–F}$ = 1.6 Hz), 138.8, 135.4 (d, $J_{C–F}$ = 5.6 Hz), 129.3 (d, $J_{C–F}$ = 2.5 Hz), 128.8, 127.5, 117.8, 100.8, 96.4 (d, $J_{C–F}$ = 191.3 Hz), 65.1, 53.3 (d, $J_{C–F}$ = 20.8 Hz), 29.3 (d, $J_{C–F}$ = 23.5 Hz), 27.2 (d, $J_{C–F}$ = 11.0 Hz), 14.2.

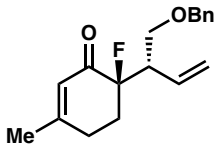
^{19}F NMR (282 MHz, $CDCl_3$): δ –168.60– –168.67 (m, 1F).

IR (Neat Film, NaCl): 2981, 2938, 1672, 1603, 1379, 1243, 1193 cm^{-1}.

HRMS (MM: ESI+): *m/z* calc'd for $C_{17}H_{20}O_2F$ $[M+H]^{+\bullet}$: 275.1442, found 275.1440.

Optical Rotation: $[\alpha]_D^{21}$ –11.2 (c 0.70, $CHCl_3$).

SFC conditions: 20% IPA, 2.5 mL/min, Chiralpak OJ-H column, l = 254 nm, t_R (min): minor = 2.25, major = 2.58.



185

(*R*)-6-((*S*)-1-(benzyloxy)but-3-en-2-yl)-6-fluoro-3-methylcyclohex-2-en-1-one (185)

Prepared from **218** (36.0 mg, 108 μmol) following General Procedure 4A using $Pd_2(dba)_3$ and **L7**. Purification by flash column chromatography (0–30% EtOAc/hexanes) afforded the title compound as a colorless oil (14.8 mg, 51.3 μmol, 48% yield, >20:1 B:L, 14.3:1 dr, 84% ee).

Crude ^1H NMR analysis reveals a B/L of 5.6:1 and a dr (B) of 12.9:1 prior to chromatography. In the tabulated NMR data for **185, the minor diastereomer is denoted.*

^{1}H NMR (400 MHz, $CDCl_3$): δ 7.36 – 7.27 (m, 5H), 5.88 – 5.74 (m, 2H), 5.34 – 5.24 (m, 0.15H (minor)), 5.17 (dd, *J* = 10.3, 1.7 Hz, 1H), 5.12 (d, *J* = 17.8 Hz, 1H), 4.50 (s, 2H), 4.45 (d, *J* = 11.8 Hz, 0.07H (minor)), 4.34 (d, *J* = 11.7 Hz, 0.07H (minor)), 3.76 (dd, *J* = 9.8, 6.7 Hz, 1H), 3.65 (dd, *J* = 9.6, 6.3 Hz, 0.07H (minor)), 3.52 (ddd, *J* = 9.8, 5.6, 0.9 Hz, 1H), 2.99 (ddt, *J* = 21.4, 9.2, 6.1 Hz, 1H), 2.91 – 2.82 (m, 0.07H (minor)), 2.53 – 2.33 (m, 3H), 2.26 – 2.14 (m, 1H), 1.96 (s, 3H), 1.93 (s, 0.19H (minor)).

^{13}C NMR (100 MHz, $CDCl_3$): δ 194.0 (d, $J_{C–F}$ = 17.9 Hz), 162.3, 138.2, 133.8 (d, $J_{C–F}$ = 4.6 Hz), 128.5, 127.8, 127.7, 125.1, 119.1, 95.6 (d, $J_{C–F}$ = 185.9 Hz), 73.3, 69.7 (d, $J_{C–F}$ = 5.7 Hz), 47.1 (d, $J_{C–F}$ = 21.4 Hz), 30.6 (d, $J_{C–F}$ = 22.7 Hz), 29.6 (d, $J_{C–F}$ = 9.5 Hz), 24.2.

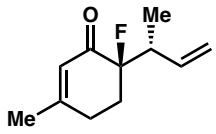
^{19}F NMR (282 MHz, $CDCl_3$): δ –167.64 – –167.85 (m).

IR (Neat Film, NaCl): 2923, 1681, 1633, 1104 cm^{-1}.

HRMS (MM: FD+): *m/z* calc'd for $C_{18}H_{21}O_2F$ $[M]^{+\bullet}$: 289.1604, found 289.1590.

Optical Rotation: $[\alpha]_D^{21}$ –34.2 (c 1.00, $CHCl_3$).

SFC conditions: 10% IPA, 2.5 mL/min, Chiralpak OJ-H column, l = 210 nm, t_R (min): minor = 4.59, major = 3.43.



187

(*R*)-6-((*R*)-but-3-en-2-yl)-6-fluoro-3-methylcyclohex-2-en-1-one (187)

Prepared from **219** (23.3 mg, 103 μmol) following General Procedure 4A using $Pd_2(pmdba)_3$ and **L3**. Purification by flash column chromatography (5–20% Et_2O/hexanes) afforded the title compound as a colorless oil (14.7 mg, 80.8 μmol, 78% yield, >20:1 B:L, >20:1 dr, 87% ee). For further characterization, the mixture of isomers was subsequently purified by C18 reverse-phase preparatory HPLC (40–65% MeCN/H_2O) to afford the major diastereomer of **187** as a single isomer.

Compound **187 was found to be volatile, avoid excessive exposure to high vacuum. Yields are corrected for trace Et_2O in sample after purification. **

^{1}H NMR (400 MHz, $CDCl_3$): δ 5.93 – 5.83 (m, 2H), 5.10 – 5.01 (m, 2H), 2.91 – 2.74 (m, 1H), 2.47 (dt, *J* = 18.9, 5.6 Hz, 1H), 2.36 (dt, *J* = 19.0, 6.5 Hz, 1H), 2.29 – 2.18 (m, 2H), 1.97 (s, 3H), 1.09 (d, *J* = 7.0 Hz, 3H).

^{13}C NMR (100 MHz, $CDCl_3$): 194.3 (d, J_{C-F} = 18.0 Hz), 162.0, 137.5, 125.4, 116.5, 95.8 (d, J_{C-F} = 184.7 Hz), 40.29 (d, J_{C-F} = 21.9 Hz), 30.5, 29.8, 29.5, 29.3, 29.2, 29.1, 14.2 (d, J_{C-F} = 5.7 Hz).

**Due to solvent contamination, there are more signals in the ^{13}C NMR than expected. **

^{19}F NMR (282 MHz, $CDCl_3$): δ –168.13– –168.31 (m, 1F).

IR (Neat Film, NaCl): 2919, 2849, 1681, 1633, 1434, 1380, 1225 cm^{-1}.

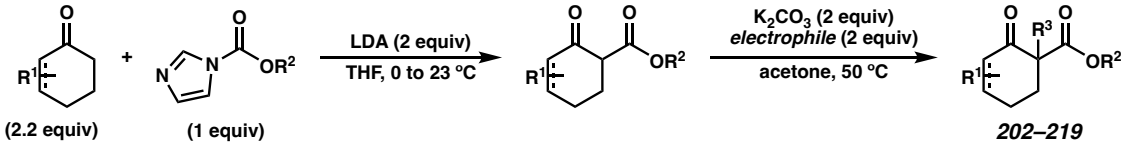
HRMS (MM: FI+): *m/z* calc'd for $C_{11}H_{15}OF$ $[M]^{+\bullet}$: 182.1107, found 182.1107.

Optical Rotation: $[\alpha]_D^{21}$ –32.3 (c 0.40, $CHCl_3$).

SFC conditions: 10% IPA, 2.5 mL/min, Chiralpak IC column, λ = 254 nm, t_R (min): minor = 4.76, major = 5.45.

Preparation of β-Ketoester Substrates

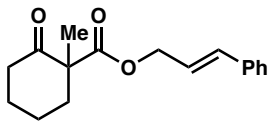
General Procedure 4B: Synthesis of β-ketoester substrates



A flame dried round bottom flask was charged with *i*-Pr_2NH (2.2 equiv) and THF (1.75 M). The solution was cooled to 0 ºC and *n*-BuLi (2.5 M in hexanes, 2.1 equiv) was added dropwise. The resultant solution was stirred for 30 min at 0 ºC. The corresponding

cyclohexenone (2.0 equiv) in THF (1.25 M) was added dropwise and stirred at 0 ºC for 30 minutes. The solution was cooled to –78 ºC, and the appropriate N-acyl imidazole (1.0 equiv) in THF (3.25 M) was added dropwise. After 2 h, the reaction was gradually warmed to 23 ºC and diluted with 2 M aqueous HCl until reaching a pH < 7. The reaction mixture was extracted three times with EtOAc. The combined organic layers were washed with brine, dried over Na_2SO_4, filtered, and concentrated under reduced pressure. The crude product was purified by flash silica gel column chromatography to afford the corresponding β-ketoester.

To a solution of β-ketoester (1 equiv) in acetone (0.5 M) is added anhydrous K_2CO_3 (2 equiv), followed by the relevant electrophile (2 equiv). The reaction is heated to 50 ºC and stirred until complete consumption of starting material is observed (typically 24–36 h). The reaction mixture is then filtered, and volatiles are removed *in vacuo*. Purification by silica gel flash column chromatography affords the desired alkylated β-ketoester.



163

cinnamyl 1-methyl-2-oxocyclohexane-1-carboxylate (163)

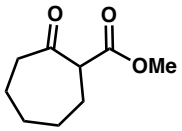
Prepared from cinnamyl 2-oxocyclohexane-1-carboxylate[19] and methyl iodide following General Procedure 4B. Purification by flash column chromatography (5–40% EtOAc/hexanes) afforded the title compound **163** as a colorless oil (0.458 g, 1.39 mmol, 84% yield).

^{1}H NMR (600 MHz, $CDCl_3$): δ 7.45 – 7.36 (m, 2H), 7.36 – 7.30 (m, 2H), 7.30 – 7.22 (m, 1H), 6.65 (d, *J* = 15.9 Hz, 1H), 6.26 (dt, *J* = 15.9, 6.5 Hz, 1H), 4.81 (ddd, *J* = 12.8, 6.4, 1.2 Hz, 1H), 4.77 (ddd, *J* = 12.8, 6.4, 1.2 Hz, 1H), 2.57 – 2.52 (m, 1H), 2.51 – 2.43 (m, 2H), 2.06 – 1.98 (m, 1H), 1.79 – 1.61 (m, 3H), 1.53 – 1.44 (m, 1H), 1.33 (s, 3H).

^{13}C NMR (101 MHz, $CDCl_3$): δ 208.3, 173.0, 136.2, 135.0, 128.8, 128.4, 126.8, 126.6, 65.9, 57.4, 40.8, 38.4, 27.6, 22.8, 21.4.

IR (Neat Film, NaCl): 2938, 1714, 1453 (m), 1142 (m), 961 (m) cm^{-1}.

HRMS (MM: FD+): *m/z* calc'd for $C_{17}H_{20}O_3$ $[M]^{+\bullet}$: 272.1412, found 272.1410.



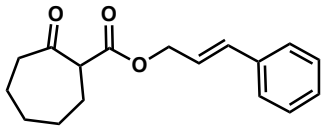
202a

methyl 2-oxocycloheptane-1-carboxylate (202a)

A flame dried round bottom flask was charged with NaH(60% dispersion in mineral oil, 2.9 g, 71 mmol, 2 equiv) and suspended with anhydrous PhMe (1.6 M). Dimethyl carbonae (9.1 mL, 108 mmol, 3 equiv) was added in one portion while stirring. The reaction mixture was heated to 80 °C and stirred. Cycloheptanone (4.2 mL, 36 mmol, 1 equiv) was added at 80 °C over 1 hour. Once H2 production ceased, the reaction was cooled to 0 °C and cautiously added 2 M HCl solution until reaching a pH <7. The aqueous layer was separated and washed with EtOAc three times. The combined organic layers were washed with dI water, dried over Mg2SO4, filtered, and concentrated *in vacuo* to afford the titled β-ketoester **202a** (5.6 g, 33 mmol, 91% yield) which was used in subsequent steps as crude.

Spectral data matches previous literature report for methyl 2-oxocycloheptane-1-carboxylate (**202a**).[20]

^{1}H NMR (600 MHz, $CDCl_3$): δ 3.72 (s, 3H), 3.55 (dd, *J* = 10.3, 4.0 Hz, 1H), 2.66 – 2.55 (m, 2H), 2.14 – 2.06 (m, 1H), 1.98 – 1.80 (m, 3H), 1.75 – 1.54 (m, 2H), 1.52 – 1.36 (m, 2H).



202b

cinnamyl 2-oxocycloheptane-1-carboxylate (202b)

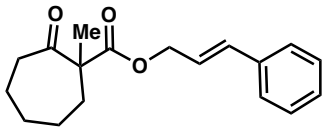
Prepared from **202a** (1.00 g, 5.89 mmol) following General Procedure 4B. Purification by flash column chromatography (0–5% EtOAc/hexanes) afforded the title compound **202b** as a colorless oil (873 mg, 3.21 mmol, 54% yield).

^{1}H NMR (400 MHz, $CDCl_3$): δ 7.34 – 7.29 (m, 2H), 7.28 – 7.22 (m, 2H), 7.22 – 7.14 (m, 1H), 6.63 – 6.49 (m, 1H), 6.20 (dtd, *J* = 16.0, 6.5, 1.2 Hz, 1H), 4.71 (dd, *J* = 6.5, 1.3 Hz, 2H), 3.53 (ddd, *J* = 10.3, 4.0, 1.2 Hz, 1H), 2.63 – 2.47 (m, 2H), 2.45 – 2.33 (m, 2H), 2.12 – 2.00 (m, 4H), 1.93 – 1.29 (m, 2H).

^{13}C NMR (101 MHz, $CDCl_3$): δ 209.1, 170.5, 136.3, 134.7, 128.7, 128.2, 126.8, 122.9, 65.8, 59.1, 43.3, 29.8, 28.2, 27.8, 24.5.

IR (Neat Film, NaCl): 3025, 2934, 2857, 1741, 1703, 1455, 1309, 1240, 1213, 1182, 966 cm^{-1}.

HRMS (MM: FD+): *m/z* calc'd for $C_{17}H_{20}O_3$ $[M]^{+\bullet}$:272.14124, found 272.14155.



202

cinnamyl 1-methyl-2-oxocycloheptane-1-carboxylate (202)

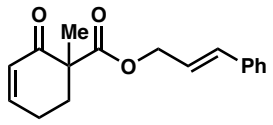
Prepared from **202b** (400 mg, 1.47 mmol) and methyl iodide following General Procedure 4B. Purification by flash column chromatography (5–10% EtOAc/hexanes) afforded the title compound **202** as a colorless oil (400 mg, 1.40 mmol, 95% yield).

^{1}H NMR (400 MHz, $CDCl_3$): δ 7.42 – 7.37 (m, 2H), 7.37 – 7.32 (m, 2H), 7.31 – 7.25 (m, 1H), 6.66 (dt, *J* = 15.9, 1.4 Hz, 1H), 6.27 (dt, *J* = 15.9, 6.4 Hz, 1H), 4.85 – 4.71 (m, 2H), 2.84 – 2.68 (m, 1H), 2.59 – 2.44 (m, 1H), 2.25 – 2.15 (m, 1H), 1.93 – 1.72 (m, 3H), 1.71 – 1.51 (m, 3H), 1.49 – 1.34 (m, 4H).

^{13}C NMR (101 MHz, $CDCl_3$): δ 210.3, 173.4, 136.2, 134.6, 128.7, 128.2, 126.7, 122.7, 65.8, 58.9, 42.1, 35.5, 30.2, 25.9, 24.8, 21.6.

IR (Neat Film, NaCl): 3025, 2933, 2860, 1732, 1710, 1448, 1256, 1230, 1150, 1103, 965 cm^{-1}.

HRMS (MM: FD+): *m/z* calc'd for $C_{18}H_{22}O_3$ $[M]^+$:286.15689, found 286.15660.



203

cinnamyl 1-methyl-2-oxocyclohex-3-ene-1-carboxylate (203)

Prepared from cinnamyl 2-oxocyclohex-3-ene-1-carboxylate (prepared following General Procedure 4B and used crude) and methyl iodide following General Procedure 4B.

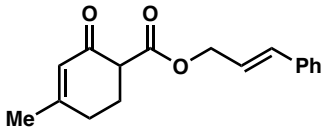
Purification by flash column chromatography (5–40% EtOAc/hexanes) afforded the title compound **203** as a colorless oil (0.48 g, 1.78 mmol, 23% yield).

^{1}H NMR (400 MHz, $CDCl_3$): δ 7.40 – 7.27 (m, 5H), 6.92 (dddd, *J* = 10.1, 4.4, 3.3, 1.0 Hz, 1H), 6.62 (d, *J* = 15.9 Hz, 1H), 6.23 (dt, *J* = 15.9, 6.3 Hz, 1H), 6.07 (ddd, *J* = 10.1, 2.4, 1.7 Hz, 1H), 4.83 – 4.70 (m, 2H), 2.57 – 2.43 (m, 2H), 2.40 – 2.30 (m, 1H), 1.92 (ddd, *J* = 14.6, 8.9, 5.2 Hz, 1H), 1.42 (s, 3H).

^{13}C NMR (100 MHz, $CDCl_3$): δ 197.0, 172.6, 149.6, 136.3, 134.5, 129.0, 128.8, 128.3, 126.8, 122.8, 65.9, 53.6, 33.5, 23.8, 20.8.

IR (Neat Film, NaCl): 3025, 1731, 1681, 1250, 1096 cm^{-1}.

HRMS (MM: FD+): *m/z* calc'd for $C_{17}H_{18}O_3$ $[M]^{+\bullet}$: 270.1256, found 270.1259.



204a

cinnamyl 4-methyl-2-oxocyclohex-3-ene-1-carboxylate (204a)

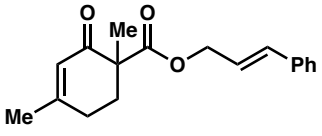
Prepared from 3-methylcyclohex-2-en-1-one and cinnamyl 1*H*-imidazole-1-carboxylate following General Procedure 4B. Purification by flash column chromatography (20% EtOAc/hexanes) afforded the title compound **204a** as a colorless oil (5.5 g, 20.3 mmol, 51% yield).

^{1}H NMR (600 MHz, $CDCl_3$): δ 7.42 – 7.36 (m, 2H), 7.32 (t, *J* = 7.6 Hz, 2H), 7.29 – 7.19 (m, 1H), 6.67 (d, *J* = 15.8 Hz, 1H), 6.28 (dt, *J* = 15.8, 6.4 Hz, 1H), 5.94 (d, *J* = 1.5 Hz, 1H), 4.82 (d, *J* = 6.4 Hz, 2H), 3.46 – 3.28 (m, 1H), 2.49 – 2.25 (m, 3H), 2.25 – 2.17 (m, 1H), 1.97 (d, *J* = 1.2 Hz, 3H).

^{13}C NMR (101 MHz, $CDCl_3$): δ 193.7, 170.2, 163.1, 136.3, 134.5, 128.7, 128.2, 126.8, 126.0, 123.0, 65.8, 52.7, 29.6, 25.6, 24.5.

IR (Neat Film, NaCl): 3026, 2935, 1737, 1666, 1445, 970 cm^{-1}.

HRMS (MM: ESI+): *m/z* calc'd for $C_{17}H_{18}O_3Na$ $[M+Na]^{+\bullet}$: 293.1148, found 293.1152.



204

cinnamyl 1,4-dimethyl-2-oxocyclohex-3-ene-1-carboxylate (204)

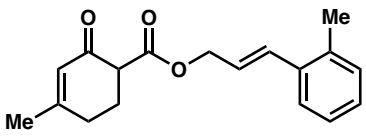
Prepared from **204a** (5.5 g, 20.3 mmol) and methyl iodide following General Procedure 4B. Purification by flash column chromatography (20% EtOAc/hexanes) afforded the title compound **204** as a colorless oil (4.5 g, 15.8 mmol, 78% yield).

^{1}H NMR (600 MHz, $CDCl_3$): δ 7.37 (d, *J* = 7.5 Hz, 2H), 7.31 (d, *J* = 7.4 Hz, 2H), 7.28 – 7.23 (m, 1H), 6.61 (d, *J* = 15.8 Hz, 1H), 6.23 (dt, *J* = 15.8, 6.4 Hz, 1H), 5.92 (s, 1H), 4.81 – 4.70 (m, 2H), 2.51 (dt, *J* = 13.3, 4.8 Hz, 1H), 2.48 – 2.39 (m, 1H), 2.25 (dt, *J* = 19.0, 5.3 Hz, 1H), 1.94 (s, 3H), 1.92 – 1.86 (m, 1H), 1.41 (s, 3H).

^{13}C NMR (101 MHz, $CDCl_3$): δ 196.7, 172.8, 161.7, 136.3, 134.3, 128.7, 128.2, 126.8, 125.7, 122.9, 65.8, 52.5, 33.3, 28.7, 24.3, 20.5.

IR (Neat Film, NaCl): 3026, 2935, 1731, 1668, 1448, 1253 cm^{-1}.

HRMS (MM: ESI+): *m/z* calc'd for $C_{18}H_{20}O_3Na$ $[M+Na]^{+\bullet}$: 307.1305, found 307.1308.



205a

(*E*)-3-(*o*-tolyl)allyl 4-methyl-2-oxocyclohex-3-ene-1-carboxylate (205a)

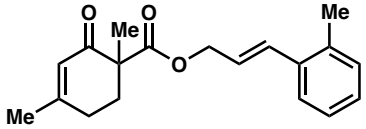
Prepared from 3-methylcyclohex-2-en-1-one and cinnamyl 1*H*-imidazole-1-carboxylate (0.94 mL, 8.3 mmol) following General Procedure 4B. Purification by flash column chromatography (25–100% CH_2Cl_2/hexanes) afforded the title compound **205a** as a yellow oil (569 mg, 2.1 mmol, 51% yield).

^{1}H NMR (400 MHz, $CDCl_3$): δ 7.46 – 7.39 (m, 1H), 7.20 – 7.10 (m, 3H), 6.88 (dt, *J* = 15.8, 1.4 Hz, 1H), 6.17 (ddd, *J* = 15.7, 6.8, 5.9 Hz, 1H), 5.98 – 5.87 (m, 1H), 4.83 (dt, *J* = 6.4, 1.3 Hz, 2H), 3.42 – 3.33 (m, 1H), 2.49 – 2.37 (m, 3H), 2.35 (s, 3H), 2.26 – 2.19 (m, 1H), 1.97 (s, 3H).

^{13}C NMR (101 MHz, $CDCl_3$): δ 193.7, 170.2, 163.1, 135.8, 135.5, 132.3, 130.4, 128.0, 126.2, 126.0, 126.0, 124.3, 66.0, 52.6, 29.5, 25.6, 24.5, 19.9.

IR (Neat Film, NaCl): 3466, 3020, 2939, 1736, 1669, 1631, 1433, 1379, 1306, 1251, 1214, 1168, 1150, 1021, 968 cm^{-1}.

HRMS (MM: FD+): *m/z* calc'd for $C_{18}H_{20}O_3$ $[M]^{+\bullet}$:284.14124, found 284.14131.



205

(*E*)-3-(*o*-tolyl)allyl 1,4-dimethyl-2-oxocyclohex-3-ene-1-carboxylate (205)

Prepared from **205a** (261 mg, 0.92 mmol) and methyl iodide following General Procedure 4B. Purification by flash column chromatography (0–20% EtOAc/hexanes) afforded the title compound **205** as a colorless oil (158 mg, 0.55 mmol, 60% yield).

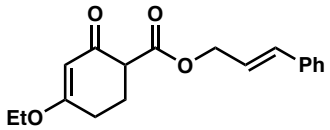
^{1}H NMR (400 MHz, $CDCl_3$): δ 7.44 – 7.37 (m, 1H), 7.20 – 7.09 (m, 3H), 6.84 (dt, *J* = 15.7, 1.5 Hz, 1H), 6.11 (dt, *J* = 15.8, 6.2 Hz, 1H), 5.92 (q, *J* = 1.4 Hz, 1H), 4.84 – 4.70 (m,

2H), 2.56 – 2.47 (m, 1H), 2.47 – 2.39 (m, 1H), 2.34 (s, 3H), 2.29 – 2.20 (m, 1H), 1.94 (s, 3H), 1.92 – 1.84 (m, 1H), 1.41 (s, 3H).

^{13}C NMR (101 MHz, $CDCl_3$): δ 196.7, 172.7, 161.7, 135.8, 135.5, 132.1, 130.4, 128.1, 126.2, 125.9, 125.7, 124.2, 65.9, 52.5, 33.3, 28.7, 24.3, 20.5, 19.9.

IR (Neat Film, NaCl): 3016, 2975, 2935, 1733, 1675, 1636, 1456, 1439, 1378, 1250, 1215, 1169, 1113, 966, 750 cm^{-1}.

HRMS (MM: FD+): *m/z* calc'd for $C_{19}H_{22}O_3$ $[M]^{+\bullet}$:298.15689, found 298.15698.



206a

cinnamyl 4-ethoxy-2-oxocyclohex-3-ene-1-carboxylate (206a)

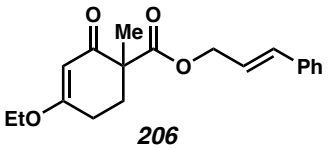
Prepared from 3-ethoxycyclohex-2-en-1-one following General Procedure 4B. Purification by flash column chromatography (10–60% EtOAc/hexanes) afforded the title compound **206a** as a colorless oil (2.13 g, 7.09 mmol, 35% yield).

^{1}H NMR (400 MHz, $CDCl_3$): δ 7.41 – 7.37 (m, 2H), 7.32 (tt, *J* = 6.5, 1.0 Hz, 2H), 7.28 – 7.23 (m, 1H), 6.67 (d, *J* = 15.9 Hz, 1H), 6.29 (dt, *J* = 15.9, 6.4 Hz, 1H), 5.40 (s, 1H), 4.82 (dd, *J* = 6.4, 1.4 Hz, 2H), 3.96 – 3.88 (m, 2H), 3.41 – 3.36 (m, 1H), 2.62 – 2.52 (m, 1H), 2.48 – 2.33 (m, 2H), 2.25 – 2.15 (m, 1H), 1.37 (t, *J* = 7.0 Hz, 3H).

^{13}C NMR (100 MHz, $CDCl_3$): δ 193.6, 177.6, 170.2, 136.2, 134.3, 128.6, 128.1, 126.7, 122.9, 102.1, 65.8, 64.6, 52.4, 27.4, 24.2, 14.1.

IR (Neat Film, NaCl): 2980, 2942, 1736, 1654, 1602, 1380, 1192 cm^{-1}.

HRMS (MM: FD+): *m/z* calc'd for $C_{18}H_{20}O_4$ $[M]^{+\bullet}$: 300.1362, found 300.1353.



206

cinnamyl 4-ethoxy-1-methyl-2-oxocyclohex-3-ene-1-carboxylate (206)

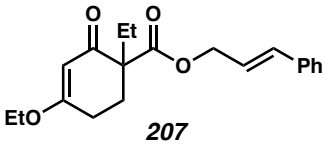
Prepared from **206a** and methyl iodide following General Procedure 4B. Purification by flash column chromatography (10–50% EtOAc/hexanes) afforded the title compound **206** as a colorless oil (0.65 g, 2.1 mmol, 63% yield).

^{1}H NMR (400 MHz, $CDCl_3$): δ 7.38 – 7.25 (m, 5H), 6.62 (d, *J* = 15.9 Hz, 1H), 6.24 (dt, *J* = 15.9, 6.3 Hz, 1H), 5.37 (s, 1H), 4.82 – 4.72 (m, 2H), 3.90 (q, *J* = 7.0 Hz, 2H), 2.61 – 2.47 (m, 2H), 2.38 (dt, *J* = 17.1, 5.3 Hz, 1H), 1.88 (ddd, *J* = 13.7, 8.5, 5.2 Hz, 1H), 1.43 (s, 3H), 1.34 (t, *J* = 7.0 Hz, 3H).

^{13}C NMR (100 MHz, $CDCl_3$): δ 196.9, 176.7, 172.9, 136.3, 134.3, 128.7, 128.2, 126.8, 123.0, 101.9, 65.8, 64.6, 52.6, 31.9, 26.6, 20.7, 14.2.

IR (Neat Film, NaCl): 2980, 2942, 1731, 1656, 1606, 1377, 1250, 1195 cm^{-1}.

HRMS (MM: FD+): *m/z* calc'd for $C_{19}H_{22}O_4$ $[M]^{+\bullet}$: 314.1518, found 314.1516.



207

cinnamyl 4-ethoxy-1-ethyl-2-oxocyclohex-3-ene-1-carboxylate (207)

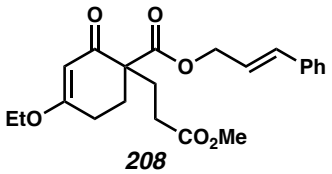
Prepared from **206a** and ethyl iodide following General Procedure 4B. Purification by flash column chromatography (5–40% EtOAc/hexanes) afforded the title compound **207** as a colorless oil (0.458 g, 1.39 mmol, 84% yield).

^{1}H NMR (400 MHz, $CDCl_3$): δ 7.38 – 7.35 (m, 2H), 7.33 – 7.29 (m, 2H), 7.27 – 7.23 (m, 1H), 6.62 (d, *J* = 15.9 Hz, 1H), 6.24 (dt, *J* = 15.8, 6.3 Hz, 1H), 5.36 (s, 1H), 4.77 (dd, *J* = 6.3, 1.4 Hz, 2H), 3.93 – 3.84 (m, 2H), 2.64 (dddd, *J* = 17.9, 9.8, 5.0, 1.2 Hz, 1H), 2.45 (dt, *J* = 13.3, 5.0 Hz, 1H), 2.36 (dt, *J* = 17.9, 5.0 Hz, 1H), 2.13 – 2.01 (m, 1H), 1.93 (ddd, *J* = 13.3, 9.6, 5.2 Hz, 1H), 1.83 (dq, *J* = 13.9, 7.5 Hz, 1H), 1.33 (t, *J* = 7.0 Hz, 3H), 0.92 (t, *J* = 7.5 Hz, 3H).

^{13}C NMR (100 MHz, $CDCl_3$): δ 196.0, 176.7, 171.8, 136.4, 134.3, 128.7, 128.2, 126.8, 123.1, 102.3, 65.7, 64.5, 56.5, 27.9, 27.1, 26.6, 14.2, 9.2.

IR (Neat Film, NaCl): 3025, 2979, 2938, 1728, 1659, 1603, 1446, 1378, 1235, 1186 cm^{-1}.

HRMS (MM: ESI+): *m/z* calc'd for $C_{20}H_{25}O_4$ $[M+H]^{+\bullet}$: 329.1747, found 329.1747.



208

cinnamyl 4-ethoxy-1-(3-methoxy-3-oxopropyl)-2-oxocyclohex-3-ene-1-carboxylate (208)

Prepared from **206a** and methyl acrylate following General Procedure 4B. Purification by flash column chromatography (5–30% EtOAc/hexanes) afforded the title compound **208** as a colorless oil (0.48 g, 1.24 mmol, 75% yield).

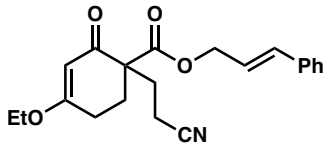
^{1}H NMR (400 MHz, $CDCl_3$): δ 7.39 – 7.35 (m, 2H), 7.34 – 7.29 (m, 2H), 7.28 – 7.23 (m, 1H), 6.62 (d, *J* = 15.9 Hz, 1H), 6.23 (dt, *J* = 15.9, 6.3 Hz, 1H), 5.36 (s, 1H), 4.82 – 4.72 (m, 2H), 3.88 (qd, *J* = 7.1, 2.0 Hz, 2H), 3.65 (s, 3H), 2.64 – 2.53 (m, 1H), 2.49 – 2.36 (m, 4H),

2.33 – 2.25 (m, 1H), 2.13 (ddd, J = 13.9, 10.0, 6.1 Hz, 1H), 1.95 – 1.87 (m, 1H), 1.34 (t, J = 7.0 Hz, 3H).

^{13}C NMR (100 MHz, $CDCl_3$): δ 195.4, 176.6, 173.7, 171.5, 136.3, 134.6, 128.7, 128.2, 126.8, 122.8, 102.2, 66.0, 64.7, 55.4, 51.8, 29.8, 29.0, 28.9, 26.4, 14.2.

IR (Neat Film, NaCl): 2946, 1737, 1731, 1659, 1651, 1606, 1246, 1192 cm^{-1}.

HRMS (MM: ESI+): *m/z* calc'd for $C_{22}H_{27}O_6$ $[M+H]^{+\bullet}$: 387.1802, found 387.1806.



209

cinnamyl 1-(2-cyanoethyl)-4-ethoxy-2-oxocyclohex-3-ene-1-carboxylate (209)

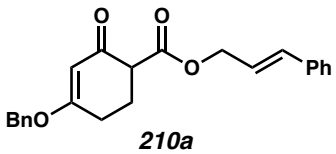
Prepared from **206a** and acrylonitrile following General Procedure 4B. Purification by flash column chromatography (5–30% EtOAc/hexanes) afforded the title compound **209** as a colorless oil (349 mg, 0.987 mmol, 59% yield).

^{1}H NMR (400 MHz, $CDCl_3$): δ 7.40 – 7.27 (m, 5H), 6.64 (d, J = 15.9 Hz, 1H), 6.23 (dt, J = 15.9, 6.5 Hz, 1H), 5.38 (s, 1H), 4.85 – 4.74 (m, 2H), 3.96 – 3.86 (m, 2H), 2.65 – 2.39 (m, 5H), 2.31 – 2.13 (m, 2H), 2.01 – 1.94 (m, 1H), 1.35 (t, J = 7.0 Hz, 3H).

^{13}C NMR (100 MHz, $CDCl_3$): δ 194.8, 176.9, 171.0, 136.1, 135.2, 128.8, 128.4, 126.8, 122.3, 119.8, 102.2, 66.4, 64.9, 55.1, 30.0, 29.4, 26.4, 14.2, 13.4.

IR (Neat Film, NaCl): 2981, 2939, 1730, 1651, 1605, 1381, 1186 cm^{-1}.

HRMS (MM: EI+): *m/z* calc'd for $C_{21}H_{23}O_4N$ $[M]^+$: 353.1629, found 353.1627.



210a

cinnamyl 4-(benzyloxy)-2-oxocyclohex-3-ene-1-carboxylate (210a)

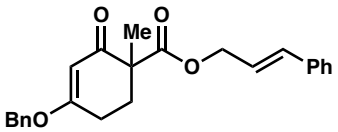
Prepared from 3-(benzyloxy)cyclohex-2-en-1-one following General Procedure 4B. Purification by flash column chromatography (10–60% EtOAc/hexanes) afforded the title compound **210a** as a colorless oil (0.79 g, 2.2 mmol, 22% yield).

^{1}H NMR (400 MHz, $CDCl_3$): δ 7.42 – 7.27 (m, 10H), 6.68 (d, *J* = 15.9 Hz, 1H), 6.29 (dt, *J* = 15.9, 6.4 Hz, 1H), 5.54 (s, 1H), 4.91 (d, *J* = 2.5 Hz, 2H), 4.83 (dd, *J* = 6.4, 1.3 Hz, 2H), 3.41 (dd, *J* = 9.0, 5.0 Hz, 1H), 2.65 (ddd, *J* = 17.5, 6.4, 5.0 Hz, 1H), 2.56 – 2.46 (m, 1H), 2.41 (dtd, *J* = 13.7, 8.7, 5.0 Hz, 1H), 2.23 (ddt, *J* = 13.5, 6.6, 5.0 Hz, 1H).

^{13}C NMR (100 MHz, $CDCl_3$): δ 193.6, 177.3, 170.1, 136.2, 134.7, 134.4, 128.8, 128.7, 128.6, 128.1, 127.9, 126.7, 122.9, 102.8, 70.8, 65.8, 52.4, 27.4, 24.2.

IR (Neat Film, NaCl): 3030, 2942, 1736, 1657, 1603, 1362, 1186, 1150 cm^{-1}.

HRMS (MM: FD+): *m/z* calc'd for $C_{23}H_{22}O_4$ $[M]^{+\bullet}$: 362.1518, found 362.1510.



210

cinnamyl 4-(benzyloxy)-1-methyl-2-oxocyclohex-3-ene-1-carboxylate (210)

Prepared from **210a** and methyl iodide following General Procedure 4B. Purification by flash column chromatography (5–30% EtOAc/hexanes) afforded the title compound **210** as a colorless oil (179 mg, 0.475 mmol, 57% yield).

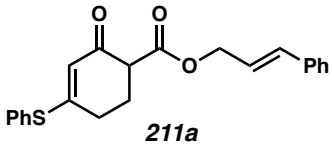
^{1}H NMR (400 MHz, $CDCl_3$): δ 7.41 – 7.26 (m, 10H), 6.63 (d, *J* = 15.9 Hz, 1H), 6.25 (dt, *J* = 15.9, 6.3 Hz, 1H), 5.52 (s, 1H), 4.89 (s, 2H), 4.83 – 4.72 (m, 2H), 2.65 (dddd, *J* = 17.6,

9.8, 4.5, 1.1 Hz, 1H), 2.56 – 2.41 (m, 2H), 1.92 (ddd, *J* = 12.8, 8.8, 4.7 Hz, 1H), 1.44 (s, 3H).

^{13}C NMR (100 MHz, $CDCl_3$): δ 196.7, 176.4, 172.8, 136.3, 135.0, 134.4, 128.9, 128.8, 128.7, 128.2, 128.0, 126.8, 123.0, 102.5, 70.8, 65.9, 52.6, 31.9, 26.6, 20.7.

IR (Neat Film, NaCl): 3027, 2935, 1730, 1659, 1607, 1251, 1189, 1170 cm^{-1}.

HRMS (MM: EI+): *m/z* calc'd for $C_{24}H_{24}O_4$ $[M]^{+\bullet}$: 376.1675, found 376.1665.



211a

cinnamyl 2-oxo-4-(phenylthio)cyclohex-3-ene-1-carboxylate (211a)

Prepared from 3-(phenylthio)cyclohex-2-en-1-one following General Procedure 4B. Purification by flash column chromatography (10–60% EtOAc/hexanes) afforded the title compound **211a** as a colorless oil (1.59 g, 4.36 mmol, 44% yield).

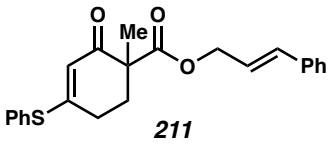
Trace starting material coeluted with **211a. The material can be carried through alkylation for **211** and separated without issue.**

^{1}H NMR (400 MHz, $CDCl_3$): δ 7.49 – 7.37 (m, 8H), 7.34 – 7.25 (m, 2H), 6.66 (d, *J* = 15.9 Hz, 1H), 6.27 (dt, *J* = 15.9, 6.3 Hz, 1H), 5.53 (s, 1H), 4.81 (dd, *J* = 6.4, 1.4 Hz, 2H), 3.41 (dd, *J* = 9.3, 4.9 Hz, 1H), 2.75 – 2.66 (m, 1H), 2.62 – 2.51 (m, 1H), 2.50 – 2.36 (m, 1H), 2.32 – 2.25 (m, 1H).

^{13}C NMR (100 MHz, $CDCl_3$): δ 190.2, 169.9, 167.5, 136.3, 135.6, 134.5, 130.5, 130.1, 128.7, 128.2, 127.7, 126.8, 122.9, 120.1, 65.9, 52.9, 28.6, 26.1.

IR (Neat Film, NaCl): 3054, 2939, 1736, 1656, 1576, 1300, 1167, 1146 cm^{-1}.

HRMS (MM: FD+): *m/z* calc'd for $C_{22}H_{20}O_3S$ $[M]^{+\bullet}$: 364.1133, found 364.1133.



211

cinnamyl 1-methyl-2-oxo-4-(phenylthio)cyclohex-3-ene-1-carboxylate (211)

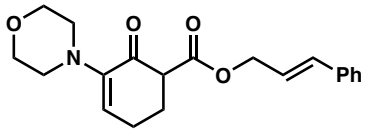
Prepared from **211a** and methyl iodide following General Procedure 4B. Purification by flash column chromatography (5–30% EtOAc/hexanes) afforded the title compound **211** as a colorless oil (232 mg, 0.853 mmol, 62% yield).

^{1}H NMR (400 MHz, $CDCl_3$): δ 7.46 – 7.27 (m, 10H), 6.62 (d, *J* = 15.9 Hz, 1H), 6.24 (dt, *J* = 15.9, 6.3 Hz, 1H), 5.52 (s, 1H), 4.81 (dd, *J* = 12.9, 6.3 Hz, 1H), 4.73 (dd, *J* = 13.0, 6.3 Hz, 1H), 2.73 – 2.64 (m, 1H), 2.59 – 2.46 (m, 2H), 2.01 – 1.93 (m, 1H), 1.41 (s, 3H).

^{13}C NMR (100 MHz, $CDCl_3$): δ 193.3, 172.5, 165.9, 136.2, 135.5, 134.3, 130.3, 129.9, 128.6, 128.1, 127.8, 126.7, 122.7, 119.9, 65.8, 52.8, 33.6, 27.6, 20.4.

IR (Neat Film, NaCl): 2934, 1729, 1655, 1577, 1303, 1250, 1167, 1108 cm^{-1}.

HRMS (MM: FD+): *m/z* calc'd for $C_{23}H_{22}O_3S$ $[M]^{+\bullet}$: 378.1290, found 378.1293.



212a

cinnamyl 3-morpholino-2-oxocyclohex-3-ene-1-carboxylate (212a)

Prepared from 2-morpholinocyclohex-2-en-1-one [21] following General Procedure 4B. Purification by flash column chromatography (30–60% EtOAc/hexanes) afforded the title compound **212a** as a colorless oil (1.34 g, 3.92 mmol, 33% yield).

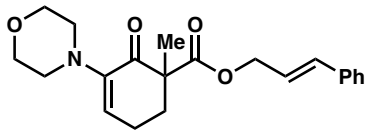
^{1}H NMR (400 MHz, C_6D_6): δ 7.16 – 7.13 (m, 2H), 7.10 – 6.98 (m, 3H), 6.43 (d, *J* = 15.9 Hz, 1H), 6.12 (dt, *J* = 15.9, 6.4 Hz, 1H), 5.22 (t, *J* = 4.5 Hz, 1H), 4.71 – 4.61 (m, 2H), 3.64

– 3.56 (m, 4H), 3.28 (dd, *J* = 9.6, 4.6 Hz, 1H), 2.67 – 2.55 (m, 4H), 2.20 – 2.12 (m, 1H), 2.02 (dq, *J* = 17.5, 4.9, 4.3 Hz, 1H), 1.81 – 1.65 (m, 2H).

^{13}C NMR (100 MHz, C_6D_6): δ 190.4, 169.7, 146.5, 136.7, 134.5, 128.8, 128.2, 127.0, 124.3, 123.4, 66.9, 65.6, 55.2, 50.3, 26.0, 23.6.

IR (Neat Film, NaCl): 3024, 2953, 2854, 1736, 1685, 1610, 1448, 1262, 1118 cm^{-1}.

HRMS (MM: ESI+): *m/z* calc'd for $C_{20}H_{24}O_4N$ $[M+H]^{+\bullet}$: 342.1700, found 342.1710.



212

cinnamyl 1-methyl-3-morpholino-2-oxocyclohex-3-ene-1-carboxylate (212)

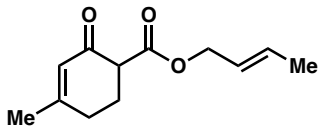
Prepared from **212a** and methyl iodide following General Procedure 4B. Purification by flash column chromatography (15–50% EtOAc/hexanes) afforded the title compound **212** as a colorless oil (0.43 g, 1.24 mmol, 81% yield).

^{1}H NMR (400 MHz, C_6D_6): δ 7.14 – 7.10 (m, 2H), 7.09 – 6.99 (m, 3H), 6.36 (d, *J* = 15.9 Hz, 1H), 6.00 (dt, *J* = 15.9, 6.4 Hz, 1H), 5.17 (ddd, *J* = 4.9, 3.5, 1.0 Hz, 1H), 4.56 (ddd, *J* = 12.9, 6.5, 1.4 Hz, 1H), 4.50 (ddd, *J* = 12.8, 6.3, 1.4 Hz, 1H), 3.67 (ddd, *J* = 11.2, 6.4, 3.0 Hz, 1H), 3.58 (ddd, *J* = 11.2, 6.4, 2.9 Hz, 1H), 2.91 (ddd, *J* = 11.5, 6.3, 2.9 Hz, 1H), 2.47 – 2.30 (m, 4H), 1.92 – 1.81 (m, 1H), 1.53 – 1.46 (m, 1H), 1.45 (s, 3H).

^{13}C NMR (100 MHz, C_6D_6): δ 192.8, 172.4, 146.9, 136.5, 134.7, 128.9, 128.6, 126.9, 123.0, 121.8, 66.9, 65.6, 54.4, 50.2, 33.3, 22.7, 20.9.

IR (Neat Film, NaCl): 2936, 2856, 1736, 1730, 1692, 1613, 1448 cm^{-1}.

HRMS (MM: ESI+): *m/z* calc'd for $C_{21}H_{26}O_4N$ $[M+H]^{+\bullet}$: 356.1856, found 356.1867.



213a

(*E*)-but-2-en-1-yl 4-methyl-2-oxocyclohex-3-ene-1-carboxylate (213a)

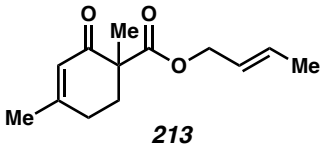
Prepared from 3-methylcyclohex-2-en-1-one following General Procedure 4B. Purification by flash column chromatography (20–40% EtOAc/hexanes) afforded the title compound **213a** as a colorless oil (1.98 g, 9.49 mmol, 63% yield).

^{1}H NMR (400 MHz, $CDCl_3$): δ 5.92 (q, *J* = 1.4 Hz, 1H), 5.84 – 5.74 (m, 1H), 5.63 – 5.54 (m, 1H), 4.58 (dt, *J* = 6.5, 1.1 Hz, 2H), 3.32 (dd, *J* = 9.6, 5.1 Hz, 1H), 2.45 – 2.27 (m, 3H), 2.21 – 2.16 (m, 1H), 1.97 (s, 3H), 1.71 (dq, *J* = 6.5, 1.2 Hz, 3H).

^{13}C NMR (100 MHz, $CDCl_3$): δ 193.8, 170.2, 163.0, 131.7, 126.0, 124.9, 66.0, 52.6, 29.5, 25.6, 24.5, 17.9.

IR (Neat Film, NaCl): 3027, 2941, 1737, 1671, 1632, 1439, 1166, 1153 cm^{-1}.

HRMS (MM: ESI+): *m/z* calc'd for $C_{12}H_{16}O_3Na$ $[M+Na]^{+\bullet}$: 231.0992, found 231.1000.



213

(*E*)-but-2-en-1-yl 1,4-dimethyl-2-oxocyclohex-3-ene-1-carboxylate (213)

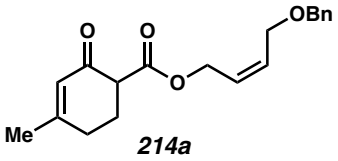
Prepared from **213a** and methyl iodide following General Procedure 4B. Purification by flash column chromatography (5–25% EtOAc/hexanes) afforded the title compound **2123** as a colorless oil (0.29 g, 1.30 mmol, 55% yield).

^{1}H NMR (400 MHz, $CDCl_3$): δ 5.89 (s, 1H), 5.74 (dqt, *J* = 15.3, 6.5, 1.2 Hz, 1H), 5.57 – 5.47 (m, 1H), 4.56 – 4.47 (m, 2H), 2.51 – 2.37 (m, 2H), 2.28 – 2.19 (m, 1H), 1.94 (s, 3H), 1.90 – 1.82 (m, 1H), 1.70 (d, *J* = 6.5 Hz, 3H), 1.37 (s, 3H).

^{13}C NMR (100 MHz, $CDCl_3$): δ 196.9, 172.8, 161.6, 131.4, 125.8, 124.8, 65.9, 52.4, 33.3, 28.7, 24.3, 20.4, 17.9.

IR (Neat Film, NaCl): 3027, 2938, 2917, 1730, 1679, 1636, 1440, 1250 cm^{-1}.

HRMS (MM: ESI+): *m/z* calc'd for $C_{13}H_{18}O_3Na$ $[M+Na]^{+\bullet}$: 245.1148, found 245.1159.



214a

***(Z)*-4-(benzyloxy)but-2-en-1-yl 4-methyl-2-oxocyclohex-3-ene-1-carboxylate (214a)**

Prepared from 3-methylcyclohex-2-en-1-one and (*Z*)-4-(benzyloxy)but-2-en-1-yl 1*H*-imidazole-1-carboxylate following General Procedure 4B. Purification by flash column chromatography (20% EtOAc/hexanes) afforded the title compound **214a** as a colorless oil (5.5 g, 20.3 mmol, 51% yield).

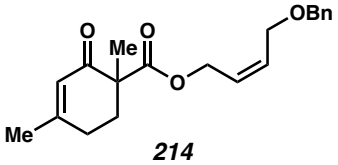
Trace starting material coeluted with **214a. The material can be carried through alkylation to yield **214** and separated without issue.**

^{1}H NMR (600 MHz, $CDCl_3$): δ 7.41 – 7.32 (m, 4H), 7.32 – 7.27 (m, 1H), 5.91 (t, *J* = 1.5 Hz, 1H), 5.86 – 5.78 (m, 1H), 5.76 – 5.63 (m, 1H), 4.72 (dd, *J* = 6.6, 1.3 Hz, 2H), 4.51 (s, 2H), 4.13 (dd, *J* = 6.2, 1.5 Hz, 2H), 3.40 – 3.21 (m, 1H), 2.48 – 2.25 (m, 5H), 2.25 – 2.14 (m, 1H), 2.05 – 1.96 (m, 4H).

^{13}C NMR (101 MHz, $CDCl_3$): δ 193.6, 170.2, 163.1, 138.1, 131.2, 128.6, 127.9, 127.8, 126.5, 126.0, 72.6, 65.8, 61.1, 52.6, 29.5, 25.6, 24.5.

IR (Neat Film, NaCl): 3457, 3031, 2936, 1738, 1667, 1453 cm^{-1}.

HRMS (MM: ESI+): *m/z* calc'd for $C_{19}H_{22}O_4Na$ $[M+Na]^{+\bullet}$: 337.1410, found 337.1415.



214

***(Z)*-4-(benzyloxy)but-2-en-1-yl 1,4-dimethyl-2-oxocyclohex-3-ene-1-carboxylate (214)**

Prepared from **214a** and methyl iodide following General Procedure 4B. Purification by flash column chromatography (20% EtOAc/hexanes) afforded the title compound **214** as a colorless oil (361 mg, 1.1 mmol, 73% yield).

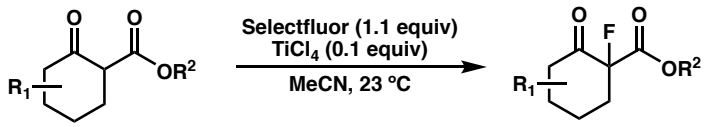
^{1}H NMR (500 MHz, $CDCl_3$): δ 7.39 – 7.31 (m, 1H), 7.31 – 7.26 (m, 1H), 5.88 (q, *J* = 1.5 Hz, 1H), 5.80 (dtt, *J* = 11.2, 6.2, 1.4 Hz, 1H), 5.70 – 5.59 (m, 1H), 4.72 – 4.59 (m, 2H), 4.11 (ddd, *J* = 6.3, 1.6, 0.8 Hz, 1H), 2.47 (dt, *J* = 13.2, 5.1 Hz, 1H), 2.43 – 2.35 (m, 1H), 2.24 (dt, *J* = 18.9, 5.2 Hz, 1H), 1.94 (d, *J* = 1.4 Hz, 1H), 1.87 (ddd, *J* = 13.2, 8.3, 5.1 Hz, 1H), 1.37 (s, 3H).

^{13}C NMR (101 MHz, $CDCl_3$): δ 196.6, 172.7, 161.6, 138.1, 131.2, 128.6, 127.9, 127.8, 126.4, 125.6, 72.6, 65.8, 61.1, 52.4, 33.2, 28.7, 24.3, 20.3.

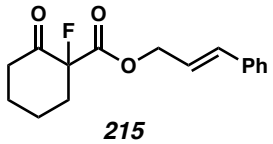
IR (Neat Film, NaCl): 3031, 2933, 1731, 1681, 1454, 1214 cm^{-1}.

HRMS (MM: ESI+): *m/z* calc'd for $C_{20}H_{24}O_4Na$ $[M+Na]^{+\bullet}$: 351.1567, found 351.1565.

General Procedure 4C: Fluorination of β-ketoesters.



To a solution of β-ketoester (1 equiv) in anhydrous acetonitrile (0.2 M) at 23 ºC is added neat titanium(IV) chloride (0.1 equiv). After 5 minutes, Selectfluor® was added in one portion. The reaction mixture is stirred at 23 ºC until complete consumption of starting material as observed by TLC (typically 2 hours). Water is then added, and the reaction mixture is extracted three times with Et_2O. The combined organic layers were washed with saturated aqueous brine, dried over anhydrous sodium sulfate, and volatiles were removed *in vacuo*. The crude reaction mixture was purified by silica gel flash column chromatography to yield the desired α-fluoro-β-ketoester.



215

cinnamyl 1-fluoro-2-oxocyclohexane-1-carboxylate (215)

Prepared from cinnamyl 2-oxocyclohexane-1-carboxylate[19] following General Procedure 4C. Purification by flash column chromatography (5–40% EtOAc/hexanes) afforded the title compound **215** as a colorless oil (0.80 g, 2.9 mmol, 75% yield).

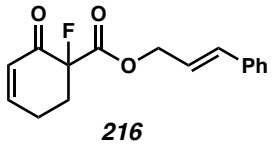
^{1}H NMR (400 MHz, $CDCl_3$): δ 7.40 (d, *J* = 7.3 Hz, 2H), 7.37 – 7.29 (m, 2H), 7.29 – 7.26 (m, 1H), 6.70 (d, *J* = 15.9 Hz, 1H), 6.29 (dt, *J* = 15.9, 6.6 Hz, 1H), 4.89 (d, *J* = 6.5 Hz, 2H), 2.81 – 2.69 (m, 1H), 2.67 – 2.56 (m, 1H), 2.57 – 2.40 (m, 1H), 2.25 – 2.11 (m, 1H), 1.99 – 1.82 (m, 4H).

^{13}C NMR (100 MHz, $CDCl_3$): δ 201.9 (d, $J_{C–F}$ = 20.0 Hz), 166.9 (d, $J_{C–F}$ = 24.9 Hz), 136.0, 135.6, 128.8, 128.5, 126.9, 121.9, 96.6 (d, $J_{C–F}$ = 197.2 Hz), 66.9, 39.7, 36.2 (d, $J_{C–F}$ = 21.7 Hz), 26.7, 21.0 (d, $J_{C–F}$ = 5.7 Hz).

^{19}F NMR (282 MHz, $CDCl_3$): δ –160.82 (ddd, *J* = 21.5, 13.5, 5.1 Hz, 1F).

IR (Neat Film, NaCl): 2943, 1731, 1457, 1281 cm^{-1}

HRMS (MM: FD+): *m/z* calc'd for $C_{16}H_{17}O_3F$ $[M]^{+\bullet}$: 276.1162, found 276.1165.



216

cinnamyl 1-fluoro-2-oxocyclohex-3-ene-1-carboxylate (216)

Prepared from cinnamyl 2-oxocyclohex-3-ene-1-carboxylate (prepared following General Procedure 4B and used crude) following General Procedure 4C. Purification by flash column chromatography (0–20% EtOAc/hexanes) afforded the title compound **216** as a colorless oil (0.54 g, 2.0 mmol, 50% yield).

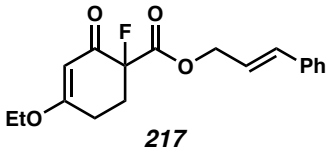
^{1}H NMR (400 MHz, $CDCl_3$): δ 7.41 – 7.37 (m, 2H), 7.35 – 7.30 (m, 2H), 7.30 – 7.26 (m, 1H), 7.10 (dt, *J* = 10.2, 4.0 Hz, 1H), 6.69 (d, *J* = 15.9 Hz, 1H), 6.27 (dt, *J* = 15.8, 6.5 Hz, 1H), 6.18 (dq, *J* = 10.2, 2.0 Hz, 1H), 4.94 – 4.84 (m, 2H), 2.72 – 2.58 (m, 3H), 2.48 – 2.39 (m, 1H).

^{13}C NMR (100 MHz, $CDCl_3$): δ 188.9 (d, *J* = 18.7 Hz), 167.0 (d, *J* = 25.9 Hz), 151.9, 135.9, 135.4, 128.7, 128.4, 127.7, 126.8, 121.8, 92.9 (d, *J* = 194.8 Hz), 66.8, 31.3 (d, *J* = 22.5 Hz), 23.3 (d, *J* = 7.2 Hz).

^{19}F NMR (282 MHz, $CDCl_3$): δ –164.30 (dd, *J* = 22.8, 12.5 Hz).

IR (Neat Film, NaCl): 3027, 2940, 1759, 1693, 1265 cm^{-1}.

HRMS (MM: FD+): *m/z* calc'd for $C_{16}H_{15}O_3F$ $[M]^{+\bullet}$: 274.1005, found 274.1004.



217

cinnamyl 4-ethoxy-1-fluoro-2-oxocyclohex-3-ene-1-carboxylate (217)

Prepared from **206a** following General Procedure 4C. Purification by flash column chromatography (0–25% EtOAc/hexanes) afforded the title compound **217** as a colorless oil (0.16 g, 0.50 mmol, 31% yield).

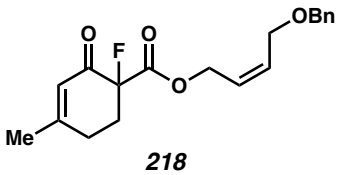
^{1}H NMR (400 MHz, $CDCl_3$): δ 7.42 – 7.35 (m, 2H), 7.36 – 7.27 (m, 2H), 7.31 – 7.22 (m, 2H), 6.68 (d, *J* = 15.9 Hz, 1H), 6.28 (dd, *J* = 16.0, 6.2 Hz, 1H), 5.46 (s, 1H), 4.94 – 4.85 (m, 2H), 3.97 (q, *J* = 7.1 Hz, 2H), 2.72 – 2.53 (m, 3H), 2.44 – 2.33 (m, 1H), 1.38 (t, *J* = 7.0 Hz, 3H).

^{13}C NMR (100 MHz, $CDCl_3$): δ 188.6 (d, $J_{C–F}$ = 18.9 Hz), 178.2, 167.7 (d, $J_{C–F}$ = 26.0 Hz), 136.1, 135.3, 128.7, 128.4, 126.9, 122.0, 101.0, 92.3 (d, $J_{C–F}$ = 193.6 Hz), 66.8, 65.3, 29.7 (d, $J_{C–F}$ = 23.0 Hz), 25.7 (d, $J_{C–F}$ = 6.0 Hz), 14.2.

^{19}F NMR (282 MHz, $CDCl_3$): δ –163.76 – –163.93 (m).

IR (Neat Film, NaCl): 2983, 2943, 1765, 1666, 1599, 1382, 1264 cm^{-1}

HRMS (MM: ESI+): *m/z* calc'd for $C_{18}H_{19}O_4FNa$ $[M+Na]^{+\bullet}$: 341.1148, found 341.1158.



218

(*Z*)-4-(benzyloxy)but-2-en-1-yl 1-fluoro-4-methyl-2-oxocyclohex-3-ene-1-carboxylate (218)

Prepared from **214a** following General Procedure 4C. Purification by flash column chromatography (10–60% EtOAc/hexanes) afforded the title compound **218** as a colorless oil (0.39 g, 1.2 mmol, 75% yield).

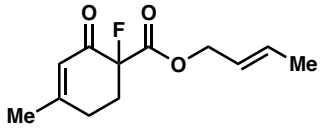
^{1}H NMR (400 MHz, $CDCl_3$): δ 7.38 – 7.27 (m, 5H), 6.00 (s, 1H), 5.89 – 5.82 (m, 1H), 5.73 – 5.66 (m, 1H), 4.79 (d, J = 6.7 Hz, 2H), 4.51 (s, 2H), 4.13 (d, J = 6.2 Hz, 2H), 2.63 – 2.33 (m, 4H), 2.03 (s, 3H).

^{13}C NMR (100 MHz, $CDCl_3$): δ 188.5 (d, $J_{C–F}$ = 18.6 Hz), 167.4 (d, $J_{C–F}$ = 25.8 Hz), 164.6, 138.1, 132.1, 128.6, 128.0, 127.9, 125.6, 124.7, 92.2 (d, $J_{C–F}$ = 194.0 Hz), 72.7, 65.8, 62.0, 31.1 (d, $J_{C–F}$ = 22.5 Hz), 28.0 (d, $J_{C–F}$ = 6.5 Hz), 24.7.

^{19}F NMR (282 MHz, $CDCl_3$): δ –165.21 (dd, J = 26.4, 12.0 Hz).

IR (Neat Film, NaCl): 2914, 1764, 1681, 1627, 1264, 1088 cm^{-1}

HRMS (MM: ESI+): *m/z* calc'd for $C_{19}H_{22}O_4F$ $[M+H]^{+\bullet}$: 333.1502, found 333.1491.



219

(*E*)-but-2-en-1-yl 1-fluoro-4-methyl-2-oxocyclohex-3-ene-1-carboxylate (219)

Prepared from **213a** following General Procedure 4C. Purification by flash column chromatography (10–60% EtOAc/hexanes) afforded the title compound **219** as a colorless oil (326 mg, 1.44 mmol, 60% yield).

^{1}H NMR (400 MHz, $CDCl_3$): δ 6.00 (s, 1H), 5.87 – 5.77 (m, 1H), 5.58 (dtq, J = 15.0, 6.7, 1.7 Hz, 1H), 4.64 (ddt, J = 6.7, 2.5, 1.2 Hz, 2H), 2.65 – 2.49 (m, 3H), 2.43 – 2.33 (m, 1H), 2.03 (s, 3H), 1.72 (d, J = 6.5 Hz, 3H).

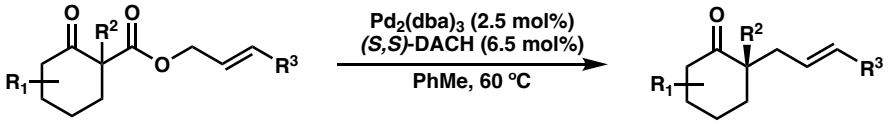
^{13}C NMR (100 MHz, $CDCl_3$): δ 188.7 (d, $J_{C–F}$ = 18.6 Hz), 167.4 (d, $J_{C–F}$ = 25.7 Hz), 164.5, 132.8, 124.7, 124.1, 92.3 (d, $J_{C–F}$ = 194.1 Hz), 67.0, 31.2 (d, $J_{C–F}$ = 22.5 Hz), 28.2 (d, $J_{C–F}$ = 6.8 Hz), 24.6, 18.0.

^{19}F NMR (282 MHz, $CDCl_3$): δ –165.04 (d, J = 22.2 Hz).

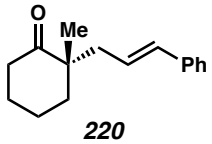
IR (Neat Film, NaCl): 3029, 2940, 1760, 1681, 1631, 1436, 1271, 1263, 1019 cm^{-1}.

HRMS (MM: ESI+): *m/z* calc'd for $C_{12}H_{15}O_3FNa$ $[M+Na]^{+\bullet}$: 249.0897, found 249.0901.

General Procedure 4D: Synthesis of Authentic Linear Samples



In a nitrogen filled glovebox, an oven-dried 1 dram vial was charged with a stir bar, $Pd_2(dba)_3$ or $Pd_2(pmdba)_3$ (2.5 μmol, 2.5 mol%), *(S,S)*-DACH (6.5 μmol, 6.5 mol%), and toluene (1.0 mL). The catalyst solution was stirred at 23 ºC for 20 min, then added to a solution of substrate in toluene (3 mL) in a 2-dram vial. The reaction vial was then sealed with electrical tape, removed from the glovebox, and heated to 60 °C for 14 h. The reaction mixture was let cool to ambient temperature, passed through a plug of silica gel, and concentrated under reduced pressure. The crude reaction mixture was purified via silica gel flash column chromatography to afford the desired linear product.



220

(*S*)-3-ethoxy-6-methyl-6-((*S*)-1-phenylallyl)cyclohex-2-en-1-one (220)

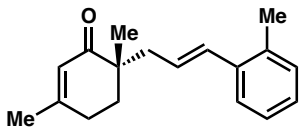
Prepared from **163** (13.6 mg, 0.05 mmol) following General Procedure 4D. Purification by preparative TLC (20% EtOAc/hexanes) afforded the title compound **220** as a colorless oil (11.2 mg, 4.9 μmol, 98% yield, 26% ee). Spectral data agrees with literature values.[22]

A racemic sample was prepared with dppf as a ligand

^{1}H NMR (600 MHz, $CDCl_3$): δ 7.33 (d, *J* = 7.1 Hz, 2H), 7.29 (t, *J* = 7.6 Hz, 2H), 7.23 – 7.17 (m, 1H), 6.40 (d, *J* = 15.6 Hz, 1H), 6.13 (dt, *J* = 15.6, 7.5 Hz, 1H), 2.52 – 2.38 (m, 4H), 1.96 – 1.68 (m, 5H), 1.67 – 1.59 (m, 1H), 1.14 (s, 3H).

^{13}C NMR (100 MHz, $CDCl_3$): δ 215.6, 137.5, 133.2 128.6, 127.3, 126.3, 125.9, 49.1, 41.4, 39.0, 38.7, 27.5, 23.1, 21.3.

SFC conditions: 10% IPA, 2.5 mL/min, Chiralpak OJ-H column, λ = 254 nm, t_R (min): minor = 3.65, major = 3.84.



222

(*S*,*E*)-3,6-dimethyl-6-(3-(*o*-tolyl)allyl)cyclohex-2-en-1-one (222)

Prepared from **205** (28.4 mg, 0.1 mmol) following General Procedure 4D. Purification by preparative TLC (10% EtOAc/hexanes) afforded the title compound **222** as a colorless oil (5.4 mg, 21 μmol, 21% yield)

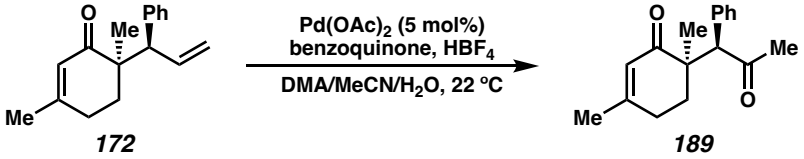
^{1}H NMR (400 MHz, $CDCl_3$): δ 7.42 – 7.35 (m, 1H), 7.17 – 7.07 (m, 3H), 6.60 (dt, *J* = 15.5, 1.4 Hz, 1H), 6.00 (dt, *J* = 15.4, 7.6 Hz, 1H), 5.85 – 5.73 (m, 1H), 2.53 (ddd, *J* = 13.7, 7.3, 1.4 Hz, 1H), 2.37 – 2.27 (m, 6H), 2.03 – 1.96 (m, 1H), 1.94 (s, 3H), 1.77 (dt, *J* = 13.7, 5.9 Hz, 1H), 1.12 (s, 3H).

^{13}C NMR (101 MHz, $CDCl_3$): δ 203.7, 160.7, 136.9, 135.1, 131.2, 130.3, 127.6, 127.2, 126.2, 125.8, 125.6, 43.8, 40.8, 33.2, 28.4, 24.2, 22.2, 20.0.

IR (Neat Film, NaCl): 3019, 2961, 2924, 2907, 2838, 1657, 1635, 1440, 1377, 1212, 968 cm^{-1}.

HRMS (MM:FD+): *m/z* calc'd for $C_{18}H_{22}O$ $[M]^{+\bullet}$:254.16707, found 254.16680.

Further Functionalization of Allylic Alkylation Products



(*R*)-3,6-dimethyl-6-((*R*)-2-oxo-1-phenylpropyl)cyclohex-2-en-1-one (189)

Prepared via literature procedure[23]: To a 1-dram vial was added $Pd(OAc)_2$ (2.8 mg, 1.25 μmol, 5.0 mol%), and benzoquinone (27.0 mg, 25 μmol, 1.0 equiv). **172** (60.1 mg, 25 μmol, 1.0 equiv) was then added in a solution of DMA/MeCN/H_2O (1.25 mL, 3.5:3.5:1 mixture). The resulting yellow solution was stirred for 18 h at 22 ºC. The reaction mixture was then poured into a separatory funnel containing Et_2O (5 mL) and water (5 mL). The aqueous phase was discarded, and the organic layer was washed 3 times with water (5 mL). The organic layer was then dried over $MgSO_4$, filtered and concentrated *in vacuo*. The resulting crude mixture was then purified via silica gel flash column chromatography (10–15% EtOAc/hexanes) to afford the title compound as a light-yellow oil (30 mg, 12 μmol, 48% yield).

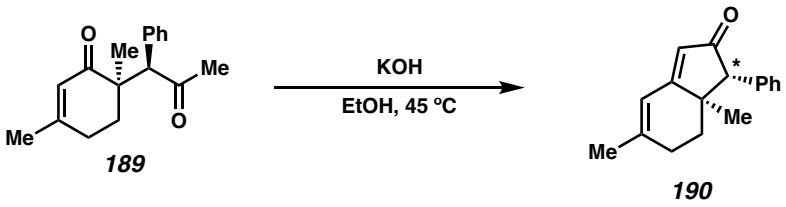
^{1}H NMR (600 MHz, $CDCl_3$): δ 7.33 – 7.20 (m, 5H), 5.69 (d, *J* = 1.9 Hz, 1H), 4.38 (s, 1H), 2.40 – 2.27 (m, 1H), 2.14 (s, 3H), 2.09 (ddd, *J* = 19.1, 5.3, 2.5 Hz, 1H), 2.01 (ddd, *J* = 13.2, 5.0, 2.5 Hz, 1H), 1.84 (s, 3H), 1.78 (ddd, *J* = 13.4, 11.7, 5.2 Hz, 1H), 1.30 (s, 3H).

^{13}C NMR (151 MHz, $CDCl_3$): δ 208.3, 202.1, 160.9, 134.8, 131.1, 128.3, 127.5, 125.0, 61.3, 48.4, 32.2, 31.1, 28.1, 24.0, 19.1.

IR (Neat Film, NaCl): 2916, 1711, 1660, 1353, 1213, 704 cm^{-1}.

HRMS (FD+): *m/z* calc'd for $C_{17}H_{20}O_2$ $[M]^{+\bullet}$: 256.1463 found 156.1467.

Optical Rotation: $[\alpha]_D^{23}$ +98.6º (c 2.42, $CHCl_3$).



(1*R*,7a*R*)-5,7a-dimethyl-1-phenyl-1,6,7,7a-tetrahydro-2*H*-inden-2-one (190)

A 1-dram vial was charged with a solution of KOH in EtOH (3M, 1 mL) and heated to 45 ºC. **189** (25.6 mg, 0.1 mmol, 1.0 equiv) was then slowly added in a solution of EtOH (0.5 mL). The resulting solution was allowed to stir at 45 ºC for 1 h. It is important to closely monitor the reaction as prolong reaction times can lead to erosion of the α-stereocenter. The reaction was then cooled to 0 ºC and quenched with HCl (1M, 3 mL) and brine (3 mL). The mixture was then extracted 3 times with diethyl ether, and the combined organic layers were dried over $MgSO_4$, filtered and concentrated *in vacuo*. The residue was then purified via silica gel flash column chromatography (20% EtOAc/hexanes) to afford the title compound as a light-yellow oil (10 mg, 42.0 μmol, 42% yield).

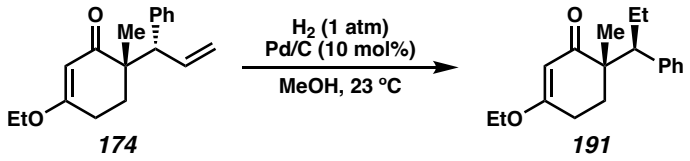
^{1}H NMR (600 MHz, $CDCl_3$): δ 7.33 (t, *J* = 7.5 Hz, 2H), 7.30 – 7.23 (m, 1H), 7.20 – 7.12 (m, 2H), 6.41 (s, 1H), 5.83 (s, 1H), 3.51 (s, 1H), 2.39 – 2.22 (m, 2H), 2.05 – 1.98 (m, 1H), 1.94 (s, 3H), 1.83 (td, *J* = 12.1, 6.2 Hz, 1H), 0.73 (s, 3H)

^{13}C NMR (100 MHz, $CDCl_3$): δ 207.0, 176.2, 149.9, 136.2, 130.3, 128.4, 127.0, 121.8, 119.6, 66.2, 44.8, 33.7, 29.5, 24.6, 23.1.

IR (Neat Film, NaCl): 3059, 2913, 1688, 1625, 1584, 1153 cm^{-1}.

HRMS (FI+): *m/z* calc'd for $C_{17}H_{18}O_3$ $[M]^{+\bullet}$: 238.13577 found 238.13732.

Optical Rotation: $[\alpha]_D^{23}$ –264.2° (c = 0.36, $CHCl_3$).



174 *191*

(*S*)-3-ethoxy-6-methyl-6-((*S*)-1-phenylpropyl)cyclohex-2-en-1-one (191)

To a solution of **174** (15.4 mg, 55 μmol, 1.0 equiv) in MeOH was added 10% Pd/C (5 mg, 5.5 μmol, 10 mol%). The mixture was sparged with N_2 for ~10 min followed by H_2 for ~10 min. The reaction was then stirred under an atmosphere of H_2 for 1 h. The reaction mixture was then filtered through a short pad of celite (~2 cm) and the celite washed with CH_2Cl_2 and the filtrate concentrated *in vacuo*. The residue was then purified via silica gel flash column chromatography (20% EtOAc/hexanes) to afford the title compound as a colorless oil (14.8 mg, 54.3 μmol, 99% yield).

^{1}H NMR (400 MHz, $CDCl_3$): δ 7.35 – 7.28 (m, 3H), 7.28 – 7.19 (m, 2H), 5.26 (d, *J* = 1.3 Hz, 1H), 3.91 (qd, *J* = 7.0, 1.3 Hz, 2H), 2.90 (dd, *J* = 10.9, 4.4 Hz, 1H), 2.64 (dddd, *J* =

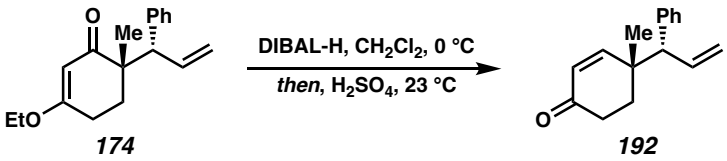
18.3, 8.2, 6.9, 1.2 Hz, 1H), 2.28 (dt, *J* = 18.3, 5.2 Hz, 1H), 1.82 – 1.67 (m, 2H), 1.67 – 1.59 (m, 2H), 1.38 (t, *J* = 7.0 Hz, 3H), 1.12 (s, 3H), 0.66 (t, *J* = 7.3 Hz, 3H).

^{13}C NMR (101 MHz, $CDCl_3$): δ 204.1, 175.4, 140.8, 130.0, 128.0, 126.5, 101.4, 64.2, 50.4, 47.3, 31.3, 26.1, 22.4, 19.5, 14.3, 13.0.

IR (Neat Film, NaCl): 2965, 2934, 2873, 1650, 1612, 1376, 1191 cm^{-1}.

HRMS (FD+): *m/z* calc'd for $C_{18}H_{25}O_2$ $[M+H]^{+\bullet}$: 273.1849 found 273.1854.

Optical Rotation: $[\alpha]_D^{21}$ +56.1° (c 1.0, $CHCl_3$).



174 ***192***

(*R*)-4-methyl-4-((*R*)-1-phenylallyl)cyclohex-2-en-1-one (192)

A solution of **174** (18.9 mg, 70 μmol, 1.0 equiv) in CH_2Cl_2 (0.7 mL) was cooled to 0 ºC in a 1-dram vial under N_2. Neat DIBAL-H (14 μL, 77 μmol, 1.1 equiv) was then added and the reaction allowed to stir at 0 ºC for 30 min. H_2SO_4 (5M, 1.4 mL) was then carefully added at 0 ºC and the reaction allowed to slowly warm to 22 ºC and stirred for 3 h. The organic layer was separated, and the aqueous phase was extracted three times with CH_2Cl_2 (2 mL). The combined organic layers were then dried over Na_2SO_4, filtered and concentrated *in vacuo*. The residue was then purified via silica gel flash column chromatography (5–20% EtOAc/hexanes) to afford the title compound as a colorless oil (9.0 mg, 40 μmol, 57% yield)

^{1}H NMR (600 MHz, $CDCl_3$): δ 7.39 – 7.28 (m, 2H), 7.25 (d, *J* = 7.2 Hz, 1H), 7.23 – 7.14 (m, 2H), 6.90 (dd, *J* = 10.3, 1.3 Hz, 1H), 6.25 (dt, *J* = 16.8, 10.0 Hz, 1H), 5.91 (d, *J* = 10.3 Hz, 1H), 5.21 (dd, *J* = 10.0, 1.7 Hz, 1H), 5.18 – 5.03 (m, 1H), 3.34 (d, *J* = 9.9 Hz, 1H), 2.53 – 2.41 (m, 2H), 2.06 (ddd, *J* = 13.6, 9.6, 5.9 Hz, 1H), 1.73 – 1.55 (m, 1H), 1.14 (s, 3H)

^{13}C NMR (101 MHz, $CDCl_3$): δ 199.5, 157.5, 140.7, 137.0, 129.2, 128.4, 127.9, 127.0, 118.4, 59.1, 39.0, 34.2, 32.8, 22.5.

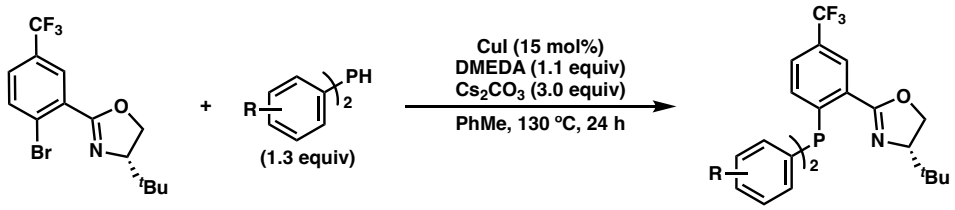
IR (Neat Film, NaCl): 3063, 3028, 2963, 1681, 1453 cm^{-1}.

HRMS (MM: FI+): *m/z* calc'd for $C_{16}H_{18}O$ $[M]^{+\bullet}$: 226.13577 found 226.13747.

Optical Rotation: $[\alpha]_D^{21}$ = +22.2° (c 0.9, $CHCl_3$).

Preparation of Novel PHOX Ligands

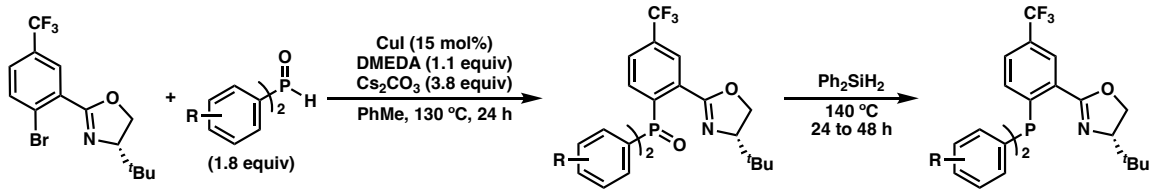
General Procedure 4E: Preparation of Novel (S)-t-BuPHOX Ligands



A flame-dried 3-neck round-bottom flask attached to a reflux condenser under nitrogen atmosphere was charged with CuI (0.15 equiv). Anhydrous toluene (0.03 M) was added followed by DMEDA (1.1 equiv), and the reaction mixture was stirred at ambient temperature for 20 minutes. To the pre-stirred catalyst solution was added the requisite aryl bromide (1.0 equiv), Cs_2CO_3 (3.0 equiv), and the aryl phosphine (1.3 equiv). Minimal additional toluene was added to rinse any solids off the sides of the flask. The reaction mixture was heated to reflux (*ca.* 130 °C) and stirred for a minimum of 21 h. Upon completion, the reaction mixture was cooled to ambient temperature, filtered through a pad

of celite, and washed with CH_2Cl_2. The filtrate was concentrated and purified by flash silica gel column chromatography.

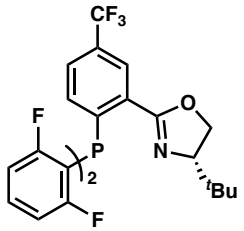
General Procedure 4F: Preparation of Novel (S)-t-BuPHOX Ligands.



A flame-dried 3-neck round-bottom flask attached to a reflux condenser was added CuI (27 mg, 0.14 mmol, 0.15 equiv) and degassed and backfilled with N_2 three times. Anhydrous toluene (0.05 M) was added followed by DMEDA (0.11 mL, 1.1 mmol, 1.1 equiv) at ambient temperature and stirred for 20 minutes. To the pre-stirred catalyst solution was added aryl bromide (333 mg, 0.95 mmol, 1.0 equiv), Cs_2CO_3 (1.2 g, 3.6 mmol, 3.8 equiv), and the aryl phosphine oxide (408 mg, 1.7 mmol, 1.8 equiv). Minimal additional toluene was added to rinse any solids off the sides of the flask. The reaction mixture was heated to reflux (*ca.* 130 °C) and stirred for a minimum of 21 h. Upon completion, the reaction flask was cooled to ambient temperature and filtered through a 2" pad of celite and washed with CH_2Cl_2. The filtrate was concentrated and purified by flash silica gel column chromatography.

The isolated Ullmann coupled phosphine oxide was placed in an oven-dried 1- or 2-dram glass vial along with a magnetic stir bar and degassed using an Argon balloon for 10 min. Ph_2SiH_2 (1.2 mL, 6.5 mmol, 7.0 equiv) was added to the reaction vial, which fully dissolved the phosphine oxide residue. The reaction vial was then placed in a pre-heated

oil bath at 140 °C and stirred until complete reduction of phosphine oxide (typically takes 24 h, sometimes 4 d). (Note: Reactions were monitored by ^{31}P NMR (in $CDCl_3$) using an aliquot of reaction mixture every 24 h.) Once complete, the reaction was cooled to ambient temperature and dry-loaded onto silica gel then purified by flash silica gel column chromatography.



L4

(*S*)-2-(2-(bis(2,6-difluorophenyl)phosphaneyl)-5-(trifluoromethyl)phenyl)-4-(*tert*-butyl)-4,5-dihydrooxazole (L4)

Prepared from bis(2,6-difluorophenyl)phosphane (190 mg, 0.74 mmol, 1.2 equiv) following General Procedure 4E. Purification by flash column chromatography (0–50% CH_2Cl_2/hexanes) afforded the title compound **L4** as a white solid (67 mg, 0.13 mmol, 20% yield).

**Note: Ullmann coupling using the aryl phosphine oxide in General Procedure 4E does not yield any product.*

^{1}H NMR (300 MHz, $CDCl_3$): δ 8.23 (dd, *J* = 4.4, 2.0 Hz, 1H), 7.61 – 7.50 (m, 1H), 7.42 – 7.26 (m, 3H), 6.83 (qd, *J* = 7.8, 2.3 Hz, 4H), 4.30 (dd, *J* = 10.1, 8.5 Hz, 1H), 4.13 (t, *J* = 8.7 Hz, 1H), 3.94 (dd, *J* = 10.1, 8.9 Hz, 1H), 0.69 (s, 9H).

^{13}C NMR (101 MHz, $CDCl_3$): δ 165.8 (td, *J* = 9.0, 3.7 Hz), 163.3 (td, *J* = 9.0, 4.1 Hz), 161.2 (d, *J* = 4.9 Hz), 140.9 (d, *J* = 28.6 Hz), 133.1, 132.1, 131.6 (dt, *J* = 28.6, 10.9 Hz),

130.5 (qd, J = 33.2, 1.6 Hz), 128.0, 126.4 (q, J = 3.7 Hz), 126.2 – 126.0 (m), 125.3, 122.6, 119.8, 114.7 – 113.3 (m), 111.9 – 111.2 (m), 68.9, 33.5, 25.8.

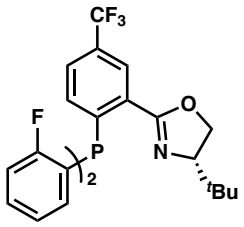
^{31}P NMR (121 MHz, $CDCl_3$): δ –55.81 – –56.51 (m).

^{19}F NMR (282 MHz, $CDCl_3$): δ –62.83 – –62.88 (m, 3F), –100.06 – –100.19 (m, 1F), –100.24 – –100.34 (m, 1F), –100.43 – –100.54 (m, 1F), –100.58 – –100.70 (m, 1F).

IR (Neat Film, NaCl): 3080, 2958, 2907, 2870, 1657, 1607, 1574, 1454, 1326, 1228, 1176, 1131, 1083, 986, 784 cm^{-1}.

HRMS (MM: FD+): *m/z* calc'd for $C_{26}H_{21}NOF_7P$ $[M]^{+\bullet}$: 527.12490, found 527.12391.

Optical Rotation: $[\alpha]_D^{21}$ +18.1° (c 0.10, $CHCl_3$)



L5

(*S*)-2-(2-(bis(2-fluorophenyl)phosphaneyl)-5-(trifluoromethyl)phenyl)-4-(*tert*-butyl)-4,5-dihydrooxazole (L5)

Prepared from bis(2-fluorophenyl)phosphine oxide (408 mg, 1.7 mmol, 1.8 equiv) following General Procedure 4F. Purification by flash column chromatography (0–50% EtOAc/hexanes) afforded the title compound **L5** as a white solid (408 mg, 0.81 mmol, 85% yield).

^{1}H NMR (500 MHz, $CDCl_3$): δ 8.28 (t, J = 2.8 Hz, 1H), 7.59 (dd, J = 8.2, 2.0 Hz, 1H), 7.41 – 7.32 (m, 2H), 7.20 (dd, J = 8.2, 3.0 Hz, 1H), 7.11 – 7.02 (m, 4H), 6.88 – 7.84 (m,

1H), 6.82 – 6.77 (m, 1H), 4.26 (dd, J = 10.1, 8.6 Hz, 1H), 4.12 (t, J = 8.6 Hz, 1H), 4.00 (dd, J = 10.1, 8.6 Hz, 1H), 0.74 (s, 9H).

^{13}C NMR (101 MHz, $CDCl_3$): δ 165.7 (dd, J = 17.9, 16.1 Hz), 163.5 – 163.0 (m), 161.3, 141.6 (d, J = 29.5 Hz), 135.0 – 134.8 (m), 134.7 – 134.4 (m), 132.3 (d, J = 21.8 Hz), 131.4 (dd, J = 25.3, 8.3 Hz), 131.0 (d, J = 33.2 Hz), 127.0 (q, J = 3.7 Hz), 126.7 (t, J = 3.5 Hz), 125.2, 124.8 (dd, J = 9.7, 3.3 Hz), 124.4 – 123.7 (m), 122.5, 68.9, 33.7, 25.8.

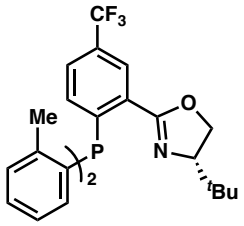
^{31}P NMR (121 MHz, $CDCl_3$): δ –32.10 (t, J = 63.2 Hz).

^{19}F NMR (282 MHz, $CDCl_3$): δ –62.90 (s, 3F), –103.64 – –103.88 (m, 1F), –103.88 – –104.11 (m, 1F).

IR (Neat Film, NaCl): 3069, 2956, 2357, 1654, 1469, 1324, 1170, 1132, 1081, 756 cm^{-1}.

HRMS (MM: FD+): *m/z* calc'd for $C_{26}H_{23}NOF_5P$ $[M]^{+\bullet}$: 491.14374, found 491.14451.

Optical Rotation: $[\alpha]_D^{22}$ –20.5° (c 0.73, $CHCl_3$)



L6

(*S*)-4-(*tert*-butyl)-2-(2-(di-*o*-tolylphosphaneyl)-5-(trifluoromethyl)phenyl)-4,5-dihydrooxazole (L6)

Prepared from di-*o*-tolylphosphane (240 mg, 1.1 mmol, 1.3 equiv) following General Procedure 4E. Purification by flash column chromatography (0–30% EtOAc/hexanes) afforded the title compound **L6** as a tan solid (130 mg, 0.27 mmol, 31% yield).

^{1}H NMR (400 MHz, $CDCl_3$): δ 8.21 (t, *J* = 2.7 Hz, 1H), 7.51 (dd, *J* = 8.1, 2.0 Hz, 1H), 7.26 – 7.16 (m, 4H), 7.11 – 6.97 (m, 3H), 6.73 – 6.64 (m, 2H), 4.13 (dd, *J* = 10.1, 8.5 Hz, 1H), 4.04 (t, *J* = 8.3 Hz, 1H), 3.94 (dd, *J* = 10.1, 8.3 Hz, 1H), 2.38 (dd, *J* = 4.1, 1.7 Hz, 6H), 0.70 (s, 9H).

^{13}C NMR (101 MHz, $CDCl_3$): δ 161.61, 143.48 – 143.01 (m), 142.75 (d, *J* = 27.4 Hz), 142.31 (d, *J* = 28.0 Hz), 135.93 – 135.60 (m), 134.81, 133.49, 133.26, 133.05, 130.85, 130.53, 130.25 (d, *J* = 4.9 Hz), 128.90 (d, *J* = 15.1 Hz), 126.81 (dq, *J* = 11.3, 3.7 Hz), 126.38 (d, *J* = 16.2 Hz), 125.30, 122.59, 68.63, 33.76, 25.79, 21.48, 21.25.

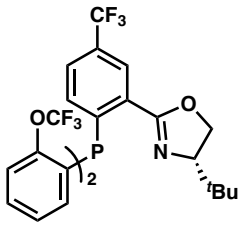
^{31}P NMR (121 MHz, $CDCl_3$): δ –20.8 (s).

^{19}F NMR (282 MHz, $CDCl_3$): δ –62.8 (s).

IR (Neat Film, NaCl): 3056, 2957, 2867, 2356, 1653, 1471, 1454, 1341, 1324, 1169, 1130, 1079, 970 cm^{-1}.

HRMS (MM: FD+): *m/z* calc'd for $C_{28}H_{29}NOF_3P$ $[M]^{+\bullet}$: 483.19389, found 483.19472.

Optical Rotation: $[\alpha]_D^{22}$ –55.4 ° (c 0.28, $CHCl_3$).



L7

(*S*)-2-(2-(bis(2-(trifluoromethoxy)phenyl)phosphaneyl)-5-(trifluoromethyl)phenyl)-4-(*tert*-butyl)-4,5-dihydrooxazole (L7)

Prepared from bis(2-(trifluoromethoxy)phenyl)phosphine oxide (700 mg, 1.9 mmol, 1.8 equiv) following General Procedure 4F. Purification by flash column chromatography (0–

50% EtOAc/hexanes) afforded the title compound **L7** as a tan solid (632 mg, 0.99 mmol, 94% yield).

^{1}H NMR (300 MHz, $CDCl_3$): δ 8.25 – 8.23 (m, 1H), 7.62 – 7.50 (m, 1H), 7.45 – 7.37 (m, 2H), 7.31 – 7.27 (m, 2H), 7.20 – 7.14 (m, 2H), 7.03 (dd, *J* = 8.2, 2.7 Hz, 1H), 6.90 – 6.74 (m, 2H), 4.21 (dd, *J* = 10.2, 8.5 Hz, 1H), 4.12 (t, *J* = 8.2 Hz, 1H), 3.98 (dd, *J* = 10.2, 7.8 Hz, 1H), 0.71 (s, 9H).

^{13}C NMR (101 MHz, $CDCl_3$): δ 161.2, 152.0, 151.9, 151.8, 151.6, 141.6, 141.3, 135.4, 135.4, 135.0, 134.5, 133.2, 133.0, 131.5, 131.2, 130.9, 130.8, 130.7, 130.5, 130.4, 130.2, 129.9, 129.7, 128.0, 127.9, 127.9, 126.9, 126.9, 126.8, 126.7, 126.7, 126.7, 125.2, 124.3, 124.3, 122.4, 121.8, 121.7, 119.6, 119.2, 119.2, 116.6, 69.0, 33.8, 25.7.

**Note: J-couplings were not determined due to complicated C-P and C-F splitting patterns.*

^{31}P NMR (121 MHz, $CDCl_3$): δ –27.4 (m).

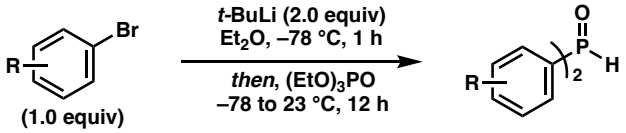
^{19}F NMR (282 MHz, $CDCl_3$): δ –56.5 (s, 6F), –62.9 (s, 3F).

IR (Neat Film, NaCl): 3062, 2964, 2870, 2363, 2342, 1653, 1472, 1326, 1251, 1216, 1200, 1168, 1160, 1128, 1081 cm^{-1}.

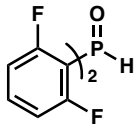
HRMS (MM: FD+): *m/z* calc'd for $C_{28}H_{23}NO_3F_9P$ $[M]^{+\bullet}$: 623.12718, found 623.12455.

Optical Rotation: $[\alpha]_D^{21}$ –20.3 ° (c 1.48, $CHCl_3$).

General Procedure 4G: Preparation of Phosphine or Phosphine Oxide Coupling Partners for Ullmann Coupling



To a flame-dried round-bottom flask was added aryl bromide (3.0 equiv) dissolved with anhydrous Et_2O (0.39 M) under a N_2 atmosphere. The solution was cooled to –78 °C and *t*-BuLi (1.7 M in pentane, 6.0 equiv) was added dropwise. Following addition, the reaction was stirred for 1 h at –78 °C. Diethyl phosphite (1.0 equiv) was added dropwise at –78 °C then allowed to warm to ambient temperature and stirred for an additional 12 h. Upon completion, the reaction was cooled to 0 °C and 1 M HCl solution was added slowly and allowed to warm to room temperature. The desired product was extracted with EtOAc three times, and the combined organic layers were washed with brine (1x), dried over Mg_2SO_4, and concentrated to dryness. The residue was purified by flash silica gel column chromatography.



223

bis(2,6-difluorophenyl)phosphine oxide (223)

Prepared from 2-bromo-1,3-difluorobenzene (3.1 mL, 27 mmol, 3.0 equiv) following General Procedure 4G. Purification by flash column chromatography (20%–50% EtOAc/hexanes) afforded the title compound **223** as a white solid (1.02 g, 3.7 mmol, 41% yield).

^{1}H NMR (300 MHz, $CDCl_3$): δ 8.70 (d, *J* = 551.5 Hz, 1H), 7.66 – 7.44 (m, 2H), 7.06 – 6.84 (m, 4H).

^{13}C NMR (101 MHz, $CDCl_3$): δ 165.2, 165.1, 165.1, 165.1, 165.1, 165.0, 162.6, 162.6, 162.5, 136.2, 136.1, 136.0, 136.0, 135.9, 135.9, 135.5, 112.6, 112.6, 112.6, 112.6, 112.5, 112.5, 112.5, 112.4, 112.4, 112.4, 112.3, 112.3.

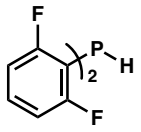
**Note: J-couplings were not determined due to complicated C-P and C-F splitting patterns.*

^{31}P NMR (121 MHz, $CDCl_3$): δ –15.72 (p, *J* = 13.9 Hz, 1P).

^{19}F NMR (282 MHz, $CDCl_3$): δ –104.46 – –104.72 (m, 4F).

IR (Neat Film, NaCl): 3082, 3037, 2397, 1614, 1582, 1460, 1271, 1231, 1209, 1124, 794 cm^{-1}.

HRMS (MM: FD+): *m/z* calc'd for $C_{12}H_7OF_4P$ $[M]^{+\bullet}$: 274.01706, found 274.01712.



224

bis(2,6-difluorophenyl)phosphane (224)

To an oven-dried 4-mL glass vial was added bis(2,6-difluorophenyl)phosphine oxide **223** (1.02 g, 3.7 mmol, 1.0 equiv) and diphenylsilane (26 mmol, 7.0 equiv). The vial was capped and sealed with electrical tape, then heated to 140 °C for 4 days. Every 24 h, an aliquot of the reaction mixture was taken and diluted with $CDCl_3$ to check for reaction completion via ^{31}P NMR. Purification by flash column chromatography (1% EtOAc/hexanes) afforded the title compound **224** as a white solid (796 mg, 3.1 mmol, 83% yield).

^{1}H NMR (300 MHz, $CDCl_3$): δ 7.36 – 7.22 (m, 2H), 6.93 – 6.77 (m, 4H), 5.48 (dp, *J* = 237.5, 4.0 Hz, 1H).

^{13}C NMR (101 MHz, $CDCl_3$): δ 165.6, 165.6, 165.5, 165.5, 165.5, 165.5, 165.4, 163.2, 163.1, 163.1, 163.0, 163.0, 163.0, 134.5, 131.9, 131.8, 131.8, 131.7, 131.7, 131.7, 131.6, 131.6, 131.6, 131.5, 128.0, 127.8, 111.6, 111.5, 111.5, 111.5, 111.4, 111.3, 111.3, 111.3, 111.3, 111.2.

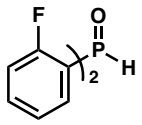
**Note: J-couplings were not determined due to complicated C-P and C-F splitting patterns.*

^{31}P NMR (162 MHz, $CDCl_3$): δ –138.98 (p, J = 8.7 Hz).

^{19}F NMR (282 MHz, $CDCl_3$): δ –100.50 – –100.68 (m, 4F).

IR (Neat Film, NaCl): 3070, 2360, 1607, 1577, 1559, 1456, 1259, 1229, 1121, 1103, 994, 782 cm^{-1}.

HRMS (MM: FD+): *m/z* calc'd for $C_{12}H_7F_4P$ $[M]^{+\bullet}$: 258.02215, found 258.02276.



225

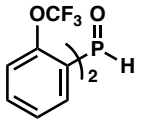
bis(2-fluorophenyl)phosphine oxide (225)

Prepared from 1-bromo-2-fluorobenzene (3.0 mL, 27 mmol, 3.0 equiv) following General Procedure 4G. Purification by flash column chromatography (20–50% EtOAc/hexanes) afforded the title compound **225** as a colorless oil that solidifies on high vacuum as a colorless solid (1.26 g, 5.3 mmol, 58% yield). Our spectral data matches previous literature report for bis(2-fluorophenyl)phosphine oxide (**225**).[24]

^{1}H NMR (300 MHz, $CDCl_3$): δ 8.38 (d, J = 517.9 Hz, 1H), δ 7.89 – 7.72 (m, 2H), 7.64 – 7.53 (m, 2H), 7.38 – 7.27 (m, 2H), 7.18 – 7.02 (m, 2H).

^{31}P NMR (121 MHz, $CDCl_3$): δ 1.22 (t, J = 12.2 Hz, 1P).

^{19}F NMR (282 MHz, $CDCl_3$): δ –107.11 – –107.48 (m, 2F).



226

bis(2-(trifluoromethoxy)phenyl)phosphine oxide (226)

Prepared from 1-bromo-2-(trifluoromethoxy)benzene (1.36 mL, 9.15 mmol, 3.0 equiv) following General Procedure 4G. Purification by flash column chromatography (20–50% EtOAc/hexanes) afforded the title compound **226** as a colorless oil (424 mg, 1.15 mmol, 38% yield).

^{1}H NMR (400 MHz, $CDCl_3$): δ 8.29 (d, J = 520.9 Hz, 1H), 7.93 (ddd, J = 14.9, 7.5, 1.7 Hz, 2H), 7.68 – 7.57 (m, 2H), 7.45 (td, J = 7.5, 1.8 Hz, 2H), 7.35 – 7.27 (m, 2H).

^{13}C NMR (101 MHz, $CDCl_3$): δ 150.3, 150.3, 134.8, 134.8, 134.0, 133.9, 126.9, 126.8, 123.7, 122.7, 121.4, 119.0, 118.9, 118.9, 118.8.

^{31}P NMR (162 MHz, $CDCl_3$): δ 6.1 (s).

^{19}F NMR (282 MHz, $CDCl_3$): δ –57.2.

IR (Neat Film, NaCl): 3071, 2376, 1596, 1478, 1444, 1253, 1208, 1089, 924, 766 cm^{-1}.

HRMS (MM: FD+): *m/z* calc'd for $C_{14}H_9O_3F_6P$ $[M]^{+\bullet}$: 370.01935, found 370.01935.

4.4.3 DETERMINATION OF ABSOLUTE AND RELATIVE STEREOCHEMISTRY BY VCD SPECTROSCOPY

Experimental Protocol

A solution of the compound of interest (45 mg/mL) in $CDCl_3$ was loaded into a front-loading SL-4 cell (International Crystal Laboratories) possessing BaF_2 windows and a 100 mm path length. Infrared (IR) and VCD spectra were acquired on a BioTools ChiralIR-2X VCD spectrometer as a set of 24 one-hour blocks (24 blocks, 3120 scans per block) in dual PEM mode. A 15-minute acquisition of neat (+)-α-pinene control yielded a VCD spectrum in agreement with literature spectra. IR and VCD spectra were background corrected using a 30-minute block IR acquisition of the empty instrument chamber under gentle N_2 purge, and were solvent corrected using a 16-hour (16 blocks, 3120 scans per block) IR/VCD acquisition of $CDCl_3$ in the same 100 μm BaF_2 cell. The reported spectra represent the result of block averaging.

Both enantiomers of compounds **186** were prepared from the *(S)* and *(R)* enantiomers of the **L3** ligand. Data were collected for both enantiomers of compounds at identical concentration and the final reported VCD spectra are the half-difference of the spectra of the compounds derived from the *(S)* minus *(R)* enantiomer of ligand.

Computational Protocol

An arbitrarily chosen enantiomer of the compound of interest was subjected to an exhaustive initial molecular mechanics-based conformational search (OPLS_2005 force field, $CHCl_3$ solvent, 10.0 kcal/mol cutoff, "Enhanced" torsional sampling) as implemented in MacroModel program.[25] The resulting ensemble of conformers was

subsequently optimized using the B3PW91 functional, cc-pVTZ(-f) basis, and implicit PBF solvation model for chloroform using the Jaguar program.[26] Harmonic frequencies computed at the B3PW91/cc-pVTZ(-f)/PBF(chloroform) level were scaled by 0.98. The resultant structurally unique conformers possessing all positive Hessian eigenvalues were Boltzmann weighted by relative free energy at 298.15 K. The predicted IR and VCD frequencies and intensities of the retained conformers were convolved using Lorentzian line shapes (γ = 4 cm^{-1}) and summed using the respective Boltzmann weights to yield the final predicted IR and VCD spectra. The predicted VCD of the opposite enantiomer was generated by inversion of sign.

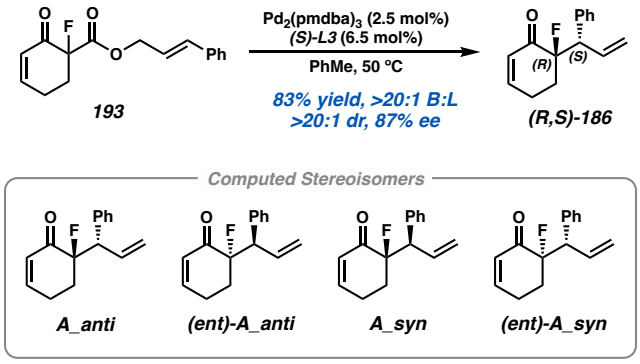


Figure 4.9. *Comparison of experimental VCD and IR spectra for product* ***186*** *to computed spectra for* ***A_anti****. Experimental IR spectrum in good agreement with computed spectrum. Experimental VCD spectrum for* ***186*** *is in excellent agreement with computed spectrum for* ***A_anti*** *with the (R,S) stereochemistry.*

Comparisons between computed spectrum of ***A_anti*** *and experimental spectra for* ***186****:*

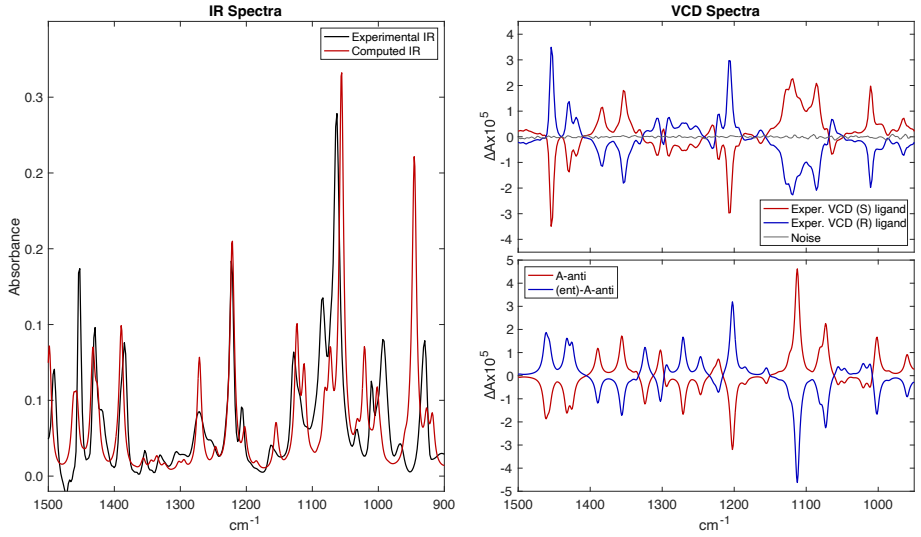


Figure 4.10. *Overlayed experimental and calculated VCD spectra for* ***(R,S)-186****.*

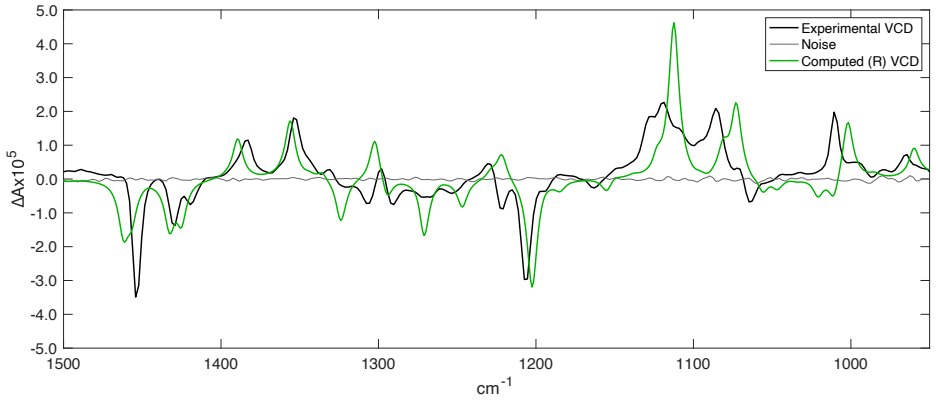
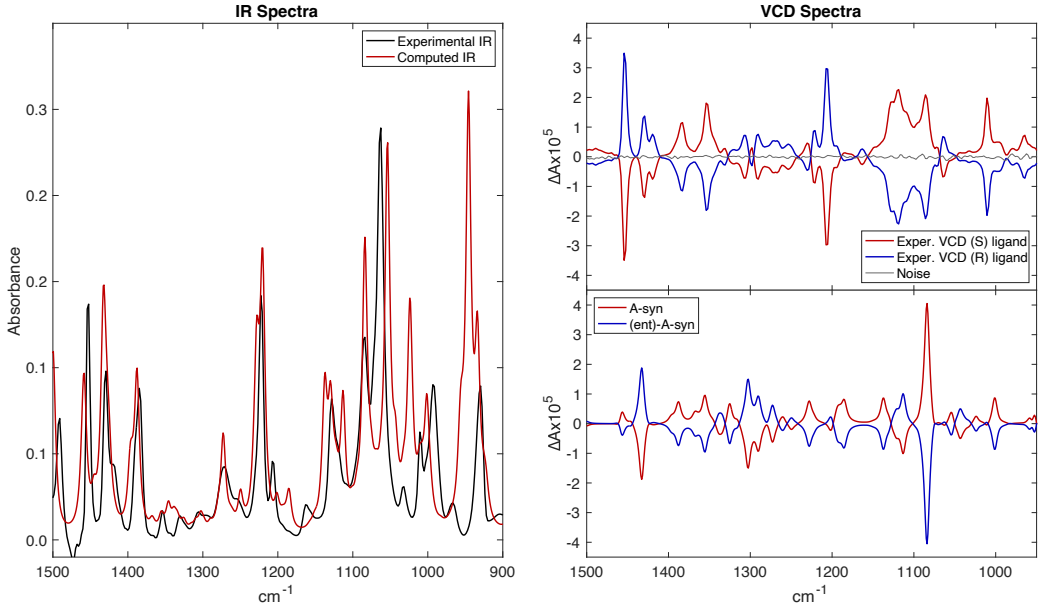


Figure 4.11. *Comparison of experimental VCD and IR spectra for product* ***186*** *to computed spectra for* ***A_syn****. Experimental spectra for* ***186*** *do not agree with computed spectrum for* ***A_syn****.*



4.4.4 COMPUTATIONAL DETAILS

General Notes

All quantum mechanics calculations were carried out with the ORCA program.[27] Geometry optimizations, harmonic frequency calculations, and single-point energy evaluations were carried out with density functional theory (DFT). The PBE0 functional[28] paired with Becke–Johnson damped D4 dispersion corrections[29], henceforth referred to as PBE0-D4, was used as it has proven a robust method for such systems in our prior studies.[30] For geometry optimization and harmonic frequency calculations, Pd is described by the def2-TZVP basis set[31] and the ECP28MWB small-core (18 explicit valence electrons) quasi-relativistic pseudopotential,[32] while carbon and hydrogen are assigned the def2-SV(P) basis. Diffuse functions are added to oxygen, nitrogen, and phosporus (ma-def2-SV(P)). Herein, we refer to this composite basis set as BS1. Geometry optimization and harmonic frequency calculations were carried out with the CPCM implicit solvation model for toluene (PhMe, $\varepsilon = 2.4$). For all calculations employing CPCM, surface charges are described by the improved Gaussian charge scheme of Neese and coworkers with a scaled Van der Waals cavity ($\varepsilon = 1.2$).[33] All Hessians were computed analytically. Stationary points are characterized by the correct number of imaginary vibrational modes (zero for minima and one for saddle points). Intrinsic reaction coordinate (IRC) analysis confirms the nature of transition states.[34] Cartesian coordinates of all optimized structures are included as ".xyz" files are available online in a compressed in a zip file format.

Electronic energies are further refined with single-point calculations employing the PBE0-D4 functional[35] and the def2-TZVPP basis set on all atoms (with the ECP28MWB

pseudopotential for Pd) with additional diffuse functions on O, P, and N (ma-def2-TZVPP). This mixed basis is henceforth referred to as BS2. Solvation was accounted for with CPCM as mentioned above (PhMe, ε = 2.4). Final Gibbs free energies were obtained by applying thermodynamic corrections obtained at the optimization level of theory to these refined electronic energies. Thermodynamic corrections from harmonic frequency calculations employ the quasi-ridged rotor harmonic oscillator approach to correct for the breakdown of the harmonic oscillator approximation at low vibrational frequencies.[36] Note that free energies remain in a 1 atm standard state as all processes modeled are unimolecular. The translational (S_{trans}) and rotational entropy (S_{rot}) contributions to the Gibbs free energy calculated for a complex in condensed phase are *ca.* 40–60% of the values obtained assuming an ideal gas.[37] As suggested in the literature, S_{trans} and S_{rot} obtained by ideal gas treatment are scaled by a factor of 0.5 to obtain the final condensed phase values.[38] Hence, the Gibbs free energy at 298.15 K is calculated as:

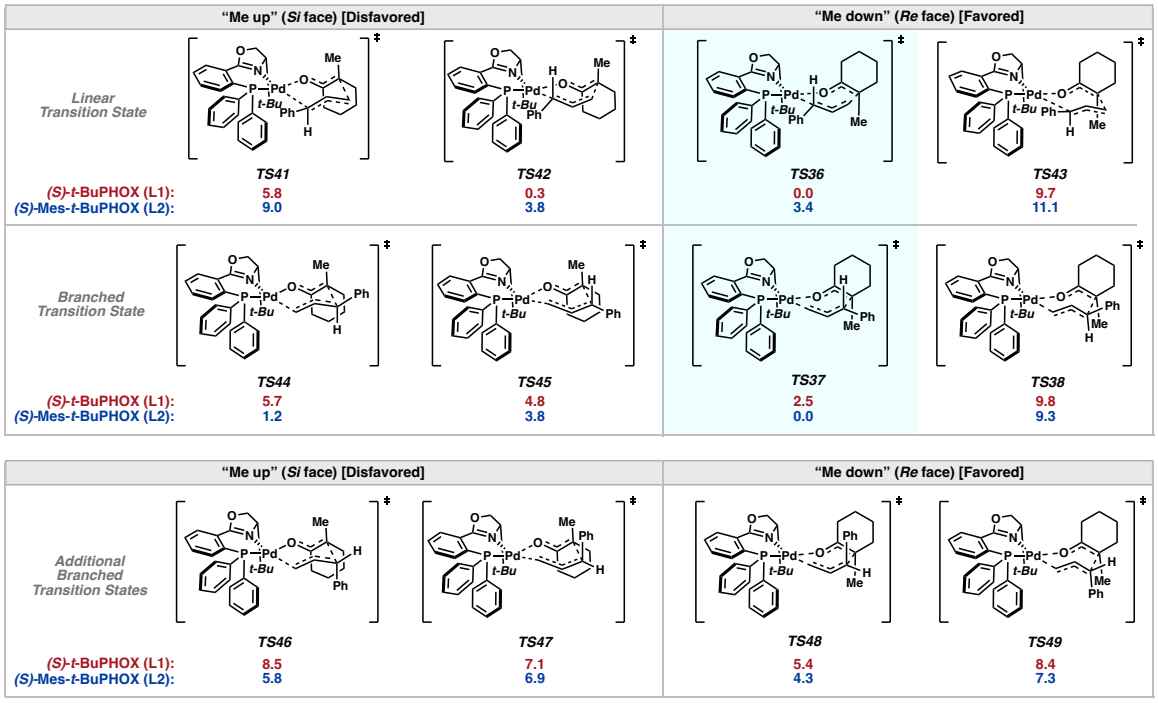
$$G^*_{solv} = E^{BS2}_{el,solv} + ZPE + E_{trans} + E_{rot} + E_{vib} + k_bT$$
$$- T\left(S_{el} + S_{vib} + \frac{1}{2}S_{trans} + \frac{1}{2}S_{rot}\right)$$

The resolution of identity (RI) and Chain-of-Spheres (COS) approximations are employed for efficient evaluation of Coulomb and exchange integrals, respectively.[39] The def2/J auxiliary basis[40] is employed for all atoms except O, N, and P, for which a suitable auxiliary was obtained via the automatic generation algorithm in the ORCA program (keyword: *AutoAux*). [41] Fine grid settings are employed in all calculations (optimization/frequency calculations: DefGrid2, single point calculations: DefGrid2).

Comparison of Barrier Heights to Inner-sphere Reductive Elimination

Various stereochemical permutations of the inner-sphere C–C bond forming transition states were explored with both the *(S)*-*t*-BuPHOX (**L1**) and *(S)*-Mes-*t*-BuPHOX (**L2**) ligands (Figure 4.12).

Figure 4.12. *Relative Gibbs free energies for various inner-sphere reductive elimination transition states with* ***L1*** *and* ***L2****. Gibbs free energies in kcal/mol computed at the PBE0-D4/BS2/CPCM(PhMe)//PBE0-D4/BS1/CPCM(PhMe) level of theory at 298.15 K.*



4.5 REFERENCES AND NOTES

(1) (a) Keith, J. A.; Behenna, D. C.; Mohr, J. T.; Ma, S.; Marinescu, S. C.; Oxgaard, J.; Stoltz, B. M.; Goddard, W. A. The Inner-Sphere Process in the Enantioselective Tsuji Allylation Reaction with *(S)-t*-Bu-Phosphinooxazoline Ligands. *J. Am. Chem. Soc.* **2007**, *129*, 11876–11877. (b) Keith, J. A.; Behenna, D. C.; Sherden, N.; Mohr, J. T.; Ma, S.; Marinescu, S. C.; Nielsen, R. J.; Oxgaard, J.; Stoltz, B. M.; Goddard, W. A. The Reaction Mechanism of the Enantioselective Tsuji Allylation: Inner-Sphere and Outer-Sphere Pathways, Internal Rearrangements, and Asymmetric C–C Bond Formation. *J. Am. Chem. Soc.* **2012**, *134*, 19050–19060. (c) Cusumano, A. Q.; Stoltz, B. M.; William A. Goddard, III. Reaction Mechanism, Origins of Enantioselectivity, and Reactivity Trends in Asymmetric Allylic Alkylation: A Comprehensive Quantum Mechanics Investigation of a C(sp3)–C(sp3) Cross-Coupling. *J. Am. Chem. Soc.* **2020**, *142*, 13917–13933. (d) McPherson, K. E.; Croatt, M. P.; Morehead, A. T.; Sargent, A. L. DFT Mechanistic Investigation of an Enantioselective Tsuji–Trost Allylation Reaction. *Organometallics* **2018**, *37*, 3791–3802.

(2) Wright, T. B.; Evans, P. A. Catalytic Enantioselective Alkylation of Prochiral Enolates. *Chem. Rev.* **2021**, *121*, 9196–9242.

(3) Trost, B. M.; Schroeder, G. M. Palladium-Catalyzed Asymmetric Allylic Alkylation of Ketone Enolates. *Chem. Eur. J.* **2005**, *11*, 174–184.

(4) For a review on Ir-catalyzed allylic alkylation see: Hethcox, J. C.; Shockley, S. E.; Stoltz, B. M. Iridium-Catalyzed Diastereo-, Enantio-, and Regioselective Allylic Alkylation with Prochiral Enolates. *ACS Catal.* **2016**, *6*, 6207–6213.

(5) (a) Yang, M.-H.; Orsi, D. L.; Altman, R. A. Ligand-Controlled Regiodivergent Palladium-Catalyzed Decarboxylative Allylation Reaction to Access α,α-Difluoroketones. *Angew. Chem. Int. Ed.* **2015**, *54*, 2361–2365. (b) Hilgraf, R.; Pfaltz, A. Chrial Bis(*N*-tosylamino)phosphine- and TADDOL-Phosphite-Oxazolines as Ligands in Asymmetric Catalysis. *Synlett* **1999**, *11*, 1814–1816. (c) Hayashi, T.; Kawatsura, M.; Uozumi, Y. Retention of Regiochemistry of Allylic Esters in Palladium-Catalyzed Allylic Alkylation in the Presence of a MOP Ligand. *J. Am. Chem. Soc.* **1998**, *120*, 1681–1687. (d) You, S.-L.; Zhu, X.-Z.; Luo, Y.-M.; Hou, X.-L.; Dai, L.-X. Highly Regio- and Enantioselective Pd-Catalyzed Allylic Alkylation and Amination of Monosubstituted Allylic Acetates with Novel Ferrocene P,N-Ligands. *J. Am. Chem. Soc.* **2001**, *123*, 7471–7472. (e) Hu, Z.; Li, Y.; Liu, K.; Shen, Q. Bis(Perfluoroalkyl) Phosphino-Oxazoline: A Modular, Stable, Strongly π-Accepting Ligand for Asymmetric Catalysis. *J. Org. Chem.* **2012**, *77*, 7957–7967.

(6) Chen, W.; Chen, M.; Hartwig, J. F. Diastereo- and Enantioselective Iridium-Catalyzed Allylation of Cyclic Ketone Enolates: Synergetic Effect of Ligands and Barium Enolates. *J. Am. Chem. Soc.* **2014**, *136*, 15825–15828.

(7) (a) Chen, J.-P.; Peng, Q.; Lei, B.-L.; Hou, X.-L.; Wu, Y.-D. Chemo- and Regioselectivity-Tunable Pd-Catalyzed Allylic Alkylation of Imines. *J. Am. Chem. Soc.* **2011**, *133*, 14180–14183. (b) Braun, M.; Laicher, F.; Meier, T. Diastereoselective and Enantioselective Palladium-Catalyzed Allylic Substitution with Nonstabilized Ketone Enolates. *Angew. Chem. Int. Ed.* **2000**, *39*, 3494–3497.

(8) (a) Behenna, D. C.; Stoltz, B. M. The Enantioselective Tsuji Allylation. *J. Am. Chem. Soc.* **2004**, *126*, 15044–15045. (b) Mohr, J. T.; Behenna, D. C.; Harned, A. M.; Stoltz, B. M. Deracemization of Quaternary Stereocenters by Pd-Catalyzed Enantioconvergent Decarboxylative Allylation of Racemic β-Ketoesters. *Angew. Chem. Int. Ed.* **2005**, *44*, 6924–6927. (c) Ngamnithiporn, A.; Iwayama, T.; Bartberger, M. D.; Stoltz, B. M. Enantioselective Synthesis of Highly Oxygenated Acyclic Quaternary Center-Containing Building Blocks via Palladium-Catalyzed Decarboxylative Allylic Alkylation of Cyclic Siloxyketones. *Chem. Sci.* **2020**, *11*, 11068–11071. (d) Alexy, E. J.; Fulton, T. J.; Zhang, H.; Stoltz, B. M. Palladium-Catalyzed Enantioselective Decarboxylative Allylic Alkylation of Fully Substituted N-Acyl Indole-Derived Enol Carbonates. *Chem. Sci.* **2019**, *10*, 5996–6000. (e) Lu, Y.; Goldstein, E. L.; Stoltz, B. M. Palladium-Catalyzed Enantioselective C(sp3)–C(sp3) Cross-Coupling for the Synthesis of (Poly)Fluorinated Chiral Building Blocks. *Org. Lett.* **2018**, *20*, 5657–5660. (f) Alexy, E. J.; Zhang, H.; Stoltz, B. M. Catalytic Enantioselective Synthesis of Acyclic Quaternary Centers: Palladium-Catalyzed Decarboxylative Allylic

Alkylation of Fully Substituted Acyclic Enol Carbonates. *J. Am. Chem. Soc.* **2018**, *140*, 10109–10112. (g) Alexy, E. J.; Virgil, S. C.; Bartberger, M. D.; Stoltz, B. M. Enantioselective Pd-Catalyzed Decarboxylative Allylic Alkylation of Thiopyranones. Access to Acyclic, Stereogenic α-Quaternary Ketones. *Org. Lett.* **2017**, *19*, 5007–5009. For comprehensive reviews, see: (h) Pàmies, O.; Margalef, J.; Cañellas, S.; James, J.; Judge, E.; Guiry, P. J.; Moberg, C.; Bäckvall, J.-E.; Pfaltz, A.; Pericàs, M. A.; Diéguez, M. Recent Advances in Enantioselective Pd-Catalyzed Allylic Substitution: From Design to Applications. *Chem. Rev.* **2021**, *121*, 4373–4505. (i) James, J.; Jackson, M.; Guiry, P. J. Palladium-Catalyzed Decarboxylative Asymmetric Allylic Alkylation: Development, Mechanistic Understanding and Recent Advances. *Adv. Synth. Cat.* **2019**, *361*, 3016–3049.

(9) (a) Prétôt, R.; Lloyd-Jones, G. C.; Pfaltz, A. Enantio- and Regiocontrol in Palladium and Tungsten-Catalyzed Allylic Substitutions *Pure Appl. Chem.* **1998**, *70*, 1035–1040. (b) Yang, X.-F.; Ding, C.-H.; Li, X.-H.; Huang, J.-Q.; Hou, X.-L.; Dai, L.-X.; Wang, P.-J. Regio- and Enantioselective Palladium-Catalyzed Allylic Alkylation of Nitromethane with Monosubstituted Allyl Substrates: Synthesis of *(R)*-Rolipram and *(R)*-Baclofen. *J. Org. Chem.* **2012**, *77*, 8980–8985.

(10) Five-membered rings failed to give high levels of regio- and stereoselectivity.

(11) In our hands, the synthesis of **L5** was easier due to faster reduction of the corresponding phosphine oxide. (see 4.4.2 for more details).

(12) $Pd_2(pmdba)_3$ was used instead of $Pd_2(dba)_3$ to allow for easier purification of the allylic alkylation product.

(13) The mechanistic implications of this result are outside the scope of this initial report. Current mechanistic studies are ongoing.

(14) Morandi, B.; Wickens, Z. K.; Grubbs, R. H. Practical and General Palladium-Catalyzed Synthesis of Ketones from Internal Olefins. *Angew. Chem. Int. Ed.* **2013**, *52*, 2944–2948.

(15) Some epimerization of the a-stereocenter was observed by 1H NMR (see 4.4.2 for more details).

(16) While the calculated dissociation energies appear to suggest that the ion pairs are inaccessible at the reaction temperature (60 ºC), the energies of each ionic species was calculated separately and stabilizing ionic interactions were not taken into account. We postulate that the error in overestimation would be comparable among the complexes with different ligands and that comparison of dissociation energies would remain valid.

(17) Pangborn, A. M.; Giardello, M. A.; Grubbs, R. H.; Rosen, R. K.; Timmers, F. J. Safe and Convenient Procedure for Solvent Purification. *Organometallics* **1996**, *15*, 1518–1520.

(18) McDougal, N. T.; Streuff, J.; Mukherjee, H.; Virgil, S. C.; Stoltz, B. M. Rapid synthesis of an electron-deficient *t*-BuPHOX ligand: cross-coupling of aryl

bromides with secondary phosphine oxides. *Tetrahedron Lett*. **2010**, *51*, 5550–5554.

(19) Linder, D.; Austeri, M.; Lacour, J. Lewis Acid/CpRu Dual Catalysis in the Enantioselective Decarboxylative Allylation of Ketone Enolates. *Org. Biomol. Chem.* **2009**, *7*, 4057–4061.

(20) Frew, A.; Proctor, G. Ring-Expansion of Carbocyclic β-Ketoesters with Acetylenic Esters. *J. Chem. Soc., Perkin Trans.* **1980**, *1*, 1245–1250.

(21) Tobias, M. A.; Strong, J. G.; Napier, R. P. Preparation of 2-substituted 2-cyclohexen-1-ones *J. Org. Chem.* **1970**, *35*, 1709–1711.

(22) Morrill, C.; Jensen, C.; Just-Baringo, X.; Grogan, G.; Turner, N.; Proctor, D. Biocatalytic Conversion of Cyclic Ketones Bearing a-Quaternary Stereocenters into Lactones in an Enantioselective Radical Approach to Medium-Sized Carbocycles *Angew. Chem. Int. Ed.* **2018**, *57*, 3692–3696.

(23) Morandi, B.; Wickens, Z.; Grubbs, R. H. "Practical and General Palladium-Catalyzed Synthesis of Ketones from Internal Olefins" *Angew. Chem. Int. Ed.* **2013**, *52*, 2944–2948.

(24) Qi, N.; Zhang, N.; Allu, S. R., Gao, J.; Guo, J.; He, Y. Insertion of Arynes into P–O Bonds: One-Step Simultaneous Construction of C–P and C–O Bonds. *Org. Lett.* **2016**, *18*, 6204–6207.

(25) **Schrödinger Release 2021-4:** MacroModel, Schrödinger, LLC, New York, NY, 2021.

(26) Bochevarov, A.D.; Harder, E.; Hughes, T.F.; Greenwood, J.R.; Braden, D.A.; Philipp, D.M.; Rinaldo, D.; Halls, M.D.; Zhang, J.; Friesner, R.A., "Jaguar: A high-performance quantum chemistry software program with strengths in life and materials sciences," *Int. J. Quantum Chem.*, **2013**, *113*, 2110-2142.

(27) (a) Neese, F. Software Update: The ORCA Program System, Version 4.0. *Wiley Interdiscip. Rev.: Comput. Mol. Sci.* **2018,** *8*, No. e1327. (b) Neese, F. The ORCA Program System. *Wiley Interdiscip. Rev.: Comput. Mol. Sci.* **2012**, *2*, 73−78.

(28) Adamo, C.; Barone, V. Toward Reliable Density Functional Methods without Adjustable Parameters: The PBE0 Model. *J. Chem. Phys.* **1999**, *110*, 6158−6170.

(29) (a) Caldeweyher, E.; Ehlert, S.; Hansen, A.; Neugebauer, H.; Spicher, S.; Bannwarth, C.; Grimme, S. A Generally Applicable Atomic-Charge Dependent London Dispersion Correction. *J. Chem. Phys.* **2019**, *150*, 154122. (b) Caldeweyher, E.; Bannwarth, C.; Grimme, S. Extension of the D3 Dispersion Coefficient Model. *J. Chem. Phys.* **2017**, *147*, 034112.

(30) Cusumano, A. Q.; Goddard, W. A. I.; Stoltz, B. M. The Transition Metal Catalyzed [s2s + s2s + p2s + p2s] Pericyclic Reaction: Woodward–Hoffmann Rules, Aromaticity, and Electron Flow. *J. Am. Chem. Soc.* **2020**, *142*, 19033–19039.

(31) Weigend, F.; Ahlrichs, R. Balanced Basis Sets of Split Valence, Triple Zeta Valence and Quadruple Zeta Valence Quality for H to Rn: Design and Assessment of Accuracy. *Phys. Chem. Chem. Phys.* **2005**, *7*, 3297–3305.

(32) Peterson, K. A.; Figgen, D.; Goll, E.; Stoll, H.; Dolg, M. Systematically Convergent Basis Sets with Relativistic Pseudopotentials. II. Small-Core Pseudopotentials and Correlation Consistent Basis Sets for the Post- *d* Group 16–18 Elements. *J. Chem. Phys.* **2003**, *119*, 11113–11123.

(33) Garcia-Ratés, M.; Neese, F. Effect of the Solute Cavity on the Solvation Energy and Its Derivatives within the Framework of the Gaussian Charge Scheme. *J. Comput. Chem.* **2020**, *41*, 922–939.

(34) Ishida, K.; Morokuma, K.; Komornicki, A. The Intrinsic Reaction Coordinate. An Ab Initio Calculation for HNC→HCN and H−+CH4→CH4+H−. *J. Chem. Phys.* **1977**, *66*, 2153−2156.

(35) Zhao, Y.; Truhlar, D. G. The M06 Suite of Density Functionals for Main Group Thermochemistry, Thermochemical Kinetics, Noncovalent Interactions, Excited States, and Transition Elements: Two New Functionals and Systematic Testing of Four M06-Class Functionals and 12 Other Functionals. *Theor. Chem. Account.* **2008**, *120*, 215–241.

(36) Grimme, S. Supramolecular Binding Thermodynamics by Dispersion-Corrected Density Functional Theory. *Chem. Eur. J.* **2012**, *18*, 9955–9964.

(37) Izato, Y.; Matsugi, A.; Koshi, M.; Miyake, A. A Simple Heuristic Approach to Estimate the Thermochemistry of Condensed-Phase Molecules Based on the Polarizable Continuum Model. *Phys. Chem. Chem. Phys.* **2019**, *21*, 18920–18929.

(38) Finkelstein, A. V.; Janin, J. The Price of Lost Freedom: Entropy of Bimolecular Complex Formation. *Protein Engineering, Design and Selection* **1989**, *3*, 1–3.

(39) Neese, F.; Wennmohs, F.; Hansen, A.; Becker, U. Efficient, Approximate and Parallel Hartree-Fock and Hybrid DFT Calculations. A 'Chain-of-Spheres' Algorithm for the Hartree-Fock Exchange. *Chem. Phys.* **2009**, *356*, 98–109.

(40) Weigend, F. Accurate Coulomb-Fitting Basis Sets for H to Rn. *Phys. Chem. Chem. Phys.* **2006**, *8*, 1057–1065.

(41) Stoychev, G. L.; Auer, A. A.; Neese, F. Automatic Generation of Auxiliary Basis Sets. *J. Chem. Theory Comput.* **2017**, *13*, 554–562.

APPENDIX 3

Spectra Relevant to Chapter 4: A Pericyclic Strategy to the Enantio- and Diastereoselective Synthesis of Vicinal Quaternary/Tertiary Stereocenters from Chiral Palladium Enolates

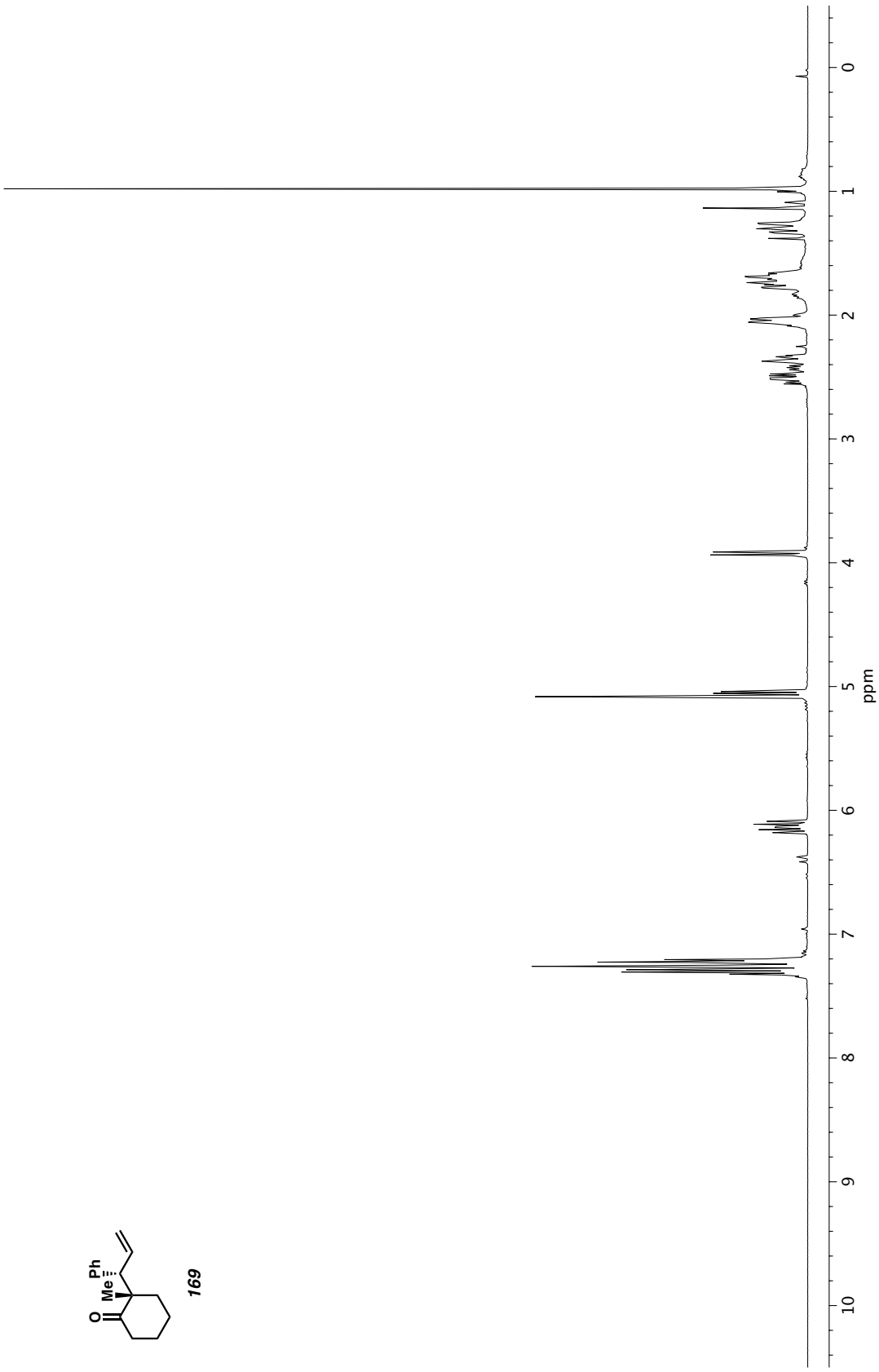


Figure A3.1. *^1H NMR (400 MHz, $CDCl_3$) of compound* ***169***.

169

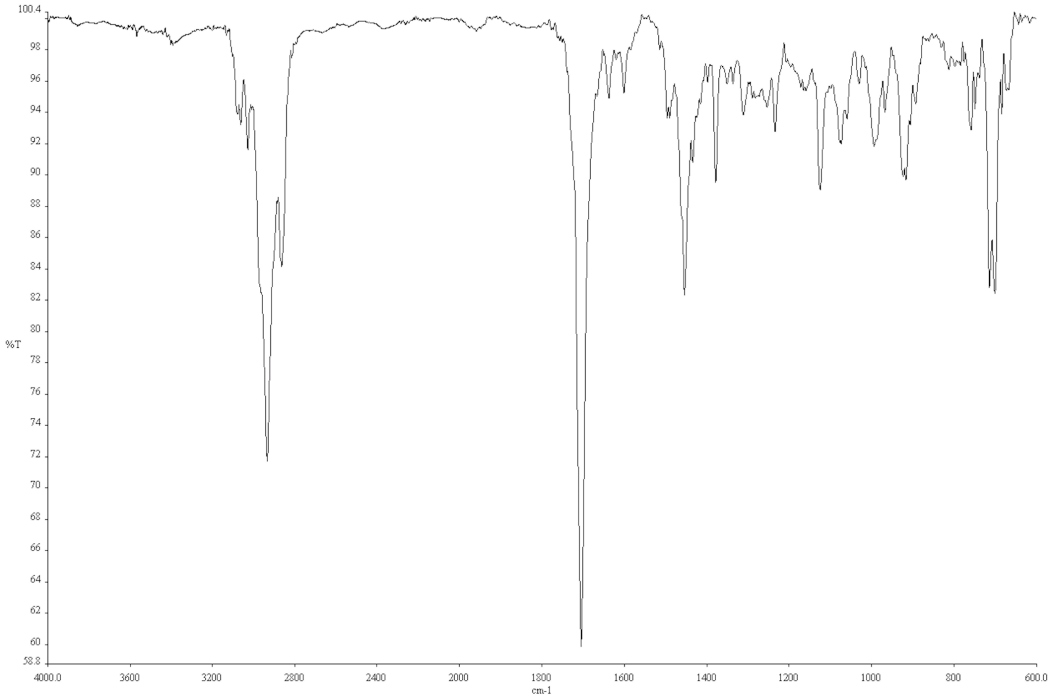


Figure A3.2. *Infrared spectrum (Thin Film, NaCl) of compound* ***169****.*

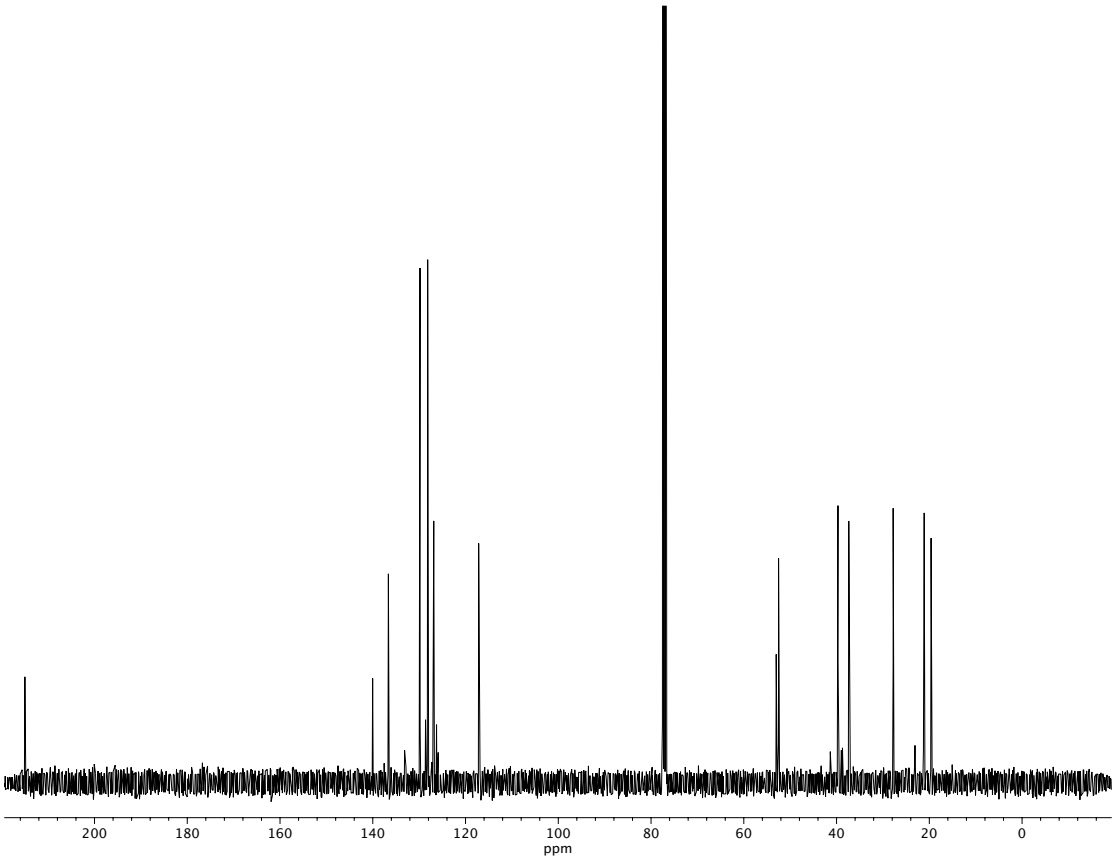


Figure A3.3. *^{13}C NMR (100 MHz, $CDCl_3$) of compound* ***169****.*

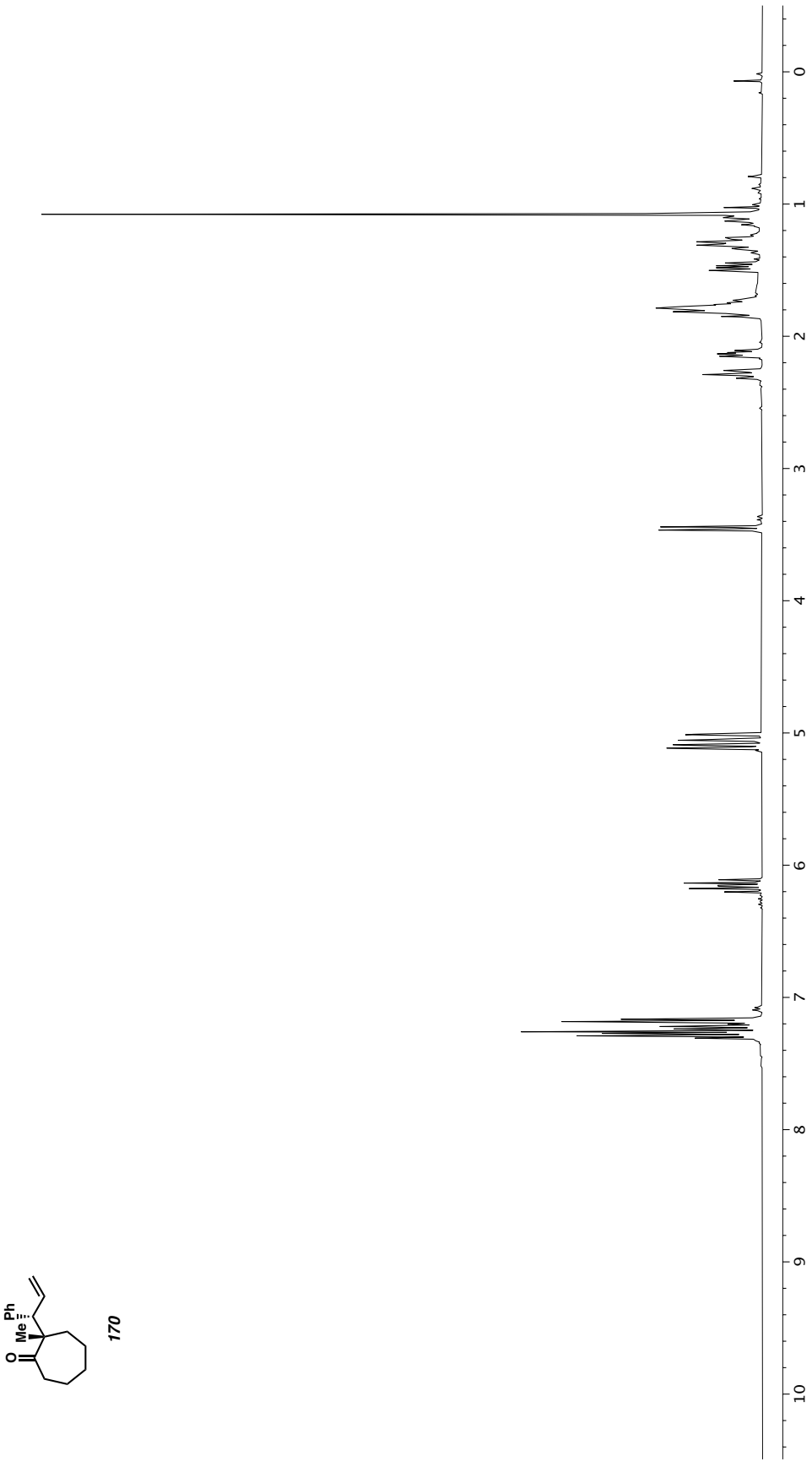


Figure A3.4. *^1H NMR (400 MHz, $CDCl_3$) of compound* ***170***.

170

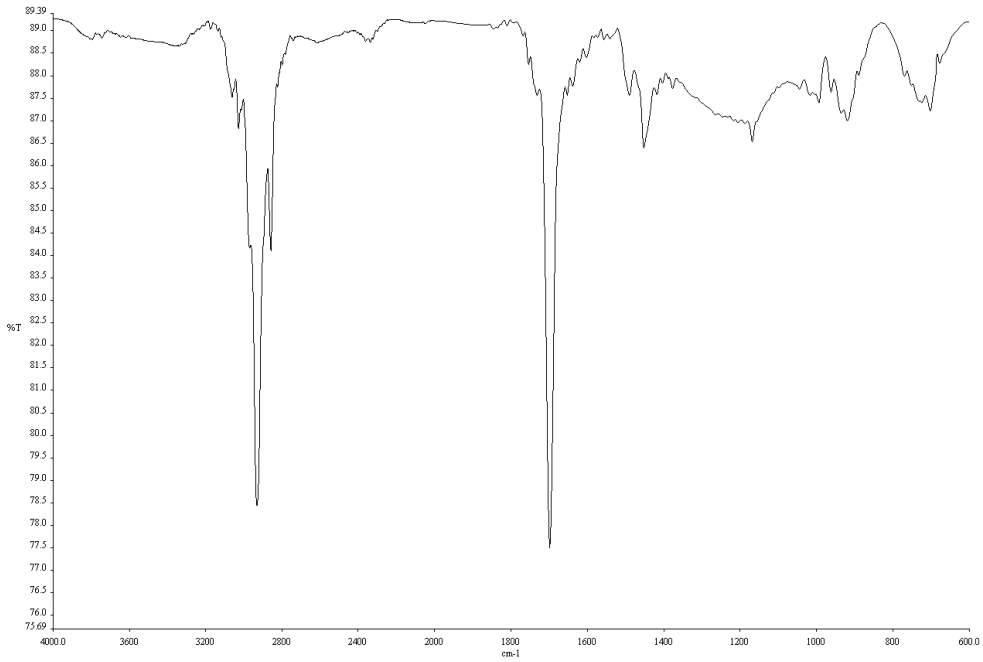


Figure A3.5. *Infrared spectrum (Thin Film, NaCl) of compound* ***170****.*

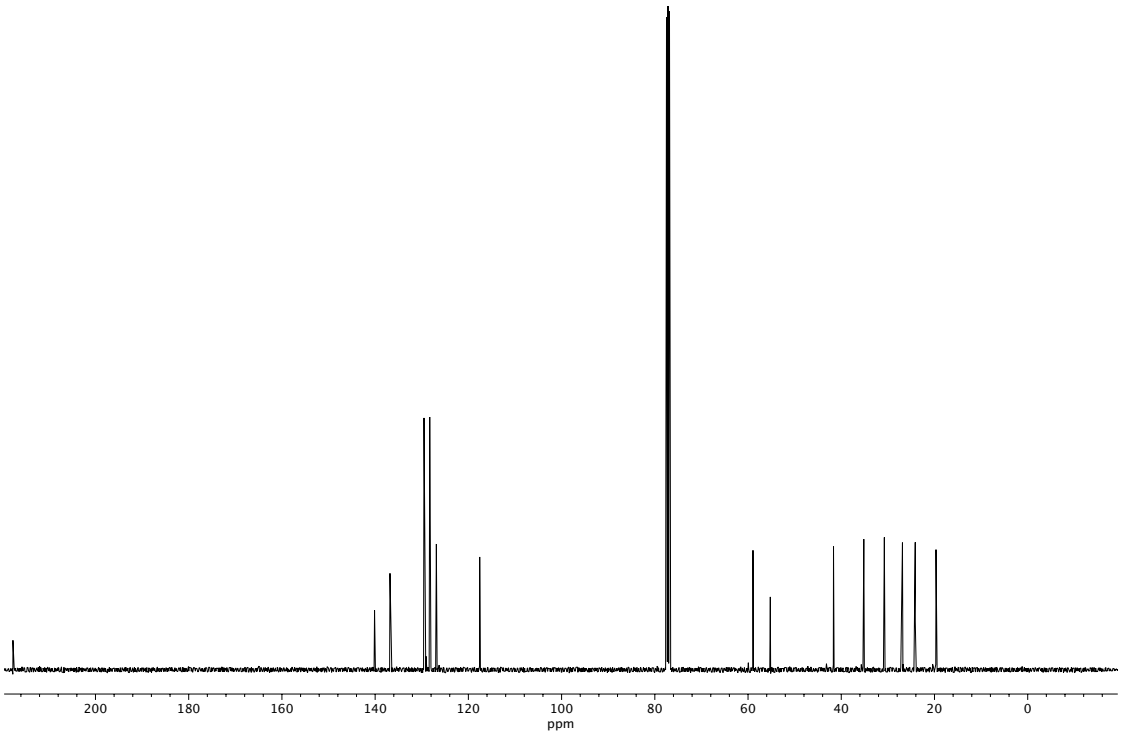


Figure A3.6. *^{13}C NMR (100 MHz, $CDCl_3$) of compound* ***170****.*

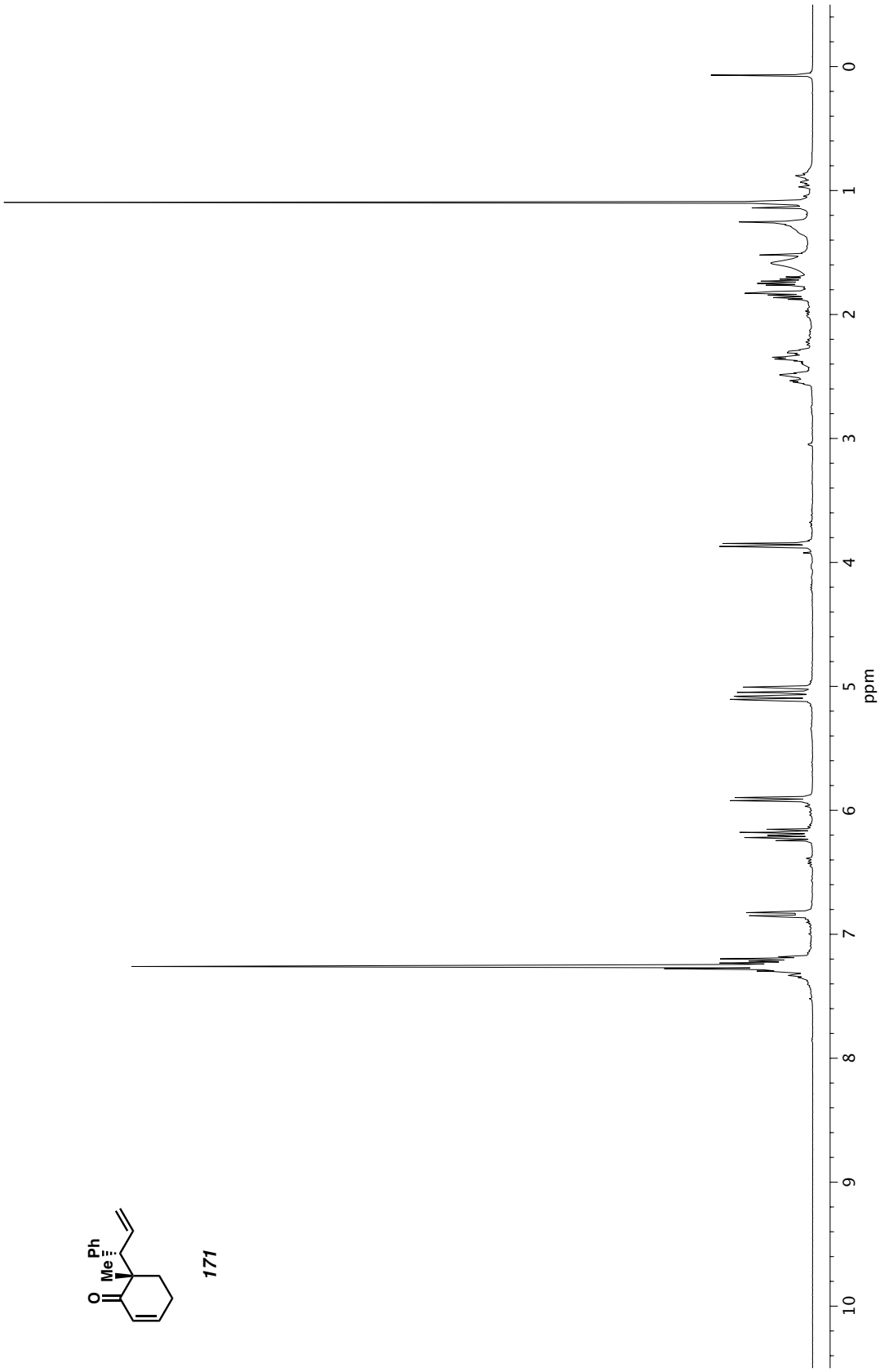


Figure A3.7. *^1H NMR (400 MHz, $CDCl_3$) of compound* ***171****.*

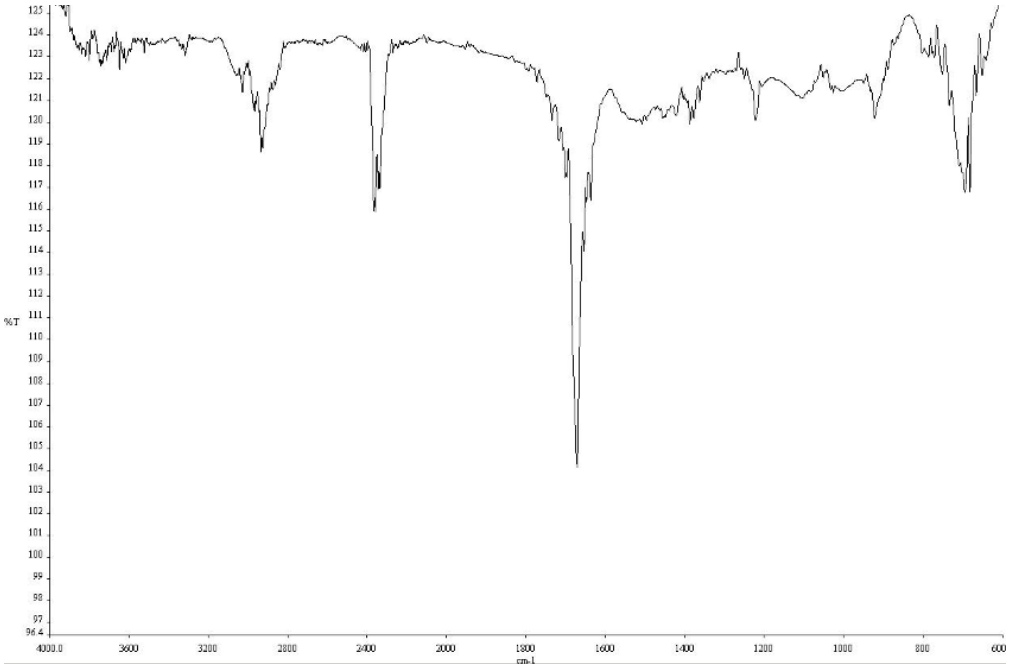


Figure A3.8. *Infrared spectrum (Thin Film, NaCl) of compound* ***171****.*

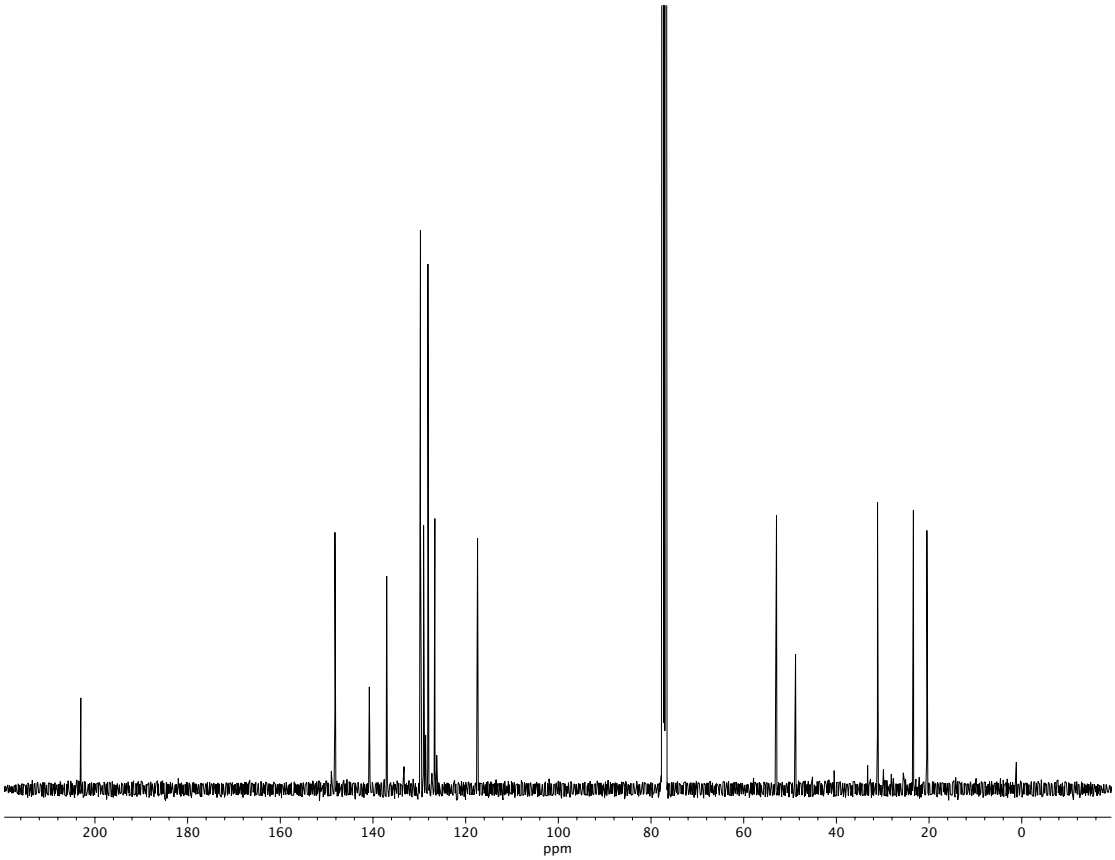


Figure A3.9. *^{13}C NMR (100 MHz, $CDCl_3$) of compound* ***171****.*

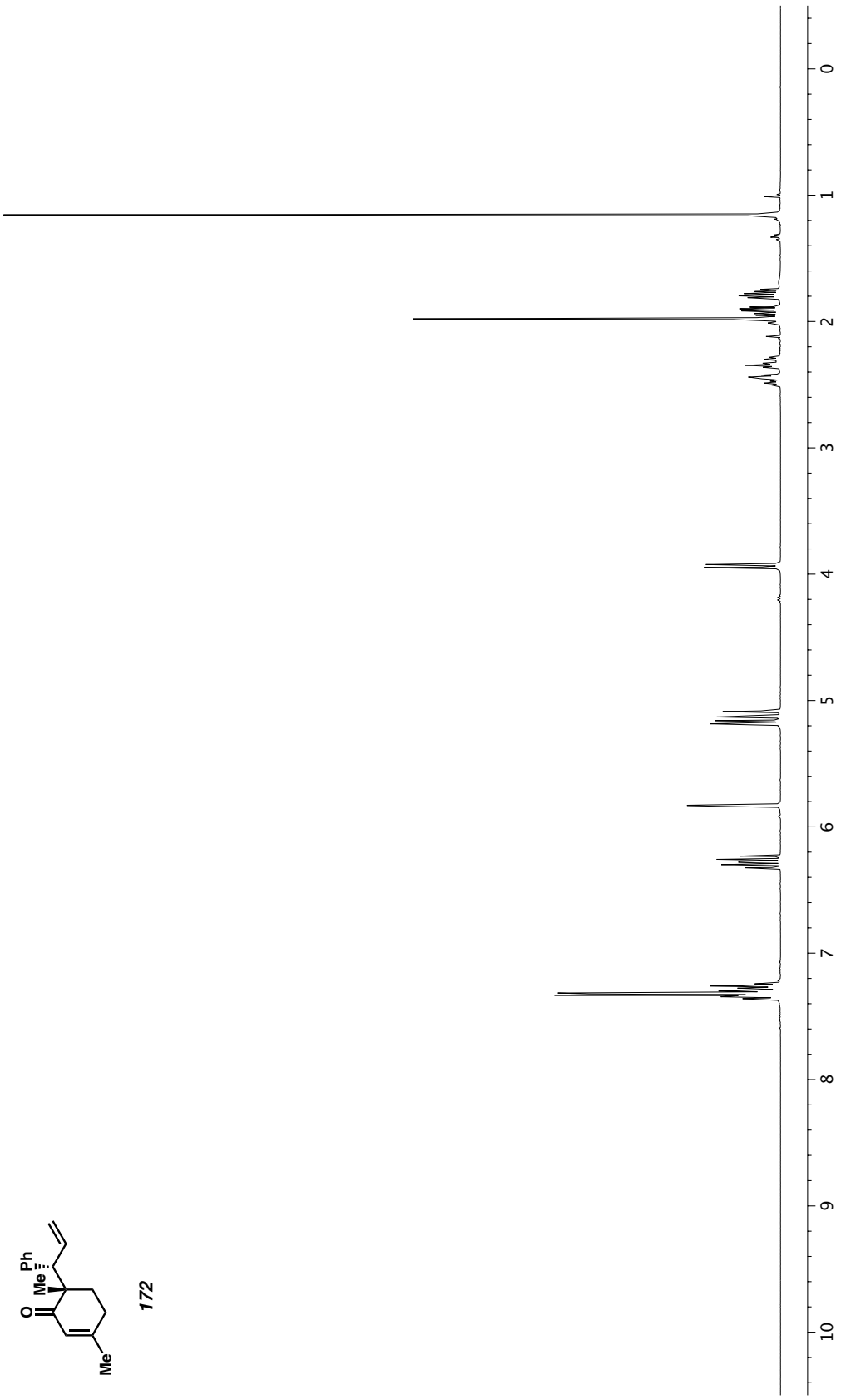


Figure A3.10. *^1H NMR (400 MHz, $CDCl_3$) of compound* ***172****.*

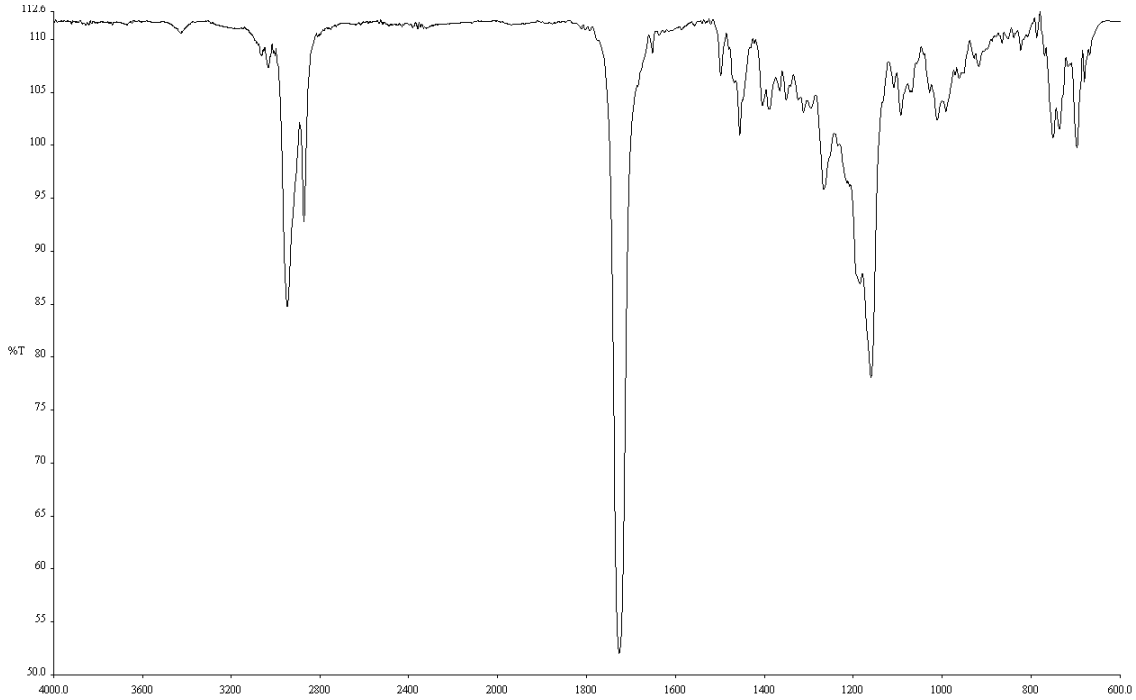


Figure A3.11. *Infrared spectrum (Thin Film, NaCl) of compound* ***172****.*

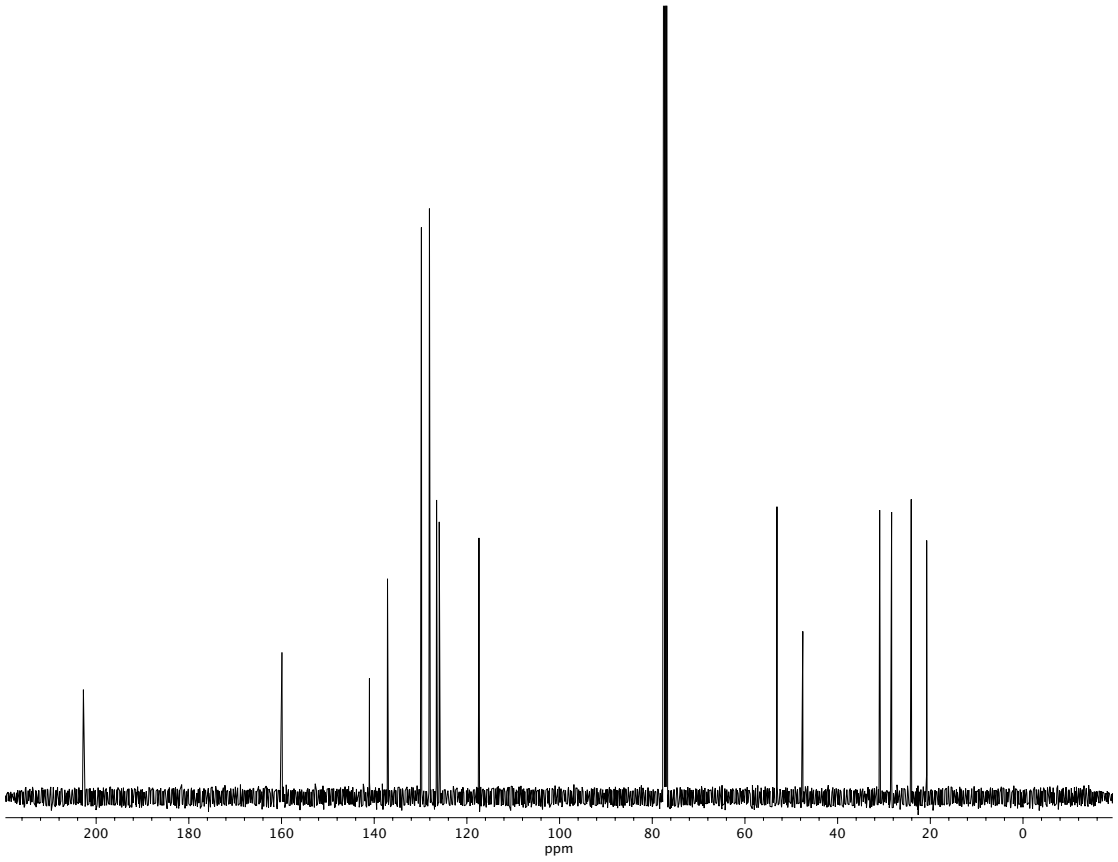


Figure A3.12. *^{13}C NMR (100 MHz, $CDCl_3$) of compound* ***172****.*

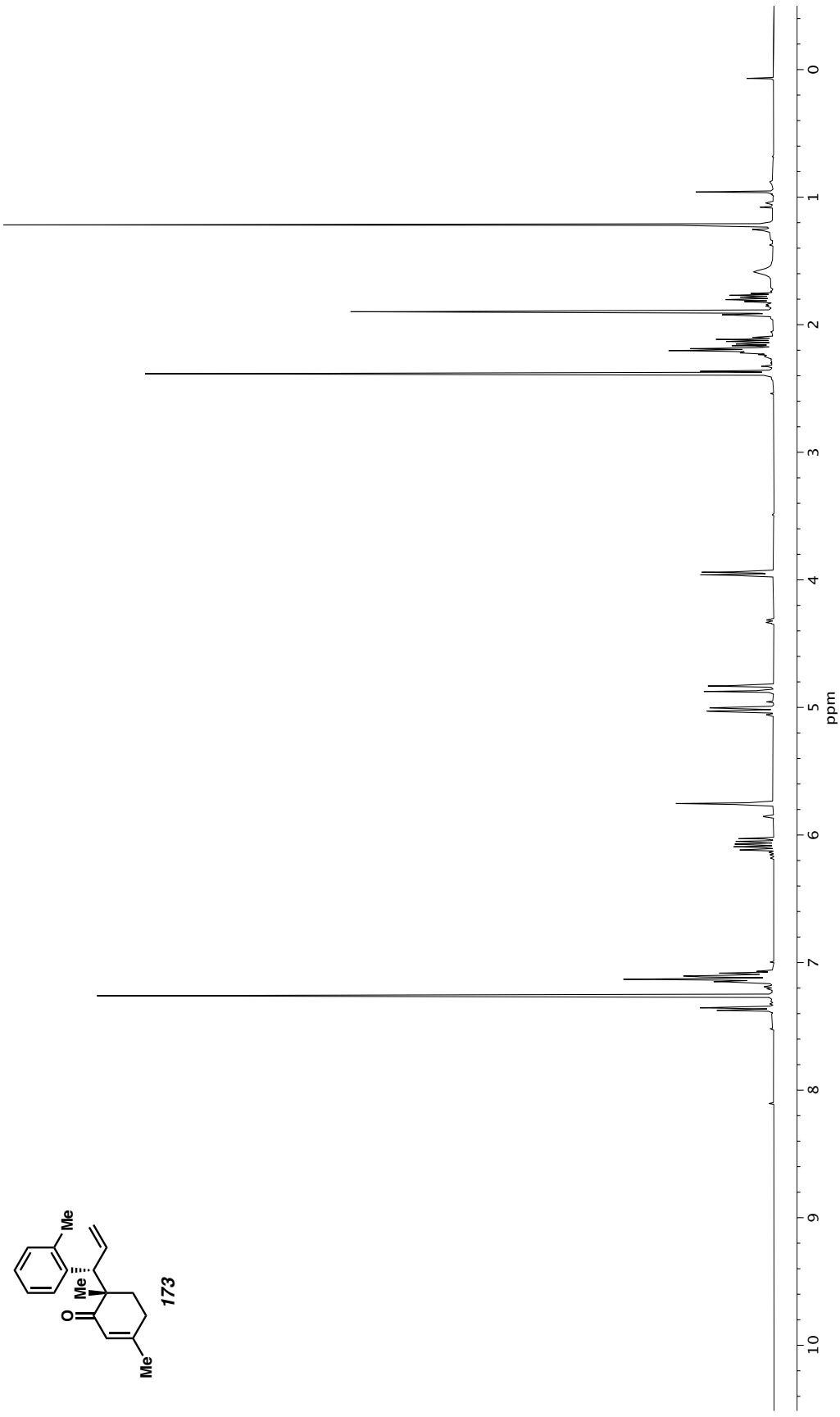


Figure A3.13. *^1H NMR (400 MHz, $CDCl_3$) of compound **173**.*

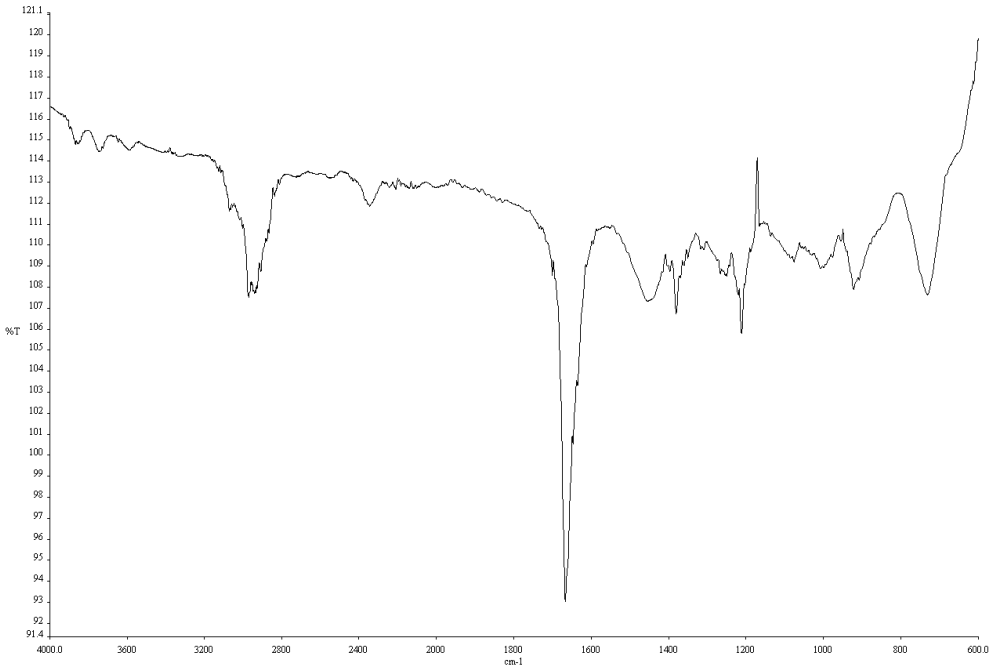


Figure A3.14. *Infrared spectrum (Thin Film, NaCl) of compound* ***173****.*

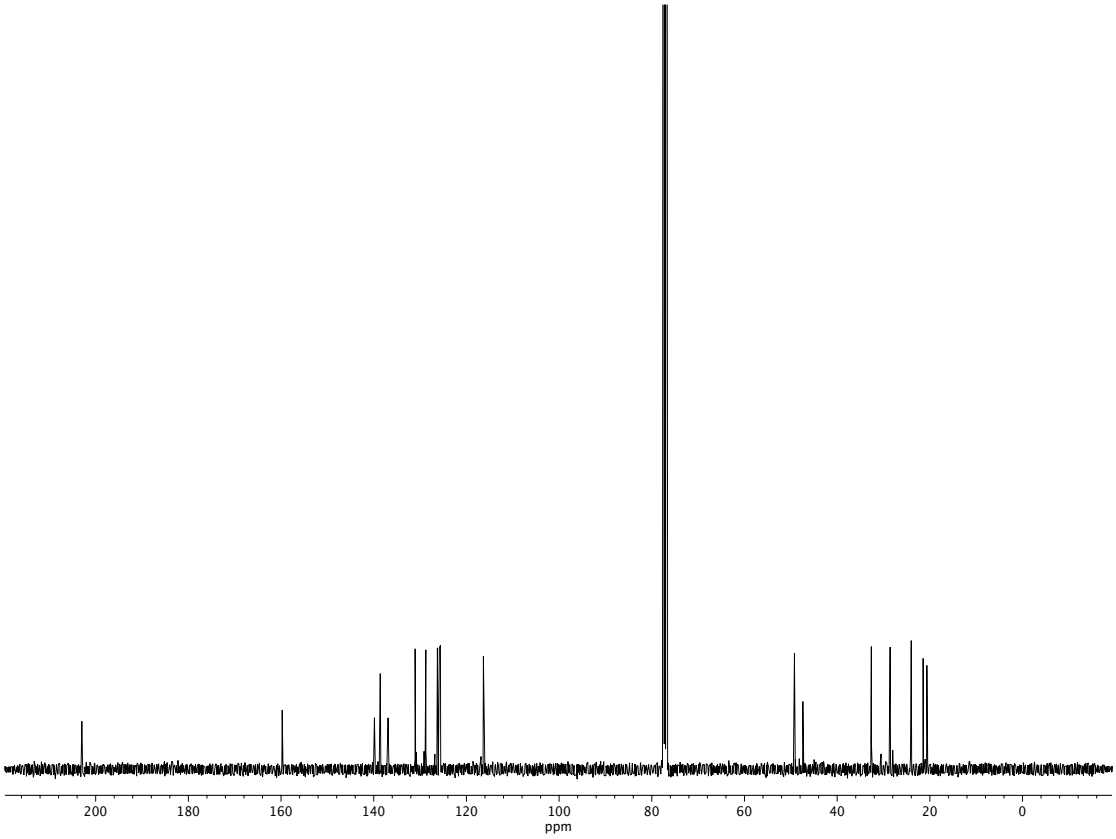


Figure A3.15. *^{13}C NMR (100 MHz, $CDCl_3$) of compound* ***173****.*

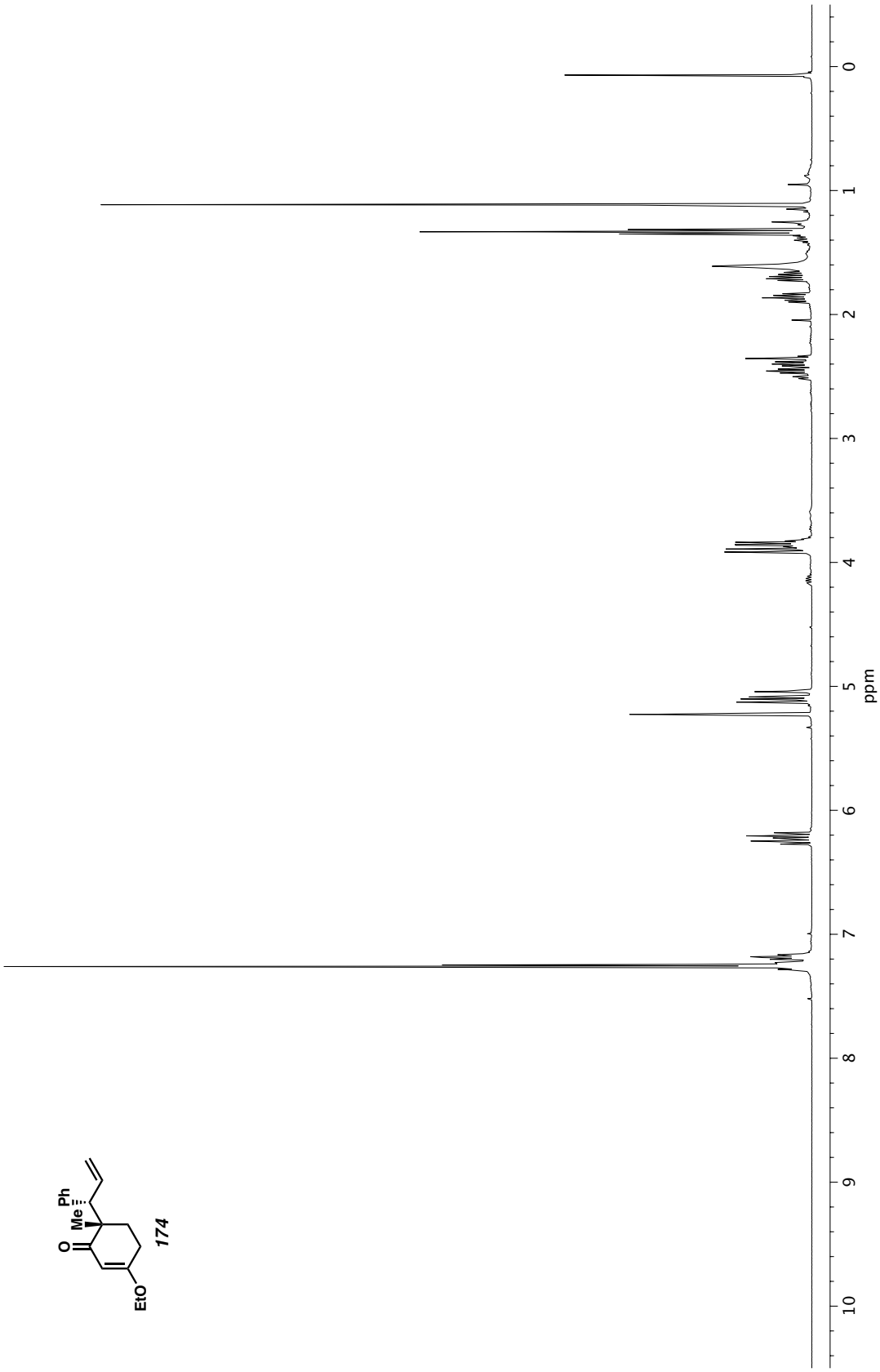


Figure A3.16. *^1H NMR (400 MHz, $CDCl_3$) of compound* ***174****.*

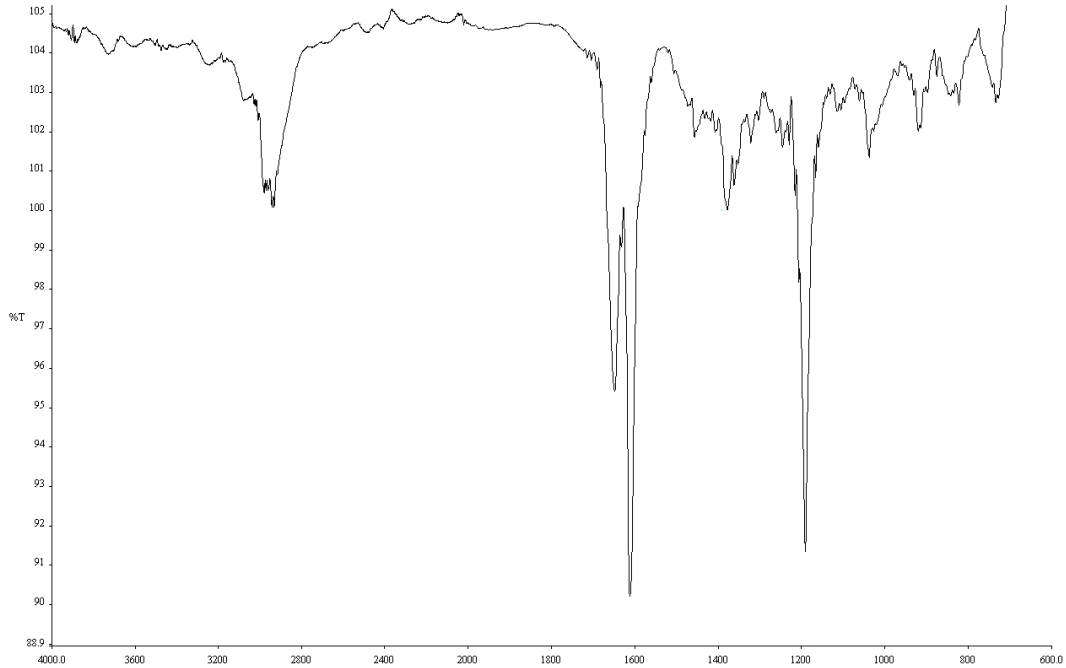


Figure A3.17. *Infrared spectrum (Thin Film, NaCl) of compound* ***174****.*

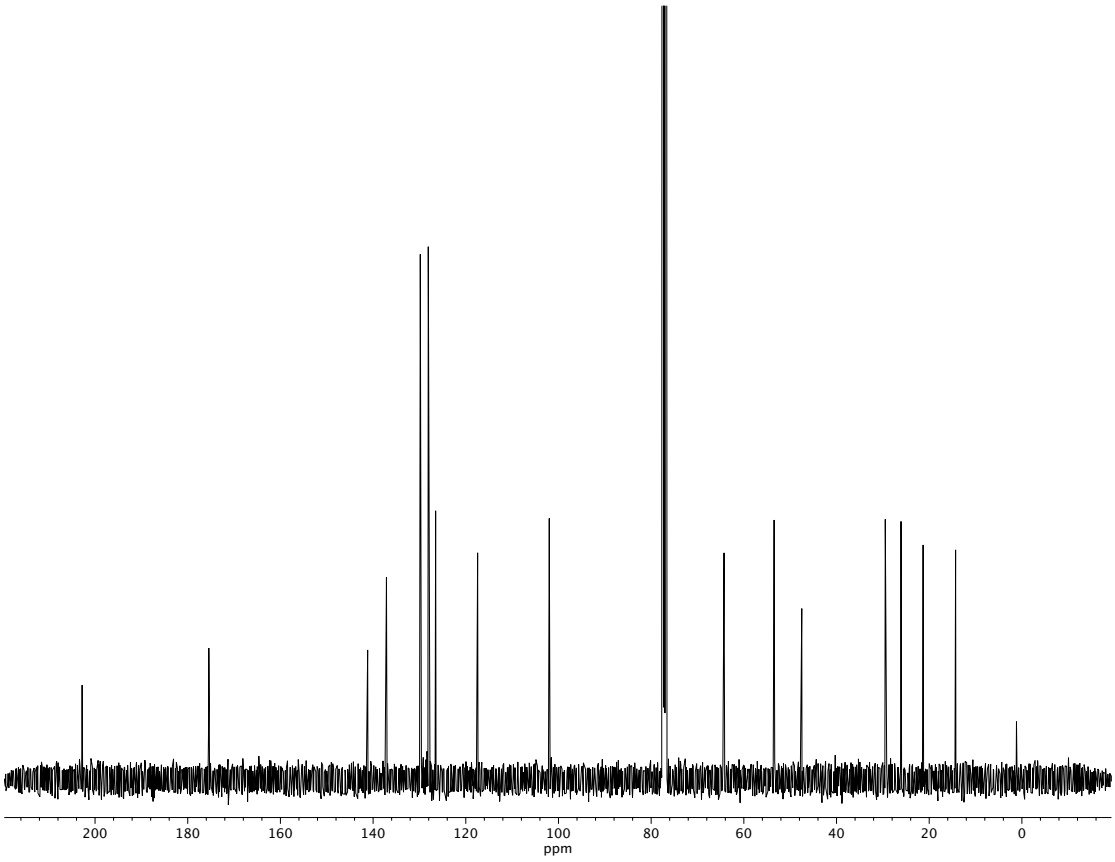


Figure A3.18. *^{13}C NMR (100 MHz, $CDCl_3$) of compound* ***174****.*

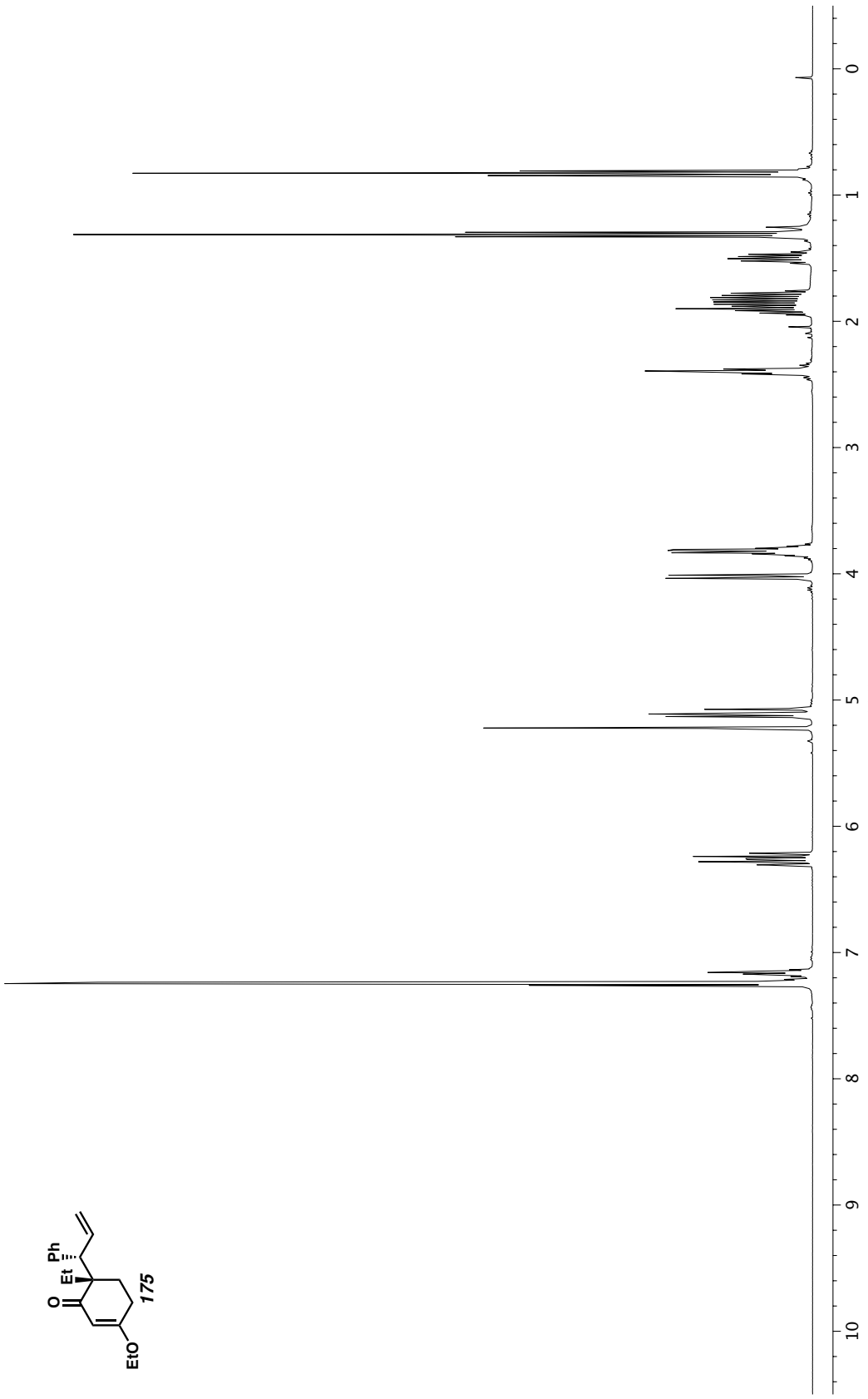


Figure A3.19. *^1H NMR (400 MHz, $CDCl_3$) of compound **175**.*

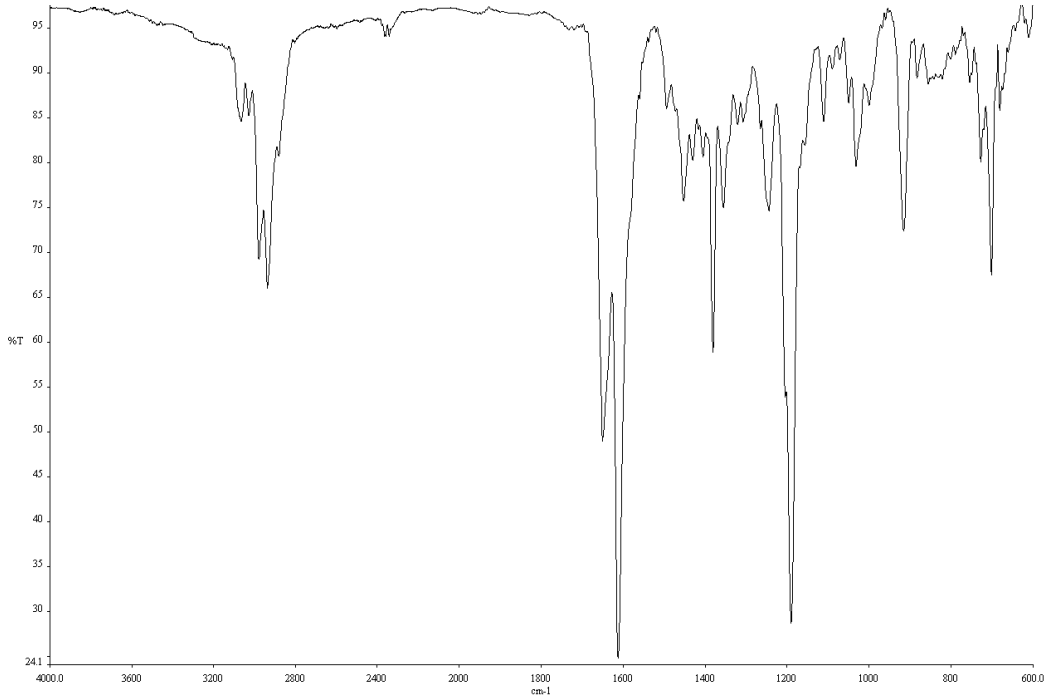


Figure A3.20. *Infrared spectrum (Thin Film, NaCl) of compound* ***175****.*

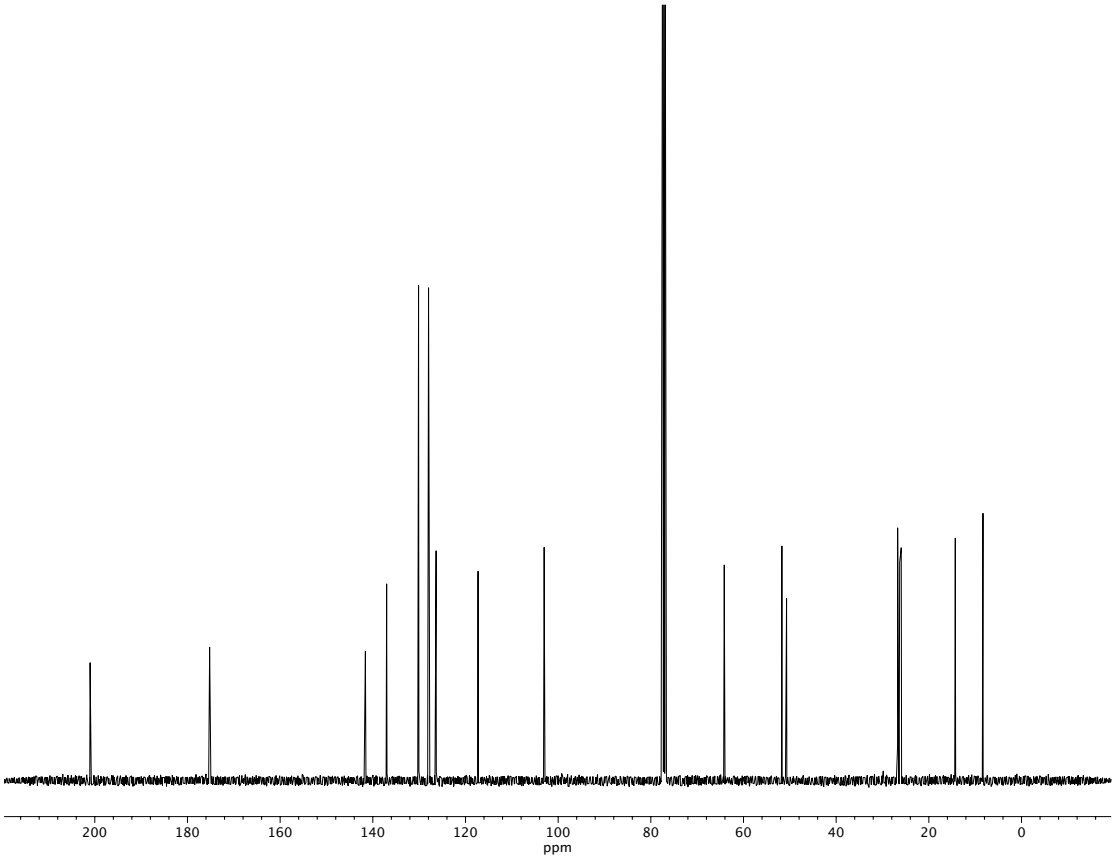


Figure A3.21. *^{13}C NMR (100 MHz, $CDCl_3$) of compound* ***175****.*

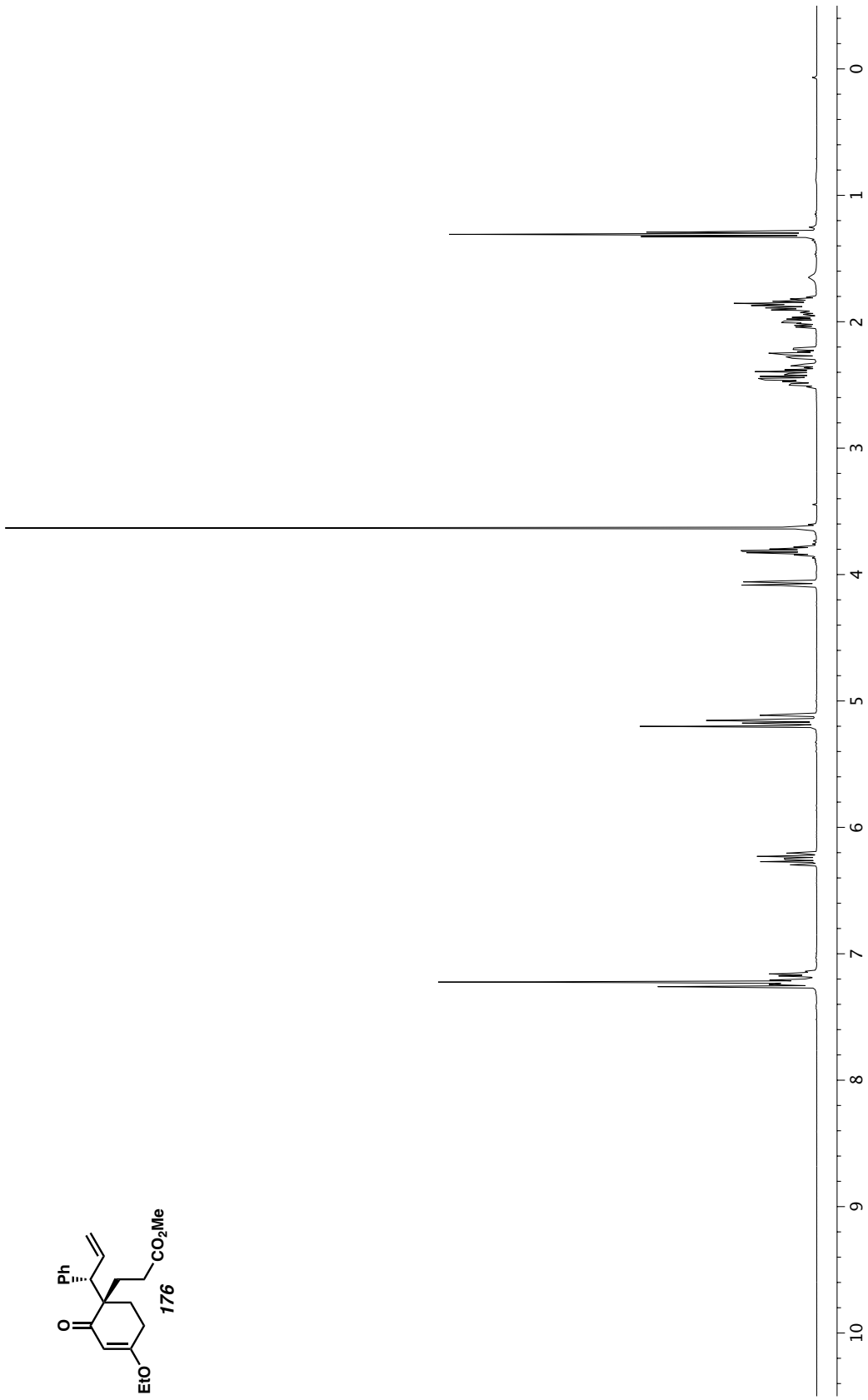


Figure A3.22. *^1H NMR (400 MHz, $CDCl_3$) of compound **176**.*

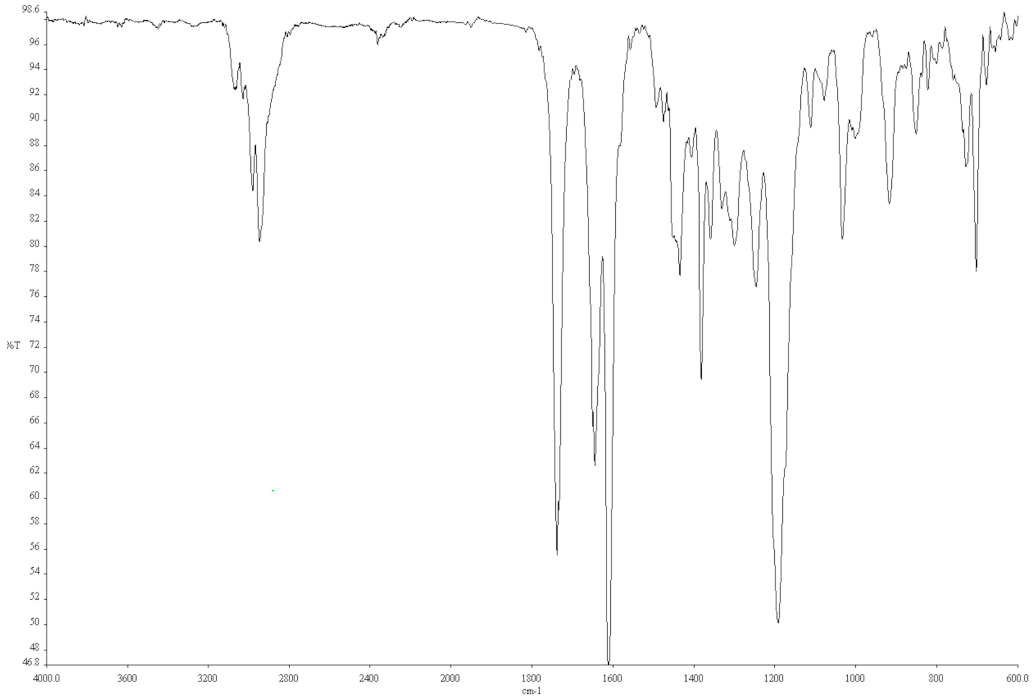


Figure A3.23. *Infrared spectrum (Thin Film, NaCl) of compound* ***176****.*

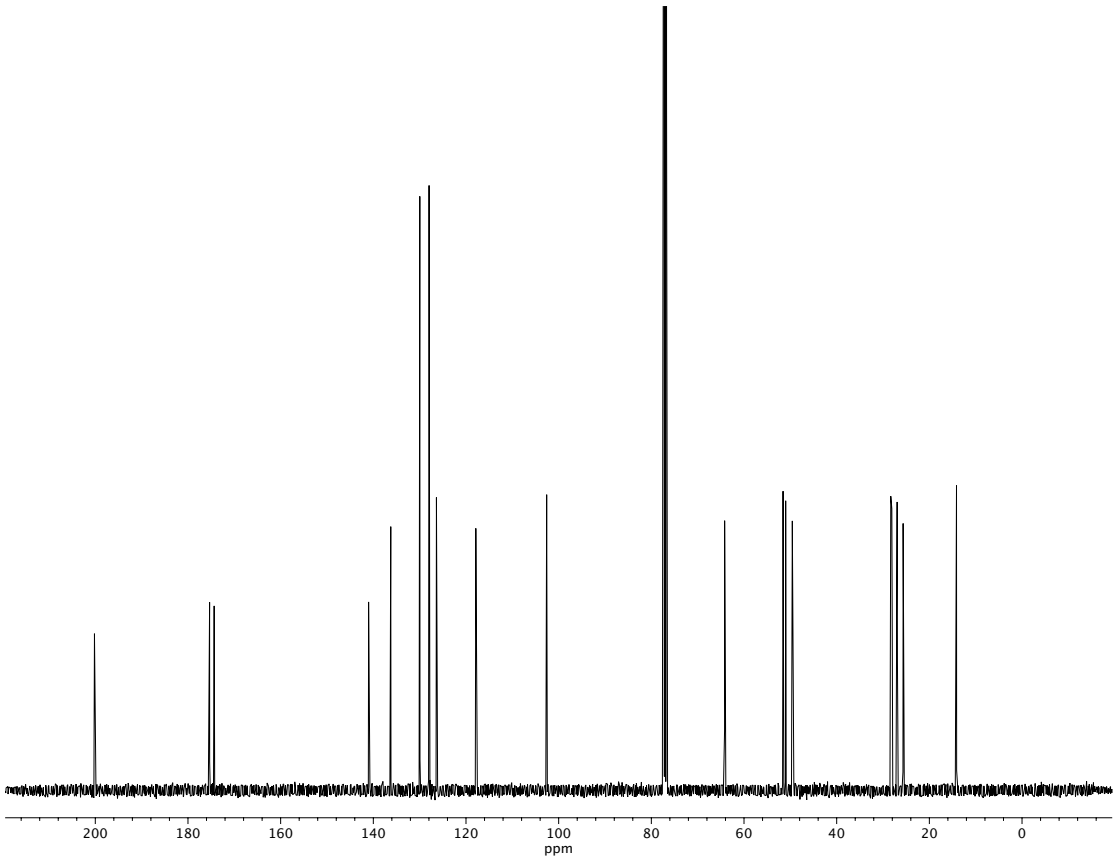


Figure A3.24. *^{13}C NMR (100 MHz, $CDCl_3$) of compound* ***176****.*

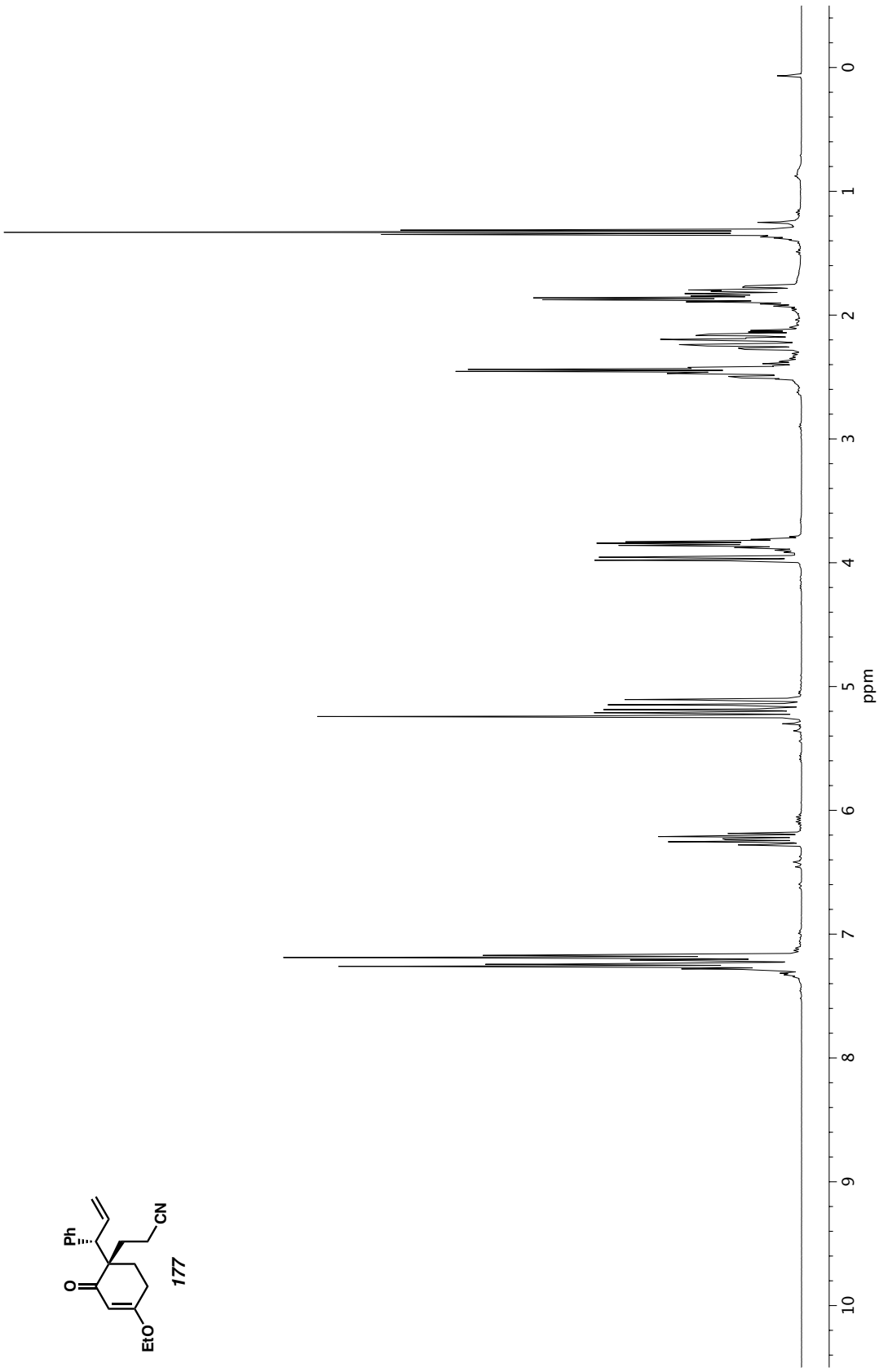


Figure A3.25. *^1H NMR (400 MHz, $CDCl_3$) of compound **177**.*

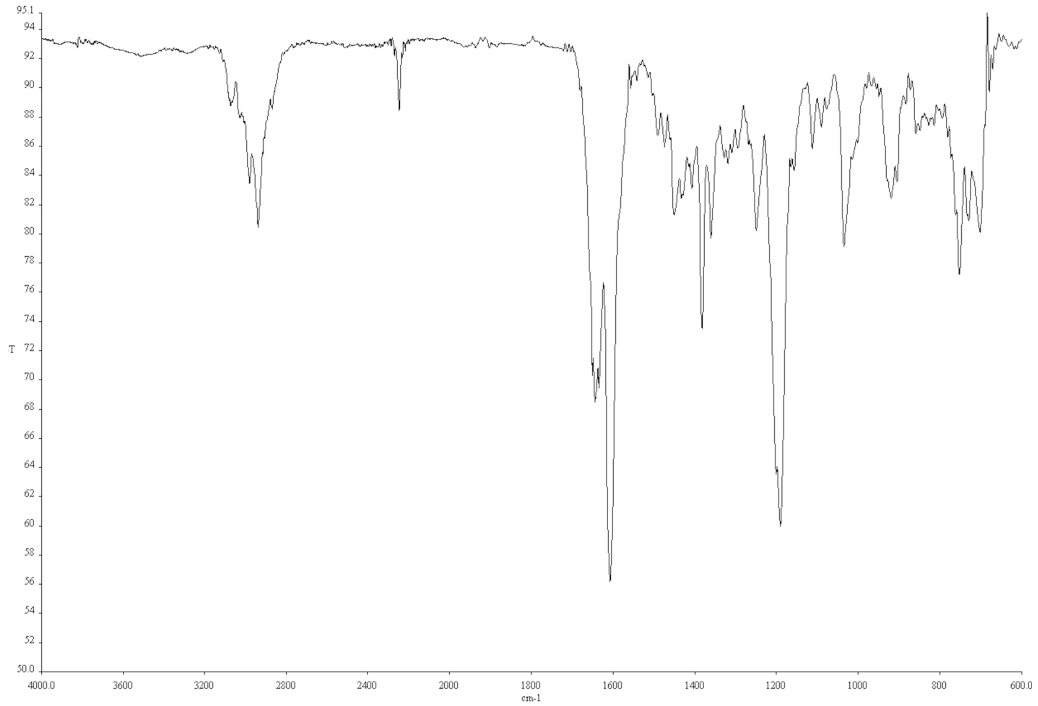


Figure A3.26. *Infrared spectrum (Thin Film, NaCl) of compound* ***177****.*

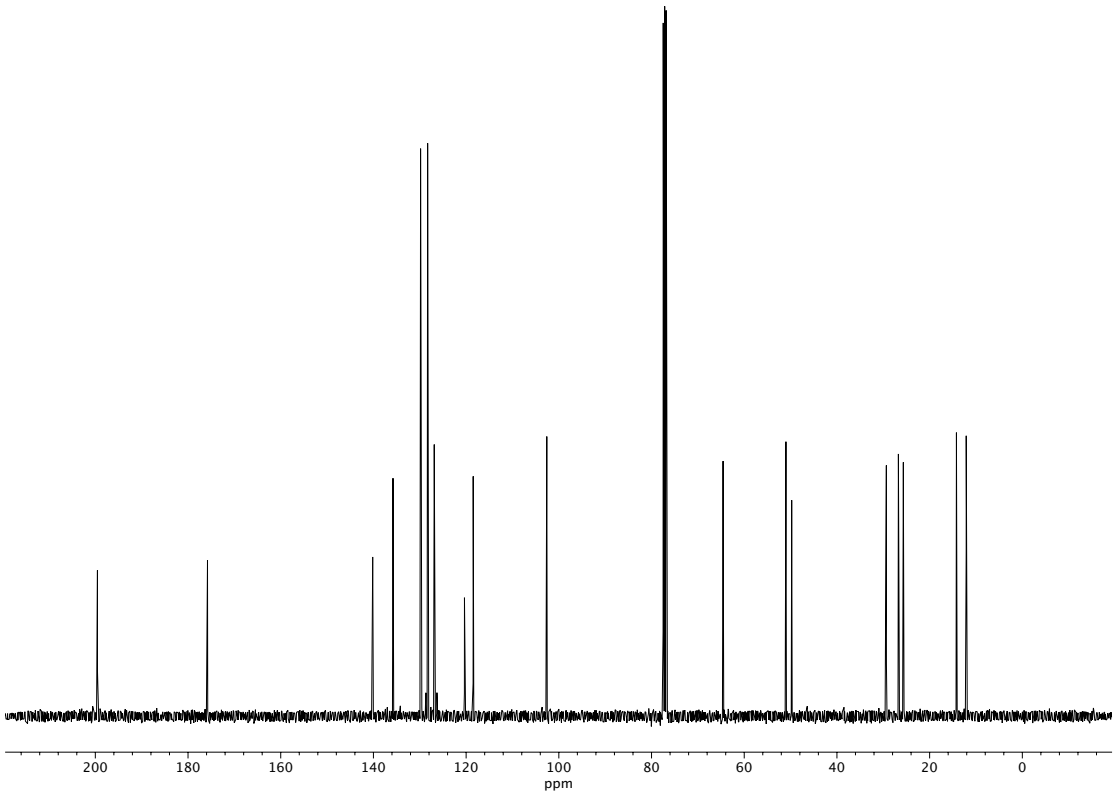


Figure A3.27. *^{13}C NMR (100 MHz, $CDCl_3$) of compound* ***177****.*

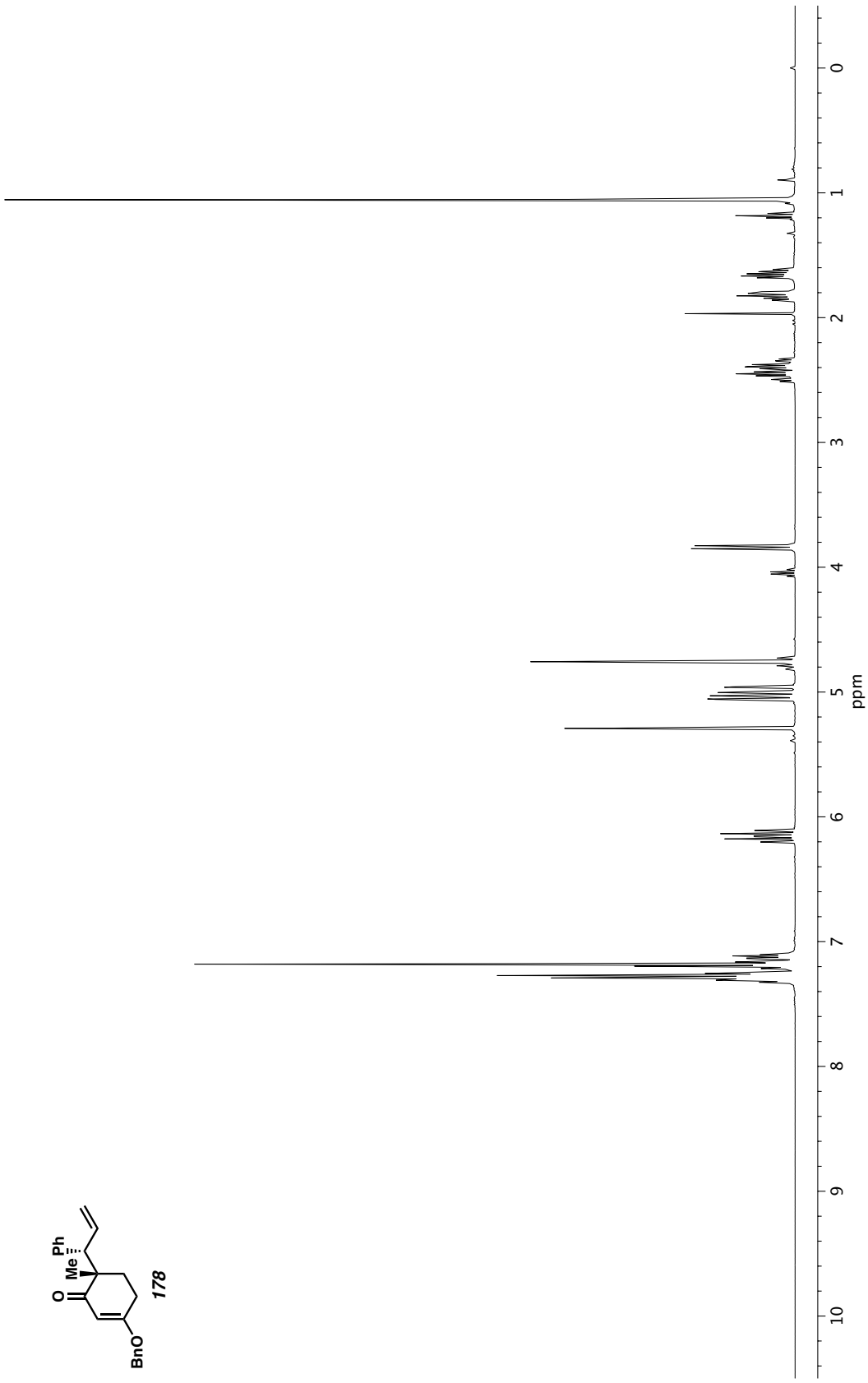


Figure A3.28. *^1H NMR (400 MHz, $CDCl_3$) of compound **178**.*

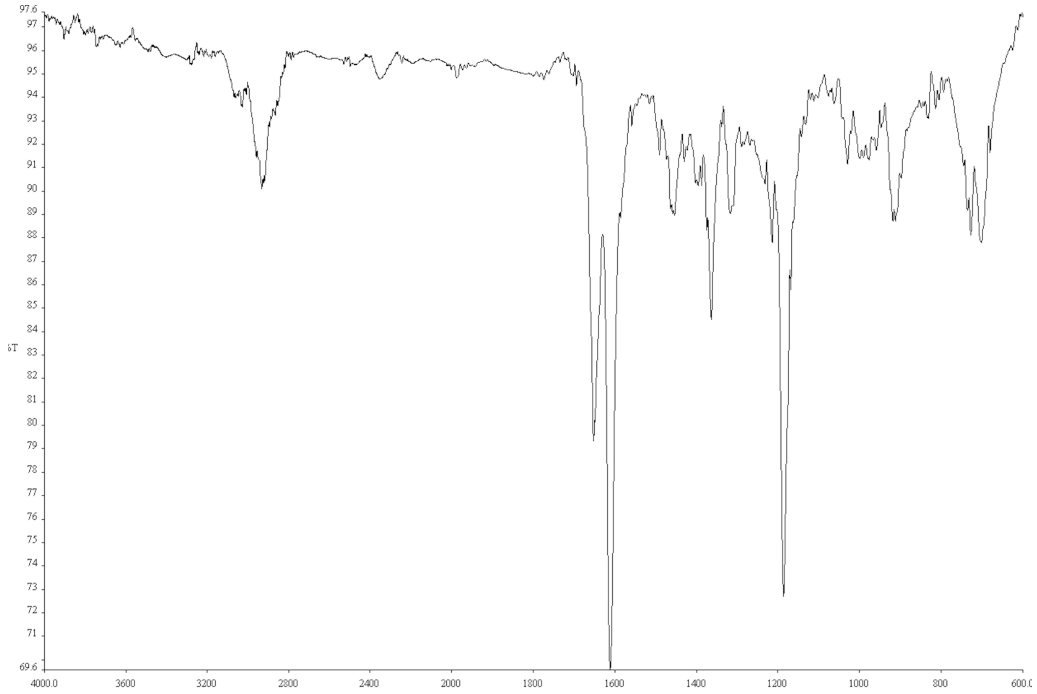


Figure A3.29. *Infrared spectrum (Thin Film, NaCl) of compound* ***178****.*

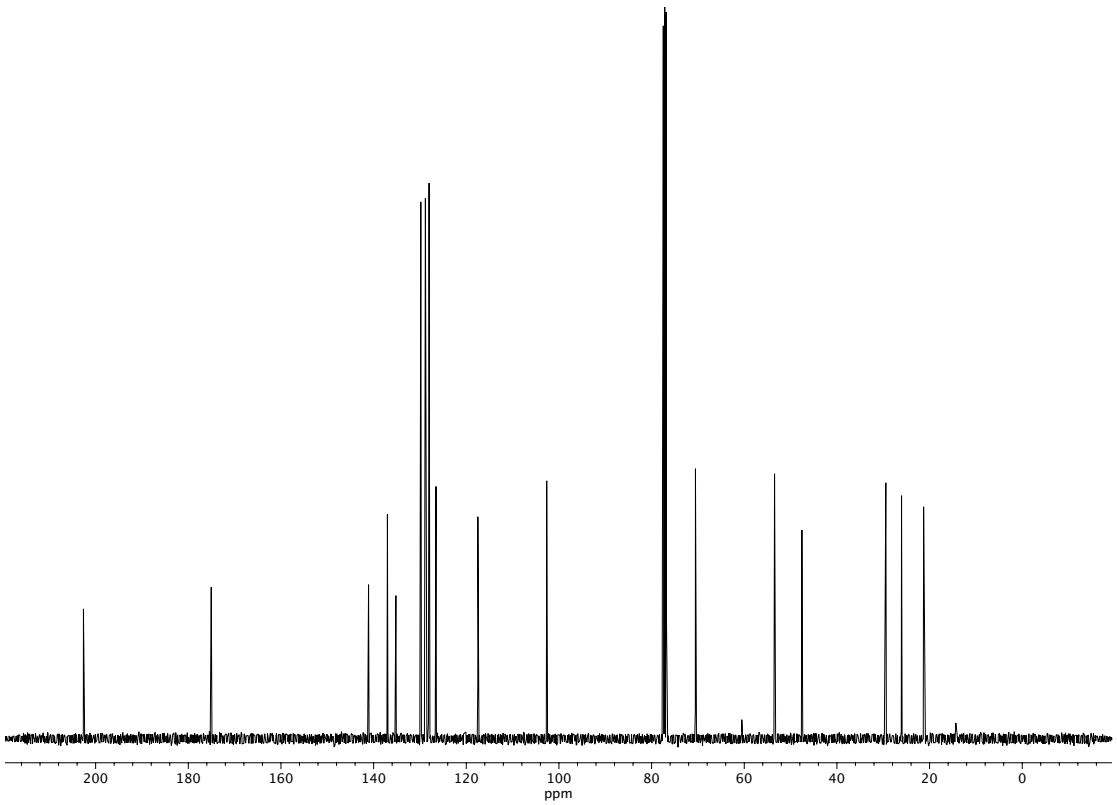
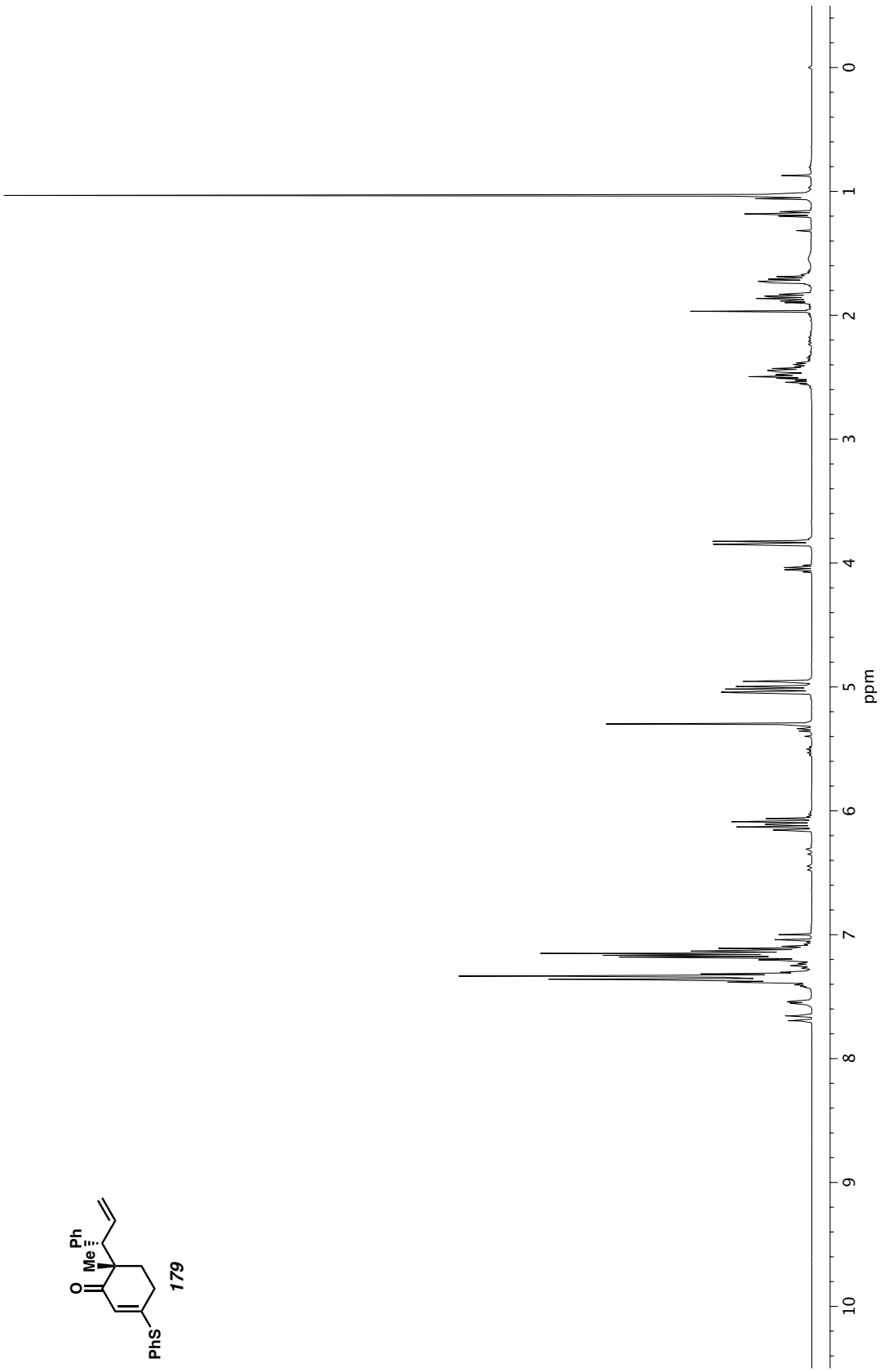


Figure A3.30. *^{13}C NMR (100 MHz, $CDCl_3$) of compound* ***178****.*



179

Figure A3.31. *^1H NMR (400 MHz, $CDCl_3$) of compound* ***179***.

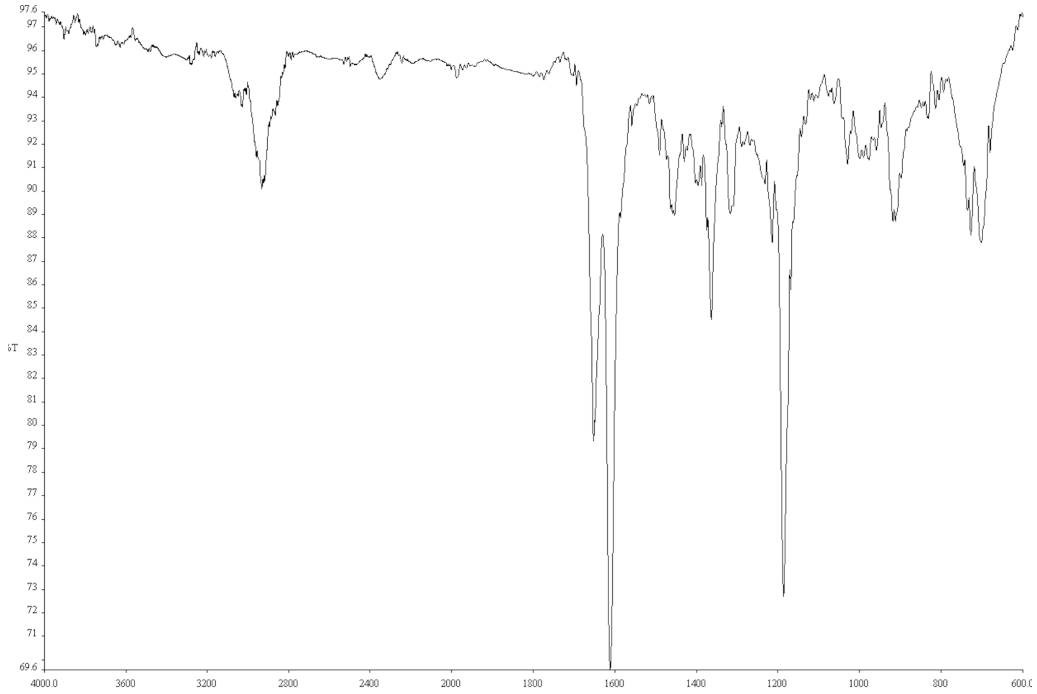


Figure A3.32. *Infrared spectrum (Thin Film, NaCl) of compound* ***179****.*

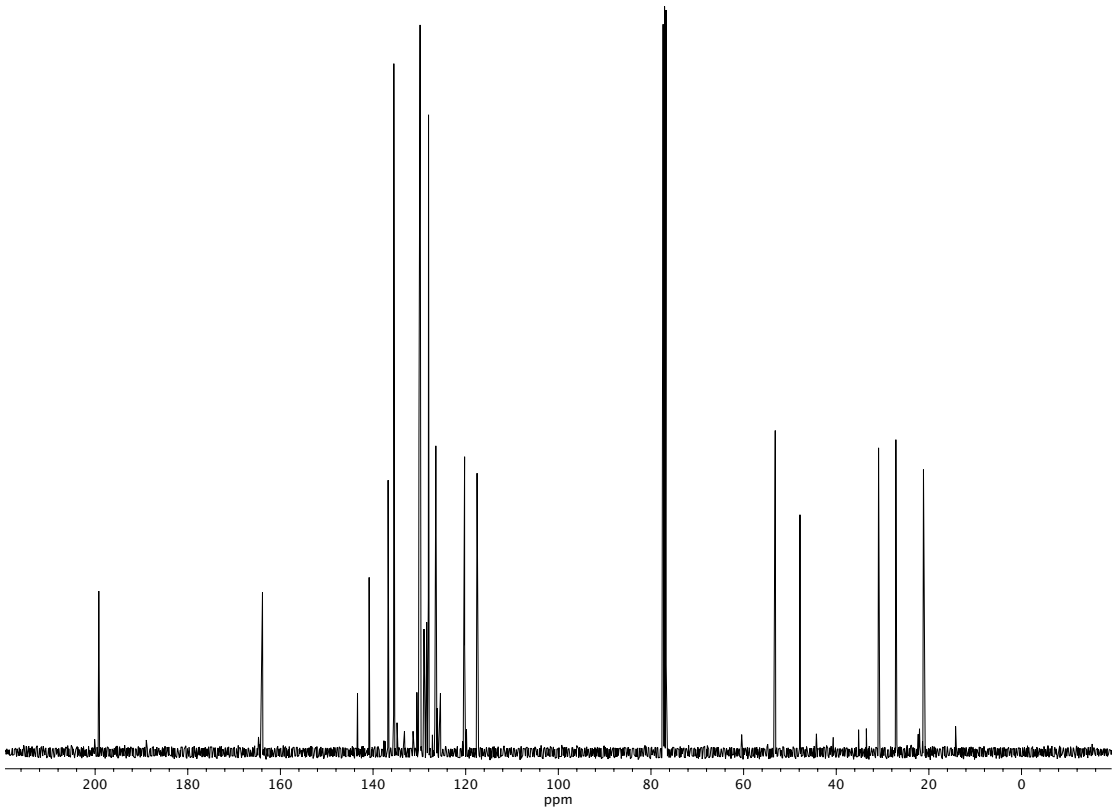


Figure A3.33. *^{13}C NMR (100 MHz, $CDCl_3$) of compound* ***179****.*

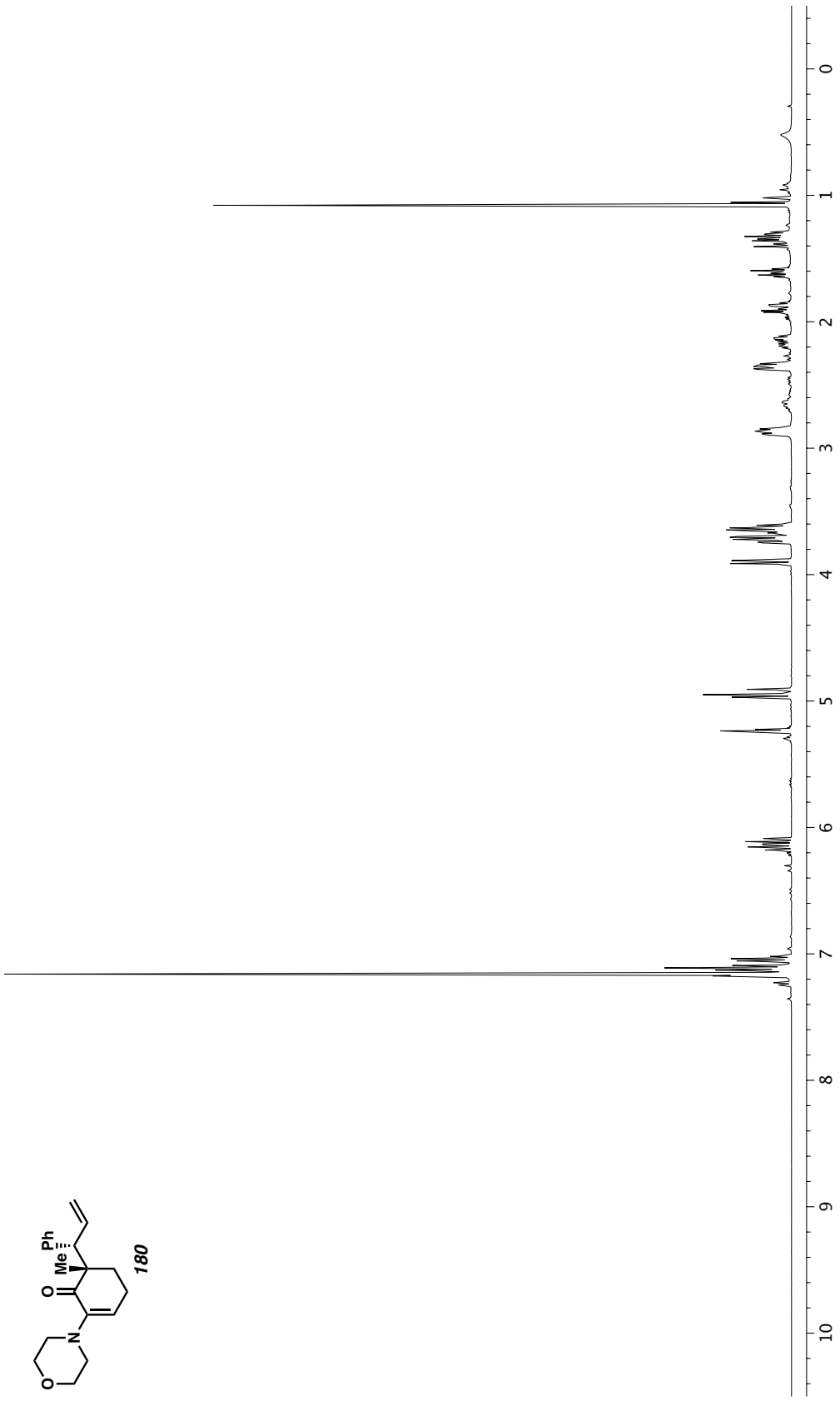


Figure A3.34. *^1H NMR (400 MHz, C_6D_6) of compound **180**.*

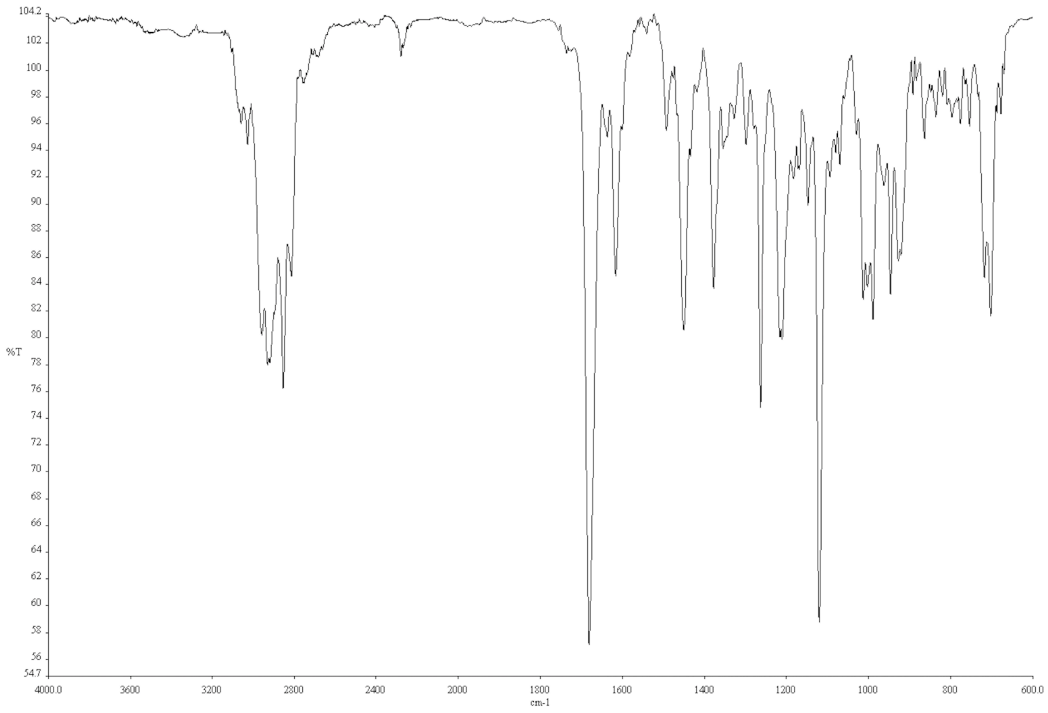


Figure A3.35. *Infrared spectrum (Thin Film, NaCl) of compound* ***180****.*

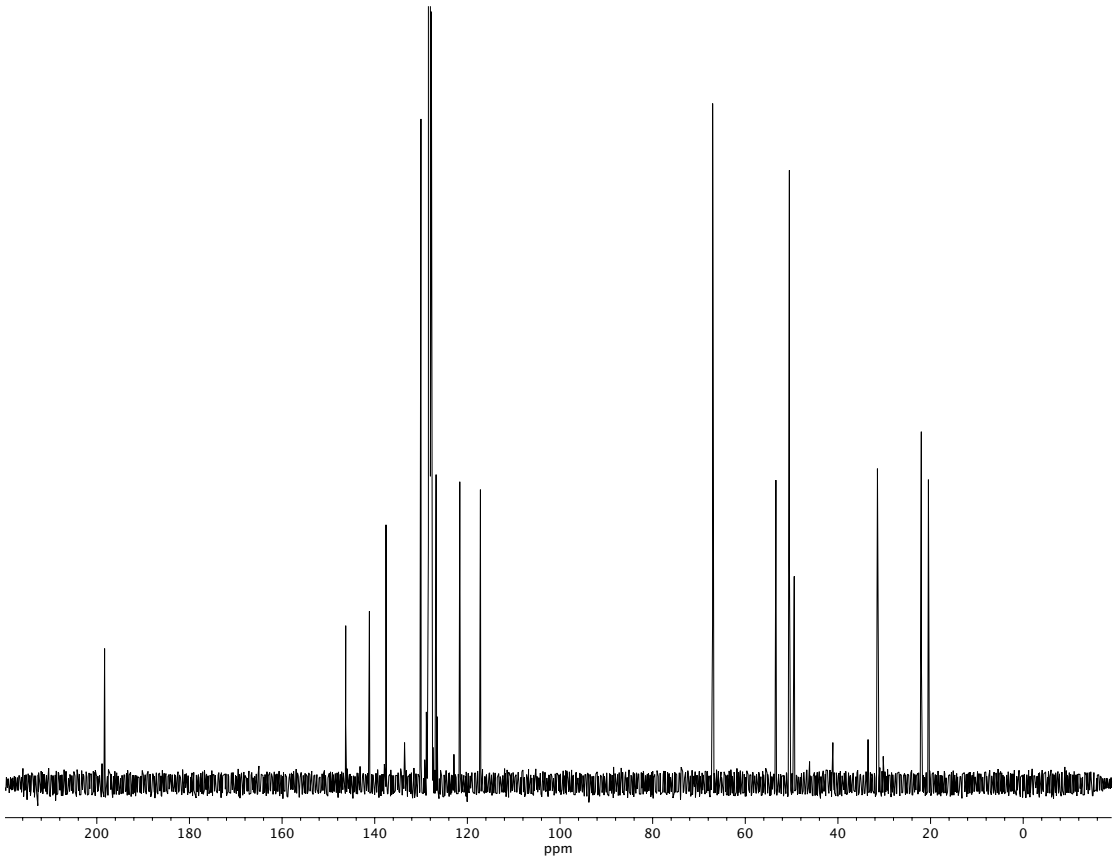


Figure A3.36. *^{13}C NMR (100 MHz, C_6D_6) of compound* ***180****.*

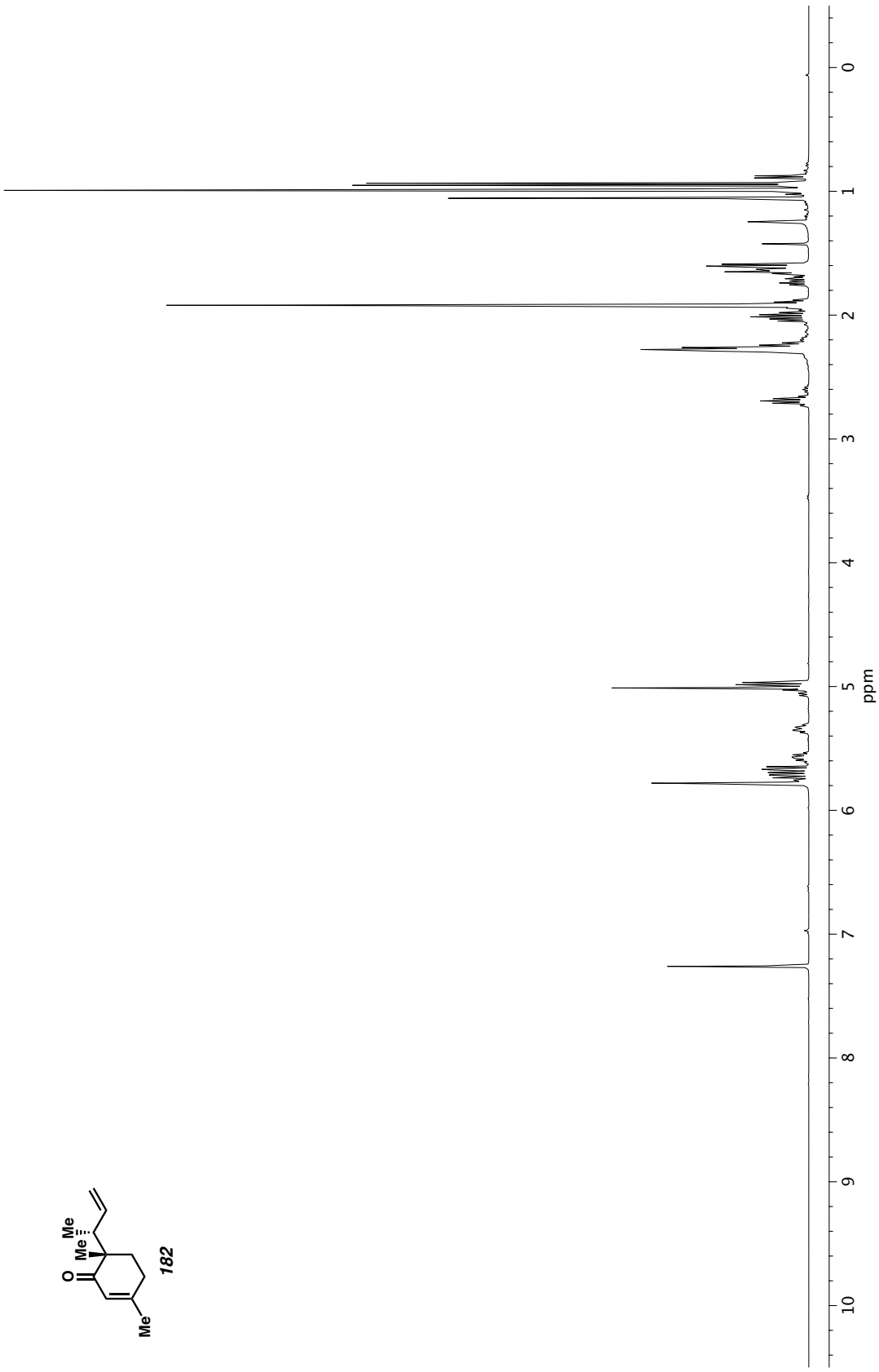


Figure A3.37. *^1H NMR (400 MHz, C_6D_6) of compound* ***182***.

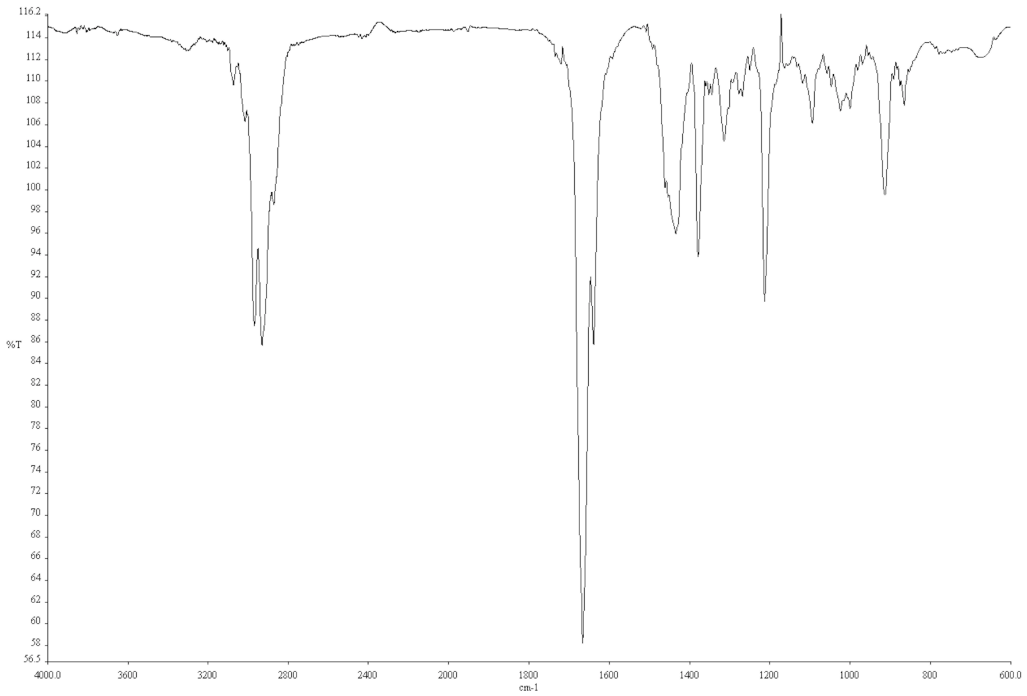


Figure A3.38. *Infrared spectrum (Thin Film, NaCl) of compound* ***182****.*

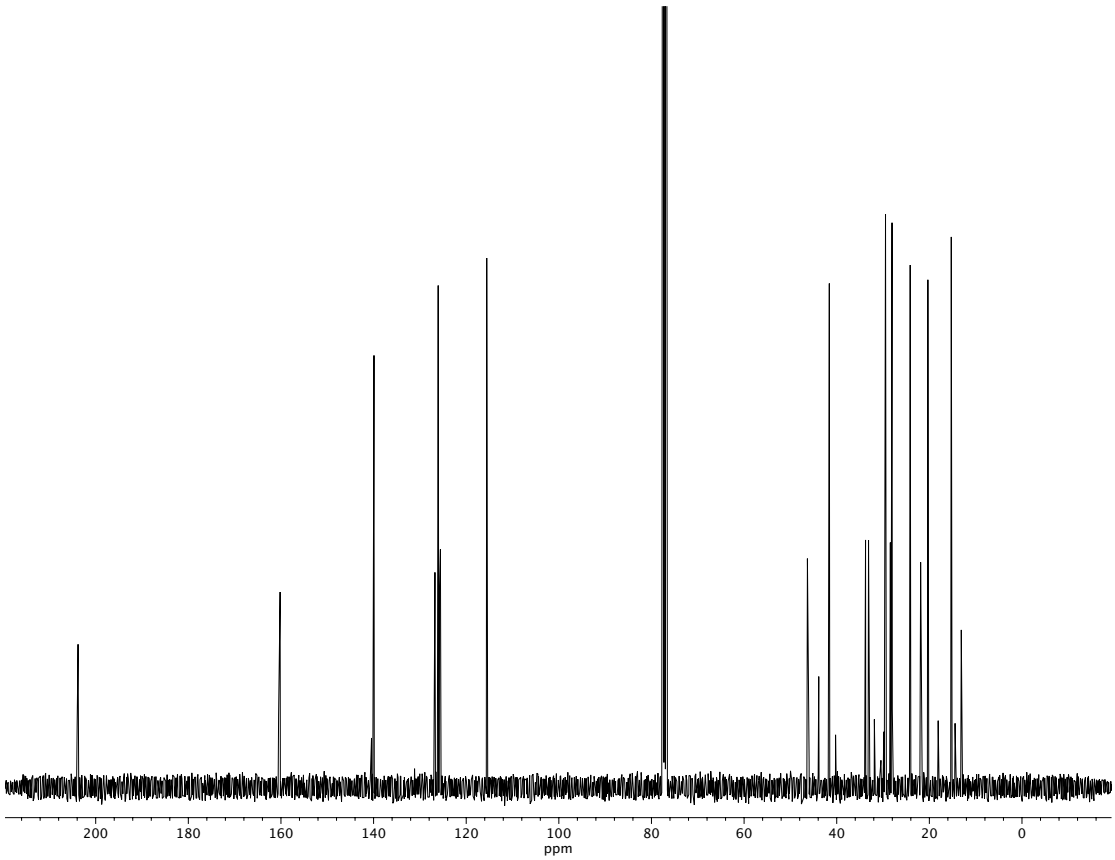


Figure A3.39. *^{13}C NMR (100 MHz, $CDCl_3$) of compound* ***182****.*

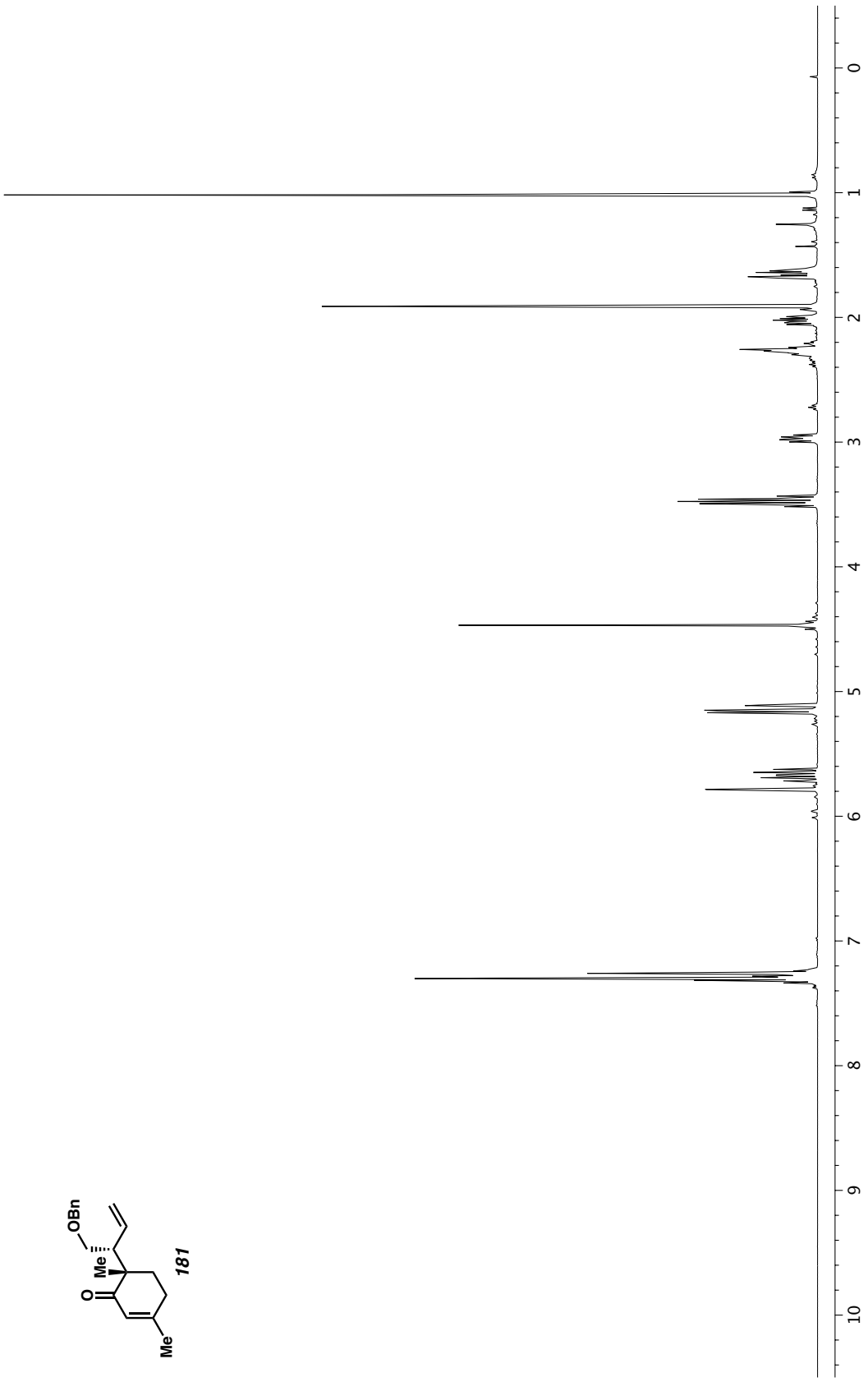


Figure A3.40. *^1H NMR (500 MHz, $CDCl_3$) of compound* ***181****.*

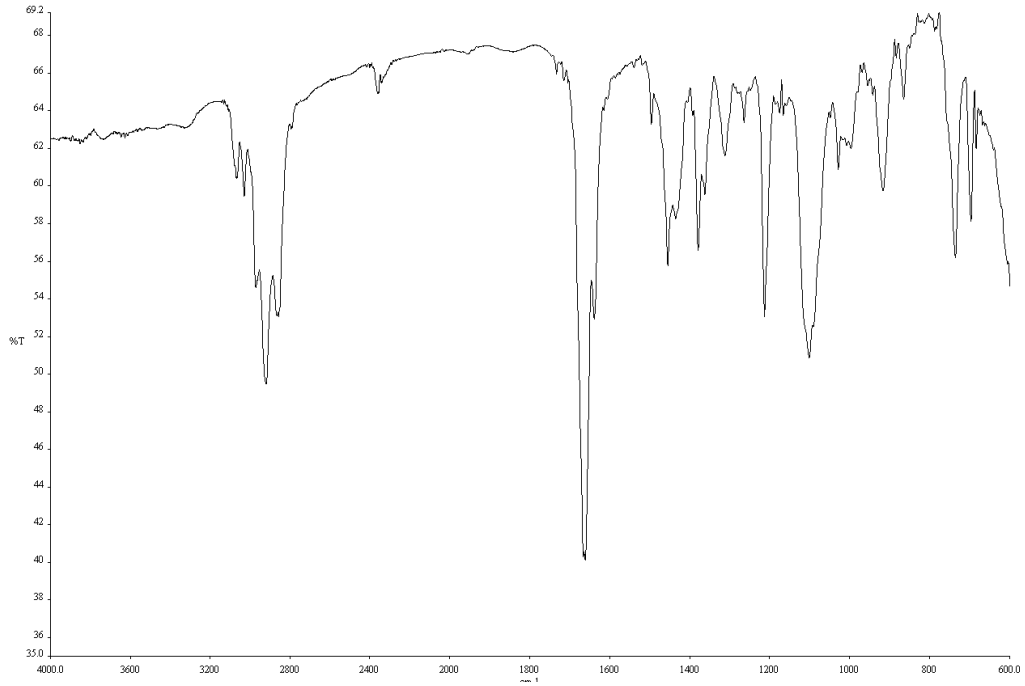


Figure A3.41. *Infrared spectrum (Thin Film, NaCl) of compound* ***181***.

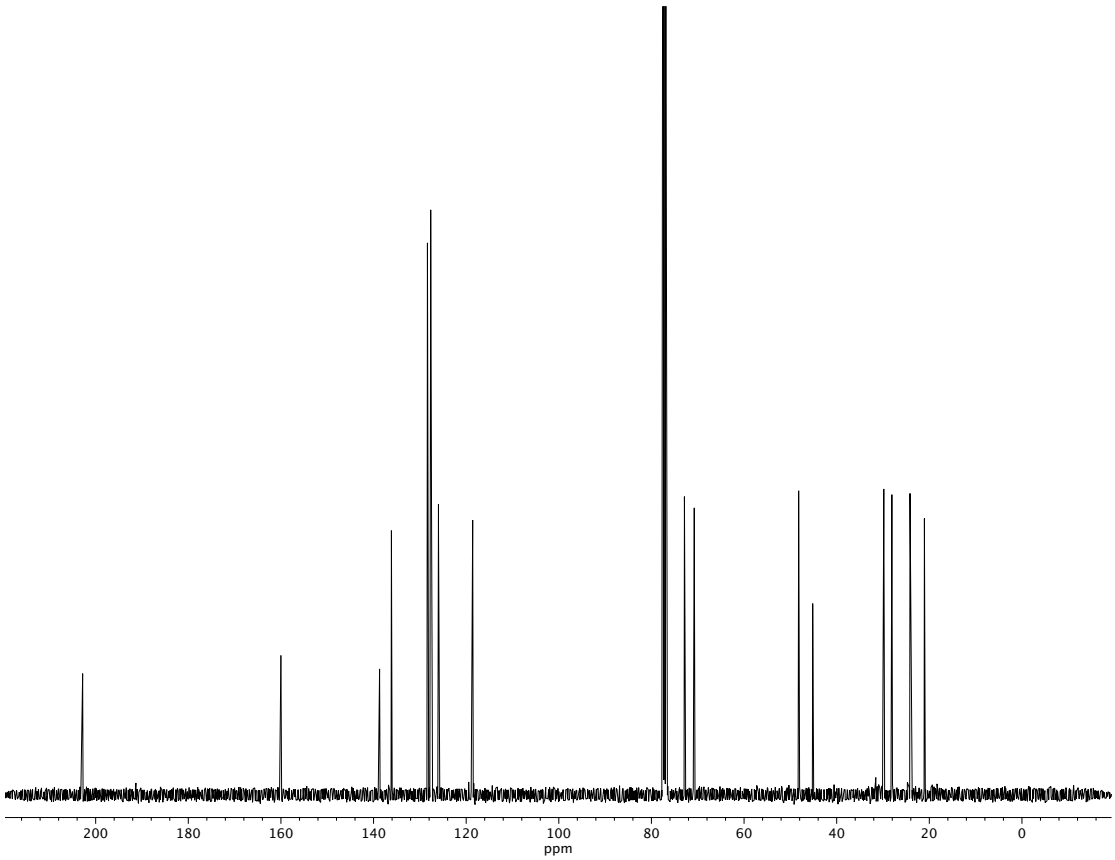


Figure A3.42. *^{13}C NMR (100 MHz, $CDCl_3$) of compound* ***181***.

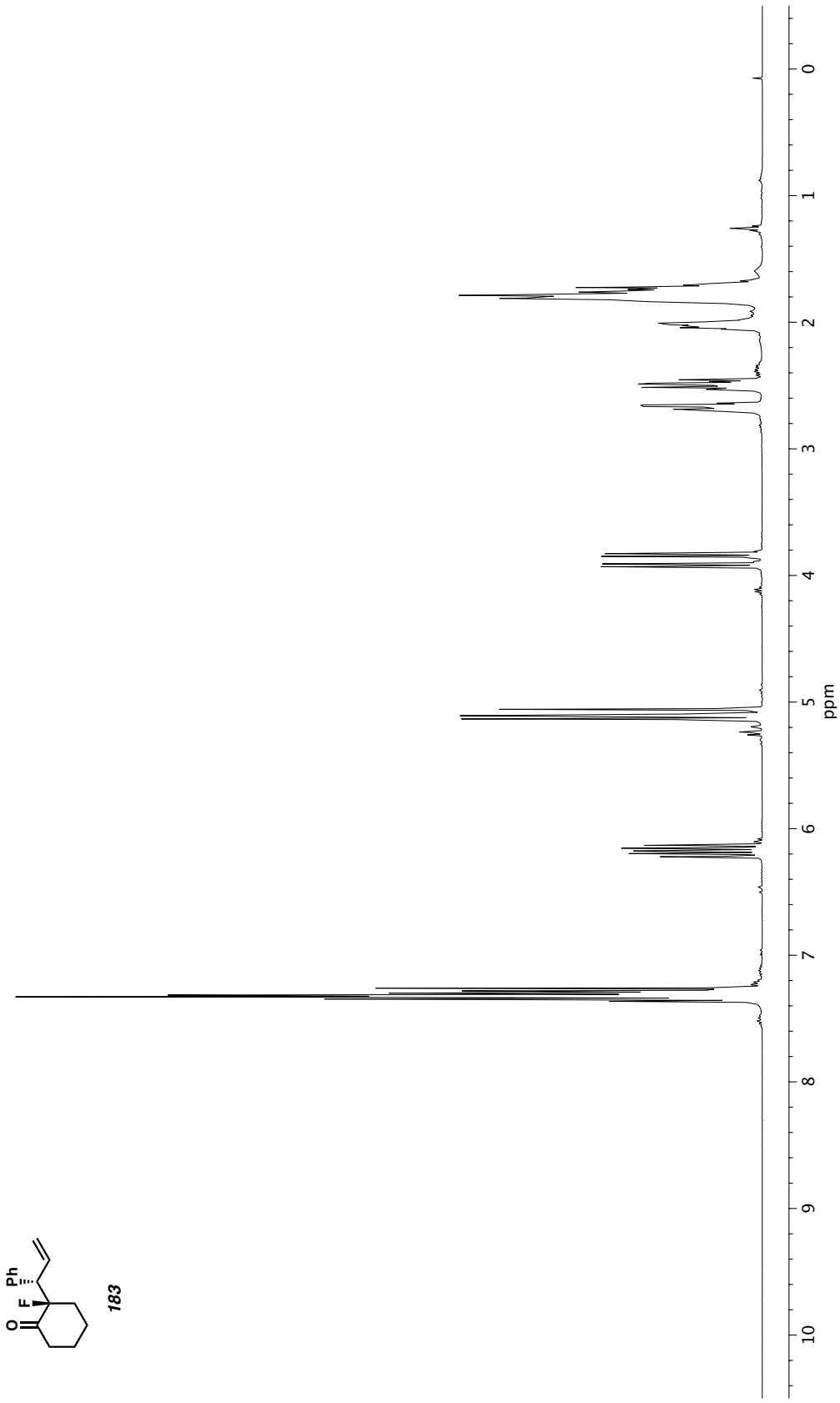


Figure A3.43. *^1H NMR (400 MHz, $CDCl_3$) of compound* ***183***.

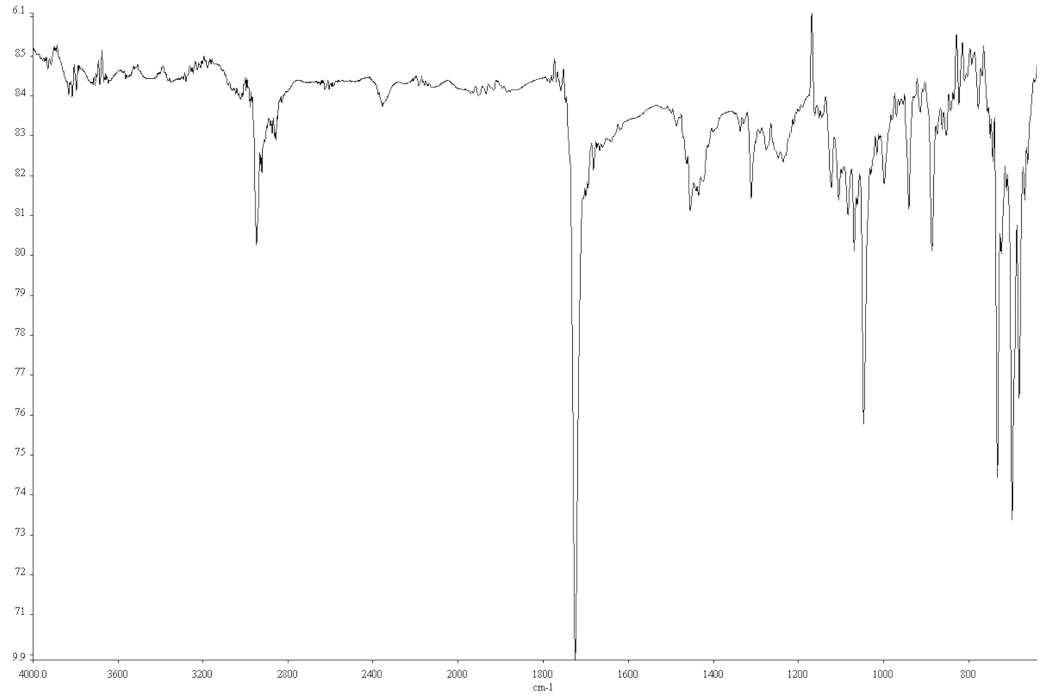


Figure A3.44. *Infrared spectrum (Thin Film, NaCl) of compound* ***183****.*

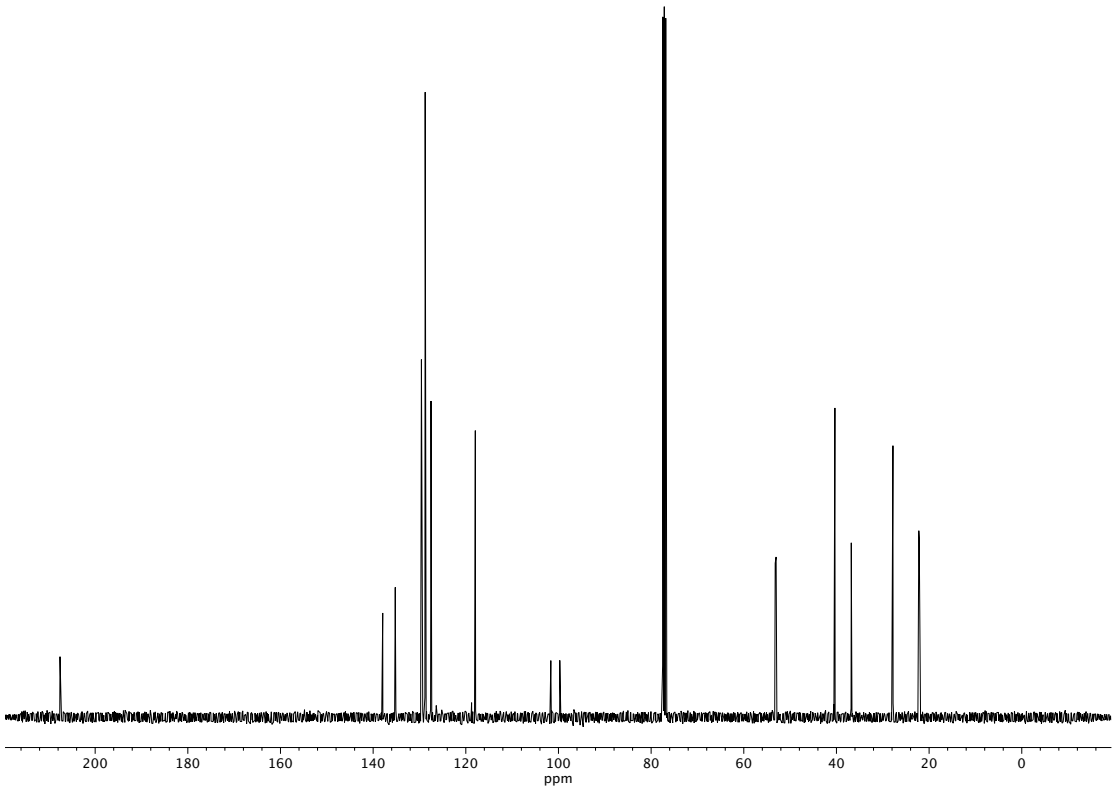


Figure A3.45. *^{13}C NMR (100 MHz, $CDCl_3$) of compound* ***183****.*

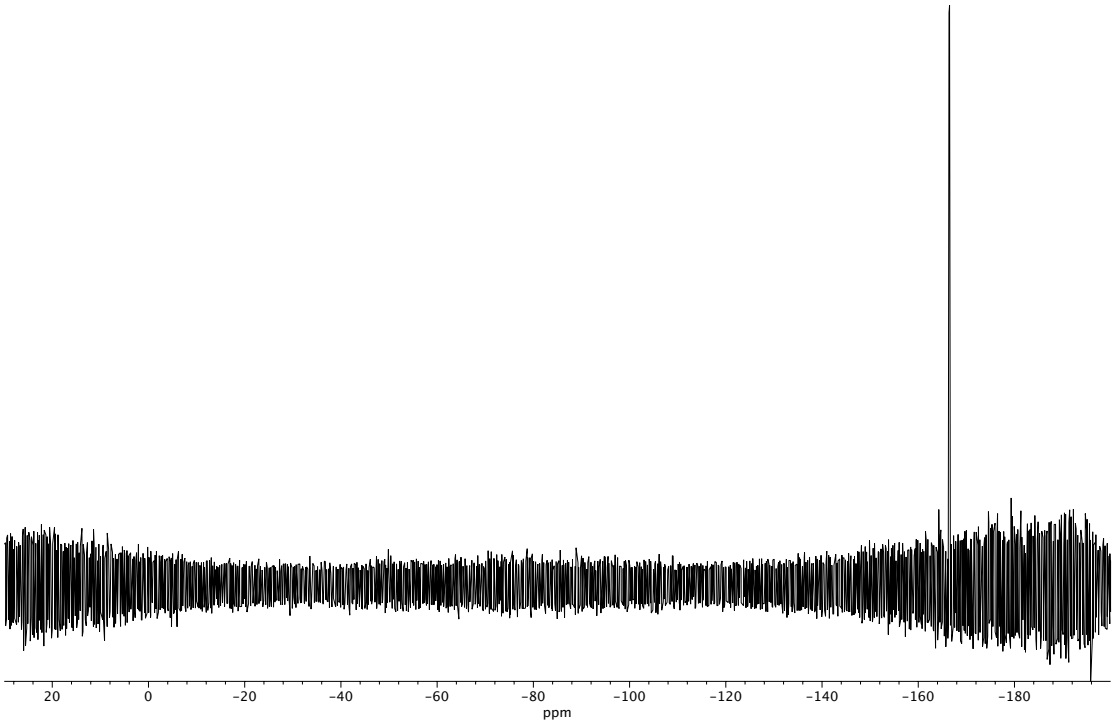


Figure A3.46. *^{19}F NMR (282 MHz, $CDCl_3$) of compound* ***183***.

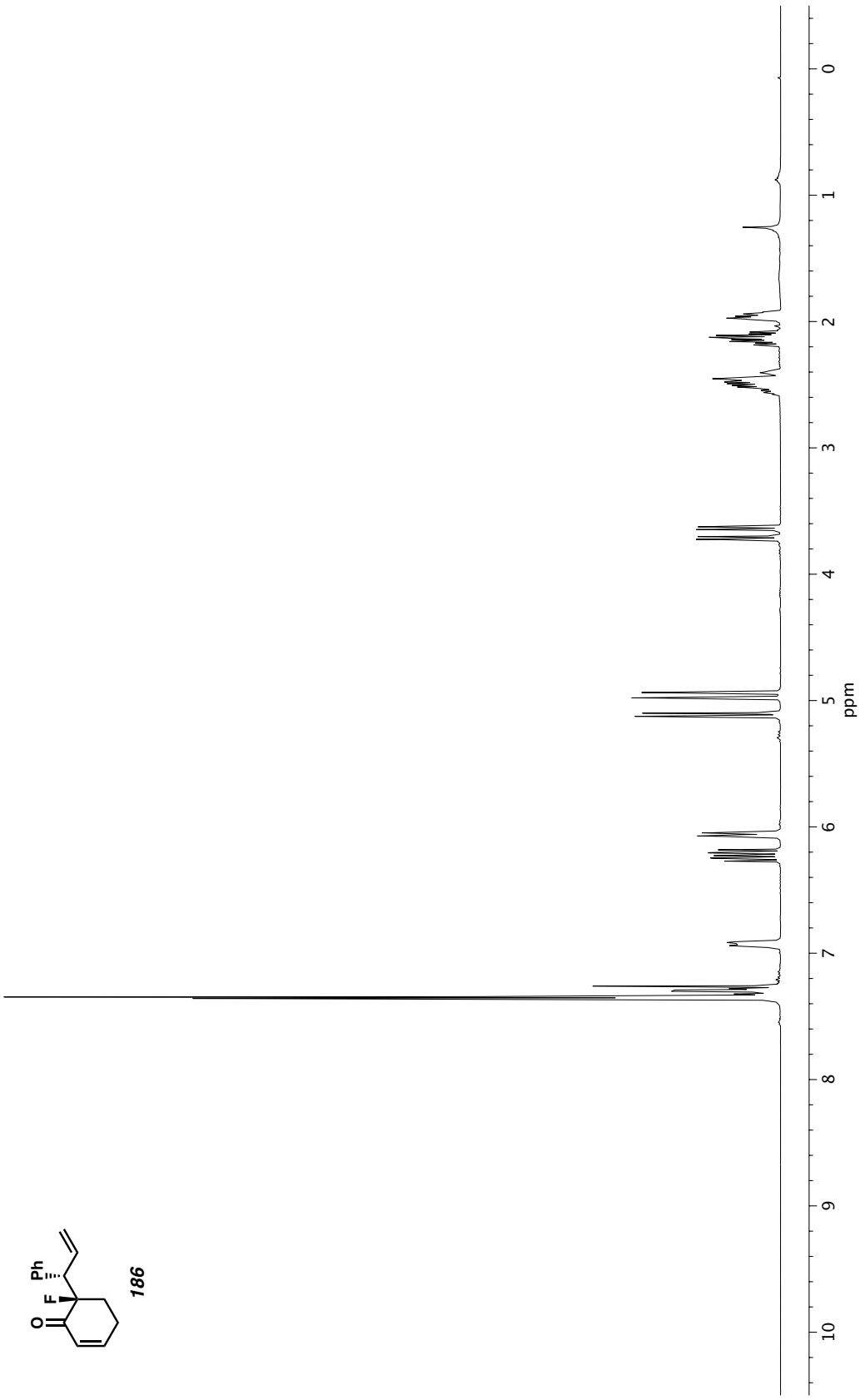


Figure A3.47. *^1H NMR (400 MHz, $CDCl_3$) of compound **186**.*

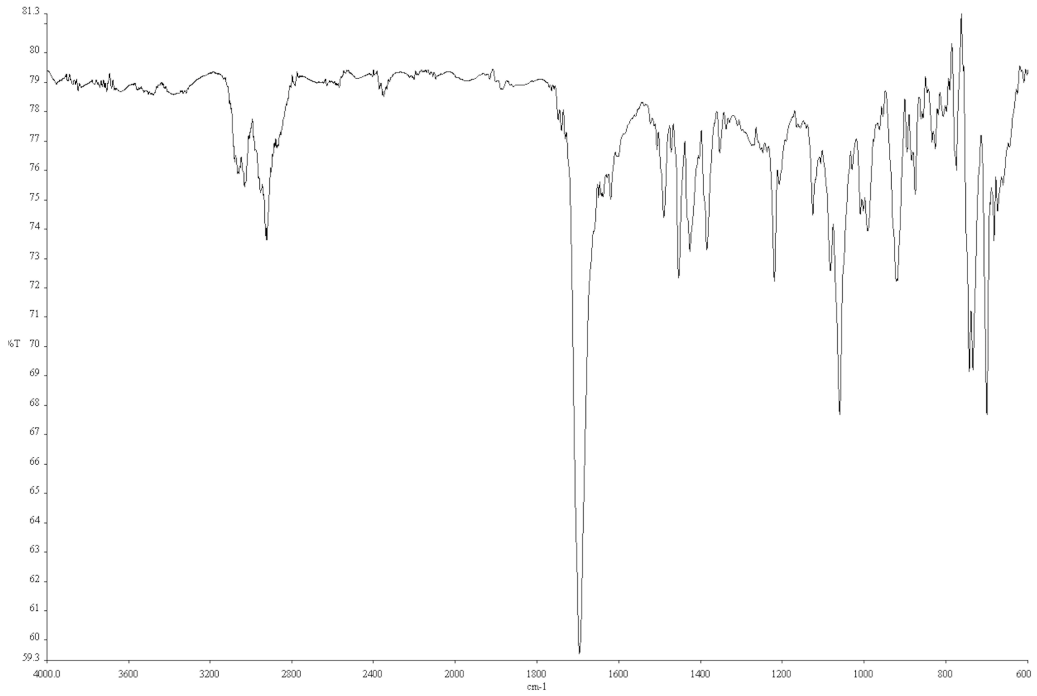


Figure A3.48. *Infrared spectrum (Thin Film, NaCl) of compound* ***186****.*

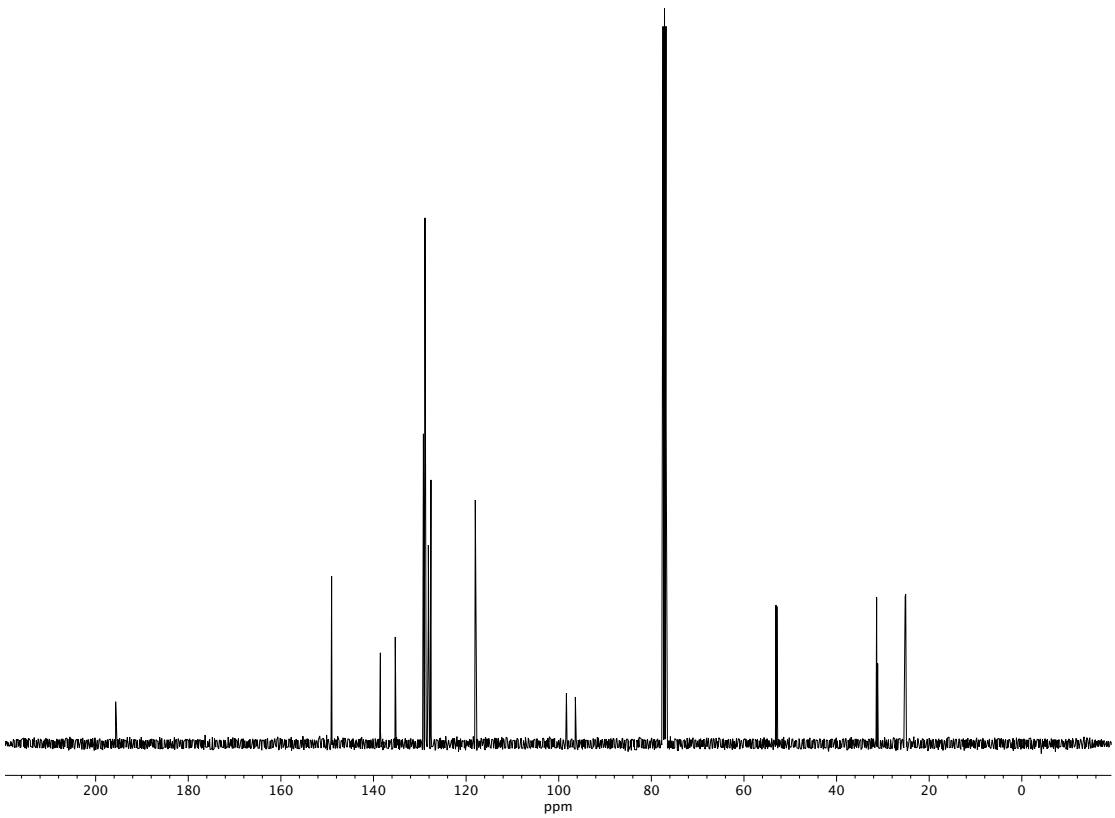


Figure A3.49. *^{13}C NMR (100 MHz, $CDCl_3$) of compound* ***186****.*

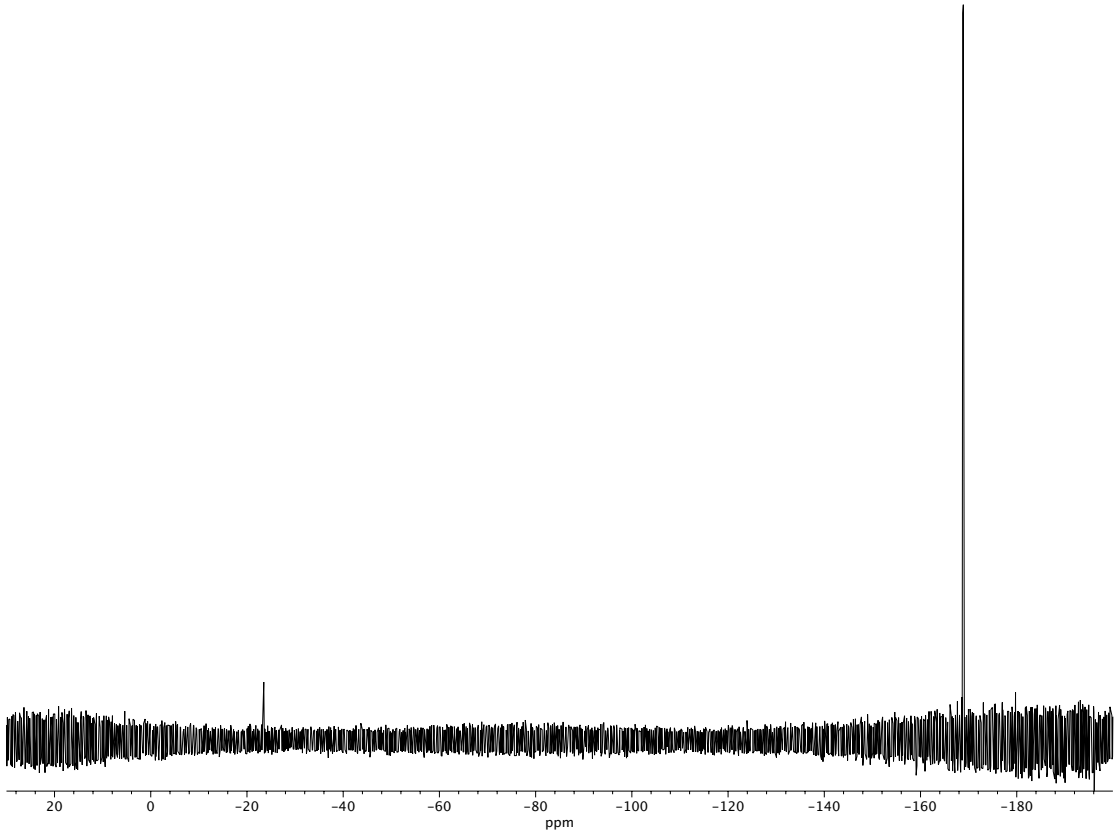


Figure A3.50. *^{19}F NMR (282 MHz, $CDCl_3$) of compound* ***186****.*

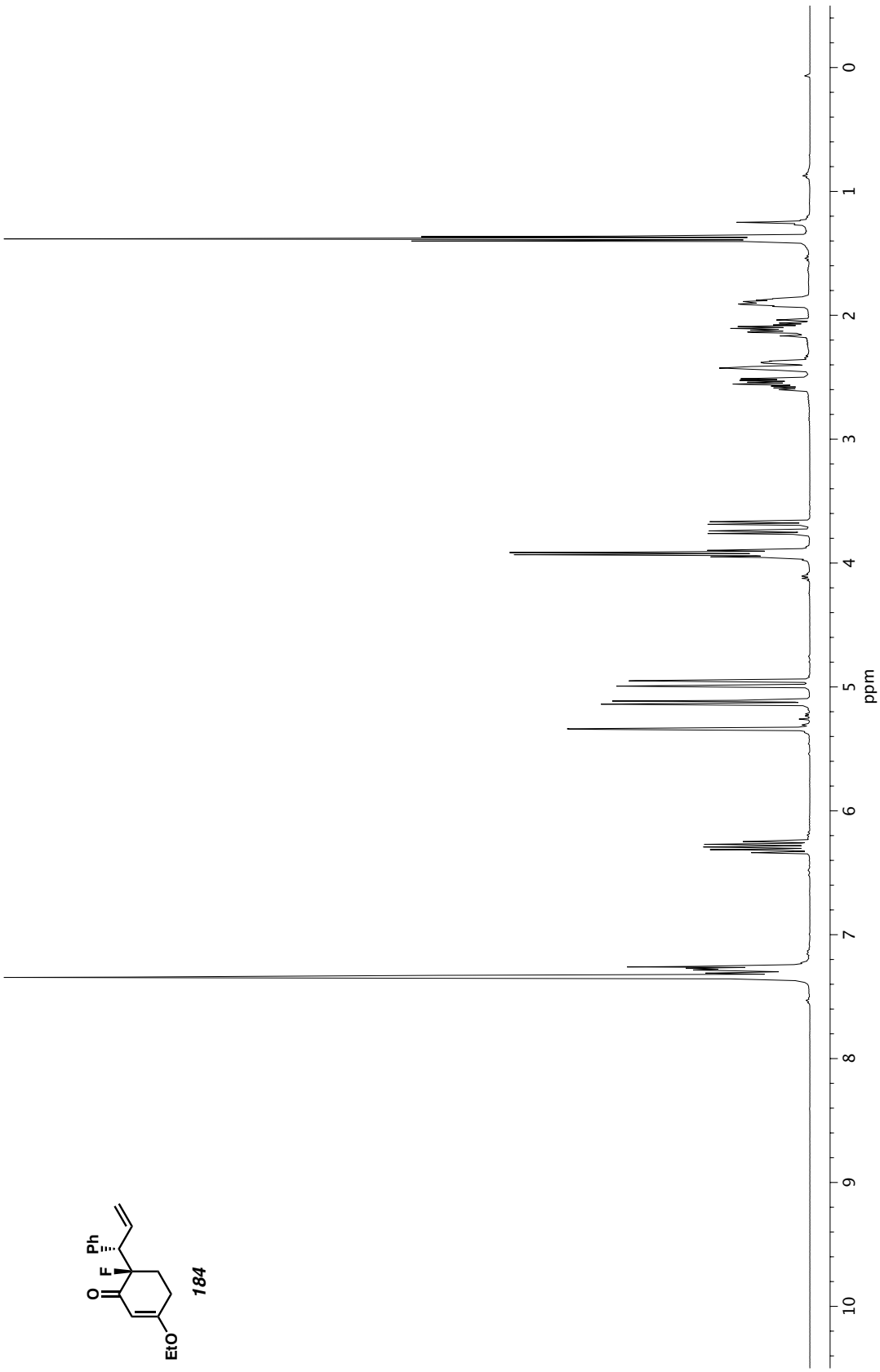


Figure A3.51. *^1H NMR (400 MHz, $CDCl_3$) of compound* ***184****.*

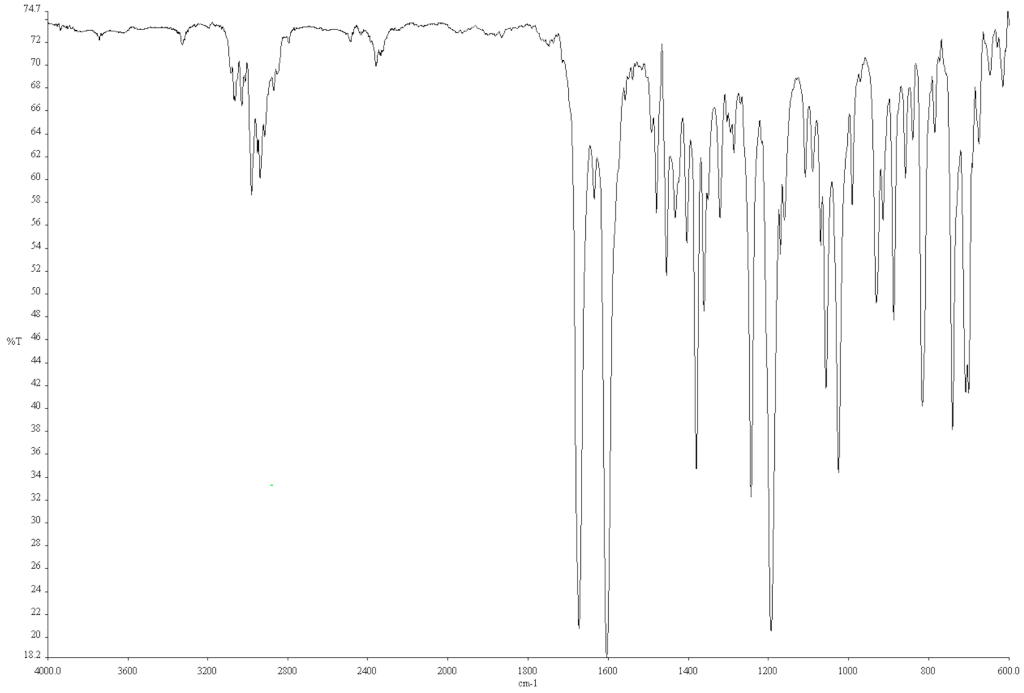


Figure A3.52. *Infrared spectrum (Thin Film, NaCl) of compound* ***184****.*

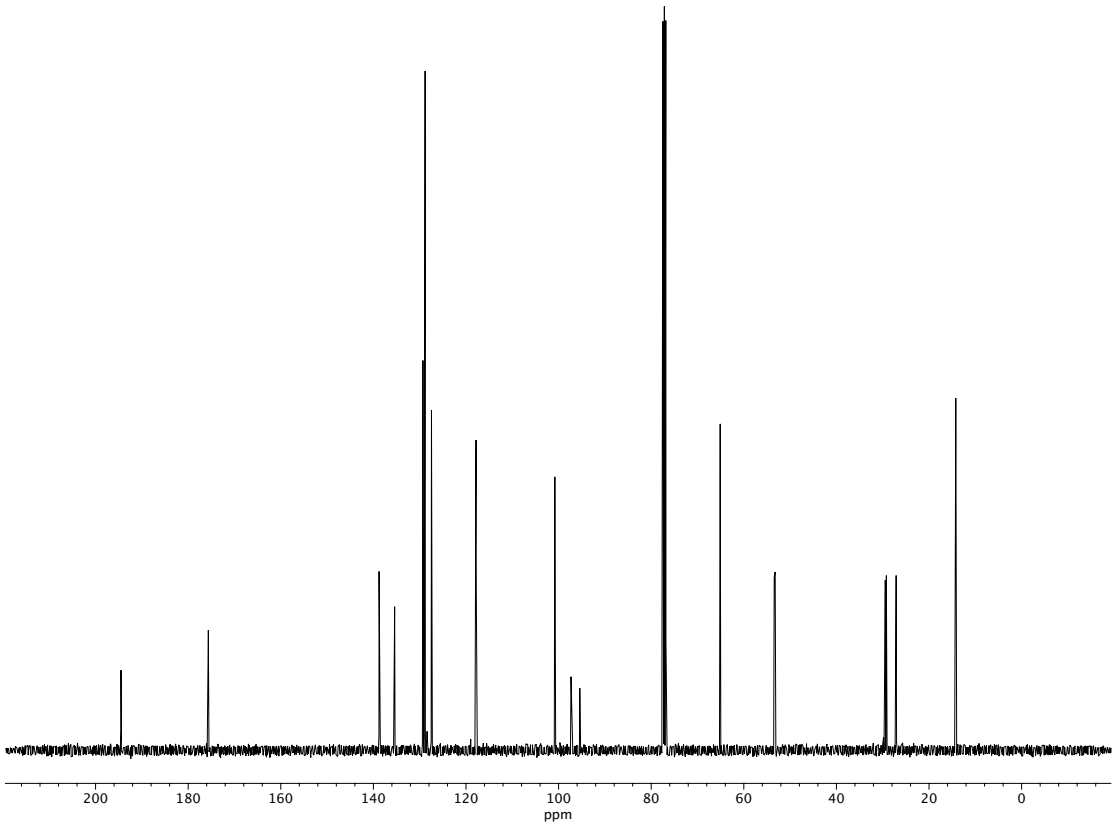


Figure A3.53. *^{13}C NMR (100 MHz, $CDCl_3$) of compound* ***184****.*

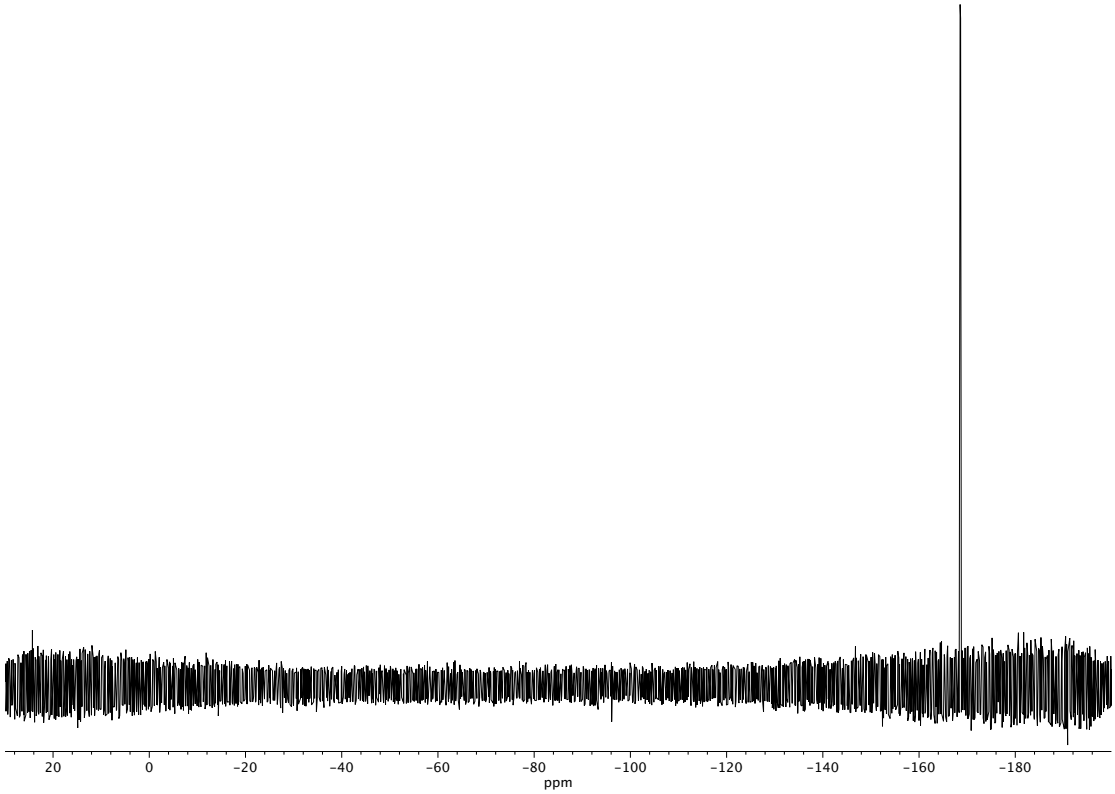


Figure A3.54. *^{19}F NMR (282 MHz, $CDCl_3$) of compound* ***184****.*

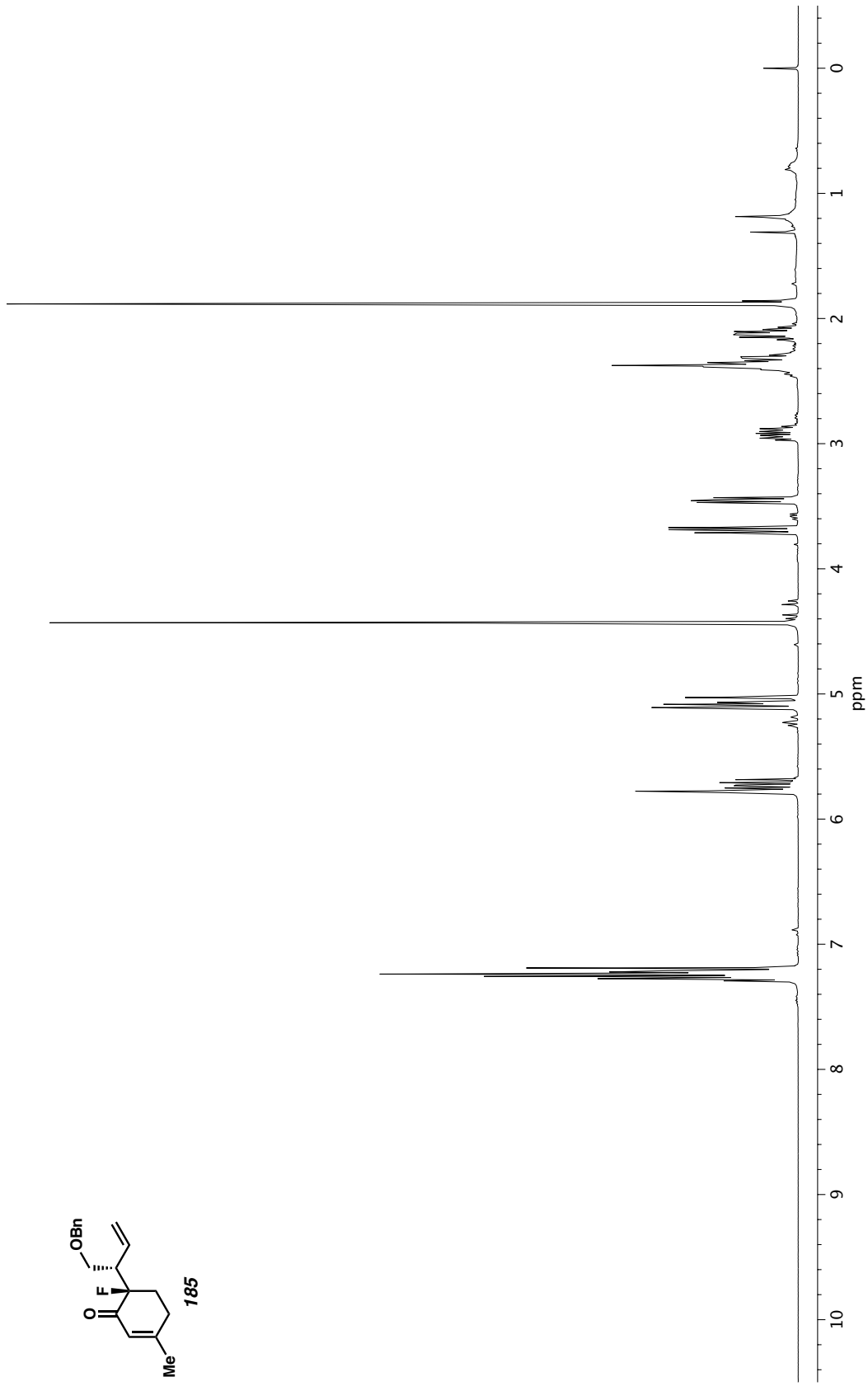


Figure A3.55. *^{1}H NMR (400 MHz, $CDCl_3$) of compound **185**.*

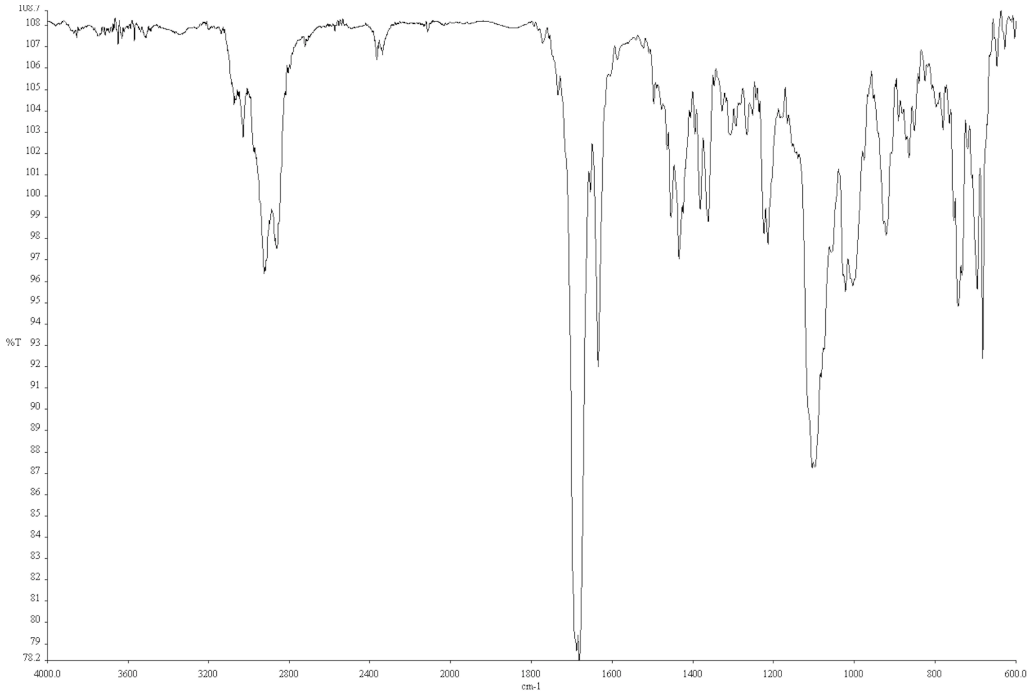


Figure A3.56. *Infrared spectrum (Thin Film, NaCl) of compound* ***185****.*

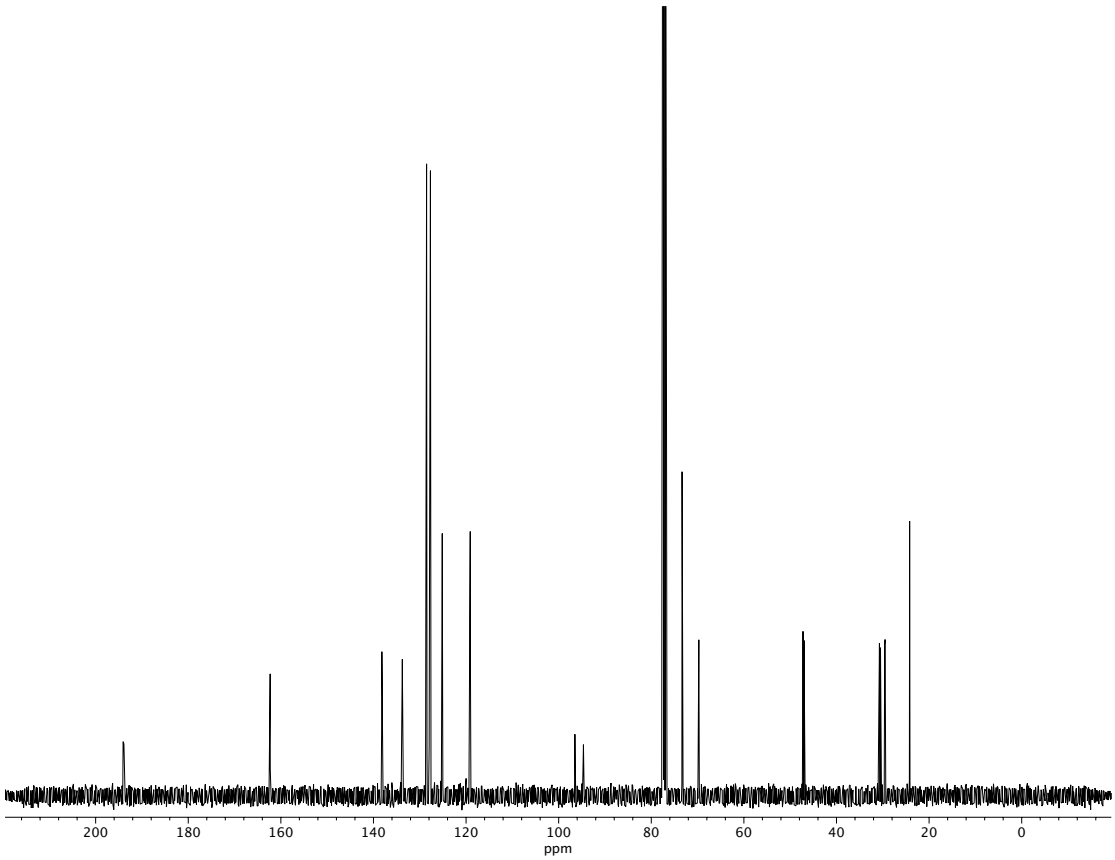


Figure A3.57. *^{13}C NMR (100 MHz, $CDCl_3$) of compound* ***185****.*

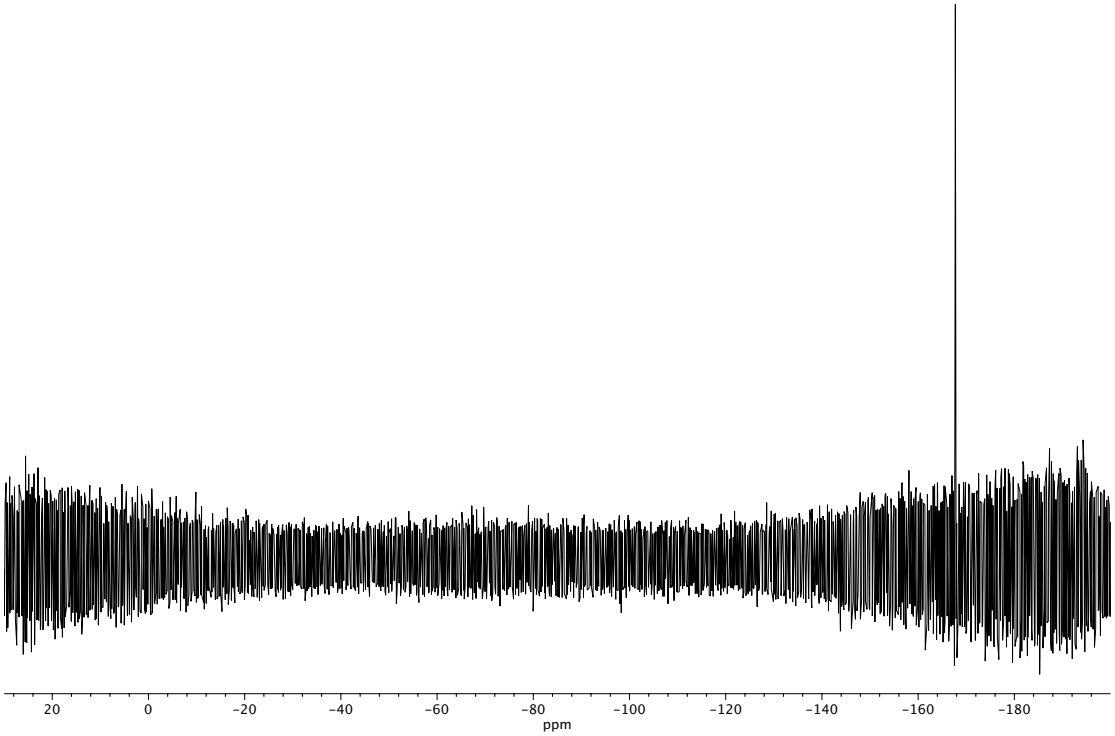
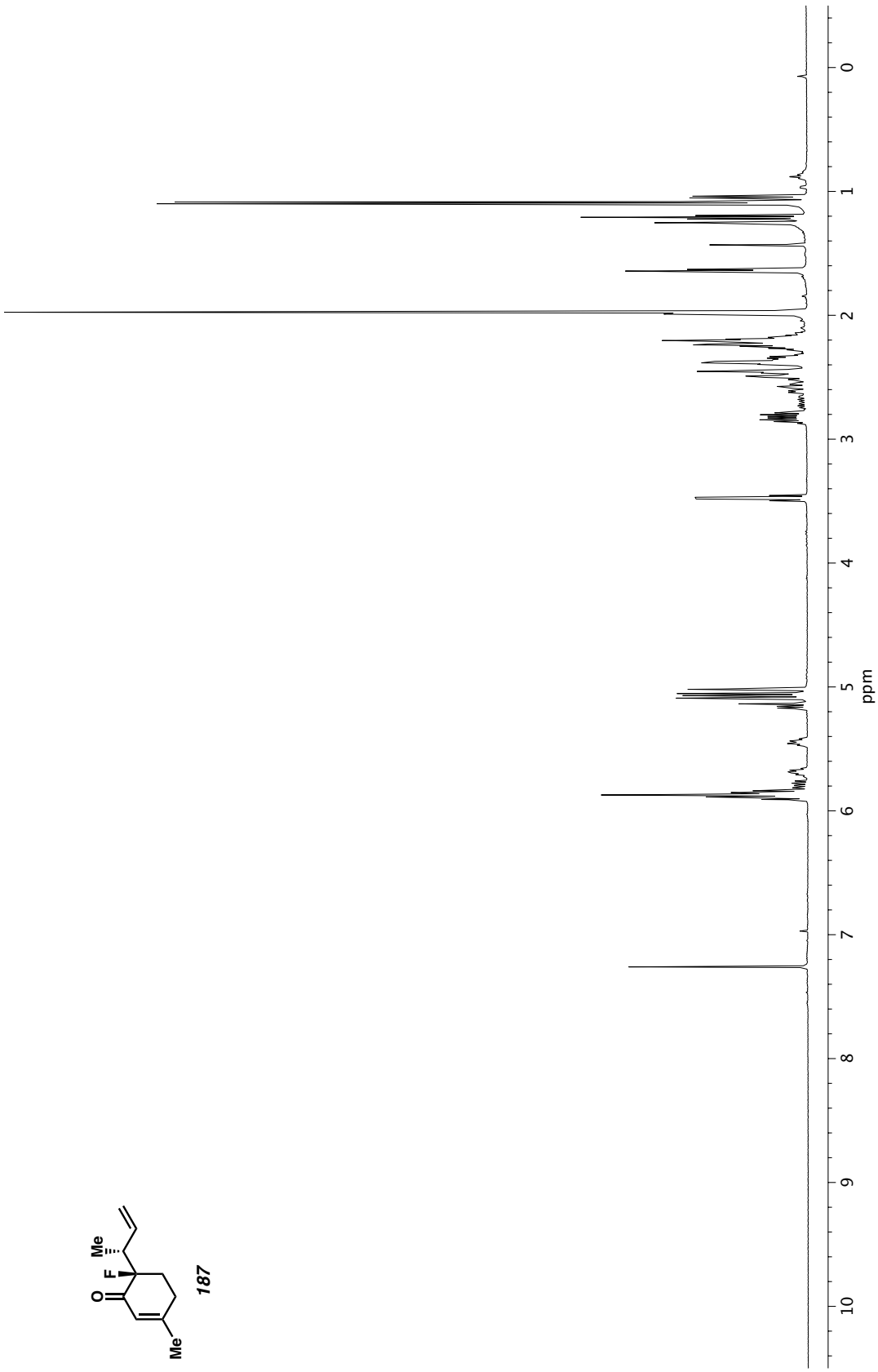


Figure A3.58. *^{19}F NMR (282 MHz, $CDCl_3$) of compound* ***185****.*



187

Figure A3.59. *^1H NMR (500 MHz, $CDCl_3$) of compound **187** (mixture).*

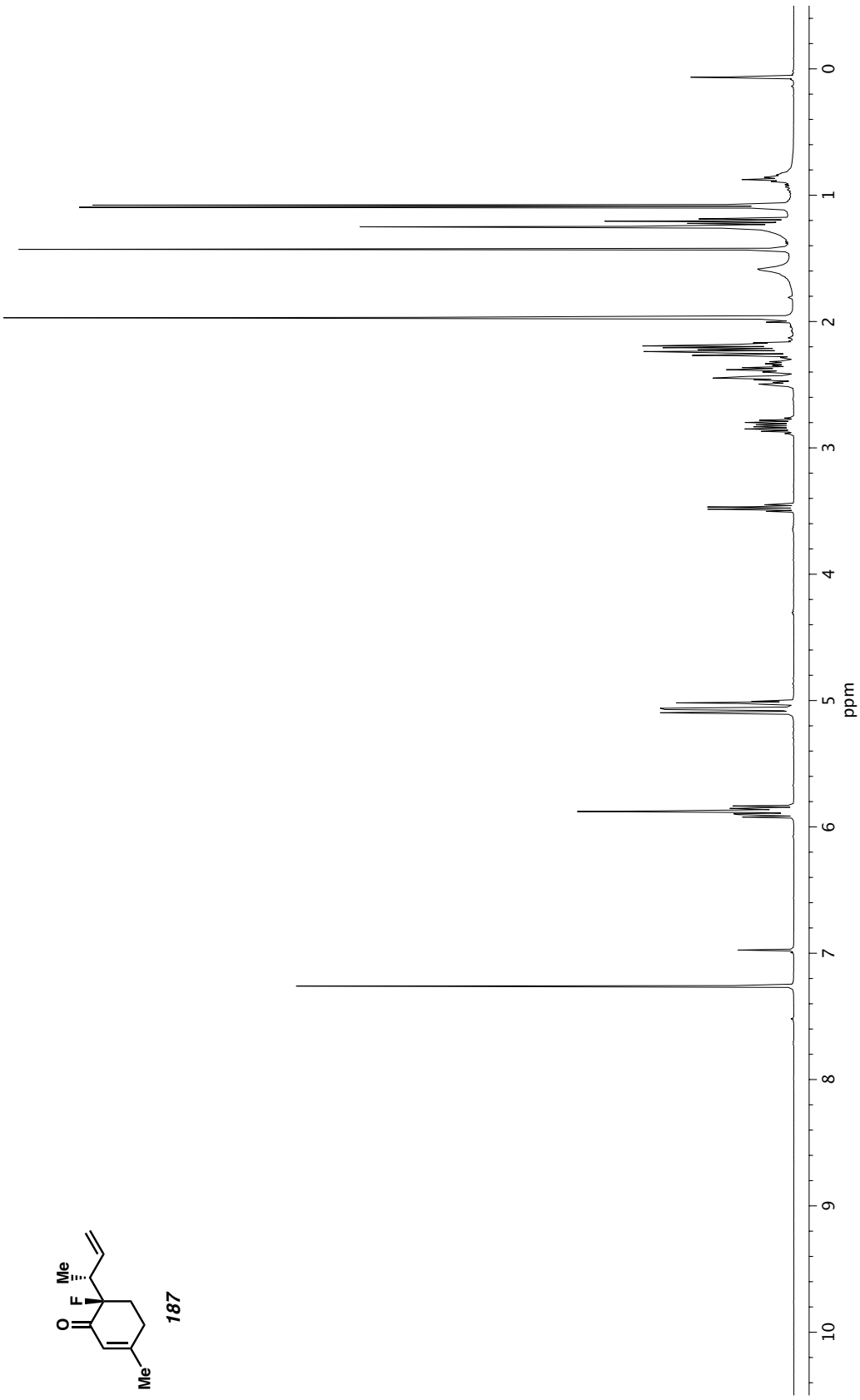


Figure A3.60. *^{1}H NMR (400 MHz, $CDCl_3$) of compound **187**.*

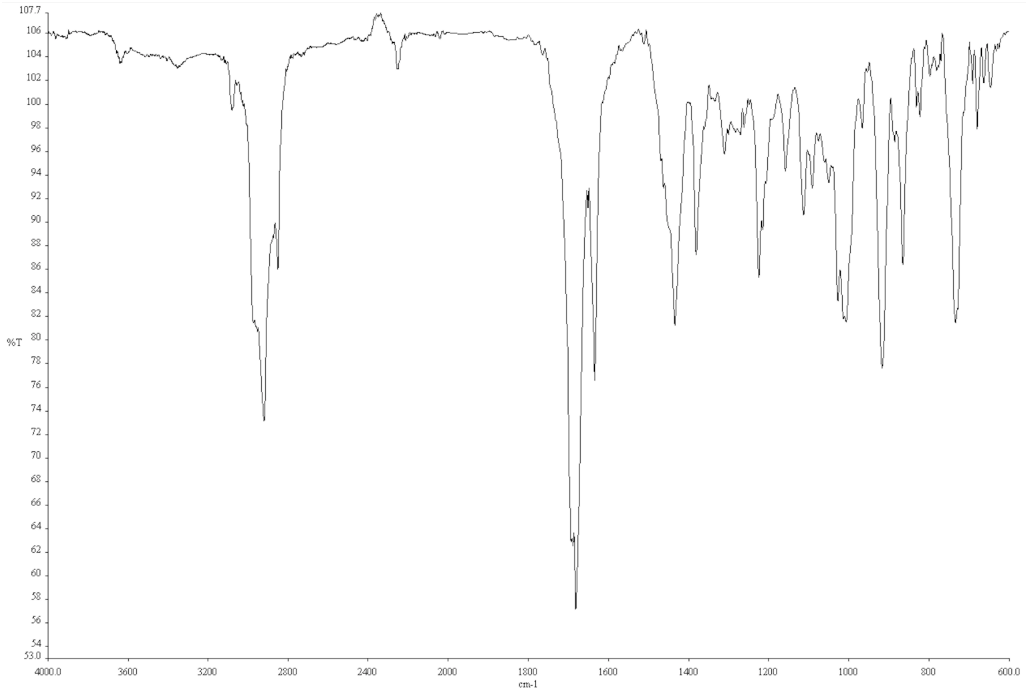


Figure A3.61. *Infrared spectrum (Thin Film, NaCl) of compound* ***187****.*

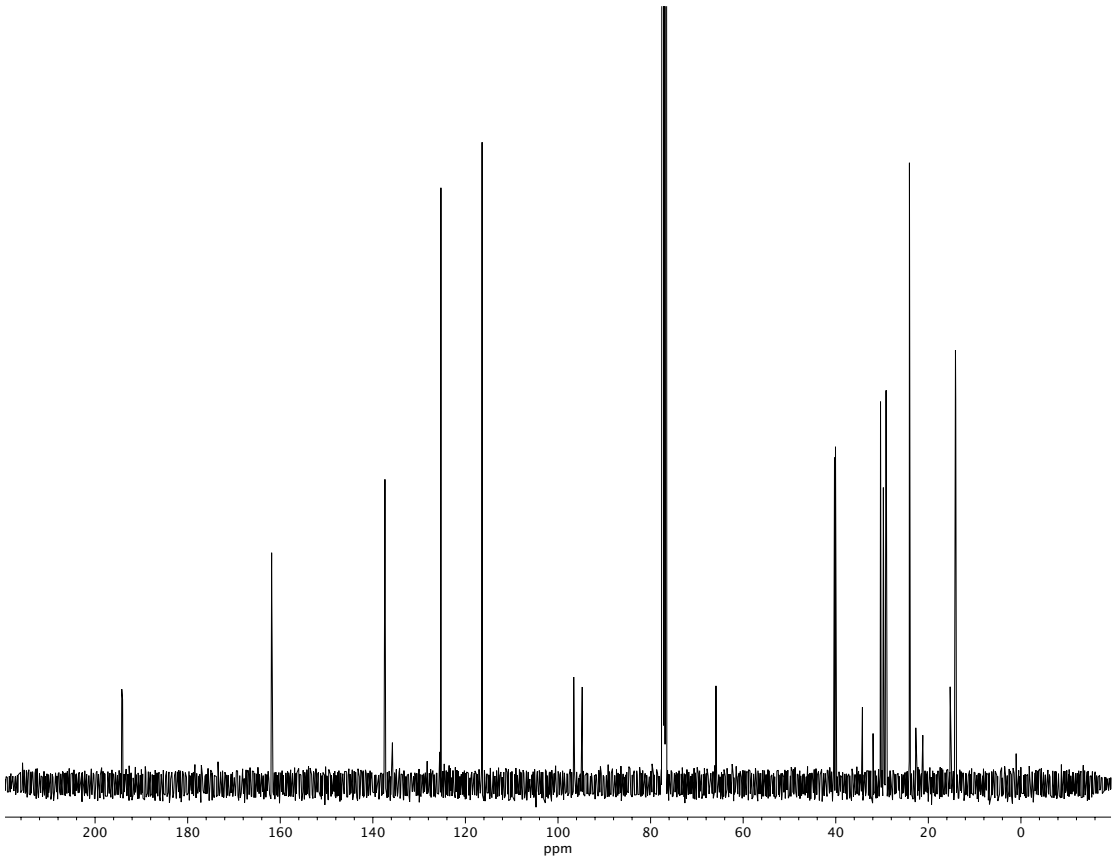


Figure A3.62. *^{13}C NMR (100 MHz, $CDCl_3$) of compound* ***187****.*

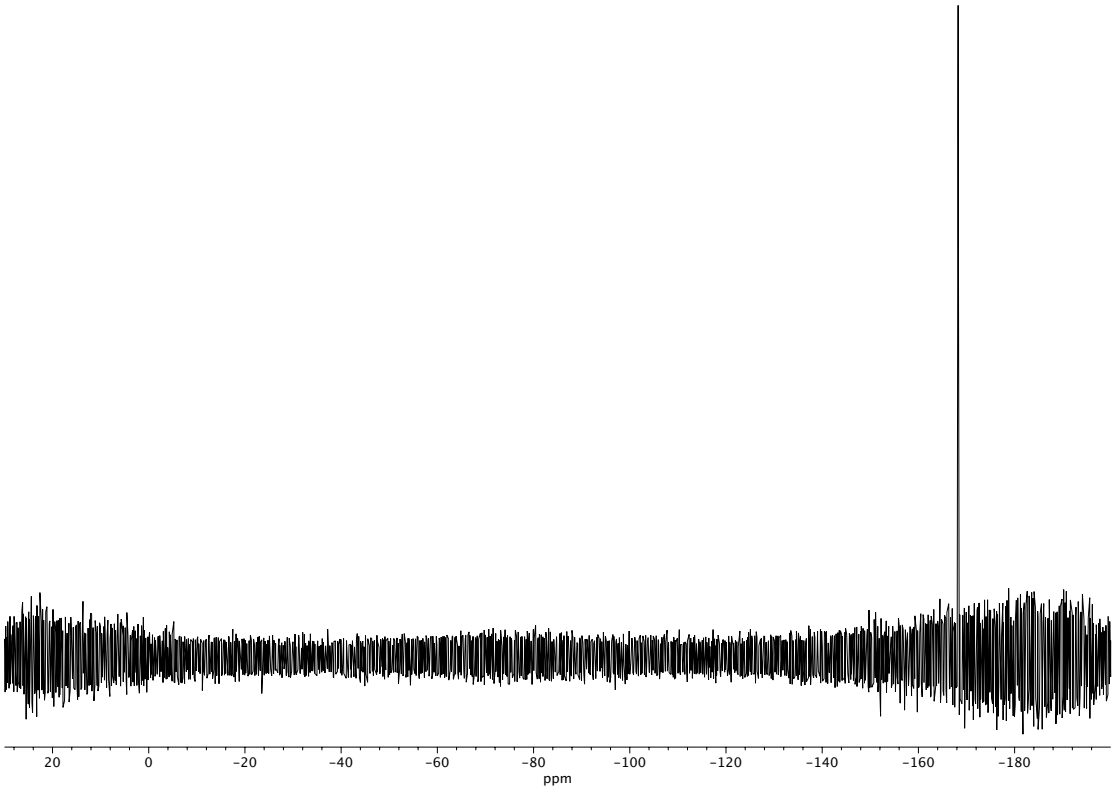


Figure A3.63. *^{19}F NMR (282 MHz, $CDCl_3$) of compound* ***187****.*

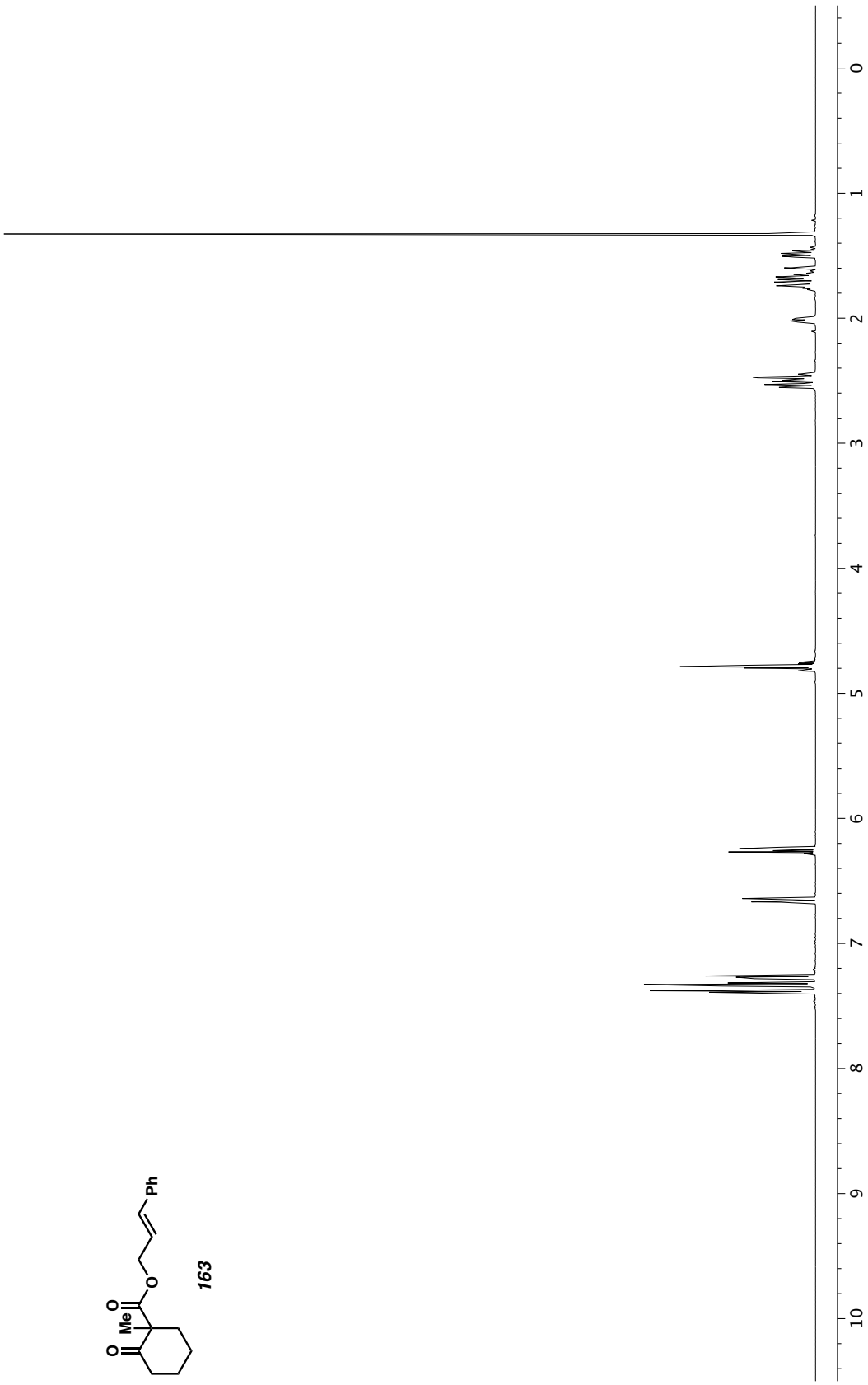


Figure A3.64. *^1H NMR (600 MHz, $CDCl_3$) of compound* ***163****.*

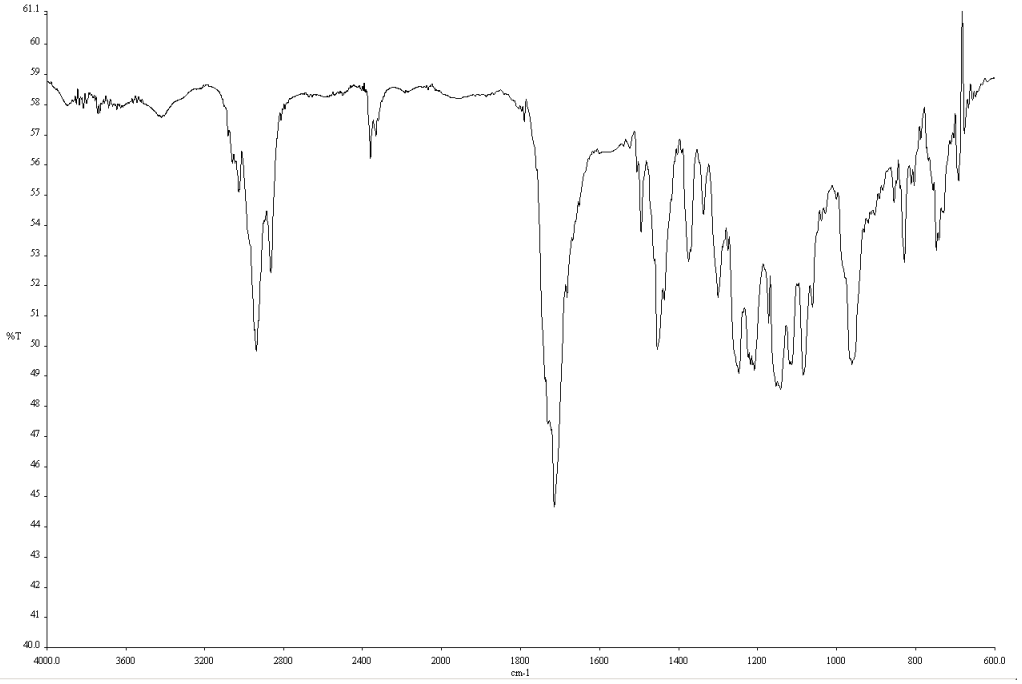


Figure A3.65. *Infrared spectrum (Thin Film, NaCl) of compound* ***163****.*

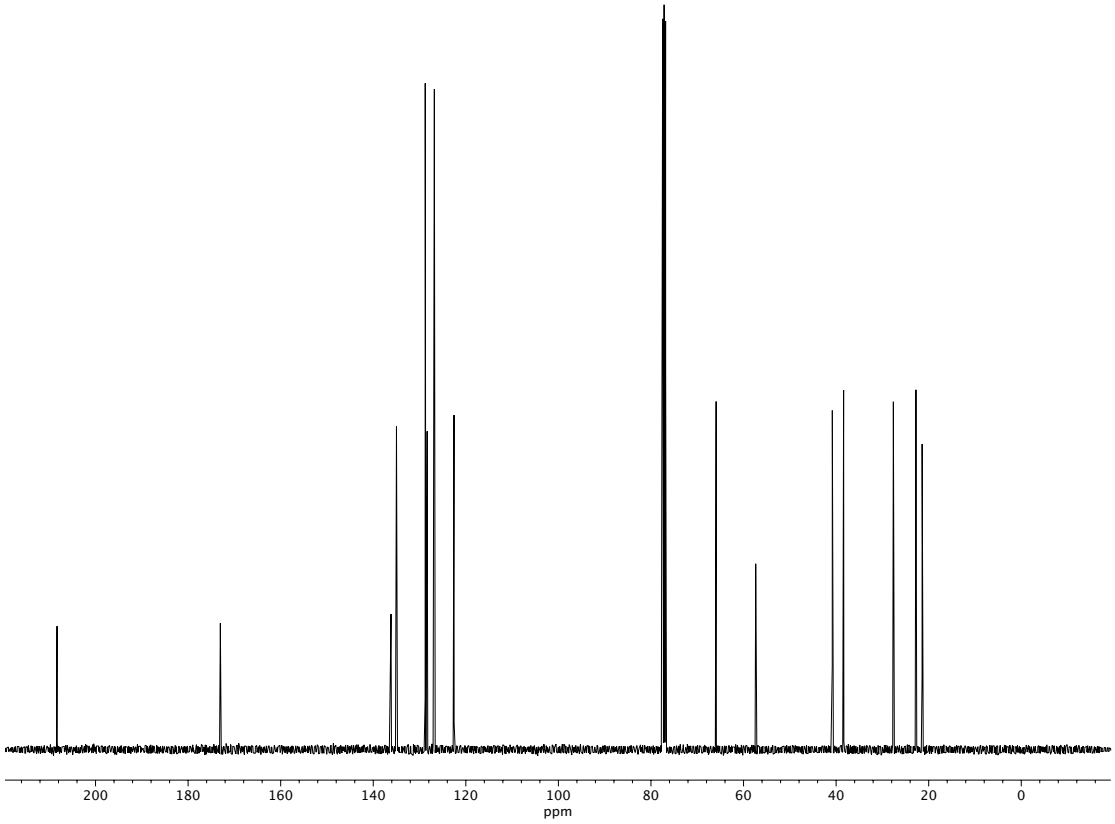


Figure A3.66. *^{13}C NMR (100 MHz, $CDCl_3$) of compound* ***163****.*

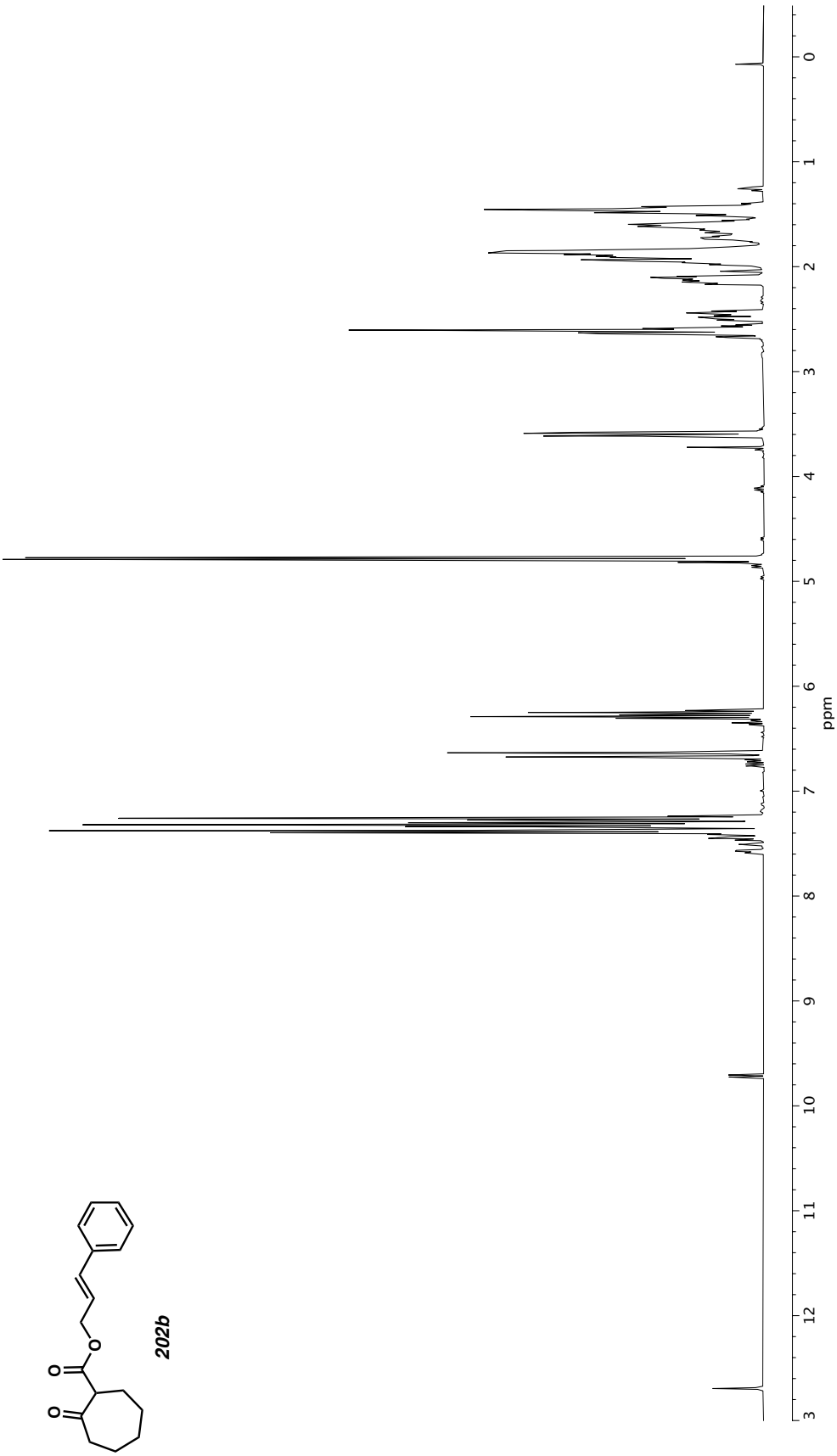


Figure A3.67. *^1H NMR (600 MHz, $CDCl_3$) of compound* ***202b****.*

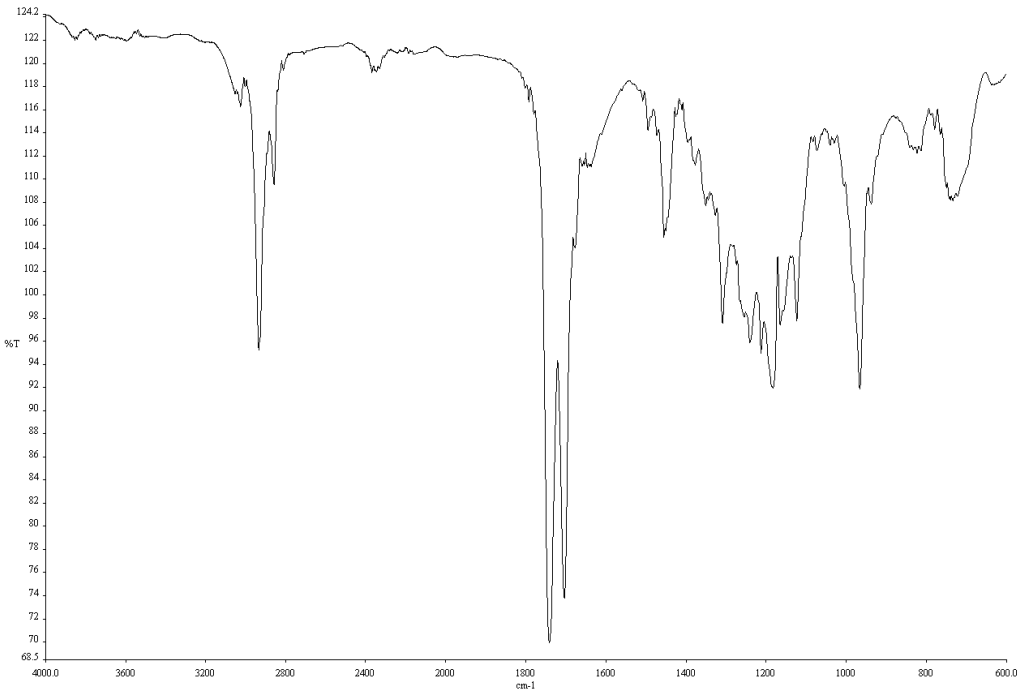


Figure A3.68. *Infrared spectrum (Thin Film, NaCl) of compound* ***202b****.*

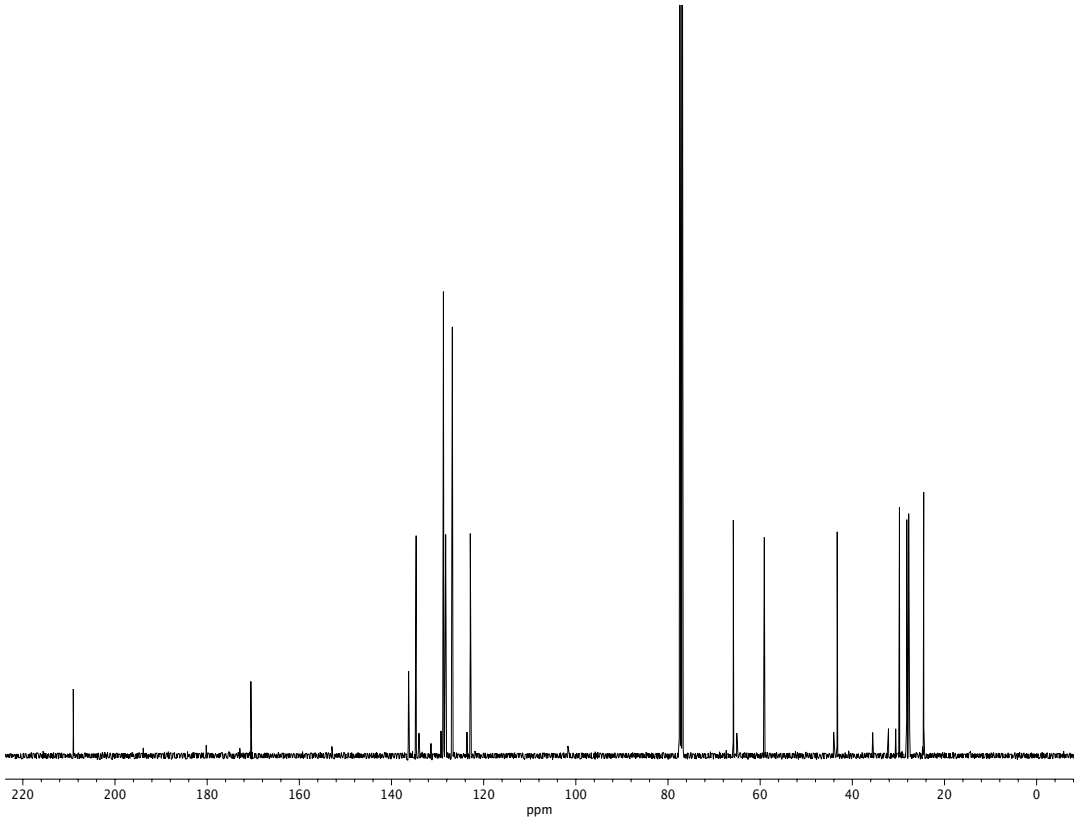
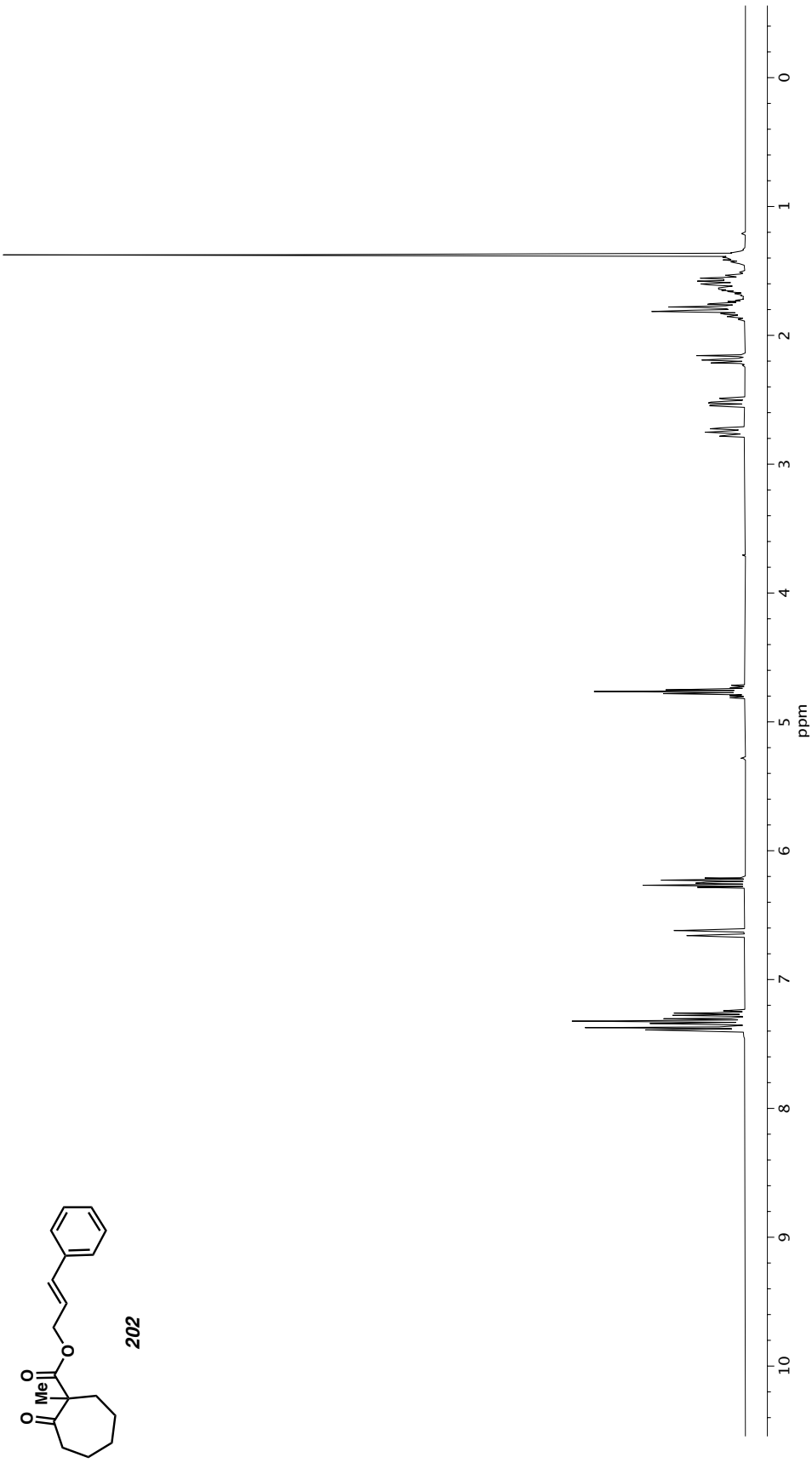


Figure A3.69. *^{13}C NMR (100 MHz, $CDCl_3$) of compound* ***202b****.*



202

Figure A3.70. *^1H NMR (600 MHz, $CDCl_3$) of compound* ***202****.*

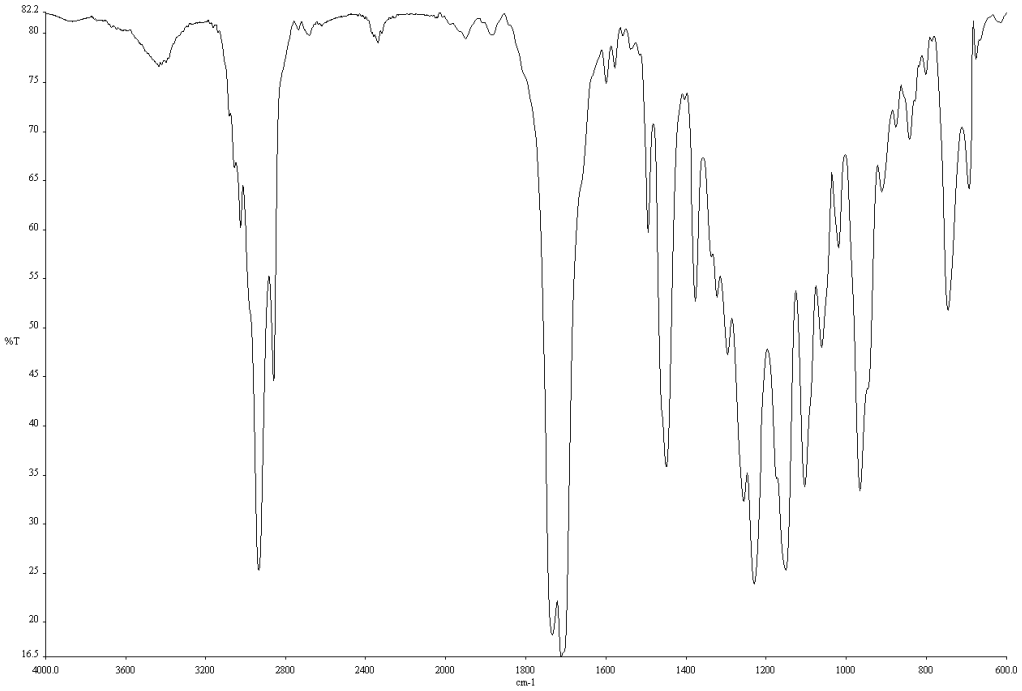


Figure A3.71. *Infrared spectrum (Thin Film, NaCl) of compound* ***202****.*

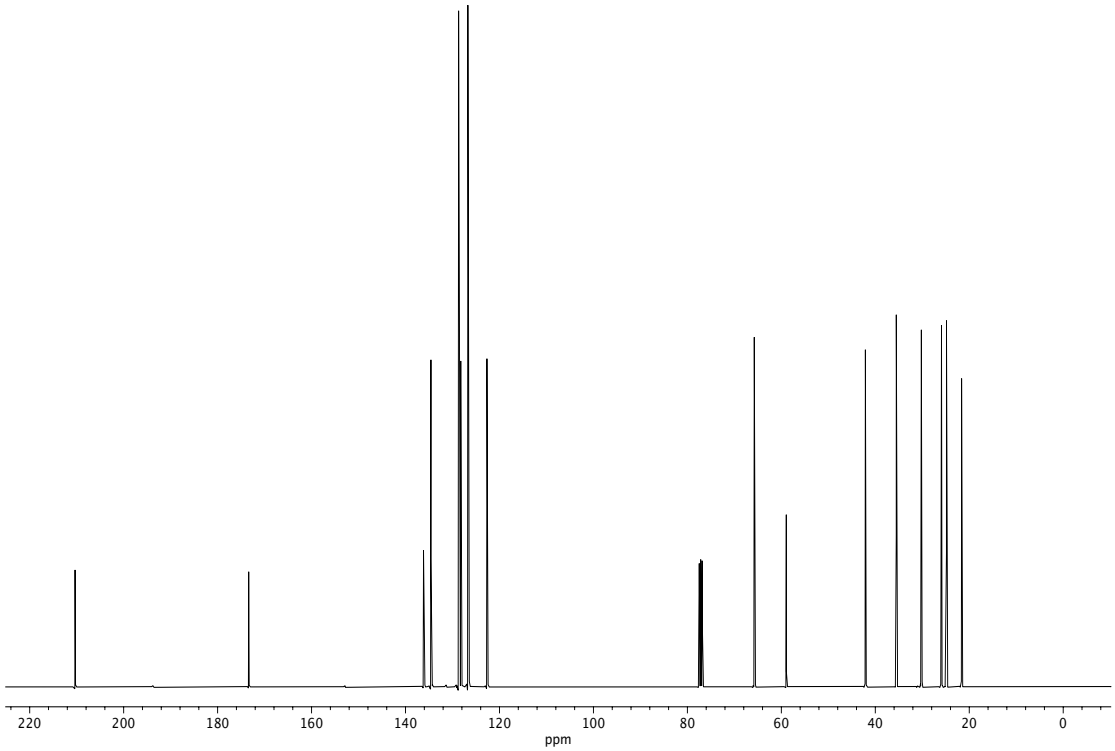


Figure A3.72. *^{13}C NMR (100 MHz, $CDCl_3$) of compound* ***202****.*

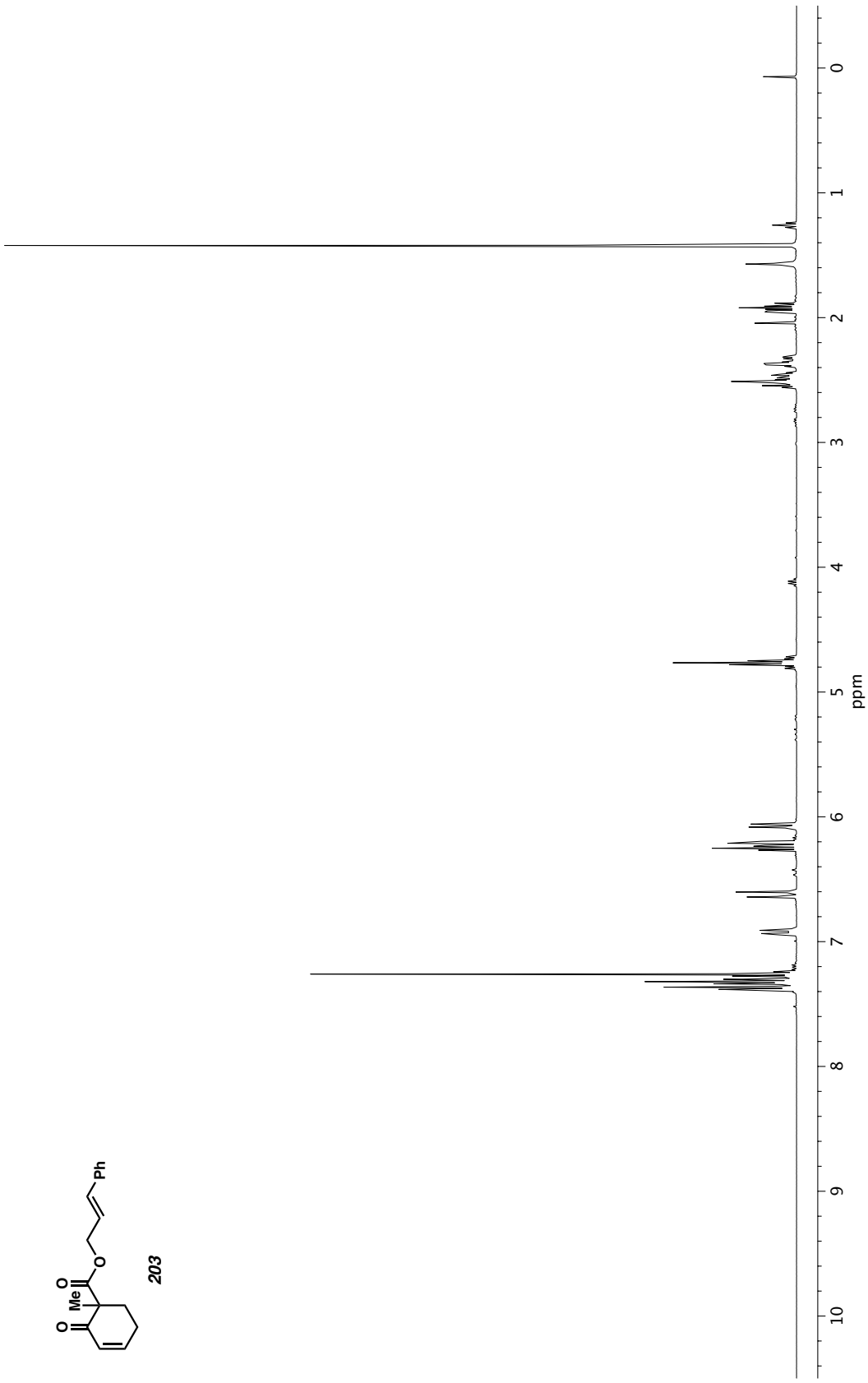


Figure A3.73. *^1H NMR (400 MHz, $CDCl_3$) of compound* ***203***.

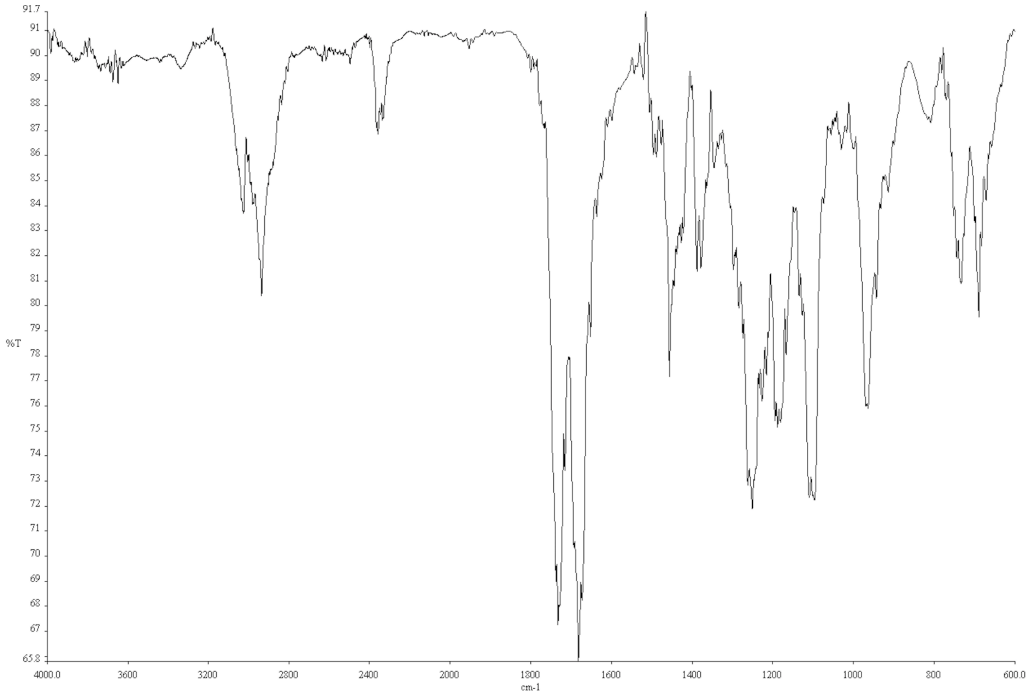


Figure A3.74. *Infrared spectrum (Thin Film, NaCl) of compound* ***203****.*

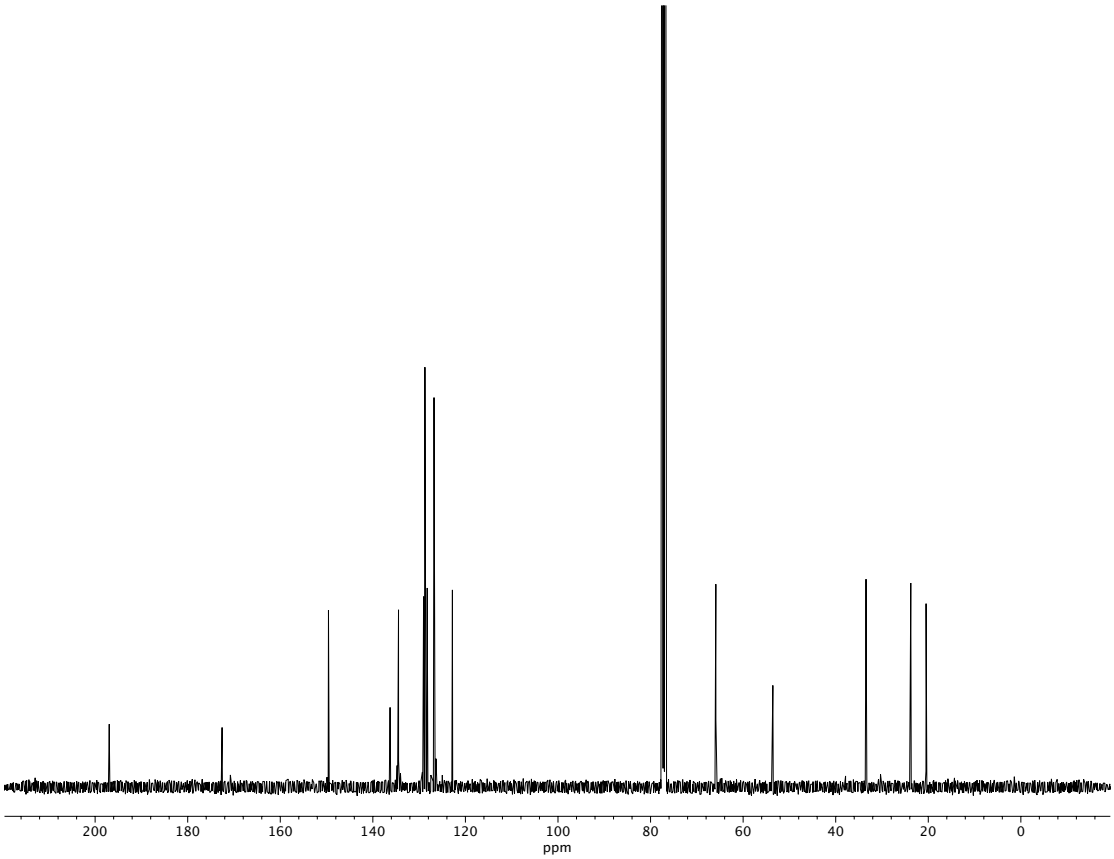


Figure A3.75. *^{13}C NMR (100 MHz, $CDCl_3$) of compound* ***203****.*

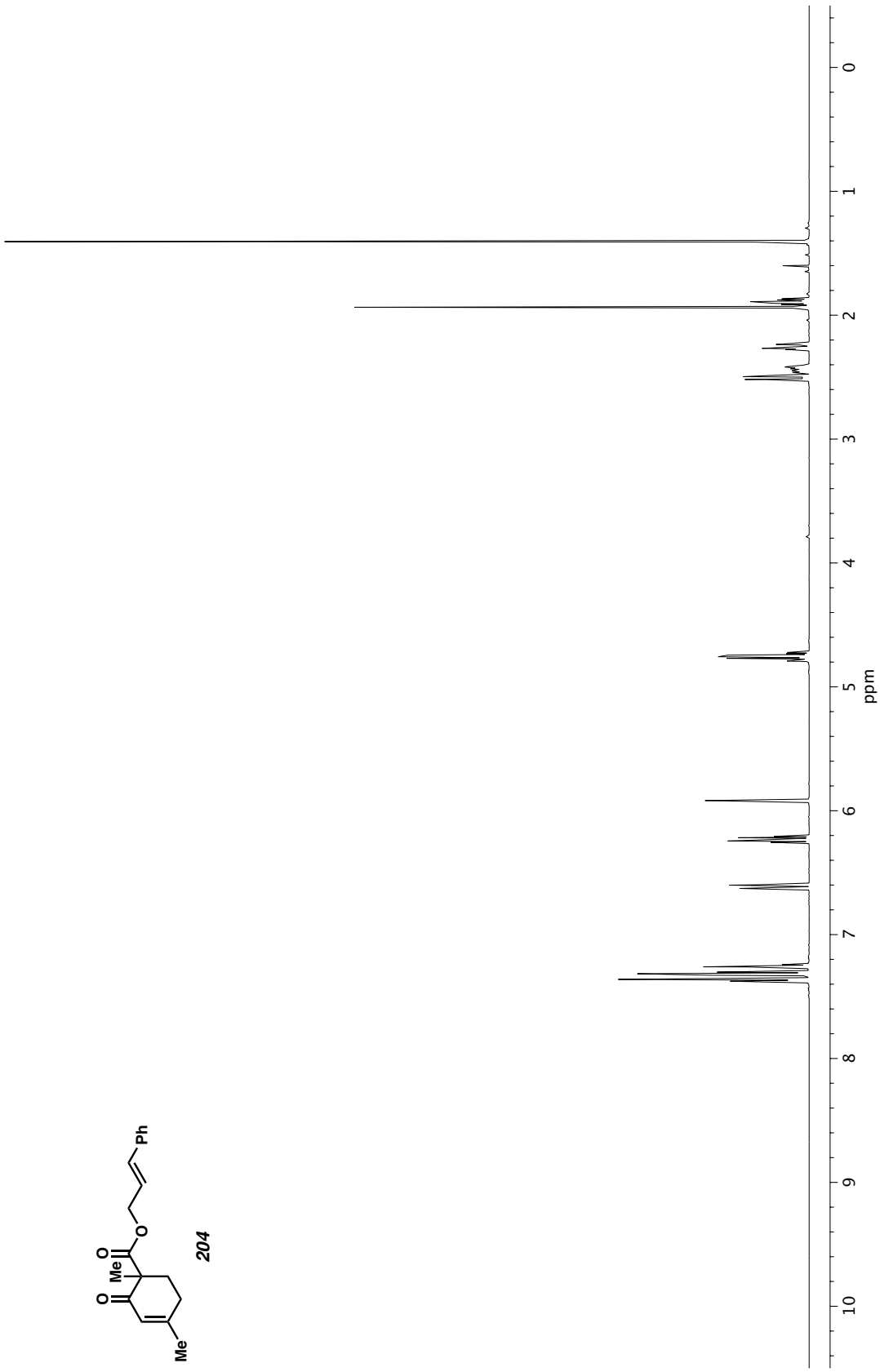


Figure A3.76. *^1H NMR (600 MHz, $CDCl_3$) of compound* ***204****.*

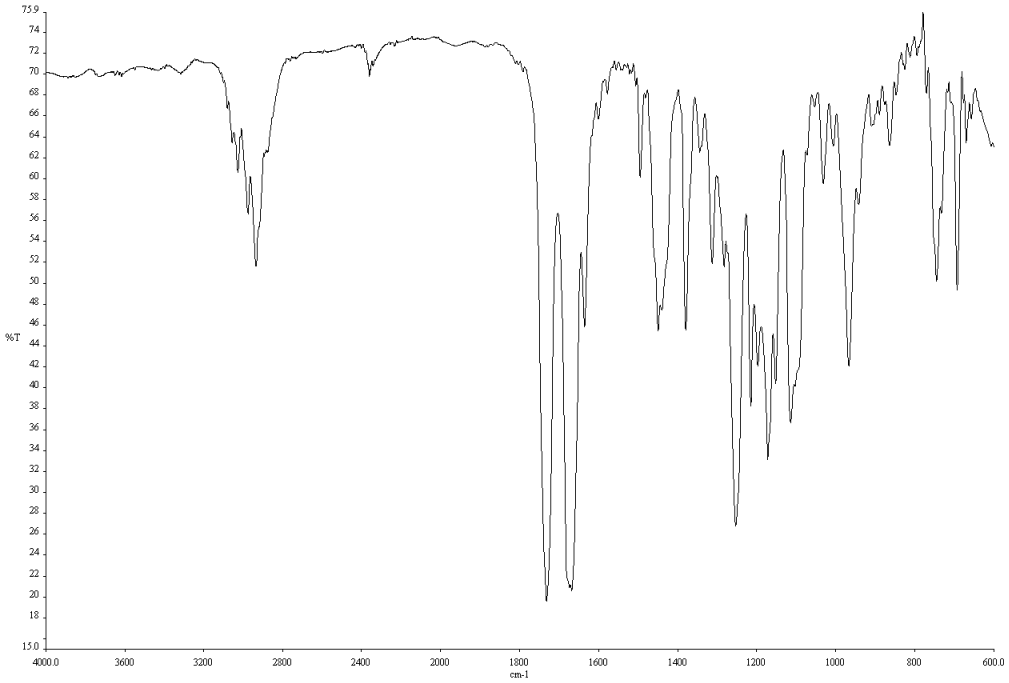


Figure A3.77. *Infrared spectrum (Thin Film, NaCl) of compound* ***204****.*

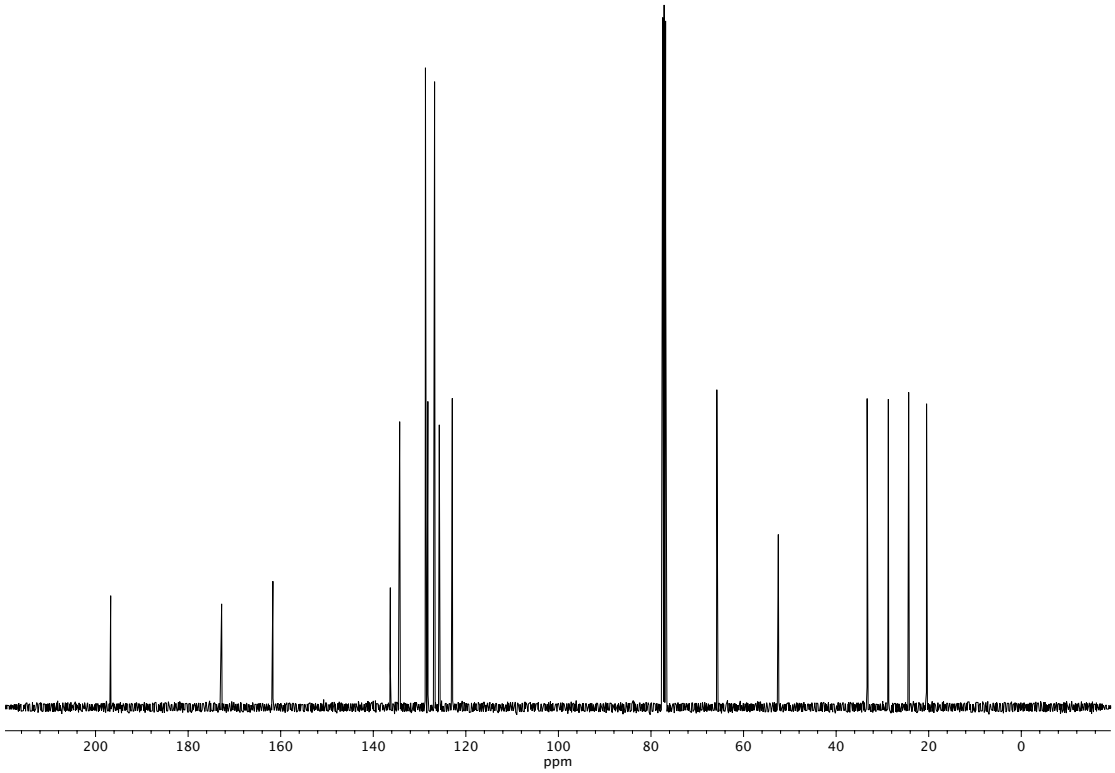


Figure A3.78. *^{13}C NMR (100 MHz, $CDCl_3$) of compound* ***204****.*

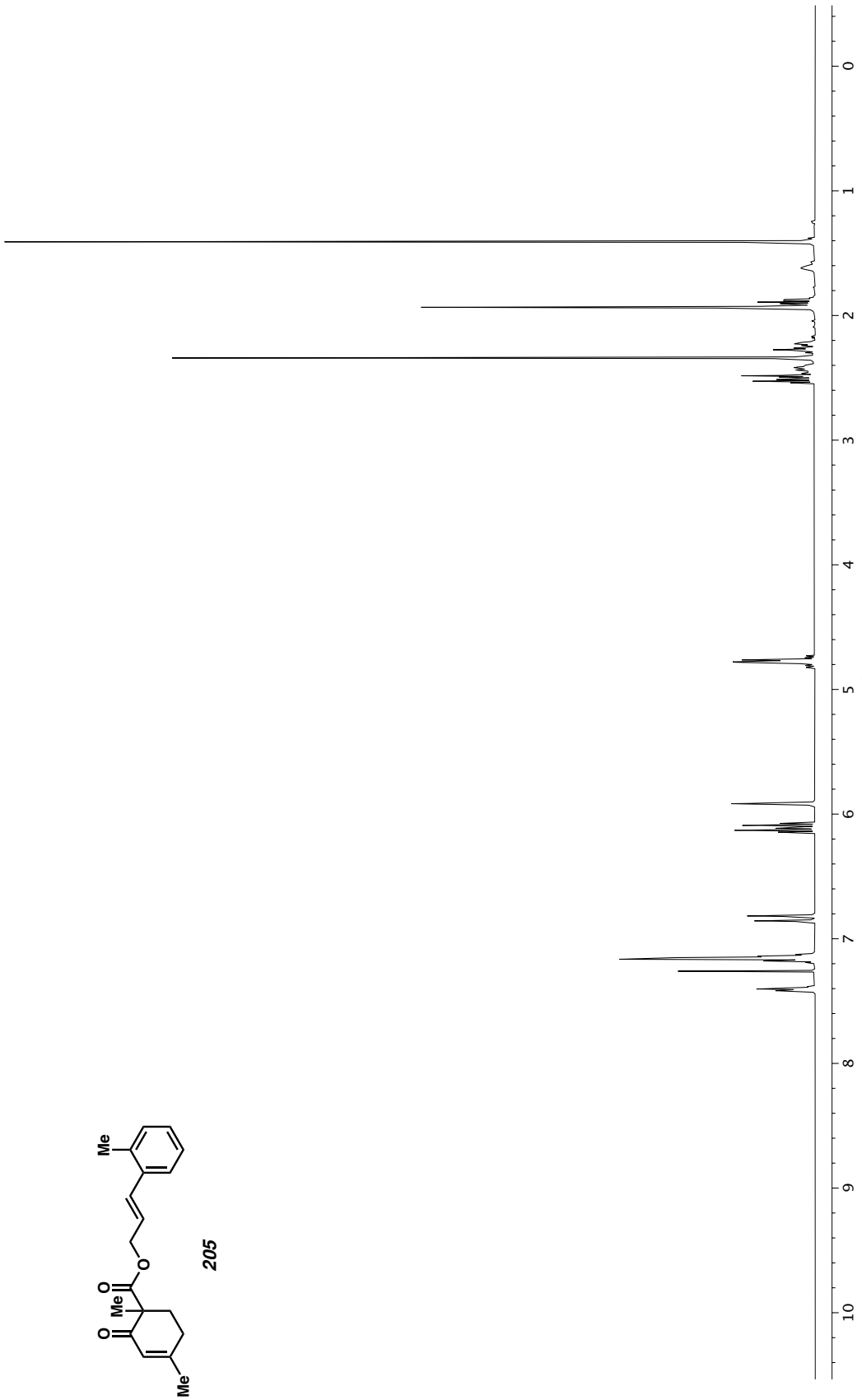


Figure A3.79. *^1H NMR (600 MHz, $CDCl_3$) of compound* ***205****.*

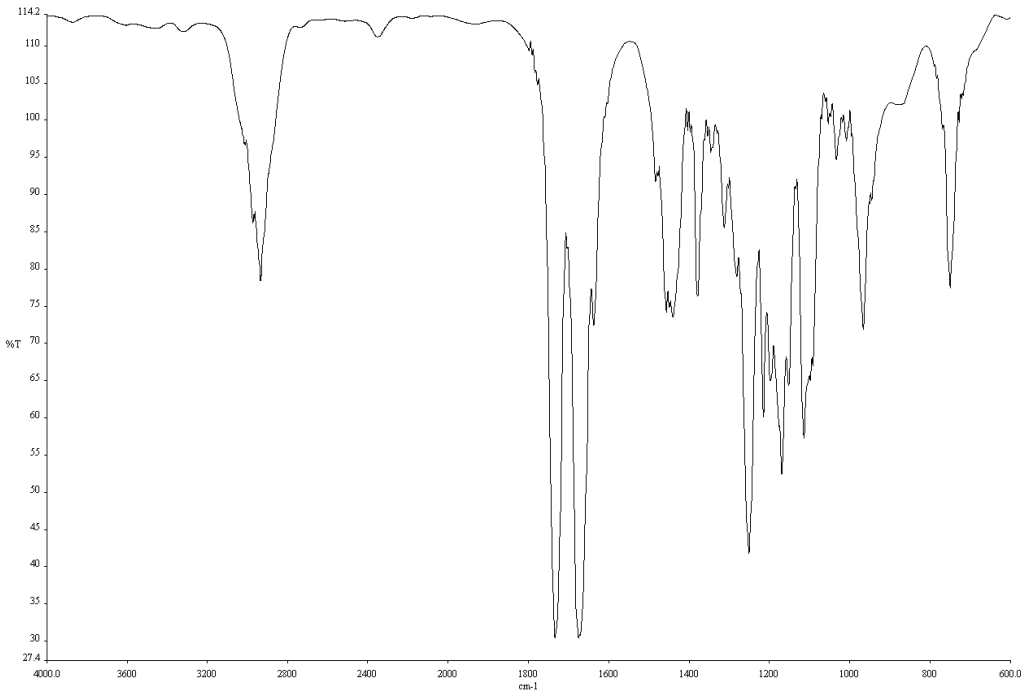


Figure A3.80. *Infrared spectrum (Thin Film, NaCl) of compound* ***205****.*

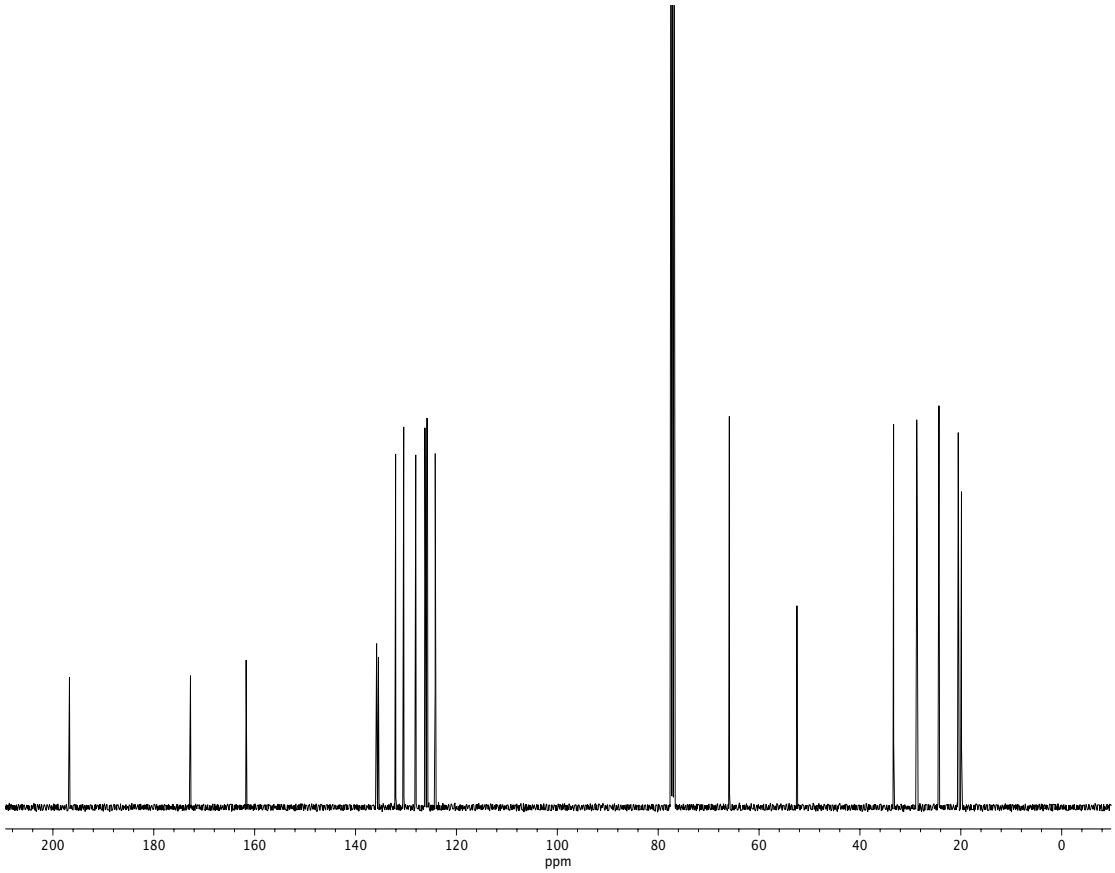


Figure A3.81. *^{13}C NMR (100 MHz, $CDCl_3$) of compound* ***205****.*

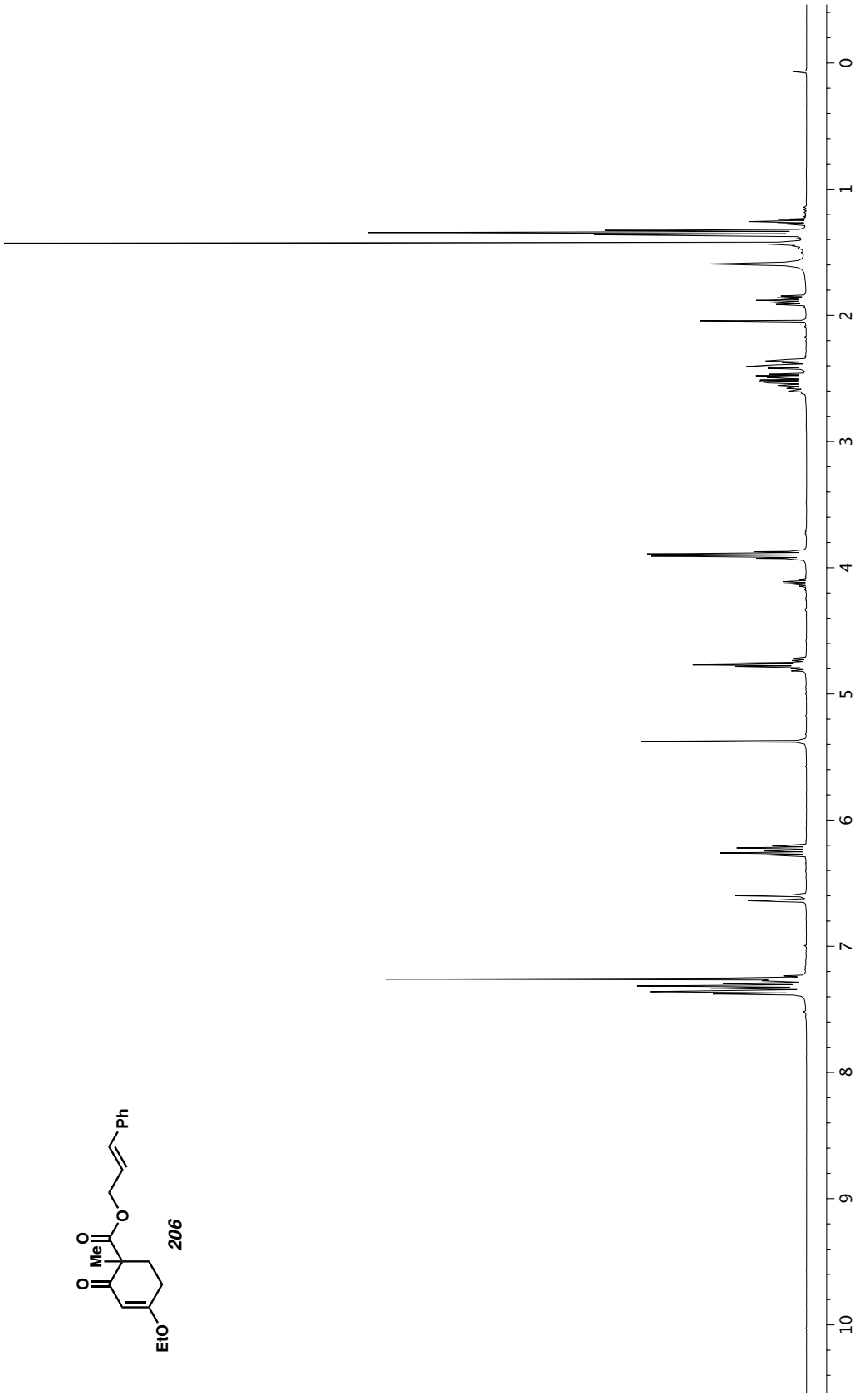


Figure A3.82. *^1H NMR (400 MHz, $CDCl_3$) of compound* ***206****.*

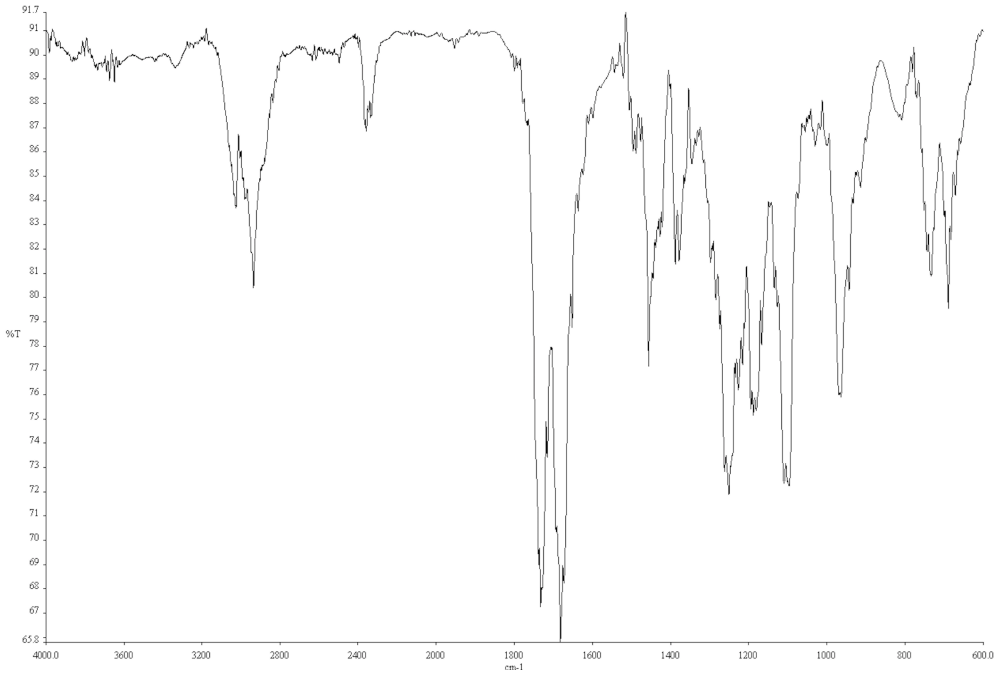


Figure A3.83. *Infrared spectrum (Thin Film, NaCl) of compound* ***206****.*

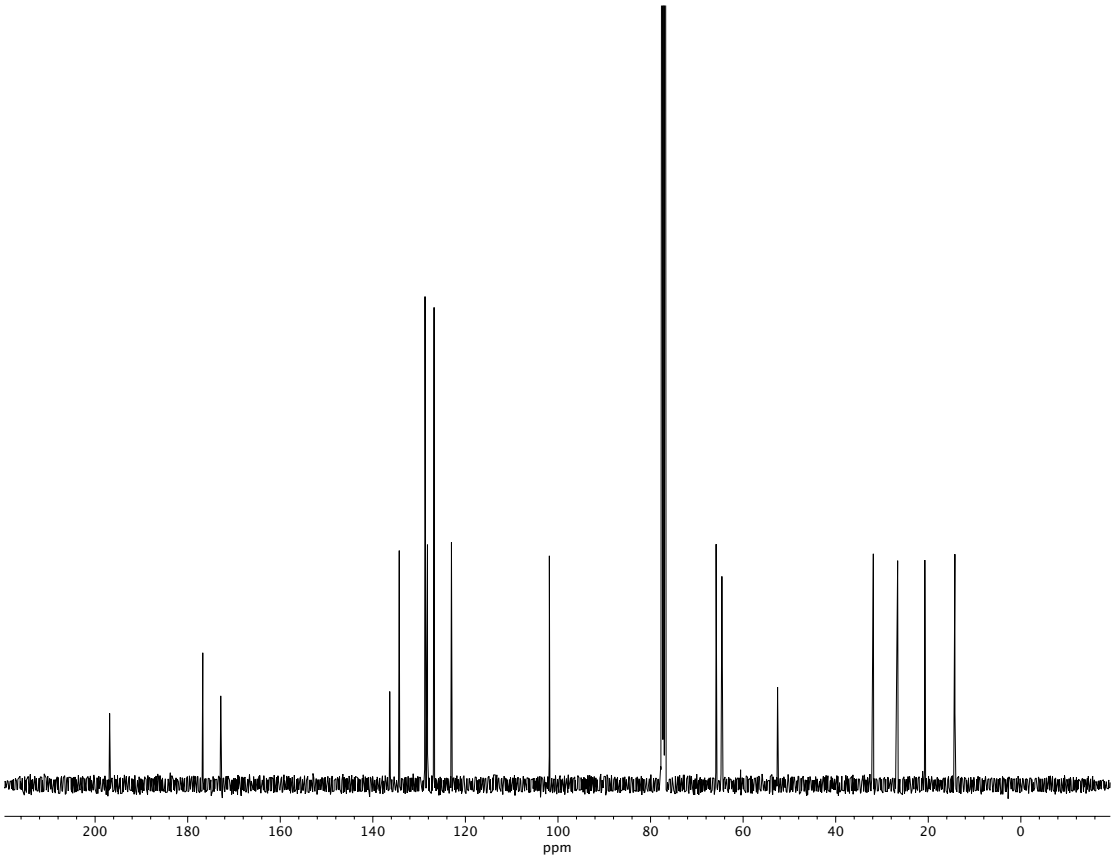


Figure A3.84. *^{13}C NMR (100 MHz, $CDCl_3$) of compound* ***206****.*

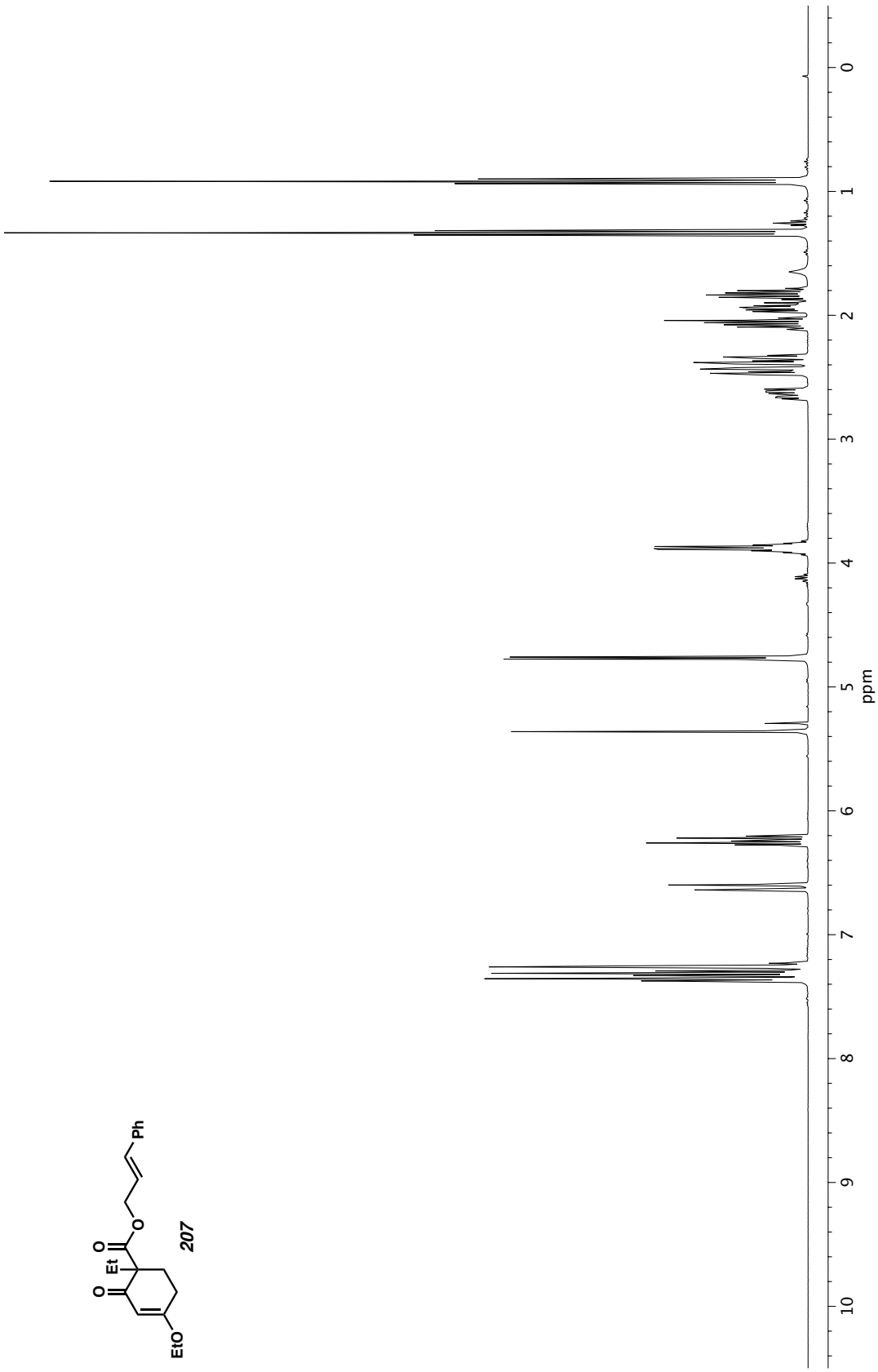


Figure A3.85. *^1H NMR (400 MHz, $CDCl_3$) of compound* ***207****.*

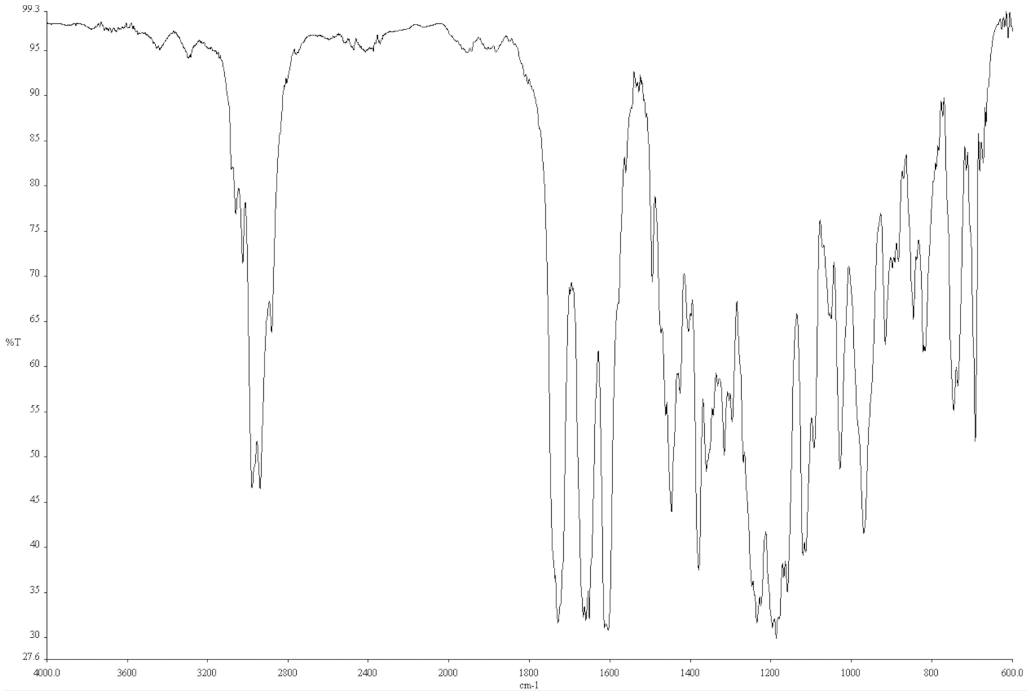


Figure A3.86. *Infrared spectrum (Thin Film, NaCl) of compound* ***207****.*

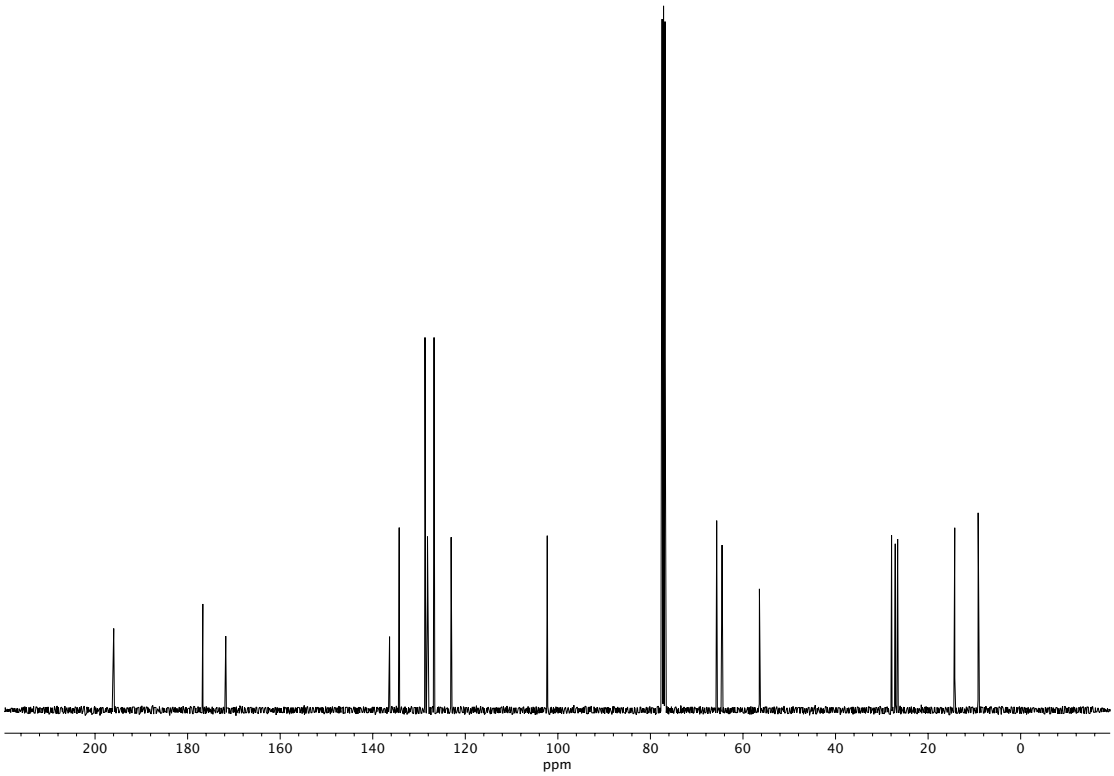


Figure A3.87. *^{13}C NMR (100 MHz, $CDCl_3$) of compound* ***207****.*

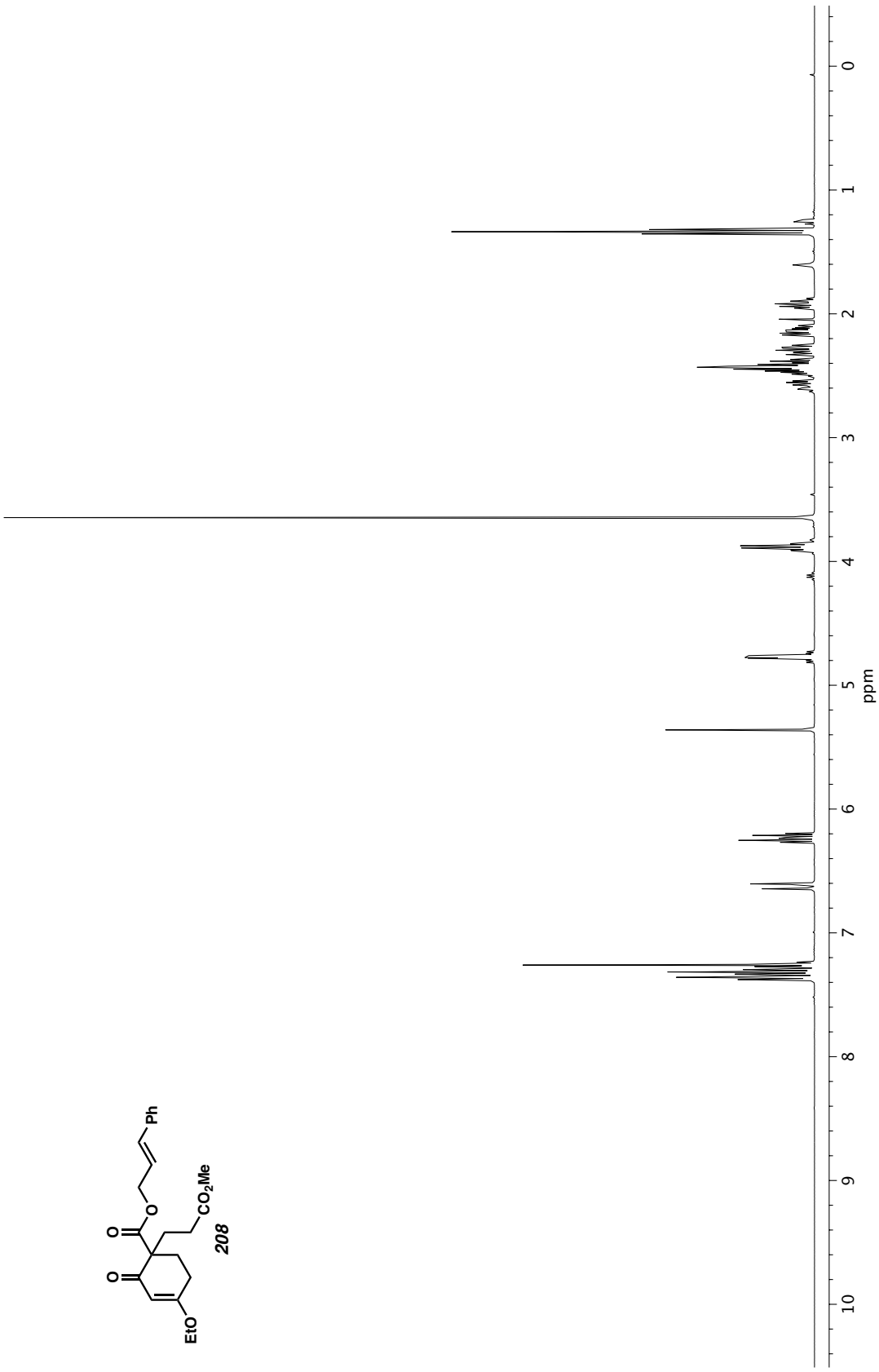


Figure A3.88. *^{1}H NMR (400 MHz, $CDCl_3$) of compound* ***208****.*

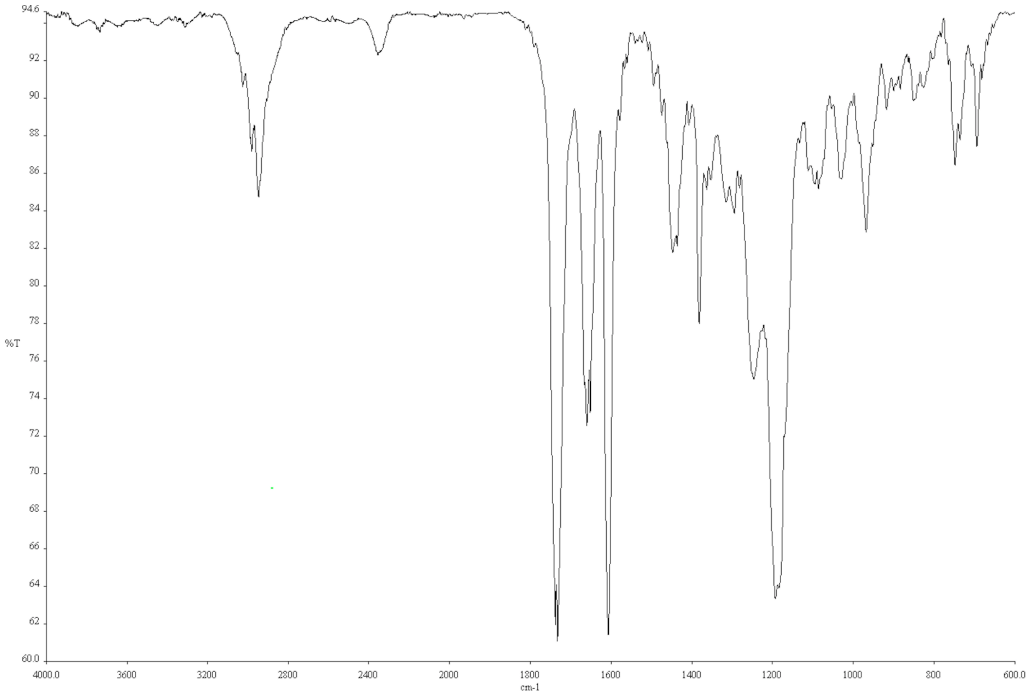


Figure A3.89. *Infrared spectrum (Thin Film, NaCl) of compound* ***208****.*

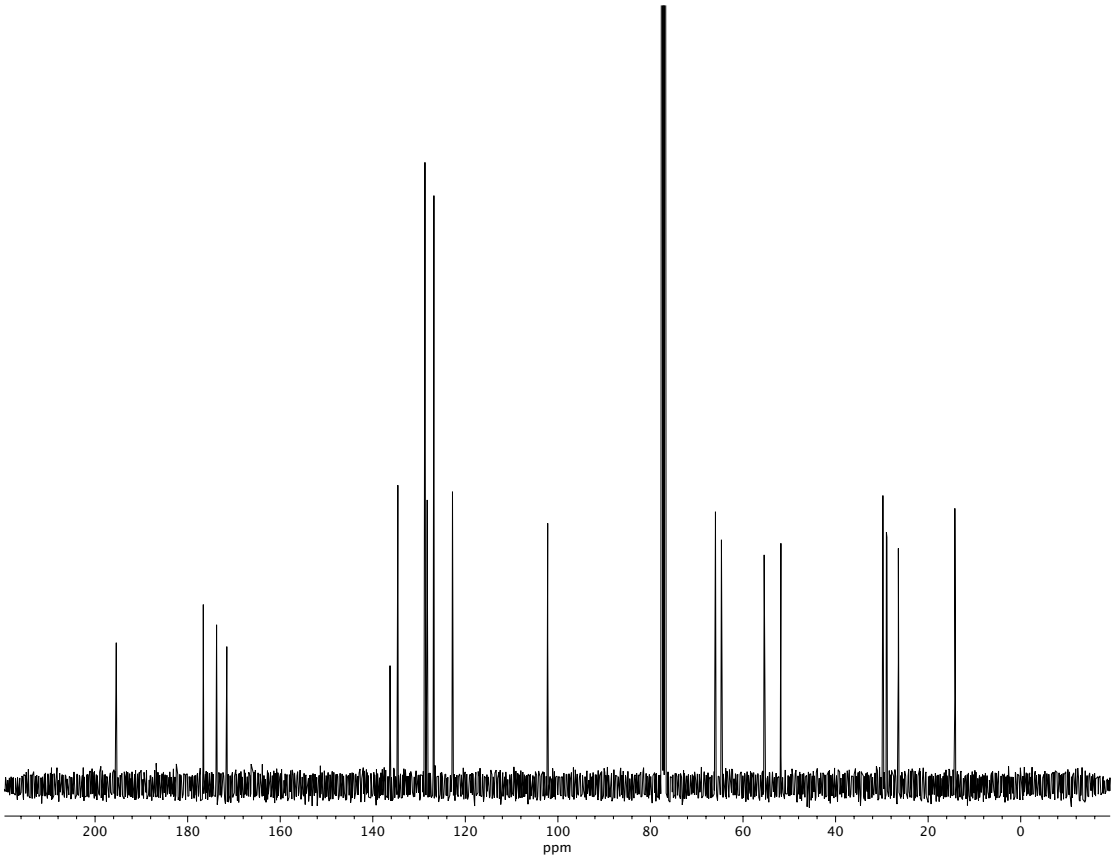


Figure A3.90. *^{13}C NMR (100 MHz, $CDCl_3$) of compound* ***208****.*

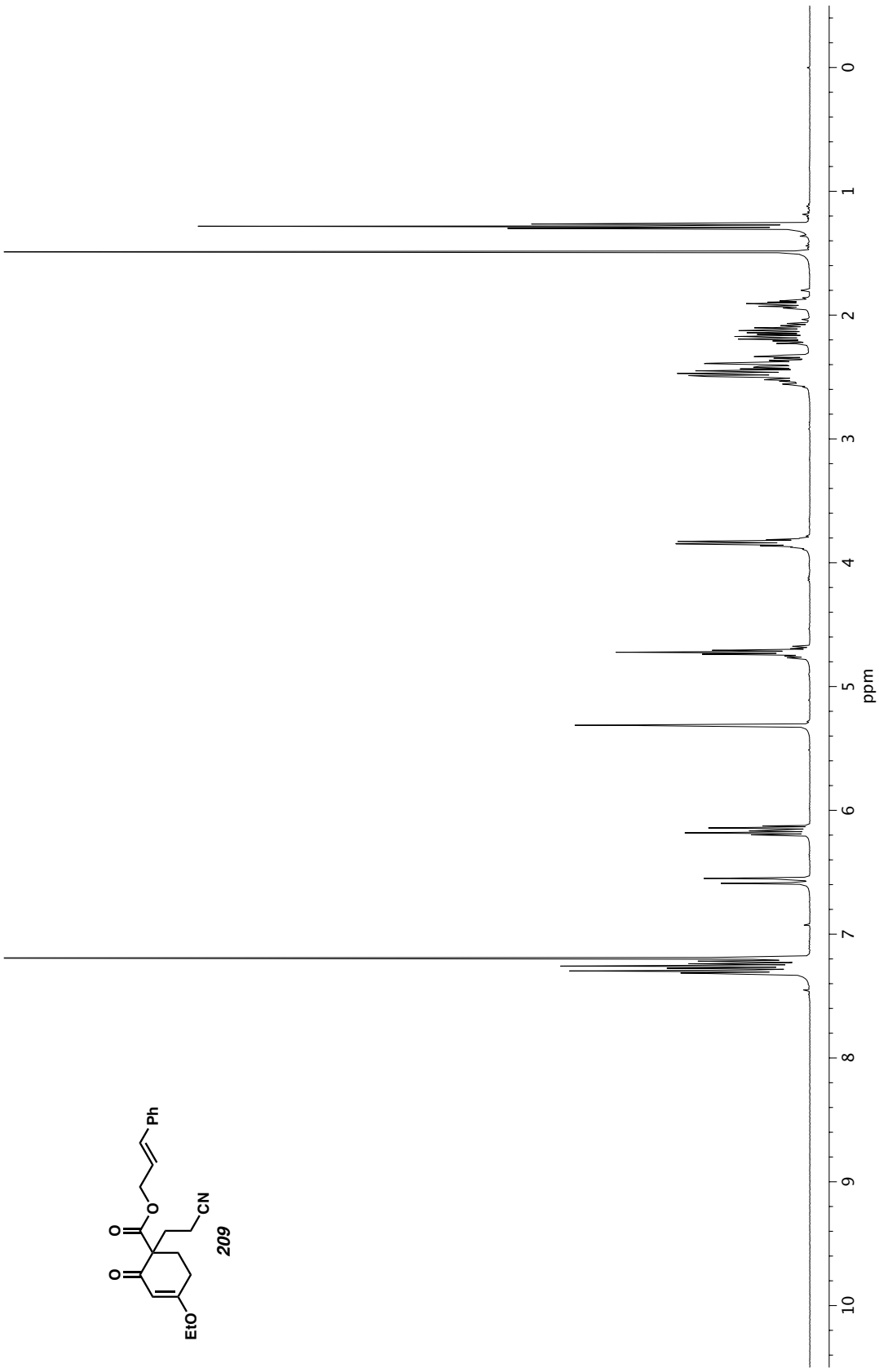


Figure A3.91. *^{1}H NMR (400 MHz, $CDCl_3$) of compound* ***209***.

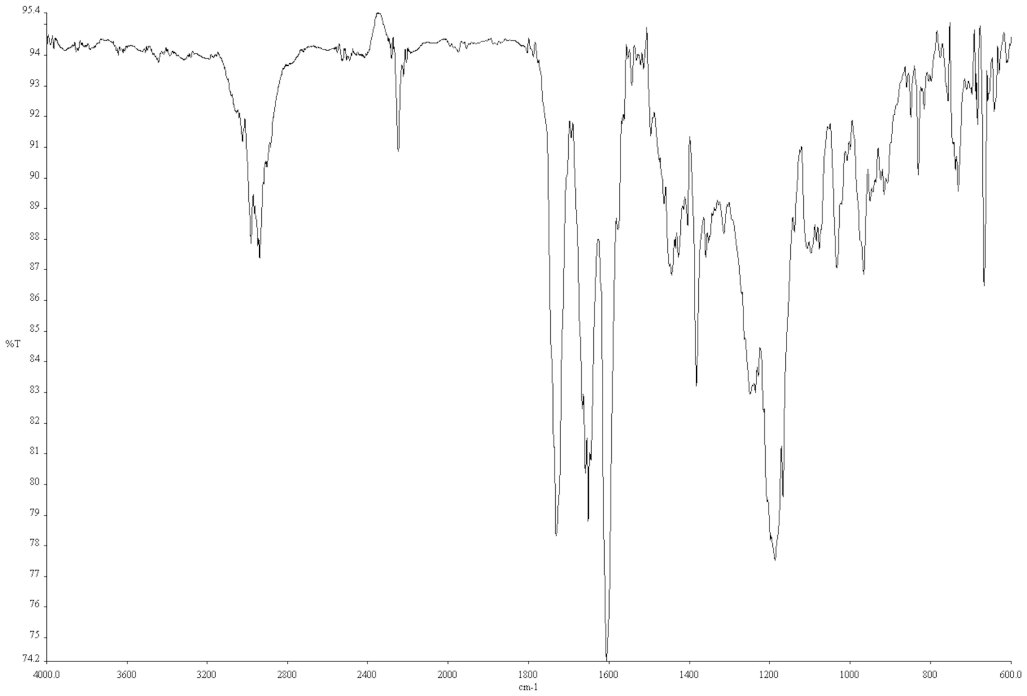


Figure A3.92. *Infrared spectrum (Thin Film, NaCl) of compound* ***209****.*

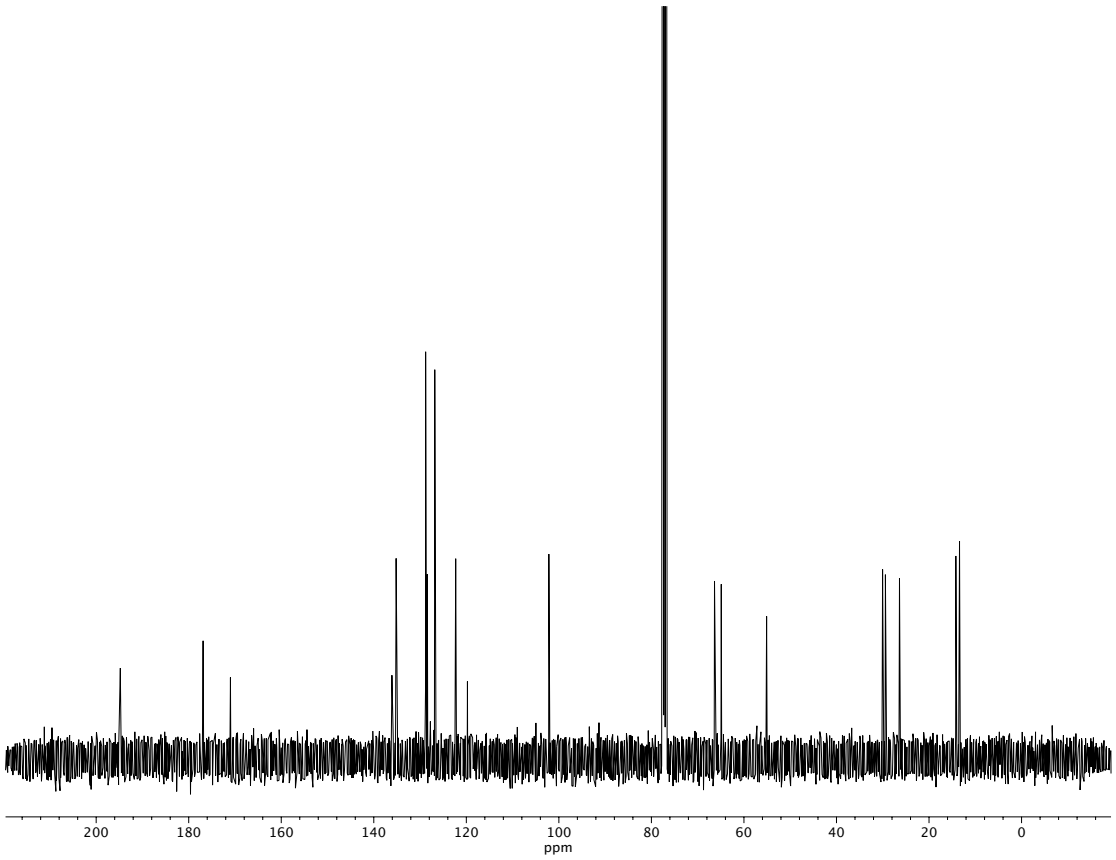


Figure A3.93. *^{13}C NMR (100 MHz, $CDCl_3$) of compound* ***209****.*

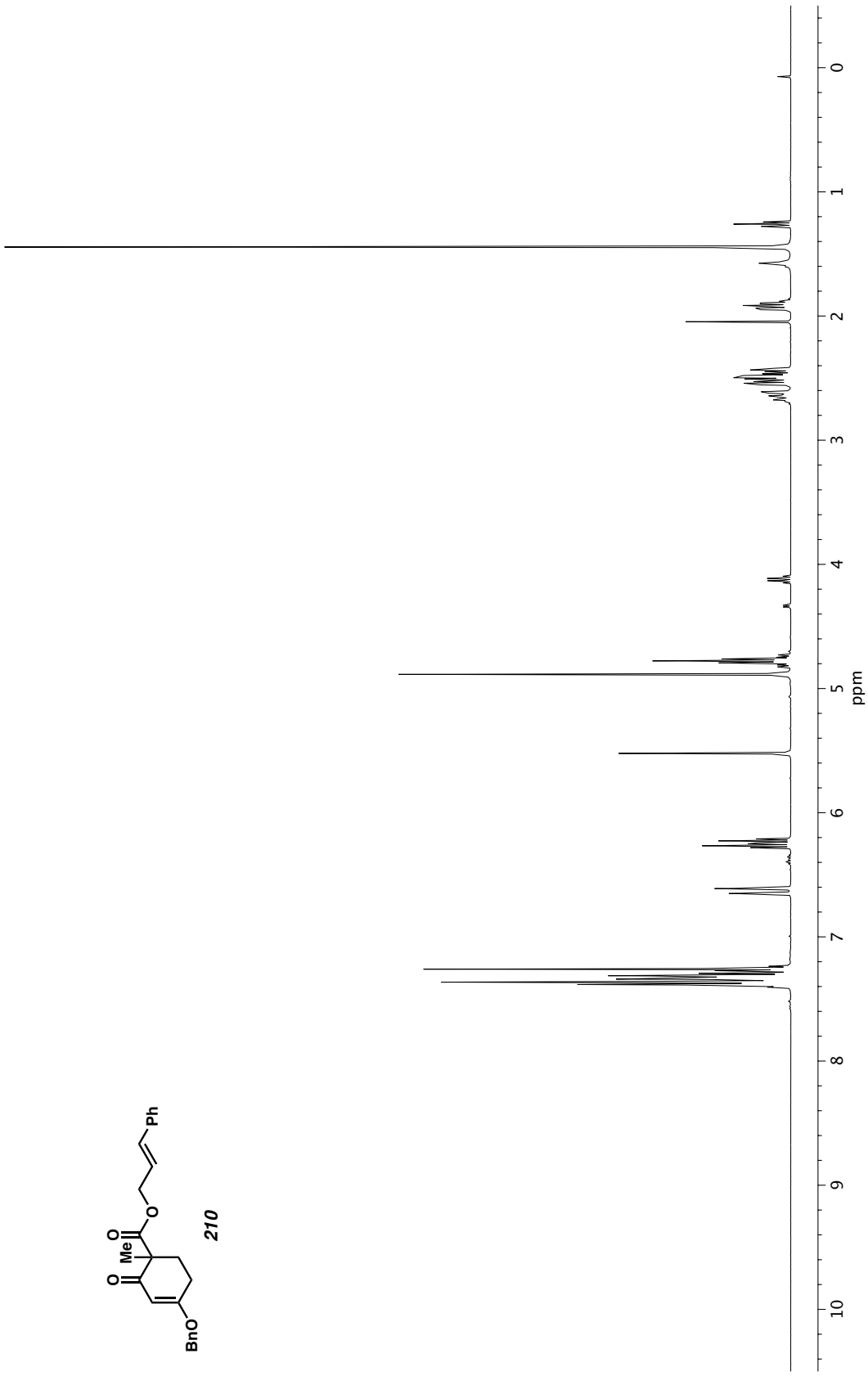


Figure A3.94. *^1H NMR (400 MHz, $CDCl_3$) of compound* ***210****.*

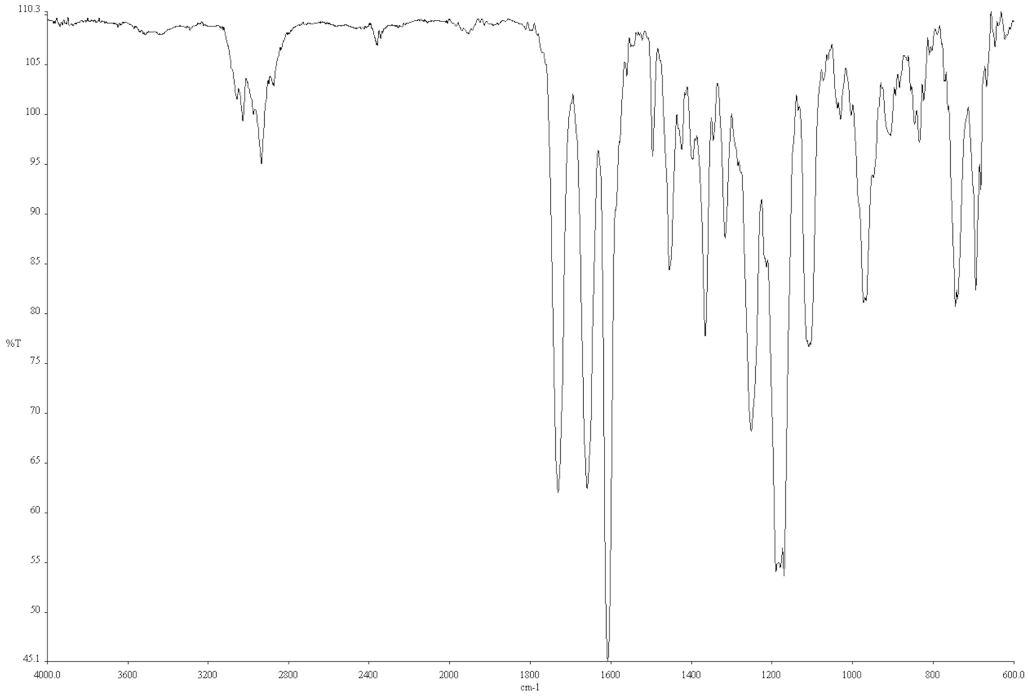


Figure A3.95. *Infrared spectrum (Thin Film, NaCl) of compound* ***210****.*

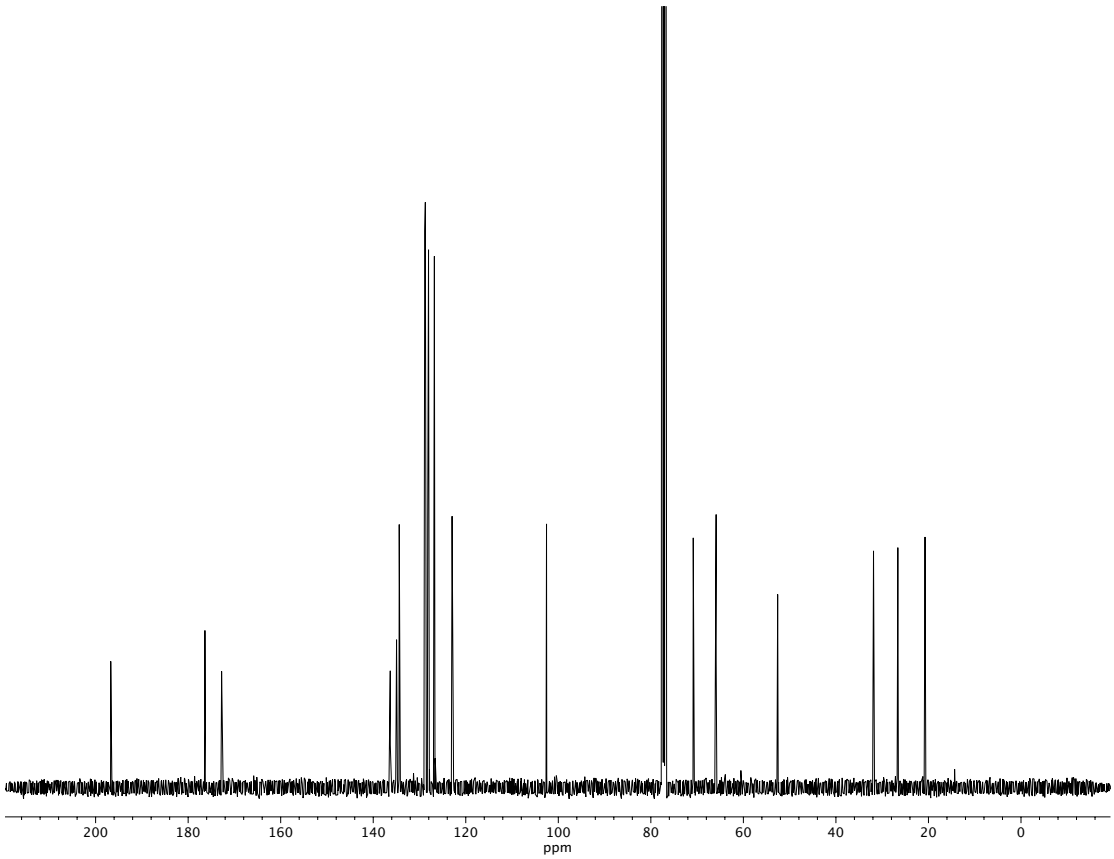


Figure A3.96. *^{13}C NMR (100 MHz, $CDCl_3$) of compound* ***210****.*

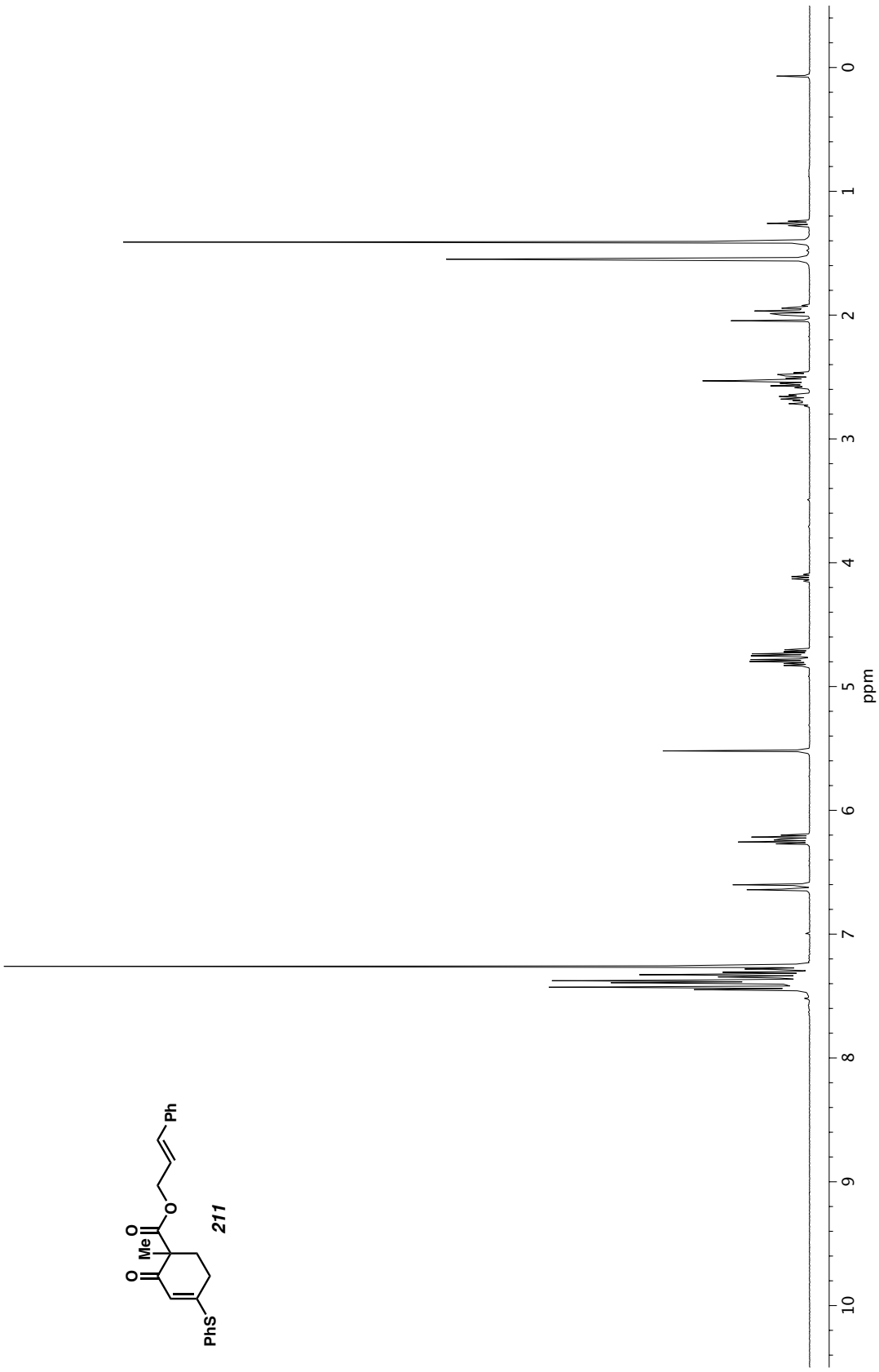


Figure A3.97. *^1H NMR (400 MHz, $CDCl_3$) of compound* ***211****.*

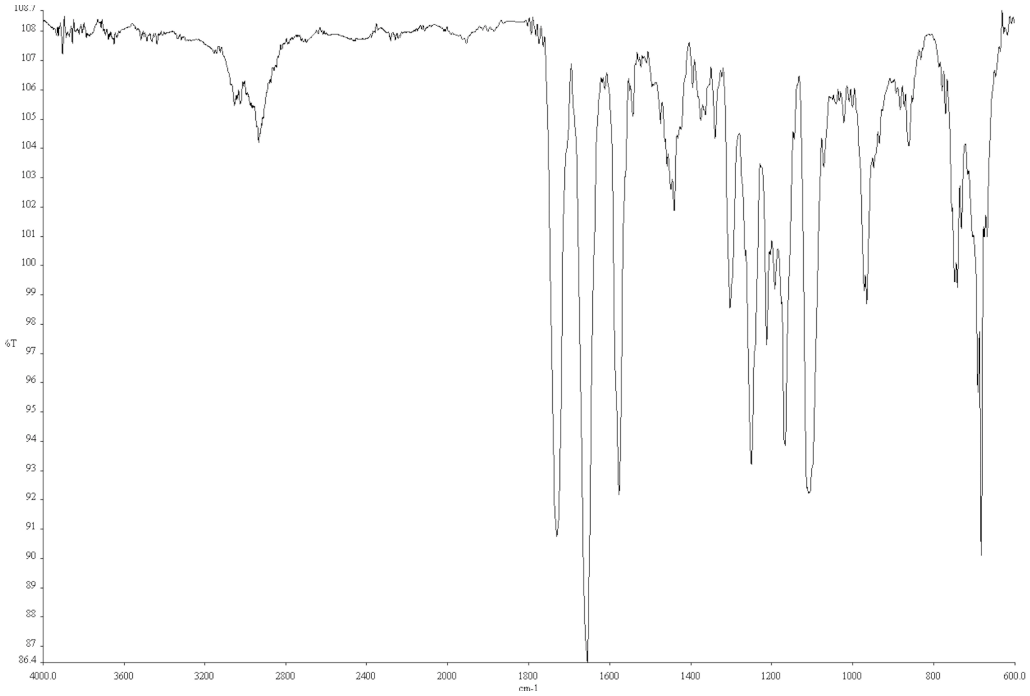


Figure A3.98. *Infrared spectrum (Thin Film, NaCl) of compound* ***211****.*

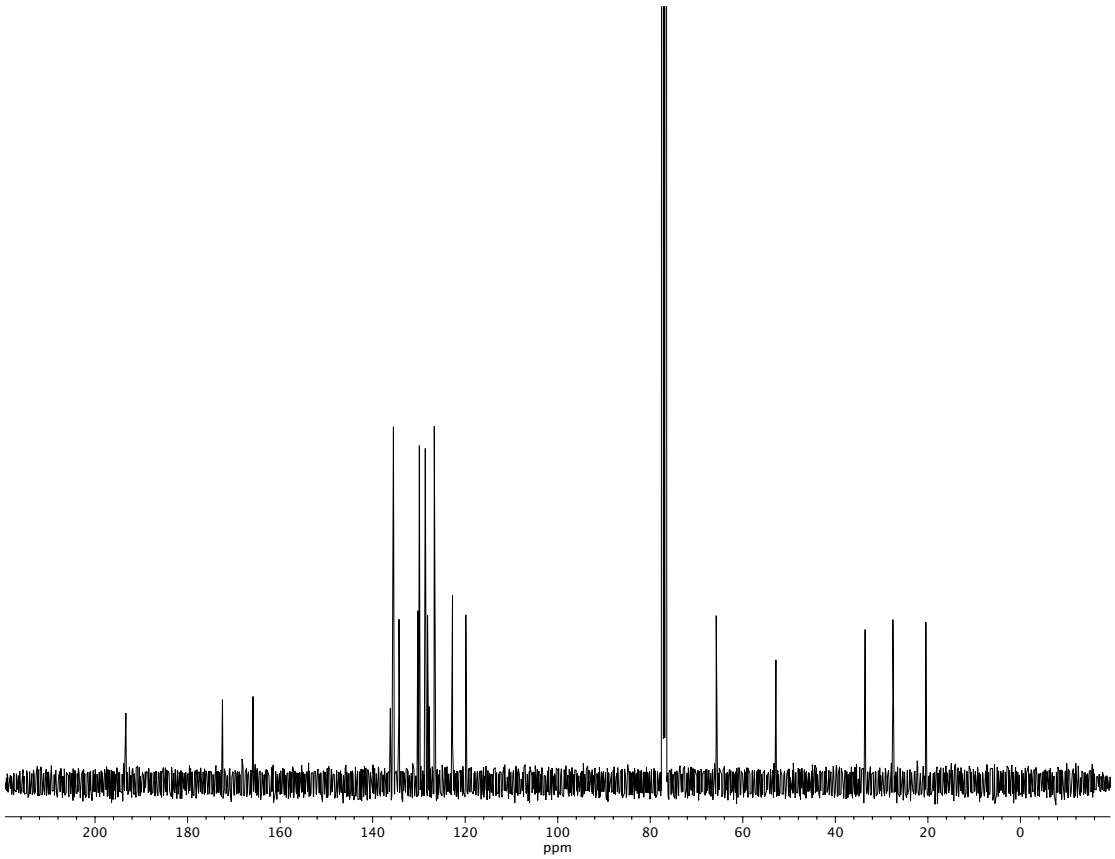


Figure A3.99. *^{13}C NMR (100 MHz, $CDCl_3$) of compound* ***211****.*

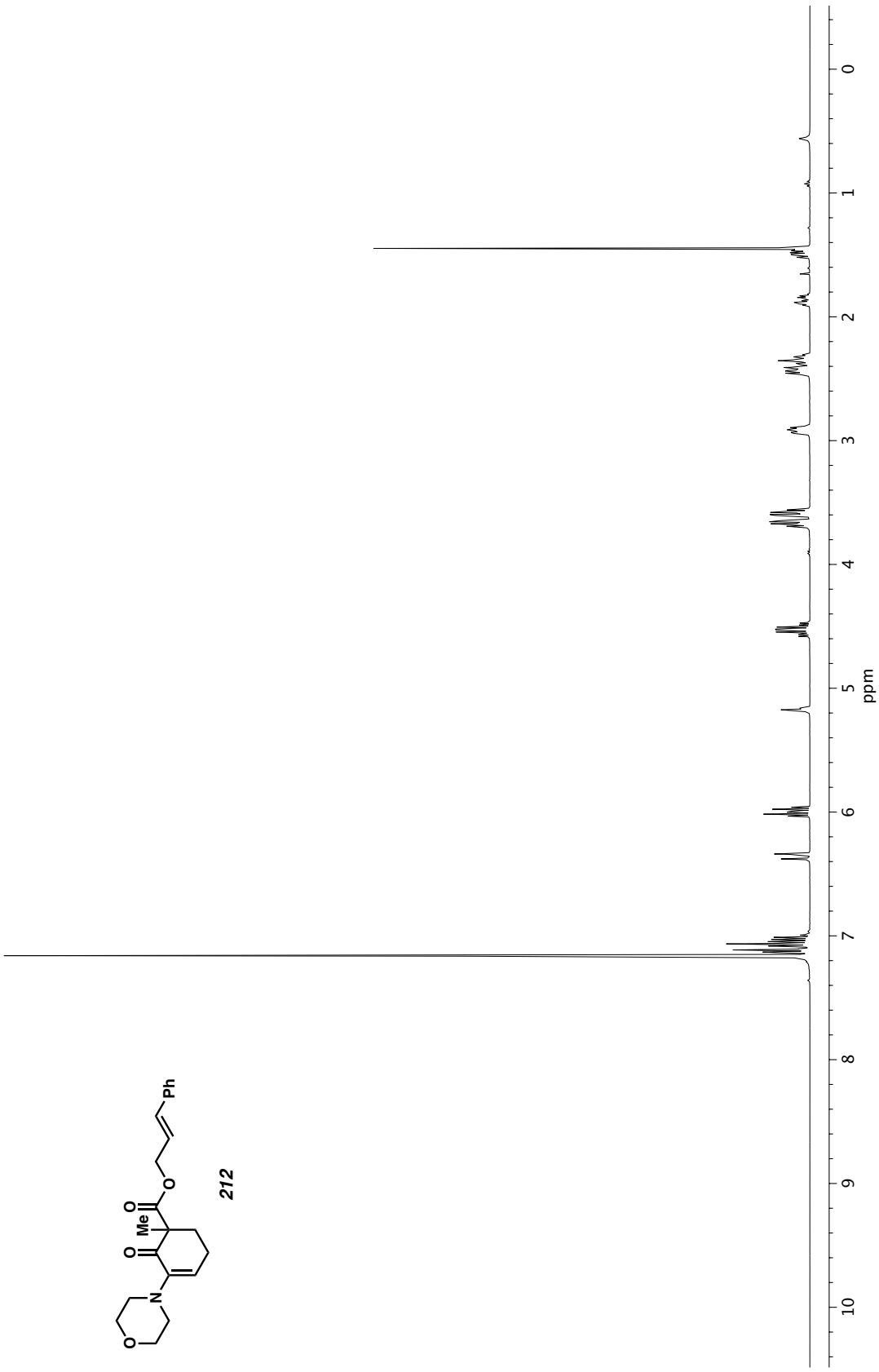


Figure A3.100. *^{1}H NMR (400 MHz, C_6D_6) of compound* ***212***.

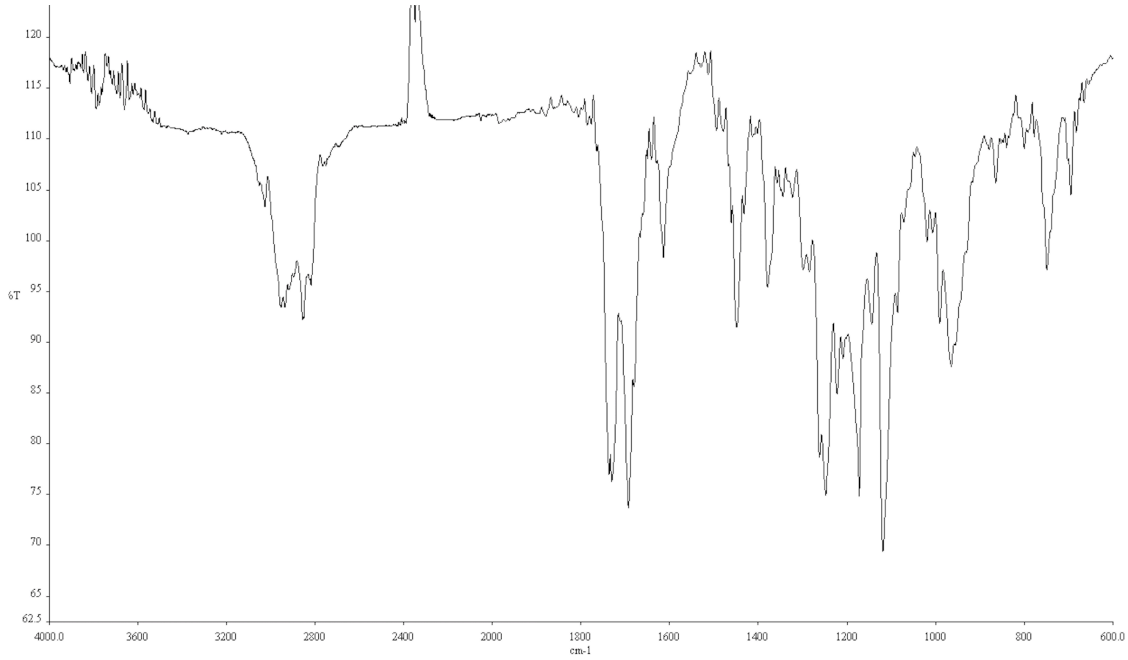


Figure A3.101. *Infrared spectrum (Thin Film, NaCl) of compound* ***212****.*

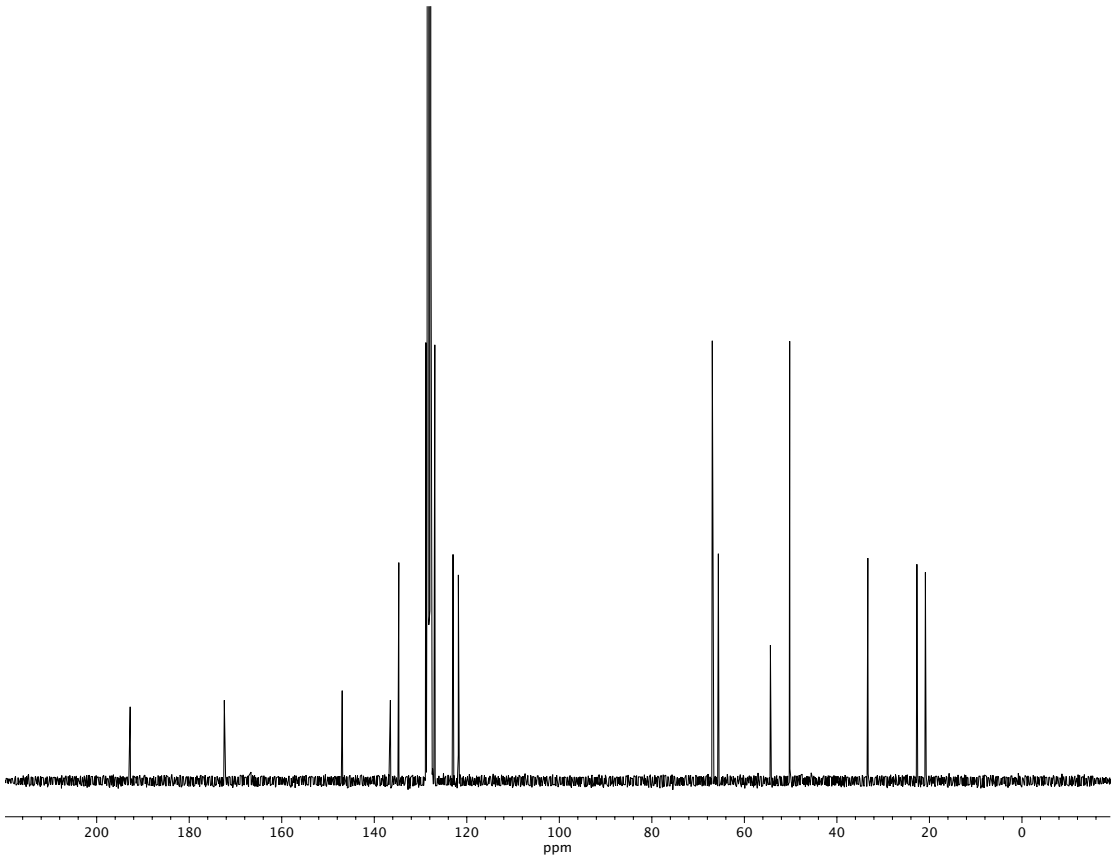


Figure A3.102. *^{13}C NMR (100 MHz, C_6D_6) of compound* ***212****.*

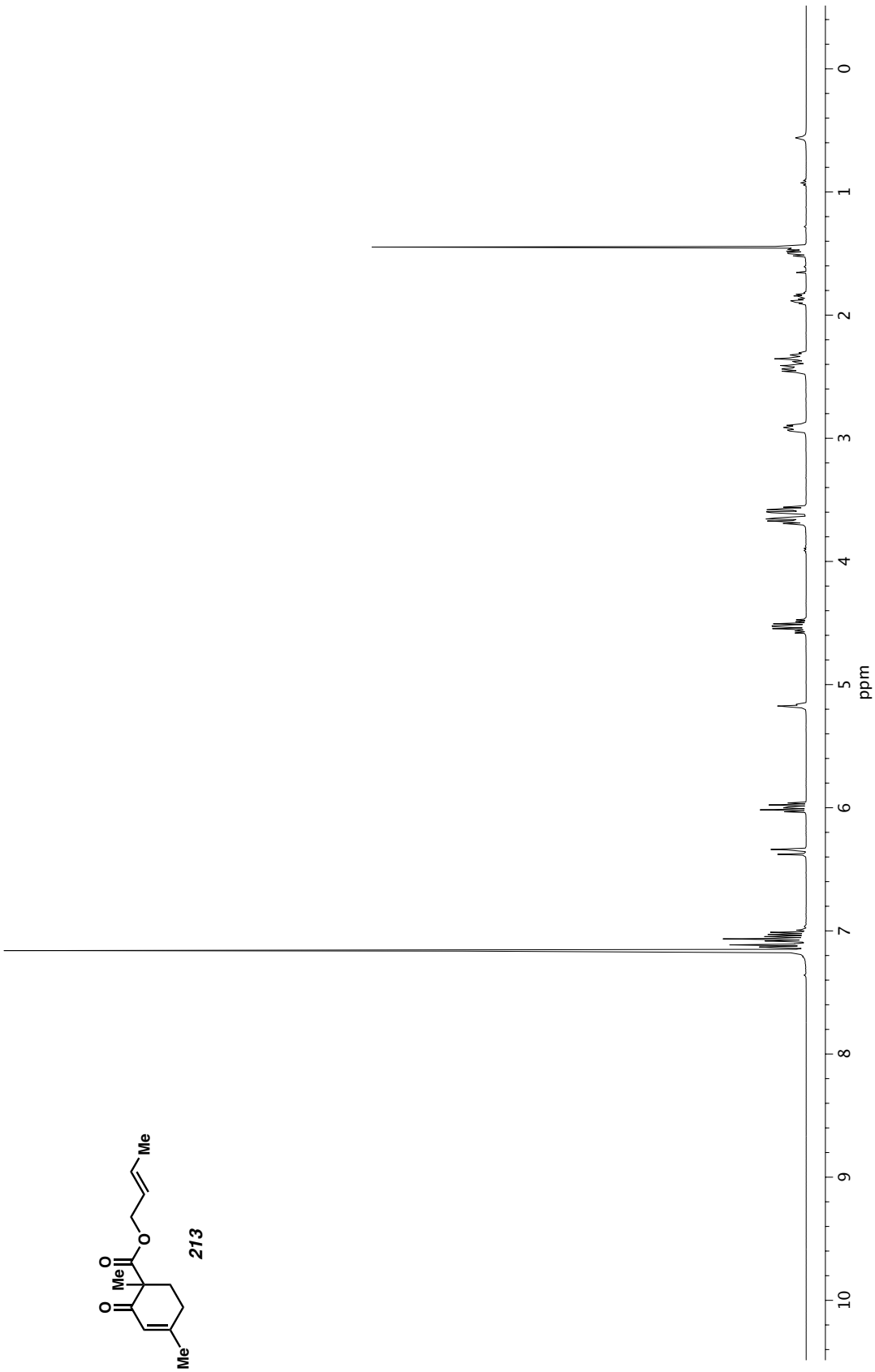


Figure A3.103. *^1H NMR (400 MHz, $CDCl_3$) of compound* ***213****.*

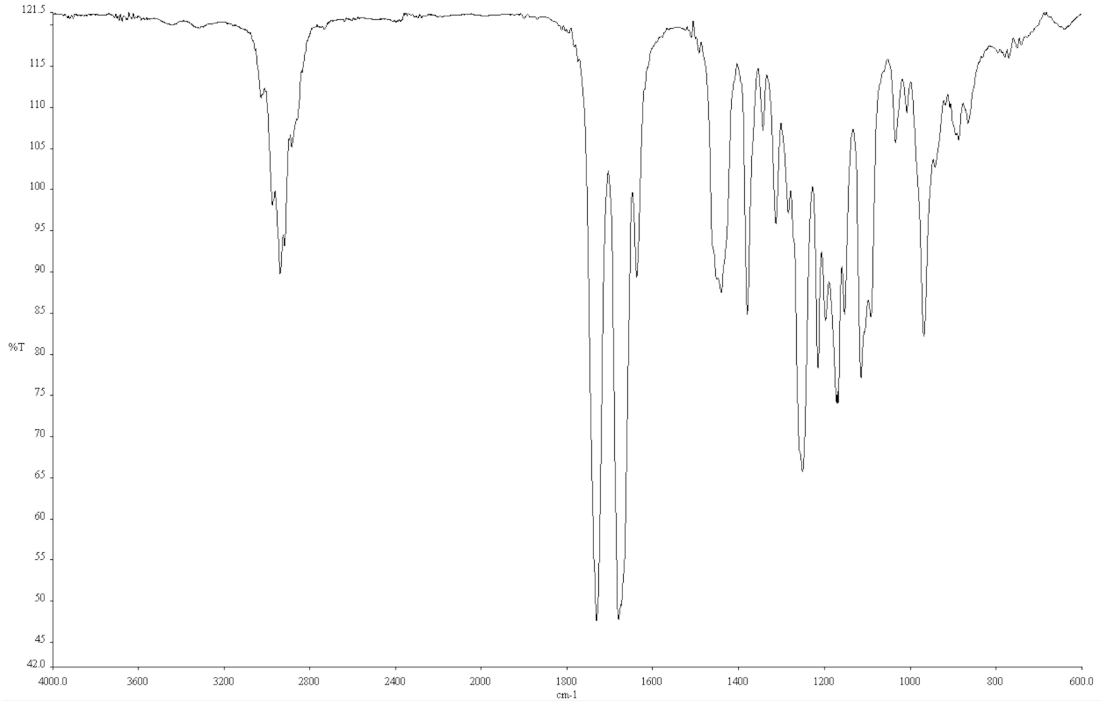


Figure A3.104. *Infrared spectrum (Thin Film, NaCl) of compound* ***213****.*

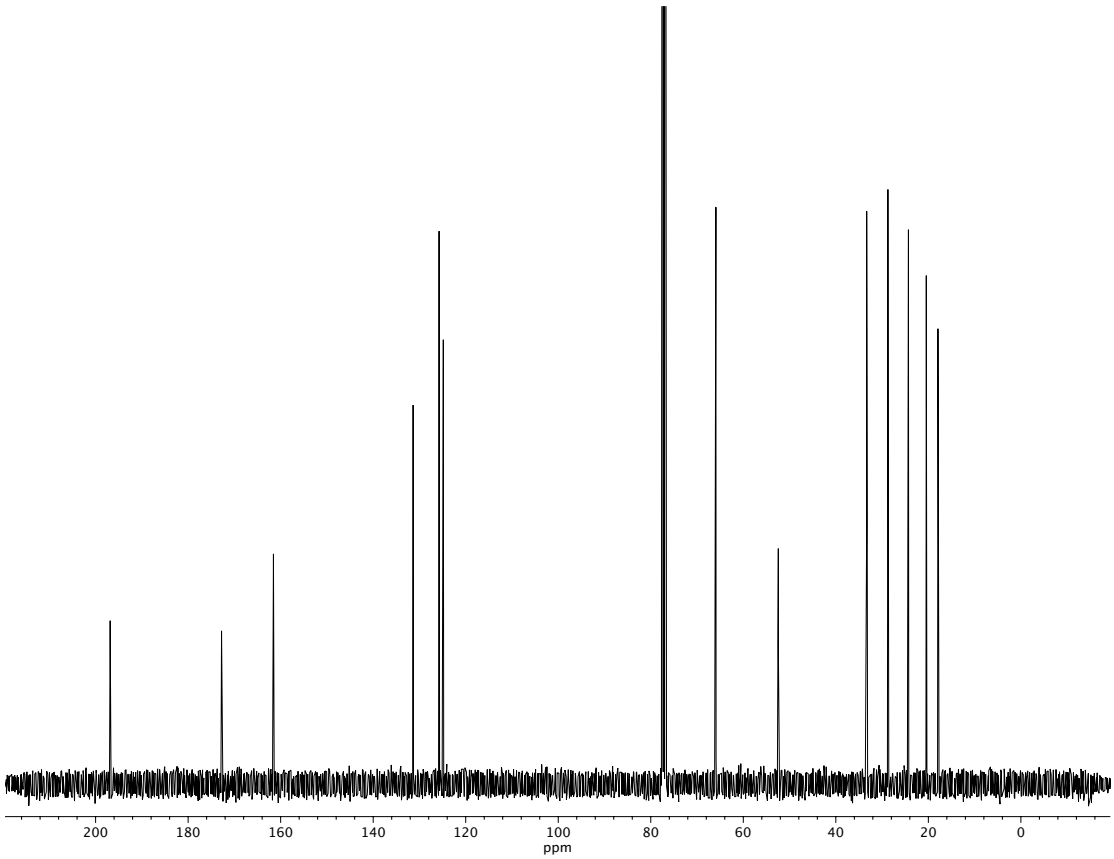


Figure A3.105. *^{13}C NMR (100 MHz, $CDCl_3$) of compound* ***213****.*

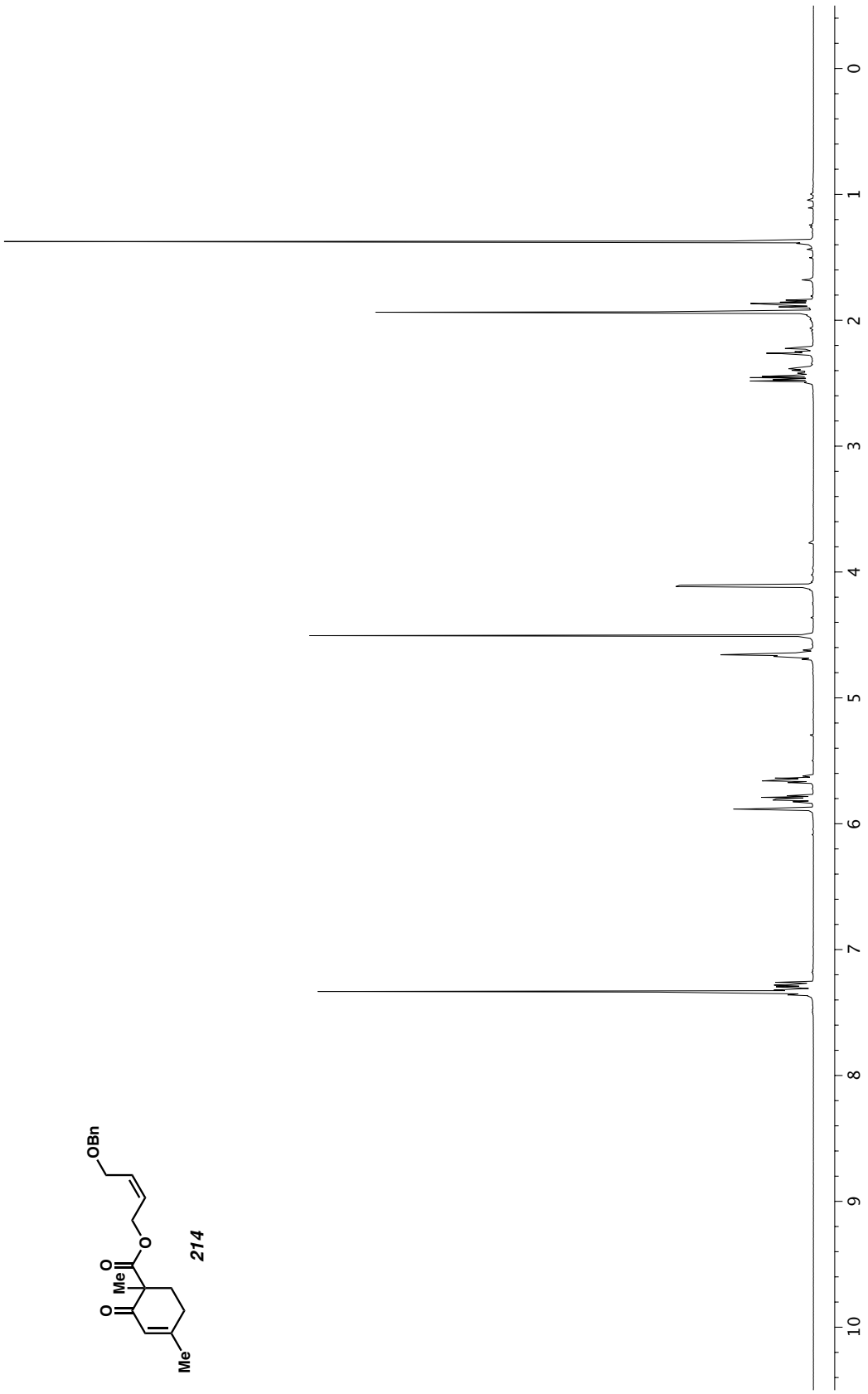


Figure A3.106. *^1H NMR (500 MHz, $CDCl_3$) of compound* ***214****.*

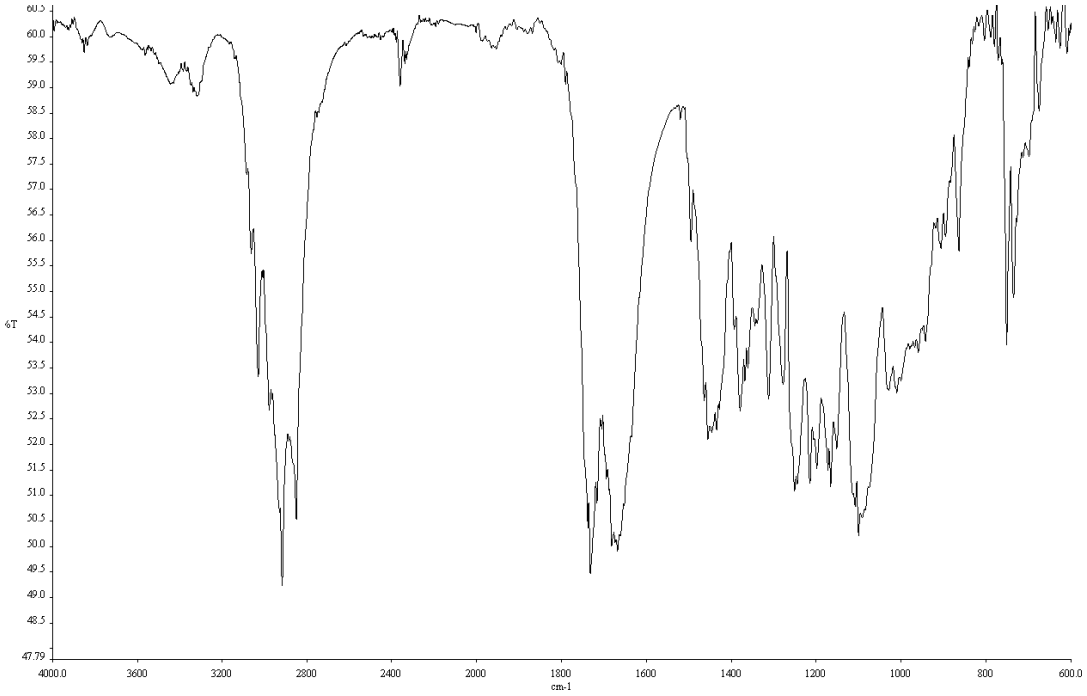


Figure A3.107. *Infrared spectrum (Thin Film, NaCl) of compound* ***214****.*

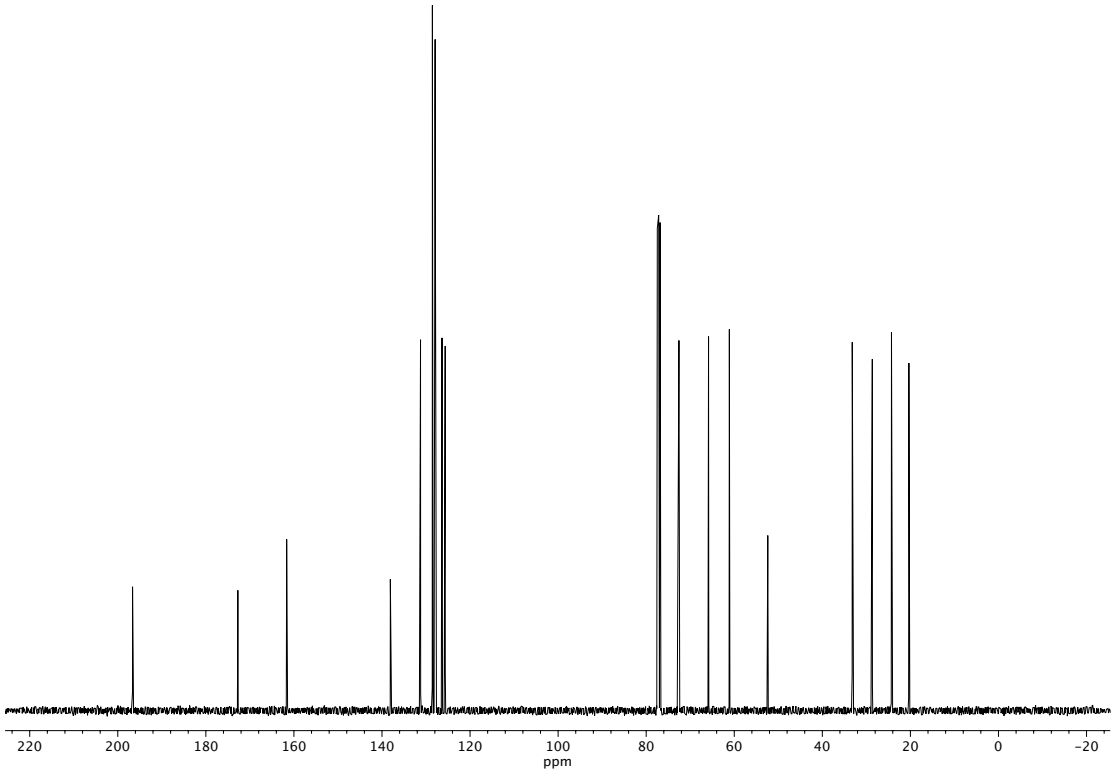


Figure A3.108. *^{13}C NMR (100 MHz, $CDCl_3$) of compound* ***214****.*

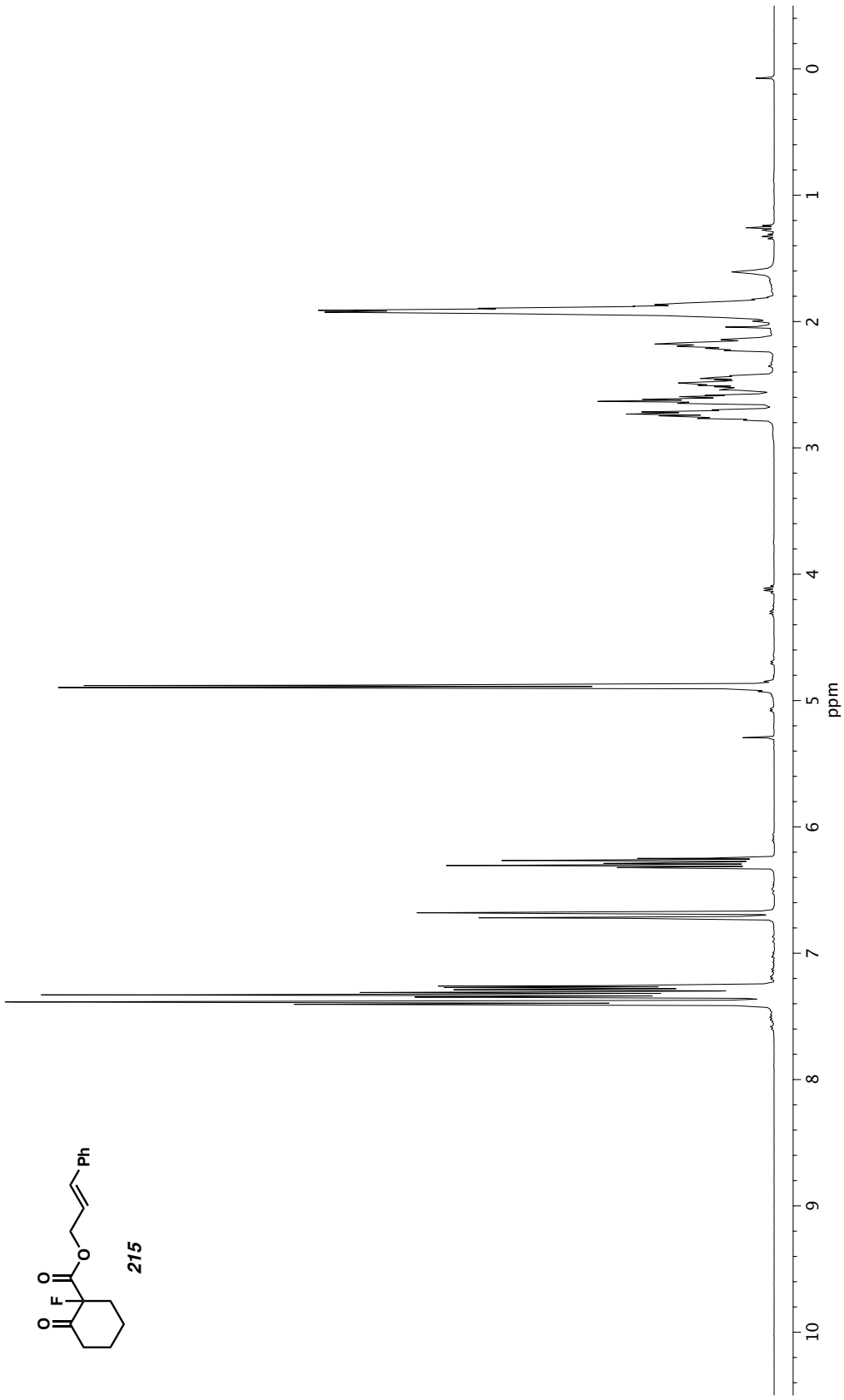


Figure A3.109. *^1H NMR (400 MHz, $CDCl_3$) of compound **215**.*

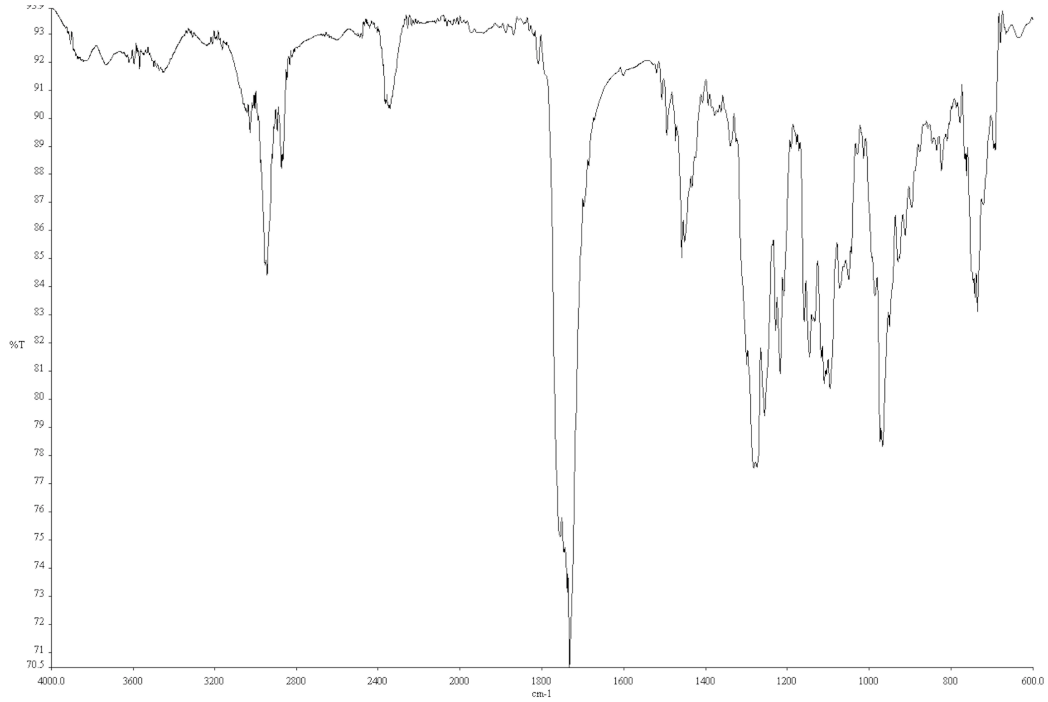


Figure A3.110. *Infrared spectrum (Thin Film, NaCl) of compound* ***215****.*

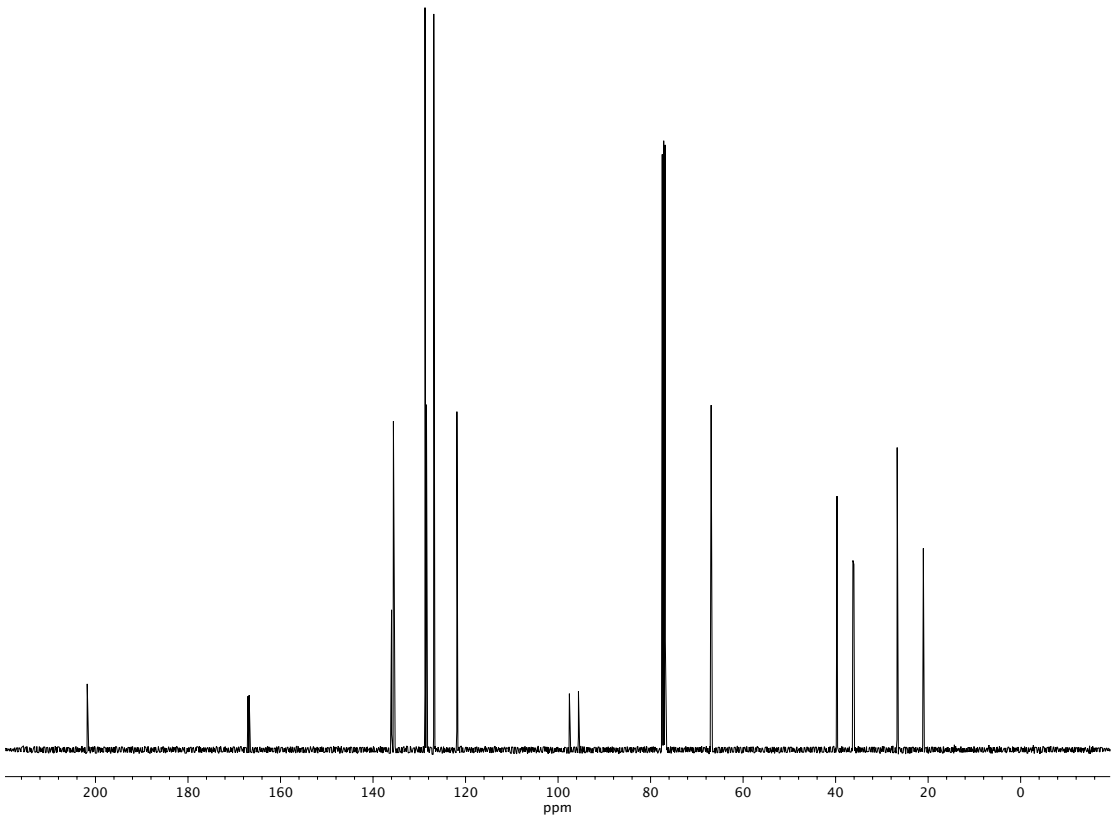


Figure A3.111. *^{13}C NMR (100 MHz, $CDCl_3$) of compound* ***215****.*

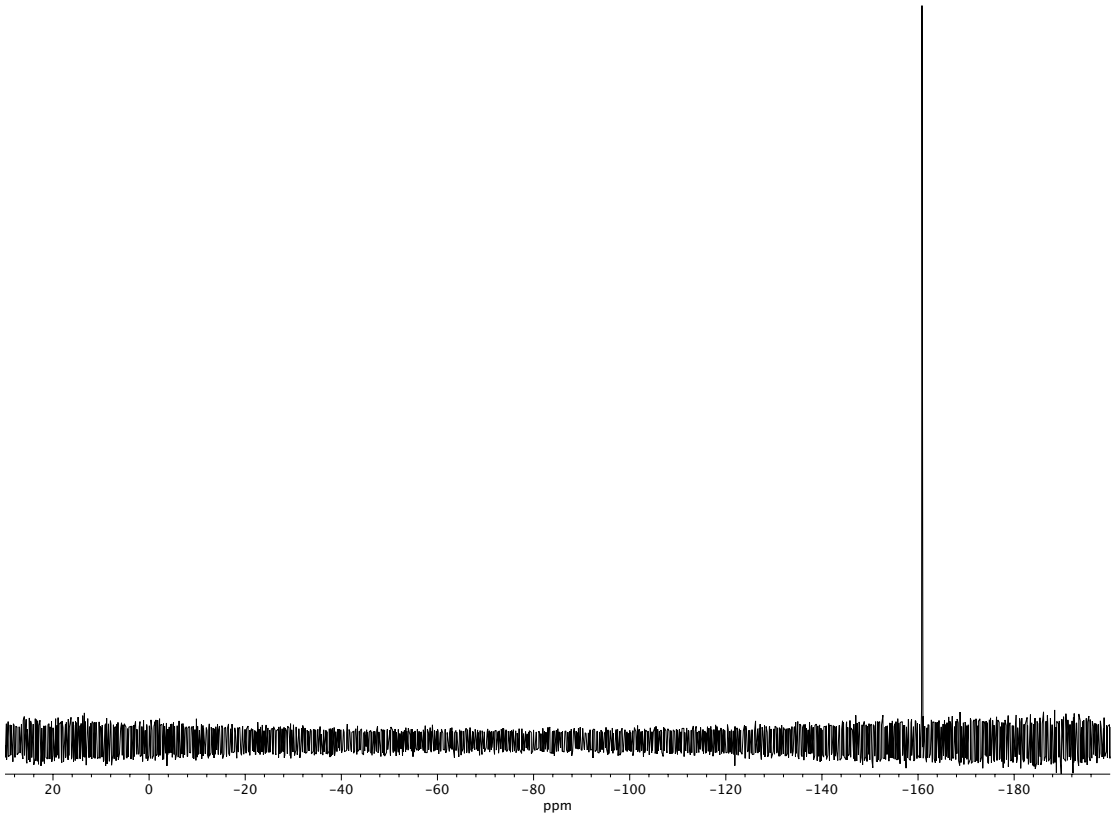


Figure A3.112. *^{19}F NMR (282 MHz, $CDCl_3$) of compound* ***215****.*

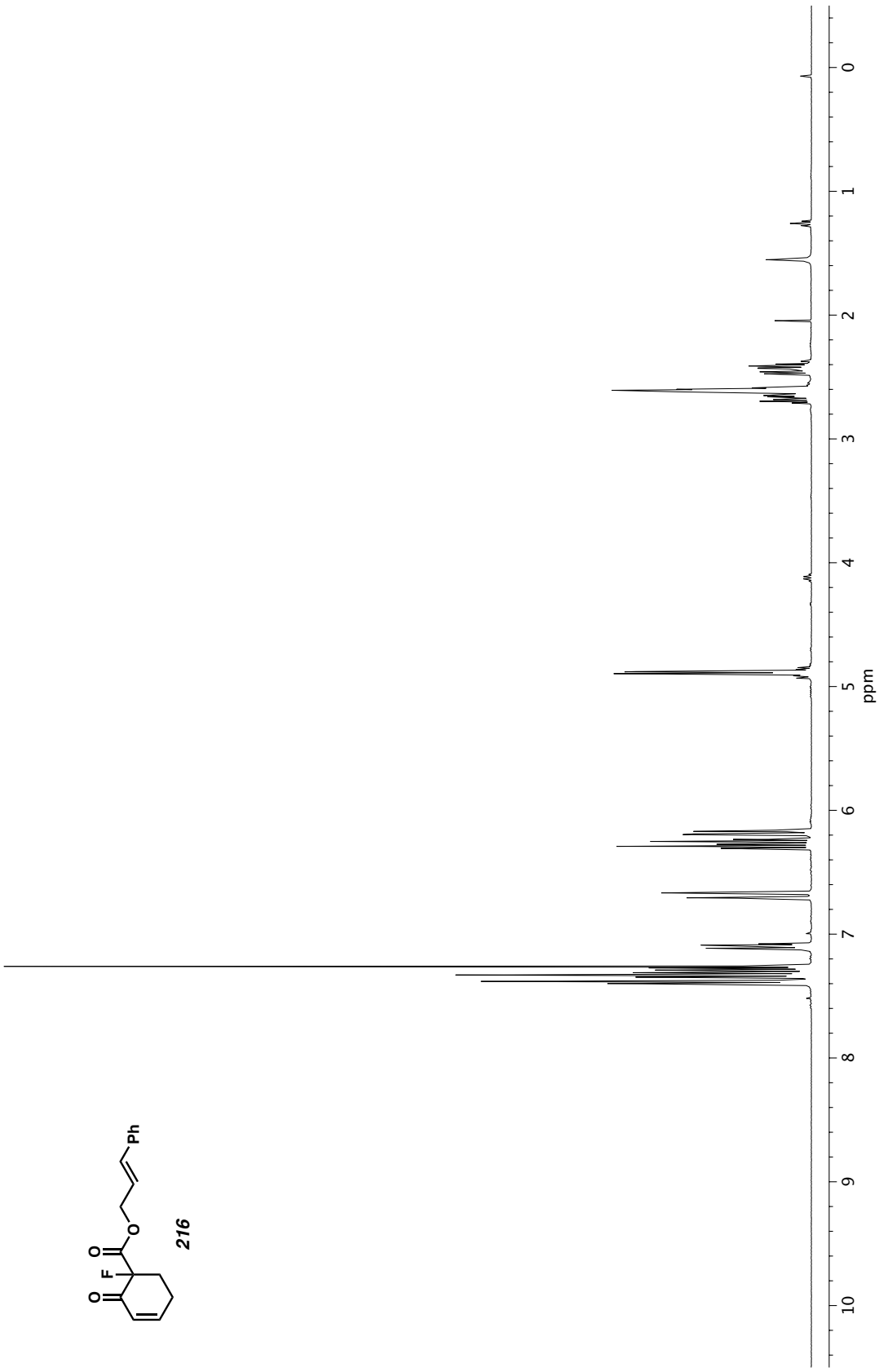


Figure A3.113. *^1H NMR (400 MHz, $CDCl_3$) of compound* ***216****.*

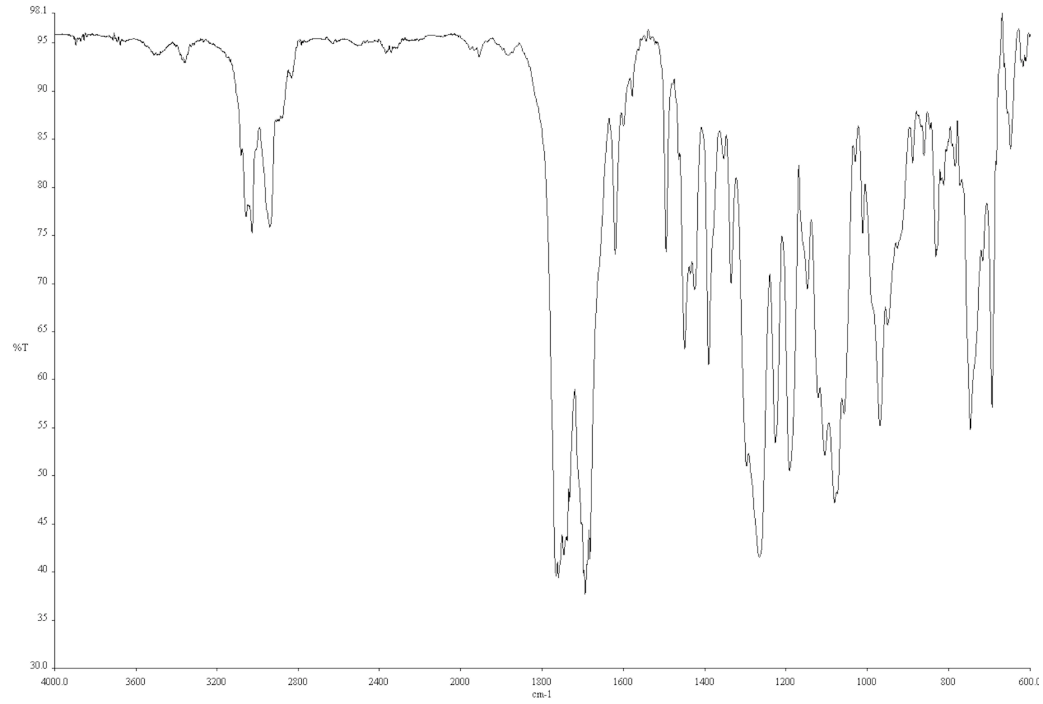


Figure A3.114. *Infrared spectrum (Thin Film, NaCl) of compound* ***216****.*

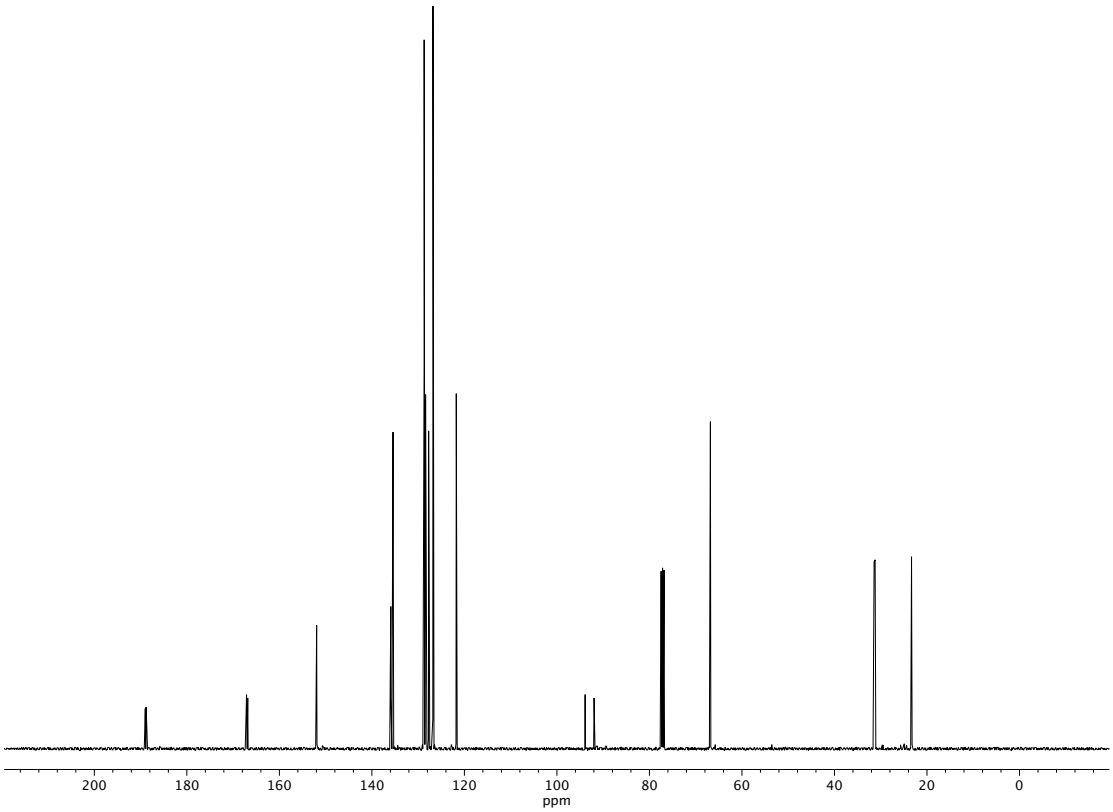


Figure A3.115. *^{13}C NMR (100 MHz, $CDCl_3$) of compound* ***216****.*

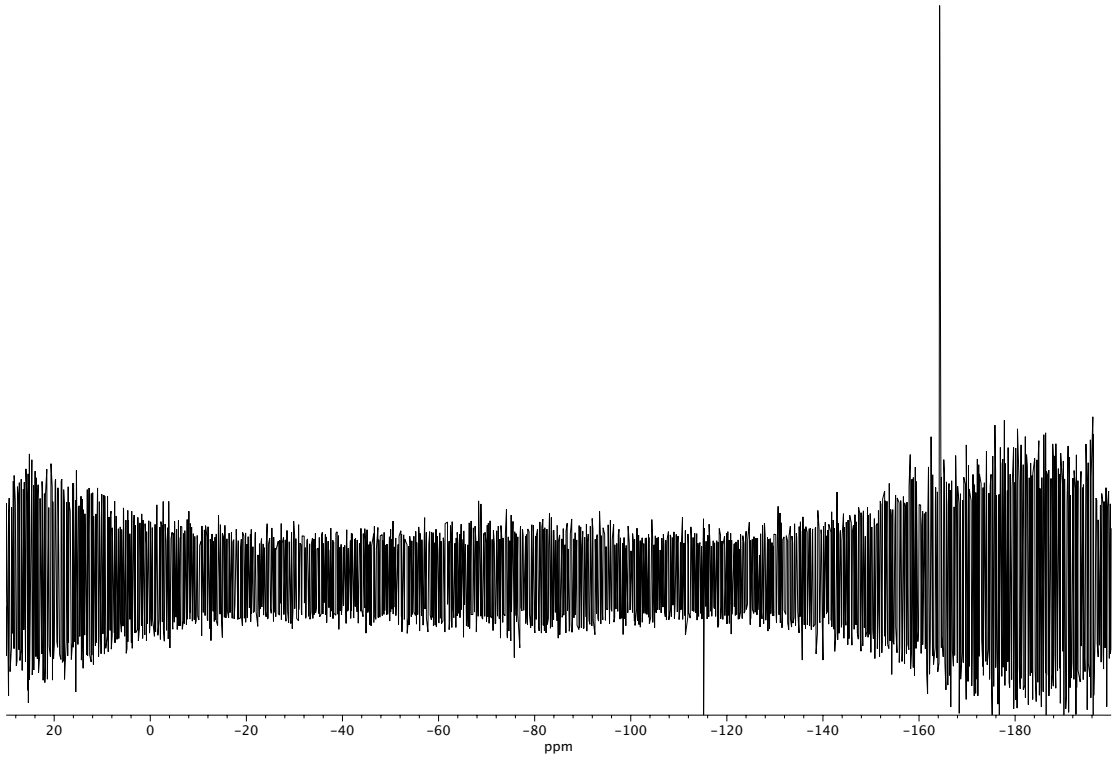


Figure A3.116. *^{19}F NMR (282 MHz, $CDCl_3$) of compound* ***216****.*

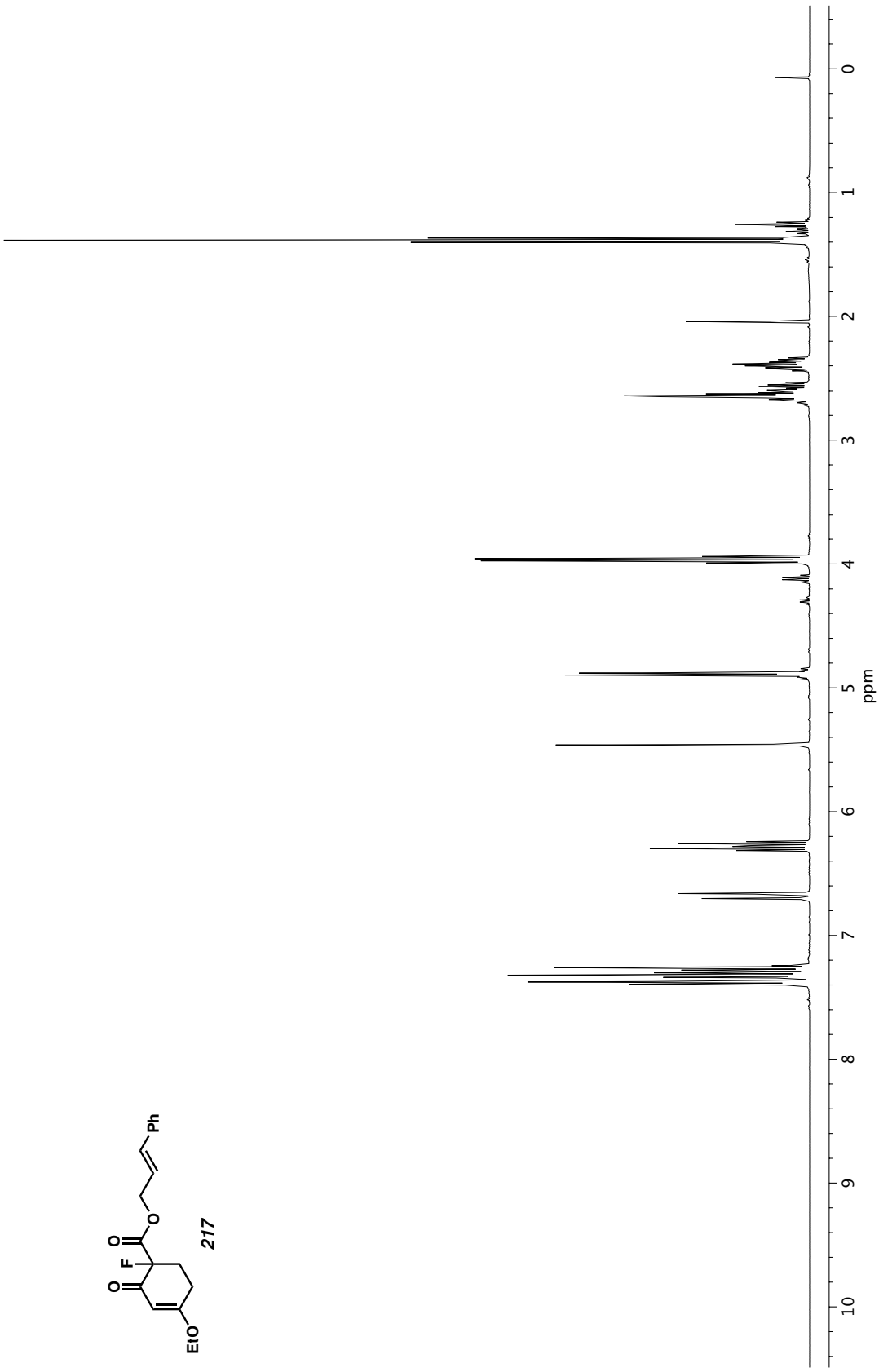


Figure A3.117. *^{1}H NMR (400 MHz, $CDCl_3$) of compound* ***217****.*

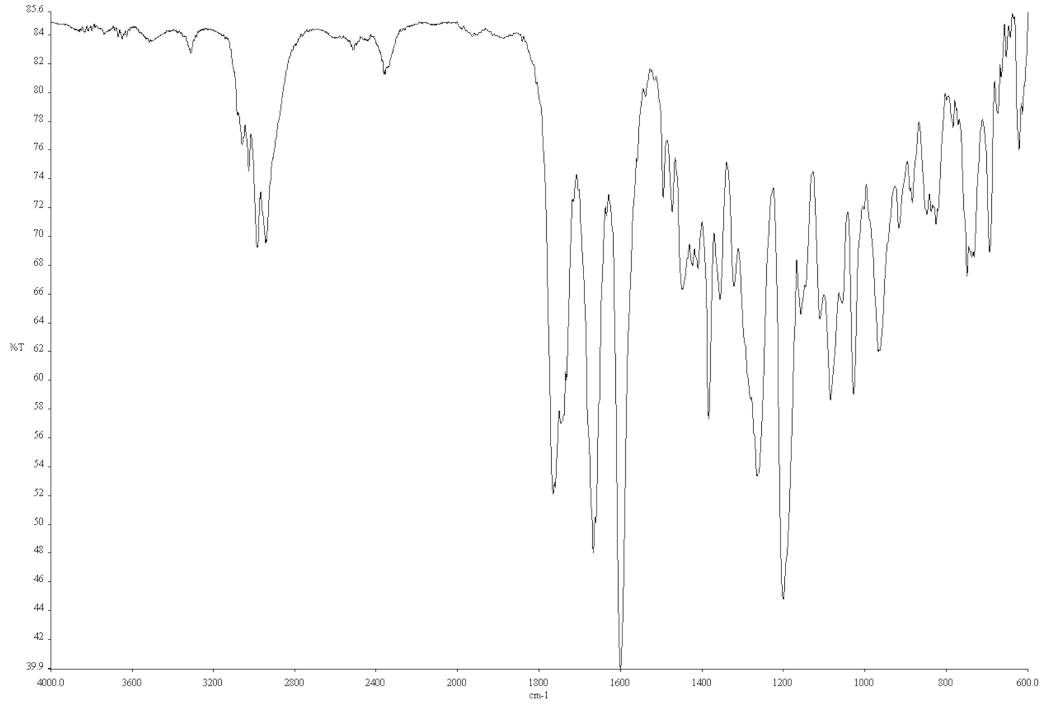


Figure A3.118. *Infrared spectrum (Thin Film, NaCl) of compound* ***217****.*

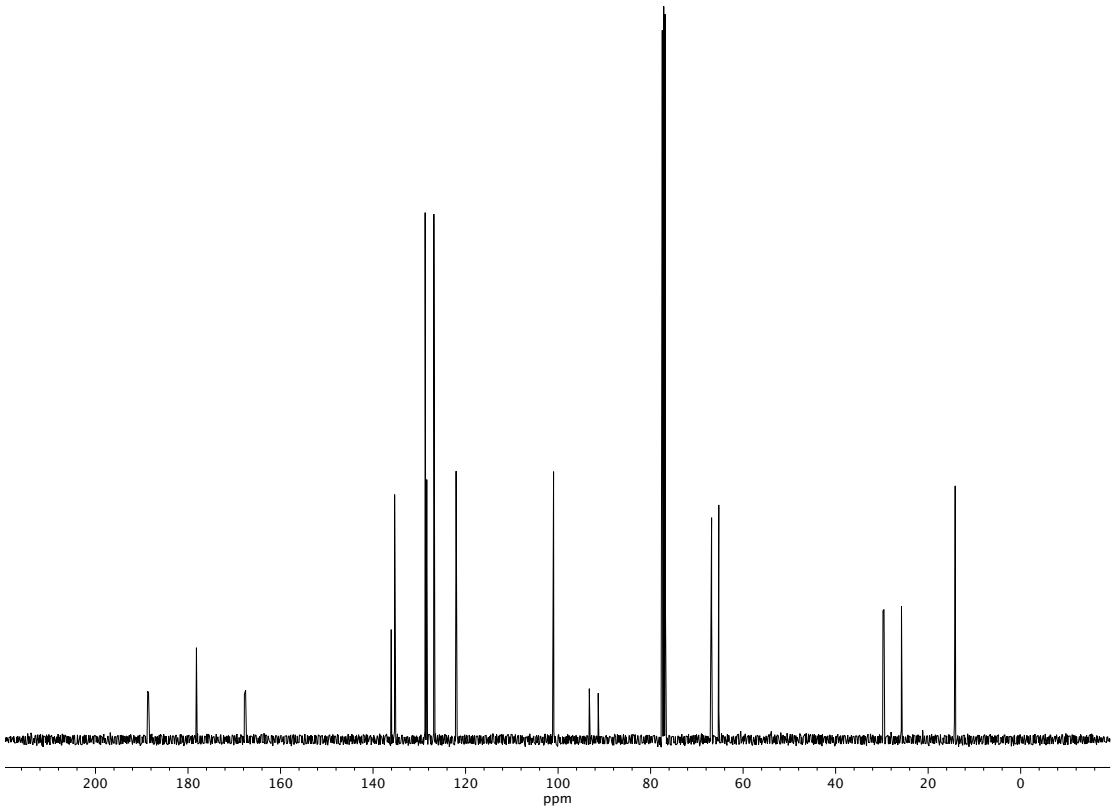


Figure A3.119. *^{13}C NMR (100 MHz, $CDCl_3$) of compound* ***217****.*

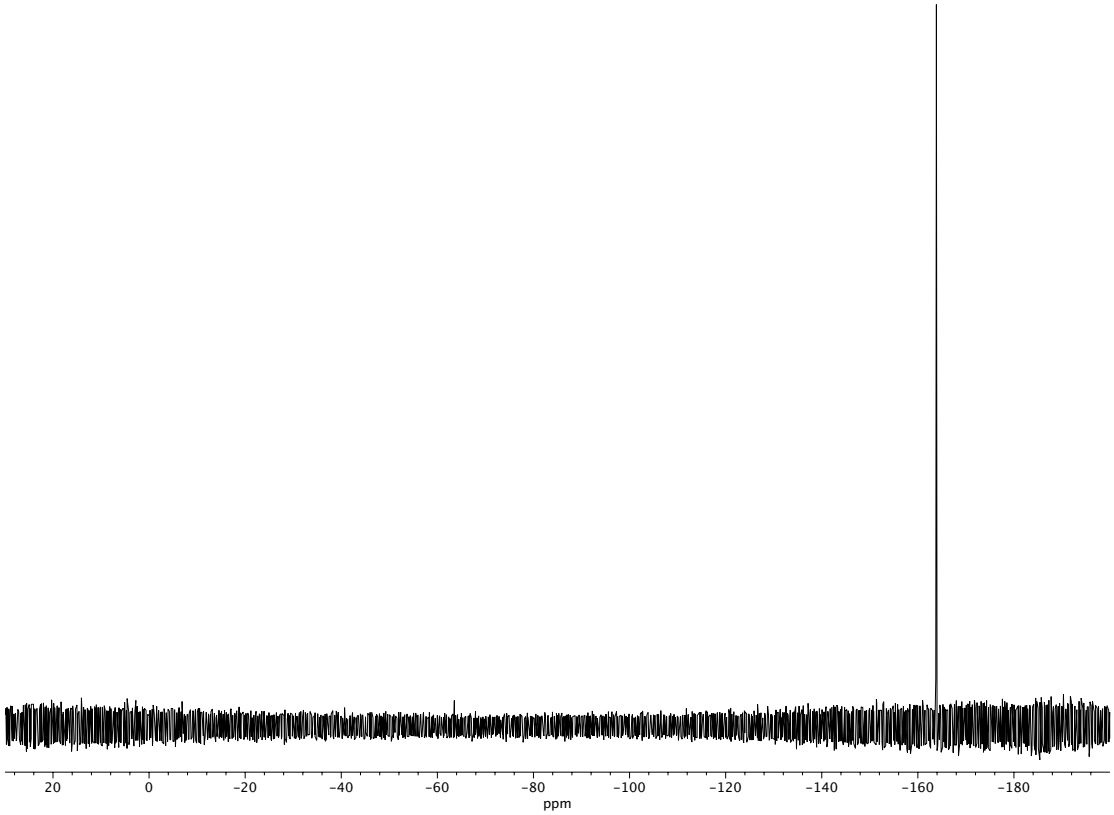


Figure A3.120. *^{19}F NMR (282 MHz, $CDCl_3$) of compound **217**.*

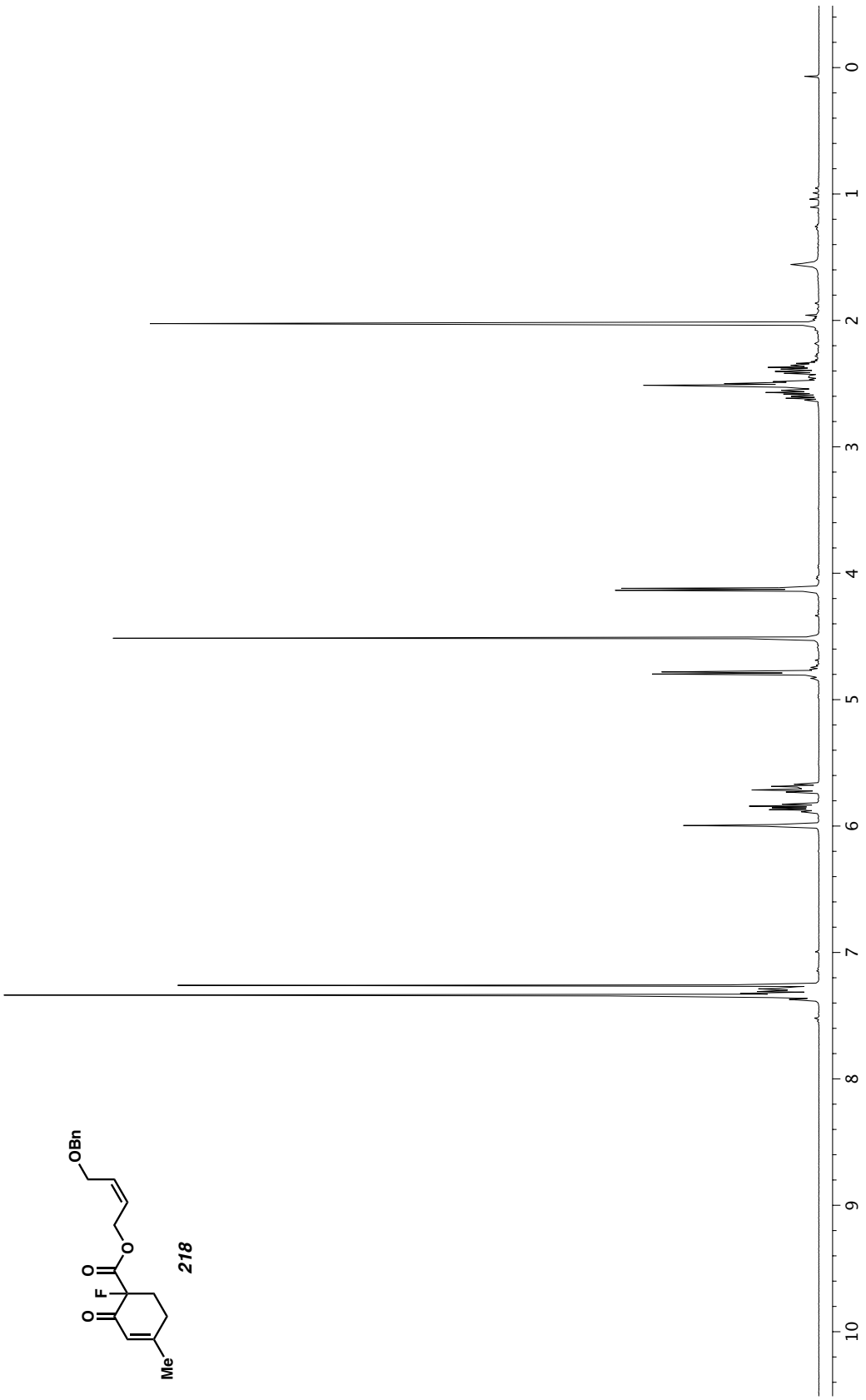


Figure A3.121. *^1H NMR (400 MHz, $CDCl_3$) of compound **218**.*

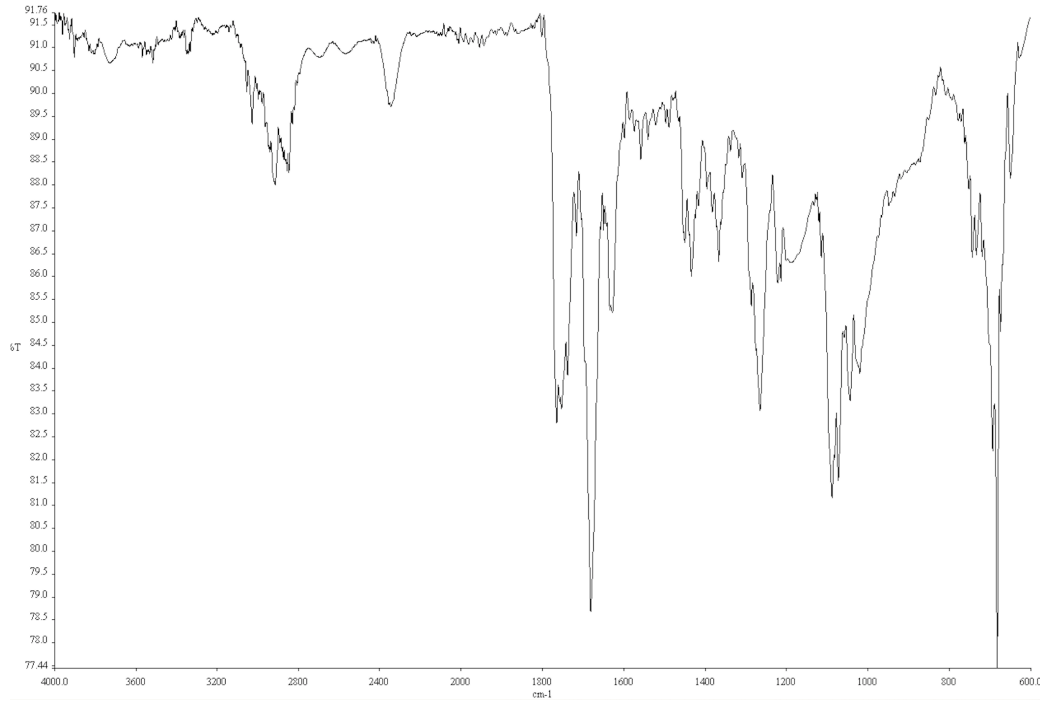


Figure A3.122. *Infrared spectrum (Thin Film, NaCl) of compound* ***218****.*

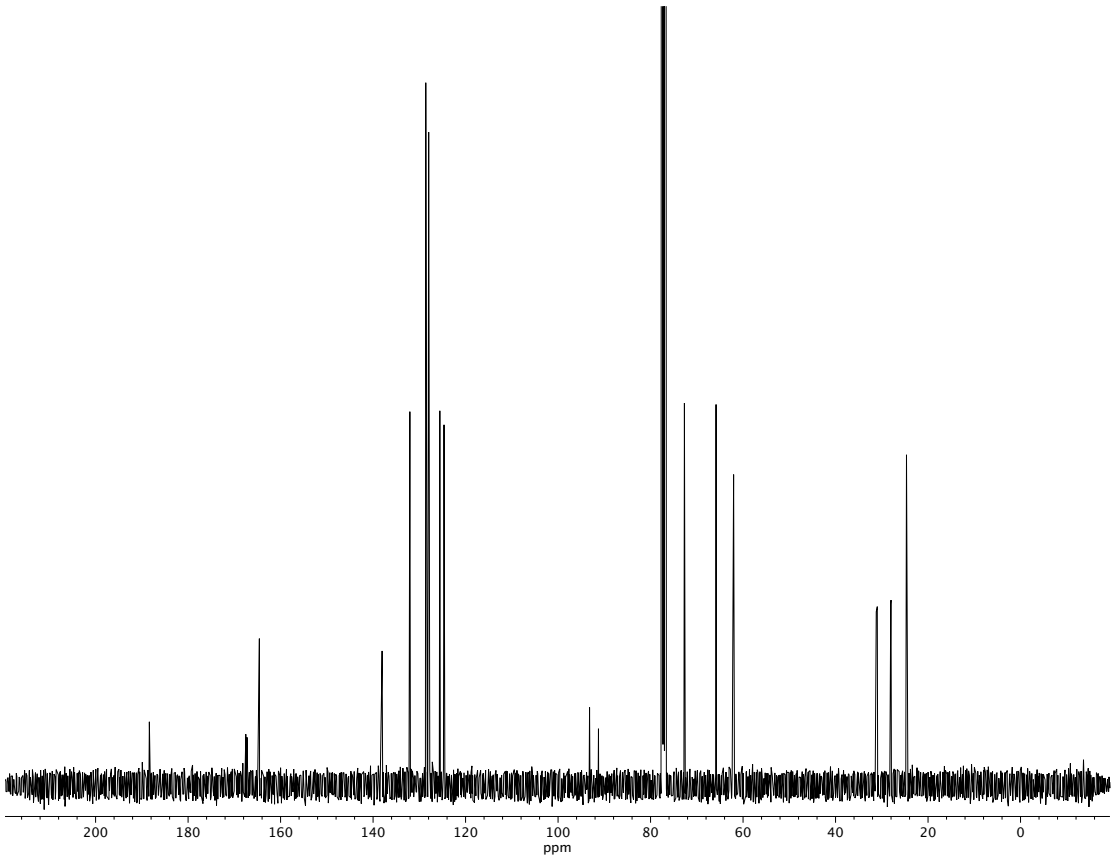


Figure A3.123. *^{13}C NMR (100 MHz, $CDCl_3$) of compound* ***218****.*

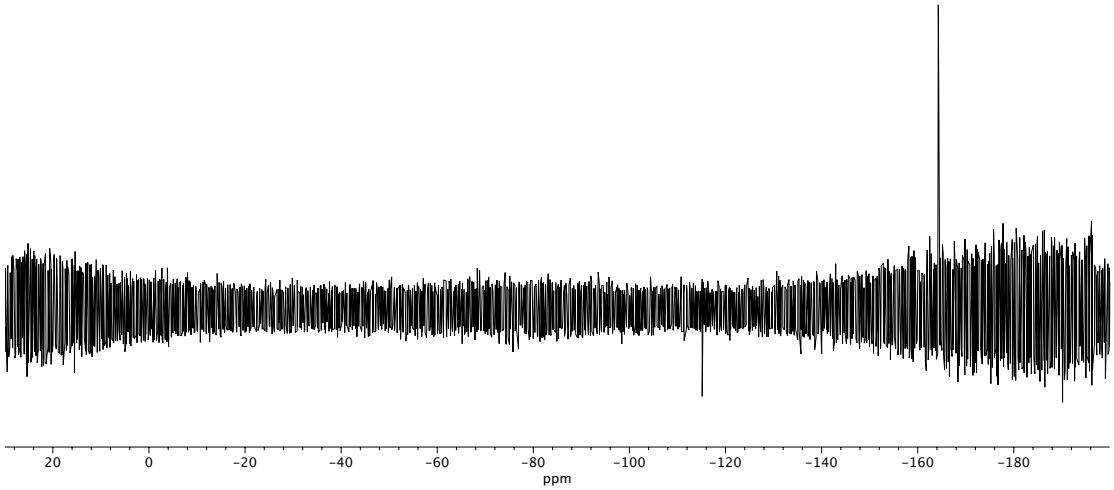
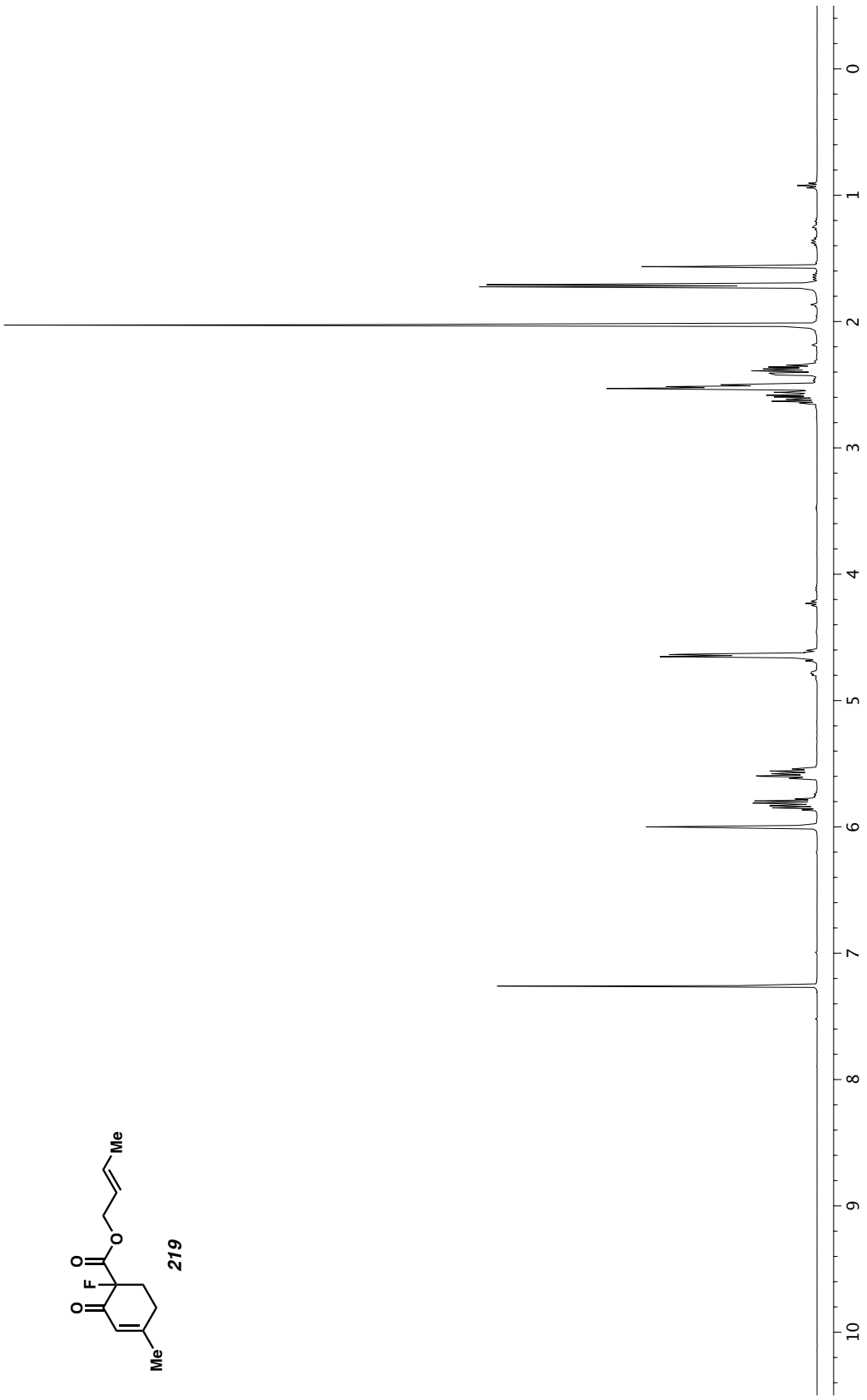


Figure A3.124. *^{19}F NMR (282 MHz, $CDCl_3$) of compound* ***218****.*



219

Figure A3.125. *^{1}H NMR (400 MHz, $CDCl_3$) of compound* ***219***.

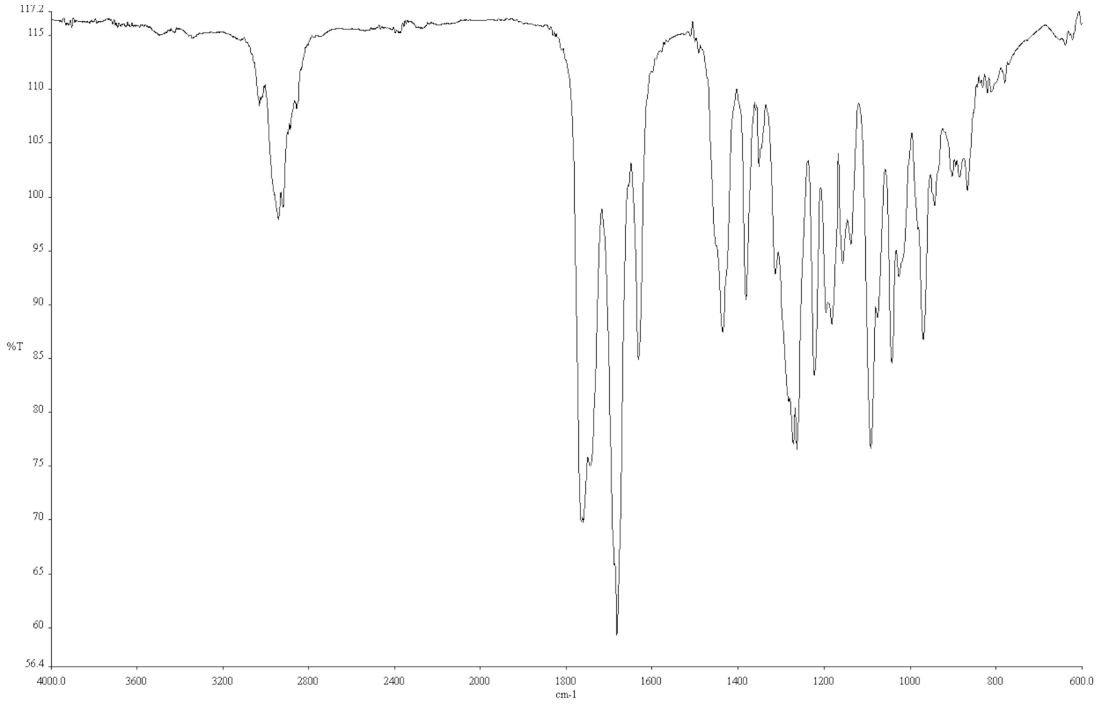


Figure A3.126. *Infrared spectrum (Thin Film, NaCl) of compound* ***219****.*

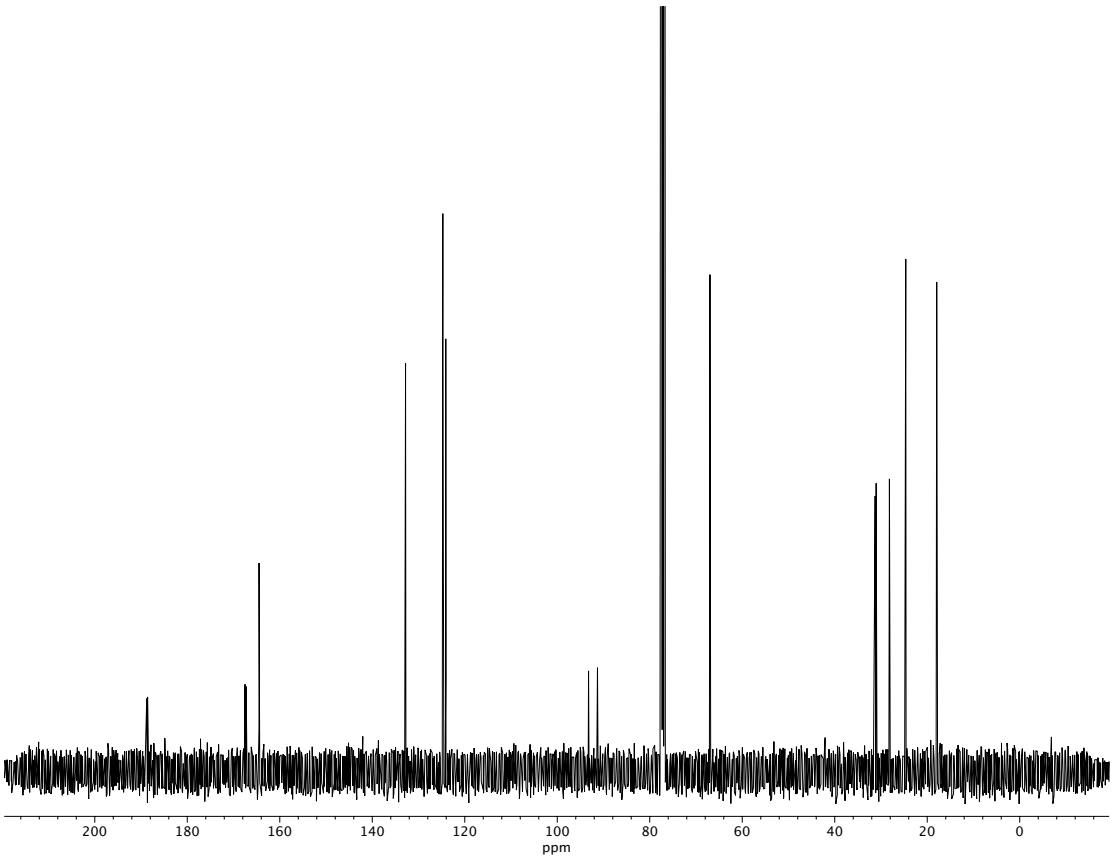


Figure A3.127. *^{13}C NMR (100 MHz, $CDCl_3$) of compound* ***219****.*

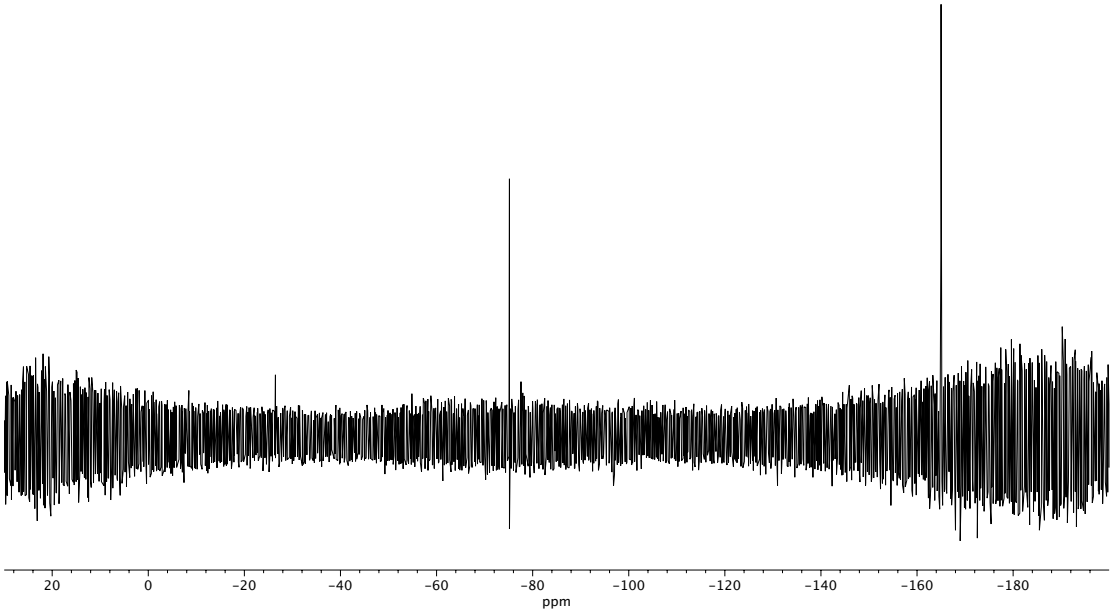


Figure A3.128. *^{19}F NMR (282 MHz, $CDCl_3$) of compound **219**.*

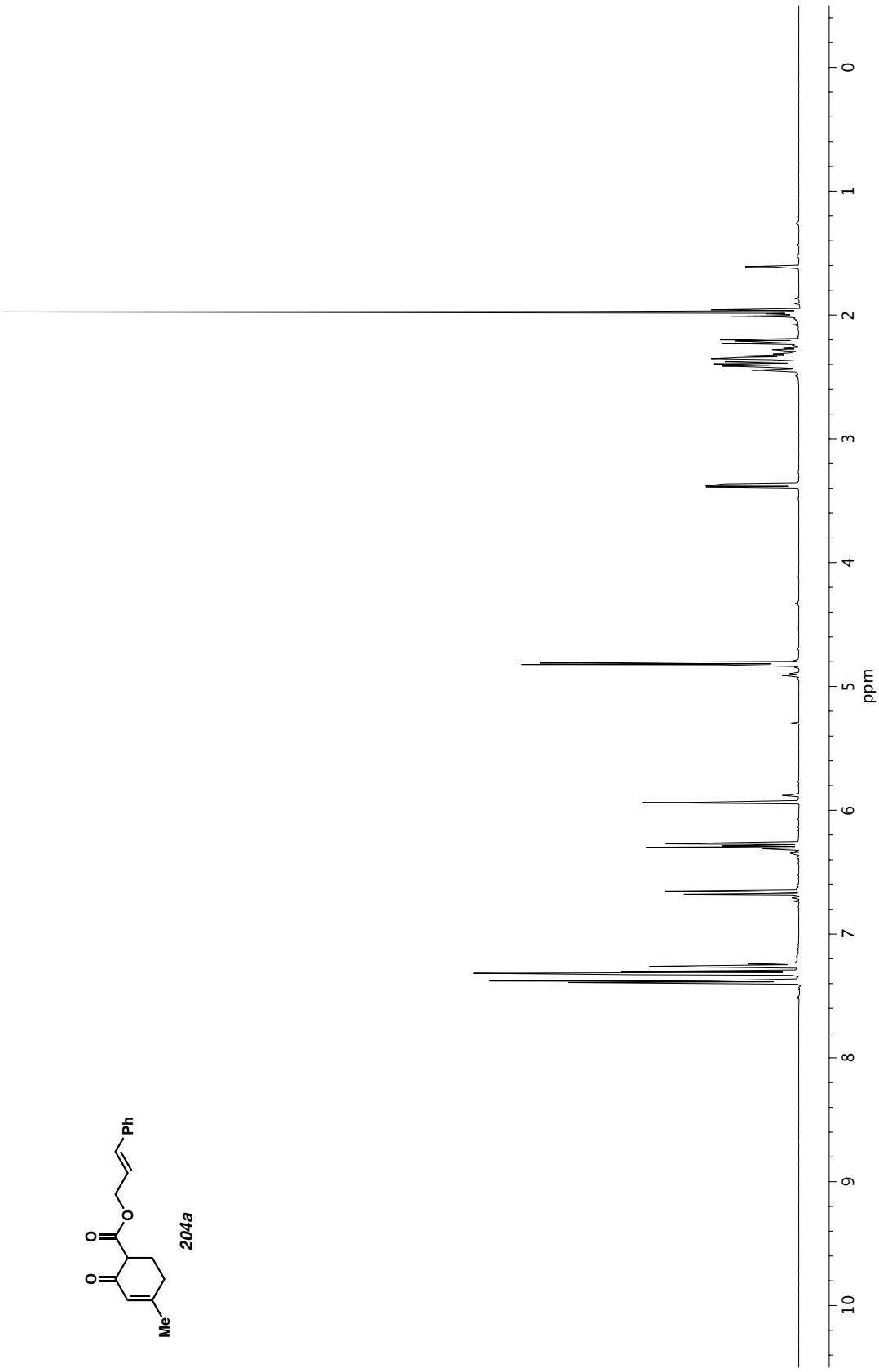


Figure A3.129. *^1H NMR (600 MHz, $CDCl_3$) of compound* ***204a***.

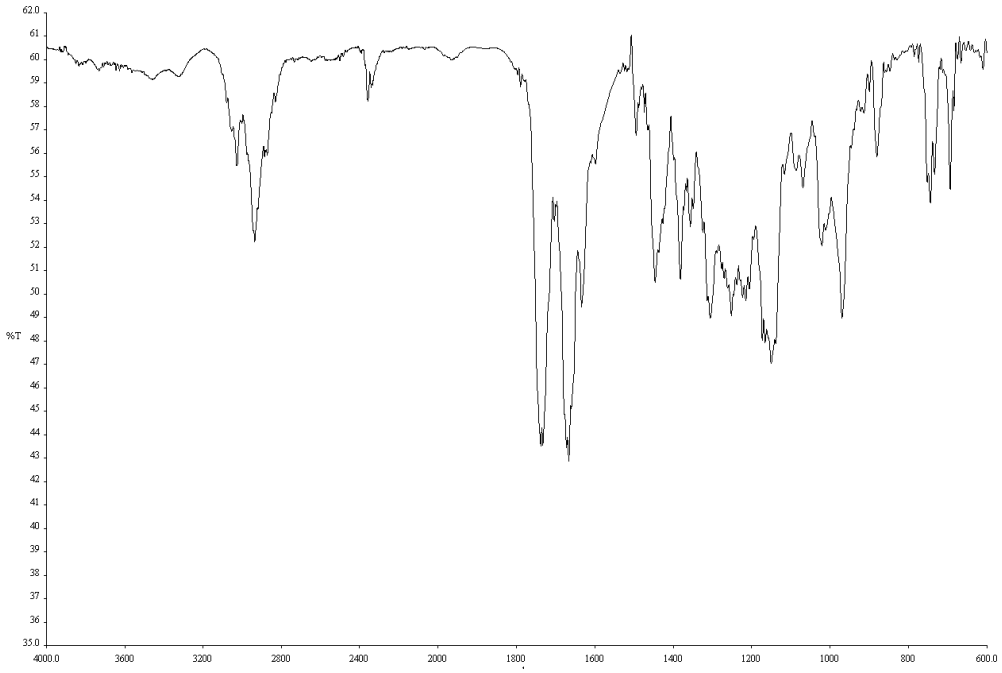


Figure A3.130. *Infrared spectrum (Thin Film, NaCl) of compound* ***204a****.*

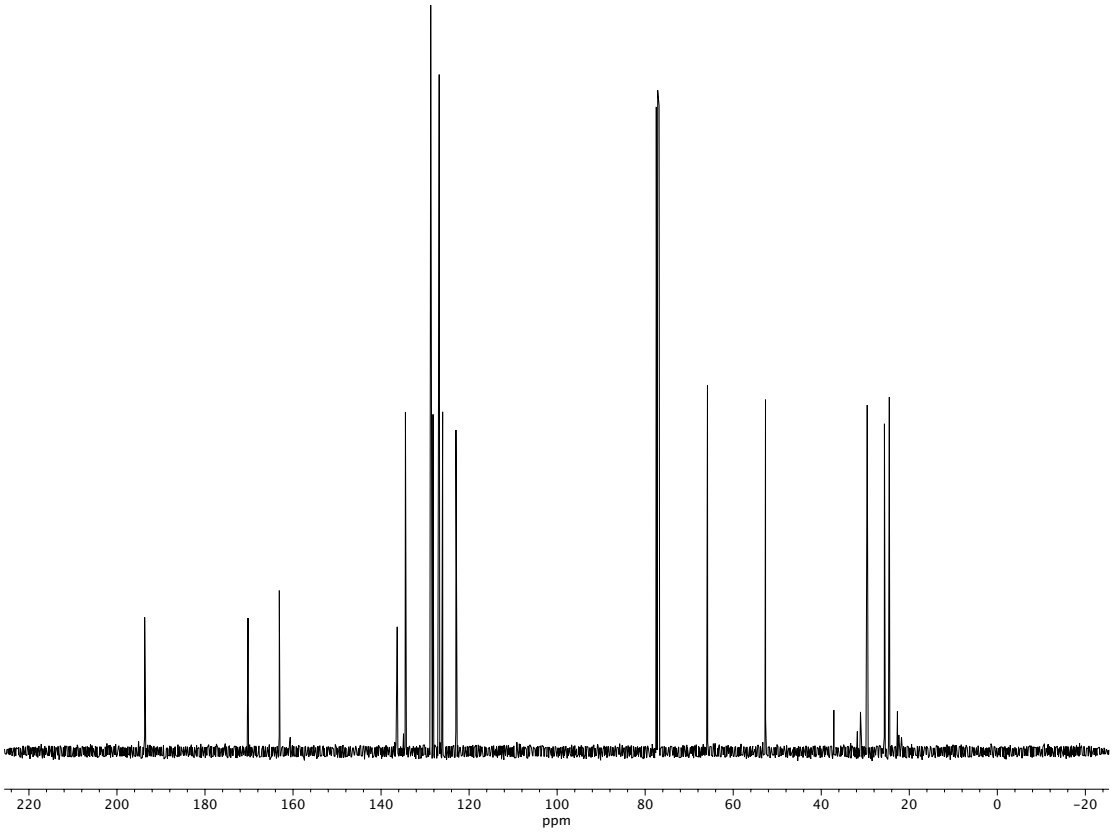


Figure A3.131. *^{13}C NMR (100 MHz, $CDCl_3$) of compound* ***204a****.*

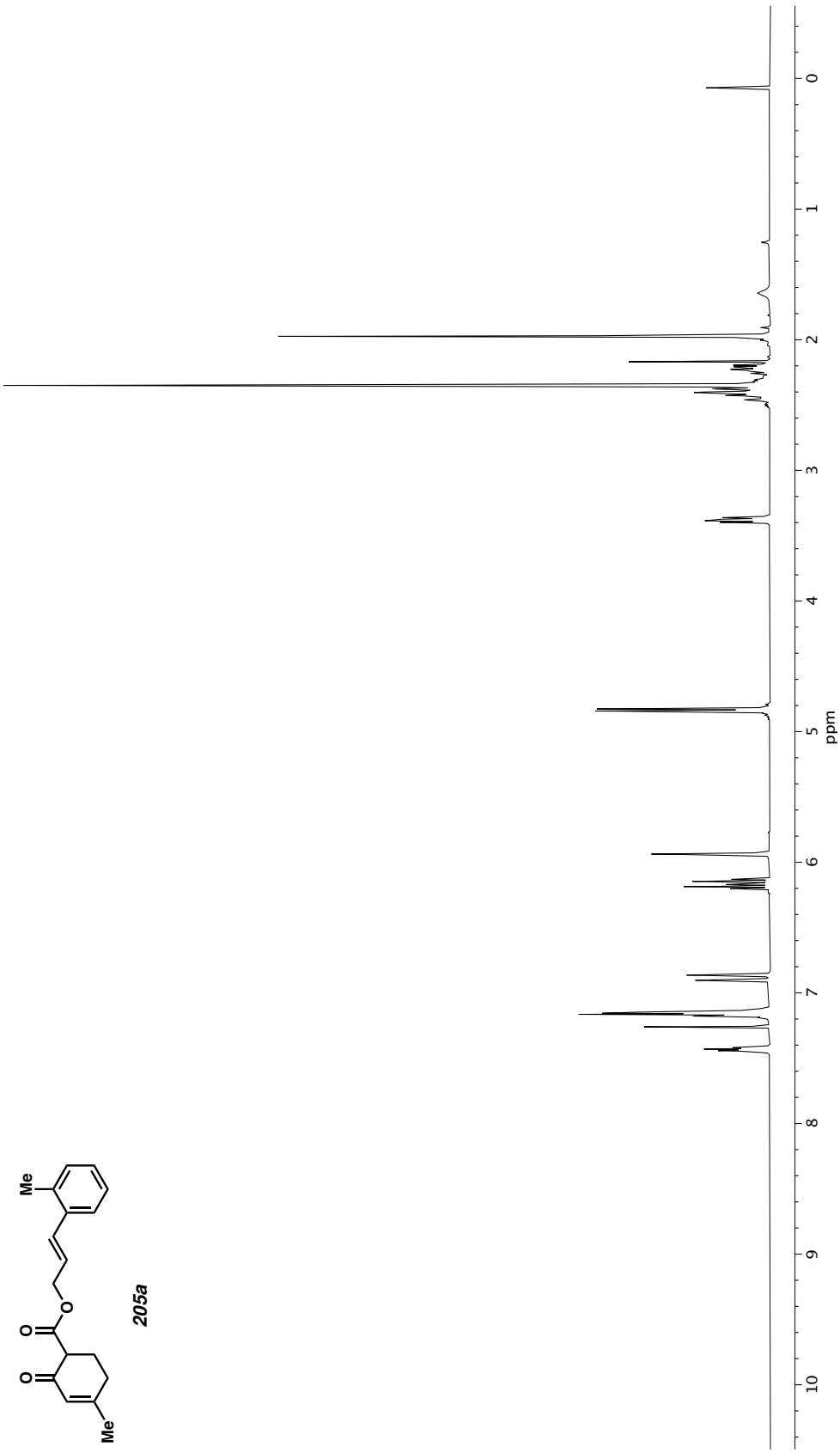


Figure A3.132. *^1H NMR (400 MHz, $CDCl_3$) of compound* ***205a***.

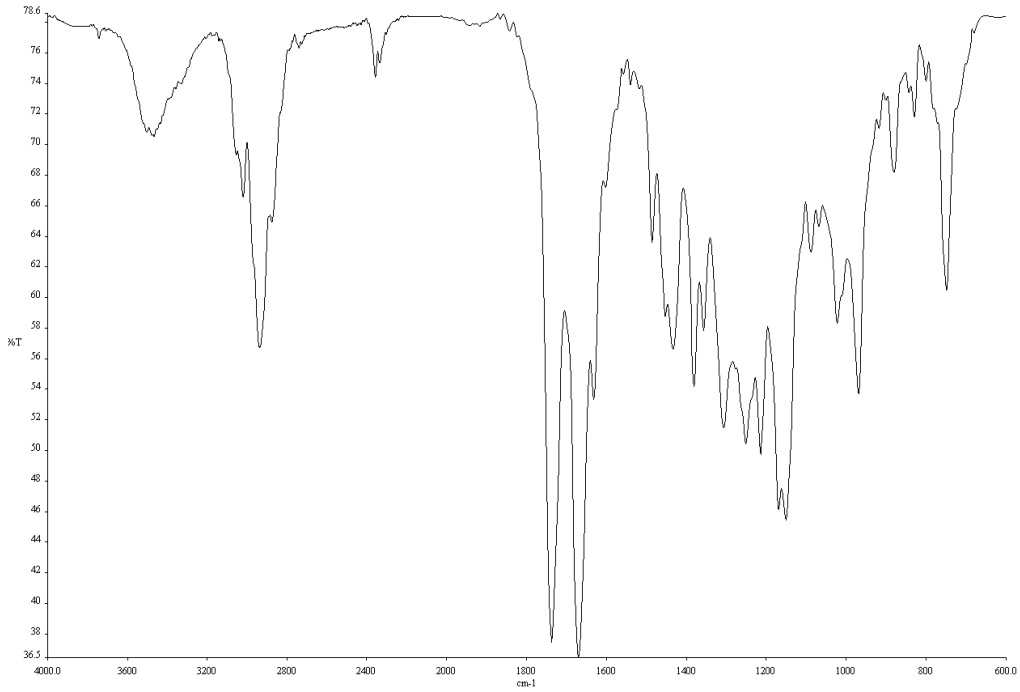


Figure A3.133. *Infrared spectrum (Thin Film, NaCl) of compound* ***205a****.*

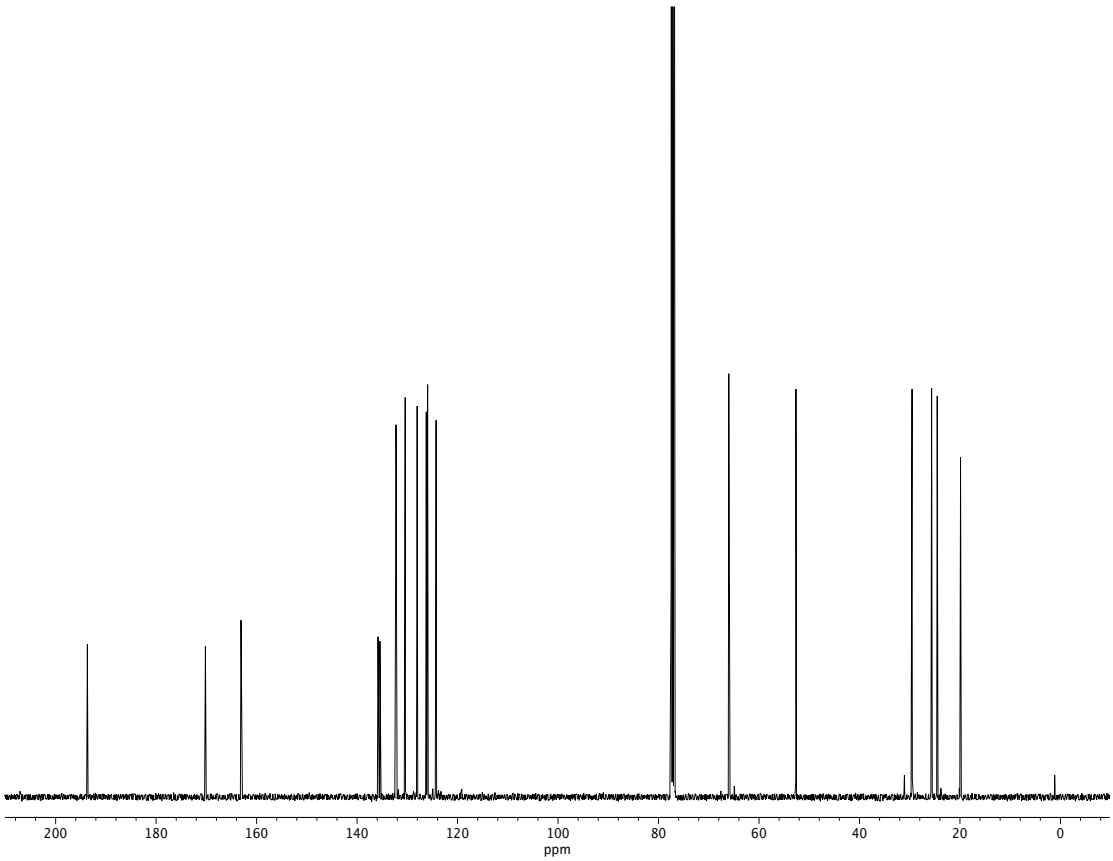


Figure A3.134. *^{13}C NMR (100 MHz, $CDCl_3$) of compound* ***205a****.*

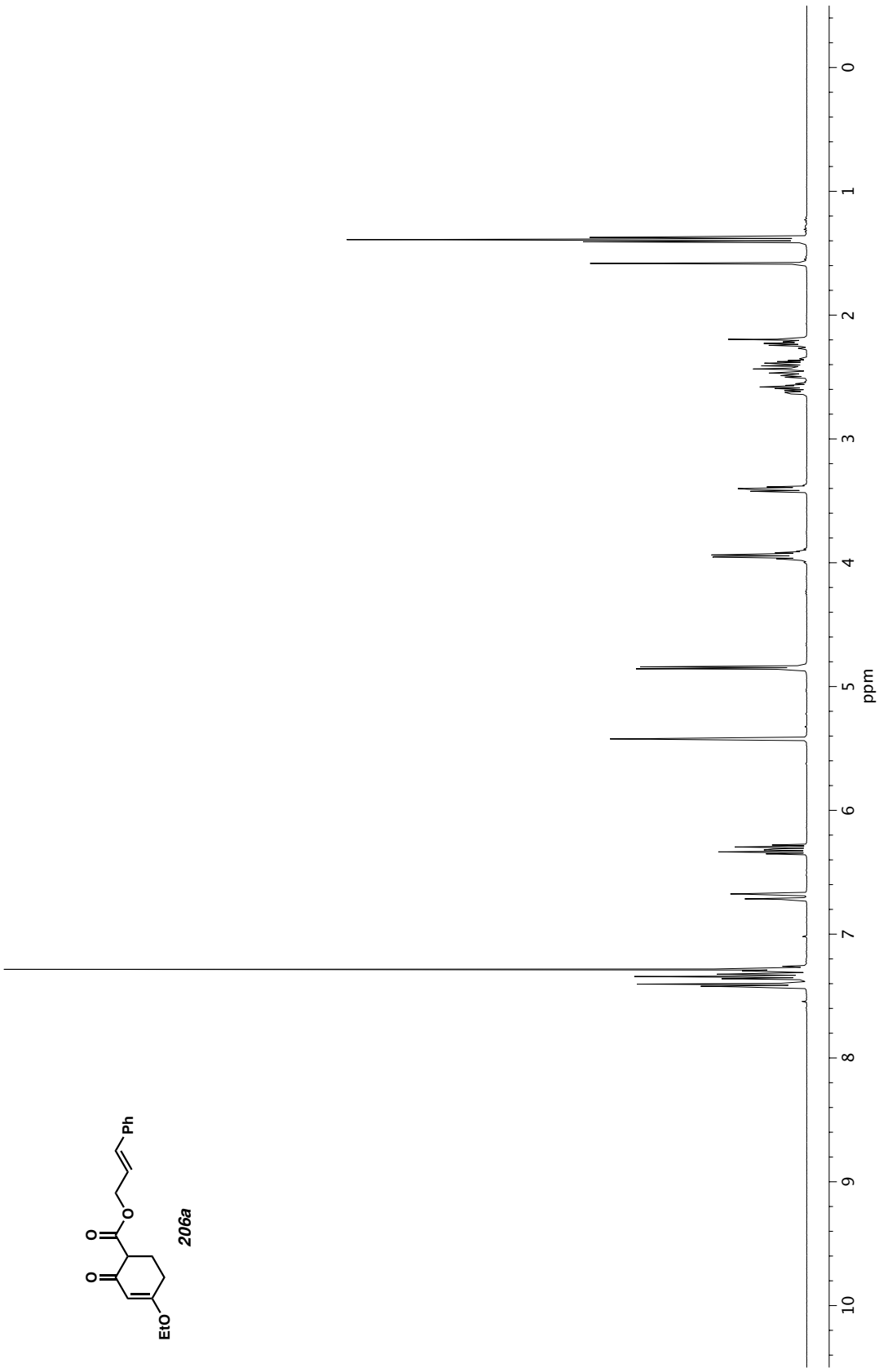


Figure A3.135. *^1H NMR (400 MHz, $CDCl_3$) of compound* ***206a***.

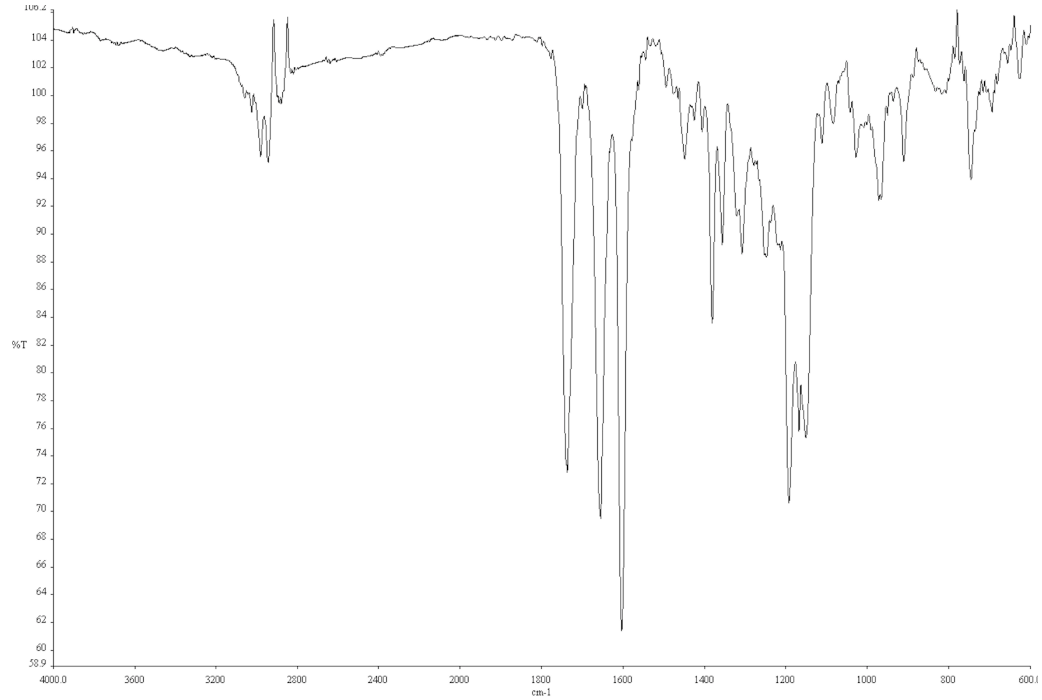


Figure A3.136. *Infrared spectrum (Thin Film, NaCl) of compound* ***206a****.*

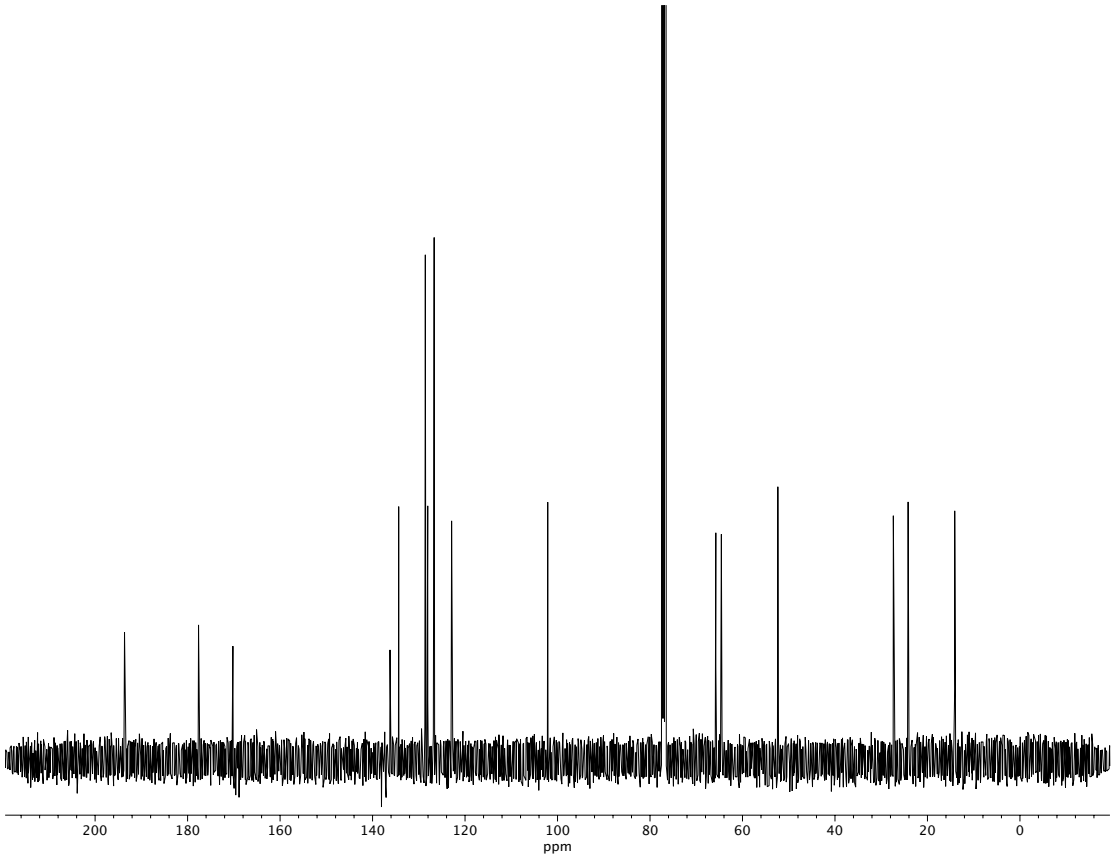


Figure A3.137. *^{13}C NMR (100 MHz, $CDCl_3$) of compound* ***206a****.*

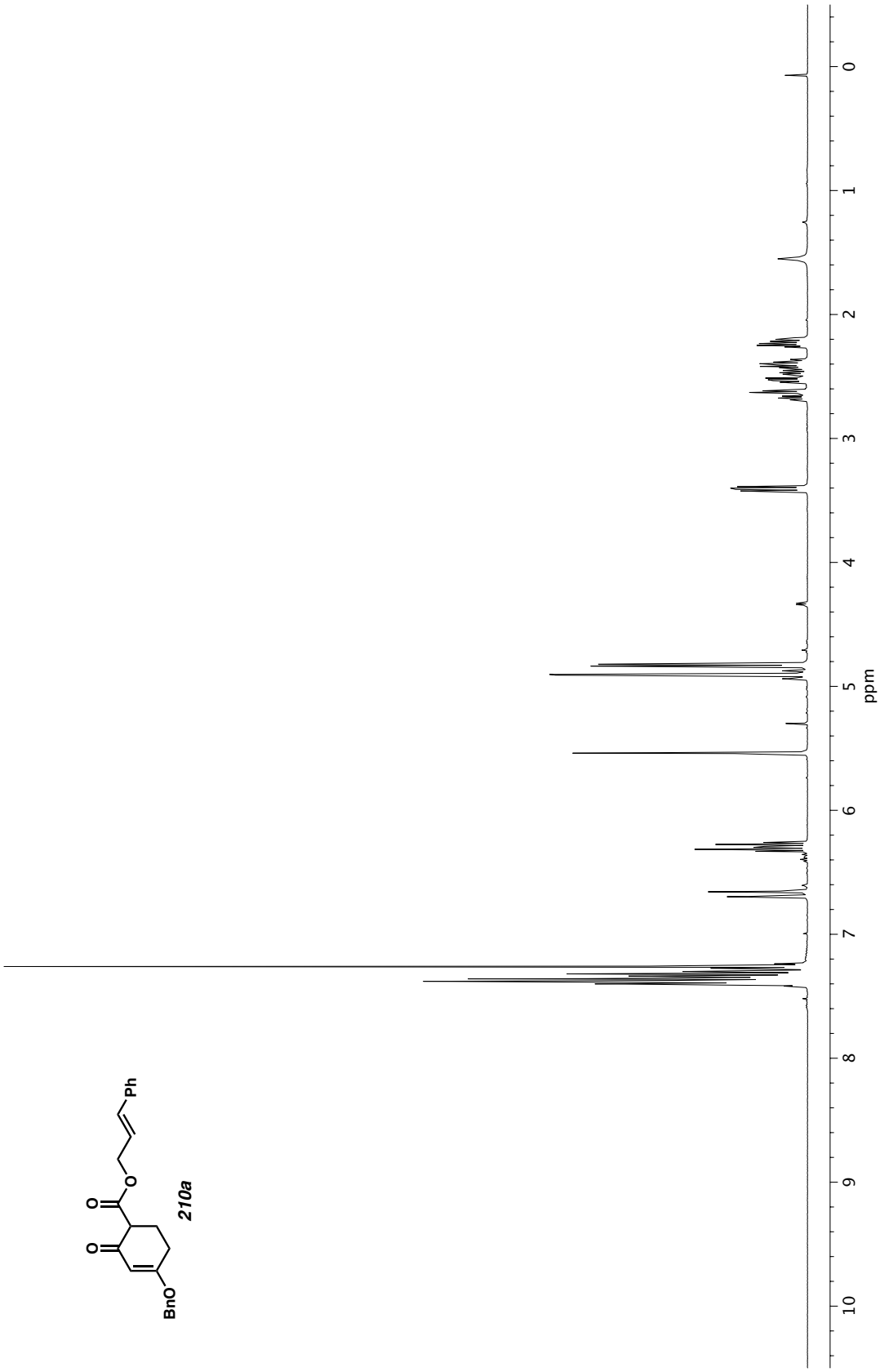


Figure A3.138. *^1H NMR (400 MHz, $CDCl_3$) of compound* ***210a****.*

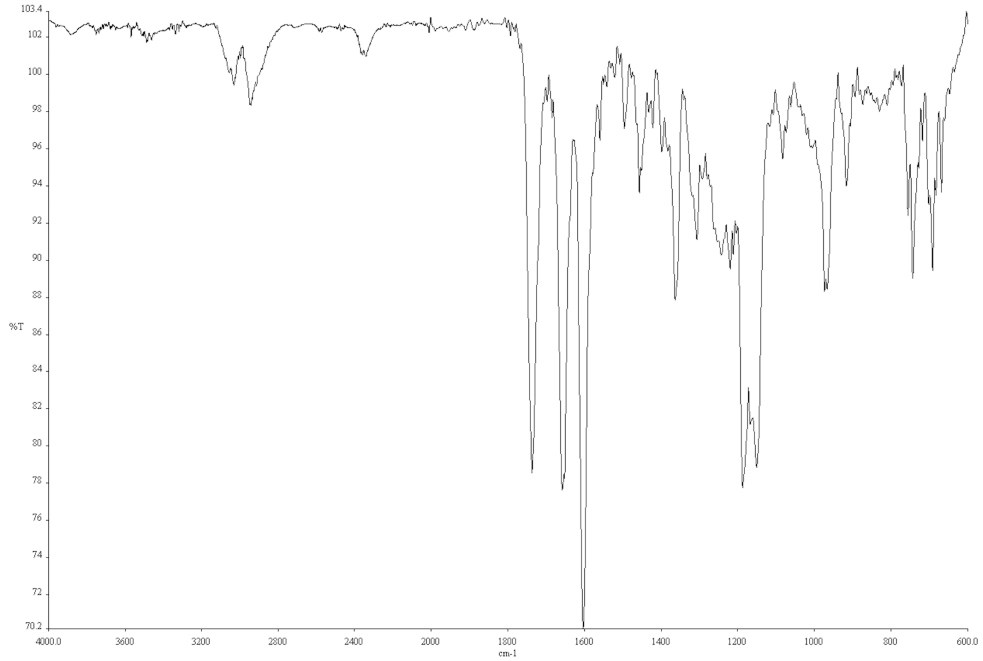


Figure A3.139. *Infrared spectrum (Thin Film, NaCl) of compound* ***210a****.*

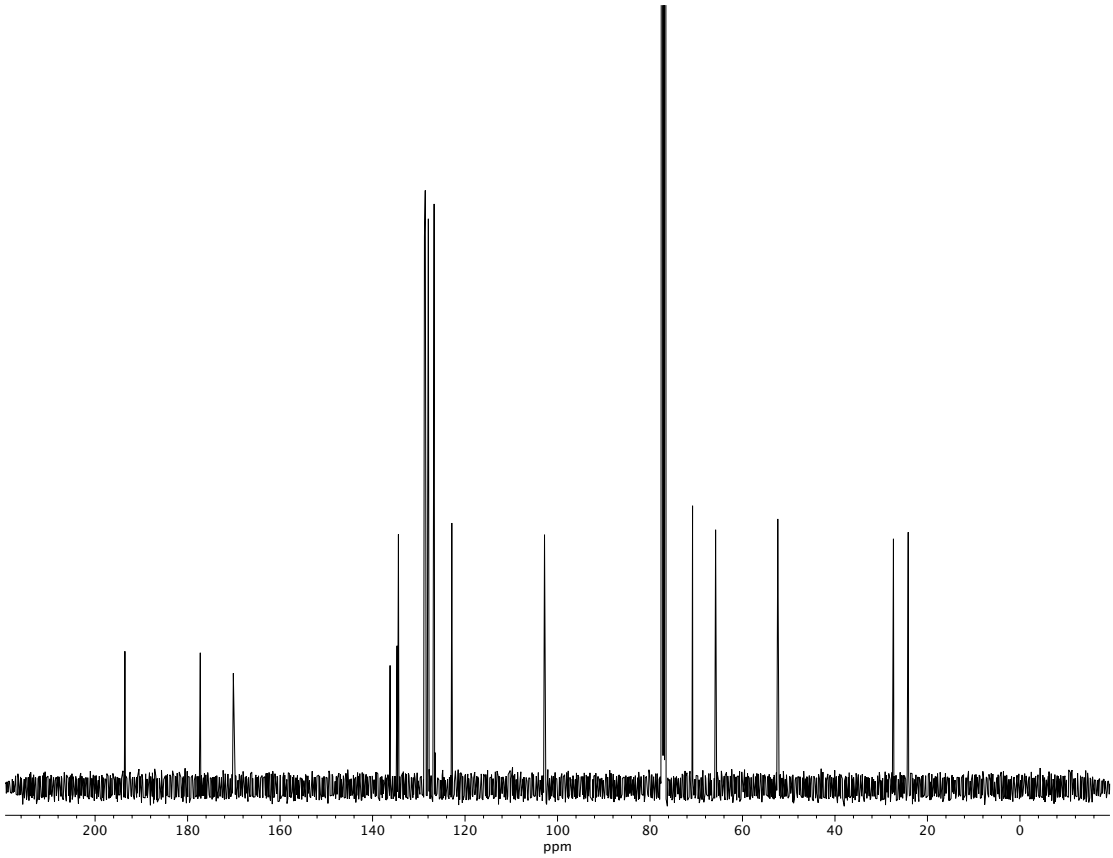


Figure A3.140. *^{13}C NMR (100 MHz, $CDCl_3$) of compound* ***210a****.*

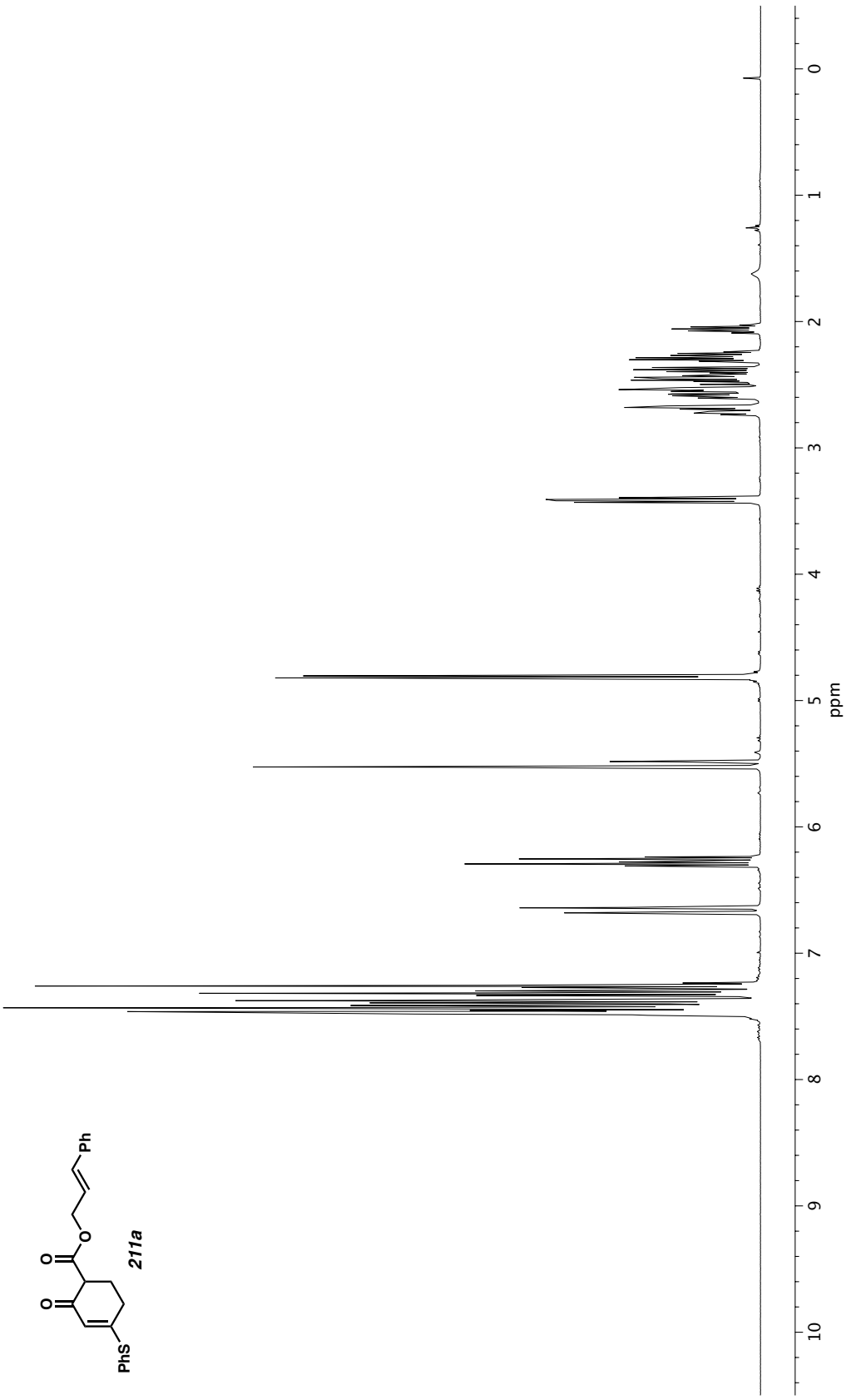


Figure A3.141. *^1H NMR (400 MHz, $CDCl_3$) of compound* ***211a****.*

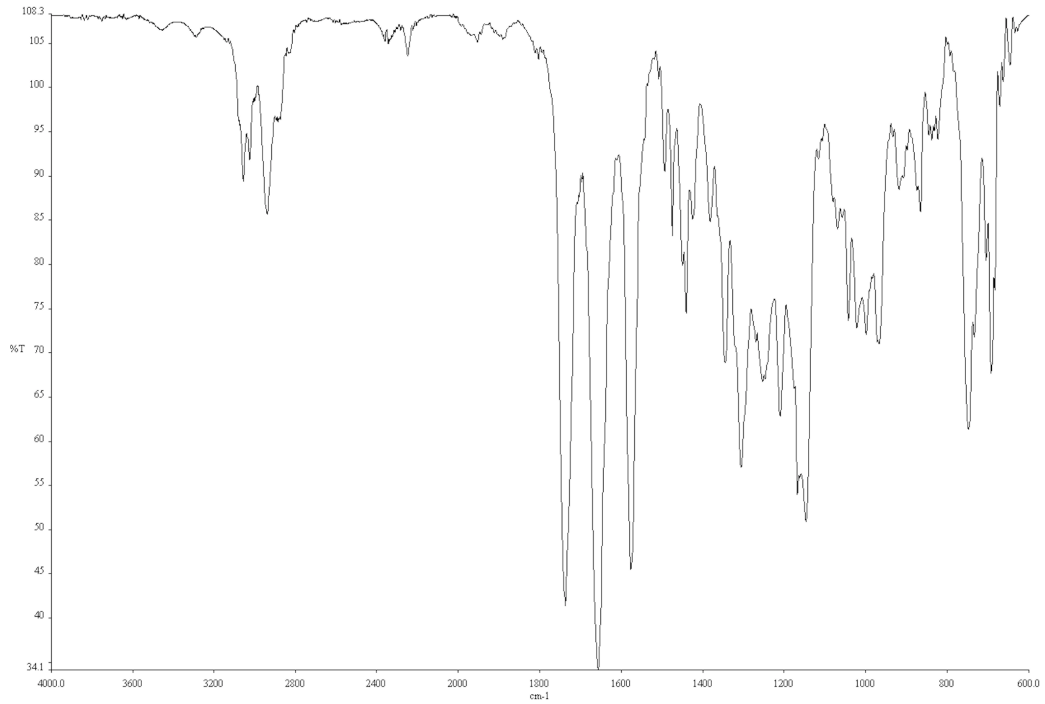


Figure A3.142. *Infrared spectrum (Thin Film, NaCl) of compound* ***211a****.*

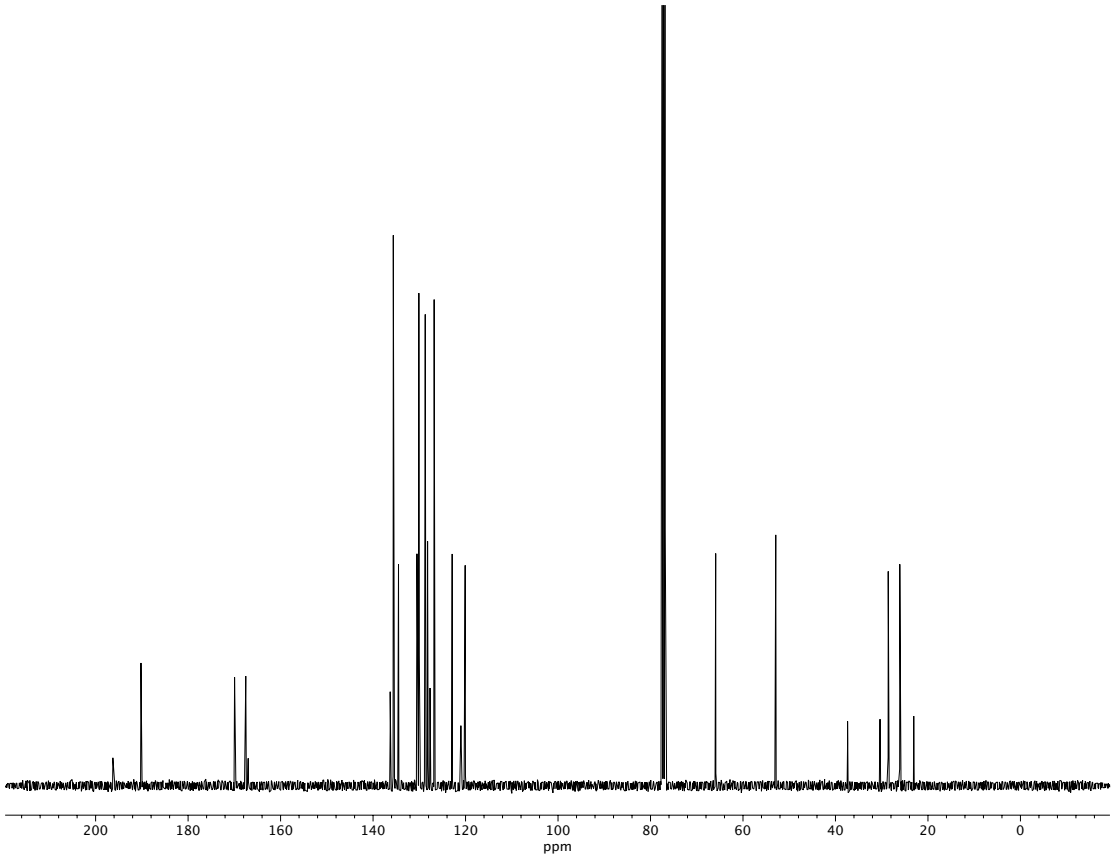


Figure A3.143. *^{13}C NMR (100 MHz, $CDCl_3$) of compound* ***211a****.*

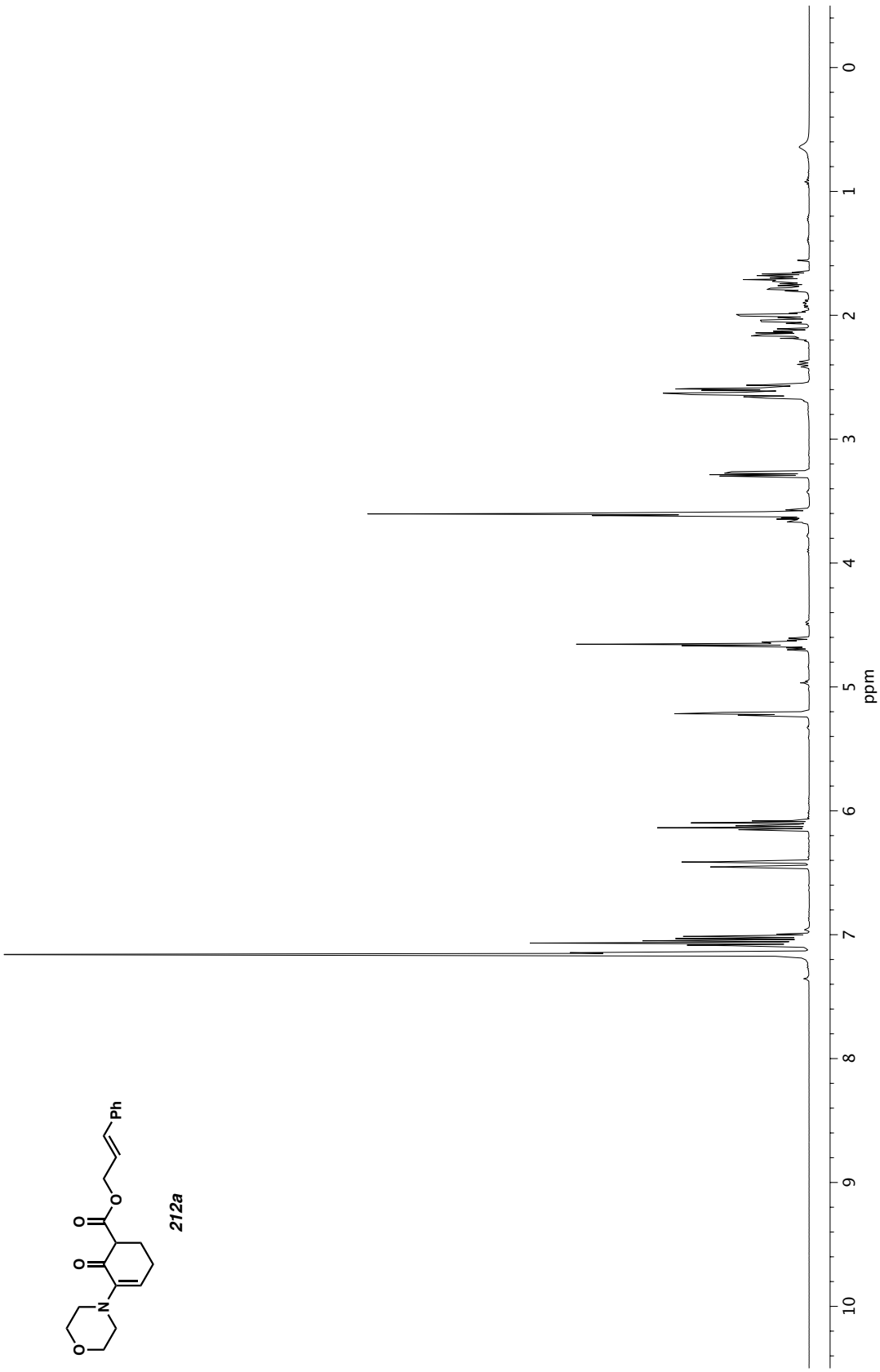


Figure A3.144. *^1H NMR (400 MHz, C_6D_6) of compound* ***212a****.*

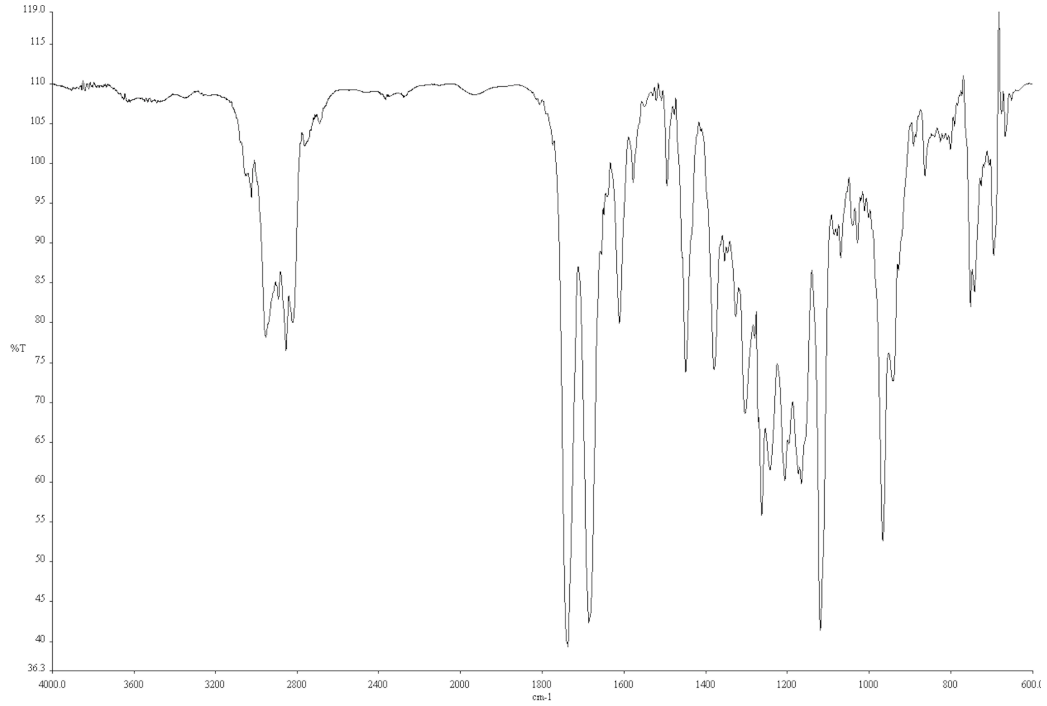


Figure A3.145. *Infrared spectrum (Thin Film, NaCl) of compound* ***212a****.*

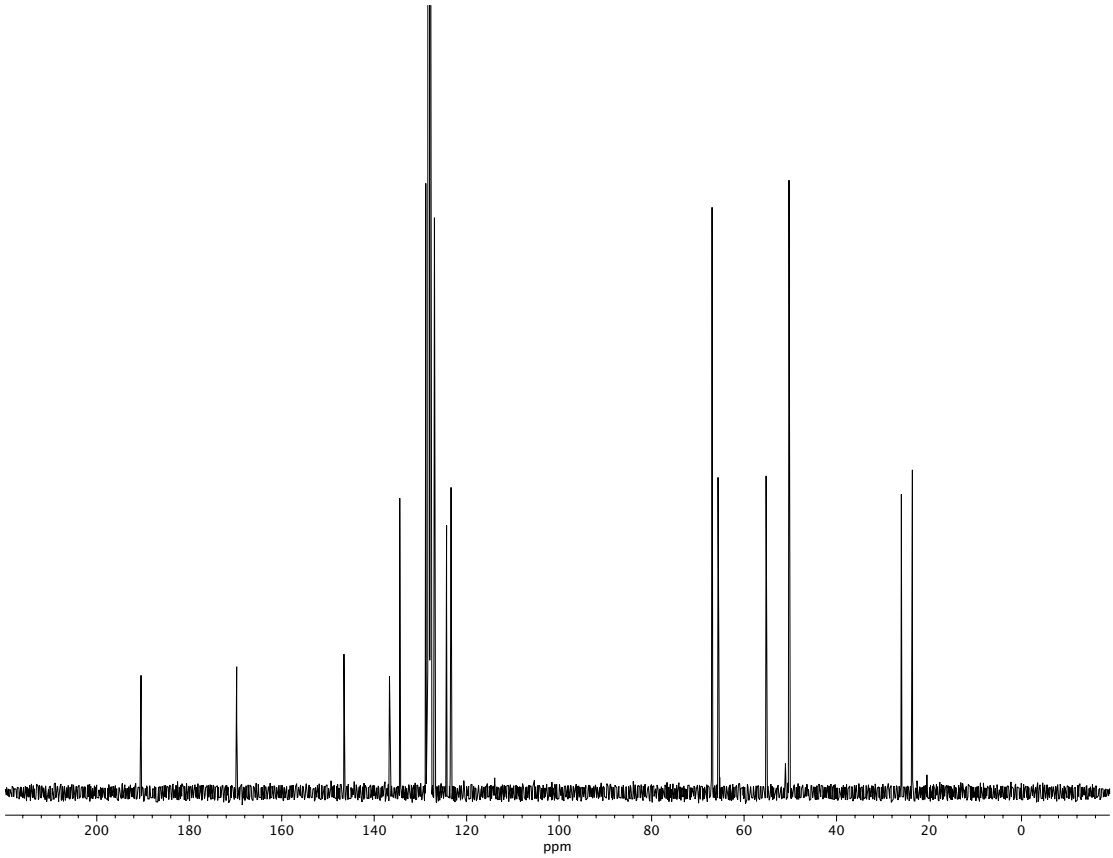


Figure A3.146. *^{13}C NMR (100 MHz, C_6D_6) of compound* ***212a****.*

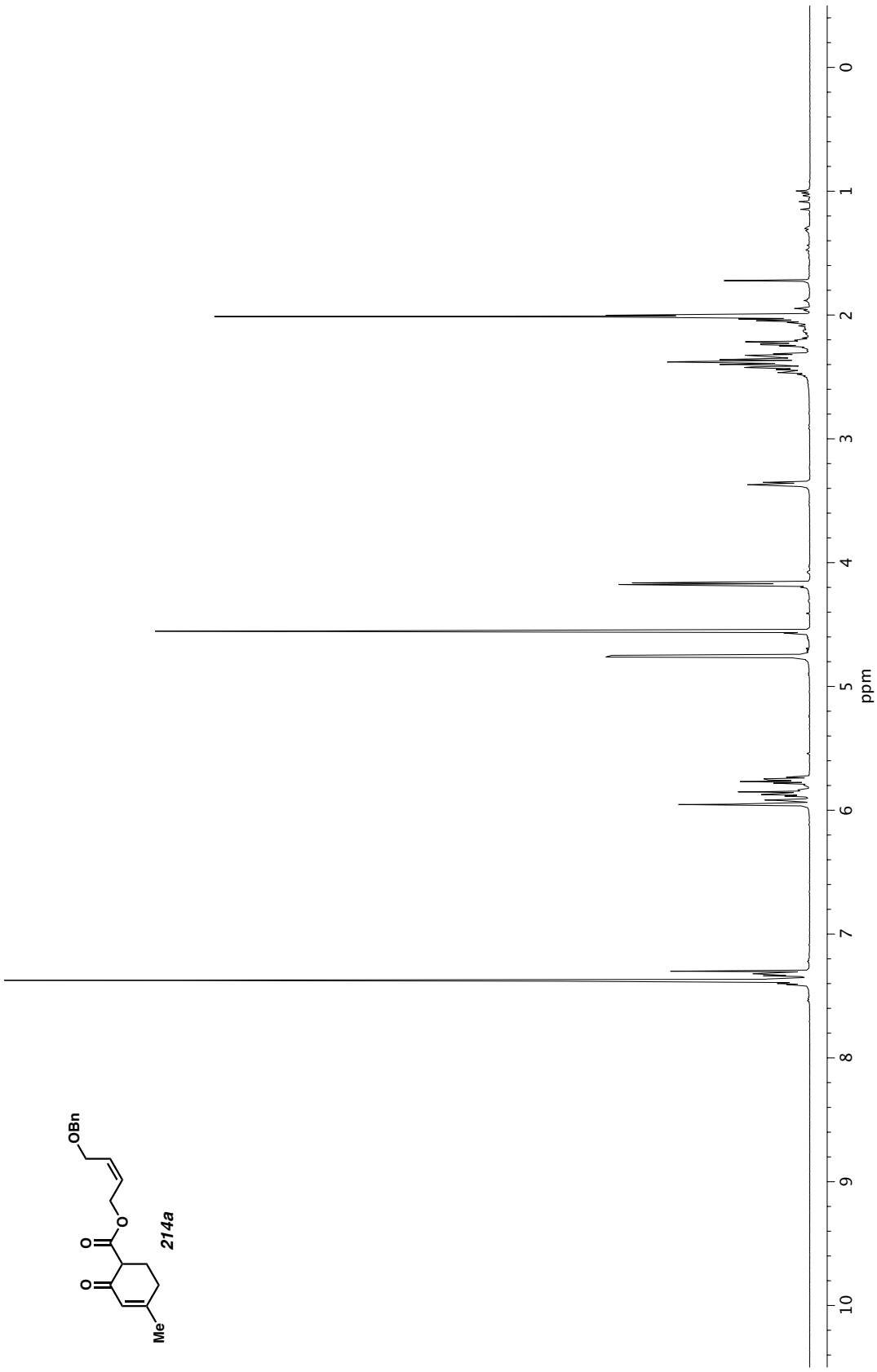


Figure A3.147. *^1H NMR (600 MHz, $CDCl_3$) of compound* ***214a****.*

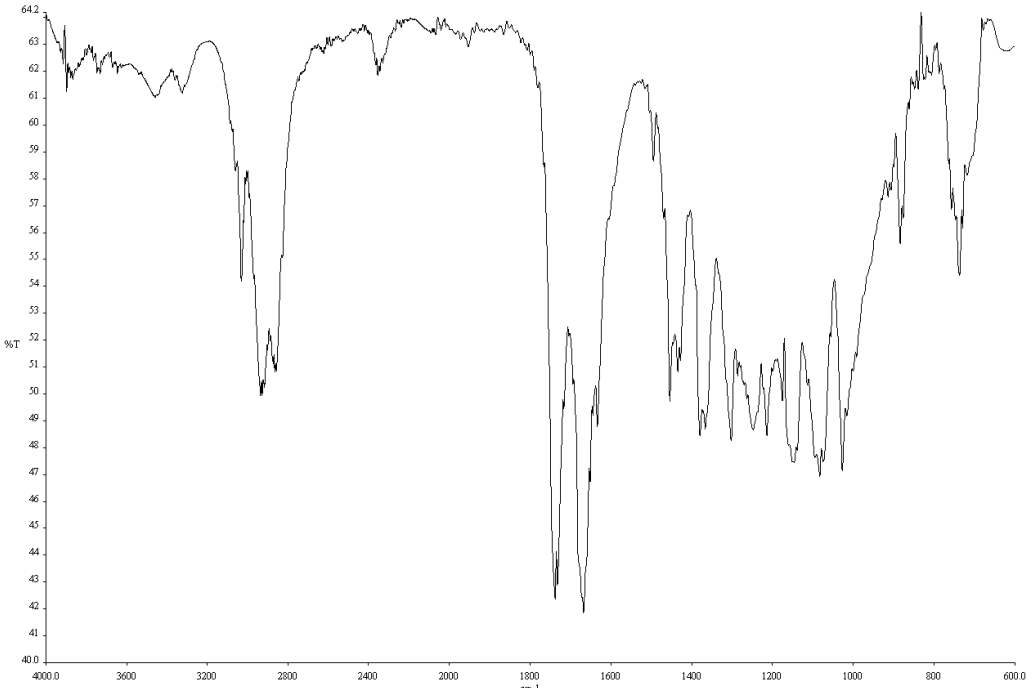


Figure A3.148. *Infrared spectrum (Thin Film, NaCl) of compound* ***214a****.*

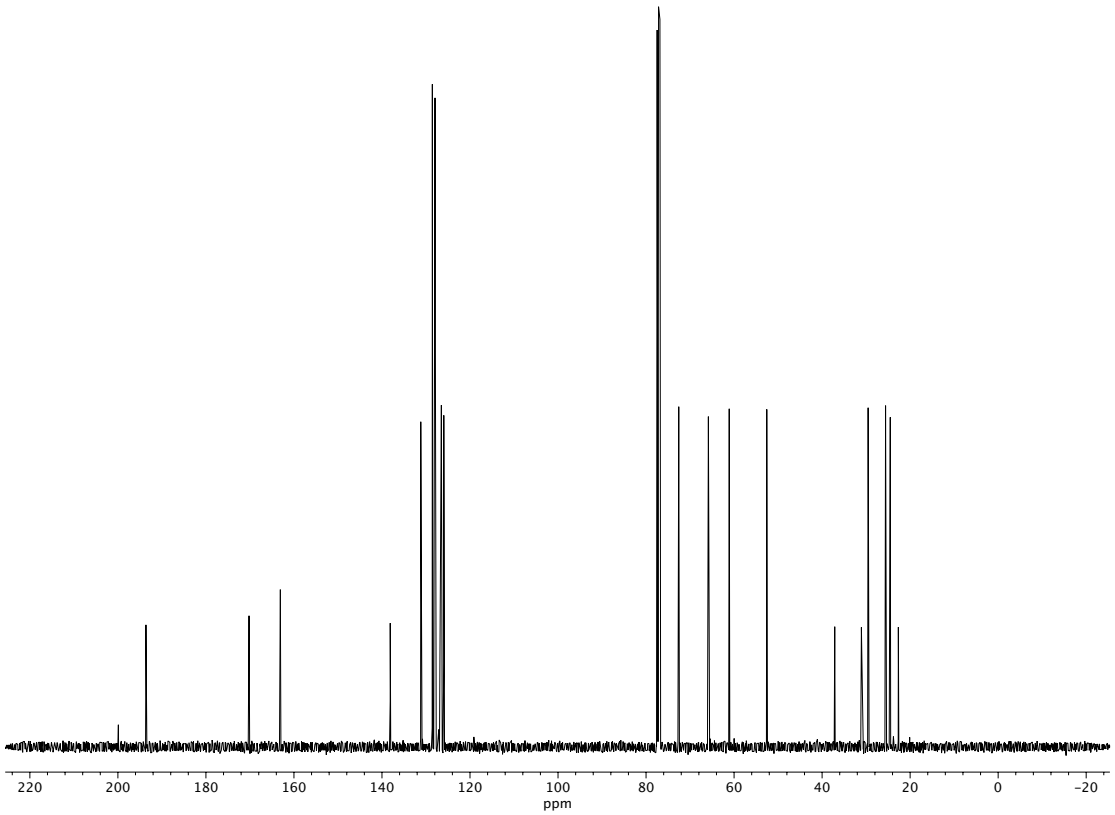


Figure A3.149. *^{13}C NMR (100 MHz, $CDCl_3$) of compound* ***214a****.*

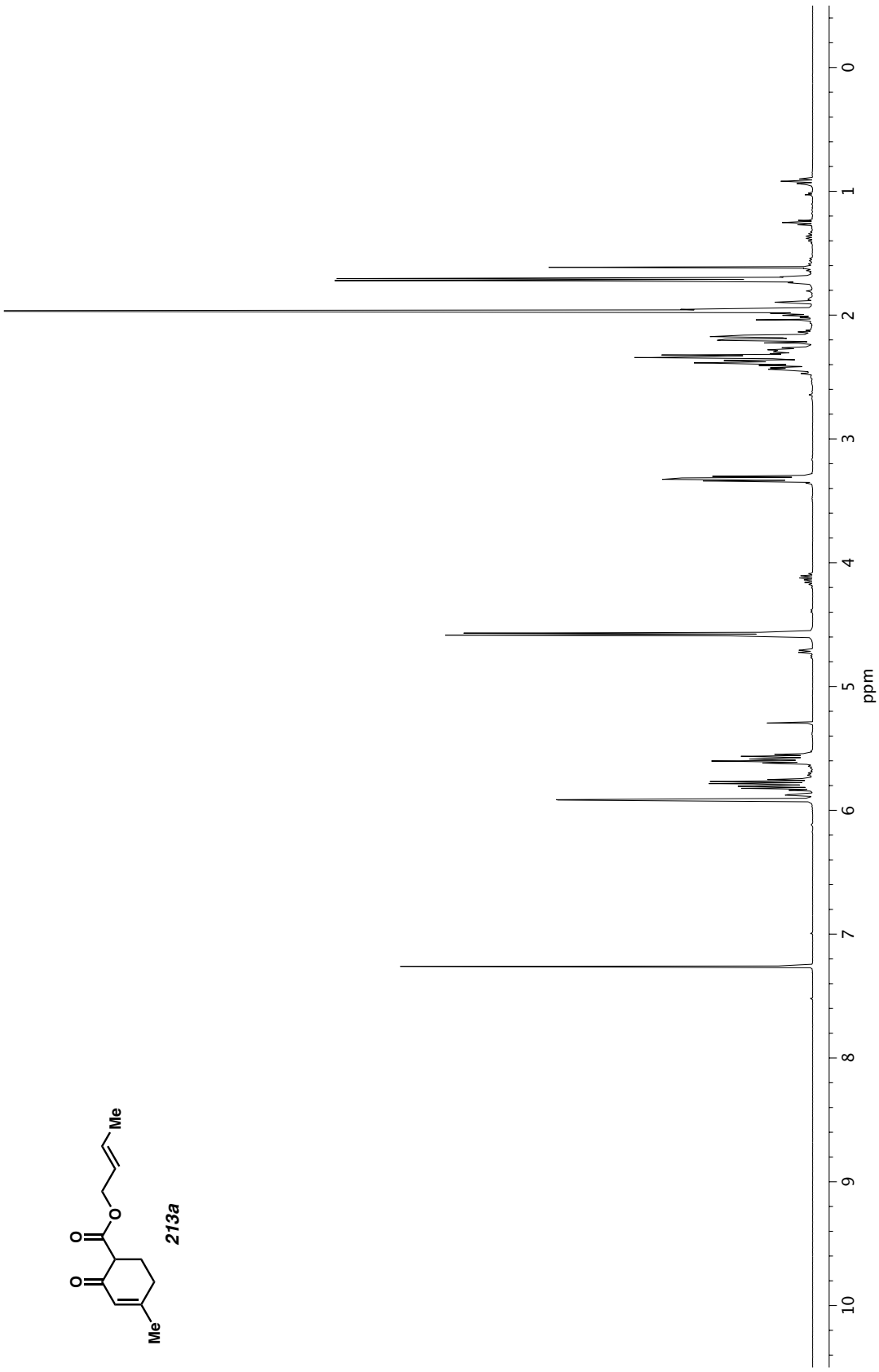


Figure A3.150. *^1H NMR (400 MHz, $CDCl_3$) of compound* ***213a***.

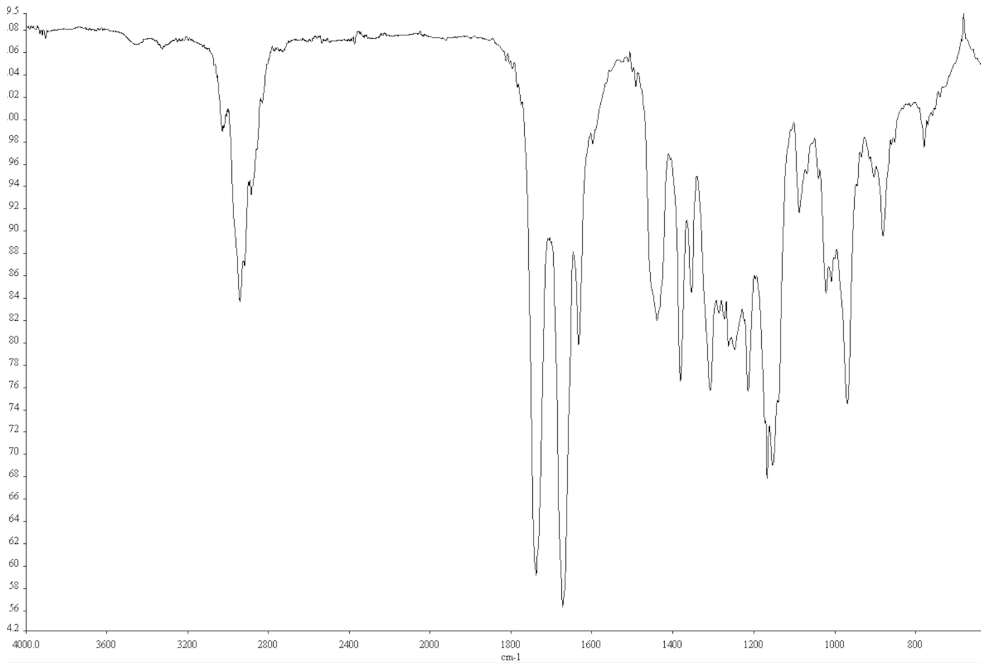


Figure A3.151. *Infrared spectrum (Thin Film, NaCl) of compound* ***213a****.*

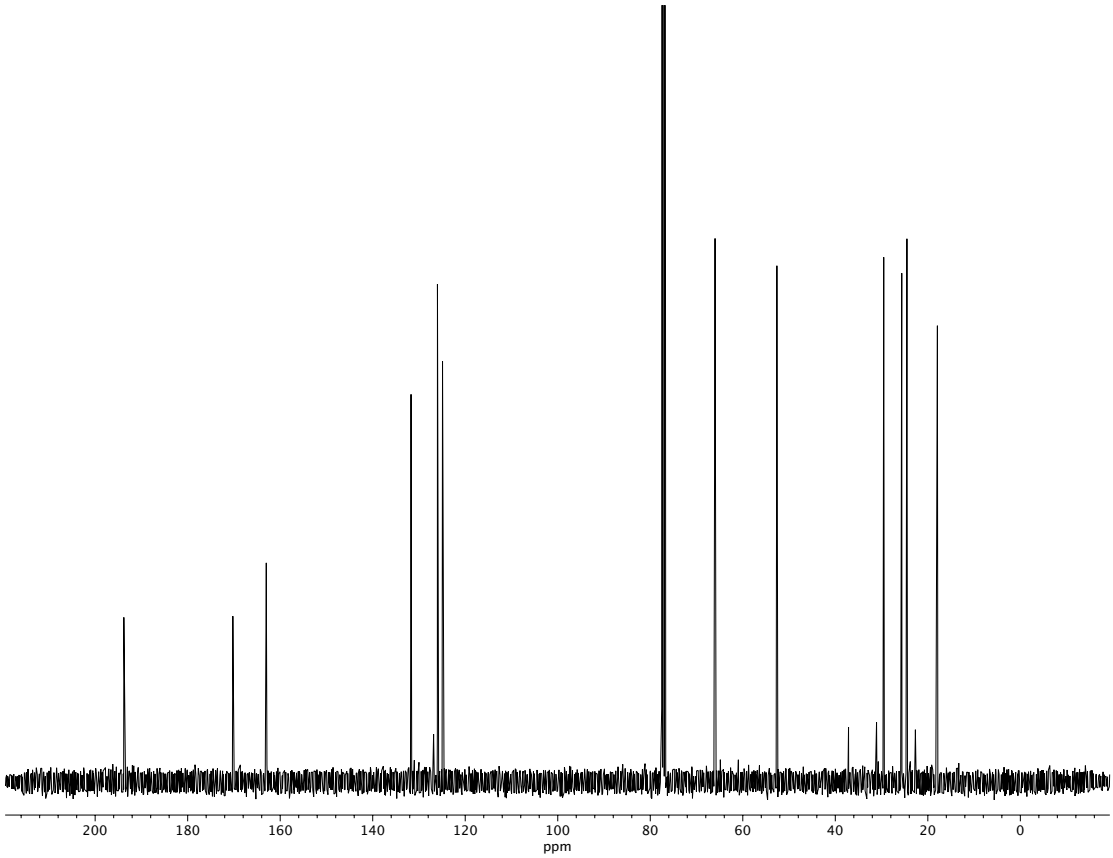


Figure A3.152. *^{13}C NMR (100 MHz, $CDCl_3$) of compound* ***213a****.*

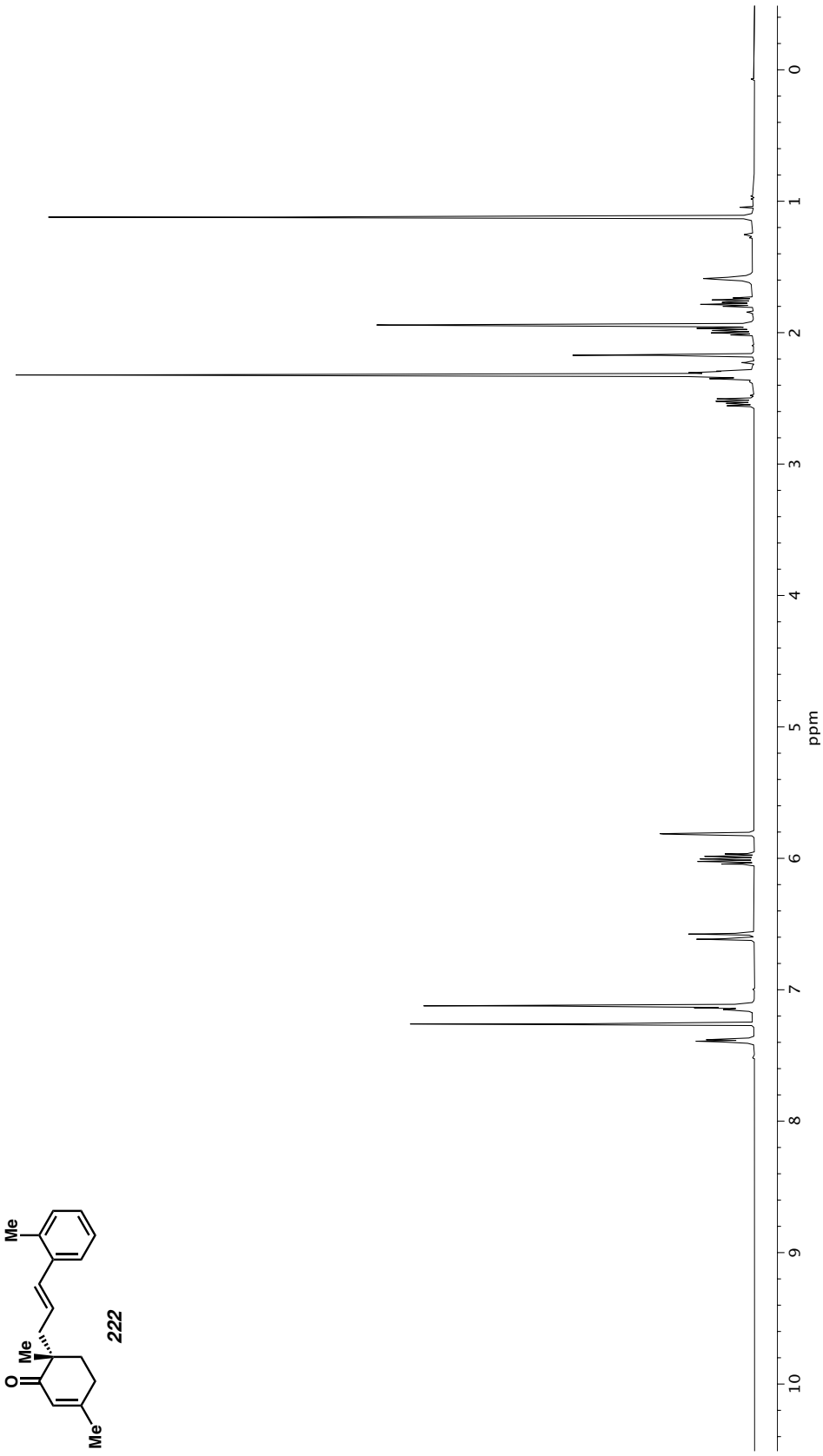


Figure A3.153. *^1H NMR (400 MHz, $CDCl_3$) of compound* ***222****.*

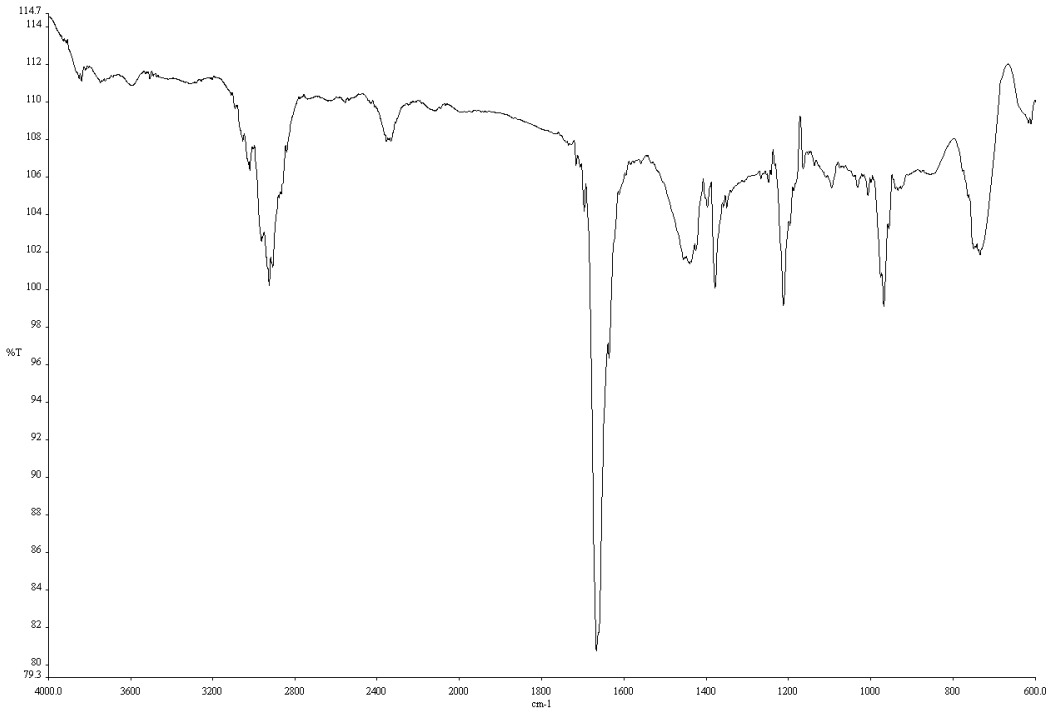


Figure A3.154. *Infrared spectrum (Thin Film, NaCl) of compound* ***222****.*

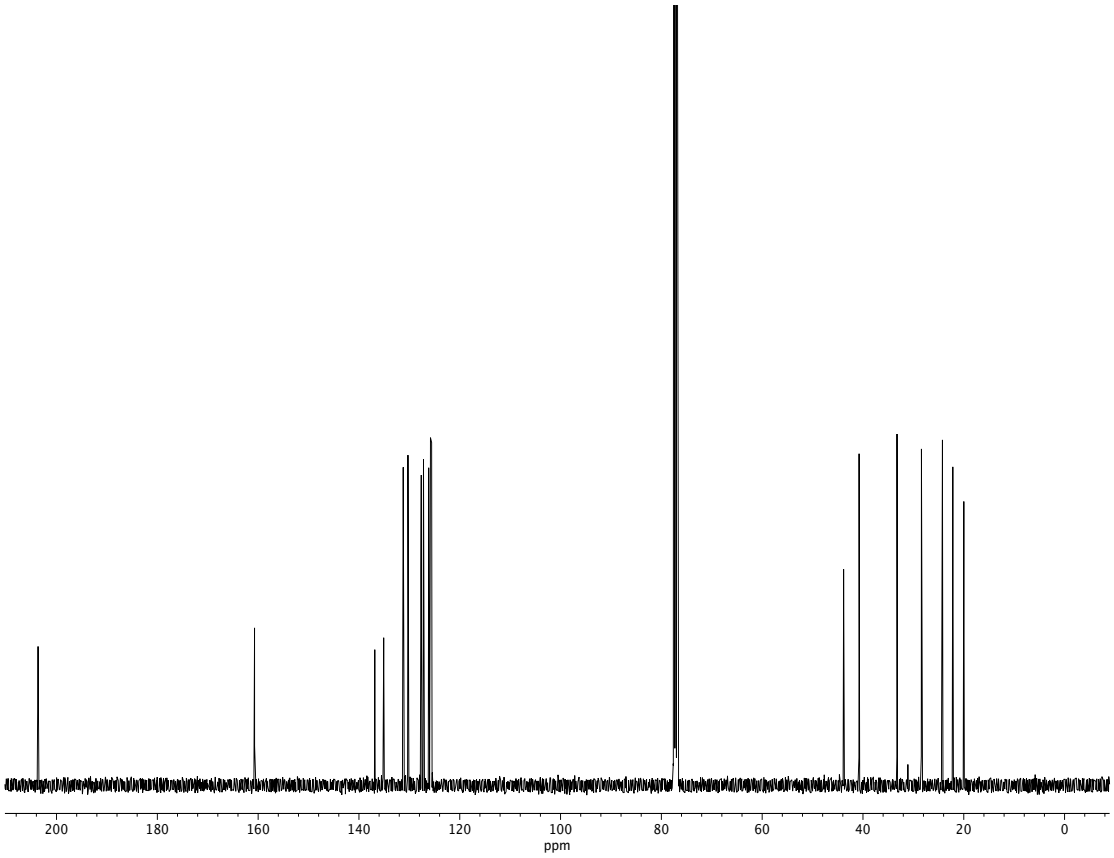


Figure A3.155. *^{13}C NMR (100 MHz, $CDCl_3$) of compound* ***222****.*

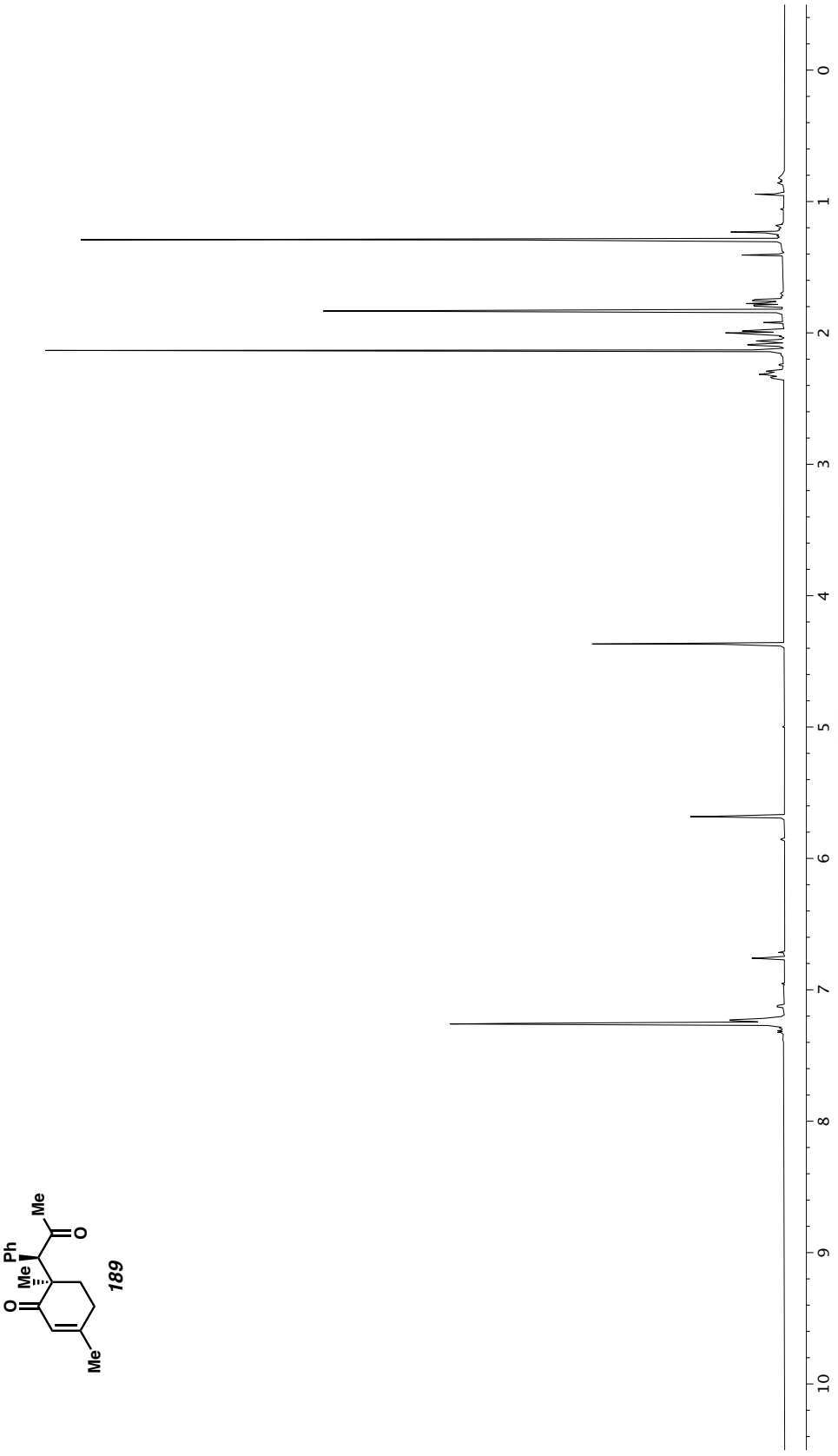


Figure A3.156. *^1H NMR (600 MHz, $CDCl_3$) of compound **189**.*

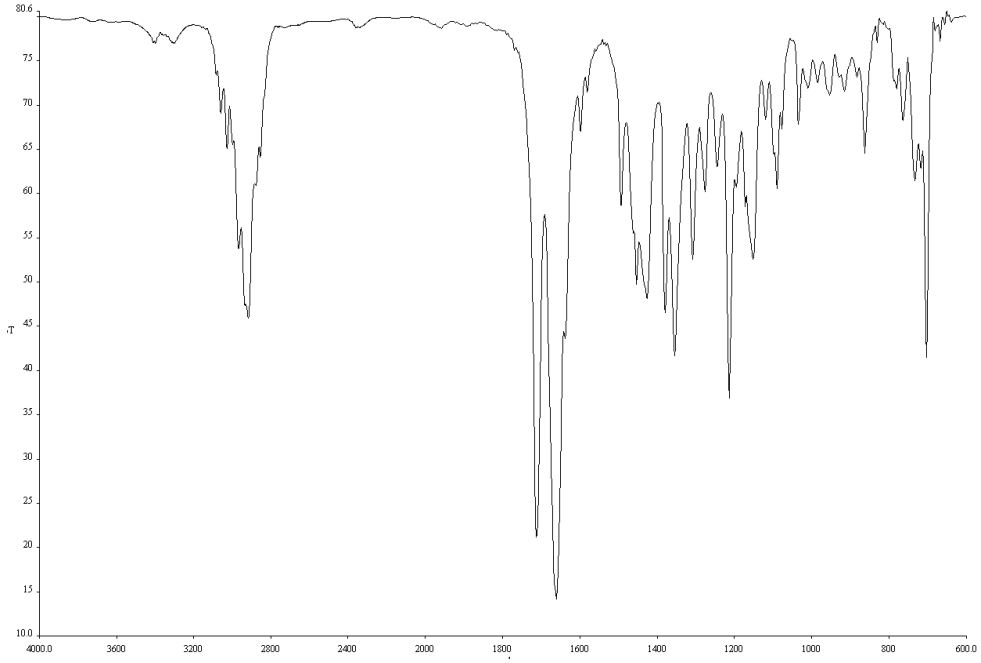


Figure A3.157. *Infrared spectrum (Thin Film, NaCl) of compound* ***189****.*

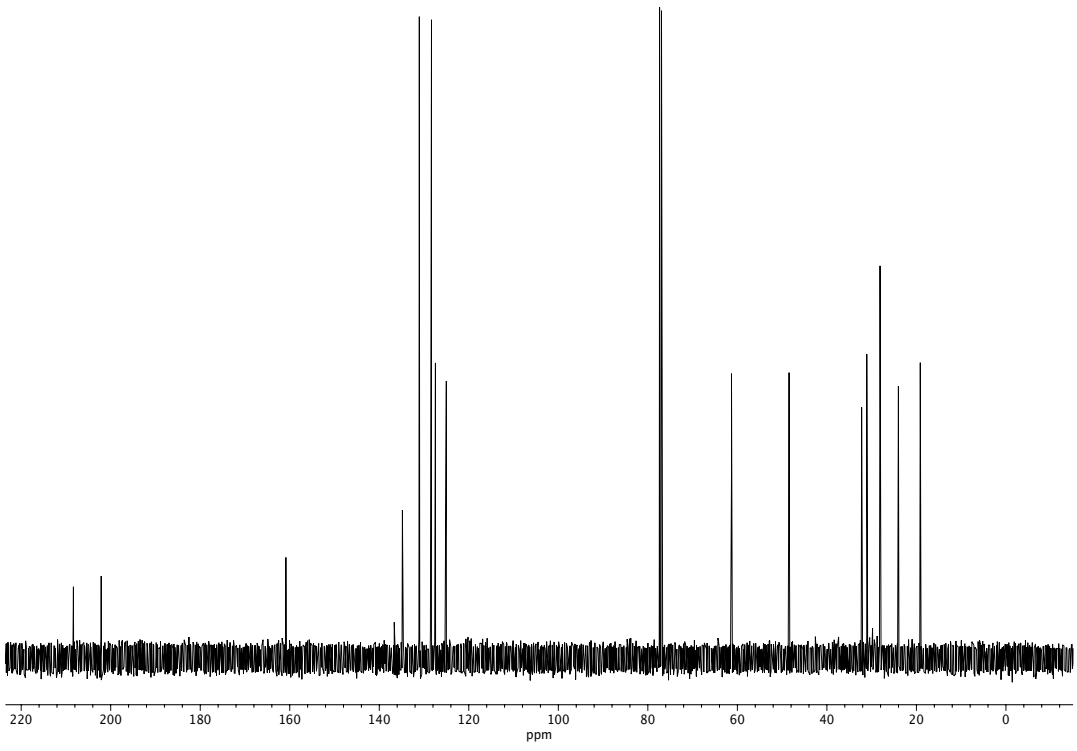


Figure A3.158. *^{13}C NMR (150 MHz, $CDCl_3$) of compound* ***189****.*

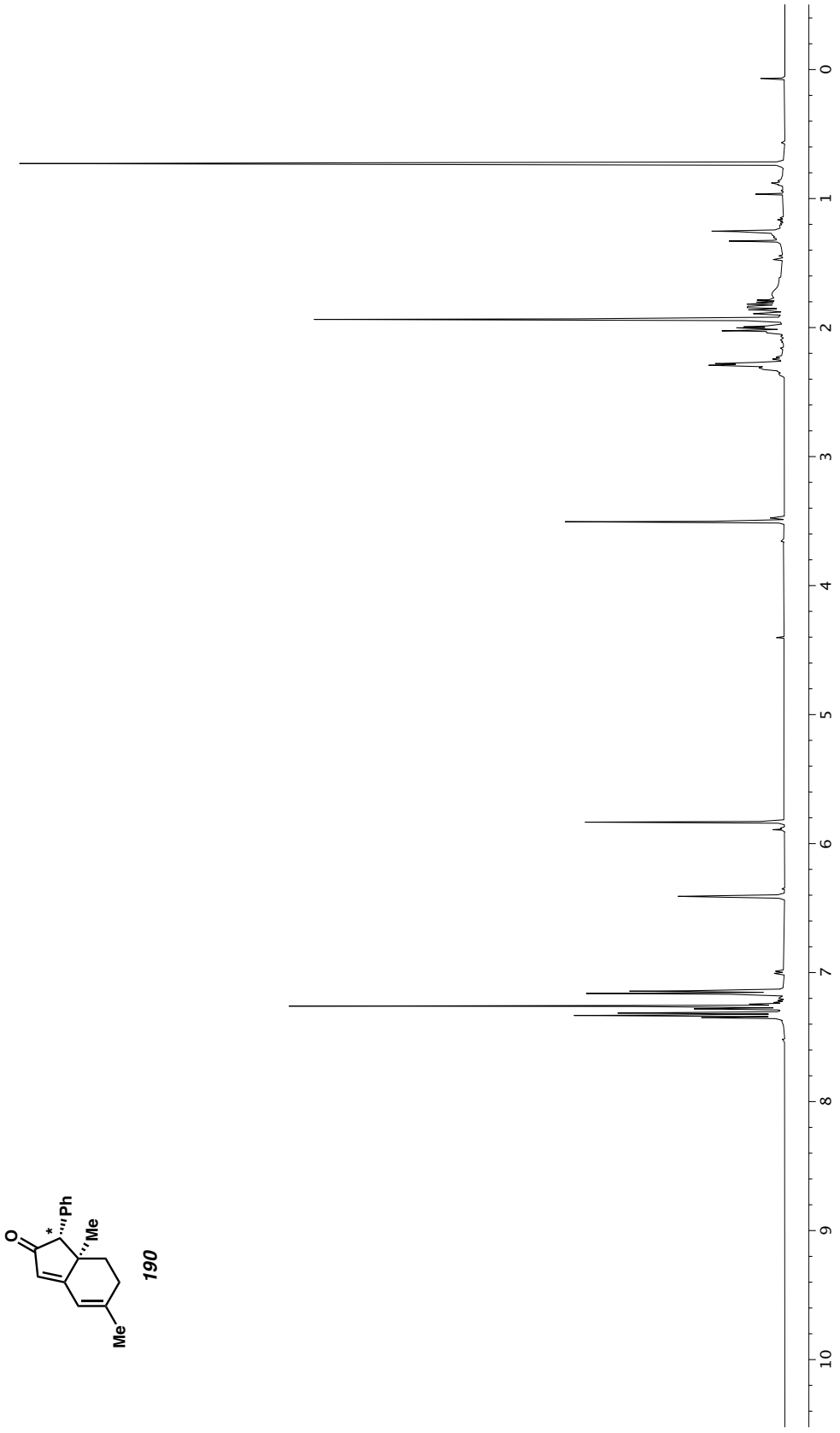


Figure A3.159. *^1H NMR (600 MHz, $CDCl_3$) of compound* ***190****.*

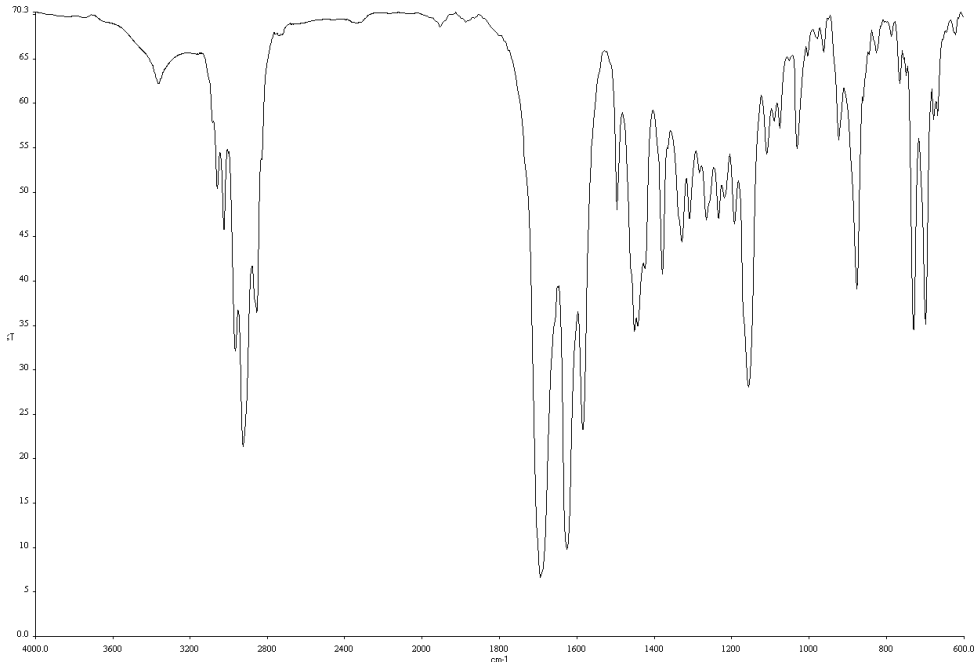


Figure A3.160. *Infrared spectrum (Thin Film, NaCl) of compound* ***190****.*

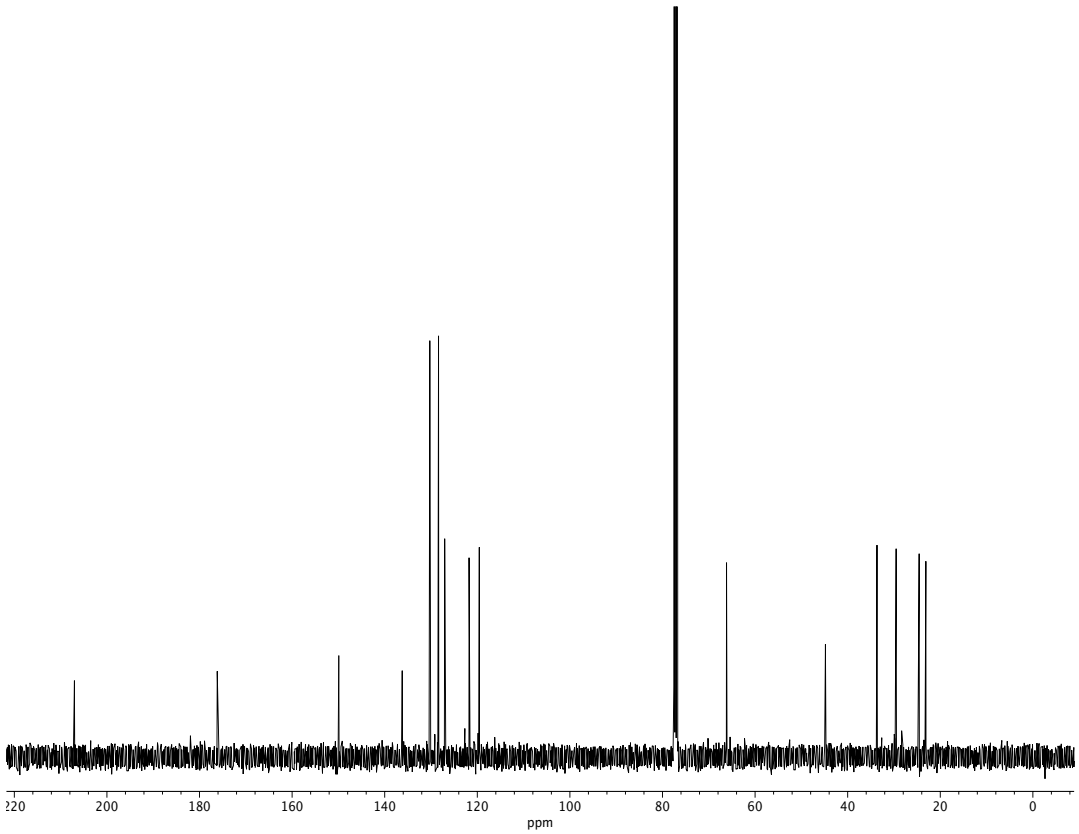


Figure A3.161. *^{13}C NMR (100 MHz, $CDCl_3$) of compound* ***190****.*

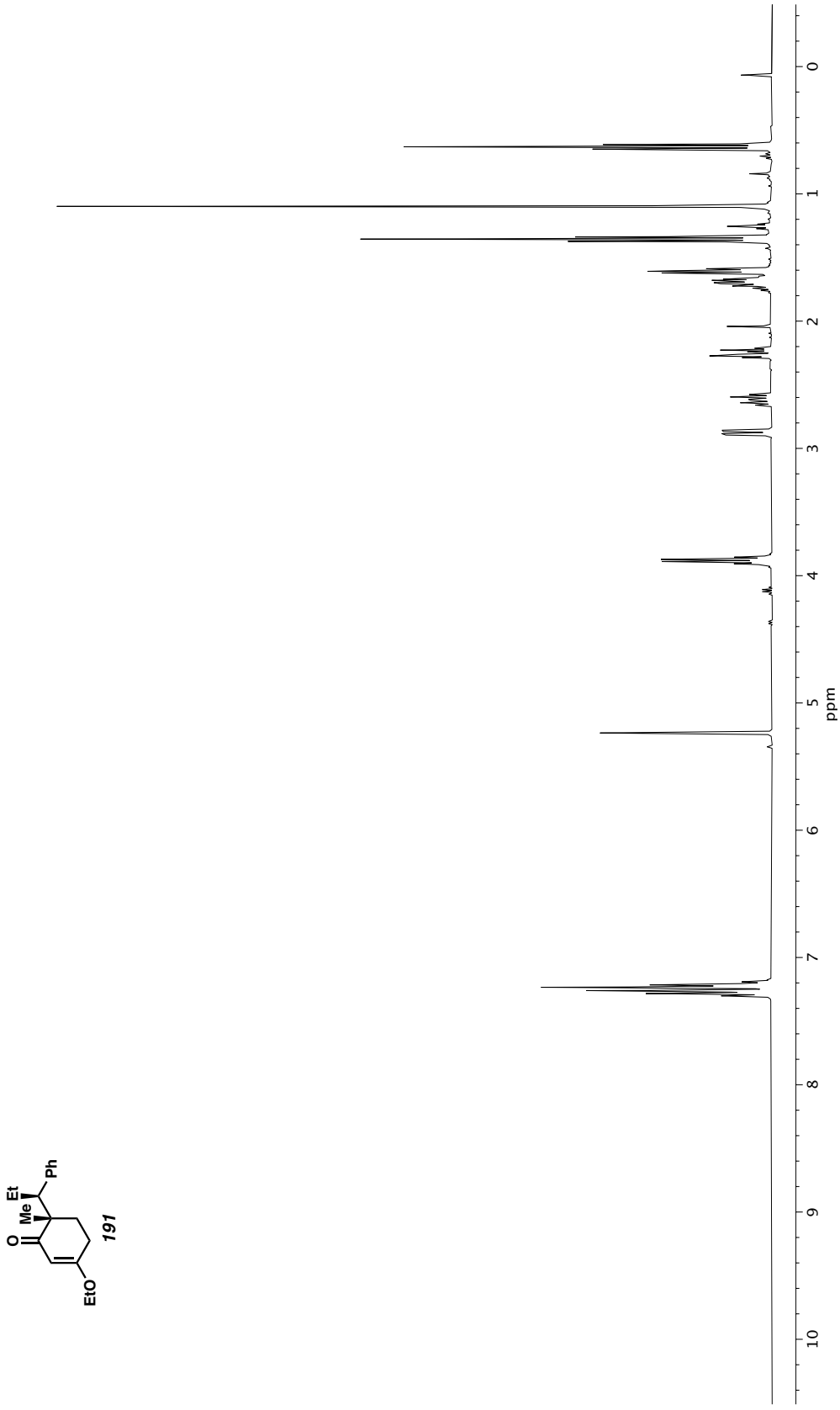


Figure A3.162. *^1H NMR (400 MHz, $CDCl_3$) of compound **191**.*

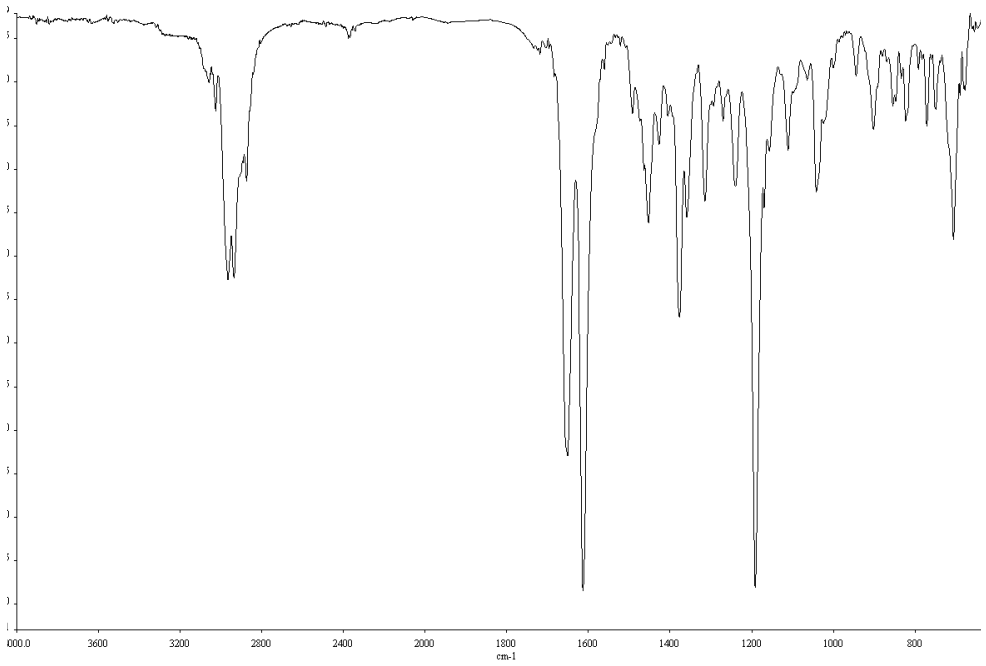


Figure A3.163. *Infrared spectrum (Thin Film, NaCl) of compound* ***191***.

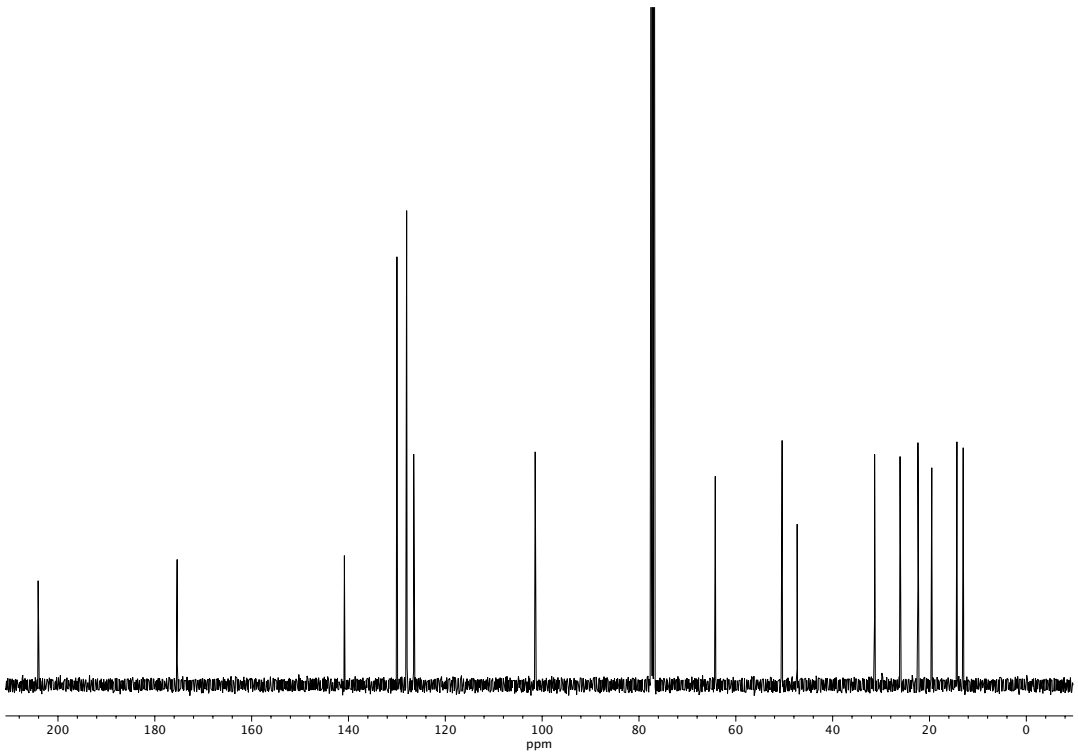


Figure A3.164. *^{13}C NMR (100 MHz, $CDCl_3$) of compound* ***191***.

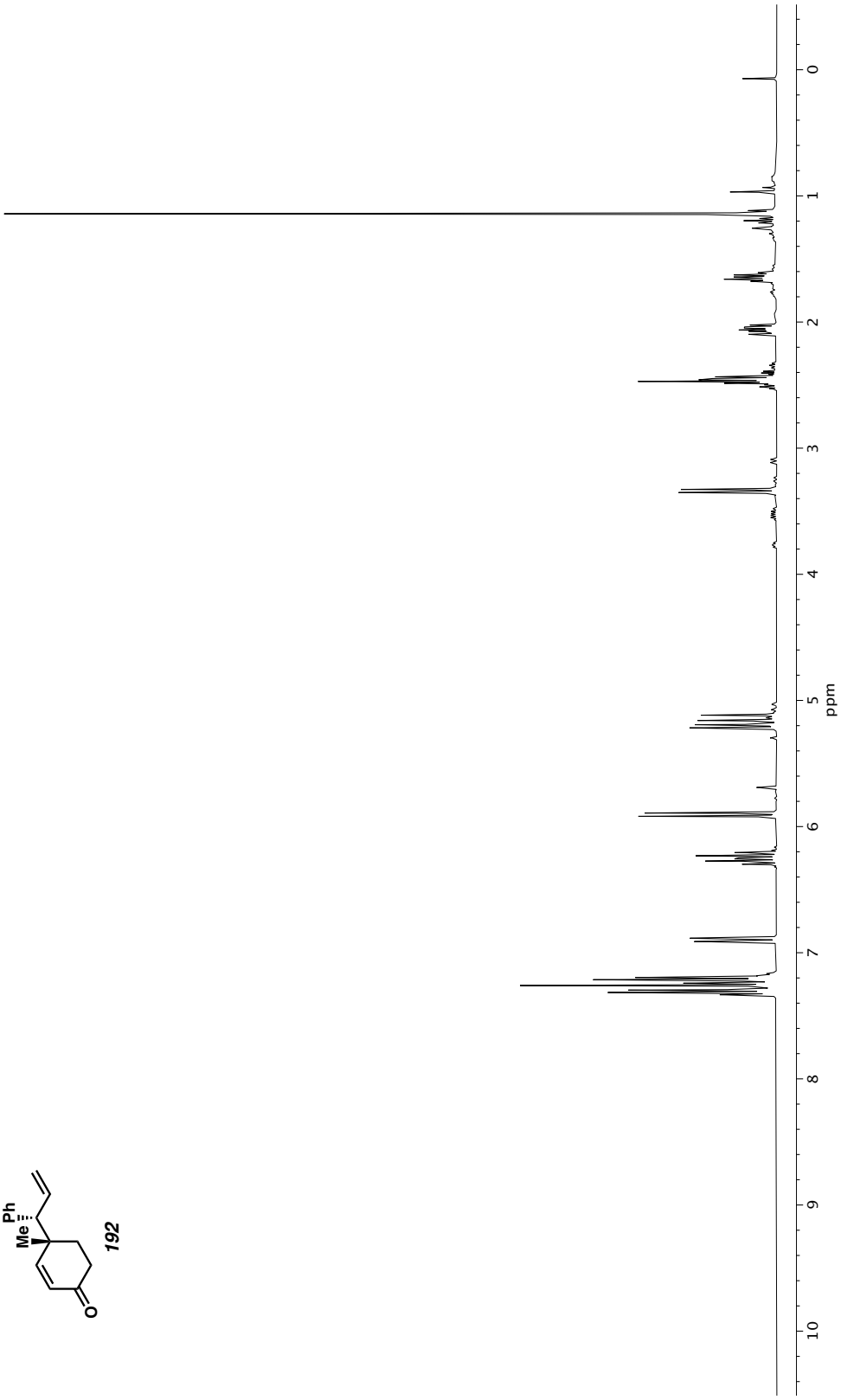


Figure A3.165. *^{1}H NMR (600 MHz, $CDCl_3$) of compound* ***192****.*

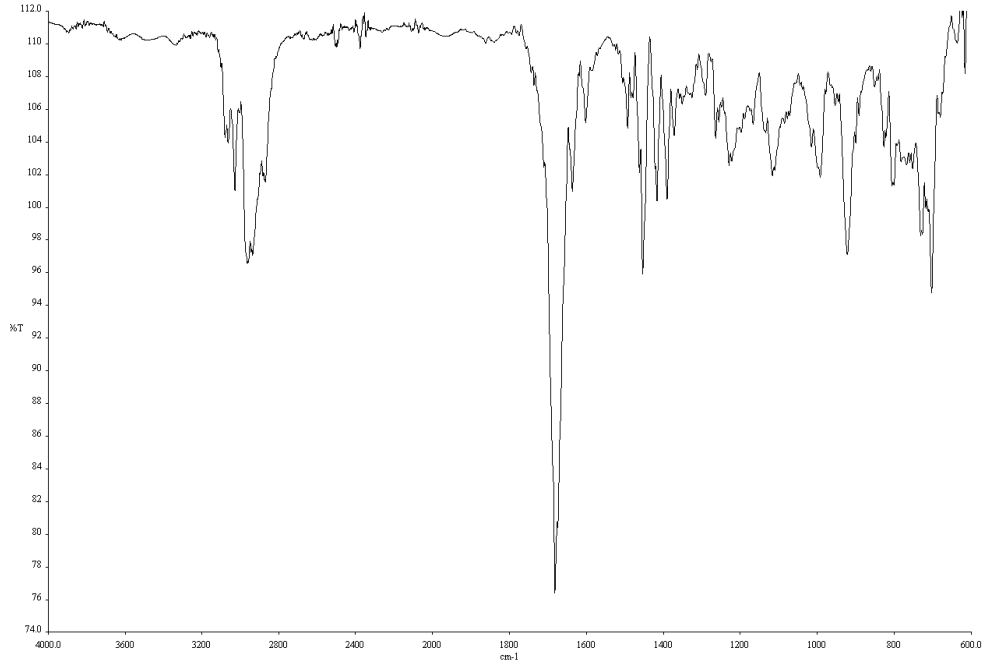


Figure A3.166. *Infrared spectrum (Thin Film, NaCl) of compound* ***192****.*

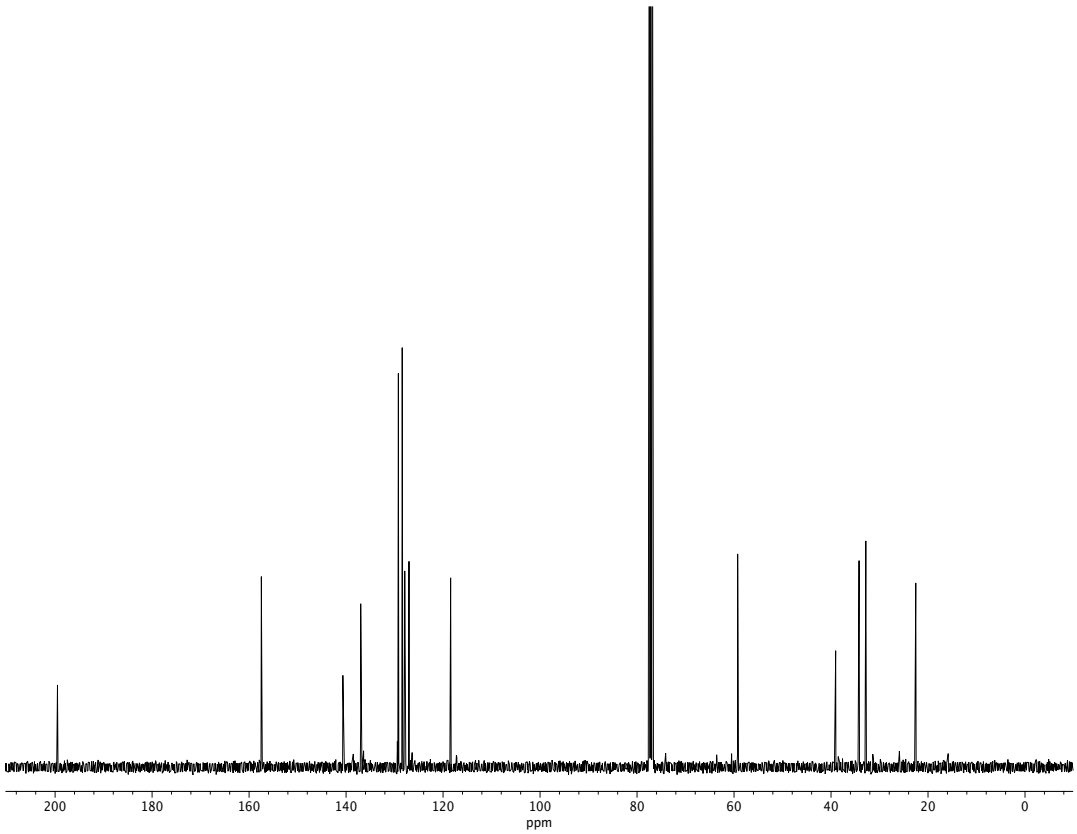


Figure A3.167. *^{13}C NMR (100 MHz, $CDCl_3$) of compound* ***192****.*

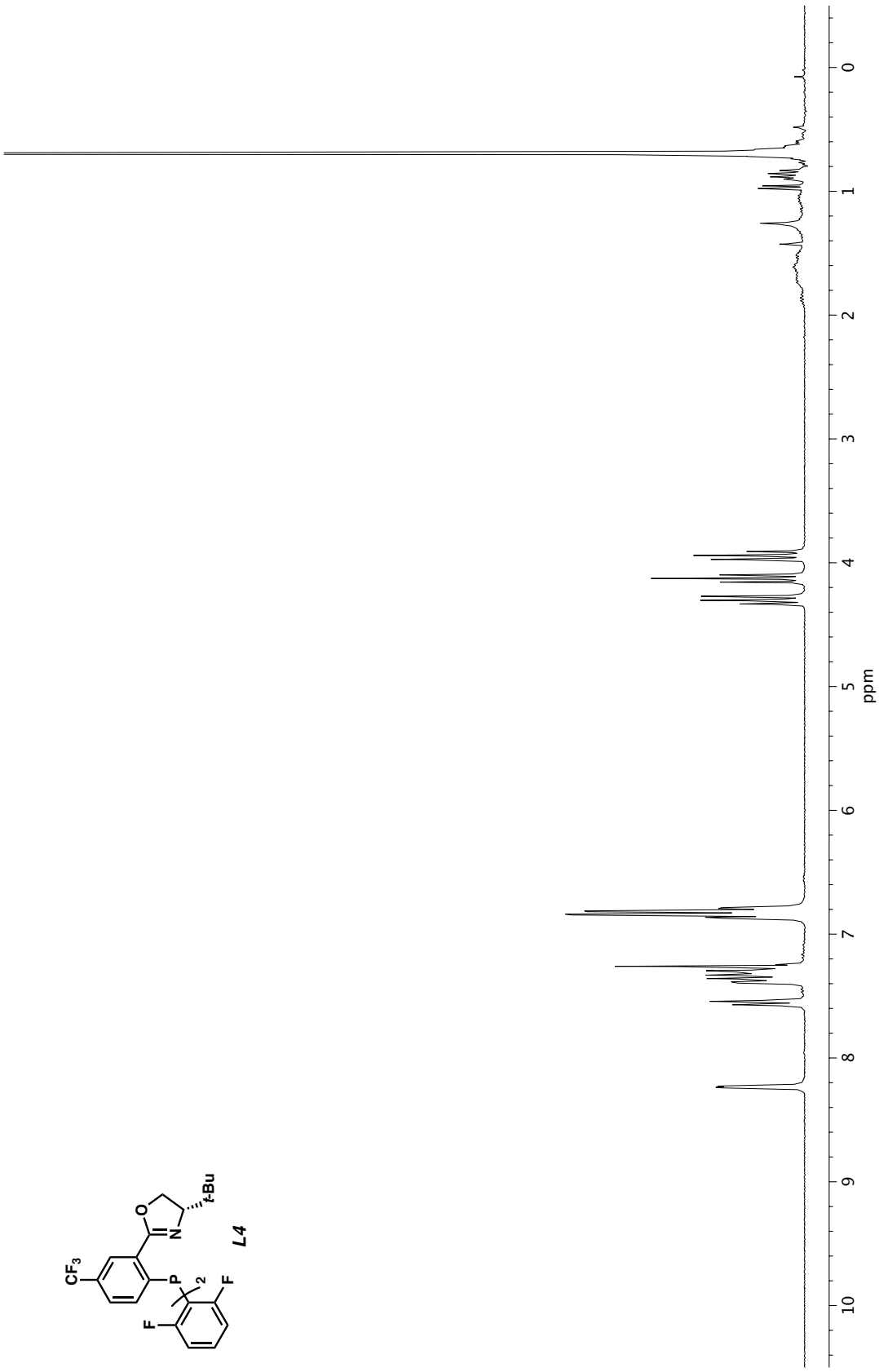


Figure A3.168. *^1H NMR (300 MHz, $CDCl_3$) of compound* ***L4****.*

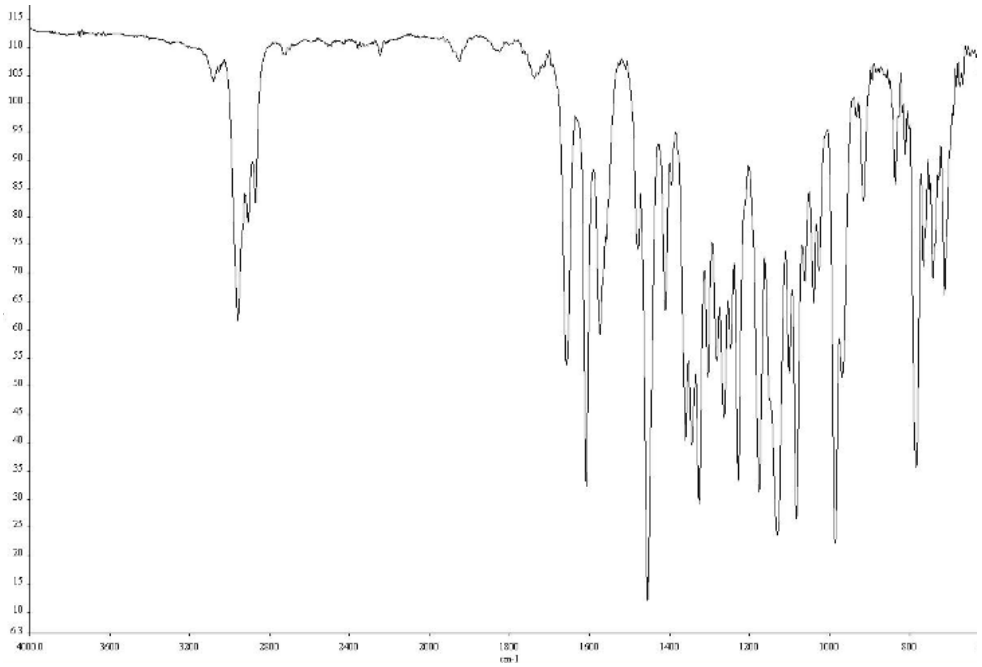


Figure A3.169. *Infrared spectrum (Thin Film, NaCl) of compound* ***L4****.*

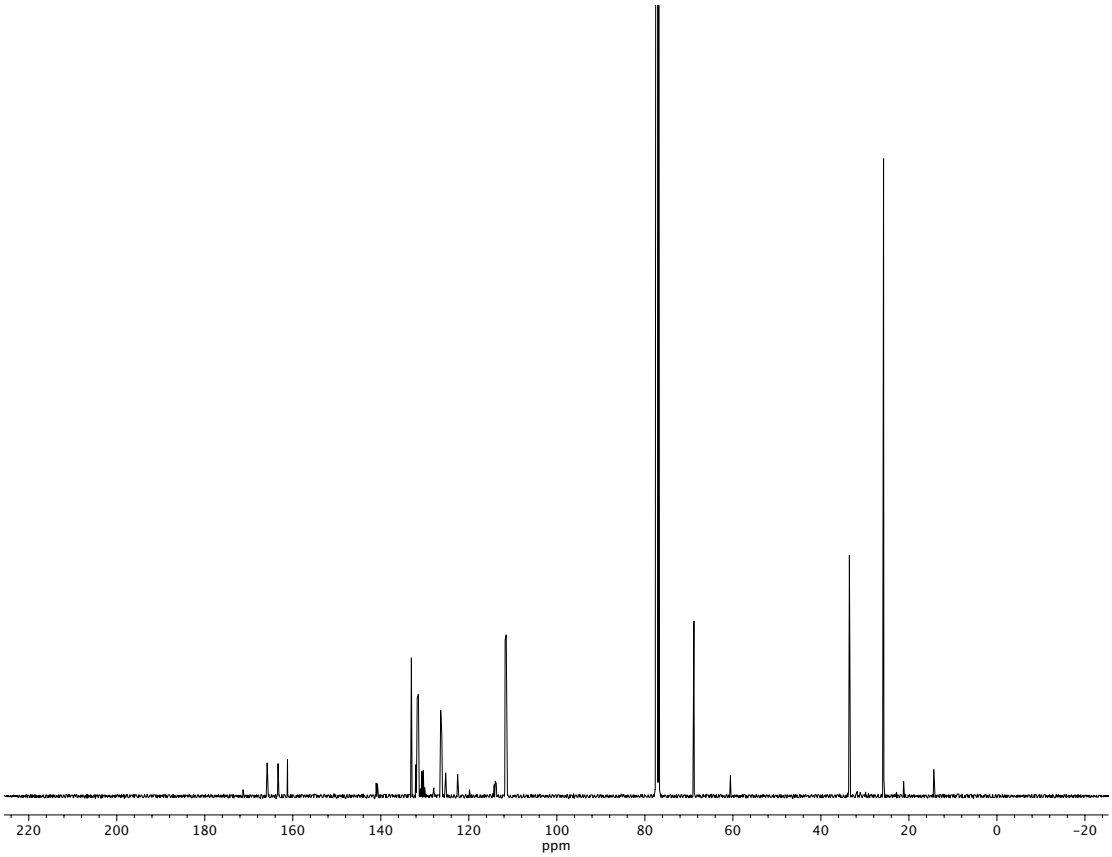


Figure A3.170. *^{13}C NMR (100 MHz, $CDCl_3$) of compound* ***L4****.*

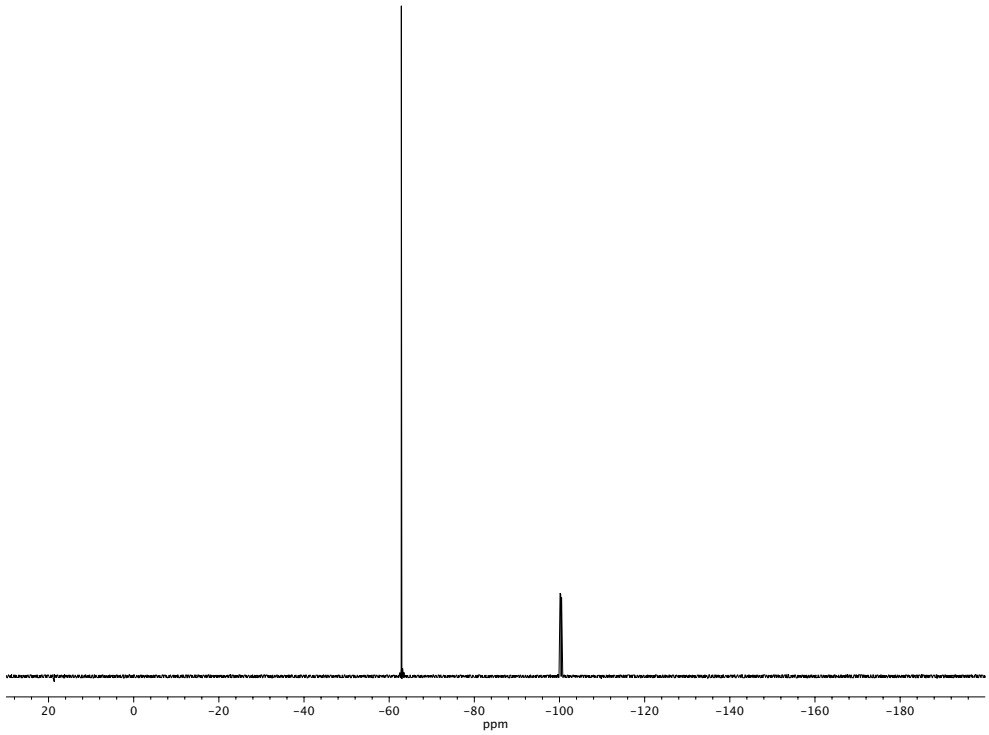


Figure A3.171. *^{19}F NMR (282 MHz, $CDCl_3$) of compound* ***L4****.*

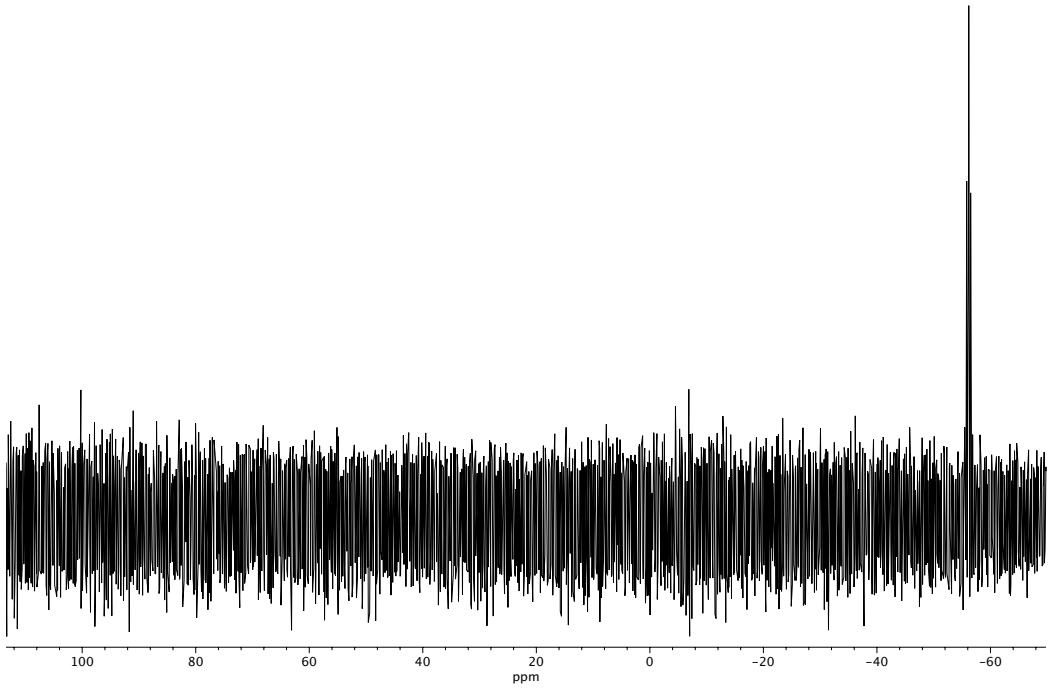


Figure A3.172. *^{31}P NMR (121 MHz, $CDCl_3$) of compound* ***L4****.*

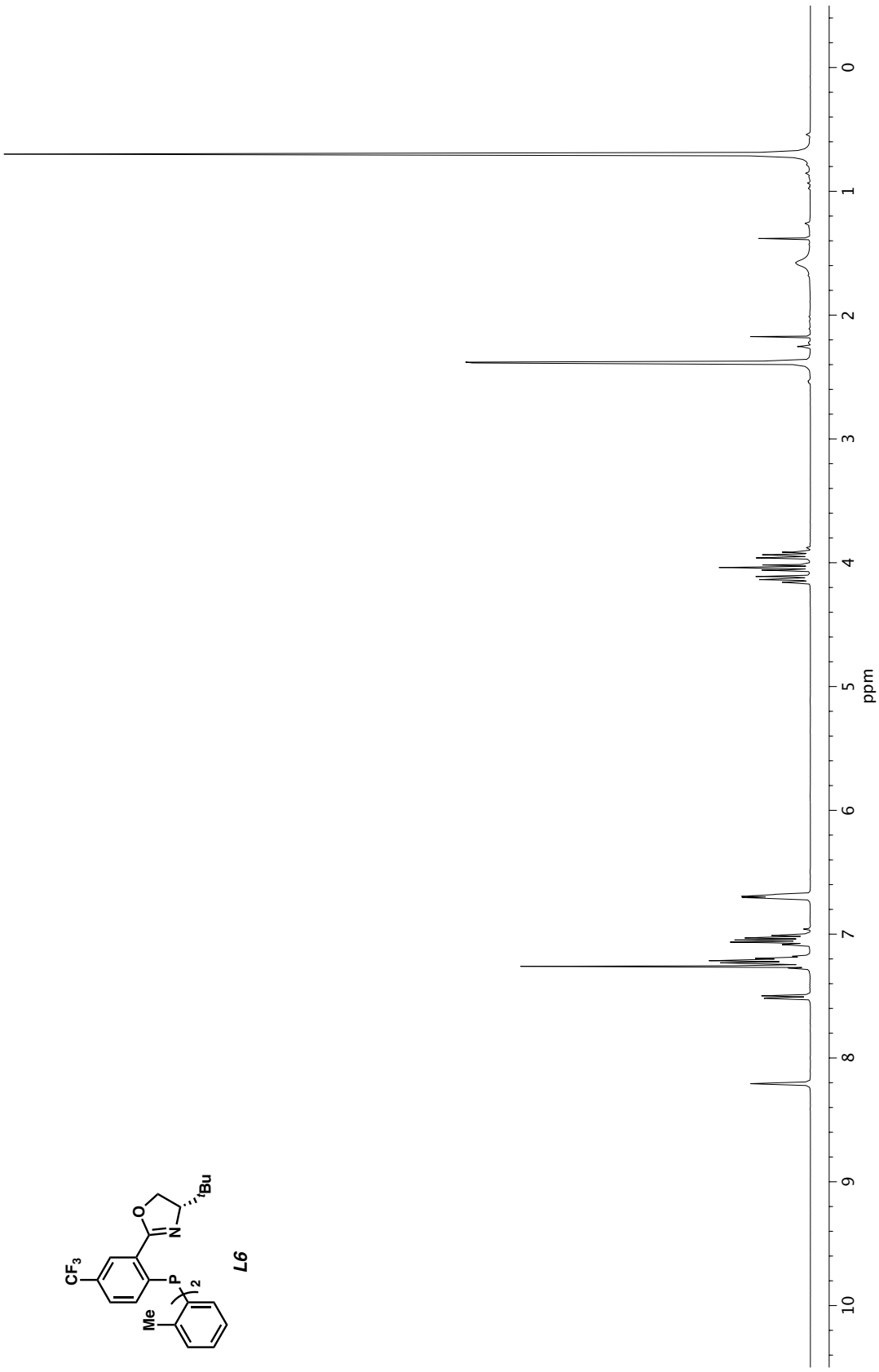


Figure A3.173. *^{1}H NMR (400 MHz, $CDCl_3$) of compound* ***L6****.*

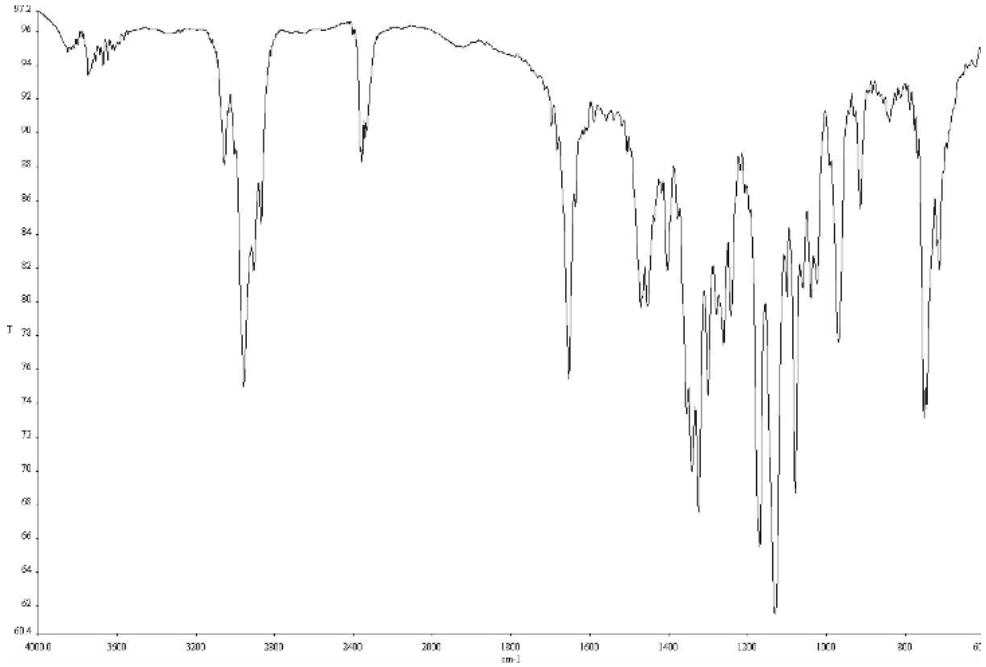


Figure A3.174. *Infrared spectrum (Thin Film, NaCl) of compound* ***L6****.*

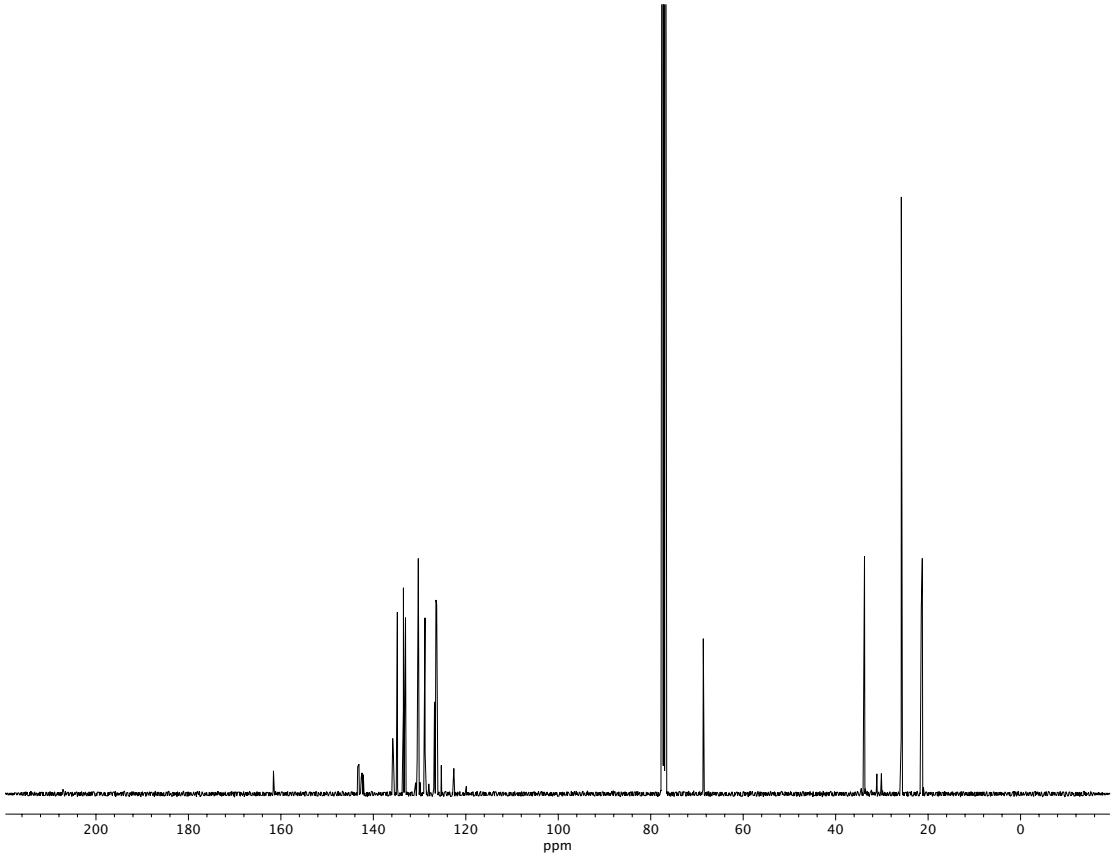


Figure A3.175. *^{13}C NMR (100 MHz, $CDCl_3$) of compound* ***L6****.*

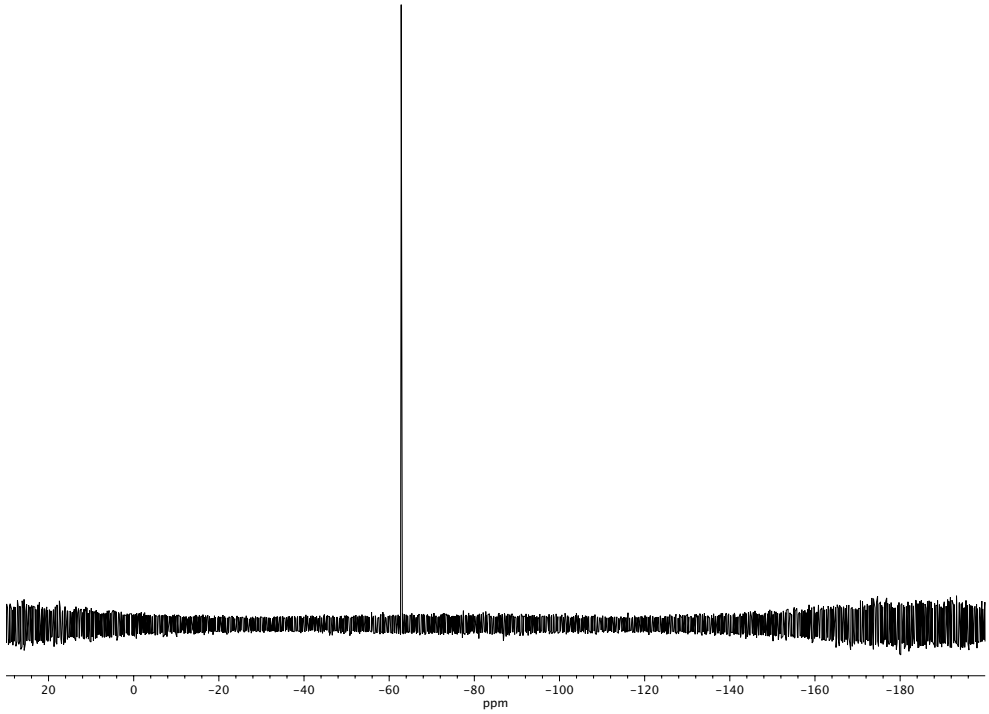


Figure A3.176. *^{19}F NMR (282 MHz, $CDCl_3$) of compound* ***L6****.*

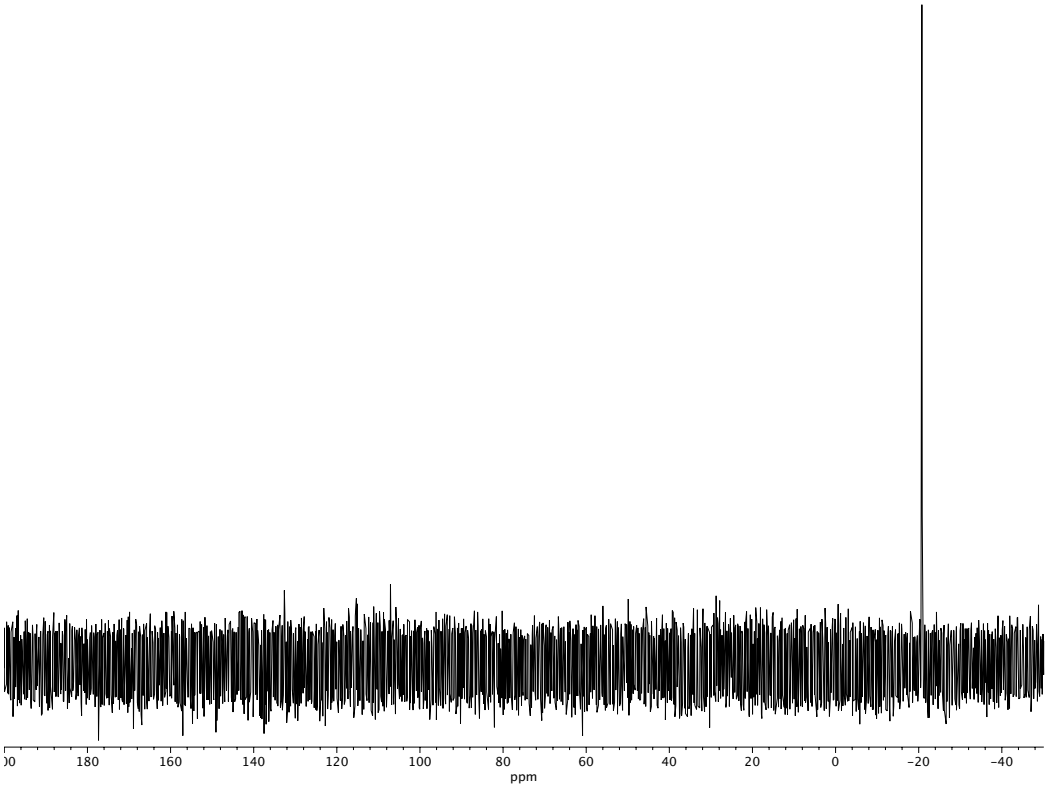


Figure A3.177. *^{31}P NMR (121 MHz, $CDCl_3$) of compound* ***L6****.*

L5

Figure A3.178. *^{1}H NMR (500 MHz, $CDCl_3$) of compound **L5**.*

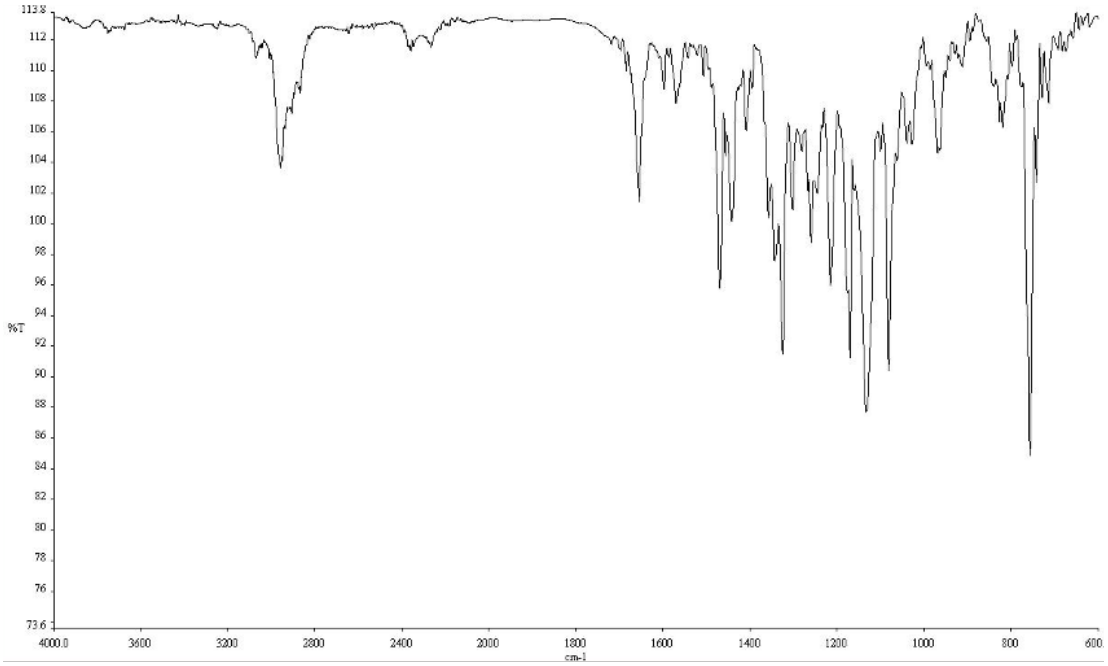


Figure A3.179. *Infrared spectrum (Thin Film, NaCl) of compound* ***L5****.*

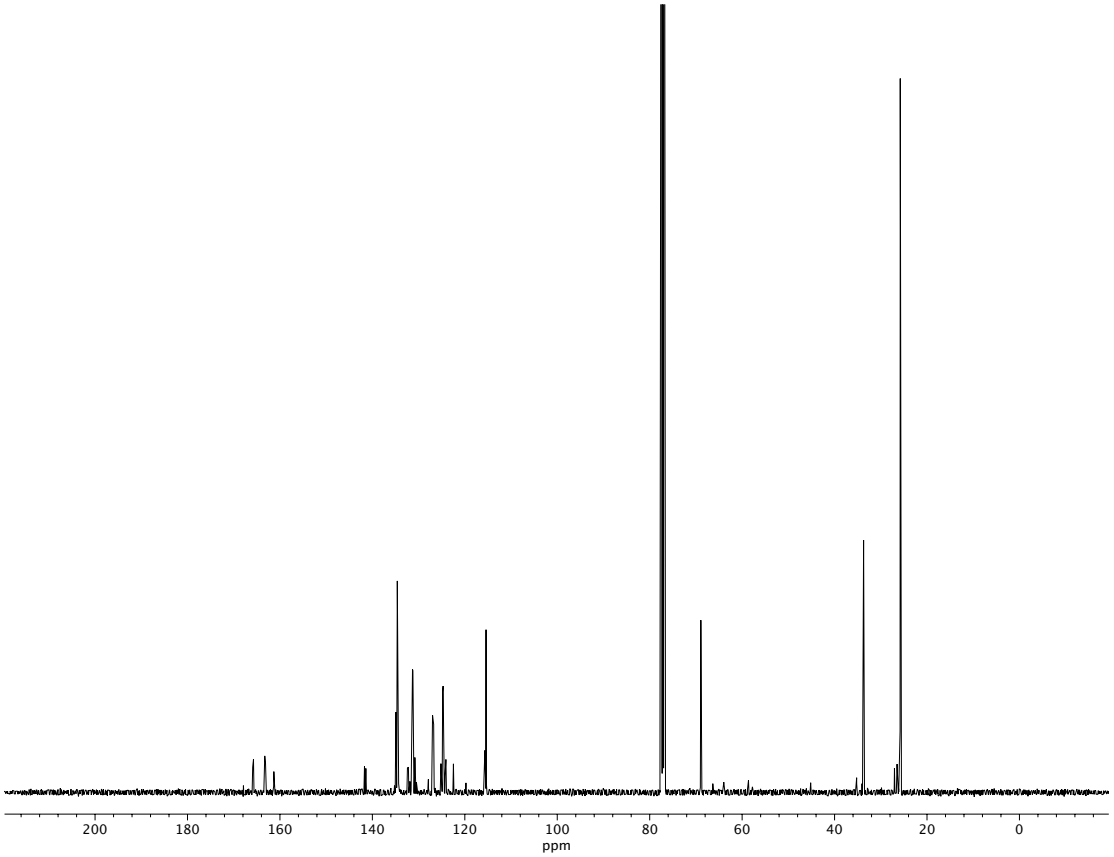


Figure A3.180. *^{13}C NMR (100 MHz, $CDCl_3$) of compound* ***L5****.*

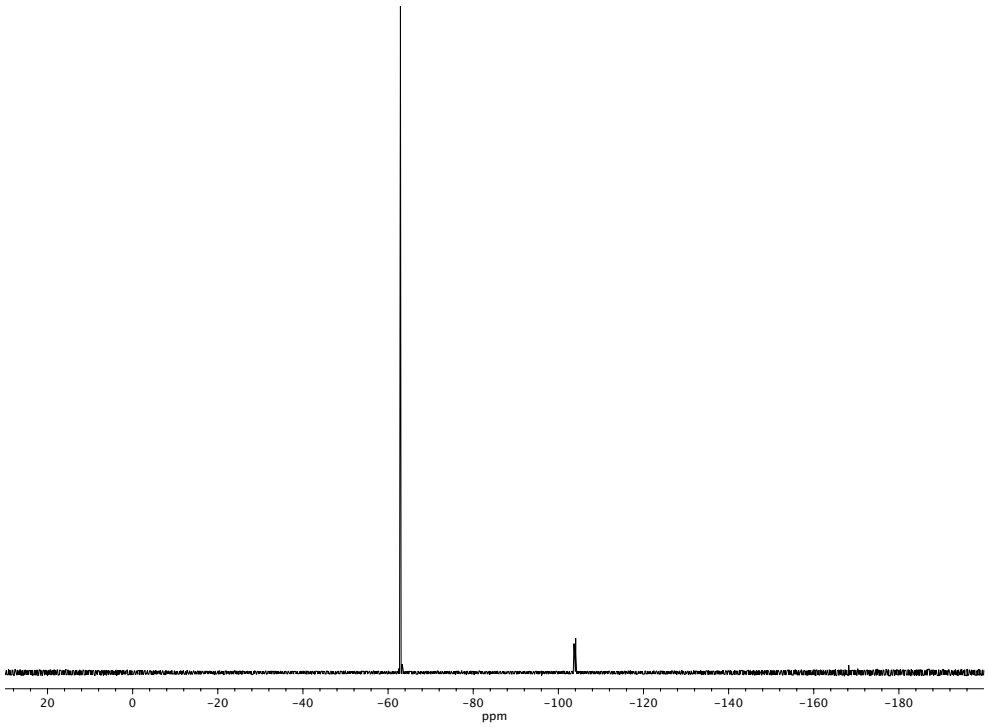


Figure A3.181. *^{19}F NMR (282 MHz, $CDCl_3$) of compound **L5**.*

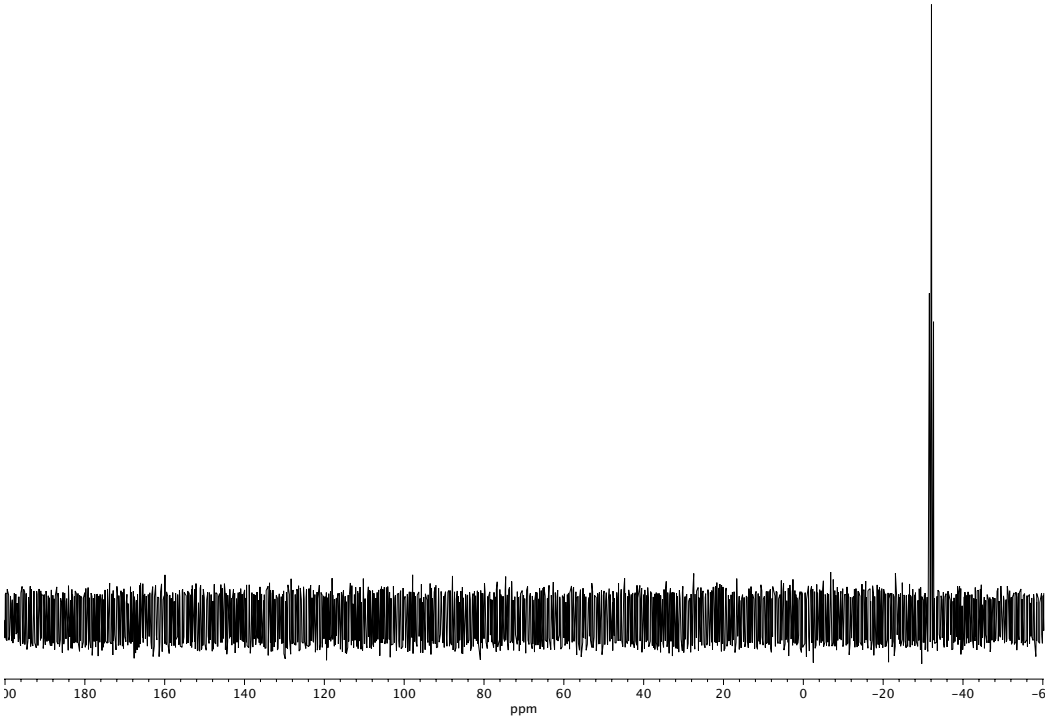


Figure A3.182. *^{31}P NMR (121 MHz, $CDCl_3$) of compound **L5**.*

Figure A3.183. *^{1}H NMR (300 MHz, $CDCl_3$) of compound **L7**.*

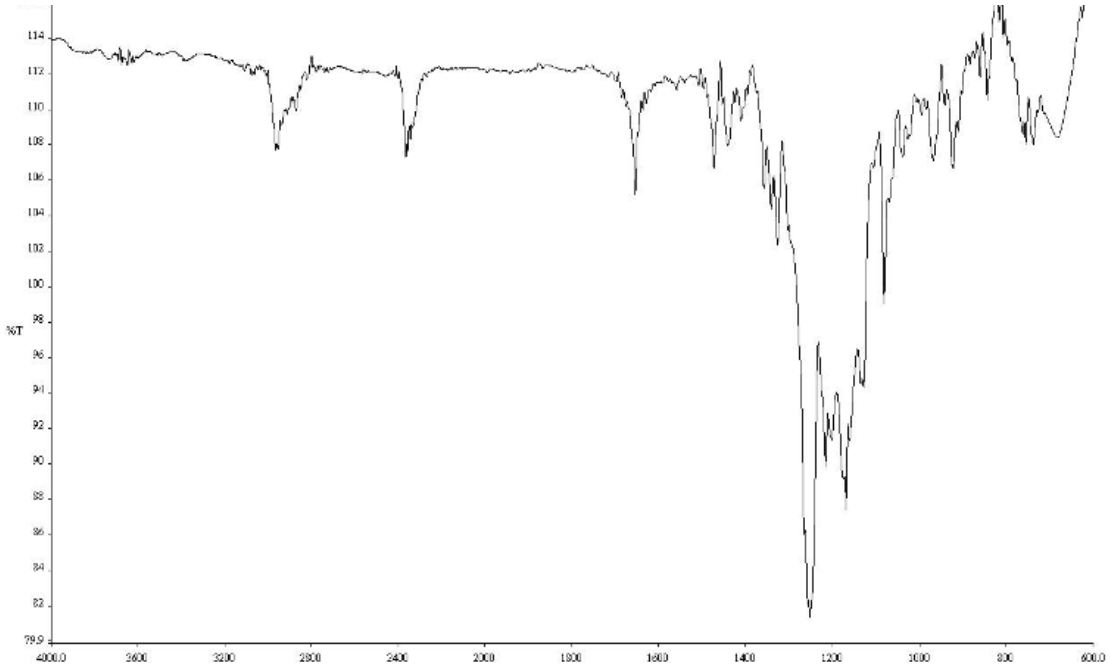


Figure A3.184. *Infrared spectrum (Thin Film, NaCl) of compound* ***L7****.*

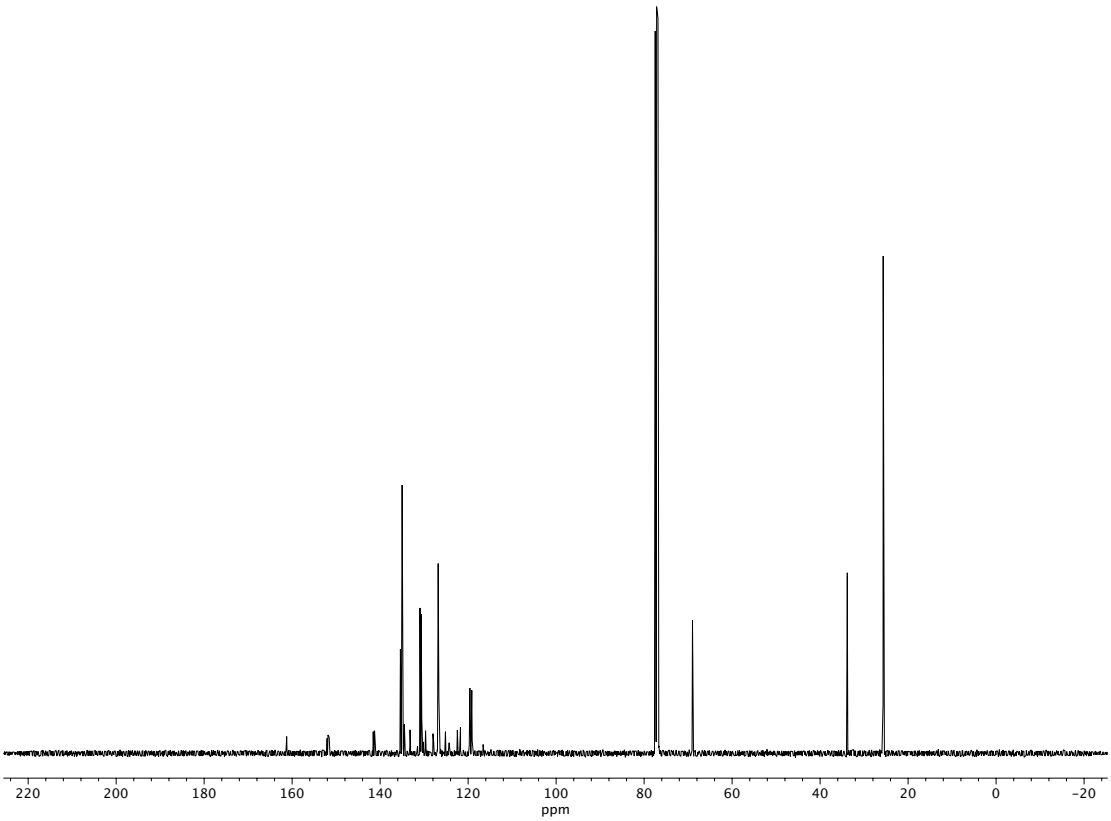


Figure A3.185. *^{13}C NMR (100 MHz, $CDCl_3$) of compound* ***L7****.*

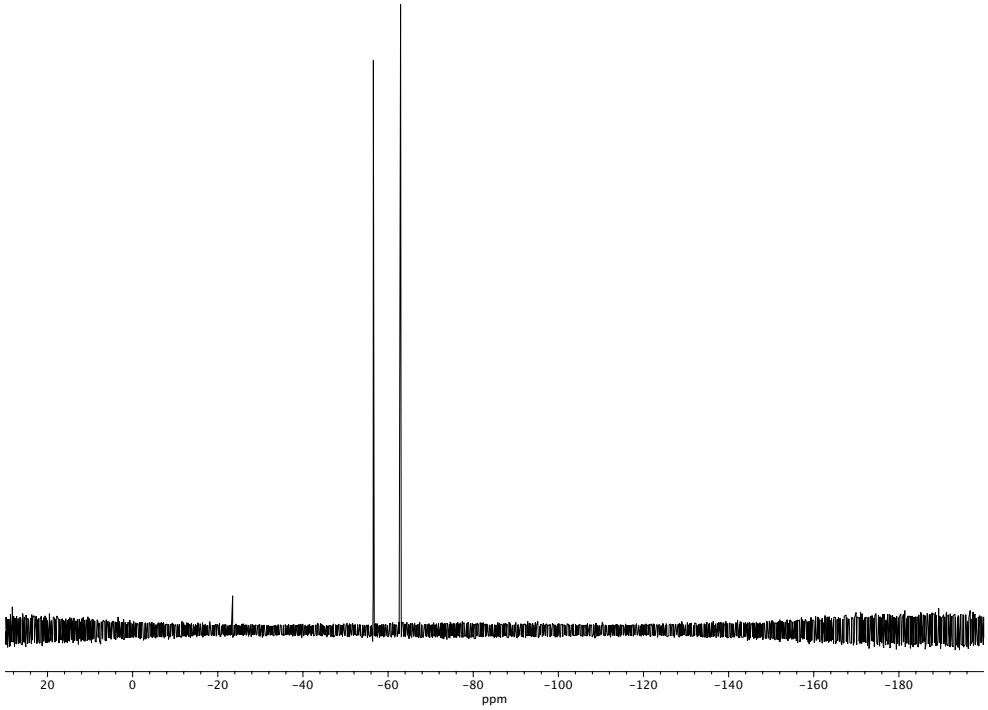


Figure A3.186. *^{19}F NMR (282 MHz, $CDCl_3$) of compound **L7**.*

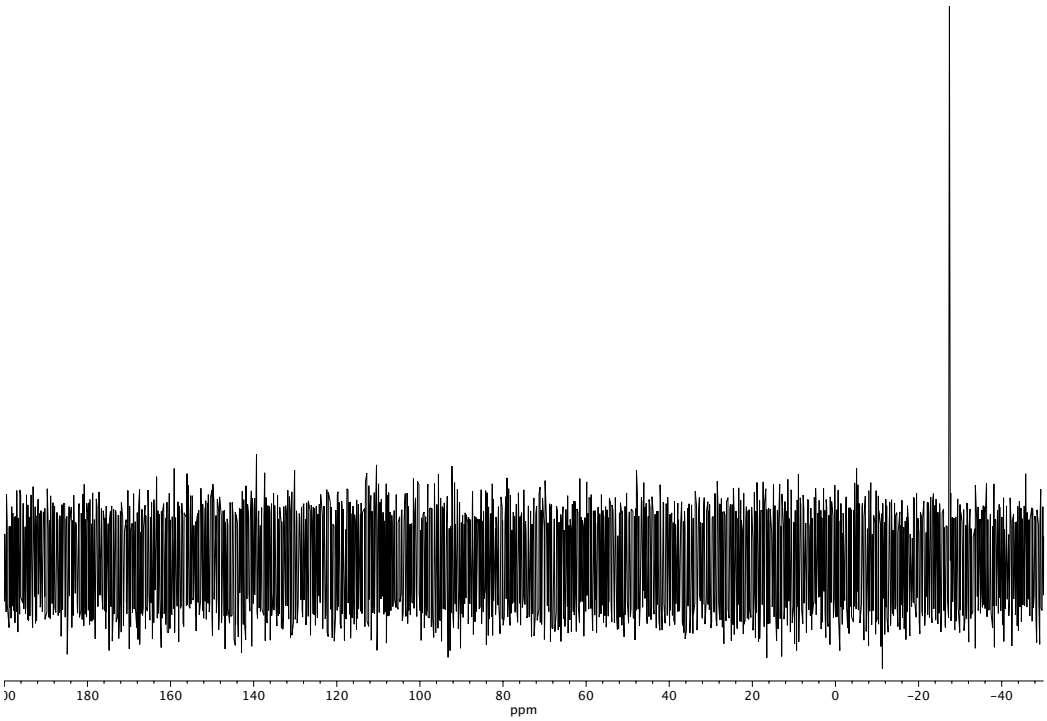


Figure A3.187. *^{31}P NMR (121 MHz, $CDCl_3$) of compound **L7**.*

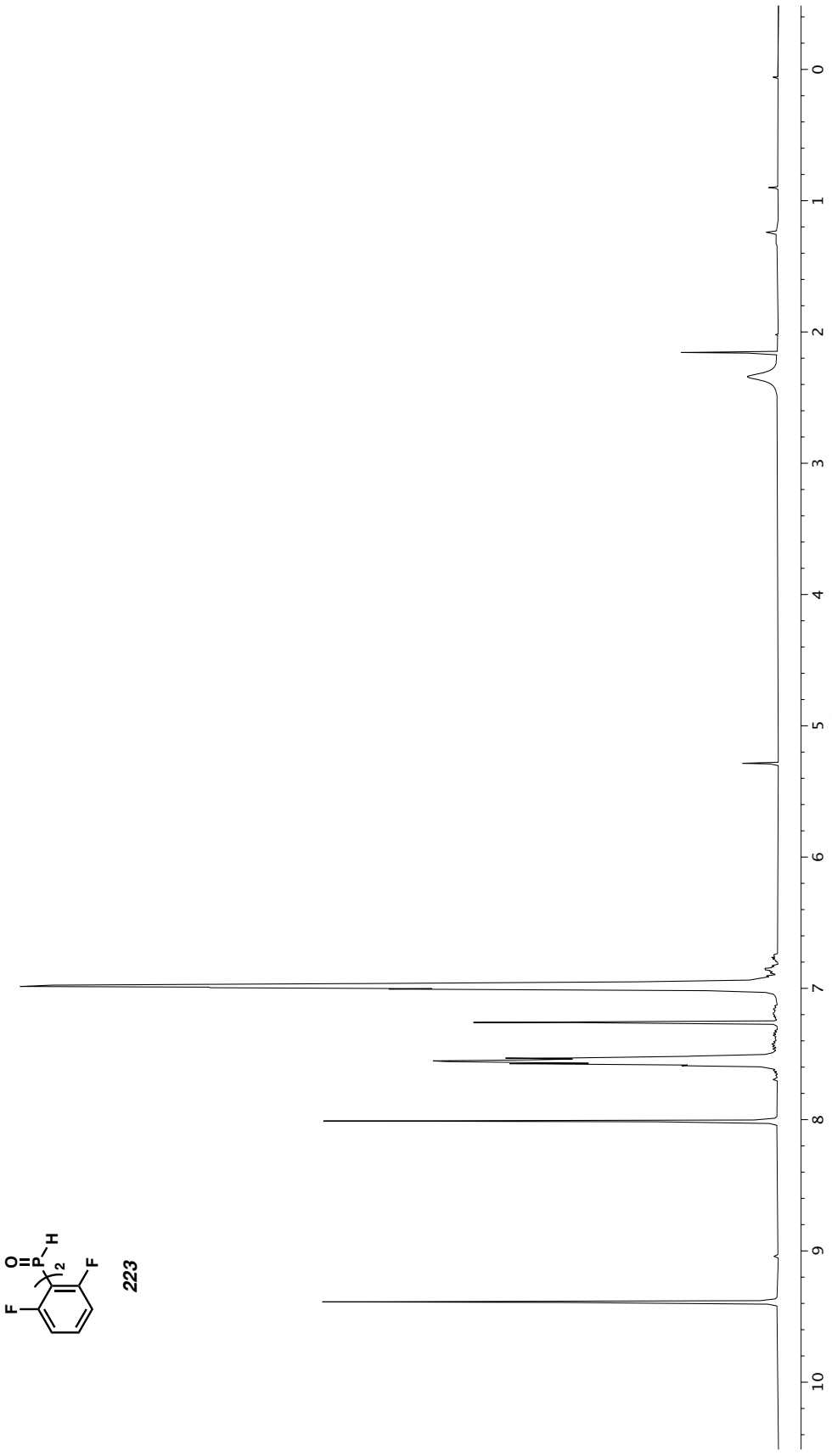


Figure A3.188. *^1H NMR (300 MHz, $CDCl_3$) of compound* ***223****.*

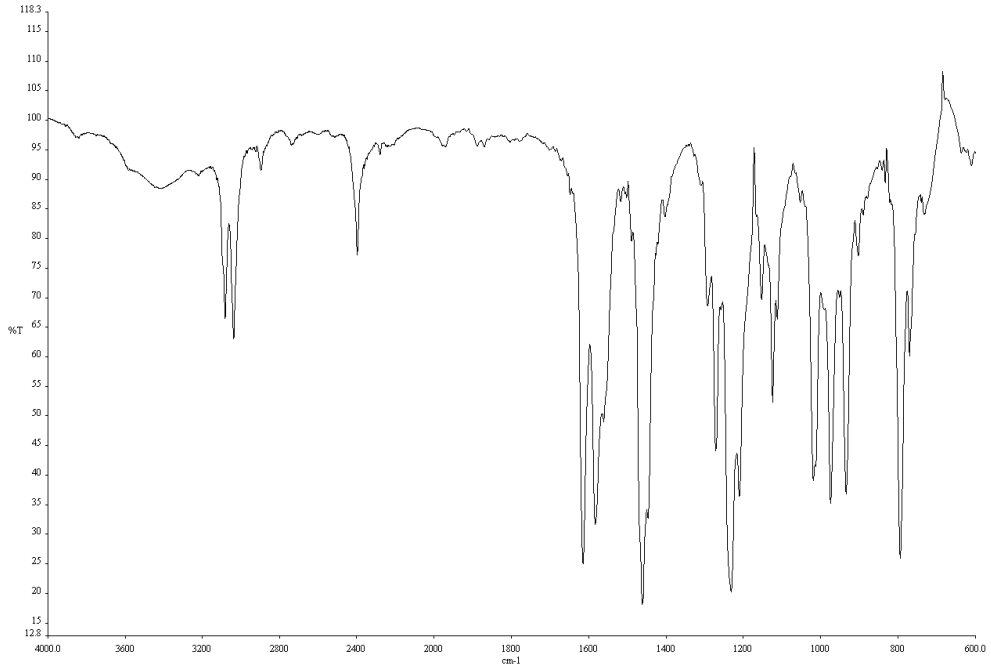


Figure A3.189. *Infrared spectrum (Thin Film, NaCl) of compound* ***223****.*

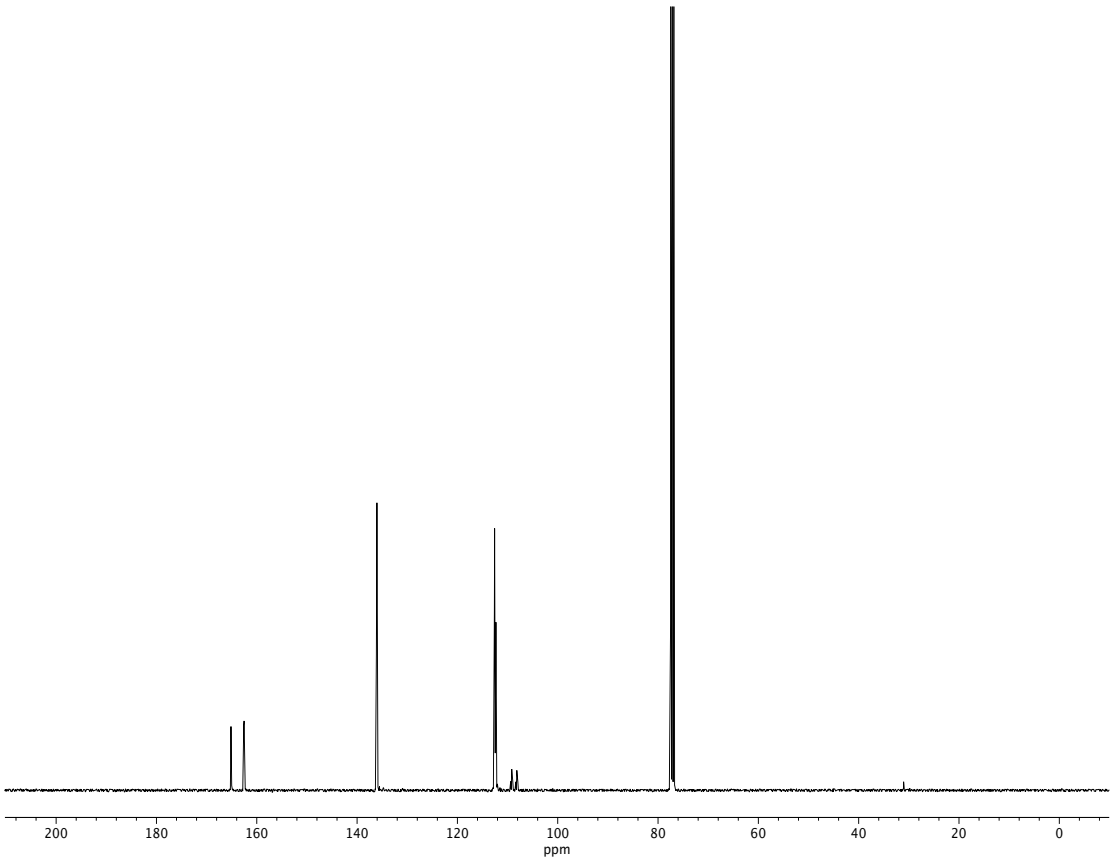


Figure A3.190. *^{13}C NMR (100 MHz, $CDCl_3$) of compound* ***223****.*

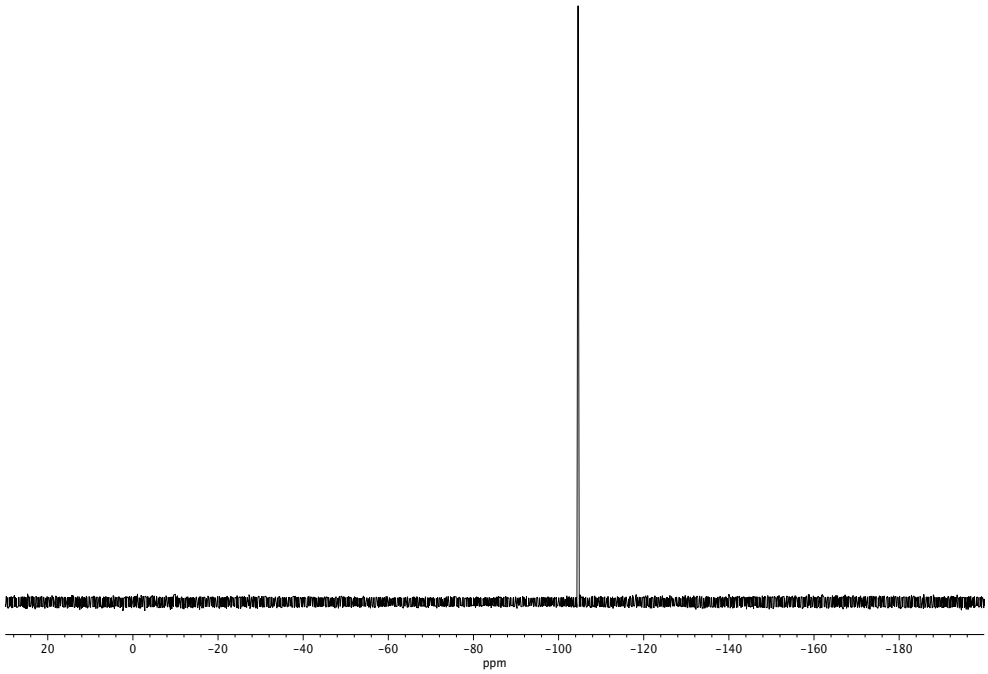


Figure A3.191. *^{19}F NMR (282 MHz, $CDCl_3$) of compound* ***223***.

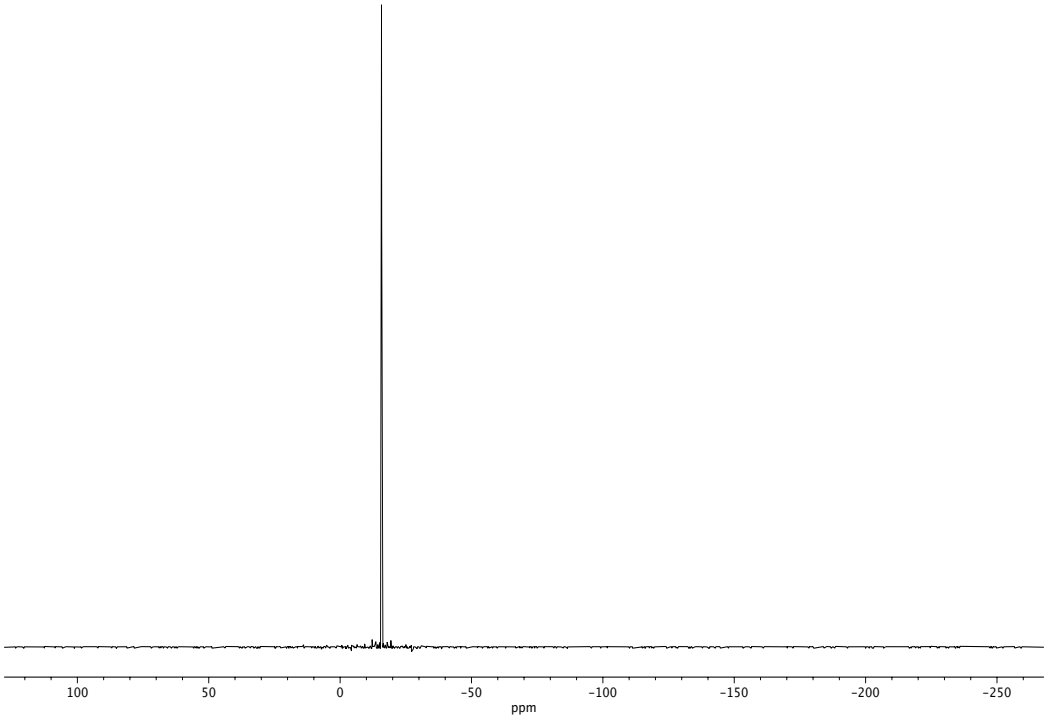


Figure A3.192. *^{31}P NMR (162 MHz, $CDCl_3$) of compound* ***223***.

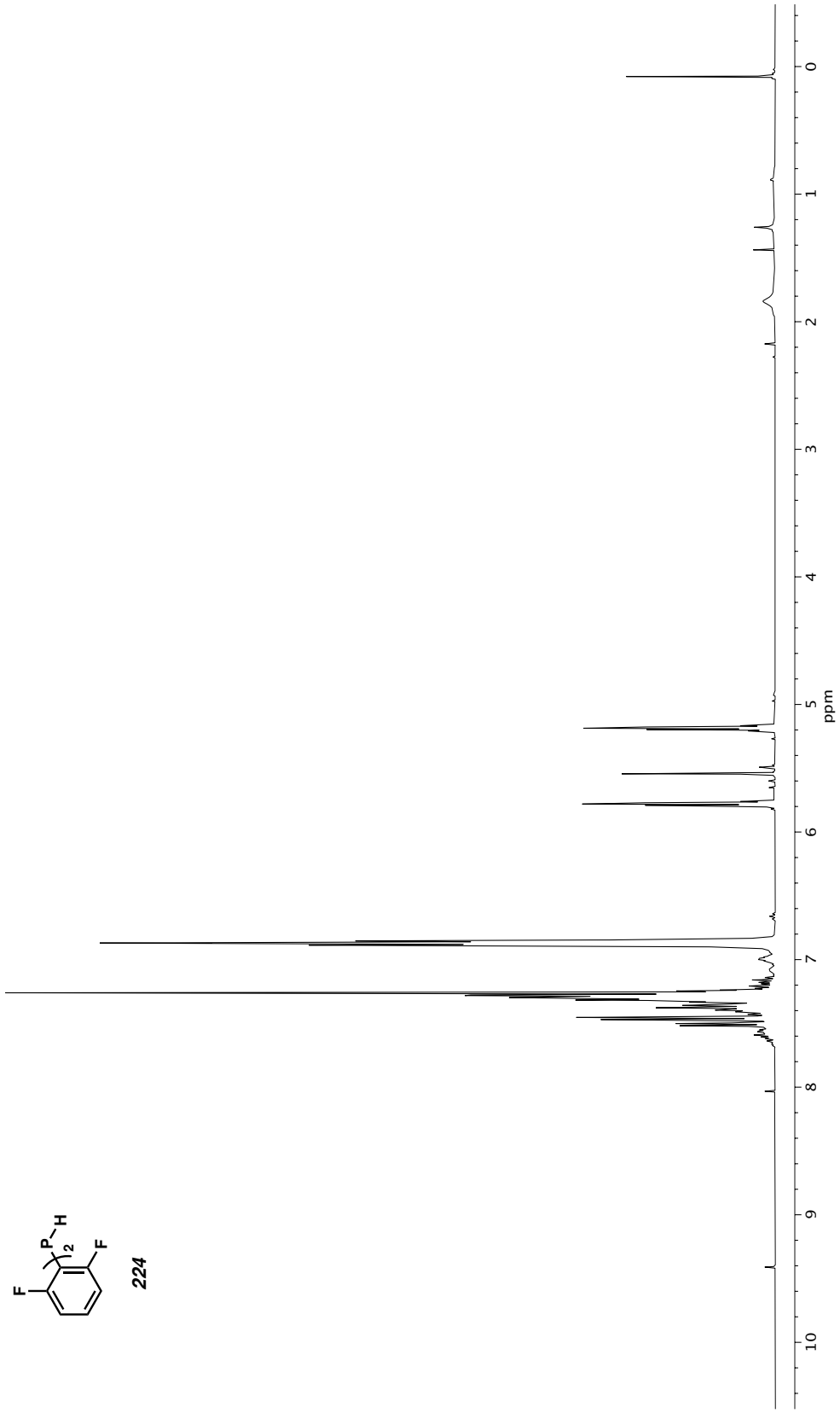


Figure A3.193. *^{1}H NMR (400 MHz, $CDCl_3$) of compound* ***224****.*

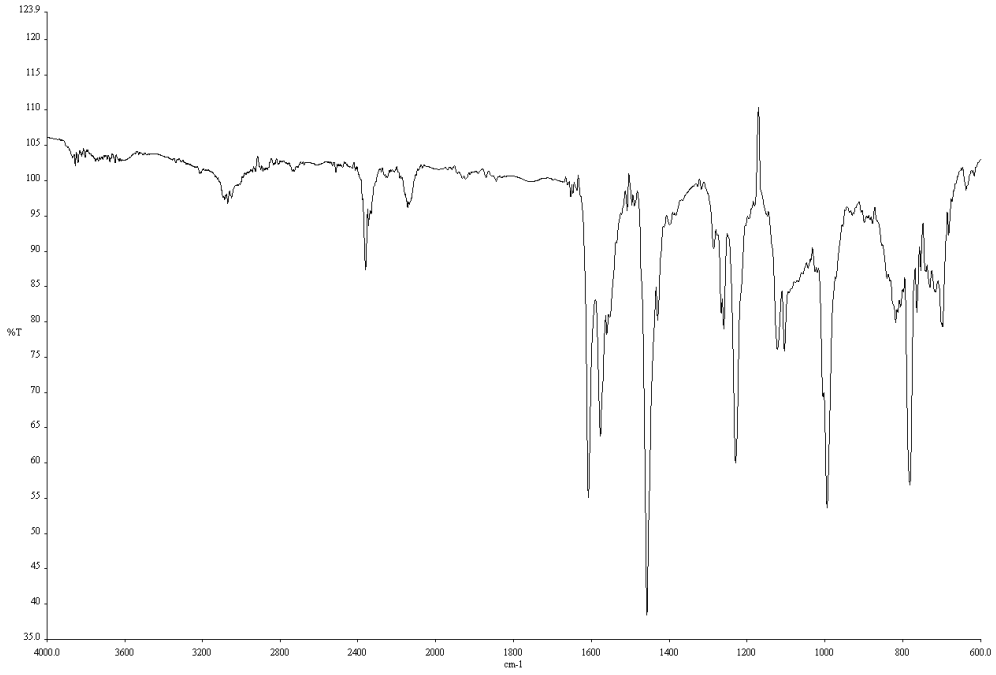


Figure A3.194. *Infrared spectrum (Thin Film, NaCl) of compound* ***224****.*

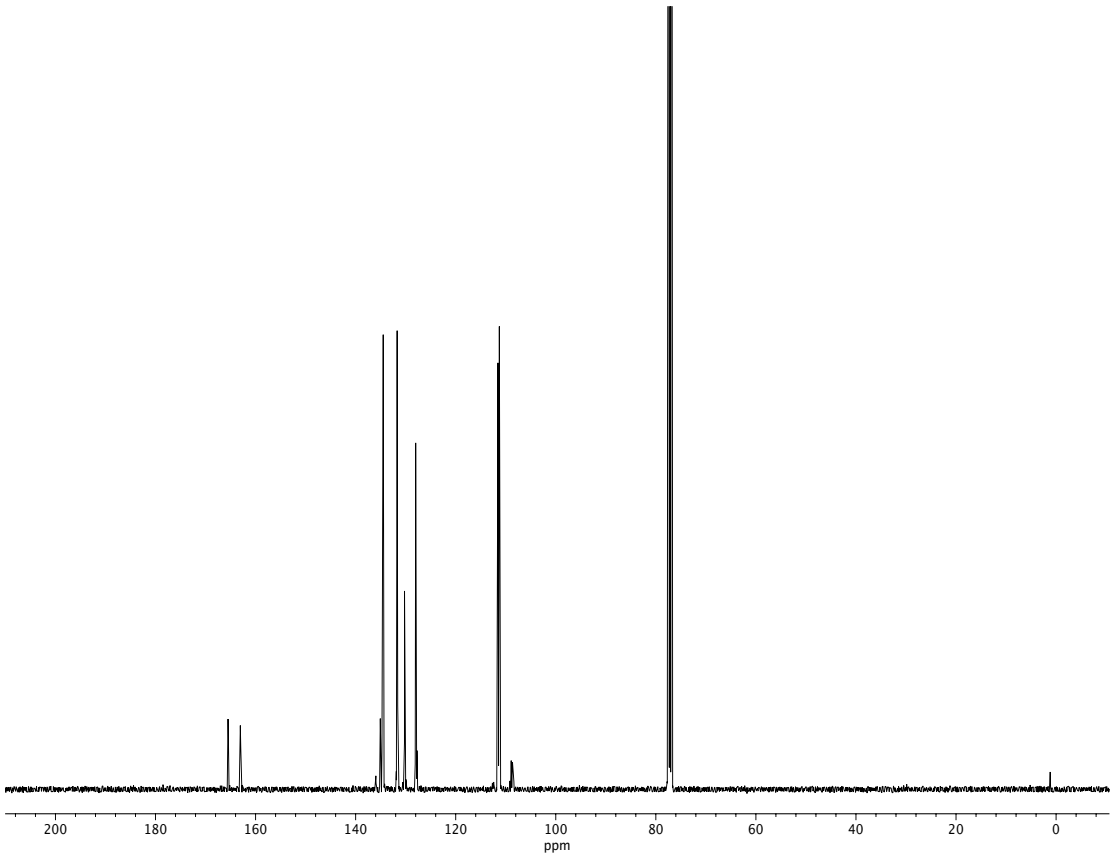


Figure A3.195. *^{13}C NMR (100 MHz, $CDCl_3$) of compound* ***224****.*

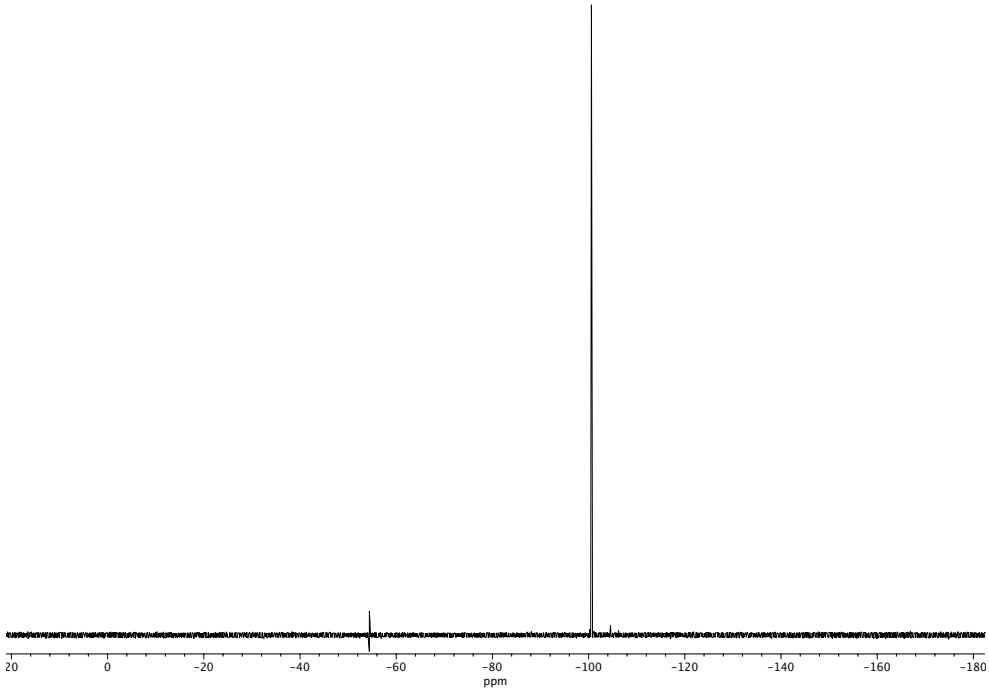


Figure A3.196. *^{19}F NMR (282 MHz, $CDCl_3$) of compound* ***224****.*

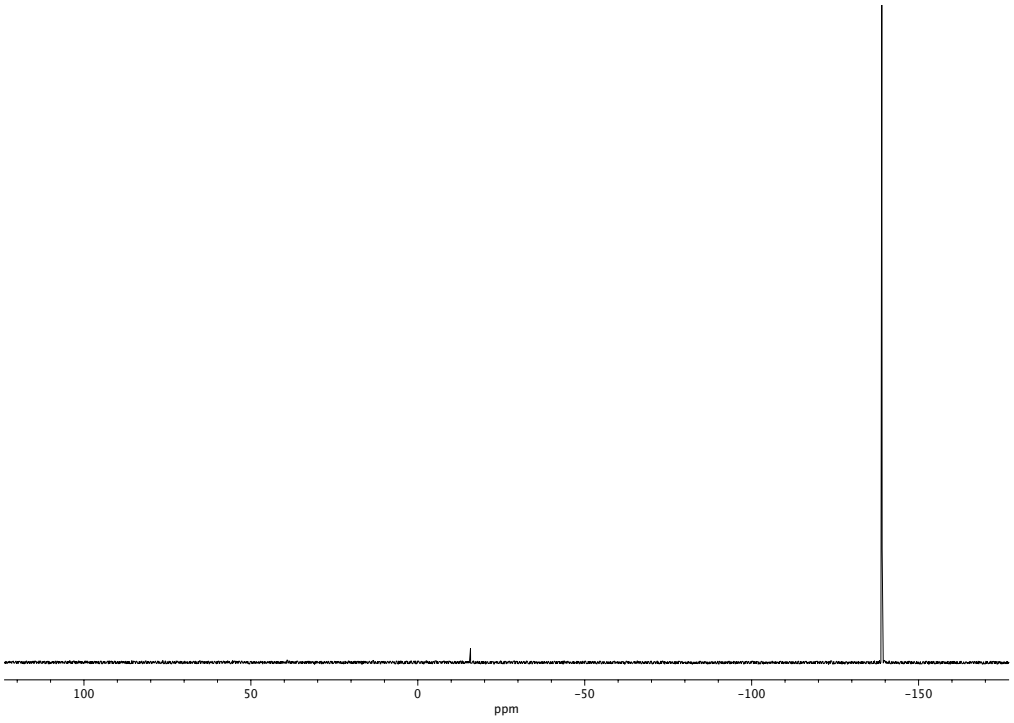


Figure A3.197. *^{31}P NMR (162 MHz, $CDCl_3$) of compound* ***224****.*

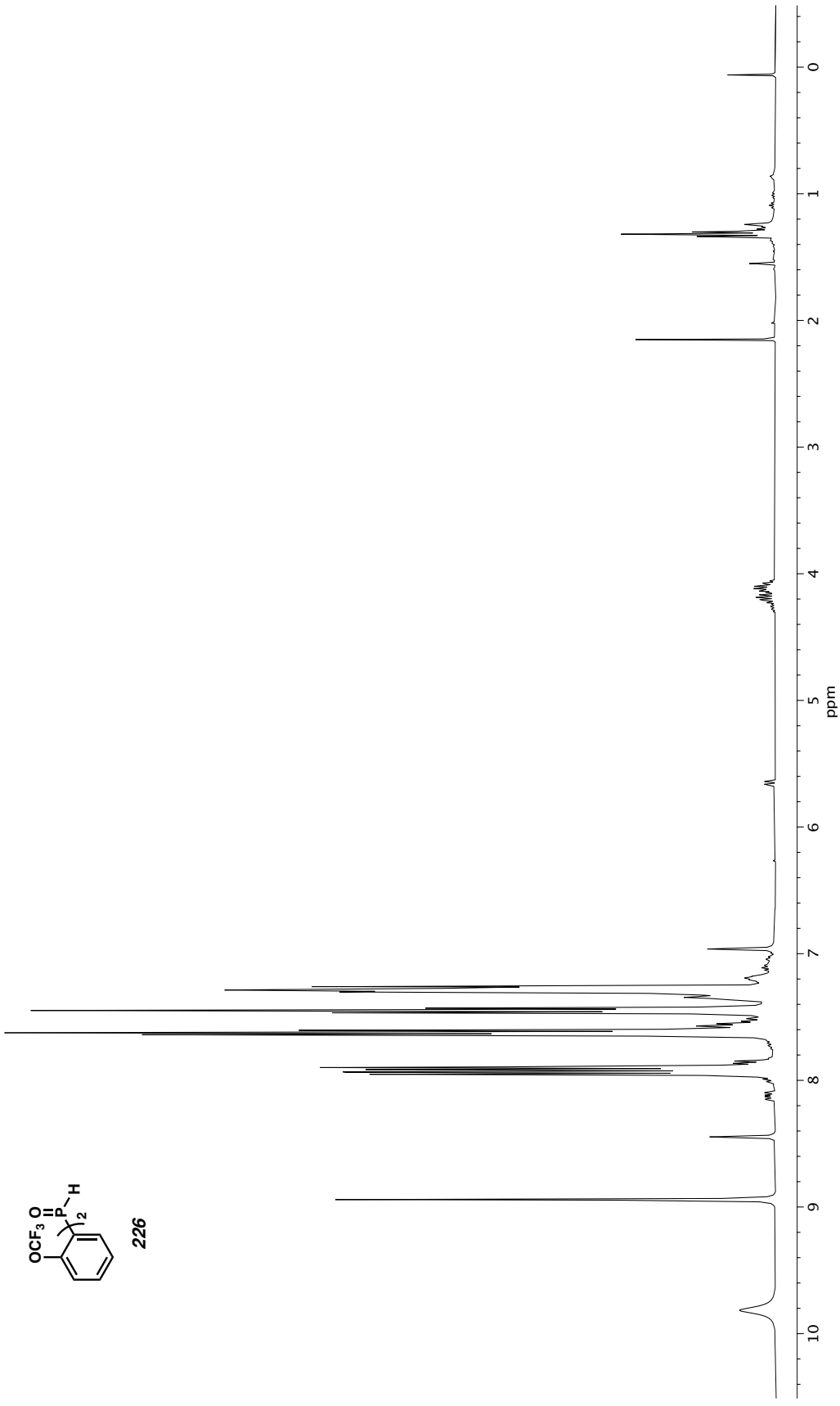


Figure A3.198. *^{1}H NMR (400 MHz, $CDCl_3$) of compound* ***226****.*

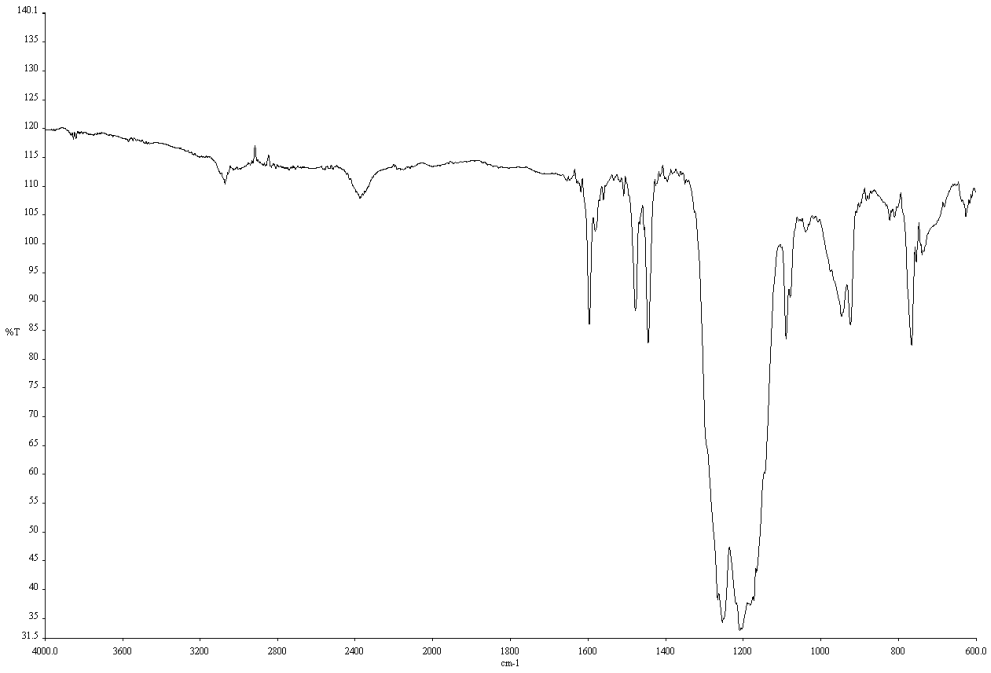


Figure A3.199. *Infrared spectrum (Thin Film, NaCl) of compound* ***226****.*

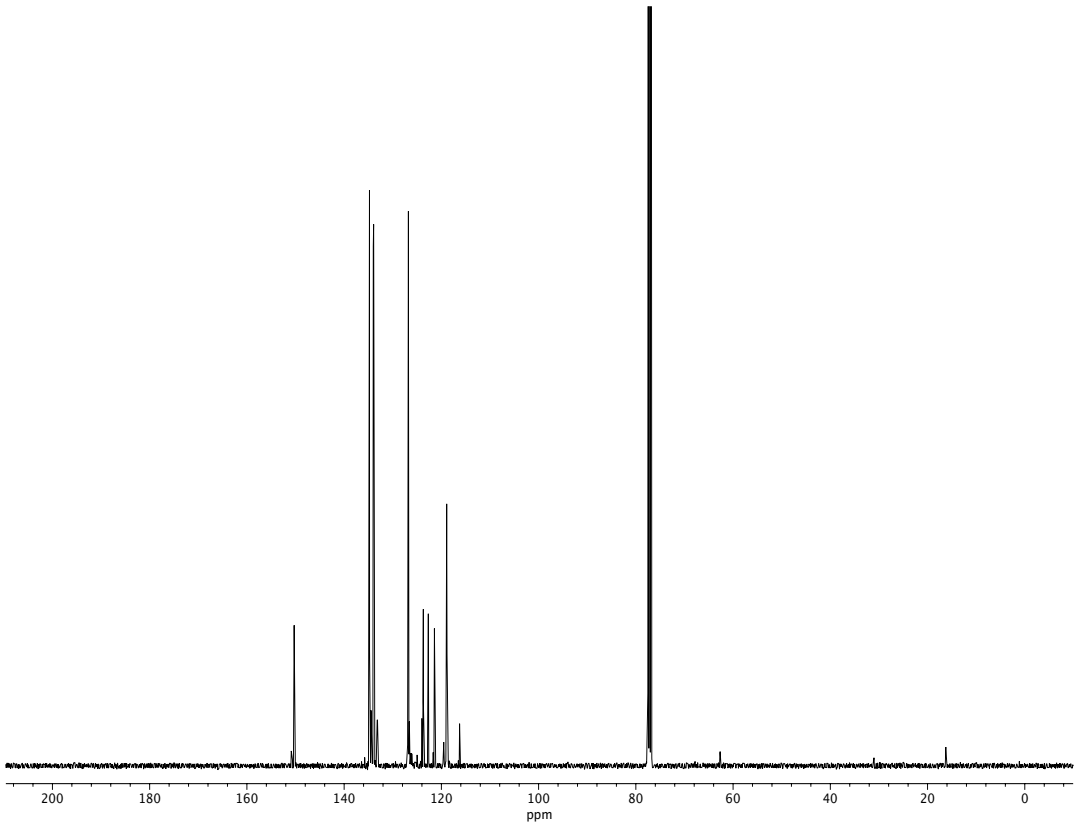


Figure A3.200. *^{13}C NMR (100 MHz, $CDCl_3$) of compound* ***226****.*

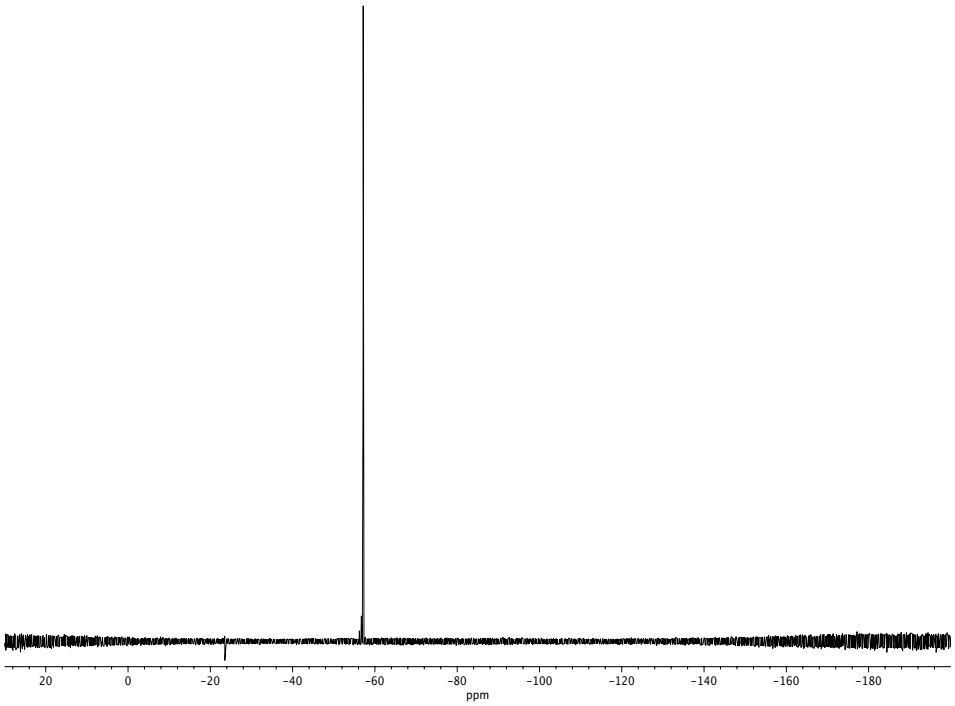


Figure A3.201. *^{19}F NMR (282 MHz, $CDCl_3$) of compound* ***226****.*

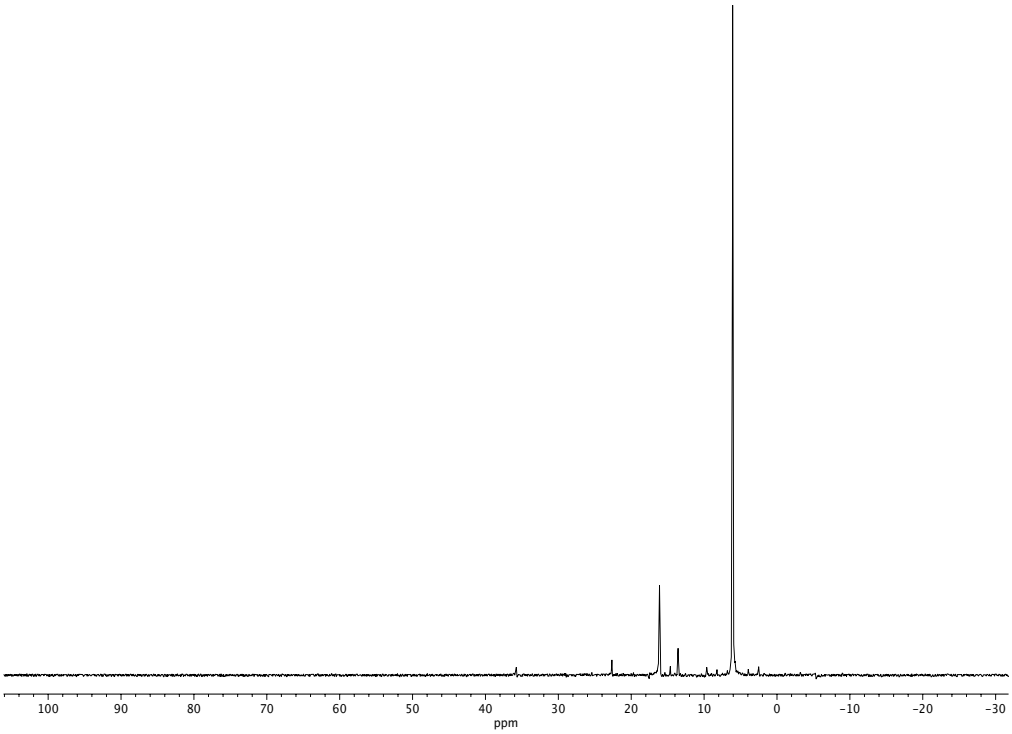


Figure A3.202. *^{31}P NMR (162 MHz, $CDCl_3$) of compound* ***226****.*

CHAPTER 5

Progress Toward the Total Synthesis of Hypermoin A†

5.1 INTRODUCTION

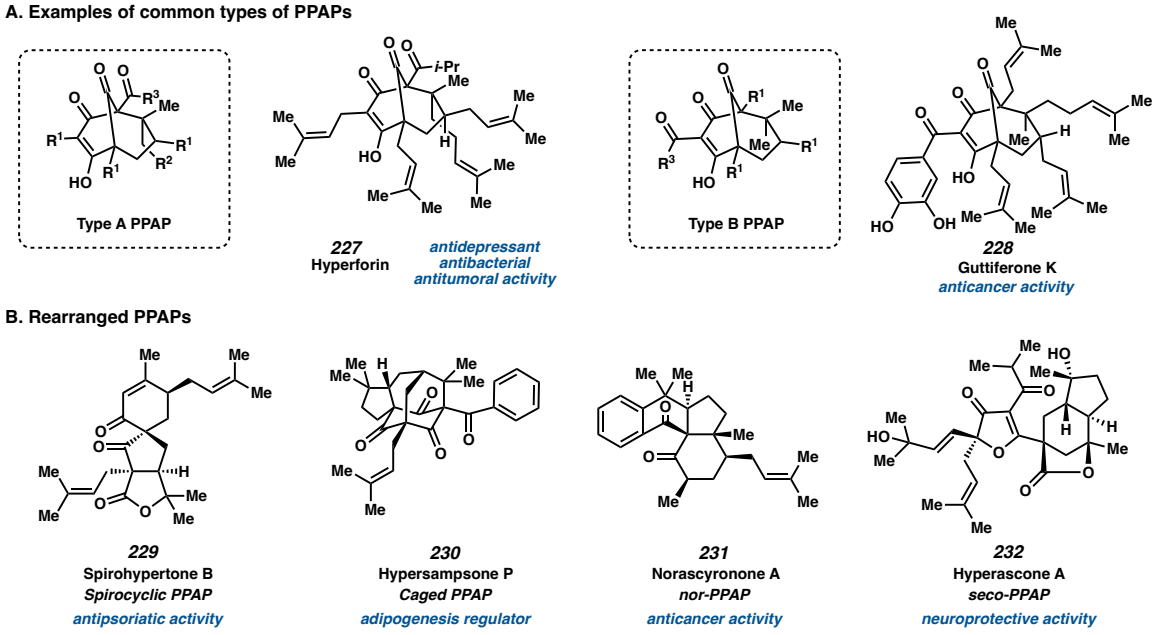
Polycyclic polyprenylated acylphloroglucinols (PPAPs) are a class of natural products with highly oxygenated cores derived from acylphloroglucinol and are often decorated with prenyl groups. Since their discovery, more than a thousand members have been isolated, and significant interest has been attracted among synthetic organic chemists and the pharmaceutical industry due to their biological properties including anti-inflammatory, antioxidant, and anticancer activities.[1,2,3,4] The majority of these structurally diverse natural products can be categorized as type A or type B PPAPs according to the acyl substitution pattern of the common bicyclo[3.3.1]nonane cores (Figure 5.1.A), and significant effort has been invested in the efficient access of these compounds to allow biological investigations of promising drug lead candidates.

In addition to type A and type B PPAPs, rearranged PPAPs also represent exciting synthetic targets (Figure 5.1.B). These natural products containing highly modified carbon skeletons, such as spirocyclic[5], caged[6], *nor*-[7], and *seco*-PPAPs[8], have displayed promising anti-psoriatic, neuroprotective, and anti-tumor activities. However, access to rearranged carbon skeletons generally require development of new synthetic strategies, as most reported syntheses of PPAPs have focused on construction of the canonical [3.3.1] bicyclic

†Unpublished research performed in collaboration with Flesch, K. N.; Patch, M. M.; Ahmad, J.; Nair, V. N.; Grogan, Z. R.; Bottcher, S. E.

core.[9] These rearranged structures therefore represent exciting targets for synthetic efforts and development of novel synthetic strategies.

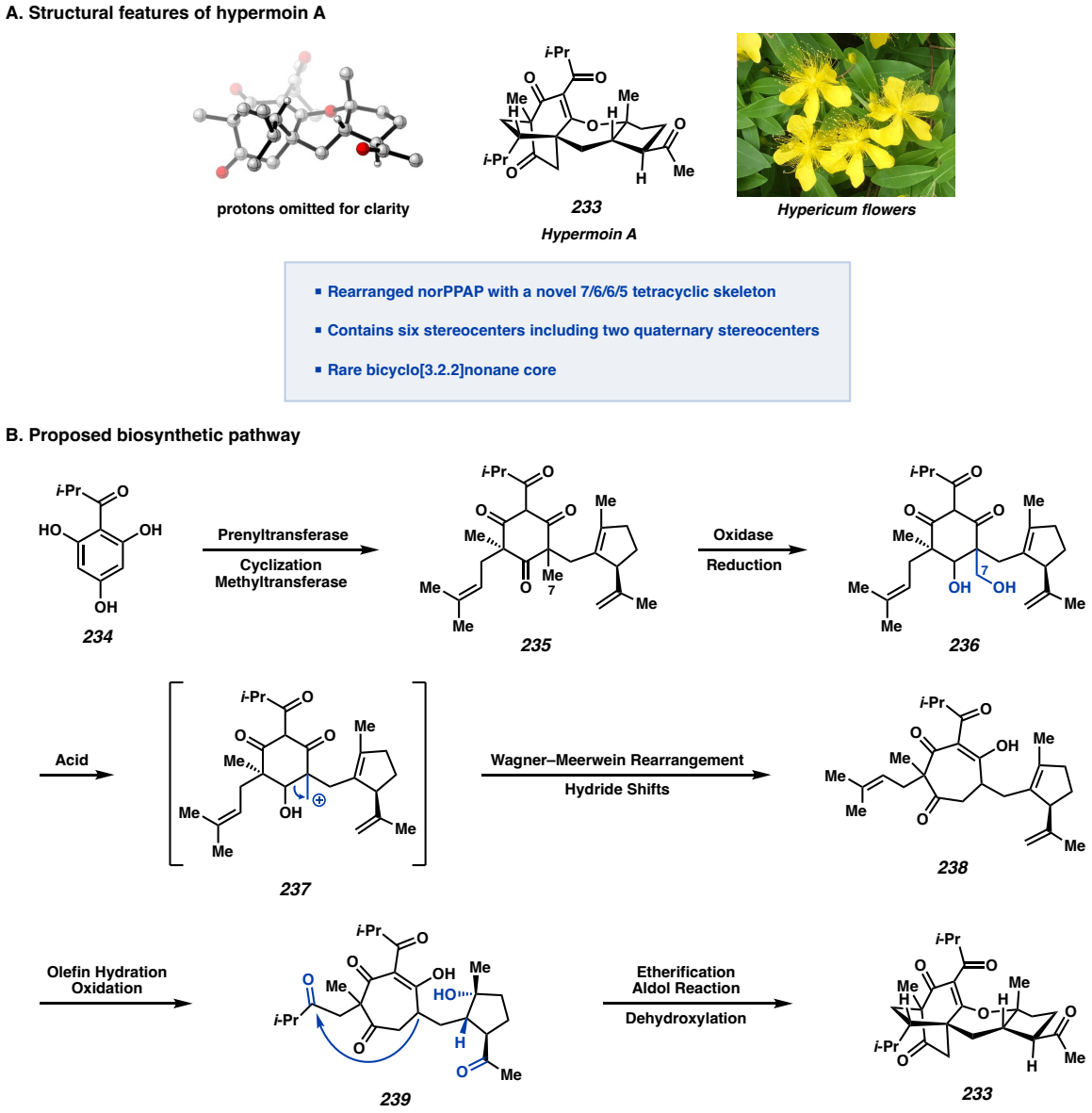
Figure 5.1. *(A) Examples of type A and type B PPAPs. (B) Common types of rearranged PPAPs.*



To this end, we identified hypermoin A (**233**) as an appealing target (Figure 5.2.A).[10] This rearranged norPPAP was isolated in 2021 from the flowers of *Hypericum monogynum* and displayed intriguing bioactivity toward reversing multidrug resistance in HepG2/ADR and MCF-7/ADR cancer cell lines. Its unique structural features include a distinct bicyclo[3.2.2]nonane core, a 7/6/6/5 tetracyclic framework, in addition to six stereocenters including two all-carbon quaternary stereocenters. The proposed biosynthesis of **233** commences with a series of prenylation, cyclization, and methylation of acylphloroglucinol **234** to yield **235** (Figure 5.2.B). Following redox reactions to afford **236**, Wagner–Meerwein rearrangement and hydride shift provides ring-expanded **238**, which can

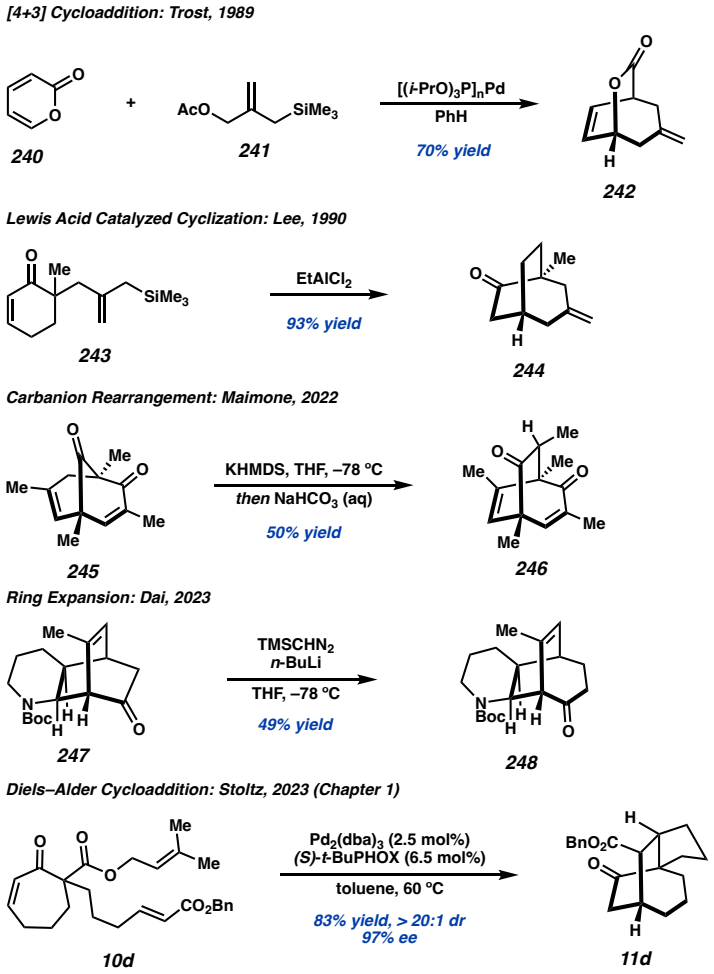
undergo subsequent olefin hydration and oxidation to **239**. Finally, etherification and intramolecular aldol reaction forges the tetracyclic core, and **233** is achieved upon dihydroxylation.

Figure 5.2. *(A) Hypermoin A. (B) Proposed biosynthesis of hypermoin A.*



A key challenge anticipated in attempting to synthesize **233** is the construction of the unusual [3.2.2] bicyclic core. In comparison with the canonical [3.3.1] bicyclic core found in most PPAP members, access to similar scaffolds remain relatively under-explored.

Figure 5.3. *Previously developed approaches to access [3.2.2] bicycles.*



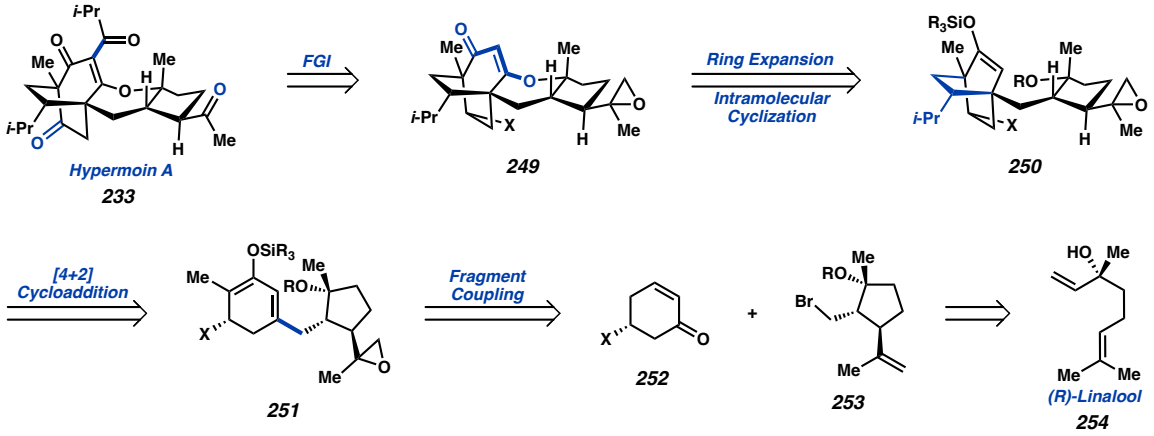
Previous research by Trost and coworkers demonstrated that bicycle **242** can be accessed through an intermolecular Pd-catalyzed [4+3] cycloaddition (Figure 5.3).[11] As shown by Lee and coworkers, a Lewis acid-catalyzed intramolecular Sakurai reaction also leads to efficient formation of bicycle **244**.[12] More recently, a distinct strategy featuring rearrangement of [3.3.1] bicycles (**245**) to yield [3.2.2] bicyclic **246** was reported by the

Maimone lab.[13] Furthermore, Dai and coworkers leveraged [2.2.2] bicycles to synthesize **248** via ring expansion.[14] Finally, our group has also developed a Pd-catalyzed asymmetric intramolecular [4+2] cycloaddition, allowing efficient construction of an enantioenriched [3.2.2] scaffold (**11d**) beginning with racemic cycloheptenone **10d** (see Chapter 1).[15] While this approach is effective in forming the desired bicyclic framework enantioselectively, its application in the synthesis of **233** would require significant manipulation of functional groups due to the position of the dienophile tether. Considering these precedented strategies, we have initially attempted to construct the [3.2.2] bicycle through intramolecular cyclization and radical cyclization (see Appendix 5) but eventually pursued a ring expansion approach most similar to that reported by the Dai group.

5.2 RETROSYNTHETIC ANALYSIS

Retrosynthetic disconnection of **233** begins with functional group interconversions and oxidations from **249** (Figure 5.4). To access the 7/6/6/5 skeleton, we propose a ring expansion–alcohol addition cascade from [2.2.2] bicycle **250**, which can be forged through a [4+2] cycloaddition employing siloxy diene **251**.

Figure 5.4. *Retrosynthetic analysis.*

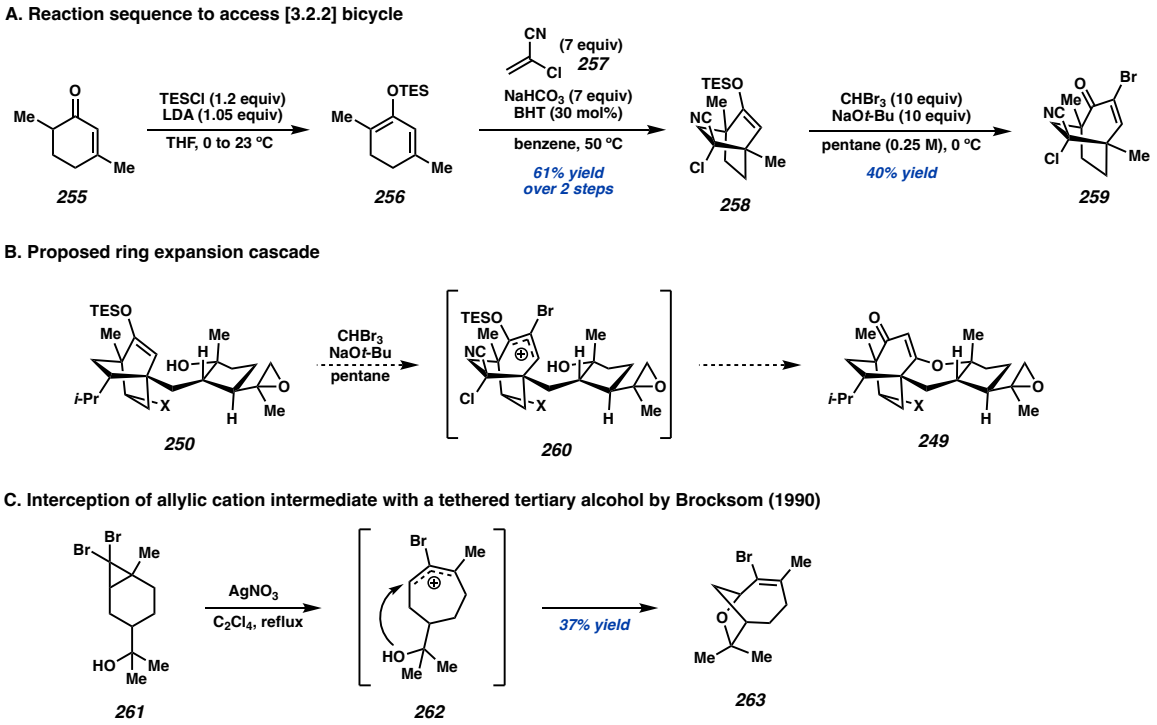


Intermediate **251** would be constructed through the coupling of enantio-enriched fragments **252** and **253** via 1,2-addition and oxidative transposition. Cyclopentane **253** can be derived from naturally occurring *(R)*-linalool (**254**).

5.3 FORMATION OF THE [3.2.2] BICYCLIC CORE

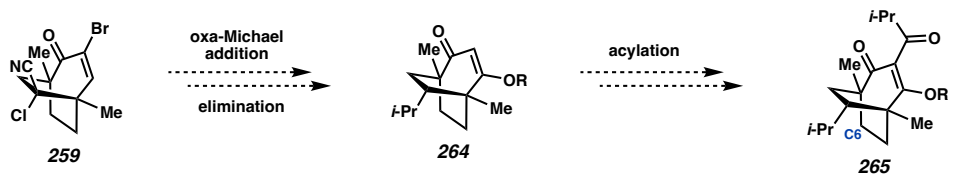
Initial assessment of the proposed route involved exploring the [4+2] cycloaddition and ring expansion sequence in a model system (Figure 5.5.A). Siloxy diene **256** was formed from enone **255**, and the subsequent [4+2] cycloaddition using ketene equivalent **257** as the dienophile proceeded smoothly with the aid of $NaHCO_3$ and butylated hydroxytoluene (BHT) as reaction additives, providing adduct **258**. We then propose the desired ring expansion can be achieved through cyclopropanation followed by ring opening to reveal

Figure 5.5. *(A) Synthesis of bicycle* ***259****. (B) Proposed ring expansion cascade. (C) Precedented interception of cationic intermediate by intramolecular nucleophiles.*



the [3.2.2] bicyclic core. We were delighted to find that using an excess of the reagents, $CHBr_3$ and NaO*t*-Bu, the ring expanded product **259** can be forged efficiently. Excitingly, we envision being able to leverage the key cationic intermediate (**260**) generated from cleavage of dibromo cyclopropanes in the ring expansion, intercepting the cation with a pendant alcohol to forge the tetrahydropyran ring (Figure 5.5.B). Previous studies have demonstrated success in similar reactions, intercepting these ring expansion cationic intermediates with intramolecular nucleophiles to form complex polycyclic structures (**263**, Figure 5.5.C).[16] Successful application of the proposed cascade would allow an efficient way to construct the complete 7/6/6/5 tetracyclic framework of hypermoin A.

Figure 5.6. *Proposed functionalization of [3.2.2] bicycle* ***259****.*

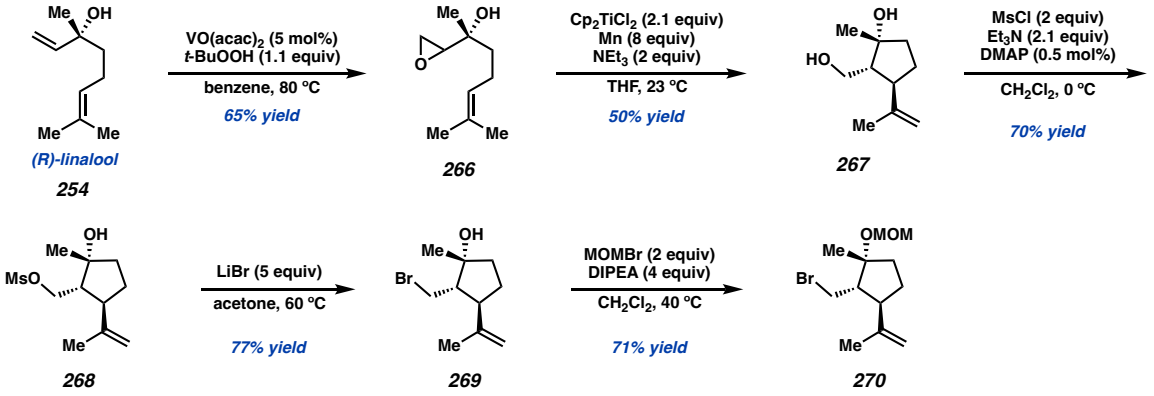


From intermediate **259**, we envision converting the α-chloro nitrile to an *i*-Pr group via a ketone intermediate, whereas the α-bromo enone can undergo oxa-Michael addition, elimination, and acylation to install the necessary functional groups on the core of hypermoin A (Figure 5.6). However, we lack a functional handle for the oxidation at the C6 position, and pre-installation of a cyclopentyl fragment (**253**) would be required to investigate the proposed ring expansion cascade.

Therefore, we aimed to explore the [4+2] cycloaddition and ring expansion sequence in a more elaborate system. We began by synthesizing cyclopentyl fragment **270** (Figure 5.7). Intermediate **267** has previously been accessed through epoxidation and radical-mediated cyclization from *(R)*-linalool (**254**).[17] The resulting primary alcohol can undergo

mesylation in 70% yield, followed by Finkelstein reaction with LiBr to forge **269**. Desired fragment **270** can then be accessed upon protection of the tertiary alcohol.

Figure 5.7. *Synthesis of cyclopentyl fragment* ***270****.*

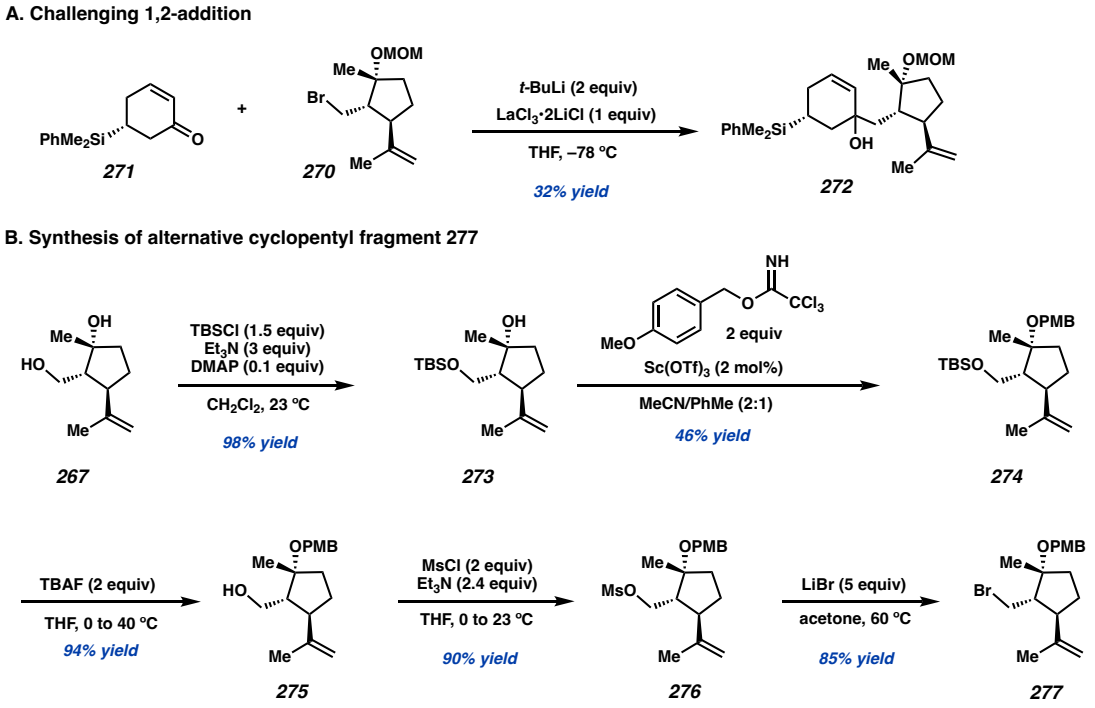


1,2-addition of **270** to chiral enone **271**[18] proved to be challenging, and we were unable to improve the yield beyond 32% despite studying different additives, varying solvents, and altering reaction temperature (Figure 5.8.A). Hypothesizing the MOM protecting group of the tertiary alcohol to be potentially problematic, we sought to examine different protecting groups. Selective silylation of the primary alcohol in intermediate **267** can be achieved in 98% yield, leaving the tertiary alcohol available for protection as a PMB ether (**274**), performed in 45% yield (Figure 5.8.B). Cleavage of the primary silyl ether was followed by the established sequence of mesylation and Finkelstein reaction to provide an analogous cyclopentyl fragment (**277**) in improved 90% and 85% yield, respectively. Optimization of the 1,2-addition using bromide **277** is underway and additional coupling strategies are also being investigated.

Despite the low yield, tertiary alcohol **272** was employed in a PDC-mediated oxidative transposition to afford enone **278** in 68% yield (Figure 5.9.A). Epoxidation of the terminal olefin was performed with the aim of protecting it from undesired cyclopropanation in the

ring expansion step later in our proposed sequence.[19] The epoxide can also serve as a functional handle for oxidative cleavage to provide the desired methyl ketone in hypermoin A. Enone **279** underwent methylation and silyl enol ether formation to furnish the requisite siloxy diene (**280**) for the proposed [4+2] cycloaddition with dienophile **257**. Unfortunately, we were unable to obtain the desired cycloadduct (**282**) but instead recovered **280**, suggesting hydrolysis of siloxy diene **281**.

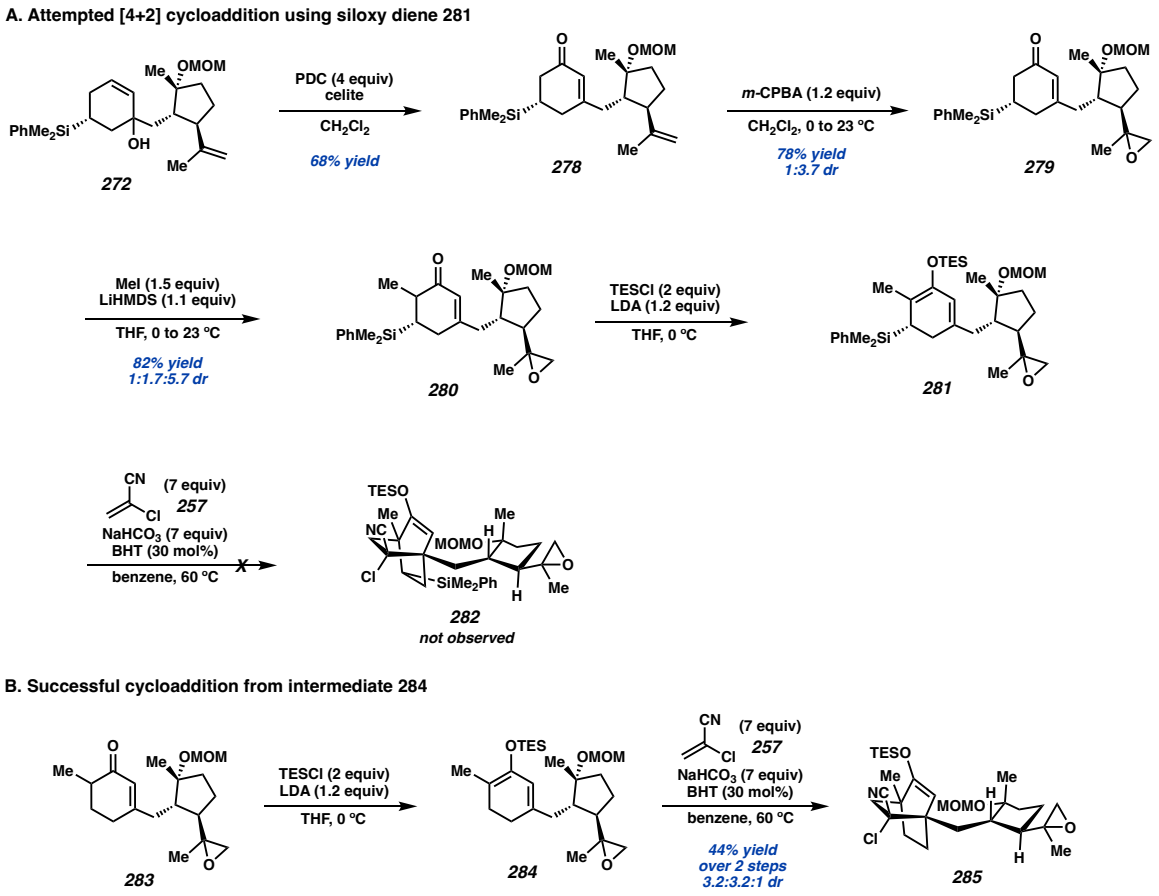
Figure 5.8. *(A) Challenging 1,2-addition to enone **271**. (B) Synthesis of PMB-protected cyclopentyl fragment **277**.*



To explore the compatibility of the diene in the cycloaddition, we performed the reaction on an analogous substrate (**283**) that does not contain the $SiMe_2Ph$ group (Figure 5.9.B). Interestingly, we were able to observe formation of the cycloadduct in 44% yield over two steps, suggesting that the $SiMe_2Ph$-incorporated substrate is likely incompatible

with the previously developed transformation. In addition, we were unable to elaborate bicyclic model **259** and install required functional groups as decomposition is observed under various reaction conditions. We attribute the undesired side reactions to the reactivity of the α-chloro nitrile moiety and decided to explore alternative dienophiles for the [4+2] cycloaddition.

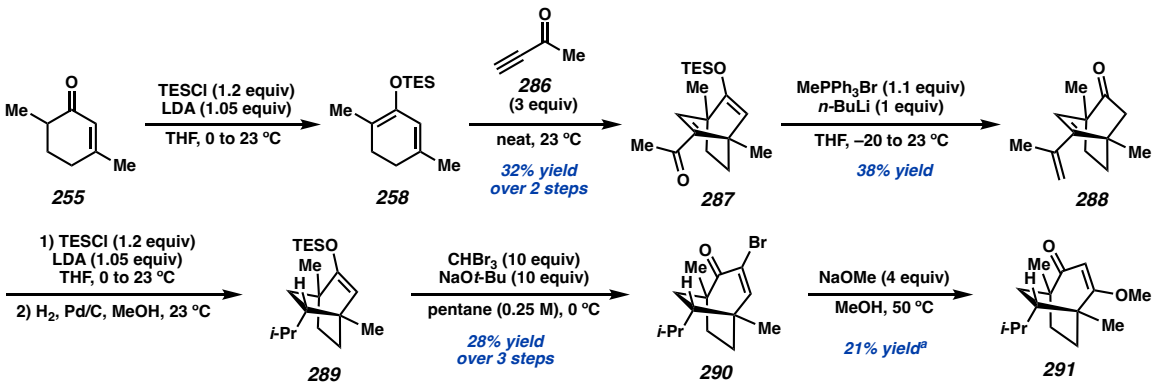
Figure 5.9. *(A) Failed attempt at [4+2] cycloaddition from substrate* ***281****. (B) Successful [4+2] reaction employing diene* ***284****.*



We sought to assess the performance of alternative dienophiles in the previously developed model system. Excitingly, ynone **286** was found to be compatible with the [4+2] reaction (Figure 5.10.B). Intermediate **287** could be further elaborated through

methylenation and selective hydrogenation to *i*-Pr incorporated **289** as a single diastereomer, with the correct stereochemistry established. It was important that the silyl enol ether be installed prior to hydrogenation to obtain the desired stereochemistry, as hydrogenation directly from ketone **288** led to a 1.5:1 mixture of diastereomers. The following ring expansion furnished the desired [3.2.2] bicycle in 28% yield over three steps, and subjection of α-bromo enone **290** to NaOMe in methanol resulted in the formation of the oxa-Michael adduct **291**.

Figure 5.10. *Cycloaddition using ynone* ***286*** *and succeeding functionalization sequence.*

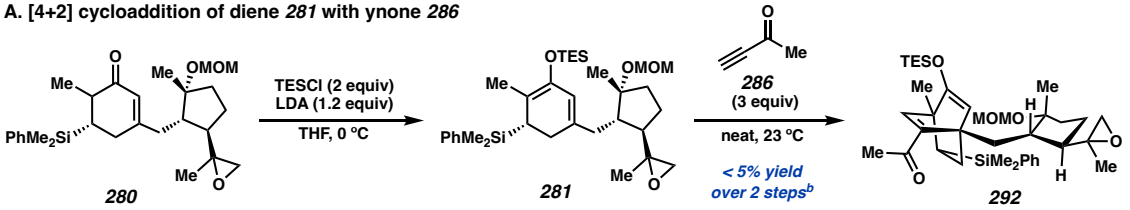


Encouraged by these results, we sought to investigate the compatibility of ynone **286** in reactions applying more elaborate substrates. Using the model system with a $SiMe_2Ph$ handle, cycloadduct **292** was observed but in extremely low yield, and significant decomposition of the siloxy diene to its enone precursor **280** was found (Figure 5.11.A). In attempt to improve this transformation, various reaction modifications were explored using a model substrate (**293**). Unfortunately, these efforts have not led to improved reaction outcome and the majority of the mass balance is attributed to recovered enone precursor and aromatization of the diene (Figure 5.11.B). We have also attempted to

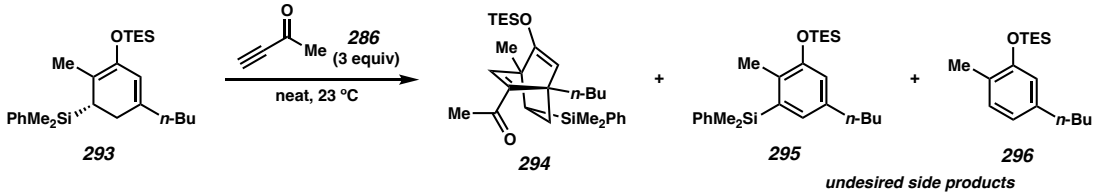
employ different oxy-substituents, including various silyl groups, acetyl, methyl, but have unfortunately either observed no formation of the desired oxy diene or observed reaction profiles without improvement.

Figure 5.11. *(A) Cycloaddition of diene* ***281*** *and ynone* ***286****. (B) Attempted optimization.*

A. [4+2] cycloaddition of diene *281* with ynone *286*



B. Optimization attempts at [4+2] cycloaddition with ynone *286*

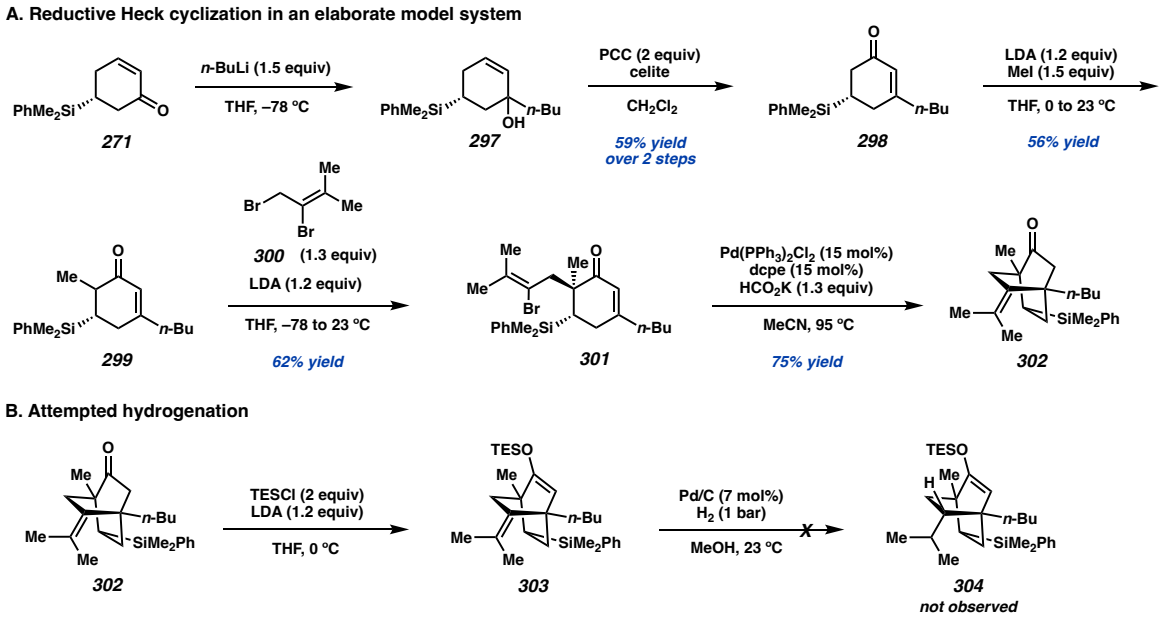


Entry	Variation to Conditions	% yield[a]	Aromatization Observed
1	none	23	trace
2	CH_2Cl_2 (1 M), 5 equiv *286*	7	Yes
3	Et_2O (1 M), 5 equiv *286*	–	Yes
4	CH_2Cl_2 (0.66 M), 5 equiv *286*, $AlCl_3$ or $BF_3{\cdot}Et_2O$ or I_2 or $TiCl_4$ (0.25 equiv)	–	No
5	10 equiv *286*, 5 equiv 2,6-lutidine	13	No
6	10 equiv *286*, 5 equiv $NaHCO_3$	19	No

Considering these challenges, we sought to develop an alternative approach to synthesizing the [2.2.2] bicycle. Model substrate **298** can be formed from enone **271** through 1,2-addition of *n*-BuLi followed by oxidative transposition (Figure 5.12.A). Methylation provides enone **299**, and subsequent treatment with LDA and prenyl dibromide **300** enabled the diastereoselective formation of vinyl bromide **301**. Subsequently, we identified that a Pd-catalyzed reductive Heck reaction can effectively form the desired [2.2.2] bicycle (**302**). We anticipated that a diastereoselective

hydrogenation of the dimethyl substituted vinylidene of silyl enol ether **303**, analogous to the previously explored strategy on model system **288**, could deliver the isopropyl group in high diastereoselectivity (Figure 5.12.B). However, the tri-substituted enol ether was reduced prior to the tetra-substituted olefin.

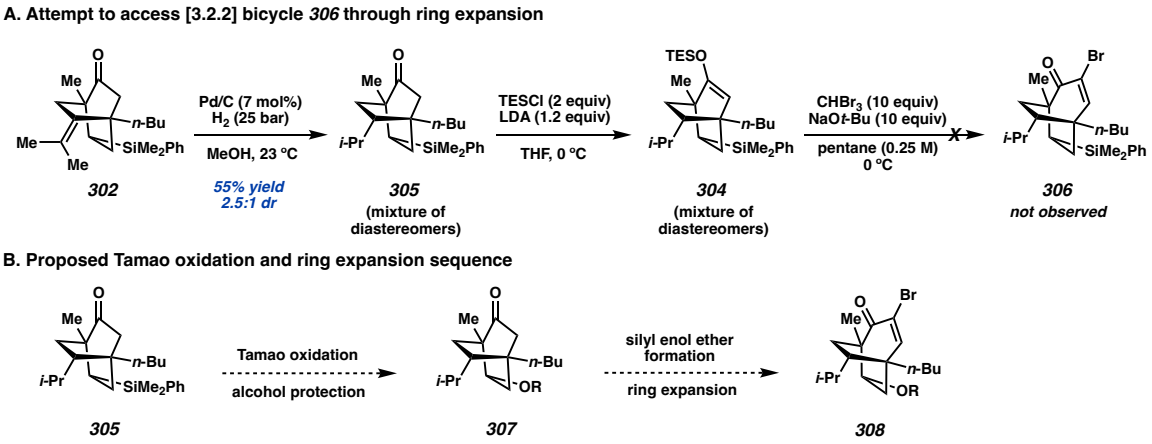
Figure 5.12. *(A) Reductive Heck cyclization as an alternative strategy for [2.2.2] bicycle formation. (B) Attempted hydrogenation to stereoselectively install isopropyl group.*



Investigations were therefore continued using ketone **302** instead, and under 25 bar pressure, the olefin can be fully reduced to the corresponding isopropyl compound **305** as a 2.5:1 mixture of diastereomers (Figure 5.13.A). Upon installation of the isopropyl group, the mixture of diastereomers (**305**) was treated with LDA and TESCl to access **304** as a mixture of diastereomers, and the proposed ring expansion was attempted. Unfortunately, formation of a [3.2.2] bicycle was not observed starting from either isopropyl compound **304** or vinylidene compound **303**. We attribute the lack of reactivity to the increased steric

hindrance of the bicyclic system, arising from the $SiMe_2Ph$ group, as the cyclopropanation–ring expansion reaction proceeded smoothly in the less congested model **289**. To approach this problem, investigations of Tamao oxidation reactions that would transform the bulky silyl group to a compact hydroxy group to reduce steric hindrance are currently underway (Figure 5.13.B).

Figure 5.13. *(A) Attempted hydrogenation and ring expansion to form* ***306****. (B) Proposed ring expansion on oxidized substrate* ***307****.*

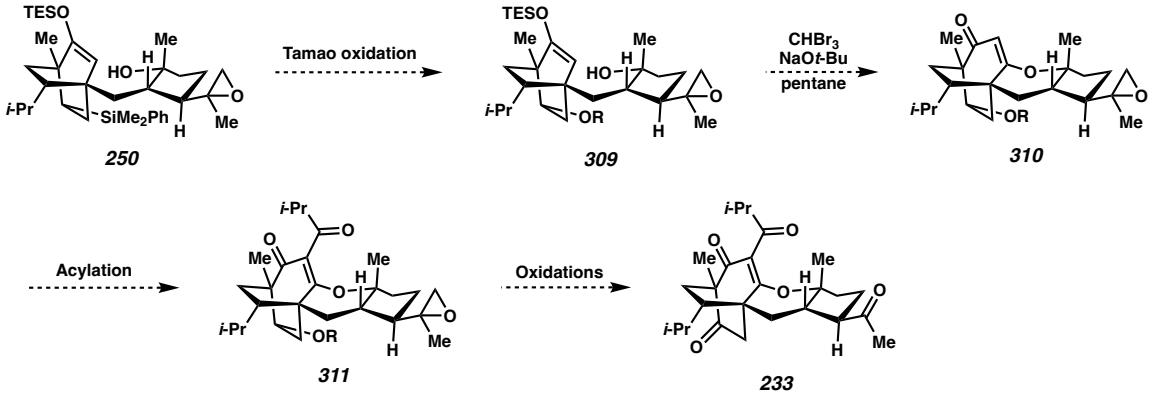


5.4 SUMMARY AND FUTURE DIRECTIONS

In summary, we have successfully developed routes to achieve a [2.2.2] bicycle, including [4+2] cycloaddition and reductive Heck cyclization, and have successfully accessed a [3.2.2] bicyclic scaffold following ring expansion in model systems. These preliminary results inform our current investigations to apply these reactions to access the bicyclic core of hypermoin A. While our first generation [4+2] cycloaddition applying ketene equivalent **257** as the dienophile and **281** as the diene led to no formation of product, we were able to identify ynone **286** as a compatible dienophile, forming a [2.2.2] bicycle

that performed efficiently in the succeeding steps in the model system. However, low yields employing diene **281** hindered further investigations of this route in more complex systems. Accordingly, we explored the reductive Heck cyclization as an alternative strategy to [2.2.2] bicycle formation and are currently working toward assessing the ring expansion reaction in this bicyclic system.

Figure 5.14. *Proposed endgame toward the synthesis of hypermoin A.*



Following successful stereoselective installation of the isopropyl moiety utilizing aforementioned strategies, we will study endgame strategies to complete the synthesis of hypermoin A (Figure 5.14). To alleviate problematic steric hindrance in the ring expansion step, we plan to perform Tamao oxidation prior to the proposed ring expansion–alcohol addition cascade. Upon construction of the tetracyclic framework, we anticipate accomplishing the synthesis through a sequence of acylation and oxidations to access hypermoin A.

5.5 EXPERIMENTAL SECTION

5.5.1 MATERIALS AND METHODS

Unless otherwise stated, reactions were performed in flame-dried glassware under a nitrogen atmosphere using dry, deoxygenated solvents. Solvents were dried by passage through an activated alumina column under argon.[20] Reaction progress was monitored by thin-layer chromatography (TLC) or Agilent 1290 UHPLC-MS. TLC was performed using E. Merck silica gel 60 F254 precoated glass plates (0.25 mm) and visualized by UV fluorescence quenching, $KMnO_4$ staining, or *p*-anisaldehyde staining. Silicycle Silia*Flash*® P60 Academic Silica gel (particle size 40–63 nm) was used for flash chromatography. Reagents were purchased from commercial sources and used as received unless otherwise stated.

^{1}H NMR spectra were recorded on a Bruker 400 MHz spectrometer and are reported relative to residual non-deuterated solvent $CHCl_3$ (δ 7.26 ppm). ^{13}C NMR spectra were recorded on a Bruker 400 MHz spectrometer (100 MHz) and are reported relative to solvent $CDCl_3$ (δ 77.16 ppm). ^{2}H NMR spectra were recorded on a Bruker 400 MHz (61 MHz) spectrometer and are reported relative to residual $CDCl_3$ (δ 7.26 ppm). Data for ^{1}H NMR are reported as follows: chemical shift (δ ppm) (multiplicity, coupling constant (Hz), integration). Multiplicities are reported as the peaks appear as follows: s = singlet, d = doublet, t = triplet, q = quartet, p = pentet, sept = septuplet, m = multiplet, br s = broad singlet, br d = broad doublet. Some reported spectra include minor impurities of water (δ 1.56 ppm), ethyl acetate (δ 4.12, 2.05, 1.26 ppm), methylene chloride (δ 5.30 ppm), acetone (δ 2.17 ppm), grease (δ 1.26, 0.86 ppm), and/or silicon grease (δ 0.07 ppm), which do not

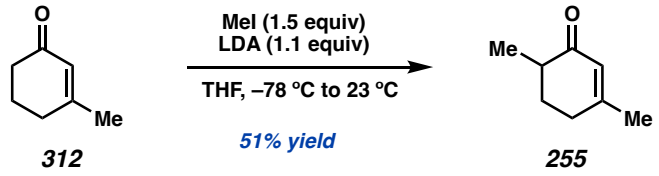
impact product assignments. Data for ^{13}C NMR are reported in terms of chemical shifts (δ ppm). ^{13}C NMR spectra of deuterated compounds are complicated by the low intensity of peaks of deuterium-substituted carbon atoms.

IR spectra were obtained by use of a Perkin Elmer Spectrum BXII spectrometer or Nicolet 6700 FTIR spectrometer using thin films deposited on NaCl plates and reported in frequency of absorption (cm^{-1}). Optical rotations were measured with a Jasco P-2000 polarimeter operating on the sodium D-line (589 nm), using a 100 mm path-length cell. High resolution mass spectra (HRMS) were obtained from the Caltech Mass Spectral Facility using a JEOL JMS-T2000GC AccuTOFTM GC-Alpha or a JEOL JMS-600H High Resolution Mass Spectrometer in field desorption (FD+) mode.

List of Abbreviations: dr – diastereomeric ratio, TLC – thin-layer chromatography.

5.5.2 EXPERIMENTAL PROCEDURES AND SPECTROSCOPIC DATA

Model System Studies: First Generation [4+2] Cycloaddition



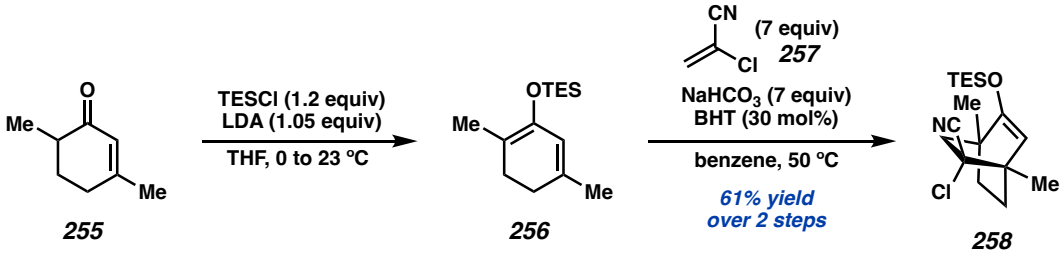
312 *255*

3,6-dimethylcyclohex-2-en-1-one (255)

A flame dried round bottom flask was charged with *i*-Pr_2NH (6.7 mL, 48 mmol, 1.2 equiv) and THF (28 mL, 1.75 M). The solution was cooled to 0 °C and *n*-BuLi (18.3 mL, 44 mmol, 1.1 equiv) was added dropwise. The resultant solution was stirred for 30 min at 0 °C. Enone **312** (4.5 mL, 40 mmol, 1.0 equiv) in THF (32 mL, 1.25 M) was added dropwise and stirring was continued at 0 °C for 30 minutes. The solution was cooled to –78 °C, and MeI (3.7 mL, 60 mmol, 1.5 equiv) was added dropwise. The reaction was gradually warmed to 23 °C.

Upon complete consumption of starting material (as determined by TLC), the reaction was diluted with a saturated solution of NH_4Cl and the product was extracted three times with EtOAc. The combined organic layers were washed with brine, dried over Na_2SO_4, filtered, and concentrated under reduced pressure. The crude product was purified by flash silica gel column chromatography (SiO_2, 5–15% EtOAc/Hexanes) to afford the corresponding methylated enone **255** as a colorless oil (2.54 g, 20.5 mmol, 51% yield).

^{1}H NMR (400 MHz, $CDCl_3$): δ 5.86 (d, *J* = 1.2 Hz, 1H), 2.45 – 2.22 (m, 3H), 2.11 – 2.02 (m, 1H), 1.95 (t, *J* = 1.1 Hz, 3H), 1.79 – 1.64 (m, 1H), 1.14 (d, *J* = 6.8 Hz, 3H).



2-chloro-1,4-dimethyl-5-((triethylsilyl)oxy)bicyclo[2.2.2]oct-5-ene-2-carbonitrile (258)

A flame dried round bottom flask was charged with *i*-Pr_2NH (5.9 mL, 42.0 mmol, 1.1 equiv) and THF (28 mL, 1.5 M). The solution was cooled to 0 ºC and *n*-BuLi (16.0 mL, 40.1 mmol, 1.05 equiv) was added dropwise. The resultant solution was stirred for 30 min at 0 ºC. Enone **255** (4.74 g, 38.2 mmol, 1.0 equiv) in THF (38 mL, 1.0 M) was added dropwise and stirring was continued at 0 ºC for 30 minutes. The solution was cooled to –78 ºC, and TESCl (7.7 mL, 45.8 mmol, 1.2 equiv) was added dropwise. The reaction was gradually warmed to 23 ºC. Upon complete consumption of starting material (as determined by TLC), the reaction was diluted with a saturated solution of NH_4Cl and the product was extracted three times with EtOAc. The combined organic layers were washed with brine, dried over

Na_2SO_4, filtered, and concentrated under reduced pressure. The crude silyloxy diene **256** was used without further purification.

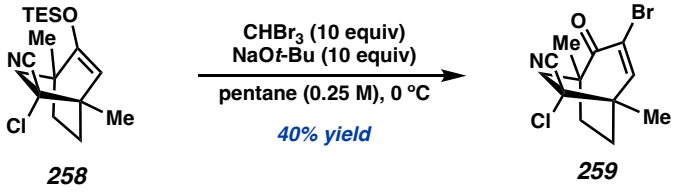
A flame dried round bottom flask was charged with crude diene **256** (9.35 g, 39.2 mmol, 1 equiv) and benzene (39.2 mL, 1.0 M) at 23 ºC. $NaHCO_3$ (23.1 g, 274 mmol, 7 equiv) and BHT (2.59 g, 11.8 mmol, 0.3 equiv) were added to the reaction mixture. Then dienophile **257** (21.9 mL, 274 mmol, 7 equiv) was added and the resulting mixture was heated to 50 ºC. Upon complete consumption of starting material (as determined by TLC), the reaction was *slowly* diluted with a saturated solution of citric acid and the product was extracted three times with EtOAc. The combined organic layers were washed with brine, dried over Na_2SO_4, filtered, and concentrated under reduced pressure. The crude product was purified by flash silica gel column chromatography (SiO_2, 0–5% EtOAc/Hexanes) to afford the corresponding bicycle **258** as a colorless oil (7.76 g, 23.8 mmol, 61% yield).

^{1}H NMR (400 MHz, $CDCl_3$): δ 4.66 (s, 1H), 2.44 (d, *J* = 14.7 Hz, 1H), 2.09 (dd, *J* = 14.7, 2.1 Hz, 1H), 1.98 – 1.85 (m, 1H), 1.52 – 1.43 (m, 3H), 1.42 (s, 3H), 1.08 (s, 3H), 0.98 (t, *J* = 7.9 Hz, 9H), 0.71 (q, *J* = 8.0 Hz, 6H).

^{13}C NMR (100 MHz, $CDCl_3$): δ 157.6, 120.3, 103.1, 63.9, 54.2, 44.5, 38.3, 33.8, 31.8, 22.0, 19.8, 6.8, 5.0.

IR (Neat Film, NaCl): 3646, 3063, 2959, 2912, 2876, 2346, 1633, 1466, 1455, 1355, 1246, 1118, 1011, 829 cm^{-1}.

HRMS (ES+): *m/z* calc'd for $C_{17}H_{28}ClNOSi$ $[M]^+$: 326.1707, found 326.1711.



258 ***259***

3-bromo-6-chloro-1,5-dimethyl-2-oxobicyclo[3.2.2]non-3-ene-6-carbonitrile (259)

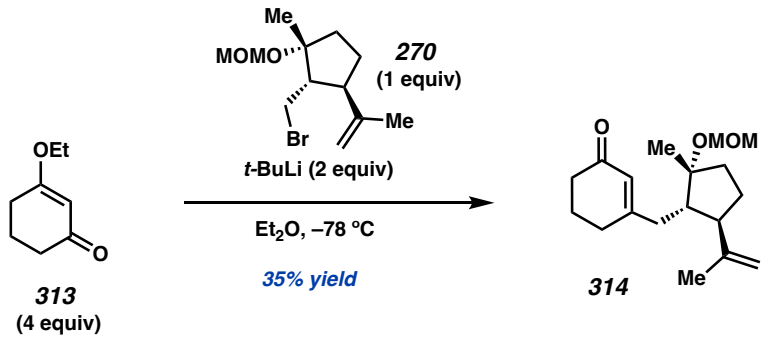
A flame dried round bottom flask was charged with silyl enol ether **258** (163 mg, 0.5 mmol, 1 equiv) and pentane (2.0 mL, 0.25 M). The resulting solution was cooled to 0 ºC and NaO*t*-Bu (480 mg, 5.0 mmol, 10 equiv) was added. Then $CHBr_3$ (0.44 mL, 5.0 mmol, 10 equiv) was added fast dropwise, rate of addition was monitored to ensure bubbling of the reaction mixture was kept to a minimum. Upon complete consumption of starting material (as determined by TLC), the reaction was *slowly* diluted with brine and the product was extracted three times with Et_2O. The combined organic layers were dried over Na_2SO_4, filtered, and concentrated under reduced pressure. The crude product was purified by flash silica gel column chromatography (SiO_2, 0–4–7% EtOAc/Hexanes) to afford α-bromo enone **259** as a white solid (60.5 mg, 0.2 mmol, 40% yield).

^{1}H NMR (400 MHz, $CDCl_3$): δ 7.18 (s, 1H), 2.75 (d, *J* = 16.0 Hz, 1H), 2.46 (dd, *J* = 15.9, 2.1 Hz, 1H), 2.17 – 1.91 (m, 3H), 1.73 – 1.67 (m, 1H), 1.65 (s, 3H), 1.30 (s, 3H).

^{13}C NMR (100 MHz, $CDCl_3$): δ 196.0, 151.5, 129.6, 118.9, 61.4, 49.0, 47.2, 46.7, 34.4, 28.0, 26.5, 25.5.

IR (Neat Film, NaCl): 3438, 2938, 2870, 2232, 1693, 1650, 1464, 1254, 850 cm^{-1}.

HRMS (FD+): *m/z* calc'd for $C_{12}H_{23}NOClBr$ $[M]^+$: 300.9869, found 300.9870.



3-(((1*S*,2*R*,5*R*)-2-(methoxymethoxy)-2-methyl-5-(prop-1-en-2 yl)cyclopentyl)methyl)cyclohex-2-en-1-one (314)

Vinylogous ester **313** (2.1 mL, 14.43 mmol, 4 equiv) was azeotroped with benzene (1 mL) 2 times and placed under high vacuum for 3 h to remove trace benzene. Alkyl bromide **270** (1.00 g, 3.61 mmol, 1 equiv, 1:4.8 ratio of *i*-Pr to isopropenyl) was azeotroped with benzene (1 mL) 2 times and placed under high vacuum for 3 h to remove trace benzene. Both vials are backfilled with N_2, then enone **313** was dissolved in Et_2O (72 mL, 0.2 M) and cooled to –78 ºC. Alkyl bromide **270** was dissolved in THF (4.5 mL, 0.8 M) and cooled to –78 ºC. *t*-BuLi (1.7 M in pentane, 4.2 mL, 2 equiv) was added dropwise and the resulting solution was stirred for 15 minutes. The alkyl Li solution was added as fast as possible via cannula to the stirring solution of **313**. Upon complete consumption of starting material (as determined by TLC), the reaction was diluted with a saturated solution of NH_4Cl and the product was extracted three times with Et_2O. The combined organic layers were washed with H_2O and brine, dried over Na_2SO_4, filtered, and concentrated under reduced pressure. The crude product was purified by flash silica gel column chromatography (SiO_2, 20% EtOAc/Hexanes) to afford enone **314** as a colorless oil (369 mg, 1.26 mmol, 35% yield,

1:5.3 ratio of *i*-Pr to isopropenyl). The mixture of *i*-Pr to isopropenyl were not separated as they can be separated during the subsequent steps.

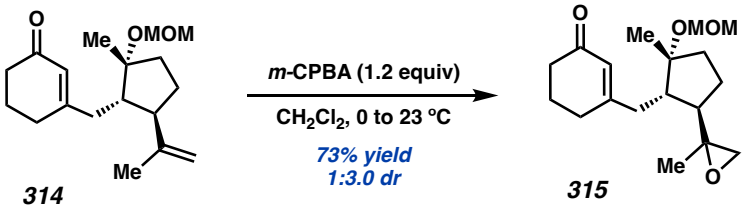
^{1}H NMR (400 MHz, $CDCl_3$): δ 5.95 (t, *J* = 1.3 Hz, 1H), 4.72 – 4.65 (m, 4H), 3.37 (s, 3H), 2.61 – 2.50 (m, 2H), 2.38 – 2.23 (m, 4H), 2.21 – 2.14 (m, 1H), 2.07 – 1.86 (m, 4H), 1.77 (ddd, *J* = 10.5, 7.0, 6.0 Hz, 1H), 1.65 (dd, *J* = 1.3, 0.8 Hz, 3H), 1.56 – 1.41 (m, 2H), 1.28 (s, 3H).

^{13}C NMR (100 MHz, $CDCl_3$): δ 199.8, 166.9, 147.3, 127.4, 111.5, 91.4, 85.4, 55.6, 52.4, 51.3, 37.4, 36.8, 36.7, 30.0, 27.9, 23.4, 22.9, 19.0.

IR (Neat Film, NaCl): 3068, 2950, 1668, 1622, 1458, 1374, 1248, 1142, 1036 cm^{-1}.

HRMS (FD+): *m/z* calc'd for $C_{18}H_{28}O_3$ $[M]^+$: 292.2033, found 292.2024.

Optical Rotation: $[\alpha]_D^{21}$ –23.2 (c 1.00, $CHCl_3$).



3-(((1S,2R,5R)-2-(methoxymethoxy)-2-methyl-5-((R)-2-methyloxiran-2-yl)cyclopentyl)methyl)cyclohex-2-en-1-one (315)

A flame dried 1 dram vial was charged with enone **314** (369 mg, 1.26 mmol, 1 equiv, 1:5.3 ratio of *i*-Pr to isopropenyl) and CH_2Cl_2 (6.3 mL, 0.2 M) and cooled to 0 ºC. *m*-CPBA (261 mg, 1.51 mmol, 1.2 equiv) was added to the reaction which was slowly warmed to 23 ºC. Upon complete consumption of starting material (as determined by TLC), the reaction was filtered over celite with CH_2Cl_2. The crude reaction mixture was diluted with approximately 1:1 $Na_2S_2O_3$ and $NaHCO_3$ solutions. The layers were separated, and the

product was extracted three times with CH_2Cl_2. The combined organic layer was washed with $NaHCO_3$ two times, washed with brine, dried over Na_2SO_4, filtered, and concentrated under reduced pressure. The crude product was purified by flash silica gel column chromatography (SiO_2, 40% EtOAc/Hexanes) to afford enone **315** as a colorless oil (284 mg, 0.92 mmol, 73% yield, 1:3.0 dr). Diastereomers are inconsequential and, therefore, are not separated.

^{1}H NMR (400 MHz, $CDCl_3$) mixture of diastereomers: δ 5.98 (t, *J* = 1.3 Hz, 0.3H, minor), 5.94 (p, *J* = 1.3 Hz, 1H, major), 4.69 – 4.61 (m, 2.7H), 3.34 (s, 4H), 2.69 – 2.47 (m, 4H), 2.41 – 2.24 (m, 6.7H), 2.08 – 1.83 (m, 6.7H), 1.81 – 1.73 (m, 0.6H, minor), 1.62 – 1.50 (m, 2.3H), 1.50 – 1.39 (m, 1.6H), 1.26 (s, 0.9H, minor), 1.26 (s, 6H, major), 1.24 (s, 0.9H, minor).

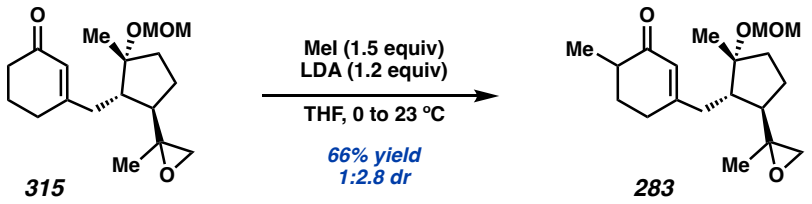
^{13}C NMR (100 MHz, $CDCl_3$) major diastereomer: δ 199.8, 166.6, 127.2, 91.4, 85.6, 58.5, 55.7, 53.1, 50.0, 49.8, 38.0, 37.5, 36.7, 29.9, 25.6, 23.1, 22.8, 19.5.

^{13}C NMR (100 MHz, $CDCl_3$) minor diastereomer: δ 199.9, 166.7, 127.2, 91.4, 85.6, 58.0, 55.7, 53.2, 50.1, 49.4, 37.5, 37.1, 36.6, 30.2, 25.3, 23.3, 22.8, 18.5.

IR (Neat Film, NaCl): 3498, 2954, 1666, 1622, 1376, 1326, 1142, 1088, 1034, 918 cm^{-1}.

HRMS (FD+): *m/z* calc'd for $C_{18}H_{28}O_4$ $[M]^+$: 308.1982, found 308.1970.

Optical Rotation: $[\alpha]_D^{21}$ –26.6 (c 1.00, $CHCl_3$).



3-(((1*S*,2*R*,5*R*)-2-(methoxymethoxy)-2-methyl-5-((*R*)-2-methyloxiran-2-yl)cyclopentyl)methyl)-6-methylcyclohex-2-en-1-one (283)

A flame dried round bottom flask was charged with *i*-Pr_2NH (0.17 mL, 1.22 mmol, 1.25 equiv) and THF (0.67 mL, 1.75 M). The solution was cooled to 0 ºC and *n*-BuLi (0.47 mL, 1.18 mmol, 1.2 equiv) was added dropwise. The resultant solution was stirred for 30 min at 0 ºC. The corresponding enone **315** (302.0 mg, 0.98 mmol, 1.0 equiv) in THF (0.78 mL, 1.25 M) was added dropwise and stirring was continued at 0 ºC for 30 minutes. MeI (0.09 mL, 1.47 mmol, 1.5 equiv) was added dropwise. The reaction was gradually warmed to 23 ºC. Upon complete consumption of starting material (as determined by TLC), the reaction was diluted with a saturated solution of NH_4Cl and the product was extracted three times with EtOAc. The combined organic layers were washed with brine, dried over Na_2SO_4, filtered, and concentrated under reduced pressure. The crude product was purified by flash silica gel column chromatography (SiO_2, 30% EtOAc/Hexanes) to afford the corresponding methylated enone **283** as a yellow oil (207 mg, 0.64 mmol, 66% yield, 1:2.8 dr). Diastereomers are inconsequential and, therefore, are not separated.

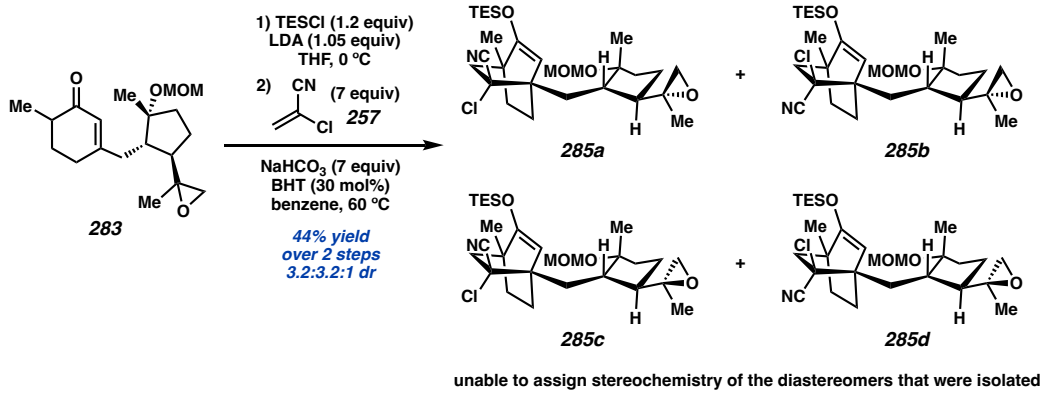
^{1}H NMR (400 MHz, $CDCl_3$) mixture of diastereomers: δ 5.96 (s, 0.3H, minor), 5.91 (s, 1H, major), 4.70 – 4.62 (m, 2.8H), 3.35 (m, 4H), 2.69 – 2.47 (m, 4H), 2.45 – 2.21 (m, 5H), 2.12 – 1.64 (m, 7H), 1.59 – 1.39 (m, 4H), 1.28 – 1.24 (m, 8H), 1.13 (d, *J* = 6.8 Hz, 4H).

^{13}C NMR (100 MHz, $CDCl_3$) mixture of diastereomers: δ 202.2, 202.2, 165.3, 126.7, 126.7, 91.4, 85.6, 85.6, 58.5, 58.5, 58.0, 55.7, 53.3, 53.2, 53.2, 50.2, 50.1, 50.1, 50.1, 49.9, 49.4, 49.4, 41.0, 40.9, 40.9, 40.8, 37.9, 37.6, 36.9, 36.7, 36.7, 31.1, 31.0, 30.9, 30.9, 30.1, 29.6, 29.4, 25.6, 25.5, 25.3, 25.2, 23.3, 23.2, 23.1, 23.1, 19.4, 18.5, 18.5, 15.2.

IR (Neat Film, NaCl): 2960, 2928, 1666, 1456, 1034 cm^{-1}.

HRMS (FD+): *m/z* calc'd for $C_{19}H_{30}O_4$ $[M]^+$: 322.2139, found 322.2127.

Optical Rotation: $[\alpha]_D^{21}$ –22.1 (c 1.00, $CHCl_3$).



(1R,4R)-2-chloro-1-(((1R,5S)-2-(methoxymethoxy)-2-methyl-5-(2-methyloxiran-2-yl)cyclopentyl)methyl)-4-methyl-5-((triethylsilyl)oxy)bicyclo[2.2.2]oct-5-ene-2-carbonitrile (285a, 285b, 285c, 285d)

A flame dried round bottom flask was charged with *i*-Pr_2NH (0.07 mL, 0.47 mmol, 1.25 equiv) and THF (0.47 mL, 1.0 M). The solution was cooled to 0 ºC and *n*-BuLi (0.18 mL, 0.45 mmol, 1.2 equiv) was added dropwise. The resultant solution was stirred for 30 min at 0 ºC. Enone **283** (120 mg, 0.37 mmol, 1.0 equiv) in THF (0.47 mL, 0.8 M) was added dropwise and stirring was continued at 23 ºC for 30 minutes. The solution was cooled to 0 ºC, and TESCl (0.13 mL, 0.74 mmol, 2 equiv) was added dropwise. Upon complete consumption of starting material (as determined by TLC), the reaction was diluted with a saturated solution of NH_4Cl and the product was extracted three times with EtOAc. The

combined organic layers were washed with brine, dried over Na_2SO_4, filtered, and concentrated under reduced pressure. The crude silyloxy diene was used without further purification.

A flame dried round bottom flask was charged with crude diene (162 mg, 0.37 mmol, 1 equiv) and benzene (0.37 mL, 1.0 M) at 23 ºC. $NaHCO_3$ (219 mg, 2.6 mmol, 7 equiv) and BHT (24.6 mg, 0.11 mmol, 0.3 equiv) were added to the reaction mixture. Then dienophile **257** (0.21 mL, 2.6 mmol, 7 equiv) was added and the resulting mixture was heated to 60 ºC. Upon complete consumption of starting material (as determined by TLC), the reaction was *slowly* diluted with a saturated solution of citric acid and the product was extracted three times with EtOAc. The combined organic layers were washed with brine, dried over Na_2SO_4, filtered, and concentrated under reduced pressure. The crude product was purified by flash silica gel column chromatography (SiO_2, 0–5–10–15–50% EtOAc/Hexanes) to afford the corresponding bicycle **285-d1**, **285-d2**, and **285-d3** as colorless oils (88.1 mg, 0.17 mmol, 44% yield, 3.2:3.2:1 dr (d1:d2:d3)). Stereochemistry of the diastereomers was not able to be assigned.

Diastereomer 1 (285-d1):

^{1}H NMR (600 MHz, $CDCl_3$): δ 4.77 (s, 1H), 4.73 – 4.68 (m, 2H), 3.40 (s, 3H), 2.80 (d, *J* = 4.7 Hz, 1H), 2.67 (d, *J* = 4.7 Hz, 1H), 2.47 (d, *J* = 14.7 Hz, 1H), 2.36 (dd, *J* = 15.2, 5.1 Hz, 1H), 2.11 (dd, *J* = 14.6, 3.2 Hz, 1H), 2.05 – 1.91 (m, 3H), 1.87 – 1.76 (m, 2H), 1.68 – 1.61 (m, 2H), 1.56 – 1.41 (m, 4H), 1.35 (s, 3H), 1.30 (s, 3H), 1.08 (s, 3H), 0.98 (t, *J* = 8.0 Hz, 9H), 0.71 (q, *J* = 7.9 Hz, 6H).

^{13}C NMR (151 MHz, $CDCl_3$): δ 158.2, 120.4, 101.5, 91.4, 85.5, 65.3, 58.1, 55.9, 54.5, 53.9, 53.9, 48.4, 48.0, 38.2, 37.1, 34.2, 33.9, 29.5, 25.3, 24.2, 19.9, 18.0, 6.8, 5.0.

IR (Neat Film, NaCl): 3504, 2958, 2878, 2358, 1734, 1628, 1460, 1282, 1038, 750 cm^{-1}.

HRMS (FD+): *m/z* calc'd for $C_{28}H_{46}ClNO_4Si$ $[M]^+$: 523.2879, found 523.2889.

Optical Rotation: $[\alpha]_D^{21}$ –5.9 (c 0.8, $CHCl_3$).

Diastereomer 2 (285-d2):

^{1}H NMR (400 MHz, $CDCl_3$): δ 4.93 (s, 1H), 4.74 – 4.68 (m, 2H), 3.39 (s, 3H), 2.82 – 2.74 (m, 2H), 2.64 (d, *J* = 4.6 Hz, 1H), 2.47 (d, *J* = 14.7 Hz, 1H), 2.14 – 1.91 (m, 3H), 1.79 (td, *J* = 9.5, 6.2 Hz, 1H), 1.67 (dqq, *J* = 14.0, 6.6, 3.2 Hz, 3H), 1.54 – 1.40 (m, 5H), 1.35 (s, 3H), 1.27 (d, *J* = 0.6 Hz, 3H), 1.09 (s, 3H), 0.98 (t, *J* = 7.9 Hz, 9H), 0.76 – 0.65 (m, 6H).

^{13}C NMR (100 MHz, $CDCl_3$): δ 157.8, 120.4, 101.4, 91.3, 86.1, 65.1, 58.1, 55.8, 55.2, 54.5, 53.6, 48.9, 47.9, 38.1, 37.0, 34.0, 33.7, 29.0, 25.2, 23.8, 19.8, 17.5, 6.8, 5.0.

IR (Neat Film, NaCl): 3466, 2958, 2930, 2878, 2358, 2342, 1734, 1632, 1460, 1036, 828 cm^{-1}.

HRMS (FD+): *m/z* calc'd for $C_{28}H_{46}ClNO_4Si$ $[M]^+$: 523.2879, found 523.2888.

Optical Rotation: $[\alpha]_D^{21}$ –13.7 (c 0.33, $CHCl_3$).

Diastereomer 3 (285-d3):

^{1}H NMR (600 MHz, $CDCl_3$): δ 5.21 (s, 1H), 4.73 – 4.67 (m, 2H), 3.40 (s, 3H), 2.52 (s, 2H), 2.47 (d, *J* = 14.6 Hz, 1H), 2.31 (dd, *J* = 15.2, 4.8 Hz, 1H), 2.18 (dd, *J* = 15.2, 3.5 Hz, 1H), 2.10 (dd, *J* = 14.8, 3.1 Hz, 1H), 2.00 – 1.87 (m, 2H), 1.86 – 1.77 (m, 2H), 1.72 – 1.64 (m, 2H), 1.53 – 1.42 (m, 4H), 1.32 (s, 3H), 1.31 (s, 3H), 1.08 (s, 3H), 0.96 (t, *J* = 7.9 Hz, 9H), 0.74 (q, *J* = 8.0 Hz, 6H).

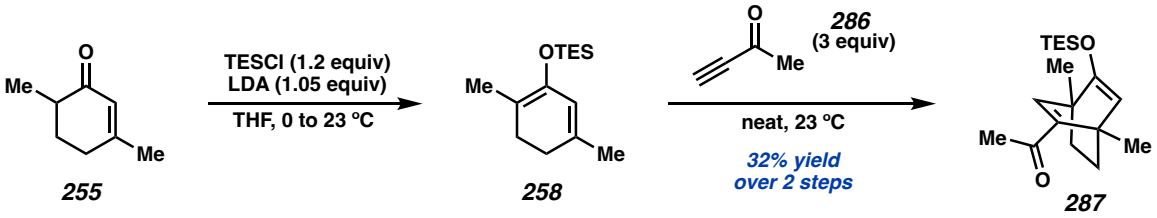
^{13}C NMR (151 MHz, $CDCl_3$): δ 157.7, 120.8, 102.1, 91.3, 86.3, 65.2, 58.1, 55.8, 54.7, 53.7, 53.3, 48.0, 47.6, 38.0, 36.7, 34.0, 34.0, 29.2, 26.0, 23.7, 20.0, 17.6, 7.2, 6.8, 6.3, 4.7.

IR (Neat Film, NaCl): 3482, 2956, 2928, 2878, 2360, 1730, 1630, 1458, 1378, 1088, 1038, 740 cm^{-1}.

HRMS (FD+): *m/z* calc'd for $C_{28}H_{46}ClNO_4Si$ $[M]^+$: 523.2879, found 523.2878.

Optical Rotation: $[\alpha]_D^{21}$ –5.8 (c 0.23, $CHCl_3$).

Model System Studies: Second Generation [4+2] Cycloaddition



1-(1,4-dimethyl-5-((triethylsilyl)oxy)bicyclo[2.2.2]octa-2,5-dien-2-yl)ethan-1-one (287)

A flame dried round bottom flask was charged with *i*-Pr_2NH (1.33 mL, 9.5 mmol, 1.1 equiv) and THF (5.7 mL, 1.6 M). The solution was cooled to 0 ºC and *n*-BuLi (3.6 mL, 9.0 mmol, 1.05 equiv) was added dropwise. The resultant solution was stirred for 30 min at 0 ºC. Enone **255** (1.07 g, 8.6 mmol, 1.0 equiv) in THF (8.1 mL, 1 M) was added dropwise and stirring was continued at 0 ºC for 30 minutes. The solution was cooled to –78 ºC, and TESCl (1.7 mL, 10.3 mmol, 1.2 equiv) was added dropwise. Upon complete consumption of starting material (as determined by TLC), the reaction was diluted with a saturated solution of NH_4Cl and the product was extracted three times with EtOAc. The combined organic layers were washed with brine, dried over Na_2SO_4, filtered, and concentrated under reduced pressure. The crude silyl oxy diene **258** was used without further purification.

A flame dried vial was charged with crude diene **258** (1 g, 4.2 mmol, 1 equiv) and 3-butyn-2-one (**286**) (1 mL, 12.8 mmol, 3 equiv) at 23 ºC and the resulting mixture was stirred at 23 ºC overnight. Upon complete consumption of starting material (as determined by TLC),

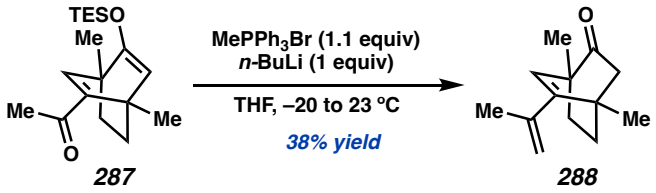
the crude product was directly purified by flash silica gel column chromatography (SiO_2, 0–5% EtOAc/Hexanes) to afford the corresponding bicycle **287** as a pale yellow oil (412.6 mg, 1.4 mmol, 32% yield).

^{1}H NMR (400 MHz, $CDCl_3$): δ 6.80 (s, 1H), 4.82 (s, 1H), 2.20 (s, 3H), 1.65 (s, 3H), 1.59 – 1.48 (m, 1H), 1.41 (s, 3H), 1.37 – 1.32 (m, 1H), 1.32 – 1.25 (m, 1H), 0.95 (t, J = 7.9 Hz, 9H), 0.71 – 0.54 (q, 6H, J = 8.3 Hz).

^{13}C NMR (100 MHz, $CDCl_3$): δ 197.7, 159.4, 152.1, 150.8, 111.2, 45.4, 43.7, 37.3, 35.5, 28.0, 22.5, 18.6, 6.8, 5.0.

IR (Neat Film, NaCl): 2932, 2870, 1724, 1676, 1596, 1450, 1366, 1254, 1196, 1080, 682 cm^{-1}.

HRMS: Mass not detected.



287 ***288***

1,4-dimethyl-5-(prop-1-en-2-yl)bicyclo[2.2.2]oct-5-en-2-one (288)

A flame dried vial was charged with $MePPh_3Br$ (64.3 mg, 0.18 mmol, 1.1 equiv) and THF (1.6 mL, 1 M). The solution was cooled to –20 ºC and *n*-BuLi (0.07 mL, 0.16 mmol, 1 equiv) was added dropwise. The resultant solution was stirred for 5 min at –20 ºC, and this solution was added dropwise to a solution of enone **287** (50 mg, 0.16 mmol, 1.0 equiv) in THF (0.5 mL, 0.33 M) at –20 ºC. The reaction mixture was warmed gradually to 23 ºC. Upon complete consumption of starting material (as determined by TLC), the reaction was diluted with water and the product was extracted three times with Et_2O. The combined

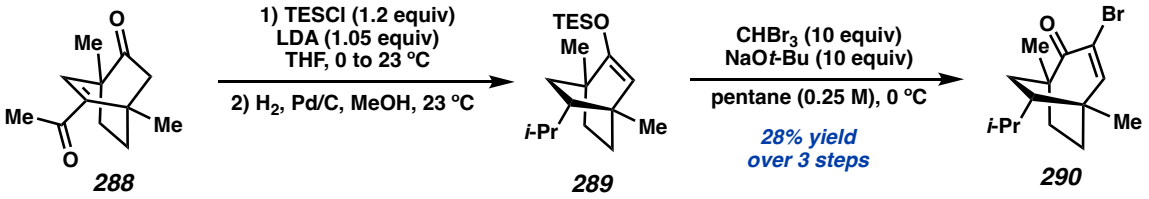
organic layers were washed with brine, dried over Na_2SO_4, filtered, and concentrated under reduced pressure. The crude product was purified by flash silica gel column chromatography (SiO_2, 0–5% EtOAc/Hexanes) to afford the corresponding bicycle **288** as a colorless oil (12 mg, 0.06 mmol, 38% yield).

^{1}H NMR (400 MHz, $CDCl_3$): δ 5.59 (s, 1H), 4.88 (dt, *J* = 3.0, 1.5 Hz, 1H), 4.69 (dq, *J* = 1.7, 0.8 Hz, 1H), 2.04 (dd, *J* = 18.2, 2.3 Hz, 1H), 1.95 (d, *J* = 18.2 Hz, 1H), 1.85 (dd, *J* = 1.6, 0.9 Hz, 3H), 1.74 – 1.67 (m, 1H), 1.62 (dd, *J* = 10.2, 2.6 Hz, 1H), 1.57 (d, *J* = 6.0 Hz, 1H), 1.54 – 1.51 (m, 1H), 1.27 (s, 3H), 1.21 (s, 3H).

^{13}C NMR (100 MHz, $CDCl_3$): δ 213.6, 154.5, 144.0, 128.0, 113.9, 49.7, 48.3, 40.0, 35.1, 31.8, 24.0, 22.7, 17.8.

IR (Neat Film, NaCl): 2950, 2876, 2344, 1700, 1672, 1452, 1416, 1186, 1120, 1006, 724 cm^{-1}.

HRMS (FI+): *m/z* calc'd for $C_{13}H_{18}O$ $[M]^+$: 190.1352, found 190.13614.



3-bromo-6-isopropyl-1,5-dimethylbicyclo[3.2.2]non-3-en-2-one (290)

A flame dried vial was charged with *i*-Pr_2NH (0.03 mL, 0.22 mmol, 1.1 equiv) and THF (0.12 mL, 1.8 M). The solution was cooled to 0 ºC and *n*-BuLi (0.082 mL, 0.21 mmol, 1.05 equiv) was added dropwise. The resultant solution was stirred for 30 min at 0 ºC. Ketone **288** (37.6 mg, 0.2 mmol, 1.0 equiv) in THF (0.2 mL, 1.0 M) was added dropwise and stirring was continued at 0 ºC for 30 minutes. The solution was cooled to –78 ºC, and

TESCl (0.04 mL, 0.24 mmol, 1.2 equiv) was added dropwise. The reaction was gradually warmed to 23 ºC. Upon complete consumption of starting material (as determined by TLC), the reaction was diluted with a saturated solution of NH_4Cl and the product was extracted three times with EtOAc. The combined organic layers were washed with brine, dried over Na_2SO_4, filtered, and concentrated under reduced pressure. The crude silyl enol ether was used without further purification.

A flame dried vial was charged with silyl enol ether (22 mg, 0.072 mmol, 1 equiv) and Pd/C (2.0 mg,10 wt%). The vial was evacuated and backfilled with H_2, and MeOH (1.2 mL, 0.06 M) was added. The reaction mixture was stirred vigorously at 23 ºC. Upon complete consumption of starting material (as determined by TLC), the reaction was filtered through a short plug of celite and concentrated under reduced pressure. The crude isopropyl compound **289** was used without further purification.

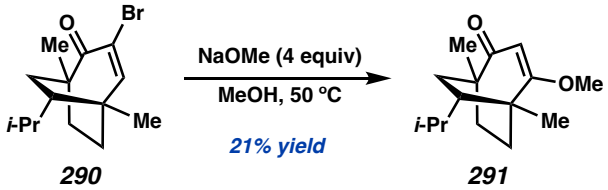
A vial was charged with silyl enol ether **289** (0.072 mmol, 1 equiv) and pentane (0.35 mL, 0.25 M). The resulting solution was cooled to 0 ºC and NaO*t*-Bu (69 mg, 0.72 mmol, 10 equiv) was added. Then $CHBr_3$ (0.067 mL, 0.72 mmol, 10 equiv) was added fast dropwise. The reaction mixture was then stirred at 23 ºC. Upon complete consumption of starting material (as determined by TLC), the reaction was diluted with brine and the product was extracted three times with Et_2O. The combined organic layers were dried over Na_2SO_4, filtered, and concentrated under reduced pressure. The crude product was purified by flash silica gel column chromatography (SiO_2, 0–5% EtOAc/Hexanes) to afford α-bromo enone **290** as a colorless oil (5.7 mg, 0.02 mmol, 28% yield).

^{1}H NMR (400 MHz, $CDCl_3$): δ 7.27 (s, 1H), 2.06 (dtq, *J* = 10.1, 7.0, 3.5 Hz, 1H), 1.79 – 1.70 (m, 1H), 1.70 – 1.58 (m, 3H), 1.57 – 1.51 (m, 1H), 1.50 – 1.43 (m, 1H), 1.38 (m, 1H), 1.23 (s, 3H), 1.23 (s, 3H), 0.86 (d, *J* = 7.0 Hz, 3H), 0.69 (d, *J* = 6.8 Hz, 3H).

^{13}C NMR (100 MHz, $CDCl_3$): δ 199.0, 159.0, 126.3, 47.8, 47.2, 42.1, 39.0, 30.2, 29.3, 27.7, 27.2, 27.0, 21.4, 17.3.

IR (Neat Film, NaCl): 2960, 2932, 2868, 1680, 1464, 1372, 1068, 850 cm^{-1}.

HRMS (FI+): *m/z* calc'd for $C_{14}H_{21}OBr$ $[M]^+$: 284.0770, found 284.0771.



290 ***291***

1-(1,4-dimethyl-5-((triethylsilyl)oxy)bicyclo[2.2.2]octa-2,5-dien-2-yl)ethan-1-one (291)

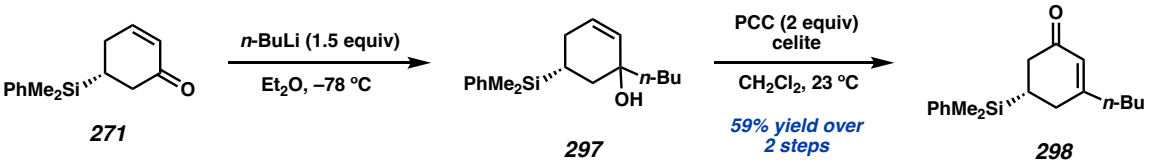
A flame dried vial was charged with α-bromo enone **290** (5.8 mg, 0.02 mmol, 1 equiv), sodium methoxide (4.4 mg, 0.08 mmol, 4 equiv), and methanol (1 mL, 0.02 M) and the resulting mixture was stirred at reflux overnight. The crude product was diluted with water, and the product was extracted three times with EtOAc. The combined organic layers were further washed with water and brine, dried over Na_2SO_4, filtered, and concentrated under reduced pressure. The crude product was purified by flash silica gel column chromatography (SiO_2, 0–10% EtOAc/Hexanes) to afford the corresponding β-methoxy enone **291** as a colorless oil (1.0 mg, 0.004 mmol, 21% yield).

^{1}H NMR (400 MHz, $CDCl_3$): δ 5.60 (s, 1H), 3.58 (s, 3H), 2.13 – 2.03 (m, 1H), 1.70 – 1.66 (m, 1H), 1.63 (dd, *J* = 10.4, 7.5 Hz, 1H), 1.54 – 1.47 (m, 1H), 1.45 (d, *J* = 11.7 Hz,

1H), 1.41 – 1.34 (m, 1H), 1.24 (s, 3H), 1.20 (s, 3H), 1.18 – 1.14 (m, 1H), 1.03 (d, J = 10.7 Hz, 1H), 0.86 (d, J = 6.9 Hz, 3H), 0.70 (d, J = 6.9 Hz, 3H).

^{13}C NMR (100 MHz, $CDCl_3$): δ 201.3, 152.7, 126.0, 55.3, 47.1, 46.5, 40.3, 37.8, 30.6, 29.5, 28.9, 27.3, 26.6, 21.8, 17.2.

IR (Neat Film, NaCl): 3516, 2937, 1681, 1463, 1109, 845 cm^{-1}.



(*S*)-3-butyl-5-(dimethyl(phenyl)silyl)cyclohex-2-en-1-one (298)

A round bottom flask was charged with chiral enone **271**[18] (1.00 g, 4.34 mmol, 1 equiv) and Et_2O (10.0 mL, 0.43 M) and cooled to –78 ºC. *n*-BuLi (2.6 mL, 6.51 mmol, 1.5 equiv) was added dropwise. Upon complete consumption of starting material (as determined by TLC), the reaction was diluted with H_2O and the product was extracted three times with Et_2O. The combined organic layers were washed with brine, dried over Na_2SO_4, filtered, and concentrated under reduced pressure. The crude allylic alcohol **297** was used without further purification.

A round bottom flask open to air was charged with celite and CH_2Cl_2 (17 mL, 0.25 M). PCC (1.87 g, 8.68 mmol, 2 equiv) was added to the slurry and stirred until the PCC is evenly dispersed. Crude allylic alcohol **297** was added to the mixture using minimal CH_2Cl_2 to transfer. Upon complete consumption of starting material (as determined by TLC), the reaction was filtered over celite with Et_2O. The crude reaction mixture was washed with 1 M NaOH, 1 M HCl, saturated $NaHCO_3$ x3, and brine. The organic layer was dried over Na_2SO_4, filtered, and concentrated under reduced pressure. The crude

product was purified by flash silica gel column chromatography (SiO_2, 10% EtOAc/Hexanes) to afford enone **298** as a colorless oil (734 mg, 2.56 mmol, 59% yield).

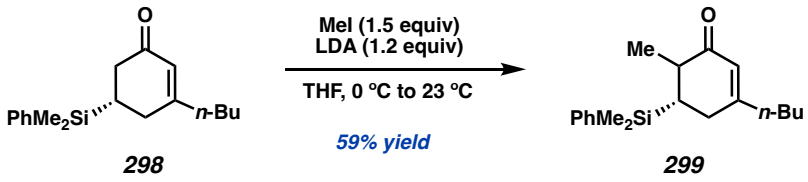
^{1}H NMR (400 MHz, $CDCl_3$): δ 7.34 – 7.27 (m, 2H), 7.24 – 7.16 (m, 3H), 5.64 (d, J = 1.1 Hz, 1H), 2.24 – 2.17 (m, 1H), 2.00 – 1.86 (m, 5H), 1.47 – 1.20 (m, 4H), 1.18 – 1.07 (m, 2H), 0.72 (t, J = 7.2 Hz, 3H), 0.15 (s, 3H), 0.15 (s, 3H).

^{13}C NMR (100 MHz, $CDCl_3$): δ 200.3, 167.5, 136.4, 134.1, 129.5, 128.1, 125.1, 38.1, 37.7, 31.0, 29.2, 23.0, 22.5, 14.0, -5.1, -5.2.

IR (Neat Film, NaCl): 2956, 2932, 2870, 2358, 1670, 1628, 1426, 1252, 1112, 816, 774 cm^{-1}.

HRMS (FD+): *m/z* calc'd for $C_{18}H_{26}OSi$ $[M]^+$: 286.1747, found 286.1756.

Optical Rotation: $[\alpha]_D^{21}$ –36.7 (c 1.00, $CHCl_3$).



298 ***299***

(5S)-3-butyl-5-(dimethyl(phenyl)silyl)-6-methylcyclohex-2-en-1-one (299)

A flame dried round bottom flask was charged with *i*-Pr_2NH (0.44 mL, 3.16 mmol, 1.25 equiv) and THF (1.8 mL, 1.75 M). The solution was cooled to 0 ºC and *n*-BuLi (1.2 mL, 3.04 mmol, 1.2 equiv) was added dropwise. The resultant solution was stirred for 30 min at 0 ºC. The corresponding enone **298** (725 mg, 2.53 mmol, 1.0 equiv) in THF (2.0 mL, 1.25 M) was added dropwise and stirring was continued at 0 ºC for 30 minutes. MeI (0.24 mL, 3.80 mmol, 1.5 equiv) was added dropwise. The reaction was gradually warmed to 23 ºC. Upon complete consumption of starting material (as determined by TLC), the reaction

was diluted with a saturated solution of NH_4Cl and the product was extracted three times with EtOAc. The combined organic layers were washed with brine, dried over Na_2SO_4, filtered, and concentrated under reduced pressure. The crude product was purified by flash silica gel column chromatography (SiO_2, 5% EtOAc/Hexanes) to afford the corresponding methylated enone **299** as a colorless oil (451 mg, 1.50 mmol, 59% yield).

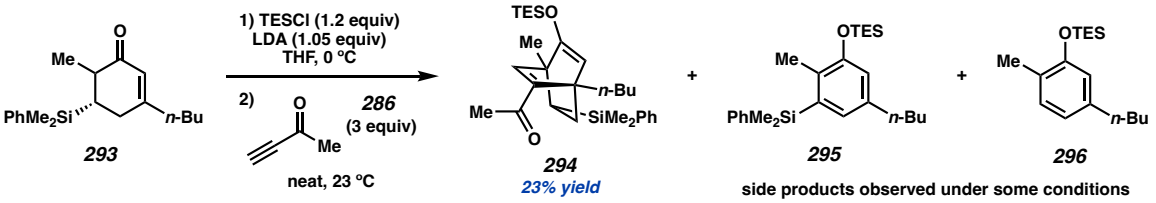
^{1}H NMR (400 MHz, $CDCl_3$): δ 7.50 – 7.46 (m, 2H), 7.39 – 7.33 (m, 3H), 5.78 (p, *J* = 1.4 Hz, 1H), 2.37 – 2.27 (m, 2H), 2.24 – 2.14 (m, 1H), 2.10 (t, *J* = 7.8 Hz, 2H), 1.47 – 1.37 (m, 3H), 1.35 – 1.24 (m, 2H), 1.13 (d, *J* = 7.0 Hz, 3H), 0.90 (t, *J* = 7.3 Hz, 3H), 0.34 (s, 3H), 0.32 (s, 3H).

^{13}C NMR (100 MHz, $CDCl_3$): δ 202.6, 165.4, 137.8, 133.9, 129.3, 128.1, 124.6, 42.0, 37.5, 30.4, 29.2, 28.9, 22.5, 16.6, 14.0, -3.2, -3.5.

IR (Neat Film, NaCl): 2958, 2930, 2860, 2358, 1668, 1426, 1252, 1112, 814 cm^{-1}.

HRMS (FD+): *m/z* calc'd for $C_{19}H_{28}OSi$ $[M]^+$: 300.1904, found 300.1900.

Optical Rotation: $[\alpha]_D^{21}$ –57.4 (c 1.00, $CHCl_3$).



1-((1*S*,8*R*)-1-butyl-8-(dimethyl(phenyl)silyl)-4-methyl-5-((triethylsilyl)oxy)bicyclo[2.2.2]octa-2,5-dien-2-yl)ethan-1-one (294)

A flame dried vial was charged with *i*-Pr_2NH (0.04 mL, 0.31 mmol, 1.25 equiv) and THF (0.15 mL, 2.0 M). The solution was cooled to 0 ºC and *n*-BuLi (0.12 mL, 0.30 mmol, 1.2 equiv) was added dropwise. The resultant solution was stirred for 30 min at 0 ºC. Enone **293** (74.9 mg, 0.25 mmol, 1.0 equiv) in THF (0.25 mL, 1.0 M) was added dropwise and

stirring was continued at 0 ºC for 30 minutes. The solution was cooled to –78 ºC and TESCl (0.05 mL, 0.30 mmol, 1.2 equiv) was added dropwise. The reaction was gradually warmed to 23 ºC. Upon complete consumption of starting material (as determined by TLC), the reaction was diluted with a saturated solution of NH_4Cl and the product was extracted three times with EtOAc. The combined organic layers were washed with brine, dried over Na_2SO_4, filtered, and concentrated under reduced pressure.

The crude diene (20.7 mg, 0.05 mmol, 1 equiv) was transferred to a vial and was placed under high vacuum to remove trace solvent and then backfilled with N_2. Dienophile **286** (12 μL, 0.15 mmol, 3 equiv) was added and the mixture was stirred neat at 23 ºC. Upon complete consumption of starting material (as determined by TLC), the reaction mixture was loaded directly onto silica for flash silica gel column chromatography (SiO_2, 0–2.5–5% EtOAc/Hexanes) to afford product **294** (5.4 mg, 0.012 mmol, 23% yield). Aromatization side products **295** and **296** were observed under some reaction conditions tested (see Table 3.1).

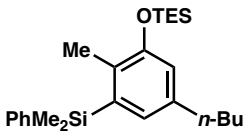
^{1}H NMR (400 MHz, $CDCl_3$): δ 7.53 – 7.47 (m, 2H), 7.36 (dd, *J* = 5.1, 1.9 Hz, 3H), 6.81 (s, 1H), 4.98 (s, 1H), 2.45 (ddd, *J* = 13.1, 11.3, 4.2 Hz, 1H), 2.24 (s, 3H), 1.69 – 1.53 (m, 2H), 1.46 – 1.33 (m, 5H), 1.29 (s, 3H), 1.05 (dd, *J* = 10.3, 3.9 Hz, 1H), 1.01 (t, *J* = 7.9 Hz, 9H), 0.96 (t, *J* = 7.2 Hz, 3H), 0.70 (m, 6H), 0.38 (s, 3H), 0.27 (s, 3H).

^{13}C NMR (100 MHz, $CDCl_3$): δ 199.2, 157.2, 154.6, 148.8, 140.5, 133.7, 128.7, 127.7, 109.9, 49.2, 47.0, 40.7, 34.3, 33.7, 29.2, 28.2, 25.9, 23.7, 19.7, 14.3, 6.8, 5.0, -2.9, -3.5.

IR (Neat Film, NaCl): 3066, 2956, 2926, 2876, 1670, 1646, 1492, 1358, 1252, 1208, 1110 cm^{-1}.

HRMS (FD+): *m/z* calc'd for $C_{29}H_{46}O_2Si_2$ $[M]^+$: 482.3031, found 482.3046.

Optical Rotation: $[\alpha]_D^{21}$ 28.3 (c 1.00, $CHCl_3$).



295

(5-butyl-2-methyl-3-((triethylsilyl)oxy)phenyl)dimethyl(phenyl)silane (295)

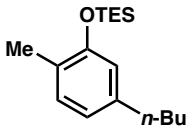
Tentative assignment. Suspected mixture of rotamers.

^{1}H NMR (400 MHz, $CDCl_3$): δ 7.47 (ddd, J = 6.2, 3.4, 2.0 Hz, 2H), 7.34 – 7.29 (m, 3H), 6.91 (d, J = 1.8 Hz, 1H), 6.67 (d, J = 1.7 Hz, 1H), 2.56 – 2.50 (m, 2H), 2.07 (s, 3H), 1.62 – 1.51 (m, 2H), 1.41 – 1.31 (m, 2H), 1.01 – 0.96 (m, 9H), 0.93 (t, J = 7.3 Hz, 3H), 0.79 – 0.70 (m, 6H), 0.55 (s, 6H).

^{13}C NMR (100 MHz, $CDCl_3$): δ 154.6, 141.4, 140.5, 139.1, 138.4, 135.0, 135.0, 132.5, 129.7, 129.7, 129.2, 128.7, 128.6, 121.0, 119.7, 36.7, 36.3, 35.1, 34.6, 23.6, 23.4, 17.5, 17.2, 15.0, 14.9, 7.7, 7.7, 6.4, 6.4, 0.4, -0.0. Additional peaks due to suspected mixture of rotamers.

IR (Neat Film, NaCl): 3066, 3046, 2956, 2930, 2876, 1562, 1458, 1410, 1282, 1248, 1142, 812, 776, 730 cm^{-1}.

HRMS (FD+): *m/z* calc'd for $C_{25}H_{40}OSi_2$ $[M]^+$: 412.2612, found 412.2612.



296

(5-butyl-2-methylphenoxy)triethylsilane (296)

^{1}H NMR (400 MHz, $CDCl_3$): δ 7.01 (dd, *J* = 7.6, 0.8 Hz, 1H), 6.67 (dd, *J* = 7.6, 1.7 Hz, 1H), 6.59 (d, *J* = 1.7 Hz, 1H), 2.52 (t, *J* = 7.6 Hz, 2H), 2.17 (s, 3H), 1.62 – 1.50 (m, 2H),

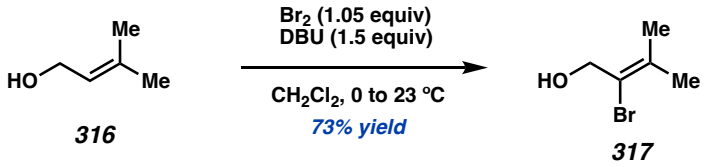
1.39 – 1.28 (m, 2H), 1.00 (t, J = 7.9 Hz, 9H), 0.92 (t, J = 7.4 Hz, 3H), 0.76 (qd, J = 7.8, 0.9 Hz, 6H).

^{13}C NMR (100 MHz, $CDCl_3$): δ 153.9, 141.6, 130.6, 125.8, 121.2, 118.7, 35.3, 33.8, 22.4, 16.4, 14.1, 6.9, 5.5.

IR (Neat Film, NaCl): 2956, 2930, 2876, 1578, 1414, 1274, 1004, 834, 732 cm^{-1}.

HRMS (FI+): *m/z* calc'd for $C_{17}H_{30}OSi$ $[M]^+$: 278.2060, found 278.2078.

Alternative Reductive Heck Cyclization Route

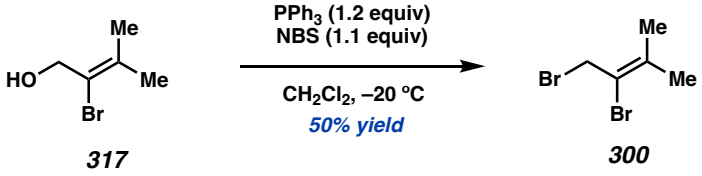


2-bromo-3-methylbut-2-en-1-ol (317)

To a flame-dried round bottom flask fitted with a stir bar and charged with prenol (1 g, 1.18 mL, 11.6 mmol, 1 equiv) in DCM (20 mL, 0.58 M) was added Br_2 (1.94 g, 0.62 mL, 12.2 mmol, 1.05 equiv) in DCM (2.5 mL, 4.9 M) at 0° C. The reaction was then stirred for 1 h at 0° C, then warmed to room temperature and stirred for another 3 h. After this, DBU (2.6 g, 2.6 mL, 17.4 mmol, 1.5 equiv) was added dropwise, upon which the reaction mixture turned dark orange. The mixture was then heated to reflux (40° C) and left to stir overnight. After this, the reaction was cooled to room temperature and quenched with a saturated solution of $Na_2S_2O_3$ dropwise until the solution turns colorless/pale yellow. The mixture was then diluted with Et_2O (10 mL) and 1M HCl (10 mL) and the phases were separated. The aqueous phase was extracted three times with Et_2O and the combined organic phases were washed with a saturated aqueous solution of $NaHCO_3$ (15 mL), dried

over Na_2SO_4 and then concentrated under reduced pressure. The resulting crude residue was purified using silica gel flash column chromatography (SiO_2, 20% EtOAc/Hexanes) to afford **317** as an oil (1.40 g, 8.5 mmol, 73%). All recorded spectra match the reported spectra.[21]

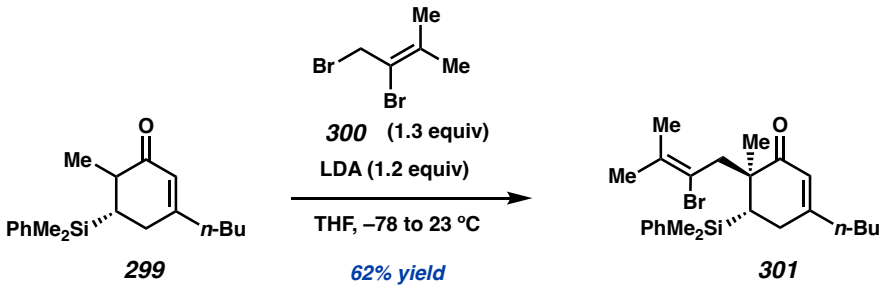
^{1}H NMR (500 MHz, $CDCl_3$): δ 4.37 (d, J = 6.5 Hz, 2H), 1.91 (s, 3H), 1.87 (s, 3H).



1,2-dibromo-3-methylbut-2-ene (300)

A flame-dried flask fitted with a stir bar was charged with bromide **317** (1.78 g, 10.78 mmol, 1 equiv) and DCM (72 mL, 0.15 M) and the mixture was cooled to –20° C. PPh_3 (3.4 g, 12.94 mmol, 1.2 equiv) and NBS (2.11g, 11.86 mmol, 1.1 equiv) were added and the reaction was stirred until completion (mixture turned yellow). The reaction was quenched with water (80 mL), the aqueous phase was extracted once with DCM (40 mL), and the organic phases were combined and dried over Na_2SO_4 and concentrated under reduced pressure. The resulting crude was purified by silica gel flash column chromatography (SiO_2, 100% hexanes) to afford **300** as a clear, colorless oil (1.24 g, 50%). Recorded spectra match those reported in the literature.[22]

^{1}H NMR (500 MHz, $CDCl_3$): δ 4.38 (s, 2H), 1.93 (s, 3H), 1.87 (s, 3H).



(5*S*,6*S*)-6-(2-bromo-3-methylbut-2-en-1-yl)-3-butyl-5-(dimethyl(phenyl)silyl)-6-methylcyclohex-2-en-1-one (301)

i-Pr$_2$NH (206.2 mg, 0.286 mL, 2.04 mmol, 1.25 equiv) was added to a flame-dried flask fitted with a stir bar and dissolved in THF (2 mL, 1.0 M) and the mixture was cooled to 0° C. *n*-BuLi (0.784 mL, 1.96 mmol, 2.5 M, 1.2 equiv) was added dropwise and the pale yellow mixture left to stir for 30 minutes at 0° C. Enone **299** (491.1 mg, 1.63 mmol, 1 equiv) in THF (1.5 mL, 1.1 M) was added dropwise and the mixture left to stir for 1 h at 0° C. After this, the reaction was cooled to – 78° C and prenyl bromide **300** (483.2 mg, 2.12 mmol, 1.3 equiv) in THF (1.5 mL, 1.9 M) was added dropwise and the reaction was warmed to room temperature overnight. The reaction was quenched with NH_4Cl (5 mL), the phases were separated and the aqueous phase was extracted three times with EtOAc (3 mL). The organic phases were combined and washed with brine (5 mL), then subsequently dried over Na_2SO_4. The organic phase was concentrated under reduced pressure, and the resulting crude was purified by silica flash column chromatography (SiO_2, 4% EtOAc/Hexanes) to afford **301** as a pale yellow, viscous oil (383.7 mg, 0.86 mmol, 62 %). **^{1}H NMR (400 MHz, $CDCl_3$):** δ 7.45 – 7.42 (m, 2H), 7.35 (qd, *J* = 4.0, 1.2 Hz, 3H), 5.84 – 5.82 (m, 1H), 2.87 (d, *J* = 14.8 Hz, 2H), 2.81 (dd, *J* = 6.6, 2.5 Hz, 1H), 2.74 (d, *J* = 14.9

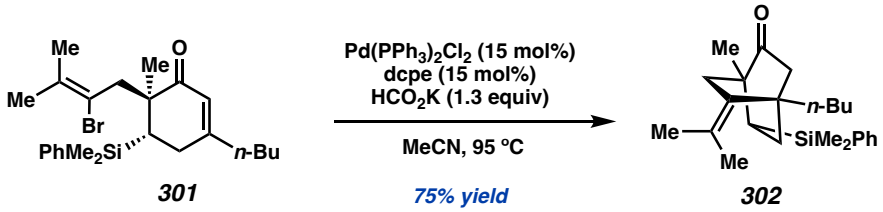
Hz, 1H), 2.12 – 2.04 (m, 4H), 1.88 (s, 3H), 1.44 – 1.34 (m, 2H), 1.34 – 1.25 (m, 2H), 1.14 (s, 3H), 0.89 (t, J = 7.2 Hz, 3H), 0.34 (s, 3H), 0.25 (s, 3H).

^{13}C NMR (100 MHz, $CDCl_3$): δ 205.2, 165.2, 141.4, 136.8, 135.3, 130.7, 129.6, 127.0, 118.0, 50.2, 46.0, 39.0, 33.2, 31.6, 30.9, 27.8, 24.2, 23.7, 23.5, 15.6, 1.6, 0.0.

IR (Neat film, NaCl): 2958, 1668, 1428, 1253, 1112, 820 cm^{-1}.

HRMS (FD+): *m/z* calc'd for $C_{24}H_{36}BrOSi$ $[M]^+$: 447.1719, found 447.1713.

Optical Rotation: $[\alpha]_D^{24}$ 58.3464 (c 0.77, $CHCl_3$).



(4*R*,7*R*)-4-butyl-7-(dimethyl(phenyl)silyl)-1-methyl-5-(propan-2-ylidene)bicyclo[2.2.2]octan-2-one (302)

To an oven-dried 2-dram vial fitted with a stir bar was added dcpe (7 mg, 15 mol%), HCO_2K (12.0 mg, 1.3 equiv) and enone **301** (50 mg, 0.1117 mmol, 1 equiv). The solids were dissolved in MeCN (2.8 mL, 0.04 M) and $Pd(PPh_3)_2Cl_2$ (11.6 mg, 15 mol%) was added. The resulting mixture was heated to 95° C and left to stir overnight, after which the previously pale-yellow mixture turned deep red. The reaction mixture was then cooled to room temperature and the crude concentrated under reduced pressure. The resulting residue was then purified by silica flash column chromatography (SiO_2, toluene) to afford **302** as a pale-yellow oil (30.3 mg, 75%).

^{1}H NMR (400 MHz, $CDCl_3$): δ 7.48 – 7.45 (m, 2H), 7.33 (dd, J = 5.0, 1.9 Hz, 3H), 2.38 (dd, J = 18.6, 3.2 Hz, 1H), 2.27 (d, J = 16.4 Hz, 1H), 2.14 (dp, J = 16.5, 2.0 Hz, 1H), 1.91

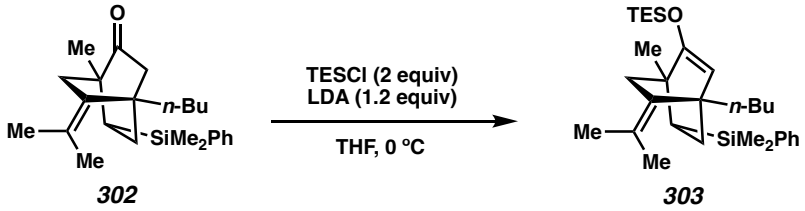
– 1.83 (m, 1H), 1.80 – 1.76 (m, 4H), 1.68 (ddd, J = 12.4, 10.2, 3.3 Hz, 1H), 1.60 (s, 3H), 1.42 – 1.33 (m, 3H), 1.28 (ddt, J = 10.4, 8.0, 3.9 Hz, 6H), 0.93 (s, 3H), 0.92 – 0.87 (m, 4H), 0.29 (s, 3H), 0.21 (s, 3H).

^{13}C NMR (100 MHz, $CDCl_3$): δ 216.9, 139.0, 133.8, 130.3, 128.9, 127.7, 123.3, 49.5, 48.1, 46.4, 43.5, 39.4, 38.1, 30.0, 27.1, 23.7, 23.3, 21.3, 20.9, 14.2, -3.2, -4.1.

IR (Neat film, NaCl): 3743, 3646, 2957, 2357, 1716, 1428, 1251, 1111, 815, 701 cm^{-1}.

HRMS (FD+): *m/z* calc'd for $C_{24}H_{36}OSi$ $[M]^+$: 368.2535, found 368.2529.

Optical Rotation: $[\alpha]_D^{23}$ 105.3987 (c 0.75, $CHCl_3$).

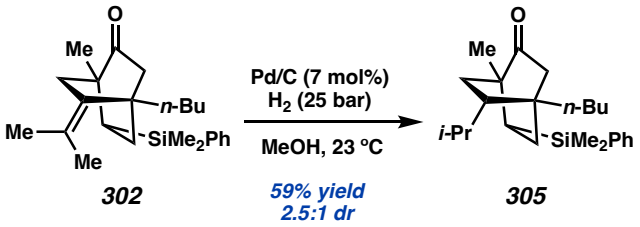


302 ***303***

((2*R*,4*S*)-4-butyl-1-methyl-8-(propan-2-ylidene)-6-((triethylsilyl)oxy)bicyclo[2.2.2]oct-5-en-2-yl)dimethyl(phenyl)silane (303)

A flame dried vial was charged with *i*-Pr_2NH (0.004 mL, 0.031 mmol, 1.15 equiv) and THF (0.016 mL, 2.0 M). The solution was cooled to 0 ºC and *n*-BuLi (0.0112 mL, 0.028 mmol, 1.05 equiv) was added dropwise. The resultant solution was stirred for 15 min at 0 ºC. Ketone **302** (10 mg, 0.027 mmol, 1.0 equiv) in THF (0.027 mL, 1.0 M) was added dropwise and stirring was continued at 0 ºC for 30 minutes. The solution was cooled to – 78 ºC and TESCl (0.004 mL, 0.036 mmol, 1.3 equiv) was added dropwise. The reaction was gradually warmed to 23 ºC. Upon complete consumption of starting material (as determined by TLC), the reaction was diluted with a saturated solution of NH_4Cl and the product was extracted three times with EtOAc. The combined organic layers were washed

with brine, dried over Na_2SO_4, filtered, and concentrated under reduced pressure. The crude product was used immediately in following reactions.

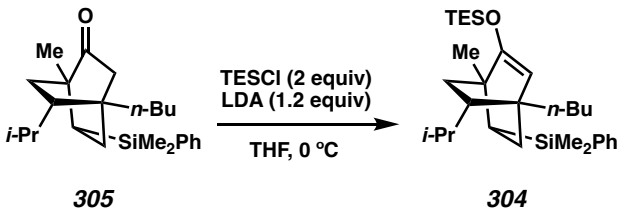


(4*R*,7*R*)-4-butyl-7-(dimethyl(phenyl)silyl)-5-isopropyl-1-methylbicyclo[2.2.2]octan-2-one (305)

A flame dried 1-dram vial was charged with ketone **302** (7.3 mg, 0.02 mmol, 1.0 equiv) in MeOH (0.3 mL, 0.07 M), followed by addition of Pd/C (10 wt%, 1.5 mg, 0.0014 mmol, 7 mol%). The vial was capped with a septum cap with an inserted vent needle, and the vial was then sealed in a hydrogenation reaction vessel, purged with H_2, and reacted overnight under an atmosphere of 25 bar H_2. The reaction mixture was then purged with N_2, filtered through a pad of celite, and concentrated under reduced pressure. The crude product was purified by flash silica gel column chromatography (SiO_2, 5–10% EtOAc/Hexanes) to afford **305** as a clear oil (4.3 mg, 0.012 mmol, 59% yield, 2.5:1 dr). Diastereomers were inseparable and relative stereochemistry was unable to be assigned.

^{1}H NMR (500 MHz, $CDCl_3$) major diastereomer: δ 7.50 – 7.44 (m, 2H), 7.37 – 7.31 (m, 3H), 2.35 (dd, J = 19.4, 3.5 Hz, 1H), 2.08 – 1.98 (m, 1H), 1.78 – 1.68 (m, 2H), 1.53 – 1.44 (m, 2H), 1.39 – 1.32 (m, 2H), 1.31 – 1.23 (m, 3H), 1.23 – 1.10 (m, 3H), 0.93 – 0.87 (m, 3H), 0.90 (s, 3H), 0.84 (d, J = 6.8 Hz, 3H), 0.80 (d, J = 6.7 Hz, 3H), 0.28 (s, 3H), 0.21 (s, 3H).

HRMS (FD+): *m/z* calc'd for $C_{24}H_{38}OSi$ $[M]^+$: 370.2686, found 370.2692.

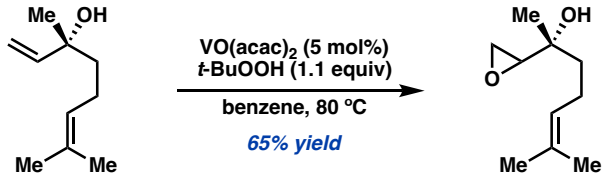


305 ***304***

(((4*R*,7*R*)-4-butyl-7-(dimethyl(phenyl)silyl)-5-isopropyl-1-methylbicyclo[2.2.2]oct-2-en-2-yl)oxy)triethylsilane (304)

A flame dried vial was charged with *i*-Pr_2NH (0.01 mL, 0.071 mmol, 1.15 equiv) and THF (0.032 mL, 2.0 M). The solution was cooled to 0 ºC and *n*-BuLi (0.026 mL, 0.065 mmol, 1.05 equiv) was added dropwise. The resultant solution was stirred for 30 min at 0 ºC. Ketone **305** (22.5 mg, 0.061 mmol, 1.0 equiv) in THF (0.064 mL, 1.0 M) was added dropwise and stirring was continued at 0 ºC for 30 minutes. The solution was cooled to –78 ºC and TESCl (0.013 mL, 0.077 mmol, 1.25 equiv) was added dropwise. The reaction was gradually warmed to 23 ºC. Upon complete consumption of starting material (as determined by TLC), the reaction was diluted with a saturated solution of NH_4Cl and the product was extracted three times with EtOAc. The combined organic layers were washed with brine, dried over Na_2SO_4, filtered, and concentrated under reduced pressure. The crude product was used immediately in following reactions.

Progress Toward Hypermoin A



(R)-linalool
254

266

(2*R*)-6-methyl-2-(oxiran-2-yl)hept-5-en-2-ol (266)

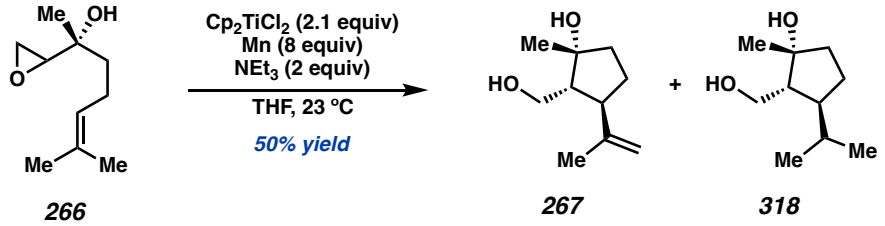
Procedure adapted from Opatz and coworkers.[17] A round bottom flask is equipped with a reflux condenser and charged with *(R)*-linalool **254** (7.1 mL, 40 mmol, 1 equiv) and benzene (154 mL, 0.26 M). The solution is heated to 65 ºC. $VO(acac)_2$ (530 mg, 2 mmol, 5 mol%) is added and the reaction mixture is heated to 80 ºC for 10 min. Then *t*-BuOOH (5.5 M in decane, 8.0 mL, 44 mmol, 1.1 equiv) was added dropwise via syringe pump over 1 h. Upon complete consumption of starting material (as determined by TLC), the reaction was cooled to 23 ºC. The reaction mixture was washed with saturated $NaHCO_3$ and brine and then dried over Na_2SO_4, filtered, and concentrated under reduced pressure. The crude product was purified by flash silica gel column chromatography (SiO_2, 20% EtOAc/Hexanes) to afford epoxide **266** as a pale yellow oil (4.39 g, 25.8 mmol, 65% yield, 1.5:1 dr). All characterization data match those reported in the literature.

Diastereomer 1:

^{1}H NMR (400 MHz, $CDCl_3$): δ 5.16 – 5.07 (m, 1H), 2.93 (dd, *J* = 3.9, 2.8 Hz, 1H), 2.85 (dd, *J* = 5.1, 2.8 Hz, 1H), 2.74 (dd, *J* = 5.1, 4.0 Hz, 1H), 2.18 – 2.07 (m, 2H), 1.69 (s, 3H), 1.62 (s, 3H), 1.65–1.55 (m, 2H), 1.32 (s, 3H).

Diastereomer 2:

^{1}H NMR (400 MHz, $CDCl_3$): δ 5.16 – 5.07 (m, 1H), 2.97 (dd, *J* = 4.1, 2.8 Hz, 1H), 2.77 (dd, *J* = 5.1, 2.8 Hz, 1H), 2.70 (dd, *J* = 5.1, 4.1 Hz, 1H), 2.18 – 2.07 (m, 2H), 1.69 (s, 3H), 1.63 (s, 3H), 1.65–1.55 (m, 2H), 1.20 (s, 3H).



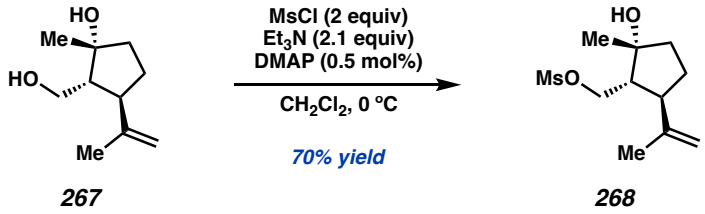
266 ***267*** ***318***

(1*R*,2*R*,3*R*)-2-(hydroxymethyl)-1-methyl-3-(prop-1-en-2-yl)cyclopentan-1-ol (267)

Procedure adapted from Opatz and coworkers.[17] A round bottom flask is charged with Mn (12.51 g, 228 mmol, 8 equiv), Cp_2TiCl_2 (14.88 g, 60 mmol, 2.1 equiv), and THF (150 mL, 0.4 M). The mixture is stirred for 30 minutes until it turns from a dark red to green color. A solution of epoxide **266** (4.84 g, 28.5 mmol, 1 equiv) and NEt_3 (7.9 mL, 57 mmol, 2 equiv) in THF (100 mL, 0.3 M) was added to the reaction mixture. Upon complete consumption of starting material (as determined by TLC), the reaction mixture was filtered to remove insoluble metals and then concentrated under reduced pressure to ~100 mL. The crude reaction mixture was diluted with Et_2O and 2N HCl and then filtered to remove the precipitate. The organic layer was separated and concentrated to approximately half the volume. 2N HCl was added and the mixture was stirred for 10 min. The mixture was separated, and the organic layer was washed with 2N HCl two times and then with brine. The organic layer was dried over Na_2SO_4, filtered, and concentrated under reduced pressure. The crude product was purified by flash silica gel column chromatography (SiO_2, 45% EtOAc/Hexanes) to afford diol **267** as an orange waxy solid (2.43 g, 14.3 mmol, 50% yield) as a mixture with the reduced compound **318**. This mixture could be used without further purification in subsequent steps. To separate the products, the mixture was dissolved in hexanes with minimal Et_2O and cooled to –20 ºC. The formed precipitate was filtered off and washed with hexanes (–20 ºC). This was repeated 2 times to yield pure **267** as a white solid (767 mg, 4.45 mmol). All characterization data match those reported in the literature.

^{1}H NMR (400 MHz, $CDCl_3$): δ 4.78 (dq, *J* = 2.5, 0.9 Hz, 1H), 4.76 (dq, *J* = 2.8, 1.5 Hz, 1H), 3.91 (dt, *J* = 11.3, 3.5 Hz, 1H), 3.72 (ddd, *J* = 11.4, 7.0, 5.1 Hz, 1H), 2.87 (dt, *J* = 10.9,

8.7 Hz, 1H), 1.95 (dtd, *J* = 12.7, 8.3, 5.8 Hz, 1H), 1.84 – 1.72 (m, 2H), 1.72 (s, 3H), 1.60 (ddd, *J* = 10.8, 5.0, 3.2 Hz, 1H), 1.55 – 1.46 (m, 1H), 1.41 (s, 3H).



267 ***268***

((1*R*,2*R*,5*R*)-2-hydroxy-2-methyl-5-(prop-1-en-2-yl)cyclopentyl)methyl methanesulfonate (268)

A round bottom flask was charged with diol **267** (757 mg, 4.45 mmol, 1 equiv), DMAP, (2.7 mg, 0.02 mmol, 0.5 mol%), and CH_2Cl_2 (23 mL, 0.2 M) and the mixture was cooled to 0 ºC. Et_3N (1.3 mL, 9.34 mmol, 2.1 equiv) was added dropwise which was followed by a dropwise addition of MsCl (0.69 mL, 8.89 mmol, 2 equiv). Upon complete consumption of starting material (as determined by TLC), the reaction mixture was washed with saturated brine two times. The organic layer was dried over Na_2SO_4, filtered, and concentrated under reduced pressure. The crude product was purified by flash silica gel column chromatography (SiO_2, 40% EtOAc/Hexanes) to afford mesylate **268** as a pale yellow oil (775 mg, 3.12 mmol, 70% yield).

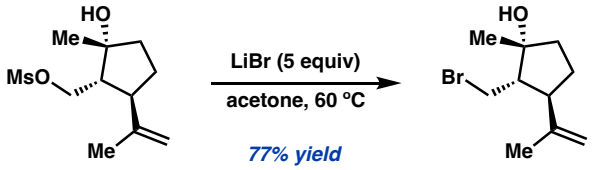
^{1}H NMR (400 MHz, $CDCl_3$): δ 4.76 (q, *J* = 1.2 Hz, 2H), 4.44 (dd, *J* = 10.1, 8.9 Hz, 1H), 4.19 (dd, *J* = 10.1, 4.1 Hz, 1H), 3.00 (s, 3H), 2.52 (dt, *J* = 11.1, 8.6 Hz, 1H), 2.02 – 1.87 (m, 2H), 1.87 – 1.73 (m, 2H), 1.70 (t, *J* = 1.1 Hz, 3H), 1.52 (dddd, *J* = 12.6, 9.3, 8.5, 6.0 Hz, 1H), 1.44 (s, 3H).

^{13}C NMR (100 MHz, $CDCl_3$): δ 145.9, 111.6, 79.6, 69.4, 50.9, 48.9, 41.7, 37.3, 28.6, 28.2, 19.0.

IR (Neat Film, NaCl): 3538, 2964, 1644, 1456, 1352, 1172, 976, 944 cm^{-1}.

HRMS (FD+): *m/z* calc'd for $C_{11}H_{20}O_4S$ $[M]^+$: 248.1077, found 248.1088.

Optical Rotation: $[\alpha]_D^{21}$ –18.4 (c 1.00, $CHCl_3$).



268 ***269***

(1*R*,2*S*,3*R*)-2-(bromomethyl)-1-methyl-3-(prop-1-en-2-yl)cyclopentan-1-ol (269)

A round bottom flask was charged with mesylate **268** (775 mg, 3.12 mmol, 1 equiv) and acetone (15.6 mL, 0.2 M). LiBr (1.36 g, 15.6 mmol, 5 equiv) was added and the solution was heated to 60 ºC. Upon complete consumption of starting material (as determined by TLC, after ~3 hours product decomposition results in lower yields), the reaction mixture was cooled to 23 ºC and concentrated. The crude residue was diluted with CH_2Cl_2 and H_2O. The product was extracted three times with CH_2Cl_2. The combined organic layers were washed with brine, dried over Na_2SO_4, filtered, and concentrated under reduced pressure. The crude product was purified by flash silica gel column chromatography (SiO_2, 10% EtOAc/Hexanes) to afford alkyl bromide **269** as a colorless oil (561 mg, 2.41 mmol, 77% yield).

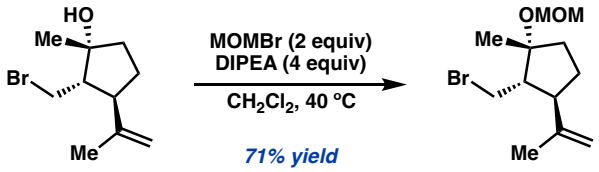
^{1}H NMR (400 MHz, $CDCl_3$): δ 4.77 (dh, *J* = 3.7, 1.1 Hz, 2H), 3.56 (dd, *J* = 10.3, 8.9 Hz, 1H), 3.42 (dd, *J* = 10.3, 3.5 Hz, 1H), 2.46 (ddd, *J* = 10.4, 9.1, 7.5 Hz, 1H), 1.98 (ddd, *J* = 11.0, 9.0, 3.5 Hz, 1H), 1.92 – 1.72 (m, 3H), 1.70 (t, *J* = 1.1 Hz, 3H), 1.51 – 1.42 (m, 1H), 1.48 (s, 3H).

^{13}C NMR (100 MHz, $CDCl_3$): δ 146.0, 111.7, 79.9, 53.4, 52.5, 41.9, 31.9, 29.7, 28.1, 19.3.

IR (Neat Film, NaCl): 3450, 3072, 2962, 2872, 1642, 1458, 1376, 1168, 896 cm^{-1}.

HRMS (FI+): *m/z* calc'd for $C_{10}H_{17}OBr$ $[M]^+$: 232.0457, found 232.0468.

Optical Rotation: $[\alpha]_D^{21}$ –16.2 (c 1.00, $CHCl_3$).



269 ***270***

(1*R*,2*S*,3*R*)-2-(bromomethyl)-1-(methoxymethoxy)-1-methyl-3-(prop-1-en-2-yl)cyclopentane (270)

A round bottom flask was charged with alcohol **269** (561 mg, 2.41 mmol, 1 equiv) and CH_2Cl_2 (12.0 mL, 0.2 M) and the mixture is cooled to 0 ºC. DIPEA (1.7 mL, 9.62 mmol, 4 equiv) was added followed by a dropwise addition of MOMBr (0.39 mL, 4.81 mmol, 2 equiv). The reaction mixture was then slowly heated to 40 ºC. Upon complete consumption of starting material (as determined by TLC), the reaction mixture was cooled to 23 ºC diluted with saturated NH_4Cl. The organic layer was washed with H_2O and brine, dried over Na_2SO_4, filtered, and concentrated under reduced pressure. The crude product was purified by flash silica gel column chromatography (SiO_2, 0–5% EtOAc/Hexanes) to afford MOM protected alkyl bromide **270** as a colorless oil (474 mg, 1.71 mmol, 71% yield).

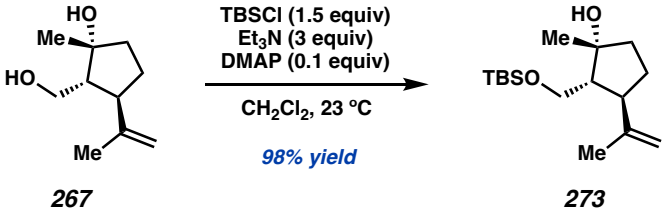
^{1}H NMR (400 MHz, $CDCl_3$): δ 4.76 (m, 2H), 4.72 (q, *J* = 7.2 Hz, 2H), 3.71 (dd, *J* = 10.2, 8.1 Hz, 1H), 3.39 (s, 3H), 3.32 (dd, *J* = 10.3, 4.0 Hz, 1H), 2.60 – 2.49 (m, 1H), 2.07 – 2.00 (m, 2H), 1.94 – 1.83 (m, 1H), 1.72 (t, *J* = 1.1 Hz, 3H), 1.64 – 1.55 (m, 1H), 1.53 – 1.41 (m, 1H), 1.49 (s, 3H).

^{13}C NMR (100 MHz, $CDCl_3$): δ 146.7, 111.5, 91.4, 85.1, 56.0, 55.6, 52.3, 37.4, 30.7, 27.8, 24.3, 19.1.

IR (Neat Film, NaCl): 3072, 2962, 1458, 1142, 1086, 1038, 918, 894 cm^{-1}.

HRMS (FI+): *m/z* calc'd for $C_{12}H_{21}O_2Br$ $[M]^+$: 276.0719, found 276.0735. Unable to obtain a mass difference <5 ppm with various ionization methods.

Optical Rotation: $[\alpha]_D^{21}$ –36.9 (c 1.00, $CHCl_3$).



267 ***273***

(1*R*,2*R*,3*R*)-2-(((*tert*-butyldimethylsilyl)oxy)methyl)-1-methyl-3-(prop-1-en-2-yl)cyclopentan-1-ol (273)

A round bottom flask was charged with alcohol **267** (100 mg, 0.587 mmol, 1 equiv) and CH_2Cl_2 (3.0 mL, 0.2 M). Et_3N (0.245 mL, 1.76 mmol, 3 equiv), TBSCl (132 mg, 0.88 mmol, 1.5 equiv) and DMAP (7.3 mg, 0.06 mmol, 0.1 equiv) were added sequentially, and the reaction mixture was allowed to stir at room temperature until full consumption of starting material (as determined by TLC). The reaction mixture was diluted with saturated NH_4Cl and extracted three times with CH_2Cl_2. The organic layer was washed with brine, dried over Na_2SO_4, filtered, and concentrated under reduced pressure. The crude product was purified by flash silica gel column chromatography (SiO_2, 5% EtOAc/Hexanes) to afford TBS protected **273** as a colorless oil (164 mg, 0.576 mmol, 98% yield).

^{1}H NMR (400 MHz, $CDCl_3$): δ 4.82 (h, *J* = 1.4 Hz, 1H), 4.72 (dq, *J* = 1.9, 0.9 Hz, 1H), 3.70 – 3.65 (m, 1H), 3.55 (dd, *J* = 10.4, 4.5 Hz, 1H), 2.54 (q, *J* = 9.1 Hz, 1H), 2.05 (td, *J* =

9.1, 4.5 Hz, 1H), 1.99 – 1.92 (m, 1H), 1.90 – 1.84 (m, 1H), 1.74 (dt, *J* = 1.4, 0.7 Hz, 3H), 1.65 – 1.56 (m, 2H), 1.38 (s, 3H), 0.89 (s, 9H), 0.06 (s, 3H), 0.05 (s, 3H).

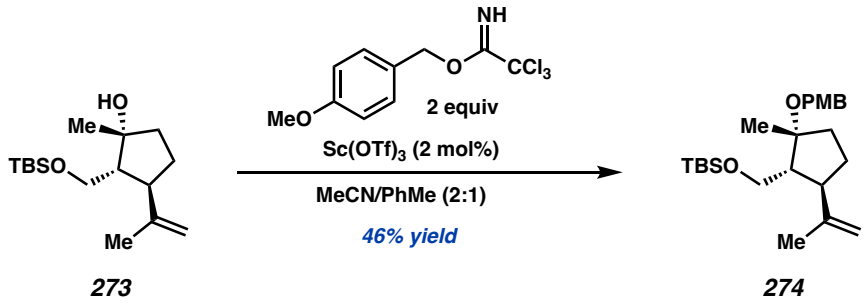
^{13}C NMR (100 MHz, $CDCl_3$): δ 144.6, 110.8, 80.8, 62.3, 50.9, 48.7, 40.9, 32.4, 27.5, 26.0, 23.5, -5.4, -5.4.

The product was isolated as a mixture with a small amount of reduced isopropyl compound, leading to some extra peaks in the NMR spectra. Regardless, the mixture can be advanced to **274 without issue.*

IR (Neat Film, NaCl): 3499, 2954, 2930, 2858, 1470, 1385, 1371, 1255, 1064, 837 cm^{-1}.

HRMS (FD+): *m/z* calc'd for $C_{16}H_{32}O_2Si$ $[M]^+$: 284.2172, found 284.2166

Optical Rotation: $[\alpha]_D^{21}$ –12.5 (c 0.64, $CHCl_3$).



273 ***274***

***tert*-butyl(((1*R*,2*R*,5*R*)-2-((4-methoxybenzyl)oxy)-2-methyl-5-(prop-1-en-2-yl)cyclopentyl)methoxy)dimethylsilane (274)**

A round bottom flask was charged with alcohol **273** (755 mg, 2.66 mmol, 1 equiv) and PhMe (53.2 mL, 0.05 M) and the mixture is cooled to 0 ºC. 4-methoxybenzyl 2,2,2-trichloroacetimidate (1.5 g, 5.31 mmol, 2 equiv) in PhMe was added dropwise, followed by dropwise addition of $Sc(OTf)_3$ (26 mg, 0.053 mmol, 2 mol%) in MeCN (0.5 mL, 0.1 M) at 0 ºC. The reaction mixture was then allowed to warm to room temperature overnight. The reaction mixture was diluted with saturated $NaHCO_3$ and extracted three times with

EtOAc. The combined organic layers were washed with brine, dried over Na_2SO_4, and concentrated under reduced pressure. The crude product was purified by flash silica gel column chromatography (SiO_2, 0–55% EtOAc/Hexanes) to afford PMB protected **274** as a colorless oil (461 mg, 1.14 mmol, 46% yield).

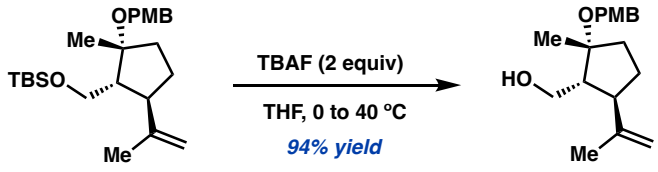
^{1}H NMR (400 MHz, $CDCl_3$): δ 7.27 – 7.20 (m, 2H), 6.88 – 6.85 (m, 2H), 4.72 – 4.68 (m, 1H), 4.70 – 4.63 (m, 1H), 4.41 (d, *J* = 11.2 Hz, 1H), 4.34 (d, *J* = 11.3 Hz, 1H), 3.95 (ddd, *J* = 10.1, 7.8, 3.8 Hz, 1H), 3.81 (s, 3H), 3.49 (dd, *J* = 10.1, 4.4 Hz, 1H), 2.51 (td, *J* = 10.3, 6.0 Hz, 1H), 2.13 – 1.99 (m, 1H), 1.95 – 1.76 (m, 2H), 1.75 – 1.71 (m, 1H), 1.71 (s, 3H), 1.47 (dd, *J* = 2.9, 1.9 Hz, 1H), 1.45 (s, 3H), 0.87 (s, 9H), 0.02 (s, 3H), 0.00 (s, 3H).

^{13}C NMR (100 MHz, $CDCl_3$): δ 148.1, 132.7, 128.4, 113.7, 110.2, 84.4, 63.5, 61.8, 55.7, 55.4, 48.8, 35.8, 28.2, 26.1, 25.5, 22.9, 19.3, 18.4, -5.2, -5.3.

IR (Neat Film, NaCl): 3513, 2938, 1514, 1242, 1042, 847 cm^{-1}.

HRMS (FD+): *m/z* calc'd for $C_{24}H_{40}O_3Si$ $[M]^+$: 404.2741, found 404.2741.

Optical Rotation: $[\alpha]_D^{21}$ –30.9 (c 0.28, $CHCl_3$).



274 ***275***

((1*R*,2*R*,5*R*)-2-((4-methoxybenzyl)oxy)-2-methyl-5-(prop-1-en-2-yl)cyclopentyl)methanol (275)

A round bottom flask was charged with **274** (126 mg, 0.311 mmol, 1 equiv) and THF (3.0 mL, 0.1 M) and cooled to 0 ºC. TBAF (1.0 M solution in THF, 0.934 mL, 0.934 mmol, 3 equiv) was added dropwise at 0 ºC, and the mixture was warmed to room temperature,

followed by stirring at 40 ºC overnight until full conversion (as determined by TLC). The mixture was cooled to room temperature, diluted with EtOAc, and washed with brine. The crude product was then dried over Na_2SO_4 and concentrated under reduced pressure. The crude product was purified by flash silica gel column chromatography (SiO_2, 0–10% EtOAc/Hexanes) to afford primary alcohol **275** as a colorless oil (84 mg, 0.29 mmol, 94% yield).

^{1}H NMR (400 MHz, $CDCl_3$): δ 7.21 (d, *J* = 8.7 Hz, 2H), 6.87 (d, *J* = 8.7 Hz, 2H), 4.79 (dq, *J* = 2.5, 0.8 Hz, 1H), 4.75 (dq, *J* = 2.9, 1.5 Hz, 1H), 4.41 (d, *J* = 10.7 Hz, 1H), 4.34 (d, *J* = 10.8 Hz, 1H), 3.89 (dd, *J* = 11.6, 2.7 Hz, 1H), 3.80 (s, 3H), 3.64 (td, *J* = 10.9, 5.7 Hz, 1H), 2.97 (dt, *J* = 10.7, 8.5 Hz, 1H), 2.15 – 2.01 (m, 1H), 1.98 – 1.90 (m, 1H), 1.72 (s, 3H), 1.68 – 1.54 (m, 3H), 1.44 (s, 3H).

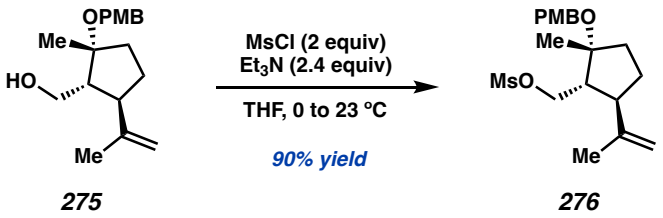
^{13}C NMR (100 MHz, $CDCl_3$): δ 159.2, 147.2, 131.2, 128.8, 114.1, 110.7, 87.6, 64.5, 64.21, 60.7, 55.4, 54.8, 46.3, 35.9, 28.3, 23.4, 19.6.

The product was isolated as a mixture with a small amount of reduced isopropyl compound, leading to some extra peaks in the NMR spectra. Regardless, the mixture can be advanced to **276 without issue.*

IR (Neat Film, NaCl): 3513, 2957, 2871, 1613, 1514, 1462, 1301, 1250, 1172, 1063, 1032 cm^{-1}.

HRMS (FD+): *m/z* calc'd for $C_{18}H_{26}O_3$ $[M]^+$: 290.1877, found 190.1875.

Optical Rotation: $[\alpha]_D^{21}$ –42.7 (c 0.66, $CHCl_3$).



275 ***276***

((1*R*,2*R*,5*R*)-2-((4-methoxybenzyl)oxy)-2-methyl-5-(prop-1-en-2-yl)cyclopentyl)methyl methanesulfonate (276)

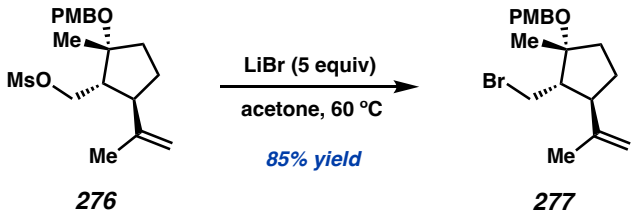
A round bottom flask was charged with alcohol **275** (100 mg, 0.344 mmol, 1 equiv) and THF (2.0 mL, 0.17 M) and the mixture is cooled to 0 ºC. Et_3N (0.115 mL, 0.825 mmol, 2.4 equiv) was added followed by a dropwise addition of MsCl (0.053 mL, 0.688 mmol, 2 equiv). The reaction mixture was stirred at 0 ºC for 15 min and then slowly warmed to room temperature. Upon complete consumption of starting material (as determined by TLC), the reaction mixture was diluted with CH_2Cl_2, washed twice with brine, dried over Na_2SO_4, filtered, and concentrated under reduced pressure. The crude product was purified by flash silica gel column chromatography (SiO_2, 0–20% EtOAc/Hexanes) to afford mesylate **276** as a colorless oil (112 mg, 0.303 mmol, 90% yield).

^{1}H NMR (400 MHz, $CDCl_3$): δ 7.24 – 7.21 (m, 2H), 6.89 – 6.86 (m, 2H), 4.79 – 4.71 (m, 2H), 4.53 (dd, *J* = 9.8, 8.3 Hz, 1H), 4.38 (d, *J* = 10.9 Hz, 1H), 4.33 (d, *J* = 10.8 Hz, 1H), 4.13 (dd, *J* = 9.8, 4.6 Hz, 1H), 3.81 (s, 3H), 2.86 (s, 3H), 2.66 – 2.53 (m, 1H), 2.20 – 2.01 (m, 2H), 1.99 – 1.83 (m, 1H), 1.72 (s, 3H), 1.65 – 1.56 (m, 2H), 1.46 (s, 3H).

^{13}C NMR (100 MHz, $CDCl_3$): δ 159.0, 146.4, 131.6, 128.8, 113.9, 111.4, 83.9, 69.8, 63.7, 55.4, 52.5, 49.2, 36.9, 35.5, 28.3, 23.1, 19.0.

IR (Neat Film, NaCl): 2959, 1613, 1514, 1358, 1249, 1175, 1032, 947, 828 cm^{-1}.

Optical Rotation: $[\alpha]_D^{21}$ –50.8 (c 0.68, $CHCl_3$).



276 ***277***

(1*R*,2*S*,3*R*)-2-(bromomethyl)-1-(methoxymethoxy)-1-methyl-3-(prop-1-en-2-yl)cyclopentane (277)

A round bottom flask with reflux condenser was charged with mesylate **276** (54.8 mg, 0.148 mmol, 1 equiv), LiBr (129 mg, 1.48 mmol, 10 equiv), and acetone (2 mL, 0.074 M). the mixture was heated to 60 ºC and stirred overnight. Upon complete consumption of starting material (as determined by TLC), the crude mixture was concentrated under reduced pressure and dissolved in a mixture of CH_2Cl_2 and water. The organic layer was washed with brine, dried over Na_2SO_4, and concentrated under reduced pressure. The crude product was purified by flash silica gel column chromatography (SiO_2, 0–5–10% EtOAc/Hexanes) to afford PMB protected alkyl bromide **277** as a yellow oil (44.3 mg, 0.125 mmol, 85% yield).

^{1}H NMR (400 MHz, $CDCl_3$): δ 7.25 (d, *J* = 6.7 Hz, 2H), 6.88 (d, *J* = 8.7 Hz, 2H), 4.76 (s, 2H), 4.42 (d, *J* = 11.0 Hz, 1H), 4.33 (d, *J* = 11.0 Hz, 1H), 3.81 (s, 3H), 3.83 – 3.74 (m, 1H), 3.32 (dd, *J* = 10.2, 4.2 Hz, 1H), 2.64 – 2.53 (m, 1H), 2.11 (ddt, *J* = 14.2, 7.6, 3.8 Hz, 2H), 1.96 – 1.79 (m, 1H), 1.72 (s, 3H), 1.61 – 1.54 (m, 2H), 1.52 (s, 3H).

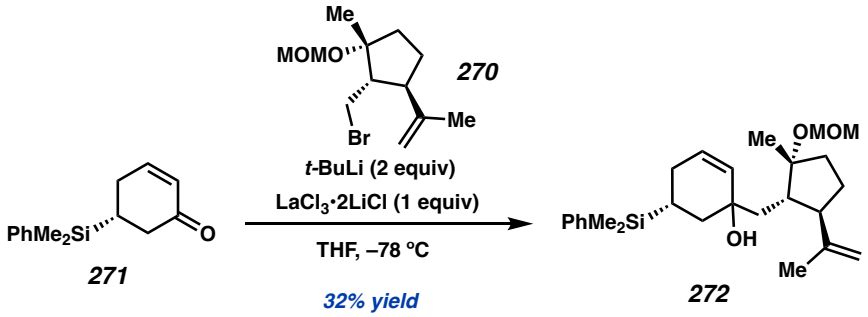
^{13}C NMR (100 MHz, $CDCl_3$): δ 158.9, 146.9, 132.0, 128.5, 113.8, 111.3, 84.3, 63.6, 56.0, 55.4, 52.2, 35.6, 31.2, 28.0, 23.2, 19.3.

**The product was isolated as a mixture with a small amount of reduced isopropyl compound, leading to some extra peaks in the NMR spectra. Regardless, the mixture can be used in subsequent steps without issue.*

IR (Neat Film, NaCl): 3073, 2960, 2871, 1613, 1513, 1462, 1455, 1380, 1249, 1063, 1041 cm^{-1}.

HRMS (FD+): *m/z* calc'd for $C_{18}H_{25}O_2Br$ $[M]^+$: 352.1032, found 352.1032.

Optical Rotation: $[\alpha]_D^{21}$ –66.2 (c 1.04, $CHCl_3$).



(5R)-5-(dimethyl(phenyl)silyl)-1-(((1S,2R,5R)-2-(methoxymethoxy)-2-methyl-5-(prop-1-en-2-yl)cyclopentyl)methyl)cyclohex-2-en-1-ol (272)

Enone **271**[18] (115.2 mg, 0.5 mmol, 1 equiv) was azeotroped with benzene (0.5 mL) 2 times and placed under high vacuum for 3 h to remove trace benzene. Alkyl bromide **270** (138.6 mg, 0.5 mmol, 1 equiv) was azeotroped with benzene (0.5 mL) 2 times and placed under high vacuum for 3 h to remove trace benzene. Both vials are backfilled with N_2, then enone **271** was dissolved in THF (2.5 mL, 0.2 M) and cooled to –78 ºC. $LaCl_3$•2LiCl (0.6 M in THF, 0.83 mL, 1 equiv) was added dropwise and the resulting solution was stirred 30 minutes. Alkyl bromide **270** was dissolved in THF (0.63 mL, 0.8 M) and cooled to –78 ºC. *t*-BuLi (1.7 M in pentane, 0.69 mL, 2 equiv) was added dropwise and the resulting solution was stirred for 15 minutes. Both solutions were warmed to –40 ºC and enone **271** and

$LaCl_3$•2LiCl solution was added as fast as possible via cannula to the stirring solution of the alkyl Li generated from **270**. Upon complete consumption of starting material (as determined by TLC), silica gel was added followed by MeOH (~0.1 mL). The slurry was filtered over celite with CH_2Cl_2, and the resulting solution was concentrated under reduced pressure. The crude product was purified by flash silica gel column chromatography (SiO_2, 10–15% EtOAc/Hexanes) to afford allylic alcohol **272** as a colorless oil (67.9 mg, 0.16 mmol, 32% yield).

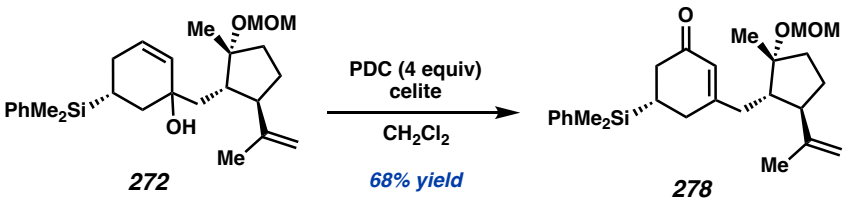
^{1}H NMR (400 MHz, $CDCl_3$): δ 7.51 – 7.46 (m, 2H), 7.36 – 7.32 (m, 3H), 5.66 (ddd, J = 10.2, 4.0, 2.8 Hz, 1H), 5.59 (dq, J = 10.2, 1.9 Hz, 1H), 4.77 (dq, J = 3.8, 1.2 Hz, 2H), 4.71 (s, 2H), 3.37 (s, 3H), 2.40 (dt, J = 10.2, 8.6 Hz, 1H), 2.01 – 1.81 (m, 5H), 1.77 – 1.68 (m, 2H), 1.67 (s, 3H), 1.65 – 1.55 (m, 3H), 1.53 – 1.40 (m, 2H), 1.26 (s, 3H), 1.14 (dddd, *J* = 14.3, 9.8, 7.2, 2.3 Hz, 1H), 0.27 (s, 3H), 0.27 (s, 3H).

^{13}C NMR (100 MHz, CDCl3): δ 148.4, 137.8, 134.7, 134.2, 134.1, 129.1, 127.9, 127.8, 127.6, 111.5, 91.7, 86.1, 70.4, 55.8, 54.3, 49.0, 40.2, 37.6, 37.2, 28.7, 26.0, 25.1, 19.5, 19.2, -5.2, -5.4.

IR (Neat Film, NaCl): 3464, 2938, 2354, 1710, 1374, 1246, 1078, 1040, 834 cm^{-1}.

HRMS (FD+): *m/z* calc'd for $C_{26}H_{40}O_3Si$ $[M]^+$: 428.2741, found 428.2740.

Optical Rotation: $[\alpha]_D^{21}$ –56.0 (c 1.00, $CHCl_3$).



(*S*)-5-(dimethyl(phenyl)silyl)-3-(((1*S*,2*R*,5*R*)-2-(methoxymethoxy)-2-methyl-5-(prop-1-en-2-yl)cyclopentyl)methyl)cyclohex-2-en-1-one (278)

A round bottom flask open to air was charged with celite and CH_2Cl_2 (0.6 mL, 0.25 M). PDC (238 mg, 0.63 mmol, 4 equiv) was added to the slurry and stirred until the PCC is evenly dispersed. Allylic alcohol **272** (67.9 mg, 0.16 mmol, 1 equiv) was added to the mixture using minimal CH_2Cl_2 to transfer. Upon complete consumption of starting material (as determined by TLC), the reaction was filtered over celite with Et_2O. The crude reaction mixture was washed with 1 M NaOH, 1 M HCl, saturated $NaHCO_3$ x3, and brine. The organic layer was dried over Na_2SO_4, filtered, and concentrated under reduced pressure. The crude product was purified by flash silica gel column chromatography (SiO_2, 10–15% EtOAc/Hexanes) to afford enone **278** as a colorless oil (45. mg, 0.11 mmol, 68% yield).

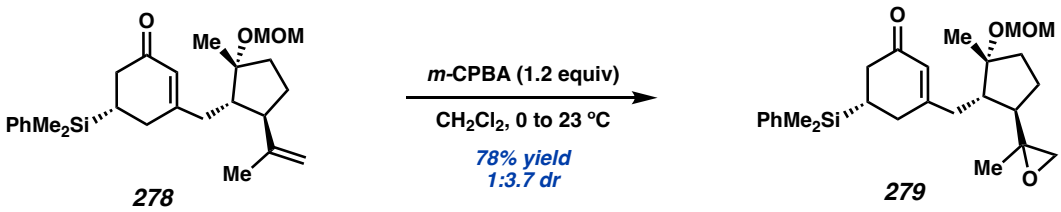
^{1}H NMR (400 MHz, $CDCl_3$): δ 7.50 – 7.45 (m, 2H), 7.40 – 7.33 (m, 3H), 5.91 – 5.85 (m, 1H), 4.66 (d, *J* = 1.0 Hz, 2H), 4.61 (ddd, *J* = 7.3, 2.2, 1.3 Hz, 2H), 3.35 (s, 3H), 2.58 – 2.45 (m, 2H), 2.35 (ddd, *J* = 16.3, 2.7, 1.7 Hz, 1H), 2.16 – 1.98 (m, 5H), 1.88 (ddt, *J* = 12.7, 10.2, 7.5 Hz, 1H), 1.68 (dt, *J* = 10.5, 6.6 Hz, 1H), 1.57 (dd, *J* = 1.4, 0.8 Hz, 3H), 1.55 – 1.37 (m, 3H), 1.25 (s, 3H), 0.32 (s, 6H).

^{13}C NMR (100 MHz, CDCl3): δ 200.0, 167.7, 147.3, 136.4, 134.0, 129.5, 128.1, 126.8, 111.5, 91.4, 85.5, 55.6, 52.3, 51.5, 37.9, 36.7, 36.6, 31.3, 28.1, 23.4, 22.8, 18.8, -5.2, -5.4.

IR (Neat Film, NaCl): 3420, 3068, 2954, 1666, 1426, 1376, 1252, 1144, 1038, 814 cm^{-1}.

HRMS (FD+): *m/z* calc'd for $C_{26}H_{38}O_3Si$ $[M]^+$: 426.2585, found 426.2582.

Optical Rotation: $[\alpha]_D^{21}$ 26.0 (c 1.00, $CHCl_3$).



(*S*)-5-(dimethyl(phenyl)silyl)-3-(((1*S*,2*R*,5*R*)-2-(methoxymethoxy)-2-methyl-5-((*R*)-2-methyloxiran-2-yl)cyclopentyl)methyl)cyclohex-2-en-1-one (279)

A flame dried 1 dram vial was charged with enone **278** (45.9 mg, 0.11 mmol, 1 equiv) and CH_2Cl_2 (0.54 mL, 0.2 M) and cooled to 0 ºC. *m*-CPBA (22.3 mg, 0.13 mmol, 1.2 equiv) was added to the reaction which was slowly warmed to 23 ºC. Upon complete consumption of starting material (as determined by TLC), the reaction was filtered over celite with CH_2Cl_2. The crude reaction mixture was diluted with approximately 1:1 $Na_2S_2O_3$ and $NaHCO_3$ solutions. The layers were separated, and the product was extracted three times with CH_2Cl_2. The combined organic layer was washed with $NaHCO_3$ two times, washed with brine, dried over Na_2SO_4, filtered, and concentrated under reduced pressure. The crude product was purified by flash silica gel column chromatography (SiO_2, 25–30% EtOAc/Hexanes) to afford enone **279** as a colorless oil (37.2 mg, 0.08 mmol, 78% yield, 1:3.7 dr). Diastereomers are inconsequential and, therefore, are not separated.

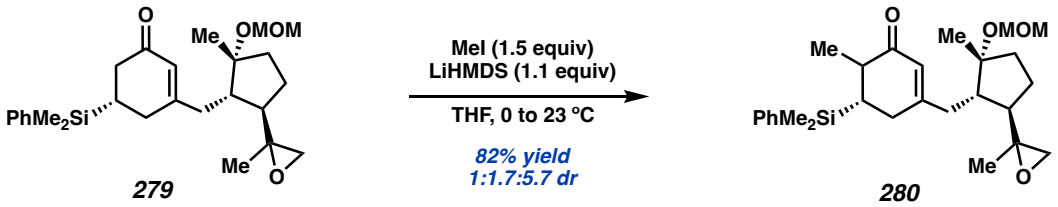
^{1}H NMR (400 MHz, $CDCl_3$) major diastereomer: δ 7.52 – 7.45 (m, 2H), 7.42 – 7.34 (m, 3H), 5.89 (d, *J* = 1.9 Hz, 1H), 4.66 – 4.60 (m, 2H), 3.33 (s, 3H), 2.62 – 2.33 (m, 4H), 2.30 – 2.10 (m, 4H), 2.07 – 1.68 (m, 3H), 1.62 – 1.50 (m, 2H), 1.51 – 1.39 (m, 2H), 1.22 (s, 3H), 1.18 (s, 3H), 0.33 (d, *J* = 2.6 Hz, 6H).

^{13}C NMR (100 MHz, CDCl3) major diastereomer: δ 199.8, 167.1, 136.2, 133.9, 129.5, 128.0, 126.5, 91.3, 85.5, 58.3, 55.6, 53.1, 50.0, 49.8, 37.9, 37.6, 36.6, 30.9, 25.4, 23.1, 22.8, 19.0, -5.3, -5.5.

IR (Neat Film, NaCl): 2954, 2354, 1730, 1666, 1250, 1144, 1038, 834 cm^{-1}.

HRMS (FD+): *m/z* calc'd for $C_{26}H_{38}O_4Si$ $[M]^+$: 442.2534, found 442.2533.

Optical Rotation: $[\alpha]_D^{21}$ 11.1 (c 1.00, $CHCl_3$).



(5*S*)-5-(dimethyl(phenyl)silyl)-3-(((1*S*,2*R*,5*R*)-2-(methoxymethoxy)-2-methyl-5-((*R*)-2-methyloxiran-2-yl)cyclopentyl)methyl)-6-methylcyclohex-2-en-1-one (280)

A flame dried round bottom flask was charged with LHMDS (107.9 mg, 0.64 mmol, 1.1 equiv) and THF (0.37 mL, 1.75 M). The solution was cooled to 0 ºC and enone **279** (259.4 mg, 0.59 mmol, 1.0 equiv) in THF (0.47 mL, 1.25 M) was added dropwise and stirring was continued at 0 ºC for 30 minutes. MeI (55 µL, 0.88 mmol, 1.5 equiv) was added dropwise. The reaction was gradually warmed to 23 ºC. Upon complete consumption of starting material (as determined by TåLC), the reaction was diluted with a saturated solution of NH_4Cl and the product was extracted three times with EtOAc. The combined organic layers were washed with brine, dried over Na_2SO_4, filtered, and concentrated under reduced pressure. The crude product was purified by flash silica gel column chromatography (SiO_2, 25% EtOAc/Hexanes) to afford the corresponding methylated enone **280** as a colorless oil

(219 mg, 0.48 mmol, 82% yield, 1:1.7:5.7 dr). Diastereomers are inconsequential and, therefore, are not separated.

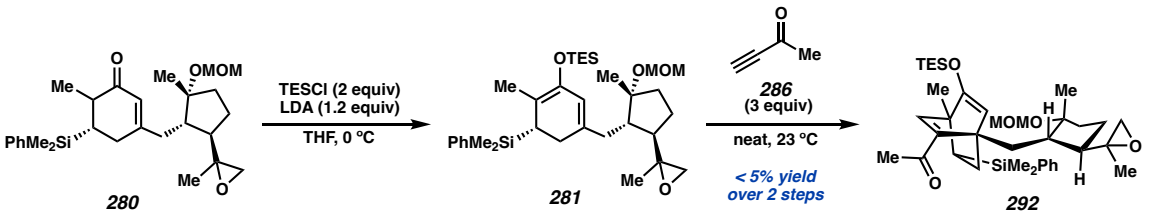
^{1}H NMR (400 MHz, $CDCl_3$) major diastereomer: δ 7.52 – 7.45 (m, 2H), 7.40 – 7.33 (m, 3H), 5.86 (s, 1H), 4.68 – 4.58 (m, 2H), 3.33 (s, 3H), 2.61 – 2.38 (m, 3H), 2.39 – 2.06 (m, 4H), 2.06 – 1.76 (m, 3H), 1.79 – 1.57 (m, 1H), 1.57 – 1.45 (m, 1H), 1.47 – 1.36 (m, 2H), 1.19 (s, 3H), 1.18 (s, 3H), 1.14 (d, J = 6.9 Hz, 3H), 0.37 (s, 3H), 0.35 (s, 3H).

^{13}C NMR (100 MHz, $CDCl_3$) all diastereomers: δ 202.0, 165.2, 137.7, 133.8, 133.7, 129.3, 129.2, 129.2, 128.0, 127.9, 125.9, 91.3, 85.3, 58.3, 57.7, 55.5, 55.5, 53.0, 52.9, 50.0, 49.8, 49.0, 42.1, 42.0, 37.2, 36.6, 36.5, 36.3, 31.6, 30.9, 30.9, 29.1, 29.0, 27.9, 25.2, 25.0, 23.2, 23.0, 22.7, 19.0, 18.3, 16.1, 15.9, 14.1, -3.0, -3.1, -3.7, -4.01, -4.03.

IR (Neat Film, NaCl): 2958, 1666, 1460, 1374, 1252, 1144, 1090, 1036, 770 cm^{-1}.

HRMS (FD+): *m/z* calc'd for $C_{27}H_{40}O_4Si$ $[M]^+$: 456.2680, found 466.2687.

Optical Rotation: $[\alpha]_D^{21}$ –1.1 (c 1.00, $CHCl_3$).



1-((1*S*,8*R*)-8-(dimethyl(phenyl)silyl)-1-(((1*R*,2*R*,5*S*)-2-(methoxymethoxy)-2-methyl-5-(2-methyloxiran-2-yl)cyclopentyl)methyl)-4-methyl-5-((triethylsilyl)oxy)bicyclo[2.2.2]octa-2,5-dien-2-yl)ethan-1-one (292)

A flame dried vial was charged with *i*-Pr_2NH (19 µL, 0.14 mmol, 1.25 equiv) and THF (0.14 mL, 1.0 M). The solution was cooled to 0 ºC and *n*-BuLi (53 µL, 0.13 mmol, 1.2 equiv) was added dropwise. The resultant solution was stirred for 30 min at 0 ºC. Enone

280 (50.0 mg, 0.11 mmol, 1.0 equiv) in THF (0.14 mL, 0.8 M) was added dropwise and stirring was continued at 23 ºC for 30 minutes. The solution was cooled to 0 ºC and TESCl (37 µL, 0.22 mmol, 2.0 equiv) was added dropwise. Upon complete consumption of starting material (as determined by TLC), the reaction was diluted with a saturated solution of NH_4Cl and the product was extracted three times with EtOAc. The combined organic layers were washed with brine, dried over Na_2SO_4, filtered, and concentrated under reduced pressure.

The crude diene **281** was transferred to a vial and was placed under high vacuum to remove trace solvent and then backfilled with N_2. Dienophile **286** (26 µL, 0.33 mmol, 3 equiv) was added and the mixture was stirred neat at 23 ºC. Upon complete consumption of starting material (as determined by TLC), the reaction mixture was loaded directly onto silica for flash silica gel column chromatography (SiO_2, 10–15–25% EtOAc/Hexanes) and the fractions containing product were them purified further via preparatory TLC (10% EtOAc/Toluene x3) to afford product **292** (less than 3.0 mg, 0.005 mmol, 4% yield, 1:1.6 dr). Diastereomers were inseparable and relative stereochemistry was unable to be assigned.

^{1}H NMR (600 MHz, $CDCl_3$) mixture of diastereomers: δ 7.47 – 7.43 (m, 4H), 7.33 – 7.29 (m, 5.6H), 6.70 (s, 0.7H, minor), 6.69 (s, 1H, major), 5.28 (s, 1H, major), 5.25 (s, 0.7H, minor), 4.79 (d, *J* = 7.1 Hz, 1H, major), 4.74 (d, *J* = 7.1 Hz, 0.7H, minor), 4.59 (d, *J* = 7.1 Hz, 0.7H, minor), 4.56 (d, *J* = 7.1 Hz, 1H, major), 3.38 (s, 2.1H, minor), 3.37 (s, 3H, major), 2.69 (q, *J* = 4.9 Hz, 2H), 2.61 – 2.54 (m, 1.6H), 2.38 (d, *J* = 4.6 Hz, 0.7H), 2.28 – 2.24 (m, 2H), 2.21 (s, 3H, major), 2.19 (s, 2.1H, minor), 2.17 – 1.91 (m, 6H), 1.80 – 1.73 (m, 1H), 1.64 (s, 1H), 1.52 – 1.32 (m, 8H), 1.31 (s, 2.1H, minor), 1.31 (s, 3H, major), 1.25

(s, 2.1H, minor), 1.24 (s, 3H, major), 1.17 (s, 2.1H, minor), 1.15 (s, 3H, major), 0.96 – 0.92 (m, 15.3H), 0.70 – 0.58 (m, 10.2H), 0.33 (s, 5H), 0.23 (s, 3H, major), 0.23 (s, 2.1H, minor). **HRMS (FD+):** *m/z* calc'd for $C_{37}H_{58}O_5Si_2$ $[M]^+$: 638.3817, found 638.3840.

5.6 REFERENCES

(1) Yang, X.-W.; Grossman, R. B.; Xu, G. Research Progress of Polycyclic Polyprenylated Acylphloroglucinols. *Chem. Rev.* **2018**, *118*, 3508–3558.

(2) Richard, J.-A.; Pouwer, R. H.; Chen, D. Y.-K. The Chemistry of the Polycyclic Polyprenylated Acylphloroglucinols. *Angew. Chem. Int. Ed.* **2012**, *51*, 4536–4561.

(3) Lin Phang, Y.; Liu, S.; Zheng, C.; Xu, H. Recent Advances in the Synthesis of Natural Products Containing the Phloroglucinol Motif. *Nat. Prod. Rep.* **2022**, *39*, 1766–1802.

(4) Ciochina, R.; Grossman, R. B. Polycyclic Polyprenylated Acylphloroglucinols. *Chem. Rev.* **2006**, *106*, 3963–3986.

(5) Duan, Y.; Sun, W.; Li, Y.; Shi, Z.; Li, L.; Zhang, Y.; Huang, K.; Zhang, Z.; Qi, C.; Zhang, Y. Spirohypertones A and B as Potent Antipsoriatics: Tumor Necrosis Factor-*α* Inhibitors with Unprecedented Chemical Architectures. *Acta Pharm. Sin. B* **2024**, *14*, 2646–2656.

(6) Zhou, H.-M.; Ye, Y.-S.; Jiang, N.-N.; Mu, R.-F.; Wang, Q.; Hu, J.; Liu, X.; Qin, W.-Y.; Xu, G.; Xiong, W.-Y. Adipogenesis Inhibitory Activity of Hypersampsone P from Hypericum Subsessile. *Nat. Prod. Bioprospect.* **2020**, *10*, 163–170.

(7) Hu, Y.-L.; Hu, K.; Kong, L.-M.; Xia, F.; Yang, X.-W.; Xu, G. Norascyronones A and B, 2,3,4-nor-Polycyclic Polyprenylated Acylphloroglucinols from Hypericum Ascyron. *Org. Lett.* **2019**, *21*, 1007–1010.

(8) Wang, S.; Shao, Y.; Tian, L.; Li, L.; Wang, S.; Wang, X.; Shen, T.; Ren, D. Two Rearranged Acylphloroglucinols with Moderate Neuroprotective Effects from *Hypericum Ascyron* Linn. *Fitoterapia* **2024**, *174*, 105852.

(9) Njardarson, J. T. Synthetic Efforts toward [3.3.1] Bridged Bicyclic Phloroglucinol Natural Products. *Tetrahedron* **2011**, *67*, 7631–7666.

(10) Zeng, Y.-R.; Li, Y.-N.; Zhang, Z.-Z.; Hu, Z.-X.; Gu, W.; Huang, L.-J.; Li, Y.-M.; Yuan, C.-M.; Hao, X.-J. Hypermoins A–D: Rearranged Nor-Polyprenylated Acylphloroglucinols from the Flowers of *Hypericum Monogynum*. *J. Org. Chem.* **2021**, *86*, 7021–7027.

(11) Trost, B. M.; Schneider, S. Pyrones as Substrates for Palladium–Catalyzed [4+3] Cycloadditions. *Angew. Int. Ed. Engl.* **1989**, *2*, 213–215.

(12) Lee, T. L.; Roden, F. S.; Yeoh, H. T.-L. Selectivity of Bifunctional Annulating Reagents; Additional Rules for Ring Closure. *Tetrahedron Lett.* **1990**, *31*, 2063–2066

(13) Sanchez, A. and Maimone, T. J. Taming Shapeshifting Anions: Total Synthesis of Ocellatusone C. *J. Am. Chem. Soc.* **2022**, *144*, 7594–7599.

(14) Cai, X.; Li, L.; Wang, Y.-C.; Zhou, J.; Dai, M. Total Syntheses of Phleghenrines A and C. *Org. Lett*. **2023**, *25*, 5258–5261.

(15) Flesch, K. N.; Cusumano, A. Q.; Chen, P.-J.; Strong, C. S.; Sardini, S. R.; Du, Y. E.; Bartberger, M. D.; Goddard, W. A.; Stoltz, B. M. Divergent Catalysis: Catalytic

Asymmetric [4+2] Cycloaddition of Palladium Enolates. *J. Am. Chem. Soc.* **2023**, *145*, 11301–11310.

(16) Brocksom, T. J.; Pesquero, E. T. C.; Lopes, F. T. The Synthesis of Chiral Cycloheptane Precursors of Guaiane Sesquiterpenes. *Synth. Commun.* **1990**, *20*, 1181–1191. Also see: a) Nishimura, T.; Unni, A. K.; Yokoshima, S.; Fukuyama, T. Concise Total Synthesis of (+)-Lyconadin A. *J. Am. Chem. Soc.* **2011**, *133*, 418–419. b) Nishimura, T.; Unni, A. K.; Yokoshima, S.; Fukuyama, T. Total Syntheses of Lyconadins A–C. *J. Am. Chem. Soc.* **2013**, *135*, 3243–3247.

(17) Langhanki, J.; Rudolph, K.; Erkel, G.; Opatz, T. Total Synthesis and Biological Evaluation of the Natural Product (−)-Cyclonerodiol, a New Inhibitor of IL-4 Signaling. *Org. Biomol. Chem.* **2014**, *12*, 9707–9715.

(18) Bolze, P.; Dickmeiss, G.; Jørgensen, K. A. Organocatalytic Asymmetric Synthesis of 5-(Trialkylsilyl)cyclohex-2-enones and the Transformation into Useful Building Blocks. *Org. Lett.* **2008**, *10*, 3753–3756.

(19) Hafeman, N. J.; Loskot, S. A.; Reimann, C. E.; Pritchett, B. P.; Virgil, S. C.; Stoltz, B. M. The Total Synthesis of (–)-Scabrolide A. *J. Am. Chem. Soc.* **2020**, *142*, 8585–8590.

(20) Pangborn, A. M.; Giardello, M. A.; Grubbs, R. H.; Rosen, R. K.; Timmers, F. J. Safe and Convenient Procedure for Solvent Purification. *Organometallics* **1996**, *15*, 1518–1520.

(21) Jacobi, P. A.; Li, Y. Enantioselective Syntheses of Ring-C Precursors of Vit. B12. Reagent Control. *Org. Lett.* **2003**, *5*, 701–704.

(22) Gatti, M.; Drinkel, E.; Wu, L.; Pusterla, I.; Gaggia, F.; Dorta, R. Efficient Ring-Closing Metathesis of Alkenyl Bromides: The Importance of Protecting the Catalyst during the Olefin Approach. *J. Am. Chem. Soc.* **2010**, *132*, 15179–15181.

APPENDIX 4

Spectra Relevant to Chapter 5: Progress Toward the Total Synthesis of Hypermoin A

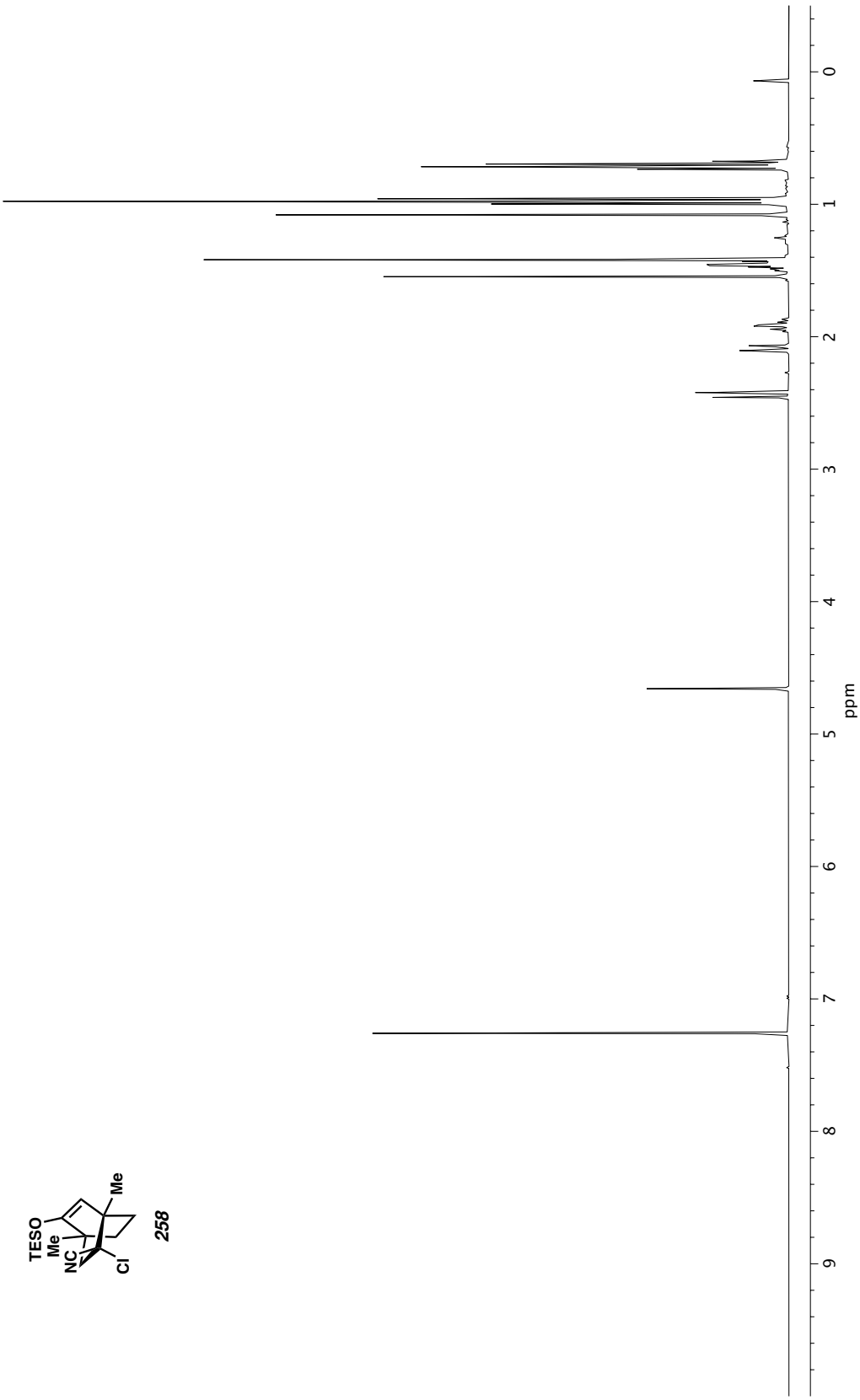


Figure A4.1. *^1H NMR (400 MHz, $CDCl_3$) of compound **258**.*

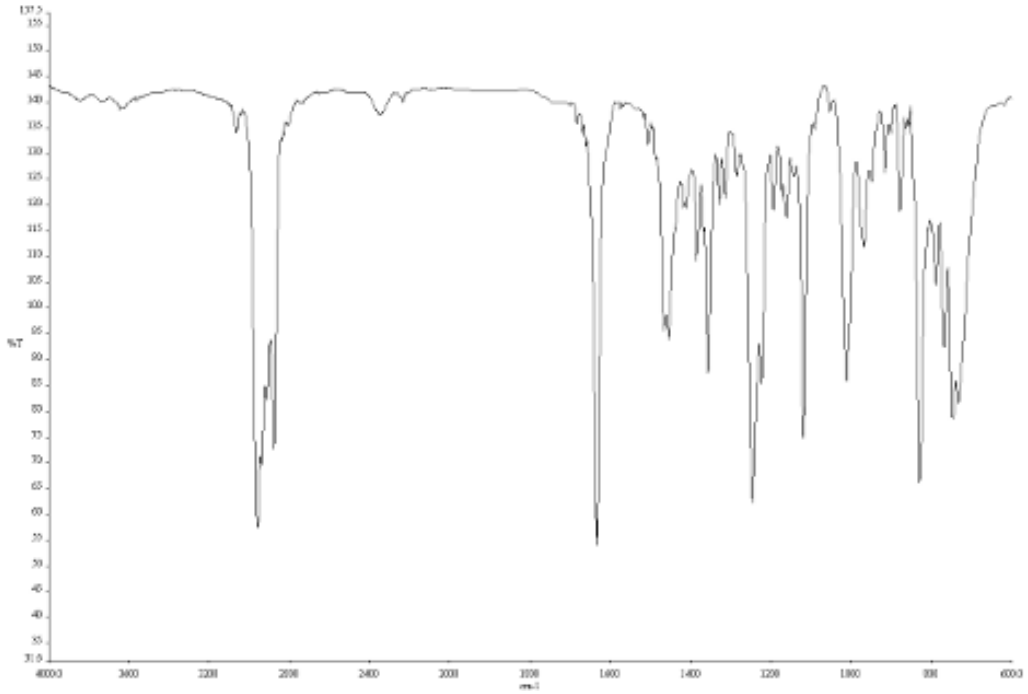


Figure A4.2. *Infrared spectrum (Thin Film, NaCl) of compound* ***258****.*

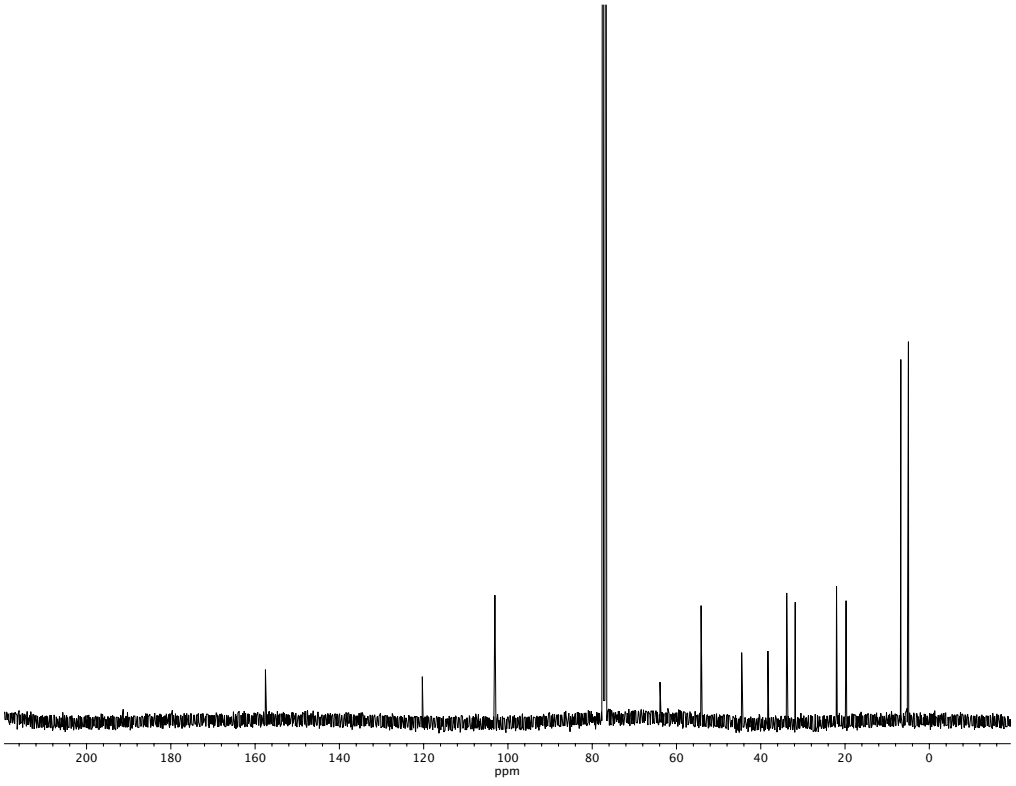


Figure A4.3. *^{13}C NMR (100 MHz, $CDCl_3$) of compound* ***258****.*

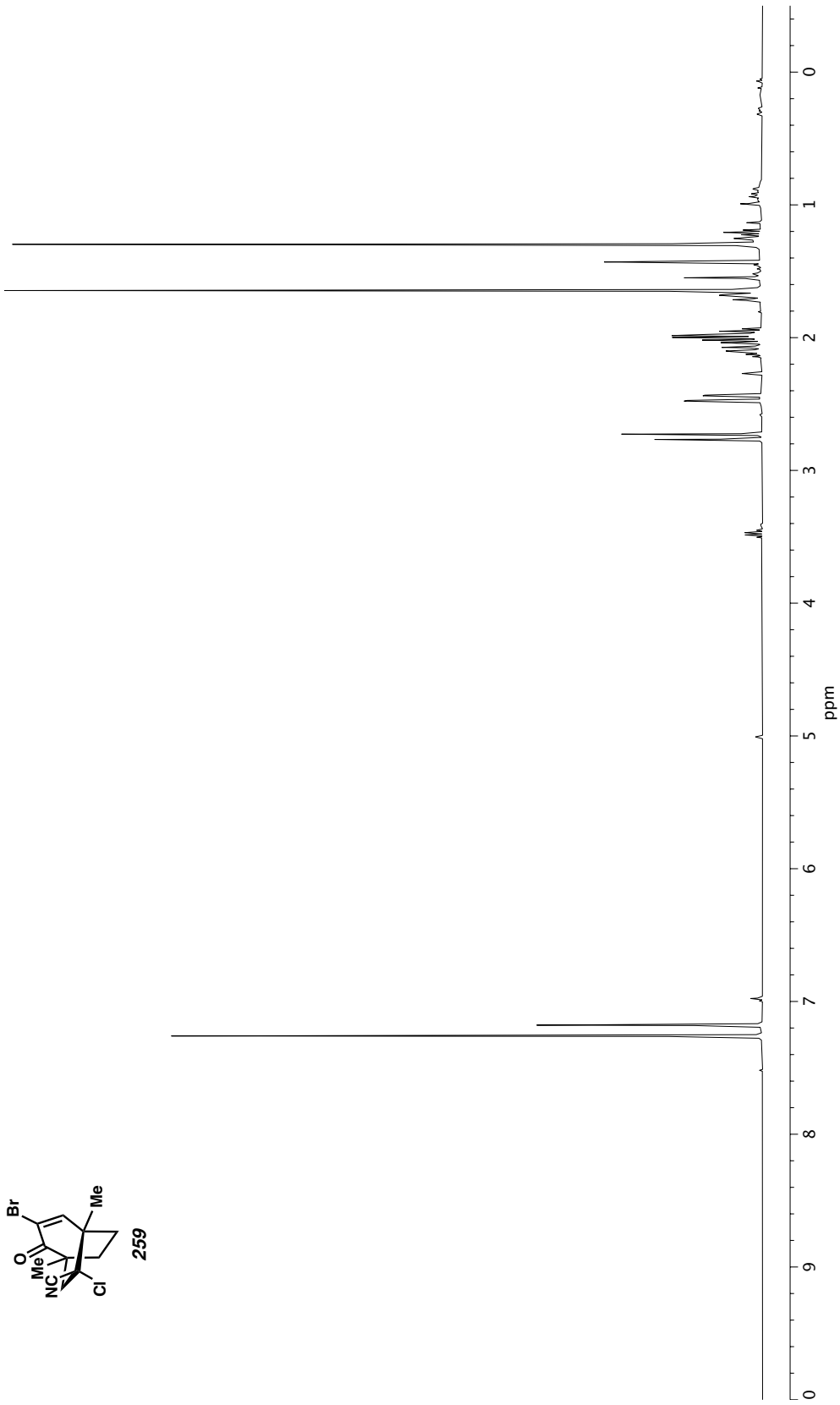


Figure A4.4. *^1H NMR (400 MHz, $CDCl_3$) of compound* ***259***.

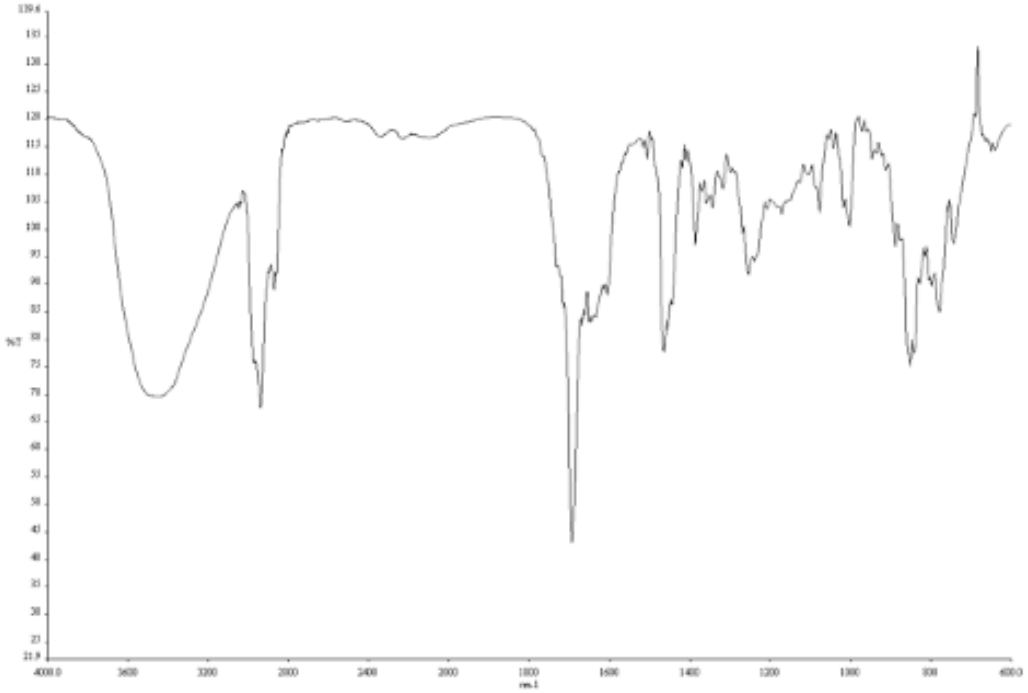


Figure A4.5. *Infrared spectrum (Thin Film, NaCl) of compound* ***259****.*

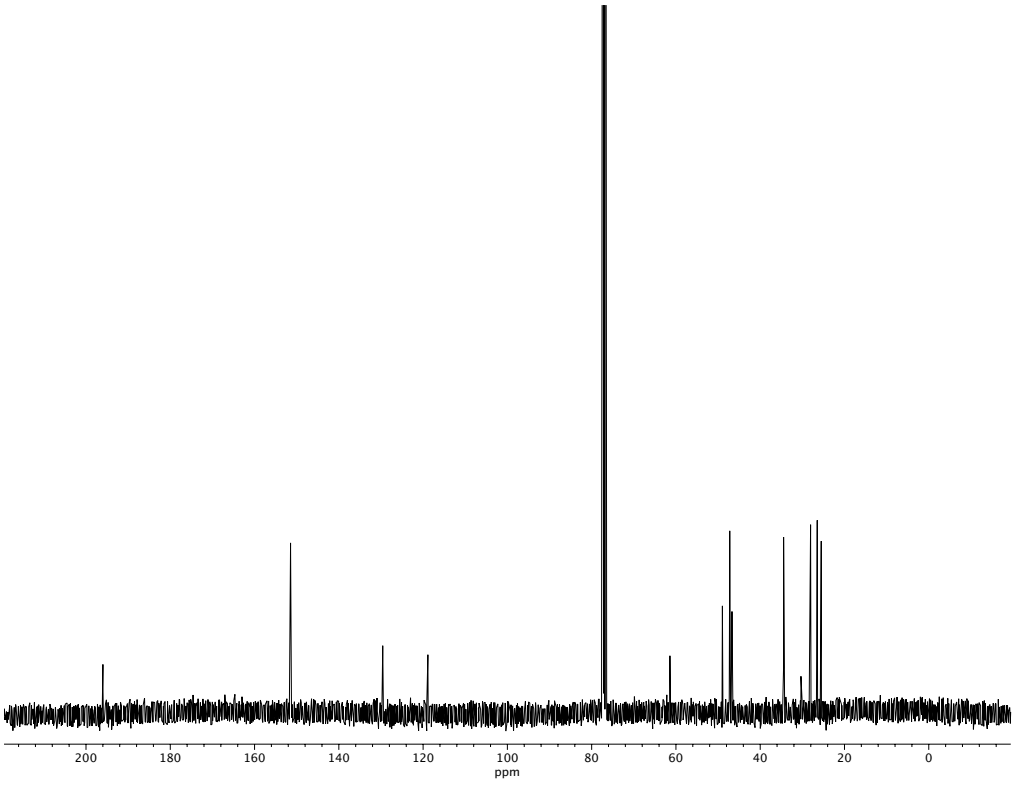


Figure A4.6. *^{13}C NMR (100 MHz, $CDCl_3$) of compound* ***259****.*

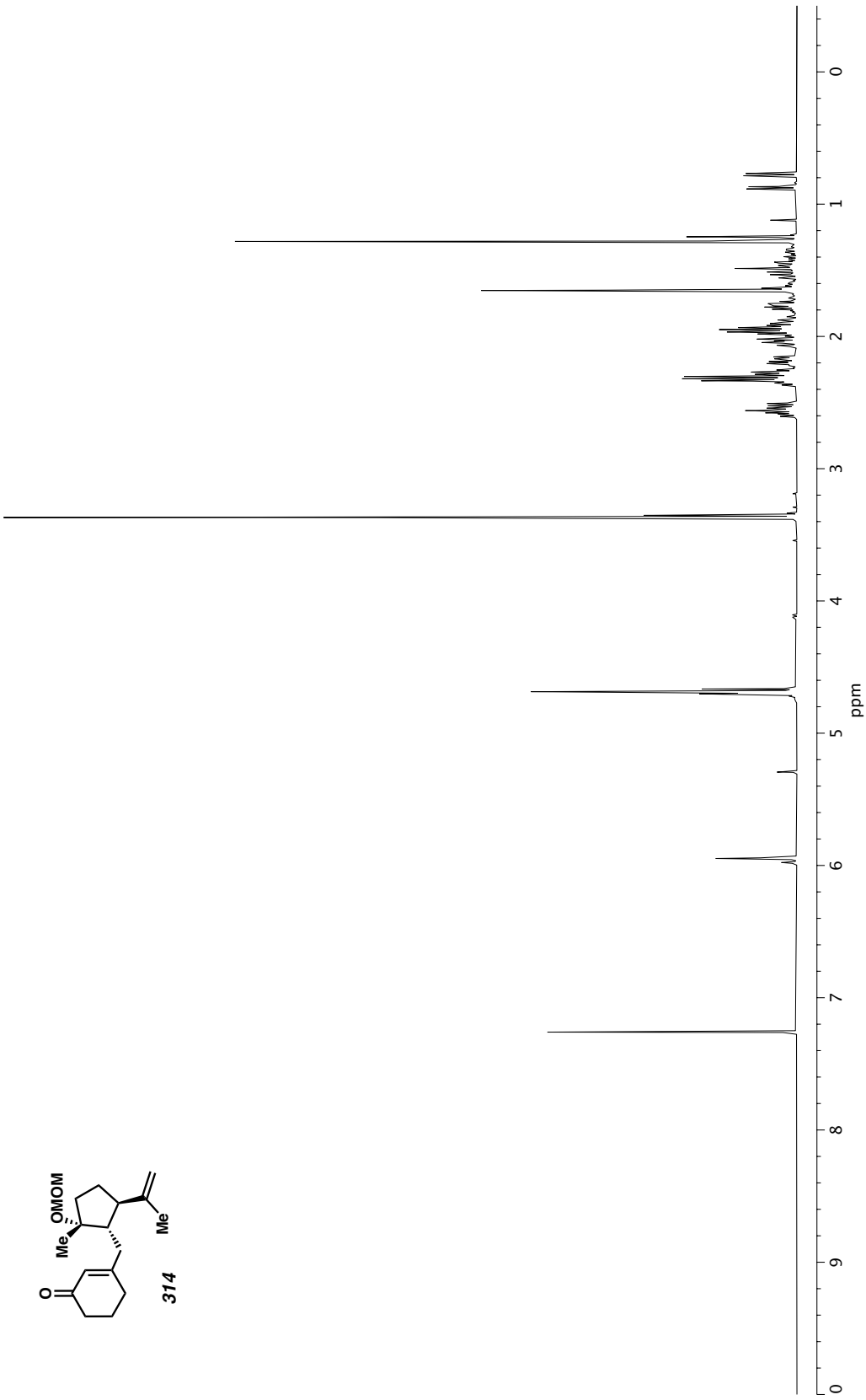


Figure A4.7. *^{1}H NMR (400 MHz, $CDCl_3$) of compound* ***314****.*

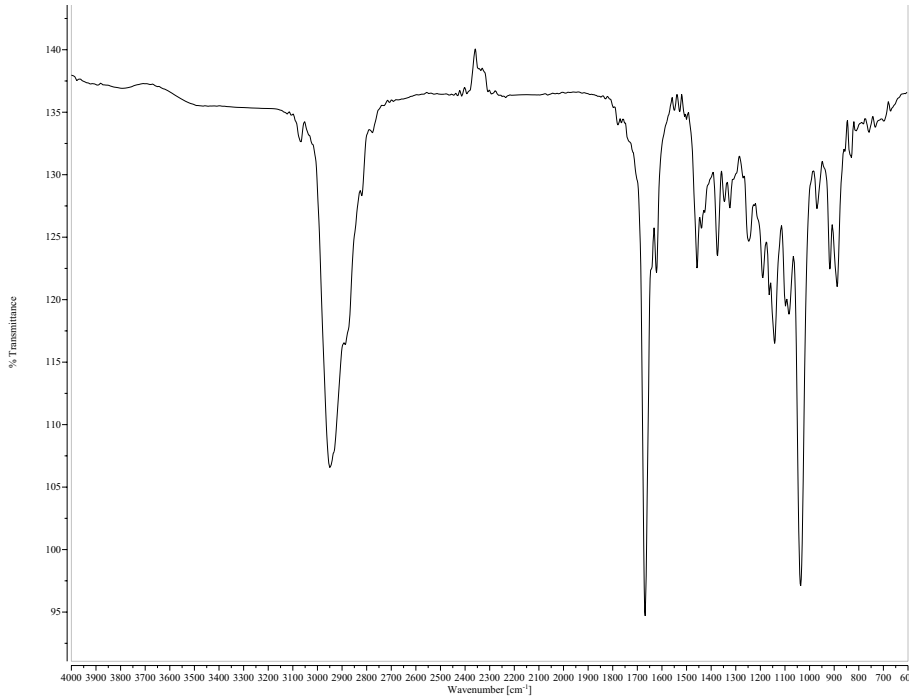


Figure A4.8. *Infrared spectrum (Thin Film, NaCl) of compound* ***314****.*

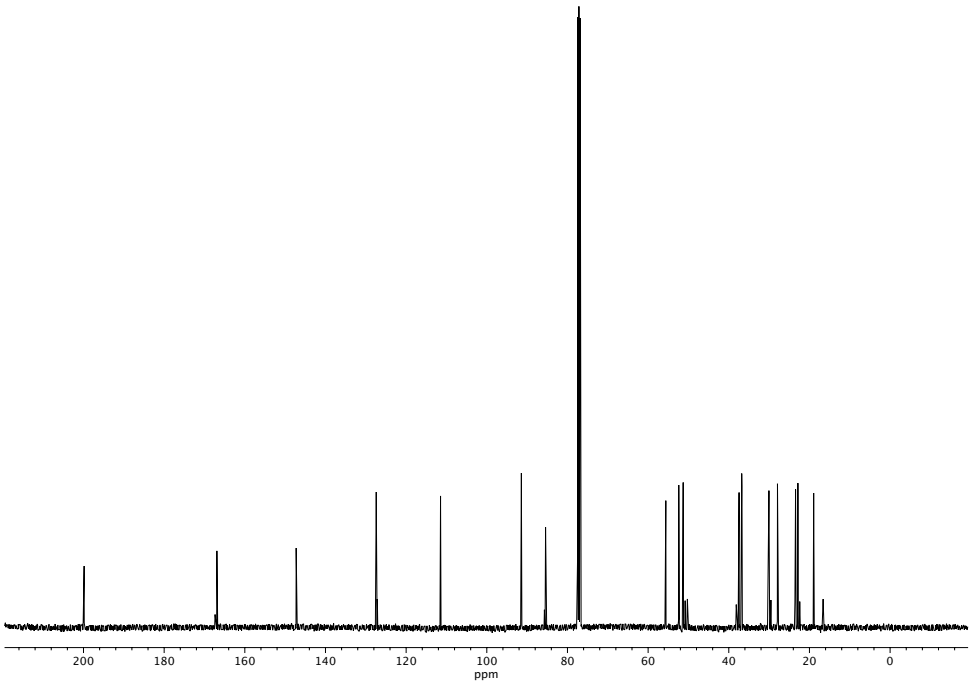
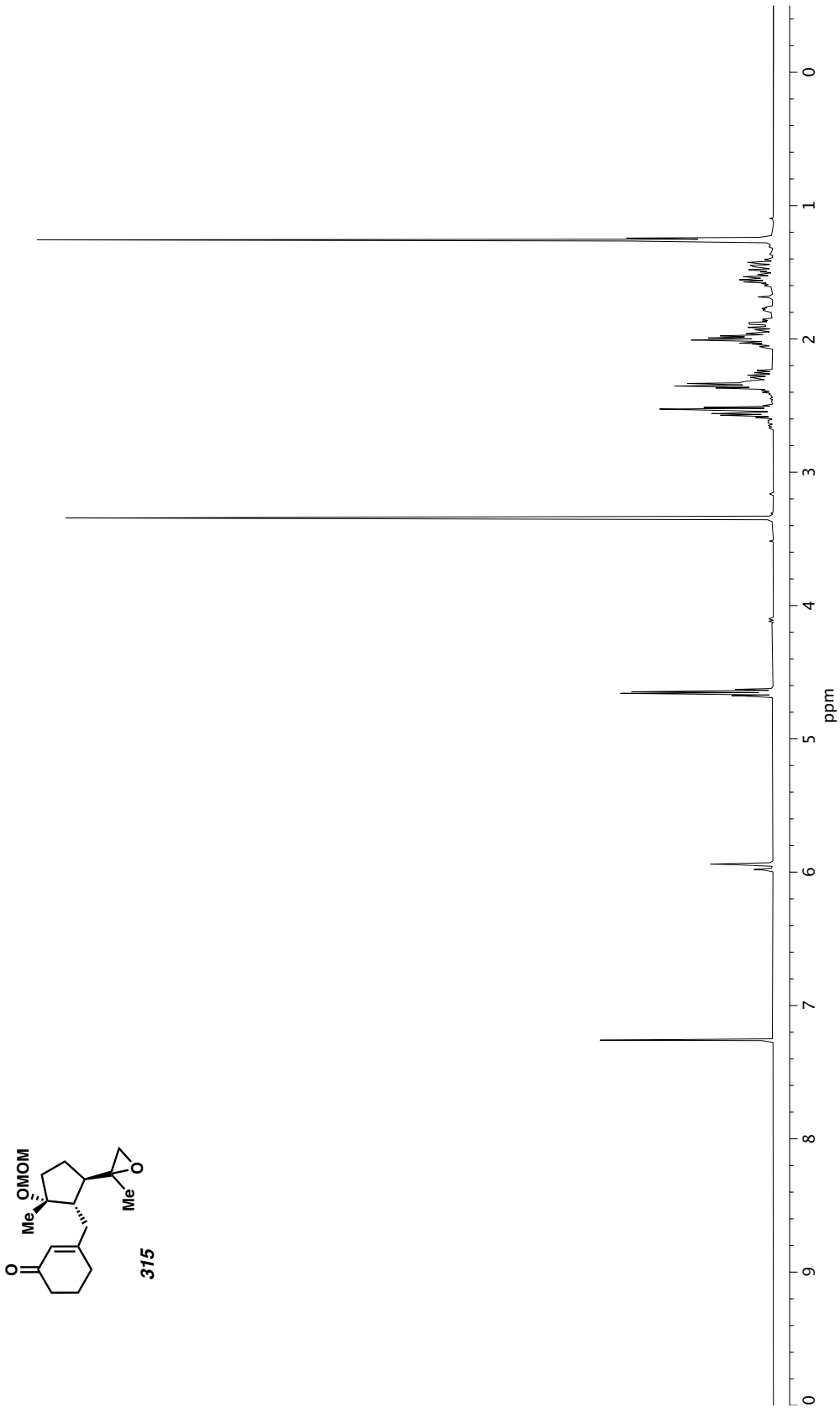


Figure A4.9. *^{13}C NMR (100 MHz, $CDCl_3$) of compound* ***314****.*



315

Figure A4.10. *^1H NMR (400 MHz, $CDCl_3$) of compound* ***315****.*

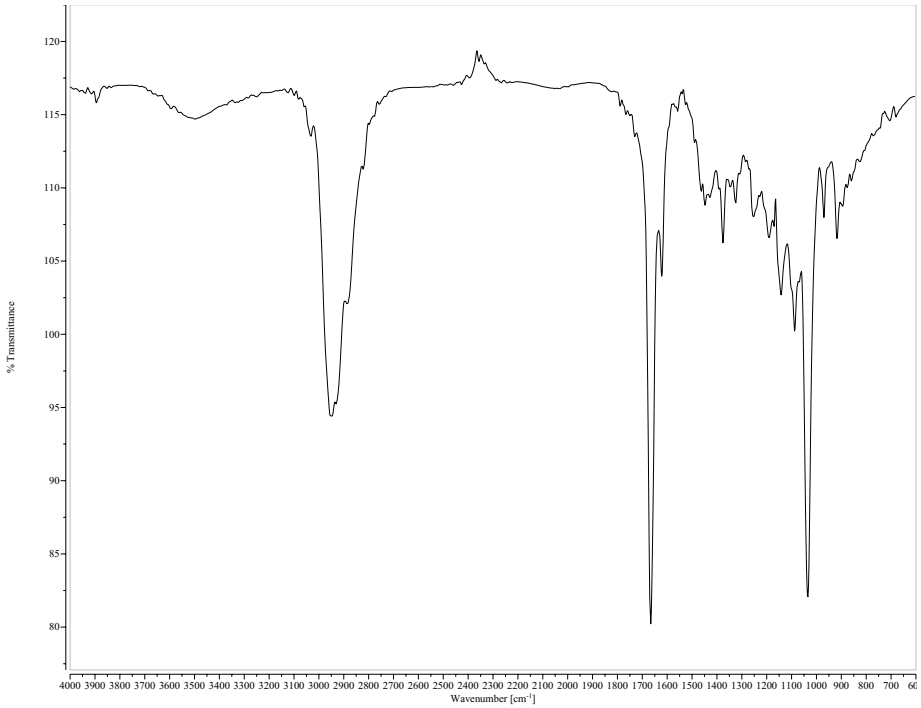


Figure A4.11. *Infrared spectrum (Thin Film, NaCl) of compound* ***315****.*

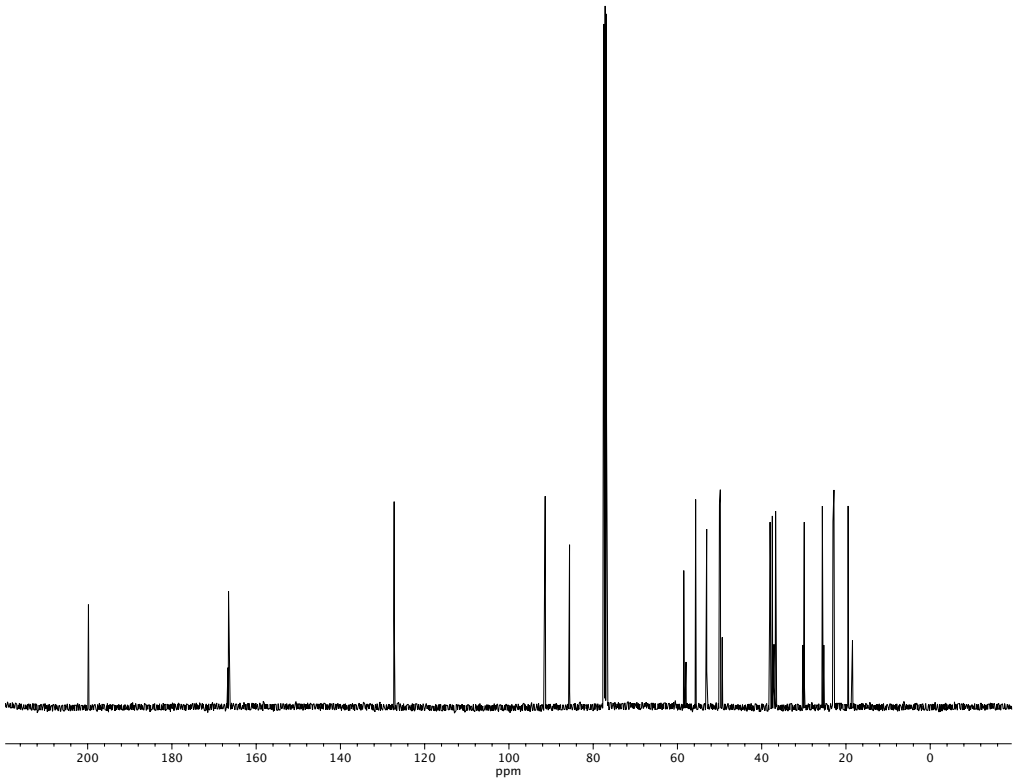


Figure A4.12. *^{13}C NMR (100 MHz, $CDCl_3$) of compound* ***315****.*

Figure A4.13. *^1H NMR (400 MHz, $CDCl_3$) of compound* ***283***.

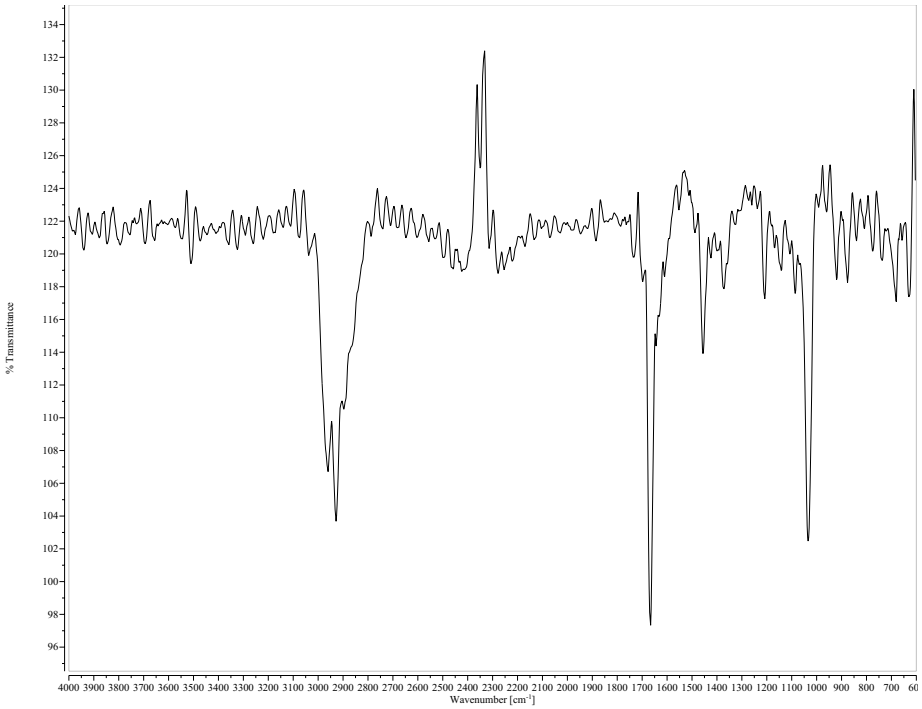


Figure A4.14. *Infrared spectrum (Thin Film, NaCl) of compound* ***283****.*

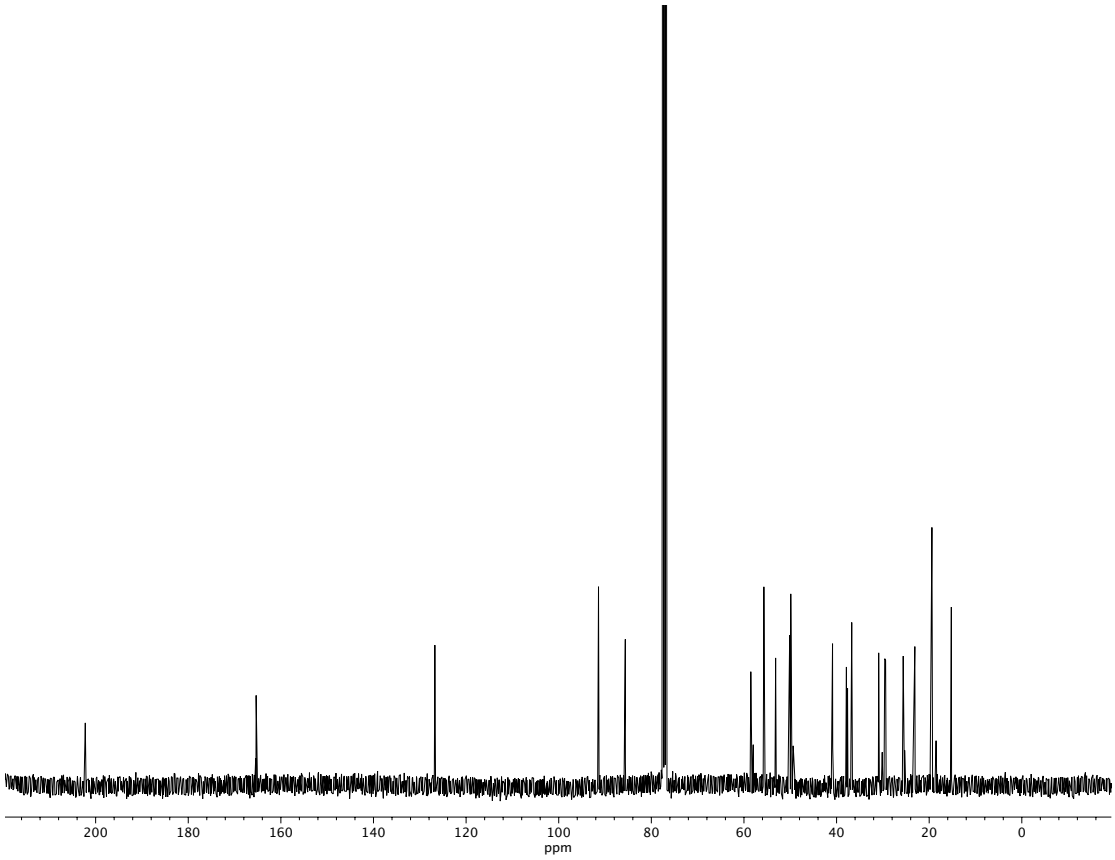


Figure A4.15. *^{13}C NMR (100 MHz, $CDCl_3$) of compound* ***283****.*

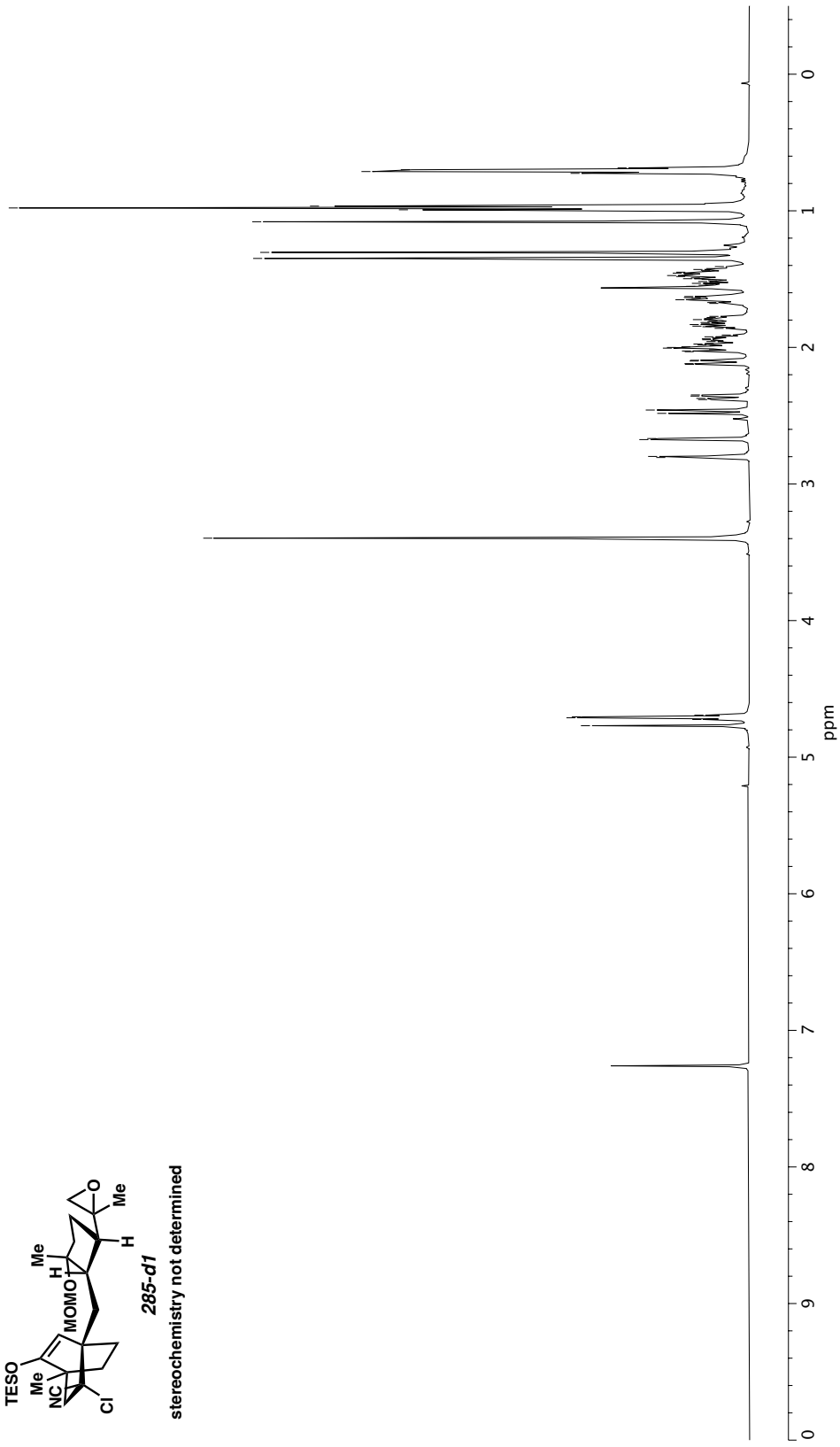


Figure A4.16. *^1H NMR (600 MHz, $CDCl_3$) of compound* ***285-d1***.

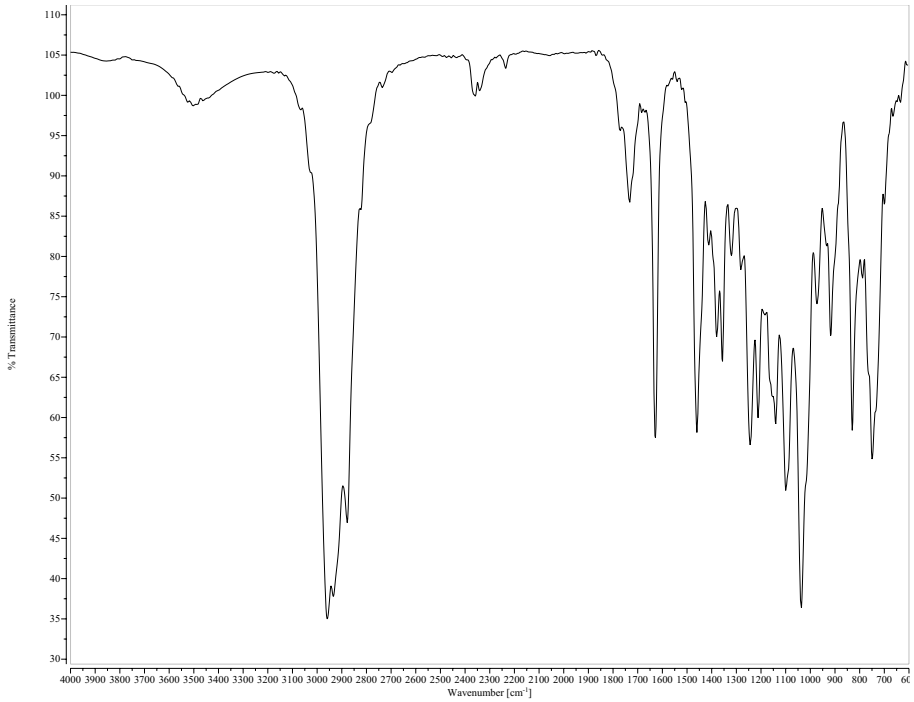


Figure A4.17. *Infrared spectrum (Thin Film, NaCl) of compound* ***285-d1***.

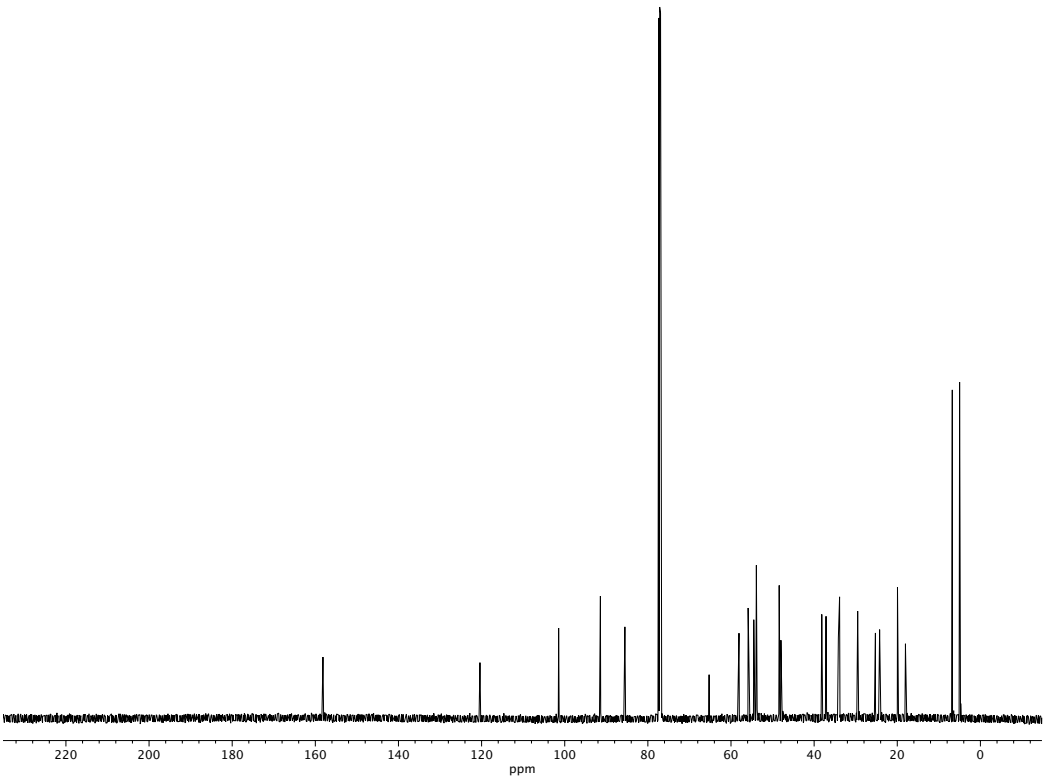


Figure A4.18. *^{13}C NMR (151 MHz, $CDCl_3$) of compound* ***285-d1***.

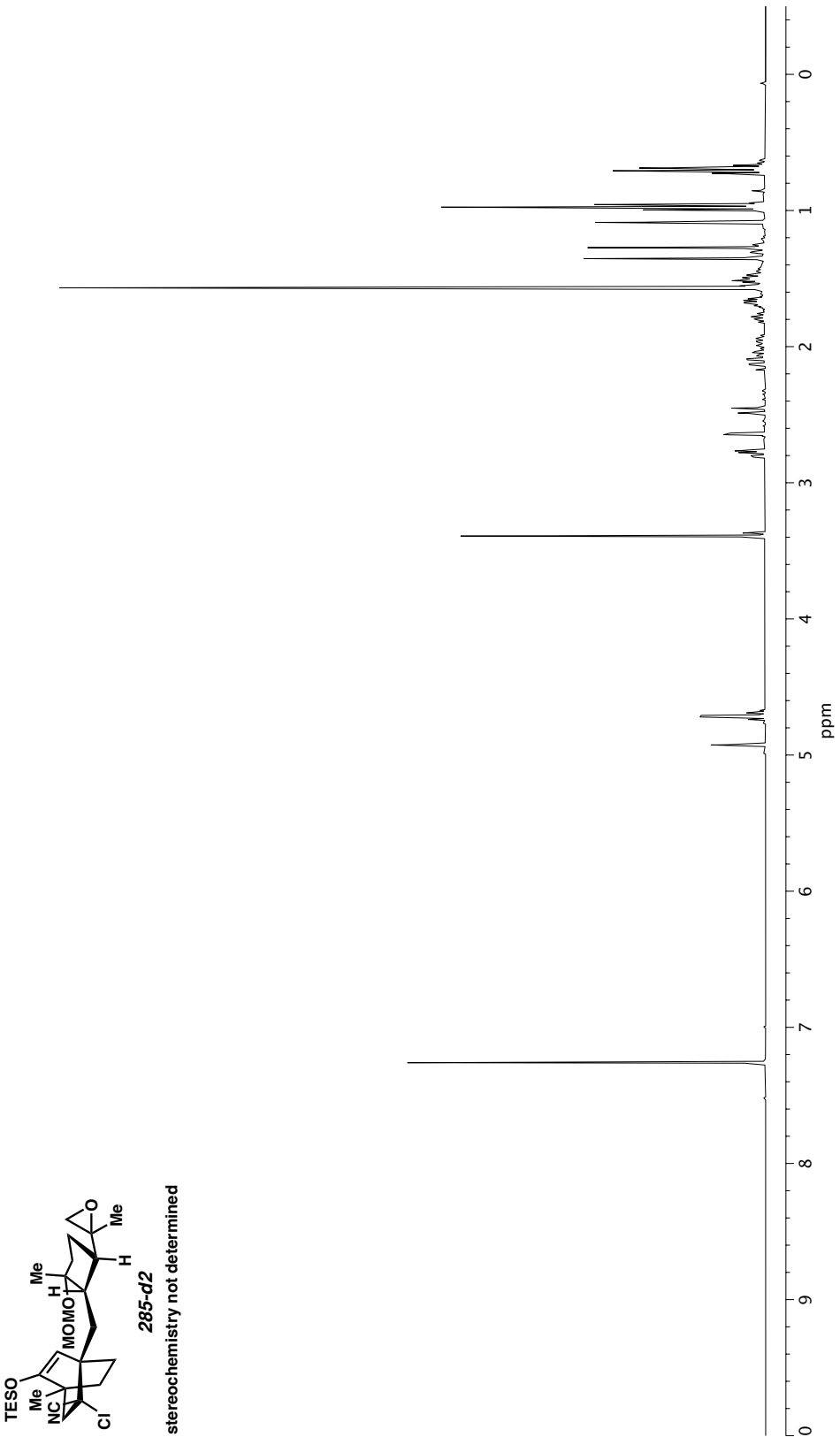


Figure A4.19. *^1H NMR (400 MHz, $CDCl_3$) of compound* ***285-d2***.

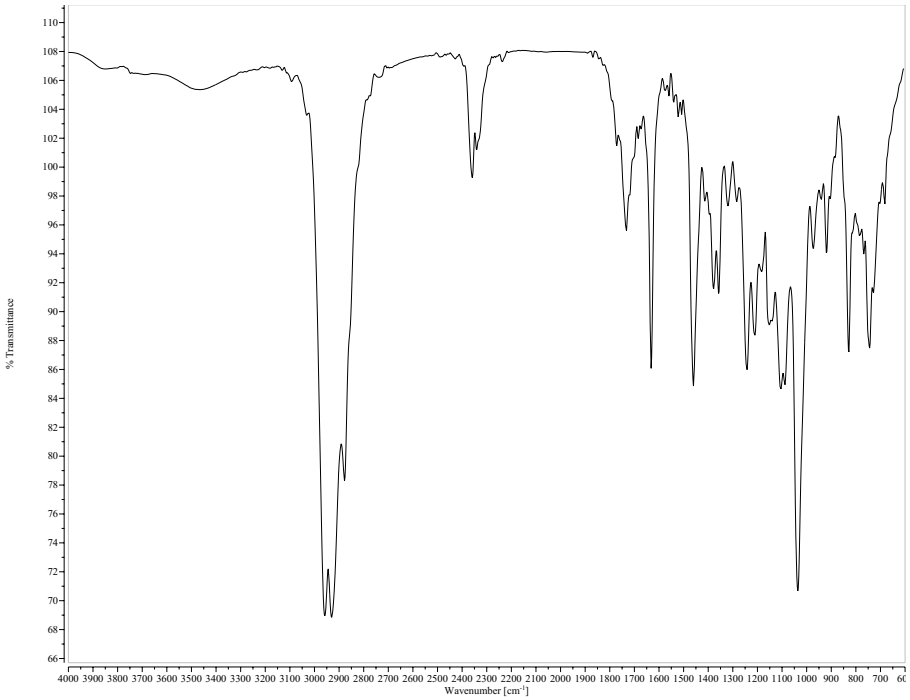


Figure A4.20. *Infrared spectrum (Thin Film, NaCl) of compound* ***285-d2****.*

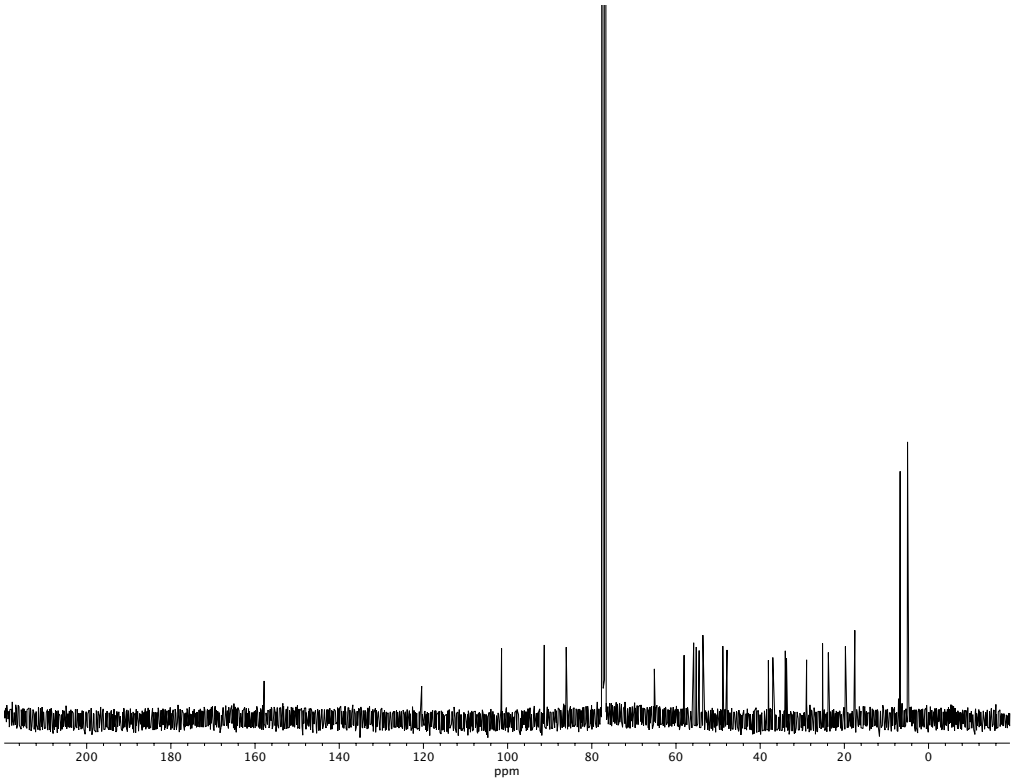


Figure A4.21. *^{13}C NMR (100 MHz, $CDCl_3$) of compound* ***285-d2****.*

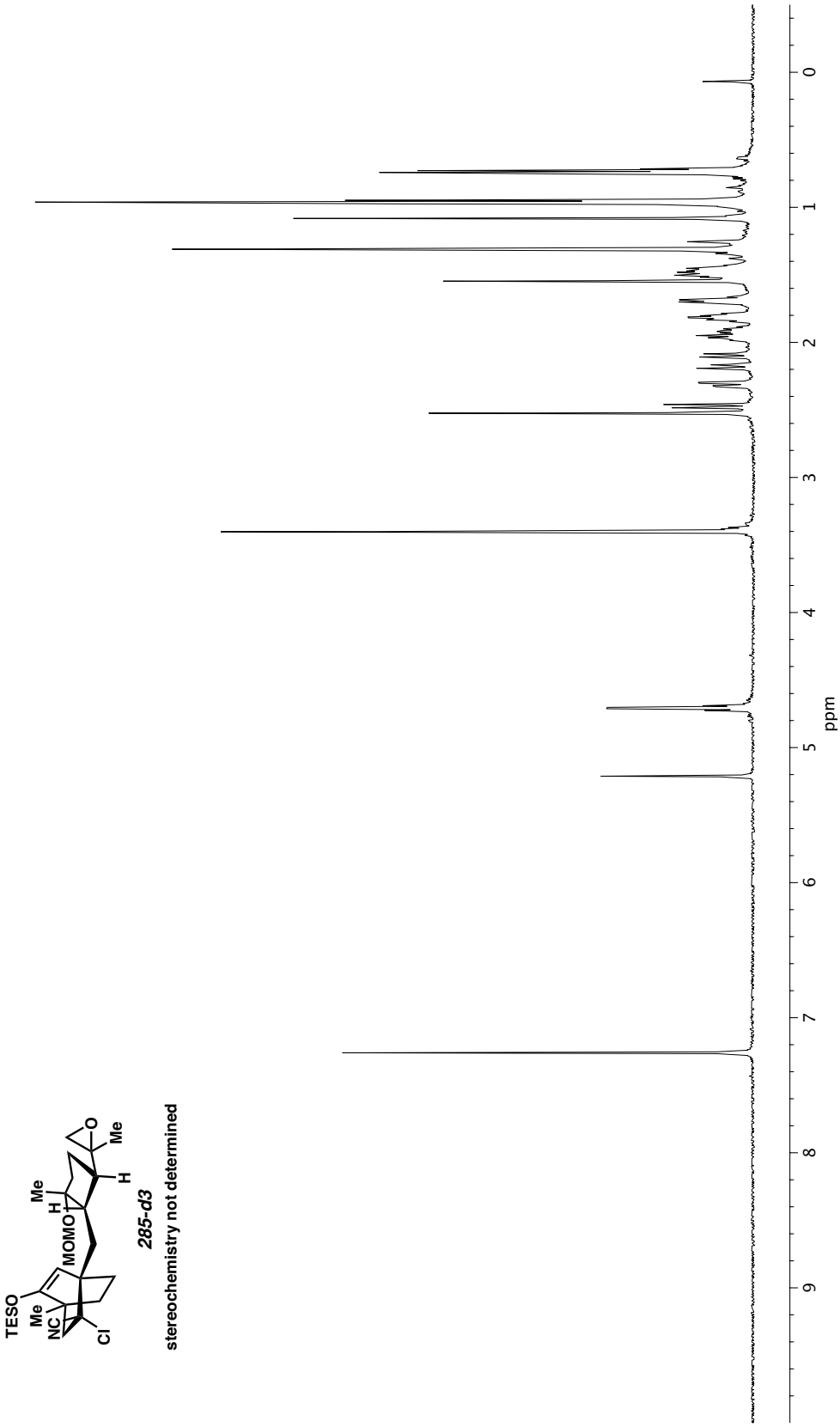


Figure A4.22. *^1H NMR (600 MHz, $CDCl_3$) of compound* ***285-d3***.

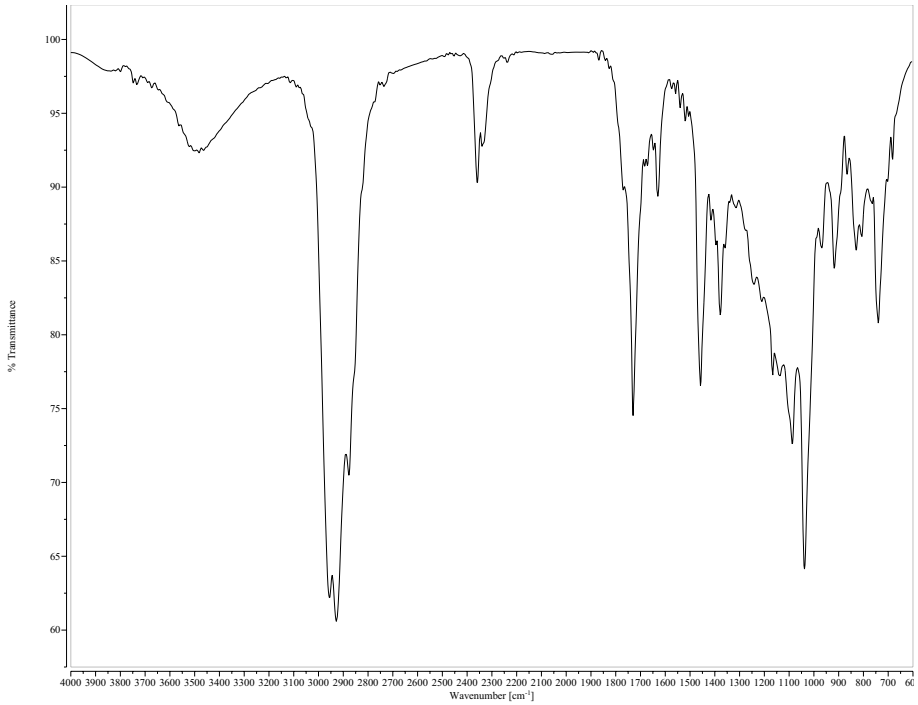


Figure A4.23. *Infrared spectrum ($CDCl_3$ solution) of compound* ***285-d3****.*

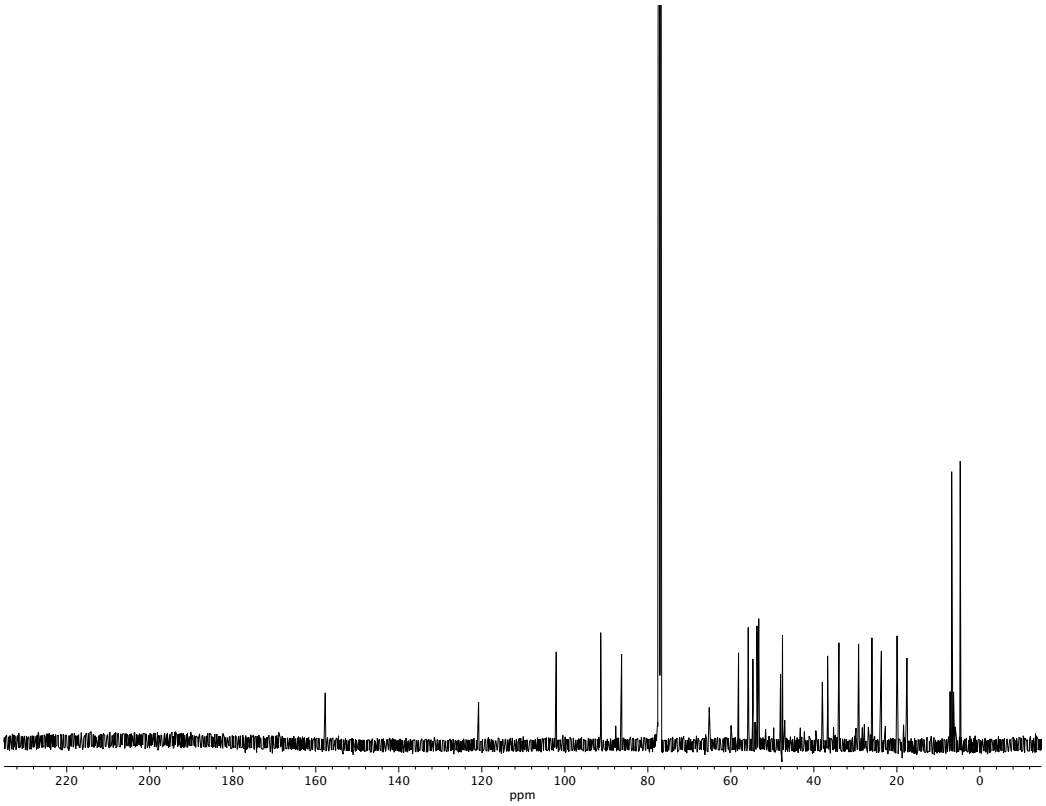


Figure A4.24. *^{13}C NMR (151 MHz, $CDCl_3$) of compound* ***285-d3****.*

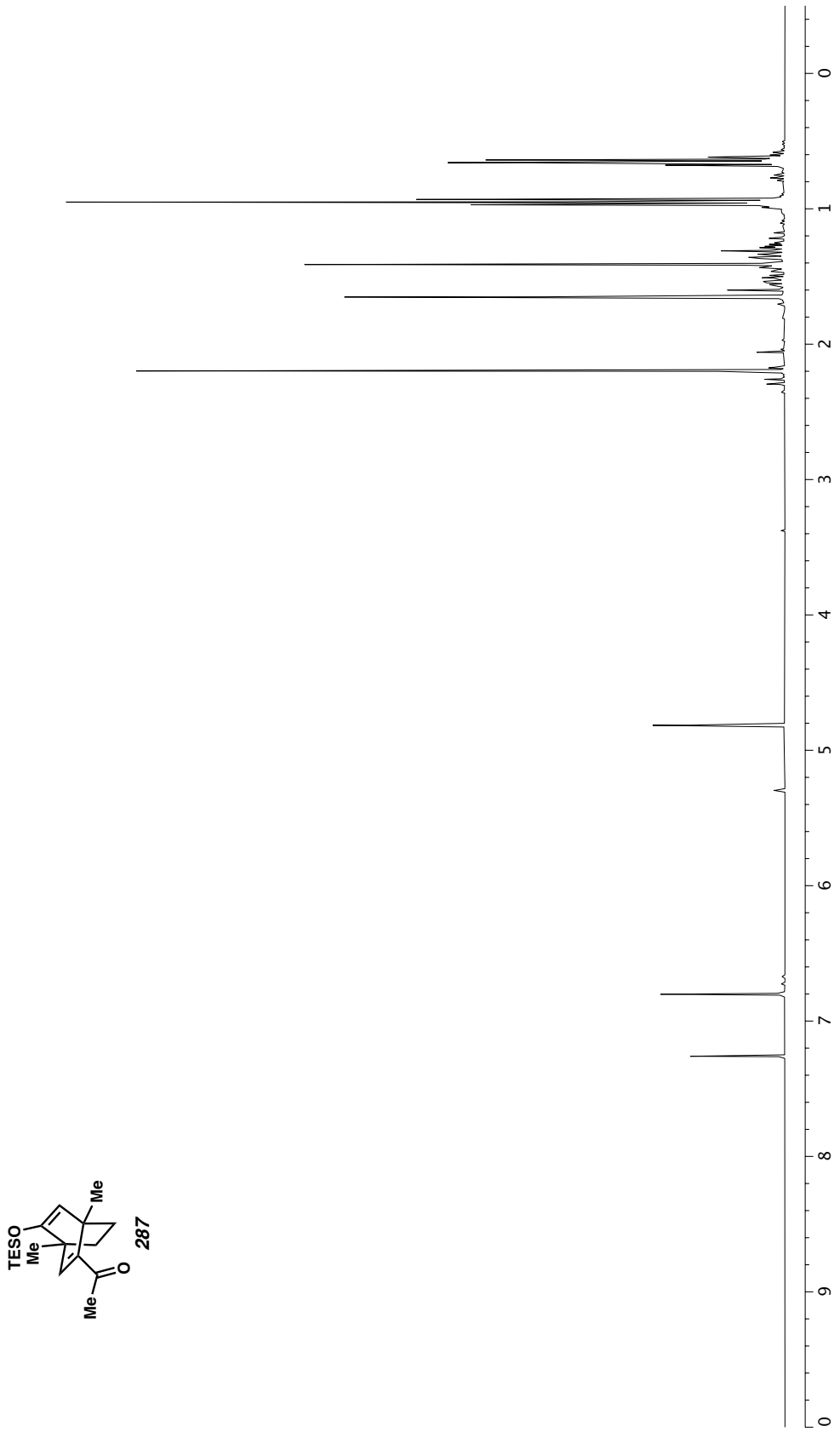


Figure A4.25. *^1H NMR (400 MHz, $CDCl_3$) of compound* ***287****.*

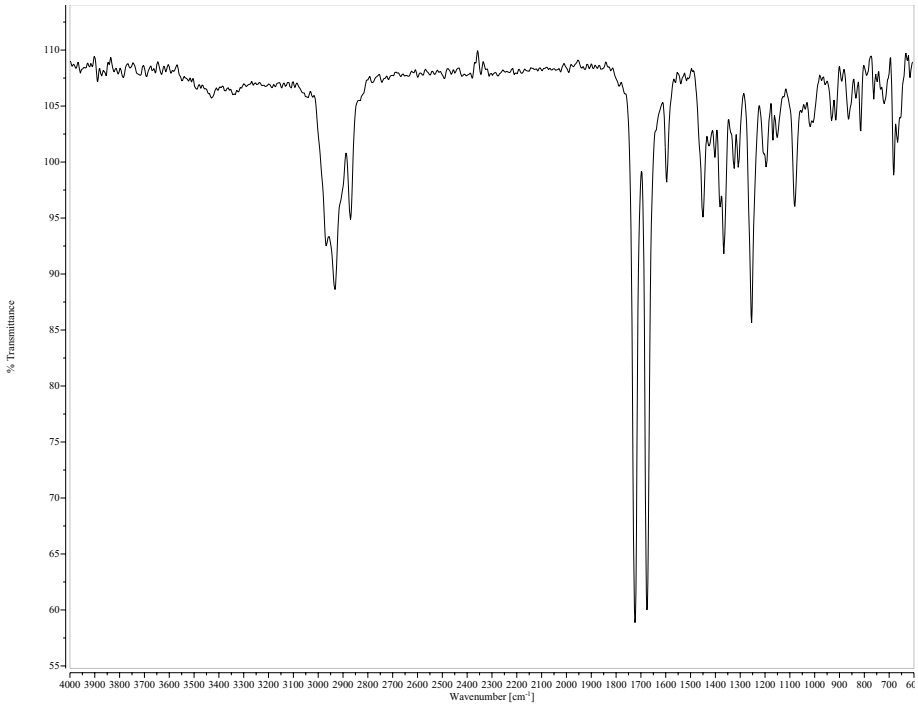


Figure A4.26. *Infrared spectrum ($CDCl_3$ solution) of compound* ***287****.*

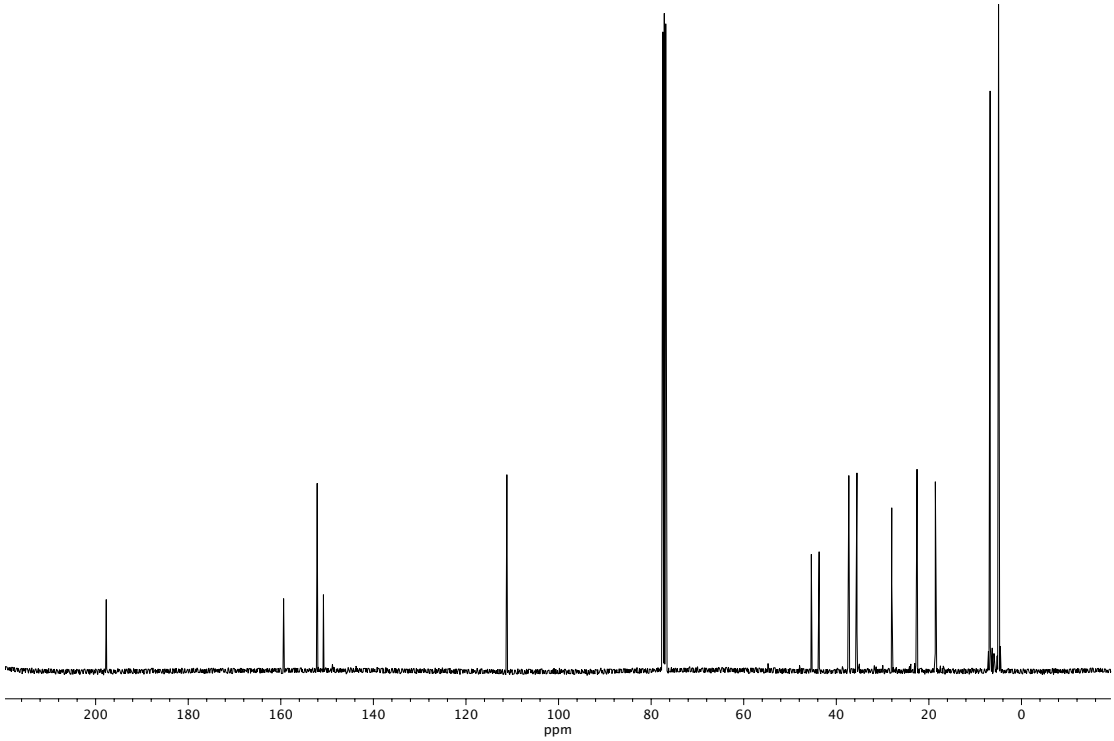


Figure A4.27. *^{13}C NMR (100 MHz, $CDCl_3$) of compound* ***287****.*

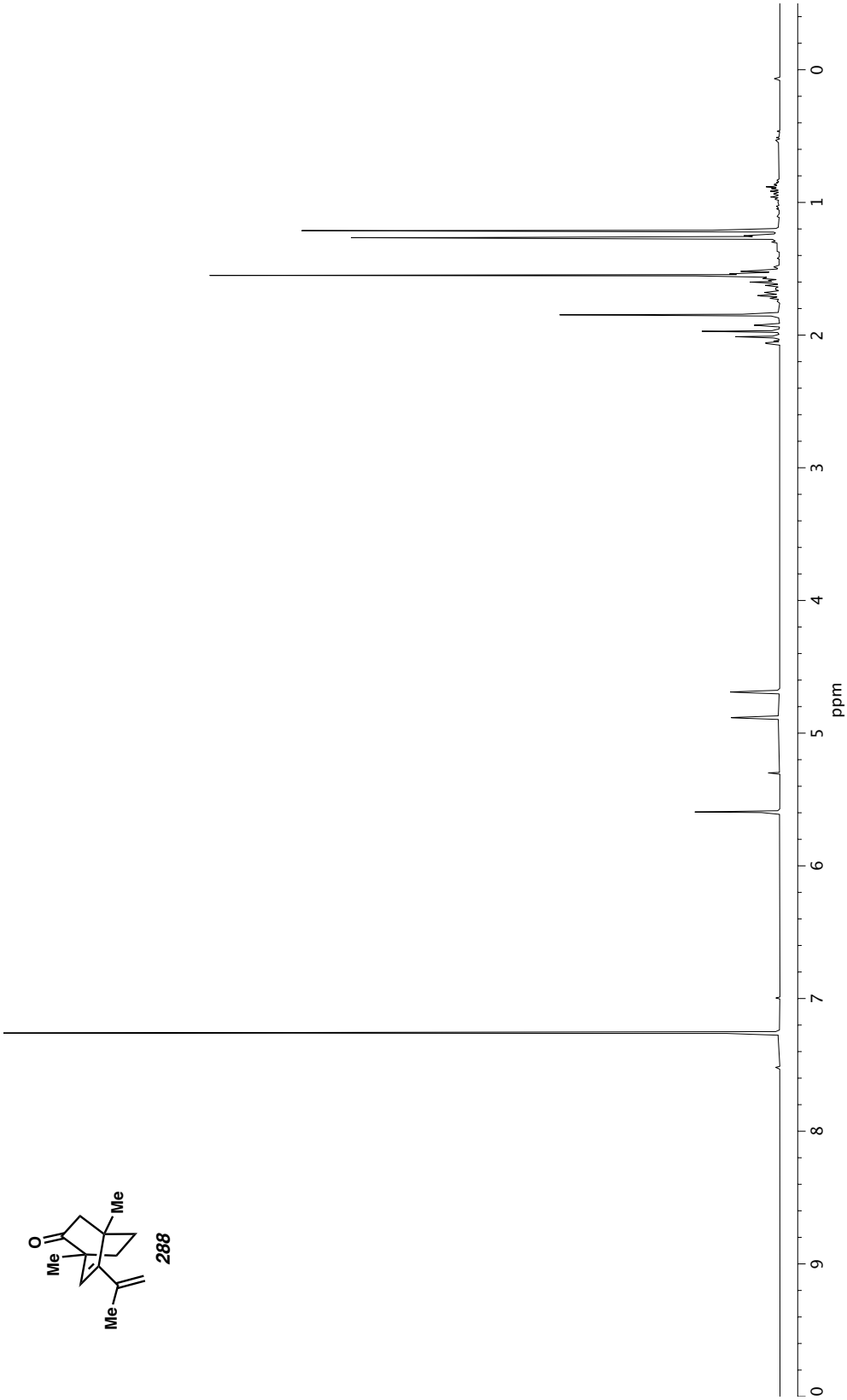


Figure A4.28. *^{1}H NMR (400 MHz, $CDCl_3$) of compound* ***288****.*

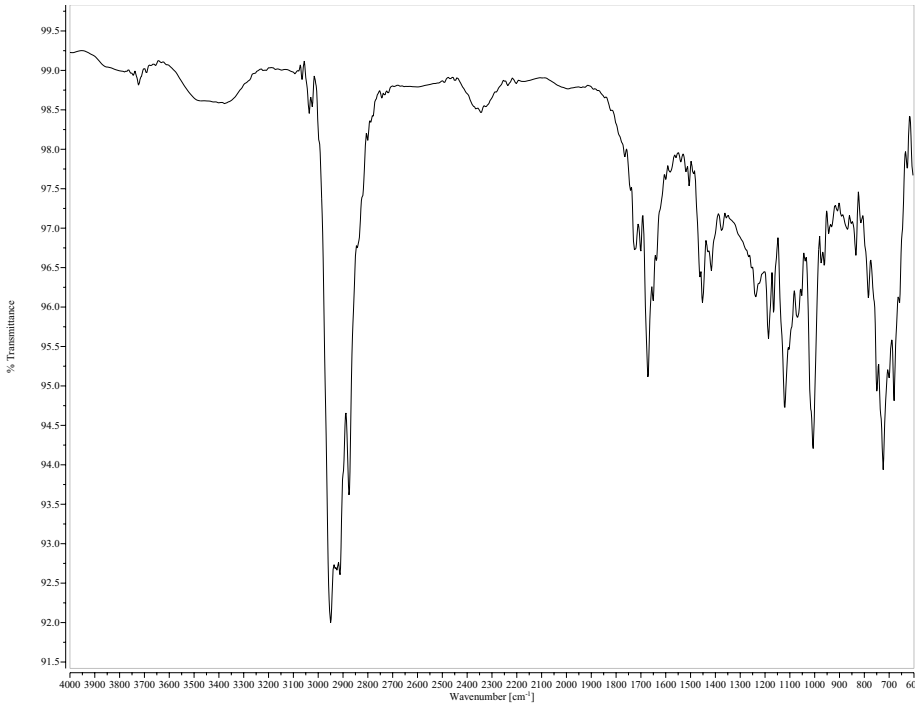


Figure A4.29. *Infrared spectrum (Thin Film, NaCl) of compound* ***288****.*

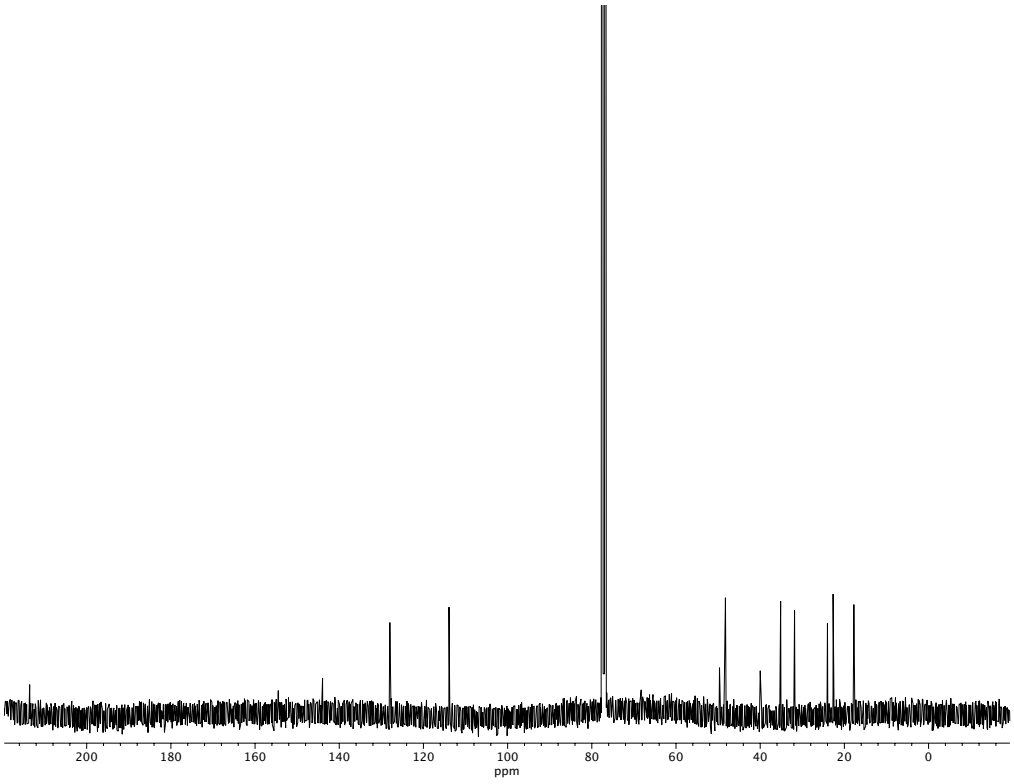
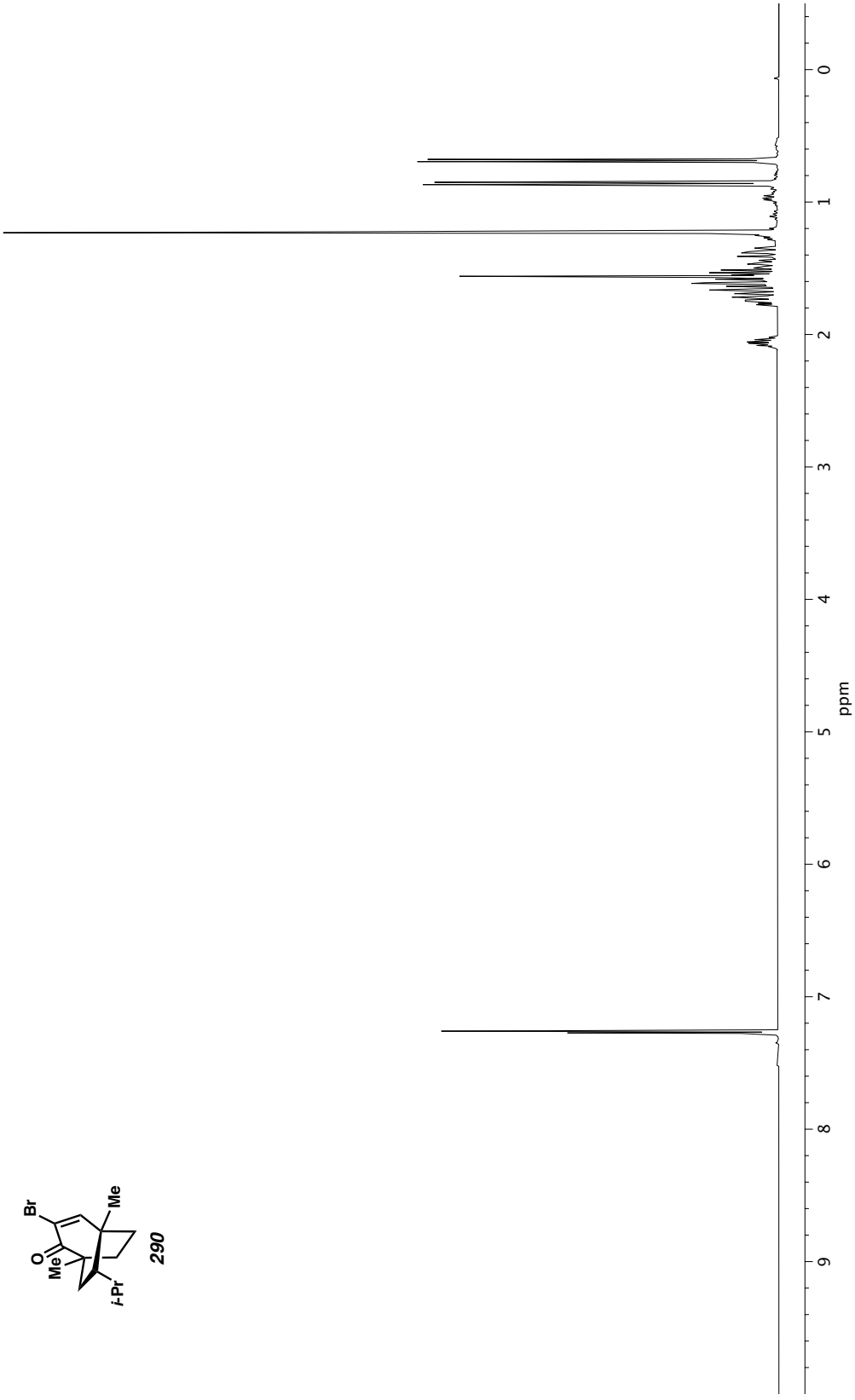


Figure A4.30. *^{13}C NMR (100 MHz, $CDCl_3$) of compound* ***288****.*



290

Figure A4.31. *^1H NMR (400 MHz, $CDCl_3$) of compound* ***290****.*

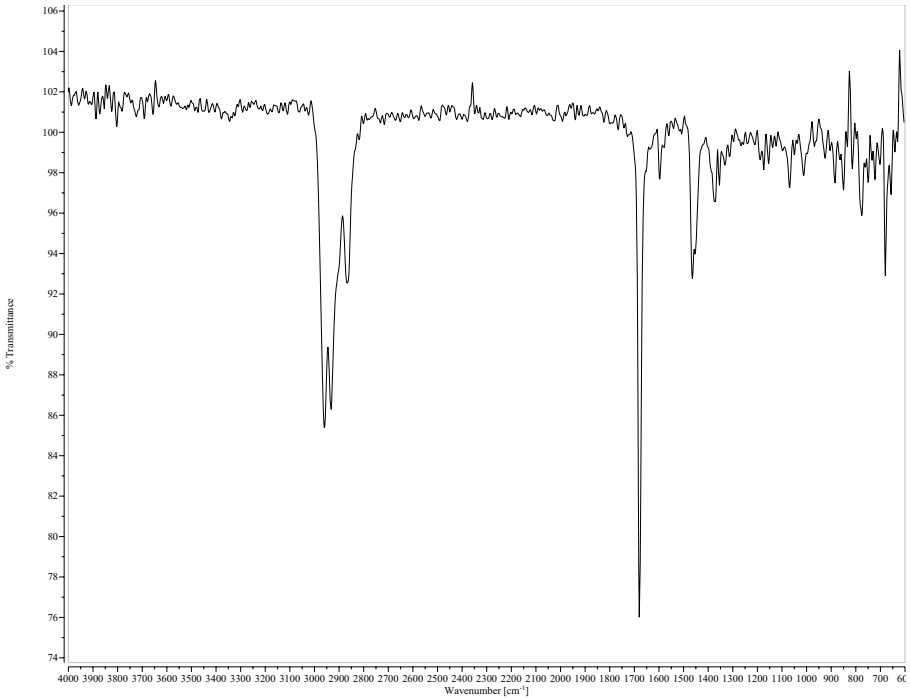


Figure A4.32. *Infrared spectrum (Thin Film, NaCl) of compound* ***290****.*

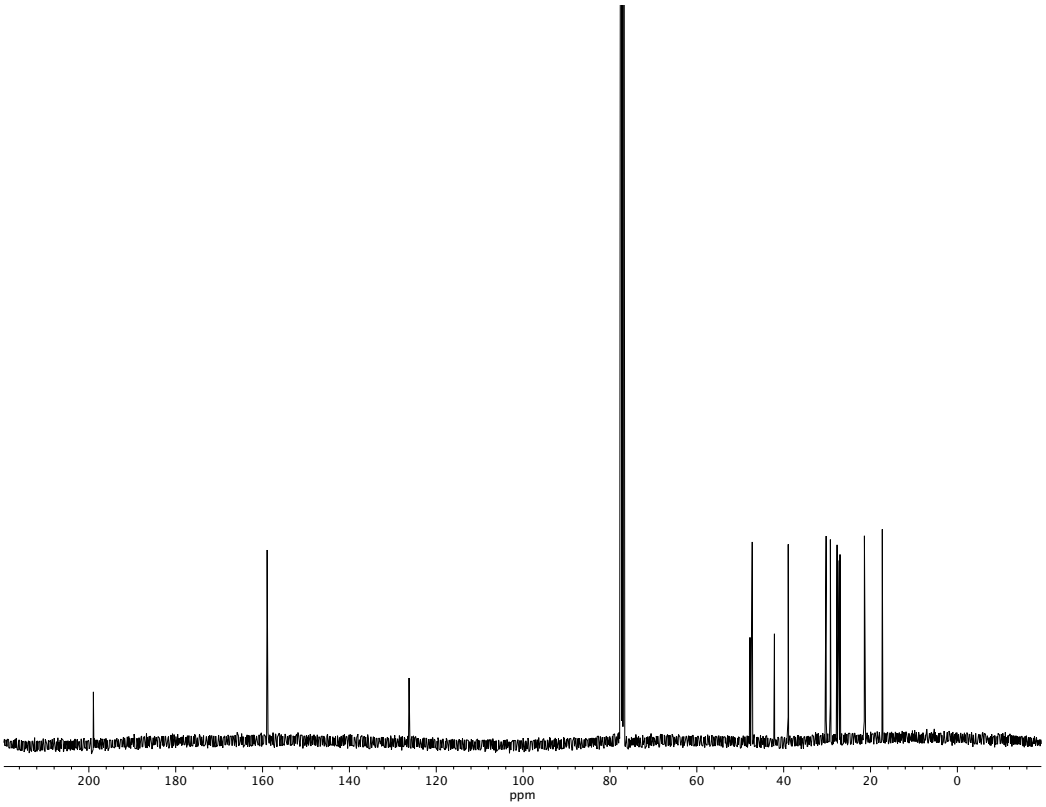


Figure A4.33. *^{13}C NMR (100 MHz, $CDCl_3$) of compound* ***290****.*

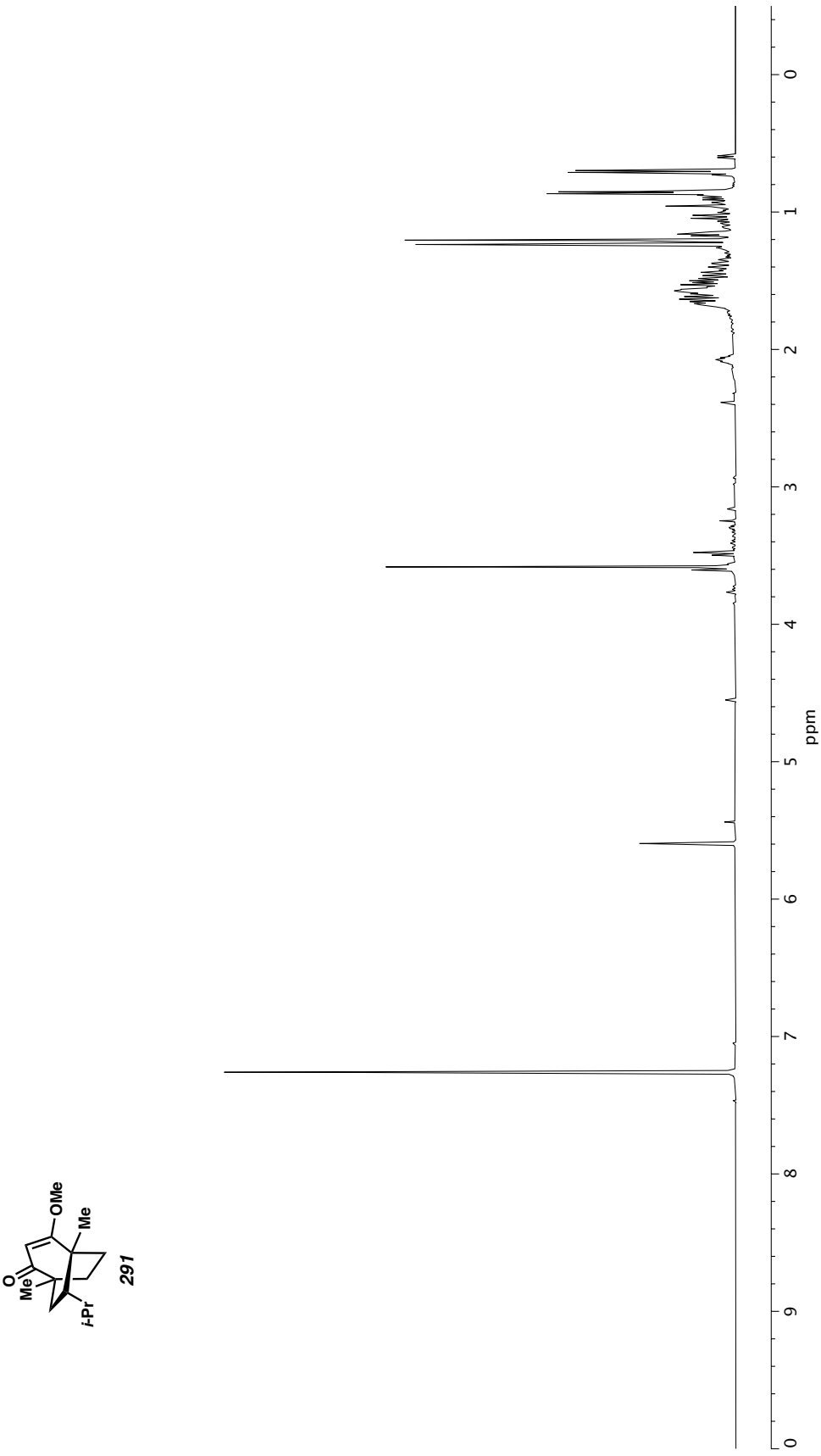


Figure A4.34. *^1H NMR (400 MHz, $CDCl_3$) of compound* ***291***.

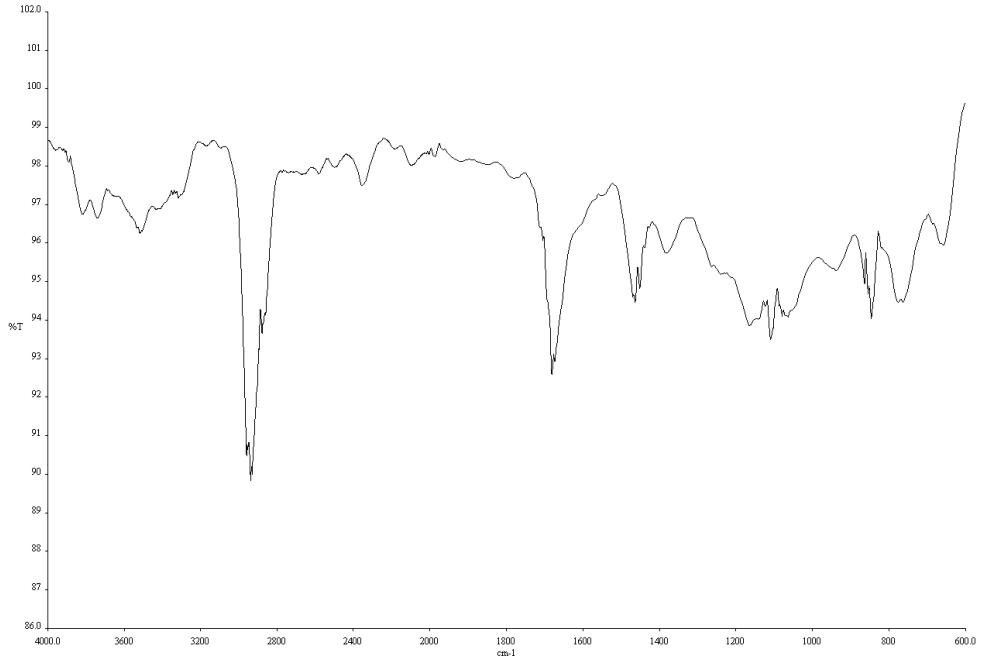


Figure A4.35. *Infrared spectrum (Thin Film, NaCl) of compound* ***291***.

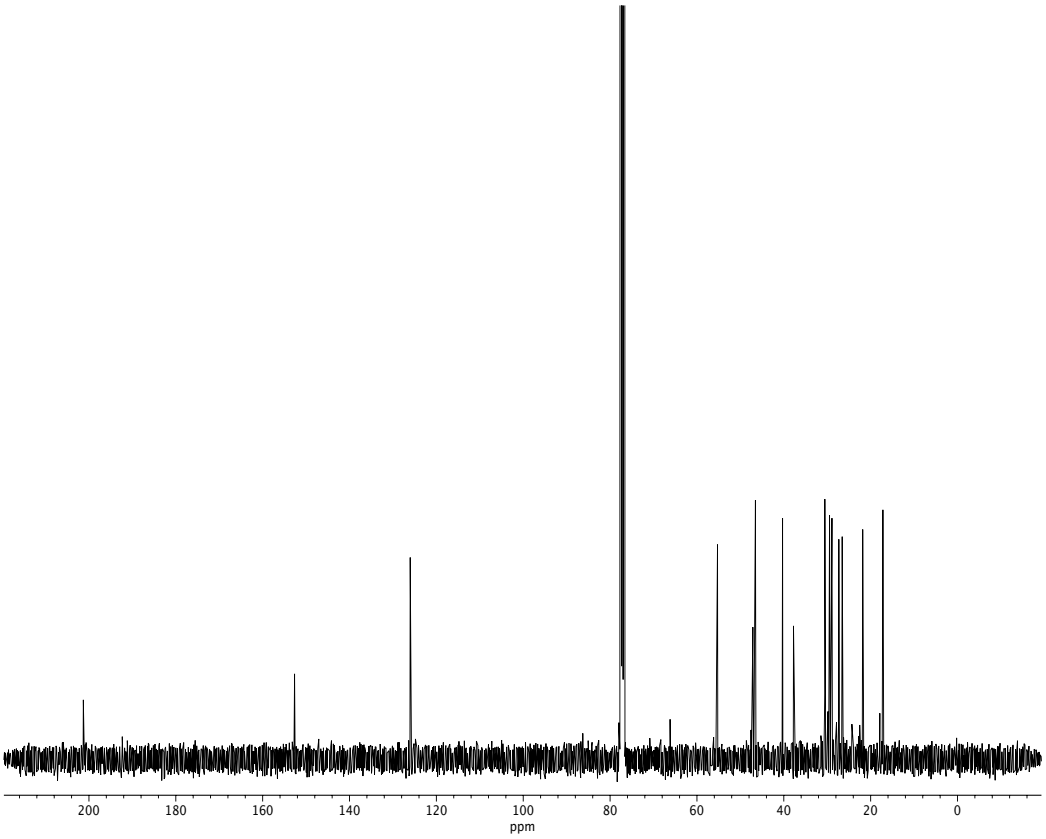


Figure A4.36. *^{13}C NMR (100 MHz, $CDCl_3$) of compound* ***291***.

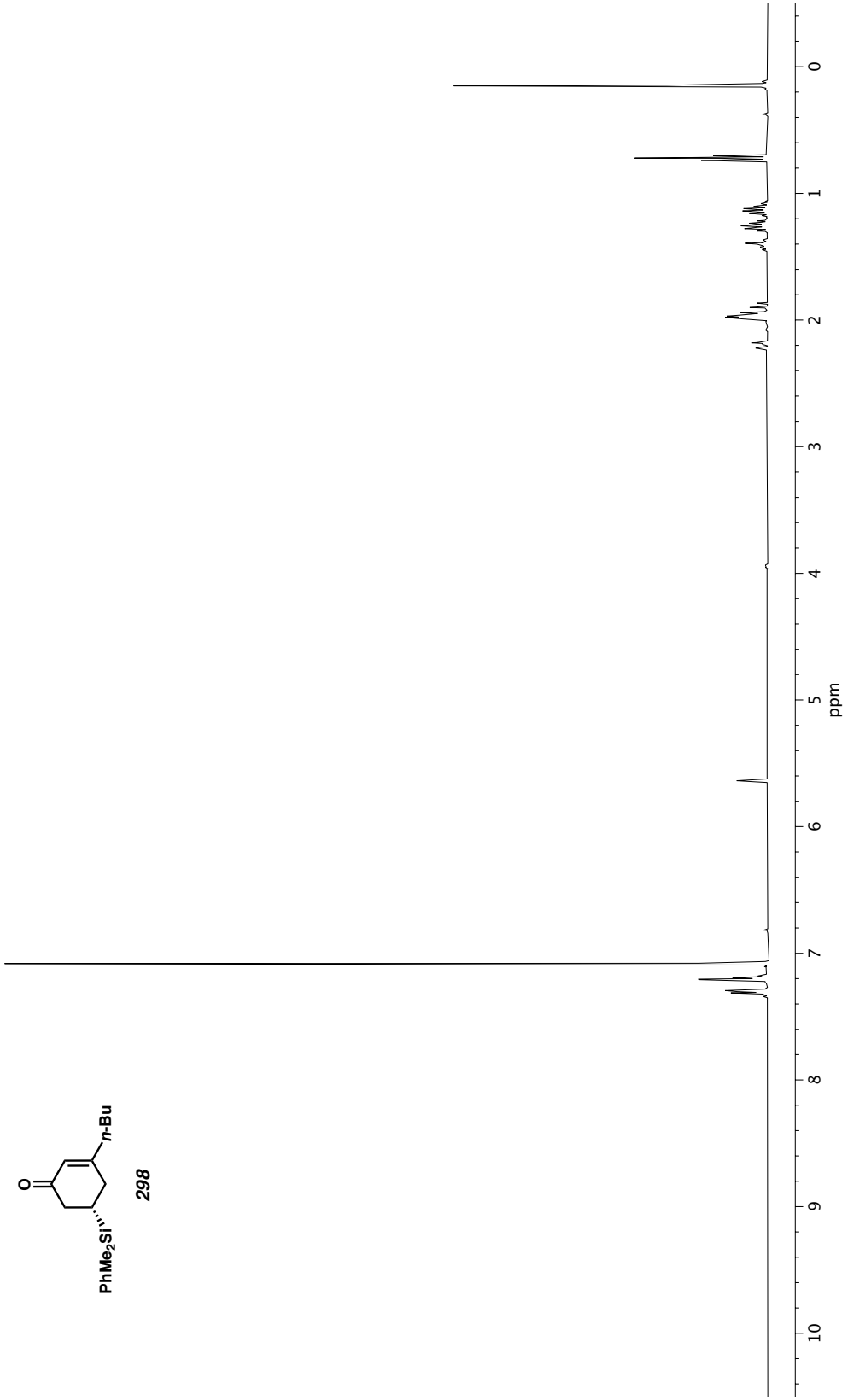


Figure A4.37. *^{1}H NMR (400 MHz, $CDCl_3$) of compound* ***298****.*

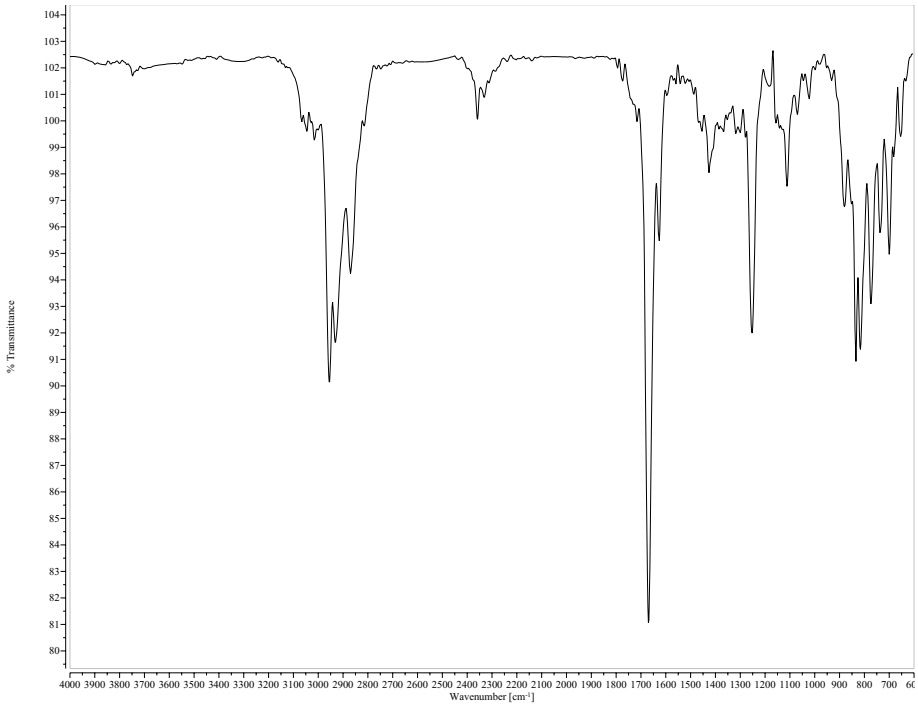


Figure A4.38. *Infrared spectrum (Thin Film, NaCl) of compound* ***298****.*

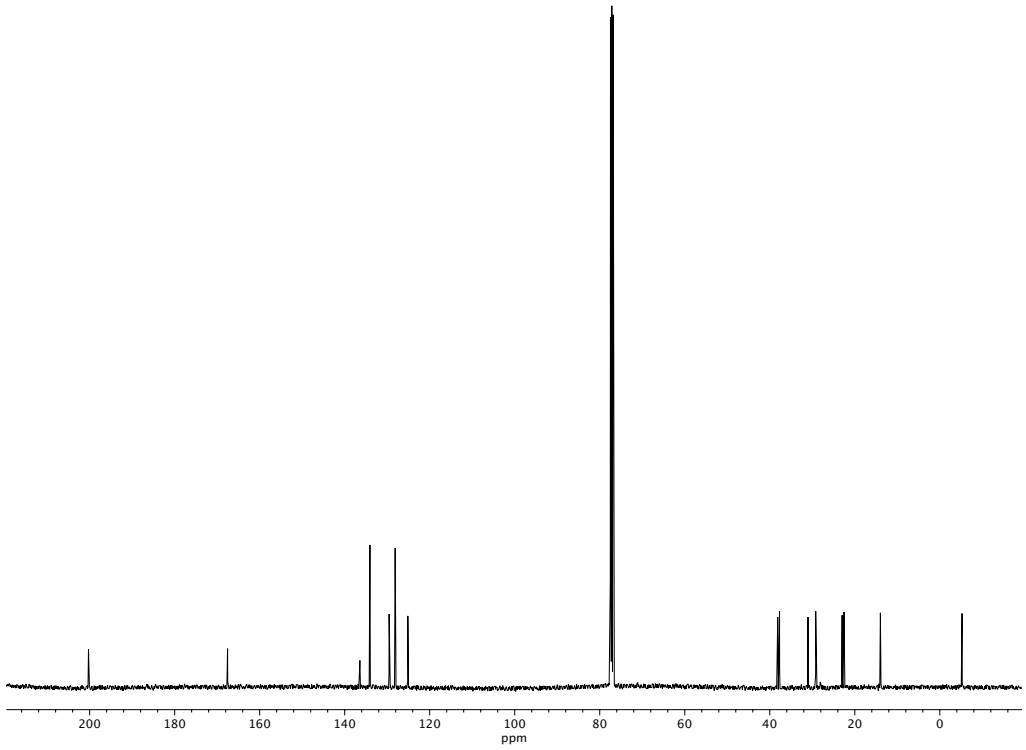


Figure A4.39. *^{13}C NMR (100 MHz, $CDCl_3$) of compound* ***298****.*

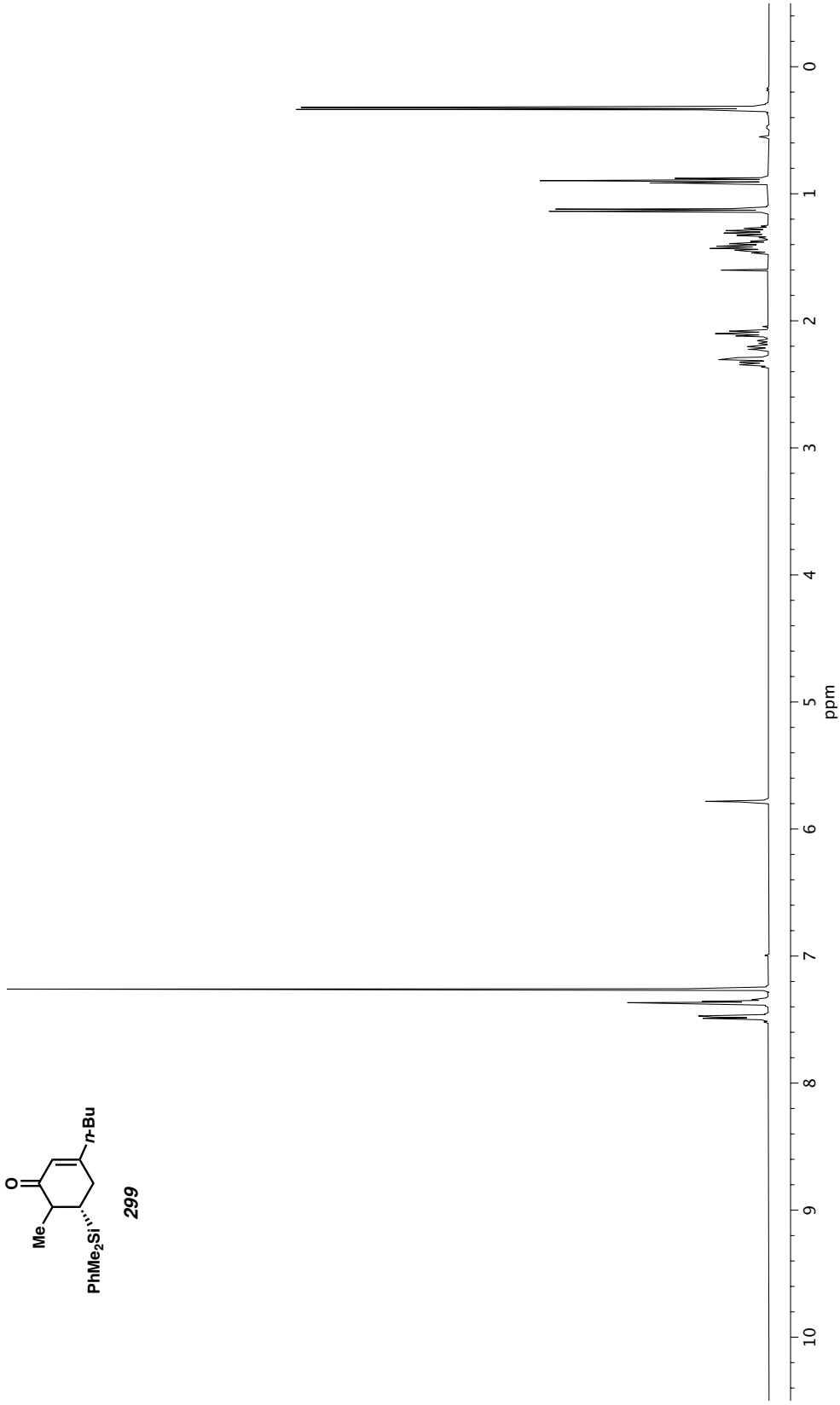


Figure A4.40. *^{1}H NMR (400 MHz, $CDCl_3$) of compound* ***299***.

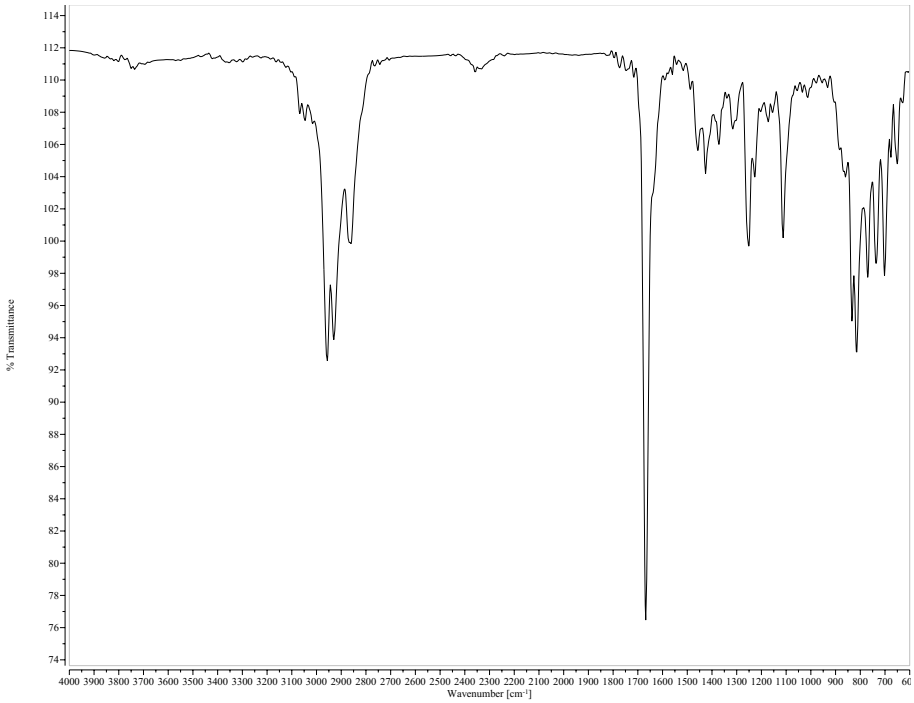


Figure A4.41. *Infrared spectrum (Thin Film, NaCl) of compound* ***299***.

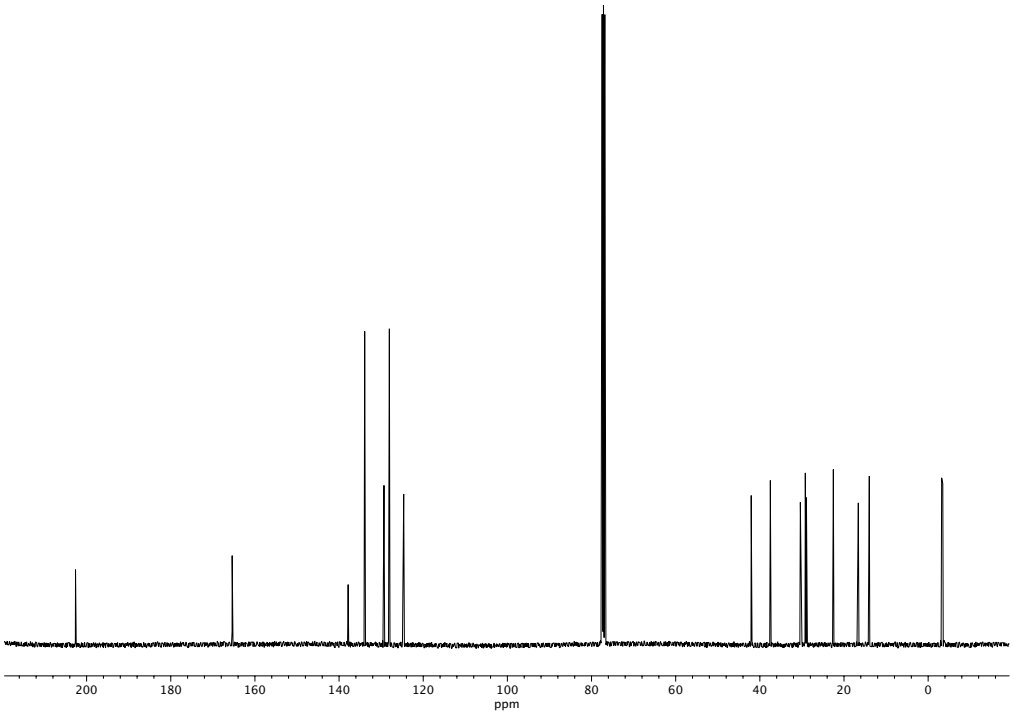


Figure A4.42. *^{13}C NMR (100 MHz, $CDCl_3$) of compound* ***299***.

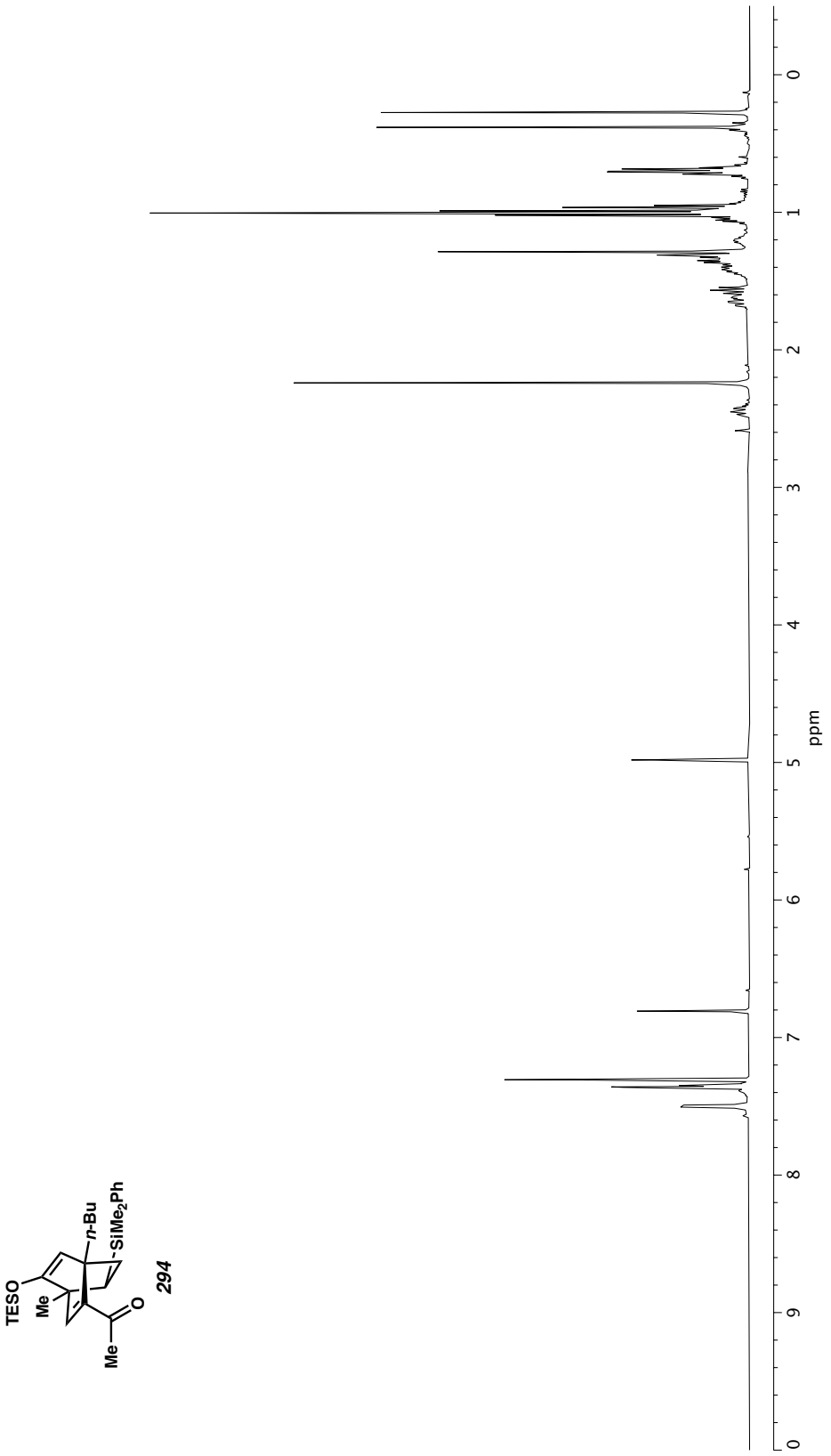


Figure A4.43. *^1H NMR (400 MHz, $CDCl_3$) of compound* ***294****.*

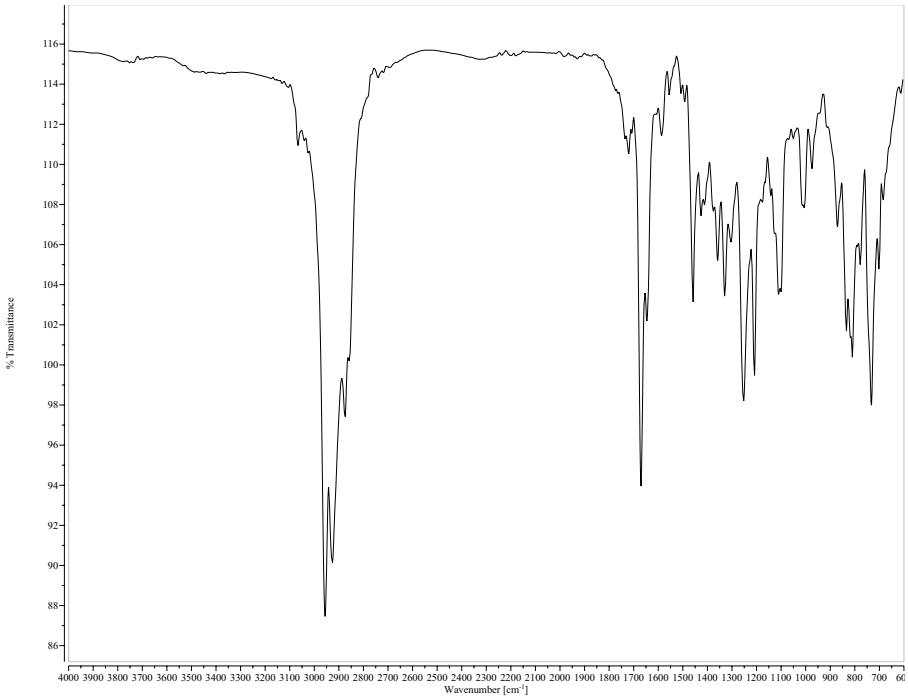


Figure A4.44. *Infrared spectrum (Thin Film, NaCl) of compound* ***294****.*

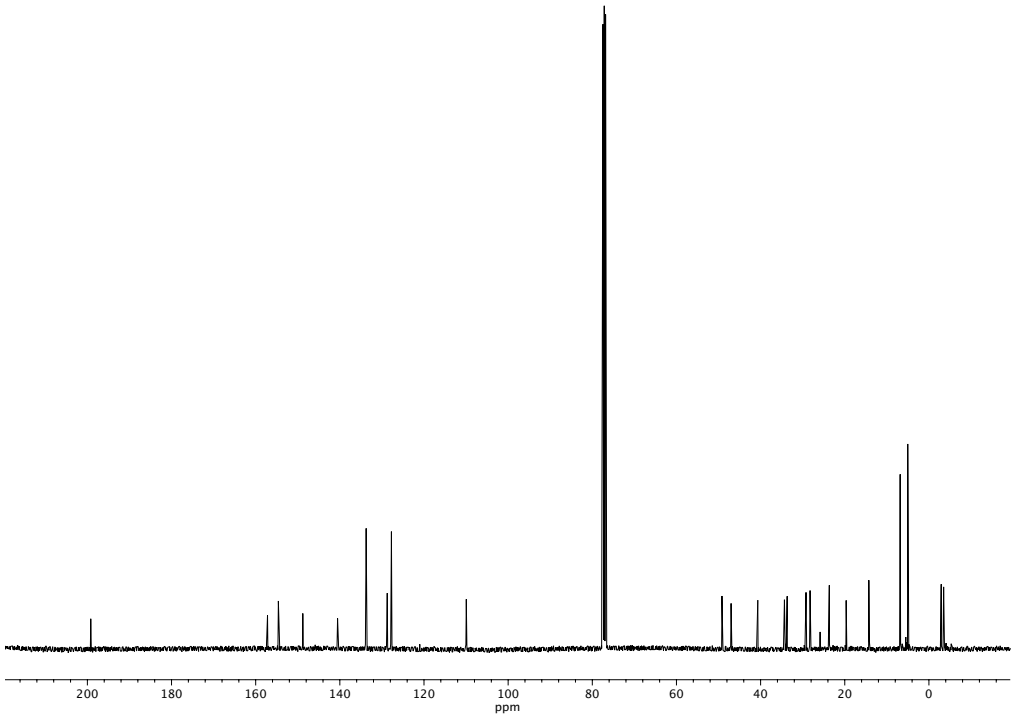


Figure A4.45. *^{13}C NMR (100 MHz, $CDCl_3$) of compound* ***294****.*

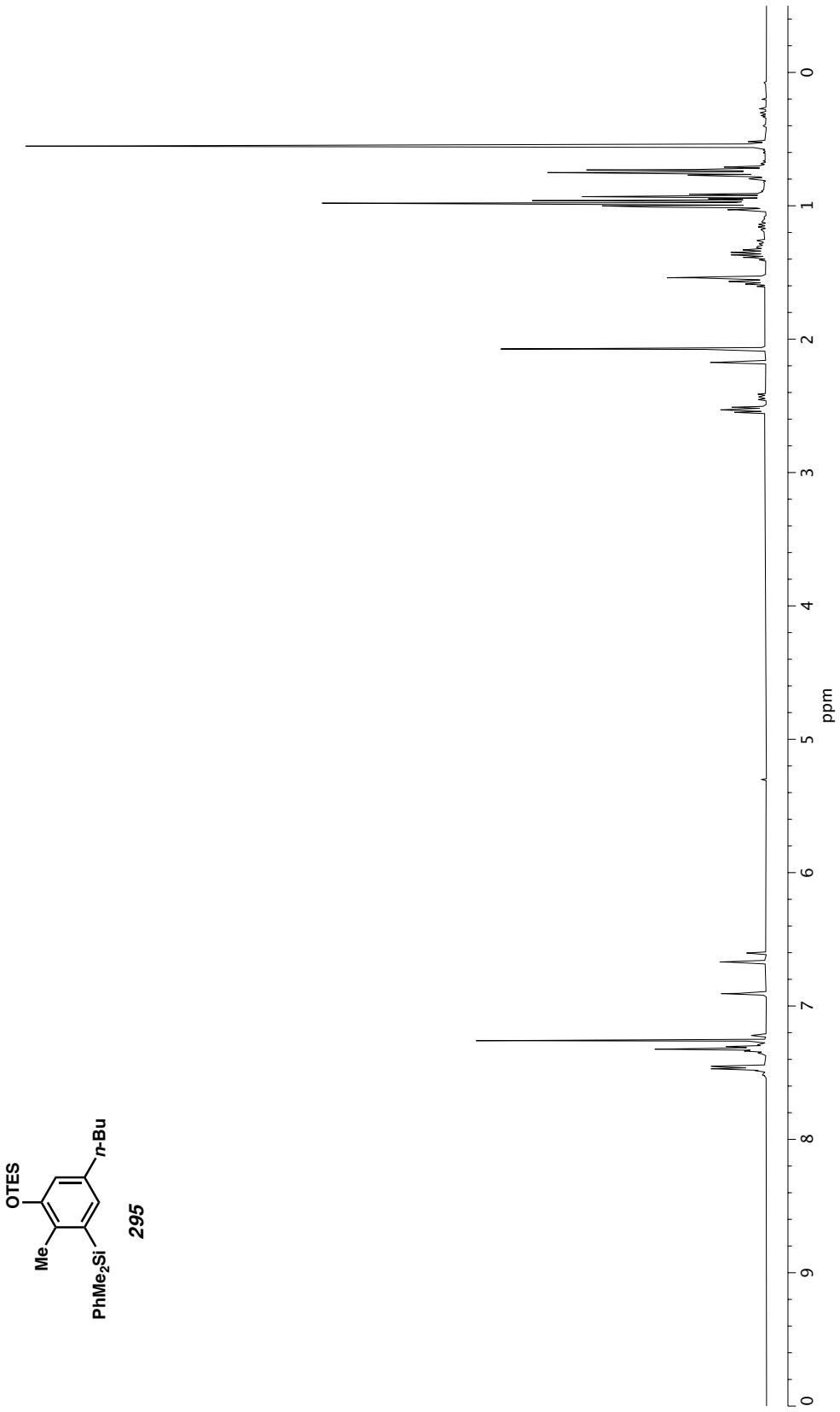


Figure A4.46. *^{1}H NMR (400 MHz, $CDCl_3$) of compound **295**.*

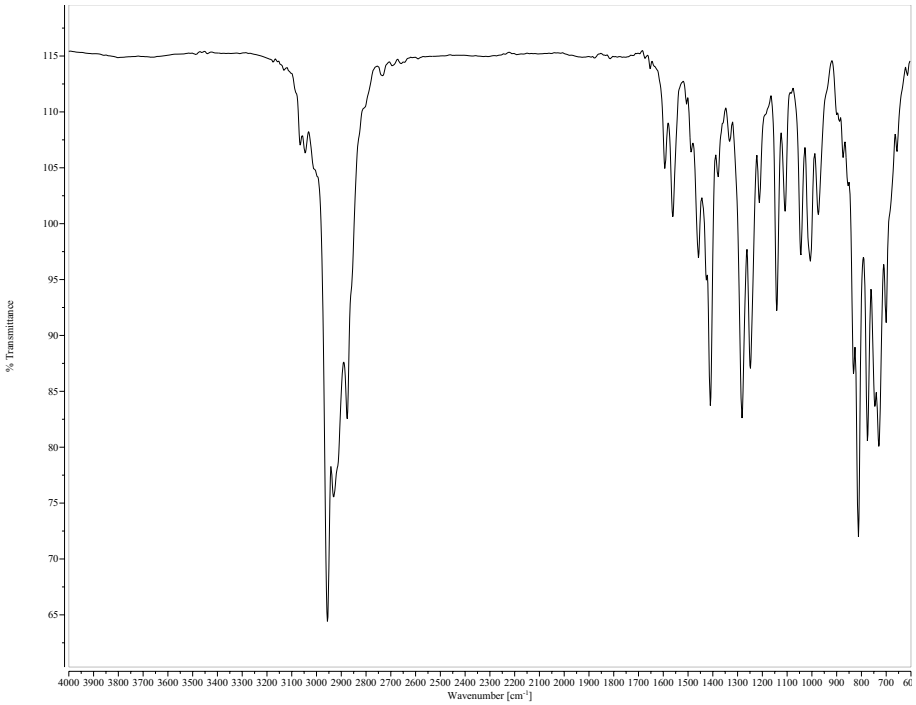


Figure A4.47. *Infrared spectrum (Thin Film, NaCl) of compound* ***295****.*

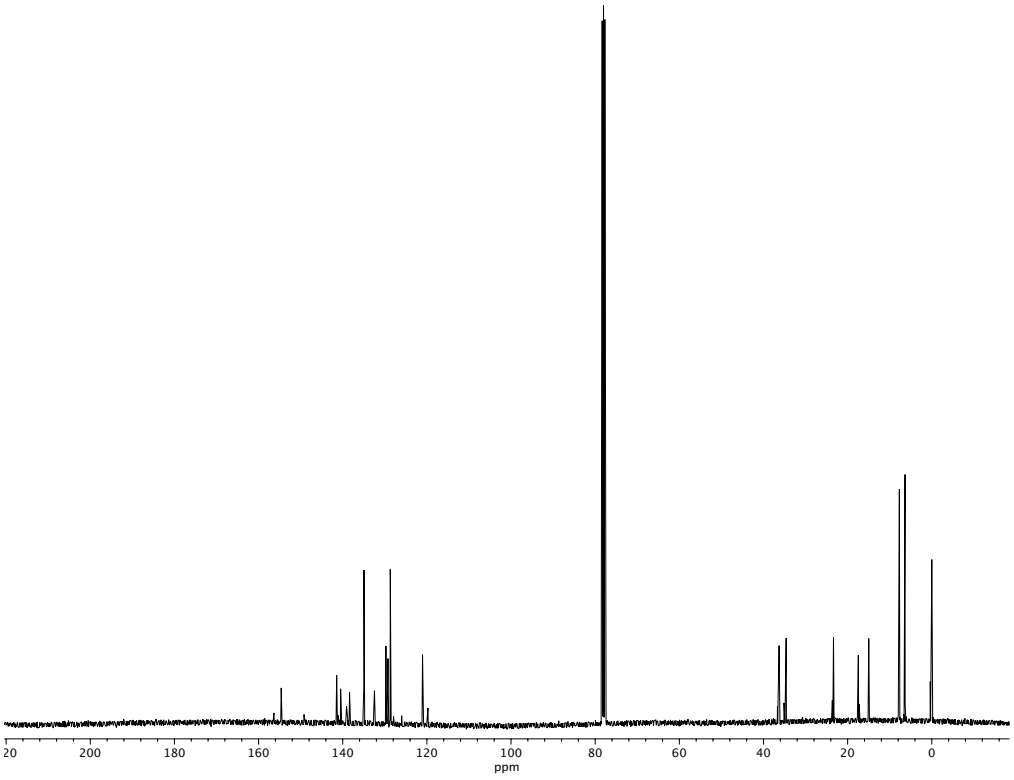


Figure A4.48. *^{13}C NMR (100 MHz, $CDCl_3$) of compound* ***295****.*

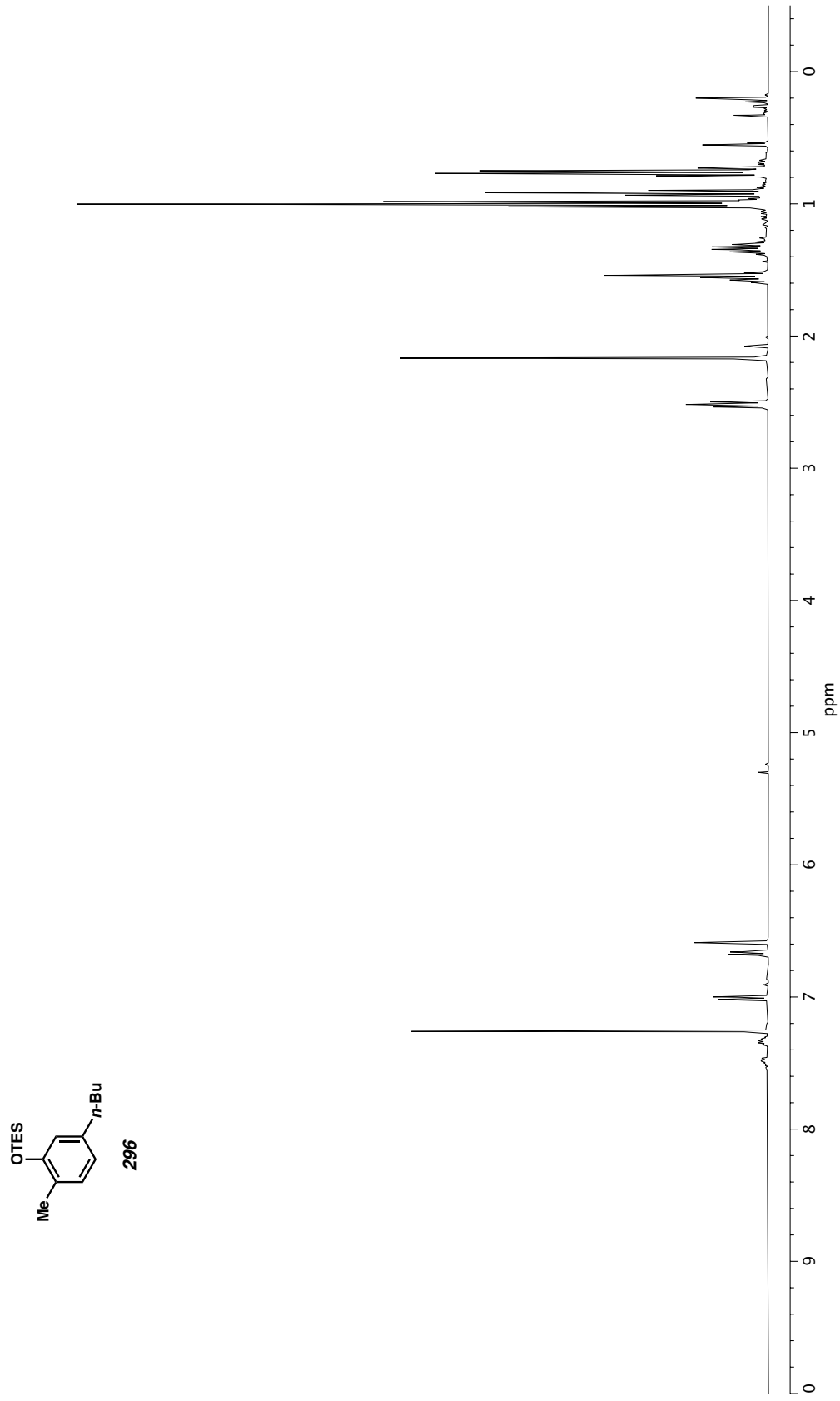


Figure A4.49. *^1H NMR (400 MHz, $CDCl_3$) of compound* ***296****.*

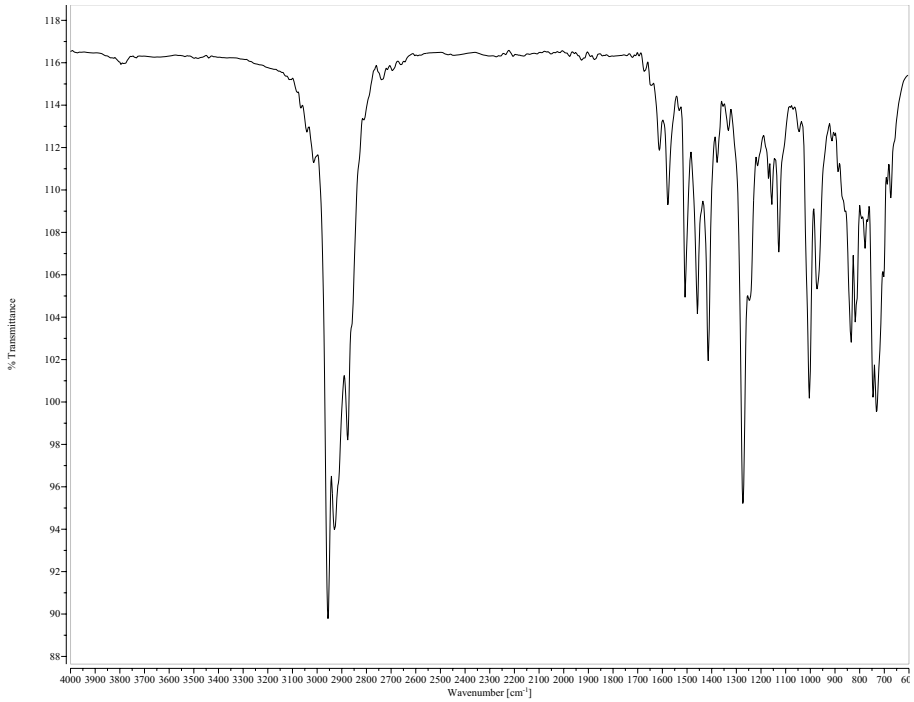


Figure A4.50. *Infrared spectrum (Thin Film, NaCl) of compound* ***296****.*

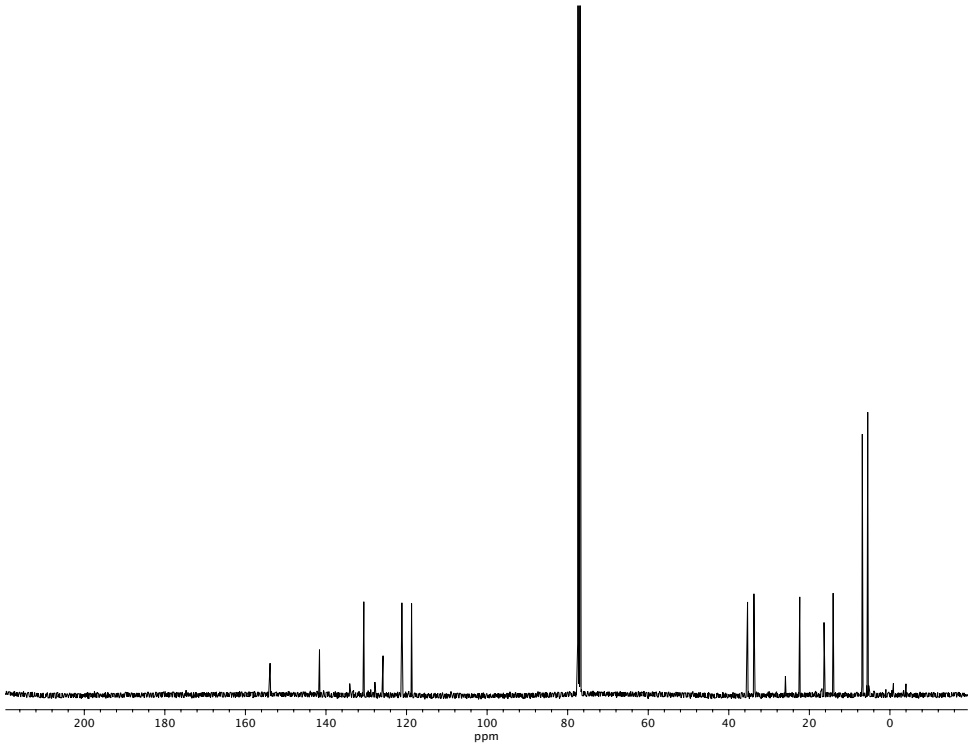


Figure A4.51. *^{13}C NMR (100 MHz, $CDCl_3$) of compound* ***296****.*

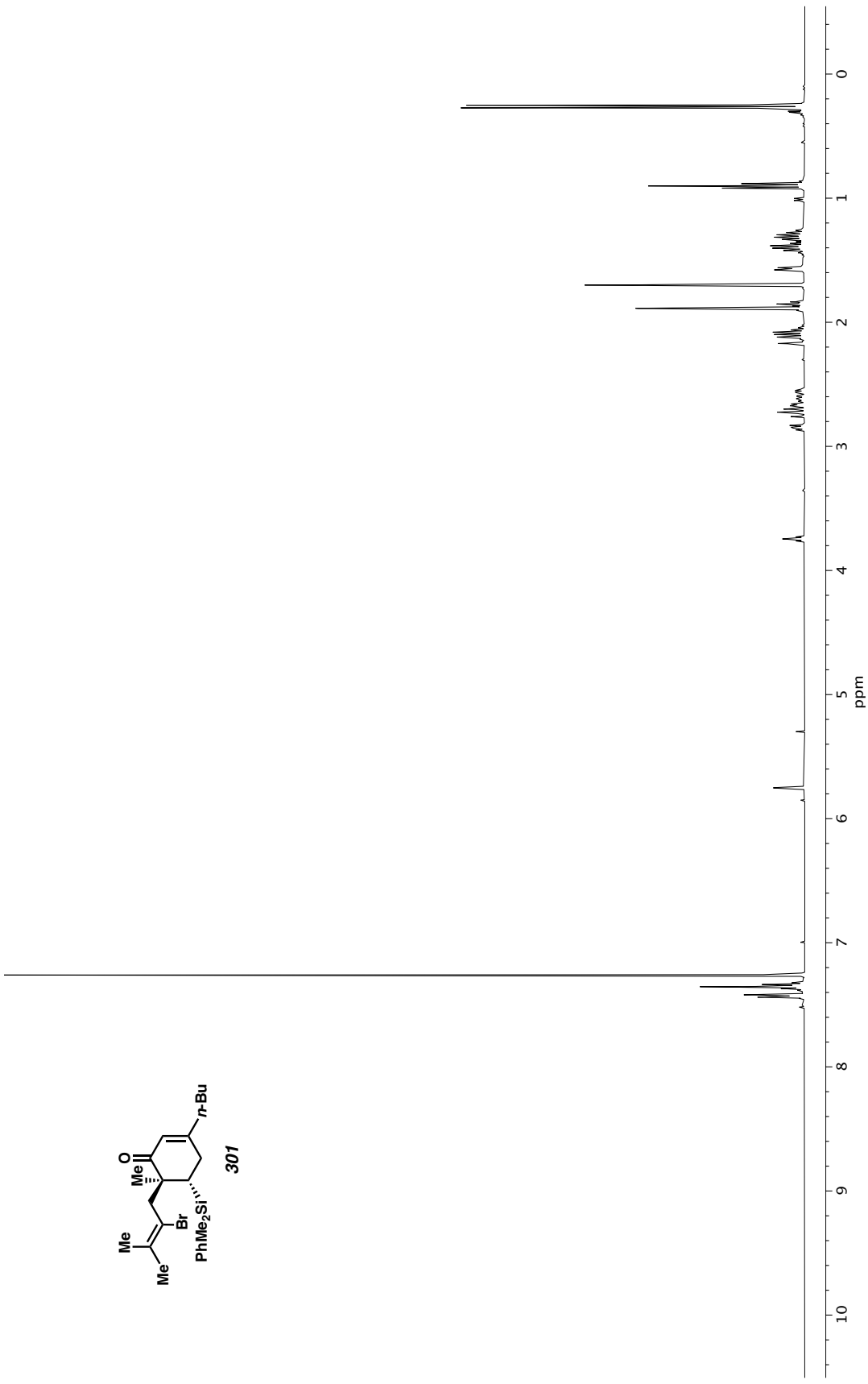


Figure A4.52. *^{1}H NMR (400 MHz, $CDCl_3$) of compound **301**.*

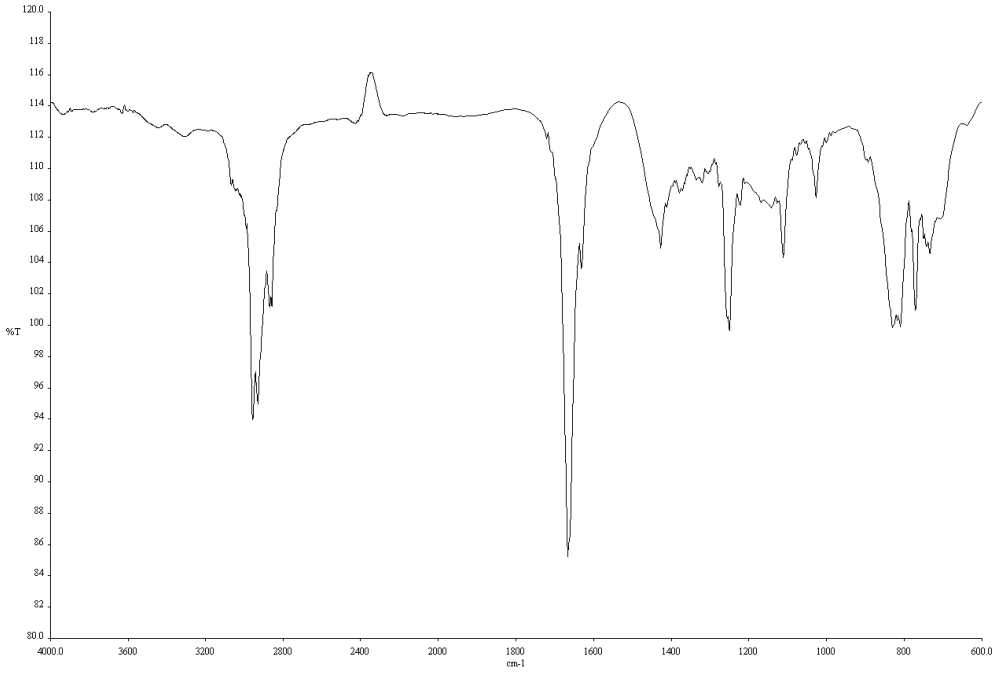


Figure A4.53. *Infrared spectrum (Thin Film, NaCl) of compound* ***301***.

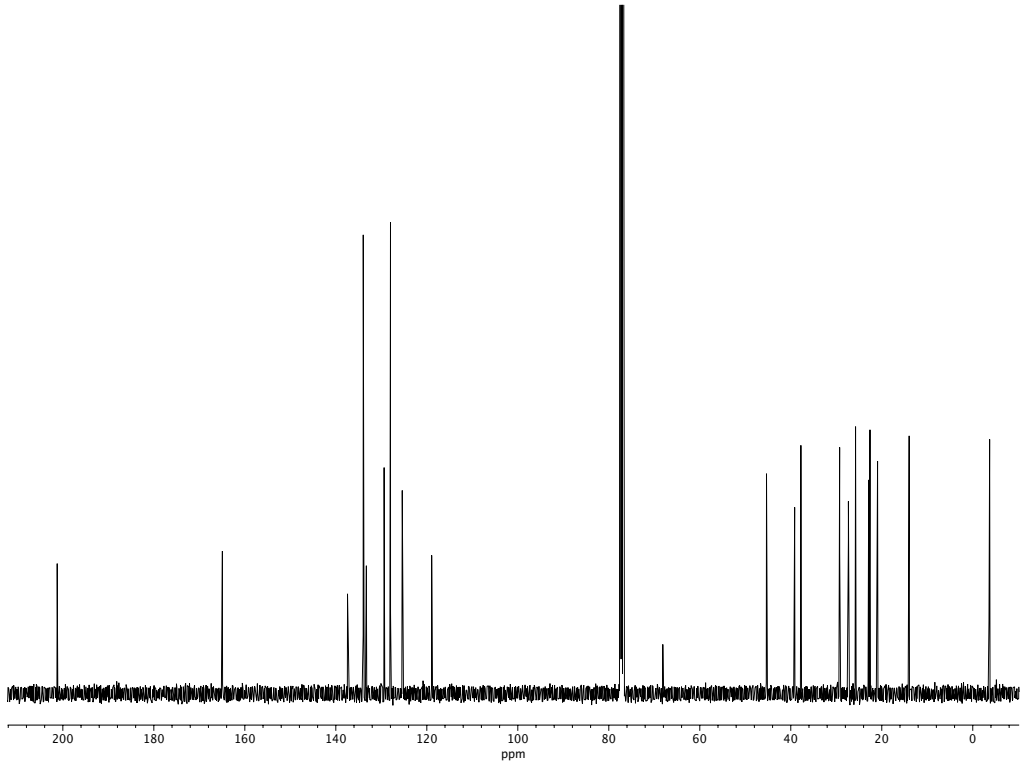


Figure A4.54. *^{13}C NMR (100 MHz, $CDCl_3$) of compound* ***301***.

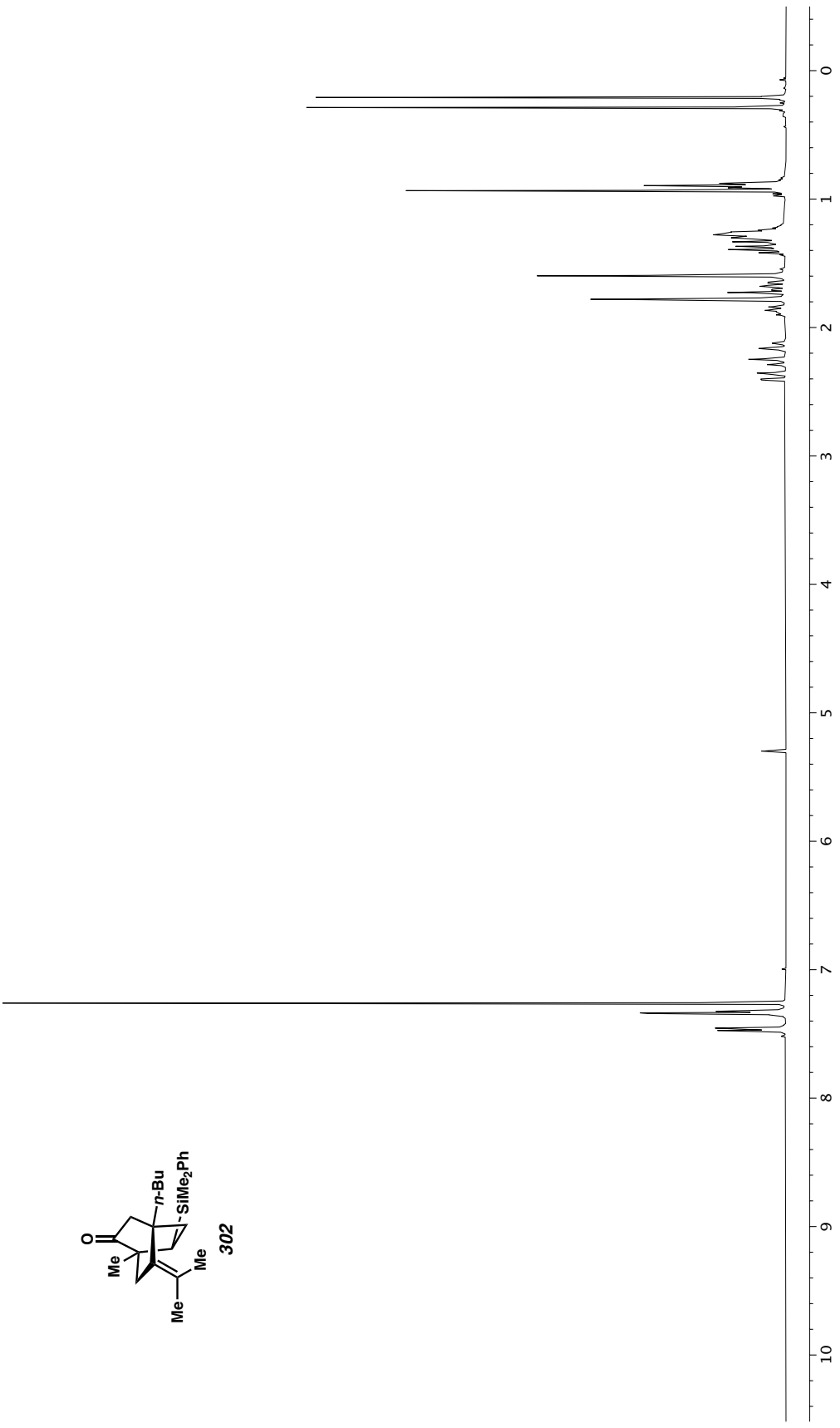


Figure A4.55. *^{1}H NMR (400 MHz, $CDCl_3$) of compound* ***302***.

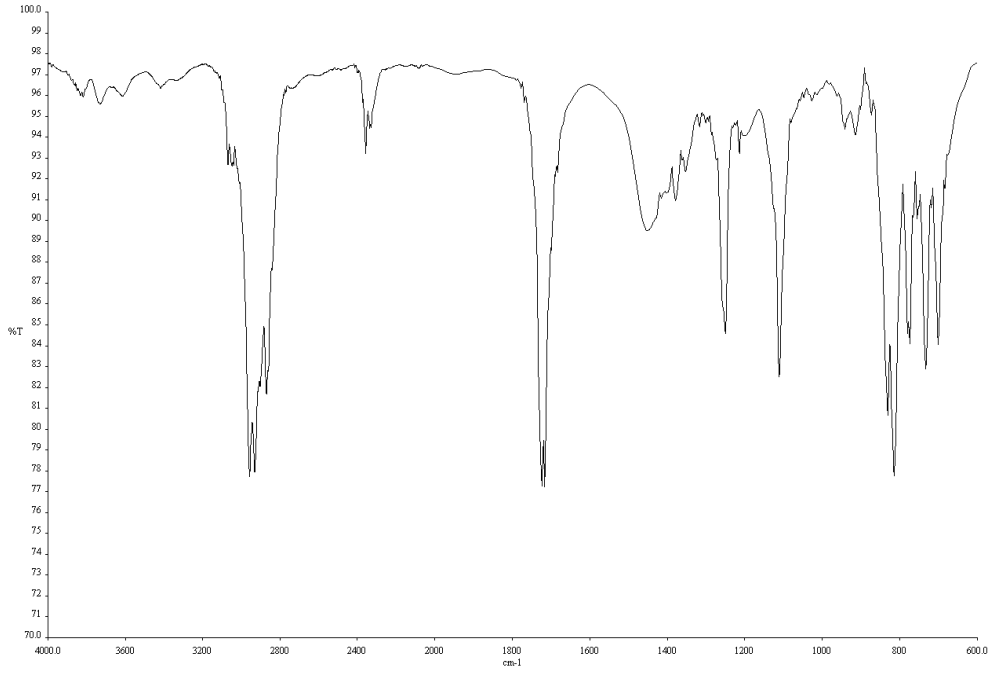


Figure A4.56. *Infrared spectrum (Thin Film, NaCl) of compound* ***302****.*

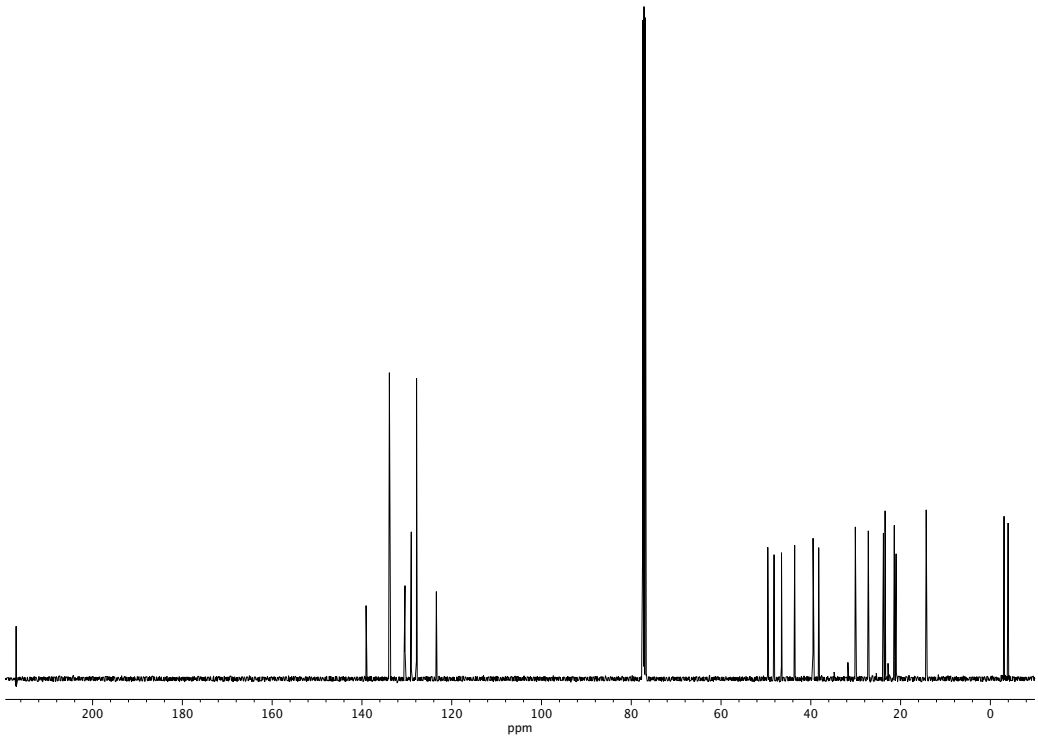


Figure A4.57. *^{13}C NMR (100 MHz, $CDCl_3$) of compound* ***302****.*

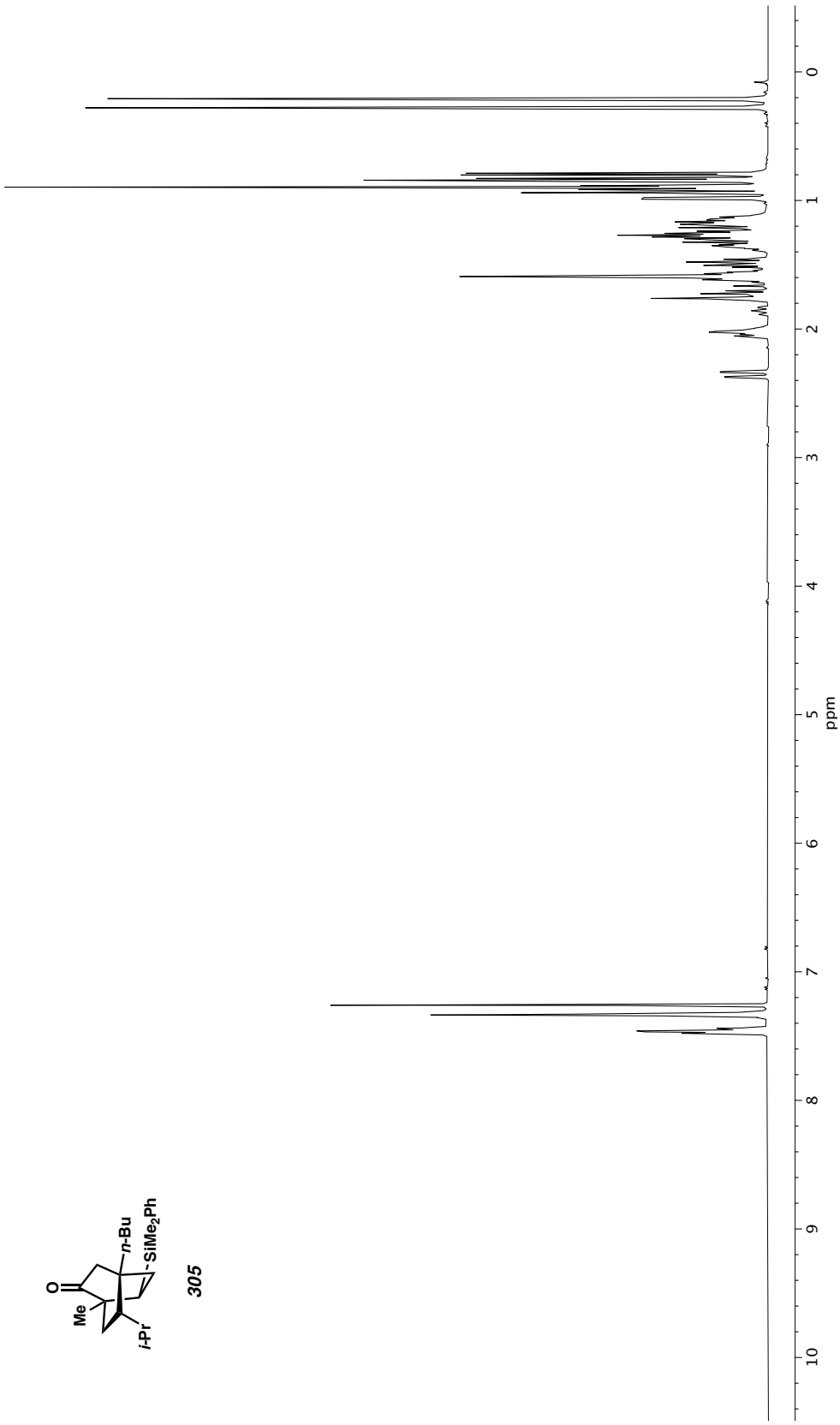


Figure A4.58. *^1H NMR (500 MHz, $CDCl_3$) of compound **305**.*

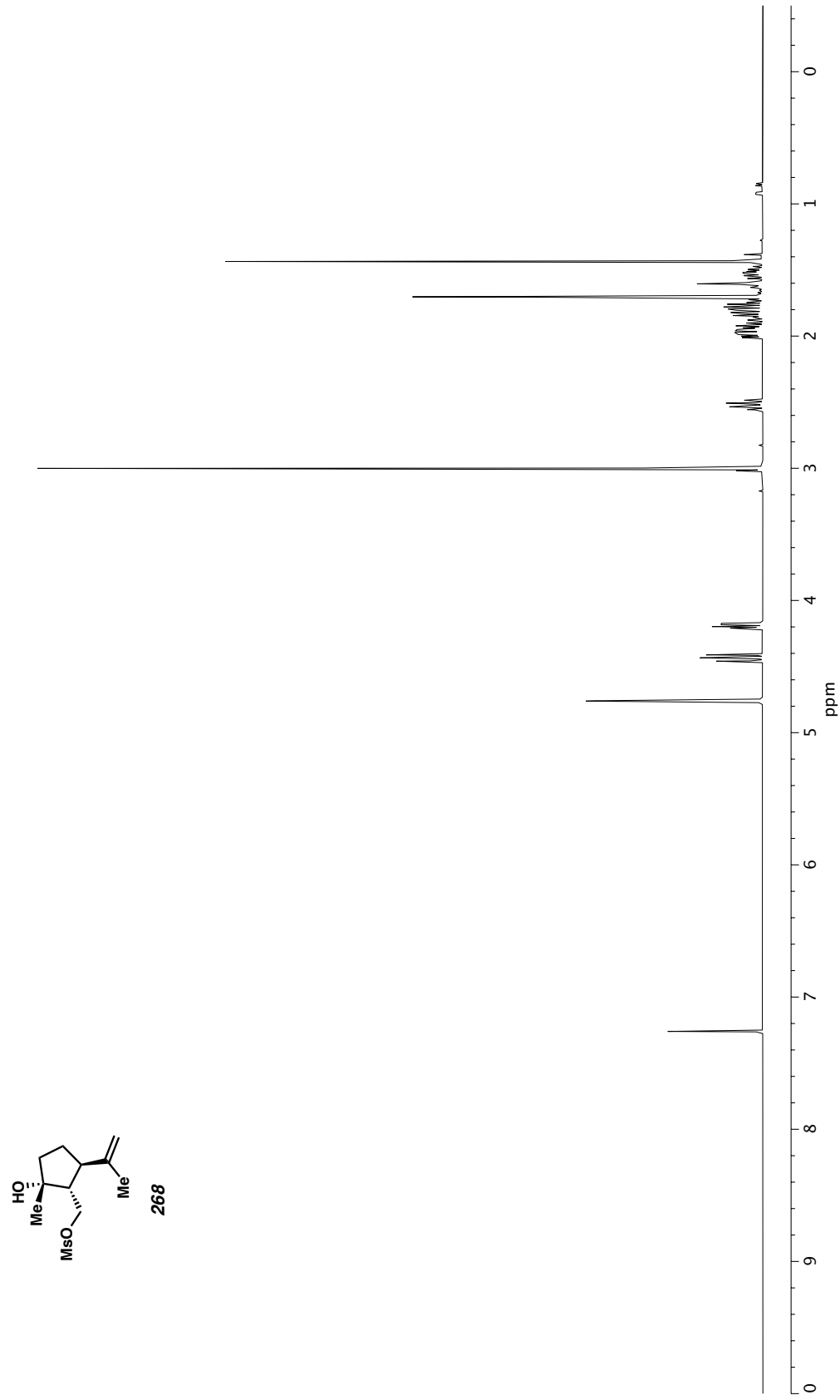


Figure A4.59. *^{1}H NMR (400 MHz, $CDCl_3$) of compound* ***268****.*

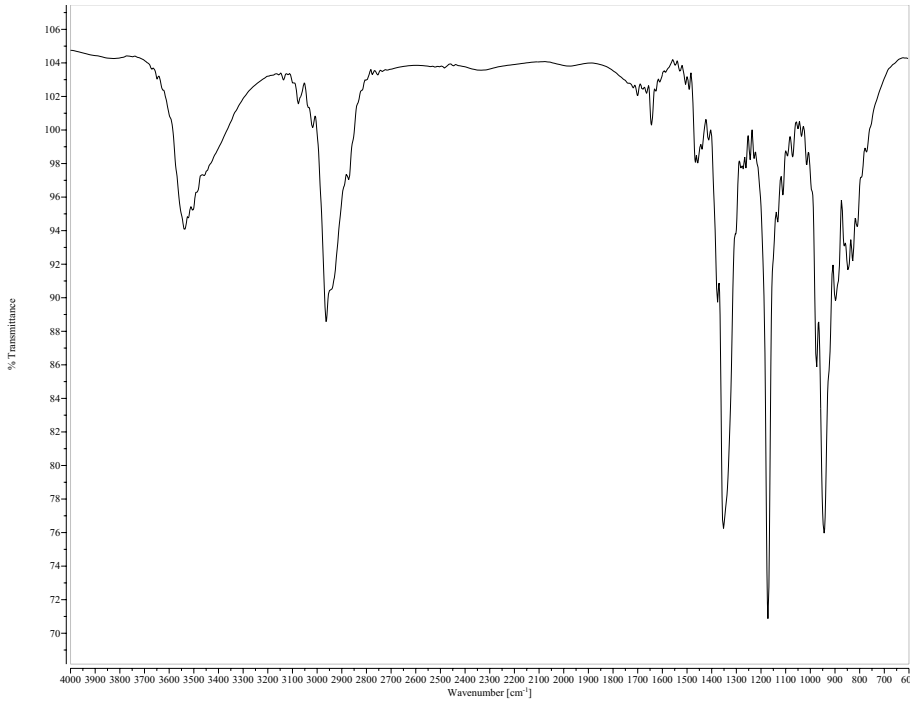


Figure A4.60. *Infrared spectrum (Thin Film, NaCl) of compound* ***268****.*

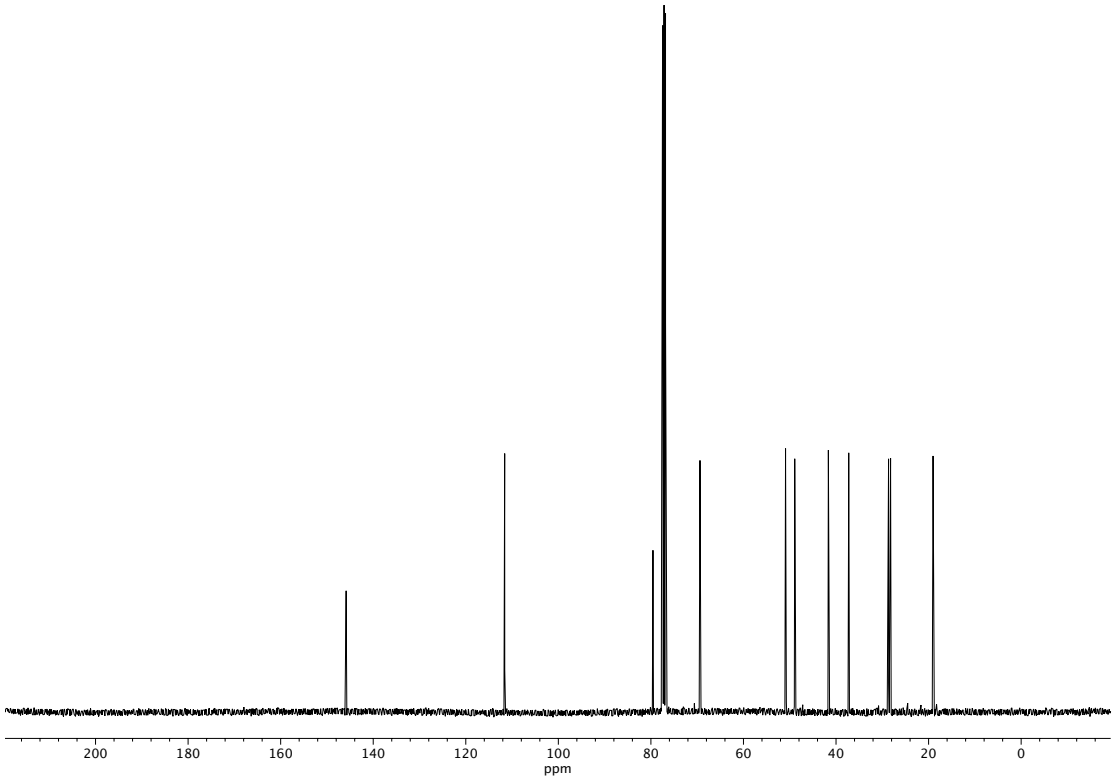
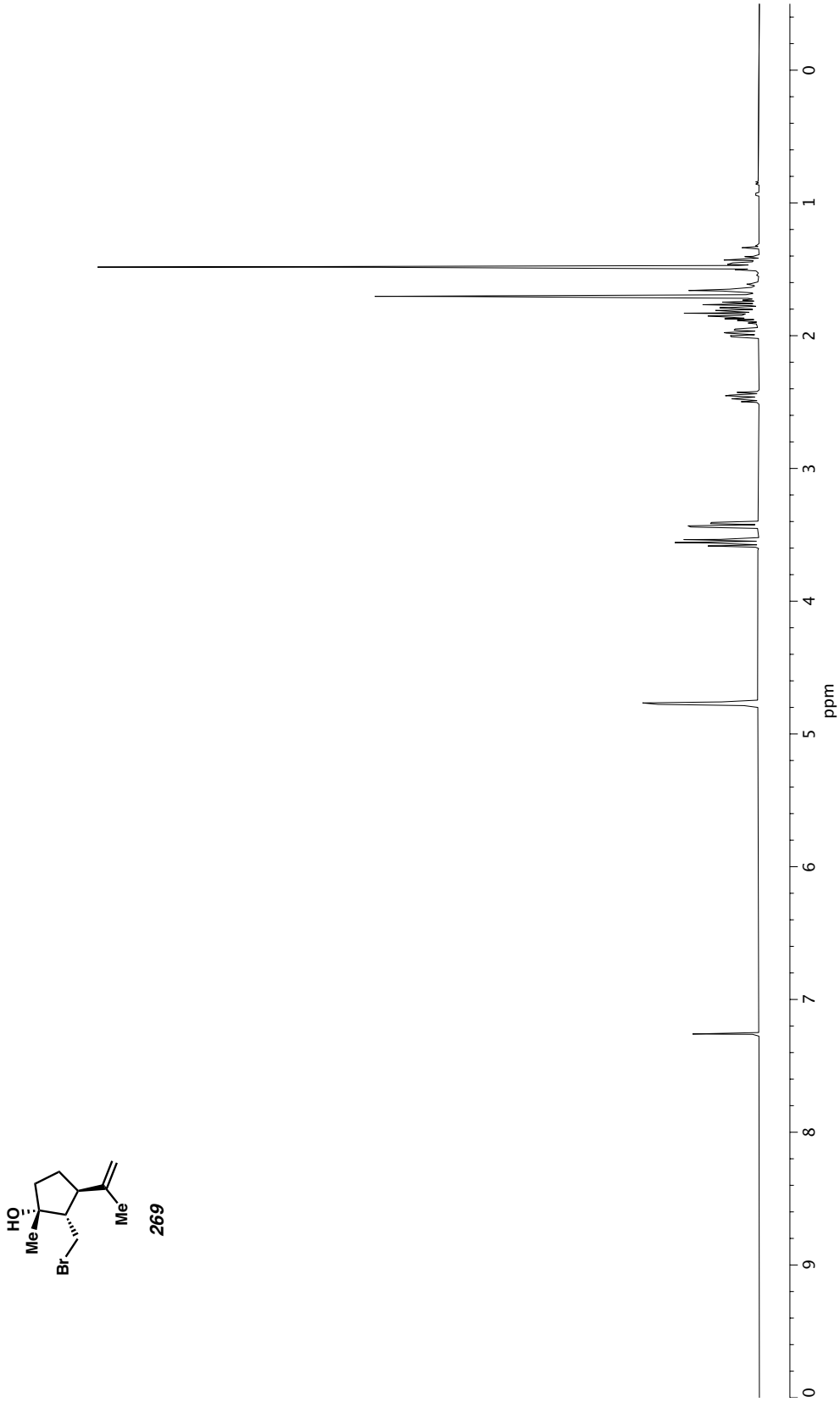


Figure A4.61. *^{13}C NMR (100 MHz, $CDCl_3$) of compound* ***268****.*



269

Figure A4.62. *^1H NMR (400 MHz, $CDCl_3$) of compound* ***269***.

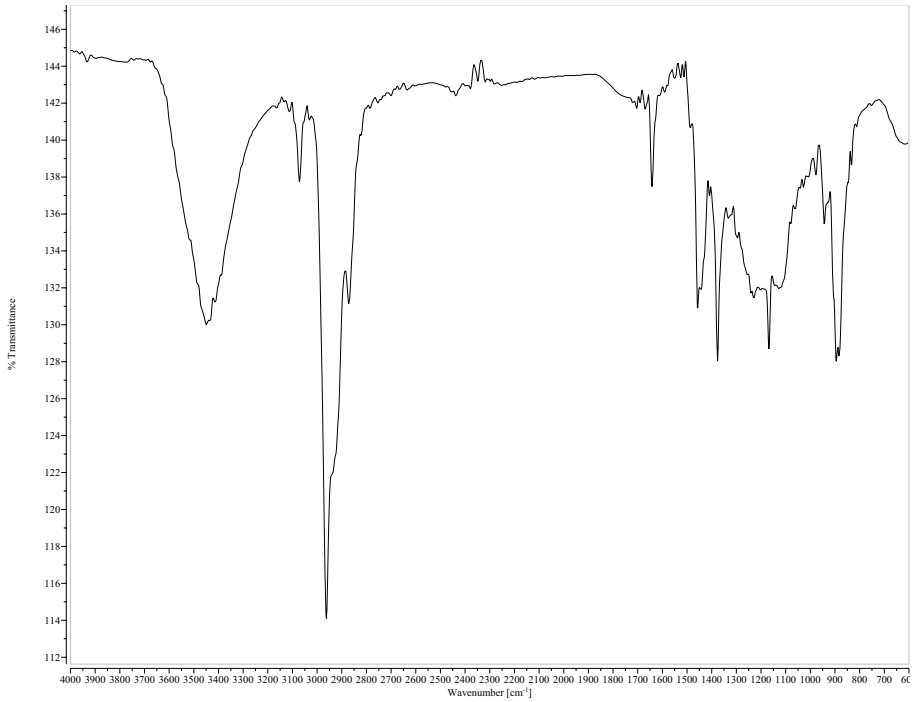


Figure A4.63. *Infrared spectrum (Thin Film, NaCl) of compound* ***269****.*

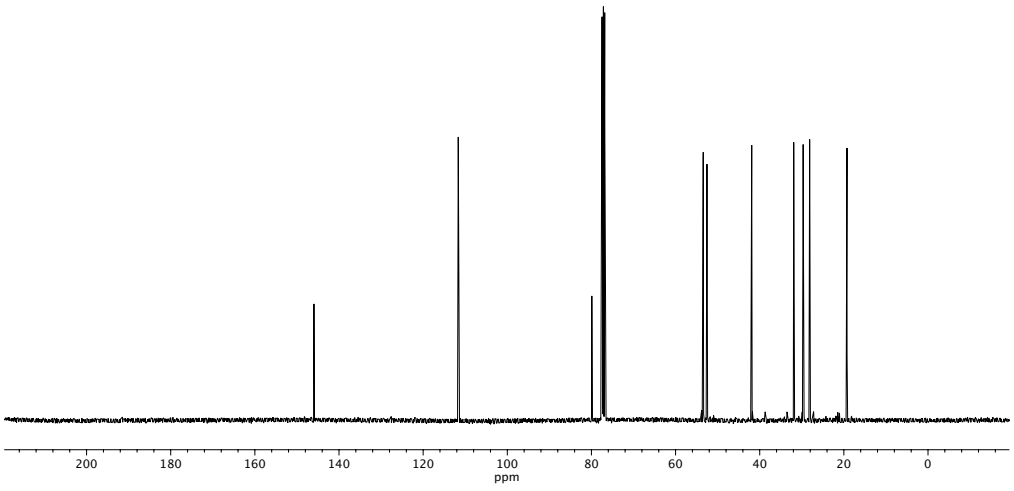
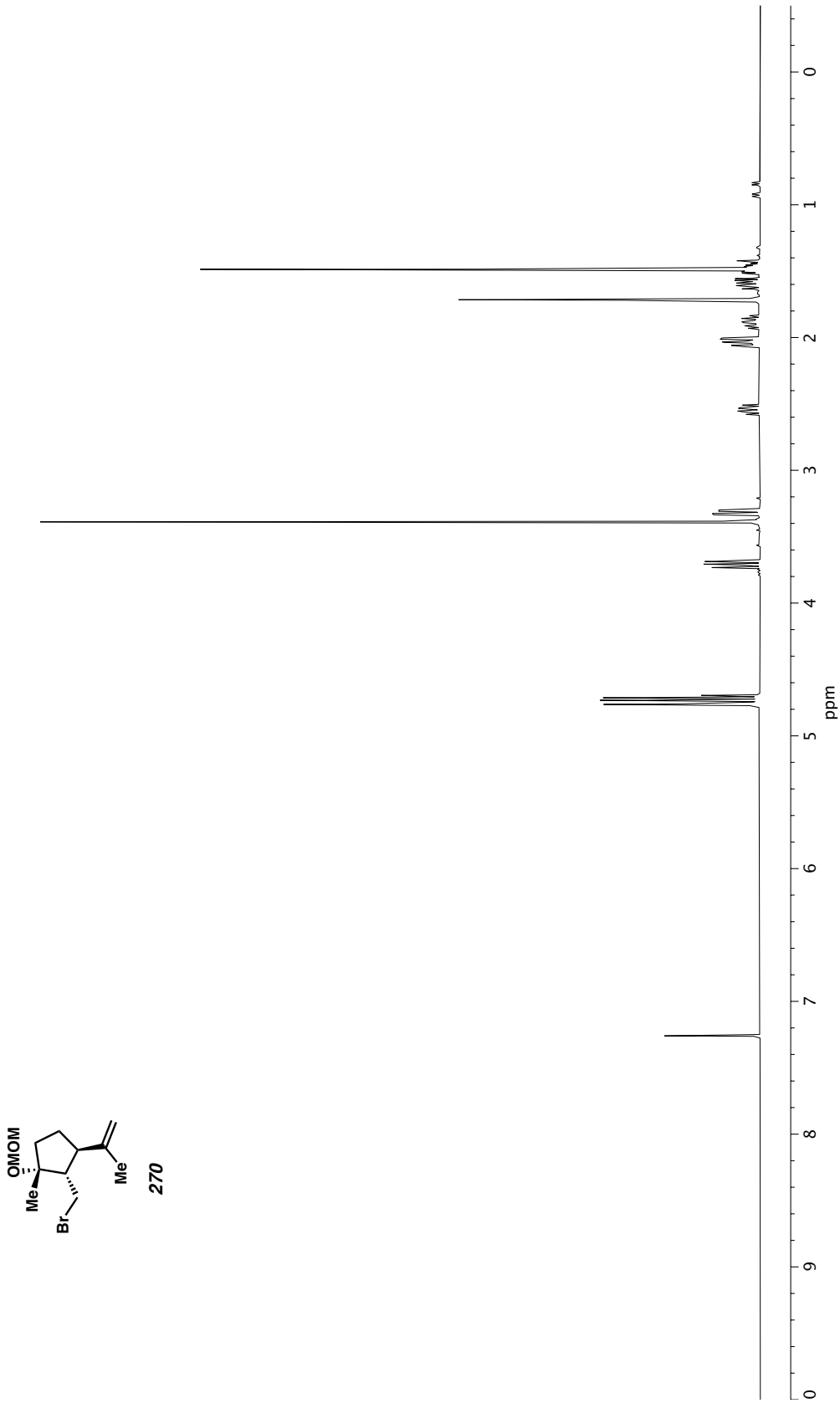


Figure A4.64. *^{13}C NMR (100 MHz, $CDCl_3$) of compound* ***269****.*



270

Figure A4.65. *^1H NMR (400 MHz, $CDCl_3$) of compound* ***270****.*

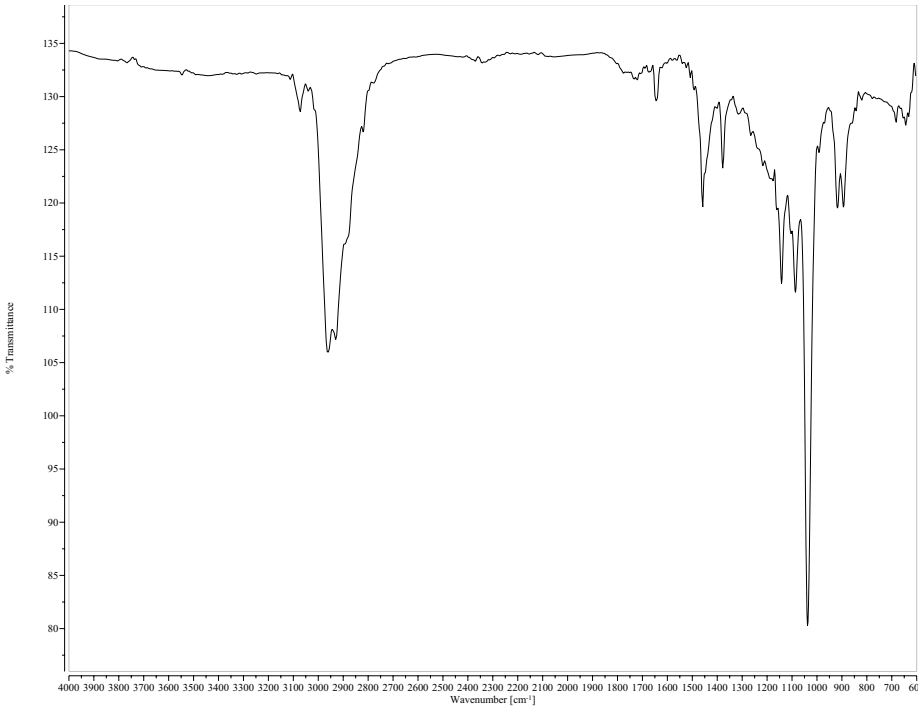


Figure A4.66. *Infrared spectrum (Thin Film, NaCl) of compound* ***270****.*

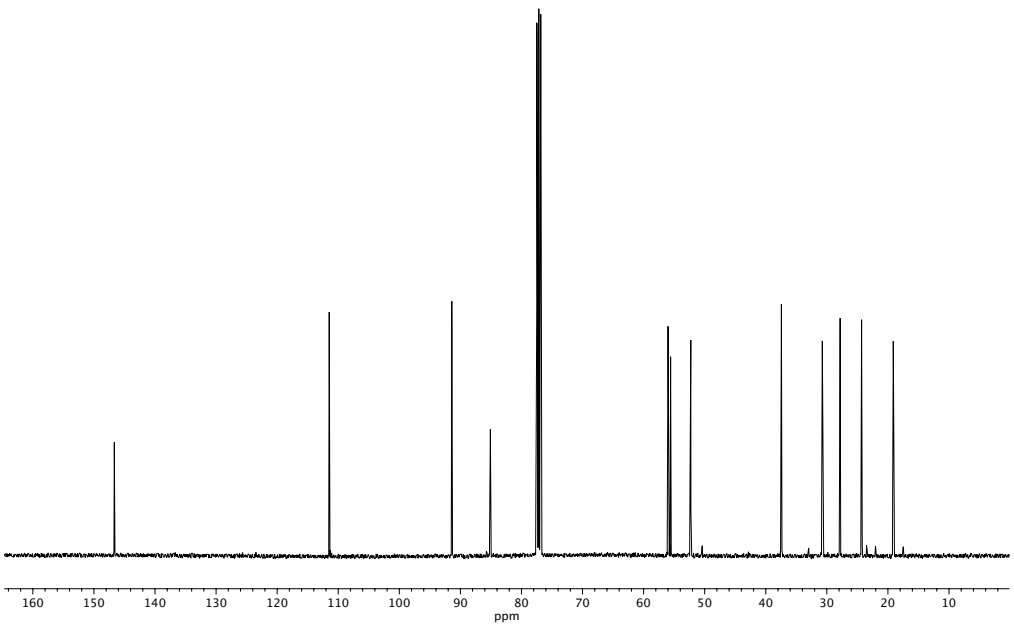


Figure A4.67. *^{13}C NMR (100 MHz, $CDCl_3$) of compound* ***270****.*

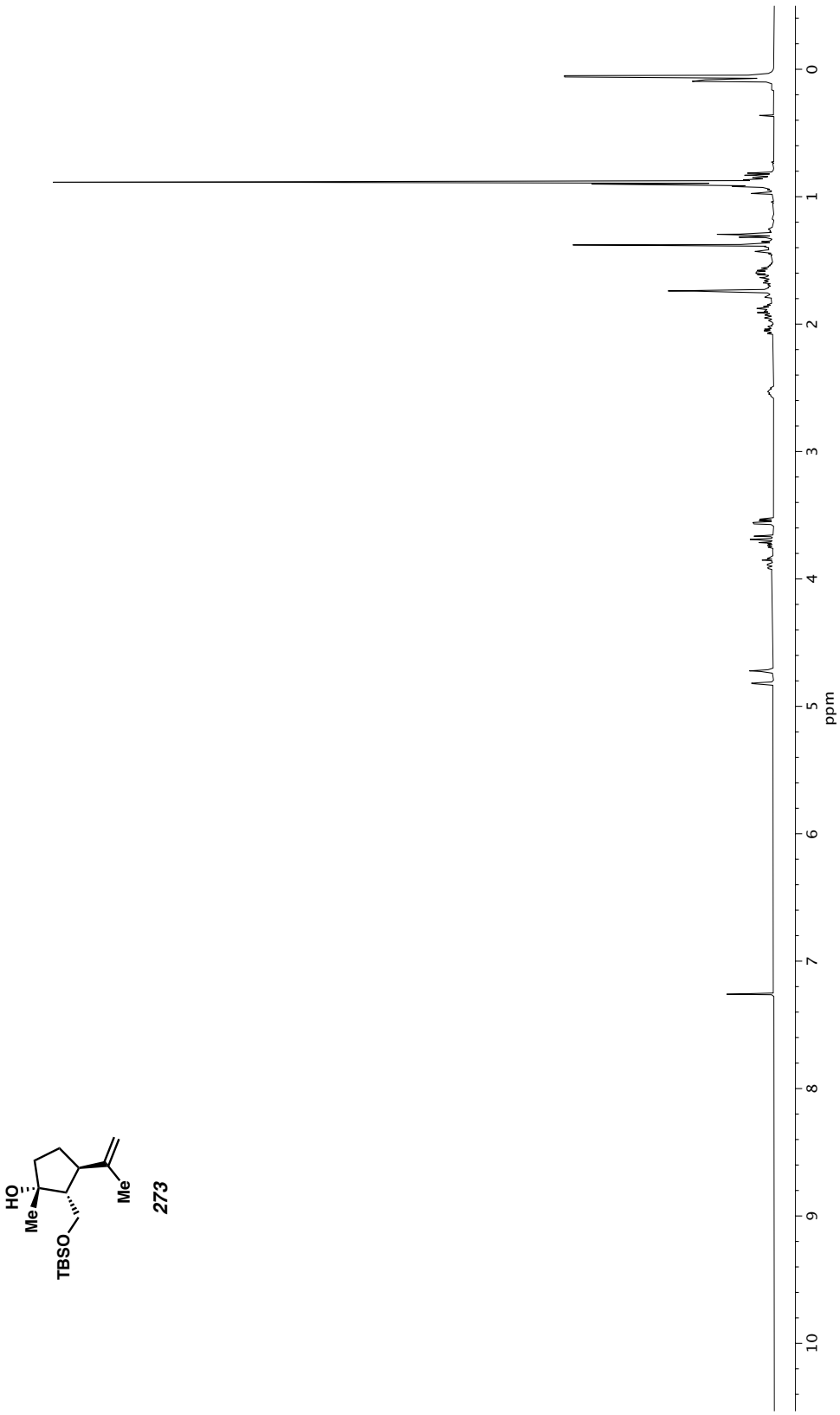


Figure A4.68. *^{1}H NMR (400 MHz, $CDCl_3$) of compound* ***273***.

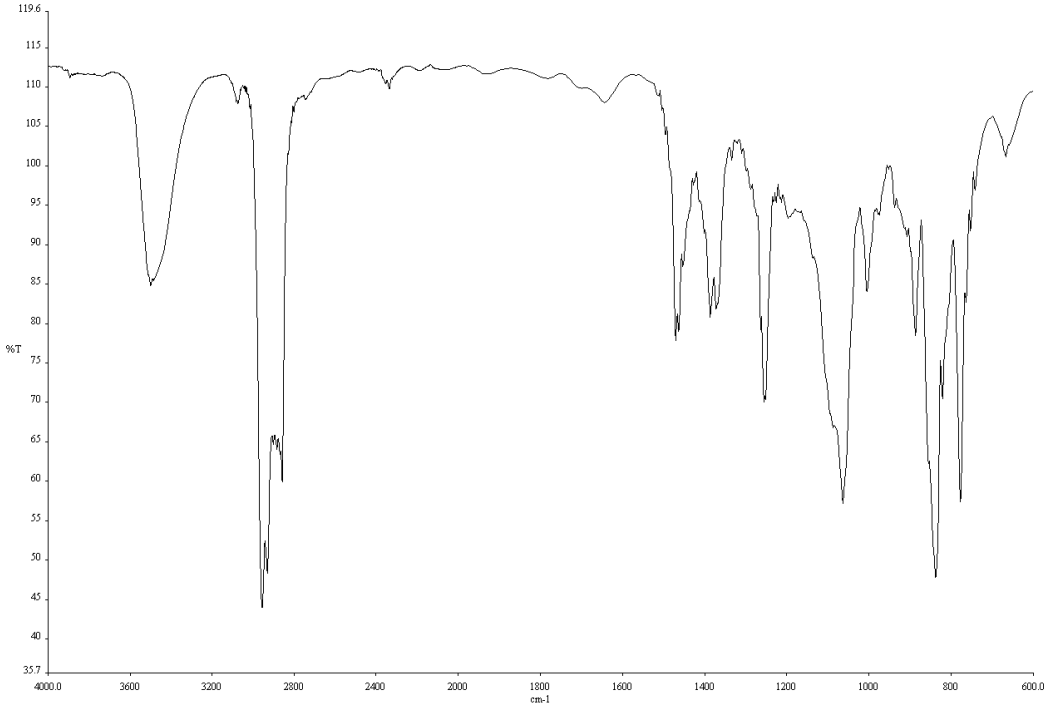


Figure A4.69. *Infrared spectrum (Thin Film, NaCl) of compound* ***273****.*

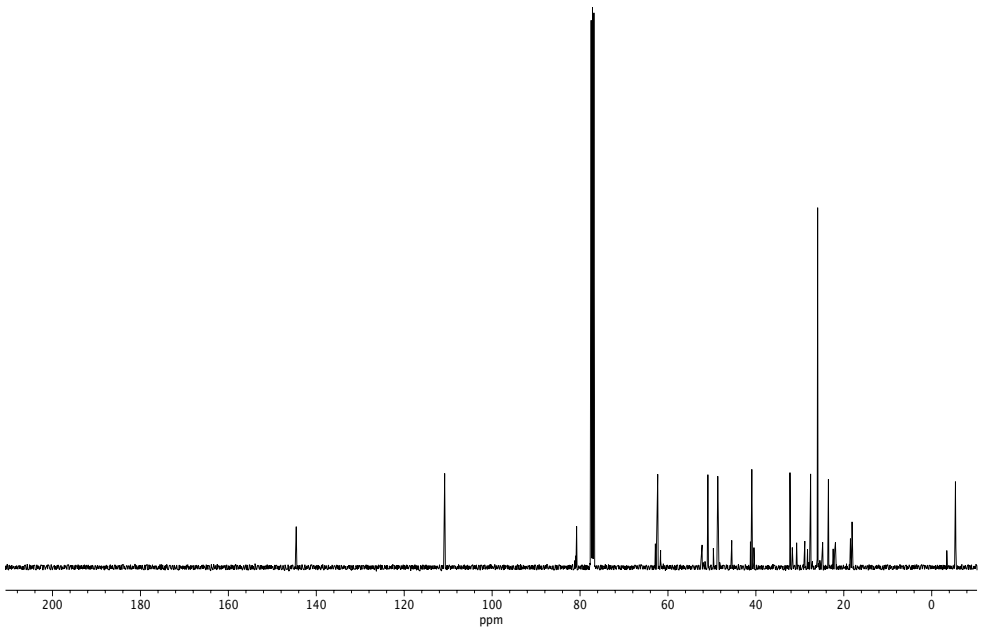


Figure A4.70. *^{13}C NMR (100 MHz, $CDCl_3$) of compound* ***273****.*

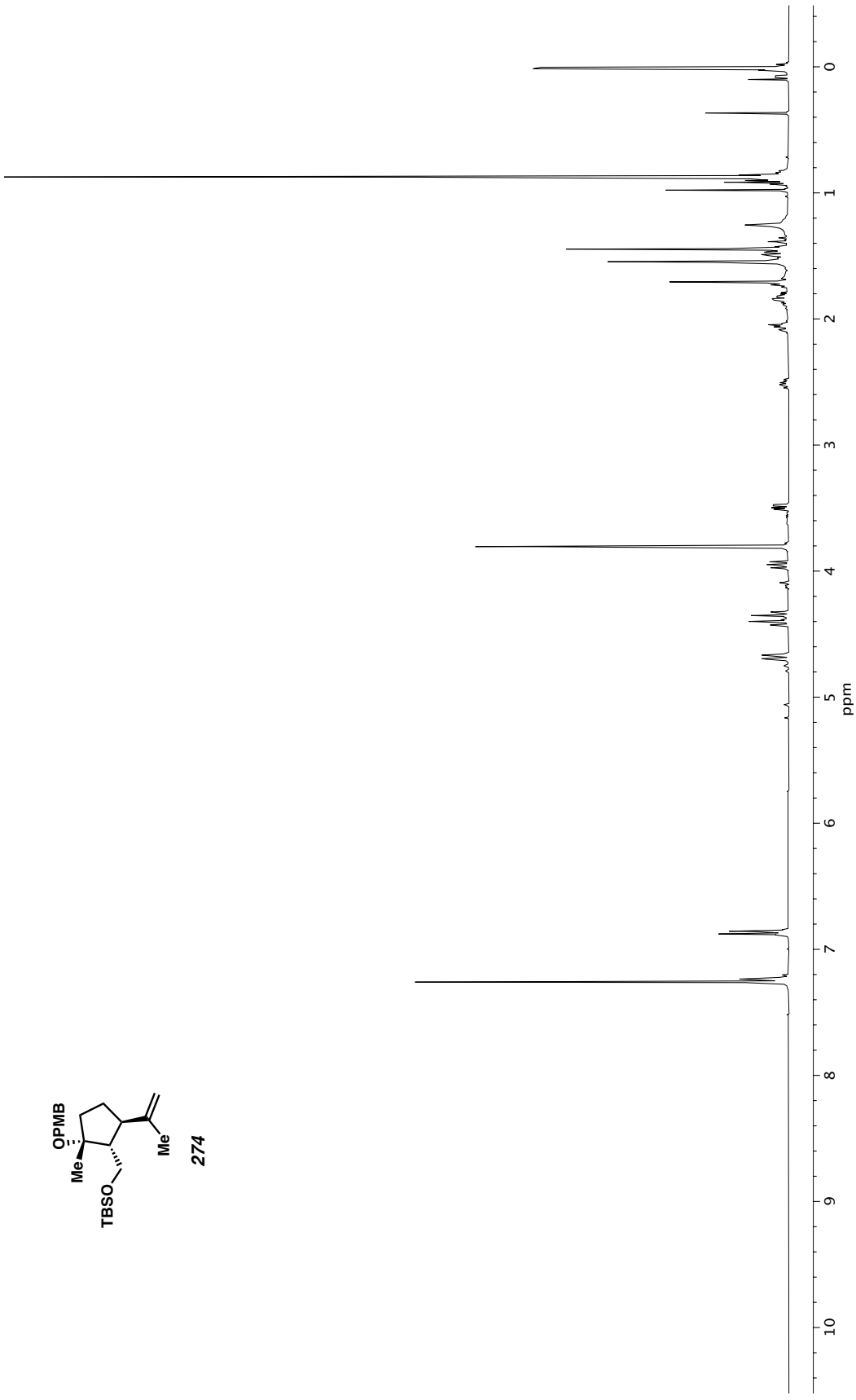


Figure A4.71. *^1H NMR (400 MHz, $CDCl_3$) of compound* ***274****.*

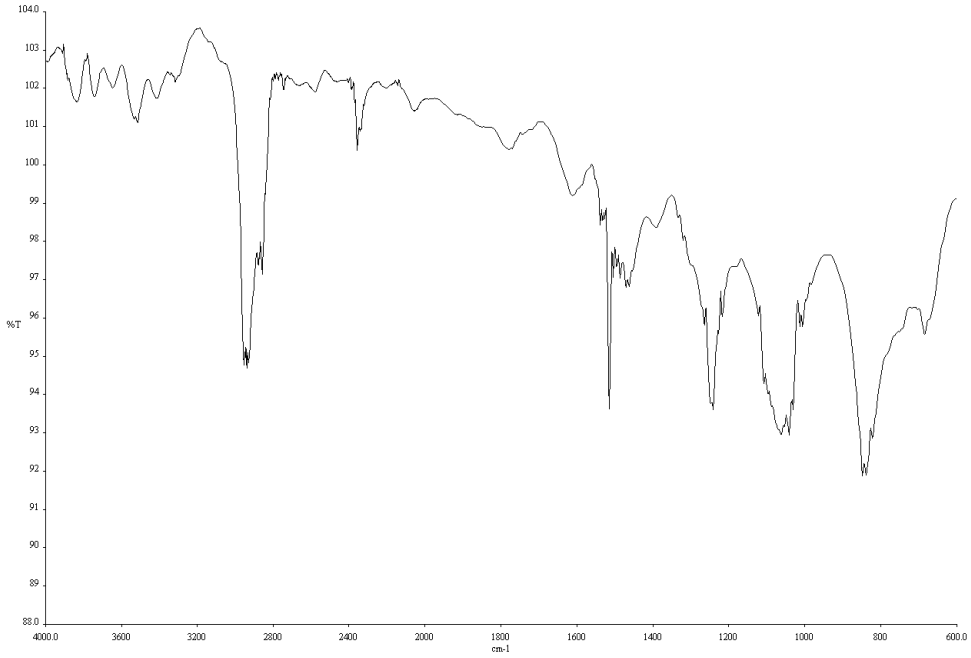


Figure A4.72. *Infrared spectrum (Thin Film, NaCl) of compound* ***274****.*

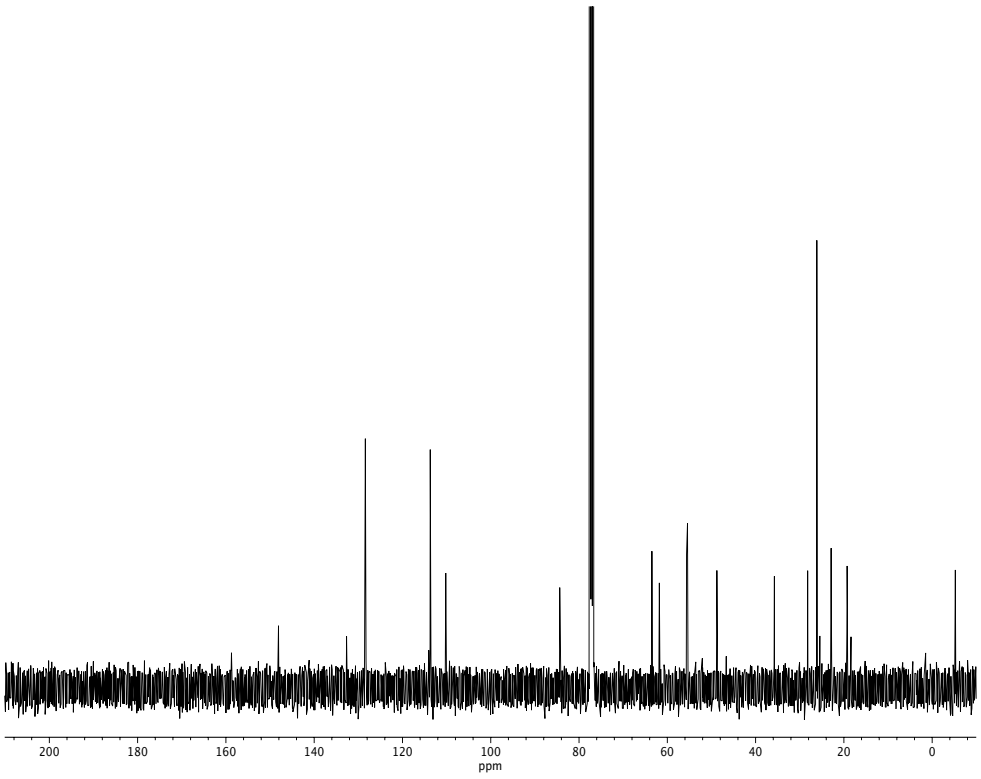
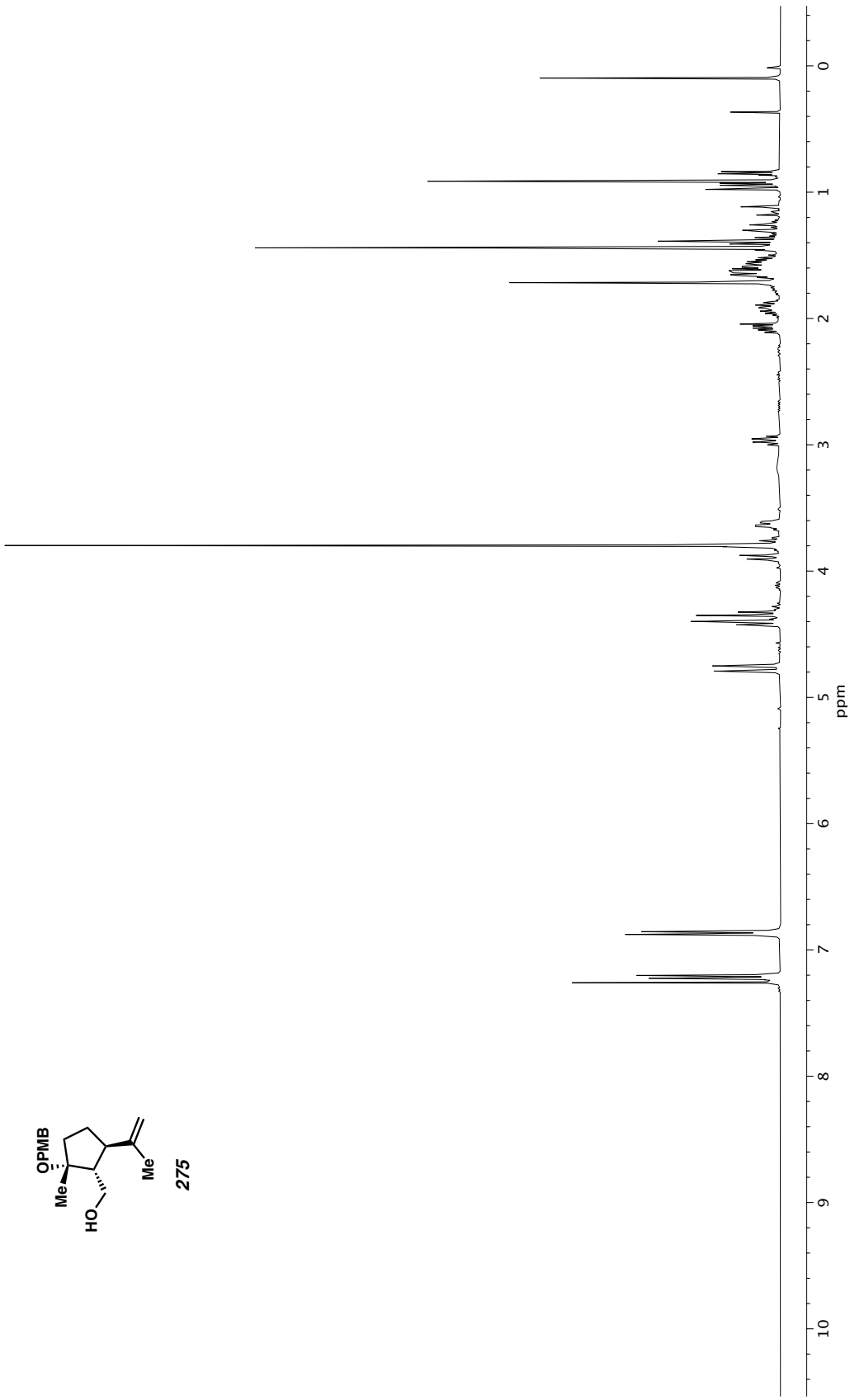


Figure A4.73. *^{13}C NMR (100 MHz, $CDCl_3$) of compound* ***274****.*



275

Figure A4.74. *^1H NMR (400 MHz, $CDCl_3$) of compound* ***275****.*

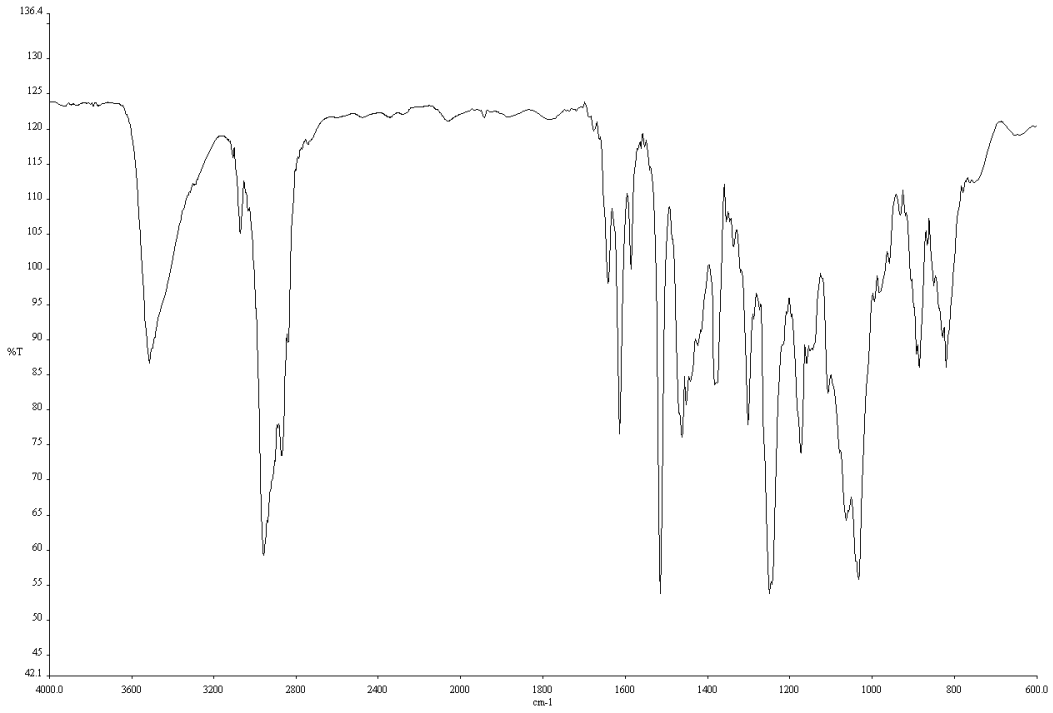


Figure A4.75. *Infrared spectrum (Thin Film, NaCl) of compound* ***275****.*

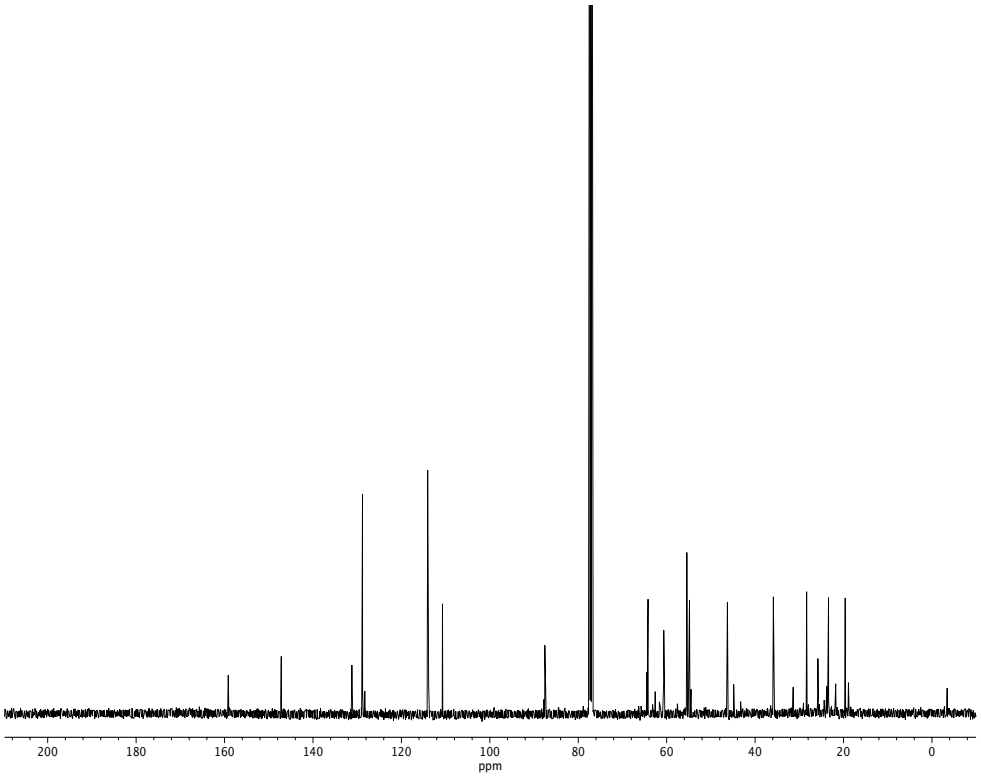


Figure A4.76. *^{13}C NMR (100 MHz, $CDCl_3$) of compound* ***275****.*

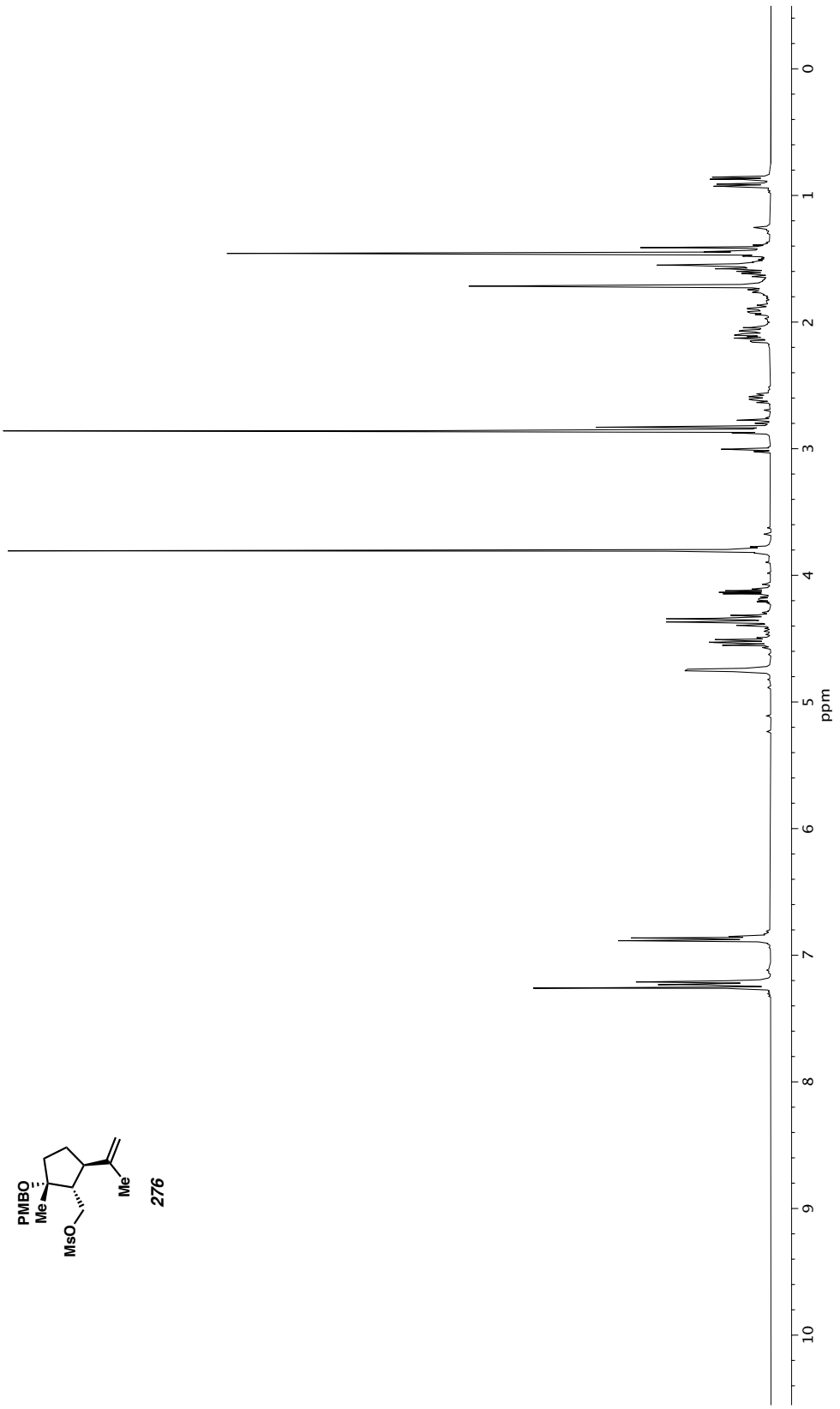


Figure A4.77. *^{1}H NMR (400 MHz, $CDCl_3$) of compound* ***276****.*

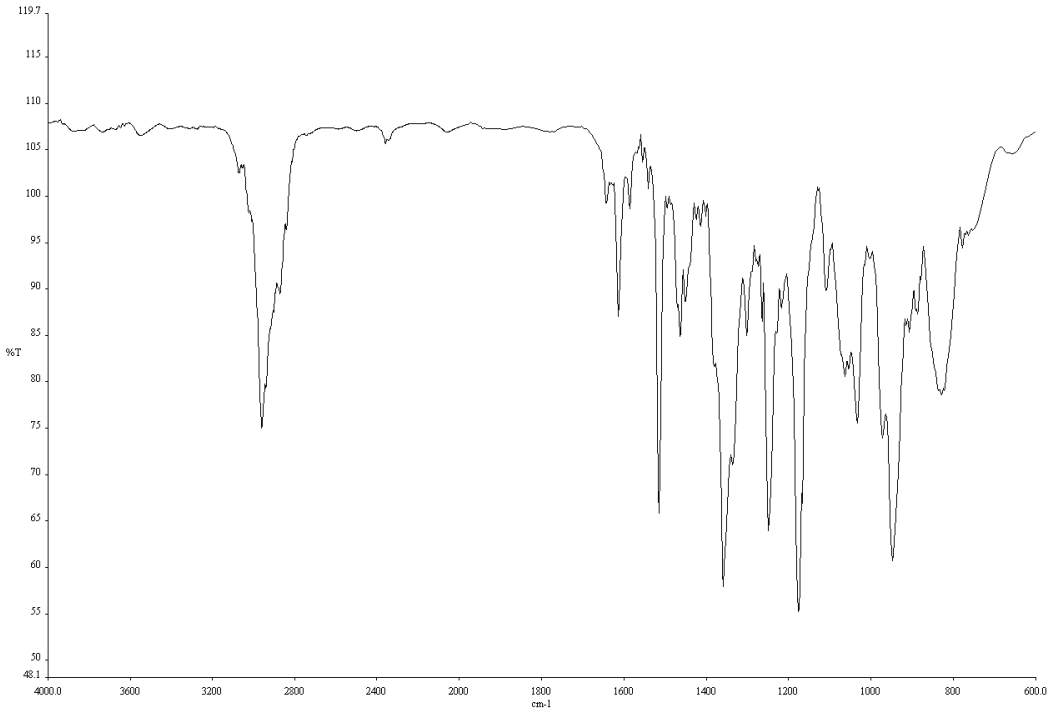


Figure A4.78. *Infrared spectrum (Thin Film, NaCl) of compound* ***276****.*

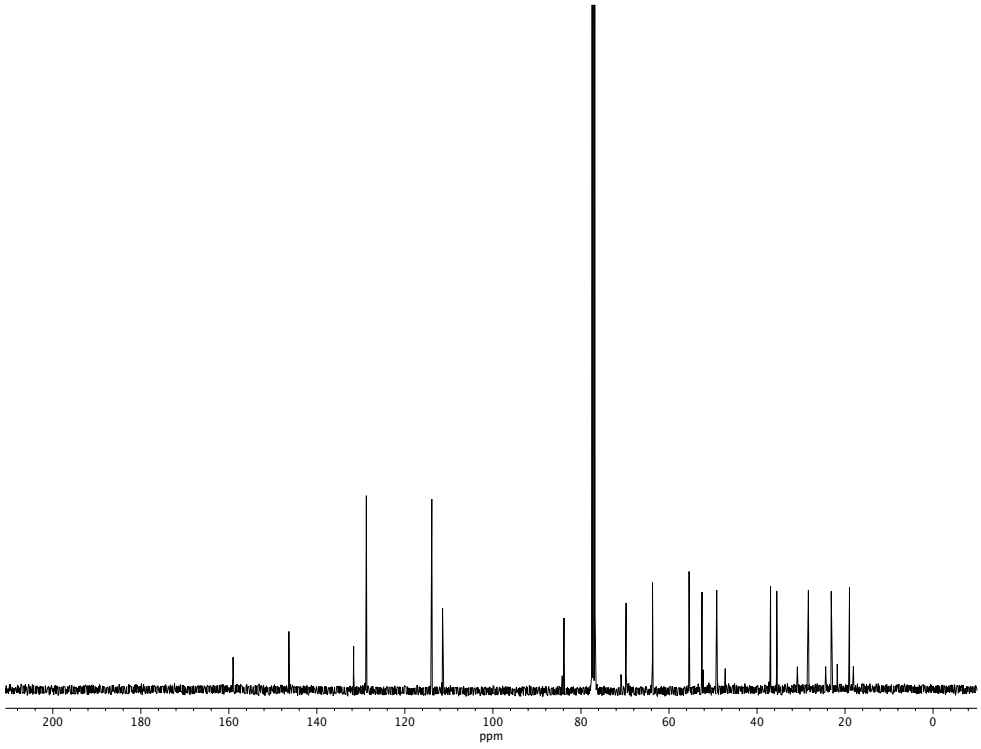


Figure A4.79. *^{13}C NMR (100 MHz, $CDCl_3$) of compound* ***276****.*

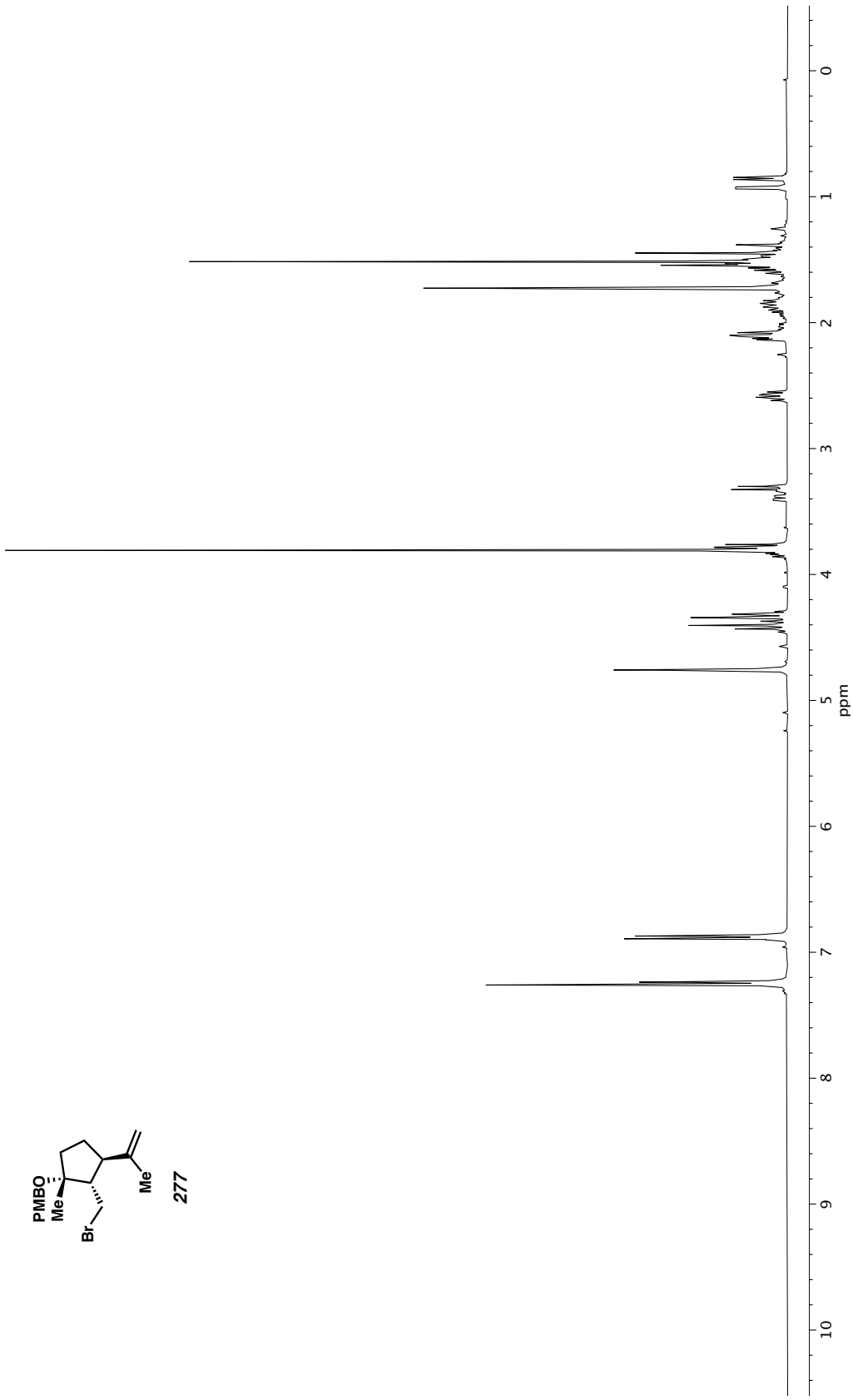


Figure A4.80. *^1H NMR (400 MHz, $CDCl_3$) of compound* ***277****.*

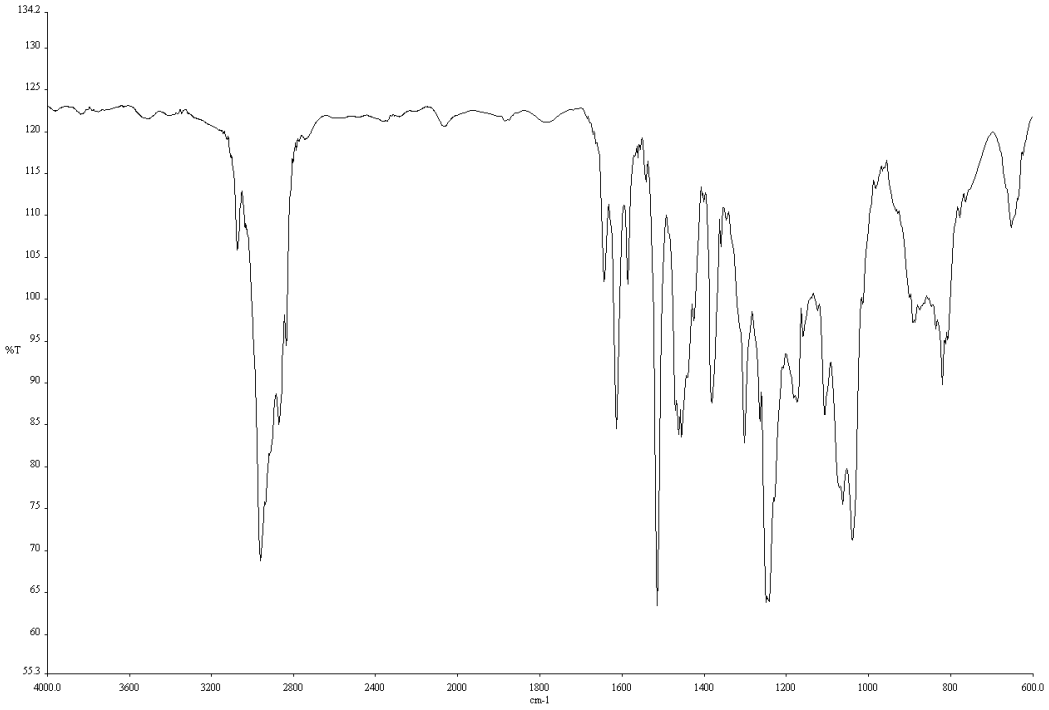


Figure A4.81. *Infrared spectrum (Thin Film, NaCl) of compound* ***277****.*

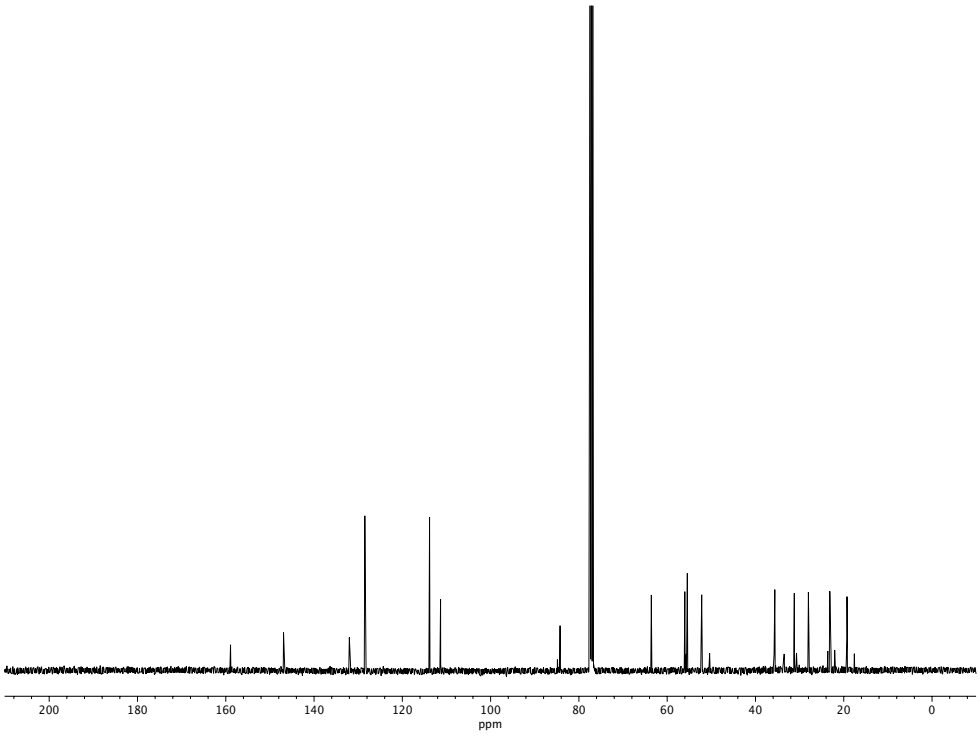


Figure A4.82. *^{13}C NMR (100 MHz, $CDCl_3$) of compound* ***277****.*

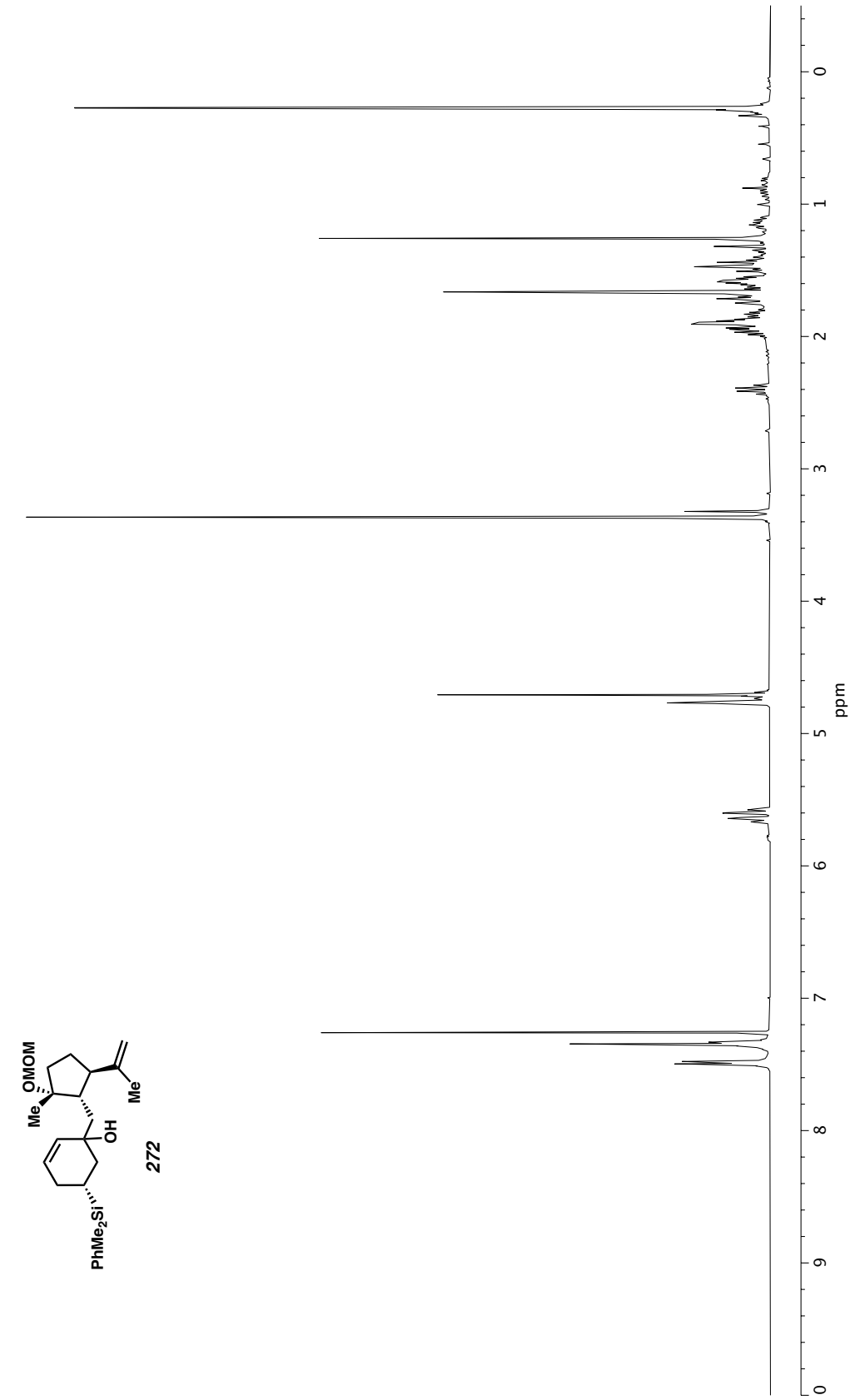


Figure A4.83. *^1H NMR (400 MHz, $CDCl_3$) of compound* ***272****.*

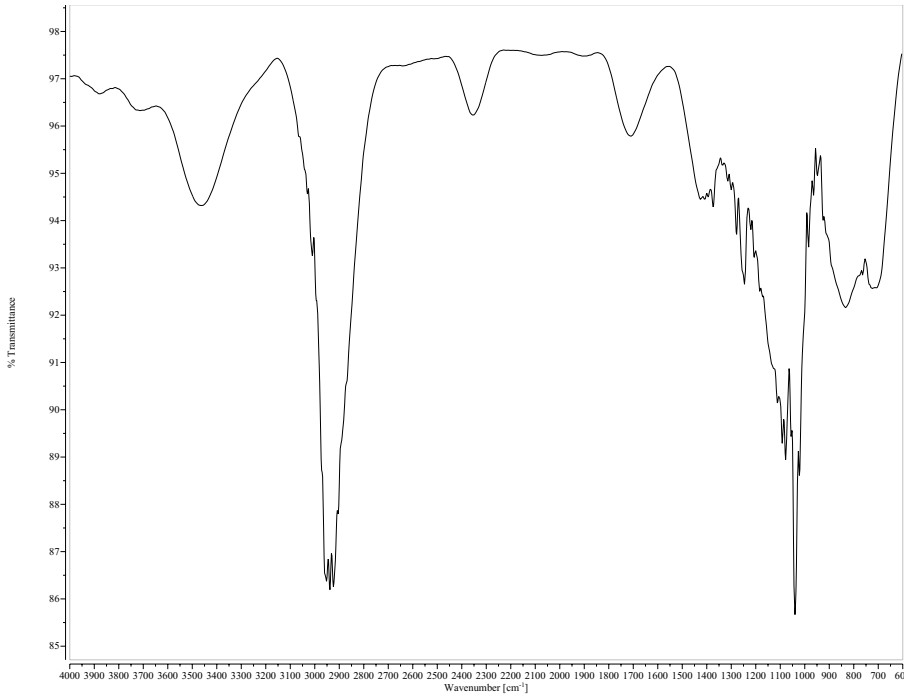


Figure A4.84. *Infrared spectrum (Thin Film, NaCl) of compound* ***272****.*

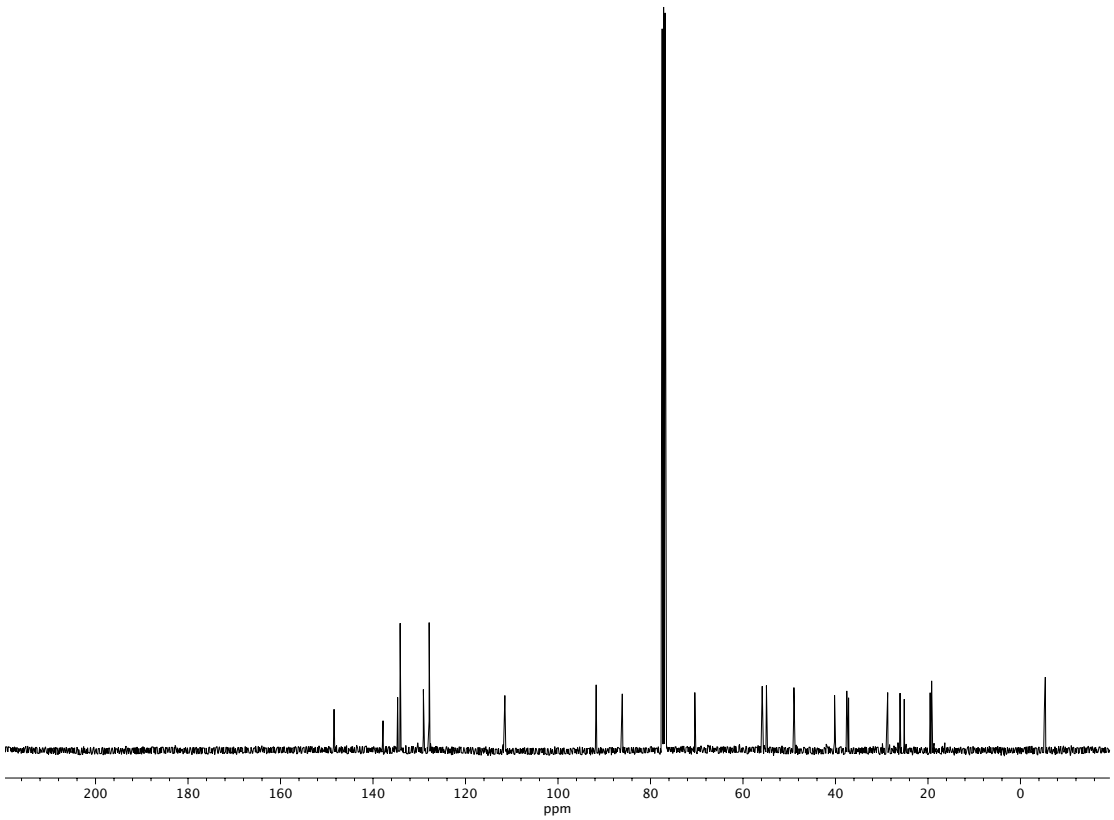


Figure A4.85. *^{13}C NMR (100 MHz, $CDCl_3$) of compound* ***272****.*

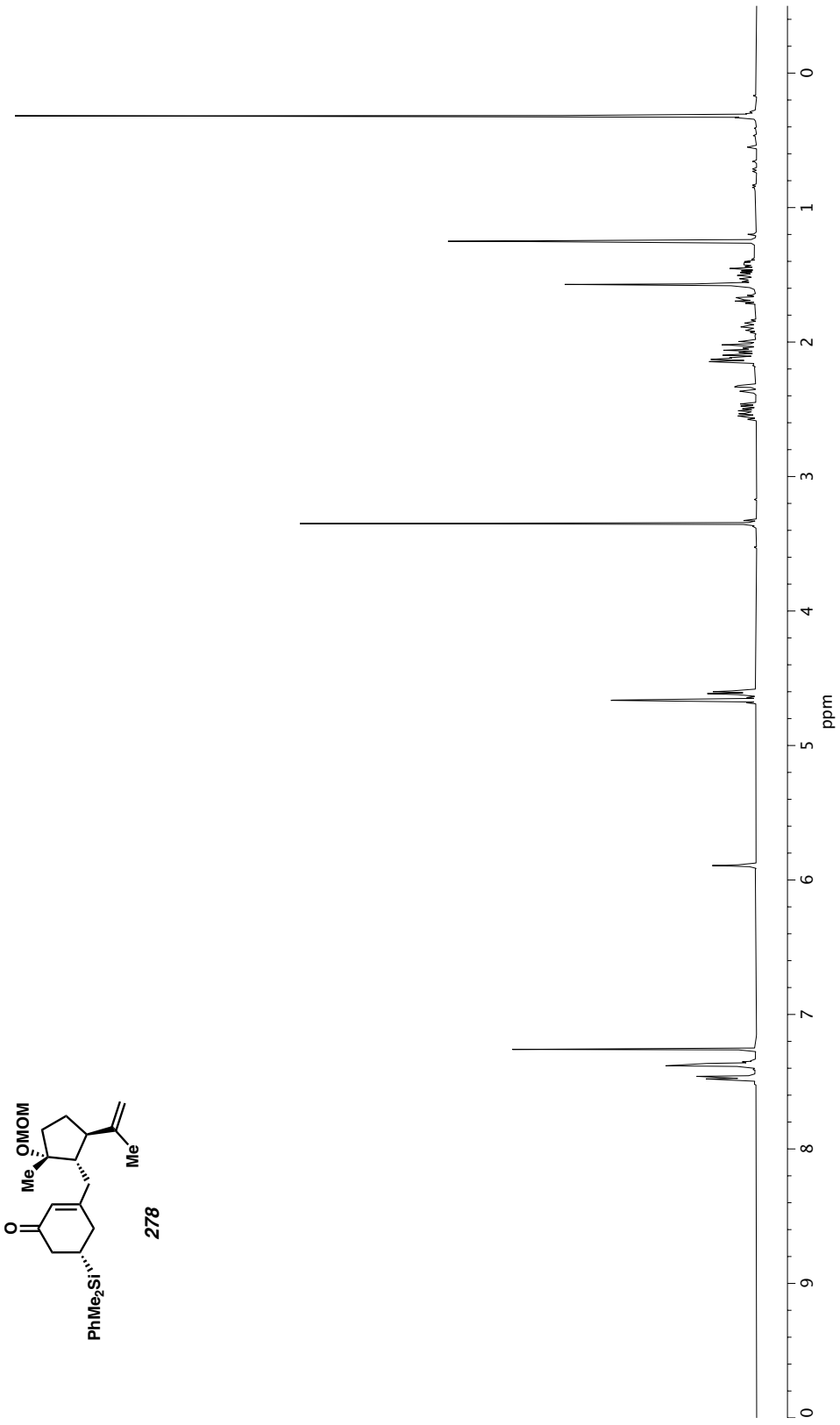


Figure A4.86. *^{1}H NMR (400 MHz, $CDCl_3$) of compound* ***278****.*

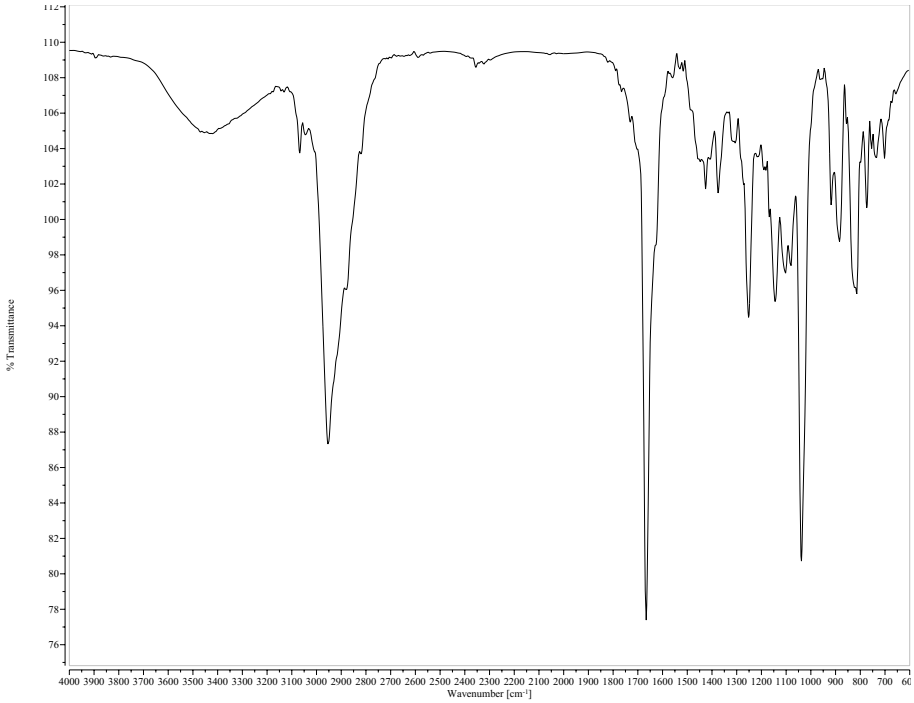


Figure A4.87. *Infrared spectrum (Thin Film, NaCl) of compound* ***278****.*

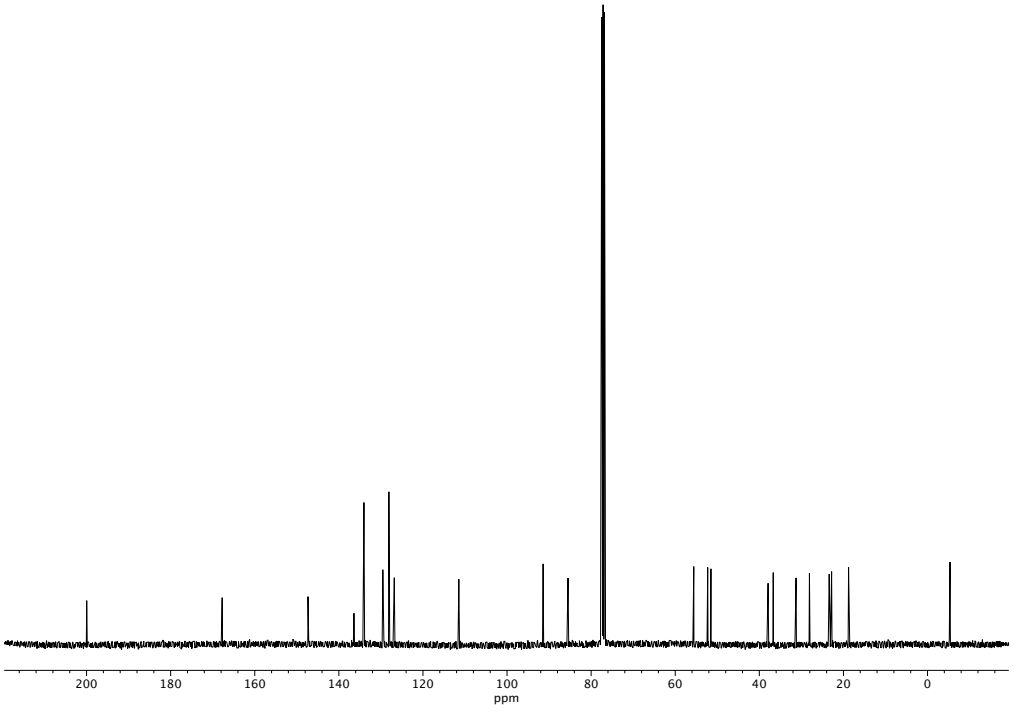


Figure A4.88. *^{13}C NMR (100 MHz, $CDCl_3$) of compound* ***278****.*

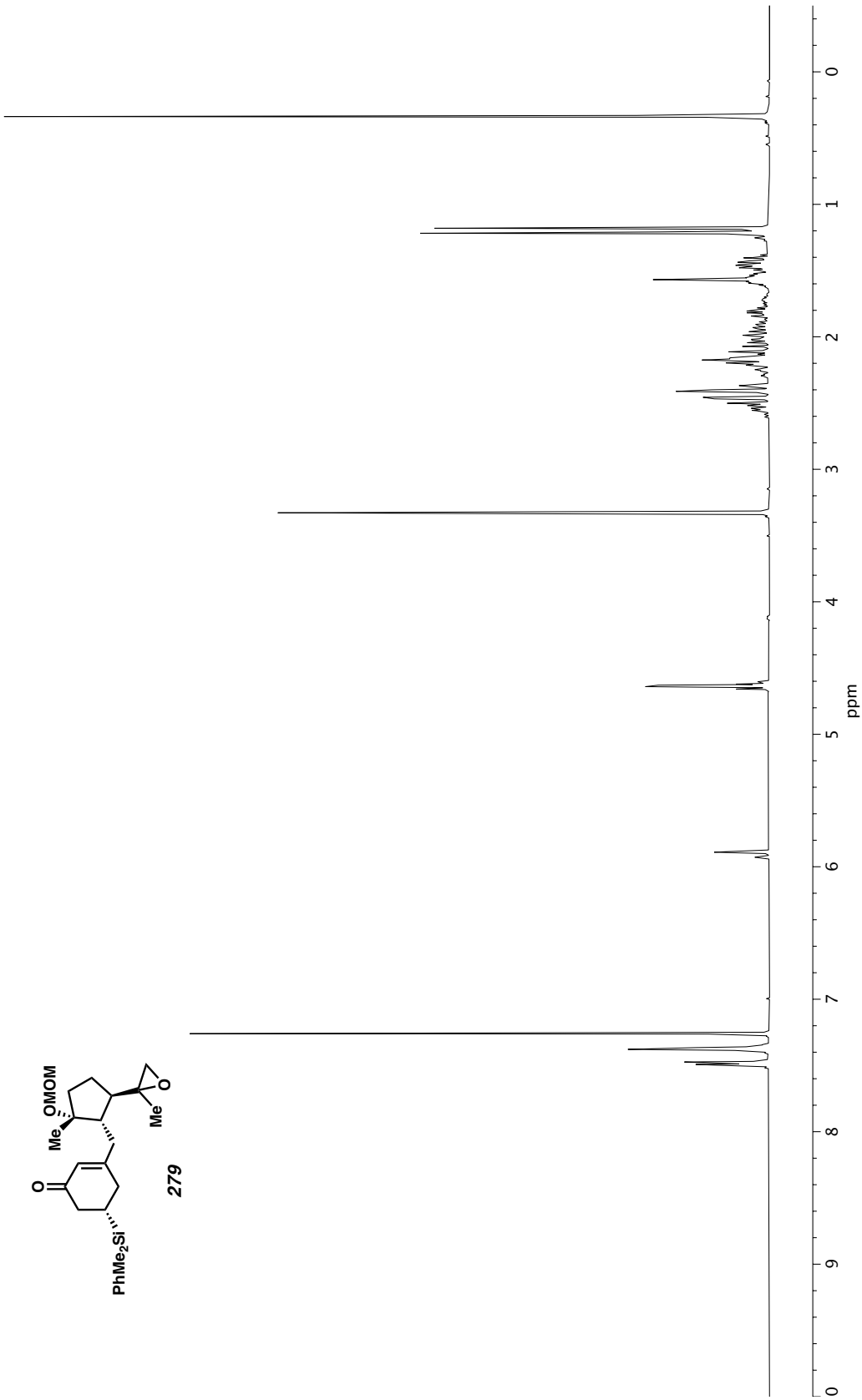


Figure A4.89. *^1H NMR (400 MHz, $CDCl_3$) of compound* ***279****.*

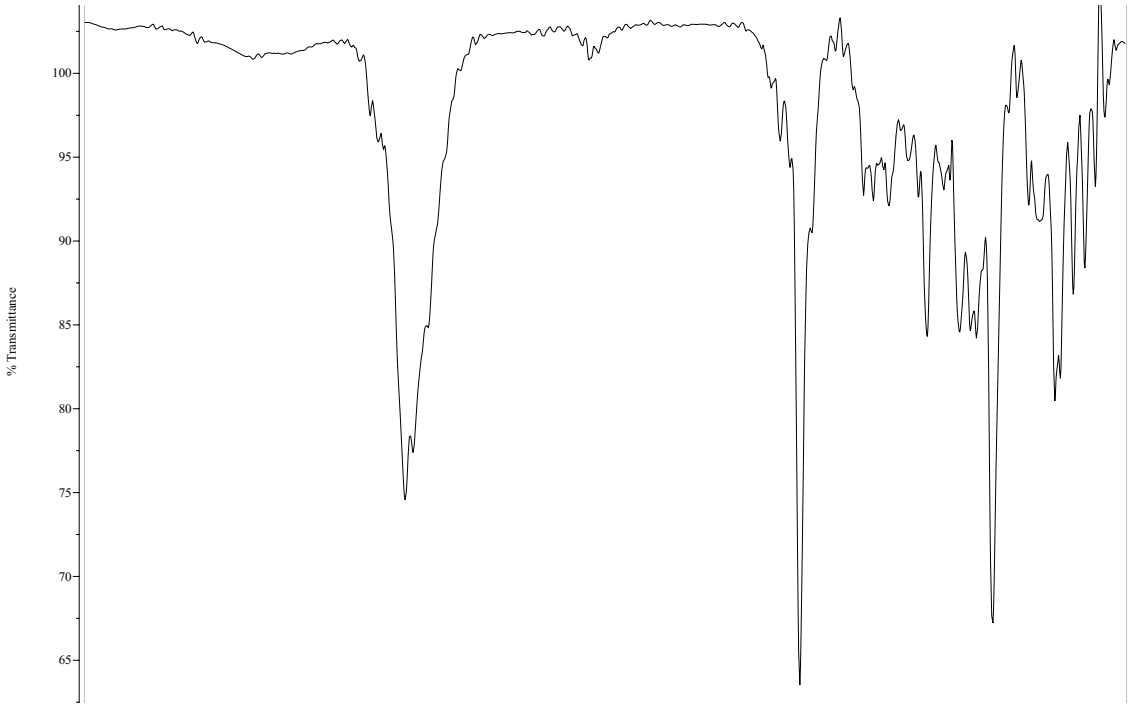


Figure A4.90. *Infrared spectrum (Thin Film, NaCl) of compound* ***279****.*

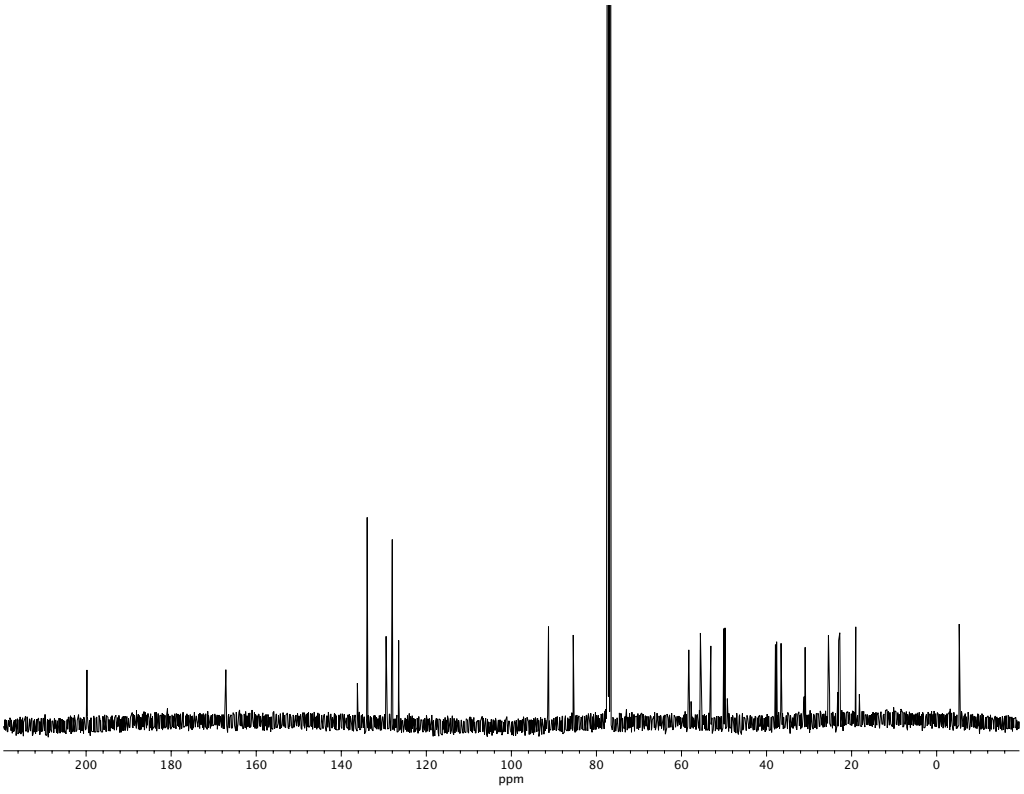


Figure A4.91. *^{13}C NMR (100 MHz, $CDCl_3$) of compound* ***279****.*

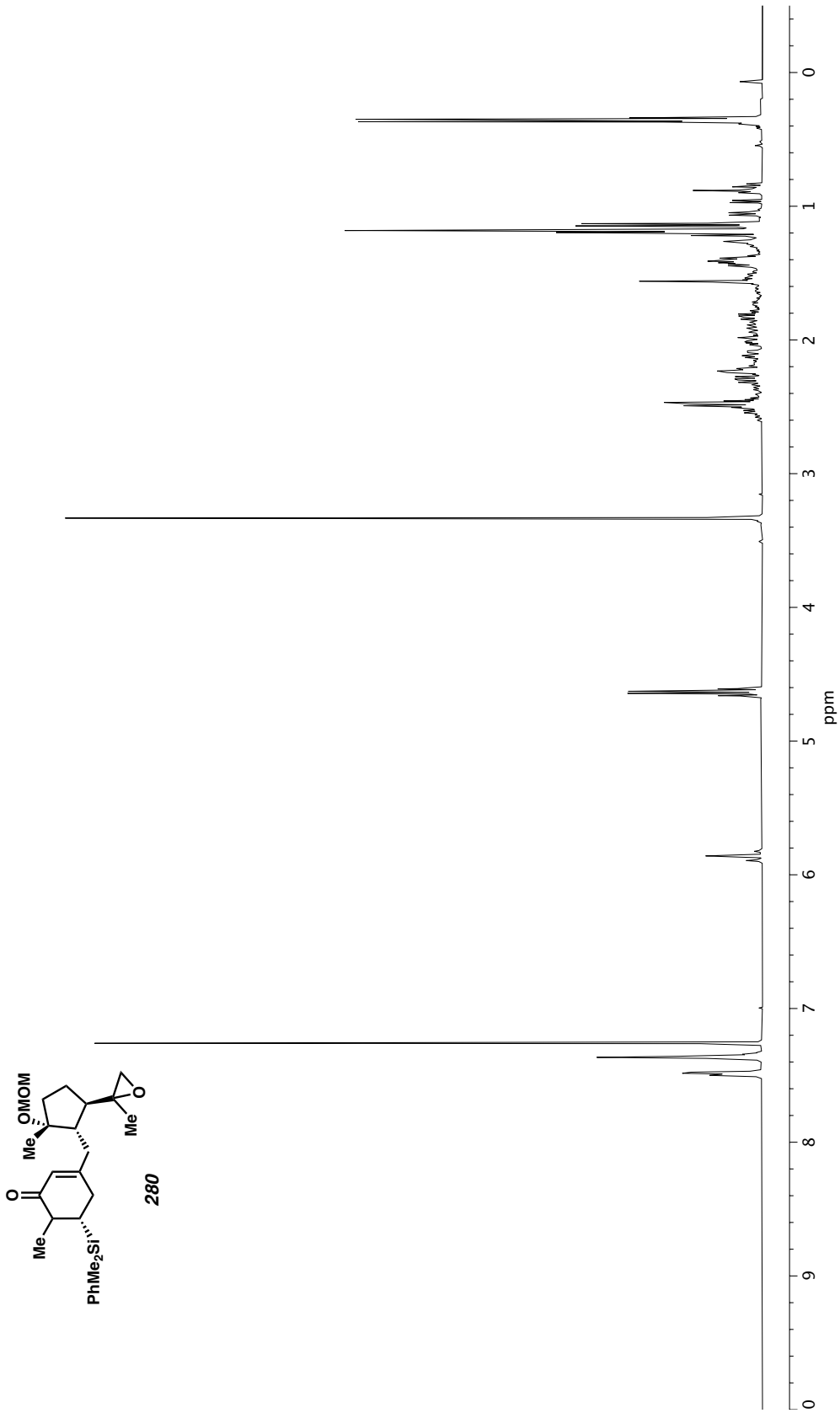


Figure A4.92. *^1H NMR (400 MHz, $CDCl_3$) of compound* ***280****.*

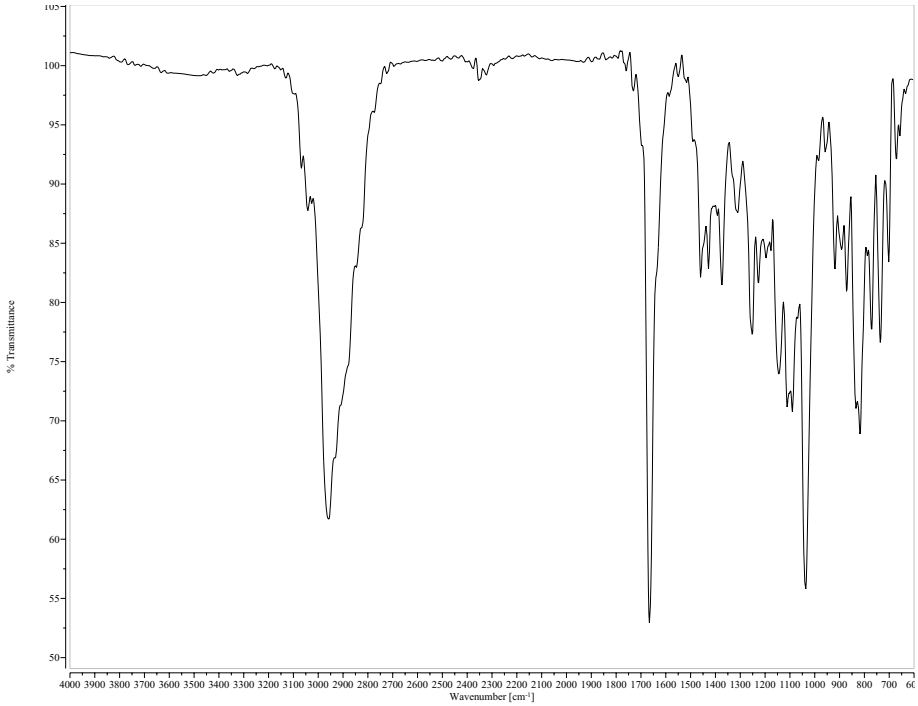


Figure A4.93. *Infrared spectrum (Thin Film, NaCl) of compound* ***280****.*

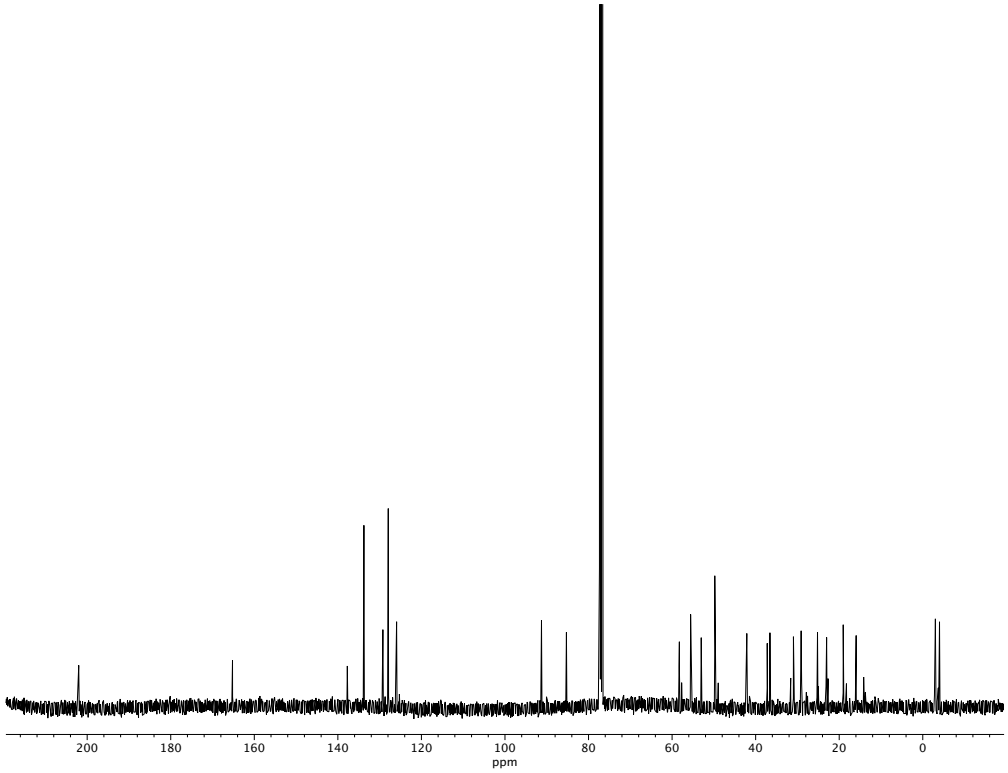


Figure A4.94. *^{13}C NMR (100 MHz, $CDCl_3$) of compound* ***280****.*

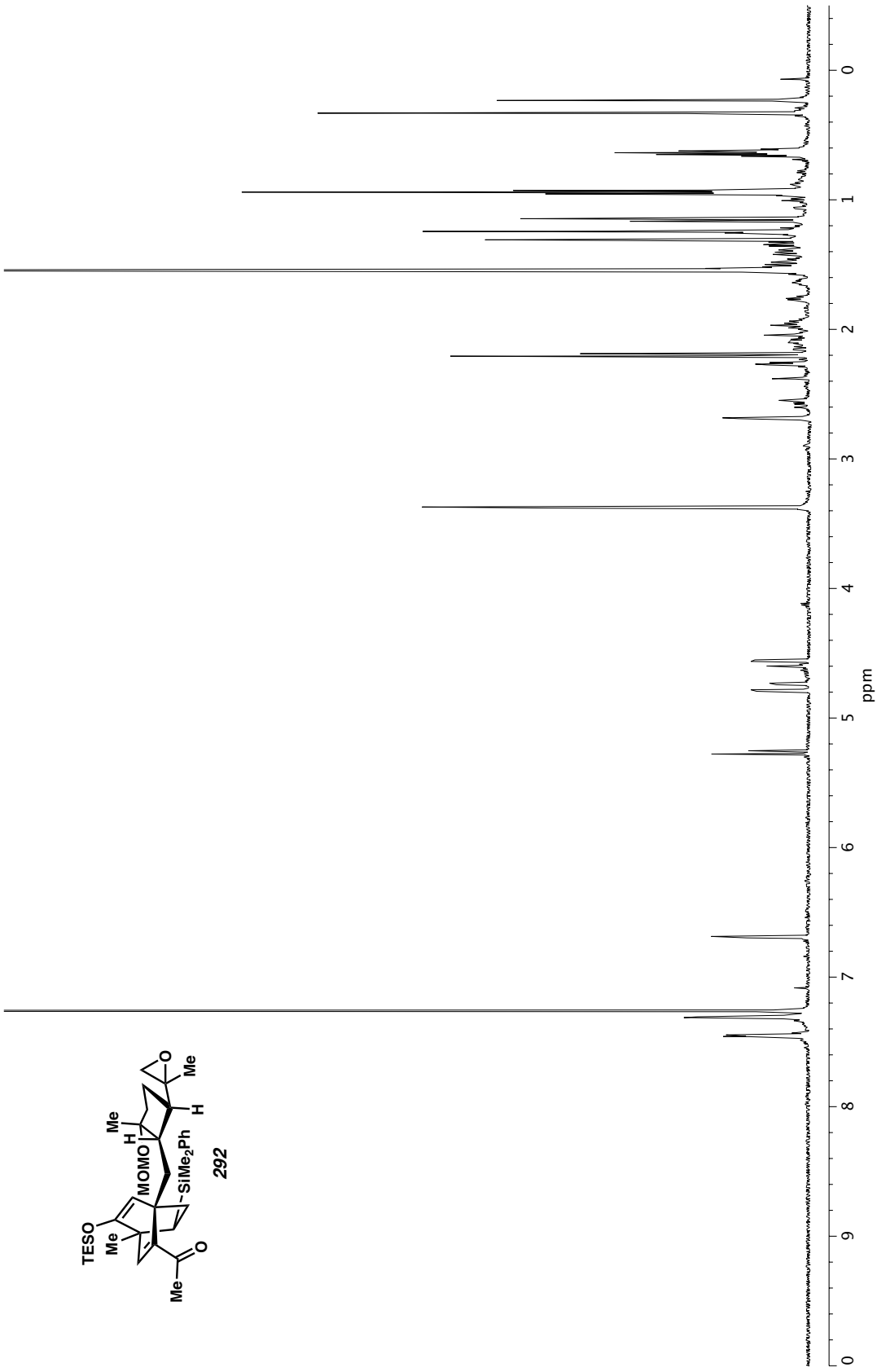


Figure A4.95. *^{1}H NMR (600 MHz, $CDCl_3$) of compound* ***292***.

APPENDIX 5

Early Strategies Toward the Total Synthesis of Hypermoin A†

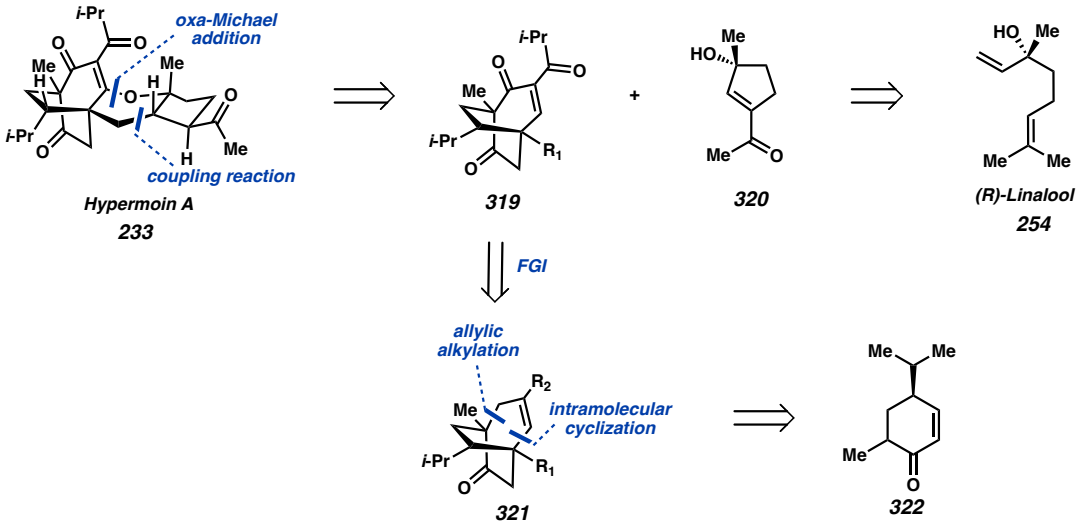
A5.1 INTRODUCTION

Throughout the development of a synthetic route toward hypermoin A (**233**), several strategies to form the [3.2.2] bicyclic core were attempted but were discontinued over the course of our studies. These strategies are detailed in this appendix.

A5.2 ALLYLIC ALKYLATION–CYCLIZATION SEQUENCE

Our first-generation retrosynthetic analysis begins with disconnection of the central six-membered ring through an *oxa*-Michael addition and a C–C bond coupling of [3.2.2] bicyclic core **319** and cyclopentyl fragment **320**, which we envisioned accessing from linalool (**254**, Figure A5.1).[1] Through functional group manipulations, **319** is anticipated

Figure A5.1. *First generation retrosynthetic analysis: allylic alkylation–cyclization.*

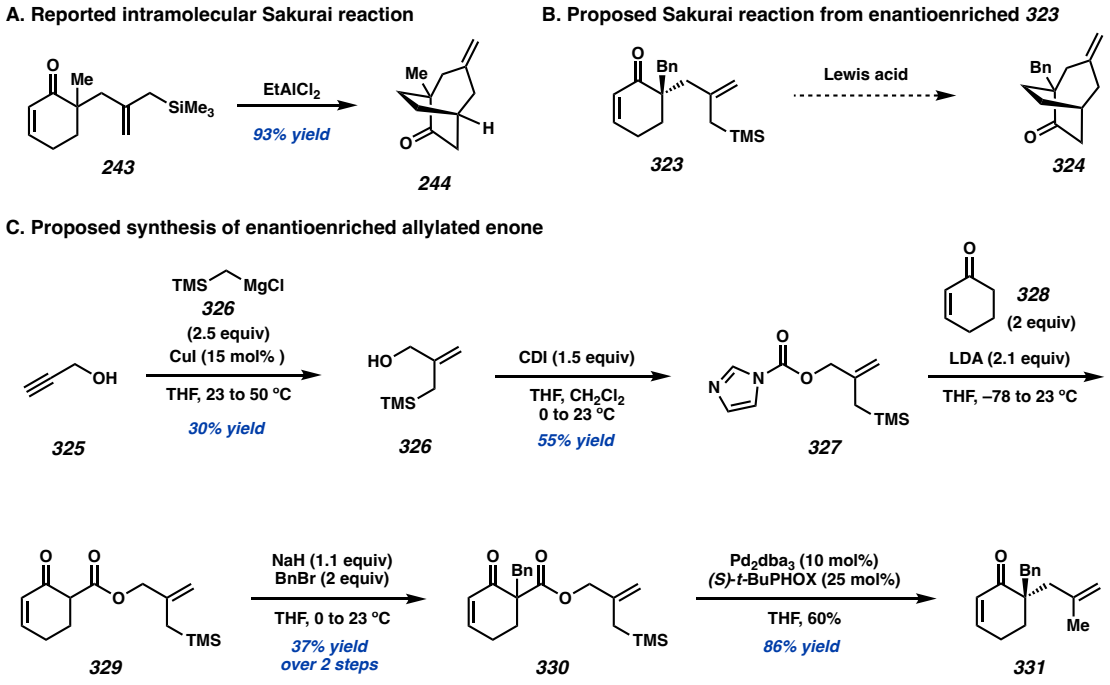


†Unpublished research performed in collaboration with Flesch, K. N.; Patch, M. M.; Ahmad, J.; Nair, V. N.; Grogan, Z. R.; Bottcher, S. E.

to be derived from intermediate **321**, which is proposed to arise from an allylic alkylation–intramolecular cyclization sequence employing cyclohexenone **322**.

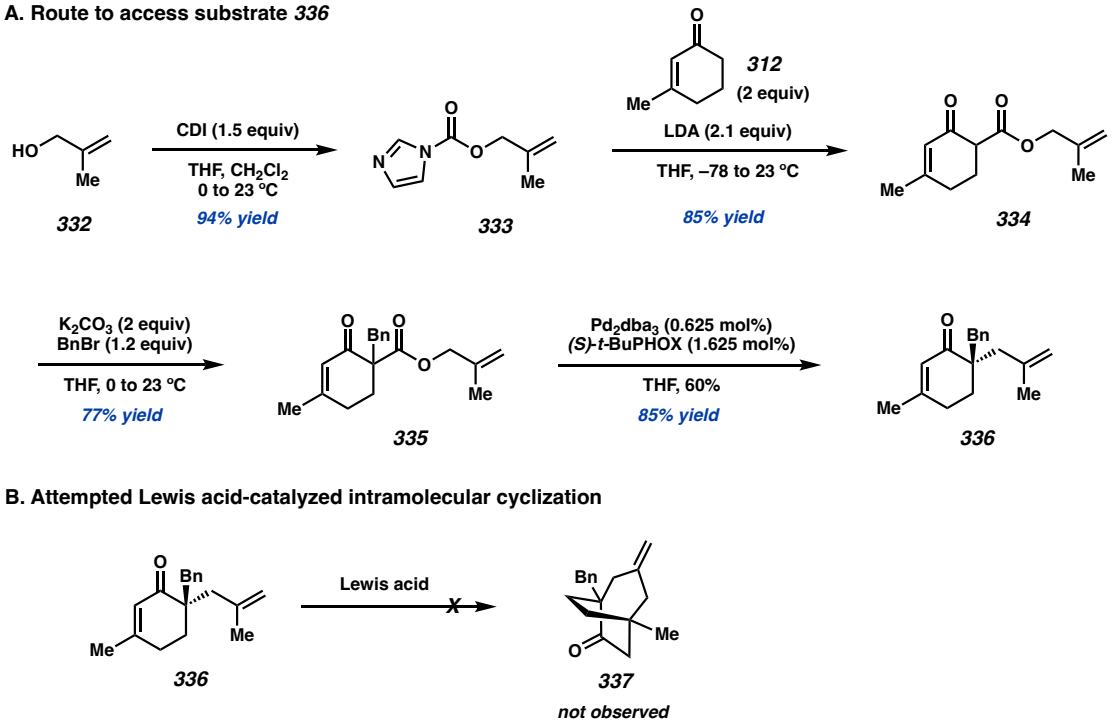
Inspired by the successful Lewis acid-catalyzed intramolecular Sakurai reaction reported by Lee and coworkers (Figure A5.2.A)[2], we planned to explore this reaction on a similar but enantioenriched substrate **323** to access **324** (Figure A5.2.B). To access substrate **323**, propargyl alcohol **325** can be reacted with Grignard reagent **326** to form allylic alcohol **326 (**Figure A5.2.C).[3] Subsequent reaction with CDI allows formation of **327**, which can undergo acylation with cyclohexenone (**328**), and benzylation of β-keto ester **329** affords substrate **330**. Unfortunately, despite attempting various reaction conditions and ligands, we were unable to access allyl enone **323** through the proposed asymmetric allylic alkylation but rather observed exclusive formation of desilylated **331**.

Figure A5.2. *(A) Reported intramolecular cyclization. (B) Proposed reaction on chiral substrate* ***323****. (C) Attempted asymmetric allylic alkylation to access* ***323****.*



Based on the observed formation of **331**, we sought to perform the intramolecular cyclization directly from substrate **336**. Through a sequence analogous to the synthesis of **331**, we were able to access enantioenriched allyl enone **336** efficiently (Figure A5.3.A). However, despite numerous attempts to catalyze the desired cyclization with $AlCl_3$, $EtAlCl_2$, $HClO_4$, and TBSOTf, we were not able to access desired product **337** (Figure A5.3.B).

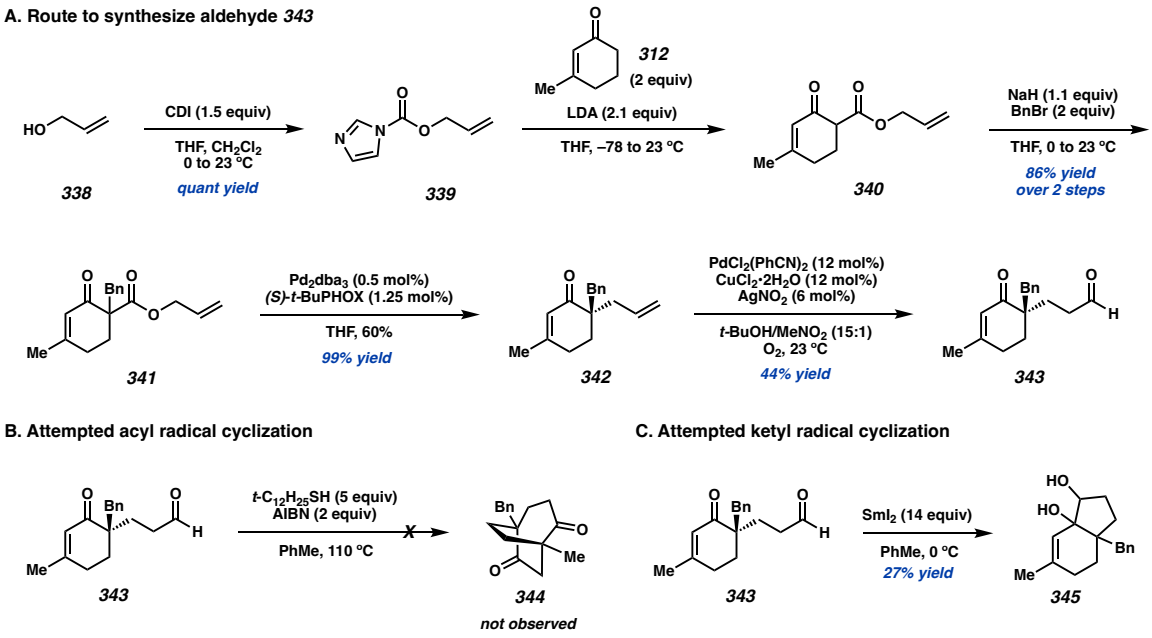
Figure A5.3. *(A) Synthesis of enone **336**. (B) Attempted Lewis acid-catalyzed intramolecular cyclization.*



Envisioning that the cyclization could occur through a radical pathway instead, we explored the application of aldehyde **343**, accessing the substrate through an analogous sequence followed by Wacker oxidation (Figure A5.4.A). While attempts to trigger cyclization from an acyl radical, initiated using thiol reagents,[4] led to no conversion of the

starting material (Figure A5.4.B), consumption of aldehyde **343** was observed when subjected to reactions with SmI_2 as the reagent.[5] Unfortunately, the 1,2-addition product (**345**) was formed exclusively, indicating that formation of the five-membered ring outcompetes the seven-membered ring formation in the 1,4-addition pathway (Figure A5.4.C). Considering the challenge associated with a competing five-membered ring formation process, exploration of this strategy was discontinued.

Figure A5.4. *(A) Synthesis of aldehyde* ***343****. (B) Attempted acyl radical cyclization. (C) Attempted ketyl radical cyclization.*

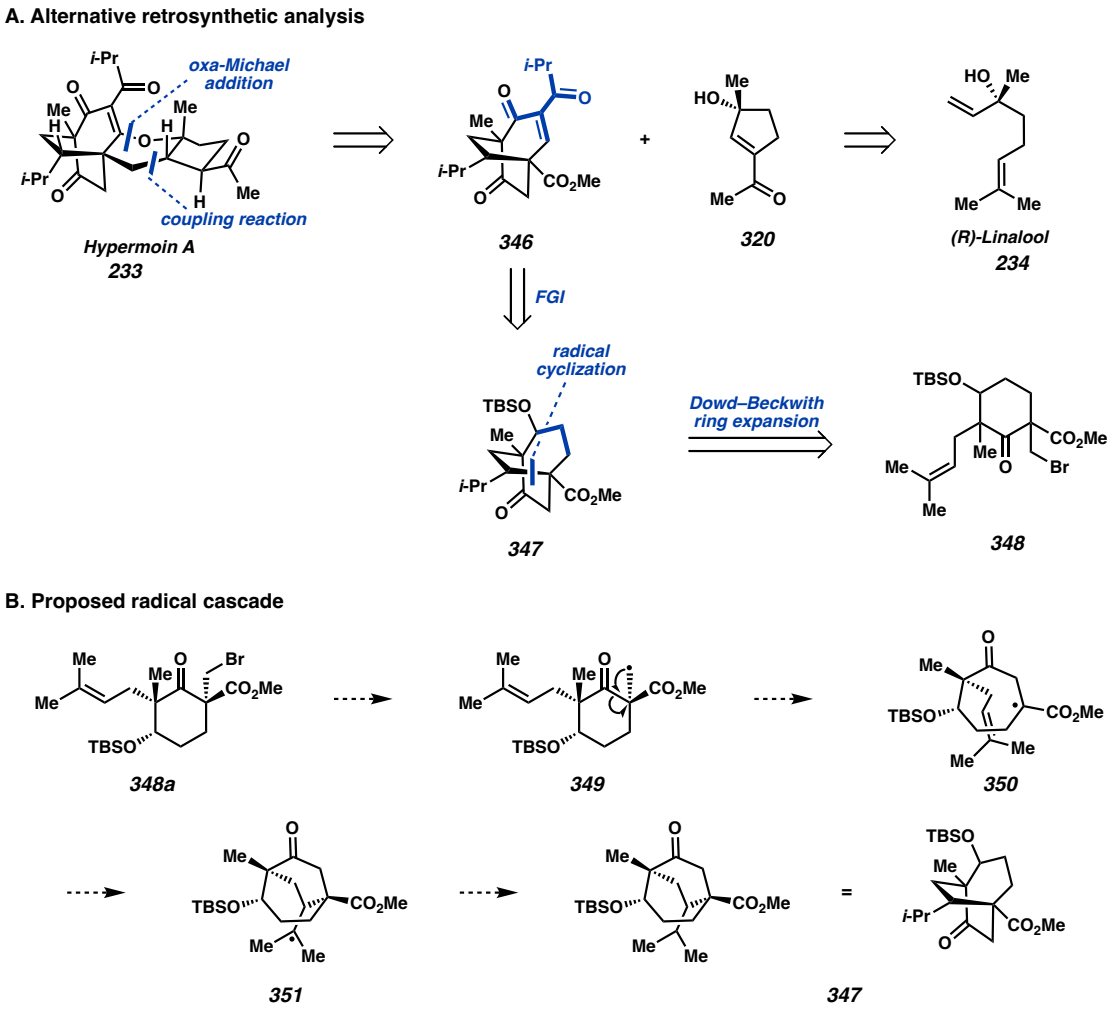


A5.3 RING EXPANSION–RADICAL CYCLIZATION SEQUENCE

To approach this challenge, we proposed pursuing an alternative retrosynthesis of [3.2.2] bicycle **346** to disconnect the C–C bond of a six-membered ring through a Dowd-Beckwith ring expansion–radical cyclization cascade from cyclohexanone **348** (Figure A5.5.A). We hypothesized that initiation of the cascade by halogen abstraction of bromide

348a and its subsequent engagement in the Dowd–Beckwith ring expansion to form cycloheptyl intermediate **350** (Figure A5.5.B). The radical intermediate is envisioned to undergo intramolecular cyclization with the prenyl group, forging the desired [3.2.2] bicyclic **347** upon hydrogen abstraction.

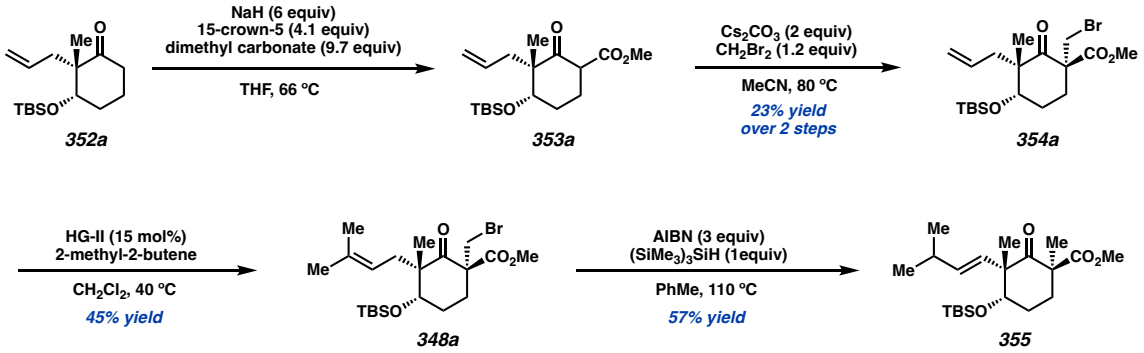
Figure A5.5. *(A) Second generation retrosynthetic analysis: radical cascade. (B) Proposed radical cascade.*



To assess the feasibility of the planned radical cascade, we sought to first access the precursor **348a**. Acylation and alkylation of ketone **352a** afford bromide **354a** in 23% yield

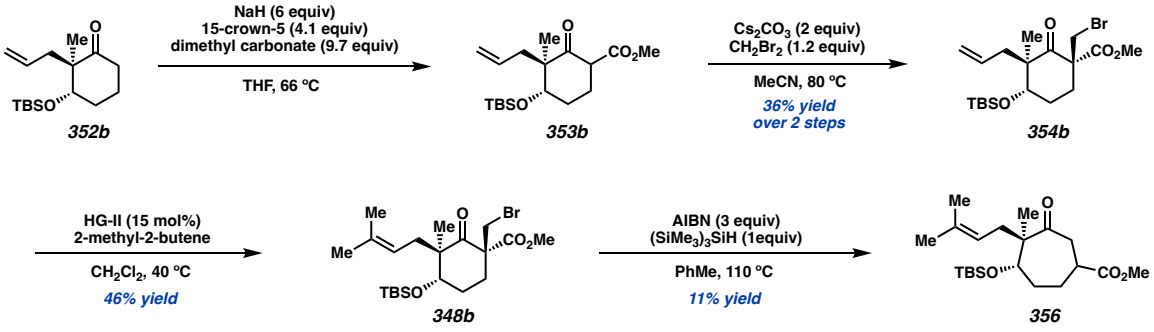
over two steps, and olefin metathesis of **354a** forges the desired precursor **348a** (Figure A5.6). However, reaction of **348a** led to the exclusive formation of olefin migration product **355**, which we attributed to a facile 1,5-HAT process between the methyl radical and the proximal prenyl group. Thus, we hypothesize that the undesired HAT can be mitigated if a different diastereomer of the radical precursor is employed.

Figure A5.6. *Synthesis of precursor* ***348a*** *and attempted radical cascade.*



The synthesis of **348b**, a different diastereomer with respect to the α-keto substituents, was therefore pursued through an analogous sequence but beginning from cyclohexanone **352b** (Figure A5.7). While subjection of **348b** to radical conditions allowed the formation of ring expanded **356**, indicating that the 1,5-HAT process was likely suppressed, premature hydrogen abstraction inhibited formation of the desired cyclization product.

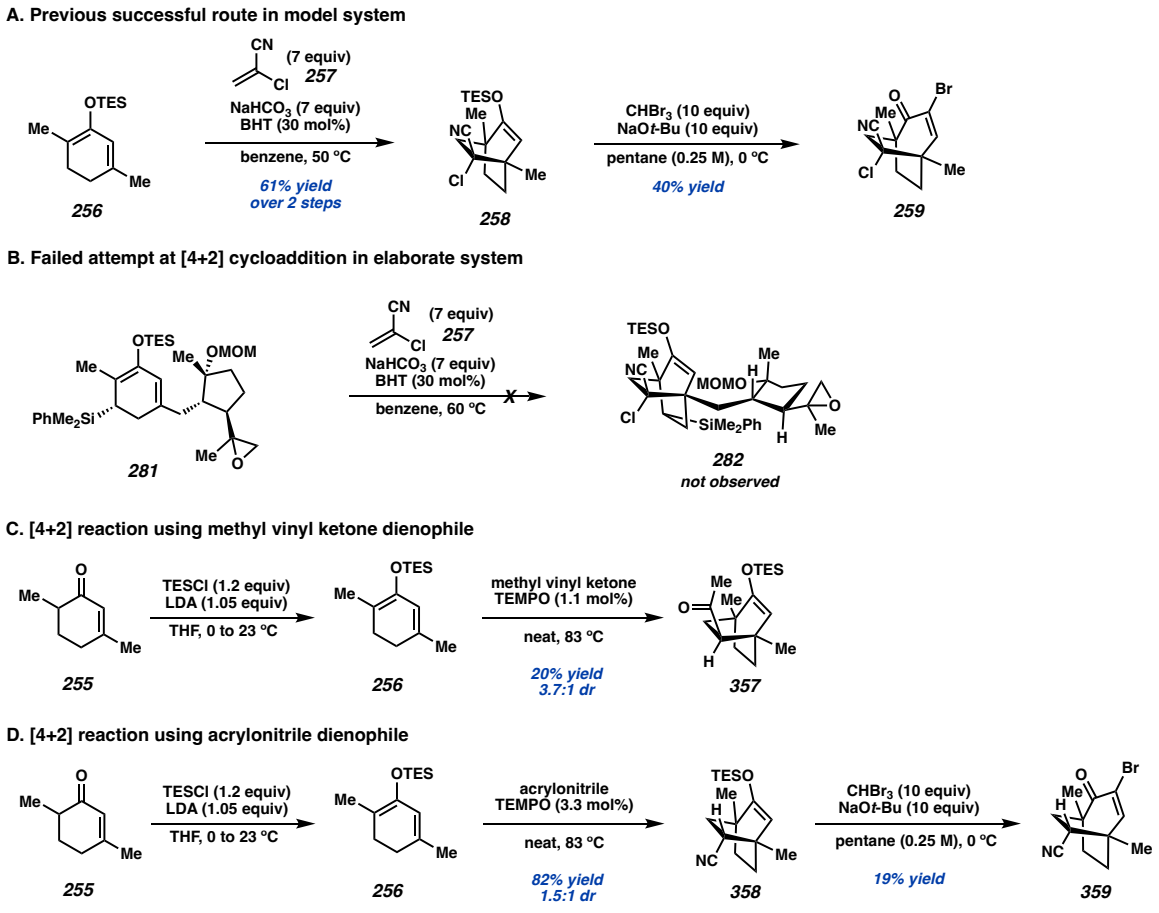
Figure A5.7. *Synthesis of precursor* ***348b*** *and attempted radical cascade.*



A5.4 INVESTIGATION OF [4+2] CYCLOADDITION DIENOPHILES

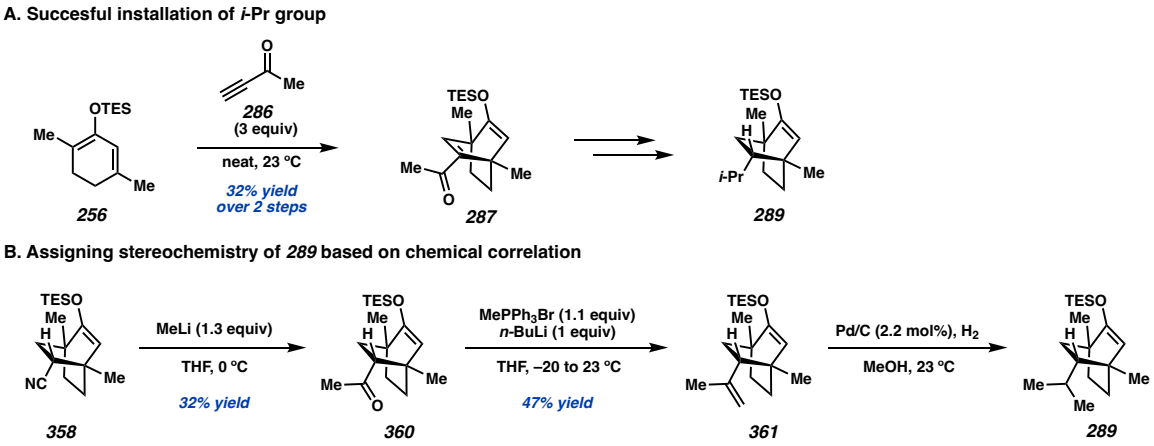
Previous investigations of a simple model system suggested [4+2] cycloaddition–ring expansion sequence to be promising for construction of the [3.2.2] bicyclic core of hypermoin A (Figure A5.8.A). However, attempts to extend this strategy to a more elaborate system were unsuccessful (Figure A5.8.B), inspiring our investigation of alternative dienophiles. In the early stages of dienophile exploration, we have attempted to employ methyl vinyl ketone and acrylonitrile as dienophiles. The reaction using methyl

Figure A5.8. *(A) Successful formation of model [3.2.2] bicycle. (B) Failed [4+2] reaction attempt with* ***281****. (C) Reaction exploration employing methyl vinyl ketone dienophile. (D) Reaction exploration employing acrylonitrile dienophile.*



vinyl ketone provided a complicated reaction profile, and desired product **357** was formed in a low 20% yield (Figure A5.8.C). While the reaction with acrylonitrile afforded product **358** in much higher 82% yield, the diastereoselectivity of the cycloaddition was low (Figure A5.8.D), which eventually led us to pursue a different dienophile. However, the major diastereomer of **358** was isolated and subsequently reacted in a ring expansion to form **359**, and its stereochemistry was confirmed by X-ray crystallography to be the desired diastereomer with respect to the α-nitrile stereocenter (see section A5.6).

Figure A5.9. *(A) Successful installation of i-Pr group. (B) Independent synthesis of* ***289*** *to assign stereochemistry.*



Further dienophile assessments revealed ynone **286** to be compatible with the reaction, ultimately affording isopropyl incorporated **289** upon functional group manipulations (Figure A5.9.A). To assign its stereochemistry, **289** was synthesized through methyl addition, Wittig olefination, and hydrogenation from **358**, the stereochemistry of which was assigned by analogy to the confirmed stereochemistry of **359** (Figure A5.9.B). The NMR spectrum of **289** (synthesized from **358**) matches that of **289** (synthesized through cycloaddition with ynone **286**), confirming the stereochemistry of the cycloadduct.

A5.5 EXPERIMENTAL SECTION

A5.5.1 MATERIALS AND METHODS

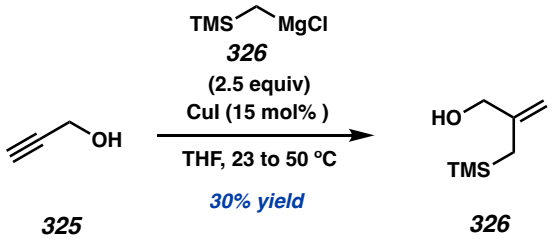
Unless otherwise stated, reactions were performed in flame-dried glassware under a nitrogen atmosphere using dry, deoxygenated solvents. Solvents were dried by passage through an activated alumina column under argon.[6] Reaction progress was monitored by thin-layer chromatography (TLC) or Agilent 1290 UHPLC-MS. TLC was performed using E. Merck silica gel 60 F254 precoated glass plates (0.25 mm) and visualized by UV fluorescence quenching, $KMnO_4$ staining, or *p*-anisaldehyde staining. Silicycle Silia*Flash*® P60 Academic Silica gel (particle size 40–63 nm) was used for flash chromatography. Reagents were purchased from commercial sources and used as received unless otherwise stated.

^{1}H NMR spectra were recorded on a Bruker 400 MHz spectrometer and are reported relative to residual non-deuterated solvent $CHCl_3$ (δ 7.26 ppm). ^{13}C NMR spectra were recorded on a Bruker 400 MHz spectrometer (100 MHz) and are reported relative to solvent $CDCl_3$ (δ 77.16 ppm). Data for ^{1}H NMR are reported as follows: chemical shift (δ ppm) (multiplicity, coupling constant (Hz), integration). Multiplicities are reported as the peaks appear as follows: s = singlet, d = doublet, t = triplet, q = quartet, p = pentet, sept = septuplet, m = multiplet, br s = broad singlet, br d = broad doublet. Some reported spectra include minor impurities of water (δ 1.56 ppm), ethyl acetate (δ 4.12, 2.05, 1.26 ppm), methylene chloride (δ 5.30 ppm), acetone (δ 2.17 ppm), grease (δ 1.26, 0.86 ppm), and/or silicon grease (δ 0.07 ppm), which do not impact product assignments. Data for ^{13}C NMR are reported in terms of chemical shifts (δ ppm).

List of Abbreviations: dr – diastereomeric ratio, TLC – thin-layer chromatography.

A5.5.2 EXPERIMENTAL PROCEDURES AND SPECTROSCOPIC DATA

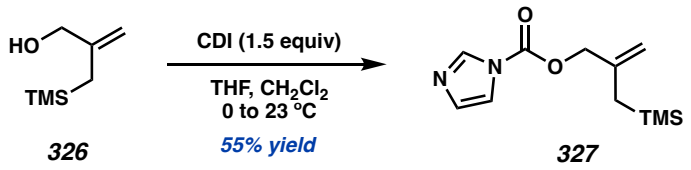
First Generation Synthesis Route: Allylic Alkylation–Cyclization Sequence



2-((trimethylsilyl)methyl)prop-2-en-1-ol (326)

A flame dried round bottom flask was charged with CuI (855 mg, 4.5 mmol, 15 mol%), (trimethylsilyl)methyl magnesium chloride (1.0 M solution in Et_2O, 75 mL, 75 mmol, 2.5 equiv) and THF (22.5 mL, 1.33 M). The mixture was stirred at room temperature for 30 min, and propargyl alcohol **325** (1.74 mL, 30 mmol, 1 equiv) was added neat. The solution was heated to 50 ºC and stirred overnight until full consumption of starting material (as determined by TLC), and the reaction was cooled to 0 ºC and quenched with saturated NH_4Cl. The aqueous layer was extracted three times with Et_2O, dried over Na_2SO_4, and concentrated under reduced pressure. The crude product was purified by flash silica gel column chromatography (SiO_2, 15% EtOAc/Hexanes) to afford the allylic alcohol **326** as a pale yellow oil (1.29 g, 8.9 mmol, 30% yield).

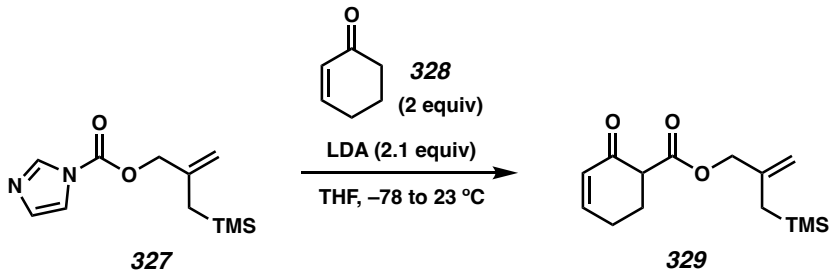
^{1}H NMR (500 MHz, $CDCl_3$): δ 4.91 (s, 1H), 4.67 (s, 1H), 3.99 (s, 2H), 1.54 (s, 2H), 0.04 (s, 9H).



2-((trimethylsilyl)methyl)allyl 1*H*-imidazole-1-carboxylate (327)

A flame dried round bottom flask was charged with 1,1'-carbonyldiimidazole (423.6 mg, 2.6 mmol, 1.5 equiv) and THF (1.3 mL, 2.0 M), and the solution was cooled to 0 ºC. a solution of alcohol **326** (150 mg, 1.74 mmol, 1 equiv) in CH_2Cl_2 (1.7 mL, 1.0 M) was added dropwise to the reaction, and the mixture was stirred at room temperature for 2 h. Upon complete consumption of starting material (as determined by TLC), the crude mixture was concentrated under reduced pressure and passed through a silica gel plug (SiO_2, 50% EtOAc/Hexanes) to afford the product **327** as a white solid (230 mg, 0.96 mmol, 55% yield).

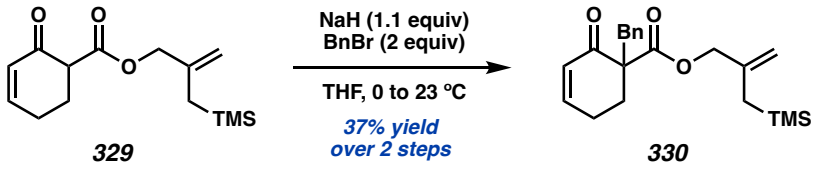
^{1}H NMR (500 MHz, $CDCl_3$): δ 8.17 (s, 1H), 7.46 (s, 1H), 7.09 (s, 1H), 4.98 (s, 1H), 4.84 (s, 1H), 4.76 (s, 2H), 1.60 (s, 2H), 0.08 (s, 9H).



2-((trimethylsilyl)methyl)allyl 2-oxocyclohex-3-ene-1-carboxylate (329)

A flame dried round bottom flask was charged with *i*-Pr_2NH (0.26 mL, 1.86 mmol, 2.2 equiv) and THF (1 mL, 1.75 M). The solution was cooled to 0 ºC and *n*-BuLi (2.5 M in hexanes, 0.7 mL, 1.78 mmol, 2.1 equiv) was added dropwise. The resultant solution was stirred for 15 min at 0 ºC. Enone **328** (0.16 mL, 1.7 mmol, 2.0 equiv) in THF (1.4 mL, 1.25

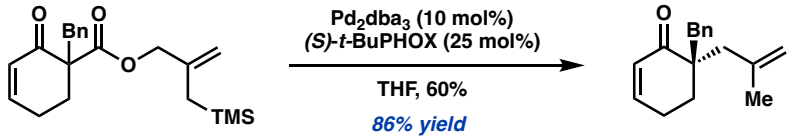
M) was added dropwise and stirring was continued at 0 ºC for 30 minutes. The solution was cooled to –78 ºC, and **327** (228.2 mg, 1.02 mmol, 1 equiv) in THF (0.3 mL, 3.25 M) was added dropwise. The reaction was gradually warmed to 23 ºC. Upon complete consumption of starting material (as determined by TLC), the reaction was diluted with a 2.0 M solution of HCl and the product was extracted three times with EtOAc. The combined organic layers were washed with brine, dried over Na_2SO_4, filtered, and concentrated under reduced pressure. Excess enone **328** was evaporated under vacuum overnight, and crude enone **329** was used without further purification.



2-((trimethylsilyl)methyl)allyl 1-benzyl-2-oxocyclohex-3-ene-1-carboxylate (330)

A flame dried round bottom flask was charged with NaH (20.2 mg, 0.51 mmol, 1.1 equiv) and THF (1.5 mL, 0.3 M). The suspension was cooled to 0 ºC, and ester **329** (116.3 mg, 0.44 mmol, 1 equiv) was added, followed by continued stirring at 0 ºC for an additional hour. BnBr (0.12 mL, 0.92 mmol, 2 equiv) was added at 0 ºC, and the reaction was warmed to room temperature overnight. Upon complete consumption of starting material (as determined by TLC), the reaction mixture was quenched with a saturated solution of NH_4Cl at 0 ºC and extracted three times with EtOAc. The organic layers were washed with brine, dried over Na_2SO_4, filtered, and concentrated under reduced pressure. The crude product was purified by flash silica gel column chromatography (SiO_2, 20% EtOAc/Hexanes) to afford enone **330** as a pale yellow oil (58.7 mg, 0.16 mmol, 37% yield).

^{1}H NMR (500 MHz, $CDCl_3$): δ 7.25 – 7.20 (m, 3H), 7.18 – 7.14 (m, 2H), 6.91 – 6.84 (m, 1H), 6.07 (ddd, *J* = 10.1, 2.8, 1.4 Hz, 1H), 4.82 (q, *J* = 1.5 Hz, 1H), 4.70 (q, *J* = 1.2 Hz, 1H), 4.48 (d, *J* = 13.6 Hz, 1H), 4.41 (d, *J* = 13.6 Hz, 1H), 3.34 – 3.23 (m, 2H), 2.52 (dddt, *J* = 20.4, 10.4, 5.3, 2.7 Hz, 1H), 2.43 – 2.35 (m, 1H), 2.34 – 2.26 (m, 1H), 1.84 (ddd, *J* = 13.7, 10.2, 5.3 Hz, 1H), 1.49 (s, 2H), 0.04 (s, 9H).

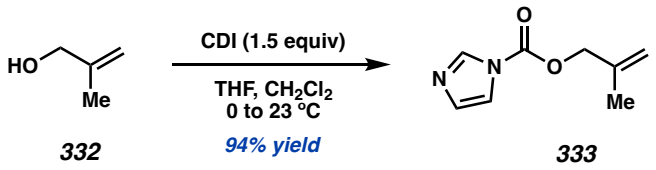


330 ***331***

(*S*)-6-benzyl-3-methyl-6-(2-methylallyl)cyclohex-2-en-1-one (331)

In a nitrogen filled glovebox, an oven-dried 2 mL vial was charged with a stir bar, $Pd_2(dba)_3$ (1.84 mg, 0.002 mmol, 10 mol %), *(S)-t*-BuPHOX (1.92 mg, 0.005 mmol, 25 mol %), and THF (0.5 mL). The catalyst solution was stirred at 23 ºC for 20 min. A solution of substrate **330** (7.13 mg, 0.02 mmol, 1 equiv) in THF (0.5 mL) was added to the vial. The resultant solution was then heated to 60 ºC overnight. The solution was then cooled to 23 ºC and concentrated under reduced pressure. The crude reaction mixture purified by preparatory TLC (SiO_2, 15% EtOAc/Hexanes) to afford enone **331** as a pale yellow oil (5.4 mg, 0.017 mmol, 86% yield).

^{1}H NMR (500 MHz, $CDCl_3$): δ 7.30 – 7.21 (m, 3H), 7.15 (d, *J* = 7.2 Hz, 2H), 6.93 – 6.86 (m, 1H), 6.03 (d, *J* = 9.9 Hz, 1H), 4.87 (s, 1H), 4.68 (s, 1H), 3.17 (d, *J* = 13.4 Hz, 1H), 2.63 (t, *J* = 13.1 Hz, 2H), 2.46 – 2.42 (m, 2H), 2.10 (d, *J* = 13.5 Hz, 1H), 1.92 (dt, *J* = 13.4, 6.4 Hz, 1H), 1.76 (dt, *J* = 12.9, 5.8 Hz, 1H), 1.68 (s, 3H).

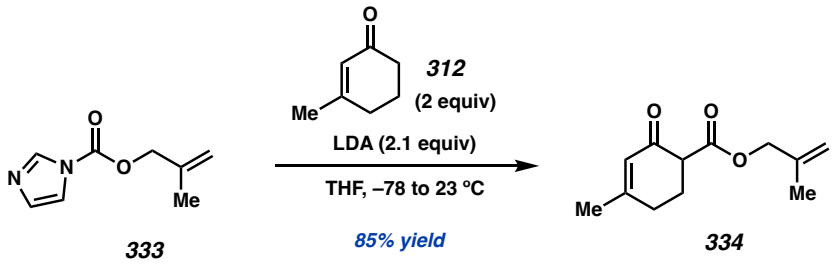


332 ***333***

2-methylallyl 1*H*-imidazole-1-carboxylate (333)

A flame dried round bottom flask was charged with 1,1'-carbonyldiimidazole (486.5 mg, 3 mmol, 1.5 equiv) and THF (1.5 mL, 2.0 M), and the solution was cooled to 0 ºC. A solution of alcohol **332** (0.17 mL, 2 mmol, 1 equiv) in CH_2Cl_2 (2 mL, 1.0 M) was added dropwise to the reaction, and the mixture was stirred at room temperature for 2 h. Upon complete consumption of starting material (as determined by TLC), the crude mixture was concentrated under reduced pressure and passed through a silica gel plug (SiO_2, 50% EtOAc/Hexanes) to afford the product **333** as a white solid (313.6 mg, 1.89 mmol, 94% yield).

^{1}H NMR (400 MHz, $CDCl_3$): δ 8.16 (t, *J* = 1.1 Hz, 1H), 7.44 (t, *J* = 1.5 Hz, 1H), 7.10 (d, *J* = 1.0 Hz, 1H), 5.09 (s, 1H), 5.06 (s, 1H), 4.81 (t, *J* = 1.0 Hz, 2H), 1.83 (s, 3H).



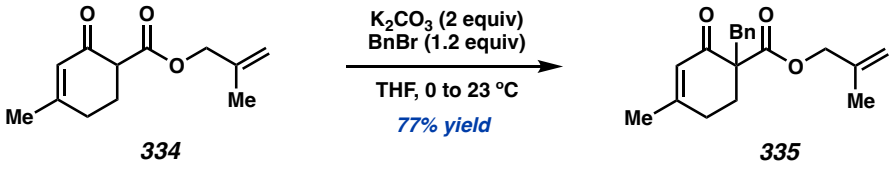
333 ***334***

2-methylallyl 4-methyl-2-oxocyclohex-3-ene-1-carboxylate (334)

A flame dried round bottom flask was charged with *i*-Pr_2NH (5.5 mL, 39.5 mmol, 2.2 equiv) and THF (10.9 mL, 1.75 M). The solution was cooled to 0 ºC and *n*-BuLi (2.5 M in hexanes, 15 mL, 37.7 mmol, 2.1 equiv) was added dropwise. The resultant solution was stirred for 15 min at 0 ºC. Enone **312** (4.1 mL, 35.9 mmol, 2.0 equiv) in THF (28.6 mL, 1.25 M) was

added dropwise and stirring was continued at 0 ºC for 30 minutes. The solution was cooled to –78 ºC, and **333** (2.98 g, 17.9 mmol, 1 equiv) in THF (5.4 mL, 3.25 M) was added dropwise. The reaction was gradually warmed to 23 ºC. Upon complete consumption of starting material (as determined by TLC), the reaction was diluted with a 2.0 M solution of HCl and the product was extracted three times with EtOAc. The combined organic layers were washed with brine, dried over Na_2SO_4, filtered, and concentrated under reduced pressure. The crude product was purified by flash silica gel column chromatography (SiO_2, 15% EtOAc/Hexanes) to afford enone **334** as a pale yellow oil (3.18 g, 15.3 mmol, 85% yield).

^{1}H NMR (500 MHz, $CDCl_3$): δ 5.93 (s, 1H), 4.99 (s, 1H), 4.93 (s, 1H), 4.62 (d, *J* = 13.1 Hz, 1H), 4.55 (d, *J* = 13.1 Hz, 1H), 3.42 – 3.34 (m, 1H), 2.45 – 2.30 (m, 3H), 2.27 – 2.17 (m, 1H), 1.98 (s, 3H), 1.76 (s, 3H).



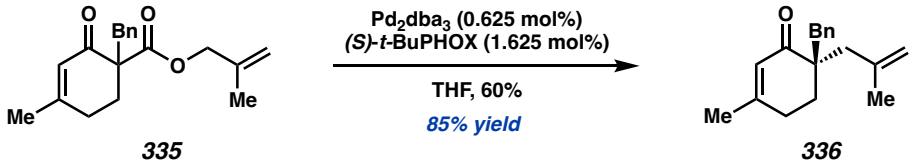
334 *335*

2-methylallyl 1-benzyl-4-methyl-2-oxocyclohex-3-ene-1-carboxylate (335)

A flame dried round bottom flask was charged with enone **334** (3.18 g, 15.3 mmol, 1 equiv) and acetone (85 mL, 0.2 M), followed by K_2CO_3 (4.23 g, 30.6 mmol, 2 equiv) and BnBr (2.2 mL, 18.3 mmol, 1.2 equiv). The reaction mixture was heated to 50 ºC and overnight. The crude mixture was filtered, and the solids were rinsed with Et_2O. The collected filtrate was concentrated under reduced pressure, and the crude product was purified by flash silica gel column chromatography (SiO_2, 20% EtOAc/Hexanes) to afford enone **335** as a pale

yellow oil (3.46 mg, 11.6 mmol, 77% yield). Some starting material (**334**) was also recovered from purification (313.7 mg, 1.5 mmol, 10% yield).

^{1}H NMR (500 MHz, $CDCl_3$): δ 7.26 – 7.18 (m, 3H), 7.17 – 7.13 (m, 2H), 5.92 (dt, *J* = 2.4, 1.2 Hz, 1H), 4.93 (s, 1H), 4.91 (s, 1H), 4.55 (d, *J* = 13.2 Hz, 1H), 4.46 (d, *J* = 13.1 Hz, 1H), 3.32 – 3.22 (m, 2H), 2.48 (dd, *J* = 18.3, 11.1 Hz, 1H), 2.35 (ddd, *J* = 13.7, 5.1, 3.0 Hz, 1H), 2.16 (dt, *J* = 19.0, 4.3 Hz, 1H), 1.90 (s, 3H), 1.81 (ddd, *J* = 13.7, 10.6, 5.3 Hz, 1H), 1.70 (s, 3H).

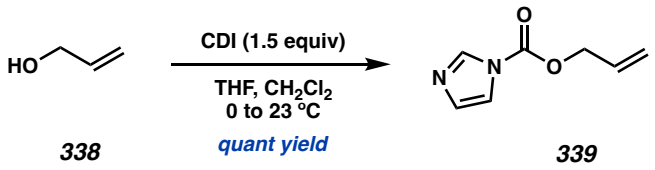


335 ***336***

(*S*)-6-benzyl-3-methyl-6-(2-methylallyl)cyclohex-2-en-1-one (336)

In a nitrogen filled glovebox, an oven-dried 2 mL vial was charged with a stir bar, $Pd_2(dba)_3$ (19.2 mg, 0.021 mmol, 0.625 mol %), *(S)-t*-BuPHOX (20.8 mg, 0.054 mmol, 1.625 mol %), and THF (11 mL). The catalyst solution was stirred at 23 ºC for 20 min. A solution of substrate **335** (1 g, 3.35 mmol, 1 equiv) in THF (32 mL) was added to the vial. The resultant solution was then heated to 60 ºC overnight. The solution was then cooled to 23 ºC and concentrated under reduced pressure. The crude reaction mixture was purified by silica gel flash column chromatography (SiO_2, 10% EtOAc/Hexanes) to afford enone **336** as a pale yellow oil (723.9 mg, 2.85 mmol, 85% yield).

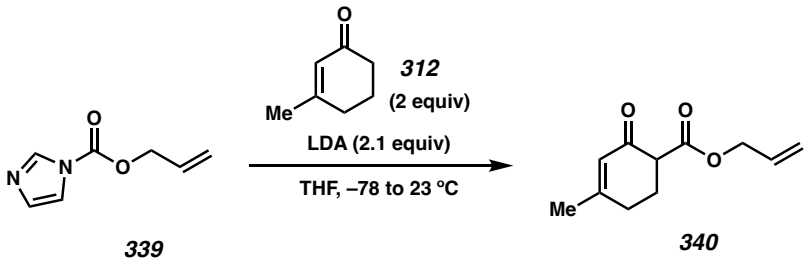
^{1}H NMR (500 MHz, $CDCl_3$): δ 7.25 – 7.16 (m, 3H), 7.15 – 7.09 (m, 2H), 5.86 (s, 1H), 4.83 (s, 1H), 4.64 (s, 1H), 3.12 (d, *J* = 13.4 Hz, 1H), 2.61 (d, *J* = 13.5 Hz, 1H), 2.56 (d, *J* = 13.4 Hz, 1H), 2.32 (t, *J* = 6.4 Hz, 2H), 2.04 (d, *J* = 13.4 Hz, 1H), 1.92 (s, 3H), 1.87 (dt, *J* = 13.4, 6.6 Hz, 1H), 1.70 (dt, *J* = 13.9, 5.9 Hz, 1H), 1.66 (s, 3H).



338 *339*

allyl 1*H*-imidazole-1-carboxylate (339)

A flame dried round bottom flask was charged with 1,1'-carbonyldiimidazole (4.87 g, 30 mmol, 1.5 equiv) and THF (1.5 mL, 20 M), and the solution was cooled to 0 ºC. A solution of alcohol **338** (1.36 mL, 20 mmol, 1 equiv) in CH_2Cl_2 (20 mL, 1.0 M) was added dropwise to the reaction, and the mixture was stirred at room temperature for 2 h. Upon complete consumption of starting material (as determined by TLC), the crude mixture was concentrated under reduced pressure and passed through a silica gel plug (SiO_2, 50% EtOAc/Hexanes) to afford the product **339** as a white solid (3.06 g, 20 mmol, quant yield). **^{1}H NMR (500 MHz, $CDCl_3$):** δ 8.16 (t, *J* = 1.1 Hz, 1H), 7.44 (t, *J* = 1.5 Hz, 1H), 7.08 (dd, *J* = 1.7, 0.9 Hz, 1H), 6.02 (ddt, *J* = 17.2, 10.4, 6.0 Hz, 1H), 5.50 – 5.36 (m, 2H), 4.90 (dt, *J* = 6.0, 1.3 Hz, 2H).

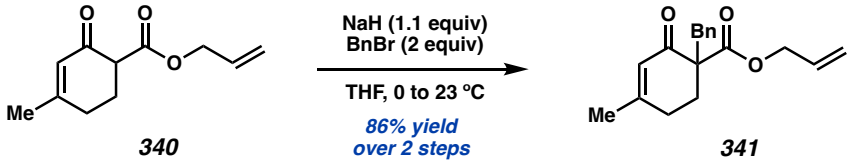


339 *340*

allyl 4-methyl-2-oxocyclohex-3-ene-1-carboxylate (340)

A flame dried round bottom flask was charged with *i*-Pr_2NH (6.1 mL, 44 mmol, 2.2 equiv) and THF (12.1 mL, 1.75 M). The solution was cooled to 0 ºC and *n*-BuLi (2.5 M in hexanes, 16.7 mL, 42 mmol, 2.1 equiv) was added dropwise. The resultant solution was stirred for 15 min at 0 ºC. Enone **312** (4.6 mL, 40 mmol, 2.0 equiv) in THF (31.9 mL, 1.25 M) was

added dropwise and stirring was continued at 0 ºC for 30 minutes. The solution was cooled to –78 ºC, and **339** (3.06 g, 20 mmol, 1 equiv) in THF (6 mL, 3.25 M) was added dropwise. The reaction was gradually warmed to 23 ºC. Upon complete consumption of starting material (as determined by TLC), the reaction was diluted with a 2.0 M solution of HCl and the product was extracted three times with EtOAc. The combined organic layers were washed with brine, dried over Na_2SO_4, filtered, and concentrated under reduced pressure. Purification of the crude product was attempted by flash silica gel column chromatography (SiO_2, 15% EtOAc/Hexanes), however a 0.7:1 mixture of enone starting material and product was obtained, and therefore this mixture was used without further purification.

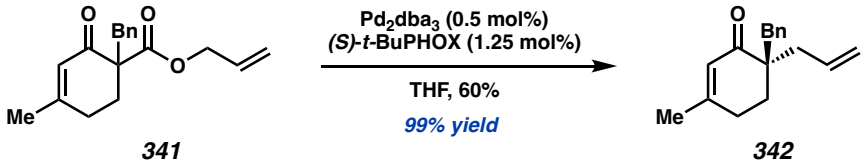


allyl 1-benzyl-4-methyl-2-oxocyclohex-3-ene-1-carboxylate (341)

A flame dried round bottom flask was charged with NaH (13.2 mg, 0.33 mmol, 1.1 equiv) and THF (2 mL, 0.3 M). The suspension was cooled to 0 ºC, and ester **340** (100 mg, 0.3 mmol, 1 equiv) was added, followed by continued stirring at 0 ºC for an additional hour. BnBr (0.07 mL, 0.6 mmol, 2 equiv) was added at 0 ºC, and the reaction was warmed to room temperature overnight. Upon complete consumption of starting material (as determined by TLC), the reaction mixture was quenched with a saturated solution of NH_4Cl at 0 ºC and extracted three times with EtOAc. The organic layers were washed with brine, dried over Na_2SO_4, filtered, and concentrated under reduced pressure. The crude product was purified by flash silica gel column chromatography (SiO_2, 20% EtOAc/Hexanes) to

afford enone **341** as a pale yellow oil (73 mg, 0.27 mmol, 86% yield based on amount of ester starting material).

^{1}H NMR (500 MHz, $CDCl_3$): δ 7.26 – 7.19 (m, 3H), 7.17 – 7.13 (m, 2H), 5.92 (s, 1H), 5.86 (ddt, *J* = 17.2, 10.8, 5.6 Hz, 1H), 5.30 – 5.21 (m, 2H), 4.59 (dq, *J* = 5.6, 1.5 Hz, 2H), 3.31 – 3.21 (m, 2H), 2.47 (dt, *J* = 11.5, 7.1 Hz, 1H), 2.35 (ddd, *J* = 13.7, 5.0, 3.1 Hz, 1H), 2.16 (dt, *J* = 19.1, 4.2 Hz, 1H), 1.90 (s, 3H), 1.81 (ddd, *J* = 13.7, 10.5, 5.3 Hz, 1H).

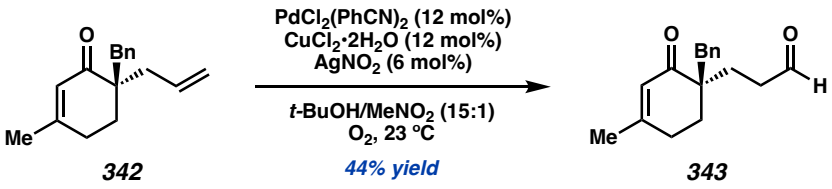


341 *342*

(*S*)-6-allyl-6-benzyl-3-methylcyclohex-2-en-1-one (342)

In a nitrogen filled glovebox, an oven-dried 2 mL vial was charged with a stir bar, $Pd_2(dba)_3$ (0.5 mg, 0.0005 mmol, 0.5 mol %), *(S)*-*t*-BuPHOX (0.6 mg, 0.00125 mmol, 1.25 mol %), and THF (0.6 mL). The catalyst solution was stirred at 23 ºC for 20 min. A solution of substrate **341** (28.4 mg, 0.1 mmol, 1 equiv) in THF (0.6 mL) was added to the vial. The resultant solution was then heated to 60 ºC overnight. The solution was then cooled to 23 ºC and concentrated under reduced pressure. The crude reaction mixture was purified by preparatory TLC (SiO_2, 20% EtOAc/Hexanes) to afford enone **342** as a pale yellow oil (23.8 mg, 0.99 mmol, 99% yield).

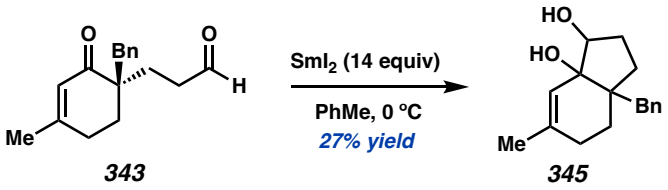
^{1}H NMR (500 MHz, $CDCl_3$): δ 7.26 – 7.17 (m, 3H), 7.14 – 7.09 (m, 2H), 5.83 (s, 1H), 5.80 – 5.71 (m, 1H), 5.12 – 5.01 (m, 2H), 3.11 (d, *J* = 13.4 Hz, 1H), 2.63 (d, *J* = 13.4 Hz, 1H), 2.43 (ddt, *J* = 13.8, 6.7, 1.3 Hz, 1H), 2.36 – 2.26 (m, 2H), 2.12 – 2.04 (m, 1H), 1.91 (s, 3H), 1.86 – 1.81 (m, 1H), 1.78 – 1.72 (m, 1H).



(*S*)-3-(1-benzyl-4-methyl-2-oxocyclohex-3-en-1-yl)propanal (179)

A flame dried round bottom flask was charged with $PdCl_2(PhCN)_2$ (141.9 mg, 0.37 mmol, 12 mol%), $CuCl_2$•$2H_2O$ (63.1 mg, 0.37 mmol, 12 mol%), $AgNO_2$ (29.2 mg, 0.19 mmol, 6 mol%), *t*-BuOH (57.4 mL, 0.05 M), and $MeNO_2$ (5.1 mL, 6 M). The mixture was stirred at room temperature for 3 min while sparging with O_2. Enone **342** (731.4 mg, 3.04 mmol, 1 equiv) was added, followed by sparging with O_2 for an additional minute. The reaction was subsequently stirred under O_2 atmosphere at room temperature overnight. The reaction mixture was diluted with H_2O and extracted three times with CH_2Cl_2, dried over Na_2SO_4, filtered, and concentrated under reduced pressure. The crude product was purified by flash silica gel column chromatography (SiO_2, 10–20% EtOAc/Hexanes with 1% Et_3N) to afford enone **343** as a pale yellow oil (342.2 mg, 1.34 mmol, 44% yield).

^{1}H NMR (500 MHz, $CDCl_3$): δ 9.74 (s, 1H), 7.25 – 7.19 (m, 2H), 7.14 – 7.07 (m, 3H), 5.83 (s, 1H), 3.08 (d, J = 13.5 Hz, 1H), 2.63 (d, J = 13.5 Hz, 1H), 2.59 – 2.50 (m, 1H), 2.43 – 2.31 (m, 3H), 1.93 (s, 3H), 1.92 – 1.85 (m, 1H), 1.85 – 1.71 (m, 3H).



7a-benzyl-5-methyl-1,2,3,6,7,7a-hexahydro-3a*H*-indene-3,3a-diol (345)

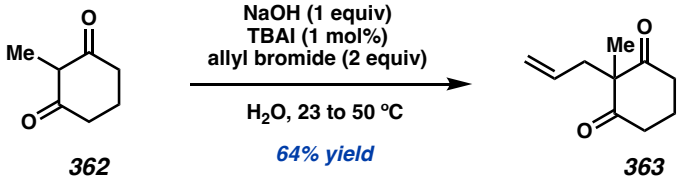
A flame dried round bottom flask was charged with aldehyde **343** (10 mg, 0.04 mmol, 1 equiv) and toluene (0.9 mL), and the solution was freeze-pump-thawed three times. The

solution was then added to SmI_2 (0.1 M solution in THF, 7 equiv, 0.28 mmol, 2.8 mL) in toluene (27.5 mL) at 0 ºC over 2 h, and another portion of SmI_2 (0.1 M solution in THF, 7 equiv, 0.28 mmol, 2.8 mL) was added after the reaction turned colorless. The reaction was then allowed to warm to room temperature and stirred for an additional 30 min. The reaction was quenched with a saturated solution of $NaHCO_3$ and the product was extracted three times with EtOAc, dried over Na_2SO_4, filtered, and concentrated under reduced pressure. The crude product was purified by preparatory TLC (SiO_2, 20% EtOAc/Hexanes) to afford diol **345** as a pale yellow oil (2.7 mg, 0.01 mmol, 27% yield). The product was isolated as a mixture of inseparable diastereomers.

^{1}H NMR (400 MHz, $CDCl_3$) mixture of diastereomers: δ 7.32 – 7.16 (m, 5H), 5.37 (s, 1H), 4.12 (dt, *J* = 10.7, 7.3 Hz, 1H), 2.95 (d, *J* = 13.4 Hz, 1H), 2.64 (d, *J* = 13.3 Hz, 1H), 2.41 – 2.31 (m, 2H), 2.19 – 1.94 (m, 2H), 1.86 – 1.77 (m, 1H), 1.73 (s, 3H), 1.72 – 1.63 (m, 1H), 1.48 – 1.38 (m, 2H), 1.23 – 1.12 (m, 1H).

^{13}C NMR (100 MHz, $CDCl_3$) mixture of diastereomers: δ 139.5, 137.3, 130.6, 128.0, 126.0, 125.6, 80.1, 45.8, 38.3, 31.2, 30.0, 28.6, 27.6, 23.4.

Second Generation Synthesis Route: Radical Ring Expansion–Cyclization Cascade



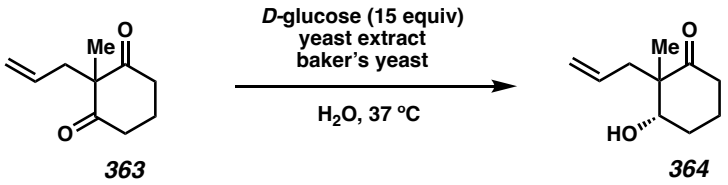
362 *363*

2-allyl-2-methylcyclohexane-1,3-dione (363)

A round bottom flask was charged with diketone **362** (5 g, 39.6 mmol, 1 equiv) and water (158 mL, 0.25 M), followed by NaOH (1.58 g, 39.6 mmol, 1 equiv) and TBAI (148 mg,

0.4 mmol, 1 mol%). The mixture was stirred at room temperature for 20 min, then allyl bromide (6.84 mL, 79.2 mmol, 2 equiv) was added ant the reaction was heated to 50 ºC. Upon complete consumption of the starting material (as determined by TLC), the product was extracted three times with EtOAc, dried over Na_2SO_4, filtered, and concentrated under reduced pressure. The crude product was purified by flash silica gel column chromatography (SiO_2, 25% EtOAc/Hexanes) to afford diketone **363** as a colorless oil (4.285 g, 25.8 mmol, 64% yield).

^{1}H NMR (400 MHz, $CDCl_3$): δ 5.65 – 5.49 (m, 1H), 5.11 – 5.01 (m, 2H), 2.73 – 2.56 (m, 4H), 2.53 (dt, *J* = 7.4, 1.2 Hz, 2H), 2.08 – 1.80 (m, 2H), 1.24 (s, 3H).

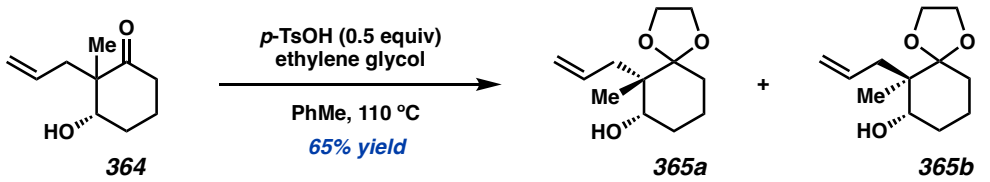


363 ***364***

(3*S*)-2-allyl-3-hydroxy-2-methylcyclohexan-1-one (364)

To an Erlenmeyer flask containing DI water (216 mL) at 37 ºC was added *D*-glucose (32.4 g, 180 mmol, 15 equiv) and yeast extract (1.08 g) with stirring. Then, baker's yeast (28.84 g) was added to this mixture, and the reaction was stirred at 30–35 ºC for an additional 30 min. Diketone **363** (2 g, 12 mmol, 1 equiv) was added subsequently, and the mixture was stirred at room temperature overnight. The reaction mixture was diluted with water (54 mL) and EtOAc. As the layers did not separate, the emulsion was filtered using a Buchner funnel. The filtrate was extracted three times with EtOAc, washed with brine, dried over Na_2SO_4, filtered, and concentrated under reduced pressure. The crude product was purified by flash silica gel column chromatography (SiO_2, 30% EtOAc/Hexanes) to afford alcohol **364** (1.686 g, 10.0 mmol, 84% yield).

^{1}H NMR (500 MHz, $CDCl_3$): δ 5.80 – 5.71 (m, 1H), 5.16 – 5.04 (m, 2H), 3.92 – 3.78 (m, 1H), 2.51 – 2.32 (m, 4H), 2.12 – 1.97 (m, 2H), 1.95 – 1.79 (m, 1H), 1.75 – 1.64 (m, 1H), 1.16 (d, *J* = 13.9 Hz, 3H).



(7*S*)-6-allyl-6-methyl-1,4-dioxaspiro[4.5]decan-7-ol (365)

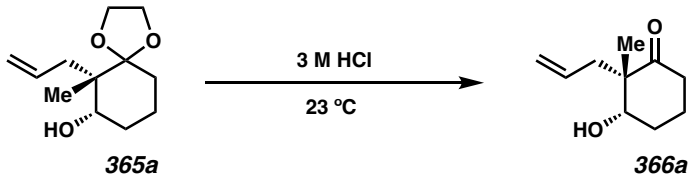
A 2-neck round bottom flask fitted with a reflux condenser and Deak–Stark apparatus was charged with *p*-TsOH•H_2O (95 mg, 0.5 mmol, 5 mol%) and ketone **364** (1.686 g, 10 mmol, 1 equiv) in toluene (154 mL, 0.065 M), followed by ethylene glycol (15.4 mL, 0.65 M). The mixture was then heated to reflux at 110 ºC for 2 h. The reaction was cooled to room temperature and quenched with a saturated solution of $NaHCO_3$. The product was extracted three times with Et_2O, dried over Na_2SO_4, filtered, and concentrated under reduced pressure. The crude product was purified by flash silica gel column chromatography (SiO_2, 10–25% EtOAc/Hexanes) to afford **365a** (509 mg, 2.39 mmol, 24% yield), **365b** (386 mg, 1.82 mmol, 18% yield), and a mixture of **365a** and **365b** (478 mg, 2.25 mmol, 23% yield). Starting material (315 mg, 1.87 mmol, 19% yield) was also covered upon purification.

365a:

^{1}H NMR (500 MHz, $CDCl_3$): δ 5.97 – 5.85 (m, 1H), 5.15 – 5.01 (m, 2H), 4.05 – 3.94 (m, 2H), 3.94 – 3.89 (m, 2H), 3.63 (t, *J* = 3.3 Hz, 1H), 2.55 (dd, *J* = 13.4, 6.8 Hz, 1H), 2.02 (dd, *J* = 13.3, 8.3 Hz, 1H), 1.86 – 1.62 (m, 4H), 1.62 – 1.51 (m, 2H), 1.03 (s, 3H).

365b:

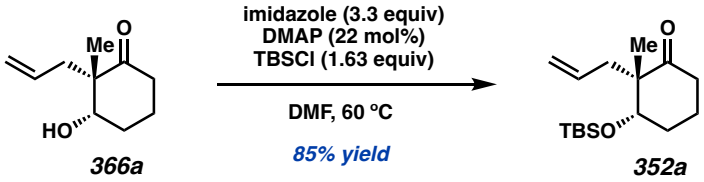
^{1}H NMR (500 MHz, $CDCl_3$): δ 6.00 – 5.88 (m, 1H), 5.13 – 4.99 (m, 2H), 4.01 – 3.89 (m, 4H), 3.72 (dd, *J* = 6.4, 2.6 Hz, 1H), 2.39 – 2.24 (m, 2H), 1.77 – 1.49 (m, 6H), 1.03 (s, 3H).



365a ***366a***

(2*S*,3*S*)-2-allyl-3-hydroxy-2-methylcyclohexan-1-one (366a)

A round bottom flask was charged with alcohol **365a** (509 mg, 2.4 mmol, 1 equiv) and HCl (3.0 M solution in water, 14.4 mL), and the mixture was stirred at room temperature until full conversion. The reaction was quenched with a saturated solution of $NaHCO_3$ and extracted three times with EtOAc, dried over Na_2SO_4, filtered, and concentrated under reduced pressure. The crude product was used without further purification.



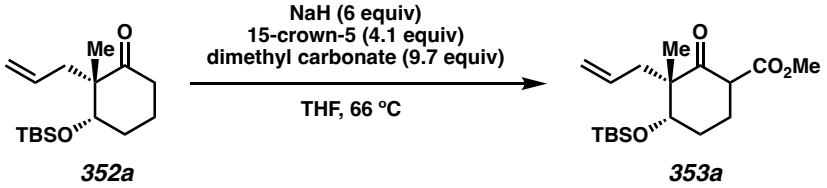
366a ***352a***

(2*S*,3*S*)-2-allyl-3-((*tert*-butyldimethylsilyl)oxy)-2-methylcyclohexan-1-one (352a)

A round bottom flask was charged with alcohol **366a** (2.4 mmol, 1 equiv), imidazole (539 mg, 7.92 mmol, 3.3 equiv), DMAP (65 mg, 0.53 mmol, 0.22 equiv), TBSCl (588 mg, 3.9 mmol, 1.63 equiv), and DMF (2.63 mL, 0.9 M). The mixture was stirred at 60 °C overnight. Upon complete consumption of the starting material (as determined by TLC), the reaction was diluted with Et_2O and quenched with a saturated solution of NH_4Cl. The product was extracted three times with Et_2O, washed with brine, dried over Na_2SO_4, filtered, and concentrated under reduced pressure. The crude product was purified by flash silica gel

column chromatography (SiO_2, 5–10% EtOAc/Hexanes) to afford **352a** as a colorless oil (579 mg, 2.05 mmol, 85% yield).

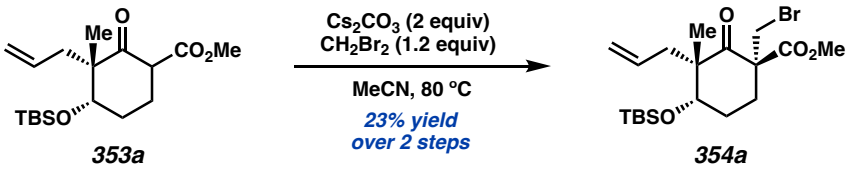
^{1}H NMR (500 MHz, $CDCl_3$): δ 5.66 (dddd, *J* = 17.0, 10.1, 7.8, 7.0 Hz, 1H), 5.08 – 4.99 (m, 2H), 3.72 – 3.65 (m, 1H), 2.49 (dd, *J* = 14.2, 7.8 Hz, 1H), 2.40 – 2.30 (m, 3H), 2.00 (dtd, *J* = 12.8, 6.4, 2.0 Hz, 1H), 1.96 – 1.89 (m, 1H), 1.89 – 1.82 (m, 1H), 1.64 – 1.52 (m, 1H), 1.09 (s, 3H), 0.90 (s, 9H), 0.07 (s, 3H), 0.06 (s, 6H).



352a ***353a***

methyl (3*S*,4*S*)-3-allyl-4-((*tert*-butyldimethylsilyl)oxy)-3-methyl-2-oxocyclohexane-1-carboxylate (353a)

A round bottom flask was charged with NaH (60% in mineral oil, 170.4 mg, 4.26 mmol, 6 equiv) and THF(0.72 mL, 0.98 M), followed by ketone **352a** (200 mg, 0.71 mmol, 1 equiv) in THF (2.5 mL, 0.28 M), 15-crown-5 (0.58 mL, 2.9 mmol, 4.1 equiv), and dimethyl carbonate (0.58 mL, 6.9 mmol, 9.7 equiv). The mixture was then heated to reflux overnight. Upon complete consumption of the starting material (as determined by TLC), the reaction was quenched with a saturated solution of NH_4Cl and the product was extracted three times with EtOAc, dried over Na_2SO_4, filtered, and concentrated under reduced pressure. The crude **353a** was passed through a short plug of silica gel and used without further purification.

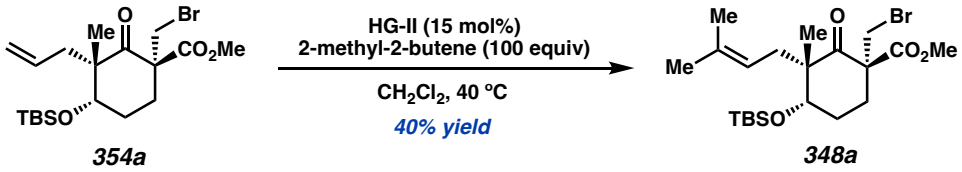


353a ***354a***

methyl (1*R*,3*S*,4*S*)-3-allyl-1-(bromomethyl)-4-((*tert*-butyldimethylsilyl)oxy)-3-methyl-2-oxocyclohexane-1-carboxylate (354a)

A flame dried vial was charged with starting material **353a** (100 mg, 0.3 mmol, 1 equiv) and MeCN (1.5 mL, 0.2 M), followed by addition of Cs_2CO_3 (195 mg, 0.6 mmol, 2 equiv) and CH_2Br_2 (0.025 mL, 0.36 mmol, 1.2 equiv). The vial was then sealed and heated to 80 ºC overnight. The reaction mixture was filtered, and the filtrate was concentrated under reduced pressure. The crude product was purified by flash silica gel column chromatography (SiO_2, 5–10% EtOAc/Hexanes) to afford bromide **354a** (30.7 mg, 0.071 mmol, 23% yield over two steps).

^{1}H NMR (500 MHz, $CDCl_3$): δ 5.77 (ddt, *J* = 17.4, 10.2, 7.4 Hz, 1H), 5.11 – 5.02 (m, 2H), 4.07 (d, *J* = 10.4 Hz, 1H), 3.88 (s, 1H), 3.72 (s, 3H), 3.39 (d, *J* = 10.4 Hz, 1H), 2.68 (d, *J* = 13.0 Hz, 1H), 2.51 (dd, *J* = 14.0, 7.6 Hz, 1H), 2.41 – 2.31 (m, 1H), 2.20 (dd, *J* = 14.0, 7.0 Hz, 1H), 1.87 (td, *J* = 13.5, 4.5 Hz, 1H), 1.76 (dt, *J* = 14.7, 3.6 Hz, 1H), 0.96 (s, 3H), 0.86 (s, 9H), 0.08 (s, 3H), 0.06 (s, 3H).



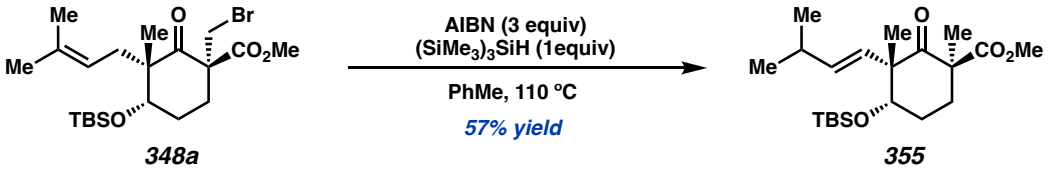
354a *348a*

methyl (1*R*,3*S*,4*S*)-1-(bromomethyl)-4-((*tert*-butyldimethylsilyl)oxy)-3-methyl-3-(3-methylbut-2-en-1-yl)-2-oxocyclohexane-1-carboxylate (348a)

A flame dried vial was charged with starting material **354a** (10 mg, 0.023 mmol, 1 equiv), HG-II catalyst (2.2 mg, 0.0035 mmol, 15 mol%), 2-methyl-2-butene (0.3 mL), and CH_2Cl_2 (0.3 mL, 0.077 M). The resulting mixture was stirred at 40 ºC overnight. The crude mixture was then filtered, and the filtrate was concentrated under reduced pressure. The crude

product was purified by preparatory TLC (SiO_2, 20% EtOAc/Hexanes) to afford bromide **348a** (4.2 mg, 0.0091 mmol, 40% yield).

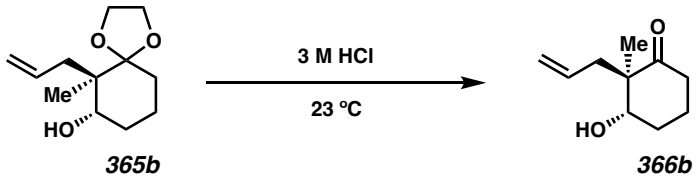
^{1}H NMR (500 MHz, $CDCl_3$): δ 5.08 (t, *J* = 7.5 Hz, 1H), 4.09 (d, *J* = 10.4 Hz, 1H), 3.95 (s, 1H), 3.73 (s, 3H), 3.39 (d, *J* = 10.4 Hz, 1H), 2.67 (d, *J* = 13.5 Hz, 1H), 2.45 (dd, *J* = 14.9, 8.4 Hz, 1H), 2.40 – 2.30 (m, 1H), 2.15 (dd, *J* = 14.5, 6.2 Hz, 1H), 1.87 (td, *J* = 13.5, 4.4 Hz, 1H), 1.78 – 1.73 (m, 1H), 1.72 (s, 3H), 1.60 (s, 3H), 0.93 (s, 3H), 0.86 (s, 9H), 0.08 (s, 3H), 0.06 (s, 3H).



methyl (1*S*,3*S*,4*S*)-4-((*tert*-butyldimethylsilyl)oxy)-1,3-dimethyl-3-((*E*)-3-methylbut-1-en-1-yl)-2-oxocyclohexane-1-carboxylate (355)

A flame dried vial was charged with starting material **348a** (10 mg, 0.02 mmol, 1 equiv), AIBN (2.2 mg, 0.058 mmol, 2.9 equiv), and toluene (0.8 mL, 0.025 M). $(SiMe_3)_3SiH$ (0.0074 mL, 0.024 mmol, 1.2 equiv) was then added to the mixture, and the vial was sealed and heated to reflux overnight. The crude mixture was then filtered, and the filtrate was concentrated under reduced pressure. The crude product was purified by preparatory TLC (SiO_2, 10% EtOAc/Hexanes) to afford product **355** (4.4 mg, 0.0115 mmol, 57% yield).

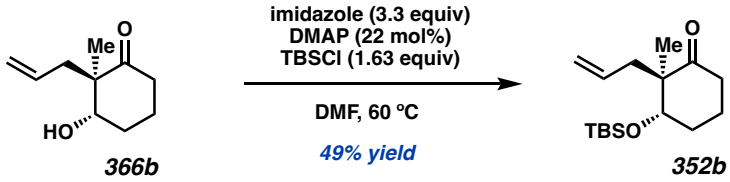
^{1}H NMR (400 MHz, $CDCl_3$): δ 6.02 (d, *J* = 16.5 Hz, 1H), 5.49 (d, *J* = 16.4 Hz, 1H), 3.82 – 3.74 (m, 1H), 3.69 (s, 1H), 2.36 (dt, *J* = 13.7, 5.3 Hz, 1H), 2.15 (ddt, *J* = 14.1, 10.6, 4.2 Hz, 1H), 1.92 – 1.67 (m, 2H), 1.32 (d, *J* = 0.9 Hz, 3H), 1.28 (d, *J* = 3.5 Hz, 3H), 1.20 (s, 3H), 1.16 (d, *J* = 6.1 Hz, 3H), 0.88 (s, 9H), 0.06 (s, 3H), 0.02 (s, 3H).



365b ***366b***

(2*R*,3*S*)-2-allyl-3-hydroxy-2-methylcyclohexan-1-one (366b)

A round bottom flask was charged with alcohol **365b** (182.2 mg, 0.9 mmol, 1 equiv) and HCl (3.0 M solution in water, 5.4 mL), and the mixture was stirred at room temperature until full conversion. The reaction was quenched with a saturated solution of $NaHCO_3$ and extracted three times with EtOAc, dried over Na_2SO_4, filtered, and concentrated under reduced pressure. The crude product was used without further purification.

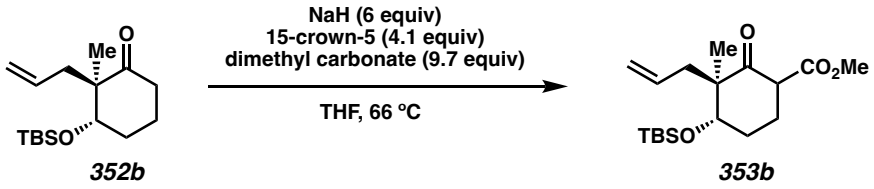


366b ***352b***

(2*R*,3*S*)-2-allyl-3-((*tert*-butyldimethylsilyl)oxy)-2-methylcyclohexan-1-one (352b)

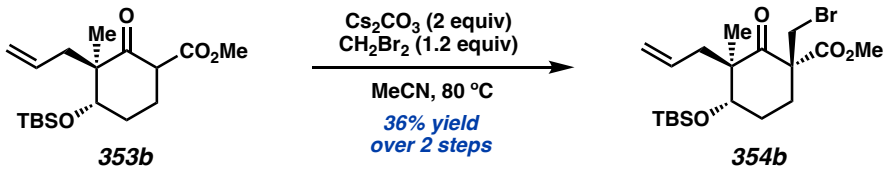
A round bottom flask was charged with alcohol **366b** (0.9 mmol, 1 equiv), imidazole (202.2 mg, 2.97 mmol, 3.3 equiv), DMAP (119.7 mg, 0.2 mmol, 0.22 equiv), TBSCl (221.6 mg, 1.47 mmol, 1.63 equiv), and DMF (1 mL, 0.9 M). The mixture was stirred at 60 ºC overnight. Upon complete consumption of the starting material (as determined by TLC), the reaction was diluted with Et_2O and quenched with a saturated solution of NH_4Cl. The product was extracted three times with Et_2O, washed with brine, dried over Na_2SO_4, filtered, and concentrated under reduced pressure. The crude product was purified by flash silica gel column chromatography (SiO_2, 5–10% EtOAc/Hexanes) to afford **352b** as a colorless oil (125.2 mg, 0.44 mmol, 49% yield).

^{1}H NMR (400 MHz, $CDCl_3$): δ 5.74 – 5.59 (m, 1H), 5.10 – 4.98 (m, 2H), 3.85 (ddd, *J* = 5.4, 2.2, 1.1 Hz, 1H), 2.47 – 2.23 (m, 4H), 2.12 – 1.97 (m, 2H), 1.80 – 1.63 (m, 2H), 1.06 (s, 3H), 0.87 (s, 9H), 0.04 (s, 3H), 0.04 (s, 3H).



methyl (3*R*,4*S*)-3-allyl-4-((*tert*-butyldimethylsilyl)oxy)-3-methyl-2-oxocyclohexane-1-carboxylate (353b)

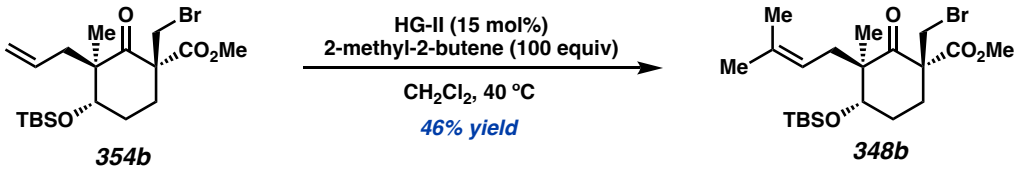
A round bottom flask was charged with NaH (60% in mineral oil, 105.6 mg, 2.64 mmol, 6 equiv) and THF(0.45 mL, 0.98 M), followed by ketone **352b** (125.2 mg, 0.44 mmol, 1 equiv) in THF (1.56 mL, 0.28 M), 15-crown-5 (0.36 mL, 1.8 mmol, 4.1 equiv), and dimethyl carbonate (0.36 mL, 4.27 mmol, 9.7 equiv). The mixture was then heated to reflux overnight. Upon complete consumption of the starting material (as determined by TLC), the reaction was quenched with a saturated solution of NH_4Cl and the product was extracted three times with EtOAc, dried over Na_2SO_4, filtered, and concentrated under reduced pressure. The crude **353b** was passed through a short plug of silica gel and used without further purification.



methyl (1*S*,3*R*,4*S*)-3-allyl-1-(bromomethyl)-4-((*tert*-butyldimethylsilyl)oxy)-3-methyl-2-oxocyclohexane-1-carboxylate (354b)

A flame dried vial was charged with starting material **353b** (0.44 mmol, 1 equiv) and MeCN (2.2 mL, 0.2 M), followed by addition of Cs_2CO_3 (286 mg, 0.88 mmol, 2 equiv) and CH_2Br_2 (0.04 mL, 0.53 mmol, 1.2 equiv). The vial was then sealed and heated to 80 ºC overnight. The reaction mixture was filtered, and the filtrate was concentrated under reduced pressure. The crude product was purified by flash silica gel column chromatography (SiO_2, 5–10% EtOAc/Hexanes) to afford bromide **354b** (67.8 mg, 0.156 mmol, 36% yield over two steps).

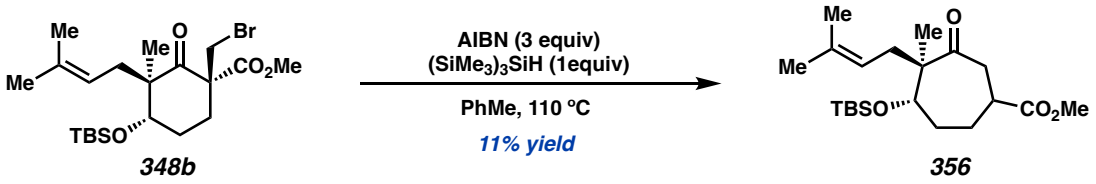
^{1}H NMR (400 MHz, $CDCl_3$): δ 5.49 (dddd, *J* = 16.7, 10.1, 8.6, 5.5 Hz, 1H), 5.14 – 4.97 (m, 2H), 4.17 – 4.07 (m, 1H), 3.87 (dd, *J* = 3.9, 1.8 Hz, 1H), 3.71 (s, 3H), 3.40 (dd, *J* = 14.4, 10.3 Hz, 1H), 2.72 – 2.61 (m, 1H), 2.48 – 2.33 (m, 1H), 2.28 – 2.15 (m, 1H), 2.13 – 2.06 (m, 1H), 1.96 (td, *J* = 13.5, 4.5 Hz, 1H), 1.72 (dtd, *J* = 14.6, 4.3, 2.8 Hz, 1H), 1.05 (s, 3H), 0.85 (s, 9H), 0.05 (s, 3H), 0.02 (s, 3H).



methyl (1*S*,3*R*,4*S*)-1-(bromomethyl)-4-((*tert*-butyldimethylsilyl)oxy)-3-methyl-3-(3-methylbut-2-en-1-yl)-2-oxocyclohexane-1-carboxylate (348b)

A flame dried vial was charged with starting material **354b** (67.8 mg, 0.156 mmol, 1 equiv), HG-II catalyst (14.7 mg, 0.023 mmol, 15 mol%), 2-methyl-2-butene (1.7 mL) and CH_2Cl_2 (1.7 mL, 0.077 M). The resulting mixture was stirred at 40 ºC overnight. The crude mixture was then filtered, and the filtrate was concentrated under reduced pressure. The crude product was purified by preparatory TLC (SiO_2, 10% EtOAc/Hexanes) to afford bromide **348b** (33.4 mg, 0.072 mmol, 46% yield).

^{1}H NMR (500 MHz, $CDCl_3$): δ 4.81 (s, 1H), 3.88 (d, *J* = 3.5 Hz, 1H), 3.74 – 3.70 (m, 1H), 3.67 (s, 3H), 3.37 (d, *J* = 10.3 Hz, 1H), 2.66 (d, *J* = 13.8 Hz, 1H), 2.47 – 2.35 (m, 1H), 2.18 – 2.07 (m, 2H), 1.93 (td, *J* = 13.5, 4.6 Hz, 1H), 1.73 (d, *J* = 3.6 Hz, 1H), 1.69 (s, 3H), 1.56 (s, 3H), 1.03 (s, 3H), 0.86 (s, 9H), 0.05 (d, *J* = 1.7 Hz, 3H), 0.03 (d, *J* = 2.3 Hz, 3H).

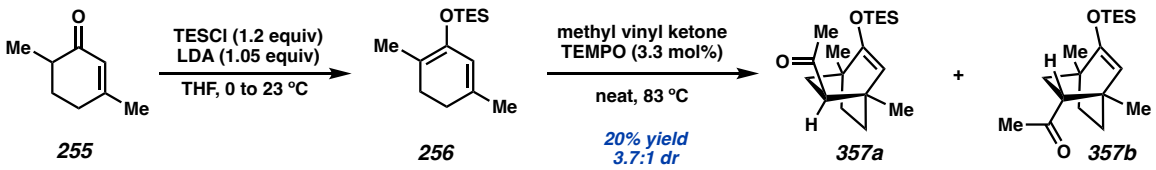


methyl (4*R*,5*S*)-5-((*tert*-butyldimethylsilyl)oxy)-4-methyl-4-(3-methylbut-2-en-1-yl)-3-oxocycloheptane-1-carboxylate (356)

A flame dried vial was charged with starting material **348b** (5 mg, 0.011 mmol, 1 equiv) in toluene (0.09 mL, 0.125 M), AIBN (5.4 mg, 0.033 mmol, 3 equiv), and $(SiMe_3)_3SiH$ (0.004 mL, 0.013 mmol, 1.2 equiv). The vial was sealed and heated to reflux overnight. The crude mixture was then filtered, and the filtrate was concentrated under reduced pressure. The crude product was purified by preparatory TLC (SiO_2, 10% EtOAc/Hexanes) to afford product **356** (0.4 mg, 0.0012 mmol, 11% yield).

^{1}H NMR (500 MHz, $CDCl_3$): δ 4.90 (s, 1H), 3.87 (s, 1H), 3.62 (s, 3H), 2.38 (d, *J* = 14.6 Hz, 2H), 2.27 (t, *J* = 13.9 Hz, 1H), 2.13 (dd, *J* = 15.1, 8.3 Hz, 1H), 2.01 (d, *J* = 15.3 Hz, 1H), 1.93 (td, *J* = 13.2, 4.1 Hz, 1H), 1.69 (s, 3H), 1.68 – 1.59 (m, 2H), 1.26 (s, 3H), 1.03 (s, 3H), 0.89 (d, *J* = 4.6 Hz, 1H), 0.86 (s, 9H), 0.04 (s, 3H), 0.03 (s, 3H).

Third Generation Synthesis Route: Diels–Alder Cycloaddition Studies



1-((1*S*,2*S*,4*S*)-1,4-dimethyl-5-((triethylsilyl)oxy)bicyclo[2.2.2]oct-5-en-2-yl)ethan-1-one (357)

A flame dried round bottom flask was charged with *i*-Pr_2NH (0.52 mL, 3.71 mmol, 1.1 equiv) and THF (2.26 mL, 1.6 M). The solution was cooled to 0 ºC and *n*-BuLi (1.36 mL, 3.4 mmol, 1.05 equiv) was added dropwise. The resultant solution was stirred for 30 min at 0 ºC. Enone **255** (400 mg, 3.22 mmol, 1.0 equiv) in THF (3.22 mL, 1 M) was added dropwise and stirring was continued at 0 ºC for 30 minutes. The solution was cooled to –78 ºC, and TESCl (3.81 mL, 10.3 mmol, 1.2 equiv) was added dropwise. Upon complete consumption of starting material (as determined by TLC), the reaction was diluted with a saturated solution of NH_4Cl and the product was extracted three times with EtOAc. The combined organic layers were washed with brine, dried over Na_2SO_4, filtered, and concentrated under reduced pressure. The crude silyl oxy diene **256** was used without further purification.

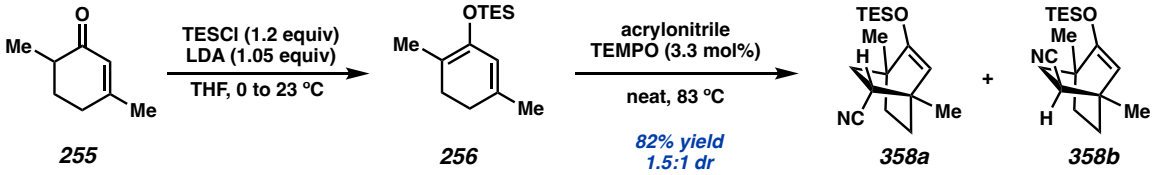
A flame dried vial was charged with crude diene **256** (23.8 mg, 0.1 mmol, 1 equiv), TEMPO (0.5 mg, 0.0011 mmol, 1.1 mol%) and methyl vinyl ketone (0.025 mL, 0.3 mmol, 3 equiv) at 23 ºC and the resulting mixture was stirred at 83 ºC overnight. Upon complete consumption of starting material (as determined by TLC), the crude product was directly purified by flash silica gel column chromatography (SiO_2, 10% EtOAc/Hexanes) to afford the corresponding bicycle **357a** (4.8 mg, 0.0156 mmol, 16% yield) and **357b** (1.3 mg, 0.0042 mmol, 4% yield).

Major diastereomer 357a:

^{1}H NMR (500 MHz, $CDCl_3$): δ 4.71 (s, 1H), 2.53 (dd, *J* = 9.8, 6.3 Hz, 1H), 2.17 – 2.09 (m, 1H), 1.90 – 1.73 (m, 2H), 1.68 – 1.62 (m, 1H), 1.44 – 1.37 (m, 1H), 1.20 – 1.14 (m, 1H), 1.11 (s, 3H), 1.10 (s, 3H), 0.99 (t, *J* = 7.8 Hz, 9H), 0.71 (q, *J* = 7.9 Hz, 6H).

Minor diastereomer 357b:

^{1}H NMR (500 MHz, $CDCl_3$): δ 4.82 (s, 1H), 2.60 (t, *J* = 8.5 Hz, 1H), 2.17 (s, 3H), 1.83 (ddd, *J* = 13.0, 9.6, 3.9 Hz, 1H), 1.53 – 1.47 (m, 2H), 1.40 – 1.28 (m, 2H), 1.15 (s, 3H), 1.13 – 1.07 (m, 1H), 1.06 (s, 3H), 0.99 (t, *J* = 7.9 Hz, 9H), 0.69 (q, *J* = 7.9 Hz, 6H).



255 ***256*** ***358a*** ***358b***

(1*R*,2*R*,4*S*)-1,4-dimethyl-5-((triethylsilyl)oxy)bicyclo[2.2.2]oct-5-ene-2-carbonitrile (358)

A flame dried round bottom flask was charged with *i*-Pr_2NH (1.3 mL, 9.28 mmol, 1.1 equiv) and THF (5.7 mL, 1.6 M). The solution was cooled to 0 ºC and *n*-BuLi (3.4 mL, 8.5 mmol, 1.05 equiv) was added dropwise. The resultant solution was stirred for 30 min at 0 ºC. Enone **255** (1.05 g, 8.45 mmol, 1.0 equiv) in THF (8.1 mL, 1 M) was added dropwise and stirring was continued at 0 ºC for 30 minutes. The solution was cooled to –78 ºC, and TESCl (1.6 mL, 10.5 mmol, 1.25 equiv) was added dropwise. Upon complete consumption of starting material (as determined by TLC), the reaction was diluted with a saturated solution of NH_4Cl and the product was extracted three times with EtOAc. The combined organic layers were washed with brine, dried over Na_2SO_4, filtered, and concentrated under reduced pressure. The crude silyl oxy diene **256** was used without further purification.

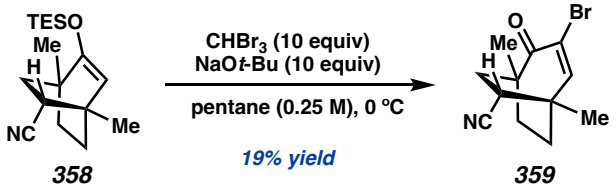
A flame dried vial was charged with crude diene **256** (714 mg, 3 mmol, 1 equiv), TEMPO (15 mg, 0.1 mmol, 3.3 mol%) and acrylonitrile (0.6 mL, 9 mmol, 3 equiv) at 23 ºC and the resulting mixture was stirred at 83 ºC overnight. Upon complete consumption of starting material (as determined by TLC), the crude product was directly purified by flash silica gel column chromatography (SiO_2, 10% EtOAc/Hexanes) to afford the corresponding bicycle **358a** as a pale yellow oil (165.1 mg, 0.57 mmol, 19% yield), **358b** as a pale yellow oil (52.9 mg, 0.18 mmol, 6% yield), and a mixture of **358a** and **358b** as a pale yellow oil (498.6 mg, 1.7 mmol, 57% yield). Ratio of diastereomers was determined based on crude ^{1}H NMR spectroscopy.

Major diastereomer 358a:

^{1}H NMR (500 MHz, $CDCl_3$): δ 4.74 (s, 1H), 2.31 (ddd, *J* = 11.7, 5.1, 2.6 Hz, 1H), 1.90 (ddd, *J* = 13.6, 9.8, 4.5 Hz, 1H), 1.80 (ddd, *J* = 13.0, 11.7, 3.5 Hz, 1H), 1.67 (dd, *J* = 13.0, 5.1 Hz, 1H), 1.58 – 1.51 (m, 1H), 1.40 (tt, *J* = 12.5, 4.0 Hz, 1H), 1.29 (s, 3H), 1.20 (tdd, *J* = 12.6, 4.5, 2.8 Hz, 1H), 1.08 (s, 3H), 0.98 (t, *J* = 7.9 Hz, 9H), 0.68 (q, *J* = 7.9 Hz, 6H).

Minor diastereomer 358b:

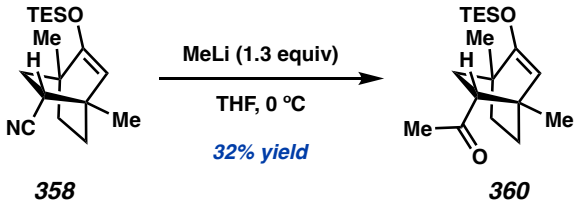
^{1}H NMR (500 MHz, $CDCl_3$): δ 4.80 (s, 1H), 2.50 (dd, *J* = 9.9, 4.5 Hz, 1H), 1.89 – 1.76 (m, 1H), 1.59 (ddd, *J* = 12.8, 4.4, 2.0 Hz, 1H), 1.41 – 1.36 (m, 2H), 1.34 (s, 3H), 1.33 – 1.28 (m, 2H), 1.10 (s, 3H), 1.00 (t, *J* = 7.9 Hz, 9H), 0.73 (q, *J* = 7.7 Hz, 6H).



(1*S*,5*R*)-3-bromo-1,5-dimethyl-2-oxobicyclo[3.2.2]non-3-ene-6-carbonitrile (359)

A flame dried round bottom flask was charged with silyl enol ether **358** (18.8 mg, 0.065 mmol, 1 equiv) and pentane (0.25 mL, 0.25 M). The resulting solution was cooled to 0 ºC and NaO*t*-Bu (62.4 mg, 0.65 mmol, 10 equiv) was added. Then $CHBr_3$ (0.057 mL, 0.65 mmol, 10 equiv) was added fast dropwise, rate of addition was monitored to ensure bubbling of the reaction mixture was kept to a minimum. Upon complete consumption of starting material (as determined by TLC), the reaction was *slowly* diluted with brine and the product was extracted three times with Et_2O. The combined organic layers were dried over Na_2SO_4, filtered, and concentrated under reduced pressure. The crude product was purified by preparatory TLC (SiO_2, 20% EtOAc/Hexanes) to afford α-bromo enone **359** as a white solid (3.3 mg, 0.012 mmol, 19% yield). The stereochemistry of this compound was confirmed through X-ray crystallography.

^{1}H NMR (500 MHz, $CDCl_3$): δ 7.31 (s, 1H), 2.78 (dd, *J* = 9.5, 7.6 Hz, 1H), 2.12 (dd, *J* = 14.9, 9.5 Hz, 1H), 1.94 (ddd, *J* = 14.9, 7.7, 1.9 Hz, 1H), 1.89 – 1.76 (m, 1H), 1.75 – 1.65 (m, 3H), 1.51 (s, 3H), 1.27 (s, 3H).



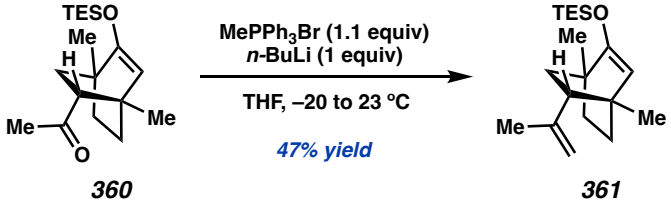
358 *360*

1-((1*S*,2*R*,4*S*)-1,4-dimethyl-5-((triethylsilyl)oxy)bicyclo[2.2.2]oct-5-en-2-yl)ethan-1-one (360)

A flame dried vial was charged with starting material **358** (165.1 mg, 0.57 mmol, 1 equiv) and THF (1.3 mL, 0.4 M). The resulting solution was cooled to 0 ºC, MeLi solution (1.6 M in Et_2O, 0.45 mL, 0.72 mmol, 1.3 equiv) was added, and the reaction was left to stir at

0 ºC for an additional hour. Upon complete consumption of starting material (as determined by TLC), the reaction was quenched with a saturated solution of NH_4Cl and the product was extracted three times with EtOAc. The combined organic layers were washed with brine, dried over Na_2SO_4, filtered, and concentrated under reduced pressure. The crude product was purified by flash silica gel column chromatography (SiO_2, 10% EtOAc/Hexanes) to afford ketone **360** (56 mg, 0.18 mmol, 32% yield).

^{1}H NMR (500 MHz, $CDCl_3$): δ 4.80 (s, 1H), 2.50 (dd, *J* = 9.9, 4.5 Hz, 1H), 1.89 – 1.76 (m, 1H), 1.59 (ddd, *J* = 12.8, 4.4, 2.0 Hz, 1H), 1.41 – 1.36 (m, 2H), 1.34 (s, 3H), 1.33 – 1.28 (m, 2H), 1.10 (s, 3H), 1.00 (t, *J* = 7.9 Hz, 9H), 0.73 (q, *J* = 7.7 Hz, 6H).

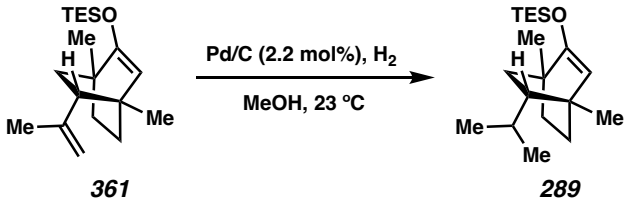


360 *361*

(((1*S*,4*R*,5*S*)-1,4-dimethyl-5-(prop-1-en-2-yl)bicyclo[2.2.2]oct-2-en-2-yl)oxy)triethylsilane (361)

A flame dried vial was charged with $MePPh_3Br$ (72 mg, 0.2 mmol, 1.1 equiv) and THF (1.8 mL, 0.11 M), and the solution was cooled to –20 ºC. *n*-BuLi (2.5 M in hexanes, 0.08 mL, 0.2 mmol, 1.1 equiv) was added subsequently, and the solution was left to stir at –20 ºC for 5 min. To a separate flame dried vial was charged ketone **360** (56 mg, 0.18 mmol, 1 equiv) and THF (0.56 mL, 0.33 M), and the solution was cooled to –20 ºC. Then, the Wittig reagent was added dropwise to the solution of **360** dropwise at –20 ºC, and the reaction was warmed to room temperature overnight. Upon complete consumption of starting material (as determined by TLC), the reaction was quenched with a dilute solution of citric

acid and the product was extracted three times with Et_2O. The combined organic layers were dried over Na_2SO_4, filtered, and concentrated under reduced pressure. The crude product was purified by flash silica gel column chromatography (SiO_2, 5% EtOAc/Hexanes), but the product was still obtained as a mixture with a slight amount of impurities. The collected **361** was used in the subsequent steps without further purification.



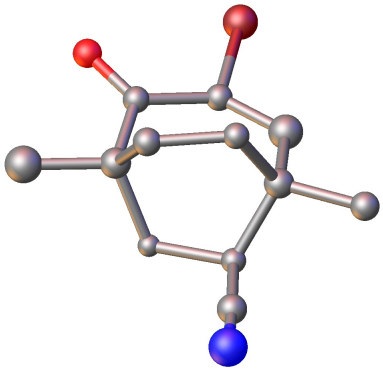
361 ***289***

(1*S*,4*S*,5*S*)-5-isopropyl-1,4-dimethylbicyclo[2.2.2]octan-2-one (289)

A flame dried vial was charged with starting material **361** (26.2 mg, 0.085 mmol, 1 equiv) and Pd/C (10 wt%, 2 mg, 0.0019 mmol, 2.2 mol%), and the vial was evacuated and backfilled with H_2. MeOH (1.2 mL, 0.07 M) was then added to the vial, and the reaction was stirred under an atmosphere of H_2 at room temperature for 1 h. Upon complete consumption of starting material (as determined by TLC), the reaction was purged with N_2 for 15 min, and the crude mixture was filtered through a short pad of celite. The filtrate was concentrated under reduced pressure, and the crude product was purified by flash silica gel column chromatography (SiO_2, 5% EtOAc/Hexanes). The collected product matches the spectrum of previously synthesized **289**.

A5.6 PRELIMINARY X-RAY CRYSTALLOGRAPHY ANALYSIS OF 359

Figure A5.10. *Preliminary picture of the structure of* ***359*** *(racemic) determined by X-ray crystallography.*



A5.7 REFERENCES

(1) Langhanki, J.; Rudolph, K.; Erkel, G.; Opatz, T. Total Synthesis and Biological Evaluation of the Natural Product (−)-Cyclonerodiol, a New Inhibitor of IL-4 Signaling. *Org. Biomol. Chem.* **2014**, *12*, 9707–9715.

(2) Lee, T. L.; Roden, F. S.; Yeoh, H. T.-L. Selectivity of Bifunctional Annulating Reagents; Additional Rules for Ring Closure. *Tetrahedron Lett.* **1990**, *31*, 2063–2066

(3) Kim, M.; Park, B.; Shin, M.; Kim, S.; Kim, J.; Baik, M.-H.; Cho, S. H. Copper-Catalyzed Enantiotopic-Group-Selective Allylation of Gem-Diborylalkanes. *J. Am. Chem. Soc.* **2021**, *143*, 1069–1077.

(4) Kim, K. E.; Stoltz, B. M. A Second-Generation Synthesis of the Cyanthiwigin Natural Product Core. *Org. Lett.* **2016**, *18*, 5720–5723.

(5) Satoh, M.; Koshino, H.; Nakata, T. Synthetic Studies on Maitotoxin. 3. Stereoselective Synthesis of the BCDE-Ring System. *Org. Lett.* **2008**, *10*, 1683–1685.

(6) Pangborn, A. M.; Giardello, M. A.; Grubbs, R. H.; Rosen, R. K.; Timmers, F. J. Safe and Convenient Procedure for Solvent Purification. *Organometallics* **1996**, *15*, 1518–1520.

APPENDIX 6

Notebook Cross-Reference for New Compounds.

Table A6.1 *Notebook cross-reference for Chapter 1.*

Compound	Notebook Ref.
10a	AQC3-189
10b	AQC5-245
10c	KNF-2-145
10d	AQC4-33
10e	CS-I-153
10f	AQC4-274
10g	AQC3-213
10h	KNF-2-219
10i	RC-I-99
10j	AQC4-109
10k	AQC3-263
10l	AQC3-277
10m	RC-I-75
10n	KNF-3-033
10o	KNF-2-207
10p	AQC4-55
10q	AQC3-281
10r	AQC4-67
10s	KNF-1-287
10t	KNF-2-157
10u	ED-2-043
11a	AQC3-291
11b	AQC5-251
11c	KNF-2-151
11d	AQC4-35_p1
11f	AQC4-19_p1
11j	AQC4-117
11k	AQC3-265B_p4
11k'	AQC3-265B_p3
11k"	AQC3-265B_p1
11l	AQC3-287
11m	RC-I-181A
11m'	RC-I-181A
11n	KNF-3-043-B
11o	KNF-2-221A
11p	AQC4-61

Compound	Notebook Ref.
11o'	KNF-2-221B
11p'	AQC4-181_p2
11q	AQC3-275_p2
11r	AQC4-69_p1
11s	KNF-1-295
11t	KNF-2-161_A
11t'	KNF-2-161_B
11u	KNF-2-229_C
12	KNF-1-289
14	KNF-1-293
17	AQC3-137
19a	AQC3-229
19d	AQC4-35-p2
19e	CS-I-163
19f	AQC4-19_p2
19g	AQC4-21
19h	KNF-3-031
19i	RC-I-119A
19m	RC-1-181A
19r	AQC4-69-p2
19t	KNF-2-161-C
19u	KNF-2-229-D
29	AQC4-75
33	CS-I-225
34	CS-I-223
35	CS-I-183
36	CS-I-271
37	CS-I-257
38	RC-I-111
39	RC-I-129
40	CS-I-51
45	RC-II-35
46	RC-II-39
47	RC-II-41
48	KNF-3-177
49	RC-I-301

50	RC-II-67
51	RC-II-65
52	RC-II-77
53	CS-I-229
54	CS-I-279
55	AQC3-187
56	AQC3-201
57	AQC3-203
58	KNF-3-029
59	KNF-1-283
60	KNF-2-155
61	KNF-2-277
62	KNF-1-275-B
63	AQC3-129
64	CS-I-217
65	CS-I-215
66	CS-I-179
67	CS-I-267
68	CS-I-249
69	AQC4-159
70	AQC3-183
71	KNF-2-121
72	KNF-2-123
73	AQC3-117
74	KNF-2-155
75	KNF-1-279
76	KNF-2-147
77	ED-2-035
78	CS-I-207
79	CS-I-203
80	CS-I-175
81	CS-I-253
82	CS-I-237
83	KNF-2-283
84	RC-I-113
D-10f	AQC4-143
D-11f	AQC4-153_p1
D-19f	AQC4-153_p2

D-56	AQC4-139
D-70	AQC4-133

Table A6.2 *Notebook cross-reference for Chapter 3.*

Compound	Notebook Ref.
126a	CS-IV-23
126b	CS-IV-99
126c	SAN-I-17
126d	CS-IV-239
126e	CS-IV-109
126f	CS-V-67
126g	CS-IV-91
126h	SAN-I-27
126i	CS-IV-295
126j	CS-V-49
126k	CS-IV-53
127a	CS-IV-45
127b	CS-IV-105-A
127c	SAN-I-21
127d	CS-IV-243-A
127e	CS-IV-115-A
127f	CS-V-79-A
127g	CS-IV-97-A
127h (d1)	CS-IV-85A-F.20-24
127h (d2)	CS-IV-85-A-F.10-11
127i (d1)	CS-IV-301-F.24-30
127i (d2)	CS-V-15-C-PTLC
127j	CS-V-53
127k	CS-IV-85-C
128	CS-IV-297
129	CS-IV-57-F.32
130a	CS-IV-195
130b	CS-IV-223
131a	CS-IV-203-A-PTLC-a
131b	CS-IV-233-A-PLC-a
132	CS-V-27
133	CS-V-33
134	CS-V-47
135	CS-V-51
136	CS-V-21
137	CS-V-81

Compound	Notebook Ref.
138	CS-V-41
145a	CS-IV-293
145b	CS-IV-139
145c	CS-IV-241
145d	CS-IV-127
146a	CS-IV-299-F.34
146b	CS-IV-143-A
146c	CS-IV-245-A
146d	CS-IV-143-D
147a	CS-IV-19
147b	SAN-I-15
147c	SAN-I-33
147d	CS-IV-83
147e	SAN-I-25
147f	CS-V-45
147g	CS-IV-49
147h	CS-IV-135
147i	CS-IV-189
147j	CS-IV-211
148	CS-IV-285

Table A6.3 *Notebook cross-reference for Chapter 4.*

Compound	Notebook Ref.
163	SRS-II-294
169	AQC5-265
170	VH-III-170
171	VH-II-197
172	AQC5-271
173	VH-III-68
174	AQC5-143
175	AQC5-201
176	AQC5-181
177	AQC5-253
178	AQC5-145
179	AQC5-147
180	AQC6-147
181	AQC6-151
182	AQC6-151
183	AQC5-267
184	AQC5-171
185	AQC5-257_p1
186	AQC5-269
187	AQC6-145_p1
189	SRS-III-207
190	SRS-III-215
191	AQC-6-93
192	AQC-6-77
202	VH-III-78
202a	VH-III-74
202b	VH-III-76
203	AQC5-65
204	SRS-III-128
204a	SRS-III-16
205	VH-III-60
205a	VH-III-59
206	AQC5-47
206a	AQC5-37
207	AQC5-193
208	AQC5-173

Compound	Notebook Ref.
209	AQC5-235
210	AQC5-117
210a	AQC5-111
211	AQC5-115
211a	AQC5-109
212	AQC6-87
212a	AQC6-83
213	AQC6-123
213a	SRS-III-30
214	SRS-III-31
214a	AQC6-113
215	AQC5-41
216	AQC5-67
217	AQC5-153
218	AQC5-103
219	AQC5-125
222	VH-III-71
223	VH-II-231
224	VH-II-254
225	VH-II-267
226	VH-II-229
L4	VH-II-264
L5	VH-II-195
L6	VH-II-281
L7	VH-II-291

Table A6.4 *Notebook cross-reference for Chapter 5.*

Compound	Notebook Ref.
255	KNF-3-233
258	KNF-4-187
259	KNF-4-119
266	KNF-8-033
267	KNF-8-035
268	KNF-8-051
269	KNF-8-057
270	KNF-8-059
272	KNF-8-061
273	MMP-I-67
274	MMP-I-143
275	MMP-I-179
276	MMP-I-181
277	MMP-I-163
278	KNF-8-063
279	KNF-8-065
280	KNF-7-231
281	KNF-7-253B1
283	KNF-8-073
285-d1	KNF-8-089-d1
285-d2	KNF-8-089-d2
285-d3	KNF-8-089-d3
287	RC-V-225
288	RC-V-189
290	RC-V-253
291	RC-VI-23
292	KNF-7-253-pTLC-B1
294	RC-V-173A_pTLCB
295	KNF-8-027B
296	KNF-0-027A
298	KNF-8-017
299	KNF-8-023
301	JA-I-153
302	JA-I-181
305	RC-VI-241
314	KNF-8-067
315	KNF-8-069

Table A6.5 *Notebook cross-reference for Appendix 5.*

Compound	Notebook Ref.
327	RC-II-127
329	RC-II-109
330	RC-II-133
331	RC-II-181
334	RC-III-47
335	RC-III-55
336	RC-III-89
341	RC-III-111
342	RC-III-117
343	RC-III-131
345	RC-III-141
348a	RC-III-217
348b	RC-III-279
352b	RC-III-257
353a	RC-III-161
353b	RC-III-263
354a	RC-III-199
354b	RC-III-271
355	RC-III-235
356	RC-III-291
357a	RC-V-73_pTLCC
357b	RC-V-73_pTLCB
358a	RC-V-273_f7
358b	RC-V-273_f2-14
359	RC-V-105
360	RC-III-275
361	RC-III-277

ABOUT THE AUTHOR

Born in Taichung, Taiwan, Ruby Pengjui Chen spent her early childhood there before relocating to Taipei, Taiwan, to complete her middle and high school education. A growing fascination with chemical reactions during middle school led to her first research endeavor in high school, investigating nanomaterials for direct methanol fuel cells in the laboratory of Professor Huan-Tsung Chang at National Taiwan University. This foundational experience inspired her to pursue a career in chemistry.

In the fall of 2017, Ruby attended University of Illinois at Urbana–Champaign as a chemistry major. As a freshman, she joined Professor Martin Burke's laboratory, working closely with Professor Daniel Blair and Dr. Andrew Blake. Her undergraduate research contributed to the development of building blocks for the efficient modular synthesis of complex targets and the synthesis of natural product derivatives designed to restore the function of transmembrane iron transporters.

Ruby subsequently pursued her graduate studies at the California Institute of Technology under the supervision of Professor Brian Stoltz. Her doctoral work encompassed the development of asymmetric transformations via chiral palladium enolate intermediates, computational mechanistic investigations, and the total synthesis of complex natural products. Following the completion of her PhD, Ruby will join Amgen in South San Francisco to begin her career as a medicinal chemist.